



INDIAN AGRICULTURAL
RESEARCH INSTITUTE, NEW DELHI.

L A R I S.

MGIPC—S1—6 AR/54—7-7-54—10,000

THE JOURNAL OF PHYSICAL & COLLOID CHEMISTRY

(Founded by Wilder D. Bancroft)

Editor

S. C. LIND

Editor for Colloid Chemistry

HARRY B. WEISER

Associate Editors

E. J. BOWEN

C. N. HINSHELWOOD

D. R. BRIGGS

C. E. MARSHALL

B. L. CRAWFORD, Jr.

J. R. PARTINGTON

J. W. WILLIAMS

Assistant Editor

LOUISE KELLEY

Volume 51

(BALTIMORE)

1947

CONTENTS

NUMBER 1, JANUARY, 1947

The Cellulose Molecule. Physical-chemical Studies. The Svedberg.....	1
Molecular-weight Determination by Light Scattering. P. Debye.....	18
The Association of Polymer Molecules in Dilute Solution. Paul Doty, Herman Wagner, and Seymour Singer.....	32
Viscosity-Molecular Weight Relationship for Cellulose Acetate. W. J. Badgley and H. Mark.....	58
Elasticity Measurements on Polychloroprenes. Per-Olof Kinell.....	70
A Statistical Theory of Discoloration for Halogen-containing Polymers and Copolymers. R. F. Boyer.....	80
Ultracentrifugal and Viscometric Studies of Amylose Acetate. Further Evidence for the Helical Structure of Amylose. Bernard A. Dombrow and Charles O. Beckmann.....	107
Effect of Molecular Association and Charge Distribution on the Gelation of Pectin. R. Speiser, M. J. Copley, and G. C. Nutting.....	117
Molecular Properties of Hemicellulose Fractions. Merrill A. Millett and Alfred J. Stamm.....	134
Sedimentation Constants of Purified Preparations of Strains of Influenza Virus. W.M. Stanley and M. A. Lauffer.....	148
On a Low-density Lipoprotein Appearing in Normal Human Plasma. Kai O. Pedersen.....	156
Ultracentrifugal and Electrophoretic Studies on Fetuin. Kai O. Pedersen.....	164
The Quantitative Interpretation of the Electrophoretic Patterns of Proteins. L. G. Longworth.....	171
Physical-chemical Characteristics of Certain of the Proteins of Normal Human Plasma. J. L. Oncley, G. Scatchard, and A. Brown.....	184
Multiple Protein Interactions as Exhibited by the Blood-clotting Mechanism. Walter H. Seegers.....	198
Hemocyanins of the Gastropods. Sven Brohult.....	206
Physicochemical Characterization of Pituitary Growth Hormone. Choh Hao Li.....	218
Mandelate as a Stabilizer of Serum Albumin. J. Murray Luck.....	229
Diffusion in Wood. H. K. Burr and Alfred J. Stamm.....	240
Micelle Structure in Aqueous Solutions of Colloidal Electrolytes. R. J. Vetter.....	262
The Morphology of Lyogels. Ernst A. Hauser and D. S. le Beau.....	278
Solubilization of Water-insoluble Dye by Pure Soaps and Detergents of Different Types. Sister Agnes Ann Green and James W. McBain.....	286
The Electrochemistry of Permselective Collodion Membranes. II. Experimental Studies on the Concentration Potential across Various Types of Permselective Collodion Membranes with Solutions of Several Electrolytes. Karl Sollner and Harry P. Gregor.....	299
The Colloid Chemistry of the Clay Mineral Attapulgit. C. E. Marshall and O. G. Caldwell.....	311
The Electrokinetic Potentials of Precipitates. L. H. Reyerson, I. M. Kolthoff, and Kieth Coad.....	321
The Effect of Heat-treatment on the Sorption-Desorption Hysteresis Characteristics of Silica Gel. W. O. Milligan and Henry H. Rachford, Jr.....	333
Communication to the Editor: The Equilibrium Spreading Coefficient of Amphipathic Organic Liquids on Water. E. Heymann and A. Yoffe.....	359
New Books:	
Surface Active Agents. By C. B. F. Young and K. W. Coons. Reviewed by J. W. McBain.....	361
Fundamentals of Physics. By Henry Semat. Reviewed by Alfred O. Nier.....	362

Studies in Biophysics: The Critical Temperature of Serum (56°). By Lecomte du Nouy. Reviewed by John D. Ferry.....	363
Qualitative Inorganic Microanalysis. By R. Belcher and Cecil L. Wilson. Reviewed by J. G. A. Griffiths.....	363
Science for Democracy. Jerome Nathanson (<i>Editor</i>). Reviewed by I. M. Kolthoff.....	363
Scientific Instruments. By Herbert J. Cooper. Reviewed by S. C. Lind.....	365
Enzymes and their Role in Wheat Technology. J. Ansel Anderson (<i>Editor</i>). Reviewed by Max Milner.....	365
Radioactivity and Nuclear Physics. By J. M. Cork. Reviewed by S. C. Lind.....	366
Tables of Fractional Powers. Reviewed by S. C. Lind.....	366
Preparation and Measurement of Isotopic Tracers. By D. Wright Wilson, A.O.C. Nier, and Stanley P. Reimann. Reviewed by S. C. Lind.....	366
Monographs on the Progress of Research in Holland during the War. Modern Development of Chemotherapy. By E. Havinga, H. W. Julius, H. Veldstra, and K. C. Winkler. Reviewed by I. M. Kolthoff.....	366
Monographs on the Progress of Research in Holland during the War. Contribution to the Physics of Cellulose Fibres. By P. H. Hermans. Reviewed by I. M. Kolthoff.....	367

NUMBER 2, MARCH, 1947

A Kinetic Study of the Urea-Formaldehyde Reaction. Lloyd E. Smythe.....	369
Aniline Formate and its Changes on Keeping. James R. Pound.....	378
Solubility and Melting Point as Functions of Particle Size. II. The Induction Period of Crystallization. Lawrence Harbury.....	382
Rates of Solution of Soaps in Water. Leo Shedlovsky, Gilbert D. Miles, and George V. Scott.....	391
Bond Energy in Diatomic Molecules from the Force Constants, Nuclear Distances, and Classical Model Theory. Melvin A. Cook.....	407
Effect of Freezing on the Stability of Colloidal Dispersions. Silica Sols--A Preliminary Report. Fred Hazel.....	415
Coordination Compounds of Boron Trichloride IV. Systems with the Propyl Chlorides. Donald Ray Martin and Albert S. Humphrey.....	425
The Rise of Air Bubbles in Lubricating Oils. J. V. Robinson.....	431
Energy Additivity in Oxygen-containing Crystals and Glasses. II. Kuan-Han Sun and Maurice L. Huggins.....	438
Stability of Synthetic Rubber Dispersions. I. Low-temperature Thickening of Neoprene Latex. H. K. Livingston.....	443
Stability of Synthetic Rubber Dispersions. II. Coagulation of Neoprene Latices by Freezing. H. W. Walker.....	451
A Spectroturbidimetric Study of the Proteins of Milk. Abraham Leviton and Harrison S. Haller.....	460
Notes on Dynamic Osmometry. K. B. Goldblum.....	474
Vapor Pressure and Heat of Vaporization of Acetylmethylcarbinol. Aaron Efron and Russell H. Blom.....	480
Studies on the Aging of Precipitates and Coprecipitation. XXXVIII. The Compressibility of Silver Bromide Powders. I. Shapiro and I. M. Kolthoff.....	483
Dimensional Stabilization of Wood. Alfred J. Stamm and Harold Tarkow.....	493
Kinetics of Homogeneous Gaseous Reactions in Flow Systems. G. M. Harris.....	505
On Unimolecular Reactions and Radioactive Transformations. George Antonoff.....	513
Isotonic Solutions: Osmotic and Activity Coefficients of Lithium and Sodium Perchlorates at 25°C. James Homer Jones.....	516
X-ray Diffraction Studies in the System $\text{Fe}_2\text{O}_3\text{-Cr}_2\text{O}_3$. W. O. Milligan and L. Merten.....	521

The Antoine Vapor-pressure Equation for Mononuclear Aromatic Hydrocarbons. Nancy Corbin, Mary Alexander, and Gustav Egloff	528
A Mathematical Approach to Reaction Mechanisms. Joseph Thie	540
Cavitation from Solid Surfaces in the Absence of Gas Nuclei. Daniel C. Pease and L. R. Blinks	556
An Unusual Liquid Interface. A. R. Olson and J. H. Hildebrand	567
Molecular Properties of Nitrocellulose. I. Studies of Viscosity. George J. Doyle, Garman Harbottle, Richard M. Badger, and Richard M. Noyes	569
Molecular Properties of Nitrocellulose. II. Studies of Molecular Heterogeneity. Robert H. Blaker, Richard M. Badger, and Richard M. Noyes	574
The Thermochemistry of Propellant Explosives. J. Taylor, C. R. L. Hall, and H. Thomas	580
Determination of the Heat of Combustion of Nitroglycerin and the Thermochemical Constants of Nitrocellulose. James Taylor and C. R. L. Hall	593
Radiation Chemistry. Milton Burton	611
New Books:	
Encyclopedia of Chemical Reactions. Compiled and edited by C. A. Jacobson. Reviewed by I. M. Kolthoff	626
Reagent Chemicals and Standards. By Joseph Rosin. Reviewed by E. B. Sandell	626
Organic Chemistry. By Paul Karrer. Translated by A. J. Mee. Reviewed by C. F. Koelsch	627
Steroid Chains as Components of Protein and Carbon Molecules. By Theodore van Schelven. Reviewed by Richard T. Arnold	627
Textbook of Physical Chemistry. By Samuel Glasstone. Reviewed by Robert Livingston	628
Currents in Biochemical Research. Edited by David E. Green. Reviewed by W. M. Sandstrom	629

NUMBER 3, MAY, 1947

Theory of the Stability of Lyophobic Colloids. E. J. W. Verwey	631
The Use of Membrane Electrodes in the Study of Soap Solutions. C. W. Carr, W. F. Johnson, and I. M. Kolthoff	636
A Limitation of the Determination of Surface Area by the "Point B" Method. Locke White, Jr	644
Solubility of Certain Amino Acids in Aqueous Solutions of Amino Acids and Peptides. Edwin L. Sexton and Max S. Dunn	648
Electron Microscope Observations of the Morphology of Several Gases Polymerized by Charged-particle Bombardment. John H. L. Watson	654
Effect of Electrolytes on the Foaming Capacity of Alpha Soybean Protein Dispersions. Joseph M. Perri, Jr., and Fred Hazel	661
Spectral Changes in Some Dye Ions and their Relation to the Protein Error in Indi- cators. Irving M. Klotz and F. Marian Walker	666
Rate of Corrosion of Lead by Hydrocarbon Solutions of Organic Acids. David Turn- bull and Delton R. Frey	681
Some E.M.F. and Conductance Measurements in Concentrated Solutions of Zinc and Calcium Chlorides. R. A. Robinson and R. O. Farrelly	704
Conductivity of Some Salts in Moist Acetone. Karol J. Mysels	708
An X-ray Diffraction Investigation of Pectinic and Pectic Acids. K. J. Palmer, R. C. Merrill, H. S. Owens, and M. Ballantyne	710
The Fractional Precipitation of Molecular-weight Species from High Polymers. Theo- ries of the Process and Some Experimental Evidence. D. R. Morey and J. W. Tamblyn	721
Note on the Relation between the Heat of Evaporation and the Surface Tension of Liquids. J. C. de Wijs	747

The Sudden Application of a Constant Shearing Motion to Anomalous Fluids. Emmett K. Carver and John R. Van Wazer.....	751
Active Magnesia. III. X-ray versus Nitrogen Adsorption Surface Areas. A. C. Zettlemoyer and W. C. Walker.....	763
Colloidal Aluminum Oxide. Arthur A. Vernon.....	768
Contributions to the Chemistry of Indium. VIII. Observations on the Formation of Magnesium Indate. Therald Moeller and J. Glenn Schnizlein, Jr.....	771
The Chlorophyll-sensitized Photooxidation of Phenylhydrazine by Methyl Red. Robert Livingston, Dorothy Sickle, and Aiji Uchiyama.....	775
Effects of High-energy Radiation on Organic Compounds. Milton Burton.....	786
Phase Boundaries in Concentrated Systems of Sodium Oleate and Water. Robert D. Vold.....	797
A New Method for Forming Sharp Boundaries in Diffusion Experiments. David S. Kahn and Alfred Polson.....	816
The Surface Tension of Liquid Crystals. Wilhelmina M. Schwartz and Hal W. Moseley.....	826
Electronic Interpretations of Organic Chemistry. II. Interpretation of the Solubility of Organic Compounds. Santi R. Palit.....	837
The Kinetics of Dissolution of Cadmium in Hydrochloric Acid. June F. Zimmerman and Hugh J. McDonald.....	857
The Longitudinal Dispersion of Infrared Rays in Polystyrenes. W. W. Lepeschkin.....	868
Longitudinal Dispersion of Infrared Rays in Optically Empty and Turbid Media, and Molecular Weights of Substances. W. W. Lepeschkin.....	875
New Books:	
Qualitative Analysis by Spot Tests. Inorganic and Organic Applications. By Fritz Feigl. Reviewed by E. B. Sandell and L. M. Kolthoff.....	884
Polarographie. Theoretische Grundlagen, Praktische Ausführung und Anwendungen der Elektrolyse mit der tropfenden Quecksilberelektrode. By J. Heyrovsky. Reviewed by I. M. Kolthoff.....	885
Elastic and Creep Properties of Filamentous Materials and Other High Polymers. By Herbert Leaderman. Reviewed by Ralph E. Montonna.....	886
Immuno-catalysis. By M. G. Sevag. Reviewed by H. O. Halvorson.....	886
Organic Preparations. By Conrad Weygand. Reviewed by Walter M. Lauer.....	887
Electronic Theory of Acids and Bases. By W. F. Luder and S. Zuffanti. Reviewed by I. M. Kolthoff.....	887
The Life of a Chemist. Memoirs of Vladimir N. Ipatieff. Edited by Xenia Jaukoff Endin, Helen Dwight Fisher, and H. H. Fisher. Translated by V. Haensel and Mrs. R. H. Lusher. Reviewed by S. C. Lind.....	889
A Laboratory Manual of Qualitative Organic Analysis. By H. T. Openshaw. Reviewed by William E. Parham.....	889
Advances in Enzymology. Vol. 6. Edited by F. F. Nord. Reviewed by W. M. Sandstrom.....	890

NUMBER 4, JULY, 1947

On the Solubility of Paraffin-chain Compounds. A. Bondi.....	891
Photoelectric Spectrophotometry. The Performance of a Quartz Double Monochromator in an Improved and More Versatile Photoelectric Spectrophotometer. F. P. Zscheile.....	903
The Decomposition of Benzoyl Peroxide. I. The Kinetics and Stoichiometry in Benzene. Benjamin Barnett and William E. Vaughan.....	926
The Decomposition of Benzoyl Peroxide. II. The Rates of Decomposition in Various Solvents. Benjamin Barnett and William E. Vaughan.....	942
Some Properties of the Radiation from Radiomanganese 54 and the Adsorption of Manganous Manganese on Hydrrous Ferric Oxide. Don H. Anderson.....	956

Studies of Aluminum Soaps. VIII. Water Sorption and Moisture Content. George W. Shreve, Harold H. Pomeroy, and Karol J. Mysels	963
The Laboratory Preparation of Alkali Metal Hydroxides by Electrolysis. A. F. Winslow, H. A. Liebhafsky, and H. M. Smith	967
Heat Guard for the McBain-Bakr Sorption Balance. Rene D. Zentner	972
Aluminum Dilaurate as Association Colloid in Benzene. James W. McBain and Earl B. Working	974
A Vapor-phase Sorption Study of Iodine and Active Magnesium Oxide Utilizing the McBain-Bakr Sorption Balance. R. C. Dunn and H. H. Pomeroy	981
Tolerance Concentrations of Radioactive Substances. Karl Z. Morgan	984
Analysis of Particle Formation and Growth by Size-frequency Determinations of the Silver Halide Precipitations of Photographic Emulsions. R. P. Loveland and A. P. H. Trivelli	1004
Communication to the Editor: A Note on the Strength of Organic Bases. Santi R. Palit	1028
New Books:	
Oxidation. A general discussion held by the Faraday Society. Reviewed by S. C. Lind	1029
Abridged Scientific Publications from the Kodak Research Laboratories. Vol. XXVII. Reviewed by S. C. Lind	1029
Reactions at Carbon-Carbon Double Bonds. By Charles C. Price. Reviewed by Richard T. Arnold	1029
Tables of Spherical Bessel Functions. Reviewed by S. C. Lind	1030
Rarer Metals. By Jack Dement and H. C. Dake. Reviewed by S. C. Lind	1030
The Chemistry of Free Radicals. By W. A. Waters. Reviewed by Richard T. Arnold	1030
Helium. By W. H. Keesom. Reviewed by S. C. Lind	1031
Nuclear Physics Tables. By J. Matlack. Reviewed by S. C. Lind	1031
An Introduction to Nuclear Physics. By S. Fluegge. Reviewed by S. C. Lind	1031
German-English Science Dictionary. By Louis DeVries <i>et al.</i> Reviewed by S. C. Lind	1031
Inorganic Chemistry. By W. Norton Jones, Jr. Reviewed by T. D. O'Brien	1032
Kinetic Theory of Liquids. By J. Frenkel. Reviewed by F. H. MacDougall	1032
Inorganic Syntheses. Vol. II. W. C. Fernelius (<i>Editor</i>). Reviewed by John C. Bailar, Jr.	1033
Physical Chemistry for Colleges. By E. B. Millard. Reviewed by William N. Lipscomb	1033
Physikalische Chemie in Medizin und Biologie. By W. Bladergroen. Reviewed by I. M. Kolthoff	1035
Organic Analytical Reagents. Vol. I. By Frank J. Welcher. Reviewed by I. M. Kolthoff	1035
Analytica Chimica Acta. Paul-E. Wenger (<i>Editor</i>). Reviewed by E. B. Sandell	1036

NUMBER 5, SEPTEMBER, 1947

Dielectrics and Rheology of Non-aqueous Dispersions. Andries Voet	1037
On a Generalization in the Diffusion Theory. Ole Lamm	1063
The Biochemistry of Plant Pigments. Wilder D. Bancroft	1078
Thin Oxide Films on Aluminum. Earl A. Gulbransen and W. S. Wyson	1087
A Study of Anhydrous Conditions in the Preparation of Lyophobic Organosols. Harrison A. Nelson	1103
Rates of Anion Exchange in Ion-exchange Resins. Robert Kunin and Robert J. Myers	1111
On the Heterogeneous Catalytic Activity of Colloidal Silver in the Production of Silver Acetate. Bal Krishna and Satyeshwar Ghosh	1130

Electrophoretic Mobilities and Fractionation of Sodium Pectinates. Wilfred H. Ward, Harold A. Swenson, and Harry S. Owens	1137
The Effects of Temperature upon the Critical Concentrations of Anionic and Cationic Detergents. H. B. Klevens	1143
Adsorption Isotherms of Mixed Vapors of Carbon Tetrachloride and Methanol on Activated Charcoal at 25°C. W. B. Innes and H. H. Rowley	1154
Adsorption Equilibria of Liquid Mixtures of Carbon Tetrachloride-Methanol with Charcoal. W. B. Innes and H. H. Rowley	1172
Experimental Arguments against the Concept of Chrome Tanning as an Adsorption Process. K. H. Gustavson	1181
The Phase Behavior of Sodium Stearate in Anhydrous Organic Solvents. Gerould H. Smith and James W. McBain	1189
A Demonstration of Some New Methods of Determining Molecular Weights from the Data of the Ultracentrifuge. W. J. Archibald	1204
New Books:	
Practical Physiological Chemistry. By Philip B. Hawk, Bernard L. Oser, and William H. Summerson. Reviewed by Charles Carr	1214
Meson Theory of Nuclear Forces. By Wolfgang Pauli. Reviewed by Edward L. Hill	1215
Fourier Transforms and Structure Factors. By Dorothy Wrinch. Reviewed by William N. Lipscomb	1215
Fundamentals of Semi-micro Qualitative Analysis. By Carl J. Engelder. Reviewed by G. B. Heisig	1216
The Problem of Reducing Vulnerability to Atomic Bombs. By Ainsley J. Coale. Reviewed by S. C. Lind	1217
Concise Chemical and Technical Dictionary. Edited by H. Bennett. Reviewed by J. Lewis Maynard	1217

NUMBER 6, NOVEMBER, 1947

Free-volume Models for Liquids. Terrell L. Hill	1219
Adsorption of Gases on Surfaces of Powders and Metal Foils. R. T. Davis, Jr., T. W. DeWitt, and P. H. Emmett	1232
Adsorption of Argon, Nitrogen, and Butane on Porous Glass. P. H. Emmett and Martin Cines	1248
Investigation of Low-temperature Nitrogen Adsorption at High Relative Pressures. James Holmes and P. H. Emmett	1262
Alteration of the Size and Distribution of Pores in Charcoals. James Holmes and P. H. Emmett	1276
Surface Complexes on Charcoal. Gas Evolution as a Function of Vapor Adsorption and of High-temperature Evacuation. Robert B. Anderson and P. H. Emmett	1308
Surface-area Measurements on Metal Spheres and on Carbon Blacks. P. H. Emmett and Martin Cines	1329
Interfacial Tension by the Ring Method: The Benzene-Water Interface. H. L. Cupples	1341
Equilibria in Silver Acetate Solutions. F. H. MacDougall and Sigfred Peterson	1346
The Shape of Heat-capacity and Equilibrium Cooling Curves in the Region of Melting of Solid Solutions. Karol J. Mysels	1361
The Molal Volumes of Aqueous Solutions of Perchloric Acid. J. Bigeleisen	1369
Some Mathematical Relations Involving the Solubility of Silver Cyanide. John E. Ricci	1375
Catalytic Oxidation of Aniline in the Vapor Phase. O. W. Brown and W. C. Frishe	1394
Coordination Compounds of Boron Trichloride. V. Relationship of Dipole Moment of Chlorides to Compound Formation. Donald R. Martin	1400
The Chemical Erosion of Steel by Hot Gases under Pressure. Richard C. Evans, F. Hubbard Horn, Zalman M. Shapiro, and Richard L. Wagner	1404

Hydrolysis of Wood Cellulose and Decomposition of Sugar in Dilute Phosphoric Acid.

Elwin E. Harris and Bill G. Lang 1430

The Solubility of Thorium Nitrate Tetrahydrate in Organic Solvents at 25°C. C. C.

Templeton and Norris F. Hall 1441

Communication to the Editor: A Note on the Oxidation of Acetoin. James R. Pound. 1449**New Books:****Characterization of Organic Compounds.** By F. Wild. Reviewed by William E.

Parham 1450

Fatty Acids, Their Chemistry and Physical Properties. By K. S. Markley. Re-

viewed by Lee Irvin Smith 1450

Actions of Radiations on Living Cells. By D. E. Lea. Reviewed by S. C. Lind . . . 1451**The Terpenes. Vol. I.** By J. L. Simonsen and L. N. Owen. Reviewed by Lee Irvin

Smith 1451

Essays in Rheology. Reviewed by John G. Kirkwood 1452**Handbook of Chemistry.** By N. A. Lange. Reviewed by H. H. Barber . . . 1452**Methods of Vitamin Assay.** Prepared and edited by the Association of Vitamin

Chemists. Reviewed by M. O. Schultze 1452

Monographs on the Progress of Research in Holland. The Wet Purification of Coal**Gas and Similar Gases by the Staatsmijnen Otto Process.** By H. A. Pieters and

D. W. van Krevelen. Reviewed by R. L. Brown 1453

Microcalorimetry. By W. S. Swietoslawski. Reviewed by F. G. Brickwedde . . 1455**Subject Index.** 1457**Author Index.** 1462**Index to Book Reviews** 1467

ERRATUM

Volume 51, Number 1, January, 1947

Page 153: The second sentence in the second paragraph under the heading "Discussion" should read: "If a mixture of two preparations . . . is subjected to ultracentrifugation . . ."

ERRATA

Volume 51, Number 2, March, 1947

Page 603: In lines 13 and 28 the word "mist" should read "rust."

ERRATUM

Volume 51, Number 2, March, 1947

Pages 580-584: All of the material beginning with the second paragraph on page 580, reading "The final products of decomposition, etc." and ending on the middle of page 581, reading "Combining equations 19, 20, 21, the following equation is obtained:" should be transferred to page 584 and inserted immediately before the equation beginning " $C_2H_4O_7N_2$."

ERRATUM

Volume 51, Number 2, March, 1947

Page 612: The last sentence in the first paragraph should read: "They are fluorescence, simple rupture, transfer of energy to another molecule or atom physically or chemically (e. g., photosensitization), and internal conversion associated with dissociation—i. e., predissociation—and internal conversion associated merely with degradation of the energy state to successively lower electronic states."

THE CELLULOSE MOLECULE¹

PHYSICAL-CHEMICAL STUDIES

THE SVEDBERG

Institute of Physical Chemistry, University of Uppsala, Uppsala, Sweden

Received August 8, 1946

In the early days of colloid chemistry polydispersity was regarded as the rule. Monodisperse systems could be obtained by special fractionation procedures (Perrin's gamboge suspensions, Odén's sulfur sols) or to a certain degree by the nuclear method (Zsigmondy's gold sols). This was still the generally recognized opinion at the time of the First Colloid Symposium, which was held here in Madison in June 1923. Three years later it was shown that a large group of colloids, the proteins, are, as a rule, monodisperse. During the following twenty years the physical chemistry of the protein molecules has been extensively studied in many laboratories (16). One of the chief centers of such studies has been here in Madison.

The fact that upon denaturation many proteins become polydisperse has often been taken as an indication that monodispersity is a characteristic of native high-molecular compounds. To a certain extent this is probably true, but polydispersity has now been found to be the rule in at least one large group of native organic colloids, *viz.*, the polysaccharides. The degree of polydispersity is, however, less high than in synthetic high polymers produced in the laboratory, such as the polyethylenes and rubbers.

In the following report a short summary will be given of the investigations carried out in Uppsala on the physical chemistry of the polysaccharide molecules, especially cellulose (2, 3, 4, 5, 6, 17). The chief experimental methods used by us are well known and will therefore be referred to only briefly.

ULTRACENTRIFUGAL SEDIMENTATION

Work of this type was started in Madison in 1923, and the method was further developed in Uppsala and in American laboratories. The type of apparatus used in Uppsala and also here in Madison for high-speed sedimentation is shown in figures 1 and 2.

The solution to be studied is enclosed in a sector-shaped cell with plane parallel windows and spun in a suitable rotor at constant speed and constant temperature. One of the chief difficulties has been the avoiding of convection currents in the solution, owing to slight thermal disturbances. In the oil-turbine ultracentrifuge this is achieved by running the rotor in hydrogen at about 15 mm. pressure, thus reducing the friction considerably and at the same

¹ Presented at the Twentieth National Colloid Symposium, which was held at Madison, Wisconsin, May 28-29, 1946.

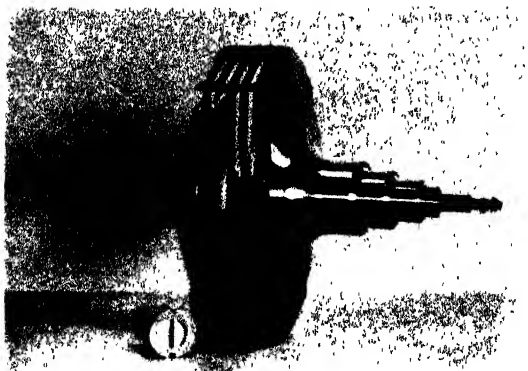


FIG. 1. Rotor and cell

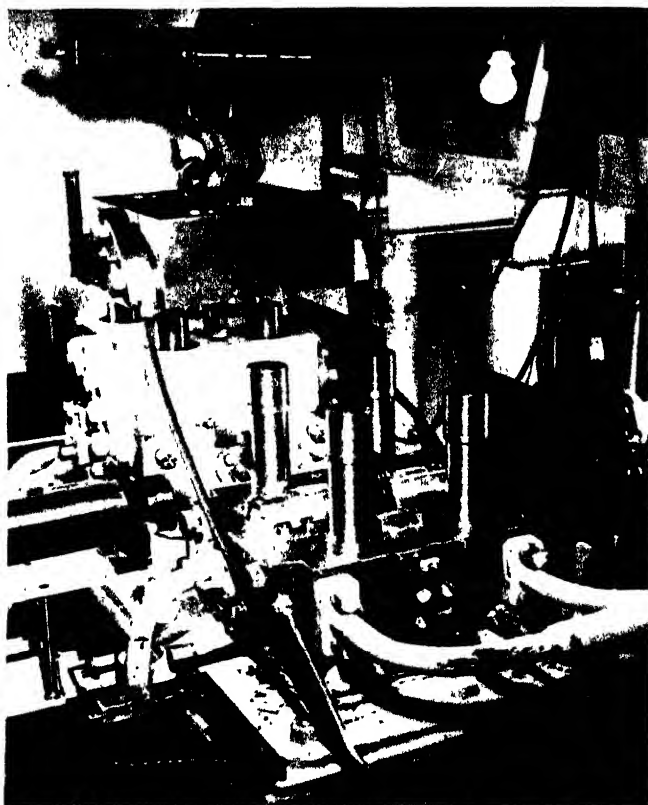


FIG. 2. The oil-turbine centrifuge

time preserving good thermal conductivity. In the air-driven ultracentrifuges used in many laboratories in this country the rotor is as a rule run in a high vacuum, but there is a certain tendency even here to go over to low-pressure hydrogen.

For measurements of sedimentation equilibrium different equipment is used, and the optimum speed is only about one-tenth of that required for the determination of the sedimentation constant. On the other hand, the sample of solution studied has to be kept spinning for a considerable length of time, at constant speed and temperature, especially in the case of thread-like molecules such as cellulose. It may take several weeks before equilibrium is reached.

In order to satisfy these requirements the rotor is arranged to rotate in hy-

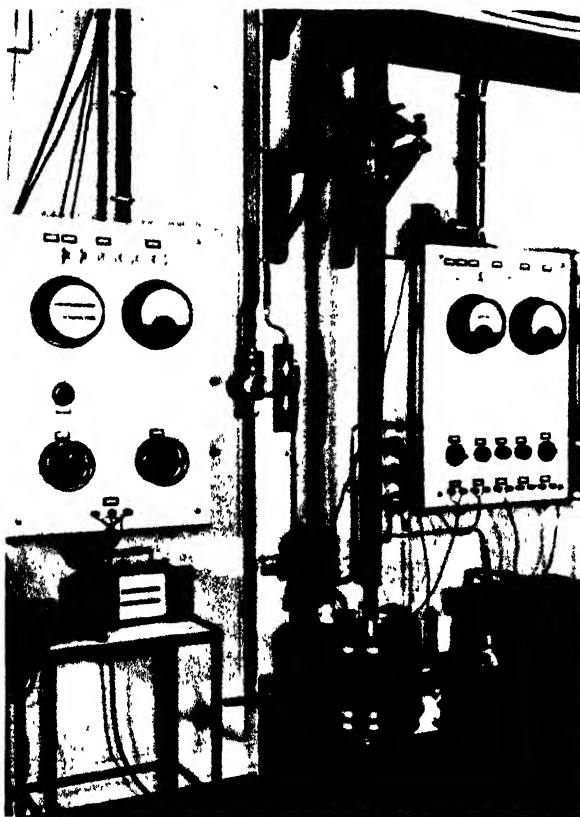


FIG. 3. The sedimentation-equilibrium centrifuge

drogen at atmospheric pressure, and the rotor casing is surrounded by a thermostated water bath (figure 3).

DIFFUSION

In the early days of ultracentrifugal studies diffusion was measured from the spreading of the sedimentation curves. I thought this a very clever feature and in a way it is, because we get the diffusion constant under exactly the same conditions with regard to temperature etc. as the sedimentation constant. On the other hand, the slightest convection disturbance or inhomogeneity with

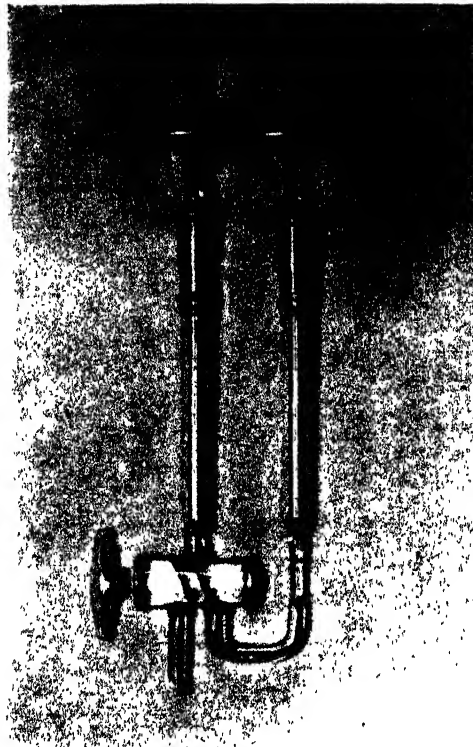


FIG. 4. Cylindrical diffusion cell

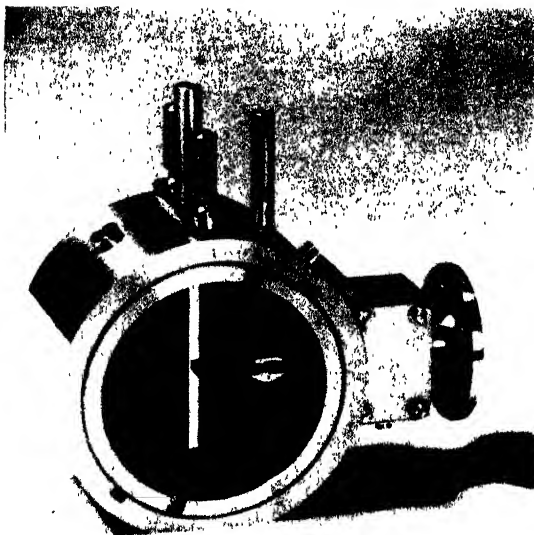


FIG. 5. Lamm's diffusion cell

regard to molecular weight will cause great errors in the diffusion constants. Nowadays, therefore, we always measure diffusion outside the centrifuge. The spreading of the sedimentation curves is, on the contrary, used for studying polydispersity.

The experimental methods used for determining diffusion constants at the time of classical physical chemistry were inconvenient and lacking in accuracy. An easier and more exact procedure was initiated during my stay at the University of Wisconsin in 1923 (14) and further developed in Upsala, especially by Lamm (10).

In the first type of apparatus (figure 4) the solution is run into the cylindrical diffusion cell beneath a layer of solvent so slowly that no mixing takes place. The second type of diffusion cell (figure 5) is arranged with a sliding horizontal dividing wall, which is withdrawn after the solvent has been placed on top of the solution. In both cases the columns of solution and solvent are high enough to be regarded as unlimited.

THE OSMOTIC BALANCE

Especially in the case of polydisperse systems is it of importance to obtain different kinds of average molecular weights. Ultracentrifugal sedimentation gives chiefly weight averages, the sedimentation-equilibrium method gives weight averages

$$M_w = \frac{\sum M_i^2 n_i}{\sum M_i n_i}$$

and so-called z averages,

$$M_z = \frac{\sum M_i^3 n_i}{\sum M_i^2 n_i}$$

while osmotic methods give number averages.

$$M_n = \frac{\sum M_i n_i}{\sum n_i}$$

Now the usual type of osmometer, where the pressure is measured by observing the height of column of solution, is not sensitive enough in the case of very dilute high-molecular solutions. And it is just within the region of low concentrations that measurements of osmotic pressure become significant.

A new procedure, using the weight instead of the height of the column, has recently been worked out in Upsala (8, 9) and has proved quite useful in the domain of low concentrations (figures 6 and 7).

A rise in height of 1 mm. in a tube of 1 cm.² area corresponds to an increase in weight of 0.1 g. (water). With a standard analytical balance it should be possible to weigh a difference in height of 0.001 mm. Certain other sources of error, however, decrease the accuracy somewhat. The influence of temperature is partly compensated by making the ratio between surface and volume equal for the solution in the osmotic cell and the solvent in the other vessel. In the present apparatus a temperature change of 0.03° introduces an error of 0.1 mg.

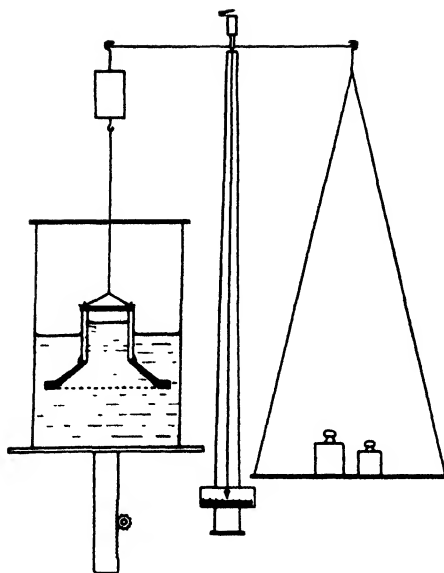


FIG. 6. Diagram of the osmotic balance

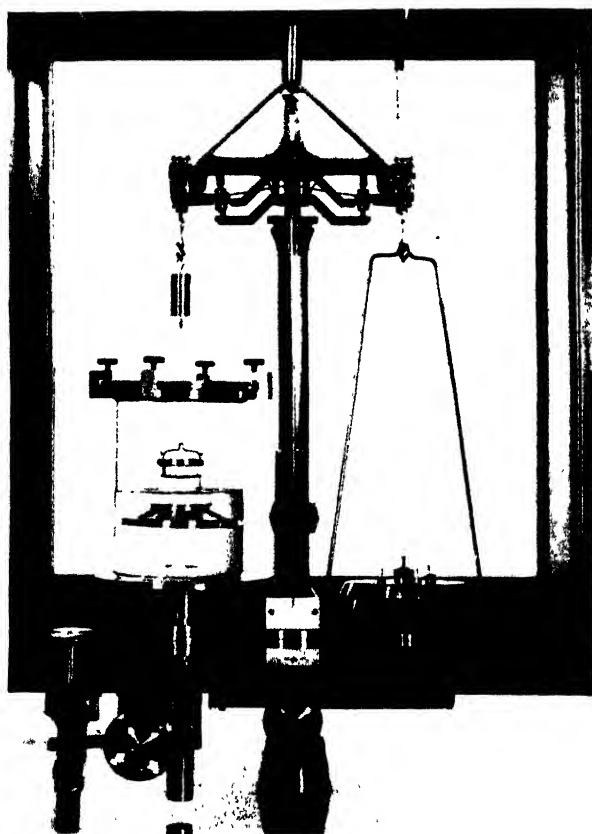


FIG. 7. Photograph of the osmotic balance with shields removed

A series of measurements is started by adjusting the outer and the inner meniscus to the same level with the balance at rest. The weight at this position is determined. The outer vessel is then moved to a position slightly away from the calculated approximate osmotic equilibrium, and the inflow or outflow of solvent is measured from time to time by weighing.

Before reviewing our work on cellulose a few measurements on monodisperse or slightly polydisperse polysaccharides may be mentioned. If larch wood is extracted with water, about 8 per cent goes into solution. Analyzed in the ultracentrifuge it is found to contain two polysaccharide components of molecular weight 16,000 and 100,000, each practically monodisperse (see figure 8).

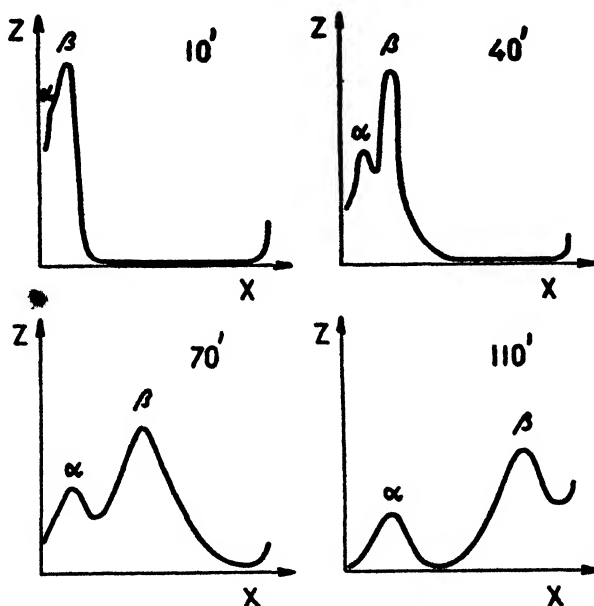


FIG. 8. Sedimentation diagram of the *Larix* polysaccharides

The water-soluble high-molecular material of the Liliaceae bulb-juices contains both polysaccharides and proteins. In figure 9 the most slowly sedimenting peaks represent polysaccharides (slightly polydisperse), the more rapidly sedimenting ones proteins.

The most widely distributed and—from a technical point of view—the most important of the polysaccharides is doubtless cellulose. In its native state cellulose is not soluble. It has to be transformed into some derivative such as the copper-cellulose complex of the Schweitzer reagent or cellulose nitrate. In the majority of cases native cellulose is linked up with some other high-molecular substance, e.g., lignin, and its liberation requires rather drastic treatment, resulting in a partial breakdown of the cellulose chains.

If spruce wood is treated directly with cuprammonium, 5–10 per cent goes into solution (figure 10, from reference 2). By treating wood with hydrochloric acid

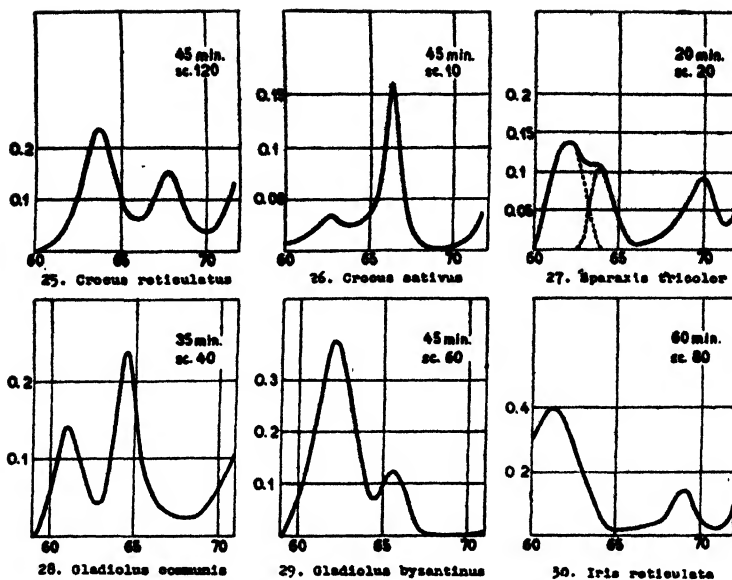


FIG. 9. Sedimentation diagram of the Liliaceae polysaccharides

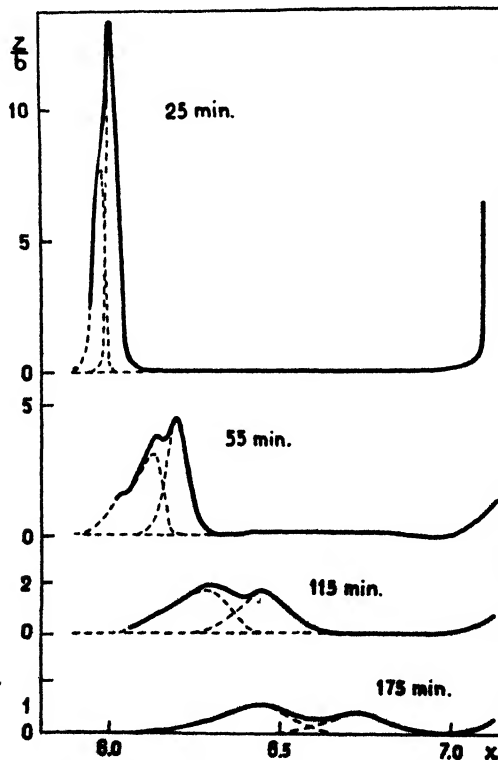


FIG. 10. Sedimentation diagrams of native wood cellulose. Two maxima: cellulose, hemicellulose and polyoses. $M_{\text{cellulose}} = 800,000$; $D.P. = 5000$. Minimum value for wood cellulose.

the lignin can be extracted and all the carbohydrates—74 per cent—are set free. After dissolving these polysaccharides in cuprammonium, the sedimentation diagrams shown in figure 11 are obtained.

Technical wood cellulose prepared according to the standard sulfite process is broken down considerably.

For substances like cellulose, where diffusion is very slow, a measure of the polydispersity can be obtained from the broadening of the sedimentation peak with distance from the center of rotation dB/dx , where B is the area of the peak divided by the height (figure 12). Figure 13 gives the dB/dx values for unbleached and bleached sulfite pulp (nitrates in acetone), and figures 14 and 15 the sedimentation diagrams for Russian unbleached linters and sulfate pulp.

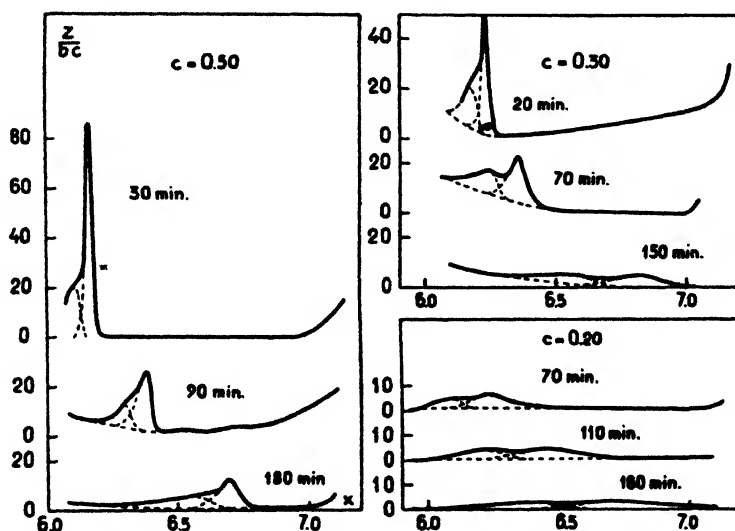


FIG. 11. Sedimentation of wood polysaccharides

The linters cellulose has a molecular weight of 1.9 million, corresponding to a *D.P.* of 6000 (15).

For the calculation of the molecular weight from the sedimentation constant s and the diffusion constant D according to the equation

$$M = \frac{RTs}{D(1 - V\rho)}$$

where R is the gas constant, T is the absolute temperature, V is the partial specific volume, and ρ is the density of the solvent, extrapolation to infinite dilution is necessary.

For the sedimentation constant this can be done by plotting s either as a function of c (figure 16) or as a function of cs (figure 17). The extrapolated value can be enclosed between two limits by plotting in the same diagram (figure 18) both s and $s\eta/\eta_0$ as a function of c (η is the viscosity of the solution at the concentration c and η_0 at infinite dilution) (8, 11, 13).

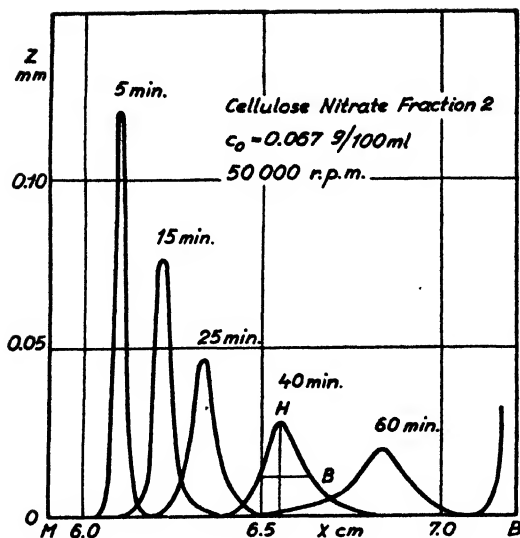


FIG. 12. Sedimentation curves for cellulose nitrate

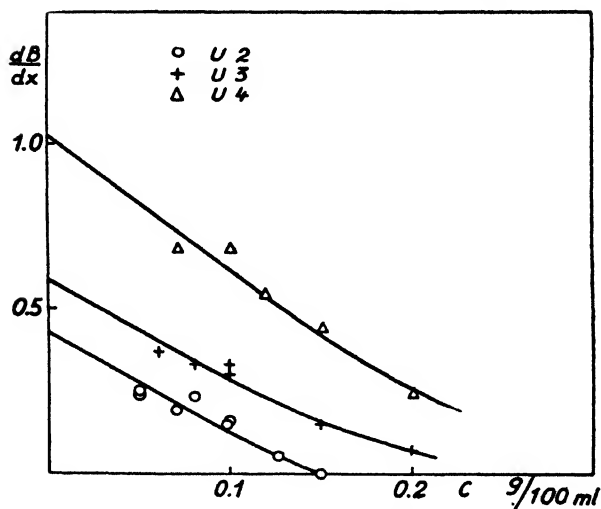


FIG. 13. Polydispersity of technical cellulose

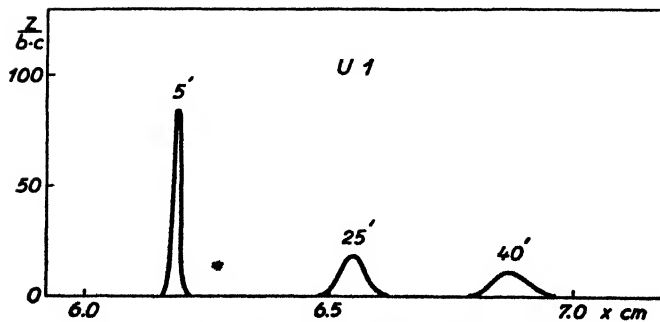


FIG. 14. Sedimentation of unbleached linters cellulose

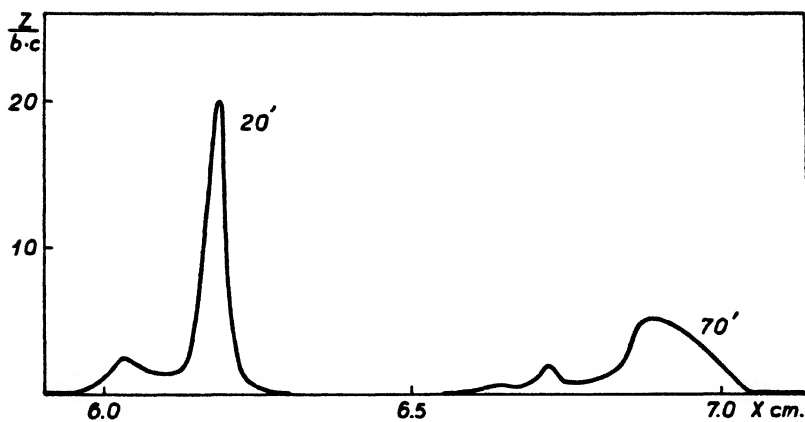
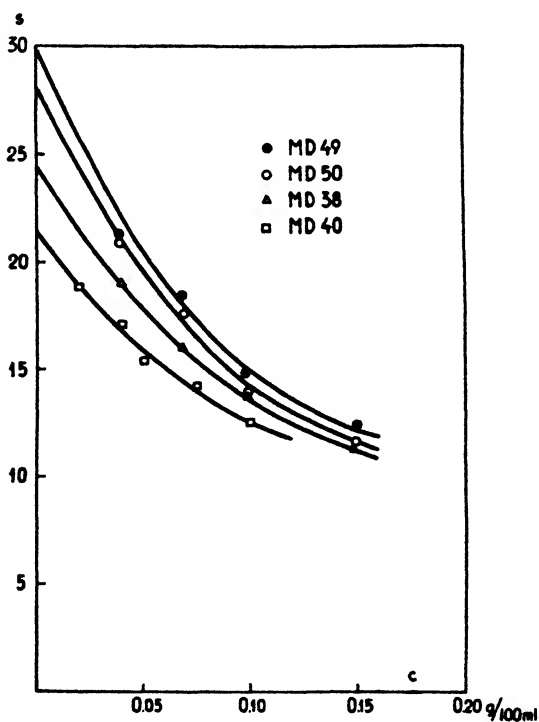


FIG. 15. Sedimentation of unbleached sulfate cellulose

FIG. 16. Extrapolation of s for cellulose nitrate in acetone as a function of c

An example of the extrapolation of diffusion constants to zero concentration is given in figure 19 (2).

In the case of a polydisperse substance the experimental diffusion curve always

has a greater height H than the corresponding normal curve (figure 20). If the diffusion constant is calculated on the one hand by means of the formula

$$D_A = \frac{A^2}{4\pi t H^2}$$

where A is the area under the diffusion curve and t the time, and on the other from

$$D_m = \frac{m_2}{2tA}$$

where

$$m_2 = \int_{-\infty}^{\infty} y |x|^2 dx$$

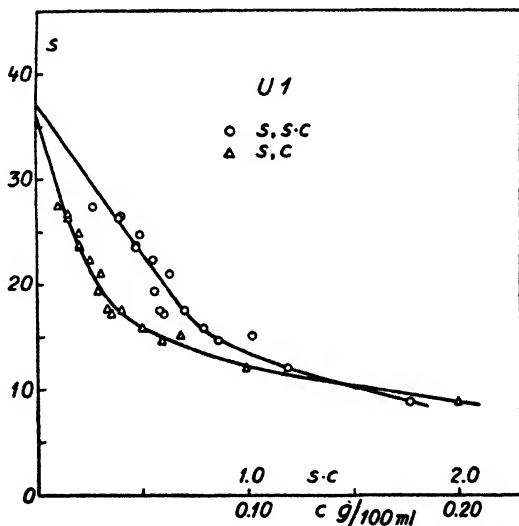


FIG. 17. Extrapolation of s for cellulose nitrate in acetone as a function of sc

(e.g., the second moment of the curve about the vertical axis through the arithmetic mean), the ratio D_m/D_A is always greater than unity for a polydisperse substance and may be taken as a measure of the polydispersity (see table 1) (1, 2).

In order to obtain reliable results the accuracy of the diffusion determinations must be very high. As a rule it is therefore preferable to use dB/dx , which is easier to determine, as a measure of polydispersity.

Mosimann (12) has noted that the sedimentation-equilibrium method cannot be used for cellulose derivatives of molecular weights higher than about 80,000, because of the deviations from the simple thermodynamic laws in the case of

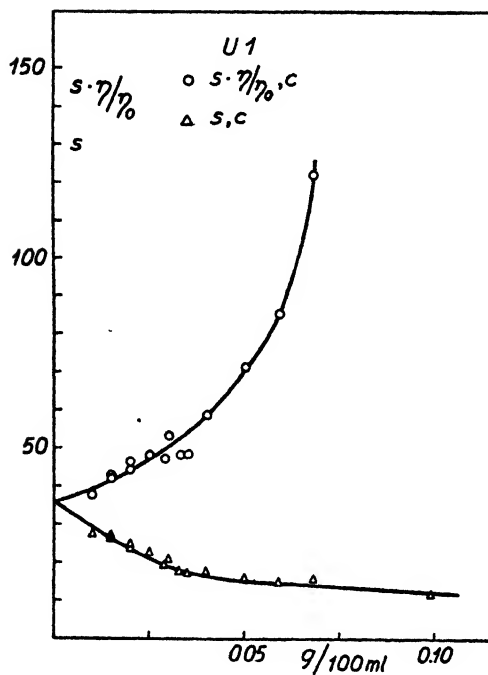


FIG. 18. Extrapolation of s and $s\eta/\eta_0$ for cellulose nitrate in acetone as a function of c

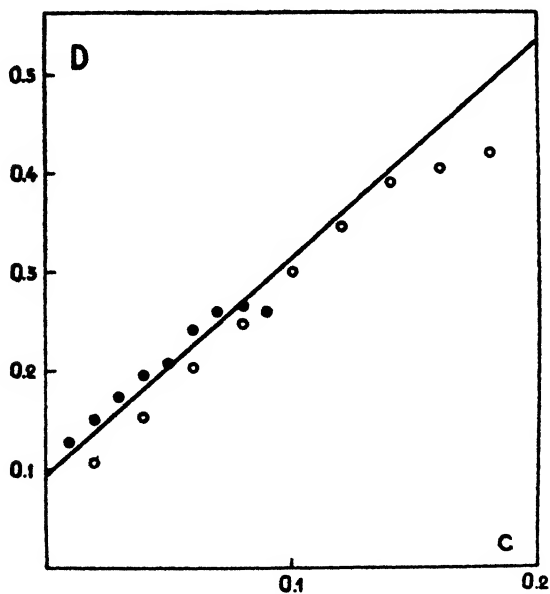


FIG. 19. Extrapolation of D for cellulose as a function of c

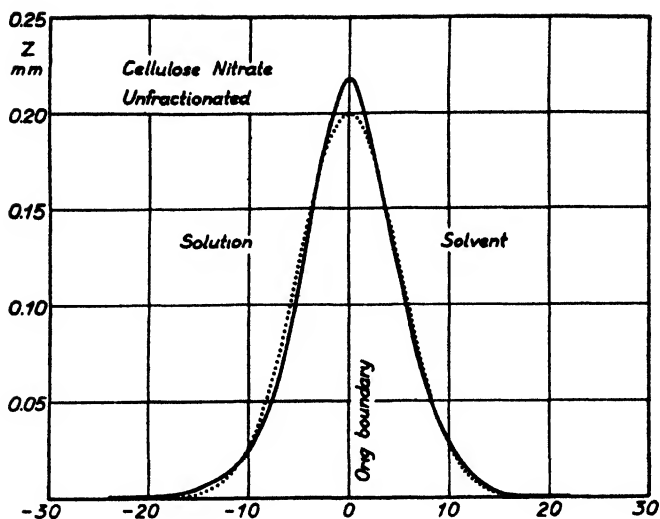


FIG. 20. Diffusion curve for cellulose nitrate

TABLE 1

Diffusion of cellulose nitrate in acetone at a concentration of 0.20 per cent

NITRATE OF	D_m	D_A	D_m/D_A
Unbleached American linters	1.42	1.29	1.10
Bleached American linters.	1.78	1.65	1.08
Chlorite-bleached linters	1.61	1.49	1.08
Sulfate cellulose	2.44	2.11	1.15
Sulfite cellulose.. . . .	2.38	2.06	1.15
Holocellulose	3.47	2.70	1.28
α -Cellulose from holocellulose	2.70	2.25	1.20
Rayon pulp No. 1	2.64	2.21	1.19
Rayon pulp No. 2	2.00	1.80	1.11
Rayon pulp No. 3	2.59	2.02	1.28
Rayon pulp No. 4	4.41	3.14	1.40
Rayon pulp No. 5	2.77	2.17	1.28
Rayon pulp No. 6	2.13	2.01	1.06

TABLE 2

Molecular weights of three nitrocelluloses

SUBSTANCE	M_w	M_z
VF 3	19,100	47,900
VF $\frac{1}{2}$	17,900	21,800
AF 1	22,700	42,800

such thread-like molecules. It should be remarked, however, that with more or less rigid linear molecules we are dealing with a distinctly unfavorable case.

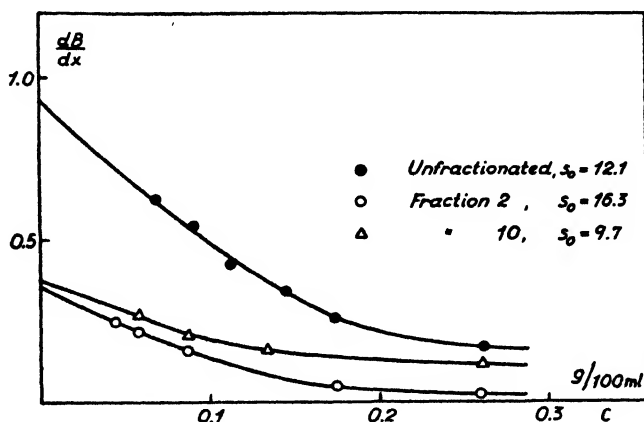


FIG. 21. Polydispersity of fractionated cellulose

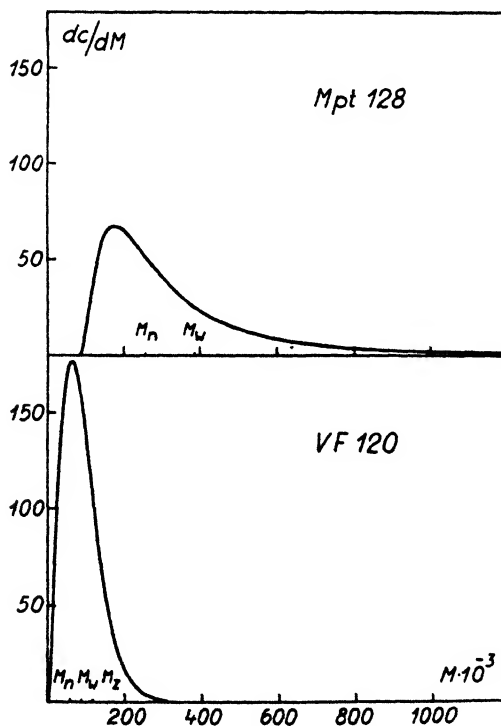


FIG. 22. Frequency curves for cellulose

Furthermore, because of the work of Wales, Bender, Williams, and Ewart it has become possible to take into substantial account the deviations from the

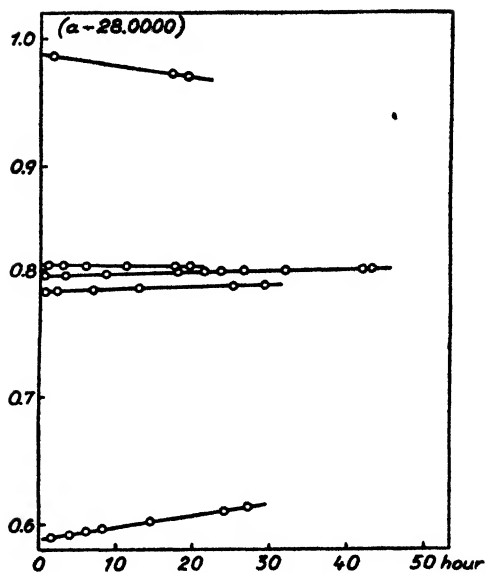


FIG. 23. Osmotic measurements on cellulose. Change of weight of cell with time.

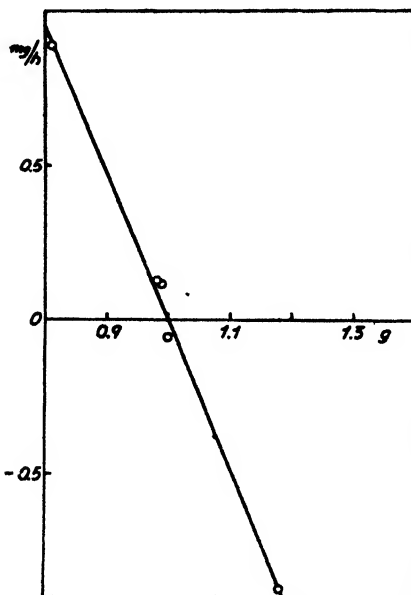


FIG. 24. Osmotic measurements on cellulose. Inflow and outflow of solvent as a function of weight.

simple thermodynamic laws, and the molecular-weight range probably will be measurably increased (18).

In table 2 the weight-average and z -average molecular weights are given for

three nitrocelluloses. The great deviations between M_w and M_n point to a high degree of polydispersity.

Many attempts have been made to determine the degree of polydispersity of cellulose by fractionating a soluble derivative such as the nitrate and measuring the molecular weight of the fractions. If the fractionation is done carefully a certain amount of information is gained, but the fractions are still polydisperse, although less so than the original material (figure 21).

Often electron-microscope studies can give information about the probable shapes of macromolecules. One recent study along these lines is that of Hambræus and Rånby (7).

The description of a polymolecular substance is not complete until the frequency curve has been obtained. The problem is a very difficult one, however, and so far only an approximate solution has been found (8). Figure 22 gives the frequency curve for two different commercial cellulose nitrates from sedimentation measurements. The different average molecular weights are indicated in the diagrams. The M_n values were obtained by means of the osmotic balance. Figures 23 and 24 give an idea of the precision of the osmotic measurements.

The study of the physical chemistry of the cellulose molecule by means of sedimentation, diffusion, and osmotic methods is beginning to yield results of interest from both a purely scientific and a technical point of view. The thread-like shape of these molecules and the polydispersity of cellulose solutions cause, however, great experimental and theoretical difficulties. The sedimentation technique as well as the diffusion and osmotic-pressure measurements have to be pushed to the utmost degree of perfection in order to give satisfactory data.

It was fortunate that the proteins and not cellulose became the testing substance for the ultracentrifugal technique. We would probably have been discouraged and given up the whole thing if, at the very beginning, we had met with such difficulties as the study of cellulose presents. After the methods had been properly developed for the mono- or paucidisperse proteins, it was a relatively simple matter to adapt them to the more complicated polydisperse systems of cellulose and its derivatives.

REFERENCES

- (1) GRALÉN, N.: Über Polydispersitätsbestimmungen aus Diffusionsmessungen nach der Lamm'schen Skalenmethode. *Kolloid-Z.* **95**, 188 (1941).
- (2) GRALÉN, N.: Sedimentation and diffusion measurements on cellulose and cellulose derivatives. Dissertation, Upsala, 1944.
- (3) GRALÉN, N., BERG, S., AND SVEDBERG, T.: Über die Polysaccharide der Eriophorum-Wolle. *Ber.* **75**, 1702 (1942).
- (4) GRALÉN, N., AND RÅNBY, B.: High-molecular wood celluloses. *The Svedberg, 1884-1944*, p. 274. Almqvist and Wiksells, Upsala (1944).
- (5) GRALÉN, N., AND SVEDBERG, T.: Soluble reserve-carbohydrates in the Liliiflorae. *Biochem. J.* **34**, 234 (1940).
- (6) GRALÉN, N., AND SVEDBERG, T.: Molecular weight of native cellulose. *Nature* **152**, 625 (1943).
- (7) HAMBRÆUS, G., AND RÅNBY, B.: Electron microscopic investigation of precipitates of cellulose nitrates. *Nature* **155**, 200 (1945).

- (8) JULLANDER, I.: Studies on nitrocellulose, including the construction of an osmotic balance. Dissertation, Upsala, 1945.
- (9) JULLANDER, I., AND SVEDBERG, T.: The osmotic balance. *Nature* **153**, 523 (1944).
- (10) LAMM, O.: Measurements of concentration gradients in sedimentation and diffusion by refraction methods. Dissertation, Upsala, 1937.
- (11) MOSIMANN, H.: Über das Sedimentationsverhalten von Nitrocellulosefraktionen und die daraus ableitbare Molekelform. *Helv. Chim. Acta* **26**, 61 (1942).
- (12) MOSIMANN, H.: Molekulargewichts- und Polydispersitätsbestimmungen an Nitrocellulosefraktionen mit Hilfe der Sedimentations-gleichgewichts-Ultrazentrifuge. *Helv. Chim. Acta* **26**, 369 (1942).
- (13) MOSIMANN, H., AND SVEDBERG, T.: Sedimentations- und Diffusions-messungen am wasserlöslichen polysaccharid aus Lärchenholz. *Kolloid-Z.* **100**, 99 (1942).
- (14) SVEDBERG, T.: *Colloid Chemistry*, 2nd edition, p. 152. The Chemical Catalog Company, Inc., New York (1928).
- (15) SVEDBERG, T.: Physikalische Chemie des Cellulosemoleküls. *Cellulosechem.* **21**, 57 (1943).
- (16) SVEDBERG, T., AND PEDERSEN, K. O.: *The Ultracentrifuge*. Oxford University Press, New York (1940).
- (17) SÄVERBORN, S.: A contribution to the knowledge of the acid polyuronides. Dissertation, Upsala, 1945.
- (18) WALES, M., BENDER, M. M., WILLIAMS, J. W., AND EWART, R. H.: Sedimentation equilibria of polydisperse non-ideal solutes. *J. Chem. Phys.* **14**, 353 (1946)

MOLECULAR-WEIGHT DETERMINATION BY LIGHT SCATTERING¹

P. DEBYE

Department of Chemistry, Cornell University, Ithaca, New York

Received August 8, 1946

I. INTRODUCTION

Non-absorbing gases or liquids are not perfectly transparent but scatter light. The main part of this light has not changed its wave length, the fraction of the intensity corresponding to the displaced spectral lines of the Raman effect is small, and the change in frequency is unimportant for the following considerations. The scattering is due to the non-homogeneous molecular structure, and we would expect that if a solvent is made more inhomogeneous by adding a solute the scattered intensity would increase. The question to be answered is how this increase in scattered intensity can be used in order to count the number of solute particles and how in appropriate cases conclusions about the structure of such particles can be drawn from observations on the angular distribution of the scattered light.

The problem can be approached either by making a detailed calculation of the

¹ Presented at the Twentieth National Colloid Symposium, which was held at Madison, Wisconsin, May 28-29, 1946.

electromagnetic field surrounding a particle in order to derive the loss of primary light energy due to its radiation (14) or by treating the effect of the molecular inhomogeneities on the light in a second approximation as due to spontaneous fluctuations of the density and the concentration in a medium which in a first approximation is considered to be perfectly homogeneous (7).

Each method has advantages and disadvantages. In the application of the direct method it is commonly considered unavoidable to start with a particle of definite shape (i.e., a sphere). It will be shown in the following that this restriction is unnecessary. This offers the advantage of drawing conclusions about the special effects related to the particle structure which will begin to occur as soon as some dimension of the particle becomes comparable to the wave length of the light. On the other hand, it becomes very difficult to extend the calculations to the case of higher concentrations, when the particles begin to interact with each other. This is not so if the method of fluctuations is applied. By this method the intimate connection between light scattering and osmotic pressure is revealed, and the effects of concentration on osmotic pressure and on light scattering can be related to each other. However, now it becomes difficult to handle larger particles.

II. SMALL PARTICLES; HIGH DILUTION

Making the decision that we will be interested only in the additional scattering due to a small amount of solute in a much larger amount of solvent, we are permitted to consider the solvent as perfectly homogeneous. The dielectric constant of this medium will be called ϵ_0 and its index of refraction (for the particular wave length which is used in a primary beam) μ_0 . The relation $\epsilon_0 = \mu_0^2$ holds, and can be considered as a definition of the dielectric constant for the frequency in question.

After the addition of the solute, we shall find regions in the solution at large mutual distances in which the dielectric (optical) properties have been changed in a way not known in detail. Each such region we call a particle.

If the solution is subjected to the influence of a homogeneous electric field of intensity F , every cubic centimeter of the solvent will acquire an electric moment

$$(\epsilon_0 - 1) \frac{F}{4\pi}$$

The homogeneous field will be disturbed in the region of the particles in a complicated way, but if we observe this effect in a point at a larger distance from the particle, the lines of force superimposed on the homogeneous field will be those of a dipole m , which can be either positive or negative, and which by its strength and direction defines the particle in all the details we need for our purpose. In general, m and F will not have the same direction, with the ultimate result that the scattered light observed under an angle of 90° with the direction of the primary beam will not be plane polarized. At the end of this paragraph we shall indicate the correction which takes care of this depolarization effect, but since in all the practical cases which have come to my attention so

far this correction is negligible, we shall from now on assume that m and F point in the same direction.

If now a volume V of solution containing n particles per cubic centimeter in high dilution is subjected to the field F , the total electric moment in the direction of F will be

$$V \left[(\epsilon_0 - 1) \frac{F}{4\pi} + nm \right]$$

which means that the dielectric constant ϵ which we observe as characteristic for the solution follows from the relation:

$$\epsilon - \epsilon_0 = 4\pi n \frac{m}{F} \quad (1)$$

Let us now suppose that the extension of the particle is so small that even at the distance where its whole disturbing effect can be described as the field of the dipole m this distance is still small compared with the wave length of the light (measured in the medium).

In order to find the radiation field surrounding the particle at larger distances we have merely to adjust it as a solution of Maxwell's equations in such a way that at small distances it equals the electrostatic field of our dipole m vibrating with the frequency of the light. This is a familiar calculation. It is found that at a large distance r (large compared with the wave length) the electric intensity E and the magnetic intensity H are

$$\begin{cases} E = m\kappa^2 \frac{\sin^2 \vartheta}{r} \cos(\omega t - \mu_0 \kappa r) \\ H = \mu_0 E \end{cases}$$

in which

$$\kappa = \frac{\omega}{v} = \frac{2\pi}{\lambda}$$

where λ = wave length in a vacuum, v = velocity of light in a vacuum, and ω = frequency of the light vibrations.

On a large sphere surrounding the dipole, with its center at the position of the dipole and its north pole at the place where the vector representing the dipole cuts through this sphere, E is in the south-north direction everywhere, and the lines of force of the magnetic field are circles of constant latitude. The angle ϑ measures the latitudes angle from the north pole, and $E = H = 0$ at both the south and the north pole.

The energy radiated per second through 1 cm.² of the sphere is represented by the time average of Poynting's vector and amounts to

$$\frac{v}{8\pi} \mu_0 m^2 \kappa^4 \frac{\sin^2 \vartheta}{r^2}$$

making the total energy loss per second and per particle equal to

$$\frac{1}{3} \frac{v}{\mu_0} \mu_0^2 m^2 \kappa^4$$

For a (polarized) primary light beam its intensity I equal to the energy carried through 1 cm.² per second, is

$$I = \frac{v}{\mu_0} \frac{\mu_0^2 F^2}{8\pi}$$

If such a beam goes through our solution, it will in the direction of propagation lose intensity according to the relation

$$-\frac{dI}{dx} = n \frac{1}{3} \frac{v}{\mu_0} \mu_0^2 m^2 \kappa^4 = \left(\frac{8\pi}{3} n \kappa^4 \frac{m^2}{F^2} \right) I$$

The quantity in brackets is what is generally called the "turbidity", to be indicated by τ . We therefore come to the conclusion that

$$\tau = \frac{8\pi}{3} n \kappa^4 \frac{m^2}{F^2} \quad (2)$$

According to equation 1 the difference in dielectric constant between the solvent and the solution is proportional to n , the number of particles per cubic centimeter, and to m/F , the electric moment characterizing the particle in a field of unit intensity. The turbidity according to equation 2 is also proportional to n , but, unlike the dielectric constant, proportional to the square of m/F . This corresponds to the fact that the change in the velocity of the light (measured by the dielectric constant) is essentially an interference effect, which involves only the amplitudes of the field, whereas the turbidity measures energy losses and therefore intensities, which are proportional to the square of the amplitude.

Like the osmotic pressure, the turbidity is proportional to the number of particles per cubic centimeter. Therefore either can be used to determine the molecular weight. However, in the first case the proportionality constant is universally the same and equal to kT (k = Boltzmann's constant; T = absolute temperature). In the second case the proportionality constant depends on the optical properties of the particle, but it can be determined unambiguously from a measurement of the change in refraction connected with a shift from the solvent to the solution. In order to express this interconnection between the two experiments which have to be carried out if the turbidity method is used, the unknown quantity m/F can be eliminated between equations 1 and 2 and we arrive at the relation (4):

$$\tau = \frac{32\pi^3}{3} \frac{\mu_0^2 (\mu - \mu_0)^2}{\lambda^4} \frac{1}{n} \quad (3)$$

where, instead of the dielectric constants, the indices of refraction, μ for the solution and μ_0 for the solvent, are introduced. For practical purposes it is customary to express n in the concentration c (in grams per cubic centimeter),

the molecular weight M , and Avogadro's number N ($N = (6.0228 \pm 0.0011) \times 10^{23}$) (1).

Relation 3 can then be written in the form

$$\frac{\tau}{c} = HM \quad (3')$$

in which the proportionality constant H must be derived from refraction measurements and is defined by the relation

$$H = \frac{32\pi^3}{3} \frac{\mu_0^2}{N\lambda^4} \left(\frac{\mu - \mu_0}{c} \right)^2 \quad (3'')$$

It has the dimension cm^2/g^2 .

The relations 3, 3', and 3'' hold for the case in which the light scattered at an angle of 90° with the direction of the primary beam is plane polarized. It can be expected that this condition is not quite satisfied, although so far a correction for depolarization has not been found necessary. If the primary light is unpolarized, the depolarization ρ of the scattered light can be measured by building the quotient of the intensity of the light which (scattered at an angle of 90°) passes a nicol with its plane of polarization coinciding with the plane of primary and secondary ray divided by the intensity passed by this nicol turned 90° . The correction factor for the molecular weight is then

$$\frac{6 - 7\rho}{6 + 3\rho}$$

and is known as Cabannes' factor (2). For $\rho = 1$ per cent the actual molecular weight is 1.56 per cent smaller than that derived from relation 3'.

III. SMALL PARTICLES; MORE CONCENTRATED SOLUTIONS

In Einstein's fluctuation theory the additional scattering from a solution as compared to that of the solvent is considered due to spontaneous fluctuations in concentration. The final result expresses that these fluctuations are the smaller in magnitude the larger the osmotic work which has to be performed in order to bring about a change in concentration. At the same time it relates the intensity of scattering also to the change in index of refraction connected with a change in concentration. The relation can be written in the form:

$$\tau = \frac{32\pi^3}{3} \frac{\mu_0^2}{N\lambda^4} \frac{(c\partial\mu/\partial c)^2}{c \frac{\partial}{\partial c} \left(\frac{P}{RT} \right)} \quad (4)$$

in which P is the osmotic pressure and $R = Nk$ is the gas constant. In most practical cases it is found that $\mu - \mu_0$ is proportional to the concentration with a high degree of precision, within the concentration range generally considered for polymer solutions. So instead of $\partial\mu/\partial c$ we can substitute $(\mu - \mu_0)/c$. The occurrence of the concentration gradient of the osmotic pressure in the denominator suggests that the reciprocal of the turbidity be considered instead of the

turbidity itself in all cases where the effect of concentration on the turbidity is to be compared with that on the osmotic pressure. So we are led to transform relation 4 into

$$H \frac{c}{\tau} = \frac{\partial}{\partial c} \left(\frac{P}{RT} \right) \quad (4')$$

in which H is the same refraction constant as defined by relation 3". Since, according to van't Hoff's law, P/RT is equal to c/M for dilute solutions, relations 3' and 4' are identical in this case.

Since it is well known that, although the deviations of van't Hoff's law for high-polymer solutions are important even at high dilutions, the osmotic pressure can be expressed adequately by a two-term expression of the form

$$\frac{P}{RT} = \frac{c}{M} + B^2c$$

we have to expect according to equation 4' that for the reciprocal specific turbidity the linear relationship

$$H \frac{c}{\tau} = \frac{1}{M} + 2Bc \quad (5)$$

will be a good approximation.

The constant B depends on the solvent. In a good solvent B is large and positive; in a poor solvent B can be zero and even negative (for the theory see references 9, 10, 12). In all practical applications of light scattering to the determination of molecular weights it has now become the custom to determine H by refraction measurements and τ for a series of concentrations, and then plot Hc/τ as a function of c . A straight line through the observed points now cuts the vertical axis of the figure at an ordinate which is equal to $1/M$ (6).² The straight-line relationship holds also for solutions containing polymers with a distribution of molecular weights. It can easily be shown from relation 4' that in this case the intercept is the reciprocal of the weight-average molecular weight (15). As an illustration figures 1 and 2 represent measurements of McCartney on polystyrene dissolved in different mixtures of a good solvent (benzene) and a precipitant (methanol). Figure 1 represents the excess turbidity (normalized in such a way that the effect of addition of methanol on the specific refractive index is eliminated) of polystyrene in solvent mixtures containing 0, 7.5, 10.0, 12.5, 15, and 22.5 volume per cent methanol. Whereas in a good solvent the

² The first application of light scattering to molecular-weight determinations in protein solutions, based on Rayleigh's theory of the scattering of a medium in which spheres are suspended, seems to be that of P. Putzeys and J. Brosteaux (Trans. Faraday Soc. **31**, 1314 (1935)). Recently a summary of a paper by H. Staudinger and I. Henel-Immendorfer (J. Makromol. **1**, 185 (1944)), entitled "Determination of molecular weights of glycogenes by the use of Rayleigh's law," came to my attention. The authors do not yet realize that the constant H can be determined experimentally without making assumptions about the particles or their so-called optical constants. See also C. V. Raman (Indian J. Phys. **2**, 1 (1927)).

turbidity increases slowly with increasing concentration, and indeed becomes essentially constant at higher concentrations, in a poor solvent the increase is more rapid and in the mixture containing the highest per cent of methanol the turbidity increases proportionally to the concentration. If these curves are converted into another set, plotting this time Hc/τ vs. c , a series of straight lines is obtained (figure 2). Thus benzene gives the steepest slope, and as the solvent gets poorer, the slope decreases until for the poorest (22.5 per cent methanol) the line is practically horizontal.

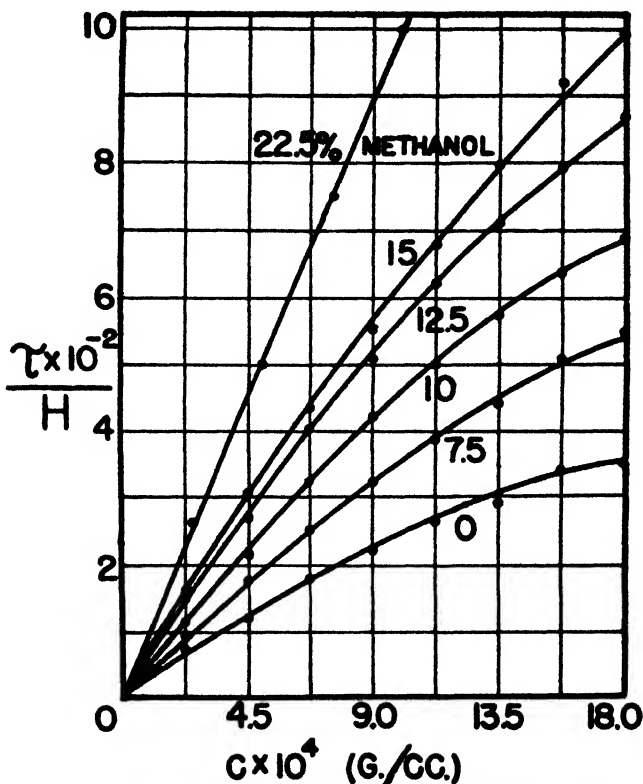


Fig. 1. Turbidity of polystyrene in benzene-methanol mixtures

A peculiar feature of the straight lines in our case is that they have not the same intercept. Considered superficially, this seems to indicate that the molecular weight increases with increasing content of non-solvent in the mixture. It can, however, be shown that the effect is due to preferential adsorption of the benzene on the polymer particle (8) and its interpretation furnishes a quantitative measurement of this preference. In simple solvents no such effect occurs, except for possible real agglomeration of the polymer particles.

IV. LARGER PARTICLES; HIGH DILUTION

The preceding has been built up on the assumption that the radiation of the particle can be represented as that of a single dipole and this implies, as we have

seen, that the dimensions of the particles are small compared with the wave length. In the case of a larger particle different parts of it will not be submitted to the same exciting field intensity either in magnitude or in phase, and at a distant point the radiation field will be made up of a superposition of waves coming from the different parts of the particle, interfering with each other. If we want to calculate the resulting radiation field according to this picture, we have not only to know what the phase differences are between the different elementary waves at the point of observation, but also what the field intensities

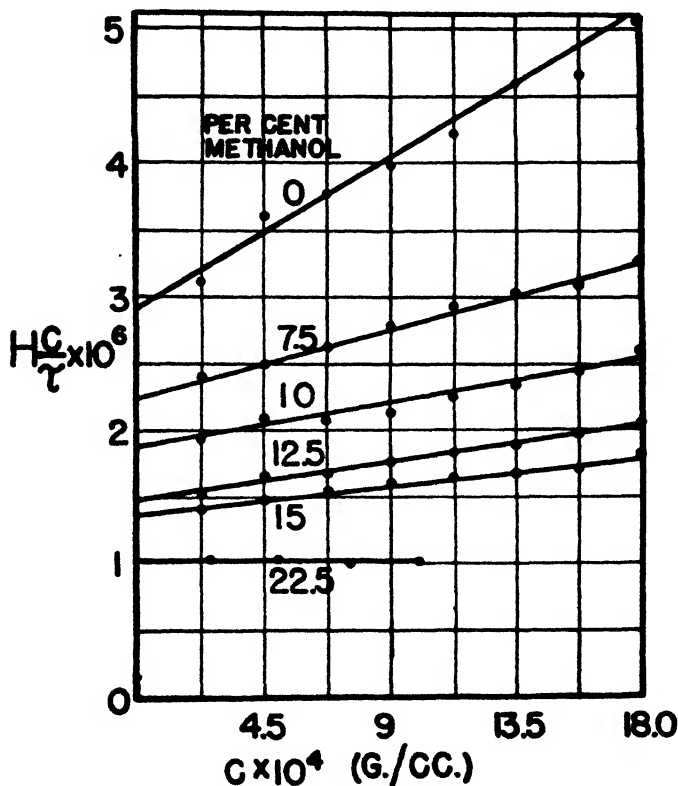


Fig. 2. Reciprocal specific turbidity of polystyrene in benzene-methanol mixtures

are in the elements of volume from which each of these waves emerges, since this determines their amplitude. In all its generality this problem can only be solved by finding an exact solution of Maxwell's equations with the proper boundary conditions. The mathematical problem is so difficult that the only case of any importance to our subject which could be treated is that of a homogeneous sphere (3, 11).³ Such a restriction to a very special form of the particle is obviously not what we want in connection with our problem.

³ For applications of these calculations see the recent articles of V. K. La Mer and Marion D. Barnes on colloidal sulfur (J. Colloid Sci. 1, 71, 79 (1946)).

Under these circumstances we propose to attack it in a different way, which eliminates the restrictions as to shape or structure of the particle from the beginning. In Mie's treatment the total radiation field is eventually represented as a superposition of fields of di-, quadru-, and higher poles all emanating from the center of the sphere. Their amplitudes and phases follow from the exact solution of Maxwell's equations. The consecutive terms of this series represent in their sequence the parts which have to be taken into account to push the representation of reality to higher and higher orders of approximation. Now the main difficulty in determining the strength of these poles lies in the fact that the original field which excites the particle is distorted by its own electromagnetic reaction. This reaction will be the stronger the more the optical constants of the particle differ from its surroundings, and the distortion of the primary field will become negligible when those differences are small. For our purpose this suggests the assumption that to a first approximation the primary field is not distorted at all. We then know right away the strength of the elementary dipoles in the different elements of volume of the particle, and it is a simple matter to calculate the result of the superposition of all the elementary waves in the point of observation. As a matter of fact, this is exactly the method of calculation followed to represent the interference effects observed with x-rays or electrons scattered by crystals, liquids, or gases. This first approximation contains from the beginning the effect of all the poles of any order, but at the same time, as a first approximation, it uses approximate values for their amplitudes and phases. Applied to a spherical particle and in a mathematical sense it amounts to a rearrangement of terms in Mie's series. The first step can be followed by a second step in which the now distorted primary field is used to calculate the excitation of the elements of the particle in a second approximation, and so on. In the following we confine our attention to the first step, not only because the higher approximations are cumbersome but mainly because in many instances and by a proper choice of solvent it is possible to make the differences in optical constants of the particle and its surroundings so small that our first approximation is adequate.

As a first example we treat the case of a flexible polymer of the familiar kind consisting of n links each of length a which can rotate freely and make an angle with each other of which the cosine is equal to p . The average square of the distance from beginning to end of such a chain is

$$R^2 = na^2 \frac{1+p}{1-p} \quad (6)$$

and the usual formula (which neglects any kind of interaction of parts of the chain on each other) representing the probability that the end point is found in a shell of radii between r and $r + dr$ with the beginning of the chain in its center is

$$w(r)4\pi r^2 dr = \left(\frac{3}{2\pi R^2}\right)^{3/2} e^{-(3/2)(r^2/R^2)} 4\pi r^2 dr \quad (6')$$

If we visualize the chain as a series of emitters, each located at the intersection of two bonds and all of the same strength, it is well known from the procedure followed in the case of x-rays that the average intensity of scattering which is to be observed in any direction is proportional to

$$I = \sum_{\mu} \sum_{\nu} \frac{\sin [\kappa s r_{\mu\nu}]}{\kappa s r_{\mu\nu}} \quad (7)$$

Here s stands for $2 \sin \frac{\vartheta}{2}$, in which ϑ is the angle between the secondary and the primary beam, $\kappa = 2 \pi / \lambda$, in which λ is the wave length as measured in the liquid surrounding the particle, and $r_{\mu\nu}$ is the distance between the emitter μ and another emitter ν . The summation goes twice over all emitters. Attention should be drawn to the fact that in equation 7 the effect of polarization has been omitted. Here and in the following the term "intensity" refers therefore to the observed intensity after correction for the influence of the polarization effect.

Relation 7 holds for a molecule of definite and unvariable shape in the average over all orientations in space which it occupies without discrimination. The only thing left to do in our case is to average relation 7 a second time over all the forms the flexible molecule can acquire with probabilities according to relations 6 and 6'. The final result is

$$I_{\text{average}} = \frac{2}{x^2} \left[e^{-x} - (1 - x) \right] \quad (8)$$

with

$$x = \frac{\kappa^2 s^2 R^2}{6} \quad (8')$$

if we normalize the average intensity so as to make it equal to unity for $x = 0$ which corresponds to $\vartheta = 0$, that is, the direction of the primary beam. Since, according to equation 8, the intensity decreases steadily with increasing x , we have to expect that in cases in which R/λ is large enough the forward scattering will exceed the backward, and experimental evidence of such an angular dissymmetry will enable us to draw conclusions about the size of the polymer molecule. For $R = 0.1 \lambda$ it follows, for instance, that the backward scattering is 8.2 per cent smaller than that in the forward direction. Our own experience, as well as that of other observers (13), seems to indicate that in many cases the dissymmetry actually observed is more pronounced than we would expect if R is calculated from the chemical structure by equation 6. This then means that the polymer chain is stiffer than free rotation combined with the assumption of negligible interaction of chain parts would lead us to expect. This is, of course, no surprise; we see the value of dissymmetry measurements in the fact that in this way we learn experimentally about the actual stiffness of the polymer chain, without having recourse to doubtful preconceived notions.

We prefer to visualize other types of polymers, like proteins, as rigid particles of definite shape. The summation of equation 7 must then be replaced by an

integration over the volume of the particle. Applied to a spherical shape (radius a) the intensity-distribution function is

$$I_{\text{average}} = \left[\frac{3}{x^3} (\sin x - x \cos x) \right]^2 \quad (9)$$

with

$$x = \kappa s a \quad (9')$$

and again normalized to $I = 1$ for $x = 0$. This relation has been used with good results in the optical analysis of rubber lattices.⁴

Formulae for other forms can easily be derived. However, from a more general point of view it seems worthwhile to present the argument in the following way: if dissymmetry measurements have been made with a rigid polymer, it will be possible to represent the (normalized) intensity as a function of s in the form

$$I = 1 - \alpha_1 s^2 + \alpha_2 s^4 - \quad (10)$$

Knowing then the coefficients α , we can ask what they tell us about the shape of the particle. If only α_1 is known or in case the two-term expression $1 - \alpha_1 s^2$ is sufficient to represent the intensity from $\vartheta = 0^\circ$ to $\vartheta = 180^\circ$, it can easily be seen that we have learned only about the average size of the particle in the following sense. It turns out that

$$\alpha_1 = \frac{\kappa^2}{3} \frac{1}{V} \int r^2 dS \quad (10')$$

in which V is the volume of the particle and r is the distance of any point in the interior of the particle from its center of gravity, whereas the integration extends over all the elements of volume dS in the interior of the particle. What we have learned then by determining α_1 is the value of the average square of all the distances within the particle from its center of gravity divided by the square of the wave length. Only if the particle is large enough, such that the two-term expression is not sufficient to represent the intensity distribution, can we learn more about the shape by light scattering. The next term tells about the average fourth power of distances within the particle and in connection with the preceding term would enable us to approximate its shape by an ellipsoid and so on.

One final remark has to be made concerning the use of formulae like equation 5 for molecular-weight determinations in cases in which a dissymmetry effect can be observed. The turbidity τ appearing in the relations of paragraph 2 has been calculated under the assumption that the particles are very small com-

⁴ McCartney has compared equation 9 with the numerical calculations of H. Blumer (Z. Physik **32**, 119 (1925)) based on Mie's formula and has found that equation 9 gives values of I_{180}/I_0 in error by less than 10 per cent for particles as large as $2a/\lambda = 1/3$ for refractive-index ratios of 1.5 and barely perceptible errors for particles even larger in the refractive-index range normally encountered in polymer solutions.

pared with the wave length. This makes the scattered intensity proportional to $\frac{1}{2}(1 + \cos^2 \theta)$, and τ of the formula can be and has been obtained by integrating over all directions in space. It is obvious that if a dissymmetry effect exists, the actual total turbidity will be diminished by the interference effect which makes the backward scattering smaller than the forward scattering. The turbidity τ appearing in the formula represents the value which would be obtained if the interference effect did not exist. Practically, the correction can easily be evaluated by comparison of the actual angular distribution with that represented by $\frac{1}{2}(1 + \cos^2 \theta)$.

V. EXPERIMENTAL ARRANGEMENTS

In the application of the turbidity method to the determination of molecular weights two measurements must be made.

Firstly, the difference between the index of refraction of the solution μ and that of the solvent μ_0 has to be measured. One single measurement at a given concentration c , say of 1 per cent, is usually sufficient, since the difference $\mu - \mu_0$ is generally very accurately proportional to c . Usually this difference is of the order 0.001 for a 1 per cent solution. The fifth decimal must be known in order to ensure an accuracy of the order of 1 per cent in the quotient $(\mu - \mu_0)/c$. In our laboratory we use a differential refractometer, consisting of a hollow large-angle prism (140° angle) which contains the solution and which is immersed in a rectangular cell containing the solvent. The cell is interposed between two lenses (focal length 70 cm.). In the focal plane of the first lens is a slit illuminated with the same monochromatic light as that used for the scattering measurements. In the focal plane of the second lens the image of the slit is observed in an eyepiece equipped with a filar micrometer. As a monochromatic light source a mercury arc, AH-4, with the appropriate light filter is used. The instrument is calibrated with sucrose solutions and water. The displacement of the slit image is proportional to $\mu - \mu_0$, and a difference of 0.001 corresponds to a displacement of 3 mm., which is amply sufficient to ensure the required accuracy.

Secondly, the turbidity must be measured. The instrument used for this purpose is so constructed that a slightly convergent beam of monochromatic light, again furnished by a mercury arc, and the appropriate filter is focused in the interior of a test tube containing the liquid, entering through the bottom of the tube. The light scattered in directions near 90° with respect to the direction of the primary beam falls on a photocell. The resulting photocurrent is amplified in a d.c. amplifier (supplied by the Photovolt Corporation, New York City) and read on a microammeter. Another photocell receives a small part of the primary light and serves as a check on the constancy of the light source. With current regulation of the mercury arc by means of a General Electric B-47 ballast lamp circuit, this arrangement gives stable, reproducible meter readings. The excess scattering of the solution as compared with the solvent is measured as the difference in reading of the microammeter for the test tube filled with solution and filled with solvent. For the most sensitive setting of the amplifier, one scale division of the microammeter corresponds to a turbidity of $5 \times 10^{-6} \text{ cm.}^{-1}$,

a result which means practically that reliable measurements can be made with solutions which scatter as little as 20 per cent more than the pure solvent. As an illustration of the high sensitivity of this method, McCartney determined the molecular weight of sucrose by 90° scattering. Figure 3 shows the close agreement between the experimental values of the turbidity and the turbidity calculated from equation 4, using osmotic-pressure data. The molecular weight calculated from experiment is 380, 10 per cent different from the osmotic-pressure molecular weight (342).

The absolute value of the turbidity is determined with the help of a standard, a solution of polystyrene in toluene of known turbidity in a sealed test tube. This standard has been calibrated with a special instrument. A monochromatic parallel beam passes first through a small rectangular cell and the light scattered under 90° by the solutions to be investigated falls on a photographic plate.

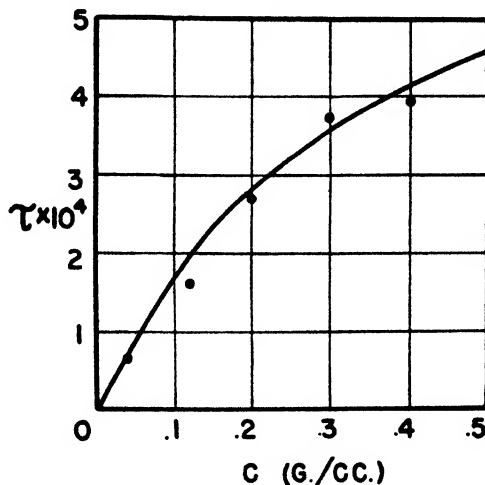


FIG. 3. Turbidity of aqueous sucrose solutions. Curve calculated from osmotic-pressure data. Points determined by 90° scattering.

After the primary light has passed this first cell it enters a second cubical cell filled with water in which a hollow cube is immersed. Three vertical sides of this cube are glass plates; the fourth vertical side is open. The light passes first the open side, is then three times reflected on the three glass sides, and eventually leaves the cube and the second cell in a direction perpendicular to the primary beam, after which it is also intercepted by the photographic plate. The reflection coefficient of each glass plate immersed in water can be calculated from the refractive indices of glass and water according to Fresnel's formula. Since this coefficient is small and since it has to be raised to the third power to account for the three reflectors, the final reflected beam has a known intensity comparable to that of the scattered beam emitted by the solution to be investigated. The intensities of the two spots on the photographic plate are finally compared with a microphotometer.

In order to indicate the order of magnitude of the effects we may mention that if a 1 per cent solution has $\mu - \mu_0 = 10^{-3}$, the refractive constant H of equation 3'' is of the order 10^{-6} cm.²/g.² This corresponds roughly, according to equation 3', to a turbidity $\tau = 10^{-3}$ reciprocal cm. for a 1 per cent solution of a polymer with the molecular weight $M = 10^6$ g.

Our dissymmetry measurements have all been made with the photographic method, although measurements with a photocell and amplifier are perfectly feasible. The second procedure now seems more advisable.

In one instrument a parallel beam of light passes through a cell and is received in a light trap. At the side of the cell is a flat glass plate. The scattered light leaves the solution through this plate and is restricted by a small circular hole in a metal plate. It is intercepted by a film which is bent to a half-circle around this opening. The blackening of the film is measured as a function of the scattering angle with a microphotometer and reverted to light intensity by the usual method. If this cell is used, corrections must be made for the effect of the refraction of the scattered light in leaving the cell in order to construct the angular distribution curve.

In another instrument a cell of octagonal cross section is used. The primary beam enters one side and leaves by the parallel side. The three other sides to the right or to the left are provided with screens, each having a small circular hole followed by a tube acting as collimator.

The scattered light leaving those tubes is again intercepted by a photographic film. In this case only the light scattered in three directions, under 45°, 90°, and 135° against the direction of the primary beam, is measured, and since it passes through the glass plates normal to their plane no corrections for refraction are indicated.

Most of the instruments have been designed by P. P. Debye (5) and constructed by our mechanician, H. Bush.

This paper is a summary, with additions and omissions, of reports submitted during the war to the Office of Rubber Reserve, Reconstruction Finance Corporation, which supports our program of research at Cornell University. Collaborators in this research were P. P. Debye, F. W. Billmeyer, Jr., J. R. McCartney, and A. M. Bueche.

REFERENCES

- (1) BIRGE, R. T.: *Rev. Modern Phys.* **13**, 233 (1941).
- (2) CABANNES, P.: *La diffusion moleculaire de la lumière*. Presses Universitaires de France, Paris (1929).
- (3) DEBYE, P.: *Ann. Physik* [4] **30**, 57 (1909).
- (4) DEBYE, P.: *J. Applied Phys.* **15**, 338 (1944).
- (5) DEBYE, P. P.: *J. Applied Phys.* **17**, 392 (1946) (description of instruments of improved design).
- (6) DOTY, P., ZIMM, B. H., AND MARK, H.: *J. Chem. Phys.* **12**, 144 (1944).
- (7) EINSTEIN, A.: *Ann. Physik* **33**, 1275-98 (1910).
- (8) EWART, R. H., ROE, C. P., DEBYE, P., AND MCCARTNEY, J. R.: *J. Chem. Phys.* **14**, 687 (1946).

- (9) FLORY, P. J.: *J. Chem. Phys.* **10**, 51 (1942).
- (10) HUGGINS, M. L.: *J. Phys. Chem.* **46**, 151 (1942).
- (11) MIE, G.: *Ann. Physik* [4] **25**, 377 (1908).
- (12) MILLER, A. R.: *Proc. Cambridge Phil. Soc.* **38**, 109 (1942); **39**, 54, 131 (1943).
- (13) STEIN, R. S., AND DOTY, P.: *J. Am. Chem. Soc.* **68**, 159 (1946).
- (14) STRUTT, J. W. (Lord Rayleigh): *Phil. Mag.* **41**, 107-20, 274-9, 447-54 (1871).
- (15) ZIMM, B. H., AND DOTY, P. M.: *J. Chem. Phys.* **12**, 203 (1944).

THE ASSOCIATION OF POLYMER MOLECULES IN DILUTE SOLUTION¹

PAUL DOTY², HERMAN WAGNER³, AND SEYMOUR SINGER⁴

Department of Chemistry, Polytechnic Institute of Brooklyn, Brooklyn 2, New York

Received August 8, 1946

The belief has developed that polymer molecules, in dilute solution at least, are always molecularly dispersed, because of the lack of refuting evidence and the attractive simplicity of the assumption. It is the purpose of this paper, however, to show that stable association of polymer molecules in solution exists under certain conditions. The work is essentially divided into two parts: in the first part the association of polyvinyl chloride in different solvent media is studied in detail by several different methods; in the second part there are described much less detailed experiments, mostly concerned with demonstrating that the stable association of polymer molecules is a general phenomenon when the system is near the point of phase separation.

I. POLYVINYL CHLORIDE

The polymers used in this part of the investigation were several fractions resulting from the fractionation of a commercial polyvinyl chloride known as Geon 101 (The Goodrich Chemical Company, Cleveland, Ohio), produced in high purity for electrical applications. The unfractionated polymer had an intrinsic viscosity in cyclohexanone at 60°C. of 0.88 and a chlorine content of 56.0 per cent compared with the theoretically expected value of 56.8 per cent.

The fractionation (1) was carried out by means of successive additions of 1-butanol to a 1 per cent solution of the polymer in cyclohexanone. Twenty-

¹ Presented at the Twentieth National Colloid Symposium, which was held at Madison, Wisconsin, May 28-29, 1946.

² Present address: Department of Colloid Science, Cambridge University, Cambridge, England.

³ Present address: Department of Chemistry, Cornell University, Ithaca, New York.

Part of this paper is from the thesis submitted by Herman Wagner in partial fulfillment of the requirements for the degree of Master of Science at the Polytechnic Institute of Brooklyn, June, 1946.

⁴ Du Pont Fellow in Chemistry, 1945-46.

three fractions were obtained. These were regrouped according to increasing viscosity, and a refractionation was performed. The viscosity distribution curve resulting from this procedure was extremely asymmetric and narrow. Fractionation by an extraction method and a selective evaporation method resulted in distribution curves of the same general shape. The fractions used here came from the first fractionation procedure described.

Unless otherwise mentioned, fraction No. 7 was used in this work. It was while investigating the temperature dependence of the osmotic pressure of this fraction dissolved in dioxane that the association was first noted. The osmotic-pressure measurements at different temperatures in several solvents were carried out as part of a thermodynamic study of heats of dilution. This work has been published (5) but is summarized below in view of its relevance to the study of association. Following this summary, the investigation of the nature of the association by means of turbidity, sedimentation in the ultracentrifuge, the angular dependence of the intensity of the scattered light, viscosity, and depolarization is discussed. An interpretation of these measurements is then presented.

A. OSMOTIC-PRESSURE MEASUREMENTS (5)

The osmotic-pressure data at different temperatures for polyvinyl chloride in cyclohexanone, butanone, and dioxane are plotted in figures 1, 2 and 3, respectively. These measurements were obtained by means of a Fuoss-Mead osmometer in a specially constructed thermostat. The number-average molecular weights calculated from the intercepts of these plots are listed in table 1. It will be noted that these molecular weights in cyclohexanone and butanone are essentially independent of temperature but differ from each other in the two solvents. In dioxane a higher molecular weight is observed at room temperature, but this decreases at temperatures above 40°C. to a value even less than was determined in cyclohexanone.

Similar measurements using fraction 12 and the unfractionated polymer dissolved in dioxane showed that the variation of molecular weight with temperature existed in other fractions and in the unfractionated polymer. The molecular weights are summarized in table 2.

During all the work the solutions were stored at room temperature. It was observed that when a dioxane solution was placed in the osmometer at a high temperature (say 70°C.), the osmotic pressure corresponding to that temperature would be exhibited as soon as a fairly reliable measurement could be made (about 5 min.). However, when the osmometer was cooled to room temperature, the osmotic pressure decreased only very slowly. If the solution was removed from the osmometer and then returned occasionally to the osmometer (at room temperature) for measurement, it was found that the osmotic pressure decreased approximately exponentially with time, requiring about a month to return to the value it originally exhibited at room temperature. This observation is relevant to the interpretation presented later.

B. LIGHT-SCATTERING MEASUREMENTS

The osmotic-pressure data reveal how the number-average molecular weight varies with temperature. It would appear that knowledge of how the weight-average molecular weight varies with temperature would be valuable. A weight-average molecular weight can be determined by the light-scattering

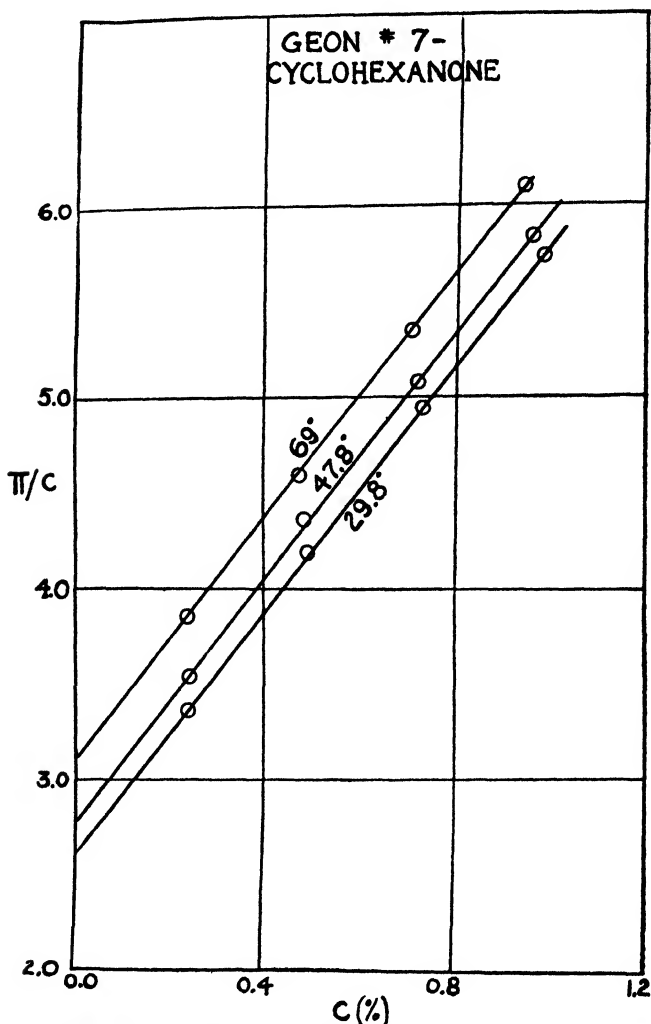


Fig. 1. Osmotic pressure of polyvinyl chloride in cyclohexanone at various temperatures

method (3, 10, 14), which involves the determination of the turbidity, of the difference in refractive index between solvent and solution, and, if the molecules exceed a few hundred Ångströms in extent, the angular dependence of the intensity of the scattered light. Moreover, the latter information can be interpreted to yield information concerning the size of the dissolved molecules.

If the intensity of the scattered light is not symmetrical about 90° , it has been reduced by the interference of light scattered from different parts of the same molecule (10). Consequently, the turbidity (as measured by scattering at 90°) is less than it would be if this interference were absent (Rayleigh scattering). The factor required to increase the measured turbidity to the value that would be exhibited if there were no intramolecular interference can be obtained from a measurement of the ratio of the intensity of the light scattered forward and backward at a pair of angles symmetrical about 90° . This ratio is designated as the dissymmetry. The measurement of this quantity, its use in correcting the

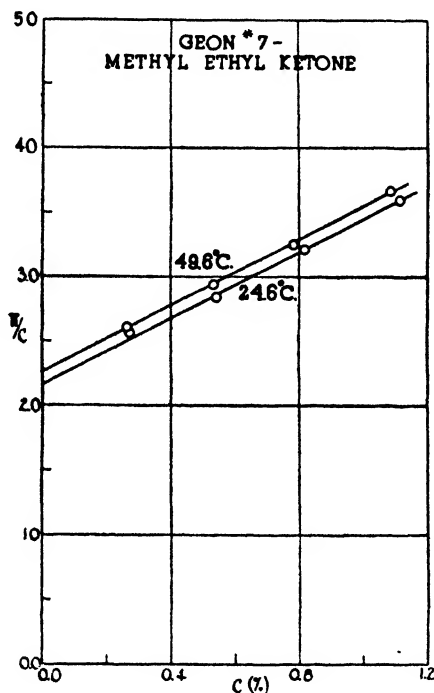


FIG. 2. Osmotic pressures of polyvinyl chloride in butanone

observed turbidity, and its interpretation in terms of molecular size are discussed in Section D of Part I.

The relation between the turbidity τ (corrected), the refractive-index increment, $\partial n/\partial c$, the concentration c , and the molecular weight M is given by

$$\frac{32\pi^3 n^2 (\partial n/\partial c)^2 c}{3\lambda^4 N_0} \frac{c}{\tau} = \frac{1}{M} + \frac{2B}{RT} c \quad (1)$$

The refractive index of the solvent is denoted by n , the wave length of light in a vacuum by λ , and Avogadro's number by N_0 . The coefficient of c/τ on the left is denoted by H . The constant B is the slope of osmotic-pressure plots,

such as in figures 1-3. Thus a plot of Hc/τ against c should give a straight line whose intercept is the reciprocal of the weight-average molecular weight.

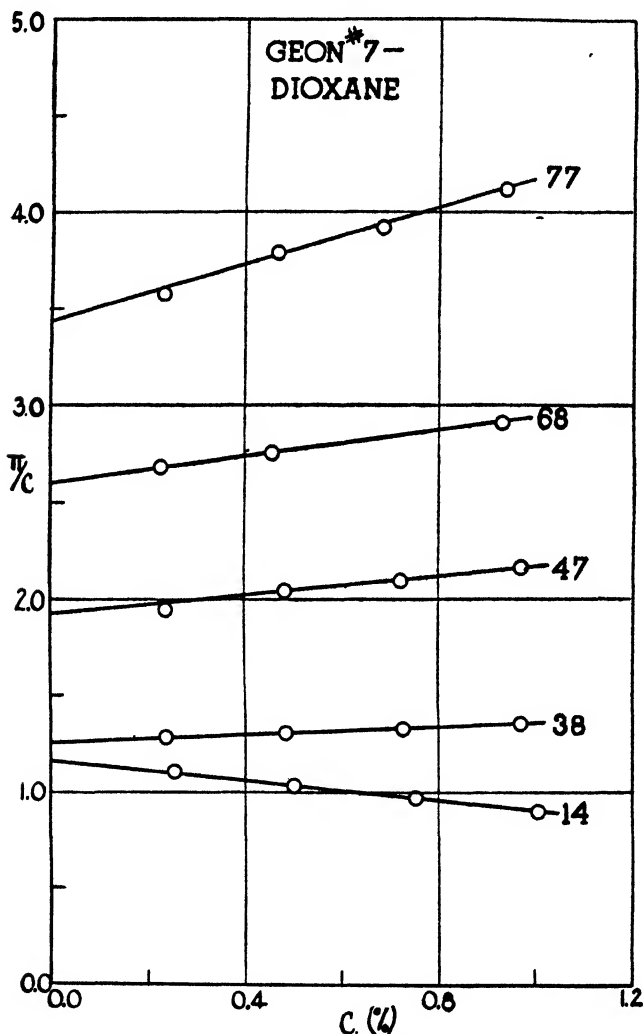


FIG. 3. Osmotic pressure of polyvinyl chloride in dioxane at various temperatures

Apparatus

For measuring the turbidity as a function of temperature a simple photo-electric instrument was constructed. A diagram of the apparatus is shown in figure 4. The source of illumination is a 100-watt AH-4 lamp (A) which is mounted in a metal housing (B). The light from this lamp is rendered parallel by a lens (C) mounted in the housing and then passes through a glass filter (D) which transmits the green mercury line (5461 Å.). This nearly parallel mono-

chromatic light is then partially reflected by means of two pieces of plate glass (E) mounted at 45° to the incident beam to a Weston photronic cell (F). The photronic cell is mounted about 6 in. away from the main part of the apparatus to minimize temperature changes due to the thermostat, since the photronic cell output is somewhat temperature sensitive. The cell is used to measure the intensity of the beam produced by the mercury lamp, since it receives a small constant fraction of this light from the two glass plates. It has a sensitivity

TABLE 1
Apparent number-average molecular weights of fraction 7

SOLVENT	TEMPERATURE	MOLECULAR WEIGHT
	$^\circ\text{C.}$	
Cyclohexanone.....	29.8	99,000
	47.8	98,500
	69.0	93,500
Butanone.....	24.6	117,000
	49.6	121,000
Dioxane.....	14.0	210,000
	38.0	211,000
	47.0	142,000
	68.0	111,000
	77.0	86,500

TABLE 2
Apparent number-average molecular weights of other polyvinyl chlorides dissolved in dioxane

POLYMER	TEMPERATURE	MOLECULAR WEIGHT
	$^\circ\text{C.}$	
Fraction 12.....	29.7	131,000
	45.7	107,000
	55.1	90,500
	70.6	84,000
Unfractionated.....	31.1	107,000
	49.9	88,000
	71.9	77,500

of about 4.4 microamperes per foot candle to white light and its response is very nearly linear, especially when there is close to zero potential difference across it. This may be accomplished by using the circuit (2, 13) shown in the lower left of figure 4. To take a reading switch S_1 is closed and the ammeter G is read. With S_1 still closed, S_2 is also closed and the ammeter is read again. If the two ammeter readings do not agree, the potential across the photronic cell is not zero and so the rheostat is adjusted until it is. This arrangement helps to increase

the sensitivity, reduce the effect of temperature variations, and increase the linearity of response.

To determine whether the response was linear, the transmission of a piece of optically flat glass, essentially a neutral filter, was measured in a photoelectric colorimeter and in this instrument. The agreement was within experimental error for this one measurement, as well as for successive measurements made with several pieces stacked together. In the latter case, the "known per cent transmission" of the glass was taken as the transmission for a single piece of the n^{th} power, where n is the number of pieces.

The major fraction of the light beam continues upward, enclosed by a wooden

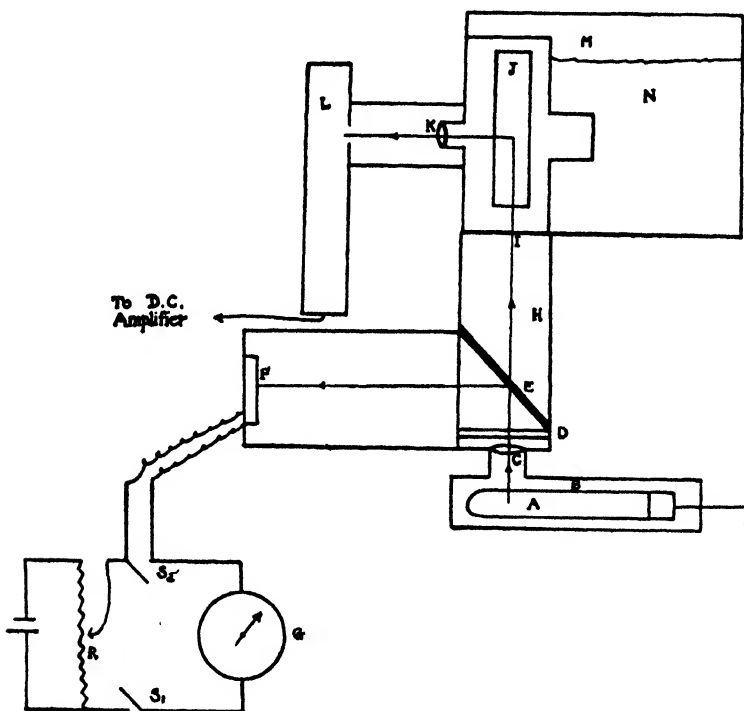


FIG. 4. The photoelectric turbidimeter

box (H) which is painted a dull flat black on the inside to reduce the stray light caused by internal reflections. It then passes through an aperture (I) so that a beam about $\frac{1}{8}$ in. in cross section enters the solution to be examined, the solution being contained in a glass cell (J). The position of the beam must be adjusted so that it passes through the center of the solution and does not hit the side of the cell.

At right angles to the cell and mounted on the outside of the thermostat is a lens (K) which serves to collect the scattered light from the sample and focus it onto the light-sensitive portion of the phototube (L). The output of the phototube is electronically amplified, and the current produced when light impinges

on the tube is determined with a sensitive galvanometer.⁵ The instrument, most sensitive to wave lengths at the lower end of the spectrum, has a sensitivity of about 2×10^{-6} foot candles per scale division in the blue region, and this may be increased tenfold by switching out the shunt across the galvanometer. Since the galvanometer has 100 divisions and can be read to about one scale division, the precision depends to a large extent on the portion of the scale used. The response of the instrument is linear, as shown in figure 5. The data were obtained in the same fashion as for the photonic cell.

The relative positions of the lens, glass cell, and phototube are so arranged that light from only the center of the solution reaches the photocell. This eliminates reflected light from the sides or corners of the glass cell. For the

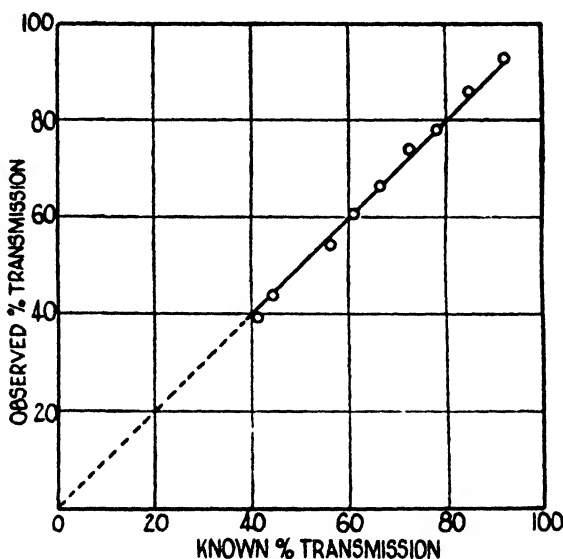


FIG. 5. Linearity of response of the phototube

same reason enough liquid must be put into the glass cell to avoid reflections from the meniscus.

The cell containing the liquid is mounted in a metal housing (M) which fits into a glass aquarium converted into a thermostated water bath (N). The temperature may be raised to about 80°C.

Operation and calibration

The instrument was calibrated indirectly. A gel of 1 per cent polystyrene in tributyl acetyl citrate was measured in a visual turbidimeter (4) which had been calibrated absolutely by using solutions and pure liquids of known turbidity. The turbidity of the gel was found to be $2.68 \times 10^{-3} \text{ cm.}^{-1}$, and the new instrument was checked before every series of readings with this secondary standard.

⁵ This entire photometer unit was purchased from the Photovolt Corporation, New York City.

The absolute value of the scattering of this gel being known, the proportionality factor between absolute scattering and instrument reading was obtained and used for all the solutions measured that day. This procedure corrects for small day-to-day variations, such as dust on the lens or on the glass plates.

To measure the turbidity of a solution, a glass cell is filled with at least 35 ml. of solution and set in place in the thermostat. Sufficient time is allowed for the solution to come to the appropriate temperature. A stop is placed in the path of the light beam and the galvanometer is adjusted to read zero. The stop is removed and the galvanometer is read again. A third reading is now taken with the stop in place again. The two dark readings are taken to be sure the amplifier has not drifted appreciably while the reading was taken. These two dark readings, which should be near zero, are averaged, and the result is subtracted from the reading obtained with the solution. Usually three such readings are taken, there being nine observations in all. The photronic cell ammeter is also read, as described above.

To calculate the absolute turbidity: Let p_s equal the galvanometer reading for the unknown solution, c_s equal the photronic cell reading when p_s was measured, p_0 equal the galvanometer reading for the standard gel, c_0 equal the photronic cell reading when p_0 was measured, and K equal the actual turbidity of the standard gel, $2.68 \times 10^{-3} \text{ cm.}^{-1}$. Then

$$\tau_0 = \frac{K p_s c_0}{c_s p_0}$$

since the response of the phototube is linear. The scattering of the solvent must be subtracted from τ_0 , the scattering of the solution, to obtain the turbidity τ , due to concentration fluctuations from which the molecular weight may be obtained. This is done by measuring τ for various concentrations, plotting Hc/τ as a function of concentration, and setting the intercept equal to $1/M_w$.

It was found necessary to filter carefully all the solutions used, since any foreign particles would obviously give erroneous results. The most prevalent and frequent contaminant was dust. All vessels were carefully rinsed and then dried by evaporation of solvents to avoid lint from the towels. The solutions were then put through sintered-glass filters, first through one of coarse or medium pore size, and then through one of fine pore size. The solutions were usually filtered directly into the glass cell in which they were to be measured, thus eliminating an intermediate step which might have caused contamination. The solution was considered dust free when no particles could be seen at right angles to an incident mercury-lamp beam.

Results

The first experiment consisted in measuring the light scattering of a 1 per cent solution (0.01 g. of polymer per cubic centimeter of solution) of fraction 7 in dioxane. The dioxane had been purified by refluxing over sodium and subsequent distillation. As the temperature of the solution was slowly raised, a sevenfold decrease in turbidity occurred between room temperature and 90°C. ,

although there was relatively little change between room temperature and 40°C. These results are shown in figure 6. A curve of the same general character resulted for fraction 12, but fraction 20, a fraction of very low molecular weight, showed very little scattering (see table 3). In every case the tempera-

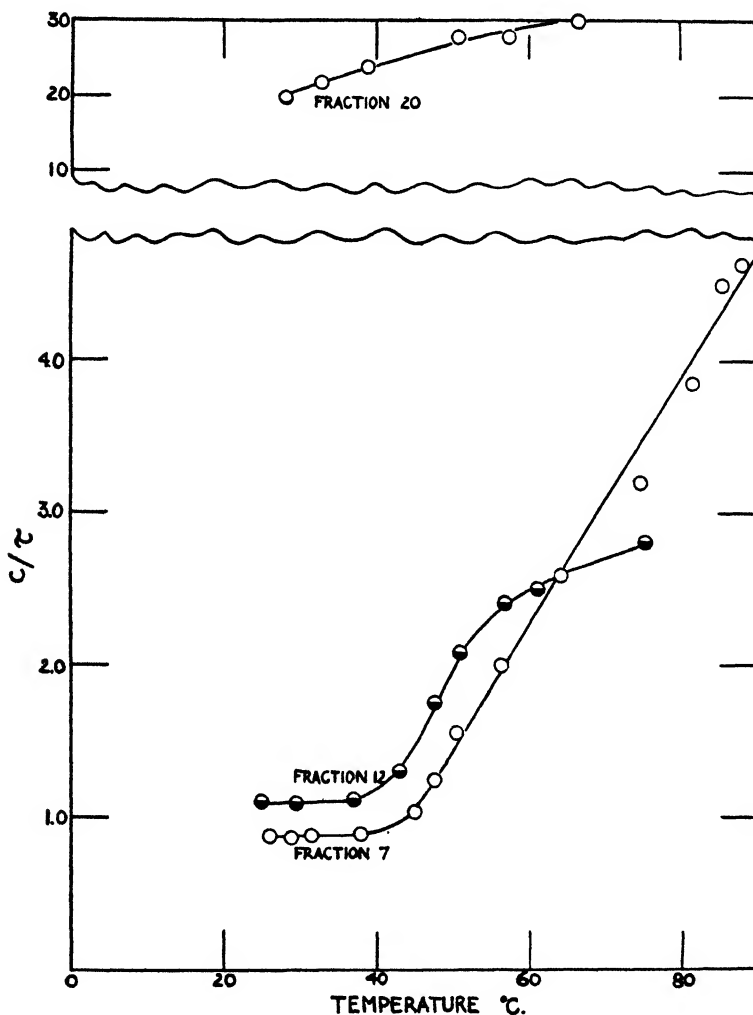


FIG. 6. Change of c/τ with temperature for fraction 7 in dioxane

ture was increased slowly, so that equilibrium was attained before a measurement was taken. It was observed that the turbidity corresponding to the higher temperature was reached at once when the solution was heated. However, when the solution was cooled from a higher temperature back to a lower temperature, the turbidity increased very slowly and required several weeks to

TABLE 3

Change of turbidity of polyvinyl chloride with temperature(a) 1 per cent solution of fraction 7 in dioxane; $Kc_0/p_0^* = 181 \times 10^{-4} \text{ cm.}^{-1}$;
solvent = $1.08 \times 10^{-4} \text{ cm.}^{-1}$

TEMPERATURE	PHOTOTUBE p_s	PHOTONIC CELL c_s	τ_0	τ	c/τ
$^{\circ}\text{C.}$			cm.^{-1}	cm.^{-1}	(g./cc.)cm.
26	59.5	94	114×10^{-4}	113×10^{-5}	0.88
29	58.5	91	116.5	115	0.865
31.5	57	89.5	116	115	0.875
38	55	88	113	112	0.89
45	46.5	87	97	96	1.04
47.5	38.5	86	98	97	1.24
50.5	30.8	86	65	64	1.56
56.5	23.3	85	51.0	50	2.00
64.5	18.8	85	39.9	38.8	2.58
75.0	15.5	85	32.7	31.6	3.21
81.5	13.2	85	27.8	26.7	3.83
86.0	11.0	85	23.4	22.3	4.50
88.0	10.5	85	22.5	21.4	4.65

(b) 1 per cent solution of fraction 12 in dioxane; $Kc_0/p_0 = 180 \times 10^{-4} \text{ cm.}^{-1}$;
solvent = $1.08 \times 10^{-4} \text{ cm.}^{-1}$

TEMPERATURE	PHOTOTUBE p_s	PHOTONIC CELL c_s	τ_0	τ	c/τ
$^{\circ}\text{C.}$			cm.^{-1}	cm.^{-1}	(g./cc.)cm.
25	48.5	95	92.5×10^{-4}	91.5×10^{-4}	1.1
29	46.5	89	95	94	1.07
37	43.5	87	91.5	90.5	1.12
43	37	87	78	77	1.3
47.5	28	86	59	58	1.75
51	23.5	86	49.5	48.5	2.08
57	20	85	43	42	2.41
61.5	19.5	84	41.7	40.7	2.50
65	18.5	83	39.9	38.9	2.58
75.5	16.5	82	36	35	2.83

(c) 1 per cent solution of fraction 20 in dioxane; $Kc_0/p_0 = 180 \times 10^{-4} \text{ cm.}^{-1}$;
solvent = $1.08 \times 10^{-4} \text{ cm.}^{-1}$

TEMPERATURE	PHOTOTUBE p_s	PHOTONIC CELL c_s	τ_0	τ	c/τ
$^{\circ}\text{C.}$			cm.^{-1}	cm.^{-1}	(g./cc.)cm.
28	3.05	91	6.0×10^{-4}	4.8×10^{-5}	20
33	2.75	87	5.7	4.5	22
39	2.65	85	5.4	4.2	24
51	2.3	84	4.8	3.6	28
57.5	2.2	83	4.8	3.6	28
66	2.1	82	4.5	3.3	30

* For an explanation of Kc_0/p_0 , see the section on apparatus.

reach the value previously exhibited at room temperature. The approach to the room-temperature value appeared to be exponential.

Turbidity was then studied as a function of concentration at 28°C., 47°C.,

TABLE 4
Change of turbidity of polyvinyl chloride (fraction 7) with concentration

PHOTOTUBE p_0	PHOTONIC CELL c_0	CONCENTRATION*	τ	c/τ	$Hc/\tau(\text{corr.}) \times 10^4$
1. Temperature = 28.5°C.; $Kc_0/p_0 = 166 \times 10^{-4} \text{ cm.}^{-1}$					
		grams/100 ml.	$\text{cm}^{-1} \times 10^4$	(g./cc) cm.	
64	89	1.00	119	0.83	0.449
60.5	88	0.833	113	0.74	0.366
56.5	86.5	0.714	107	0.665	0.322
50	85	0.526	96	0.55	0.240
44	84	0.430	86	0.50	0.210
33	83	0.296	65	0.46	0.173
M_w					16,700,000
2. Temperature = 48°C.; $Kc_0/p_0 = 181 \times 10^{-4} \text{ cm.}^{-1}$					
40	87	0.979	81.5	1.20	0.54
35	86	0.815	72.0	1.13	0.51
32	85	0.700	66.5	1.05	0.46
26	85	0.515	53.4	0.97	0.40
24	85	0.450	49.3	0.92	0.38
18	85	0.311	36.6	0.84	0.32
M_w					4,500,000
3. Temperature = 63°C.; $Kc_0/p_0 = 164 \times 10^{-4} \text{ cm.}^{-1}$					
27	97	0.962	44.7	2.15	0.86
24.5	96	0.801	40.8	1.97	0.81
22	90	0.686	39.0	1.78	0.76
18	87	0.506	32.7	1.55	0.68
15	85	0.413	28.2	1.47	0.65
11.5	85	0.285	20.7	1.33	0.60
M_w					2,040,000

* Concentrations must be corrected for the change in density as the temperature is increased. The density of dioxane at 29°, 48°, 51°, and 63°C. is 1.0218, 0.9997, 0.9964, and 0.9832 g./cc., respectively.

† Corrections for dissymmetry at 48°C. were obtained by an interpolation procedure, as explained in section D.

and 63°C., to determine how the molecular weight varied with temperature. In tables 4 and 5 Hc/τ (corr.) indicates that τ is corrected for dissymmetry.

The term denoted by H in equation 1 must be evaluated. The refractive-index increment, $\partial n/\partial c$, was determined by measuring the refractive-index differ-

ences between dioxane and a 1 per cent solution of fractions 7 and 12 in dioxane by means of a Pulfrich refractometer with a divided cell. For fractions 7 and 12 the refractive-index increment was found to be 0.0850 and 0.0865 (g./cc.)⁻¹, respectively, at a wave length of 5461 Å. The quantity H is evaluated: for fraction 7, $H = 9.0 \times 10^{-7}$; for fraction 12, $H = 9.3 \times 10^{-7}$.

In figures 7 and 8 Hc/τ is plotted against c in accordance with equation 1.

TABLE 5
Change of turbidity of polyvinyl chloride (fraction 12) with concentration

PHOTOTUBE p_0	PHOTONIC CELL c_0	CONCENTRATION	τ	c/τ	$Hc/\tau(\text{corr.}) \times 10^4$
1. Temperature = 28.5°C.; $Kc_0/p_0 = 176 \times 10^{-4}$					
		grams/100 ml.	cm. ⁻¹	(g./cc.)cm.	
44	87	1.000	87.6×10^{-4}	1.16	0.593
41	85	0.833	84.0	0.99	0.498
39	85	0.714	79.8	0.89	0.425
32.5	84	0.526	67.2	0.78	0.34
28.5	84	0.430	58.8	0.73	0.30
22	82	0.296	46.2	0.64	0.236
M_w					12,500,000
2. Temperature = 51°C.; $Kc_0/p_0 = 180 \times 10^{-4}$					
25	92	0.977	48.0×10^{-4}	2.07	0.97
22	89	0.814	43.2	1.87	0.905
20	88	0.698	39.3	1.78	0.805
15.5	86	0.514	30.6	1.67	0.721
13	84	0.420	27.0	1.55	0.644
9.9	83	0.289	20.1	1.43	0.578
M_w					2,400,000
3. Temperature = 62.5°C.; $Kc_0/p_0 = 181 \times 10^{-4}$					
19.5	92	0.962	37.8×10^{-4}	2.55	1.03
16	90.5	0.686	31.2	2.22	0.98
13.5	89	0.506	26.1	1.93	0.834
11.5	88	0.413	22.8	1.82	0.79
8.9	87	0.285	17.4	1.65	0.71
M_w					1,780,000

The values of τ corrected for dissymmetry are used. It is noted that the intercepts, which are numerically equal to the reciprocal of the molecular weights, vary with temperature similarly to the case of osmotic pressure. The molecular weights for these two samples at the different temperatures are listed in table 6.

By means of two minor approximations it is possible to transform the curve of c/τ shown in figure 6 into a plot of molecular weight *versus* temperature.

First it must be assumed that the dissymmetry of a 1 per cent solution varies linearly with temperature above 40°C. but is constant below that temperature. Secondly, the approximation is made that the Hc/τ plot has a slope independent of temperature. On this basis we can immediately correct the turbidity for

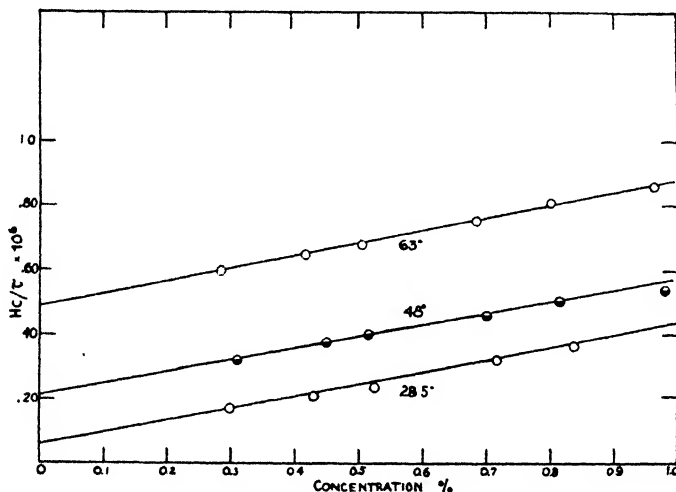


FIG. 7. Plot of turbidity data for fraction 7 in dioxane at various temperatures

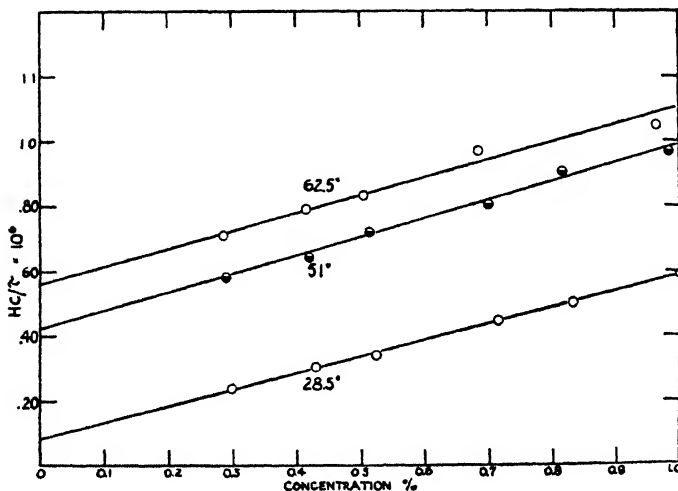


FIG. 8. Plot of turbidity data for fraction 12 in dioxane at various temperatures

dissymmetry and multiply the c/τ value thus obtained by H . If the average increase of Hc/τ in the concentration range 0–1 per cent in the plots in figure 7 is subtracted, there is obtained a curve representing Hc/τ at zero concentration *versus* temperature. The reciprocal of this curve is the weight-average molecular

weight. The final curve is shown in figure 9, where the number-average molecular weights (osmotic pressure) are shown on an enlarged scale.

The great difference between the number-average and the weight-average molecular weights as shown in figure 9 is striking. The changes brought about by increasing temperature are parallel in the two plots: no change up to about 40°C., then a sharp drop which begins to level off near 60°C. The obvious conclusion to be drawn from this is that the molecular-weight distribution is not a simple continuous distribution expected of a fraction but rather a very broad and perhaps discontinuous distribution. Moreover, the behavior shown in figure 9 suggests that the high-molecular-weight components break up into a low-molecular-weight species upon heating. In order to test this hypothesis and to gain more information, some ultracentrifuge studies were carried out.

TABLE 6
*Variation of weight-average molecular weights with temperature for
fractions 7 and 12 in dioxane*

FRACTION	TEMPERATURE	MOLECULAR WEIGHT
	°C.	
7.....	28.5	16,700,000
	48	4,500,000
	63	2,040,000
12.....	28.5	12,500,000
	51	2,400,000
	62.5	1,780,000

C. ULTRACENTRIFUGAL STUDIES

The ultracentrifuge is able to give sedimentation diagrams which are essentially plots of the concentration gradient in the solution *versus* distance from the axis of rotation. If there are two very different molecular-weight species in a solution, each will sediment with its own rate and create its own concentration gradient. The area under such a gradient curve is proportional to the concentration of that species in the original solution. Therefore, if there is a discontinuous distribution of molecular weights of fraction 7 in dioxane, the sedimentation diagrams should show two or more distinct maxima, and if association is the cause of the effects just described it is expected that the areas under the maxima should reflect the changes attendant upon heating the solution.

Fortunately, in order to obtain sedimentation diagrams of the dioxane solutions of polyvinyl chloride at different temperatures, it is not necessary to operate the centrifuge at elevated temperatures for, as previously noted, the change in molecular weight brought about by heating persists essentially unchanged for several hours after the solution is cooled. Thus if the solution is observed in the ultracentrifuge shortly after heating to a certain temperature for over 15 min., the results should not be significantly different from those obtained by actually operating the ultracentrifuge at the elevated temperature.

The ultracentrifuge used in these experiments is an air-driven Beams-Pickels model; our installation is described in detail elsewhere (11). The optical method in use is the Philpot modification of the schlieren method which permits visual observation of the course of an experiment.

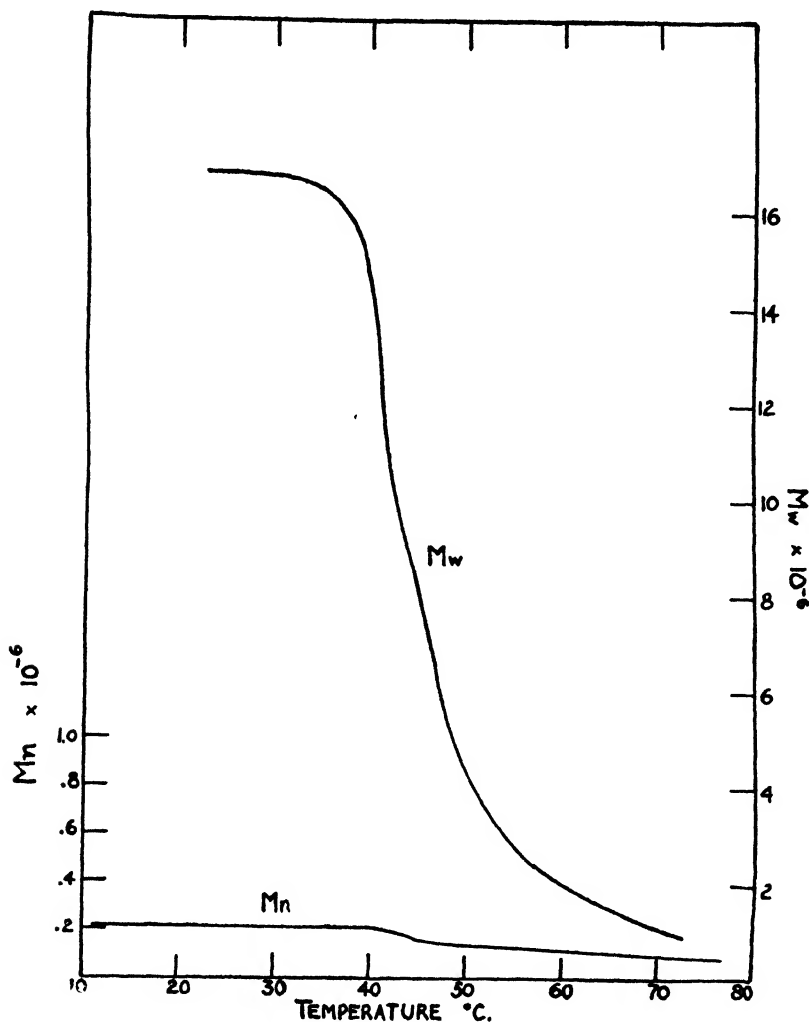


FIG. 9. Number-average and weight-average molecular weights of fraction 7 in dioxane as a function of temperature.

Two runs on a 1 per cent solution of fraction 7 in dioxane, one at 25°C., the other at 25°C. after the solution had been heated at 76°C. for 1 hr., were performed. In figure 10 two pictures taken at comparable times and speeds show the results obtained. Sedimentation is taking place from right to left, the species under the left peak being of larger molecular weights. A definite shift from the

larger to the smaller molecular-weight species upon heating is evident. Measurement of the areas gave the results in table 7. The great asymmetry of the curve of the heavier species indicates considerable skewness in the molecular-weight distribution of that group of components.

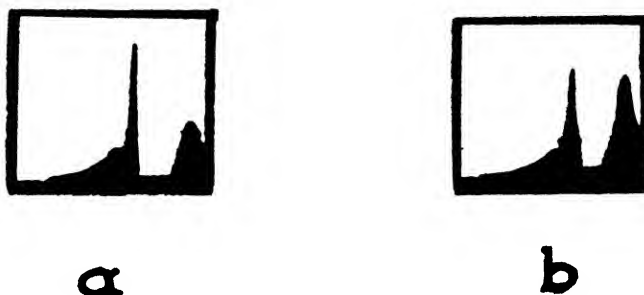


FIG. 10. Sedimentation diagrams of fraction 7 in dioxane at (a) 25°C. and (b) 76°C. Sedimentation proceeds toward the left.

TABLE 7

Relative concentrations of the two molecular-weight species in fraction 7—dioxane and fraction 7—butanone solutions as a function of temperature

SOLVENT	TEMPERATURE	HEAVIER COMPONENT	LIGHTER COMPONENT
	°C.	per cent	per cent
Dioxane.....	25	62	38
	76	41	59
Butanone.....	25	11	89
	76	9	91

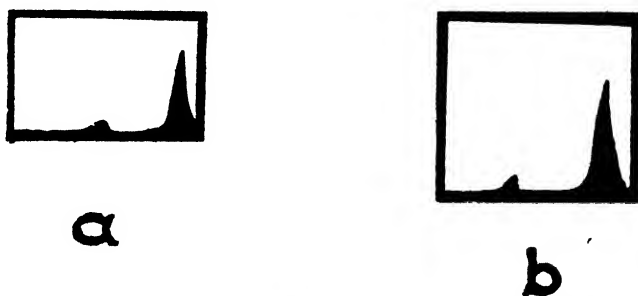


FIG. 11. Sedimentation diagrams of fraction 7 in butanone at (a) 25°C. and (b) 76°C. Sedimentation proceeds toward the left.

A 0.53 per cent solution of fraction 7 in butanone was studied under similar circumstances and showed no significant change in the relative amounts of the two species with heating; moreover, a much smaller amount of associated polymer exists in butanone than in dioxane (figure 11). It should be emphasized that

the observed number-average molecular weights prohibit the identification of the two peaks in the butanone diagram with those in the dioxane diagram. The quantity of the large-molecular-weight component in dioxane at 76°C. appears to be much larger than in butanone, yet at approximately these temperatures the number-average molecular weight in dioxane is 86,500 whereas in butanone it is 120,000.

These sedimentation experiments thus confirm the hypothesis that in dioxane some of the molecules are associated into clusters which break up somewhat on heating and re-form slowly when cooled. The remaining portion of the investigation is concerned with obtaining some information concerning the nature of the clusters.

D. DISSYMMETRY OF THE RADIATION ENVELOPE (3, 10, 14)

If the largest average dimension of a dissolved particle exceeds a few hundred Ångströms, the intensity of the light scattered from it will not be symmetrical about 90° (from the incident beam) because of the destructive interference of light scattered from different portions of the same molecule. This effect is conveniently characterized by the ratio of the intensities of the light scattered forward and backward at two angles symmetrical about 90°. This ratio is the dissymmetry at the given angles and serves as a useful measurement of particle or molecular size when evaluated by extrapolation to infinite dilution.

The dissymmetry can also be used to determine the amount by which the 90° scattering has been diminished by the interference effect. Consequently, the observed turbidity can be augmented to that which would have been observed if the molecules had been compact enough to give symmetrical Rayleigh scattering. It is in this manner that the turbidities in section B have been corrected for use in equation 1.

The dissymmetry of dioxane solutions of fraction 7 was determined for a number of concentrations at 25°C. and after heating to 64°C. for a few minutes. The results are plotted in figure 12. For the correction of turbidities observed at 48°C. an interpolation is made (dotted line). The limiting dissymmetry for the unheated sample is 2.63, compared with 2.02 for the heated sample. This shows that the average molecular size is smaller after heating. An indication of how much smaller may be gained from the following considerations. First, since the dissymmetry is a weight-average effect, the observed change does not seem to be of the same order of magnitude as the change in weight-average molecular weight that was observed. Secondly, the variation of dissymmetry with a characteristic dimension has been worked out for models such as spheres, rods, and random coils (4, 6, 14). The latter model is probably the nearest approximation for our purpose. In terms of a model random coil a dissymmetry of 2.03 (for a wave length in air of 5461 Å.) corresponds to a value of 1700 Å. for the root-mean-square separation of the ends of the coil; a dissymmetry of 2.63 corresponds to 2150 Å. It thus appears that the average molecular or cluster size does not greatly diminish upon heating.

From another point of view, consider the difference in molecular weight be-

tween two random coils exhibiting the observed dissymmetries. The molecular weight is proportional to the mean-square separation of the ends for a random coil. Consequently, the molecular weight of a random coil with a dissymmetry of 2.62 is 60 per cent greater than of one with a dissymmetry of 2.03. Since

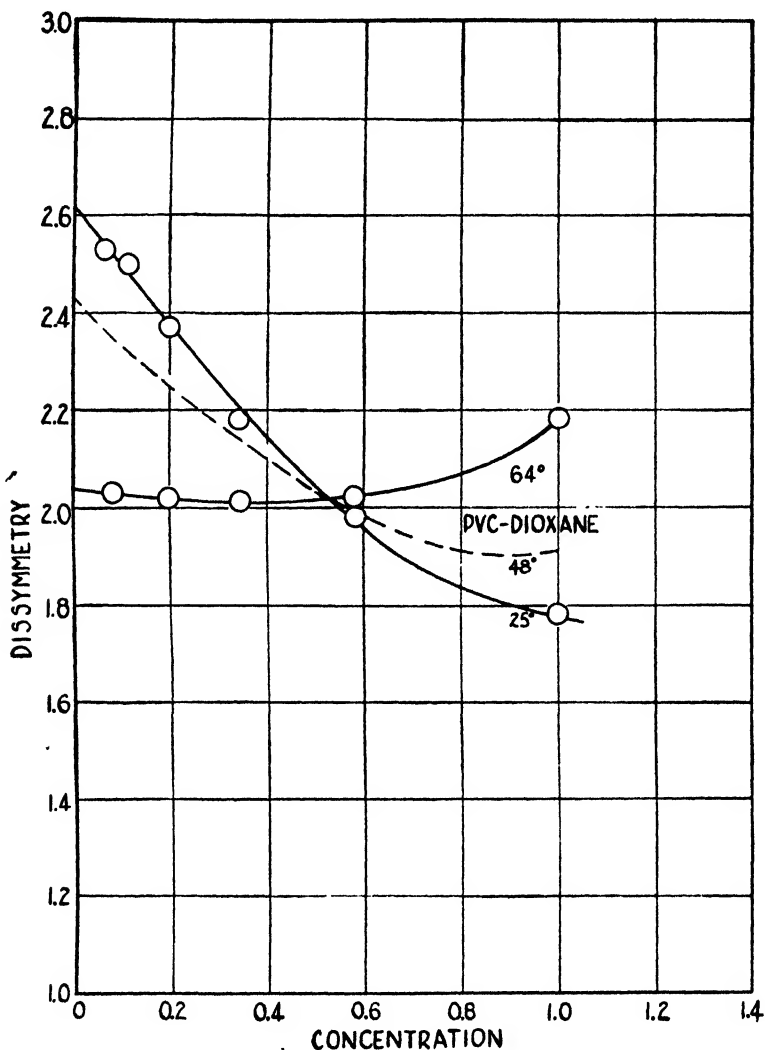


FIG. 12. Dissymmetry of fraction 7 in dioxane at various temperatures. The values at 48°C. are interpolated.

the observed change in weight-average molecular weight between 25°C. and 63°C. was found to be about *eightfold*, we can conclude that the small difference in dissymmetry observed at these two temperatures indicates that the cluster and the individual molecules are of about the same size, that is, have the same

average extent in space. This would require that the cluster be considerably more closely coiled than the individual molecule.

E. VISCOSITY

Additional evidence favoring the view that the cluster is approximately the same size and hence more densely coiled than the individual molecule is obtained from an examination of the variation of specific viscosity with temperature. The specific viscosity of both fraction 7 and the unfractionated polymer in dioxane was determined at 26°C. and at 60°C. The solutions measured at 26°C. had, of course, been stored at this temperature for the previous month. The results of the measurements are shown in figure 13, where η_{sp}/c is plotted against concentration. It is at once apparent that the specific viscosity is practically unchanged when the temperature is increased from 25°C. to 60°C.,

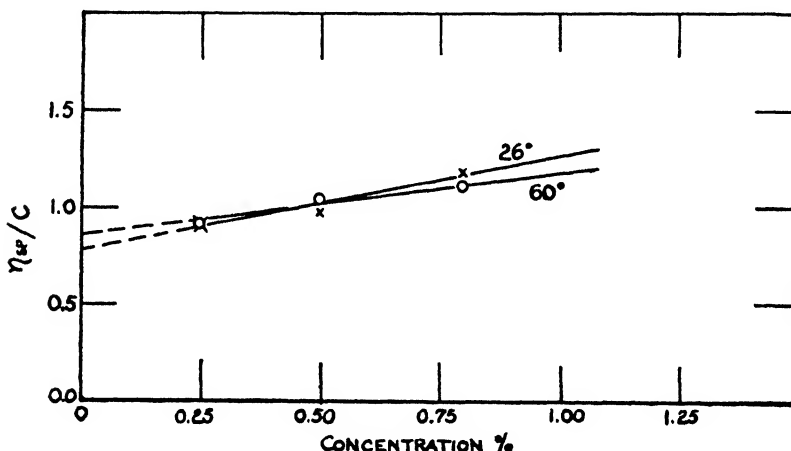


Fig. 13. Viscosity of fraction 7 in dioxane at two temperatures

whereas the same increase in temperature produces an eightfold decrease in the weight-average molecular weight. In fact, the change in the specific viscosity and the intrinsic viscosity is fractionally less in the case of the dioxane solution than in the case of cyclohexanone or butanone solutions. The unlikely possibility that the clusters were broken up in the shear field of the capillary tube was eliminated by demonstrating that the turbidity of a solution was the same before and after passage through a thin capillary.

The view is taken that the fact that the specific viscosity is essentially unchanged when the amount of association is altered is coincidental and not particularly significant. The important feature is that the observed viscosity is very considerably less than would have been predicted if the configuration of the molecules in the cluster were nearly identical with the configuration of the individual molecule except for the effect of molecular weight. For example, if the association were of the end-to-end type, then the viscosity would surely

have been decreased several fold when the associated molecules were broken up. Here in the viscosity measurements there is evidence that the cluster must be of about the same size as the individual molecules, for it is the largest average dimension more than any other factor which determines the specific viscosity. Consequently, it appears that the molecules are so highly coiled and packed in the cluster that the viscosity is greatly reduced and by coincidence is nearly equal to that of the unassociated molecules at the same weight concentration.

F. DEPOLARIZATION OF SCATTERED LIGHT⁶

A study of the depolarization of light scattered laterally from polymer solutions, using both polarized and unpolarized incident light, has been shown to yield useful qualitative information on the shape of dissolved molecules. The only feature of this type of investigation (7) which we have used here is that of measuring the depolarization ratio when the incident light is vertically polarized. The depolarization ratio in this case is a measure of the anisotropy of the

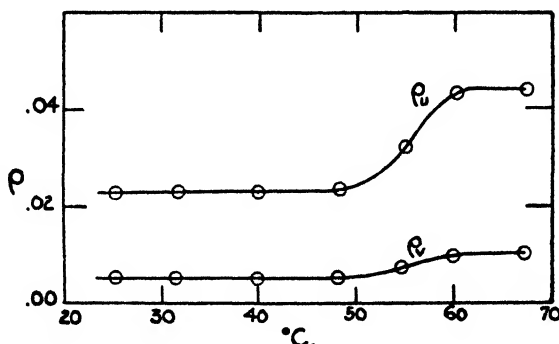


FIG. 14. Depolarization ratio for vertically polarized and unpolarized light as a function of temperature for fraction 7 in dioxane.

molecule. In figure 14 the ratio of the horizontal to the vertical component, that is, the depolarization ratio ρ_v , of the light scattered from a 1 per cent solution of fraction 7 in dioxane is plotted as a function of increasing temperature. We note that in the vicinity of 40–50°C. ρ_v increases significantly. This reflects an increase in the anisotropy of the scattered particles. Since the number of individual molecules has increased over this temperature range, it appears that the individual molecules exhibit greater anisotropy than the cluster. This behavior is consistent with the picture that the clusters are more closely packed, homogeneous particles than are the individual molecules. That is, if a cluster of molecules is of about the same size as a chain-like molecule, it is to be expected that the single molecule is more anisotropic. The evidence from depolarization supports this view.

⁶ The authors are indebted to Mr. S. J. Stein for these measurements.

G. DISCUSSION

Investigation of the forces holding the molecules together in the cluster has not been carried out. However, in view of the observations described above, certain explanations of the phenomenon can be eliminated and a self-consistent description can be postulated.

Is it possible to explain the observed behavior by assuming that there is a dynamic equilibrium between individual molecules and a cluster composed of a number of molecules? Such an explanation is fundamentally incompatible with two observations. First, it was noted both with osmotic pressure and turbidity that the equilibrium value of either of these quantities was obtained at once upon heating but, upon cooling, a very long time was required for the return of either of these properties to its equilibrium value at the lower temperature. This microscopic irreversibility cannot result from a dynamic equilibrium where individual molecules would be associating and clusters would be breaking up at a reasonably fast rate.

The second objection to the hypothesis of dynamic equilibrium is found in the straight lines obtained in the osmotic-pressure plots at any temperature measurement, for if this association resulted from a dynamic equilibrium the equilibrium constant, being defined in terms of the concentrations, would demand that the apparent molecular weight would vary enormously with the concentration. This would lead to strongly curved lines of π/c versus c .

The alternative explanation requires that the equilibrium be of the static type, and that the temperature dependence of the amount of association result from the presence of secondary bonds of many different strengths. In other words, if the points of binding in the cluster are of different strengths, then upon heating the dioxane solution to, say, 45°C., about the weakest 15 per cent of the secondary bonds would be broken and a certain number of individual molecules set free. Upon heating to a higher temperature, the weakest fraction of the secondary bonds remaining would be broken and more individual molecules would result. When the solution cooled, the individual molecules would return to clusters only when the portions of the molecule in which the secondary binding could arise diffuse together. Such a diffusion-controlled reaction would, of course, be very slow. The spectrum of secondary bond strengths required in this description may perhaps arise from a coöperative phenomenon, in which regions of varying length of the polymer chains could fit together in such a sterically favorable pattern as to enhance greatly the dipole-dipole interaction or hydrogen bonding. The strength of such an attachment would depend upon the length of the chains participating at the region of binding. It thus appears that qualitatively the observations on polyvinyl chloride solutions can be explained if the association originates in secondary bonds of varying degrees of strength.

From the sedimentation diagrams it would appear that a significant critical number of molecules are necessary to form a cluster, because there is always a large gap between the two peaks, indicating the absence of clusters of intermedi-

ate size. There is some basis for further speculation, but in view of the complexity of the phenomenon it would scarcely serve a useful purpose.

II. ASSOCIATION IN POOR SOLVENT MEDIA

It is natural to inquire whether or not the association which is so marked in solutions of polyvinyl chloride in dioxane might be a general phenomenon, especially in poor solvents or solvent-non-solvent mixtures. The striking opalescence of some polymer solutions when near the phase-separation point (as, for example, in fractionation by precipitation) suggests the possibility of association. On the basis of the experiments described in Part I, it is clear that the phenomenon is greatly enhanced if the solution near the precipitation point is allowed to remain at a low temperature (for example, room temperature)

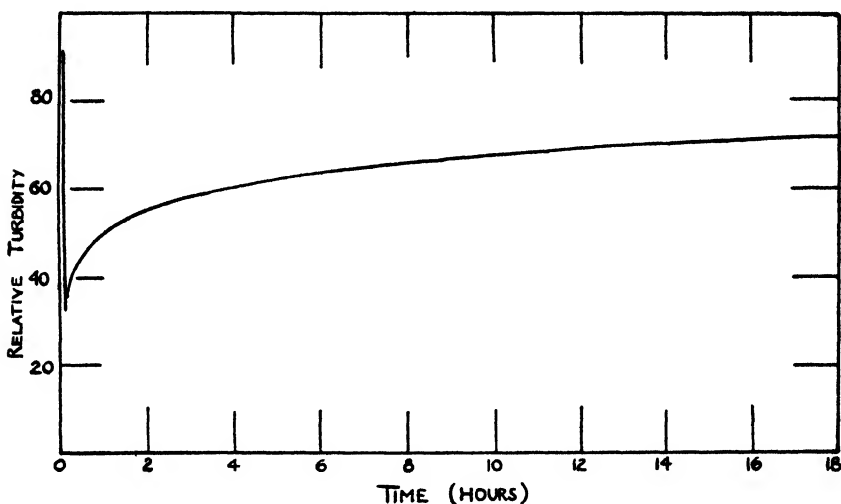


Fig. 15. Relative turbidity as a function of time for a polyvinyl chloride-acetate copolymer in butanone. The sharp minimum in turbidity occurred upon heating the solution to 70°C. for 3 min.

for several weeks preceding investigation. On this basis, association has been observed in several solutions other than those of polyvinyl chloride. An investigation of association in polystyrene solutions (8) will be described in a forthcoming publication. Here we shall describe qualitative experiments with polyvinyl chloride-acetate copolymer and cellulose acetate.

A solution of polyvinyl chloride-acetate copolymer containing 5 per cent of polyvinyl acetate was dissolved in butanone to make a 1 per cent solution. Methanol was added until the solution was very close to the phase-separation point. It was then heated to about 60°C. for several minutes and stored in a 27°C. thermostat for 2 weeks. After this time its relative turbidity was observed; it was then heated to 70°C. for 3 min. and cooled to 30°C. Its relative turbidity was followed throughout these manipulations and for some time after cooling. The results are summarized in figure 15. The relative turbidity

diminished about threefold upon heating and upon cooling returned exponentially to its original value. These results are qualitatively the same as those observed in solutions of polyvinyl chloride in dioxane, except that the return to the original turbidity value was rather slow. Other polyvinyl chloride-acetate copolymers behaved qualitatively in the same manner when treated similarly.

It is perhaps of interest to record what happened when an acetone solution of cellulose acetate was treated in this manner. A solution of a fraction of cellulose acetate with molecular weight of about 100,000 was dissolved in a 10:23 acetone-methanol mixture to give a concentration of 0.15 per cent and after heating was stored in a thermostat at 27°C. for 10 days. At the end of this time there was no apparent phase separation, yet the observed absolute turbidity and dissymmetry indicated a molecular weight of several million. The solution was slowly heated in the turbidimeter, whereupon its turbidity gradually diminished to 60 per cent of its room-temperature value when the temperature of the solution had reached 52°C. Upon cooling to 30°C., the turbidity had returned to 85 per cent of its original value and 10 min. later the turbidity had completely returned to its original value. Thus, the association was not greatly broken up by heating. Acetone was then added to the solution in order to adjust the acetone-methanol ratio to 10:20. The solution was then heated and stored in a thermostat at 27°C. for 10 days. After this time it was observed that the absolute turbidity was not significantly different from what it was previously, but upon heating and cooling the turbidity was reduced threefold and returned to its room-temperature value very slowly, exhibiting behavior quite similar to that shown in figure 15.

These experiments tend to emphasize that near the phase-separation region there can be stable association of the molecules. The existence of association probably plays an important rôle in fractionation procedures. The very narrow asymmetric distribution curves obtained for polyvinyl chloride mentioned previously can probably be traced to the association which was always taking place in varying amounts as the fractionation proceeded. All errors produced in this manner would of course tend to give a distribution curve that was too narrow. It would appear that in fractionation carried out by phase-separation procedures the length of time during which the two phases are allowed to be in contact should be a compromise between the time required for the attainment of equilibrium and the time in which a significant amount of association will take place.

In the course of investigations of cellulose acetate fractions in various solvent media, it was discovered that in methyl cellosolve association existed. Osmotic-pressure measurements on fraction 9 in acetone gave a molecular weight of 53,000 (9). When the same fraction was studied in methyl cellosolve, a number-average molecular weight of 74,400 was obtained. These osmotic data are illustrated in figure 16. Further indication of association in this solvent was given by the ultracentrifuge. In figure 17b diagrams of this fraction sedimenting in acetone at a speed of 720 R.P.S. are recorded. It is to be noticed that the peak remains relatively sharp over an hour of sedimentation; in figure 17a we have

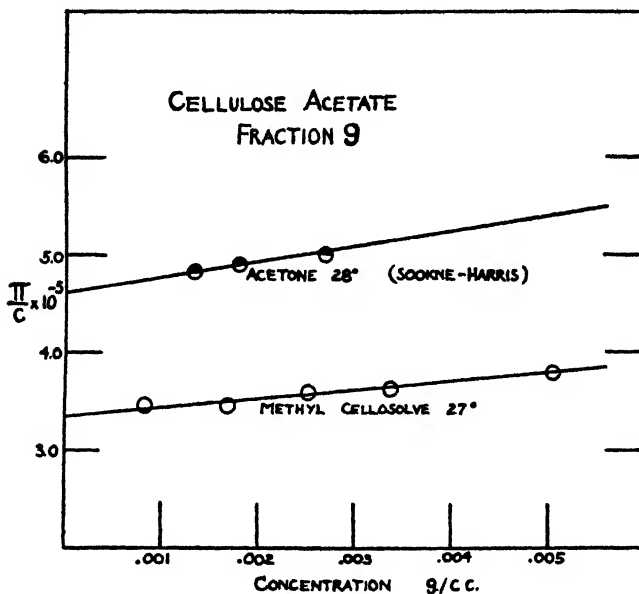


FIG. 16. Osmotic pressure of a Sookne and Harris cellulose acetate fraction in two different solvents.

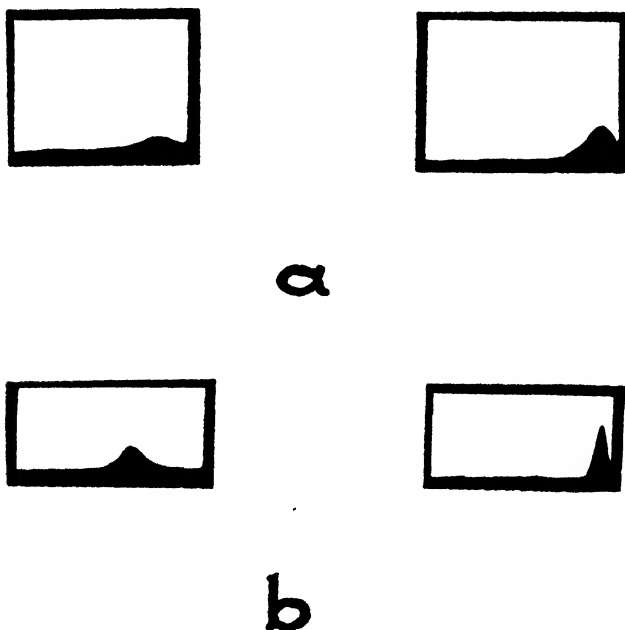


FIG. 17. Sedimentation diagrams of the cellulose acetate fraction of figure 16, at 0.3 per cent concentration in (a) methyl cellosolve and (b) acetone. In each pair, the diagram at the right is the earlier one, and sedimentation is taking place towards the left.

represented the same fraction sedimenting in methyl cellosolve. Here the rapid spread of the curve in 18 min. of sedimentation at 500 r.p.s. indicates considerable polymolecularity as well as increased molecular weights.

Somewhat similar association appears to be present in ethyl cellulose dissolved in pure hydrocarbon solvents, according to the osmotic-pressure data of Steurer (12).

SUMMARY

Association of polyvinyl chloride molecules in dilute dioxane solution is demonstrated by osmotic-pressure, light-scattering, and ultracentrifugal measurements. The association persists in butanone solution and is characterized by a rapid partial dissociation upon heating and a slow (diffusion-controlled) return to equilibrium association after cooling. Dissymmetry, depolarization, and viscosity measurements indicate that the molecular clusters are composed of many molecules but are much more densely packed, so that the sizes of the cluster and of the individual molecule are of the same order of magnitude. Some of the requirements of the binding forces are discussed.

Qualitative experiments indicate that cluster formation occurs in varying degrees in other polymer-solvent systems, especially near the phase-separation regions. Association in polyvinyl chloride-acetate copolymers and cellulose acetate is described, and the significance of this evidence for fractionation procedures is mentioned.

REFERENCES

- (1) AUERBACH, V.: Ph.D. Thesis, Polytechnic Institute of Brooklyn, 1945.
- (2) CAMPBELL, N. R., AND FREETH, M. K.: *J. Sci. Instruments* **11**, 125 (1934).
- (3) DEBYE, P.: *J. Applied Phys.* **15**, 456 (1944).
- (4) DEBYE, P.: Lecture, Polytechnic Institute of Brooklyn, November 21, 1944.
- (5) DOTY, P., AND MISHUCK, E.: *J. Am. Chem. Soc.*, in press.
- (6) DOTY, P., AFFENS, W. A., AND ZIMM, B. H.: *Trans. Faraday Soc.*, in press.
- (7) DOTY, P., AND KAUFMAN, H. S.: *J. Phys. Chem.* **49**, 583 (1945).
- (8) EDELSON, D.: B. S. Thesis, Polytechnic Institute of Brooklyn, 1946.
- (9) SOOKNE, A., AND HARRIS, M.: *Ind. Eng. Chem.* **37**, 475 (1945).
- (10) STEIN, R. S., AND DOTY, P.: *J. Am. Chem. Soc.* **68**, 159 (1946).
- (11) STERN, K. G., SINGER, S., AND DAVIS, S.: *Polymer Bull.* **1**, 31 (1945).
- (12) STEURER, E.: *Z. physik Chem.* **A190**, 1, 16 (1941).
- (13) WOOD, L. A.: *Rev. Sci. Instruments* **7**, 157 (1936).
- (14) ZIMM, B., STEIN, R. S., AND DOTY, P.: *Polymer Bull.* **1**, 90 (1945).

VISCOSITY-MOLECULAR WEIGHT RELATIONSHIP FOR CELLULOSE ACETATE¹

W. J. BADGLEY AND H. MARK

*Institute of Polymer Research, Polytechnic Institute of Brooklyn, Brooklyn, New York**Received August 8, 1946*

INTRODUCTION

The problem of relating the molecular weight of a high polymer to the intrinsic viscosity of its solution has been the subject of many investigations. The early work of Staudinger (17) resulted in the empirical equation

$$\eta_{sp}/c = KM \quad (1)$$

where K = a constant. It must be kept in mind that this expression was obtained for polymers whose molecular weights were sufficiently low to allow for their measurement by cryoscopic experiments. The question arises as to the validity of the results obtained by the extrapolation of this equation to much higher molecular-weight ranges.

During recent years, the publication of data for a rather wide variety of polymer-solvent systems (1, 4, 6, 13) has indicated that a more general equation is needed. The equation suggested in 1938 (12)

$$[\eta] = KM^a \quad (2)$$

where

$$[\eta] = \lim_{c \rightarrow 0} (\eta_{sp}/c)$$

is found to be more applicable to describing the intrinsic viscosity-molecular weight relation for a wide variety of materials. The exponent a of equation 2 is a function of the geometry of the molecule in solution and has values between 0.5 and 2 for tightly curled and rigidly extended molecules, respectively (7). Table 1 lists values of a for various polymer-solvent systems. The wide variation in value from system to system in a molecular-weight range above about 50,000 indicates the necessity for the use of equation 2.

The facts that for low-molecular-weight materials an a of unity is satisfactory and that for higher molecular-weight regions the a values are, for the most part, different from unity, would suggest that there may be a gradual change in the magnitude of a as one investigates the fractions of a polymer over a very wide range of molecular weight. Unfortunately there exists, at present, an insufficient amount of data to test this possibility for the several polymers. However, it is the purpose of this paper to show, for a series of cellulose acetate fractions in acetone and in methyl cellosolve, that the linearity of the $[\eta]$ - M plot and of the

¹ Presented at the Twentieth National Colloid Symposium, which was held at Madison, Wisconsin, May 28-29, 1946.

$\log [\eta] - \log M$ plot, as predicted by equations 1 and 2, does not exist except for relatively narrow ranges of molecular weight.

EXPERIMENTAL

Material

A sample of Waynesboro Acetate, with the following analysis

Moisture.	3.5 per cent
Combined acetic acid	54.50 per cent
24 per cent viscosity	360
Ash	0.03 per cent

was fractionated according to the procedure outlined by Sookne, Harris, Rutherford, and Mark (16). The first (or zero) fraction, containing a high percentage of insolubles, was discarded. In an attempt to have each fraction as homogene-

TABLE 1
a values for several systems

SYSTEM	<i>a</i>
Cellulose nitrate-acetone	1.00*
Polyisobutylene-diisobutylene	0.64†
Polyvinyl acetate-acetone	0.67‡
Cellulose-cuprammonium oxide	0.72§
Polyvinyl chloride-cyclohexanone	1.0¶

* H. Mosiman (Helv. Chim. Acta **26**, 61 (1943)) and N. Gralén (Inaugural Dissertation, Upsala, 1944) give values somewhat less than 1.0.

† P. J. Flory: J. Am. Chem. Soc. **65**, 372 (1943).

‡ A. Matthes: J. prakt. Chem. **162**, 245 (1943).

§ From data of Gralén: Inaugural Dissertation, Upsala, 1944.

¶ D. J. Mead and R. Fuoss: J. Am. Chem. Soc. **64**, 277 (1942).

ous as possible, refractionation was made three times. Of the resulting thirty fractions, eight were so chosen as to represent the entire molecular-weight range. Each of the selected fractions was dissolved in acetone. The solutions were filtered through a sintered-glass filter plate and the acetate was reprecipitated with ethanol. The samples were dried in a vacuum at 55°C. for 24 hr. Solutions of 1 per cent were made up in acetone, and aliquot portions were diluted to obtain the desired concentrations.

VISCOSITY

Viscosity measurements were made in Ostwald viscosimeters at 26.5°C. $\pm 0.05^\circ$. The time of efflux for pure solvent at this temperature was about 80–90 sec. for all the viscosimeters. Values of $[\eta]$ were obtained by plotting η_{sp}/c versus c and extrapolating to $c = 0$.

Data for the values of η_{sp} for cellulose acetate in methyl cellosolve had been obtained previously at about 0.2 per cent concentration. One fraction was

dissolved in methyl cellosolve and the k' for the system was determined. Assuming that the same k' held for all fractions, the values of $[\eta]$ were calculated from the equation:

$$\eta_{sp}/c = [\eta](1 + k'\eta_{sp}) \quad (3)$$

Osmotic-pressure measurements were made in a Fuoss-type osmometer at room temperature—about 25°C. All measurements were made by the static method, using denitrated nitrocellulose membranes (5). These membranes were found to be satisfactory for molecular weights as low as 30,000, i.e., no diffusion of solute was observed. As a check, several of the measurements were made again, using the dynamic technique (5). Agreement between the static and dynamic methods was excellent,—less than 0.02 cm. difference in all cases. Molecular weights were determined by graphical extrapolation of the π/c - c plots to zero concentration.

RESULTS AND DISCUSSION

The viscosity data for the fractions are given graphically in figure 1, where η_{sp}/c is plotted against c . Since it is to be expected (11) that divergence from linearity may result in the higher concentration ranges (particularly for the species of higher molecular weight), the measurements were made in as dilute a solution as would be favorable for reasonable precision. The linearity of the plot attests to the applicability of the Huggins equation

$$\eta_{sp}/c = [\eta] + [\eta]^2 k' c \quad (4)$$

over the concentration range investigated. Some indication of the similarity of hydrodynamic nature of the various fractions is given by the approximate constancy of k' most of the range.

The osmotic data are given in figure 2. According to the equation of Flory (3) and Huggins (9)

$$\frac{\pi}{c} = \frac{RT}{M} + \frac{RT}{V_1 d_2^2} (0.5 - \mu) c \quad (5)$$

it would be expected that for a series of fractions of the same thermodynamic behavior in a given solvent, the value of the slope and hence the μ value should be constant. This is readily seen from the plots of figure 2. Values of μ for the entire series, as calculated from the slope, are 0.42 ± 0.007 . Table 2 lists the value of the intercept of the π/c - c plot as obtained from graphical extrapolation, together with the corresponding values for the number-average molecular weights of the fractions, \bar{M}_n . It must be mentioned that it is difficult to evaluate, precisely, the molecular weight of the highest fractions, since a small error in the measurement of the osmotic head constitutes a rather large percentage error in the value of π/c . This is particularly true in the regions of low concentration.

HOMOGENEITY OF FRACTIONS

Before relating the number-average molecular weight to that average obtained from viscosity measurements, it is necessary to consider the effect of hetero-

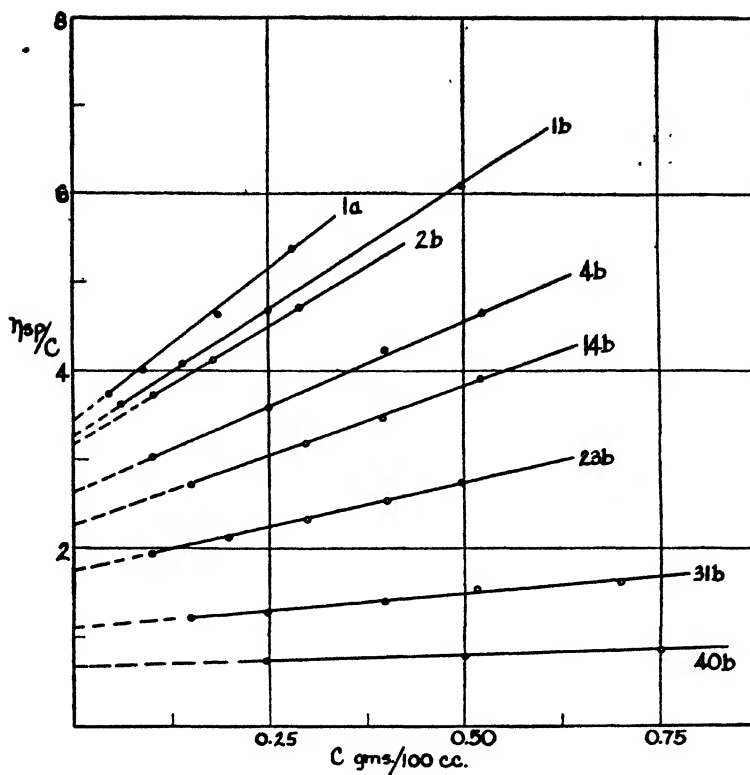


FIG. 1. Viscosity data for cellulose acetate fractions in acetone at $26.5^{\circ}\text{C.} \pm 0.05^{\circ}$ (according to Huggins' equation).

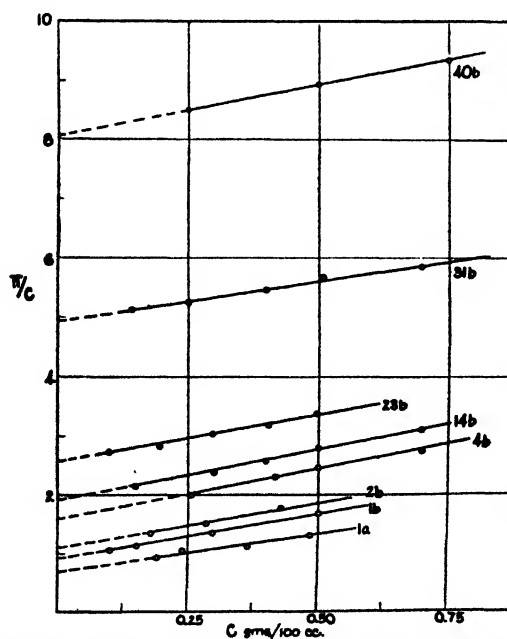


FIG. 2. Osmotic-pressure data for cellulose acetate fractions in acetone at room temperature ($\approx 25^{\circ}\text{C.}$).

geneity of the samples. As has been pointed out by Kraemer (10), the osmotic pressure gives a number average, while the viscosity measurement gives an average which is usually close to the weight average. Since the greatest contribution to the former average results from the presence of the smaller solute molecules while the larger molecules contribute to the latter, no satisfactory relationship may be established unless the measured samples are relatively uniform with respect to chain length. The closest approach to a sharp distribution of molecular weight is possible through several careful refractionations of the sample to be measured. Although it is not possible to obtain perfect homogeneity, some idea of the heterogeneity may be obtained through a comparison of the weight average as measured by light scattering or in the ultracentrifuge

TABLE 2
Osmotic-pressure data for the cellulose acetate-acetone system

FRACTION	$\left(\frac{\pi}{c}\right)_{c=0}$	M_n
1a.	0.70	360,000
1b.	0.92	275,000
2b.	1.10	230,000
4b.	1.60	158,000
14b.	1.90	133,000
23b.	2.55	99,000
31b.	4.93	52,000
40b.	8.05	31,000

TABLE 3
Comparison of M_w and M_n values

FRACTION	M_w	M_n	M_w/M_n
8b.	173,000	(163,000)*	1.06
14b.	135,000	133,000	1.01
18b.	77,000	(75,000)	1.02

* Values in brackets were determined from viscosity measurements by the use of equation 6.

and the number average as measured in the osmometer. For a uniform, homogeneous system, the ratio M_w/M_n will be unity. The more heterogeneous the system, the larger the value of the ratio. The results of some light-scattering experiments by Stein and Doty (18) on several of the fractions led to the values for the ratio given in table 3.

VISCOSITY AND MOLECULAR WEIGHT

Figure 3 gives a plot of $\log [\eta]$ versus $\log M$ for both the cellulose acetate-acetone and cellulose acetate-methyl cellosolve systems. The straight line represents the Staudinger equation. The results in both cases indicate that the viscosity increment falls off with increasing molecular weight—the deviation

occurring at a molecular weight of about 100,000. Unfortunately, it is not possible to compare the curves for the two solvent systems, since the viscosity measurements in methyl cellosolve were made at a somewhat higher temperature. The important point is, however, that both these curves indicate that the simple equations (1 and 2) cannot represent the $[\eta]$ - M relationship over the entire range. Since, as has been mentioned before, there exists some doubt concerning the absolute value of the molecular weight of the highest fractions, the data in figure 3 have been plotted so that the shaded area represents the limit of error on the basis of the ability to evaluate the osmotic head to ± 0.02 cm. It is seen that any values of molecular weight calculated from viscosity data by

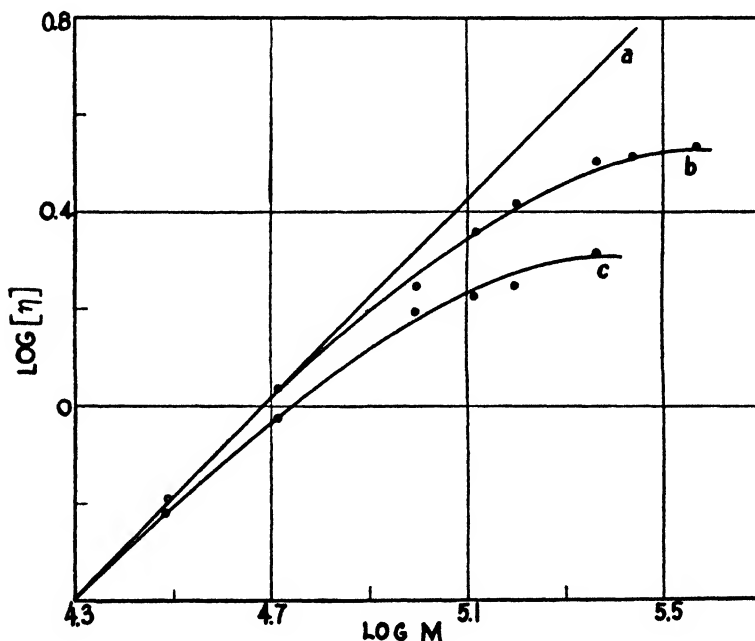


FIG. 3. Log $[\eta]$ -log M plots for cellulose acetate in several solvents. Curve a, according to the Staudinger equation; curve b, experimental values for cellulose acetate in acetone; curve c, experimental values for cellulose acetate in methyl cellosolve.

means of the Staudinger equation would be much higher than observed values. It has been determined that the curve as drawn through the experimental points may be well represented by an equation of the form:

$$[\eta] = KM^a - K' M^{2a} \quad (6)$$

While it is difficult to evaluate the constants precisely, owing to poor precision in the high-molecular-weight range, the following values are given tentatively:

$$a = 1 \quad K = 2.09 \times 10^{-5} \quad K' = 0.315 \times 10^{-10}$$

In table 4 are listed the values of the molecular weights of the several samples, as well as the observed intrinsic viscosities and those calculated from the

Staudinger equation and from equation 2, with $a = 0.83$ and $K = 3.01 \times 10^{-4}$. As would be expected, these two equations fit only certain regions of the $[\eta]$ - M plot. About three or four different a and K values would be necessary to describe the entire molecular-weight range. This would adequately explain the apparent discrepancies in the a values thus far encountered for the cellulose acetate-acetone system.

From equation 7, however, it may be seen that in the range of low molecular weight the second term is relatively small and the equation reduces to that of Staudinger, which would be expected to hold, at least approximately, for the low-molecular-weight species. This is also in agreement with the recent investigations of Sookne and Harris (16), who report an a value of 1.0 for the cellulose acetate-acetone system for molecular weights up to about 130,000. With increasing molecular weight, the deviations from equation 1 become significant (compare $[\eta]$ calculated from equations 1 and 2 with the observed value for molecular weight 360,000). From time to time there has been presented an

TABLE 4
Viscosity and molecular-weight values for cellulose acetate

FRACTION	$[\eta]$	M	$[\eta]$ CALCULATION I	$[\eta]$ CALCULATION II	$[\eta]$ CALCULATION III
1a.....	3.45	360,000	8.15	5.71	3.36
1b.....	3.29	275,000	5.68	4.31	3.35
2b.....	3.16	230,000	4.81	3.76	3.15
4b.....	2.60	158,000	3.30	2.72	2.52
14b.....	2.23	133,000	2.78	2.42	22.2
23b.....	1.73	99,000	2.09	1.88	1.78
31b.....	1.10	52,000	1.09	1.10	1.01
40b.....	0.65	31,000	0.65	0.95	0.62

opportunity to check this equation against the molecular-weight value obtained from light-scattering experiments. The agreement in all cases has been very satisfactory.

THE SHAPE FACTOR

Although no completely satisfactory theory has been developed to account for the shape of long-chain molecules in solution, it is of interest to consider the results of the above experiments in terms of the shape of the solute molecules. By assuming that a molecule has a certain shape in solution, Huggins (8) has calculated the viscosity increment produced by a chain molecule made up of a certain number of hydrodynamic units. Under the conditions that the solute molecule be large, and that Brownian movement predominate markedly over the velocity gradient, he has deduced that the following relations hold:

$$\eta_{sp}/c = kn^2 \text{ for rigid rods} \quad (7)$$

$$\eta_{sp}/c = kn \text{ for random coils} \quad (8)$$

(n = the number of hydrodynamic units per chain and hence is proportional to the molecular weight.)

If it is considered that the cellulose acetate molecule is a relatively extended molecule, then from these expressions and our experiments, several conclusions may be drawn.

(1) That the same elongated shape persists over the entire molecular-weight range. In this instance it is possible that at high values of the velocity gradient there would be an orientation of the molecule in the direction of flow, with a corresponding decrease in the value of the viscosity. This would result, on correction, in a raising of the η_{sp} values for the low-molecular-weight species. However, since, as Lyons (11) has pointed out, the effect of velocity gradient becomes relatively negligible at low concentrations, very dilute solutions have been used. Further, the measurements have been made in viscosimeters of small capillary diameter, so that the time of flow shall be long and hence $\bar{\beta}$ shall be small.²

TABLE 5
Relative viscosities at several concentrations as a function of $\bar{\beta}$

β (sec. ⁻¹)		600	900	1500	1800	2100
FRACTION	CONCENTRATION	RELATIVE VISCOSITIES				
II(a).....	0.125			1.48	1.48	1.48
	0.250		2.16	2.17	2.17	2.14
	0.375	3.08	3.09	3.06	3.04	3.04
23(c).....	0.3		1.76	1.76		1.68
	0.4		2.05	2.04	2.00	
	0.6	4.38	4.15			

The dependence of relative viscosity on the mean velocity gradient has been determined for a low- and a high-molecular-weight fraction with values of $\bar{\beta}$ varying between 600 and 5800 sec.⁻¹ These data are given in table 5.

From the values of η_{rel} for fraction II(a) it may be seen that the effect of the gradient up to $\bar{\beta} = 2100$ is small and would have little effect on the value of the intrinsic viscosity as calculated from this data. The same may be said for the data for fraction 23(c) up to $\bar{\beta} = 1500$ if the concentrations used are less than 0.6 g. per 100 cc. In any case, for the fractions of lower molecular weight the slope of the η_{sp}/c - c plot is sufficiently flat to allow for the extrapolation of valid $[\eta]$ values, particularly if the η_{sp}/c values at low concentrations (below 0.5 g. per 100 cc.) are given sufficient weight in the determination of the curve.

(2) That as the molecule becomes increasingly larger, its general architecture changes, i.e., branching occurs. This change in shape could adequately account for a gradual falling off of the viscosity increment provided the degree of branch-

$$^2 \bar{\beta} = \frac{8}{3} \frac{V}{r^2 t}$$

ing increased with molecular weight. It would be expected, however, that under such conditions there should also be a gradual change in the solubility characteristics of the solute as the molecular weight increased. In any case, there should be a rather marked difference in the solubility behavior of the low and high fractions. Such a difference should be reflected in the thermodynamic constant μ ,

$$\mu = \beta + \alpha/RT \quad (9)$$

where β = entropy contribution and α = heat contribution, since, while the second term in equation 9 should most probably remain constant, the entropy term, β , would be different (2). It may be seen from a consideration of the osmotic-pressure data in figure 2 that the slopes, and consequently the μ values, are constant for all the fractions within experimental error.

(3) That as the molecule becomes larger, it becomes more and more curled up, eventually approaching a more or less spherical shape. This picture is consistent

TABLE 6*
Dimensions of cellulose acetate molecules

FRACTION	MOLECULAR WEIGHT	ROOT-MEAN-SQUARE DISTANCE BETWEEN ENDS		
		Assuming rigid rod	Assuming random coil	Computed from molecular weight
		<i>A.</i>	<i>A.</i>	<i>A.</i>
8b	163,000	1900	1340	3100
14b	135,000	1900	1340	2400
18b	75,000	1550	1120	1440
32b	65,000	1550	1120	1250
31b	52,000	1380	960	1000

* R. Stein and P. Doty: J. Am. Chem. Soc. **68**, 159 (1946).

with the idea of a molecule with a relatively high rotational restriction between adjacent segments. This change in over-all shape from an elongated, quite rigid, rod-like particle to one which, at sufficiently high molecular weight, would be matted, would account for the falling off of the viscosity increment, since after a sufficiently matted particle had been formed, an increase of molecular weight would effect little change in the over-all shape and hence would result in a variation of the value of the exponent in equation 2 toward zero.

Some corroborating evidence for the change in shape as a function of molecular weight may be obtained from the experiments of Stein and Doty (18) on the angular dependence of light scattering. They have measured five of the above fractions over the molecular weight range 52,000 to 163,000. From the ratio of the forward and backward angle scattering they have determined that at about 80,000 molecular weight, the cellulose acetate molecules take on a less extended shape. The data are given in table 6.

It may be seen that values for the three low-molecular-weight fractions correspond within experimental error to the calculated values, while values for

samples 8b and 14b are considerably less than that for the completely stretched-out molecule. This change at about 80,000 corresponds remarkably well to the point at which deviation from the Staudinger equation begins (see figure 3).

In an attempt to place the evaluation of the shape factor on a somewhat more quantitative basis, Simha (14) and Kraemer (10) have developed equations of a semiempirical nature, relating the intrinsic viscosity to the axial ratio (length/diameter) of the molecule. Although the basic assumption (i.e., that the molecules, in solution, may be considered comparable to an ellipsoid of revolution which, hydrodynamically, produces the same effect as the molecule) is such as to disallow a comparison of different solute species, it seems quite reasonable that this treatment may give some semiquantitative information concerning the relative shape of a series of fractions of the same material. In the following treatment of the viscosity data we have used the curve of Simha relating axial ratios to intrinsic viscosity under the condition that there existed complete Brownian movement. It should be stated that over the range of

TABLE 7
Dimensions of cellulose acetate molecules in acetone, from viscosity measurements

FRACTION	$[\eta]_v$	LENGTH (X-RAY)	LENGTH	DIAMETER
		A.	A.	A.
40b	0.97	595	434	12.4
31b	1.58	1000	628	13.4
23b	2.53	1910	938	15.1
14b	3.28	2560	1130	15.7
4b	3.86	3040	1285	16.3
2b	4.60	4430	1556	17.9
1b	4.83	5300	1676	18.8
1a	5.00	6920	1861	20.4

observed intrinsic viscosities, the value of the axial ratio, f , would be somewhat larger if Brownian movement were not complete. In the calculation of the viscosity in terms of volume concentration of solute, Kraemer's (10) value of 0.68 for the partial specific volume of cellulose acetate in acetone was used.

From the equation

$$[\eta]_v = \nu(f) \quad (10)$$

it may be deduced that the length, l , of a molecule with an axial ratio $f = l/d$ may be expressed as

$$l = \frac{\sqrt[3]{6f^2M}}{\pi N_A \rho} \quad (11)$$

where M = molecular weight, N_A = Avogadro's number, and ρ = density.

Table 7 lists the various observed and calculated values for the series of fractions in acetone. Similar values are given in table 8 for the cellulose acetate-methyl cellosolve system.

Values of l (x-ray) as given in column 3 of tables 7 and 8 were calculated using a monomer length of 5.1 Å. Comparison of these values with those obtained from viscosity measurements indicates that the molecule in the low-molecular-weight range is rather rigidly extended, i.e., the magnitudes of l (x-ray) and $l_{[\eta]}$, are comparable. However, with increasing molecular weight the x-ray and viscosity values diverge markedly. The results indicate that for molecular weight 360,000 the molecule is equivalent, hydrodynamically, to an ellipsoid of

TABLE 8
Dimensions of cellulose acetate molecules in methyl cellosolve

FRACTION	$[\eta]$	LENGTH (X-RAY)	LENGTH	DIAMETER
		$A.$	$A.$	$A.$
40b.....	0.88	595	415	12.6
31b.....	1.38	1000	582	13.8
23b.....	2.28	1910	890	15.4
14b.....	2.46	2560	1025	17.1
4b.....	2.58	3040	1090	17.6
2b.....	3.06	4430	1315	19.3

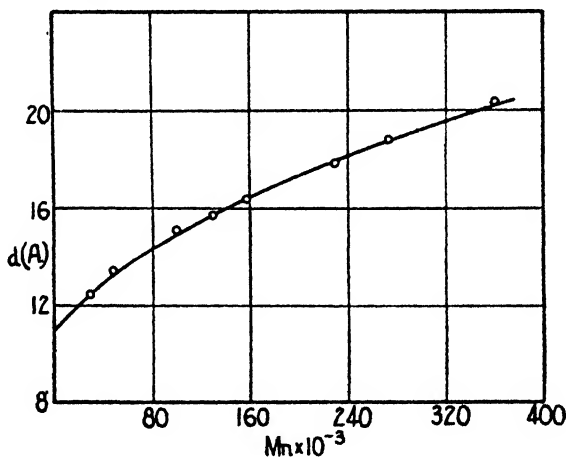


FIG. 4. Plot of the apparent diameter of the cellulose acetate molecule (calculated from viscosity values in acetone) as a function of the molecular weight.

revolution the ratio of whose major and minor axes is about 0.14 that of the completely extended molecule, while for molecular weight 31,000 the ratio of curled to fully extended is greater than 0.5.

Although, as has been mentioned before, the temperature at which the viscosity measurements were made on the cellulose acetate-methyl cellosolve system was about 5°C. higher than that for the acetone system, a comparison of the values of l and d indicates that the shape of the solute molecule does not change markedly when one passes from a good solvent ($\mu = 0.43$ for acetone) to a poorer one

($\mu = 0.49$ for methyl cellosolve), i.e., for fraction 14b of molecular weight 133,000, l equals 1130 Å. in acetone and 1025 Å. in methyl cellosolve. This observation has been made by Doty (18) during an examination of the shape of the vinylite VYNW molecule in several solvents, as determined by light-scattering measurements. On this basis it would appear that the differences in viscosity are due to a marked degree to the extent of solvation or desolvation of the solute molecule.

In figure 4 are plotted the values of the diameter of the cellulose acetate molecule, in terms of the hydrodynamically equivalent ellipsoid of revolution *versus* the number-average molecular weight. While it is realized that the Simha equation holds only for axial ratios above $\cong 10$, it is rather surprising to note that the curve may be extrapolated to zero molecular weight, yielding a value of d equal to about 11 Å., which, according to the x-ray experiments, is a reasonable value for the diameter of the monomer unit.

SUMMARY

Experimental values for intrinsic viscosity and molecular weight for the cellulose acetate-acetone and the cellulose acetate-methyl cellosolve systems, over a wide molecular-weight range, show that the simple equations relating these two quantities are inadequate.

An empirical equation is suggested, which represents the data with an average deviation of 3 per cent over the entire molecular-weight range. The constants K and K' and the exponent a have tentatively been evaluated as 2.09×10^{-5} , 0.315×10^{-10} , and 1, respectively.

An attempt has been made to relate these measurements with the work of Simha and Kraemer on the axial ratios of molecules. The results indicate that in the regions of lower molecular weight the molecule is rather rigidly extended, but that as the molecular weight increases the molecule takes on a more spherical shape.

Calculation of the diameter of the hydrodynamically equivalent ellipsoid of revolution yields reasonable values.

REFERENCES

- (1) BARTOVICS, A., AND MARK, H.: J. Am. Chem. Soc. **65**, 1901 (1943).
- (2) DOTY, P. M.: Private communication.
- (3) FLORY, P. J.: J. Chem. Phys. **9**, 660 (1941); **10**, 51 (1942).
- (4) FLORY, P. J.: J. Am. Chem. Soc. **65**, 372 (1943).
- (5) FUOSS, R., AND MEAD, D. J.: J. Phys. Chem. **47**, 59 (1943).
- (6) GRALÉN, N.: Inaugural Dissertation, Upsala, 1944.
- (7) HUGGINS, M. L.: J. Phys. Chem. **42**, 911 (1938); **43**, 439 (1939).
- (8) HUGGINS, M. L.: In *Cellulose and Cellulose Derivatives*, Emil Ott (Editor). Interscience Publishers, Inc., New York (1943).
- (9) HUGGINS, M. L.: J. Phys. Chem. **46**, 151 (1942).
- (10) KRAEMER, O.: J. Franklin Inst. **231**, 1 (1941).
- (11) LYONS, W.: J. Phys. Chem. **13**, 43 (1945).
- (12) MARK, H.: *Die feste Körper*, page 103. S. Hirzel, Leipzig (1938).
- (13) MEYER, K.: Helv. Chim. Acta **23**, 1063 (1940).
- (14) SIMHA, R.: J. Chem. Phys. **13**, 188 (1945).

- (15) SOOKNE, A., AND HARRIS, M.: *Ind. Eng. Chem.* **37**, 475 (1945).
- (16) SOOKNE, A., HARRIS, M., RUTHERFORD, H. A., AND MARK H.: *J. Research Natl. Bur. Standards* **29**, 123 (1942).
- (17) STAUDINGER, H.: *Die hochmolekularen organischen Verbindungen*. J. Springer, Berlin (1932).
- (18) STEIN, R., AND DOTY, P.: *J. Am. Chem. Soc.* **68**, 159 (1946).

ELASTICITY MEASUREMENTS ON POLYCHLOROPRENES¹

PER-OLOF KINELL

University of Upsala, Upsala, Sweden

Received August 8, 1946

During the last fifteen years great interest has been directed toward the physicochemical behavior of synthetic high-molecular compounds; this is perhaps especially true of rubber-like materials. The main problem here is to get a proper understanding of the factors which determine the specific property of high elasticity. Many investigations have appeared in this field, and a short review of the modern theories is given below. It seems, however, that comparatively little attention has been devoted to the influence of the different sizes of the macromolecules on the network structure in the polymer and to the extent to which the molecular weight determines the elastic properties. The purpose of this paper is to give a brief account of some preliminary attempts to study the building up of network structures by means of molecular-weight determinations and especially to establish the relation between the size of the macromolecules in solution and the constants characterizing the network structure.

The most fundamental difference between the elastic properties of ordinary solid bodies such as metals and of rubber-like materials is that on isothermal stretching at constant volume in the case of solids the change in entropy is zero but for rubbers the change in internal energy is zero. This means that in solids the stress causes a deformation of the molecular structure in such a manner that the ordered state is not disturbed. In rubber-like materials there is no deformation of chemical bonds or valence angles but only a rearrangement of the segments in the molecular chains as a result of free rotation about single carbon-carbon bonds. It must, however, be emphasized that these conditions, i.e.

$$(\partial \Delta S / \partial \Delta l)_T = 0 \quad \text{and} \quad (\partial \Delta E / \partial \Delta l)_T = 0$$

(S = entropy, E = internal energy, l = length of specimen, and T = absolute temperature) are valid only for ideal substances. In real matter the changes in free energy are due to changes both in entropy and in internal energy.

It is a well-known fact that high-molecular compounds with thread-shaped

¹Presented at the Twentieth National Colloid Symposium, which was held at Madison, Wisconsin, May 28-29, 1946.

molecules crystallize when they are stretched to high elongations. According to the ability of the macromolecules to fit into a crystal lattice, the ordered state can be more or less pronounced. Mark (8, 9) has pointed out that the free energy can have its absolute minimum either in the initial unstretched state or in the final arrangement of the system in the stretched state. The main factors influencing the position of the minimum are the molecular attraction between the chains, the temperature, other external forces, and the above-mentioned ability of fitting geometrically into a lattice. The initial state can be assumed to consist of curled-up chains, and represents in the case of large intramolecular forces a stable state. The final arrangement is determined by the mutual attraction between adjacent chains caused by intermolecular forces. If these forces are small, we have a condition typical of rubber-like materials. The chains have a tendency to return to their original states.

The stretching of such a material involves first of all a breaking down of the internal crystallization. The molecules are brought into a more probable position and, depending upon the strength of the intramolecular forces, the gain in entropy is small or large in comparison with the loss in potential energy. The relative values of entropy and internal energy depend upon the substance in question. Evidently one must always bear in mind that at the start of the stretching of a *rubber* specimen a certain part of the force exerted is used up in breaking down certain bonds (hydrogen bonds) between chain segments.

The gain in entropy on stretching was first calculated by Kuhn (6, 7), Wall (14), and Guth and Mark (4). The calculations are based on a statistical study of the possible configurations of the chain molecules. The probability $p(x, y, z)$ of the molecular chain having components of length x, y, z , respectively, along each of the three coordinate axes is

$$p(x, y, z) dx dy dz = \frac{\beta^3}{\pi^{3/2}} e^{-\beta^2(x^2+y^2+z^2)} dx dy dz \quad (1)$$

where

$$\frac{1}{\beta^2} = \frac{2}{3} \cdot l_c^2 \cdot Z \frac{1 + \cos \theta}{1 - \cos \theta} \quad (2)$$

Here l_c is the carbon-carbon bond distance, Z the number of links in the chain, and $180^\circ - \theta$ the valence angle. Using the assumptions (cf. Kuhn (7)) that all molecules have the same chain length, that the extension of the length components of each molecule changes in the same ratio as the components of length of the macroscopic rubber, and that the volume of the rubber remains unchanged, Wall obtains from formula 1 the following expression for the change in entropy:

$$\Delta S = -\frac{1}{2} N_0 k \left(\alpha^2 + \frac{2}{\alpha} - 3 \right) \quad (3)$$

where N_0 is the number of molecules, k is Boltzmann's constant, and $\alpha = 1 + \gamma$, where γ equals the fractional extension. Now the following thermodynamical relationship is valid in the case of reversible stretching

$$\kappa = (\partial \Delta E / \partial \Delta l)_T - T(\partial \Delta S / \partial \Delta l)_T \quad (4)$$

It is the force κ which keeps the rubber specimen in the stretched state. Observing that $\gamma = \Delta l/l_0$ (l_0 = original length) one obtains from equations 3 and 4

$$\kappa = (\partial \Delta E / \partial \Delta l)_T + NkT(\alpha - 1/\alpha^2) \quad (5)$$

or, since $Nk = R\rho/M$,

$$\kappa = (\partial \Delta E / \partial \Delta l)_T + \frac{RT\rho}{M}(\alpha - 1/\alpha^2) \quad (5')$$

The force κ refers to the original cross section, N is the number of molecules per cm.³, ρ is the density of rubber, and M is the molecular weight. The expression $(\partial \Delta E / \partial \Delta l)_T$ represents the part of the force exerted which causes changes in internal structure, i.e., deformation of bonds and valence angles. In order to get a complete description of the stress-strain curves it would be necessary to make certain assumptions about the nature and magnitude of the forces which cause these deformations.

Flory and Rehner (2) have carried out a statistical treatment on a three-dimensional network model, and have succeeded entirely in avoiding the assumptions of Kuhn and Wall regarding the manner in which the chain-length distribution is transformed by macroscopic deformation of the rubber sample. The expression for ΔS is quite the same as equation 3, but in this case M in equation 5' must be the molecular weight of the part of the macromolecule between two points of cross-linkage, i.e., an average molecular weight of an elastic unit. Using the cross-linked network model Flory and Rehner have also studied the swelling of rubber (3) and obtain, in the case of swelling equilibrium with a pure solvent, the following expression for the molecular weight:

$$M_c = \frac{\rho V_1 v_2^{1/3}}{K v_2^2/2 + \ln(1 - v_2) + v_2} \quad (6)$$

where ρ is the density of rubber, V_1 the molar volume of the solvent, v_2 the volume fraction of polymer in the swollen gel, and K a quantity which depends upon the heat of mixing. Thus it is possible to obtain values of M in two different ways, according as the process is stretching or swelling.

Huggins (5) has recently developed a theory of rubber elasticity based on hypothetical model substances consisting of a large number of like systems, each being in equilibrium between two states with different arrangements of the atoms. He obtains rather complicated expressions for the stress-strain dependence. The discussions in this paper have hitherto been based upon relation 5' only. But at higher elongations especially, Huggins' treatment seems to be preferable.

As to the influence of molecular weight, i.e., the length of the macromolecules, on the elastic properties, Mark (9) points out that the material must have a certain degree of polymerization and that this minimum degree depends upon the substance. Thus, for polyhydrocarbons the tenacity below a polymerization degree of 80 is negligible. Above 80 it increases roughly proportionally to the chain length, and at about 250 the curves begin to flatten out. First at poly-

merization degrees of about 700 is the tenacity no longer dependent upon the chain length. The shape of the distribution curve also influences the mechanical properties. Small amounts of low-molecular-weight materials (polymerization degree below 150) have an especially detrimental effect, and it is therefore necessary to have a comparatively low degree of polydispersity.

Another important question is the branching and cross-linking of the chains. It has not been possible to make any clear-cut decision on this problem, but a low degree of branching probably has very little effect on mechanical properties. Highly branched chains and cross-linked molecules, on the other hand, give a very hard and stiff material. The very few measurements in this field do not tell us much about the real network structure and how molecules with different chain lengths build up the network. It is therefore of interest to obtain experi-

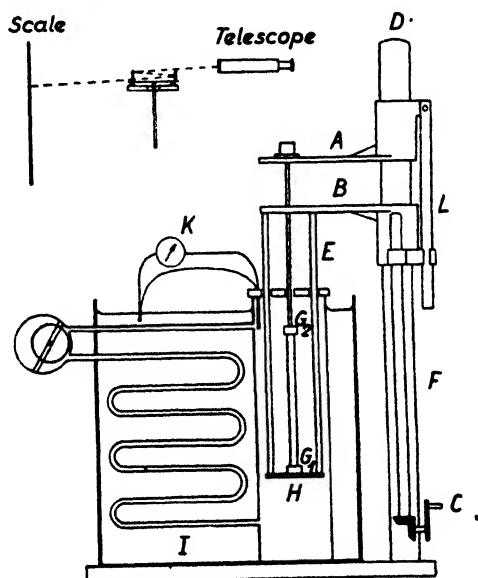


FIG. 1. Dynamometer for elasticity measurements (Polanyi)

mental data on a range of synthetic materials with different molecular weights and to follow the change in elasticity from the unvulcanized to the vulcanized state.

In order to obtain stress-strain curves for the rubber samples a Polanyi dynamometer (12) was constructed. Meyer and Ferri (11) have used a similar apparatus. The main features of the dynamometer are seen in figure 1. Two arms A and B (with a framework) are movable on a steel rod D. During the measurements A is fixed and B moved downwards or upwards by means of a screw F and a handle C, causing the rubber specimen between the clamps G_1 and G_2 to stretch or unstretch. On A a steel spring rests on two steel knife edges. At each end the spring carries a small mirror, and as the spring bends these mirrors incline towards each other. The bending of the spring is de-

pendent upon the tension set up in the specimen, and by observing an illuminated scale at a distance of about 2 m. from the apparatus through a telescope it is possible to follow the displacement of the scale image. By calibrating the scale in force units, one can thus obtain the total force exerted on the spring. The initial and actual lengths of the specimen can be read off on a scale L (a cathetometer has recently been constructed for the length measurements and this is an obvious improvement). The stretching occurs in an air thermostat (H), and the air is heated by means of a coil (I) immersed in a water thermostat. A positive displacement pump effects the circulation. The temperature in H is measured by means of a thermocouple and a galvanometer (K). During the measurements the specimen can be observed through glass windows in the thermostats.

As shown by Meyer (10), with this apparatus it is possible to calculate the quantities ΔE and ΔS from the stress-temperature curves. Such measurements have not yet been made. Only in a few cases has the relation between stress and temperature been investigated.

The following rubber samples were used: *Sample I*: unvulcanized polychloroprene from homogeneous polymerization; molecular weight from sedimentation and diffusion in chloroform about 130,000. *Sample II*: unvulcanized polychloroprene (neoprene E); molecular weight from sedimentation and diffusion in chloroform about 204,000. *Sample III*: unvulcanized polychloroprene from emulsion polymerization; as the sample is soluble in chloroform only up to 32 per cent the molecular weight has not been determined; the sample contains 2 per cent sulfur. *Sample IV*: vulcanized rubber; this sample was only used to compare the unvulcanized and vulcanized states. The molecular weights for I and II were taken from an investigation of a large number of different polychloroprenes carried out by I. Svedberg and the author (not yet published).

From samples I and II rubber specimens were prepared according to Treloar (13), except that the samples were dissolved in chloroform. The thickness of the films was about 0.5 mm. Samples III and IV were in the form of thin sheets. In measuring the stress it was necessary to let such a long time elapse that the relaxation process had time to end completely. After 15–20 min. the stress was constant within a few tenths of a per cent.

As samples I–III are unvulcanized it is not to be expected that the stretching procedure is reversible in a thermodynamic sense. The hysteresis losses are very large too, as is seen from table 1 containing the values for samples II (different cycles) and III (different temperatures). The shapes of the curves for sample II and sample III (29.2°C.) are shown in figure 2. The similarity between the curves for sample II and those obtained by Bostrom (1) for raw rubber (smooth sheets) is obvious, and it can therefore be assumed that even in the case of polychloroprene the large hysteresis loss for the first cycle is due to a structure which is broken down when the rubber is first extended. The curve for sample III is not so steep at low elongations and is in this respect more similar to that of vulcanized rubber. From this and the smaller values for the hysteresis losses the conclusion can be drawn that the addition of sulfur to the polymeriza-

tion mixture causes a slight vulcanization or, in other words, a more network-like structure. As can be expected, the hysteresis losses decrease with increasing temperature.

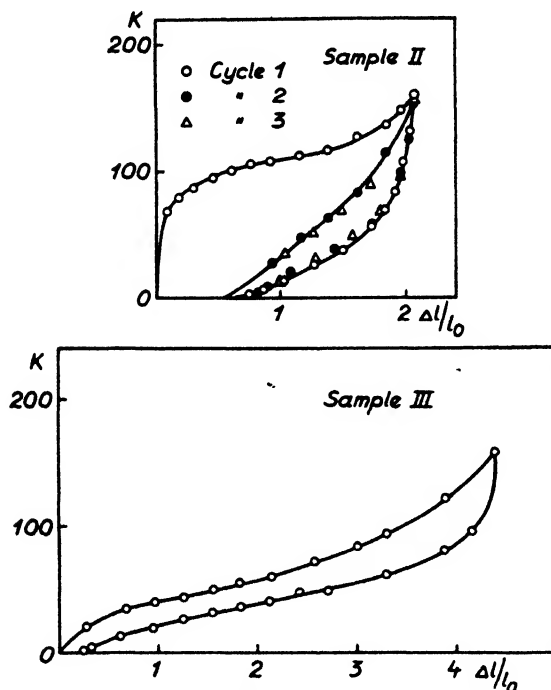


FIG. 2. Stress-strain curves and hysteresis cycles for samples II and III. κ is the force in grams per millimeter.

TABLE 1
Hysteresis losses for polychloroprenes

SAMPLE	TEMPERATURE	RELATIVE ELONGATION	HYSTERESIS LOSSES
	°C	per cent	per cent
II { first cycle	20.0	2.07	75.5
	20.0	2.07	37.4
	20.0	2.07	34.5
III, first cycle	29.2	4.37	35.9
	31.2	4.89	40.5
	34.5	4.54	29.3
	37.4	4.57	26.7
	39.8	4.51	20.3

The stress-strain curves obtained for samples I-IV are shown in figures 2 and 3. The stress is referred to the original cross section of the specimen. Es-

pecially for unvulcanized rubber is it difficult to reproduce the curves. If the measurements are carried out on specimens of different sizes, the stress changes within 10 per cent. For vulcanized rubber the reproducibility is fairly good. Starting from these curves formula 5' has been used to get values of M . The expression $(\partial\Delta E/\partial\Delta l)_T$ has been assumed to be a constant and also calculated under this assumption. Evidently this is only a very crude approximation, especially for the first and last parts of the curves, as is seen from figure 4, where the stress has been plotted *versus* the expression $\alpha - 1/\alpha^2$ for samples I and IV and the straight lines correspond to formula 5'. It must be emphasized that on the whole it is incorrect to use this formula, if the constants are to express changes

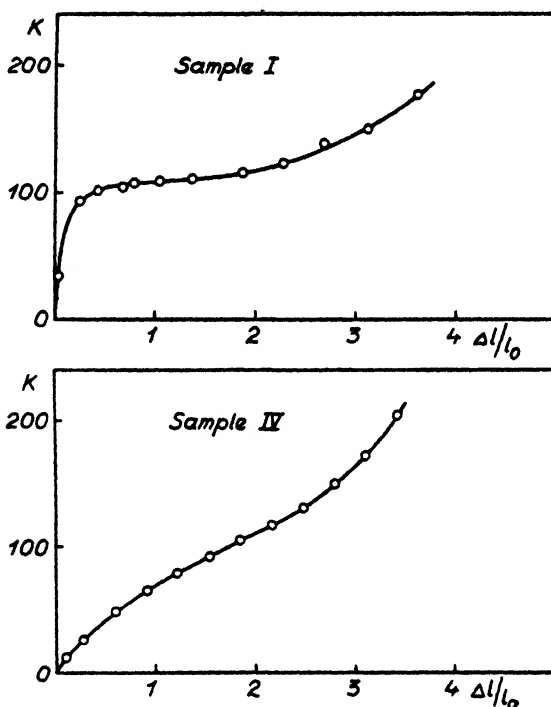


FIG. 3. Stress-strain curves for samples I and IV

in thermodynamic quantities for a reversible process. Yet it is suitable to use such an equation, which is based on certain assumptions about internal network structure, to characterize the elastic nature of the material, especially as it describes the behavior of vulcanized rubber fairly well up to rather high elongations (*cf.* figure 4). The values obtained are given in table 2.

The expression $(\partial\Delta E/\partial\Delta l)_T$ cannot—as just pointed out—be constant for the whole curve. As the curves for samples I and II are very steep at low elongations, the modulus is very high. The values 11×10^7 dynes/cm.² and 10×10^7 dynes/cm.², respectively, are calculated and are, compared to sample III (0.7×10^7 dynes/cm.²), of another magnitude. Thus it can be assumed that in certain

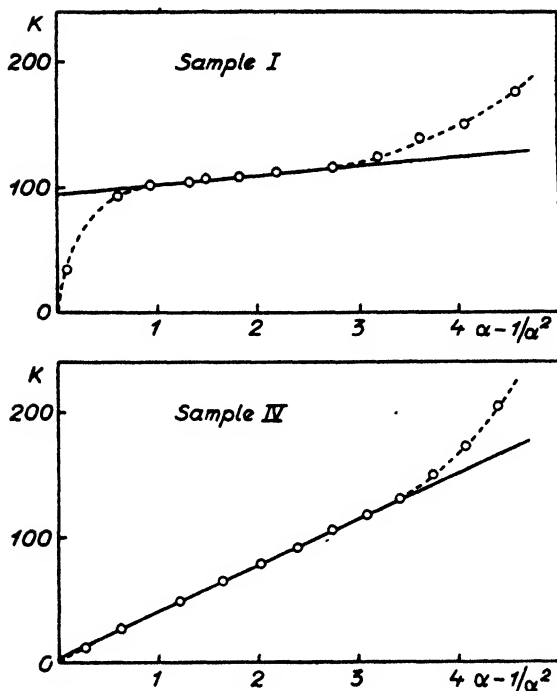
FIG. 4. The force κ plotted against $\alpha - 1/\alpha^2$ for samples I and IV

TABLE 2
Values of $(\partial \Delta E / \partial \Delta l)_T$ and M according to formula 5'

SAMPLE	TEMPERATURE	$(\partial \Delta E / \partial \Delta l)_T$	M
	°C.	g.-cm./cm.^2	
I.....	25.0	8520	42,200
	25.0	7860	35,200
	25.0	9520	44,200
		8630	40,500
II.....	20.0	8400	21,000
III.....	29.2	1430	22,100
	31.2	1470	16,500
	34.5	2000	24,300
	37.4	1690	27,800
	39.8	1810	33,200
	43.0	1930	41,400
IV.....	25.0	350	8,500

points of the material crystallization has occurred. This crystallization must be less pronounced the more the rubber is vulcanized; furthermore it probably depends on time. This follows from figure 2, where the curves corresponding to

the second and third time loading of the specimen do not exhibit any steep behavior. The values of $(\partial\Delta E/\partial\Delta l)_T$ determined from equation 5' in the manner shown above can to some extent illustrate the degree of initial crystallization. From the values for sample III there seems to be some temperature dependence, but this cannot be further discussed until more experiments have been carried out. It seems very unlikely that the degree of crystallization should increase with increasing temperature.

The values of M in table 2 show an evident change from the unvulcanized to the more vulcanized state. It is interesting to see that samples I and II, which have almost the same values of $(\partial\Delta E/\partial\Delta l)_T$, have such different values of M . If M is related to the part of the macromolecule between two points of cross-linkage, the number of those points are on an average per molecule for sample I equal to 3 and for sample II equal to 10. Sample II should consist of a more perfect network structure compared to sample I. As both samples are

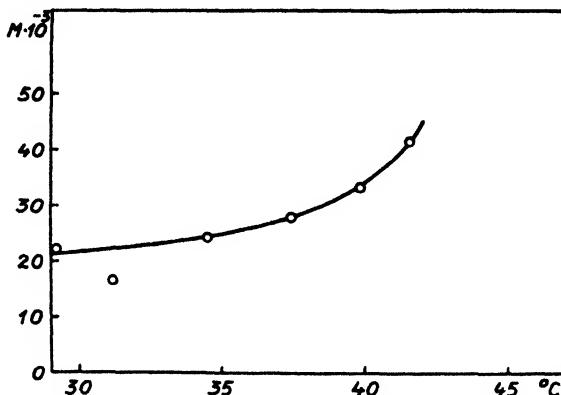


FIG. 5. M as a function of temperature

unvulcanized in the common sense, it is probable that sample II has a larger content of μ -polymer. For sample III the values of M increase with the temperature; this may be an indication that the forces in a point of cross-linkage in this case are very weak and cannot withstand the increased heat motion of the molecular segments. Hence the length of the molecule between adjacent points of cross-linkage increases. This increase seems to be more pronounced at higher temperatures, as is seen from figure 5.

For the determination of M it is also possible to use equation 6. Investigations in this direction are in progress.

Naturally it is very difficult to draw conclusions valid for the substances in question. Firstly, the expressions upon which the conclusion are based only give an approximate description of the material in certain respects and do not account for such phenomena as plastic flow, etc. Secondly, the substances are not well defined as to the types of polymers. It seems, however, from the results obtained in this investigation that certain comparisons can be made between

different substances and that further work will show the possibilities of getting better knowledge of the factors determining the transition from the unvulcanized to the vulcanized state.

SUMMARY

A brief survey of modern opinion as to the nature of the rubber-like state in certain high polymers is given. The behavior of unvulcanized and vulcanized rubber samples has been investigated with a Polanyi dynamometer. By means of Wall's formula for entropy changes on stretching, certain constants characterizing the samples have been calculated. The use of these constants for comparison purposes has been discussed.

This investigation is a part of a fundamental research program on synthetic rubber carried out at the request of the Governmental Commission of Industry in Sweden and under the guidance of Professor The Svedberg.

The author wishes to express his sincere thanks to Professor The Svedberg for his very kind interest and for the many facilities put at the author's disposal.

REFERENCES

- (1) BOSTROEM, S.: *Kolloidchem. Beihefte* **26**, 439 (1928).
- (2) FLORY, P. J., AND REHNER, J., JR.: *J. Chem. Phys.* **11**, 512 (1943); *Ann. N. Y. Acad. Sci.* **44**, 419 (1943).
- (3) FLORY, P. J., AND REHNER, J., JR.: *J. Chem. Phys.* **11**, 521 (1943).
- (4) GUTH, E., AND MARK, H.: *Monatsh.* **65**, 93 (1934).
- (5) HUGGINS, M. L.: *J. Polymer Sci.* **1**, 1 (1946).
- (6) KUHN, W.: *Kolloid-Z.* **67**, 2 (1934).
- (7) KUHN, W.: *Kolloid-Z.* **76**, 258 (1936).
- (8) MARK, H.: *Am. Scientist* **31**, No. 2 (1943).
- (9) MARK, H.: In *The Chemistry of Large Molecules*, R. E. Burk and O. Grummitt (*Editors*), p. 33. Interscience Publishers, Inc., New York (1943).
- (10) MEYER, K. H.: *High Polymers. Vol. IV. Natural and Synthetic High Polymers*, p. 153, Interscience Publishers, Inc., New York (1942); cf. MEYER, K. H., AND MARK, H.: *Hochpolymere Chemie*, Vol. II, p. 143, Akademische Verlagsgesellschaft m.b.H., Leipzig (1940).
- (11) MEYER, K. H., AND FERRI, G.: *Helv. Chim. Acta* **18**, 570 (1935).
- (12) POLANYI, M.: *Z. tech. Physik* **6**, 121 (1925).
- (13) TRELOAR, L. R. G.: *Trans. Faraday Soc.* **36**, 538 (1940).
- (14) WALL, F. T.: *J. Chem. Phys.* **10**, 485 (1942).

A STATISTICAL THEORY OF DISCOLORATION FOR HALOGEN-CONTAINING POLYMERS AND COPOLYMERS¹

R. F. BOYER

*Physical Research Laboratory, The Dow Chemical Company, Midland, Michigan**Received August 8, 1946*

INTRODUCTION

The tendency of halogen-containing polymers to lose a part of their halogen through the catalytic action of light, heat, or chemical reagents has long been recognized. The changes in color and mechanical properties accompanying this degradation reaction were almost sufficient in the early days to militate against the use of such polymers.

However, technological advances resulting from better control of the purity of raw materials, improved techniques of fabrication, and the employment of special light- and heat-stabilizing agents have so improved the situation that this problem is now mainly one of academic interest (28). And in proportion, as the practical aspects of the problem were solved, the academic side of the problem received more and more emphasis.

In brief, the systematic degradation of halogenated polymers with special reagents has been used to furnish important clues about the structures of high polymers. This field of inquiry is best exemplified by the results of Marvel and coworkers (26, 27), who have studied the effects of zinc on polyvinyl chloride and vinyl chloride-vinyl acetate copolymers. This experimental work, in conjunction with the theoretical conclusions of Flory (12), Wall (45), and Simha (36), has established, among other things, that polyvinyl chloride possesses a head-to-tail structure. While this technique has not been too successful with copolymers (26), it does constitute an important tool for studying high polymers in general.

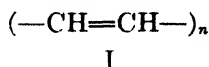
Other efforts in the same direction include Staudinger and Feisst's treatment of polyvinylidene chloride with phosphorus and hydrogen iodide in an unsuccessful attempt to obtain a pure, long-chain, soluble, hydrocarbon residue which would offer some clue as to the structure of the original polymer (41). The relationship between formation of hydrogen chloride and electrical conductivity, as well as color in polyvinyl chloride, was reported by Fuoss (15), while Lichtenberger and Naftali (24) described the results of systematic attacks on chlorinated rubber by pyridine. Numerous other references to the problem have appeared from time to time (33, 40).

Ironically enough, this tendency to lose the halogen acids has even been used to advantage. Thus, Dinsmore (8) has shown how vinylidene chloride polymers can be vulcanized, presumably by virtue of the unsaturated system formed on loss of hydrogen chloride. Even prior to this, Ostromyslenskii (34) had prepared rubber-like products by the action of zinc on polyvinyl halides.

¹ Presented at the Twentieth National Colloid Symposium, which was held at Madison, Wisconsin, May 28-29, 1946.

A more recent ingenious application of degradation has been made by Land and Rogers (22), who found that dehydration of oriented polyvinyl alcohol films caused a slight darkening and the onset of a strong positive dichroism, that is, an ability to polarize light. They postulated the existence of oriented polyene groups, $(-\text{CH}=\text{CH}-)_n$, to account for this selective absorption of light in a given direction.

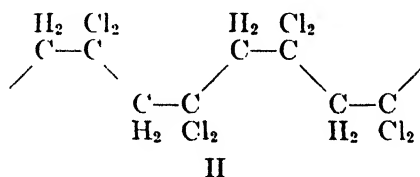
The present report attempts to extend the theory of such effects by deriving an explicit connection between loss of hydrogen chloride and formation of color in polyvinylidene chloride and its copolymers. The theory should be applicable to other halogen-containing polymers if suitable account is taken of their physical and chemical characteristics. Similarly, it should apply to polyvinyl alcohol which can lose water, and to polyvinyl acetate which can lose acetic acid. Our work is based on the suggestion by Marvel, Sample, and Roy (27) that color formation is the result of polyene structures of the type



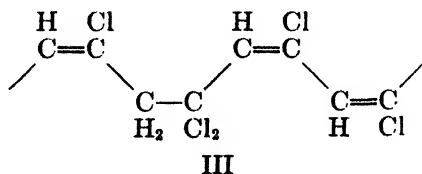
where n is an integer, which develops on loss of hydrogen chloride.

STATISTICAL TREATMENT OF LOSS OF HYDROGEN CHLORIDE

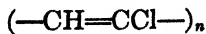
Polyvinylidene chloride might be pictured to have a chain structure of the type:



as indicated from x-ray diffraction studies by Frevel (13), whose principal conclusions have been given by Reinhardt (35). Because of the disposition of the hydrogen and chlorine atoms, hydrogen chloride will tend to be lost from a monomer unit, and not between two adjacent monomer units. Moreover, after one hydrogen chloride molecule has been removed from a monomer unit, the remaining chlorine atom is stabilized by the double bond (11), and there should be little tendency for the same monomer to lose a second molecule of hydrogen chloride. Thus a polyvinylidene chloride molecule which has lost hydrogen chloride through exposure to light, heat, or chemical reagents might have a local structure such as:



If this hydrogen chloride is lost at random along the length of the chain, there will result structures of the type:



IV

where n may assume integral values. In fact, there should be a distribution of n values given by probability laws and depending on the fraction, p , of all monomer units which have lost a molecule of hydrogen chloride.

Briefly, assuming an infinitely long polymer chain with hydrogen chloride lost at random, the probability that a given unsaturated system is formed consisting of n double bonds in conjugation is:

$$P_n(p) = (1 - p^2)p^n \quad (1)$$

This equation follows at once from the theory of probability for successive events (3). n double bonds, each of probability p , must be formed in successive monomer units along the chain, while at each end of this conjugated system is a monomer which has not lost a hydrogen chloride molecule, and for which the probability is $(1 - p)$. p is equivalent to the extent of the degradation reaction; thus, if 40 per cent of the original monomers have lost hydrogen chloride, then the probability that any monomer selected at random in the polymer chain is unsaturated is 0.4.

Incidentally, the assumption of a finite molecular weight, which would be around 20,000 for the polymers under consideration, will not greatly alter the results. The exact equation which accounts for chain length will be given later as equation 7a.

Figure 1 summarizes some of the pertinent features of equation 1 by plotting the percentage of all double bonds which reside in structures of complexity n as a function of the extent of degradation. In the beginning most of the double bonds are isolated, and it is not until an extensive degree of degradation has occurred that complex double-bond systems occur with appreciable frequency.

The probable nature of the double-bond arrangements having been described as a function of the known loss of hydrogen chloride, the next problem is to correlate these structures with color or light absorption. The connection between structure and color in organic compounds has been summarized in excellent reviews by Brode (4) and Lewis and Calvin (23). In particular, both authors treat in detail the extensive and pertinent series of measurements carried out by Hausser, Kuhn, and coworkers on a variety of polyene compounds, $R(-C=C-)_nR'$. Of greatest interest are the diphenylpolyenes, which have been studied out to $n = 7$ (17). Lewis and Calvin have shown that for these compounds, the square of the wave length of the first absorption maximum increases linearly with n , while the intensity of absorption (as measured by the maximum extinction coefficient) is also a linear function of n . Still other examples of linear conjugated systems are well known; β -carotene, for example, with its vivid yellow color, has eleven double bonds in conjugation. Sticher

and Piper (42) have polymerized phenylacetylene to obtain reddish colored polymers. Tuttle and Jacobs (44) have prepared polymers of phenoxyacetylene possessing a red color with an absorption maximum at 4200 Å. They believe this product to be a polyene, since it developed a characteristic blue color in the presence of antimony trichloride.

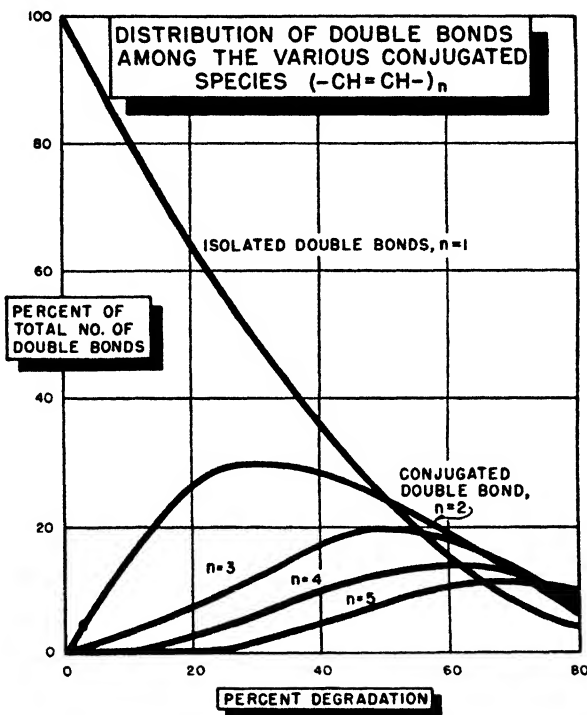


FIG. 1. Distribution of double bonds among the various conjugated species, $(-\text{CH}=\text{CH}-)_n$, for random loss of hydrogen chloride.

TESTING THE THEORY

Knowing the complexity of double-bond systems which might be expected in a degraded polymer, and knowing the general light-absorption characteristics of such polyenes, it should be possible to test the theory. With this end in mind, the following simple experiment was carried out. A vinylidene chloride-12 per cent vinyl chloride copolymer was refluxed for 8 hr. in dioxane at atmospheric pressure in the presence of an excess of zinc powder. The zinc had first been treated with hydrochloric acid to remove impurities (27), and then washed with water and dioxane. The zinc exerted a catalytic action in removing hydrogen chloride from the polymer, and the boiling solution gradually acquired a yellow color. After 8 hr. the solution was filtered and diluted with an equal volume of water to precipitate the polymer. The dioxane-water mixture was colorless but slightly hazy. The polymer was washed with methanol and

acetone. The dried degraded polymer, which now had a brownish color, was redissolved in dioxane to give a 1 per cent solution. Incidentally, this degraded polymer was much more soluble than the original material. The light-absorption curve of this solution for a thickness of 9.5 mm. is plotted in figure 2. The absorption curve is extremely broad and relatively free from any fine details.

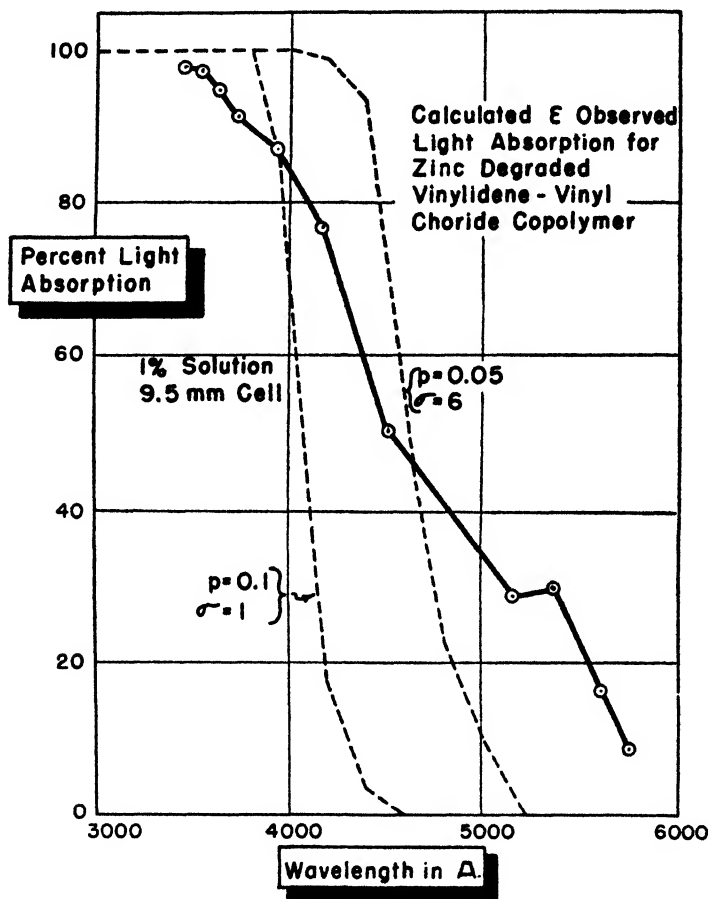
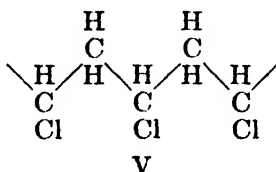


FIG. 2. The curve marked $p = 0.1$ was calculated for a 10 per cent random loss of hydrogen chloride; the curve marked $p = 0.05$ assumes a 5 per cent non-random loss of hydrogen chloride. σ greater than unity implies a preferential building up of long conjugated systems.

This is what might be expected if the absorption resulted not from a single color body but from the superimposed effects of many types of absorbers. The polymer showed chlorine analyses of 71.18 per cent and 69.58 per cent before and after degradation, a result which indicated that the zinc treatment had removed hydrogen chloride from approximately 10 per cent of the monomers.

Several words of explanation might be in order at this point concerning the choice of experimental conditions. Marvel, Sample, and Roy (27) had shown

that the effect of zinc on polyvinyl chloride is to remove chlorine atoms in pairs, with the consequent formation of cyclopropane rings along the polymer chain. Marvel stated that no color developed in the presence of zinc (25). However, on treatment of their polymer with caustic, a reddish brown polymer was formed (27). This action of zinc is what might be expected from the known x-ray structure of polyvinyl chloride (14).



With polyvinylidene chloride, as given by formula II, it is apparent that this same type of action is not very probable. Thus, the fact that zinc promotes removal of hydrogen chloride from polyvinylidene chloride is at least in agreement with Frevel's structure.

The choice of a vinylidene chloride copolymer was dictated by the following considerations: Melt viscosity studies by McIntire (29) had indicated that polyvinylidene chloride and its copolymers with small amounts of vinyl chloride behaved as linear polymers, whereas polyvinyl chloride seemed to be highly branched. The 12 per cent vinyl chloride copolymer used here was chosen then because it was believed to be a linear polymer and because it was soluble in dioxane at its boiling point. Pairs of vinyl chloride units along the copolymer chain should be relatively infrequent, and one would not expect much action of the type that occurs between zinc and polyvinyl chloride. It should be stated that measurements of bromine absorption on the degraded polymer indicated that roughly 1 per cent of hydrogen chloride had been lost. Infrared examination of the degraded polymer did not furnish any conclusive results about the amount of unsaturation, although it did reveal considerable C=O.

Assuming that p in equation 1 is 0.1, values of P_n were calculated. The concentration of polymer in the solution measured for light absorption was 10 g. per liter, or approximately 10/90 base moles per liter. The concentration in moles per liter of a conjugated material of complexity n would therefore be $10P_n/90$.

This value can then be substituted in the expression

$$I = I_0 10^{-\epsilon cd/2.30} \quad (2)$$

where c is the concentration in moles per liter, d is the cell thickness, and ϵ is the molar extinction coefficient of the diphenylpolyenes as given by Hausser, Kuhn, and Smakula (17). The calculated optical density at any wave length is:

$$D_\lambda = \log_{10} I_0/I = \sum_{n=1}^{\infty} 0.106\epsilon_n P_n \quad (3)$$

where the summation includes all polyenes which absorb at that wave length. In this manner the theoretical curve for 10 per cent degradation as shown in

figure 2 (with $\sigma = 1$) was obtained. The general agreement with the observed absorption curve is not too good. In general, theory predicts too much absorption at the shorter wave lengths, and not enough at the longer wave lengths.

There are several principal difficulties with the theory thus far. In the first place, the diphenylpolyenes are likely not good models to use for light absorption. They have terminal phenyl groups which are lacking in the polymer. This would make the agreement even poorer, although our degraded polymer had $C=O$ groups which might compensate to some extent for the lack of phenyl

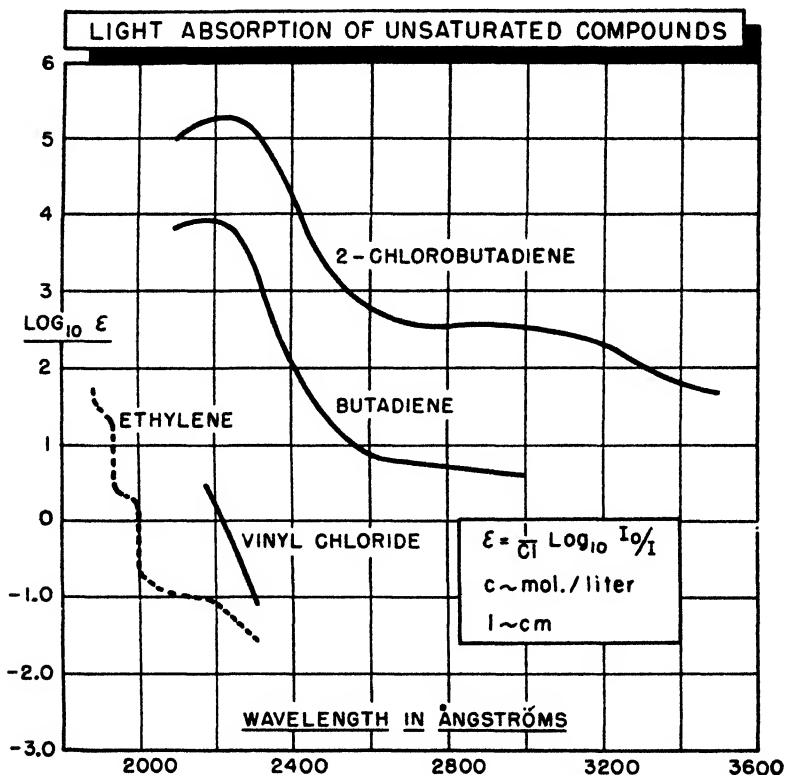


FIG. 3. Light-absorption curves on unsaturated compounds corresponding to the units formed in degraded vinyl chloride and vinylidene chloride polymers and copolymers.

groups. Actually, Kuhn and Grundmann (21) have prepared polyenes of $n = 4$ and 6 with terminal methyl groups. Such materials absorb in approximately the same spectral region but have smaller extinction coefficients than the corresponding diphenylpolyenes. Thus, the polyene chain itself is apparently much more important than the terminal group when n is large.

An even more important difference is that our degraded polymer has chlorine groups spaced regularly along the polyene chains. It might be expected that these chlorine atoms would shift the absorption curve to longer wave lengths (6).

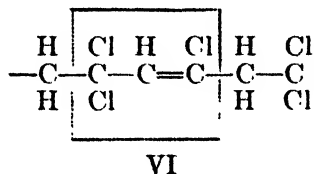
Figure 3, for example, compares the light-absorption characteristics of ethylene (39), vinyl chloride,² butadiene,² and 2-chlorobutadiene.³ Chlorine substitution causes both a shift toward longer wave length and a more intense absorption.

Walsh (46), in commenting on the spectrum of vinyl chloride, points out that its ionization limit and electronic levels are at longer wave lengths than for ethylene, despite the high electronegativity of chlorine. His proposed explanation is based on the resonance occurring between the π electrons of the $C=C$ double bond and the non-bonding p/π lone-pair electrons on the chlorine atoms. The spectra of the *cis*- and *trans*-dichloro-, dibromo-, and diiodoethylenes (18) show a progressive broadening toward longer wave lengths as the weight of the substituent atom increases, even though the position and height of the maxima are roughly the same.

Moreover, the various polyene systems in a single polymer chain do not exist as separate molecules, and therefore will have some inductive effect on each other. Brode and Tryon have found that the absorption spectra of non-conjugated, unsaturated fatty acids vary with the number of double bonds present (5). Jeffrey (19) has noted from x-ray studies that the single bond midway between the two double bonds in geranylamine hydrochloride is considerably shorter than a normal single bond, and that it behaves as if partly conjugated with the other two double bonds in the molecule. Pertinent ultraviolet-absorption studies have been made by Bateman and Koch (2).

Another aspect of this problem is the influence of isomeric structure on the light absorption. Mulliken (32) has calculated, for example, that a polyene in its most elongated form (*trans, trans, trans*), will show greater absorption than the same chain in a more *cis*-like form. It is not known, of course, just what shape such partially degraded polymers of the type we are discussing here would assume, although there would likely be a mixture of isomers present. The coexistence of many values of n and the possibility of mixed isomers for each value of n probably account for the complete lack of detail in the absorption curves of degraded polymers.

There is one other possibility, perhaps even more important than any thus far considered,—namely, that the loss of hydrogen chloride along the chain is not completely random. Drake suggested (9) that once a double bond forms anywhere along the chain, a structure of the allyl chloride type results:



¹ The light-absorption data on vinyl chloride and butadiene were obtained from L. G. Reinhardt, Spectroscopy Division, The Dow Chemical Company.

² The light-absorption curve on 2-chlorobutadiene was furnished through the courtesy of Dr. J. B. Nichols, Experimental Station, E. I. du Pont de Nemours & Co., Wilmington, Delaware.

The chlorine atom of allyl chloride is quite labile because of the inductive effect of the double bond. Conant, Kirner, and Hussey reported, for example, that in a reaction with sodium iodide, allyl chloride was seventy-nine times more reactive than *n*-propyl chloride (7). While the structure pictured above is complicated by extra chlorine atoms, it might be anticipated that an adjacent double bond would form more quickly than would an isolated bond. The theory for such a non-random loss of hydrogen chloride follows:

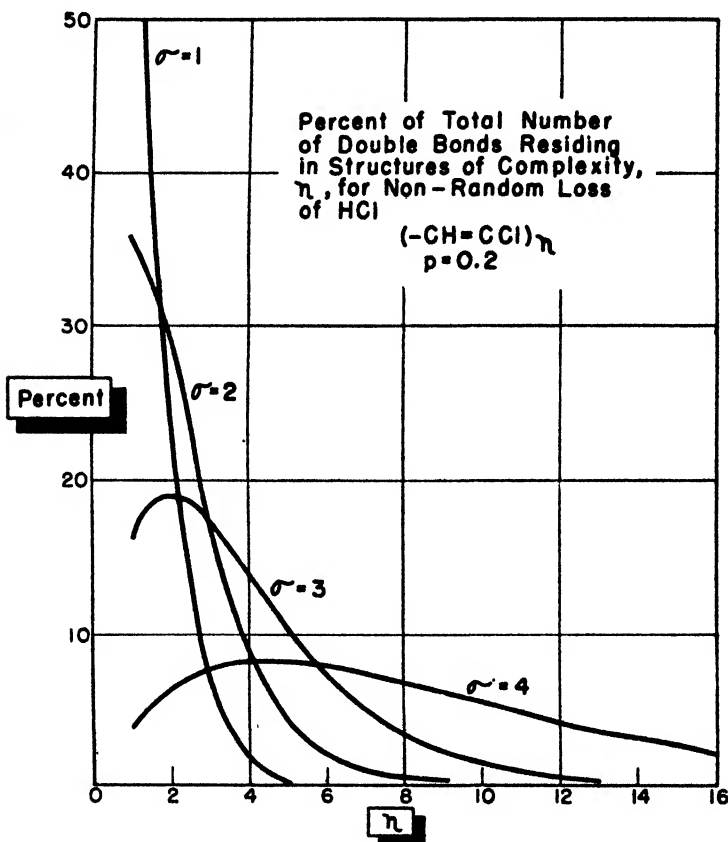


FIG. 4. Distribution of conjugated systems for 20 per cent loss of hydrogen chloride with increasing degrees of departure from random loss of hydrogen chloride (increasing values of σ).

If σ is the relative reactivity of an adjacent hydrogen chloride molecule, so that σp is the probability of forming a double bond in conjugation to an existing double bond, then the probability, $P_n(p, \sigma)$, of obtaining n double bonds in conjugation is:

$$P_n(p, \sigma) = [(1 - \sigma p)^2 / \sigma] (\sigma p)^n \quad (4)$$

Actually, this inductive effect is unidirectional but the net result is that a conjugated system would tend to propagate itself at the expense of isolated double bonds. Figure 4 illustrates calculations based on equation 4, when p is 0.2 and σ assumes various values. It is readily apparent that long conjugated systems can form quite readily. Figure 5 is a plot of the number-average value of n as a function of the extent of reaction, p , for several values of σ . This number

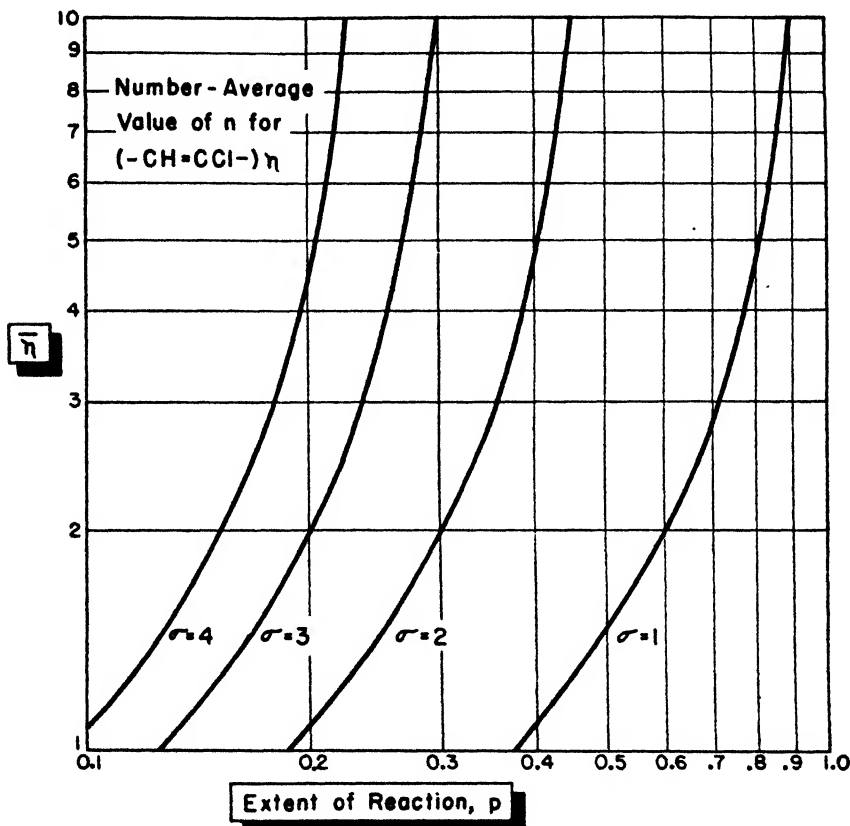


FIG. 5. Number-average length of conjugated systems as a function of the fraction of available hydrogen chloride lost for several values of σ .

average, n , is an expression of the complexity of the conjugated double-bond systems, and is given by

$$\bar{n} = 1/\ln_e(\sigma p) \quad (5)$$

Color calculations based on equation 4 for $p = 0.05$ and $\sigma = 6$ are shown in figure 2. For this case we included in the calculations an assumed light-absorption curve for diphenylpolyene corresponding to $n = 8$. A somewhat similar light-absorption curve would appear in figure 2 for $p = 0.01$, $\sigma = 50$. No special significance other than that of curve fitting can be attached to these

latter two results. One reason why the calculated absorption curves end abruptly at 5200 Å. is the lack of absorption data on the diphenylpolyenes for n greater than 7. Kuhn (20) reports absorption maxima at 5300, 4930, and 4620 Å. for the $n = 11$ diphenylpolyene, but does not give an absorption curve. He also reports $n = 15$ with an absorption maximum at 5700 Å., which might account for the observed absorption of figure 2 out to 6000 Å.

Positional isomerization of double bonds is another reaction which can increase the degree of conjugation. Isolated double bonds along the chain would conceivably migrate and either form a conjugated system or extend an existing one. Such reactions usually require catalytic conditions (38), but might proceed under ultraviolet light. This predilection for isomerization might cause the hydrogen chloride on a monomer adjacent to an existing double bond to be more readily removed.

Any such isomerization tendency would increase the average length of the polyene systems. It would act in both directions along the chain, whereas the allyl chloride effect should be unidirectional. Asinger (1), incidentally, recommends the use of silver stearate for cleaving halogen acids from alkyl halides of high molecular weight without shifting of the double bond.

In the case of exposure to light, it will be precisely those regions of the chain which have already developed unsaturation and conjugation that will absorb radiant energy most strongly and over a progressively widening spectral band. This localization of absorbed energy may then promote unsaturation in adjacent monomers, again promoting the formation of long conjugated systems.

Thus, in concluding this section, one can say that probability theory coupled with the known absorption spectra of long conjugated polyene compounds can account for the general nature of color formation in degraded polyvinylidene chloride. Chemical and isomeric differences between the studied polyenes and the degraded polymers, inductive effects of one conjugated system upon another one along the same polymer chain, and the influence of unsaturation in promoting loss of hydrogen chloride from an adjacent monomer unit (allyl chloride effect) are all unknown factors. These three factors acting concurrently should serve to extend the calculated absorption further toward the red end of the spectrum, and hence into better agreement with observation.

Incidentally, this method of calculating the color of degraded polymers gives an interesting interpretation of two important characteristics of vinylidene chloride and vinyl chloride polymers. The first question is: Why should these materials darken in sunlight since they do not contain chromophoric groups which would be expected to absorb radiant energy present in sunlight (wave lengths longer than 2900 Å.)? A simple calculation, based on equation 1 and the known light absorption of polyenes, shows that if a chlorinated polymer loses only a few hundred parts per million of hydrogen chloride during manufacture and processing, then the observed light absorption of freshly molded polymer, as reported by Matheson and Boyer (28), is readily explained. Such a loss of hydrogen chloride is not unreasonable with commercial molding and extrusion temperatures in excess of 100°C. |

The second point is this: Matheson and Boyer (28) have suggested that esters of maleic and aconitic acid stabilize vinylidene chloride polymers by undergoing a Diels-Alder condensation with conjugated double-bond systems formed in the degraded polymer. The solid polymer contains 1700/97 moles per liter of monomer units, and therefore the total number of pairs of double bonds would be

$$(1700/97)(P_2 + P_3 + 2P_4 + 2P_5 + 3P_6 + \dots) \quad (6)$$

where the P 's are probabilities given by equation 1. For a polymer which has lost 10 per cent of hydrogen chloride, the above equation predicts a requirement of 0.15 mole or 3 weight per cent of tributyl aconitate. This is the correct order of magnitude for the amount of such stabilizer described in one patent (16). This does not prove the proposed mechanism and may merely be a coincidence. Actually, the unsaturated ester would have to react with only an occasional pair of conjugated double bonds to lessen the color markedly.

COPOLYMERS OF HALOGENATED WITH NON-HALOGENATED MONOMERS

We wish now to extend the results of the previous section to the case of copolymers between halogenated and non-halogenated monomers. In general, the second monomer should be one that does not lose hydrogen chloride, acetic acid, water, hydrogen cyanide, or in any way develop unsaturation. Ideal comonomers for this purpose would be ethylene, isobutylene, styrene, the acrylates, and the methyl methacrylates.

It is immediately evident on qualitative grounds that such neutral monomers interspersed at random along a polymer chain will have several important effects on the discoloration resulting from the loss of hydrogen chloride. In general, they will prevent the formation of certain long conjugated systems that might otherwise occur, they will limit the maximum size of long conjugated systems, and they will tend to inhibit inductive action between adjacent conjugated systems. Thus, for a given loss of hydrogen chloride, such a copolymer should not develop as deep a red color as the pure halogenated polymer. The hydrogen chloride which is lost is channeled, so that short conjugated systems should form with greater ease. Figure 6 shows light-absorption curves on a series of unstabilized vinylidene chloride-ethyl acrylate copolymers which were exposed in the form of 0.007-in. films to a Fadeometer for 24 hr. The beneficial action of the neutral comonomer is readily apparent.

Figure 7 is a calculated plot of the average length of the uninterrupted vinylidene chloride chains as a function of the mole fraction of vinylidene chloride in the copolymer. Identical results hold for all other copolymer systems which are ideal. The ethyl acrylate copolymer was chosen for study because it is believed to be ideal, that is, the copolymer formed has approximately the same composition as the monomer mixture, and is independent of the per cent yield. As figure 7 indicates, a fairly large proportion of the vinylidene chloride chains is necessary to reduce the average length of the vinylidene chloride chains to a safe level as regards the possibility of developing long unconjugated systems. Moreover, these are number-average values, and while there will be many

shorter chains, there will also be an appreciable number of chains up to five times the average length. Figure 7 was calculated by using an expression given by Stockmayer (43). If the copolymer is not ideal, and, for example, vinylidene chloride monomer enters the copolymer more rapidly than the acrylate does, the

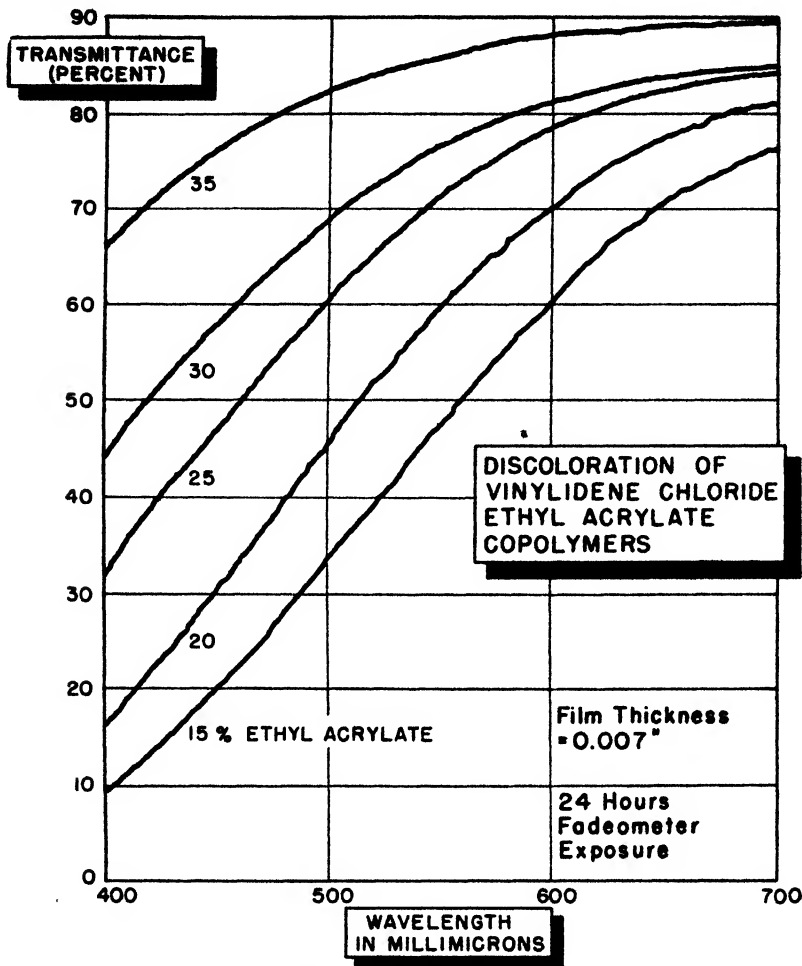


FIG. 6. Beneficial effect of increasing amounts of neutral comonomer (ethyl acrylate) on the light stability of vinylidene chloride-ethyl acrylate copolymers. These films did not contain a light stabilizer.

average length of vinylidene chloride chains will be even longer, as shown by the upper curves of figure 7.

In general, as the proportion of acrylate in the copolymer increases, there will exist long runs of acrylate chains which do not contribute their maximum possible amount to the desired stabilizing action except by acting as a diluent. A desired copolymer would be one containing exactly one or two acrylates

between every three to four vinylidene chloride units along the chain. The precise effect of the neutral monomer on double-bond formation will be apparent from quantitative calculations to be given later.

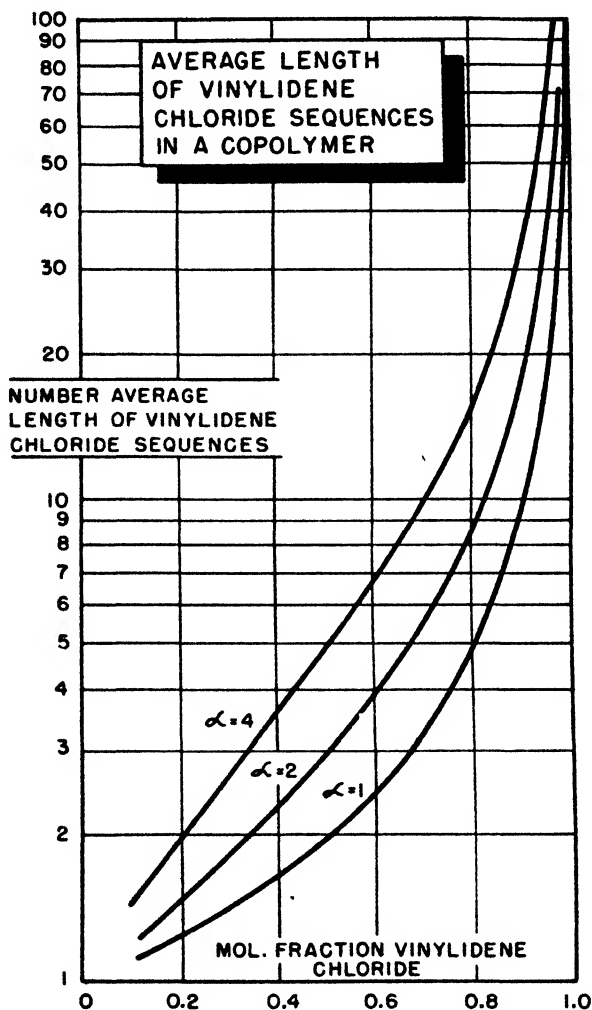


FIG. 7. Effect of monomer composition on the average length of the vinylidene chloride sequences. α measures the preferential tendency of a vinylidene chloride monomer to add onto a copolymer chain which has an active vinylidene chloride group at the growing end of the chain.

In attempting to develop a statistical theory⁴ for the loss of hydrogen chloride from such copolymers, we have made the following simplifying assumptions, some of which are admittedly artificial:

⁴ The author is indebted to R. Simha for the derivation of equations 7-12, as well as equations 15-18.

(1) The copolymer is ideal in that the two monomers enter the chain at random.

(2) All copolymer chains have the same length or degree of polymerization, L .

(3) Hydrogen chloride is lost at random.

(4) Only one hydrogen chloride molecule can be removed from each vinylidene chloride monomer.

If x is the mole fraction of vinylidene chloride units in the copolymer, the acrylates will divide these chlorides up into runs of length t . Simha (37) has shown that

$$N(t) = N(1 - x)x^t[2 + (L - t - 1)(1 - x)] \quad (7a)$$

for $t \leq L - 1$, and

$$N(L) = Nx^L \quad (7b)$$

for $t = L$, where $N(t)$ is the number of runs of consecutive vinylidene chlorides of length t , L is the degree of polymerization of the copolymer chain, and N is the total number of such chains. From now on the acrylates can be ignored, and attention focused only on polyvinylidene chloride chains possessing a distribution of chain lengths as defined by equations 7a and 7b.

From these vinylidene chloride polymers a fraction, p , of the hydrogen chloride is removed by some physical means. p is defined as the ratio of the total number of hydrogen chloride molecules removed (or the total number of unsaturated monomers formed) to the total number of vinylidene chloride monomers present. This action is equivalent to forming a new copolymer, so to speak, between vinylidene chloride and its unsaturated product, $-\text{CH}=\text{CCl}-$. What is now required is the number, $M_n(t, p)$, of runs of conjugated chains of length, n , as a function of t and p . By analogy with equations 7a and 7b,

$$M_n(t, p) = N(t)(1 - p)p^n[2 + (t - n - 1)(1 - p)] \quad (8a)$$

for $n \leq t - 1$ and

$$M_t(t, p) = N(t)p^t \quad (8b)$$

for $n = t$.

However, runs of conjugated double bonds of length n can exist in vinylidene chloride chains of lengths $t_1, t_2 \dots t_L$, so that, following Montroll (30), the total number, $M_n(p)$, of conjugated systems of length n as a function of the degree of unsaturation, p , is given by

$$M_n(p) = \sum_{t=n}^{t=L} M_n(t, p) \quad (9)$$

$$= N(n)p^n \quad (10a)$$

$$+ \sum_{t=n+1}^{L-1} M_n(t, p) \quad (10b)$$

$$+ NX^L p^n(1 - p)[2 + (L - n - 1)(1 - p)] \quad (10c)$$

Expression 10a refers to a run of n double bonds for $t = n$; expression 10c refers to a run of n double bonds in pure polyvinylidene chloride; and expression 10b covers all intermediate cases. $N(n)p^n$ in equation 10a is, from equation 7a:

$$N(n)p^n = N(1-x)x^n p^n [2 + (L-n-1)(1-x)] \quad (11)$$

Equation 10b is obtained by substituting equation 7a in equation 8a, whence

$$\sum_{t=n+1}^{L-1} M_n(t, p) = N(1-x)(1-p)p^n \sum_{t=n+1}^{L-1} x^t [2 + (L-t-1)(1-x)] \cdot [2 + (t-n-1)(1-p)] \quad (12)$$

The quantity within the summation sign can be expanded and then summed according to methods given by Montroll and Simha (31). However, the final expression appeared at first to be extremely awkward for purposes of calculation, and quite sensitive to small arithmetical errors. Fortunately, these calculations could be carried out rather conveniently with punched-card computing machines (10), and this has been done,⁵ using standard IBM (International Business Machine) equipment. L , the degree of polymerization, was taken as 100, corresponding to a molecular weight of approximately 10,000. The actual molecular weight for copolymers of vinylidene chloride and ethyl acrylate is probably several times this value. However, with L greater than 100 the work on the machines would have multiplied many fold, and the final answers would not have been greatly different. Calculations were completed for the following conditions:

$$\begin{aligned} x &= 0.98, 0.95, 0.90, 0.85, 0.75, 0.65 \\ p &= 0.05, 0.15, 0.30, 0.45, 0.60 \\ n &= 1, 3, 5, 7, 9 \end{aligned}$$

The IBM machines also handled the calculations for equation 11. The three terms which were finally added up to give the total number of conjugated systems of length n are, of course, equations 10c, 11, and 12. Thus, calling $M_n(p)$ the total number of conjugated systems of length n when the extent of degradation is p , we have

$$M_n(p) = \text{equation 10c} + \text{equation 11} + \text{equation 12} \quad (13)$$

The logarithm of $M_n(p)$ plotted against n for n equal to 1, 3, 5, 7, and 9 gave straight lines. Thence, values of $M_n(p)$ for n equal to 2, 4, 6, 8, 10, 11, and 12 could be obtained very readily. The complete set of values of $M_n(p)$ is listed in table 1.

Figure 8 is a plot showing the individual contributions of the three terms in equation 13 to $M_n(p)$ for the particular case where $p = 0.30$ and $n = 1$. Similar results would hold for other values of p and n . The extension of this curve to values of x smaller than 0.65 was obtained by the use of equations 15 and 16,

⁵ The writer is indebted to John Milliman and D. B. Ovait, who interpreted this problem for use on the IBM machines and then carried out the calculations.

TABLE I
*Values of $M_n(p)/N$ for various extents of chlorine loss, p , and various mole fractions of vinylidene chloride, x^**

p	x	$x \rightarrow 1.0$	0.98	0.95	0.90	0.85	0.75	0.65
0.05	1	4.51	4.441	4.363	4.105	3.898	3.474	3.043
	2	2.24×10^{-1}	2.15×10^{-1}	2.12×10^{-1}	1.77×10^{-1}	1.60×10^{-1}	1.31×10^{-1}	1.02×10^{-1}
	3	1.11×10^{-2}	1.04×10^{-2}	9.52×10^{-3}	8.15×10^{-3}	6.89×10^{-3}	4.78×10^{-3}	3.15×10^{-3}
	4	5.47×10^{-4}	5.45×10^{-4}	4.60×10^{-4}	2.90×10^{-4}	2.80×10^{-4}	1.74×10^{-4}	9.52×10^{-5}
	5	2.70×10^{-5}	2.78×10^{-5}	2.20×10^{-5}	1.095×10^{-5}	1.097×10^{-5}	6.59×10^{-6}	2.80×10^{-6}
0.15	1	10.86	10.74	10.512	10.117	9.729	8.861	7.98
	2	1.69	1.60	1.52	1.485	1.26	9.71×10^{-1}	8.20×10^{-1}
	3	2.39×10^{-1}	2.28×10^{-1}	2.10×10^{-1}	1.81×10^{-1}	1.551×10^{-1}	1.099×10^{-1}	7.41×10^{-2}
	4	3.56×10^{-3}	3.20×10^{-3}	2.95×10^{-3}	2.38×10^{-3}	1.98×10^{-3}	1.22×10^{-3}	7.30×10^{-4}
	5	5.28×10^{-4}	4.79×10^{-4}	4.12×10^{-4}	3.22×10^{-4}	2.46×10^{-4}	1.36×10^{-4}	6.86×10^{-5}
	6	7.85×10^{-4}	6.92×10^{-4}	5.60×10^{-4}	4.15×10^{-4}	3.03×10^{-4}	1.48×10^{-4}	6.48×10^{-5}
	7	1.166×10^{-4}	1.03×10^{-4}	8.05×10^{-5}	5.55×10^{-5}	3.78×10^{-5}	1.59×10^{-5}	6.22×10^{-6}
0.30	1	14.82	14.77	14.687	14.473	14.247	13.60	12.7
	2	4.40	4.40	4.20	3.90	3.62	3.02	2.43
	3	1.314	1.252	1.17	1.034	9.06×10^{-1}	6.68×10^{-1}	4.72×10^{-1}
	4	3.88×10^{-1}	3.72×10^{-1}	3.33×10^{-1}	2.82×10^{-1}	2.30×10^{-1}	1.61×10^{-1}	9.32×10^{-2}
	5	1.153×10^{-1}	1.061×10^{-1}	9.31×10^{-2}	7.37×10^{-2}	5.77×10^{-2}	3.40×10^{-2}	1.75×10^{-2}
	6	3.42×10^{-3}	3.10×10^{-3}	2.62×10^{-3}	2.05×10^{-3}	1.43×10^{-3}	7.61×10^{-4}	3.29×10^{-4}
	7	1.017×10^{-3}	8.97×10^{-4}	7.41×10^{-4}	5.29×10^{-4}	3.69×10^{-4}	1.64×10^{-4}	6.21×10^{-5}
	8	3.02×10^{-3}	2.65×10^{-3}	2.13×10^{-3}	1.41×10^{-3}	9.50×10^{-4}	3.59×10^{-4}	1.12×10^{-4}
	9	8.95×10^{-4}	7.46×10^{-4}	6.00×10^{-4}	3.74×10^{-4}	2.34×10^{-4}	7.8×10^{-5}	2.51×10^{-5}

0.45	1	13.83	13.997	14.225	14.511	14.731	14.813	14.8
	2	6.17	6.00	6.00	6.90	5.65	4.92	4.33
	3	2.76	2.669	2.548	2.332	2.115	1.652	1.236
	4	1.224	1.17	1.10	9.25 $\times 10^{-1}$	8.11 $\times 10^{-1}$	5.57 $\times 10^{-1}$	3.61 $\times 10^{-1}$
	5	5.45 $\times 10^{-1}$	5.09 $\times 10^{-1}$	4.56 $\times 10^{-1}$	3.74 $\times 10^{-1}$	3.03 $\times 10^{-1}$	1.85 $\times 10^{-1}$	1.032 $\times 10^{-1}$
	6	2.43 $\times 10^{-1}$	2.22 $\times 10^{-1}$	1.98 $\times 10^{-1}$	1.48 $\times 10^{-1}$	1.17 $\times 10^{-1}$	6.15 $\times 10^{-2}$	3.01 $\times 10^{-2}$
	7	1.084 $\times 10^{-1}$	9.69 $\times 10^{-2}$	8.17 $\times 10^{-2}$	6.02 $\times 10^{-2}$	4.36 $\times 10^{-2}$	2.09 $\times 10^{-2}$	8.63 $\times 10^{-3}$
	8	4.82 $\times 10^{-2}$	4.25 $\times 10^{-2}$	3.52 $\times 10^{-2}$	2.38 $\times 10^{-2}$	1.66 $\times 10^{-2}$	6.79 $\times 10^{-3}$	2.42 $\times 10^{-3}$
	9	2.14 $\times 10^{-2}$	1.845 $\times 10^{-2}$	1.462 $\times 10^{-2}$	9.65 $\times 10^{-3}$	6.21 $\times 10^{-3}$	2.23 $\times 10^{-3}$	7.16 $\times 10^{-4}$
0.60	1	9.89	10.256	10.815	11.677	12.459	13.613	14.699
	2	5.88	5.96	6.06	6.255	6.40	5.985	5.71
	3	3.49	3.477	3.445	3.335	3.177	2.72	2.192
	4	2.075	2.02	1.94	1.80	1.62	1.19	8.60 $\times 10^{-1}$
	5	1.232	1.18	1.098	9.55 $\times 10^{-1}$	8.11 $\times 10^{-1}$	5.358 $\times 10^{-1}$	3.262 $\times 10^{-1}$
	6	7.32 $\times 10^{-1}$	6.90 $\times 10^{-1}$	6.15 $\times 10^{-1}$	5.12 $\times 10^{-1}$	4.15 $\times 10^{-1}$	2.29 $\times 10^{-1}$	1.27 $\times 10^{-1}$
	7	4.35 $\times 10^{-1}$	4.00 $\times 10^{-1}$	3.50 $\times 10^{-1}$	2.73 $\times 10^{-1}$	2.06 $\times 10^{-1}$	1.001 $\times 10^{-1}$	4.83 $\times 10^{-2}$
	8	2.58 $\times 10^{-1}$	2.30 $\times 10^{-1}$	1.96 $\times 10^{-1}$	1.48 $\times 10^{-1}$	1.05 $\times 10^{-1}$	4.45 $\times 10^{-2}$	1.88 $\times 10^{-2}$
	9	1.535 $\times 10^{-1}$	1.35 $\times 10^{-1}$	1.11 $\times 10^{-1}$	7.77 $\times 10^{-2}$	5.25 $\times 10^{-2}$	1.89 $\times 10^{-2}$	7.49 $\times 10^{-3}$
	10	8.99 $\times 10^{-2}$	7.60 $\times 10^{-2}$	6.30 $\times 10^{-2}$	4.12 $\times 10^{-2}$	2.68 $\times 10^{-2}$	8.72 $\times 10^{-3}$	2.92 $\times 10^{-3}$
	11	5.39 $\times 10^{-2}$	4.50 $\times 10^{-2}$	3.55 $\times 10^{-2}$	2.20 $\times 10^{-2}$	1.31 $\times 10^{-2}$	3.87 $\times 10^{-3}$	1.14 $\times 10^{-3}$
	12	3.20 $\times 10^{-2}$	2.65 $\times 10^{-2}$	2.00 $\times 10^{-2}$	1.17 $\times 10^{-2}$	6.60 $\times 10^{-3}$	1.69 $\times 10^{-3}$	4.48 $\times 10^{-4}$

* x = mole fraction of vinylidene chloride.

given in the appendix. The over-all behavior shown in figure 8 is what would be expected according to the distribution of chain lengths in a copolymer, as defined by figure 7.

Figure 9 shows how the distribution of conjugated systems changes for three different copolymers ($x = 1.0, 0.85$, and 0.65) for $p = 0.60$. It is very evident

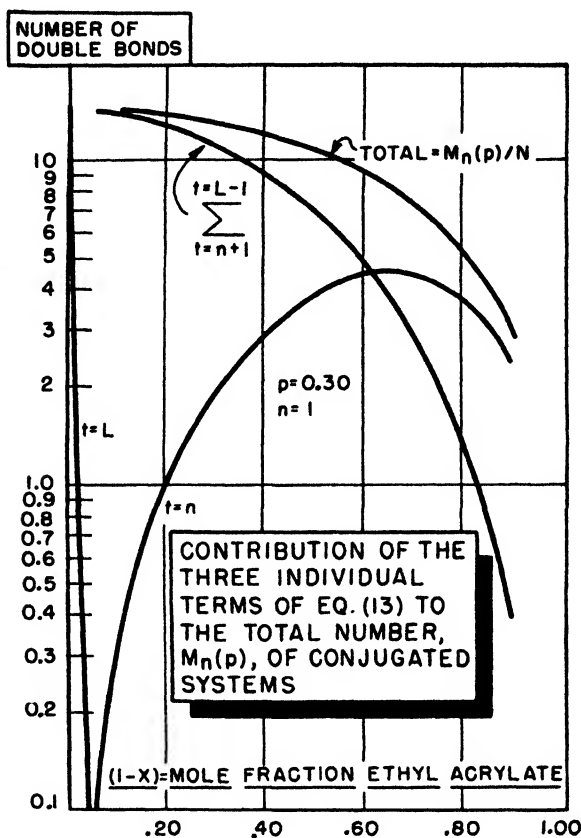


FIG. 8. Top curve is total number of isolated double bonds ($n = 1$) for 30 per cent loss of hydrogen chloride as a function of copolymer composition. The $t = L$ curve gives the number of double bonds occurring in pure polyvinylidene chloride; $t = n$ is the number of double bonds which occur in single vinylidene chloride monomers isolated between comonomer units. The remaining curve gives the number of double bonds occurring in all other sequences of vinylidene chloride units.

that increasing amounts of the neutral comonomer shift the distribution in favor of shorter conjugated systems, and hence at the expense of those long conjugated systems which cause a more intense visible color. Qualitatively, the theory is in accord with experimental results of the type shown in figure 6.

It does not appear worthwhile to attempt any calculations of the actual color, or light transmission, of degraded copolymers in view of the moderate success obtained on pure polymers. Most of the factors, such as the allyl chloride

effect, influence of chlorine atoms on light absorption, isomerization, and inductive effects, would be operating in copolymers, although to a lesser extent. It being assumed that visible coloration arises from values of n greater than 3, figure 10 shows the per cent of all double bonds which would occur in conjugated structures of n greater than 3 for different amounts of degradation and different amounts of neutral monomer. Figure 11 is a similar plot for n greater than 5.

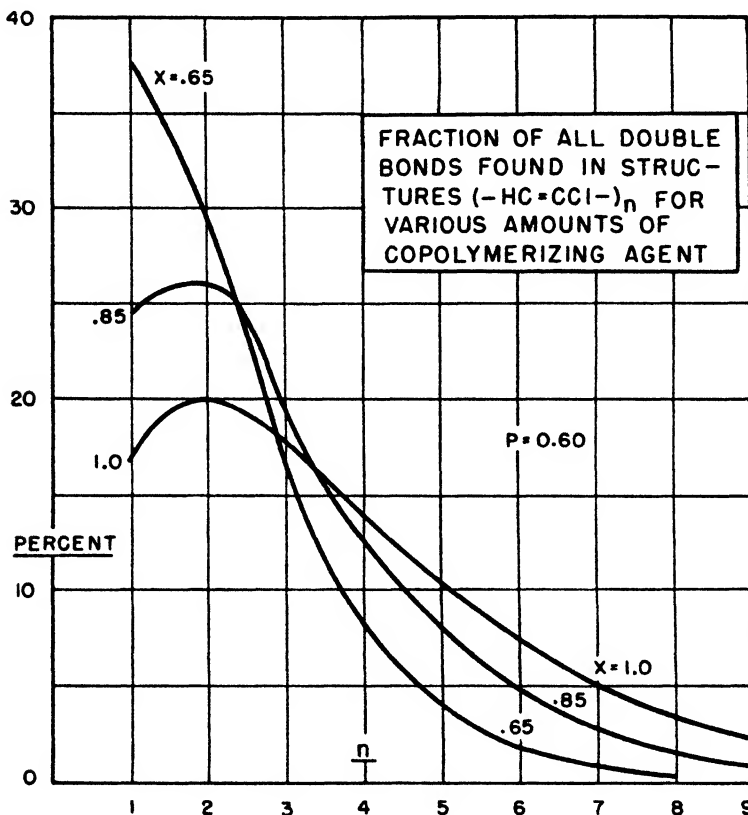


FIG. 9. Distribution of conjugated systems for 60 per cent loss of hydrogen chloride at three different mole fractions, x , of vinylidene chloride. Random loss of hydrogen chloride.

The per cent values given on the ordinates of figure 10 were obtained from the values in table 1 by performing the operation:

$$\text{Per cent} = \left[\frac{\sum_{n=4}^{n=L} nM_n(p)}{\sum_{n=1}^{n=L} nM_n(p)} \right] 100 \quad (14)$$

Figure 12 gives the percentage of all double bonds which are found in conjugated structures longer than a given value of n for values of n from 3 to 10. p was taken as 0.60. The increasing slope of these lines as n is made greater emphasizes in still another way the pronounced rôle of a neutral comonomer in reducing the number of long conjugated systems.

One might summarize these results by pointing out that there are three different ways in which a neutral comonomer will benefit the light and heat stability of a copolymer.

(1) With increasing amounts of neutral monomer present, the number of active (vinylidene chloride) monomers per chain decreases, and is given by Lx . Therefore, when several copolymers with different values of x are subjected to

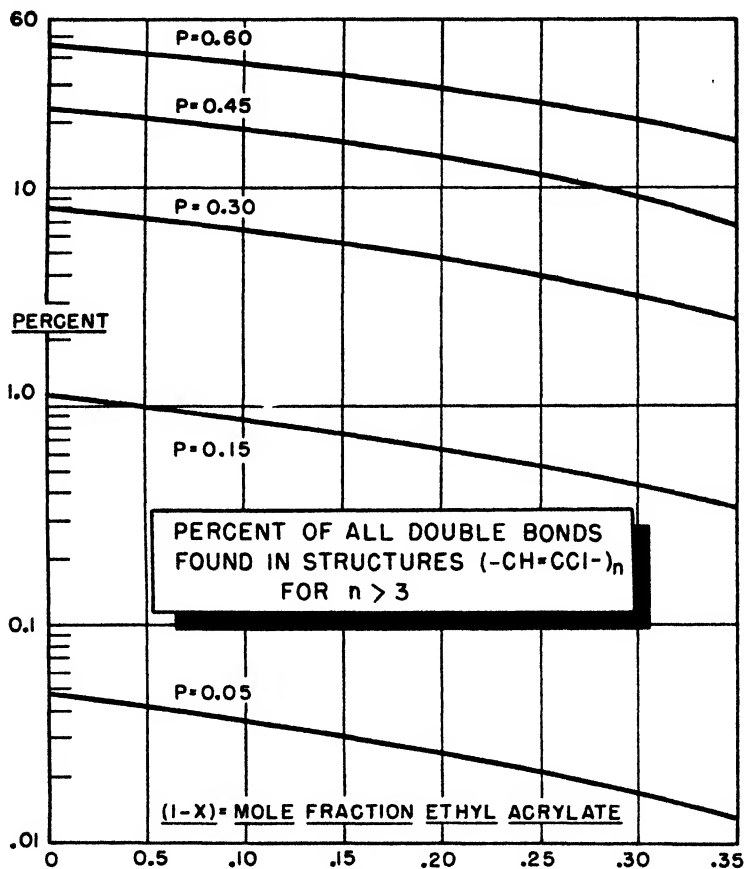


FIG. 10. Per cent of all double bonds found in conjugated structures longer than $n = 3$, for hydrogen chloride losses ranging from 5 to 60 per cent. The smaller the ordinates, the smaller would be the visible discoloration of the copolymer. Random loss of hydrogen chloride.

the same light or heat source, or to the same concentration of reagent, there will be fewer double bonds formed because of the law of mass action. In other words, p will decrease as x decreases, the exact relationship depending on the order of the reaction.

(2) Even when the reaction conditions for several copolymers are varied until p is the same in each case, the total number of double bonds will be smaller the

smaller the value of x . This total number of double bonds, given by equation 17, is Lpx per copolymer chain.

(3) Finally, for the same extent of degradation, p , the number of long conjugated systems is greatly reduced, as shown by table 1 and figures 9 to 12. However, when the extent of degradation is increased so as to give the same value of Lpx for two copolymers, then the conjugated systems formed in each copolymer are identical. Thus, pure polyvinylidene chloride degraded 10 per cent ($px = 0.10$), should possess the same conjugated groups as a 10 per cent

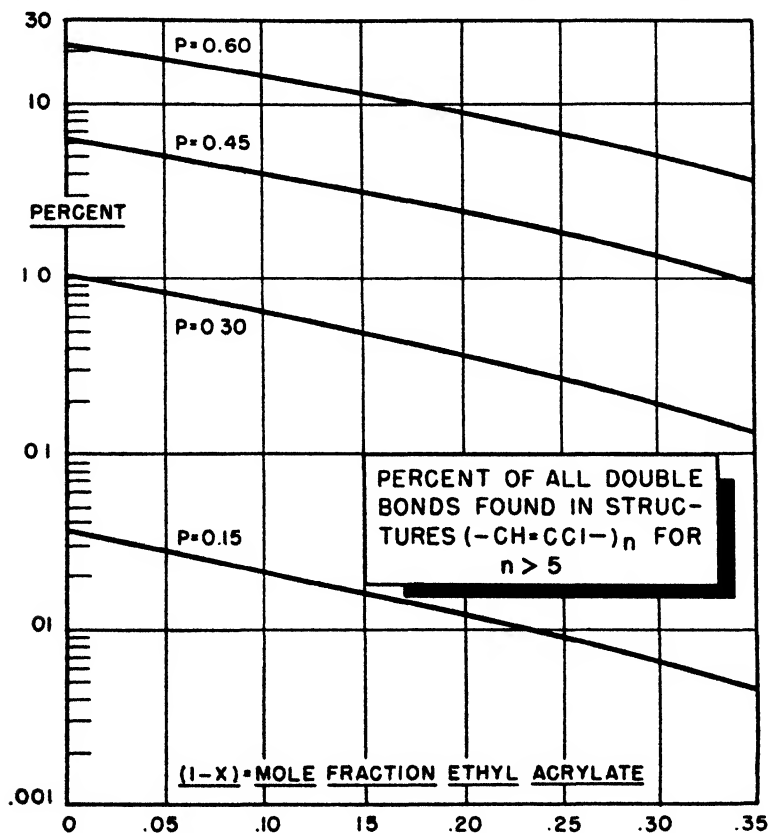


FIG. 11. Per cent of all double bonds found in conjugated systems longer than $n = 5$. The hydrogen chloride loss (from 15 to 60 per cent) is assumed to occur at random.

vinylidene chloride-90 per cent ethyl acrylate copolymer which has been fully degraded ($px = 0.10$). In the former case, even though space is available, long conjugated systems do not form frequently because of the small probability for their occurrence. In the latter case, the probability of a large number of double bonds in conjugation is high, but there is no place for them to form. Hence, their net frequency is again small. As equation 16 will emphasize, the only factor governing the nature of a conjugated system is the product (px). Even when the conjugated systems are identical in theory, they need not be so

in practice; and the color of the two copolymers would almost certainly be different. For small values of x (say less than 0.10), it will not be possible to realize large values of px even when the copolymer is fully degraded.

Table 2 presents some numerical examples chosen to illustrate the three principles outlined above. Results are listed on the number of active monomers, the number of degraded monomers, and the number of conjugated systems of

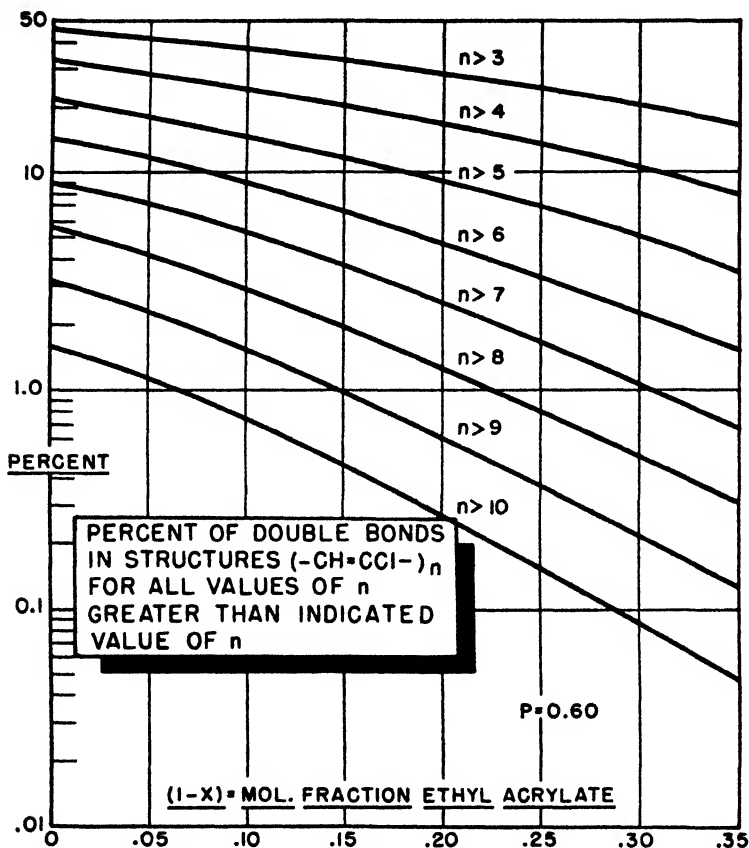


FIG. 12. Per cent of all double bonds found in structures longer than the indicated value of n for 60 per cent hydrogen chloride lost at random. Increasing values of n correspond to light absorption moving toward the red end of the spectrum.

various lengths, n , for $x = 1.0, 0.90$, and 0.45 , with $p = 0.30$ and 0.45 . All quantities are given for a single copolymer chain. Comparison of columns (a), (b), and (c) with one another and comparison of columns (d), (e), and (f), as a second group, shows the marked decrease in the longer conjugated systems as x decreases. However, comparison of column (b), for which $Lpx = 27$, with column (f), for which $Lpx = 29.25$, shows approximately the same number of conjugated systems, even though x has decreased from 0.90 to 0.65.

Thus far, nothing has been said about the theory of non-random loss of

hydrogen chloride in copolymers. By analogy, one might guess that a very good first approximation could be obtained by using in the copolymer equations a modified value, p' , for the degradation, where $p' = \sigma p$. p is the actual degradation and σ is again a measure of the tendency for conjugated chains to propagate themselves. The values of $M_n(p)$ thus obtained should be divided by σ to yield the desired answer.

TABLE 2

Effect of a neutral comonomer in reducing the total number of double bonds and the number of long conjugation systems in a copolymer

Mole fraction vinylidene chloride . . .	1.00	0.90	0.65
Number of active monomers, Lx , per chain	100	90	65
Number of degraded monomers, Lpx , per chain:			
$p = 0.30$	30	27	19.5
$p = 0.45$	45	40.5	29.25
Number of conjugated systems, $M_n(p)/N$, per chain:			
$p = 0.30, n = 1$	(a) 14.82	(b) 14.47	(c) 12.70
3	1.31	1.03	0.472
5	0.115	0.00737	0.0175
7	0.0102	0.00529	0.000620
9	0.000895	0.000374	0.0000250
$p = 0.45, n = 1$	(d) 13.83	(e) 14.51	(f) 14.80
3	2.76	2.33	1.236
5	0.545	0.374	0.103
7	0.108	0.0602	0.00863
9	0.0214	0.00965	0.000716

Various side reactions, such as chain scission, cross-linking, and oxidation, have been ignored, except to point out the presence of some $C=O$ groups in one experimental sample. While these factors are important commercially where one is dealing with a molded sample, they can be reduced in importance in a laboratory study by working at sufficient dilution with inert atmospheres.

SUMMARY

Starting with the assumption of Marvel, Sample, and Roy that discoloration in degraded polyvinyl halides arises from polyene structures of the type $(-CH=CH-)_n$, a statistical calculation has been made of the expected distribution of n values, both for random and for non-random loss of hydrogen chloride. Next, using the known light-absorption characteristics of polyene compounds, the expected color or light transmission curve of a degraded polymer is computed. Comparison of theory with an experiment on vinylidene chloride-vinyl chloride copolymer indicated fair agreement.

Next, the theory was extended to cover copolymers between a reactive monomer (vinylidene chloride) and a stable monomer (ethyl acrylate), where the presence of a neutral group in the copolymer chain greatly reduced the number of long conjugated systems. No color calculations were attempted with copolymers, although a number of quantities related to color were presented in graphical form. The important parameter for copolymers is px , the product of fraction of hydrogen chloride removed and mole fraction of chlorine-containing monomer. All degraded copolymers for which px is the same should have the same distribution of conjugated systems, although not necessarily the same color.

It will be realized that the results presented here on chlorine-containing polymers and copolymers are applicable to polyvinyl acetate, polyvinyl alcohol, and other polymers which can lose molecules to form double bonds along the chain.

This material was first presented in part before a Colloquium at the Department of Physics, Case School of Applied Science, in the Spring of 1942, and in part before the Midland Section of the American Chemical Society on April 1, 1943.

I should like to express appreciation first to Professor H. Mark, who called our attention to the Marvel, Sample, and Roy theory of discoloration in polyvinyl halides, and second, to Dr. R. Simha for his help on the mathematical equations used in the copolymer section, as well as for a critical reading of the manuscript. I am also indebted to Dr. L. K. Frevel, Dr. L. A. Matheson, and Mr. R. C. Reinhardt for stimulating discussions concerning this material.

REFERENCES

- (1) ASINGER, F.: Ber. **75B**, 660 (1942).
- (2) BATEMAN, L., AND KOCH, H. P.: J. Chem. Soc. **1945**, 216.
- (3) BOND, W. N.: *Probability and Random Errors*, Edward Arnold and Company, London (1935). The type of statistics employed is identical with that used by Flory (J. Am. Chem. Soc. **58**, 1877 (1936)) for calculating molecular-size distributions in linear condensation polymers.
- (4) BRODE, W. R.: *Chemical Spectroscopy*, particularly Chap. VII. John Wiley and Sons, Inc., New York (1939).
- (5) Reference 4, figure 7.21.
- (6) BRODE, W. R.: J. Applied Phys. **10**, 758 (1939).
- (7) CONANT, J. B., KIRNER, W. R., AND HUSSEY, R. E.: J. Am. Chem. Soc. **47**, 488 (1925).
- (8) DINSMORE, R. P.: *Modern Plastics* **21**, 88 (December, 1943); see also Canadian patent 433,186.
- (9) DRAKE, L. R. (The Dow Chemical Company): Private communication. This same effect was subsequently noted by C. S. Marvel and E. C. Horning, Chap. 8, "Synthetic Polymers", p. 754 in Vol. I, 2nd edition of *Organic Chemistry, an Advanced Treatise*, Henry Gilman (Editor), John Wiley and Sons, Inc., New York (1943).
- (10) ECKERT, W. J.: *Punched Card Methods in Scientific Computation*. Thomas J. Watson Astronomical Computing Bureau, Columbia University, New York (1940).
- (11) FIESER AND FIESER: *Organic Chemistry*, p. 152. D. C. Heath and Company, Boston, Massachusetts (1944).
- (12) FLORY, P. J.: J. Am. Chem. Soc. **61**, 1518 (1939).
- (13) FREVEL, L. K. (The Dow Chemical Company): Unpublished observations.

- (14) FULLER, C. S.: Chem. Rev. **26**, 161 (1940).
- (15) FUOSS, R. M.: Trans. Electrochem. Soc. **74**, 110 (1938).
- (16) HANSON, A. W., AND GOGGIN, W. C.: U. S. patent 2,273,262 (February 17, 1942).
- (17) HAUSSE, K. W., KUHN, R., AND SMAKULA, A.: Z. physik. Chem. **B29**, 384 (1935).
- (18) *International Critical Tables*, Vol. V, p. 368, fig. 43. McGraw-Hill Book Company, Inc., New York (1929).
- (19) JEFFREY, G. A.: Proc. Roy. Soc. (London) **A183** (1945); see also BATEMAN, L., AND JEFFREY, G. A.: J. Chem. Soc. **1945**, 211.
- (20) KUHN, R.: Angew. Chem. **50**, 707 (1937).
- (21) KUHN, R., AND GRUNDMANN, C.: Ber. **71A**, 442 (1938).
- (22) LAND, E. H., AND WEST, C. D.: "Dichroism and Dichroic Polarizers" in Vol. VI of *Colloid Chemistry*, Jerome Alexander (Editor). Reinhold Publishing Corporation, New York (1946).
- (23) LEWIS, G. N., AND CALVIN, M.: Chem. Rev. **25**, 273 (1939).
- (24) LICHTENBERGER, J., AND NAFTALI, M.: Rub. Chem. Tech. **13**, 133 (1940); original in Bull. soc. ind. Mulhouse **115**, 169 (1939).
- (25) MARVEL, C. S.: Private communication. See also MARVEL, C. S., AND RIDDLE, E. H.: J. Am. Chem. Soc. **62**, 2666 (1940), where it is shown that zinc removes hydrogen bromide from polyvinyl bromide.
- (26) MARVEL, C. S., JONES, G. D., MASTIN, T. W., AND SCHERTZ, G. L.: J. Am. Chem. Soc. **64**, 2356 (1942).
- (27) MARVEL, C. S., SAMPLE, J. H., AND ROY, M. F.: J. Am. Chem. Soc. **61**, 3241 (1939).
- (28) MATHESON, L. A., AND BOYER, R. F.: Manuscript in preparation.
- (29) MCINTIRE, O. R. (The Dow Chemical Company): Unpublished observations.
- (30) MONTROLL, E.: J. Am. Chem. Soc. **63**, 1215 (1941), Equation (14).
- (31) MONTROLL, E., AND SIMHA, R.: J. Chem. Phys. **8**, 721 (1940), especially the appendix.
- (32) MULLIKEN, R.: J. Chem. Phys. **7**, 570 (1939).
- (33) OSTROMISLENSKII, I.: J. Russ. Phys. Chem. Soc. **44**, 204, 240 (1912).
- (34) OSTROMISLENSKII, I.: German patent 264,123 (1913); Chem. Zentr. **84**, II, 1187 (1913).
- (35) REINHARDT, R. C.: Ind. Eng. Chem. **35**, 422 (1943).
- (36) SIMHA, R.: J. Am. Chem. Soc. **63**, 1479 (1941).
- (37) Reference 36, Equation (1a).
- (38) SLOBODIN, YA. M.: J. Gen. Chem. (U.S.S.R.) **6**, 129 (1936).
- (39) SNOW, C. P., AND ALLSOPP, C. B.: Trans. Faraday Soc. **30**, 93 (1934).
- (40) STAUDINGER, H., BRUNNER, M., AND FEISST, W.: Helv. Chim. Acta **13**, 805 (1930).
- (41) STAUDINGER, H., AND FEISST, W.: Helv. Chim. Acta **13**, 832 (1930).
- (42) STICHER, J., AND PIPER, J. D.: Ind. Eng. Chem. **33**, 1567 (1941).
- (43) STOCKMAYER, W. H.: J. Chem. Phys. **13**, 199 (1945).
- (44) TUTTLE, W. P., JR., AND JACOBS, T. L.: Abstracts of papers presented at the Buffalo Meeting of the American Chemical Society, Sept. 7-11, 1942, Page 13M. (University of California, Los Angeles.)
- (45) WALL, F. T.: J. Am. Chem. Soc. **62**, 803 (1940); **63**, 821 (1941).
- (46) WALSH, A. D.: Trans. Faraday Soc. **41**, 35 (1945).

APPENDIX

After the machine calculations on copolymers were completed, Simha⁴ derived several pertinent equations which would serve to simplify any further calculations. The summation in equation 12 can be written as:

$$\sum_{t=n+1}^{L-1} M_n(t, p) = N(1-p)p^n \{x^{n+1} [2(L-n) - x(1+p)(L-n-2)] - X^L [(L-n+1) - p(L-n-1)]\} \quad (15)$$

The complete expression for $M_n(p)$, which is the sum of equations 10c, 11, and 12, is given by

$$M_n(p) = N(1 - px)(px)^n[2 + (L - n - 1)(1 - px)] \quad (16a)$$

for $n = L - 1$ and by

$$M_n(p) = N(px)^L \quad (16b)$$

for $n = L$. The similarity in form between this equation and equation 7, which holds for the degradation of pure polymer, is rather surprising. Moreover, one can see at once from equation 16 why a plot of $\log M_n(p)$ should be linear with respect to n .

Next, two expressions connected with the total number of double bonds are useful:

$$\sum_{n=1}^L nM_n(p) = NLpx \quad (17)$$

This is, so to speak, the normalization equation which accounts for all of the double bonds regardless of the complexity of the structures in which they reside. The total number of double bonds up to a certain length, $n = k$, of the conjugated chains is:

$$\sum_{n=1}^{n=k} nM_n(p) = N\{Lpx - (px)^{k+1}[L + k(L - 1 - k)(1 - px)]\} \quad (18)$$

These results can be extended one step further to yield two useful equations. The ratio of equation 18 to equation 17, called f , is the fraction of all double bonds contained in structures up to size $n = k$.

$$f = 1 - (px)^k[L + k(L - 1 - k)(1 - px)]/L \quad (19)$$

The fraction, F , of all double bonds contained in structures for n greater than k is, of course, given by

$$F(n > k) = 1 - f(n \leq k) \quad (20)$$

It is evident from equations 19 and 20 why the semilogarithmic plots of figures 10 and 11 should be very nearly linear.

ULTRACENTRIFUGAL AND VISCOMETRIC STUDIES OF
AMYLOSE ACETATES¹

FURTHER EVIDENCE FOR THE HELICAL STRUCTURE OF AMYLOSE

BERNARD A. DOMBROW AND CHARLES O. BECKMANN

*Department of Chemistry, Columbia University, New York 27, New York**Received August 8, 1946*

The suggestion that the amylose molecule has a helical structure is certainly one of the most interesting that has been put forth in connection with the study of starch. Enzymatic studies have led many investigators to the conclusion that the starch molecule is constructed in a manner that would permit a unit of six glucose molecules to be split out during degradation in order to explain the preponderance of hexasaccharides that are found after the limited treatment of starch with α -amylase from malt (20). The formation of cyclohexaamylose and cycloheptaamylose by the enzyme of bacillus macerans lends credence to the idea that the starch chain is helical, with six or seven glucose units per turn (10). In 1939, Freudenberg and coworkers (11) constructed a model of a linear starch molecule from Stuart atomic models and concluded that the helical structure was extremely plausible. Six glucose residues could be fitted into one turn without strain and produced a helix with a diameter of 13 Å. and a length of 7.5–8 Å. per turn. Caesar and Cushing (7), using Fisher–Hirschfelder models, confirmed these general conclusions and pointed out that the model was flexible. The recent studies of Rundle and French (22) and the x-ray diffraction of the amylose–iodine complex show that a helix of a diameter of 12.97 Å. and of a length of 7.91 Å. per turn is the best representation of the molecule.

The x-ray evidence of Rundle and French establishes the model quite definitely for the amylose–iodine complex in the solid state. The model cannot, however, be assumed to represent the molecule in solution without further evidence. The problem of determining the shape of a molecule in solution is a difficult one both in theory and in practice. One is limited from the outset by the fact that theories have been developed only for regular shapes like the sphere and ellipsoids of revolution. It is necessary therefore to assume that the molecule in question conforms to one of these shapes. A helix, of course, is more closely approximated by a cylinder than by a prolate spheroid, but the method suggested by Burgers (6) for converting an ellipsoid to a hydrodynamically equivalent cylinder has shown on closer examination to be impossible when a simple factor is used, as suggested.

The ratio of the dimensions of the ellipsoid of revolution equivalent to the molecular shape can be obtained from viscosity data, using the equation of Simha (25), and from ultracentrifugal data, using the equation of Perrin (21). In addition, one obtains the molecular weight from the ultracentrifugal data,

¹ Presented at the Twentieth National Colloid Symposium, which was held at Madison, Wisconsin, May 28–29, 1946.

which enables one to calculate the characteristic dimensions of the model and not only the ratio of dimensions.

Amylose obtained directly from starch is somewhat heterogeneous with respect to molecular weight. By combining the essential features of Meyer's extraction (13, 14, 15, 16, 18) and Schoch's (23) butanol precipitation methods, Kerr (12) has succeeded in producing a so-called "crystalline amylose." By carrying out repeated crystallizations from water saturated with butanol, amyloses which are practically homogeneous can be obtained. Three crystalline amyloses prepared from tapioca, corn, and potato starches were prepared by this method and used in the present study. The extent of fractionation in the process is so extensive, however, that the amyloses can no longer be considered as typical of the parent starches but must be regarded only as particular specimens useful for a physical-chemical study. Because the amyloses have a limited solubility in water, they were converted to triacetates and studied in methyl acetate and tetrachloroethane.

TABLE 1
Analytical data on amylose and amylose acetates

SOURCE OF AMYLOSE	CODE (3)	IODINE ABSORBED	β -AMYLASE CONVERSION	ACETYL CONTENT OF AMY- LOSE TRIACETATE
		<i>per cent</i>	<i>per cent</i>	<i>per cent</i>
Tapioca.....	KA5	18.6	88-90	43.9
Corn	KA3	18.9	93-95	44.0
Potato.....	KA4	19.1	97	44.0
				44.8 (theory)

EXPERIMENTAL

Preparation and analyses of samples

The amyloses were tested for purity by the potentiometric iodine titration method of Bates, French, and Rundle (1). The results in table 1 indicate a purity of 97-100 per cent. The titration curve for the amylose from corn starch indicated some heterogeneity of that sample. The conversion of the amyloses to maltose with the enzyme β -amylase was not complete (table 1) but compared favorably with other samples. Apparently, the difficulty of complete conversion is due to retrogradation, as was pointed out by Kerr and Steverson (12).

The three amyloses were acetylated according to the procedure of Mullen and Pacsu (19). This method can be carried out without degradation of the starch and produces acetates in better than 90 per cent yield. The per cent of acetyl was determined by the method of the same authors (19) and is also given in table 1.

Sedimentation and diffusion method

The sedimentation-velocity measurements were made on solutions of the amylose acetates in methyl acetate at various concentrations to permit extrapolation to zero concentration. The instrument used was the air-driven ultra-

centrifuge described by Beckmann and Landis (2). The Lamm (28) scale method was used to follow the sedimenting boundary, and the data were evaluated in the usual manner by plotting the scale-line displacement, Z , against the distance from the center of rotation, x , as shown in figure 1, a typical graph of results. The sedimentation constants were calculated by plotting the logarithm of

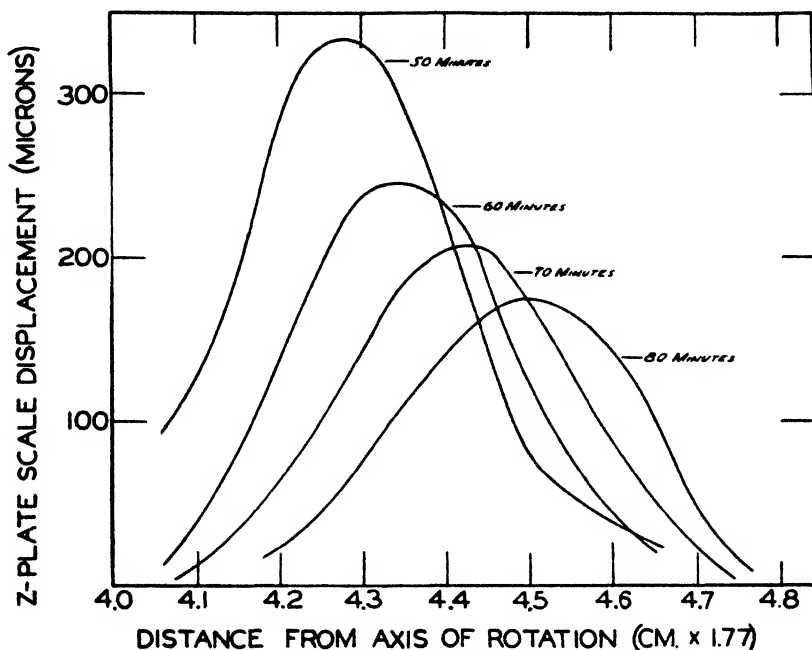


Fig. 1. Sedimentation curves for KA4 in methyl acetate (0.70 per cent)

the position of the maximum, x_m , of each curve, i.e., the sedimenting boundary, against time, determining the slope and using the equation:

$$\frac{d \log x_m}{dt} = \frac{\omega^2 s}{2.3}$$

where ω is the angular velocity of the rotor in radians per second. This method enables a calculation of s to within 5 per cent. The summary of the data is given in table 2.

The value of the sedimentation constant at zero concentration was determined by plotting s against the concentration c and extrapolating (figure 2). The error in this procedure may amount to 20 per cent and in this particular case did not warrant plotting the reciprocal of s against c , the more desirable method from a theoretical point of view (3, 5). In fact, this would have given too much weight to the least precise point at the lowest concentration.

The diffusion measurements were carried out in a Tiselius electrophoresis cell by Mr. Jerome L. Rosenberg, and the results are described in a paper by Beckmann and Rosenberg (3) under the code symbols given in table 1. The

TABLE 2
Amylose acetates in methyl acetate

AMYLOSE ACETATE	CONCENTRATION	(R.P.S.)	S_{20}^0 (S) *	S_{25}^0 (S)
	grams/100 cc.			
Tapioca.....	0.70	1080	8.6	9.1
	0.35	1020	9.6	10.1
	0.00		10.7	11.2†
Corn.....	0.80	1020	6.5	6.8
	0.70	1080	6.7	7.1
	0.35	1020	8.4	8.9
	0.00		9.9	10.5†
Potato.....	0.70	900	7.0	7.4
	0.50	1020	7.2	7.6
	0.35	900	7.2	7.6
	0.00		7.5	7.9†

* (S) = Svedbergs = 10^{-13} c.g.s. (sec.).

† Extrapolated.

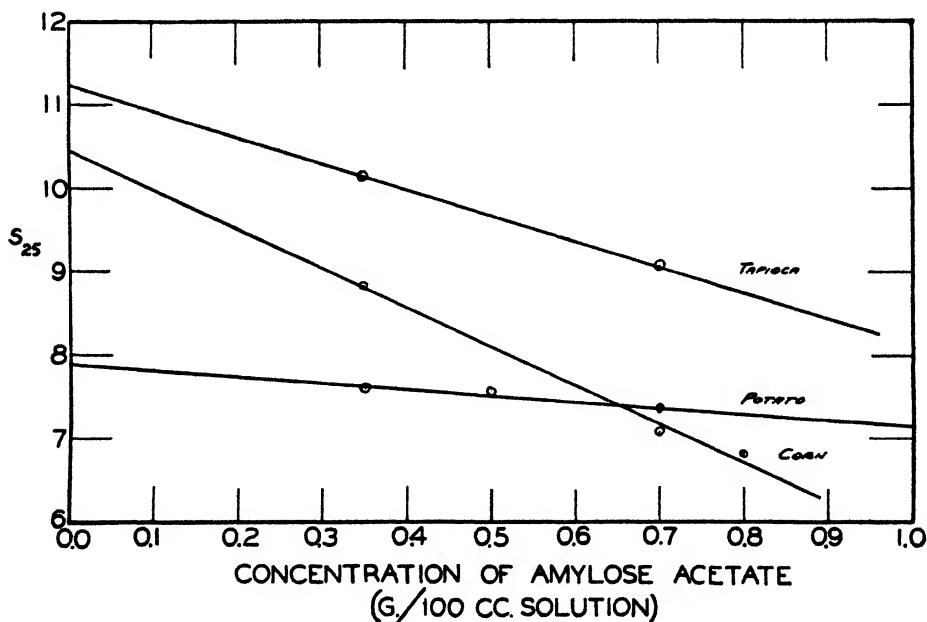


FIG. 2. Sedimentation constant at 25°C. versus concentration for amylose acetate

results compare favorably with those obtained from the sedimentation curves and thus offer additional evidence for the homogeneity of the samples.

The partial specific volumes of the amylose acetates were determined from density measurements and were calculated according to the method described

by Kraemer (27). The values for all three amylose acetates in methyl acetate were the same,—namely, 0.71.

Viscosity measurements

Viscometric measurements were made at 25°C. in Bingham (4) viscometers, which were chosen so that the time of flow was at least 100 sec. for the pure solvents. At each concentration, five different air pressures in the range 100–150 cm. of water were used. In each case, the product of pressure and time of flow was constant, indicating that the flow was Newtonian. Relative and specific

TABLE 3
Amylose acetates in methyl acetate

TYPE OF AMYLOSE	CONCENTRATION	η_r	η_{sp}	$\frac{\eta_{sp}}{c}$
	<i>grams/100 cc.</i>			
Tapioca	1.00	2.33	1.33	1.33
	0.70	1.84	0.84	1.20
	0.40	1.43	0.43	1.08
	0.00			0.91*
Corn	1.00	1.68	0.68	0.68
	0.50	1.31	0.31	0.62
	0.00			0.56*
Potato	1.00	1.49	0.49	0.49
	0.50	1.23	0.23	0.46
	0.00			0.43*

* Extrapolated.

viscosities were calculated in the usual way. Extrapolation to zero concentration yielded intrinsic viscosities and from these and the partial specific volume, \bar{V} , of the solute, the viscosity increments, ν , defined by Simha (25), were calculated according to the equation:

$$\nu = \frac{1}{\bar{V}} \left(\frac{\eta_{sp}}{c} \right)_{c=0} \quad (1)$$

The data are summarized in table 3 and figure 3.

DISCUSSION AND CALCULATIONS

With the data at hand, there are two methods available for the calculation of the dimensions of the ellipsoid which is hydrodynamically equivalent to the molecule under consideration. The one method depends on the calculation of the form factor f/f_0 (where f is the molar frictional coefficient of the solute and f_0 is the molar frictional coefficient for a solute composed of spherical molecules

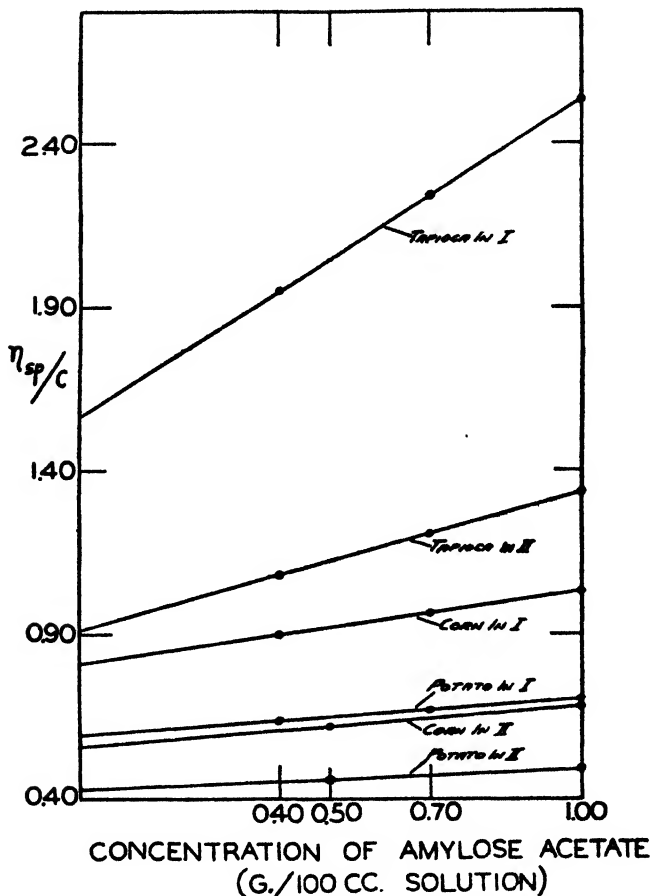


FIG. 3. η_{sp}/c versus concentration for amylose acetate in two solvents: I, *s*-tetrachloroethane; II, methyl acetate.

of molecular weight identical with that of the solute) from the sedimentation-diffusion data. It can be shown that:

$$\begin{aligned} \frac{f}{f_0} &= \left(\frac{4}{3}\right)^{1/3} \frac{1}{6\eta} \left(\frac{RT}{\pi N}\right)^{2/3} \left(\frac{1 - V\rho}{D^2 s V}\right)^{1/3} \\ &= 2.152 \times 10^{-8} \left(\frac{1}{D^2 s}\right)^{1/3} \end{aligned} \quad (2)$$

where η is the viscosity of the solvent, R and T have their usual significance, N is Avogadro's number, V is the partial specific volume of the solute, ρ is the density of the solvent, D is the diffusion coefficient, and s is the sedimentation constant. The numerical coefficient of the second line is the value of all the constant quantities for a system of amylose triacetate in methyl acetate at 25°C. From f/f_0 one can calculate the ratio of length to diameter, i.e., L/d , of

the ellipsoid by means of Perrin's equation (21). The second method is due to Simha (25) and enables one to calculate L/d from the viscosity increment, ν .

For the calculation of absolute values of L and d , both methods require, of course, a knowledge of the molecular volume which is obtained from M , the molecular weight, and V , the partial specific volume. In the present work, M is obtained from Svedberg's equation,

$$M = \frac{RTs}{(1 - V\rho)D}$$

using the extrapolated values of s and D . A summary of the pertinent data and the values of L/d calculated by both methods are given in table 4.

TABLE 4
The ratio L/d for amylose acetates

SOURCE OF AMYLOSE	$s_{25} \times 10^{13}$	$D_{25} \times 10^7$	M	f/f_0	ν	L/d	
						Perrin	Simha
Tapioca	11.2	4.2	187,000	3.70	128	82.0	41.5
Corn	10.5	6.8	108,000	2.74	79	42.5	31.0
Potato	7.9	8.0	69,000	2.70	61	41.2	26.5

The discrepancy between the two sets of values of L/d is great. The value obtained from Perrin's equation is burdened with all the errors of the sedimentation method. The value obtained from Simha's equation is probably more reliable because of the high precision of viscosity measurements. Because of the necessity of using the molecular weight from the sedimentation-velocity method in either case for the calculation of the absolute values of L and d , both values of the ratio are used in the following calculation.

By equating the measured molecular volume with that of the model (a prolate spheroid) one obtains:

$$\frac{MV}{N} = \frac{\pi}{6} Ld^2 = \frac{\pi}{6} \left(\frac{L}{d}\right) d^3$$

and on solving for d , one obtains:

$$d = \left[\frac{6MV}{\pi N} \times \frac{1}{L/d} \right]^{1/3}$$

This procedure is valid, of course, only if solvent molecules are not entrapped in the helix. Examination of a Fisher-Hirschfelder model of the acetylated helical amylose indicated that the methyl acetate molecule would not fit in the helix. It can be seen from this equation that the minor diameter of the ellipsoid depends only on the cube root of the value of L/d . A discrepancy of a factor of 2 in the two values of L/d for the tapioca amylose reduces therefore to a discrepancy of 1.25 in the two corresponding values of d .

With a knowledge of both L/d and d , one can calculate L . From the molecular

weight of the amylose triacetate and of the monomer ($M = 288$) one can calculate the degree of polymerization and the effective length per glucose unit. The results of these calculations are given in table 5. Similar calculations can be made on the assumption that the molecule is an oblate spheroid. These lead, however, to the physically unlikely result that the molecule is a disk with a thickness of about 1.6–2.8 Å.

The systematic difference between the two sets of values for the diameters of the molecules eludes us at the present time. Experimental error is not entirely responsible for the deviations. There is most certainly a theoretical difficulty as well. However, the fact that good agreement on the size and shape of protein molecules (8) is obtained from various methods leads one to the conclusion that the values in table 5 are essentially correct. Furthermore, the agreement with values calculated from the x-ray data of French and Rundle (10) is satisfactory. French and Rundle assign a value of 13 Å. to the diameter of the helical amylose molecule. If one adds to this an estimated contribution of the acetyl group of from 2.7 Å., a minimum value, to 5.4 Å., a maximum value (the value depending

TABLE 5
Values of L and d for amylose acetates

SOURCE OF AMYLOSE	DEGREE OF POLYMERI- ZATION	FROM PERRIN'S L/d			FROM SIMHA'S L/d		
		d	L	A. per monomer	d	L	A. per monomer
		Å.	Å.		Å.	Å.	
Tapioca...	649	17.2	1410	2.17	21.5	892	1.37
Corn	376	17.8	757	2.01	19.8	614	1.63
Potato	240	15.5	639	2.66	18.0	477	1.99

on the orientation of the groups), one arrives at the values 15.7–18.4 Å. for the diameter of the amylose triacetate molecule; this closely approximates the values reported here.

In addition, the values obtained for the contribution of each glucose unit to the length of the molecule (given in table 5 as A. per monomer) are physically reasonable. The x-ray value (10, 22) for this parameter is reported as 1.31 Å. Those reported here are larger but are still much less than the value 5.15 Å. which one would expect for the completely extended molecule.

This general agreement between the x-ray data and the hydrodynamic data is not fortuitous. The results of Signer and v. Tafel (24) on methyl cellulose in water are comparable to those of this report. By the procedure outlined above, the corresponding values for methyl cellulose have been calculated and are reported in table 6. In this case, also, the agreement with x-ray data is satisfactory. Meyer and Mark (17) assign a value of 8.25 Å. to the width of the cellulose molecule. If to this is added the contribution of the methyl group, which is estimated at 1.7 Å., a value of approximately 10 Å. is obtained. The contribution of each glucose to the length of the molecule approaches the x-ray value of 5.15 Å. The agreement in this case appears to be better when L and d

are calculated from Simha's equation. The values obtained for the length of the molecule from Perrin's equation are larger than bond distances would allow. Signer and v. Tafel report their samples to be polydisperse, and because of the uncertainty that this produces in the molecular weight one hesitates to argue the superiority of one equation over another. Using either method leads to results that are reasonable in the light of experimental error.

Because the largest experimental error in the present work is associated with the sedimentation constant, it is interesting to calculate what experimental values of s would be obtained if the amylose acetate molecule were (1) completely extended and (2) more irregularly curled. For this purpose it is most convenient to use the approximate form of Perrin's equation which was developed by

TABLE 6
Values of L and d for methyl cellulose

SAMPLE	M	DEGREE OF POLY- MERIZA- TION	FROM PERRIN'S EQUATION					FROM SIMHA'S EQUATION				
			f/f_0	L/d	d	L	A. per mono- mer	ν	L/d	d	L	A. per mono- mer
II	38.100	202	4.5	120	9.0	1084	5.4	304	68	10.9	749	3.71
III	24.300	130	3.9	92	8.5	777	6.0	207	55	10.0	550	4.23
IV	14.100	78	3.0	52	8.4	436	5.6	118.5	40	9.1	365	4.68

Simha (26). Combining this equation with equation 2 gives d as a function of s and D :

$$d = G s^{0.878} D^{1.156}$$

where G is a constant for a particular system. If we assume D constant because of its relatively high precision, we can calculate s as a function of d . For the tapioca amylose acetate, the assumption of complete extension would make d about 10 A. The calculated value of s in this case is 4.4 Svedbergs. If a d of 25 A. is assumed for the irregular coil, the calculated value of s becomes 21.4 Svedbergs. On comparison with the experimental value of 11.2 Svedbergs, these forms of the molecule are untenable. A highly solvated and randomly kinked molecule is not entirely excluded by the results of this study, but until a theory of sedimentation of such a molecule is developed, no comparison between theory and experiment can be made.

Meyer, Bernfeld, and Hohenemser (14) have reported the molecular weight of a corn amylose acetate as 78,000. This result was obtained by using the intrinsic viscosity and Staudinger's equation:

$$M = K \left(\frac{\eta_{sp}}{c} \right)_{c \rightarrow 0}$$

in which the constant K has a value 7.4×10^4 . The viscosity measurements were carried out in tetrachloroethane. For comparison, the viscosities of the

amylose acetates of this work were measured in the same solvent. Using the value of $K = 7.4 \times 10^4$, the molecular weights of the amylose acetates from tapioca, corn, and potato starches are calculated to be 115,000, 60,000, and 44,000, respectively. These values are lower than those obtained from sedimentation-diffusion measurements by a factor of approximately 1.66. From the description of the preparation of Meyer's amylose it appears likely that the sample which was used to obtain the value of K from an osmotically determined molecular weight was polydisperse. The value of K thus obtained will be low, because the osmotic molecular weight of a polydisperse system is lower than the viscosity molecular weight. A sedimentation-diffusion molecular weight more nearly approaches the latter, and it is suggested therefore that the value of K be taken as 1.2×10^5 .

It should be emphasized that the amyloses studied were not representative of their source. Other results obtained in this laboratory on unfractionated samples confirm the order of decreasing size reported by Foster and Hixon (9),—namely, potato, tapioca, and corn.

SUMMARY

1. From sedimentation-velocity, diffusion, and viscosity measurements on very homogeneous samples of amylose triacetates, the dimensions of the ellipsoids of revolution which are hydrodynamically equivalent to the shape of the molecules are calculated.

2. The resulting dimensions are compatible with the helical model of amylose which has been established for the solid amylose-iodine complex by x-ray methods.

The authors are greatly indebted to Dr. Ralph W. Kerr of the Corn Products Refining Company, Argo, Illinois, for the samples of crystalline amyloses and to the Corn Industries Research Foundation for a gift that in part supported this research.

REFERENCES

- (1) BATES, F. L., FRENCH, D., AND RUNDLE, R. E.: J. Am. Chem. Soc. **65**, 142 (1943).
- (2) BECKMANN, C. O., AND LANDIS, Q.: J. Am. Chem. Soc. **61**, 1504 (1939).
- (3) BECKMANN, C. O., AND ROSENBERG, J. L.: Ann. N. Y. Acad. Sci. **46** (5), 329 (1945).
- (4) BINGHAM, E. C.: *Fluidity and Plasticity*. McGraw-Hill Book Company, Inc., New York (1922).
- (5) BRYCE, H. G., Dissertation, Columbia University, New York, 1943. See also GRÄN, N.: Inaugural Dissertation, Upsala, 1944.
- (6) BURGERS, J. M.: *Second Report on Viscosity and Plasticity*. Amsterdam (1938).
- (7) CAESAR, G. V., AND CUSHING, M. L.: J. Phys. Chem. **45**, 776 (1941).
- (8) COHN, E. J., AND EDSALL, J. T.: *Proteins, Amino Acids and Peptides*, p. 520. Reinhold Publishing Corporation, New York (1943).
- (9) FOSTER, J. F., AND HIXON, R. M.: J. Am. Chem. Soc. **65**, 618 (1943).
- (10) FRENCH, D., AND RUNDLE, R. E.: J. Am. Chem. Soc. **64**, 1651 (1942).
- (11) FREUDENBERG, K., SCHAAF, E., DUMPERT, G., AND PLOETZ, T.: *Naturwissenschaften* **27**, 850 (1939).
- (12) KERR, R. W., AND STEVERSON, G. M.: J. Am. Chem. Soc. **65**, 193 (1943).

- (13) MEYER, K. H., AND BERNFELD, P.: *Helv. Chim. Acta* **23**, 875 (1940).
- (14) MEYER, K. H., BERNFELD, P., AND HOHENEMSER, W.: *Helv. Chim. Acta* **23**, 885 (1940).
- (15) MEYER, K. H., BERNFELD, P., AND WOLFF, E.: *Helv. Chim. Acta* **23**, 854 (1940).
- (16) MEYER, K. H., BRENTANO, W., AND BERNFELD, P.: *Helv. Chim. Acta* **23**, 845 (1940).
- (17) MEYER, K. H., AND MARK, H.: *Z. physik. Chem.* **132**, 115 (1929).
- (18) MEYER, K. H., WETHEIM, M., AND BERNFELD, P.: *Helv. Chim. Acta* **23**, 865 (1940).
- (19) MULLEN, J. W., II, AND PACSU, E.: *Ind. Eng. Chem.* **34**, 1209 (1942).
- (20) MYRBÄCK, K., ÖRTENBLAD, B., AND AHLBORG, K.: *Biochem. Z.* **307**, 49 (1940).
- (21) PERRIN, F.: *J. phys. radium* [7] **7**, 1-11 (1936).
- (22) RUNDLE, R. E., AND FRENCH, D.: *J. Am. Chem. Soc.* **65**, 1707 (1943).
- (23) SCHOCH, T. J.: *J. Am. Chem. Soc.* **64**, 2957 (1942).
- (24) SIGNER, R., AND TAFEL, P. v.: *Helv. Chim. Acta* **21**, 535-45 (1938). See also SVEDBERG, T., AND PEDERSEN, K.: *The Ultracentrifuge*, p. 436, Oxford University Press, New York (1940).
- (25) SIMHA, R.: *J. Phys. Chem.* **44**, 25 (1940). See also MEHL, J. W., ONCLEY, J. L., AND SIMHA, R.: *Science* **92**, 132 (1940).
- (26) SIMHA, R.: *J. Chem. Phys.* **13**, 188 (1945).
- (27) SVEDBERG, T., AND PEDERSEN, K. O.: *The Ultracentrifuge*, p. 57 (article by E. O. Kraemer). Oxford University Press, New York (1940).
- (28) SVEDBERG, T., AND PEDERSEN, K. O.: *The Ultracentrifuge*, p. 253 (article by O. Lamm). Oxford University Press, New York (1940).

EFFECT OF MOLECULAR ASSOCIATION AND CHARGE DISTRIBUTION ON THE GELATION OF PECTIN¹

R. SPEISER, M. J. COPLEY, AND G. C. NUTTING

Eastern Regional Research Laboratory,² Philadelphia 18, Pennsylvania

Received August 8, 1946

When a polymer solution gels, a liquid solution incapable of withstanding shear stress is transformed into a "solid" solution which is rigid and elastic. The requirement for such a transformation is the ability of the polymer molecules to form an extended three-dimensional network which is sufficiently rigid to support shear, yet is capable also of incorporating mobile solvent molecules within interstices of the structure. Two sorts of gels may be distinguished: (1) irreversible gels, stable to heat and additional solvent, in which the polymer molecules are cross-linked by covalent bonds; and (2) reversible gels, dispersible upon heating and usually soluble in excess solvent, in which cross-links are secondary valence or ionic bonds.

The definition of a gel of type 1 is not ambiguous. To illustrate, if vulcanized rubber is placed in benzene, it swells until the elastic reaction of the rubber gel

¹ Presented at the Twentieth National Colloid Symposium, which was held at Madison, Wisconsin, May 28-29, 1946.

² One of the laboratories of the Bureau of Agricultural and Industrial Chemistry, Agricultural Research Administration, United States Department of Agriculture.

just equals the osmotic pressure of the benzene, and gel and solvent achieve an equilibrium not affected by excess solvent. Heating upsets the equilibrium, changing the amount of benzene imbibed by the rubber, but the gel does not disperse.

Type 2 gels behave in a considerably more complex fashion. Recognizing the gel may sometimes be difficult, because the transition point between gel and solvated precipitate of the gelling agent is ill defined. Recourse to a purely thermodynamic definition of the gel is not satisfactory, because reactions that govern the formation and stability of these gels are often slow and as yet quantitatively unpredictable. For a polymeric gelling agent of this type, which is effective at concentrations less than 1 per cent and still yields gels rigid enough to be easily measured (as on a Delaware jelly-strength tester (14), the general requirement is a high molecular weight and a polymer surface capable of forming numerous intermolecular secondary valence bonds. In some substances—pectin, for example—dipole interaction leads to hydrogen bonding, and coulombic forces lead simultaneously to ionic bonding. In any event the polymer has only limited solubility in the solvent, so that although there are enough intermolecular contacts to form a rigid gel, the numerous voids and the high affinity of the solvent for the polymer make it possible for the gelling agent to contain a considerable volume of solvent. The number of intermolecular contacts necessary before a gel structure can be considered a precipitate is arbitrary, and depends upon the means used to define and measure gel properties.

Aqueous solutions of pectin and the pectinic acids give gels of type 2 above. The aggregative tendency of a pectic material depends upon its degree of esterification (λ) (3) and the nature of the aqueous solution used as solvent. It has been shown previously (1, 2, 4, 12) that two sub-types of pectic gels can be prepared: (1) a hydrogen-bonded gel, conventionally incorporating 65 per cent sugar; and (2) an ionic-bonded gel made with a multivalent ion such as Ca^{++} .³ Optimum strength of hydrogen-bonded pectin and pectinic acid gels depends principally upon the molecular weight. However, optimum strength of calcium pectinate gels is influenced strongly also by the mode of pectin deesterification. Enzyme-deesterified pectinic acids make weaker gels than do acid- (4, 12) or alkali-deesterified pectinic acids (7). Table 1 shows that while Sample H89C (enzyme deesterified) had a higher molecular weight than H84D (acid deesterified), the H84D calcium gel was the stronger. Significantly, also, the enzyme-deesterified pectinic acid gave the stronger sugar gel (compare again H89C and H84D in table 1). In earlier communications (2, 12), this difference in gelling behavior was attributed to a difference in the homogeneity of λ among the molecules making up the pectinic acid samples, the enzyme-deesterified preparations being the less homogeneous.

In this paper, experimental evidence obtained by electrophoresis measurements

³ Although calcium pectinate gels incorporating no sucrose or other hydrogen-bonding agent can be made, it is advantageous for some purposes to use both sucrose and calcium salt in the gel composition (4). In this paper the calcium pectinate gels ("calcium gels") contained 35 per cent sucrose, and the "sugar gels" contained 65 per cent sucrose.

that substantiates this hypothesis is given. In addition, pectin gel quality is correlated with data on turbidity, viscosity, and solubility and with the relation of pectinic acid solubility to the ionic equilibria among pectinic acid, calcium pectinate, hydrogen ions, and calcium ions.

TABLE 1
Strength of pectinic acid gels

SAMPLE	λ	MODE OF DEESTERIFICA- TION	GEL STRENGTH (CM. OF WATER)		MOLECULAR WEIGHT*	
			Sugar gel	Calcium gel	M_w	M_n
H84	0.80	None	61	0	105,000	83,400
H84D	0.32	Acid	20	30	80,800	57,200
H89C	0.35	Enzyme	47	13	102,000	76,700
H85C	0.39	Acid	60	57		
H87C	0.36	Enzyme	135	52†		
H59	About 0.30	Acid	72	56	199,000	143,000
H74	About 0.30	Enzyme	24	4	162,000	64,400

* Molecular weight of the nitrate (12, 13) This molecular weight $\times 0.73$ = molecular weight of the pectinic acid. M_w and M_n are the weight- and number-average molecular weights.

† All but the H87C calcium gel were made with 1 g. of pectinic acid. The H87C calcium gel was made with 2 g., in order to obtain a measurably strong calcium gel.

EXPERIMENTAL

Apple pectins alone were used. Their preparation has been described (13), as have also the preparation and strength measurement of the gels (4). Stress-strain relations were obtained by means of a Delaware jelly-strength tester (14). The plunger was graduated so that the total stress, expressed as centimeters of water pressure, could be measured as a function of the depression of the plunger into the gel surface. Stress-strain cycles were determined at a constant rate of stress. The ratio, total pressure/plunger depression ($\tan \theta$ in table 8), is proportional to the elastic modulus of the gel. No attempt was made to define this quantity more rigorously, since the required information regarding the mechanical behavior could be gained from the elastic modulus thus defined, without further mathematical treatment.

Solubility measurements

Dilute (about 4 per cent) solutions of pectinic acids of various λ , both acid and enzyme deesterified, were dried slowly in a convection oven at 80°C. Resulting films were ground and sieved through an 80-mesh screen. To measure the solubility of these materials, the neutralization equivalent was first determined by potentiometric titration with 0.01 *N* sodium hydroxide. Two-gram samples were shaken for 2 hr. with 100 g. of water in a water bath at constant temperature. The mixture was centrifuged, and the concentration of dissolved pectin then determined by titration with 0.01 *N* sodium hydroxide. The weight of dissolved pectin was calculated from the formula relating the weight of pectin to the neutralization equivalent of the sample.

Electrophoresis

Mobility patterns were obtained with a Tiselius-Klett apparatus equipped with the schlieren-scanning device of Longworth (9). The water bath was maintained at 0.5°C. Five-tenths per cent pectin solutions in 0.1 *N* sodium acetate + 0.01 *N* acetic acid buffer were dialyzed against the buffer for 2 days. Two changes of the buffer were made during the dialysis.

RESULTS AND DISCUSSION

Association and gel formation in the absence of calcium ions

Gel strength and rigidity, and stability toward syneresis are closely related to the solubility of the pectinate in the gel medium. Interpretation of the gelling tendency of pectic materials may be better understood if the solubility is con-

TABLE 2

*Solubility of partially soluble pectinic acids in water at 27°C. in the presence of solid phase**

SAMPLE	WEIGHT OF SAMPLE	SOLUTION A: CONCENTRATION OF DISSOLVED PECTINIC ACID	SOLUTION A DILUTED 1 TO 10 AND REEQUILIBRATED WITH SOLUTE: CONCENTRATION OF PECTINIC ACID
		grams per liter	grams per liter
H84G.....	12.18	1.569	0.167
H91D.....	14.798	4.69	0.487
H91E.....	1.722	0.349	0.033

* Pectinic acids of the weight listed in the second column were shaken for 2 hr. with 1 liter of water at 27°C.

sidered both when the sample is a dry powder or film and also when a large proportion of solvent (a gel mixture) is initially present.

Solubility behavior exhibited by a high polymer such as pectinic acid differs fundamentally from that of a simple substance like sodium chloride. A saturated solution of salt in the presence of solid salt is in thermodynamic equilibrium. If water is added, sufficient salt dissolves to saturate the solution again. In other words, the concentration of dissolved salt attains the same equilibrium value upon dilution when excess solid is present. If an equal volume of water is added to such a system and reequilibrated, the amount of salt in solution is twice that in the original solution.

A solution of a slightly soluble pectinic acid with excess solid does not act in this manner. Upon addition of solvent no more pectin dissolves, so that the concentration decreases in the same ratio as the dilution increases (table 2). It is evident that the soluble portion of the pectinic acid is *leached out* by the water. Pectinic acid behaves thus because dispersion and solution of its aggregates is a mechanical process of prying apart the molecules that compose them. Water must be able to enter interstices of the aggregates and so solvate the pectinic acid molecules that swelling and eventual solution can occur. Solubility behavior of this sort depends upon the molecular rigidity, the perfection of spatial

ordering, and the magnitude of intermolecular forces. The crystalline phase of a high polymer is usually less soluble than the amorphous phase. In the crystalline regions the chains of a linear polymer like pectinic acid are well aligned, and the maximum number of cross-bonds (hydrogen bonds) per unit length of the molecule is formed. If the molecules are long and rigid (and experimental evidence supports this view (8, 10)), a considerable amount of work is required to separate them, because nearly all the hydrogen bonds between chains must be ruptured simultaneously. For this reason, pectic substances with low λ , and consequently a high concentration of strongly interacting carboxyl groups, tend to crystallize upon precipitation or drying and form relatively insoluble aggregates.

If there are bulky side groups, or if irregularities of a sufficiently high degree are present in the polymer chains, a lesser extent of crystallization results, and

TABLE 3
Solubility of acid-deesterified pectinic acids
Two-gram samples shaken with 100 g. water for 2 hr. at 27°C. and 100°C.

SAMPLE	ASH	λ	BALLAST CON- TENT	AMOUNT DISSOLVED AT 27°C.	AMOUNT DISSOLVED AT 100°C.
	<i>per cent</i>		<i>per cent</i>	<i>per cent</i>	<i>per cent</i>
H91	0.25	0.75	22.2	100	100
H91A	0.22	0.57	15.0	100	100
H91C	0.20	0.35	14.5	100	100
H91D	0.40	0.24	8.2	31	100
H91E	0.53	0.11	4.7	20	50
H91K	0.37	0.03	0.9	5	39

aggregates that admit solvent freely are formed. Such aggregates contain a higher proportion of material that can be leached out. Examples are pectinic acids with high λ and high non-galacturonide or "ballast" content (12).

Data of tables 3 and 4 show that acid deesterification, which simultaneously removes ballast and methyl ester groups, effects a greater decrease in solubility than does enzyme deesterification, which leaves the ballast content essentially unchanged. A high content of electrolyte such as sodium chloride promotes solubility. Preparations H88F and H89F, containing about 5 per cent ash, were readily soluble although almost completely deesterified. De-ashing to less than 0.5 per cent reduced their solubility considerably. The electrolyte promotes dissociation of the carboxyl groups and so not only decreases the number of strong hydrogen bonds but creates ionized groups which repel one another. When a solution of a very low ester pectinic acid, relatively free of electrolyte and ballast (H91K), is evaporated slowly, so that extensive hydrogen bridging between carboxyls can take place, the resulting film is crystalline, as revealed by x-ray diffraction, and is so closely packed as not to dissolve completely even in 10 per cent sodium hydroxide.

One of the practical factors discouraging the use of very low ester pectinic

acids has been their limited solubility. It is now obvious that control of the degree of lateral interaction among the pectinic acid molecules, by choice of enzyme rather than acid deesterification, by incorporating electrolyte or other diluent, and by rapid precipitation and drying, can largely remove this limitation.

The tendency of pectinic acids to form aggregates and separate from dilute solution is indicated by the optical quality of the solutions. Table 5 shows the dependence of solution turbidity on λ for acid- and enzyme-deesterified pectinic acids. The aggregates formed irreversibly, since turbidity did not disappear on dilution. It is noteworthy that all the enzyme-deesterified materials gave turbid solutions. This is thought to reflect heterogeneity in λ among the molecules, with the result that those of very low λ and correspondingly great tendency to associate (which are present in every solution) precipitate and contribute the observed cloudiness. Lowering the pH increases the turbidity, and the lower λ is, the greater is the effect.

TABLE 4
Solubility of enzyme-deesterified pectinic acids
Two-gram samples shaken with 100 g. water for 2 hr. at 27°C.

SAMPLE	ASH	λ	BALLAST CONTENT	AMOUNT DISSOLVED AT 27°C.	AMOUNT OF DE-ASHED MATERIAL* DISSOLVED AT 27°C.
	<i>per cent</i>		<i>per cent</i>	<i>per cent</i>	<i>per cent</i>
H91F	0.31	0.55	18.3	100	
H91G	0.51	0.45	17.4	100	
H91H	0.55	0.33	19.7	100	
H91I	0.62	0.23	16.4	100	100
H91J	1.01	0.14	16.2	100 (cloudy)	85 (cloudy)
H88F	4.69	0.03	21.5	100	70 (about)
H89F	4.95	0.04	19.1	100	74

* De-ashed to 0.5 per cent.

Roughly paralleling the turbidity is the viscosity behavior, for with decreasing λ a pronounced viscosity maximum appears near pH 1.5 (figure 1). The origin of both pH effects is attributed to an increase in the number of undissociated carboxyl groups. The viscosity maxima observed for high λ pectinic acids at pH values above 4 are due to electrokinetic effects, since the maxima disappear when 0.1 *N* sodium chloride is present. The low pH maxima persist in 0.1 *N* sodium chloride, so cannot have their origin in electrokinesis.

The formation of pectin gels in concentrated solutions of sugar, glycerol, and glycol at pectin concentrations of less than 1 per cent is often interpreted as a precipitation of the pectin due to preferential solvation of the water by the polyhydroxy compounds. Although, thermodynamically, the addition of a gelling agent may lead to enough change in the activity of the polymer to cause precipitation, it is unlikely that in the case of pectin the mechanism of stable gel formation is one of dehydration alone. It is more probable that sucrose and similar compounds form bridges between the rather stiff pectin molecules (8, 10)

TABLE 5

*Turbidity of 4 per cent aqueous solutions of pectinic acid at 15°C.**

SAMPLE	λ	TURBIDITY†
Acid deesterification		
H91.....	0.75	—
H91B.....	0.57	—
H91C.....	0.35	—
H91D.....	0.24	++
H91E.....	0.11	+++
H91K.....	0.03	++++
Enzyme deesterification		
H91F.....	0.55	+
H91G.....	0.45	+
H91H.....	0.33	++
H91I.....	0.23	++
H91J.....	0.14	++

* Partially soluble samples were either heated to dissolve them or partially neutralized and the electrolyte then removed by passage through ion-exchange columns. The solutions were filtered hot and then kept overnight in a refrigerator.

† Turbidity estimated by visual observation. Solutions marked — were clear.

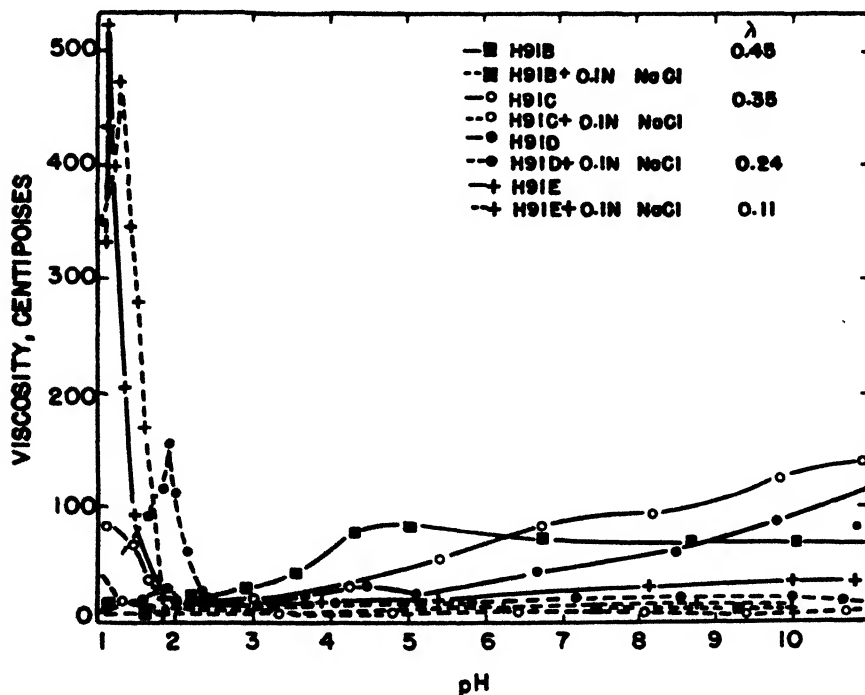


FIG. 1. Effect of pH on the viscosity of acid-deesterified pectinic acids, in the presence and absence of 0.1 *N* sodium chloride. Concentration of pectin, 1 per cent. Measurements made at 12 P.M. with No. 2 rotor of Brookfield viscosimeter.

and are able to stabilize a gel structure because of the large total number of hydrogen-bonding groups they present. As λ is decreased, the number of pectin carboxyl groups that can contribute to hydrogen bonding increases, making the effectiveness of the added hydrogen-bonding agents greater (4). Less sugar is then necessary to produce a gel. At very low λ the tendency of pectinic acid to associate with itself is so great that considerable syneresis of the gels takes place.

Sugar gels of high λ when immersed in a large volume of water dissolve from the surface, the gels retaining their cohesion and shape until completely dissolved. Gels of low λ act similarly at pH's greater than about 2. At lower pH's the gels do not dissolve, but the sugar diffuses out, leaving behind the skeleton gels of insoluble pectin.

TABLE 6

*Effect of methyl ester content of pectinate on optimum calcium-to-pectinate ratio and gel strengths of gels made from enzyme- and acid-deesterified pectinic acids**

CH ₃ O	GEL STRENGTH	CALCIUM/PECTINATE RATIO AT OPTIMUM	METHOD OF PREPARATION
<i>per cent</i>	<i>cm. H₂O</i>		
8	16	0.040	Enzyme
7	26	0.020	Enzyme
6	33	0.019	Enzyme
5	37	0.017	Enzyme
7.7	8	0.073	Acid
6.1	270	0.070	Acid
4.9	180	0.038	Acid
4.4	110	0.029	Acid
3.8	84	0.023	Acid

* Data from Hills, White, and Baker (4).

Solubility of pectinic acids in the presence of calcium ions

It has been demonstrated that the ability of dilute pectin solutions to form calcium gels, both in the presence and in the absence of hydrogen-bonding agents, depends upon λ (2, 3, 4). In 1 per cent solution, pectins with λ greater than about 0.5 do not gel with calcium ion alone. When λ is between about 0.5 and 0.25, stable calcium gels are formed, whereas when λ is less than 0.25, the tendency to synerize is great. The lower λ is, the smaller is the amount of calcium ion required to form the gel of optimum strength. Otherwise expressed, the "calcium tolerance" decreases with decreasing λ . This is illustrated by table 6. In this table, per cent methoxyl has been used instead of λ , since carboxyl contents necessary for computation of λ are not available.

Viscosity changes with λ and calcium-ion concentration much as does gelling power. Figures 2 and 3 give data, respectively, for acid- and enzyme-deesterified pectinic acids. Precipitation of calcium pectinate causes the viscosity decrease at the right of the maxima. In practical gel-making, less calcium ion than corresponds to the maxima would be used to avoid cloudiness and syneresis.

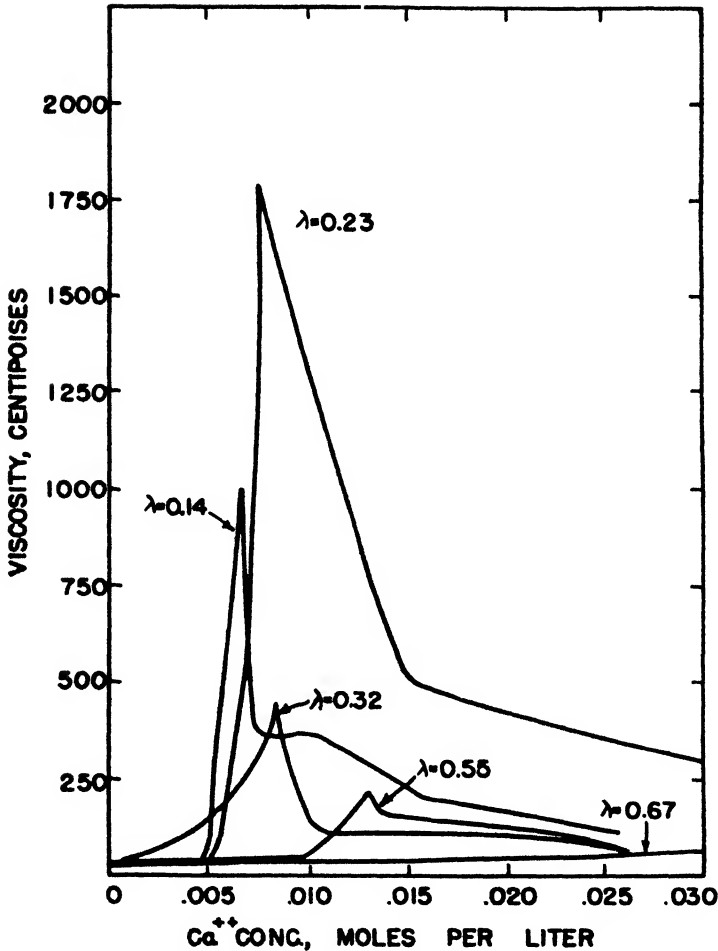


FIG. 2. Effect of calcium chloride concentration on the viscosity of acid-deesterified pectinic acids. Concentration of pectin, 0.25 per cent. Measurements made at 12 R.P.M. with No. 3 rotor of Brookfield viscosimeter.

If the mass-action law is followed, the equilibrium among calcium ion, hydrogen ion, pectinic acid, and calcium pectinate should be expressed by the equation

$$\frac{(\text{Ca}^{++})}{(\text{calcium pectinate})} = \frac{K_2}{K_1^2} \frac{(\text{H}^+)^2}{(\text{pectinic acid})^2} \quad (1)$$

in which K_1 is the dissociation constant for pectinic acid (treated as a monobasic acid), and K_2 is the dissociation constant for calcium pectinate. The equation indicates an increase in the calcium tolerance of pectinic acid solutions as the pH is lowered. This expectation is realized experimentally. Table 7 shows for a typical pectinic acid, H91C', that equation 1 describes the equilibrium up to the gel point, since the ratio K_2/K_1^2 , is approximately constant to this point.

An explanation of the decreased calcium-ion tolerance with decreasing λ may be sought in the graphs of pH *versus* total calcium-ion concentration in figure 4. It is evident that for equal additions of calcium ion, the lower λ is, the greater is

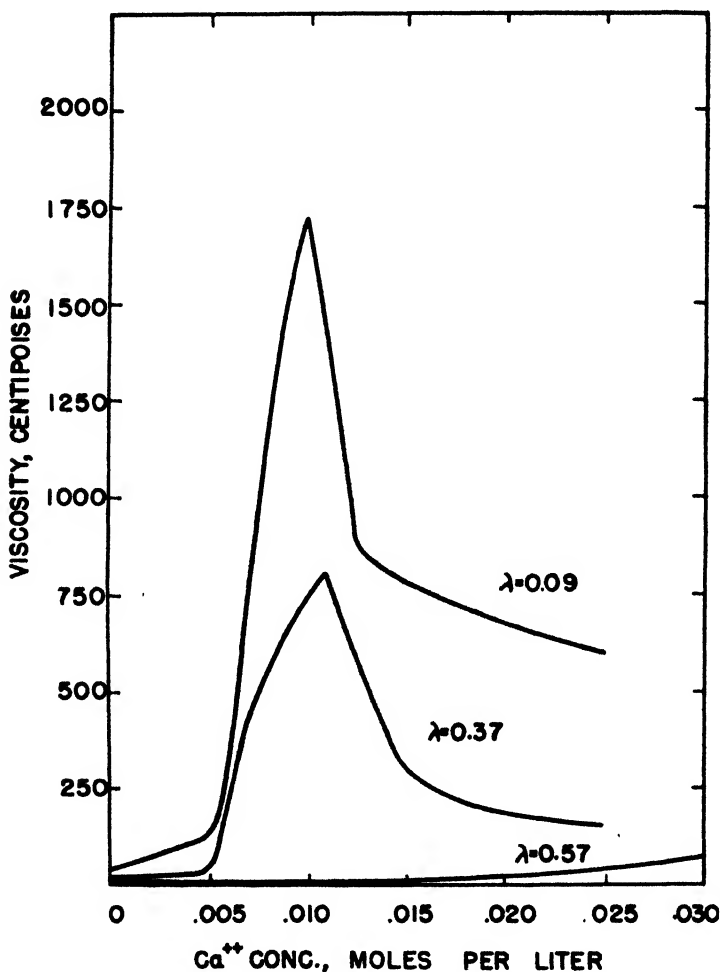


FIG. 3. Effect of calcium chloride concentration on the viscosity of enzyme-deesterified pectinic acids. Concentration of pectin, 0.25 per cent. Measurements made at 12 R.P.M. with No. 3 rotor of Brookfield viscosimeter.

the drop in pH. This means that there is a progressive increase in the amount of bound calcium ion and consequent liberation of hydrogen ion.

The nature of the interaction between pectinic acid and calcium ion is further revealed by the following observations. A calcium pectinate gel incorporating no hydrogen-bonding agent was not visibly altered by 72 hr. immersion in 15 volumes of distilled water. However, when sodium oxalate was added to the water, the calcium ions which linked the pectinic acid molecules were removed

by precipitation as the oxalate ions diffused into the gel, and the gel dissolved. Evidently the calcium ion is so firmly bound to the carboxyl groups that it cannot diffuse out of the gel, and since osmotic pressure is insufficient to force more water into the gel, the calcium-ion concentration within the gel is unchanged, and the gel is stable even in the presence of a considerable excess of solvent. In this respect, calcium gels are different from sugar gels. Oxalate ions are able to move fairly freely into the gel and, by sequestering much of the calcium, promote its dissolution. Like the oxalate, but less effectively, hydrogen ions can also remove calcium from the gel network, with the result that it disintegrates and dissolves.

TABLE 7
Calcium pectinate-pectinic acid equilibrium (sample H91C)

TOTAL Ca^{++} ADDED	INCREASE IN $(\text{H}^+)^*$	$\frac{K_2}{K_1^2}$
<i>moles per liter</i>	<i>moles per liter</i>	
3×10^{-4}	0.91×10^{-4}	51.5
6.01	1.37	48.5
9.01	1.79	52.3
12.02	2.35	47.2
18.03	2.71	60.9†
36.06	3.99	68.0
54.09	4.92	71.5
84.14	5.91	79.4
120.20	6.22	110.0

* Calcium pectinate concentration assumed equal to $\frac{1}{3}\Delta(\text{H}^+)$.

† Gelation occurred at this point.

Charge distribution and gel formation

As stated earlier, the inferior strength of enzyme-deesterified calcium pectinate gels was thought to reflect a peculiar distribution in the degree of esterification among the pectinate molecules (2), that is, because the action of pectinesterase may be highly selective, some molecules of a pectinic acid sample are demethylated to a very different degree from others. Acid and alkali presumably remove ester groups at random, so that λ for each individual molecule is about the same as the average λ for the entire preparation. Enzyme deesterification would then produce a broad distribution in λ , as compared with acid deesterification.

The electrophoretic mobility of a pectin molecule is proportional to $\alpha(1 - \lambda)$, where α is the degree of dissociation. Heterogeneity in λ should then be revealed in electrophoresis patterns. Figures 5 and 6, for acid- and enzyme-deesterified pectinic acids, show the expected broader distribution in mobility in the enzyme-treated preparations. Owens (7) recently has made similar observations on citrus pectin. He has fractionated enzyme-deesterified pectins by chemical means, and has found marked differences in λ among the fractions.

Ascending boundaries in figure 6, D and E, obtained from enzyme-deesterified

pectinic acid, demonstrate the presence of a small amount of a second component. The mobility of the second component is greater in figure 6D and less in figure 6E than the mobility of the principal component. We have also observed ascending boundaries in which three components were present. This is apparently a consequence of the non-random nature of pectin demethylation by enzymes.

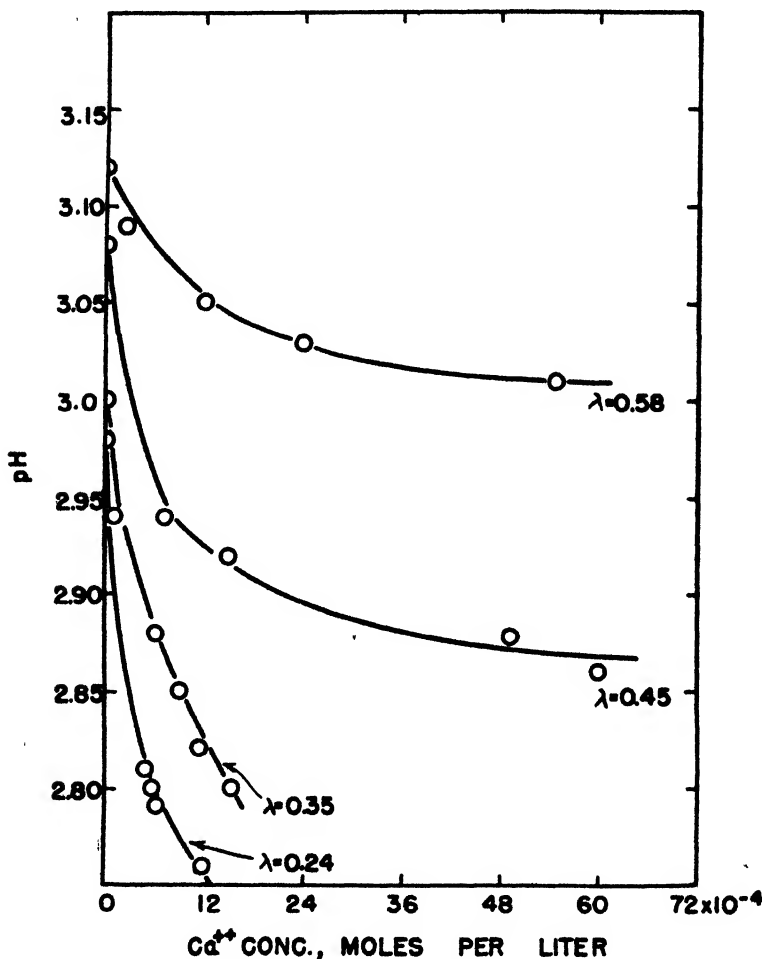


FIG. 4. Effect of calcium chloride on the pH of pectinic acids of various λ . Concentration of pectin, 0.2 per cent.

Explanation of the difference in gel strength between 65 per cent sugar and 35 per cent sugar-calcium pectinate gels shown in tables 1 and 6 can now be based on two experimental facts: (1) The amount of calcium ion required for maximum strength decreases with λ . (2) For a given λ all the molecules are not deesterified to the same extent, the deviation from the average being much greater in enzyme- than in acid-deesterified pectinic acids. Consequently, since nearly all the molecules have the same λ , a single calcium concentration is

optimum for an acid-deesterified pectinic acid. However, a single calcium concentration is not optimum for all the molecules of an enzyme-deesterified pectinic acid. The fraction of low λ requires less calcium than the fraction of high λ , so an intermediate calcium concentration would precipitate the former

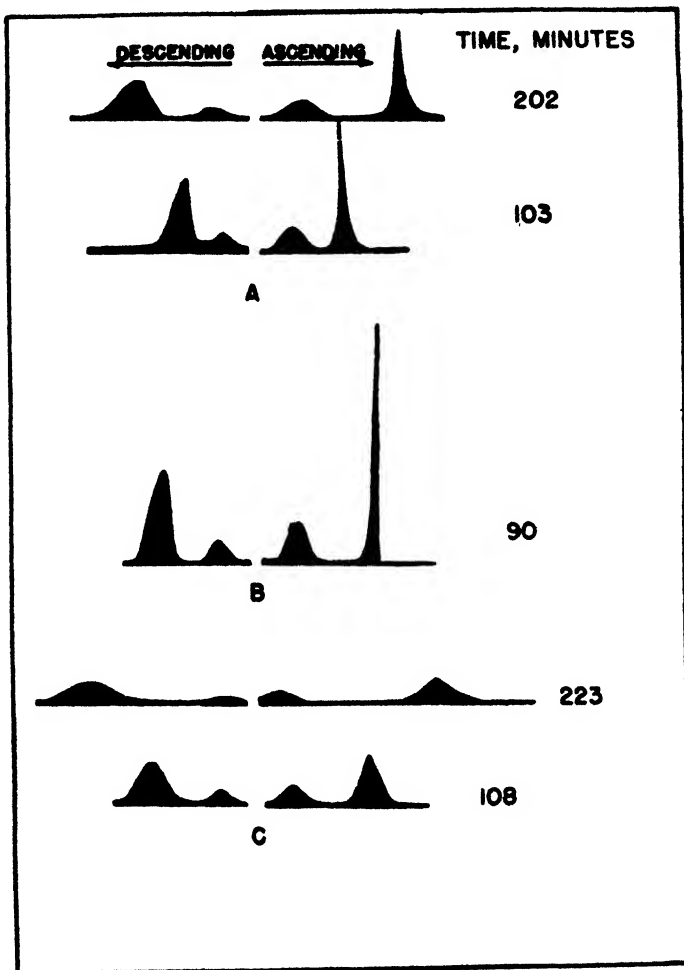


FIG. 5. Electrophoresis patterns of pectic materials
 A: H84, the original pectin, $\lambda = 0.80$, pH = 5.7
 B: H84D, acid deesterified, $\lambda = 0.32$, pH = 5.7
 C: H89C, enzyme deesterified, $\lambda = 0.35$, pH = 5.7

while incompletely cross-linking the latter. This would make gels of low strength. An experiment performed by Hills (2) illustrates the point. Two pectinic acids produced by acid deesterification, with methoxyl contents of 3.3 and 5.7 per cent, gave calcium gels with strengths of 88 and 89 cm. The pectinic acids were mixed in equal amounts. The methoxyl content of the mixture was 4.5 per cent, and the distribution in λ was no longer sharp but resembled that of an enzyme-

deesterified pectin. Significantly, the calcium gel strength was only 44, or half that of the gel made from each constituent of the mixture. A similar mixture made with enzyme-deesterified pectinic acids did not give a correspondingly

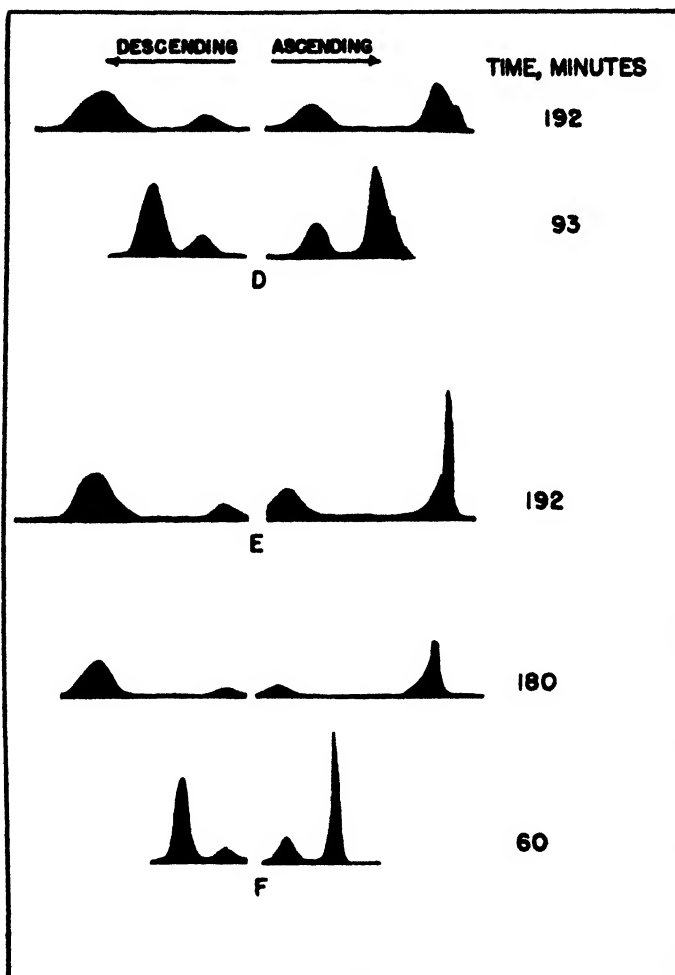


FIG. 6. Electrophoresis patterns of pectinic acids
 D: H88C, enzyme deesterified, $\lambda = 0.35$, pH = 5.6
 E: H91I, enzyme deesterified, $\lambda = 0.23$, pH = 5.6
 F: H59, acid deesterified, $\lambda = \text{ca. } 0.35$, pH = 5.8

weakened gel. This result was expected, since initially the enzyme-treated pectins were heterogeneous in λ .

As the average λ becomes small, the distribution in λ among the molecules of enzyme-deesterified pectinic acids inevitably becomes more homogeneous, and the gel strength rises until syneresis reverses the trend (table 6). Electrophoresis patterns demonstrate directly the increased homogeneity, Sample H91I with

$\lambda = 0.23$ giving much sharper peaks than enzyme-treated preparations of greater λ .

The possibility should be mentioned that non-random demethylation by an enzyme may result in giving part of a pectinic acid molecule the properties of pectic acid and part the properties of a high-ester pectin. Such a condition would also contribute to the observed differences in solubility, viscosity, electrophoretic mobility, and gel behavior of acid- and enzyme-deesterified pectinic acids, although to a smaller extent than the heterogeneity in λ discussed above. Jansen and MacDonnell (5) have accumulated impressive experimental evidence that hybrid pectic acid-pectin molecules actually result from pectase action.

Influence of molecular weight

The strength of calcium pectinate gels depends upon molecular weight, λ , and the calcium-binding power. During acid deesterification there is simultaneous progressive molecular degradation (12). In a λ series (table 6) the initial strength, which expresses the effect of high molecular weight, is at first exceeded despite degradation, because of the overbalancing effect of the increased number of strong ionic cross-links made possible as λ is lowered. Ultimately, the molecular-weight effect, partly obscured, it is true, by precipitation and syneresis, again predominates, and the gel strength falls. Similar behavior is shown in the viscosity curves of figure 2.

Controlled enzyme deesterification leads to little chain degradation, so the molecular weight is nearly independent of λ (12). Therefore gel strength (table 6) and viscosity (figure 3) increase with decreasing λ . Gel syneresis is here less troublesome because the large content of ballast material represses association.

Bond types and the elastic properties of pectin gels

Observed gel elasticity must arise from bending of the pectin molecules and deformation of three-dimensional interweaving networks of multilaterals of different size and shape made by hydrogen and calcium-ion bridges between portions of the pectin chain.

In 65 per cent sugar gels hydrogen bridges alone are active. Because of the predominant proportion of sugar and the large size and low mobility of its molecules in comparison with water, the bridges between pectin molecules must be principally through sugar. To form a gel, the pectin molecules need nowhere be in contact or even close to one another. Consequently, it might be expected that the sugar gels would be easily deformed and relatively elastic. In calcium pectinate gels the most effective cross-bonds are calcium-ion bonds between carboxyls. Since the bond distances are short, the pectin molecules must approach very closely at these tie points. The bonds are strong and not distensible. An inelastic, rather brittle gel results, as is shown in table 8. Recoverable deformation is only about one-half that of sugar gels, although the strength of calcium pectinate gel may be as great or even greater. Also characteristic of a brittle material are the high values of $\tan \theta$ and the small work of deformation.

$\tan \theta$, which is analogous to an elasticity modulus, gives an approximately

straight line when plotted against the ultimate strength for a series of sugar gels. Owens and Maclay (9) found that plots of shear modulus *versus* ultimate strength are also linear. This means that the modulus of rigidity is a measure of the strength of a 65 per cent sugar pectin gel, just as it is for gelatin gels (11). There is not even approximate linearity between strength and $\tan \theta$ for calcium pectinate gels, and this makes an analysis of their mechanical behavior considerably more difficult.

TABLE 8
Mechanical properties of pectin gels

SAMPLE	CH ₂ O	WEIGHT OF PECTIN	TAN θ §	ULTIMATE STRENGTH	REVERSIBLE DEFORMATION¶
	<i>per cent</i>	<i>grams</i>		<i>cm. H₂O</i>	<i>per cent</i>
Sugar gels (65%):					
E35-1*	8.06	1	32.5	156.0	About 60
-12.....	8.06	0.6	23.3	112.0	54
-13.....	8.06	0.6	23.0	114.0	52
H59-11†	4.53	1	17.0	72.0	43
-12.....	4.53	1	17.2	67.0	40
-14.....	4.53	2	21.3	150	59
-15.....	4.53	2	20.0	170	58
H74-18‡	4.50	1	5.6	8	Very low
-19.....	4.50	1	4.1	11.5	Very low
-21.....	4.50	2	13.4	47.6	43
-22.....	4.50	2	13.3	50.5	32
Sugar-calcium pectinate gels (35%):					
H59-1†	4.53	2	50.0	56	25
-2.....	4.53	2	62.5	48	37

* Unmodified pectin.

† Acid-deesterified pectinic acid.

‡ Enzyme-deesterified pectinic acid.

§ $\tan \theta = \frac{\text{pressure in cm. H}_2\text{O}}{\text{displacement in mm.}}$; obtained graphically.

¶ Gel deformed under a stress of 30 cm. H₂O and then allowed to recover at zero load.

Per cent reversible deformation = $\frac{\text{reversible deformation} \times 100}{\text{total deformation}}$

It is worthy of note, finally, that for sugar gels of increasing strength, permanent flow decreases and reversible deformation increases.

SUMMARY

1. The solubility of pectic materials is an index to their gel-forming ability. Solubility in general decreases with the degree of esterification, λ . Because of their higher content of non-uronide material, enzyme-deesterified pectinic acids are more soluble than acid-deesterified pectinic acids.

2. Molecular association in pectinic acid solutions is also expressed by the development of turbidity and heightened viscosity.

3. The quantity of divalent ion (Ca^{++}) necessary to form a gel of a given strength decreases with λ , reflecting the increased possibility of forming cross-links between carboxyl groups of adjacent pectinic acid molecules.

4. Electrophoresis diagrams for acid- and enzyme-deesterified pectinic acids show the latter to be more heterogeneous in the distribution of λ among its molecules. This heterogeneity is principally responsible for the low strength of gels made from enzyme-deesterified pectinic acids.

5. Calcium pectinate gels are characteristically brittle as compared with hydrogen-bonded pectinate gels.

We should like to thank Robert C. Warner for his aid in the electrophoresis work.

REFERENCES

- (1) BAKER, G. L., AND GOODWIN, M. W.: Delaware Agr. Expt. Sta., Bull. **234** (1941).
- (2) HILLS, C. H., MOTTERN, H. H., NUTTING, G. C., AND SPEISER, R.: "Factors influencing the behavior of pectinate gels," presented before the Division of Agricultural and Food Chemistry at the 108th meeting of the American Chemical Society, New York City, September 13, 1944.
- (3) HILLS, C. H., AND SPEISER, R.: Science **103**, 166 (1946).
- (4) HILLS, C. H., WHITE, J. W., JR., AND BAKER, G. L.: Proc. Inst. Food Tech. **1942**, 47.
- (5) JANSEN, E. F., AND MACDONNELL, L. R.: Arch. Biochem. **8**, 97 (1945).
- (6) LONGSWORTH, L. G.: J. Am. Chem. Soc. **61**, 529 (1939).
- (7) OWENS, H. S.: Private communication.
- (8) OWENS, H. S., LOTZKAR, H., SCHULTZ, T. H., AND MACLAY, W. D.: J. Am. Chem. Soc. **68**, 1628 (1946).
- (9) OWENS, H. S., AND MACLAY, W. D.: J. Colloid Sci. **1**, 313 (1946).
- (10) PALMER, K. J., AND HARTZOG, M. B.: J. Am. Chem. Soc. **67**, 2122 (1945).
- (11) SHEPPARD, S. E., AND SWEET, S. S.: J. Am. Chem. Soc. **43**, 539 (1921).
- (12) SPEISER, R., AND EDDY, C. R.: J. Am. Chem. Soc. **68**, 287 (1946).
- (13) SPEISER, R., EDDY, C. R., AND HILLS, C. H.: J. Phys. Chem. **49**, 563 (1945) (Fig. 11).
- (14) TARR, L. W.: Delaware Agr. Expt. Sta., Bull. **142** (1926).

MOLECULAR PROPERTIES OF HEMICELLULOSE FRACTIONS^{1,2}MERRILL A. MILLETT³ AND ALFRED J. STAMM⁴*Forest Products Laboratory,⁵ Forest Service, U. S. Department of Agriculture**Received August 8, 1946*

INTRODUCTION

Conventional pulping processes and the Cross and Bevan method for analytically isolating cellulose from lignocellulosic materials leave the higher-molecular-weight portion of the cellulose as a solid residue, dissolving out the lignin and at least part of the hemicelluloses. These treatments are so drastic that they simultaneously degrade both the solid cellulosic fractions and the hemicelluloses that are put into solution. Ritter and Kurth (20) developed a means of isolating holocellulose, the solid fraction of lignocellulosic materials comprising all of the cellulose and the hemicelluloses. The procedure was modified by Van Beckum and Ritter (24) to make the method more practical.

The holocellulose method of isolating cellulose and hemicellulose not only isolates them in a single solid fraction but also reduces to a minimum the degradation of both the cellulose and the hemicelluloses. For example, the alpha cellulose content of pulps based on the original weight of the dry extracted wood seldom exceeds 30 per cent. Yields of alpha cellulose from holocellulose on the same basis may be as high as 50 per cent. Hemicelluloses isolated from pulp as beta and gamma cellulose thus contain not only the natural hemicelluloses of the wood but also degradation products of alpha cellulose.

Alpha cellulose has been intensively studied both as to its chemical constitution and its physical-chemical properties, such as molecular weight, size, and shape. Most studies of the hemicelluloses have been primarily concerned with the chemical identification of the various polysaccharides present, that is, hexosans, pentosans, uronic acids, and the simple sugars or sugar derivatives that could be isolated from them. A few molecular-weight measurements have been made by Kraemer (6) on beta and gamma celluloses. These values, as previously indicated, are for hemicellulose fractions containing degraded cellulose.

This paper is concerned with the physical-chemical properties obtained in studies at the Forest Products Laboratory on the hemicellulose fractions of aspen holocellulose through the use of as many of the classical methods as could

¹ Presented at the Twentieth National Colloid Symposium, which was held at Madison, Wisconsin, May 28-29, 1946.

² Thesis submitted by Merrill A. Millett to the Graduate School of the University of Wisconsin in partial fulfillment of the requirements for the degree of Doctor of Philosophy, 1943.

³ Chemist.

⁴ Chief, Division of Derived Products.

⁵ Maintained at Madison 5, Wisconsin, in cooperation with the University of Wisconsin.

be applied. Fractional extraction procedures were used to obtain the following four fractions (11):

Fraction I—soluble in hot water

Fraction II—soluble in 1 per cent sodium hydroxide

Fraction III—soluble in 5 per cent sodium hydroxide

Fraction IV—residue (represents alpha cellulose and more difficultly soluble hemicellulose)

Fraction I, being water soluble, lends itself most readily to the greatest number of classical methods for obtaining molecular properties and thus received the most study.

PREPARATION OF MATERIAL

Holocellulose was prepared from aspen sawdust by a modification of the method of Van Beckum and Ritter (24), involving alternate chlorination of the sawdust in saturated chlorine water and extraction of the chlorinated lignin with a 3 per cent hot alcoholic monoethanolamine solution. Satisfactory lignin removal, as evidenced by the lack of color formation when treated with the amine solvent, was obtained after about five cyclic treatments. The extracted holocellulose was washed thoroughly first with 95 per cent alcohol to remove the solvent and then with ether, and finally was dried in a vacuum oven at 70°C.

In the work covered by this research four different batches of holocellulose were prepared and were designated A to D. Osmotic-pressure measurements were made on each batch as it was prepared, in order to correlate the results with those of the particular molecular-weight method for which it was prepared. In addition to the usual extraction treatment for lignin removal, batches C and D were given a 20-min. bleach with 25 cc. of saturated calcium hypochlorite solution dissolved in 2 gallons of cold distilled water. The holocellulose obtained by this method was considerably whiter than that prepared without the final bleach.

FRACTIONATION OF HOLOCELLULOSE

Fraction I—soluble in hot water

Fifty to 100 g. of holocellulose were covered with sufficient water to form a thin suspension and heated to 90–95°C. for 15 min. with constant stirring. The material was then filtered on a Buchner funnel. A second extraction was made under the same conditions, and the two filtrates were combined and concentrated to a volume of 100 cc. by vacuum distillation, using a water pump. The concentration of water-soluble material in this solution was about 0.5 to 1.0 per cent, depending on the initial amount of holocellulose used, and represented about 2 per cent of the original holocellulose, or about twice that amount of the non-alpha cellulosic part of the holocellulose. In order to prevent mold growth, a few crystals of β -chloronaphthalene were added to the solution. Concentrations

were determined by the evaporation of a 10-cc. portion at 70°C., followed by final drying in a vacuum oven at 70°C.

Fraction II—soluble in 1 per cent sodium hydroxide

The residue from fraction I was suspended in a 1 per cent solution of sodium hydroxide for 3 days at room temperature with frequent stirring. After filtering, the dissolved material was precipitated with alcohol, filtered, and freed from salts by suspending it in water, acidifying with hydrochloric acid, adding alcohol, and again filtering. After thorough washing with alcohol, it was dried in a vacuum oven at 70°C. This fraction represented about 1 per cent of the original holocellulose.

Fraction III—soluble in 5 per cent sodium hydroxide

The residue from fraction II was suspended for 3 days in a 5 per cent sodium hydroxide solution, after which the dissolved material was isolated in the same manner as in fraction II. This fraction represented about 7 per cent of the original holocellulose.

MOLECULAR PROPERTIES OF THE WATER-SOLUBLE FRACTION

Osmotic pressure

Osmotic-pressure measurements were made in an all-glass osmometer of the static type, using a collodion membrane. The membrane was supported on an alundum crucible bottom, which was cemented to the osmometer.

The osmometer was filled completely with a solution of known concentration, so that the liquid level extended several centimeters up the capillary (approximately 15 cc. of solution required). The osmometer was then placed in a large test tube of distilled water held in a thermostated bath at 25°C. \pm 0.05°. The water in the test tube was agitated by means of a small glass motor-driven stirrer. When thermal equilibrium was established, the stopcock on the side-arm filling tube was closed, and the rise of the liquid up the capillary was observed every 15 or 30 min. until no further rise was noted.

If the capillary rise is plotted against time, the position of maximum osmotic pressure may be found by extrapolation. About 5 to 8 hr., depending on the thickness of the membrane, are required before a reliable extrapolation can be made. Check runs were made by opening the stopcock for a few minutes to allow the solution in the capillary to drop down to its starting position and then closing it again. Even after three repeated measurements, the maximum capillary rise was nearly the same as on the first run. The effectiveness of the collodion as a semipermeable membrane was evidenced by the fact that this maximum capillary rise could be maintained for several days with no apparent decrease.

Figure 1 shows a typical pressure-time curve obtained with a concentration of 0.144 g. per 100 cc. of solution. The osmotic pressure reached in 3 hr. was only 4 per cent below that obtained at the end of 13 hr. By using a value of

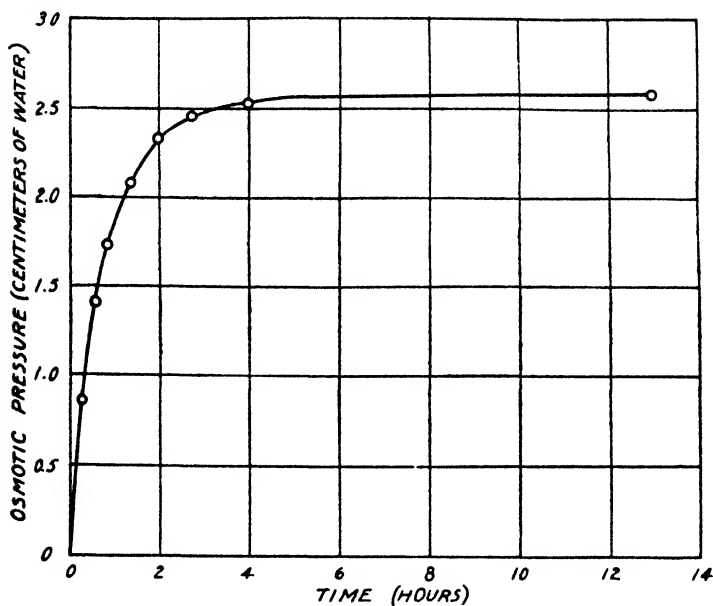


FIG. 1. Relation of osmotic pressure to time for water-soluble fraction of hemicellulose (0.144 g. per 100 cc.).

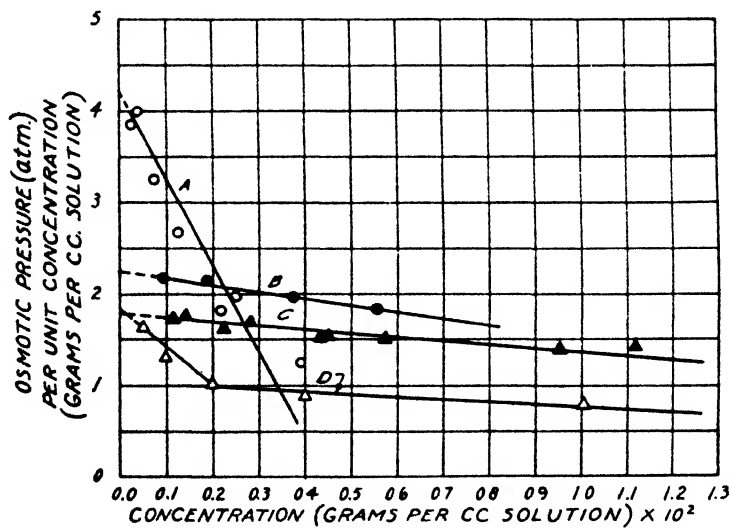


FIG. 2. Change in osmotic pressure per unit concentration with concentration. Data from four different hemicellulose preparations.

2.6 cm. as the maximum osmotic pressure and substituting into the van't Hoff equation

$$P = \frac{CRT}{M}$$

where P is in atmospheres, R in cc.-atmospheres, and C in grams per cubic centimeter, a molecular weight of 13,900 is obtained for the water-soluble fraction.

The minimum concentration for which reasonably accurate osmotic-pressure readings could be made with this osmometer was about 0.025 per cent. At this dilution check runs on different fillings of solution could be made to an accuracy of 10–15 per cent. At concentrations in the neighborhood of 0.1 per cent, check runs agreed within 1 to 2 per cent.

Figure 2 shows the generally accepted method of obtaining molecular weight by a plot of osmotic pressure per unit concentration against the concentration and extrapolating to zero concentration. Straight lines are obtained throughout the concentration range used, although the intercept at zero concentration is somewhat different for the different batches of holocellulose. Also, the line representing batch D has a definite break to a steeper slope at a concentration of 0.2 per cent. The limiting molecular weights determined for the four batches were as follows:

BATCH	MOLECULAR WEIGHT FROM INTERCEPT ON P/C vs. C CURVE
A.....	6,000
B.....	11,000
C.....	13,600
D.....	13,700

Equilibrium centrifuge

Sedimentation-equilibrium studies were made on the water-soluble fraction of holocellulose batches A, B, and C, using the scale-displacement method. In making the measurements, it was found that a concentration of from 2 to 3 per cent had to be used in order to get sufficient refractive-index differences between the solvent and solution. A temperature of $25^{\circ}\text{C.} \pm 0.05^{\circ}$ was maintained in the bath around the rotor, and a rotor speed of 12,000 R.P.M. was used. Under these conditions equilibrium was established in about 10 days.

Table 1 shows the molecular weights found for the three solutions as a function of the distance from the center of rotation. The constancy of the molecular weights throughout the depth of the cell indicates a remarkable homogeneity for a material of this kind, and the results are in good agreement with those obtained from osmotic-pressure data.

Viscosity

Viscosity measurements on the various holocellulose fractions and on their acetylated derivatives were made in a viscometer having a flow time of 332 sec. for water under a pressure of 20 cm. of mercury. The viscometer was rigidly mounted in a thermostated water bath held at $25^{\circ}\text{C.} \pm 0.05^{\circ}$. The applied air pressure was controlled by means of a reducing valve and was connected in parallel to the viscometer and to from one to four air escape bubblers that

contained water and were connected in series with one another. By adjusting the reducing valve so as to maintain a constant bubble rate, pressures of about 10, 20, 30, and 40 cm. of mercury could be obtained and held constant to 0.02 cm. of mercury, as measured by means of a cathetometer. The readings were reproducible in subsequent measurements to 0.03 to 0.05 cm. of mercury.

Flow measurements were made in both directions in the viscometer, and the flow times used in the calculations were averages of these two values. Over the concentration range used, the straight-line proportionality between time of flow and concentration indicated that the solutions obeyed Poiseuille's law. All solutions, prior to use, were filtered through a fine-pored, fritted-glass filter.

TABLE 1

Molecular weights determined by the equilibrium ultracentrifuge method at various distances from the center of rotation

BATCH A			BATCH B		BATCH C	
Distance from center of rotation	Molecular weight		Distance from center of rotation	Molecular weight	Distance from center of rotation	Molecular weight
	Run 1	Run 2				
mm			mm.		mm.	
50.0	11,500	12,500	50.5	8,040	56.5	10,500
49.5	11,400	10,200	50.0	8,300	55.5	6,500
49.0	11,000	9,850	49.5	9,000	54.5	5,350
48.5	10,300	9,400	49.0	9,370	53.5	5,200
48.0	8,600	9,500	48.5	9,130	52.5	4,920
47.5		9,600	48.0	10,000	51.5	5,530
47.0		8,750	47.5	9,380	50.5	5,140
					49.5	4,550

Figure 3 shows the curves for the specific viscosity divided by concentration (η_{sp}/C) plotted against concentration, where C is expressed in grams per cubic centimeter. The experimental error in measuring the specific viscosity at concentrations below 0.1 per cent is such that these values are not given much weight in drawing the curves. The straight line representing the values for holocellulose batch C extrapolates to an η_{sp}/C value of 62, or 0.062 when C is expressed in grams per liter; similarly, the extrapolated value for batch D is 0.054. Substituting these values into the Staudinger equation

$$\eta_{sp}/C = K_m P \quad (2)$$

and using his K_m value of 11×10^{-4} , obtained for methyl cellulose in water (22), the degree of polymerization (P) for the two batches is 56 and 50, respectively.

The basic repeating unit of cellulose is the glucose anhydride unit, but from the work of Mitchell and Ritter (11) it is known that the water-soluble fraction of maple holocellulose contains about 50 per cent xylan, about 17 per cent uronic acid anhydride, and about 25 per cent hexosan. By use of their analytical data, an average of 149 was obtained for the unit weight of this fraction. Resulting molecular weights for batches C and D are 8350 and 7450, respectively, values

which are in good agreement with those obtained osmotically and by means of sedimentation equilibrium.

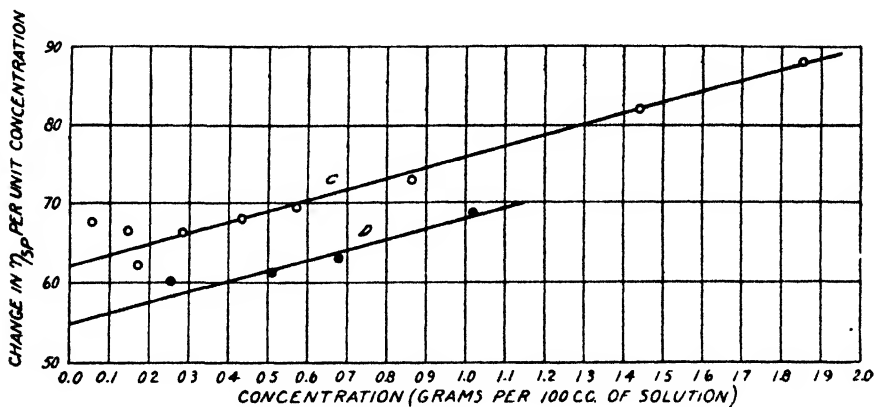


FIG. 3. Change in specific viscosity per unit concentration plotted against concentration for the water-soluble fraction from holocellulose batches C and D.

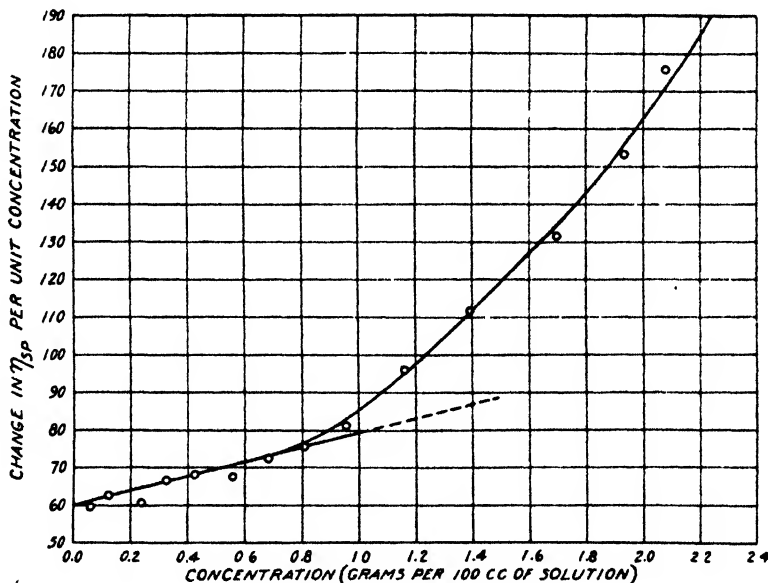


FIG. 4. Change in specific viscosity per unit concentration plotted against concentration for the acetylated water-soluble fraction from holocellulose batch C dissolved in chloroform.

The water-soluble fraction, acetylated by the pyridine-acetic anhydride method of Hibbert (5), was completely soluble in chloroform. Figure 4 shows the η_{sp}/C versus C curve for the acetylated material prepared from holocellulose batch C. Above a concentration of 0.8 per cent the curve exhibits a sharp rise in η_{sp}/C with increasing concentration, in contrast to the curves for the water-

soluble material, which were linear up to the maximum concentration used. Extrapolation of the straight-line portion below this point gives a value of 0.060 for η_{sp}/C at 0.0 concentration. Using a K_m value of 6.3×10^{-4} , given by Staudinger for triacetyl cellulose (22), a degree of polymerization of 95 is obtained. This is almost twice that obtained for the original water-soluble material, a result which is highly improbable. The degree of polymerization should be somewhat less because of degradation occurring during the acetylation. An earlier paper by Staudinger (21) gave a K_m of 11×10^{-4} , which is the same as that used for the water-soluble fraction. The degree of polymerization would then be 55, or about the same as for the unacetylated water-soluble material and would yield a molecular weight of 13,200, based on an acetyl content of 38 per cent, as experimentally determined. Since the theoretical acetyl content for the diacetyl derivative is 37 per cent, whereas for the triacetyl derivative it is 47 per cent, it is apparent that the major portion of the material is in the form of the diacetyl derivative.

The residue obtained by evaporation of chloroform from the solutions used in the previous measurements was deacetylated in absolute alcohol by means of metallic sodium. After neutralization and thorough washing with alcohol, the material was dissolved in water and viscosity measurements were made. A linear curve was obtained up to the maximum concentration used (about 1.1 per cent), and an extrapolated η_{sp}/C of 0.072 was obtained, a value which yielded a degree of polymerization of 65 and a molecular weight of 9700, in good agreement with the original water-soluble material.

Several osmotic-pressure measurements made at concentrations below 0.5 per cent gave a limiting molecular weight of 8500. These results show that the acetylation procedure used was so mild that little, if any, degradation occurred—a conclusion also reached by Kraemer (6).

Spreading measurements

A series of spreading measurements was made, using a Langmuir-type torsion wire film balance. It was found that the acetylated derivative spread nicely from a chloroform solution onto a water surface, but no satisfactory substrate was found for the unacetylated material.

A 0.032 per cent solution of the acetylated water-soluble holocellulose from batch C was prepared, and an amount containing 7.56×10^{-5} g. of solute was added to the trough. Figure 5 shows the pressure-area curve obtained. The shape of the curve is similar to that obtained for stearic acid, in having a long straight-line portion, and extrapolates to a value of 30 A.² per repeating unit. The second curve in figure 5 is for a more dilute solution, and again a limiting value of 30 A.² was obtained. Similar pressure-area curves for the acetylated material from holocellulose batch D gave 25 A.² as the limiting area per repeating unit.

From the weight and area of the film at zero pressure and a density of 1.5, a film thickness of 8.8 A. is obtained. The cross-sectional area per molecule of fifty repeating units would be 50 by 30 by 10^{-16} , or 1500 by 10^{-16} sq. cm.

which, when multiplied by the thickness, gives a volume of $13,000 \times 10^{-24}$ cc. Assuming that the molecule is rod-like in shape and has a radius of 4.4×10^{-8} cm. (half the spreading thickness), a length of 217×10^{-8} cm. is obtained. This gives an axial ratio of about 25 to 1, indicating a rather short molecular chain.

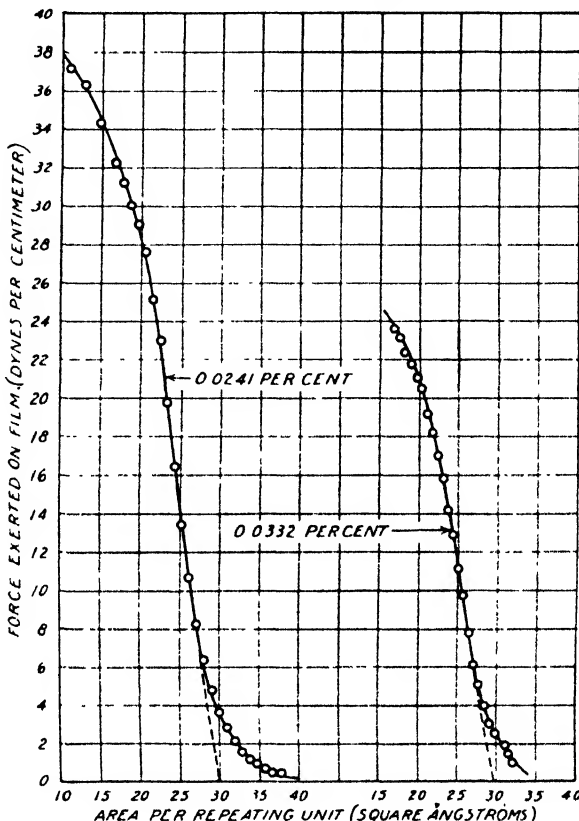


FIG. 5. Film pressure plotted against cross-sectional area for 7.56×10^{-6} and 5.48×10^{-6} g. of the acetylated water-soluble fraction of holocellulose batch C, spread on a water surface.

Diffusion

The diffusion constant of the water-soluble holocellulose fraction was determined by the membrane-diffusion method, using fritted Pyrex diffusion cells of the type developed by Northrup and Anson (14), McBain and coworkers (8, 9, 10), and Mouquin and Cathcart (12). They were standardized with 0.1 *N* potassium chloride, the diffusion constant of which was 1.631×10^{-5} sq. cm. per second at 25°C. (10). Concentrations were determined interferometrically. Using this value for *D*, the cell constants were determined by means of the equation:

$$KD = \frac{\log C_0 - \log(C_0 - 2C)}{T_E} \quad (3)$$

where K is the cell constant, C_0 the initial concentration, and C the concentration of the liquid surrounding the cell after time T_E (10). K , having been determined in this way, can be applied to any other diffusion measurement made in the same cell. A preliminary test of the cells with various concentrations of sucrose gave a molecular weight of 350 on extrapolation to zero concentration of the curve relating the concentration to the diffusion constant.

The diffusion constant of the water-soluble fraction of holocellulose batch D was determined for concentrations ranging from 0.766 to 2.226 per cent. Extrapolation of the diffusion-concentration curve to zero concentration gave a diffusion constant of 0.16×10^{-5} sq. cm. per second. Substitution of this value into the Stokes-Einstein equation for spherical particles:

$$D = \frac{RT}{N} \times \frac{1}{6\pi\eta r} \quad (4)$$

where R is expressed in ergs, T is the absolute temperature, N is Avogadro's number, η is the absolute viscosity of water in poises, and r is the particle radius in centimeters, gave a molecular radius of 15.2×10^{-8} cm. The molecular weight M can then be calculated from the equation:

$$M = 4/3\pi r^3 d N \quad (5)$$

where $4/3\pi r^3$ is the particle volume and d is the density. A molecular weight of 12,500 is thus obtained, which is in rather good agreement with that found by the other methods.

The assumption that the water-soluble hemicellulose molecule is spherical, however, is at variance with that made for the calculation of molecular weights from Staudinger's viscosity equation. There it was assumed that the material was similar to cellulose, which is known to be a linear molecule, and the K_m value of cellulose was used. This gave a degree of polymerization of about 50. If the molecular chain were made up entirely of glucose anhydride units, which have a b/a ratio of 1 to 1 (length to thickness), the b/a ratio for the water-soluble fraction would be about 50 to 1. Actually, owing to the presence of about 50 per cent pentosans, the ratio would be less than this, perhaps 30 or 40 to 1. Spreading data indicated a ratio of 25 to 1. There is some evidence (25) that the hemicellulosic chains may be branched, a factor which, together with solvation effects, might well bring the shape factor still lower.

Some of the various equations used in correcting for molecular dissymmetry in the calculation of molecular weights from diffusion data were tested for the calculation of the b/a ratio.

For randomly oriented rods (Kuhn) (4, 7):

$$\eta_{sp} = 2.5G + G/16 (b/a)^2 \quad (6)$$

For randomly oriented particles in which $b \gg a$ (Eisenschitz) (3, 4):

$$\eta_{sp} = G \times \frac{(b/a)^2}{15(\ln 2(b/a) - 3/2)} \quad (7)$$

For randomly oriented rods (Onsager) (4, 15):

$$\eta_{sp} = 0.107G \times \frac{(b/a)^2}{\ln b/a} \quad (8)$$

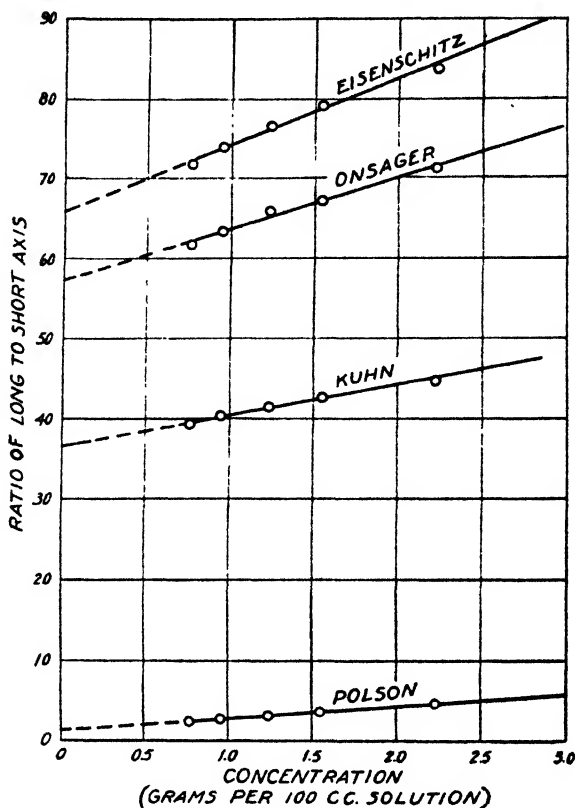


FIG. 6. Axial ratios calculated from four dissymmetry equations plotted against the concentration of the water-soluble fraction from holocellulose batch D.

Empirical equation (Polson) (4, 17):

$$\eta_{sp} = 4G + 0.098(b/a)^2 \quad (9)$$

in which G is the volume fraction of the solute in milliliters per milliliter of solution, η_{sp} is the specific viscosity, and (b/a) is the axial ratio. All of these equations represent extensions of the Einstein equation for spherical particles, $\eta_{sp} = 2.5\theta$ (2), where θ is the volume fraction occupied by the solute.

In figure 6 the variation of the b/a ratio with concentration is shown for each of the preceding equations. Extrapolation to zero concentration gives for the limiting values of b/a :

Eisenschitz	66.0
Onsager.....	57.5
Kuhn	36.5
Polson.....	1.5
Experimental	25.0

The last value is that estimated from spreading data. The assumption is made that the unacetylated material has the same b/a ratio as the acetylated material.

Perrin (16) has developed an equation that gives the ratio of the frictional coefficient of a prolate spheroid of revolution to that of a spherical particle of the same weight in terms of the axial ratio:

$$f/f_0 = \frac{\sqrt{1 - (b/a)^2}}{(b/a)^{2/3} \ln \frac{1 + \sqrt{1 - (b/a)^2}}{b/a}} \quad (10)$$

where f/f_0 is the ratio of the frictional coefficients. Polson (18) and Neurath (13) have developed similar equations.

Solution of the Perrin equation for the preceding axial ratios gives the following f/f_0 ratios:

Eisenschitz	3.34
Onsager	3.13
Kuhn	2.56
Polson	0.945
Experimental	2.18

Substitution of these values for f/f_0 into the Svedberg equation (23):

$$f/f_0 = \frac{RT/D}{6\pi\eta N \left(\frac{3M\bar{V}}{4\pi N} \right)^{1/3}} \quad (11)$$

where R is in ergs, D is the diffusion constant, η is the solvent viscosity, M is the molecular weight, and \bar{V} is the solute specific volume, gave the following molecular weights:

Eisenschitz	340
Onsager	413
Kuhn	770
Polson	14,900
Experimental	1,200

In comparing these molecular weights with those obtained by the previous methods, it is evident that only the Polson equation (9) gives a result that is at all comparable. This equation was found to hold well for nearly all proteins (4), and since proteins usually have a small b/a ratio, the foregoing results indicate a small b/a ratio for the water-soluble fraction of holocellulose. As was shown previously, the assumption that the molecule is spherical ($b/a = 1$) leads to a molecular weight of 12,500. Assuming that the ratio is 6, a molecular weight of 7350 is obtained, a value which is in somewhat better agreement with the average results obtained from the other methods.

MOLECULAR PROPERTIES OF THE ALKALI-SOLUBLE FRACTIONS

Viscosity measurements

The fraction soluble in 1 per cent sodium hydroxide was found, after isolation, to be soluble in 0.5 per cent sodium hydroxide, and the fraction soluble in 5 per cent sodium hydroxide was soluble in 2 per cent sodium hydroxide. Both

fractions gave linear η_{sp}/C versus C curves up to the maximum concentrations used (about 1.5 per cent) which, on extrapolation to $C = 0$, gave η_{sp}/C values of

TABLE 2

Comparison of the molecular properties of aspen hemicelluloses determined by various methods

HEMICELLULOSE FRACTION	PROPERTY	METHOD	RESULTS
Water soluble	Molecular weight	Osmotic pressure	11,000
	Molecular weight	Sedimentation equilibrium	8,000
	Molecular weight	Viscosity ($K_m = 11 \times 10^{-4}$)	8,000
	Molecular weight	Diffusion (spherical particle)	12,500
	Molecular weight	Diffusion (axial ratio = 6)	7,400
	Molecular weight	Chemical (iodine No.) (11)	2,000
Acetylated water soluble	Molecular weight	Viscosity ($K_m = 11 \times 10^{-4}$)	13,000
	Molecular size	Spreading ($D.P. = 50$)	8.8 A. x 15,000 A. ²
	Shape factor	Spreading ($D.P. = 50$)	25 to 1
Deacetylated water soluble	Molecular weight	Viscosity ($K_m = 11 \times 10^{-4}$)	10,000
	Molecular weight	Osmotic pressure	8,500
1 per cent sodium hydroxide soluble	Molecular weight	Viscosity ($K_m = 11 \times 10^{-4}$)	8,000
	Molecular weight	Chemical (iodine No.) (11)	4,000
Acetylated 1 per cent sodium hydroxide soluble	Molecular weight	Viscosity ($K_m = 16 \times 10^{-4}$)	13,500
	Molecular weight	Spreading ($D.P. = 56$)	7.8 A. x 1900 A. ²
	Shape factor	Spreading ($D.P. = 56$)	40 to 1
5 per cent sodium hydroxide soluble	Molecular weight	Viscosity ($K_m = 11 \times 10^{-4}$)	8,000
	Molecular weight	Chemical (iodine No.) (11)	10,000
Acetylated 5 per cent sodium hydroxide soluble	Molecular weight	Viscosity ($K_m = 16 \times 10^{-4}$)	13,600
	Molecular size	Spreading ($D.P. = 59$)	8.7 A. x 1900 A. ²
	Shape factor	Spreading ($D.P. = 59$)	29 to 1
Beta cellulose	Molecular weight	Viscosity ($\frac{D.P.}{\eta} = 260$) (6)	3,000-15,000
Gamma cellulose	Molecular weight	Viscosity ($\frac{D.P.}{\eta} = 260$)	3,000

0.056 and 0.062, respectively. Taking K_m as 11×10^{-4} , degrees of polymerization of 50 and 56 were obtained, which gave molecular weights of 7500 and 7850, respectively, for the fractions soluble in 1 per cent and 5 per cent sodium hydroxide. These results are in close agreement with those obtained for the

water-soluble fraction. Apparently, the solubility difference between the three fractions is one of chemical constitution and not one of molecular weight.

Acetylation of both fractions gave material that was only 50 per cent soluble in chloroform, the undissolved portion being only swollen by the solvent. Extrapolation of the straight-line portions of the η_{sp}/C versus C curves to $C = 0$ gave η_{sp}/C values of 0.090 and 0.095, respectively, for the fractions soluble in 1 per cent and 5 per cent sodium hydroxide. Using $K_m = 11 \times 10^{-4}$, which was the same as used for the acetylated water-soluble fraction, polymerization degrees of 82 and 86 were found, which correspond to a molecular weight of about 19,800 for both fractions. Here again is evidence that the Staudinger constant varies considerably with different materials and cannot be used as a universal constant. A K_m value of about 16×10^{-4} would give degrees of polymerization for these fractions more in keeping with that found for the unacetylated material.

Spreading measurements

The acetylated material from the fractions of holocellulose which were soluble in 1 per cent and 5 per cent sodium hydroxide, respectively, spread nicely on the water surface from a chloroform solution. Pressure-area curves, obtained on the film balance, extrapolated to 34 and 29 sq. A., respectively. Both of these values are in good agreement with those found for the acetylated water-soluble fractions.

Assuming a density of 1.5, film thicknesses of 7.8×10^{-8} and 8.7×10^{-8} cm. were obtained. The molecular volume for both fractions is $14,850 \times 10^{-24}$ cc. which, on assumption of a molecular radius equal to one-half the film thickness, gave molecular lengths of 310×10^{-8} cm. and 250×10^{-8} cm., respectively, and shape factors of 40 to 1 and 29 to 1. These calculations are based on a K_m of 16×10^{-4} , used in calculating molecular volumes.

SUMMARY AND CONCLUSIONS

Aspen sawdust, extractive-free, was delignified by alternate chlorination and extraction with monoethanolamine. The holocellulose so obtained was separated into four main fractions: (1) a water-soluble fraction; (2) a fraction soluble in 1 per cent sodium hydroxide; (3) a fraction soluble in 5 per cent sodium hydroxide; and (4) a residue consisting mainly of alpha cellulose. Molecular properties of the first three fractions were determined by as many of the classical methods as could be applied. Table 2 presents a summary of the results obtained.

REFERENCES

- (1) ADAM, N. K.: *The Physics and Chemistry of Surfaces*, Chap. II. Oxford University Press, London (1930).
- (2) EINSTEIN, A.: Ann. Physik [4] **19**, 289 (1906); **34**, 591 (1911).
- (3) EISENSCHITZ, R.: Z. physik. Chem. **A163**, 133 (1933).
- (4) FRIEDMAN, L., AND RAY, B. R.: J. Phys. Chem. **46**, 1140 (1942).
- (5) HIBBERT, H.: Can. J. Research **15B**, 490 (1937).
- (6) KRAEMER, E. O.: Ind. Eng. Chem. **30**, 1200 (1938).
- (7) KUHN, W.: Z. physik. Chem. **A161**, 1 (1932).
- (8) MCBAIN, J. W.: J. Am. Chem. Soc. **55**, 545 (1933).

- (9) MCBAIN, J. W., DAWSON, C. R., AND BARKER, H. A.: *J. Am. Chem. Soc.* **56**, 1021 (1934).
- (10) MCBAIN, J. W., AND LIU, T. H.: *J. Am. Chem. Soc.* **53**, 59 (1931).
- (11) MITCHELL, R. L., AND RITTER, G. J.: *J. Am. Chem. Soc.* **62**, 1958 (1940).
- (12) MOUQUIN, H., AND CATHCART, W. H.: *J. Am. Chem. Soc.* **57**, 1791 (1935).
- (13) NEURATH, H.: *J. Am. Chem. Soc.* **61**, 1842 (1939).
- (14) NORTHRUP, J. H., AND ANSON, M. L.: *J. Gen. Physiol.* **12**, 543 (1929).
- (15) ONSAGER, L.: *Phys. Rev.* **40**, 1029 (1932).
- (16) PERRIN, J.: *J. phys. radium* **7**, 1 (1936).
- (17) POLSON, A.: *Kolloid-Z.* **88**, 51 (1939).
- (18) POLSON, A.: *Nature* **137**, 740 (1936).
- (19) RITTER, G. J.: *Ind. Eng. Chem., Anal. Ed.* **1**, 52 (1929).
- (20) RITTER, G. J., AND KURTH, E. F.: *Ind. Eng. Chem.* **25**, 1250 (1933).
- (21) STAUDINGER, H.: *Trans. Faraday Soc.* **29**, 26 (1933).
- (22) STAUDINGER, H.: *Papier-fabr.* **36**, 381 (1939).
- (23) SVEDBERG, T.: *Proc. Roy. Soc. (London)* **B127**, 1 (1939).
- (24) VAN BECKUM, W. G., AND RITTER, G. J.: *Paper Trade J.* **105**, 127 (1937).
- (25) WHITE, E. V.: *J. Am. Chem. Soc.* **64**, 302, 2836 (1942).

SEDIMENTATION CONSTANTS OF PURIFIED PREPARATIONS OF STRAINS OF INFLUENZA VIRUS^{1,2}

W. M. STANLEY AND M. A. LAUFFER³

Department of Animal and Plant Pathology, The Rockefeller Institute for Medical Research, Princeton, New Jersey

Received August 8, 1946

INTRODUCTION

During the course of a comprehensive investigation of influenza virus, carried out with a view to the development of useful vaccines (7), a study was made of the biophysical properties of purified influenza virus preparations obtained by means of differential centrifugation (3). Electron micrographs of preparations of the PR8 strain showed slightly irregular, spherical particles with an average diameter of 115 m μ . The sedimentation rate was found to vary inversely with the concentration of virus, and this was found to be due to the variation of solution viscosity with concentration. When purified preparations were examined at high concentrations in the ultracentrifuge there was observed, in addition to the virus, a more slowly sedimenting component. The amount of this component was found to vary from preparation to preparation and from strain to strain of virus. It was separated from the virus and was found to possess no virus ac-

¹ Presented at the Twentieth National Colloid Symposium, which was held at Madison, Wisconsin, May 28-29, 1946.

² The work described in this paper was done under a contract, recommended by the Committee on Medical Research, between the Office of Scientific Research and Development and The Rockefeller Institute for Medical Research.

³ Present address, University of Pittsburgh, Pittsburgh, Pennsylvania.

tivity (6). However, this material was found to possess a very high viscosity; hence the viscosity of the usual preparations of influenza virus can be explained as being due in large part to the presence of the more slowly sedimenting component.

Sedimentation studies on influenza virus in sucrose solutions of varying densities showed a non-linear dependence of sedimentation rate upon solvent density, indicating that the density in solution increases with increasing sucrose concentration (3). However, similar studies carried out in bovine albumin solutions showed a linear relationship between rate of sedimentation and solvent density (4). The results indicated that the density of the PR8 strain of influenza virus is about 1.1, and that the virus particles contain about 60 per cent by weight of water (3, 4).

Several strains of influenza virus are known (1). Most of these fall into two groups, Type A strains, of which PR8 is a representative, and Type B strains, of which Lee is a representative. Under comparable conditions, the sedimentation constants of the PR8 and Lee strains are about 700 and 800 S, respectively (3, 5, 7). Since the Type A strains and the Type B strains do not cross-immunize (1), it is necessary to have representatives of both present in a vaccine in order to secure protection against influenza virus strains of these two common types. During studies on the preparation of such vaccines it was noted that the completed vaccine showed only a single sedimenting boundary in the ultracentrifuge, despite the fact that it contained equal parts of Type A and Type B strains with sedimentation constants of about 700 and 800 S, respectively (6). The sedimentation constant of the material in the vaccine had a value intermediate between those of the separate components of the vaccine. Because it seemed unusual for components having sedimentation constants of about 700 and 800 S to yield a mixture showing only a single sedimenting boundary with an intermediate sedimentation constant, further studies of the sedimentation behavior of strains and of mixtures of strains of influenza virus were carried out. The results of this study are reported in the present paper.

EXPERIMENTAL

In order to establish the reproducibility of the sedimentation behavior of different strains of influenza virus, samples of Lee virus, the only Type B strain studied, were obtained from three different laboratories and used as inocula. Preparations made in this laboratory were found, under comparable conditions, to yield sedimentation constants essentially identical with that of the Lee virus customarily used in this laboratory. In addition, samples of PR8 virus from three different laboratories were found to yield preparations which possessed the same sedimentation constant, under comparable conditions, as that of the PR8 virus customarily used in this laboratory. Other representatives of Type A virus, such as F12, WS, and swine, were found to possess sedimentation constants which varied considerably from preparation to preparation. However, when these were corrected for solution viscosity (3), values essentially identical with that of the PR8 strain were obtained. It appears that the Lee, as well as

the Type A strains, tends to contain different but characteristic amounts of the low-molecular-weight impurity possessing a high viscosity. Preparations of the F12 strain tend to contain the largest amount of this impurity. The swine, WS, and Lee preparations tend to contain smaller amounts and the PR8 preparations the smallest amount of this impurity. Highly viscous material of low molecular weight has been separated and purified from normal allantoic fluid and from preparations of Lee, PR8, and F12 viruses (2, 3, 6). The properties of the materials from the different sources appear to be quite similar. When such materials from normal allantoic fluid or from Lee virus preparations were added to purified PR8 virus preparations, they were found to decrease the sedimentation constant of the PR8 virus. Because of the large effect on the rate of sedimentation which can accompany an increase in viscosity, and because of the fact that different virus preparations can contain different amounts of this highly viscous impurity, it is obvious that it is necessary to correct the sedimentation constants of influenza virus preparations for the viscosity of the solution if results that are directly comparable are to be obtained.

The first vaccine used in these studies, which has been described earlier (6), was prepared from Lee, PR8, and Weiss influenza virus materials produced in chick embryos and concentrated and purified by means of two cycles of differential centrifugation. The intrinsic viscosities of the Lee, PR8, and Weiss virus preparations, before incorporation into a vaccine, were found to be 34.8, 16.1, and 39.9. Since highly purified preparations of PR8 influenza virus have been found to have an intrinsic viscosity as low as 11.3, these results indicate that the three preparations contain impurities possessing a high viscosity. The amount of this impurity appeared to be low in the PR8 virus preparation and somewhat higher in the other two preparations. The sedimentation constants of the Lee, PR8, and Weiss preparations at a concentration of 2.5 mg. per cubic centimeter in 0.05 *M* phosphate buffer and corrected for solution viscosity (3) were found to be 832, 719, and 700 S, respectively. A formalinized mixture consisting of two parts of Lee virus, one part of PR8 virus, and one part of Weiss virus was found to show a single sedimenting boundary in the ultracentrifuge with a sedimentation constant, corrected for solution viscosity, of 790 S. In experiments with individual strains the addition of formalin at the concentration usually used in vaccines, 1 part per 2000 or less, was not found to affect the sedimentation constant of the virus.

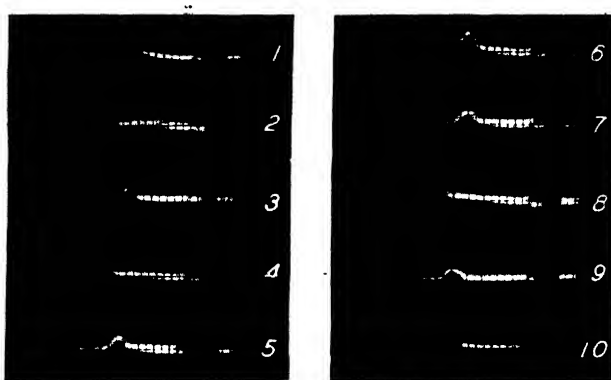
The second vaccine, which was manufactured by a commercial biological company, was prepared in a manner comparable to that of the first vaccine. The Lee, PR8, and Weiss preparations were examined at a concentration of about 4 mg. per cubic centimeter and found to have sedimentation constants, not corrected for solution viscosity, of 755, 620, and 698 S, respectively. The formalinized mixture of these components was found to show a single sedimenting boundary with a sedimentation constant, not corrected for solution viscosity, of 699 S. A third vaccine was prepared by another commercial biological company by means of a single cycle of differential centrifugation. The Lee, PR8, and Weiss virus preparations were examined at a concentration of 2 mg. per cubic

TABLE 1
The sedimentation of influenza A and influenza B virus preparations before and after mixing

VIRUSES USED	INFLUENZA A					INFLUENZA B					MIXTURE				SOLVENT	
	Virus concentration	$\frac{\eta}{\eta_0}$	S_{20}^{w*}	$S_{20}^{w*} \frac{\eta^*}{\eta_0}$	Reference to figure	Virus concentration	$\frac{\eta}{\eta_0}$	S_{20}^{w*}	$S_{20}^{w*} \frac{\eta^*}{\eta_0}$	Reference to figure	Concentration of each virus	$\frac{\eta}{\eta_0}$	S_{20}^{w*}	$S_{20}^{w*} \frac{\eta^*}{\eta_0}$		Reference to figure
PR8 No. 1 and Lee No. 1	2.5	1.041	663	690		2.5	1.091	730	796		5	1.168	612	715	1	0.05 M phosphate, pH 7
											2.5	1.08	669	721		0.05 M phosphate, pH 7
PR8 No. 2 and Lee No. 2	5	1.112	625	695	3	5	1.243	667	830	2	2.5	1.172	626	734	4	0.1 M phosphate, pH 7
											1.25		657		5	0.1 M phosphate, pH 7
WS No. 1 and Lee No. 3	5.1	1.17	576	674	9	5.1	1.14	703	802	8	2.5		478		6	1.0 M sodium chloride
											2.5		652		7	0.1 M phosphate, pH 9
											2.55	1.15	569	656	10	0.1 M phosphate, pH 7

*Svedberg units.

centimeter and found to have sedimentation constants, not corrected for solution viscosity, of 781, 679, and 697 S, respectively. The formalinized mixture of



The figures show one, usually the fourth, of a series of photographs, taken at 5-min. intervals during sedimentation at 11,100 R.P.M. in an ultracentrifuge, of the Svensson schlieren diagrams of different preparations of influenza virus. The preparations are described in the text of the paper. The sedimentation-constant determinations were made by Mr. H. K. Schachman. s_{η} indicates that the sedimentation constant has been corrected for solution viscosity.

FIG. 1. Mixture containing 5.0 mg. of a purified preparation of Lee influenza virus and 5.0 mg. of a purified preparation of PR8 influenza virus per cubic centimeter in 0.05 *M* sodium phosphate at pH 7. The picture is the third in the series. $s_{\eta} = 715$ S.

FIG. 2. Purified preparation of Lee influenza virus at a concentration of 5 mg. per cubic centimeter in 0.1 *M* phosphate buffer at pH 7. $s_{\eta} = 830$ S.

FIG. 3. Purified preparation of PR8 influenza virus at a concentration of 5 mg. per cubic centimeter in 0.1 *M* phosphate buffer at pH 7. The picture is the third in the series. $s_{\eta} = 695$ S.

FIG. 4. Mixture containing equal parts of the Lee and PR8 influenza virus preparations described in figures 2 and 3. $s_{\eta} = 734$ S.

FIG. 5. Same as figure 4 except at a concentration of 1.25 mg. per cubic centimeter for each virus preparation. The picture is the third in the series. $s_{20}^w = 657$ S.

FIG. 6. Same as figure 4 except in 1.0 *M* sodium chloride. $s_{20}^w = 478$ S.

FIG. 7. Same as figure 4 except at pH 9. The picture is the third in the series. $s_{20}^w = 652$ S.

FIG. 8. Purified preparation of Lee influenza virus at a concentration of 5.1 mg. per cubic centimeter in 0.1 *M* phosphate buffer at pH 7. $s_{\eta} = 802$ S.

FIG. 9. Purified preparation of WS influenza virus at a concentration of 5.1 mg. per cubic centimeter in 0.1 *M* phosphate buffer at pH 7. $s_{\eta} = 674$ S.

FIG. 10. Mixture containing equal parts of the Lee and WS influenza virus preparations described in figures 8 and 9. $s_{\eta} = 840$ and 656 S.

these components showed a single sedimenting boundary which possessed a sedimentation constant, not corrected for solution viscosity, of 747 S.

In order to secure additional information concerning the sedimentation behavior of strains of influenza virus, preparations of the Lee strain of influenza B virus and the PR8 strain of influenza A virus were studied in the ultracentrifuge before mixing and after mixing. The virus preparations were obtained by two

cycles of differential centrifugation. Two different preparations of each virus were studied. The results obtained are shown in table 1. It can be seen that even though the two PR8 preparations had much lower sedimentation rates than the two Lee preparations, in both experiments the mixtures showed single boundaries corresponding to sedimentation constants of intermediate values. The substitution of molar sodium chloride for tenth molar phosphate buffer did not result in resolution of the components. Similar results were obtained when the solvent was adjusted to pH 9 and also when the concentration of the phosphate buffer at pH 7 was increased to 1.0 molar. Sedimentation diagrams for the virus preparations before mixing and after mixing are shown in figures 1 to 7, inclusive. The virus or mixture represented in each figure can be identified by referring to table 1.

In order to determine whether a different representative of the Type A virus would behave in a manner similar to that of the PR8 strain when mixed with the Lee strain of influenza B virus, freshly prepared samples of Lee virus and of the WS strain of influenza A virus were examined. The results obtained with these viruses before and after mixing are also shown in table 1. It can be seen that in this case, the mixture was resolved into two components in the ultracentrifuge, with corrected sedimentation constants of 656 and 840 S. Sedimentation diagrams of the two viruses and of the mixture are reproduced in figures 8, 9, and 10. The results indicate that, whereas the mixture of Lee and PR8 viruses has only a single sedimenting boundary, the mixture of Lee and WS viruses is resolved into two sedimenting components.

DISCUSSION

The inability to resolve mixtures of PR8 and Lee viruses into two separate boundaries with the ultracentrifuge is possibly the result of the natural heterogeneity of the preparations. The size of the influenza virus particle is such that the diffusion rate must be negligible. Therefore, the boundary spreading observed in sedimentation studies with virus purified by centrifugation must be due to heterodispersity. It was estimated in a previous study that the sedimentation rate of centrifugally purified preparations of the PR8 strain of influenza A virus could be characterized by a mean value of 722 Svedberg units with a standard deviation of about 8 per cent of the mean (3). Sharp and co-workers reported qualitatively similar heterodispersity for PR8, swine, and Lee influenza viruses (5). The results shown in the present report indicate comparable degrees of heterogeneity.

For the purpose of understanding the effect of heterodispersity upon resolvability in the ultracentrifuge, let it be supposed that a virus preparation consists of a family of particles distributed, with respect to sedimentation rate, according to the normal law. If a mixture of two preparations with mean sedimentation rates of 700 and 800 S, respectively, and with standard deviations of 8 per cent of the means are subjected to ultracentrifugation, roughly one-sixth of the particles in the fast-moving population will sediment with rates below 736 S and roughly one-sixth of the particles from the more slowly sedimenting popula-

tion will sediment with rates greater than 756 S. About one-fourth of the faster moving population will sediment more slowly than this latter rate. Thus, it is obvious even at the qualitative level that it will be impossible to separate absolutely two such populations, no matter how extensive the centrifugation. It can be shown readily by graphical means that two normal curves, each with a standard deviation of 8 per cent of its mean and with means at 700 and 800 S, respectively, will overlap considerably. They add up to a curve with a single maximum which is only slightly different in shape from a normal curve with a mean of 750 S and a standard deviation of 11 per cent. Only a fairly sensitive optical system, such as the scale system, would be capable of distinguishing between the curve obtained as the sum of the two normal curves and the normal curve constructed about the new mean. The schlieren system used in these studies is not capable of such a sensitive resolution. Thus, it should be expected that a mixture of two viruses, one with a mean sedimentation rate of 700 S and a standard deviation of 8 per cent and the other with a mean rate of 800 S and a standard deviation of 8 per cent, would sediment with a single boundary indistinguishable by other than very sensitive means from that of a single population with a mean rate of 750 S and a standard deviation of 11 per cent. In a general sort of way, the results obtained with mixtures of PR8 and Lee influenza viruses are consistent with the interpretation that they cannot be resolved into two boundaries because the sedimentation rates of their respective populations overlap too much.

It can be shown by a simple application of calculus that, when two normal curves with the same areas and the same standard deviations, but constructed about different means, are added, a curve with a single maximum will be obtained if the difference between the means is less than the sum of the two standard deviations. On the other hand, if the difference between the two means is greater than the sum of the two standard deviations, the curve obtained by adding the two normal curves will have two maxima, separated by a minimum. In other words, it will resemble a bi-modal frequency distribution. When a curve of this latter type is obtained in an ultracentrifugation experiment, it is fairly obvious evidence for two sedimenting populations. However, when a curve of the former type is obtained, it is not easy to estimate whether one or more than one population is present. The situation is qualitatively similar, though somewhat more complex, when the standard deviations of the two populations are not identical. However, the mathematical treatment for the simplified case is adequate to illustrate that the ability or lack of ability to resolve a mixture of two populations in the ultracentrifuge into a bi-modal diagram depends upon the relationship of the difference between the mean sedimentation rates of the two populations to the sum of their standard deviations. In the example chosen for analysis in the preceding paragraph, the sum of the standard deviations exceeded the difference between the means by only a small amount. If a mixture were made of two virus populations in which either the difference between the mean rates was slightly more or the sum of the standard deviations slightly less than in the example chosen, then the two populations

could be resolved readily with the ultracentrifuge. It is entirely possible that an interpretation of this sort can explain the ability to resolve a mixture of WS and Lee viruses even though mixtures of PR8 and Lee viruses cannot be resolved.

The relationship of the difference between the mean sedimentation rates and the sum of the standard deviations encountered in mixtures of two preparations of influenza virus may be in such a critical state that only a small shift of either will determine whether or not the mixture is readily resolvable. The accuracy of the data presented in figures 1 to 10 is not such as to afford an opportunity for a really critical test of the theory here presented. However, the explanation suggested for the ability to resolve mixtures of Lee and WS but not mixtures of Lee and PR8 viruses does seem to be both possible and plausible.

The viscosity of purified influenza virus preparations appears to be dependent largely upon the presence of a highly viscous impurity of lower molecular weight. The amount of this impurity present in purified virus preparations tends to be characteristic of the strain of the virus, but the amount can also vary from preparation to preparation of the same virus strain, hence it is necessary in all cases to correct for the solution viscosity in order to secure sedimentation constants that are directly comparable. However, it seems unlikely that this impurity or the viscosity effects which it produces can provide an explanation for the present results, for in some instances preparations of Lee and PR8 viruses possessing essentially the same intrinsic viscosity were mixed and yet failed to show the presence of two sedimenting boundaries in the ultracentrifuge. It is obvious that additional studies on the physicochemical properties of the different strains of influenza virus are indicated.

SUMMARY

Mixtures of purified preparations of PR8 and Weiss influenza viruses, which belong to Type A and possess sedimentation constants near 700 S, with Lee influenza virus, a Type B virus with a sedimentation constant of about 800 S, show only a single sedimenting boundary in the ultracentrifuge with an intermediate sedimentation constant. Similar results were obtained with mixtures of PR8 and Lee influenza viruses. The mixtures of PR8 and Lee influenza viruses also showed only a single sedimenting boundary when studied at different concentrations, in 1.0 *M* sodium chloride, in 1.0 *M* phosphate buffer at pH 7, or in 0.1 *M* phosphate buffer at pH 9. However, when a preparation of WS influenza virus, another Type A strain possessing a sedimentation constant, corrected for solution viscosity, of 674 S, was mixed with a preparation of Lee influenza virus possessing a sedimentation constant, corrected for solution viscosity, of 802 S, two sedimenting boundaries with corrected sedimentation constants of 656 and 840 S were observed. The inability to resolve mixtures of equal concentrations of PR8 and Lee viruses can be explained on the basis of the assumption that both virus populations are heterodisperse with respect to sedimentation rate and that the difference between the mean sedimentation rates is less than the sum of the standard deviations of the two distributions. The ability to resolve the mixture of the WS and the Lee strains, when present in equal concentrations,

can be explained on the assumption that the difference between the mean sedimentation rates is somewhat more than the sum of the standard deviations of the two distributions. Earlier studies indicating the advisability of correcting sedimentation constants of influenza virus preparations for solution viscosity, because of the presence in such virus preparations of variable amounts of a viscous impurity, have been confirmed.

REFERENCES

- (1) FRANCIS, T., JR.: Harvey Lectures **37**, 69 (1941).
- (2) KNIGHT, C. A.: J. Exptl. Med. **80**, 83 (1944).
- (3) LAUFFER, M. A., AND STANLEY, W. M.: J. Exptl. Med. **80**, 535 (1944).
- (4) SHARP, D. G., TAYLOR, A. R., McLEAN, I. W., JR.: BEARD, D., AND BEARD, J. W.: Science **100**, 151 (1944).
- (5) SHARP, D. G., TAYLOR, A. R., McLEAN, I. W., JR., BEARD, D., AND BEARD, J. W.: J. Biol. Chem. **156**, 585 (1944).
- (6) STANLEY, W. M.: J. Exptl. Med. **79**, 267 (1944).
- (7) STANLEY, W. M.: J. Exptl. Med. **81**, 193 (1945).

ON A LOW-DENSITY LIPOPROTEIN APPEARING IN NORMAL HUMAN PLASMA¹

KAI O. PEDERSEN

*Institute of Physical Chemistry, University of Upsala, Upsala, Sweden**Received August 8, 1946*

At the beginning of the 1930's von Mutzenbecher (6) made a study of several normal sera in the ultracentrifuge. Amongst other things he found that when the same serum was investigated at different concentrations the ratio albumin/globulin, calculated from the sedimentation diagrams, increased with increasing serum concentration.

In 1933-34 McFarlane (5) studied a number of different dilutions of various sera, and obtained results in concordance with those of von Mutzenbecher. The same was also the case for "artificial sera" made from mixtures of serum albumin and serum globulin. No reasonable explanation for this concentration effect has so far been given.

McFarlane also noticed the presence of a component with a sedimentation constant between those for albumin and globulin; he named this the "X-protein." It was generally most distinct in the concentrated human sera, but disappeared into the "albumin" peak in the dilute ones. Although the concentration of the X-protein in normal human serum amounted to 20-30 per cent of the total protein, McFarlane did not succeed in isolating this substance, nor did he observe

¹ Presented at the Twentieth National Colloid Symposium, which was held at Madison, Wisconsin, May 28-29, 1946.

it in the albumin or the globulin fractions obtained by precipitation with ammonium sulfate. A reëxamination of McFarlane's sedimentation diagrams from the normal globulin fractions shows, however, the presence of a slower moving component which McFarlane assumed to be serum albumin. According to the author's experience, serum albumin is not precipitated by half-saturated ammonium sulfate unless the pH of the mixture is adjusted to 5 or below. A protein with properties in the ultracentrifuge similar to those of McFarlane's X-protein is precipitated, however, by 45–60 per cent saturated ammonium sulfate. Since McFarlane did not wash his precipitate, a small amount of albumin might have been present in this in the form of mother liquor, but this cannot account for the large quantity of substance sedimenting more slowly than the normal globulin, in one case 43 per cent and in another 22. The major part of this component must undoubtedly have consisted of the "X-protein." Likewise, in the sedimentation experiments with the albumin fraction, some X-protein surely must have been hidden in the "albumin peak."

In the following, some studies on the nature of this X-protein will be given.

THE INFLUENCE OF VARIOUS SALTS ON THE APPEARANCE OF THE X-PROTEIN

Several years ago, it was found by the author (4, 10) that the sedimentation diagram for human serum was extremely sensitive to small variations in the salt concentration of the solution, especially when the concentration is close to that prevailing under physiological conditions. A more systematic study with various salts was then started (8).

Figure 1 shows the effect of varying the concentration of added potassium chloride. It is seen that the diagram is most sensitive to small changes in the salt concentration when this is between 0.15 and 0.35 *M* potassium chloride.

When the influence of the nature of the salt was studied further, it was found that some salts already showed very pronounced effects at low concentrations, while others were apparently not capable, within reasonable salt concentrations, of affecting human serum. Simultaneous investigations on other sera—cow, horse, rabbit, and pig—did not reveal any salt effect.

Different electrophoretically isolated fractions from human serum were also investigated with respect to the salt effect. It was found that the ($\beta + \gamma$)-globulin fraction contained one component with $s_{20} \sim 7$ S, another component whose sedimentation constant varied with the salt concentration ($3 < s_{20} < 5$), and finally some inhomogeneous material. When the γ -globulin fraction was examined alone in the ultracentrifuge, it showed mainly the normal globulin sedimentation with $s_{20} \sim 7$ S independent of the salt concentration. It can be concluded, therefore, that the labile X-protein is a β -globulin (see 10, page 400).

Attempts to correlate the effect with chemical and physical properties of the salt solutions were in vain until finally it was found that the whole effect was dependent upon the density of the solution. A given density would produce almost the same effect on the sedimentation diagram irrespective of the salts present. This means that the whole effect is due to a difference in specific volume between the albumin and the X-protein. It means also that when

the sedimentation constant is calculated in the routine way, an incorrect value for s_{20} is obtained.

In figure 2 the routine calculated sedimentation constants for both the albumin and the X-protein (β -globulin) peak have been plotted against the density of the solvent. For both peaks the line of regression has been determined. It is seen that the albumin line is almost parallel to the abscissa, as it should be if the right value for V is used. (In fact, the correct value for albumin is $V = 0.736$.) For the X-protein, however, s_{20} varies very strongly with the density, which means that its specific volume must be quite different from 0.75, and close

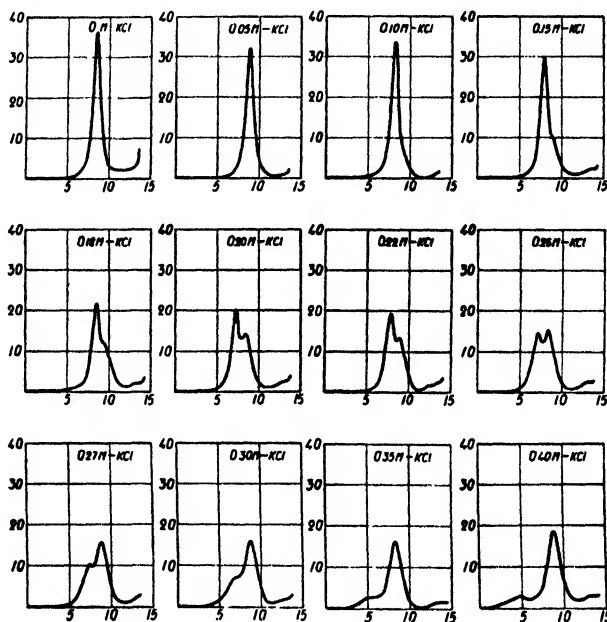


FIG. 1. The effect of varying the concentration of potassium chloride on the sedimentation diagram for normal human serum. All diagrams recalculated to the same theoretical scale distance; 1-mm. exposures taken 130 to 145 min. after reaching full speed; mean temperature = 27°C.; serum concentration = 0.4 C_0 .

to 1. As the line of regression for the X-protein crosses the abscissa between 1.03 and 1.04, it means that in solution with densities above 1.04 the X-protein will rise to the top of the cell instead of sediment toward the bottom. The low density of the X-protein has been used in the isolation of this protein.

THE INFLUENCE OF THE SERUM CONCENTRATION ON THE APPEARANCE OF THE X-PROTEIN

It has been found that the size of the X-protein peak, for a given salt concentration, depended upon the serum concentration. In order to study this phenomenon, a normal human serum and the corresponding plasma were dialyzed against a citrate-phosphate buffer of such a density that the X-protein and the

albumin peaks could be easily measured separately from the sedimentation diagrams. A number of solutions with concentration varying from about 2 per cent to about 5 per cent were then studied in the ultracentrifuge. Some of the sedimentation diagrams from the experiments on serum are given in figure 3, and all the results have been summarized in figure 4.

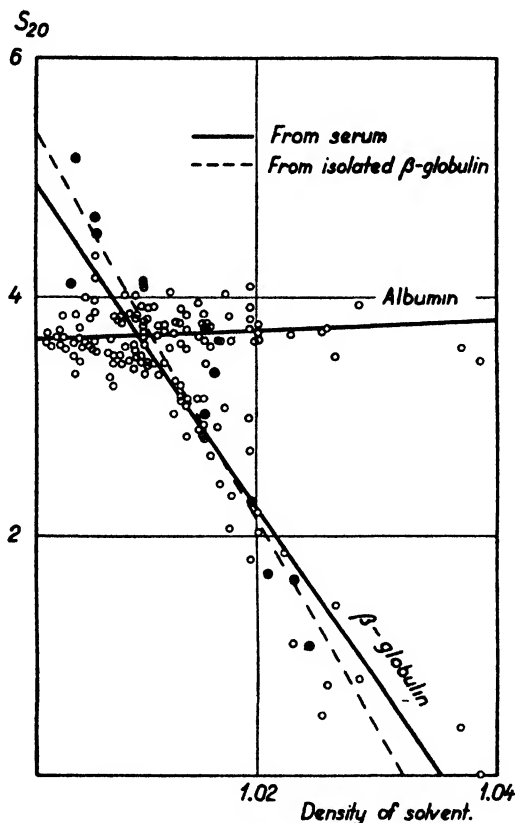


FIG. 2. The variation of s_{20} for albumin and β -globulin (X-protein) with the density of the solution. In this calculation a specific volume of 0.75 has been assumed for both proteins. \circ refers to values obtained in runs with serum. Serum concentration = 0.4 C_0 . \bullet refers to values from runs on X-protein isolated as described on page 160.

From figure 3 it is seen that the X-protein is not visible in the lowest concentration, but is very distinct in the 5 per cent solution. From figure 4 it is seen that the total protein concentration calculated from the sedimentation diagram increases proportionally with Δn , as it should do. For the albumin and the globulin, however, this is not the case; their increase is less than what could be expected. The X-protein, on the other hand, does not start until Δn is about 0.0035, but its concentration then increases linearly with Δn of the solution. It therefore seems likely that some albumin and globulin in the more concentrated solutions enter into the X-protein complex.

This view is also strengthened by the finding that if purified human globulin is added to a fresh solution of human serum, the X-protein peak increases, whereas the normal globulin peak augments much less than expected. If the

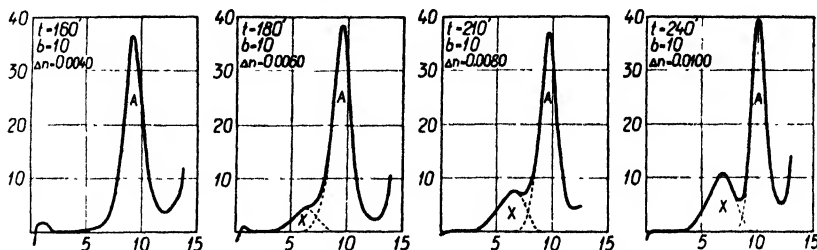


FIG. 3. Variation of sedimentation diagram of human serum with protein concentration. The diagrams have all been reduced to the same protein concentration and scale distance, so that they are strictly comparable. t gives the time in minutes after the centrifuge has reached full speed, b is the scale distance, and Δn is the measured difference between the refractive index of the protein solution and that of the buffer solution. X = X-protein; A = albumin.

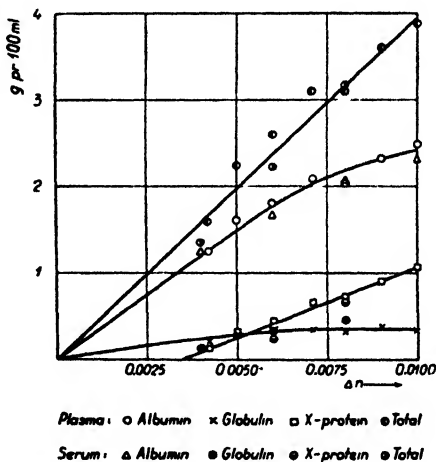


FIG. 4. Variation of the concentration of the individual components of human serum and plasma with Δn for the solution, as calculated from the sedimentation diagram. For the calculation of the protein concentration from the sedimentation diagram, it has been assumed that $\Delta n = 0.00189$ was equal to a protein concentration of 1 g. protein per 100 ml. of solution.

serum is old or if a globulin other than human is used, the normal globulin peak is enlarged exactly as one would expect.

ISOLATION OF THE X-PROTEIN FROM HUMAN SERUM

As mentioned earlier, the low density of the X-protein may be used for its isolation. If 35 ml. of normal human serum is mixed with 25 ml. of saturated magnesium sulfate no precipitation takes place usually, but if this solution is spun in an air-driven centrifuge at 27,000 R.P.M. for 6 hr., an oily layer will

collect at the top of the centrifuge tubes. This oil consists mainly of the X-protein. It may be further purified by resuspension in half-saturated magnesium sulfate and respinning in the centrifuge, but a large amount of X-protein is lost by this procedure, probably owing to the splitting off of albumin and globulin from the X-protein.

If such a purified X-protein solution is dialyzed against 0.2 *M* sodium chloride and studied in the ultracentrifuge, it shows a sedimentation diagram like the left-hand one in figure 5; the sedimentation constant for the main peak corresponds almost to that for albumin. If, however, the density of the solution is increased, as in the right-hand diagram, the peak splits into two peaks, one sedimenting as albumin and the other, marked β , at a slower rate.

A number of experiments have been carried out in solutions of X-protein isolated in the manner just described. In figure 2 the routine values obtained for

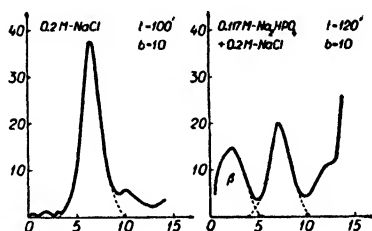


FIG. 5. Sedimentation diagrams from runs with an X-protein isolated from human serum.

s_{20} for this β -globulin have been plotted against the density of the solution. The dotted line gives the line of regression for this component. From this a value of $V = 0.97$ is calculated for the hydrated particle. The partial specific volume of the unhydrated particle is probably lower.

From the line of regression we obtain a value of $s_{20} = 5.9$ S in water. If it be assumed that the particle is spherical, we have a particle weight of about 1.9×10^6 .

A diffusion experiment, made on the same material, gave $D_{20} = 1.7 \times 10^{-7}$. From this value, $s_{20} = 5.9$ S and $V_{20} = 0.97$, a particle weight of 2.6×10^6 is obtained for the hydrated X-protein.

The phosphorus content of the X-protein is very high, and it has been estimated that between 20 and 45 per cent of the X-protein consists of phosphatides (8). These values are much higher than those given by Blix *et al.* (3) for electrophoretically prepared β -globulin. Recently, however, still higher values for the phosphatide content of a β_1 -globulin from human plasma have been found at the Harvard Medical School (7), and this β_1 -globulin shows the same properties as the X-protein. In connection with the method of isolating the X-protein just described, it may be of interest to note the following: It has always been found (8) that in the range 0.5 to 0.6 saturation with ammonium sulfate (pH above 5) the precipitates are very difficult to clear with the centrifuge. They generally rise to the top of the centrifuge tubes, and it is necessary to filter the

solutions in order to collect these fractions. Electrophoretic examination showed that they were rich in β_1 - and β_2 -globulins, but in addition both albumin and α -globulin were always present. A similar low-density protein has recently been described by Adair and Adair (1), but this protein must, according to their serological tests, probably have been a comparatively pure β -globulin.

DISCUSSION

From what has been said above it appears most likely that the X-protein in human serum is a reversible dissociable compound consisting of β -globulin and variable amounts of albumin, γ -globulin, and lipids. In concentrated serum it will contain rather large amounts of albumin and globulin, but as the serum is diluted or the X-protein is purified, the albumin and the globulin are split off.

If the albumin and the globulin are taken up by the X-protein, one would expect that the sedimentation constant for the X-protein compound would increase parallel with the increase in its content of the more dense proteins. So far, however, no such increase has ever been observed.

According to some recent experiments by Blix and the author, the electrophoresis diagram for human serum is hardly changed when the lipids are extracted according to Blix (2), but the sedimentation diagram is much altered in so far as the X-protein has completely disappeared from the diagram. As at the same time the albumin peak has increased, it must be supposed that the main part of the β -globulin, after extraction, sediments at the same rate as the albumin. Thus in this case it is only the centrifuge that can tell us whether or not some change in the protein solution has occurred.

The presence of the X-protein can only be demonstrated in fresh human serum. As the serum becomes old it loses its ability to form an X-protein. This sensitivity of the X-protein is after all due to the lipid part of the compound, where reesterification and hydrolysis may take place, thus giving rise to new substances with different properties (e.g., lecithin \rightarrow lysolecithin, etc.). Oxidation of the unsaturated fatty acid component of the phosphatides also seems possible. That changes, for instance in the lecithin part, actually destroy the X-protein, both in serum and in the isolated state, has recently been shown by Petermann (9). She found that after treatment with lecithinase the X-protein component disappeared from the sedimentation diagram both of isolated X-protein and of whole serum. In the first case both the albumin and the globulin peaks are twice as large after the treatment as before. In the whole serum only the globulin peak was increased after the treatment.

The amount of X-protein seems to vary very much from individual to individual, but for a given individual it seems to be rather constant. There seems perhaps to be rather little X-protein in the blood from persons in the teens.

So far no sera other than human have shown the presence of an X-protein. As, however, it is known—for example, from the work of McFarlane (5)—that the increase in the globulin peak is less than proportional to the increase in serum concentration, while the opposite holds for the “albumin” peak, it must be supposed that part of the globulin and the albumin, in these sera too, combine

with the β -globulin to form some kind of an X-protein; but its sedimentation properties are such that this component will be hidden in the "albumin" peak.

In an investigation still in progress the author has found that although the fractions precipitated between 0.45 and 0.6 saturated ammonium sulfate may sediment at a rate equal to that for serum albumin or slower, they show diffusion constants considerably lower than that for the albumin. Values as low as $D_{20} = 3 \times 10^{-7}$ have been observed.

From the ease with which the X-protein takes up certain proteins and lipids it may be supposed that it plays a very important rôle in the transport function of the blood.

SUMMARY

The labile X-protein in human plasma, first described by McFarlane, has been shown to be a lipoprotein, β -globulin, with density close to 1.

The particle weight for this compound is of the order 10^6 .

In concentrated serum the X-protein complex furthermore contains considerable amounts of both albumin and γ -globulin.

The expenses connected with this study have been defrayed by grants from the Nobel Fund and the Rockefeller Foundation.

REFERENCES

- (1) ADAIR, G. S., AND ADAIR, MURIEL E.: J. Physiol. **102**, 17P (1944).
- (2) BLIX, G.: J. Biol. Chem. **137**, 495 (1941).
- (3) BLIX, G., TISELIUS, A., AND SVENSSON, H.: J. Biol. Chem. **137**, 485 (1941).
- (4) JERSILD, M., AND PEDERSEN, K. O.: Acta Path. Microbiol. Scand. **15**, 426 (1938).
- (5) MCFARLANE, A. S.: Biochem. J. **29**, 407, 660 (1935).
- (6) MUTZENBECHER, P. VON: Biochem. Z. **266**, 226 (1933).
- (7) ONCLEY, J. L., SCATCHARD, G., AND BROWN, A.: J. Phys. Colloid Chem. **51**, 184 (1947).
- (8) PEDERSEN, K. O.: *Ultracentrifugal Studies on Serum and Serum Fractions*. Almqvist and Wiksells, Upsala (1945).
- (9) PETERMANN, MARY L.: J. Biol. Chem. **162**, 37 (1946).
- (10) SVEDBERG, T., AND PEDERSEN, K. O.: *The Ultracentrifuge*, p. 398. Oxford University Press, New York (1940).

ULTRACENTRIFUGAL AND ELECTROPHORETIC STUDIES
ON FETUIN¹

KAI O. PEDERSEN

*Institute of Physical Chemistry, University of Upsala, Upsala, Sweden**Received August 8, 1946*

It has long been known that there is some difference between the sera (and plasma) from the new-born animal and that from the adult. In the former case the serum contains less globulin than in the latter. According to earlier investigations by, among others, Howe (2), the proportions between the various globulin fractions are different in the two instances. A few years ago some publications appeared dealing with the electrophoresis of serum from new-born and young animals. They all show the presence of large amounts of α -globulin, small amounts of β -globulin, and the absence of γ -globulin in the sera of the new-born calf (1, 3) and foal (8). It was not, however, until the present author (5, 6, 7) started a series of fractionation experiments on calf serum and studied the fractions obtained in the ultracentrifuge that it was realized that a protein entirely different from the known albumins and globulins was present in these sera. Later on it was found that the new protein was present in still larger amounts in some fetal plasma, and the name fetuin was proposed (5).

The presence of fetuin in certain fetal and embryonic sera may also explain some earlier unpublished experiments from Upsala. Thus, Svedberg and Andersson several years ago found that the "albumin peak" in the sedimentation diagram from embryonic chicken sera was very asymmetric and gave a comparatively low value for the sedimentation constant, just as one would expect in case fetuin were present. Later on, in 1939, M. E. Adair, G. S. Adair, and the author found a similar behavior of the sera from sheep's fetus. Recently Moore *et al.* (4) have followed the change taking place in the plasma of the developing chick and pig embryo with age.

PREPARATION OF FETUIN

The first preparation of fetuin was made from pooled calf serum (age below 1 week). At that time, however, the existence of fetuin was not known and the preparation was carried out in the hope of getting fractions rich in α - or β -globulin.

The serum was diluted with an equal volume of 0.2 *M* sodium chloride containing enough sulfuric acid to change the pH of the solution to about 6. Addition of saturated ammonium sulfate solution to 0.33 Am_2SO_4 and to 0.35 Am_2SO_4 ² only produced a few inconsiderable flakes. The ammonium sulfate concentration was then increased to 40 per cent and a heavy precipitate $\text{g}_{1\epsilon 1}$ was formed. It was twice resuspended in 0.43 Am_2SO_4 and centrifuged down.

¹ Presented at the Twentieth National Colloid Symposium, which was held at Madison, Wisconsin, May 28-29, 1946.

² By "0.35 Am_2SO_4 " is meant a solution that in a total of 100 ml. contains 35 ml. of 4 *M* ammonium sulfate.

The mother liquor was brought to $0.45 \text{ Am}_2\text{SO}_4$, whereby $g_{2\epsilon_1}$ was formed. It was twice washed with $0.47 \text{ Am}_2\text{SO}_4$. The supernatant from the precipitation of $g_{2\epsilon_1}$ was finally brought to $0.50 \text{ Am}_2\text{SO}_4$ and yielded $g_{3\epsilon_1}$, which was washed twice with $0.53 \text{ Am}_2\text{SO}_4$. In figure 1 the sedimentation diagrams for the three fractions are given. Besides the fetuin and the normal globulin the two first solutions also contained 10 and 5 per cent, respectively, of a heavy component ($s_{20} \sim 20 \text{ S}$).

Electrophoretic examination of $g_{1\epsilon_1}$ showed that it contained large amounts of a substance with the mobility of an α_2 - or β_1 -globulin. As the solution appeared very turbid, this was first taken as a further criterion that the main

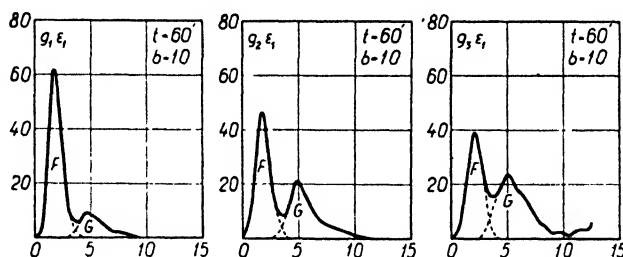


FIG. 1. Sedimentation diagrams for the globulin fractions of calf serum, showing the fetuin (F) and the globulin (G) peaks. The 20-component has already sedimented to the bottom of the cell. As is evident from the diagrams, the appearance of the globulin peak indicates that much inhomogeneous material sediments together with this protein. The concentrations of the sedimented solutions were, from left to right, 2.7, 2.6, and 2.9 per cent. The sedimentation diagrams have all been reduced to an initial concentration of 1 per cent.

component was one of the lipoproteins. A large part of the turbidity could, however, be precipitated by dialysis against 0.2 M sodium dihydrogen phosphate. The main part of the remaining turbidity could be removed by spinning the solution in an air-driven centrifuge for 4 hr. at $27,000 \text{ R.P.M.}$

Various attempts to purify this fetuin solution by refractionations were not very successful. The best solution was run at different concentrations in the centrifuge and gave for infinite dilution $s_{20} = 3.38 \text{ S}$.

$\Delta n \times 10^5 \dots$	1059	537	265	132
$s_{20} \dots$	2.16	2.76	3.06	3.23

The variation of the sedimentation constant with concentration is quite remarkable for a protein of such a low molecular weight.

A number of different experiments were carried out to find the best conditions for preparing the fetuin from calf serum.

One way of doing it was first to precipitate to $0.60 \text{ Am}_2\text{SO}_4$ at pH 6, wash the precipitate thoroughly, and then extract the precipitate with $0.50 \text{ Am}_2\text{SO}_4$, $0.45 \text{ Am}_2\text{SO}_4$, $0.40 \text{ Am}_2\text{SO}_4$, $0.35 \text{ Am}_2\text{SO}_4$, and finally with 0.2 M sodium chloride.

The result was not good, however; the relative fetuin content was less than in the earlier experiments and the amount of inhomogeneous material was higher.

The attempt was made to eliminate the inhomogeneous material by first dialyzing the serum against a dilute phosphate buffer (0.01 *M* sodium dihydrogen phosphate). A heavy precipitate also came down, and it was extremely inhomogeneous according to the sedimentation diagrams. From the supernatant a comparatively pure fetuin could be prepared.

As, however, at that time it was supposed that the fetuin had its isoelectric point at about pH 5 and the normal globulin had its isoelectric point somewhere

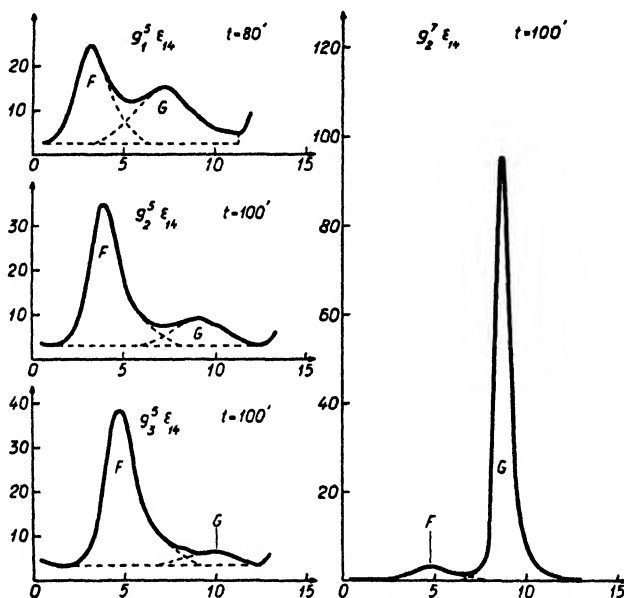


FIG. 2. Sedimentation diagrams for the globulin fractions from calf serum precipitated between 0.33 and 0.40 Am_2SO_4 . All diagrams have been reduced to the same protein concentration ($\Delta n = 0.00200$). The main part of the fetuin is precipitated at pH 5 (left-hand diagrams), while almost pure globulin is precipitated at pH 7 (right-hand diagram).

around pH 7, it was thought worthwhile to try to remove the fetuin at pH 5 and the normal globulin at pH 7. A series of experiments was then carried out with precipitation at alternating pH values. The serum was first diluted with an equal volume of 0.2 *M* sodium chloride and its pH changed to 5. It was then mixed with ammonium sulfate to 0.33 Am_2SO_4 and the precipitate $g_1^5 \epsilon_{14}$ was obtained. The pH was then changed to 7, but the solution remained clear. Changing the pH back to 5 and increasing the salt concentration to 0.37 Am_2SO_4 produced another precipitate, $g_2^5 \epsilon_{14}$. Upon changing the pH to 7 the precipitate $g_3^5 \epsilon_{14}$ resulted. The pH was again changed back to 5 and the salt concentration increased to 0.40 Am_2SO_4 , whereupon $g_2^5 \epsilon_{14}$ was formed. Figure 2 shows the sedimentation diagrams from these four fractions. From these, it is quite evident that there is preferential precipitation of fetuin at pH 5, and of normal

globulin at pH 7. A refractionation of the fractions $g_{2\epsilon_{14}}^5$, $g_{2\epsilon_{14}}^7$, and $g_{3\epsilon_{14}}^5$ did not result in any appreciable improvement in the purity of the fetuin or of the globulin.

There seems, however, to be at least one more possibility of improving the purity of the fetuin preparation, as it has been found in other experiments (7) that the solubility of the fetuin decreases with increase in temperature, whereas the globulin is more soluble at room temperature than in the cold room. By running the fractionation according to the scheme: $g_1^7 \rightarrow g_1^5 \rightarrow g_2^7 \rightarrow g_2^5 \rightarrow g_3^7 \rightarrow g_3^5 \rightarrow$, etc. and by taking the precipitates at pH 7 in the cold ($+1^\circ$ to $+5^\circ\text{C}.$) and the precipitates at pH 5 at room temperature ($\sim +20^\circ\text{C}.$), the precipitation of the fetuin should be favored at pH 5 and suppressed at pH 7 and *vice versa* for the globulin.

So far the scheme has not yet been seriously tested, as in the meanwhile it was found that it was a much simpler matter to prepare the fetuin from fetal serum.

For this preparation the fetal serum is first diluted with an equal volume of 0.2 M sodium chloride; then ammonium sulfate is added until a concentration of 0.45 Am_2SO_4 is reached. The precipitate is thoroughly washed twice by resuspension with 0.50 Am_2SO_4 .

The main contaminant in a fetuin solution prepared in this way was ordinarily a high-molecular component with $s_{20} \sim 20$ S. It can be considerably reduced in amount by spinning the fetuin solution for several hours in an air-driven centrifuge at 27,000 R.P.M.

All attempts to crystallize the fetuin have so far been in vain.

THE SEDIMENTATION CONSTANT³

A large number of sedimentation experiments has been carried out in the ultracentrifuge on solutions of fetuin. The results of these experiments have been summarized in figure 3. In this figure the measured s_{20} has been plotted against the fetuin concentration, as calculated from the sedimentation diagram. The fetuin concentration has been expressed in Δn , the increase in refractive index due to the presence of fetuin.

As there appeared to be some difference between the sedimentation properties of calf fetuin and that of fetal fetuin, separate values for s_{20} at infinite dilution have been calculated. Also, in the case of the fetal fetuin there seems to be some difference between the values obtained from different preparations. Thus some preparations (ζ_1 to ζ_4) gave values quite different from those obtained with the calf fetuin; another, ζ_8 , gave values close to those for calf fetuin.

For the different cases, the line of regression and the coefficient of correlation, r , have been calculated. These values were:

For calf fetuin:

$$s_{20} = 3.28 - 200 \cdot \Delta n \quad r = 0.86$$

³ All the sedimentation constants are given in Svedberg units, S.

For bovine fetal fetuin:

$$\begin{aligned} s_{20} &= 3.09 - 145 \cdot \Delta n & r &= 0.89 & \zeta_1 - \zeta_4 \\ s_{20} &= 3.23 - 200 \cdot \Delta n & r &= 0.99 & \zeta_8 \end{aligned}$$

Parallel with the difference in sedimentation these fetuins also show differences in other properties, such as diffusion constants, partial specific volume, and phosphorus content.

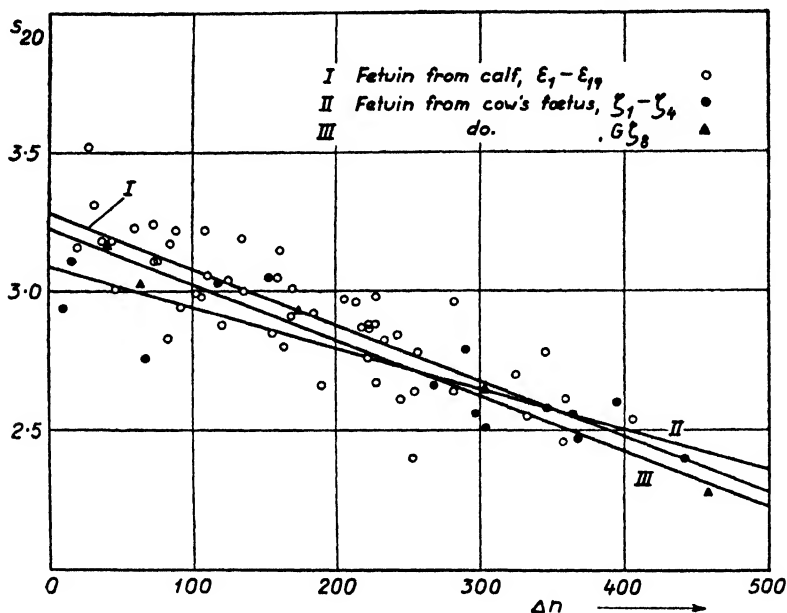


FIG. 3. Variation of s_{20} with concentration of fetuin, as measured from the sedimentation diagrams.

A series of experiments recently carried out on fetuin from sheep's fetus gave the following results:

$\Delta n \times 10^6$	163	130	114	82	65	33
s_{20}	3.05	3.03	3.09	3.09	3.23	3.23

For the line of regression and the coefficient of correlation the following were found:

$$s_{20} = 3.28 - 164 \cdot \Delta n \quad r = 0.88$$

The sedimentation constant at infinite dilution is thus the same as for calf fetuin, but the slope is somewhat different.

THE DIFFUSION CONSTANT⁴

Several diffusion experiments have been carried out on fetuin prepared from both calf and fetal sera. None of the solutions have, however, been 100 per cent pure; they have all contained some amount of the 20-component. By examining the same sample in the ultracentrifuge, it is possible, however, to calculate how much of the 20-component there is present along with the fetuin.

It was found very important always to clear the samples in the air-driven centrifuge at 27,000 R.P.M. for some hours before using them in diffusion experiments in order to remove any coarse disperse material present.

Two diffusion measurements were made on calf fetuin. From the sedimentation diagram it was found that the sample consisted of 89 per cent fetuin and 11 per cent of the 20-component. The diffusion constants were (7) for $\Delta n = 0.00138$, $D_A = 4.65$ and $D_m = 5.08$. After the curves had been corrected for the presence of the 20-component (tentative value $D_{20} = 1.65$), D_{20} for the fetuin was found to be $D_A = 5.68$ and $D_m = 5.51$.

The same solution was also run at a concentration corresponding to $\Delta n = 0.00250$. The original values were then $D_A = 4.48$ and $D_m = 5.10$; after correction for the presence of the 20-component, D_{20} for the fetuin was found to be $D_A = 5.35$ and $D_m = 5.72$. The best value for the diffusion constant of calf fetuin would probably be $D_{20} = 5.5$.

Several diffusion experiments were carried out on fetal fetuin, some of them in order to determine the variation of the diffusion constant with the fetuin concentration. The experiments were, however, not sufficiently accurate to detect any such variation. The two most reliable experiments gave $D_A = 4.62$ and $D_m = 4.91$, and $D_A = 4.89$ and $D_m = 4.69$, respectively. After the correction for the presence of only 2 per cent of the 20-component, these values changed to $D_A = 4.85$, $D_m = 4.98$, and $D_A = 4.96$ (D_m not calculated). As the most reasonable value for the diffusion constant of fetal fetuin we may take (preparation ζ_4) $D_{20} = 5.0 \times 10^{-7}$.

PARTIAL SPECIFIC VOLUME; NITROGEN AND PHOSPHORUS CONTENT⁵

For the calf fetuin $V_{20} = 0.714$ was found. For the fetal fetuin two rather different values were obtained. Thus the ζ_4 preparation gave $V_{20} = 0.69_2$, while ζ_8 gave $V_{20} = 0.71_2$ or almost the same as for the calf fetuin.

The nitrogen and phosphorus contents of the same two preparations were also quite different. For the ζ_4 preparation the values found were 12.3 g. nitrogen per 100 g. protein and 188 mg. phosphorus per 100 g. protein, while for ζ_8 the values were 13.4 g. nitrogen and 101 mg. phosphorus, respectively,—a considerable difference.

⁴ All the diffusion constants are expressed in units of 10^{-7} .

⁵ The author is indebted to Professor Carl Drucker and to Mrs. Brita Wikén, Upsala, for carrying out the determinations of the partial specific volume and of the nitrogen and phosphorus contents, respectively.

TABLE 1
Electrophoretic mobility of fetuin from cow's fetus
Temperature, +0.4°C.

BUFFER	pH	$\mu \times 10^5$
0.033 M Na ₃ citrate + 0.8 M H ₃ citrate + 0.1 M NaF....	2.85	+0.62
0.1 M Na acetate + 0.45 M H acetate + 0.1 M NaF.....	3.75	-0.09
0.1 M Na acetate + 0.15 M H acetate + 0.1 M NaF... ..	4.31	-0.75
0.1 M Na acetate + 0.03 M H acetate + 0.1 M NaF....	4.88	-1.60
0.07 M NaH ₂ PO ₄ + 0.01 M Na ₂ HPO ₄ + 0.1 M NaF.....	5.97	-2.68
0.04 M NaH ₂ PO ₄ + 0.02 M Na ₂ HPO ₄ + 0.1 M NaF ..	6.48	-3.09
0.004 M NaH ₂ PO ₄ + 0.032 M Na ₂ HPO ₄ + 0.1 M NaF. ..	7.36	-3.41

Isoelectric point at pH 3.5.

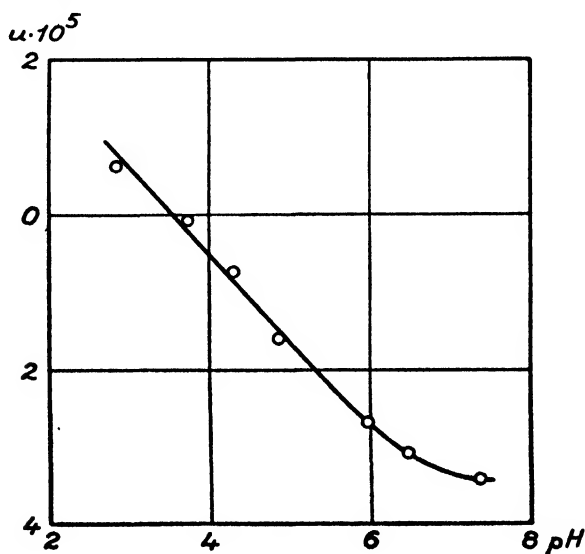


FIG. 4. Variation of the electrophoretic mobility of fetuin with pH. Ionic strength of solution 0.2.

MOLECULAR WEIGHT

For the molecular weights of the fetuin of different origin we find:

For fetuin from calf:

$$s_{20} = 3.28, D_{20} = 5.5, \text{ and } V_{20} = 0.714 \text{ give } M = 50,600$$

For fetuin from cow's fetus:

$$s_{20} = 3.09, D_{20} = 5.0, \text{ and } V_{20} = 0.692 \text{ give } M = 48,700$$

THE ISOELECTRIC POINT OF FETUIN

The electrophoretic mobility of fetuin was determined in a number of different buffer solutions, as shown in table 1. In figure 4 the mobility is plotted against pH. It is seen that the isoelectric point is at pH 3.5. This is an exceptionally

acid value for a plasma protein, where all the globulins have their *I.P.*'s above pH 5 and the albumin has an *I.P.* of 4.8.

SUMMARY

Methods for preparing fetuin from calf and fetal sera have been described.

The sedimentation constant for fetuin varies strongly with concentration. For infinite dilution s_{20} seems to vary somewhat with the origin of the fetuin, but the molecular weight always comes out at about 50,000.

Fetuin has its isoelectric point at pH 3.5, which is a very acid value for a plasma protein.

The expenses connected with this study have been defrayed by grants from the Nobel Fund and The Rockefeller Foundation.

REFERENCES

- (1) CLEMENTE, C. L. SAN, AND HUDDLESON, J. F.: Mich. State College Agr. Exptl. Sta., Tech. Bull. **182**, 3 (1943).
- (2) HOWE, P. E.: J. Biol. Chem. **49**, 115 (1921); **53**, 479 (1922).
- (3) JAMESON, E., ALVAREZ-TOSTADO, C., AND SORTOR, H. H.: Proc. Soc. Exptl. Biol. Med. **51**, 163 (1942).
- (4) MOORE, D. H., SHEN, S. C., AND ALEXANDER, C. S.: Proc. Soc. Exptl. Biol. Med. **58**, 307 (1945).
- (5) PEDERSEN, K. O.: In *The Svedberg 1884-1944*, p. 490. Almqvist and Wiksells, Upsala (1944).
- (6) PEDERSEN, K. O.: Nature **154**, 575 (1944).
- (7) PEDERSEN, K. O.: *Ultracentrifugal Studies on Serum and Serum Fractions*. Almqvist and Wiksells, Upsala (1945).
- (8) POLSON, A. G.: Nature **152**, 413 (1943).

THE QUANTITATIVE INTERPRETATION OF THE ELECTROPHORETIC PATTERNS OF PROTEINS¹

L. G. LONGSWORTH

Laboratories of The Rockefeller Institute for Medical Research, New York, New York

Received August 8, 1946

INTRODUCTION

In the moving-boundary method as adapted by Tiselius (14) for the analysis of protein mixtures, the initial boundary is formed between the two solutions that result from the dialysis of the protein solution against a large volume of an appropriate buffer solution. The diffusible buffer ions are then present on both sides of the initial boundary at concentrations corresponding to a Donnan equilibrium. On passage of the current this boundary generally splits into a number of separate boundaries, one of which remains near the initial boundary

¹ Presented at the Twentieth National Colloid Symposium, which was held at Madison, Wisconsin, May 28-29, 1946.

position while the others move away from this position at different rates. At each of the moving boundaries the concentration of one of the protein components varies from a constant value below the boundary to zero above and is thus said to disappear in the boundary. Moreover, the variation of the refractive index with the height due to the disappearance of this species may be recorded photographically by either the schlieren-scanning or the cylindrical-lens method (7). In the complete pattern each boundary appears as a separate peak whose area is proportional to the difference of refractive index between the two solutions forming the boundary.

At pH values not too different from the isoelectric pH the equivalent weights of most proteins are large in comparison with those of the buffer ions. Consequently, a relatively low equivalent concentration of protein may still be one at which this constituent makes a major contribution to the density and refractive index of the solution. The conductance, on the other hand, is determined largely by the buffer ions. Thus the limiting case is approached in which one of the solutions meeting at the original boundary contains small concentrations of one, or more, species in a large excess of other ions, whereas only the dominant species are present in the other end solution and at the same concentrations. The dominant species, the buffer ions, then insure throughout the boundary system a uniform electric field in which the constituents at low equivalent concentrations, the protein ions, drift. At a moving boundary in which a protein ion disappears there are then no superimposed gradients of other species, and the area of the corresponding peak in the pattern is a direct measure of the concentration of the disappearing species. Moreover, in this case the boundary pattern is independent of the direction in which the current is passed. Consequently, if boundaries are formed initially in each of the two sides of the U-shaped channel of the Tiselius cell, as is the usual procedure, the pattern obtained from one side is the mirror image of that from the other side. Such patterns may be said to be *enantiographic*. This limiting or ideal case is the basis of the current method for obtaining what will be called the *apparent* composition of a protein mixture. In this approximate method the superimposed gradients are ignored, and the relative concentration of a component is taken as the ratio of the area of the peak in the pattern due to this component to the sum of the areas due to all constituents. A glance at the deviations of almost any pair of patterns from enantiography will convince one, however, that actual systems may approach, but do not attain, the ideal conditions. With the aid of the moving-boundary theory developed by Kohlrausch (5) and Weber (16), and recently extended by Dole (4) and Svensson (11, 12, 13), it is the purpose of this report to compute the behavior of some typical systems and to compare the results with experiment.

THREE-ION SYSTEMS

Since the theory assumes that the relative ion mobilities are constant throughout the system, it is applicable to protein ions only insofar as the presence of the buffer electrolytes insures a uniform pH and hence a constant protein-ion mobility. In Dole's theory the displacements of the boundaries and the composi-

tions of the solutions formed by their separation are computed from the relative mobilities and concentrations of the two solutions forming the original boundary, the so-called end solutions. The inverse problem of computing the mobilities and concentrations of the ions in the end solutions from the boundary pattern is, however, the one that arises in the electrophoretic analysis of protein mixtures. As a matter of fact this problem is not solvable in the general case without additional information and even then the computations are laborious. Although results for more complex mixtures will be presented later in this paper, it is only in the case of a three-ion system that simple relations are obtained. A single protein dissolved in a buffer having a pH at which the conductance of the hydrogen-ion constituent can be neglected is an important special case of such a system.

Notation

In this paper A, B, C' . . . will refer to cations whose mobilities, u , are in the order $u_A > u_B > u_C$. . . while R, S, T . . . indicate anions for which $|u_R| > |u_S| > |u_T|$ The mobility of one species relative to that of another taken as unity is called the relative mobility and is denoted as r . Both the relative and absolute mobility and the concentration of a given ion retain the sign of the charge on that species. The initial boundary is indicated by separating with a dash, —, the symbols for the ions in the two end solutions. In the system that develops on passage of the current a moving boundary is denoted by an arrow, \rightarrow , while a double colon, $::$, will be used for the concentration boundary remaining near the site of the original boundary. The current is always taken as flowing from left to right, and the solutions meeting at the boundaries will be denoted by Greek letters in the order of decreasing density. Owing to the nature of the end solutions in the case of proteins, no difficulty will be experienced in determining this order, since the protein components disappear progressively with increasing height at each moving boundary and thus the density decreases with the number of species in a solution. The end solution containing the protein ions is thus always the α solution.

Except at low ionic strengths the mobility of the protein ion is generally less in magnitude than that of either the buffer cation or anion and these are denoted, therefore, as A and R, respectively. At pH values below its isoelectric pH the protein ion is the cation B, whereas above this pH it is the anion S. Here the protein solution will be taken as ABR, since the necessary modifications when the protein is an anion will be obvious. As will be shown below, the buffer acid, or base, may be considered as part of the solvent if it is uncharged. The special case in which the buffer acid and its conjugate base are both charged, e.g., the H_2PO_4^- and HPO_4^{2-} ions in phosphate buffers, offers no difficulty if the concentration and mobility of the buffer-ion constituent are used.

In that side of the channel in which the protein ions descend the boundary system for three ions is $\text{AR}(\gamma) :: \text{AR}(\beta) \rightarrow \text{ABR}(\alpha)$, whereas in the other side it is $\text{ABR}(\alpha) :: \text{ABR}(\beta) \rightarrow \text{AR}(\gamma)$. Wherever it is necessary in order to avoid confusion, the subscripts r (rising) and d (descending) will be added to distinguish between the two systems.

The protein mobility

At the descending boundary $\alpha\beta$ in the system $AR(\gamma) :: AR(\beta) \rightarrow ABR(\alpha)$ the protein ion B disappears from the end solution α of known conductance, κ^α . Its mobility, u_B , in this solution may be computed (9) directly with the aid of the relation, $u_B = v^{\alpha\beta}\kappa^\alpha$, in which $v^{\alpha\beta}$ is the displacement, in milliliters, of the first moment of the gradient curve per coulomb of electricity passed. Although the $\alpha\beta$ boundary is generally diffuse, the modern schlieren methods for recording the refractive-index gradients usually make it possible to locate this moment with an uncertainty of less than 0.03 mm. If the boundary moves 3 cm., for example, this represents an error of 0.1 per cent in the mobility. If the mobility of the protein in pure buffer solution is required, determinations are made at two or more protein concentrations and extrapolated.

The buffer-concentration boundary

The earlier designation (8) of the buffer-concentration boundary $\beta\gamma$ as the ϵ boundary was unfortunate, since it has been confused with the moving boundaries due to the serum globulins that are also identified with Greek letters. The corresponding boundary in the other side of the channel, heretofore called the δ boundary, will be termed the protein-concentration boundary. In the ideal case that the relative mobilities of all species are constant throughout the channel, the buffer- and protein-concentration boundaries are stationary. In real systems they generally move slightly on passage of the current.

Since the protein solution α is prepared by dialysis against a large excess of the buffer solution γ , its composition is not arbitrary but is given, to a close approximation, by the first term in the expansion of the Donnan equation, i.e.

$$C_A^\alpha = C_A^\gamma - \frac{1}{2}C_B^\alpha \quad (1)$$

$$C_R^\alpha = C_R^\gamma - \frac{1}{2}C_B^\alpha \quad (2)$$

With the aid of these relations and the electroneutrality conditions, $\Sigma C_i = 0$, the Kohlrausch regulating functions (4, 5) of the two end solutions become

$$\omega^\gamma = \frac{C_A^\gamma}{r_A} + \frac{C_R^\gamma}{r_R} = C_A^\gamma \left(\frac{1}{r_A} - \frac{1}{r_R} \right)$$

and

$$\omega^\alpha = \frac{C_A^\alpha}{r_A} + \frac{C_B^\alpha}{r} + \frac{C_R^\alpha}{r_R} = \omega^\gamma + \frac{1}{2}C_B^\alpha \left(\frac{2}{r_B} - \frac{1}{r_A} - \frac{1}{r_R} \right)$$

Since $\omega^\alpha/\omega^\gamma$ is the dilution factor for all species at the concentration boundaries in both sides of the channel and occurs frequently in the theory, it will be designated ξ .

$$\xi = \frac{\omega^\alpha}{\omega^\gamma} = 1 + \left(\frac{r_B - r_R}{r_B} \frac{r_A}{r_A - r_R} - \frac{1}{2} \right) \frac{C_B^\alpha}{C_A^\gamma} \quad (3)$$

At sufficiently low protein concentrations ξ becomes unity and deviations therefrom are, therefore, a measure of the divergence of real systems from the ideal behavior that is assumed in the usual electrophoretic analysis.

In the case of the buffer-concentration boundary the difference in refractive index is

$$n^{\beta} - n^{\gamma} = K_{AR}(C_A^{\beta} - C_A^{\gamma}) = K_{AR}(\xi - 1)C_A^{\gamma} \\ = K_{AR} \left(\frac{r_B - r_R}{r_B} \frac{r_A}{r_A - r_R} - \frac{1}{2} \right) C_B^{\alpha} \quad (4)$$

where K_{AR} is the increment of refractive index per equivalent of AR. At a given pH and ionic strength the area of the buffer-concentration peak in the pattern is thus proportional to the protein concentration.

In the special case that the mobilities of the buffer ions are equal, i.e., $r_A = -r_R$, equation 4 becomes

$$n^{\beta} - n^{\gamma} = K_{AR} C_B^{\alpha} r_A / 2r_B \quad (5)$$

At a constant ionic strength and protein concentration of p grams per 100 ml. of solution, both C_B^{α} and r_B vary with the pH. This variation is due to the change of the valence, z_B , of the protein ion. Since C_B^{α} is directly proportional to z_B

TABLE 1

The buffer-concentration boundary in a three-ion system

Ovalbumin in 0.1 *N* sodium acetate at pH 3.92 ($e = 2.34 \times 10^{-4}$): $r_{Na} = 1.000$,
 $r_{Ac} = -0.7875$, $r_{protein} = 0.1392$, $K_{AR} = 0.01235$

1	p (grams per 100 ml.)	0.64	1.36	2.74
2	C_B^{α} (equivalents per liter)	0.00150	0.00318	0.00641
3	$n^{\beta} - n^{\gamma}$ (equation 4)	0.000060	0.000127	0.000255
4	$n^{\beta} - n^{\gamma}$ (observed)	0.00004 _s	0.00012 _s	0.00024 ₇
5	c (computed)	0.0001 _s	0.00022 ₇	0.00022 ₇

and r_B is approximately so, and they occur in equation 5 as the ratio, compensation occurs. With a given buffer salt $n^{\beta} - n^{\gamma}$ should, therefore, be almost independent of the pH.

The variation of $n^{\beta} - n^{\gamma}$ with the ionic strength at constant pH and protein concentration, p , is more obscure. In this case z_B , and hence C_B^{α} , generally increases with increasing ionic strength (2, 6), whereas the relative mobility of the protein ion decreases (15). Both of these effects should, if K_{AR} is independent of the salt concentration, cause $n^{\beta} - n^{\gamma}$ to increase somewhat with increasing ionic strength.

Although the foregoing conclusions appear to be in accord with experiment, no data of sufficient precision to test equation 4 are available except for a variation of the protein concentration at constant pH and ionic strength (9). The results of this test are summarized in table 1. The equivalent concentrations of protein, line 2, are given by the relation, $C_B^{\alpha} = 10pe$, where e is the net charge in Faraday equivalents per gram of protein and is taken from the titration data of Cannan, Kibrick, and Palmer (2). Although the molecular weight, M , of the protein is not required for the computation of C_B^{α} , if M for ovalbumin (15) is 45,000 the valence of these ions in the present example is $z_B = Me = 10.5$.

The relative mobilities of table 1 are based on the measured value, u_B , for the protein ion, the conductance, κ^γ , of the buffer solution, and the cation transference number, T , of 0.1 *N* sodium acetate, i.e.,

$$u_A = 1000\kappa^\gamma T/FC_A^\gamma \quad \text{and} \quad u_R = 1000\kappa^\gamma(1 - T)/FC_R^\gamma$$

Since κ^γ is the conductance of sodium acetate in the presence of acetic acid, provision is thereby made for the effect on the buffer-ion mobilities of the viscosity due to the weak buffer acid. In any given system allowance can also be made as follows for the viscosity due to the protein. Since u_R/u_A is taken as equal to $(T - 1)/T$ throughout the system, the specific conductance of the protein solution may be written

$$1000\kappa^\alpha/F = C_A^\alpha u_A + C_B^\alpha u_B + C_R^\alpha u_A(T - 1)/T$$

and may be solved for u_A .

Since refractive-index differences, as computed from pattern areas, are uncertain by at least 1×10^{-5} , the agreement between the observed and computed values of $n^\beta - n^\gamma$ (lines 3 and 4 of table 1) is essentially complete. A conductometric analysis of the β solution after its removal from the channel would doubtless yield a more precise value for C_A^β than the refractometric method and will be used in the future.

If the procedure is reversed and the net charge, e , computed from the observed values of $n^\beta - n^\gamma$, the results given in the last line of table 1 are obtained. It is clear that this affords a method for the determination of the net charge on the protein that compares favorably with the value, 0.000234, obtained from titration data.

The ratio of the displacements of the rising and descending boundaries

In the other side of the channel where the system is $ABR(\alpha) :: ABR(\beta) \rightarrow AR(\gamma)$, the protein ion B disappears in the rising boundary $\beta\gamma$. The displacement of this boundary is given by the relation $u_B = v^{\beta\gamma}\kappa^\beta$. Since the β solution has been formed by the passage of the current its conductance, κ^β , is not known and the rising boundary cannot, therefore, be used for direct mobility measurements.

In terms of the relative conductances, σ , and mobilities, r , the relations at the rising and descending boundaries are

$$r_B = v_d^{\alpha\beta}\sigma_d^\alpha \quad \text{and} \quad r_B = v_r^{\beta\gamma}\sigma_r^\beta$$

Since the α solution is the same in both sides of the channel, $\sigma_d^\alpha = \sigma_r^\alpha$ and $v_r^{\beta\gamma}/v_d^{\alpha\beta} = \sigma_r^\alpha/\sigma_r^\beta$. The ratio of the relative conductances at either concentration boundary is also the dilution factor, ξ , from which

$$v_r/v_d = \xi \tag{6}$$

where the superscripts have been dropped, since there is only one moving boundary in each side of the channel with three-ion systems. With the aid of this

relation values of v_r/v_d for the solutions listed in table 1 were computed and are given in the second line of table 2. The agreement with the observed values in the third line is poor.

In seeking to explain this discrepancy it will be recalled that the theory assumes the constancy of the relative ion mobilities. The deviation of v_r/v_d from unity predicted by equation 6 is due to the stronger field, i.e., lower conductance, in the solution above the protein-concentration boundary resulting from the dilution at this boundary. Equation 6 may thus be said to correct for the conductivity change at this boundary. It does not provide, however, for any change in the relative mobility of an ion. If, for example, the pH is different on the two sides of the protein-concentration boundary the mobility of the protein ion, relative to the mobilities of the buffer ions, is also different. A correction for such a pH effect may be made as follows.

The influence of pH gradients

Evidence to be presented below indicates that the concentration of the weak buffer acid, HR, remains constant throughout the boundary system. In the diluted protein solution β the concentration of the buffer salt AR differs, however,

TABLE 2

The displacement ratio of the rising and descending boundaries in a three-ion system
Ovalbumin in 0.1 N sodium acetate at pH 3.92

1	p	0.64	1.36	2.74
2	v_r/v_d (equation 6)	1.048	1.103	1.207
3	v_r/v_d (observed)*	1.091	1.180	1.333
4	v_r/v_d (corrected for pH effect)	1.078	1.166	1.341

* These values differ slightly from those previously published (9), since here the boundary position is correctly taken as the position of the first moment of the gradient curve instead of the bisecting ordinate that was used in the earlier work.

from the concentration of this material in the original protein solution α . For small variations in composition the relation

$$\text{pH} = \text{const.} + \log (C_{\text{AR}}/C_{\text{HR}})$$

may be assumed and the difference of pH across the protein-concentration boundary is

$$\text{pH}^\alpha - \text{pH}^\beta = \log (C_{\text{A}}^\alpha/C_{\text{A}}^\beta) = \log \xi$$

Since $\xi > 1$ the pH of the solution above this boundary is less than that underneath. Below the isoelectric pH the protein-ion mobility increases with decreasing pH, and these ions thus move faster above the $\alpha\beta$ boundary than below it. If $du/d\text{pH}$ is the slope of the mobility curve at the pH in question

$$r_{\text{B}}^\beta/r_{\text{B}}^\alpha = 1 - (1/u_{\text{B}})(du_{\text{B}}/d\text{pH}) \log \xi \quad (7)$$

and the value of v_r/v_d given by equation 6 must be increased by this factor. At pH 3.92 and 0.1 N, $(1/u_{\text{B}})(du_{\text{B}}/d\text{pH}) = -3.8$ for ovalbumin (6) and the cor-

rected values of v_r/v_d are given in the last line of table 2. The improved agreement with the observed values constitutes part of the evidence for the validity of the assumption that the concentration of the weak buffer acid remains essentially uniform throughout the system. Additional evidence has been obtained as follows:

If, prior to forming the boundaries, the protein solution is diluted by the factor ξ with a solution of HR at the concentration C_{HR} , the concentration boundaries are eliminated from the resulting patterns. In the case of a buffer system in which the acid and its conjugate base are both charged, e.g., phosphate buffers, the dilution is made with water. This is a useful device in counter-current electrolysis where one of the concentration boundaries would normally be drawn into the bottom section of the cell, thereby initiating convection.

TABLE 3
The protein-concentration boundary in a three-ion system
Ovalbumin in 0.1 *N* sodium acetate at pH 3.92

1	p	0.64	1.36	2.74
2	$n^\alpha - n^\beta$ (equation 9)	0.000114	0.000351	0.001085
3	$n^\alpha - n^\beta$ (observed)	0.00015 ₈	0.00049 ₄	0.00149 ₆
4	$n^\alpha - n^\beta$ (corrected for pH effect).	0.000146	0.000476	0.001509

The protein-concentration boundary

If the pH change at the protein-concentration boundary is ignored, the expression for the difference in refractive index becomes

$$n^\alpha - n^\beta = K_{AR}(C_A^\alpha - C_A^\beta) + K_{BR}(C_B^\alpha - C_B^\beta) \quad (8)$$

$$= [K_{AR}C_A^\gamma + (K_{BR} - \frac{1}{2}K_{AR})C_B^\alpha](1 - 1/\xi) \quad (9)$$

The equivalent refraction, K_{BR} , is that of the protein salt, ovalbumin acetate in the present example. Its relation to the specific refraction, k , of the isoelectric protein is

$$k(1 + ae)p = K_{BR}C_B^\alpha$$

where a is a constant for a given buffer salt (1). The product ae represents a small correction for the effect of the charge, e , of the protein ion on its refractivity and for the refractivity of the buffer ions that balance this charge.

The values of $n^\alpha - n^\beta$ given in the second line of table 3 were computed with the aid of equation 9 for the solutions of table 1. As in the case of the boundary displacement ratio before correction for the pH effect, the agreement with the observed values, line 3, is poor. The increased mobility of the protein ions at the lower pH of the β solution leads, however, to a concentration, $C_B^{\beta*}$, that must satisfy, approximately, the relation $C_B^{\beta*}r_B^\beta = C_B^\beta r_B^\alpha$. In order to correct for the pH effect, C_B^β in equation 8 is replaced by $C_B^{\beta*}r_B^\alpha/r_B^\beta$, where r_B^α/r_B^β is given by equation 7. The values obtained in this manner, line 4 of table 3, are in good

agreement with those observed. In a more exact treatment of the problem the concentrations of the buffer ions in the β solution would also be adjusted to preserve electrical neutrality, but the effect of this adjustment on the refractive index of the solution is small.

Although there is a similar pH change at the buffer-concentration boundary, the relative mobilities of the buffer ions are not appreciably altered thereby. It is for this reason that an analysis of the buffer solution below this boundary probably affords the most direct method for determining, with the aid of moving boundaries, the net charge on the protein.

The conductivity and pH effects

The conductivity and pH changes at the boundaries do not always combine, as in the examples given above, to decrease the enantiography of the patterns

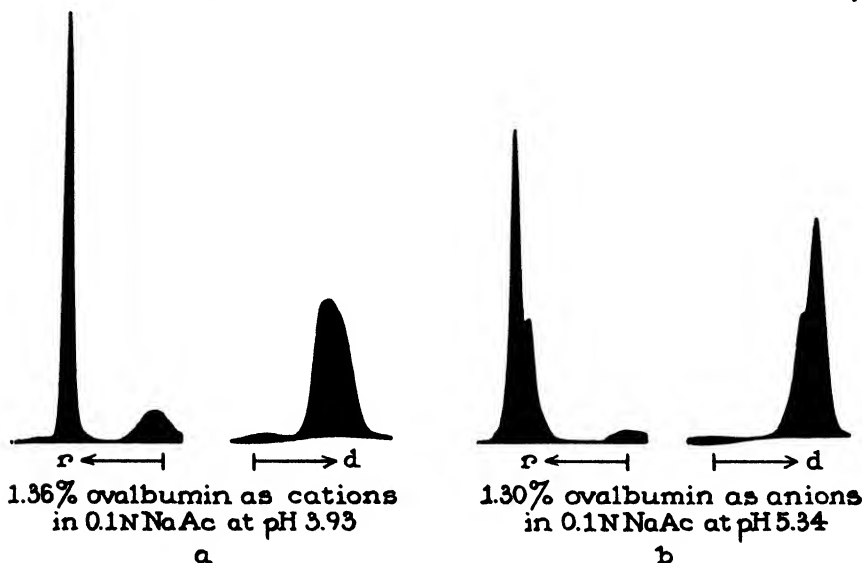


FIG. 1

from the two sides of the channel. Above the isoelectric pH of the protein the coefficient $(1/u)(du/dpH)$, equation 7, is positive and the pH effect then tends to cancel the conductivity effect. In buffers of the uncharged-acid type, the patterns obtained above the isoelectric pH tend to be more nearly mirror images of each other than below this pH. This is illustrated in figure 1, where the patterns at *a* are those of the 1.36 per cent ovalbumin solution of table 1, whereas a similar concentration, 1.30 per cent, of this protein in a 0.1 *N* sodium acetate buffer at pH 5.34 gave the patterns of figure 1*b*. Even when allowance is made for the inhomogeneity of this protein at the higher pH, the increased enantiography of the patterns when the protein is an anion is clearly evident.

The deviations from enantiography shown here are those most commonly encountered. If, however, the buffer is of the uncharged-base type, e.g., glycine hydrochloride, a reversal in the sign of the pH effect can be expected.

Sharpening and spreading of the moving boundaries

An additional deviation from enantiography illustrated in figure 1 is the relative sharpness of the rising boundary. If the conductivity is lower behind a moving boundary than ahead of it, the boundary generally spreads less rapidly than from diffusion alone and is thus sharper than if the conductivity change aids diffusion. If A and R are the buffer ions, the conductance increases with increasing height at each moving boundary in both sides of the channel (13). A rising boundary thus tends to be sharper than the corresponding descending one. If, however, the mobility of the protein ion is greater than that of the buffer ion of the same sign, the conductivity change is reversed and the rising boundary then becomes, in the absence of a pH effect, the diffuse one.

As is apparent in figure 1a the pH change may also enhance the sharpening effect of the conductivity change at the rising boundary and the spreading effect of this change at the descending boundary or, as in figure 1b, the pH effect may partially counteract the conductivity effect. In at least one system that the author has studied, namely, 0.1 *M* sodium hydroxide, 0.2 *M* glycine, 0.05 *M* glutamic acid (α)-0.1 *M* sodium hydroxide, 0.2 *M* glycine (γ), the pH effect outweighed the conductivity change so that the sharp boundary moved into the solution with the low conductance. In the case of a 0.3 per cent solution of ovalbumin in 0.01 *N* sodium diethylbarbiturate at pH 8.6 the conductivity effect is so small, since the protein and diethylbarbiturate ions have the similar mobilities of -10.8×10^{-5} and -11.9×10^{-5} , respectively, that the pH effect dominates and causes the descending boundary to be the sharp one.

SYSTEMS CONTAINING TWO OR MORE PROTEINS

In the absence of sufficiently precise data on mixtures of two or more proteins it has appeared most practicable to compute, with the aid of Dole's theory, the pattern characteristics for hypothetical systems. If these patterns are then analyzed in the conventional manner the apparent compositions may be compared with those assumed in making the computations and the differences will indicate the errors in the apparent values.

The hypothetical mixture selected for the computations consists of the two proteins, S and T, each at a concentration of 1 per cent, with relative mobilities of $r_s = -0.3$ and $r_T = -0.15$ and equivalent concentrations of $C_s = -0.0036$ and $C_T = -0.0018$. Insofar as it is permissible to lump the serum globulins together as the single component, T, such a solution could represent serum, diluted with two to three volumes of buffer, at pH 8.6 in which the albumin-globulin ratio is unity.

The results of the computations for this protein mixture in 0.1 *N* solutions of the sodium salts of the commonly used buffers are given in table 4. As is clear from the second column of the table, the buffer anions in the first column are arranged in the order of increasing negative mobility. The equivalent refractions of the buffer salts in column 3 were measured at 0°C. in a hollow-prism cell with the aid of the schlieren-scanning camera (7).

As in the case of a single protein (13) the displacement ratios for the fast boundary, column 4 of table 4, and for the slow one, column 5, increase as the buffer anion mobility, $|r_R|$, increases. In a given buffer this ratio is greater for the slow than for the fast boundary and is in accord, therefore, with experiment. In an analysis of twenty-five human plasmas, diluted 1 to 3 in a 0.1 *N* sodium diethylbarbiturate buffer at pH 8.6, Dole (3) obtained 1.06 as the average displacement ratio for the albumin boundary and 1.13 for the globulin boundaries

TABLE 4

Results of computations for a mixture of the two proteins S and T in 0.1 N solutions of sodium buffer salts

Data assumed: $r_{Na} = 1$; $r_s = -0.3$; $r_T = -0.15$; $C_s = -0.0036$; $C_T = -0.0018$

(1)	(2)	(3)	(4)	(5)	(6)
Buffer ion, R	$-r_R$	K_{AR}	$v_r^\beta / v_d^\alpha \beta$	$v_r^\beta / v_d^\beta \gamma$	$-v_d^\beta \gamma \sigma^\alpha$
Diethylbarbiturate	0.4640*	0.04055	1.0371	1.085	0.1471
Lactate	0.5795†	0.01914	1.0443	1.111	0.1459
Glycinate	0.7098†	0.01746	1.0515	1.138	0.1444
Acetate	0.7825‡	0.01235	1.0550	1.150	0.1437
Phosphate (dibasic)	1.1008*	0.01484	1.0595	1.189	0.1411
Chloride	1.6810*	0.01120	1.0844	1.257	0.1381
	(7) (8) CONCENTRATION BOUNDARIES, $\Delta n \times 10^6$		(9) (10) PER CENT OF S		(11) AVERAGE ERROR
	Buffer	Protein	Rising	Descending	per cent
Diethylbarbiturate	268	473	52.55	50.28	1.42
Lactate	155	412	53.47	50.93	2.20
Glycinate	166	473	54.16	51.50	2.83
Acetate	126	458	54.69	51.81	3.25
Phosphate (dibasic)	176	543	55.67	52.59	4.13
Chloride	176	649	57.12	53.44	5.28

* From transference measurements at 0.1 *N* and 0.5°C.

† Assuming additivity of ion conductances at 0.1 *N* and 0.5°C.

‡ From transference measurements at 0.1 *N* and 25.0°C.

If the mobility of the slow protein, T, is computed from the displacement of the slow, descending boundary and the known conductance of the protein solution α , the (relative) values of column 6 are obtained. In the limit of vanishingly small concentrations of protein all of the figures in this column would have the assumed value of -0.15 . The deviations from this are a measure of the errors that are made in the conventional method of determining this mobility.

The computed differences in refractive index at the concentration boundaries, columns 7 and 8 of table 4, indicate the magnitude of these effects in different buffers.

Of most interest, however, are the effects of the superimposed gradients at a boundary due to ions other than the one that disappears. These cause the relative concentration of the fast component S to appear greater than the assumed

value of 50 per cent. Moreover, in the examples of table 4 the error increases with increasing mobility of the buffer anion and is more serious in the pattern of the rising boundaries, column 9, than in that of the descending boundaries, column 10. If the apparent composition from the two patterns is averaged, the deviation from the true value of 50 per cent is then given in column 11.

The available results on mixtures of proteins are in qualitative accord, at least, with the theory as represented by the computations of table 4. As equation 3 indicates, the regulating functions for the two end solutions approach equality as the ratio of the protein to the buffer salt concentration approaches

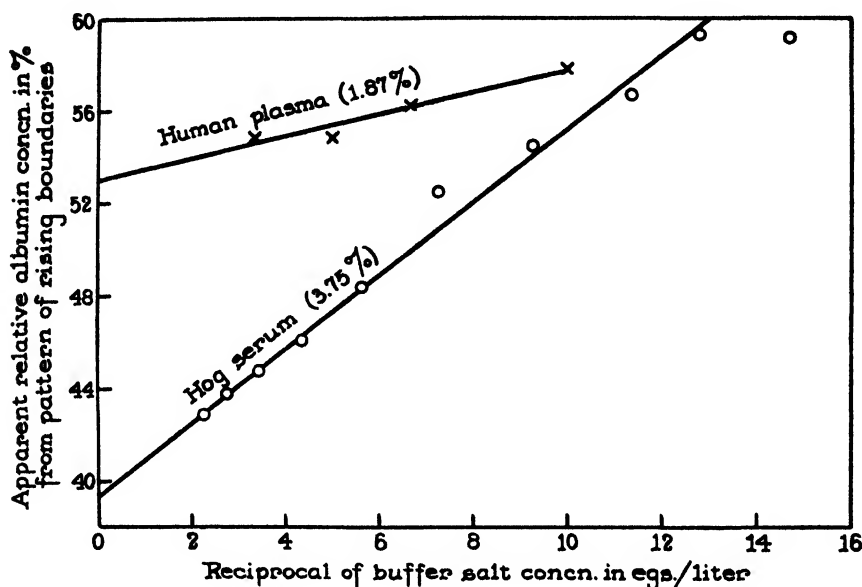


FIG. 2

zero. Thus the true composition of a protein mixture may be obtained by extrapolation of the apparent composition either to zero protein concentration at constant ionic strength or to infinite salt concentration at constant protein content. Both methods have been used. Thus Svensson (11) analyzed a hog serum at a total protein concentration of 3.75 per cent in a 0.068 *N* sodium phosphate buffer at pH 7.7 to which increasing amounts of sodium chloride were added. From the patterns of the rising boundaries he found the apparent albumin content to decrease from 59.1 per cent with no added sodium chloride to 42.9 per cent when the concentration of this salt was 0.37 *N*, whereas the corresponding variation in the patterns of the descending boundaries was from 51.9 per cent to about 44 per cent. These results are in accord with the computations of table 4 insofar as the theory predicts larger errors from the rising-boundary pattern than from that of the descending boundaries and also the relatively large errors to be expected in phosphate-chloride buffers. However, with increasing salt concentration the apparent composition approaches the true value asymp-

totically and the plot used by Svensson is not suitable for extrapolation. As equation 3 suggests and as is shown by the circles in figure 2, a plot of his apparent values against the reciprocal of the salt concentration is approximately linear and extrapolates to an albumin content of 39.4 per cent.

With the aid of a 0.1 *N* sodium diethylbarbiturate buffer at pH 8.6 Perlmann and Kaufman (10) have studied the apparent composition of a human plasma with varying amounts of added sodium chloride. As would be expected from table 4 for this buffer and as is shown graphically by the crosses of figure 2, they observed errors similar to those of Svensson but of smaller magnitude. They also studied the same plasma at different concentrations of total protein. At a constant buffer salt concentration of 0.1 *N* they observed a change in the apparent albumin content from 58.2 to 54.6 per cent as the absolute protein concentration was reduced from 2.66 to 1.0 per cent. In this case the variation was approximately linear and extrapolated to the same albumin content, 53 per cent, as do the crosses of figure 2. Although additional experiments of this type will be necessary in order to establish the relative merits of the two methods of extrapolation, it is clear that a determination of the true composition of a protein mixture will involve at least two experiments in which either the protein concentration or the salt concentration is varied.

SUMMARY

With the aid of the moving-boundary theory developed by Vincent P. Dole the electrophoretic behavior of some typical protein systems has been computed and compared with experiment. Satisfactory agreement is obtained in the case of a single protein if a correction is made for the pH changes at the boundaries as well as for the conductivity changes predicted by the theory. In the case of solutions containing more than one protein both the computations and the available experimental results indicate that appreciable errors may be made in the usual electrophoretic analysis of such mixtures. Procedures for minimizing these errors are suggested.

REFERENCES

- (1) ADAIR, G. S., AND ROBINSON, M. E.: *Biochem. J.* **24**, 993 (1930).
- (2) CANNAN, R. K., KIBRICK, A., AND PALMER, A. H.: *Ann. N. Y. Acad. Sci.* **41**, 243 (1941).
- (3) DOLE, V. P.: *J. Clin. Investigation* **23**, 708 (1944).
- (4) DOLE, V. P.: *J. Am. Chem. Soc.* **67**, 1119 (1945).
- (5) KOHLRAUSCH, F.: *Ann. Physik* **62**, 209 (1897).
- (6) LONGSWORTH, L. G.: *Ann. N. Y. Acad. Sci.* **41**, 267 (1941).
- (7) LONGSWORTH, L. G.: *Ind. Eng. Chem., Anal. Ed.*, **18**, 219 (1946).
- (8) LONGSWORTH, L. G., AND MACINNES, D. A.: *Chem. Rev.* **24**, 271 (1939).
- (9) LONGSWORTH, L. G., AND MACINNES, D. A.: *J. Am. Chem. Soc.* **62**, 705 (1940).
- (10) PERLMANN, G. E., AND KAUFMAN, D.: *J. Am. Chem. Soc.* **67**, 638 (1945).
- (11) SVENSSON, H.: *Arkiv Kemi, Mineral. Geol.* **17A**, No. 14, 1 (1943).
- (12) SVENSSON, H.: *Arkiv Kemi, Mineral. Geol.* **21B**, No. 5, 1 (1945).
- (13) SVENSSON, H.: *Arkiv Kemi, Mineral. Geol.* **22A**, No. 10, 1 (1946).
- (14) TISELIUS, A.: *Trans. Faraday Soc.* **33**, 524 (1937).
- (15) TISELIUS, A., AND SVENSSON, H.: *Trans. Faraday Soc.* **36**, 16 (1940).
- (16) WEBER, H.: *Die partiellen Differential-Gleichungen der mathematischen Physik*, 5th edition, Chap. 24. Braunschweig (1910).

PHYSICAL-CHEMICAL CHARACTERISTICS OF CERTAIN OF THE PROTEINS OF NORMAL HUMAN PLASMA^{1,2,3}J. L. ONCLEY, G. SCATCHARD, AND A. BROWN⁴*Harvard Medical School, Boston, Massachusetts, and Massachusetts Institute of Technology, Cambridge, Massachusetts**Received August 8, 1946*

During a study of the separation of normal human plasma proteins by a low-temperature ethanol fractionation procedure (6, 22, 29), certain components have been isolated in pure form and others in varying degrees of purity. We have studied many of these products, and have attempted to characterize certain of them by physical-chemical methods.

Studies of the electrophoretic behavior of plasma and plasma fractions have indicated the presence of at least seven protein components: albumin, fibrinogen, and α_1 -, α_2 -, β_1 -, β_2 -, and γ -globulins (3, 15, 31). Studies in the ultracentrifuge have indicated that four main components are normally present: "albumin" ($s_{20,w} = 4.6$), "X-protein" ($s = 6$),⁵ "globulin" ($s = 7$), and "20-component" ($s = 20$) (16, 18, 23). Certain components with sedimentation constants between 7 and 20 have been observed during studies of plasma fractions. These components have been arbitrarily classified into two groups: those with sedimentation constants between 8 and 11, and those with constants between 12 and 18.

Studies of the concentrations of each of these ultracentrifuge components in the various fractions obtained during alcohol fractionation of normal human plasma (6, 22) have been carried out, and are recorded graphically in figure 1. For comparison, we have recorded the distribution of the electrophoretic components in a similar manner in figure 2. The height of each bar represents the weight of that fraction obtained during fractionation. For fraction V several bars are placed side by side and the heights should be added together, this fraction representing 48 per cent of the plasma protein (by weight), or 31.5 g. per liter. A comparison of figures 1 and 2 indicates that there is no simple corre-

¹ Presented at the Twentieth National Colloid Symposium, which was held at Madison, Wisconsin, May 28-29, 1946.

² This work was carried out under a contract, recommended by the Committee on Medical Research, between the Office of Scientific Research and Development and Harvard University.

³ This is paper Number 50 in the series "Studies on Plasma Proteins" from the Harvard Medical School, Boston, Massachusetts, on products developed by the Department of Physical Chemistry from blood collected by the American Red Cross.

⁴ Present address: Research and Development Laboratory, Carbide and Carbon Chemicals Corporation, South Charlestown, West Virginia.

⁵ "X-protein", unlike the other components of plasma, was found by Pedersen (23) to have a specific volume very near unity, and accordingly to have an uncorrected sedimentation constant very sensitive to the density of the solvent. In 0.5 *M* sodium chloride solution, a sedimentation constant of about 2.9 is observed. Because of this "density effect" of X-protein, it can easily be differentiated from other components.

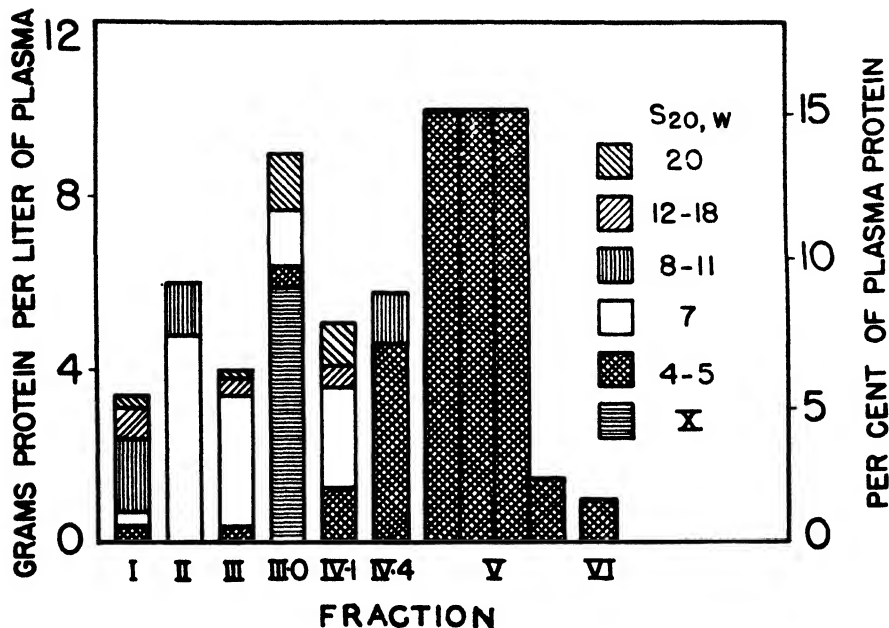


FIG. 1. Distribution of ultracentrifuge components of normal human plasma into fractions obtained by low-temperature ethanol precipitation (see text for detailed description).

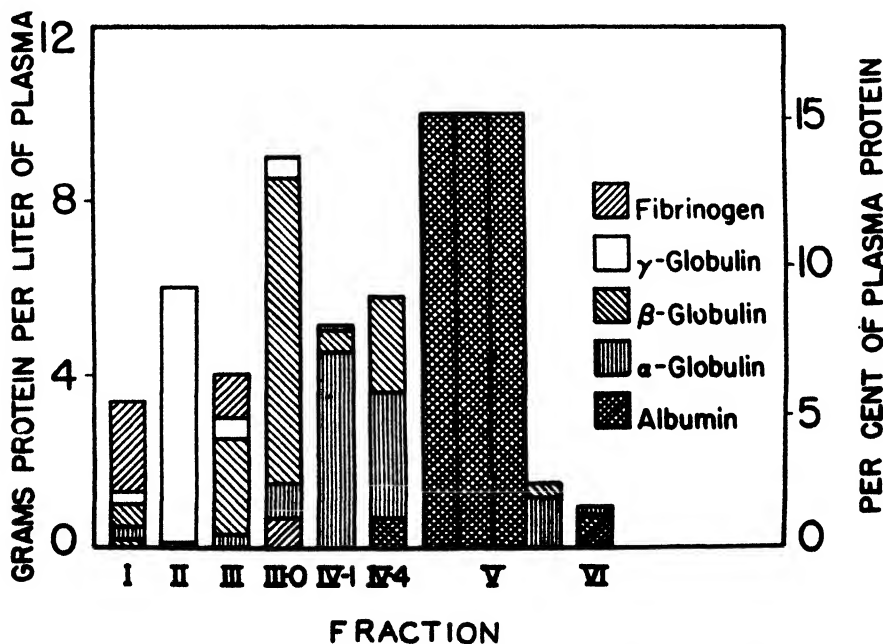


FIG. 2. Distribution of electrophoretic components of normal human plasma into fractions obtained by low-temperature ethanol precipitation (see text for detailed description). This material was taken largely from Table IX of reference 5.

spondence between the electrophoretic and the ultracentrifugal components. Studies of these fractions and certain subfractions obtained by further fractionation have led to the identification of a number of components, however, and certain of these components have been studied by other methods if they were obtained in sufficient purity.

METHODS

Most of the osmotic pressures were measured in an osmometer of the Hepp type (8, 12), modified so that the capillary was perpendicular and the osmometer could be placed in a water thermostat, with a collodion or cellophane membrane. Some were measured in a thimble-type cell (27) with a collodion membrane. Smoothed values were obtained by plotting P/c vs. c or vs. P , whichever gave the straighter line. The molecular weight was determined from the extrapolated value of P/c at c or P equal to zero.

The viscosities were measured in an Ostwald viscometer. Values were extrapolated using the function $H = (\ln \eta/\eta_0)/c$, plotting H vs. c or vs. $\ln \eta/\eta_0$, whichever gave the straighter line; the intrinsic viscosity, H_0 , was taken as the extrapolated value of H at c or $(\ln \eta/\eta_0)$ equal to zero. Here η is the viscosity of the protein solution, η_0 the viscosity of the solvent (usually 0.15 M sodium chloride), and c is the protein concentration in grams per 100 cc. of solution. Values of the Einstein viscosity coefficient, F , were calculated from the intrinsic viscosity, H_0 , and the partial specific volume, V_1 , using the equation $F = 100 H_0/V_1$.

The partial specific volume of the protein was calculated from a plot of w_1 vs. V , where w_1 is the weight fraction of protein and V is the specific volume of the solution.⁶ The partial specific volume appeared to be independent of the concentration of protein over the range we have investigated.

The sedimentation constants were measured in an air-driven ultracentrifuge (1, 26) equipped with a modified Philpot schlieren optical system (25). The measurements were made in a cell 1.65 cm. high, whose center was 6.5 cm. from the axis of rotation. A speed of 54,000 R.P.M. was used, and the average temperature was about 25°C. Values of the sedimentation constant were determined from the slope of a plot of $\log x_i$ vs. t_i^2 , where x_i is the distance from the axis of rotation to the center of the schlieren peak, and t_i^2 is the time of centrifugation, corrected for variation of viscosity of the solvent medium with temperature. The sedimentation constants have been reduced to the value in a solvent of the density and viscosity of water at 20°C., $s_{20,w}$ (30), and are recorded in Svedberg units.

Estimates of f/f_0 values from intrinsic-viscosity studies have been made. These estimates involve the important assumptions that (1) the molecules behave as rigid elongated ellipsoids of revolution, obeying the Simha equation for viscosity (17, 28) and the Perrin equation for f/f_0 (13, 24),⁷ and (2) the amount of hydration is approximately known. The second of these assumptions is of less significance and only becomes of importance if a high degree of

⁶ See pp. 57-66 of reference 30.

⁷ See p. 41 of reference 30 for tabulated values.

TABLE 1

Osmotic-pressure studies of various plasma proteins

PROTEIN	SOLVENT	TEMPERATURE <i>t</i>	CONCENTRATION <i>c</i>	OSMOTIC PRESSURE <i>p</i>	<i>P/c</i>	MOLECULAR WEIGHT <i>M</i>
		°C.	grams per 100 cc.	mm. H ₂ O		
α_1 -Lipoprotein (182, IV-1, 1)	0.15 M NaCl	37	8.33	226	27.1	(78,000)
			5.62	163	29.0	
			4.07	127	31.2	
			2.75	86	31.2	
			1.40	46	32.9	
			0	0	(34.0)	
α_1 -Lipoprotein (184, IV-1, 1)	0.15 M NaCl	37	5.12	90	17.6	(109,000)
			3.41	68	20.0	
			1.70	37	21.8	
			0	0	(24.2)	
α_2 -Globulin (A191C, IV-6-2)	0.15 M NaCl	37	12.42	626	50.4	(600,000)
			8.42	290	34.4	
			5.46	130	23.8	
			4.35	89	20.2	
			2.14	25	11.8	
			1.14	14	12.2	
α_1 Globulin (A191C, IV-7W)	0.15 M NaCl	37	0	0	(4.8)	93,000
			15.57	937	60.2	
			9.83	476	48.4	
			6.51	295	45.3	
			5.14	200	38.9	
			2.83	97	34.3	
β_1 -Lipoprotein (Lot 2)	0.15 M NaCl	37	0	0	(28.5)	(250,000)
			5.43	45	8.3	
			4.17	37	8.9	
			3.24	30	9.3	
γ -Globulin (172-2, II-1,2)	0.15 M NaCl	37	0	0	(10.4)	140,000
			19.27	453	23.5	
			12.35	253	20.5	
			5.81	112	19.3	
γ -Globulin (172-2, II-3)	0.15 M NaCl	37	0	0	(18.6)	200,000
			18.67	500	26.8	
			12.11	232	19.2	
			5.90	94	15.8	
γ -Globulin (SW1, II-3)	0.15 M NaCl	37	0	0	(13.3)	155,000
			16.99	426	25.1	
			11.22	229	20.4	
			5.61	104	18.5	
			3.47	64	18.5	
			0	0	(17.0)	

TABLE 1—(Continued)

PROTEIN	SOLVENT	TEMPER- ATURE <i>t</i>	CONCEN- TRATION <i>c</i>	OSMOTIC PRESSURE <i>p</i>	<i>P/c</i>	MOLECULAR WEIGHT <i>M</i>
		°C.	grams per 100 cc.	mm. H ₂ O		
γ-Globulin (S74A, II-1, 2)	0.15 <i>M</i> NaCl	25	19.63	562	28.6	156,000
			9.63	174	18.1	
			7.36	124	16.9	
			4.94	83	16.8	
			2.40	39	16.4	
			0	0	(16.2)	
Fibrinogen (167, I-2)	0.05 <i>M</i> sodium citrate buffer, pH 6.4	37	8.54	112	13.1	580,000
			5.21	37	7.0	
			2.83	17	6.2	
			0	0	(4.5)	

accuracy is demanded, since the relations between f/f_0 and the viscosity coefficient F depend upon solvation and the form of the ellipsoid but to a limited extent. We have assumed that 0.2 g. of water is bound by 1 g. of protein in all cases but that of the β_1 -lipoprotein, and that the ellipsoids are elongated. This is the shape and amount of hydration obtained for serum albumin and certain other proteins from dielectric-dispersion studies (20). In the case of the β_1 -lipoprotein we have calculated the hydration from specific-volume measurements which are reported in a later section of this paper.

PROPERTIES OF COMPONENTS

Results of the osmotic-pressure, viscosity, specific-volume, and sedimentation-constant studies of various plasma fractions are recorded in tables 1 to 4.

Albumin

Fraction V, containing about 98 per cent of albumin (6), and crystallized albumin, containing not more than a few tenths of a per cent of globulin (5), have been studied. Studies in the ultracentrifuge usually show less than 2 per cent of material with sedimentation constants different from that found for albumin. Osmotic-pressure studies, which have been reported elsewhere (27), indicated a molecular weight of 69,000. Viscosity measurements yield an intrinsic viscosity of 0.042. A partial specific volume of 0.733, in good agreement with the value of 0.736 reported by Pedersen (23), has been obtained from density measurements. The sedimentation constant at zero protein concentration was found to be about 4.6, again in agreement with Pedersen's value (23). The diffusion constant is less accurately known. Preliminary measurements have led to a tentative value^a of 6.1 for $D_{20,w}$. Pedersen (23) reports a value of 5.9,

^a All diffusion constants are reduced to $D_{20,w}$, and recorded in units 10^7 times the c.g.s. unit.

TABLE 2
Viscosity studies of various plasma proteins

PROTEIN	SOLVENT	TEMPER- ATURE <i>t</i>	CONCEN- TRATION <i>c</i>	RELATIVE VISCOSITY η/η_0	$\ln (\eta/\eta_0)$	H
		°C.	<i>grams per 100 cc.</i>			
Albumin (cryst.) (HA42)	0.15 <i>M</i> NaCl	37	25.0	5.75	1.750	0.070
			17.7	2.82	1.037	0.059
			11.3	1.78	0.576	0.051
			0	1.00	0	(0.042)
Albumin (185, V)	0.15 <i>M</i> NaCl	37	19.58	3.48	1.250	0.064
			14.06	2.25	0.812	0.058
			9.17	1.61	0.474	0.052
			0	1.00	0	(0.042)
α_1 -Lipoprotein (182, IV-1, 1)	0.15 <i>M</i> NaCl	37	8.33	2.42	0.884	0.106
			5.47	1.59	0.464	0.086
			2.62	1.22	0.199	0.076
			0	1.00	0	(0.066)
α_1 -Lipoprotein (184, IV-1, 1)	0.15 <i>M</i> NaCl	37	5.12	1.68	0.519	0.101
			3.41	1.35	0.300	0.088
			1.70	1.14	0.131	0.074
			0	1.00	0	(0.066)
α_2 -Globulin (A191C, IV-6-2)	0.15 <i>M</i> NaCl	37	19.33	16.9	2.823	0.146
			12.76	5.09	1.628	0.128
			8.42	2.64	0.973	0.116
			0	1.00	0	(0.092)
β_1 -Globulin (A191C, IV-7W)	0.15 <i>M</i> NaCl	37	23.06	9.30	2.230	0.096
			15.57	3.40	1.224	0.079
			9.83	1.93	0.660	0.067
			5.14	1.36	0.306	0.060
β_1 -Lipoprotein (Lot 2)	0.15 <i>M</i> NaCl	37	0	1.00	0	(0.055)
			5.43	1.28	0.248	0.046
			3.24	1.15	0.142	0.044
			0	1.00	0	(0.041)
γ -Globulin (172-2, II-1, 2)	0.15 <i>M</i> NaCl	37	19.27	11.85	2.475	0.128
			12.35	3.56	1.270	0.103
			5.81	1.59	0.464	0.080
			0	1.00	0	(0.059)
γ -Globulin (172-2, II-3)	0.15 <i>M</i> NaCl	37	18.67	13.52	2.600	0.140
			12.11	3.94	1.370	0.113
			5.90	1.68	0.519	0.088
			0	1.00	0	(0.065)
γ -Globulin (SW1, II-3)	0.15 <i>M</i> NaCl	37	11.22	3.29	1.190	0.106
			5.61	1.61	0.476	0.085
			3.47	1.31	0.270	0.079
			0	1.00	0	(0.071)

TABLE 2—(Continued)

PROTEIN	SOLVENT	TEMPERATURE <i>t</i>	CONCENTRATION <i>c</i>	RELATIVE VISCOSITY η/η_0	$\ln(\eta/\eta_0)$	<i>H</i>
		°C.	grams per 100 cc.			
γ -Globulin (179, II-1, 2)	0.15 <i>M</i> NaCl	37	16.2	6.53	1.876	0.116
			11.98	3.45	1.227	0.103
			7.85	1.98	0.685	0.087
			5.08	1.50	0.402	0.079
			0	1.00	0	(0.059)
γ -Globulin (179, II-1, 2)	0.15 <i>M</i> NaCl	0	16.2	13.43	2.598	0.159
			11.96	4.90	1.590	0.133
			7.91	2.33	0.846	0.107
			5.12	1.62	0.484	0.094
			0	1.00	0	(0.065)
γ -Globulin (179-II-3)	0.15 <i>M</i> NaCl	37	15.3	6.90	1.932	0.126
			10.4	2.81	1.034	0.099
			6.72	1.79	0.582	0.087
			0	1.00	0	(0.069)
γ -Globulin (179-II-3)	0.15 <i>M</i> NaCl	0	15.44	15.88	2.765	0.179
			10.39	4.02	1.390	0.134
			6.75	2.03	0.710	0.105
			0	1.00	0	(0.084)
γ -Globulin (66, II-1, 2)	0.15 <i>M</i> NaCl	37	20.68	20.01	2.997	0.145
			15.04	6.37	1.852	0.123
			9.45	2.58	0.947	0.100
			4.82	1.49	0.396	0.082
			0	1.00	0	(0.062)
Fibrinogen (167, I-2)	0.05 <i>M</i> sodium citrate buffer (pH = 6.4)	37	2.93	2.35	0.856	0.293
			1.58	1.52	0.416	0.263
			1.16	1.34	0.293	0.253
			0	1.00	0	(0.228)

for this quantity. Using $s = 4.6$, $D = 6.1$, and $V = 0.733$, we calculate a molecular weight of 69,000.

γ -Globulin

A number of γ -globulin preparations (9, 22) have been studied, several of which contained over 98 per cent of a single electrophoretic component. The principal impurities were albumin and β -globulin. The preparations all contained less than 0.06 per cent of cholesterol, and approximately 1 per cent of carbohydrate (6).⁹ We have found a value of 0.739 for the partial specific

⁹ The γ -globulin prepared electrophoretically and studied by Blix, Tiselius, and Svensson (J. Biol. Chem. 137, 485 (1941)) contained considerably more cholesterol (0.1–0.7 per cent) and carbohydrate (3 per cent).

TABLE 3
Specific-volume studies of various plasma proteins

PROTEIN	SOLVENT	TEMPERATURE <i>t</i>	CONCENTRA- TION % $\times 100$	SPECIFIC VOLUME <i>V</i>	PARTIAL SPECIFIC VOLUME <i>V</i> ₁
		°C.	grams per 100 g		
Albumin (cryst.) (179, 5X)	Water	25	5.76	0.9874	0.733
			2.30	0.9967	
			1.17	0.9998	
			0	1.0029	
α_1 -Lipoprotein (182, IV-1, 1)	0.15 <i>M</i> NaCl	37	8.45	0.9857	0.841
			5.52	0.9905	
			2.63	0.9949	
			0	(1.0006)	
α_2 -Globulin (A191C, IV-6-2)	0.15 <i>M</i> NaCl	25	9.56	0.9663	0.693
			6.69	0.9755	
			4.70	0.9820	
			2.94	0.9872	
β_1 -Globulin (A191C, IV-7W)	0.15 <i>M</i> NaCl	37	0	0.9966	0.725
			6.01	0.9840	
			5.44	0.9858	
			4.28	0.9887	
β_1 -Lipoprotein (Lot 2)	0.15 <i>M</i> NaCl	25	3.28	0.9918	0.950
			2.43	0.9940	
			0	1.0006	
			5.40	0.9941	
β_1 -Globulin mixture (lot 2)	0.15 <i>M</i> NaCl	25	2.16	0.9956	0.745
			1.08	0.9961	
			0	0.9966	
			4.90	0.9843	
γ -Globulin (179, II-1, 2)	0.15 <i>M</i> NaCl	25	1.96	0.9915	0.739
			0.79	0.9945	
			0	0.9966	
			4.45	0.9846	
γ -Globulin (179, II-3)	0.15 <i>M</i> NaCl	25	4.06	0.9862	0.739
			2.45	0.9903	
			1.77	0.9917	
			0.89	0.9940	
γ -Globulin (179, II-3)	0.15 <i>M</i> NaCl	25	0.76	0.9946	0.739
			0	0.9966	
			5.03	0.9836	
			3.36	0.9879	
γ -Globulin (179, II-3)	0.15 <i>M</i> NaCl	25	2.01	0.9915	0.739
			1.62	0.9924	
			0.80	0.9946	
			0.66	0.9950	
γ -Globulin (179, II-3)	0.15 <i>M</i> NaCl	25	0	0.9966	0.739

TABLE 4
Sedimentation-constant studies of various plasma proteins

PROTEIN	SOLVENT	CONCENTRATION	SEDIMENTATION CONSTANT	
		<i>c</i> <i>grams per 100 cc.</i>		
Albumin (cryst.) (HA42)	0.15 <i>M</i> NaCl	2.0	3.9	
		1.0	4.9	
		0.5	4.5	
		0.25	4.6	
Albumin (cryst.) (179)	0.15 <i>M</i> NaCl	1.4	4.4	
		1.0	4.7	
		0.5	4.2	
α_1 -Lipoprotein (184, IV-1, 1)	0.50 <i>M</i> NaCl	2.5	3.8	
		1.0	4.8	
		0.5	4.9	
α_1 -Lipoprotein (182, IV-1, 1)	0.15 <i>M</i> NaCl	1.0	4.5	
α_1 -Lipoprotein (S362, IV-1-1W)	0.15 <i>M</i> NaCl	1.0	4.5	
α_2 -Globulin (AVL54, IV-6-2)	0.15 <i>M</i> NaCl	3.3	5.7*	
		2.0	6.9*	
		1.0	7.0*	
		0.6	8.6*	
α_2 -Globulin (A191C, IV-6-2)	0.15 <i>M</i> NaCl	4.0	4.5*	
		1.0	7.0*	
		0.5	8.1*	
α_2 -Globulin (S366-1, IV-6-2)	0.15 <i>M</i> NaCl	5.2	4.1*	
		3.5	5.2*	
		2.0	7.3*	
		1.0	8.0*	
β_1 -Globulin (A191C, IV-7W)	0.15 <i>M</i> NaCl	4.0	4.6	
		2.0	5.0	
		1.0	5.1	
		0.5	5.6	
β_1 -Globulin (S366-1, IV-7W)	0.15 <i>M</i> NaCl	2.5	4.5	
		2.0	5.0	
		1.0	5.5	
		0.5	5.0	
β_1 -Globulin mixture (S366, III-0-Ba)	0.15 <i>M</i> NaCl	2.3	7.3	16.2
		1.0	7.1	18.8
		0.5	7.5	20.9
β_1 -Globulin mixture (S366, III-0-Bb)	0.15 <i>M</i> NaCl	2.0	6.6	16.1
		1.9	6.9	18.1
		1.0	7.0	19.8
		0.6	7.2	19.8

TABLE 4—*Concluded*

PROTEIN	SOLVENT	CONCENTRATION <i>c</i>	SEDIMENTATION CONSTANT <i>s</i> _{10,w}	
		grams per 100 cc		
β_1 -Lipoprotein (lot 1)	0.50 <i>M</i> NaCl	3.4	2.3*	
		1.7	2.5*	
		0.8	2.8*	
		0.5	2.9*	
γ -Globulin (S35, II-1, 2)	0.15 <i>M</i> NaCl	7.8	4.8	
		6.5	4.8	
		5.0	5.6	6.7*
		2.5	5.8	7.9*
		1.6	6.7	9.8*
		1.0	7.2	9.8*
		0.5	6.9	9.8*
		0.25	7.3	10.3*
γ -Globulin (L498, II-1, 2)	0.15 <i>M</i> NaCl	6.9	4.7	6.2*
		5.1	5.6	7.4*
		3.5	6.0	8.1*
		1.7	6.7	9.6*
		0.8	6.9	9.6*
		0.4	7.1	10.3*
Fibrinogen (167, I-2)	0.05 <i>M</i> sodium citrate buffer, pH 6.4	2.0	7.0	
		1.0	8.3	
		0.5	8.5	

* This fraction is rather heterogeneous and the sedimentation constant listed here represents only an average value.

volume, considerably larger than the value 0.718 reported by Pedersen (23). The ultracentrifuge studies indicated that only 75–85 per cent of these preparations sediments with a constant of the magnitude usually assigned to the globulin of serum or plasma (*ca.* 7). The remaining material is somewhat heterogeneous, but has a mean sedimentation constant considerably larger. Extrapolation of these two sedimentation constants yields values of about 7.2 and 10 at zero protein concentration. Pedersen (23) gives 7.1 and Bridgman (2) 7.3 for the sedimentation constant of γ -globulin.

There is considerable variation in the viscosity measurements of different preparations, but a value of 0.067 for the intrinsic viscosity is obtained from averaging all the results. Since this value is obtained from preparations containing about 20 per cent of the component with a sedimentation constant of 10, it must be corrected before it can be properly applied to the γ -globulin component with $s = 7$. The $s = 10$ component could represent (1) a component composed of two molecules of the $s = 7$ component associated end to end, (2) a component of the same molecular weight as the $s = 7$ component but spherical in shape, or (3) some other component entirely unrelated to the size and shape of the

$s = 7$ component. We have taken the first of these possibilities as the most likely, which would give an intrinsic viscosity of about 0.06 for the $s = 7$ component. Additional data are required before the other possibilities may be eliminated. Studies of diffusion constant would be of considerable value in interpreting these results. Bridgman (2) has studied the diffusion constants of preparations of γ -globulin prepared by these methods, and reports $D_A = 3.81$ and $D_m = 3.57$. Pedersen (23) gives the values $D_A = 3.99$ and $D_m = 4.01$ for his preparations of γ -globulin (which may contain a very different amount of

TABLE 5

Protein components of normal human plasma characterized by physical-chemical methods

ELECTROPHORETIC COMPONENT	FRACTION†	AP-PROXI-MATE AMOUNT IN PLASMA	SEDI-MENTA-TION (CON STANT 570.0)	SPECIFIC VOLUME V	INTRIN-SIC VIS-COSITY $H_0 \times 10^5$	FRIC-TIONAL RATIO f/f_0	MOLECULAR WEIGHT M	APPROXIMATE DIMENSIONS	
								Length	Diam-eter
		grams per liter						A.	A.
Albumin.....	V	32	4.6	0.733	4.2	1.28	69,000	150	38
α_1 -Globulin.....	IV-1	2*	5.0	0.841	6.6	1.38	230,000	300	50
α_2 -Globulin.....	IV-6	1	9.	0.693	9.2	1.58	(300,000)		
β_1 -Globulin ...	IV-7	2	5.5	0.725	5.5	1.37	90,000	190	37
β_1 -Globulin .	III-0, III-2	2	7.	0.74			(150,000)		
β_1 -Globulin .	III-0	1	20.	0.74			(500,000-1,000,000)		
β_1 -Globulin	III-0	2*	2.9†	0.950	4.1	1.7†	1,300,000	185	185
β_2 -Globulin.	III-1	2	7.				(150,000)		
γ -Globulin. . .	II	5	7.2	0.730	6.	1.38	156,000	235	44
γ -Globulin ..	II	1	10.				(300,000)		
Fibrinogen....	I-2	2	9.		25.	1.98	400,000	700	38

* These two globulins are lipoproteins containing 35 per cent lipid for the α_1 -globulin and 75 per cent lipid for the β_1 -globulin. The other components contain little or no lipid.

† This is the sedimentation constant obtained in 0.5 M sodium chloride solution, when corrected in the usual manner. The f/f_0 value given here is the value for sedimentation, correcting for the partial specific volume of the hydrated protein (0.97), using the equation of Kraemer (equation 124, p. 65, reference 30). A solvation of 0.6 g. of water per gram of protein was used for this calculation, and the molecule was assumed spherical.

‡ These designations of the various fractions, and especially the designations used in tables 1-4, are those employed during the development of new fractionation processes. Because of the large number of components being separated from fractions III and IV, a revised terminology will be introduced when a definitive process is at hand.

$s = 10$ component, since he used an entirely different method of preparation and does not refer to this component in his studies). The assumption that the $s = 10$ component is a double molecule of the $s = 7$ component leads to values of $D_A = 3.9$ and $D_m = 4.0$ for the mixtures we have been considering, taking the dimensions we have calculated for the $s = 7$ component (table 5).

β -Globulin

A considerable number of components whose electrophoretic behavior is that of either β_1 - or β_2 -globulin have been separated from certain fractions. Most

of the β -globulin is found in fractions III, III-0, and IV-4, with a smaller amount in fractions IV-1 and V.

Fraction III-1, obtained from fraction III (22), contains somewhat more than half β_2 -globulin, and most of this fraction is found to have a sedimentation constant of about 7. There would thus seem to be evidence for the existence of a component having the electrophoretic mobility of β_2 -globulin and $s = 7$, but more purified samples of this component have not been studied in our laboratory.¹⁰ Studies of fraction III-1 would seem to indicate that this component probably has a conventional partial specific volume, and the viscosities of solutions would indicate that the molecules were not unusually asymmetrical. A tentative estimate of molecular weight of about 150,000 has thus been made, but we have no further data to evaluate this value.

Fraction III-2, also obtained from fraction III (22), contains about one-half β_1 -globulin. Certain subfractions of this material have contained as much as 80 per cent of β_1 -globulin. This fraction also has a large percentage of a component with sedimentation constant of about 7, and leads us to postulate a β_1 -globulin with these properties.

Fraction III-0 contains 70–80 per cent of β_1 -globulin, and certain euglobulin subfractions of this material contain over 90 per cent of β_1 -globulin (21). These subfractions have been further separated by spinning in the preparative ultracentrifuge to yield solutions containing (1) 90–100 per cent of β_1 -lipoprotein; (2) a mixture of components with $s = 7$ (70 per cent) and 20 (25 per cent), but over 85 per cent β_1 -globulin and containing less than 2 per cent of lipid; (3) over 80 per cent of an $s = 20$ β_1 -globulin component containing practically no lipid. The β_1 -lipoprotein component was found to contain about 75 per cent lipid and only about 4 per cent nitrogen (21), and ultracentrifuge studies show that it has the properties of the "X-protein" of McFarlane (16) and Pedersen (23). A partial specific volume of 0.950 and an intrinsic viscosity of 0.041 were obtained for this material. We have calculated the hydration, w , of the β_1 -lipoprotein from the equation (19)

$$w = (V_h - V_1)/(V_0 - V_h)$$

where V_h , V_1 , and V_0 are the specific volumes of the hydrated protein, the anhydrous protein, and water, respectively. Using $V_h = 0.97$, $V_1 = 0.95$, and $V_0 = 1.00$, this yields $w = 0.6$ for the hydration of this molecule,¹¹ in good agreement with the value obtained from the intrinsic viscosity, assuming that the molecule is spherical and hydrated. Osmotic-pressure studies indicated a much lower molecular weight for this component than is obtained from the other studies, and also indicated considerable leakage through collodion membranes impermeable to other plasma proteins. Since there should have been no leakage of a molecule of this size, the assumption was made that the osmotic pressure of this component was due to smaller molecules, very probably of lipid,

¹⁰ More highly purified samples of this component have been obtained by H. F. Deutsch, R. A. Alberty, and L. J. Gosting at the Department of Chemistry, University of Wisconsin (see *J. Biol. Chem.* **165**, 21 (1946)).

¹¹ See p. 31 of reference 23 for the evaluation of V_h .

in equilibrium with the β_1 -lipoprotein. Partial specific volumes have been evaluated for the β_1 -globulin mixture of the $s = 7$ and $s = 20$ components, indicating a normal value of 0.745. Physical-chemical studies on the solution containing a high concentration of the $s = 20$ component have been limited to ultracentrifuge and electrophoretic measurements, since a great deal of denaturation of this component upon dilution has been observed.

A component from fraction IV-4 (29) has been isolated in a subfraction containing 70 per cent β_1 -globulin, and with $s = 5.5$. Measurements of intrinsic viscosity and partial specific volume yield values of 0.055 and 0.725, respectively, while osmotic-pressure studies indicate a molecular weight of about 90,000.

α -Globulin

Most of the α -globulin is found in fractions IV-1 and IV-4, with smaller amounts in fractions V and III-0 and traces in fractions I, III, and VI.

An α_1 -lipoprotein containing about 35 per cent lipid has been separated from fraction IV-1 in a nearly homogeneous subfraction, as revealed by either electrophoresis or ultracentrifugation (7). The sedimentation constant of this material is near 5.0, and the partial specific volume is 0.841. Studies of intrinsic viscosity give a value 0.066, while osmotic-pressure studies show a fairly large P/c ratio with considerable leakage through the collodion membranes. As was the case with the β_1 -lipoprotein, these osmotic-pressure results could be explained if a small concentration of lipid were in equilibrium with the α_1 -lipoprotein, and hence the lower estimate of the molecular weight obtained in this manner has not been considered.

An α_2 -globulin has been separated from fraction IV-4, with an electrophoretic purity of 90–95 per cent (29). This material has a somewhat smaller specific volume, 0.693, than is usually found for protein molecules, and a high viscosity and low osmotic pressure. It contains a number of somewhat poorly characterized components when studied in the ultracentrifuge. The average sedimentation constant, extrapolated to zero concentration, is of the order of 9. These measurements indicate that this fraction has a rather large molecular weight, perhaps about 300,000.

Fibrinogen

A purified fibrinogen has been prepared from fraction I (10). Over 90 per cent of this material was clotted by thrombin. Approximately 90 per cent of this preparation had a sedimentation constant of about 9 when extrapolated to zero protein concentration. An intrinsic viscosity of about 0.23 was observed for this fraction. Since some of this preparation seemed to consist of smaller molecules than fibrinogen, we have assumed 0.25 to be an approximate value for the intrinsic viscosity of fibrinogen. A length of about 700 Å. has been estimated from double refraction of flow measurements (11), assuming a rigid ellipsoidal model for the molecule. Combination of viscosity and sedimentation-constant measurements, with the same assumptions about the shape of the molecules, gives an equatorial diameter of about 38 Å. These estimates of the dimensions of fibrinogen yield a molecular weight of about 400,000. The os-

otic-pressure studies of this preparation indicated a somewhat larger molecular weight. Both of these estimates are lower than the molecular weight of 700,000 estimated from a combination of sedimentation and diffusion-constant measurements by Holmberg (14).

SUMMARY

The physical-chemical properties of the various plasma components have been summarized in table 5, together with an estimate of the amount present in plasma. These properties are not precisely known in many cases, but must be regarded as our best estimates at the present time. Further studies with more highly purified fractions will be required to evaluate these properties more accurately. At that time it will also be essential to obtain estimates for the diffusion constants of these components, as well as other studies to confirm the size and shape estimates.

The approximate dimensions of most of these components have been calculated, assuming that the molecules are rigid ellipsoids with hydration to the extent of 0.2 g. of water per gram of protein (except β_1 -lipoprotein which binds 0.6 g. of water). Such calculations are, of course, much too simple to represent accurately the dimensions of the molecules, but even preliminary estimates of these quantities are useful in interpreting the physiological behavior of proteins.

The variations in these physical-chemical properties of certain of these plasma proteins are unusually large. For example, the spread from 0.693 to 0.950 for the partial specific volumes of these proteins is greater than usually ascribed to proteins from all sources. The intrinsic viscosity of β_1 -lipoprotein is unusually low for a protein of such high molecular weight. The wide range of the physical-chemical properties of plasma proteins does not seem so unusual, however, if we consider the wide range of functions of these proteins and the unusual composition of many of the molecules. A more complete knowledge of both the physical-chemical and the chemical characteristics of these proteins is one of the essentials to our understanding of their function.

REFERENCES

- (1) BAUER, J. H., AND PICKELS, E. G.: J. Exptl. Med. **65**, 565 (1937); see also pp. 191-212 of reference 30.
- (2) BRIDGMAN, W. B.: J. Am. Chem. Soc. **68**, 857 (1946).
- (3) COHN, E. J.: Chem. Rev. **28**, 395 (1941).
- (4) COHN, E. J., AND EDSALL, J. T.: *Proteins, Amino Acids and Peptides as Ions and Dipolar Ions*. Reinhold Publishing Corporation, New York (1943).
- (5) COHN, E. J., HUGHES, W. L., JR., AND WEARE, J. H.: In preparation.
- (6) COHN, E. J., STRONG, L. E., HUGHES, W. L., JR., MULFORD, D. J., ASHWORTH, J. N., MELIN, M., AND TAYLOR, H. L.: J. Am. Chem. Soc. **68**, 459 (1946).
- (7) COHN, E. J., STRONG, L. E., BLANCHARD, M. H., AND BICK, M.: Personal communication.
- (8) DAVIS, B. D.: Personal communication.
- (9) DEUTSCH, H. F., GOSTING, L. J., ALBERTY, R. A., AND WILLIAMS, J. W.: J. Biol. Chem. **164**, 109 (1946).
- (10) EDSALL, J. T., MORRISON, P. R., AND MILLER, S. G.: In preparation.
- (11) EDSALL, J. T., FOSTER, J. F. AND SCHEINBERG, H.: In preparation.

- (12) HEPP, O.: *Z. ges. exptl. Med.* **99**, 709 (1935).
- (13) HERZOG, R. O., ILLIG, R., AND KUDAR, H.: *Z. physik. Chem.* **A167**, 329 (1933).
- (14) HOLMBERG, C. G.: *Arkiv. Kemi, Mineral. Geol.* **17A**, No. 28 (1944).
- (15) LONGSWORTH, L. G.: *Chem. Rev.* **30**, 323 (1942).
- (16) MCFARLANE, A. S.: *Biochem. J.* **29**, 407, 660, 1175, 1202 (1935).
- (17) MEHL, J. W., ONCLEY, J. L., AND SIMHA, R.: *Science* **92**, 132 (1940).
- (18) MUTZENBECHER, R. VON: *Biochem. Z.* **266**, 226, 250, 259 (1933).
- (19) ONCLEY, J. L.: *Ann. N. Y. Acad. Sci.* **41**, 138 (1941).
- (20) ONCLEY, J. L.: *Chem. Rev.* **30**, 433 (1942); see also chapter 22 of reference 4.
- (21) ONCLEY, J. L., MELIN, M., AND GROSS, P. M., JR.: In preparation.
- (22) ONCLEY, J. L., MELIN, M., RICHERT, D. A., CAMERON, J. W., AND GROSS, P. M., JR.: In preparation.
- (23) PEDERSEN, K. O.: *Ultracentrifugal Studies on Serum and Serum Fractions*. Almqvist and Wiksells Boktryckeri AB, Upsala, Sweden (1945).
- (24) PERRIN, F.: *J. phys. radium* [7] **7**, 1 (1936).
- (25) PHILPOT, J. ST. L.: *Nature* **141**, 283 (1938).
- (26) PICKELS, E. G.: *Rev. Sci. Instruments* **9**, 358 (1938); **13**, 426 (1942).
- (27) SCATCHARD, G., BATCHELDER, A. C., AND BROWN, A.: *J. Clin. Investigation* **23**, 458 (1944); *J. Am. Chem. Soc.* **68**, 2320 (1946).
- (28) SIMHA, R.: *J. Phys. Chem.* **44**, 25 (1940).
- (29) STRONG, L. E., SURGENOR, D. M., TAYLOR, H. L., AND COHN, E. J.: Personal communication.
- (30) SVEDBERG, T., AND PEDERSEN, K. O.: *The Ultracentrifuge*. Oxford University Press, New York (1940).
- (31) TISELIUS, A.: *Biochem. J.* **31**, 1464 (1937).

MULTIPLE PROTEIN INTERACTIONS AS EXHIBITED BY THE BLOOD-CLOTTING MECHANISM¹

WALTER H. SEEGER²

College of Medicine, Wayne University, Detroit, Michigan

Received August 8, 1946

There is now emerging, from the researches of the past century, a tangible concept of a whole system of protein interactions involved in the blood-clotting mechanism. An undertaking of these reactions will lead to new viewpoints in protein chemistry. From the advances and contributions already made, it is apparent that the techniques of physical chemistry in conjunction with quantitative measurements of protein reactivity will be drawn upon heavily for the elucidation of the problems involved. It is the purpose of this paper to organize the existing information as briefly as possible, to show the relationships of the components of the system, and to incorporate new contributions from our labora-

¹ Presented at the Twentieth National Colloid Symposium, which was held at Madison, Wisconsin, May 28-29, 1946.

² This work was aided by a grant from the Research Department, Parke, Davis, and Company, Detroit, Michigan.

tory. If it is obvious that this field of knowledge is incomplete, it is not so much a reflection on the labors of the past, as an indication that previous efforts have born fruit and that the opportunities for future investigators are promising.

I. A SYSTEM OF INTERACTIONS

The reactions under consideration are correlated in figure 1. Prothrombin, a glycoprotein (35), reacts with thromboplastin, a macromolecular lipoprotein (6, 7, 8), to yield thrombin (33) and perhaps other products not identified as yet. The reaction requires the presence of calcium ion (1, 15) in optimum concentration. Only strontium can serve as a substitute, and even it is not as efficient as calcium (23). It has been shown that the reaction is stoichiometric (26) in

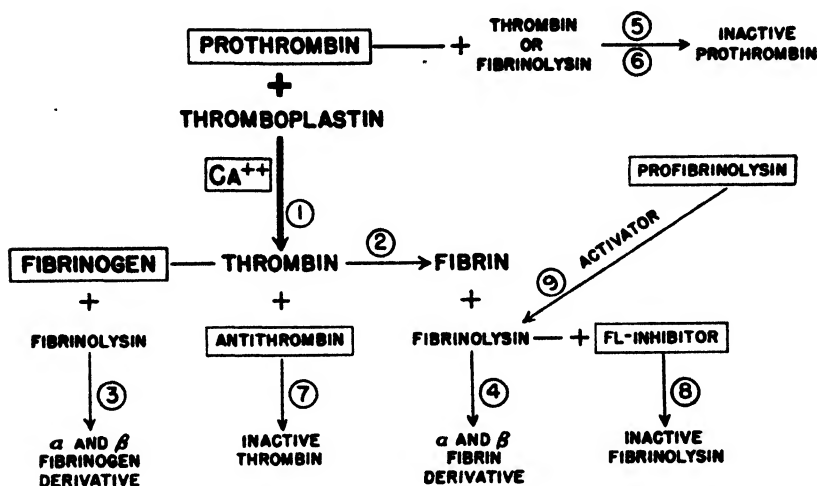


FIG. 1. Correlation of protein interactions involved in the blood-clotting mechanism

character, can be blocked with inorganic salts (23) in moderately high concentration, and also with heparin (22) and an unidentified blood plasma factor (5). Either of the latter two factors alone is without effect (5, 25, 30).

In a second reaction the newly formed enzyme thrombin transforms a large (12) long (17) protein molecule, fibrinogen, into insoluble fibrin. The latter is essentially crystalline in structure (2, 14, 16, 20, 21, 41, 43, 44), and its amino acid composition is known (4). Inorganic salts tend to inhibit the reaction (38). Calcium ion, though not essential, favors the rate (38) of fibrin formation and probably gives a more insoluble fibrin (3, 34). Various colloids also speed up the reaction (38). It has been shown that a certain amount of thrombin disappears with fibrin formation (19, 32, 46). Later, in this paper, data will be presented to show that this is incidentally due to adsorption of thrombin on fibrin and is not a part of the basic mechanics of fibrinogen and thrombin interactions.

In another reaction a plasma-derived protein, fibrinolysin, acts on fibrinogen and decomposes it into at least two protein derivatives (42). The reaction has

many similarities to equation 4, in which the solid fibrin clot is also attacked by fibrinolysin. In the latter case there are also at least two decomposition products (42), and since it is likely that they are the same derivatives as those obtained from fibrinogen, it is possible to use this information in explaining reaction 2. We have discovered that this same fibrinolysin will also destroy prothrombin (equation 6). This topic will be discussed in succeeding paragraphs.

It has also been shown, with the use of purified systems, that thrombin destroys prothrombin as represented by equation 5 (27). The complication extends even farther. Both fibrinolysin and thrombin, which are destructive to prothrombin, can be destroyed by a specific factor, which is in each instance another plasma protein. The specific plasma factor which destroys thrombin (equation 7) is plasma antithrombin, a factor long recognized but still not isolated. The reaction is greatly accelerated by heparin (31, 37), but the quantity of thrombin which can be destroyed by a given amount of antithrombin is definitely limited (40). In the case of fibrinolysin the specific inhibitor normally present in plasma (equation 8) alters fibrinolysin in such a manner as to make it incapable of attacking fibrinogen, fibrin (10, 29), or, as will be shown below, prothrombin.

Finally, fibrinolysin has its origin in profibrinolysin (9, 11, 24, 28), a plasma protein. The best experiments completed to date indicate that activation of profibrinolysin is probably accomplished by a specific activator (10), as represented by equation 9. Such an activator can be prepared from streptococci (18, 28). This activation is in a sense the counterpart of prothrombin activation by thromboplastin, as represented by equation 1. Eventually it will be necessary to explain how the animal organism provides for the activator when it is needed. Just as platelets and tissue extracts supply thromboplastin for the activation of prothrombin (33, 45), a special source of fibrinolysin activator must be present in some tissue(s), in which, however, it has not been recognized as yet. In the laboratory, chloroform serves the purpose of an activator (13).

II. COEXISTENCE

In the organization plan of figure 1 calcium ion and certain proteins have been enclosed in rectangles. This designates factors which coexist in plasma. Although each of these protein molecules has reactive groups, their properties are such that they will not react with each other. Now, let us consider what is involved when prothrombin is activated to thrombin. (1) It must be altered, at some point in the molecule, by thromboplastin. (2) It can attack fibrinogen. (3) It can attack prothrombin. (4) It can no longer be destroyed by fibrinolysin. (5) It can be destroyed by antithrombin. A single protein and its derivative are thus seen to be involved in a variety of reactions, and the whole system is interrelated in such a manner as to suggest common configurational patterns. Similarly, when profibrinolysin is activated the following is involved: (1) It must be altered, at some point in the molecule, by profibrinolysin activator. (2) It can attack fibrinogen. (3) It can dissolve fibrin. (4) It can destroy prothrombin. (5) It can itself be destroyed by fibrinolysin inhibitor.

Until something is known about the kinetics of these reactions and the size and shape of the molecules involved, both before and after the various reactions, it is not likely that satisfactory explanations will be derived only from studies of $-\text{NH}_2$, $-\text{S}-\text{S}-$, $-\text{COOH}$, aromatic hydroxyl, phosphoric ester, guanidonium, or imidazole groups.

III. ADSORPTION OF THROMBIN ON FIBRIN

The protein preparations used and the methods developed for measuring their reactivity have already been described. Bovine prothrombin (35, 36, 41),

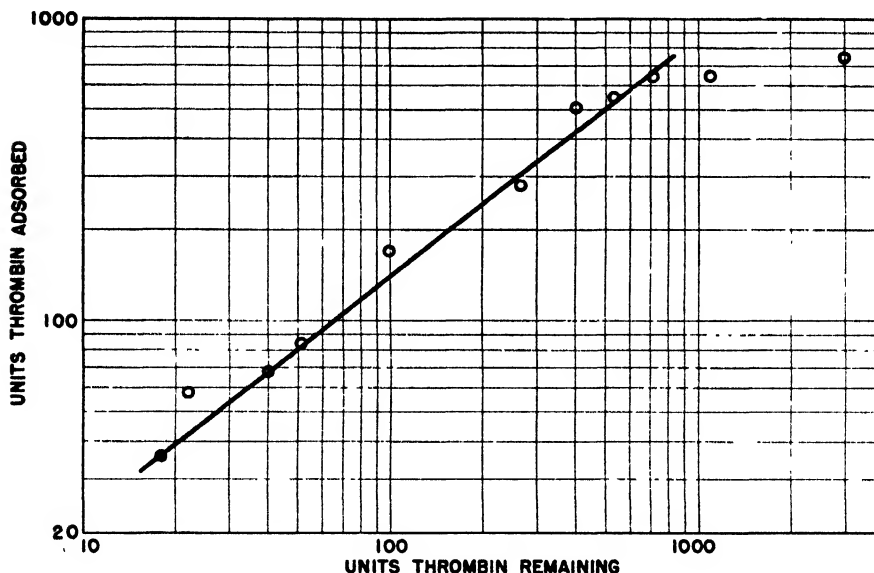


FIG. 2. Quantity of thrombin remaining when various concentrations of thrombin are used to clot 1 cc. of a 1 per cent fibrinogen solution. With very high concentrations of thrombin, clotting is too rapid for thorough mixing and consequently two points on the curve are obviously irregular.

thrombin (35, 36, 39, 41), fibrinogen (42), and fibrinolysin (24) were prepared and determined quantitatively (23, 24, 38, 42, 47).

To a series of test tubes containing 1 cc. of the fibrinogen (1 per cent in 0.9 per cent sodium chloride) was added 1 cc. of thrombin solution of various known concentrations. Mixing was done as rapidly as possible. After 10 min. the resulting fibrin clot was removed with a glass rod, and the remaining thrombin activity was measured. In all cases the remaining fluid volume was considered to be 2 cc. The amount of thrombin remaining bears a logarithmic relationship to the amount removed by the fibrin (figure 2). This is the relationship expected in adsorption phenomena and consequently constitutes presumptive evidence that the thrombin was removed by adsorption.

To give further support to this conclusion the thrombin can be eluted in a

special way: namely, with the aid of fibrinolysin, which has recently been prepared in concentrated form (24). Instead of removing the fibrin clot by mechanical means, it can be removed with fibrinolysin according to equation 5 of figure 1. One cubic centimeter of thrombin (3320 units) was mixed with 1 cc. of fibrinolysin, and then 1 cc. of fibrinogen was also added. A clot formed immediately and within 8 min. was dissolved by the fibrinolysin. Analysis showed 3300 units of thrombin in solution. When 1 cc. of the thrombin from the same thrombin stock solution was mixed with 1 cc. of fibrinogen, only 2000 units of thrombin could be accounted for after removal of the clot by mechanical means. It can, therefore, be concluded that thrombin is adsorbed on fibrin during the clotting process.

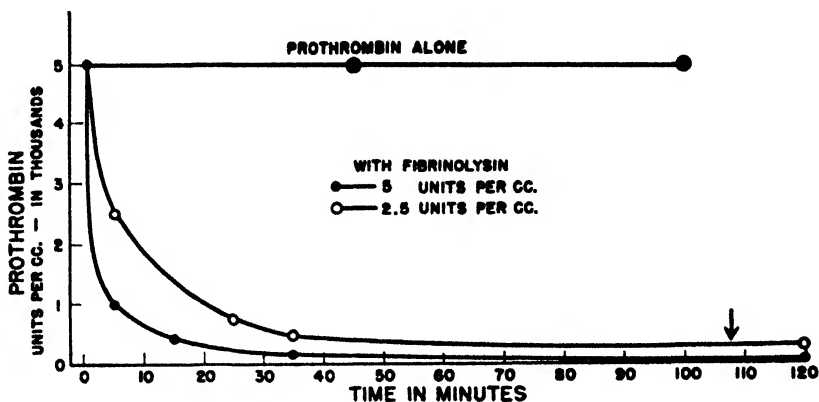


FIG. 3. Inactivation of purified prothrombin with fibrinolysin, derived from plasma, at room temperature, pH 7.2, and in 0.9 per cent sodium chloride solution.

The above experiment also proves the important fact that fibrinolysin does not destroy thrombin. This could not have been predicted, since the circumstances are quite different in the analogous case of prothrombin.

IV. REACTION OF PROTHROMBIN WITH FIBRINOLYSIN

The fact that fibrinolysin will destroy prothrombin was discovered by serendipity. The rate of prothrombin disappearance is shown in figure 3.

With the lower concentration of fibrinolysin used in these experiments some prothrombin remained even after 2 hr., but it can be shown that the remainder was altered. It is far more refractory to the action of thromboplastin (equation 1, figure 1) than ordinary purified prothrombin or native plasma prothrombin. To describe such altered prothrombin we propose to use the term *paraprothrombin*. It is one of the subtle changes in the protein molecule which can be detected by a study of reaction rates. For unavoidable reasons the analytical methods which must be used are not entirely satisfactory, but are quite adequate to prove the point.

V. PARAPROTHROMBIN

To demonstrate the existence of paraprothrombin two solutions are needed: (1) purified prothrombin, and (2) prothrombin acted upon by fibrinolysin specifically as indicated at the point of the arrow on figure 2. Each prothrombin preparation is suitably diluted so that reaction 2 can be employed to follow the rate of reaction 1 (figure 2). In other words, the two-stage analytical technique (47) is applied to such diluted solutions.

The purified prothrombin is completely activated within 15 min. (figure 4). In contrast, the fibrinolysin-treated prothrombin continues to be converted to thrombin over a period of more than 30 min. The reaction rate with thromboplastin is thus seen to be retarded. To appreciate the magnitude of the differ-

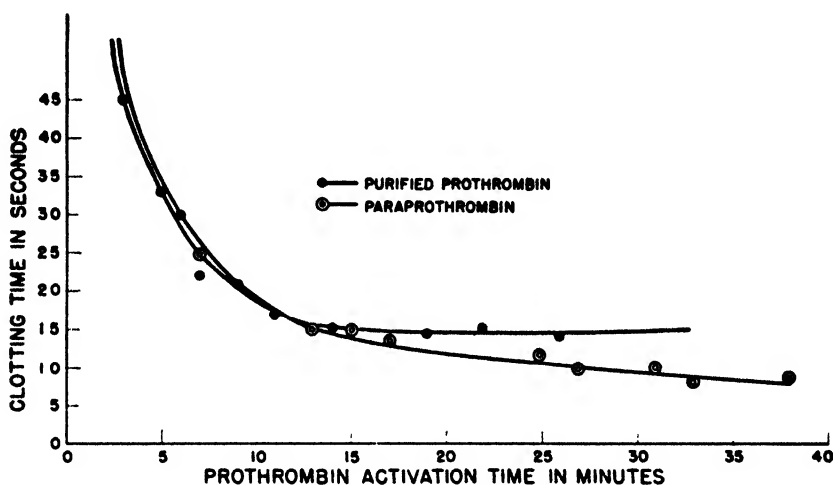


FIG. 4. Comparison of activation rate of purified prothrombin and purified prothrombin treated with fibrinolysin, at room temperature.

ence between the two curves in figure 4 it must be realized that a clotting time of 5 sec. involves more than twice as much thrombin as a clotting time of 15 sec.

VI. QUANTITY OF PROTHROMBIN DESTROYED BY FIBRINOLYSIN

One aspect of the destruction of prothrombin by fibrinolysin is atypical when compared with more familiar reaction types. Prothrombin seems to be resistant to small amounts of fibrinolysin. It is efficiently but incompletely destroyed by intermediate quantities, and rather inefficiently and still incompletely destroyed by strong solutions of fibrinolysin. The data are presented in table 1. With 0.2 unit of fibrinolysin no prothrombin activity was lost and no paraprothrombin could be detected. With 0.8 unit of fibrinolysin, 2100 units, or approximately half the prothrombin was destroyed and paraprothrombin was present. Nevertheless a tenfold increase in fibrinolysin concentration still did not result in the destruction of all the prothrombin. These relationships are similar to adsorption reactions, in which adsorption is proportionately greater from very dilute

solutions than from more concentrated solutions. The destruction ("adsorption") of prothrombin is proportionately greater with small amounts of fibrinolysin than with larger amounts of fibrinolysin. Such a relationship between proteins has been encountered previously: namely, in the case of the inactivation of thrombin by antithrombin. The latter reaction (equation 7, figure 1) also follows logarithmic relationships (40).

VII. FIBRINOLYSIN INHIBITOR, FIBRINOLYSIN, AND PROTHROMBIN

We have been able to confirm the observation that blood plasma contains a powerful inhibitor (10, 29) which is capable of destroying fibrinolysin so that

TABLE 1

Quantity of prothrombin destroyed by various amounts of fibrinolysin, with 15-min. prothrombin activation time

PROTHROMBIN	FIBRINOLYSIN	PROTHROMBIN DESTROYED	REMARKS
<i>units per cc.</i>	<i>units per cc.</i>	<i>units per cc.</i>	
4000	0.2	None	No paraprothrombin
4000	0.4	None	
4000	0.6	450	
4000	0.8	2100	Some paraprothrombin
4000	2.0	2950	
4000	4.0	3725	
4000	6.0	3800	Much paraprothrombin
4000	8.0	3850	
4000	10.0	3880	

the latter can no longer attack fibrinogen or fibrin. It remains to be shown, however, whether or not the inhibitor can also protect prothrombin from being inactivated by means of fibrinolysin. A number of experiments have been performed and they all show that the inhibitor does furnish protection. One of these was the following: 1 cc. of plasma was mixed with 1 cc. of fibrinolysin solution (60 units per cubic centimeter) and allowed to stand 1 hr. Then 6000 units of dry prothrombin were dissolved in the mixture. The prothrombin retained its full potency for several hours. Without the plasma inhibitor this amount of fibrinolysin destroys most of the prothrombin within 10 min. (figure 2, and table 1).

SUMMARY

Prothrombin can be destroyed by fibrinolysin and during the destruction an intermediate, paraprothrombin, is formed. The inactivation of prothrombin is proportionately greater with small amounts of fibrinolysin than with more concentrated quantities.

Fibrinolysin inhibitor protects prothrombin from being destroyed by fibrinolysin.

Thrombin is not destroyed by fibrinolysin.

When thrombin clots fibrinogen, some of the thrombin is adsorbed on fibrin. It can be recovered by dissolving the clot with fibrinolysin.

The physical-chemical characteristics of most of the proteins provided for the blood-clotting mechanism have not been determined. That is also true for the reaction products. Since most of these proteins exhibit activity, further study of such activity in conjunction with studies of physical-chemical characteristics presents a unique opportunity for broadening our understanding of protein interactions and protein structure.

REFERENCES

- (1) ARTHUS, M., AND PAGES, C.: *Arch. physiol. norm. path.* **2**, 739 (1890).
- (2) BAILEY, K., ASTBURY, W. T., AND RUDALL, K. M.: *Nature* **151**, 716 (1943).
- (3) BOSWORTH, A. W.: *J. Biol. Chem.* **20**, 91 (1915).
- (4) BRAND, E., KASSELL, B., AND SAIDEL, L. J.: *J. Clin. Investigation* **23**, 437 (1944).
- (5) BRINKHOUS, K. M., SMITH, H. P., WARNER, E. D., AND SEEGER, W. H.: *Am. J. Physiol.* **125**, 683 (1939).
- (6) CHARGAFF, E., ZIFF, M., AND MOORE, D. H.: *J. Biol. Chem.* **139**, 383 (1941).
- (7) CHARGAFF, E., MOORE, D. H., AND BENDICK, A.: *J. Biol. Chem.* **145**, 593 (1942).
- (8) CHARGAFF, E., BENDICK, A., AND COHEN, S.: *J. Biol. Chem.* **156**, 161 (1944).
- (9) CHRISTENSEN, L. R.: *J. Gen. Physiol.* **28**, 363 (1945).
- (10) CHRISTENSEN, L. R., AND MACLEOD, C. M.: *J. Gen. Physiol.* **28**, 559 (1945).
- (11) CHRISTENSEN, L. R.: *J. Bact.* **47**, 65 (1944).
- (12) COHN, E. J., ONCLEY, J. L., STRONG, L. E., HUGHES, W. L., JR., AND ARMSTRONG, H. S., JR.: *J. Clin. Investigation* **23**, 417 (1944).
- (13) DELEZENNE, C., AND POZERSKI, E.: *Compt. rend. soc. biol.* **55**, 690 (1903).
- (14) EBBECKE, U., AND KNUCHEL, R.: *Arch. ges. Physiol. (Pflüger's)* **243**, 65 (1940).
- (15) FERGUSON, J. H.: *Physiol. Rev.* **16**, 640 (1936).
- (16) FERGUSON, J. H., AND RALPH, P. H.: *Am. J. Physiol.* **138**, 648 (1943).
- (17) FOSTER, J. F., SCHEINBERG, H., AND EDSALL, J. T.: *Federation Proc.* **3**, 57 (1944).
- (18) GARNER, R. L., AND TILLET, W. S.: *J. Exptl. Med.* **60**, 239 (1934).
- (19) HOWELL, W. H.: *Am. J. Physiol.* **26**, 453 (1910).
- (20) HOWELL, W. H.: *Am. J. Physiol.* **40**, 526 (1916).
- (21) HOWELL, W. H.: *Am. J. Physiol.* **35**, 143 (1914).
- (22) HOWELL, W. H., AND HOLT, E.: *Am. J. Physiol.* **47**, 328 (1918).
- (23) LOOMIS, E. C., AND SEEGER, W. H.: *Arch. Biochem.* **5**, 265 (1944).
- (24) LOOMIS, E. C., GEORGE, C., JR., RYDER, A., AND NIEFT, M. L.: *Arch. Biochem.*, in press.
- (25) MELLANBY, J.: *Proc. Roy. Soc. (London)* **B116**, 1 (1934).
- (26) MERTZ, E. T., SEEGER, W. H., AND SMITH, H. P.: *Proc. Soc. Exptl. Biol. Med.* **42**, 604 (1939).
- (27) MERTZ, E. T., SEEGER, W. H., AND SMITH, H. P.: *Proc. Soc. Exptl. Biol. Med.* **41**, 657 (1939).
- (28) MILSTONE, H.: *J. Immunol.* **42**, 109 (1941).
- (29) OPIE, E. L.: *Physiol. Rev.* **2**, 552 (1922).
- (30) QUICK, A. J.: *Proc. Soc. Exptl. Biol. Med.* **35**, 391 (1936).
- (31) QUICK, A. J.: *Am. J. Physiol.* **123**, 712 (1938).
- (32) RETTGER, L. A.: *Am. J. Physiol.* **24**, 406 (1909).
- (33) SCHMIDT, A.: *Arch. ges. Physiol. (Pflüger's)* **6**, 413 (1872).
- (34) ROBBINS, K. C.: *Am. J. Physiol.* **142**, 581 (1944).
- (35) SEEGER, W. H.: *J. Biol. Chem.* **136**, 103 (1940).
- (36) SEEGER, W. H., AND SMITH, H. P.: *J. Biol. Chem.* **140**, 677 (1941).
- (37) SEEGER, W. H., WARNER, E. D., BRINKHOUS, K. M., AND SMITH, H. P.: *Science* **96**, 300 (1942).

- (38) SEEGERS, W. H., AND SMITH, H. P.: Am. J. Physiol. **137**, 348 (1942).
- (39) SEEGERS, W. H., AND MCGINTY, D. M.: J. Biol. Chem. **146**, 511 (1942).
- (40) SEEGERS, W. H., AND SMITH, H. P.: Proc. Soc. Exptl. Biol. Med. **52**, 159 (1943).
- (41) SEEGERS, W. H., LOOMIS, E. C., AND VANDENBELT, J. M.: Arch. Biochem. **8**, 85 (1945).
- (42) SEEGERS, W. H., NIEFT, M. L., AND VANDENBELT, J. M.: Arch. Biochem. **7**, 15 (1945).
- (43) STÜBEL, N.: Arch. ges. Physiol. (Pflüger's) **181**, 285 (1920).
- (44) TOCANTINS, L. M.: Am. J. Physiol. **114**, 709 (1936).
- (45) TOCANTINS, L. M.: Medicine **17**, 155 (1938).
- (46) WILSON, S. J.: Arch. Internal Med. **69**, 647 (1942).
- (47) WARNER, E. D., BRINKHOUS, K. M., AND SMITH, H. P.: Am. J. Physiol. **114**, 667 (1936).

HEMOCYANINS OF THE GASTROPODS¹

SVEN BROHULT

The Institute of Physical Chemistry, University of Upsala, Upsala, Sweden

Received August 8, 1946

Svedberg and collaborators (9, 13, 16) have shown that the hemocyanins are giant molecules with molecular weights from about half a million up to about ten million. They have also found that the hemocyanins may dissociate into well-defined submultiples upon a change in the pH, this dissociation often being reversible.

Among the hemocyanins the largest molecular weights are observed for the Gastropods (9). The dissociation reactions of these hemocyanins have been investigated more in detail (3, 4). It was then found that for certain species (e.g., *Helix pomatia*) the dissociation depends not only upon the pH but also upon the nature and the amount of electrolytes or non-electrolytes present in the solution. For other species (e.g., *Paludina vivipara*) the dissociation is influenced only by the pH.

Helix pomatia hemocyanin (abbreviation, H.P.h.) and some other hemocyanins of the Gastropods have been investigated by the author (3) and by Borgman and the author (4, 5). *Paludina vivipara* hemocyanin (abbreviation, P.V.h.) has been studied by Ekvall and the author (7, 6).

I. MOLECULAR WEIGHT AND MOLECULAR SHAPE

The molecular constants have been determined for the two species *Helix pomatia* and *Paludina vivipara*.

A. Molecular weight

The sedimentation constant, *s*, the diffusion constant, *D*, and the partial specific volume, *V*, are given in table 1 for H.P.h. and P.V.h. and for their

¹ Presented at the Twentieth National Colloid Symposium, which was held at Madison, Wisconsin, May 28-29, 1946.

dissociation products. The molecular weight was calculated from the formula of Svedberg (12):

$$M = \frac{RTs}{D(1 - V\rho)}$$

The values are found in table 1. It has not been possible to isolate the first dissociation component of P.V.h. and to determine its molecular weight, since this component only appears in a very narrow pH region.

It follows from table 1 that the dissociation products correspond to one-half and one-eighth of the original molecule. The molecular constants of the two species of hemocyanins are equal within the limits of experimental error.

TABLE 1

Molecular constants of Helix pomatia and Paludina vivipara hemocyanins and their dissociation products

SPECIES	$(S_{20})_0^*$	D_{20}	V_{20}	M	f/f_0	L_1^\dagger	L_2^\ddagger
		$10^{-7}cm$				A	A
<i>Helix pomatia</i>	103.0	1.07	0.738	8.91×10^6	1.45	1130	890
	65.7	1.41	0.738	4.31×10^6	1.40	820	890
	19.7	1.77	0.738	1.03×10^6	1.79	820	960
<i>Paludina vivipara</i>	102.5	1.09	0.738	8.70×10^6	1.43	1090	
	64.5		0.738				
	21.8	1.79	0.738	1.13×10^6	1.72	790	

* $(S_{20})_0$, the sedimentation constant at zero concentration, is expressed in Svedbergs (S).

† Length of the molecules from f/f_0

‡ Length of the molecules from stream double refraction.

B. Molecular shape

(1) Frictional ratio, f/f_0

It is possible to calculate the lengths, L , of the hemocyanins and their dissociation products from the frictional ratio, f/f_0 , by assuming that the molecules are unhydrated and that they behave hydrodynamically like oblong ellipsoids of revolution (16). The values of f/f_0 and the lengths, L , appear in tables 1 and 2 ($L = L_1$ in table 1). The calculated minor axes, d , are given in table 2.

(2) Stream double refraction

Snellman and Björnsthål (11) have determined the lengths of H.P.h. and its dissociation products by stream double refraction, assuming that the molecules behave like cylinders. The values of L are given in tables 1 and 2. ($L = L_2$ in table 2.) L and M being known, the minor axes, d , may be calculated (table 2).

It may be concluded from the figures in table 1 that the wholes, halves, and eighths are equal in length. The dissociation down to eighths therefore probably occurs parallel to the longer axes (*cf.* Polson (10)).

(3) Electron micrographs

In order to obtain correlation between sedimentation, diffusion, and stream double refraction experiments, Borgman and the author have taken a large

TABLE 2

Molecular dimensions of Helix pomatia hemocyanin and its dissociation products

METHOD	COMPONENT	LENGTH OF MOLECULES, L	d^*	L/d
		$A.$	$A.$	
f/f_0	Wholes	1130	136	8.3
Stream double refraction.	Wholes	890	125	7.1
Electron microscope { Fig. 1	Wholes	(480)†	(135)†	(7.4)
		(1140)†	154	
Monolayers	Wholes		($d_1 = 150$)‡ $d_2 = 71$	
f/f_0	Halves	820	111	7.4
Stream double refraction	Halves	890	87	10.2
f/f_0	Eighths	820	54	15.2
Stream double refraction	Eighths	960	41	23.4
Monolayers	Eighths		38	

* d = minor axes of the molecules; d_1, d_2 = minor axes (unequal in length); d_1 = width of the molecule; d_2 = thickness of the molecule.

† The determinations are uncertain.

‡ The width d_1 is calculated on the assumption that the wholes are rectangular prisms.

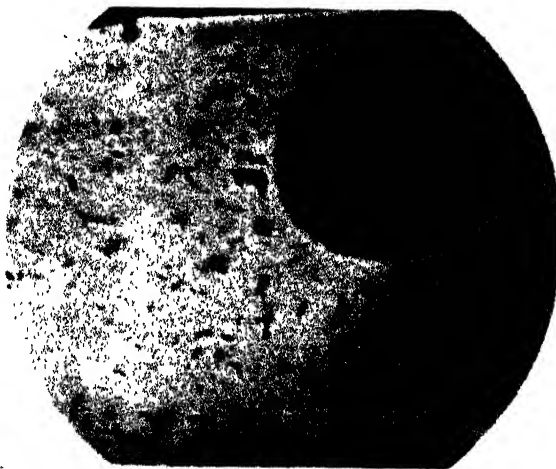


FIG. 1. Electron micrograph of *Helix pomatia* hemocyanin. Concentration 4×10^{-7} g. per milliliter. Magnification electron optically 35,000:1.

number of electron micrographs without getting, however, entirely reproducible results. In several cases micrographs like that in figure 1 have been obtained. The lengths vary from 380 to 580 A. (mean value 480 A.) and the widths from

100 to 165 Å. (mean value 135 Å.). In one case a micrograph like that in figure 2 was obtained.

The filaments observed in figure 2 are probably hemocyanin molecules associated end to end. The median value of the width of the filament is 154 Å. (computed from nine filaments each of them measured at ten different places). The lengths of the filaments vary from 2000 to 7000 Å., and it seems possible to arrange them in three groups, probably corresponding to threads of two, four, and six hemocyanin molecules (thirty filaments have been measured). On this assumption the length of the hemocyanin molecule may be calculated to be 1140 Å.



FIG. 2. Electron micrograph of *Helix pomatia* hemocyanin. Concentration 4×10^{-7} g per milliliter. Magnification electron optically 35,000:1.

(4) Thickness of monolayers

Trurnit and Bergold (17) have measured the thickness of monolayers of H.P.h. and its dissociation products. The monolayer was deposited on a metal according to the method of Blodgett (1) and Blodgett and Langmuir (2). Trurnit and Bergold found thicknesses varying between 38 and 71 Å.

These investigators assume that the hemocyanin molecules, when adsorbed on the metal, are transformed to quadratic or rectangular prisms. The eighths which are supposed to give quadratic prisms will have a quadratic section with a side of 37.5 Å. (890 Å. is used as the height of the prism). If the eighths, which are of the same length as the wholes, are arranged in two quadratic groups of four, we get whole molecules with rectangular sections having the sides d_1 and d_2 equal to 150 Å. and 75 Å.

There exists a certain agreement between the above assumption and the experimental data, since all measured thicknesses of the monolayers lie between 75 Å. and 37.5 Å.

(5) Comparison between the different methods

The lengths of the molecules calculated from the frictional ratio agree rather well with those obtained by the stream double refraction (tables 1 and 2). Since a calculation from the frictional ratio, f/f_0 , is valid only for unhydrated molecules, it may be concluded that there is no considerable hydration of the hemocyanin components.

It should be of great importance to compare the molecular sizes obtained by indirect methods with those estimated directly from electron micrographs. As already mentioned, reproducible micrographs have not yet been obtained. The disagreement between the length estimated from figure 1 and that obtained from stream double refraction is too large to permit the assumption that the particles observed are single molecules. Besides, if they were single molecules, their thickness would be more than twice that observed by Trurnit and Bergold (table 2). Therefore the particles in figure 1 probably are some split products of the original hemocyanin. The length estimated from figure 2 is too uncertain to permit a comparison with other values.

The width of the filaments in figure 2 is somewhat larger than that obtained by the first two methods (table 2). One must consider that some deformation may occur when the hemocyanin solution is evaporated on a film of cellulose nitrate before the exposure to the electron beams. The preparations of samples for electron micrographs and of monolayers are similar, and we might expect a certain agreement in the results. It is also found (table 2) that the width calculated from measurements of monolayers agrees with that estimated from the filaments in figure 2.

II. DISSOCIATION AND ASSOCIATION REACTIONS

A. *Helix pomatia* hemocyanin

(1) Dissociation upon change in pH

The H.P.h. may, upon a change in the pH, dissociate into halves, eighths, and lower components. Near the isoelectric point only whole molecules exist, provided the salt concentration is not too high (see figure 5). If the solution is not too acid or too alkaline, the dissociation reaction is reversible (Svedberg and Heyroth (15); Eriksson-Quensel and Svedberg (9)).

The sedimentation diagram of a hemocyanin solution at pH 7.2 appears in figure 3. A certain amount of "intermediate compounds"—with no definite boundary—is found between the peaks corresponding to whole and half molecules. We assume that these "intermediate compounds" are composed of swelling whole molecules. The assumed mechanism is shown schematically in figure 4.

The original hemocyanin molecule where the halves are close to each other is indicated in the figure by 1. With successively increasing distance between the halves, molecules such as 2 and 3 may be obtained. The forces between the fragments are still great enough to keep them together. The solvent may to some extent pass through molecules such as 2 and 3 during the sedimentation,

and therefore a decrease in the sedimentation constant is to be expected until freely sedimenting half molecules (4 and 4') occur. The mechanism described above gives a plausible explanation of the existence of "intermediate compounds." The swelling of the molecule may be the first step in the dissociation process.

By diffusion experiments we have tried to prove the assumption that the swelling of the molecule is a process preceding the dissociation. The diffusion constant of the "intermediate compounds" should be lower than that of the

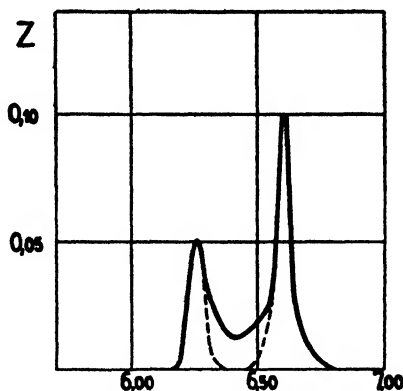


FIG. 3. Sedimentation diagram by the refraction method, showing the "intermediate compounds".

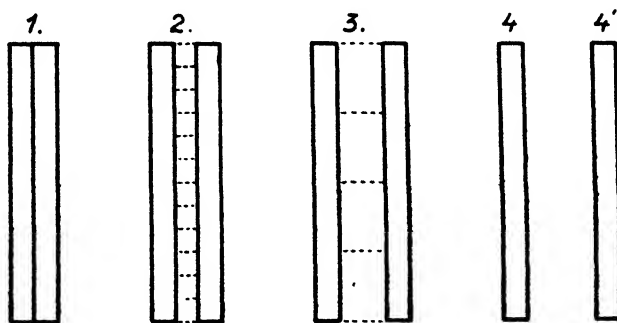


FIG. 4. Swelling of the hemocyanin molecule. 1, whole molecule; 2 and 3 "intermediate compounds"; 4 and 4', half molecules.

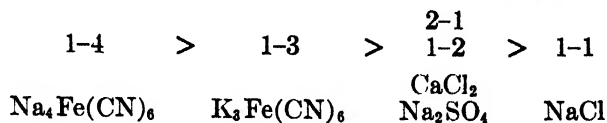
whole molecules. A hemocyanin solution containing 49 per cent wholes, 22 per cent halves, and 29 per cent "intermediate compounds" gave a diffusion constant, D , equal to 1.07. Accordingly, the diffusion experiment supports the assumption of the "intermediate compounds" being swelling molecules, as the diffusion constant of wholes is 1.07 and that of halves is 1.41.

(2) Dissociation by electrolytes

The H.P.h. is dissociated not only by a change in the pH but also by addition of electrolytes (3, 6). The dissociation effect increases in general with the

amount and with the valence of the ions, both cation and anion being of importance. Certain ions, however, have special effects, particularly in high concentrations.

In dilute salt solutions the dissociation caused by different types of salts is as follows, the valence combinations being arranged in decreasing order of effect:



The valence rule does not apply to the 2-2 valent magnesium sulfate.

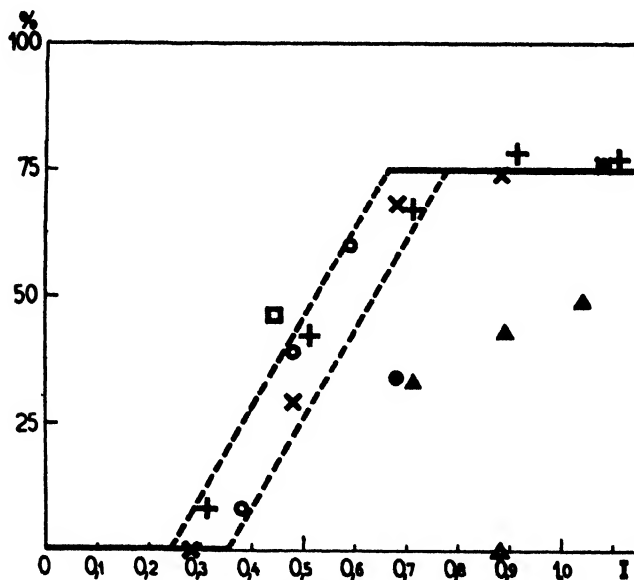


FIG. 5. Dissociation into half molecules as a function of the ionic strength, I , of the solvent. \times , sodium chloride buffered with acetate; $+$, sodium chloride buffered with phosphate; \circ , sodium ferrocyanide buffered with acetate; \square , potassium ferricyanide buffered with acetate; \bullet , calcium chloride buffered with acetate; Δ , sodium sulfate buffered with phosphate; \triangle , magnesium sulfate buffered with acetate. The experiment was carried out in the pH region 5.0–6.0, where no dissociation occurs at ionic strengths below 0.2.

In figure 5 the proportion of half molecules is plotted against the ionic strength of the solvent.

This figure shows that no further dissociation takes place when the hemocyanin is dissociated to 75 per cent. In solutions of sodium chloride, sodium ferrocyanide, and potassium ferricyanide the dissociation is about equal, the ionic strength being the same.

The dissociating effect of concentrated salt solutions differs widely with the salt used. In concentrated solutions of sodium chloride and sodium ferrocyanide, no further dissociation occurs when the half molecules amount to 75 per cent

of the hemocyanin. Dissociation to eighths and lower components takes place when concentrated solutions of calcium chloride are used, while an association to whole molecules occurs in concentrated solutions of sodium sulfate (3).

(3) Dissociation by non-electrolytes

The H.P.h. is also dissociated by non-electrolytes such as sugars, glycerol, and urea (3). The effect is, however, in general less pronounced than with electrolytes.

(4) The hemocyanin of *Helix pomatia* is composed of two kinds of molecules

When the H.P.h. is dissociated by addition of salts, e.g., sodium chloride (figure 5), the dissociation increases with the concentration of the electrolyte and suddenly ceases when 75 per cent of the hemocyanin is dissociated. No further dissociation occurs upon increasing the concentration of the electrolyte. The hemocyanin behaves as if it were composed of two different kinds of molecules: one, A, whose concentration is 75 per cent and which is dissociated by electrolytes, and another, B, which is not dissociated. The existence of two kinds of molecules, A and B, has been proved by the following experiments.

(a) *Separation by centrifugation*: A separation has been done with the preparative centrifuge of Beams. The hemocyanin solution used for the experiment was one where the dissociation had reached its maximum value, i.e., 75 per cent. By repeated centrifugation it was possible to obtain two solutions, one containing only half molecules and one containing whole and half molecules in about equal proportions (figure 6).

The dissociation properties of these solutions as a function of the concentration of electrolytes are given in figure 7, together with those of the original solution. This figure shows that we have obtained two solutions differently influenced by electrolytes: one which can be completely dissociated into half molecules, and one where the dissociation is less than in the original solution. The first solution contains only molecules of kind A; the second one has a larger amount of kind B than the original solution (cf. also 4).

(b) *Precipitation by ammonium sulfate*: The hemocyanin ordinarily precipitates between 0.40 and 0.45 Am_2SO_4 .² The precipitation is so carried out that seven fractions are obtained. The deposits are redissolved and dialyzed against a buffer (1 *M* sodium chloride + 0.08 *M* acetates), where the original hemocyanin is dissociated to 75 per cent. By sedimentation analysis it was found that the hemocyanin of the first fraction was dissociated only to 60 per cent and the hemocyanin of the last fraction was completely dissociated to half molecules. This experiment shows that the properties of the two kinds of molecules, A and B, differ so widely that they—although equal in size—can be fractionated by ammonium sulfate.

(c) *Mixed molecules*: The two kinds of hemocyanin molecules, A and B, can both be dissociated into eighths by a change in the pH. The eighths originating

² 0.40 Am_2SO_4 designates a solution that in a total of 100 ml. contains 40 ml. of 4 *M* ammonium sulfate.

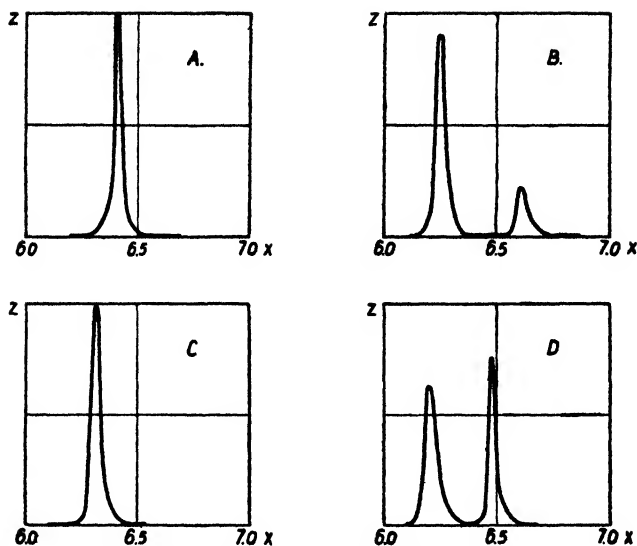


FIG. 6. Sedimentation diagrams showing the separation of the two kinds of hemocyanin molecules. A: original hemocyanin; whole molecules; buffer, 0.2 *M* sodium chloride + 0.08 *M* acetates; pH, 5.3. B: original hemocyanin; maximum dissociation by electrolytes; buffer, 1.00 *M* sodium chloride + 0.08 *M* acetates; pH, 5.2. C: separated hemocyanin; same buffer as in B; the solution contains only half molecules. D: solution of the redissolved centrifuge deposit; same buffer as in B. Concentration of the hemocyanin about 0.3 per cent.

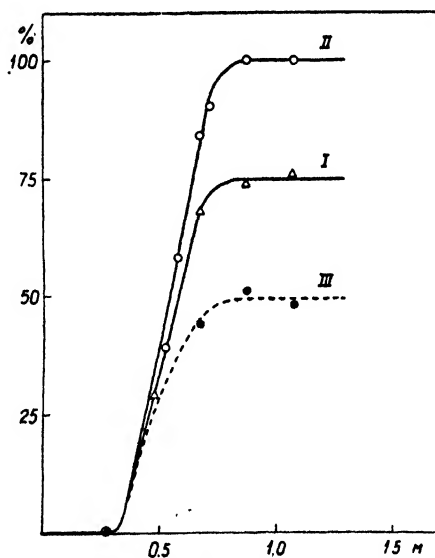


FIG. 7. Dissociation into half molecules as a function of the molarity, *M*, of sodium chloride. Curve I, original hemocyanin; curve II, hemocyanin of kind A, completely dissociated into half molecules when the concentration of the salt is above 0.8 *M*; curve III, solution of the redissolved deposit containing the kinds A and B in about equal proportions.

from A and those from B should have different properties. When eighths are reassociated to wholes, we might expect mixed hemocyanin molecules. It was now found that reassociated hemocyanin molecules have other dissociation properties than the original hemocyanin. A reassociated hemocyanin was dissociated to 88 per cent by addition of electrolytes instead of 75 per cent for the original hemocyanin (*cf.* also 4).

B. Paludina vivipara hemocyanin

(1) Dissociation by change of pH

The P.V.h. dissociates like H.P.h. into halves and eighths by a change in the pH (*cf.* 8). The halves appear in a very narrow pH region (pH 7.2–7.8) and

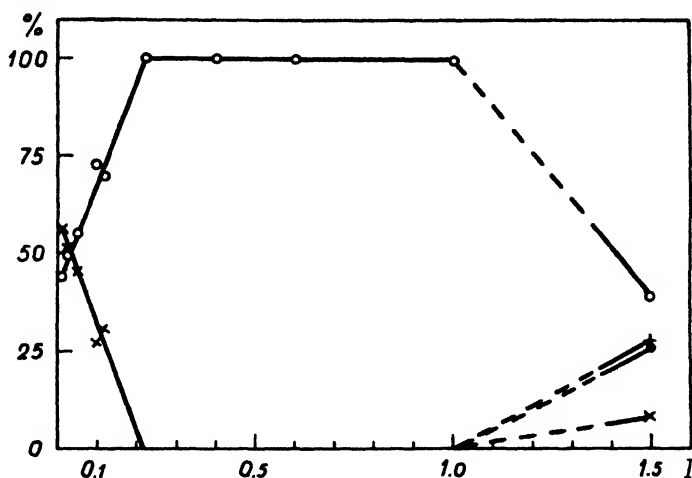


FIG. 8. *Paludina vivipara* hemocyanin. Percentage of different components as a function of the ionic strength, I . \circ , percentage of wholes; \times , percentage of halves; $+$, percentage of eighths; \bullet , percentage of association products. Solvent: sodium chloride + phosphate buffer of pH 7.5.

always together with whole molecules or with wholes and eighths. Eighths occur in the pH region 7.7–10. Lower—not well-defined—components than eighths are observed on the alkaline side. Coagulation takes place on the acid side, starting at pH 4.5.

(2) Effect of electrolytes

Contrary to H.P.h. the P.V.h. is not dissociated by electrolytes. The effect of salt is quite different: association occurs instead of dissociation.

(a) *Association in dilute salt solutions:* The effect of the addition of sodium chloride appears in figure 8, where the hemocyanin solution investigated had a pH of 7.5. At ionic strength below 0.05, wholes and halves have about the same concentration. Upon increasing the ionic strength, association to whole

molecules occurs. Between ionic strengths of 0.2 and 1.0 only whole molecules appear in the sedimentation diagram.

(b) *Association in concentrated salt solutions*: New components of 120–130 S appear in concentrated salt solutions and probably correspond to double hemocyanin molecules. This association is always accompanied by a dissociation into halves and eighths (figure 8). The association phenomenon has been observed in the pH region 7.0–8.0. In some cases association products of 140–160 S have been found.

III. COMPARISON BETWEEN HEMOCYANINS OF THE GASTROPODS

Borgman and the author (4) have studied the influence of electrolytes also on some other hemocyanins of the Gastropods and found that this influence was very different for different species. The hemocyanins investigated may be classified in two groups (table 3): one where dissociation occurs both on the addition of electrolytes and upon a change in the pH, and one where dissociation takes place only upon a change in the pH.

TABLE 3
Dissociation brought about by change in the pH and by electrolytes

	SPECIES	pH	ELECTROLYTES
I	<i>Helix pomatia</i>	Dissociation	Dissociation to 75 per cent
	<i>Helix hortensis</i>	Dissociation	Dissociation to 30 per cent
	<i>Helix arbustorum</i>	Dissociation	Dissociation to 100 per cent
II	<i>Paludina vivipara</i>	Dissociation	No dissociation
	<i>Littorina littorea</i>	Dissociation	No dissociation
	<i>Buccinum undatum</i>	Dissociation	No dissociation

Svedberg and collaborators (9, 14) have found that the sedimentation constant and the dissociation upon change in pH show many regularities indicative of biological kinship. Considering the influence of electrolytes, the maximum dissociation differs widely from one species to another (table 3) and this difference may also be biologically interesting.

SUMMARY

1. The hemocyanins of *Helix pomatia* and *Paludina vivipara* have served as prototypes in this investigation.
2. The molecular constants of these hemocyanins are given in table 1 and are equal within the limits of experimental error. The first and the second dissociation products correspond to halves and eighths of the original molecule.
3. The wholes, halves, and eighths are equal in length. The dissociation therefore probably occurs parallel to the longer axis.
4. Lengths and widths obtained from the frictional ratio, from stream double refraction, from electron micrographs, and from measurements of monolayers are collected in table 2. A fairly good agreement is found between the different values.

5. The first step in the dissociation process probably is a swelling of the hemocyanin molecule.

6. The hemocyanin of *Helix pomatia* is dissociated not only by a change in the pH but also by the addition of electrolytes. The dissociation effect increases with the valence of the ions, both cation and anion being of importance.

7. The hemocyanin of *Helix pomatia* is composed of two kinds of molecules: one, A, whose concentration is 75 per cent and which is dissociated by electrolytes, and another, B, which is dissociated only by a change in the pH. A has been isolated by centrifugation and by precipitation with ammonium sulfate. B has been enriched from 25 to 50 per cent.

8. The *Paludina vivipara* hemocyanin is dissociated by a change in the pH. The addition of electrolytes causes association instead of dissociation.

The author wishes to express his sincere gratitude to the Head of the Institute, Professor The Svedberg, for his kind interest in this work and for the facilities which were placed at his disposal.

The expenses of this investigation were defrayed by grants from the Rockefeller Institute and the Nobel Fund of Chemistry.

REFERENCES

- (1) BLODGETT, K. B.: J. Am. Chem. Soc. **57**, 1007 (1935).
- (2) BLODGETT, K. B., AND LANGMUIR, I.: Phys. Rev. **51**, 964 (1937).
- (3) BROHULT, S.: Nova Acta Reg. Soc. Sci. Upsaliensis [4] **12**, No. 4 (1940).
- (4) BROHULT, S., AND BORGMAN, K.: In *The Svedberg 1884-1944*, pp. 429-37. Almquist and Wiksells, Upsala (1944).
- (5) BROHULT, S., AND BORGMAN, K.: Unpublished work.
- (6) BROHULT, S., AND CLAESSON, S.: Nature **144**, 111 (1939).
- (7) BROHULT, S., AND EKWALL, P.: Unpublished work.
- (8) EKWALL, P.: Finska Kemistsamfundets Medd. **51**, 67 (1942).
- (9) ERIKSSON-QUENSEL, I.-B., AND SVEDBERG, T.: Biol. Bull. **71**, 498 (1936).
- (10) POLSON, A.: Kolloid-Z. **88**, 51 (1939).
- (11) SNELLMAN, O., AND BJÖRNSTÅHL, Y.: Kolloid-Beihefte **52**, 403 (1941).
- (12) SVEDBERG, T.: Zsigmondy Festschrift (Erg. Bd. zu Kolloid-Z. **36**) 53 (1925).
- (13) SVEDBERG, T.: Ind. Eng. Chem., Anal. Ed. **10**, 113 (1938); Kolloid-Z. **85**, 119 (1938).
- (14) SVEDBERG, T., AND HEDENIUS, A.: Biol. Bull. **66**, 191 (1934).
- (15) SVEDBERG, T., AND HEYROTH, F. F.: J. Am. Chem. Soc. **51**, 550 (1929).
- (16) SVEDBERG, T., AND PEDERSEN, K. O.: *The Ultracentrifuge*. Oxford University Press, New York (1940).
- (17) TRURNIT, H. J., AND BERGOLD, G.: Kolloid-Z. **100**, 177 (1942).

PHYSICOCHEMICAL CHARACTERIZATION OF PITUITARY GROWTH HORMONE^{1,2}

CHOH HAO LI

*The Institute of Experimental Biology, University of California, Berkeley, California**Received August 8, 1946*

INTRODUCTION

Since the hormones thus far isolated and purified from the anterior hypophysis are proteins, progress in the techniques of handling and characterizing them has significantly assisted studies of the physicochemical nature of these substances. Indeed, physical methods such as electrophoresis and the ultracentrifuge have been of prime importance in the isolation of the pituitary protein hormones.

At present we are certain that at least six hormones exist in extracts of the anterior pituitary. Biological rôles of these hormones enable us to divide them into two groups: (a) gonadotropic hormones—the follicle-stimulating (FSH), interstitial-cell-stimulating (ICSH or LH), and lactogenic hormones (prolactin); (b) metabolic hormones—the thyrotropic, adrenocorticotropic (ACTH), and growth hormones. From their known chemical characteristics, we may classify them into two types of proteins: (a) glycoproteins—the thyrotropic, follicle-stimulating, and interstitial-cell-stimulating hormones; (b) simple proteins—the lactogenic, adrenocorticotropic, and growth hormones.

Four of these hormones have been isolated in pure form: namely, the lactogenic (7, 22), interstitial-cell-stimulating (8, 17), adrenocorticotropic (9, 16), and growth hormones (6). The purity of these protein preparations has in each case been established by their behavior in electrophoresis, ultracentrifuge, diffusion, and solubility studies. Both the follicle-stimulating (4) and the thyrotropic hormones (2) have been highly purified but not yet isolated.

In 1921, Evans and Long (3) injected a simple saline extract of ox pituitary glands into normal rats and found that the growth of the animals was accelerated and the final body weight heavier than that of the controls. Later, Smith (19), using hypophysectomized rats, showed that the growth of these animals was resumed when the same anterior pituitary extract was given them. Thus, the existence of a growth hormone in extracts of the pituitary was indicated. The isolation of the hormone in apparently pure form has only recently been accomplished (6). This paper aims to present data concerning the physicochemical characterization of the growth hormone.

HORMONE PREPARATIONS

Growth hormone preparations were isolated from freshly dissected ox anterior pituitary glands according to the method previously described (6). The success

¹ Presented at the Twentieth National Colloid Symposium, which was held at Madison, Wisconsin, May 28-29, 1946.

² This work was aided by grants from the Research Board of the University of California and from the Rockefeller Foundation, New York, New York.

of the method depends on the following solubility characteristics of the hormone: (a) in impure state, the hormone is precipitated after long-continued dialysis against water; (b) at pH 7.0, the hormone is soluble in 0.8 *M* but insoluble in 1.65 *M* ammonium sulfate; (c) at pH 4.0, the hormone is soluble in 0.10 *M* but insoluble in 5.0 *M* sodium chloride; (d) the contaminating proteins are insoluble at pH 5.5 and pH 8.8 in the absence of electrolytes, whereas the growth hormone is soluble under these conditions; and (e) in the absence of salt, the hormone possesses a minimum solubility at pH 6.8, which is shown to be its isoelectric point.

All preparations employed were found to be homogeneous in the Tiselius electrophoresis apparatus, using the scanning optical method of Longworth with at least two buffers of different pH. Figure 1 reproduces typical patterns secured in the electrophoresis experiments, patterns indicating the single nature of the protein. Solubility studies were also employed in establishing the homogeneity of the hormone preparations (see figure 2). It has already been shown

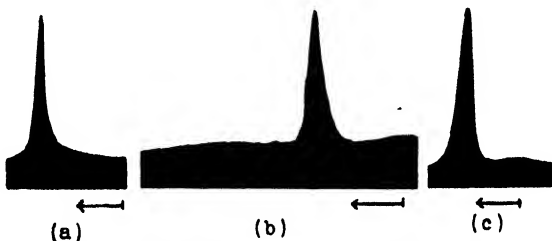


FIG. 1. Electrophoresis patterns of growth hormone in buffers of 0.10 ionic strength. (a) acetate buffer, pH 4.0; potential gradient about 6 volts per centimeter; 120 min. electrolysis. (b) acetate buffer, pH 4.95; potential gradient about 2.5 volts per centimeter; 540 min. electrolysis. (c) barbiturate buffer, pH 9.60; potential gradient about 2.5 volts per centimeter; 360 min. electrolysis.

in a previous paper (6) that 0.01 mg. daily for 10 days (nine injections) of such a growth hormone preparation causes an average of 10 g. increase in the body weight³ of hypophysectomized female rats.

³ We have recently injected the growth hormone into normal-plateau female rats for 435 days; the daily dose was increased gradually from 0.4 mg. to 2.0 mg. It was found that the animals gained weight continuously, although the growth rate became slower in the later period of hormone injections. Figure 3 presents the growth curves of a typical injected rat and a control. It can be seen that the body weight of the rat increases from 270 g. to 664 g., whereas the control gains only 42 g.

A similar experiment with hypophysectomized female rats, 26–28 days old and 12–14 days postoperative, also indicates that the growth hormone can induce continuous growth in such animals and that there is no sign of refractoriness up to over 200 days of injections. The daily dose required in this experiment is much less than that for the normal rats; it changes from an initial dose of 0.10 mg. to 0.20 mg. in the later period of the experiment. Though the experiments with hypophysectomized animals are still in progress, we wish to present at this time the growth rate of an injected rat and its control in figure 4. It is apparent that the growth hormone can cause continuous body growth in both hypophysectomized and normal rats.

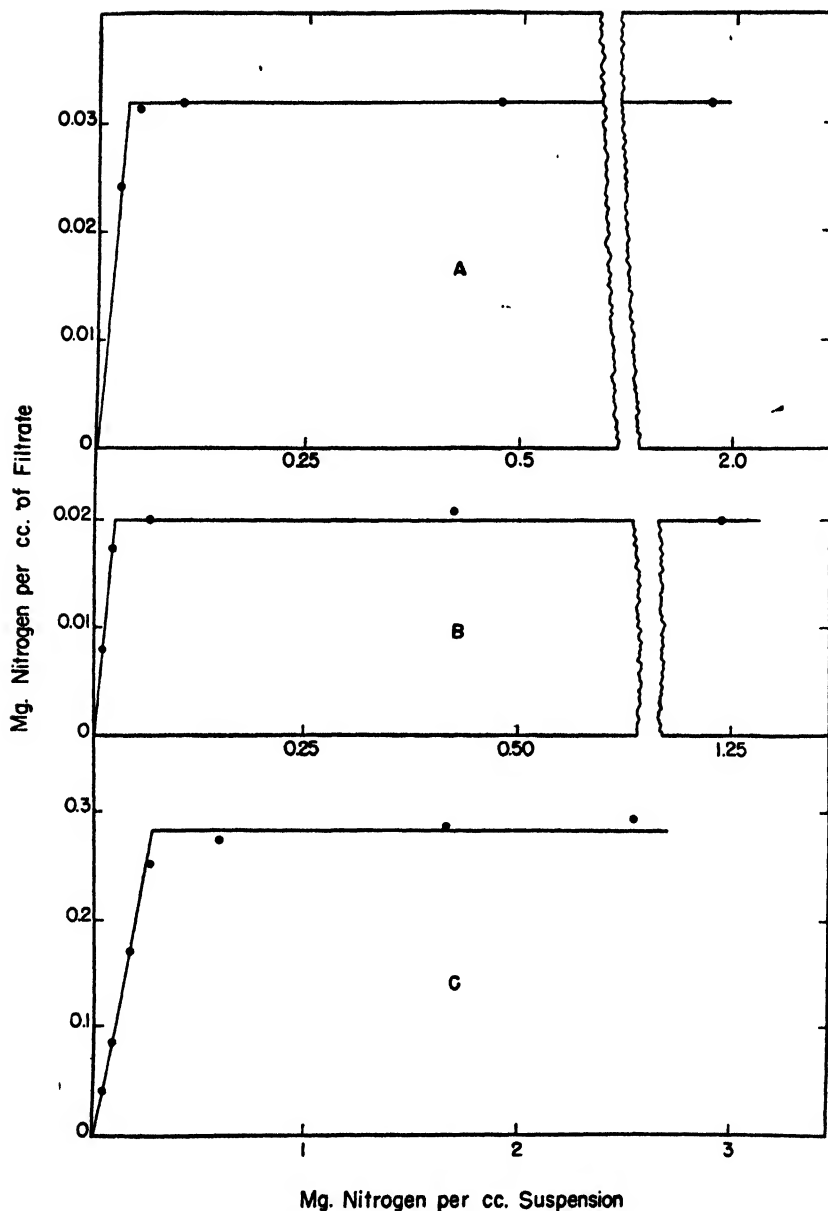


FIG. 2. Solubility curves of the growth hormone in various solvents at 5°C. (A) Distilled water, pH 7.1; (B) 4.8 *M* sodium chloride in 0.07 *M* phosphate buffer, pH 5.7; (C) 3.8 *M* sodium chloride in 0.07 *M* phosphate buffer, pH 6.4.

VISCOSITY

Viscosity measurements were performed in an Ostwald viscometer, as described by Neurath *et al.* (13). A working volume of 25 cc. was employed; the time of flow was determined within an accuracy of ± 0.05 sec. At least six

measurements were made in each run. A water bath at $25.00^{\circ}\text{C.} \pm 0.05^{\circ}$ was used. The protein solution was dialyzed for at least 24 hr. against the buffer before the viscosity determinations. Density determinations were made in a pycnometer of 9-cc. volume at 25°C. The micro-Kjeldahl method was used to determine the nitrogen content in the solution; protein concentration was computed from these determinations, using the conversion factor 100/15.5.

The results of viscosity measurements in borate buffer of pH 9.70 and ionic strength 0.10 are presented in table 1. It will be seen that a straight-line relationship exists between the relative viscosity and the protein concentration. The last column in the table gives the computed intrinsic viscosity,

$$(\eta/\eta_0 - 1)1000/cV_1$$

V_1 , the partial specific volume, is calculated from the density data and found to be 0.76.

TABLE 1

Relative viscosity of the hypophyseal growth hormone at 25°C. in borate buffer of pH 9.7 and ionic strength 0.10

CONCENTRATION OF PROTEIN PER LITER OF SOLUTION	DENSITY	RELATIVE VISCOSITY	INTRINSIC VISCOSITY
<i>grams</i>			
10.80	1.00505	0.0664	8.05
10.10		0.0586	7.64
8.65	1.00458	0.0480	7.30
6.20	1.00401	0.0372	7.87
4.05	1.00357	0.0230	7.47
2.05	1.00310	0.0117	7.50
Mean \pm standard deviation			7.64 \pm 0.11

As seen in table 1, the average intrinsic viscosity of the growth hormone is 7.64. If, as an approximation, the hydration is neglected, the apparent molecular shape could be estimated with the Simha equation (18). Thus, the ratio of major to minor axes of the hormone is 6.3, assuming that the molecule is a prolate ellipsoid. By substitution of this value for b/a into Perrin's equation (14), the dissymmetry constant, f/f_0 , for the hormone becomes 1.31. It is therefore apparent that even with 100 per cent hydration, the growth hormone molecule must be far from spherical in shape.

When a 1.0 per cent solution of the growth hormone was dialyzed against acetate buffer⁴ of pH 4.0 and ionic strength 0.10 for 72 hr. or longer at $2-3^{\circ}\text{C.}$, the protein solution became slightly opalescent and exhibited a Tyndall effect, indicating perhaps that the protein was denatured and the molecules aggregated. The viscosity of such solutions⁵ was measured, and it was found that

⁴ The buffer was prepared by mixing 334 cc. of 1 *M* acetic acid and 65 cc. of 1 *M* sodium hydroxide and diluting with water to 2 liters containing 7 g. sodium chloride.

⁵ Before the protein solution became opalescent, its viscosity was measured; the computed intrinsic viscosity is 7.58, a value which does not differ from that secured in borate buffer at pH 9.7.

the relative viscosity was actually increased. It may be noted in table 2 that when the protein concentration was varied from 0.203 to 0.940 per cent, the intrinsic viscosity increased from 20.2 to 27.1. Such changes in intrinsic viscosity with concentration suggest that some dissociation has occurred in the more dilute solutions. From the increased intrinsic viscosity in acetate buffer of pH 4.0 as compared with that at pH 9.7, the interpretation of an elongation of the protein molecule may be suggested.

In order to ascertain the degree of aggregation of the hormone molecules in acetate buffer of pH 4.0 and ionic strength 0.1, we have determined the osmotic pressure of the solution at 2°C. by the method of Burk and Greenberg (1). It was found that a 1.53 per cent solution gave a pressure of 3.80 cm. H₂O; the molecular weight of the hormone is thus computed to be 96,600, a value which is appreciably higher than that determined for the native protein (6).

TABLE 2

Relative viscosity of the hypophyseal growth hormone at 25°C. in acetate buffer of pH 4.0 and ionic strength 0.10

CONCENTRATION OF PROTEIN PER LITER OF SOLUTION	DENSITY	RELATIVE VISCOSITY	INTRINSIC VISCOSITY
<i>GRAMS</i>			
9.40	1.00455	0.1785	27.1
5.64	1.00335	0.1033	26.2
3.38	1.00260	0.0522	22.1
2.03	1.00221	0.0288	20.2

From the foregoing it is clear that a considerable alteration of the growth hormone molecule has occurred in an acetate buffer of pH 4.0. It was not felt to be altogether unlikely that a corresponding change in its biological activity could be detected. When the denatured hormone was assayed in hypophysectomized female rats at a daily dose of 0.10 mg. for a 10-day period (nine injections), an average body growth (ten rats) of 18.5 g. was obtained, while the native hormone caused an increase of body weight of 20.0 g. under similar conditions. It may therefore be said that the growth-promoting action of the hormone is essentially unchanged even though osmotic-pressure and viscosity measurements indicate that definite changes have occurred in the protein molecule.

One may note here that insulin films retain the original biological activity (15) and that denatured pepsin possesses the same peptic potency as the native enzyme (20). On the other hand, the dissociation of tobacco mosaic virus with urea causes the disappearance of biological activity (5). It is therefore apparent that in some instances the biologic activity of biologically active proteins is not dependent on molecular size and shape but that in other instances this is the case. The present experiments indicate that the growth hormone belongs to the former group.

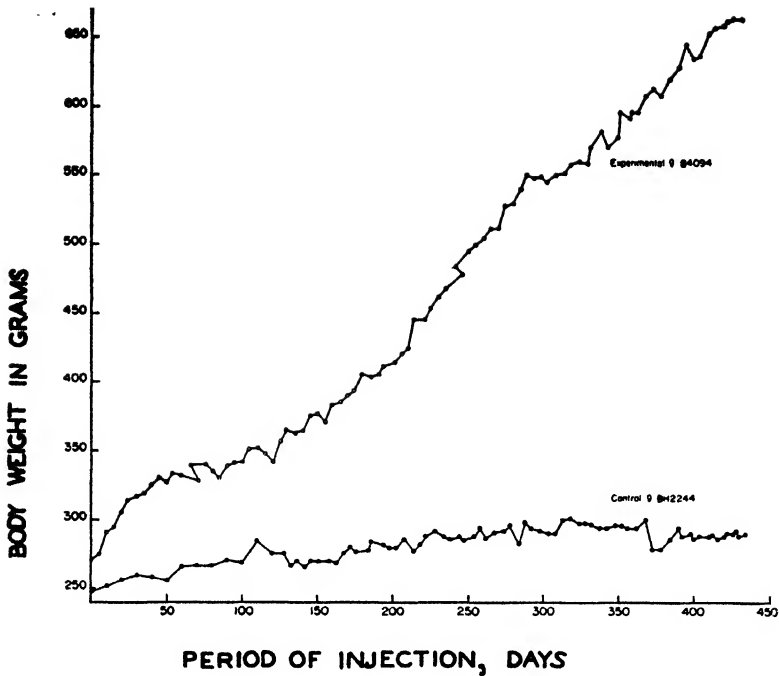


FIG. 3. Growth curves of normal-plateau female rats. The experimental animal received daily 0.40 mg. growth hormone the first 23 days, 0.60 mg. daily the next 68 days, 1.0 mg. daily the next 33 days, 1.5 mg. daily the next 115 days, 2.0 mg. daily the last 193 days; no injections on Sundays. The control rat received no injections.

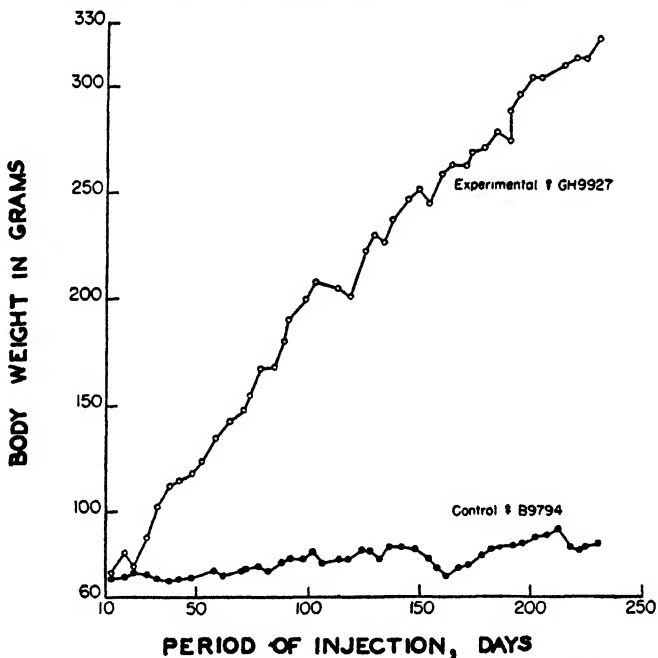


FIG. 4. Growth curves of hypophysectomized female rats. The experimental animal received 0.10 mg. of growth hormone daily for the first 140 days and then the daily dose was increased to 0.20 mg.; no injections on Sundays. The control received no injections.

DIFFUSION

The diffusion measurements of the growth hormone were carried out at 2°C. in the Tiselius electrophoresis cell, as suggested by Longsworth (10). The protein solution (*ca.* 0.5 per cent) was thoroughly dialyzed against the buffer before use. The buffer was prepared with borate having a pH of 9.70 and an ionic strength of 0.10. Five diffusion patterns, as shown in figure 5, were taken at different time intervals. The diffusion curves were enlarged, and the areas

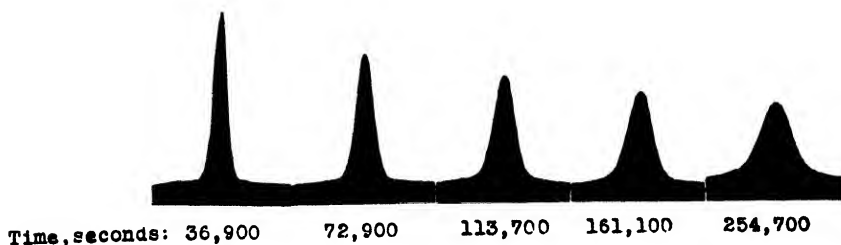


FIG. 5. Diffusion patterns of growth hormone in borate buffer of pH 9.70 and ionic strength 0.10 at 2°C.

TABLE 3

Diffusion measurements of the hypophyseal growth hormone at 2°C.

<i>t</i>	<i>A</i>	<i>H_m</i>	<i>A/H_m</i>	<i>D' × 10⁷</i>
<i>seconds</i>	<i>cm.²</i>	<i>cm.</i>	<i>cm.</i>	<i>cm.²/second</i>
36,900	1.204	3.550	0.339	2.46
72,900	1.262	2.562	0.492	2.64
113,700	1.314	2.150	0.611	2.62
161,100	1.350	1.825	0.739	2.70
254,700	1.398	1.512	0.924	2.76
<i>D', mean</i>				2.64
<i>D_{20° w}</i>				7.15

under the curves measured with a planimeter. The diffusion coefficient was computed by the maximum ordinate-area method (12):

$$D = \frac{A^2}{H_m^2 4\pi t} K^2 \quad \text{or} \quad D' = \frac{D}{K^2} = \frac{A^2}{H_m^2 4\pi t} \quad (1)$$

Here *A* is the area under the curve, *H_m* the maximum height, *t* the time in seconds, and *K* the optical conversion factor. The results are summarized in table 3. If the diffusion behavior of the protein obeys equation 1, a plot of *A/H_m* against \sqrt{t} should be a straight line. Figure 6 illustrates that such a relationship exists, indicating the monodispersity of the growth hormone. As shown in table 3, after the necessary corrections are made, *D_{20° w}* for the growth hormone becomes 7.15×10^{-7} sq. cm. per centimeter.

From the diffusion coefficient and dissymmetry constant it should be possible to calculate the molecular weight by equation 2,

$$M = \frac{R^3 T^3}{162 \pi^2 \eta_0 N^2} \cdot \frac{(f_0 f)^3}{D^3 V_1} \quad (2)$$

where M is the molecular weight, T the temperature, η_0 the viscosity of the solvent, and N Avogadro's number. Substituting the value f_0/f for growth hormone as estimated from viscosity measurements together with its diffusion coefficient into equation 2, we find the molecular weight for growth hormone to be 39,300. In previous studies (6) we had measured the osmotic pressure

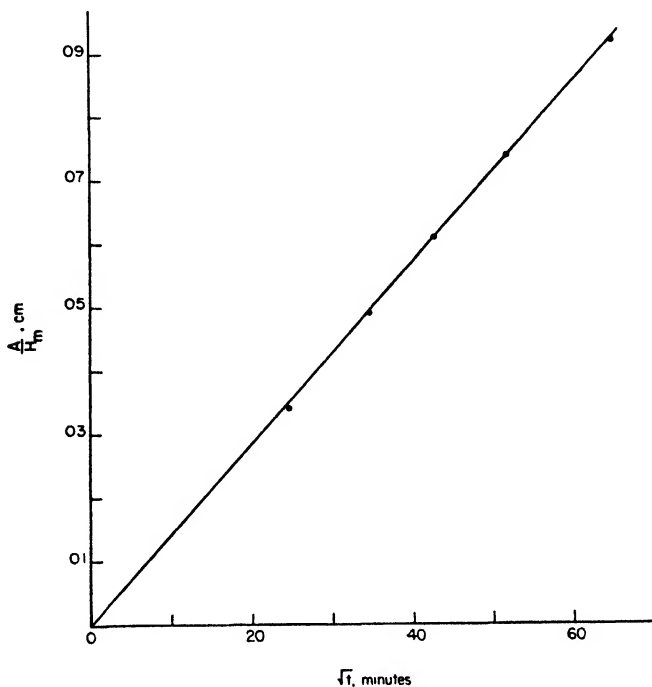


FIG. 6. A plot of A/H_m against \sqrt{t} from the diffusion data of growth hormone at 2°C.

of growth hormone solutions and computed the molecular weight to be 44,250. Since experimental errors in the diffusion and viscosity data would be greatly magnified in equation 2, the molecular weight of the growth hormone computed from the diffusion-viscosity data should be considered in satisfactory agreement with that derived from osmotic pressure.

SULFUR DISTRIBUTION

The colorimetric method of McCarthy and Sullivan (11) was used for the determination of methionine, while cystine was estimated by the procedure of Sullivan, Hess, and Howard (21). The protein samples were digested with 6 M hydrochloric acid at 115°C. for a period of from 15 to 40 hr. The digested

solutions were decolorized with charcoal (norit), filtered, and diluted to proper concentrations for amino acid determinations. The Cenco photometer with proper filters was employed for color comparisons.

The results are summarized in table 4. It may be noted that four growth hormone preparations were employed and that the results obtained from them are in fair agreement. Thus, the growth hormone contains 3.06 per cent methionine and 2.25 per cent cystine. From these values, the total sulfur in the hor-

TABLE 4
Methionine and cystine content of the hypophyseal growth hormone

PREPARATION NO.	AMOUNT USED	PERIOD OF DIGESTION	METHIONINE	CYSTINE
	mg.	hr.	per cent	per cent
12A	75.0	15.0	3.40 (2)*	2.20 (2)
98P	100.0	25.0	3.00 (2)	2.15 (2)
41P	100.0	15.0	2.92 (4)	2.30 (2)
50P	38.0	40.0	3.06 (1)	2.50 (1)
Mean \pm standard deviation			3.06 \pm 0.08	2.25 \pm 0.05

* Values in parentheses indicate number of determinations.

TABLE 5
Molecular weight of the hypophyseal growth hormone computed from analytic data

CONSTITUENT	AMOUNT	MINIMUM MOLECULAR WEIGHT	COMPUTED MOLECULAR WEIGHT			
	per cent					
Tryptophan . . .	0.92	22,200	44,400 (2)*	22,200 (1)	66,600 (3)	88,800 (4)
Cystine	2.25	10,680	42,720 (4)	21,360 (2)	64,080 (6)	85,440 (8)
Methionine . . .	3.06	4,876	43,884 (9)	19,504 (4)	68,264 (14)	87,768 (18)
Tyrosine	4.30	4,214	42,140 (10)	21,070 (5)	67,424 (16)	88,494 (21)
Glutamic acid . .	13.40	1,098	43,920 (40)	21,960 (20)	65,880 (60)	87,838 (80)
Sulfur	1.30	2,466	44,388 (18)	22,194 (9)	66,582 (26)	88,776 (36)
Average value			43,575	21,381	66,471	87,852
Standard deviation			378	420	583	516

* Values in parentheses are the assumed number of molecules or atoms.

none is computed to be 1.25 per cent. Since the hormone has no cysteine and since its sulfur content is 1.30 per cent, as determined by the Carius method (6b), it may be said that the cystine and methionine content accounts for the total sulfur in the molecule within the limits of experimental error.

We have previously reported (6b) that the growth hormone contains 0.92 per cent tryptophan, 4.30 per cent tyrosine, and 13.4 per cent glutamic acid. It seems worth while to utilize these values, together with those for cystine and methionine, in calculating the minimal molecular weight of the growth hormone.

Table 5 presents such computations. It may be noted that the smallest standard deviation from the mean is obtained by assuming that the hormone contains two molecules of tryptophan, four molecules of cystine, nine molecules of methionine, ten molecules of tyrosine, forty molecules of glutamic acid, and eighteen atoms of sulfur. It is thus reasonable to assume that the minimal molecular weight of the growth hormone is 43,600, a value which agrees well with that estimated from osmotic-pressure determinations. It need not be emphasized, perhaps, that the validity of such minimal molecular weight computations depends on the purity of the protein preparation and the accuracy of the analytic data. However, since the molecular weights as obtained from osmotic-pressure, vis-

TABLE 6
Physicochemical data on the hypophyseal growth hormone

Carbon, per cent	46.35
Hydrogen, per cent	7.07
Sulfur, per cent	1.30
Nitrogen:	
Dumas, per cent	15.65
Kjeldahl, per cent	15.50
Amino nitrogen, per cent	0.76
Amide nitrogen, per cent	1.20
Number of acid groups per 10 ⁴ g. protein	9.80
Number of base groups per 10 ⁴ g. protein	13.40
Tyrosine, per cent	4.30
Tryptophan, per cent	0.92
Cysteine, per cent	0.00
Cystine, per cent	2.25
Methionine, per cent	3.06
Glutamic acid, per cent	13.40
Molecular weight:	
Osmotic pressure	44,250
Diffusion-viscosity	39,300
Analytical data	43,600
Isoelectric point, pH	6.85
Diffusion constant, $D_{20^\circ, w} \times 10^7$	7.15
Partial specific volume, V_1	0.76
Intrinsic viscosity, $(\eta/\eta_0 - 1)1000/cV_1$	7.64
Dissymmetry constant, (f/f_0)	1.31

cosity-diffusion, and analytical data are in fair agreement, the growth hormone would appear to be monomolecular in solution.

Table 6 summarizes the known physicochemical data for the hypophyseal growth hormone.

SUMMARY

1. The viscosity of pituitary growth hormone solutions has been measured in an Ostwald viscometer at 25°C. In borate buffer of pH 9.70 and ionic strength 0.10, the intrinsic viscosity of the hormone is 7.64; the dissymmetry constant is 1.31.

2. The hormone is denatured in acetate buffer of pH 4.0 and ionic strength 0.10, as judged by increase in the intrinsic viscosity and molecular weight, but its growth-promoting action is essentially unchanged.

3. The partial specific volume of the hormone is 0.760 cc. per gram at 25°C.

4. The diffusion constant (referred to pure water at 20°C.) is 7.15×10^{-7} sq. cm. per second, as determined by the free-diffusion technique in the electrophoresis apparatus.

5. The cystine and methionine content has been determined. The total sulfur in the molecule is accounted for by 3.06 per cent methionine and 2.25 per cent cystine.

6. The molecular weight computed from viscosity and diffusion data is 39,300, while the minimal molecular weight as derived from analytical data is 43,600.

REFERENCES

- (1) BURK, N. F., AND GREENBERG, D. M.: *J. Biol. Chem.* **87**, 197 (1930).
- (2) CIERESZKO, L. S.: *J. Biol. Chem.* **160**, 585 (1945).
- (3) EVANS, H. M., AND LONG, J. A.: *Anat. Record* **21**, 62 (1921).
- (4) (a) GREEP, R. O., VAN DYKE, H. B., AND CHOW, B. F.: *J. Biol. Chem.* **133**, 289 (1940).
(b) FRAENKEL-CONRAT, H., SIMPSON, M. E., AND EVANS, H. M.: *Ann. Facultad de Medicina, Montevideo* **25** (1940).
- (5) LAUFFER, M. A., AND STANLEY, W. M.: *Science* **89**, 2311 (1939).
- (6) (a) LI, C. H., AND EVANS, H. M.: *Science* **99**, 183 (1944).
(b) LI, C. H., EVANS, H. M., AND SIMPSON, M. E.: *J. Biol. Chem.* **159**, 353 (1945).
- (7) LI, C. H., LYONS, W. R., AND EVANS, H. M.: *J. Gen. Physiol.* **23**, 433 (1940); *J. Am. Chem. Soc.* **62**, 2925 (1940); *J. Biol. Chem.* **139**, 43 (1941); *J. Gen. Physiol.* **24**, 303 (1941).
- (8) LI, C. H., SIMPSON, M. E., AND EVANS, H. M.: *Science* **90**, 355 (1940); *Endocrinology* **27**, 803 (1940); *J. Am. Chem. Soc.* **64**, 367 (1942).
- (9) (a) LI, C. H., SIMPSON, M. E., AND EVANS, H. M.: *Science* **96**, 450 (1942).
(b) LI, C. H., EVANS, H. M., AND SIMPSON, M. E.: *J. Biol. Chem.* **149**, 413 (1943).
- (10) LONGSWORTH, L. G.: *Ann. N. Y. Acad. Sci.* **41**, 267 (1941).
- (11) MCCARTHY, T. E., AND SULLIVAN, M. X.: *J. Biol. Chem.* **141**, 871 (1941).
- (12) NEURATH, H.: *Chem. Rev.* **30**, 357 (1942).
- (13) NEURATH, H., COOPER, G. R., AND ERICKSON, J. O.: *J. Biol. Chem.* **138**, 411 (1941).
- (14) PERRIN, F.: *J. phys. radium* **7**, 1 (1936); see also LAUFFER, M. A.: *Chem. Rev.* **31**, 561 (1944).
- (15) ROTHEN, A., CHOW, B. F., GREEP, R. O., AND VAN DYKE, H. B.: *Cold Spring Harbor Symposia Quant. Biol.* **9**, 272 (1941).
- (16) SAYERS, G., WHITE, A., AND LONG, C. N. H.: *J. Biol. Chem.* **149**, 2125 (1943).
- (17) (a) SHEDLOVSKY, T., ROTHEN, A., GREEP, R. O., VAN DYKE, H. B., AND CHOW, B. F.: *Science* **92**, 178 (1940).
(b) CHOW, B. F., VAN DYKE, H. B., ROTHEN, A., AND SHEDLOVSKY, T.: *Endocrinology* **30**, 635 (1942).
- (18) SIMHA, R.: *J. Phys. Chem.* **44**, 25 (1940).
- (19) SMITH, P. E.: *J. Am. Med. Assoc.* **88**, 158 (1927).
- (20) STEINHARDT, J.: *J. Biol. Chem.* **123**, 543 (1938).
- (21) SULLIVAN, M. X., HESS, W. C., AND HOWARD, H. W.: *J. Biol. Chem.* **145**, 621 (1942).
- (22) WHITE, A., BONSNES, R. W., AND LONG, C. N. H.: *J. Biol. Chem.* **143**, 447 (1942).

MANDELATE AS A STABILIZER OF SERUM ALBUMIN¹

J. MURRAY LUCK

*Biochemical Laboratory, Department of Chemistry, Stanford University, California**Received August 8, 1946*

In several recent papers (1, 2, 3, 4, 6) we have reported on various aspects of the phenomenon of stabilization of serum albumin solutions by non-polar anions. The initial studies were restricted to the effects of the lower fatty acids, the lower alkyl sulfonates, several salts of aromatic acids, and a few simple organic salts. The investigations were concerned with the temperature at which, under certain defined conditions, aqueous solutions of serum albumin coagulated or formed light-scattering material. Figures 1 and 2 will serve to illustrate the results obtained. Attention should be drawn in particular to the mandelate and caprylate curves of figure 2, the caprylate curve being the uppermost dotted line. In an extension of these studies it seemed desirable to learn something of the association, if any, which was presumed to exist between the stabilizer and the albumin. For this purpose ultrafiltration and electrophoretic studies were pursued. As for the former, we were surprised to find that while caprylate under the conditions of these experiments was quite considerably bound by the protein, the binding of mandelate, as also of butyrate, was comparatively slight: 7 per cent of total mandelate was bound by 5 per cent bovine serum albumin from a solution which contained initially 0.04 *M* mandelate; somewhat less than 20 per cent was bound by an albumin solution of 16.5 per cent. The corresponding figures for 0.04 *M* caprylate at the same pH and sodium chloride content were 30 and 72 per cent, respectively. In other words, the concentration of mandelate in the ultrafiltrate from a solution containing 5 per cent albumin was only slightly less than its concentration in the parent solution from which the ultrafiltrate had been derived. This dissimilarity in behavior of caprylate and mandelate led us to pursue the other studies reported in this present paper, the objective being to compare in various ways the stabilizing properties of mandelate and caprylate. By way of further explanation it might be pointed out that caprylate was selected as a reference standard because of the very considerable body of information that has now been accumulated concerning its effects on serum albumin. Caprylate is also assumed to be representative of the lower fatty acids, which differ from one another only quantitatively, the effects in question being observed to vary in gradual progression with increase in chain length. Mandelate became an object of study in the first place because of the consideration that is being given to it for incorporation as a stabilizer in serum albumin solutions of low sodium chloride content.

MATERIALS AND METHODS

The serum albumin solutions were prepared as described in previous papers. Amorphous and crystalline bovine albumin and amorphous human serum al-

¹ Presented at the Twentieth National Colloid Symposium, which was held at Madison, Wisconsin, May 28-29, 1946.

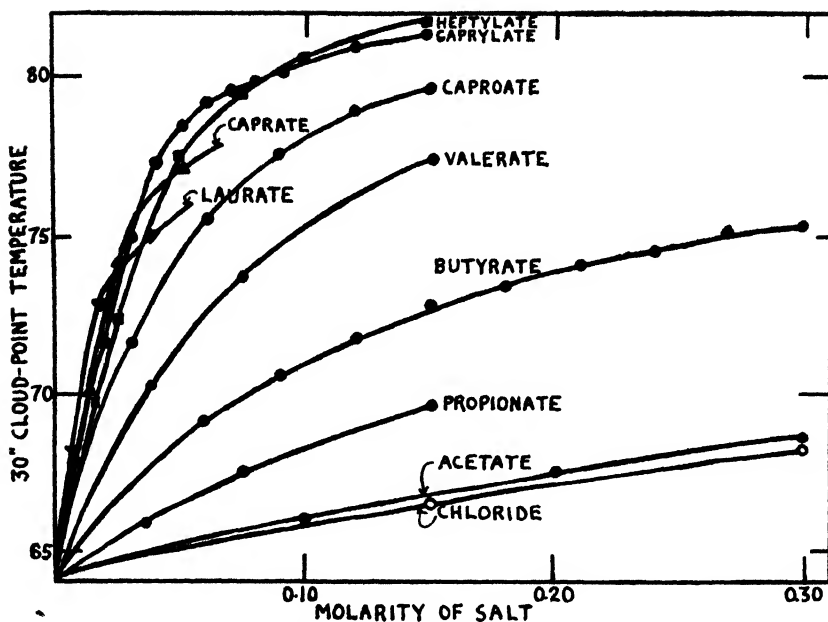


FIG. 1. The stabilization of serum albumin to heat by the sodium salts of fatty acids

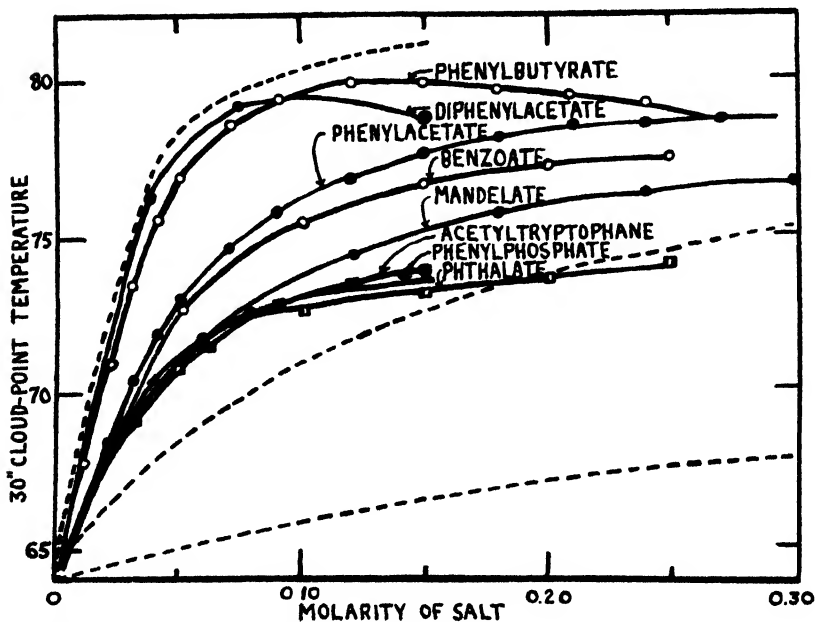


FIG. 2. The stabilization of serum albumin to heat by the sodium salts of various aromatic acids. The three broken lines, reading from the bottom, are for sodium chloride, butyrate, and caprylate, respectively.

bumin were used. The crystalline preparations were homogeneous, as determined by electrophoretic analysis, while the amorphous albumin preparations contained not more than 2 per cent of alpha and beta globulins as the sole protein impurity. The proteins used were obtained through the courtesy of the Armour Laboratories, the Cutter Laboratories, and the Department of Physical Chemistry, Harvard Medical School.

Cloud-point (thermal stability) studies were carried out as described in a recent paper (3), using 25 g. per cent solutions of human serum albumin.

Viscosity determinations were made with Ostwald viscosity pipets at a temperature of $30^{\circ}\text{C.} \pm 0.01^{\circ}$. The water times, at 30°C. , of the pipets used with 2 g. per cent solutions of albumin were from 60 to 85 sec. Nine of the pipets (of the eleven used) had water times of 75 ± 5 sec. The pipets were thoroughly cleaned with a dilute Nacconol solution between determinations, exhaustively rinsed with dilute acetic acid and water, and finally dried in a current of dry air at room temperature.

All solutions used in the viscosity experiments were 0.1 *M* in sodium chloride except those reported upon in figures 5 and 6, which were 0.01 *M*. The pH of all such solutions was 7.8, though not verified by direct determination in all individual cases.

In the experiments involving time of interaction (figure 3 and figures 7 to 11) care was exercised to make sure that the solutions employed were at thermal equilibrium before mixing. The urea and sodium chloride, comprising one solution at 30°C. , were mixed with the protein solution at 30°C. , the time of mixing being recorded as zero time. As soon thereafter as possible, 6-ml. aliquots were pipetted into flasks, again at 30°C. , containing either 0.2 ml. of stabilizer (caprylate or mandelate) or 0.2 ml. of water. After stirring, 5-ml. portions were pipetted into the viscosimeters and the viscosities determined immediately. From 30 to 50 sec. necessarily elapsed after taking an aliquot before the flow-time measurement could be commenced. The control solutions differed in that the stabilizer was mixed in with the urea, sodium chloride, and protein at zero time and the time of interaction between the stabilizer and other constituents increased progressively up to 24 hr.

Viscosity measurements were discontinued if any particulate matter appeared.

The electrophoretic studies were carried out with a Tiselius apparatus, using the scanning method of Longworth. All analyses were made at pH 7.7, a phosphate concentration ($\text{Na}_2\text{HPO}_4 + \text{NaH}_2\text{PO}_4$) of 0.025 *M*, and enough sodium chloride together with the sodium salt of the fatty acid to yield a molarity for these two components together of 0.13 *M* and a constant ionic strength throughout of 0.2. All mobilities were corrected to the viscosity of water. Hydrogen-ion concentrations were determined at room temperature; the conductivity and viscosity measurements were made on the protein solutions at 0.6°C. after prolonged dialysis until equilibrium requisite for electrophoresis was attained. The potential gradients used for all the runs came within the range of 4 to 6 volts per centimeter. The ascending and descending boundaries were quite symmetrical and indicated a high state of homogeneity. Only the mobilities of the de-

scending boundaries were used in the calculations. The albumin mobility in the control samples was uniformly 5.2×10^{-5} cm./sec./volt./cm.

The details of the ultrafiltration studies will be presented in a paper which is now in preparation. It is sufficient to point out here that cellophane membranes treated according to the method of McBain and Stuewer (5) were used.

In addition to viscosity determinations, attempts were made by the method of papain digestion (6) to throw additional light on the state of the stabilized molecule. Since these experiments are incomplete, it is sufficient to point out that they are proceeding according to the technique previously set forth by Rice *et al.* (6).

RESULTS

The electrophoretic studies revealed an effect of mandelate upon the mobility of serum albumin appreciably greater than we would have expected from the ultrafiltration results. The mobilities corrected to solutions of the viscosity of

TABLE 1

Effects of mandelate and of caprylate on the mobility of human serum albumin
Cutter albumin (run F); all solutions 0.5 per cent in albumin, pH 7.7, ionic strength 0.2; mobilities corrected to water at 0.6°C.

CONCENTRATION OF MANDELATE OR CAPRYLATE	MOBILITY	
	Mandelate	Caprylate
<i>M</i>	cm /sec./volt/cm. $\times 10^5$	cm /sec./volt/cm. $\times 10^5$
0.00	5.21	5.2
0.02		5.92
0.04	5.87	6.12
0.06	6.03	6.66
0.08	6.46	6.77
0.10	6.52	6.87

water² are presented in table 1. Reference to the paper by Ballou *et al.* (2) reveals the effect of mandelate upon the mobility of serum albumin to be slightly greater than that of heptoate.

We next sought to compare the effects of caprylate and mandelate on solutions of urea-denatured serum albumin. Figure 3 serves to illustrate the over-all effects of these substances on the relative viscosity of 2 per cent solutions of serum albumin in which the only variable was the time which elapsed after adding urea. It might be added that in the absence of urea the effects of mandelate and caprylate upon the viscosity of serum albumin are comparatively small in the concentration used. As will be evident from the results of other experiments presently to be reported upon, the principal fact that emerges from this experiment is the failure of mandelate in the concentration employed to prevent as effectively as does caprylate the increase in viscosity brought about by urea

² It should be pointed out that the viscosity correction with mandelate is comparatively great; the uncorrected values revealed a very slight effect indeed.

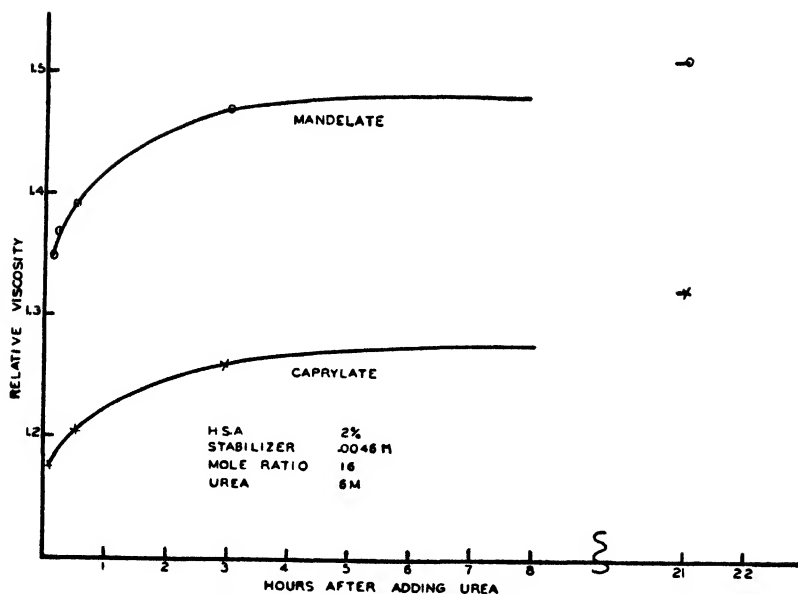


FIG. 3. The effects of caprylate and mandelate on the viscosity of human serum albumin in 6 M urea.

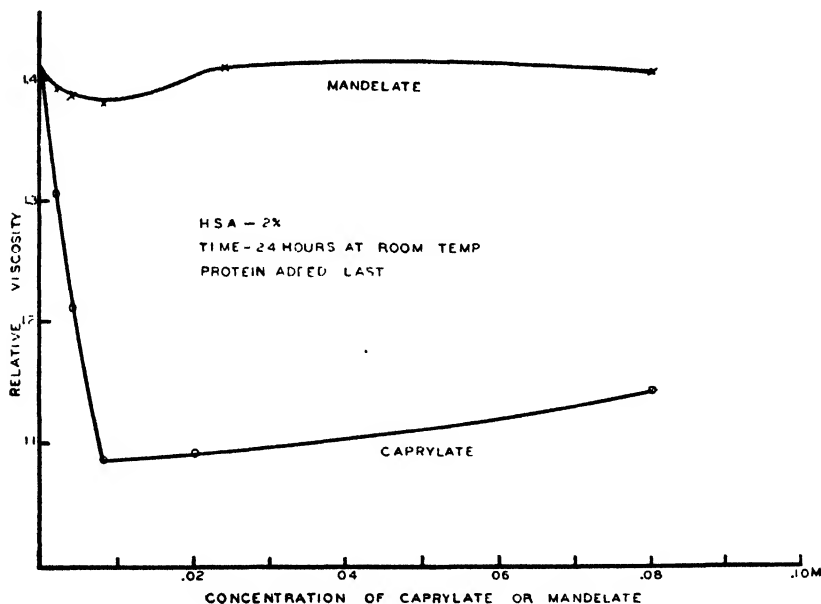


FIG. 4. The effects of caprylate and mandelate on the denaturation of human serum albumin by 6 M urea. The protein was added last and the viscosity determinations were made after 24 hr. further standing at room temperature.

denaturation. Figure 4 presents the results of a closely related experiment in which the mandelate and caprylate in the presence of human serum albumin and

6 *M* urea were permitted to react for 24 hr. at room temperature before the viscosity measurements at 30°C. were made. Here the sole variable is the concentration of stabilizer. As previously reported by Boyer *et al.*, caprylate was found to prevent very effectively the apparent denaturation of albumin by urea which would otherwise result in a high viscosity value. The effect of caprylate is maximal between 0.01 *M* and 0.05 *M*. In sharp contrast to the findings with caprylate, mandelate shows no such protection against denaturation. The slight dip in the concentration curve with very low concentrations of mandelate has been repeatedly confirmed and is roughly analogous to the much greater decrease observed with caprylate. The failure of mandelate to stabilize effec-

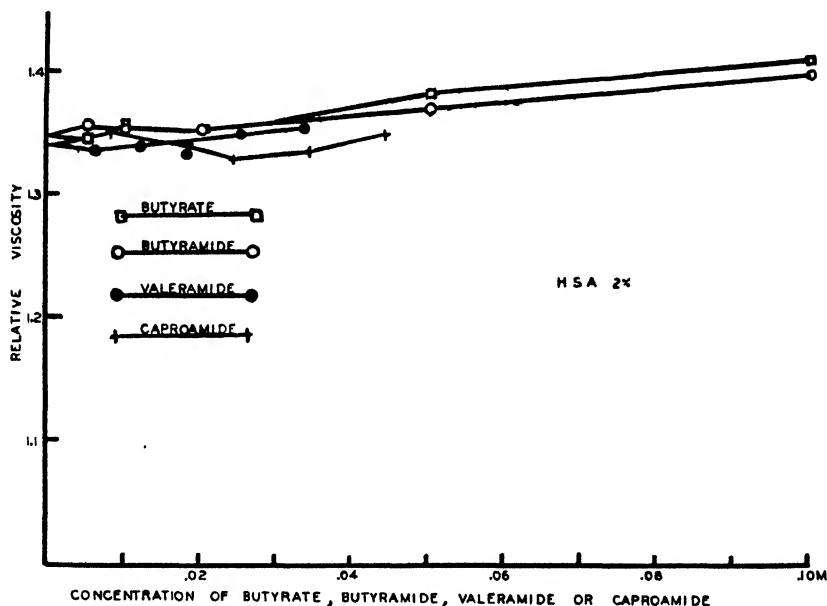


FIG. 5. The effects of butyrate, butyramide, valeramide, and caproamide on the denaturation of human serum albumin by 6 *M* urea. The protein was added last and the viscosity determinations were made after 24 hr. further standing at room temperature.

tively the albumin molecule against urea denaturation is paralleled by butyrate, butyramide, valeramide, and caproamide, results of which are presented in figure 5. Figure 6 serves as a control experiment in which the viscosity values for protein-mandelate systems at two different levels of protein concentration are reported upon. The divergence between the two upper curves (one broken) is indicative of the slight stabilization induced by mandelate.

Bovine albumin was used in this experiment instead of human serum albumin, but it is proper to mention that the differences in behavior of human and bovine serum albumin in viscosity studies such as these have not been found to be of sufficient magnitude to affect the conclusions drawn.

Another comparison of caprylate and mandelate stems from observations

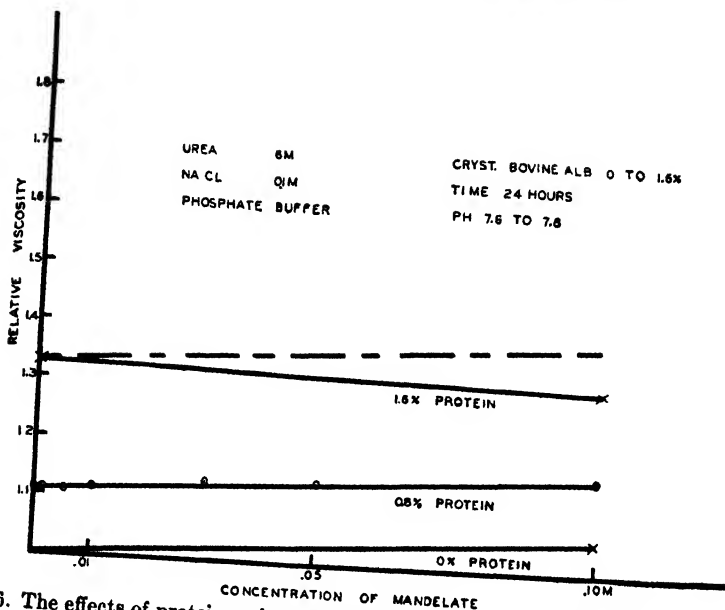


Fig. 6. The effects of protein and mandelate concentration on the viscosity of solutions of human serum albumin denatured by 6 *M* urea. The protein was added last, and the viscosity determinations were made after 24 hr. further standing at room temperature.

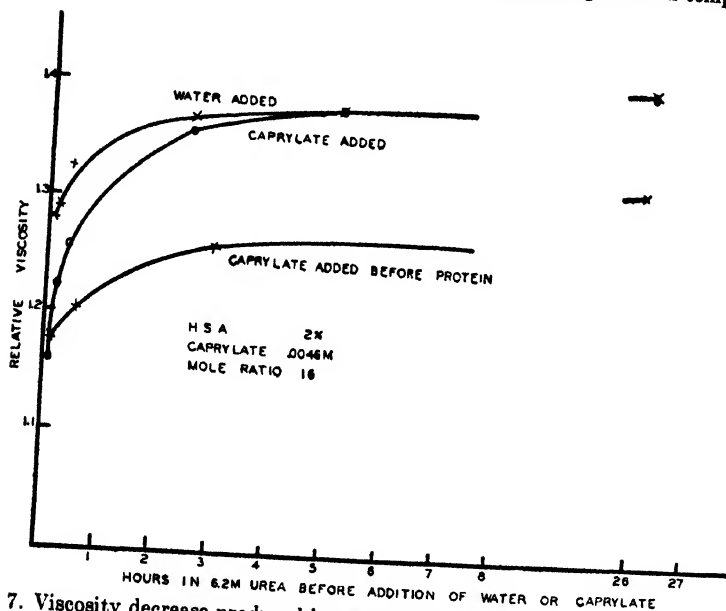


Fig. 7. Viscosity decrease produced by caprylate after exposure of albumin to urea for various time intervals. To solutions of human serum albumin in 6.2 *M* urea, sufficient water or sodium caprylate solution was added at various time intervals to give a solution of the final composition indicated above. The third curve, reproduced from figure 3, is a control.

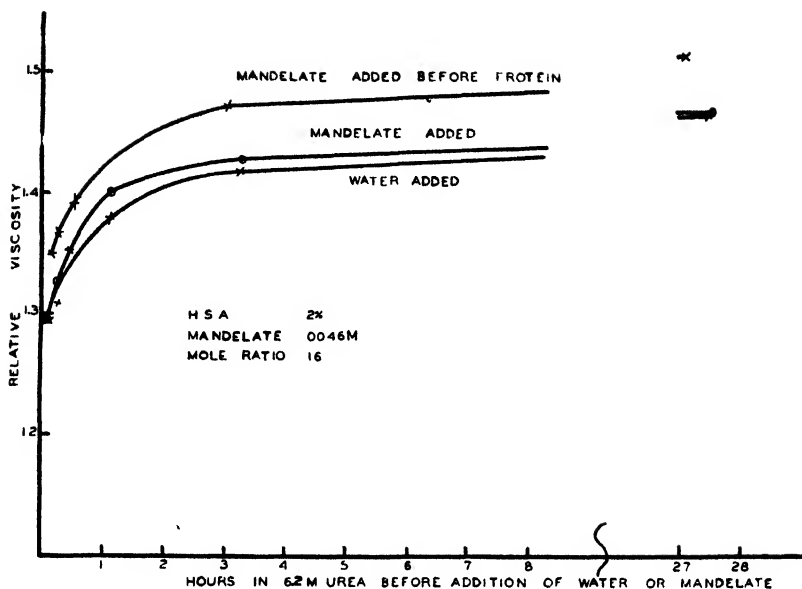


FIG. 8. Viscosity effects produced by mandelate after exposure of albumin to urea for various time intervals. To solutions of human serum albumin in 6.2 *M* urea, sufficient water or sodium mandelate solution was added at various time intervals to give a solution of the final composition indicated. The third curve, reproduced from figure 3, is a control.

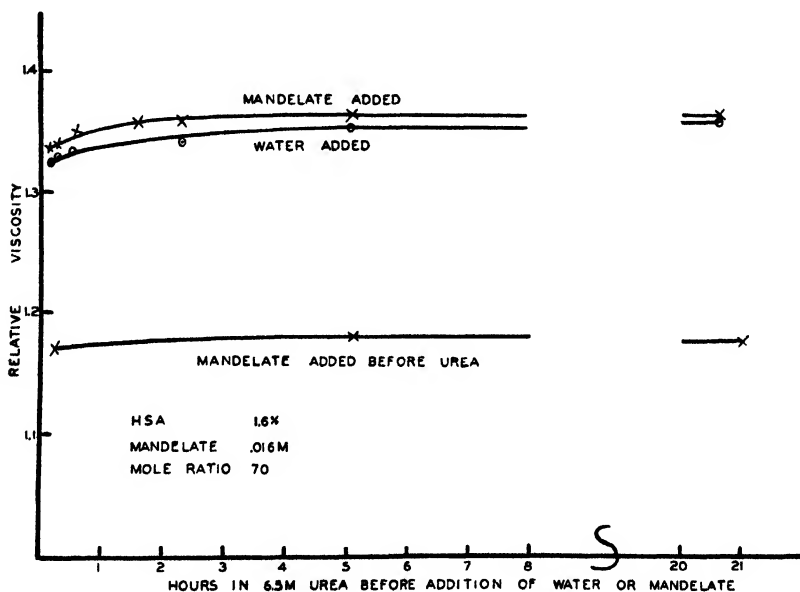


FIG. 9. Effects of a higher mole ratio of mandelate to albumin and of time of exposure to urea on the relative viscosity of human serum albumin solutions. The third curve, a type of control, suggests an apparent stabilization.

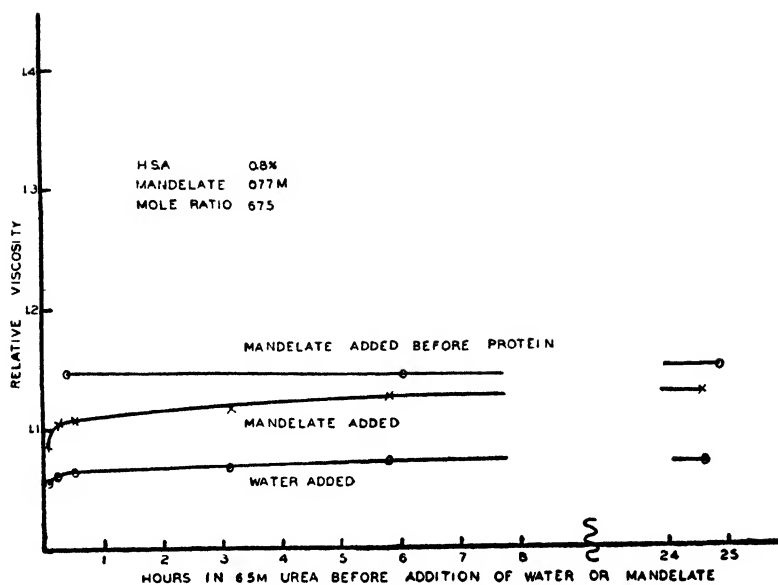


FIG. 10. Effects of a very high mole ratio of mandelate to albumin, and of time of exposure to urea, on the relative viscosity of human serum albumin solutions.

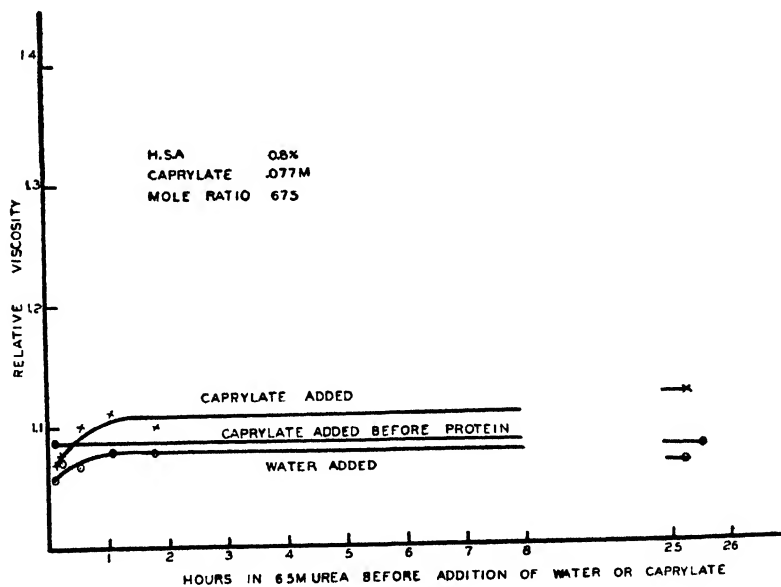


FIG. 11. Effects of a very high mole ratio of caprylate to albumin, and of time of exposure to urea, on the relative viscosity of human serum albumin solutions.

previously reported, in which caprylate added subsequent to the mixing of protein and urea was found to maintain the viscosity of the solution at a value inter-

mediate between that of the stabilized native protein and that of the urea-denatured protein. Figure 7 illustrates the results obtained with caprylate, in which it will be noted that addition of the stabilizer a few minutes after addition of the urea results in a quite low value for the relative viscosity of the solution. Included in this figure is a third curve comparable to figure 3, in which the caprylate and urea were first mixed, protein was then added, and the reaction permitted to proceed for 1, 2, 3, or 24 hr. as indicated on the curve.³ Figure 8 presents the results of a comparable experiment with mandelate. A comparison of figures 7 and 8 necessitates the conclusion that whatever may be the denaturing effect of urea, this is further enhanced by mandelate irrespective of whether the mandelate be added after the urea and protein have been mixed or whether the protein be added last under circumstances which permit the urea molecules and mandelate ions to have an equal opportunity to react with the albumin. It will be noted, incidentally, that in the experiments presented in figures 7 and 8 the mole ratio of stabilizer to albumin is low: 16 to 1. At a higher mole ratio (70 to 1) (figure 9) the results are qualitatively similar to those presented in figure 8. The third curve in figure 9 shows that mandelate added to the protein prior to the urea in a final concentration of 0.016 *M* and measured at various intervals thereafter appears to have prevented viscosity increases otherwise to be observed. At a high mole ratio of 675 to 1 (figure 10), this time with a serum albumin concentration of 0.8 per cent, the effects observed were similar to those reported upon in figure 8 (mole ratio 16 to 1) with the single qualification that the apparent denaturing effect of mandelate under these conditions is even more pronounced. It might be mentioned that caprylate in a sufficiently high concentration appears to be likewise denaturing in effect (figure 11).

CONCLUSION

Tentatively we are inclined toward the conclusion that mandelate, unlike caprylate in corresponding low concentrations, does not stabilize serum albumin in the closed native configuration. It appears to act rather as a solubilizing agent, effecting a solvation of the partially extended form of the partially denatured molecule and preventing the formation of light-scattering particles of protein under the conditions of an ordinary thermal-stability test. This conclusion is supported by the results of experiments on the rate of digestion of the native and urea-denatured forms of serum albumin in the presence of caprylate or mandelate. If caprylate be added a few minutes after urea (the latter in an overall concentration of 6 *M*) is added to serum albumin, it is found that the rate of digestion by papain is quite low, indeed approaching that of the native molecule. This was reported by Rice *et al.* (6) and has been confirmed by Miss Carol Moore. In comparable experiments in which mandelate instead of caprylate was added to the urea-denatured protein it has been found that the rate of digestion by

³ In the control, unlike the two experimentals, the mandelate was present for an increasing period of time (up to 24 hr.). In the two experimentals the viscosity determinations were made within a minute or two of adding the mandelate in water. The requirements of the experiment were such as to render this difference in treatment unavoidable.

papain is quite high,—approaching the digestion rate of the denatured protein rather than that of the native protein. We conclude that while caprylate added promptly to urea-denatured albumin causes a closure of the molecule, mandelate on the contrary permits the papain-reactive groups, exposed by 6 *M* urea, to remain exposed. The closure of the molecule or envelopment of these groups is not in evidence. This conclusion is subject to the qualification that caprylate and mandelate may be inhibitory to papain. A study of this question is now in progress.

The work described in this paper was done under a contract, recommended by the Committee on Medical Research, between the Office of Scientific Research and Development and Stanford University.

Grants-in-aid from the Rockefeller Foundation and the Cutter Laboratories are gratefully acknowledged.

The present paper constitutes a brief summary of several aspects of investigations which have been pursued with the collaboration of G. A. Ballou, P. D. Boyer, Carol Moore, and L. H. Noda. The recent viscosity work has been carried out by E. L. Duggan with the technical assistance of Jean Legg and the electrophoretic studies on mandelate by C. Alvarez Tostado with the technical assistance of Inger Jorgensen.

REFERENCES

- (1) BALLOU, G. A., BOYER, P. D., LUCK, J. M., AND LUM, F. G.: *J. Biol. Chem.* **153**, 589 (1944).
- (2) BALLOU, G. A., BOYER, P. D., AND LUCK, J. M.: *J. Biol. Chem.* **159**, 111 (1945).
- (3) BOYER, P. D., BALLOU, G. A., AND LUCK, J. M.: *J. Biol. Chem.* **162**, 199-208 (1946).
- (4) BOYER, P. D., LUM, F. G., BALLOU, G. A., LUCK, J. M., AND RICE, R. G.: *J. Biol. Chem.* **162**, 181-97 (1946).
- (5) MCBAIN, J. W., AND STUEWER, R. F.: *J. Phys. Chem.* **40**, 1157 (1936).
- (6) RICE, R. G., BALLOU, G. A., BOYER, P. D., LUCK, J. M., AND LUM, F. G.: *J. Biol. Chem.* **158**, 609 (1945).

DIFFUSION IN WOOD¹H. K. BURR² AND ALFRED J. STAMM*Forest Products Laboratory³, Forest Service, U. S. Department of Agriculture**Received August 8, 1946*

INTRODUCTION

Diffusion processes are of great importance in wood technology. The seasoning (drying) of wood involves diffusion, as does the treatment of wood with preservatives, fire retardants, antishrink and seasoning chemicals, and the penetration of chips with reagents prior to pulping. Until recently these processes have been studied only empirically. A fundamental understanding of the basis of diffusion and flow phenomena in wood should hence be of great practical value.

In an as yet unpublished Department of Agriculture bulletin, Stamm (10) has derived theoretical expressions for the rates of passage of liquids, vapors, and dissolved materials through softwoods (coniferous or needle-leaved trees) in the longitudinal and transverse directions under various conditions of temperature, moisture content, and pressure from capillary structure considerations. These equations involve quantities which have had to be estimated in an indirect fashion from limited data, part of which is of doubtful accuracy. The purpose of the present work was twofold: (1) To check the diffusion values predicted by Stamm's equations by measurements of diffusion constants in softwoods and in regenerated cellulose; (2) by similar measurements on selected hardwoods (deciduous or broadleaved trees) to determine to what extent these same equations may be used for hardwoods.

Because of the complexity and variability of the structure of the hardwoods, Stamm (10) found it necessary to confine his analysis to the case of the simpler softwoods, such as the pines, spruces, hemlocks, and firs.

The softwoods are made up chiefly of wood fibers, or tracheids, which are hollow cellulosic tubes, tapered and closed at both ends, and something between rectangular and elliptical in cross section. Their length averages about 3.5 to 4.0 mm. and their diameter about 0.030 to 0.035 mm. These fibers are laid down in fairly regular radial rows, with their long axes parallel to that of the tree. The tapered ends of the fibers overlap longitudinally by about one-fourth their length. The summerwood fibers are smaller than the springwood and are somewhat flattened in the radial direction, thus forming the visible annual rings. The fiber walls are made up almost entirely of cellulose and hemicellulose, which

¹ Presented at the Twentieth National Colloid Symposium, which was held at Madison, Wisconsin, May 28-29, 1946.

Thesis submitted by H. K. Burr to the University of Wisconsin in partial fulfillment of the requirements for the degree of Doctor of Philosophy, September, 1941.

² Present address: Western Regional Research Laboratory, Bureau of Agricultural and Industrial Chemistry, U. S. Department of Agriculture, Albany, California.

³ Maintained at Madison 5, Wisconsin, in cooperation with the University of Wisconsin.

comprise about 70 per cent of the dry weight of the wood. The fibers are cemented together by a membrane material consisting of lignin.

A number of the softwoods also contain vertical and horizontal resin ducts, but these are usually clogged with resin. As their contribution to diffusion and flow is small, their effect was neglected in the calculations.

About 1 or 2 per cent of the void volume of softwoods is in the form of wood rays. These are bundles of cells somewhat similar to the tracheids, but oriented radially and communicating with the fibers by simple pits. They have also been neglected in Stamm's theoretical calculations.

Each fiber cavity has between 50 and 300 "bordered pits" communicating with adjacent fiber cavities and concentrated on the radial faces and tapered ends of the fibers. The pit chamber is roughly in the form of a truncated cone, the smaller end opening into the fiber cavity and the larger end closed by the pit membrane. The pit membrane is three or four times as large in diameter as the pit opening. The pit membrane, a continuation of the middle lamella, has a central thickened portion, the torus, surrounded by a portion perforated by permanent pores and, in the presence of swelling agents, transient capillaries as well. The term "transient" is here used to designate capillaries which exist only when the membrane or cell wall is swollen.

The fiber walls consist of long fibrils oriented at a slight angle to the fiber axis and wrapped by a layer of other fibrils practically at right angles to them. The fibrils consist of smaller "fusiform bodies," which, in turn, are composed of micelles and single primary-valence chains of cellulose. X-ray studies have shown that, when water is adsorbed by cellulose, it is concentrated between the micelles rather than within them. In the presence of a swelling medium, the cell wall will have a transient capillary structure in the form of the intermicellar space. Small molecules can diffuse through this fine cell-wall structure.

The capillaries in softwoods through which most of the passage occurs are the fiber cavities, the pit chambers, the permanent pores and transient capillaries in the pit membranes, and the transient capillaries of the cell wall. By analogy with an electrical resistance network, the fiber cavities can be considered as connected in series with the pit chambers and the pores and transient capillaries of the pit membranes. In parallel with the pit structure are the transient cell-wall capillaries, and in parallel with these combined paths is the continuous path through the cell walls. This structure is illustrated diagrammatically in figure 1. In other words, passage may occur (1) through a fiber cavity, into a pit chamber, through a permanent or transient pore in the pit membrane and into the next pit chamber and fiber cavity; (2) through a fiber cavity and through the swollen cell wall into the next fiber cavity; or (3) continuously through the cell-wall capillaries.

In order to calculate the net "conductivity" of this net work, three dimensions must be known for each of the structural units (fiber cavities, pit chambers, pit-membrane pores, and cell-wall capillaries). These are: (1) average effective capillary length, (2) number of capillary lengths per unit distance, and (3) effective capillary cross section.

The first case considered by Stamm (10) is that of the diffusion of a solute through wood completely filled with water. In this case:

$$D_l = 1/R_l = \frac{1}{R_a + \frac{1}{\frac{1}{\frac{1}{1/R_b + 1/R_c} + R_d} + 1/R_f}} + 1/R_f \quad (1)$$

where D_l = longitudinal diffusion constant relative to the dimensions of the swollen wood,

R_l = total resistance of the network in the longitudinal direction per centimeter cube,

R_a = resistance of the fiber cavities,

R_b = resistance of the permanent pit-membrane pores,

R_c = resistance of the transient pit-membrane capillaries,

R_d = resistance of the pit chambers,

R_e = resistance of the cell-wall capillaries to passage from one fiber cavity to the next, and

R_f = resistance of the capillaries of the cell wall to continuous passage through them.

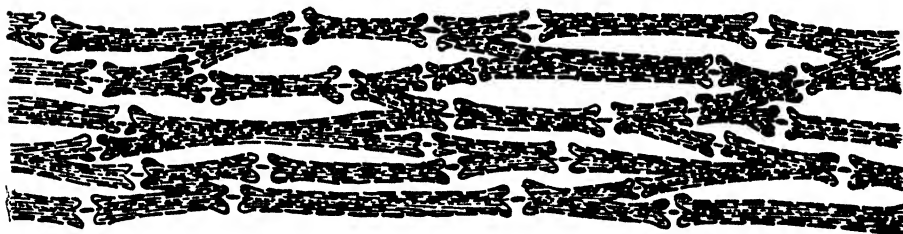


FIG. 1. Diagrammatic sketch of a swollen tangential section of a softwood

Each resistance term includes D_0 in the denominator, where D_0 is the diffusion constant for the bulk liquid.

Substitution of typical values for a softwood with a specific gravity of 0.365 gives $D_l = 0.651D_0$, $D_t = 0.0466D_0$, and $D_l/D_t = 14.1$. Figure 2 shows the variation of these quantities with specific gravity.⁴ In the longitudinal direction, the contribution of the continuous path through the cell wall is negligible, and the resistance of the fiber cavities is great compared with that of the pit structures and the cell-wall capillaries. Longitudinal diffusion, then, is limited by the void cross section of the fiber cavities, and since this is inversely proportional to the specific gravity of the wood, the plot of D_l/D_0 against specific gravity is nearly a straight line. In the transverse direction, the contribution

⁴ Unless otherwise specified, the specific gravity of wood is taken as the oven-dry weight of a sample divided by its volume at or above the fiber-saturation point.

of the continuous path through the cell wall is about 3 per cent of the total. The pit resistance is approximately twice that of the cell-wall capillaries, and their combined resistance is much greater than that of the fiber cavities. D_t/D_0 falls rather sharply with increasing specific gravity in the low-specific-gravity region, but a roughly linear relationship exists between them above a specific gravity of about 0.3. In consequence, the ratio D_i/D_t is fairly constant in the

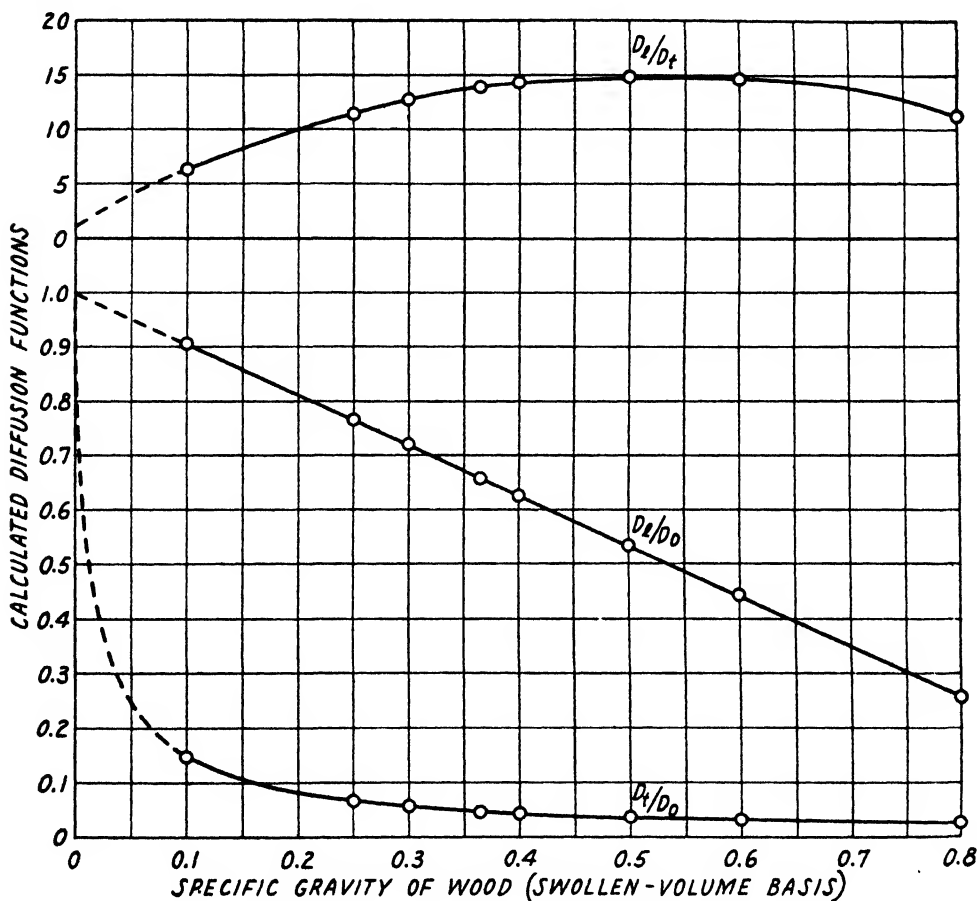


FIG. 2. Calculated diffusion functions relative to bulk diffusion for the passage of solutes with molecules the size of the water molecule through water-saturated wood of different specific gravities (from the calculation of Stamm (10)).

range of specific gravities normal for softwoods. While D_t will depend to a certain extent upon factors which are independent of the specific gravity, variations in these quantities among the common softwoods appear to be minor (10).

In deriving the equation for D_i it was assumed that the fiber cavities were long cylindrical tubes. If account is taken of the two- or threefold variation in cross section of a cavity along its length, D_i will be reduced by between 11 and 25 per cent.

The data of Cady and Williams (3) for the longitudinal diffusion of glycerol, lactose, and urea into Western red cedar, white fir, and Western hemlock (which have specific gravities of 0.425, 0.350, and 0.441, respectively) are lower than the theoretical values calculated from equation 1 by amounts ranging from 6.7 to 19.4 per cent. The data of Stamm (9) for the relative electrical conductivity in the fiber direction of wood saturated with dilute salt solutions are lower than the theoretical by 11.2 to 20.8 per cent. Several softwoods with specific gravities between 0.290 and 0.526 were used. Both these sets of measurements are in excellent agreement with the theoretical values when the effect of non-uniform bore is taken into account.

Diffusion measurements in the radial and tangential directions were made by Cady⁵ and, though subject to considerable experimental error, confirm the values calculated from equation 1. No difference within experimental error was found between the diffusion constants in the radial and the tangential directions. A few data for the relative electrical conductivity of wood in the tangential direction were also obtained by Stamm (9). He obtained an experimental value of $D_t/D_0 = 0.046$ for slash pine (specific gravity 0.430), and 0.037 for Douglas fir (specific gravity 0.326). The corresponding theoretical values are 0.041 and 0.052. These limited data indicate that equation 1 will serve to approximate transverse diffusion constants.

The drying of wood is a much more complicated phenomenon. Tuttle (13), Sherwood (8), and Kollmann (5, 6) have treated moisture gradients and drying rates by Fourier analysis as though it were a simple diffusion problem. But Stillwell (12) and Martley (7) have shown that this assumption is not strictly valid.

In the first place, the dimensions of the wood vary from lamina to lamina, owing to the moisture-content gradient. In the second place, there are three different driving forces operating during the drying of wood. Above the fiber-saturation point, liquid flows through the coarse capillaries toward the drying surface owing to capillary forces, and vapor moves through the same structure owing to a relative vapor-pressure gradient caused by the depression of vapor pressure in the smaller capillaries. Below the fiber-saturation point, the drying process is controlled by diffusion, but while the vapor is moving under the vapor-pressure gradient, there is also a movement of bound water through the cell wall under a moisture-content gradient. Cases have been recorded (1) in which these two gradients act in opposite directions. The resultant movement in such cases seems to be controlled chiefly by the vapor-pressure gradient.

In spite of these complications it is possible to treat the drying process by a method similar to that used for the diffusion of a solute through wood saturated with solvent by considering laminae of 0, $\frac{1}{4}$, $\frac{1}{2}$, $\frac{3}{4}$, and 1 times the moisture content at the fiber-saturation point on the basis of volume of water per unit volume of swollen wood substance.

⁵ Thesis entitled "Molecular diffusion into wood," submitted by L. C. Cady to the University of Wisconsin in partial fulfillment of the requirements for the degree of Doctor of Philosophy and filed in the Library of the University of Wisconsin, August, 1934.

EXPERIMENTAL

Four types of measurements were made. The electrical conductivities of several species of woods saturated with salt solutions were determined. The ratios of these values to the conductivities of the solutions with which the samples were in equilibrium were assumed to be equal to the corresponding diffusion constants relative to unit dimensions of the wood. Direct measurements of relative diffusion constants were made in order to check the validity of this assumption. A series of microscopic measurements was made on a number of

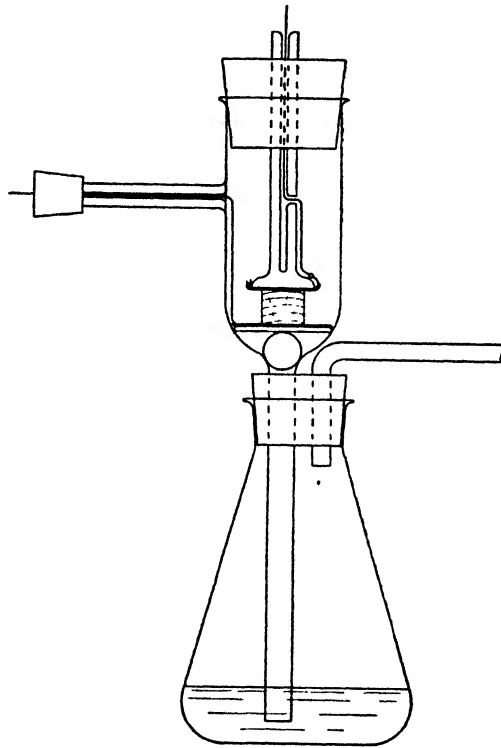


FIG. 3. Cell for the measurement of electrical conductivities of cubes of wood saturated with aqueous solutions. Cube is shown in position for measurement.

different species in order to determine to what extent certain of the structural dimensions differed from those taken by Stamm as typical of softwoods. Finally, measurements of the rate of transfusion of water vapor through wood and through regenerated cellulose were made, using the method of the steady state.

Electrical conductivity

The capillary structure of wood, which permits the migration of ions in an electric field, was assumed to be the same as that which permits the diffusion of similar ions under a concentration gradient, provided surface conductance

effects are negligible and in both cases the wood is completely filled with liquid. If this is true, the relative conductivity, k/k_0 , defined as the ratio of the conductivity of the solution-saturated wood to that of the bulk solution with which it is in equilibrium, may be taken as identical to the relative diffusion constant, D/D_0 . Since conductivity measurements are more easily and more accurately made than direct diffusion measurements, relative conductivities were determined and tentatively treated as relative diffusion constants.

The cell illustrated in figure 3 was constructed of Pyrex glass. It consists of an upper chamber connected by a tube running through a rubber stopper with the bottom of a 200-cc. Erlenmeyer flask. A horizontal tube makes it possible to blow liquid from the flask into the upper chamber without opening the cell. The electrodes were of platinum foil mounted on glass supports. The disk which holds the lower electrode rests on a glass ball, permitting it to tilt slightly as necessary. From time to time the electrodes were coated with platinum black by electrodeposition. Between runs, they were ordinarily kept covered with distilled water or with solution.

The cell was mounted in a water-jacketed air bath, the temperature of which was thermostatically controlled at $30^\circ\text{C} \pm 0.1^\circ$. Resistance measurements were made with a bridge consisting of two fixed resistances and a resistance box having a range of 1 to 11,110 ohms. A 1000-cycle microphone hummer served as a source of alternating voltage, and a telephone headset as a detector. Resistances could be determined to ± 0.2 per cent or better.

For filling the samples with solution, the cube of wood was first dried to constant weight in an oven at 105°C . It was then placed in a bottle, and the pressure was reduced to 1 mm. Hg or less for a period found to be sufficient for nearly complete evacuation of the sample, usually 2 days. Without permitting air to enter the vessel, freshly boiled solution was allowed to run in and the vacuum was released, thus forcing the liquid into the coarse capillary structure by atmospheric pressure. Precautions were taken to prevent the sample from floating to the surface of the liquid. Two weeks or more was allowed for equilibration, and at the end of that time the samples were again weighed and their dimensions measured. The void volume of the cubes was calculated from the following equation:

$$V_f = 1 - g(1/g_a + m/\rho) \quad (2)$$

where g = green-volume specific gravity,

g_a = apparent specific gravity of pure wood substance as measured by the displacement of water,

m = weight of the liquid in the sample divided by the dry weight of the sample, and

ρ = density of the solution.

If the void volume was not less than 3 per cent, the cubes were returned to the liquid for another period.

For the conductivity measurements on regenerated cellulose, pieces of sheet cellulose acetate 0.025 cm. thick were deacetylated by treatment for a week

with 3 per cent sodium hydroxide in methyl alcohol. The regenerated cellulose was then soaked in frequently changed distilled water until no more alkali was leached out. Squares of the material approximately 1 cm. on a side were cut out and transferred to 0.10 *N* potassium chloride solution, and several days were allowed for equilibration before measurements were made.

To measure the conductivities of wood samples, a cube of wood approximately 1 cm. on an edge and previously filled with solution to a void volume of 3 per cent or less was placed in the upper chamber of the cell, and some of the solution with which it was in equilibrium was placed in the lower flask. The thermostat doors were closed and liquid was blown into the upper chamber until it completely covered the cube and electrodes. After 1 hr., the level of the solution was lowered again, the cell was opened, and the cube centered on the lower electrode with its longitudinal axis vertical. The cork stopper was replaced and the upper electrode pressed firmly down upon the cube, where it was held by friction on the cork. Solution was forced into the upper chamber again and maintained there for 15 to 20 min., when it was again withdrawn. Exactly 5 min. later, the resistance of the block was determined. In a similar manner, values for the radial and tangential resistances were obtained, except that the 1-hr. temperature equilibrium period was omitted. Readings could be checked within 3 per cent. The specific conductivity in each of the structural directions of the cube was calculated from the dimensions of the cube. The bulk conductivity, k_0 , was determined in a conductivity cell which had been calibrated against a 0.10 *N* solution of potassium chloride.

An error of considerable magnitude was introduced by the film and meniscus of solution which remained on the cube and electrodes even after the drainage period. The film acted as a resistance in parallel with that of the sample, and the meniscus which formed on each electrode effectively shortened the cube in the direction in which the measurement was being made. Using a technique which eliminated the meniscus effect, Stamm (9) had found it possible to assign a resistance to the film, but this method could not be applied to the present problem. In order to correct for both factors, five longitudinal, five radial, and four tangential conductivities were measured on cubes of various species between dry or nearly dry electrodes. Each cube was shaken to remove excess liquid, and the electrodes were dried with a stream of air. The resistance of the cube was determined and the process repeated until successive readings were approximately constant. A corrective factor, C , was determined by which the conductivity measured between wet electrodes was to be multiplied in order to get the true conductivity. A plot of C against k/k_0 showed no definite relationship between the two quantities, and although the factor for the longitudinal direction was higher than for the transverse, the radial and tangential factors were approximately the same. The longitudinal factor averaged 0.878, with a standard deviation of 0.019; the transverse factor averaged 0.701, with a standard deviation of 0.065. All measured longitudinal conductivities were then multiplied by 0.88 and all transverse values by 0.70. The conductivities of a cube as measured between dry electrodes depended to such an extent upon electrode

pressure and the degree to which the cube and electrodes had been dried that it was felt advisable to use wet electrodes and a standardized drainage time and apply an average corrective factor rather than to measure conductivities between the dry electrodes directly.

Resistances measured at 60 cycles were found to be identical to those at 1000 cycles. Measurements on cubes of Western white pine filled with distilled water and with solutions containing various concentrations of potassium chloride showed that 0.10 *N* was a concentration sufficient to render surface conductance effects negligible. Accordingly, all conductivity data reported here are for cubes filled with 0.10 *N* potassium chloride.

Table 1 gives the relative conductivities of samples of the heartwood of Western white pine (*Pinus monticola*), Western hemlock (*Tsuga heterophylla*), and Douglas fir (*Pseudotsuga taxifolia*). These values are also plotted in figure 4, together with the curves calculated from Stamm's equations. It is to be noted that all the longitudinal values fall within the limits predicted on the assumption that there is a two- to threefold variation in the fiber-cavity diameter along

TABLE 1

Electrical conductivities relative to the bulk conductivity of the solution for the longitudinal, radial, and tangential directions of softwood cubes completely filled with 0.10 N potassium chloride

SPECIES	SPECIFIC GRAVITY	k_l/k_0	k_r/k_0	k_t/k_0
Western white pine	0.352	0.54	0.032	0.031
Douglas fir	0.478	0.43	0.022	0.025
Douglas fir	0.475	0.42	0.020	0.022
Western hemlock	0.414	0.46	0.031	0.024
Western hemlock	0.420	0.47	0.029	0.024

its length (10). On the other hand, the transverse values are lower than those predicted by from 26 to 46 per cent. For the pine and hemlock, the radial values are somewhat higher than the tangential, while in the case of Douglas fir the tangential values are the higher.

Similar measurements were made on samples of the heartwood and sapwood of the following hardwood species: black tupelo (*Nyssa sylvatica*), also known as blackgum in the lumber trade; sweetgum (*Liquidambar styraciflua*); Southern magnolia (*Magnolia grandiflora*); American sycamore (*Platanus occidentalis*); sugar maple (*Acer saccharum*); and Northern red oak (*Quercus borealis*). These data are tabulated in table 2 and plotted in figures 5 and 6. The values enclosed in parentheses were obtained on cubes which became distorted upon swelling,—an indication that some form of collapse had occurred in the drying of the wood.

The longitudinal values fall somewhat below the theoretical curve even when allowance is made for a threefold variation in the fiber-cavity diameter, but they do fall roughly along a line parallel to that predicted. The fact that these

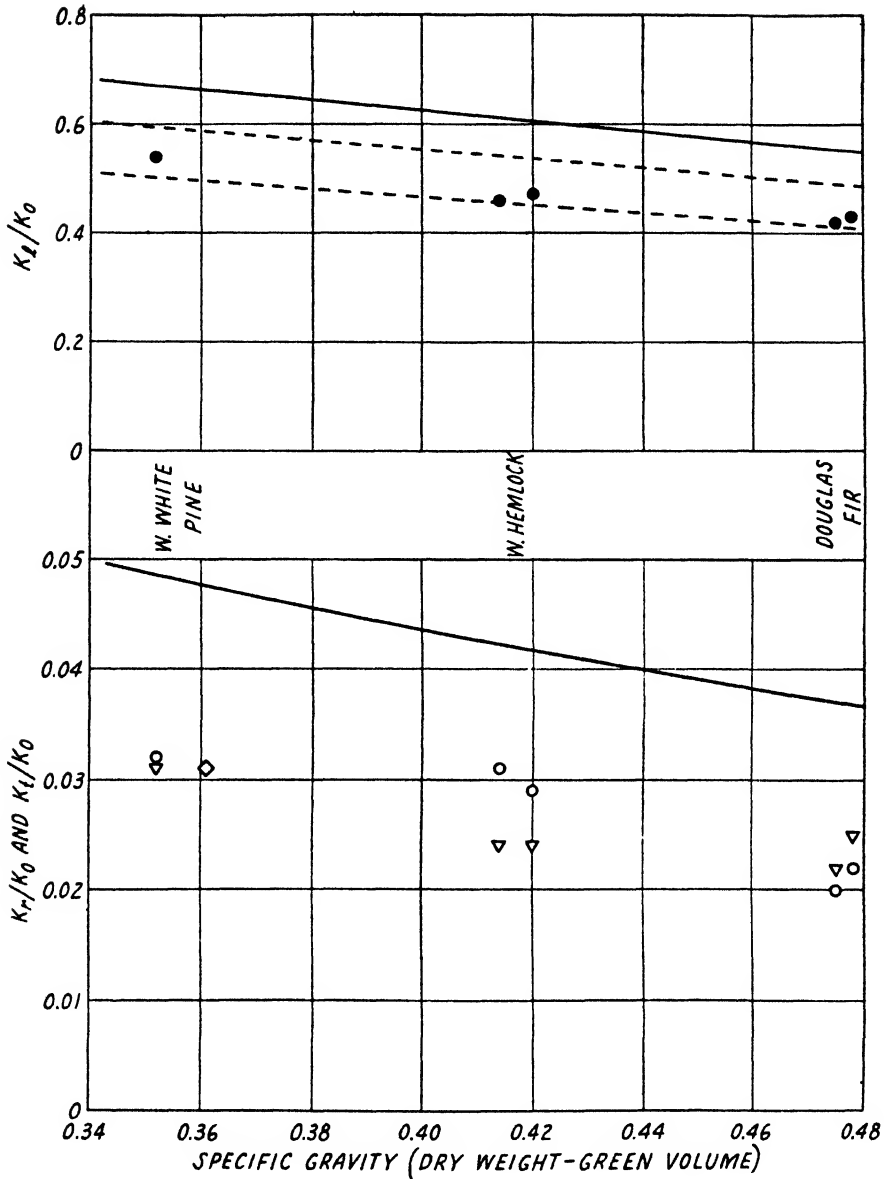


FIG. 4. Relative electrical conductivities for three softwoods. Solid lines calculated from Stamm's equation with no correction. Dotted lines (upper) represent values with minimum taper correction and (lower) values with maximum taper correction. ●, longitudinal values; ○, radial values; ▽, tangential values; ◇, relative diffusion constant from actual diffusion measurements in the tangential direction.

deviations from the uncorrected calculated values are greater than those obtained for softwoods can be justified by the microscopic measurements, which indicate a significantly greater taper of hardwood as compared to softwood

fibers. The transverse values are widely scattered, but, in general, the highest conductivities are found in the low-specific-gravity range and the lowest values in the high-specific-gravity range. Exactly one-half the points fall above the

TABLE 2

Relative electrical conductivities in the longitudinal, radial, and tangential directions of hardwoods completely filled with an approximately 0.1 N solution of potassium chloride

SPECIES	SPECIFIC GRAVITY	k_l/k_0	k_r/k_0	k_t/k_0
Sugar maple:				
Sapwood	0.588	0.32	0.044	0.024
Sapwood	0.580	0.33	0.039	0.020
Heartwood	0.591	0.30	0.035	0.023
Heartwood	0.568	0.29	0.024	0.017
Black tupelo:				
Sapwood	0.495	0.40	0.050	0.029
Sapwood	0.464	0.40	0.052	0.032
Sapwood	0.455	0.42	0.056	0.035
Sapwood	0.450	0.44	0.055	0.024
Heartwood	0.560	0.30	0.043	0.023
Heartwood	0.527	0.29	0.055	0.041
Heartwood	0.504	0.37	0.061	0.044
Sweetgum:				
Sapwood	0.424	0.46	0.055	0.027
Sapwood	0.413	0.44	0.062	0.026
Heartwood	0.435	0.20*	0.044*	0.024*
Heartwood	0.389	0.48	0.081	0.051
Southern magnolia:				
Sapwood	0.440	0.41	0.081	0.055
Sapwood	0.374	0.47	0.068	0.038
Heartwood	0.472	0.33	0.079	0.056
Heartwood	0.433	0.40	0.057	0.038
American sycamore:				
Sapwood	0.433	0.38	0.051	0.030
Sapwood	0.484	0.40	0.053	0.033
Heartwood	0.475	0.13*	0.023*	0.016*
Red oak:				
Heartwood	0.480	0.24	0.015	0.013
Heartwood	0.531	0.26	0.025	0.015
Heartwood	0.622	0.19	0.011	0.009

* Values obtained from cubes deformed by collapse during drying.

theoretical curve and half below. In every case the radial conductivity exceeds the tangential, the ratio, k_r/k_t , being 2.3 for one sample of sweetgum. The average of the transverse values for all the sapwood samples is 3.5 per cent higher

than that for all the heartwood samples excepting the red oak cubes, while the average specific gravity is 5.7 per cent lower. Correction being made for the difference in average specific gravity, the difference between the average trans-

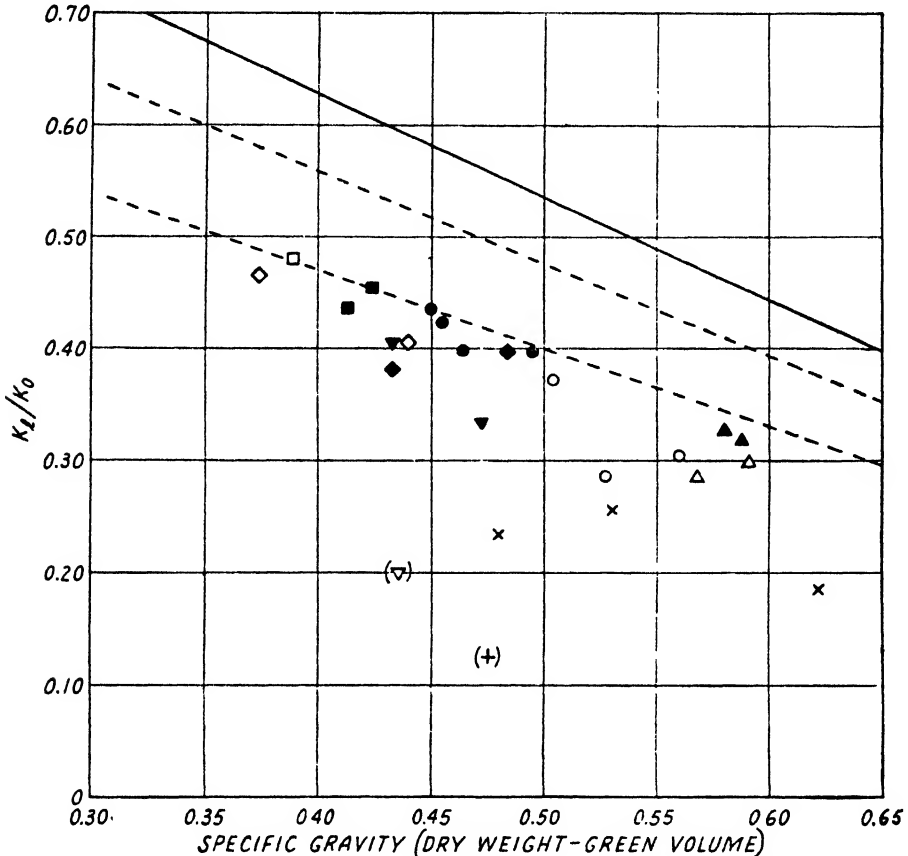


FIG. 5. Longitudinal relative electrical conductivities for several hardwoods. Solid curve calculated from Stamm's equation for softwoods (10) with no correction. Dotted lines (upper) represent values with minimum taper correction and (lower) values with maximum taper correction for softwoods (10). Values in parentheses obtained from cubes deformed by collapse during drying.

- | | |
|---------------------------|--------------------------------|
| ▲, sugar maple sapwood | □, ▽, sweetgum heartwood |
| △, sugar maple heartwood | ◇, Southern magnolia sapwood |
| ●, black tupelo sapwood | ▼, Southern magnolia heartwood |
| ○, black tupelo heartwood | ◆, American sycamore sapwood |
| ■, sweetgum sapwood | +, American sycamore heartwood |
| | ×, red oak heartwood |

verse relative conductivities of the sapwood and heartwood samples is less than 1 per cent.

The fact that, in all the samples tested except Douglas fir, the radial conductivity exceeded the tangential can probably be explained by the presence of

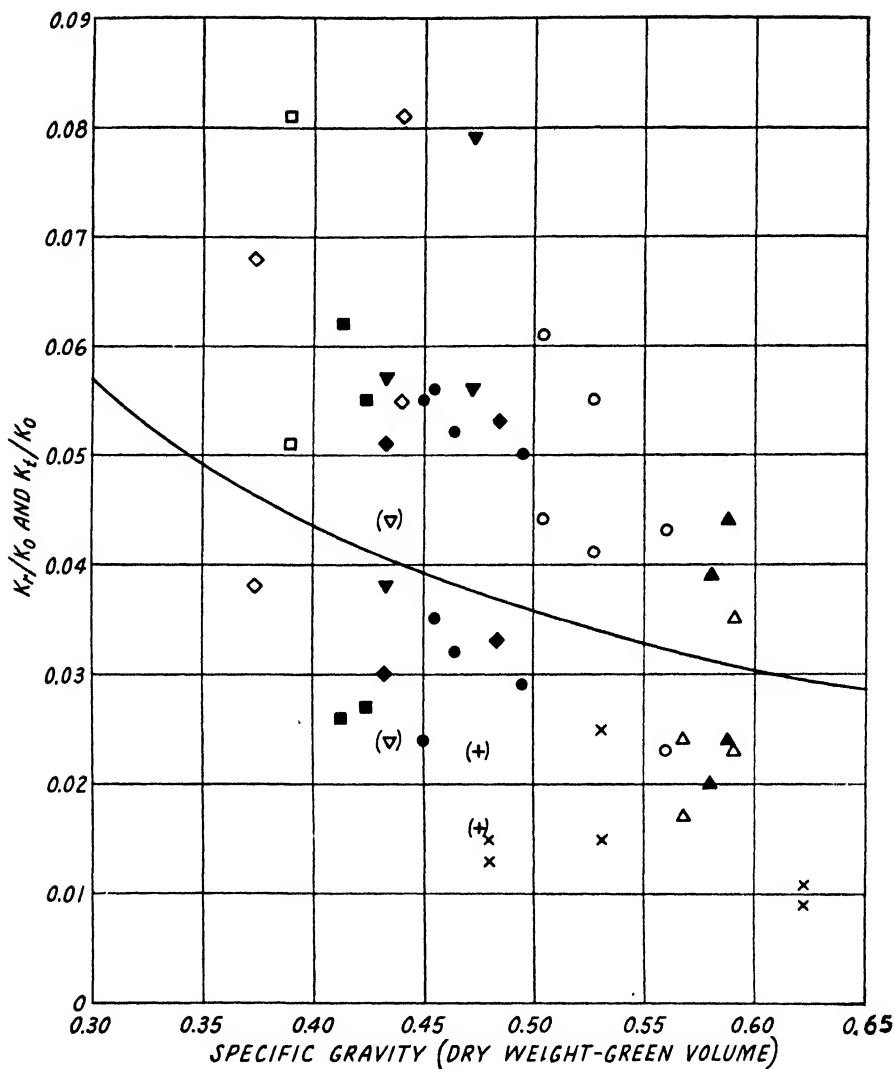


FIG. 6. Transverse relative electrical conductivities for several hardwoods. Curve calculated from Stamm's equation (10). Upper point of each pair represents radial value; lower point represents tangential value. Values in parentheses obtained from cubes deformed by collapse during drying.

- | | |
|---------------------------|--------------------------------|
| ▲, sugar maple sapwood | □, ▽, sweetgum heartwood |
| △, sugar maple heartwood | ◇, Southern magnolia sapwood |
| ●, black tupelo sapwood | ▽, Southern magnolia heartwood |
| ○, black tupelo heartwood | ◆, American sycamore sapwood |
| ■, sweetgum sapwood | +, American sycamore heartwood |
| | ×, red oak heartwood |

wood rays and, in the case of pine, also by the presence of radial resin ducts. The contribution of these structures was necessarily neglected by Stamm because of

the mathematical difficulties which they would introduce. Rays are generally more numerous in the case of hardwoods than of softwoods, a fact which will account for the higher value of k_r/k_t . The tangential conductivities for the hardwoods fall roughly as far below the theoretical curve as do those for the softwoods. This suggests that, on the assumption that the radial structures can be neglected, the transverse values calculated by Stamm should be reduced by 30 to 40 per cent. This discrepancy is probably due to errors in his estimation of the resistances of the submicroscopic capillaries of the pit membranes and the cell walls.

A rough value was obtained for the relative conductivity of sheets of regenerated cellulose in equilibrium with 0.10 *N* potassium chloride solution and having a moisture content of 88 per cent. Because of the nature of the material, it was necessary to measure the resistance of piles of the sheet cellulose between nearly dry electrodes. With piles measuring 0.20, 0.325, and 0.80 cm. in height, values of 0.11, 0.097, and 0.098 were obtained for the relative conductivity. The value taken as an average was 0.10.

Direct measurements of solute diffusion

In order to test the validity of the assumption that relative conductivities may be taken as equal to the corresponding relative diffusion constants, two types of experiments were made. In the first, sodium chloride was allowed to diffuse from a concentrated solution into wood filled with water and the resulting salt concentrations at different depths were obtained by sectioning the wood and analyzing for chloride ion volumetrically. Four blocks of Western white pine approximately 20.6 cm., 7.9 cm., and 4.7 cm. in the longitudinal, radial, and tangential directions, respectively, were filled with water by the method used in the electrical conductivity experiments. After 8 months' soaking, the void volume remained at 3.1 to 6.1 per cent. The ends were dipped in a molten mixture of equal parts of beeswax and rosin to minimize longitudinal diffusion and were then placed in a tall glass jar containing approximately 10 liters of 1.5 *N* sodium chloride solution. An electric stirrer was operated constantly. Blocks were removed at the end of 84, 132, and 228 hr. As each block was removed, 8 cm. of wood was cut from each end and 3 cm. from each edge. The resulting block was then divided in half by a cut parallel to the longitudinal face, and from the two final blocks tangential sections were split off with a chisel so mounted as to insure accurate sectioning. Each section was immediately placed in a flask with about 200 cc. of distilled water in order to remove the salt. The leaching process continued for 2 days or more at an elevated temperature and with occasional swirling of the flasks. The solution was then decanted and analyzed for chloride with 0.10 *N* silver nitrate. The wood sections were dried at 105°C. for 24 hr. and weighed.

From the dry weights of the sections, the green-volume specific gravity, and the known total tangential dimension of the block, it was possible to calculate the thickness and the volume of each section. A step diagram was then constructed, the width of each step corresponding to the thickness of the section,

and the height to the salt concentration in terms of grams per cubic centimeter of solution. Four such diagrams were thus obtained for each original block, since diffusion had occurred through both tangential faces of each of the two central blocks. One such set of diagrams is shown in figure 7.

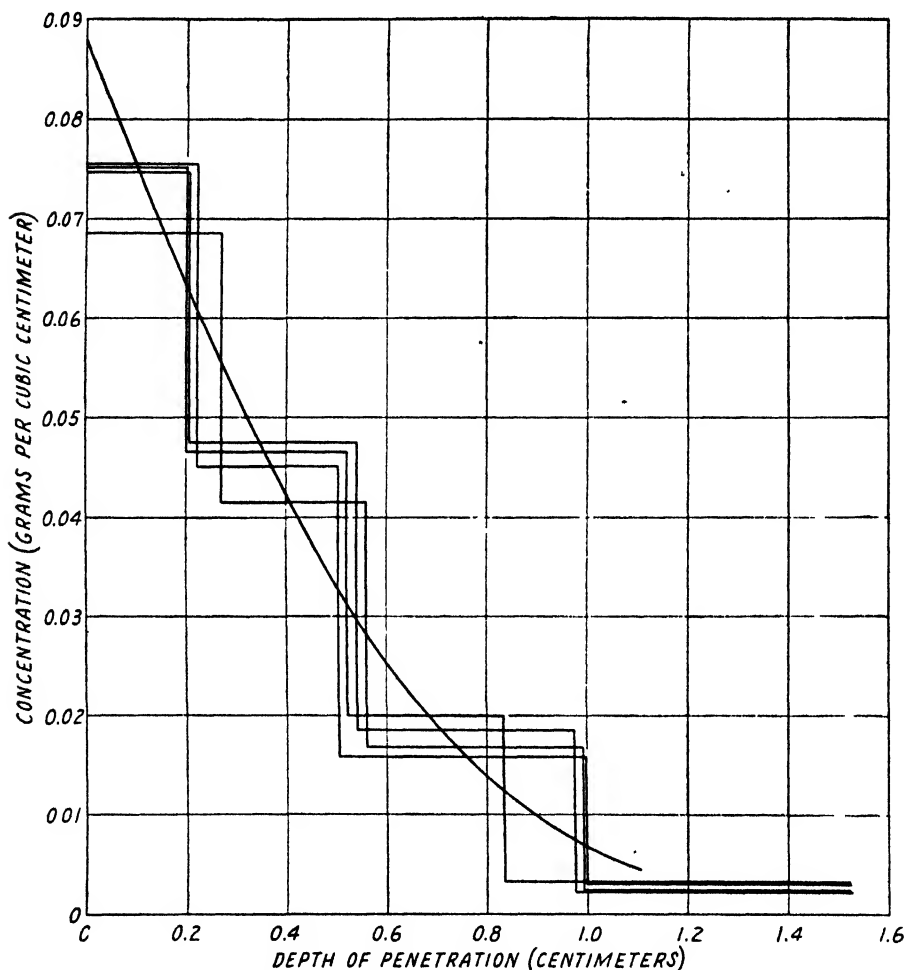


FIG. 7. Step diagram showing penetration of sodium chloride into a block of Western white pine after 132.5 hr. $T = 26.7^{\circ}\text{C}$. $C_0 = 0.0880$ g. per cubic centimeter. The theoretical curve corresponds to a diffusion constant of 4.70×10^{-7} cm.² per second with respect to unit dimensions of the wood, or a relative diffusion constant of 0.031.

The mean external salt concentration for each block was determined by interpolating between the original and final concentrations of the brine, allowance being made both for the varying number of blocks in the solution and for the fact that the amount of salt absorbed varies as the square root of the time.

Theoretical distribution curves were calculated from the following formula:

$$C/C_0 = 1 - 2/\sqrt{\pi} \int_0^{x/2\sqrt{Dt}} e^{-\beta^2} d\beta \quad (3)$$

where C = concentration of salt at any point within the wood,

C_0 = external salt concentration,

x = distance from the tangential face in centimeters,

D = diffusion constant in cm^2 per second, and

t = time in seconds.

The curve corresponding to a diffusion constant of $3.36 \times 10^{-7} \text{ cm}^2/\text{sec.}$ fitted

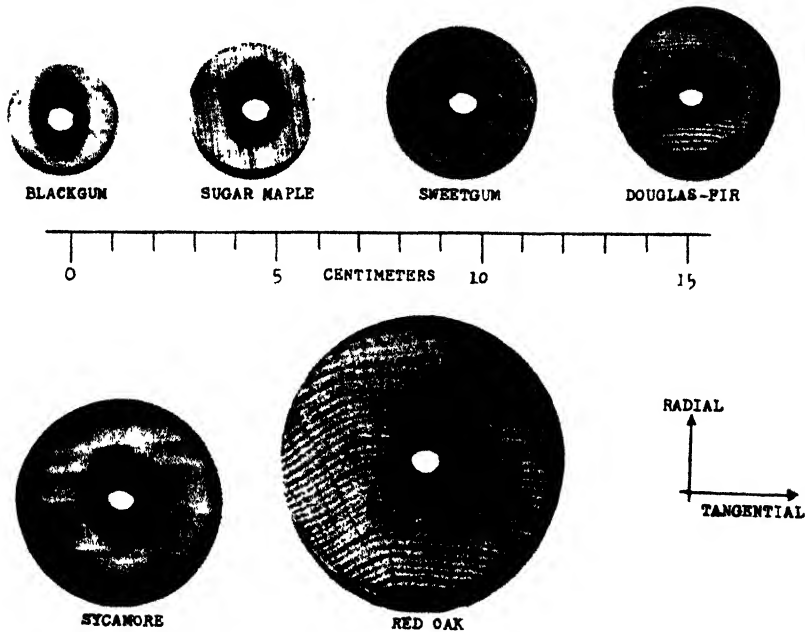


FIG. 8. Photograph of disks showing relative rates of diffusion in the radial and tangential directions.

all the step diagrams with fair accuracy. This value is divided by the fractional volume of liquid in the wood minus the 6 per cent by weight which is regarded as bound in a monomolecular film (10). This translates the diffusion constant to the basis of the bulk dimensions of the wood and yields a value for D of 4.75×10^{-7} . Clack (4) found the integral diffusion constant for 1.5 N sodium chloride at 18°C . to be 1.21×10^{-6} . Multiplying this value by the ratio of the absolute temperatures and the inverse ratio of the viscosities of water at 26.7° and 18°C . gives an approximate value for D_0 of 1.52×10^{-6} at the higher temperature. D_t/D_0 is thus equal to 0.031, in good agreement with the transverse relative conductivity for Western white pine of slightly lower specific gravity. This value is included in figure 4.

Because of the unexpectedly large differences between radial and tangential conductivity found among the hardwoods, the following method was used to show whether such differences exist under diffusion conditions. Thin transverse disks of five hardwoods and of Douglas fir were filled with water and interleaved with a layer of rosin-beeswax mixture. A central hole was cut through the entire pile with a No. 3 cork borer. The disks were then clamped between two brass plates and placed under water to prevent drying. By means of a hole in each plate, a concentrated solution of ferric chloride was passed through the disks at a rate of about 0.5 cc. per minute for a period of 4 days. At the end of that time, the channel was flushed out with water and the wax peeled from the disks. The ferric ion was then precipitated within the wood by soaking overnight in concentrated ammonium hydroxide. The disks were then stained superficially by dipping in slightly acidified potassium ferrocyanide solution. Figure 8 shows these disks. As can be seen, radial diffusion took place more rapidly than tangential except in the cases of red oak and Douglas fir, where the reverse was true. Also to be noted is the irregular pattern found particularly on the red oak. By cutting the disks radially and tangentially through the central hole and measuring the distance to which the ferric salt had diffused in sufficient concentration to produce a visible stain, the following rough values for D_r , D_t were obtained:

SPECIES	D_r D_t
Black tupelo	3 6
Sugar maple	2 8
Sweetgum	1 9
Douglas fir	0 6
American sycamore	1 4
Red oak	0 9

These are the squares of the ratios of the measured depths of penetration, but they can only be regarded as qualitative. It was very difficult to measure the limit of the "visible stain," and the irregular stain pattern shows that the diffusion along a single arbitrary line may be quite different from the average in a large sample. Nevertheless, the results, except in the case of red oak, are in qualitative agreement with the results of the conductivity measurements.

Microscopic examination of thin sections cut from the Douglas-fir disks showed that diffusion had proceeded much more rapidly through the springwood than through the summerwood. This fact further illustrates the highly variable nature of wood as a diffusion medium.

Similar examination of sections from the black tupelo disk did not show any greater concentration of Prussian blue in the fibers adjacent to wood rays than in those midway between the rays. This is not surprising however, in view of the fact that every fiber is in contact with ray cells at several points along its length even though these rays may not be included in a single thin section. Measurements to be described in the next section show that, in hardwoods, the

average number of fibers per centimeter is less in the radial direction than in the tangential. This means that fewer pits and cell walls have to be traversed than when passage occurs parallel to an annual ring and so helps to explain the fact that the radial is greater than the tangential diffusion constant.

Microscopic measurements on hardwoods

The theoretical curves obtained by Stamm were based on average structural dimensions for the simpler softwoods. It was expected that the corresponding dimensions for hardwoods might be different. Furthermore, the presence of longitudinally oriented pores or "water vessels" in hardwoods would tend to modify the diffusion process. It was particularly desired to determine approximate values for the average number of fibers traversed per centimeter in the transverse directions, for the average double cell-wall thickness, and for the fractional volume of the pores.

Measurements were made from photomicrographs of transverse sections of red oak, sugar maple, black tupelo, sweetgum, Southern magnolia, and American sycamore filed in the library of the U. S. Forest Products Laboratory and from slides prepared from swollen cross sections of the same red oak that was used in the studies of electrical conductivity and moisture transfusion.

Although it was not known what method was used in preparing the slides from which the photomicrographs were made, it was assumed that the sections were in the fully swollen condition or nearly so.

In each case, values were obtained directly for the average number of fibers in the radial and tangential directions by counting the fibers over a known distance. The fractional-pore volume was estimated from the diameters and number of pores per unit area. Average values were calculated from several measurements made at random throughout various portions of the annual ring. Values for the average thickness of the double cell wall were obtained from the average number of fibers per square centimeter, the fractional-pore volume, and the total void volume of the wood at the fiber-saturation point as calculated from equation 2. Since the actual green specific gravities of the woods from which the photomicrographs were made were unknown, an average value for each species was used as follows:

Red oak	0.565
Sugar maple	0.560
Black tupelo	0.460
Sweetgum	0.440
Southern magnolia	0.460
American sycamore	0.456

The data are recorded in table 3, together with the values used by Stamm in his calculations for softwoods.

These three important quantities vary appreciably from species to species, and, to judge from the data for red oak and Douglas fir, from sample to sample

and even from point to point within a single small sample. This appreciable variation between samples and species makes generalizations difficult. There seems to be a greater variation in the number of fibers per centimeter for these hardwoods than for the softwoods tabulated by Stamm (10) and also a greater variation in the relative number of fibers per centimeter in the radial and tangential directions.

The most striking difference between softwoods and hardwoods is that the former contain no pores, or large continuous water vessels, whereas the latter contain an appreciable fractional void volume made up of these large capillaries which varies appreciably from species to species. Because of this, the simple relationship between average double cell-wall thickness and the specific gravity used by Stamm (10) does not apply for hardwoods. The double cell-wall thick-

TABLE 3

Structural dimensions of certain hardwoods and of Douglas fir and average values for softwoods used in calculations

WOOD	NUMBER OF FIBERS PER CENTIMETER IN TANGEN- TIAL DIREC- TION	NUMBER OF FIBERS PER CENTIMETER IN RADIAL DIRECTION	DOUBLE CELL-WALL THICKNESS	FRACTIONAL- PORE VOLUME	SPECIFIC GRAVITY
			<i>microns</i>		
Red oak	700	570	5.3	0.11	0.565
Red oak 109A	635	495	5.1	0.19	0.480
136A	670	505	5.4	0.11	0.531
57A	600	580	6.7	0.15	0.622
Sugar maple	850	600	5.1	0.12	0.560
Black tupelo	310	240	11.0	0.36	0.460
Sweetgum .	375	235	9.0	0.36	0.440
Southern magnolia	375	270	9.0	0.29	0.460
American sycamore .	335	225	11.0	0.48	0.456
Douglas fir	345	315	7.1	0.00	0.430
Extreme springwood	300	265	4.5		
Extreme summerwood	385	500	14.0		
Softwoods (average) (17)	300	300	7.2*	0.00	

* Value for a softwood with a specific gravity of 0.365.

ness for hardwoods may be appreciably greater than the value for softwoods of the same specific gravity.

No means has as yet been devised for measuring pit-membrane pore cross sections of hardwood. Add to this the fact that the effectiveness of the pores themselves cannot be approximated without further knowledge of the nature of their walls and of the films, "tyloses," that exist within them, and it is not surprising that the hardwoods have diffusion values that vary by as much as 100 per cent from the theoretical values for softwoods.

Moisture-transfusion measurements

In order to obtain experimental values for the drying diffusion constant, the method of the steady state was employed. The apparatus, described in more

detail in another paper (2), is similar to the ordinary cup type of moisture-transfusion cell, except that an internal magnetic stirrer was incorporated to insure gentle agitation of the saturated salt solution and the air within the cell. Without such stirring, the rate of transfusion was low by as much as 40 per cent, depending on the nature and thickness of the membrane and the vapor-pressure gradient.

In practice, the apparatus was placed in a room with constant relative humidity and a constant temperature of 80°F. The cells were rotated continuously, and a fan was used to blow air across the upper surfaces of the membranes. The cells were weighed once a day until the rate of change in weight was constant. In the case of wood membranes, it was necessary to repair the wax seal several times until the wood had reached an equilibrium warp. When a cell had reached a constant rate of weight change, the membrane was removed, its thickness measured with a dial gauge or a micrometer, and a sample quickly cut from it for measurement of the average moisture content and the specific gravity at moisture content of test. The diffusion constant was calculated from the following equation:

$$D = \frac{mh}{A(d_2 - d_1)gt} \quad (4)$$

where D = the diffusion constant in cm.² per second,
 m = the change in weight,
 h = the thickness,
 d_2 and d_1 = the moisture contents of the material in equilibrium with the relative vapor pressures inside the cell and outside the cell, respectively,
 g = the dry weight of the sample divided by the volume at the moisture content of test, and
 t = the time in seconds.

Values of d_2 and d_1 for cellophane were obtained from the data of Urquhart, Bostock, and Ekersall (14). Values for red oak were measured by determining the vapor-pressure isotherm at 26.7°C. in a series of humidity rooms; values for the other woods were obtained from the data of Stamm and Loughborough (11).

In table 4 are recorded the measured diffusion constants for samples of three different species of wood. The samples marked "(comp.)" had been compressed to a high density. The three red oak samples marked "(green)" had not been dried previous to the measurements. All the other samples had been dried to approximately 6 per cent moisture content and then brought to equilibrium with a relative humidity of 97 per cent. Also included in table 4 are values for D_t for red oak obtained in other Forest Products Laboratory research and calculated from the rate of drying of samples cut from the same boards as those used in the moisture-transfusion measurements. These diffusion constants, which had to be translated into c.g.s. units, are not strictly comparable to the steady-state values, as they were measured at 46.1°C. and with a surface equilibrium moisture content of 14 to 16 per cent. Furthermore, the true drying diffusion

constant for these samples may be as much as 40 per cent higher than the calculated values, because an optimum rate of air circulation could not be obtained.

In table 5 are given the diffusion constants measured for 600-gauge cellophane which had been soaked in several changes of distilled water in order to remove the glycerol used as a plasticizing agent. Included in the table are the theoretical relative diffusion constants of Stamm for longitudinal and transverse diffusion through systems of oriented micelles. The measured values are somewhat

TABLE 4

Radial drying diffusion constants relative to the dimensions of wood for blackgum, basswood, and red oak at 80°F. (26.7°C.)

WOOD	THICK- NESS	RELATIVE VAPOR- PRESSURE GRADIENT	AVERAGE MOISTURE CONTENT	SPECIFIC GRAVITY	DIFFUSION CONSTANT		
					From steady- state measure- ments	From Stamm's theoret- ical cal- culations (17)	From rate of moisture loss in seasoning
					$D_t \times 10^6$		
	cm		per cent				
Black tupelo	0.169	1.00-0.80	17.0	0.409	1.8	2 0	
Black tupelo	0.319	1.00-0.80	17.0	0.409	1.9	2 0	
Black tupelo (comp.)	0.079	1.00-0.80	16.8	0.803	0 30	0 52	
Black tupelo (comp.)	0.137	1.00-0.80	17.0	0.963	0.18	0.15	
Basswood	0.251	1.00-0.80	17.8	0.408	2 2	2 0	
Basswood (comp.)	0 100	1 00-0.80	17.9	0.992	0.20	0 14	
Red oak (green)	0 662	1.00-0.30	32.5	0.480	0 71	1 5	0.55
Red oak (green)	0 666	1.00-0.30	34.6	0.531	0.87	1 3	0 53
Red oak (green)	0.682	1.00-0.30	31 6	0.622	0.74	1.1	0 42
Red oak (dried)	0.680	1.00-0.30	21 0	0 480	1.09	1.5	
Red oak (dried)	0.684	1.00-0.30	18.5	0.531	0.99	1.3	
Red oak (dried)	0.677	1.00-0.30	19.1	0.622	0.77	1.1	

TABLE 5

Experimental and theoretical relative diffusion constants for cellophane

RELATIVE VAPOR- PRESSURE GRADIENT	AVERAGE MOISTURE CONTENT	D/D_w (EXPERIMENTAL)	THEORETICAL (10)	
			In fiber direction	Across fibers
	per cent			
0.91 to 0.65	17	0.006	0.0067	0.0034
0.65 to 0.33	11	0.004	0.0027	0.0014

higher than the theoretical, but the agreement is reasonably good when account is taken of the difference in structure between regenerated cellulose and the oriented cellulose as it exists in the cell wall of wood.

SUMMARY AND CONCLUSIONS

Measurements were made of relative electrical conductivities in the three structural directions on samples of various species of wood, in an effort to test the theoretical calculations of Stamm (10). The longitudinal relative conduc-

tivities of three softwoods are in good agreement with the values predicted for the diffusion constants relative to the dimensions of the wood, while the transverse conductivities are low by from 26 to 46 per cent but follow the predicted trend with specific gravity. In the case of hardwoods, the longitudinal values are slightly lower than those predicted but lie along a curve parallel to the theoretical one. It is shown that the fiber cavities of hardwoods are less uniform in bore than those of the softwoods, a fact which may account for this discrepancy. The transverse relative conductivities are widely scattered but are equally divided above and below the theoretical curve. In the case of Douglas fir, the tangential conductivity is appreciably greater than the radial, while in all the other species studied the radial exceeds the tangential, the ratio exceeding 2:1 for certain hardwood samples. No appreciable difference was found between the conductivities of sapwood and heartwood among the hardwoods tested. It is suggested that the high radial conductivity of hardwoods is due to the abundance of wood rays and that the tangential conductivity of Douglas fir is augmented by checks localized at or near the sharp transition in the annual ring.

By a direct measurement of the rate of diffusion of sodium chloride tangentially into Western white pine and by qualitative demonstration of the ratio of radial to tangential diffusion in several hardwoods and Douglas fir, it is shown that the relative electrical conductivity is equal to the relative diffusion constant.

Microscopical measurements of the number of fibers per centimeter in the radial and tangential directions, of the double cell-wall thickness, and of the fractional-pore volume of hardwoods show a wide variation in these quantities and indicate why the equations of Stamm, derived for the simpler softwoods, apply with less consistency to the hardwoods.

Measurements of the rate of transfusion of water vapor through red oak, basswood, black tupelo, and compressed basswood and black tupelo are in fairly good agreement with theoretical values. Similar measurements on regenerated cellulose confirm the order of magnitude of the value for the effective fractional cross section of the transient capillaries in the cell wall estimated by Stamm.

REFERENCES

- (1) BABBITT, J. D.: *Can. J. Research* **18A**, 105 (1940).
- (2) BURR, H. K., AND STAMM, A. J.: *Ind. Eng. Chem., Anal. Ed.* **13**, 655 (1941).
- (3) CADY, L. C., AND WILLIAMS, J. W.: *J. Phys. Chem.* **39**, 87 (1935).
- (4) CLACK, B. W.: *Proc. Phys. Soc. (London)* **29**, 49 (1917).
- (5) KOLLMANN, F.: *Forsch. Gebiete Ingenieurw.* **6**, 169 (1935).
- (6) KOLLMANN, F.: *Forsch. Gebiete Ingenieurw.* **7**, 113 (1936).
- (7) MARTLEY, J. F.: *Dept. Sci. Ind. Research (Brit.) Tech. Paper No. 2* (1926).
- (8) SHERWOOD, T. K.: *Ind. Eng. Chem.* **21**, 12 (1929).
- (9) STAMM, A. J.: *J. Phys. Chem.* **36**, 312 (1932).
- (10) STAMM, A. J.: "Passage of Liquids, Vapors, and Dissolved Materials through Softwoods," *U. S. Dept. Agr. Bull.*, in press.
- (11) STAMM, A. J., AND LOUGHBOROUGH, W. K.: *J. Phys. Chem.* **39**, 121 (1935).
- (12) STILLWELL, S. T. C.: *Dept. Sci. Ind. Research (Brit.) Tech. Paper No. 1* (1926).
- (13) TUTTLE, F.: *J. Franklin Inst.* **200**, 609 (1925).
- (14) URQUHART, A. R., BOSTOCK, W., AND EKER-SALL, N.: *J. Textile Inst.* **23**, T135 (1932).

MICELLE STRUCTURE IN AQUEOUS SOLUTIONS OF COLLOIDAL ELECTROLYTES¹R. J. VETTER²*Chemistry Department, University of Wisconsin, Madison, Wisconsin**Received August 8, 1946*

INTRODUCTION

Two hypotheses, one by McBain (19) and the other by Hartley (8), have been developed to explain the behavior of aqueous solutions of colloidal electrolytes. Both points of view state that the unusual concentration dependencies of properties such as osmotic pressure, equivalent conductivity, density, and others result from the aggregation of large organic ions to form colloidal micelles. The two hypotheses differ in the structural details and properties of the micelles, and in the nature of the equilibrium between micelles and simple ions.

The purpose of this paper is to contribute to the discussion of micellar structure with the aid both of new experimental observations and of a reëxamination of a few observations published by other investigators.

The colloidal electrolyte chosen for study was the sodium salt of sulfonated di(2-hexyl) succinate, which is known commercially as Aerosol MA. This compound is characterized by having its hydrophilic ionizing group at approximately the mid-point of the molecule. It was of interest for this reason because most of the work in this field had been confined to electrolytes in which the hydrophilic group is at the end of a linear chain structure.

Experimental measurements were made of the density and viscosity behavior of Aerosol MA in aqueous solutions and also of the rate of diffusion in aqueous sodium chloride solvents. The measurements were extended over an appreciable range of concentration.

Several papers (6, 20) describing some of the solution properties of Aerosol MA have appeared since the work reported here was initiated. They show that the "Aerosol"-type compounds are colloidal electrolytes, and that the "Aerosols" and other branched-chain compounds differ from members of the straight-chain type in the degree to which certain properties depend upon chain length (21).

EXPERIMENTAL

Purification of Aerosol MA

A commercial sample was obtained which contained about 1 per cent impurities, these being chiefly water and about 0.1–0.2 per cent sodium sulfate.³ The

¹ Presented at the Twentieth National Colloid Symposium, which was held at Madison, Wisconsin, May 28–29, 1946.

This paper is based on a thesis submitted by R. J. Vetter to the Faculty of the University of Wisconsin in partial fulfillment of the requirements for the degree of Doctor of Philosophy, June, 1944.

² Present address: E. I. du Pont de Nemours & Co., Inc., Richmond, Virginia.

³ The sample and its analysis were obtained through the kindness of Mr. C. A. Sluhan of the American Cyanamid and Chemical Corporation.

inorganic impurities were removed by filtration of a purified-dioxane solution followed by evaporation at 100°C. with the ultimate use of high vacuum. The resulting material was white and odorless; it was stored over phosphorus pentoxide at room temperature.

The use of a more elaborate procedure has been described (6) but it was not felt justified, because Aerosol MA undergoes carboxy-ester hydrolysis in aqueous solution.

Preparation of solutions

All solutions were prepared by weight, other than those for diffusion studies, and the Aerosol MA was allowed to dissolve at room temperature. Solutions used for density and viscosity measurements were made with freshly boiled, double-distilled conductivity water. The aqueous sodium chloride solvents used for diffusion measurements contained ordinary distilled water and Baker's analyzed salt.

Turbidity developed several hours after preparation in salt-free solutions containing less than 2.2-2.5 per cent Aerosol MA. More concentrated solutions remained clear for months, but on dilution below 2.2-2.5 per cent at any time after several hours' aging they immediately became turbid. With aqueous sodium chloride solvents the Aerosol MA concentration at which turbidity appeared decreased with increasing salt concentration. The effects of turbidity and aging on density and viscosity were indetectably small; their effect on diffusion behavior is described below.

A plausible explanation for the appearance of turbidity is that water-insoluble 2-hexanol is formed by ester hydrolysis, for it is known that the pH of an Aerosol MA solution gradually decreases with time. In a sufficiently concentrated solution the colloidal micelles present solubilize the alcohol but in a more dilute solution, where colloid does not exist, the alcohol separates into a finely divided second phase which causes turbidity. This second phase is presumably stabilized by the emulsifying action of the detergent. The effect of sodium chloride on the concentration dependence of turbidity is associated with the ability of added salt to reduce the critical concentration for micelle formation (see below).

For density measurements each solution was prepared directly from detergent and water and was used within 24 hr. after preparation.

For viscosity measurements all but three solutions were prepared by dilution of a more concentrated solution. Referring to the order given in table 3, the first seven, the next two, and the last twelve solutions form the three dilution series. In several of these solutions, the solute had been dissolved for as long as 1 week.

For diffusion measurements separate solutions of Aerosol MA and sodium chloride, prepared by weight, and water were mixed volumetrically. The volumetric mixing was the more convenient for insuring equal concentrations of sodium chloride in the two solutions employed in the differential-diffusion measurements. Some of the aqueous Aerosol solutions were allowed to stand as long as 2 weeks prior to use, but no aging effect could be detected within limits of experimental error.

Density measurements

Two pycnometers were used, one a 60-cc. Ostwald-Sprengler type and the other a 26-cc. instrument of the type described by Tennent and Vilbrandt (28). Measurements were made at $25.00^{\circ}\text{C} \pm 0.01^{\circ}$.

Precautions were taken with respect to rinsing and wiping the pycnometers prior to weighing, tempering in the balance case, double weighings, the buoyant effect, use of a similarly constructed counterweight for the pycnometer (second type only), sensitivity of balance, and calibration of weights. Weighings were reproducible to ± 0.1 mg.

The partial specific volumes of the Aerosol MA were calculated by a modification of the second (graphical) method of Lewis and Randall (18). The volume of the solution per gram of water was computed for each concentration, and the difference between adjacent values was divided by the difference in concentrations expressed as fractions. The values of partial specific volume thus obtained were assigned to the means of the two concentrations. This method has the advantage of simplicity and the disadvantage that very small errors in the data are greatly magnified. It is also an integral rather than a differential method.

Viscosity measurements

Viscosities were measured in an Ostwald viscometer at $25.00^{\circ}\text{C} \pm 0.02^{\circ}$. The flow time for water was 375.1 sec. The viscometer was calibrated with water and two sucrose solutions; it was found that the kinetic-energy correction amounted to less than 1 part in 1000 and it was therefore neglected.

Diffusion measurements

Rates of diffusion were measured at $25.00^{\circ}\text{C} \pm 0.02^{\circ}$ in an all-glass cell of the type described by Svedberg (26), with the aid of the scale-line displacement method of Lamm (16). In all experiments the solute was allowed to diffuse from a more to a less concentrated solution.

RESULTS

Partial specific volume

The data show that two transition ranges of concentration exist in which the partial specific volume changes abruptly and between which it remains constant. This behavior is illustrated in figure 1; the experimental density data are given in table 1 and the derived values of partial specific volume in table 2.

The concentration at which the first transition sets in has been called the "critical concentration for micelle formation" and is about 1.0 per cent Aerosol MA. This value agrees with the result of Haffner, Piccione, and Rosenblum (6), who found a sharp downward break in the equivalent conductivity-concentration curve at 1.1 per cent Aerosol MA. The first transition range appears to extend to about 2.5 per cent, but since an integral rather than a differential method was used to calculate partial specific volume, it is probable that the transition range is somewhat narrower than indicated by figure 1.

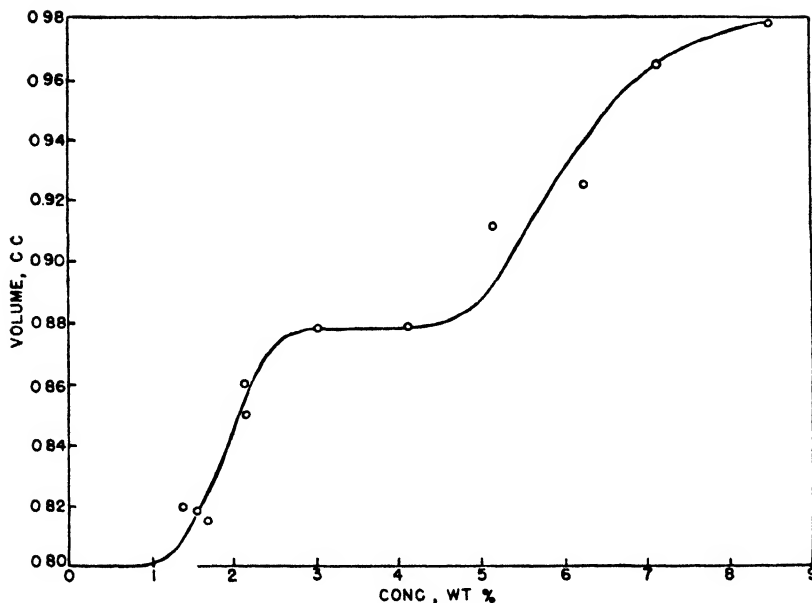


FIG. 1. The variation of the partial specific volume with concentration in aqueous solutions of Aerosol MA at 25°C.

TABLE 1

Density data and derived quantities for Aerosol MA in water at 25.00°C \pm 0.01°

CONCENTRATION	DENSITY (ABSOLUTE)	VOLUME OF SOLUTION PER GRAM OF WATER
<i>weight per cent</i>		<i>cc</i>
0.000	0.99704	1.00296
0.475 ₅ *	0.99806	1.00673
0.609 ₄	0.99823	1.00786
0.690 ₉ *	0.99848	1.00849
0.930 ₈ *	0.99897	1.01043
1.219 ₅ *	0.99949	1.01287
1.448 ₇	0.99995	1.01475
1.871 ₀	1.00086	1.01819
2.329 ₅	1.00169	1.02213
2.416 ₇	1.00190	1.02282
3.599 ₂	1.00401	1.03319
4.589 ₀	1.00597	1.04188
5.666 ₆	1.00796	1.05170
6.758 ₇	1.01005	1.06181 ₅
7.534 ₂	1.01139	1.06930
9.479 ₄	1.01508	1.08831

* Values obtained in the 60-cc. Ostwald-Sprengel pycnometer.

The second transition range begins at about 4.5 per cent. Although the data are not extensive enough at higher concentrations to show the attainment of a second range of constant partial specific volume, they indicate a trend in this

direction. Hess, Philippoff, and Kiessig (13) found two transition ranges of concentration in measuring the densities of aqueous solutions of an homologous series of soaps, provided the molecule contained six or more carbon atoms. They found also that the appearance of long-spacing x-ray diffraction began at the same concentration where the second transition of partial specific volume set in. These investigators regard this concentration as a second critical point.

The lack of agreement in figure 1 between the curve and the points at 5.13 and 6.21 per cent can be accounted for by an error in estimating either the density or the concentration of but one solution, that at 5.667 per cent. A change of either 15 parts per 100,000 in density or 2 parts per 1000 in concentration would bring the two points in figure 1 to close coincidence with the curve as drawn.

TABLE 2
Partial specific volume of Aerosol MA in water at 25.00°C. \pm 0.01°

CONCENTRATION	PARTIAL SPECIFIC VOLUME
<i>weight per cent</i>	<i>cc. per gram</i>
0.00-1.0	0.800
1.33	0.820
1.54	0.817
1.66	0.815
2.10	0.859
2.14	0.848
3.01	0.877
4.09	0.878
5.13	0.912
6.21	0.926
7.15	0.965
8.51	0.977

Viscosity

The relative viscosity-concentration curve, figure 2, shows a break at 1.1 per cent Aerosol MA, in agreement with the density and cited conductivity measurements. The general shape of the curve is quite similar to that found generally for aqueous solutions of colloidal electrolytes (23); the gentle upward curvature with relative viscosities above about 1.1 is the result of mutual interference between colloidal particles in motion during flow.

The absence of a second break in the curve corresponding to that found with density measurements is suggested but not proven because the measurements do not extend to high enough concentrations.

The experimental viscosity data are given in table 3.

Diffusion

It was necessary to measure the rate of diffusion by the differential rather than the integral method because turbidity appeared at low concentrations of

Aerosol MA which made it difficult, or impossible, to measure the displacement of the scale lines.

Aerosol MA diffused in a manner which closely approximated that theoretically expected for free diffusion, as can be seen from figure 3, in which "normalized" diffusion curves are compared with the theoretical curve (16). Deviations oc-

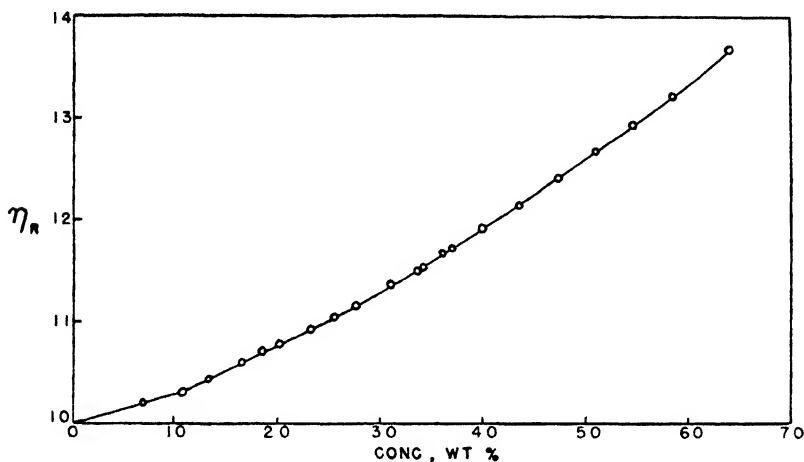


FIG. 2. The variation of the relative viscosity with concentration in aqueous solutions of Aerosol MA at 25°C.

TABLE 3

Viscosities of aqueous solutions of Aerosol MA relative to water at 25.00°C. ± 0.02°

CONCENTRATION	RELATIVE VISCOSITY	CONCENTRATION	RELATIVE VISCOSITY
<i>weight per cent</i>		<i>weight per cent</i>	
0.000	1.000	3.386 ₈	1.150 ₂
0.709 ₄	1.021 ₉	3.619 ₉	1.164 ₄
1.054 ₉	1.031 ₈	3.423 ₂	1.153 ₂
1.313 ₀	1.043 ₃	3.709 ₇	1.170 ₇
1.652 ₀	1.059 ₆	3.996 ₉	1.190 ₆
1.849 ₄	1.068 ₉	4.349 ₀	1.214 ₁
2.036 ₄	1.076 ₄	4.718 ₂	1.238 ₉
2.297 ₆	1.091 ₄	5.092 ₈	1.265 ₄
2.548 ₀	1.103 ₄	5.453 ₁	1.291 ₄
2.775 ₄	1.114 ₉	5.847 ₆	1.320 ₁
3.101 ₉	1.135 ₃	6.376 ₁	1.361 ₇

curring in that the maximum height of the curve was slightly greater than ideal and also in that the curves were slightly skewed. The degree of skewness increased the lower the concentration of the less concentrated solution. From the shape of the "normalized" curves it is probable that calculation of the diffusion coefficient by the method of slope and area would yield too low a value and that use of the method of (second) moments would give too high a value. It was

found that in all but two of sixteen experiments this order was obtained, and it is considered that the average of the values given by the two methods is more nearly correct than either of the two separately. In most of the experiments the two methods gave values which agreed to within 10 per cent, so the average may be regarded as accurate to about 5 per cent or less.

The turbidity appearing at low concentrations of the less concentrated solution began in the cell at a level slightly above the diffusion boundary and continued on into the remainder of the dilute solution. With increasing time the boundary of the turbid region receded away from the diffusion boundary. Attending the appearance of turbidity, the form of the diffusion curve changed in the manner

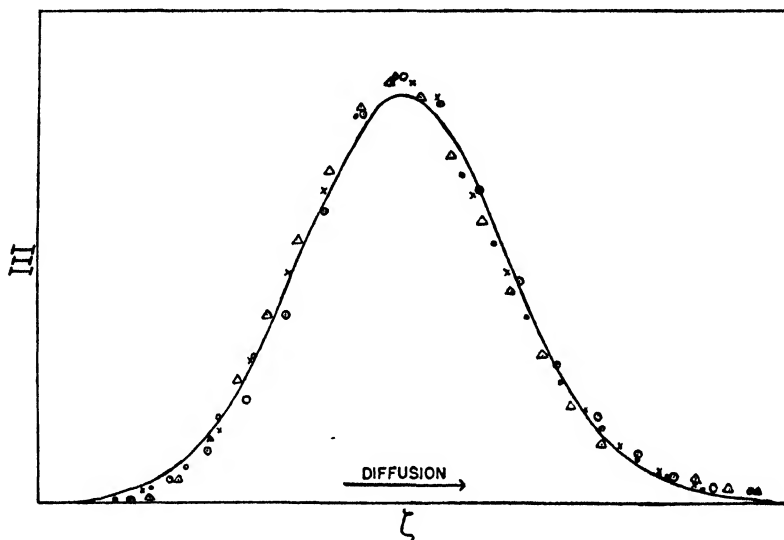


FIG. 3. The variation of the scale-line displacement with distance in the diffusion cell for the differential-diffusion behavior of Aerosol MA in aqueous sodium chloride solutions. The curve represents the ideal behavior in free diffusion and the various sets of points represent "normalized" experimental curves taken at various times after formation of the boundary.

shown by figure 4. This curve was obtained 12 hr. after the diffusion boundary was formed between 1.0 and 0.5 per cent solutions of Aerosol MA in 0.128 *N* sodium chloride.

The anomalous shape of this curve was probably the result, first, of the separation of 2-hexanol in the less concentrated solution and second, of its progressive solubilization as Aerosol MA diffused into the turbid region.

Three factors were found to affect the rate of diffusion in clear solutions: (1) the average Aerosol MA concentration of the two solutions used in the experiment; (2) the difference between the detergent concentrations of the two solutions; (3) the concentration of sodium chloride. The first factor was studied systematically at one constant set of values for the second and third variables,

but only a few other experiments were made which show trends in the effects of these variables separately.

The effect of varying the first factor while keeping the other two constant is to cause an initial decrease of diffusion coefficient with increasing concentration.

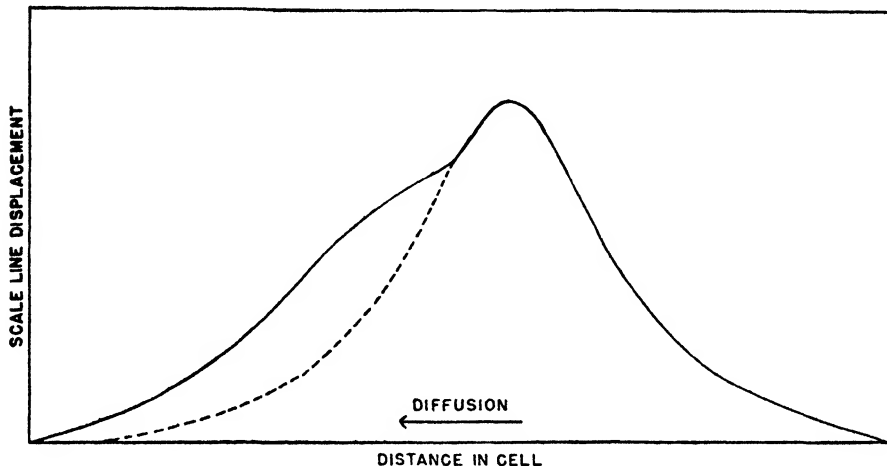


FIG. 4. The anomalous diffusion behavior of Aerosol MA at low concentrations in differential-diffusion experiments. The solid curve is that obtained experimentally, and the dotted curve is that to be expected in the absence of turbidity.

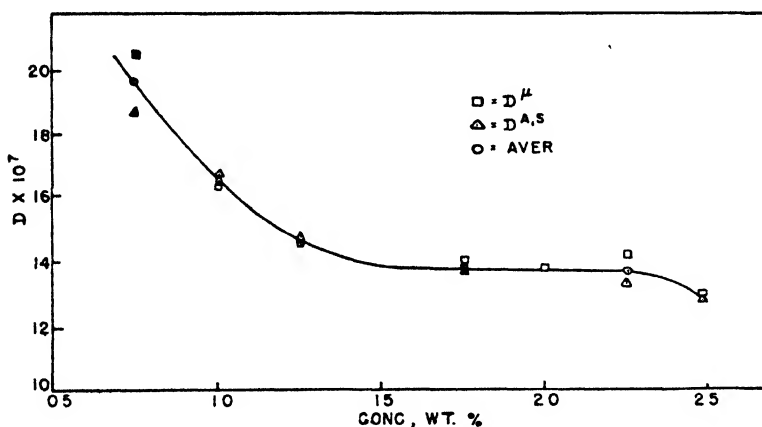


FIG. 5. The variation of the differential-diffusion coefficient with concentration of Aerosol MA in 0.257 *M* sodium chloride. Diffusion coefficients calculated by the method of moments (D^{μ}) and the method of area and slope ($D^{A,S}$). The concentration difference between the two solutions is 0.5 per cent Aerosol.

This is followed by a concentration region in which the diffusion coefficient is constant. At sufficiently high concentrations there is indication that the diffusion rate again falls off with concentration. This behavior is shown in figure 5,

the points of which are marked with an asterisk in table 4. The initial fall, followed by a region of constant diffusion coefficient, is in agreement with the observations of Hakala (7), Lamm (17), and Hartley and Runnicles (11), who measured the diffusion rate of various straight-chain colloidal electrolytes in the presence of swamping electrolyte.

Increasing the concentration of swamping electrolyte was studied at two average concentrations of Aerosol MA. The results show that the diffusion coefficient decreases with increasing salt concentration. From experiments 1 and 2 and experiments 6 and 7 in table 4 it is seen that at 0.75 per cent Aerosol

TABLE 4

The differential diffusion of Aerosol MA in aqueous sodium chloride solutions at 25°C.

NO.	c	c_1	c_2	NaCl	D^μ	$D^{A,S}$	D (AVERAGE)
				N			
1	0.75	1.00	0.50	0.180	29.9	23.3	26.6
2a	0.75	1.00	0.50	0.257	21.6	19.6	18.8*
2b	0.75	1.00	0.50	0.257	19.5	17.8	
3	1.00	1.25	0.75	0.257	16.4	16.7	16.5 ₆ *
4	1.25	1.50	1.00	0.257	14.6	14.4	14.5*
5	1.25	2.00	0.50	0.257	16.7	15.0	15.8
6a	1.50	2.00	1.00	0.257	15.3	15.1	15.4
6b	1.50	2.00	1.00	0.257	16.4	14.8	
7	1.50	2.00	1.00	0.514	13.8		
8a	1.75	2.00	1.50	0.257	14.0	13.9	
8b	1.75	2.00	1.50	0.257	14.0	13.5	13.8 ₆ *
9	2.00	2.25	1.75	0.257	13.4	(16.9)	13.4*
10	2.25	2.50	2.00	0.257	14.2	13.2	13.7*
11	2.50	2.75	2.25	0.257	12.9	12.8	12.8 ₆ *
12a	2.50	3.00	2.00	0.386	8.2	7.8	
12b	2.50	3.00	2.00	0.386	8.2	7.9	8.0

c_1 and c_2 are the concentrations of colloidal electrolyte in the more and in the less concentrated solutions, respectively; c is the average of these two. Aerosol MA concentration is given in weight per cent and that of the sodium chloride in normality. D^μ and $D^{A,S}$ are the diffusion coefficients in 10^{-7} cm.² per second as calculated by the methods of second moments and of area and slope, respectively.

* Points plotted in figure 5.

MA the diffusion coefficient is more sensitive to addition of salt than at 1.50 per cent.

The effect of increasing the difference between detergent concentrations of the two solutions seems to be dependent on the absolute values of the concentrations, but the data at hand do not present a clear picture. Comparing the result of experiment 6 with the diffusion coefficient to be expected from figure 5 and also comparing experiments 4 and 5, it is seen that increasing the concentration difference increases the rate of diffusion. There is some uncertainty connected with this point, because on this basis it would be expected that experiment 6 should show a larger value of diffusion coefficient than experiment 4. At higher

concentrations of Aerosol MA increasing the concentration difference and the salt concentration together causes a decrease in the rate of diffusion, as is apparent from experiments 11 and 12. For reasons outlined below, it seems probable that either one of these factors separately would have had the same effect, although to a lesser extent than both together.

DISCUSSION

Some insight as to the average size, shape, and weight of colloidal particles can be obtained from a combination of diffusion, viscosity, and density data (27c). In general, the estimation of molecular-kinetic parameters from these measurements is accompanied by some uncertainty, for several reasons. First, a model for the colloidal structure need be assumed which is amenable to mathematical analysis of its hydrodynamic properties. Second, with models other than spheres, the effects of shape and solvation have not been separated (2). Third, hydrodynamic analyses of concentration effects have not been successful beyond very dilute solutions except for the case of spherical particles. Fourth, the calculation of particle weights from the above measurements involves transposition from the volume to the weight basis with the aid of the partial specific volume, the assumption being that this quantity is an estimate of the density of the colloidal phase. With the exception of the last factor, these uncertainties are greatly reduced if there is evidence that the colloidal particles are spherical in shape.

The shape of the particles, or micelles, in aqueous colloidal electrolyte systems is thought by Hartley to be spherical. He believes also that the radius of the spherical micelle is constant over a range of concentrations above a critical concentration for micelle formation and that the radius is approximately equal to the stretched-out length of the aggregating chain ions. McBain, on the other hand, suggests that two colloidal micelles co-exist, the one being a small spherical micelle and the other a larger lamellar structure whose over-all shape is, presumably, not spherical. The two types are in equilibrium with simple ions and with each other. The size of the lamellar micelle increases gradually with concentration and is believed to be responsible for the diffraction of x-rays which is observed at higher concentrations. The various facts which support these two points of view have been reviewed in detail elsewhere (8, 9, 19).

Neither of these two theories, nor any of the various modifications of them which have been suggested (12, 25), is capable of explaining adequately all the experimental observations. McBain has not discussed a second critical concentration, although he extends his analysis to concentrations beyond this point. Hartley has not attempted to explain the x-ray diffraction observed, which occurs only at concentrations above the second critical concentration (12, 25); for this reason, his theory can be regarded only as an explanation of the facts below this concentration.

The measurements reported in this paper do not extend appreciably beyond the second critical concentration, and the interpretations to follow are confined to concentrations below this point. It is shown that with this restriction a

slight modification of the Hartley picture is better able to explain the facts than is the McBain viewpoint.

The constancy or the variability of micelle size in the range between the first and second critical concentrations is a pertinent test of the Hartley and McBain theories. Three lines of evidence may be cited—namely, diffusion, osmotic-pressure, and viscosity measurements—to show that micelle size is constant in this range.

The diffusion behavior of colloidal electrolytes may be used to estimate micelle size only if the measurements are made in the presence of sufficient swamping electrolyte to eliminate the small-ion charge effect (11, 27a). Such measurements have been made by Hartley and Runnicles (11), Lamm (17), Hakala (7) and the writer, as reported in the present paper. All of these investigators found that after an initial range in which the diffusion coefficient decreased with increasing concentration, another range followed in which the diffusion coefficient was constant. This behavior indicates constancy of micelle size, micelle shape, and degree of solvation in this second range of concentrations if these three factors do not change simultaneously in such a manner that they neutralize their separate effects. This latter possibility seems highly improbable.

The McBain and Brady analysis of the osmotic pressures of colloidal electrolyte systems (21) indicates that the number of molecules per micelle (the aggregation number) depends only on the structural type of the aggregating molecules and not on their molecular length. McBain and Brady make the following statement:

"Consider reactions of the type $aA + bB = A_aB_b$ for different substances at molalities m and m' and m'' , etc., such that α , the fraction of total A in the complex, has the same value for all. Then g likewise will be the same provided that the equilibrium constants are functionally the same even if in general numerically different, that is, if a and b are the same for all the substances."

They support this statement with experimental evidence. Assuming its validity, one may conclude either that a true equilibrium between simple ions and micelles does occur, in which event the aggregation number and hence the micelle size is constant with concentration, or that the concentration dependencies of the parameters a and b are functionally the same for all substances of the same structural type. The former possibility seems more probable.

The intrinsic viscosity of colloidal solutions is regarded as a measure of either the size (14) and/or the shape (24) of the colloidal units, depending on the model chosen. With an ellipsoid of revolution as model, for which a sphere is a unique case, constancy of intrinsic viscosity indicates constancy of shape as well as degree of solvation. This model may be assumed as a close approximation to colloidal electrolyte micelles, in view of the diffusion work cited above. It is clear that if colloid does not exist below a critical concentration for micelle formation, the ordinary method of plotting reduced viscosity⁴ against concentration and taking the intercept on the ordinate axis as the intrinsic viscosity will

⁴ The reduced viscosity is the quantity η_{sp}/c .

not apply. The analyses of Grindley and Bury (5) and of Wright and Tartar (29) indicate that the concentration of simple ions reaches an approximate saturation value at the first critical concentration; hence, the solution at this concentration may be taken as the solvent for the colloidal micelles. The intrinsic viscosity characterizing the micelles can then be evaluated by computing the viscosities of solutions more concentrated than the critical concentration relative to that of the latter solution and at the same time subtracting the critical from the higher concentration values.

Upon applying this adjusted viscosity analysis to the measurements of Wright and Tartar (29), who studied aqueous solutions of sodium dodecyl sulfonate, it is found that the intrinsic viscosities at 40°, 50°, 60°, and 70°C. are 10.3, 10.4, 10.1, and 10.0, respectively. This is to say that the intrinsic viscosities are independent of temperature within experimental error. This result seems readily understandable on the basis of a spherical micelle whose radius is controlled by the length of the aggregating molecule, but is difficultly reconcilable with the suggestion of an equilibrium between two considerably different types of micelle, especially since the critical concentration is temperature dependent.

From the considerations outlined above, it is concluded that a single spherical micelle of constant size exists in the region between the first and second critical concentrations. The mass-action treatment of Grindley and Bury (5) indicates that micelle formation begins at a critical concentration and that micelle size increases to a maximum over a short transition range of concentration.

The amount of solvent kinetically associated with the spherical micelles can be estimated by comparing the intrinsic viscosity with the value 2.5, which has been shown to be characteristic of unsolvated spheres (3, 4). This is conveniently effected by computing the "hydrodynamic volume" of Kraemer and Sears (15). The intrinsic viscosity of Aerosol MA in aqueous solution is found to be 4.05; hence the "hydrodynamic volume" is $4.05 \cdot 2.5 = 1.62$. This value indicates that about 38 per cent of the volume of the colloidal unit is kinetically associated solvent. Indirect evidence for an appreciable degree of solvation may be inferred from the variation of partial specific volume with concentration. Over the range of concentration studied it increases by more than 20 per cent of its value in very dilute solutions; in view of the fact that the fusion of salts involves a volume change of about 10 per cent (1) it seems highly improbable that a change in excess of 20 per cent for Aerosol MA can be accounted for on the basis of its space requirements alone. Rather it suggests that the formation of micelles is attended by a change in the structure of the solvent, that is, by an interaction between micelles and solvent.

The radius of spherical colloidal particles can be calculated from the diffusion coefficient with the aid of the Stokes equation (27b). A comparison of the radius found by this method with that predicted for the model proposed is a test of the validity of the model. The longest chain leading away from the sulfonic group in Aerosol MA contains seven methylene groups and one carboxy-ester linkage, the length of which, including the sulfonic group, is 15 Å. if one takes 109° 28' as the angle between all atomic bonds. Assuming the amount of associated

solvent, as estimated from the "hydrodynamic volume," to be layered on the exterior of the micelle, the predicted radius is 17.6 Å. The value of the diffusion coefficient in the range 1.50–2.25 per cent Aerosol MA in 0.257 *N* sodium chloride is 13.8×10^{-7} cm.² per second, which yields the value 17.3 Å. for the radius of the micelle.

The effects on diffusion coefficient of swamping electrolyte concentration and the difference in Aerosol MA concentrations of the two solutions used in the experiment were mentioned above. They present pertinent questions regarding the characterization of the colloidal micelle by the diffusion coefficient chosen in the preceding paragraph. The effects of varying the concentration difference were observed with solutions in the neighborhood of the critical concentrations where the size of the micelle is changing with concentration. Similarly, the effects of varying swamping electrolyte concentration can be associated with changes in the critical concentrations due to addition of more salt (8, 19). It is clear, assuming Hartley's point of view, that in order to estimate the size of the micelle, both solutions used in the diffusion experiment must be in the range of fully formed micelles. From inspection of figure 5, the experiments at 1.75, 2.00, and 2.25 per cent Aerosol MA in 0.257 *N* sodium chloride seem to meet this requirement. From the constancy of the diffusion coefficient, it may be inferred that the salt was present in sufficiently high concentration to eliminate the small-ion charge effect; additional evidence for this statement is supplied by the measurements of Hakala (7), who studied the diffusion coefficient of sodium lauryl sulfate as a function of swamping electrolyte concentration.

The very close agreement between the observed and calculated values for the radius of Aerosol MA micelles is probably fortuitous. First, the value of "hydrodynamic volume" calculated pertains to salt-free solutions, whereas the diffusion coefficient was measured in salt solution. If the viscosities had been measured in the latter solution, it is probable that the "hydrodynamic volume" would have been reduced, because the effect of salt is to reduce the electroviscous effect (2). Second, it seems improbable that the paraffin–water interface in the micelle should be perfectly sharp, as is implied by assuming exterior layering of the associated solvent. Rather it seems more probable that water penetrates the micelles in the neighborhood of the interface. Both these factors tend to reduce the expected radius of the micelle below the value 17.6 Å., but it is evident from the length of the aggregating molecule that the lower limit is 15.0 Å.

Experimental evidence suggesting penetration of water within the micelles of straight-chain colloidal electrolytes may be cited by comparing the "hydrodynamic volume" of sodium dodecyl sulfonate with that to be expected on the basis of the diffusion coefficient of the closely similar sodium lauryl sulfate. Hakala's measurements (7) of the latter compound indicate a (spherical) micelle radius which is about 20 per cent greater than the maximum length of the molecule, leading to an expected "hydrodynamic volume" of about 1.7 on the basis of exterior layering of the associated solvent. Wright and Tartar's viscosity measurements (29) show that the "hydrodynamic volume" of sodium dodecyl sulfonate is actually 4.0, which is to say that solvation accounts for 75 per cent

of the micelle volume. In order to retain the proposed micelle model, it seems necessary to assume that solvent penetrates the paraffin portion of the micelle to an appreciable extent. If this is the case, it is probable that the density distribution of solvent within the micelle decreases with depth of penetration and that the core of the micelle is practically pure paraffin in nature. This picture represents a slight modification of the point of view of Hartley, who suggests that the paraffin water interface extends over the length of, say, two water molecule diameters (9).

The difference between the contributions of solvent to the micellar volumes of Aerosol MA and sodium dodecyl sulfonate, 38 and 75 per cent, respectively, is probably associated with the difference in structure between the two molecules. The radius of the Aerosol micelle is determined by the length of the longer of two chains leading away from the ionic group, but the shorter chain is also imbedded in the micelle. It is clear that the presence of the shorter chain will reduce the volume of solvent which can cluster around the ionic group, and, on the basis of the structure proposed above, it should also reduce the volume within the micelle which might otherwise be available for penetrating solvent. Were it not for the fact that the aggregation numbers of straight-chain and branched-chain electrolyte differ (21), it would be easy to test the validity of this explanation with the data at hand for the two compounds.

Further evidence for the Hartley micelle, as modified above, is suggested by the work of McBain and Johnson (22), who studied the solubilization of the water-insoluble dye Orange OT in aqueous solution by four potassium soaps. The results show that for soaps containing eight, ten, twelve, and fourteen carbon atoms, respectively, the amounts of dye solubilized per mole of soap are in the proportions 1:2.14:6.48:11.61.⁵ McBain and Brady's analysis (21) indicates that the aggregation numbers of these four soaps are equal, and from this it follows that the above proportions give directly the relative amounts of dye solubilized per micelle.

It seems generally accepted that in solubilization of the type studied by McBain and Johnson the dye dissolves in the paraffinic interior of the micelle (10, 19). To account for the quantitative data cited above it is necessary that a proposed structure for the micelle enable one to correlate the chain length of the soap molecules with the effective paraffinic volume of the micelle.

According to the modified Hartley structure it follows that the effective paraffinic nature of the micelle diminishes with distance from the center because of the attendant increasing frequency of water molecules. The volume of the effective paraffinic portion should consequently be proportional to the third power of an adjusted chain length of the soap molecule. By a process of trial and error it was found that if the number of carbon atoms per soap molecule in the above series were reduced by three and the resulting series 5, 7, 9, and 11 raised to the third power, the volumes obtained are in the proportions 1:2.74:5.83:10.65. Considering the approximate nature of the treatment, these ratios are in good agreement with those found experimentally by McBain and Johnson.

⁵ The original figures have been modified at the suggestion of Sister Agnes Green.

Objections to the micelle structure outlined might be raised on the grounds that penetration of water within the micelle would reduce the decrease of free interfacial energy attending micelle formation. While this may be true, penetration of water would also reduce the repulsion between the like-charged ionized groups on the surface of the micelle.

The aggregation number of Aerosol MA micelles may be estimated approximately with the aid of the diffusion coefficient, partial specific volume, and "hydrodynamic volume" on the basis of the modified Hartley micelle. The equation relating aggregation number with these parameters is:

$$\text{Aggregation number} = VD/HM$$

where V = volume of micelle,

D = density of aggregating ions in micelle,

H = "hydrodynamic volume," and

M = molecular weight of Aerosol MA

There are several approximations involved in the use of this equation. The one perhaps of chief concern is that the partial specific volume is assumed to be a measure of the density of the detergent molecules in the colloidal phase. It was indicated above that the magnitude of the change in this formal quantity strongly suggests that a change in the structure of the solvent attends micelle formation. If this is the case, the observed partial specific volume of the solute is not a true estimate of the density of the colloidal phase. In this connection, Adams (1) has shown how the solute density can be estimated with the aid of pressure-density-concentration studies.

Several other approximations enter because both the density and the viscosity measurements were made in salt-free solutions, whereas the diffusion coefficient pertains to salt solutions of the detergent. Considering the fact that a 5 per cent error in estimating the diffusion coefficient causes a 16 per cent error in the calculated micellar volume, the writer is inclined to the viewpoint that the errors involved in the approximations mentioned will not seriously reduce, in the relative sense, the precision of estimating the aggregation number.

Using the values 17.3 Å. for the micelle radius, 1.62 for the "hydrodynamic volume," 0.878 for the partial specific volume, and 388.4 for the molecular weight of the Aerosol MA, one obtains the value 23.6 for the aggregation number.

SUMMARY

1. Measurements of the densities and viscosities of aqueous solutions of purified Aerosol MA have been carried out over an appreciable concentration range. The diffusion behavior of Aerosol MA micelles in aqueous sodium chloride solutions has also been investigated.

2. The "critical concentration for micelle formation" in aqueous solution is about 1.1 per cent Aerosol MA, and the probable existence of a second critical concentration at about 5 per cent in aqueous solution is indicated.

3. The diffusion coefficient and the partial specific volume are constant in a concentration range between the first and second critical points.

4. A micelle-structure hypothesis has been proposed for the concentration range between the first and second critical points which is a modification of the spherical-micelle picture of Hartley. The modification is that solvent penetrates the micelle to an extent which depends on the distance from the center of the micelle.

5. In the concentration range between the first and second critical points Aerosol MA micelles contain about twenty-four detergent molecules which, on a volume basis, constitute about 62 per cent of the micelle, the remainder being solvent.

The writer wishes to express his gratitude to Professor J. W. Williams, under whose direction this work was carried out.

REFERENCES

- (1) ADAMS, L. H.: J. Am. Chem. Soc. **53**, 3769 (1931).
- (2) COHN, E. J., AND EDSALL, J. T.: *Proteins, Amino Acids and Peptides*, p. 522. Reinhold Publishing Corporation, New York (1943).
- (3) EIRICH, F.: Kolloid-Z. **74**, 276 (1936).
- (4) EIRICH, F.: Kolloid-Z. **81**, 7 (1937).
- (5) GRINDLEY, J., AND BURY, C. R.: J. Chem. Soc. **1929**, 679.
- (6) HAFFNER, F. D., PICCIONE, G. A., AND ROSENBLUM, C.: J. Phys. Chem. **46**, 662 (1942).
- (7) HAKALA, N. V.: Dissertation, University of Wisconsin, 1943.
- (8) HARTLEY, G. S.: *Aqueous Solutions of Paraffin-Chain Salts*, Actualités scientifiques et industrielles No. 387. Hermann et Cie., Paris (1936).
- (9) HARTLEY, G. S.: Kolloid-Z. **88**, 22 (1939).
- (10) HARTLEY, G. S.: "Solvent Action of Detergent Solutions", in *Wetting and Detergency*. Chemical Publishing Company, Inc., New York (1937).
- (11) HARTLEY, G. S., AND RUNNICES, D. F.: Proc. Roy. Soc. (London) **A168**, 420 (1938).
- (12) HESS, K.: Fette u. Seifen **49**, 81 (1942).
- (13) HESS, K., PHILIPPOFF, W., AND KIERSIG, H.: Kolloid-Z. **88**, 40 (1939).
- (14) HUGGINS, M. L.: J. Phys. Chem. **42**, 911 (1938); **43**, 439 (1939).
- (15) KRAEMER, E. O., AND SEARS, G. R.: J. Rheol. **1**, 231 (1930).
- (16) LAMM, O.: Nova Acta Reg. Soc. Sci. Upsaliensis **4**, No. 6, 10 (1937).
- (17) LAMM, O.: Kolloid-Z. **98**, 45 (1942).
- (18) LEWIS, G. N., AND RANDALL, M.: *Thermodynamics and the Free Energy of Chemical Substances*, p. 36. McGraw-Hill Book Company, Inc., New York (1923).
- (19) MCBAIN, J. W.: In Alexander's *Colloid Chemistry*, Vol. 5. Reinhold Publishing Corporation, New York (1944).
- (20) MCBAIN, J. W., AND BOLDUAN, O. E. A.: J. Phys. Chem. **47**, 94 (1943).
- (21) MCBAIN, J. W., AND BRADY, A. P.: J. Am. Chem. Soc. **65**, 2072 (1943).
- (22) MCBAIN, J. W., AND JOHNSON, K. E.: J. Am. Chem. Soc. **66**, 9 (1944).
- (23) PHILIPPOFF, W.: *Viskosität der Kolloide*. J. W. Edwards, Ann Arbor, Michigan (1944); originally published in Germany in 1940.
- (24) SIMHA, R.: J. Chem. Phys. **13**, 188 (1945).
- (25) STAUFF, J.: Kolloid-Z. **89**, 224 (1939).
- (26) SVEDBERG, T.: Zsigmondy Festschrift (Erg. Bd. zu Kolloid-Z. **36**), p. 53 (1925).
- (27) SVEDBERG, T., AND PEDERSEN, K. O.: *The Ultracentrifuge*, Oxford University Press, Oxford and New York (1940): (a) p. 23; (b) p. 38; (c) p. 42.
- (28) TENNENT, H. G., AND VILBRANDT, C. F.: J. Am. Chem. Soc. **65**, 424 (1943).
- (29) WRIGHT, K. A., AND TARTAR, H. V.: J. Am. Chem. Soc. **61**, 544 (1939).

THE MORPHOLOGY OF LYOGELS¹

ERNST A. HAUSER

Massachusetts Institute of Technology, Cambridge, Massachusetts

AND

D. S. LE BEAU

*Midwest Rubber Reclaiming Company, East St. Louis, Illinois**Received August 8, 1946*

In March 1915, Wo. Ostwald's book, *The World of Neglected Dimensions* (11), was published. Over twenty years later, v. Buzágh made the following statements in the preface to his book, *Colloid Systems* (3): "It is no coincidence, but neither is it to be ascribed to any artificially forced tendency, that 'The World of Neglected Dimensions' has become, in two short decades, 'The World of Not-to-be-Neglected Dimensions'."

However, if one scans the literature of the past ten years as far as it pertains to matter which must be classified as colloidal, one often wonders if the following statements, also taken from v. Buzágh's preface, have been overlooked: "It is a mistake for the physical chemist to doubt that colloid science has justified its existence, to fail to recognize its aims, and to hold the opinion that the classical laws of physical chemistry can be directly applied to colloid phenomena, and that an explanation of these phenomena is automatically provided by the atomic theory. A knowledge of pure physics and chemistry is necessary to enable us to judge when we are confronted with colloid phenomena for which the classical principles of physical chemistry provide no explanation."

While the discovery of the ultramicroscope by Zsigmondy (14) and Siedentopf (12) and others has enabled us to study colloidal sols and some of their properties visually, the same can not be said for typical lyogels. The optical principle on which the standard ultramicroscopic illumination is based calls for a very thin preparation of uniform thickness. Besides this, the matter under observation must be discontinuous or embedded in another continuous medium which permits passage of light. Therefore, it is not possible to study the actual structure or morphology of lyogels by the use of a standard ultramicroscope.

When, only a few years ago, the electron microscope was for the first time applied to the study of lyogels—as, for example, soaps—the pioneers in this field of research also introduced a new technique for the preparation of specimens (10). A few years later it was applied to the study of the structure of hevea rubber (4).

It seemed that we had finally been able to offer a visual proof for the differences in properties exhibited by various fractions of hevea rubber and the changes it undergoes during vulcanization. From the point of view of the colloid chemist, however, the changes in the properties of the lyogels due to electron bombardment and the high vacuum could not be overlooked. But the results had demon-

¹ Presented at the Twentieth National Colloid Symposium, which was held at Madison, Wisconsin, May 28-29, 1946.

strated that the technique used for the preparation of the specimens was just what thus far had been lacking in the ultramicroscopy of lyogels. Now it was possible to prepare samples with such density differences that an ultramicroscopic effect could be obtained, if ultra-illumination by incident light was applied instead of the customary dark-field illumination.

It must of course be realized that the power of resolution of the ultramicroscope is by far less than that of the electron microscope. Comparative studies, however, have shown that, as far as the general morphology of lyogels is concerned, this difference in resolving power is not of primary importance, because it constitutes a difference in degree only.

Since details of the technique as well as some results have already been published (5, 6, 7), further discussions can be limited to new observations and deductions drawn therefrom.

So far it had been assumed that the spherules observed in preparations for electron- or ultramicroscopy of natural rubber and some synthetic elastomers (4, 5) were due to low-molecular-weight fractions of the hydrocarbons, and that the filaments represented the high-molecular-weight fractions. Besides this, it was assumed that these formations occurred instantaneously. More detailed studies of cryptostegia rubber—a hydrocarbon polymer which is characterized by a large fraction of low as well as of high molecular weight polymer and only a very small fraction of intermediate molecular sizes (6)—have shown that the formation of the spherules is not instantaneous (figures 1, 2, 3, 4).² It is well known that unvulcanized natural rubber under stress exhibits plastic flow. It is a well-established fact that if rubber is stretched to a fixed extension, a decrease in tension occurs with time. This phenomenon is known as relaxation or elastic recovery. The degree of this change depends on the temperature at which the tests are carried out. As pointed out by Treloar (13), the tension for a given elongation will be greater at 25°C. than at 50°C. The films were deposited on the wire screens at a temperature as close to 25°C. as possible. Upon evaporation of the solvent the film is undoubtedly under a certain amount of strain. This must cause the long-chain molecular fractions to be aligned to a certain extent. This will cause the shorter chains to be squeezed out. Such a phenomenon, which might be compared to syneresis, must be time consuming by virtue of its nature. The microscopic technique offers the first visual proof of the phenomenon of plastic flow and elastic recovery. The same has also been observed with preparations of some of the other elastomers of synthetic or natural origin. However, balata and gutta-percha, which are known to be low-molecular-weight polymers, do not show this phenomenon (figures 5, 6). Spherules can only be found after very prolonged storage of the preparation. The films are coarse and of ragged contours, and even fine filaments are rarely observed.

It is well established that both natural rubber as well as balata and gutta-percha consist of the same chemical building unit (isoprene). However, natural

² All illustrations are prints from Kodachrome A or Ansco color-reversible films (6). The magnifications of figures 1-4, 7-15, and 17-19 are approximately 4000 \times , the magnification of figure 16 is 1500 \times .

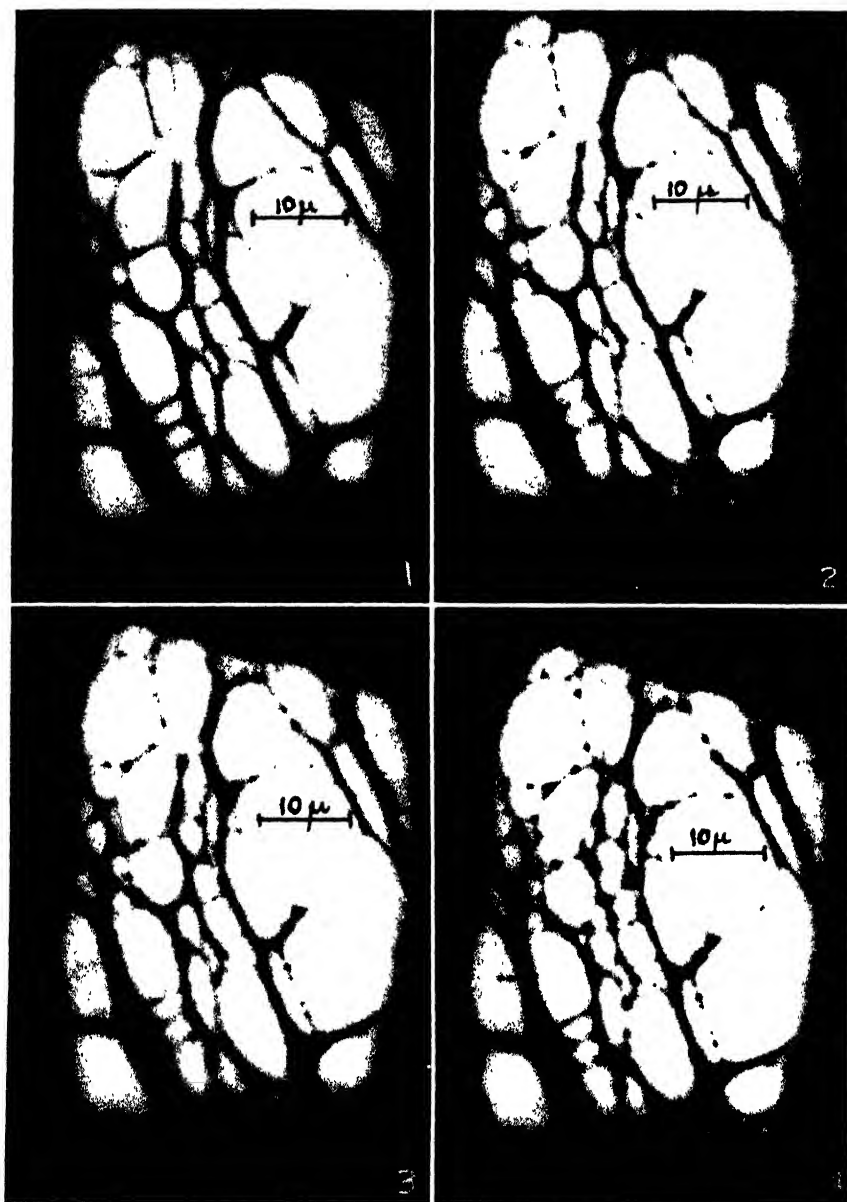


FIG. 1. *Cryptostegia grandiflora* rubber (fresh preparation)

FIG. 2. *Cryptostegia grandiflora* rubber (after 5 hr. storage)

FIG. 3. *Cryptostegia grandiflora* rubber (after 10 hr. storage)

FIG. 4. *Cryptostegia grandiflora* rubber (after 20 hr. storage)

rubber crystallizes in the *cis* configuration, whereas gutta-percha and balata crystallize in *trans* configuration. It is also well known that gutta-percha has a much higher melting point than natural rubber and that it becomes elastic only

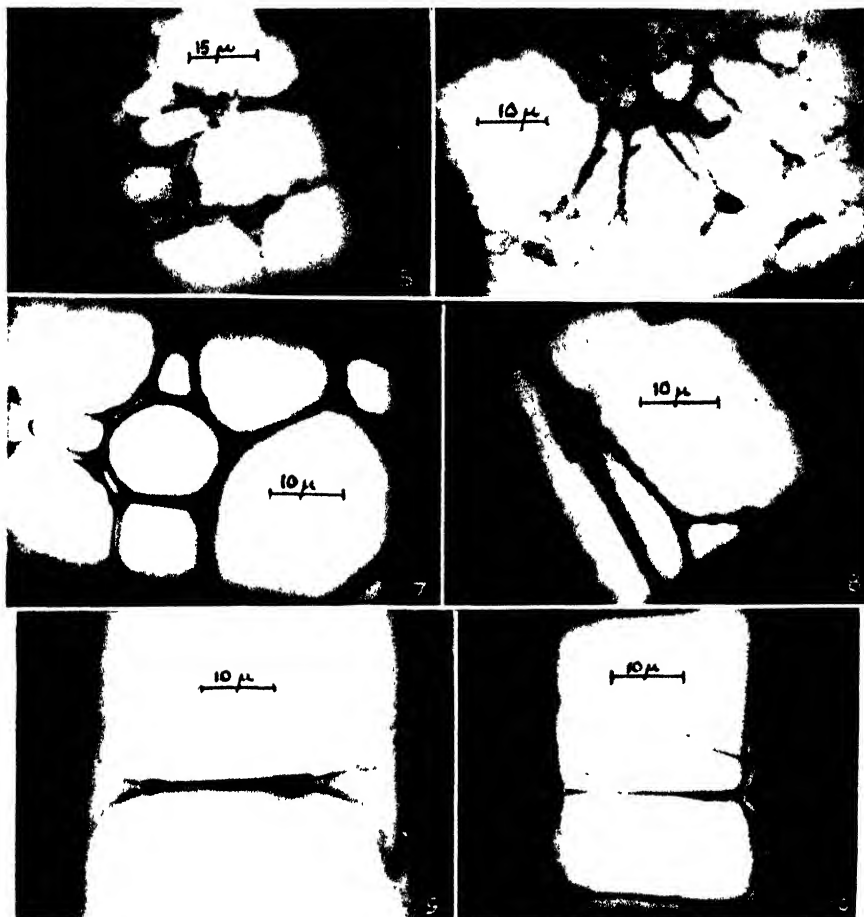


FIG. 5. Balata.

FIG. 6. Gutta-percha (preparation 4 weeks old).

FIG. 7. Neoprene GN (original).

FIG. 8. Neoprene GN (milled 10 mm).

FIG. 9. Polyisobutylene (fresh preparation).

FIG. 10. Polystyrene.

at temperatures above its melting point. Accepting the hypothesis that chain-bond oscillation alone is responsible for the melting of these crystallites, then the question arises why the rotation around the single bonds does not occur with equal ease at the same temperature in natural rubber as in gutta-percha and balata. In the rubber chain, the methyl group stands in a slightly different



position than in gutta-percha. For rubber the angle $\text{—C}=\text{CH—}$ has been measured to be 115° , whereas for gutta-percha it amounts to 125° . Furthermore, in rubber, because of its *cis* double-bond configuration, no obstruction to vibration is offered such as can be found in gutta-percha (2). These theoretical concepts, largely based on x-ray diffraction studies, now seem to be corroborated by the ultramicroscopic studies. The greater freedom of motion of the rubber hydrocarbon polymers having the *cis* configuration is reflected in their flow and syneresis, as observed in the cryptostegia preparations, and the lack or long delay in the occurrence of these two phenomena in the *trans* configurations, as encountered in the gutta-percha and balata preparations.

Polychloroprene also crystallizes in the *trans* configuration. Therefore, its molecular structure and its morphology should correspond to that obtained from gutta-percha. This, however, is not the case. Although the film deposited on the wire screen breaks into fibres, spherules have also been found either upon previous mastication of the polymer or after prolonged storage of the preparation. This apparent discrepancy nevertheless again checks with the theoretical concept that the chlorine atom is farther removed from the hydrocarbon chain than the methyl group in gutta-percha. Thus, chain-bond rotation and molecular oscillation are facilitated, permitting a greater freedom of movement which results in the structures observed in the ultramicroscopic studies (figures 7, 8).

The same considerations can be applied to polyisobutylene (figure 9). Here flow can be noticed even in a polymer of an average molecular weight of 300,000 (Staudinger), although a greater time interval for the flow to occur seems to be necessary. This is not surprising, if the chemical structure and configuration of the polymer are taken into consideration.

It is interesting to note that so far it has been impossible to obtain any polyisobutylene pictures in the electron microscope.

Polystyrene (obtained by polymerization at 80°C . without the addition of catalyst), as well as polymethyl methacrylate, does not show any properties of flow even if the preparation is stored for a very long time (figures 10, 11). This again is in line with the theoretical concept of the molecular structures of these polymers. In the case of polystyrene, the presence of the rather bulky phenyl group attached to the flexible chain probably does not permit perfect geometrical alignment and free movement (9), and in the case of polymethyl methacrylate the two methyl groups will also tend to block any alignment and orientation. This is substantiated by the fact that so far no x-ray fiber diagrams have been obtained for these polymers (9).

So far we have only discussed the application of this new technique to the study of high polymers, but it is equally applicable to certain proteins. Figure 12 shows the coarse and brittle bands obtained from rat tail tendons dissolved in 0.5 per cent acetic acid.

Several years ago McBain and collaborators (10) published the first electron-microscope pictures of fatty acid salts. Although the ultramicroscopic technique for obvious reasons cannot compare in its resolving power with the electron

microscope, it offers, as previously stated, the advantage of time studies which are of particular importance for freshly prepared specimens. Thus, it was found that soap, deposited from water solution on the wire support by dipping and drying at room temperature and observed under the microscope immediately thereafter, will form threads and spherules (figure 13). However, if the specimen is aged, the same kind of thorny configurations as obtained by the electron microscope become evident (figure 14). The formation of the soap films depends on the concentration of the soap solution, varying also with the kind of soap used, and is well above the so-called critical concentration for micelle formation.

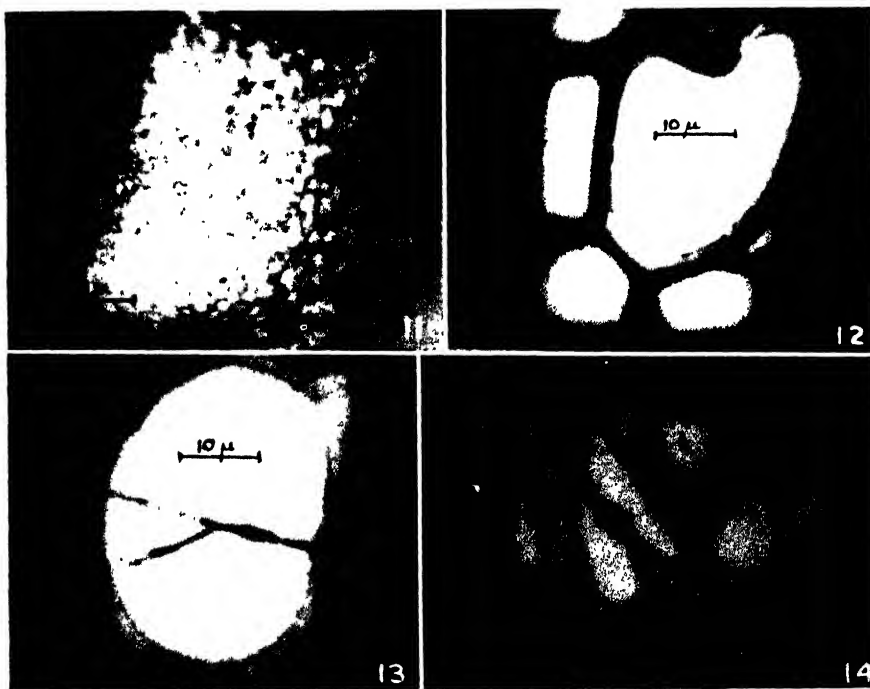


FIG. 11 Polymethyl methacrylate

FIG. 12 Rat tail tendon

FIG. 13. Sodium oleate (fresh)

FIG. 14 Sodium oleate (after 48 hr. storage)

It was considered of interest to study the cationic soaps in the same manner. Carefully prepared cetyltrimethylammonium chloride, bromide, and iodide were subjected to ultramicroscopic observations. Cetylpyridinium chloride (figure 15) resembles anionic soaps in its morphology, although the threads are not as pronounced. Cetylpyridinium bromide (figure 16) shows films only, which upon bursting do not exhibit threads. Cetylpyridinium iodide (figure 17) will not even form films but crystallizes instantaneously. The same phenomenon can be observed with the cetyltrimethylammonium cationic soaps (figures 18, 19).

It is known that the reduction in surface tension of these compounds follows

the periodic order of the halide anions (8). This has been explained by the degree of hydration of these ions as calculated by Born (1). According to the heats of hydration, the chloride ion must be considered more hydrophilic than the bromide ion, and the latter more hydrophilic than the iodide ion.

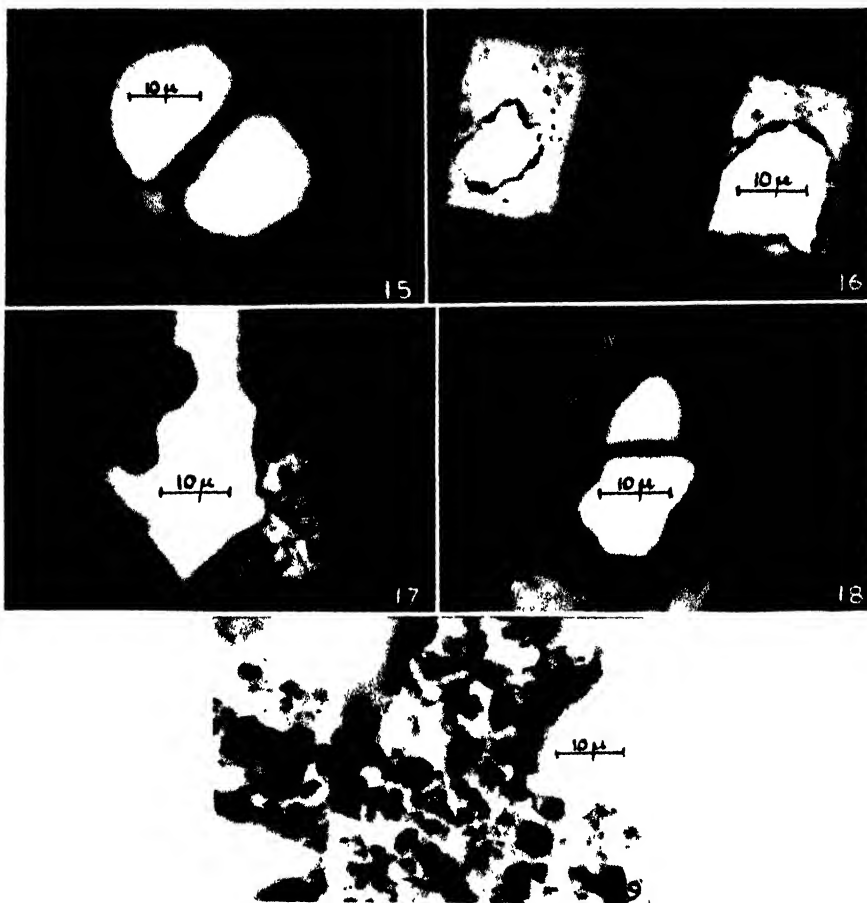


FIG. 15. Cetylpyridinium chloride

FIG. 16. Cetylpyridinium bromide

FIG. 17. Cetylpyridinium iodide

FIG. 18. Cetyltrimethylammonium chloride

FIG. 19. Cetyltrimethylammonium iodide

These studies, as well as recent observations on several silicone resins and hydro- and organogels of colloidal clays, have offered an interesting visual evidence that the morphological differences found in lyophilic colloids and the changes they undergo during storage or by chemical or physical influences must be considered primarily a function of the degree of solvation and not only of their chemical composition.

The results furthermore visually demonstrate the great effect which seemingly minor changes in the structural configuration of chemically identical compounds or small differences in their composition exert on the lyophilic character of colloids and their importance to the properties they exhibit.

SUMMARY

The application of ultramicroscopy by incident light in studying the morphology of lyogels is discussed. Special attention is paid to organophilic elastomers and plastics and to lyophilic anionic and cationic soaps. The changes these gels undergo during storage are critically reviewed, and an explanation is offered for their similar morphology on the basis of colloid-chemical reasoning.

REFERENCES

- (1) BORN, M.: *Ber. deut. physik. Ges.* **21**, 679 (1919).
- (2) BUNN, C. W.: *Proc. Roy. Soc. (London)* **A180**, 82 (1942).
- (3) BUZÁGH, A. v.: *Colloid Systems*. The Technical Press, London (1937).
- (4) HALL, C. E., HAUSER, E. A., *et al.*: *Ind. Eng. Chem.* **36**, 634 (1944).
- (5) HAUSER, E. A., AND LE BEAU, D. S.: *Ind. Eng. Chem.* **37**, 786 (1945); **38**, 335 (1946); *J. Am. Chem. Soc.* **68**, 153 (1946); *J. Phys. Chem.* **50**, 171 (1946).
- (6) HAUSER, E. A., AND LE BEAU, D. S.: *India Rubber J.* **110**, 169 (1946).
- (7) HAUSER, E. A., AND LE BEAU, D. S.: *Rubber Age* **59**, 67 (1946).
- (8) HAUSER, E. A., AND NILES, G. E.: *J. Phys. Chem.* **45**, 954 (1941).
- (9) MARK, H.: *The Chemistry of Large Molecules*, p. 33. Interscience Publishers, Inc., New York (1943).
- (10) MARTON, L., MCBAIN, J. W., AND VOLD, R. D.: *J. Am. Chem. Soc.* **63**, 1990 (1941).
- (11) OSTWALD, W.: *Die Welt der vernachlässigten Dimensionen*. Th. Steinkopff, Dresden (1915).
- (12) SIEDENTOFF, H.: *J. Roy. Microscop. Soc.*, page 573 (October, 1903).
- (13) TRELOAR, L. R. G.: *Trans. Faraday Soc.* **36**, Part 4, 538 (1940).
- (14) ZSIGMONDY, R.: *Ann. Physik (Drude's Ann.)* **10**, 1 (1903).

SOLUBILIZATION OF WATER-INSOLUBLE DYE BY PURE SOAPS
AND DETERGENTS OF DIFFERENT TYPES¹

SISTER AGNES ANN GREEN

Department of Chemistry, Immaculate Heart College, Los Angeles, California

AND

JAMES W. MCBAIN

*Department of Chemistry, Stanford University, California**Received August 8, 1946*

INTRODUCTION

Among the interesting and characteristic properties of detergents, the phenomena of solubilization are at present the most challenging from the viewpoint of theory. Emphasis is placed upon the need for interpretable data by the rapidly increasing use of solubilization in such industrial processes as emulsion polymerizations, the dyeing of rayon, and the preparation of lubricants. Solubilization (1) consists in the spontaneous passage of a substance insoluble in a pure solvent into a dilute solution of a detergent in that solvent to form a thermodynamically stable solution. The saturation value is constant at any given concentration of detergent under conditions of constant temperature and pressure, whether the end point is approached from undersaturation or oversaturation.

The immediate purposes of the following experiments were to study the effect of changes in the detergent molecule itself on solubilizing power, and to observe the effects of the presence of certain organic liquids. To this end, a study of several aqueous systems of pure soaps, commercial detergents, and a non-ionic detergent was made in the presence of the same saturant, Orange OT (1-*o*-tolylazo-2-naphthol). This dye was chosen as a non-polar crystalline substance, insoluble in water but whose solubility in the detergent solutions is great enough to be easily measured, while not of sufficient magnitude to alter the properties and the micellar constitution of the solutions. The experimental method was that described in a former paper (3).

EXPERIMENTAL RESULTS

Potassium and sodium soaps as solubilizers

Measurements were made on potassium and sodium laurates and on potassium and sodium oleates over as complete a concentration range as the solubility of the soaps themselves would permit. The results are given in tables 1 to 4. A comparison of the solubilizing capacity of the two laurate soaps below 0.25 *N* is represented in figure 1. In this range it is plainly evident that the sodium laurate is more effective per gram-molecular weight than the potassium laurate.

¹ Presented at the Twentieth National Colloid Symposium, which was held at Madison, Wisconsin, May 28-29, 1946.

TABLE 1

Solubilization of Orange OT in aqueous solutions of potassium laurate at 25°C.

VOLUME CONCENTRATION OF SOAP	DYE PER 100 CC OF SOLUTION	DYE PER MOLE OF KC_{12}	MOLAR RATIO DYE/SOAP $\times 10^3$
<i>N</i>	<i>mg.</i>	<i>grams</i>	
0.001	0		
0.010	0.02	0.020	0.076
0.025	0.44	0.176	0.67
0.049	2.28	0.462	1.76
0.098	8.15	0.833	3.18
0.125	12.12	0.970	3.70
0.250	25.95	1.038	3.96
0.500	52.20	1.048	4.00
0.820	85.40	1.043	3.98
1.000	107.60	1.076	4.10

TABLE 2

Solubilization of Orange OT in aqueous solutions of sodium laurate at 25°C.

VOLUME CONCENTRATION OF SOAP	DYE PER 100 CC OF SOLUTION	DYE PER MOLE OF NaC_{12}	MOLAR RATIO DYE/SOAP $\times 10^3$
<i>N</i>	<i>mg.</i>	<i>grams</i>	
0.001	0.03	0.30	1.14*
0.005	0.095	0.19	0.72
0.010	0.260	0.26	0.99
0.025	0.950	0.380	1.45
0.050	3.65	0.730	2.78
0.075	7.45	0.998	3.80
0.100	14.45	1.445	5.50
0.150	23.05	1.535	5.85
0.200	35.10	1.750	6.67†

* Believed to include suspending action (3).

† From supersaturation.

TABLE 3

Solubilization of Orange OT in aqueous solutions of potassium oleate at 25°C.

VOLUME CONCENTRATION OF SOAP	DYE PER 100 CC OF SOLUTION	DYE PER MOLE OF KC_{18}	MOLAR RATIO DYE/SOAP $\times 10^3$
<i>N</i>	<i>mg.</i>	<i>grams</i>	
0.0001	0.04	4.00	15.25*
0.0010	0.21	2.10	8.00
0.0025	0.68	2.72	10.37
0.0125	3.38	2.70	10.29
0.125	33.75	2.70	10.29
0.250	67.00	2.67	10.21
0.500	141.00	2.82	10.75

* Believed to include suspending action.

TABLE 4

Solubilization of Orange OT in aqueous solutions of sodium oleate at 25°C.

VOLUME CONCENTRATION OF SOAP	DYE PER 100 CC. OF SOLUTION	DYE PER MOLE OF NaC_{18}	MOLAR RATIO DYE/SOAP $\times 10^3$
<i>N</i>	<i>mg.</i>	<i>grams</i>	
0.0001	0.01	1.00	3.81
0.0010	0.14	1.40	5.34
0.0025	0.56	2.24	8.54
0.005	1.25	2.50	9.53
0.010	2.90	2.90	11.06
0.025	7.50	3.00	11.44
0.050	15.00	3.00	11.44
0.10	30.0	3.00	11.44
0.20	59.0	2.95	11.26
0.30	100.5	3.35	12.77

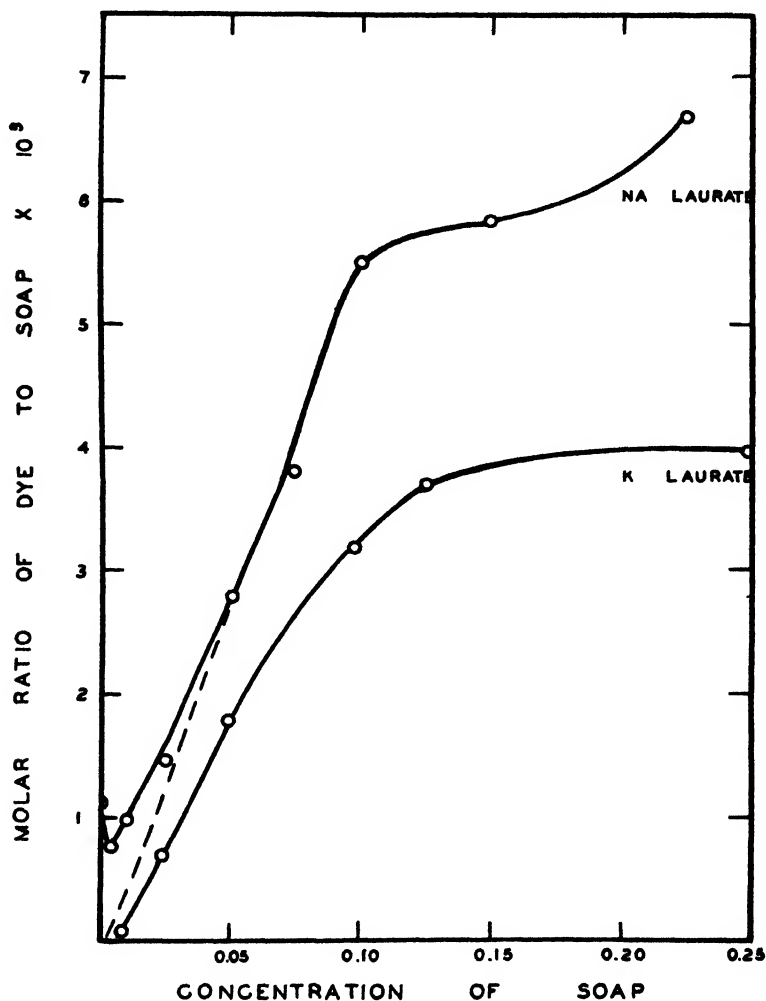


FIG. 1. Solubilization of Orange OT by sodium and potassium laurates

A steep rise in the curve, marking the greatest increase in the amount of dye solubilized per mole of potassium laurate, occurs in the interval from 0.01 *N* to 0.10 *N*, the same region where the conductance (8) and osmotic coefficients (2) indicate a transition from the behavior of a strong electrolyte to that of a colloidal electrolyte. In the case of the sodium laurate, it is difficult to decide whether its own limited solubility prevented it from reaching an even higher maximum representing full colloidal form. Its greatest rate of change in solubilizing ability per mole also occurs in the same concentration range as that of potassium laurate.

A comparison of the relative solubilizing power of potassium and sodium oleates below 0.125 *N* is given in figure 2, again illustrating the superior solubilizing power of the sodium soap. The greater regularity of the sodium oleate curve

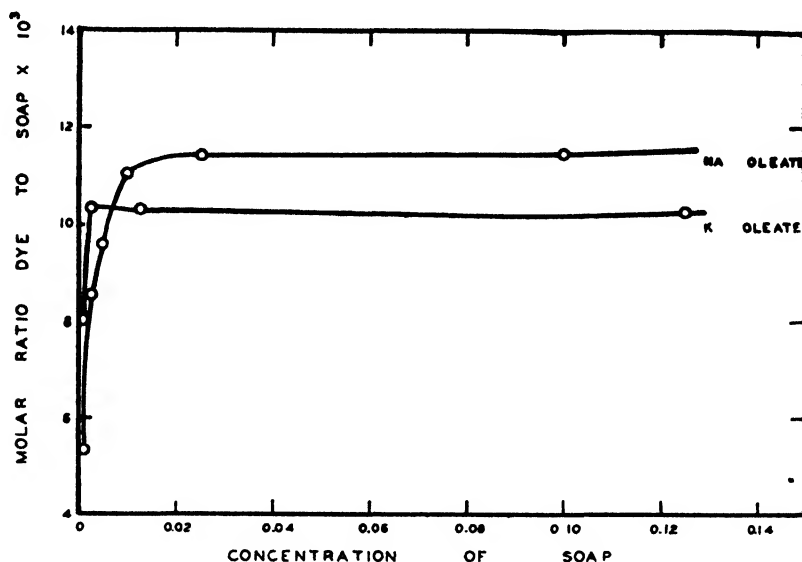


FIG. 2. Solubilization of Orange OT by sodium and potassium oleates

is attributed to the greater purity of this product, which was prepared from specially purified oleic acid (13). The other soaps were prepared from Kahlbaum's best fatty acids without further purification.

In figure 3, both the oleates and the laurates, within the range 0.01 *N* to 1.0 *N*, are represented on the same graph. This brings out the superiority of the oleates, representing greater chain length and unsaturation in the soap molecule. This figure also shows the greater effectiveness of both the sodium soaps as compared with the potassium soaps. Apparently, then, solubilization is not entirely dependent upon the length of the hydrocarbon chain of the detergent molecule. Since this difference can only be due to the polar end of the molecule, some dipole attraction must enter into the process of solubilization, if only in its influence on the colloidal structure of the soap solutions.

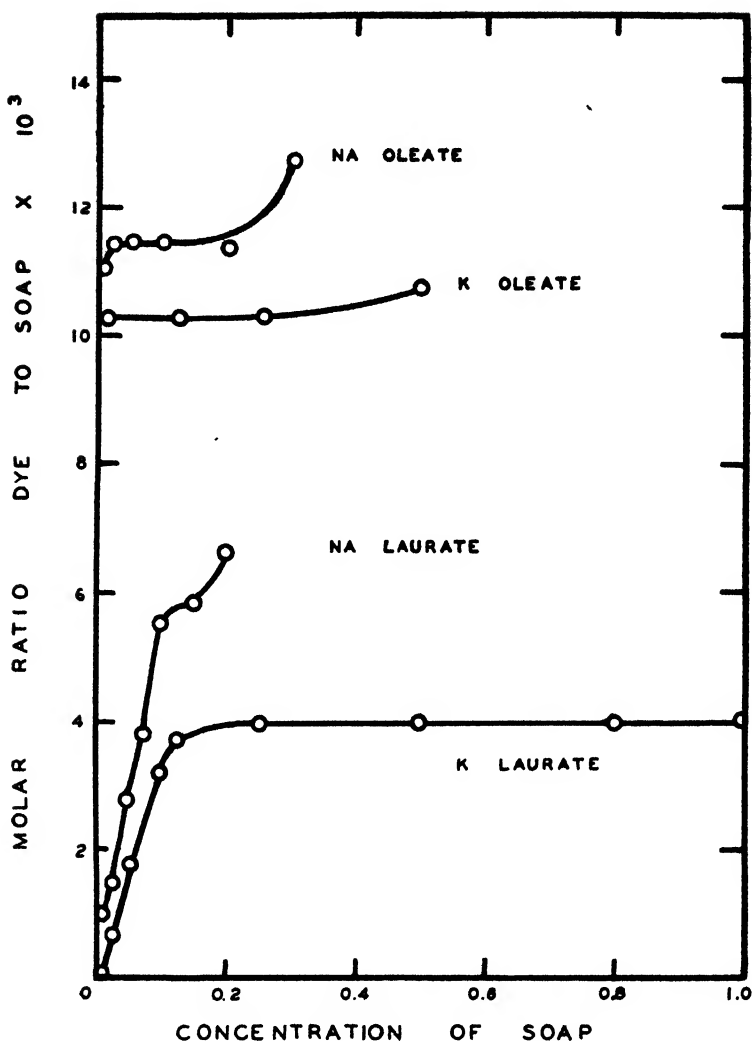


FIG. 3. Comparison of solubilization by sodium and potassium oleates and laurates

A cation-active detergent

The detergent properties of dodecylamine hydrochloride are of special interest, because its paraffin chain is in the cation part of the molecule. The charge, then, upon the ion containing the large organic group, and hence upon the micellar formation in solution, is opposite in sign from that in the ordinary soaps, the salts of fatty acids, and that in lauryl sulfonic acid. By measuring the solubilizing capacity of solutions of these detergents for Orange OT, a comparison was obtained between cation- and anion-active detergents containing the paraffin chain of twelve carbon atoms in their organic radicals. The data obtained from measurements on solutions made from the pure crystalline do-

decylamine hydrochloride, as prepared by P. H. Richards (7), are given in table 5 and represented graphically in figure 4. The extent of the curve is again limited by the solubility of the soap itself at 25°C. The greatest increase in solubilization occurred in the same region where the conductance curve showed the greatest change (12),—namely, in the interval from 0.01 *N* to 0.05 *N*.

TABLE 5
Solubilization of Orange OT by dodecylamine hydrochloride at 25°C.

VOLUME CONCENTRATION OF DETERGENT	DYE PER 100 CC. OF SOLUTION	DYE PER MOLE OF DETERGENT	MOLAR RATIO DYE/SOAP $\times 10^3$
<i>N</i>	mg.	grams	
0.001	0		
0.010	0.06	0.06	0.23
0.025	1.925	0.77	2.94
0.050	6.94	1.39	5.29
0.075	11.19	1.49	5.69
0.100	18.25	1.83	6.96
0.150	28.50	1.90	7.24
0.200	47.50	2.38	9.05

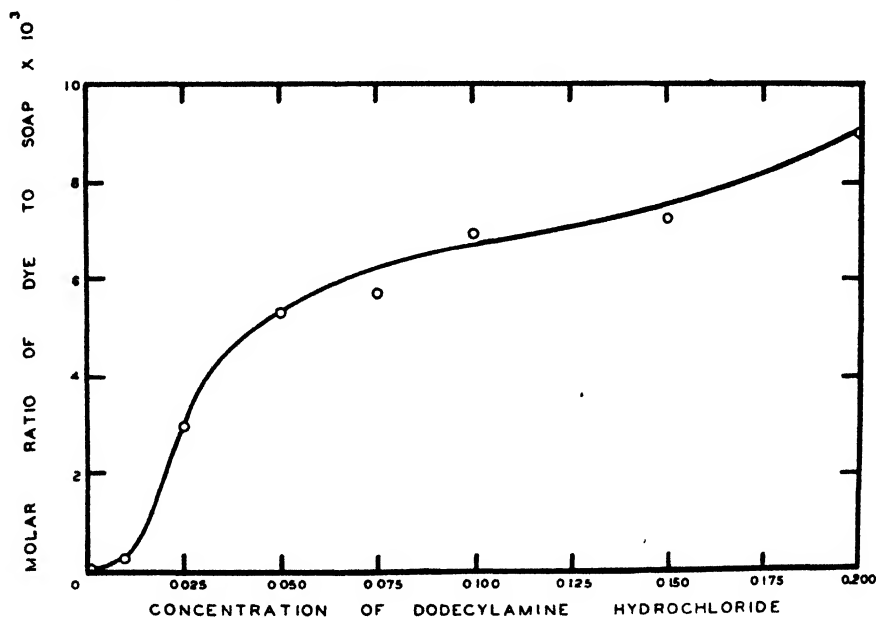


FIG. 4. Solubilization of Orange OT by dodecylamine hydrochloride

Lauryl sulfonic acid, prepared by M. E. Synerholm according to the method of Noller and Gordon (10), was used in making the measurements recorded in table 6 and in figure 5. The greater solubility of the compound made possible measurements at much higher concentrations than have been previously re-

ported (6). The increase in solubilizing ability was found to be greatest in the interval between 0.01 and 0.05 *N*, which again coincides with the interval of greatest change in the conductance curve (9), exhibiting in both the typical behavior of a colloidal electrolyte.

TABLE 6
Solubilization of Orange OT by lauryl sulfonic acid solutions at 25°C.

VOLUME CONCENTRATION OF DETERGENT	DYE PER 100 CC. OF SOLUTION	DYE PER MOLE OF DETERGENT	MOLAR RATIO DYE/SOAP $\times 10^3$
<i>N</i>	<i>mg.</i>	<i>grams</i>	
0.001	0.0275	0.275	1.05
0.010	0.685	0.685	2.61
0.05	9.00	1.80	6.86
0.10	17.13	1.72	6.54
0.20	36.13	1.81	6.92
0.50	91.00	1.82	6.94
0.727	165.00	2.27	8.64
0.74	171.0	2.31	8.81

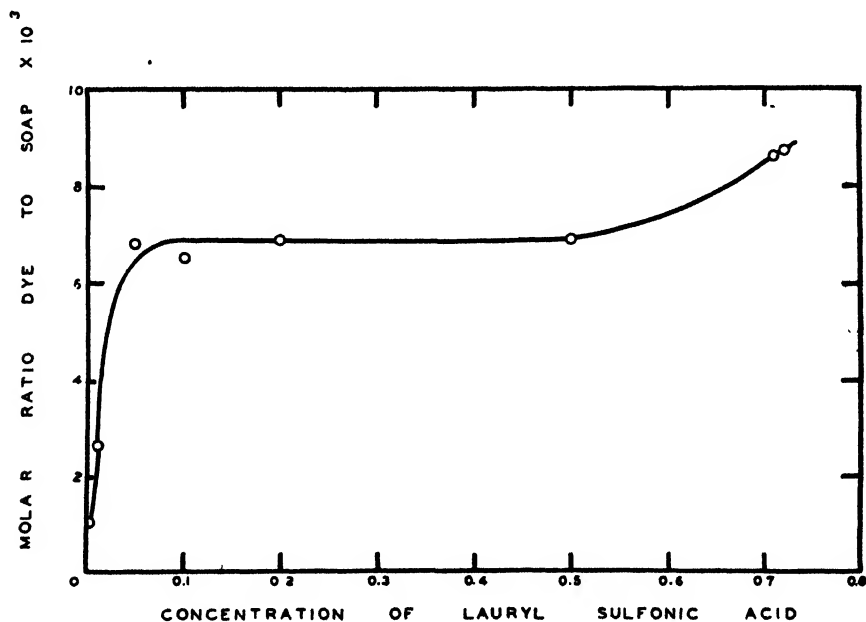


FIG. 5. Solubilization of Orange OT by lauryl sulfonic acid.

These measurements showed that the cation-active detergent, dodecylamine hydrochloride, possesses greater solubilizing ability than that of the neutral anion-active detergents, potassium and sodium laurates, containing the same number of carbon atoms. It was only slightly more effective than lauryl sulfonic acid, which was also better than the laurates.

A non-ionic detergent, Triton X-100

Triton X-100 is a commercial product (Röhm and Haas Company), a high-molecular-weight derivative of polyethylene oxide, which does not ionize in

TABLE 7
Solubilization of Orange OT in aqueous solutions of Triton X-100

PERCENTAGE COMPOSITION BY WEIGHT	DYE PER 100 CC	DYE PER GRAM OF DETERGENT	APPROXIMATE NORMALITY*	DYE PER MOLE OF DETERGENT	MOLAR RATIO DYE/DETERGENT $\times 10^3$
	mg.	mg.	N	grams	
0.0176	0.012	0.68	0.0003	0.04	0.156
0.10	0.305	3.05	0.0017	1.83	6.98
0.50	1.95	3.90	0.0083	2.34	8.92
1.00	4.05	4.05	0.0167	2.43	9.27
2.00	8.50	4.25	0.033	2.55	9.72
5.00	21.65	4.33	0.083	2.60	9.91
10.00	44.87	4.49	0.167	2.69	10.25
30.00	142.5†	4.75	0.5	2.85	10.8
100.00	1949. ‡	19.49		11.69	44.57

* Calculation of normality based upon molecular weight of 600, determined by freezing-point measurements in benzene. Unpublished work of Dr. E. Gonick.

† A measurement by Arthur G. Wilder, Stanford University, which fits the extrapolated curve for these data, shown in figure 7.

‡ Units of this measurement are milligrams of dye per 100 g. of detergent.

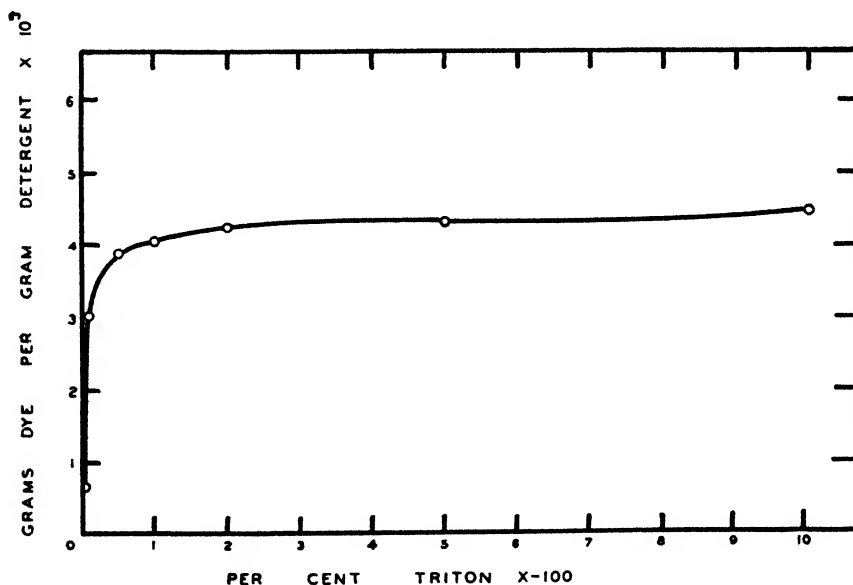


FIG. 6. Solubilization of Orange OT by aqueous solutions of Triton X-100

solution. However, the measurements given in table 7 proved its solubilizing capacity to be high, and the shape of the curve below 10 per cent, shown in

figure 6, is very similar to those of the colloidal electrolytes. A measurement was made of the solubility of the dye in the pure Triton X-100, a liquid, which showed its solvent power to be four or five times its solubilizing power, per weight

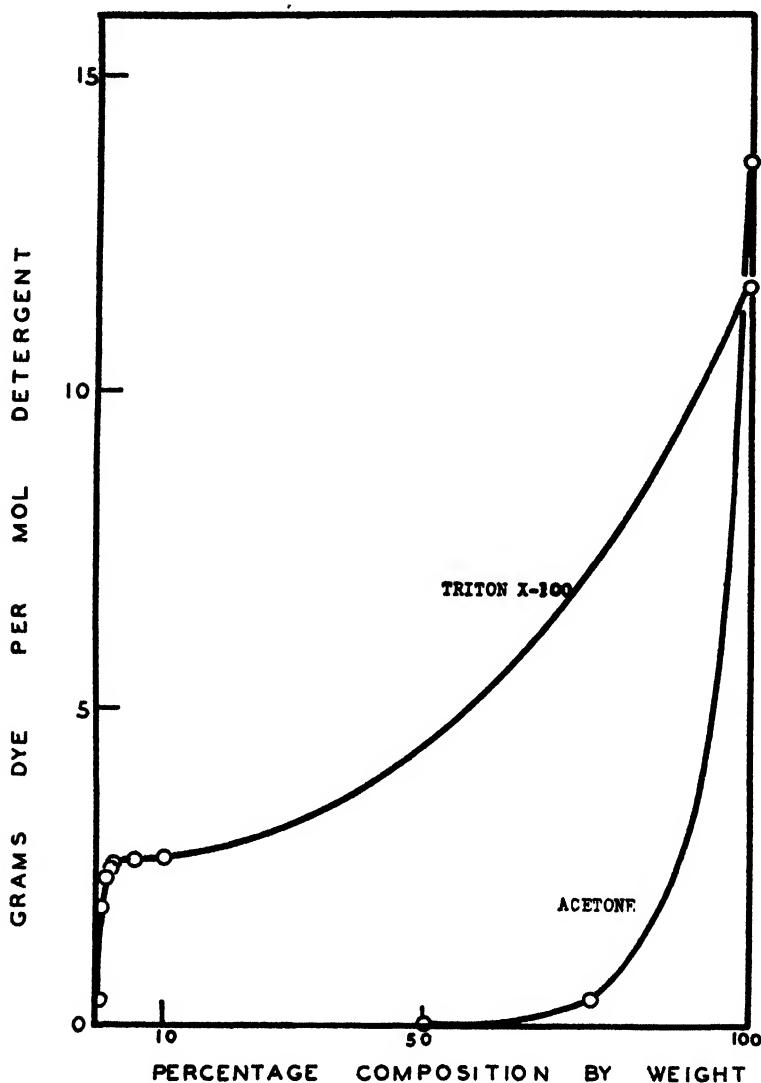


FIG. 7. Solubilization *versus* solvent action in solutions of Triton X-100 and acetone. Solubility of Orange OT in acetone from measurements by R. C. Merrill, Jr.

of detergent. This is shown in figure 7, with an extrapolated line for the intermediate compositions, many of which set into rigid gels. In this figure, the solubility of Orange OT in pure acetone and in aqueous solutions of acetone is also represented, in order to bring out the difference between the behavior of a solvent and of a solubilizer.

The solubilizing power of aqueous solutions of Triton X-100 indicates some kind of colloid formation. This is supported by unpublished measurements by Dr. Gonick in these laboratories. For example, one of these measurements showed that a 0.100 *m* solution, assuming the molecular weight to be 600, produced a freezing-point lowering in water solution of 0.032°, indicating a molecular weight of 3484, definite evidence of a high degree of association. Although solutions of Triton X-100 were found to be excellent solubilizers, a 2 per cent solution of carbowax, also a polyethylene oxide polymer, showed no solubilizing action on Orange OT, but exhibited instead a high foaming and flotation action.

TABLE 8

Effect of organic liquids on solubilization of Orange OT by 0.2 N potassium laurate

ADDED HYDROCARBON...	BENZENE	TOLUENE	HEXANE	ALCOHOL*	NONE
Amount of hydrocarbon in 25 cc. of solution, cc.	0.094	0.052	0.098	1.25	
Dye per 100 cc. of solution, milligrams..	27.50	29.25	33.50	17.50	20.46
Dye per mole of soap, grams	1.375	1.462	1.675	0.921	1.023
Molar ratio dye/soap $\times 10^3$	5.24	5.57	6.38	3.51	3.90
Molar ratio hydrocarbon/soap	0.21	0.098	0.15	4.28	

* Absolute ethyl alcohol.

TABLE 9

Solubility of Orange OT in the pure organic solvents

SOLVENT	MOLECULAR WEIGHT	d	MOLECULAR VOLUME	DYE PER 100 CC.	DYE PER MOLE	MOLAR RATIO DYE/SOLVENT $\times 10^3$
				grams	grams	
Benzene	78.11	0.879	88.9	62.5	5.55	21.2
Toluene.. . . .	92.13	0.866	106.4	65.0	6.92	26.4
Alcohol	46.07	0.789	58.4	2.725	0.16	0.61
n-Hexane	86.14	0.662	130.1	5.438	0.71	2.70

Effect of solvents on the solubilizing ability of soap solutions

It is a well-established fact (1, 7) that many organic liquids have a measurable solubility in soap solutions. In order to determine whether detergent solutions containing solubilized organic liquids are better or poorer solvents for a water-insoluble crystalline dye, the following measurements were made. The organic liquid was incorporated in 0.2 *N* potassium laurate solutions, in amounts in the case of hydrocarbons equal to 75 per cent of the saturation value determined by Richards (7). The dye was added to these clear solutions, and the saturation value determined in the usual manner (3). The results are given in table 8. Similar measurements were made with 0.1 *N* potassium oleate, and the same trends were observed. The solubility of the dye in the pure solvents themselves was determined and is recorded in table 9; the results brought out the fact that the variations apparent in table 8 were not due to actual solution of the dye in

the added solvent. Alcohol, a good solvent for the dye, caused a *decrease* in the solubilizing power of the soap solution. The hydrocarbons, which themselves are solubilized, caused a notable increase when present only in small amounts.

Solubilization by three sodium naphthenates

The following experiments were carried out in order to observe how naphthenate soaps of different molecular weights compared among themselves and with other detergents in the solubilization of Orange OT. The soaps were prepared by neutralizing with sodium hydroxide three fractions of naphthenic acids obtained from the Standard Oil Company of California. The acid numbers and the average equivalent weights of these fractions were determined by electro-

TABLE 10

Solubilization of Orange OT by three sodium naphthenates of different equivalent weights

CONCENTRATION OF NAPHTHENATE	LIGHT NAPHTHENATE (236.4 equivalent weight)			MEDIUM NAPHTHENATE (303 equivalent weight)			HEAVY NAPHTHENATE (334.9 equivalent weight)		
	Dye per 100 cc.	Dye per equivalent weight	Ratio $\times 10^3$	Dye per 100 cc.	Dye per equivalent weight	Ratio $\times 10^3$	Dye per 100 cc.	Dye per equivalent weight	Ratio $\times 10^3$
<i>N</i>	mg.	grams		mg.	grams		mg.	grams	
0.005	0			0.553	1.106	4.22*	0.775	1.55	5.91
0.01				1.53	1.53	5.83*	1.60	1.60	6.10
0.05	0.275	0.055	0.21	3.25	0.65	2.48	8.00	1.60	6.10
0.10	1.25	0.125	0.48	6.69	0.669	2.55	15.50	1.55	5.91
0.15	2.05	0.137	0.52						
0.20	3.25	0.163	0.62						
0.25	5.60	0.224	0.85	24.5	0.98	3.74	41.25	1.65	6.29
0.50	11.75	0.235	0.90	47.0	0.94	3.58	102.50	2.05	7.82
0.75	25.00	0.333	1.30						
0.99	35.68	0.361	1.38						
1.00				98.0	0.98	3.74			
1.27				132.5	1.047	4.91			

* Believed to include suspending action (3).

titration and were found to have the following equivalent weights: 214.4, 281.0, and 332.9. The procedure for the colorimetric determination of the dye had to be modified because of the color of the naphthenate solutions. The dye was extracted with benzene in the case of the naphthenate of lowest molecular weight. This procedure was unsatisfactory for the other two, owing to the formation of permanent emulsions which could not be broken conveniently by centrifuging. Hence, a colorimetric comparison of a dilution of the solution saturated with dye was made with the same dilution of the original solution. The results are given in table 10, and also shown graphically in figure 8. The solubilizing power of the naphthenates was found to increase very greatly with their equivalent weights, in a manner similar to the behavior of the soaps of the fatty acids (3, 4), but not in the same series. The naphthenates are not as

effective as the fatty acid soaps, since the naphthenate with the average equivalent weight of 303 has a saturation ratio of 3.74×10^{-3} at 0.25 *N*, which compares with 3.96×10^{-3} for 0.25 *N* potassium laurate, a soap of lower molecular weight (238.4). Hence the condensation of the saturated paraffin chain into rings decreases the solubilizing ability of the soap. There is an advantage, however, in the greater solubility of these sodium soaps, in that higher concentrations can be employed.

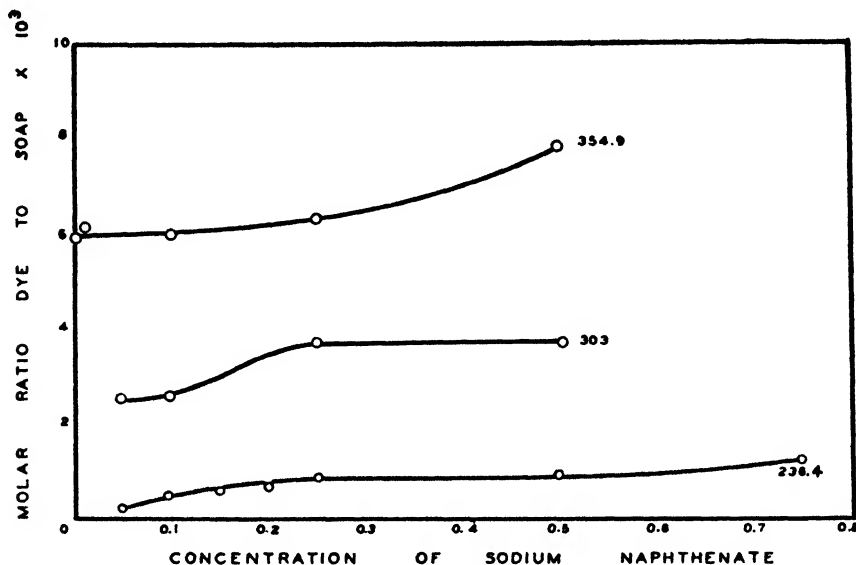


FIG. 8. Solubilization of Orange OT by three sodium naphthenates of different molecular weights.

Solubilization in benzene

Many detergents which are solubilizers in water have also been shown to be effective in other solvents (5). The following simple experiment was performed to show that the amount of methylene blue which can be solubilized by soap in benzene is much greater than that which could possibly be dissolved by the benzene in a colorless form (11). Excess methylene blue was agitated in thiophene-free benzene, and then allowed to stand for 20 hr. The dye settled, and half of the colorless upper portion, 20 cc., was then removed by pipet and placed in a second bottle. The same amount of sodium oleate, 0.05 g., was added to both bottles, which were then agitated for 24 hr. at 25°C. A blue-violet color developed in the first bottle, which contained the excess dye in contact with the benzene-soap solution; no color was visible in the bottle containing the benzene, which was removed from contact with the dye. A small amount of water extracted the color in its normal hue from the former, but remained colorless in the latter.

SUMMARY

A study has been made of the comparative effectiveness of potassium and sodium soaps as solubilizers. Measurements were made on potassium and sodium laurates and oleates. The sodium soaps were found to be better solubilizers for the water-insoluble dye 1-o-tolylazo-2-naphthol (Orange OT) per gram-molecular weight of soap.

Measurement of the solubilizing ability of the cation-active detergent, dodecylamine hydrochloride, showed it to be greater than that of the neutral anion-active detergents, the laurates, containing the same number of carbon atoms. Its effect is comparable to that of lauryl sulfonic acid, which was re-investigated in order to obtain a complete curve over its entire range of solubility at 25°C.

The solubilizing power of the non-ionic detergent, Triton X-100, was studied, and the similarity of its solubilization curve to that of the colloidal electrolytes indicated the highly colloidal nature of its water solutions. Its solubilizing power per unit weight of detergent in a 10 per cent solution is only about one-fourth its solvent power for the dye in anhydrous form.

The effect of simultaneously solubilized organic liquids on the solubilization of a dye was found to be dependent on the nature of the added liquid. Benzene, toluene, and *n*-hexane in small amounts were found to increase the solubilization of the dye from 30 to 50 per cent (synergistic effect); 5 per cent ethyl alcohol was found to decrease it (antergistic effect), although anhydrous alcohol itself is a good solvent for the dye.

The relative solubilizing abilities of three sodium naphthenates of different molecular weights were measured. They varied with their equivalent weight, the higher having very much the greater solubilizing power for the dye. Compared with the fatty acid soaps of similar molecular weights, the naphthenates are not as effective as solubilizers, but they have a higher range of solubility.

REFERENCES

- (1) MCBAIN, JAMES W.: "Solubilization and Other Factors in Detergent Action," in *Advances in Colloid Science*, E. O. Kraemer (Editor), Vol. I, pp. 99-142. Interscience Publishers, Inc., New York (1942).
- (2) MCBAIN, JAMES W., AND BOLDUAN, O. E. A.: *J. Phys. Chem.* **47**, 94 (1943).
- (3) MCBAIN, JAMES W., AND GREEN, SISTER AGNES ANN: *J. Am. Chem. Soc.* **68**, 1731 (1946).
- (4) MCBAIN, JAMES W., AND JOHNSON, K. E.: *J. Am. Chem. Soc.* **66**, 9 (1944).
- (5) MCBAIN, JAMES W., MERRILL, R. C., JR., AND VINOGRAD, J. R.: *J. Am. Chem. Soc.* **62**, 2880 (1940).
- (6) MCBAIN, JAMES W., MERRILL, R. C., JR., AND VINOGRAD, J. R.: *J. Am. Chem. Soc.* **63**, 670 (1941).
- (7) MCBAIN, JAMES W., AND RICHARDS, PAUL H.: *Ind. Eng. Chem.* **38**, 642 (1946).
- (8) MCBAIN, M. E. LAING: *J. Phys. Chem.* **47**, 196 (1943).
- (9) MCBAIN, M. E. L., DYE, W. B., AND JOHNSON, S. A.: *J. Am. Chem. Soc.* **61**, 3210 (1939).
- (10) NOLLER, CARL R., AND GORDON, J. J.: *J. Am. Chem. Soc.* **55**, 1090 (1933).
- (11) PALIT, S. R.: *Nature* **153**, 317 (1944).
- (12) RALSTON, A. W., HOERR, C. W., AND HOFFMAN, E. J.: *J. Am. Chem. Soc.* **64**, 97 (1942).
- (13) VOLD, ROBERT D., AND MONTGOMERY, REBA: Communication from the University of Southern California, 1945.

THE ELECTROCHEMISTRY OF PERMSELECTIVE COLLODION MEMBRANES. II

EXPERIMENTAL STUDIES ON THE CONCENTRATION POTENTIAL ACROSS VARIOUS TYPES OF PERMSELECTIVE COLLODION MEMBRANES WITH SOLUTIONS OF SEVERAL ELECTROLYTES¹KARL SOLLNER AND HARRY P. GREGOR²*Department of Physiology, University of Minnesota, Minneapolis 14, Minnesota**Received August 8, 1946*

I

In the first paper (17) of this series a study was made of the rates at which final stable concentration potentials with various electrolytes are established across several types of permselective collodion membranes. The present paper is an experimental study of the final concentration potentials established by various electrolytes at different concentrations across several types of permselective collodion membranes. All measurements reported in this paper represent final and stable potential values.

The concentration potential across a membrane is a function of the nature, the concentration ratio, and the absolute concentrations of the electrolyte solutions separated by that membrane. In a systematic investigation it is therefore necessary to measure the concentration potentials arising with a variety of electrolytes at several concentration levels. With the exception of the cases in which ideal ionic membrane selectivity prevails, the latter is strictly defined only with concentration ratios which differ infinitesimally from unity. In experimental work the concentration ratio of the two solutions, therefore, should be as small as practicable; following an established procedure (6, 7, 8, 9, 12, 16) the concentration ratio 1:2 was used in the present investigation.

II

The significance and the physical meaning of experimental concentration potentials measured across ion-selective membranes can be visualized only by reference to the theoretical limits within which the properties of real membranes are confined.

With membranes of high ionic selectivity by far the more important of these limits is the (calculated) potential, E_{\max} , which would arise if the membrane behaved under a given set of conditions as an ideal membrane for the reversible transfer of the critical ion. The critical ion in the case of electronegative membranes such as collodion membranes is the cation. The non-critical ion (the anion in the present case) is assumed to contribute nothing to the transport of electricity across the membrane; the concentration potential is defined only by the activities of the critical ion at the two sides of the membrane.

¹ Presented at the Twentieth National Colloid Symposium, which was held at Madison, Wisconsin, May 28-29, 1946.

² Present address: Polytechnic Institute of Brooklyn, Brooklyn 2, New York.

The other limit is the potential which would arise across a membrane which does not show any ion selectivity of its own; this lower limit therefore is the liquid junction potential E_l arising from free, unhindered diffusion in the absence of any membrane. This criterion is of particular interest where a low degree of ionic selectivity of the membrane prevails.

The two limiting values of the concentration potential can be calculated with considerable accuracy from available data.

The calculations of the *theoretically possible maximum values of the concentration potential*, E_{\max} , are based on the general equation

$$E_{\max} = \frac{RT}{z_+ F} \ln \frac{a_+^{(2)}}{a_+^{(1)}} \quad (1)$$

z_+ being the valency of the critical ion and $a_+^{(1)}$ and $a_+^{(2)}$ its activities $c_+^{(1)} \cdot \gamma_+^{(1)}$ and $c_+^{(2)} \cdot \gamma_+^{(2)}$ in the two solutions. In the case of uni-univalent electrolytes, the mean activity coefficients were used ($a_+ = a_{\pm}$). With the uni-bivalent electrolyte potassium sulfate the activity coefficient for the critical ion, the potassium ion, is calculated assuming that the activity coefficient of a given ion is determined only by the total ionic strength of the solution, s ($s = \frac{1}{2} \sum c_i z_i^2$). Then γ_{K^+} in a solution of potassium sulfate is the same as γ_{K^+} in a potassium chloride solution having the same ionic strength. The individual ion-activity coefficient of the potassium ion, γ_{K^+} , in solutions of potassium chloride is equal to the mean activity coefficient γ_{KCl} .³

The majority of the numerical values necessary for these calculations were taken preferentially from Harned and Owen (3), MacInnes (5), and the *International Critical Tables* (4), intermediate data being interpolated graphically.

The maximum concentration potential can be calculated with considerable accuracy. The probable error in the case of potassium chloride and lithium chloride is undoubtedly considerably smaller than the accuracy of our experimental determinations. Although the calculated values in the case of potassium sulfate and hydrochloric acid may contain some small systematic error, it seems safe to assume that it is insignificant compared with the accuracy and reproducibility of the experimental data which are reported below.

The potential arising from diffusion in free solution, that is, the liquid-junction potential c_2/c_1 , was calculated from the equation

$$E_{l(\text{calc})} = \frac{t_+}{z_+} \frac{RT}{F} \ln \frac{a_+^{(2)}}{a_+^{(1)}} - \frac{t_-}{z_-} \frac{RT}{F} \ln \frac{a_-^{(2)}}{a_-^{(1)}} \quad (2)$$

where $E_{l(\text{calc})}$ is the liquid-junction potential, t_+ and t_- the transference numbers of cation and anion within the membrane, $a_+^{(1)}$ and $a_+^{(2)}$ the single ion activities of the cations, and $a_-^{(1)}$ and $a_-^{(2)}$ the single ion activities of the anions in the solutions (1) and (2).

³ For example, a 0.01 *M* potassium sulfate solution, the ionic strength of which is 0.03, has the same γ_{K^+} as a potassium chloride solution of ionic strength 0.03, the concentration of the latter solution being 0.03 *M*. The γ_{K^+} of a 0.03 *M* potassium chloride solution is 0.848; therefore the γ_{K^+} in a 0.01 *M* potassium sulfate solution is assumed to be 0.848.

For uni-univalent electrolyte we assumed $a_+ = a_- = a_{\pm}$. Since $t_+ + t_- = 1$, equation 2 becomes

$$E_{l(\text{calc})} = (2t_+ - 1) \frac{RT}{F} \ln \frac{a_+^{(2)}}{a_+^{(1)}} \quad (3)$$

In the case of the uni-bivalent electrolyte potassium sulfate, it is necessary to use equation 2 and the single ion activities defined and calculated respectively as described farther above.

The numerical values of t_+ were taken preferentially from the before-mentioned reference tables.⁴

The accuracy of the computed $E_{l(\text{calc})}$ values is probably about as high as the accuracy and reproducibility of most of our corresponding measurements. With electrolytes other than potassium chloride, systematic errors of at least 0.10 millivolt may occur.

III

The degree of the ionic selectivity of the permselective collodion membranes is so great and the accuracy and reproducibility of the measured concentration potentials is so high that the full value of the assembled experimental data cannot be utilized unless proper corrections are made for the asymmetry of the two liquid-junction potentials potassium chloride–agar bridge | electrolyte c_1 and electrolyte c_2 | potassium chloride–agar bridge. The customary neglect of these corrections is not justified in the case of the permselective membranes.⁵

The best way to eliminate this difficulty would consist in the outright experimental elimination wherever possible of the two doubtful liquid-junction potentials by the use of specific reversible electrodes, such as the Ag | AgCl or the Hg | Hg₂SO₄ electrodes. (In cases where such specific electrodes are available their use seems indicated in further work.) For the present investigation we had recourse to the following method which, although not completely free from objections, seems to be sufficiently satisfactory for the purpose on hand, no corrections being attempted in the case of potassium chloride.

The electromotive forces $E_{l(\text{exp})}$ were measured which arise in diffusion chains without membranes which were otherwise identical with those used for the measurement of the concentration potentials across membranes. These experimental values of the liquid-junction potential $E_{l(\text{exp})}$ were compared with the corresponding calculated values of the liquid-junction potentials $E_{l(\text{calc})}$, and the difference between these two values is taken as the correction.

⁴ Equations 2 and 3 assume that the transfer numbers are independent of concentration. This assumption, as can be seen from the last column of table 1, is not quite correct. Therefore in calculating the liquid-junction potential, values of t_+ were used which correspond to the mean concentration of each concentration ratio.

⁵ We also feel that the introduction of this correction in many of the published data on membrane potentials with electrolytes other than potassium chloride would bring these data more closely in line with one another and also into better agreement with theoretical considerations.

If an experimental value was, e.g., lower than the calculated one, the difference had to be added to the measured concentration potential across a membrane in order to arrive at the corrected, true value of the latter. All data referring to the concentration potentials ϵ across membranes which are given in table 1 are corrected in this manner.

IV

The technique used for the measurement of the concentration potential ϵ across the membranes was the same as that described in the preceding paper: saturated calomel electrode | potassium chloride saturated | saturated potassium chloride-agar bridge | electrolyte c_2 | membrane | electrolyte c_1 | saturated potassium chloride-agar bridge | potassium chloride saturated | saturated calomel electrode.

In all instances the final stable concentration potentials ϵ were determined with all the precautions discussed in the preceding paper.

As in the case of the rate experiments (17), the membranes prior to the measurements had been aged by about 3 days' immersion in 0.1 *N* potassium chloride solutions. Occasional repetitions of previously made determinations which were interspersed between later experiments showed that the membranes did not undergo any detectable change in the course of the various consecutive experimental series.

The electrolytes used were potassium chloride, lithium chloride, potassium sulfate, and hydrochloric acid. The investigated concentration ranged from 0.002 *N*/0.001 *N* to 0.4 *N*/0.2 *N*.

In addition to the three types of membranes Ox 8 — Hum 43, Ox 12 — Hum 43 and Ox 10 — Hum 43 — Alc 65 for which the time studies on the concentration potential have been reported (17), membrane Ox 14 — Hum 58 has also been used in the present work.

All measurements reported below in table 1 for one type of membranes were performed successively with a single membrane, except in one case (Ox 14 — Hum 58) where the original membrane broke accidentally and had to be replaced by a second specimen which, as shown by repeat experiments, had within the limits of experimental error the same properties as the original one.

The reproducibility of the measurements was about ± 0.10 millivolt, except in the case of the highest concentrations of hydrochloric acid where the error may be as high as 0.30 millivolt. In this latter case the measurable potential changes appreciably with time when the potassium chloride-agar bridges are inserted in the solutions, so that here the error may be quite significant.⁶

To determine the liquid-junction potential $E_{l(\text{exp})}$ the membrane-free chains: saturated calomel electrode | potassium chloride saturated | saturated potassium chloride-agar bridge | electrolyte c_2 | electrolyte c_1 | saturated potassium

⁶ The instability of the concentration potential in this case is of course not due to a lack of definition of the situation at the membrane, but to a lack of stability of the two liquid-junction potentials: saturated potassium chloride-agar bridge | electrolyte c_2 and saturated potassium chloride-agar bridge | electrolyte c_1 . The same difficulty, of course, arises also when the liquid-junction potential $E_{l(\text{exp})}$ without a membrane is measured.

chloride-agar bridge | potassium chloride saturated | saturated calomel electrode were measured for all the electrolytes at the same concentrations as were used with the membranes. A simple W-shaped tube with the glass stopcock in the middle proved satisfactory for these measurements. Otherwise the instruments used and the technique employed were the same as were used for the determination of the concentration potentials across membranes.

At medium and higher concentrations the measurements were reproducible within about 0.10 millivolt, except at the highest concentration of hydrochloric acid. At the lowest concentrations the resistance of the system was too high for best performance of the potentiometer used; $E_{l(\text{exp})}$ was difficult to measure with the usual accuracy and the errors may be greater than 0.10 millivolt in some instances.

In table 1 below are given the values of the liquid-junction potential, $E_{l(\text{exp})}$, as measured in the manner outlined, together with the corresponding calculated values, $E_{l(\text{calc})}$, and their differences Δ , the correction which must be applied to the experimentally determined value of the concentration potential.

Table 1 gives for four different electrolytes the following experimental and calculated data at the temperature $25.00^\circ\text{C.} \pm 0.05^\circ$. Column 1 presents the concentrations c_2 and c_1 of the electrolyte solutions used in equivalents per liter; column 2 gives the theoretically possible maximum value of the concentration potential E_{max} calculated as outlined in the preceding section; columns 3, 4, 5, and 6 present the concentration potentials ϵ across the various membranes corrected as outlined above; column 7a gives the calculated liquid-junction potential $E_{l(\text{calc})}$ which would arise in free solution, computed as indicated before; column 7b gives the liquid-junction potential $E_{l(\text{exp})}$ as measured; column 7c gives Δ , the difference between 7a and 7b, which has been applied to the figures given in columns 3, 4, 5, and 6.

The data presented in table 1 are given in figure 1 in the form of graphs to facilitate their visualization and evaluation.

Following a previously established convention (6, 12, 16) the concentration c_1 indicated in the graphs refers to the more dilute solution;⁷ plotted in this man-

⁷ The conventional plot of concentration potentials against the lower concentration is arbitrary. This procedure involves an appreciable error unless the concentration ratios used closely approach the 1:1 ratio. The physical properties of the membranes which are represented by the experimental data correspond to a concentration which lies somewhere between the two concentrations used. The use of the mean concentration for reference value, which was suggested by Michaelis (7, 8, 9), unfortunately has not been accepted by the later investigators.

The mean concentration, although a better choice than the lower concentration, is, however, not necessarily the correct reference concentration; the latter can be assumed to lie nearer to the more dilute concentration (1).

With a 2:1 concentration ratio of the two solutions the error which is introduced by the conventional assumptions is not too great for the purpose at hand; the curves in figure 1 under no circumstances could require a shift of more than $\frac{1}{4} \log 2$ (this is 0.15 unit) to the left.

For the comparison of the different membranes and various electrolytes the arbitrary selection of c_1 as the reference concentration is of course inconsequential.

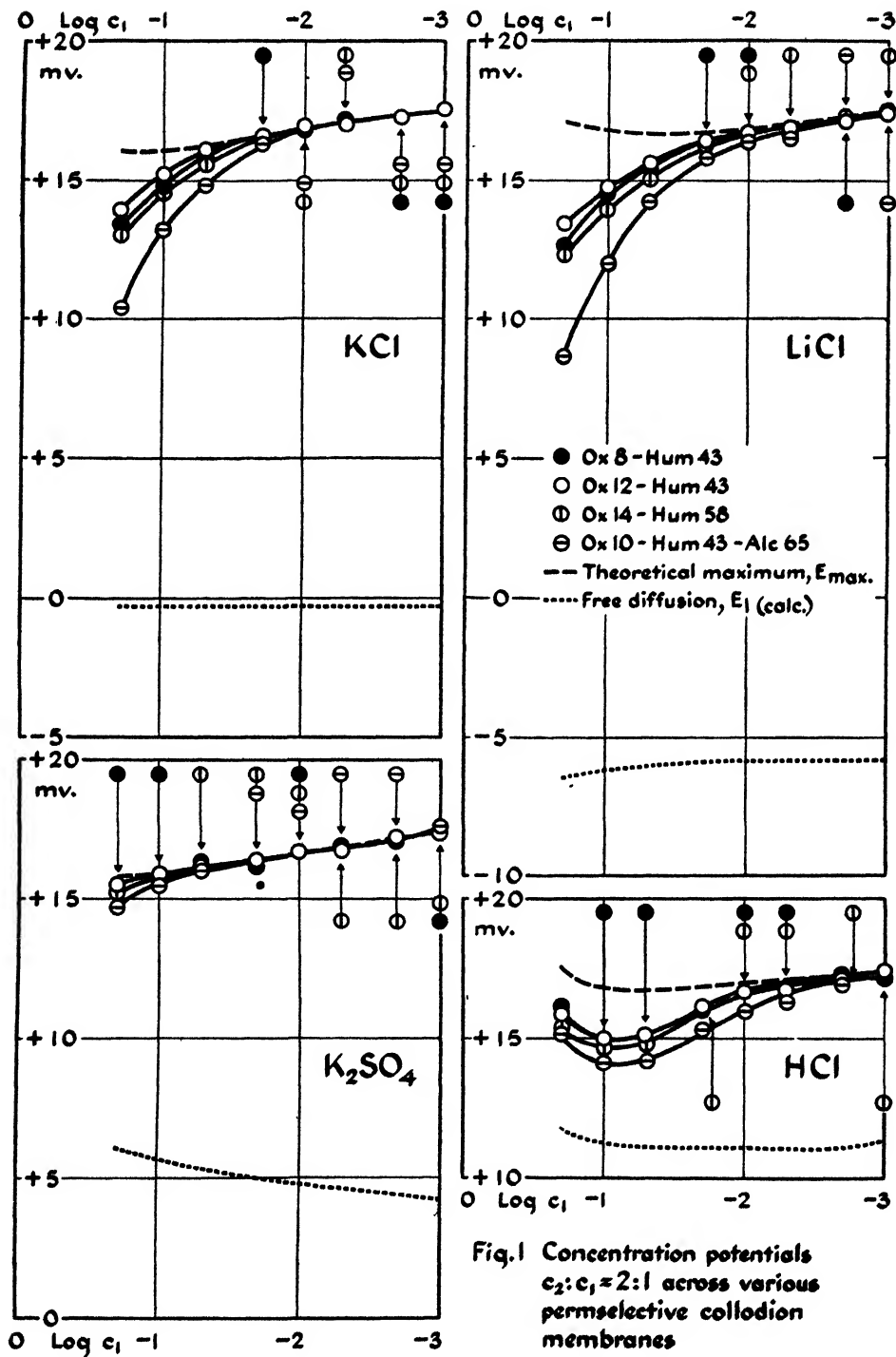


Fig.1 Concentration potentials $c_2:c_1=2:1$ across various permselective collodion membranes

TABLE 1

Concentration potentials E ($c_2:c_1 = 2:1$) of several electrolytes across various permselective collodion membranes

1	2	3	4	5	6	7a	7b	7c
CONCENTRATION OF ELECTROLYTE	THEORETICAL MAXIMUM	MEMBRANE Ox 8 — Hum 43	MEMBRANE Ox 12 — Hum 43	MEMBRANE Ox 14 — Hum 58	MEMBRANE Ox 10 — Hum 43 — Alc 65	DIFFUSION POTENTIAL E_I IN FREE SOLUTION		
$c_2:c_1$	E_{max}	ϵ	ϵ	ϵ	ϵ	E_I (calculated)	E_I (experimental)	Δ

A. Potassium chloride

equiv./liter	m.v.	m.v.	m.v.	m.v.	m.v.	m.v.	m.v.	m.v.
0.002/0.001	17.5	17.5	17.5	17.5	17.5	-0.3		nil
0.004/0.002	17.3	17.3	17.3	17.3	17.3	-0.3		nil
0.01/0.005	17.1	17.1	17.0	17.1	17.1	-0.3		nil
0.02/0.01	16.9	16.9	17.0	16.9	16.9	-0.3		nil
0.04/0.02	16.6	16.6	16.6	16.5	16.4	-0.3		nil
0.1/0.05	16.3	16.0	16.1	15.6	14.8	-0.3		nil
0.2/0.1	16.1	14.8	15.2	14.5	13.2	-0.3		nil
0.4/0.2	16.0	13.4	13.9	13.0	10.4	-0.3		nil

B. Lithium chloride

	m.v.	m.v.	m.v.	m.v.	m.v.	m.v.	m.v.	m.v.
0.002/0.001	17.5	17.5	17.4	17.5	17.4	-5.8	-5.7	-0.1
0.004/0.002	17.3	17.1	17.1	17.2	17.2	-5.8	-5.7	-0.1
0.01/0.005	17.1	16.7	16.9	16.9	16.6	-5.8	-5.6	-0.2
0.02/0.01	16.9	16.7	16.7	16.7	16.4	-5.8	-5.6	-0.2
0.04/0.02	16.7	16.4	16.4	16.3	15.8	-5.9	-5.5	-0.4
0.1/0.05	16.5	15.4	15.6	15.0	14.2	-6.0	-5.4	-0.6
0.2/0.1	17.0	14.5	14.7	13.9	12.0	-6.3	-5.1	-1.2
0.4/0.2	16.9	12.6	13.4	12.3	8.7	-6.5	-4.7	-1.8

C. Potassium sulfate

	m.v.	m.v.	m.v.	m.v.	m.v.	m.v.	m.v.	m.v.
0.002/0.001	17.4	17.4	17.4	17.4	17.5	4.2	4.2	0.0
0.004/0.002	17.1	17.1	17.2	17.1	17.2	4.4	4.3	+0.1
0.01/0.005	16.9	16.9	16.8	16.8	16.9	4.6	4.5	+0.1
0.02/0.01	16.7	16.7	16.7	16.7	16.6	4.8	4.6	+0.2
0.04/0.02	16.4	16.2	16.4	16.4	16.4	5.0	4.8	+0.2
0.1/0.05	16.1	16.2	16.1	16.2	16.0	5.4	4.9	+0.5
0.2/0.1	15.9	15.9	15.9	15.7	15.5	5.7	5.0	+0.7
0.4/0.2	15.8	15.5	15.5	15.2	14.7	6.1	5.1	+1.0

D. Hydrochloric acid

	m.v.	m.v.	m.v.	m.v.	m.v.	m.v.	m.v.	m.v.
0.002/0.001	17.4	17.2	17.4	17.2	17.3	11.3	11.3	0.0
0.004/0.002	17.3	17.2	17.1	17.1	17.0	11.2	11.2	0.0
0.01/0.005	17.1	16.8	16.8	16.8	16.3	11.1	11.1	0.0
0.02/0.01	17.0	16.7	16.7	16.7	16.0	11.1	10.6	+0.5
0.04/0.02	16.8	16.1	16.2	16.1	15.3	11.0	10.2	+0.8
0.1/0.05	16.8	15.1	15.1	14.8	14.2	11.1	9.8	+1.3
0.2/0.1	16.8	15.0(?)	15.0(?)	14.6(?)	14.1(?)	11.1	9.0(?)	+2.2(?)
0.4/0.2	17.6	16.0(?)	15.9(?)	15.4(?)	15.2(?)	11.8	8.0(?)	+3.8(?)

ner the data become easily comparable to many analogous data published in the literature.

In many instances the experimental concentration potentials obtained with different membranes and the same electrolyte coincide. In order to make the graphic representation of these points feasible, the expedient has been chosen in figure 1 of plotting some of the points not in their proper position but of arranging them outside the curves and indicating their proper position by arrows.

V

The first impression one gains when looking at the data of table 1 and figure 1 is that of their high degree of regularity and consistency. In the subsequent publication an attempt will be made to apply to these data two kinds of objective quantitative considerations, one of these already used in principle by Michaelis (7, 8, 9, 10), the other one developed to utilize fully for the elucidation of membrane action the experimental data given here. In the present paper we shall evaluate these data merely in the conventional qualitative and semiquantitative manner.

The criterion for this is the difference between the calculated theoretically possible maximum values E_{\max} and the corresponding experimental concentration potentials ϵ . The greater the difference between two corresponding such values, the lower is the "ionic selectivity" of a membrane under the particular conditions.

When considering the data presented in table 1 and figure 1 the emphasis may be placed on the one hand on the comparison between the different membranes; on the other hand, one may focus one's attention on the differences between the various electrolytes.

With regard to the former problem it is evident that with the lowest concentrations used all membranes behave as ideal—at least within the limits of experimental error. The differences between the various membranes become apparent in the differences of the concentrations at which a significant deviation of the experimental from the calculated concentration potential can be observed. The disparity between the membranes of the various types is most pronounced with the highest concentrations investigated, except in the case of hydrochloric acid, which shows a peculiar behavior (see below).

Any comparison therefore has to be based preferentially on the results obtained with the medium high and the highest concentrations.

Although the concentration potentials across membranes Ox 8 — Hum 43 and Ox 12 — Hum 43 coincide with both potassium sulfate and hydrochloric acid within the limits of experimental error,⁸ the ionic selectivity of the membranes follows the sequence: membrane Ox 12 — Hum 43, Ox 8 — Hum 43, Ox 14 —

⁸ This observation probably is explained by the fact that on the one hand membrane Ox 8 — Hum 43 is less highly oxidized than membrane Ox 12 — Hum 43, and on the other hand it is of lesser porosity; these two antagonistic factors seem to compensate each other within the limits of experimental error.

Hum 58, Ox 10 — Hum 43 — Alc 65, the latter membrane having the lowest degree of ionic selectivity. This sequence of ionic selectivities of the different membranes is identical with that found previously (2) with 0.1 *N* potassium chloride/0.01 *N* potassium chloride.

One may turn now to the other part of the conclusions which can be drawn from the data presented in table 1 and figure 1—namely, a comparison of the effects which are observed with the solutions of various electrolytes.

For a detailed comparison of the various electrolytes one must keep in mind the limits of the accuracy of the calculated as well as of the experimental data. Some discretion must be used not to transgress the inherent limits of the usefulness of these values in any attempt to establish minor differences between various electrolytes. Differences between calculated and experimental concentration potentials of ± 0.20 millivolt can hardly be taken as significant; discrepancies of this magnitude may easily be due to a combination of limited experimental accuracy and systematic error in the computation and correction methods used. For this reason any conclusions which are drawn with respect to the differences of behavior of different electrolytes should be based primarily on the trend of the curves over wide concentration ranges and on the data obtained with higher (> 0.05 *N*) concentrations.

It is immediately evident from table 1 and figure 1 that the agreement between the calculated and the experimental concentration potentials is best with potassium sulfate. In other words, the ionic selectivity of the membranes is highest in this case, far surpassing that observed with the other electrolytes. The ionic membrane selectivity with potassium chloride, while being considerably less than with potassium sulfate, is decidedly greater than with lithium chloride. The behavior of hydrochloric acid deviates from that of the neutral salts potassium chloride and lithium chloride, in that the membrane selectivity is not quite as high at medium concentrations as with the neutral salts; at the highest concentrations, on the contrary, the selectivity of the membrane in the case of hydrochloric acid is higher than with potassium chloride and lithium chloride.

With the membrane of the highest ionic selectivity reported on in this paper (membrane Ox 12 — Hum 43), ideal ionic selectivity within the limits of the error of experiments and computations is observed with potassium sulfate at all concentrations up to 0.2/0.1 *N*; with potassium chloride, lithium chloride, and hydrochloric acid this limit is approximately 0.04/0.02, 0.02/0.01, and 0.004/0.002, respectively. With the membranes of lesser ionic selectivity these figures are correspondingly lower, but even with the alcohol-swelled membrane Ox 10 — Hum 43 — Alc 65 ideal ionic selectivity exists with potassium sulfate up to a concentration of 0.1/0.05 *N*.

These results, generally speaking, are in agreement with the concept put forward by Michaelis (7) that electrical and steric pore blocking account for the characteristic ionic selectivity of membranes of porous character.

According to the theory which has been stated of late more precisely (6, 11, 12, 13, 16, 18), the electrochemical structure of an electronegative membrane is due to the presence of an essentially constant number of anionic groups perma-

nently built into the walls of the pores of the membranes; these groups, carboxyl groups in the case of collodion membranes (6, 11, 12, 14, 15, 16), are compensated for electrically by the same species of cations as that present in the adjacent solutions. Since the "degree of dissociation" of these surface compounds does not vary appreciably with the different alkali ions, the electrical situation at the pore walls is very similar in the various neutral electrolyte solutions.⁹

In acid solution the surface carboxyl groups are combined with hydrogen ions as counter ions; the resulting free carboxylic acids cannot be expected to act like strong electrolytes. The electrochemical structure of the membranes in acid solution, at all concentrations except perhaps the very lowest, therefore, must be expected to differ considerably from that existing with fair uniformity in all neutral solutions where the acidic (anionic) surface groups with their counter ions, K^+ or Li^+ , act as strong electrolytes (16).

Let us consider now in the light of the above-outlined theory the results obtained with the various electrolytes, focussing our attention first on the neutral salts.

In the case of potassium sulfate, the electrical and the steric blocking reinforce one another. The sulfate ion is prevented from penetrating the membrane both on account of its size and on account of the electric repulsion which arises between the fixed negative groups at the pore walls and its two negative charges. On account of its double charge alone the sulfate ion would be screened out much more effectively than ions which carry single charges only, such as the chloride ion.

With potassium chloride the steric factor does not play an important rôle, since potassium and chloride ions have very nearly the same size; only the electric factor of pore blocking is operative. In the case of lithium chloride the steric factor of pore blocking on account of the greater size of the hydrated lithium ion results in a lower degree of ionic selectivity of the membrane as compared with potassium chloride; certain pathways across the membrane which are accessible on a purely steric basis to potassium and chloride ions are inaccessible to the lithium ion.

The behavior of the membranes with hydrochloric acid cannot be interpreted in the same straightforward manner as that of the neutral salts. On the basis of steric considerations only, one would expect that the hydrogen ion would go particularly easily across the membrane; in other words, one would expect the situation to be somewhat similar to that observed with potassium sulfate, where the cation is much smaller than the anion. This, however, is obviously not the case; the different electrochemical structure (and its dependence upon concentration) which prevails in acid solution must be considered. The lower degree of dissociation of the electrochemically active surface compounds within acid solution results in an electrochemical structure of the membrane under considera-

⁹ Some pores of a membrane for geometrical reasons may not be available for the one or the other species of ions of an electrolyte; nevertheless, those critical acidic (anionic) wall groups which are operative are compensated for electrically by the cation of the electrolyte under consideration.

tion which is analogous to that prevailing in neutral solution with membranes having a smaller surface concentration of potentially dissociable anionic groups; for the case of the collodion membrane this means that the behavior of a highly oxidized membrane in acid solution is similar to that shown in neutral solution by less highly oxidized membranes.

The above-outlined explanation of membrane behavior in acid solution cannot, as it seems, be applied to the highest acid concentrations for which data are available if the latter are taken at their face value. At the highest acid concentrations used the membrane selectivity is slightly greater than at lower concentrations. An explanation of this latter observation is still missing. It may possibly be due to a systematic error in the measurement or the computation of the liquid-junction potential (or a combination of these two factors) which was used as a correction for the measured empirical values of the concentration potential. However, there is no proof that this situation really prevails. It is equally possible that some unknown physical factor causes the apparent anomaly. Only further experiments will permit a decision regarding this question.¹⁰

The concentration range of useful highest ionic selectivity of these membranes can be expanded to an appreciable extent beyond that indicated in table 1 and figure 1 by keeping the concentration at the one side of the membrane fairly low, e.g., ten or one hundred times lower than that of the more concentrated solution. With this precaution the membrane selectivity as determined by potential measurements can be fully satisfactory with electrolyte concentrations considerably higher than is indicated by the above presented experimental data with the 2:1 concentration ratio. This fact is well known from measurements with the 10:1 concentration ratio of the characteristic concentration potential 0.1 *N* potassium chloride/0.01 *N* potassium chloride and analogous measurements with other electrolytes.

The higher degree of membrane selectivity observed under these conditions can be explained in the following manner. The permselective collodion membranes are relatively thick, about 40 μ . When one side of the membrane is in contact with a sufficiently dilute solution, an adjacent layer of the membrane retains a very high degree of ionic selectivity. This layer of the membrane is not greatly influenced by the presence of a relatively concentrated solution on the other side of the membrane, although the layer of the membrane which is in immediate contact with this solution may show a somewhat impaired degree of ionic selectivity.

As was pointed out above, all the potential measurements and calculated

¹⁰ In this connection it is interesting to note that Michaelis, Ellsworth, and Weech (8) with membranes much denser than the permselective membranes have found a much higher membrane selectivity with hydrochloric acid than with the alkali halides, the investigated concentration range being from 0.02 *N*/0.01 *N* to 0.16 *N*/0.08 *N*. A final explanation of this discrepancy between the results of the above-mentioned authors and our own data is still lacking. It probably has to be looked for in the much smaller size of the majority of the pores of the membranes used by Michaelis and collaborators. As will be shown in a later paper, a similar discrepancy exists between the two sets of data in the case of the membrane resistance.

potential values dealt with in this paper have a definite limitation in significance. Each individual calculated or experimental potential value has a probable error of 0.10 millivolt; in a few instances even more. Although this situation is somewhat ameliorated by the fact that the consistent trend of curves has a greater significance than the individual numerical values, small deviations of the membranes from ideal selectivity, small differences between different membranes, and minor differences between different electrolytes can better be established by methods other than direct potential measurements. As such methods one may mention the combination of "leak" (2) and resistance (2) measurements, studies on the transfer of ions in an electric field across the membranes (7, 10), studies of both the rates of cation *and* anion exchange across the membranes, carried out preferentially with tracer elements¹¹ and others.

SUMMARY

1. Concentration potentials of potassium chloride, lithium chloride, hydrochloric acid, and potassium sulfate solutions across several types of permselective collodion membranes were measured at several concentration levels between 0.001 *N* and 0.4 *N*, the concentration ratio being 2:1.

2. The experimentally obtained concentration potentials are compared with the calculated values of the concentration potentials which would arise with membranes of ideal ionic selectivity, in other words, with the potential which would originate if the membranes would act as ideal reversible electrodes for the critical (cat)ion.

3. The agreement between the calculated and the experimental concentration potentials in all instances is closest with the more dilute solutions. With the membrane of the highest ionic selectivity reported on in this paper (membrane Ox 12 — Hum 43), ideal ionic selectivity within the limits of the error of the experiments and computations ± 0.2 millivolt is observed with potassium sulfate at all concentrations up to 0.2/0.1 *N*; with potassium chloride, lithium chloride, and hydrochloric acid this limit is approximately 0.04/0.02, 0.02/0.01, and 0.004/0.002, respectively. With the membranes of lesser ionic selectivity these figures are correspondingly lower.

4. The results are in agreement with the fixed-charge theory as applied to membranes of porous character. Also, the existing differences in behavior between neutral electrolytes on the one side and hydrochloric acid on the other side can be explained essentially on the basis of this theory, by reference to the changed electrochemical structure of the membranes in acid solution owing to a lower degree of dissociation of the electrically active surface compounds.

REFERENCES

- (1) GREGOR, H. P.: Ph. D. Thesis, University of Minnesota, 1945.
- (2) GREGOR, H. P., AND SOLLNER, K.: *J. Phys. Chem.* **50**, 53 (1946).
- (3) HARNED, H. S., AND OWEN, B.: *The Physical Chemistry of Electrolyte Solutions*. Reinhold Publishing Corporation, New York (1943).

¹¹ The reasons for this latter restriction will become apparent in a forthcoming paper on the bi-ionic potential.

- (4) *International Critical Tables*, Vol. VI. McGraw-Hill Book Company, Inc., New York (1929).
- (5) MACINNES, D. A.: *The Principles of Electrochemistry*. Reinhold Publishing Corporation, New York (1943).
- (6) MEYER, K. H., AND STEVERS, J.-F.: *Helv. Chim. Acta.* **19**, 649, 665 (1936).
MEYER, K. H. *Trans. Faraday Soc.* **33**, 1073 (1937).
- (7) MICHAELIS, L.: *Bull. Natl. Research Council*, No. **69**, 119 (1929), *Kolloid-Z.* **62**, 2 (1933).
- (8) MICHAELIS, L., ELLSWORTH, R. McL., AND WEECH, A. A.: *J. Gen. Physiol.* **10**, 671 (1927).
- (9) MICHAELIS, L., AND WEECH, A. A.: *J. Gen. Physiol.* **11**, 147 (1927).
- (10) MICHAELIS, L., WEECH, A. A., AND YAMATORI, A.: *J. Gen. Physiol.* **10**, 685 (1927).
- (11) SOLLNER, K.: *J. Phys. Chem.* **49**, 47 (1945).
- (12) SOLLNER, K.: *J. Phys. Chem.* **49**, 171 (1945).
- (13) SOLLNER, K.: *J. Phys. Chem.* **49**, 265 (1945).
- (14) SOLLNER, K., ABRAMS, I., AND CARR, C. W.: *J. Gen. Physiol.* **24**, 467 (1941).
- (15) SOLLNER, K., ABRAMS, I., AND CARR, C. W.: *J. Gen. Physiol.* **25**, 7 (1941).
- (16) SOLLNER, K., AND CARR, C. W.: *J. Gen. Physiol.* **28**, 1 (1944).
- (17) SOLLNER, K., AND GREGOR, H. P.: *J. Phys. Chem.* **50**, 470 (1946).
- (18) TEORELL, T.: *Proc. Soc. Exptl. Biol. Med.* **33**, 282 (1935); *Proc. Natl. Acad. Sci. U. S.* **21**, 152 (1935).

THE COLLOID CHEMISTRY OF THE CLAY MINERAL ATTAPULGITE^{1, 2}

C. E. MARSHALL AND O. G. CALDWELL

Department of Soils, Missouri Agricultural Experiment Station, Columbia, Missouri

Received August 8, 1946

Attapulgite, the most recently characterized of the clay minerals, is of especial interest to colloid chemists. Its colloid-chemical properties have been little investigated, but sufficient is known of its structure to act as a stimulus to further research. It affords a beautiful example of the close relationship between atomic structure and colloidal properties in the group of the silicates.

In 1935 de Lapparent (6) decided that a certain fuller's earth from Attapulgus, Georgia, and a similar clay from Mormoiron, France, were quite distinct from the clays of the montmorillonite group in spite of some similarity in chemical composition. Both were hydrous aluminum magnesium silicates, but the x-ray data and thermal dehydration curves indicated that the new clays were more closely related to the hydrous magnesium silicate sepiolite (or meerschaum) than to montmorillonite. Further work by de Lapparent (7, 8) and by Longchambon (9, 10) strongly suggested that attapulgite and sepiolite are members

¹ Presented at the Twentieth National Colloid Symposium, which was held at Madison, Wisconsin, May 28-29, 1946.

² Contribution from the Department of Soils of the Missouri Agricultural Experiment Station, Journal Series No. 1007.

of an isomorphous series structurally related to the amphiboles, sepiolite being the magnesium end member of the series. Finally, in 1940 Bradley (1) made a detailed x-ray study of attapulgite which confirmed its similarity to the amphiboles and gave us a clear picture of its structure, with only minor details still uncertain.

The ideal cell formula given by Bradley for the magnesium end member of the attapulgite series is $(\text{OH}_2)_4(\text{OH})_2\text{Mg}_5\text{Si}_8\text{O}_{20} \cdot 4\text{H}_2\text{O}$, which may be compared with the ideal formula of the amphibole tremolite $(\text{OH})_2\text{Ca}_2\text{Mg}_5\text{Si}_8\text{O}_{22}$. In each case long double chains of composition Si_4O_{11} run parallel to the fibre axis. In the typical amphiboles these are cemented together only by cations such as magnesium and calcium appropriately distributed along the axis. In attapul-

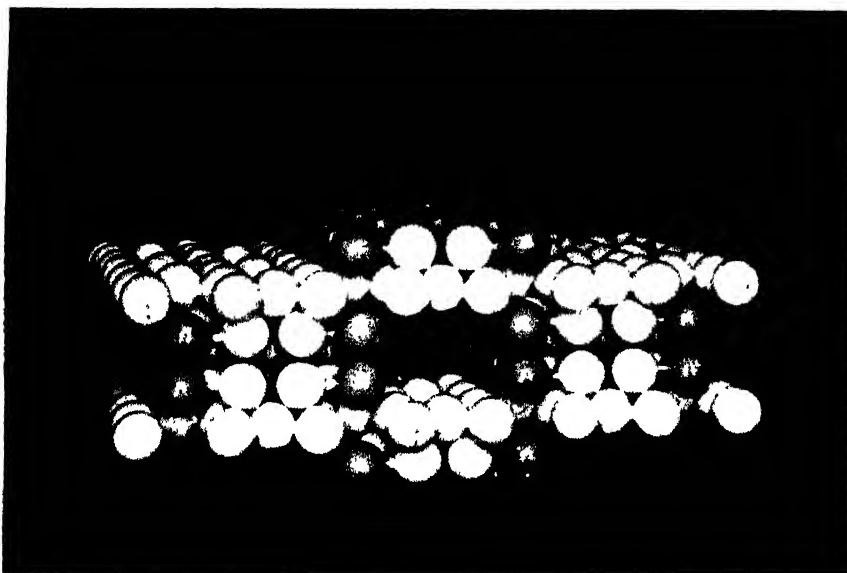


FIG. 1. Model of attapulgite structure. View along amphibole-like chains. Silica sheets horizontal. Larger spheres oxygen and hydroxyl. Smaller spheres magnesium or aluminum. Silicon not shown.

gite, however, the Si_4O_{11} units are also joined through shared oxygen atoms. This has an interesting consequence. A complete planar sheet of oxygen atoms is thus produced, these being arranged exactly as in the micas and in the other clay minerals. However, the silicon atoms associated with the oxygen sheet are not all on one side, as is the case with the micas, talc, pyrophyllite, and the micaceous clays. Instead, they form long strips, each an amphibole unit wide, alternately on the two sides of the oxygen sheet. Correspondingly, the magnesium-aluminum-oxygen units are placed also in strips parallel to the fibre axis. The result is that channels about one amphibole unit wide and one brucite unit high run parallel to the fibre axis (figure 1). These channels have no interconnections of comparable size. Each is bounded by oxygen atoms of the silica sheets on two sides and by hydroxyl groups, or strongly polarized water molecules

of the brucite layers on the others. The idealized structure pictures these walls as electrically neutral. However, as we shall see later, departures from the ideal composition may cause a net negative charge to reside on the framework and this must be balanced by cations in the channels.

The free cross section of the channels is about 3.7 Å. by 6.0 Å., large enough therefore to admit molecules of considerable size. In the natural clay loosely held water molecules occupy a considerable part of this space. On dehydration at moderate temperatures they are removed, but the structure remains essentially intact, just as it does in the zeolites. There is neither a gradual shrinkage such as occurs with clays of the montmorillonite group nor the sudden collapse which is characteristic of halloysite. Attapulgite differs from the zeolites in that most of the charge on the silica chain framework is balanced by structural brucite layers, leaving only a very small residue to be balanced by mobile cations. In the zeolites the whole of the charge on the framework is balanced by such cations. In attapulgite the channels are appreciably larger than those of the zeolites, which, according to Hey (4), range around 2.9–3.5 Å. in diameter.

Unfortunately, practically nothing is known of the sorption of organic molecules by attapulgite. Bradley (2) has made the very significant observation that the action of ethylene glycol is to cause a reduction in the mean refractive index instead of an increase. This would imply that loosely held water molecules are removed without corresponding replacement by the glycol.

DETAILED COMPOSITION IN RELATION TO STRUCTURE

The silica can conveniently be related to a sheet of composition $(\text{Si}_2\text{O}_3)_n$, in which the tetrahedral silicon positions are in strips alternately on both sides of the oxygen sheet. Taking the unit of pattern as containing eight silicon positions, examination of available analyses shows a deficit of silicon, amounting to 0.3 to 0.6 atom. On the assumption that these tetrahedral positions are filled by aluminum, this part of the lattice would thereby acquire a negative charge of 0.3 to 0.6 equivalent. In the strips containing magnesium and aluminum there are five octahedral positions. Magnesium atoms occupy 1.5–2 of these, aluminum 1.7–1.9, iron (ferric and ferrous) about 0.3–0.5, with small quantities of titanium and manganese. Some calcium not removed by electro dialysis probably belongs here also. The sum of the charges is generally somewhat greater than ten; hence, as compared with $\text{Mg}_5\text{Si}_5\text{O}_{20}(\text{OH})_2$, this part of the structure has a net positive charge. However, it is less in magnitude than the negative charge of the silicon layers by about 0.2 to 0.3 equivalent. This can therefore be regarded as the net negative charge per lattice unit. It is balanced by cations which are in part readily exchangeable and in part closely associated with the lattice. The former generally predominate, so that normally we have an exchange capacity amounting to about 0.14 to 0.16 equivalent per unit cell or 21 to 24 milliequivalents per 100 g. of clay. This is much lower than the values found for clays of the montmorillonite group, which range from 60 to 120 milliequivalents per 100 g. The question therefore arises as to whether there is real proof that the exchange properties are a consequence of a net negative charge

on the lattice or whether they could not be ascribed to unsatisfied valencies at edges and corners of the particles. It will be shown below that the chemical evidence strongly favors the former view.

PARTICLE SIZE, DISTRIBUTION, AND SHAPE

Although sepiolite (meerschau) has long been known as a microscopically fibrous mineral, the elongated character of attapulgite particles was not fully realized until they were fractionated and examined in the electron microscope (12). The particle-size distribution below 2μ equivalent diameter of the particular attapulgite sample³ examined by the authors is given in table 1. For this determination and for the accumulation of the fractions for further study the two-layer method was used. The tube centrifuge (11) with glycerol-water (1:4 by volume) as the lower liquid gave the fractions 2μ – 0.5μ and 0.5μ – 0.2μ , whilst the Sharples supercentrifuge (14) gave the final separation into 0.2μ – 0.05μ and $<0.05\mu$ fractions. The specific gravities and mean refractive indices

TABLE 1

Particle-size distribution below 2μ , specific gravities, and mean refractive indices of attapulgite

FRACTION	PERCENTAGE OF THE CLAY < 2μ	SPECIFIC GRAVITY	MAIN REFRACTIVE INDEX
μ	<i>per cent</i>		
2–0.5	18.9	2.30	1.542
0.5–0.2	51.4	2.28	1.550
0.2–0.05	26.3	2.30	1.550
<0.05	3.5	2.06	1.558

as determined on very dilute suspensions in aqueous potassium mercuric iodide (3) are also included in table 1.

The electron-microscope pictures of these fractions are shown in figures 2–5 (12). The general impression one obtains is that the particles are lath-like. Single particles of appreciable width are often very faint, whereas narrower particles are much blacker, suggesting that they are laths seen on edge. It is clear from the photographs that the mean length of the particles varies much less than their settling velocities. The smallest particles of the coarsest fraction, whose settling velocity corresponds to an equivalent diameter of 500μ , are about 1.22μ in length and 63μ in width. On the other hand, the largest particles of the finest fraction, corresponding to 50μ equivalent diameter, are about 645μ long and 17μ wide. The other variable, the thickness, is hard to determine with precision, but some guidance is afforded by the mineral impurity present, whose form is more or less isometric, by a consideration of the relative electron penetration. In the $<50\mu$ fraction the faint laths lying flat are certainly less than 15μ and very probably less than 10μ in thickness; in the coarser fractions practically none is thicker than 30μ .

If one takes individual laths and calculates the most probable mean settling velocity, using the formulae of Müller (13), cases are frequently found in which

³ Sample kindly furnished by the Attapulgus Clay Company, Attapulgus, Georgia.



FIG. 2 Attapulgite clay fraction 2-0.5 μ equivalent spherical diameter. Dimension shown = 1 μ .



FIG. 3. Attapulgite clay fraction 0.5-0.2 μ equivalent spherical diameter

the value is below the theoretical minimum for the fraction. A similar situation was noticed by Kelly and Shaw (5) in the case of halloysite, which is also lath-like. They suggest that to some extent an overlapping of fractions may occur, owing

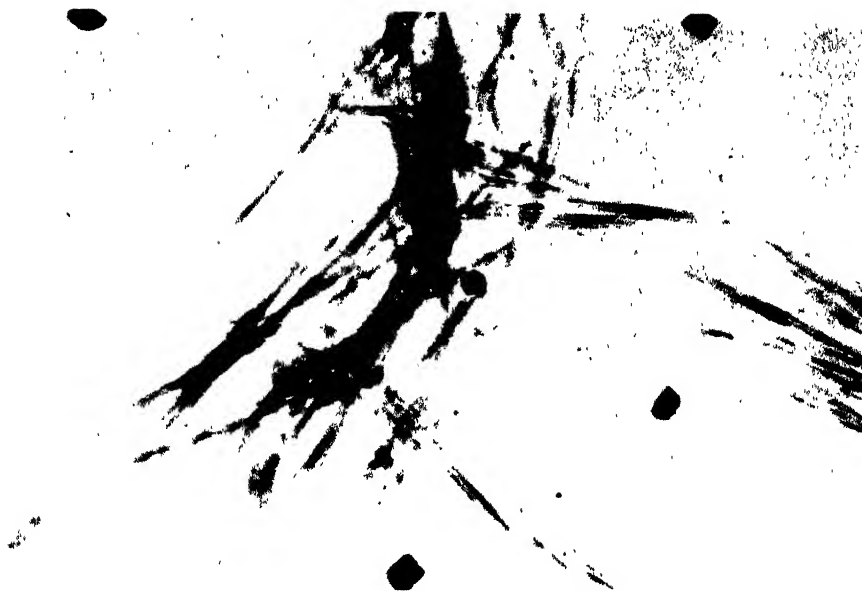


FIG. 4. Attapulgite clay fraction $0.2-0.05 \mu$ equivalent spherical diameter



FIG. 5. Attapulgite clay fraction $<0.05 \mu$ equivalent spherical diameter

to different orientations of individual particles during fractionation. The procedure was probably quite reliable in other respects, since the isometric mineral

impurities fall into the correct fractions. To some extent also there may have been temporary association of particles during fractionation. Attapulgit is extremely sensitive to coagulation and readily forms temporary associations of particles which can be broken up by shaking. Even the pure sodium-saturated clay shows this property at concentrations of 0.5 per cent and over.

STABILITY AND CATION-EXCHANGE PROPERTIES

The original clay sample was essentially saturated with calcium. On electrodialysis this calcium was readily replaced by hydrogen, smaller quantities of magnesium, sodium, lithium, aluminum, and iron appearing also at the cathode. After about 10 hr. the rate of removal fell off considerably, indicating that the simple replacement of the cations by hydrogen was essentially complete. However, prolongation of the treatment over 968 hr. brought out considerable amounts of calcium, magnesium, aluminum, and iron at a slow but steady rate. At the same time silicon was liberated and accumulated in both the cathode and the anode chambers. It is evident that slow decomposition of the lattice follows

TABLE 2

Base-exchange capacity of attapulgit fractions (in milliequivalents per 100 g., ignited basis)

FRACTION	AMMONIUM (pH 7.0)	CALCIUM (pH 5.0)	CALCIUM (pH 7.0)	CALCIUM (pH 9.0)
μ				
2 -0.5	18.0	21.4	22.8	24.2
0.5-0.2	19.0	19.2	21.2	21.2
0.2-0.05	22.2	22.7	23.5	25.3

upon preparation of the hydrogen clay. Fragments of the lattice are carried to the anode or cathode according to their predominant charge.

The hydrogen attapulgit gives a pH which varies from 3 to 4, according to the concentration of the suspension used. It is readily reproducible over short periods of time, but eventually it rises, indicating internal attack upon the lattice. After 197 days an 0.835 per cent suspension gave a pH of 4.76, whereas during the first 2 hr. it had remained constant at 3.90.

The base-exchange capacity of three fractions of attapulgit was determined by repeated treatment with 0.1 *N* ammonium acetate at pH 7 and with 0.1 *N* calcium acetate at pH 5, 7, and 9. The results are given in table 2.

It is evident that the increase in exchange capacity with diminishing particle size is small, just as is the case with the montmorillonite clays. The kaolinite clays, whose exchange capacity may primarily be ascribed to negative charges at broken edges, show essentially complete dependence of capacity upon particle size. The small increase due to change of pH from 5 to 9 is also significant. The montmorillonite clays behave similarly, whereas the kaolinite clays show a greater proportionate increase. The data presented thus lend support to the idea that the exchange cations are held by virtue of ionic replacements in the lattice itself.

ELECTROCHEMICAL CHARACTERISTICS

The fact that freshly electrodialyzed attapulgite gives pH values in the range 3-4 shows that as a colloidal acid it is of comparable strength to the clays of the montmorillonite group. Titration curves have been obtained for attapulgite, using various monovalent and divalent bases, but because of the small quantities available only concentrations below 0.5 per cent were investigated. The curves were thus particularly sensitive to the presence of small amounts of impurities, and further work at a variety of concentrations is needed. When monovalent bases were used, no inflection points corresponding to an exchange capacity of 20-25 milliequivalents were found. However, an inflection on the alkaline side corresponded to about 50 milliequivalents. Calcium and barium gave two inflections, the first at 20-25 milliequivalents and the second at about 50.

The best comparison with other clays is afforded by the calculated fraction active, derived from pH determinations on the electrodialyzed clays and from

TABLE 3

Electrochemical characteristics of attapulgite in comparison with those of other clay minerals

CLAY	CON- CENTRATION	EXCHANGE CAPACITY	FRACTION ACTIVE		
			H	K	Na
	<i>per cent</i>	<i>milliequiv. per 100 g.</i>			
Attapulgite.....	0.356	22	0.128	0.456	
Kaolinite.....	10.00	2.5	0.011	0.266	0.288
Nontronite.....	0.275	70	0.066	0.250	
Montmorillonite.....	0.300	100	0.061		0.178

measurements of potassium-ion activity on the corresponding potassium clays. From the available measurements on different clays those have been selected in which the measured cationic activities were not too widely different. The results are assembled in table 3. The dissociation of hydrogen ions from freshly electrodialyzed attapulgite is considerably greater than for montmorillonite and nontronite, suggesting that it is the strongest colloidal acid amongst the clays. The potassium clay is also more extensively dissociated than the others. We may conclude that attapulgite is a colloidal electrolyte in the strict sense of the term. It possesses a mechanism for ionization which is conditioned by the molecular structure, all units of which are accessible to molecules and ions of the outer solution. Further work on its electrochemical properties should be of great interest.

PROPERTIES OF CLAY FILMS

In the investigation of the three clays attapulgite, nontronite, and saponite, the dehydration curves at various temperatures were determined by drying down a small quantity of clay suspension in a crucible and heating in an oven or

furnace. Under these circumstances the same clay film was employed for all points on the curve. When the data were examined it was found that at each temperature, and especially for those below 500°C., the moisture content of the sample was higher than had been expected from data in the literature. If, however, the clay film were detached from the crucible, ground by hand in an agate mortar, and reheated, normal values were obtained. The difference was very large. At 110°C., in the clay as powdered for analysis 16 per cent moisture was present, whilst the film came to equilibrium at about 24 per cent moisture. All fractions behaved in the same way and gave closely agreeing dehydration curves. At 400°C. data from the literature indicated that attapulgite retained only 4–5 per cent water, whereas the films contained 8–10 per cent. It would seem therefore that the extra water which is enmeshed in the structure of the film is held by bonding energies which are of the same order of magnitude as those of water molecules held inside the clay particles. This conclusion holds

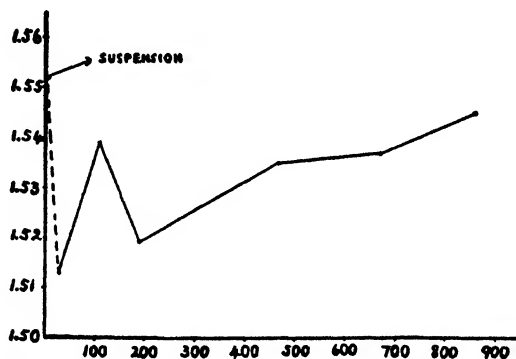


Fig. 6. Mean refractive index of attapulgite films (determined in oils) in relation to temperature of preheating.

not only for attapulgite but for the clays of the montmorillonite group also. For these platy clays it is readily understood. Films formed by slow drying show excellent orientation parallel to the surface. The spaces between initially separate plates steadily diminish with diminishing water content and the film shrinks in thickness. Eventually the spaces become of the same order of magnitude as those which initially separated the lattice units. From this point onwards a clear distinction between intramolecular and extramolecular water is lost.

Attapulgite, however, is not a swelling clay and might be expected to show some deviations from the above pattern. The optical properties, in conjunction with the dehydration curves, enable us to interpret its behavior.

Suspensions of attapulgite clay, on mixing with concentrated potassium mercuric iodide solution, show a relatively high mean refractive index. An air-dried film shows a much lower value. On heating the film to 110°C. the mean refractive index rises, although not to the value of the suspension. At 200°C. the mean index has fallen again; but for higher temperatures it rises slowly (figure 6). Two effects cause these variations. Shrinkage of the water film

between particles or shrinkage of the lattice causes a rise in the mean refractive index of the film. On the other hand, loss of water from fixed channels causes a lowering of the index, just as is found in the case of the zeolites. Between the air-dry condition (50 per cent humidity at 30°C.) and 110°C., shrinkage of the water film between particles more than counterbalances the loss of water from the fixed channels within the particles. Between 110°C. and 200°C. the latter process predominates. From 200°C. onwards shrinkage of the water film plus possible shrinkage of the lattice itself cause a rise in refractive index.

In spite of the fact that the lattice channels seem to be of adequate size, attapulgite rehydrates very slowly. For this reason if a suspension is dried, ground, and resuspended in water the new suspension will give a much lower mean refractive index in potassium mercuric iodide solution than the original. Clays of the montmorillonite group, similarly treated, return to the original values. This provides a simple optical test to distinguish between them.

The lath-shaped character of the attapulgite particles might seem to favor an aggregation into a brush-heap type of gel. This is probably the case for gels formed by random coagulation, but in the films prepared by the settling and drying of stable suspensions an extensive degree of orientation is present. This shows itself in their optical properties. Negative birefringence is present which is easily measured when the films are viewed on edge. The interference figure is biaxial with a small optic axial angle. Bradley's x-ray data indicate that in such films we have not only an orientation of rods parallel to the film surface, but that one axis at right angles to the fibre length is preferred over the other in this orientation. As would be expected, this axis lies in the plane of the oxygen sheets and corresponds to the width of the lath. Thus the orientation finally achieved, though not perfect, largely corresponds to that given by the montmorillonite clays, whose oxygen sheets also lie approximately parallel to the film surface.

From the above outline of what has been done it will be evident that attapulgite clay is an extremely attractive material for colloid-chemical research and that much remains to be investigated.

REFERENCES

- (1) BRADLEY, W. F.: *Am. Mineral.* **25**, 405 (1940).
- (2) BRADLEY, W. F.: *Am. Mineral.* **30**, 704 (1946).
- (3) CALDWELL, O. G., AND MARSHALL, C. E.: *Univ. Missouri Agr. Expt. Sta., Research Bull.* **354** (1942).
- (4) HEY, M. H.: *Mineralog. Mag.* **24**, 99 (1935).
- (5) KELLY, O. J., AND SHAW, B. T.: *Soil Sci. Soc. Am. Proc.* **7**, 58 (1942).
- (6) LAPPARENT, J. DE: *Compt. rend.* **201**, 481 (1935).
- (7) LAPPARENT, J. DE: *Z. Krist.* **97**, 237 (1937).
- (8) LAPPARENT, J. DE: *Z. Krist.* **98**, 233 (1938).
- (9) LONGCHAMON, M.: *Compt. rend.* **203**, 672 (1936).
- (10) LONGCHAMON, H.: *Compt. rend.* **204**, 55 (1937).
- (11) MARSHALL, C. E.: *J. Soc. Chem. Ind.* **50**, 457T (1931).
- (12) MARSHALL, C. E., HUMBERT, R. P., SHAW, B. T., AND CALDWELL, O. G.: *Soil Sci.* **54**, 149 (1942).
- (13) MÜLLER, H.: *Kolloidchem. Beihefte* **27**, 233 (1928).
- (14) WHITESIDE, E. P., AND MARSHALL, C. E.: *Soil Sci. Soc. Am. Proc.* **4**, 100 (1939).

THE ELECTROKINETIC POTENTIALS OF PRECIPITATES¹

L. H. REYERSON, I. M. KOLTHOFF, AND KIETH COAD

*School of Chemistry, University of Minnesota, Minneapolis 14, Minnesota**Received August 8, 1946*

Studies on the aging of precipitates by Kolthoff and his collaborators have shown that there is a very rapid exchange of ions between the precipitate and the solution during the early stages of the process. There is also evidence of ion exchange and the perfection of the crystals even after a week's time. It was therefore felt that the surfaces which exhibit such changes might show similar changes in other surface properties, such as the electrokinetic potential. The following study was begun in the hope that by electrokinetic measurements it would be possible to obtain further insight into the mechanism of the aging of precipitates. The results did show that the lattice ions of the precipitated salt have a definite electrokinetic-potential-determining effect. Certain non-lattice ions also exhibited a positive effect, but it was not possible to obtain positive results that showed the aging process.

The only previous investigations of a similar nature were those of Ruysen (6) and Julien (1). Ruysen measured the electrokinetic or zeta potential of aged barium sulfate in pure water, in aqueous solutions of barium chloride up to 0.001 molar, and in solutions of 50 per cent ethyl alcohol containing barium chloride up to 0.001 molar concentration. Julien studied the electrokinetic behavior of silver bromide. Most of his experiments were carried out with a capillary of silver bromide, but he did measure the streaming potential of precipitated silver bromide which had been packed in a diaphragm. His results for the precipitate were not very reproducible; hence he concluded that the most reliable data were obtained with the capillary of silver bromide. In the present work not only was barium sulfate further investigated but lead chromate and silver bromide were also studied.

EXPERIMENTAL

The investigation was conducted along lines similar to previous studies in this laboratory, as reported by Smith and Reyerson (7). Three different types of cells were constructed and used in the streaming-potential measurements. Their designs are shown in figure 1. The electrodes for each cell are designated E, and their perforation is shown diagrammatically in the figure. In the case of cell A the electrodes used were either gold, silver, copper, or silver-silver chloride. In cell B only platinum was used, while in cell C copper, silver, or silver-silver chloride was used. Cell A was very similar to the cells used in the previously reported study (7). This cell was difficult to pack with the pre-

¹ Presented at the Twentieth National Colloid Symposium, which was held at Madison, Wisconsin, May 28-29, 1946.

For the sake of brevity the two papers read at the Symposium have been combined.

precipitates and tended to leak under the pressures needed for steady potential measurements. Satisfactory experimental results could be obtained only with such great difficulty that cell B was constructed as described by Lauffer and Gortner (5). This cell gave some satisfactory results, but there was difficulty in keeping the ground-glass joints tight under pressure. Cell C was then constructed and it proved to be satisfactory. In the figure D represents the packed precipitate diaphragm in each case.

To develop a streaming potential the solution was forced under measured pressure from one reservoir to the other. The pressures were corrected for differences in solution levels. Figure 2 shows the general scheme of forcing the

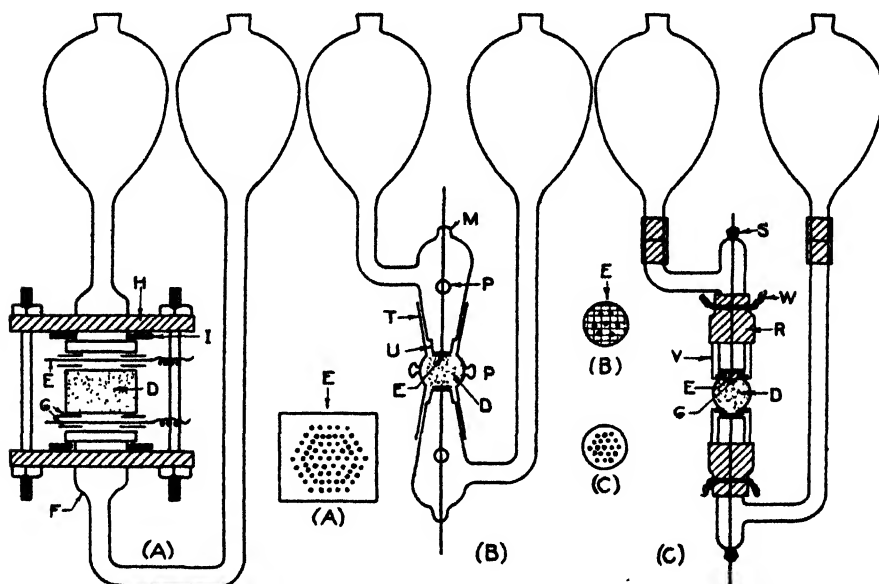


FIG. 1. Cells for measuring streaming potentials

liquid through the diaphragm. The three-way stopcocks (T) make it possible to force the liquid through the diaphragm in either direction. The mercury manometer M was used to measure the pressure maintained by the nitrogen from tank N. Reservoir B was used to give the system a large gas volume, as compared to the volume change produced by the flow through the diaphragm. During the early part of this investigation the potential developed by streaming the liquid through the packed precipitate under constant pressure was measured by essentially the same vacuum-tube potentiometric device as described by Smith and Reyerson. However, for this work it was found that the potentials developed could be accurately determined with a good potentiometer and a highly sensitive galvanometer. The same ratios of E/P were obtained using either instrument. Furthermore, careful study showed that polarization of the cells was no factor when a galvanometer having a sensitivity of 0.022 microampere per scale division was used as a null instrument.

Three different samples of barium sulfate were used. The material studied most completely was an aged barium sulfate having particles ranging from 1–5 microns in cross section. It was prepared by allowing 0.1 *M* potassium sulfate and 0.1 *M* barium chloride to mix slowly in boiling water. The solutions were delivered under the surface of the boiling water, which was stirred vigorously. The precipitate was left in contact with the mother liquor for 24 hr. and then filtered. Microscopic examination showed the particles to be in the above-mentioned size range, and they appeared to be reasonably perfect rhombohedra. One sample of very fine analytical grade of barium sulfate (M) was used in a few experiments and some high-grade natural baryte was ground and separated into suitable sizes by graded sieves. The lead chromate was prepared from

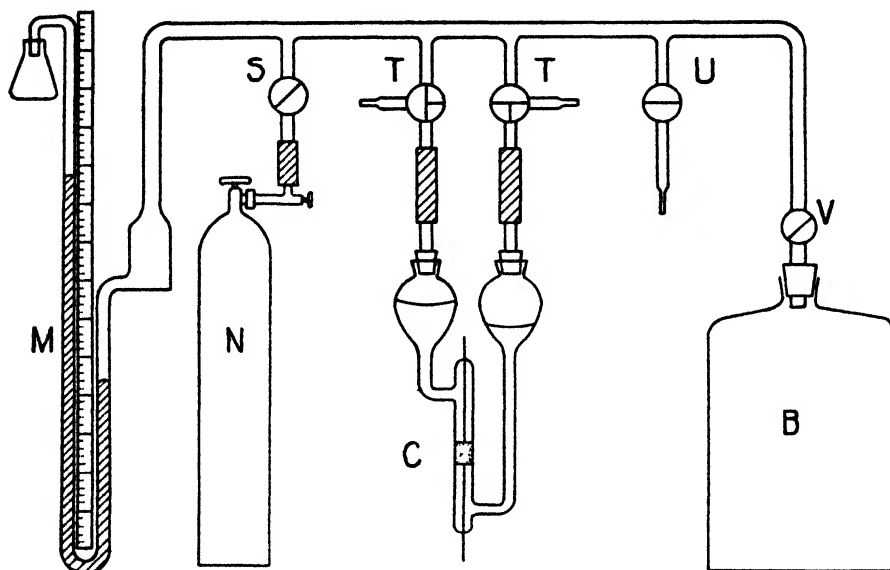


FIG. 2. Pressure system

natural krokoite in the same manner. Two samples of silver bromide were used. One was an analytical grade which was found to have the size of particles desired, and the other was prepared by fusing silver bromide and then scratching the surface of the fused solid in close parallel lines with a needle and then cross hatching until enough fine particles had been obtained. This method was found necessary because of the extreme softness of the salt.

In any given run it was necessary not only to measure the pressures applied and the potentials developed between the two electrodes but also to measure the specific conductance of the solutions in the pores of the diaphragm. A sensitive conductivity bridge similar to that described by Smith and Reyerson (7) was built, and the cell constants for each packed diaphragm were determined by using 0.1 or 0.01 *M* potassium chloride solutions. From the measurements of the pressure driving the liquid, the potential developed, and the specific conductance of the liquid in the diaphragm, it was possible to calculate the electro-

kinetic or zeta potential from the equation

$$\zeta = \frac{4\pi NKE}{DP}$$

where N is the viscosity, D the dielectric constant, P the measured pressure, E the measured potential, and K the specific conductance of the solution in the diaphragm. The values of N and D were taken from standard tables.

RESULTS

Several runs were made upon freshly precipitated barium sulfate, but the method of obtaining sufficiently large particles for the satisfactory use of the

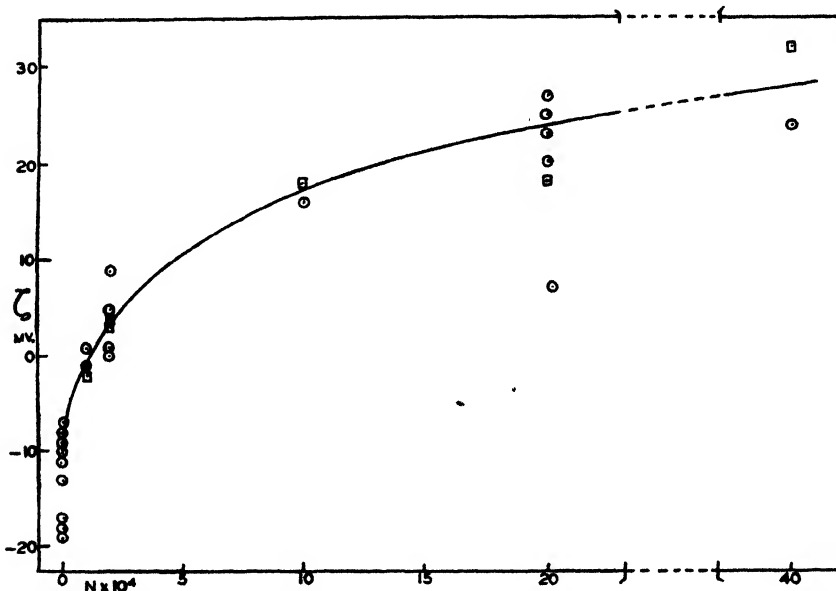


FIG. 3. Zeta-potential values for aged barium sulfate in aqueous solutions of barium salts, showing reproducibility.

diaphragms apparently gave rise to crystals which gave no different potentials with time. At least in the present investigation no positive results were obtained which showed that the zeta potential changed with aging. However, the results on aged barium sulfate were quite reproducible, as is indicated in figure 3. Here all of the results obtained on aged barium sulfate in aqueous solutions of barium salts are given. The result which deviated most from the others at a given concentration was obtained on a packed diaphragm which showed that definite channeling had occurred. The largest error in the measurements lies in the determination of the ratio E/P . Figure 4 shows two typical curves for the determination of E/P . The upper figure gives the results for barium sulfate, using 0.001 N hydrochloric in cell A, and the lower one is for barium sulfate, using 0.001 M barium chloride in cell C. The negative pressures are merely

used for the reversal of liquid flow through the diaphragm. Since the potentiometric measuring system was not reversed, the results appear as indicated. Figures 5 to 9 give the curves for changing zeta potentials in various solutions of electrolytes using barium sulfate, lead chromate, and silver bromide as precipitated salts. The zeta-potential values each represent the average of several determinations, and it is believed that the curves represent the behavior of the electrokinetic potential of the crystalline salts studied. The reproducibility

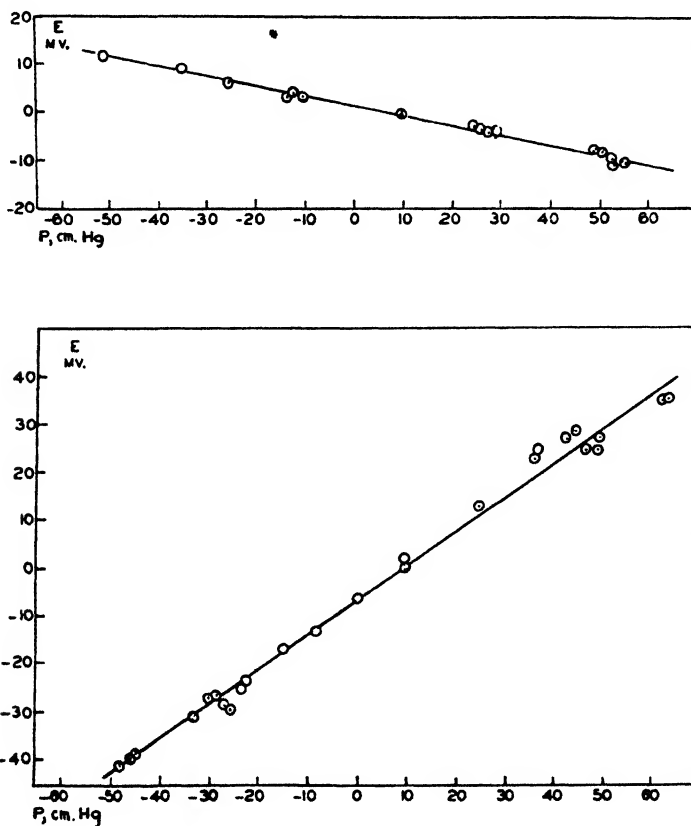


FIG. 4. Typical determinations of E/P

of the values of the zeta potential was found to be good, since the results from the different cells using different electrical methods were found to be in good agreement, as is shown in figure 3.

DISCUSSION

1. The product "aged barium sulfate" has a negative zeta potential in water. This potential remains negative upon the addition of "indifferent electrolytes" like alkali chlorides and hydrogen chloride. The fact that hydrogen chloride has about the same effect as an alkali chloride shows that the electrokinetic

potential of the glass of the measuring cell is not involved in the measurements. Barium salts decrease the negative charge and even at very small concentrations impart a positive potential to the barium sulfate, which increases with increasing concentration of barium. The barium ions behave like typical "potential-determining ions" in this respect. Lead ions, which fit in the lattice of barium sulfate, also behave as potential determining, as is evident from the fact that lead nitrate in water charges the barium sulfate positively. Dilute solutions of thorium chloride in water also charge the solid positively. This does not necessarily mean that the thorium ions behave like potential-determining ions. The thorium chloride is strongly hydrolyzed, and the positively charged colloidal thorium hydroxide particles may deposit on the negatively charged surface of the barium sulfate, thus changing the surface of barium sulfate into one of thorium hydroxide.

Alkali sulfates and copper sulfate increase the negative charge of the barium sulfate. The change of the potential caused by the potential-determining sulfate ions is, however, much less than that caused by barium ions.

It is peculiar that potassium citrate increases the negative charge of barium sulfate much more than water does. In this respect, *the citrate ions behave as potential-determining ions, although they do not* fit in the lattice of barium sulfate. As a matter of fact, the large effect of citrate was anticipated, since barium sulfate can be peptized in water by the addition of citrate, but not of sulfate. Apparently, citrate ions can form a negatively charged complex with barium ions. This complex ion may be formed on the surface by adsorption of citrate ions on the barium sulfate.

Potassium ferrocyanide in water slightly increases the negative potential of barium sulfate until a minimum value is obtained at a concentration of about $2.5 \times 10^{-4} M$.

2. The zeta potentials were also determined in 50 per cent alcohol. It was found by Kolthoff and MacNevin (3) that at the same final concentration the adsorption of barium salts and of potassium bromate is much greater from 50 per cent ethanol than from water. From the present work it is seen that at very small concentrations, barium nitrate and chloride have a much greater effect upon the zeta potential in 50 per cent ethanol than in water. The zeta potential increases rapidly until a final value of about 35 to 40 millivolts is reached. This value is higher than that attained in water. Lithium and potassium sulfates increase the negative potential of barium sulfate in 50 per cent ethanol. Again, the effect of sulfate at small concentrations is much more pronounced in 50 per cent ethanol than in water.

Indifferent electrolytes like potassium chloride and bromate decrease the originally negative potential, as was to be expected.

Some of our results are at variance with measurements reported by Ruyssen (6). This author made a few measurements of the electrokinetic potential of barium sulfate in 50 per cent ethanol. His product was prepared in a similar way as our "aged product." The maximum value of the electrokinetic potential of barium sulfate in aqueous barium chloride was found by Ruyssen to be + 41.2 millivolts (0.001 M barium chloride), while in 50 per cent ethanol the maximum

value was +88 millivolts. We found in aqueous barium chloride a maximum value of about 25 millivolts and in 50 per cent ethanol a maximum of 33 millivolts. Qualitatively, our results agree with those of Ruyssen regarding the effect of alcohol upon the zeta potential of barium sulfate in barium chloride solutions.

On the other hand, the values of the zeta potential measured by Ruyssen in potassium chloride and bromate solutions in 50 per cent ethanol differ not only in number but also in *sign* from our values, although Ruyssen's data in aqueous potassium chloride solutions are very similar to ours. In $5 \times 10^{-4} M$ potassium

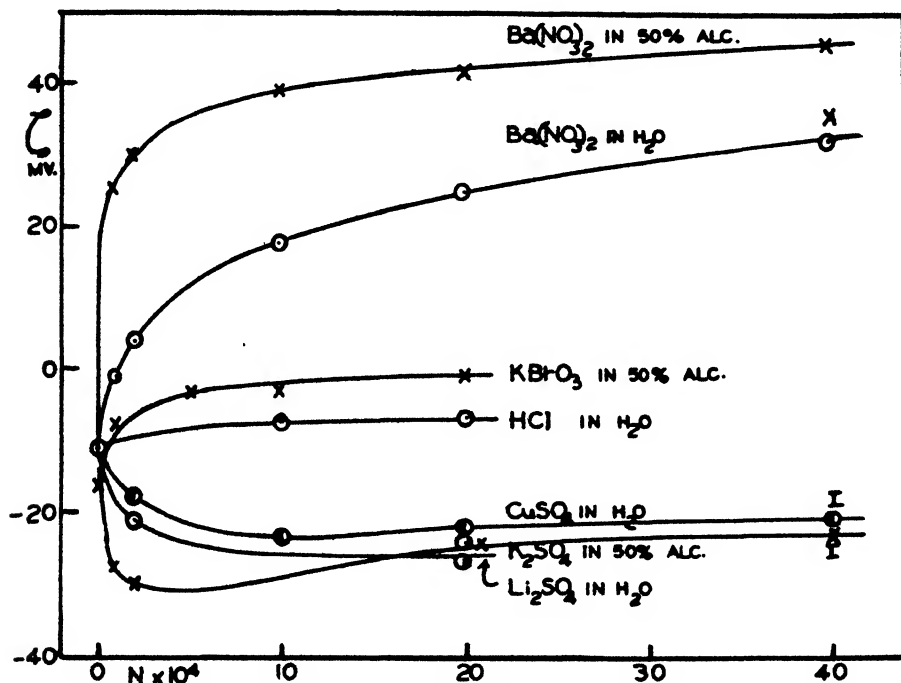


FIG. 5. Zeta potential of aged barium sulfate in solutions of its potential-determining ions.

chloride solution in 50 per cent ethanol Ruyssen found the abnormally large value of +44 millivolts, whereas our value of the zeta potential was about -4 millivolts. We also found in all concentrations of potassium bromate in 50 per cent ethanol a negative value of the zeta potential (see figures 5 and 6), whereas Ruyssen found at all concentrations ($2 \times 10^{-5} M$ to $2.5 \times 10^{-3} M$) positive values varying between +19 and +30 millivolts.

There is no plausible reason why barium sulfate should become positively charged in potassium chloride or bromate solutions in 50 per cent ethanol. Since all values (also in barium chloride) measured by Ruyssen in this solvent are much more positive than ours, we suspect that a systematic error must have been introduced in his measurements in 50 per cent ethanol.

3. Our results show that the "primary stability" (8) of a colloid is not solely

determined by the adsorption of salts which have an ion in common with the lattice or which contain an ion which fits in the lattice of the precipitate. In the first place, attention is called to the fact that barium nitrate and chloride at the same concentration have almost the same effect upon the zeta potential. Still, barium nitrate is much more strongly adsorbed from 50 per cent ethanol than is barium chloride.

Unpublished results obtained in this laboratory revealed that in 50 per cent ethanol potassium sulfate is adsorbed much more strongly on barium sulfate than is barium chloride.

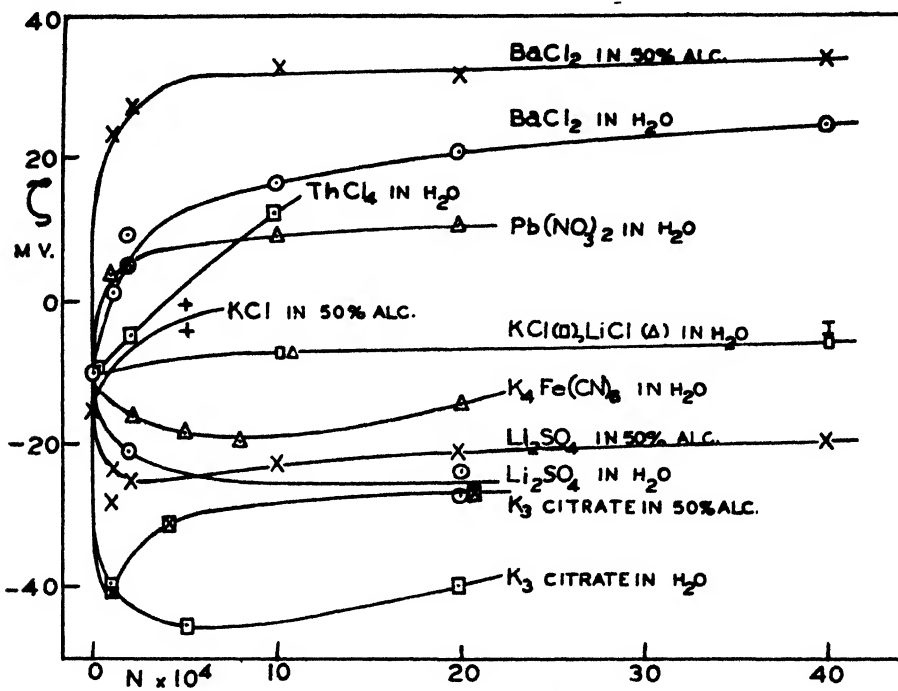


FIG. 6. Zeta potentials of aged barium sulfate in solutions of various electrolytes

In spite of this behavior it is found that the stability of a suspension of barium sulfate in 50 per cent ethanol is greatly increased by the addition of barium chloride, whereas *sulfates have a flocculating effect*.

It is also to be noted that in 50 per cent ethanol potassium bromate has about the same effect upon the zeta potential as potassium chloride, in spite of the fact that the former is much more strongly adsorbed than the latter.

Our study brings to light the fact that there is no simple relation between the effect of salts upon the primary stability of a barium sulfate suspension and their adsorbabilities on the precipitate.

From the experimental results in this paper we are led to the conclusion that in a consideration of the primary stability of colloids and the peptizing effect of salts, we have to distinguish between an adsorption of ions on an "active sur-

face" and on the "normal surface." A salt like potassium bromate is markedly adsorbed from 50 per cent ethanol, but this adsorption does not affect the zeta potential. Apparently, both the potassium and the bromate ions are adsorbed in equal amounts on the normal surface of barium sulfate. Such an adsorption does not change the charge of the precipitate. We shall call it "*equivalent adsorption*."

Adsorption on active surface of salts which contain a potential-determining ion, on the other hand, results in an incorporation of the potential-determining ions in (or on) the lattice, while the ions of opposite charge remain in the diffuse double layer in the liquid phase. This type of adsorption, which we designate

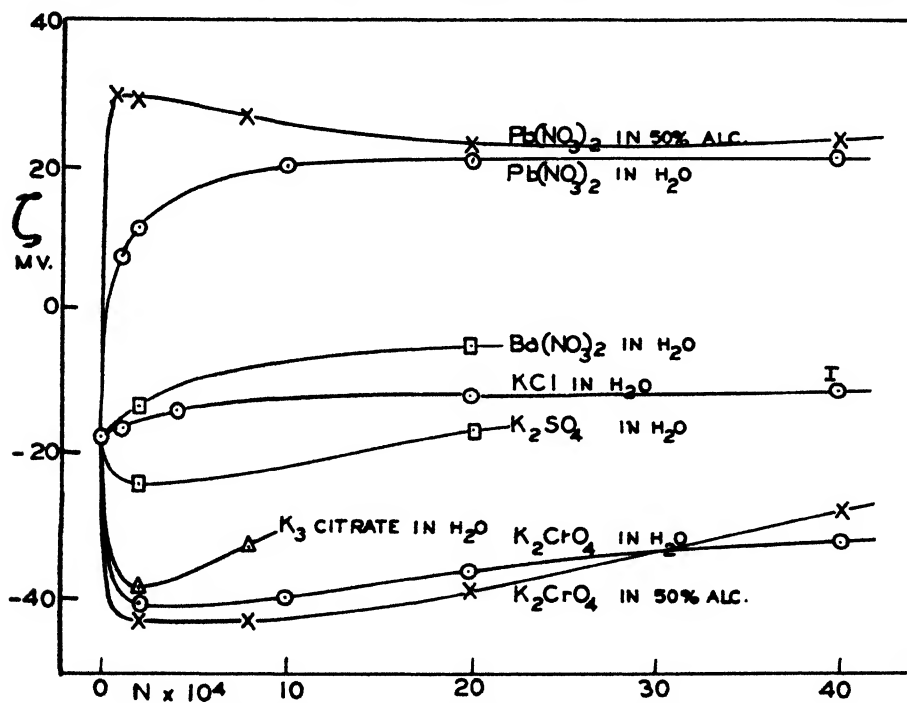


FIG. 7. Zeta potentials of natural lead chromate (krokoite)

distribution adsorption, determines the primary stability of colloids. Only when we are dealing with this kind of adsorption, which results in an increase of the number of one kind of lattice ions or other potential-determining ions in the lattice, can we expect an effect upon the primary stability of the colloidal suspension. Apparently, then, the barium salts give a marked distribution adsorption in addition to equivalent adsorption. The oppositely charged citrate ions behave in a similar way. Sulfates, on the other hand, show little distribution adsorption, but mainly equivalent adsorption.

The difference in the behavior of the lattice ions barium and sulfate is unexplained. It is very peculiar that in the case of lead chromate just the opposite result is found. In the absence of a protecting colloid it is possible to prepare a

colloidal solution of lead chromate in an excess of chromate ions, but not in an excess of lead (2). In agreement with this behavior it was found in the present study that chromate ions in water increased the negative potential of natural lead chromate (krokoite) to -40 millivolts, while lead ions only raised the potential to $+20$ millivolts (figure 7).

4. In other respects the behavior of krokoite was similar to that of barium sulfate, also with regard to the effect of ethanol. Citrate ions again behaved as potential-determining ions. They did not increase the negative charge of krokoite as much as chromate ions, while in the case of barium sulfate the effect of citrate was greater than that of sulfate.

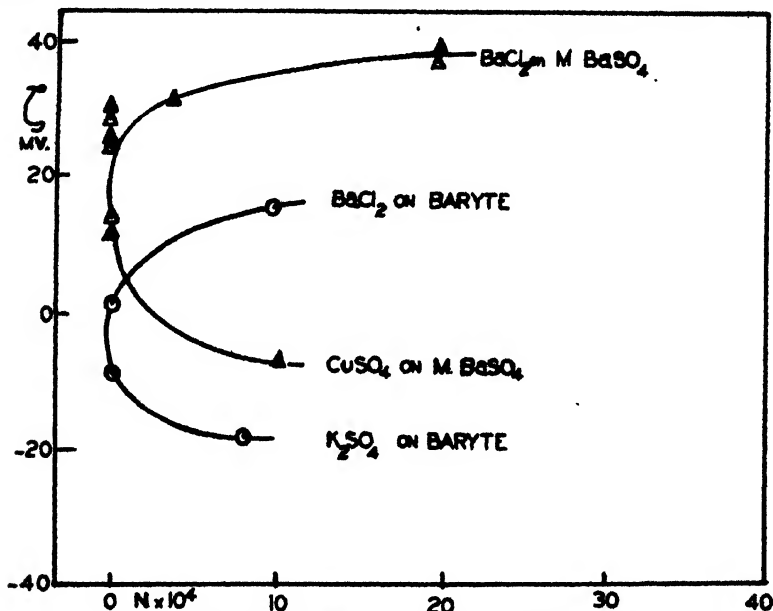


FIG. 8. Zeta potentials of other types of barium sulfate

The sulfate ion, which is isomorphous with the chromate ion, behaves like a potential-determining ion on lead chromate. Barium ions portray a similar tendency, although the krokoite could not be charged positively by the addition of barium nitrate.

5. Qualitatively, the electrokinetic behavior of the very finely divided sample of chemically pure barium sulfate and of the coarse particles of natural baryte (figure 8) was found similar to that of the precipitated barium sulfate of intermediate size. Contrary to the results of Kruyt and Ruyssen (4) it was found that the natural baryte particles could be charged positively by barium chloride, even in aqueous solutions. Kruyt and Ruyssen conclude that the surfaces of the more perfect crystals of the natural baryte behave like that of an "indifferent paraffin" wall. We have not been able to confirm this, even though the particles of our natural product were very coarse and had a size between 100 and 175 microns.

Although the results obtained with precipitates of lead chromate are not included in this paper, it is of significance to note that qualitatively the natural mineral krokoite (particle size 100 to 150 microns) behaved similarly to precipitates of lead chromate of fine particle size as far as the electrokinetic behavior is concerned.

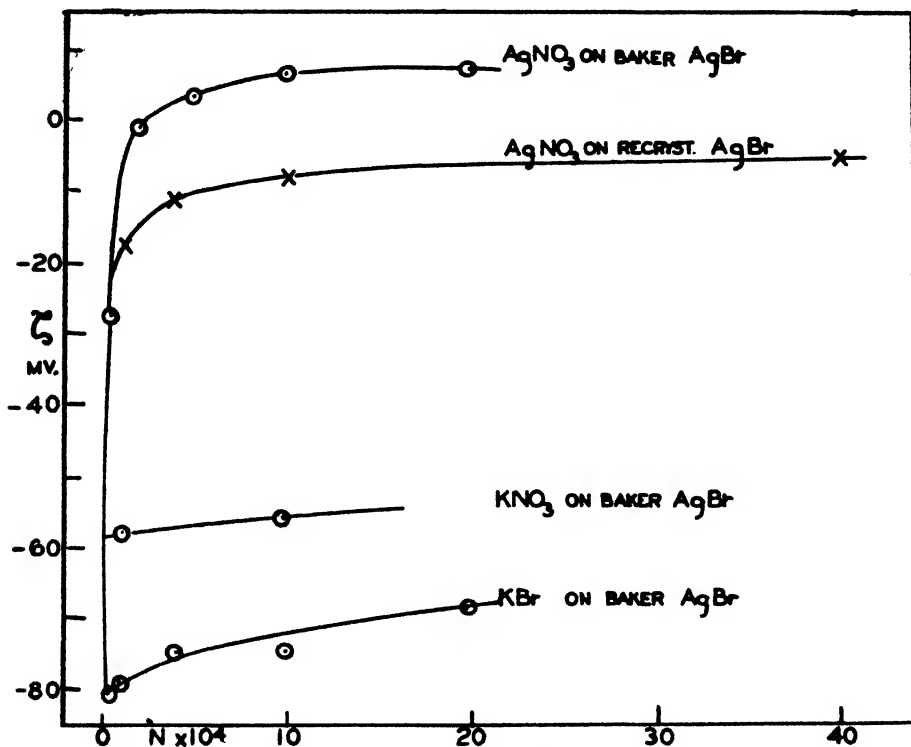


FIG. 9. Zeta potentials of silver bromide

The krokoite certainly did not behave like a "paraffin wall", and its electrokinetic potential was affected in the expected way by the addition of potential-determining ions.

The different products of silver bromide used in this study showed a large negative electrokinetic potential of the order of -60 ± 10 millivolts in water or in dilute aqueous solutions of potassium nitrate. Only the commercial product (precipitate), analytical grade, could be assigned a slight positive potential (+7 millivolts) by the addition of silver nitrate (figure 9). On the other hand, the fused and recrystallized products of silver bromide could not be charged positively by silver nitrate. Still, the silver ions behaved as typical potential-determining ions in as far as they decreased the zeta potential of recrystallized silver bromide from a value of -76 millivolts to a much more positive value of -15 millivolts in $4 \times 10^{-5} M$ silver nitrate. Potassium nitrate of the same concentration had hardly any effect upon the zeta potential. In this respect the behavior of fused or recrystallized silver bromide is quite different from that

reported by Julien (1), who found that fused silver bromide behaved like paraffin regarding the effect of silver nitrate and other salts upon its zeta potential.

We are not able to explain the difference in behavior found by Julien and that described in this paper.

SUMMARY

1. Citrate ions behave much more effectively as potential-determining ions on the surface of barium sulfate than sulfate ions. This is contrary to the classical view. Citrate also acts as a potential-determining ion on the surface of lead chromate.

2. There is no direct relation between the adsorbability of a salt on the surface of barium sulfate and its peptizing effect upon the colloidal precipitate. It is suggested that distinction should be made between adsorption on an "active surface" and on a "normal surface" and that the primary stability of a colloid is determined mainly by adsorption on an active surface (distribution adsorption).

3. Barium ions have a peptizing effect on colloidal barium sulfate and sulfate ions a flocculating effect. On the other hand, lead ions flocculate colloidal lead chromate and chromate ions stabilize it. This behavior of these ions is reflected by their effect upon the electrokinetic potential of barium sulfate and of lead chromate.

4. At the same concentration the effect of potential-determining ions upon the zeta potentials of barium sulfate and lead chromate is much greater in 50 per cent ethanol than in water. The difference is especially pronounced at small concentrations.

5. Lead ions behave as potential-determining ions on the surface of barium sulfate, while barium and sulfate ions behave like potential-determining ions on the surface of lead chromate (ion isomorphism).

6. Contrary to results of Kruyt and Ruysen it was found that particles of the natural product baryte qualitatively showed an electrokinetic behavior similar to that of precipitates of varying size and age.

7. Silver bromide samples showed a large negative electrokinetic potential in water or in dilute potassium nitrate solutions. Only precipitated silver bromide could be assigned a slight positive potential in silver nitrate solutions, but fused and recrystallized products remained negatively charged. Still, silver ions distinguished themselves as potential-determining ions insofar as they decreased the zeta potential in a very pronounced way.

REFERENCES

- (1) JULIEN, P. F.: Thesis, Utrecht, 1933, H. J. Paris, Amsterdam.
- (2) KOLTHOFF, I. M., AND EGGERTSEN, F. T.: *J. Phys. Chem.* **46**, 458 (1942).
- (3) KOLTHOFF, I. M., AND McNEVIN, WM.: *J. Am. Chem. Soc.* **55**, 1543 (1936).
- (4) KRUYT, H. R., AND RUYSEN, R. G.: *Koninkl. Akad. Wetenschappen Amsterdam* **37**, 498 (1934).
- (5) LAUFFER, M. A. AND GORTNER, R. A.: *J. Phys. Chem.* **42**, 641 (1938).
- (6) RUYSEN, R. G.: *J. Phys. Chem.* **44**, 265 (1940).
- (7) SMITH, G. W. AND REYERSON, L. H.: *J. Phys. Chem.* **38**, 133 (1934).
- (8) VERWEY, E. J. W.: *Chem. Rev.* **16**, 363 (1935).

THE EFFECT OF HEAT-TREATMENT ON THE SORPTION-DESORPTION HYSTERESIS CHARACTERISTICS OF SILICA GEL¹

W. O. MILLIGAN AND HENRY H. RACHFORD, JR.

*Department of Chemistry, The Rice Institute, Houston, Texas**Received August 8, 1946*

The characteristic hysteresis loop obtained from the isothermal sorption and desorption of vapors on porous substances was first observed in 1896 by van Bemmelen (2, 3) in his classical work on the silica-water system. The occurrence of sorption-desorption hysteresis has been referred to as the "van Bemmelen phenomenon" (18).

Numerous investigators (6, 8, 13, 14, 17) have verified the experimental existence of the sorption-desorption hysteresis phenomenon in many hydrous oxide-water systems, including silica gel. In contrast to the results of other investigators, Patrick (12) reported that a commercial silica gel gave no hysteresis loop when examined in a special apparatus in which elaborate precautions were taken to ensure the removal of inert gases. The sample of commercial silica gel was heated to 350°C. and was carried through several cycles of alternate evacuation and sorption of water vapor at 20°C. The isotherms obtained after this exhaustive treatment were reversible and showed no trace of a hysteresis loop. Patrick was of the opinion that these results demonstrated conclusively that sorption-desorption hysteresis was caused by the presence of air or other inert gases. However, Bartell and Almy (1), Foster (7), Lambert and Foster (8), and others observed that drastic evacuation at high temperatures does not eliminate the hysteresis loop.

Pidgeon (13) pointed out that in the experiments reported by Patrick a large volume of silica gel (about 1200 ml.) was examined in a relatively small apparatus. Pidgeon expressed the opinion that this procedure might result in tracing simultaneously the sorption and desorption curves regardless of whether the gel was decreasing or increasing in water content. In order to test this assumption, Pidgeon carried out extremely careful isotherms on silica gel, using a McBain-Baker silica-spring balance under conditions such that the volume of gel was very small as compared with the volume of the apparatus. From the observed hysteresis loop, Pidgeon concluded that the van Bemmelen phenomenon has an experimental reality. In order to test the effect of large volumes of gel, Pidgeon also placed 20 g. of gel within his apparatus, but weighed on the McBain-Baker balance only a 0.5-g. quantity. Under these conditions, the hysteresis loop was diminished or eliminated. These results appear to offer conclusive evidence that the apparent reversibility of the isotherms reported by Patrick was inherent in the experimental technique employed. However, as has been pointed out by Brunauer (4), the shapes of the silica gel isotherms reported by Patrick are

¹ Presented at the Twentieth National Colloid Symposium, which was held at Madison, Wisconsin, May 28-29, 1946.

modified from the usual S-shaped curves found by all other investigators, to curves of the Langmuir type. This suggests that the silica gel examined by Patrick's collaborators may have been different from the usual silica gels.

More recently, Taylor (15) obtained isosteres for the system silica gel-water, and did not detect any appreciable hysteresis.

In this laboratory it has been found possible to diminish drastically or to eliminate the hysteresis characteristics of a number of hydrous oxide gels by treatment prior to their precipitation (19, 20).

In this present work sorption-desorption isotherms have been obtained for a series of silica gels which had been subjected to systematic heat-treatments from room temperature to about 1000°C.

EXPERIMENTAL

Preparation of samples

A quantity of moist, commercial silica gel which had not been previously heated above room temperature was allowed to come to equilibrium with the moisture in the atmosphere. After several days the air-dried lumps of translucent or faintly opalescent gel were crushed to a white powder.

Preliminary experiments suggested that the gel was very sensitive to marked changes in humidity, and therefore elaborate precautions were taken to ensure that all portions of the gel were treated exactly alike, except for the temperature of heat-treatment. Twelve separate portions of the air-dried gel were exposed to a current of air saturated with water vapor. The samples were weighed twice weekly until no further change in weight occurred. After approximately 6 weeks the samples came to constant weight, and were heated for periods of 2 hr. at the following temperatures, respectively: 30°, 200°, 300°, 400°, 450°, 500°, 600°, 650°, 725°, 790°, 880°, and 930°C. After the heat-treatment, the gels were allowed again to come to equilibrium with the water vapor in the atmosphere. In preliminary experiments with a series of samples which were not subjected to these elaborate precautions, the resulting isotherms were somewhat erratic.

APPARATUS

Complete sorption-desorption isotherms at 12.00°C. were obtained for the twelve heat-treated samples in an apparatus already described (11). The temperature was kept constant to within 0.001°C. During sorption or desorption, care was taken to add or remove exceedingly small increments or decrements of water vapor, in order that the successive points on the curves be obtained under substantially isobaric conditions. As in the work of Pidgeon, the total volume of gel was very small (about 1.8 ml. for six samples), whereas the volume of the apparatus was large (about 7 liters). The samples were not subjected to a further heat-treatment within the apparatus, (a) since several investigators (1, 7, 8) have demonstrated that such a procedure does not appreciably modify the hysteresis characteristics of silica gel, and (b) since we were concerned with examining the samples as they exist after the careful heat-treatments described

above. Following the same procedure used previously in this laboratory, the samples were thoroughly evacuated at 12.00°C., after which the sorption branch of the isotherm was first obtained, and then the desorption branch. A vacuum of 5-10 millimicrons as measured by a calibrated ionization gauge was attained during the evacuation. The twelve complete isotherms are given in figures 1-12

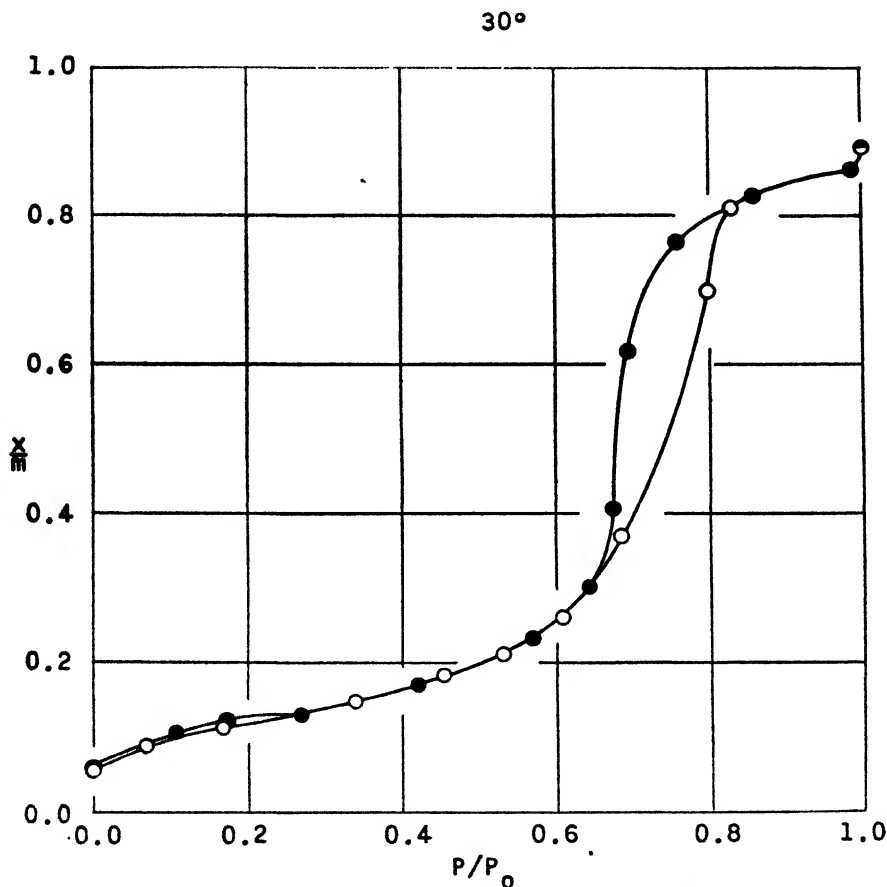


Fig. 1. Sorption-desorption isotherm for silica gel at 30°C.

X-RAY EXAMINATION

The samples described above were examined by the standard x-ray diffraction method, using Cr K α x-radiation. All of them were found to be amorphous to x-rays. From previous x-ray diffraction work on the same gel, it was known that a much longer heating period is required to transform the amorphous silica to α -cristobalite even at temperatures as high as 950°C.

DISCUSSION

It will be noted that the characteristic hysteresis loop is not destroyed by moderate or even excessive heat-treatment. Indeed there is some evidence

that heating to temperatures of about 400–600°C. actually increases the area within the loop.

In figures 13–23 is plotted the volume of adsorbed water per gram of sample (V/m) against pore size as calculated from the Kelvin equation (16):

$$\ln P - \ln P_0 = -2\gamma V/rRT$$

200°

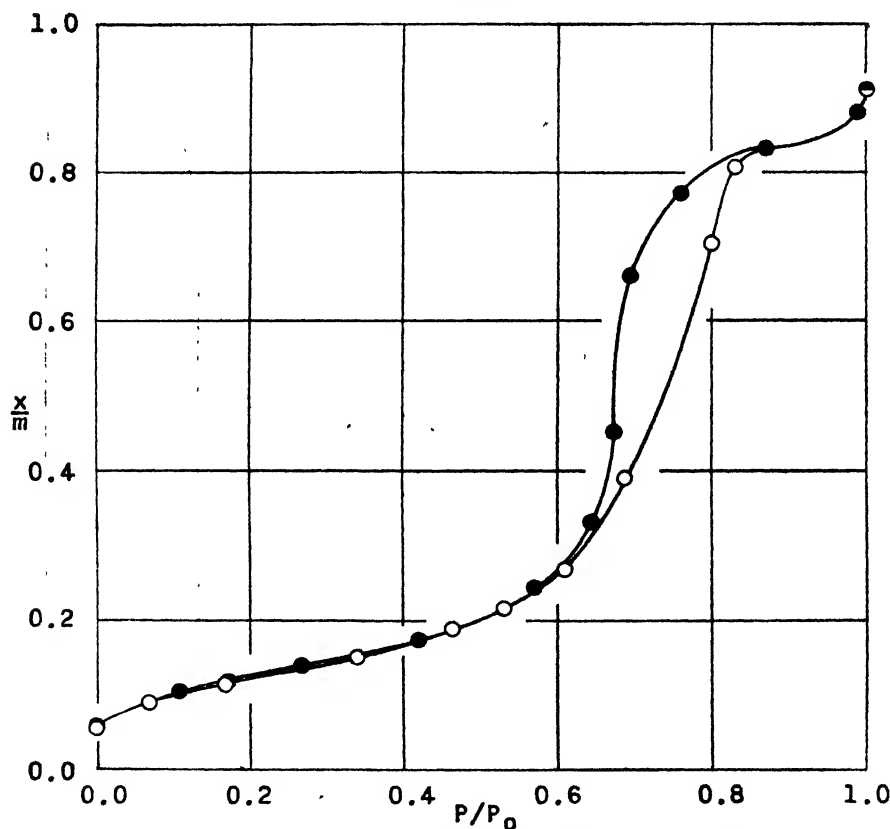


FIG. 2. Sorption-desorption isotherm for silica gel at 200°C.

where γ = surface tension,
 V = molal volume of water,
 T = absolute temperature,
 R = gas constant,
 r = radius of assumed pore,
 P = observed vapor pressure, and
 P_0 = vapor pressure of water at 12.00°C.

No attempt was made to correct the radius of the pores for mono- or multi-layers of water upon the walls of the pores. In figures 13–23 is also plotted dV/dr as a function of pore radius, according to well-known methods (cf. Bushey

(5, 10)). It is convenient to assume that these curves are a measure of the frequency of occurrence of pores of various sizes. The height of the peak may be assumed to approximate the number of pores of the most frequent size.

It will be noted that heat-treatment of the original gel does not appreciably modify the distribution or the size of the pores, but does appear to diminish their number. Any attempt at this time to postulate a mechanism for the decrease in number of pores would be premature.

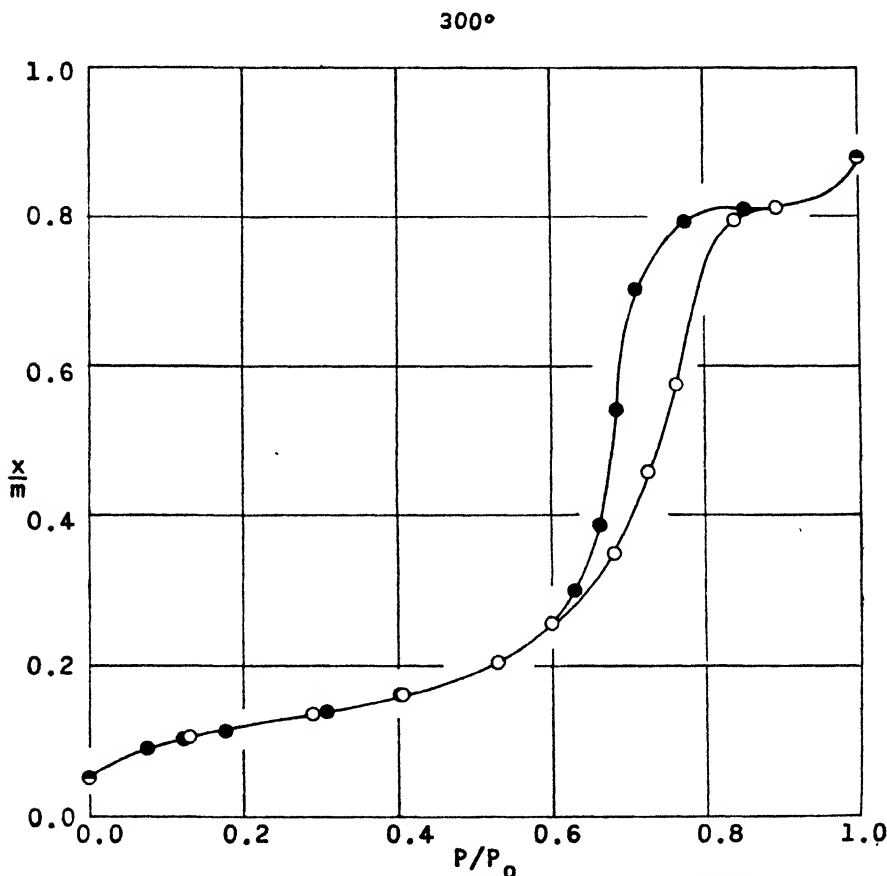


FIG. 3. Sorption-desorption isotherm for silica gel at 300°C.

In figure 24 is given the surface area of the various samples as a function of temperature of heat-treatment. The surface areas have been calculated according to the standard BET (4) and Harkins and Jura (4) methods. The results of the calculations by these two independent methods (*cf.* 9) agree quite well. It is apparent from the results that heat-treatment at temperatures around 200°C. actually increases the available surface slightly, and that additional heat-treatment at more elevated temperature decreases the available surface in a regular manner. It is believed that these results, as well as previous

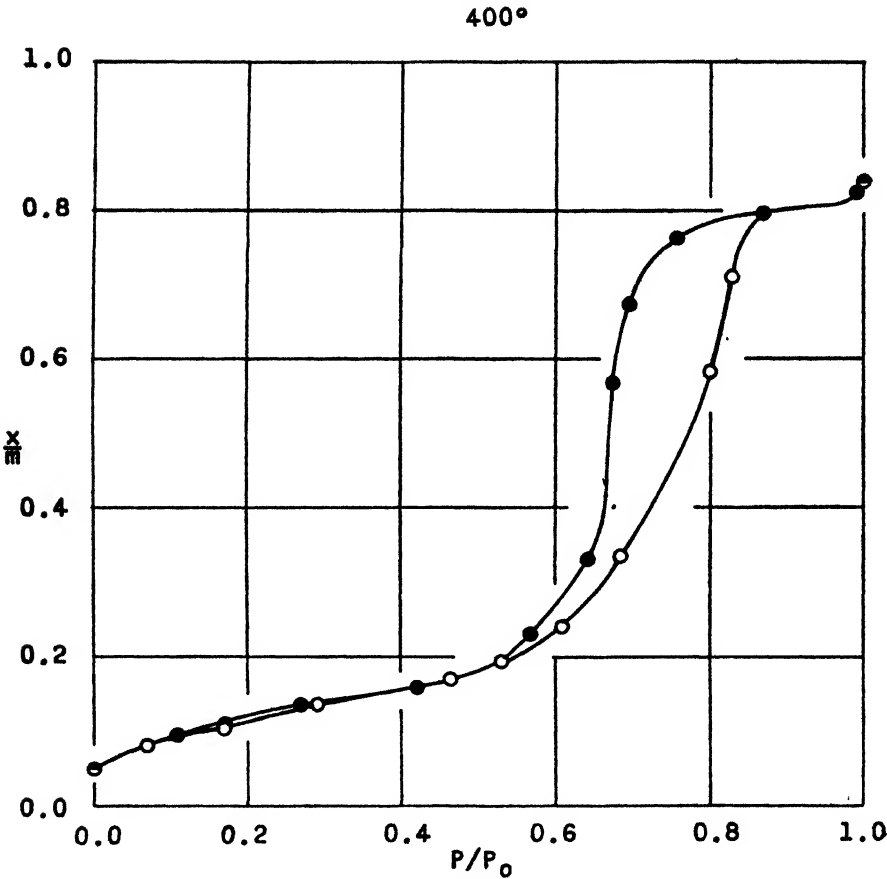


FIG. 4. Sorption-desorption isotherm for silica gel at 400°C.

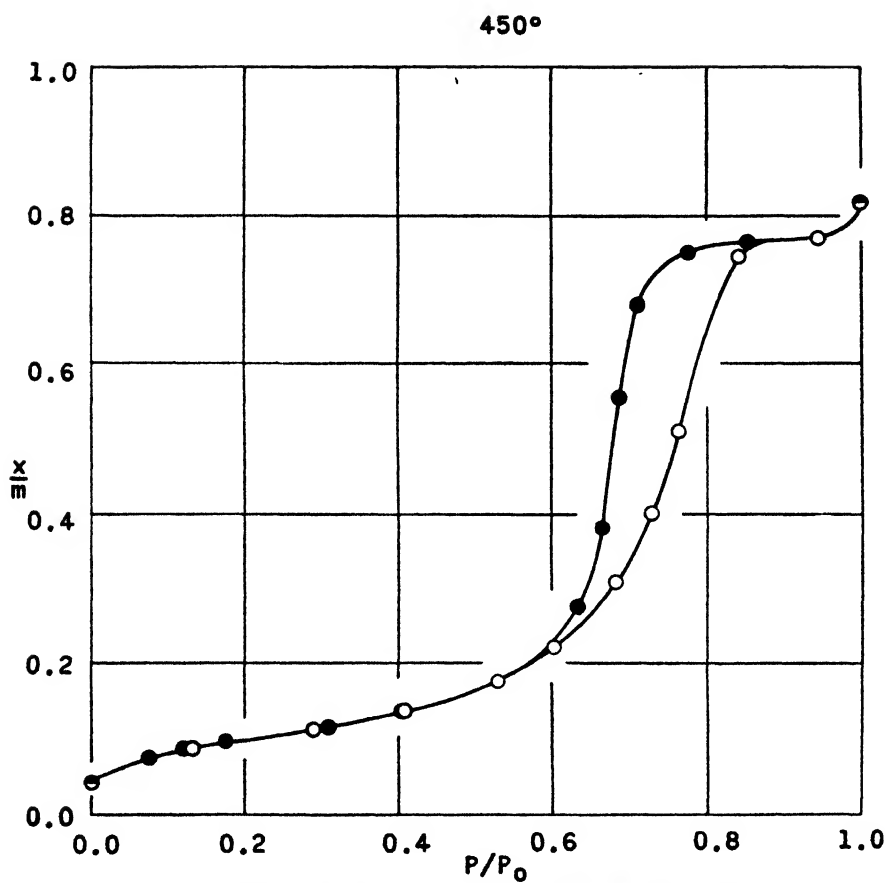


FIG. 5. Sorption-desorption isotherm for silica gel at 450°C.

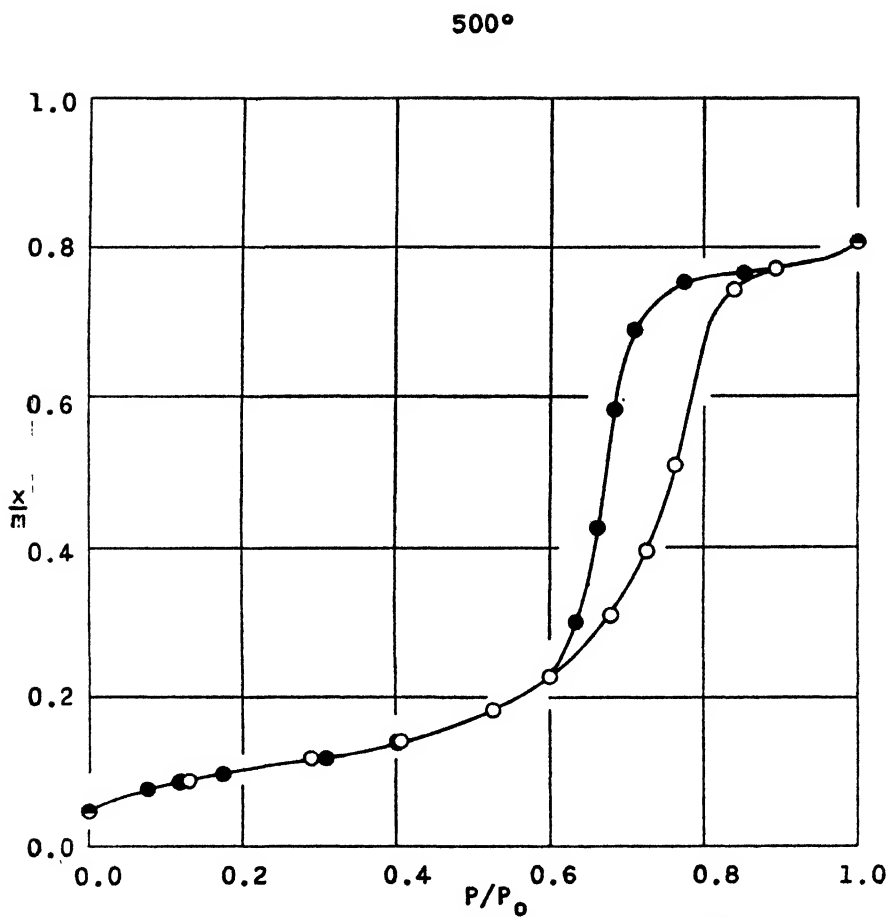


FIG. 6. Sorption-desorption isotherm for silica gel at 500°C.

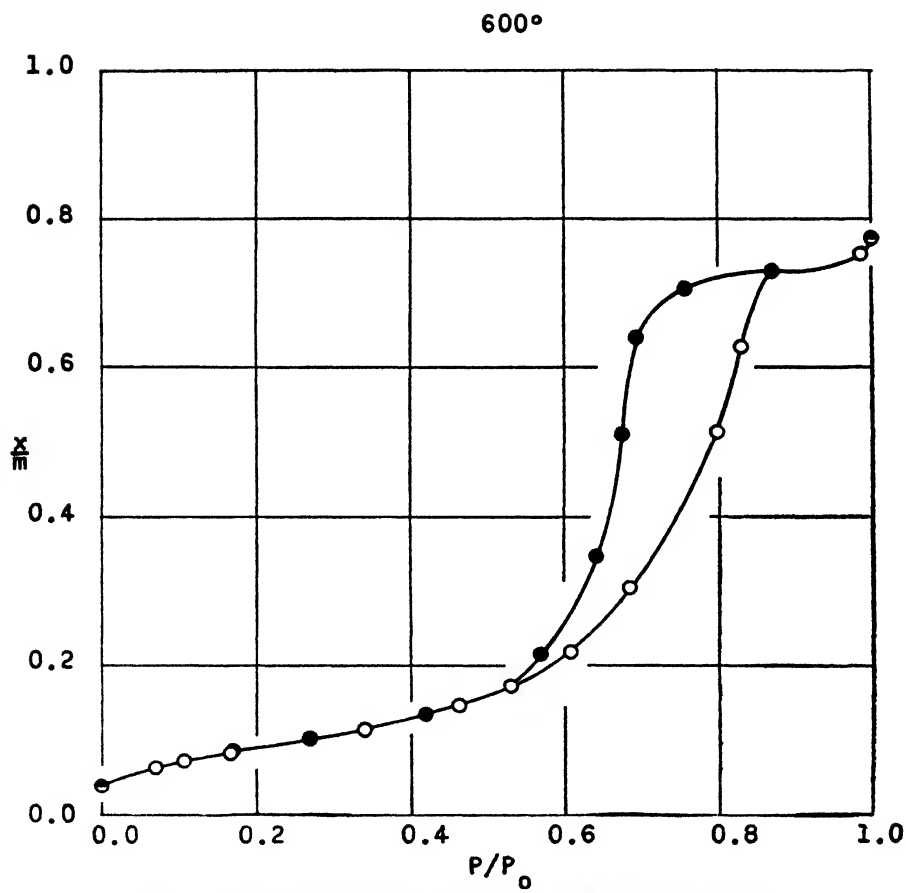


FIG. 7. Sorption-desorption isotherm for silica gel at 600°C.

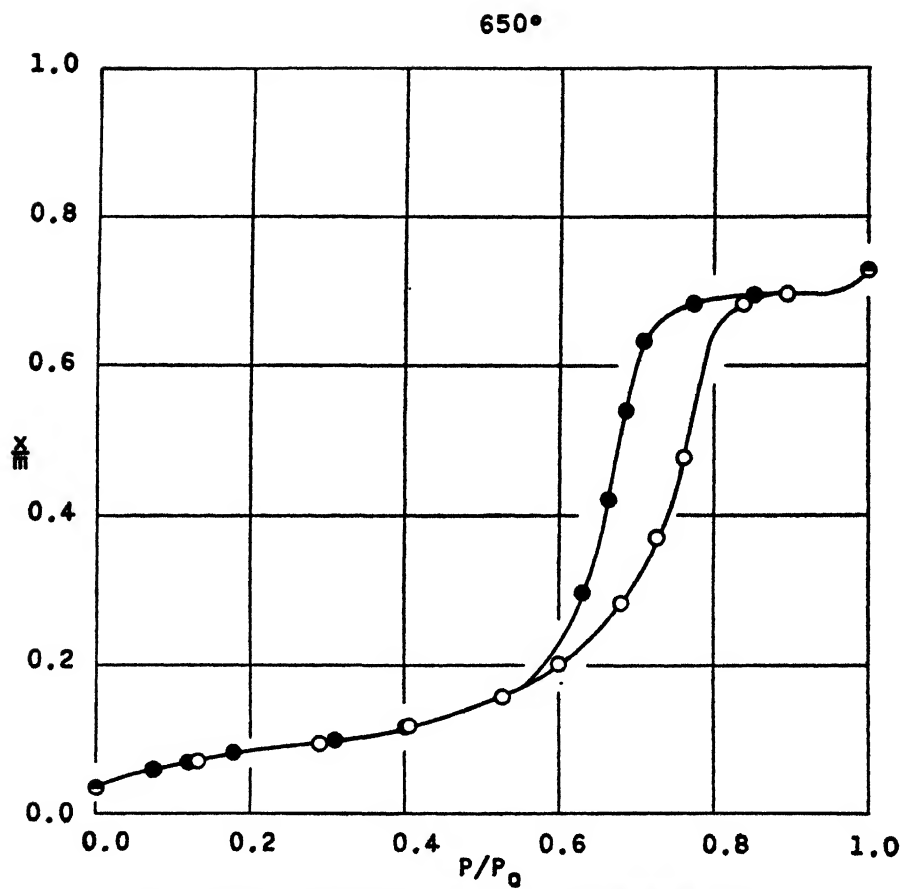


FIG. 8. Sorption-desorption isotherm for silica gel at 650°C.

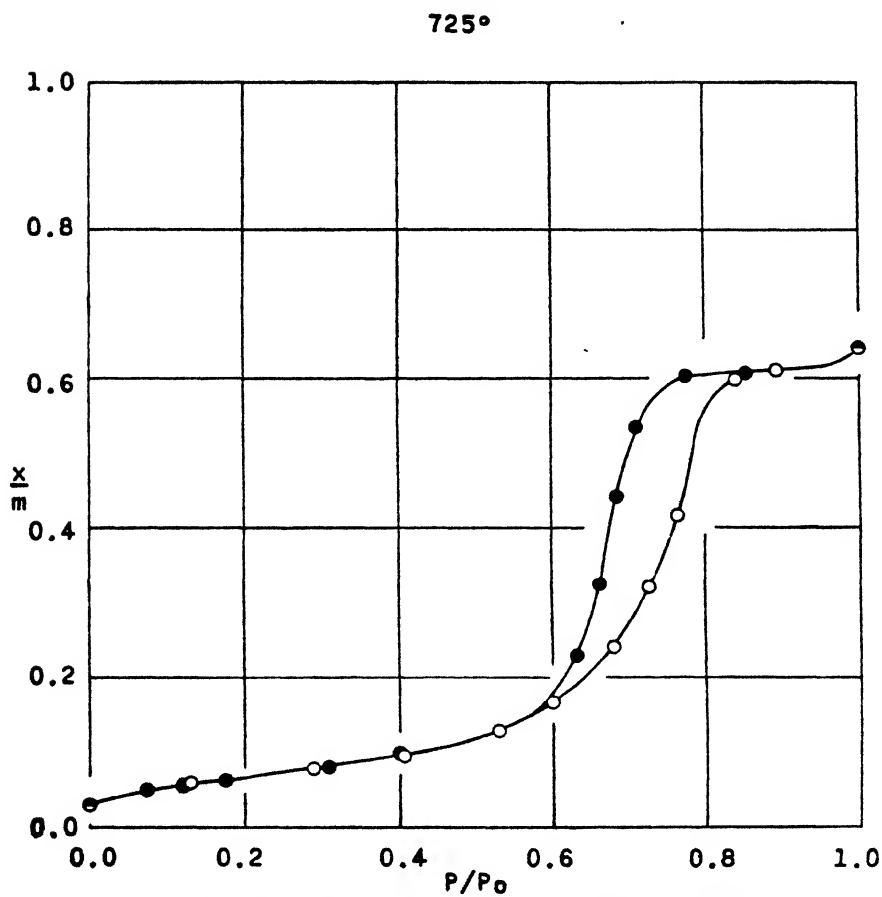


FIG. 9. Sorption-desorption isotherm for silica gel at 725°C.

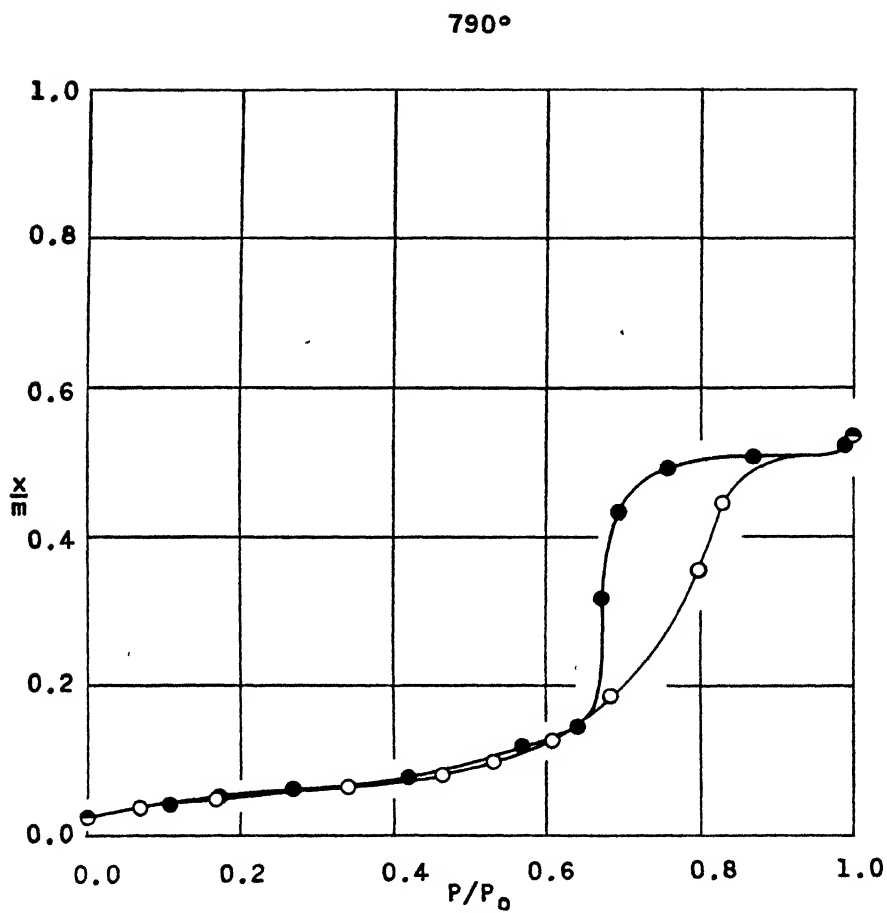


Fig. 10. Sorption-desorption isotherm for silica gel at 790°C.

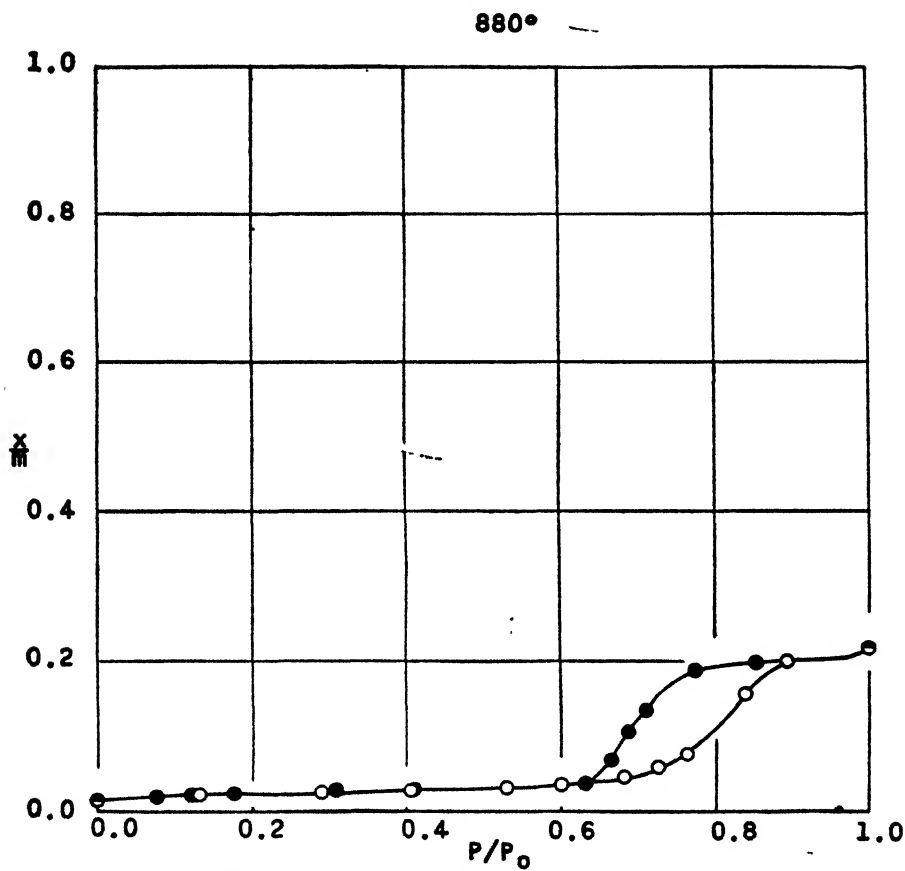


FIG. 11. Sorption-desorption isotherm for silica gel at 880°C.

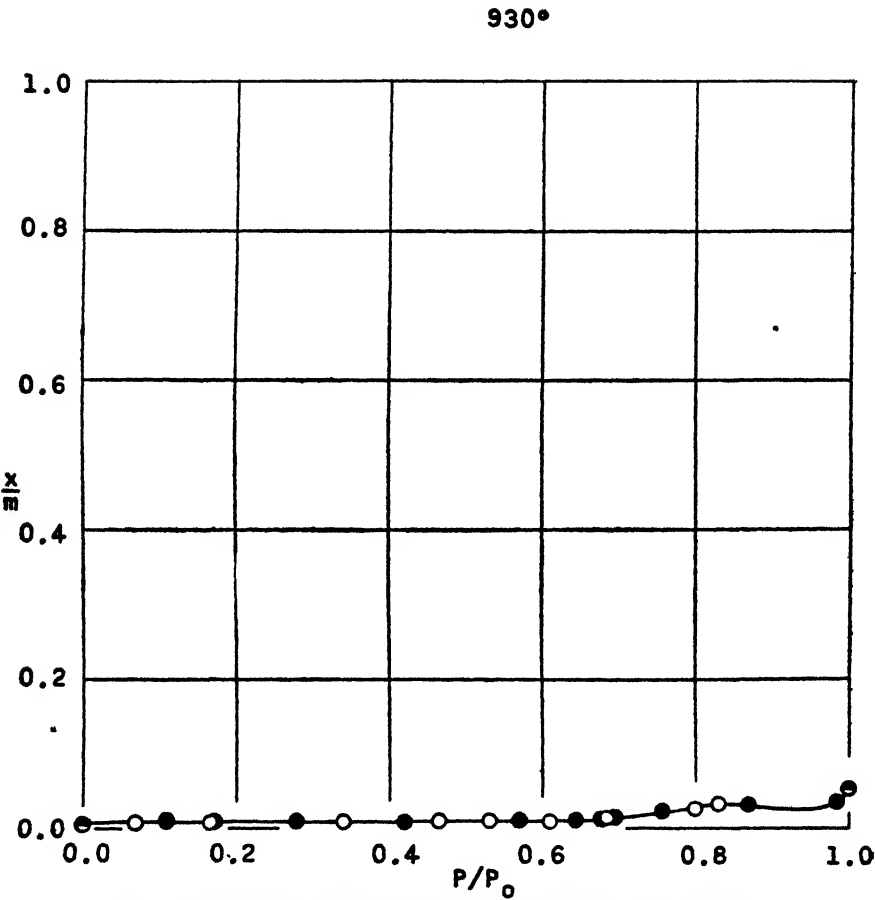


FIG. 12. Sorption-desorption isotherm for silica gel at 930°C.

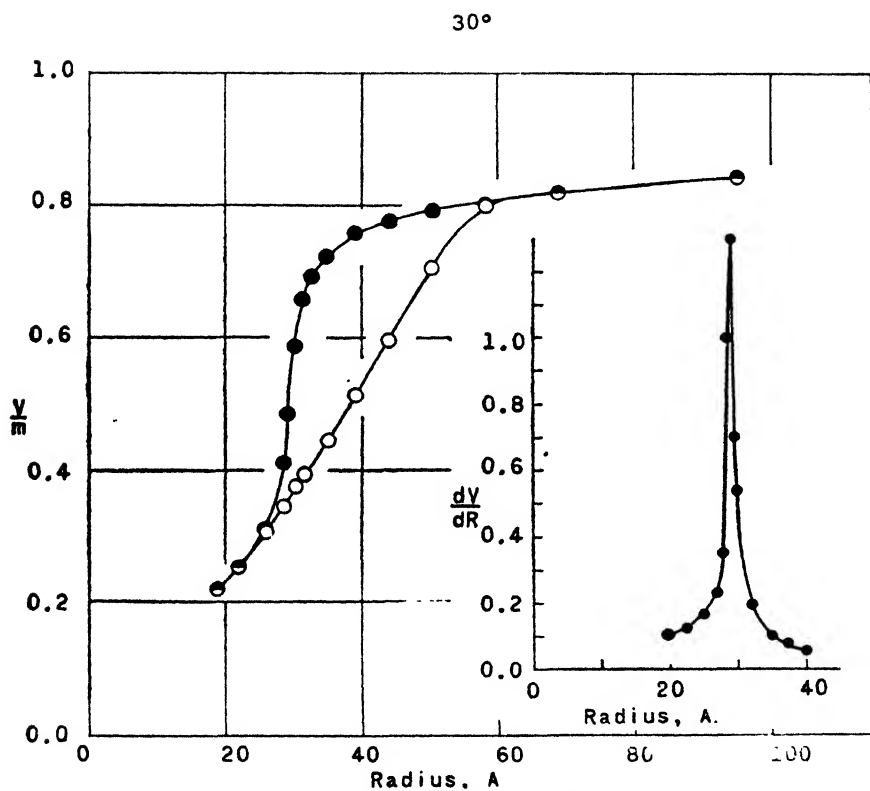


FIG. 13. Pore-distribution curve for silica gel at 30°C.

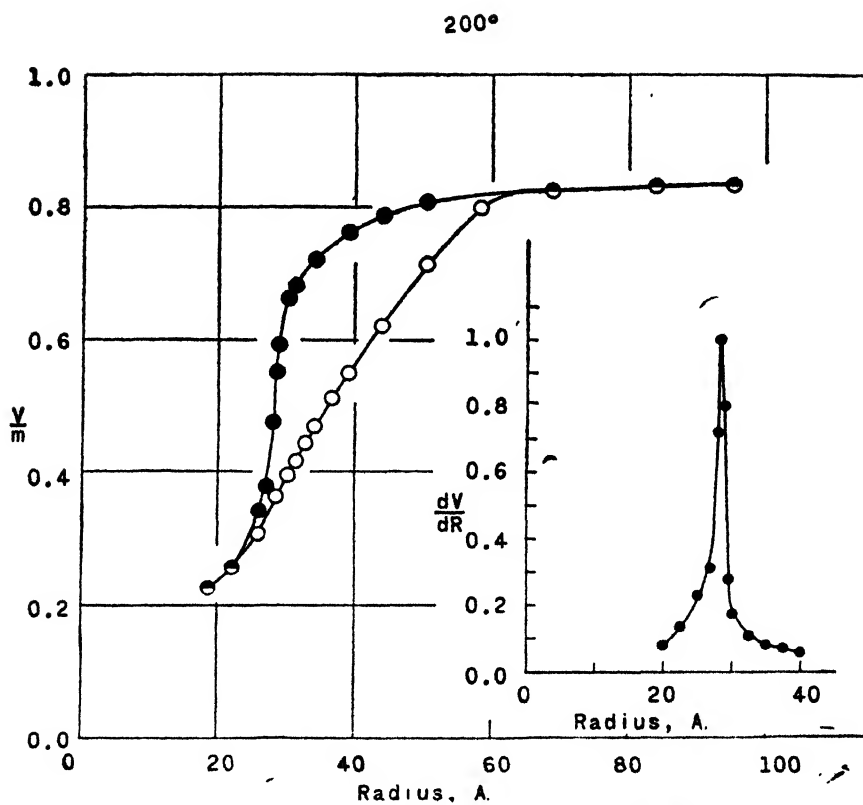


FIG. 14. Pore-distribution curve for silica gel at 200°C.

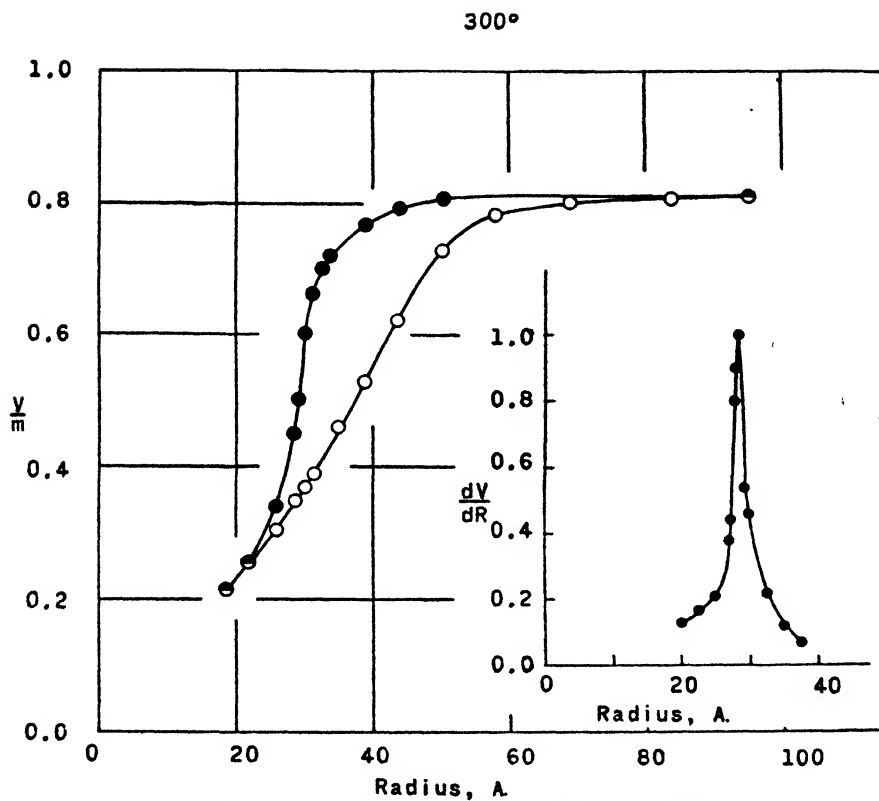


FIG. 15. Pore-distribution curve for silica gel at 300°C.

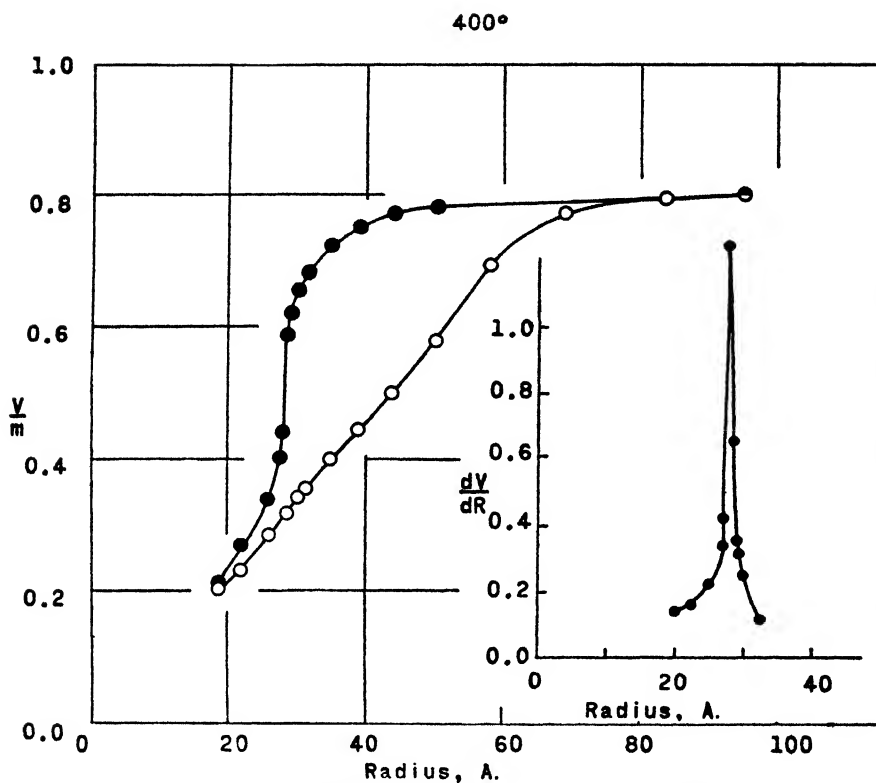


FIG. 16. Pore-distribution curve for silica gel at 400°C.

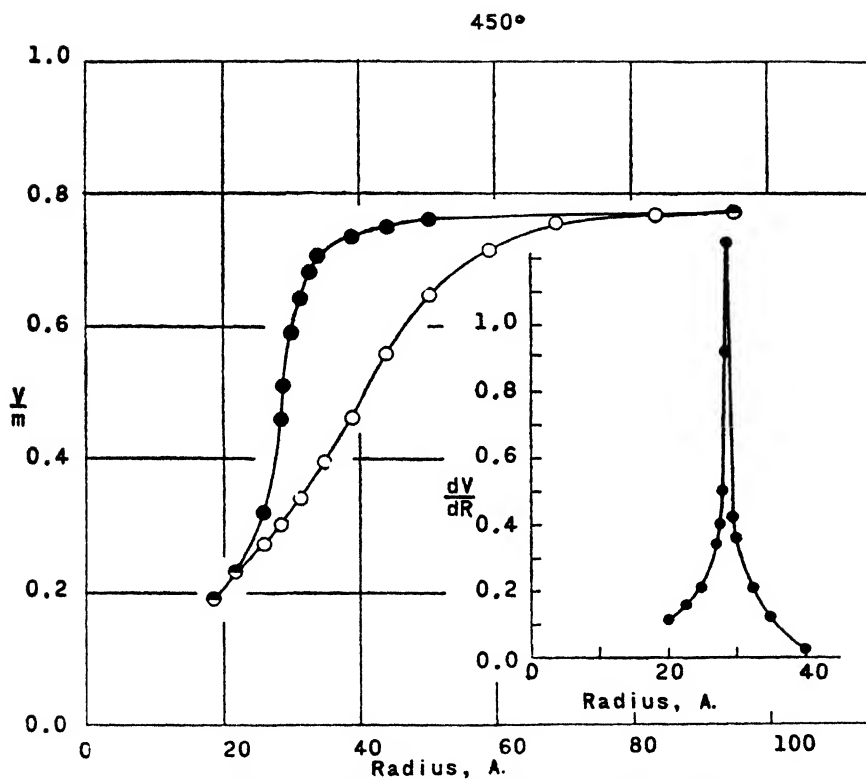


FIG. 17. Pore-distribution curve for silica gel at 450°C.

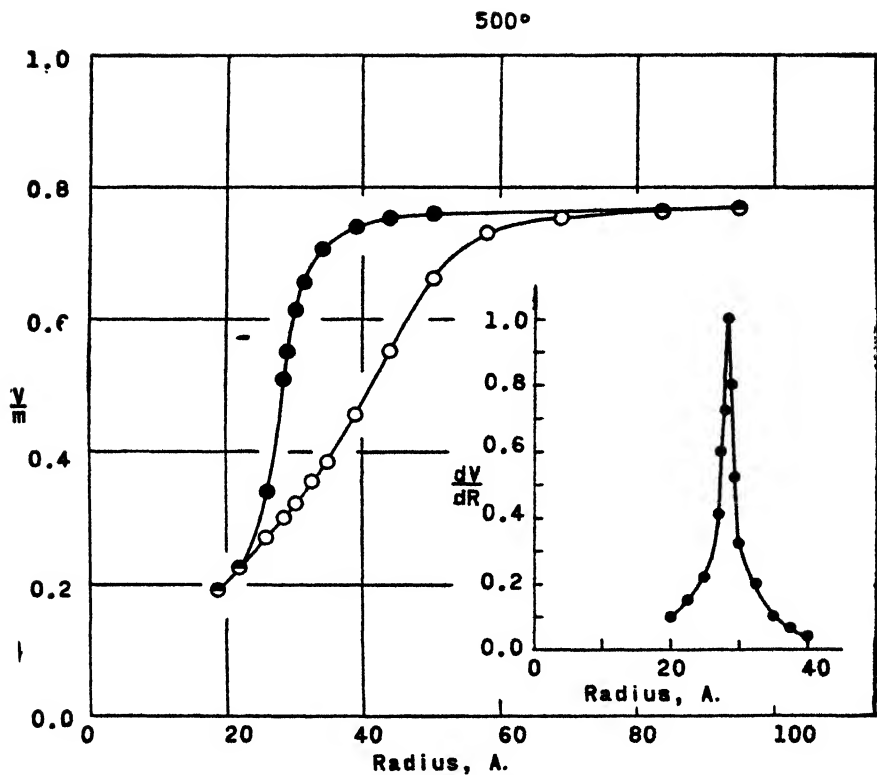


FIG. 18. Pore-distribution curve for silica gel at 500°C.

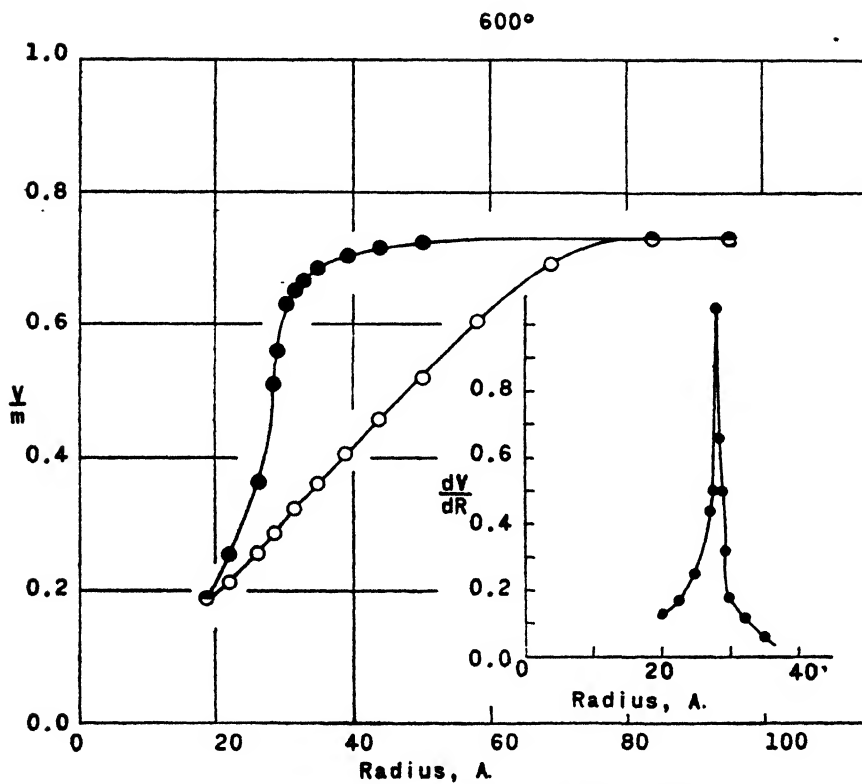


FIG. 19. Pore-distribution curve for silica gel at 600°C.

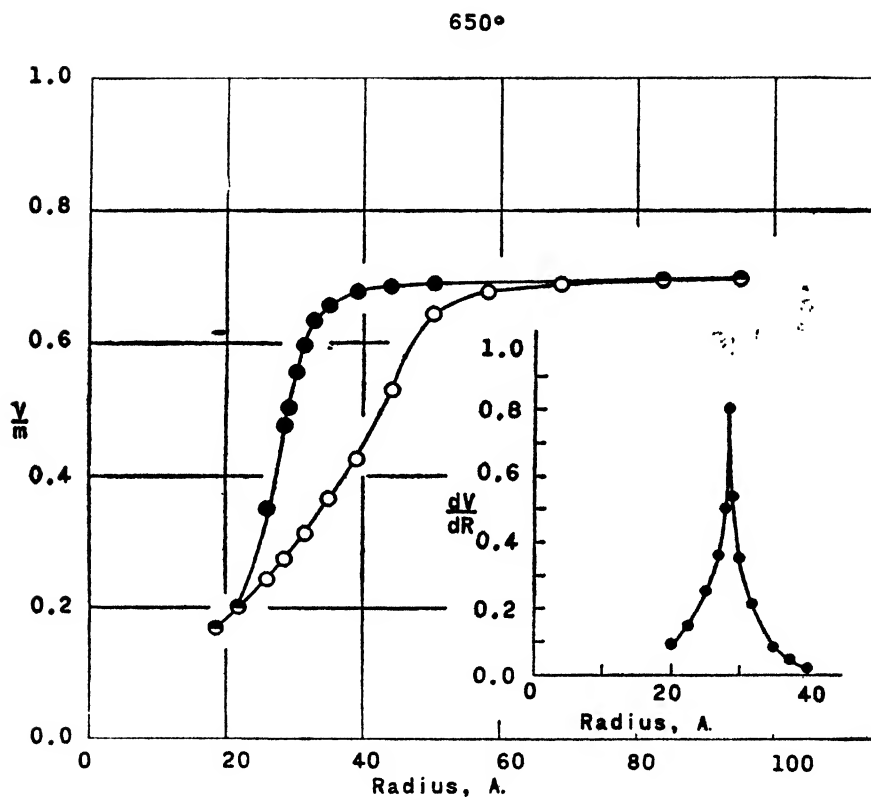


FIG. 20. Pore-distribution curve for silica gel at 650°C.

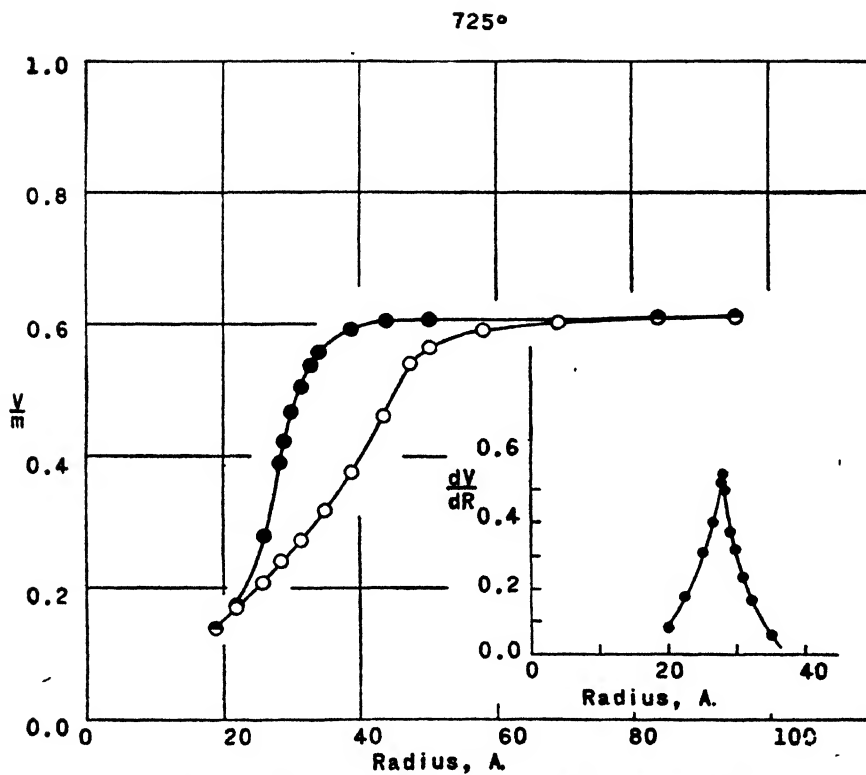


FIG. 21. Pore-distribution curve for silica gel at 725°C.

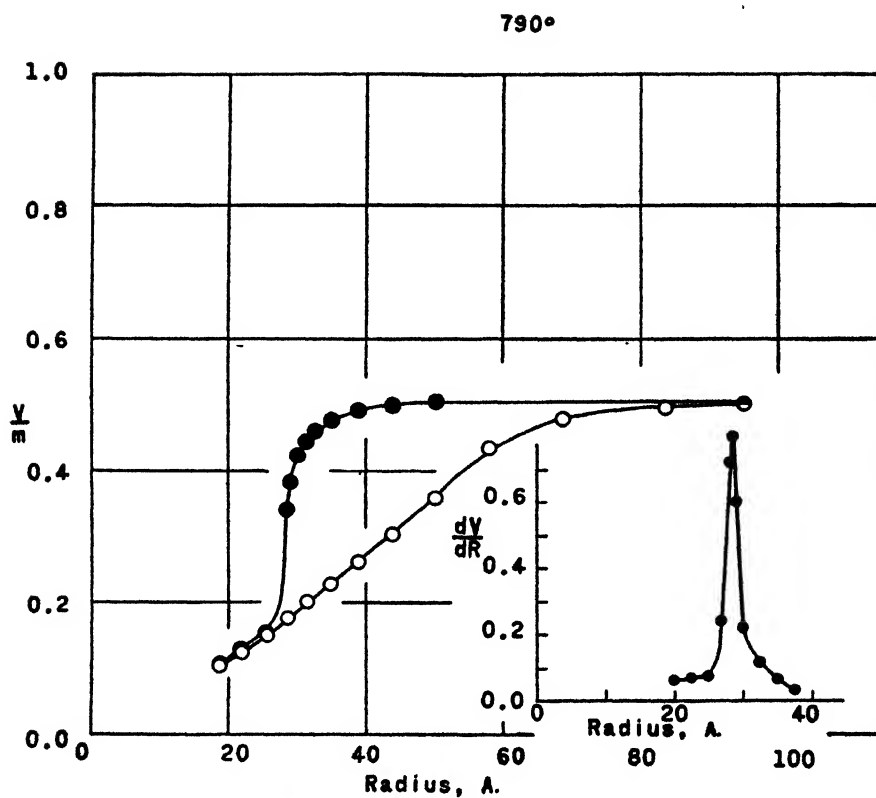


FIG. 22. Pore-distribution curve for silica gel at 790°C.

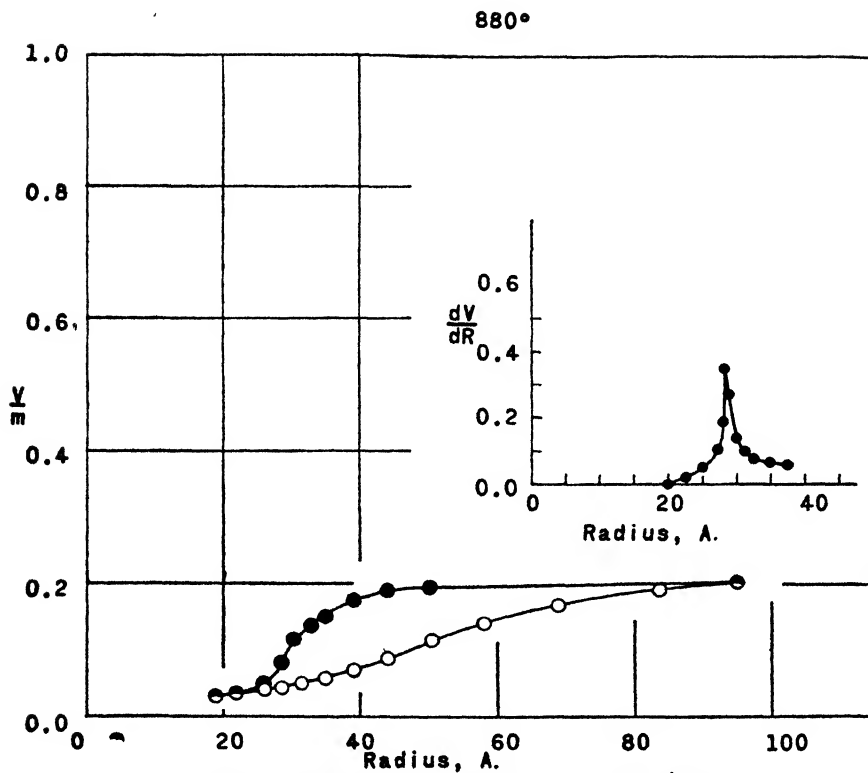


FIG. 23. Pore-distribution curve for silica gel at 880°C.

results (19, 20) from this laboratory, wherein hysteresis was diminished or eliminated by treatment of the solutions prior to precipitation of the gels, will be helpful in evaluating the various theories of hysteresis which have been proposed by other investigators.

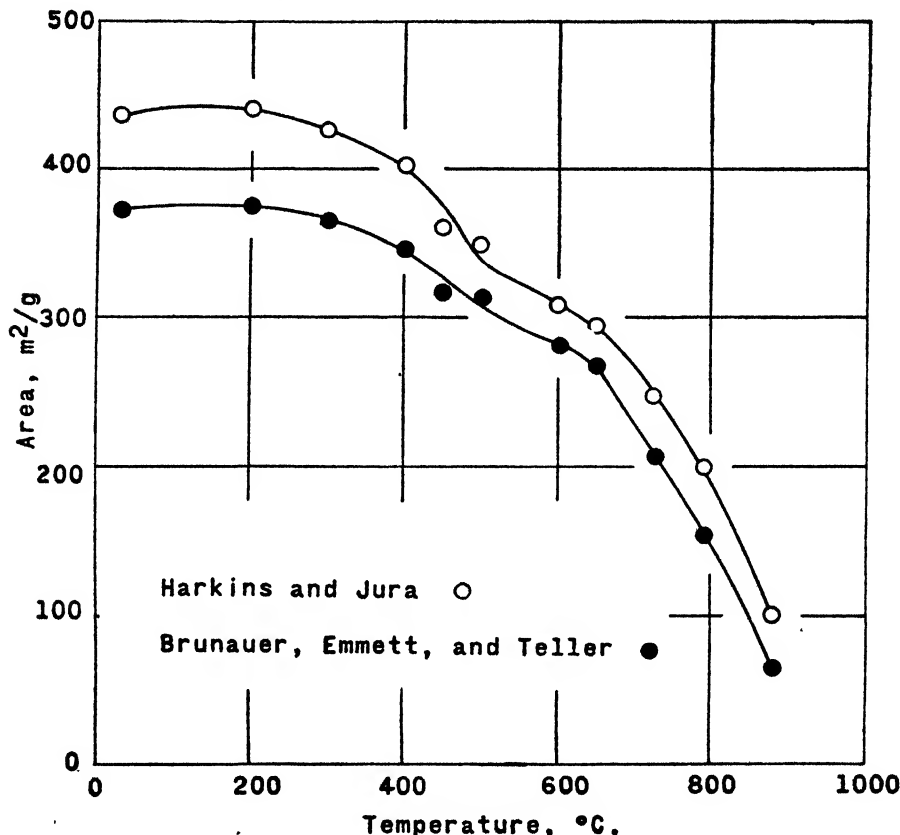


FIG. 24. Surface area of silica gels as a function of temperature of heat-treatment

REFERENCES

- (1) BARTELL AND ALMY: *J. Phys. Chem.* **36**, 475 (1932).
- (2) VAN BEMMELN: *Z. anorg. allgem. Chem.* **13**, 233 (1897).
- (3) VAN BEMMELN: *Die Adsorption*. T. Steinkopff, Dresden (1910).
- (4) BRUNAUER: *The Adsorption of Gases and Vapors. I. Physical Adsorption*. Princeton University Press, Princeton, New Jersey (1943).
- (5) BUSHEY: Thesis, The Rice Institute, 1944.
- (6) COHAN: *J. Am. Chem. Soc.* **66**, 98 (1944).
- (7) FOSTER: *Proc. Roy. Soc. (London)* **A146**, 129 (1934).
- (8) LAMBERT AND FOSTER: *Proc. Roy. Soc. (London)* **A134**, 246 (1932).
- (9) LIVINGSTON: *J. Chem. Phys.* **12**, 466 (1944).
- (10) MILLIGAN AND BUSHEY: Results presented before the Division of Colloid Chemistry at the 108th Meeting of the American Chemical Society, which was held in New York City, September 11-15, 1944.

- (11) MILLIGAN, WEISER, AND SIMPSON: Results presented before the Division of Colloid Chemistry at the 105th Meeting of the American Chemical Society, which was held in Detroit, Michigan, April 12-16, 1943.
- (12) PATRICK: Colloid Symposium Monograph 7, 129 (1930).
- (13) PIDGEON: Can. J. Research 10, 713 (1934).
- (14) RAO: J. Phys. Chem. 45, 500 (1941).
- (15) TAYLOR: Ind. Eng. Chem. 37, 849 (1945).
- (16) THOMSON: Phil. Mag. [4] 42, 448 (1871).
- (17) URQUHART: J. Textile Ind. 20, 117 (1929).
- (18) WEISER, MILLIGAN, AND COPPOC: J. Phys. Chem. 43, 1109 (1939).
- (19) WEISER, MILLIGAN, AND HOLMES: J. Phys. Chem. 46, 586 (1942).
- (20) WEISER, MILLIGAN, AND SIMPSON: J. Phys. Chem. 46, 1051 (1942).

COMMUNICATION TO THE EDITOR

THE EQUILIBRIUM SPREADING COEFFICIENT OF AMPHIPATHIC ORGANIC LIQUIDS ON WATER¹

H. L. Cupples (J. Phys. Chem. 50, 283 (1946)) has again taken exception to our reasoning concerning the equilibrium spreading coefficient (J. Phys. Chem. 49, 239 (1945)). In his opinion we err in assuming that W'_A is the work of adhesion between the organic bulk phase and the interfacial layer of the amphipathic compound.

In an earlier communication Cupples (J. Phys. Chem. 48, 75 (1944)) has agreed with us that

$$F'_s = \gamma'_w - \gamma'_o - \gamma'_{wo} = W'_A - W'_c$$

However, since $W'_c = 2\gamma'_o$, it follows that

$$W'_A = \gamma'_w + \gamma'_o - \gamma'_{wo}$$

where γ'_{wo} is the interfacial tension between the mutually saturated phases, γ'_o the surface tension of the bulk phase of the amphipathic organic compound saturated with water, and γ'_w the surface tension of the aqueous phase, saturated with, and *having a surface film of, the amphipathic compound* with the hydrocarbon chains turned upward and a pressure corresponding to the equilibrium surface pressure. W'_A is thus the change in free surface energy which occurs on bringing the two mutually saturated phases in contact, i.e., on establishing contact between the organic bulk phase and the monolayer in the surface of the aqueous phase. For this reason the cross-section BB' in Fig. 1 of our paper is assumed to be above the oriented layer; (we have not shown in Fig. 1 the oriented layer which, in the equilibrium state, also extends over the water surface). H. L. Cupples has apparently overlooked in his criticism that, in the evaluation of W'_A , we are concerned with an aqueous phase which is fully saturated with the

¹ Received September 17, 1946.

amphipathic compound and therefore has a surface film of the latter at a pressure corresponding to the equilibrium pressure.

A similar reasoning is implied by W. D. Harkins, discussing the "final" spreading coefficient of heptyl alcohol on water in his article, "General Thermodynamic Theory of Spreading" (J. Chem. Phys. **9**, 559 (1941)), to which reference was made in our paper. It is clear from the discussion that Harkins envisages separation in a plane corresponding to that of cross-section BB' in Fig. 1 of our paper.

Finally, the choice of cross-section BB' as the plane of separation above the oriented interfacial layer, and beyond the range of influence of the water molecules in the aqueous phase, is indicated by the actual behavior of the systems involved. When a drop of oleic acid is brought on a water surface, it will spread to a duplex film first, but soon contraction occurs to lenses whilst a monolayer is left in the water surface. Moreover, if the water surface is covered by a monolayer of oleic acid and a drop of oleic acid is placed on it, the drop will not spread but remain as a lens. This behavior is obviously due to the fact that the work of cohesion of the oleic acid bulk phase is greater than the work of adhesion between the bulk phase and the oleic acid monolayer in the water surface.

Cupples has also objected to the derivation of our equation 4. Now W'_A is the work involved in separating the organic bulk phase from the monolayer in the water surface *which is oriented*. This means that W'_A is equivalent to the work of cohesion

$$W'_c = W_c^H + W'_p \quad (2a)$$

except that, on separation, it is necessary only to orient the layer of molecules at the surface of the bulk phase, since the layer on the water surface is already oriented. Therefore the work of orientation included in W'_A is about one-half of that included in W'_c , though this is only approximate for reasons set out in our previous publication. Thus

$$W'_A \cong W'_c - \frac{W'_p}{2}$$

and by equation 2a we obtain

$$W'_A \cong W_c + \frac{W'_p}{2} \quad (4)$$

The notation in this communication is the same as that used previously (J. Phys. Chem. **49**, 239 (1945)).

Chemistry Department,
Melbourne University
Melbourne, Australia
and

Trinity College, Cambridge, England

E. HEYMANN.
A. YOFFE.

NEW BOOKS

Surface Active Agents. By C. B. F. YOUNG AND K. W. COONS. Brooklyn, New York: The Chemical Publishing Company, Inc., 1945. Price: \$6.00.

This book has been criticized as being largely a compilation from trade catalogs and similar sources. However, it has its definite uses, as the authors point out, by calling the attention of industrial chemists to concrete examples of surface phenomena which have been turned to useful account. Many such instances have been developed, such as household recipes or trade or family secrets, where the originators did not know the reasons for the use of the ingredients they utilized. The authors rightly emphasize that reference to such examples can be stimulating in suggesting ideas about the reader's own industrial problems. It is somewhat like the stimulus which any scientist or industrialist receives by visiting a factory in some unrelated industry, which nevertheless suggests ideas which he can develop in his own field.

The book cannot be taken as a piece of careful scientific writing. For example, on page 4, under the heading "Definitions", the definition of surface-active agents, the subject of the book itself, is "Compounds which cause variations in either interfacial tension or surface tension." The authors do not mean this as a scientific statement. It is either meaningless or untrue. The authors had just before pointed out that sodium chloride is not a surface-active agent, although it does raise the surface tension of water. Practically all dissolved substances and many insoluble substances cause variations, either plus or minus, in the surface tension of water; and therefore all are included in the "definition", although this is by no means the intention of the authors.

Again, on the same page, the authors state that the forces between molecules are equal in all directions, whereas the most significant feature of surface phenomena is the orientation of molecules caused by the unequal distribution of molecular forces around the different parts of the same molecule. On the following page, "work" is expressed in "dynes per centimeter."

Incorrect or misleading statements such as those just cited are not uncommon in scientific writing, and lend support to the allegation that scientists as a rule are uneducated men. The fault must lie in the system of education in the science departments of our universities. For the convenience of instructors, too much reliance is placed upon the true or false system of examinations. The more intelligent pupils realize that they are being forced to give answers that are not strictly true but have to be fitted into the Procrustean framework provided by the busy examiner. It is seldom that a pupil is required to produce a piece of rigorous scientific writing in which each statement is true to the best of his knowledge and power of expression. However, this is no valid reason why professors or trained industrial chemists or scientists in general should be careless of the truth.

Nevertheless the vitality of the scientific method and the permanence of demonstrable fact are such that man's material achievements have been accomplished in spite of half-truths and imperfect theory. The purest scientist has to reflect that much of current theory which he is teaching, viewed in the light of previous history, will prove to be imperfect or erroneous and only the stubborn scientific facts will endure. However, this is no reason for publishing statements that are obviously untrue or misleading or not expressed to the best of one's ability.

The book brings together a lot of information of proven utility. It begins with a chapter on the "Theory of Surface Tension", already commented upon. Next is a detailed account of "Determination of Surface Tension", and much of the illustrative material is taken from the authors' own work. The reader will be dismayed and bewildered by figures 6 and 7, which indicate that none of the methods of determining the surface tension of water give the value recorded in the *International Critical Tables* or *Landolt-Börnstein* but that, depending upon the six methods given, the surface tension of water varies between 68.9 and 91.3. Furthermore, when the dissolved substance is added, in figure 7, some of the methods

show a rapid diminution of surface tension, others an increase above that of water. . . . What is truth?

The remainder of Part I is frankly mainly a condensation from a well-known symposium, but includes a convenient listing of commercial wetting agents and detergents.

Part II has a chapter each on "Emulsions"; "Plating, Metal Cleaning, Pickling and Etching"; "Cosmetics"; "Leather"; "Flotation"; "Inks"; "Application of Surface Tension to Textiles"; "Cutting and Soluble Oils"; "Adhesives"; "Foods"; "Lubrication"; and "Soldering, Brazing and Welding"—all with illustrative formulae and a modicum of theory. This constitutes the brief compendium of practical information taken from these various fields. Much of it remains a challenge to the scientist.

J. W. MCBAIN.

Fundamentals of Physics. By HENRY SEMAT. 593 pp. New York: Farrar and Rinehart, 1946. Price: \$4.00.

In the preface the author indicates that this text is intended as a first-year college physics text for students having different degrees of preparation. The most advanced mathematics employed is trigonometry and this very sparingly. Each of the thirty-two chapters includes a set of questions and a set of problems. The questions should be useful to the student in his studying and in many cases will be valuable for stimulating class discussions. The problems are fairly simple, generally involving the application of only a single principle. Answers are given to all odd-numbered problems; answers to the remaining problems can be obtained.

The text contains a liberal number of carefully worked illustrative examples. Both the metric and English systems of units are employed. To avoid confusion in the discussion of mass, weight, and subsequent topics in mechanics, the only units of force mentioned are the dyne and pound; gram force and poundal are avoided entirely. The entire discussion of Newton's laws and the definition of mass and force are clearer than those found in most elementary texts. In the section on electricity and magnetism, the electrostatic, electromagnetic, and practical systems of units are employed in their appropriate places.

Some of the more fundamental derivations of elementary physics are omitted. For example, the relation between period, displacement, and acceleration for a simple harmonic motion is not discussed. The formula for the period of a simple harmonic motion is stated but not derived. In the section on rotational motion extensive use is made of the formula relating to torque, moment of inertia, and angular acceleration of a rigid body free to rotate about a fixed axis without attempting to derive it. The same statement may be made about the use of the theorem for computing the moment of inertia about an axis parallel to one through the center of mass. No attempt is made to derive the relation between focal length and object and image distance for a lens or spherical mirror, although considerable use is made of the equation. Again, in the section on electricity a whole chapter is devoted to alternating current circuits, including series circuits containing resistance inductance and capacitance. The circuits are solved by the familiar vector diagram method. However, nowhere in the text is mention made of the generation of a sinusoidal curve by a rotating vector. The expression for conductive reactance is used without explanation of its origin.

In spite of some of these shortcomings, the book should be very useful as a beginning text. Presentation of material is in a straightforward and logical manner. Explanations are generally clear and concise. Because of the rather elementary approach to most topics its level is too low for use by engineering students, unless the course were followed by one employing a more mathematical treatment.

A few errors are to be found. On page 125 a slip has been made in writing the last equation. In several places on page 359 inductive reactance is written in place of capacitive reactance.

ALFRED O. NIER.

Studies in Biophysics: The Critical Temperature of Serum (56°). By LECOMTE DU NOUY. vi + 185 pp. New York: Reinhold Publishing Corporation, 1945. Price: \$3.50.

This book describes the effects of heat-treatment on the properties of serum of the horse, rabbit, and other animals. Representative data from thousands of very careful measurements of viscosity, optical rotation and rotatory dispersion, light scattering, depolarization of scattered light, sedimentation of precipitates, electrical conductivity, pH, interfacial tension, interaction with ether, and ultraviolet-light absorption are cited to show that above 56° irreversible changes take place in serum, the more rapidly the higher the temperature.

Some of the observed changes are interpreted as representing an increase in volume of protein molecules by hydration. Many readers probably will be skeptical of the enormous values of hydration deduced. Following recent theoretical developments to which the author has not referred, they may prefer to interpret increases in viscosity in terms of changes in shape, and increases in light scattering and depolarization in terms of aggregation.

The introduction contains some interesting remarks concerning the author's philosophy of experimentation. The style of the book is lucid and expressive.

JOHN D. FERRY.

✓ *Qualitative Inorganic Microanalysis. A Short Elementary Course.* By R. BELCHER AND CECIL L. WILSON. 18 x 12 cm.; viii + 68 pp. London, New York, and Toronto: Longmans, Green and Company, 1946. Price: 2/6d.

Microanalytical methods have advantages over the well-known procedures of ordinary qualitative analysis, and not least amongst the benefits to students is the training in manual dexterity which is so valuable in experimental research. The authors describe in detail how the experimentalist can make very simply from glass tubing much of the apparatus required, and a chapter is devoted to the minutiae of its manipulation in a variety of tests. The scheme for the qualitative analysis of mixtures of the commoner cations is based on the use of hydrogen sulfide and the zirconium separation for phosphates. A procedure avoiding the use of hydrogen sulfide is also presented. The chapter of tests for acid radicals and the table of preliminary tests might well be expanded. The book contains twenty-eight excellent diagrams to which frequent references in the text would be facilitated by giving the numbers of the pages on which they appear, as well as the figure numbers. Errors are few, but "sulphite" is out of position near the bottom of the table on page 31.

The book is good value for the money and should be in the hands of all who are learning and practising chemistry.

J. G. A. GRIFFITHS.

✓ *Science for Democracy.* Edited and with an introduction by JEROME NATHANSON. 170 pp. Morningside Heights, New York: King's Crown Press, 1946. Price: \$2.50.

Especially during the war period many natural scientists have become more conscious than ever of the social implications of science. Through science mankind has gained control over man. No wonder that many scientists feel that it is their human duty to offer their aid in the settlement of sociological problems of national and international scope. The book under discussion deals with the social implications of science, the social obligations of scientists, and the application of scientific methods to sociological problems.

The book is a very timely one and should be a source of inspiration to those scientists who are socially minded. The book is devoted to the following topics: "Science in the National Economy; "The Challenge of Science to Social Thinking;" "Does Private Industry Threaten Freedom of Scientific Research;" and "The Role of Science in the Determination of Democratic Policy."

As can be suspected from the titles, the book is partly of a philosophic and partly of a practical nature. The Introduction, by J. Nathanson, excels in clear statements. Some

of these are quoted below, partly because of their own value and partly because they reflect upon the nature of the papers and the discussions found in the book.

"The papers and discussions which follow are an attempt to grapple with the problem of making the scientific habit of mind an integral part of the democratic process. In the months that have elapsed since the first atom bomb fell on Hiroshima, the physicists have learned some of the hard lessons of political responsibility and political activity. . . .

"Aware of the social implications of their professional work, they (scientists) have left the laboratory for the public forum, and in doing so, they have themselves received a further education. . . .

"And unless all scientists are united in the realization that their futures are inseparable from the future of the democratic cause, they will themselves help dig the grave of free inquiry. . . ."

The "hot" problem of "planning in science" is touched upon already in the Introduction: "The chief problem of our time is how to plan our economic and social life without sacrificing freedom. To say that planning necessarily leads to serfdom is as ridiculous as to say that using our heads necessarily means tying our hands. We can use both our heads and our hands. We can plan our national and international life intelligently and increase human freedom. The problem is how to do it. That is a problem of intelligence, or organizing knowledge, in a word, of science. . . . In the second place, scientists are obliged to see that their knowledge functions in government, insisting wherever and whenever possible that they are not subservient employees of government employees, but their colleagues in planning policy."

Lack of space does not permit a lengthy discussion of the many valuable papers presented in this book. The controversial subject "Science in the National Economy" is discussed in three papers: "Science and Human Welfare" by P. B. Sears, "The Scientific Spirit and Economic Dogmatism" by J. Frank, and "The Gentlemen Talk of Science" by R. S. Lynd. In his well-documented and tolerant paper Judge Frank takes exception to Hayek: "Because in the lands from which they fled, a robust democratic faith never took root, Teutonic refugees, like Hayek, fail to comprehend the American democratic tradition."

The questions raised by Lynd give much thought for reflection. "All this raises the question: whose business is science? In a democracy there ought to be only one possible answer to that question. You may ask: where are the scientists themselves in all this? . . . Our fates as scientists depend not upon men of good will, but upon the outcome of the contemporary struggle for power."

Why not recognize the contributions of scientists to society as the realistic Russians do?

In the part dealing with "Challenge of Science to Social Thinking" Dr. Gerald Wendt states: "But one thing is certain, it will be infinitely harder for the unscientific public to readjust its thinking than it was for the scientist. Thus the basic challenge of science to society lies in the need of constant readjustment to change."

"Does private industry threaten freedom of scientific research?" is answered by an emphatic "No" by Dr. Langsdorf. "But I do not know of any instance of suppression, or attempted suppression, of research in the physical sciences because someone felt that vested interests might be threatened." Many scientists, including your reviewer, will not agree with Dr. Langsdorf's statement. In this connection, Dr. H. Grundfest's paper and especially his discussion of the question "Does industry threaten freedom of research by various forms of monopoly and cartel practice?" is of particular interest.

The main bulk of the book is devoted to symposia on "Freedom of Scientific Research" and "The Role of Science in Determination of Democratic Policy."

The papers and the discussions in the book exemplify the true spirit of democracy, which makes a free exchange of thoughts and opinions among intellectual leaders possible.

On page 166 Mr. Putnam defines the conference as an instrument for action to extend the application of scientific method as a means of promoting democracy. However, the means of promoting scientific thinking among the masses is barely touched upon. It is true that newspapers, magazines, and the radio successfully popularize science, thus con-

tributing to an increasing appreciation of science by the public. However, the kind of information supplied is mainly of a factual nature. What we need particularly in a growing democracy is the more general adoption of the objective, unbiased way of scientific thinking by all groups of the population. This teaching of the method of scientific thinking should be an essential part of the general program of teaching of science.

I. M. KOLTHOFF.

✓ *Scientific Instruments.* By HERBERT J. COOPER. 305 pp. Brooklyn, New York: The Chemical Publishing Company, Inc., 1946. Price: \$6.00.

Those who are interested in instrumentations will find this a most useful book. As the author states, it is not intended as a manual giving the operating details of a given instrument or its use, but rather to present the broad principles of instrumentation in many different fields of science. The specialist will not find anything he doesn't know about his own instrument but will find out about the other man's.

The book is divided into five sections: optical instruments, measuring instruments, navigation and surveying instruments, liquid testing, and miscellaneous. Each of these sections treats a number of instruments. Electrical instruments, including electrometers and Geiger counters, are not treated.

S. C. LIND.

Enzymes and their Role in Wheat Technology. Edited by J. ANSEL ANDERSON. American Association of Cereal Chemists Monograph Series, Vol. I. ix + 371 p. 215 Fourth Avenue, New York 3, New York: Interscience Publishers, Inc., 1946. Price: \$4.50.

This monograph brings together the current fundamental knowledge of certain enzyme systems and the rôle of such systems in wheat technology. Following an introductory chapter by Sandstrom on the general chemistry of enzymes, the specific enzyme systems considered have been treated from two aspects: a critical review of the general knowledge in each field, followed by a chapter on the specific rôle of the enzyme system in wheat technology.

Chapters by Caldwell and Adams and by Kneen and Sandstedt deal with the amylases, which system, incidentally, has been the most clearly elaborated of the various enzymes of importance to cereal chemists. Following these, Longenecker reviews the general field of the esterases, while in the succeeding chapter Sullivan deals with their rôle in milling and baking. The section by Barron on oxidizing enzyme systems is a condensed but excellently written discussion on this complex subject. The following chapter by Sullivan discusses the present limited knowledge on these enzymes in relation to wheat and flour. The general field of proteases is comprehensively reviewed by Balls and Kies, and the technological application of these enzymes to baking is discussed by Hildebrand. Werkman has given an up-to-date review on alcoholic fermentation and has presented a lucid discussion of the intermediary mechanisms and phosphorylation. The last chapter, by Atkin, Schultz, and Frey, deals with the practical aspects of yeast fermentation as applied to bread doughs. Thus, fifteen recognized authorities on enzymes and their technological applications have contributed the eleven chapters which make up this volume.

The reader is struck by the disproportion in our present knowledge between the comparatively well elaborated and organized information on enzymes from animal sources and their rôle in the intermediary metabolism of such tissues, and the sparsity of similar information on enzymes from plant sources. In clearly raising this point, this volume should serve as a guide and a challenge to the majority of biochemists who have been interested in plants only as sources of certain enzymes and who have disregarded the integrated rôle of such enzymes in the intermediary metabolism of plants or the nature of their action in plant products.

This book is a timely contribution to enzymology and will be of interest to both the research worker and the technologist. The bibliographies at the end of every chapter as

well as the author and subject indexes make this book exceedingly useful as detailed source material. Few inaccuracies or errors were found.

MAX MILNER.

Radioactivity and Nuclear Physics. By J. M. CORK. 175 pp. Ann Arbor, Michigan: Edwards Brothers, 1946. Price: \$3.50.

In a very acceptable way this volume bridges over from the classical natural radioactivity to the new nuclear physics. Its timely appearance will make it doubly welcome. The greatly enhanced interest in nuclear reactions makes it important for students and research workers alike to have an up-to-date volume giving principles and experimental data in convenient form.

The work is intended primarily for students. Each chapter ends with a few questions and problems admirably chosen to emphasize the most pertinent points. The drawings and tables are exceptionally clear. The importance of the subject is worthy of a more permanent form of binding and reproduction, but owing to the large volume of data that should soon be released in this field, the present form should suffice in the interim. The lithoprinting is excellent.

A rather long list of errata accompanies the volume. A few minor typographical errors still remain.

The various chapters treat successively: natural radioactivity; the detection of radiation; apparatus for induced radioactivity, including the cyclotron, betatron, and synchrotron; alpha, beta, and gamma radiation; neutrons; protons; deuterons; cosmic radiation; nuclear fission and some applications of radioactivity in astronomy, botany, chemistry, engineering (radiography and thickness measurement), metallurgy (atomic diffusion), medicine (therapy, specific absorption, and tracers), mineralogy (coloring of crystals), zoology (mutations). Two important omissions are luminous paints and the chemical effects of radiation.

S. C. LIND.

Tables of Fractional Powers. Prepared by the Mathematical Tables Project under the sponsorship of the National Bureau of Standards. 489 pp. New York: Columbia University Press, 1946. Price: \$7.50.

The present volume, begun under the auspices of the Works Progress Administration for the City of New York, has been completed with the support of the Office of Scientific Research and Development under the direction of Lyman J. Briggs of the Bureau of Standards and Arnold N. Lowan, Project Director.

In Part I the values of A^x for fixed bases and variable exponents are given to fifteen decimal places. In Part II the function X^a , for variable bases and the frequently occurring exponents $\pm 1/2$, $\pm 1/3$, $\pm 2/3$, $\pm 1/4$, $\pm 3/4$, are tabulated also to fifteen places.

S. C. LIND.

Preparation and Measurement of Isotopic Tracers. By D. WRIGHT WILSON, A. O. C. NIER, AND STANLEY P. REIMANN. viii + 108 pp. Ann Arbor, Michigan: J. W. Edwards, 1946. Price: paper bound, \$1.80.

This work is a symposium prepared in lithoprint for the Isotope Research Group. It contains eight chapters by different authorities. It is intended to acquaint biologists and chemists with the methods of preparation and analysis of isotopes, especially carbon and hydrogen.

With the great present interest in and importance of this subject this timely symposium will greatly aid research workers who are using tracer elements in solving problems in chemistry or biology. Both stable and radioactive isotopes are treated.

S. C. LIND.

Monographs on the Progress of Research in Holland during the War. Modern Development of Chemotherapy. By E. HAVINGA, H. W. JULIUS, H. VELDSTRA, AND K. C. WINKLER.

op. New York and Amsterdam: Elsevier Publishing Company, 1946. Price: \$3.50. Although the scientific journals in this country were published uninterruptedly during the war, very few papers of a fundamental nature appeared, partly because of the fact that the scientists who were leaders in academic research were engaged full time in secret work for the government. In the ex-occupied countries in Europe there is naturally a large urge of getting acquainted with the progress of research in this country during the war. It is not recognized by these European scientists that most of the research carried out in the U. S. during the war is only now being released for publication. Thus, the main bulk of research carried out in the U. S. during the war will become available simultaneously to all scientists over the world. On the other hand, we in this country have a hard time getting acquainted with the continental European scientific literature published during the war. It is hardly possible for any productive scientist to find the time for reading a host of back-journals published during the war period. The only possible convenient way of getting acquainted with the progress of science in the occupied countries is by review papers published in suitable journals or in the form of monographs.

From this viewpoint the appearance of a series of monographs on the progress of research in Holland should be extended a hearty welcome. Unfortunately, the aims and scope of the present series seem to be quite different from those which your reviewer would formulate. Dr. R. Houwink and Dr. J. A. A. Ketelaar, editors of the series, in their Foreword: "The purpose of this series on . . . is to show the work of the scientists in the Netherlands have remained active during the five years of German occupation."

Instead of publishing an unlimited number of monographs, which would have served the appreciation of Dutch scientific contributions and would have made the scientists outside of Holland better acquainted with the progress of research in this country, a relatively small number of brief comprehensive reviews, each volume covering the progress in one main field—e.g., the various fields of chemistry, physics, physiology, etc.—had been made available. The editors have chosen the publication of twenty-eight monographs, with "other volumes in preparation."

The title of the present volume, *Modern Developments in Membrane Research*, is misleading, since the contents are confined almost entirely to research on the membranes of cells. This information is made available for the first time in a book form.

The above general comments apply to the whole series of the book under consideration. Since it emphasizes the work of the authors, who are leaders in the field in Holland; the series is of considerable interest from that of standard monographs. Also, the English is excellent, and frequently unusual words, such as "membrane," "isotonic," etc., are noticed.

The book is divided into two parts. "The Mechanism of the Action of the Sulphonamide, *p*-Aminobenzoic Acid," "Chemical Investigations," "Pharmacological Investigations," and "Mycotherapy, Investigations on Antimicrobial Agents." This last chapter (pages 158-75) deals with the interesting new antimicrobial substance "Nystatin" with the formula $C_{47}H_{81}O_{17}$, which has been isolated by van Luyk from *Penicillium notatum*. The new substance is hailed in Holland as an important agent in skin infections, especially in superficial mycoses.

For the reader of this Journal the part dealing with physicochemical investigations is of interest. In this part data on electrometric titrations (acid-base), ultraviolet-absorption spectra, surface activity of and formation of monolayers of amides are presented and the mechanism of the action of *p*-aminobenzoic acid and amides is discussed. The surface activity of the compounds is estimated from depression of the polarographic oxygen maximum. The authors do not realize that interpretation of their results in 0.1 N potassium chloride is obscured by the fact that the hydroxyl ions during its reduction, which ions neutralize substances with acidic character.

I. M. KOLTHOFF.

Monographs on the Progress of Research in Holland. Contribution to the Physics of Cellulose. By P. H. HERMANS. Communication No. 21 from the Institute for Cellulose

Research of the AKU and Affiliated Companies, Utrecht. 221 pp. Amsterdam and New York: The Elsevier Publishing Company, Inc., 1948. Price: \$4.00.

This book is one of a series of *Monographs on the Progress of Research in Holland*. In the preceding review your reviewer has expressed his opinion about the publication of an unlimited number of monographs on certain subdivisions of various specific subjects.

The present volume contains the following chapters: "General Theoretical Background," "Survey of the Fibre Material Used," "Studies in Sorption" (Including Heat of Sorption), "Studies in Density," "Studies in Refractive Power and Double Refraction," and "X-ray Studies on Orientation." In the appendix Dr. J. J. Hermans presents a note on the theory of sorption, a mathematical section giving the relation between the main polarisabilities of the fibre and the orientation of its structural elements, and another section on the relation between the distribution of the orientation of paratropic planes and the optical constants of the crystalline material.

The last twenty pages are devoted to a brief description of the experimental methods used in the text.

The book is written in a clear and thought-provoking style. It is of interest not only to specialists in the field of cellulose but to all those interested in the properties of crystalline and amorphous solids.

A considerable part of the work had not been published previously, a fact which accounts for the presentation of many detailed experimental data. As a communication from the Institute for Cellulose Research of AKU it is quite a success, giving a constructive critical discussion, based on experimental evidence, of *capita selecta* of the subject of cellulose fibres.

However, as a separate book it would have gained in value and prestige if the author had published his experimental work in one of the technical journals and had confined himself in a monograph to a critical discussion of the entire field, taking into account the American and English literature to which he did not have access during the war. Numerous references are made to the German literature during the war period, including the year 1944.

I. M. KOLTHOFF.

A KINETIC STUDY OF THE UREA-FORMALDEHYDE REACTION

LLOYD E. SMYTHE

Department of Inorganic and Physical Chemistry, University of Sydney, N.S.W., Australia

Received November 8, 1946

INTRODUCTION

The purpose of this investigation was to obtain kinetic data for the reaction between urea and formaldehyde in aqueous solution within defined conditions of hydrogen-ion concentration. An investigation of the initial reaction between equimolecular proportions of urea and formaldehyde was the primary object, subsequent polymerization being neglected.

It was early recognized (3, 4, 6, 9) that the resultant products and course of the urea-formaldehyde reaction depend on: (a) the hydrogen-ion concentration, (b) the relative proportions of reactants, (c) the temperature, (d) catalysts, if present. These criteria are critical and are responsible for the diversity of products obtained by the various investigators.

Most of the information concerning this reaction is of a qualitative nature, only a small proportion of the published data relating to physicochemical and quantitative aspects.

Walter and Gewing (10) have made an analytical study of the water and formaldehyde lost during the condensation process, and work by Dixon (2), de Chesne (1), Redfarn (8), and others has been concerned with the polymerization of the initial dimethylol- and monomethylolureas formed. The preliminary formation and rate of formation of these substituted ureas is therefore of importance with regard to subsequent polymerization and the course of the reaction.

To avoid unnecessary complications, aqueous formaldehyde solutions adjusted to pH 7.0 ± 0.05 and aqueous urea solutions (pH 8.66) were used. By employing equimolecular proportions of the reactants in aqueous solution, the reaction may be followed by estimating the decrease in concentration of formaldehyde with time. In addition, samples were taken during each reaction and the products were identified.

Owing to the critical nature of the reaction, buffering of the reaction solution was not employed, lest the buffer have some catalytic effect on the reaction. It was hoped that changes in pH during the course of the reaction might possibly be correlated with the reaction mechanism. For this reason strict control of the pH was employed and all changes were noted during each reaction.

MATERIALS AND EXPERIMENTAL DETAILS

(1) *Urea*: An 8 *M* aqueous solution (480.48 g. per liter) prepared from recrystallised n.p. quality urea was used. It was checked for urea content and tested for impurities (e.g., heavy metals). The pH was 8.66.

(2) *Formaldehyde solution*: This was prepared by distilling paraformaldehyde with 3 *N* sulfuric acid. The aqueous distillate was diluted to the required

strength with distilled water and tested for possible sulfate contamination. The acidity of the solution was determined as follows: A 100-ml. sample of the formaldehyde solution was run into a 500-ml. Erlenmeyer flask, 10 ml. of $N/2$ sodium hydroxide was added, and the excess sodium hydroxide was then back-titrated with $N/2$ sulfuric acid, using methyl red as the indicator. Then:

$$\frac{10(\text{base titer} \times \text{normality } H_2SO_4)}{\text{normality } NaOH} = \text{ml. } N/2 \text{ NaOH used}$$

$$1 \text{ ml. } N/2 \text{ NaOH} \equiv 0.02302 \text{ g. HCOOH}$$

$$\therefore \text{ per cent } CH_2O \text{ by volume (g./100 ml.)} = \text{ml. } N/2 \text{ NaOH used} \times 0.02302$$

This determination of acidity (usually 0.01–0.03 per cent by volume) was necessary for adjustment of the formaldehyde solution to $pH 7.0 \pm 0.05$. The calculated volume of $N/2$ sodium hydroxide solution was added before the formaldehyde content of the solution was determined. Final adjustments gave a formaldehyde content of 24.024 per cent by volume (8 M solution) of $pH 7.0 \pm 0.05$.

(3) *Estimation of formaldehyde content of solution:* The formaldehyde content of such a solution was estimated as follows: 1 ml. of the solution was run into a 100-ml. Erlenmeyer flask and approximately 10 ml. of distilled water was added. Three drops of bromophenol blue indicator were then added, followed by 10 ml. of a 10 per cent by weight aqueous hydroxylamine hydrochloride solution. The flask was then rotated to mix the contents well and allowed to stand for 20 min. The free hydrochloric acid was then estimated by titration with $N/2$ sodium hydroxide solution, the end point (purple) being determined with the aid of a standard color. The percentage by volume of formaldehyde is given by the expression:

$$\frac{3.0 \times \text{ml. titrant} \times \text{normality } NaOH}{\text{ml. of sample used}}$$

(4) *Estimation of free formaldehyde during the course of the reaction:* Samples of the reaction mixture were taken at intervals with the aid of a vacuum sampler and immediately cooled to $20^\circ C$. by immersion in ice water. This was carried out quickly in order to check the reaction. The requisite sample (usually 5 ml.) was then measured by a pipet into a 100-ml. Erlenmeyer flask, 10 ml. of water added, and three drops of bromophenol blue indicator, followed by 10 ml. of 10 per cent by weight hydroxylamine hydrochloride solution. From the time of adding the latter solution to the time of commencement of titration must be 30 sec., the flask being gently shaken during that time. The titration of the free hydrochloric acid with $N/2$ sodium hydroxide was immediately commenced at the end of this 30-sec. period and completed in 1–2 min. The 30-sec. period is timed from the mid point of the time taken for the pipet to deliver 10 ml. The end point (purple) was matched against a standard. The above procedure must

be strictly followed, otherwise the estimation will be inaccurate, for reasons to be described. It was found that:

$$x \text{ ml. } N/2 \text{ NaOH} + 4 \text{ per cent of } x = \text{ml. } N/2 \text{ NaOH (titrant)}$$

(to be used in the calculation below)

$$\text{Per cent free CH}_2\text{O by volume} = \frac{\text{ml. titrant} \times \text{normality NaOH} \times 3}{\text{ml. of sample used}}$$

The above method was devised after difficulty in reproducing results. Reaction samples were affected by the hydrochloric acid liberated in the reaction between hydroxylamine hydrochloride and formaldehyde. The actual figure obtained for the titrant varied very greatly, depending upon how long the sample was allowed to stand after adding the hydroxylamine hydrochloride, and before the titration was commenced. Numerous experiments were carried out concerning this variance in results; the findings are summarized in the next section.

(5) *Experiments relating to the method for the estimation of free formaldehyde:* Figure 1 illustrates the general findings of experiments concerning the estimation of formaldehyde (free) in: (a) pure formaldehyde solutions; (b) the urea-formaldehyde reaction mixtures; (c) pure formaldehyde solution containing some monomethylolurea.

Curve a: The per cent of formaldehyde by volume is plotted against the time in minutes the sample was allowed to stand before titrating and after mixing with the hydroxylamine hydrochloride solution. This curve was found to be characteristic. In this particular experiment the room temperature was 19.1°C., the strength of the pure formaldehyde solution 21.7 per cent CH₂O by volume (checked by two methods), and the sample taken was 1 ml.

Curve b shows the variation in figures obtained when a 5-ml. sample of a urea-formaldehyde reaction mixture is allowed to react at varying times with the hydroxylamine hydrochloride solution. It will be seen that curve b does not flatten out as in the case of curve a. Also, the percentage of formaldehyde found varies greatly with time. The actual percentage of free formaldehyde by the method in (4) above is taken to be 1.08. In the experiment on which curve b is based, 1 mole of formaldehyde and 1 mole of urea, each as 12 per cent by volume concentration in the mixture, were allowed to stand for 12 hr. to allow the reaction product to be formed. The estimation was then commenced with nine 5-ml. samples. Repeat experiments showed the curve to be characteristic.

Curve c shows the variation in the estimation of the "free" formaldehyde content of a solution of pure formaldehyde containing some added monomethylolurea. Uncombined formaldehyde was 21.5 per cent by volume of the mixture, combined formaldehyde 3.9 per cent by volume of the mixture, and total formaldehyde 25.4 per cent by volume of the mixture. This curve also was characteristic of repeat experiments performed with formaldehyde solution and added monomethylolurea.

A consideration of the experiments and curves a, b, and c showed: (1) the method in (4) can be used for the estimation of free formaldehyde in urea-formaldehyde reaction mixtures. (2) The accuracy of the estimation, when the technique has been mastered, is the best attained to date. (3) The method is not recommended when the percentage of formaldehyde is less than 1.

(6) *Apparatus and working details:* The reaction was studied at 10°C. intervals from 30° to 60 C. A glass electrode pH meter was used for pH determinations, and the accuracy of the determinations was ± 0.05 pH. The reactions were carried out in a 1-liter three-necked flask and maintained at the required temperature $\pm 0.1^\circ\text{C}$. by an electric immersion heater in an oil bath and governed by a

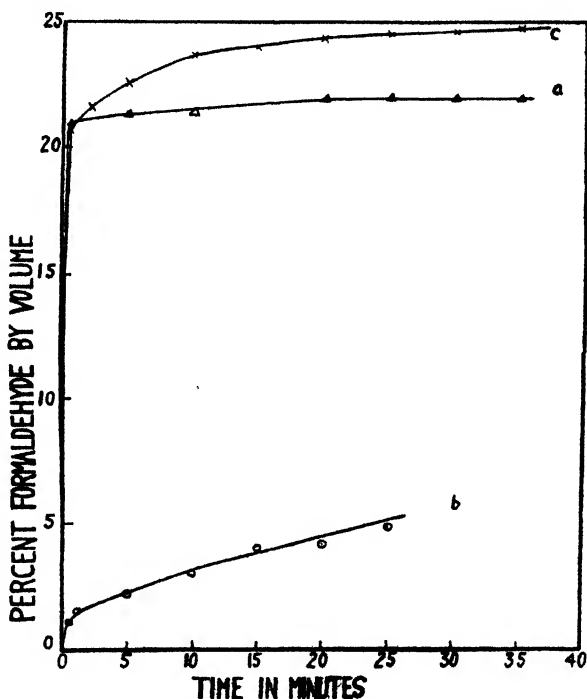


FIG. 1. Factors influencing the estimation of free formaldehyde in reaction mixtures

toluene regulator. The bath consisted of light paraffin, and efficient stirring for the bath and reaction vessel was provided by an electric motor driving glass stirrers. A standard mercury-in-glass solid-stem thermometer was used, and the necessary corrections were applied. The reaction vessel was fitted with stirrer, thermometer, vacuum sampler, cooling or heating coil, and condenser.

The measured volume of formaldehyde solution was introduced into the flask and allowed to reach the required temperature. When the temperature was steady the measured volume of urea solution, previously adjusted to the required temperature, was quickly added with the aid of reduced pressure. The time of mixture of the urea and formaldehyde solutions was taken as the mid point of the time required to add the urea solution. The slightly exothermic

reaction necessitated temperature control with the aid of the cooling coil within the reaction vessel.

RESULTS OF THIS INVESTIGATION

Experiments at 30°C.: The reaction was between 250 ml. of formaldehyde solution and 250 ml. of urea solution. The initial concentration of formaldehyde in the mixture was 12.01 per cent by volume. Experiment No. 17 is typical (see table 1).

In this experiment $a = 2.52$ from * in table 1, and $t =$ the figure in the column (seconds) minus 300. It was found that the initial reaction upon mixing the

TABLE 1

Results of experiment No. 17

$t = 30^\circ\text{C}.$; k (observed) at $30^\circ\text{C} = 5.5 \times 10^{-6}$ liters/gram-mole second

TIME	pH	PER CENT CH_2O BY VOLUME	x	$a - x$	$k \times 10^6$
<i>sec.</i>					
0	4.95	12.01			
300	5.10	7.57*			
600	5.18	7.26	0.10	2.42	5.46
1200	5.31	6.72	0.28	2.24	5.51
1800	5.45	6.24	0.44	2.08	5.59
3600	5.60	5.19	0.79	1.73	5.48
5400	5.76	4.44	1.04	1.48	5.47
7200	5.87	3.87	1.23	1.29	5.48
9000	5.98	3.42	1.38	1.14	5.52
10800	6.03	3.06	1.50	1.02	5.56
12600	6.09	2.79	1.59	0.93	5.51
14400	6.15	2.55	1.67	0.85	5.53

$$k = \frac{1}{ta} \cdot \frac{x}{a - x}$$

a = initial concentration of formaldehyde in gram-moles per liter.

$a - x$ = free formaldehyde in gram-moles per liter.

t = time in seconds.

solutions was of greater rapidity than the subsequent reaction. A further noticeable feature was the drop in pH to 4.95 immediately upon mixing the solutions. It was found that no constant applicable to any reaction order could be derived unless the initial reaction (first 300 sec.) were disregarded. Even if the temperature were lowered or the reaction conducted using more dilute solutions, this initial reaction could not be followed. It appears that the reaction for the first 5 min. is approximately fourteen times faster than for the second 5 min. The change in pH during these two periods is in each case of the order of 0.05 pH. The change in velocity therefore must be attributed to the instantaneous change in pH upon mixing the solutions. The initial stage in such reactions, in order to be followed, would require an accurate method for the estimation of free formaldehyde in very dilute solutions.

The product isolated at 14,400 sec. was identified as monomethylolurea (mp. $111^\circ\text{C}.$, corrected) obtained in 95 per cent yield. No dimethylolurea was

TABLE 2
Results of experiments 33a and 33b
 $t = 30^{\circ}\text{C}.$

c	$t_{\frac{1}{2}}$	$k = \frac{1}{t_{\frac{1}{2}}c}$
gram-moles/liter	sec.	10^4 liters/gram-mole second
(a) 4	1920	1.30
(b) 2	3900	1.28

TABLE 3
Results of experiment No. 23
 $t = 40^{\circ}\text{C}.$; k (observed) at $40^{\circ}\text{C}.$ = 11.8×10^{-5} liters/gram-mole second

TIME	pH	PER CENT CH_3O BY VOLUME	x	$a - x$	$k \times 10^4$
sec.					
0	4.95	12.01			
300	5.30	7.02*			
600	5.47	6.48	0.18	2.16	11.87
900	5.60	6.03	0.33	2.01	11.69
1800	5.80	4.98	0.68	1.66	11.66
3600	6.05	3.66	1.12	1.22	11.88
5400	6.17	2.91	1.37	0.97	11.83
7200	6.28	2.43	1.53	0.81	11.71
9000	6.38	2.07	1.65	0.69	11.74
10800	6.45	1.83	1.73	0.61	11.77
12600	6.50	1.59	1.81	0.53	11.87

* $a = 2.34$.

TABLE 4
Results of experiment No. 29
 $t = 50^{\circ}\text{C}.$; k (observed) at $50^{\circ}\text{C}.$ = 24.5×10^{-5} liters/gram-mole second

TIME	pH	PER CENT CH_3O BY VOLUME	x	$a - x$	$k \times 10^4$
sec.					
0	4.95	12.01			
300	4.40	6.22*			
600	5.57	5.40	0.27	1.80	24.15
1200	5.95	4.26	0.65	1.42	24.55
1800	6.28	3.51	0.90	1.17	24.78
3600	6.42	2.21	1.30	0.77	24.70
5400	6.52	1.74	1.49	0.58	24.35
7200	6.60	1.38	1.61	0.46	24.50
9000	6.67	1.14	1.69	0.38	24.68

* $a = 2.07$.

present in sufficient quantity to be detected. The observed figure for the bi-molecular constant, given above table 1, is the average of four independent experiments; this also applies to the constants for 40° , 50° , and $60^{\circ}\text{C}.$

This second-order reaction was also confirmed by determining how the time of half-completion of the reaction varied with concentration of initial reactants. Experiments No. 33a and 33b at 30°C. illustrate this (see table 2).

Experiments at 40°C.: What has been said with regard to the experiments at 30°C. applies also at this temperature. Monomethylolurea was again the exclusive product at 12,600 sec. A greater increase in pH toward the bottom of the table is noticeable. Experiment No. 23 is illustrated in table 3.

Experiments at 50°C.: As at 30°C. and 40°C., monomethylolurea was obtained in almost theoretical yield from sample No. 8. Experiment No. 29 is illustrated in table 4.

TABLE 5
Results of experiment No. 38

$t = 60^\circ\text{C}.$; k (observed) at $60^\circ\text{C}.$ = 50.1×10^{-5} liters/gram-mole second

TIME	pH	PER CENT CH_2O BY VOLUME	x	$a - x$	$k \times 10^6$
sec.					
0	4.96	12.01			
300	5.90	5.65*			
600	6.10	4.83	0.46	1.61	50.6
1200	6.40	3.03	0.87	1.01	50.8
1800	6.50	2.24	1.10	0.78	50.0
3600	6.60	1.38	1.42	0.46	49.8
5400	6.65	0.96	1.56	0.32	50.8

* $a = 1.88$.

Experiments at 60°C.: As at the other temperatures studied, monomethylolurea was obtained in almost theoretical yield from sample No. 6. Experiment No. 38 is illustrated in table 5.

DISCUSSION OF RESULTS

Considering the general bimolecular course of the reaction, no relation was found connecting the velocity constant with the change in hydrogen-ion concentration. It will be seen in tables 1 to 5 that the constants are steady over a change in pH of 1.

The variation with temperature of the velocity constant for a thermal reaction occurring in solution is expressed by:

$$k = Ze^{-E/RT}$$

or

$$\ln k = Z - \frac{E}{RT}$$

Plotting $\ln k$ against $1/T$ (see figure 2), the Arrhenius equation takes the form:

$$\ln k = 14.61 - \frac{14,700}{RT}$$

when $E = 14,700$ cal. and the collision number $Z = \text{approximately } 2.2 \times 10^6$.

The low values of E and Z are interesting in the light of current theories regarding bimolecular reactions in solution. The deviation of the reaction from the ideal behavior of the simple collision theory introduces the probability factor P and

$$k = PZe^{-E/RT}$$

P in the case of the reaction studied is approximately 2×10^{-6} . The P factor may be interpreted in terms of vibrational and rotational partition functions and

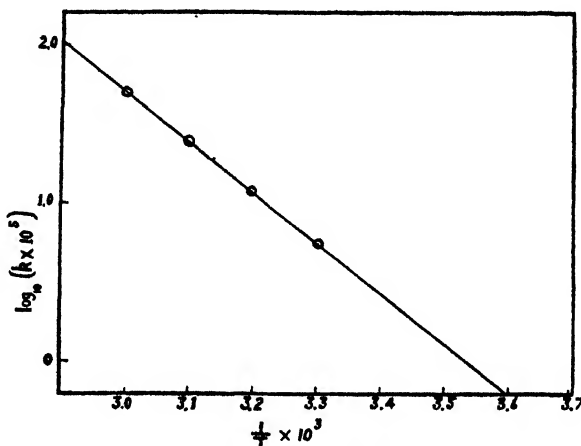


FIG. 2. Plot of $\ln k$ against $1/T$

according to the statistical theory in the case of two non-linear polyatomic molecules.

$$P \approx \left(\frac{f_v}{f_r} \right)^5$$

If the reactant molecules have to be placed together in a particular way before reaction, the probability of the formation of the activated complex will be less, and when a linear complex is formed the rate should be less by a factor of f_v/f_r than for a non-linear complex, assuming that the activation energy is the same in each case. The formation of the activated complex from two polyatomic molecules is accompanied by the formation of five new vibrational degrees of freedom and a translational degree of freedom along the reaction coordinate, this of course being accompanied by the disappearance of three translational and three rotational degrees of freedom (5).

In this case, the low probability factor that is found may be due to restrictions on the molecule, making the energy transitions necessary for the formation of the activated complex. The initial rapid reaction rate appears to be intimately related to this subsequent slow bimolecular reaction and involves a consideration of the changes in hydrogen-ion concentration noted.

Possibly the rate of reaction is dependent on the ionization of the urea, in turn

dependent upon the hydrogen-ion concentration. Initially, therefore, the reaction in the first instance may be a normal one where

$$\text{Ion}^{\pm} + \text{molecule}^0 = \text{normal rate}$$

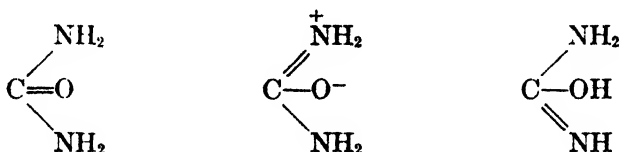
$$E \approx 22,000 \text{ cal.}$$

$$Z \approx 2.8 \times 10^{11}$$

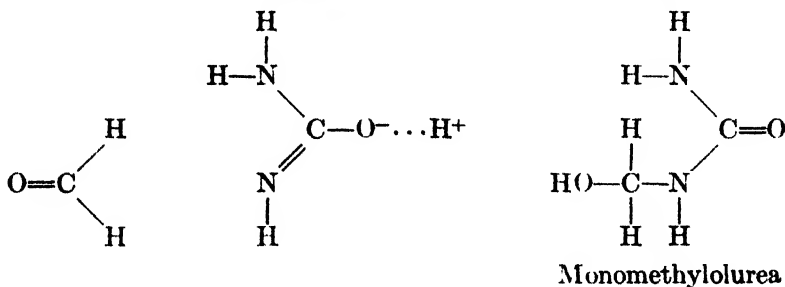
Consideration of tables 1 to 5 shows that the hydrogen-ion concentration is increased by 10^2 initially. Thereafter increases are of a smaller order.

As the main reaction is of the slow bimolecular type the course would appear to be *via* neutral molecules, one of them, urea, necessarily assuming the suitable reacting condition prior to the formation of the activated complex. This condition of urea appears to be the rate-determining factor.

Urea in solution may be regarded as an equilibrium mixture of the forms:



The normal rate of reaction may depend on the migration of hydrogen ion from the hydroxyl group of the tautomeric form of urea, leading to an activated complex and subsequent rearrangement to monomethylolurea:



According to Lecher (7), migration of the hydrogen ion from the hydroxyl group to the imino group is more likely than migration to the amino group. The fact that monomethylolurea is the exclusive product under the conditions studied suggests that two identical amino groups are not involved in the reaction. The rate of reaction then appears to be closely associated with the condition of the urea molecule, which is in turn influenced by hydrogen-ion concentration.

SUMMARY

1. The reaction between urea and formaldehyde in aqueous solution within defined conditions has been shown to be mainly of the slow bimolecular variety.

2. Determined values for E , Z , and P are given and discussed in the light of present knowledge regarding bimolecular reactions in solution.

3. A method for estimating the free formaldehyde during the course of a urea-formaldehyde reaction is presented.

In conclusion I wish to express my thanks to Dr. T. Iredale for valuable advice and discussion.

REFERENCES

- (1) DE CHESNE, E. B.: *Kolloid-Beihefte* **36**, 387 (1932).
- (2) DIXON, A. E.: *J. Chem. Soc.* **113**, 238 (1918).
- (3) EINHORN, A., AND HAMBURGER, A.: *Ber.* **41**, 24 (1908).
- (4) EINHORN, A.: *Ann.* **343**, 207 (1905); **361**, 113 (1908).
- (5) GLASSTONE, S., LAIDLER, K. J., AND EYRING, H.: *The Theory of Rate Processes*, pp. 18-20. (1941).
- (6) GOLDSCHMIDT, C.: *Ber.* **29**, 2438 (1896); *Chem.-Ztg.* **46**, 460 (1897); *J. Chem. Soc.*, **74**, 178 (1898).
- (7) LECHER, H.: *Ann.* **438**, 154 (1920); **445**, 35 (1925); **455**, 139 (1927).
- (8) REDFARN, C. A.: *Brit. Plastics* **5**, 288 (1933).
- (9) SCHEIBLER, H., AND COWORKERS: *Z. angew. Chem.* **41**, 1305 (1928).
- (10) WALTER, G., AND GEWING, M.: *Kolloid-Beihefte* **34**, 163 (1936).

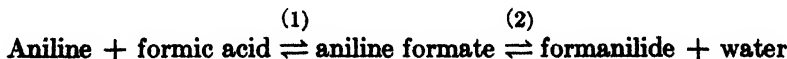
ANILINE FORMATE AND ITS CHANGES ON KEEPING

JAMES R. POUND

The School of Mines, Ballarat, Victoria, Australia

Received September 24, 1946

A study of the system aniline-formic acid-water was made in 1934 by A. M. Wilson and the present writer (1). The conditions under which crystals of aniline formate were obtainable at room temperatures were indicated, and also the changing of these crystals into formanilide and water. There are two equilibria involved:



These affect both the liquid mixtures and the solid crystals of aniline formate.

I. CHANGES IN THE CRYSTALS ON KEEPING

The original colorless crystals of aniline formate become in a few days sticky, then they often completely liquefy, then crystals of formanilide separate, and finally the whole re-solidifies. These changes generally are retarded in the presence of a drying agent. After twelve years four sealed samples of such crystals were re-investigated. There were determined (a) the "free formic acid" (by direct titration with alkali), (b) the "combined formic acid" (by boiling with excess alkali and back-titration by acid), and (c) the total aniline (by the bromate method). (b) indicates the formanilide content, and (a) the aniline formate

content (plus the excess actual formic acid, if any). The results are given in table 1. The designations of the samples are the same as given in the previous paper. (The per cent by weight of "free formic acid" in aniline formate is 33.1 per cent; formanilide gives per cent "combined formic acid" = 38.0 per cent and "combined aniline" = 76.8 per cent.)

Samples F and G were from the same parent lot of crystals, and samples P and R from another such lot. Sample F had re-solidified some time before seven years; the final solid might have been expected to contain moisture, but the analysis showed that it was 100 per cent formanilide, and it had the highest melting point of the samples.

TABLE 1
Changes in aniline formate crystals over a period of time

SAMPLE	KEPT	AFTER TIME	"FREE FORMIC ACID" <i>per cent</i>	CONDITION OF SAMPLE
F.....	In sealed tube (by itself)	1 day	32.5	Colorless crystals
		13 days	7.9	Liquid
		12 yr.	0	White and gray crystals, fairly loose; m.p. 47°C.
G.....	Over H ₂ SO ₄	1 day	32.5	Colorless crystals
		13 days	28.8	Sticky
		12 yr.	3.6	Dry compact creamy solid; m.p. 33°C.
P.....	Over P ₂ O ₅	0	33.8	Colorless crystals
		9 days	31.2	Slightly sticky
		12 yr.	2.0	Dry compact creamy solid; m.p. 42°C.
R.....	Over H ₂ SO ₄	0	33.8	Colorless crystals
		7 days	32.2	Slightly sticky
	Over P ₂ O ₅	12 yr.	0	Very hard compact whit- ish lump; m.p. 44°C.

Sample G became "damper" or stickier after several weeks, and slightly yellowish; "drier" and more opaque after twelve months, and there was a sublimate above the sample (possibly of aniline sulfate). The final solid contained 11 per cent of aniline formate and 89 per cent of formanilide.

Sample P became "damper" for a couple of months, then drier and seemed dry after a year; the final solid contained 6 per cent of aniline formate and 94 per cent of formanilide.

Sample R was kept over sulfuric acid for the first 9 days, then over phosphorus pentoxide; it became "damper" from the first day and was completely liquid on the tenth day, recrystallizing after two months; it remained solid thenceforth, but became slightly discolored with time. The final solid was 100 per cent formanilide.

F and R, which at one stage were completely liquid, had changed completely to formanilide; but G and P, which were never completely liquid, had not done so. The rate of change to formanilide was fastest for F.

II. CHANGES IN THE LIQUID MIXTURES ON KEEPING

These changes have been indicated in the previous paper. Certain mixtures of aniline, formic acid, and water separated on keeping into two layers; others remained homogeneous for periods up to a year (at least).

(a) *In the homogeneous mixtures* the percentage of free formic acid diminished with time and reached an equilibrium value after 15 or 20 days. In the mixtures 10, 32, 35, and 39 (which are referred to in the previous paper) the percentages of free formic acid after one year (actually 314 to 369 days) were 24.2, 33.9, 40.6, and 62.1, respectively,—all being within a few tenths of 1 per cent of the values quoted before. Mixture 38, which was originally 62.6 per cent formic acid, 17.7 per cent aniline, and 19.7 per cent water, gave after the days indicated in [] the following per cent free formic acid (): [0], (62.6); [1], (61.0); [4], (58.0); [11], (56.1); [16], (55.6); and [319], (55.8). The last figures indicate that the liquid then had the composition: formanilide, 18.4 per cent; aniline formate, 5.4 per cent; actual formic acid, 53.8 per cent; water, 22.4 per cent. When equilibrium was reached in the above five mixtures and in mixtures 3 and 6 (*q.v.*) there were present finally 61–22 per cent actual formic acid, 2–6 per cent aniline formate, 18–49 per cent anilide, and 14–44 per cent water. The actual aniline in the solution was always taken as 0; or the aniline was present wholly as anilide and as formate, there being always formic acid in excess.

In the final solutions the ratio

$$\frac{\text{Per cent free formic acid}}{\text{Per cent combined formic acid}}$$

varied from 2 to 8. The ratio

$$\frac{\text{Per cent anilide} \times \text{per cent water}}{\text{Per cent aniline formate}}$$

varied from 76 to 261 (mean 173), and this roughly substantiates the second equilibrium (equilibrium 2). The ratio

$$\frac{\text{Per cent actual formic acid}}{\text{Per cent aniline formate}}$$

varied from 16 to 4.5, and this substantiates the first equilibrium (equilibrium 1), assuming some small constant value for the per cent actual aniline.

(b) *Heterogeneous mixtures:* Many mixtures of aniline, formic acid, and water, though homogeneous at first, separated in time into two layers. This separation is associated with the formation of formanilide (see reference 1), and it occurs in several days. Seven such separated systems were analyzed: one, 37 days after separation; the other six, twelve years after separation, all being kept in sealed glass tubes. The analyses of four of the six long-term samples are given in

table 2; and the other samples gave similar results. The equilibria then are attained in the course of days, rather than years.

The first four columns of table 2 give the primary results, and the last five columns the calculated constituents. In all the layers the per cent actual formic acid and/or the per cent aniline is zero; in other words, as either the acid or the aniline is in excess, the calculation is so adjusted. By the method of analysis adopted it is not possible to discriminate more exactly between the actual formic acid and the acid present as aniline formate,—both “acids” being included in the “free formic acid.”

TABLE 2

Data regarding mixtures of formic acid, aniline, and water after separation into two layers

SAMPLE NUMBER	RELATIVE WEIGHTS	FREE ACID	COMBINED ACID	TOTAL ANILINE	ACTUAL ACID	ANILINE FORMATE	ANILIDE	ANILINF	WATER
		<i>per cent</i>	<i>per cent</i>	<i>per cent</i>	<i>per cent</i>	<i>per cent</i>	<i>per cent</i>	<i>per cent</i>	<i>per cent</i>
16 Original mixture*	100	10.5		58.4					31.1
Aqueous layer	31	0.5	0.5	4.1	0	1.5	1.3	2.1	95.1
Aniline layer	69	0	15.1	85.0	0	0	39.7	54.5	5.8
17 Original mixture	100	19.5		60.1					20.4
Aqueous layer	25	0.6	1.2	4.1	0	2.3	3.1	0	94.6
Aniline layer	75	0.2	24.8	76.5	0	0.6	65.2	25.9	8.3
18 Original mixture	100	30.5		37.6					31.0
Aqueous layer	38	5.8	2.2	6.9	14.6	3.6	5.8	0	76.0
Aniline layer	62	10.8	27.2	57.2	9.7	3.4	71.6	0	15.1
8 Original mixture	100	33.2		45.9					20.9
Aqueous layer	24	14.9	2.5	6.2	14.4	1.7	6.6	0	77.3
Aniline layer	76	10.2	27.9	57.6	10.1	1.8	73.5	0	14.6

* By synthesis.

The per cent of aniline formate is always small, and this carries the largest proportional error. In the “aqueous layers” the ratio per cent formanilide/per cent aniline formate averages 2, but in the “aniline layers” this ratio is 50 or more. In the aqueous layers the ratio

$$\frac{\text{Per cent formanilide} \times \text{per cent water}}{\text{Per cent aniline formate}}$$

averages 175 (as in the homogeneous mixtures), but in the “aniline” layers it is 300 and over. The formation of formanilide is thus most complete in the absence of water. The ratio

$$\frac{\text{Per cent actual formic acid in the aqueous layer}}{\text{Per cent actual formic acid in the “aniline” layer}} = 1.5$$

The "total aniline" and the "combined formic acid" or "anilide" are ten to seventy times more abundant in the "aniline" layers than in the aqueous layers, but the "free formic acid" is more evenly distributed (1:1 to 2:1).

This work completes the previous investigation. It proves that the transformation of crystals of aniline formate to formanilide is often very slow, being retarded if free water is absent. In the liquid mixtures of formic acid, aniline, and water the two equilibria concerned are completed in one or two weeks; thereafter the four or five constituents remain mixed indefinitely. When such liquid mixtures separate into two layers, equilibrium is again attained, with the formanilide and aniline preponderating in the lower layers.

REFERENCE

- (1) WILSON, A. M., AND POUND, J. R.: J. Phys. Chem. **39**, 709 (1935).

SOLUBILITY AND MELTING POINT AS FUNCTIONS OF PARTICLE SIZE. II¹

THE INDUCTION PERIOD OF CRYSTALLIZATION

LAWRENCE HARBURY

Kentucky Color and Chemical Co., Inc., Louisville, Kentucky

Received September 17, 1946

I. INTRODUCTION

Fischer (2) found for several easily soluble salts,² as well as for poorly soluble salts³ and also for an organic acid such as oxalic acid, an induction period of crystallization from supersaturated solutions. This period of induction must be passed before the separation of a new phase becomes traceable. It varies from substance to substance, but, when appropriate conditions are taken care of, it satisfies in each case the relation:

$$C\sqrt{I} = \text{constant} \quad (1)$$

In this formula C stands for the degree of supersaturation, c/c_0 , and I for the corresponding period of induction. The function indicates a rapid decrease of the period of induction with increase of the degree of supersaturation. Such a behavior has also been found, for other substances, by Gapon (3).

II. SOME THEORETICAL ASPECTS OF THE INDUCTION LAW

When endeavoring to find out the reason for the behavior expressed by formula 1, let us restrict ourselves first to a consideration of the spontaneous formation of

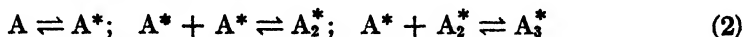
¹ For the first paper on this topic see Harbury (5).

² Such as K_2SO_4 , $K_2Cr_2O_7$, $(NH_4)_2C_2O_4 \cdot H_2O$, and $(NH_4)_2SO_4 \cdot FeSO_4 \cdot 6H_2O$.

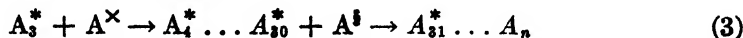
³ Such as Ag_2CrO_4 , $BaSO_4$, $SrSO_4$, $CaSO_4 \cdot 2H_2O$, $CaCO_3$, PbI_2 , Ag_2SO_4 , $PbSO_4$, $PbCrO_4$, and $MgC_2O_4 \cdot 2H_2O$.

"wall germs"⁴ in a very strongly supersaturated solution of a substance A, and let us assume, for the present, that such a solution is free from impurities that could influence the value of I .

Considering the formation of the new phase as the result of a "stepwise process of chemical fixation,"⁵ it is possible to split the process of growth into two types of chain reactions, *viz.*: (1) that of the germ formation:



and (2) that of the growth of nuclei of crystals:



Somewhat different schemes might also be suggested,⁶ but the above will do for the present. In view of the very high degree of supersaturation of the systems considered,⁷ it is assumed⁸ in schemes 2 and 3 that already a favorably orientated aggregate of three molecules may serve as an effective germ. Once this is formed, the fate of the separation of the crystalline state is sealed. The chain reactions (scheme 3) then proceed to the right to a sweeping extent in accordance with their own laws of germ and crystal growth, *i.e.*, autocatalytically in the beginning, but with a brake put on subsequently when, owing to the separation of the new solid phase, the concentration of the solute decreases.

Thus it is in the first place scheme 2 which is interesting. It is the bringing about of one, or a few, favorably orientated A_3^* aggregate(s) which controls the period of induction, *i.e.*, the reaction involves in that interval only the conversion of a small number of molecules and hence does not change—practically speaking—either the concentration of A, or that of A^* and A_2^* .⁹

Let us look a little closer to the consequences. A wall action being assumed, it is important to pay attention to the way and extent to which the wall is covered with activated molecules and molecule aggregates of A. In case selective adsorption is completely absent, the pattern on the wall will be comparable to that of a cross section of the liquid. Almost 100 per cent thereof should be considered as occupied by molecules of the solvent and the solute. These, as such, have no constructive significance for possible germ formation. It is only at relatively widely separated places that the cross section (or wall) will be occupied by favorably activated and orientated molecules (or ions) of A^* .¹⁰ The presence on the wall of A_2^* aggregates of the appropriate type will be quite exceptional. No doubt the pattern changes all the time. Whereas, at any moment, part of the activated molecules and double molecules will be leaving the imaginary cross section (or solid wall), another number is supplied from elsewhere. The pattern

⁴ For this notion see page 197 of reference 5.

⁵ Cf. Koessel (7).

⁶ See Section IX.

⁷ So high that the state of supersaturation cannot be maintained indefinitely.

⁸ Compare the previous paper (5).

⁹ This is so, since, for reasons indicated in the previous paper and somewhat extended below, $C_A \gg C_{A^*} \gg C_{A_2^*} \gg C_{A_3^*}$.

¹⁰ Cf. page 195 of reference 5.

of occupation by such activated single and double molecules is a changing disorderly one which is controlled only by the law of chance.

Let us suppose, in order to give the idea a more concrete form, that the average density D of occupation of the wall with activated single molecules A^* amounts to 5×10^{-6} . This will then mean that only one A^* molecule will be present, and occupy one place, in a section of a monomolecular layer having, e.g., 2×10^6 places available for occupation, though the location of such single A^* molecule may vary in course of time. The part of such a section occupied by activated double molecules A_2^* will then amount to around 2×10^{-10} ; for more generally it is known¹¹ that the fraction f of the surface which is occupied by aggregates of n molecules is determined—in the case of a very sparse density D of occupation—by the formula:

$$f = p \cdot \frac{D^n}{n!} \quad (4)$$

in which p amounts to ca. 7 for an aggregate of two molecules ($n = 2$), and to ca. 70 for an aggregate of three molecules ($n = 3$).

The average density of occupation f_3 for activated aggregates of three molecules hence amounts to

$$70 \cdot \frac{1}{2^3} \cdot \frac{10^{-15}}{3 \times 2} = \text{ca. } 10^{-15}$$

i.e., a value which is negligible for all practical purposes.¹²

This density of occupation, no doubt, would be somewhat larger if it were justifiable also to consider aggregates with abnormally large distances between the constituting molecules. Experience, however, in the field of recrystallization phenomena has shown that the growth power, even of crystals, is already detrimentally impaired by a small amount of stretching, whereas their susceptibility to physical or chemical attack is enhanced.

III. INFLUENCE OF SELECTIVE ADSORPTION

When looking for possibilities of a somewhat greater density of occupation, it is better to drop the assumption of selective adsorption being absent. As a matter of fact, the general case will be that the wall *does* adsorb selectively. The

¹¹ Cf. Reinders and Hamburger (8).

¹² In this use of formula 4 the wall is supposed to be impermeable. For this reason, and in anticipation of what follows, the occupation with aggregates has been calculated at one side of the solid wall. In the case of poorly soluble substances the density of occupation by activated single and double molecules will be still smaller. In the case of a substance like calcium carbonate the solubility at room temperature is only of the order of 1 mg. per 100 cc. The average occupation of a cross section by A molecules only amounts to 10^{-4} in case the supersaturation (c/c_s) amounts to 10. Clearly, the density of occupation by activated single molecules is still smaller by far. In the case of poorly soluble substances, however, the energy of solvation tends to be smaller. A smaller energy of activation therefore being required, the percentage of A^* , as compared with that of A , may be shifted so that the activated form A^* may be somewhat favored.

average period of occupation by A_2^* molecules, moreover, will in any case be greater than that of A^* molecules, whereas that of A_2^* aggregates will surpass the average period of adsorption of A_2^* molecules. Especially in the case of a very high degree of supersaturation, can such an opportunity for the formation of one or more three-molecule aggregates develop that a favorably orientated specimen gets an opportunity for further growth before becoming detached from its base (the helping wall) or being split up, owing to the action of the solvent. For the rest, however, only factors of proportionality change thereby. Owing to the low density of occupation, a linear proportionality remains true—applying with fair approximation—between on the one hand the concentrations of A^* , A_2^* , and A_3^* , respectively, prevailing in the adsorption layer, and on the other hand the corresponding concentrations in the liquid, even though the latter change functionally with the degree of supersaturation of non-activated A initially applied.

As has been explained, the formation of A_3^* aggregates will become practically effective for a progressive germ growth *when their (very) concentration on the wall surpasses a threshold value. The time required therefor will then tend to increase inversely with the third power of C_A , and since—practically speaking—the concentration of the solute does not change during the induction period, there will be an inverse proportionality with the third power of the degree of supersaturation $C' (= c/c_0)$ with which we started.*

IV. INFLUENCE OF IMPURITIES

It was assumed in the above that any impurity capable of changing the induction period I would be absent. Obviously this assumption is untenable. Traces of impurities are always present, and even a content thereof far below the limit of analytical detection may have a great influence on I . It is true that reproducible values for I have been found in carefully handled experiments, but this only indicates that the content of impurities, influencing I , has been kept as reproducible as other experimental conditions (such as temperature, type of wall surface, volume of the liquid, etc.).

It is necessary, therefore, to consider the possible effect of a blocking, deactivation, or corrosion of A^* , A_2^* , A_3^* , on account of impurities, and especially by those contaminations that are readily adsorbed by the wall.

It must, then, be kept in mind that it is exactly in the initial stages of a stepwise growth that the reactivity changes with leaps and bounds, the change being the greatest when passing from A^* to A_2^* , and being markedly less when passing from A_2^* to A_3^* , the last one being the least vulnerable of the three links considered in the formation of a smallest effective germ.

In the sequence of reactions of scheme 2 however, the possibilities of blocking, deactivation, or other actions, tending to eliminate a normal behavior of A^* , are not of paramount significance. This is so because the ratio of A^* units to the number of A_2^* or A_3^* aggregates is large, and, moreover, because the ratio C_A/C_{A^*} is very large, so that the time to make up for A^* losses on the wall (by way of the reaction $A \rightleftharpoons A^*$) will also be small.

It is a different story for A_2^* , the stock of which, present on the wall, is only small. Paralysis of the greater part thereof practically cancels the in any case small chance of A_2^* formation.

In the above, a substantial staying time was attributed to A_2^* aggregates. But a still greater staying time and life expectancy must be attributed to the combination of A_2^* with adsorbed impurities.

By now the formation of a sufficient amount of A_2^* —required first to “neutralize” impurities, and second to provide for a threshold concentration of free A_2^* building units qualified to form A_2^* —becomes the bottleneck in the complex of chain reactions and controls the induction period. Hence this period becomes practically determined by the rate of A_2^* formation, which is proportional to C_{A^*} , and hence to C_A^2 or C^2 .

Where reproducibility of the experiments is secured, the amount of A_2^* required for fixation of impurities, and the supply of the indicated threshold surplus, will be the same for every repetition of the trial.

It thus follows that the induction period involved therewith should be inversely proportional to the square of the concentration of the solute. Hence, the order of the reaction is one less than was found before, when we still placed A_2^* in the center of our attention.¹³ This order, moreover, need not change if the n value of the critical germ size A_n were to exceed somewhat the figure 3.

V. CONCERNING THE APPLICABILITY OF THE RELATION $C\sqrt{I} = \text{CONSTANT}$ TO STATIONARY SATURATED SOLUTIONS

An attempt has also been made to extend the empirically established relation between C and I to fields in which the degree of supersaturation is held within such limits that the supersaturation can be upheld indefinitely. When a trace of inoculating material is added to such supersaturated solutions, reproducible induction periods could be ascertained which, again, satisfied the relation $C\sqrt{I} = \text{constant}$. This plainly confirms the presence and influence of “reproducible contaminations.” Their ability to paralyze substantially the surface of the material used for inoculation would explain why it is that, even in the presence of such material, effective germ action and crystal growth do not start at once in the moderately supersaturated system. The author would not know of another way of explaining the phenomenon of the very substantial periods of induction which systematically occur in such type of systems when brought into contact with a few tiny crystals that were intended to serve as centers of crystallization.

It must be inferred that on their infected surfaces, too, a sufficient number of activated A molecules and aggregates have to be formed, and the question can be raised what critical size of the two-dimensional germ will apply here.

¹³ Examining this interpretation more closely, it may also be argued that on the one hand the combination of A_2^* with a contaminating molecule is of a more lasting nature than the combination of A^* with such a molecule. On the other hand, the chance that contaminating molecules may block larger growth-active aggregates entirely rapidly decreases with increasing size and number of these particles, and finally becomes negligible in systems with only small traces of impurities.

Without a supply of a small amount of inoculating material, the spontaneous formation of relatively large aggregates would have been required to effect crystallization, since the type of system considered in this section is assumed to have only a moderate degree of supersaturation. However, when we study an inoculated system, in which the action of the surface of inoculation is substantially but not entirely paralyzed, a two-dimensional germ growth thereon will be decisive. For this a type of scheme like that of scheme 2 will again be applicable, and the smallest growth-active aggregate used need not be much larger than A_s^* .

As far as the period of induction is concerned, it can be stated once more that, in the presence of traces of blocking impurities, this will be mainly determined by C_A^* . Owing to the only moderate degree of supersaturation to which this section is restricted, the concentration of A^* spontaneously formed on the substantially blocked surface of the inoculating material will tend to be still smaller than was the case before,¹⁴ whereas (residual) blocking effects have again to be compensated for in order that a threshold value of an appropriate number of free A_2^* aggregates be obtained. This is required for a further stepwise growth of these fundamental building units of germs and pro-germs. Consequently, a relation of the type $C\sqrt{I} = \text{constant}$, or of a cognate type, will remain applicable. The further inference is that I should be considered as mainly representing a period of blockade and incubation. In line therewith is the fact that I can be extended enormously by deliberately supplying impurities of a type that is readily adsorbed. Contrariwise, I is found capable of a substantial decrease when substances are added that activate or, in some effective way, are capable of taking care of adsorbed contaminations.

VI. VERY HIGH DEGREES OF SUPERSATURATION

When a very high degree of supersaturation exists, and blocking impurities have been removed as much as possible, the induction period may practically vanish. In the case of very high C_A values it may be, moreover, that the state of solvation of the molecules of the solute undergoes a change, which in turn affects requirements of orientation and activation. In case the energy of activation decreases from E^* to E^X ($E^X < E^*$), the fraction of A molecules transformed into the A^X state may increase, and hence the chance of formation of aggregates may improve in an accelerated way with increasing concentrations.

VII. TECHNOLOGICAL SIGNIFICANCE OF MOBILITY ON CRYSTAL SURFACES, AND OF BLOCKING AGENTS

In the preceding discussion we did not exclude some degree of mobility in the border film on a "wall" or crystal surface. Means can be employed to increase such mobility. When, e.g., a crystal of bitter salt is dropped into a highly supersaturated solution of this substance, a tail of small crystals is formed in its wake. Obviously, part of the small germs, as they are formed on the

¹⁴ Hence, compensation is required by means of a stronger fixation to the more similar lattice of the inoculating crystal.

crystal surfaces, are removed therefrom, owing to the friction with the liquid.^{15,16} Freed, they grow to independent small crystals. For the same reason a much larger number of crystals separates from a supersaturated solution that is kept in motion, than from one that is kept at rest.

Again the number and size of crystals formed from supersaturated solutions in motion may be changed by blocking agents. More or less continuous industrial processes have been developed in which supersaturated solutions are supplied to or formed in a system in which an optimum (small) concentration of well-defined blocking agents is maintained. These factors can be used with great advantage in order, e.g., to control the formation of an approximately uniform size of crystals of desired dimensions.¹⁷

The stabilization of supersaturated solutions is also a field of some technical importance, with which we hope to deal at a later time. The more general cases are those of stabilizing unstable phases or modifications, if these possess advantageous properties, or the controlled transformation of unstable systems to more stable ones having preferred properties. Transformations can be delayed or, practically speaking, be completely halted by means of blocking "holding agents," chilling, etc. On the other hand, they can usually be accelerated by appropriate changes in factors such as temperature, acidity, the supply of catalysts (e.g., nuclei of crystallization), or the supply of agents capable of removing (or "neutralizing") blocking agents. Applied chemistry and metallurgy are making ever-increasing use of these ways and means. The policies applied in particular instances are adjusted to the properties which are considered as being most advantageous for the application of the final product.

VIII. CRYSTAL SHAPE

It is a remarkable feature that the solid phase separating from supersaturated solutions or undercooled melts tends to crystallize at first in the form of needles and networks of needles (dendrites). This is even the case when crystallization takes place in the regular system. It is here, too, that the induction period of the infected crystal exerts its influence. Growth of lattice layers takes place at the expense of the nearest solute molecules (or ions), and the degree of supersaturation is thereby locally decreased. Owing to blocking contaminations, the growth of a small crystal, even if belonging to the regular crystal system, will be unequal in various directions, and the first products of crystallization will have more or less the form of amicroscopic needles. The pinnacle of each growing tiny needle, however, can be reached from many more sides than is the case elsewhere on the crystallite surface, and solute withdrawn at or near this point from the liquid phase can be made up most readily by diffusion. In consideration of the fact that the period of induction is inversely proportional to the square of the degree of supersaturation, local concentration differences will

¹⁵ In industrial processes where many crystals are held in motion, friction between them may also give rise to new nuclei of crystallization.

¹⁶ It has been demonstrated (4) that also (dry) polishing of ground crystal aggregates gives rise to the removal of small aggregates and to relatively sweeping surface changes.

¹⁷ See, for example, Berkhoff (1) and Van Aken (10).

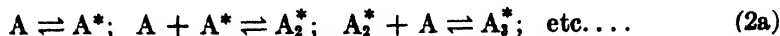
be of marked influence on the local rate of growth. In the presence of strongly blocking impurities, the induction period will be very substantially extended, and the phenomenon of unequal growth rates, leading to needles, will tend still more to manifest itself. To this effect factors such as lattice defects and local tensions may also contribute, whatever their cause may be.

In the course of time, and with increasing chances of blockade, crystal pinacles will also be subject to a hampering of growth by contamination. When this is the case, other places on the needle surface will become candidates for comparatively preferred growth. Thus, places of hampered and of preferred growth change with time. Consequently, crystallization in the form of needles and dendrites will dominate the picture. In the long run this may change again when recrystallization becomes an effective factor. In the case of slow crystallization from slightly supersaturated solutions that are kept at rest, or in properly adjusted slow motion, the latter factor may even become the dominating one (almost) from the outset. In any case, the use of carefully purified solutions will favor the separation of the new phase in the shape of regularly formed crystals. But this is often far from easy to control, since impurities that we are accustomed to calling small, owing to the impossibility of their detection or estimation by means of analytical procedure, may still exert a marked influence on the shape, size, and quality (lattice defects) of crystals. The influence of the adsorption of traces of foreign substances on crystal surfaces may also lead to more sweeping effects, such as crystallization in an abnormal symmetry class and/or abnormal degrees of solvation, etc. These interesting phenomena constitute quite an extended field, to which a number of other investigators have already paid attention.¹⁸

IX. CONCLUDING REMARKS

A significant element in the line of reasoning followed in the preceding sections is the acceptance of the notion of a genetic building-up process based on simple reaction chains. Contrariwise, a notion—as suggested, e.g., by Tammann—is rejected, according to which the incidental, simultaneous, and favorable encounter of an odd 8 molecules would be required as a basic condition for germ formation. At least in the case of supersaturated solutions of substances with not too simple molecular and lattice structures, such an assumption seems unacceptable.

No doubt one may consider variations of scheme 2, e.g., of the following form:



In the case, however, of long induction periods of germ formation, it is not held acceptable for easily soluble substances to assume a dominating participation of inactivated A molecules in the process of germ formation. And in cases where the induction period practically vanishes,¹⁹ one would rather think, as previously indicated, of a decrease in the required energy of activation.

¹⁸ Cf., for example, Tertch (9) and Kohlschütter and coworkers (6).

¹⁹ At very high concentrations of the solute.

A relatively long period of induction is often found to be followed by a relatively substantial velocity of crystallization.²⁰ This can easily be understood. Whereas, in the case of germ formation, a large energy of activation is required per molecule, much less activation is required when attachment takes place to a relatively large aggregate with a well-built lattice. This applies especially in the case of the so-called repeated stepwise attachment. The exposed surface, moreover, being incomparably larger in the case of progressive crystallization than in the case of germ formation, this is an additional factor in favor of comparatively rapid crystal growth.

It was in connection with the smaller energy of activation that in scheme 3 (see page 383) the symbols A^{\times} and A^{\ddagger} were introduced, corresponding to such energies of activation that $E^* > E^{\times} > E^{\ddagger}$.

X. SUMMARY

It is shown that the empirically established relation $C\sqrt{I} = \text{constant}$, between the induction period of crystallization, I , and the degree of supersaturation, C , of a supersaturated solution can be explained by taking into account the paramount significance of (activated) double molecules in the process of germ formation.

The shape (needles and dendrites) in which a new crystalline phase tends to separate initially from unstable systems can be connected with the existence of periods of induction, varying with factors such as the degree of instability, the unavoidable presence of blocking "impurities", stresses, and lattice defects.

The technological significance of supplying to unstable systems blocking (or unblocking) agents in controlled small concentrations is pointed out. Such measures are significant, in addition to the control of other factors, such as the degree of instability (degree of supersaturation, undercooling, etc.), the temperature, the acidity, the presence of nuclei of crystallization, agitation (whereby mobility on "interfaces" may be increased and regulated), and other measures, applied in order to obtain best results. The actual policy followed in any particular process must be properly adjusted to the type of process (e.g., continuous or discontinuous) and the desired properties of the final product.

REFERENCES

- (1) BERKHOFF, G.: Chem. Weekblad **35** (1938); paper on the crystallization of technical products, particularly of ammonium sulfate, forming a contribution to a symposium on *Solutions and Solubility*, Leyden, 1938, pp. 154-63.
- (2) FISCHER, W. M.: Z. anorg. Chem. **145**, 316 (1925).
- (3) GAPON, E. N.: J. Soc. Chim. Russ. **61**, 1721, 1730, 2319 (1929).
- (4) HAMBURGER, L.: Z. Metallkunde **25**, 29, 53 (1933).
- (5) HARBURY, L.: J. Phys. Chem. **50**, 190 (1946).
- (6) KOHLSCHÜTTER, V., AND COWORKERS: Helv. Chim. Acta **8**, 457, 470 (1925).
- (7) KOSSEL, W.: *Die molekularen Vorgänge beim Kristallwachstum*. Hirschel, Leipzig (1928).

* Provided one has refrained from deliberately adding substances which put a serious brake on crystal formation.

- (8) REINDERS, W., AND HAMBURGER, L.: *Rec. trav. chim.* **50**, 479, 481 (1931); *Chem. Weekblad* **30**, 126 (1933).
- (9) Cf., e.g., TERTSCH, H.: *Trachten der Kristalle*. Springer, Berlin (1926).
- (10) VAN AKEN, J. S. A. J. M. (to De Directie van de Staatsmijnen in Limburg): British patent 511,390 (1939); German patent 715,758 (1941).

RATES OF SOLUTION OF SOAPS IN WATER¹

LEO SHEDLOVSKY, GILBERT D. MILES, AND GEORGE V. SCOTT

Colgate-Palmolive-Peet Company, Jersey City, New Jersey

Received October 22, 1946

I. THEORETICAL FACTORS WHICH DETERMINE THE RATE OF SOLUTION OF SOLIDS IN LIQUIDS

Heterogeneous rates of solution, such as the rate of solution of a solid in a liquid (3), range from extremely slow rates to an upper limit determined by the velocity with which the reagent or solvent can reach the solid surface or the product leave it under definite stirring conditions. Such cases may be considered as consisting of two consecutive steps, one at the interface, and the other the rate of transfer of solute from the surface. The over-all rate is determined by the slower step; consequently, if the process at the surface is much more rapid than the other processes, this will have no appreciable influence on the observed rate, which is controlled by diffusion. This theory considers the velocity component of turbulence perpendicular to the interface to be a negligible factor in transporting the dissolved substances to and from the surface as compared to transport by diffusion.

As King (3) points out, this means that the thickness of the layer in which diffusion is important varies not only with the stirring speed, but also with the diffusion coefficient of the reagent or solute. If this coefficient is high, the point at which diffusion becomes comparable to convection will be at a greater distance from the solid surface than if the coefficient is low.

The rates of solution of solids in liquids usually follow a first-order equation:²

$$\frac{dc}{dt} = \frac{KA}{V} (C_s - C) \quad (1)$$

where K is determined by the stirring conditions or the linear speed of the liquid just past the solid, the composition of the surface, and the temperature, which

¹ Presented before the Division of Colloid Chemistry at the 110th Meeting of the American Chemical Society, Chicago, Illinois, September 9, 1946.

² Except where the activity coefficients are constant or equal to 1, the diffusion rates are determined not by differences in concentrations, but by differences in activities, since such rates are governed by differences in the free energy between two points in the solution. However, since suitable data on activity coefficients are not available, concentrations are referred to throughout this paper.

in turn affects the solubility, C_s . For soaps, the increase in C_s with increase in temperature is very considerable, especially above the so-called Krafft point. It will be noted that C_s must be known to calculate K .

II. METHOD OF CALCULATING SOLUBILITIES FROM RATE MEASUREMENTS

The following derivation leads to a method of calculating C_s from rate measurements:

- C = concentration of solute,
 C_s = concentration of solute in saturated solution,
 t = time,
 A = surface area of substance dissolving, and
 v = volume of solution.

$$\frac{kA}{v} (t_2 - t_1) = \ln \frac{(C_s - C_1)}{(C_s - C_2)} \quad (2)$$

$$e^{[(kA/v)(t_2-t_1)]} = \frac{C_s - C_1}{C_s - C_2} \quad (3)$$

$$C_s = \frac{C_2 e^{[(kA/v)(t_2-t_1)]} - C_1}{e^{[(kA/v)(t_2-t_1)]} - 1} \quad (4)$$

$$C_s = \frac{C_4 e^{[(kA/v)(t_4-t_3)]} - C_3}{e^{[(kA/v)(t_4-t_3)]} - 1} \quad (5)$$

$$\frac{C_2 e^{[(kA/v)(t_2-t_1)]} - C_1}{C_4 e^{[(kA/v)(t_4-t_3)]} - C_3} = \frac{e^{[(kA/v)(t_2-t_1)]} - 1}{e^{[(kA/v)(t_4-t_3)]} - 1} \quad (6)$$

Take

$$(\Delta t) = (t_2 - t_1) = (t_4 - t_3) \quad (7)$$

and equation 6 becomes

$$\frac{C_2 e^{[(kA/v)(\Delta t)]} - C_1}{C_4 e^{[(kA/v)(\Delta t)]} - C_3} = 1$$

$$e^{[(kA/v)(\Delta t)]} = \frac{C_3 - C_1}{C_4 - C_2} \quad (8)$$

$$\frac{kA(\Delta t)}{2.303v} = \log \frac{C_3 - C_1}{C_4 - C_2} \quad (9)$$

From equation 2

$$\frac{kA\Delta t}{2.303v} = \log \frac{C_s - C_1}{C_s - C_2} = \log \frac{C_3 - C_1}{C_4 - C_2} \quad (10)$$

$$\frac{C_3 - C_1}{C_4 - C_2} = \frac{C_s - C_1}{C_s - C_2} = R \quad (11)$$

$$C_s = \frac{C_1 - RC_2}{1 - R} = \frac{RC_2' - C_1}{R - 1} \quad (12)$$

C_s can be calculated from rate measurements by applying equations 11 and 12.

III. PREVIOUS WORK ON RATE OF SOLUTION OF SOAPS

Previous work on the rate of solution of soap in water has been fragmentary; in most cases the surface area of the substance dissolving and the linear speed of liquid past the solid, which is a function of the rate of agitation, were not adequately controlled.

In 1911 Shukov and Shestakov (6) measured the time required to dissolve fixed weights of commercial soaps. They did not control the surface area of their specimens, and the linear rate of flow of water past the surface cannot be estimated.

S. Kawai (1) reported the selective solution of a mixed soap made from tallow and coconut oil. The soap was kept in distilled water at various temperatures for different periods of time. The neutralization values of the fatty acids of the dissolved soap decreased with rise in temperature while the iodine numbers increased, from which it was concluded that soaps of lower members of the series of saturated fatty acids, such as sodium laurate, and of unsaturated fatty acids, such as sodium oleate, were selectively dissolved.

Sauer and Burek (5) determined the rate of solution of sodium palmitate, sodium stearate, and sodium oleate, as well as of six commercial soap samples. In their experiments, equal parts of dried soap and water were pressed in a mold to form a cylinder with the end surface smooth. A stream of water at constant temperature and rate of flow was passed over the surface of the test piece, whose surface was kept constant. The soap concentration was determined by titration with 0.01 *N* hydrochloric acid. During the first 4 min. the rates of solution for sodium palmitate were somewhat slower than later. They attributed this to the necessity of soaking the surface before a steady rate was obtained. The rate of solution for the palmitate increased with greater rates of flow, but this rise was not uniform and reached a maximum. They note that this may be due to the relative importance of the rate of soaking and the loss of soap by mechanical transfer at higher rates of flow. For sodium stearate, no maximum solution rate was shown at any particular rate of flow. Although the volume rate of flow was given, the description of the apparatus does not permit a calculation of the relative linear speeds of flow, which would be necessary for comparisons with other methods.

C. Stiepel (7) described a method for determining the rate of solution and amount of foam obtained with soap solutions, but he did not report any data. In his method the soap was tied in a linen bag and agitated at constant temperature and rate of stirring in a small glass churn for a fixed time interval. The amount of soap dissolved was estimated by filtering and acidifying a measured volume of solution and determining the amount of fatty acids liberated. It appears that the area of the test piece and the rate of flow of liquid over it cannot be suitably controlled by this method.

IV. PROCEDURE

We have devised the following method for measuring the rates of solution of soaps under controlled conditions.

The soaps were prepared according to the methods described by Miles and Ross (4). The equivalent weight by titration with 0.5 normal hydrochloric acid to a bromocresol green end point in all cases corresponded to the theoretical values within better than 1 per cent and the amount of free alkali was less than 0.1 per cent.

Cylinders of the material were prepared by compressing the powdered sample in an iron mold at 10,000 lb. per square inch. A hole was drilled in the briquet, which was clamped in a holder made in the form of a threaded bolt with rubber and brass washers at the ends. The samples were rotated in glass electrolytic

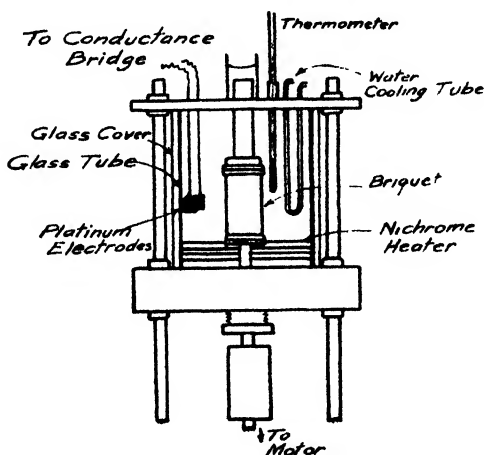


FIG. 1. Rate-of-solution apparatus

conductivity cells (figure 1) containing platinum electrodes coated with platinum black. The volume of the cells was 270 and 285 cc.

The electrolytic conductivity of the solution was measured as function of the time with a 1000-cycle conductivity bridge (Industrial Instruments Model RC-IB) which gave a precision of ± 0.5 per cent. The time was measured with a stopwatch, and the temperature with a mercury thermometer graduated in 0.1°C . The temperature of the solution was maintained within $\pm 0.05^\circ\text{C}$. during the run by adjusting the current through an asbestos-covered, nichrome-wire heater which was wrapped around the outside of the conductivity cell (figure 1).

Usually each run was continued for about an hour, after which a fresh briquet was started in a soap solution somewhat more dilute than the last point obtained in the previous run. In this way, as complete a rate curve as desired was obtained in sections. An important limitation for the length of time of a run was the necessity of avoiding too large a change in the diameter of the test cylinder.

The electrolytic conductivity of solutions of known concentrations was measured using the Industrial Instruments dipping-type cell, having a constant of 1.0, and by comparison of several solutions with the cylinder-type cell (figure 1) a conversion factor was determined. On this basis, the concentrations were obtained from the conductivities.

We had found in previous experiments that, owing to absorption of water by the soap, the rate of solution of a cylinder which had been previously soaked in water was usually slower than that of a fresh sample. All rate experiments except several preliminary runs were always started with a cylinder which had not been used before.

For rate-of-solution measurements of soap, starting with solutions containing soaps, salts, and alkalies, the apparatus shown in figure 1 was used, but the rate was not followed by the conductometric method. A cylinder of sodium palmitate was rotated in the solution for 35 min., and then the total solids in an aliquot of the final solution were determined by evaporation to dryness. From this value and from a blank determination without soap, the amount of soap dissolved was calculated.

Measurements of pH were made using the Beckman Model G pH meter equipped with a type E glass electrode, which is stated to be relatively free from sodium salt error at high pH values. The solutions were heated to 65°C. and the pH readings were obtained with the temperature compensator at 40°C. Such readings were adequate for our purposes, since we were concerned only with a constant pH or relative changes in pH.

For the rate measurements in which the interferometer was used, 2-cc. aliquots were withdrawn from the solution, at intervals during the run, and immediately replaced with 2 cc. of distilled water at the same temperature. The aliquots were acidified and extracted with petroleum ether (Skellysolve A) in 50-cc. separatory funnels. The Skellysolve phase was separated from the aqueous portion, dried, and evaporated. The residual fatty acid was placed in an oven at 80°C. for 20 min. and then dissolved in 5.00 cc. of chloronaphthalene (Halowax 1000). This solution was compared in the Zeiss interferometer cell with a standard chloronaphthalene solution containing a trace of fatty acid. From a calibration curve previously determined by a similar treatment of soap solutions of known concentrations, the amount of soap present in the aqueous aliquots could be calculated.

It is required that the bath liquid for the interferometer have a refractive index close to that of the solvent used in the cell; otherwise the illuminated part of the fields for the upper and lower bands do not lie one above the other. Therefore, chloronaphthalene was used as a solvent and in the bath of the interferometer.

Leaching experiments were carried out with a cylinder made from a mixture of 65 per cent sodium palmitate and 35 per cent sodium laurate. This cylinder was rotated in water for various periods of time and various temperatures, and at the end of each run, a 100-cc. aliquot was transferred to a tared flask and evaporated. The flask was then placed in an oven at 105°C. until constant weight was attained. The residue was redissolved and titrated with 0.1 N

hydrochloric acid, using bromocresol green as indicator. The mean molecular weight of the soap in the residue is equal to the weight of the residue divided by the equivalents of hydrochloric acid. This value is compared with the mean molecular weight of the original soap mixture.

The cell shown in figure 1 was used for estimating the apparent solubilities of pure soaps directly. The concentration changes were determined conductometrically, and the final concentrations were checked in each case by evaporating an aliquot to dryness and weighing the residue. Soap solutions of various concentrations were prepared at a temperature several degrees higher than that of the test and allowed to cool slowly to the desired temperature. A definite drop in electrolytic conductivity over a period of 30 min. at constant temperature was taken as a sign that the solubility of the soap had been exceeded. After a series of approximations of the concentration which first shows a definite drop in conductivity, a solution which is not saturated was prepared. The conductivity of this solution did not change during a 30-min. period at constant temperature. After the solution had been heated to a temperature several degrees higher, 25 cc. was removed. The required volume of a 2.0 per cent solution of the soap and sufficient hot distilled water were added to make up the original volume and increase the concentration 0.05 per cent. By repeating this procedure the concentration of the solution was increased by 0.05 per cent increments until the conductivity definitely dropped during a 30-min. period at constant temperature.

For the preliminary measurements of the rate of solution of benzoic acid in water, a stainless-steel cylinder was partly covered with a strip of adhesive tape whose length was equal to the circumference of the cylinder. A layer of reagent-grade benzoic acid was put on by dipping in molten benzoic acid at about 135–140°C. The rest of the procedure was the same as in the electrolytic method described for soaps.

V. RESULTS

A. Rate of solution and solubility of benzoic acid

The properties of soap solutions are obviously different from those of benzoic acid, but this acid is well suited to test the method for determining rates of solution and solubility (C_s) as estimated from equations 11 and 12. For this purpose the rate of solution of benzoic acid in water was determined.

Two experiments at average peripheral speeds of 9700 and 10,200 cm. per minute at 25.0°C. gave rates which followed the first-order equation (equation 2). Figure 2 indicates the rate curve at a peripheral speed of 9700 cm. per minute.

C_s at 25°C., calculated from equations 11 and 12, gives a mean value of 0.0270 mole per liter, which is 2.2 per cent less than the value (0.0276) given by Kendall and Andrews (2).

B. Rate of solution and calculated solubility of soaps in water

The method was then applied for the determination of the rate of solution and calculated solubility of pure soaps at various temperatures.

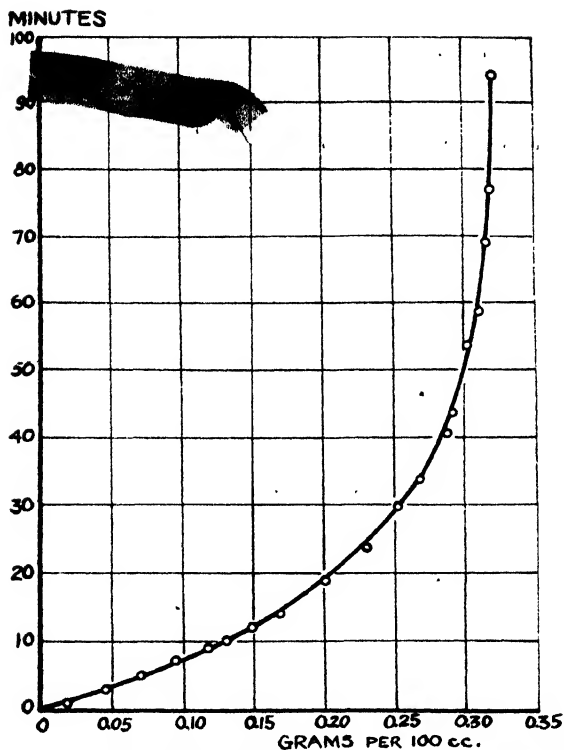


FIG. 2. Rate of solution of benzoic acid at 25°C. $V = 400$ cc., $D = 2.45$ cm., $L = 4.35$ cm., $S = 9700$ cm. per minute.

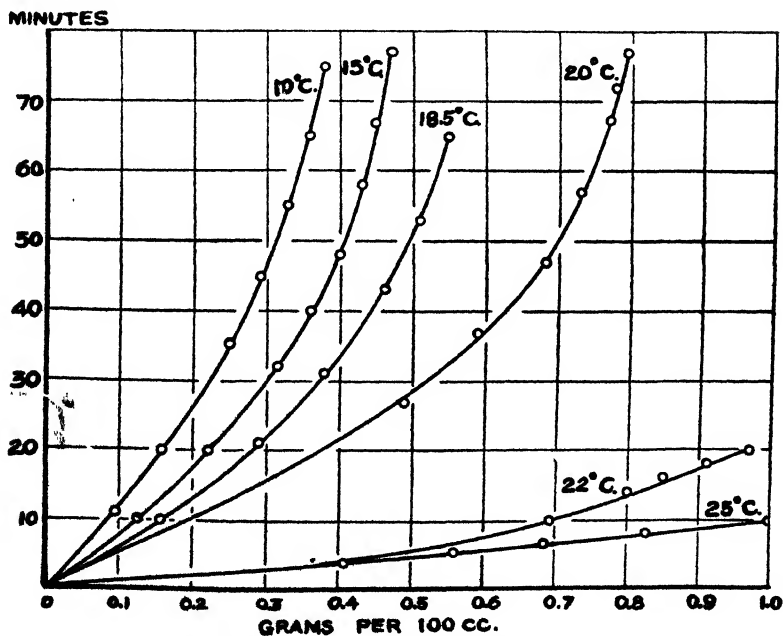


FIG. 3. Rate of solution of sodium laurate

Figure 3 shows rate curves for sodium laurate. These data were plotted on a larger scale and calculations made from the most representative curve.

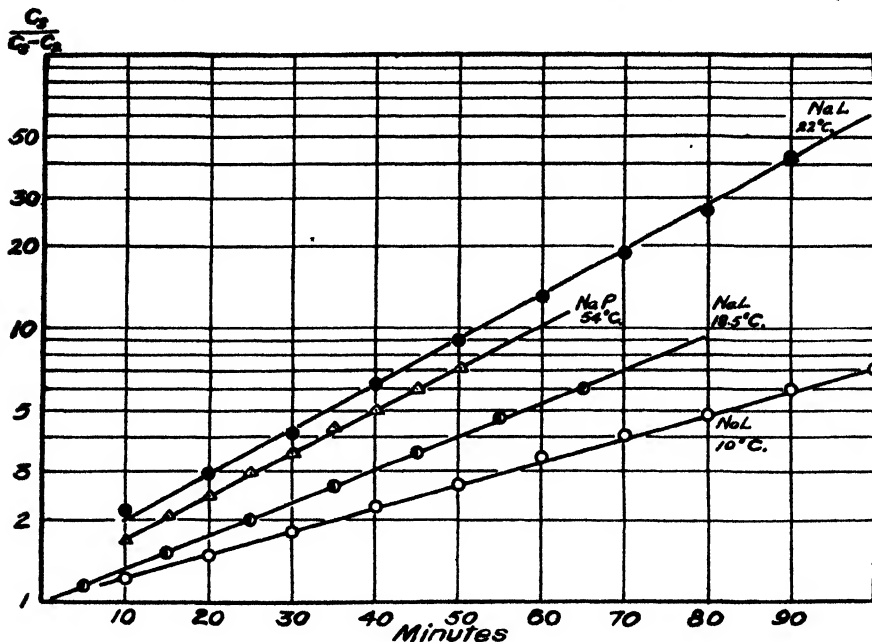


Fig. 4. $\log \frac{C_s}{C_s - C_1}$ against t for rate experiments for sodium laurate and sodium palmitate

TABLE 1

Rate of solution and calculated solubility of sodium palmitate (1.2 per cent water)

TEMPERATURE	$\frac{t_2/t_1}{t_1/t_2}$	k^*	C_s	C_s
°C.		cm./min.	g./100 cc	millimoles/liter
49.0	1.9	0.78	0.16	5.7
52.0	2.0	0.21	0.44	15.6
53.0	1.95	0.20	0.55	19.5
54.0	2.0	0.28	0.62	22.0
55.0	2.0	0.24	0.88	31.2
56.0	2.0	0.29	1.1	39.0
56.5	2.0	0.24	1.4	39.5
57.0	2.0	0.19	2.0	71.0

* k was corrected for an equivalent peripheral speed of 8700 cm. per minute.

From equation 2 it is apparent that a plot of $\log \left(\frac{C_s - C_1}{C_s - C_2} \right)$ against $(t_2 - t_1)$ is a straight line with slope $kA/2.3v$, and $k = 2.3(\text{slope})V/A$.

Figure 4 is a plot of $\log \left(\frac{C_s - C_1}{C_s - C_2} \right)$ against $(t_2 - t_1)$ for some typical rate ex-

periments for sodium laurate and sodium palmitate. From equation 2, $t_1 = 2t_2$, a relationship frequently used to test whether rate data follow a first-order equation.

Table 1 shows the rate constants obtained from the slopes of the straight lines of the plot of $\log \left(\frac{C_s - C_1}{C_s - C_2} \right)$ against $(t_2 - t_1)$ and the calculated values of C_s at temperatures from 49°C. to 57°C. It will be seen that the ratio of t_1/t_2 is nearly 2 in all cases. This constant ratio, as well as the excellent linearity of the plot of $\log \left(\frac{C_s - C_1}{C_s - C_2} \right)$ against $(t_2 - t_1)$, is taken as evidence that the rates follow the first-order equation.

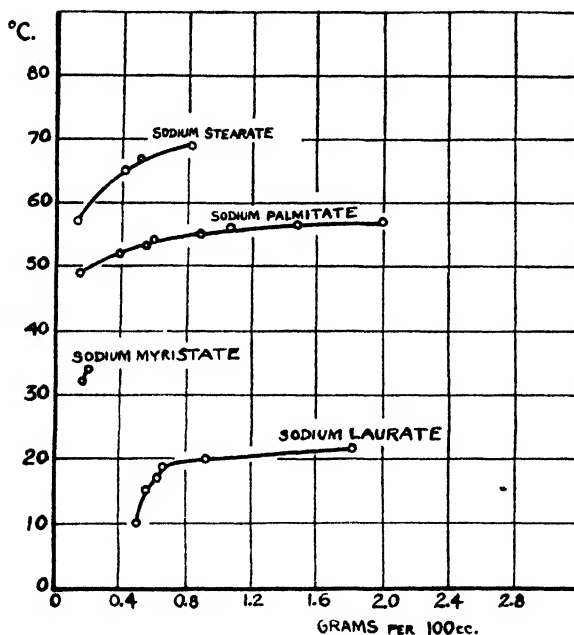


FIG. 5. Calculated solubilities from rate measurements

Figure 5 indicates the values of the saturation concentrations (C_s) which are approached at various temperatures. These values were calculated from equations 11 and 12.

C. Effect of addition of salts and soap to initial solution on rate of solution of sodium palmitate

Some measurements of the rates of solution of soap were made starting with solutions to which soaps, salts, and alkalies had been added. It was found that 0.295 g. of sodium palmitate per 100 cc. dissolved in 35 min. in an initial solution of sodium laurate containing enough sodium hydroxide to raise the pH to 11.0 (1.8 milliequivalents sodium laurate + 0.32 milliequivalent sodium hydroxide per 100 cc.) at 52°C., whereas only a negligible amount of sodium palmitate

(0.003 g. per 100 cc.) was dissolved in 35 min. in an initial solution of pH 11.0 and containing sodium chloride and sodium hydroxide with the same total equivalent concentration of sodium salt as the previous laurate solution.

Figure 6 indicates the decrease in the amount of sodium palmitate dissolved at 52°C. when the concentration of sodium chloride is increased at a fixed pH. The pH was 11.0 when solutions were at 65°C. and measured as noted in Section IV.

Three experiments where different amounts of sodium hydroxide were added to the initial solutions showed that the effect of increase in pH was not large enough to obscure the retarding effect of increased concentration of sodium salt. In all

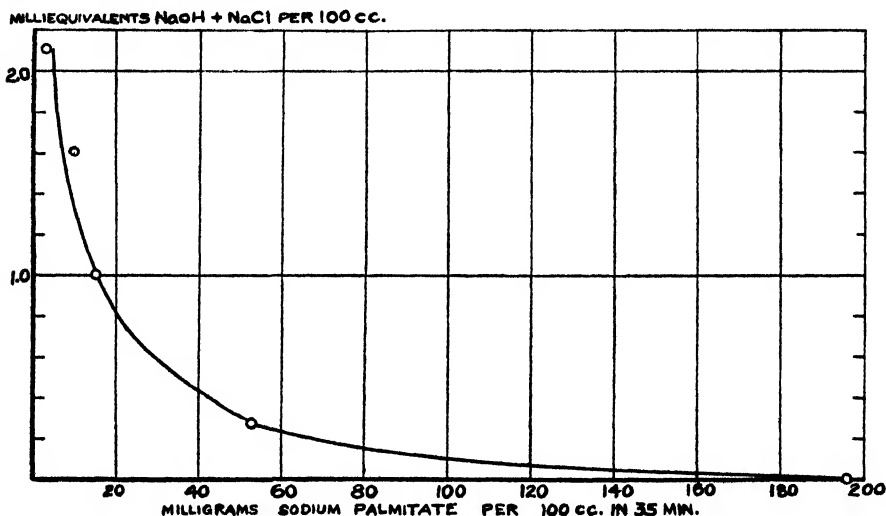


FIG. 6. Rate of solution of sodium palmitate in sodium hydroxide + sodium chloride solution at 52°C. 0.27 milliequivalent of sodium hydroxide per 100 cc. of initial solution.

these cases, the amount of sodium palmitate dissolved was much less than in water at the same temperature.

The difference between the effect of potassium chloride when compared with sodium chloride in the initial solution is seen in figure 7. The initial solutions were adjusted to pH 11.0 by adding sodium hydroxide.

Figure 8 records the influence of potassium chloride on the amount of sodium palmitate dissolved at 40°C. where the initial solution was adjusted to pH 10.8–10.9 (at 65°C.) with potassium hydroxide. At 40°C. only a negligible amount of sodium palmitate would be dissolved in 35 min. in distilled water, but appreciable amounts are dissolved in the presence of potassium salts. If increasing amounts of potassium hydroxide and no chloride are used, the increase is only slightly greater than for solutions having the same equivalent total potassium salt concentration with a fixed low potassium hydroxide concentration. The pH of the initial solution appears to be relatively unimportant.

The curve for concentration against temperature (figure 9) has the same

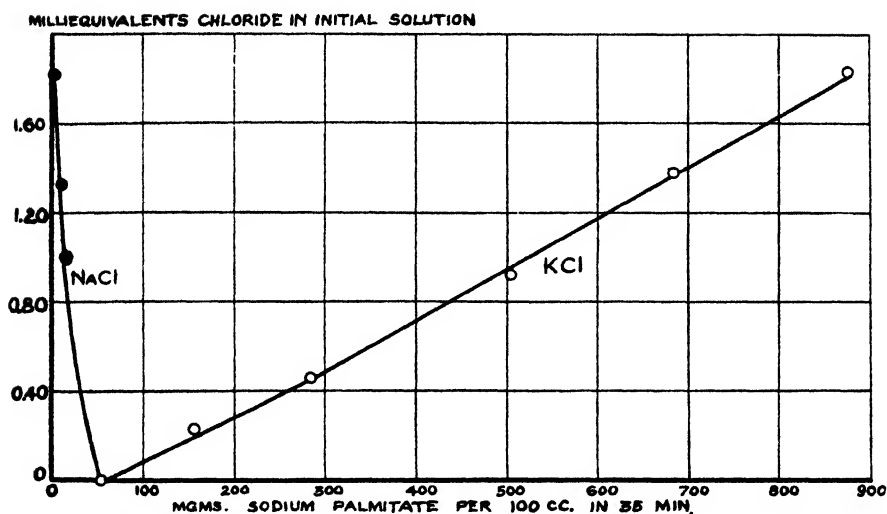


FIG. 7. Rate of solution of sodium palmitate in sodium chloride or potassium chloride solution at 52°C. pH of initial solutions adjusted to 11.0 by addition of 0.27-0.29 milliequivalent of sodium hydroxide per 100 cc.

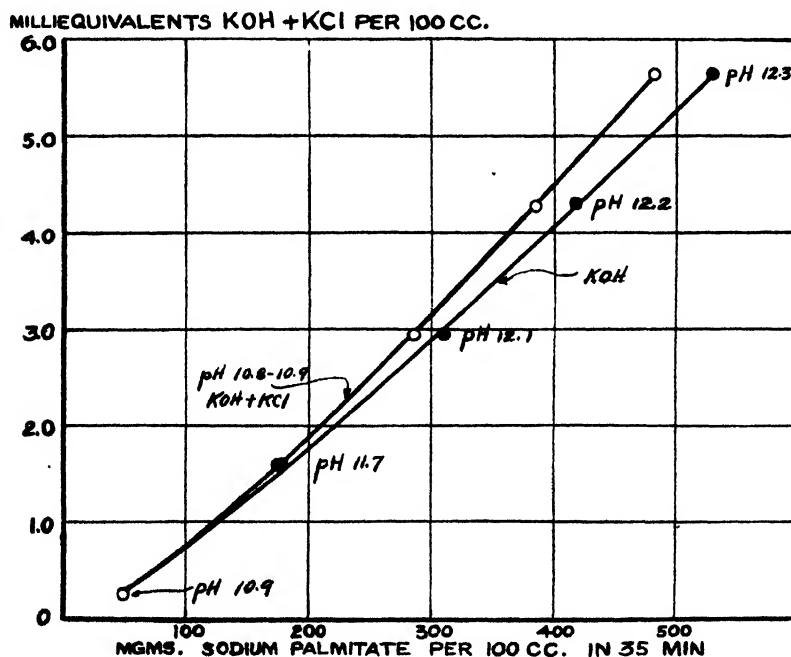


FIG. 8. Rate of solution of sodium palmitate in potassium hydroxide + potassium chloride solution at 40°C. 0.26 milliequivalent of potassium hydroxide per 100 cc. of initial solution.

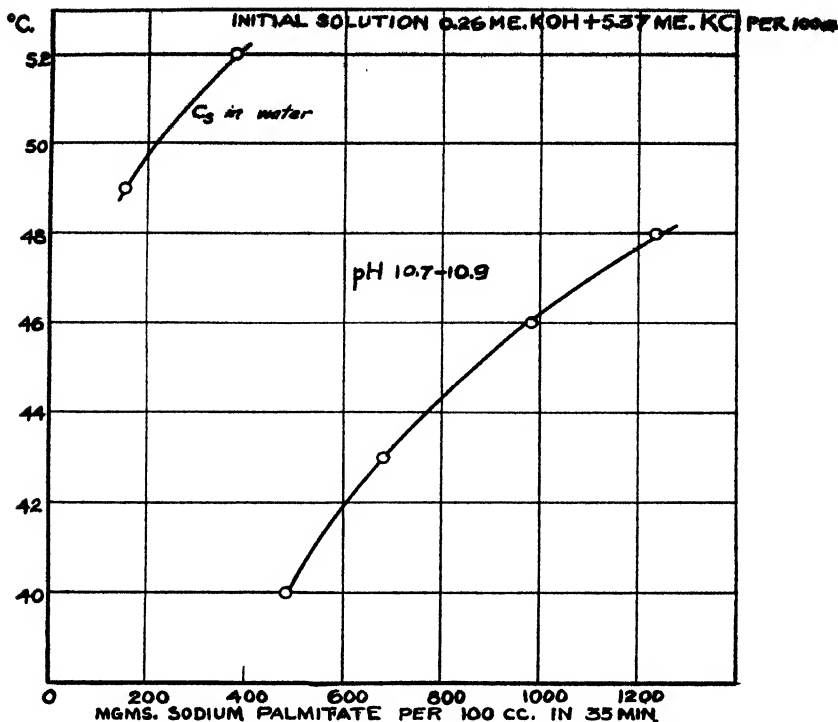


FIG. 9. Effect of temperature on rate of solution of sodium palmitate in potassium hydroxide + potassium chloride solution. Initial solution contained 0.26 milliequivalent of potassium hydroxide + 5.37 milliequivalents of potassium chloride per 100 cc.

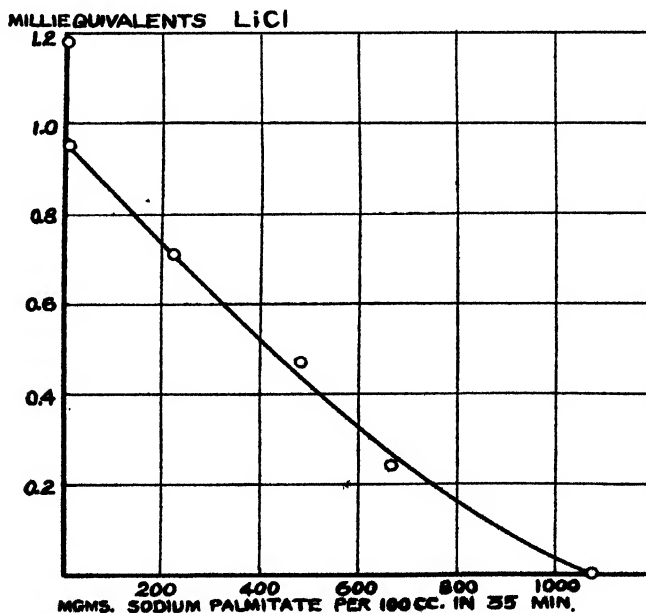


FIG. 10. Rate of solution of sodium palmitate in lithium hydroxide + lithium chloride at 57°C. Initial solution contained 0.30 milliequivalent of lithium hydroxide.

general shape as the saturation concentration (C_s value) against temperature for pure soaps in distilled water. For reference the calculated saturated concentrations (C_s values) of sodium palmitate are shown at two temperatures.

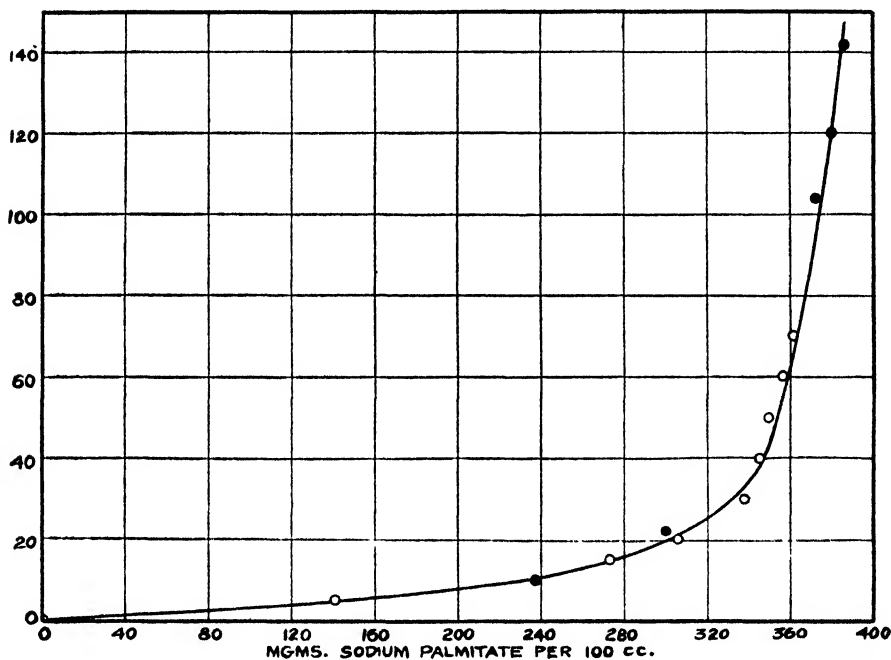


FIG. 11. Rate of solution of sodium palmitate in potassium hydroxide + potassium chloride at 40°C. Concentrations from interferometer. Initial solution contained 0.26 milliequivalent of potassium hydroxide + 2.68 milliequivalents of potassium chloride per 100 cc.

TABLE 2

Leaching experiments with a mixture of 35 per cent sodium laurate + 65 per cent sodium palmitate

EXPT.	TEMPERATURE	TIME OF RUN	CONCENTRATION IN GRAMS OF SOLIDS PER 100 CC.	MOLECULAR WEIGHT	REMARKS
	cc.	min.			
1	45	$\frac{1}{2}$	0.241	254	
2	40	1	0.160	252	
3	36	6		237	
4a	30	50			
4b	39	40		204, 206 286, 284	Continuation of 4a Cylinder scrapings

Several measurements (shown in figure 10) with initial solutions containing lithium hydroxide and lithium chloride indicate the marked decrease in the amount of sodium palmitate dissolved in 35 min. at 57°C. In these experiments most of the solutions had to be filtered before analysis.

TABLE 3
Rate of solution of mixed soaps

SOAP COMPOSITION	GRAMS DISSOLVED IN 10 MIN. AT							
	57°C.	60°C.	63°C.	64°C.	65°C.	66°C.	67°C.	69°C.
90% sodium stearate + 10% sodium oleate	0.15	0.22	0.33		0.62			
90% sodium stearate + 10% sodium laurate	0.12	0.18		0.29		0.40		
Sodium stearate	0.08				0.21		0.22	0.47

TABLE 4
Solubilities of sodium soaps

SOAP	TEMPERATURE	CS FROM RATE OF SOLUTION	SOLUBILITY FROM DIRECT METHOD
	°C.	g./100 cc.	g./100 cc.
Sodium oleate	3.0		4 (approx.)
Sodium laurate	3.0		0.60-0.70
	5.0		0.75
	10.0	0.49	0.77
	11.0		0.9
	12.0		1.0
	15.0	0.56	
	17.0	0.62	
	18.5	0.66	1.20
	20.0	0.92	
	22.0	1.81	
Sodium myristate	30.0		0.15
	32.0	0.16	0.25
	34.0	0.20	0.31
	36.0		0.55-0.60
	37.0		0.80
	38.0		1.0
	39.0		1.3
	40.0		1.7
Sodium palmitate	49.0	0.16	
	52.0	0.44	0.33-0.36
	53.0	0.55	
	54.0	0.62	0.60-0.65
	55.0	0.88	0.91-0.92
	56.0	1.1	
	56.5	1.4	
	57.0	2.0	
Sodium stearate	57.0	0.12	0.10-0.12
	65.0	0.40	0.30
	67.0	0.50	
	68.6		0.6
	69.0	0.85	

It appeared desirable to determine a complete rate curve for one case for solutions containing potassium salts. A rate curve (figure 11) was obtained for dissolving sodium palmitate at 40°C. in an initial solution with 2.69 milliequivalents of potassium chloride (0.2 per cent) and 0.26 milliequivalent of potassium hydroxide (pH 10.8). Owing to the high electrolyte concentration of the initial solution, the conductometric method could not be applied, and the Zeiss interferometer was used for the determination of the amount of soap dissolved.

Calculating the apparent solubility C_s from equations 11 and 12 gives a value of 0.405 g. of sodium palmitate per 100 cc. A plot of $\log \left(\frac{C_s - C_1}{C_s - C_2} \right)$ against $(t_2 - t_1)$ gives an excellent straight line for all points over 30 min., and this is evidence that the rate follows the first-order equation after 30 min. As in previous experiments, the rate for the first 30 min. is faster than that obtained later.

From titrations, sodium laurate gave a molecular weight of 224 (theoretical, 222), sodium palmitate gave 280 (theoretical, 280), and the mixture of 35 per cent sodium laurate plus 65 per cent sodium palmitate gave 254 (theoretical, 255).

In table 2, experiments 3 and 4a followed by 4b indicate selective leaching of the more soluble sodium laurate, which was accompanied by the formation of a rough pitted surface on the cylinder. In experiment 3, small pieces of solid were broken off the cylinder.

Rate-of-solution measurements were made for several soap mixtures. These data are compared from the 10-min. values in table 3. It can be seen that the increase in the amount dissolved in 10 min. is greater for the mixture containing the more soluble sodium oleate than for the one with sodium laurate.

In table 4 the solubilities obtained from rate measurements are listed with those obtained by the direct method, where a decrease in conductance at constant temperature was taken as a criterion of saturation.

VI. DISCUSSION

It is apparent that diffusion rates control the rates of solution of soaps, since they are in accord with equation 2. In some cases, the rates during the early part of the experiments are faster. For example, in figure 4 the line for sodium laurate (22°C.) and sodium palmitate (54°C.) has a greater slope up to 10 min. This is not in accord with the results of Sauer and Burck (4), where initial rates of sodium palmitate were slower than those obtained after 4 min. The decrease in rates which we have found during the initial part of the run may be attributed to the change in the soap sample on soaking. The formation of hydrolysis products of the soap containing more fatty acids leads to a constant but slower rate than that obtained in the earlier part of the run.

Since rates of solution of soaps sometimes do not become constant until after the first 10–20 min., a comparison of the amounts dissolved in a fixed period of time greater than 20 min. includes an over-all rate.

The rate of solution and therefore the solubility of sodium palmitate is increased considerably by starting with an initial solution of sodium laurate at pH 11.0, when compared with an initial solution of sodium chloride at the same pH.

This increase may be due to a solubilization of sodium palmitate by the sodium laurate solution.

The rates of solution of sodium palmitate in salt solutions are apparently influenced in the direction of the solubility of the mixed soap which is formed in the solution. Lithium soaps are less soluble than sodium soaps, and lithium chloride retards the rate of solution of sodium palmitate, whereas potassium soaps are more soluble than the corresponding sodium soaps, and potassium salts increase the rate of the solution of sodium palmitate. In all these cases, the saturated layer, as well as the final solution, may be considered to be of a composition which corresponds to the sodium soap, the soap of the salt used in the initial solution, and the products of hydrolysis.

For soap mixtures, selective leaching of the more soluble constituent has been shown. This effect becomes more pronounced as the length of the rate experiment is increased. The formation of a rough pitted surface which eventually tends to break off in lumps is visual evidence of how such a leaching process can take place with soap cylinders.

The solubilities obtained from rate measurements (figure 5) show an abrupt break for sodium laurate as the temperature is increased, but this break is somewhat less pronounced for the soaps of higher molecular weight. Only two points are shown for sodium myristate. At temperatures above 34°C. the rate curves plotted like those shown in figure 3 gave points of inflection followed by a flattening of the curve and then a slow rise in slope. This was shown to be due in part to a progressive effect of soaking the briquet and aging the solution, but a series of relatively short runs did not entirely eliminate this effect. For this reason solubility calculations for sodium myristate could not be made from rate measurements above 34°C.

Since soaps form colloidal solutions whose properties may vary with the method of preparation as well as the age of the solution, it is difficult to apply the same methods for determining solubility as are commonly used for other materials. Consequently, the direct estimates made of the concentration of the saturated solutions would be expected to be particularly susceptible to variations in the procedure. A comparison was made of the solubilities obtained by the direct method with the values of C_s obtained from rate measurements (table 4). It can be seen that for sodium palmitate, the values obtained by the two methods differ by as much as 25 per cent. For the other soaps, the differences are much greater. The solubilities obtained by the direct method are not as clearly defined as the values of C_s obtained from rate measurements which are considered as representing the concentration of soap in all forms present in the saturated solution which is approached in the experiment.

VII. SUMMARY

A method for determining the rate of solution of soaps in water was applied to sodium soaps of pure fatty acids and to several mixed soaps at temperatures from 10°C. to 70°C. Soap cylinders were rotated at constant speed in a thermostated cell. The amount of soap dissolved was obtained from electrolytic

conductivity, from evaporation of a solution to dryness, or by the use of an interferometer.

In most cases, the rates follow a first-order equation, from which the saturation concentration which is approached can be calculated. These values were compared with estimates obtained from the electrolytic conductivities of soap solutions of increasing concentrations.

Some typical rates of solution are shown for one soap in other soap solutions and in alkali chloride solutions at various pH values. Sodium chloride and lithium chloride decrease the rate of solution of sodium palmitate, whereas potassium chloride increases the rate.

The authors acknowledge and express their appreciation to Conrad W. Jakob, who made many of the measurements reported.

REFERENCES

- (1) KAWAI, S.: J. Soc. Chem. Ind. Japan **33**, Suppl. binding 244-5 (1930).
- (2) KENDALL, J., AND ANDREWS, J. C.: J. Am. Chem. Soc. **43**, 1545-60 (1921).
- (3) KING, C. V.: J. Am. Chem. Soc. **57**, 828-31 (1935).
- (4) MILES, G. D., AND ROSS, J.: J. Phys. Chem. **48**, 280-90 (1944).
- (5) SAUER, E., AND BURCK, W.: Angew. Chem. **48**, No. 11, 171-4 (1935).
- (6) SHUKOV, K. A., AND SHESTAKOV, P. I.: Seifensieder-Ztg. **38**, 982-3 (1911).
- (7) STIEPEL, C.: Allgem. Oel-u. Fett-Ztg. **32**, 63-5 (1935).

BOND ENERGY IN DIATOMIC MOLECULES FROM THE FORCE CONSTANTS, NUCLEAR DISTANCES, AND CLASSICAL MODEL THEORY¹

MELVIN A. COOK

*Eastern Laboratory, Explosives Department, E. I. du Pont de Nemours and Company, Inc.,
Gibbstown, New Jersey*

Received September 24, 1946

A theory of the chemical bond was presented recently (2, 3) which accounts for binding energy as a type of resonance interaction between the nuclei and the valence electrons. Nuclear vibration is considered to be accompanied by pulsations of the orbits of the valence electrons, the pulsation frequency being equal to w_0 , the vibration frequency. In fact, this is really the only factor according to the theory which contributes strength to the bond in those molecules formed "adiabatically", i.e., without electronic transitions. The average kinetic energy T in the molecule is assumed, in accordance with the theory and with results obtained in the treatment (2) of the hydrogen molecule and the

¹ Presented before the Division of Physical and Inorganic Chemistry at the 110th Meeting of the American Chemical Society, Chicago, Illinois, September 10, 1946.

hydrogen molecule ion, to be the same as in the separate atoms constituting the molecule except when bond formation is accompanied by a change in the electronic configuration. T appears to be intimately associated with the field of the particle, i.e., with the quantum state. Hence the bond energy under adiabatic formation is evidently equal to the decrease in the average potential energy, \bar{V} , occurring in bond formation. One might say, although somewhat ambiguously, that the bond energy is entirely potential energy. These conditions are introduced as basic postulates in the present discussion, in which we attempt to develop the bond strength in terms of the experimental force constants and bond distances.

DEVELOPMENT OF EQUATIONS

The energy relations in diatomic molecules at the various stages of vibration may be shown as follows:

Nuclear distance	$R + x_{02}$	R	$R + x_{01}$
T (kinetic energy)	$-E_a + D_0$	$-E_a$	$-E_a - D_0$
V (potential energy)	$2E_a$	$2E_a + D_0$	$2E_a + 2D_0$
E (total energy)	$E_a + D_0$	$E_a + D_0$	$E_a + D_0$

where R is the nuclear equilibrium distance, x_{02} and x_{01} are the amplitudes in the opposite phases of vibration, D_0 is the bond energy, and E_a is the sum of the energies of the separate atoms. If, for the purpose of analysis, the real system may be replaced by a series of vibrationless models of varying nuclear distances, the following relations may be obtained:

$$F_0 R = D_0 \pm \tilde{w}_0 \quad (2a)$$

$$F_2(R + x_{02}) = 2D_0 \quad (2b)$$

$$F_1(R + x_{01}) = 0 \quad (2c)$$

Here \tilde{w}_0 is the vibrational energy, and F_0 , F_1 , and F_2 are forces determined by the methods of reference 2, which must now be applied to equilibrate the nuclei at the equilibrium, maximum, and minimum distances, respectively. The term \tilde{w}_0 appears in equation 2a to account for the fact that at the equilibrium position the nuclei have acquired a kinetic energy $\frac{1}{2}h\nu_0$. From an examination of the solutions (2) of H_2^+ and H_2 it appears that the sign of \tilde{w}_0 in equation 2a is determined by the particular instantaneous configuration determining the minimum energy, which may occur at either the inner or the outer extremity of vibration (2). For example, in H_2^+ the minimum energy is determined at the outer extremity and we find that

$$\frac{1}{2}g_0e^2/\bar{r}_0 = D_0 + \tilde{w}_0 = F_0 R$$

In H_2 , on the other hand, it appears at the opposite side of the equilibrium position and

$$\frac{1}{2}g_0e^2/\bar{r}_0 = D_0 - \tilde{w}_0 = F_0 R$$

To determine the sign of \tilde{w}_0 in equation 2a requires a detailed analysis of the model in each molecule.

Combining equations 2a and 2b we obtain

$$\{(F_2 - F_0)R \pm \tilde{w}_0\}(R + x_{02})/(R - x_{02}) = D_0 \quad (3)$$

The externally applied constraints required in the hypothetical vibrationless systems are shown (2) to take the place of the effects of orbit pulsations, although we must recognize certain distortions brought about by the fact that the orbital radii are not the same in the vibrationless models as in the real system, since the external constraint virial must be added. Thus, from equation 2c it is evident that the vibrationless model requiring no externally applied constraint has a nuclear distance of $R + x_{01}$, i.e., the method of analysis results in an artificial shift of the equilibrium position from R to $R + x_{01}$. Conversely one may say that the setting up of orbital pulsations synchronous with nuclear oscillations will have the effect of shifting the equilibrium position toward greater values of R , a condition which is readily apparent in the classical model treatments of the hydrogen molecule and the molecule ion. While the linear law $f(x) = -kx$ is known to hold as a close approximation in the nuclear oscillator, it does not express the relations between the artificial constraints F_0 , F_1 , and F_2 of the vibrationless models. However, for a known function $f(x)$ one may evidently determine the nature of the distortions and $F(y)$ of the virtual system. (Here y is the displacement measured from $R + x_{01}$, where $F_1 = 0$.) Employing the difference $F_2 - F_0$ under certain conditions appears to avoid any distortional effects of the method of analysis and one may express it by $f(x_{02})$. It evidently is the same as though the equilibrium had not been shifted artificially from its true position at R . We may thus replace $F_2 - F_0$ in equation 3 by kx_0 , and x_{02} by x_0 , giving:

$$(kx_0R \pm \tilde{w}_0)(R + x_0)/(R - x_0) = D_0 \quad (4)$$

It remains therefore to establish under what conditions this substitution may be considered valid. As a matter of interest one may show that equation 4, used without further restriction, gives reasonably accurate bond energies for a number of molecules. However, it does not explain isotopic effects and in some cases leads to errors in D_0 amounting to perhaps 20 per cent. Evidently its failure in any case is due to the non-linearity of the nuclear oscillator.

For H_2^+ the equation $\frac{1}{2}ge^2/\bar{r} = R'F$ of reference 2 gives 4.43×10^{-12} ergs for RF_0 and 8.40×10^{-12} ergs for $F_2(R + x_0)$, taking \bar{r} as 0.483 Å., as required by the total energy obtained in the analysis. Dividing the first result by R and the second by $R + x_0$ gives 4.14×10^{-4} and 6.77×10^{-4} dynes for F_0 and F_2 , respectively, and $F_2 - F_0$ then amounts to 2.63×10^{-4} dynes. The value kx_0 obtained from the linear law and the experimental force constant is 2.55×10^{-4} dynes. Similar agreement is obtained in the hydrogen molecule. These results were obtained by employing x_0 from the linear law. The lack of distortion in $F_2 - F_0$ is due, as a matter of fact, to the use of this value, the value determined in reference 2 for x_0 being distorted by approximately $2\frac{1}{2}$, and to the correction of

the orbit radius for the effect of the external constraint virial. For a reduced mass of 1.0 (defined here as $2m_1m_2/(m_1 + m_2)$, where the m 's are in atomic weight units so that M is 1.0 for H_2 and H_2^+), we actually find a distortion in $F(y)$ in the inner branch ($F_0 - F_1$) amounting approximately to the factor $2^{\frac{1}{2}}$. This is the distortional factor to be expected from the consideration that the artificial shift of the equilibrium position from its true position to $R - x_0$ gives a potential difference for a displacement $y = 2x_0$ (measured by the linear law) of $2kx_0^2$, which is twice the sum of the potential differences in the two branches in the real case. Since V varies as x^2 and F as x , evidently the force function $F(y)$ in the inner branch thus involves the factor $2^{\frac{1}{2}}$ as a distortional factor, the distortions having been corrected in the $F_2 - F_0$ branch by the form of the equation and the substitution. That this is the case is illustrated by the fact that

$$(R + x_0)/(R - x_0) \approx 2^{\frac{1}{2}}$$

in the hydrogen molecule and the molecule ion. This ratio, according to equations 2, should equal

$$(F_0 \pm \tilde{w}_0/R)/((F_2 - F_0) \pm \tilde{w}_0/R)$$

Equating this to $(D_0/D_e)^{\frac{1}{2}}$ times the distortional factor $2^{\frac{1}{2}}$ and generalizing on the empirical basis of the results obtained in other molecules such as oxygen and chlorine to include molecules in which M is greater than 1.0, we obtain

$$(R + M^{\frac{1}{2}}x_0)/(R - M^{\frac{1}{2}}x_0) = (2D_0/D_e)^{\frac{1}{2}} \quad (5)$$

Judging by its success in reproducing results in the treatments of reference 2 and its quite close agreement with experiment in most diatomic molecules, equation 5 may be regarded as the criterion for the validity of the substitution of kx_0 for $F_2 - F_0$, i.e., for the validity of the linear law.

The amplitude, assuming equations 4 and 5 to be correct, evidently does not vary appreciably with M . This, in fact, was implied in the treatments of reference 2. Hence, anharmonic and distortion effects must apparently counter the implied linear law relation $x_0 \propto 1/M^{\frac{1}{2}}$. Equations 4 and 5 may thus be used to compute D_0 even in those molecules where the linear law substitution will be shown by equation 5 to be inapplicable. This may be done by simply converting to the reduced mass for which the linear law is valid by means of equation 5, the harmonic oscillator relation for $M^{\frac{1}{2}}x_0$ in terms of \tilde{w}_0 , namely,

$$M^{\frac{1}{2}}x_0 = 8.162 \times 10^{-8}/w_0^{\frac{1}{2}}$$

and the experimental force constant. There is some evidence however, e.g., in such molecules as bromine, iodine, and hydrogen iodide, that this criterion for correcting for non-linearity may not be quite correct, particularly when very large changes in M are needed to render the linear approximation valid. In bromine and iodine, where M must be lowered 50 per cent or more to satisfy equation 5, it leads to values 0.14 and 0.23 e.v., respectively, too high. Values 0.11 and 0.07 e.v. too low are obtained from equation 4 without correcting M by equation 5. When the corrected M 's are within reason however, this procedure appears quite satisfactory.

RESULTS

Table 1 gives a comparison between experimental and calculated data for some homonuclear diatomic molecules. The experimental data were taken from Herzberg (4), and where discrepancies in experimental data existed, data by Sponer (7) and Bichowsky and Rossini (1) are also shown. In cases where the experimental data were regarded as uncertain they are enclosed in brackets or otherwise described as in the references. Diatomic carbon and phosphorus are the only cases where serious discrepancies exist, and in these cases the experimental data

TABLE 1
Diatomic molecules of like atoms (energy in e.v.)

MOLECULE	w_0	R	D_0^*	D_0	D_0 (EXPERIMENTAL)
	cm. ⁻¹	Å.			
Br ₂	322	2.28	1.86	2.11 ± 0.03	1.97
C ₂	1630	1.31	4.93	4.41 ± 0.13	3.6†
Cl ₂	561	1.99	2.50	2.53 ± 0.04	2.48
H ₂	4280	0.74	4.02	4.47	4.48
D ₂	3055	0.74	3.30	4.54	4.56
H ₂ ⁺	2235	1.07	2.57	2.63	2.65
I ₂	214	2.67	1.47	1.77 ± 0.02	1.54
Li ₂	349	2.67	0.87	0.84 ± 0.03	1.14
K ₂	92.3	3.92	0.35	0.46 ± 0.01	0.51
Na ₂	158	3.08	0.49	0.63 ± 0.01	0.76
N ₂	2345	1.10	7.65	7.14 ± 0.17	7.38
N ₂ ⁺	2191	1.12	7.10	6.45 ± 0.16	6.35
O ₂	1568	1.21	4.93	5.05 ± 0.10	5.09
O ₂ ⁺	1860	1.12	5.93	6.05 ± 0.13	6.48
P ₂	778	1.89	3.65	3.38 ± 0.05	5.03†
S ₂	723	1.89	3.33	3.18 ± 0.05	<3.6†
Se ₂	391	2.16	2.35	2.67 ± 0.04	2.7
Te ₂	250	2.59	1.85	2.13 ± 0.02	2.3†

* D_0^* is the value obtained from equation 4 without applying the criterion for linearity, i.e., equation 5.

† Sponer (7) gives C₂, (5.5); S₂, 4.45; Te₂, (2.0). Bichowsky and Rossini (1) list values leading to 1.84 e.v. for P₂. Other data were taken from Herzberg (4).

are certainly open to question. Since the sign of \tilde{w}_0 in equation 4 is uncertain except in H₂ and H₂⁺, we have simply indicated the limits of this correction in the tables.

In the treatment of diatomic molecules having atoms of unequal mass it is evident that x_0 is not derived accurately when reduced mass is used directly. Apparently in addition to the quantum condition $\frac{1}{2}h\tilde{w}_0 = \frac{1}{2}kx_0^2$, the equation $m_1x_1^2 = m_2x_2^2$ should also apply, as though each particle were quantized separately. Here x_1 and x_2 are the amplitudes contributed by each atom, the total amplitude being $x_1 + x_2 = x_0$. Hence the direct calculation of x_0 seems to necessitate the reversion to real masses. However, the simplest equivalent procedure and the one which allows the use of reduced mass and equation 5 unaltered is as follows:

The molecule is first treated as a homonuclear molecule of $M = m_1$, and then as one of $M = m_2$, converting \tilde{w}_0 in each case by means of the force constant. The two values of x_0 thus obtained may then be simply averaged to give the true x_0 corresponding to the value of M satisfying equation 5. When large corrections for anharmonicity are necessary, an ambiguity arises as to how much correction to apply to each atom. We have adopted here the procedure of applying all of it first to one atom and then to the other and averaging the results. In some cases this is not possible however, and the correction must then be applied all on

TABLE 2
Hydrides

MOLECULE	w_0	R	D'_0	D_0	D_0 (EXPERIMENTAL)
	cm. ⁻¹	A.			
AgH ¹	1726	1.62	2.19	(2.5) \pm 0.14	(2.3)
Al ²⁷ H ¹	1653	1.65	2.29	2.43 \pm 0.13	<3.07
AuH ¹	2261	1.52	2.97	(3.5) \pm 0.16	(3.6)*
B ¹¹ H ¹	(2317)	1.23	3.04	3.17 \pm 0.17	<3.49
Be ⁹ H ¹	2023	1.34	2.71	2.71 \pm 0.15	(2.2)*
CH ¹	2778	1.12	3.54	3.71 \pm 0.21	3.47
CuH ¹	1903	1.46	2.35	2.63 \pm 0.15	(3.0)*
CaH ¹	1280	2.00	1.83	1.98 \pm 0.09	\leq 1.70*
H ¹ H ²	3722	0.74	3.65	4.50	4.51
H ¹ Cl ³⁵	2937	1.27	4.16	4.48 \pm 0.21	4.43
H ¹ Br.....	2605	1.41	3.55	(3.84) \pm 0.19	3.60
HI.....	2270	1.60	3.18	(3.44) \pm 0.16	2.75*
H ¹ F ¹⁹	4050	0.92	5.10	6.39 \pm 0.31	6.4
MgH ¹	1463	1.73	2.03	2.14 \pm 0.10	<2.5
N ¹⁴ H ¹	(3300)	1.04	4.30	4.64 \pm 0.24	(3.4)*
O ¹⁶ H ¹	3650	0.97	4.63	(4.95) \pm 0.27	4.3*
ZnH ¹	1553	1.60	1.92	(2.2) \pm 0.12	0.85
(ZnH ¹) ⁺	1877	1.51	2.41	(2.6) \pm 0.15	(2.5)

* Sporer (7) lists AuH, (3.9); BeH, (2.4); CuH, 3.2; NH, (4.2). Bichowsky and Rossin¹ (1) give 1.88 for CaH, 4.4 for NH, and 5.04 e.v. for OH. Hulbert and Hirschfelder (6) use 3.05 e.v. for HI, a value which they credit to Crist.

one atom. It is only for molecules requiring large corrections and for which the atomic weight of one of the atoms is large that such difficulties may be encountered; in these cases we have shown the calculated results in brackets. Table 2 shows the results obtained in some hydrides; in most cases the calculated and experimental data agree as well as might be expected, considering the uncertainties in the experimental data. The hydrides of zinc, cadmium, and mercury are exceptions, for in these cases $D_0(\text{calcd.})$ is more than twice as large as $D_0(\text{exptl.})$. Such cases are in fact anticipated in the theory and may possibly be explained on the basis of nonadiabatic formation, i.e., electronic transitions corresponding to the "promoted electrons" of the Hund-Mulliken theory. It is of interest that the corresponding molecule ions of these hydrides do not appear abnormal in this respect. In OH, NH, and CaH the theoretical values are

higher than the experimental values proposed by Herzberg (4), but are in good agreement with data given by Bichowsky and Rossini (1). A discrepancy exists also in hydrogen iodide, part of which may be due to an error in correcting for the large non-linearity factor in this molecule.

Table 3 lists data on various oxides, nitrides, sulfides, and halides. Only in a few of these molecules are the experimental data known with sufficient accuracy to provide reliable comparisons. The alkali halides constitute marked discrepancies, the accepted bond strengths being two or three times larger than the computed ones. Supposedly, the alkali halides have so-called ionic bonds and are therefore non-adiabatic, involving direct electron transfer from the alkali to

TABLE 3
Oxides, nitrides, sulfides, and halides

MOLECULE	ν_0	R	D'_0	D_0	D_0 (EXPERIMENTAL)
	<i>cm.⁻¹</i>	<i>A.</i>			
AlO	970	1.62	3.54	3.34 ± 0.07	(4.2)*
BeO	1475	1.33	4.22	4.12 ± 0.10	(5.7)
BO	1874	1.20	5.78	5.50 ± 0.12	(9.1)*
CaO	837	(1.75)	3.31	3.25 ± 0.06	(3.6)
CO	2155	1.13	6.90	6.50 ± 0.15	(9.144)*
(CO) ⁺	2196	1.11	6.88	6.50 ± 0.15	(6.5)
NO	1890	1.15	5.95	5.84 ± 0.13	5.29
PO	1224	1.45	4.56	4.50 ± 0.08	(6.2)
SO	1118	1.49	4.13	4.11 ± 0.07	4.00*
CN	2055	1.17	6.50	5.98 ± 0.14	(5.96)*
BeF	1256	1.36	3.48	3.60 ± 0.08	(5.4)*
CaF	855	(2.02)	4.01	3.40 ± 0.06	3.15*
ICl	383	2.32	1.96	2.30 ± 0.06	2.15
NaCl	379	2.51	1.57	1.57 ± 0.03	4.25

* Spomer's (7) data are: AlO, (7?); CO, (9.6); SO, 5.05; CN, (6.7); BeF, (6.0); CaF, (3.5). Bichowsky and Rossini (1) give 5.98 e.v. for BO.

the halide atom. However, there is definitely no evidence in the force constants and the bond distances for other than normal homopolar binding in these molecules. Usually when the bond energy differs appreciably from the simple arithmetic mean of the corresponding bond energies in the homonuclear molecules represented in the molecule, the bond distance also differs from the arithmetic mean of the corresponding homonuclear molecules, but in the opposite sense. Just how direct electron transfer in the ionic bond can result in a binding energy several times larger than in homopolar binding without becoming evident in either the force constant or the bond distance seems rather difficult to explain. The strong deviations from the arithmetic mean bond energies in CH, HF, HCl, HBr, NH, and CO, for example, are quite evident in the bond distances and force constants. When there is an excess in bond energy the bond distance is contracted and the force constant increased, and *vice versa*, as might be expected. In sodium chloride, however, there is only the slightest contraction in the bond

length (2.51 *vs.* 2.53 Å.) but a threefold increase in the bond energy. The calculated value which is in close agreement with the arithmetic mean of $D_0(\text{Na}_2)$ and $D_0(\text{Cl}_2)$ would thus seem to be near the correct value. Another example of interest is hydrogen iodide, which in showing a bond contraction from the arithmetic mean of about 6 per cent would be expected to have a bond strength in excess of 3.0 e.v., in accord with the computed value but contrary to the experimental value listed by Herzberg. It is of course possible that non-adiabatic effects may influence the bond energy without becoming evident in the force constant and bond distance.

The value 6.5 ± 0.15 e.v. for CO, while in poor agreement with Herzberg's value 9.144 e.v., is in much better agreement with Schmidt and Gerð's value 6.89 e.v. Such a low value, however, incurs difficulties in explaining the bond energies in CN, $(\text{CO})^+$, and C_2 , the computed values in the first two being in excellent agreement with Herzberg's data. If CO is actually related to N_2 , i.e., is a member of the same isoelectronic sequence, it should be expected to have a lower bond energy because of its lower force constant and slightly larger bond distance. We are thus inclined toward the value 6.89 e.v. In this case the agreement in CN and $(\text{CO})^+$ would probably have to be explained as due to electron transitions involving the same states as were used in assigning the experimental values, the true bond energies being lower. The alternative would of course be to consider CO to involve the electron transition and to accept the value 9.144 e.v. as the correct one.

In conclusion it may be well to emphasize that the experimental methods of dissociation spectra for bond energies are really reliable only in establishing an upper limit in most cases (and a lower limit corresponding to the highest observed vibrational level). In view of the good agreement obtained in the majority of cases therefore, the comparisons appear to provide substantial support of the validity of the classical model theory.

REFERENCES

- (1) BICHOWSKY, F. R., AND ROSSINI, F. D.: *The Thermochemistry of the Chemical Substances*. Reinhold Publishing Corporation, New York (1936).
- (2) COOK, M. A.: *J. Chem. Phys.* **13**, 262 (1945).
- (3) COOK, M. A.: *J. Chem. Phys.* **14**, 62 (1946).
- (4) HERZBERG, G.: *Molecular Spectra and Molecular Structure*, Vol. I. Prentice-Hall, New York (1939).
- (5) HERZBERG, G.: *Chem. Rev.* **20**, 145 (1937).
- (6) HULBERT, H. M., AND HIRSCHFELDER, J. O.: *J. Chem. Phys.* **9**, 61 (1941).
- (7) SPONER, H.: *Molekülspektren und ihre Anwendung auf chemische Probleme. Vol. I. Tabellen*. J. Springer, Berlin (1935).

EFFECT OF FREEZING ON THE STABILITY OF COLLOIDAL DISPERSIONS¹

SILICA SOLS—A PRELIMINARY REPORT

FRED HAZEL

*Department of Chemistry and Chemical Engineering, University of Pennsylvania,
Philadelphia, Pennsylvania*

Received October 1, 1946

Several investigators have frozen silica sols and reported the behavior on melting. The literature is not extensive, however, and it gives a somewhat confused picture. Failure to induce flocculation by freezing a sodium silicate solution (1) caused stress to be laid on the purity of the colloidal system (5), it being shown that dialyzed silica sols were susceptible to flocculation (2, 6). Djatschkowsky (3) found, on the other hand, that partial dialysis may be more effective than extended dialysis in promoting flocculation.

The present investigation consisted of a study of the factors which influence the flocculation of silica sols by freezing. The aid afforded by exchange resins in the preparation of the sols greatly increased the number of systems of considerable purity that could be investigated. Prepared by ion exchange the sols did not have their electrolyte content increased but they did experience an increase in hydrogen-ion activity. The latter proved to be a decisive factor, and it has been found that modification of silicate solutions with various substances which lower their pH can result in systems which are unstable to freezing. None of the systems have been dialyzed, and in those cases where soluble substances were added the electrolyte content was increased.

The present report is confined to systems prepared with exchange resins.

EXPERIMENTAL

The sols were prepared by adding measured volumes of sodium silicate² solutions to weighed portions of ion-exchange resins³ in the hydrogen form. The systems were permitted to stand at room temperature with stirring for 20 min., after which they were filtered and their pH measured with a Leeds and Northrup pH meter.

Ten-cc. portions of sol of known pH and concentration were frozen, while being stirred, in an alcohol-water bath maintained at $-10^{\circ}\text{C.} \pm 0.4^{\circ}$ with dry ice. The apparatus is shown in figure 1. The freezing point was reached in about 2 min., after which there was a gradual fall of temperature to that of the bath,

¹ Presented at the Symposium on the Stability of Colloidal Dispersions, which was held under the auspices of the Division of Colloid Chemistry at the 110th Meeting of the American Chemical Society, Chicago, Illinois, September, 1946.

² The sodium silicate was the commercial grade, N brand, and was supplied by The Philadelphia Quartz Company.

³ The resins were supplied by The Dow Chemical Company (Nalcite MX) and The Resinous Products Company (IR 100-H).

requiring about 12.5 min. The temperature-time relationships are given in figure 2.

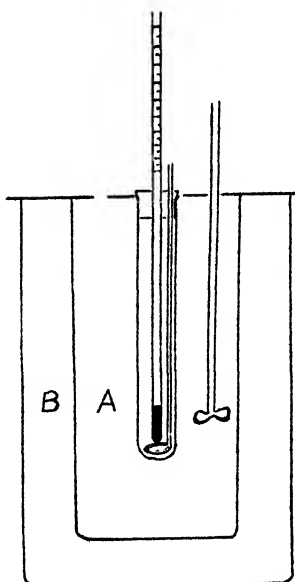


FIG. 1. The freezing apparatus: A, alcohol-water freezing bath; B, glass wool

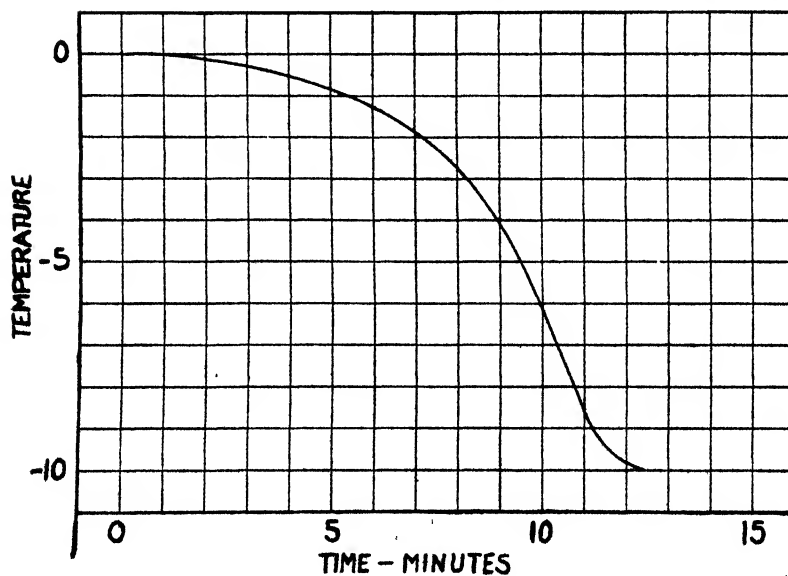


FIG. 2. Temperature-time relationships after freezing

At the end of the freezing time the tube was removed from the bath and held under a tap of running water until its contents melted. The system was stirred

during melting. The pH was measured and the amount of flocculation as judged from the optical density was noted. This is recorded as numbers, in which the number 4 corresponds to maximum flocculation.

The following factors were investigated: hydrogen-ion concentration of the sol; time kept in the frozen state; effect of repeated freezing; age of the sol; age of the stock solution; and concentration of the sol.

RESULTS

Figure 3 shows that 15 min. in the freezing bath produced flocculation at all pH values investigated except between 2.5 and 3.5 pH in systems containing 2.5 per cent silica. These data are suggestive of an irregular series with a zone of no flocculation separating the two flocculation zones.

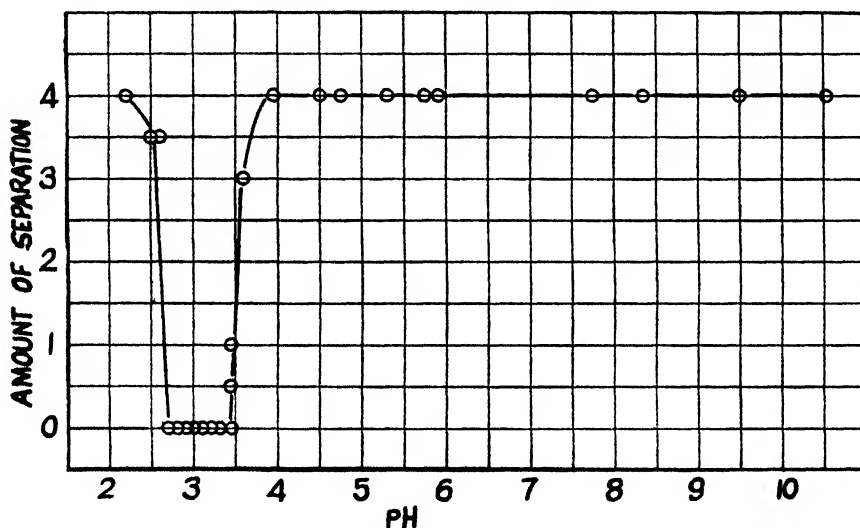


FIG. 3. Results of freezing for 15 min. at various pH values

Figure 4 shows that the resistance to flocculation prevailed on freezing for 30 min., although the range of pH over which there was no flocculation was narrowed somewhat. This indicates an increased tendency to flocculate with increase in freezing time.

Figure 5 shows that the sols were most susceptible to flocculation above a pH of 5, while at a pH of 3 they were most resistant. In the former case a 5-min. freezing period in which the temperature did not fall below about -1°C . was sufficient to produce flocculation.

The effects of several 15-min. freezing periods on sols of pH 2.75 and pH 3.0 are shown in figure 6. One 30-min. period had flocculated the system of lower pH. With repeated freezing, stepwise flocculation occurred with this system. The treatment was without effect with the sol of pH 3.0.

The effect of the age of the sol is illustrated in figure 7, where it is revealed that the tendency to flocculate increases with age. Portions of the systems were

frozen 15 min. when freshly prepared. Other portions were allowed to stand at room temperature for varying lengths of time and then frozen for 15 min.

The age of the stock solution from which the sols were prepared affected their tendency to flocculate when they were at pH values which corresponded to

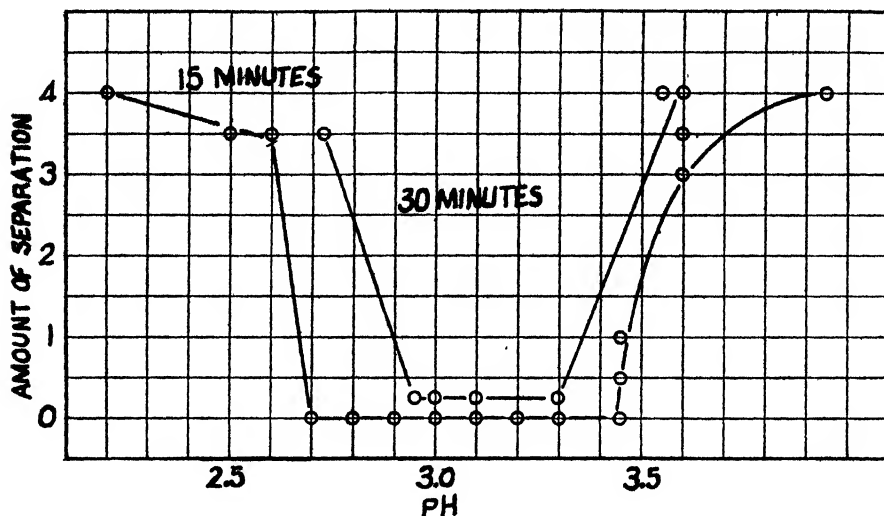


FIG. 4. Results of freezing for 15 min. and for 30 min. in the zone of no flocculation

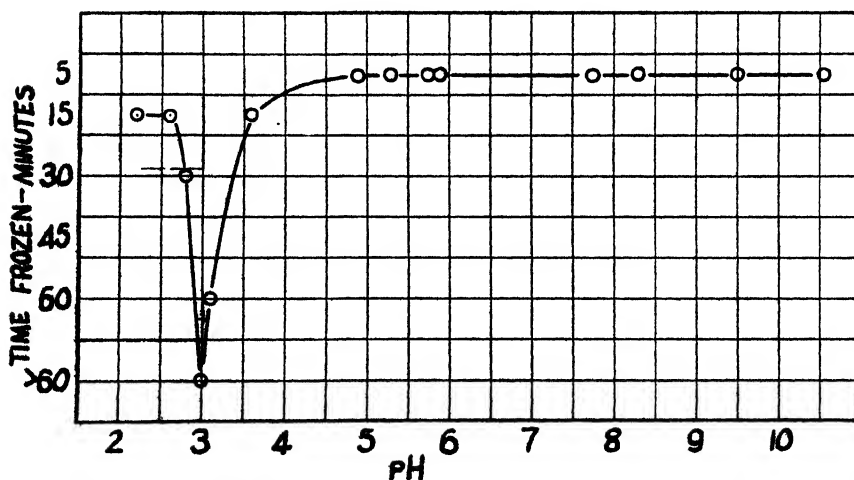


FIG. 5. Time required for coagulation by freezing at various pH values

transitions between zones of no flocculation and complete flocculation. This effect, which may be described by the word "memory," is illustrated in figure 8 for sols of pH 2.6 and in figure 9 for sols of pH 3.6. With systems on either side of the transition pH, the age of the stock solution is without effect. This is revealed in figure 10 with sols of pH 2.2 and 2.7.

Figure 11 gives information on the effect of concentration on the low-temperature behavior of the system. It is shown that decreasing the silica concentration extends the zone of no flocculation to higher pH values.

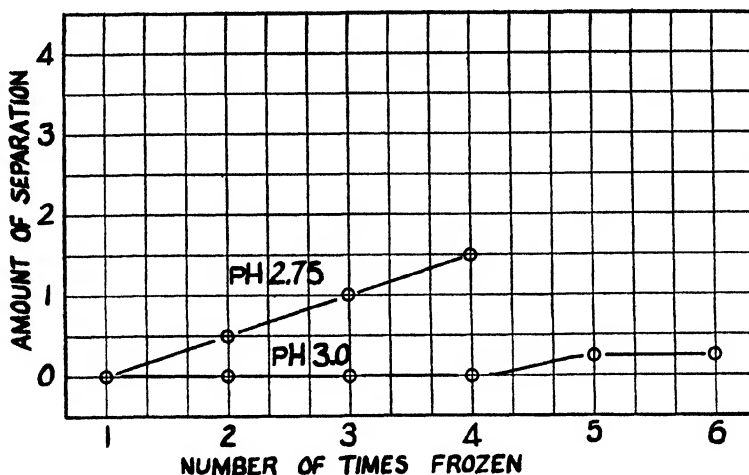


FIG. 6. Effect of cyclic freezing and thawing on the flocculation of two sols in the zone of no flocculation.

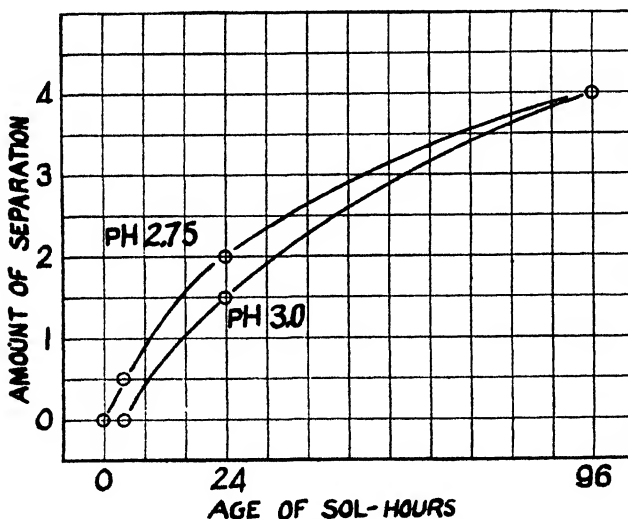


FIG. 7. Effect of age of the sol on the tendency to flocculate

In figure 12 flocculation data are compared with the mobility values for silica sols at the same hydrogen-ion activities. The mobilities were determined previously (4). It is evident that the two distinct flocculation zones, while resembling an irregular series, are not founded on the recharging of the silica.

Small increases in pH were observed to accompany freezing of the sols. In

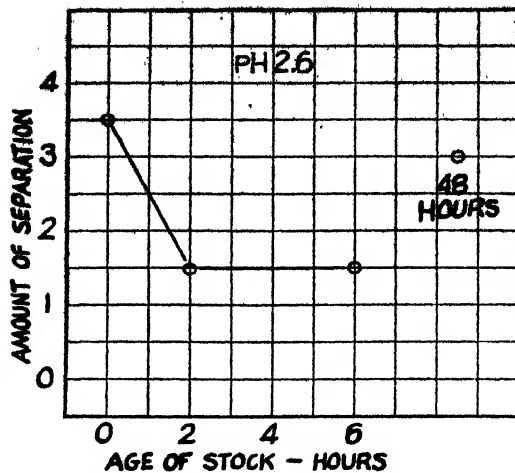


FIG. 8. Effect of age of the stock solution on the flocculation of sols of pH 2.6

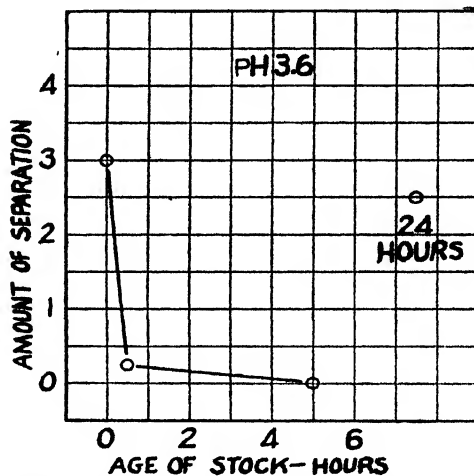


FIG. 9. Effect of age of the stock solution on the flocculation of sols of pH 3.6

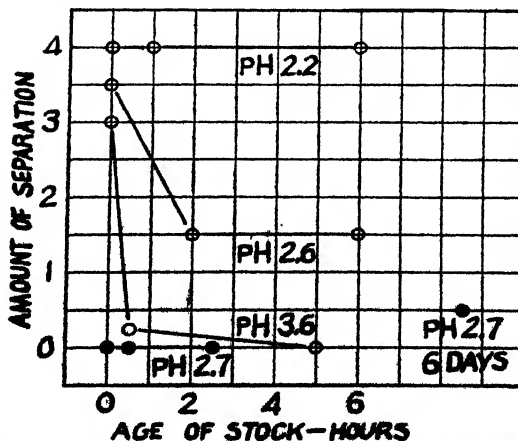


FIG. 10. Effect of age of the stock solution on the flocculation of sols at several pH values

forty experiments they ranged between 0.10 and 0.20 units and averaged 0.16. The pH changes were independent of freezing time, amount of flocculation, and age of the stock solution. In experiments involving repeated freezing, smaller

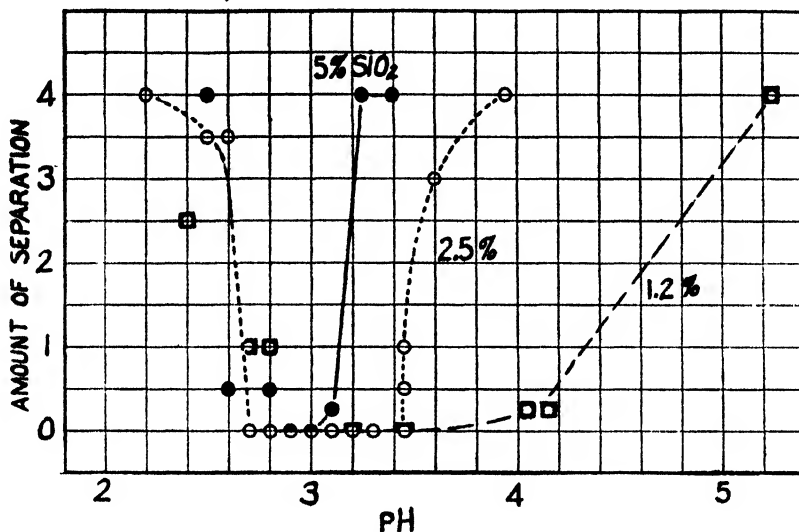


FIG. 11. Effect of concentration of silica on the zone of no flocculation

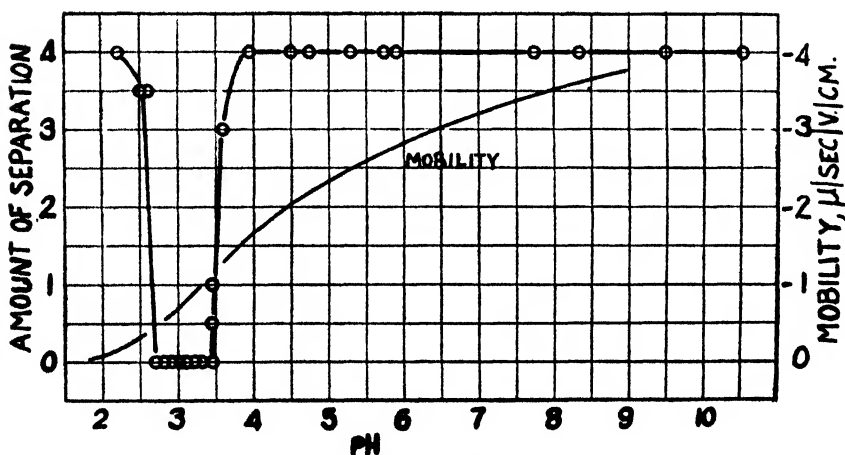
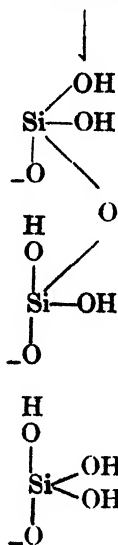
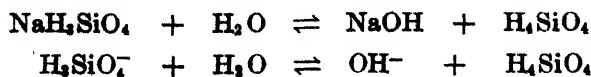


FIG. 12. Comparison of the degree of flocculation of silica sols by freezing with their mobilities at several pH values.

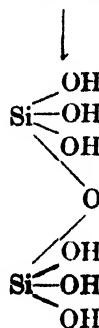
pH increases occurred on the second and subsequent freezings than on the first. The cause of the pH increases was not established, but it was not due to aging of the sol. Systems which had stood for 30 min. at room temperature showed much smaller increases, these ranging from 0.0 to 0.05 pH units.

DISCUSSION

The silicate solution employed in this study contained 3.3 moles of silica to every mole of sodium oxide. In terms of molecules this composition lies between that represented by NaH_2SiO_4 and H_4SiO_4 . The strong alkaline reaction of the solution suggests the equilibrium given below.



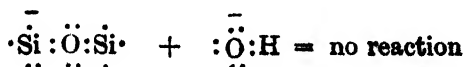
A



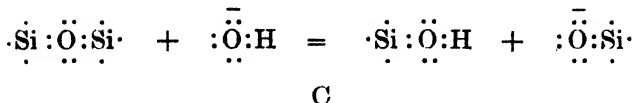
C

It is probable that the structures A and C more nearly represent the nature of the solutions than do simple molecules. During freezing the concentration of the dispersed silica is effectively increased, producing a condition favorable for particle growth by condensation. This process may involve the formation of oxygen bridges and in the case of A, hydrogen bridges. Particles formed by the growth of A are charged, while those from C are neutral. Flocculation results when the particles formed by freezing are not dispersed on melting.

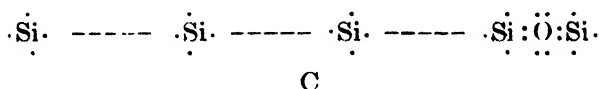
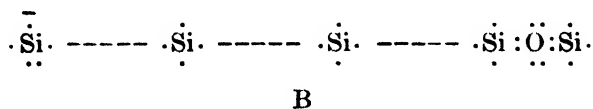
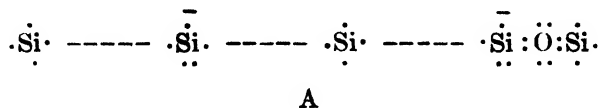
Hydroxyl ions dissolve, or disperse, the flocs by breaking oxygen bridges between the silicon atoms. This reaction depends not only on the hydroxyl-ion concentration but also on the charge on the particles. The latter tends to inhibit the dispersing action because of electric repulsion between the hydroxyl ions and the charge on the particles. Thus, a concentration of these ions which will break the bond in C will not attack A because of the charge on the structure near the point of attack. This is illustrated in the following:



A



Both the charge on the particles and the hydroxyl-ion concentration decrease with pH (figure 12). At very high alkalinities, such as those which prevail in unmodified silicate solutions, the flocs are dispersed despite their large charge. As the hydroxyl-ion concentration is reduced, the charge on the particles decreases. In effect this amounts to a shifting of the charge to a greater distance from the point of attack, as indicated below in a comparison of structures B and A, causing it to be more soluble in hydroxyl ions.



In the present work it was found (figure 3) that flocculation on melting remained complete at pH values above about 3.5. At this pH, for the systems containing 2.5 per cent silica frozen for 15 min. at $-10^{\circ}\text{C}.$, the bonds holding the structures together were so weak that even the low concentration of hydroxyl ions present in the system was enough to dissolve them. The balance between these forces was so nearly complete when this range was entered that the precipitate dissolved slowly rather than disappearing at once on melting. With further decrease in pH there was no flocculation until a pH of about 2.6 was reached. Under these conditions the hydroxyl-ion concentration had been diminished to such an extent that it no longer was able to dissolve the structures even though the charge had been reduced further. Accordingly, flocculation again became considerable.

The other results of this study can be explained on the basis of the above mechanism. The formation of particles by condensation requires time. The effect of this is most noticeable in the pH region where there is no flocculation after a 15-min. freezing period at $-10^{\circ}\text{C}.$ In these cases (figures 4 and 5) an increase in time of freezing increases the stability of the structures and increases their tendency to flocculate.

Condensation occurs in modified silicates at room temperature but much more slowly than when the systems are frozen.⁴ Moreover, the same rules which

⁴ Condensation is faster at room temperature than it is at any temperature between this and the freezing point, e.g., $5^{\circ}\text{C}.$ The increase in structure formation by freezing is not due to the prevailing low temperature but rather to an increase in the concentration of the silica and the promotion of oxygen bridges by removal of water.

apply to condensation by freezing hold at the higher temperature. Thus, there is a connection between the stabilities of the structures which are formed and the pH of the system. Separation of the structures by gel formation or by flocculation was at a minimum in both cases at about a pH of 3. When a fresh sol with a pH of 3 was frozen, the structure which formed dissolved completely on thawing. On the other hand, freezing of a sol of the same pH which had aged for several days and as a result undergone considerable condensation, caused complete flocculation (figure 7). The effects produced by repeated freezing and thawing (figure 6) appear to be merely the sum of the effects produced in the separate freezing periods, taking into account the age of the sol in the melted condition.

The stabilities of the structures increase with concentration of silica, a result which follows from greater opportunities for bonding. The experimental results (figure 11) reveal that at a pH of 4 the structure formed from the system containing 1.2 per cent silica dissolved on thawing, while those formed from 2.5 per cent and 5 per cent dispersions remained flocculated. The 5 per cent system was flocculated at pH values above 3.2. The stabilities of the structures increase sharply above a pH of 5. Flocculation has been produced in systems containing only a few parts per million of silica when the freezing was conducted in the pH range of 5.7 to 7.1.

The data in figures 8, 9 and 10 relate to the effect of the age of the stock solution on the behavior of the sols. In the preparation of the stock solutions by the addition of water to the parent silicate, the equilibria that are present in the latter are disturbed. The hydrolysis appears to take place slowly, and as a result the fresh stock solutions contain metastable structures. These are converted slowly to more stable structures through an intermediate form and, conveyed to the sols, introduce different flocculation characteristics. The nature of the stock solution does not change greatly with age and the effects are observed only under favorable conditions, *viz.*, at hydrogen-ion activities which correspond to a transition between a zone of no flocculation and one of complete flocculation. It is possible that the behavior may be influenced by the parent silicate, particularly its ratio and age. This phase of the study has not been investigated fully.

SUMMARY

1. Silica sols, prepared by the interaction of sodium silicate solutions with ion-exchange resins, have been frozen at -10°C .
2. The effects of the following factors on the degree of flocculation were studied: hydrogen-ion activity of the sol; time kept in the frozen state; age of the sol; concentration of the sol; repeated freezing; age of the stock solution of silicate.
3. It was found with systems containing 2.5 per cent silica frozen for 15 min. that a zone of no flocculation occurred at a pH between about 2.5 and 3.5.
4. Dilution of the sol caused the zone of no flocculation to be extended to higher pH values.
5. The systems showed an increased tendency to flocculate when aged before

freezing. The tendency to flocculate was increased, also, by extending the time the systems were held in the frozen state.

6. The age of the stock solution was found to have an effect on the sols prepared from it when the pH values of the latter were just outside the pH range of no flocculation. Flocculation passed through a minimum with increase in age of the stock solution at pH values corresponding to transitions between maximum and minimum flocculation.

The author wishes to acknowledge the assistance given him in this work by The Philadelphia Quartz Company.

REFERENCES

- (1) BOBERTAG, FEIST, AND FISCHER: Ber. **41**, 3675 (1908).
- (2) BRUNI: Ber. **42**, 563 (1909).
- (3) DJATSCHKOWSKY: Kolloid-Z. **54**, 278 (1931).
- (4) HAZEL: J. Phys. Chem. **42**, 409 (1938).
- (5) LOTTERMOSER: Ber. **41**, 3976 (1908).
- (6) LOTTERMOSER AND LANGENSCHIEDT: Kolloid-Z. **58**, 336 (1932).

COÖRDINATION COMPOUNDS OF BORON TRICHLORIDE. IV

SYSTEMS WITH THE PROPYL CHLORIDES

DONALD RAY MARTIN AND ALBERT S. HUMPHREY

Noyes Chemical Laboratory, University of Illinois, Urbana, Illinois

Received September 3, 1946

A survey of the literature reveals that few chlorine-containing compounds form coördination compounds with boron trichloride (4). In the previous paper of this series (6) it was observed that methyl chloride does not form a coördination compound with boron trichloride, whereas ethyl chloride does. It was proposed to study the behavior of the next higher members of the alkyl chloride series with respect to the donor properties of the chlorine atom. The purpose of this paper was to conduct this study by means of thermal analyses of the systems propyl chloride-boron trichloride and isopropyl chloride-boron trichloride.

The apparatus and procedure employed in this study have been described previously (1, 2, 5, 6), with the exception of the technic used for the establishment of the mole fractions. Inasmuch as all three components are liquids at the temperature of melting ice, the calibrated flasks were always filled with gas to a pressure at least 15 mm. below the vapor pressure of the gas at 0°C.

Two thermal analyses were made of each system, using components which were purified by fractional distillation under different pressures. The check

analyses are indicated by asterisks in the data listed in tables 1 and 2 and by solid circles in the phase-rule diagrams depicted in figures 1 and 2.

The boron trichloride used in these studies was prepared by allowing boron trifluoride to react with sublimed aluminum chloride (3) and was purified by fractional distillation.

The propyl chlorides were obtained from the Eastman Kodak Company and were purified similarly by fractional distillation.

TABLE 1
Data for the system n-propyl chloride-boron trichloride

MOLE FRACTION OF BCl ₃	FREEZING POINT	EUTECTIC TEMPERATURE
±0.010	±0.4	±0.4
	—°C.	—°C.
0.000*	122.3	
0.062*	123.7	
0.100	126.0	142.0
0.145	127.3	
0.149*	129.1	
0.202	130.5	
0.251*	131.9	
0.302	134.0	
0.351	135.9	142.0
0.372		141.7
0.400	139.2	
0.450*	137.3	141.8
0.495*	132.2	141.9
0.525	129.3	141.8
0.550*	127.5	141.8
0.600	123.6	
0.649*	120.5	
0.701	116.8	
0.702	118.2	
0.751*	115.6	
0.800	113.0	
0.851*	111.7	
0.900	108.6	
0.951*	108.0	
1.000*	107.2	
1.000	106.7	

* = check analyses.

THE SYSTEM PROPYL CHLORIDE-BORON TRICHLORIDE

There is no evidence for the formation of a compound between propyl chloride and boron trichloride at low temperatures. The thermal analyses data shown in table 1 and depicted in figure 1 indicate that no maximum exists but only a eutectic point which lies at 42.4 ± 1.0 mole per cent boron trichloride and at $-141.8^\circ\text{C.} \pm 0.4^\circ$.

The freezing points of the purified samples of boron trichloride were observed as -106.7°C. and $-107.2^{\circ}\text{C.} \pm 0.4^{\circ}$.

The freezing point of the purified propyl chloride was found to be $-122.3^{\circ}\text{C.} \pm 0.4^{\circ}$. Considerable difficulty was experienced in the determination of this freezing point, owing to the tendency of the propyl chloride to form a glass. The value obtained is 0.5°C. higher than the accepted value of Timmermans (7) of -122.8°C.

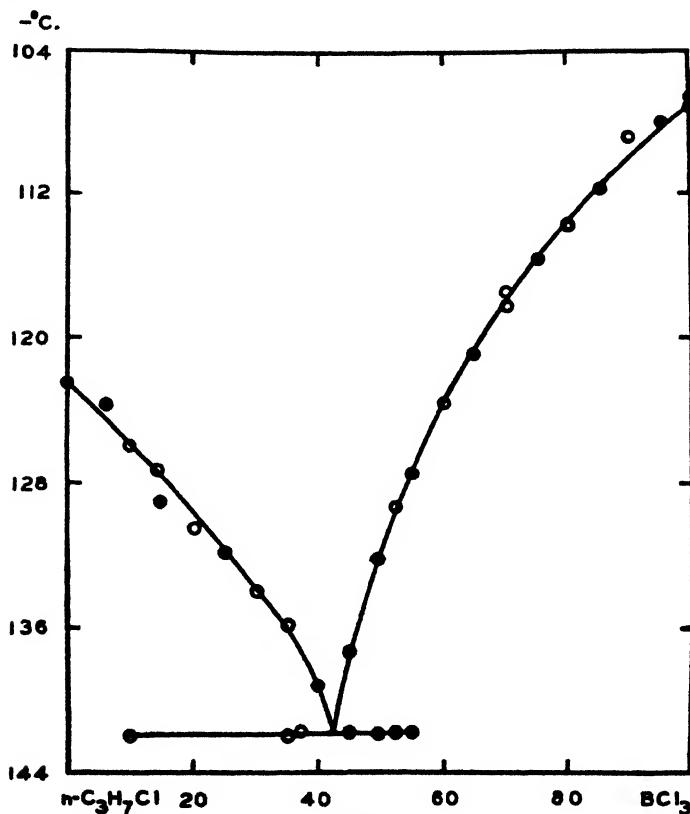


Fig: 1

Some trouble was encountered in the determination of the freezing points of the mixtures having a composition of less than 50 mole per cent boron trichloride, owing to severe supercooling coupled with a tendency towards glass formation. This difficulty was particularly acute between 15 and 35 mole per cent boron trichloride.

THE SYSTEM ISOPROPYL CHLORIDE-BORON TRICHLORIDE

The freezing points of the purified samples of boron trichloride used for this system were found to be -107.0°C. and $-107.3^{\circ}\text{C.} \pm 0.4^{\circ}$.

The samples of purified isopropyl chloride were observed to have freezing points of -117.5°C. and -117.8°C.

The data recorded in table 2 and delineated in figure 2 indicate a maximum at 25.0 mole per cent boron trichloride, corresponding to the compound most simply expressed as $(i\text{-C}_2\text{H}_7\text{Cl})_3\text{:BCl}_3$. The freezing point of the compound is $-105.0^\circ\text{C.} \pm 0.4^\circ$.

TABLE 2
Data for the system isopropyl chloride-boron trichloride

MOLE FRACTION OF BCl_3	FREEZING POINT	EUTECTIC TEMPERATURE
± 0.009	± 0.4	± 0.4
	$-^\circ\text{C.}$	$-^\circ\text{C.}$
0.000	117.5	
0.000*	117.8	
0.047	118.3	
0.098*	113.3	
0.104	113.8	118.3
0.149	111.2	118.7
0.197*	107.3	
0.235*	105.3	
0.242*	105.0	
0.294	105.4	
0.297*	105.9	
0.346	106.0	
0.397*	106.8	
0.445	107.7	
0.496*	109.0	
0.546	110.6	
0.596*	111.9	
0.633	112.7	114.8
0.664	113.8	
0.690	114.8	
0.725*	114.7	
0.750*		114.6
0.777	113.1	
0.825*	112.8	
0.861*	110.6	
0.899	109.4	
0.929	108.0	
0.950*	107.8	
0.980*	106.9	
1.000	107.0	
1.000	107.3	

* = check analyses.

Minima exist on each side of the maximum, occurring at 6.4 ± 0.9 mole per cent boron trichloride and $-118.5^\circ\text{C.} \pm 0.4^\circ$ and at 70.7 ± 0.9 mole per cent boron trichloride and $-114.7^\circ\text{C.} \pm 0.4^\circ$.

Consideration of the maxima in the systems involving ethyl chloride (6) and

isopropyl chloride with boron trichloride, with respect to their flatness and the temperature at which they exist, indicates that the isopropyl chloride-boron trichloride compound is more stable than the ethyl chloride-boron trichloride compound.

It is well known that isopropyl compounds are more reactive than the corresponding *n*-propyl derivatives. It is not surprising therefore that the chlorine atom of isopropyl chloride coördinates with the boron atom of boron trichloride, although the chlorine atom in *n*-propyl chloride does not.

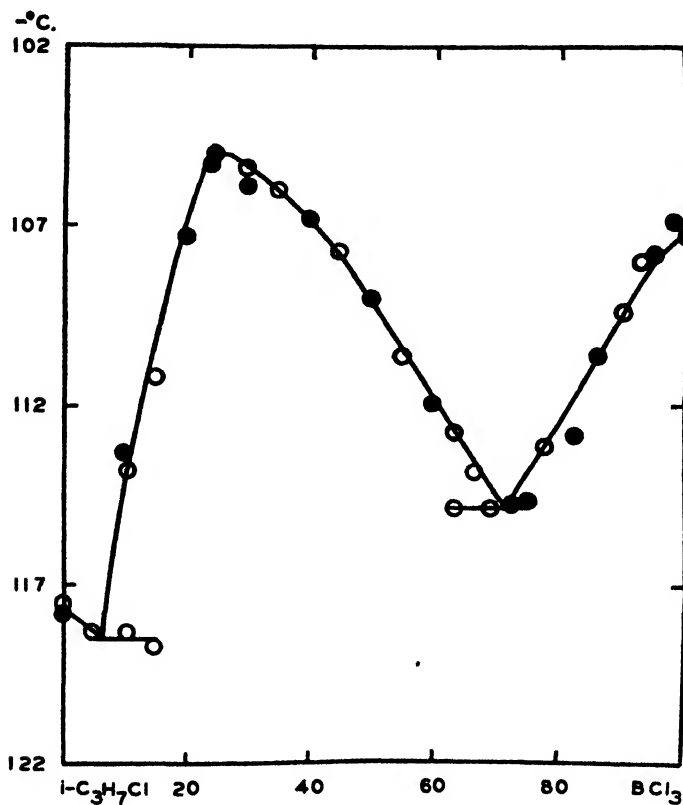
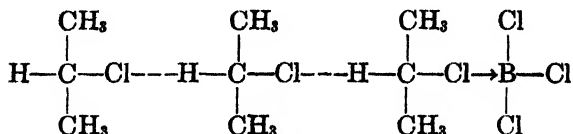


FIG. 2

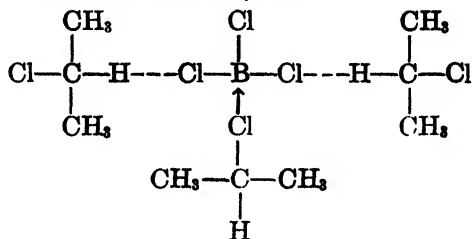
However, it is surprising that a compound having 3 moles of isopropyl chloride to 1 mole of boron trichloride should exist, rather than the simplest possibility of a 1:1 molecular ratio. This becomes more apparent when consideration is given to the bonding forces at play in the compound. One molecule of isopropyl chloride undoubtedly coördinates through its chlorine atom to the boron atom of boron trichloride. The two additional molecules of isopropyl chloride can be accounted for only by hydrogen bonding. This hydrogen bonding might take place between the hydrogen atom on the secondary carbon atom of isopropyl

chloride and the chlorine atom of another isopropyl chloride giving rise to a trimer, thus:



An objection to this proposed structure is that there is no experimental evidence to indicate that isopropyl chloride is associated in the liquid state at low temperatures.

Another possible structure to account for this compound involves the assumption that the hydrogen bonding takes place between the hydrogen atoms on the secondary carbon atoms of the isopropyl chloride molecules and the chlorine atoms of the boron trichloride molecule, thus:



Inasmuch as the chlorine atoms around the boron atom are at the corners of a tetrahedron in coordination compounds of boron trichloride, it is difficult to understand why three molecules of isopropyl chloride would not attach themselves to the three chlorine atoms of the boron trichloride by hydrogen bonds instead of only to two.

SUMMARY

1. The thermal analysis of the system propyl chloride-boron trichloride disclosed only a eutectic point at 42.4 ± 1.0 mole per cent boron trichloride and at $-141.8^\circ\text{C.} \pm 0.4^\circ$.
2. The freezing point of propyl chloride was found to be $-122.3^\circ\text{C.} \pm 0.4^\circ$, a value which is higher than the accepted value in the literature.
3. The thermal analysis of the system isopropyl chloride-boron trichloride revealed a maximum at 25.0 ± 0.9 mole per cent boron trichloride and at $-105.0^\circ\text{C.} \pm 0.4^\circ$, corresponding to the compound most simply expressed as $(i\text{-C}_3\text{H}_7\text{Cl})_3\text{:BCl}_3$. Minima exist on each side of the maximum, one at 6.4 ± 0.9 mole per cent boron trichloride and $-118.5^\circ\text{C.} \pm 0.4^\circ$ and the other at 70.7 ± 0.9 mole per cent boron trichloride and $-114.7^\circ\text{C.} \pm 0.4^\circ$.

REFERENCES

- (1) BOOTH, H. S., AND MARTIN, D. R.: J. Am. Chem. Soc. **64**, 2198-2205 (1942).
- (2) BOOTH, H. S., AND MARTIN, D. R.: Chem. Rev. **33**, 57-88 (1943).
- (3) GAMBLE, E. L., GILMONT, P., AND STIFF, J. F.: J. Am. Chem. Soc. **62**, 1257-8 (1940).
- (4) MARTIN, D. R.: Chem. Rev. **34**, 461-73 (1944).
- (5) MARTIN, D. R.: J. Am. Chem. Soc. **67**, 1088-91 (1945).
- (6) MARTIN, D. R., AND HICKS, W. B.: J. Phys. Chem. **50**, 422-7 (1946).
- (7) TIMMERMANS, J.: Bull. soc. chim. Belg. **27**, 334-43 (1913).

THE RISE OF AIR BUBBLES IN LUBRICATING OILS

J. V. ROBINSON¹*Department of Chemistry, Stanford University, California**Received July 15, 1946*

It was the purpose of the experiments described in this report to expose the mechanism by which additives in a lubricating oil stabilize the "emulsified" air incorporated into the oil circulated through a high-speed gear pump. By measuring the velocity of rise of air bubbles in a column of quiescent oil, with and without additives, the presence or absence of thick layers of liquid on the bubble surface and moving with the bubbles could be ascertained. The presence of such thick layers of liquid moving with the bubbles in oils containing additives is demonstrated in the experiments described in this report, and their absence is demonstrated in an oil containing no additives.

SYMBOLS

Stokes's law: $V = 2ga^2(d_1 - d_2)/9\eta$ V = velocity of fall of spherical body in viscous medium (cm./sec.), g = acceleration of gravity = 980 dynes per gram, a = radius of spherical body (cm.), d_1 = density of spherical body (g./cc.), d_2 = density of medium (g./cc.), η = absolute viscosity of the medium (poises), d_o = density of the oil (0.9 g./cc. at 25°C.), d_a = density of the air (0.00129 g./cc. at 25°C.), d_{ao} = effective density of air bubble surrounded by a rigid shell of oil, r_a, D_a = radius and diameter, respectively, of the air bubble, measured optically, r'_a, D'_a = radius and diameter, respectively, of the air bubble, calculated from Stokes's law from its observed velocity of rise, r_{ao}, D_{ao} = radius and diameter, respectively, of the rigid shell of oil surrounding the air bubble, v_a = volume of air bubble = $4\pi r_a^3/3$, v_o = volume of the rigid oil shell around the air bubble, $v_{ao} = v_a + v_o$, ν = kinematic viscosity of the liquid medium or oil (Stokes), $= \eta/d_2$ or η/d_o .

THEORY OF THE RISE OF AIR BUBBLES THROUGH OIL

Applying Stokes's law to the rise of air bubbles through oil, d_1 becomes d_a , d_2 becomes d_o , and a becomes r'_a . Within 0.1 per cent, $(d_a - d_o) = -d_o$. This approximation permits the substitution of the kinematic viscosity, ν , for

¹Present address: The Mead Corporation, Chillicothe, Ohio.

$\eta/(d_1 - d_2)$. With these substitutions, the equation may be solved for the square of the bubble diameter:

$$(D'_a)^2 = 18\nu V/g = 0.01836\nu V$$

In oils containing no additives, the velocity of rise of air bubbles was proportional to the square of the observed diameter, in accordance with Stokes's law. In oils containing additives an abnormally slow rise was observed, which may be accounted for by assuming that the air bubble is accompanied by a shell of oil (or additive, or both), thus increasing the resistance to passage of the bubble with no compensating increase in the oil displacement. It is desired to calculate the apparent radius of this shell.

The effective density of the bubble with its shell is $d_{ao} = (v_a d_a + v_o d_o)/v_{ao}$. Considering the bubble as truly spherical, $v_a = 4\pi r_a^3/3$, $v_{ao} = 4\pi r_{ao}^3/3$, and $v_o = 4\pi(r_{ao}^3 - r_a^3)/3$. Stokes's law becomes

$$V = 2gr_{ao}^2(d_o - d_{ao})/9\eta = 2g(d_o - d_a)r_a^3/9\eta r_{ao}$$

and

$$r_{ao} = 2g(d_o - d_a)r_a^3/9\eta V$$

Substituting ν for η/d_o , and the approximation $(d_o - d_a) = d_o$, then $r_{ao} = 2gr_a^3/9\nu V$.

However, $9\nu V/2g = (r'_a)^2$; whence $r_{ao} = r_a^3/(r'_a)^2$. That is, the radius of the rigid shell of oil carried along by the air bubble is equal to the ratio of the cube of the observed radius of the air bubble divided by the square of the apparent radius calculated from the observed velocity of rise substituted into Stokes's law. Similarly, $D_{ao} = D_a^3/(D'_a)^2$.

The ratio $D_a^2/(D'_a)^2$ is the factor by which the observed diameter is multiplied to obtain the outside diameter of the rigid shell of liquid carried by the air bubble. The proportion of this shell is thus indicated for any size of bubble.

EXPERIMENTAL METHOD

Into oil contained in a 100-ml. graduated cylinder immersed in a water thermostat, air bubbles were released from an extended syringe pipet. Through a window in the back of the thermostat, illumination was provided by a lamp. Through another in front, the rate of rise of the air bubbles was observed. The time was measured for the passage of a bubble between each pair of 10-ml. graduations (equal to 1.90 cm.), using two stopwatches to make the record continuous. The bubble diameter was measured by comparison of its image with a calibrated ocular micrometer set in a travelling telescope, at a magnification of about ten times. The telescope was used also to measure the vertical distance between the graduations on the cylinder. In the case of large bubbles, the diameter could be measured only once or twice during the rise, and the measurement required rapid manipulation. With small bubbles there was ample time for the observation, and the diameter of the bubble was measured between each pair of graduations.

The temperature was read from a thermometer graduated in $0.1^{\circ}\text{C}.$, immersed in the oil. Owing to absorption of heat from the illuminating lamp, the temperature of the oil rose about $0.2^{\circ}\text{C}.$ per hour during the observation.

The bubbles were formed in a capillary tube, with a U-turn on the end, which was inserted to the bottom of the cylinder. Bubbles were released from the tip when the plunger of the connected syringe was gently pressed. The position of the jet with respect to the cylinder wall is critical. If it is too far from the cylinder wall, the bubbles cannot be seen clearly; if it is too close to the wall, the bubbles run into the wall, according to Bernoulli's theorem.

There are many sources of possible error in the measurements. The bubble diameter was measured with a maximum error, for the smallest bubbles, approaching 5 per cent. The magnification of observed horizontal diameter by the curved wall of the cylinder was neglected; it varied if the bubbles deviated from

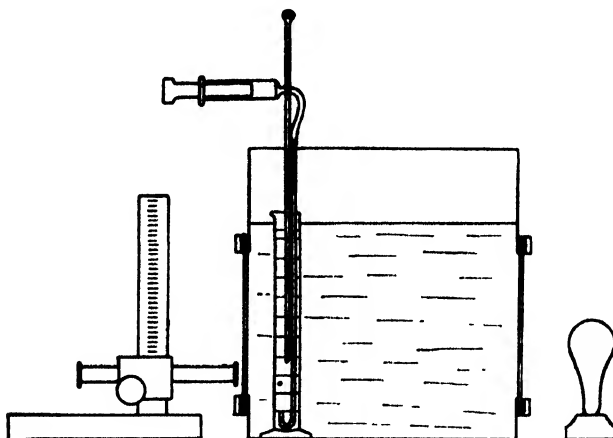


FIG. 1. The apparatus

the same vertical path in their upward journey. Owing to velocity pressure, the bubbles are actually not quite spherical. Unfortunately, these two errors are additive. The timing of the bubbles was accurate to better than 1 per cent. The greatest error is caused by the convection currents in the oil. Despite 9 in. of water between the oil column and the light source, appreciable radiation was absorbed, causing small density and viscosity gradients in the oil. The relative viscosities of the oils used in the calculations were carefully checked and found precise within 5 per cent.

Because of these variations and the small magnitude of the effect being sought, a large number of data were necessary for valid comparison.

RESULTS AND DISCUSSION

The rise of bubbles in four oils was observed. One was a lubricating oil containing no additives. Two others were the same oil to which foam-inhibiting compounds were added. The fourth was an oil containing lubricating additives.

The results of the measurements are expressed by the ratio $D_a^2/(D'_a)^2$. This ratio of the square of the observed diameter to the calculated bubble diameter is also the ratio of the observed to the calculated velocity of bubble rise and in addition the ratio of the outside diameter of a shell of oil carried by the bubble to the diameter of the bubble itself. Provided the absolute values of all constants used are exact and the measurements accurate, this ratio must be unity unless there is some difference between the bubble in actuality and a smooth sphere rising through a Newtonian liquid.

The results are summarized in table 1, in which are shown average values, the average deviation from the average, and the number of determinations averaged (in parentheses). In oil A, containing no additives, bubbles behaved as expected, the rate of rise being directly proportional to the observed diameter. The data were homogeneous. The difference between the ratio of the squared diameters and unity in the case of oil A is ascribed to the accumulated absolute errors in the

TABLE 1
*Averaged values of $D_a^2/(D'_a)^2$ **

Oil A, containing no additives....	0.879 ± 0.033 (45)
Oil A, containing 0.075 per cent glycerol and 0.025 per cent Aerosol OT	2.08 ± 0.23 (16)†
Oil A, containing 0.1 per cent of Dow Corning Fluid Type 200	1.35 ± 0.15 (24)
Oil B, containing lubricating additives	1.02 ± 0.07 (17)

* Figures in the table are averaged values of $D_a^2/(D'_a)^2$, plus or minus the average deviation from average, giving the number of measurements averaged in parentheses.

† The oil column was not thermostated when these data were obtained, but the oil temperature was measured.

constants used and in the measurements themselves. Such errors should appear approximately proportionately in the other values in table 1, so that the relative values are significant.

A phenomenon not shown by the averaged data is that the velocity of the bubbles rising through oils containing additives, in particular oil B, became slower as the bubbles rose. This effect was completely absent in oil A, which contained no additives. Care was taken to avoid having the bubbles rise too close to the wall, which they would then tend to approach, causing a decreasing velocity similar to that observed. It is considered likely that the adsorbed material on the bubble, and hence the diameter of the shell moving with the bubble, increases as the bubble travels. Data illustrating the phenomenon are shown in table 2. These are consistent with the direct observation that the additive material in oil B is greatly concentrated in the liquid collected when the froth formed by air bubbles rising through a column of the oil is collected and segregated.

To illustrate further the homogeneity of the measurements and the absence of a changing velocity with time of rise, data for oil A containing no additive are shown in table 3. From the data in tables 2 and 3, the method of calculation may be followed in detail.

These phenomena are of great interest theoretically as regards the structure of liquids. The additives in the oils add a shell to the air bubbles which can have a

TABLE 2
Rise of air bubbles through oil B

INTERVAL (GRADUATIONS)*	TIME	VELOCITY (l')	OBSERVED DIAMETER (D_a)	TEMPERATURE	VISCOSITY (ν)	VELOCITY AT 25°C	CALCULATED DIAMETER SQUARED (D_a') ² $\times 10^{-4}$	RATIO OF SQUARED DIAMETERS $\frac{(D_a)^2}{(D_a')^2}$
	sec.			°C.				
20 to 30	21.8	0.0872		23.9	11.05	0.0925	176.4	0.921
30 to 40	23.5	0.0808	0.1273	23.9	11.05	0.0857	163.5	0.992
40 to 50	25.4	0.0749	0.1253	23.9	11.05	0.0795	151.6	1.04
50 to 60	29.0	0.0655	0.1234	23.9	11.05	0.0695	132.5	1.15
60 to 70	33.0	0.0575	0.1216	23.9	11.05	0.0610	116.3	1.27
70 to 80	37.5	0.0506	0.1234	23.9	11.05	0.0537	102.6	1.48
20 to 30	25.8	0.0736		23.4	11.35	0.0806	154	0.936
30 to 40	27.8	0.0684		23.4	11.35	0.0749	143	1.01
40 to 50	31.0	0.0614		23.4	11.35	0.0672	128	1.13
50 to 60	35.5	0.0535	0.1198	23.4	11.35	0.0584	111	1.30
60 to 70	41.6	0.0456	0.1160	23.4	11.35	0.0498	95.0	1.41
70 to 80	45.4	0.0419	0.1140	23.4	11.35	0.0457	87.2	1.49
20 to 30	41.6	0.0456		23.3	11.45	0.0502	95.8	0.943
30 to 40	46.0	0.0413		23.3	11.45	0.0455	86.9	1.04
40 to 50	54.6	0.0342	0.0950	23.3	11.45	0.0377	72.0	1.25
50 to 60	59.2	0.0321		23.3	11.45	0.0354	67.5	1.23
60 to 70	74.6	0.0255	0.0912	23.3	11.45	0.0280	53.5	1.56
70 to 80	82.7	0.0230		23.3	11.45	0.0253	48.3	1.73
20 to 30	59.8	0.0318		23.7	11.17	0.0342	65.3	1.03
30 to 40	67.0	0.0284	0.0817	23.7	11.17	0.0305	58.2	1.15
40 to 50	75.6	0.0252	0.0799	23.7	11.17	0.0270	51.5	1.24
50 to 60	89.5	0.0212	0.0779	23.7	11.17	0.0228	43.5	1.40
60 to 70	112.0	0.0170	0.0760	23.7	11.17	0.0183	34.9	1.66
70 to 80	121.1	0.0157	0.0760	23.7	11.17	0.0169	32.2	1.79
20 to 30	78.4	0.0242		23.5	11.30	0.0263	50.2	1.04
30 to 40	89.1	0.0214	0.0722	23.5	11.30	0.0232	44.3	1.18
40 to 50	100.4	0.0189	0.0722	23.5	11.30	0.0205	39.2	1.33
50 to 60	120.9	0.0157	0.0703	23.5	11.30	0.0171	32.6	1.51
60 to 70	155.6	0.0122	0.0685	23.5	11.30	0.0133	25.4	1.85
70 to 80	169.2	0.0112	0.0665	23.5	11.30	0.0121	23.1	1.91

* Each group of data set off by spaces represents a single bubble, observed over different intervals.

diameter half again as great as the air bubble itself. This must mean that a gel-like structure, possibly a plastic solid, extends from the air interface far into the oil. The great extent of this structure (great in terms of molecular size)

may be due principally to the motion of the bubbles. Similar experiments on the adsorption of solutes in aqueous solutions show that the concentration ad-

TABLE 3
Rise of air bubbles through oil A

INTERVAL (GRADUATIONS)*	TIME	VELOCITY (V)	OBSERVED DIAMETER (D_b)	TEMPERA- TURE	VISCOSITY (ν)	VELOCITY AT 25°C.	CALCULATED DIAMETER SQUARED (D_b') ² $\times 10^{-4}$	RATIO OF SQUARED DIAMETERS $\frac{(D_b')^2}{(D_b)^2}$
	<i>sec.</i>			<i>°C.</i>				
20 to 30	18.4	0.1032		24.1	8.87	0.1090	168	0.858
30 to 40	18.4	0.1032		24.1	8.87	0.1090	168	0.858
40 to 60	36.3	0.1046	0.1198	24.1	8.87	0.1104	170	0.846
60 to 70	19.2	0.0990		24.1	8.87	0.1046	161	0.869
70 to 80	19.0	0.1000	0.1179	24.1	8.87	0.1057	163	0.853
50 to 60	19.6	0.0969	0.1140	24.7	8.55	0.0985	151.8	0.856
20 to 30	21.0	0.0905		24.7	8.55	0.0920	141.8	0.917
30 to 50	40.0	0.0950	0.1140	24.7	8.55	0.0966	149.0	0.872
50 to 70	38.6	0.0986	0.1102	24.7	8.55	0.1003	154.5	0.792
70 to 80	20.8	0.0914		24.7	8.55	0.0930	143.2	0.850
30 to 40	30.2	0.0629	0.0912	24.7	8.55	0.0640	98.6	0.844
40 to 50	30.5	0.0623		24.7	8.55	0.0634	97.6	0.853
50 to 60	30.4	0.0625	0.0912	24.7	8.55	0.0636	98.0	0.850
60 to 70	31.8	0.0597	0.0912	24.7	8.55	0.0608	93.6	0.889
20 to 30	37.8	0.0503		22.1	9.95	0.0595	91.6	0.871
30 to 40	37.7	0.0504		22.1	9.95	0.0596	91.9	0.869
50 to 60			0.0893	22.1	9.95			
60 to 70	40.6	0.0468		22.1	9.95	0.0554	85.5	0.893
70 to 80	41.0	0.0464	0.0874	22.1	9.95	0.0549	84.6	0.902
20 to 30	45.0	0.0422	0.0760	24.1	8.87	0.0450	69.4	0.833
40 to 50	46.2	0.0411	0.0760	24.1	8.87	0.0439	67.5	0.855
50 to 60	47.3	0.0402	0.0760	24.1	8.87	0.0425	65.5	0.882
60 to 70	48.6	0.0390	0.0741	24.1	8.87	0.0412	63.5	0.866
70 to 80	50.4	0.0377	0.0722	24.1	8.87	0.0398	61.4	0.852
20 to 30	64.0	0.0297		24.1	8.87	0.0314	48.4	0.895
30 to 40	65.7	0.0289	0.0665	24.1	8.87	0.0305	47.0	0.921
40 to 50	66.2	0.0287	0.0646	24.1	8.87	0.0303	46.6	0.896
50 to 60	67.1	0.0283	0.0646	24.1	8.87	0.0299	46.1	0.907
60 to 70	70.4	0.0270	0.0626	24.1	8.87	0.0285	44.0	0.894
70 to 80	71.1	0.0267	0.0589	24.2	8.81	0.0282	43.5	0.796

* Each group of data set off by spaces represents a single bubble, observed over different intervals.

sorbed on the surface of moving bubbles may be from twice to many times the concentration adsorbed on a plane quiet surface at equilibrium (2, 3).

The wholly or partially immobilized liquid may contain chains of oriented molecules of additive extending outwards from a primary sorbed layer on the surface of the bubble, as suggested independently by McBain (2) and by Hardy (1) in 1927. This may well be supplemented by cybotactic arrangement of the hydrocarbon molecules in the same region, as McBain has also suggested. The practical significance of the observations is that the reluctance of finely "emulsified" air to separate in lubricating oils containing additives has been accounted for.

CONCLUSIONS

In the oils containing additives, there is a thick shell of material surrounding moving air bubbles, which moves with the bubbles, impeding their passage through the oil.

SUMMARY

The rates of rise of small air bubbles, up to 2 mm. in diameter, were measured at room temperature in an oil containing no additives, in the same oil containing foam inhibitors, and in an oil containing lubricating additives. The apparent diameter of the air bubbles was measured visually through an ocular micrometer on a travelling telescope.

Additives in lubricating oils may impede the escape of small bubbles from the oil, by forming shells of liquid with a quasi-solid or gel structure around the bubbles.

The bubbles in the oil containing no additives obeyed Stokes's law, the rate of rise being proportional to the square of the apparent diameter and inversely proportional to the viscosity of the oil.

The bubbles in the oils containing additives rose more slowly than predicted by Stokes's law from the apparent diameter, and the rate of rise decreased as the length of path the bubbles travelled increased.

A method is derived for calculating the thickness of the liquid shell which would have to move with the bubbles in the doped oils to account for the abnormally slow velocity. The maximum thickness of this shell, calculated from the velocities observed, was equal to the bubble radius.

The information contained in this paper was obtained in connection with an investigation sponsored and financed by the National Advisory Committee for Aeronautics and carried out under the supervision of Professor James W. McBain.

REFERENCES

- (1) HARDY, W. B.: *J. Gen. Physiol.* **8**, 641 (1927).
- (2) MCBAIN, J. W., AND DAVIES, GEORGE P.: *J. Am. Chem. Soc.* **49**, 2230 (1926).
- (3) MCBAIN, J. W., AND WOOD, L. A.: *Proc. Roy. Soc. (London)* **A174**, 286 (1940).

ENERGY ADDITIVITY IN OXYGEN-CONTAINING CRYSTALS AND GLASSES. II¹KUAN-HAN SUN² AND MAURICE L. HUGGINS*Kodak Research Laboratories, Rochester, New York**Received September 17, 1946*

In recent papers (2, 3) it has been shown that the energies of dissociation of simple and complex oxides into the gaseous ions of their component elements are approximately additive, conforming to the relationship

$$E_i \approx \sum_M m_M \epsilon_M \quad (1)$$

where E_i is the "ionic dissociation energy" of the compound (or glass) $M_m M'_m M''_m \cdots O_n$ and ϵ_M is a constant characteristic of element M. This constant may be thought of as the average contribution of one gram-atom of element M to the total energy of dissociation into gaseous ions of compounds or glasses in which each M atom is surrounded by a shell of oxygen atoms. No assumption regarding the nature of the forces (ionic or covalent) holding the M atoms to these oxygens is involved. Differences in the number of oxygens around each M in different compounds or glasses produce departures from strict additivity, but the deviations are not great.

A large part of the magnitude of each ϵ_M value can be attributed to the energies of formation of the gaseous ions, M^{+v} and O^{-2} , from the uncharged gaseous atoms, M and O. In studying other factors affecting the magnitudes of the energy constants, it is of interest to subtract the contributions of these atomic ionization energies—in other words, to compute and compare energy constants, ϵ'_M , for dissociation into gaseous uncharged atoms, rather than ions.

The ϵ'_M values are related to the ϵ_M values by the following equation:

$$\begin{aligned} \epsilon'_M &= \epsilon_M + Qf[M^{+v}, \text{gas}] - Qf[M, \text{gas}] + \frac{v}{2}\{Qf[O^{-2}, \text{gas}] - Qf[O, \text{gas}]\} \\ &= \epsilon_M + Qf[M^{+v}, \text{gas}] - Qf[M, \text{gas}] - 83 v \end{aligned} \quad (2)$$

Here v is the valence of the atom M in the compounds or glasses being considered and Qf designates the heat of formation, obtainable from Bichowsky and Rossini's valuable tabulation (1).

Table 1 lists values of ϵ'_M , together with the values of ϵ_M from which they were computed by means of equation 2. Some additional ϵ'_M values are included, for elements for which the data on ionization energies of the gaseous elements required for the computation of ϵ_M are not available. The equation used for

¹ Communication No. 1107 from the Kodak Research Laboratories.

² Present address: Research Laboratory, Westinghouse Electric and Manufacturing Company, East Pittsburgh, Pennsylvania.

TABLE 1
Ionic and atomic dissociation constants*

M	ϵ_M	ϵ_M'
	kg.-cal.	kg.-cal
<i>Monovalent:</i>		
H, in $M(OH)_2$	515	118
H, in $MHCO_3$	501	104
H, in $MHSO_4$	490	93
H, in $H_2M_2O_7$	489	92
H, average.....	500	103
Li.....	351	144
Na.....	322	120
K.....	299	115
Rb.....	295	115
Cs.....	288	114
Cu.....	295	131
Ag.....	346	88
Rh.....	316	154
Tl.....	309	250
NH ₄	151 - c	68 - c'
<i>Divalent:</i>		
Be.....	1141	250
Mg.....	912	222
Ca.....	839	257
Sr.....	800	256
Ba.....	768	260
Zn.....	941	144
Cd.....	883	119
Hg.....	907	68
V.....	901	240
Mn.....	895	196
Fe.....	919	189
Co.....	1118	171
Ni.....	929	166
Cu.....	860	146
Rh.....		198
Pd.....	978	161
Sn.....	882	200
Pb.....	829	145
<i>Trivalent:</i>		
B.....	2047	356
Al, in $M_2Al_2O_7$	1878	402
Al, in $M_2Al_2Si_2O_7$	1793	317
Al, in $M_2M_2(SO_4)_2$	1721	245
Al, average.....	1797	321
Sc.....	1563	362
Y.....	1566	399
La.....		406
Ga.....	1827	267
In.....	1722	259
Tl.....	1734	187

TABLE 1—*Continued*

M	ϵ_M	ϵ'_M
	kg.-cal.	kg.-cal.
<i>Trivalent—Continued:</i>		
N.....	2555	194
As.....	1767	193
Sb.....	1614	164
Bi.....	1526	147
V.....	1691	337
Cr.....	1695	279
Mn.....		233
Fe.....		287
Co.....		239
Ni.....		223
Rh.....		241
Au.....		171
<i>Tetravalent:</i>		
C.....	4208	471
Si.....	3172 — 123 N_{Si}	466 — 123 N_{Si}
Si, average.....	3128	424
Ti.....	2882	435
Zr.....	2637	485
Th.....		516
Sn.....	2769	278
Pb.....	2835	232
V.....		393
Mo.....		406
W.....		457
U.....		593
Se.....		249
Te.....		269
Mn.....		309
Ru.....		289
Ir.....		286
<i>Pentavalent:</i>		
N.....	6831	276
P.....	4870 — 530 N_P	575 — 530 N_P
P, average.....	4720	425
V.....	4564	449
As.....	4507	349
Sb.....	4250	339
Bi.....		281
<i>Hexavalent:</i>		
S.....	7195	439
Cr.....		443
Mo.....		553
W.....		622
U.....		725
Se.....	6886	349
Te.....	6167	407

TABLE 1—*Concluded*

M	ϵ_M	ϵ'_M
	kg.-cal.	kg.-cal.
<i>Heptavalent:</i>		
Cl.....	9948	353
Mn.....		405
I.....		357
<i>Octavalent:</i>		
Os.....		452

* c denotes the heat of formation of NH_4^+ (gas) from hypothetical NH_4 metal.

c' denotes the heat of formation of NH_4 (gas) from hypothetical NH_4 metal.

N_{Si} denotes the ratio of silicon atoms to oxygen atoms in the compound or glass.

N_{P} denotes the ratio of phosphorus to oxygen atoms in the compound or glass.

computing ϵ'_M from the Qf data for a simple crystalline oxide (M_mO_n) is

$$\begin{aligned}\epsilon'_M &= \frac{1}{m} Qf[\text{M}_m\text{O}_n, \text{crystal}] - Qf[\text{M}, \text{gas}] - \frac{n}{m} Qf[\text{O}, \text{gas}] - \frac{m+n}{m} RT \\ &= \frac{1}{m} Qf[\text{M}_m\text{O}_n, \text{crystal}] - Qf[\text{M}, \text{gas}] + 29.3v - 0.6\end{aligned}\quad (3)$$

For a complex oxide, the equation is similar but slightly more complicated.

Just as approximate *ionic* dissociation energies, E_i , may be computed additively from the ϵ_M values by equation 1, so *atomic* dissociation energies, E_a , may be computed additively from the ϵ'_M values. Mathematically expressed:

$$E_a \approx \sum_M m_M \epsilon'_M \quad (4)$$

The ϵ'_M values are all much lower than the corresponding ϵ_M values, a result of the fact that large amounts of energy are required to remove the valence electrons from the more metallic atoms and add them to oxygen atoms, forming O^{2-} ions. Dissociation of an oxide into isolated neutral atoms requires less energy than dissociation into isolated ions.

The ϵ'_M values for Groups I to IV of the Periodic Table are plotted in figure 1. The most striking regularity is the regular increase in ϵ_M with increase in valence, measuring the increase in attraction energy for oxygen as the kernel charge is increased.

Another generalization, obvious from the figure, is that with increasing atomic number ϵ'_M decreases within the *b* subgroups and increases within the *a* subgroups (except in Subgroup Ia, in which it remains practically constant). The decrease in the *b* subgroups may be related to the decrease in binding energy as the atomic number increases. For these elements, which tend (more than do the *a* subgroup elements) to form covalent bonds, the coordination number is practically independent of atomic number. For the elements in the *a* subgroups, however, the binding is largely ionic, and increasing atomic number is accompanied by increasing size and increasing coordination number. This more

than counteracts the probable decrease in attraction energy *per oxygen neighbor* as the atomic number increases within each group.

The constants for the elements of higher valence change less regularly with atomic number than do those for the elements represented in the figure, for various reasons. The experimental data are more sketchy. The tendency to

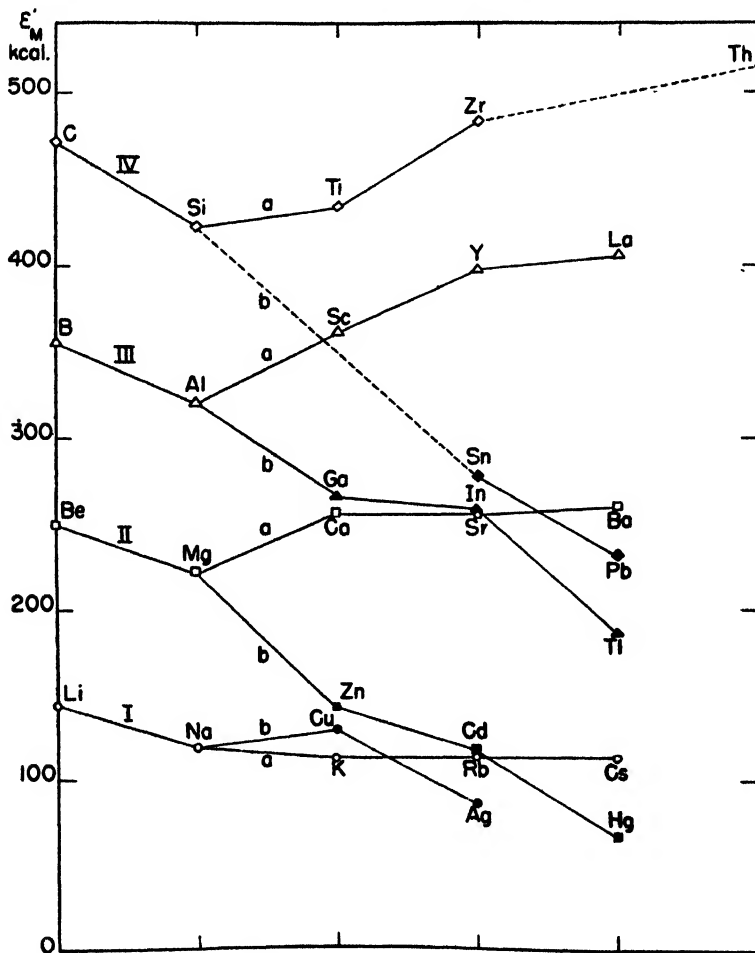


Fig. 1. Atomic dissociation constants for elements in Groups I to IV of the Periodic Table, when exhibiting their normal valences.

form covalent bonds is strong, resulting in the formation of groups of atoms (ions) and more variation in energy content from compound to compound. The electronic structures of the atoms play a greater rôle. Because of these complications, further discussion of the dissociation energy constants for the higher valence elements will not be attempted at this time. For similar reasons, discussion of the data for the transition elements and for atoms in states other than those in which they exhibit their normal valence will also be omitted.

SUMMARY

Energies of dissociation of simple and complex oxides into their component atoms, like the corresponding ionic dissociation energies, are approximately additive. A table of characteristic constants for use in computing these atomic dissociation energies is presented. Certain relationships to the Periodic Table are noted: in particular, the increase in the magnitude of the constant with increase in valence and its regular increase and decrease with atomic number in the *a* and *b* subgroups, respectively.

REFERENCES

- (1) BICHOWSKY, F. R., AND ROSSINI, F. D.. *The Thermochemistry of the Chemical Substances*. Reinhold Publishing Corporation, New York (1936).
- (2) HUGGINS, M. L., AND SUN, K.-H.. *Trans. Soc. Glass Tech.* **28**, 463 (1944); *J. Am. Ceram. Soc.* **28**, 149 (1945).
- (3) HUGGINS, M. L., AND SUN, K.-H.. *J. Phys. Chem.* **50**, 319 (1946).

STABILITY OF SYNTHETIC RUBBER DISPERSIONS. I

LOW-TEMPERATURE THICKENING OF NEOPRENE LATEX^{1,2}

H. K. LIVINGSTON

*Jackson Laboratory, E. I. du Pont de Nemours and Company, Wilmington, Delaware**Received October 1, 1946*

INTRODUCTION

Neoprene latex of 50 per cent neoprene concentration is quite fluid and deviates only slightly from the ideal or Newtonian flow characteristics. The viscosity of Neoprene Latex Type 571 at 25°C. is 7–9 centipoises, but if the latex is cooled into the temperature range 0–10°C., at some point in this temperature range (the exact temperature depending on factors to be discussed) an abrupt change in the character of the latex takes place. The latex becomes of a paste-like consistency with a very high yield point and viscosity. Typical data showing this transition, as given in an earlier paper (8), are reproduced in table 1.

In view of this marked change in viscosity, Neoprene Latex Type 571 cannot be considered to be stable below 10°C., if "stability" is defined in the broad sense. However, the instability is not of the type that produces coagulation of the colloidal system. This is in contrast to the behavior of synthetic rubber latices cooled below 0°C. At sub-zero temperatures, instability takes the form of

* ¹Contribution No. 53 from Jackson Laboratory, E. I. du Pont de Nemours and Company.

²Presented at the Symposium on the Stability of Colloidal Dispersions, which was held under the auspices of the Division of Colloid Chemistry at the 110th Meeting of the American Chemical Society, Chicago, Illinois, September, 1946.

coagulation, as discussed in the second paper of this series (15). The change that occurs at temperatures above 0°C. is completely reversible and resembles in some respects a sol \rightarrow gel phase transition. The transition occurs at the same temperature, or at least within a temperature range of no more than 0.5°C., on cooling or warming. The only change that takes place in the latex while it is in the paste form is a slow separation of serum (i.e., the latex creams (8)). As far as can be determined, Neoprene Latex Type 571 can be held at 0°C. indefinitely without harmful effects. In the longest test that has been run under controlled conditions, a sample of latex was held at 0°C. for 75 days without any change in properties.

Some of the other synthetic latices have the same temperature sensitivity as Neoprene Latex Type 571 and undergo a liquid-paste transition at these low temperatures. This effect was first reported by Bächle (1) for Buna (butadiene

TABLE 1
The effect of temperature on the viscosity of Neoprene Latex Type 571
Data obtained with the conicylindrical viscosimeter (14)

TEMPERATURE	LIMITING VISCOSITY	YIELD POINT*
°C.	centipoises	mg./cm. ³
30	6.8	6
25	7.6	6
20	8.5	6
15	9.3	6
10	6800	75

* These values differ slightly from those given in reference 8. In that reference, the yield points were calculated by comparison with results obtained with the Jordan-Brass-Roe capillary viscosimeter (7). The results given above were obtained by calculations based on the instrument constants, and are believed to be more accurate.

polymer) latices. The thickening observed with Buna latices made from emulsions stabilized with alkylnaphthalenesulfonic acids as emulsifying agents was made the basis of a German patent in which the latex was concentrated by filtering, centrifuging, or pressing after it had been thickened by cooling (9). Thickening below 7°C. has also been reported to occur with the American latex GR-S No. 3 (3, 6).

EXPERIMENTAL

The transition of neoprene latex from liquid to paste resembles in a general way the change that takes place in lubricating oils at the pour point. It was found that the transition point could be determined with sufficient accuracy for most purposes by a modification of the A.S.T.M. pour-point test for lubricating oils (A.S.T.M. Designation D 97-39).

The standard pour-point bottles (4-oz. capacity, 5½ in. high) were filled to a depth of 2 in. with latex, and a thermometer was introduced with the bulb just covered by the latex. Crushed ice was packed around the bottle and the latex

was allowed to cool until it ceased to pour when the bottle was tilted through 90°. Since the latex around the bulb would be the last to reach the transition temperature, the thermometer reading when no liquid latex remained corresponded to the true transition temperature.

An alternate method for determining transition temperatures makes use of the conicylindrical viscosimeter (14). Latex is placed in a viscosimeter that has a water jacket and is cooled below the transition temperature. Under these conditions quite a large torque must be applied to the rotor to produce even a slow rotation. With an instrument that has the dimensions given by Mooney and Ewart (14), a load of 200 g. will produce approximately 0.01 revolution of the rotor per second with Neoprene Latex Type 571 below the transition point, as compared with 10 R.P.S. for the same latex above the transition point. If this high load is applied to a paste which is then allowed to warm up by increasing the temperature of the water circulating through the jacket, the rotor will suddenly begin to rotate rapidly at the moment that the latex reaches the transition point. This change is easily recognized, and if the latex is warming up gradually so that the thermometer reading represents the latex temperature, this method may give a very accurate measure of the transition point. It is difficult, however, to obtain a satisfactory approach to temperature equilibrium throughout the apparatus while raising the temperature.

FACTORS AFFECTING THICKENING

The transition temperature increases with increasing latex concentration and with increasing alkalinity of the aqueous phase. This is in agreement with Bächle's observations on Buna latex (1). Neoprene Latex Type 571 is polymerized at 50 per cent concentration and a pH of approximately 12.4. It contains 4.5 per cent rosin soap (based on the neoprene) in addition to amine stabilizers and inorganic catalysts. If it is made at a lower pH or lower concentration, the liquid \rightarrow paste transition temperature is lowered. The addition of water to the finished latex lowers the transition temperature, while the addition of a dilute sodium hydroxide solution raises it markedly (see table 2).

The addition of small amounts of non-ionic surface-active agents will prevent the thickening of Neoprene Latex Type 571 at all temperatures at which it is safe from freezing. Apparently this remarkable effect has not been reported before. Results obtained with a variety of non-ionic surface-active agents are given in table 3.

The effective agents are of two classes: the amphoteric long-chain compounds typified by betaine derivatives, and the polyethylene glycol esters or ethers made by condensing ethylene oxide with long-chain acids or alcohols. All these compounds can be considered to be non-ionic surface-active agents. Anionic surface-active agents, such as sodium lauryl sulfate or Daxad-11 (a formaldehyde-naphthalenesulfonic acid condensation product), have little or no effect on the thickening point. Cationic agents could not be tested; they are incompatible with Neoprene Latex Type 571, since it is stabilized with an anion-active material.

The explanation of the effect of the non-ionic agents on latex thickening seems

TABLE 2

The effect of dilution and of sodium hydroxide on the thickening point of Neoprene Latex Type 571

ADDED MATERIAL	GRAMS ADDED PER 100 GRAMS LATEX	THICKENING POINT
		°C.
None.		5
Water.....	2	4
4.5 per cent NaOH.....	2	5
Water.....	4	4
4.5 per cent NaOH.....	4	12
Water.....	10	2
4.5 per cent NaOH.....	10	18
Water.....	20	-1

TABLE 3

The effect of non-ionic surface-active agents on the thickening point of Neoprene Latex Type 571

SURFACE-ACTIVE AGENT	GRAMS ADDED PER 100 G. NEOPRENE	GRAMS WATER ADDED PER 100 G NEOPRENE	THICKENING POINT
			°C.
None.....			5
Nonaethylene glycol monolaurate.....	0.5	2	Below 0
C-Cetylbetaine.....	0.5	4	0
Tween 20*	1.0	4	Below 0
Tween 80†	1.0	4	Below 0
Emulphor O‡.....	0.8	5	Below 0
Triton NE§.....	1.0		0

* Tween 20 = sorbitan monolaurate condensed with an alkylene oxide.

† Tween 80 = sorbitan monooleate condensed with an alkylene oxide.

‡ Emulphor O = condensation product from 17 moles ethylene oxide and 1 mole cetyl alcohol.

§ Triton NE = 33 per cent aqueous solution with an ethylene oxide-lauryl alcohol condensation product as the active ingredient.

TABLE 4

The effect of rosin soap on the viscosity of Neoprene Latex Type 571 at various temperatures
Data obtained with the conical cylindrical viscosimeter (14)

	T = 11°C.		T = 25°C.		T = 49°C.	
	η^*	F	η	F	η	F
Untreated latex.....	13.8	6	9.2	6	6.7	6
20 parts latex + 1 part Dresinate X + 1 part water	16.4	13	22.4	58	23.4	143
20 parts latex + 1 part Dresinate X + 0.02 part NaOH + 0.98 part H ₂ O	21.1	7	17.6	22	29.0	166

* η = limiting viscosity in centipoises.F = yield point in mg./cm.²

to lie in their influence on the phase changes that take place in the rosin soap. This will be discussed in the next section.

The viscosity-temperature relationships of neoprene latex are affected by the concentration of the dispersing agent (rosin soap) as well as by the water, alkali, and non-ionic soap concentrations. If the rosin soap concentration is 0.1 part or more per part of neoprene, and the total solids is maintained at 50 per cent, the viscosity of Neoprene Latex Type 571 goes through a minimum as the temperature is lowered. Typical viscosity data for Latex Type 571, untreated or with large amounts of rosin soap added, are given in table 4.

BEHAVIOR OF SOAP SOLUTIONS

Conover states that the change which takes place in GR-S latices at 40°F. "actually is only the thickening and subsequent immobility of the excess soap" (3). We have undertaken a study of the changes that take place on cooling aqueous rosin soap systems resembling those used in Neoprene Latex Type 571. We have found definite changes to occur in the turbidity of the soap solutions, and consider this to be much more significant than the relatively minor changes in the viscosity of the solutions that were observed. It seems very likely that the paste transition, at least in the case of neoprene latex, is not due to the thickening of the excess soap. Instead, it appears to occur at the temperature at which the transition from a clear to a turbid solution occurs. The detailed investigations were carried out with two standard solutions:

SOLUTION A	SOLUTION B
4.5 g. sodium rosinate*	4.5 g. sodium rosinate*
0.5 g. sodium hydroxide	0.3 g. sodium hydroxide
95 g. water	95 g. water
pH = 12.7	pH = 12.4

* Dresinate X, a product of the Hercules Powder Company, was used.

The viscosities of the two solutions were the same at 20°C. On cooling to 7°C. solution B increased in viscosity, while the *apparent* viscosity of solution A decreased. However, solution A became turbid at 12°C. This turbidity is due to the formation of curd fibers in the solution, as has been described by Darke, McBain, and Salmon (4). Since the viscosity was determined by using the mixture of liquid and curd fiber, it does not represent the true solution viscosity.

There was a pronounced time lag in the phase transition of curd fiber formation. For example, if solution A was divided into two parts, and one part was warmed until clear and homogeneous while the other part was cooled below 12°C. so as to make the solution turbid and produce curd fibers, it was found that the portion containing curd fibers retained the fibers when held at 15°C. for 1 hr. and did not become clear and homogeneous until warmed to 20°C. But the portion that was homogeneous remained so (i.e., no curd fibers formed) when held at 15°C. for 1 hr. This tendency for soap solutions to become supersaturated with respect to

curd fiber has been reported by McBain, Burnett, and Elford as being very common with the fatty acid soaps (10, 11, 12).

As an aid to the understanding of the behavior of rosin soap, we have prepared a phase diagram that affords a qualitative representation of the system sodium hydroxide-rosin soap-water. The diagram (figure 1) is of the type given by McBain and Burnett for sodium laurate (11). It will be seen that the region of isotropic solutions is a very narrow one, and that the addition of very much sodium hydroxide brings about separation into two phases. This is due to the salting-out effect of salts on soaps. Sodium chloride has the same effect as

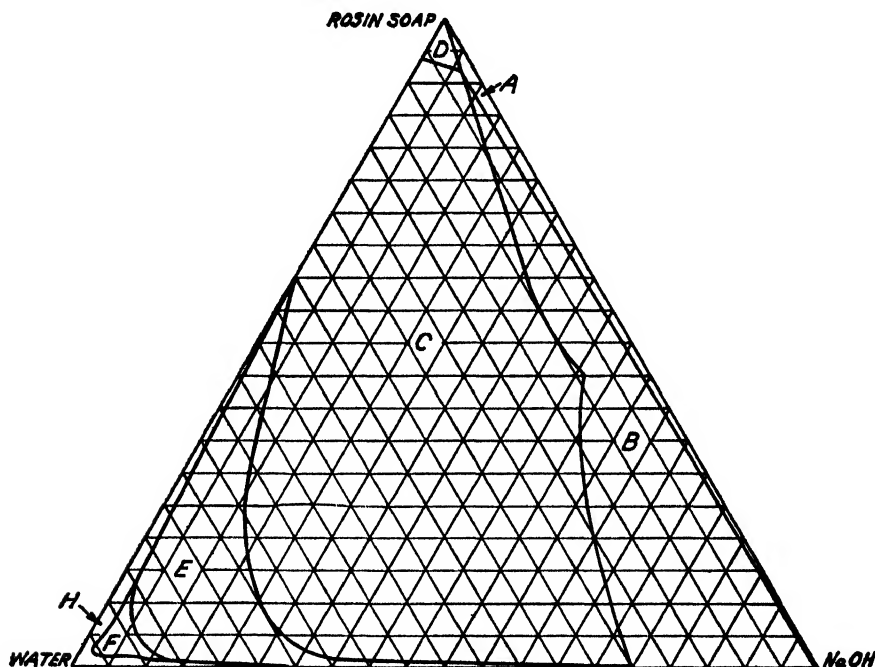


FIG. 1. Phase diagram showing qualitatively the phase relationships in the system rosin soap-sodium hydroxide-water at 10-80°C. Phases: A, sodium hydroxide + curd; B, sodium hydroxide + curd + lye; C, curd + lye; D, dehydrated curds; E, neat soap + lye; F, curds + isotropic solution; H, homogeneous isotropic solution.

sodium hydroxide in the phase diagram. This is in agreement with the results of McBain and Pitter (13) with fatty acid soaps. They found that sodium hydroxide, sodium chloride, and many other sodium salts have the same qualitative effect on soap-water systems.

No attempt has been made to supply an exact terminology for differentiating between the various solid phases of rosin soap (phases A to E, figure 1). For the fatty acid soaps, the number of solid phases is variously given as four (5) or seven (2). It is possible that the situation in rosin soap is of similar complexity. For our purposes, however, the transition to isotropic solutions appears to be the one of most importance.

The temperature of curd fiber formation in rosin soap solutions is lowered by the addition of non-ionic surface-active agents in the same way that the paste-formation temperature of neoprene latex is lowered. All of the surface-active agents listed in table 2 would lower the temperature of curd formation in solutions A or B. This effect of non-ionic soaps on the phase transitions of anionic soaps has not been reported before to our knowledge. Typical data appear in table 5.

TABLE 5

The effect of non-ionic surface-active agents on the solubility of rosin soap

Solution	A	C	D	E	F
<i>Parts by weight:</i>					
Rosin soap*	4.5	4.5	4.5	4.5	4.5
NaOH	0.5	0.5	0.5	0.5	0.5
Water	95	94.5	94	94.5	94
Nonathylene glycol monolaurate		0.5	1.0		
C-Cetylbetaine				0.5	
Emulphor O					1.0
T_i (temperature at which an isotropic solution formed on warming), °C.	20	11	5	9	2

* Dresinate X was used.

DISCUSSION

The similarity between the low-temperature phase transitions observed with Neoprene Latex Type 571 and with rosin soap solutions of approximately the same constitution as the aqueous phase in the neoprene latex offers strong evidence that the two transitions are interrelated. The points of similarity are: (1) Both transitions occur at approximately the same temperature for solutions of the same pH and rosin concentration. (2) In both cases, the transition temperature is lowered by the addition of non-ionic surface-active agents.

A possible explanation for the interrelation is that the curd fibers, when reinforced by the presence of a large number of colloid particles, as in neoprene latex, form a network of considerable solidity and greatly increase the yield point and viscosity of the colloidal system.

The high-temperature thickening of latices with high soap concentrations, reported in table 4, is very likely due to a second transition, such as F \rightarrow E (see figure 1), but no detailed study of this problem has been made.

An interesting corollary of this theory is that if the type of soap in a given latex is known, it should be possible to determine the concentration of soap by observing the temperature of the transition to the paste phase, and comparing this temperature with the transition temperatures for a series of soap solutions at the same pH. Attempts have been made to use this method to estimate soap concentrations, but the temperature of the H \rightarrow F transition (see figure 1) is much more sensitive to sodium hydroxide concentration than to soap concentration, at

least for soap concentrations over 2 per cent. As a result, it is difficult to make accurate measurements of soap concentration. Furthermore, sodium chloride or non-ionic soaps in the latex would interfere with this type of determination.

The phase transition should be accompanied by a latent heat. McBain (10) reports that heat evolution has been observed to accompany the formation of soap curds. We have not noticed any break in the time-temperature curve when warming paste latex to above the transition temperature. However, the method used was not accurate enough to pick up the small heat effect that would result from the melting of a portion of the rosin soap, where the total rosin soap concentration is only 2 per cent of the total latex weight.

CONCLUSION

The instability of neoprene latices manifested by abrupt thickening at low temperatures is not an evidence of incipient coagulation, but rather the result of phase transitions occurring in the aqueous soap solutions that form the dispersing phase.

REFERENCES

- (1) BÄCHLE: *Kautschuk* **13**, 174 (1937).
- (2) BUERGER, SMITH, RYER, AND SPIKE: *Proc. Natl. Acad. Sci. U. S.* **31**, 226 (1945).
- (3) CONOVER: *Rubber Age* **58**, 207 (1945).
- (4) DARKE, MCBAIN, AND SALMON: *Proc. Roy. Soc. (London)* **A98**, 395 (1921).
- (5) FERGUSON, ROSEVEAR, AND STILLMAN: *Ind. Eng. Chem.* **35**, 1005 (1943).
- (6) HOWLAND, PEAKER, AND HOLMBERG: *India Rubber World* **109**, 579 (1944).
- (7) JORDAN, BRASS, AND ROE: *Ind. Eng. Chem., Anal. Ed.* **9**, 182 (1937).
- (8) LIVINGSTON: *Ind. Eng. Chem.* **39**, (1947).
- (9) LUDWIG AND MEIS: German patent 727,534 (October 1, 1942).
- (10) MCBAIN: *Third Report on Colloid Chemistry*, p. 2. British Association for the Advancement of Science (1920).
- (11) MCBAIN AND BURNETT: *J. Chem. Soc.* **121**, 1320 (1922).
- (12) MCBAIN AND ELFORD: *J. Chem. Soc.* **1926**, 421.
- (13) MCBAIN AND PITZER: *J. Chem. Soc.* **1926**, 893.
- (14) MOONEY AND EWART: *Physics* **5**, 350 (1934).
- (15) WALKER: *J. Phys. Colloid Chem.* **51**, 451 (1947).

STABILITY OF SYNTHETIC RUBBER DISPERSIONS. II

COAGULATION OF NEOPRENE LATICES BY FREEZING^{1, 2}

H. W. WALKER

*Jackson Laboratory, E. I. du Pont de Nemours and Company, Wilmington, Delaware**Received October 1, 1946*

The freezing of selected polychloroprene (2-chloro-1,3-butadiene), dispersions provides a rapid and economical method for coagulating the polymer without the introduction of foreign material (1, 6). This operation is the primary step in a continuous process for the regular production of commercial types of dry neoprene, such as GR-M and GR-M 10. Although the coagulation by freezing of natural rubber latex has been known for a long time (4), it is not known to form a part of any commercial operation employing rubber latex and no study of the subject appears to have been reported. In developing the commercial process for coagulating neoprene by freezing, some of the many variations for making emulsion polymer that might influence the instability of frozen neoprene latices have been examined. Brief attempts have been made to determine the cause for the breaking of rubber latices by freezing. This paper is a preliminary report of some of the results obtained.

The plant process for isolating neoprene from polymerized emulsions consists essentially in freezing a thin film of the dispersion on the surface of a brine-cooled rotating drum partly submerged in a tank of the latex. The film is conveyed from the unfrozen latex by the rotation of the drum, remains in contact with the cold surface for complete coagulation during about one-half a revolution at 1 to 1.5 R.P.M., and is removed by a scraper held tangentially against the drum. The frozen film is thawed by warm water and the coagulum freed from soluble material by washing. That the polymer be completely coagulated to avoid loss in the wash water is important. Passage through squeeze rolls removes the excess water, and conveyance through a hot-air chamber dries the film.

APPARATUS AND PROCEDURE

A laboratory apparatus designed to reproduce the plant coagulating conditions is shown in the schematic drawing of figure 1. By means of this assembly thin frozen films from small amounts of polymer dispersions were formed under controlled conditions and could be held, prior to examination, at fixed low temperatures. A 3 x 20 cm. Monel-metal tube, A, on which the films were frozen was maintained at a constant temperature by refluxing *s*-dichlorotetrafluoroethane. The refrigerant was recycled at a reduced pressure through a

¹Contribution No. 54 from Jackson Laboratory, E. I. du Pont de Nemours and Company.

²Presented at the Symposium on the Stability of Colloidal Dispersions, which was held under the auspices of the Division of Colloid Chemistry at the 110th Meeting of the American Chemical Society, Chicago, Illinois, September, 1946.

vapor outlet, B, and an eight-coil copper condenser, C, cooled by a solid carbon dioxide-acetone bath. The vapor outlet and condenser tubing, D, were constructed of thin-walled 9.5-mm. copper tubing. Gate valves (1, 2, 3) served to shut off the system when not in use. The reduced pressure under which the refrigerant boiled was attained by attachment at L to a vacuum line, regulated by an air bleed, H, through a 2.5 x 60 mm. column of mercury, G, open to an

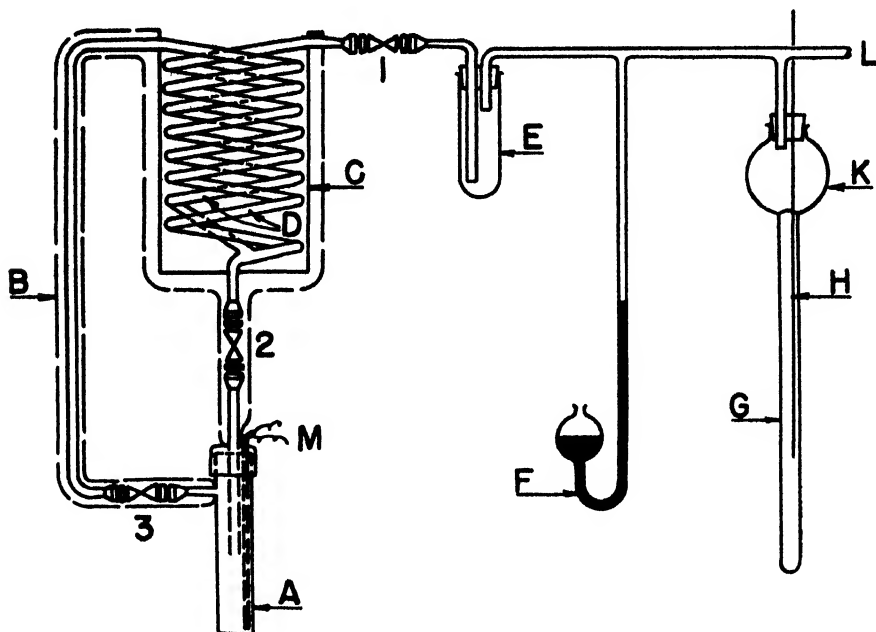


FIG. 1. Constant-temperature cooling tube and assembly for forming frozen films of latex in thin films.

TABLE 1

Temperature-vapor pressure relationship for s-dichlorotetrafluoroethane

TEMPERATURE	PRESSURE	LATENT HEAT OF EVAPORATION
°C.	mm. Hg	cal. per gram
-15	345	34.5
-20	275	
-25	215	
-30	170	35.7

expansion flask, K, of 1000-ml. capacity, and measured by a manometer, F. The reduced pressure was imposed upon the system through a second copper coil welded near the base of the condenser coil. Trap E was inserted in the vacuum line for testing the efficiency of the condensing bath.

The temperatures maintained within the freezing tube were measured by a potentiometer connected with the thermocouple, M. Representative temperatures attained and the corresponding operating pressures, together with the latent heat of evaporation, are given in table 1.

The pressure on the cooling system was adjusted to give the desired temperature, and a short time was allowed for the refrigerant to reach a steady state of reflux. Any frost that collected on the freezing tube was removed with acetone and wiped dry just before use. A frozen film of latex was formed by raising a small beaker of latex, previously cooled to 2–4°C., around the cold Monel tube. The thickness of the film deposited from a given dispersion varies with the temperature of the tube and with the time of immersion, as shown in figure 2. The

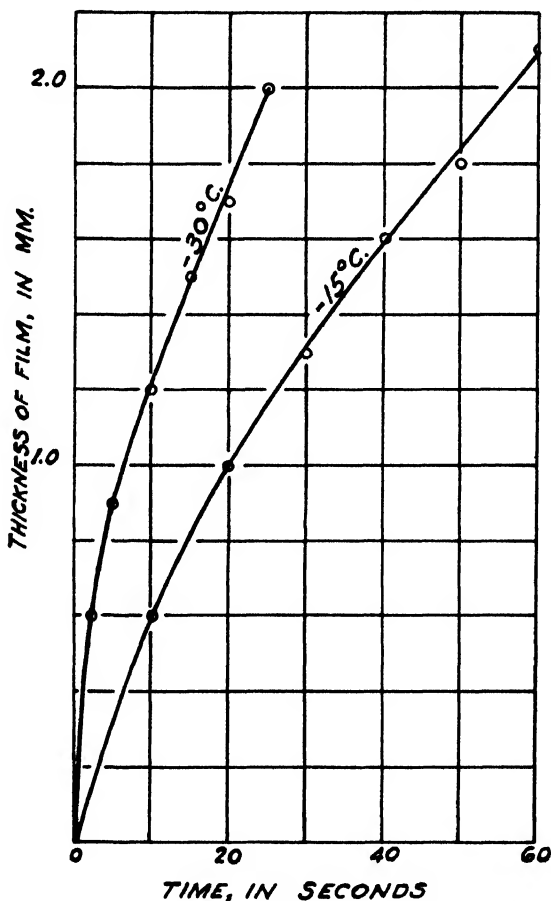


FIG. 2. Variation of film thickness with time of immersion in 20 per cent neoprene latex

relationship is not linear, owing to the decreased heat transfer through films of increasing thickness. The film thickness was measured by micrometer calipers whose contact points had been cooled to prevent local thawing of the film at the areas of contact. Thawing of the films after various time intervals was accomplished by chipping a portion of the film onto a warmed black Bakelite plate. The completeness of the coagulation was estimated by noting the amount of coagulum present and the turbidity of the serum exuded from the thawed film. In most cases clear serums were obtained with complete coagulation. In doubt-

ful instances the presence of polymer in a turbid serum could be detected by treating a drop of the serum with alcohol or sodium chloride solution.

In general, synthetic rubber latices coagulate more rapidly by freezing than does natural rubber latex, as shown in table 2. The time of immersion to form the films was 10 sec. at -15°C .

FACTORS AFFECTING COAGULATION

Studies made by this procedure and observations from other experiments described later reveal that the rate of coagulation of neoprene dispersions varies with the temperature of the frozen film and the nature of the stabilizing agent. The rate at which a quickly frozen film is thawed influences the amount of coagulation. The pH of the latex and the nature of the polymerization regulator used are factors that, in combination with certain stabilizing agents, affect the coagulation rate. Coagulation in the cases examined was independent of the

TABLE 2

*Comparison of selected latices: time for complete coagulation in 0.6-mm. films at -15°C .
20 per cent latices used*

DISPERSED PHASE	STABILIZING AGENT	TIME
		<i>min</i>
Natural rubber.... .	Natural proteins-resins-ammonia	>65
Butadiene-methyl methacrylate copolymer	Oleyl diethyl ethylenediamide hydrochloride	1-2
Neoprene	Oleyl acetate sodium sulfate	<1

concentration of the stabilizing agent, the age of the latex, the amount of monomer present, and the presence of solvents, such as benzene.

The rate of coagulation, expressed as the time for complete coagulation, in a frozen film of 0.6-mm. thickness at -15°C . formed from selected neoprene latices under varying pH conditions is shown in table 3. These dispersions were made by emulsifying 100 parts of chloroprene in 400 parts of a 1 per cent solution of the stabilizing agent containing the polymerization regulators specified and polymerizing at 25°C . to a 90 per cent or higher conversion. When sulfur was used as the polymerization regulator, it was added to the chloroprene before emulsification. The latices examined over the pH range from 2 to 10 were acidified with 10 per cent hydrochloric acid and adjusted to the neutral point and made alkaline with 10 per cent ammonia solution.

The latices stabilized with the sulfonates and sulfates exhibit a uniformly rapid coagulation rate on either the acid or the alkaline side under these freezing conditions. Latices stabilized with sodium rosinate or oleate coagulate more slowly, while the dispersions of the cetyl alcohol-ethylene oxide condensation product coagulate at a still slower rate. The effect of alkali in the cetyltrimethylammonium bromide-sulfur dioxide dispersion is reversible, i.e., a dispersion that took 600 sec. to coagulate when alkaline coagulated in 60 sec. when acidified,

but required the longer period when again made alkaline. The coagulation rate is increased by lowering the temperature. For example, at -30°C . the alkaline cetyltrimethylammonium bromide-sulfur dioxide latex coagulated in 20 sec., and the acid and alkaline latices containing the quaternary salt with thioglycolic acid-hydrogen sulfide in 60 sec. Polymerization regulators such as thiophenol, thioglycolic acid-hydrogen sulfide, sulfur dioxide, and sulfur, that have reacted with the polymer or may be present in small amounts, usually have no influence. However, cetyltrimethylammonium bromide in combination with sulfur dioxide gives a much less stable acid latex than when combined with thioglycolic acid and

TABLE 3
Effect of stabilizing agent on coagulation of neoprene latices at -15°C .
0.6-mm. films from 20 per cent latices

STABILIZING AGENT	POLYMERIZATION REGULATOR*	pH OF LATEX	TIME FOR COMPLETE COAGULATION seconds
<i>Anionic type:</i>			
Abietene sodium sulfonate	A	2-10	20
Cetyl sodium sulfate	A, B	2-10	20-40
Oleyl acetate sodium sulfate	A, B, C, D	2-10	20
Sodium oleate	D	10	200-300
Sodium rosinate	D	12	200-300
<i>Cationic type:</i>			
Cetyltrimethylammonium bromide	A	2-10	900
Cetyltrimethylammonium bromide ..	B	2	30
Cetyltrimethylammonium bromide	B	7-10	600
<i>Non-ionic type:</i>			
Cetyl alcohol-ethylene oxide condensation product	D	5	>1200

* Polymerization regulators, per cent based on chloroprene: A, 0.75 per cent thioglycolic acid + 0.06 per cent hydrogen sulfide; B, 4 per cent sulfur dioxide; C, 1 per cent thiophenol; D, 0.75 per cent sulfur.

hydrogen sulfide, owing probably to the formation of a sulfur dioxide reaction product.

Dispersions made with from 0.5 to 5.0 per cent of oleyl acetate sodium sulfate, those made with 1 per cent of this agent in which the polymerization was stopped at 53, 70, and 90 per cent conversions, respectively, and contained the residual monomer, and those to which 1 and 3 parts of a solvent, such as benzene, were added per 100 parts of polymer coagulated at -15°C . in 20 sec. The effect of benzene was examined because it is often desirable to add chemicals to the latex as emulsified benzene solutions. Aging latices stabilized with oleyl acetate sodium sulfate for six weeks had no effect on their rate of coagulation.

COAGULATION AND ICE FORMATION

A relationship between the extent of coagulation and the formation of ice crystals might be considered a factor in the transformation of a polymer in a

frozen film from a dispersed state to a coagulated condition. The breaking of oil emulsions by freezing has been ascribed to the withdrawal of water from the films between touching droplets by crystallization as ice (5). Therefore, a second method was applied for determining the stability of frozen latices that also included a calorimetric measurement of any crystallized water present. Approximately 40 g. of a latex of known composition, weighed to 0.1 g. in a 75-ml. test tube, was immersed in a constant-temperature alcohol-solid carbon dioxide bath. After being cooled and held at the bath temperature for a period, the tube with the frozen latex was transferred to a calorimeter for measurement of its heat absorption as the system attained equilibrium.

In view of the type of data desired, a very simple calorimeter was used. It consisted of a jacketed Dewar flask (a 1-qt. wide-mouth Thermos bottle), holding about 700 g. of water heated to 46–48°C. and equipped with a thermometer reading to 0.1°C. and a stirrer. The amount of crystallized water present was calculated from the heat absorbed by the fusion of the ice. This was taken as the difference between the total heat given up by the calorimeter in warming the frozen mass and the heat absorbed by the latex constituents exclusive of any ice-melting process. The heat-capacity constants for the calorimeters having been measured using water only, subsequent determinations of the amount of crystallized water present could be reproduced within ± 2 per cent.

The values obtained for the extent of the crystallization of the water are not absolute; they probably deviate as much as 5 per cent from the correct values, but are useful in determining a general relationship between coagulation and ice formation. Heat-capacity values at low temperature for neoprene and the non-polymer constituents of the latices are not available, so approximate constants for dry neoprene and smoked sheet rubber were determined with water mixtures of the shredded polymers in the calorimeters and used in the calculations. The extent of coagulation of the polymer was measured, when necessary, by diluting the thawed latex in water, collecting the coagulated polymer, and drying on a small mill.

The neoprene latices used in these determinations were prepared by emulsifying 100 parts of chloroprene in 100 parts of approximately 4 per cent aqueous solutions of the stabilizing agents and polymerizing at 40°C., except in the case of the Emulphor O emulsion which was polymerized at 20°C. The sodium rosinate latex contained residues of inorganic polymerization initiators and amine stabilizers, and the Emulphor O latex only the inorganic material. The dry solids content of the latices ranged from 46 to 50 per cent.

Typical results of the measurements are summarized in table 4. Coagulation by freezing has occurred in no case in the absence of ice formation. In two cases (experiments 10 and 6), natural rubber latex and Emulphor O stabilized neoprene latex, both of which represent relatively stable colloidal systems at moderate freezing temperatures, no coagulation was obtained at -10°C. and -12°C. , even though most of the water was crystallized. However, both of these latices were coagulated in a short time by freezing when the temperature was lowered to

$-42^{\circ}\text{C}.$ (experiments 11 and 7). In the case of a latex stabilized with Daxad-11, which remained fluid and showed no ice formation or coagulation at $-8^{\circ}\text{C}.$ under supercooled conditions (experiment 3), slight agitation at this freezing temperature induced both crystallization and coagulation (experiment 4). The coagulation followed the formation of ice. A partial crystallization of the water with a lag in the coagulation of the polymer is also shown in experiment 1 by the latex stabilized with cetyltrimethylammonium bromide cooled at $-12^{\circ}\text{C}.$ for 21 min. The coagulation and ice formation are complete in a longer freezing period (experiment 2). The rate at which ice formation takes place in the

TABLE 4
Coagulation of polymer and ice formation in latices
40 g. of latex immersed in cold bath and thawed in calorimeter

STABILIZING AGENT	COAGU- LATION	WATER CRYSTAL- LIZED	BATH TEMPER- ATURE	TIME OF IMMER- SION	REMARKS
	<i>per cent</i>	<i>per cent</i>	$^{\circ}\text{C}.$	<i>min.</i>	
<i>A. Neoprene latices:</i>					
Expt.					
1 Cetyltrimethylammonium bromide	32	65	-12	21	
2 Cetyltrimethylammonium bromide . . .	100	95	-12	30	
3 Daxad-11*	Nil	Nil	-8	37	Supercooled liquid
4 Daxad-11	37	53	-8	37 + 12	Above liquid solidified
5 Daxad-11.	100	93	-8	48	Supercooling avoided
6 Emulphor O†	Nil	94	-12	27	
7 Emulphor O	100	95	-42	90	
8 Sodium rosinate	Nil	Nil	-5	68	Firm paste
9 Sodium rosinate	100	92	-10	30	
<i>B. Natural rubber latex:</i>					
10 Natural proteins	Nil	87	-10	32	
11 Natural proteins	90	93	-42	90	

* Daxad-11 = sodium salt of naphthalenesulfonic acid-formaldehyde condensation product.

† Emulphor O = cetyl alcohol-ethylene oxide condensation product.

latices is dependent upon the temperature and the extent of agitation, and may vary with the composition of the latex. Coagulation of the polymer follows the crystallization of the water at a slower rate, depending upon the temperature at which the latex is frozen and the nature of the stabilizing agent. Once a coherent mass of polymer is formed, the particles remain in contact and appear as a coagulum on thawing.

A cross section of the chloroprene polymer coagulated by freezing in the test tube exhibits a pseudocrystalline structure resembling spherulites. Its appearance is confirming evidence that the formation of the coagulum followed the path of formation of the water crystals from the colder outer portion of the tube toward the center. In partially coagulated specimens the uncoagulated portions of

the latex were at the center of the cylinder, that portion of the mass which was the last to freeze.

RATE OF THAWING

Although latices are coagulated by freezing at temperatures such as $-10^{\circ}\text{C}.$ to $-45^{\circ}\text{C}.$, polymer remains dispersed in films of latex quickly frozen at lower temperatures. When such films are thawed rapidly the polymer is found to be largely dispersed, but it appears as a coagulum after slow thawing. This pronounced effect of the rate of thawing of films formed at $-60^{\circ}\text{C}.$ and below is illustrated by the following examples. The sodium rosinate neoprene latex containing 50 per cent solids was frozen in a film 1 mm. thick on a metal tube cooled to $-60^{\circ}\text{C}.$ After standing at this temperature for from 5 min. to 3 hr. the tube was emptied of the cooling mixture (alcohol-carbon dioxide) and plunged into water at $50^{\circ}\text{C}.$ The polymer in all cases was largely dispersed. A very thin layer of coagulated polymer remained next to the tube. When a portion of the frozen film was chipped from the cooling tube and dropped at once into heated water, complete dispersion of the polymer took place. Calorimetric measurement of a quantity of the frozen film showed ice present. In contrast to this, a similar film formed and held at $-60^{\circ}\text{C}.$ was completely coagulated when allowed to warm up slowly during a 3-min. interval. A chip from this same film was observed to disperse completely when dropped into hot water. Natural rubber latex containing 20 per cent solids behaved similarly when films quickly frozen at $-60^{\circ}\text{C}.$ were thawed rapidly and slowly. In another experiment the sodium rosinate latex was cooled to $-186^{\circ}\text{C}.$ by dropping from a pipet into liquid nitrogen to form pellets 2 mm. in diameter. After standing in the liquid nitrogen for 2.5 hr. and being placed in hot water, the pellets were only partially coagulated, but they were found to be completely coagulated when thawed in cool water. The neoprene latex frozen in the $-60^{\circ}\text{C}.$ bath in a test tube or as a shallow layer inside the metal tube was entirely coagulated when thawed in hot water.

It would appear that at extremely low temperatures the dispersed polymer in a thin film of latex assumes a fixed metastable condition before coalescence can occur.

DISCUSSION

The coagulation rate is slow relative to the rate of formation of a hard brittle latex film in which the mobility of the polymer particles is greatly limited. On rapid thawing, the polymer is released and redisperses before it can coagulate. On slow thawing, the increased mobility of the particles in a temperature range below the melting point causes an irreversible coagulation. Thick films or masses of latex enclosed in a glass or metal container are coagulated on cooling in a $-60^{\circ}\text{C}.$ bath because the low heat transfer through these specimens allows time for coagulation to take place before the latex is thoroughly cooled and converted to a brittle solid.

The disruption of aqueous dispersions by freezing with an accompanying crystallization of the water has been observed before. Rochow and Mason (6) conclude that the breaking of oil emulsions by freezing may be ascribed to the following causes, in sequence:

1. Withdrawal of water by crystallization as ice.
2. Establishment of contact between adjacent films of emulsifier, with loss of the orienting influence of water.
3. Diffusion of the emulsifier in the film away from these thick regions.
4. Decrease in film area and coalescence of droplets as soon as thawing of the ice permits them to change shape.

Doan and Baldwin (3) state that in the destruction of fat emulsion brought about by the unagitated freezing of cream, the pressure developed by the congealing water is the causative factor of most importance. Additions of sugar to cream limit the amount of pressure developed in freezing, owing to the smaller size of ice crystals. de Vries and Beumde-Nieuwland (2) noted that natural rubber latex is slow to coagulate at -15°C . and described the inner structure of the frozen mass as white threads with ice crystals between. When the ice melts, the threads of rubber bind together to form a coherent coagulum from which clear serum is exuded.

The coagulation of the polymer by slow thawing in the experiments at -60°C . seems to preclude the possibility that by quick low-temperature freezing the formation of smaller ice crystals prevents coagulation with rapid thawing. If this were the case, that part of the frozen film in contact with the freezing tube should contain water crystals still smaller in size than those on the outer portion and be the source of the redispersing polymer in a rapid thawing process. Furthermore, if the smaller crystals existed they would persist during the short period at the slow thawing rate until the melting point was reached, and complete redispersion rather than complete coagulation should be observed.

An explanation of the coagulation by freezing of neoprene and other rubber latices should consider such factors as the formation of ice in the frozen latex, the influence of the stabilizing agent on the rate of coalescence of the polymer particles, and the relationship between the rate of coalescence and the freedom of movement of the particles at low temperatures. A tentative, simplified explanation is that, on freezing, a large portion of the water content of a latex forms ice and causes a high local concentration of the polymer in the amorphous network surrounding the water crystals. Coagulation occurs if the stabilizing agent is incapable of preventing a coalescence of the polymer particles under these conditions. Different rates of coagulation at fixed moderate freezing temperatures arise from differences in the stabilizing action of the specific agent with which a latex is stabilized. Temperature is a contributing factor in a given latex; the decreased mobility and kinetic energy of the polymer in the solidified amorphous soap-water phase, as the temperature is lowered, tend to increase the attractive forces between the particles. However, at extremely low temperatures the individual polymer particles may assume a fixed configuration in a hard brittle film before they can coalesce and thus remain dispersed in a well-frozen condition.

SUMMARY

1. An apparatus and method are described for measuring the stability of frozen latices in thin films.
2. The influence of some of the variations in making emulsion polychloroprene on the coagulation by freezing have been examined.
3. The rate of coagulation by freezing of rubber latices varies principally with the temperature and the nature of the latex-stabilizing agent.
4. Polymer remains dispersed in films quickly frozen at extremely low temperatures.
5. The rate of thawing of films formed from latices by quick freezing at very low temperatures has a pronounced effect on the coagulation of the polymer.
6. A tentative explanation of the coagulation of latices by freezing is presented.

The author wishes to express his appreciation to A. F. Benning for suggesting the design of the constant-temperature cooling tube and for supplying the refrigerant.

REFERENCES

- (1) CALCOTT, W. S., AND STARKWEATHER, H. W.: U. S. patent 2,187,146 (January 16, 1940).
- (2) DE VRIES, O., AND BEUMÉE-NIEUWLAND, N.: *Arch. Rubbercultuur* **12**, 675-82 (1928); *Chem. Abstracts* **23**, 1771.
- (3) DOAN, F. J., AND BALDWIN, F. BRUCE, JR.: *J. Dairy Sci.* **19**, 225 (1936); *Chem. Abstracts* **30**, 4227.
- (4) EATON, B. J., AND GRANTHAM, J.: *J. Soc. Chem. Ind.* **35**, 722 (1916).
- (5) ROCHOW, T. G., AND MASON, C. W.: *Ind. Eng. Chem.* **28**, 1296 (1936).
- (6) STARKWEATHER, H. W., AND YOUKER, M. A.: *Ind. Eng. Chem.* **31**, 934 (1939).

A SPECTROTURBIDIMETRIC STUDY OF THE PROTEINS OF MILK¹

ABRAHAM LEVITON AND HARRISON S. HALLER

*Division of Dairy Research Laboratories, Bureau of Dairy Industry,
U. S. Department of Agriculture, Washington, D. C.*

Received September 17, 1946

Light in its passage through a suspension of dielectric spheres suffers an attenuation in intensity due to scattering. Theoretical formulae governing this phenomenon have been worked out from different points of view by Rayleigh (8), Mie (4), Einstein (3), Smoluchowski (9), Debye (2), and others.

We have used as the basis of our work the theoretical treatment due to Mie, inasmuch as the general theory as worked out by him appeared to be the one most intimately concerned with the particular problem of this report.

¹ Presented before the Division of Colloid Chemistry at the 110th Meeting of the American Chemical Society, Chicago, Illinois, September, 1946.

Milk is a complex colloidal system. It is not only a polydisperse, but also a multicomponent system. Its chief colloidal constituent is lipid in character and constitutes approximately 30 per cent by weight of the solids of milk. The greater part of this constituent is easily separated from whole milk, and there remains as a result of such separation skim milk, which, if the separation is carried out in a high-speed cream separator, contains approximately 0.05 per cent of lipid substances soluble in ether.

The predominant colloid in skim milk is a calcium caseinate-phosphate complex. Ramsdell and Whittier (7) found that the complex centrifuged out of skim milk by means of a Sharples supercentrifuge contained 95.2 per cent of calcium caseinate, of which 94 per cent was casein. Svedberg and Fåhræus (11), in a report based on preliminary ultracentrifugal studies, concluded that the radii of particles of skim milk have an order of magnitude of 10–70 $m\mu$ (millimicrons). Nichols *et al.* (5) showed that the majority of the particles were less than 100 $m\mu$ in radius, and that they ranged in size from molecular dimensions to a radius of 100 $m\mu$. A mean radius of about 45 $m\mu$ was obtained. During the course of the experiment, about 15 per cent of the suspended material, based on light-absorption measurements, was removed from the field of observation. The particles in this group were thought to consist of fat, leucocytes, calcium phosphate, and large aggregates of calcium caseinate.

From the standpoint of turbidimetric analysis, the colloidal system skim milk is complicated, but not too complicated to discourage an attempt at analysis. If the particles for which Nichols obtained a distribution curve are assumed to be dielectric spheres, each with the same refractive index, and if, furthermore, the actual distribution curve representing the true relation of weight of material to radius rather than the weight optical relation is also characterized by a single maximum, then application of the Mie theory of light scattering to light-absorption data over the range 360 to 1000 $m\mu$ should yield information relating not only to the value of the weight-mean molecular weight, but possibly also to a distribution curve. A complicating factor, of course, is the contribution to scattering of the coarser particles of skim milk comprised in the fraction responsible for 15 per cent of the light absorption in the experiments of Nichols. A reasonable assumption regarding the particles of this fraction is that the attenuation coefficient, except for the occurrence periodically of rather flat maxima, is independent of wave length. This assumption is based on the Mie theory as it applies to large transparent dielectric spheres and to relatively smaller particles, the refractive indices of which are quite large compared with water.

EXPERIMENTAL

Measurements of light absorption were made with a Beckman spectrophotometer. Cells the windows of which were 1 cm. apart were used. The photocells were fixed by means of a spacer at approximately 20 cm. from the absorption cells, and the scattered light striking the sensitive element was further restricted by the introduction of a circular aperture $3/32$ in. in diameter in front of the

shutter of the photocell block. The influence of secondary radiation is quite marked and may contribute as much as 179 per cent to the intensity of the transmitted light when the absorption cells are placed in juxtaposition with the photocell block and no aperture is used. Suspensions were prepared from fresh separator-prepared skim milk by dilution with water. In the experiments the particles comprising the suspended phase were precipitated at -17°C . by the addition of 90 parts by volume of methanol to 10 parts of skim milk, and suspensions were prepared by addition of cold water to the wet precipitate. Removal of methanol was accomplished by distillation under high vacuum at temperatures significantly below room temperature. Evaporation was carried to the point at which the sample began to freeze.

In some experiments no attempt was made to remove the alcohol, and all solutions under study were adjusted to the same methanol concentration.

Refractive-index measurements were made on solutions of the reconstituted proteins freed of methanol, and a correction was made for the contribution to the refractive index of occluded solids. An Abbé refractometer was employed, and measurements were made in a room the temperature of which was thermostatically controlled at 20.0°C . The partial specific volume was determined from the change of density with concentration at 20°C .

Preliminary experiments with skim milk showed that following dilution a holding period of 3 hr. at the temperature of measurement was necessary before the turbidity ceased to diminish and reached a constant value. These experiments also indicated that in the presence of methanol, there was a gradual but slow increase in turbidity with age, and for suspensions containing methanol it was necessary to apply small corrections to the measured turbidity values.

Solids were determined by drying to a constant weight in a vacuum oven.

RESULTS

The experimental results are presented in the various figures. Figure 1 presents a compilation of formulae due to Mie. For spherical particles the optical density is a function basically of four variables: the wave length of incident light *in vacuo*, the refractive index of the solvent, the refractive index of the particle, and the radius of the particle. The attenuation function may be written in a number of ways, and that part of formula I outside of the summation sign may be written as a function of any integral power of the wave length merely by multiplication of the coefficients contained in the summation by some power of α . Inasmuch as the attenuation due to scattering by the protein complex of milk appeared to follow an inverse fourth power law with respect to wave length, the form adopted for purposes of discussion contains the reciprocal of the fourth power of the wave length outside of the summation sign. C is the concentration of scattering units of the same kind and M is their molecular or particle weight. The original formula contains the concentration expressed in terms of relative volume, and the particle size in terms of volume. In converting to weight units one introduces the square of the partial specific volume, and in assuming that the number of particles is given by the weight of

the particles divided by the molecular weight, one introduces the molecular weight and Avogadro's number. The coefficients included in the summation are numbers and are evaluated by substitution of values for m and α in equations derived by Mie. m is the ratio between the refractive index of the particle and that of water; for purposes of simplification it is assumed that the ratio is independent of wave length. The refractive index of the particle is calculated on the basis that the refractive index of the suspension under study is equal

$$2.303K = \frac{24\pi^4 m_0^4}{\lambda^4 N_0} MC\phi^2 \sum_1^\infty \nu \frac{|a_\nu|^2 + |p_\nu|^2}{2\nu + 1}$$

$$|a_\nu| = \frac{|A_\nu|}{2\alpha^3}; \quad p_\nu = \frac{|P_\nu|}{2\alpha^3}$$

$$\alpha = \frac{2\pi m_0 r}{\lambda}$$

$$2.303K = \frac{24\pi^3 m_0}{\lambda^4 N_0} MC\phi^2 \left(\frac{m^2 - 1}{m^2 + 2} \right)^2$$

$$m_0 = 1.333; \quad m = \frac{1.56}{1.333} = 1.17; \quad \phi = 0.7235$$

$$K = \frac{4\pi\alpha^2 m_0}{2.303\lambda} \phi C (|a_1|^2 + |p_1|^2 + \frac{2}{3} |a_2|^2)$$

$$M = \frac{9.42 \times 10^{22}}{C} \frac{d \log \frac{I_0}{I}}{d \frac{1}{\lambda^4}}$$

Fig. 1 Compilation of formulac due to Mie

to the product of the refractive index and the partial volume of water, plus the product of the refractive index and the partial volume of the suspended phase.

Thus

$$m_{\text{solution}} = m_{\text{particle}} \times \phi \times w + m_{\text{water}} (1 - \phi \times w)$$

where ϕ and w = respectively, the partial specific volume, and the concentration of the suspended phase in grams per milliliter.

The value for the refractive index of the suspended phase obtained by this procedure rounded off to two decimal places is 1.56, and the value for m , the relative index, is 1.17. In connection with the value 1.56, it was found that fragments of the glassy solid obtained by drying the alcohol-precipitated and washed solids of skim milk possessed a refractive index of 1.55. The value for casein given in the literature is 1.55. Allowing for a contraction of about 5 per cent, such as casein undergoes when it is dissolved, the value 1.56 calculated for the refractive index of the suspended phase in solution is in agreement with that measured in air.

The general formula proposed by Mie reduces to that (see the fourth formula in figure 1) first given by Rayleigh for very small values of α , that is, when the ratio between the radius of the particles and the wave length of light used approaches zero. Under these conditions the value of the coefficients A_n , for which n is greater than 1 approaches zero, and the values of all coefficients P_n , approach zero. $|A_1|$ approaches the value $2\alpha^3 \frac{m^2 - 1}{m^2 + 2}$, and the equation then takes the form that is commonly used. If all particles of a suspension scatter according to this limiting law, then the plot of the optical density against the reciprocal of the fourth power of the wave length should yield a straight line passing through the origin when extrapolated. The slope of this line under

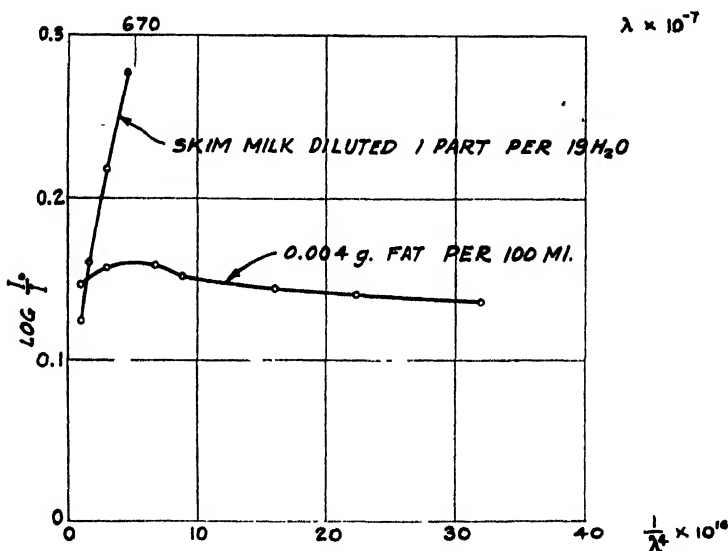


Fig. 2. Turbidity curves for skim milk and diluted cream

these circumstances is proportional to the product of the molecular weight and the concentration.

In figure 2 optical density is plotted against the reciprocal of the fourth power of the wave length for diluted skim milk and diluted 40 per cent cream. The cream sample was prepared by the dilution of freshly prepared 40 per cent cream to 1 per cent, and the homogenization three times at 40°C. of the 1 per cent emulsion. The emulsion was then reduced in concentration by dilution to contain 0.004 g. fat per 100 ml. In the plots the ordinates are exaggerated in order to bring out the maximum at 670 mμ in the curve representing the turbidity of the cream sample. This maximum probably corresponds to the transmission minimum at approximately 420 mμ observed by Stratton and Houghton (10) for a fog composed of particles $2.5 \pm 0.5 \mu$ in diameter. Theoretically, the maximum probably corresponds to the maximum at $\alpha = 15$ in the theoretical absorption curve for fogs. It is readily seen that, in agreement with theory,

the curve for the relatively coarse lipid particles is easily distinguishable from that representing the protein complex of milk. It is characterized by a rather flat maximum and for practical purposes the attenuation by the lipid particles of milk may be considered to be independent of wave length. In qualitative agreement with theory, the attenuation due to the protein complex of milk appears to vary or rather to approach a condition at the longer wave length in which it varies as the inverse fourth power of the wave length. As the wave length decreases, the rate of change of turbidity diminishes, and this phenomenon too is in qualitative agreement with theory.

Figure 2' contains three curves, one representing the attenuation due to the suspended particles of diluted skim milk, another that due to the suspended particles of dilute homogenized cream, and the third the attenuation due to the particles of a composite sample of dilute skim milk and cream. The points cover a range of wave lengths extending from 840 to 1000 $m\mu$. Over this range,

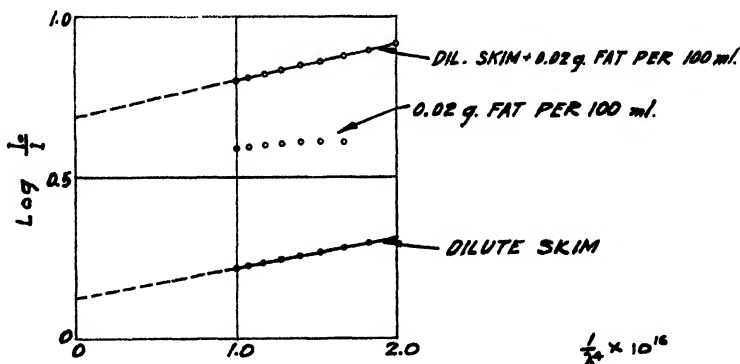


FIG. 2'. Influence of fat globules on turbidity

the optical density of the two dilute skim milk samples varies as the inverse fourth power of the wave length. The lines extrapolated to the ordinate axis cut the axis at two points. The difference between the optical densities corresponding to these points should be equal to the extrapolated value of the optical density of the dilute cream sample. The actual difference in optical density is 0.56. The extrapolated optical density of the cream sample is 0.56. Here, as in the preceding figure, the curve representing the optical density of the cream sample is approximately parallel to the $1/\lambda^4$ axis.

The extrapolated value for the optical density of the dilute skim milk sample is 0.125. The ratio between this value and the extrapolated optical density of the cream sample multiplied by the lipid concentration of the cream sample is equal to 0.004 g. of fat per 100 ml. Multiplying by 12.5, the dilution factor for the skim milk, one obtains a value of 0.05 g. of fat per 100 ml. of skim milk. This is in excellent agreement with the value obtained for the fat concentration in skim milk.

It is seen at once that the application of the spectroturbidimetric method provides a result of practical significance in that a simple means for the measure-

ment of fat concentration in milk and derived products becomes available. Such application to the skim milk sample of figure 2 is predicated on two assumptions: One assumption is that the particle-size distribution in the lipid phase of skim milk parallels the distribution in homogenized dilute cream. This is borne out by the experimental results and also by microscopic observation of the particles in the two samples. The other assumption is that in the range of wave lengths under observation only the lipid phase contributes particles of the wave length. This assumption is also borne out by the results.

It is interesting to speculate on the significance of the maximum in the curve for the dilute cream sample. The location of this maximum with precision in

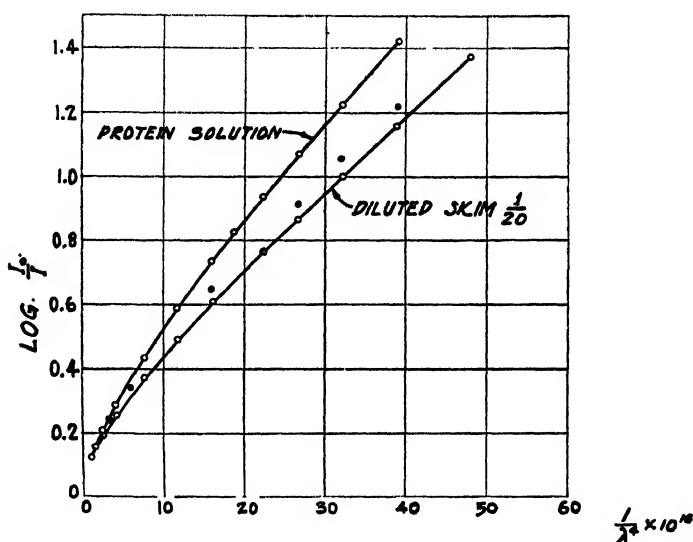


FIG. 3. Turbidity of reconstituted protein suspension and skim milk

analyses of milk and cream should, when the Mie coefficients are elaborated for the fat phase, afford a simple means for the evaluation of some sort of an average value for the radius of the fat particles, and possibly also the establishment of a distribution curve.

In figure 3 is shown a plot of the optical density against the inverse fourth power of the wave length for two samples, one for diluted skim milk and the other for a reconstituted suspension containing the alcohol-precipitated proteins of skim milk. The protein suspension was reconstituted to have the same turbidity at 1000 m μ as the dilute skim milk sample. Analysis for total solids indicated that the optical density values for the skim milk sample required a correction in order to facilitate comparison. The corrected values are given by the black circles. These points and those on the turbidity curve for the protein suspension refer then to the same concentration of alcohol-precipitable solids. In the range of longer wave lengths the curves approach one another. As the wave length decreases there is an increasing divergence. If the convergence at long

wave lengths may be taken to indicate that the weight-mean molecular weights of the two suspensions are equal, then the greater rate of change in the slope of the curve for skim milk may be taken to indicate greater non-uniformity in particle size. This condition would be met if alcohol precipitation resulted in the formation of agglomerates of relatively large and relatively small particles which upon dissolution in water yielded particles intermediate in size. This is not an unreasonable hypothesis.

One cannot but be impressed by the linear character of segments of both curves. In the skim milk curve, for example, over a range of values of $1/\lambda^4$ from 15×10^{16} to 50×10^{16} , corresponding, respectively, to wave lengths of 510 and 370 $m\mu$, respectively, the curve connecting the various points is a straight line.

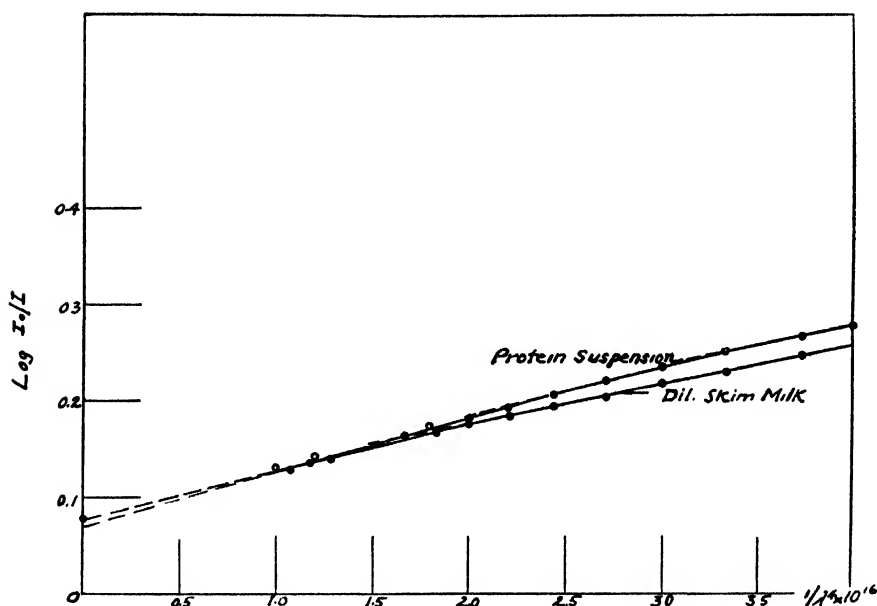


FIG. 4. Turbidity curves for reconstituted protein solution and skim milk

Figure 4 presents a close-up view of both curves in the range of wave lengths extending from 700 to 1000 $m\mu$. The open circles represent the corrected values for the optical density of the skim milk sample, and these points fall on the curve for the reconstituted protein suspension. The extrapolated optical density value is approximately 0.075, and this corresponds to a fat concentration of 0.05 per cent in the skim milk from which both samples were derived. The identity of this value for both samples shows that in alcohol precipitation the fat phase is precipitated along with the proteins.

Both curves consist of straight-line segments. The first change in slope occurs at approximately 800 $m\mu$ in both curves. In the curve belonging to the protein suspension an additional break is observable at 740 $m\mu$. There is a strong temptation to associate the sharpness of the break with the levelling off of optical

density values in the curve of figure 2, representing the change of optical density with wave length due to the lipid phase.

The value of this slope is related to an average value of the particle weight which may appropriately be designated, for reasons which will appear later, as an optical weight-mean particle weight. If the scattering coefficients for all of the particles comprising a distribution are equal to $\left(\frac{m^2 - 1}{m^2 + 2}\right)^2$, then the attenuation in intensity follows the Rayleigh equation and the optical weight-mean particle weight becomes equal to the weight-mean particle or molecular

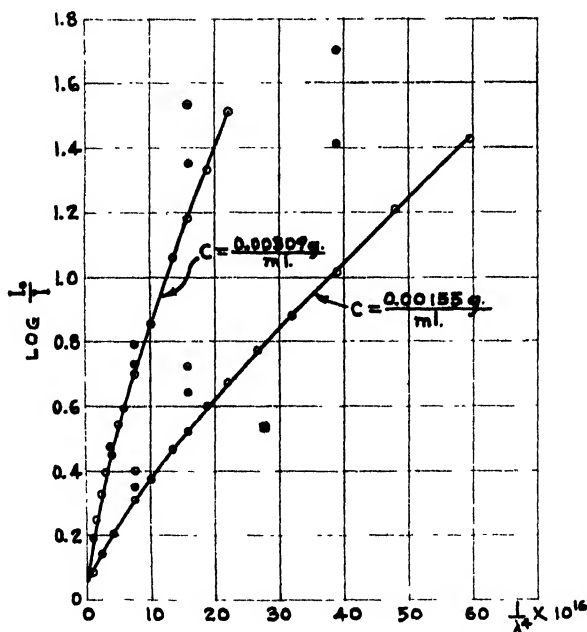


Fig. 5. Turbidity of milk proteins in 5 per cent methanol

weight. If this assumption is made, a value of 2.15×10^8 is obtained as the mean molecular weight of the particles comprising the alcohol-precipitated solids. This corresponds to a radius of $40 \text{ m}\mu$, and is not an unreasonable value. Recently Oster (6) has published values obtained by similar measurements on solutions of tobacco mosaic virus. For one sample a value for the diameter of $100 \text{ m}\mu$ was obtained, in good agreement with the results of electron microscope and ultracentrifugation studies. One is also struck by the fact that the break in his curve occurs at about $800 \text{ m}\mu$, corresponding to the wave length at which the break occurs in the curve for the particles in skim milk.

Figure 5 contains the plot of two curves. These represent the turbidities of solutions prepared from the alcohol-precipitated solids of skim milk. No attempt was made in the preparation of the solutions to remove occluded alcohol, and instead the solutions were adjusted to the same methanol concentration,

5 per cent. The mean molecular weight of the particles in suspension containing 0.00319 g. per ml. of precipitated solids calculated from the slope of the curve in the near infrared is 2.92×10^5 . The mean molecular weight in the suspension diluted to contain 0.00155 g. per ml. of precipitated solids is 2.68×10^5 . The decrease of mean molecular weight with dilution, a decrease which is even more marked when skim milk itself is diluted, is probably due to disaggregation or dissociation effects which take place upon dilution. The curves appear to consist of straight-line segments, and for this reason analysis is made more difficult. In the figure, the half-shaded circles represent points corresponding to turbidity values calculated on the assumption that the suspension is a monodisperse one, the particles of which possess a molecular weight equal to the mean molecular weight. It is also assumed that the Rayleigh equation is applicable over the entire spectral range. The fully shaded circles represent points corresponding to turbidity values calculated according to the complete theory of Mie. It is at once evident that the suspensions under consideration are polydisperse. It also appears that, in order to correct for the marked deviation in the short-wave-length region of the theoretical curve for a monodisperse suspension from the experimental curve, the distribution curve must be one in which the non-uniformity coefficient is high, that is, the maximum value of the rate of change of molecular weight with concentration should correspond to a weight less than the weight-mean molecular weight, and the maximum should be approached sharply from the region of relatively small particle sizes, and gradually from the region of relatively large sizes. Although it is possible to compare theoretical absorption curves derived from a variety of distribution curves with the experimental curve, no such attempt was made. It was thought desirable first to obtain more data based on fractions of various sized particles obtained by alcohol precipitation. Preliminary experiments have indicated the possibility of separating the relatively coarse particles of skim milk to leave a residue for which the attenuation curve is linear from 500 to 1000 $m\mu$.

It was also considered doubtful that analyses could be carried out unambiguously by neglect of particles larger in radius than 100 $m\mu$. The data obtained by Nichols *et al.* point to the existence of a single maximum in the distribution curve in the range of particle sizes up to a radius of 100 $m\mu$. If the particles comprising this distribution could be separated as a group, it should be decidedly advantageous to establish a distribution curve. However, in view of the fact reported by Nichols *et al.* that a not insignificant proportion of the suspended material had left the field of observation in their experiments, and mindful of the significance in attenuation measurements of these relatively large particles, it was considered discretionary not to stretch the interpretation of our data.

Figure 6 shows that part of the curves of figure 5 which was used in the calculation of mean molecular weights. Here, as in other curves already discussed, one is struck by the linearity of the relation between optical density and the inverse fourth power of the wave length, and the abrupt change in slope at $\lambda = 800 m\mu$.

Again, a value of 0.05 per cent is obtained for the concentration of lipid substances in the skim milk from which the suspended material was derived.

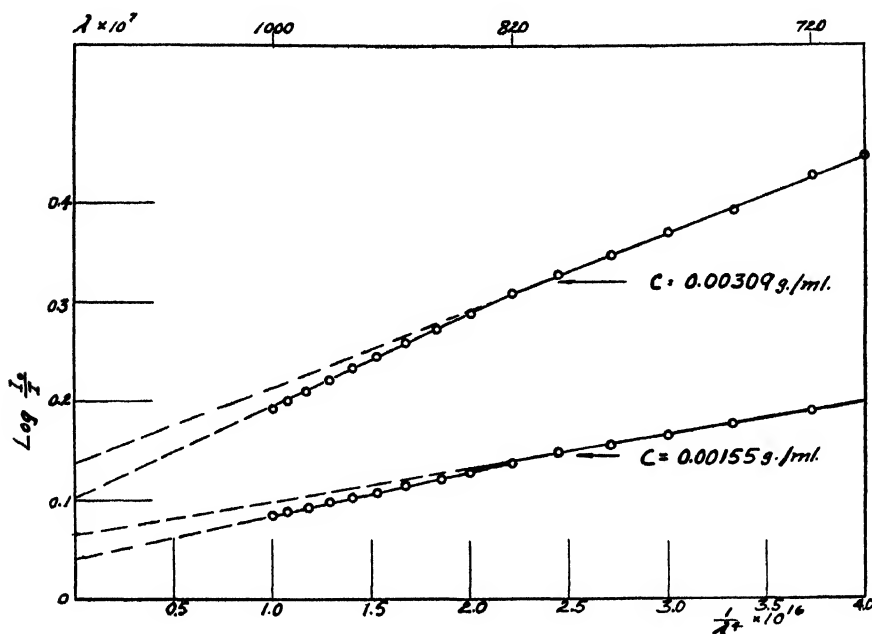


FIG. 6. Turbidity of milk proteins in 5 per cent methanol

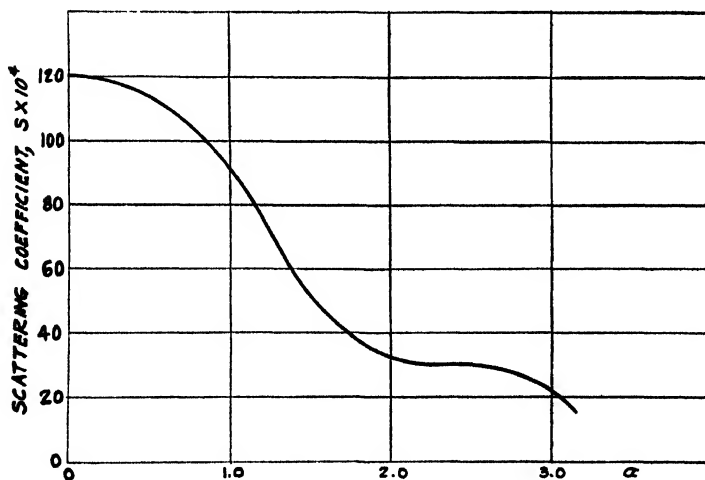


FIG. 7. Scattering coefficients for $\alpha = 0$ to $\alpha = 3.0$

The theoretical coefficients designated in this report as scattering coefficients are plotted in figure 7 against $2\pi \frac{m_0 r}{\lambda} = \alpha$. These coefficients have been evaluated over a range of values of α extending from $\alpha = 0$ to $\alpha = 3$ for spherical

particles of refractive index 1.56. The calculations were carried to seven decimal places. For values of α greater than 1, excellent agreement was found between the calculated values given in this report and those given by Casperson (1). Casperson's table shows a maximum whose value is 1.50×10^{-2} at $\alpha = 0.50$. This does not conform to our calculations. A number of maxima have been obtained between $\alpha = 0$ and $\alpha = 0.5$ with the use of the unexpanded periodic functions given by Mie in conjunction with fifth-place sine and cosine tables. However, if the expanded forms of these functions are used and if the calculations are carried to seven decimal places, a smooth curve is obtained. The general formulae for the calculation of the scattering coefficients are:

$$S = \sum_2^{\infty} \nu \frac{|a_\nu|^2 + |p_\nu|^2}{2\nu + 1}$$

$$|a_\nu| = \frac{|A_\nu|}{2\alpha^3}; \quad |p_\nu| = \frac{|P_\nu|}{2\alpha^3}$$

$$A_\nu = (2\nu + 1)i^\nu \frac{D'_\nu B_\nu \beta + D_\nu B'_\nu \alpha}{C'_\nu B_\nu \beta + C_\nu B'_\nu \alpha}$$

$$P_\nu = -(2\nu + 1)i^\nu \frac{D_\nu B'_\nu \beta + D'_\nu B_\nu \alpha}{C_\nu B'_\nu \beta + C'_\nu B_\nu \alpha}$$

$$\alpha = \frac{2\pi m_0 r}{\lambda}; \quad \beta = m\alpha$$

For $m = 1.17$ and for values of α extending from $\alpha = 0$ to $\alpha = 3$, coefficients A_ν , and P_ν , corresponding to values of ν greater than 2 and 1, respectively, may be neglected. D_ν is a periodic function of α , and D'_ν is its derivative. B_ν and B'_ν are corresponding functions of β . C_ν is a function of α yielding for all values of ν and α complex numbers, and C'_ν is its derivative.

Examination of the scattering curve indicates that not only in the vicinity of $\alpha = 0$, but also in the vicinity of the range $\alpha = 2.0$ to $\alpha = 2.8$, is the attenuation proportional to the inverse fourth power of the wave length. What is characteristic of attenuation due to Rayleigh scattering is not so much the proportionality to the inverse fourth power of the wave length of the attenuation coefficient, but rather the value of the scattering coefficient which for Rayleigh scattering is equal to $\left(\frac{m^2 - 1}{m^2 + 2}\right)^2$. For scattering in the vicinity $\alpha = 2$ to $\alpha = 2.8$, the attenuation is also proportional to the inverse fourth power of the wave length, but the value of the scattering coefficient is equal to $0.25\left(\frac{m^2 - 1}{m^2 + 2}\right)^2$. Thus, for particles $240 \text{ m}\mu$ in radius, a linear relation should be found to hold in the wave-length range 1000 to $715 \text{ m}\mu$. At $715 \text{ m}\mu$ a levelling off in the curve should occur, and the attenuation coefficient should approach a nearly constant value showing fluctuations about a mean. The existence of such a relation may serve to explain the discontinuities in the attenuation curve for the particles of skim milk. If the particles of skim milk contained, in addition to those

distributed between $r = 0$ and $r = 100 \text{ m}\mu$, a group distributed in the vicinity of $r = 300 \text{ m}\mu$, then as the wave length was decreased, a linear relation would be observed up to the point at which α became equal to 2.8 for the largest particles. Here, as the attenuation due to the large particles became nearly independent of wave length, a change in slope would occur in a manner conforming to our experimental data. Thus the existence of a linear relation is not in itself justification for the calculation of a weight-mean molecular weight. What is justified is the calculation of a relation

$$\frac{\sum M_i^2 n_i S_i}{\sum M_i n_i}$$

where M_i , n_i , and S_i refer to the molecular weight, the number, and the scattering coefficient of particles of species i . Here S_i is independent of wave length, and the value of the summation calculated from the slope of the line may be designated as an optical weight-mean molecular weight. Only if certainty exists that the value of the scattering coefficients for all particles under consideration approximates $\frac{(m^2 - 1)^2}{(m^2 + 2)^2}$ is the value obtained from the slope of the line equal to the weight-mean molecular weight.

In connection with the shape of the transmission curve for fog particles of more than one size, Stratton and Houghton observed that, contrary to a decrease in transmission with an increase in wave length as anticipated by the theoretical transmission for a single particle, no change in transmission was observed. This they attributed to the fact that fog particles of more than one radius contributed to the attenuation. It may be that the points of transition in the slope of the curves obtained in our study are due to groups of particles each group of which contains particles of more than one size. As a possible explanation of our results this requires further study.

SUMMARY

Spectroturbidimetric studies have been made of diluted skim milk, homogenized diluted cream, and suspensions of the alcohol-precipitated solids of skim milk. What appears to be a curve the slope of which diminishes as the inverse fourth power of the wave length increases, upon closer examination plots best as a series of line segments. Extrapolation of the segment corresponding to the range of wave lengths $\lambda = 800$ to $\lambda = 1000$ to the optical density axis yields a value for optical density which coincides with the optical density of the lipid material of the sample. The possible application of spectroturbidimetric methods to the determination of fat in milk is discussed.

The attenuation curve for homogenized dilute cream is characterized by a maximum at $670 \text{ m}\mu$. It is easily distinguished from the curve for the non-lipid solids of skim milk and, in agreement with the general theory of Mie, the attenuation coefficient is very nearly independent of wave length. It is suggested that the determination of the magnitude of optical density and the position of the maximum should furnish information concerning particle size, and particle-size distribution, once the Mie coefficients are evaluated.

The linearity in the near infrared curve showing the relation between the attenuation coefficient and the inverse fourth power of the wave length permits the calculation of an average value for the "molecular" weight of the particles of skim milk. This average value is designated as an optical weight-mean molecular weight, and its value for skim milk diluted to 1/20 its original solids concentration is 2.2×10^8 . This value corresponds to a radius of 40 m μ . A mean radius of 40–50 m μ was obtained by Nichols *et al.* for the calcium caseinate complex in skim milk on the basis of ultracentrifugal studies.

■ Alcohol precipitation of the suspended material of milk at -17°C . results in the formation of a precipitate which when dispersed in water yields a stable suspension. This suspension contains the fat phase of skim milk. The optical weight-mean molecular weight of the particles of this suspension is equal to 2.2×10^8 , the value obtained for the particles of skim milk. Although the attenuation curves coincide in the far red and in the near infrared end of the spectrum, the curve for the suspension of alcohol-precipitated solids diverges from that for skim milk. This is taken to indicate greater uniformity in particle size in the suspension of alcohol-precipitated solids.

A method for obtaining fractions the particles of which vary in size is briefly referred to. Preliminary experiments indicate that the attenuation curve for a residual fraction from which the coarse particles had been eliminated was linear from 500 to 1000 m μ .

The abrupt change in slope at various points in the attenuation curve as a result of which the curve appears to consist of line segments is explained on the basis of the possible presence of particles in the size range 200 to 300 m μ radius.

Scattering coefficients for particles of refractive index 1.56 are given for values of α extending from $\alpha = 0$ to $\alpha = 3$. It is shown that not only in the vicinity of $\alpha = 0$ but also in the vicinity of $\alpha = 2.5$, the values of the scattering coefficients are independent of the value of α . Rayleigh scattering is characterized by a constant value of the scattering coefficient of $\left(\frac{m^2 - 1}{m^2 + 2}\right)^2$.

In the vicinity of $\alpha = 2.5$, the scattering coefficient is $0.25 \left(\frac{m^2 - 1}{m^2 + 2}\right)^2$. The shapes of the experimental curves are discussed in terms of the theoretical scattering coefficients.

REFERENCES

- (1) CASPERSON, T.: *Kolloid-Z.* **60**, 151 (1932).
- (2) DEBYE, P.: *Ann. Physik* **30**, 57 (1909).
- (3) EINSTEIN, A.: *Ann. Physik* **33**, 1275 (1910).
- (4) MIE, G.: *Ann. Physik* **25**, 377 (1908).
- (5) NICHOLS, J. B., BAILEY, E. D., HOLM, G. E., GREENBANK, G. R., AND DEYSHER, E. F.: *J. Phys. Chem.* **35**, 1303 (1931).
- (6) OSTER, G.: *Science* **103**, 306 (1946).
- (7) RAMSDELL, G. A., AND WHITTIER, E. O.: *J. Biol. Chem.* **154**, 413 (1944).
- (8) RAYLEIGH, LORD (J. W. STRUTT): *Phil. Mag.* **47**, 377 (1899).
- (9) SMOLUCHOWSKI, M. V.: *Ann. Physik* **25**, 205 (1908).
- (10) STRATTON, J. A., AND HOUGHTON, H. G.: *Phys. Rev.* **38**, 159 (1931).
- (11) SVEDBERG, T.: *Kolloid-Z.* **51**, 10 (1930).

NOTES ON DYNAMIC OSMOMETRY

K. B. GOLDBLUM

*Plastics Laboratory, General Electric Company, Pittsfield, Massachusetts**Received August 26, 1948*

During considerable work on the determination of molecular weights by the dynamic osmometric method of Fuoss and Mead (1), a few peculiarities of the osmometer itself as well as the need for thermostating the instrument were observed. The peculiarities and means for eliminating their effects are given below as helpful hints for those who might be troubled with the same difficulties.

PLATE THICKNESS

The early osmometers used in the laboratory were built from $\frac{5}{16}$ -in. stainless-steel plates. It was found that with the partial bolt circle of the Fuoss and Mead design, a bending of the plates could be detected when the bolts were tightened. Under this condition the membrane was free to move perceptibly, with the result that the determinations were uncertain. The changes suggested to correct this condition are the following: (1) to make the instrument from plates at least 1 in. thick; (2) to design a complete bolt circle to insure uniform pressure on the membrane. However, from work with an osmometer made of heavier plate ($1\frac{1}{8}$ in. thick), it has been found that the complete bolt circle is desirable but not absolutely necessary.

VALVE AND STEM MATERIAL

The material making up the valve blocks and the stems in the early osmometers was brass for the blocks and stainless steel for the stems. Much difficulty was experienced in keeping this combination leak-tight. It was found that the brass seats were deformed easily and that good closure was almost impossible. A much better combination was obtained by the use of hardened tool steel for the blocks and by continuing the use of stainless-steel valve stems. The valve seats were ground and lapped, with the result that tight valves were realized.

STAND PIPES

The fragility and frequent breakage of the glass stand pipes on the side arms of the osmometer were aggravating factors. The replacement of the glass with stainless-steel pipe spun to the same dimensions solved this problem.

CONSTANT TEMPERATURE

It had been found that temperature control was one of the major problems in osmometric measurements. The need for holding a particular temperature within small limits is of twofold importance. In the first place, the temperature effect on the π/C vs. C curve (π is the osmotic pressure and C is the concentration) is quite marked, especially where the degree of solvation of the polymer is high and quite temperature dependent. In this case, the π/C vs. C curve is not hori-

zontal but has a positive slope. This slope will vary with temperature. Thus if the temperature of the instrument is different each time that measurements are made on the same solution, the π/C values will be different. So, in order to obtain a curve that can be extrapolated to a value of $(\pi/C)_0$ which will have some significance, it is necessary to make all measurements at the same temperature.

RANGE OF TEMPERATURE VARIATION

The second point is the need to hold the constant temperature within certain small limits. The closed side of the osmometer acts as a pycnometer to temperature changes. These slight volume changes are reflected, highly magnified, in the movement of the level of the liquid in the closed-side capillary tube. Diffusion of the solvent through the membrane tends to cancel part of the change and restore the equilibrium conditions. However, if the temperature drift is rapid, the diffusion process is too slow to take care of it.

Data were collected on a thermostatted osmometer in which the water-bath temperature was regulated to a range of 0.045°C . at 30°C . and in which the heater was on for 6 min. and off for 6 min. These data showed that the closed-side capillary level varied about 1.2 mm. over the 0.045°C . range. The accuracy of reading the capillary levels was about in the range of 0.1 to 0.2 mm. Thus a temperature control within a range of 0.004°C . was indicated.

MEANS OF THERMOSTATTING THE OSMOMETER

Aside from the necessity of holding a constant temperature within narrow limits, there were several mechanical considerations in the design of a thermostatted osmometer. The direct immersion of the osmometer in a bath was rejected, because of the necessity for a complicated system for the side arms through the walls of the bath container as well as the fact that each membrane change, when necessary, would be a time-consuming operation. The use of a water jacket covering each plate of the instrument seemed to be a solution that would be practical. The jackets could be designed so that the membrane could be changed without disturbing the water jackets and *vice versa*.

OSMOMETER BODY DESIGN

Such an osmometer was designed (see figures 1 and 2). The body of the osmometer has several modifications of the Fuoss and Mead design. The full bolt circle which was displaced 22.5° has been already discussed. The other change concerned the welding on of a block of metal for the side-arm connections. This was done to allow more of the plate to be covered by the water jacket. This change necessitated the drilling of the outlet to the side arm at an angle similar to that for the outlet to the capillary tube above.

WATER JACKET DESIGN

The water jacket was designed (see figure 3) so that an area larger than that of the working area of the interior of the instrument was covered on the outer plate. The jacket had two sets of bolt holes around the periphery. The larger set

corresponded to the bolts holding the osmometer plates together and was drilled large enough so that the heads of these (Allen) bolts go through freely. The smaller set of holes was for the bolts that hold the jacket and its gasket to each plate. Thus, if the membrane needs attention, it can be reached by unloosening the large bolts without interfering with the water jacket. Conversely, if one or

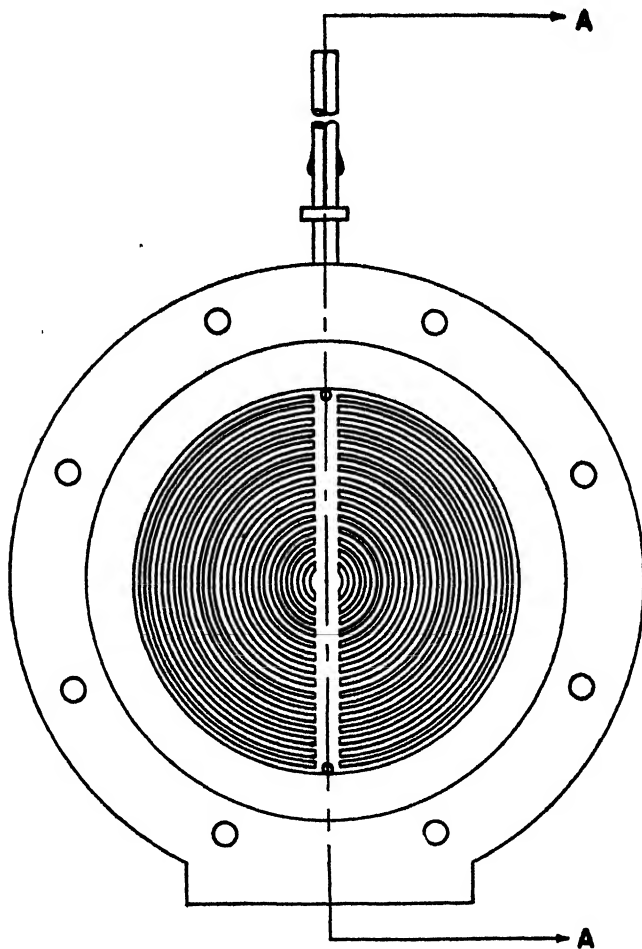


FIG. 1. Osmometer plate

the other of the water jackets needs repair, it may be fixed without disturbing the membrane.

In order to minimize the effect of changes in room temperature, the jacketed osmometer was packed in waste in a wooden box. This box had slots cut in the sides to allow for the side arms. The cover had holes and slots for the thermometer, capillaries, and the rubber tubing through which the circulating water was conducted.

GUIDE PINS

The original osmometer design showed guide pins to assist in putting the two plates together without cutting the membrane. In the modified design there

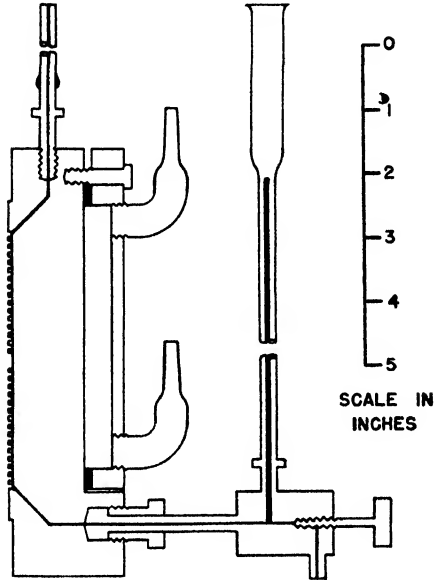


FIG. 2. Section of osmometer plate through A-A

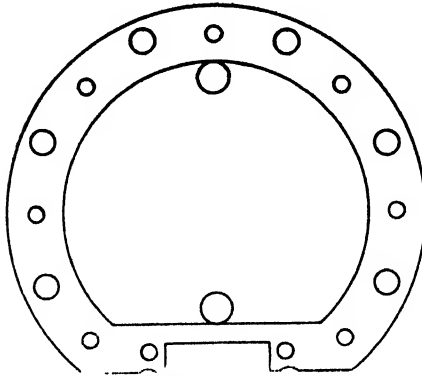


FIG. 3. Water jacket plate

was no space on the bolt circle to have guide pins without weakening the construction. Therefore, two pins were made of steel threaded at the ends to fit into the tapped holes for the large bolts. The shanks of these pins were made without heads and with rounded tips so that they could be screwed into holes in the bolt ring 180° apart and used as guide pins. After several of the large bolts were tightened in place, these pins could be removed and the bolts put in their places.

CONSTANT-TEMPERATURE BATH AND CONTROL

A large Pyrex jar 12 in. in diameter and 18 in. high filled with distilled water containing a slightly alkaline sodium chromate solution to minimize corrosion was

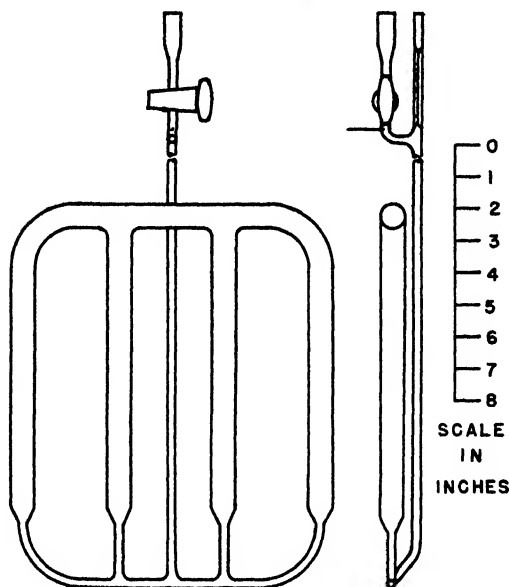


FIG. 4. Glass thermoregulator

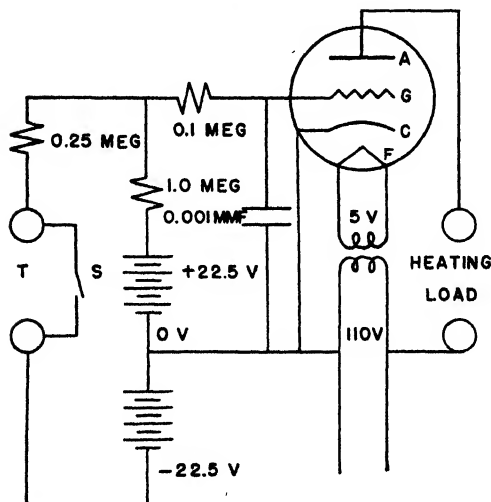


FIG. 5. Thyatron control circuit

set up with a laboratory-size Lightnin Mixer for good agitation. The circulation to the osmometer jackets was maintained by a small Eastern Laboratories centrifugal pump. The bath was covered with a $\frac{1}{4}$ -in. Textolite panel, suitably

cut out for the various connections. This minimized evaporation and helped to maintain constant conditions.

The temperature control was maintained by means of a specially designed Pyrex-glass thermoregulator (see figure 4), which can be built by a glassblower. Contact in the capillary was obtained through a 0.010 in. tungsten wire mounted on a threaded screw for ease in positioning. The other contact is through the platinum wire shown in the side arm. In conjunction with the thermoregulator, a thyratron tube control circuit¹ was used (see figure 5). The tube was a GE FG 57 thyratron tube. The filament transformer can be a 5-volt or 6.3-volt filament transformer. The one actually used was a Utah Radio Products 6.3-volt make. The battery used was a No. 5156 Burgess 45-volt type with a center tap to give the plus and minus 22.5 volts. The resistors and capacitor were of the conventional radio type. In figure 5, A, G, C, and F are the anode, grid, cathode, and filament, respectively, of the tube. The thermoregulator is denoted by T, and the short-circuit switch to protect the tube during the warm-up period (300 sec.) is shown as S.

A Cenco 125-watt knife-edge heater in the bath in series with a variable resistance was connected to the load side of the thyratron circuit to furnish the necessary heat. The bath was maintained at 30.00°C. on a thermometer graduated in 0.1°C. and calibrated by the National Bureau of Standards. The choice of 30.00°C. was made so that, except in rare instances in the summer months when room temperature might exceed this, no internal cooling coils would be necessary.

SUMMARY

The complete installation as outlined above has functioned satisfactorily. The temperature control exceeded expectation; the range found was 0.002°C. Many difficulties of osmometry that plague the operator in making determinations have been removed or their effect has been minimized.

REFERENCE

- (1) FUOSS, R. M., AND MEAD, D. J.: *J. Phys. Chem.* **47**, 59 (1943).

¹ Modeled after data in a written communication from Dr. D. J. Mead, General Electric Research Laboratory, Schenectady, New York.

VAPOR PRESSURE AND HEAT OF VAPORIZATION OF
ACETYLMETHYLCARBINOLAARON EFRON AND RUSSELL H. BLOM¹*Northern Regional Research Laboratory,² Peoria, Illinois**Received September 3, 1946*

Values for the vapor pressure of acetylmethylcarbinol at several temperatures have been reported (2), but they appear to be abnormally high. This substance is produced as a by-product in the fermentation of carbohydrates to butylene glycol; in developing a method for separating the two materials by distillation it became necessary to measure the vapor pressure of acetylmethylcarbinol and to calculate its heat of vaporization.

METHOD AND MATERIAL

Vapor pressures were determined by means of an isoteniscope, and the static method of Smith and Menzies (3) was used. This method was chosen because it affords two important advantages: (1) the vapor of the material is prevented from coming in contact with the confining atmosphere, a practical necessity in the case of acetylmethylcarbinol, since some oxidation to diacetyl takes place under commercial grades of nitrogen or carbon dioxide; and (2) dissolved gases and traces of other materials more volatile than that under investigation are removed easily or proved to be absent.

The acetylmethylcarbinol used was obtained by melting acetylmethylcarbinol dimer under carbon dioxide. The preparation of the dimer from D-(—)-2,3-butyleneglycol has been reported previously (1). Before the sample used for the vapor-pressure determinations was melted, it was dried over magnesium perchlorate.

The isoteniscope was heated in a liquid bath consisting of a 3-liter beaker containing dibutyl phthalate. The liquid was stirred mechanically and maintained at the desired temperature ($\pm 0.02^\circ\text{C}$.) by means of a controlled electric-resistance heater. Temperatures were measured with a thermometer graduated to tenths of a degree, and pressures were measured by means of an open-leg manometer and a Fortin-type barometer. Corrections were made for the emergent thermometer stem, and the mercury heights were reduced to 0°C . in the usual manner. Temperatures and pressures were measured with probable accuracies of $\pm 0.1^\circ\text{C}$. and ± 1 mm., respectively.

The temperature range from 99°C . to 144°C . was traversed three times, twice with ascending and once with descending temperatures, and several measurements were made during each traverse. All determinations were made on one filling of the isoteniscope. The sample was boiled out strongly before

¹ Present address: Mold Bran Company, Inc., Eagle Grove, Iowa.

² One of the laboratories of the Bureau of Agricultural and Industrial Chemistry, Agricultural Research Administration, U. S. Department of Agriculture.

the first traverse and at intervals during each traverse to remove dissolved gases and diacetyl.

EXPERIMENTAL RESULTS

The experimental results are presented in table 1, which also gives the traverse in which each observation falls.

The data are plotted in figure 1, with vapor pressure on the logarithmic scale against the reciprocal of the absolute temperature. Data obtained from the

TABLE 1
Vapor pressure of acetylmethylcarbinol

t_{obed}	P_{obed}	TRAVERSE NUMBER	$t_{\text{obed}} - t_{\text{sealed}}^*$	$P_{\text{obed}} - P_{\text{sealed}}^*$
°C.	mm. Hg		°C.	mm. Hg
99.28	193.2	1	-0.4	2
99.30	193.0	2	-0.4	2
99.40	186.6	3	0.7	-4
107.84	258.2	2	-0.4	3
109.76	270.8	1	0.1	-1
112.73	293.5	3	0.6	-6
116.88	349.7	2	-0.7	7
124.44	435.5	1	-0.2	4
124.57	446.4	2	0.8	10
128.05	468.5	3	1.0	-14
131.75	551.0	2	-0.6	10
137.60	645.8	2	-0.3	6
141.64	742.5	1	-1.3	24
141.79	718.4	2	0.2	-3
141.94	728.8	1	-0.3	6
141.94	735.2	2	-0.5	12
143.62	701.6	3	2.8	-57
143.72	682.1	3	3.9	-78

* From $\log P_{\text{mm}} = 7.922 - \frac{2101}{t + 273.1}$, using t_{obed} to calculate P_{sealed} and P_{obed} to calculate t_{sealed} .

first and second traverses were found to agree closely. The vapor pressures observed in the last traverse were somewhat lower than those obtained in the preceding determinations, possibly because of the rather long exposure of the sample to high temperatures and the consequent formation of higher-boiling polymeric substances.

SUMMARY

The equation,

$$\log P_{\text{mm}} = 7.922 - \frac{2101}{T} \quad (370^\circ < T < 420^\circ)$$

was fitted to the data in figure 1. The data obtained from the first and second traverses at pressures below 700 mm. were believed to be the most reliable, and hence were given the greatest weight in fitting the curve.

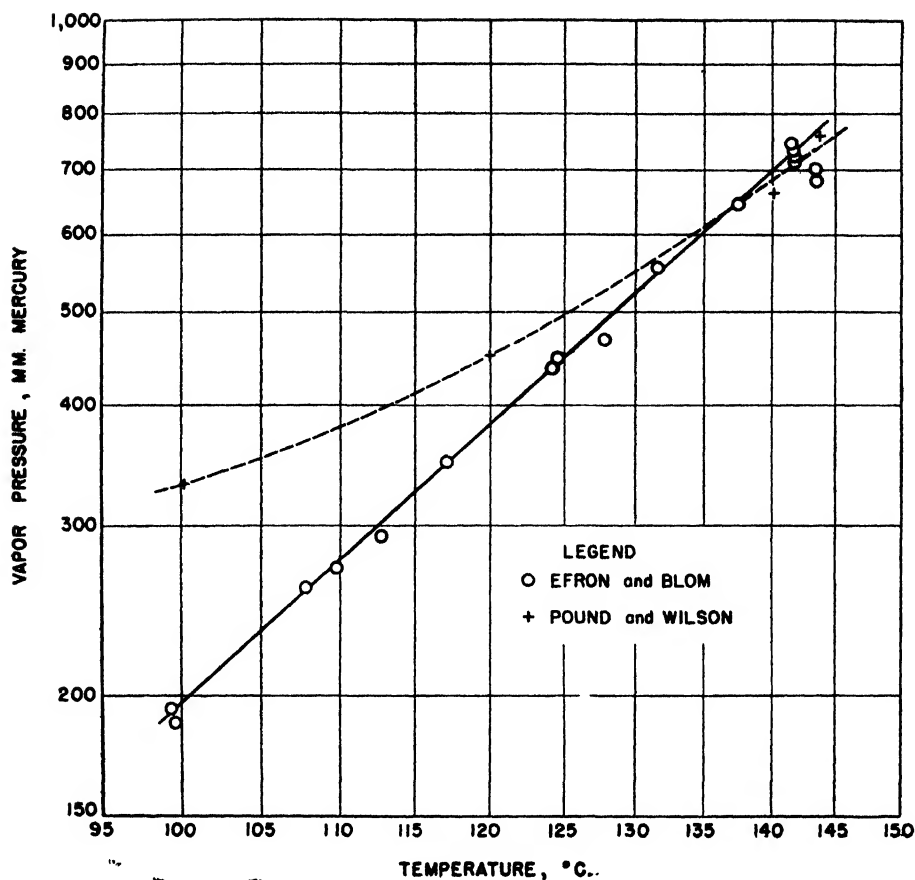


FIG. 1. Vapor pressure of acetylmethylcarbinol

TABLE 2

Vapor pressure of acetylmethylcarbinol

TEMPERATURE	FOUND AND WILSON (2)	EFRON AND BLOM
°C.	mm. Hg	mm. Hg
0	162	1.7*
20	168	5.7*
60	210	41.0*
100	330	195
120	449	378
140	664	693
143.6		760
144	760	

* Extrapolated values.

The average heat of vaporization in the range 99–144°C. was calculated from the integrated Clausius–Clapeyron equation, and found to be 109 cal. per gram, with a probable accuracy of ± 5 cal.

Compared with the vapor-pressure data reported by Pound and Wilson (2), the present results are much lower, especially at the lower temperatures, as may be seen from table 2 and figure 1.

The higher values obtained by the previous investigators may have resulted from the presence of diacetyl in the acetylmethylcarbinol which they used.

REFERENCES

- (1) BLOM, R. H., AND EFRON, AARON: *Ind. Eng. Chem.* **37**, 1237 (1945).
- (2) POUND, J. R., AND WILSON, A. M.: *J. Phys. Chem.* **39**, 1135 (1935).
- (3) SMITH, ALEXANDER, AND MENZIES, A. W. C.: *J. Am. Chem Soc.* **32**, 1413 (1910).

STUDIES ON THE AGING OF PRECIPITATES AND COPRECIPITATION. XXXVIII

THE COMPRESSIBILITY OF SILVER BROMIDE POWDERS¹

I. SHAPIRO AND I. M. KOLTHOFF

School of Chemistry, University of Minnesota, Minneapolis 14, Minnesota

Received November 8, 1946

Although considerable experimentation has been carried out on the loose packing of powders (4), few data are available on the effect of pressure upon the bulkiness of powders. Balshin (2) and coworkers, working in the field of powder metallurgy, have attempted to correlate the apparent specific volume of powders with externally applied pressures but have met with little success. By applying the concept of fluid mechanics to this problem, Balshin proposed the following expression,

$$\log p = -LV_0 + C \quad (1)$$

where p is the pressure applied, V_0 is the apparent specific volume of the powder, and L and C are constants. In practice it was found that the values of L and C were not constant but varied with the conditions of the experiments and the powder. The application of hydrostatics to this problem cannot be considered valid since, as Wretblad and Wulff (9) have pointed out, the compression of a liquid implies an elastic deformation, whereas the pressing of a powder mass is primarily a plastic deformation.

A more satisfactory approach to this general problem is through a study of

¹ This paper is based on a thesis submitted by Isadore Shapiro to the Graduate Faculty of the University of Minnesota in partial fulfillment of the requirements for the degree of Doctor of Philosophy, August, 1944.

the packing of particulate matter. The apparent density, ρ_a , of a powder mass can be expressed in terms of the true density, ρ_s , of the solid and the fraction of voids or porosity, P_0 , present in the mass by the following relation:

$$\rho_a = \rho_s(1 - P_0) \quad (2)$$

The apparent density is thus defined as the bulk weight of a unit volume of a packing. The value of P_0 (condition of no external pressure upon the powder) depends upon the particle size (if below a critical value (8)), the size distribution, the shape and porosity of the individual particles (aggregates), and the type of

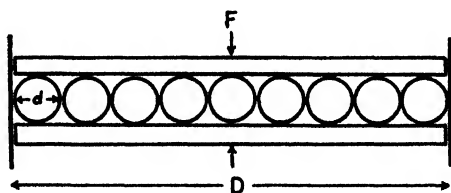


FIG. 1. Compression of a packed layer of spheres

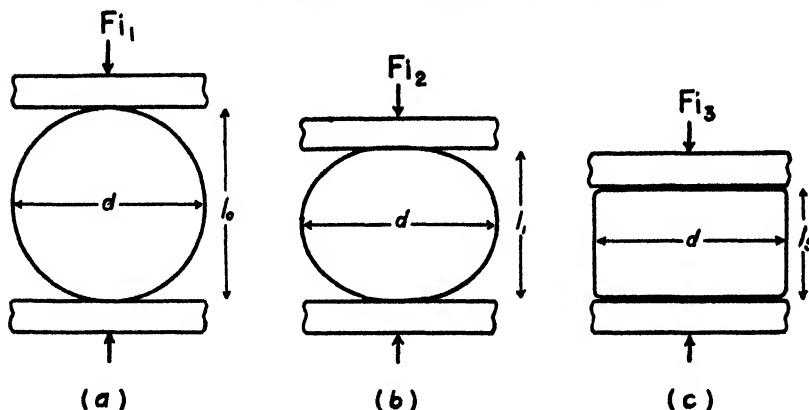


FIG. 2. Compression of a plastic sphere: (a) initial stage; (b) intermediate stage; (c) final stage.

packing of the particles in the container. For uniform solid spheres placed in a hexagonal close-packed arrangement the porosity is 25.95 per cent.

When an external pressure is applied to a powder mass in a die, the apparent density of the powder will increase and approach the true density of the solid as a limit. The ease with which the apparent density approaches the limiting value will depend upon the material being compressed, i.e., its plasticity and surface development. As the powder is compressed, the "effective value" of P_0 in equation 2 will decrease and approach zero, so the porosity P at any pressure p will be related by

$$P = \frac{\rho_s - \rho_a}{\rho_s} = P_0 \times f(p) \quad (3)$$

where $f(p)$ can be determined experimentally.

From geometric considerations of a packing of spheres of uniform size the value of P_0 should be independent of the actual particle size of the spheres but the pressure function $f(p)$ will depend materially upon the size of the spheres. As an example, consider one layer of uniform spheres of diameter d in a cylinder of diameter D pressed between two plates with a force F , such as represented in figure 1. The number of spheres in a close-packed arrangement will be

$$\frac{\pi}{4 \times 0.866} \left(\frac{D}{d}\right)^2$$

so the force per particle, F_i , will be

$$F_i = \frac{F}{\frac{\pi}{4 \times 0.866}} \frac{d^2}{D^2} \quad (4)$$

Focusing our attention on one sphere such as that in figure 2(a), it is obvious that only a small area of the sphere is sustaining the load. The localized pressure at the point of contact between the plate and the sphere will be

$$p_i = \frac{4 \times 0.866 F d^2}{\pi a_i D^2} \quad (5)$$

where a_i is the area of contact. Since the elastic limit of a plastic material is usually small, the loading of the particles or spheres will produce a plastic deformation. Figure 2 represents the progress of the deformation under various loads. Let l_0 be the distance between the plates before loading (figure 2(a)) and let l_i be the minimum distance between the plates for the plastic deformation (figure 2(c)); these values determine the limits for the apparent density of the material. The porosity of the packing, using l_0 as the length, is P_0 , and the porosity decreases to zero as the length decreases to l_i . It is evident that the porosity, which is a measure of the deformation, depends upon the localized pressure such as expressed in equation 5. From this latter equation it is deduced that the deformation will be less for a packing of smaller-size spheres under the same external load. Since in practice the particles of a powder are seldom spherical but are irregular in shape, the equations can be made applicable by introducing a shape factor (5).

The effect of pressure upon a powdered material under conditions of varying particle sizes can be studied conveniently in conjunction with the "aging process" of the material, because of its correlation with growth and perfection of the particles (6). For silver bromide powders of various history and age it has been found experimentally that the change in porosity with pressure can be expressed by

$$\frac{dP}{dp} = -kP \quad (6)$$

The constant k can be called the "coefficient of powder compressibility," and its value depends upon the physical characteristics of the powder. Integrating equation 6 and combining with equation 3 gives the relation:

$$p_a = p_0(1 - P_0 e^{-kp}) \quad (7)$$

In connection with equation 6 it is interesting to note that Athy (1) has found that the compaction of shale beneath the earth's surface can be given by

$$P = P_0 e^{-bz} \quad (8)$$

where P is the porosity of shale at depth z below the surface, P_0 is the porosity of surface clays, and b is a constant. This agreement of experimental findings for two different materials, both of which are considered very plastic, is significant.

EXPERIMENTAL

Silver bromide powders: The preparation of silver bromide powders aged in different ways and the subsequent measurement of their compressibilities are described in detail in the thesis upon which this paper is based. All chemicals were of C. P. quality or better, and conductivity water was used throughout the experiments. The silver bromide was precipitated by adding 0.4 N silver nitrate solution to an equivalent amount of 0.4 N potassium bromide solution with vigorous stirring. All preparations and the handling of the silver bromide were carried out in photographically inactive red light. The precipitates were washed immediately on a sintered-glass filter with large quantities of water, then with acetone, and finally with thiophene-free benzene. Dry air was passed through the material until the odor of benzene was no longer perceptible. The powder was aged by heating portions to various temperatures.

Fused product (series 1): Silver bromide was placed in a Pyrex tube in a well of a copper-block furnace and heated to 450°C. (the melting point of silver bromide is about 426°C.). A constant stream of bromine vapor was maintained over the silver bromide to prevent loss of bromine from the salt. The molten salt was cooled slowly to room temperature, crushed, ground in an agate mortar, and sieved with standard screens. Samples whose particle size ranged from 8 to 10 mesh are designated as 1a; 10–14 mesh, 1b; 14–20 mesh, 1c; and a mixture of the above three samples in approximately equal proportions by weight is designated as 1d.

Well-aged product (series 2): The silver bromide was heated at 375°C. for 2 hr. in the presence of bromine vapor in the same furnace as used above. This product was powdered and sieved with standard screens. Samples whose particle size ranged from 8 to 10 mesh are designated 2a; 10–14 mesh, 2b; 14–20 mesh, 2c; and 20–28 mesh, 2d. (The screened particles of the various powders and also those of less aged products are in reality aggregates of minute particles, but because of the cohesive forces holding them together, they can be treated as individual porous particles for the time being.)

Aged product (series 3): The precipitated silver bromide was heated for 4 hr. at 110°C. without bromine vapor present. The particle size of the sample was 14–20 mesh.

Fresh product (series 4): In this case the silver bromide powder received no further treatment after being air-dried. The sample used shortly after preparation is designated 4a; that aged for three weeks at room temperature in the dry state, 4b. These powders were not sieved.

Measurement of powder compressibility: Approximately 10-g. samples of the silver bromide powders were weighed accurately and placed in a cylindrical die whose cross-sectional area was 2.38 sq. cm. The powder was compacted to pellets by applying pressure to a piston in the die by means of a hydraulic press. The pressure, whose range was up to 3000 atm., was read on a calibrated gauge. The lengths of the pellets at the various pressures were measured with a cathetometer (± 0.02 mm.), and the final dimensions were checked with a micrometer after the pellets had been removed from the die and reweighed. The apparent density is calculated from the weight of the pellet and the volume occupied by the pellet in the die.

Apparent density of the uncompressed powders in air and water: Although the actual particle sizes of the silver bromide powders were not measured directly, relative values of particle size were obtained by density measurements. The densities of the uncompressed powders of the various silver bromide samples were measured (a) with a pycnometer, using water at 25°C. as the liquid medium, and (b) by weighing four hundred particles from each screened particle-size group. The pycnometer densities are designated as $(\rho_a)_w$, apparent density in water;

TABLE 1
Apparent densities of uncompressed silver bromide powders

AGE OF SAMPL.	$(\rho_a)_w$	$(\rho_a)_A$
Fused (1)	6.42	7.4
Well-aged (2).	6.04	5.1
Aged (3)	6.13	3.5
Fresh (4)	5.88	1.8

and the weighed-sized particle densities as $(\rho_a)_A$, apparent density in air. The values are tabulated in table 1. The accepted value of the true density of (fused) silver bromide is 6.478 g./cc. (3). The values of table 1 can be interpreted on the basis of views postulated in connection with the "aging of precipitates" (see the review of aging phenomena (6)). Freshly precipitated silver bromide consists of aggregates of microscopically and submicroscopically highly imperfect particles which are capable of aging in the dry state (7). The irregularities on the surface of the primary particles are capable of keeping the particles separated, with a resultant low apparent density ($(\rho_a)_A$, table 1). Roller (8) also has found that exceedingly minute particles of various materials bulk greater than particles of correspondingly larger size. When the powders are heated to elevated temperatures, the active surface decreases as a result of the manifestation of the surface mobility of the ions. The perfection of the surface aids in the cementing together of the particles. Thus the values of $(\rho_a)_A$ increase with the age of the powder. The high value of 7.4 g./cc. for the apparent density of the fused powder is explained by the fact that this value was calculated on the basis of a spherical particle, whereas it was observed that the powdered fused particles were oblong in shape.

The pycnometer densities of the aggregates are all smaller than the true

density of silver bromide; evidently all of the entrapped air in the powder is not displaced by the water. A growth or perfection of the particles, which is accompanied by a decrease in the specific surface of the powder, accounts for the

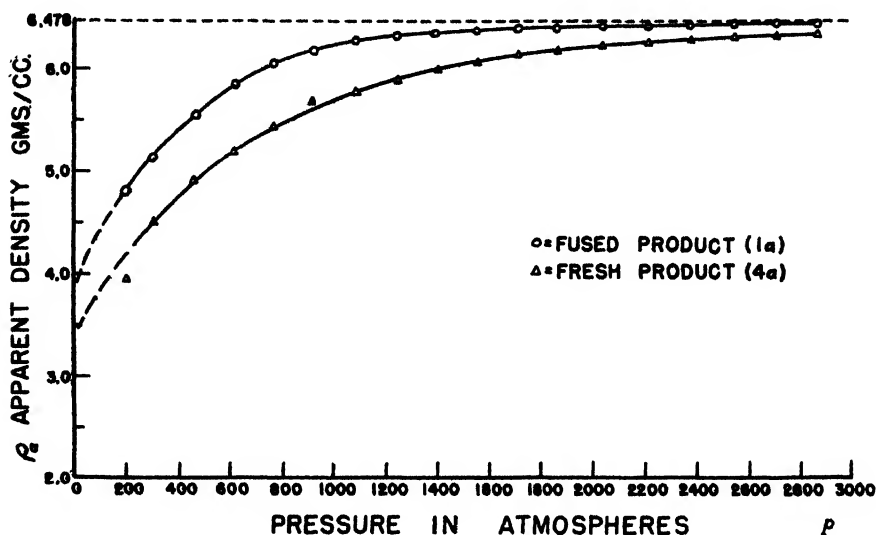


Fig. 3. Effect of pressure on apparent density of silver bromide powders

TABLE 2
Apparent densities and porosities of fused silver bromide pellets

<i>P</i>	1a: FUSED; 8-10 MESH; 11.256 G.; 25°C.		1b: FUSED; 10-14 MESH; 11.640 G.; 25°C.		1c: FUSED; 14-20 MESH; 10.900 G.; 25°C.		1d: FUSED; MIXED SIZE; 11.270 G.; 25°C.		1aa: FUSED; 8-10 MESH; 95°C.	
	ρ_a	<i>P</i>	ρ_a	<i>P</i>	ρ_a	<i>P</i>	ρ_a	<i>P</i>	ρ_a	<i>P</i>
<i>atm.</i>		<i>per cent</i>		<i>per cent</i>		<i>per cent</i>		<i>per cent</i>		<i>per cent</i>
205	4.81	25.7	4.79	26.0	4.81	25.7	5.02	22.5	5.18	20.0
304	5.13	20.9	5.11	21.1	5.06	21.9	5.29	18.4	5.45	15.9
465	5.56	14.2	5.58	13.9	5.52	14.8	5.73	11.6	5.88	9.25
616	5.86	9.55	5.89	9.09	5.83	10.0	5.95	8.16	6.15	5.06
770	6.05	6.61	6.05	6.61	6.01	7.23	6.11	5.68	6.29	2.90
925	6.18	4.60	6.18	4.60	6.18	4.60	6.18	4.60	6.38	1.51
1085	6.28	3.06	6.27	3.21	6.25	3.52	6.30	2.75	6.40	1.20
1245	6.33	2.28	6.33	2.28	6.32	2.44	6.38	1.51	6.45	
1400	6.35	1.98	6.38	1.51	6.35	1.98	6.40	1.20		

increase in values of $(\rho_a)_w$ with the heat-treatment of the powder. Actually it was found that the specific surface, as determined by the adsorption of wool violet on the various silver bromide powders when the surface is saturated with dye, decreases with the "age" (including heat-treatment) of the products. Thus the particle size of the primary particles increases with the "age" (heat-treatment) of the powder.

COMPRESSIBILITY OF THE POWDERS

The effect of pressure upon the apparent density of a pellet of fresh and fused product of silver bromide is shown in figure 3. It is observed that the apparent

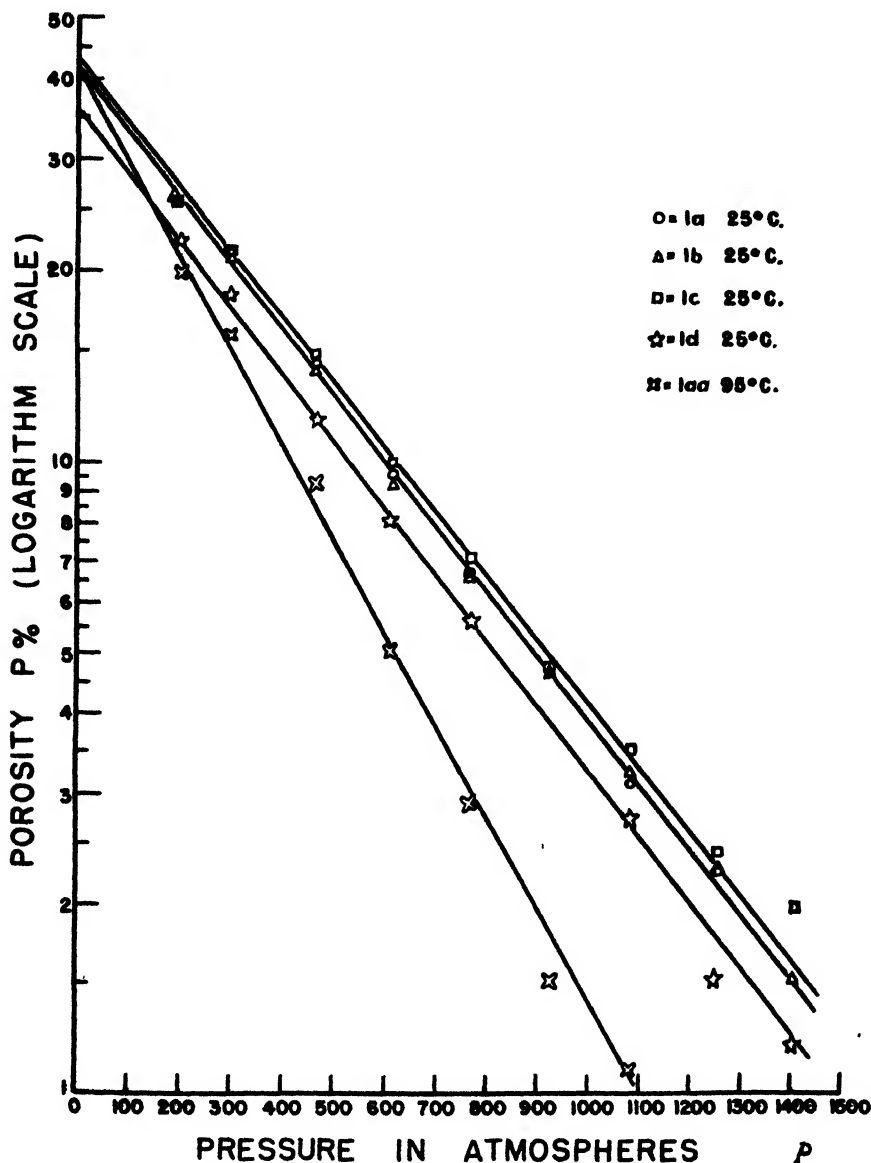


FIG. 4. Compressibility of silver bromide powders (prepared from fused samples)

densities of pellets of both products approach the true density of the silver bromide as a limit within the pressure range of the experiments. Since the apparent density of the powder at high pressures is within a few per cent of the true density, the accuracy of the values for porosity at the extremely high

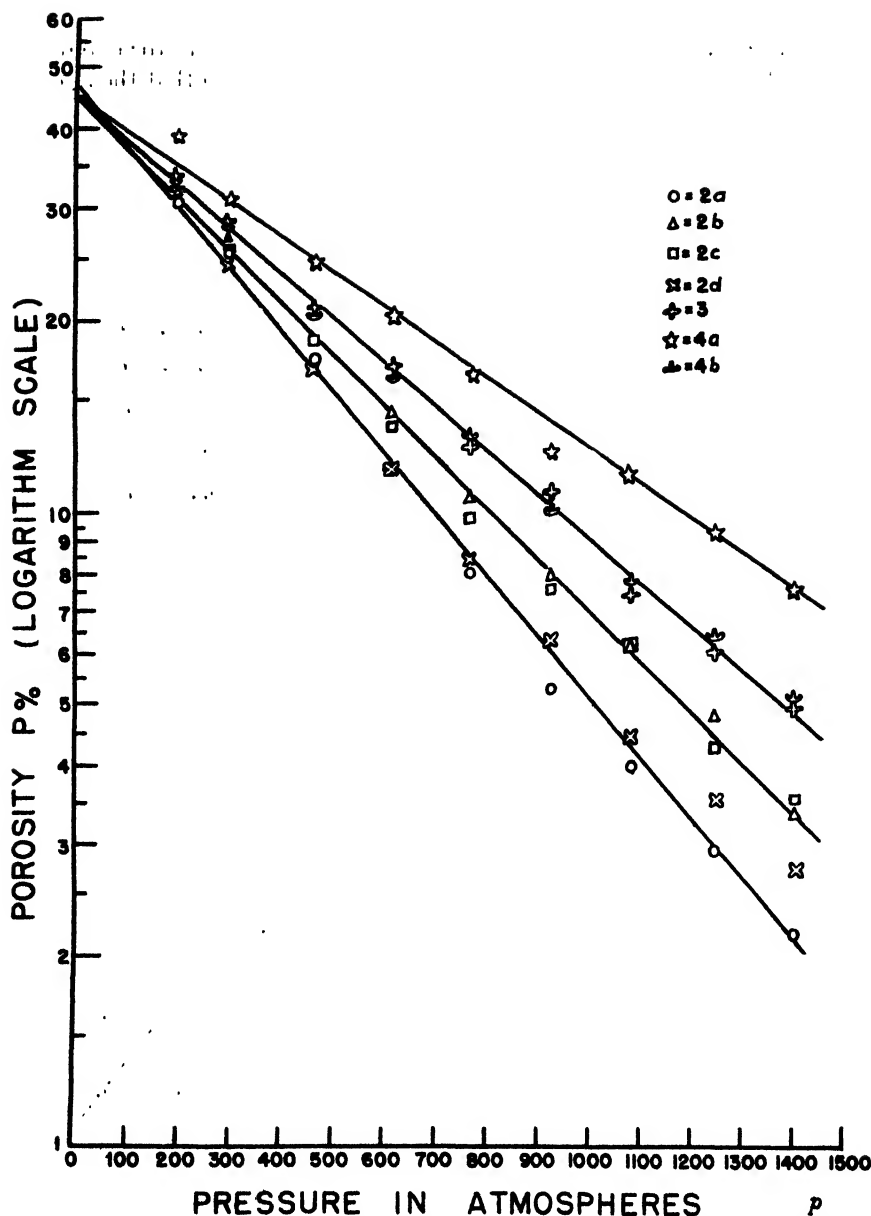


Fig. 5. Compressibility of silver bromide powders (fresh and heated products)

pressures is not as high as the values at the lower pressures. Therefore, in calculating the porosity of the pressed pellets only the values obtained in the first half of the pressure range will be considered here.

The apparent densities and porosities of the fused powders (pellets) at various pressures are tabulated in table 2 and the porosities are plotted in figure 4.

The porosity is the value calculated with the aid of equation 3 multiplied by 100. For the sake of brevity the tabulation of the rest of the data found with the other samples has been omitted. The data are given in the thesis of the junior author and are plotted in figure 5. The values of k , the coefficient of powder compressibility, and P_0 (in per cent) (equation 7) for the various samples have been calculated from the lines given in figures 4 and 5 and are tabulated in table 3. When these experimentally determined values are introduced into equation 7, the calculated apparent density fits closely the experimental values over the entire pressure range indicated in figure 3.

Whenever powders are compacted under pressure, the friction between the particles of the powder tends to oppose the transmission of this pressure throughout the entire mass. Immediately after the application of pressure, the powder directly beneath the movable piston will be under a greater internal pressure than the powder near the fixed piston in the die, so that under the condition of constant volume between the pistons, the externally applied pressure will decrease slowly with time. However, by using a die with a large cross-sectional area as compared to the length of pellet in the die, and by increasing continuously the applied pressure with time to a predetermined value, one can obtain very easily a condition of pressure equilibrium throughout the mass of powder (as evidenced by no further decrease in pressure with time). These precautions have been observed in all of the above experiments. The effect of entrapped air in the pellets has been reduced to a minimum by having the movable piston slightly undersize and by applying the pressure slowly. While the effect of entrapped air may become appreciable at the high pressures, it is of little importance in the pressure range considered here.

EFFECT OF TEMPERATURE UPON COMPRESSIBILITY

Some experiments were carried out with the powder of the fused product at room temperature (25°C.) and at 95°C. Representative data for such experiments are given in table 2 (1a, 1aa) and figure 4. It is observed that the value of P_0 remains unchanged, but that the value of k increases materially with temperature. This finding is in accord with the fact that the plasticity of materials increases with temperature.

DISCUSSION OF RESULTS

Experimentally it has been shown that the relation between the apparent density of a compressed silver bromide powder and the pressure under various conditions of the powder can be expressed by equation 7. A comparison of the curves in figures 4 and 5 shows that the slopes of the curves remain essentially unchanged for any given condition of "age" of the powder and that the initial porosity P_0 is the same for samples of particles of uniform size but decreases for samples composed of particles of different size. In the latter case the smaller particles can fill some of the voids between the larger particles and thereby increase the efficiency of the packing.

From figure 5 and table 3 it is seen that the value of k increases with the "age" of the powder. Previously it was pointed out that the particle size of the

powder increases with "age"; therefore the effect of particle size upon compressibility agrees experimentally with the theoretical considerations given at the beginning of this paper.

The values of P_0 in table 3 are characteristically constant and evidently depend upon the geometric shape of the particles. A packing of irregular-shaped particles will favor a more loose packing than, for example, a packing of uniform-size spheres. The porosity of a packing of uniform spheres in a regular arrangement can vary from 26 per cent (hexagonal close-packed system) to 47.6 per cent (cubic loose-packed), so a value for P_0 of *ca.* 43 per cent for compressed silver bromide powders is substantially in agreement with theoretical values. It is emphasized here that the values of P_0 in table 3 have been obtained by extrapolation of high-pressure data and should not be used directly in equation 2

TABLE 3
Coefficients of powder compressibility at 25°C.

SAMPLE ¹	P_0 (GRAPH)	k
	<i>per cent</i>	<i>atm.</i>
1a	41.6	2.38×10^{-3}
1b	41.6	2.38
1c	43.0	2.38
1d	36.4	2.43
1aa*	42.2	3.51
2a	49.0	2.23
2b	45.2	1.86
2c	45.2	1.86
2d	49.0	2.23
3	43.8	1.58
4a	45.4	1.33
4b	43.8	1.58

* At 95°C.

unless the powder is tamped into the mold or die. For just a loose packing of the powder in a container (no external pressure) the value of the apparent density given by equation 2 is related closely to values of $(\rho_a)_A$ in table 1. The difference between values of P_0 with and without pressure is greatest for the fresh powders and arises from the fact that the forces separating the primary particles in the aggregates are overcome even with only slight pressures.

SUMMARY

The compressibility of silver bromide powders can be expressed empirically by the equation

$$P = P_0 e^{-kp}$$

in which P_0 is the initial (extrapolated) porosity at zero applied pressure and P the porosity at a pressure p .

The value of k increases with the particle size (or decreasing surface develop-

ment) of the primary particles in the powder and/or the temperature at which the compression takes place. The variation of k with particle size has been anticipated from theoretical considerations.

The values of P_0 have been shown to be essentially independent of the condition of "age" of the compressed powders.

Compressibility data of tampered powders give insight into the degree of aging of silver bromide.

REFERENCES

- (1) ATHY, L. F.: Bull. Am. Assoc. Petroleum Geol. **14**, 1 (1930).
- (2) BALSHIN, M. YU: Vestnik Metalloprom. **18**, 124 (1938) (in Russian).
- (3) BAXTER, G., AND HINES, M.: Am. Chem. J. **31**, 220 (1904).
- (4) DALLA VALLE, J. M.: *Micrometrics*, p. 100. Pitman Publishing Company, New York (1943).
- (5) GREEN, HENRY: J. Franklin Inst. **204**, 713 (1927).
- (6) KOLTHOFF, I. M.: Tekniska Samfundets Handlingar **3**, 119 (1939).
- (7) KOLTHOFF, I. M., AND O'BRIEN, A. S.: J. Chem. Phys. **7**, 401 (1939).
- (8) ROLLER, PAUL S.: Ind. Eng. Chem. **22**, 1206 (1930).
- (9) WULFF, J.: *Powder Metallurgy*, p. 45. American Society for Metals (1942).

DIMENSIONAL STABILIZATION OF WOOD¹

ALFRED J. STAMM AND HAROLD TARKOW

Forest Products Laboratory,² Forest Service, U. S. Department of Agriculture

Received October 1, 1946

All known processes for stabilizing the dimensions of wood involve either (a) coatings which block the entrance and exit of water but do not change the hygroscopicity of the wood, (b) bulking agents which tend to keep wood in a swollen state, or (c) chemical agents which react with the hydroxyl groups of the cellulose, lignin, or both and replace them with less polar groups, thus reducing the hygroscopicity of the wood.

PREVIOUSLY REPORTED METHODS

Most of the efforts that have been made to stabilize the dimensions of wood involve the use of external or internal coatings. Unfortunately, all known coatings that will adhere to wood allow the passage of some moisture. Internal coatings are, in general, less effective than external coatings, as it is impossible to coat all the microscopically visible capillary structure completely. One thick continuous surface film is more effective in blocking the passage of water than numerous imperfect internal films. Good surface coatings, such as synthetic-

¹ Presented before the Division of Colloid Chemistry at the 110th Meeting of the American Chemical Society, Chicago, Illinois, September, 1946.

² Maintained at Madison, Wisconsin, in coöperation with the University of Wisconsin.

resin varnishes and aluminum paints, do retard the rate of moisture absorption sufficiently to minimize the steepness of moisture gradients in the wood and subsequently reduce the stresses which cause grain raising, warping, and checking (2, 6). They do not, however, prevent the aggravating swelling of drawers and doors that occurs during prolonged periods of high relative humidity.

Another approach to the stabilization of the dimensions of wood is to keep the wood in a partially or completely swollen state. When wood is treated with a concentrated solution of a hygroscopic salt (8) or sugar (1, 11), the chemical retains more water in the wood than would normally be retained at the prevailing relative humidity. When the wood is dried, shrinkage does not commence until the relative humidity falls below that in equilibrium with the salt or sugar solution within the cell walls (8, 11). The final oven-dry shrinkage is also reduced by an amount equal to the bulk of chemical held in the cell-wall structure. Wood so treated, however, is wet and sticky at the higher relative humidities, it is subject to leaching, and it is less strong than dry wood. For these reasons this method of stabilizing the dimensions of wood has never been commercialized.

If a water-insoluble material could be deposited within the cell-wall structure, the bulking effect might be made more practical. This can be accomplished by either of two methods: (a) replacement of water with a mutual solvent for water and the wax or resin with which the wood is to be treated, followed by replacement of the mutual solvent with the wax or resin; or (b) insolubilizing a water-soluble material within the cell-wall structure. Procedure (a) has been successfully carried out on small specimens of wood, using ethylene glycol monoethyl ether as the intermediate replacing agent and various waxes as the final bulking agent (9, 13). This method, although reasonably effective in reducing the swelling and shrinking, is, however, too involved for commercial use. The second method, by which phenolic resins have been formed within the intimate cell-wall structure of wood, has proven quite practical, using an unpolymerized phenol-formalin-catalyst mix or a water-soluble phenol-formaldehyde resinoid of sufficiently low molecular weight to penetrate the cell-wall structure and sufficiently polar to bond to the active groups of the wood (16). This treatment resulted in Impreg (16) and Compreg (17), resin-treated uncompressed wood and compressed wood, respectively, which found war use as aircraft carrier decking, housings for electrical control equipment, propellers, antenna masts, bearing plates, and forming dies, and which show promise of more extended peacetime uses.

Both phenol and formaldehyde and their initial water-soluble condensation product are selectively adsorbed by wood and, as a result, swell wood in their aqueous solutions more than wood is swollen by water alone. It is believed that, when the resin is formed by the application of heat, they remain chemically bonded to the hydroxyl groups of both cellulose and lignin. It thus appears that the dimensional stabilization of wood obtained by forming the resin within the wood is due to both a bulking effect and a chemical combination. The relative importance of each factor is still unknown.

The only dimension-stabilizing treatment thus far reported that can be explained only on the chemical basis is that obtained by heating wood under conditions such that water of constitution is lost. Under these conditions it is believed that water splits out between two hydroxyl groups on adjacent cellulose chains and that an ether bridge is formed (10, 12, 14). Stabilization presumably results from a combination of the reduction in hygroscopicity and the bridging. This means of stabilizing the dimensions of wood is the cheapest so far developed, but, unfortunately, some carbonization and oxidation, which accompany the desired reaction, cause significant losses in strength properties. The strength loss can be minimized by heating the wood in the absence of air in a molten bath (10, 12).

ACETYLATION

The chief disadvantage of stabilizing the dimensions of wood by forming synthetic resins within the structure is that the resins embrittle the wood appreciably. For some uses, such as in aircraft, this is very serious. Efforts were therefore made to find some other bulking agent which preferably reacts with the hydroxyl groups of wood and which does not embrittle the wood. Acetylation appeared to be a likely means of accomplishing this.

Acetylation as it is normally practiced on cellulose with acetic anhydride requires a swelling agent, such as acetic acid, to open up the structure and a catalyst, such as sulfuric acid, to promote the esterification reaction. Mineral acids, however, promote hydrolysis and breakdown of the cellulose chains. This hydrolytic effect, if kept within bounds, is not harmful in plastic and rayon manufacture, but it would defeat one of the chief objectives of acetylating wood by breaking the structural bonds and embrittling the fiber.

Pyridine is known to catalyze the acetylation of cellulose with acetic anhydride. It is effective, however, only when the cellulose has been previously subjected to a strong alkali treatment resulting in hydrate cellulose, or when the water in swollen cellulose is replaced by pyridine (4, 7). This replacement is necessary, as pyridine itself is a poor swelling agent for cellulose. Acetic acid could not be used as the swelling agent, owing to the fact that pyridine reacts with acetic acid to form pyridine acetate. Staudinger (18) showed that acetylation of cellulose, using the pyridine replacement method of Hess (4), does not break down the cellulose chains.

Preliminary experiments on wood showed that it is unlike cellulose in that pyridine swells wood 25 to 30 per cent more than it is swollen by water. It thus appeared that the alkali treatment or replacement steps would not be necessary. This proved to be the case. Small sections of sugar maple about $\frac{1}{8}$ in. thick in the fiber direction were acetylated by immersing them in acetic anhydride-pyridine mixtures for various periods of time at various temperatures. Acetyl contents of 20 per cent were readily obtained under the more favorable conditions, and reductions in equilibrium swelling to 30 per cent of normal (70 per cent anti-shrink efficiency). This liquid-phase treatment, however, requires the take-up of a large excess of acetylating solution to assure uniform acetylation, followed

by subsequent removal of this large excess. Vapor-phase acetylation was hence tried. This proved equally successful in stabilizing the dimensions of wood, with much less take-up of chemical. In the acetylation of Sitka spruce, the take-up of solution was 227 per cent of the weight of the wood by the liquid-phase treatment and only 50 per cent of the weight of the wood by the vapor-phase method. In both cases a 21 per cent acetyl content resulted. Because of this the major part of the experimental work was carried out by the vapor-phase method.

Treating equipment

The preliminary vapor-phase treatments were made on small sections of wood merely suspended over the acetylation mixture in glass cylinders. Later acetylation studies were made in a wooden cabinet 26 by 22 by 18 in. that was lined with stainless steel and provided with stainless-steel steam coils near the bottom of the cabinet, and a stainless-steel pan over the coils with a drain for introducing and removing the acetylating liquid, a stainless-steel fan for circulation of the vapor given off from the pan, and glass rods located at the top of the cabinet from which the sheets of veneer to be treated were suspended. An exhaust tube to which a condenser might be connected insured the operation of the equipment at atmospheric pressure.

Treating variables

Although reasonable variations in the moisture content of the wood do not affect the rate or degree of acetylation by the vapor-phase method at atmospheric pressure, it is desirable to have the wood quite dry to avoid an excessive reaction of acetic anhydride with water. A moisture content of about 2 per cent, which is not difficult to attain commercially in veneer, was used in most of the experiments.

The rate of vapor-phase acetylation is determined by the rate of diffusion of vapors into wood. As diffusion varies as the square of the thickness, the acetylation time will increase rapidly with increases in thickness. Experience showed that the process should be confined to veneer of $\frac{1}{8}$ -in. thickness or less or solid wood only a few inches long in the fiber direction to maintain practical treating times.

Species that have been successfully acetylated in veneer form are yellow birch, sugar maple, mahogany, sweetgum, yellow poplar, basswood, Douglas fir, Sitka spruce, and white spruce. Balsa was acetylated in blocks $\frac{1}{2}$ in. thick in the fiber direction. Softwoods (needle-bearing trees) required a higher degree of acetylation than hardwoods (broadleaf trees) to attain the same antishrink efficiency (percentage reduction in shrinkage) under equilibrium conditions. This is shown in figure 1 for a dense hardwood (sugar maple), a low-density hardwood (balsa), and Sitka spruce, a typical softwood. The time required to obtain a degree of acetylation that gives 70 per cent antishrink efficiency (70 per cent reduction in swelling and shrinking under equilibrium conditions) decreases with increasing temperature. At 90°C. about 6 hr. are required to

treat $\frac{1}{8}$ -in. hardwood veneers to a 20 per cent acetyl content, using a vapor-generating solution of 20 per cent pyridine in acetic anhydride. A higher concentration of pyridine reduces the treating time only slightly. Softwoods, under the same conditions, require 10 to 12 hr. for adequate acetylation to attain the same antishrink efficiency (25 per cent acetyl content). With softwoods,

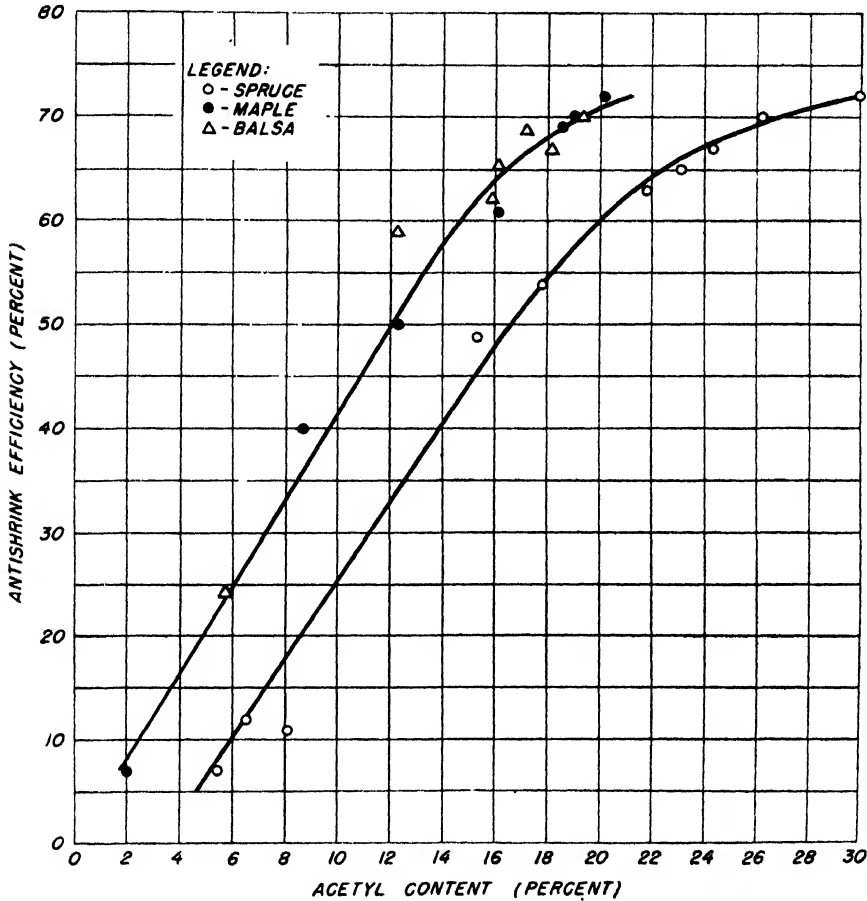


FIG. 1. Relationship between the acetyl content and the antishrink efficiency for several species of wood.

however, increasing the concentration of pyridine to 50 per cent in the liquid phase has a pronounced effect in reducing the time for adequate acetylation.

Properties

Acetylated veneer looks practically like untreated veneer. Some species appear slightly bleached, especially after exposure to ultraviolet light. Birch, on the other hand, is often but not always darkened by the treatment but bleaches on exposure to ultraviolet light. The grain of acetylated veneer may be some-

what more raised than that of untreated wood. If, however, it is pressed at as low a pressure as 100 pounds per square inch and 150°C., the surface becomes and remains extremely smooth.

Antishrink efficiencies of 70 per cent, measured between the water-soaked and oven-dry conditions or between high and low relative humidities, are readily obtained (figure 1). In some instances, antishrink efficiencies as high as 82 per cent have been obtained. These values are slightly higher than the values of 65 to 75 per cent obtainable with phenolic resins (16), 50 per cent obtainable with urea resins, and 40 to 60 per cent obtainable by heat (12). By acetylation the reductions in hygroscopicity are slightly less than the antishrink efficiencies, as is shown in table 1. Acetylated wood differs from resin-treated wood in that the communicating capillary structure is not blocked by a deposited material. Acetylated wood, therefore, takes up liquid water within the coarse capillaries about as readily as does untreated wood.

Acetylated wood shows considerable resistance to wood-destroying organisms. Acetylated balsa blocks exposed to *Poria versicolor* for three months in laboratory

TABLE 1

Percentage reduction in hygroscopicity and antishrink efficiency of acetylated Sitka spruce (30 per cent acetyl content) between the oven-dry condition and various relative humidities

RELATIVE HUMIDITY AT 80°F.	REDUCTION IN HYGROSCOPICITY	REDUCTION IN SWELLING
per cent	per cent	per cent
30	75	81
65	63	78
80	63	76
95	67	77

culture test showed no decay, whereas the untreated controls lost as much as 50 per cent of their weight. Acetylated sweetgum and yellow poplar veneer sheets, together with untreated controls, were subjected to 97 per cent relative humidity and 26.7°C. After several months the controls were coated with bluestain, whereas the treated veneer was free from stain.

Acetylated birch panels were inserted in termite-infested soil. After two years, the treated panels showed no signs of attack, whereas the controls showed moderate to bad attack. Acetylated wood was also found resistant to marine borers.

Esters of organic compounds are known to be susceptible to hydrolysis. Tests were therefore made to determine the chemical permanence of acetylated wood. Small specimens of acetylated birch were subjected to ten cycles of relative humidity change from 97 to 30 per cent at 26.7°C. for a period of four months. No change in antishrink efficiency was observed. Acetylated birch specimens were suspended over a saturated solution of sodium chloride (75 per cent relative humidity) at 80°C. for 3½ days. No change in antishrink efficiency resulted. Thin sections of acetylated birch were immersed in a 9 per cent aqueous solution of sulfuric acid for 18 hr. at room temperature. After the

acid had been washed out, tests of antishrink efficiency and acetyl content indicated that no ester hydrolysis had occurred. When the same test was made at 40°C. the antishrink efficiency dropped from 75 to 65 per cent.

Acetylated birch panels that had been suspended in the warm saline waters of the Gulf of Mexico for two years showed no damage due to marine borers, whereas the controls were badly attacked. This resistance to borers indicates that loss of acetyl groups due to hydrolysis could not have been large.

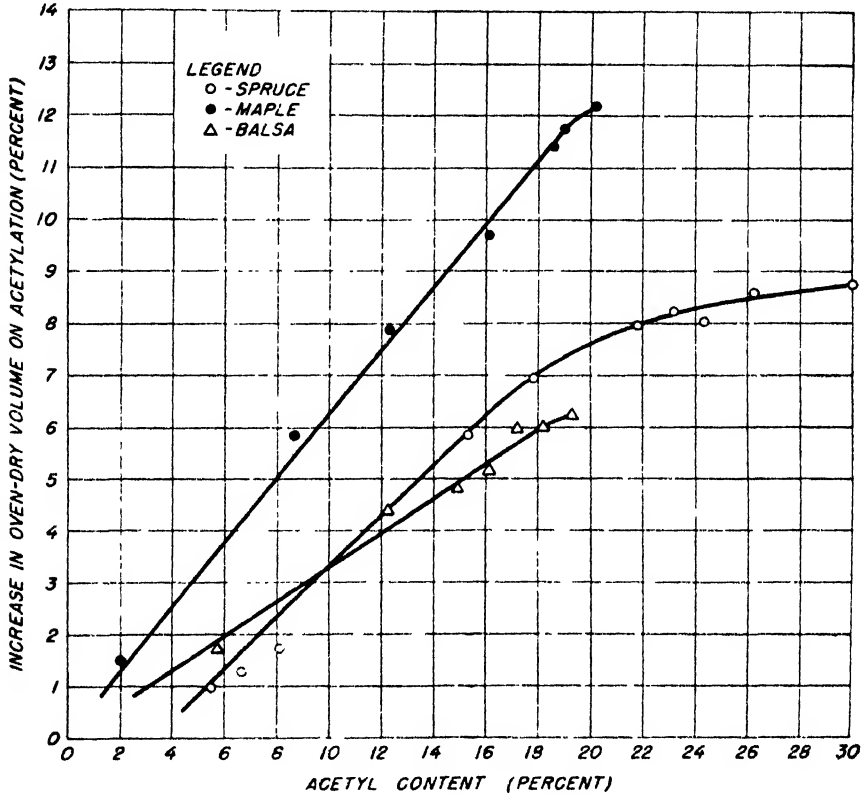


FIG. 2. Relationship between the acetyl content and the percentage increase in oven-dry volume.

Acetylation has a bulking effect upon wood. As a result, the oven-dry dimensions of wood increase with an increase in acetyl content (figure 2). The bulking effect for a fixed acetyl content also increases with an increase in the specific gravity of the wood. This is due to the facts that bulking is directly proportional to the amount of acetyl groups taken up by the cell-walls, and that any fixed acetyl content on a weight basis means a higher acetyl content per unit volume of wood for the heavier woods. Because of this, a species with high specific gravity is increased less in specific gravity as a result of a fixed degree of acetylation than a species of lower specific gravity (figure 3). At an acetyl

content of 20 per cent, for example, the oven-dry specific gravity of maple is increased by 8 per cent, that of spruce by 12 per cent, and that of balsa by 14 per cent. When based on the weight and volume under normal conditions, the

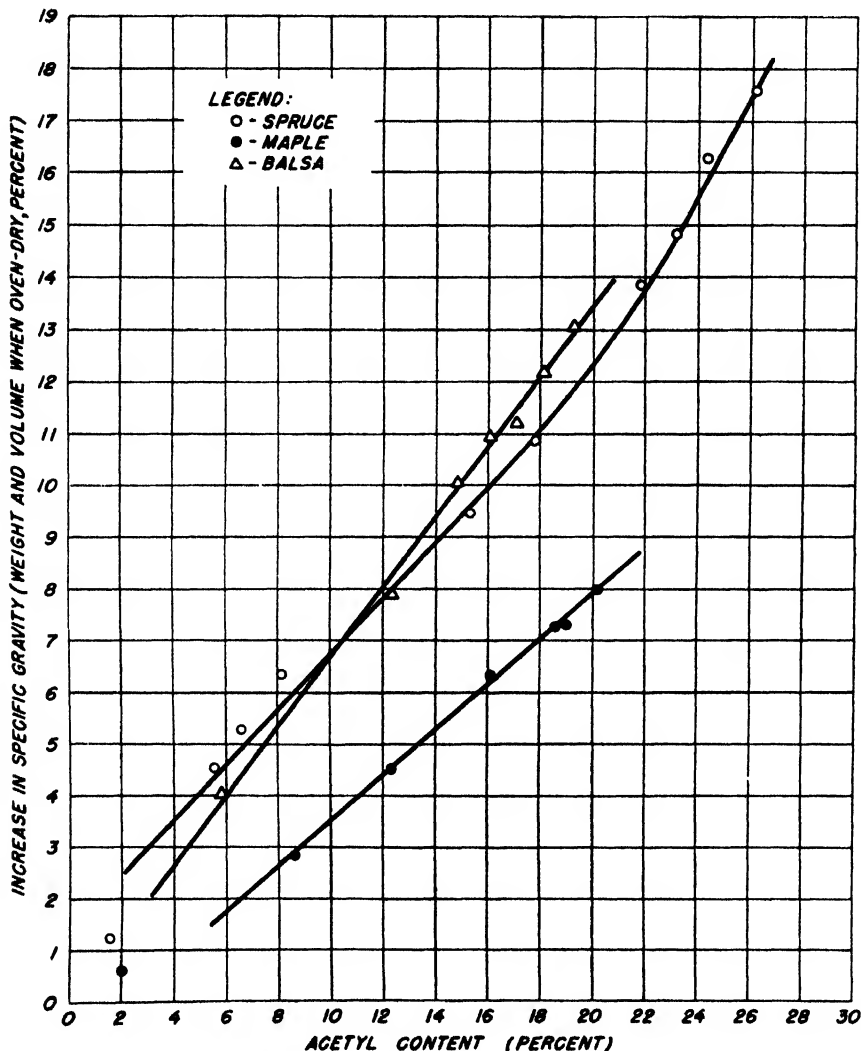


FIG. 3. Relationship between the acetyl content and the percentage increase in specific gravity.

percentage increases in specific gravity are less than those based on oven-dry weight and volume. At 65 per cent relative humidity, for example, untreated spruce has a moisture content of 12 per cent, whereas spruce with an acetyl content of 20 per cent, having an antishrink efficiency of 60 per cent and a reduction in hygroscopicity of 50 per cent, has a moisture content of 6 per cent. Under

these conditions, the increase in specific gravity at test over that of untreated wood is 9 per cent rather than 12 per cent. Similarly, the specific gravity increase of maple at test (65 per cent relative humidity) is only 5 per cent, in contrast to 8 per cent for the dry wood.

The limited strength tests that have been made to date indicate that dry acetylated wood has practically the same strength properties as the untreated controls except in the case of toughness. The toughness is either unaffected or is increased by as much as 20 per cent. The strength properties in equilibrium with high relative humidities should, in general, be improved because of the lower moisture content of the acetylated material.

Mechanism of stabilization

Table 2 gives data to show that the dimensional stabilization of wood attained by acetylation is primarily due to a bulking effect. Although acetylation appreciably increases the oven-dry dimensions of wood, originally having the same

TABLE 2
Volumetric changes in the system acetylated spruce-water

PROPERTY	UNTREATED WOOD	ACETYLATED WOOD
Oven-dry volume of spruce before acetylation, cc.	5.71	5.73
Subsequent acetyl content, per cent by weight.	0.00	28.6
Oven-dry volume after acetylation, cc.	5.71	6.23
Water-swollen volume, cc.	6.45	6.47
Volume change on immersion in water, cc.	0.74	0.24
Antishrink efficiency, per cent	0	70
Total volume change (acetyl and water), cc.	0.74	0.74

dry untreated volume, the water-swollen dimensions of the untreated and the acetylated wood are practically identical.

It may be argued that the replacement of the hydroxyl groups by the acetyl groups causes the stabilization as a result of the replacement of hydrophilic groups by less hydrophilic groups. Evidence, however, has been accumulated which suggests that the reduced polarity is not so probable a cause of stabilization as the bulking effect. Wood was acetylated, propionylated, and butyrylated. If stabilization resulted from the replacement of hydroxyl groups by the acyl group (acetyl, propionyl, or butyryl) for a given acyl content, the acetylated wood should have the greatest antishrink efficiency, the butyrylated wood should have the lowest, and that of the propionylated wood should lie between that of the acetylated wood and the butyrylated wood. This would be so because of the increasing molecular size and, therefore, because of the decreasing number of hydroxyl groups replaced as the molecular size of the acyl group increases.

Actually, all three treated specimens have the same antishrink efficiency. Yet only two-thirds of the hydroxyl groups replaced in acetylated wood are replaced in butyrylated wood. Thus it seems that the extent of stabilization obtained by acylating wood depends primarily on the bulk of the acyl groups

laid down per unit weight of wood. The single curve of figure 4 in which the volume of the acyl groups (acetyl, propionyl, or butyryl) per unit weight of wood is plotted against the antishrink efficiency holds for acetylated, propionylated, and butyrylated wood. The calculated specific volume of the acetyl group, the

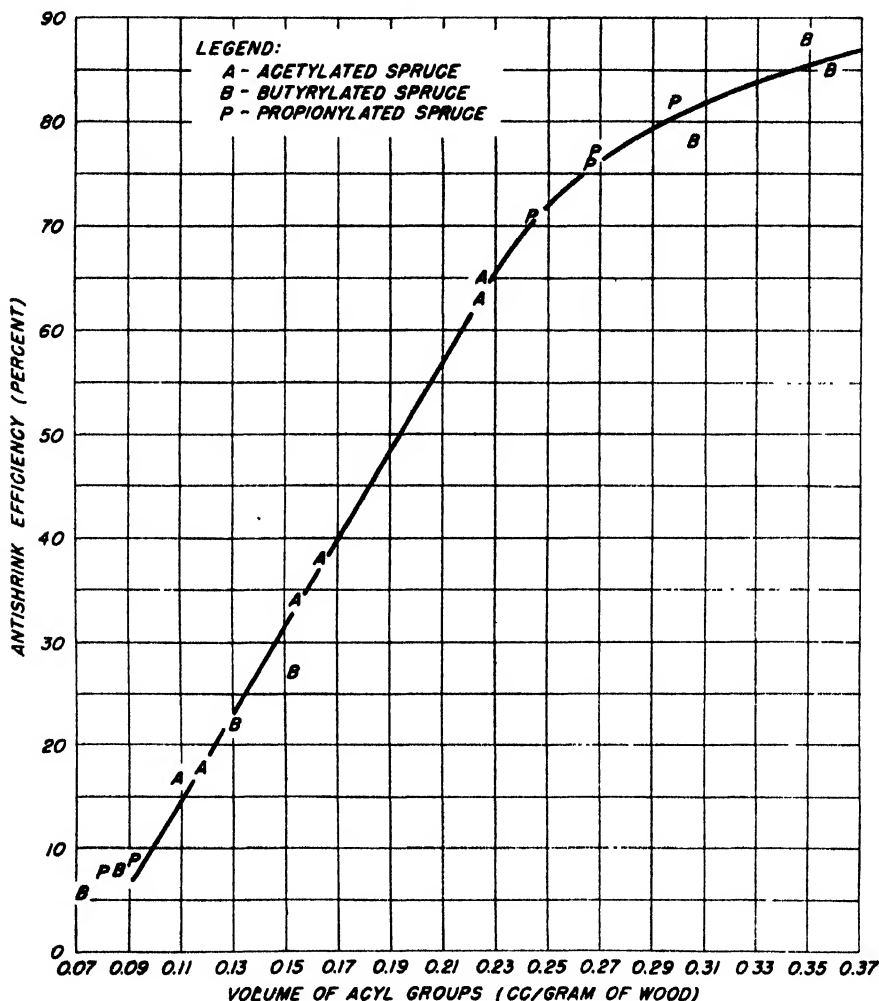


FIG. 4. Relationship between volume of acyl groups per gram of wood and the antishrink efficiency.

propionyl group, and the butyryl group used in the calculations is 0.902, 1.00, and 1.055 cc. per gram, respectively.

The bulking effect expressed as the increase in oven-dry volume caused by acetylation is, in general, equal to the volume of the acetyl groups. This is shown in figure 5, in which the volume of the acetyl groups per gram of wood is plotted against the external volumetric swelling of the wood. The volume of the

acetyl groups was obtained by multiplying their weights by their calculated specific volume. The slope of the curves for spruce and maple is unity, as is the case for normal woods swelling in water, the volume of liquid taken up adding its volume to that of the cell wall and the fiber cavities changing an insignificant

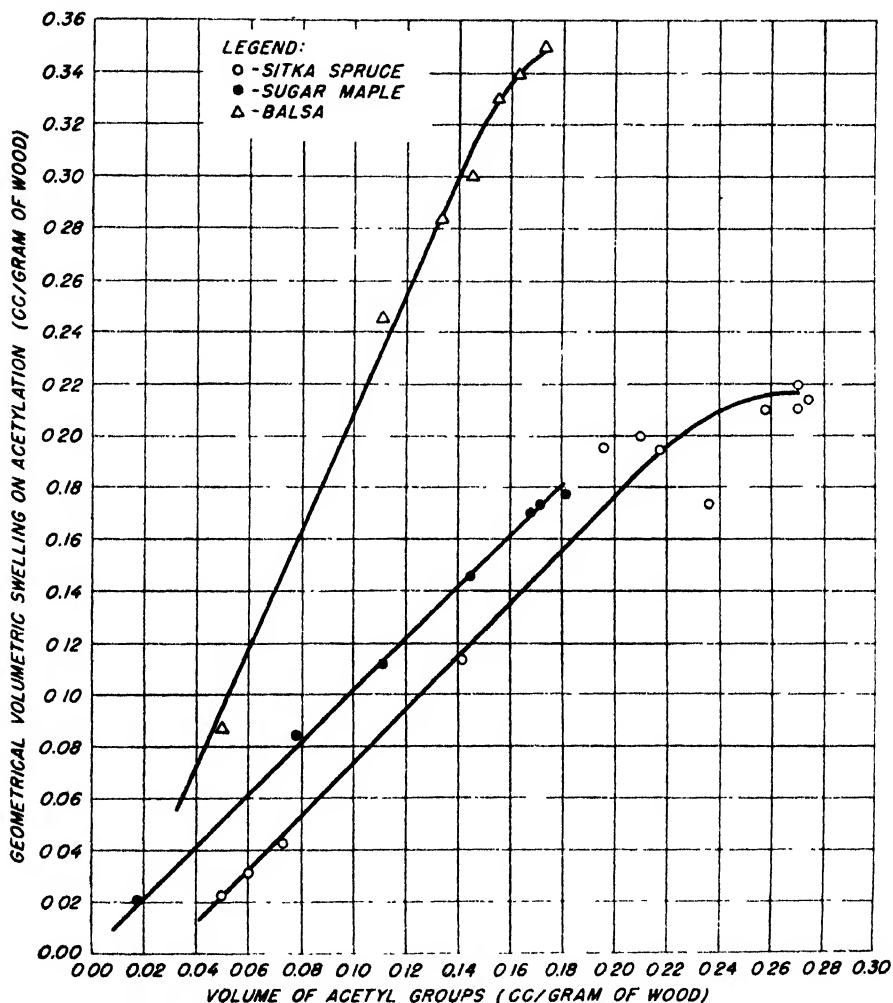


FIG. 5. Relationship between the volume of the acetyl groups and the external volumetric swelling.

amount in size (15). Balsa is abnormal in that the slope of the curve is about 2; that is, the increase in external volume is about twice the volume of acetyl groups taken up. Swelling of balsa in water is similarly abnormal. Swelling of balsa must be accompanied by an increase in the volume of the fiber cavities.

These data all indicate that the dimensional stabilization imparted to wood is due to a bulking effect which reduces the shrinkage. The fact that the acetyl

groups become chemically bonded to the wood throughout the cell-wall structure rather than merely being mechanically deposited within the cell wall apparently is of little importance in imparting dimensional stability to the wood. It may, however, be of considerable importance from the standpoint of permanence.

Harrison (3) has recently reported the hygroscopicity of partially acetylated, butyrylated, and stearoylated pulps. On comparing the hygroscopicity of such acylated pulps in which the same percentage of hydroxyl groups had been replaced, he finds a pronounced reduction in hygroscopicity as the size of the acyl group increases. Harrison believes this is due to an increasing hydrophobic character of the acyl group with increasing size.

Another explanation is offered, based on the bulking action of the acyl groups. It is assumed that the reduction in hygroscopicity of partially acylated pulp is equal to the volume of the acyl group laid down in the cell walls of the pulp. In other words, the total swelling that cellulose undergoes on partial acylation plus subsequent water gain remains constant regardless of the nature of the acyl group and regardless of the acyl content, provided this content is below such an

TABLE 3
Reduction in hygroscopicity of pulp on acylation

ACYL GROUP	ACYL CONTENT	VOLUME OF ACYL GROUP	HYDROXYLS REPLACED	REDUCTION IN HYGROSCOPICITY
	<i>weight per cent of pulp</i>	<i>cc. per 100 g. pulp</i>	<i>per cent of total number</i>	<i>per cent</i>
Acetyl...	22.3	20.1	28.0	25
Butyryl.....	16.3	17.2	12.4	25
Stearoyl.....	17.3	19.5	3.5	25

amount where no disruption or polymorphic change (5) in the cellulose can occur. Table 3 has been constructed from Harrison's data.

It will be noted that all acylated pulps have the same hygroscopicity, even though 28 per cent of the total number of hydroxyl groups are replaced by acetyl groups, 12.4 per cent replaced by butyryl groups, and only 3.5 per cent replaced by stearyl groups. On the other hand, it will be noted that the *volume* of the acyl groups laid down in the pulp seems to be approximately the same. Thus the hygroscopicity of partially acylated pulp seems to be governed primarily by the volume of the acyl group laid down rather than by the number of hydroxyl groups which have been replaced. It should be emphasized that this relationship holds only providing the volume of the acyl group is not sufficient to change the polymorphic configuration of the cellulose unit cell. For greater acyl contents, the assumption no longer holds that the total swelling on acylation and moisture gain remains constant. At these higher acyl contents, volumetric changes in the size of the unit cell of cellulose complicate the calculations.

CONCLUSIONS

It has been shown that wood can be acetylated by a vapor-phase treatment with acetic anhydride and pyridine so as to avoid breakdown of the wood struc-

ture. This treatment gives the highest degree of dimensional stabilization on a moisture equilibrium basis thus far obtained. The resulting ester is quite stable. Unlike other dimension-stabilizing treatments, the wood is not embrittled. It has other strength properties about the same as those of untreated wood. It is highly resistant to decay, termites, and marine borers. The dimensional stabilization is primarily due to a bulking effect by the acetyl groups, which causes an increase in the dry dimensions without increasing the wet dimensions.

REFERENCES

- (1) BATESON, B. A.: Chem. Trade J. **105** (8) (2724), 93 (1939).
- (2) BROWNE, F. L.: Ind. Eng. Chem. **25**, 835 (1933).
- (3) HARRISON, J. J.: Paper Trade J. **119**, 28 (1944).
- (4) HESS, K.: Ber. **61**, 1460 (1928).
- (5) HESS, K., AND TROGUS, C.: Z. physik. Chem. **B15**, 157 (1932).
- (6) HUNT, G. M.: U. S. Dept. Agr. Circ. No. **128** (1930).
- (7) MULLEN, J. W., AND PACSU, E.: J. Am. Chem. Soc. **63**, 1487 (1941).
- (8) STAMM, A. J.: J. Am. Chem. Soc. **56**, 1195 (1934).
- (9) STAMM, A. J.: U. S. patent 2,060,902 (November, 1936).
- (10) STAMM, A. J.: U. S. patent 2,296,316 (September, 1942).
- (11) STAMM, A. J.: Ind. Eng. Chem. **29**, 833 (1937).
- (12) STAMM, A. J., BURR, H. K., AND KLINE, A. A.: Ind. Eng. Chem. **38**, 630 (1946).
- (13) STAMM, A. J., AND HANSEN, L. A.: Ind. Eng. Chem. **27**, 1480 (1935).
- (14) STAMM, A. J., AND HANSEN, L. A.: Ind. Eng. Chem. **29**, 831 (1937).
- (15) STAMM, A. J., AND LOUGHBOROUGH, W. K.: Trans. Am. Soc. Mech. Engrs. **63**, 329 (1942).
- (16) STAMM, A. J., AND SEBORG, R. M.: Ind. Eng. Chem. **31**, 897 (1939).
- (17) STAMM, A. J., AND SEBORG, R. M.: Trans. Am. Inst. Chem. Engrs. **37**, 385 (1941).
- (18) STAUDINGER, H.: Ann. **529**, 219 (1937).

KINETICS OF HOMOGENEOUS GASEOUS REACTIONS IN
FLOW SYSTEMS

G. M. HARRIS

*Department of Chemistry, University of Saskatchewan, Saskatoon, Saskatchewan, Canada**Received November 8, 1946*

INTRODUCTION

A review of the literature indicates that a number of special cases of the kinetics of flow systems have from time to time been the subject of theoretical treatment. Recently, general discussions have been given by two authors (3, 6), but their concern was primarily with applications to large-scale industrial operations. It is the purpose of the present paper to reexamine and elaborate the theory of reactions in flow systems, with special regard to the requirements of experimenters in the field of the kinetics of homogeneous gaseous reactions.

Many years ago, both Bodenstein (2) and Langmuir (7) drew attention to the

necessity for modification of the forms of the usual static-system kinetic equations for uni- and bimolecular reactions, when the latter take place under flow conditions. These altered expressions were based on the assumptions that no change in volume of the reacting mixture took place during reaction, and that the velocity of flow of the gases was slow enough, as compared to the rate of molecular diffusion, so that complete and instantaneous mixing of the reactants could be presumed throughout the reaction space. This work underlines the two complicating factors which distinguish the kinetic treatment of flow-system reactions from their static analogues:

(1) Reactions in flow systems in general occur at constant pressure, as compared to the constant-volume conditions of static systems. Thus, in the former case, when the number of moles of reacting mixture undergoes a change as reaction proceeds, the resulting continuous volume change considerably complicates the definition of the concentration terms in the kinetic equation. This factor will hereafter be referred to simply as the "volume effect."

(2) Exclusive of the "volume effect," the concentration gradient of the reactants along the reaction path is a function not only of the streaming velocity of the gas mixture, but also of the lateral rate of diffusion of reactant molecules. This factor will be identified in the subsequent text as the "diffusion effect."

The general problem is not so difficult of solution if the "diffusion effect" is entirely neglected, and only the "volume effect" considered. On these terms, Benton (1) has defined an expression for the rate constant of the general unimolecular reaction $A \rightarrow nC$, while other workers (8, 9) have derived rate expressions applicable to particular bimolecular reactions. The "diffusion effect" has been rigorously dealt with by Förster and Geib (5) for the simple reaction $A \rightarrow B$. The highly involved mathematical form of their result for all but the simple boundary conditions (i.e., $D = 0$ and $D = \infty$, where D is the coefficient of diffusion) renders it impossible to define the rate constant in terms of experimentally measurable factors except in the two extreme cases mentioned. Recently, Hurlburt (6) has formulated an equation on quite general terms, using hydrodynamical theory, which attempts to allow for both the "volume effect" and the "diffusion effect." However, the complicated nature of the diffusion term in his fundamental differential equation allows its rigorous solution only for the simple case $A \rightarrow B$, for which Hurlburt's integrated expression is identical in form with that previously derived by Förster and Geib (5).

Bearing in mind the discussion given in the foregoing paragraphs, it is seen that the extent of the present inquiry may well be limited by the two following criteria:

(1) Previous calculations (5, 6) have shown that it is mathematically impractical to attempt to allow for all possible fractional contributions of the "diffusion effect" in deriving general expressions for the rate constants of reactions in flow systems. It is consequently reasonable to confine attention to the two boundary conditions stated by Förster and Geib—the conditions of (a) very rapid or (b) very slow diffusion, as compared to the molecular displacements resulting from the streaming of the gases through the reactor. The first of these

extreme cases may be realized experimentally in a system which combines relatively slow rates of flow, large reactor cross-section, low pressure, and high temperature (4). The opposites of these factors favor the slow diffusion extreme.

(2) Generally speaking, consideration of the kinetics of homogeneous gaseous reactions may be confined in practice to the types $A \rightarrow nC$ and $A + B \rightarrow nC$, since it is an accepted fact that very few reactions of higher than the second order occur by a simple collision process. In the reaction types given, C can be taken to represent all species of product molecules collectively.

The two above-stated criteria define four distinct reaction types, which may now be analyzed in detail. A uniform system of symbolism has been adopted for use throughout the succeeding calculations, as follows:

N_{A_0}, N_{B_0} = number of moles of reactants A or B entering reactor per second,
 N_A, N_B, N_C = number of moles of reactants A or B or of products C leaving the reactor per second,

V_0 = velocity of flow of entering mixture (liters per second),

V_e = velocity of flow of effluent mixture (liters per second),

C_A, C_B, C_C = concentrations of reactants A or B or of products C, as defined in the discussion, and

n = number of moles of product formed per mole of a given reactant undergoing reaction.

It will be assumed in every case that the reaction is caused to cease immediately after the reactants leave the reaction zone, either by a sudden temperature decrease, or by removal of one or more of the reactants (e.g., by "freezing out" in a trap). Since the quantities which are usually most convenient to measure in experimental work of this nature are the rates of inflow of the reactants and the rate of formation of one or more of the products, all final expressions are given in terms of N_{A_0}, N_{B_0} , and N_C .

CASE I. FIRST-ORDER REACTION: NEGLIGIBLE DIFFUSION

This case, as mentioned above, has been dealt with by Benton (1), and the essentials of his derivation differ little from that given here. In each element of reaction space, the rate of reaction is given by:

$$\frac{dN_A}{dt} = -k_1 N_A$$

The volume V occupied by the mixture of reactants and products at any time t is, on the assumption of the perfect gas laws:

$$V = \frac{RT}{p} (N_A + N_C) = \frac{RT}{p} \left[N_{A_0} + \left(\frac{n-1}{n} \right) N_C \right]$$

since $N_A = N_{A_0} - \frac{1}{n} N_C$. In this equation, T and p are the temperature and pressure of the reaction zone, respectively. V is seen to be defined also as the volume of mixture which passes through any sectional plane of the reactor in unit time.

Consider the volume V of reacting mixture to pass through an element of the reaction chamber of volume dV_R . Its time in the volume element of the reactor is:

$$dt = \frac{dV_R}{V}$$

Combining the above expressions, it is seen that:

$$\frac{dN_A}{dt} = V \frac{dN_A}{dV_R} = -k_1 N_A$$

and

$$\frac{1}{n} \frac{dN_C}{dV_R} = k_1 \left(\frac{p}{RT} \right) \left[\frac{\left(N_{A_0} - \frac{1}{n} N_C \right)}{N_{A_0} + \left(\frac{n-1}{n} \right) N_C} \right]$$

When the latter equation is integrated, with the condition that $N_C = 0$ when $V_R = 0$, the result is:

$$k_1 = \left(\frac{RT}{p} \right) \left(\frac{1}{V_R} \right) \left[n N_{A_0} \ln \frac{N_{A_0}}{N_{A_0} - \frac{1}{n} N_C} - \left(\frac{n-1}{n} \right) N_C \right]$$

or, since $\frac{N_{A_0} RT}{p} = V_0$ (assuming the perfect gas laws),

$$k_1 = \left(\frac{V_0}{V_R} \right) \left[n \ln \frac{N_{A_0}}{N_{A_0} - \frac{1}{n} N_C} - \left(\frac{n-1}{n} \right) \frac{N_C}{N_{A_0}} \right] \quad (1)$$

CASE II. FIRST-ORDER REACTION: COMPLETE DIFFUSION

Here the composition of the effluent gas mixture is the same as the composition of the mixture at any point within the reaction zone. The concentration of product C in the effluent gases is proportional to the time t spent by the mixture in the reactor and to the concentration of reactant A; i.e., $C_C = tk_1 C_A$. Thus, since $C_C = N_C/V_0$, and $C_A = N_A/V_0$, the number of moles of C collected in unit time is given by the expression $tk_1 N_A$. Since the average time spent by each element of the reacting mixture in the reactor is given by $t = V_R/V_0$, the rate constant for the reaction is:

$$k_1 = \frac{N_C}{tN_A} = \frac{V_0 N_C}{V_R N_A}$$

also,

$$N_A = N_{A_0} - \frac{1}{n} N_C$$

and

$$V_* = V_0 \left(\frac{N_A + N_C}{N_{A0}} \right) = V_0 \left[1 + \left(\frac{n-1}{n} \right) \frac{N_C}{N_{A0}} \right]$$

Whence

$$k_1 = \left(\frac{V_0}{V_R} \right) \left(\frac{N_C}{N_{A0} - \frac{1}{n} N_C} \right) \left[1 + \left(\frac{n-1}{n} \right) \frac{N_C}{N_{A0}} \right] \quad (2)$$

CASE III. SECOND-ORDER REACTION: NEGLIGIBLE DIFFUSION

This situation can be dealt with adequately in a manner analogous to case I above. The result obtained covers the special examples considered by Pease (8) and by Sherwood and Reed (9) and can be shown to be identical in form with the equation derived hydrodynamically by Hurlburt (6) for the corresponding general case.

Consider the reaction $A + B \rightarrow nC$. In each element of reactor along the path of flow, the rate of reaction is given by:

$$\frac{dC_A}{dt} = -k_2 C_A C_B$$

in which C_A and C_B are the concentrations of the reactants in the element of reactor under consideration. If V represents the volume occupied by reactants and products at any time of reaction, C_A and C_B can be replaced by $\frac{N_A}{V}$ and $\frac{N_B}{V}$, and the differential equation becomes:

$$\frac{dN_A}{dt} = -k_2 \frac{N_A N_B}{V}$$

Assuming the perfect gas laws, V is defined by the following relation:

$$\begin{aligned} V &= \frac{RT}{p} (N_A + N_B + N_C) \\ &= \frac{RT}{p} \left[N_{A0} + N_{B0} + \left(\frac{n-2}{n} \right) N_C \right] \end{aligned}$$

since $N_A = N_{A0} - \frac{1}{n} N_C$ and $N_B = N_{B0} - \frac{1}{n} N_C$. Here again, T and p are the temperature and pressure of the reaction mixture.

As in case I, $dt = \frac{dV_R}{V}$, and the expression takes the form:

$$\frac{1}{n} \frac{dN_C}{dV_R} = k_2 \left(\frac{p}{RT} \right)^2 \frac{\left(N_{A0} - \frac{1}{n} N_C \right) \left(N_{B0} - \frac{1}{n} N_C \right)}{\left[N_{A0} + N_{B0} + \left(\frac{n-2}{n} \right) N_C \right]^2}$$

This equation can be integrated, and, on application of the limit $N_C = 0$ when $V_R = 0$, gives, for $N_{A_0} \neq N_{B_0}$:

$$k_2 = \left(\frac{V_0^2}{V_R} \right) \left[\frac{(n-2)^2}{(N_{A_0} + N_{B_0})^2} \left(\frac{1}{n} N_C \right) + \alpha \ln \left(\frac{N_{A_0}}{N_{A_0} - \frac{1}{n} N_C} \right) - \beta \ln \left(\frac{N_{B_0}}{N_{B_0} - \frac{1}{n} N_C} \right) \right] \quad (3a)$$

where α and β are constants defined by:

$$\alpha = \left(\frac{1}{N_{B_0} - N_{A_0}} \right) \left[1 + (n-2) \frac{N_{A_0}}{N_{A_0} + N_{B_0}} \right]^2$$

$$\beta = \left(\frac{1}{N_{B_0} - N_{A_0}} \right) \left[1 + (n-2) \frac{N_{B_0}}{N_{A_0} + N_{B_0}} \right]^2$$

For the special case of $N_{A_0} = N_{B_0}$, the integrated form is:

$$k_2 = \left(\frac{V_0^2}{V_R} \right) \left[\frac{(n-2)^2}{(N_{A_0})^2} \left(\frac{1}{n} N_C \right) + \frac{N_C}{N_{A_0} \left(N_{A_0} - \frac{1}{n} N_C \right)} + \frac{2n(n-2)}{N_{A_0}} \ln \left(\frac{N_{A_0} - \frac{1}{n} N_C}{N_{A_0}} \right) \right] \quad (3b)$$

CASE IV. SECOND-ORDER REACTION: COMPLETE DIFFUSION

This type is analogous to case II. Again, the composition of the effluent gases is the same as the composition of the reacting mixture anywhere within the reaction zone. The concentration of C in the outflowing gas is proportional to the time the mixture has remained within the reactor, and to the concentrations of reactants; i.e.:

$$C_C = k_2 t C_A C_B$$

The terms C_A , C_B , C_C are equivalent to N_A/V_e , N_B/V_e , and N_C/V_e , where V_e is the volume of mixture issuing from the reactor per unit time at the temperature and pressure of the reactor. Also, the average time of reaction t equals V_R/V_e , so the equation above becomes:

$$k_2 = \frac{V_e^2}{V_R} \cdot \frac{N_C}{N_A N_B} = \frac{V_e^2}{V_R} \cdot \frac{N_C}{\left(N_{A_0} - \frac{1}{n} N_C \right) \left(N_{B_0} - \frac{1}{n} N_C \right)}$$

since $N_A = N_{A_0} - \frac{1}{n} N_C$ and $N_B = N_{B_0} - \frac{1}{n} N_C$, as before. Furthermore:

$$V_e = V_0 \left(\frac{N_A + N_B + N_C}{N_{A_0} + N_{B_0}} \right) = V_0 \left[1 + \left(\frac{n-2}{n} \right) \frac{N_C}{N_{A_0} + N_{B_0}} \right]$$

Thus, for $N_{A_0} \neq N_{B_0}$,

$$k_2 = \left(\frac{V_0^2}{V_R}\right) \left[\frac{N_C}{\left(N_{A_0} - \frac{1}{n} N_C\right) \left(N_{B_0} - \frac{1}{n} N_C\right)} \right] \left[1 + \left(\frac{n-2}{n}\right) \frac{N_C}{N_{A_0} + N_{B_0}} \right]^2 \quad (4a)$$

When $N_{A_0} = N_{B_0}$, the equation is:

$$k_2 = \left(\frac{V_0^2}{V_R}\right) \left[\frac{N_C}{\left(N_{A_0} - \frac{1}{n} N_C\right)^2} \right] \left[1 + \left(\frac{n-2}{n}\right) \frac{N_C}{2N_{A_0}} \right]^2 \quad (4b)$$

DISCUSSION

Considerable simplification of the expressions derived in the above analysis results for certain special conditions. In the first place, if no volume change is involved in the reactions (i.e., $n = 1$ in cases I and II, $n = 2$ in case III and IV), the equations reduce to the following forms:

Case I:

$$k_1 = \left(\frac{V_0}{V_R}\right) \ln \left(\frac{N_{A_0}}{N_{A_0} - N_C} \right) \quad (5)$$

Case II:

$$k_1 = \left(\frac{V_0}{V_R}\right) \left(\frac{N_C}{N_{A_0} - N_C} \right) \quad (6)$$

Case III:

$$k_2 = \left(\frac{V_0^2}{V_R}\right) \left(\frac{1}{N_{B_0} - N_{A_0}} \right) \left[\ln \frac{N_{A_0}(N_{B_0} - \frac{1}{2}N_C)}{N_{B_0}(N_{A_0} - \frac{1}{2}N_C)} \right]; \quad (N_{A_0} \neq N_{B_0}) \quad (7a)$$

OR

$$k_2 = \left(\frac{V_0^2}{V_R}\right) \left[\frac{N_C}{N_{A_0}(N_{A_0} - \frac{1}{2}N_C)} \right]; \quad (N_{A_0} = N_{B_0}) \quad (7b)$$

Case IV:

$$k_2 = \left(\frac{V_0^2}{V_R}\right) \left[\frac{N_C}{(N_{A_0} - \frac{1}{2}N_C)(N_{B_0} - \frac{1}{2}N_C)} \right]; \quad (N_{A_0} \neq N_{B_0}) \quad (8a)$$

OR

$$k_2 = \left(\frac{V_0^2}{V_R}\right) \left[\frac{N_C}{(N_{A_0} - \frac{1}{2}N_C)^2} \right]; \quad (N_{A_0} = N_{B_0}) \quad (8b)$$

It is immediately apparent that these simplified equations are, when mixing is negligible (i.e., cases I and III), identical in form with the integrated forms of the corresponding expressions for static systems. However, for the complete mixing examples (cases II and IV), the forms are seen to be quite different.

Additional simplification results if the percentage of reaction is small, say of

the order of less than 10 per cent. With such a stipulation, the rate-constant equations given above become further reduced as follows:

Cases I and II:

$$k_1 = \left(\frac{V_0}{V_R} \right) \left(\frac{N_C}{N_{A_0}} \right) \quad (9)$$

Cases III and IV: ($N_{A_0} \neq N_{B_0}$)

$$k_2 = \left(\frac{V_0^2}{V_R} \right) \left(\frac{N_C}{N_{A_0} N_{B_0}} \right) \quad (10)$$

Cases III and IV: ($N_{A_0} = N_{B_0}$)

$$k_2 = \left(\frac{V_0^2}{V_R} \right) \left(\frac{N_C}{N_{A_0}^2} \right) \quad (11)$$

Obviously, it is immaterial in this situation whether mixing in the reactor is considered negligible or complete.

The author takes pleasure in expressing his appreciation to his colleague, Professor J. W. T. Spinks, for helpful discussions and advice in the preparation of this article.

REFERENCES

- (1) BENTON, A. F.: J. Am. Chem. Soc. **53**, 2984 (1931).
- (2) BODENSTEIN, M., AND WOLGAST, K.: Z. physik. Chem. **61**, 422 (1908).
- (3) DENBIGH, K. G.: Trans. Faraday Soc. **40**, 352 (1944).
- (4) FARKAS, A., AND MELVILLE, H. W.: *Experimental Methods in Gas Reactions*, p. 296. The Macmillan Company, New York (1939).
- (5) FORSTER, VON TH., AND GEIB, K. H.: Ann. Physik **20**, 250 (1934).
- (6) HURLBURT, H. M.: Ind. Eng. Chem. **36**, 1012 (1944); **37**, 1063 (1945).
- (7) LANGMUIR, I.: J. Am. Chem. Soc. **30**, 1742 (1908).
- (8) PEASE, R. N.: see J. Am. Chem. Soc. **51**, 3470 (1929).
- (9) SHERWOOD, T. K., AND REED, C. E.: *Applied Mathematics in Chemical Engineering*, p. 57. The McGraw-Hill Book Company, Inc., New York (1939).

ON UNIMOLECULAR REACTIONS AND RADIOACTIVE TRANSFORMATIONS

GEORGE ANTONOFF

*Department of Chemistry, Fordham University, New York, New York**Received March 22, 1946*

Following the publication by the author of an article on unimolecular reactions (1), there ensued an exchange of letters; ultimately two letters were published by Luder (5, 6) and one by Glasstone (4), the latter of whom invited the readers to disregard the author's statements on unimolecular and first-order reactions.

In view of the highly confused state of the subject, the author wishes to make the following statement. He finds it difficult to teach kinetics because in most textbooks the definitions are different, if they are given at all, and to his knowledge he is not alone, many other people complaining about the confused state of the subject.

In his paper the author took the same view as expressed by Lind in his article on radioactivity in Taylor's *Treatise on Physical Chemistry* (7, page 1724).

The well-known exponential expression used in radioactivity, according to Lind, "is the ordinary equation for unimolecular reaction, and in fact, represents the most perfect case, and, as is sometimes maintained, may represent the only true case of unimolecular change."

In the following, the theory will be discussed as the author understands it. It should be mentioned that, for reasons which will be explained later, he uses in this paper the terms "unimolecular reaction" and "first-order reaction" indiscriminately.

It is a well-known fact that when the student of physical chemistry approaches the treatise on rate he is informed that the expression for first-order reactions is

$$-\frac{dC}{dt} = KC \quad (1)$$

where C is the concentration, t is time, and K is a constant. The popular definition of a first-order reaction is so worded that it involves concentration; hence the above mathematical expression is the logical result. When he investigates radioactive decay, he is informed that the rate is given as

$$-\frac{dN}{dt} = KN \quad (2)$$

where N is the number of particles reacting, and that here the rate is independent of concentration. If he investigates further he learns that, strictly speaking, volume is not a necessary factor in expressing first-order reactions, and that it would seem more precise to express the rate in terms of number. The question then arises in his mind, "Why have two expressions for identical phenomena? Why treat a first-order reaction and radioactive decay separately?"

It is our contention that the expression $-dN/dt$ could very well substitute for both reactions and more clearly express their rate. We contend that $-dN/dt$ is the simpler expression and that all others can be reduced to it by cancellations of unnecessary terms on both sides of equation 1.

The above expression (equation 2) in integrated form will be

$$N = N_0 e^{-kt}$$

where N_0 is the number of particles initially present, and N their number at a time t .

The exponential equation will be equally well satisfied if we write $C = C_0 e^{-kt}$, where C_0 is the initial concentration, and C is the concentration at time t .

One could also write $G = G_0 e^{-kt}$, where G_0 is the number of grams initially present, and G the number at time t .

The latter expression can be written

$$N \times 1.65 \times 10^{-24} \times M = N_0 \times 1.65 \times 10^{-24} \times M \times e^{-kt}$$

where N and N_0 are as above, 1.65×10^{-24} is the mass of the hydrogen atom in grams, and M is the molecular weight.

If one divides both sides by V , the volume, the equation is then expressed in concentrations.

In all cases, on cancellation, what remains is always:

$$N = N_0 e^{-kt}$$

It is the fundamental equation and its rate, $-dN/dt$, is the velocity of a reaction having a definite physical meaning, and is independent of concentration. All other expressions, such as $-dC/dt$ or $-dC_0/dt$, can be regarded only as multiples of it, and should be used only with special care.

Expression 1 is objectionable because it conveys the idea to a student that the velocity of the reaction depends upon concentration, whereas in reality it does not. That much the student can understand, but the theory upheld by Luder and Glasstone is too contradictory to be taught, as can be seen from the following: Both of them cite in their respective letters (4, 6) the textbooks of the latter (3) but do not specify any pages. In the index the heading "Unimolecular reactions" refers to page 1028. One finds there actually the word "unimolecular" mentioned more than once but without any definition or explanation. On page 1031 in the section on pseudo-unimolecular reactions there is the sentence "... each act of decomposition involves one molecule only." This might be regarded as a suitable definition of a unimolecular reaction but it is not clear whether it is intended to mean that, because the reaction



involves two molecules according to Luder, with whom Glasstone agrees completely, and they both call it unimolecular.

On page 1085 Glasstone (3) says, "For unimolecular changes, or more explicitly for those of first order, the time taken to reduce the concentration of reactant by a

definite fraction is independent of that concentration; for a given mass of gas, the *amount decomposed in unit time*, i.e., *the rate of reaction*,¹ will, therefore, be independent of the volume." Here the rate of reaction as he defines it would be, in our notation:

$$-\frac{dG}{dt}$$

In his letter (4) the rate is:

$$-\frac{dC}{dt}$$

On page 1024, in a footnote, he says that the rate, velocity, and speed are used indiscriminately and should be regarded as synonymous, but surely two different expressions used for the rate by the same author are not synonymous.

Want of convention and of clear-cut definitions leads in the hands of some other writers to such inaccuracies as the following: $-dC/dt$ is described as the rate, and the rate is said to be proportional to the *amount* of matter reacting.

In our notation it would mean:

$$-\frac{dC}{dt} = kG$$

which is inconsistent with both equations 1 and 2. There is another point difficult to understand.

Luder says that radioactive decay is not a first-order process in concentration. Glasstone agrees with him completely, and yet on page 1027 he says, "The decay of a radioactive element may be regarded as a first-order process."

Thus it appears that the order depends on the letter used in the equation. If it is written with N , it is not first order; if for the same process C is used, it is the other way about.

It should be added that Luder does not read rightly the exponential equation used in radioactivity. It is not stated in terms of weight, as he says, but number. Besides, it is expressed in terms of the number present at any time, and not decomposed, as Luder says.

In view of the above, the author cannot recognize as valid the method of Glasstone and Luder for discriminating between unimolecular and first-order reactions.

CONCLUSION

The coefficient $-dN/dt$ is the only proper expression for the velocity of first-order reactions.

Radioactive changes and first-order reactions must be classed together, being subject to the same law, as stated in the article by Lind (7, page 1724).

Want of proper definitions in chemical kinetics is the cause of the confused state of the subject.

¹ Italics inserted by the author.

Indiscriminate use of the expressions "speed," "velocity," and "rate" without giving definition to these terms leads to confusion, of which the theory upheld by Luder and Glasstone is a manifestation.

REFERENCES

- (1) ANTONOFF, G.: *J. Chem. Education* **21**, 420 (1944).
- (2) ANTONOFF, G.: *J. Chem. Education* **22**, 98 (1945).
- (3) GLASSTONE, S.: *Text-book of Physical Chemistry*. D. Van Nostrand Company, Inc., New York (1940).
- (4) GLASSTONE, S.: *J. Chem. Education* **22**, 201 (1945).
- (5) LUDER, W. F.: *J. Chem. Education* **21**, 559 (1944).
- (6) LUDER, W. F.: *J. Chem. Education* **22**, 201 (1945).
- (7) TAYLOR, H. S.: *A Treatise on Physical Chemistry*, 2nd edition, Vol. II. D. Van Nostrand Company, Inc., New York (1931).

ISOTONIC SOLUTIONS: OSMOTIC AND ACTIVITY COEFFICIENTS OF LITHIUM AND SODIUM PERCHLORATES AT 25°C.¹

JAMES HOMER JONES

*Department of Chemistry, Indiana University, Bloomington, Indiana**Received September 3, 1946*

The activity coefficients of lithium and sodium perchlorates up to 1 molal have been determined from freezing-point measurements by Scatchard and coworkers (4). No measurements at 25°C. are available in the literature. The present investigation determines the osmotic and activity coefficients of the two salts at 25°C. and over a much wider concentration range—about 0.2–6.5 molal for sodium perchlorate and 0.2–4.5 molal for lithium perchlorate.

The method used is the familiar isopiestic vapor-pressure measurement developed by Robinson and Sinclair and perfected by Robinson (3). The reference salt is sodium chloride, the activity and osmotic coefficients of which have been tabulated by Stokes and Levien (5). The apparatus, except for some modification, has been described previously (1). An all-brass desiccator about 8 in. in diameter and 6 in. deep replaced the one previously used, and a new rocking device was installed. This furnished a much superior heat reservoir and helped to moderate the effect of small fluctuations of temperature in the thermostat.

EXPERIMENTAL

Purification of materials

c. P. anhydrous sodium perchlorate was recrystallized from isobutyl alcohol, washed with anhydrous ether, and dried at 100°C. The material was then crushed in an agate mortar, dried at 250°C., and stored in a vacuum desiccator over anhydron. The lithium perchlorate was made according to the method

¹ Presented before the Division of Physical and Inorganic Chemistry at the 110th meeting of the American Chemical Society, Chicago, Illinois, September, 1946.

used by Scatchard and coworkers (4) for their freezing-point measurements. It was fused at 300°C. to remove the last traces of moisture before each solution was prepared. c. p. sodium chloride was precipitated by hydrochloric acid, recrystallized twice from conductivity water, and dried at 100°C. It was then crushed in an agate mortar and finally dried in a muffle furnace at 500–600°C.

Preparation of solutions

All solutions were made to predetermined concentrations by weighing both dry salt and water. The solutions were added to the vapor-pressure cups from a weight buret, the weight of the sample being determined by difference. The

TABLE 1
Concentrations of the isotonic solutions

<i>m</i> /NaCl	<i>m</i> /LiClO ₄	RATIO	<i>m</i> /NaCl	<i>m</i> /NaClO ₄	RATIO
0.2267	0.2178	1.0410	0.2003	0.2013	0.9951
0.2415	0.2315	1.0431	0.2415	0.2433	0.9926
0.2459	0.2361	1.0423	0.2458	0.2473	0.9940
0.3935	0.3695	1.0650	0.4241	0.4283	0.9902
0.4283	0.4000	1.0707	0.6186	0.6284	0.9845
0.5855	0.5389	1.0864	0.8557	0.8730	0.9802
0.6343	0.5785	1.0964	1.0328	1.0574	0.9767
0.8462	0.7598	1.1138	1.1208	1.1522	0.9728
1.0429	0.9208	1.1326	1.3415	1.3800	0.9721
1.3796	1.1898	1.1595	1.0486	1.4562	0.9673
1.8530	1.5572	1.1899	1.5493	1.6018	0.9672
1.9720	1.6448	1.1996	1.7295	1.8016	0.9598
2.093	1.734	1.2067	2.213	2.336	0.9474
2.648	2.144	1.2351	2.467	2.634	0.9400
3.234	2.561	1.2628	2.825	3.037	0.9302
3.633	2.841	1.2788	2.845	3.057	0.9305
4.064	3.149	1.2906	3.234	3.508	0.9219
4.480	3.439	1.3027	3.633	3.990	0.9105
4.585	3.513	1.3050	4.064	4.513	0.9005
5.308	4.038	1.3151	4.480	5.032	0.8914
5.585	4.230	1.3203	4.585	5.159	0.8890
			5.308	6.075	0.8738
			5.585	6.436	0.8678

precision in weight was at least 0.5 mg. The final weight of the solution after equilibrium had been established was obtained by subtracting the known weight of the cup from the final weight of cup plus sample. The cups were provided with covers to reduce loss of water after they had been removed from the reaction vessel. Experiment has shown that the loss of weight from removal until time of weighing was usually of the order of 1 mg. or less. The final concentration of each solution was computed from the known initial concentration, the weight of the sample, and the loss or gain of water.

DATA OBTAINED

The concentrations of the isotonic solutions are collected in table 1. In most of the cases at least two duplicate cups were used, and so the recorded concentra-

tions are the average of the two. These agreed with each other for the most part within 0.05 per cent.

TREATMENT OF DATA

The osmotic coefficients of lithium and sodium perchlorates were calculated from the isopiestic ratios and known values for sodium chloride, using the equation

$$\phi_x = \frac{m_{\text{NaCl}}}{m_x} \phi_{\text{NaCl}}$$

The osmotic coefficients for sodium chloride were taken from the tabulation by Stokes and Levien.

The activity coefficients were computed from the osmotic coefficients, using the method outlined by Harned and Owen (1). The equation used was

$$-\ln \gamma_{\pm} = (1 - \phi) + 2 \int_0^m \frac{(1 - \phi)}{m^{1/2}} dm^{1/2} \quad (1)$$

The activity coefficients for sodium perchlorate up to 1 molal were also computed by the original equation of Robinson, where the subscript x refers to sodium

$$\log \gamma_x = \log \gamma_r + \log m_r/m_x + \frac{2}{2.3026} \log \int_0^a \frac{\left(\frac{m_r}{m_x} - 1\right)}{a^{1/2}} da^{1/2} \quad (2)$$

perchlorate and r to sodium chloride. The answers by both equations were identical. Very good agreement should be expected, since the value of the integral in equation 2 up to experimental concentrations is very small and could be missed by several per cent without affecting the answer appreciably. This is certainly not the case with salts such as lithium perchlorate, where the integral has a quite large value.

To evaluate the integral in equation 1, it is necessary to use some extrapolation equation based on theory, since the value of the function $\frac{1 - \phi}{m^{1/2}}$ is so susceptible to experimental errors in dilute solutions. Such an equation may be derived from the Debye-Hückel theory in the form of $1 - \phi = 0.3888\sigma_m m^{1/2}$. The evaluation of σ_m depends on the finding of a suitable λ parameter (distance of closest approach of the ions) from the experimental data at the lower concentrations. For sodium perchlorate, the five lower concentrations gave a value of $\lambda = 4.4$ Å. (Ångström units). For lithium perchlorate, however, a very high value of 7–8 Å. was indicated. This value is too high, indicating that the solutions at the lower concentrations do not approach the theoretical value closely enough to be used. Since lithium perchlorate has activity coefficients close to those of lithium iodide, for which a value of λ of 5.5 Å. has been suggested, this value was also chosen as λ for lithium perchlorate. A linear term in con-

centration was then added to the limiting equation to make it fit the experimental data at the lower concentrations. The extrapolation was then made with the equation:

$$1 - \phi = 0.3888 \sigma_m m^{1/2} - 0.148m$$

The σ_m values for various values of m were taken by interpolation from the table given by Harned and Owen (1).

TABLE 2
Activity and osmotic coefficients

m	NaClO_4		LiClO_4	
	ϕ	γ	ϕ	γ
0.2	0.9190	0.728	0.9575	0.792
0.3	0.9142	0.701	0.9710	0.792
0.4	0.9115	0.681	0.9855	0.799
0.5	0.9102	0.667	0.9995	0.808
0.6	0.9096	0.656	1.0135	0.821
0.7	0.9100	0.647	1.0285	0.836
0.8	0.9110	0.640	1.0430	0.851
0.9	0.9122	0.634	1.0575	0.869
1.0	0.9135	0.629	1.0720	0.888
1.2	0.9166	0.621	1.1030	0.930
1.4	0.9202	0.616	1.1350	0.978
1.6	0.9244	0.612	1.1680	1.031
1.8	0.9290	0.610	1.2025	1.090
2.0	0.9338	0.608	1.2375	1.156
2.4	0.9445	0.608	1.3175	1.316
2.7	0.9528	0.610	1.3680	1.440
3.0	0.9618	0.612	1.4210	1.585
3.4	0.9742	0.617	1.4935	1.803
3.7	0.9836	0.622	1.5450	1.984
4.0	0.9925	0.627	1.5985	2.170
4.5	1.0090	0.637	1.6515	2.415
5.0	1.0250	0.649		
5.5	1.0412	0.662		
6.0	1.0570	0.675		
6.5	1.0745	0.691		

The activity and osmotic coefficients of sodium and lithium perchlorates are tabulated in table 2.

DISCUSSION OF RESULTS

The general trend of the variation of activity coefficients with concentration can best be illustrated graphically. Figure 1 shows such a graph.

In behavior these two salts are quite different. The activity coefficients of lithium perchlorate are distinguished by their high values. They pass through a minimum at about 0.2 molal, or just at the edge of the experimental region,

and increase rapidly with concentration. Among the uni-univalent electrolytes measured, these activity coefficients are exceeded only by those of lithium iodide and hydriodic acid. The value of the activity coefficient in a 0.2 molal solution at its freezing point is 0.805. The value of 0.792 at 25°C. and 0.2 molal is in the right direction and of the correct order of magnitude.

The activity coefficients of sodium perchlorate go through a long flat minimum between 2 and 3 molal. The value of the activity coefficient in a 0.2 molal solution at its freezing point is 0.720. The value of 0.728 at 0.2 molal and 25°C.

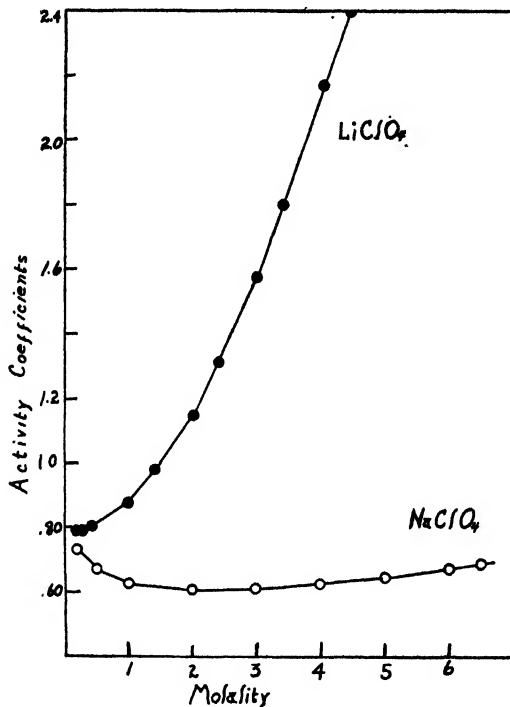


FIG. 1

is also in the right direction, and the difference is of the order of magnitude expected.

SUMMARY

The concentrations of isotonic solutions of sodium perchlorate-sodium chloride and lithium perchlorate-sodium chloride were determined from approximately 0.2-5.5 molal sodium chloride.

From the data obtained and the known values for the osmotic and activity coefficients of the reference salt, the corresponding values for sodium and lithium perchlorates were computed. Check computations on sodium perchlorate were made by two independent methods.

REFERENCES

- (1) HARNED, H. S., AND OWEN, B. B.: *The Physical Chemistry of Electrolytic Solutions*. Reinhold Publishing Corporation, New York (1943).
- (2) JONES, J. H.: *J. Am. Chem. Soc.* **65**, 1353 (1943).
- (3) ROBINSON, R. A., AND SINCLAIR, D. A.: *J. Am. Chem. Soc.* **56**, 1830 (1934).
- (4) SCATCHARD, G., PRENTISS, S. S., AND JONES, P. T.: *J. Am. Chem. Soc.* **50**, 803 (1934).
- (5) STOKES, R. H., AND LEVIEN, B. J.: *J. Am. Chem. Soc.* **68**, 333 (1946).

X-RAY DIFFRACTION STUDIES IN THE SYSTEM $\text{Fe}_2\text{O}_3\text{--Cr}_2\text{O}_3$ ¹

W. O. MILLIGAN AND L. MERTEN

*Department of Chemistry, The Rice Institute, Houston, Texas**Received October 8, 1946*

An unusual mutual protective action has been observed in mixed gels of cupric and ferric oxides (4) and of nickel and aluminum oxides (5). In both oxide pairs, the constituents mutually protected each other against crystallization, even at high temperatures. Thus ferric oxide prevented or retarded the crystallization of cupric oxide, and nickel oxide prevented marked crystallization of aluminum oxide in samples heated below 1000°C. for a period of 2 hr.

In this paper these results have been extended to include the system $\text{Fe}_2\text{O}_3\text{--Cr}_2\text{O}_3$, in which the components are closely similar in crystal structure and in lattice constants.

EXPERIMENTAL

Preparation of samples

Mixed gels of hydrous ferric and chromic oxides were prepared by the addition of an equivalent amount of ammonium hydroxide to mixtures of solutions of ferric nitrate (0.5 *M* with respect to Fe_2O_3) and chromic nitrate (0.5 *M* with respect to Cr_2O_3), using a rapid mixing device described elsewhere (10).

The amounts of the ferric and chromic nitrate solutions were chosen so that there was obtained a series of eleven samples containing 0, 10, 20, 30, 40, 50, 60, 70, 80, 90, and 100 mole per cent of ferric oxide. The dual gels were washed in a centrifuge until the supernatant liquid no longer gave a test for nitrate ions. After the moist gels were dried in air at room temperature, separate portions of each of the samples were heated for 2-hr. periods at various temperatures.

In a similar manner, a second series of eleven gels was prepared, using sodium hydroxide as the precipitant.

In order to attempt to ascertain any possible effect of adsorbed sodium hydroxide or silica from the alkali solution employed, separate experiments were

¹ Presented before the Division of Colloid Chemistry at the 109th Meeting of the American Chemical Society, which was held in Atlantic City, New Jersey, April 8-12, 1946.

carried out, using redistilled ammonium hydroxide as the precipitant. Small amounts (about 1 per cent) of (a) sodium hydroxide and (b) dialyzed silica sol were deliberately added to moist chromic oxide gels prepared as described above. The treated gels were allowed to dry in air at room temperature and were heated for periods of 2 hr. at 400°C. and 450°C.

X-ray diffraction analysis

X-ray diffraction patterns were obtained for the air-dried and heat-treated mixed oxide gels described above, using chromium K_{α} x-radiation. The K_{β} x-radiation was removed by vanadium pentoxide filters.

TABLE 1
Fe₂O₃-Cr₂O₃ gels precipitated by ammonia

SAMPLE NUMBER	MOLE PER CENT		RESULTS OF X-RAY ANALYSIS			
	Fe ₂ O ₃	Cr ₂ O ₃	Air-dried	300°C.	350°C.	400 and 500°C.
1 .	100	0	Amorphous	Crystalline	Crystalline	Crystalline
2 . .	90	10	Amorphous	Amorphous	Crystalline	Crystalline
3. . .	80	20	Amorphous	Amorphous	Amorphous	Crystalline
4 . . .	70	30	Amorphous	Amorphous	Amorphous	Crystalline
5. . . .	60	40	Amorphous	Amorphous	Amorphous	Crystalline
6. . . .	50	50	Amorphous	Amorphous	Amorphous	Crystalline
7. . . .	40	60	Amorphous	Amorphous	Crystalline	Crystalline†
8 . . .	30	70	Amorphous	Amorphous	Amorphous	Crystalline
9	20	80	Amorphous	Amorphous	Crystalline	Crystalline
10.	10	90	Crystalline*	Amorphous	Crystalline	Crystalline
11.	0	100	Crystalline†	Amorphous	Crystalline	Crystalline

* Faint but broad lines of a new crystalline phase.

† Intense and sharper lines of this new crystalline phase.

‡ 400°C. sample very faintly crystalline.

The results of the x-ray examination are given in tables 1 to 3. Some of the diffraction patterns are given in chart form in figures 1 to 3.

DISCUSSION

Samples precipitated by ammonium hydroxide

All of the air-dried samples were found to be amorphous to x-rays (table 1, figure 1) except the gels containing 100 and 90 per cent chromic oxide. The x-radiogram observed for the air-dried pure chromic oxide gel is distinct from the pattern of anhydrous chromic oxide and does not appear to correspond to the x-radiogram reported by Simon, Fischer, and Schmidt (7) for $\text{Cr}_2\text{O}_3 \cdot \text{H}_2\text{O}$ prepared in a bomb at high temperature and pressure. The x-ray diffraction data of these investigators were presented in the form of an unlabeled chart, from which quantitative values for the interplanar spacings cannot be obtained. However, from a consideration of the relative intensities of the lines, it does not appear likely that the new x-radiogram for hydrous chromic oxide gel corresponds to

this monohydrate. Hydrous chromic oxide gels previously prepared in this laboratory (11) and reported in the literature (for a survey consult reference 8) have been found to give amorphous x-ray and electron-diffraction patterns. Hydrous chromic oxide gels precipitated by sodium hydroxide and described

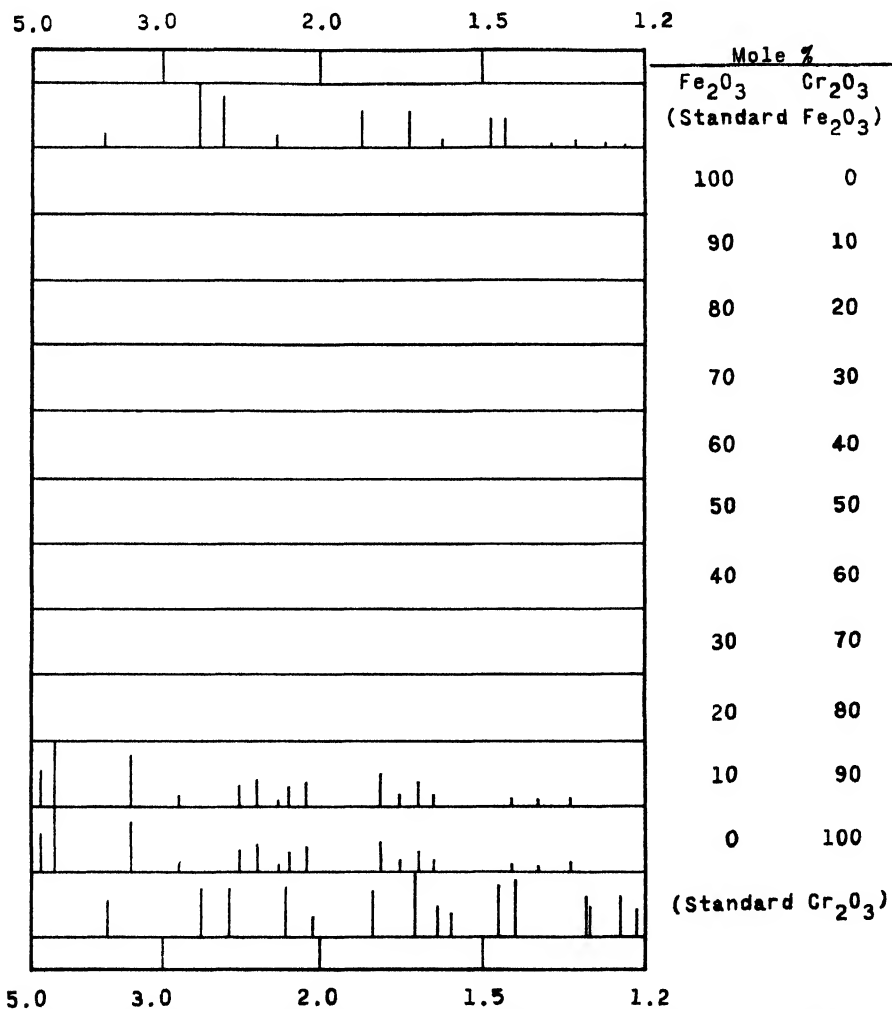


FIG. 1. X-ray diffraction patterns of $\text{Fe}_2\text{O}_3\text{-Cr}_2\text{O}_3$ gels precipitated by ammonia and dried in air.

below are likewise amorphous to x-rays. In contrast to the above results, Baccaredda and Beati (1) reported that a chromic oxide gel gave an electron-diffraction pattern closely similar to the pattern of $\alpha\text{-Al}_2\text{O}_3 \cdot 3\text{H}_2\text{O}$. The pattern reported in this present paper does not agree exactly with the interplanar spacing reported by Baccaredda and Beati, but the pattern does resemble very closely the x-radiogram of bayerite.

It will be noted that the gels exhibiting this new crystalline phase were prepared from neutral or slightly acid solution, suggesting that this phase may be a basic salt. In order to test this possibility a chromic oxide gel was prepared as described above from chromic chloride. The x-radiogram of the gel made from the chloride agreed exactly with that of the gel made from the nitrate. These results suggest that the new crystalline phase is not a basic salt, since it is unreasonable that a basic chromium nitrate and a basic chromium chloride would exhibit identical x-radiograms. The x-radiogram of the new crystalline phase does not agree with the pattern of possible impurities such as ammonium nitrate.

It will be noted from table 2 that this crystalline phase decomposed around 50–60°C., in contrast to the behavior of $\alpha\text{-Al}_2\text{O}_3 \cdot 3\text{H}_2\text{O}$ (2, 9), and the resulting

TABLE 2
Heat-treatment of chromic oxide gel

TEMPERATURE °C.	RESULTS OF X-RAY ANALYSIS	
	Precipitated by ammonia	Precipitated by sodium hydroxide
[Air-dried]	Crystalline*	Amorphous
50	Crystalline*	
100	Amorphous	
150	Amorphous	
200	Amorphous	
300	Amorphous	Amorphous
350	Crystalline†	
400	Crystalline†	Crystalline‡
500	Crystalline†	Crystalline‡

* New low-temperature crystalline phase, found in gels precipitated by ammonia.

† Cr_2O_3 .

‡ Cr_2O_3 + new high-temperature crystalline phase, found in gels precipitated by sodium hydroxide.

product remained amorphous at temperatures as high as 300°C. These data suggest that the new gel is not a hydrous form of a second crystalline modification of Cr_2O_3 .

By a process of elimination, and because of the close similarity to the x-radiogram of bayerite, it is suggested that the new chromic oxide gel is actually a hydrate. Isobaric dehydration studies for the conclusive identification of this hydrate are in progress.

It will be noted in table 1 that more than 10 mole per cent of ferric oxide retards or prevents the crystallization of the new chromic oxide crystalline phase, and that all other members of the series are amorphous to x-rays, in confirmation of previous x-ray and electron-diffraction results obtained in this laboratory (11). Heat-treatment at various temperature levels (table 1 and figures 2 and 3) resulted in the formation of crystalline products which consist of solid solutions of $\alpha\text{-Fe}_2\text{O}_3$ and Cr_2O_3 . The observed variations in interplanar spacings agree

closely with the results obtained by Passerini (6) and Wretblad (12) for the mixed oxides heated to higher temperatures.

Marked mutual protection is observed at temperatures as high as 350°C . As little as 30 mole per cent of Cr_2O_3 retards or prevents crystallization of

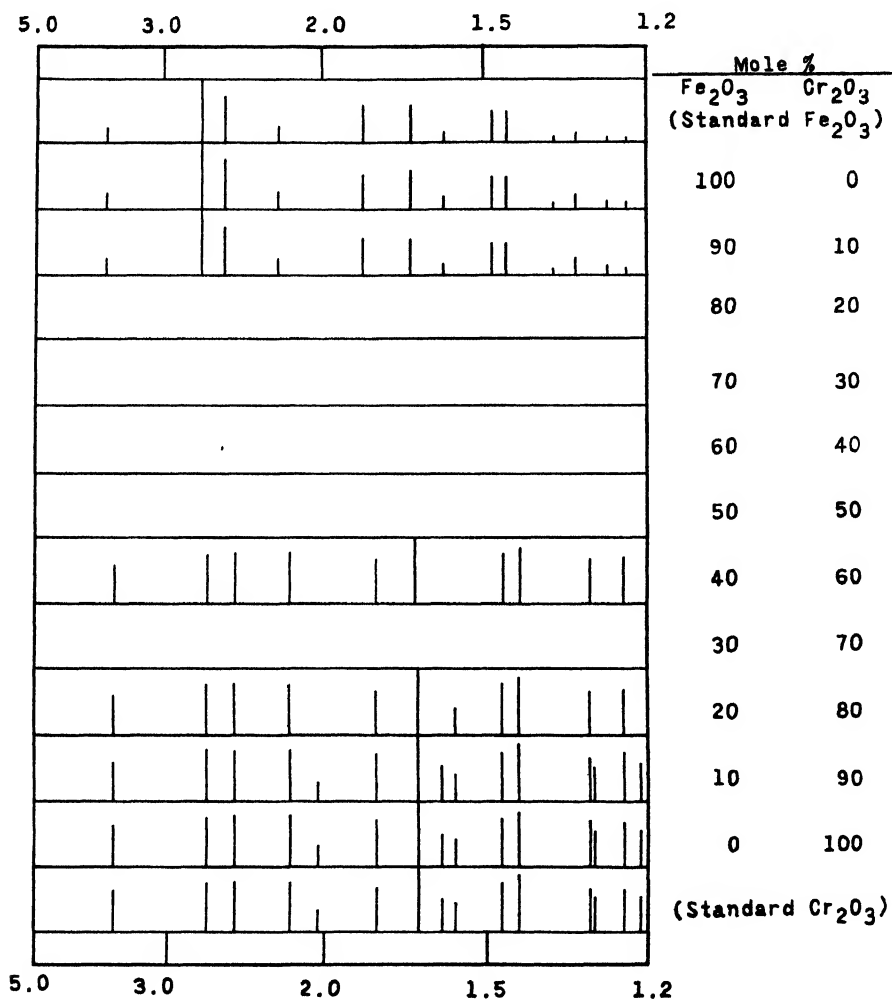


FIG. 2. X-ray diffraction patterns of $\text{Fe}_2\text{O}_3\text{--Cr}_2\text{O}_3$ gels precipitated by ammonia and heated at 350°C .

$\alpha\text{-Fe}_2\text{O}_3$, whereas 40 or 50 mole per cent of Fe_2O_3 retards the crystallization of Cr_2O_3 .

Samples precipitated by sodium hydroxide

The x-radiograms of the air-dried samples of the series of dual gels precipitated by sodium hydroxide were found to be entirely amorphous. No indication was

found of the new crystalline phase observed in the chromic oxide gels precipitated by ammonium hydroxide. Some of the air-dried gels were also examined using chromium K_{α} x-radiation rendered monochromatic by means of a quartz crystal monochromator. An exposure time of 24–100 hr. was required. The resulting

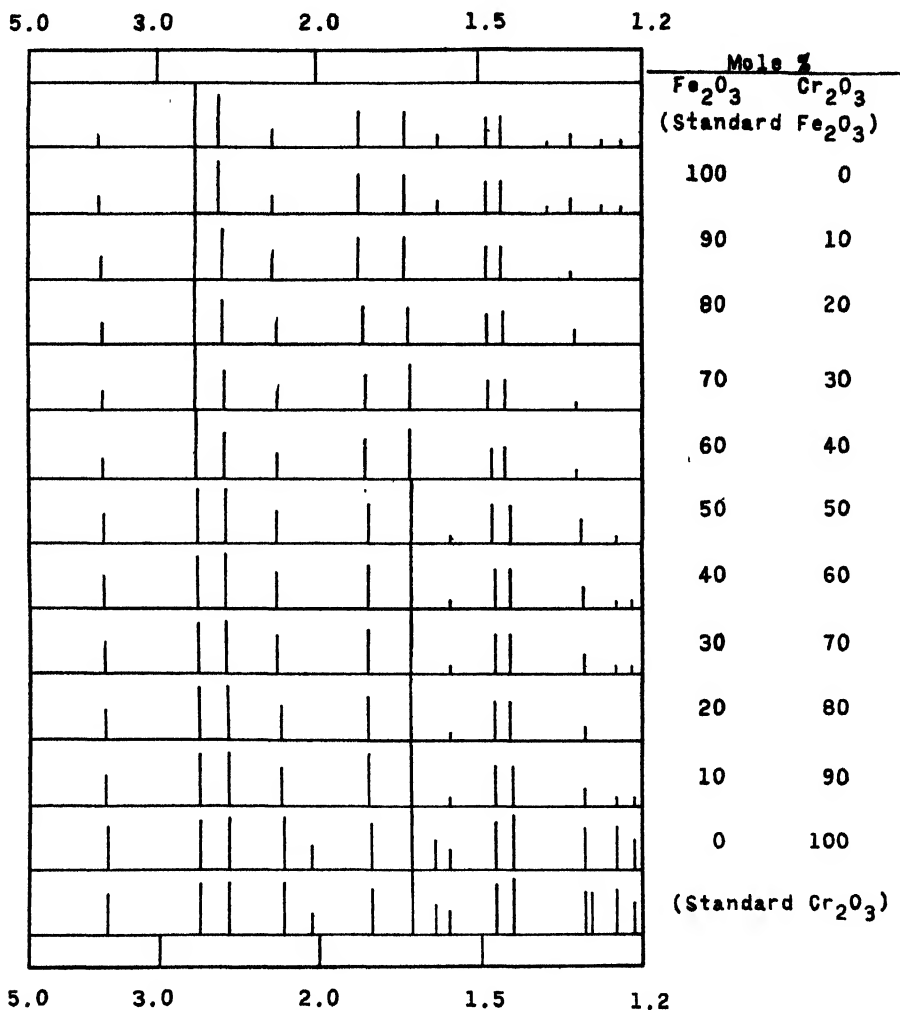


FIG. 3. X-ray diffraction patterns of Fe_2O_3 - Cr_2O_3 gels precipitated by ammonia and heated at 500°C .

x-radiograms were of the amorphous type. There was little or no evidence of more than one or two amorphous bands.

The x-ray results for the samples heat-treated at 300°C . demonstrate that the gels remain amorphous at a higher temperature level than was found for the series of gels precipitated by ammonium hydroxide. At 400°C . the phenomenon of mutual protection is observed clearly (table 3). All of the results suggest

that the series of gels precipitated by sodium hydroxide crystallizes at much higher temperatures than the series of gels precipitated by ammonium hydroxide.

X-radiograms of the samples deliberately contaminated with silica or sodium hydroxide show that a small amount of silica (about 1 per cent) retards the crystallization of pure chromic oxide, whereas small amounts of sodium hydroxide (about 1.0 per cent) engender a new crystalline anhydrous phase to be discussed below. It will be recalled that Götte (3) observed that small amounts of silica will retard the crystallization of ferric oxide. This present work extends the protective action of small amounts of silica to dual systems of chromic and ferric oxides.

It will be noted from table 3 that the gels precipitated by sodium hydroxide and containing 50-100 per cent chromic oxide develop at temperatures of 400-500°C.

TABLE 3
 $\text{Fe}_2\text{O}_3\text{-Cr}_2\text{O}_3$ gels precipitated by sodium hydroxide

SAMPLE NUMBER	MOLE PER CENT		RESULTS OF X-RAY ANALYSIS			
	Fe_2O_3	Cr_2O_3	Air-dried	300°C.	400°C.	500°C.
1	100	0	Amorphous*	Amorphous	Amorphous	Crystalline
2	90	10	Amorphous	Amorphous	Amorphous	Crystalline
3	80	20	Amorphous*	Amorphous	Amorphous	Crystalline
4	70	30	Amorphous	Amorphous	Amorphous	Crystalline
5	60	40	Amorphous*	Amorphous	Crystalline	Crystalline
6	50	50	Amorphous	Amorphous	Amorphous	Crystalline†
7	40	60	Amorphous*	Amorphous	Crystalline†	Crystalline†
8	30	70	Amorphous	Amorphous	Amorphous	Crystalline†
9	20	80	Amorphous*	Amorphous	Crystalline†	Crystalline†
10	10	90	Amorphous	Amorphous	Crystalline†	Crystalline†
11	0	100	Amorphous*	Amorphous	Crystalline†	Crystalline†

* Using quartz-crystal monochromator.

† Very faint pattern.

‡ $\text{Fe}_2\text{O}_3\text{-Cr}_2\text{O}_3$ pattern plus lines of new crystalline phase.

a new crystalline pattern in addition to the standard pattern of chromic oxide. Pure chromic oxide gel deliberately contaminated with about 1 per cent sodium hydroxide likewise exhibits this new pattern. The possibility has been considered that this pattern is for a new crystalline form of chromic oxide engendered by the presence of the sodium, analogous to the formation of $\beta\text{-Al}_2\text{O}_3$ in the presence of sodium. Another possibility is the formation of a sodium chromite. The identification of these extra diffraction lines will require a careful study of the system $\text{Cr}_2\text{O}_3\text{-Na}_2\text{O}$.

REFERENCES

- (1) BACCAREDDA AND BEATI: *Atti X° congr. intern. chim.* **2**, 99 (1935).
- (2) FRICKE AND SEVERIN: *Z. anorg. allgem. Chem.* **205**, 287 (1932).
- (3) GÖTTE: *Z. physik Chem.* **45B**, 223 (1940).
- (4) MILLIGAN AND HOLMES: *J. Am. Chem. Soc.* **63**, 149 (1941).

- (5) MILLIGAN AND MERTEN: J. Phys. Chem. **50**, 465 (1946).
- (6) PASSERINI: Gazz. chim. ital. **60**, 544 (1930).
- (7) SIMON, FISCHER, AND SCHMIDT: Z. anorg. allgem. Chem. **185**, 107 (1930).
- (8) WEISER: *Inorganic Colloid Chemistry. Vol. II. The Hydrous Oxides and Hydroxides.* John Wiley and Sons, Inc., New York (1935).
- (9) WEISER AND MILLIGAN: J. Phys. Chem. **38**, 1175 (1934).
- (10) WEISER AND MILLIGAN: J. Phys. Chem. **40**, 1071 (1936).
- (11) WEISER AND MILLIGAN: J. Phys. Chem. **44**, 1081 (1940).
- (12) WRETBAD: Z. anorg. allgem. Chem. **189**, 329 (1930).

THE ANTOINE VAPOR-PRESSURE EQUATION FOR MONONUCLEAR AROMATIC HYDROCARBONS

NANCY CORBIN, MARY ALEXANDER, AND GUSTAV EGLOFF

Universal Oil Products Company, Chicago, Illinois

Received September 24, 1946

The present study was undertaken to determine whether the variation of the constants of the Antoine equation

$$\log p = A - \frac{B}{t + C} \quad (1)$$

with the number of carbon atoms could be utilized to predict vapor pressures and boiling points of compounds for which experimental data are inadequate. The results indicate that these properties can be reasonably predicted for the normal alkylbenzene series and the 2-methyl-2-phenylalkane series. For other types of alkylbenzenes the variations are too great to permit satisfactory use. The vapor pressure and boiling point can, however, be estimated for phenyl-substituted normal alkanes if the boiling point at 760 mm. is known.

The Antoine equation is valid over a greater pressure range than is the widely used equation

$$\log p = A - \frac{B}{T} = A - \frac{B}{t + 273.16} \quad (2)$$

where p = pressure in mm., T = absolute temperature, and t = temperature in °C.

A plot of the reciprocal of the absolute temperature against the logarithm of the pressure usually exhibits a slight curvature, which increases at lower pressures. Although the linear equation represents the data quite well between about 200 and 800 mm., it cannot be extended much below 200 mm. A more convenient representation of vapor-pressure data is given by the Antoine equation when the constant C is chosen to give as nearly a linear function as possible in the pressure range under consideration. This equation makes possible the use of data between about 800 mm. and 10 mm.

When precise vapor-pressure data are available, the value of the constant C may be accurately evaluated (3, 4). However, the equation is useful even though the data are insufficient to evaluate C accurately, because the value of 230 for C gives a good representation of vapor-pressure data for many compounds (3).

The wider range of validity of equation 1 as compared with equation 2 markedly increases the number of mononuclear aromatic hydrocarbons for which pressure-temperature relationships may be determined. During a recent critical evaluation (2) of physical constants of these hydrocarbons, it was found that vapor-pressure data between 700 and 200 mm. were lacking for a large number of compounds, thus precluding the possibility of evaluating the constants of equation 2. For many of these compounds, however, data were available at 10 to 100 mm. and at or near 760 mm., permitting evaluation of constants of the Antoine equation.

A recent study of vapor pressures and boiling points of some paraffin, alicyclic, and alkylbenzene hydrocarbons (4) indicates that within a homologous series the values of the constants B and C of the Antoine equation vary in a regular manner with the number of carbon atoms. In the present study the variation of constants A and B with the number of carbon atoms was investigated for two homologous series of mononuclear aromatic hydrocarbons.

METHODS AND RESULTS

Experimental data for all the compounds studied except the first three members of the n -alkylbenzene series were insufficient to permit evaluation of constant C . The values of C for these three compounds (4) indicate that C decreases with increasing number of carbon atoms, and is approximately 200 for n -alkylbenzenes of about eleven carbon atoms. In order to determine the variation of constants A and B with the number of carbon atoms, calculations were carried out by the method of least squares with C taken as 200, 210, 220, and 230. The vapor-pressure data were taken from Willingham *et al.* (4) for the first three compounds, and from Egloff (2) for the rest of the compounds. A plot of B versus n (the number of carbon atoms) indicates that a linear relation in the form

$$B = a + bn \quad (3)$$

is adequate. One compound, n -pentylbenzene, deviated widely from what would be expected on the basis of the other values (figure 1) and was therefore given a low weight in the calculations. The first three compounds of the series were given high weights, because of the quality and completeness of the data.

Constants a and b of equation 3 were evaluated by the method of least squares for each of the four values of C used. These constants were found to be simple functions of C , expressed by the following equations:

$$a = -4.280 - 3.24934C + 0.023688C^2 \quad (4)$$

$$b = 66.9456 + 0.29508C \quad (5)$$

Values of a and b computed from the experimental data, and values calculated from equations 4 and 5 at the four values of C used in this study are shown in table 1.

Values of constant B computed from the experimental data and values calculated in two different ways are shown in table 2. The columns headed " B (calculated) (1)" contain values of B computed from equation 3 and the "observed" values of a and b in table 1. The columns headed " B (calculated) (2)" contain values of B computed from equation 3 and the "calculated" values of a and b in table 1.

Constant A was evaluated by the method of least squares from the experimental vapor-pressure data and the final calculated values of B .

A plot of the resulting values showed A to be a simple function of n . This function has the form

$$A = k + rn + qn^2 \quad (6)$$

TABLE 1
Constants of the B versus n equation

C	a (EXPERIMENTAL)	a (CALCULATED)	b (EXPERIMENTAL)	b (CALCULATED)
200	292.897	293.392	125.9075	125.9626
210	359.509	358.022	129.2433	128.9134
220	425.902	427.389	131.3699	131.8643
230	501.990	501.494	135.0348	134.8151

As was the case with B , constants k , r , and q of equation 6 are functions of C and may be expressed by equations 7, 8, and 9.

$$k = 4.072733_6 + 0.0012556_6 C + 0.04429_6 C^2 \quad (7)$$

$$r = 0.025332 + 0.0012497 C - 0.0_5105 C^2 \quad (8)$$

$$q = 0.003453 - 0.0_44684_6 C + 0.0_61825 C^2 \quad (9)$$

Values for k , r , and q computed from the experimental data and those based on equations 7, 8, and 9 at the four values of C used in this study are shown in table 3.

Values of A computed from the experimental data, using the final calculated values of B , are compared in figure 2 and table 4 with the values of A calculated from equation 6, using the calculated constants in table 3.

Aside from the normal alkylbenzenes, the only homologous series on which sufficient data were available for calculation of A and B as a function of n was the 2-methyl-2-phenylalkane series. Adequate vapor-pressure data have been recorded in the literature for only four members of this series, and one of these compounds deviated widely from the expected values for A and B . The extensive calculations carried out for the n -alkylbenzene series were therefore not carried out for the 2-methyl-2-phenylalkane series. Constants A and B were

TABLE 2
Values of B for n -alkylbenzenes

No.	C = 200			C = 210			C = 220			C = 230		
	B (experi- mental)	B (calculated) (1)	B (calculated) (2)	B (experi- mental)	B (calculated) (1)	B (calculated) (2)	B (experi- mental)	B (calculated) (1)	B (calculated) (2)	B (experi- mental)	B (calculated) (1)	B (calculated) (2)
7. . .	1170.913	1174.721	1175.130	1257.682	1261.383	1260.416	1349.515	1349.730	1350.439	1443.439	1445.709	1445.200
8. . .	1304.508	1300.629	1301.093	1394.935	1390.627	1389.329	1485.660	1481.100	1482.303	1583.748	1580.744	1580.015
9. . .	1426.108	1426.536	1427.055	1517.677	1519.870	1518.243	1604.166	1612.470	1614.168	1709.426	1715.778	1714.830
10. . .	1552.438	1552.444	1553.018	1651.493	1649.113	1647.156	1747.912	1743.840	1746.032	1858.337	1850.813	1849.645
11. . .	1750.641	1678.351	1678.981	1857.814	1778.356	1776.069	1972.363	1875.210	1877.896	2081.698	1985.848	1984.460
12. . .	1837.340	1804.259	1804.943	1944.173	1907.600	1904.983	2054.030	2006.580	2009.761	2166.645	2120.883	2119.275
13. . .	1913.091	1930.166	1930.906	2019.662	2036.843	2033.896	2120.742	2137.950	2141.625	2229.192	2255.918	2254.090
14. . .	2050.895	2056.074	2056.868	2160.482	2166.086	2162.810	2272.544	2269.319	2273.489	2387.818	2390.952	2388.905
15. . .	2163.873	2181.981	2182.831	2273.590	2295.330	2291.723	2386.251	2400.689	2405.354	2501.380	2525.987	2523.721
Stand- ard devia- tion of B		± 6.750			± 7.521			± 9.443			± 9.707	
Stand- ard de- viation of b		± 0.233			± 0.248			± 0.312			± 0.320	

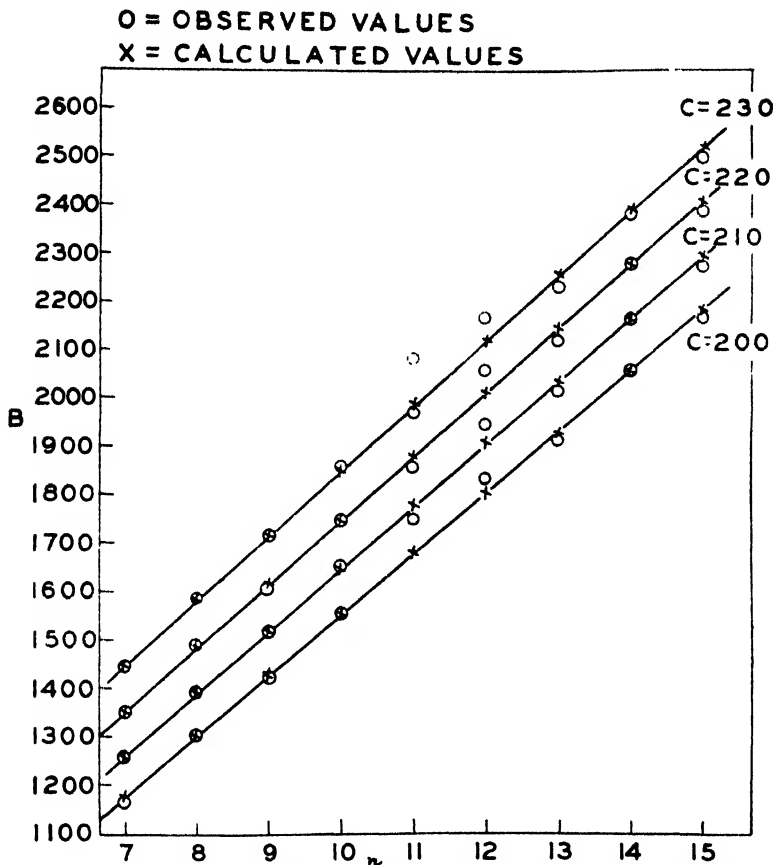


FIG. 1. Values of constant B of the Antoine equation as a function of the number of carbon atoms for 1-phenylalkanes.

TABLE 3

Constants of the A versus n equation

C	$\overset{\overset{h}{\mid}}{\text{(EXPERIMENTAL)}}$	$\overset{\overset{h}{\mid}}{\text{(CALCULATED)}}$	$\overset{\overset{r}{\mid}}{\text{(EXPERIMENTAL)}}$	$\overset{\overset{r}{\mid}}{\text{(CALCULATED)}}$	$\overset{\overset{q}{\mid}}{\text{(EXPERIMENTAL)}}$	$\overset{\overset{q}{\mid}}{\text{(CALCULATED)}}$
200	6.095773	6.095664	0.071107	0.071078	0.001383	0.001384
210	6.289501	6.289830	0.062557	0.062645	0.001667	0.001664
220	6.493183	6.492855	0.053278	0.053190	0.001977	0.001980
230	6.704629	6.704739	0.042686	0.042715	0.002334	0.002333

evaluated at $C = 200$ and $C = 230$, and their relation to n was determined. Both A and B were found to be substantially linear functions of n , as expressed by the following equations:

$$\left. \begin{aligned} A &= 6.07272 + 0.070027n \\ B &= 399.278 + 103.9747n \end{aligned} \right\} C = 200 \quad (10)$$

$$(11)$$

TABLE 4
Values of A for 1-phenylalkanes

n	C = 200		C = 210		C = 220		C = 230	
	A (experimental)	A (calculated)	A (experimental)	A (calculated)	A (experimental)	A (calculated)	A (experimental)	A (calculated)
7.....	6.66395	6.66103	6.81178	6.80988	6.96570	6.96221	7.11654	7.11806
8.....	6.74825	6.75286	6.89171	6.89749	7.04098	7.04510	7.19791	7.19577
9.....	6.85329	6.84747	6.99329	6.98838	7.13894	7.13195	7.28252	7.27815
10.....	6.94036	6.94484	7.07657	7.08268	7.21775	7.22276	7.35722	7.36519
11.....	7.04502	7.04499	7.17896	7.18027	7.31793	7.31753	7.45539	7.45690
12.....	7.14230	7.14790	7.27451	7.28119	7.41171	7.41626	7.54742	7.55327
13.....	7.26756	7.24357	7.39839	7.38543	7.53407	7.51895	7.66842	7.65431
14.....	7.35815	7.36202	7.48763	7.49300	7.62210	7.62560	7.75546	7.76002
15.....	7.47197	7.47323	7.60126	7.60391	7.73532	7.73621	7.86836	7.87039

O=OBSERVED VALUES
X=CALCULATED VALUES

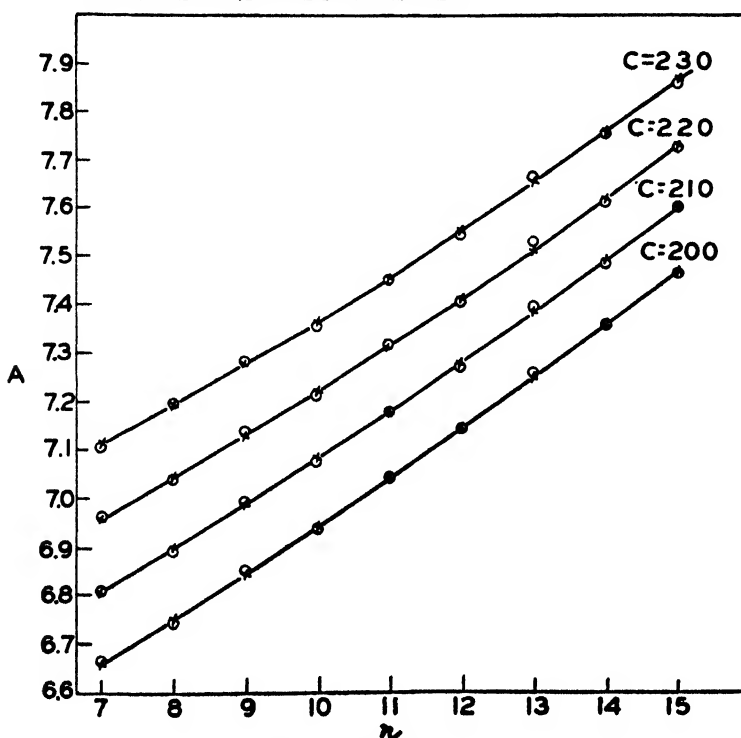


FIG. 2. Values of constant A of the Antoine equation as a function of the number of carbon atoms for 1-phenylalkanes.

$$A = 6.64523 + 0.057424n \quad C = 230 \quad (12)$$

$$B = 650.878 + 108.3732n \quad C = 230 \quad (13)$$

Experimental and calculated values of constants A and B are shown in table 5.

APPLICATION OF THE RESULTS

By means of the Antoine equation and values for its constants calculated from equations 3 through 13, the vapor pressure over a considerable temperature range, or the boiling point at any pressure between 10 and 800 mm., may be calculated for the compounds covered by this study, using any desired value of C between 200 and 230. By extrapolation vapor pressures and boiling points of higher members of the two series may be estimated. The reliability of

TABLE 5
Values of A and B for the 2-methyl-2-phenylalkane series

n	C = 200				C = 230			
	A (experimental)	A (calculated)	B (experimental)	B (calculated)	A (experimental)	A (calculated)	B (experimental)	B (calculated)
10	6.78032	6.77299	1438.418	1439.025	7.22836	7.21947	1734.036	1734.610
11	6.83318	6.84302	1648.561	1543.000	7.26497	7.27689	1968.121	1842.983
13	7.00098	6.98307	1752.095	1750.949	7.40891	7.39174	2060.687	2059.730
14	7.05542	7.05310	1854.385	1854.924	7.45201	7.44916	2167.718	2168.103

TABLE 6
Boiling points at low pressures of higher n-alkylbenzenes

n	p	t (EXPERIMENTAL)	t (CALCULATED)
	mm	$^{\circ}C.$	$^{\circ}C.$
18.	13	179-180	181.7
	12	183-185	179.7
	9	172-173	172.8
19.....	10	188-189.5	186.8
20.....	9	195-196	195.2
22.....	16	235-237	230.1
	15	230	228.4
24.....	15	249	246.8

extrapolations cannot be definitely ascertained until accurate experimental data are available beyond the range covered in this study. However, some indication of the accuracy of extrapolated values may be obtained from data already at hand. Boiling points at low pressure have been recorded for several higher *n*-alkylbenzenes (2) and a comparison of the values for observed and calculated boiling points given in table 6 shows agreement which is as good as could be expected on the basis of the inconsistency of the experimental values.

Prediction of vapor pressures of compounds for which experimental data are lacking is limited to members of the two homologous series covered in this study.

In an effort to enlarge the scope of the applicability of the Antoine equation to other types of aromatic hydrocarbons, the relation of constant B to the normal boiling point was investigated. As a basis for comparison, the final calculated values of B at $C = 230$ were plotted against the boiling points (computed from the calculated values of A and B) for n -alkylbenzenes of from seven to twenty-two carbon atoms. In the same way a plot of B versus boiling point was made for the four tertiary alkylbenzenes covered in this study.

In both series, B was found to be a function of the boiling point. The relationships are expressed by the following equations:

For n -alkylbenzenes:

$$B = 421.037 + 8.5331t - 0.02187t^2 + 0.045101t^3 \quad C = 200 \quad (14)$$

$$B = 441.297 + 12.3392t + 0.03976t^2 + 0.048066t^3 \quad C = 230 \quad (15)$$

TABLE 7
Normal alkanes with a phenyl substituent

COMPOUND	BOILING POINT °C.	C = 200			C = 230		
		B (experi- mental)	B (calculated)	ΔB	B (experi- mental)	B (calculated)	ΔB
Isopropylbenzene	152.3	1395.352	1393.580	+1.772	1670.777	1683.192	-12.415
2-Phenylbutane	172.8	1513.165	1505.768	+7.397	1819.278	1802.391	+16.887
2-Phenylhexane	210.6	1712.206	1724.661	-12.455	2020.985	2029.780	-8.795
3-Phenylpentane	188.4	1647.706	1593.577	+54.129	1966.774	1894.031	+72.743
3-Phenylhexane	210.5	1712.669	1724.051	-11.382	2019.505	2029.148	-9.643

For 2-methyl-2-phenylalkanes:

$$B = 559.197 + 4.8768t + 0.001772t^2 \quad C = 200 \quad (16)$$

$$B = 817.540 + 5.0833t + 0.001846t^2 \quad C = 230 \quad (17)$$

where t = the boiling point at 760 mm.

These equations reproduce the final calculated values of B with standard deviations of ± 5.888 at $C = 200$ and ± 11.929 at $C = 230$ for the n -alkylbenzenes, and ± 5.842 at $C = 200$ and ± 6.089 at $C = 230$ for the 2-methyl-2-phenylalkanes.

The values for constant B for a number of alkylbenzenes of types not included in the series were computed from the available vapor-pressure data (2), and were compared with the values of B calculated from equations 14 through 17. These comparisons are shown in tables 7 to 13.

From table 7 it is apparent that the position of substitution of the phenyl group in normal alkanes has little effect on the value of B as a function of the boiling point. Thus, the value of constant B for any phenyl-substituted normal alkane whose boiling point at 760 mm. is known may be calculated from equa-

tion 14 or 15. Constant A may then be evaluated from B and the boiling point. Using these values, the vapor pressure at a variety of temperatures or the boiling point at pressures between 800 and 10 mm. may be estimated.

TABLE 8
Phenyl-substituted branched-chain alkanes with no quaternary carbon atoms

COMPOUND	BOILING POINT	$C = 200$			$C = 230$		
		B (experi- mental)	B (calcu- lated)	ΔB	B (experi- mental)	B (calcu- lated)	ΔB
	°C.						
1-Phenyl-2-methylpropane..	170.1	1564.458	1490.829	+73.629	1886.919	1786.683	+100.236
1-Phenyl-2-methylbutane...	194.1	1984.059	1626.445	+357.614	2357.013	1928.126	+428.887
1-Phenyl-2-methylpentane..	205.0	1959.654	1690.764	+268.890	2308.688	1994.704	+313.984
1-Phenyl-3-methylpentane..	221.3	1895.023	1791.918	+103.105	2236.417	2098.165	+138.252
1-Phenyl-3,7-dimethyl- octane.....	275.0	2334.478	2174.720	+159.758	2700.886	2505.015	+195.871
2-Methyl-4-phenylpentane..	197.9	1754.821	1650.033	+104.788	2089.567	1953.934	+135.633

TABLE 9
Phenyl-substituted alkanes with the phenyl group on a quaternary carbon atom

COMPOUND	BOILING POINT	$C = 200$			$C = 230$		
		B (experi- mental)	B (calcu- lated)	ΔB	B (experi- mental)	B (calcu- lated)	ΔB
	°C.						
2,3-Dimethyl-2-phenyl- pentane.....	223.4	1743.569	1737.110	+6.459	2050.281	2045.278	+5.003
2,4-Dimethyl-2-phenyl- pentane.....	217.7	1780.437	1704.857	+75.580	2098.097	2011.662	+86.435
2,3-Dimethyl-2-phenyl- hexane.....	236.7	1773.163	1812.815	-39.652	2080.898	2124.183	-43.285
2,4-Dimethyl-2-phenyl- hexane.....	238.7	1812.562	1824.254	-11.692	2121.950	2136.104	-14.154
2,5-Dimethyl-2-phenyl- hexane.....	236.9	1893.138	1813.959	+79.179	2215.900	2135.541	+80.359
2-Methyl-2-phenyl-3-ethyl- pentane.....	236.7	1811.934	1812.815	-0.881	2127.454	2124.183	+3.271
3-Methyl-3-phenylpentane..	205.7	1672.445	1637.333	+35.112	1983.983	1941.284	+42.699
3-Ethyl-3-phenylpentane...	224.4	1763.785	1742.781	+21.004	2072.596	2051.188	+21.408
4-Methyl-4-phenylheptane..	243.5	2001.237	1851.746	+149.491	2340.981	2164.179	+176.802
3-Ethyl-3-phenylhexane...	239.4	1929.422	1828.261	+101.161	2252.213	2140.877	+111.336
2-Methyl-3-ethyl-3-phenyl- pentane.....	239.4	1898.196	1828.261	+69.935	2222.261	2140.280	+81.981

Branching of the side chain in alkylbenzenes has a pronounced influence on constant B , as can be seen from table 8. The effect in every case is to increase the value of B beyond what would be expected from the boiling point.

Compounds with five carbon atoms in the side chain appear to be anomalous. In all cases the value of constant B is higher than would be anticipated from other compounds of similar structure. Whether these compounds really are anomalous, or whether inaccurate data lead to a high result in every case, is a question which cannot be settled without further experimental study.

TABLE 10
Dialkylbenzenes

COMPOUND	BOIL- ING POINT °C.	$C = 200$			$C = 230$		
		B (experi- mental)	B (calcu- lated)	ΔB	B (experi- mental)	B (calcu- lated)	ΔB
<i>o</i> -Xylene	144.4	1389.839	1350.814	+39.025	1641.010	1636.832	+4.178
<i>m</i> -Xylene	139.1	1324.977	1322.404	+2.573	1604.941	1605.811	-0.870
<i>p</i> -Xylene	138.3	1314.736	1317.819	-3.083	1593.319	1600.636	+7.317
1-Methyl-2-ethylbenzene..	164.9	1533.909	1462.223	+71.686	1852.682	1756.479	+96.203
1-Methyl-4-ethylbenzene. .	162.1	1480.387	1446.898	+33.489	1795.734	1740.223	+55.511
1-Methyl-2-propylbenzene	182.5	1524.316	1560.031	-35.715	1828.797	1859.138	-30.341
1-Methyl-4-propylbenzene .	183.1	1601.148	1563.422	+37.726	1921.089	1862.671	+58.418
1-Methyl-3-isopropyl- benzene	175.4	1502.280	1520.216	-17.936	1804.897	1817.545	-12.648
1-Methyl-4-isopropyl- benzene.	176.9	1522.305	1528.582	-6.277	1834.727	1826.304	+8.423
1 Methyl-4- <i>n</i> -butylbenzene.	196.7	1743.884	1641.603	+102.281	2074.805	1943.828	+130.977
1-Methyl-4- <i>sec</i> -butyl- benzene	196.0	1531.460	1637.511	-106.051	1823.839	1939.591	-115.752
1-Ethyl-4-isopropylbenzene	197.0	1624.469	1643.359	-18.890	1940.180	1945.646	-5.466
1-Methyl-3- <i>n</i> -pentyl- benzene	215.5	1883.185	1754.854	+128.331	2218.337	2061.044	+157.293
1,3-Dipropylbenzene . . .	216.5	1799.909	1761.080	+38.829	2119.088	2067.496	+51.592
1,4-Dipropylbenzene . . .	221.1	1820.378	1790.014	+30.364	2139.084	2097.506	+41.578
1,3-Diisopropylbenzene . .	204.0	1668.748	1684.775	-16.027	1987.794	1988.508	-0.714
1,4-Diisopropylbenzene . .	208.9	1641.135	1714.305	-73.170	1946.545	2019.062	-72.517
1-Methyl-4-hexylbenzene .	237.0	2038.504	1894.116	+144.388	2385.633	2206.014	+179.619
1-Methyl-4- <i>n</i> -heptyl- benzene	265.1	2076.637	2096.671	-20.034	2413.151	2420.742	-7.591
1,4-Di- <i>n</i> -butylbenzene . . .	260.0	1868.330	2057.913	-189.583	2174.428	2379.223	-204.795
1- <i>n</i> -Butyl-4- <i>sec</i> -butyl- benzene	251.3	1815.262	1993.926	-178.664	2119.662	2311.143	-191.481
1,4-Di- <i>sec</i> -butylbenzene . .	238.0	1768.933	1900.894	-131.961	2043.539	2213.116	-169.577
1,4-Di- <i>sec</i> -pentylbenzene .	265.0	2076.745	2095.902	-19.157	2403.804	2419.916	-16.112

Table 9 shows results of calculations for compounds containing a quaternary carbon atom. The deviations from expected values of B are variable in sign, but in general of lesser magnitude than the deviations of branched-chain alkylbenzenes with no quaternary carbon atoms. However, in most cases the experimental values of B are outside the limits of error, and therefore reliable estimates of vapor pressure or boiling points cannot be made for compounds of this type.

TABLE 11
Trialkylbenzenes

COMPOUND	BOILING POINT	C = 200			C = 230		
		B (experi- mental)	B (calcu- lated)	ΔB	B (experi- mental)	B (calcu- lated)	ΔB
	°C.						
1,2,4-Trimethylbenzene....	169.3	1504.680	1486.414	+18.266	1802.342	1782.033	+20.309
1,3,5-Trimethylbenzene....	164.7	1492.804	1461.127	+31.677	1798.617	1755.318	+43.299
1,2-Dimethyl-4-ethyl- benzene.....	187.6	1697.641	1589.001	+108.640	2025.570	1889.249	+136.321
1,4-Dimethyl-2-ethylben- zene.....	185.4	1576.274	1576.463	-0.189	1891.973	1876.245	+15.728
1-Ethyl-2,4-dimethyl- benzene.....	185.6	1573.613	1577.600	-3.987	1886.326	1877.428	+8.898
1-Propyl-2,4-dimethyl- benzene.....	208.1	1623.338	1709.452	-86.114	1921.854	2014.039	-92.185
1,3-Dimethyl-5-propyl- benzene.....	208.0	1639.806	1709.846	-69.040	1942.103	2013.413	-71.310
1,2-Dimethyl-4-isopropyl- benzene.....	199.2	1707.126	1656.283	+50.843	2027.510	1959.026	+68.484
1-Isopropyl-2,4-dimethyl- benzene.....	194.5	1643.294	1628.770	+14.524	1959.705	1930.535	+29.170
1-Methyl-2-ethyl-4-iso- propylbenzene.....	209.3	1858.677	1716.737	+141.940	2192.967	2021.578	+171.389
1,2,4-Triethylbenzene....	217.5	1795.765	1767.328	+28.437	2117.928	2073.973	+43.955
1,3,5-Triethylbenzene....	216.2	1757.350	1759.209	-1.859	2075.473	2065.558	+9.915
1-Methyl-2-propyl-4-iso- propylbenzene.....	225.2	1945.121	1816.230	+128.891	2285.989	2124.744	+161.245
1,2,4-Triisopropylbenzene.	240.4	1886.892	1917.280	-30.388	2208.405	2230.405	-22.000

TABLE 12
Tetra-, penta-, and hexaalkylbenzenes

COMPOUND	BOILING POINT	C = 200			C = 230		
		B (experi- mental)	B (calcu- lated)	ΔB	B (experi- mental)	B (calcu- lated)	ΔB
	°C.						
1,2,3,4-Tetramethyl- benzene.....	205.1	1664.915	1691.364	-26.449	1963.095	1995.325	-32.230
1,2,3,5-Tetramethyl- benzene.....	197.1	1694.254	1643.945	+50.309	2016.391	1946.253	+70.138
1,3,5-Trimethyl-2-ethyl- benzene.....	210.5	1726.588	1724.051	+2.537	2042.005	2029.148	+12.857
1,2,4-Trimethyl-5-ethyl- benzene.....	209.0	1729.434	1714.913	+14.521	2048.333	2019.690	+28.643
Pentamethylbenzene.....	231.9	1928.210	1859.990	+68.220	2262.259	2170.334	+91.925
1,2,3,4-Tetraethylbenzene..	253.5	1955.655	2009.862	-54.207	2276.144	2328.045	-51.901
1,2,4,5-Tetraisopropyl benzene.....	258.4	1994.270	2045.948	-51.678	2313.049	2366.049	-53.000
Hexapropylbenzene.....	333.5	2636.639	2726.739	-90.100	3002.576*	3118.228	-115.652

* Boiling point for C = 230 is 332.9°C.

Tables 10, 11, and 12 show observed and calculated values of constant B for polysubstituted benzenes with no branched-chain substituents. The values of B for the xylenes are based on excellent data (4), and indicate that B is very nearly the same for dialkylbenzenes as for hypothetical n -alkylbenzenes of the same boiling point. Values of B for all other polyalkylbenzenes are based on scant data (2), often only two or three values. The differences between experimental and calculated values of B are in most cases large, but up to a boiling point of about 240°C. the deviations apparently have a random distribution. Above 240°C. all experimental values are lower than the calculated ones. Up to this temperature it is probable that predictions of vapor pressures or of boiling points at reduced pressures for polyalkylbenzenes on the basis of the calculated values of constant B will be no less accurate than much of the existing data.

Table 13 compares values of B computed from experimental data with those calculated from the boiling points and equations 16 and 17, for a few di- and trialkylbenzenes with one tertiary side chain. The deviations are too great to

TABLE 13
Polyalkylbenzenes with one tertiary substituent

COMPOUND	BOILING POINT °C.	$C = 200$			$C = 230$		
		B (experi- mental)	B (calcu- lated)	ΔB	B (experi- mental)	B (calcu- lated)	ΔB
1-Methyl-4- <i>tert</i> -butylben- zene.....	190.2	1650.078	1550.868	+99.210	1968.556	1851.165	+117.391
1- <i>tert</i> -Butyl-2,4-dimethyl- benzene.....	212.8	1740.805	1677.383	+63.422	2058.938	1983.026	+75.912
1,3-Dimethyl-5- <i>tert</i> -butyl- benzene.....	204.9	1769.857	1632.849	+137.008	2101.151	1936.611	+164.540
1- <i>n</i> -Butyl-4- <i>tert</i> -butyl- benzene.....	249.0	1818.146	1883.386	-65.240	2124.373	2197.735	-73.362

permit reliable estimation of vapor pressures or boiling points for this type of compound.

The only classes of compounds for which reliable estimates of vapor pressures or of boiling points at pressures between 10 and 800 mm. can be made in the absence of any experimental data are the normal alkylbenzenes and the 2-methyl-2-phenylalkanes. Estimation of boiling points at reduced pressures can be made for phenyl-substituted alkanes with the phenyl group not in the 1-position and for polyalkylbenzenes with no branched-chain or tertiary substituents if the boiling points at 760 mm. are known.

SUMMARY

Constants A and B of the Antoine equation

$$\log p = A - \frac{B}{t + C}$$

have been evaluated and related to the number of carbon atoms at several values of C for the normal alkylbenzene series and the 2-methyl-2-phenylalkane series. The relationship of A and B to C has been evaluated for the normal alkylbenzene series.

Applications of the results for the prediction of vapor pressures at different temperatures or boiling points at pressures of 10 to 800 mm. are discussed.

REFERENCES

- (1) ANTOINE, C.: *Compt. rend.* **107**, 681 (1888).
- (2) EGLOFF, G.: *Physical Constants of Hydrocarbons*, Vol. III. Reinhold Publishing Corporation, New York (1946).
- (3) THOMSON, G. W.: *Chem. Rev.* **38**, 1 (1946).
- (4) WILLINGHAM, C. B., TAYLOR, W. J., PIGNOCCO, J. M., AND ROSSINI, F. D.: *J. Research Natl. Bur. Standards* **35**, 219 (1945).

A MATHEMATICAL APPROACH TO REACTION MECHANISMS

JOSEPH THIE

University of Dayton, Dayton, Ohio

Received July 15, 1946

INTRODUCTION

Several articles (3, 6, 7, 9, 10) have already been written in which chemical equations are treated in a purely mathematical manner. However, there is more to be said about this subject, especially regarding the occurrence of intermediates and practical applications. The purpose of this article is fourfold:

- A. To give a rule for determining whether or not a given group of intermediates can occur alone in the production of a given reaction.
- B. To give a method of obtaining all possible component equations containing a given group of intermediates which have been postulated for a certain reaction.
- C. To give a method of obtaining all possible mechanisms by which a given group of intermediates, postulated for a certain reaction, can occur.
- D. To apply these new principles to practical problems of the kinetics of chemical reactions.

METHOD AND EXAMPLES

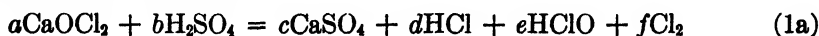
Concerning those groups of intermediates which may occur alone (i.e., those for which mechanisms can be written containing only those intermediates and terms found in the original equation) we have the following principle: All those groups of intermediates, and only those, may occur along which, when inserted into a given equation, yield a resulting equation having the following properties: (I) It has all the terms of the original equation and one or more additional

terms. (II) It can be balanced by an infinite number of non-multiple sets of coefficients.

Whether an equation has property II can be discovered by writing its set of simultaneous algebraic equations. Porges (7) illustrates this algebraic balancing. As an example of the above principle consider the reaction:



Let the intermediate, Cl_2 , be postulated as a solitary one. We insert it in the original equation as stated above:



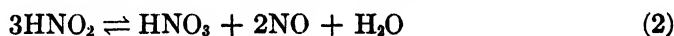
The only way in which this can be balanced is

a	b	c	d	e	f
1	1	1	1	1	0

Since equation 1a contains no terms in addition to the terms in equation 1 (and also since 1a can be balanced in only one way), Cl_2 cannot occur as a solitary intermediate. If the original reaction occurs as stated and if there is experimental evidence for the occurrence of Cl_2 as an intermediate in this reaction, then another intermediate must exist.

Though in the above example no ions were present, the same results are obtained if an ionic equation is used. The only difference occurs in the algebraic balancing of the equation. Ionic equations have an additional algebraic equation obtained from the conservation of charge.

As another example of the above principle we shall consider the reaction:



N_2O_4 is a logical intermediate to postulate and it is therefore desirable to know if it can occur alone, and what are all the possible mechanisms if it is permitted to occur.

The first step is to insert the intermediate in the original equation as stated above:



Two of the infinite number of non-multiple sets of coefficients of this equation are:

a	b	c	d	e
5	3	4	1	-1
5	-1	2	3	2

Since equation 2a fulfills properties I and II, N_2O_4 can occur as a solitary intermediate in the production of the original equation.

Next it is desired to find the totality of mechanisms. It is a fact that all equations capable of being balanced in an infinite variety of non-multiple ways, and only these equations, have a certain property. They can be resolved into

two or more simpler equations containing no new terms. The totality of these component equations is found by writing the set of algebraic equations corresponding to the equation which is being resolved (i.e., begin to balance the equation algebraically). The unknowns are individually set equal to zero, and in each case the remaining unknowns are solved for. If we apply this to equation 2a to discover the totality of its component equations, we shall consequently also have all possible "intermediate equations" of 2.

The simultaneous equations corresponding to equation 2a are:

$$a = b + 2d$$

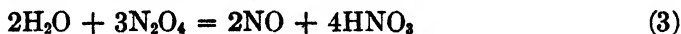
$$a = b + c + 2e$$

$$2a = 3b + c + d + 4e$$

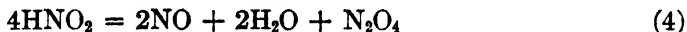
Let $a = 0$ and solve for b , c , d , and e :

$$b = 4, c = 2, d = -2, e = -3$$

The component equation is therefore:



Let $b = 0$ and solve for a , c , d , and e . The component equation is therefore:



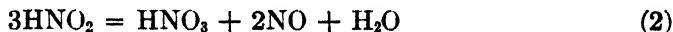
When $c = 0$ the equation is:



When $d = 0$ the equation is:



When $e = 0$ the equation is:

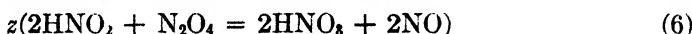
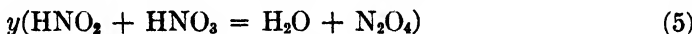
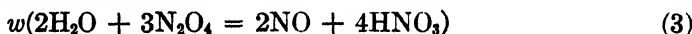


None of the five preceding equations can be balanced in an infinite variety of ways, and therefore none can be further resolved. (This is not always the case, and whenever possible each component equation must be resolved into its own component equations.) Therefore equations 2, 3, 4, 5, and 6 are the totality of component equations of 2a. It is impossible to write any other equation containing only these terms. The totality of the component equations of 2 is therefore 2a, 3, 4, 5, and 6. Therefore all possible mechanisms of equation 2 involving only the intermediate N_2O_4 consist of various combinations of equations 2a, 3, 4, 5, and 6.

The next step is to eliminate as many of these equations as possible. Equation 2a can be eliminated because it can be represented by simpler equations. We must keep all the others, unless it can be said with certainty that one or more of them cannot occur to the right and cannot occur to the left under the conditions of the experiment. However, in this particular case if a reaction does not

occur in just one direction it can be dropped. The reason is that equation 2 is reversible, and therefore all reactions of the mechanism must be reversible. However, none from the group 3, 4, 5, and 6 can even now be eliminated.

The last step is to find all possible mechanisms given by the remaining component equations. To do this it is necessary to use the following algebraic method: Set up all the equations thus:



w , x , y , and z may be any positive number, negative number, or zero. Utilizing the fact that the sum of these four equations is equation 2, we can obtain algebraic equations involving these unknowns. In order for the coefficient of HNO_2 to be 3 in the sum, the following must be true:

$$4x + y + 2z = 3$$

Similarly we get these other algebraic equations, one for each compound:

$$4w - y + 2z = 1$$

$$2w + 2x + 2z = 2$$

$$-2w + 2x + y = 1$$

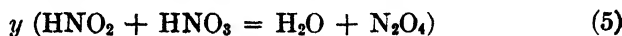
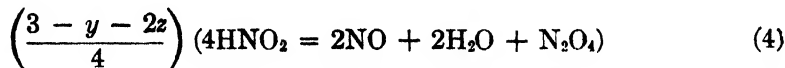
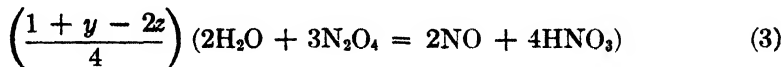
$$3w - x - y + z = 0$$

Actually, there are only two independent equations:

$$4x + y + 2z = 3$$

$$4w - y + 2z = 1$$

Solving for w and x and substituting above, we can express mechanisms consisting of four equations in terms of two parameters:

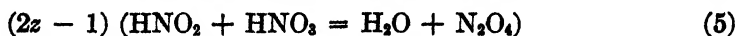


To obtain all mechanisms consisting of three equations, we individually set the four unknowns equal to zero and solve for a mechanism in each case. If $w = 0$ we have the two independent equations:

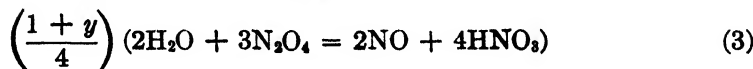
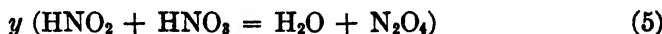
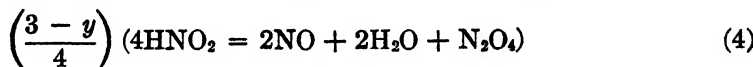
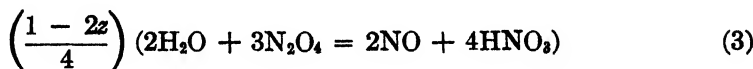
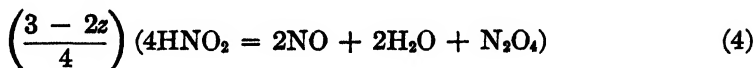
$$4x + y + 2z = 3$$

$$-y + 2z = 1$$

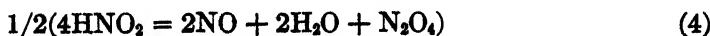
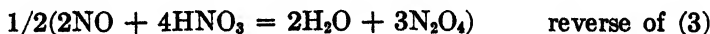
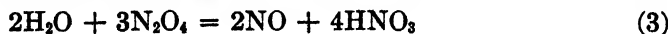
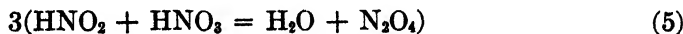
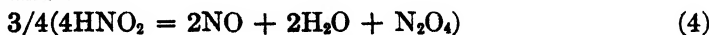
The corresponding mechanism is (actually a one-parameter family of mechanisms)

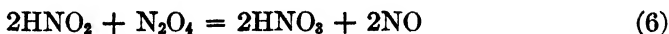
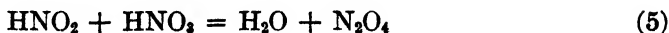


By setting individually the other unknowns equal to zero, three other one-parameter families of mechanisms consisting of three equations are had:



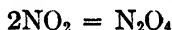
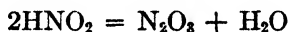
To obtain all mechanisms consisting of two reactions we individually set all possible pairs of the unknowns equal to zero and solve for a mechanism in each case. The mechanisms are:



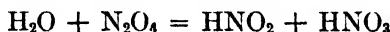
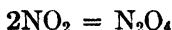
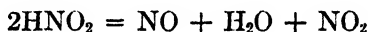


Up to this point the analysis of equation 2 has been purely mathematical. All possible mechanisms have been given, and it is impossible to write another way in which N_2O_4 can occur unless other intermediates are introduced. Now is the time to apply chemical principles to the above mechanisms.

What is sought is the simplest mechanism that conforms to experimental facts. Regarding the simplicity of the above mechanisms it is readily seen that the last three mechanisms are the simplest. (High coefficients and fractional coefficients of other mechanisms make them more complex. However $1/2$ is a permissible coefficient of N_2O_4 because of the rapid equilibrium between it and NO_2 .) Abel and Schmid (2) gave the third from the last mechanism. They showed that it consisted of a rate-determining step and a rapid equilibrium and that it conformed to rate measurements. They reduced its high order by suggesting the following:



However, the order can also be reduced in the following way, provided it conforms to experimental facts:



The general approach to discovering a reaction mechanism is the following: Let all possible intermediates be selected and let them be m in number. Postulate all possible groups of intermediates: namely, each one separately, all combinations of two, all combinations of three, etc. The total number of combinations is $2^m - 1$. In each of the $2^m - 1$ cases determine all possible mechanisms. With every mechanism present by which the reaction could occur, one has merely to eliminate the undesirable and choose the best by application of chemical principles and experimental facts.

Numerous simplifications illustrated below make this general approach rather simple in many cases without too much loss of generality. The principal simplification, and one which can be made without any loss of generality, is to postulate immediately all m intermediates in the first group. The resulting mechanisms will constitute all mechanisms by which the equation could proceed (i.e., all possible mechanisms in each of the $2^m - 1$ cases are obtained).

The advantages of this general method are obvious. The only thing that can prevent the discovery of the mechanism is that totally unknown species occur as intermediates. If the general approach is not used, then one cannot be certain that the mechanism he presents is the actual mechanism. For example, though his mechanism might conform to experimental facts, other mechanisms which he did not consider could also conform to these facts. As of now the investigator cannot say anything about the uniqueness of the reaction mechanism he presents. However, if this truly scientific method of formulating mechanisms is used rather than the trial and error method of formulating mechanisms (before testing them experimentally), then one can state how unique his mechanism is.

As another example, consider the catalytic decomposition of hydrogen peroxide by the bromine-bromide couple. The net reaction is:

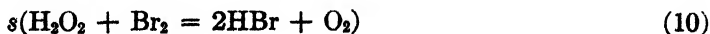
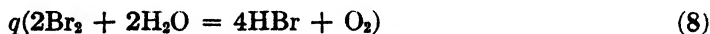


According to the general approach in discovering a reaction mechanism, we must first formulate all possible intermediates. By formulating all plausible intermediates considerable simplicity is gained at little loss of generality. These intermediates are HBr, Br₂, HBrO, HBrO₂, HBrO₃, and HBrO₄. (At least the first two must be postulated, because it is an experimental fact that an aqueous solution containing H₂O₂, O₂, HBr, and Br₂ reaches a steady state with respect to HBr and Br₂, and consequently these compounds are definitely involved in the reaction mechanism.)

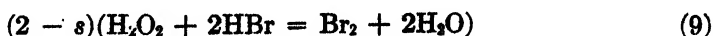
The next step in the general procedure is to insert all the intermediates into the original equation (since this will give us precisely the same results as considering each of the $2^m - 1 = 63$ cases separately). However, let us first look for all mechanisms in which only the intermediates HBr and Br₂ appear, since these are actually present in the solution. Later, mechanisms containing one or more of the oxy acids can be sought. Inserting these in equation 7:

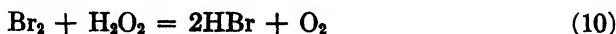
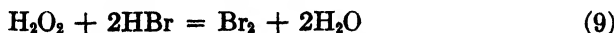
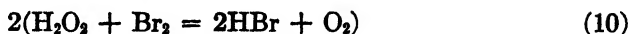
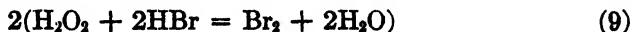
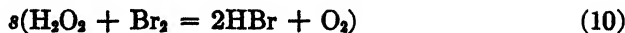


From this equation the totality of component equations of 7 are found to be the following:



The "a" equation can always be eliminated, and then all possible mechanisms of equation 7 are found by the algebraic method to be the following:





The simplest of these is the last one, and it is the one which Bray and Livingston (4) have shown to be consistent with rate data:

$$\begin{aligned} \frac{d(\text{Br}_2)}{dt} &= k_1(\text{H}_2\text{O}_2)(\text{H}^+)^2(\text{Br}^-)^2 \\ -\frac{d(\text{Br}_2)}{dt} &= k_2(\text{H}_2\text{O}_2)(\text{Br}_2) \end{aligned}$$

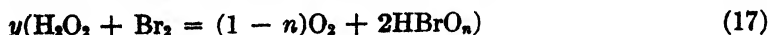
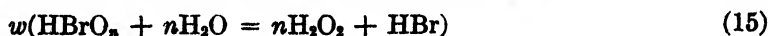
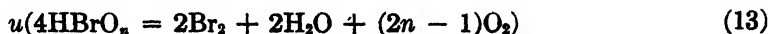
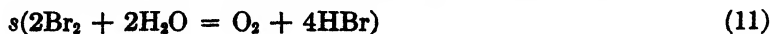
and at the steady state

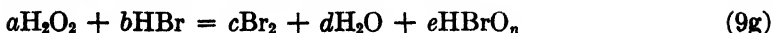
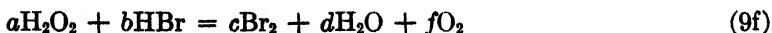
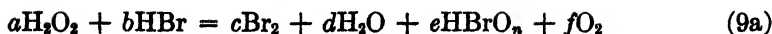
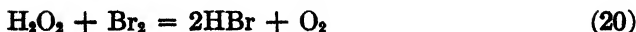
$$k_1(\text{H}_2\text{O}_2)(\text{H}^+)^2(\text{Br}^-)^2 = k_2(\text{H}_2\text{O}_2)(\text{Br}_2)$$

$$\frac{(\text{Br}_2)}{(\text{H}^+)^2(\text{Br}^-)^2} = \frac{k_1}{k_2} = \text{a constant}$$

Since experimental facts show that reactions 9 and 10 are two compensating reactions in the decomposition of hydrogen peroxide, we may now separately investigate each of these to see if they take place in steps.

Let us first consider reaction 9. The plausible intermediates are HBrO , HBrO_2 , HBrO_3 , HBrO_4 , and O_2 . Let us look for those mechanisms in which only one of the oxy acids of bromine appears, since mechanisms containing two or more are complex in comparison. Thus the intermediates may be represented by the pair HBrO_n and O_2 (where $n = 1, 2, 3$, or 4). Inserting both in equation 9, we find the following to be the totality of component equations:





The last nine equations can be dropped for the following reasons: equation 19 is the decomposition of peroxide; equation 20 is the same as equation 10, the other compensating reaction. The others can be resolved into simpler equations.

To obtain all possible mechanisms we write the following equations:

$$2t + 4u - v + w - 2x - 2y - 2z = 0$$

$$s + nt + (2n - 1)u + (1 - n)y = 0$$

$$-nw + (2n - 1)x + y + nz = 1$$

$$-4s - 2t - (2n - 1)v - w - (2n - 2)z = 2$$

$$-2s + 2u - nv - x - y - nz = 1$$

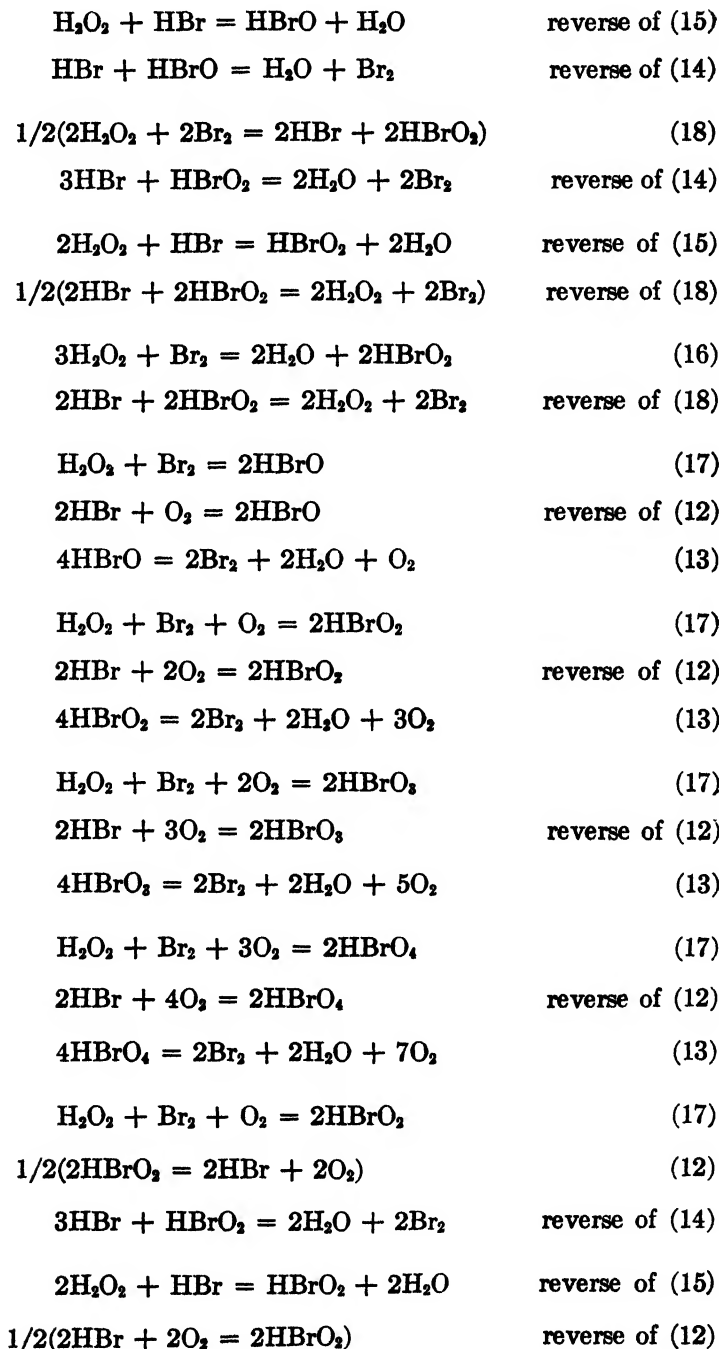
$$-2s + 2u - nv - nw + (2n - 2)x = 2$$

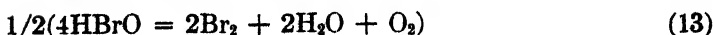
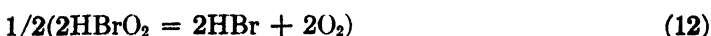
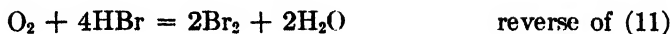
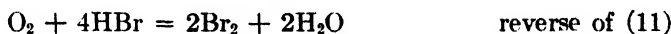
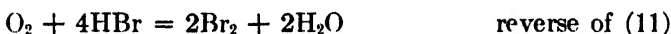
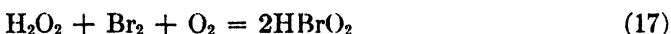
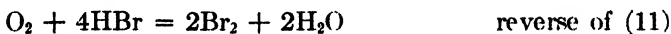
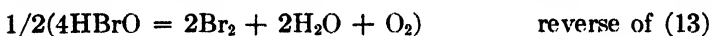
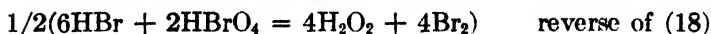
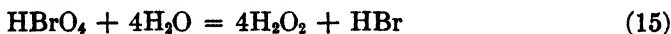
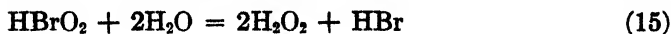
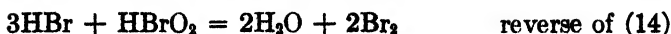
If we set six unknowns equal to zero and do this for all combinations of six unknowns, then we obtain all mechanisms consisting of two equations; if we set five unknowns equal to zero and do this for all combinations of five unknowns, then we obtain all mechanisms consisting of three equations, etc.

Each time the simultaneous equations are solved, four possibilities present themselves: (1) A unique solution in terms of numbers, n , or both. (2) A solution in terms of unknowns, together with or without n and numbers. (3) Inconsistent equations: case A: n must equal 1, 2, 3, or 4 in order for a solution to exist; case B: n must equal some number other than 1, 2, 3, or 4 in order for a solution to exist; case C: the equations are inconsistent for all values of n . Only in cases 1, 2, and 3A will the solution be considered.

After all such solutions are written, all the mechanisms can be immediately written, but many will be quite complex. We can eliminate the more complex by listing only those consisting of three or less equations, and only those in which the variables corresponding to them—namely, s , t , u , v , w , x , y , and z —assume the values ± 1 or $\pm 1/2$ in cases where no terms (except O_2 and Br_2 , which may

have 1/2 as a coefficient) will have fractional coefficients. The following are all such mechanisms:

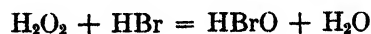
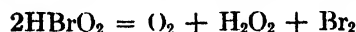
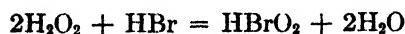
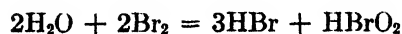
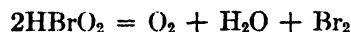
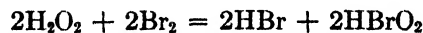
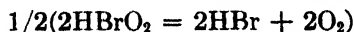
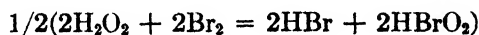
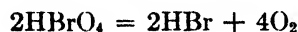
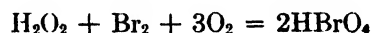
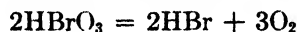
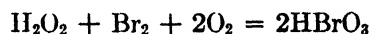
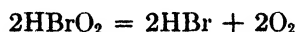
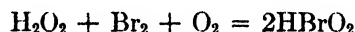
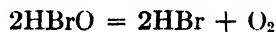


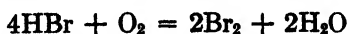
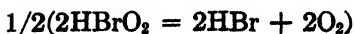
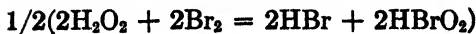
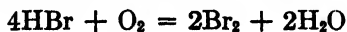
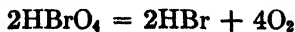
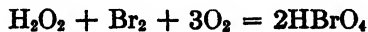
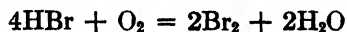
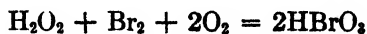
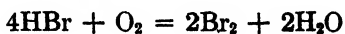
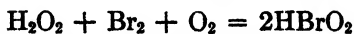
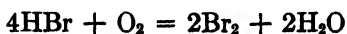
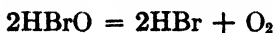
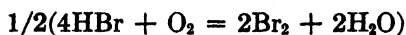
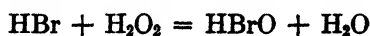
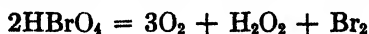
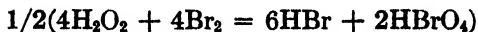
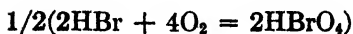
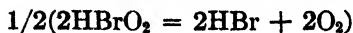
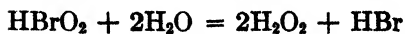
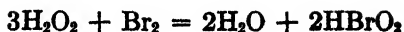
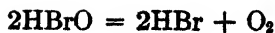


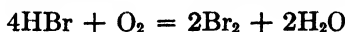
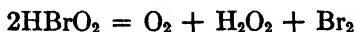
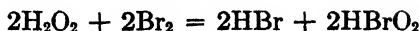
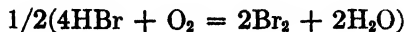


It is easily seen that the first mechanism is the simplest, and it was the one given by Bray and Livingston (4). It consists of a rapid equilibrium and a rate-determining step, and conforms to rate measurements. However we add to their results here, showing that there is no other mechanism as simple for the intermediates postulated.

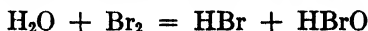
Let us now treat in the same way the other compensating reaction in the catalytic decomposition of hydrogen peroxide,—namely, reaction 10. Let the intermediates be H_2O and HBrO_n . If the same simplifications are made as in the case of 9, the following are the resulting mechanisms of 10:







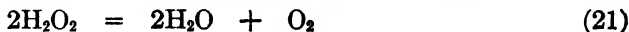
The eighth mechanism was given by Bray and Livingston (4) in the form



the last equation being the sum of two equations. The mechanism consists of a rapid equilibrium and a rate-determining step and conforms to rate data.

If the catalytic decomposition of hydrogen peroxide by the chlorine-chloride couple is studied as above, the same results are obtained as in this bromine case. Livingston and Bray (5) investigated this experimentally.

As our next example let us consider the catalytic decomposition of hydrogen peroxide by the iodine-iodide couple. The original reaction is again

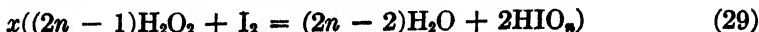


The plausible intermediates are HI, I₂, and HIO_n. We can proceed as in the bromine case and consider first only HI and I₂. However, none of the mechanisms obtained are consistent with the rate equations given by Abel (1):

$$-\frac{d(\text{H}_2\text{O}_2)}{dt} = k_1(\text{H}_2\text{O}_2)(\text{I}^-)$$

$$-\frac{d(\text{H}_2\text{O}_2)}{dt} = k_2(\text{IO}^-)(\text{H}_2\text{O}_2)$$

However, the general procedure is to consider all three intermediates at once. Doing this we obtain the following as the component equations of 21, after dropping those which can be further resolved:

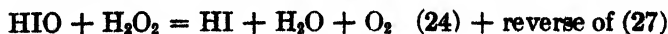
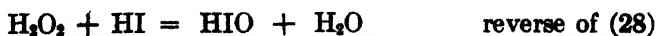




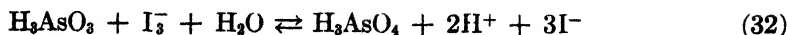
Making the same simplifications regarding the mechanisms to be listed as were made above, the following are the mechanisms (given in algebraic form):

$$\begin{aligned} r &= 1; s = 1 \\ n &= 2; t = 1/2; w = -1 \\ n &= 2; q = -1; t = 1; z = 1 \\ n &= 4; q = -1; t = 1/2; z = 1/2 \\ n &= 2; q = -1/2; u = 1/2; z = -1 \\ n &= 2; q = 1; v = -1; w = -1 \\ n &= 4; q = 1; v = -1; z = 1/2 \\ n &= 4; q = 1; w = -1; z = -1/2 \\ n &= 3; q = 1; x = 1; z = -1 \\ n &= 3; q = 1; y = -1; z = 1 \\ n &= 1; v = 1; t = 1; x = 1 \\ n &= 2; r = 1; t = 1/2; z = 1/2 \\ n &= 2; r = 1; y = -1; z = 1 \\ n &= 2; s = -1; t = 1; x = 1 \\ n &= 1; s = 1; v = -1; w = -1 \\ n &= 2; s = 1; v = -1; z = 1/2 \\ n &= 2; s = 1; w = -1; z = -1/2 \\ n &= 2; s = 1; x = 1; z = -1 \\ n &= 2; t = -1; u = 1; z = 1 \\ n &= 2; t = -1; u = 1; z = 1 \\ n &= 2; t = 1/2; v = -1; z = 1 \\ n &= 2; t = 1/2; x = 1; z = -1/2 \\ n &= 2; u = -1; y = -1; z = 1/2 \\ n &= 1; u = 1; x = 1; y = 1 \end{aligned}$$

The mechanism $n = 1; s = 1; v = -1; w = -1$ was given by Abel (1) and in the form:



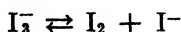
As a final example consider the reaction



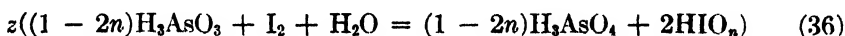
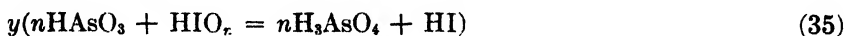
which for the purpose of mathematical analysis can be written in a simpler form



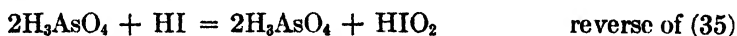
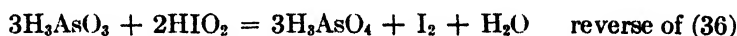
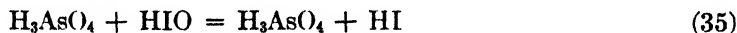
because of the rapid equilibrium



The plausible intermediate is HIO_n , and we shall consider only mechanisms in which no more than one oxy acid of iodine appears. The following are the component equations of 33, after dropping those which can be further resolved:



The following are all the mechanisms in which x , y , and z are only ± 1 .



Roebuck (8) gave the first mechanism as being consistent with rate data. Here we show that it is the simplest possible mechanism for the intermediates postulated.

SUMMARY

We have set forth principles and methods which aid in the problem of determining the mechanism of a reaction. For any reaction it is now possible to write a series of mechanisms which contains the actual mechanism unless an unknown compound occurs as an intermediate. (This will be true only when generality is not sacrificed by making simplifying assumptions.) Several examples have illustrated this. It was possible to state in these examples how unique the accepted mechanisms are.

The author is very much indebted to Dr. William Hamill of the University of Notre Dame for his many suggestions made in the development of the subject matter treated here.

REFERENCES

- (1) ABEL, E.: *Z. physik. Chem.* **136**, 161 (1928).
- (2) ABEL, E, AND SCHMID, H.: *Z. physik. Chem.* **132**, 56 (1928); **134**, 279 (1928); **136**, 153 (1928).
- (3) BOTTOMLEY, J.: *Chem. News.* **37**, 110 (1878).
- (4) BRAY, W. C., AND LIVINGSTON, R. S.: *J. Am. Chem. Soc.* **45**, 1251 (1923).
- (5) LIVINGSTON, R. S. AND BRAY, W. C.: *J. Am. Chem. Soc.* **47**, 2069 (1925); **48**, 405 (1926).
- (6) MCGAVOCK, W. C.: *J. Chem. Education* **22**, 269 (1945).
- (7) PORGES, A.: *J. Chem. Education* **22**, 266 (1945).
- (8) ROEBUCK, J. R.: *J. Phys. Chem.* **6**, 365 (1902); **9**, 727 (1905).
- (9) STANDEN, A.: *J. Chem. Education* **22**, 461 (1945).
- (10) STEINBACH, O. F.: *J. Chem. Education* **21**, 66 (1944).

CAVITATION FROM SOLID SURFACES IN THE
ABSENCE OF GAS NUCLEI¹DANIEL C. PEASE² AND L. R. BLINKS*The Hopkins Marine Station of Stanford University, Pacific Grove, California**Received April 2, 1946*

INTRODUCTION

In general, the literature on cavitation and bubble formation presents a very confusing picture. On the one hand, modern theoretical work by Doring (3), Furth (4), Piccard (7), and Harvey *et al.* (5) has indicated that cavitation and bubble formation cannot be accounted for on the basis of random thermal movements in homogeneous solutions unless relatively enormous superheating, supersaturation, or negative tension is established. On the other hand, most experimental work, including that with supersonic vibrations (and everyday laboratory experience), suggests that cavitation and bubble formation require no great driving force. To be sure, Kenrick *et al.* (6) have heated water to 270°C. (54 atm. absolute pressure) before it exploded, and have supersaturated water with oxygen, nitrogen, and carbon dioxide at 100 atm. without producing bubbles when the sample was decompressed. Clare (1) apparently sometimes accomplished supersaturation with oxygen to 250 atm. without bubbles being formed. Dixon (2) achieved negative tensions of up to 150 atm. before a

¹ The work described in this paper was done under a contract, recommended by the Committee on Medical Research, between the Office of Scientific Research and Development and Stanford University.

The work of Harvey and his collaborators progressed simultaneously with our own, and a free exchange of ideas sometimes made the question of priority difficult. One of the authors (D. C. P.) worked with Dr. Harvey's group for the first year of their activity, and the experiments reported here followed naturally upon their work.

² Present address: Anatomy Department, School of Medicine, University of Southern California, Los Angeles, California.

column of water broke (a column of plant sap broke at 207 atm.). Furthermore, laboratory experience does often demand the use of "boiling chips" to prevent considerable superheating.

Much of this confusion has resulted because it has not been generally realized that there are two distinct problems here. One concerns the nature and stability of gas masses which persist in fluids and on surfaces, and can and do act as nuclei for cavitation and bubble formation. When nuclei are present, bubbles can be expected when the driving forces are very low. The other problem, considered in this paper, deals with cavitation and consequent bubble formation *de novo*, in the absence of any preëxisting gas phase.

It has been the considerable recent contribution of Harvey *et al.* (5) to demonstrate experimentally that most commonly observed instances of cavitation and bubbling depend, in fact, upon the presence of gas nuclei. In a dramatic experiment they took a sample of water in a glass tube and subjected it to high hydrostatic pressure in order to force all preëxisting gas masses into solution and thus have a system entirely devoid of gas nuclei. "Water so treated has remarkable properties. It can be heated above 200°C. without bursting into vapor. When intense high frequency sound waves are passed through, no cavitation occurs, and no bubbles arise. Finally, if exhausted to the vapor pressure of water, moderate knocks have no effect and only a very severe blow will cause bubbles to form."

Harvey and coworkers deduce that a bubble nucleus is a gas mass trapped in a crack or depression on a hydrophobic surface. As a consequence, it can have a negative surface curvature (concave) at the fluid interface. Then surface tension will always tend to sustain or enlarge the gas mass, and a true equilibrium state can exist so that the nucleus can persist indefinitely. Thus, dust particles and container walls are a potential source of nuclei which will almost invariably be present unless special precautions are taken. It was only on the basis of the above work that it became possible knowingly to take adequate steps to remove all preëxisting gas nuclei. Thus true cavitation could be studied with this potential source of serious confusion eliminated.

EXPERIMENTAL

1. General method

To produce tension in fluids we adopted the general method of Harvey *et al.* (5), which consisted simply in striking the container wall with an iron hammer. If the fluid column was 4–5 in. high, it was set in motion by the pressure pulse, with a consequent negative component resulting from the inertia. The elastic bounce of the container wall away from the moving column of fluid was an additional component. We have no way of knowing how large a tension is possible with this procedure, but it may be considerable very locally. We did have the empirical knowledge that the force was much more than adequate to produce clouds of bubbles from nuclei which were still stable in air-saturated water exhausted down to its vapor pressure. And we could also observe very large (1 cm.) cavities form and quickly collapse at the vapor pressure of the water

when the system was largely degassed. The tension produced proved completely adequate to make a number of very clear distinctions. The technique was employed throughout because of its great simplicity. In all cases the pressure corresponded to the vapor pressure of the fluid in question, or 2–3 mm. Hg (whichever was greater). Pyrex glassware was employed throughout, and was kept clean and wet by soaking until use with concentrated sulfuric acid saturated with potassium dichromate.

2. Water in glass and rubber

As previously mentioned, Harvey *et al.* (5) discovered that a water sample in a clean glass tube could be exposed to high hydrostatic pressure and then evacuated down to its vapor pressure without giving rise to any bubbles. Nor would bubbles appear when the tube was hit sharp blows with a metal hammer. We have repeated this basic experiment many times, deliberately hitting various sorts of glass tubes at the vapor pressure of water with harder and harder blows until the tubes shattered. We go further than Harvey in saying that when additional precautions are taken (which will be obvious later), we never obtained any cavitation or bubble formation in such previously pressurized systems (12,000 lb./in.² applied for 5 min.). The tension developed by the hammer blows was simply inadequate to tear the water away from the glass in the absence of gas nuclei. On three occasions, though, the glass cracked on the inside, but the crack did not extend through the wall. Cavities and bubbles did form in these tubes, suggesting the momentary existence of a much greater tension. It is probable that a very great tension existed momentarily, for the water molecules presumably could not move rapidly enough to fill the crack as it expanded.

We wanted a more rigorous test of the behavior of water when all nuclei were absent. We took a wide-bore tube, and built up a very thick latex rubber plug at one end by repeated dipping. The glass-rubber junction caused trouble until the rubber was run far up within the tube on the first dip. Such a tube, filled with water, was first pressurized and then exposed to a vacuum corresponding to the vapor pressure of the water. Extremely hard hammer blows on the rubber diaphragm did not produce cavitation except in so far as there was surface splashing. Cast latex tubes, filled with water and sealed, and then pressurized, were similarly resistant to the hardest blows that we could deliver to them *in vacuo*. Such pressurized gum rubber appears milky, and is apparently entirely hydrophilic.

The primary conclusion upon which the rest of the work is predicated is that in the absence of a free gas phase (gas nuclei), water itself does not cavitate unless large tensions are produced. Nor does water tear away from a wet glass or gum rubber interface without the application of very considerable force.

Aside from using hydrostatic pressure, it seemed likely that all gas nuclei might be removed by making the system essentially gas-free. A wide-bore tube, 2–3 ft. long and with 4–5 in. of water in it, was clamped upright and kept continuously evacuated with an aspirator pump. At the same time a hammer activated by a solenoid repeatedly hit the bottom of the tube at the rate of one blow per

second. At first, of course, great clouds of bubbles appeared from nuclei. As the gas left the solution, their growth rate became slow and the bubbles remained small, but persisted as centers from one blow to the next. Depending upon the blow intensity and the characteristics of the tube, after perhaps 20–40 min. the water in the tube would stop cavitating entirely. And once stopped, the cavitation could not be started again with any blow that did not shatter the tube! So much gas had been removed from solution that not only were the nuclei dissolved, but also there was insufficient gas to sustain a vapor cavity as a nucleus from one second to the next. In other words, bubbles once formed had a life of less than 1 sec.

Gentle heating to produce boiling *in vacuo* greatly accelerated the removal of dissolved gas. Then a stage could be reached quite rapidly when a continuous vapor column had to be maintained or boiling would stop, cavitation could not be induced, and the water could be superheated at least 60–80°C. without boiling. (Probably much greater superheating could have been attained, but no particular attempts were made in this direction.) This method of removing gas nuclei was in all respects as effective as the hydrostatic pressure procedure. The only important difference was that the system was necessarily degassed, while pressure allowed the use of supersaturated solutions.

3. Organic liquids in glass

Even though glassware be cleaned with hot concentrated sulfuric acid–dichromate mixture and kept continuously wet until use, it will inevitably carry micronuclei when water is the fluid phase used. This is not the case with several organic fluids which we have tested in contact with glass. One can take a dry glass tube and fill it with paraffin oil, a melted fatty acid (capric or caprylic), or ether, and nuclei will not be retained in the system. The pouring may trap a few nuclei or discrete bubbles, but if the system is evacuated the bubbles will rise to the surface. A few judicious taps will then enlarge all existing nuclei and remove them from the system as bubbles. From then on no cavitation or bubbles can be produced by any amount of striking (except possibly in ether, where unduly high vapor pressures can be produced).

Thus we had a third method of working with systems free of nuclei. This is thought to depend upon the different physical relations at the air–liquid–glass interface when the liquid is not water. The contact angle was small or zero with these organic fluids, so that the negative curvatures necessary to sustain nuclei were not possible. The surface tension at the convex surface then promptly drove any gas mass into solution. Solvent action may have added to their effectiveness in removing any adherent oil or grease films. Presumably any three-phase system with a sufficiently great spreading coefficient of fluid on solid would behave in the same manner.

We have, now, the important conclusion that these organic compounds, like water, will not cavitate or bubble without large driving forces when gas nuclei are absent. We have also found that ether, at least, can be greatly superheated under these conditions.

4. *Solid surfaces; various crystals*

Having several experimental means of removing gas nuclei, we were now in a position to study the properties of other solid-liquid interfaces. We could work with systems that were either supersaturated or essentially gas-free. We found that the presence of a variety of different solid surfaces allowed very easy cavitation without preëxisting gas nuclei being present.

First of all, it was found that when different crystals were precipitated from their own nucleus-free melt or solution, cavitation frequently could be obtained without the slightest difficulty. The crystallization was accomplished by a slight change in temperature. The effect was completely reversible, and upon remelting or redissolving the crystals, the sample invariably returned to its original condition, lacking nuclei. This work is summarized in table 1.

A glance at table 1 will show that no matter how formed, and irrespective of the fluid medium, the organic crystals always allowed easy cavity formation, even in the absence of dissolved air and in the presence of only a *very few, very small* crystals. The ionic salt crystals behaved differently, in that large numbers of crystals ordinarily had to be formed before cavitation could be induced. Rochelle salt gave an intermediate effect, as might be expected from its structure.

In the above experiments crystals were always formed in a medium known to be free of nuclei, but the results were extended by taking preformed crystals and applying procedures presumably capable of removing all nuclei. Thus, water suspensions of crystalline cholesterol, iodoform, and calcium carbonate, and very thin cast sheets of paraffin, were exposed to 12,000 lb./in.² hydrostatic pressures overnight, or for 2-3 days, to remove existing nuclei. The pressurized samples of cholesterol, iodoform, and paraffin cavitated as soon as they could be tested at reduced pressures. The calcium carbonate cavitated with some difficulty. Exactly the same effects were observed when the nuclei were presumably destroyed by removing the dissolved air, for cavitation continued indefinitely with the first group of substances, and erratically and occasionally with calcium carbonate.

A more conclusive experiment was performed by actually cooling and solidifying melted paraffin under water while it was continuously exposed to 12,000 lb./in.² pressure. This treatment, even when followed by subsequent repressurization, did not prevent easy cavitation from the solid paraffin surface.

The nature of the solid surface was obviously of great importance in these experiments. Experiments were performed which gave considerably deeper insight into the essential requirement of easy cavitation. It was observed early that actively melting or dissolving crystals would no longer allow cavitation by our methods. This phenomenon was specifically observed and studied with crystals of capric and caprylic acids and of ethyl cinnamate in their own melts, and with crystals of succinic acid and potassium dichromate in saturated solution. The results suggested that unstable surfaces were not favorable for cavitation, and this thought was confirmed by a much more precise study of the capric acid crystal-melt system.

A heavy sludge of cavitating capric acid crystals was prepared in its own melt. The system, at 3 mm. Hg pressure, and while being continuously struck, was gently warmed to start melting the crystals. Cavitation stopped, and the

TABLE 1
Cavitation brought about by the formation of crystals

COMPOUND	CRYSTALS FORMED IN	MEDIUM		CAVITATION ORDINARILY REQUIRING	
		Air-saturated	Gas-free	Few crystals	Many crystals
Capric acid.....	Melt	+	+	+	
	Water suspension	+	+	+	
Caprylic acid.....	Melt	+		+	
	Water suspension	+		+	
Paraffin.....	Saturated paraffin oil	+		+	
Ethyl cinnamate	Melt		+	+	
	Small drop under water		+	+	
Bromoform.....	Small drop under water		+	+	
Succinic acid.....	Saturated solution	+	+	+	
Rochelle salt.....	Saturated solution		+	Intermediate	
Potassium nitrate.....	Saturated solution		+		+
Potassium dichromate.....	Saturated solution		+		+
Potassium sulfate.....	Saturated solution		+		+

Cavitation was possible when crystals of the above compounds were formed in glass-fluid systems which were known to be previously free of all gas nuclei, and which did not allow cavitation. The ionic mineral salts, however, did not ordinarily allow cavitation until heavy sludges of crystals were present. The other compounds allowed cavitation in the presence of a *very* few, *very* minute crystals, except in the case of Rochelle salt. The latter compound more nearly resembled the other organic compounds than the inorganic, but the effect was intermediate and not entirely definitive. When heavy sludges were required, it is possible that enormous supersaturations produced bubbles as trapped fluid cores proceeded to solidify. This possible source of error could hardly have been involved in the results with the organic compounds.

temperature was lowered slightly so that the crystals were in equilibrium with their own melt. This equilibrium was maintained for 45 min. without the production of a cavity, in spite of the many crystals present. The temperature was then dropped only 0.2°C., and a slow growth phase started which was

barely visible. But cavities appeared at once as soon as the tube was gently tapped.

We conclude that in this sort of an equilibrium system there are no stable surfaces at all, any more than there are when crystals are rapidly melting or dissolving. It appears that a stable surface with "fixed" molecules is an essential requirement for easy cavitation.

5. Stearate monolayer surfaces and the effects of added substances

The above experiments were all of a qualitative nature. It was desirable to develop a semiquantitative technique so that different surfaces could be more precisely compared. These ends were accomplished by using stearate monolayers³ as the basic surface, which could then be modified by the addition of other substances soluble in water.

It was first of all determined that water in stearate-coated tubes cavitated very easily even after treatment with 12,000 lb./in.² hydrostatic pressure applied for days. Also, similarly coated tubes of water continued to cavitate indefinitely after the removal of dissolved gas at the vapor pressure of the water. These were the standard treatments which removed all nuclei and prevented cavitation in similar systems lacking the stearate.

The hammer blow striking the tube was activated by a solenoid. By simply altering the current flow through the solenoid, the intensity of the blow could be varied at will. The frequency of cavitation resulting from striking could be correspondingly altered from 0-100 per cent (of course each tube had its own absolute characteristics).

In making an experiment, the stearate-coated tube with 4-5 in. of water in it would be exhausted with an aspirator pump and repeatedly struck with the hammer for a half-hour or more until we were sure the system was essentially gas-free. The blow intensity would then be adjusted so that the cavitation frequency was known to be within the range from 70-90 per cent. It was then possible to test the effect which various added substances had upon this frequency of cavitation. These were added in solution, and the system once more exhausted and struck until gas-free before determining the new frequency.

³ A saturated solution of ferric stearate in benzene was the source of the stearate monolayers (Langmuir method). The same solution was used throughout, so that any impurities were constant. In applying these layers the history of the glass was very important. Best results were obtained when the glass was either freshly fused and kept hot until application, or was soaked overnight with 0.1 *M* barium hydroxide and then washed and completely dried by evacuation and heat. Even repeated washings with pure benzene would not remove the stearate monolayers applied thus from solution. But simply to remove the excess ferric stearate, the tubes were given two washings with pure benzene, dried, and then washed with a good lather of Ivory soap. Tubes prepared in this manner were "hydrophobic", and the water contact angle would be about 40°. It should be noted, however, that the monolayers applied from solution were presumably open-work structures, for the contact angle never approached the high values of a complete monolayer or a crystalline surface. From our point of view the important fact was that we were able to put monolayer patches of stearate on the glass to give hydrophobic loci where the stearate "tails" were in contact with water and the polar "heads" were in turn fixed to the glass.

It was found that various substances, upon addition to the fluid phase, greatly reduced the cavitation frequency. The data are summarized in table 2.

It can be seen in table 2 that the cavitation frequency was reduced much as the expected van der Waals association between stearate and added substance was increased. Substances such as *n*-butyl alcohol, leucine, or gelatin offered a large degree of "protection." All of these substances have polar groups included in the molecule, which would not take part in the association and would

TABLE 2

Effectiveness of various agents in reducing the cavitation frequency from stearate monolayers

CHAIN LENGTH	ALCOHOL	EFFECT	COMPOUND	EFFECT
1	Methyl	0	Gelatin (dilute)	+++
			Egg albumin (dilute)	++
2	Ethyl	0	Potassium butyrate	0
	Isopropyl	+	Sodium benzoate	0
	Tert.-Butyl	++	Sodium stearate	+++
			Sulfonated soap	+++
3	Propyl	+	<i>l</i> -Leucine	+++
	Isobutyl	++	Alkaline leucine	+
	<i>sec</i> -Butyl	++	Glycine	++
4	<i>n</i> -Butyl	+++	Glycerol	+(+)
			Ethylene glycol	0(+)
			Phenol	++
			2 per cent ammonia	0
			Potassium chloride	0

This table indicates the effectiveness of various agents in reducing the cavitation frequency from stearate monolayers when they were added to the water phase. The strength of the hammer blow was adjusted to give a known cavitation frequency from 70-90 per cent before the addition was made. The symbol 0 means that there was no significant effect of the added agent. The other symbols refer to orders of magnitude, with + indicating a small, but significant, effect, a cavitation frequency reduced to about 10-20 per cent. ++ indicates a very decided effect with the frequency reduced about a hundredfold to 1 per cent, and +++ indicates about a thousandfold reduction in frequency.

No specific concentrations were used, the attempt being simply to add a great excess for sorption on the stearate. Whenever solubilities allowed it, 5-10 per cent by volume was added; in other cases solutions were very nearly saturated unless specifically designated.

be presented to the water phase. But they all also have substantial non-polar chains for association with the non-polar fraction of the stearate molecules.

Stearate-coated tubes were tested after the addition of each of the lower alcohols with informative results. Methyl and ethyl alcohols offered no protection, *n*-butyl alcohol excellent protection, with *n*-propyl alcohol intermediate. Here we have serial differences depending upon chain length. But the mass of the non-polar fraction is also important, as can be seen by comparing the

series with two-carbon chains, for ethyl alcohol was ineffective, while isopropyl and tertiary butyl alcohols gave increasing protection in that order.

All of these effects were entirely reversible. Invariably, when the added substance was washed off and removed, the stearate-coated tube returned to its original cavitation frequency. But it was not always easy to remove an added substance. For instance, a tube that had had leucine or *n*-butyl alcohol in it could be flushed with running water overnight and would still not show its original characteristics. This was fortunately not true of a simple soap, which apparently would replace these added substances on the stearate, and then be quickly washed off itself. Application of a good lather of Ivory soap, followed by a few rinses, always returned the tube to its original condition, except possibly after the use of proteins. Thus a tube could be used many times. (Sulfonated soaps offered good protection in themselves, but did not rinse off easily.)

It must be noted and emphasized, however, that we have not been able to add any substance to the aqueous phase which offered complete protection against cavitation from the stearate monolayer. The cavitation frequency could be reduced more than a thousandfold, but it none the less occurred at a finite rate. We must assume that we were dealing with equilibrium conditions; that not all of the stearate chains would be associated with the added substance at any given moment, and thus there was no complete coverage and protection.

If the behavior of a stearate monolayer could be modified by the addition of various substances, so should gross crystal surfaces. Here it was much harder to standardize conditions, but the essential experiments of the stearate series have been performed using suspended cholesterol crystals as the hydrophobic solid surface. The results seemed identical, although obtained with less comparative exactitude. There was no doubt, though, that *n*-butyl alcohol, leucine, and soap gave a very great degree of protection.

DISCUSSION RELATIVE TO GAS NUCLEI

Our most basic finding is that certain types of stable solid surfaces are essential prerequisites for easy cavitation in the absence of gas nuclei. Since Harvey *et al.* (5) have made it amply clear that cavitation will occur without difficulty from gas nuclei, it is important to consider whether or not preëxisting nuclei could have survived our treatments. The most convincing experiments are certainly those with stearate monolayers, for here it seems incredible that preëxisting gas nuclei could have withstood the great hydrostatic pressures that were applied, since every crack necessarily must have been exposed to the fluid phase. As far as gross crystals are concerned, they were often used with their own melts as the fluid phase. Under such circumstances there was no possibility of supporting the negative gas curvatures which are prerequisite for stable nuclei.

The possibility that nuclei formed *de novo* on some types of solid surfaces requires more serious consideration. Harvey *et al.* (5) assume that minute vapor cavities might form as a result of statistical fluctuations of the molecules. They go on to calculate the very limited conditions whereby such a cavity might become a stable nucleus by acquiring gas from solution. To begin with,

most of our systems which have given easy cavitation do not fall within these limited conditions. But a much more serious objection questions their assumption that statistical fluctuations of molecules will produce vapor cavities at all at any finite rate. The experimental evidence denies this, for such cavities would allow tears to start in the body of a fluid, and slight tension should produce cavitation without any difficulty. Yet we now know that water in a clean glass tube will not cavitate when the gas nuclei are removed. And we must remember that Dixon (2) achieved tensions that often exceeded 100 atm. before the water column broke. These tensions were built up relatively slowly, and would not have been possible if minute cavities had been constantly forming. Similarly, Kenrick *et al.* (6) would not have been able to superheat water to 270°C. if there had been spontaneous cavities.

A more difficult suggestion to rule out supposes that first of all a sorption process concentrates gas molecules from the fluid on certain types of solid surfaces. And then, conceivably, statistical fluctuations of the concentrated molecules might form a nucleus *de novo*. However, the work with "gas-free" systems makes this most unlikely, and there do not appear to be any theoretical or experimental reasons for believing that this sort of molecular concentration would be possible. Furthermore, we can fall back on the work of Kenrick *et al.* (6) and Clare (1), who often did not obtain bubbling when water saturated at 100–250 atm. was decompressed. This is indicative of the driving forces that would be required, and thus we do not believe that we can account for our results on any basis which involves gas nuclei.

CONCLUSIONS

We believe that when we have produced cavitation under the described conditions, we have done so by quite literally starting a tear where no gas phase existed before. We presume that the tensions applied as driving forces were small (a few atmospheres at most). Thus any tear must have started at a very "weak" locus where the intermolecular forces momentarily approached zero.

We have found that a solid surface is a prerequisite for easy cavitation. And certainly, "hydrophobic" surfaces with exposed non-polar groups allowed tears to start most easily. Indeed, it is doubtful that any other sort of surface would allow this easy cavitation, for impurities, as well as other explanations, could account for any cavitation which required a heavy sludge of crystals. It is not likely that the ionic crystal surfaces allow easy cavitation *per se*. Rather, they should probably be grouped with glass as non-cavitating surfaces.

We can ask ourselves why it is that fluctuating intermolecular forces only approach zero when non-polar groups are fixed on solid surfaces. A reasonable explanation supposes that a "fixed" molecule is less able to follow the thermal movements of the fluid molecules around it. If the forces of adhesion are low to begin with, such as van der Waals forces, it would seem that there can be a momentary escape of a fluid molecule away from the attractive sphere of the associated fixed molecule. Thus a hole quite literally comes into existence.

These conditions were realized when hydrocarbon chains were exposed on solid surfaces. Then the nature of the fluid made little if any difference.

Fluid systems, chemically identical with those allowing cavitation in the presence of a solid surface, did not cavitate. So the corollary of the above conclusions is that holes do not actually develop in the body of a fluid even when the cohesive forces are low. It seems that any particular fluid molecule tends to follow the thermal movements of all others around it. This it must do by moving sufficiently on its own account so that all of the molecules involved stay within one another's spheres of attractive force. There is no "escape," so that the cohesive forces do not approach zero, and a tear cannot be started easily.

Furthermore, there was no cavitation from "solid" surfaces which were presumably unstable enough to allow some molecular displacement. Thus we were not able to start a tear from the surface of dissolving or melting crystals, or unstable crystals in temperature equilibrium with their melt. And the protective action of a layer associated by van der Waals forces presumably also resulted from the mobility of the associated molecules.

From our own experiments we are not able to say how much tension would be required to tear the body of a fluid. We have not been able to do it by our procedures. But we have already referred to experiments in the literature reporting high values of applied tension, superheating, and supersaturation. These allow us to say that the force required cannot be less than 100–200 atm. in the case of water, and that it is of the same order of magnitude for some organic compounds. If one examines the methods employed by these workers, it is obvious that the techniques of all involved some previous pressurization. One can see in retrospect that they were dealing unknowingly with systems free of gas nuclei. Thus their results are a valid indication of the forces necessary to produce true cavitation. But even these values may be much too low for the body of a fluid because of contamination, or because at best there was a glass–fluid interface which seems likely to be "weaker" than the body of the fluid.

The theoretical treatments of the subject mentioned in the introduction are substantiated in principle by our work. What we may designate as true cavitation is not possible without large driving forces being applied, unless certain types of solid surfaces are included in the system. What has usually been encountered experimentally is a false cavitation in which the cavities were derived from preëxisting gas nuclei rather than *de novo*.

SUMMARY

The literature on cavitation has been confused because means have not been available to distinguish experimentally between false cavitation from preëxisting gas nuclei, and true cavitation *de novo* in the absence of any gas phase. Three procedures are described which remove all gas nuclei. Under these circumstances, water–glass systems will not cavitate unless forces of at least 100–200 atm. are applied. On the other hand, we find very easy cavitation when molecules with non-polar hydrocarbon groups are "fixed" on solid surfaces, either

on a crystal face or spread as monolayer patches on glass. The nature of the fluid phase then makes little qualitative difference. Substances which associate with the non-polar surface groups by van der Waals forces, and then present polar groups to the fluid phase, prevent easy cavitation in so far as equilibrium conditions allow a greater or lesser coverage.

Since certain types of solid surfaces are essential prerequisites for easy cavitation, we conclude that fluctuating intermolecular forces can approach zero only under very limited conditions. This happens only in those molecular combinations where the forces are relatively low irrespective of the phase relationships. We believe that when we have produced cavitation in the absence of gas nuclei, we have quite literally torn the fluid away from the solid, the tear beginning at a "weak" locus where non-polar groups were exposed on the solid surface. There, only, fluid molecules momentarily can escape the attraction of fixed molecules which are unable to follow their movements. Conversely, in the body of any fluid, or at such solid-liquid interfaces where the attractive forces greatly exceed van der Waals forces, molecules are unable to separate sufficiently far to get out of one another's attractive spheres even momentarily, and large forces must be applied to initiate a tear.

REFERENCES

- (1) CLARE, N. D. Trans. Roy. Soc. Canada [3] **19**, 32 (1925).
- (2) DIXON, H. H., Proc. Roy. Soc. Dublin [NS] **14**, 229 (1914).
- (3) DORING, W. Z. physik. Chem. **36**, 371 (1937); **38**, 292 (1937).
- (4) FURTH, R. Proc. Cambridge Phil. Soc. **37**, 252 (1941).
- (5) HARVEY, E. N., *et al.* J. Cellular Comp. Physiol. **24**, 1, 23 (1944), J. Am. Chem. Soc. **67**, 156 (1945).
- (6) KENRICK, F. B., *et al.* J. Phys. Chem. **28**, 1297, 1308 (1924).
- (7) PICCARD, J. Proc. Mayo Clinic **16**, 700 (1941).

AN UNUSUAL LIQUID INTERFACE

A. R. OLSON AND J. H. HILDEBRAND

Department of Chemistry, University of California, Berkeley, California

Received October 22, 1946

Two well-behaved immiscible liquids usually arrange themselves in the container in two horizontal layers with the denser liquid underneath; consequently a system such as the one depicted in figure 1, where one liquid forms a column inside the other, has been rather startling to most people who have seen it, physical chemists included. (The bottle is shown immersed in a larger vessel of water in order to give a truer picture of its contents.) The original bottle has indeed often served as a final examination question for a course in surface phenomena, and few students have been able to state all of the essential condi-

tions. These are as follows: (a) The inner liquid must be slightly denser than the outer. (b) The outer phase must preferentially wet the (glass) container. (c) The surface tension of the outer phase must be greater than the vector sum of the surface tensions of the inner phase and of the interface in order to hold the denser liquid on the surface. (d) The volume of the outer phase must not be so great as to pinch off the vase-shaped inner phase; otherwise one would have the

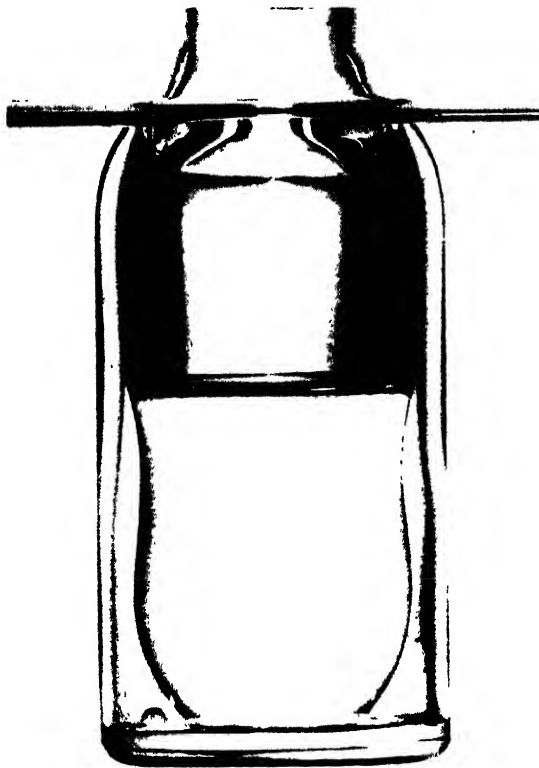


FIG. 1

more familiar case of a concavo-convex lens of the denser liquid left on the surface of the lighter.

These conditions are fulfilled in the system shown in figure 1 by an outer phase of water and an inner phase of a solution of carbon tetrachloride and benzene with a density slightly greater than 1. Other combinations could readily be selected to reproduce the essential conditions stated above.

MOLECULAR PROPERTIES OF NITROCELLULOSE. I

STUDIES OF VISCOSITY¹

GEORGE J. DOYLE, GARMAN HARBOTTLE, RICHARD M. BADGER, AND
RICHARD M. NOYES

*Gates and Crellin Laboratories of Chemistry, California Institute of Technology, Pasadena,
California*

Received September 3, 1946

INTRODUCTION

Probably the procedures most commonly used for the characterization of samples of high polymers involve measurements of viscosity on solutions of these polymers. Many of the procedures which are used commercially involve measurements on concentrated solutions, because results of great use in the empirical characterization of samples can be obtained from experiments in which the control of conditions need not be inconveniently precise. However, more valuable results from the theoretical standpoint can be obtained from measurements of viscosity on very dilute solutions and the extrapolation of the data to infinite dilution.

In the course of studies of the properties of nitrocellulose we have had occasion to measure the viscosities of dilute and concentrated solutions of several nitrocelluloses in various solvents and have developed procedures for the empirical correlation of results obtained under different conditions. The use of these measurements for evaluating molecular weights will be discussed in a subsequent paper.

EXPERIMENTAL PROCEDURE

Materials

Technical butyl acetate was dried over calcium oxide and fractionally distilled under reduced pressure. The middle fraction, which boiled at 53°C. at 55 mm. pressure, was used for the solvent in the experiments described below.

Chemically pure acetone was stored for a day with potassium permanganate and distilled. The distillate was dried over potassium carbonate, decanted into a flask containing anhydrous calcium sulfate, and redistilled. The resulting material was used for studies of dilute solutions; untreated acetone was used for preparing the concentrated solutions, which were intended to resemble those used in standard commercial measurements of viscosity.

The alcohol used in preparing the concentrated solutions was commercial 95 per cent ethanol denatured with about 4 per cent by volume of methanol.

Most of the nitrocelluloses used in these studies were representative commercial samples with various properties.

¹ Contribution No. 1076 from the Gates and Crellin Laboratories of Chemistry, California Institute of Technology.

This paper is based in whole or in part on work done for the Office of Scientific Research and Development under Contract OEMsr-881 with the California Institute of Technology.

Method of measurement

The viscosities of dilute solutions in purified acetone and butyl acetate were measured at 25°C. with previously calibrated Ostwald-type capillary viscometers.

Concentrated solutions were prepared to contain 10 per cent of nitrocellulose in a solvent mixture prepared from 10 parts (by weight) of denatured alcohol and 90 parts of acetone. The viscosities of these solutions were measured with a capillary-type viscometer of special design (2) instead of with the falling-ball viscometer used commercially (3).

RESULTS AND DISCUSSION

The "intrinsic viscosity", $[\eta]$, of a solute in a particular solvent is defined by the expression

$$[\eta] = \lim_{c \rightarrow 0} \frac{\eta_{sp}}{c} = \lim_{c \rightarrow 0} \frac{\ln \eta_{rel}}{c} \quad (1)$$

in which η_{rel} = relative viscosity = $\eta_{solution}/\eta_{solvent}$,
 η_{sp} = specific viscosity = $\eta_{rel} - 1$, and
 c = concentration in grams per 100 ml.

The precise determination of the intrinsic viscosity of a nitrocellulose involves making measurements at several concentrations and extrapolating the results to infinite dilution. However, if the dependence of viscosity on concentration is known with sufficient precision, it is possible to calculate the intrinsic viscosity from the result of a single measurement on a solution of moderate concentration such that the viscosity can be determined with good precision. The equation of Martin (1) is the most satisfactory expression that we have found for the dependence of viscosity on concentration up to about 1 per cent of nitrocellulose. This equation states that

$$\log \frac{\eta_{sp}}{c} = \log [\eta] + k[\eta]c \quad (2)$$

in which k is a constant dependent upon the solvent and upon the chemical composition but not the molecular weight of the solute.

The precision with which this equation fits the data is illustrated in table 1. In this table the results of measurements on solutions of four representative nitrocelluloses are presented with the intrinsic viscosities obtained by extrapolating these results to infinite dilution. In the last column of the table are presented the intrinsic viscosities calculated from individual measurements by equation 2 with the use of $k = 0.22$ if the solvent is acetone and $k = 0.18$ if it is butyl acetate.² The calculated intrinsic viscosities agree with the extrapolated values

² Subsequent experiments with other preparations of the same solvents indicated different but self-consistent values of k in the neighborhood of 0.2. The differences were not enough to cause serious errors in intrinsic viscosities calculated with the use of equation 2, but they do suggest that viscometric measurements in pure solvents are very sensitive to small traces of impurities and that each preparation should be checked before equations are applied blindly to measurements made with it.

TABLE 1
Dependence of viscosity of nitrocellulose solutions on concentration

NITROCEL- LULOSE NUMBER	NITROGEN	SOLVENT	INTRINSIC VISCOSITY $[\eta]$ (EXTRA- POLATED)	CONCEN- TRATION, c	SPECIFIC VISCOSITY, η_{sp}	INTRINSIC VISCOSITY $[\eta]$ (CALCULATED)
	<i>per cent</i>			<i>g./100 ml.</i>		
1087.....	11.99	Acetone	0.667	4.029	7.339	0.566
				3.022	4.408	0.588
				2.015	2.355	0.618
				1.007	0.884	0.633
				0.403	0.304	0.659
	11.89	Butyl acetate	0.848	4.022	10.34	0.733
				3.017	6.031	0.756
				2.011	3.072	0.782
				1.006	1.136	0.801
				0.402	0.376	0.813
2917.....	11.89	Acetone	2.81	1.007	10.37	2.64
				0.756	5.925	2.73
				0.504	2.994	2.85
				0.252	1.024	2.82
				0.100	0.325	2.81
	13.26	Butyl acetate	3.99	0.804	10.91	3.75
				0.603	6.122	3.81
				0.402	3.052	3.89
				0.201	1.099	3.91
				0.080	0.363	3.94
10405.....	13.26	Acetone	3.00	1.007	12.40	2.84
				0.756	6.768	2.91
				0.504	3.351	3.04
				0.252	1.131	3.04
				0.101	0.355	3.02
	13.94	Butyl acetate	4.30	0.704	11.33	4.39
				0.528	6.019	4.32
				0.352	2.960	4.37
				0.352	3.002	4.41
				0.176	1.046	4.30
2465.....	13.94	Acetone	6.25	0.070	0.348	4.34
				0.504	14.65	6.08
				0.378	7.746	6.20
				0.252	3.441	6.17
				0.126	1.175	6.24
	13.94	Butyl acetate	8.66	0.050	0.366	6.19
				0.402	14.90	8.56
				0.302	7.894	8.63
				0.201	3.709	8.73
				0.101	1.281	8.75
				0.040	0.398	8.56

at least within 3 per cent, provided c is less than 0.5 g./100 ml. The value of k appears to be independent of nitrogen content for nitrocelluloses containing from 12 to 14 per cent of nitrogen.

The results of measurements of intrinsic viscosity on butyl acetate and acetone solutions of several representative nitrocelluloses are presented in table 2. The data indicate that the ratio of the intrinsic viscosities in these solvents is 1.40 ± 0.04 for commercial nitrocelluloses having intrinsic viscosities greater than about 1. The value of the ratio appears to fall off for low-viscosity nitrocelluloses. These results are in qualitative agreement with those of Staudinger and Sorkin (4) for the ratios of viscosities of nitrocellulose fractions, but the absolute values of the ratios found by them were less than the values observed by us.³

TABLE 2
Comparative viscosities of nitrocelluloses in butyl acetate and in acetone

NITROCELLULOSE NUMBER	NITROGEN	INTRINSIC VISCOSITY IN BUTYL ACETATE, [η] _{bu ac}	INTRINSIC VISCOSITY IN ACETONE, [η] _{ace}	RATIO [η] _{bu ac} /[η] _{ace}
	<i>per cent</i>			
1948.....	11.82	0.83	0.64	1.29
1087.....	11.99	0.85	0.67	1.27
3875.....	10.93	1.64	1.20	1.37
3293.....	11.95	1.87	1.37	1.36
2936.....	12.17	2.35	1.69	1.39
5251.....	12.55	3.89	2.84	1.37
2917.....	11.89	3.99	2.81	1.42
6278.....	13.40	4.22	3.07	1.37
5250.....	12.55	4.26	3.05	1.40
10405.....	13.26	4.30	3.00	1.43
10411.....	13.23	4.45	3.12	1.43
5248.....	13.42	4.85	3.43	1.41
5167.....	13.46	4.87	3.50	1.39
5246.....	13.45	4.92	3.44	1.43
2465.....	13.94	8.66	6.25	1.39

The data presented do not show any systematic dependence of the ratio of intrinsic viscosities in the two solvents upon the nitrogen content of the nitrocellulose. Evidently such an effect, if present, cannot be very large. Its presence cannot, however, be entirely excluded, since in the materials available for measurement high nitrogen content tended to be accompanied by high viscosity, and low nitrogen content by low viscosity.

The viscosities of 10 per cent solutions of several nitrocelluloses in 10:90 alcohol-acetone were measured in stokes, and the results were used to calculate the viscosities in Hercules smokeless seconds (2). The results of these measure-

³ Subsequent experiments with other preparations of the same solvents indicated self-consistent values of the ratio nearer to the values observed by Staudinger and Sorkin. The intrinsic viscosity in at least one of these solvents appears to be very dependent upon the presence of small amounts of impurities.

ments are compared in table 3 with the intrinsic viscosities of the same nitrocelluloses in acetone. The data can be fitted empirically by an equation of the form

$$\log V = 3.55 \log [\eta] - 0.71 \quad (3)$$

in which V is the viscosity in Hercules smokeless seconds. The values of V calculated by means of this expression are presented in the last column of table 3. They indicate that it is not possible from the results of measurements on dilute solutions to predict the viscosities of concentrated solutions within the apparent accuracy of experimental determinations, but that it is nevertheless possible to obtain a reasonably satisfactory correlation between the results of measurements of the two types.

TABLE 3
Comparative viscosities of dilute and concentrated solutions of nitrocellulose

NITROCELLULOSE NUMBER	NITROGEN	VISCOSITY, V , IN HERCULES SMOKELESS SECONDS	INTRINSIC VISCOSITY IN ACETONE, [η]	VISCOSITY, V (CALCULATED)
	<i>per cent</i>			
1948.....	11.82	0.04	0.64	0.04
3875.....	10.93	0.33	1.20	0.37
3293.....	11.95	0.50	1.37	0.59
2936.....	12.17	1.24	1.69	1.26
8432.....	12.67	7.8	2.65	6.2
2917.....	11.89	12.0	2.81	7.6
6278.....	13.40	10.0	3.07	10.5
10411.....	13.23	10	3.12	11.0
5248.....	13.42	14.2	3.43	15.5
5246.....	13.45	13	3.44	15.8

SUMMARY

Measurements of viscosity have been made on dilute solutions of several nitrocelluloses in acetone and in butyl acetate, and it has been found that the results can be expressed by an equation of the form

$$\eta_{\text{rel}} = 1 + [\eta]c \times 10^{k[\eta]c}$$

in which η_{rel} is the relative viscosity of the solution, $[\eta]$ is the intrinsic viscosity of the solute, and c is the concentration in grams per 100 ml. The constant k is close to 0.2 for both acetone and butyl acetate and appears to vary for different preparations of solvent.

The ratio of the intrinsic viscosities in butyl acetate and in acetone is about 1.40 for nitrocelluloses having intrinsic viscosities greater than about 1, but the value of the ratio appears to fall off for low-viscosity nitrocelluloses. The value of this ratio appears to vary for different preparations of solvents but is constant within about ± 0.04 for measurements made with specific preparations.

The viscosity of a nitrocellulose in Hercules smokeless seconds can be estimated approximately from its intrinsic viscosity in acetone by means of the expression

$$\log V = 3.55 \log [\eta] - 0.71$$

in which V is the viscosity in smokeless seconds.

We are indebted to Messrs. Robert H. Blaker, John Hardy, Earl Hoerger, and Thomas J. O'Neill for assistance in the measurements. We are also indebted to Dr. Robert B. Corey for helpful suggestions during the progress of the research.

REFERENCES

- (1) PFEIFFER, G. H., AND OSBORN, R. H.: In *Cellulose and Cellulose Derivatives*, Emil Ott (Editor), p. 966. Interscience Publishers, Inc., New York (1943).
- (2) SHOEMAKER, D. P., HOERGER, EARL, NOYES, R. M., AND BLAKER, R. H.: Ind. Eng. Chem., Anal. Ed. **19**, in press (1947). The *smokeless second* is defined in respect to the standard falling-ball viscometer, but the solution employed contains 10 per cent by weight of nitrocellulose in a solvent consisting of 10 parts (by weight) of acetone and 10 parts of denatured alcohol. The viscosity in poises is approximately equal to this time multiplied by the factor 3.77.
- (3) SPEICHER, J. K.: Cellulose **1**, 232-4 (1930).
- (4) STAUDINGER, H., AND SORKIN, M.: Ber. **70**, 1993 (1937).

MOLECULAR PROPERTIES OF NITROCELLULOSE. II

STUDIES OF MOLECULAR HETEROGENEITY¹

ROBERT H. BLAKER, RICHARD M. BADGER, AND RICHARD M. NOYES

Gates and Crellin Laboratories of Chemistry, California Institute of Technology, Pasadena, California

Received September 3, 1946

INTRODUCTION

Of the methods currently employed for determining the average molecular weights of high polymers, procedures involving measurements of osmotic pressure and viscosity are probably the most frequently used. These procedures require comparatively simple apparatus and are capable of precision satisfactory for many purposes; however, they lead to different results when used for measurements on mixtures of polymeric species of different molecular weight.

When measurements of osmotic pressure on solutions of a polymeric mixture

¹ Contribution No. 1077 from the Gates and Crellin Laboratories of Chemistry, California Institute of Technology.

This paper is based in whole or in part on work done for the Office of Scientific Research and Development under Contract OEMsr-881 with the California Institute of Technology.

are extrapolated to infinite dilution, the results can be used to calculate the number-average molecular weight defined by the relation

$$\bar{M}_n = \frac{1}{\sum f_i/M_i} \quad (1)$$

in which \bar{M}_n is the number-average molecular weight, f_i is the fractional weight of the i^{th} species in the mixture, and M_i is the molecular weight of the i^{th} species. In this average the lower-molecular-weight material has a predominant effect, and traces of material of very high molecular weight have little influence.

When measurements of viscosity are made on similar solutions, the data cannot necessarily be related to the molecular weight of the solute by any simple expression (3); however, for many straight-chain polymers the following empirical equation is found to hold reasonably well:

$$[\eta] = K_s \bar{M}_w/M_0 \quad (2)$$

In this so-called Staudinger expression K_s is a constant dependent upon the polymeric material and the solvent but independent of molecular weight, M_0 is the molecular weight of the monomeric unit in the polymer, \bar{M}_w is the weight-average molecular weight defined by the relationship

$$\bar{M}_w = \sum f_i M_i \quad (3)$$

and $[\eta]$ is the "intrinsic viscosity" of the solute defined by the relationship

$$[\eta] = \lim_{c \rightarrow 0} \frac{\ln \eta_{\text{rel}}}{c} \quad (4)$$

where η_{rel} is the viscosity of the solution relative to that of pure solvent and c is the concentration in grams per 100 ml. The weight-average molecular weight as defined by expression 3 is predominantly influenced by the presence of material of high molecular weight.

The number-average and weight-average molecular weights of a sample are equal only if the sample is molecularly homogeneous; otherwise the ratio of the weight-average to the number-average molecular weight is greater than unity, and its magnitude may be taken as a rough measure of the heterogeneity of the sample. In cases where the molecular-weight distribution function has a single broad maximum of the kind obtained in the polymerization of a monomer or in the degradation of a single high polymer (4), the ratio may be expected to be slightly less than two. Other forms of distribution function yield larger values of the ratio, but it seems probable that values in excess of two will only be encountered in practice when the distribution function has more than one maximum.

We have made measurements of osmotic pressure on acetone solutions of several supposedly homogeneous nitrocellulose fractions of different molecular weights and have used the results to evaluate K_s for nitrocellulose containing about 13.4 per cent of nitrogen. With the aid of data reported by previous workers we have used our results to calculate K_s as a function of nitrogen content

and have studied the molecular heterogeneities of various nitrocelluloses by means of measurements of number-average and weight-average molecular weights on samples prepared from different sources.

It should be emphasized that a polymeric mixture is not completely characterized by determinations of its weight-average and number-average molecular weights, for identical values of these quantities can be obtained with different molecular distribution functions. The object of the determinations described below is to obtain approximate information about molecular heterogeneity by procedures which are much simpler than the extensive fractionations necessary for determining complete molecular distribution functions.

EXPERIMENTAL

Materials

The nitrocellulose fractions used in the evaluation of the Staudinger constant, K_s , were prepared by Dr. J. W. Williams and coworkers at the University of Wisconsin. The fractionation procedure involved dissolving a sample of nitrocellulose in a mixture of 3 parts (by volume) of commercial 95 per cent alcohol and 5 parts of acetone and then precipitating part of the sample by the addition of ligroin under controlled conditions. The fractions from the first precipitations were refractionated by the same procedure. The final fractions are thought to be more nearly homogeneous with regard to nitrogen content and molecular weight than most other nitrocellulose samples that have been available for such studies.

The nitrocellulose samples used in the studies of heterogeneity were taken from standard commercial lots prepared for use in the manufacture of smokeless powder.

The acetone used for solvent in the osmometric and viscometric studies was purified by the procedure described in the first paper of this series (1).

Osmometric measurements

Measurements of osmotic pressure were made with static osmometers modeled after the one described by Wagner (6). The capillary rise of the solution in the osmometer was corrected for with the use of an open section of capillary immersed in the solvent by a procedure similar to that developed independently by Zimm and Myerson (8).

Commercial cellophane was the most satisfactory membrane material investigated. The only pretreatment given to the cellophane was to soak it in distilled water for at least 12 hr. before it was used and to wash out the water with acetone at the time the osmometer was being assembled. Membranes treated in this way were satisfactory for use with nitrocelluloses having average molecular weights greater than 20,000, but a few per cent of samples of lower average molecular weight diffused through the membranes.

The data were treated by plotting the osmotic pressure, π , divided by the concentration, c , against concentration and extrapolating the curve to a value of

π/c at infinite dilution. This type of plot does not differ significantly from a straight line and has a slope which, within the limits of experimental error, is independent of the molecular weight of solute but is different for different solutes or solvents (2). The molecular weight of the sample was calculated by the equation

$$\bar{M}_n = \frac{RT}{\lim_{c \rightarrow 0} (\pi/c)} \quad (5)$$

in which T is the absolute temperature, R is the gas constant in 100 ml. atm./mole degree, and the other quantities have been defined previously.

TABLE I
Staudinger constants for nitrocellulose fractions in acetone

FRACTION NUMBER	NITROGEN	NUMBER-AVER- AGE MOLECULAR WEIGHT, \bar{M}_n (OSMOTIC VALUE)	DEGREE OF POLYMERIZATION	INTRINSIC VISCOSITY	STAUDINGER CONSTANT $K_s \times 10^4$
	<i>per cent</i>				
S-3,4	13.36	41,000	144	1.32	9.15
S-1,1-4	13.44	64,700	227	2.24	9.88
P-3,2	13.41	130,800	459	4.37	9.52
P-4,2	13.42	216,400	759	6.83	9.00
Average					9.39

Viscometric measurements

Measurements of viscosity were made with Ostwald-type capillary viscometers, and the intrinsic viscosities of the solutes were calculated by the procedure described in the first paper of this series (1).

RESULTS AND DISCUSSION

Evaluation of Staudinger constant

The results of measurements of osmotic pressure and viscosity on four nitrocellulose fractions are presented in table 1. The data indicate that the Staudinger relation is obeyed within the probable accuracy of the measurements by nitrocelluloses having molecular weights between 40,000 and 200,000.

The value of the constant presented in table 1 is valid only for use with nitrocellulose samples containing about 13.4 per cent of nitrogen, and then only if the solvent is purified acetone and if the viscosities are measured at 25°C. In order to obtain values applicable to all nitrocelluloses, we have used the data of Wannow (7). He nitrated cellulose to various degrees under conditions such that the degrees of polymerization of the products were the same as indicated by osmotic-pressure measurements. By means of measurements of viscosity on these samples he was able to express the fractional change in K_s with change in

nitrogen content, but he was not able to obtain an absolute value for K , because his samples were not molecularly homogeneous. With the use of the value of K , for nitrocellulose containing 13.4 per cent of nitrogen obtained from table 1 and with the data of Wannow we have calculated values of K , for various nitrogen contents from 10.7 to 13.6 per cent and have plotted the results in figure 1.

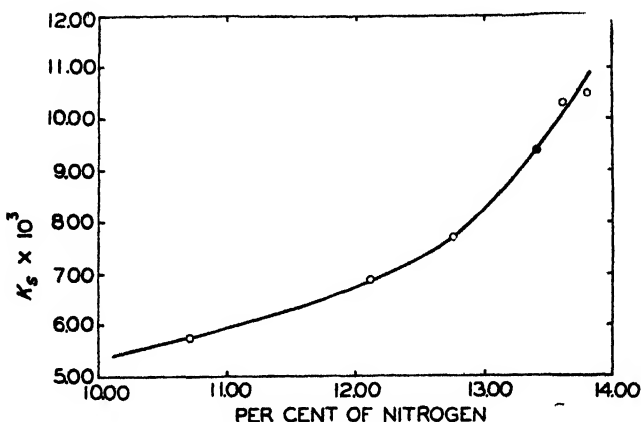


FIG. 1. Dependence of Staudinger constant in acetone on nitrogen content of nitrocellulose. ●, determined in these laboratories; ○, calculated from the data of Wannow with the use of the other point.

TABLE 2
Heterogeneities of commercial nitrocelluloses

NITROCELLULOSE NUMBER	SOURCE	NITROGEN	NUMBER- AVERAGE MOLECULAR WEIGHT, \bar{M}_n	INTRINSIC VISCOSITY, [η]	DEGREE OF POLYMERIZA- TION	WEIGHT- AVERAGE MOLECULAR WEIGHT, \bar{M}_w	\bar{M}_w/\bar{M}_n
		<i>per cent</i>					
6278... ..	Wood	13.40	43,300	3.07	327	93,100	2.15
8432.....	Wood	12.67	41,600	2.65	351	96,000	2.31
10405.....	Wood	13.26	44,200	3.00	333	94,200	2.13
5167.....	Cotton	13.46	65,900	3.50	365	104,200	1.58
5168.....	Cotton	12.60	53,400	2.85	383	104,200	1.95
10411.....	Cotton	13.23	56,700	3.12	351	98,700	1.74

It should be emphasized that the curve presented in figure 1 is very approximate and can probably be refined by subsequent experiments. The absolute values of all points are based on the assumption that the fractions used in these experiments were molecularly homogeneous, and the relative values of the Staudinger constant taken from Wannow's data are based on the assumption that the distribution of molecular species was the same in each of his samples. This second assumption is not necessarily justified by the fact that the number-average degrees of polymerization of all Wannow's samples were virtually identical.

Molecular heterogeneity of commercial nitrocelluloses

Measurements of osmotic pressure and viscosity were made on dilute acetone solutions of six commercial nitrocelluloses, three of which had been prepared from wood pulp and three from cotton linters. The results of these measurements were used to calculate the weight-average and number-average molecular weights of these samples by the procedures described above, and the data are presented in table 2.

The results demonstrate that the nitrocelluloses prepared from wood are distinctly more heterogeneous than those prepared from cotton. It is interesting to note that the heterogeneities of the homogeneously nitrated samples containing about 12.6 and 13.4 per cent of nitrogen are not significantly different from those of the nitrocelluloses containing about 13.2 per cent of nitrogen, which were blended from materials of the other two types. Since the samples studied in table 2 were all prepared to be of approximately the same viscosity or weight-average molecular weight, the greater heterogeneity of these particular wood nitrocelluloses is probably due to the presence of a considerable fraction of low-molecular-weight material. These observations are consistent with those reported by other workers (5).

SUMMARY

The absolute value of the Staudinger constant for nitrocellulose in acetone has been determined by means of measurements of osmotic pressure and of viscosity and by the use of data previously reported in the literature.

Measurements of number-average and weight-average molecular weights on six commercial nitrocelluloses indicate that materials prepared from wood pulp are distinctly more heterogeneous molecularly than those prepared from cotton linters.

We are indebted to Dr. J. W. Williams for the nitrocellulose fractions which rendered this investigation possible. We are also indebted to Dr. Robert B. Corey for helpful suggestions during the progress of the research.

REFERENCES

- (1) DOYLE, G. J., HARBOTTLE, GARMAN, BADGER, R. M., AND NOYES, R. M.: *J. Phys. Colloid Chem.* **51**, 569 (1947).
- (2) HUGGINS, M. L.: *J. Am. Chem. Soc.* **64**, 1712 (1942).
- (3) HUGGINS, M. L.: *Ind. Eng. Chem.* **35**, 980 (1943).
- (4) MONTROLL, E. W., AND SIMHA, R.: *J. Chem. Phys.* **8**, 721 (1940).
- (5) OTT, EMIL: *Advancing Fronts in Chemistry. Vol. I. High Polymers*, Sumner B. Twiss (Editor), pp. 83-5. Reinhold Publishing Corporation, New York (1945).
- (6) WAGNER, R. H.: *Ind. Eng. Chem., Anal. Ed.* **16**, 521 (1944).
- (7) WANNOW, H. A.: *Kolloid-Z.* **102**, 29 (1943).
- (8) ZIMM, B. H., AND MYERSON, I.: *J. Am. Chem. Soc.* **68**, 911 (1946).

THE THERMOCHEMISTRY OF PROPELLANT EXPLOSIVES

J. TAYLOR, C. R. L. HALL, AND H. THOMAS

*Research Department, Imperial Chemical Industries, Limited, Explosives Division,
Stevenston, Ayrshire, Scotland**Received March 27, 1946**Revised copy received October 9, 1946*

The normal method of determining the heat of combustion of an organic substance is, of course, to burn it with gaseous oxygen in a suitable calorimetric bomb. In the case of certain explosive substances, such as cordite and propellant powders, for example, in which exothermic reaction can be brought about without supplying any free oxygen, it is the usual practice to explode them in special calorimetric bombs capable of withstanding high pressures, and to measure directly the heat produced by the explosion. At the same time the total gas volume and the permanent-gas volume produced by the explosion can be ascertained. The heat produced per gram of explosive is termed "the calorific value."

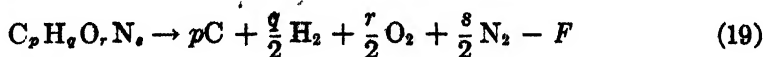
The final products of decomposition thus derived theoretically will not, in general, coincide with those obtained in practice, but they may be transformed into the practical products by a simple water-gas reaction involving a negligible heat change. The heat evolution or absorption as calculated in the above arbitrary manner will consequently be the same as that in the practical case.

QUANTITATIVE TREATMENT FOR ANY COMPOUND

Consider the case of any compound $C_pH_qO_rN_s$, which is the type usually dealt with in propellants. Let F be the molecular heat of formation in calories at constant volume and 33°C . The compound may be explosive or non-explosive, but it is assumed that it can be made to react in the calorimetric bomb as a component of an explosive mixture, the final gaseous products being the water-gas constituents and nitrogen, as already described.

The heat liberation will be independent of the mechanism of decomposition of the compound and explosive, and will depend solely on the final state. Moreover, if the water is considered in the liquid state, as it is in the calorimetric bomb, the heat liberation will be independent of the actual relative concentrations of hydrogen, water, carbon monoxide, and carbon dioxide within the limits of accuracy set by the heat liberation in the water-gas reaction.

On this basis the hypothetical decomposition of the compound $C_pH_qO_rN_s$ may now be discussed. The initial decomposition may be regarded purely hypothetically as

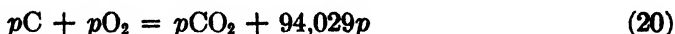


The carbon, hydrogen, and oxygen will intercombine with one another or with the molecules of the decomposed explosive or with the water-gas constituents. There are a number of ways in which combination may take place, as follows:

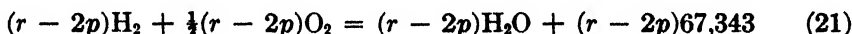
- (1) $C + O_2 \rightarrow CO_2$
- (2) $C + \frac{1}{2}O_2 \rightarrow CO$
- (3) $C + CO_2 \rightarrow 2CO$
- (4) $C + H_2O \rightarrow CO + H_2$
- (5) $H_2 + CO_2 \rightarrow H_2O + CO$
- (6) $H_2 + \frac{1}{2}O_2 \rightarrow H_2O$
- (7) $CO + \frac{1}{2}O_2 \rightarrow CO_2$

It is always possible, however, to transform the products of the final results of intercombination into the products of any other intercombination by a simple water-gas reaction, so that according to the established theorem it is only necessary to consider one mode of decomposition in order to derive a quantitative expression for the molecular calorific value (water liquid) of the compound.

Any of the above reactions would serve for the present purposes, but the carbon dioxide and water reactions may be chosen, namely:



and



Combining equations 19, 20, and 21, the following equation is obtained:

The thermochemical constants of propellants are widely used for ballistic calculations and control of manufacture, and it is of importance to be able to calculate them for any composition and to predict the effect of any change of constituent. The present paper describes a simple method for calculating the calorific values for propellants. This method has been in extensive use for fifteen years in the Research Department of Imperial Chemical Industries Ltd., Explosives Division, and has proved to be both convenient and accurate in use.

Whilst the method was primarily developed for use with propellant explosives, it has wider applications to any assembly in which the products are hydrogen, water, carbon dioxide, carbon monoxide, and nitrogen, and provides an alternative method to the normal one for determining approximately the heats of combustion or formation of organic compounds including non-explosive compounds.

THERMOCHEMICAL CONSIDERATIONS

Modern propellants largely consist of colloidal mixtures of nitroglycerin and nitrocotton, with the addition of various organic compounds as stabilizers and coolers.

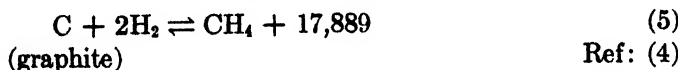
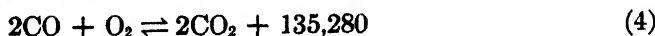
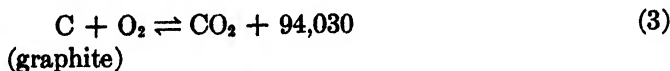
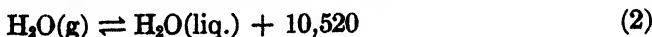
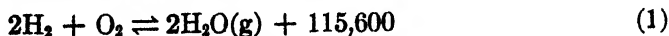
Such propellants contain insufficient oxygen in their constitution to oxidize

fully the carbon and hydrogen, and it is established that the reactions occurring in their gaseous products are governed primarily by the water-gas reaction:

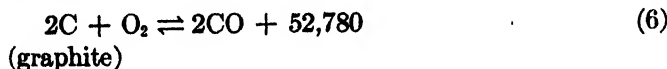


A small amount of methane is produced by a secondary action during cooling and this must be corrected for. In addition, certain explosives can deposit carbon during explosion and this must be carefully watched in any experimental work.

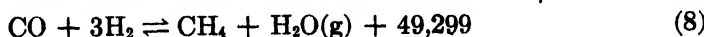
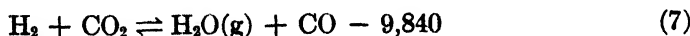
Thus, the gaseous products can be regarded as consisting almost uniquely of carbon monoxide, carbon dioxide, hydrogen, water, and nitrogen, the relative concentrations of the first four gases being determined by the water-gas equilibrium constant corresponding to the "freezing-out" temperature. In the ensuing thermochemical considerations for such a gaseous assembly the following thermal equations are utilized, the heats of reaction being expressed in calories at 25°C. and constant pressure as given by Rossini (5, 6).



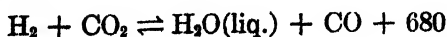
Ref: (4)



Hence:

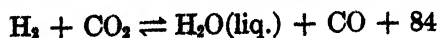


Consider now the gaseous products of a propellant fired in a calorimetric bomb. The experimental result obtained will be a calorific value (water liquid) corresponding to certain gaseous products. If the relative concentrations of the gaseous products are imagined as being altered, then the change must take place according to the water-gas equilibrium but, as in the case considered the final state of the water is liquid, the equation governing the heat change will be, from equations 7 and 2:

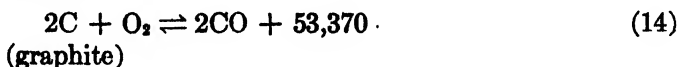
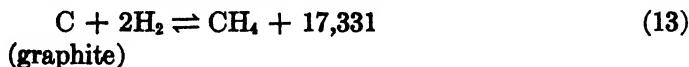
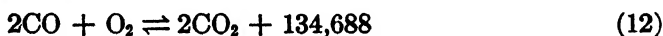
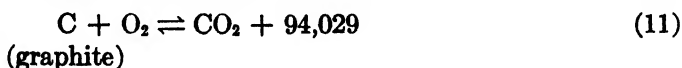
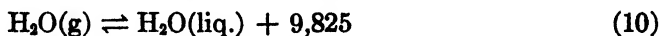
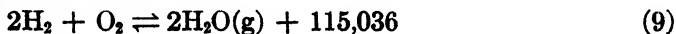


at constant pressure.

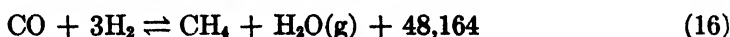
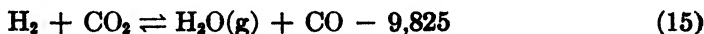
In a calorimetric-bomb system, however, the reaction occurs at constant volume, and for such conditions the water-gas equation becomes:



The heat exchange in the water-gas reaction depends on the latent heat of vaporization of the water, and it is obviously possible by choosing a suitable temperature to make the heat liberation zero. Actually, at 33°C. in constant-volume conditions, there is no heat evolved or absorbed in the water-gas reaction, when the water formed is considered in the liquid phase. It may be concluded, therefore, that the calorific value of a propellant at constant volume and at 33°C., with the water produced in the liquid state, is quite accurately independent of the composition of the resultant gaseous products. It is obviously advantageous to use 33°C. as a datum temperature for calculations. It is also advantageous to make all the calculations under the constant-volume conditions which apply to the calorimetric bomb. Consequently the thermal data given by Rossini have been suitably corrected to apply to constant-volume conditions at 33°C., the equations now reading as follows:



so that, from these equations:



THERMOCHEMISTRY OF A MIXTURE OF PROPELLANTS

The deduction which we have just made above may be stated in another form, as follows:

The calorific value at constant volume and 33°C. (water liquid) of a propellant explosive is unaffected by any reaction which may be brought about among the gaseous molecules according to the water-gas reaction.

This theorem enables some important deductions about the calorific value of mixtures to be made.

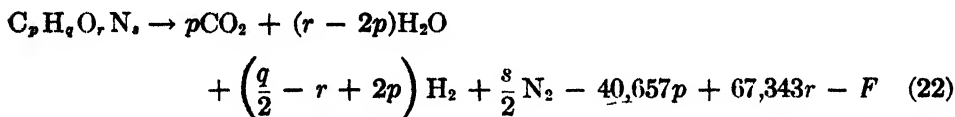
If a composite propellant comprising a parts of composition A of calorific value Q_A (water liquid), b parts of composition B of calorific value Q_B , and so on, is made, then the final calorific value of the composite powder is given by

$$Q = \frac{aQ_A + bQ_B + cQ_C + \cdots + mQ_M}{a + b + c + \cdots + m} \quad (17)$$

or with obvious notation

$$Q = \frac{\sum nQ_N}{\sum n} \quad (18)$$

The calorific value (water liquid) of a propellant is thus an additive property of the calorific values of its components. Equation 18 introduces a great simplification and enables the calorific value (water liquid) of many types of propellants and mixtures to be determined from a few known values. It might be thought that only mixtures of explosives could be treated in this manner, but this is not so, for the treatment can be applied to a mixture of a propellant explosive with non-explosive organic substances provided, as will be shown, suitable negative calorific values are adopted for the non-explosive constituents. Any constituent of the propellant may be considered as decomposing and reacting with the gaseous products in any manner whatever provided the final products are hydrogen, water, carbon dioxide, carbon monoxide, and nitrogen. This decomposition will be characterized by an evolution or absorption of heat which may be calculated, if the heat of formation of the substance in question is known.



The gaseous products given in equation 22 may be considered to undergo a water-gas reaction without evolution or absorption of heat, until the actual composition corresponding to the practical case is achieved. The molecular calorific value (water liquid) of the compound at constant volume and 33°C. is therefore given by the expression:

$$q_H = -40,657p + 67,343r - F \quad (23)$$

Finally, the calorific constant h for the substance may be defined as the heat evolved or absorbed on decomposition in calories per 0.01 g. of the substance at constant volume and 33°C. (water liquid) as follows:

$$h = \frac{q_H}{100 \times \text{gram-molecular weight}} \quad (24)$$

It should be noted that the molecular calorific value, q_H , may assume positive or negative values according as heat is evolved or absorbed on decomposition and reaction of the compound. For the purposes of calculating the calorific values of propellants then, the calorific constant h as defined by equation 24 may be used in conjunction with a simple extension of equation 18. It follows directly that the calorific value (water liquid) in calories per gram of a propellant explosive is given by the expression:

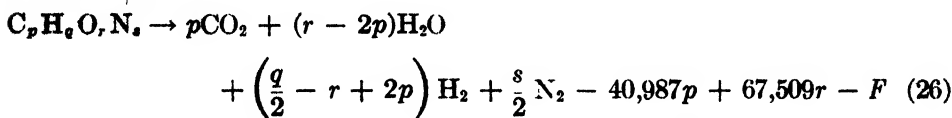
$$Q = \sum (h_s) \text{ (per cent S)} \quad (25)$$

where h_s , the calorific constant of each of the constituents, may be determined experimentally or calculated in a simple manner.

In the calculations based on the heats of formation as published in the litera-

ture, it is assumed that the compound is contained in the propellant in its normal physical state.

The experimentally determined values of the calorific value are obtained at a mean temperature of 17°C. Two methods are available for relating the theoretically calculated value of q_H to the experimentally observed value. Firstly, the experimentally observed value of q_H at 17°C. may be corrected to apply to 33°C. This calculation requires a knowledge of the specific heat of the compound and of the gaseous products. Alternatively, the molecular calorific value, q_H , may be calculated at 17°C. Thus, proceeding as in equations 19, 20, 21, and 22, with the corresponding heats of reaction at 17°C., then the following equation is obtained:



The gaseous products given in equation 26 may be transformed into the actual gaseous products by the water-gas reaction. At 17°C. and constant volume, with the water considered as liquid, the water-gas reaction becomes:



For one particular compound there are two extreme cases which must be considered; firstly, one in which the products consist of water and carbon monoxide, and secondly, one in which the products consist of hydrogen and carbon dioxide. It follows therefore that the maximum scatter in the calorific value of a pro-

pellant at 17°C. due to the water-gas reaction is $(p + \frac{q}{2})169$ cal. The mean of

these two molecular calorific values is therefore correct to within $\pm \frac{1}{2}\left(p + \frac{q}{2}\right)169$.

For the generalized case of the compound $\text{C}_p\text{H}_q\text{O}_r\text{N}_s$ this mean molecular calorific value is given by

$$\bar{q}_H = -40,515p + 85\frac{q}{2} + 67,440r - F \quad (28)$$

and for any particular experimental observation at 17°C.

$$q_H = \bar{q}_H \pm \frac{1}{2}\left(p + \frac{q}{2}\right)169 \quad (29)$$

By means of this equation the experimental value of the calorific value is related to the theoretical value, so that the heat of formation of the compound may be calculated.

The calorific effect of any substance added to a propellant may be readily calculated by means of equation 25. Thus consider a propellant powder A of calorific value (constant volume, water liquid) Q_1 and let Q_2 be the corresponding

calorific value of an intimate mixture of $(100 - p)$ per cent of A and p per cent of a substance B. Then from equation 25:

$$Q_2 = \frac{(100 - p)}{100} Q_1 + ph \quad (32)$$

If the heat of formation of the substance is known, then by means of equations 28 and 24 the value of h may be calculated.

Conversely, the heat of formation of the substance may be calculated from the experimentally determined h value.

It is to be observed however, that the heat of formation of the substance as generally reported in the literature refers to the ordinary state, and this may not correspond exactly to the value of the heat of formation for the substance when incorporated in the propellant powder, since its physical condition may be different.

In the calorimetry of propellant powders, it is preferable therefore to use values for h which have been experimentally determined from finished propellant powders. The values actually observed for various substances will now be considered.

The calorific values of the propellant powders were experimentally determined in a specially designed calorimetric bomb. The calorimetric bomb and its accessories together with the experimental technique employed are described elsewhere (8).

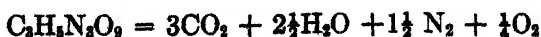
Nitroglycerin

It is of fundamental importance in the present work that the calorific effect of nitroglycerin contained in propellant powders should be carefully determined. The calorific values of a large number of propellants consisting of nitroglycerin, nitrocellulose, and ethyl centralite or mineral jelly were therefore determined experimentally in the calorimetric bomb. It would appear from a careful analysis of the results so obtained that the calorific effect of nitroglycerin varies slightly with the physical condition of the nitroglycerin in the propellant, and that it is highest and of almost uniform value in well-gelatinized powders.

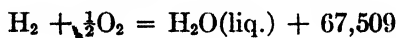
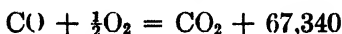
In actual practice propellants are almost all of the type characterized by the stable high nitroglycerin calorific constant. The effect, however, is important, since a value for the calorific constant h for nitroglycerin must be selected for use in the thermochemical calculations.

From consideration of the experimental results the figure of 17.55 cal. for 0.01 g. (at 17°C.) has been selected for the calorific constant of nitroglycerin as describing its behavior in normal propellants and in matured propellants whether of the solvent or the non-solvent type.

It has been established (8) that nitroglycerin alone decomposes as follows in the calorimetric bomb:



and the heat evolved at constant volume is 366.6 kg.-cal. per mole (water liquid). Further, the liberated oxygen will be available to oxidize carbon monoxide to carbon dioxide or hydrogen to water as follows:

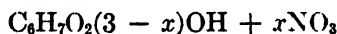


Thus the mean quantity of heat liberated by the available oxygen is 33,712 cal. It follows therefore that the theoretical calorific effect of nitroglycerin in propellants is 400.3 kg.-cal. per mole, or 17.63 cal. per 0.01 g. (at 17°C.). The agreement between the theoretical and experimental values for the calorific constant of nitroglycerin is very satisfactory.

Nitrocellulose

The experimentally determined calorific values and gas volumes have been reported in a recent communication (8).

It is reasonable to suppose a formula of $\text{C}_6\text{H}_{10}\text{O}_5$ or $\text{C}_6\text{H}_7\text{O}_2(\text{OH})_3$ for cellulose, and nitrocellulose may then be considered as being formed by replacing the OH groups by NO_2 groups. The general formula for a nitrocellulose is then



where x lies between the extreme values of 0 and 3.

Let p be the per cent by weight of nitrogen in the nitrocellulose considered; then it may be shown that the gram-atoms of carbon, hydrogen, oxygen, and nitrogen per kilogram of nitrocellulose are:

$$\bar{C} = 37.024 - 1.1891p$$

$$\bar{H} = 61.698 - 2.6959p$$

$$\bar{O} = 30.849 + 0.43675p$$

$$\bar{N} = 0.71429p$$

and consequently the gas volume per gram of nitrocellulose of p per cent nitrogen is:

$$V = 1520.3 - 48.837p$$

The p per cent nitrogen is, of course, the true nitrogen content of the nitrocellulose and if the analytical nitrogen figures observed are systematically different from these, then there will be a systematic error in the calculations of the gas volume.

The results show excellent agreement between the gas volumes as measured directly and as calculated from this equation. For the nitrocelluloses of higher nitrogen content (13.16 per cent and 13.24 per cent) the measured gas volumes are greater than those calculated from the nitrometer nitrogen figure. This slight discrepancy may be due to nitrometer nitrogen determination or to a slight inaccuracy in the methane determinations.

The relation between the finally corrected calorific value and the nitrogen content of the nitrocellulose is linear, and this fact may be used as a very stringent test of the theory. Since the relation between the calorific value and the nitrogen content is linear, the intercept of the graph on the axis of ordinates (calorific values) must represent the calorific effect of a nitrocellulose of zero nitrogen content, i.e., cellulose. The heat of combustion of cellulose at constant pressure and 18°C. is 4181 cal. per gram (3). From this value, and by equations 23 and 24, the calculated calorific constant per gram of cellulose is 834.8 cal. at 18°C. In order to obtain the linear relation between the calorific value and the nitrogen content, one more point must be considered. It is convenient to consider the extreme point: namely, the nitrocellulose containing 13.24 per cent nitrogen and of calorific value of 1060 cal. per gram. The linear relation is then given by:

$$Q_{18^\circ\text{C.}} = 143.5p - 834.8 \quad (33)$$

where $Q_{18^\circ\text{C.}}$ is the calorific value (constant volume, water liquid) of pure dry gelatinized nitrocellulose of p per cent nitrogen. The very satisfactory fit of the experimental values shows that there is little doubt of the substantial accuracy of the theory.

If M is the gram-molecular weight of the nitrocellulose, then from equation 26:

$$\frac{\bar{q}_H}{M} = -40,515 \frac{p}{M} + 42.5 \frac{q}{M} + 67,440 \frac{r}{M} - \frac{F}{M} \quad (34)$$

\bar{q}_H/M is the calorific value (water liquid) of 1 gram of the substance at constant volume, usually denoted by \bar{Q}_L , while p/M and q/M are the number of gram-atoms of carbon and hydrogen in 1 gram of the substance. F/M is the heat of formation per gram at a constant pressure of 1 atm. and 18°C.

If the general formula for nitrocellulose is taken to be $\text{C}_6\text{H}_7\text{O}_2(3-x)(\text{OH}) + x\text{NO}_2$, as before, then the values of p/M etc. can be expressed in terms of P , the percentage of nitrogen in the nitrocellulose, by the following equations:

$$\frac{p}{M} = 0.037024 - 0.0011891P$$

$$\frac{q}{M} = 0.061698 - 0.0026959P$$

$$\frac{r}{M} = 0.030849 + 0.00043675P$$

On substituting these values of p/M etc. in equation 34 we obtain:

$$\bar{Q}_L = 583 + 77.6P - \frac{F}{M} \quad (35)$$

Thus, knowing the calorific value of the nitrocellulose and the percentage of nitrogen which it contains, equation 35 may be used to calculate the heat of

formation per gram of the nitrocellulose at constant pressure. It is considered that this is a superior method to determining the heat of formation from the heat of combustion of the nitrocellulose in excess of oxygen, since the heat of combustion is about four times the heat of formation, while the calorific value is generally less than twice the heat of formation. The method has also the advantage of eliminating the uncertainty caused by the formation of oxides of nitrogen when the burning takes place in excess of oxygen.

It has been shown that the experimentally determined calorific values of the dry gelatinized nitrocelluloses may be expressed by a linear equation (33). On eliminating \bar{Q}_L , between equations 33 and 35, the following expression is obtained for the heat of formation of dry gelatinized nitrocellulose

$$\frac{F}{M} = 1417.8 - 65.8P \text{ cal. per gram} \quad (36)$$

at a constant pressure of 1 atm. and 17°C.

The heats of formation at constant pressure of the various nitrocelluloses examined as calculated from this equation are set out in table 1.

TABLE 1
Heats of formation of nitrocellulose

PERCENTAGE BY WEIGHT OF NITROGEN IN THE NITROCELLULOSE	HEAT OF FORMATION OF NITROCELLULOSE AT CONSTANT PRESSURE AND 18°C
<i>per cent</i>	<i>cal /g</i>
12.10	621.6
12.65	585.4
13.16	551.9
13.24	546.6

Graphite

By calculation from equations 24 and 29 the h value for pure graphite is -33.76 ± 0.07 cal. The graphite used in propellants is of a good commercial quality, and may contain up to 10 per cent mineral matter. The experimental value of h for graphite should therefore be numerically less than -33.76 but greater than -30.38 cal.

An intimate mixture of 95 per cent of a propellant (which consisted of 50 per cent of nitroglycerin and 50 per cent of guncotton) and 5 per cent graphite was prepared, and its calorific value determined in the calorimetric bomb. The calorific value of the propellant itself was also determined experimentally, and yielded the result 1385.5 cal. per gram (constant volume, water liquid). The calorific value of the mixture was 1148, so that, using equation 32:

$$1148 = 0.95 \times 1385.5 + 5h$$

whence $h = -33.64$ cal. The agreement between the theoretical and experimental values is therefore satisfactory.

Dinitrotoluene

An intimate mixture of 95 per cent of the propellant powder of the last example and 5 per cent of dinitrotoluene was prepared, and its calorific value determined in the calorimetric bomb. The resulting experimental value for the constant h was 1.30 cal. By means of equation 14 the heat of formation of dinitrotoluene at constant pressure is determined as 8.8 kg.-cal. per mole; consequently the heat of combustion of dinitrotoluene to carbon dioxide, water (liq.), and nitrogen at constant pressure and 20°C. is 853.8 kg.-cal. per mole. Garner and Abernethy (2) report a direct experimental value of 852.8 kg.-cal. per mole for this heat of combustion. A direct experimental value of 856.5 kg.-cal. per mole has also been reported (7). The agreement between the values is reasonably satisfactory. In our calculations a specific heat of 0.3 cal. per gram per °C. has been assumed for dinitrotoluene; only negligible errors are introduced by this assumption.

Dibutyl phthalate

The calorific constant, h , of this compound was found by calorimetric investigation of a propellant containing 2 per cent of dibutyl phthalate. A value of -20.2 cal. was thus determined. Consequently, the calculated heat of formation at constant pressure and 17°C. of dibutyl phthalate is 1820 kg.-cal. per mole, and the heat of combustion to carbon dioxide, water (liq.), and nitrogen is 2070 kg.-cal. per mole. The corresponding heats of combustion reported in the literature are 2058 kg.-cal. per mole (1) and 2160 kg.-cal. per mole (7).

It may be considered therefore that the value obtained in the present work is fairly close to the true heat of combustion of dibutyl phthalate.

Methyl centralite

The effect of methyl centralite on the calorific value of propellant powders was investigated in the usual manner, and the value of -23.8 cal. found for the calorific constant, h .

A direct determination of the heat of combustion of methyl centralite was carried out in our own laboratories and resulted in the value of 1948.5 kg.-cal. per mole. The heat of combustion calculated from the calorific constant, h , is 1930 kg.-cal. per mole at 17°C. and constant pressure. The results are therefore in reasonable agreement.

Ethyl centralite

A similar investigation on ethyl centralite resulted in a value of -24.4 cal. for the calorific constant, h . This corresponds to a heat of combustion of 2253 kg.-cal. per mole at 17°C. and constant pressure. The corresponding value of the heat of combustion of ethyl centralite derived by direct experiment was 2264.6 kg.-cal. per mole.

The experimental values of the calorific constant, h , for some of the compounds used in propellant explosives are set out in table 2.

Thus, consider a propellant explosive of "dry" composition: nitrocellulose

(13.08 per cent nitrogen), 65 per cent; nitroglycerin, 30 per cent; mineral jelly, 5 per cent. The volatile matter is 0.37 per cent and the "ash" 0.16 per cent. Assume (as is justified by experience) that the volatiles are half water and half acetone; then the reduced composition is: nitrocellulose, 64.66 per cent; nitroglycerin, 29.84 per cent; mineral jelly, 4.97 per cent; moisture, 0.19 per cent; acetone, 0.18 per cent; ash, 0.16 per cent, and by direct application of the present theory and the given experimental h values the calorific value of this composition is given by:

$$\begin{aligned}\bar{Q}_L &= 10.45 \times 64.66 + 17.60 \times 29.84 - 34.60 \times 4.97 - 19.80 \times 0.18 \\ &= 1027.5 \text{ cal. per gram}\end{aligned}$$

The experimentally observed calorific value of this composition corrected for methane formation is 1027 cal./g. at 17°C., in agreement with the calculated values.

TABLE 2
Values of h for some compounds used in propellant explosives

SUBSTANCE	h IN CALORIES PER 0.01 G. AT 17°C.
Nitrocellulose (13.1 per cent nitrogen)	+10.48
Nitroglycerin	+17.60
Mineral jelly	-34.60
Acetone	-19.80

CALCULATION OF THE GAS VOLUME GIVEN BY A POWDER

Since the gaseous products of propellant powders, when corrected for the small quantities of methane formed, contain only carbon dioxide, carbon monoxide, water (vapor), hydrogen, and nitrogen, no alteration in the volume of the gases can take place due to interaction of the constituent gases, since any such change must be finally in the nature of a water-gas reaction,—namely,



and this reaction involves no increase or diminution of volume.

It is evident, therefore, that the total gas volume in molecules per gram of the propellant powder as derived experimentally (corrected for any methane formation) does correspond exactly with the number of molecules. It follows that the total gas volume, V_T cc. per gram of powder at N.T.P. (corrected for any methane formed) is given by the expression

$$V_T = 22.4(\bar{C} + \frac{1}{2}\bar{H} + \frac{1}{2}\bar{N}) \quad (37)$$

where \bar{C} , \bar{H} , \bar{N} are the gram-atoms of carbon, hydrogen, and nitrogen contained in 1 kg. of the powder.

Furthermore, the gas volume is an additive property of the gram-atoms of carbon, hydrogen, and nitrogen contained in the constituents of the powder,

and as a consequence equation 37 may be expressed more simply in terms of the percentages of nitroglycerin, nitrocotton, etc. in the composition, as follows:

$$V_r = \Sigma(V_s)(\text{per cent } S)/100$$

where V_s is the gas volume constant characteristic of the substance S .

The calculation of the constant V_s for most compounds is direct and simple. The constant V_s has been designated the "gas volume constant" of the compound, and defines the gas volume in cubic centimeters given by 0.01 g. of the compound when contained as a constituent of a propellant explosive.

SUMMARY

A method has been developed for calculating the calorific values and gas volumes of modern propellant explosives. It has been established that, when such propellants are fired in a calorimetric bomb, the explosion products consist almost uniquely of carbon dioxide, carbon monoxide, hydrogen, water (liquid), and nitrogen. The final equilibrium is therefore determined by the well-known water-gas reaction, and the present thermochemical considerations are applicable to any such gaseous assembly. It has been shown that with the water considered in the liquid phase, and under constant-volume conditions, then the heat exchange in the water-gas reaction is very small, and in fact, at 33°C. is zero. This fact forms the basis of the present work, and by its application a calorific constant may be defined for the organic compounds used in propellants. Further, the calorific value of a mixture of such compounds may be expressed by a simple additive law of these calorific constants and the composition.

The method has proved both convenient and accurate in use, while it may also be employed as an alternative method for determining approximately the heats of combustion and formation of organic compounds.

The theoretical and quantitative development of the theory is given. Applications of the method to the determinations of the heats of formation and combustion of organic compounds are discussed, while a typical example of its application to normal propellants is also given and detailed consideration has been given to nitrocellulose.

REFERENCES

- (1) AMBLER, H. R.: *J. Soc. Chem. Ind.* **55**, 291 (1936).
- (2) GARNER, W. E., AND ABERNETHY, C. L.: *Proc. Roy. Soc. (London)* **99**, 213 (1921).
- (3) *International Critical Tables*.
- (4) PROSEN, E. J.: *J. Research Natl. Bur. Standards* **34**, 263 (1945).
- (5) ROSSINI, F. D.: *J. Research Natl. Bur. Standards*, **22**, 407 (1939).
- (6) ROSSINI, F. D.: *J. Research Natl. Bur. Standards*, **34**, 143 (1945).
- (7) SCHMIDT, A.: *Sprengstoffe* **29**, 259 (1934).
- (8) TAYLOR, J., AND HALL, C. R. L.: *J. Phys. Colloid Chem.* **51**, 593 (1947).

DETERMINATION OF THE HEAT OF COMBUSTION OF NITROGLYCERIN AND THE THERMOCHEMICAL CONSTANTS OF NITROCELLULOSE

JAMES TAYLOR AND C. R. L. HALL

*Research Department, Imperial Chemical Industries Limited, Explosives Division,
Stevenston, Ayrshire, Scotland*

Received January 14, 1946

Revised copy received October 9, 1946

An important section of explosives technology is the calculation of calorific values, of both simple explosive substances and mixtures. For this purpose, reliable figures for the heat of combustion of nitroglycerin and calorific values and gas-volume constants of nitrocelluloses of varying nitrogen content are required. Since considerable discrepancies exist among published values, it was felt that experiments should be carried out in a modern propellants calorimetric installation in order to determine reliable figures. The present paper describes these investigations.

The calorimetric apparatus is a modification of that developed by Research Department, Woolwich (now Armaments Research Department) about ten years prior to the war. The authors have pleasure in acknowledging the origin of the methods and apparatus design, and are indebted to the Chief Scientific Officer, Ministry of Supply, for permission to publish them. The design of apparatus to be described differs somewhat from the original Woolwich apparatus, but the method of experiment is essentially the same as the original Woolwich method and differs only in a few details. The apparatus has been used for over fifteen years with satisfactory results and a considerable body of data obtained under identical conditions.

GENERAL DESCRIPTION OF METHOD

The method used is applicable to explosive substances such as cordite which react without additional oxygen, that is to say, substances which contain their own oxygen. The explosive is fired in a bomb of 124-cc. capacity, a charge of 12.4 g. normally being used, yielding a pressure of the order of 5 tons per square inch. In the case of powerful detonating explosives such as nitroglycerin, somewhat reduced charges (approximately 7 g.) have been used. Ignition of the charge is brought about by electrolytic gas fired by a fine heated wire. The rise of temperature is determined in a suitable calorimeter, and afterwards the volume of gas and the amount of water produced by the explosive are measured. The apparatus actually determines what is termed in explosives technology "the calorific value of the explosive," that is, the number of calories per gram of explosive produced when it is exploded without oxygen, other than what it contains itself.

DESCRIPTION OF APPARATUS

(a) *Calorimetric bomb*: The particulars of design of the calorimetric bomb are given in figure 1. The bomb is constructed almost entirely of Vibrac steel, which possesses important properties for high-pressure work.

(b) *The water calorimeter and calorimeter container*: The water calorimeter and calorimeter container are shown in figures 2 and 3, respectively. This apparatus does not incorporate any original features.

(c) *Thermostatic bath*: The calorimeter container is fixed in a constant-temperature water bath. Stirring is by air, and a continuous circulation of water from the bottom to the top of the bath is maintained.

(d) *Thermometers*: The special thermometers used were made of carefully selected lengths of glass tubing and conform to the following specifications: range, 12°C., graduated in 0.01°C.; filled with nitrogen at 60 mm. pressure; length, 29 in. One of the thermometers has been graduated every quarter of a degree, to 0.02°C., by the National Physical Laboratory, and the other thermometers have been graduated from this.

(e) *Apparatus for generating electrolytic gas*: The electrolytic gas is generated by the electrolysis of a 0.25 per cent solution of baryta water by means of a current density of about 0.3 amp./cm.² A T-piece is used for connecting the bomb and the vacuum pump to the electrolytic gas apparatus, and a phosphorus pentoxide drying tube and a flame trap are connected between the gas reservoir and the T-piece.

(f) *Apparatus for determining the permanent-gas volume*: The familiar mercury manometer type of gas-measuring device has been adopted for use in the present investigation, using a cathetometer for determining the mercury levels accurately.

(g) *Apparatus for determining water*: The apparatus consists of a trap which is immersed in a thermos flask containing a freezing mixture of acetone and solid carbon dioxide. For the purpose of weighing, the ends of the trap are closed with small rubber caps similar to that used for covering the valve outlet nipple of the bomb.

WATER EQUIVALENT OF THE CALORIMETRIC BOMB

(a) *Apparatus*: The water equivalent of the calorimetric bomb is determined by an electrical method. Figure 4 indicates the circuit used. The heater element is a nichrome wire, 25 gauge, about a yard in length, wound in the form of a spiral. Resistance of the coil is of the order of 6 ohms, and it is conditioned for use before a determination by glowing out for a long period in nitrogen.

(b) *Experimental procedure*: The temperature-time curve is taken with two thermometers in the usual manner; simultaneously the voltage drop across the 0.1-ohm standard resistance and the bomb terminals is recorded at intervals of about 10 sec. The time at which the switch S is opened and the current cut off is noted. The temperature-time curve is taken concurrently with the current-voltage readings, and readings are continued after switching off the current until the usual constant temperature rise per minute is obtained. The point of extrapolation is determined experimentally from the graph of the temperature-

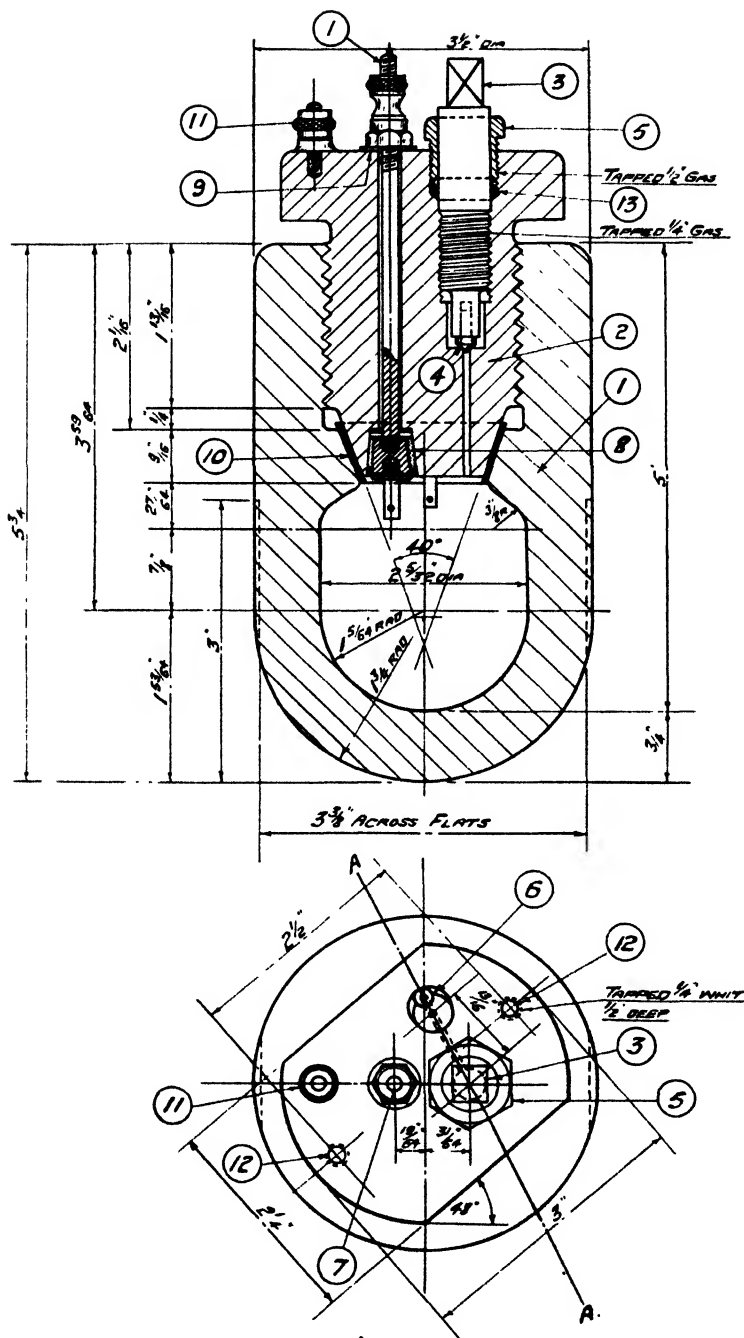


FIG. 1. Bomb calorimeter. 1, body (Vibrac steel); 2, plug (Vibrac steel); 3, valve spindle (M.S.); 4, valve (Vibrac steel); 5, gland (gun metal); 6, nozzle (M.S. with lead washer); 7, electrode (cast steel with two nuts and end piece as shown); 8, cone and washer (Bakelite; six cones, six washers); 9, washer (fibre); 10, obturation cone (copper); 11, standard terminals No. 8 B.A. (brass); 12, lifting rods (M.S.).

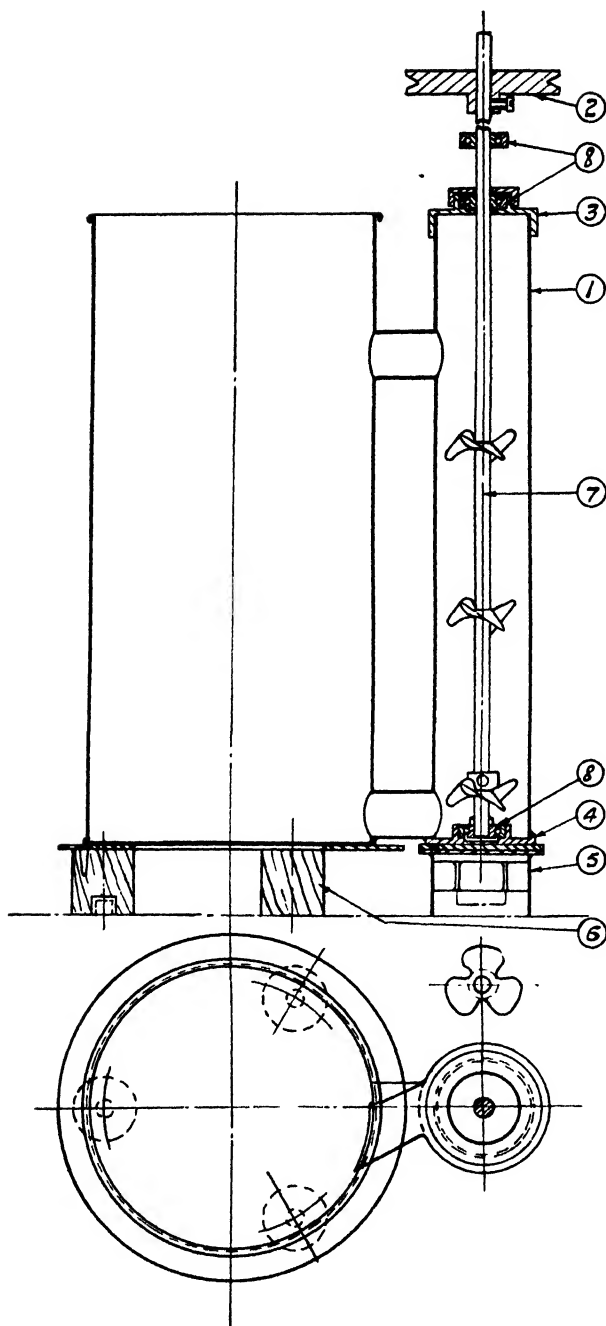


FIG. 2. Water calorimeter 1, calorimeter container (copper); 2, pulley (brass); 3, top cover (brass); 4, bottom cover (brass; soldered to 1); 5, small support (brass and fibre); 6, large support (brass and wood); 7, stirrer (steel and brass); 8, Hoffmann bearings (type S-1 Hoffman small journal bearing).

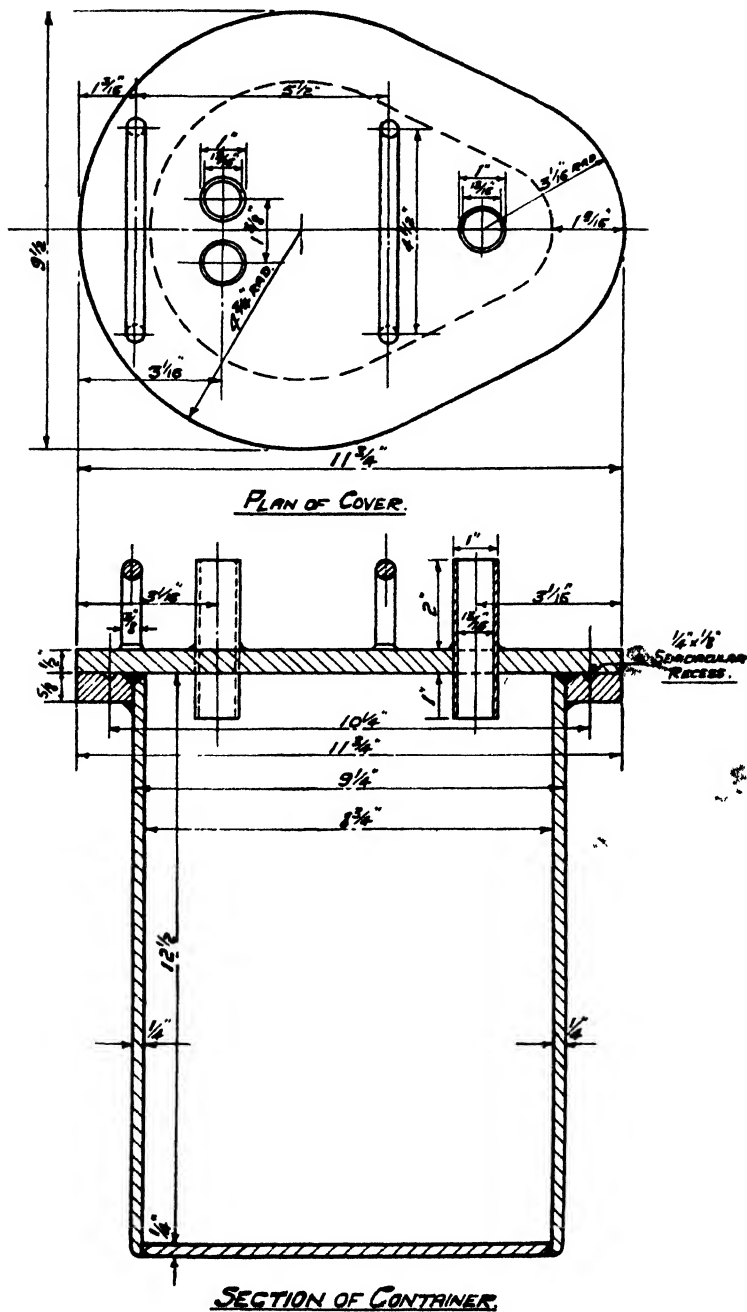


FIG. 3. Container for calorimeter

time curve, so that the temperature rise can be deduced. The electrical energy input is derived from summation of the products of the average current in the circuit and voltage across the bomb terminals in the usual manner.

The method of determining the "true" temperature rise is exactly the same in principle as that used in the case of determinations on explosive compounds, but (see later) the point of "extrapolation" is determined for each experiment separately by the graphical method of equal areas.

THERMOMETRY

The method of calorimetric thermometry used is an adaptation of the Regnault correction curve method which will be clear from figure 5.

The form of the temperature-rise curve $ABCD$ is the same from experiment to experiment, for a given type of bomb; consequently, the point of extrapolation at which the ordinate XY is constructed may be determined once and for all for any given installation. Figure 5 shows the result for one installation and

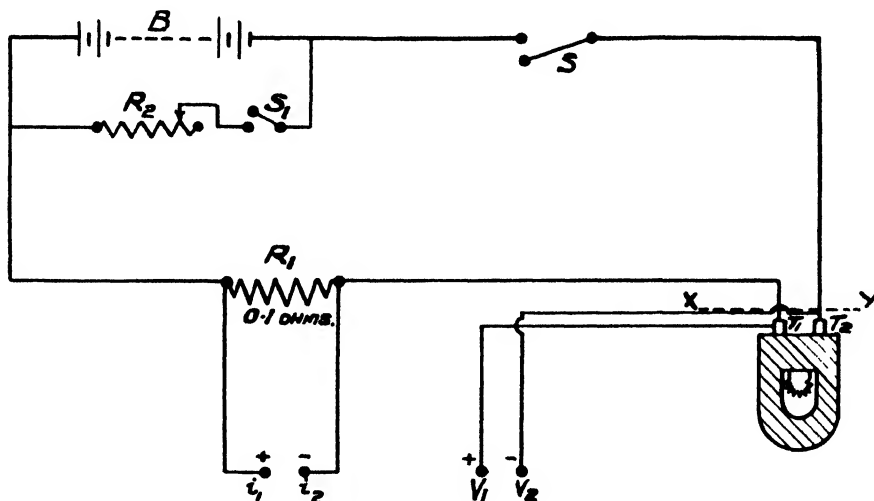


FIG. 4. Working diagram for determination of water equivalent

determines that the ordinate XY must be constructed on the graph at the time 2 min. after firing.

Thus, in any actual calorimetric determination, the portions AB and CD only are found experimentally. The rise of temperature each minute is observed before firing. This determines AB . When the rise of temperature with time is constant, the charge is fired, and the instant t of firing is noted. About 20 min. after firing the readings of the thermometers with time are again taken each minute. This determines the portion CD of the temperature-time curve. Hence the temperature rise represented by the ordinate XY may be readily calculated.

PART I: NITROGLYCERIN

Experimental method

In the initial experiments commercial Grade A nitroglycerin which had been carefully dried over sulfuric acid for some days was used. An accurately weighed

charge of about 7 g. of nitroglycerin was introduced into the calorimetric bomb, which was fastened up, evacuated, and filled with electrolytic gas. Experiment showed that 2 atm. of electrolytic gas were required to ignite the charge. Ignition was uncertain when smaller pressures of electrolytic gas were used. With very small charges of nitroglycerin (of the order of 1 g.) deposition of carbon was

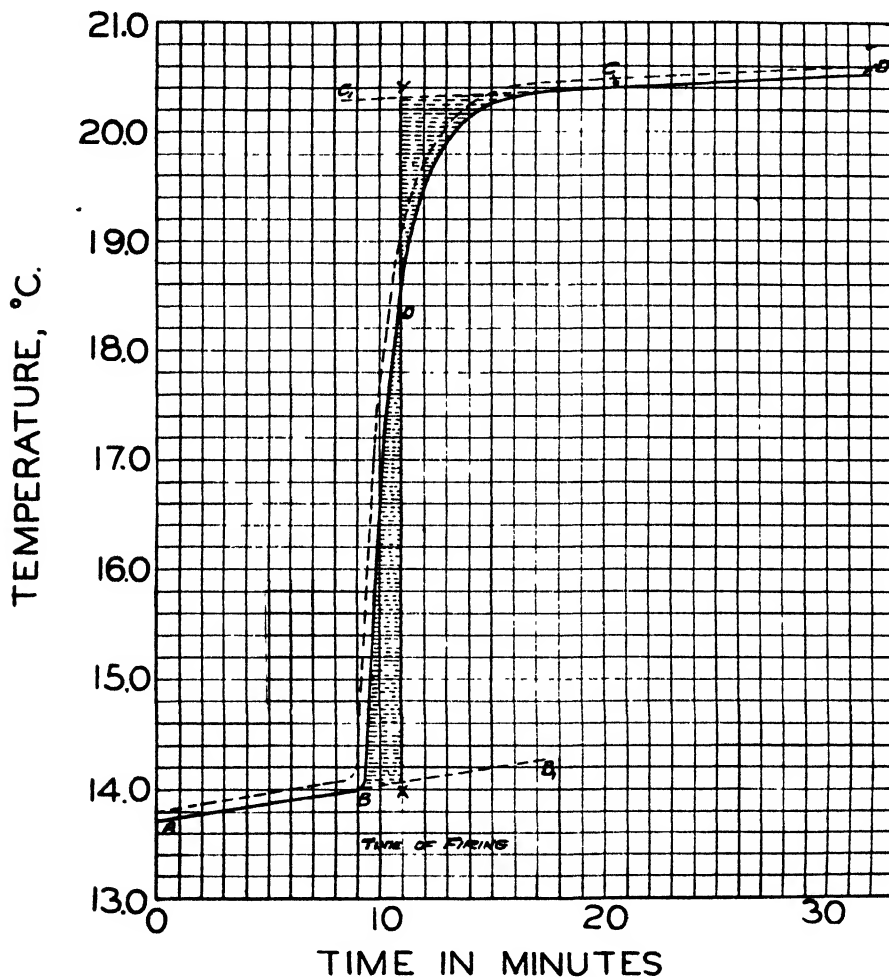


FIG. 5. Temperature-rise curve—interpolation method

liable to occur, but with higher charges decomposition was found to be complete. In order to ensure adequate ignition a fine nickel wire was soldered to the firing pins as igniter. The firing wires were connected to a switch, ammeter, and fuse box. The fuse wire was burnt out first, so that the Eureka wire just reached a sufficiently high temperature to initiate the electrolytic gas. This system gave an almost constant heat yield.

It is assumed that the electrolytic gas combines to form water according to the equation:



and thereafter functions as an inert material. The correction on the observed calorific value due to the firing of the electrolytic gas is -16 cal. (water liquid). No correction is required for the permanent-gas volume or the gas analysis, but if the water in the bomb is determined directly, then 0.005 g. must be subtracted from the figure obtained for the water per gram of charge.

On firing a charge of nitroglycerin of the order of 7 g. the inside of the bomb was found to be rusted. Six successive shots were fired, care being exercised between shots to keep the surface of the bomb in constant condition by drying the bomb by evacuation. After six shots, it was considered that the inside surface of the bomb would be conditioned, and actual determinations were made. Five shots yielded the following results (calories per gram of nitroglycerin, constant volume, water liquid, at $18^\circ\text{C}.$): (1) 1631.2 , (2) 1636.2 , (3) 1638.2 , (4) 1632.5 , (5) 1640.5 ; *mean* = 1635.7 .

From these observations it appears that either there is no further oxidation of the surface of the bomb, or that there is a small constant oxidation produced by each shot. Another sample of carefully dried nitroglycerin was obtained, and only one shot was fired in the unoxidized bomb before determinations were made. The results of successive determinations were (calories per gram of nitroglycerin, constant volume, water liquid, at $18^\circ\text{C}.$): (1) 1683.4 , (2) 1702 , (3) 1690.4 , (4) 1679.3 , (5) 1672.8 , (6) 1670.2 , (7) 1698 , (8) 1679 , (9) 1662.2 , (10) 1666 , (11) 1666 , (12) 1654.4 , (13) 1653.5 , (14) 1658 , (15) 1656.3 , (16) 1658.6 , (17) 1660.2 .

It will be observed that, within limits, the calorific values drop until an almost constant value is obtained. This proves that initially the oxidation of the bomb is considerable, and that, finally, it falls to either zero or some minimum and almost constant value.

The divergencies in the above results were attributed, after investigation of possible causes, to the variation of the amount of solder used in fixing the firing wire, this solder being oxidized by the free oxygen liberated on decomposition of the nitroglycerin. In subsequent experiments, therefore, a minimum and constant amount of solder was used. A little soft packing and mica were used in the firing-pin system, and any shot fired immediately after a change of packing was neglected.

Experiments on "pure" nitroglycerin

A few pounds of nitroglycerin were specially prepared from double-distilled glycerol and specially pure acids. The preparation was carried out very carefully and the product was thoroughly washed with water and dried. The final drying was carried out over sulfuric acid. It may be concluded, therefore, that the nitroglycerin produced was of a very high grade.

Initially some experiments were carried out in the oxidized bomb without

careful attention to the reduction of the quantity of solder to a minimum. The results were (calories per gram of nitroglycerin, constant volume, water liquid): (1) 1634.8, (2) 1633.8, (3) 1646.2, (4) 1669.4, (5) 1637.7, (6) 1634.1, (7) 1636.5.

The solder was then reduced to a minimum and constant quantity and the following values were obtained: (1) 1626.3, (2) 1626.8, (3) 1625.5, (4) 1624.7, (5) 1624.6. It will be observed that these results are lower and much more regular than the previous ones. Prior to firing these latter shots forty charges of nitroglycerin in all had been fired successively in the bomb; consequently there was a very good protective coating on the inside, and very little rusting per shot can be anticipated.

The volume of gas liberated and the amount of water produced in each determination were found by the methods already described. The following results were obtained. Permanent gases at N.T.P. (cc./g. of nitroglycerin): 465.5, 465.1, 466.4, 466.7, 468.5, 466.4, 467.2. Water (g./g. of nitroglycerin): 0.2017, 0.2015, 0.1991, 0.2000, 0.1980, 0.1976. The average results of these determinations, together with their probable errors, were as follows: calorific value (constant volume, water liquid, at 18°C.) = 1625.6 ± 0.4 cal. per gram of nitroglycerin. Permanent gases = 466.5 ± 0.5 cc. per gram of nitroglycerin at N.T.P. Water = 0.1996 ± 0.0007 g. per gram of nitroglycerin.

Experimental precision

The probable error of the arithmetic mean value of the observed calorific value of nitroglycerin has been calculated as ± 0.4 cal. It is considered that this figure represents the order of reproducibility of the experimental results. In addition, the errors introduced in the measurement of the water equivalent of the calorimeter, in the system of thermometry employed, and other errors inherent in bomb calorimetry must be examined. Washburn (12) has considered these latter corrections in detail. A consideration of all these factors has shown that the finally recorded calorific value of nitroglycerin is correct to within 2.5 parts in 1000.

Consideration of results on "pure" nitroglycerin

The known data for pure nitroglycerin, assuming decomposition into water (liq.), carbon dioxide, nitrogen, and oxygen without any deposition of carbon or formation of oxides of nitrogen are:

EMPIRICAL FORMULA	PERMANENT GASES: CC. PER GRAM AT N.T.P.	WATER	TOTAL GASES: CC. PER GRAM AT N.T.P.
	cc.	g / g.	cc.
$C_3H_5(NO_2)_3$	468.6	0.1982	715.4

The measured volume of permanent gases is 2 cc. less than that for the nitroglycerin molecule. This was confirmed by repetition of the gas-volume results. The interpretation of this deficiency is that either there are products other than water (liq.), carbon dioxide, nitrogen, and oxygen in the products of explosion or

that some of the gas has disappeared by chemical action or absorption at the bomb surface.

Analysis of explosion gases

Analysis of the explosion gases by means of an Ambler gas analysis apparatus failed to disclose any constituents other than carbon dioxide, oxygen, and nitrogen.

In order to test for carbon monoxide specific tests using all gases from shots were carried out. A very dilute solution of palladium chloride was made and divided into three equal portions: (1) reserved for standard comparison, (2) used for testing the nitroglycerin explosion gases, and (3) used for a check test on M.D. cordite explosion gases containing 40 per cent of carbon monoxide. Three liters of gas from a nitroglycerin shot were bubbled through the second portion of the palladium chloride solution, and 10–15 cc. of the M.D. cordite gas was bubbled through the third portion of the solution. Portion 3 of the solution was definitely darkened due to precipitation of palladium, whilst no observable difference was found between portions 1 and 2 after bubbling the nitroglycerin explosion gases through portion 2. It may be concluded, therefore, that carbon monoxide is absent from the nitroglycerin explosion gases considered in these experiments.

In order to test for nitric oxide and nitrogen dioxide, the gas from a shot (3 1.) was bubbled through a saturated solution of ferrous sulfate. No brown coloration of the system was observed. The liquor was drawn off from the bomb and filtered and tested for nitric acid, but the result was negative.

From these results, it appears that the explosion gases from nitroglycerin fired under the present conditions consist uniquely of carbon dioxide, oxygen, water, and nitrogen.

Quantitative estimation of the constituents of the explosion gas

Attempts were made to determine the percentage of carbon dioxide in the explosion gases gravimetrically by absorption in potash. This method proved to be unsuccessful, because the gas from one shot required a "bubbling-through" period of 3 hr., and during this time there was an appreciable absorption of gas at the inside surface of the bomb with formation of iron oxide and carbonate, for the gases are at high pressure in the bomb. The absorption of gas in the bomb was proved by carrying out measurements of the permanent-gas volume with continued times of standing of the gases in the bomb at high pressure. Normal measurements in the bomb yielded a mean gas volume of 466.5 cc./g. Fired charges which had stood for $3\frac{1}{4}$ hr. before measurement was carried out gave 451.5 and 458.8, a mean of 455 cc./g. When the gas from a charge was allowed to flow into a gas-volume apparatus at the same rate as bubbling through the potash solution in a carbon dioxide determination, the gas volume measured was 455.2 cc./g. It is evident, therefore, that this method of gravimetrically estimating the carbon dioxide in the explosion gases is unsatisfactory.

Subsequently, "fresh" explosion gases were used and analyzed volumetrically

with as high a degree of precision as possible. A constant-pressure gas-analysis apparatus was developed for this purpose and every care was taken in making up and using the reagents. The carbon dioxide was removed by absorption in potash. The oxygen was absorbed in alkaline pyrogallol and the gas was subsequently washed with cuprous ammoniacal solution to remove any traces of carbon monoxide which might have been produced in the pyrogallol reaction. The results of the gas analyses on two different shots were:

	CO ₂	O ₂	N ₂ (BY DIFFERENCE)
	<i>per cent</i>	<i>per cent</i>	<i>per cent</i>
(1) ..	63.04	4.92	32.04
(2) ..	63.17	4.87	31.96
Mean .	63.10	4.90	32.00

The breakdown of the molecular substance $C_3H_5(NO_3)_3$ would yield the analysis:

CO ₂	O ₂	N ₂
<i>per cent</i>	<i>per cent</i>	<i>per cent</i>
63.17	5.26	31.57

On the assumption that the sample is pure nitroglycerin, it appears that there is very little carbon dioxide absorbed during calorimetric determination, but that there is an appreciable percentage of oxygen absorbed, presumably to form mist on the surface of the bomb. It will be observed that about 0.1 per cent of the carbon dioxide is absorbed and 7 per cent of the free oxygen. Now the volumes of carbon dioxide and oxygen contained in 1 g. of the explosion gases are 296.0 and 24.6 cc., respectively. Consequently, there are 0.3 cc. of carbon dioxide and 1.7 cc. of oxygen absorbed by reaction in the bomb, i.e., the total absorption is 2 cc. per gram of explosion gases. The permanent gases per gram of pure nitroglycerin without absorption are 468.6 cc. The figure reduced by absorption will, therefore, be 466.6 cc., which corresponds exactly with the average figure for the permanent gases found experimentally for the sample of nitroglycerin investigated in the present experiments.

Further, the average water determined experimentally was 0.1996 g. per gram of nitroglycerin and the figure for the molecular substance $C_3H_5(NO_3)_3$ is 0.1982 g. per gram; the difference is +0.7 per cent, but the limits 0.1996 ± 0.002 are well within the theoretical values. It is considered that the slightly high value of the water, as found experimentally, is due to absorption of water from the air in the mist coating and some of this is removed by evacuation when the water is determined after a shot.

From the above-described results, it may be legitimately concluded that the sample of nitroglycerin examined corresponded very closely to the molecular substance, and that it decomposed on explosion under the present conditions

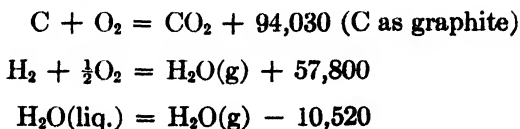
into carbon dioxide, oxygen, water, and nitrogen, of which a part of the oxygen reacted with the surface of the bomb to form oxides of iron and a part of the carbon dioxide to form iron carbonate. The effect of these secondary reactions is to alter very slightly the composition of the explosion gases and to decrease the permanent gas volume by 2 cc. per gram.

The effect of these secondary reactions on the heat evolution produced by explosion of the nitroglycerin must be considered. It may be assumed that the oxygen forms either Fe_2O_3 or Fe_3O_4 . The heat evolved when 1 cc. of oxygen is oxidized to these, produces 5.7 and 5.9 cal., respectively. A mean figure of 5.8 cal./cc. of oxygen absorbed may be accepted without appreciable error. The disappearance of 1.7 cc. of oxygen would entail an evolution of approximately 10 cal. It may be assumed that the carbon dioxide forms ferrous carbonate by reaction with ferrous oxide. This reaction evolves 1 cal. per cc. of carbon dioxide, i.e., $1/3$ cal. for the 0.33 cc. of carbon dioxide actually absorbed. The total heat evolved due to absorption of oxygen and carbon dioxide is approximately 10.5 cal. per gram of nitroglycerin explosion gases. The calorific value found experimentally for "pure" nitroglycerin was 1625.6 cal. per gram. Thus the calorific value corrected for these secondary reactions is 1615 cal. per gram. This figure is considered as the most probably correct one for the heat of combustion of nitroglycerin at constant volume at a temperature of 20°C . with the water in the liquid state. It is improbable that the corrections for oxygen and carbon dioxide formation are in error by more than 1 or 2 cal.

Thermochemical data for "pure" nitroglycerin

Accepting this value for the heat of combustion of "pure" nitroglycerin under the specified conditions, then the heat of combustion at constant pressure and heats of formation of "pure" nitroglycerin may be readily calculated.

Rossini's (10) critically reviewed values of the heats of reaction for the fundamental reactions have been used in these calculations. Rossini's values in calories at constant pressure and 25°C . are:



The calculated thermochemical data for "pure" nitroglycerin are set out in table 1.

Comparison with previous investigations

In table 2 a summary of the heats of combustion of nitroglycerin published by previous investigators is given. The heats of formation given by previous investigators are presented in table 3.

The figures of Sarrau and Vieille, Rinkenbach, and Macnab are experimental, whereas all the others appear to have been calculated from the heats of formation of glycerin and nitric acid, etc., and some of these are obviously in error

because the authors have failed to take into account the fact that the nitration of glycerin is, itself, an exothermic reaction. Sarrau and Vieille used a platinum-

TABLE 1
Thermochemical data for nitroglycerin at 20°C.

THERMOCHEMICAL CONSTANT	CALORIES PER GRAM		KILOGRAM-CALORIES PER MOLE	
	Water liquid	Water vapor	Water liquid	Water vapor
Heat of combustion, at constant pressure	1603	1486	363.8	337.4
Heat of combustion, at constant volume	1615	1505	366.6	341.6
Heat of formation, at constant pressure	391		88.8	
Heat of formation, at constant volume	370		83.9	

TABLE 2
Heats of combustion of nitroglycerin

AT CONSTANT VOLUME AT 20°C				REFERENCE
Calories per gram		Kilogram-calories per mole		
Water liquid	Water vapor	Water liquid	Water vapor	
1579	1478	358.5	335.6	Berthelot (1)
1600		363.3		Sarrau and Vieille (11)
1630.4		370.25		Rinkenbach (9)
1589	1470	360.8	333.7	Escales (3)
	1455		330.4	Kast (5)
1580		358.8		Brunswick (2)
1595		362.1		Naoum (8)
1652		375.1		Macnab (6)

TABLE 3
Heats of formation of nitroglycerin at constant pressure and 20°C.

CALORIES PER GRAM	KILOGRAM-CALORIES PER MOLE	REFERENCE
Water liquid	Water liquid	
432	98.0	Berthelot (1)
416	94.4	Reichsanstalt (4)
415	94.2	Brunswick (2)
416	94.4	Kast (5)
435.7	98.9	Escales (3)
381.6	86.6	Rinkenbach (9)

lined bomb so that no oxidation of the surface would occur, but the charges used were small and it is not unlikely that a little carbon deposition occurred.

Macnab, on the other hand, used a steel bomb and did not allow for surface oxidation of the bomb. His result is, therefore, almost certainly too high. Rinkenbach does not describe his experimental method and it is not possible, therefore, to judge of the accuracy of his determinations.

It is considered that the careful experimental procedure adopted in the present investigation, together with the application of recently revised thermochemical data, has resulted in the determination of the most probably correct values for the heats of combustion and formation of nitroglycerin.

PART II: NITROCELLULOSE

Experimental method

Preparation of the nitrocellulose: The analytical data for the nitrogen and ash of the unprecipitated and precipitated samples of the nitrocelluloses investigated are set out in table 4. The nitrocelluloses examined, with the exception of sample D which was tested in the unprecipitated condition, were treated in the following manner: The nitrocotton was first dried, and sufficient of this

TABLE 4
Analytical data for the unprecipitated and precipitated samples of nitrocellulose

SAMPLE	UNPRECIPITATED		PRECIPITATED	
	Nitrogen (ash-free)	Ash	Nitrogen (ash-free)	Ash
	<i>per cent</i>	<i>per cent</i>	<i>per cent</i>	<i>per cent</i>
A	13.10	0.40	13.16	0.20
B	12.73	0.30	12.65	0.07
C	12.16	0.36	12.10	0.07
D	13.24	0.35		

nitrocotton for the calorific determinations was wetted with an equal weight of alcohol (66 O.P.) and then dissolved in acetone, 4 g. of nitrocellulose in 100 cc. of acetone. The solution was filtered twice through glass wool and the nitrocellulose precipitated in a considerable excess of well-agitated distilled water. This precipitated nitrocellulose was washed in four changes of distilled water, and boiled for 2 hr. in distilled water. It was then drained and as much of the water squeezed out as possible. Finally the product was dried, first for 7 hr. at a temperature of 80°C., and secondly, in a vacuum for 6 hr. at a temperature of 80°C. to 85°C. in order to remove all traces of solvent.

In the case of sample C the solution was centrifuged for 2 hr. before precipitation, in addition to the above treatment.

From table 4 it will be observed that in the case of samples B and C practically ash-free nitrocellulose has been obtained, but in the case of sample A only 50 per cent of the original ash has been removed. All thermochemical results have been corrected for the ash content.

Moisture conditioning of the nitrocellulose: In order that the moisture of the

nitrocellulose used for a calorimetric determination could be accurately known, it was necessary to bring the nitrocellulose into such a condition that no change in its moisture content would take place whilst the charge was being weighed out and the bomb loaded.

This was achieved by spreading the nitrocellulose on trays and exposing it to the atmosphere so that its moisture could come into equilibrium with the atmospheric humidity. It was conditioned in this manner for 1 or 2 days before the calorimetric determinations were commenced and was left exposed throughout the whole series of experiments. With the nitrocellulose in this condition it is assumed that the moisture of the charge taken for a calorimetric determination was identical with that of a sample weighed out at the same time for moisture determination.

Method of charging the calorimetric bomb: A charge of the conditioned nitrocellulose was weighed out into a weighing bottle and then introduced into the calorimetric bomb through a glass funnel. Any nitrocellulose left adhering to the weighing bottle and glass funnel was allowed for by reweighing.

The calorimetric bomb was then connected to a weighed trap, as used for the water determination, and evacuated. The water drawn off was caught in the trap; its weight could be found by reweighing the trap after it had acquired room temperature and air at atmospheric pressure and humidity introduced. The time required to evacuate the bomb was noted, and a blank experiment performed for the same length of time with the valve closed. By this means, any moisture that has condensed in the trap due to a very slight leak can be allowed for and the moisture drawn off from the nitrocellulose in the calorimetric bomb accurately determined.

At the same time as the charge for the calorimetric determination was weighed out, a sample was taken for moisture determination. Hence by this means the initial moisture of the charge was known, and the moisture lost due to evacuation was known, therefore the actual moisture of the nitrocellulose in the calorimetric bomb could be calculated.

Mode of producing ignition: Several methods were tried out before a satisfactory mode of ignition of the nitrocellulose was obtained. Finally the following method was adopted. Fine tungsten wire was connected to copper extension rods fitted to the firing pins. The tungsten wire was coated with a mixture of 40 per cent tetrazene and 60 per cent potassium perchlorate, having a calorific value of 1290 cal. per gram at constant volume.

The wire, which was soldered to the ends of the copper extension rods, was coated in the following manner: It was first dipped in a fairly thin solution of nitrocellulose in acetone, and then into a small pile of the above mixture. This was repeated until the wire was coated with the mixture, and it was finally dipped in the nitrocellulose solution so as to obtain a protective covering of nitrocellulose, and thus prevent the particles of the initiating composition being brushed off when the wire came in contact with the main charge in the calorimetric bomb.

The weight of coating used was of the order of 0.001 g. and the charge of nitrocellulose 5 g., so that the heat put into the bomb due to firing, per gram of

TABLE 5
Experimental data observed for nitrocellulose, sample A

EXPERIMENTAL CALORIFIC VALUE; CON- STANT VOL- UME, WATER LIQUID AT TEMPERATURE OF EXPERIMENT	CALORIFIC VALUE; WATER LIQUID AT TEMPERATURE OF EXPERIMENT (CORRECTED FOR MOISTURE AND ASH)	EXPERI- MENTAL GAS VOLUME AT N.T.P.	WATER	TOTAL GASES AT N.T.P.	TOTAL GASES AT N.T.P. (CORRECTED FOR MOISTURE AND ASH)	MOISTURE OF NITROCELLU- LOSE WHEN WEIGHED OUT	MOISTURE OF NITROCEL- ULOSE IN BOMB AFTER EVACUATION
<i>cal./g.</i>	<i>cal./g.</i>	<i>cc./g.</i>	<i>g./g.</i>	<i>cc./g.</i>	<i>cc./g.</i>	<i>per cent</i>	<i>per cent</i>
1044.5	1052.5	693	0.1530	883.5	883	0.96	0.59
1043	1049	693	0.1507	880.5	882	0.77	0.39
1038.5	1048.5	692	0.1519	881.0	880.5	0.95	0.77
1035	1045					0.97	0.80
1039.5	1051					1.05	0.92
1046	1056	691.5				1.05	0.81
1038.5	1050.5	690	0.1555	883.5	881.5	1.15	0.97
1044	1053.5	692.5	0.1520	881.5	880.5	1.18	0.78
1040.5	1053	690.5	0.1536	882.0	880.5	1.20	1.03
1040	1052	690.5	0.1532	881.5	880	1.14	1.00

TABLE 6
Experimental data observed for nitrocellulose, sample B

EXPERIMENTAL CALORIFIC VALUE; CON- STANT VOL- UME; WATER LIQUID AT TEMPERATURE OF EXPERIMENT	CALORIFIC VALUE; WATER LIQUID AT TEMPERATURE OF EXPERIMENT (CORRECTED FOR MOISTURE AND ASH)	EXPERI- MENTAL GAS VOLUME AT N.T.P.	WATER	TOTAL GASES AT N.T.P.	TOTAL GASES AT N.T.P. (CORRECTED FOR MOISTURE AND ASH)	MOISTURE OF NITROCELLU- LOSE WHEN WRIGHT OUT	MOISTURE OF NITROCEL- ULOSE IN BOMB AFTER EVACUATION
<i>cal./g.</i>	<i>cal./g.</i>	<i>cc./g.</i>	<i>g./g.</i>	<i>cc./g.</i>	<i>cc./g.</i>	<i>per cent</i>	<i>per cent</i>
968	984.5	708	0.1584	905	900.5	1.88	1.61
961.5	978.5	707	0.1551	900	894.5	1.79	1.73
961.5	978.5	709.5	0.1579	906	900.5	1.88	1.68
959.5	975.5	708	0.1587	905	900	1.85	1.65
966.5	984.6	708	0.1595	906.5	901	1.93	1.75
963.5	980.5	707	0.1603	906.5	901	2.00	1.68

TABLE 7
Experimental data observed for nitrocellulose, sample C

EXPERIMENTAL CALORIFIC VALUE; CON- STANT VOL- UME; WATER LIQUID AT TEMPERATURE OF EXPERIMENT	CALORIFIC VALUE; WATER LIQUID AT TEMPERATURE OF EXPERIMENT (CORRECTED FOR MOISTURE AND ASH)	EXPERI- MENTAL GAS VOLUME AT N.T.P.	WATER	TOTAL GASES AT N.T.P.	TOTAL GASES AT N.T.P. (CORRECTED FOR MOISTURE AND ASH)	MOISTURE OF NITROCELLU- LOSE WHEN WEIGHED OUT	MOISTURE OF NITROCEL- ULOSE IN BOMB AFTER EVACUATION
<i>cal./g.</i>	<i>cal./g.</i>	<i>cc./g.</i>	<i>g./g.</i>	<i>cc./g.</i>	<i>cc./g.</i>	<i>per cent</i>	<i>per cent</i>
880	901	736	0.1584	933	926.5	2.42	2.30
881.5	900.5	736	0.1584	933	927	2.21	2.09
882	903.5	735.5	0.1588	933	926	2.59	2.36
876.5	898	737	0.1590	935	928.5	2.52	2.33
882	900	737	0.1571	932.5	926.5	2.11	2.01

nitrocellulose, was 0.3 cal. This quantity was subtracted from the observed calorific value to correct for the heat input due to firing.

TABLE 8
Experimental data observed for nitrocellulose, sample D

EXPERIMENTAL CALORIFIC VALUE; CON- STANT VOL- UME; WATER LIQUID AT TEMPERATURE OF EXPERIMENT	CALORIFIC VALUE; WATER LIQUID AT TEMPERATURE OF EXPERIMENT (CORRECTED FOR MOISTURE AND ASH)	EXPERI- MENTAL GAS VOLUME AT N.T.P.	WATER	TOTAL GASES AT N.T.P.	TOTAL GASES AT N.T.P. (CORRECTED FOR MOISTURE AND ASH)	MOISTURE OF NITROCELLU- LOSE WHEN WEIGHED OUT	MOISTURE OF NITROCEL- LULOSE IN BOMB AFTER EVACUATION
<i>cal./g.</i>	<i>cal./g.</i>	<i>cc./g</i>	<i>g./g.</i>	<i>cc./g</i>	<i>cc./g</i>	<i>per cent</i>	<i>per cent</i>
1038.5	1051.5	684.5	0.1568	879.5	879	1.04	0.93
1050.5	1064.5	686	0.1535	877	876.5	1.12	1.02
1044	1058.5	684	0.1545	876	875	1.18	1.07
1050	1065.0	681	0.1554	874.5	874	1.20	1.08
1043.5	1060.5	681.5	0.1548	874	872	1.40	1.30
1031	1046.5	681	0.1552	874	872.5	1.31	1.21

TABLE 9
Mean values of determined calorific values and gas volumes

NITROCELLULOSE SAMPLE	CALORIFIC VALUE; WATER LIQUID AT TEMPERATURE OF EXPERIMENT	TOTAL GASES AT N.T.P.
	<i>cal./g.</i>	<i>cc./g</i>
A	1051.0	881
B.	980.5	899.5
C	900.5	927
D	1060	874

In obtaining the averages for sample D, the lowest calorific determination (1046.5) and the highest gas-volume determination (879) have been omitted.

TABLE 10
Finally corrected calorific values and gas volumes of nitrocelluloses

SAMPLE	\bar{Q}_L CALORIFIC VALUE; WATER LIQUID, AT 0°C. (CORRECTED FOR METHANE FORMATION)	V TOTAL GASES AT N.T.P. (CORRECTED FOR METHANE FORMATION)
	<i>cal./g.</i>	<i>cc./g</i>
A	1054	883.5
B	982	902.5
C	902	929.5
D	1063	876.5

Experimental results

The experimental results obtained for the nitrocelluloses examined are set out in tables 5, 6, 7, and 8. In order to obtain the calorific value, at the tem-

perature of experiment, and total gases for pure dry, ash-free, nitrocellulose from the experimental figures, the data must be corrected for ash and residual moisture, and the former also corrected for the heat put in due to firing. The corrected values so obtained are also set out in the tables, while the mean of these values are collected in table 9. The calorific values and total gases corrected for methane formation are given in table 10.

The relation between the finally corrected calorific value and the nitrogen content of the nitrocellulose is shown in figure 6; the relation is linear. Milus (7) determined the calorific value of various nitrocelluloses of plant manufacture in a calorimetric bomb and analyzed the explosion gases. His results are in satisfactory agreement with those obtained in the present investigation.

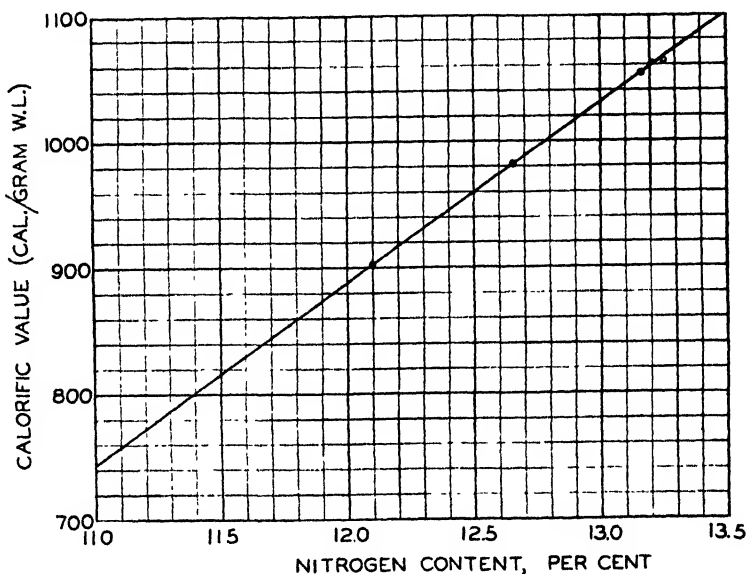


FIG. 6. Relation between the calorific value (water liquid) and the nitrogen content of pure dry nitrocellulose.

SUMMARY

The heat of combustion of nitroglycerin of a high degree of purity has been determined experimentally in a calorimetric bomb. The calorimetric bomb, which is a modification of that originally designed by Research Department, Woolwich, has been briefly described. Careful analysis of the explosion gases under the chosen conditions of experiment indicate that the gases consist uniquely of carbon dioxide, water, and nitrogen. It is considered that the finally reported value of the heat of combustion of nitroglycerin is accurate to within about 2.5 parts in 1000. The results are compared with those of the early investigators.

It is concluded that the heat of combustion of nitroglycerin at 20°C. is 1615 cal. per gram at constant volume (water liquid); this is equivalent to $\frac{341.6}{366.6}$ kg.-cal. per mole.

The calorific value and gas-volume constants of a series of precipitated nitro-celluloses of varying nitrogen content have also been directly determined. It has been shown that the calorific value varies linearly with the nitrogen content of the nitrocellulose.

The authors are indebted to Dr. H. Thomas for his assistance in preparing the data for this report.

REFERENCES

- (1) BERTHELOT, M.: *Sur la force des matières explosives*. Gauthiers-Villars, Paris (1883).
- (2) BRUNSWIG, H.: *Explosivstoffe*, p. 70. G. J. Göschen'sche, Leipzig (1909).
- (3) ESCALES, R.: *Nitroglycerin und Dynamit*, p. 169. Von Veit, Leipzig (1908).
- (4) JAHRESBER. N. Chemisch-Techn. Reichsanstalt, p. 94 (1924-1925).
- (5) KAST, H.: *Spreng- und Zündstoffe*, p. 70. Friedr. Vieweg und Sohn, Braunschweig (1921).
- (6) MACNAB, W.: Proc. Roy. Soc. (London) **56**, 8 (1894).
- (7) MILUS, P. R.: Ind. Eng. Chem. **29**, 492 (1937).
- (8) NAČUM, P.: *Nitroglycerin und Nitroglycerin-Sprengstoffe*, p. 133. J. Springer, Berlin (1924).
- (9) RINKENBACH, W. H.: Ind. Eng. Chem. **18**, 1195 (1926).
- (10) ROSSINI, F. D.: J. Research Natl. Bur. Standards **22**, 407 (1939).
- (11) SARRAU, E. AND VIEILLE, M.: Compt. rend. **93**, 269 (1881).
- (12) WASHBURN, E. W.: J. Research Natl. Bur. Standards **10**, 525 (1933).

RADIATION CHEMISTRY^{1, 2}MILTON BURTON³*Clinton Laboratories, Monsanto Chemical Company, Oak Ridge, Tennessee**Received August 27, 1946*

NATURE OF RADIATION CHEMISTRY

In classical chemistry the branch of chemical kinetics concerned with the interaction of ordinary energetic "emanations" and matter is called photo-

¹ Summary of paper presented at the Symposium on Nuclear Chemistry which was held under the auspices of the Division of Physical and Inorganic Chemistry at the 109th Meeting of the American Chemical Society, Atlantic City, New Jersey, April 10, 1946.

² This paper includes references to the work of many collaborators as well as others, both at the Metallurgical Laboratory of the University of Chicago and at Clinton Laboratories, Oak Ridge, Tennessee. None of such work yet appears in the open literature. Material here reported is for the most part qualitative, and there are certain evident hiatuses of subject matter. An effort is made, however, to give due credit by indication in footnotes of the names of the investigators. Thus, when the literature does become freely available, the references may be identified. The list of names is regrettably incomplete, primarily because not all studies are here reported. It would be futile to attempt an acknowledgment of the contributions of Dr. James Franck, who was a constant advisor and consultant

chemistry. The emanations, photons, are of a type associated with transitions between energy states of the external electrons of atoms and molecules. The wave lengths of effective photons range from the near infrared for some photographic processes (i.e., 10,000 Å.) to a lower limit in the far ultraviolet (of the order of 1000 Å.) for some absorption-spectra studies and for some investigations of ionic crystals. The corresponding energy range is approximately 1.2 to 12 e.v. In these cases, in spite of the fact that details are well understood in only a few of them, the primary processes involved are rather simple. The absorbing molecule is raised to an excited state from which various changes occur in times which are of the order of one vibration period (10^{-13} sec.) or considerably longer. Dependent on the molecules, competition favors one or the other of processes which are distinguished in part by the time required for their completion. They are fluorescence, simple rupture, transfer of energy to another molecule or atom physically or chemically (e.g., photosensitization), and internal conversion associated merely with degradation of the energy state to successively lower electronic states.

In the field of atomic energy we have a corresponding branch of chemical kinetics, concerned with the interaction of extremely energetic "emanations" and matter. In the atomic energy projects it has, for want of a better name, been called radiation chemistry. The "emanations" are of a type or energy ordinarily associated with nuclear transitions in either natural or induced radioactive or fission processes. By extension of this idea, radiation thus includes alpha and beta particles and gamma radiation (found in radioactivity), neutrons and fission recoils, and fast protons, deuterons, electrons, and x-radiation produced by various instrumental means.

The energy range for these studies is determined by the interests of the investigator and by the radiation sources available. Some work has been done with 170-kv. cathode rays (11) and there have been studies with x-rays of somewhat higher corresponding energy. This is the lower end of the spectrum of radiations studied in radiation chemistry.⁴ The usual particles or radiations studied begin in that energy range for some slow betas and soft gammas, and extended up to 20 m.e.v. in studies of the effects of neutrons, betas, and gammas, and up to 100 m.e.v. for some of the fission recoils.

While the particles (i.e., photons) of photochemistry cause, in the first instance, only excitation of one molecule, those of radiation chemistry cause not only excitation but ionization of many molecules. The average energy required per ionization act for most substances studied in the gas phase is in the range 30 to 35 e.v. Except in chain reactions, usually no more than a few molecules are chemically converted per ion-pair produced.

on most of the work. For the most part, references are to work performed in the Radiation Chemistry Sections at Chicago and at Oak Ridge. The locale of other work is indicated.

* Present Address: Department of Chemistry, University of Notre Dame, Notre Dame, Indiana.

⁴ However, investigations at lower energies, e.g., on chemical effects of accelerated protons of 200–800 e.v. (see I. Amdur and H. Perlman: *J. Chem. Phys.* **8**, 7 (1940)) can be very useful for radiation chemistry in the interpretation of details of mechanism.

In photochemistry we emphasize the rôle of the photon by reporting results in terms of the quantum yield, γ . In radiation chemistry, there has been a tendency, somewhat justified in practice, to report yields in terms of the number of molecules converted per ion-pair produced—the so-called M/N ratio (8). This method of expression neglects the fact that, in condensed systems certainly, the value of N is essentially an assumed one based on the idea that the average energy, E_{av} , required per ionization process is precisely that determined for the gas phase, perhaps only of a similar (not even the identical) substance. Also, the M/N method of expression introduces a variety of scales of reference, depending on the various substances studied, for E_{av} is different for different substances. Furthermore, its use suggests an idea which remains to be proved—that the ionization process is at the root of all radiation chemical reactions. Alternative methods of representation of yields have been used in the Radiation Chemistry Sections: either G , the number of molecules converted or produced per 100 e.v., or, a form of expression favored by some, the energy in electron volts required to convert or produce one molecule.

RADIATION SOURCES

The magnitude of the Plutonium Project made accessible for its purposes instruments which had simply not been previously available for the work of earlier investigators. Cyclotron sources of high-voltage deuterons were used at the University of Chicago and the University of Michigan, and of high-energy neutrons at Washington University and the University of California at Berkeley. Van de Graaff generators at the Massachusetts Institute of Technology, the University of Chicago, and the University of Notre Dame were also available; these were used as sources both of high-voltage x-rays and of electron beams. The latter type of instrument is rather interesting because of the monochromatic nature of its beam, and because of the high power levels at which it is possible to operate. The x-ray instrument at the Chicago Tumor Institute and the betatron at the University of Illinois were also employed in a preliminary way. The need for this wide range of instruments will appear in the subsequent discussion.

In addition, the pile itself (i.e., the atomic energy plant) and products from the pile were both important sources of radioactivity. The flexibility of operations made possible by the availability of these sources is pointed up by the fact that a gram of radium, which only the rarer investigator might afford in the past, in secular equilibrium dissipates energy at the rate of 0.12 watt, while the piles in actual use for the production of plutonium operate at many thousands of kilowatts (13). Radioactive fission products from such piles were correspondingly useful, for they could be concentrated to give intensities of radiation from radioactive sources far exceeding any of the past.

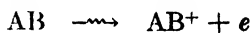
DETAILED EFFECTS OF HIGH-ENERGY RADIATION

In the pile itself, all radiations associated with atomic energy are potentially effective. Figure 1 shows the regions in a graphite pile in which the major

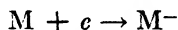
Casual perusal reveals that all the phenomena of photochemistry are necessarily present. Very energetic radiation produces not only excitation but also ionization and, as in the case of fast neutrons, sometimes simple elastic scattering.

The phenomena ensuant on molecular excitation are no different in radiation chemistry from what they are in photochemistry. Since they are subjects which have been extensively, if not exhaustively, discussed in another setting, they will be touched on only lightly here. They are among the lesser complexities of radiation chemistry, knowledge of which is necessarily precedent to the understanding of any particular chemical reaction. Thus, while there are perhaps four or five cases of thermal and photochemical reactions whose mechanisms are thought to be thoroughly understood, the best that can be said for the complicated processes of radiation chemistry is that some of their outlines are apparent.

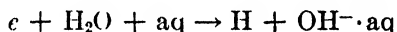
High-energy particles and radiations all produce ionization (as well as excitation) of the molecules or atoms with which they interact.⁶



The electron travels several hundred molecular diameters after its liberation before it comes to rest either to discharge a positive ion or to form a negative ion,



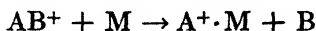
where M may be AB or some other molecule. In water (i.e., where M is H₂O) this may be an intermediate step but the over-all reaction is



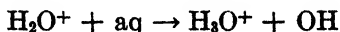
In general, after the primary acts in which electrons are released and trapped at some remote point, the succeeding processes in which the ions concerned may become involved depend on their nature and their stability in their environment. The nature of the general environmental conditions surrounding ions requires prime consideration. At one time it was thought that the small mobility of gaseous ions in an electric field (unaccountable by simple kinetic theory assuming ordinary molecular diameters) indicated that in reality the diameters were abnormally large and represented a cluster of a central ion and associated neutral molecules held thereto by strong polarization forces. Ultimately, it was established that the phenomenon could be explained in terms of drag exerted on the ions by dipole forces set up in the molecules through whose neighborhood they drift (10). Meanwhile, however, the idea of clustering had given birth to the cluster theory of radiation chemistry. Lind noticed the many instances where M/N exceeded unity and suggested the idea that energy liberated in neutralization of the ion caused dissociation of the surrounding cluster of molecules (8(b)). The preferred notion now is that small values of M/N in excess of unity indicate merely the production of a few free atoms or radicals per ionization act (3), as well as a possible contribution by excited molecules.

⁶ The symbol $\xrightarrow{\gamma}$ in radiation chemistry has a significance parallel to $\xrightarrow{h\nu}$ in photochemistry.

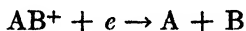
The new point of view does not deny the existence of weakly held clusters (with energy of attachment of the order of thermal motion) (3) nor does it neglect the further possibility of two other significant phenomena. In certain cases, e.g., where AB or M may strongly solvate a dissociation product of AB⁺, the existence of clusters in liquid or in gas may affect the course of reaction considerably, yielding



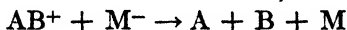
as, for example, in water



instead of the significant reaction where solvation does not occur: namely,



or



(3)

Furthermore, there may be a slight distinction between a free atom or radical liberated (by neutralization of an ion) when clustering does not occur and when it does. In the latter case the atom or radical escapes through an envelope of oriented molecules. That there is a significance in this fact has not been established.

The important point is that reactions of the class of reaction 3 constitute one of the important groups in radiation chemistry. The mechanism in this group of reactions is that radiation causes ionization and that ultimately a positive ion is discharged by an electron or negative ion. The electron moves to the positive ion in a time so short that the constituent atoms remain substantially undisplaced (Franck-Condon principle); the energy of neutralization thus appears as excitation of the products. In effect, some of the atoms or radicals are left in positions corresponding to energy states above the dissociation limit for the bond concerned. Dissociation results as in reaction 3. Dissociation of M itself in this process is unlikely.

A complete discussion of all types of chemical phenomena associated with radiation-chemical processes is inappropriate here. It is proper to say that usual considerations of free radical chains apply and that, in radiation chemistry, there are phenomena of sensitization (i.e., by ions) similar to photosensitization by excited molecules. Recombination of primary products (i.e., free atoms or radicals) plays the usual rôle. However, radiation-induced back-reaction involving product molecules plays a more significant rôle in radiation-chemical reactions than in other classes of reactions. In photochemistry it is frequently possible to choose radiation of wave length which will not affect the product. In radiation chemistry this procedure is never possible. Thus, a steady state dependent on the variety of circumstances of the investigation is usually to be found (particularly for inorganic systems) in radiation chemistry.

Energetic heavy-charged particles, such as alphas, deuterons, or protons, rarely make direct nuclear impact but cause ionization of the molecules with which they "collide." As is generally the case for any incident charged particles, the electrons thus liberated move several hundred molecular diameters from the incident beam. However, such heavy particles cause a relatively large number of ions per unit path length. A deuteron of high energy would ionize about one in five molecules in its track in water. Thus, for heavy-particle irradiation part of the primary products is concentrated in a restricted locale with an inhomogeneous distribution.

An energetic electron or beta, unlike a heavier particle, ionizes about on the average one in five hundred molecules in its track in water. Consequently, the primary effects of fast electrons are diffuse and overlap between tracks, and, unlike the case for heavy particles, the distribution of primary products is essentially homogeneous both along and transverse to the beam.

Gamma rays and x-rays interact with molecules to produce ions and energetic electrons. The latter, in turn, are responsible for the major portion of the observed effects. Thus, it is possible to simulate effects of gammas or x-rays by use of an electron beam from a Van de Graaff generator. However, there is an important difference. Whereas the half-thickness for 1-m.e.v. x-rays is 12 cm. of water, and the x-rays give up energy in any conveniently short distance (e.g., 1 cm.) fairly uniformly, an electron of the same energy penetrates only about 0.5 cm. and gives up most of its energy in an element of path somewhat below the surface. Therefore, where homogeneity of effect is essential, an electron beam cannot be used to simulate gamma rays. This consideration is not usually important, but for cases where it is, the Plutonium Project has sufficient radioactive fission product on hand to supply an adequate concentration of gamma or beta rays. Usually, however, instrumental sources suffice. For example, exposures may be made 2 cm. before the target of the Notre Dame generator at a rate of x-ray dosage of 7×10^5 r./min. If a really high rate of energy dissipation is required, the direct use of the electron beam can increase it by a factor of 10^5 .

Fast neutrons, which are not absorbed in the process, scatter the nuclei with which they collide. The amount of energy transmitted in an elastic scattering process is given by the relation

$$\Delta E/E_0 = 2A/(A + 1)^2$$

where $\Delta E/E_0$ is the arithmetical average fractional decrease in energy of the neutron and A is the atomic weight of the element of the atom concerned.

The form in which energy appears in an ejected atom depends on the energy and the nature of the incident particle; part may be kinetic and part may be in the form of excitation of its electronic system. In general, two types of impacts are involved in this effect: primary scattering by fast neutrons and secondary scattering by scattered ions or atoms. The impact of the neutron and the effect of the neutron, unlike that of charged particle radiation, are exclusively on the nucleus. If the energy of the incident neutron is low enough, the velocity

of the ejected nucleus will be in turn sufficiently low so that its electronic cloud will remain with it. For sufficiently high velocities of the incident neutron, the velocity of the ejected nucleus will be such that it leaves one or more electrons behind it. The result may be that in the first case all of the energy of the neutron is transmitted as kinetic energy and, in the second case, the energy may be transmitted to a major degree in the form of electronic excitation or ionization. The threshold value for the latter process depends on the element concerned, and according to our theory is by no means sharp. The diffuseness of the threshold confuses the effort to calculate *a priori* the number of atoms displaced by fast neutron bombardment. Resort to experiment is essential.

The secondary processes involving the particle ejected by a fast neutron depend strongly on the mass of the particle. Figure 2 indicates the variety of effects produced by the fast ions in passage through a substrate. They may waste their energy in the production of excited molecules or they may produce ions with one or more of the electrons removed. On the other hand, a fast neutron may possess only sufficient energy to expel an atom uncharged from its lattice position; this atom may in turn by head-on collision displace other atoms from their lattice positions. Such a process involves maximum utilization of the kinetic energy of the neutron for production of displaced atoms. The probability of this ideal process decreases with decreasing size of the atoms involved. For small atoms the threshold energy above which a considerable fraction of the neutron energy is converted into excitation and ionization is quite small. In consequence, in the case of very light elements or compounds of such elements, the principal effect will be of a type not purely characteristic of fast-neutron effects. In water, for example, the effect would be nearly like that of an incident proton beam. As the atomic weight of the element involved increases, the fraction of energy transmitted per collision decreases and the threshold below which the energy is transmitted nearly entirely as kinetic energy increases. The magnitude of the effect will obviously reach a maximum at intermediate atomic weights which, comparatively speaking, are rather low. We shall return to a discussion of these effects in connection with solids.

DISCOMPOSITION IN SOLIDS⁷

The effect of fast neutrons on solids was first considered by E. P. Wigner *in extenso* in 1942. He showed that on theoretical grounds, fast neutrons should cause displacement of relatively light atoms from their lattice positions. Such discomposition is to be expected in the case of all substances containing elements of low atomic weight. However, the chance of a back-reaction, in which the atom returns to its original lattice position or to a similar lattice position, will depend on the nature of the solid involved. In a compact solid of maximum density, it is possible that an ejected atom may come to rest in an interstitial

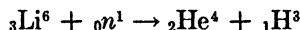
⁷ M. G. Bowman, S. G. Davis, J. Franck, M. Goldberger, S. Gordon, R. C. Hirt, E. J. Hochanadel, B. Leaf, R. J. Maurer, A. J. Miller, R. S. Mulliken, T. J. Neubert, A. Novick, R. A. Penneman, F. D. Rossini (National Bureau of Standards), J. Royal, F. Seitz, R. T. Schenck, E. Teller, A. R. Van Dyken, P. H. Yuster, and E. P. Wigner.

position, but that it will be under such great forces in that position that the application of only moderate energy may cause it to move to a more stable trap—e.g., a hole of a type created in the moment of its ejection. Another phenomenon which may exist in back-reaction is that of instantaneous annealing. We would expect that solids of low melting point, particularly those which are soft to begin with, might not display a detectable discomposition effect, even after prolonged irradiation with fast neutrons.

Both the short space allotted and the security restrictions still in force at the time of preparation of this paper prevent discussion of the effects observed in various substances, and the characteristics of those effects.^{7, 8} At this time we can say merely that the effects are real and interesting, and provide a very fruitful field for further investigation. So far as the research work in radiation chemistry is concerned, discomposition is one of the most interesting effects detected. It was found, for example, that the electric resistance, elasticity, and heat conductivity of graphite all change with exposure to intense neutron radiation.

COLORATION OF IONIC CRYSTALS

Another interesting effect produced in solids is illustrated in the case of lithium fluoride.⁹ The Li^6 isotope undergoes a reaction,



This reaction is by slow-neutron bombardment and is exothermal to the extent of 4.6 m.e.v. (9). All this energy is effective in the production of precisely the same types of changes in crystals as is produced by ultraviolet light or by x-rays or by electron bombardment—namely, the coloration of crystals, which was so thoroughly studied before and during the recent war by various groups associated with Hilsch and Pohl, Mott and Gurney, Schneider, Seitz, and others. The interesting thing here is that the existence of this neutron reaction exaggerates the effect produced in the crystal. Thus lithium fluoride, when exposed in the pile, gives a great variety of effects, at least one of which is completely transient in nearly all other materials. The nature of the spectrum after lithium fluoride bombardment is shown in figure 3. The F and F' designations are according to the terminology of Hilsch and Pohl. The F absorption band is supposed to be characteristic of a single electron trapped at a negative-ion vacancy, while the visible F' band is attributed to the looser binding of two electrons trapped in such a vacancy. In lithium fluoride, unlike most other alkali halides, the F' band is fairly stable at room temperature. The M and R bands are identified according to the terminology of Seitz and his coworkers. M -centers are believed to be aggregates of two halogen-ion vacancies and one positive-ion vacancy to which an electron is attached. R -centers are pairs of halogen-ion vacancies to which one or two electrons are attached.

⁸ I. Estermann, S. N. Foner, G. I. Kirkland, J. Koehler, O. Stern, and others of the Carnegie Institute of Technology.

⁹ R. A. Penneman.

THE SPECIAL CASE OF WATER AND AQUEOUS SYSTEMS¹⁰

In pure water and selected aqueous solutions we have an illustration of the general class of effects of radiation on inorganic compounds containing mainly covalent bonds. The over-all reactions are:

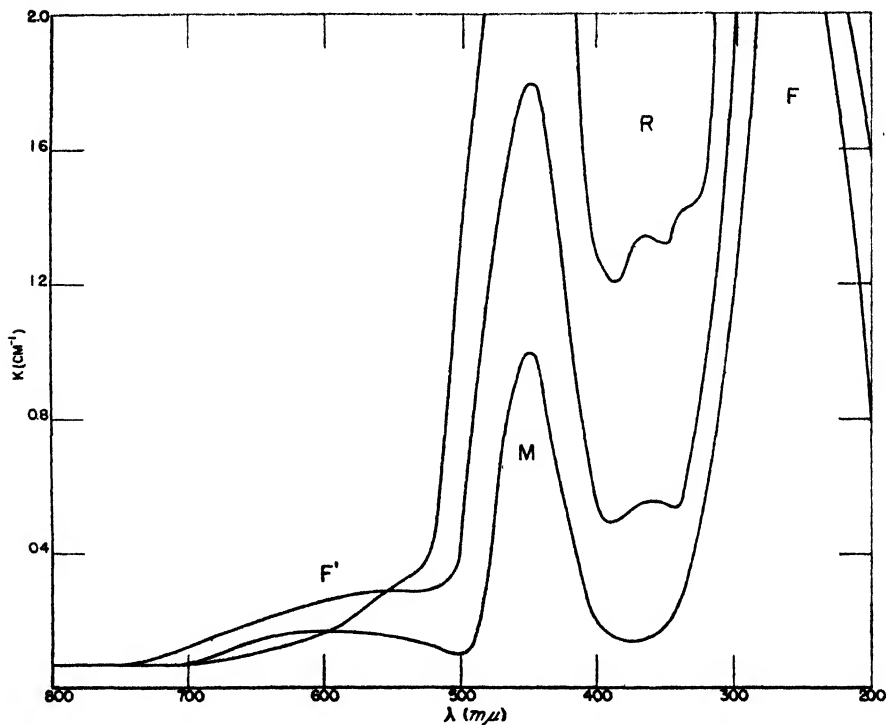


FIG. 3. Absorption spectrum of irradiated lithium fluoride

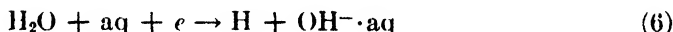
The situation in the vapor is not greatly different from that in the liquid. Using xenon as sensitizer, Günther and Holzapfel (6) found M/N for the decomposition by small dosages of x-rays to be as high as 1.0 (i.e., $G \approx 3$) with clear indication that the yield was greatly decreased by back-reaction. In the liquid, the magnitude of the observable effects depends not only on the radiation but on the method of detection of the effects. When heavy-particle radiation is employed, there is no difficulty in detection of decomposition, but reported data correspond to yields for decomposition, G (decomposition), ranging from 0.07 (deuteron

¹⁰ A. O. Allen, M. G. Bowman, J. W. Boyle, W. R. Burns, C. V. Cannon, S. G. Davis, R. Fearing, J. A. Ghormley, S. Gordon, R. C. Hirt, C. J. Hochanadel, J. P. Howe, R. Livingston, A. Krueger, A. J. Miller, R. A. Penneman, E. Shapiro, L. Treiman, and M. Tetenbaum.

bombardment) where the products are kept in solution¹¹ to 2.3 (alpha bombardment), where the gas is evolved at low pressure (2). With x-rays most investigators have failed to detect an effect, but values of G as high as 2 are reported when gas is evolved at low pressure (7). In the Plutonium Project it has been found that G (decomposition) on electron bombardment in a burst of 0.01 sec. is 0.5, based on hydrogen peroxide determination, with no oxygen formed. On the other hand, in continuous bombardment at low pressure large amounts of gas, including oxygen, are evolved and G (decomposition) is initially 0.3, decreasing to zero at relatively low gas pressure,¹² depending on the intensity of irradiation. The effect of fission recoils on pure water is not readily determinable. However, studies made in uranium solutions indicate an initial G (decomposition) value of 3. All the results are interpretable on the basis of the ideas of the primary effects already set forth. They are summarized by the forward reactions



and at a remote point



as well as the direct reaction in acidic system



The forward reaction



occurs on every collision, but the reaction



proceeds with some activation energy, E_a , and consequently conditions for the production of hydrogen peroxide will be most favorable in those special regions where OH exists in unusually high local concentration. This condition occurs most favorably in the ion track of heavy particles. The back-reaction



occurs with no E_a , and the recombination reaction



with but small E_a . Thus conditions which remove product gas instantaneously or favor reaction 9 and disfavor reaction 11 increase G (decomposition). The former favorable effect is seen in those cases of electron and x-radiation where the product gas is rapidly removed. Reaction 9 occurs most favorably on heavy-

¹¹ A. Krueger.

¹² J. A. Ghormley.

particle irradiation. When the exposure is rapidly interrupted, adequate time is provided for removal of hydrogen while OH is still at a low concentration, thus disfavoring reaction 11. In a detailed discussion of the influence of radiation on water, the effect of HO_2 , formed by the action of free H on O_2 , must be considered.

In general, it must be realized that in aqueous systems containing low concentration of solute or suspended (biological) material, the significant primary effects observed on the other component are those of the free atoms and radicals (including HO_2 when air is present or, after the initial stage, when oxygen has been produced).

ORGANIC MATERIALS¹³

Organic materials quite naturally have engaged the interest of many investigators far prior to this project. For example, the work of Schoepfle and Fellows with 170-kv. cathode rays (11) developed several significant points. In general,

TABLE 1
Irradiation of various hydrocarbons with 170-kv. cathode rays
(Schoepfle and Fellows: Ind. Eng. Chem. **23**, 1396 (1931))

HYDROCARBON	GAS OBTAINED IN 30 MIN.
	cc.
<i>n</i> -Hexane	57.6
<i>n</i> -Heptane	51.4
<i>n</i> -Octane	48.3
<i>n</i> -Decane.	41.6
<i>n</i> -Tetradecane	34.9

aromatic compounds yield less gas than do saturated aliphatics, while unsaturated aliphatics yield an intermediate quantity.

Data on similar substances of varying molecular weight indicate a "cage effect" of magnitude increasing with molecular size. Escape of large molecules from the cage becomes less probable and consequently there is less decomposition. However, this interpretation of the effect of molecular size must not be accepted too unwarily. An alternative explanation is given by a new principle involving the ionic discharge equation (equation 3) already discussed. The larger the molecule (AB) the less difference there will be between the atomic configuration of the ion and that of the uncharged molecule and the more likely will be discharge without decomposition. Table 1 illustrates the magnitude of this effect.

The effect of molecular configuration on the nature of the products is shown in some similar studies on octanes by the same authors. Table 2 shows a decrease of hydrogen yield with increasing complexity, while the yield of methane increases with number of methyl groups. The decrease in yield of hydrogen and increase in yield of non-volatile substances were not understood. Franck has

¹³ J. W. Burr, R. A. Day, J. V. Flanagan, W. M. Garrison, A. H. Germany, C. J. Hochanadel, A. J. Miller, and R. Schlegel.

now suggested an explanation based on increased probability of internal conversion with molecular complexity (see introductory remarks on photochemistry). With increased probability of internal conversion there should be less hydrogen production (which takes place largely *via* free atom splits) and greater opportunity for increased yield of large molecules (not radicals) as primary decomposition products in a manner similar to predissociation by rearrangement in photochemistry.

Measurement of the yield of gas alone tends to be a deceptive measure of the amount of chemical change in organic compounds. Table 3 summarizes briefly some detailed studies on the effect of 2.5 to 2.8 m.e.v. electrons on a selected variety of substances. The gas yield was substantially all hydrogen.

TABLE 2
Irradiation of some octanes with 170-kv. cathode rays
(Schoepfle and Fellows; Ind. Eng. Chem. **23**, 1396 (1931))

OCTANE	TOTAL GAS	H ₂	CH ₄	NON-VOLATILE
	cc	cc	cc.	cc
<i>n</i> -Octane ..	48.3	38.8	1.4	8.1
2,5-Dimethylhexane	49.8	21.0	5.8	23.0
2,2,4-Trimethylpentane ..	50.3	17.6	7.6	25.1

TABLE 3
*Effect of fast-electron irradiation on liquid hydrocarbons**

COMPOUND	<i>G_g</i> (MOLECULES GAS PER 100 E.V.)	<i>G_p</i> (MOLECULES LIQUID CONVERTED TO POLYMER PER 100 E.V.)
Benzene	0.04	0.5
<i>n</i> -Heptane ..	4.2	1.7
Cyclohexane	4.0	1.2
Cyclohexene	1.0	4.2
Methylcyclohexane ..	4.5	4.2
Toluene	0.09	0.7

* J. V. Flanagan, C. J. Hochanadel, and R. A. Penneman.

The results are not altogether startling. As might have been expected, the low yield of gas in the aromatic compounds did not completely represent the situation. Polymerization of a considerably greater order was simultaneously occurring. The result confirms a notion that the low yield of gas in the case of benzene is in part resultant from the frequent closely adjacent formation of C₆H₆ and C₆H₇ after the process of ionic discharge. The latter radicals may enter into "polymerization reactions" with each other as well as unconverted benzene molecules. The benzene case will be discussed in greater detail in a subsequent paper.

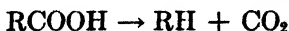
In general, it appears from table 3 that unsaturation tends to decrease the gas yield and to increase the degree of polymerization, while introduction of a

single aliphatic group into the benzene ring boosts the gas yield markedly. Unsaturated aliphatics tend to give lower gas yields, for the simple reason that unsaturated bonds tend to capture free atoms and radicals. This fact may be used to reduce gas yields in certain instances where hydrogenous materials are required but where gas production might be undesirable.

Recently, a group at the Massachusetts Institute of Technology (12) has been studying the effects of radon alphas and high-voltage deuterons on the decomposition of fatty acids. From the point of view of the simple principles with which this paper is concerned, their most important observation was the relative simplicity of the products from larger molecules. For example, hydrogen, carbon dioxide, carbon monoxide, and methane are all produced in *approximately* equal amount in the decomposition of acetic acid. When palmitic acid is reached, only the first two are among the major gaseous products; the liquid product is principally *n*-pentadecane. A naive examination of the problem would have led to the expectation of an increasingly wide variety of products with increase in size and complexity of the parent molecule. The converse phenomenon is, however, to be expected generally in radiation chemistry phenomena.

The principle involved in cases such as these is that already suggested in the interpretation of the results of table 1. The larger the molecule AB involved in reactions such as 3, the more closely does the atomic configuration of AB correspond to that of AB⁺. As a result, although after reaction 3 the molecule AB usually contains sufficient excess energy for rupture of one or more bonds, the energy is insufficiently localized for such rupture to occur within one vibration period. For rupture into free radicals or atoms energy must localize in the bond in a typical predissociation process (1), which may require 10⁻¹⁰ sec. or more. There are two results consequent on this fact.

In the first place, the process of relocation of the potential energy of the molecule (and ensuing rearrangement of the atoms) may lead to decomposition to ultimate molecules before rupture can occur. There is an increasing body of evidence that this is a very important process in many cases where free-radical decomposition had been assumed as the only important mechanism (*cf.* 4, 5). When rearrangement decomposition is concerned, it usually occurs by a preferred path, e.g., to form carbon monoxide and alkanes in decomposition of aliphatic aldehydes and ketones, and, apparently, in the decomposition of fatty acids to form carbon dioxide and the largest possible alkane in the primary act by the straightforward process



Another factor requiring consideration is the effect of liquid state upon the yield. Since internal conversion of energy and the ensuing predissociation process take >10⁻¹⁰ sec. and collision in the liquid occurs practically in every vibration period (≈10⁻¹³ sec.), there is a good probability that energy will leak from the excited molecule without decomposition. This is an old and well-understood phenomenon in reaction kinetics and photochemistry. It plays an important rôle in the radiation chemistry of large molecules because, to a greater extent than in the other cases, the potential energy is not localized in any part

of the molecule during the excitation process. Thus, decomposition yield in radiation-induced reactions of large molecules in the liquid state is considerably reduced and this reduction in yield occurs to a greater extent with increase in molecular size.

Consequently, we see well illustrated in radiation chemistry the principle of the effect of molecular size. It leads to the twofold conclusion that increase of molecular size decreases yield and increases the ratio of the relative probabilities of ultimate molecule decomposition by a preferred route and of free-radical decomposition by a variety of (almost indiscriminate) routes.

SUMMARY

In the atomic energy pile and in the subsequent processes for separation of plutonium and fission products from parent uranium, quantities and intensities of radiation far exceed those from any previously known natural source. The term "radiation," as here used, includes also high-energy particles; the radiations whose chemical effects had to be determined in advance of operations included betas, gammas, fast neutrons, and fission recoils as well as others. Sources of radiation used in the work included cyclotrons, Van de Graaff generators, betatrons, x-ray machines, and piles. A new *discomposition* effect in solids was discovered. Typical results on solids, water, and organic compounds are reported. The first important step (other than simple excitation) in radiation chemistry processes is ionic discharge. The ensuing chemical processes depend on the nature of the medium. There are three principles which seem to govern: the Franck-Condon principle, the principle of increased probability of internal conversion with increase in molecular complexity (Franck), and the principle that the ionic configuration is more nearly like that of the uncharged molecule the greater the size of that molecule. Illustrative examples are cited.

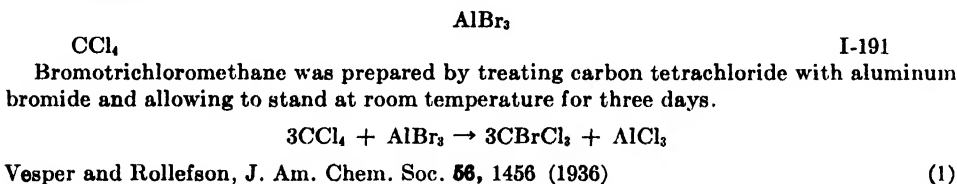
REFERENCES

- (1) Cf BURTON, M., AND ROLLEFSON, G. K.: J. Chem. Phys. **6**, 416 (1938).
- (2) DUANE, W., AND SCHEUER, O.: Le radium **10**, 33 (1913).
- (3) EYRING, H., HIRSCHFELDER, J. O., AND TAYLOR, H. S.: J. Chem. Phys. **4**, 479, 570 (1936).
- (4) Feldman, M. H., BURTON, M., RICCI, J. E., AND DAVIS, T. W.: J. Chem. Phys. **13**, 440 (1945).
- (5) GARRISON, W. M., AND BURTON, M.: J. Chem. Phys. **10**, 730 (1942).
- (6) GÜNTHER, P., AND HOLZAPFEL, L.: Z. physik. Chem. **B42**, 346 (1939).
- (7) GÜNTHER, P., AND HOLZAPFEL, L.: Z. physik. Chem. **B49**, 303 (1941).
- (8) LIND, S. C.: *The Chemical Effects of Alpha Particles and Electrons*, 2nd edition, The Chemical Catalog Company, Inc., New York (1928): (a) p. 100; (b) Chap. 11.
- (9) LIVINGSTON, M. S., AND HOFFMAN, J. G.: Phys. Rev. **50**, 401 (1936).
- (10) LOEB, L. B.: *Fundamental Processes of Electrical Discharge in Gases*, Chap. 1. John Wiley and Sons, Inc., New York (1939).
- (11) SCHÖEPFLE, C. S., AND FELLOWS, C. H.: Ind. Eng. Chem. **23**, 1396 (1931).
- (12) Cf. SHEPPARD, C. W., AND WHITEHEAD, W. L.: Bull. Am. Assoc. Petroleum Geol. **30**, 32 (1946).
- (13) SMYTH, H. D.: *Atomic Energy for Military Purposes*, 6.41, p. 104. The Princeton University Press, Princeton, New Jersey (1945).

NEW BOOKS

✓ *Encyclopedia of Chemical Reactions*. Vol. I. Aluminum, Antimony, Arsenic, Barium, Beryllium, Bismuth, Boron and Bromine. Compiled and edited by C. A. JACOBSON, Professor of Chemistry, West Virginia University. 804 pp. New York: Reinhold Publishing Corporation, 1946. Price: \$10.00.

The editor, the associate editors, and the staff of one hundred seventeen persons who have been assigned the task of preparing the abstracts deserve praise and gratitude from all chemists for making available a compilation of practically all the published chemical reactions of inorganic compounds, which are described briefly and expressed in equation form with a reference to the original literature. The manner of presentation is best illustrated by an example:



In this example, AlBr_3 is the reactant and CCl_4 the reagent.

In the Introduction the Editor-in-chief states, "We also want to apologize for the imperfections that may be found herein. The critic may take a more tolerant attitude when he realizes that the entire work was built by volunteer help, and that most of this help had very little previous training for the abstracting job."

Indeed, it is deplorable that Dr. Jacobson did not have at his disposal the aid of more skilled coöperators who could have presented the material in a more critical form (see, e.g., reactions I-4, and I-5, or still worse the formation of aluminum sulfide in reaction I-241 on page 74, or the compound $\text{Al}_2\text{O}_3 \cdot 6\text{HCN}$ in I-80 on page 38)

The presentation could have been simplified if reactions of the aquoaluminum ion had been given instead of the reaction of several aluminum salts in water with various reagents. In this connection the analytical chemist is disappointed in not having available the reaction of aluminum ions with a host of organic reagents. The precipitation of aluminum hydroxide from aqueous solutions of aluminum salts with various reagents is given in a very incomplete form. Again, all these reactions should be given under the heading of the aquoaluminum ion. The formation of aluminum lakes is not found in the book

For the other elements treated in Volume I similar shortcomings and omissions could be stated.

The book would gain in usefulness if all the information supplied by the abstractors were coördinated by experts. If this were done the book could develop into a monumental contribution to the inorganic chemical literature.

I. M. KOLTHOFF.

✓ *Reagent Chemicals and Standards*. By JOSEPH ROSIN. Second edition. x + 542 pp. New York: D. Van Nostrand Co., Inc., 1946. Price: \$7.50.

Approximately fifty new reagents have been added in the second edition of this book. Among these are aluminum oxide for chromatography and various organic reagents such as dithizone and *o*-phenanthroline. The book thus reflects some of the progress which has been made in the field of analysis in the ten years that have elapsed since the first edition appeared. Many of the directions for testing have been revised in accordance with more satisfactory procedures now available.

This work may be recommended as the most comprehensive of its kind. Completeness is an unattainable ideal in a book of this type, and one can hardly expect to find tests de-

scribed for all impurities that may be encountered in reagents. However, it would seem to be preferable in a future edition to include tests for specific heavy metals such as copper, zinc, and lead in a good many reagents for which only the general hydrogen sulfide test is given at present. Moreover, inclusion of directions for the assay of more organic reagents, such as dithizone and thioglycolic acid, would be helpful.

E. B. SANDELL.

Organic Chemistry. By PAUL KARRER, Professor at the University of Zurich. Second English edition (based on the eighth (1942) German edition), translated by A. J. Mee. 7 x 10 in.; 953 pp. New York City: Elsevier Publishing Company, Inc., 1946. Price: \$7.50.

Like its predecessor, this new edition of a well-known book presents in a descriptive way representative facts from the immense body of data considered of interest and importance by the classical organic chemist. In addition to covering fundamentals in a systematic and interesting fashion, it deals with probably a wider range of subjects than any other single volume on organic chemistry. Thus it is of value to a student or to a research worker who may wish to become acquainted with a field outside that in which he is expert. It contains comparatively few (166) references to the original literature, but this is more than compensated for by numerous references to texts in specialized subjects. It is well indexed.

In order to give the book its comprehensive character, some sacrifice in detail has necessarily been made, and a specialist may be disappointed with the treatment which has been given to the subject of his particular interest. Such disappointment will be least for a chemist dealing with natural products, and greatest for a physico-organic chemist, inasmuch as some topics (terpenes, sterols, vitamins, etc.) are particularly well done, while kinetics, thermodynamics, catalytic action, reaction mechanisms, electronic formulations, etc., are practically ignored.

The author's attitude toward theoretical discussions (and the level attained in them) is typified in the following quotation from the chapter on fuchsone dyes (page 592), concerning the structure of salts derived from aminotriphenylcarbinols.

"The problem resolves itself into whether the carrier of the positive charge in these compounds is nitrogen or carbon

"There is no space to discuss this question, which is not by any means solved. Indeed its importance is easily over-estimated. Both formulae (quinoid immonium salt and benzenoid carbonium salt), like all our structural formulae, can only give an approximate idea of the affinity relationships within the molecule, and leave out of consideration the forces between atoms which are not directly linked with each other. It is quite possible that in the dye salts and dye bases of the triphenylmethane dyes, in one case the nitrogen and in other cases the carbon gives up an electron, and thus becomes the bearer of the charge of the positive ion."

Such adherence to the principles of classical structural theory characterizes all of the author's work. In the book under consideration, this leads to an excellent organization of the material, and gives it both a form easily understood by any chemist and an aspect of comfortable authority.

Readers who are not able to carry on research themselves will find the book a valuable source of information within the limits noted above. Of those who are in a position to do original work, some will be stimulated by it to continue advances along classical lines, others to produce theoretical interpretations of data it contains.

The work of the translator, that of the composer, and that of the printer are of excellent quality.

C. F. KOELSCH.

Steroid Chains as Components of Protein and Carbon Molecules. By THEODORE VAN SCHELVEN. 15 x 25 cm.; 62 pp.; 3 fig. Amsterdam (Holland): Kosmos Publishing Company, 1946. Price: \$3.00.

The author of this booklet is a man of rare ability and unusual courage. In addition to the present volume he has turned out three other works under the following titles: *Weiss Magnetons as Components of Nuclear and Subnuclear Structures* (1945); *Experiments on the Presence of Carcinogenic Compounds in Human Surroundings* (1946); and *An Introduction to Definitive Philosophy and Basic Psychology* (1946).

van Schelven has recognized the incomplete state of our knowledge of protein structure and the difficulty of isolating these substances from their native habitats without modification. "Assuming that the protein has a regular structure and is built up of more or less congruent hydrocarbon units, the problem is to find the configuration in which the atoms of the amino acids in proteins may be arranged in a regular manner in some geometrical pattern." He suggests "that the native protein is a quadric structure." "This elongated, rectangular tube consists of 4 side walls, 4 flat steroid poly-chrysane chains, perpendicular to each other. Living protein may be a micellar aggregate of these prismatic, quadrangular, parallel molecular tubes arranged in a regular mosaic", etc. It is apparent that the author is entranced with the prevalence of six-membered rings in organic compounds and uses this common structural feature as a basis for the statement that steroids are "protein fossils" which conserve "many peculiarities typical for protein tetracts."

Unfortunately the author discusses a wide variety of topics only remotely related to the central thesis. Aside from a few typographical mistakes, the reader soon becomes aware of some obvious errors in the text. Steroids are written as polyhydrochrysanes rather than cyclopentanophenanthrenes, and proposals concerning the chemistry of tricyclo(2,2,2,2)-decane indicate a serious lack of background in fundamental organic chemistry.

His suggestion that "it may be possible to extend the physical theories of relativity, statistics, quanta, and wave mechanics to atoms underlying the phenomena of life" is well within the realm of possibility. Most readers, I believe, would be happy if, within their natural lifetimes, it will be possible to calculate "from scratch" the result of the simplest reactions of organic compounds.

In spite of the interesting geometrical pattern proposed for proteins in their native state, the reviewer found himself exhausted after being exposed to this maze of facts and fancies.

RICHARD T. ARNOLD.

✓ *Textbook of Physical Chemistry.* By SAMUEL GLASSTONE. Second edition. 6 x 9½ in.; xiii + 1320 pp. New York: D. Van Nostrand Co., Inc., 1946. Price: \$9.00.

In preparing the second edition of this well-known text, the author has introduced few important changes. The general organization is the same, and most of the chapters are substantially unchanged. The total number of pages has been increased from 1289 to 1320. A slight saving of space has been effected by reducing the scale of a few diagrams, particularly in the first chapter. The book has been "modernized" by introducing brief discussions of such topics as the meson, Nier's mass spectrograph, nuclear isomerism, plutonium, the atomic bomb, etc. The thermodynamic symbols and terminology have been altered to conform to the conventions of Lewis and Randall. One exception is that the term "thermodynamic potential" and the symbol μ have been retained in preference to Lewis' "partial molal free energy" and \bar{F} . In chapter VIII the present edition is in agreement with standard American usage in that the adjective molar is substituted for molecular, as in molar volume, molar refraction, etc. The order of presentation has been changed in the section on electromotive force and the discussion somewhat amplified. In several chapters the subheadings have been simplified. On the whole, the modifications are not of such a nature as to change the popularity of this text. Its supporters will probably remain as ardent as before and its critics as unconvinced of its merits.

The present edition is clearly printed on white opaque paper. One unfortunate consequence of the use of heavier paper is that the thickness of the volume has been increased from about 2½ to 3½ in., and its weight from 3½ to 5½ pounds. The present book is so unwieldy that it is to be hoped that thinner paper will be used in future editions and printings.

ROBERT LIVINGSTON.

Currents in Biochemical Research. DAVID E. GREEN, *Editor*. 486 pp. New York: Interscience Publishers, Inc., 1946. Price: \$5.00.

This volume consists of thirty-one chapters on particular fields of biochemistry. Each essay presents a condensed but very readable sketch of the current situation and many include suggestive speculations on possible future tendencies in the field. The authors, all of whom are specialists and current workers in their respective fields, have presented the material in lucid style and have generally omitted experimental details and data. However, in most cases ample citations are appended.

It is not possible to comment on the several chapters, but the scope of the collection is indicated by the titles. Genes and biochemistry are discussed by G. W. Beadle; the viruses by W. M. Stanley; photosynthesis and the production of organic matter by H. Gaffron; bacterial cells by René J. Dubos; the nutrition of plants by D. R. Hoaglund; the biological significance of the vitamins by C. A. Elvehjem; and vitamin research by Karl Folkers. The essay on quantitative analysis in biochemistry comes from the pen of D. D. Van Slyke. The field of the enzymes is considered under several captions: the peptide bond by J. S. Fruton, metabolic processes by F. Lipmann, carbon dioxide assimilation by S. Ochoa, mucolytic enzymes by K. Meyer, intermediate metabolism by K. Bloch, and a general survey of biochemistry from the enzymatic standpoint by the editor. The hormones are generally surveyed by B. A. Houssay, while G. Pincus describes the steroid hormones and K. V. Thimann writes on plant hormones. Fundamental redox principles are discussed by L. Michaelis and mesomeric concepts by H. M. Kalchauer. The applications of physical methods include viscometry by M. A. Lauffer, isotopic techniques by D. Rittenberg and D. Shemin, and x-ray diffraction on fibrous proteins by I. Fankuchen and H. Mark. Chemotherapy in cytochemistry is presented by R. D. Hotchkiss, immunochemistry by M. Heidelberger, the chemical mechanism of nervous action by D. Nachmansohn, biochemical antagonisms by D. W. Wooley, and biochemical aspects of pharmacology by A. D. Welch and E. Bueding. The subject of some biochemical problems posed by a disease of muscles is discussed by C. L. Hoaglund, and a general paper on physiology and biochemistry by C. H. Best covers the phases of biochemistry applied to medicine. The last two articles are wider in their scope: W. B. Sebrell discusses the social aspects of nutrition and L. C. Dunn has a stimulating article on the support and organization of science and research in the United States.

We commend the editor and the writers for a most readable, informative, and stimulating collection of essays.

W. M. SANDSTROM.

THEORY OF THE STABILITY OF LYOPHOBIC COLLOIDS¹

E. J. W. VERWEY

*Natuurkundig Laboratorium der N. V. Philips' Gloeilampenfabrieken,
Eindhoven, Holland*

Received November 14, 1946

Hamaker (4) has given a general theory of the stability of lyophobic colloids in terms of potential curves, giving the potential energy of two particles with respect to each other as a function of their mutual distance. He considered different types of potential curves, all being a superposition of an attractive potential due to London-van der Waals forces between the particles and a repulsive potential due to the interaction of the double layers surrounding the particles. He gave expressions for the London-van der Waals potential for various cases (two spherical particles, two parallel plates, etc.).

The theory of the interaction of the double layers, however, offered considerable difficulties. This is especially shown by the circumstance that later work by different authors led to completely divergent results. Hamaker gave only a rough estimate of the double-layer interaction potential but assumed it to be repulsive for all distances between the particles. Hamaker's conclusions have been challenged by Langmuir, who argues that a system of charged colloidal particles and oppositely charged counter ions will show an attraction between the particles for certain distances. An entirely different point of view is presented in the work of Levine and Dube, and in that of Corkill and Rosenhead. They consider different cases, but in both instances the conclusion is reached that even for the case of two particles, attractive forces may result from the double-layer interaction.

We have been reconsidering this problem (8, 9, 10, 11), and a brief outline of our results is given here. Full details are to be published in book form (12).

It occurred to us that the conclusions of those authors who find an attraction between the particles ought to be incorrect, as the net result of an interaction under reversible conditions will generally be a partial suppression of the double-layer charge. This will especially be true for lyophobic colloidal particles, for which the double-layer potential is fixed by the concentration of the potential-determining ions in the sol medium, and therefore will be independent of the particle distance. The double layer is formed autogenously when the particles are brought into contact with the solution. This formation is accompanied by a decrease of the free energy of the system. The interaction of two double layers must therefore be associated with an increase of the free energy, leading to a repulsion between the particles.

This could be confirmed quantitatively by a careful consideration of the free

¹ Presented at the Symposium on the Stability of Colloidal Dispersions, which was held under the auspices of the Division of Colloid Chemistry at the 110th Meeting of the American Chemical Society, Chicago, Illinois, September, 1946.

energy of a system of particles surrounded by an electrolytic double layer. The theory has been applied to a number of special cases, e.g., two flat plates parallel to each other, two spherical particles, and a hexagonal pattern of parallel cylinders. In most cases we started from the complete differential equation determining the electrical potential in the electrolytic solution in the neighborhood of the particles. For a single flat double layer this equation leads to the well known Gouy-Chapman theory of the diffuse double layer. In some cases we also tried a better approach to the electrical conditions in the double layer, similar to Stern's theory. In colloidal systems containing a small amount of electrolyte, the thickness of the double layer will generally be smaller than the particle dimensions. The linear approximation used in the Debye-Hückel

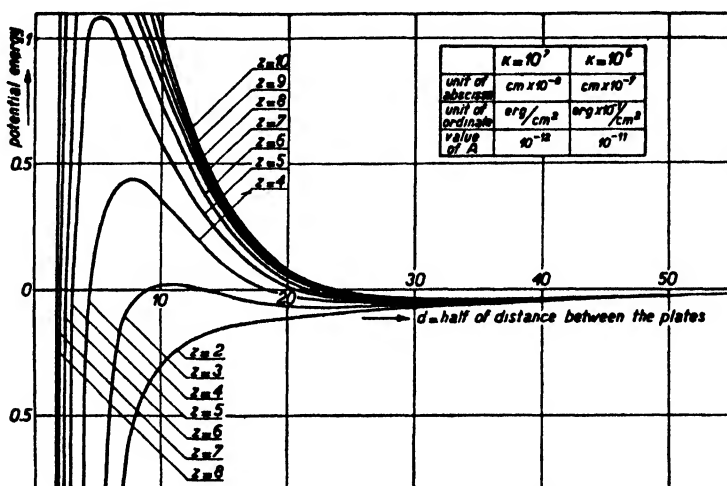


FIG. 1. Potential energy vs. distance for two parallel plates in a solution of monovalent ions, for different values of the double-layer potential, z , measured in units kT/e (see text).

theory of electrolytes cannot be applied in such systems, as it would lead to completely unsatisfactory results.

Calculating in this way the repulsive potential between the plates or particles, and adding the London-van der Waals attractive potentials as calculated by Hamaker, we found potential vs. distance curves of the type given in figure 1. The graph refers to the case of two parallel plates in a solution of monovalent ions and shows a set of curves with increasing values of the double-layer potential, z , measured in units kT/e ($z = 1$ means therefore 25.6 mv. at room temperature, $z = 2$ is 51.2 mv., etc.). The units of the coordinates depend on the electrolyte concentration, n , measured by Debye's well-known quantity $\kappa = (8\pi n e^2 / \epsilon kT)^{1/2}$; $\kappa = 10^7$ holds approximately for a 0.1 n solution, $\kappa = 10^6$ for 0.001 n , etc. A is a proportionality factor for the London-van der Waals potential; it will depend on the nature of the participating atoms, but for most colloidal systems it appears to be in the neighborhood of a few times 10^{-12} .

We note the following features:

1. For small values of the double-layer potential the London-van der Waals potential appears to prevail for all plate distances. The plates (or particles) will be attracted when they approach each other and the corresponding colloidal systems will flocculate.

2. For sufficiently large values of the double-layer potential the repulsion due to the interaction of the double layers appears to dominate for intermediate distances (in the neighborhood of $\kappa d = 1$) and the curves show a more or less pronounced maximum. The resulting potential barrier, if sufficiently high with respect to kT , will prevent agglomeration of the particles and the colloidal system will behave as a stable sol.

3. The curves showing a maximum have two regions for which the London-van der Waals potential again prevails: *viz.*, for very small distances, and for comparatively large distances.

The weak minimum at large distances will be of importance if its depth is larger than kT . The curves of figure 1 have been calculated under the assumption that the London-van der Waals potential between two atoms is proportional to r^{-6} . Later on, doubt arose as to whether this law would still be correct for large distances between the atoms, of the order of magnitude of the wave lengths corresponding to the fundamental frequencies of the atoms (say 10^{-5} cm.). Casimir has therefore reconsidered the theory of van der Waals forces, including retardation, and found that for large distances the potential decays much more rapidly (approaching an r^{-7} law). The actual minima are therefore still weaker than those in figure 1. Provisional calculations suggest that minima larger than kT can only be expected in certain favorable cases; for instance, in the case of blade-shaped particles (approximated by the case of two flat plates) or cylindrical particles of sufficient size when oriented parallel to each other. The phenomena observed in aged ferric oxide sols by Heller (5) and Zocher and in tobacco mosaic virus sols by Bernal and Fankuchen (1) must probably be explained in this way (formation of tactoids).

The theory shows that in systems containing sufficiently small amounts of electrolytes the height of the potential maximum may very easily reach a value of several times kT . The influence of the electrolyte concentration is shown by figure 2, for a rather low value of the double-layer potential ($z = 1$, i.e., the surface potential is 25.6 mv.). The graph refers to the case of two spherical particles with radius $a = 10^{-5}$ cm., using the London-van der Waals constant $A = 10^{-12}$; $s = R/a$ is the distance between the particle centers measured in units a . It is seen that with increasing values of κ , i.e., with increasing electrolyte concentration, the potential barrier shifts gradually to smaller particle distances and is finally entirely suppressed. This behavior is obviously associated with the circumstance that for larger electrolyte concentrations the charge in the liquid is so strongly concentrated in the neighborhood of the surface of the particles that the repulsive field of the double layers falls entirely within the attractive sphere of the van der Waals forces and can no longer be active.

The curves obtained for two spherical particles are not much different from

those for two flat plates, so that, especially if the particles are not extremely small, the case of two plates can often be used as a first approximation. For large values of the double-layer potential we may then derive a very simple expression for the electrolyte concentration for which the maximum in the potential curve touches the axis of abscissas, i.e., an approximate value of the electrolyte concentration for which the maximum will be insufficient to prevent agglomeration. This concentration is known as the flocculation value, and it is a well-known fact that it depends strongly on the valency of the ions with a

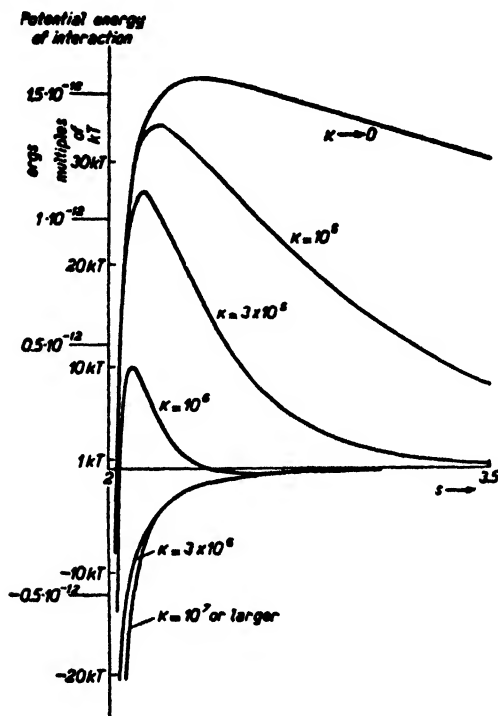


FIG. 2. Potential energy of interaction *vs.* distance between centers of two spherical particles (in units of particle radius $a = 10^{-5}$ cm., for $z = 1$), showing the influence of electrolyte concentration.

charge opposite to that of the particles (Schultze-Hardy rule). The simplified theory leads to the result that for monovalent, divalent, and trivalent ions the flocculation concentrations should be in a ratio

$$1:(1/2)^6:(1/3)^6 = 100:1.6:0.13$$

which is very close to the actual ratio found for all sorts of colloidal systems.

Although the theory appears to be in agreement with various colloid-chemical data, a large amount of work remains to be done to fit the complicated facts into the theory. One handicap in making comparisons with experimental data is that the potential drop in the diffuse layer has usually been calculated from elec-

trophoretic data. We know now that the ζ -potentials calculated in this way are more or less incorrect, because we cannot neglect the relaxation effect in electrophoresis. The interesting phenomena discussed by Stamberger (coagulation by stirring (7)) must be directly associated with this effect, as it seems rather certain that they must be explained by a local decrease of the potential barrier between the particles caused by a lagging behind of the charge in the liquid phase when a particle is in motion with respect to the surrounding liquid. The theory may be especially useful in considering in more detail the phenomena of thixotropy and tactoid formation as discussed by Heller (5). It seems worthwhile to study more closely the significance of the quantity ζ^2/κ put forward by Eilers and Korff, and discussed in the present symposium in the paper by Graham (3).

For further details we refer to the papers previously cited (8-12). There we have also considered extensively the work of previous authors, including some who have been mentioned above. We wish to add that an essentially correct theory for the interaction of two double layers can be found in earlier papers (2) by the Russian author Deryagin, though worked out in an unsatisfactory manner. It should also be mentioned that Langmuir, in the last part of his well-known paper (6) on tactoids and coacervation, gives a correct expression for the repulsive force between two plates, which can be directly derived from our more general theory.

SUMMARY

The theory of the interaction of the double layers has been reviewed in relation to the stability of lyophobic colloids. It is concluded that the interaction must be associated with an increase of the free energy, leading to a repulsion between the particles. The repulsive potential calculated from a consideration of the free energy for certain special cases has been combined with the London-van der Waals attractive potential calculated by Hamaker to obtain curves of potential *vs.* distance. Predictions based on these curves appear to agree well with various experimental data. For example, the influence of electrolyte concentration and of the valencies of the ions on flocculation is satisfactorily explained in terms of the theory, although many complicated phenomena remain to be correlated with it.

REFERENCES

- (1) BERNAL, J. D., AND FANKUCHEN, I.: *J. Gen. Physiol.* **25**, 111-20, 147 (1941).
- (2) DERYAGIN, B.: *Acta Physicochim. U.R.S.S.* **10**, 333 (1939); *Trans. Faraday Soc.* **36**, 203 (1940).
- (3) GRAHAM, D. P.: The Contribution of Solvation to the Stability of Anthraquinone Vat Dye Suspensions; Paper No. 32 of the Symposium on the Stability of Colloidal Dispersions, which was held under the auspices of the Division of Colloid Chemistry at the 110th Meeting of the American Chemical Society, Chicago, Illinois, September 1946.
- (4) HAMAKER, H. C.: *Chem. Weekblad* **35**, 47 (1938); (English language) Symposium on Lyophobic Colloids.
- (5) HELLER, W.: Thixotropy, Tactoid Formation, Syneresis, and Other Colloid Phe-

- nomena, and their Dependence on Colloid Stability; Paper No. 27 of the Symposium on the Stability of Colloidal Dispersions, which was held under the auspices of the Division of Colloid Chemistry at the 110th Meeting of the American Chemical Society, Chicago, Illinois, September, 1946.
- (6) LANGMUIR, I.: *J. Chem. Phys.* **6**, 873 (1938).
 - (7) STAMBERGER, P.: Flocculation of Lyophobic Dispersions by Slow Mechanical Stirring; Paper No. 33 of the Symposium on the Stability of Colloidal Dispersions, which was held under the auspices of the Division of Colloid Chemistry at the 110th Meeting of the American Chemical Society, Chicago, Illinois, September, 1946.
 - (8) VERWEY, E. J. W.: *Chem. Weekblad* **39**, 563 (1942).
 - (9) VERWEY, E. J. W.: Contribution to a symposium held by the Nederlandsche Chemische Vereniging on July 3-4, 1944.
 - (10) VERWEY, E. J. W.: *Philips Research Reports* **1**, 33 (1945).
 - (11) VERWEY, E. J. W., AND OVERBEEK, J. TH. G.: *Trans. Faraday Soc.*, in press.
 - (12) VERWEY, E. J. W., AND OVERBEEK, J. TH. G., with the collaboration of K. van Nes: *Theory of the Stability of Lyophobic Colloids*, in press. Elsevier Publishing Company, Amsterdam, Holland.

THE USE OF MEMBRANE ELECTRODES IN THE STUDY OF SOAP SOLUTIONS¹

C. W. CARR, W. F. JOHNSON, AND I. M. KOLTHOFF

*School of Chemistry, Institute of Technology, University of Minnesota,
Minneapolis, Minnesota*

Received November 14, 1946

I. INTRODUCTION

In studies of the properties of soap solutions several different physicochemical methods have been applied. These methods include such diverse measurements as that of the electrical conductance, the degree of solubilization of an oil or dye, the freezing-point lowering, the viscosity, and the surface tension of the solutions. The present paper is concerned with the use of recently developed membrane electrodes (1, 2, 4, 8) for the determination of the cation and anion activity in soap solutions. The collodion membranes are negatively charged in electrolyte solutions and behave as electrodes for cations in much the same way as the glass electrode behaves toward hydrogen ions. Similarly, the protamine-collodion membranes, being positively charged, behave as anion electrodes. These membranes differ from the glass electrode in that they are not specific for any one ion. For that reason they cannot be used for determining directly the activity of one ion in the presence of another of the same sign. However, they have been applied with success to a number of solutions containing a single electrolyte (3).

Since the membranes are not always perfectly selective, especially at concen-

¹This investigation was carried out under the sponsorship of the Office of Rubber Reserve, Reconstruction Finance Corporation, in connection with the synthetic rubber program of the United States Government.

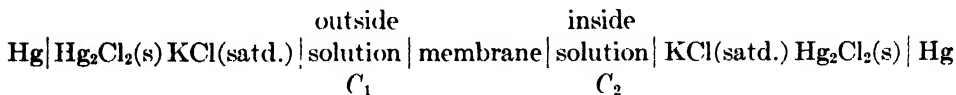
trations above 0.05 *N*, the simplest method to determine ionic activities is by means of a potentiometric titration. The solution of unknown concentration is placed on one side of the membrane and a known volume of water on the other side. A strong solution of known concentration of an electrolyte which has the ion whose activity is to be determined in common with the electrolyte studied is added to the water from a buret. It is not necessary that the ions of opposite charge in the unknown and known be the same. After each addition of electrolyte the membrane potential is measured, and the addition of electrolyte is continued until the potential changes in sign. The point of zero potential indicates that the activity of the ion being measured is the same on both sides of the membrane. At the point of zero potential the activity of the ion under consideration is equal to that of the same ion in the outside solution. From the volume and concentration of strong electrolyte added to a given volume of water the concentration of this electrolyte at the zero-point potential is calculated, and from this concentration the activity of the ion under investigation is estimated.

EXPERIMENTAL PROCEDURE

The membranes used in this work were prepared as described by Sollner and coworkers (1, 2, 4, 8). They are bag-shaped, being formed over 25 x 100 mm. test tubes, and hold about 30 ml. of solution.

A known volume of water is added to a beaker of such size that the beaker is about one-half to two-thirds filled. In most of the experiments a 250-ml. beaker filled with 150 ml. of water was used. Next, the membrane is filled with the solution to be investigated. About two-thirds of its length is immersed in the beaker containing the water, and the membrane is then clamped in position. For a clamp a wooden test tube holder held to a ring stand with a right-angle clamp is convenient.

The temperature is measured and titration is started. The electrolyte solution used as titrant should be at least ten times as concentrated as the solution being titrated, to avoid the addition of excessively large volumes needed to reach the end point. After each addition the E.M.F. of the system is determined:



In our measurements a Leeds & Northrup Type K potentiometer was used. The saturated calomel electrodes are connected with the two solutions by means of specially constructed agar bridges saturated with potassium chloride. These bridges are made with 3-mm. glass tubing, and the tips which make contact with the solutions are about 1 mm. in diameter. The small contact area is necessary to minimize the diffusion of potassium chloride into either solution. To minimize this diffusion still further, the bridges are removed from the two solutions after each measurement of the potential and placed in saturated potassium chloride solution. Just before use they are wiped dry and placed in the solutions being measured.

As more and more electrolyte is added to the outside solution, the potential decreases until it reaches zero, changes sign, and begins to increase. The end point, which is the point of zero potential, is determined graphically. The membrane potential is plotted on the linear axis of semilogarithmic paper and the concentration of the outside solution is plotted on the logarithmic axis.

The slope of the lines obtained with the negative membranes is close to 55 mv. at 25°C. for a tenfold change in concentration when the membranes are perfectly cation-selective. Since this is not always true, especially at concentrations above 0.05 *M*, the slopes will tend to be slightly less than 55 mv. With the positive membranes the largest slope that has been obtained is 53 mv. For the titrations with either type of membrane it is not necessary that the maximum slope be obtained. It is only necessary that it be constant in the concentration range near the end point.

Materials used

The soap solutions used were in all cases prepared by the neutralization of the fatty acid with an equivalent amount of standard aqueous base. The capric, lauric, and myristic acids were obtained from the Eastman Kodak Company. The oleic acid was a sample of 97 per cent purity supplied to us by Dr. W. C. Ault of the Department of Agriculture, Eastern Regional Research Laboratory. The sodium rosinate was made from a sample of dehydrogenated rosin acid, obtained from the Hercules Powder Company, which was mostly a mixture of dihydroabietic acid, tetrahydroabietic acid, and dehydroabietic acid.

EXPERIMENTAL RESULTS

The first titration carried out was with a solution of sodium laurate of known concentration. Freshly prepared 0.01 *M* sodium laurate was placed inside a negative membrane, and a known volume of water was placed outside, using 0.1 *M* sodium laurate as the titrating solution. The results are plotted graphically in figure 1. The concentration of sodium laurate in the outside solution at the end point is found to be 0.0101 *M*, in good agreement with the known concentration (0.0100 *M*) of the inside solution.

To determine whether or not the counter ion was of any influence in these dilute solutions, another titration was carried out using 0.02 *M* laurate in the inside and 0.2 *M* sodium chloride instead of laurate as the titrating solution. The results are also shown in figure 1. In this titration the concentration of sodium chloride at the end point was found to be 0.0201 *M*. Thus the sodium-ion activity in 0.0200 *M* sodium laurate is the same, at least within 1 or 2 per cent, as in 0.0200 *M* sodium chloride.

After these preliminary experiments the cation activity of several soap solutions was determined. The solution in question was titrated with standard sodium or potassium chloride solution. A sample calculation of the cation activity coefficient is as follows: In the titration of 0.1 *M* sodium laurate the concentration of sodium chloride at the end point was 0.0512 *M*. The sodium-ion activity in this solution is 0.0430. The activity coefficient of the sodium ion in 0.1 *M* sodium laurate then is $0.043/0.1 = 0.43$.

The results obtained with the several soap solutions are shown in figure 2, in which the activity coefficient of the cation is plotted against concentration. A similar curve for sodium chloride is also included for comparison. The values used for this electrolyte are those given by Lewis and Randall (5).

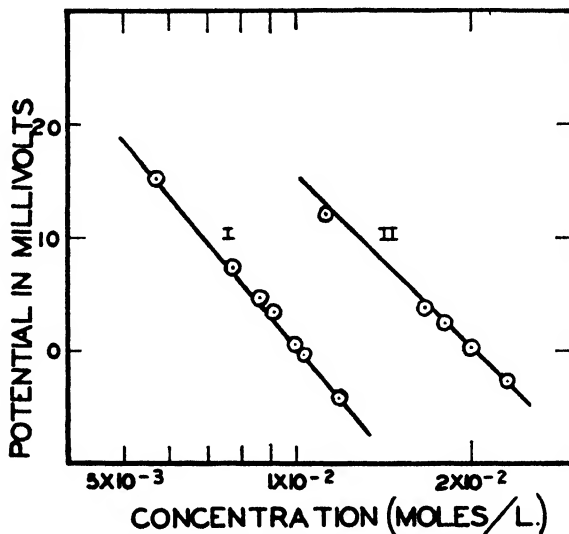


FIG. 1. Potentiometric titrations of sodium laurate solutions with the use of membrane electrodes. Curve I, 0.01 *M* sodium laurate titrated with 0.1 *M* sodium laurate; curve II, 0.02 *M* sodium laurate titrated with 0.2 *M* sodium chloride.

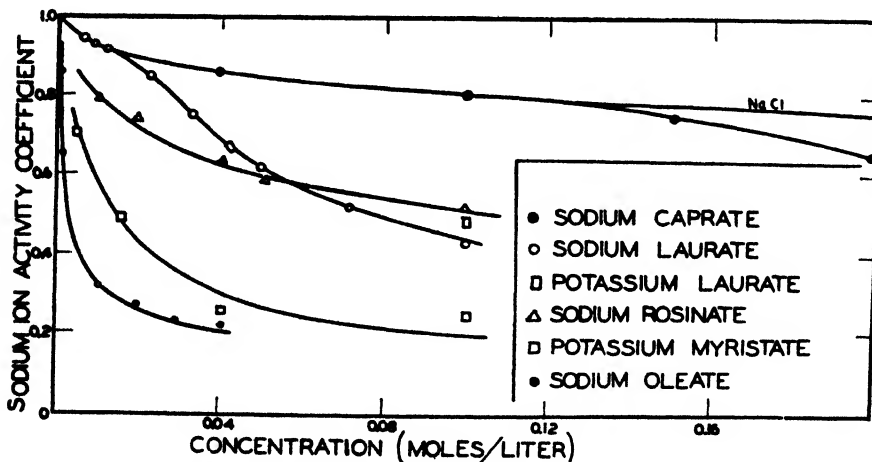


FIG. 2. Sodium-ion activity coefficients in various soap solutions

The curves in figure 2 show that the cation activity in soap solutions below the critical point is the same as in solutions of strong uni-univalent electrolytes. When the critical point is reached, however, the cation activity begins to drop below that of a strong uni-univalent electrolyte. This drop in activity indicates

that as the soap concentration increases beyond the critical concentration a large fraction of the sodium ions becomes inactivated with the formation of lamellar micelles and does not contribute to the sodium-ion activity measured in the soap solution.

A rough estimate of the activity of the sodium ions in the dissolved soap micelles can be made as follows. The critical concentration of sodium laurate is approximately 0.02 *M*. The activity coefficient of sodium ions in this solution corresponds to an activity of sodium ions of 0.018. In the concentration range between 0.02 *M* and 0.04 *M* sodium laurate, the activity of the sodium ions increases from 0.018 to 0.027. Assuming that the un-micellized concentration of sodium laurate remains unaltered above the critical concentration, we find that an increase of the concentration of the micellized soap from 0 (0.02 *M* sodium laurate) to 0.02 (0.04 *M* sodium laurate) gives rise to an increase in the sodium-ion activity of 0.009. This would correspond to an "average activity coefficient" of the sodium ions of the micellized soap of 0.45. Making similar calculations

TABLE 1

The critical concentration in several soap solutions as determined by two different methods

SOAP	MEASUREMENT OF Na ⁺ ACTIVITY	COAGULIZATION OF DMAB
Sodium caprate.	0.10	0.105
Sodium laurate.	0.02	0.023
Potassium myristate	0.003	0.005
Sodium oleate	<0.001	<0.001
Sodium rosinate	—	—

over the ranges 0.04–0.06 *M*, 0.06–0.08 *M*, and 0.08–0.10 *M*, we find values for such "activity coefficients" of 0.35, 0.25, and 0.20, respectively.

It should be realized that these values are only very approximate and that part of the un-micellized soap may become micellized above the critical concentration. However, the figures show that a large fraction of the sodium ions becomes inactive when the concentration of the soap micelles increases.

In earlier work McBain and Betz (6) and McBain and Williams (7) have measured the hydrogen-ion activity in micellized solutions of sulfonic acids. The hydrogen-ion activity coefficient decreased much more abruptly and to much lower values than in corresponding concentrations of hydrochloric acid, but there was no indication that the activity coefficient of the hydrogen ion shows an abrupt decrease at the critical concentration.

In order to show that equilibrium is established quickly when a micellized soap solution is diluted below the critical concentration, a reverse titration was carried out in which 0.01 *M* sodium chloride was placed inside of a membrane and water outside. As titrating solution 0.2 *M* sodium laurate was used. From the measured potential after each addition of sodium laurate, the sodium-ion activity for the sodium laurate at the several different concentrations was calcu-

lated. The equation² used in this calculation is

$$E \text{ (mv.)} = 59.1 \log_{10} \frac{(A_{\text{Na}^+})_i}{(A_{\text{Na}^+})_0}$$

The complete titration was carried out in 20 min., the final concentration of sodium laurate in the outside solution being 0.1 *M*. When the sodium-ion activity coefficient was plotted against concentration, the curve obtained was identical with the curve given in figure 2 with sodium laurate as the inside solution.

When the concentration of the soap is increased above the critical concentration, equilibrium is also established rapidly.

It was of interest to measure the change of the anion activity in solutions of sodium laurate and caprate by using positive protamine-collodion membranes. These investigations are of a preliminary nature only. The results are reported below.

In a typical experiment 0.002 *M* sodium laurate was used in the inside of the membrane. To a given volume of water on the outside of the membrane known volumes of 0.2 *M* sodium laurate were added from a buret, and the E.M.F. of the cell was measured after each addition. The results are presented graphically by curve I of figure 3. The slope of the curve is 53 mv. for a tenfold change in concentration, the maximum that can be obtained with the protamine-collodion membrane using strong electrolytes. Also the point of zero potential (end point) was reached when the concentration of the second solution became equal to 0.002 *M*. As the concentration in the second solution was increased further, the slope of the curve began to decrease markedly and finally changed sign at 0.005 *M*. At about 0.02 *M*, zero potential was reached again, and further increase of the concentration resulted in a continued change of the E.M.F. in the same direction. Curves II and III obtained with 0.008 *M* sodium caprate and 0.02 *M* sodium caprate, respectively, in the inside of the membrane showed a behavior very similar to that found with the sodium laurate. In these experiments the titrations were made with 0.2 *M* sodium caprate. From the E.M.F. of the cell the laurate-ion activity has been calculated at different concentrations of sodium laurate, and this activity is plotted in figure 4 against the soap concentration.

It is seen that the activity goes through a maximum at about 0.006 *M*. The anionic activity in 0.02 *M* sodium laurate is apparently the same as in 0.002 *M* sodium laurate, and the activity in 0.03 *M* sodium laurate is considerably less than in 0.003 *M* sodium laurate.

The results cannot be interpreted at present in a satisfactory way. From solubilization and other methods it is quite evident that the critical concentration of sodium laurate is 0.024 *M*; therefore, one would expect that the laurate-

²This calculation is not exact, especially when the ratio of the sodium activities is greater than 5. In addition to the possible imperfect selectivity mentioned above, there is a small error in the measured value of *E*, owing to diffusion potentials at the agar bridge-solution interface.

ion activity in 0.02 *M* sodium laurate solution would be about equal to that of the sodium ions. Actually, the experiments indicate that the laurate-ion activity in 0.02 *M* solution is only 0.0018, whereas the sodium-ion activity is about 0.017.

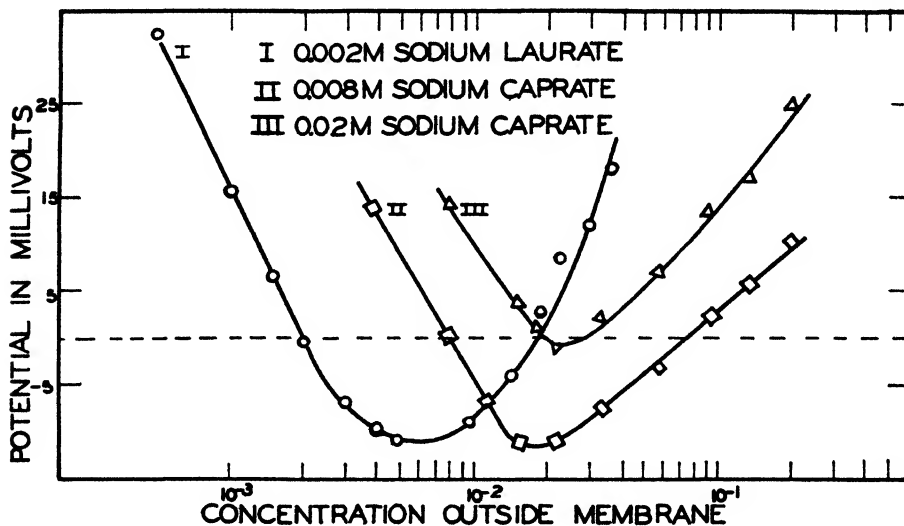


FIG. 3. Potentiometric titration of the anions in solutions of sodium laurate and sodium caprate.

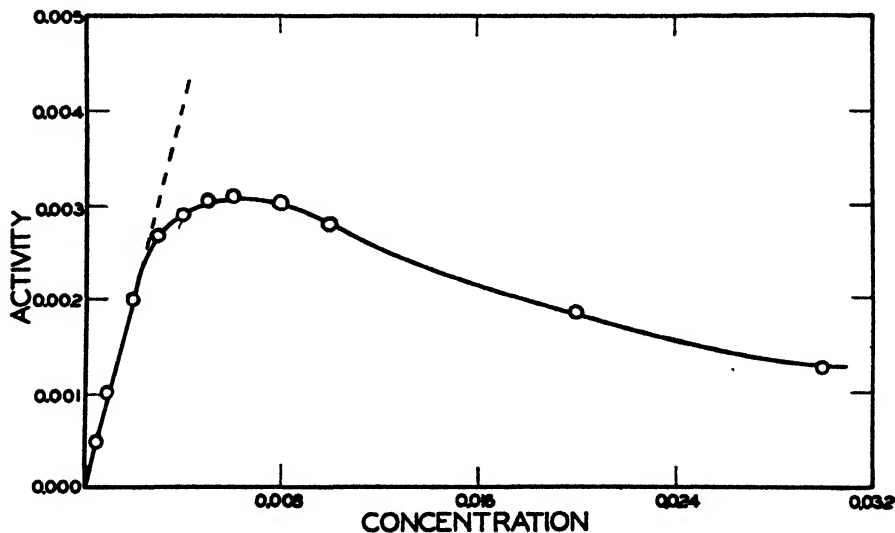


FIG. 4. Comparison of the anion concentration and apparent activity in solutions of sodium laurate (as determined with protamine-collodion membranes).

The considerable association of the anions below the critical concentration as indicated by the positive-membrane E.M.F. measurements is not found by other physical chemical properties. The E.M.F. measurements indicate that the

activity of the caprate ions in 0.1 *M* sodium caprate is equal to only 0.007. Such a low activity would correspond to a very high degree of association of the anions. On the other hand, the freezing point of 0.1 *M* sodium caprate was found to be practically identical with the freezing point of 0.1 *M* sodium chloride, indicating that at 0.1 *M* concentration the sodium caprate still behaves like a strong uni-univalent electrolyte. This disagreement casts some doubt on the reliability of the anion activity in soap solutions as measured by the positive collodion membranes. The membranes were tested by using solutions of sodium acetate and were found to behave normally. The acetate solutions had a pH close to 7, as they had not been prepared in carbon dioxide-free water. There is a possibility that the high pH in the soap solutions is responsible for the abnormal behavior found, though it is difficult to account for the fact that up to approximately 0.015 *M* sodium caprate the anion activity was the same as in a strong uni-univalent electrolyte of the same concentration. It seems unlikely that the peculiar results can be attributed to the fact that the positive membranes are being discharged by the soap anions, because the membranes obtained their final potential almost immediately after changing the soap concentration on the outside of the membrane. Upon removal from the soap solution the membranes functioned normally with solutions of ordinary uni-univalent strong electrolytes.

It is planned to investigate the positive membranes in non-hydrolyzed solutions of sodium alkyl sulfates and sulfonates in order to test whether the high concentration of hydroxyl ion is responsible for the behavior of the positive membranes.

SUMMARY

Recently developed collodion membranes have been used to determine ion activities in fatty acid soap solutions.

With the use of negative collodion membranes the cation activity in solutions of sodium and potassium soaps has been determined over wide ranges of concentration. It has been found that up to the critical point in a given concentration of a soap, the cation activity is the same as that at the same concentration of alkali chlorides. At the critical concentration the cation activity coefficient begins to decrease markedly with a further increase in concentration. This behavior is in accordance with what would be predicted from other measurements of physical properties of soap solutions, such as conductance and freezing-point lowering.

A few measurements have also been made with positive collodion membranes of the activity of the anions in dilute solutions of sodium laurate and sodium caprate. From these experiments it is indicated that in very dilute solutions the apparent anion activity changes in the same way as in solutions of strong uni-univalent electrolytes. However, long before the critical concentration is reached the apparent anion activity decreases very strongly. Further studies are planned to test the positive membranes for use with soap solutions.

REFERENCES

- (1) CARR, C. W., GREGOR, H. P., AND SOLLNER, K.: *J. Gen. Physiol.* **28**, 179 (1945).
- (2) CARR, C. W., AND SOLLNER, K.: *J. Gen. Physiol.* **28**, 119 (1944).
- (3) GREGOR, H. P.: Ph. D. Thesis, University of Minnesota, 1945.

- (4) GREGOR, H. P., AND SOLLNER, K.: J. Phys. Chem. **50**, 53, 88 (1946).
- (5) LEWIS, G. N., AND RANDALL, M.: *Thermodynamics*, p.382. McGraw-Hill Book Company, Inc., New York (1923).
- (6) McBAIN, J. W., AND BETZ, M. D.: J. Am. Chem. Soc. **57**, 1905 (1935).
- (7) McBAIN, J. W., AND WILLIAMS, R. C.: J. Am. Chem. Soc. **55**, 2250 (1933).
- (8) SOLLNER, K.: J. Am. Chem. Soc. **65**, 2260 (1943).

A LIMITATION OF THE DETERMINATION OF SURFACE AREA BY THE "POINT B" METHOD^{1, 2}

LOCKE WHITE, JR.

Southern Research Institute, Birmingham, Alabama

Received November 20, 1946

In the first successful method of the determination of surface area by the physical adsorption of gas, Emmett and Brunauer (3) established empirically that the beginning of the straight-line portion of the standard S-shaped adsorption isotherm corresponded to unimolecular covering of the surface of the adsorbent. Subsequently, these authors, together with Teller (2), developed a theory of multimolecular physical adsorption which predicted that a straight line should result if the data were plotted in a specified form, and that both the heat of adsorption and the volume corresponding to unimolecular covering of the surface could be calculated from the slope and intercept of the line. Surface areas determined by the empirical method, commonly referred to as the "point B" method, and by the theoretical (or B.E.T.) method were found to be in satisfactory agreement.

The B.E.T. method is usually to be preferred for surface-area measurements. A relatively small number of points is sufficient to determine the straight line, whereas the precise location of point B requires a large number of measurements. In some cases, in which the isotherm is convex to the pressure axis even at low pressures, point B cannot be located at all, but the B.E.T. method still gives useful results.

It has thus far been assumed in the literature that the methods are of equivalent accuracy, so long as an S-shaped isotherm is available. The purpose of this paper is to indicate that the existence of an S-shaped isotherm in physical adsorption is not a sufficient condition that point B correspond to unimolecular covering of the surface. The discrepancy was first observed experimentally, in a case in which the surface areas calculated by the two methods differed in the

¹ The work reported here was part of a project sponsored by Core Laboratories, Inc., Dallas, Texas.

² Presented at the Symposium on Gas Adsorption, which was held under the auspices of the Division of Colloid Chemistry at the 110th Meeting of the American Chemical Society, Chicago, Illinois, September, 1946.

ratio of about three to two. The theory of multimolecular adsorption was then examined in an attempt to establish the conditions under which the two methods would agree.

No rigorously straight region is exhibited when the adsorbed volume is plotted as a function of pressure in the ordinary isotherm, on the basis of the B.E.T. equation. Expressed analytically, in no extended region is $\partial V/\partial P$ recognizably constant, and therefore the B.E.T. theory makes available no analytical expression for the location of point *B*. However, an upper limiting value for point *B* is given by the inflection point of the curve. That is, point *B* must necessarily be lower than the inflection point, and whatever maximum conditions apply to the location of the inflection point must also apply to point *B*.

Let us express the B.E.T. equation in the following form:

$$V = \frac{V_m C \phi}{(1 - \phi)[1 + (C - 1)\phi]} \quad (1)$$

with

$$\phi = P/P_0$$

and

$$C = \frac{a_1 b_2}{a_2 b_1} \exp (E_1 - E_L)/RT \sim \exp (E_1 - E_L)/RT$$

From this, we derive that

$$\partial^2 V/\partial \phi^2 = 2V_m C \left[\frac{(C - 1)^2 \phi^3 + 3(C - 1)\phi - C + 2}{\{(1 - \phi)[1 + (C - 1)\phi]\}^3} \right] \quad (2)$$

Since *C* can be zero only in a trivial case, and since the denominator can not become infinite, the inflection point, at which $\partial^2 V/\partial \phi^2$ is zero, must be located where ϕ satisfies the condition that

$$(C - 1)^2 \phi^3 + 3(C - 1)\phi - C + 2 = 0 \quad (3)$$

The physical meaning of ϕ requires that the solution of interest here be located in the range $0 \leq \phi \leq 1$.

We are concerned here with the ratio of the volume adsorbed at the inflection point to that adsorbed at unimolecular covering, which ratio we call V_i/V_m . The point *B* method is accurate when V_B/V_m is unity (V_B being volume adsorbed at point *B*). But since $V_i > V_B$, only when V_i/V_m is somewhat greater than unity can the point *B* method be valid.

Because there is no simple expression for V_i/V_m as a function of *C*, the dependence is shown in figure 1, obtained by solving equation 3 for each of several values of *C*, and by substituting these values of ϕ into the B.E.T. equation to obtain V_i/V_m for corresponding values of *C*. This plot indicates that the point *B* method is distinctly in error when $C \leq 9$, and is in question when *C* is somewhat larger. Actually, however, the range of values of *C* for which the point *B* method may be in error is not wide, its lower limit being determined by the fact that

the isotherm, when C is as low as about 5, is so nearly convex over its entire length that point B can not be located. As C becomes larger, the transition from concave to straight region becomes more clearly marked. Thus, the sharper is the transition, the more confidence one may place in the point B method.

That the discrepancy does exist is shown in figure 2, the isotherm for carbon tetrachloride on a sample of sandstone at 0°C . Included in the graph are both

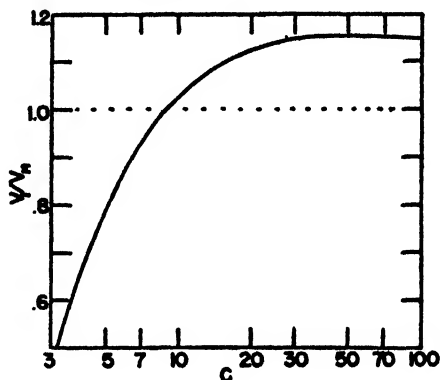


FIG. 1. Ratio of volume adsorbed at inflection point of isotherm to volume adsorbed at unimolecular covering, as function of C .

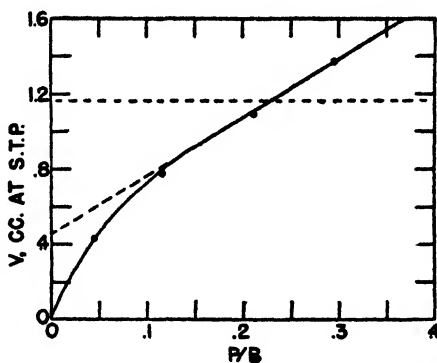


FIG. 2. Adsorption isotherm of carbon tetrachloride on sandstone at 0°C .

the experimental points and the curve calculated from the B.E.T. theory, using for V_m and C the values determined from the B.E.T. treatment of the experimental data. These values are $V_m = 1.66$ cc. at S.T.P., and $C = 11.38$. The dotted line is at $V = V_m$. It is clear that the experimental isotherm is in agreement with that predicted by B.E.T. theory, and yet that the adsorbed volume at point B is distinctly less than V_m .

A similar case occurred among the comparisons quoted by Brunauer, Emmett, and Teller in their first paper on multimolecular adsorption (2). V_m for butane on a sample of silica gel was 28.1 cc. by the empirical method and 58.2 cc. by the

theoretical. At that time the authors stated that they had no explanation for the discrepancy. Brunauer (1), in his book on physical adsorption, attributes it to the difficulty in locating point *B*. In this case *C* was only about 4.6, and it is true that point *B* could hardly be located with any confidence. But it is also clear from the treatment given here that a somewhat larger value of *C* would have produced a fairly distinct point *B*, which, however, would have led to an erroneous value for V_m .

It is interesting to observe that the value of *C* is also the limiting factor in an experimental simplification proposed by Brunauer and Emmett. In determining surface area it is usually valid, they say, to take a single point at a relative pressure of about 0.3, and to use it and the origin to determine the straight line of the B.E.T. method. If such a procedure is employed, using a point at a relative pressure of 0.3, we may express the apparent slope of the B.E.T. line by the following method:

Since

$$\begin{aligned}\frac{\Delta y}{\Delta x} &= \frac{\text{intercept} + (\text{true slope})\Delta x}{\Delta x} \\ \text{Apparent B.E.T. slope} &= \frac{1/V_m C + (0.3)(C - 1)/V_m C}{0.3} \\ &= \frac{C + 2.33}{V_m C}\end{aligned}$$

Then, since V_m is the reciprocal of the sum of the slope and the intercept of the line, we obtain for the apparent V_m :

$$V'_m = V_m \frac{C}{C + 2.33}$$

Thus the accuracy of the simplification is determined by the value of *C*.

SUMMARY

Because the B.E.T. equation permits no analytical location of point *B*, the inflection point of the isotherm is taken as an upper limiting value for point *B*. The volume adsorbed at the inflection point is greater than V_m only when *C* > 9. Therefore, the point *B* method is accurate only when *C* is somewhat larger than 9.

REFERENCES

- (1) BRUNAUER, S.: *The Adsorption of Gases and Vapors*, Vol. I, p. 292. Princeton University Press, Princeton (1945).
- (2) BRUNAUER, S., EMMETT, P. H., AND TELLER, E.: J. Am. Chem. Soc. **60**, 309 (1938).
- (3) EMMETT, P. H., AND BRUNAUER, S.: J. Am. Chem. Soc. **59**, 1553 (1937).

SOLUBILITY OF CERTAIN AMINO ACIDS IN AQUEOUS SOLUTIONS OF AMINO ACIDS AND PEPTIDES^{1,2}EDWIN L. SEXTON³ AND MAX S. DUNN*Department of Chemistry, University of California, Los Angeles, California**Received October 22, 1946*

It has been pointed out by Cohn (4) that small molecules of known structure should be investigated as a necessary first step toward an understanding of the interactions of ions and dipolar ions in biological systems. Simple systems of this type which have been studied by Cohn and coworkers (5, 6) include: asparagine with alanine, glycine, α -amino-*n*-butyric acid, diglycine, and lysyl-glutamic acid; cystine with glycine, alanine, α -amino-*n*-butyric acid, diglycine, and valine. The solubility relations of the analogous systems norvaline with glycine and glutamic acid with glycine, diglycine, and triglycine have been investigated in the present work.

PREPARATION OF AMINO ACIDS AND PEPTIDES

Glycine: Commercial material was recrystallized three times from water and alcohol. Analysis: less than 0.004 per cent of chloride, P_2O_5 , heavy metals, iron, or ammonia. N (Kjeldahl): milliequivalents found, 2.266; milliequivalents calculated, 2.266.

l(+)-Glutamic acid: Commercial monosodium glutamate was converted to *l(+)*-glutamic acid and the latter was recrystallized twice from water and twice from water and alcohol. Analysis (formol titration with the glass electrode): milliequivalents found, 2.378; milliequivalents calculated, 2.379. The specific rotation in 6 *N* hydrochloric acid given below agreed closely with the values obtained with other samples of purified *l(+)*-glutamic acid prepared in the authors' laboratory.

$$[\alpha]_D^{22.4} = \frac{+1.265 \times 100}{4.00 \times 1.0125} = +31.30^\circ$$

dl-Norvaline: The synthetic material was recrystallized three times from water and alcohol. Analysis: less than 0.004 per cent chloride, P_2O_5 , heavy metals, iron, or ammonia. N (Kjeldahl): milliequivalents found, 6.110; milliequivalents calculated, 6.119.

Diglycine: This material, prepared by the acid hydrolysis of diketopiperazine, was recrystallized twice from water and methanol. Analysis: less than 0.004 per cent of chloride, P_2O_5 , heavy metals, iron, or ammonia. Formol titration

¹Paper No. 37. For Paper No. 36 see Dunn *et al.* (8). This work was aided by grants from the Gelatin Products Corporation, Merck and Company, Inc., and the University of California.

²From a thesis submitted by Edwin L. Sexton to the Faculty of the Graduate School in partial fulfillment of the requirements for the degree of Master of Arts, June, 1942.

³Present address: Best Foods, Inc., Buffalo, New York.

with the glass electrode: milliequivalents_{found}, 2.165; milliequivalents calculated, 2.168.

Triglycine: This material was prepared by the reaction of chloroacetyl chloride, diglycine, and sodium hydroxide. The intermediate product, chloroacetyl-glycylglycine, was recrystallized from water. Analysis (titration with the glass electrode): milliequivalents found, 1.958; milliequivalents calculated, 2.057. A mixture of the purified intermediate and concentrated aqueous ammonia was allowed to stand 4 days at room temperature, and the crystalline product was recrystallized twice from water and methanol and three times from water. Analysis: less than 0.004 per cent chloride, P_2O_5 , heavy metals, iron, or ammonia. Formol titration with the glass electrode: milliequivalents found, 2.109; milliequivalents calculated, 2.112.

EXPERIMENTAL PROCEDURE

An appropriate volume of the solution of the solvent amino acid in carbon dioxide-free distilled water, an excess of the solute amino acid, and ten pieces of 3-mm. glass rod were transferred to an oil sample bottle of 120-ml. capacity. Adequate precautions were taken to prevent leakage, and the bottle was placed in the rotator of a thermostated bath maintained at $25.00^\circ\text{C.} \pm 0.01^\circ$.

TABLE 1

Electrometric titration of l(+)-glutamic acid in aqueous solutions of glycine and glycine peptides

GLUTAMIC ACID	2.51 M GLYCINE	0.970 M DIGLYCINE	0.179 M TRIGLYCINE
Milliequivalents found	2.158	2.173	1.391
Milliequivalents present	2.160	2.171	1.395
Milliequivalents found (per cent of theoretical)	99.9	100.2	99.7

In order to determine the minimum time for equilibration, bottles were removed from the thermostat at 24-hr. intervals, and the concentration of amino acids was measured. Although the values were constant in all cases after 24 hr., the glutamic acid systems were equilibrated for 72 hr. and the norvaline systems for 48 hr. Since the same results were found with the glutamic acid systems after 5 days and with the norvaline systems after 96 hr., it was concluded that bacterial decomposition during these periods was negligible.

It was shown in preliminary experiments that glutamic acid could be determined accurately in solutions of glycine and glycine peptides by electrometric titration with the sensitive glass-electrode apparatus described by Robertson (12). These data are given in table 1.

Glycine in the solutions was determined essentially by Bergmann and Niemann's (1) trioxalatochromiate method. Although Block (2) determined glycine in the complex either by Van Slyke amino nitrogen or Kjeldahl analysis, only the latter procedure gave satisfactory results in the present experiments. The

TABLE 2
l(+)-Glutamic acid-glycine-water

GLYCINE SOLUTION	<i>l(+)-GLUTAMIC ACID-GLYCINE SOLUTION</i>			
	Density (25°C.)	pH	Glycine	<i>l(+)-Glutamic acid</i>
<i>molarity</i>			<i>moles per 1000 g. water</i>	<i>moles per 1000 g. water</i>
0.000	0.9982	3.40	0.00	0.05912
0.100	1.0020	3.55	0.09566	0.06184
0.300	1.0090	3.73	0.3072	0.07131
0.500	1.0170	3.80	0.5134	0.08137
0.800	1.0230	3.93	0.8308	0.09048
1.000	1.0321	3.98	1.032	0.09674
1.500	1.0470	4.13	1.594	0.1135
2.000	1.0605	4.20	2.180	0.1307
2.500	1.0754	4.32	2.821	0.1475
3.000	1.0890	4.39	3.475	0.1617

TABLE 3
l(+)-Glutamic acid-diglycine-water

DIGLYCINE SOLUTION	<i>l(+)-GLUTAMIC ACID-DIGLYCINE SOLUTION</i>			
	Density (25°C.)	pH	Diglycine	<i>l(+)-Glutamic acid</i>
<i>molarity</i>			<i>moles per 1000 g. water</i>	<i>moles per 1000 g. water</i>
0.000	0.9982	3.40	0.00	0.05912
0.100	1.0046	3.82	0.09681	0.06472
0.500	1.0282	4.17	0.5217	0.09973
1.000	1.0539	4.38	1.076	0.1375
1.500	1.0805	4.50	1.586	0.1675

TABLE 4
l(+)-Glutamic acid-triglycine-water

TRIGLYCINE SOLUTION	<i>l(+)-GLUTAMIC ACID-TRIGLYCINE SOLUTION</i>			
	Density (25°C.)	pH	Triglycine	<i>l(+)-Glutamic acid</i>
<i>molarity</i>			<i>moles per 1000 g. water</i>	<i>moles per 1000 g. water</i>
0.000	0.9982	3.40	0.00	0.05912
0.0700	1.0045	3.78	0.06773	0.06986
0.1400	1.0077	3.96	0.1336	0.08125
0.2100	1.0138	4.02	0.2003	0.08987
0.3000	1.0191	4.10	0.2827	0.10025

TABLE 5
dl-Norvaline-glycine-water

GLYCINE SOLUTION	<i>dl-NORVALINE-GLYCINE SOLUTION</i>			
	Density (25°C.)	pH	Glycine	<i>dl-Norvaline</i>
<i>molarity</i>			<i>moles per 1000 g. water</i>	<i>moles per 1000 g. water</i>
0.000	1.0101	6.96	0.00	0.7204
0.500	1.0242	6.65	0.5107	0.7178
1.000	1.0357	6.49	1.033	0.7081
1.800	1.0576	6.35	1.878	0.6946
2.300	1.0701	6.28	2.546	0.6489
3.000	1.0745	6.28	2.746	0.6133

total-nitrogen values obtained by Kjeldahl analysis were reproducible to 1.0 per cent. The same recovery factor, 81.2 per cent, was found in the analysis of 1 *M* solutions of glycine containing 0, 4.80, and 14.56 per cent of *dl*-norvaline.

The concentration of the amino acids in the various solutions was calculated from the densities of the solutions and the content of glutamic acid, glycine, and total nitrogen. The solubility data obtained are shown in tables 2-5.

DISCUSSION

Advantage has been taken in the present studies of the equation utilized by Cohn (3) and coworkers in their investigations of dipolar ion interactions:

$$(\bar{F}_e - \bar{F}_e^0)/2.303RT = \log N/N_0 + K_s C = K_r(D_0/D)C$$

$(\bar{F}_e - \bar{F}_e^0)$ is the change in partial molal free energy of the solute amino acid due to electrostatic forces, N is the mole fraction of the solute in a solution of dielectric constant D and concentration C of another dipolar ion, N_0 is the mole fraction of the solute in water of dielectric constant D_0 , K_s is a salting-out constant which increases with the length of the hydrocarbon side chain, and K_r is a constant derived from electrostatic forces.

In systems where K_s is appreciable, $K_r - K_s$ may be approximated from the value of the limiting slope of the curve resulting from a plot of N/N_0 against C . For systems in which K_s is small in comparison to K_r , the value $K_r - K_s$ is given by the ordinate where D_0/D equals unity for the straight line obtained by plotting $\log \frac{N/N_0}{C}$ against D_0/D . The value for $K_r/2$ is given by the ordinate where D_0/D equals 0.5.

The possibility of altered solubilities due to compound formation between dipolar ions may be neglected, since von Przylecki *et al.* (11) have shown by electrometric titration evidence that compound formation does not occur in the systems under investigation. Change in solubilities resulting from shifts in ionic equilibria of dipolar ions because of changes in pH were not significant in experiments with the *dl*-norvaline-glycine system, which was investigated only at pH levels in close proximity to the isoelectric points of these amino acids. It was necessary, however, to correct the concentrations of dipolar ions in the glutamic acid-glycine and glutamic acid-glycine peptide systems for the concentrations of the ionic species present, since the solubility measurements were made over a range of pH values.

The corrected concentrations of dipolar ions were calculated from the appropriate mass-action expressions of these equilibria, the activity coefficients given by Hoskins, Randall, and Schmidt (9) and Smith and Smith (14), and the dissociation constants given by Schmidt and Miyamoto (13) and Nims and Smith (10). It was assumed that the experimental pH values were a measure of $\log 1/a_{H^+}$. The observed pH values ranged from 5.96 to 6.25 for 0.04625-3.130 *M* glycine and from 5.52 to 5.62 for 0.5680-0.7770 *M* diglycine solutions. The pH of 0.06521-0.3000 *M* triglycine solutions was 5.46.

The values of the dielectric constants of the several systems were calculated

from the values for the dielectric increment (δ) given by Wyman and McMeekin (15) and Devoto (7). K_s , K_r , and $K_r - K_s$ were calculated by Cohn's methods. A summary of these calculations is given in table 6. Since $K_r - K_s$ is relatively small for the *dl*-norvaline-glycine system, it was not feasible to calculate the individual K_r and K_s values. A plot of $\log N/N_0$ against concentration of

TABLE 6
Dipolar ion system constants

DIPOLAR ION SYSTEM	$K_r - K_s$	K_r	K_s	DIELECTRIC INCREMENT	DIPOLE MOMENT, $\mu \times 10^{18}$ E.S.U.
<i>dl</i> -Norvaline-glycine.....	-0.010			22.6	15
<i>l</i> (+)-Glutamic acid-glycine.....	0.282	0.224	0.068	22.6	15
<i>l</i> (+)-Glutamic acid-diglycine....	0.802	0.780	0.066	70.6	26
<i>l</i> (+)-Glutamic acid-triglycine.....	1.415	0.780	0.653	113	32

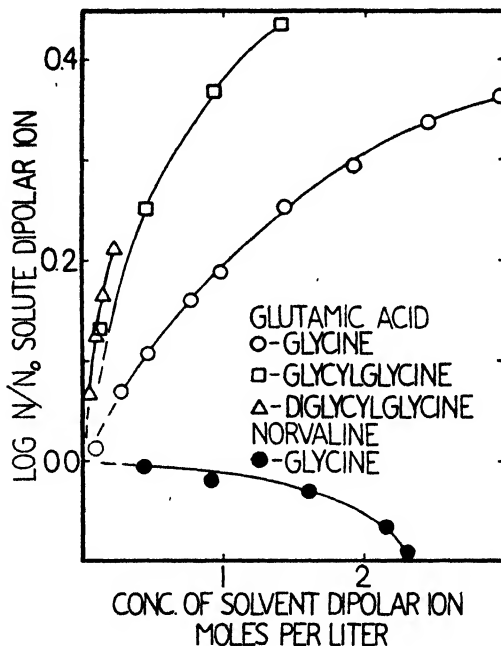


FIG. 1. Plot of $\log N/N_0$ against concentration of glycine and glycine peptides

glycine and glycine peptides is given in figure 1, and a plot of $1/C \log N/N_0$ against D_0/D is shown in figure 2.

It may be noted that the substitution of a carboxyl for a terminal methyl group has not only changed the sign of the limiting slope of the curve but has resulted in a 28.4-fold increase in the absolute value of the slope. These results would indicate that the change in free energy as measured by $K_r - K_s$ is a function of the second power of the dipole moment. In analogous systems containing

asparagine or cystine Cohn has found that the first, rather than the second power was involved. It was expected that studies would be made of the influence of different terminal groupings on dipolar ion interactions, but it seemed desirable to present the present experimental data, since this work cannot be continued for an indeterminate time.

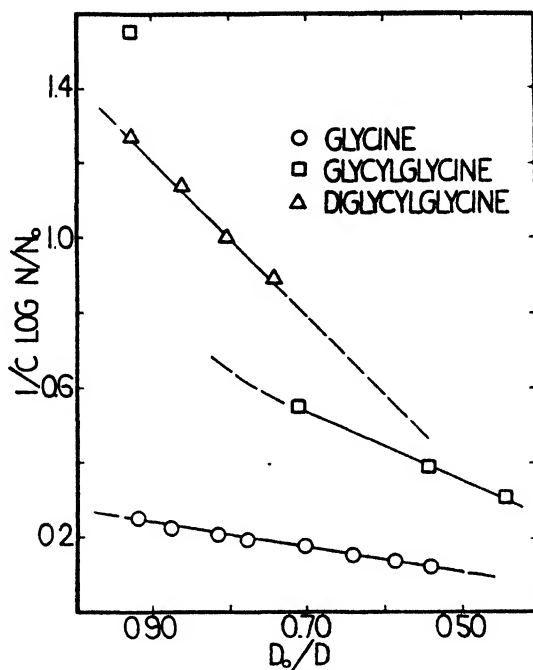


FIG. 2. Plot of $1/C \log N/N_0$ against D_0/D

SUMMARY

Solubility relations have been determined for the systems *dl*-norvaline-glycine, *l*(+)-glutamic acid-glycine, *l*(+)-glutamic acid-diglycine, and *l*(+)-glutamic acid-triglycine. An interpretation has been made of dipolar interactions occurring in these systems in terms of the concentration of dipolar ions, dielectric and other constants which were calculated from the experimental data, and an equation relating these factors. It has been shown that substitution of a carboxyl for a terminal methyl group caused a change in sign of the limiting slope and greatly increased the absolute value of the slope of the curve relating $\log N/N_0$ and C . It was found, also, that the change in free energy as measured by $K_r - K_s$ was a function of the second power of the dipole moment.

REFERENCES

- (1) BERGMANN, M., AND NIEMANN, C.: *J. Biol. Chem.* **122**, 577 (1938).
- (2) BLOCK, R.J., AND BOLLING, D.: *The Determination of the Amino Acids*, p. 51. Burgess Publishing Company, Minneapolis (1940).

- (3) COHN, E.J.: In Cohn and Edsall's *Proteins, Amino Acids and Peptides as Ions and Dipolar Ions*, p. 217. Reinhold Publishing Corporation, New York (1943).
- (4) COHN, E.J., McMEEKIN, T.L., AND BLANCHARD, M.H.: *Compt. rend. trav. lab. Carlsberg* **22**, 142 (1938).
- (5) COHN, E.J., McMEEKIN, T.L., AND BLANCHARD, M.H.: *J. Gen. Physiol.* **21**, 651 (1938).
- (6) COHN, E.J., McMEEKIN, T.L., FERRY, J.D., AND BLANCHARD, M.H.: *J. Phys. Chem.* **43**, 169 (1939).
- (7) DEVOTO, G.: *Gazz. chim. ital.* **61**, 897 (1931).
- (8) DUNN, M.S., CAMIEN, M.N., SHANKMAN, S., AND BLOCK, H.: *Archiv. Biochem.*, in press.
- (9) HOSKINS, W.M., RANDALL, M., AND SCHMIDT, C.L.A.: *J. Biol. Chem.* **88**, 215 (1930).
- (10) NIMS, L.F., AND SMITH, P.K.: *J. Biol. Chem.* **101**, 401 (1933).
- (11) PRZYLECKI, S.J. VON, CICHONCKA, J., HOFER, E., AND RAFOLOWSAK, H.: *Biochem. Z.* **299**, 230 (1938).
- (12) ROBERTSON, G.R.: *Ind. Eng. Chem., Anal. Ed.* **3**, 5 (1931).
- (13) SCHMIDT, C.L.A., AND MIYAMOTO, S.: *J. Biol. Chem.* **99**, 335 (1933).
- (14) SMITH, P.K., AND SMITH, E.R.: *J. Biol. Chem.* **121**, 607 (1937).
- (15) WYMAN, J., AND McMEEKIN, T.L.: *J. Am. Chem. Soc.* **55**, 908 (1933).

ELECTRON MICROSCOPE OBSERVATIONS OF THE MORPHOLOGY OF SEVERAL GASES POLYMERIZED BY CHARGED- PARTICLE BOMBARDMENT

JOHN H. L. WATSON¹

Plant Research Department, Shawinigan Chemicals Ltd., Shawinigan Falls, Quebec, Canada

Received January 2, 1947

The polymerization of certain gases and vapors when bombarded by charged atomic particles is a well-known phenomenon (1, 2). Interest in the microphysical structure of cuprene, as a polymer of acetylene formed in the presence of a cuprous oxide catalyst, led to electron microscope examination of cuprene formed by charged-particle bombardment (3). Extension of these observations for cuprene, and for polymerized hydrogen cyanide and cyanogen gases is given here.¹

The corona cuprene samples were received as brittle semi-transparent sheets, which were ground and mounted as a dry powder for microscope examination. This cuprene was formed in a semi-corona, cold discharge in a cylindrical glass tube with a central aluminum electrode. The polymer was taken from the deposit found on the inner wall surrounding the electrode.

The alpha-ray cuprene sample used here is similar to that described elsewhere (3). The polymer was deposited upon the sides of a large glass flask

¹ The author is indebted for the samples to Dr. S. C. Lind, Dean of the Institute of Technology, University of Minnesota, and Dr. George Glockler of the Department of Chemistry and Chemical Engineering, Iowa State University. The "corona" cuprene samples were obtained from Dr. Glockler and the other samples from Dr. Lind.



FIG. 1 Corona cuprene magnification, 10,000 \times

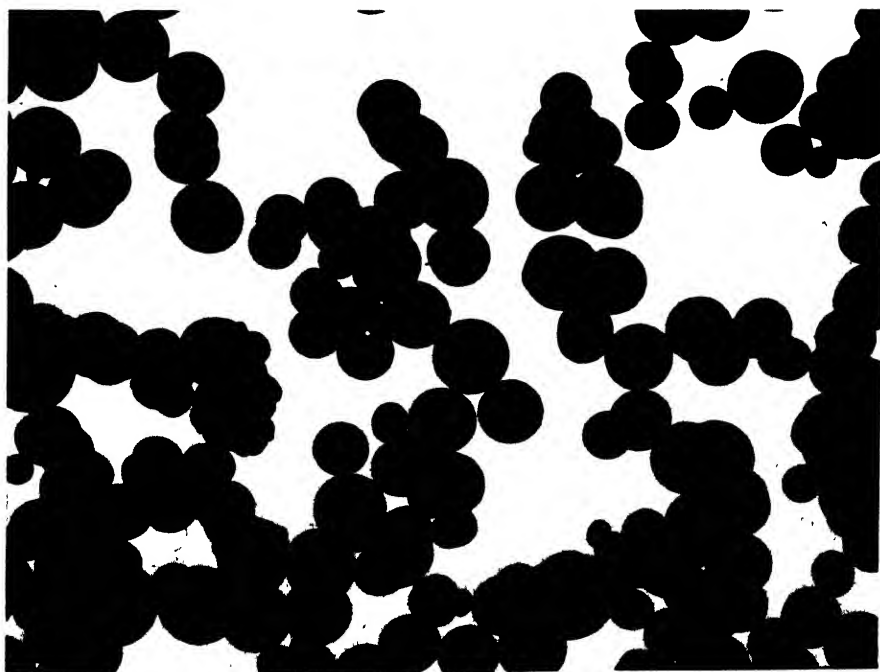


FIG. 2. Alpha-ray cuprene: magnification, 10,000 \times

and was easily scraped off as a fine soft powder, ideal for electron microscope examination. The cyanogen polymer also occurred as an easily mounted, soft powder, but the hydrogen cyanide polymer was fixed firmly to the glass walls and was scraped off with difficulty for examination. None of these samples had been exposed to oxidation.

Typical electron micrographs of the four polymers are reproduced in the figures. In figure 1 the corona cuprene is observed to be composed of broken flakes and pieces. These are seen to possess a very fine structure, not resolvable

TABLE 1
Particle size of alpha-ray cuprene

SPECIMEN POSITION	MEAN PARTICLE DIAMETER	STANDARD DEVIATION
	<i>mμ</i>	<i>mμ</i>
A	660	190
B	750	250
C	800	200

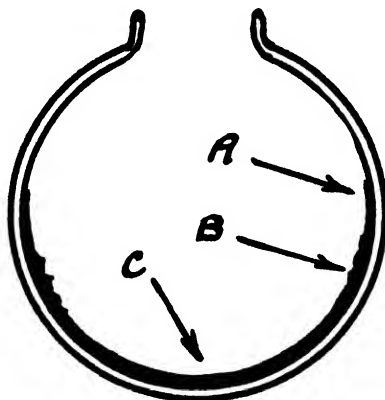


FIG. 3. Diagram of flask containing alpha-ray cuprene deposit showing areas from which samples were taken.

in the micrographs. Such a structure film would be expected if the polymer originally deposited as a very fine particle mist, the particles probably existing in a semi-liquid state. The same type of structure is detected in deposits taken from other positions in the tube.

The alpha-ray cuprene examined and illustrated in figure 2 is identical with the samples reported in reference 3. If bombardment with secondary radiation makes any changes in the chemical formula of the polymer, the differences are not rendered visible in the micrographs. There is a suggestion in table 1 that the particle size of this acetylene polymer increases as the specimen is taken from areas situated toward the bottom of the flask. This would indicate that the particles formed in space fall out under gravity, effecting a partial

separation of particle sizes. Figure 3 shows a drawing of the bulb with approximate specimen positions marked as A, B, and C.

Cuprene formed by alpha-ray bombardment of acetylene in the presence of hydrogen gas and formed similarly in the presence of krypton possesses the same morphological characteristics in both cases as the normal alpha-ray cuprene. However, particle sizes vary and are given for all samples in table 2.

It is interesting to note at this point that *three distinct* cuprene structures exist, depending upon the method of preparation. Although the structure of catalytic cuprene is quite complex, it may be said in general to be a tubular fibre and a solid (3). The alpha-ray cuprene has a round-particle structure,

TABLE 2
Particle size data for several gases polymerized by alpha-ray bombardment

SAMPLE	MEAN PARTICLE SIZE	STANDARD DEVIATION
	<i>mμ</i>	<i>mμ</i>
Cuprene (the arithmetic mean of values in table 1)	740	210
Cuprene (in presence of hydrogen)	720	180
Cuprene (in presence of krypton)	500	200
Hydrogen cyanide polymer	540	200
Hydrogen cyanide polymer (in presence of xenon)	760	140
Cyanogen polymer decomposed to paracyanogen	85	50
Cyanogen polymer (in presence of nitrogen)	130	90

the particles being joined by short thick necks. This cuprene seems to exist in some type of semi-liquid state. The corona cuprene is a solid and in electron micrographs appears to be composed of thin sheets possessing very fine structure.

Although the polymerization mechanism for the formation of the hydrogen cyanide and the cyanogen polymers is probably similar to that for alpha-ray cuprene, the appearance in electron micrographs is quite different. Figure 4 is typical of the hydrogen cyanide, and figures 7 and 8 of the cyanogen polymers.

In the hydrogen cyanide polymer there is a wide variety of particle shapes and sizes, but the particle edges are smooth, indicating a strong possibility that the particles are all reproduced with the same appearance they had when deposited. In table 2 the mean sizes quoted are for the smaller round particles only. No differences in appearance are observed in a sample of this polymer prepared in the presence of xenon. Several extremely large round particles were observed. These have diameters as large as 10 microns, and their shapes

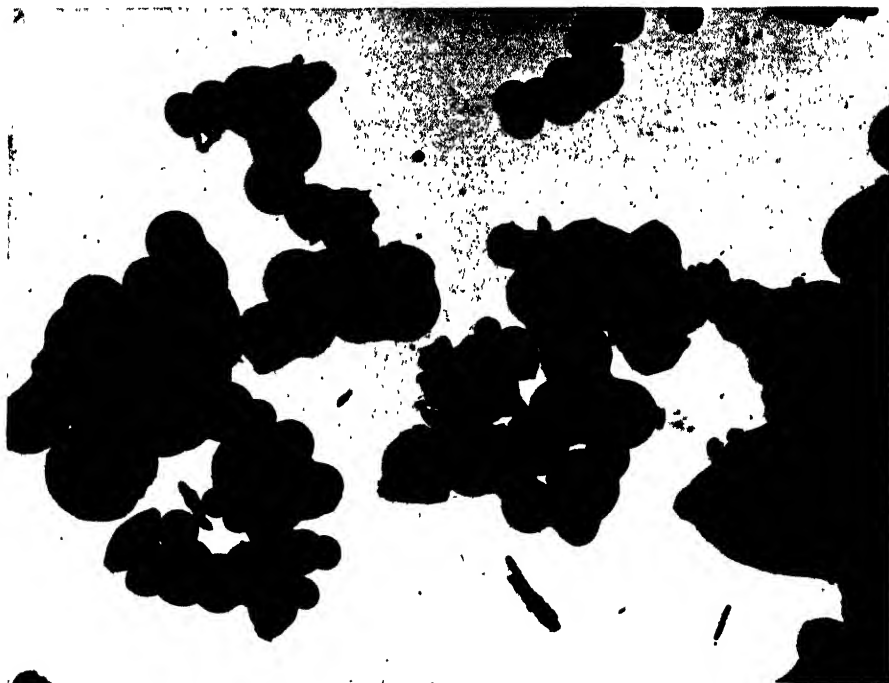


FIG. 4. Hydrogen cyanide polymer made by alpha-ray bombardment of the gas. Magnification, 10,000 \times .



FIG. 5. Hydrogen cyanide polymer made by alpha-ray bombardment of the gas in the presence of xenon. This particular field shows a large particle before electron bombardment in the electron microscope. Magnification, 3800 \times .

FIG. 6. The same particle shown in figure 5 has become two under electron bombardment in the microscope. Magnification, 3800 \times .

oscillate under the electron beam like a suspended liquid droplet. One large particle became two under these circumstances, as in figures 5 and 6. Fine unresolved structure is visible in fragments of these large particles.

Figure 7 shows a typical field of cyanogen polymer made by alpha-ray bombardment of the gas. This sample has been decomposed to paracyanogen. The morphology here is quite different from that in any of the other materials. The ultimate particle size is much reduced and the larger units are all agglomerations of smaller particles.

Figure 8 is a micrograph of alpha-ray cyanogen polymer formed in the presence of nitrogen. The material is quite similar to that in figure 4, but in addition there are larger particles which cannot be counted as agglomerates and which

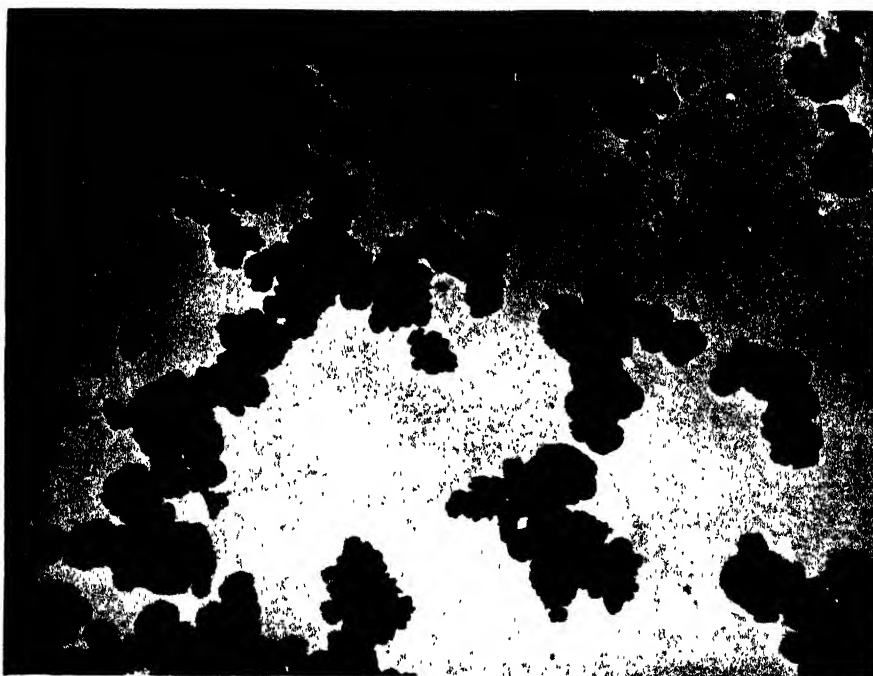


FIG. 7. Cyanogen polymer, decomposed to paracyanogen, made by alpha-ray bombardment of the gas. Magnification, 10,000 \times .

consequently contribute to an increased particle size. These are not smooth and therefore do not resemble the particles of cuprene. They must possess some agglomeration structure, although it is not made clearly evident in the micrographs.

These samples each yield high-contrast electron micrographs. Since only the lightest atoms are present in their structure, the density of the particles must be relatively high to cause such efficient electron scattering.

Different conditions of preparation of alpha-ray cuprene do not result in any striking morphological differences. The same may be said for the hydrogen cyanide polymers, but there is some indication that this is not so with cyanogen, where the appearance is different in the two samples.

By reference to electron micrographs it is possible to distinguish alpha-ray cuprene from corona and catalytic cuprene, and cuprene in general from both the hydrogen cyanide and cyanogen polymers.

There is a possibility that both alpha-ray cuprene and the hydrogen cyanide polymers exist as viscous quasi-liquids, whereas the corona and catalytic cuprene and the cyanogen polymer have the physical appearance of solids in the micrographs.

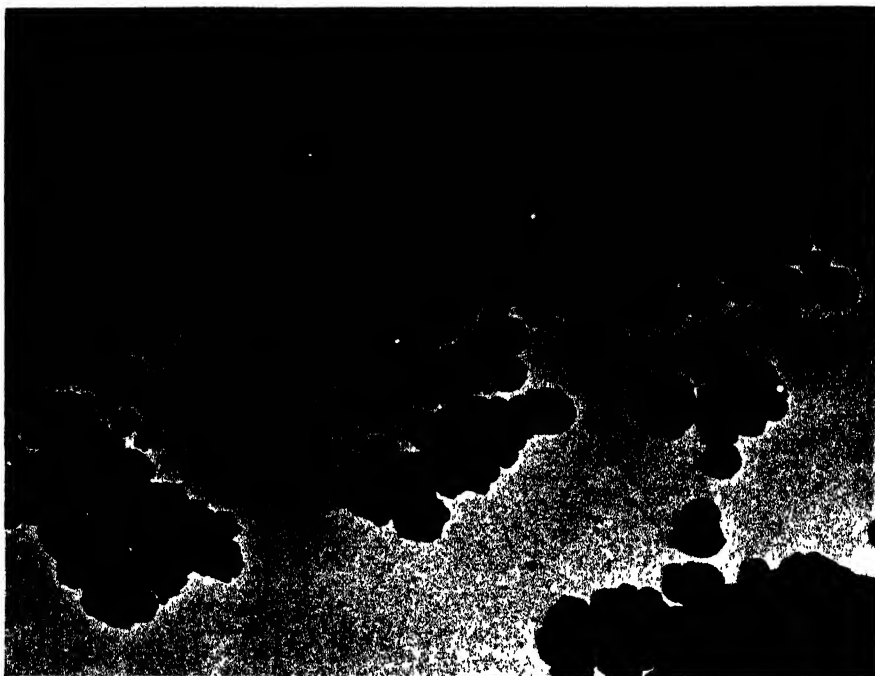


FIG. 8. Cyanogen polymer made by alpha-ray bombardment of the gas in the presence of nitrogen. Magnification, 10,000 \times .

Each of these polymerized gases is deposited in a fine particle form by alpha-ray bombardment. The hydrogen cyanide tends to depart slightly from this general observation.

SUMMARY

Electron micrographs are reproduced of acetylene, hydrogen cyanide, and cyanogen polymers formed under different conditions by charged-particle bombardment of the respective gases. Three types of cuprene can be distinguished from electron micrographs. The polymers formed from the three gases by alpha-ray bombardment are distinguishable by their physical appearance. There is evidence that alpha-ray cuprene and hydrogen cyanide polymer exist as viscous quasi-liquids, whereas the corona and catalytic cuprene and cyanogen polymer appear to be solids. Each of the polymers is deposited in a fine particle

form from charged-particle bombardments. Statistical data concerning the particle sizes are given.

REFERENCES

- (1) GLOCKLER, GEORGE, AND WALZ, ALVIN E.: *Trans. Electrochem. Soc.* **88**, 63 (1945).
- (2) LIND, S. C., AND BARDWELL, D. C.: *J. Am. Chem. Soc.* **48**, 1556 (1925).
- (3) WATSON, J. H. L., AND KAUFMANN, C.: *J. Applied Phys.* **17**, 996 (1946).

EFFECT OF ELECTROLYTES ON THE FOAMING CAPACITY OF ALPHA SOYBEAN PROTEIN DISPERSIONS¹

JOSEPH M. PERRI, JR.,² AND FRED HAZEL

Department of Chemistry and Chemical Engineering, University of Pennsylvania, Philadelphia, Pennsylvania

Received November 14, 1946

Alpha soybean protein is insoluble in water but it may be dispersed by the addition of bases such as sodium or calcium hydroxide. The dispersions are capable of producing stable foams. This property, which is not an unusual one for systems of this class, may be attributed to the surface activity of the protein. Since both the solubility and the nature of the adsorbed layer of proteins are influenced by pH changes and by the presence of salts in solution (1), these factors would be expected to have an influence on the foaming properties. In the following, the observations which have been made on the effect of electrolytes and pH on alpha soybean protein foams are reported.

EXPERIMENTAL

Preparation of the protein dispersions

Thirty grams of alpha protein were dispersed in 2 liters of a 0.5 per cent sodium hydroxide solution. The protein was precipitated by adjustment of the pH to 4.1, using hydrochloric acid. The precipitate was allowed to settle and the supernatant siphoned off. Sodium hydroxide was added to a suspension of the precipitated protein to effect solution at a pH of 11. Toluene was added as a preservative, and the solution was dialyzed in the cold until the diffusate gave a negative test for chloride ions with silver nitrate and was neutral to litmus paper. This solution was layered with toluene and stored in a refrigerator. Withdrawal for use was made by insertion of the tip of a pipet into the body of the solution.

¹ Presented before the Division of Colloid Chemistry at the 110th Meeting of the American Chemical Society, Chicago, Illinois, September, 1946.

² Present address: National Foam System, Inc., Packard Building, Philadelphia, Pennsylvania.

Preparation of the foaming solutions

For electrolyte studies: The desired volume of protein solution was added to a 250-cc. volumetric flask. This volume was diluted with distilled water and the calculated volume of electrolyte solution added. Distilled water was added to the mark. The electrolyte solutions were prepared from Baker's Analyzed salts.

For pH studies: Sodium hydroxide and hydrochloric acid were used for pH adjustment. A Leeds & Northrup glass-electrode pH meter was used for determination of the hydrogen-ion activities.

The apparatus and technique for determining foaming capacities have been described previously (6). In the individual determinations, nitrogen gas was passed through 150 cc. of the solution until an equilibrium had been established between foam formation and foam decay, as indicated by the constant volume of the remaining solution. The values given in the tables express the number of cubic centimeters of solution converted into foam by 1 g. of protein nitrogen.

RESULTS

The effect of pH on the foaming capacity of soybean protein is shown in table 1. The data are plotted in figure 1. The solution used in this experiment contained 0.0761 g. of nitrogen per liter and had an initial pH of 7.15. It was prepared by a dilution of a stock solution containing 1.586 g. of nitrogen per liter. The latter was prepared by the method described in the experimental section.

The effects of electrolytes on the foaming capacity of soybean protein solutions are shown in the following tables. The data in tables 2 and 3 were obtained with a solution prepared by dilution of a stock solution of pH 8.3 which contained 1.387 g. of nitrogen per liter.

Table 2 shows the effect of the valency of the cation of the added salt³ on the foaming capacity of the protein.

Table 3 shows the effect of cation lyotropy of the alkali metals on the foaming capacity of the protein.

Table 4 shows the effect of anion lyotropy on the foaming capacity. The

³ Neutral salts were employed as electrolytes with dilute protein solutions. This tended to keep pH changes accompanying mixing at a minimum. A measure of the extent of the latter is given by the following data, obtained in a preliminary experiment with a dilute protein solution of pH 6.75 and sodium chloride.

MOLARITY OF SODIUM CHLORIDE	pH OF SYSTEM
0.0	6.75
0.01	6.7
0.1	6.35
0.5	6.0
1.0	6.0

The above would indicate that the effects observed on the foaming were due to the presence of neutral salts and not to pH changes.

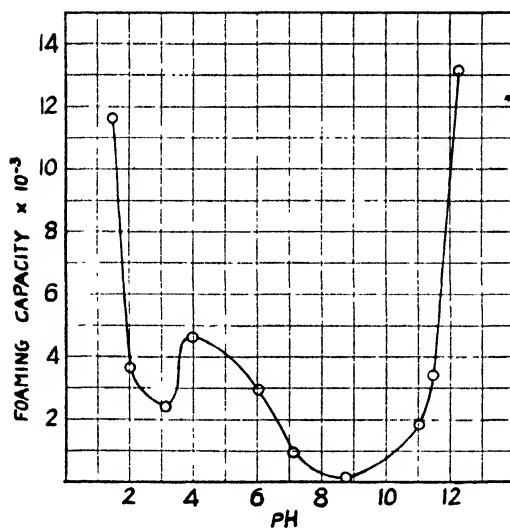


FIG. 1. Effect of pH on foaming capacity

TABLE 1
Effect of pH on the foaming capacity

pH	FOAMING CAPACITY PER GRAM OF NITROGEN
	cc
1.5*	11,650
2.05	3,680
3.15	2,450
4.0	4,640
6.1	2,980
7.15	960
8.8	180
11.05	1,840
11.5	3,420
12.3*	13,130

* These two systems had the same ionic strength with respect to added electrolyte: 0.057.

TABLE 2
Effect of valence of cation of added salt

MOLARITY OF ADDED SALT	FOAMING CAPACITY PER GRAM OF NITROGEN		
	NaCl	CaCl ₂	LaCl ₃
	cc.	cc.	cc.
0.0	120	120	120
0.0001	300	1,570	2,870
0.001	1,320	8,490	*
0.01	7,360	*	6,910
0.5	42,050	42,050	†

* Coagulated, making determinations impossible.

† Not investigated.

protein solution employed was of the same concentration and from the same source as the one used in the pH investigation. It had a pH of 7.15.

TABLE 3
Effect of cation lyotropy of added salt

MOLARITY OF ADDED SALT	FOAMING CAPACITY PER GRAM OF NITROGEN		
	NaCl	LiCl	KCl
	cc.	cc.	cc.
0.001	1,320	1,200	1,200
0.01	7,360	7,620	8,110
1.0	55,120	63,750	51,230

TABLE 4
Effect of anion lyotropy of added salt

MOLARITY OF ADDED SALT	FOAMING CAPACITY PER GRAM OF NITROGEN		
	$\frac{1}{2}$ K ₂ SO ₄	KCl	KCNS
	cc.	cc.	cc.
0.01	11,030	9,810	9,282
0.1	23,110	19,260	15,930
1.0	63,050	63,050	13,660

DISCUSSION

The dispersions prepared by the interaction of sodium hydroxide with soybean protein and employed in the present study were complex mixtures in which the particle size probably varied from the molecular to the colloidal range. Addition of electrolytes would be expected to affect not only the behavior of the individual components, e.g., the spreading (1) and charge of the molecular components and the stability⁴ and charge of the larger "colloidal" particles, but also the distribution of the components with respect to particle size. Despite the complexity of the system, several previously reported behaviors of proteins and/or colloidal systems are suggested by the foaming data given in the experimental section.

The amphoteric nature of soybean protein is revealed by the data in figure 1. Maxima in foaming capacity were found to occur at the extremities of the pH range and at the isoelectric point. Similar maxima have been reported for the spreading of certain proteins (2). Since the particle size was at a maximum and the charge was at a minimum at the isoelectric point, while the reverse was true

⁴ From the electrokinetic point of view, soybean protein dispersions are intermediate between hydrophobic colloids and hydrophilic colloids. Systems which are hydrophobic are characterized by a high critical potential (7), while strictly hydrophilic systems do not precipitate when the electric charge is reduced to zero (3). Soybean protein, on the other hand, does precipitate at its isoelectric point.

both at high and low pH values, the occurrence of minima at intermediate hydrogen-ion activities is not entirely surprising.

The data in table 2 show that the effect of valency on the foaming capacity resides in the cation. This result may be associated with the fact that the protein particles were negatively charged. With no electrolyte in the system the foaming capacity was very low, possibly because of the strong repulsion of the relatively large particles present at the interface. Addition of a small amount of each of the electrolytes (equivalent to a concentration of 0.0001 *M*) increased the foaming capacity and revealed a marked valence effect of the type encountered in electrokinetic behavior. The particles were discharged completely at a concentration of 0.001 *M* in the case of the lanthanum chloride system and precipitation occurred. Calcium ions, being less effective, did not discharge the particles completely until a higher concentration, 0.01 *M*, had been reached.

A comparison of the foaming capacities of the systems in the presence of 0.01 *M* sodium chloride and 0.01 *M* lanthanum chloride reveals the striking fact that the two electrolytes were about equally effective in the production of a stable foam. In both cases, the protein particles were charged and repulsive forces operated between them to about the same extent in the interface. The sign of the charge on the particles was opposite, however, and was due to the recharging⁵ of the lanthanum chloride system to the positive form which gave it stability and made possible the determination of the foaming capacity.

It may be noted, also, from the data in table 2 that an increase in concentration from 0.01 *M* to 0.5 *M* stabilized the system toward calcium chloride. The cause of the stabilization was different, however, than with lanthanum chloride. Calcium ions did not recharge the particles, for the latter were isoelectric as nearly as could be determined, at both 0.01 *M* and 0.5 *M*. The increased stability in this case must be ascribed to a peptization or salting in of the protein particles by the additional electrolyte.

Table 3 shows that the effectiveness of monovalent cations on the foaming capacity follows the lyotropic series $\text{Li} > \text{Na} > \text{K}$, and was observable only at the highest electrolyte concentrations.

The lyotropic effect of anions on the foaming capacity was operative at much lower concentration of electrolyte than that of the cations. This type of behavior is frequently encountered and remains unexplained (8). The data in table 4 show the effect of the chloride to be small in comparison with that of the sulfate. The latter was so marked that lyotropy appeared even in the 0.01 *M* solutions. On the other hand, the presence of thiocyanate resulted in the

⁵ The isoelectric point of soybean protein is shifted markedly by electrolytes. Thus, in the presence of 0.01 *M* lanthanum chloride the shift was from a pH of 4.1 to about 7. While a shift in the isoelectric point of a protein by salts is not a unique phenomenon (5), the magnitude of the shift is much greater than is found with proteins and more nearly resembles the behavior of a hydrophobic sol (4). Sols of the latter type are readily recharged by polyvalent strongly adsorbable ions of opposite sign.

production of a solution of comparatively low foaming capacity. This was evident especially at the highest concentration employed.

SUMMARY

1. The effects of electrolytes and of hydrogen-ion concentration on the foaming properties of alpha soybean protein dispersions have been investigated.

2. At low concentrations, the valence of the cation was found to have a marked effect on foam formation in the series potassium chloride, calcium chloride, lanthanum chloride.

3. Lyotropic effects were observed with both cations and anions.

4. The hydrogen-ion concentration was found to influence the foaming capacity strongly. A maximum was found to occur at the isoelectric point (pH 4.1), while minima were shown to exist at pH 3.15 and pH 8.8.

REFERENCES

- (1) ADAM: *The Physics and Chemistry of Surfaces*, 3rd edition, p. 87 et seq. Oxford University Press, London (1941).
- (2) Reference 1, p. 91.
- (3) HARDY: *J. Physiol. Chem.* **24**, 288 (1899).
- (4) HAZEL AND AYRES: *J. Phys. Chem.* **35**, 3148 (1931).
- (5) HAZEL AND KING: *J. Phys. Chem.* **39**, 515 (1935).
- (6) PERRI AND HAZEL: *Ind. Eng. Chem.* **38**, 549 (1946).
- (7) POWIS: *Z. physik. Chem.* **89**, 186 (1915).
- (8) SCHMIDT: *The Chemistry of the Amino Acids and Proteins*, p. 340. Charles C. Thomas, Springfield, Illinois (1938).

SPECTRAL CHANGES IN SOME DYE IONS AND THEIR RELATION TO THE PROTEIN ERROR IN INDICATORS¹

IRVING M. KLOTZ AND F. MARIAN WALKER

Department of Chemistry, Northwestern University, Evanston, Illinois

Received October 30, 1946

INTRODUCTION

It has been pointed out by Sørensen (14) that the presence of proteins may introduce large errors in the determination of pH by colorimetric methods. The magnitude of this protein error has been found to depend on the particular indicator involved as well as on the nature and concentration of the protein and on the pH of the solution (2, 3, 4, 10, 11, 15, 16). Thus, for example, the error for neutral red in globulin solutions is opposite in sign to and of much greater magnitude than that for phenol red in the same solutions (10). Similarly, for either of these two indicators the direction of the error in globulin

¹ This investigation was supported by a grant-in-aid from the Abbott Fund of Northwestern University.

solutions is opposite to that in albumin solutions, and with either protein the magnitude of the error increases with increasing concentration (10). The pH effect is illustrated particularly well by Danielli's investigations (4), in which it has been found that bromocresol green shows protein errors as large as 1.1 unit in 1 per cent ovalbumin solutions at pH's below about 4.8 but no errors at higher pH's.

Even the early investigators realized that the protein error must be related in some way to adsorption of the dye by the protein molecule. Clark (1), on the other hand, emphasized that the protein would affect the activity coefficients of the indicator ions and in that way displace the equilibrium in one direction or the other. No attempt was made, however, to systematize the many diverse phenomena which had been observed.

It remained for Hartley (6) to point out that large protein errors are observed in solutions in which the protein and one of the indicator ions are of opposite charge. The large electrostatic forces between the oppositely charged entities lead to adsorption of the indicator ion by the protein, with a consequent displacement of the equilibrium between the acidic and basic forms of the indicator. Thus, the general inapplicability of the azo indicators in protein solutions is to be attributed to the fact that the acid form is electrically neutral, whereas the base form is anionic and hence strongly adsorbed by positively charged proteins on the acid side of their isoelectric points. Similarly, the disappearance of the error with bromocresol green in ovalbumin solutions above pH 4.8 is due to the fact that this pH corresponds to the isoelectric point of this protein, and in more basic solutions the latter acquires a negative charge which repels the dye anions.

While Hartley's "sign rule" serves as a very useful principle in systematizing the different observations on protein errors, and, in particular, in predicting the usefulness or inapplicability of a new indicator, there are, nevertheless, a number of anomalies which are difficult to explain by this rule. Serum albumin, for example, causes a protein error with phenol red (10), despite the fact that all species are anionic in nature at the pH used. It is unlikely that this error is due to an effect on the activity coefficients of the indicator ions, since the phenomenon is observed even in very dilute solutions of the protein. Apparently some hitherto unrecognized factor must enter in these anomalous situations.

The experiments described in this paper show that many anionic indicators can combine with specific proteins even when the latter are negatively charged. The primary effect of this combination in pH determinations is, of course, a displacement of the equilibrium between the acidic and basic forms of the indicator. In addition, however, this complex formation produces pronounced changes in the spectrum of the adsorbed species, so that an additional contribution to the protein error may come from this source. Hartley (10) also realized that the spectrum of an adsorbed dye might differ from that of the free molecule, but he undertook no direct investigation of this effect. Thiel and Schulz (16) did observe some anomalies in the spectrum of methyl orange in protein solutions

at pH's from 2 to 5, the transition region for this indicator, but an investigation in solutions of pH 7 to 12, containing only the dye anion, revealed no differences between the spectra in pure solution and in the presence of casein, egg albumin, and Witte peptone, respectively. In this paper conclusive evidence is presented for such spectral alterations in serum albumin solutions, and some of the factors affecting the magnitude of these deviations are considered.

EXPERIMENTAL

Absorption spectra

The absorption of light by the dye solutions was determined with the Beckman spectrophotometer in a room at approximately 25°C. One-centimeter cells were used and extinction coefficients, ϵ , were calculated from the familiar equation

$$\epsilon = \frac{1}{cd} \log_{10} (I_0/I)$$

where I_0 is the intensity of the light passing through the solvent, I the intensity of the light passing through the solution, c the molar concentration of the solute, and d the thickness of the absorption cell in centimeters.

Reagents

The dyes and indicators which have been investigated, together with their structural formulas and purities, are listed in table 1.

Crystalline bovine serum albumin and purified bovine γ -globulin were furnished through the courtesy of the Armour Laboratories. Purified human serum albumin was generously supplied by the American Cyanamid Company.

The gelatin was Eastman "purified calfskin gelatin" with an isoelectric point of 4.7 and an ash content of 0.023 per cent.

Sodium dodecyl sulfate was a specially purified sample generously supplied by the Fine Chemicals Division of the du Pont Company.

RESULTS AND DISCUSSION

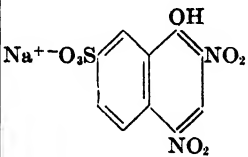
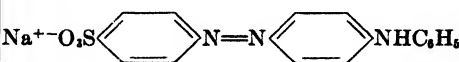
For each of the dyes investigated there is a distinct alteration of the spectrum upon the addition of serum albumin, even in very dilute solutions, as is evident from figures 1 to 11. With azosulfathiazole, for example, a significant depression in absorption was observed with as little as 0.01 per cent albumin. With the other dyes only experiments with 0.2 per cent albumin were carried out, but the magnitude of the observed changes indicates that about 0.01 per cent would be sufficient to change the spectrum for each dye, except, perhaps, prontosil (figure 5) and 2,6-dinitrophenol (figure 8).

The change in spectrum on the addition of protein cannot be attributed to a disturbance in the polymer-monomer equilibrium of the dye anions, for among the dyes investigated no such micelle formation is to be found in the concentration region investigated. The optical density is a linear function

TABLE 1
Dyes and indicators

SUBSTANCE	FORMULA	PURITY
		<i>per cent</i>
Orange I†	$\text{Na}^+ \text{O}_3\text{S} \text{---} \text{C}_6\text{H}_4 \text{---} \text{N}=\text{N} \text{---} \text{C}_6\text{H}_3\text{OH}$	92.5*
Orange II†	$\text{Na}^+ \text{O}_3\text{S} \text{---} \text{C}_6\text{H}_4 \text{---} \text{N}=\text{N} \text{---} \text{C}_6\text{H}_3\text{HO}$	95*
Amaranth† (FD and C Red #2)	$\text{Na}^+ \text{O}_3\text{S} \text{---} \text{C}_6\text{H}_4 \text{---} \text{N}=\text{N} \text{---} \text{C}_6\text{H}_3\text{HO} \text{SO}_3^-\text{Na}^+ \text{SO}_3^-\text{Na}^+$	90.0
Azosulfathiazole§	$\text{CH}_3\text{CONH} \text{---} \text{C}_6\text{H}_3\text{OH} \text{SO}_3^-\text{Na}^+ \text{---} \text{N}=\text{N} \text{---} \text{C}_6\text{H}_4 \text{SO}_2\text{NHR}$	97.2‡
Prontosil§	$\text{H}_2\text{N} \text{---} \text{C}_6\text{H}_4 \text{---} \text{N}=\text{N} \text{---} \text{C}_6\text{H}_4 \text{SO}_2\text{NH}_2$	"Pharmaceutical quality"
Methyl orange	$\text{Na}^+ \text{O}_3\text{S} \text{---} \text{C}_6\text{H}_4 \text{---} \text{N}=\text{N} \text{---} \text{C}_6\text{H}_4 \text{N}(\text{CH}_3)_2$	Reagent grade
Methyl red	$\text{C}_6\text{H}_4 \text{---} \text{N}=\text{N} \text{---} \text{C}_6\text{H}_4 \text{N}(\text{CH}_3)_2$	Reagent grade
2,6-Dinitrophenol	$\text{HO} \text{---} \text{C}_6\text{H}_3\text{NO}_2$	"Highest purity"¶
Bromocresol green	$\text{HO} \text{---} \text{C}_6\text{H}_2\text{Br}_2 \text{---} \text{CH}_2 \text{---} \text{C} \text{---} \text{CH}_2 \text{---} \text{C}_6\text{H}_2\text{Br}_2 \text{---} \text{O} \text{---} \text{C}_6\text{H}_4 \text{SO}_3\text{H}$	"Highest purity"¶

TABLE 1—*Continued*

SUBSTANCE	FORMULA	PURITY
Naphthol yellow S .		per cent Standard commercial sample
Tropeolin OO.		Standard commercial sample

* Purity determined by titanium chloride titration.

† Kindly supplied by the National Aniline Division of the Allied Chemical and Dye Corporation.

‡ Purity determined by methylene blue titration.

§ Kindly supplied by the Winthrop Chemical Company.

¶ Preparation from the Eastman Kodak Company.

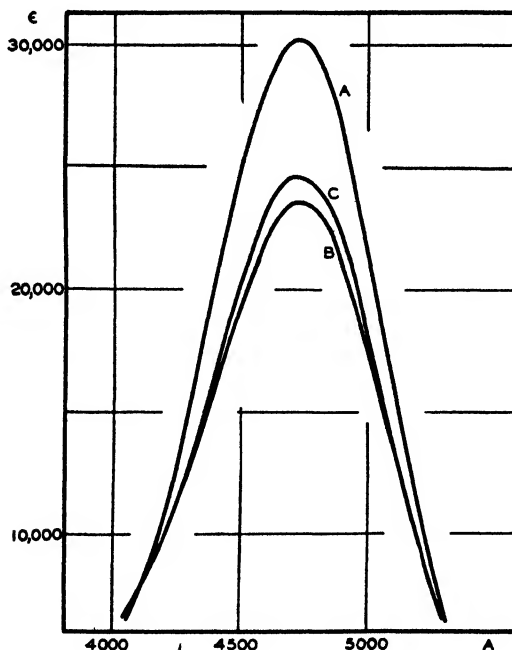


FIG. 1. Absorption spectra of orange I. A, buffer, pH 6.81; B, buffer + bovine albumin (0.2 per cent), pH 6.81; C, buffer + bovine albumin + potassium biphthalate ($0.98 \times 10^{-3}M$), pH 6.63.

of the concentration, at least up to 10^{-4} molar, for orange I, orange II, methyl orange, azosulfathiazole, and bromocresol green, respectively, a behavior indicative of the absence of dimerization. These examples include a variety of

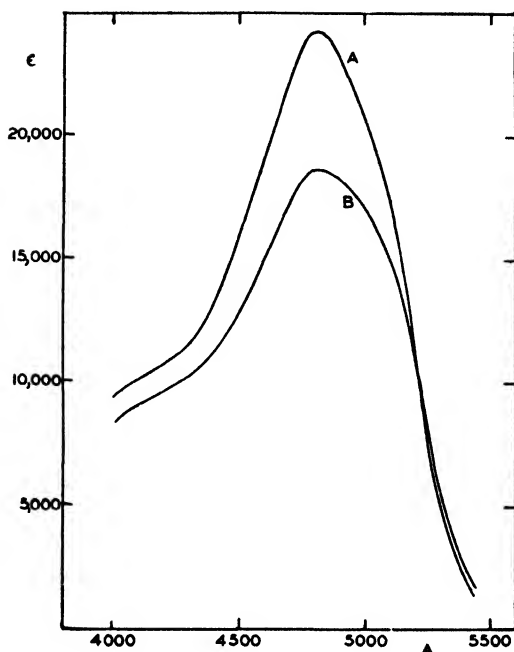


FIG. 2. Absorption spectra of orange II. A, buffer, pH 6.83; B, buffer + bovine albumin (0.2 per cent), pH 6.83.

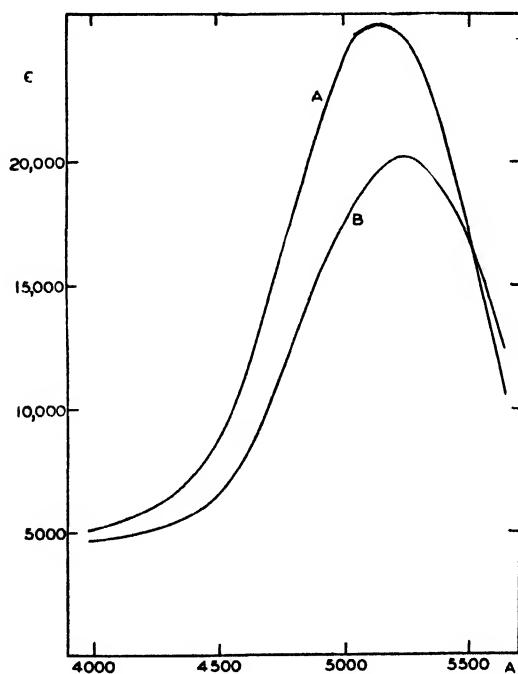


FIG. 3. Absorption spectra of amaranth. A, buffer, pH 6.86; B, buffer + bovine albumin (0.2 per cent), pH 6.86.

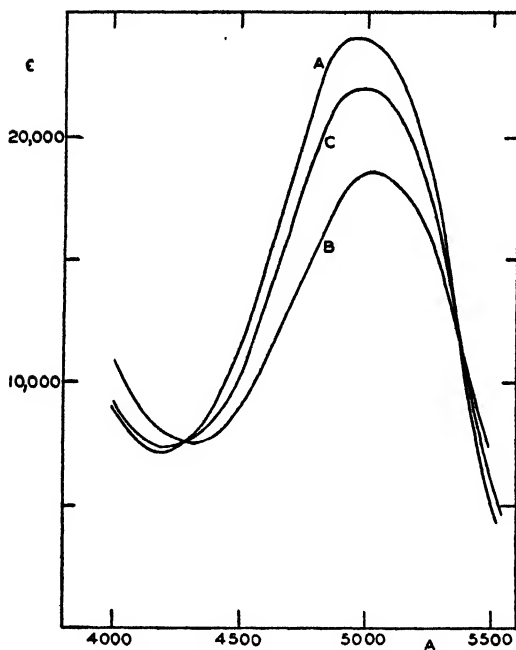


FIG. 4. Absorption spectra of azosulfathiazole. A, buffer, pH 6.92; B, buffer + bovine albumin (0.2 per cent), pH 6.90; C, buffer + bovine albumin + potassium biphthalate.

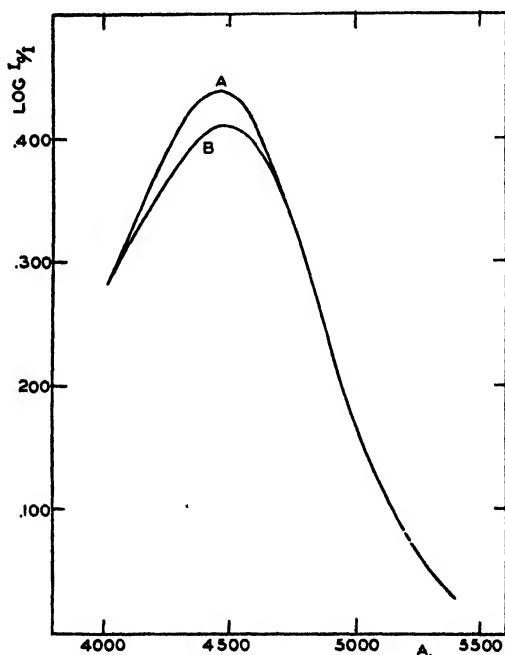


FIG. 5. Absorption spectra of prontosil (saturated solution at 25°C.). A, buffer, pH 5.76; B, buffer + bovine albumin (1.00 per cent), pH 5.69.

structural configurations and ionic charges so that the substances which have not been tested, being of similar nature, would be expected to behave similarly.

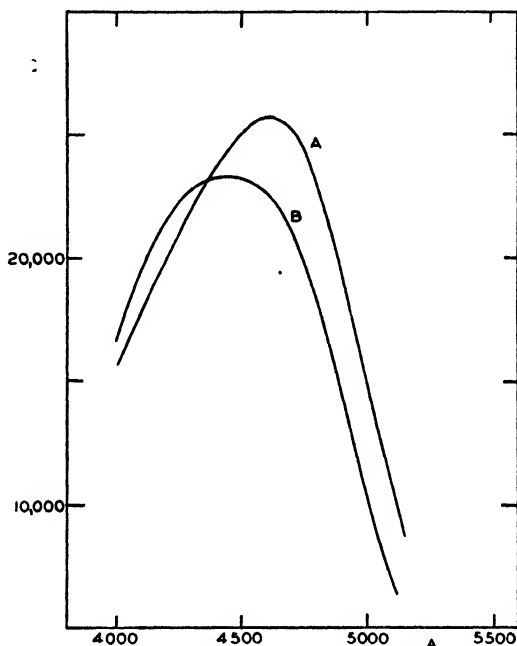


FIG. 6. Absorption spectra of methyl orange. A, buffer, pH 6.84; B, buffer + bovine albumin (0.2 per cent), pH 6.83.

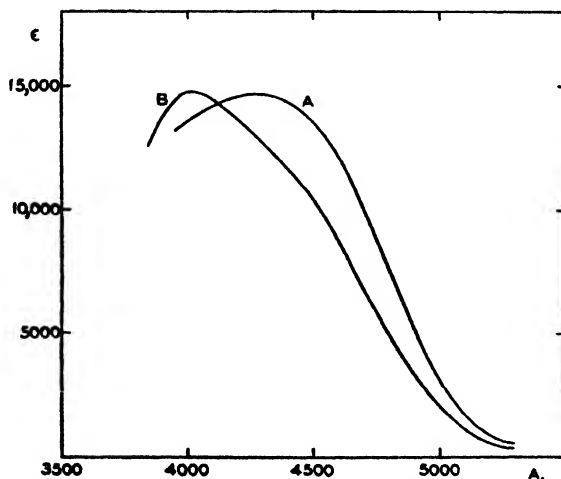


FIG. 7. Absorption spectra of methyl red. A, buffer, pH 7.33; B, buffer + bovine albumin (0.2 per cent), pH 7.31.

Only amaranth has a higher charge than any of the compounds mentioned (three SO_3^- groups), but this property would decrease any propensity toward micelle formation (9).

In the solutions used the pH was always above 5, so that the albumin was on the alkaline side of its isoelectric point and hence negatively charged. Similarly for each dye, the pH was chosen so that practically all of the material was in the anionic form. Under these circumstances one would predict the absence of any interaction between dye and protein. The spectral changes, however, are clear indications of the presence of a specific interaction between the large and small molecules, interactions which are so strong that they overcome the repulsion between the ions of similar charge.

That the anionic dyes can be bound by the negatively charged albumin has been verified by direct dialysis-distribution studies on orange I, orange II, azo-sulfathiazole, methyl orange, and bromocresol green. The results for one of these, methyl orange, are summarized in figure 12. Clearly, very large fractions

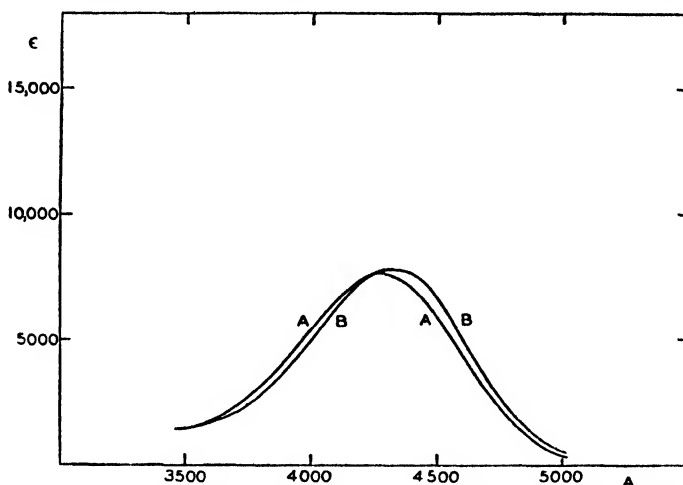


FIG. 8. Absorption spectra of 2,6-dinitrophenol. A, buffer, pH 7.62; B, buffer + human albumin (0.2 per cent), pH 7.59.

of the indicator anion combine to form a complex with the albumin, even in solutions of the order of 10^{-6} molar. Such complex formation would have a pronounced effect on the equilibrium between the acid and base forms of the indicator. This disturbance of the equilibrium, coupled with the change in the spectrum of the adsorbed form, may introduce a large error in a colorimetric determination of pH, despite the fact that the dye and protein have the same charge.

All of the azo dyes, with the possible exception of methyl red, show lower maxima in the presence of albumin than in its absence. The two nitrophenol derivatives (figures 8 and 10), on the other hand, have significantly higher maxima in the presence of protein. The two dyes whose spectra show the smallest alteration on the addition of albumin are prontosil and 2,6-dinitrophenol. These are also the two compounds which lack a sulfonate or carboxylate substituent, each of which, as has been shown previously (7), contributes very strongly to the

formation of a stable protein-anion complex. Apparently prontosil and 2,6-dinitrophenol are not strongly bound by the albumin. This has been verified in the case of prontosil by the observation that spectral changes are still observed when the protein concentration is increased from 0.2 to 1 per cent, whereas

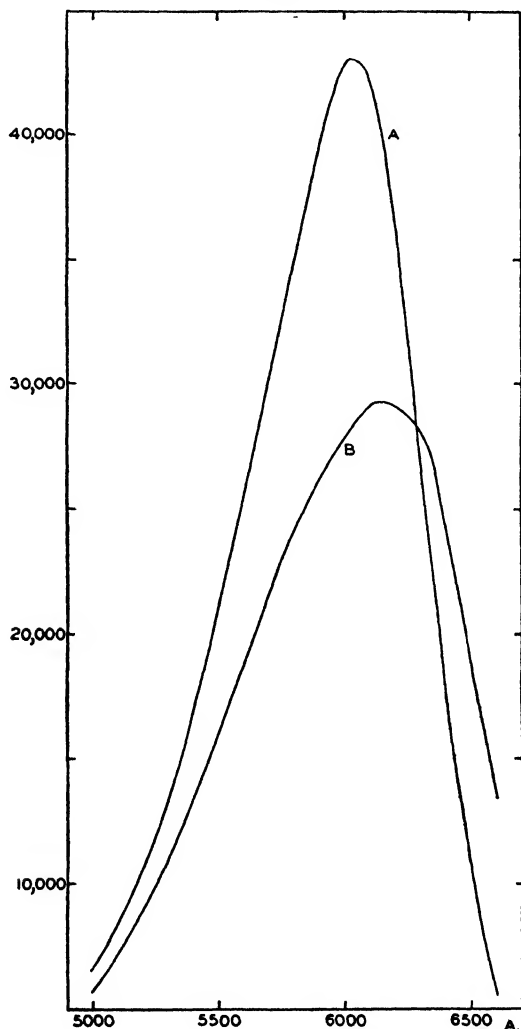


FIG. 9. Absorption spectra of bromocresol green. A, buffer, pH 6.92; B, buffer + bovine albumin (0.2 per cent), pH 6.92.

in the case of methyl orange or azosulfathizole, increases in protein content beyond about 0.2 per cent produce no further alterations (7). In the case of the dinitrophenol, the presence of only a single aromatic ring would also tend to decrease the strength of the protein-dye bond (8). The basis of Sørensen's observation that the protein error is generally smaller with indicators of simpler constitution thus becomes clear.

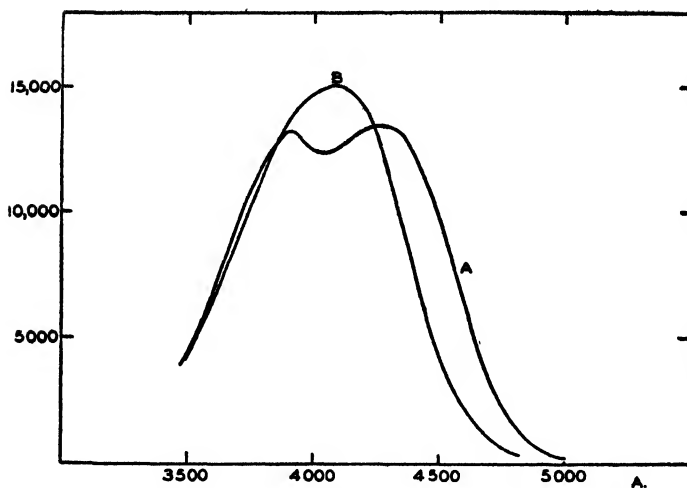


FIG. 10. Absorption spectra of naphthol yellow S. A, buffer, pH 7.63; B, buffer + bovine albumin (0.2 per cent), pH 7.59.

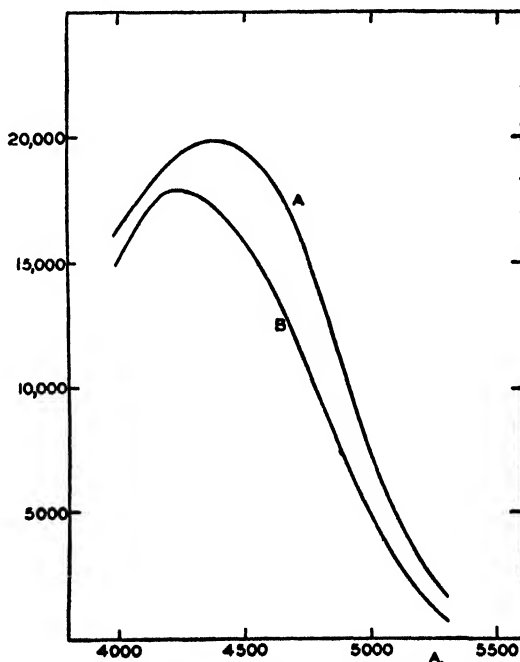


FIG. 11. Absorption spectra of tropaeolin OO. A, buffer, pH 7.63; B, buffer + bovine albumin (0.2 per cent), pH 7.60.

Despite the common binding group among the sulfonated dyes, the shift in wave length of the peak in the presence of protein differs from one compound to another. Thus in methyl orange (figure 6) and tropeolin OO (figure 11) the

shift is toward shorter wave lengths, and in azosulfathiazole (figure 4) and amaranth (figure 3) toward longer wave lengths, whereas orange I (figure 1) and orange II (figure 2) show no significant shift. Apparently the relative effect of the protein on the energies of the ground and excited states of the dyes is dependent on the nature of the entire molecule and not only on the character of the binding sulfonate group.

The anion-anion interaction between protein and dye is a very specific effect, and so far at least, has been observed only with serum albumin, either bovine or human. Sodium dodecyl sulfate, which in the micellar state in aqueous solution has a molecular weight of 20,000 (12), produces no alteration in the spectrum of azosulfathiazole, for example. Similarly, gelatin does not affect the spectrum of methyl orange or azosulfathiazole even in solutions containing

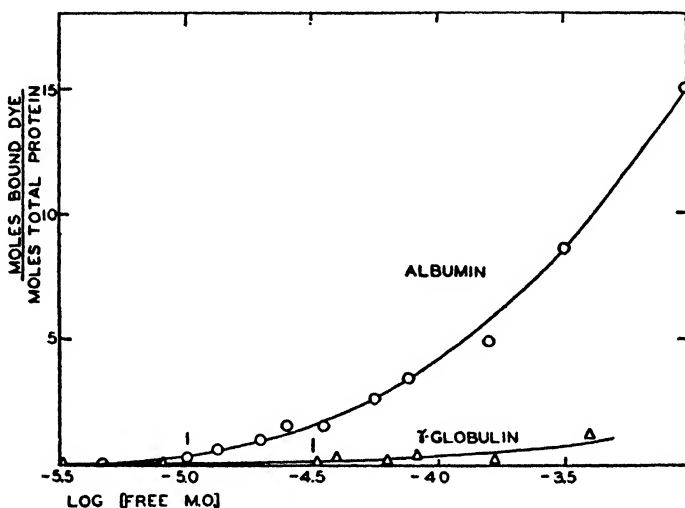


FIG. 12. Binding of methyl orange by bovine serum proteins

as high as 1 per cent of this protein, a concentration which is approximately five times as much as is necessary to produce a maximum effect with bovine albumin. The spectra of methyl orange in solutions of bovine γ -globulin at a concentration of 0.2 per cent and at pH's of 6.9 and 7.4 have been examined also, but no significant protein effect has been observed. Concurrently, dialysis-distribution experiments, using methyl orange, have been carried out with this globulin. The absence of any appreciable binding (figure 12) is evident. Only in concentrated solutions is a significant amount of methyl orange bound and even then the fraction in the complex is only a small part of that free in solution. The failure of Thiel and Schulz (16) to observe any effect on the light absorption of methyl orange on the addition of egg albumin, casein, or Witte peptone, respectively, must also be due to this same cause—the inability of these substances to bind the dye.

The extreme specificity of the anion-anion interaction is illustrated further

by a comparison of the effects of bovine and human serum albumin. With the former protein in solutions of methyl orange or azosulfathiazole, the spectral depression is essentially the same at all pH's from 5 to 9. Quite the contrary is observed in methyl orange solutions containing human serum albumin, as is illustrated in figure 13. At a pH of 6.89, the addition of the albumin produces only a very slight decrease in absorption at the shorter wave lengths, whereas

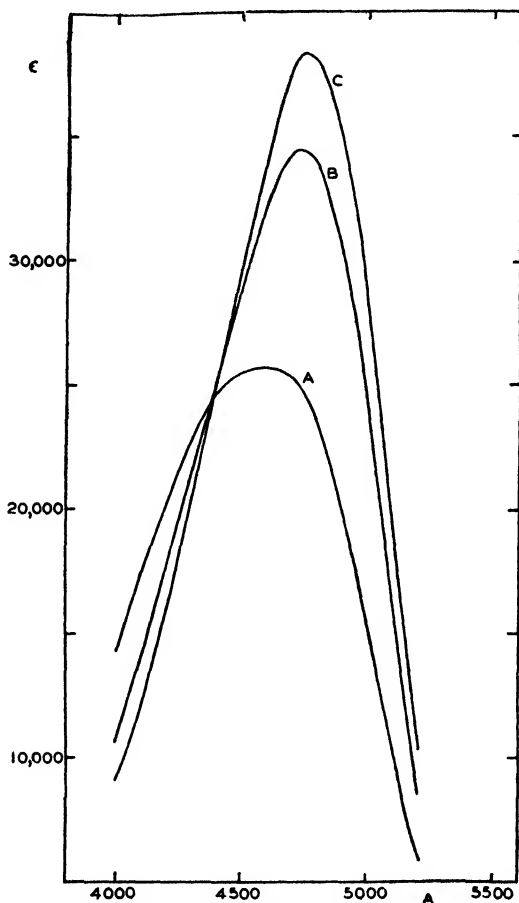


FIG. 13. Absorption spectra of methyl orange in 0.2 per cent human albumin. A, pH 6.89; B, pH 7.61; C, pH 9.16.

at a pH 7.61 there is a very pronounced increase in absorption. This increased absorption is even more pronounced at pH 9.16.

While direct binding studies with human albumin are incomplete as yet, the indications are that the results will not parallel the spectral changes. The extent of binding of methyl orange at pH 6.8 is almost the same as that at pH 7.6, despite the very pronounced difference in spectral behavior at these two pH's. The change in spectrum with decreased acidity seems to be due, therefore, to some change in the protein molecule, for the dye itself is not affected by pH

changes in this region. The region near pH 7 does correspond to the pK of the imidazolium group of the histidine residue in the protein and it may be that after the removal of the hydrogen ion, the ring —NH group of histidine is capable of forming a hydrogen bond with the dimethylamine substituent of methyl orange and thereby affecting the resonance within the dye ion. Some special interaction of this type, with pronounced structural specificity, is also indicated by the fact that with azosulfathiazole, human albumin produces spectral effects which are entirely analogous to those of bovine albumin.

In any event it is quite clear that the dependence of the protein error on pH observed by Danielli (4) is not the only type which may exist. In Danielli's experiments the error disappears entirely when the isoelectric point of the protein is passed and all species are in anionic form. In the experiments described here, however, where specific protein-dye interactions occur, the magnitude of the error may vary greatly with pH, despite the fact that the sign of the charge on the protein, or dye, undergoes no change.

The magnitude of the shift in spectrum on addition of serum albumin, and hence also the protein error, may depend on the particular buffer present in the solutions. A typical reversal of the spectrum of the protein-anion complex toward that of the free dye by the addition of potassium acid phthalate is illustrated in figure 4. The phthalate ion is only one of many organic anions which are capable of reversing this spectral shift (7). As has been shown previously (7), the cause of the reversal is the displacement of the dye anion by the organic anion. Since the degree of displacement depends on the nature and concentration of the organic ion, the magnitude of the protein error will be a function of the type and strength of the buffer in which the measurements are made.

CONCLUSIONS

The results of the experiments reported here, as well as those of previous investigations, indicate that the effect of proteins on colorimetric pH determinations may be the resultant of a variety of causes.

(1) The protein may adsorb an indicator ion of opposite charge, aided by electrostatic attraction, and thereby disturb the equilibrium between the acidic and basic forms of the indicator (6) or that between the dye micelle and the individual ions (5, 13).

(2) Specific attractive forces may lead to complex formation between protein and indicator ion even when both have the same electrical charge and hence a strong electrostatic repulsion. The equilibria of the indicator would be affected just as in (1).

(3) The protein may alter the activity coefficients of the indicator ions (1). This effect would be particularly important in concentrated solutions.

(4) The pH at the surface of the protein may differ from that in the bulk of the solution (4). Danielli has indicated how this difference may be calculated from the electrical charges on the protein.

(5) The spectrum of the dye in combination with the protein may differ from that of the free dye.

Since most of these effects depend on specific interaction constants, it is im-

possible, at least at present, to predict *a priori* the net error to be expected from a given protein in a particular solution. Insofar as colorimetric pH determinations are concerned, these studies serve to emphasize that the extrapolation of a set of observed errors from one protein to another, or from one pH to another, or even from one buffer to another at the same pH, may lead to very gross mistakes.

SUMMARY

Spectral changes on the addition of serum albumin have been observed for eleven indicators and dyes, including orange I, orange II, amaranth, azosulfathiazole, prontosil, methyl orange, methyl red, 2,6-dinitrophenol, bromocresol green, naphthol yellow, and tropeolin OO. These changes have been observed at relatively high pH values, where both protein and dye are negatively charged, and have been attributed to specific protein-dye interactions. Concurrent dialysis-equilibrium experiments have been carried out with some of these indicator ions and they have shown directly that albumin binds large fractions of the dye ions.

The effect of these specific protein-indicator interactions on colorimetric pH determinations is discussed, together with those of other factors previously recognized in the literature.

REFERENCES

- (1) CLARK, W. M.: *The Determination of Hydrogen Ions*, pp. 184-8. The Williams & Wilkins Company, Baltimore (1928).
- (2) CLARK, W. M., AND LUBS, H. A.: *J. Bact.* **2**, 1, 109, 191 (1917).
- (3) COHEN, B.: U. S. Public Health Service, Pub. Health Rept. **41**, 3051 (1926).
- (4) DANIELLI, J. F.: *Biochem. J.* **35**, 470 (1941).
- (5) GUTBIER, A., AND BRINTZINGER, H.: *Kolloid-Z.* **41**, 1 (1927).
- (6) HARTLEY, G. S.: *Trans. Faraday Soc.* **30**, 444 (1934).
- (7) KLOTZ, I. M.: *J. Am. Chem. Soc.* **68**, 2299 (1946).
- (8) KLOTZ, I. M., WALKER, F. M., AND PIVAN, R. B.: *J. Am. Chem. Soc.* **68**, 1486 (1946).
- (9) KORTUM, G.: *Z. physik. Chem.* **B34**, 255 (1936).
- (10) LEPPER, E. H., AND MARTIN, C. J.: *Biochem. J.* **21**, 356 (1927).
- (11) PALITZSCH, S.: *Compt. rend. trav. lab. Carlsberg* **10**, 162 (1911).
- (12) PUTNAM, F. W., AND NEURATH, H.: *J. Biol. Chem.* **159**, 195 (1945).
- (13) SHEPPARD, S. E., AND GEDDES, A. L.: *J. Chem. Phys.* **13**, 63 (1945).
- (14) SØRENSEN, S. P. L.: *Biochem. Z.* **21**, 131 (1909).
- (15) ST. JOHNSTON, J. H., AND PEARD, G. T.: *Biochem. J.* **20**, 816 (1926).
- (16) THIEL, A., AND SCHULZ, G.: *Z. anorg. allgem. Chem.* **220**, 225 (1934).

RATE OF CORROSION OF LEAD BY HYDROCARBON SOLUTIONS OF ORGANIC ACIDS

DAVID TURNBULL AND DELTON R. FREY¹*Department of Chemistry and Chemical Engineering, Case School of Applied Science, Cleveland, Ohio**Received October 30, 1946*

INTRODUCTION

In an earlier paper (3) from this laboratory the rate of corrosion of lead was studied in relatively concentrated (0.04 to 0.25 molar) solutions of organic acids in hydrocarbons under conditions in which the test piece was stationary with respect to the reaction vessel and the solution around it was mildly agitated by having the vessel in a mechanical shaker during the test. Results of this investigation showed that for this experimental arrangement the rate of corrosion was controlled primarily by the concentration of molecular oxygen or organic peroxide and was nearly independent of acid concentration over wide limits (0.03 to 0.25 molar). Denison (1) had previously reported that the rate of corrosion of lead in oils was controlled by the concentration of peroxides formed during oxidation of the lubricant and independent of acid number after an appreciable quantity of acid had been formed. He proposed a two-step mechanism for the corrosion of lead: (1) oxidation of lead to lead oxide by organic peroxides, (2) reaction of lead oxide with organic acid to form a lead salt soluble in the lubricant. Denison's experimental procedures were basically similar to those employed in this laboratory. Later, employing the same experimental techniques, Prutton, Turnbull, and Frey (4) demonstrated that organic oxidizing agents in the general sense, such as quinones and oxynitro compounds, acted in conjunction with organic acids to accelerate the corrosion rate of lead in hydrocarbon solvents.

Although in most of these studies (some of the non-peroxidic oxidizing agents excepted) the rôle of organic acids in controlling the corrosion rate was secondary, it appeared advisable to reinvestigate their rôle, using experimental conditions which would minimize diffusion of reactant into the surface layer as a rate-controlling factor.

This investigation was undertaken for the purpose of studying the effect of acid structure and concentration upon the corrosion rate of lead in hydrocarbon solvents using a fixed oxidizing agent—namely, air at atmospheric pressure—and conditions which served to reduce the depth of the diffusion layer surrounding the test specimen. Reduction of the depth of the diffusion layer was accomplished by rotating the test specimen at a high speed. This effect has been discussed at length by a number of investigators (2, 5).

¹ Present address: Anderson-Pritchard Oil Corporation, Cyril, Oklahoma.

EXPERIMENTAL PROCEDURE

Materials

Cylindrical test pieces of lead were prepared by casting Baker's analytical reagent grade granular lead in Pyrex tubes *in vacuo*. Test pieces were constructed to average about 1 in. in length and $\frac{3}{8}$ in. in diameter.

Organic acids employed were all c.p. grade acids obtained from the Eastman Kodak Company or Eimer and Amend. Traces of certain impurities in the high-molecular-weight acids used had a very marked influence on the corrosion rates. This phenomenon and the methods of further purification will be discussed in the section on results.

Benzene and xylene were the solvents used. c.p. grade materials were obtained from the J. T. Baker Chemical Company and further purified immediately before use by distillation from metallic sodium.

Apparatus

Figure 1 is a cross section showing the essentials of the construction of the stirring mechanism and the manner in which the lead test piece was supported and attached thereto. All parts were drawn according to the scale indicated on the diagram.

By regulating the speed of the electric motor with a variable transformer it was possible to vary the rotational speed from 1200 to 2000 R.P.M. with the gear ratio 36 to 18 as shown, and from 250 to 1000 R.P.M. when the gears were interchanged to make the ratio 18 to 36.

During a part of the investigation the lead test piece was supported on a bakelite shaft, so that no metal parts other than lead were in contact with the solution. Results obtained with bakelite shafts, however, did not differ perceptibly from those obtained with steel, so that the latter were used throughout most of the investigation, since their greater mechanical strength was desirable at high rotational speeds.

Test solutions were maintained at a constant temperature by immersing the reaction vessel to its neck in an oil bath maintained at a constant temperature ($\pm 0.2^\circ$) by means of a Cenco "Quickset" bimetallic regulator which activated a relay powered by a Rectran, both supplied by the American Instrument Company. Heat was supplied by a 1000-watt Aminco flexible-type immersion heater.

Procedure

A 180-ml. Soxhlet flask containing 160 ml. (accurately measured) of the solution to be used was placed in the constant-temperature bath directly below the shaft F, to which the steel shaft S, holding the lead cylinder, was to be attached. After the solution had reached the bath temperature, the shaft S with the lead piece supported on it was attached in the manner indicated by figure 1. Bath and stirring mechanism were arranged so that the lead piece was completely immersed in the solution after attachment. Upon setting the shaft in rotation,

timing was begun with a stop watch. After a specified interval the rotation was stopped and the lead piece detached. It was then rinsed successively with benzene and isopropyl ether, after which its surface was wiped with a clean

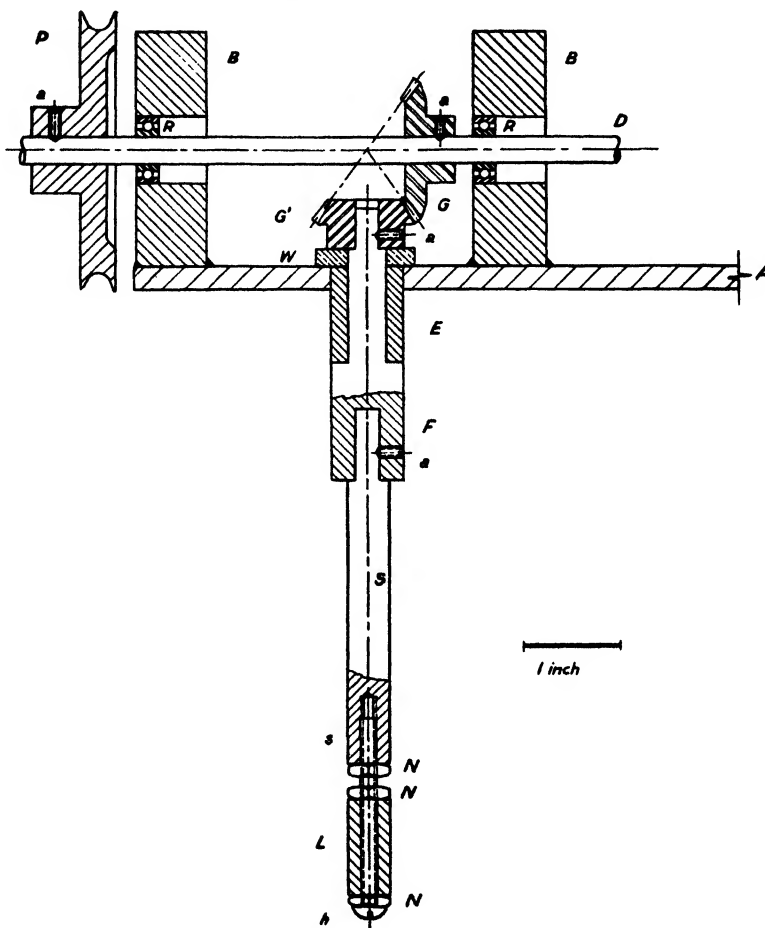


FIG. 1. The apparatus. P, 3-in. pulley from which a belt was passed to a 2-in. pulley powered by a $\frac{1}{4}$ -h.p. electric motor; B, steel blocks $\frac{3}{4}$ in. x $1\frac{1}{2}$ in. x $2\frac{1}{2}$ in., welded to steel plate; A, steel plate $\frac{1}{4}$ in. thick by $2\frac{1}{2}$ in. wide mounted over a constant-temperature bath; R, ball-bearing races shrunk-fit into steel blocks; D, $\frac{1}{2}$ -in. steel shaft; a, set screws; G, G', brass bevel gears, 18 teeth in G' and 36 in G, 48 pitch; F, steel shaft; W, $\frac{1}{8}$ -in. brass washer; E, brass bearing shrunk-fit into steel plate; S, steel shaft; s, steel screw; h, screw head; N, steel nuts seated on steel washers; L, lead test piece.

lintless towel. After its weight loss had been determined, it was replaced in the apparatus and rotated for another specified interval. This procedure of rinsing and weighing the test piece several times during the course of an experiment was justifiable, provided no protective film was removed in the cleaning operation. Actually, a number of experiments were carried out in which the corrosion rate

was found to be independent of the time interval chosen for the weighings. Also, kinetic data to be reported in the results gave further confirmation that the corrosion rate for most of the experiments was determined by the nature of the solution rather than by accumulation of surface films on the lead.

RESULTS

It will be convenient to consider the results of these experiments on the basis of the assumption that the corrosion rate was directly proportional to acid concentration. Since the concentration of the oxidizing agent was constant at all times, any term in the rate expression dependent upon it will be included in the rate constant. On the basis of these assumptions the following expression for corrosion rate may be formulated:

$$\frac{dw}{dt} = k'AC \quad (1)$$

where w = total weight loss in time t ,
 A = area of test piece, and
 C = concentration of acid at time t .

It is convenient to express the concentration of acid in terms of the weight loss of the metal sample. Thus, if C_0 is the initial concentration of acid, this may react with w_0 grams of lead, which will be given by the following relation:

$$w_0 = gC_0V \quad (2)$$

where g = weight of lead which reacts with 1 mole of acid and V = volume of solution in liters. At any time t the concentration of acid will then be given by

$$C = \frac{w_0 - w}{gV} \quad (3)$$

Substituting equation 3 into equation 1 we have:

$$\frac{dw}{dt} = \frac{k'A}{gV} (w_0 - w) \quad (4)$$

Integrating equation 4 and applying the condition that $w = 0$ when $t = 0$, we have:

$$\frac{k'}{g} = \frac{2.303V}{At} \log \frac{w_0}{w_0 - w} \quad (5)$$

Setting $k'/g = k$:

$$k = \frac{2.303V}{At} \log \frac{w_0}{w_0 - w} \quad (6)$$

Product of corrosion of lead by organic acids

In an earlier publication (3) it was reported that in the corrosion of lead by organic acids the normal salt PbA_2 , where A represents the acid radical, was

formed. This was established by comparing the weight of the salt which could be crystallized out of solution at room temperature after corrosion at a higher temperature with the weight of metal lost. Under the conditions of those experiments the acid was present in considerable excess, so that if a basic salt had formed in the corrosion process, the normal salt would have been precipitated out at the lower temperature.

Kinetic and analytical evidence obtained in the present investigation points to basic lead salts rather than to normal salts as the direct product of corrosion in xylene or benzene solutions at temperatures of 70° to 80°C. At room temperature the normal salt may ultimately be precipitated out of the mixture, however, providing there is considerable excess of acid.

In order to deduce the nature of the corrosion product from kinetic evidence dw/dt may be plotted against w . Then, if equation 4 represents adequately the corrosion rate, a straight line should be obtained having a slope = $-kA/gV$ and an intercept kAw_0/gV . By dividing the intercept by the slope, w_0 is found. Then, if W represents the gram-atomic weight of lead, w_0/WC_0V should give the ratio of lead atoms to acid radicals in the molecule of the corrosion product.

This method of evaluating the ratio of lead corroded to acid consumed is illustrated in figures 2, 2a, 3, and 3a. For example, in figure 2 the corrosion loss of a lead test piece in a benzene solution initially 0.0050 molar in butyric acid at 70°C. is plotted against time. Then, in order to arrive at figure 2a, the slope of this curve was evaluated graphically at various even values of the time and plotted against the corresponding weight loss for the point under consideration, as shown in figure 2a. It is clear from figures 2a and 3a, which are typical of the results obtained, that a linear relation holds between dw/dt and w as required by equation 4 until the reaction is at least 70 per cent completed. In these experiments a stirring speed of 1925 R.P.M. was employed. Table 1 summarizes the results of these determinations.

When carefully purified stearic and palmitic acids were used in the corrosion studies, it was necessary to use a small amount of acetic acid as a catalyst in order to obtain a rapid corrosion rate. From the results of table 1 it is clear that the formula of the corrosion product was determined primarily by the initial concentration of acid used and was little affected by the changes in solvent, temperature, and molecular weight of acid employed. For initial acid concentrations of 0.01 to 0.005 mole per liter a mean ratio of 1.43 ± 0.03 moles of acid per gram-atom of lead was found, while for initial acid concentrations of 0.002 mole per liter a mean ratio of 1.23 ± 0.04 was obtained. This suggested that basic salts rather than the normal salt were the direct products of corrosion under these conditions. In the more concentrated solutions studied an empirical formula of $PbA_{1.43}(OH)_{0.57}$ (or $PbA_{1.43}O_{0.28}$) was indicated, while for the 0.002 normal solutions a formula of $PbA_{1.23}(OH)_{0.77}$ (or $PbA_{1.23}O_{0.38}$) was indicated.

In order to establish further evidence for the formation of basic lead salts in these experiments, corrosion products were isolated from the reaction mixture and analyzed for lead by an ash method, which gave results accurate to within 1 per cent. In these experiments lead test pieces were rotated for a 2-hr. period

in 168 cc. of a benzene solution 0.0095 molar in lauric acid and 0.00028 molar in acetic acid at 70°C. From the number of the equivalents of acid initially present

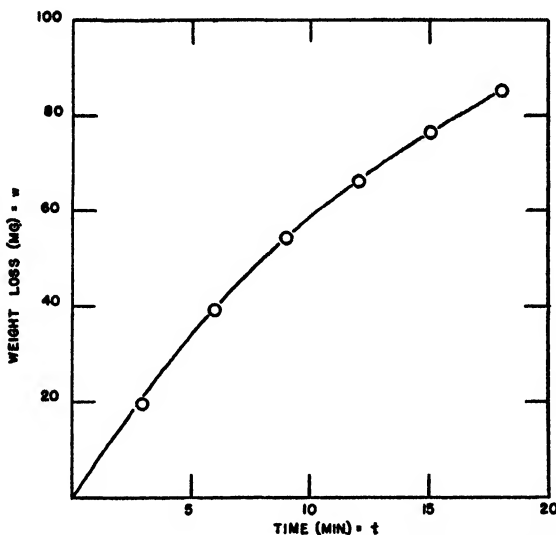


FIG. 2. Corrosion loss of lead in 0.0050 *M* butyric acid in benzene at 70°C.

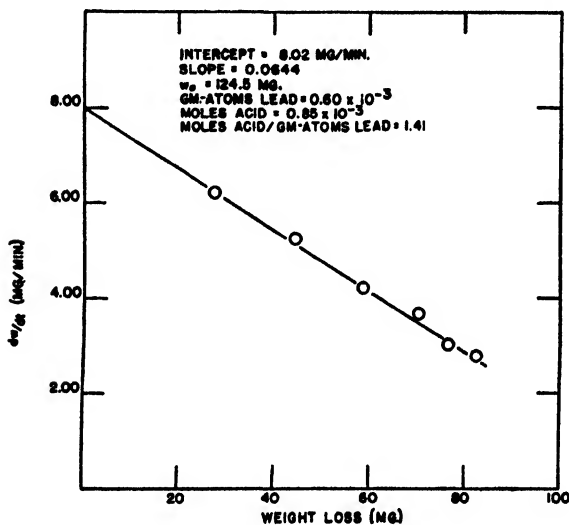


FIG. 2a. Rate of corrosion of lead in 0.0050 *M* butyric acid in benzene at 70°C. as a function of corrosion loss.

the amount of lead which would have dissolved had the reaction gone to completion could be calculated on the basis of either normal salt (PbA_2) or basic salt formation. Actually, an amount of lead was dissolved in substantial excess of that which would have dissolved had a normal salt been formed. When the

reaction was stopped and the solutions had cooled to room temperature, a small amount of a white crystalline solid crystallized out. This was filtered and found

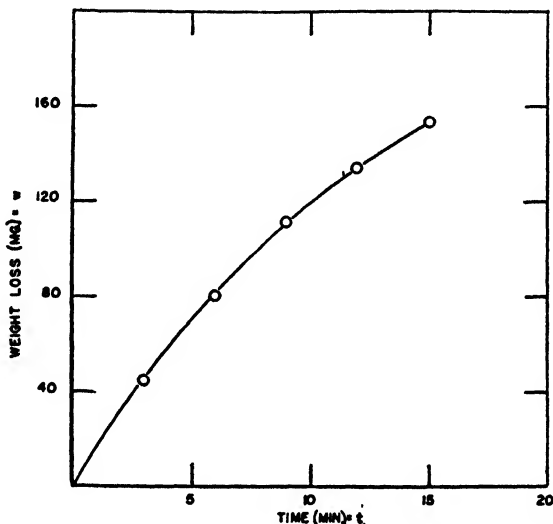


FIG. 3. Corrosion loss of lead in 0.0095 *M* butyric acid in xylene at 78°C.

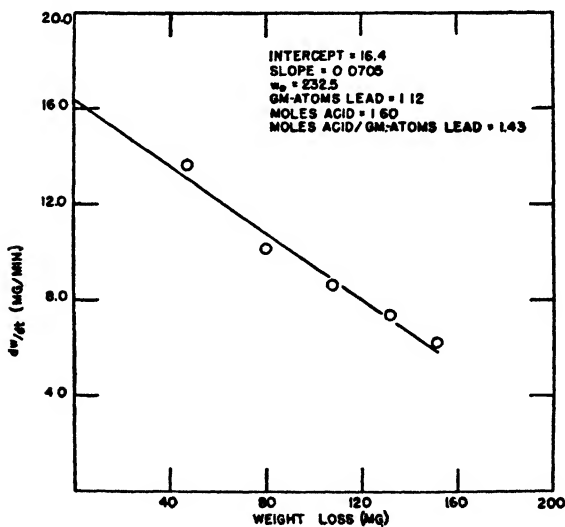


FIG. 3a. Rate of corrosion of lead in 0.0095 *M* butyric acid in xylene at 78°C. as a function of corrosion loss.

to contain 34.0 ± 0.2 per cent lead, a value in good agreement with the per cent of lead in the normal salt, 34.1. However, only about 21 per cent of the lead which had dissolved could be accounted for in this manner, while the remainder stayed in solution in the form of some salt which was benzene soluble at room

temperature. This was in accord with other observations made in this laboratory, that if the corrosion reaction in xylene or benzene solution was stopped while the amount of remaining acid was in considerable excess of that required to form the normal salt, an amount of this salt could be crystallized out at room temperature equivalent to the quantity of lead dissolved; if the reaction was permitted to proceed nearly to completion, however, little or no salt of any kind could be crystallized out when the solution was cooled and permitted to remain at room temperature for a long period.

After the normal salt had separated from the solutions, benzene was removed from the filtrate by distillation from a water bath. No phase separation was observed during the course of the benzene removal. When nearly all the benzene had been removed, a light brown syrupy liquid remained which finally set to an amorphous solid upon standing. This residue was found on ashing to contain

TABLE 1

Ratio of acid radicals to lead atoms found in the corrosion product for the reaction between lead and organic acid in a hydrocarbon solvent as evaluated by a kinetic method

TEMPERATURE	SOLVENT	ACIDS		INITIAL ACID CONCENTRATION		MOLES ACID PER GRAM-ATOM OF LEAD
		1	2	1	2	
°C.						
70	Benzene	Butyric		0.00190		1.25
70	Xylene	Butyric		0.00190		1.22
78	Xylene	Butyric		0.00190		1.22
70	Benzene	Butyric		0.00475		1.42
70	Benzene	Butyric		0.00502		1.43
70	Xylene	Butyric		0.00480		1.38
78	Xylene	Butyric		0.00475		1.51
78	Xylene	Butyric		0.0095		1.43
78	Xylene	Stearic	Acetic	0.0095	0.00031	1.47
78	Xylene	Palmitic	Acetic	0.0095	0.00031	1.41

39.4 ± 0.2 per cent lead, as compared with 41.2 per cent which would have been expected if all of the benzene had been removed. Table 2 summarizes the results of these analyses for two different experiments. These results offer further support for the hypothesis that basic lead salts rather than the normal salt are formed in the corrosion process. These salts apparently have the proximate formula $\text{PbA}_{1.5}(\text{OH})_{0.5}$ (or $\text{PbO} \cdot 3\text{PbA}_2$), are low melting, and in contrast to the normal salt (which is benzene soluble at 70°C. but only very slightly soluble at room temperature) are quite soluble in benzene at room temperature.

By heating together proper proportions of lead hydroxide and lauric acid it was possible to prepare basic salts with properties identical to those isolated from the reaction mixture insofar as they were examined. For example, when lead hydroxide and lauric acid were heated together in the molar proportion of 2 to 3 at 110°C. for 14 hr., a syrupy liquid was formed which was very similar in appearance to the residue isolated from the reaction mixture; this preparation was benzene soluble at room temperature and an ash determination showed that

it contained 39.3 ± 0.1 per cent lead, a value which compared well with 40.3 per cent lead required by the formula $\text{Pb}_2(\text{OH})\text{A}_3$, where A represents the laurate radical. Further, it was found possible to prepare a basic lead laurate which was low melting and benzene soluble at room temperature by heating together in a similar manner a 1:1 molar proportion of lead hydroxide and lauric acid.

Thus kinetic evidence, analysis and properties of products isolated from the reaction mixture, and synthesis of materials having properties like those isolated from the reaction mixture all point to basic lead salts having formulae ranging from $\text{Pb}_2(\text{OH})\text{A}_3$ to $\text{Pb}(\text{OH})\text{A}$ as the product of reaction between lead and dilute solutions of organic acids in xylene or benzene in the temperature range 70° to 100°C .

Effect of speed of rotation of test piece upon corrosion rate

It will be shown later in this paper that butyric acid was one of the most reactive of the acids studied. Therefore, since a diffusion process was more

TABLE 2

Amounts and composition of lead salts recovered from reaction mixture of lead and benzene solution of 0.0095 molar lauric acid and 0.00028 molar acetic acid at 70°C .

RUN NUMBER	ACID INITIALLY ADDED	LEAD DISSOLVED	LEAD LAURATE RECOVERED	LEAD FOUND IN LEAD LAURATE	LEAD IN RESIDUE	ACID IN RESIDUE	ACID PER GRAM-ATOM OF LEAD IN RESIDUE	LEAD IN RESIDUE
	moles	gram-atoms	moles	weight per cent	gram-atoms	moles	moles	weight per cent
1	0.00165	0.001028	0.000201	33.9	0.00083	0.00125	1.51	39.2
2	0.00165	0.001005	0.000224	34.0	0.00078	0.00120	1.54	39.6

likely to be rate controlling for this acid than for the less reactive acids, an investigation was made on the effect of rotational speed upon the corrosion rate constant. Rotational speed was varied between 375 R.P.M. and 1925 R.P.M., corresponding to a radial velocity range from approximately 1100 to 5800 cm. per minute. Butyric acid solutions were made up in xylene and experiments were carried out at 78°C . Under these conditions it was found that equation 4 satisfactorily represented the reaction rate when the concentration of butyric acid was 0.01 mole per liter or below. Rate constants were calculated using equation 6. Since it was found that the length of the test piece did not diminish appreciably over extended periods of time, while the diameter of the test piece decreased uniformly as corrosion proceeded, the apparent surface area was calculated from the area of the cylinder wall, while those of the ends, which were always covered by washers, were neglected. Rate constants evaluated for different test pieces having areas differing by a factor from 1 to 2 generally agreed to within ± 5 per cent.

Figure 4 shows the rate constants plotted against stirring speed. Above a rotational speed of 500 R.P.M. there is no marked change in the rate constant. Therefore, it may be concluded that above this rotational speed diffusion is only

a secondary factor in determining the corrosion rate. Unless otherwise specified, all the results reported in this paper were taken using a rotational speed of 1925 R.P.M.

Effect of acid concentration on corrosion rate

Organic acids studied in this investigation could be classified into two groups according to their reactivity. Group I consisted of acids which were very reactive in dilute solutions (0.01 molar or less) and were typified by acetic, butyric, and benzoic acids. Acids falling in this group were all appreciably soluble in water and exhibited acid strengths which were of the order of that of acetic acid or stronger. Group II acids were relatively unreactive in dilute solutions and were typified by lauric, stearic, and naphthenic acids, and phenol. Acids in

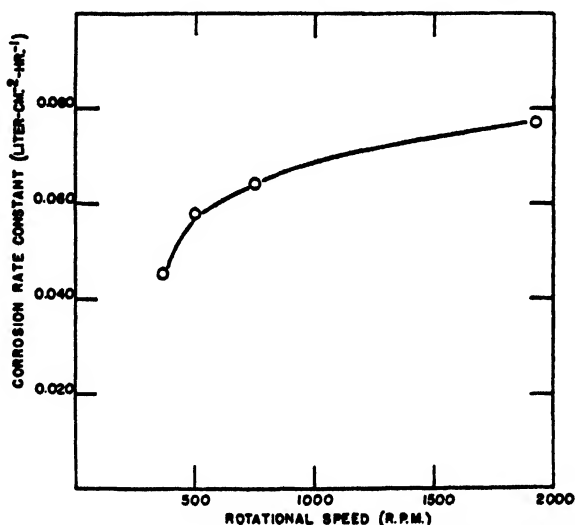


FIG. 4. Effect of rotational speed upon corrosion rate constants of lead in dilute (0.005 to 0.01 *M*) solutions of butyric acid in xylene at 78°C.

this group were generally either water insoluble, or if water soluble, were very weak, such as phenol.

Group I acids

In studying acids in this group five tests each of 3–5 min. duration were usually made with a particular solution. Thus the total period of the experiment was about 15–25 min., and this was sufficiently long so that the reaction was well past the half-life period. Rate constants were then evaluated using equation 6. Constants calculated in this way (w_0 was determined in the manner already outlined) generally deviated by no more than ± 3 per cent from the average.

Table 3 summarizes the rate constants found for butyric acid in xylene and benzene solutions at 70°C. and in xylene solutions at 78°C. for different con-

centrations of acid. From these results it may be seen that the corrosion rate constants for butyric acid are virtually independent of acid concentration for concentrations of 0.01 molar and below at 78°C., and for concentrations of 0.005 molar and below at 70°C. These results are in agreement with the requirements of equations 4 and 6. At 70°C. the mean rate constant in benzene was about 15 per cent higher than in xylene, showing that the effect of changing solvent in this case was not marked. It is also apparent that the temperature coefficient for the reaction in xylene in this range was not appreciable.

At concentrations of acid greater than 0.01 mole per liter at 78°C. (0.005 mole per liter at 70°C.) the rate constant decreased markedly and, in fact, the actual reaction rate was less in a more concentrated solution. This can be shown most conveniently by considering the variation of kC_0 , which is directly propor-

TABLE 3
Corrosion rate constants, k , for lead in butyric acid solutions
Rotational speed of lead test piece = 1925 R.P.M.

SOLVENT	TEMPERATURE	INITIAL ACID CONCENTRATION	AVERAGE	OVER-ALL AVERAGE k
	°C.	M	liter $cm.^2$ $hr.^{-1}$	
Benzene	70	0.00095	0.0915	0.090
		0.00190	0.0894	
		0.00475	0.0855	
		0.0095	0.0388*	
Xylene	70	0.00192	0.0756	0.0784
		0.00480	0.0814	
Xylene	78	0.00095	0.0776	0.0780
		0.00190	0.077	
		0.00475	0.075	
		0.0095	0.0822	

* Not included in calculating over-all average.

tional to the reaction rate dw/dt when $t = 0$, with C_0 . When equation 4 is satisfied, kC_0 is a linear function of C_0 for the results presented, excepting at concentrations greater than 0.005 mole per liter in benzene at 70°C. Under these conditions for $C_0 = 0.00475$, $kC_0 = 4.06 \times 10^{-4}$, and for $C_0 = 0.0095$, $kC_0 = 3.68 \times 10^{-4}$. This effect was also observed for xylene solutions at 78°C. Thus, for some measurements taken at 500 R.P.M., kC_0 was a linear function of C_0 to a concentration of 0.01 mole per liter. Beyond this concentration deviations from linearity were very marked, and for a C_0 value of 0.025 mole per liter kC_0 was only two-thirds as great as its value at 0.0100 mole per liter.

Xylene solutions of acetic acid showed a very marked reactivity toward lead in very dilute solutions, 0.003 mole per liter or less, but above this concentration the corrosion rate fell off sharply and became very small in more concentrated solutions. This is shown in figure 5, in which kC_0 is plotted against C_0 . At concentrations lower than that at which the maximum rate was attained, no

visible film was apparent on the test piece, while at higher concentrations the presence of an adherent gray film covering the whole surface was readily apparent. Thus, the lower reaction rate at higher concentrations may be attributed to the protective action of a solid film not present at lower concentrations. It is possible that at concentrations below the maximum, soluble basic acetates are formed, while at higher concentrations acetates which are less basic and less soluble in xylene are formed. Normal lead acetate is only slightly soluble in xylene at 78°C.

Table 4 summarizes the corrosion rate constants and the corrosion rates in xylene at 78°C. for the three reactive acids studied. This table shows that for lower concentrations there is little difference in the reactivity of the three acids. There is considerable difference in the C_0 value at which kC_0 is no longer a linear

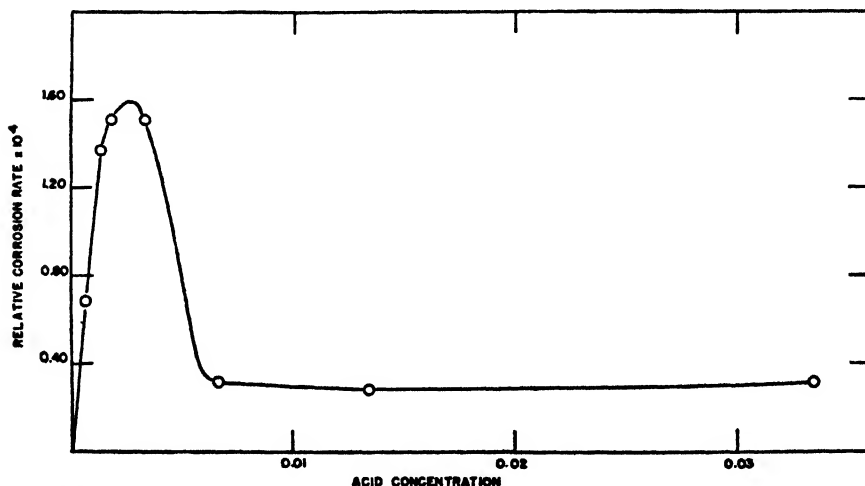


FIG. 5. Variation of reaction rate of lead with acetic acid solutions in xylene at 78°C. as a function of acetic acid concentration.

function of C_0 . For acetic acid this is about 0.002 molar, for benzoic acid between 0.005 and 0.01 molar, and for butyric acid between 0.01 and 0.02 molar.

Group II acids

Lauric acid exhibited a reactivity toward lead which was typical of the behavior of the acids which were not particularly reactive at lower concentrations. C.P. lauric acid as purchased proved to have substantial reactivity down to very low concentrations. However, when this acid was further purified it was found to be only about $\frac{1}{10}$ as reactive as butyric acid in xylene solutions at 78°C. for a concentration of 0.01 mole per liter. Further purification was effected by two methods, each of which gave a product which behaved similarly. In the first method a given amount of the acid was dissolved in ethyl alcohol and sufficient water was then added to precipitate out most of the acid. After filtration the precipitate was vacuum dried and retained in a desiccator until its

use was required. In the second method 100 cc. of a 0.25 molar solution of the acid in benzene or xylene was made up. This was then extracted with four 100-cc. portions of distilled water. After extraction the solution was dried over anhydrous sodium sulfate and filtered. After filtration the concentration of acid was ascertained, and the desired solutions for the corrosion measurements were prepared by diluting this solution with the amounts of pure solvent necessary to give the concentration desired. After the recrystallized acid or extracted solution had been prepared, it was necessary to use caution in order to prevent them from becoming contaminated again. Thus, if the stopper of a glacial

TABLE 4

Summary of corrosion rate constants and relative corrosion rates for lead in xylene solutions of Group I acids at 78°C.

Speed of rotation = 1925 R.P.M.

ACID	INITIAL CON- CENTRATION OF ACID	AVERAGE k	$kC_0 \times 10^4$	OVER-ALL AVERAGE k FOR C_0 VALUES WHERE kC_0 IS LINEAR FUNC- TION OF C_0
	<i>M</i>	<i>liter cm.⁻²hr⁻¹</i>		
Acetic	0.00067	0.102	0.685	0.102
	0.00134	0.102	1.37	
	0.00191	0.079	1.51	
	0.00335	0.045	1.50	
	0.00670	0.0048	0.32	
	0.0135	0.0021	0.28	
	0.0335	0.00095	0.32	
Butyric	0.00095	0.0776	0.736	0.0780
	0.00190	0.077	1.46	
	0.00475	0.075	3.56	
	0.0095	0.0822	7.80	
Benzoic	0.00190	0.0985	1.87	0.103
	0.00475	0.108	5.14	
	0.0095	0.074	7.03	

acetic acid bottle was brought near to recrystallized acid left exposed, its reactivity toward lead might be increased by a large factor (10 or more). All of the other higher-molecular-weight acids were further purified by one of the above methods, although in some instances the behavior of the purified acid was no different from that of the c.p. acid as purchased (e.g., Eastman's stearic acid, Eimer and Amend's oleic acid). Phenol was further purified by redistillation.

For Group II acids correlation of the relative corrosion rates, kC_0 , with acid concentration proved to be more illuminating than comparison of the rate constants. Figure 6 shows relative corrosion rates plotted against concentration for three typical Group II acids. These results show that the corrosion rate is

quite low below a certain "critical concentration," which is about 0.035 mole per liter for lauric acid. Above this concentration the rate rises very sharply and rapidly to a value which increases only very slowly with concentration and which was of the same order of magnitude for the three acids studied. This limiting rate was of the same order of magnitude, although about 25–30 per cent lower, as the maximum corrosion rate attained in butyric acid solutions under the same conditions. Other high-molecular-weight acids studied (including oleic, palmitic, naphthenic, and capric) exhibited relative corrosion rates which varied in a similar manner with concentration. There appeared to be a rough correlation between critical concentration and molecular weight of the acid (within a homologous series); as the molecular weight increased the critical concentration generally was higher. Heptylic and caproic acids proved to be borderline acids

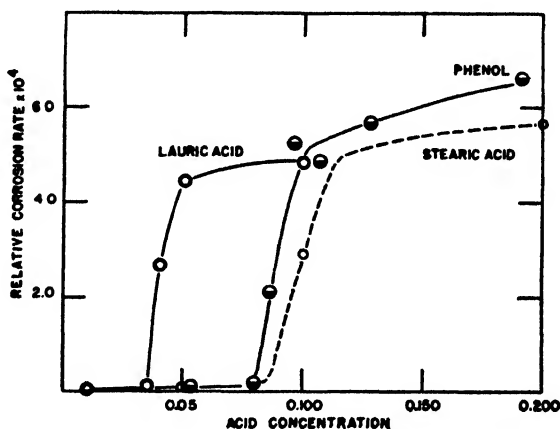


FIG. 6. Relative rates of corrosion of lead in xylene solutions of Group II acids at 78°C: as a function of acid concentration.

which exhibited no well-defined critical concentration. However, the rate constant did increase with increasing concentration of acid.

To study the effect of temperature on the critical concentration proved to be a difficult problem, because of the difficulty in choosing a solvent or acid which did not oxidize to some extent at a high temperature to give Group I acids which might either cause rapid corrosion or catalyze corrosion by Group II acids. Thus, in either xylene or *n*-hexadecane solutions of lauric acid no critical concentration was observed at 140°C., a result which might be attributed to (1) a decrease or complete disappearance of the critical concentration, (2) oxidation of the solvent to Group I acids, (3) oxidation of lauric acid to a Group I acid. With solutions of phenol in biphenyl a well-defined critical concentration was observed at 140°C. However, this may have been due to the unlikelihood of such a solution oxidizing to a Group I acid. Further, it will be seen that Group I acids have no catalytic effect upon the corrosion of lead by phenol solutions. Figure 7 shows a comparison of the corrosion rates of lead in these solutions at two temperatures. At 100°C. it is seen that the critical concentration is greater

than 0.02 molar and less than 0.03 molar, while at 140°C. it is between 0.007 and 0.01 molar. Thus it appears that with increasing temperature the critical concentration is decreased to a large extent.

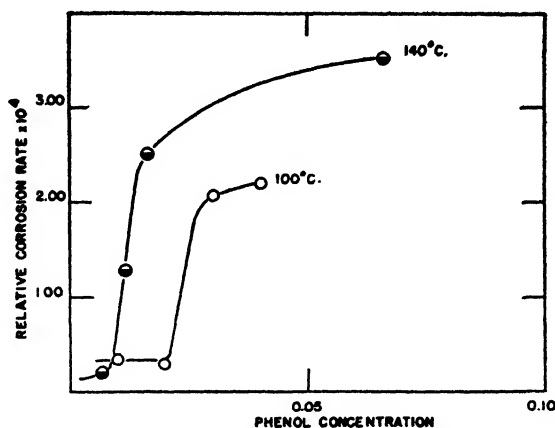


FIG. 7. Relative rates of corrosion of lead in biphenyl solutions of phenol

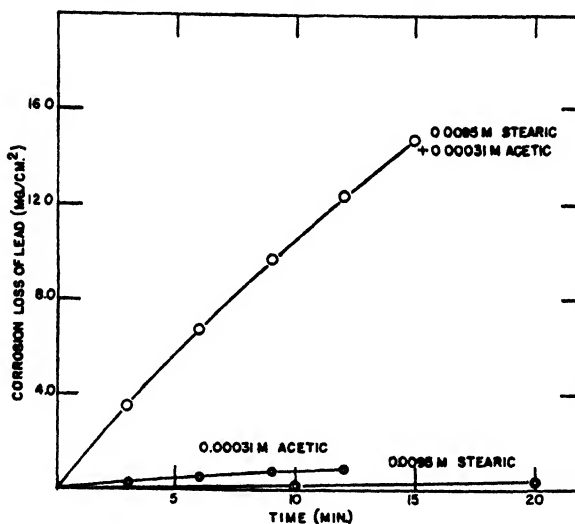


FIG. 8. Corrosion losses of lead in xylene solutions at 78°C., showing catalytic effect of acetic acid on corrosion by stearic acid.

Catalytic effect of Group I acids upon corrosion rates by Group II acids

When a small amount of a Group I acid was added to a solution of a Group II acid whose concentration was much less than the critical, the corrosion rate of lead was increased by a large factor (10 to 60). In experiments studying this effect the concentration of Group I acid was maintained low enough so that only a negligible quantity of lead could have been dissolved by the Group I acid acting by itself. This effect is illustrated graphically in figure 8, which shows

the striking catalytic effect of acetic acid on the rate of corrosion of lead by stearic acid. In this experiment only 1.1 mg./cm.² of lead could have been dissolved through the action of acetic acid alone. Equation 4 proved to be a satisfactory rate equation for corrosion by these solutions, where the initial concentration of Group II acid did not exceed 0.01 molar, until the reaction was at least 70 per cent completed.

Table 5 summarizes the relative corrosion rates of 0.01 molar solutions of various Group II acids in xylene at 78°C. with and without the addition of 0.00031 molar acetic acid. For the higher-molecular-weight acids the corrosion rates have been increased by a factor of 40 to 60. Also the rates for 0.01 molar solutions of the higher-molecular-weight acids from lauric to stearic are about $4.6 \pm 0.4 \times 10^{-4}$ in the presence of acetic acid. It is noteworthy that neither acetic acid nor the other Group I acids have any measurable catalytic effect upon the rate of corrosion of lead by phenol solutions.

TABLE 5

Relative corrosion rates of various 0.01 molar solutions of Group II acids with and without the addition of acetic acid as a catalyst

GROUP II ACID	RELATIVE CORROSION RATE (kC_0) $\times 10^4$	
	No added acetic acid	With 0.00031 molar acetic acid
Heptylic.....	1.21	7.6
Capric.....	0.10	6.1
Naphthenic.....	0.11	5.2
Lauric.	0.088	4.4
Palmitic... . .	0.080	4.95
Oleic	0.083	4.2
Stearic.	0.087	4.85

Other Group I acids, such as butyric and benzoic, also had a very pronounced positive catalytic effect upon the corrosion rate of Group II acids. Butyric acid was not as effective a catalyst as acetic acid, however. For example, in a 0.01 molar stearic acid solution a small concentration of butyric acid raised the corrosion rate to only about 60 per cent of what it would have been if a comparable amount of acetic acid had been used.

A considerable number of experiments were made in order to study the catalytic effect of acetic acid on corrosion by 0.01 molar lauric acid solutions as a function of acetic acid concentration. Xylene was again used as the solvent and a temperature of 78°C. was employed. Concentrations of acetic acid ranging from 3×10^{-5} to about 4×10^{-4} were used. In figure 9 the relative corrosion rate kC_0 (where C_0 equals the initial concentration of lauric acid) is plotted against acetic acid concentration. Below an acetic acid concentration of 3×10^{-5} molar the acetic acid has little catalytic effect. When the concentration was greater than this, a catalytic effect was observed. Above a concentration of 2×10^{-4} molar there was only a small increase in catalytic effect with further increase in acetic acid concentration.

When the concentration of catalyst acid was maintained at a constant value it was observed that kC_0 was a linear function of C_0 , where C_0 = concentration of

Group II acid, with no intercept as required by equation 4 when C_0 did not exceed 0.01. When C_0 was greater than 0.01, kC_0 increased less rapidly and started to approach a limiting value. This is illustrated in figure 10, where

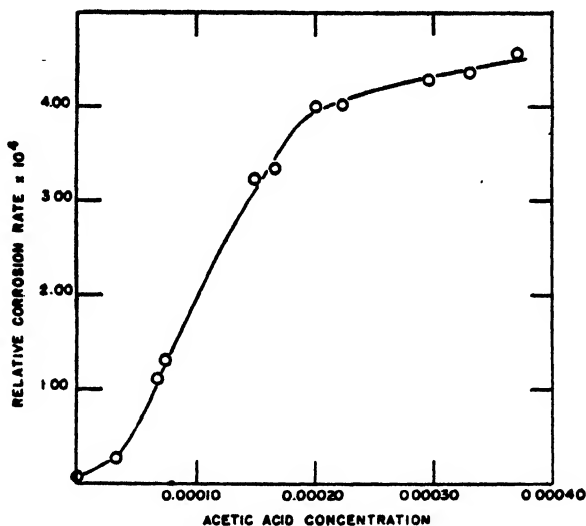


FIG. 9. Relative rates of corrosion of lead in 0.0095 *M* lauric acid solutions in xylene at 78°C. as a function of acetic acid concentration.

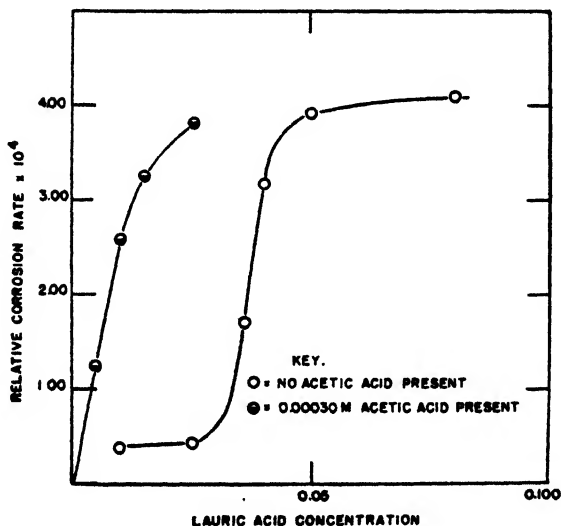


FIG. 10. Relative rates of corrosion of lead in *n*-hexadecane solutions at 100°C. as a function of lauric acid concentration with and without acetic acid present.

kC_0 for the corrosion of lead in *n*-hexadecane solutions of lauric acid with and without acetic acid at 100°C. is plotted against lauric acid concentration. From this figure it may be seen that the primary function of the acetic acid catalyst is to reduce effectively the critical concentration of lauric acid to a negligible value.

From the results of studies in *n*-hexadecane at 100°C. it is clear that the pronounced catalysis of lead corrosion due to Group I acids obtains up to this temperature. Using such solvents as *n*-hexadecane and xylene, however, it was difficult to decide whether or not the catalytic effect persisted at higher temperatures. As explained above, measurements in these solvents at 140°C. are of doubtful significance, owing to oxidation of the solvent during the course of the experiment. In biphenyl solutions however, proof was obtained that Group I acids had a catalytic effect on lead corrosion, although it was not as pronounced as at lower temperatures, since at the higher temperature the uncatalyzed reaction proceeded at a more rapid rate. Table 6 gives some relative corrosion rates measured in biphenyl solution at 140°C. At this temperature benzoic rather than acetic acid was chosen as a catalyst, owing to the volatility of acetic acid. It is seen that benzoic acid increases the lead corrosion rate in biphenyl by a factor of 3 to 4 at 140°C.

TABLE 6
Relative corrosion rates of lead in biphenyl solutions of fatty acids

TEMPERATURE °C.	GROUP II ACID	CATALYST ACID	INITIAL ACID CONCENTRATION		RELATIVE CORROSION RATE (<i>k</i> C ₀) × 10 ⁴
			Group II acid	Catalyst acid	
			<i>M</i>	<i>M</i>	
100	Lauric	None	0.0100		0.25
140	Lauric	None	0.0100		1.02
140	Lauric	Benzoic	0.0100	0.0005	2.96
140	Stearic	None	0.0100		0.88
140	Stearic	Benzoic	0.0100	0.0005	3.34

Dependence of corrosion rate upon concentration of oxidizing agent

In the experiments described above a constant concentration of a particular oxidizing agent was used: namely, air at atmospheric pressure. As already pointed out, it has been confirmed that the presence of an oxidizing agent was necessary in order for lead corrosion to take place at an appreciable speed in hydrocarbon solvents. Previous measurements had been made employing concentrations of acids considerably greater than those used in this investigation and using conditions under which diffusion of the oxidizing agent into the metal surface might be the rate-controlling factor. Now the question arises, with diffusion largely eliminated as a rate-controlling step, what is the dependence of the corrosion rate of lead upon the concentration of oxidizing agent? This question was partially answered by running corrosion experiments on stearic acid solutions in benzene and xylene at 70°C. and 78°C., respectively, through which pure oxygen was passing. Rates of corrosion found checked those observed using air as the oxidizing agent, within experimental error. These results were not considered entirely conclusive, however, since in the dynamic experimental system which was used the effective concentration of oxygen in the vapor phase was not known with certainty. To obtain results which were more conclusive, *tert*-butyl hydroperoxide, one of the most reactive oxidizing agents studied in the earlier investigation, was added in a definite concentration,

thus permitting a close control of the concentration of oxidizing agent. Also, quinone was used as an oxidizing agent in a number of experiments. Table 7 gives the results obtained using other oxidizing agents. It is seen from table 7 that addition of *tert*-butyl hydroperoxide did not alter the rate of the acetic acid-catalyzed corrosion of lead to any very significant extent. In view of earlier investigations on the rôle of oxidizing agents (3, 4) this might be considered surprising. However, this result must indicate that with experimental conditions chosen so that diffusion was not an important rate-determining factor, the corrosion rate must be nearly independent of the concentration of the more active oxidizing agents, such as oxygen or *tert*-butyl hydroperoxide, when they are present in excess of some critical value. In this connection it may be pointed out that the corrosion rate was insignificant when no oxidizing agent was present,

TABLE 7

Relative corrosion rates of lead in xylene solutions of fatty acids at 78°C. in presence of the oxidizing agents in addition to air

REAGENTS			INITIAL CONCENTRATION			RELATIVE CORROSION RATE $\times 10^4$
Group II acid	Catalyst acid	Oxidizing agent	Group II acid	Catalyst acid	Oxidizing agent	
Lauric	Acetic	Air	<i>M</i>	<i>M</i>		
Lauric	Acetic	<i>tert</i> -Butyl hydroperoxide	0.0095	0.00031	750 mm.	4.19
			0.0095	0.00031	0.0190 <i>M</i>	4.25
Lauric	Acetic	<i>tert</i> -Butyl hydroperoxide	0.0095	0.00031	0.0380 <i>M</i>	3.76
Lauric		Air	0.0095		750 mm.	0.09
Lauric		<i>tert</i> -Butyl hydroperoxide	0.0095		0.0380 <i>M</i>	0.30
Lauric		Quinone	0.0095		0.00095 <i>M</i>	0.495
Lauric		Quinone	0.0095		0.00190 <i>M</i>	0.99

either with the semi-static tests previously used or with the dynamic conditions of these experiments. In this investigation an atmosphere essentially free of oxygen could be obtained by carrying out the reaction in a two-necked flask fitted with an oil seal through which the shaft containing the test piece was passed, and a gas inlet through which nitrogen of high purity (99.99 per cent) was passed. In view of the results of these experiments it seems likely that for the more highly reactive oxidizing agents used in the previous investigations the corrosion rate was controlled by diffusion, although for the less reactive of these it was probably controlled by chemical reaction.

With no catalyst acid present and for a lauric acid concentration below the critical (0.01 molar), added *tert*-butyl hydroperoxide had some accelerating effect upon the corrosion rate, although, as may be seen from table 7, it was not sufficient to make the rate any more than $\frac{1}{12}$ as great as for the acetic acid-catalyzed reaction.

In one of the previous papers (4) it was suggested that the intermediate product of reaction following oxidation might be similar for oxygen and *tert*-butyl hydroperoxide, so that it must not be considered surprising that little

difference was observed in their behavior in these experiments. In the earlier investigation a mechanism was postulated for the corrosion reaction in which quinone served as the oxidizing agent, which was definitely different from that postulated for oxygen and hydroperoxides. Therefore some experiments were made in which quinone, recrystallized from alcohol, was added, but with oxygen still present. With catalyst acid present quinone had little appreciable effect, but with no catalyst acid present and for a lauric acid concentration of 0.01 *M* (less than the critical) the corrosion rate was definitely increased (see table 7) and for quinone concentrations of 0.002 molar or less appeared to be directly proportional to quinone concentration. It may be concluded, therefore, that the mechanism of corrosion involving quinone as an oxidizing agent is definitely different from that involving oxygen and is not interfered with by the latter.

DISCUSSION

From the results of this investigation a number of generalizations may be made about the corrosion rate of lead in hydrocarbon solutions of organic acids where diffusion has been largely eliminated as a rate-controlling step and where a comparatively active oxidizing agent, air at atmospheric pressure or *tert*-butyl hydroperoxide, is used, namely:

1. For organic acid solutions of 0.01 molar or less in the temperature range from 70–80°C. the direct products of corrosion are basic lead salts ranging in composition from $\text{PbA}_{1.5}(\text{OH})_{0.5}$ to $\text{PbA}_{1.2}(\text{OH})_{0.8}$, where A represents the acid radical. These compositions did not appear to be greatly affected by solvent, temperature, or molecular weight of the acid, but became more basic as the acid concentration was lowered.

2. Acids were divided into two groups, I and II, according to their behavior:
 - (a) Group I acids were either comparatively strong organic acids such as benzoic and *o*-toluic or comparatively low-molecular-weight carboxylic acids, including formic through butyric at least. For very dilute solutions of these acids the corrosion rate of lead was directly proportional to the concentration of the acid and the corrosion rate constant did not depend to a marked extent upon the nature of the acid or temperature. For higher concentration of acid (in excess of 0.003 molar for acetic and in excess of 0.01 molar for butyric) the corrosion rate was no longer directly proportional to acid concentration, and in fact, for acetic and butyric acids it decreased with increasing concentration in a certain range.

- (b) Group II acids included phenol and the high-molecular-weight carboxylic acids studied, capric through stearic and oleic. At temperatures of 100°C. or below for dilute solutions the corrosion rate of lead was comparatively low (about $\frac{1}{80}$ to $\frac{1}{100}$ as great as for Group I acids). When a certain critical concentration (0.035 molar for lauric acid and 0.08 molar for phenol in xylene solution at 78°C.) was exceeded however, the corrosion rate rose very rapidly and in a brief span of concentration attained a value which increased only very slowly with increasing acid concentration and which approached the order of magnitude of the maximum rates attained by the Group I acids. Critical concentrations were somewhat dependent upon the nature of the solvent,

decreased with increasing temperature, and generally increased with increasing molecular weight of the carboxylic acids. With increasing temperature the corrosion rate attained before the critical concentration was exceeded was generally increased to a considerable extent.

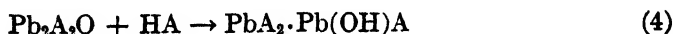
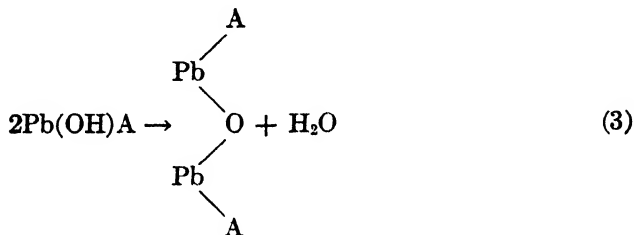
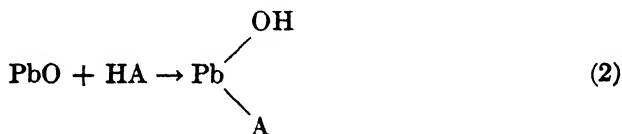
3. Very small amounts (2×10^{-4} moles per liter of acetic acid) of Group I acids have a marked catalytic effect (amounting to a factor of 40–60 in many instances) upon the rate of corrosion of lead in solutions of Group II acids, excepting phenol, at concentrations below their critical. It appears that the Group I acid effectively reduces the critical concentration of Group II acids to a value not detectably different from zero, so that the corrosion rate finally attained will not be significantly different from that attained by the Group II acid at a concentration greater than the critical in the absence of a catalyst acid.

4. Small concentrations of Group I acids have no detectable catalytic effect upon the rate of corrosion of lead in phenol solutions.

5. Although the corrosion rate is negligible in the absence of oxygen or other oxidizing agents the corrosion rate is independent of oxygen pressure in excess of that supplied by air and, excepting for Group II acids below their critical concentration, is independent of concentration of *tert*-butyl hydroperoxide added in the presence of air.

6. Below the critical concentration of Group II acids the corrosion rate was proportional to quinone concentration where the concentration of the latter did not exceed 0.002 molar.

Formation of basic lead salts during the corrosion reaction may take place in one of two ways: either the normal salt is formed directly and is then quickly hydrolyzed by any water which might be present to the basic salt, or it may form without the direct intervention of water by a series of reactions like the following:



If the above mechanism or a similar one is accepted, the fifth generalization made above would require that step 1 should be rapid in comparison with one of the following steps. Where the reaction rate is proportional to acid concentration, either step 2 or 4 might then be rate controlling.

With transport by diffusion not important, proportionality of the corrosion rate to acid concentration might be established by one of the following reaction steps: (1) adsorption of acid into a surface layer, (2) chemical reaction of acid with some oxidized form of lead in the surface layer. In view of the very small temperature coefficient of the reaction, it seems likely that the reaction rate was controlled by step 1 or by a step very similar in nature to 1.

In order to develop a satisfactory theory for the corrosion of lead in hydrocarbon solutions, it is necessary to explain the existence of a critical concentration for Group II acids and the catalytic effect of small concentrations of Group I acids upon corrosion by Group II acids. Two explanations for this have occurred to the authors. These are offered with the realization that other theories might be advanced which would explain the experimental results thus far obtained equally well. These theories are as follows:

(1) An intermediate in the corrosion process may be a solid film which is soluble in dilute solutions of Group I acids but insoluble in Group II acids until a critical concentration is exceeded. Such an insoluble film might consist of lead compounds of well-known properties, such as basic carboxylates, lead oxide, lead hydroxide, or basic lead carbonate. On the other hand, such a compound might be a surface compound having properties different from those of the known compounds of lead.

(2) It may be necessary for a critical concentration of organic acid in an adsorbed surface layer to be exceeded before corrosion can proceed rapidly. This layer should be more polar in character than the solution and may be composed of lead compounds like those listed in the preceding paragraph plus water, acid, hydrocarbon, and oxygen. Group I acids may be more highly adsorbed in such a polar layer than Group II acids, and thus a very low critical concentration in the solution might give a concentration in the adsorbed layer sufficient to exceed that required for reaction, while a much higher concentration of Group II acid might be required. For very dilute acid solutions the corrosion rate might be determined by the rate of adsorption of acid into the polar layer, which would in turn be controlled by the concentration of acid in solution.

On the basis of the second theory, catalysis by Group I acids might be effected by the following mechanism: (1) Group I acid is adsorbed in surface layer in excess of critical concentration. (2) Group I acid reacts with surface oxide (or hydroxide) to form basic lead salt of Group I acid. (3) Lead salt of Group I acid reacts with Group II acid to form basic lead salt of this acid and regenerate Group I acid. (4) Salt of Group II acid is desorbed and diffuses into solution.

According to this theory corrosion by phenol could not be catalyzed by Group I acids, since over-all free-energy considerations would not be likely to permit regeneration of Group I acid by step 3, in view of the weak relative acidity of phenol in comparison with carboxylic acids. This consideration would not bar step 3 for Group II carboxylic acids, since these have acid strengths of the

same order as Group I acids, and their concentration in the body of the solution greatly exceeded that of Group I acid.

In order to test the first theory, a study was made of the properties of various solid films which might have been formed and their interaction with the various solutions tested. It appeared that an insoluble basic salt film was rather unlikely, since a salt as basic as lead monohydroxy monolaurate proved very soluble in hydrocarbon solvents. In order to test the possibility that such a film might be normal lead hydroxide or normal lead oxide, c.p. powders of these materials were compacted in a mold by mechanical pressure into cylindrical forms through which holes were drilled in order to accommodate them to the stirring mechanism used for pure lead. Their solubilities in various fatty acid solutions were then tested under the same dynamic conditions in which the corrosion of lead was measured in these solutions. Both of these compounds dissolved at a fairly rapid rate in dilute solutions of Group II acids, and no critical concentration in excess of 0.005 *M* acid had to be exceeded. Furthermore, addition of a small concentration of acetic acid accelerated the solution rate by a factor no greater than 1.5.

There was some possibility that an insoluble film accounting for the results might be the basic lead carbonate. It appeared that a film having the properties of a basic carbonate accumulated in solutions of Group II acids below their critical concentration. However, this theory was discounted for two reasons: (1) when carbon dioxide-free air was passed through the acid solutions, in the course of the corrosion experiments, the corrosion rate was no different from that found in ordinary air; in these experiments no visible film was observed on lead pieces at acid concentrations lower than the critical. (2) Although the basic carbonate proved to be less soluble in xylene solutions of fatty acids (at 78°C.) than lead oxide or hydroxide, its solubility rate in Group II acids was not affected by Group I acids, nor was evidence found for a critical concentration. In view of these results on the solubility rates of lead compounds, the theory that the corrosion rate of lead is conditioned by the formation of an intermediate insoluble film of one of these compounds appears to be doubtful. In this connection it might, of course, be argued that, in view of the effect of traces of impurities on the corrosion rate of the acids, traces of catalytic impurities were present in the c.p. compounds used. However, laboratory preparations of lead hydroxide and lead oxide behaved in the same way as the c.p. materials purchased. Also, lead oxide exhibited the same solubility behavior after having been heated for a $\frac{1}{2}$ -hr. period at a temperature in excess of 500°C.

It seems that if the critical concentration and catalytic phenomena are to be explained on the basis of a film theory, the film must consist of a surface compound having properties different from those of known lead compounds.

A serious objection to the polar film explanation is that if the surface concentration of Group II acid is not sufficient to make reaction with the intermediate surface lead oxide possible, it might be even less likely to react with the intermediate basic salt of the Group I acid. However, it is likely that surface forces may alter the possibilities of chemical reaction somewhat. It is reasonable

to suppose that the surface interaction with a surface lead oxide should be stronger than with a basic salt.

Two explanations may be offered for the tendency of the corrosion rate to approach a constant value independent of further increase in acid concentration for high concentrations of acid. First, if the reaction takes place in an adsorbed surface layer it is possible that this layer becomes saturated with reactant in higher acid concentrations. Second, the corrosion rate may be controlled by the rate of desorption of reaction product.

This investigation has shown that in the corrosion of lead in relatively dilute (0.001 to 0.05 molar) acid solutions of hydrocarbon solvents, where experimental conditions are chosen so that a reactive oxidizing agent is present above a critical concentration and so that diffusion of reagent is not important as a rate-controlling step, the corrosion rate is determined primarily by the concentration and nature of the acid present. In another paper the authors will discuss the applicability of the findings of this investigation to the corrosion of copper-lead bearings.

The authors extend their appreciation to the Lubri-Zol Corporation, which sponsored this work. They have had the benefit of the continued interest and helpful advice of Dr. C. F. Prutton in working on this problem.

Their appreciation is also extended to Mrs. Anne Lodge, Mr. George Dlouhy, and Miss Marjorie Palenschat for analytical assistance in this study.

REFERENCES

- (1) DENISON, G. H.: *Ind. Eng. Chem.* **36**, 477 (1944).
- (2) KING, C. V.: *J. Am. Chem. Soc.* **57**, 828 (1935).
- (3) PRUTTON, C. F., FREY, D. R., TURNBULL, D., AND DLOUHY, G.: *Ind. Eng. Chem.* **37**, 90 (1945).
- (4) PRUTTON, C. F., TURNBULL, D., AND FREY, D. R.: *Ind. Eng. Chem.* **37**, 917 (1945).
- (5) ROLLER, P. S.: *J. Phys. Chem.* **39**, 221 (1935).

SOME E.M.F. AND CONDUCTANCE MEASUREMENTS IN CONCENTRATED SOLUTIONS OF ZINC AND CALCIUM CHLORIDES

R. A. ROBINSON AND R. O. FARRELLY

Department of Chemistry, Auckland University College, New Zealand

Received August 7, 1946

In a recent issue of this Journal, Mead and Fuoss (5) have described some viscosity and conductance measurements on concentrated solutions of zinc and calcium chlorides. Some similar measurements made in these laboratories should therefore be of interest. It is well known that the activity coefficient of an electrolyte in a mixed salt solution of constant total ionic strength varies with the individual electrolyte concentration in a very simple way. The work

of Güntelberg and of Harned (3) has established that in a mixture of two electrolytes at constant total ionic strength, the following relation holds:

$$\log \gamma_1 = \log \gamma_1^0 + kx$$

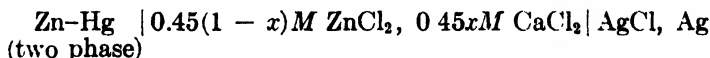
where γ_1^0 is the activity coefficient of salt 1 in the absence of salt 2, and γ_1 is the activity coefficient of salt 1 in the presence of a fraction x of salt 2. Hawkins (4) has shown the rule to hold in hydrochloric acid-uniunivalent halide mixtures of total molarity as high as 6 M .

We have made measurements of the activity coefficient of zinc chloride in mixtures with calcium chloride of constant total molarity. Zinc chloride was prepared by the solution of zinc oxide in hydrochloric acid, and, after analysis, the addition of sufficient hydrochloric acid to give the correct stoichiometric ratio of zinc to chloride. Calcium chloride was prepared by threefold recrystallization of the best grade of analytical reagent. In the first series of measure-

TABLE 1

x	E	$E' - ax$	Δ
			<i>mv.</i>
0	1.03329	1.03329	0
0.0915	1.03430	1.03307	-0.05
0.2110	1.03596	1.03292	+0.02
0.3210	1.03769	1.03272	+0.03
0.4200	1.03952	1.03252	+0.01
0.5090	1.04146	1.03232	-0.02
0.5746	1.04314	1.03216	-0.06
0.6922	1.04714	1.03200	0

ments, mixtures were made of 0.45 M zinc chloride with 0.45 M calcium chloride in different ratios and the E.M.F. of the cell:



measured at 25°C. The cells were similar to those used by Robinson and Stokes (6) and the silver-silver chloride electrodes were of the Carmody type (1). The E.M.F. of the cell is:

$$E = E^0 - RT/2F \cdot \ln \gamma_{\text{Zn}} \gamma_{\text{Cl}}^2 m_{\text{Zn}} m_{\text{Cl}}^2$$

The chloride concentration is constant at 0.90 M and the zinc-ion concentration is 0.45(1 - x) M . Consequently,

$$E = E^0 - RT/2F \cdot \ln (0.45 \times 0.90^2) - RT/2F \cdot \ln (1-x) - 3RT/2F \cdot \ln \gamma_{\text{ZnCl}_2}$$

Putting

$$\log \gamma_{\text{ZnCl}_2} = \log \gamma_{\text{ZnCl}_2}^0 + kx$$

we get:

$$E + 0.02958 \log (1-x) = E' - ax$$

where

$$E' = E^0 - RT/2F \cdot \ln (0.45 \times 0.90^2) - 3RT/2F \cdot \ln \gamma_{\text{ZnCl}_2}^0$$

and $a = 3RTk/2F$ are constants for this series of measurements.

In table 1 are given the measured E.M.F.'s of the cell for different values of x and the derived values of $E' - ax$. In the last column are given the differences (in millivolts) between the observed values of $E' - ax$ and those calculated from:

$$E' - ax = 1.03329 - 0.00186x$$

TABLE 2

x	E	$E' - ax$	Δ
			mv.
0	0.98001	0.98001	0
0.0994	0.98140	0.98005	-0.39
0.2188	0.98330	0.98013	-0.83
0.3237	0.98539	0.98036	-1.05
0.4223	0.98771	0.98066	-1.18
0.5011	0.99001	0.98108	-1.11
0.5701	0.99256	0.98172	-0.76
0.6433	0.99604	0.98280	0

TABLE 3

x	E	$E' - ax$	Δ
			mv.
0	0.94480	0.94480	0
0.1012	0.94691	0.94554	-2.80
0.1718	0.94873	0.94631	-4.52
0.2907	0.95258	0.94817	-6.84
0.3161	0.95283	0.94795	-7.95
0.4482	0.96008	0.95244	-8.10
0.4714	0.96180	0.95362	-7.73
0.5046	0.96443	0.95541	-7.11
0.5232	0.96643	0.95691	-6.27
0.5729	0.97187	0.96094	-3.98
0.6120	0.97635	0.96419	-2.11
0.6730	0.98280	0.96844	0

This column indicates that the law of linear variation of $\log \gamma$ with x holds within the experimental errors of these measurements.

A second series of measurements was made in which the total concentration of zinc chloride + calcium chloride was 2.5 M , with the results shown in table 2. To obtain values of Δ , $E' - ax$ was calculated from:

$$E' - ax = 0.98001 + 0.00434x$$

The deviation of $\log \gamma_{\text{ZnCl}_2}$ from linearity is appreciable.

A third series of measurements was made at a constant total molarity of 5 M ,

TABLE 4

CONCENTRATION	κ	d	λ
<i>moles/liter</i>			
0.787	0.1261	1.152	40.1
0.849	0.1290	1.170	38.0
0.927	0.1325	1.189	35.7
1.005	0.1356	1.205	33.7
1.203	0.1415	1.239	29.4
1.399	0.1452	1.264	26.0
1.566	0.1463	1.281	23.4

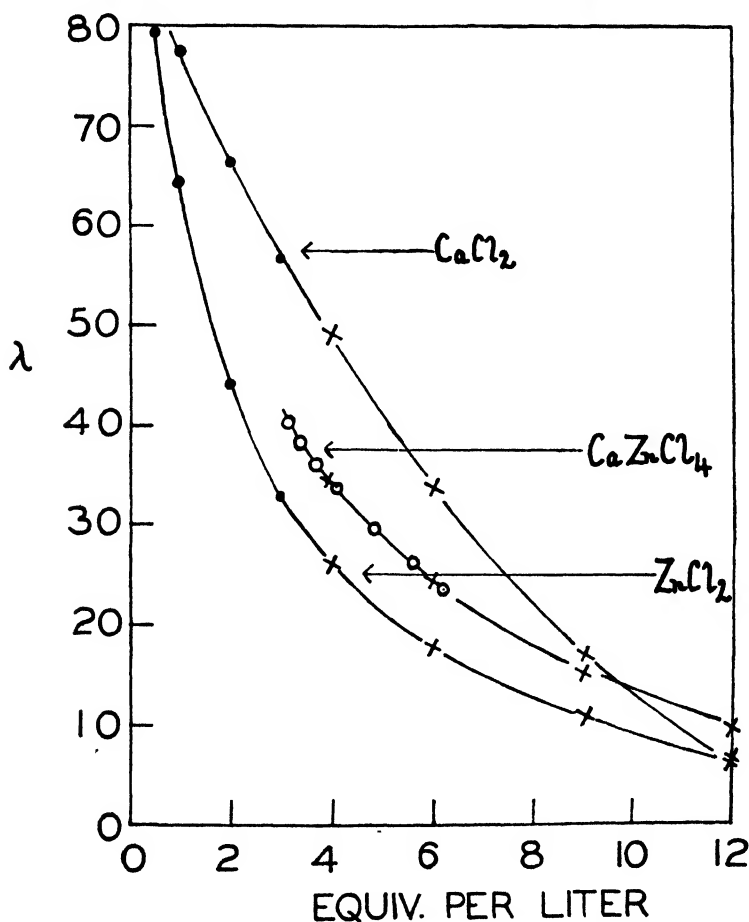


FIG. 1. Equivalent conductances of zinc chloride, calcium chloride, and equimolar mixtures at 25°C. ●, I.C.T. data; ×, Mead and Fuoss; ○, this paper.

with the results given in table 3. Values of Δ were obtained by putting $\alpha = -0.03512$. These measurements were of an exploratory nature, and we do not pretend that they attained the high degree of accuracy of the work of Harned

and Güntelberg. Nevertheless, the deviation from linearity indicated by these Δ -values is very large and beyond the experimental error. It may be pointed out that Harned and Harris (2) found a maximum deviation from linearity of 1.95 mv. for sodium hydroxide-sodium chloride mixtures at a total molarity of 5 *M*. The deviations found for zinc chloride-calcium chloride mixtures are much larger and, we suggest, can be accounted for by the formation of complex ions, such as ZnCl_4^{--} , in these solutions.

We have also made a few measurements of the density and conductance of equimolar mixtures of these salts at 25°C., as shown in table 4. Concentrations in the first column have been expressed as moles of either salt per liter, but the equivalent conductances have been evaluated with a concentration unit based on $(0.5 \text{ CaCl}_2 + 0.5 \text{ ZnCl}_2)$. A graphical comparison of these equivalent conductances (figure 1) with those of the single salts suggests that zinc chloride and calcium zinc chloride belong to the same family, while the behavior of calcium chloride is different. This would be consistent with the formulation $\text{Zn}(\text{ZnCl}_4)$ and $\text{Ca}(\text{ZnCl}_4)$ for zinc chloride and the mixed salt, respectively.

REFERENCES

- (1) CARMODY, W. R.: *J. Am. Chem. Soc.* **51**, 2901 (1929).
- (2) HARNED, H. S., AND HARRIS, J. M.: *J. Am. Chem. Soc.* **50**, 2633 (1928).
- (3) HARNED, H. S., AND OWEN, B. B.: *The Physical Chemistry of Electrolytic Solutions*, Chap. 14. Reinhold Publishing Corporation, New York (1943).
- (4) HAWKINS, J. E.: *J. Am. Chem. Soc.* **54**, 4480 (1932).
- (5) MEAD, D. J., AND FUOSS, R. M.: *J. Phys. Chem.* **49**, 480 (1945).
- (6) ROBINSON, R. A., AND STOKES, R. H.: *Trans. Faraday Soc.* **36**, 740 (1940).

CONDUCTIVITY OF SOME SALTS IN MOIST ACETONE¹

KAROL J. MYSELS²

Department of Chemistry, Stanford University, California

Received December 3, 1946

In 1932 Lannung (1) studied the solubility of certain salts in acetone by measuring the conductivity of saturated solutions, both "anhydrous" and containing small amounts of water. He found varying conductivities and varying susceptibilities to water. A reëxamination of Lannung's data suggests a somewhat different interpretation and also a simple method for determining moisture in acetone.

¹ Study conducted under contract OEMsr-1057 between Stanford University and the Office of Emergency Management, recommended by Division 11.3 of the National Defense Research Committee, and supervised by Professor J. W. McBain.

² Present address: Department of Chemistry, New York University, University Heights, New York 53, New York.

The salts studied by him fall into two classes. Saturated solutions of cesium iodide and sodium bromide have a high conductivity in "anhydrous" acetone which is relatively little affected by added moisture. All others have relatively low conductivities strongly affected by traces of moisture as shown in figure 1,

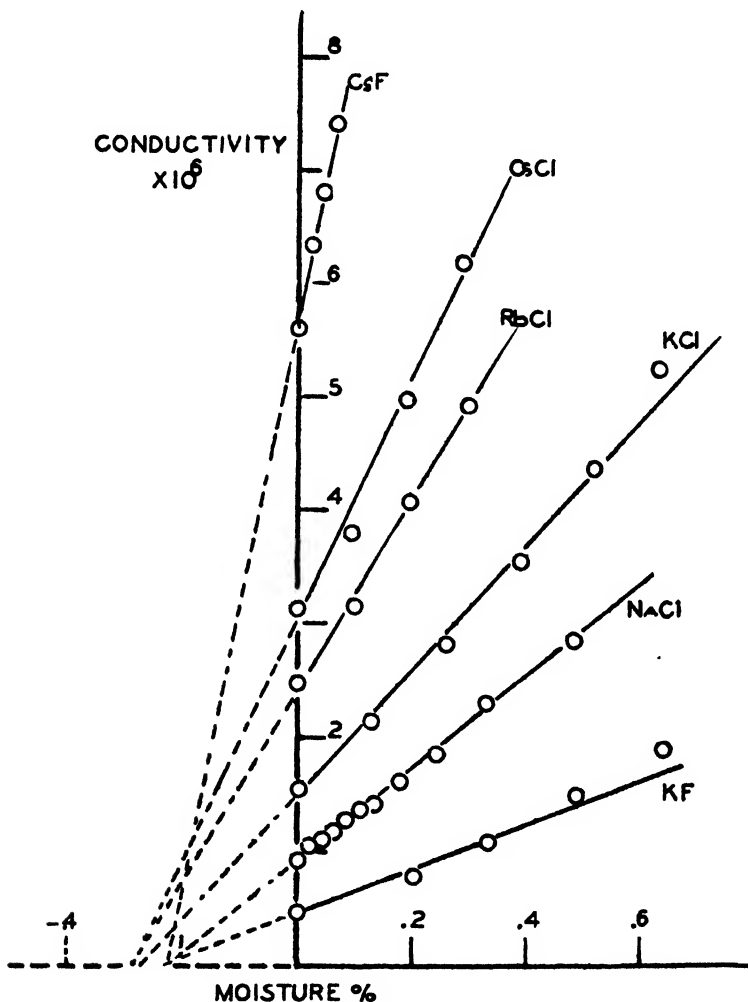


FIG. 1. Conductivity of some salts in moist acetone

on which Lannung's data are replotted. The conductivities of these latter solutions increase linearly with moisture content, as has been pointed out by Lannung, but furthermore they all extrapolate to zero conductivity at a moisture content of 0.2–0.3 per cent less than Lannung's "anhydrous" acetone.

This coincidence suggests strongly that the conductivity of saturated solutions of these salts is actually close to zero in *really* anhydrous acetone and that Lannung's anhydrous acetone contained 0.2–0.3 per cent of moisture. In view of

the difficulty of drying acetone (2) and Lannung's method of drying (distillation from potassium carbonate and protection by calcium chloride), it would be surprising if a much higher degree of dryness were obtained. Lannung's own criterion of dryness—conductivity of saturated sodium chloride solution—suggests a variation of 0.05 per cent moisture in the acetone used.

If this view is correct, the conductivity of saturated solutions of a salt such as cesium fluoride would be a simple and sensitive method of determining traces of moisture in acetone and their conductivity in anhydrous acetone would be of a smaller order of magnitude than reported by Lannung.

REFERENCES

- (1) LANNUNG, A.: *Z. physik. Chem.* **161**, 255, 269 (1932).
- (2) TIMMERMANS, J., AND GILLO, L.: *Roczniki Chem.* **18**, 812 (1938).

AN X-RAY DIFFRACTION INVESTIGATION OF PECTINIC AND PECTIC ACIDS

K. J. PALMER, R. C. MERRILL, H. S. OWENS, AND M. BALLANTYNE

Western Regional Research Laboratory,¹ Albany, California

Received January 2, 1947

It has been recognized for some time (10) that pectinic acid is composed of an essentially linear polygalacturonide chain of length sufficient for the production of fibers. However, the only published x-ray data on fibers of this important natural high polymer are those of Wuhrmann and Pilnik (19).

In 1933 Van Iterson and Corbeau (18) obtained optically negative, uniaxial, birefringent fibers by spinning concentrated aqueous solutions of commercial citrus pectin into an alcohol-ether mixture. These authors claimed that x-ray photographs of these fibers showed the presence of oriented crystallites. Henglein and Schneider (7) have since reported that x-ray photographs of nitropectin fibers show weak crystallite orientation. Kringstad and Lunde (9) have published a power photograph of a pectinic acid, but they gave neither the values of the spacings nor data from which they could be calculated. Astbury and Bell (2) have reported results obtained by K. L. Scott on commercial lemon pectin.

Only Wuhrmann and Pilnik (19) have attempted to deduce any structural information from their x-ray photographs. These authors suggest, on the basis of the x-ray patterns obtained from oriented films and fibers of pectinic and pectic acids, that the fiber identity period is about 8.8 Å. In the present paper it will be shown that this value is too small, the fiber identity period actually being about 13 Å. This value of 13 Å. is similar to that found to occur in sodium pectate (14, 15).

¹ Bureau of Agricultural and Industrial Chemistry, Agricultural Research Administration. U. S. Department of Agriculture.

The present paper is concerned with an analysis and interpretation of data obtained from x-ray patterns of pectinic acids (from 11 to ~ 1 per cent methoxyl content) and pectic acid (< 1 per cent methoxyl content), in the form of both powders and fibers. Although a method has been developed which produces fibers having a rather high degree of molecular orientation, the quantity of diffraction data obtained is unfortunately still meager. This has been partially compensated for by studying the variation of the x-ray patterns with moisture and methoxyl content. In spite of the lack of general information with regard to the chemical structure of pectin, the x-ray data obtained allow some interesting conclusions to be drawn regarding the configuration of the polygalacturonide chain.

EXPERIMENTAL

The commercial citrus and apple pectins were deashed by means of ion-exchange resins as described in the literature (12). The rest of the samples were kindly supplied by Dr. T. H. Schultz and H. Lotzkar and were prepared as follows: Samples L51 and L65 were extracted from lemon peel at pH 3.5 with three volumes of water containing 12 g. of "sodium hexametaphosphate" (Calgon) per kilogram of peel for 20 min. at 90–95°C. The filtered extract was precipitated in ethanol at pH 1.0 to 1.5. The precipitate was washed with 55 per cent ethanol until free of chloride, then hardened with 95 per cent ethanol, and dried *in vacuo* at 60°C. The other samples were deesterified by citrus pectinesterase acting *in situ* in lemon peel, as described previously (13). Deashing was accomplished in the same way as for samples L51 and L65. Samples L43 and L69 were extracted by the procedure of Baier and Wilson (3). Sample L43C was precipitated in neutral alcohol and received no deashing treatment.

The analytical and viscosity data given in table 1 were obtained by methods previously described (12). The per cent water in the equilibrated samples was determined by measuring the loss in weight of samples dried *in vacuo* at 70°C. for 16 hr. X-ray photographs of the powders were taken after the samples had been equilibrated with an atmosphere having a relative humidity of 49 per cent by means of a vacuum desiccator containing the proper concentration of sulfuric acid. Column 6 of table 1 gives the per cent water sorbed by these samples when in equilibrium with an atmosphere having a relative humidity of 49 per cent. Column 2 of table 1 gives the methoxyl content and column 3 the ash content of the samples. The per cent uronide is given in column 4 for those samples for which this data is known, while column 5 lists the values of the intrinsic viscosity.

The fibers were prepared by using 2–4 per cent solutions which had been freed from bubbles and suspended solids by centrifugation. The resulting solution was forced through a 1-mm. round orifice into a coagulating bath composed of an equal-volume mixture of alcohol and ether. The fibers were usually partially dehydrated for 5–15 min. in an alcohol bath and then suspended in air to dry. During drying they were stretched by adding small weights. The dry fibers were then given an additional stretch, varying between 40 and 100 per cent, by suspending them with weights attached in the vapor of a boiling alcohol-water mixture. The ratio of alcohol to water was found to be very critical

for a given fiber with a given weight attached. In general, the latitude of the alcohol concentration between no stretch and elongation until break was only about 2-3 per cent. The per cent elongation could be controlled by using intermediate concentrations. In our particular arrangement, using six fibers about 0.5 mm. in diameter and with a 100-g. weight attached, the optimum concentration of alcohol in the liquid was found to lie between 4 and 7 per cent.

TABLE 1
Analytical data on pectinic and pectic acid samples

SAMPLE	CH ₂ O	ASH	URONIC ACID ANHYDRIDE	INTRINSIC VIS- COSITY	WATER CONTENT AT R.H. 49 PER CENT
	<i>per cent</i>	<i>per cent</i>	<i>per cent</i>		<i>per cent</i>
L51.....	10.9	0.4		9.3	17.4*
Commercial citrus pectin (deashed).....	10.7	0.2	85	4.2	15.8†
L65.	10.5	1.0	80	7.9	18.2*
L25	10.7	0.6	80	8.7	16.0†
L25	10.7	0.6	80	8.7	15.8†
Commercial apple pectin (deashed).....	10.9	0.2	84	6.4	16.5*
L64	7.4	0.4	79‡	5.5	18.0*
					18.6*
					16.6†
L37P.....	5.8	0.4	80‡	5.8	17.7*
					16.0†
L81	4.5	0.5	80‡	5.2	18.2*
					16.3†
L67	2.7	0.3	81‡	3.5	18.4*
					15.8†
L66	1.4	0.7	82‡	2.2	16.0†
L43	0.6	0.4	82	4.2	16.6†
L43C	0.6	15.0			23.4*
L69	0.7	0.2	82	3.7	18.3*
					15.5†

* Desorption.

† Sorption.

‡ Estimated.

The density was determined by suspension in a toluene-ethylene bromide mixture. The values found are listed in the bottom row of table 2. The density found by this method is in good agreement with that found for powdered pectin by the helium gas displacement method (17). The value 1.18 for the specific gravity of orange pectin at 20°C. (11) is either an apparent bulk specific gravity or too low because of incomplete penetration of sample by the pycnometer liquid.

X-ray photographs of the fibers were made in the usual way with $\text{CuK}\alpha$ radiation filtered through thin nickel foil. The powders, after being brought to equilibrium with an atmosphere having a relative humidity of 49 per cent, were quickly placed in methyl methacrylate capillaries. The capillaries were sealed to a close-fitting copper wire at one end and sealed off at the other end by means of melted beeswax. The methyl methacrylate capillaries were made by the method of Fricke and coworkers (5).

RESULTS

The x-ray patterns of powders of the various pectinic and pectic acids are similar in general appearance (figure 1). Lower methyl ester content, however, usually gives rise to somewhat sharper rings, as would be expected because

TABLE 2

X-ray spacings and density of pectinic and pectic acids in equilibrium at 49 per cent relative humidity

	L25 (ALCOHOL PRECIPITATED)	L25 (HUMIDIFIED)	COMMERCIAL CITRUS PECTIN (ALCOHOL PRECIPITATED)	COMMERCIAL CITRUS PECTIN (HUMIDIFIED)	COMMERCIAL APPLE PECTIN (HUMIDIFIED)	L51	L65	L64	L37P	L81	L67	L66	L43	L43C	L69
X-ray spacing in Å.	7.06	11.0 6.84	7.10	10.85 6.84	6.84	6.94	6.89	6.80	6.72	6.70	6.63	6.60	6.61	7.11 4.37*	6.58
	4.18 3.03	4.22 3.06	4.18 3.04	4.18 3.09	4.20 3.05	4.18 3.06	4.23 3.09	4.18 3.05	4.15 3.03	4.16 3.02	4.15 3.03	4.16 3.01	4.14 3.05	4.19 2.98	4.12 2.98
ρ (grams per cc.).	1.50	1.49		1.49	1.50	1.49	1.54	1.51	1.50		1.54	1.53		1.52	

* Measurement made at sharp inner edge of reflection.

† Measurement made at center of reflection.

the more uniform chains can pack together in a more regular manner. In general, only three distinct rings have been observed from deashed high-molecular-weight pectinic and pectic acids, although under proper conditions one or more additional rings appear. For example, when a high-molecular-weight pectic acid, which gives the usual x-ray pattern showing three rings, is heated for several hours at 80°C ., the resulting heat-degraded pectin, after careful washing with water to remove any low-molecular-weight products, gives an x-ray pattern which exhibits as many as fifteen sharp rings. These heat-degraded products are now under investigation, and the results will be published in the near future. The three distinct characteristic rings consist of an intense, rather diffuse inner ring, a moderately intense, rather sharp intermediate ring, and a weak outer ring (figure 1). The spacings calculated for these rings for the samples listed in table 1 are given in table 2.

The first column of table 2 lists the x-ray spacings obtained from a pectinic acid sample (L25) which had been precipitated in ethyl alcohol. Column 2 shows the spacings obtained from the same sample after it had been placed in a desiccator containing pure water for 24 hr. (hereinafter referred to as humidified), and then brought to equilibrium with an atmosphere having a relative humidity of 49 per cent.

It has been shown (8) that pectins contain sorbed alcohol when precipitated with ethanol. It has also been shown (8) that this sorbed alcohol is removed by humidification. The differences in x-ray spacings listed in columns 1 and 2 of table 2 are therefore due to the presence of sorbed alcohol. Columns 3 and 4 illustrate this same effect for a commercial citrus pectin.

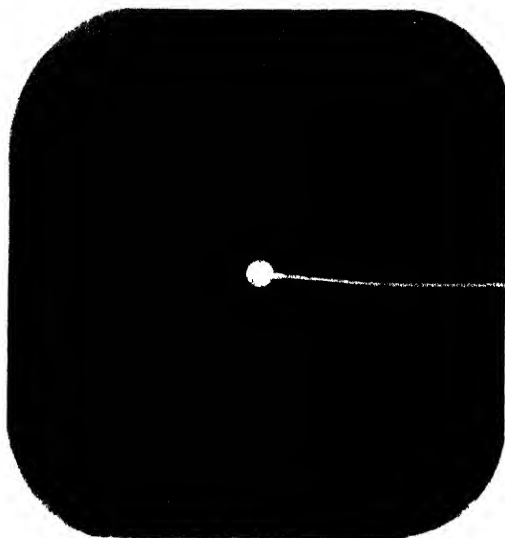


FIG. 1. X-ray diagram of powdered pectic acid

A comparison of the values in columns 13 and 14 shows the effect of having ash present. The intermediate ring obtained from sample L43C (15 per cent ash) has a sharp inner edge which corresponds to a spacing of 4.37 Å. The center of this ring corresponds to a spacing of about 4.19 Å. It is interesting that three prominent reflections in sodium pectate (15) occur at 7.00, 4.37, and 4.17 Å. This particular high-ash-containing pectic acid, therefore, probably contains an appreciable amount of pectic acid in the form of the sodium salt. High ash contents as well as partial degradation may account for the large number of reflections which have been reported for pectinic and pectic acids by some previous investigators. In particular, we have not been able to confirm the presence of the very intense reflection at 22 Å. reported by Astbury and Bell (2).

Table 2 also shows the effect on the spacings due to variation in methoxyl content for samples which were in equilibrium with an atmosphere having a

relative humidity of 49 per cent and had the water contents listed in the last column of table 1. A plot of the interplanar spacing obtained from the intense inner ring *versus* methoxyl content at a constant water content of 16 per cent is shown in figure 2. This latter spacing is also a function of the water content. The effect of moisture, however, will be considered in more detail in another place (16). One other point of interest is illustrated by the two samples L25 and commercial citrus pectin. When these samples are humidified and then placed in an atmosphere having a humidity of 49 per cent until their weight becomes constant, both exhibit inner rings which correspond to spacings of about 10.9 Å. (table 2). When these samples are dried in a 70°C. vacuum oven and then brought to equilibrium at 49 per cent relative humidity, the inner

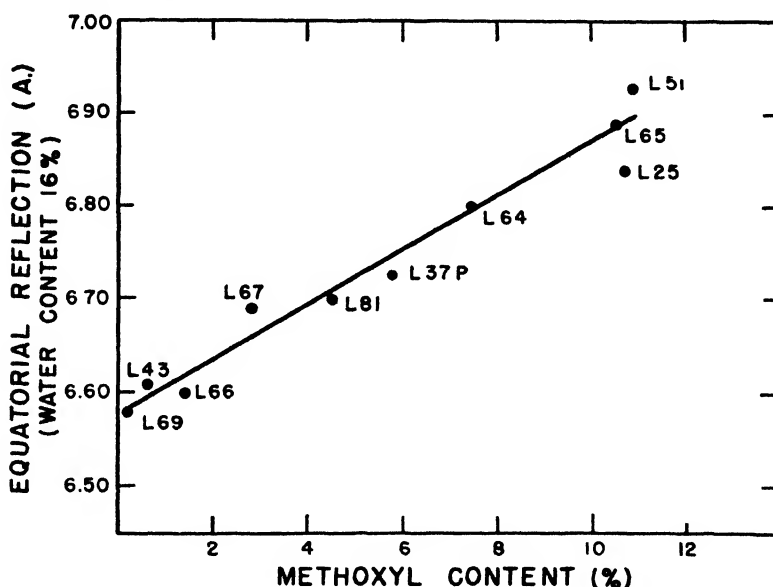


FIG. 2. Plot of intense equatorially accentuated x-ray reflection against methoxyl content for samples having a moisture content of 16 per cent.

ring is no longer observed. This effect is reproducible on subsequent cycles. The 10.9 spacing probably results from the higher degree of crystallinity made possible because the hydrated chains are free to move with respect to one another and therefore assume a more regular arrangement.

The fiber diagram of pectic acid L69, which is typical of those obtained from the other samples, is reproduced in figure 3 and data are given in table 3. It is evident from this photograph that the 6.5–6.9 Å. ring becomes equatorially accentuated, while the two rings at approximately 4 Å. and 3 Å. become meridionally accentuated. In addition, the most highly oriented fibers exhibit an additional meridionally accentuated arc giving a spacing of about 6.1 Å. and a very diffuse equatorial spot. This latter spot is very difficult to measure accurately, because it blends in with the small angle scattering resulting from the small size of the

crystallites. The x-ray spacings obtained from the fiber photographs of this pectic acid and a pectinic acid which has a methoxyl content of 4.4 per cent are listed in table 3. Columns 4 and 5 of table 3 give the visually estimated intensities and the layer line, respectively, on which the reflection occurs.



FIG. 3. X-ray photograph of pectic acid fiber. Fiber axis vertical; $\text{CuK}\alpha$ radiation; camera distance 5.0 cm.

TABLE 3
X-ray spacings of a pectinic acid and a pectic acid fiber

PECTINIC ACID L61: 4.4 PER CENT CH_3O , 2.7 PER CENT ASH; $\rho =$ 1.55 G./CC.	ORIENTATION OF REFLECTION*	<i>I</i> (ESTIMATED)†	LAYER LINE	PECTIC ACID L69: 0.7 PER CENT CH_3O , 0.2 PER CENT ASH; $\rho = 1.59$ G./CC.
(12.65)	E very diffuse	M	0	(13.08) very diffuse
6.76	E diffuse	VS	0	6.51 diffuse
6.12	M	VW	2	6.15
4.14	M	S	3	4.15
3.01	M	MW	4	3.00

* E is equatorial; M is meridional.

† VS = very strong; S = strong; M = medium; MW = medium weak; VW = very weak.

In agreement with the results reported by Wuhrmann and Pilnik (19) and Van Iterson (18), we have found that fibers made from pectinic and pectic acids all have a negative sign of birefringence with respect to the fiber axis when viewed in air. Sodium pectate fibers are also negative (15). This is in contrast to the positive sign of cellulose, alginic acid, and sodium alginate fibers. This point will be discussed below.

DISCUSSION

On the assumption that the chain molecules align themselves parallel to the direction of elongation, it follows that the equatorially accentuated reflection giving a spacing of 6.5–6.9 Å. is related to the interchain separation. This is substantiated by the fact that this reflection varies with the methoxyl, alcohol, and water contents, whereas the meridionally accentuated reflections are essentially invariant.

From the position and length of the three meridional arcs it follows that those reflections must arise from planes which are either perpendicular, or very nearly so, to the fiber axis. The determination of the fiber axis identity period is, unfortunately, not straightforward, because the position of the layer lines cannot be determined with certainty. However, it is obvious that the three meridionally accentuated reflections lie on different layer lines. It follows, therefore, from an inspection of the values listed in table 3 that the fiber axis identity period cannot be less than three times the value of the 4 Å. spacing. There are several reasons for suspecting that the actual value of the identity period is somewhat larger than this and is in fact very nearly equal to that found for sodium pectate (15),—namely, 13.1 Å.

The reasons for this latter conclusion are that sodium pectate has a prominent reflection at 4.17 Å. with hexagonal indices (103) which both becomes oriented and has the same general appearance as the 4 Å. spacing obtained from the pectinic acids. Of more importance, however, is the fact that when sodium pectate is precipitated rapidly from solution, a product is obtained which gives a diffraction pattern consisting of two prominent rings. The appearance of this photograph is very similar to that obtained from the pectinic acids. The intense outer ring corresponds to a spacing of 4.17 Å., in very good agreement with the value obtained from the similar ring in the pectinic acids. It is unlikely that the identity period along a single chain in this quickly precipitated sodium pectate is any different than it is in oriented fibers; it seems more likely that, owing to the rapid precipitation, the carboxyl groups (and therefore the sodium atoms) in adjacent chains are not arranged with sufficient regularity with respect to one another to allow the (003) reflection to appear.²

The tendency for the polygalacturonide chains to assume a crystalline arrangement is greatest in the case of the sodium salt and least when the carboxyl groups are esterified, as in high-methoxyl pectinic acids. For this reason and also because of the variable distribution in electron density, resulting from the random distribution of methoxyl groups, the (003) reflection does not appear even in fairly well oriented fibers made from pectinic acids. So far we have

² The sodium pectate sample can readily be made to give a pattern on which the (003) reflection appears by merely humidifying it. The hydrated chains are evidently able to move with respect to one another until the carboxyl groups on adjacent chains take up positions opposite one another. When a sufficient degree of crystalline regularity is attained, then, because of the threefold screw symmetry of the chains, a strong (003) reflection appears.

not observed any reflections which can be unequivocally indexed as (001) from pectic acid fibers either. This is presumably due to the strong interaction between the polygalacturonic acid chains resulting from the presence of the free carboxyl groups, which prevents the chains from having the mobility necessary to assume a crystalline arrangement. This strong interaction between the polygalacturonic acid chains also accounts for the low solubility of pectic acid in water compared to the high-methoxyl pectinic acids.

There is one additional piece of evidence favoring the assumption that the fiber identity period in the pectinic and pectic acids is approximately the same as in sodium pectate. When x-ray diffraction patterns were taken of a highly oriented sodium pectate fiber at different stages of hydration, it was observed that the (003) reflection gradually disappeared and the (103) reflection (4.17 Å.) became relatively much more intense. The position of the (003) reflection, however, did not vary with water content as long as it could be observed. The photograph of completely dry sodium pectate has, like the photograph obtained from rapidly precipitated sodium pectate, the same general appearance as the photographs of pectinic acids.

All of the evidence so far obtained, therefore, points to the conclusion that the fiber identity period of the polygalacturonide chain is more or less constant and has a value of about 13 Å. Wuhrmann and Pilnik suggest that the fiber identity period of the polygalacturonide chain is about 8.8 Å. Evidently their fibers and films were not sufficiently well oriented for them to observe the meridional reflection at 6.1 Å. which rules out this possibility.³

An identity period of 13 Å. excludes the possibility of there being only two pyranose units in the identity period. The most reasonable assumption is that the polygalacturonide chain has the symmetry of a threefold screw axis. The identity period of about 13 Å. is then to be expected if the pyranose rings have the *trans* configuration suggested for sodium pectate (14, 15) and alginic acid (1). It is of interest in this connection that $3/2$ times 8.7, the identity period for the twofold alginic acid chain, is 13.05 Å., a value which is in good agreement with the value found for sodium pectate and postulated for the pectinic acids.

The variation of the equatorially accentuated x-ray reflection with methoxyl content, shown in figure 2, is for samples which contain 16 per cent water, this value being taken from plots of x-ray spacings *versus* moisture content. From figure 2 it is evident that the *d*-value calculated from the equatorial reflection is approximately a linear function of the methoxyl content and increases about 0.3 Å. on going from pectic acid to a pectinic acid having a methoxyl content of 11 per cent. A methoxyl content of 11 per cent corresponds to about 76 per cent of the carboxyl groups being esterified, when, as is the case for the pectinic acids under discussion, the non-uronide content is about 18 per cent. On the

³ Because of the importance of this 6.1 Å. meridional reflection in the deduction of the fiber identity period, it was considered desirable to obtain an x-ray photograph using strictly monochromatic radiation. This was done by reflecting the x-ray beam from the cleavage face of rock salt. The resulting photograph distinctly showed the presence of the 6.1 Å. meridional reflection.

assumption that the straight-line relationship shown in figure 2 holds for complete esterification (14.5 per cent), the increase in the x-ray spacing in going from 0 to 14.5 per cent methoxyl would be about 0.4 Å. Since complete esterification would correspond to one methyl group per five atoms along the chain, this increase of 0.4 Å. is in good agreement with the difference of 0.3 Å. found to occur between the *d*-values of polybutadiene and polyisoprene (6). The number of methyl groups per chain atom in these two cases is 0 and 1/4.

It is interesting that the equatorially accentuated x-ray reflection varies in a continuous manner with the methoxyl content. This is a result of the fact that the x-ray reflection is a measure of the average interchain separation. In the case of the pectinic acids the actual interchain distance probably varies from point to point by as much as a few tenths of an Ångström, owing to the random distribution of methoxyl groups. This causes the equatorial reflection to be quite diffuse. The equatorial reflection from pectic acid is sharper, in agreement with the expectation that there is probably less variation in interchain separation because of the more uniform chains.

The equatorial reflection is always considerably more diffuse than the meridional reflection, a result which indicates that the crystalline regions are considerably longer than they are wide. This conclusion is in agreement with the optical studies carried out by Van Iterson (18) and Wuhrmann and Pilnik (19) on pectin fibers. They determined the birefringence of pectin fibers immersed in media of different refractive index. From these results they were able to show that the intrinsic birefringence of pectin fibers is negative with respect to the fiber axis, but that the form birefringence is positive. In other words, the crystallites are rod shaped. Rod-shaped particles have also been found to occur in pectinic acid solutions by Boehm (4), who studied their flow birefringence.

The reason for the negative intrinsic birefringence of pectinic acid fibers is not known at the present time. The negative sign cannot be due to the presence of the methoxyl groups, as has been suggested (4), because pectic acid also has a negative sign. It is unlikely that the negative sign can be due to the presence of carboxyl groups or the serpentine-like configuration of the chain, because alginic acid, which appears to have a similar chain configuration (1), has a positive sign of birefringence with respect to the fiber axis.

One difference between pectinic acid and alginic acid is that the pyranose ring in the former has the α -*d*-configuration, while in the latter the ring has been shown to have the β -*d*-configuration. In pectinic acid, therefore, the C—O bonds on the first and second carbon atoms project out on the same side of the pyranose ring, while in alginic acid, as in cellulose, these two bonds project out on opposite sides of the pyranose ring. This difference may account for the fact that the polarizability is larger in a direction perpendicular to the chain axis than parallel to the chain axis in pectinic acid, whereas the reverse is true for both alginic acid and cellulose.

SUMMARY

X-ray photographs have been taken of pectinic and pectic acids in the form

of both powders and fibers, and their interplanar spacings have been recorded. The variation in x-ray spacings with methoxyl content has been determined.

A fiber identity period of about 13 Å. has been found for the polygalacturonide chain in all the pectinic and pectic acids so far investigated. The interchain separation increases from approximately 6.6 Å. to 6.94 Å. when the methoxyl content varies from 0 to 11 per cent.

The sign of intrinsic birefringence of pectinic and pectic acid fibers is negative. This is in contrast to fibers of alginic acid and sodium alginate, which are positive. A structural reason for the negative sign of birefringence is suggested.

REFERENCES

- (1) ASTBURY, W. T.: *Nature* **155**, 667 (1945).
- (2) ASTBURY, W. T., AND BELL, F. O.: *Tabulae Biologicae* (Haag) **17**, 96 (1939).
- (3) BAIER, W. E., AND WILSON, C. W.: *Ind. Eng. Chem.* **33**, 287 (1941).
- (4) BOEHM, G.: *Arch. exptl. Zellforsch. Gewebezücht.* **22**, 520 (1938-39).
- (5) FRICKE, R., LOHRMANN, O., SCHRODER, W., WEITBRECHT, A., AND SAMMET, R.: *Z. Elektrochem.* **47**, 374 (1941).
- (6) FULLER, C. S., FROSCH, C. J., AND PAPE, N. R.: *J. Am. Chem. Soc.* **62**, 1905 (1940).
- (7) HENGLEIN, F. A., AND SCHNEIDER, G.: *Ber.* **69B**, 309 (1936).
- (8) JANSEN, E. F., WAISBROT, S. W., AND RIETZ, E.: *Ind. Eng. Chem.* **16**, 523 (1944).
- (9) KRINGSTAD, H. VON., AND LUNDE, G.: *Kolloid-Z.* **83**, 202 (1938).
- (10) MEYER, K. H.: *Natural and Synthetic High Polymers*, p. 363. Interscience Publishers, Inc., New York (1942).
- (11) OHN, A.: *Ind. Eng. Chem.* **18**, 1295 (1926).
- (12) OWENS, H. S., LOTZKAR, H., MERRILL, R. C., AND PETERSON, M.: *J. Am. Chem. Soc.* **66**, 1178 (1944).
- (13) OWENS, H. S., MCCREADY, R. M., AND MACLAY, W. D.: *Ind. Eng. Chem.* **36**, 936 (1944).
- (14) SCHULTZ, T. H., LOTZKAR, H., OWENS, H. S., AND MACLAY, W. D.: *J. Phys. Chem.* **49**, 554 (1945).
- (15) PALMER, K. J., AND HARTZOG, M. B.: *J. Am. Chem. Soc.* **67**, 1865 (1945).
- (16) PALMER, K. J., AND LOTZKAR, H.: *J. Am. Chem. Soc.* **67**, 884 (1945).
- (17) PALMER, K. J., AND HARTZOG, M. B.: *J. Am. Chem. Soc.* **67**, 2122 (1945).
- (18) PALMER, K. J., MERRILL, R. C., AND BALLANTYNE, M.: In preparation.
- (19) PALMER, K. J., SHAW, T. M., AND BALLANTYNE, M.: *J. Polymer Sci.*, in press.
- (20) VAN ITERSON, G., JR.: *Chem. Weekblad* **30**, 2 (1933).
- (21) WUHRMANN, K., AND PILNIK, W.: *Experientia* **1**, 330 (1945).

THE FRACTIONAL PRECIPITATION OF MOLECULAR-WEIGHT SPECIES FROM HIGH POLYMERS

THEORIES OF THE PROCESS AND SOME EXPERIMENTAL EVIDENCE¹D. R. MOREY AND J. W. TAMBLYN²*Kodak Research Laboratories, Rochester, New York**Received January 8, 1947*

The phenomenon of longer chains being less soluble than shorter ones of like structure has been known for some time, and has been utilized for the separation of chains on a length basis. The reasons for such behavior have been much less known and understood than the empirical applications, and it is only recently that theoretical frameworks have been found which coördinate the facts.

We limit our discussion here to the case when the chains differ in length but not in over-all composition. Chains of differing chemical structure will have differing solubility properties on this account, and these two effects may, for certain solvents, oppose each other; for other solvents they may act in the same direction.³

At the present time there are three distinct theories accounting for the selective precipitation of different molecular-weight species from solution.⁴ The earliest theory is that proposed by Schulz (25), who treated the problem by considering the distribution of polymer between solution and precipitate to be governed by

¹ Communication No. 1133 from the Kodak Research Laboratories.

² Present address: Tennessee Eastman Corporation, Kingsport, Tennessee.

³ When it is known that the polymer varies in composition (as, for example, in degree of esterification), then fractions obtained by a precipitation fractionation should be analyzed to show that there is no progressive change in composition, and hence separation on a length basis only. Otherwise, conclusions as to molecular-weight distribution are in error. In this paper, some reverse-order precipitation effects are described. We base their explanation upon the differential solubility of end groups, as compared to inner segments. If this is correct, then these effects in a way might be classed as due to differences in composition. But this is a difference of composition which is itself a direct function of chain length, whereas other compositional differences so far recognized are not necessarily related to chain length.

⁴ Several other methods of fractionating polymers have been used, but the standard and most widely used method remains that of fractional precipitation and is the method specifically considered in the three theories. The various methods, and the uses to which they have been applied, are described in a comprehensive review of the literature on high-polymer fractionation, recently published by Cragg and Hammerschlag (4).

Some rather extravagant claims for fractionation by extraction from a "coacervate" have been made by Gavoret and Duclaux (10) on a fractionation of polyvinyl acetate. However, there seems to be a confusion, in the stating of their concentration units, between "grams" and "grundmols". Correcting for this, we note that their separation of molecular weights is like that which we have obtained on several fractionations of polyvinyl acetate, using the precipitation method. On a different polymer we have carried out parallel fractionations, using the standard method and the "coacervate" method of these authors. Besides finding this latter technique very time consuming, we found the resultant fractions to be less well separated than those from fractional precipitation.

the relative energies in the two phases and the Boltzmann probability for such energies. The thermodynamic approach has been developed by Flory (7), Gee (11), and Huggins (14). Both entropies and heats of mixing are calculated for the solution and precipitate phases; these are then used in the thermodynamics of equilibrium between two phases. A treatment which considers the mechanics of the start of aggregation of precipitation as a reversible reaction in equilibrium was recently proposed by Morey (18) and is further elaborated in this paper.

The theory of Schulz, while open to criticism, also deserves a favorable word for being the first vigorous attack on the problem, and for stimulating interest in the theoretical aspects of polymer fractionation. The basis of the theory is laid in a Brønsted-Boltzmann expression for the distribution of a substance in two immiscible solvents. Representing by E the energy difference per molecule of the material on passing from the first solvent to the second, and by a_1 and a_2 the activities in the two liquids,

$$\frac{a_1}{a_2} = K'e^{-E/kT}$$

Schulz assumes that the activities may be replaced by the actual concentrations, C_1 and C_2 . This is reasonable at low concentrations, but is questionable at higher concentrations and when the polymer is no longer molecularly dispersed, but aggregated. It is further assumed that the two immiscible solvents may be replaced, in theory, by the solution and precipitate, considering the latter as a fluid. The specific application to high polymers comes in defining E as proportional to the number of monomer units in the chain, and the proportionality factor to be a linear function of the per cent of precipitant, P , which has been added to the solvent. Hence:

$$\frac{C_1}{C_2} = K''e^{-(A+BP)(M/kT)}$$

For the study of precipitation and fractionation phenomena, a very convenient parameter is the per cent of precipitant just at the moment of precipitation; put in another way, the saturated state and the values of concentration, precipitant, and temperature which produce the saturated state form a readily measurable set of parameters. We shall henceforth designate the concentration of polymer (of a given molecular weight) in solution which produces saturation as C_γ , and the per cent of precipitant which corresponds to this same state of saturation as P_γ .

One more assumption is now made by Schulz,—namely, that the concentration of polymer in the precipitated phase, C_2 , is constant. This is known to be in error to some extent; the lower-molecular-weight precipitates are less swollen than the precipitates of longer chains. Fortunately for the theory, the error in this assumption is counterbalanced by the opposing error introduced when concentrations are made to replace activities. Schulz thus arrives at:

$$C_\gamma = Ke^{-(A+BP_\gamma)(M/kT)} \quad (1)$$

wherein K , A , and B are constants. At constant temperature, this expression leads to two consequences which may be tested experimentally: (a) for constant molecular weight, P_r is linearly related to $\log C_r$; (b) with the concentration at saturation the same, for each different species precipitated, P_r is linearly related to $1/M$.

Experiments will be presented later in the paper, but at this point we may note some of the results: Deduction (a) is found to be true, while (b) is only approximated. Aside from the explicit assumptions already cited, there are two which are implicit. It will be noted that the energy difference between solution and gel is made proportional to the molecular weight. This has the effect of stating, when the equation is applied to the very start of precipitation, that in the precipitate, the longer the chain, the greater the number of secondary links to other chains. This is certainly the case for large-size particles or aggregates, but in the initial coalescence only a few secondary cross links are required to establish a nucleus or embryo aggregate, this number being nearly independent of chain length. Indeed, the probability of establishing these first links is related to the chain length, but this probability is not to be confused with the number of links required for initial coalescence. This latter factor is the one which must be considered if phase separations are to be noted experimentally by the first signs of optical haze. The other implicit assumption has already been noted by Flory and Huggins, and is the neglect of effects due to the entropy of mixing of polymer and solvent.

THERMODYNAMIC THEORY

The thermodynamic approach is a quite general study of phase relationships, out of which as particular cases can be derived both fractionation by successive precipitation from solution, and fractionation by extraction from a highly swollen gel. The outline is as follows: The partial molal free energy of the solvent, $\Delta\bar{F}_1$, and its activity, a_1 , are expressed by the fundamental relation:

$$\Delta\bar{F}_1 = RT \ln a_1 = \Delta\bar{H}_1 - T\Delta\bar{S}_1 \quad (2)$$

and similarly for the polymer:

$$\Delta\bar{F}_2 = RT \ln a_2 = \Delta\bar{H}_2 - T\Delta\bar{S}_2 \quad (3)$$

To predict a separation of phases requires a knowledge of these partial molal free energies; hence, the partial molal heats of mixing and the partial molal entropy changes, on passing from one phase to another, must be calculated. For the heat term, those who use the thermodynamic approach take the form as given by Scatchard (23), and by differentiating with respect to the mole fraction of solvent or polymer, obtain:

$$\Delta\bar{H}_1 = BV_1\phi_2^2 \quad \Delta\bar{H}_2 = BV_2\phi_1^2 \quad (4)$$

V_1 and V_2 are the molar volumes, ϕ_1 and ϕ_2 are the volume fractions which the solvent and polymer occupy in the whole system, and B is a constant.

The entropy term is obtained from the Boltzmann definition of entropy as the

logarithm of probability. The problem then becomes one of counting all the different ways in which polymer and solvent molecules can be arranged. This is a somewhat difficult procedure, and requires a number of assumptions as to the randomness of mixing, the absence of aggregation, the degree of flexibility of the chains, etc. Some of these assumptions have been further considered by Flory (9), Alfrey and Doty (1), and by Schuchowitzky (24). The counting method is based upon the regarding of the system of solvent and polymer as an assembly of lattice points or holes into each of which may be placed a solvent molecule or an equal-sized polymer segment. The segments of a chain must be placed in neighboring lattice points, although not in a straight line. For rubber, one might expect free bending at each union between monomer units, but for cellulose derivatives, one must assume that, on the average, β monomer units must be placed in a straight line before a kink occurs. By this means, variations in chain flexibility are recognized and incorporated into the theory. These entropy calculations result finally in the expressions for the partial molal free energies:

$$\Delta\bar{F}_1 = \frac{RT}{\beta} \left[\frac{\beta BV_1}{RT} \phi_2^2 + \ln \phi_1 + \left(1 - \frac{V_1}{V_2} \right) \phi_2 \right] \quad (5)$$

$$\Delta\bar{F}_2 = RT \left[\frac{\beta BV_2}{RT} \phi_1^2 + \ln \phi_2 + \left(1 - \frac{V_2}{V_1} \right) \phi_1 \right] \quad (6)$$

The coefficient BV_1/RT is, following Huggins, denoted by μ . The effect of β is to emphasize the heat term at the expense of the entropy term. For solutions of rubber in toluene, Flory (8) indicates that a value of $\beta = 5$ brings agreement with experiment, while a value of 8 is found for polystyrene in toluene. On the basis of a following discussion on the lack of flexibility found for cellulose acetate, a value of $\beta = 50$ for cellulose derivatives seems like a reasonable guess.

Having obtained equations 5 and 6, the next problem is to calculate the amounts of the components which bring about the appearance of a precipitate. Because of the complexity of equations 5 and 6 this is not simple analytically, but the method is graphically illustrated in figure 1. If a solution phase and a gel phase are in equilibrium, then the partial molal free energy (activity) of the solvent which is present in the solution equals the partial molal free energy (activity) of the solvent which finds itself in the gel. If $\Delta\bar{F}_1$ is plotted against the volume fraction of solvent, it will be found to increase with larger amounts of the solvent. If this curve rises continuously, then two phases are not found, for there are not two different values on the volume fraction axis for which the same partial molal free energy exists. But for certain values of $\beta\mu$, the curves show a maximum and a minimum. Then two phases can appear, and at different values of the volume fraction, equal partial molal free energies are found.

A similar curve can be plotted for $\Delta\bar{F}_2$, as shown in figure 1, and the same equilibrium condition must be met for two stable phases to appear; that is, a horizontal line must cut this curve also at more than one point. In one and the same solution, these equilibrium conditions must also begin simultaneously;

this condition requires drawing vertical lines. It will be found that there is only one place in which the two horizontal and the two vertical lines can be put together to form a rectangle with corners on the curves. The compositions determined by the positions of the two vertical lines then give the "critical" compositions at which a phase first appears or disappears. These critical compositions can then be plotted against $\beta\mu$ or against the per cent of precipitant

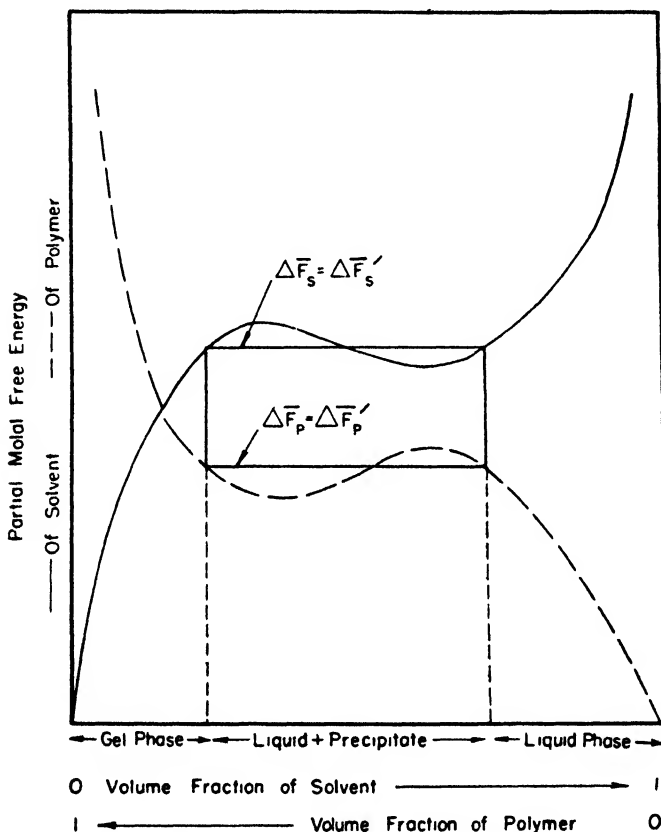


Fig. 1. Appearance of phases in relation to the partial molal free energies of the components

added to the solution, as in figure 2. (It can be shown that the percentage of precipitant is approximately proportional to $\log \beta\mu$.)

Such a curve gives the limiting compositions at which a change in the number of phases takes place. This curve represents the case when the polymer is considered to be of only one molecular weight; for each different molecular weight there is a characteristic curve, as shown in figure 3, and as determined by the ratio V_2/V_1 , appearing in equations 5 and 6.

With the aid of figure 3, the essential features of fractionation can be deduced. For fractionation by precipitation, we deal with the portions of the curves in figure 3 which are below the peaks or extreme left parts of the curves. Put in

another way, if one species forms a precipitate, it must be denser and richer in polymer than the phase from which it came. This means entering the two-

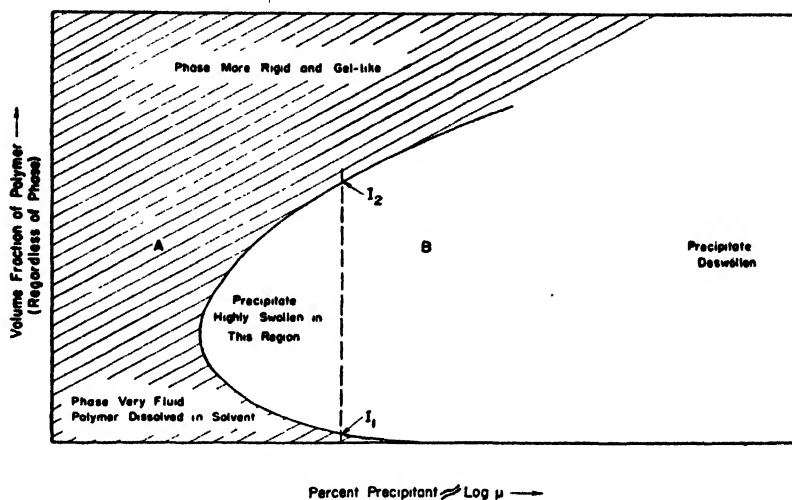


FIG. 2. Region of single and double phases in relation to the amount of precipitant. Phases for a single molecular weight: A, one phase only; B, two coexisting phases, the compositions of which are given at intersection points such as I_1 , I_2 .

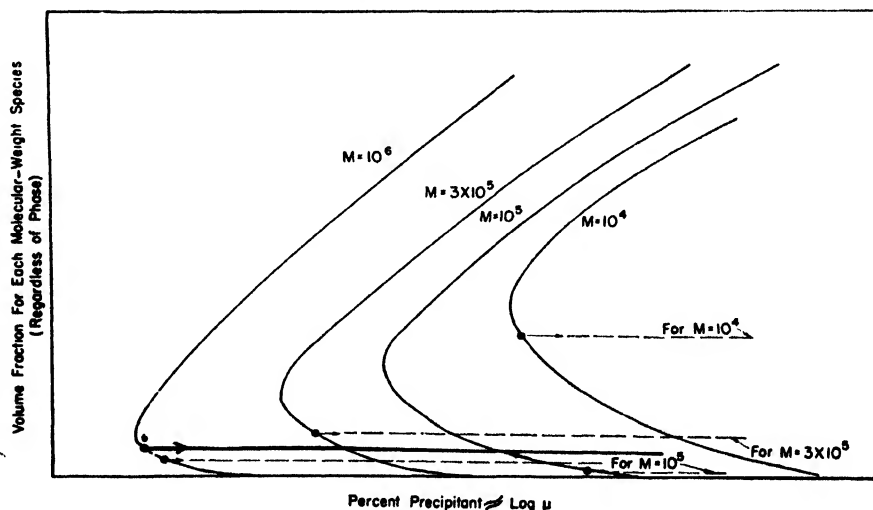


FIG. 3. Double phase regions for varying molecular weights. Possible courses of fractionation: ●——, all species present in equal amounts, ○——, a possible mass distribution.

phase region from below rather than from above the left-sided peak; otherwise the process is more a syneresis than a precipitation. The inclined straight lines on figure 3 show the order in which the various species would begin precipitating, as one continuously added precipitant. They are not quite horizontal,

since the concentration of polymer decreases as precipitant is added. (They would be horizontal if the experiment were carried out by lowering the temperature.) If the species in the polymer were all present in the same amount, precipitation would proceed as indicated by the solid line. But if the species have a non-uniform distribution, which is generally the case, then precipitation takes place by following the various dashed lines, which start out from different concentration values, on the M curves. (The values of molecular weights shown in figure 3 have no quantitative significance; they indicate the direction of dependence on M .) It is seen that the concentration, as well as the identity, of a species determines the precipitation point, and that a species of low molecular weight may start precipitating before one of higher molecular weight if the former is present in much greater amounts. The starting distribution thus plays a part in determining the purity of fractions, and necessitates a refractionation when abrupt changes in distribution are present. This effect of a low species precipitating before a higher one, owing to distribution, is not to be confused with the true reverse-order effect (20), which is still found when the species are made to have equal concentrations.

As to fractionation by extraction, this too is predicted by this outline of phase relationships, as has been pointed out by Scott (26). This comes about by starting, on figure 3, on the right-hand side, and drawing lines approximately horizontal, cutting across the phase separation boundaries. The line proceeds to the left as more solvent is added, and the low-molecular-weight fraction is seen to enter the solution phase first.

Returning to fractional precipitation, and the use of the lower portions of the phase separation boundaries, the authors have constructed such curves from experimental data and have used them to deduce the distribution curves of cellulose acetate butyrate polymers (19). The distribution was obtained both by a graphical use of the phase boundary curves and by an analytical procedure. Figure 4 shows one of the nomograms used. The curved lines, plotted for molecular-weight intervals of 10,000, show where each particular species will begin to precipitate. The diagram is calculated for a fixed value of initial concentration of the whole polymer, including all species. The straight lines fix the precipitation point for a given species when present in varying fractions of the total polymer. Thus, if a molecular weight of 100,000 was the only species present, the line $C_M/C_{ZM} = 1$ would fix the per cent precipitant. If the amount of that species present was only 0.1 of the total, then the line $C_M/C_{ZM} = 1$ would be followed. Since figure 4 is constructed using a low value of polymer concentration, it may be regarded as a high magnification of the lower part of figure 3.

Phase-change boundary curves for polyethylene in various solvents have been published recently by Richards (21), showing the shape of curve to be dependent upon solvent power.

THE RELATIVE IMPORTANCE OF THE ENTROPY CONTRIBUTION

We have seen that a large portion of the thermodynamic development has been concerned with including entropy effects. The size of error which may

result from such a lack of entropy terms must depend, however, upon the type of polymer molecule, and one can make a rough separation of polymer solutions

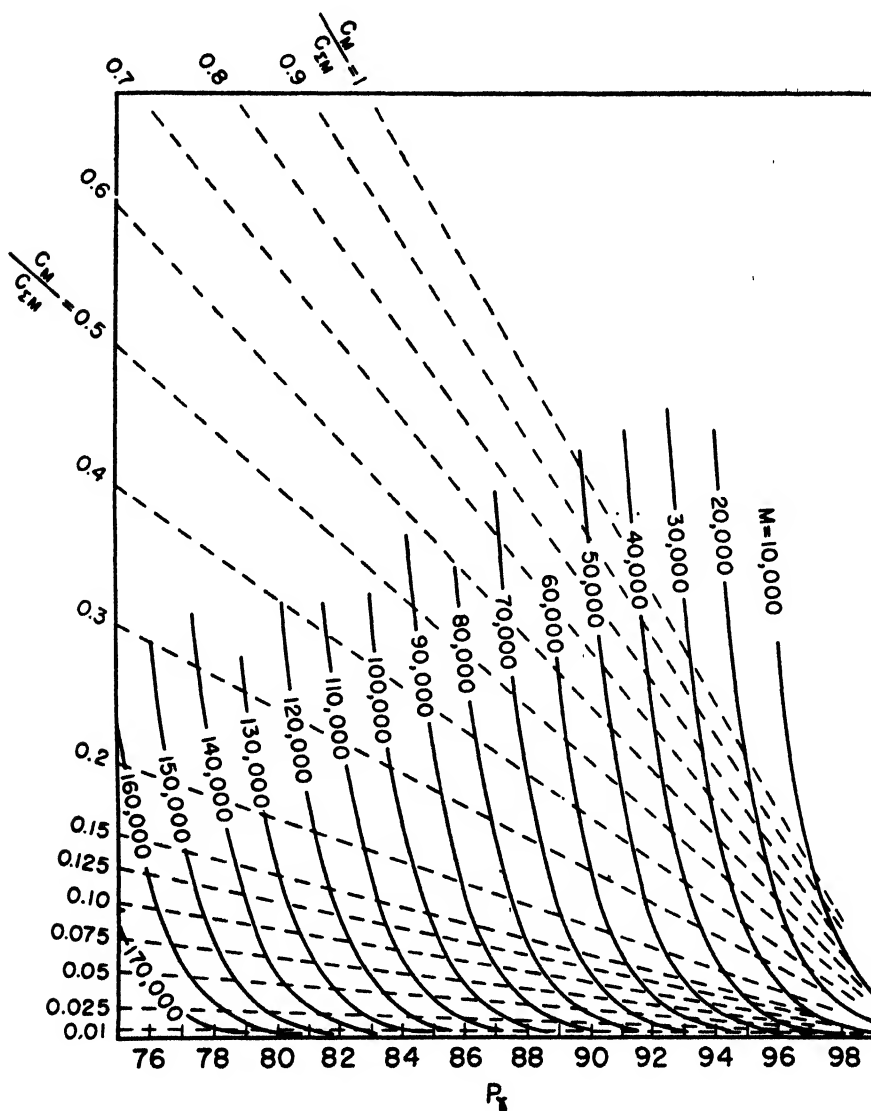


FIG. 4. Phase separation limits for cellulose acetate butyrate. Solvent, acetone; precipitant, 3:1 (by volume) mixture of ethyl alcohol and water.

into two classes: (1) Relatively uncross-linked rubber and other hydrocarbons with large flexibility at each segment; (2) cellulose esters and other relatively rigid chains, for which entropy effects are less pronounced and interaction effects strong. Rubber molecules in solution may have such high kinking that the

distance between ends may be only one-tenth the extended length, but considering cellulose esters, recent evidence is that the entropy effects must be much smaller. Thus, in a study of cellulose acetate in acetone, Stein and Doty (29) conclude that "the smaller molecules of cellulose acetate are approximately fully extended in acetone solution, but that the longer ones are bent in gentle waves." From other optical measurements, Doty and Kaufmann (5) conclude that cellulose acetate chains are relatively rigid, and mention calculations by R. M. Simha indicating that such chains in solution have approximately half the extended length. Further evidence that specific interaction effects, rather than entropy effects, play the chief rôle for the solutions of cellulose esters is given by the large differences in fractionating behavior obtained by the use of varied types of precipitants (20). Recent work of Doty, Wagner, and Singer (6) shows that association may take place before the visual turbidity point is reached, and that such associations may be quite stable. This condition gives a different statistical counting than an ideally random solution, and a lowered entropy contribution.

We must not, therefore, expect Schulz's theory to hold for rubber, but when applied to cellulose derivatives, its shortcomings as regards a lack of entropy terms are not so significant. On the other hand, the thermodynamic treatment needs a careful weighting of the entropy contribution before it is applied specifically to cellulose derivatives. In the equilibrium rate theory which is now discussed, entropy is not calculated directly. Its effects are not completely ignored, however, since the probability of collision enters into the calculations.

PRECIPITATION AS A REVERSIBLE REACTION CONSIDERED FROM THE KINETIC VIEWPOINT

A step common to the three theories is that of defining precisely the state of saturation. The measurable factors which define such a state are the per cent of precipitant (P_γ), the temperature (T), the concentration (C_γ), and the molecular weight (M_i) of the dissolved polymer. In actual practice, a measure of this state is best obtained by carrying a little beyond saturation, so that precipitation has proceeded enough to give a measurable turbidity. We inquire, therefore, into the mechanics of the process of forming the first small aggregates. The initial step of aggregation consists in two chains coming together and remaining attached for at least a time, until two other chains shall have formed a similar union. We assume that for such a union it is not necessary that the chains be completely joined through all the possible secondary links, but that only a relatively few junction points, n in number, suffice for such an embryo aggregate. The rate at which one chosen chain will be able to find another and establish with it the necessary n bonds is inversely proportional to n , and since the n bonds must all be between the same two chains, not simply n bonds anywhere in solution, then the rate is proportional to the chain lengths M_i and M_j of the pair of molecules uniting.⁵ The rate will also be proportional to the number of other

⁵ This number n is not to be confused with the total number of bonds which may develop upon subsequent further growth of the aggregate; it represents a minimum number of link-

chains in solution from which one particular M_i can choose a partner. The number of such chains is proportional to the weight concentration of polymer, C_γ , divided by the average molecular weight. Then the rate of aggregation for a particular chain molecule is:

$$(\text{rate})_i = D/n \cdot M_i M_j C_\gamma / M_a \quad (7)$$

where D is a constant, including a diffusion coefficient. The rate for all possible pairs of chains thus is:

$$(\text{rate})_{\Sigma i} = D/n \cdot M_i^2 \cdot M_j^2 \cdot C_\gamma^2 / M_a^2 \quad (8)$$

We shall now assume that all the different M values indicated may be replaced by the number average, M_a . D may be further defined as proportional to the square root of the absolute temperature, and inversely proportional to both chain length and viscosity of the solvent, since both factors result in lessened mobility.⁶ Since the viscosity factor is temperature dependent, this would require further evaluation if the theory is tested by temperature experiments. However, most available data are taken at fixed temperature. Thus

$$(\text{rate})_{\Sigma i} = \frac{BT^{1/2} M_a C_\gamma^2}{\eta n} \quad (9)$$

B being a constant.

This rate is calculated on the assumption that all bondings are equally effective, whether arising from segments within the chain or from end groups. But there is a growing body of evidence showing that end groups, while few in number, may exert, under proper conditions, appreciable influence. In considering the solubility of a long chain, it is not to be considered as a homogeneous unit. Just as with the fatty acids, wherein some of the valuable lubricating and surface-active properties are due to different behaviors of carboxyl and hydrocarbon ends, so also the action of end groups can be differentiated from that of inner segments of a polymer chain. This has been recognized by others; for example, Highfield (12) showed that solvents for cellulose nitrate contain polar and non-polar groups, and considered that each was necessary to solvate different parts of the polymer. Staudinger and Heuer (28) considered that the aromatic and paraffinic portions of polystyrene retain their own characteristic solubility when polymerized. It is reported (15) that the use of potassium persulfate as catalyst in the polymerization of polyethylene forms associative end groups; when these were hydrolyzed off, the polymer had a much lower melting point. The marked

ages which create a nucleus capable of further growth and sharing in the turbidity by which P_γ is detected. There may well be long portions of chains in this embryonic nucleus which float freely in the solution without at first being linked to each other. For these reasons, n is to a first approximation independent of molecular weight, although the probability of attaining n is related to molecular weight. It was pointed out earlier in the paper that Schulz's theory contains a confusion of these considerations.

⁶ D is inversely proportional to the first power of chain length for chains of slight kinking, but to a fractional power between $\frac{1}{2}$ and 1 if the chains show much coiling.

influence of traces of metallic ions (calcium, magnesium) present in water used for washing newly acetylated cellulose is well recognized commercially (31). The increased viscosity which is known to result ("salt effect") has been ascribed to calcium bridges forming complexes of chains (22). This increased viscosity appears with acetone as solvent, but not with acetic acid, according to Lohmann (17). This requirement of particular groups and particular solvating medium has also been found necessary for the reverse-order precipitation effect (20).

We therefore return to the calculation of the aggregation rate, to include a separate term for end groups. Since the size of a linear chain determines the number of inner segments but has nothing to do with the number of ends of the chain, the quantities M_i and M_e , which appear in equations 7, 8, and 9, do not affect the contribution of end groups to the aggregation rate. The combined rate thus becomes:

$$\text{Aggregation rate} = \frac{BT^{\frac{1}{2}}C_{\gamma}^2M_e + fBT^{\frac{1}{2}}C_{\gamma}^2M_a^{-2}}{\eta n} \quad (10)$$

where f is a weighting factor which weighs the relative bonding strength or importance of end-containing bonds, as compared to segment-segment bonds, in imparting stability to the embryo aggregate; f thus varies with the solvent-precipitant system chosen.

We now equate the rate of aggregation to the rate of solution,⁷ the latter being due to secondary bonds receiving excess thermal energies:

$$\frac{BT^{\frac{1}{2}}C_{\gamma}^2}{\eta n} (M_e + f/M_a^2) = e^{-E_s/kT} + fe^{-E_e/kT} \quad (11)$$

B may be further defined at this point to absorb the additional constants introduced. The weighting factor f appears on the right-hand side also, since if it is concluded that end groups are important in forming an aggregate, then the breaking of an end-containing bond will be equally important for the disappearance of the aggregate.

The terms E_s and E_e are the dissociation energies of the segment-segment and the end-containing bonds. These energies are dependent upon the kind of neighbors which surround the segments in question; when, for example, the neighbors are all solvent molecules, this energy drops below a value necessary

⁷ A similar theoretical approach, applied to the theory of melting of fatty acids, has already been used by King and Garner (16). These authors equate the probability that a molecule will collide with and join to the solid surface, to the probability that it will be removed by receiving thermal activation energy equal to the heat of crystallization. The probability of adsorption is placed in inverse relation to the chain length, so that

$$K/M = e^{-Q/RT}$$

is obtained. The second paper deals with the question of the molecule being rod-shaped or kinked, and for the latter case the probability of adsorption is a more complicated function of M . These authors have also assigned a different effectiveness to terminal groups, as compared to inner groups, in holding chains together, and show that these have different values of heats of solution.

for the continued existence of the bond. As precipitant molecules enter the sphere of neighbors, the bond energy rises. We shall assume that E_s is linear with P_γ :

$$E_s = sP_\gamma - U_s \quad (12)$$

where U_s is a constant related to the energy of association between segment and solvent. The proportionality function s could be further defined in terms of cohesive energy densities of polymer, solvent, and precipitant. This is not essential to the present development of this theory, and we shall amplify s only to account for its dependence upon concentration. For low polymer concentrations, the bonds in the embryo aggregate are surrounded for the most part by small-molecule material. As the concentration increases, however, we must take into account the fact that segments from still other chains form part of the shell of neighbors around the secondary link in question. This will have the effect of aiding the precipitation, so that we shall assume

$$E_s = S_s P_\gamma (1 + C_\gamma/100) - U_s \quad (13)$$

and similarly

$$E_s = S_s P_\gamma (1 + C_\gamma/100) - U_s \quad (14)$$

expressing C_γ in grams per 100 g. of solution.

Equations 11, 13, and 14 may now be applied to specific conditions. Considering normal-order precipitation, in which end groups play no significant part, f is assigned a very small value. Then

$$\begin{aligned} C_\gamma^2 &= \frac{\eta n}{BT^{\frac{3}{2}} M_a} e^{-s_s P_\gamma (1 + C_\gamma/100)/kT} e^{U_s/kT} \\ &\simeq \frac{\eta n}{BT^{\frac{3}{2}} M_a} e^{-s_s P_\gamma/kT} e^{U_s/kT} \end{aligned} \quad (15)$$

for concentrations below 10 per cent. In agreement with common experimental knowledge, equation 15 predicts: (a) with increasing molecular weight, a decrease in the concentration at which precipitation begins; (b) with increasing amount of precipitant, a decrease in the concentration needed for saturation; (c) for some (but not all) systems, an increase in the concentration needed for saturation, with increasing temperature. Two other predictions are made, for which the experimental evidence is less well known: (d) At a fixed molecular weight, there is a linear relation between $\log C_\gamma$ and P_γ . (It is not the initial concentration, but the actual concentration at each precipitation point which must be used.) Schulz has already established the validity of prediction (d), and with a few exceptions, we have confirmed it in numerous examples, two of which are illustrated in figures 5 and 6. (e) At a fixed value of C_γ , there is a linear relation between $\log 1/M$ and P_γ .

To test (e), one must adjust C_γ to come out the same at each precipitation point, or else calculate what the value of P_γ would be at the chosen C_γ . Predic-

tion (e) is important for determining the correctness of this theory as compared to that of Schulz, the latter predicting linearity between $1/M$ and P_γ . We have carefully examined the available data, which are presented graphically in

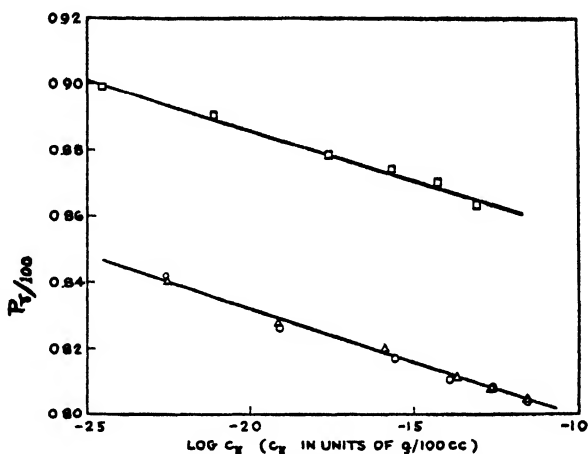


FIG. 5. P_γ - $\log C_\gamma$ relation for cellulose acetate butyrate. \circ , unfractionated ($\bar{M}_n = 71,000$); Δ , fraction B₂ ($\bar{M}_n = 126,000$); \square , fraction D₂ ($\bar{M}_n = 54,000$). Solvent, acetone; precipitant, 3:1 (by volume) mixture of ethylalcohol and water.

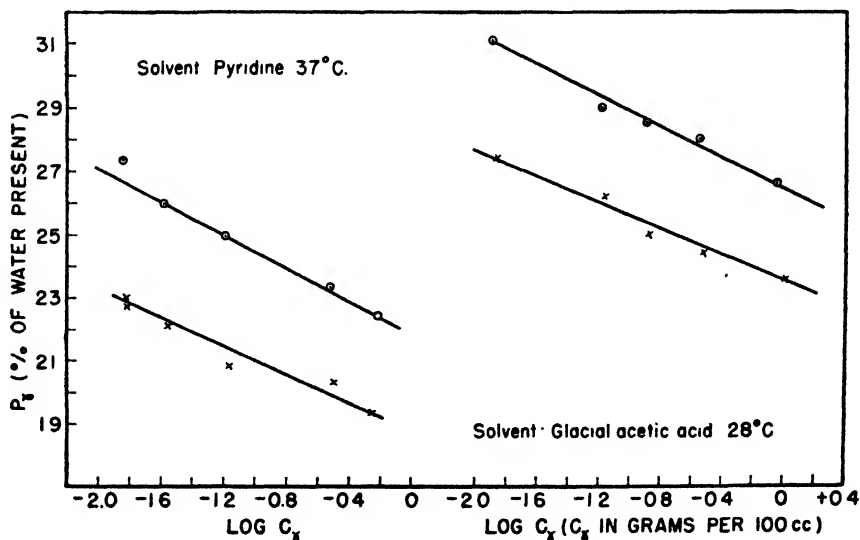


FIG. 6. P_γ - $\log C_\gamma$ relation for cellulose acetate butyrate fractions. \times , 164,000; \circ , 48,000.

figures 7 to 14. In figure 7 are presented the data which are the most favorable to the $1/M$ relation. Good straight lines, over the range covered, are seen. However, the range of $1/M$ is limited, and when data covering a wider range are plotted, as in figure 8, then the linearity is seen to exist only for higher molecular

weights, while the $\log 1/M$ form gives linearity for the lower range. It may be concluded that for the polystyrene-benzene-methyl alcohol system, an inter-

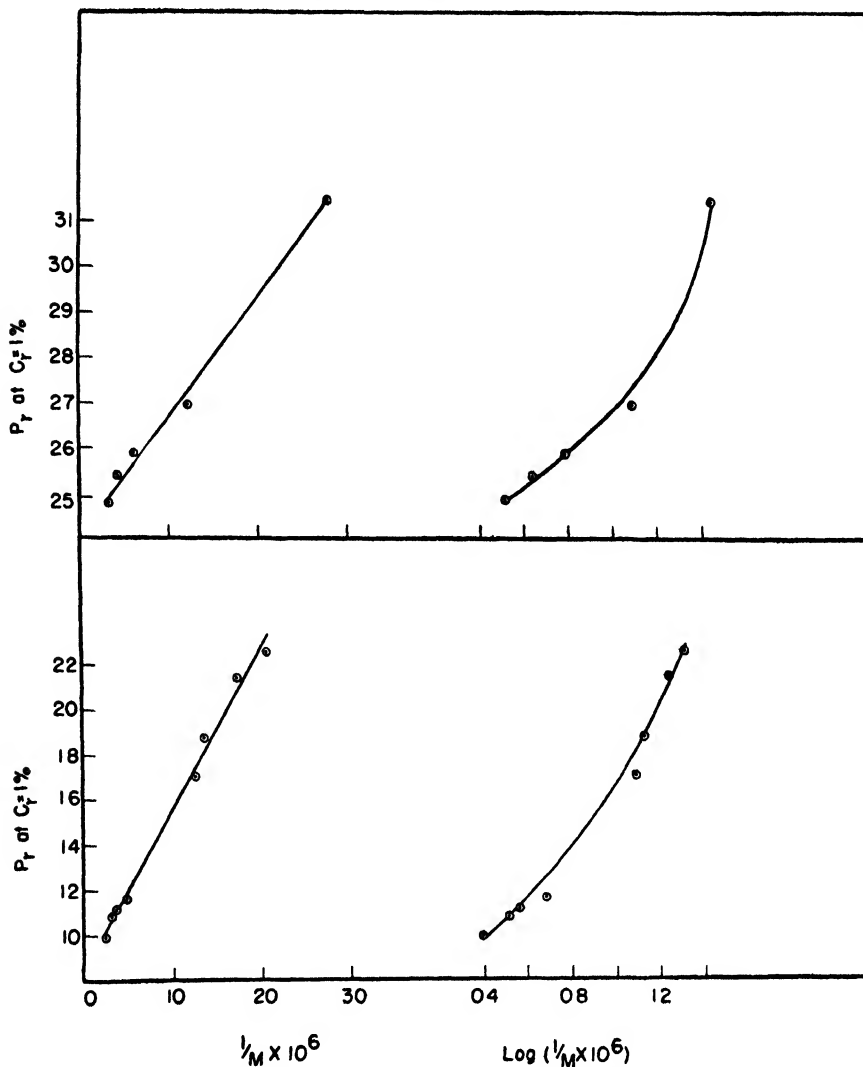


FIG. 7. P_γ - $1/M$ and $\log 1/M$ relations for polystyrene and nitrocellulose. Top: polystyrene; solvent, benzene; precipitant, methyl alcohol. Data of Schulz and Jirgensons (Z. physik. Chem. **B46**, 114 (1940)). Bottom: nitrocellulose; solvent, acetone; precipitant, water. Data of Schulz and Jirgensons.

mediate degree of dependence on $1/M$ is correct. Later data of Schulz and Jirgensons (25) also deviated from the $1/M$ form, and these authors suggested as a modification that P_γ should be linear with $1/M^{2/3}$. This form does, in fact, fit the data of figures 9 and 10, both of which show $1/M$ and $\log 1/M$ to be approaching a fit from opposite directions.

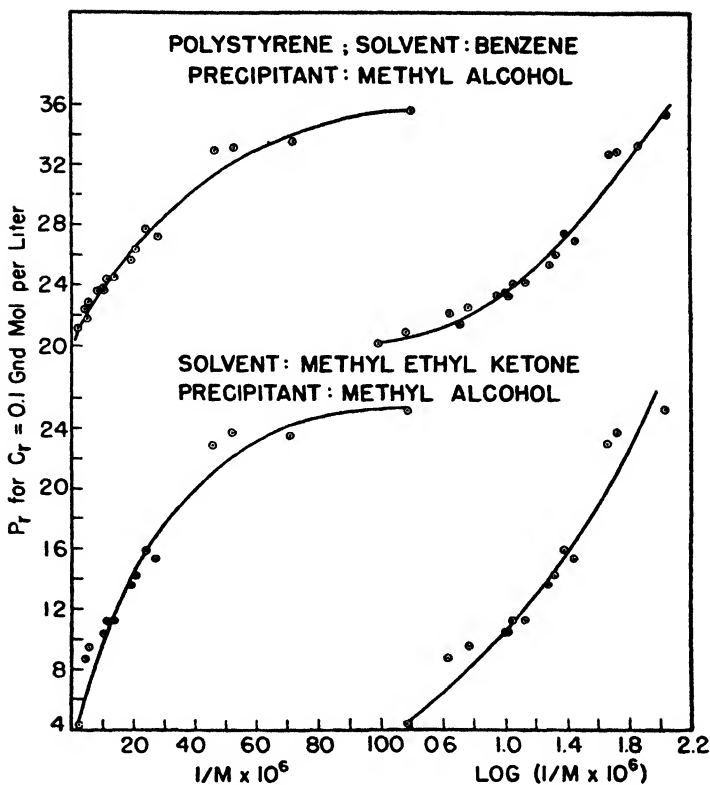


FIG. 8. P_T - $1/M$ and $\log 1/M$ relations for polystyrene. Combined data of Schulz (Z. physik. Chem. **A179**, 321 (1937)) and of Staudinger and Heuer (Z. physik. Chem. **A171**, 144 (1934)).

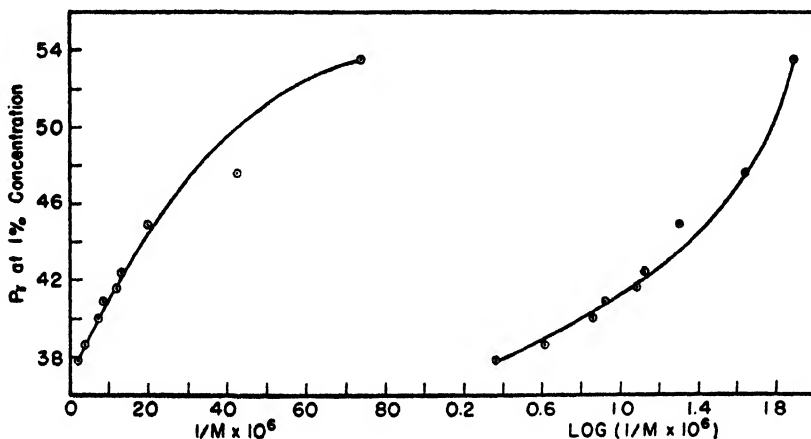


FIG. 9. P_T - $1/M$ and $\log 1/M$ relations for polymethyl methacrylate. Solvent, benzene; precipitant, cyclohexane. Data of Schulz and Jirgensons (Z. physik. Chem. **B46**, 114 (1940)).

Figures 11 and 12 show a marked superiority of the $\log 1/M$ form. Figure 13, plotted with the aid of additional data on the effect of concentration, kindly furnished us by Dr. W. O. Baker, shows again a departure from linearity at low

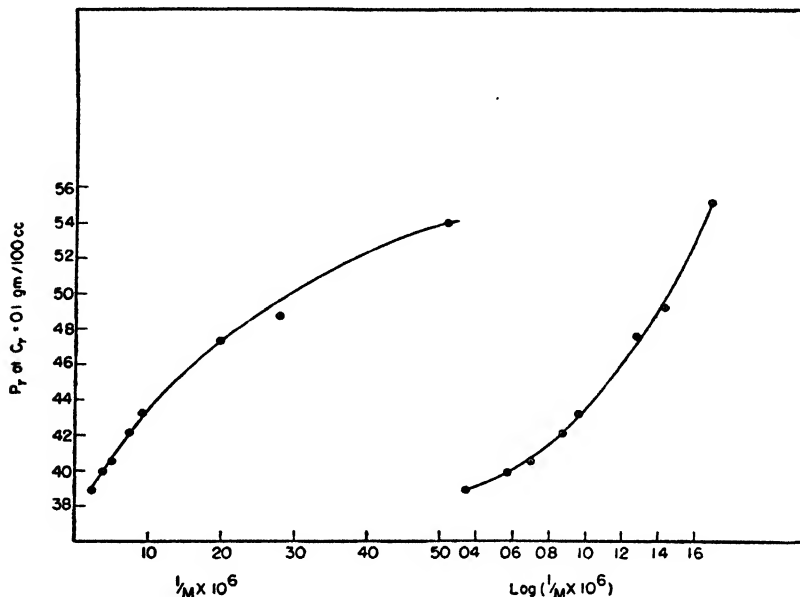


FIG. 10. P_T - $1/M$ and $\log 1/M$ relations for glycogen. Solvent water; precipitant, methyl alcohol. Data of E. Husemann (J. prakt. Chem. **153**, 173 (1941)).

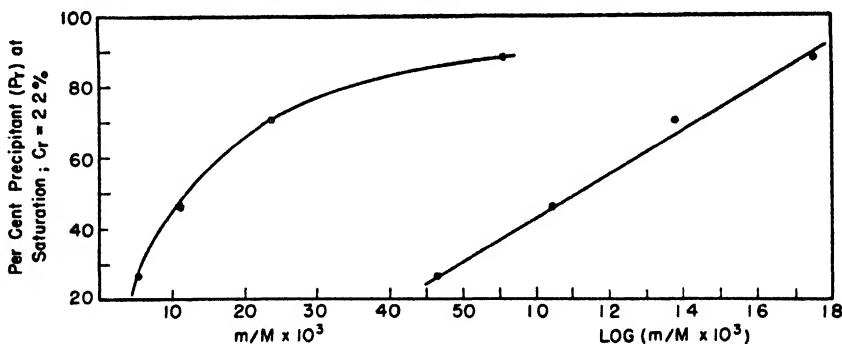


FIG. 11. P_T - $1/M$ and $\log 1/M$ relations for polyoxyethylenes. Solvent, methyl alcohol; precipitant, ether. Data of Lovell and Hibbert (J. Am. Chem. Soc. **61**, 1916 (1939)).

molecular weights when using the $1/M$ form, while the \log form fits reasonably well. In figure 14 the \log form is only approximately correct, but obviously gives a better fit than does $1/M$. It may be concluded that the linearity of P_T with $\log 1/M$ is approximated sufficiently well to establish the first-order correctness of the rate theory.

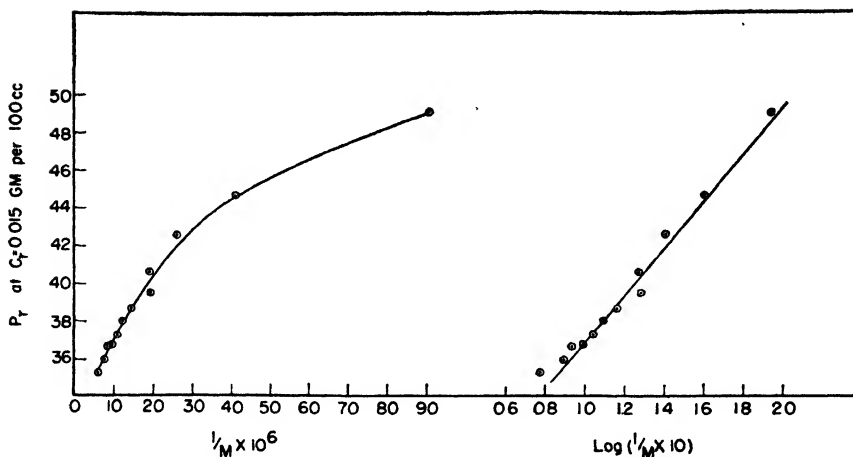


FIG. 12. P_r - $1/M$ and $\log 1/M$ relations for cellulose acetate (40.4 per cent acetyl) fractions. Solvent, acetone; precipitant, water.

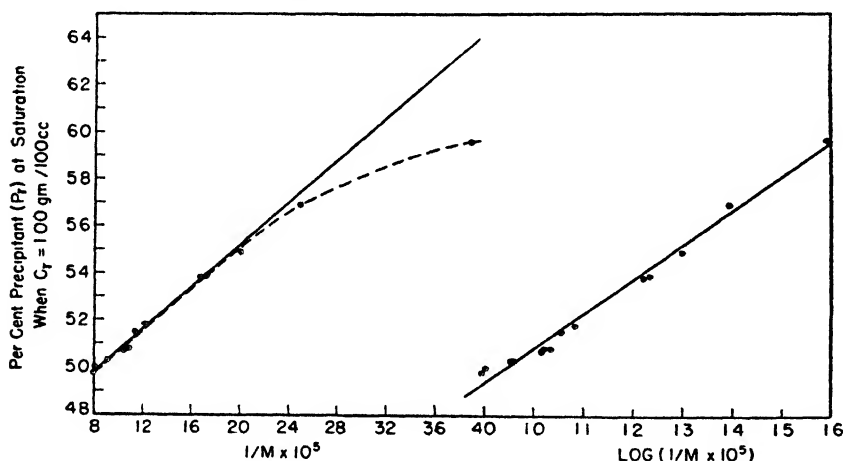


FIG. 13. P_r - $1/M$ and $\log 1/M$ relations for polyundecanoates. Solvent, chloroform; precipitant, methyl alcohol. Data of Baker, Fuller, and Heiss (*J. Am. Chem. Soc.* **63**, 2142 (1941)).

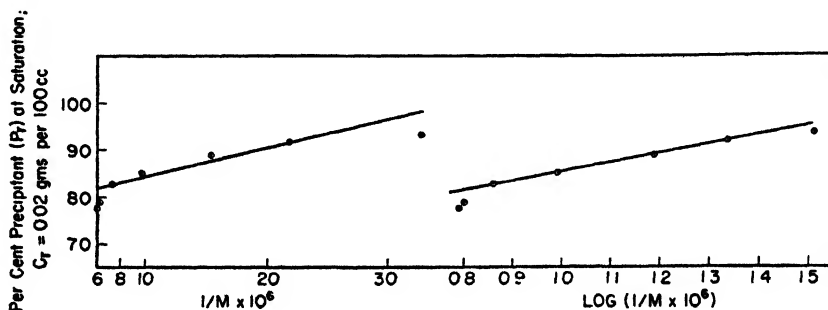


FIG. 14. P_r - $1/M$ and $\log 1/M$ relations for cellulose acetate butyrate fractions. Solvent, acetone; precipitant, 3:1 (by volume) mixture of ethyl alcohol and water.

REVERSE-ORDER PRECIPITATION

We now inquire into the consequences of choosing a system of polymer, solvent, and precipitant in which the end groups are particularly active. This corresponds, in the general equation (equation 11), to making the weighting factor f large. In the extreme case, we neglect terms not containing f and obtain, for lower concentrations:

$$C_\gamma^2 = \frac{\eta n M_a^3}{BT^{\frac{1}{2}}} e^{U_s/kT} e^{-S_s R_\gamma/kT} \quad (16)$$

We see that with increasing molecular weight, the concentration required for saturation *increases*; put another way, the shortest chains will precipitate first. That there are rather unique cases of this has already been reported (20). Fur-

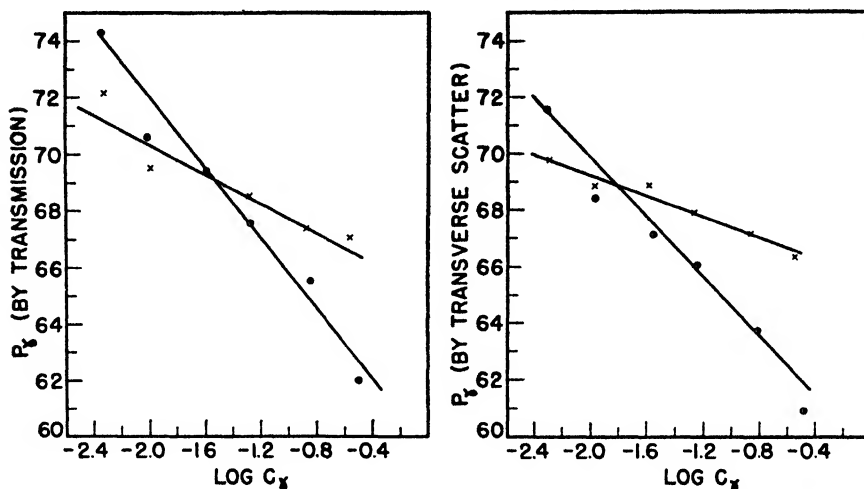


FIG. 15. Reverse-order precipitation as a function of concentration. Cellulose acetate butyrate fractions; glacial acetic acid-isopropyl ether system; 11°C. O, $M_n = 48,000$; X, $M_n = 164,000$.

ther study of the effect, as it appears with cellulose acetate butyrate solutions and isopropyl ether as precipitant, has shown that it is not a temperature-dependent phenomenon, but does depend strongly upon the concentration of the polymer solution used. This is illustrated in figure 15. At a quite dilute concentration, approximately 0.03 per cent, the two lines, each corresponding to a different molecular-weight fraction, cross. At this point, both species precipitate at the same value of P_γ . For concentrations lower than this, the fractions precipitate in normal manner. For concentrations higher than this, however, the low-molecular-weight component precipitates before the higher, and indeed the divergence is more and more marked as higher concentrations are used.⁸

The two graphs in figure 15 refer to different optical means of detecting the

⁸ These same two fractions and solvent are shown in figure 6, wherein with water as precipitant, normal-order precipitation is seen for all concentrations.

initial turbidity. Figure 16 shows that an increase of temperature, for both the normal- and the reverse-order regions, increases the over-all solubility, but does not destroy the reverse-order effect nor its dependence upon concentration. Figure 17 again illustrates the rôle of concentration, this time with acetone as solvent and using additional fractions.

Before accepting an explanation of this reverse-order effect based upon a more abstruse matter such as the end-group hypothesis advanced here, it is desirable to know that no other analytic factor is responsible. We have determined (30)

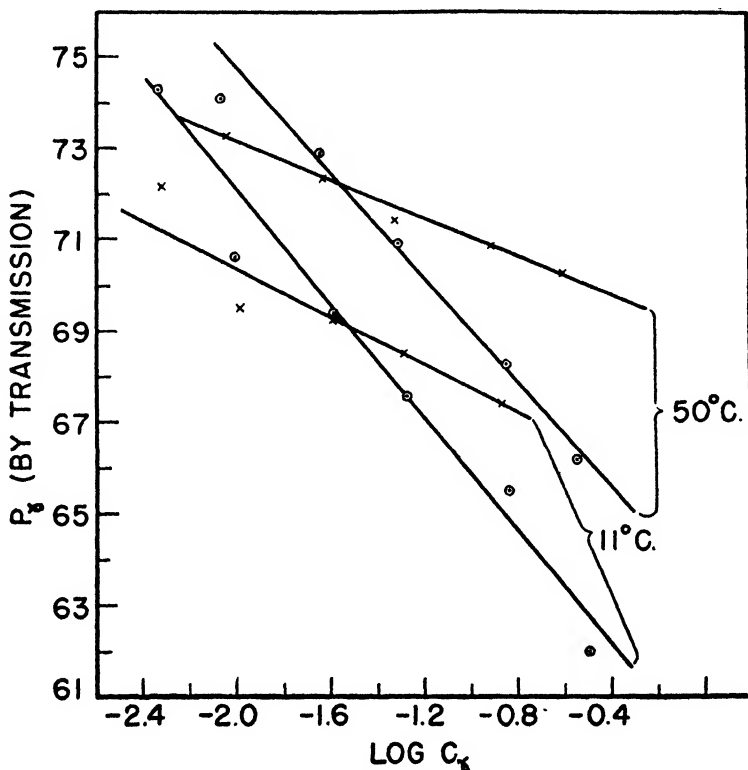


FIG. 16. Reverse-order precipitation independent of temperature. Cellulose acetate butyrate fractions; glacial acetic acid-isopropyl ether system. \circ , $M_n = 48,000$; \times , $M_n = 164,000$.

that the acetyl and butyryl contents of the fractions employed were the same within the accuracy of analysis, approximately 0.5 per cent. Ash analysis, made on another set of fractions of the same polymer, gave the results in table 1. It is seen that with the exception of the higher ash content collected in the first fraction, the ash content is essentially independent of molecular weight; hence the reverse-order effect is hardly to be ascribed to a progressive change in total ash content. This is more apparent when it is recalled that the reverse-order effect was obtained on several pairs of fractions taken from the range encompassed by fractions 2 and 7 of table 1. Accepting the view that end groups are

responsible, then there should be some change of analysis with molecular weight, but its detection would require still more precise analytic procedure, and not

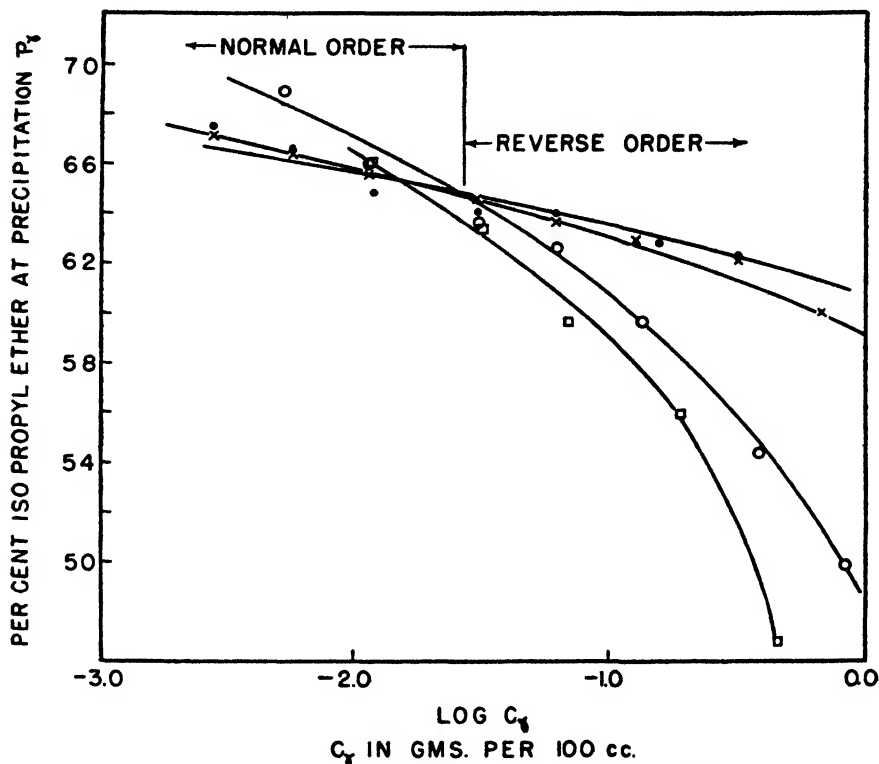


Fig. 17. Reverse-order precipitation for various fractions. Cellulose acetate butyrate fractions. Solvent, acetone. ●, $M_n = 164,000$ (A_2); ○, $M_n = 48,000$; ×, $M_n = 164,000$ (blend M); □, $M_n = 20,000$.

TABLE 1
Ash analysis of cellulose acetate butyrate fractions

FRACTION NO.	INHERENT VISCOSITY $\{\eta\}_{c=0.25}$	INORGANIC MATERIAL
		weight per cent
1.....	2.84	0.092 ± 0.002
2.....	2.64	0.031 ± 0.006
3.....	2.49	0.029 ± 0.002
4.....	2.32	0.030 ± 0.002
5.....	1.98	0.028 ± 0.002
6.....	1.57	0.028 ± 0.002
7.....	0.84	0.034 ± 0.002
8.....	0.75	0.016 ± 0.006
Unfractionated original.....	1.70	0.036 ± 0.002

necessarily an analysis for ash unless it were proven that inorganic material is a unique constituent of the end group.

The reverse-order effect is associated with the formation of aggregates in their early stages of growth, and is picked up at lower concentrations, the more sensitive the detecting arrangement is for observing the first signs of precipitation. In our apparatus, sensitivity was greatest for the observation of transverse scatter, and next for observation of the first detectable drop in transmission. Finally, a point was measured where gross precipitation started. Figure 18 shows how the point of appearance of reverse-order precipitation depends upon how far precipitation is allowed to proceed, or how large the aggregates are allowed to grow. This is shown in a different way in figure 19, where the actual rise of turbidity is plotted against precipitant added. At high concentrations, the low-molecular-weight material shows the first rise of turbidity. It is interesting to note, however, that when precipitation is allowed to proceed to the growth

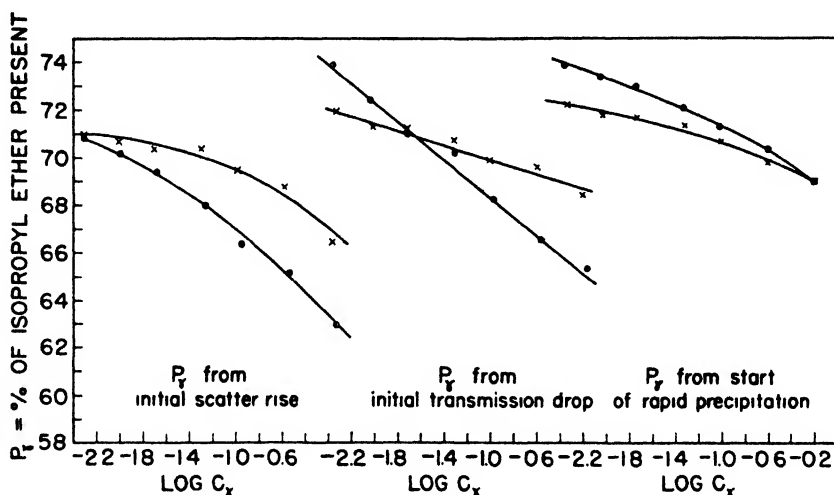


FIG. 18. Reverse-order precipitation as a function of extent of aggregation. Cellulose acetate butyrate fractions. Solvent, pyridine. \circ , $M_n = 48,000$; \times , $M_n = 164,000$.

of large particles, the longer chains again become more able to precipitate first. Thus, a fractionation designed to obtain species in reverse order must keep the "cuts" which are removed small.

Equation 16 predicts the appearance of reverse-order precipitation, but does not explain its dependence upon concentration. It is necessary to connect E_s more fully with the state of aggregation to do this. For those bonds which lie in the center of an aggregate or micelle, the type of solvation is likely to be different from that for those bonds which are on the surface. For very small aggregates, where the ratio of volume to surface is still small, this difference may produce marked effects in the value of the average solvation and the E_s value to be chosen.

Going back to equation 11, we might also expect to find cases where f is intermediate in value, the end and segment bondings both contributing to aggregation. Then over a limited range, precipitation should occur without

preference as to molecular weight. Such a case has recently been reported by Battista and Sisson (2). In such cases, it is evident that any computation of a "distribution" curve of molecular weights is in gross error.

The evidence so far presented on the appearance of reverse-order precipitation has been on dilute solutions, examined optically. It would, therefore, be more convincing if an actual physical separation of fractions were accomplished, with first fractions being examined and found to be of lower molecular weight. This has been done, with the results given in tables 2 and 3. We have seen that the appearance of reverse order is associated with high concentrations. Several fractionations were therefore carried out, at varying concentrations, with typical results shown in table 2. At lower concentrations, the fractions appear normally, and a separation is obtained similar to that which holds when a more

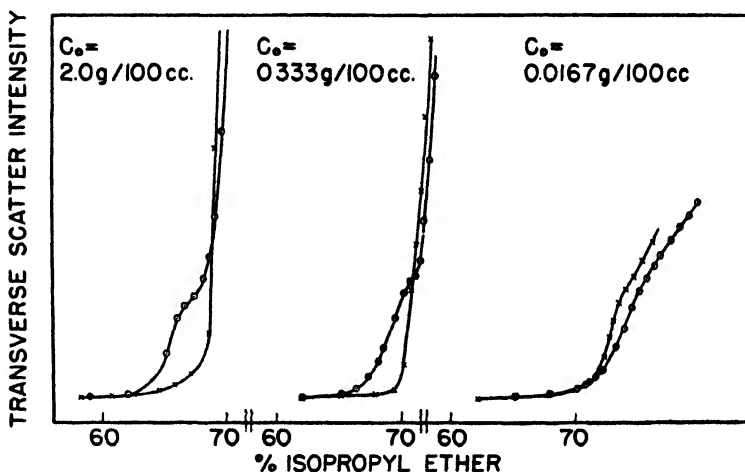


FIG. 19. Course of precipitation, in a reverse-order system, for various concentrations Cellulose acetate butyrate fractions. Solvent, pyridine. ○, $M_n = 48,000$; ×, $M_n = 164,000$.

usual precipitant, such as water, is used. At 10 per cent starting concentration, lower fractions are found to separate first, and then as fractionation proceeds, normal order again sets in. Further examples of this are given in table 3, wherein results on fractionating from other solvents, but still using a precipitant specific for reverse order, are shown.

EFFICIENCY OF FRACTIONATION

These data again illustrate the importance of careful choice of solvent and precipitant, for efficiency in separation. The use of a higher concentration, if a system with reverse-order tendencies were chosen, would thus lead to an apparently less efficient normal-order fractionation. The lower efficiency would be due not to higher concentrations *per se* as the prime cause, but to enhancement of the end-group effect. Efficiency is of practical importance, and it is proper

that in the course of the development of theories, this should be examined. However, it is striking that in the discussion of efficiencies, so much attention

TABLE 2
Fractionation of cellulose acetate butyrate
Solvent, acetone; precipitant, isopropyl ether

STARTING CONCENTRATION: 1.25 G./100 CC.			STARTING CONCENTRATION: 10.0 G./100 CC.		
Fraction No.	Weight per cent	$\{\eta\}_c = 0.25$	Fraction No.	Weight per cent	$\{\eta\}_c = 0.25$
1	4.3	2.88	1	4.7	1.70
2	4.1	2.76	2	2.1	1.83
3	14.9	2.48	3	1.9	2.12
4	17.9	2.11	4	11.1	2.30
5	19.9	1.80	5	9.9	2.10
6	13.3	1.40	6	12.5	1.98
7	9.7	1.08	7	12.6	1.87
8	6.9	0.78	8	10.0	1.82
9	9.0	0.43	9	8.7	1.69
			10	8.0	1.54
			11	5.0	1.36
			12	3.5	1.16
			13	3.5	0.97
			14	6.5	0.69

TABLE 3
Fractionation of cellulose acetate butyrate

FROM 5 PER CENT SOLUTION IN PYRIDINE PRECIPITANT, ISOPROPYL ETHER			FROM 5 PER CENT SOLUTION IN GLACIAL ACETIC ACID PRECIPITANT, ISOPROPYL ETHER		
Fraction No.	Weight per cent	$\{\eta\}_c = 0.25$	Fraction No.	Weight per cent	$\{\eta\}_c = 0.25$
1 + 2	1.1	1.61	1	1.0	1.63
3	1.1	2.03	27	1.78
4	3.3	2.99	39	1.58
5	9.3	2.65	48	1.48
6	13.6	2.28	5	2.8	2.06
7	15.7	2.03	6	6.7	2.67
8	15.6	1.79	7	17.5	2.21
9	12.1	1.50	8	15.8	1.93
10	8.1	1.24	9	16.2	1.71
11	5.4	1.11	10	13.7	1.34
12	5.1	0.94	11	7.0	1.17
13	4.4	0.74	12	6.4	0.95
14	5.2	0.52	13	9.9	0.69

has been paid to the concentration, while the importance of the proper choice of system has not been understood. Howlett and Urquhart (13) examined a number of solvent-precipitant combinations, for cellulose acetate, and chose the

system which spread out the fractions over the greatest range of per cent precipitant; this has the advantage that less precision is required in adding the proper amount for approximately equal fractions. Similar considerations influenced the choice made by Blease and Tuckett (3) for their fractionation of polyvinyl acetate.

But this goal of spreading the fractions over a wide range of precipitant, while desirable in itself, still leaves unanswered and unproved the crux of the matter: to obtain fractions which are spaced in molecular weights. As Battista and Sisson have shown, there is a distinction to be drawn between mere mass separations and species separations.

As to the use of low concentrations, one must critically determine whether or not the gains predicted by approximate theory are really of such magnitude as to justify the attendant disadvantages, and this should be done by experiment. It has been our opinion, expressed earlier, that too much emphasis has been laid on extremely low concentrations (20). It is of interest to note that a fractionation of nitrocellulose was carried out by Spurlin (27) from a 10 per cent acetone solution, and a good degree of molecular weight separation reported. Further experimental evidence dealing with the fractionation of butyl rubbers has been reported to us by Dr. J. Rehner, Jr. With his kind permission the following passage is quoted from one of his communications to us:

"We have on several occasions carried out fractionations in parallel starting with polymer concentrations ranging from about 0.25 per cent to about 2 per cent, and have found little or no difference in the results. While emphasis has been placed for some years on the necessity of employing high dilutions for good fractionation, our results showed that, at least for the polymers worked with, this did not appear to be a vital factor; we found careful temperature control to be far more important. The relatively minor importance of concentration on efficiency of fractionation agrees with your recently reported findings with cellulose acetate."

The expressions for denoting efficiency, as deduced by Schulz and Flory, are not so much concerned with the concentration as they are with the volume fraction of the precipitated phase; these efficiency measures state that the separability rises with the log of the ratio of solution to precipitate volumes. In other words, efficiency is concerned more with taking small cuts or fractions, and hence a larger number of fractions, than it is with the over-all concentration.

Referring again to figures 3 and 4, it is seen that if one of the dashed lines is followed corresponding to increasing the amount of precipitant, but followed for only a short distance (small cut), then one particular species is most active in precipitation. But if the same line is followed a long distance (large cut), then so many phase boundaries are crossed that the net result is an average composition of lesser homogeneity. Our physical means of distinguishing one chain length from another do not permit us to go on indefinitely recognizing length differences; we soon come to a point where we consider neighboring chains to be identical. This means, on the basis of figures 3 and 4, that letting P_1 vary over a still shorter range (smaller cut) does not produce any recognizable

increase in homogeneity, and hence there is a practical limit to the number of fractions to be taken out.

Diagrams such as figure 3 show the left-hand peaks to occur at rather low concentrations. There is a tendency to regard this as additional evidence for the idea that only at very low concentrations can efficient fractionation be obtained. It must be kept in mind, however, that the ordinate scale of volume fraction (or concentration) of such diagrams applies to each particular molecular species being considered at the moment, not to the mixture of all species. In precipitation, it is true that a species is not one pure molecular weight, but a band of neighboring sizes which are not distinguishable; these can then be considered to interact. But when the molecular weights are far enough apart, then, for reasonably low concentrations, such separated species act quite independently.⁹ Therefore, in a broad distribution, a concentration of say 10 per cent for the whole mixture means something like 1 per cent on each particular curve of figure 3.

Concentrations which are above the left-hand peaks of these curves are too high, but it is hardly a valid argument against the efficiency of a precipitation process to point to conditions where such a process is no longer taking place and where actually *syncrexis* is occurring.

SUMMARY

Existing theories accounting for the selective precipitation of increasing chain lengths are reviewed. These theories are: (a) that of G. V. Schulz, a treatment based upon considering the potential energy of a chain molecule when in the solution or in the precipitate phase; (b) a thermodynamic treatment, developed by Flory, Gee, and Huggins, in which a calculation of activities is made and used to predict phase separation conditions; and (c) a theory in which the precipitate phase is considered as a consequence of the opposing rates of solution and aggregation.

With this last theory, by including a separate term for the influence of end groups, the type of fractionation in which short chains are less soluble than the long ones can be accounted for. This reverse-order effect is further studied and shown to be independent of temperature but dependent upon concentration. The opposing rate theory is shown to be in accord also with experimental data on normal-order precipitations.

The efficiency of fractionation is also discussed from the viewpoint of these studies.

⁹ In an experimental proof of this, the concentration of the high fraction must be adjusted to the same value, upon the addition of a low fraction, that it had in the comparison titration. It is incorrect to take the same concentration for the mixed species. This would lead to an apparent enhancement of long-chain solubility by the presence of short chains, when the effect is actually one of variation of titration point with concentration. In a study of such mixtures by thermodynamic theory, the same precautions hold; the volume fraction of the species being considered to precipitate must not be confused with the combined volume fraction of all polymer components.

REFERENCES

- (1) ALFREY, T., AND DOTY, P. M.: J. Chem. Phys. **13**, 77 (1945).
- (2) BATTISTA, O. A., AND SISSON, W. A.: J. Am. Chem. Soc. **68**, 915 (1946).
- (3) BLEASE, R. A., AND TUCKETT, R. F.: Trans. Faraday Soc. **37**, 571 (1941).
- (4) CRAGG, L. H., AND HAMMERSCHLAG, H.: Chem. Rev. **39**, 79 (1946).
- (5) DOTY, P. M., AND KAUFMAN, H. S.: J. Phys. Chem. **49**, 583 (1945).
- (6) DOTY, P. M., WAGNER, H., AND SINGER, S.: J. Phys. Colloid Chem. **51**, 32 (1947).
- (7) FLORY, P. J.: J. Chem. Phys. **9**, 660 (1941); **10**, 51 (1942); **12**, 425 (1944).
- (8) FLORY, P. J.: J. Chem. Phys. **10**, 57 (1942).
- (9) FLORY, P. J.: J. Chem. Phys. **13**, 453 (1945).
- (10) GAVORET, G., AND DUCLAUX, J.: J. chim. phys. **42**, 41 (1945).
- (11) GEE, G.: Trans. Faraday Soc. **38**, 276 (1942).
- (12) HIGHFIELD, A.: Trans. Faraday Soc. **22**, 57 (1926).
- (13) HOWLETT, F., AND URQUHART, A. R.: J. Textile Inst. **37**, T89 (1946).
- (14) HUGGINS, M. L.: J. Chem. Phys. **9**, 440 (1941); J. Phys. Chem. **46**, 151 (1942); Chap. 9B of *Cellulose and its Derivatives*, Emil Ott (Editor), Interscience Publishers, Inc., New York (1943).
- (15) I. G. Report: Modern Plastics **23**, 153 (1946).
- (16) KING, A. M., AND GARNER, W. E.: J. Chem. Soc. **1934**, 1449; **1936**, 1368.
- (17) LOHMANN, H.: J. prakt. Chem. **155**, 301 (1940).
- (18) MOREY, D. R.: A.A.A.S. Conference on High Polymers, Gibson Island, Maryland, July, 1946.
- (19) MOREY, D. R., AND TAMBLYN, J. W.: Meeting of the Division of High-Polymer Physics, Rochester, New York, 1944; J. Applied Phys. **16**, 419 (1945).
- (20) MOREY, D. R., AND TAMBLYN, J. W.: J. Phys. Chem. **50**, 12 (1946).
- (21) RICHARDS, R. B.: Trans. Faraday Soc. **42**, 10 (1946).
- (22) ROGOVIN, S., AND SCHLACHOVER, M.: Kolloid-Z. **78**, 224 (1937).
- (23) SCATCHARD, G.: Chem. Rev. **8**, 321 (1931).
- (24) SCHUCHOWITZKY, A.: Acta Physicochim. U.R.S.S. **20**, 887 (1945).
- (25) SCHULZ, G. V.: Z. physik. Chem. **A179**, 321 (1937) (with B. Jirgensons); **B46**, 122 (1940).
- (26) SCOTT, R. L.: J. Chem. Phys. **13**, 178 (1945).
- (27) SPURLIN, H. M.: Ind. Eng. Chem. **30**, 538 (1938).
- (28) STAUDINGER, H., AND HEUER, W.: Z. physik. Chem. **A171**, 146 (1934).
- (29) STEIN, R. S., AND DOTY, P. M.: J. Am. Chem. Soc. **68**, 166 (1946).
- (30) TAMBLYN, J. W., MOREY, D. R., AND WAGNER, R. H.: Ind. Eng. Chem. **37**, 573 (1945).
- (31) U. S. patents 2,126,488-9.

NOTE ON THE RELATION BETWEEN THE HEAT OF EVAPORATION
AND THE SURFACE TENSION OF LIQUIDS

J. C. DE WIJS

*Mr. Franckenstraat 10, Nijmegen, Holland**Received January 22, 1947*

Some time ago the author proved (1)¹ a relation between the heat of evaporation of liquids and the temperature:

$$L = k(T_k - T)^m \quad (1)$$

in which L is the total heat of evaporation at the temperature T and T_k the critical temperature, while k and m are two constants dependent on the nature of the substances under investigation; the value of m is about 0.4. This formula holds good for a great number of liquids between their melting point and their critical temperature, but not for the liquid gases.

There is also a formula of the same form as mentioned above for another important property of liquids. In connection with his thermodynamic theory of capillarity, van der Waals has given an exponential function for the surface tension, σ , for liquids up to the critical point (4):

$$\sigma = A(T_k - T)^n \quad (2)$$

in which A is a constant, dependent on the nature of the substances, while the exponent n should be the same for all sorts of liquids very near the critical temperature, namely, $n = 1.5$; in reality, for the so-called normal substances, $n = 1.25$ on the average at lower temperatures, and for the liquid gases the value of n varies from 0.8 to 1.33.

When we now combine these two formulas, it is obvious that this is possible in various ways. In the first place we can eliminate the temperature, so that we obtain a relation between the heat of evaporation and the surface tension which is *independent* of the temperature. From these two formulas it follows that:

$$T_k - T = \left(\frac{L}{k}\right)^{1/m} \quad \text{and} \quad T_k - T = \left(\frac{\sigma}{A}\right)^{1/n}$$

and therefore

$$\left(\frac{L}{k}\right)^{1/m} = \left(\frac{\sigma}{A}\right)^{1/n}$$

or

$$L = B\sigma^p \quad (3)$$

if $B = k/A^p$ and $p = m/n$.

¹ Other authors have also made use of the same formula, some with the same exponent for all substances, others with a special exponent for each one.

In the second place we are able to combine both formulas in such a way that we get another relation between L and σ , but one which is, in contrast to equation 3, *dependent* on the temperature.

When we divide equation 1 by equation 2 we get:

$$\frac{L}{\sigma} = \frac{k}{A} \cdot \frac{(T_k - T)^m}{(T_k - T)^n}$$

or

$$\frac{L}{\sigma} = C(T_k - T)^q \quad (4)$$

if $C = k/A$ and $q = m - n$.

TABLE 1

Ethyl alcohol

$B = 68.105$; $C = 274.2$; $p = 0.3922$; $q = -0.6071$

T	$T_k - T$	σ	L		Δ	L/σ		Δ
			Observed	Equation 3		Observed	Equation 4	
40	203.1	20.20	218.7	221.4	+2.7	10.82	10.89	+0.07
60	183.1	18.43	213.4	213.6	+0.2	11.58	11.59	+0.01
80	163.1	16.61	206.4	205.0	-1.4	12.43	12.42	-0.01
100	143.1	14.67	197.1	195.3	-1.8	13.44	13.49	+0.05
120	123.1	12.68	184.2	184.4	+0.2	14.52	14.76	+0.24
140	103.1	10.59	171.1	171.8	+0.7	16.15	16.44	+0.29
160	83.1	8.45	156.9	157.3	+0.4	18.57	18.75	+0.18
180	63.1	6.23	139.2	139.6	+0.4	22.35	22.19	-0.16
200	43.1	3.99	116.6	117.2	+0.6	29.22	27.97	-1.25

Instead of combining the formula for the heat of evaporation with those of van der Waals for surface tension, one can also combine formula 1 with the formula of Eötvös for the molecular surface energy:

$$\sigma V^{2/3} = k(T_k - T)$$

in which $V^{2/3}$ is the molecular volume at temperature T . We then do not obtain the relations between L and σ only, but instead of this, between L , σ , and V (this is, however, not the theme of this paper).

When we wish to examine formulas 3 and 4, it is obvious that this is possible only for substances for which the heat of evaporation as well as the surface tension are known in a wide range between the melting point and the critical temperature. The substances for which both series of data are known are, with the exception of the liquid gases, chiefly organic compounds (alcohols, esters, benzene, and some others). For most of them the data for L and σ are known up to a few degrees below the critical point, but, because it is very difficult to obtain accurate values for σ close to the critical temperature, we find ourselves obliged to finish our calculations some tens of degrees below this point.

TABLE 2

Ethyl acetate

$$B = 34.14; C = 336.4; p = 0.3340; q = -0.8073$$

T	$T_k - T$	σ	L		Δ	L/σ		Δ
			Observed	Equation 3		Observed	Equation 4	
80	170.1	16.32	85.78	86.34	+0.56	5.257	5.320	+0.063
100	150.1	13.98	82.15	81.98	-0.17	5.875	5.887	+0.012
120	130.1	11.75	77.53	77.38	-0.15	6.598	6.621	+0.023
140	110.1	9.57	72.74	72.23	-0.51	7.600	7.567	-0.033
160	90.1	7.48	65.91	66.43	+0.52	8.812	8.890	+0.078
180	70.1	5.51	59.87	60.08	+0.21	10.86	10.95	+0.09
200	50.1	3.64	52.71	52.31	+0.40	14.48	14.25	-0.23
220	30.1	1.96	42.63	42.54	-0.09	21.75	21.52	-0.23

TABLE 3

Benzene

$$B = 37.43; C = 438.9; p = 0.3170; q = -0.8526$$

T	$T_k - T$	σ	L		Δ	L/σ		Δ
			Observed	Equation 3		Observed	Equation 4	
80	208.5	20.28	95.45	94.28	+1.17	4.706	4.627	-0.079
100	188.5	18.02	91.41	90.93	-0.48	5.071	5.039	-0.032
120	168.5	15.71	86.58	87.36	+0.78	5.511	5.538	+0.027
140	148.5	13.45	82.82	83.10	+0.28	6.158	6.170	+0.012
160	128.5	11.29	78.94	78.75	-0.19	6.993	6.987	-0.006
180	108.5	9.15	74.62	73.84	-0.78	8.155	8.060	-0.095
200	88.5	7.17	68.81	68.52	-0.29	9.598	9.601	+0.003
220	68.5	5.25	62.24	62.27	+0.03	11.85	11.95	+0.10
240	48.5	3.41	54.11	54.54	+0.43	15.87	16.04	+0.17
260	28.5	1.75	43.82	44.44	+0.62	25.04	25.0	+0.16

TABLE 4

SUBSTANCE	p	q
Ether.	0.31	-0.87
Carbon tetrachloride	0.30	-0.85
Methyl alcohol.	0.38	-0.63
Ethyl alcohol	0.39	-0.61
Methyl formate	0.33	-0.83
Ethyl acetate	0.33	-0.81
Acetic acid	0.20	-0.91
Benzene.	0.32	-0.85

For the heat of evaporation there are available the measurements of Sydney Young and coworkers as published by Mills (2), while for the surface tension the data are taken from the well-known investigations of Ramsay and Shields (3).

For testing the formulas we have calculated for several substances the constants B , C , p , and q and with these the values of L in equation 3 and of L/σ in equation 4, which have been compared with the observed values. It is obvious that the values of the constants are dependent on the nature of the substances in general and, so far as B and C are concerned, also on the units in which the heat of evaporation and the surface tension are expressed. In tables 1-3 L is given in calories per gram and σ in dynes per centimeter.

It appears from these tables that in all cases the agreement between the observed and calculated values for L and L/σ , respectively, is very satisfactory. Most of the differences (Δ) for both equations are not higher than 1 per cent, which is of about the same order as the accuracy of formulas 1 and 2. Owing to the fact that near the critical point it is difficult to obtain exact values of σ , the differences in this region are somewhat greater, more especially for equation 4. Besides the examples given above, about the same agreement for the formulas has been found for other substances, such as ether, carbon tetrachloride, methyl alcohol, acetic acid, and methyl formate.

As follows from the deductions of the two equations, the values for the exponents p and q are given by those of m and n . With the average value for $m = 0.4$ and $n = 1.25$, we have $p = m/n = 0.32$ and $q = m - n = -0.85$. As table 4 shows, this holds good for the normal substances, but not for those, such as the alcohols and acetic acid, which are complex in the liquid state, as is mostly found for empirical relations.

SUMMARY

Two empirical relations between the heat of evaporation and the surface tension of liquids are given.

REFERENCES

- (1) DE WIJS, J. C.: *Rec. trav. chim.* **62**, 459 (1943).
- (2) MILLS, J. E.: *J. Am. Chem. Soc.* **31**, 1099 (1909).
- (3) RAMSAY, W., AND SHIELDS, J.: *Z. physik. Chem.* **12**, 433 (1893).
- (4) VAN DER WALLS, J. D.: *Z. physik. Chem.* **13**, 716 (1894).

THE SUDDEN APPLICATION OF A CONSTANT SHEARING MOTION
TO ANOMALOUS FLUIDS¹EMMETT K. CARVER AND JOHN R. VAN WAZER²*Department of Manufacturing Experiments, Eastman Kodak Company, Rochester, New York**Received September 17, 1946*

INTRODUCTION

Solutions of high polymers are often found to exhibit a more firm or rigid structure when they are allowed to stand undisturbed for a time. This effect is evidenced experimentally by the phenomena of thixotropy, false body (6), and transient elasticity (4). Several years ago at the Eastman Kodak Company, during the investigation of the rheological properties of thickened petroleum fractions, an experimental study was made of the transition between this rested structure and the one found in flow. A continuous photographic record was made of the force set up by the sudden application of a constant shearing motion to a fluid contained in a concentric cylinder viscosimeter.

APPARATUS

The viscosimeter of the rotating-cup type was constructed on the bed of a jeweler's lathe that had been mounted with the bearing end down (see figure 1). A synchronous motor (A) originally designed for use with a Cine Kodak Special Camera was geared to the lathe shaft, on top of which a carefully machined steel cup (B) was centered. Within the cup (height, 5.30 cm.; diameter, 2.54 cm.) (see figure 2) was a hollow brass cylinder filled with chloroform³ and joined to a heavy torsion rod (C) which was clamped at the lathe tailpiece (D). Two inner cylinders (height, 2.35 cm.; diameters, 2.30 and 1.60 cm.) and several torsion rods were used in these experiments. A small plane mirror was affixed to the torsion rod so that a torque applied to the rod might be measured by the rotation of a beam of light. By using a stiff torsion rod and a mirror, the motion of the inner cylinder on the application of a torque could be made negligibly small. At the bottom of the inner cylinder a small rod protruded to fit into a short sleeve on the bottom of the cup. This lower bearing prevented the materials from dragging the inner cylinder from its central position. In order to keep the material from crawling up the central wire, a cover (E) was used on top of the outer cylinder or cup. This cover was pierced with a hole just large enough to allow the torsion wire freedom to twist without friction. The period of vibration of the inner cylinder and torsion rod used for most of the work reported here was 0.011 sec.

An apparent rate of shear at the wall of the inner cylinder of 24 sec.⁻¹ to 422 sec.⁻¹ was obtainable with the different gear combinations. The gears built

¹ Presented before the Division of Colloid Chemistry at the 110th Meeting of the American Chemical Society, which was held in Chicago, Illinois, September, 1946.

² Present address: Rumford Chemical Works, Rumford, Rhode Island.

³ This served merely to weight the cylinder without adding to the moment of inertia.

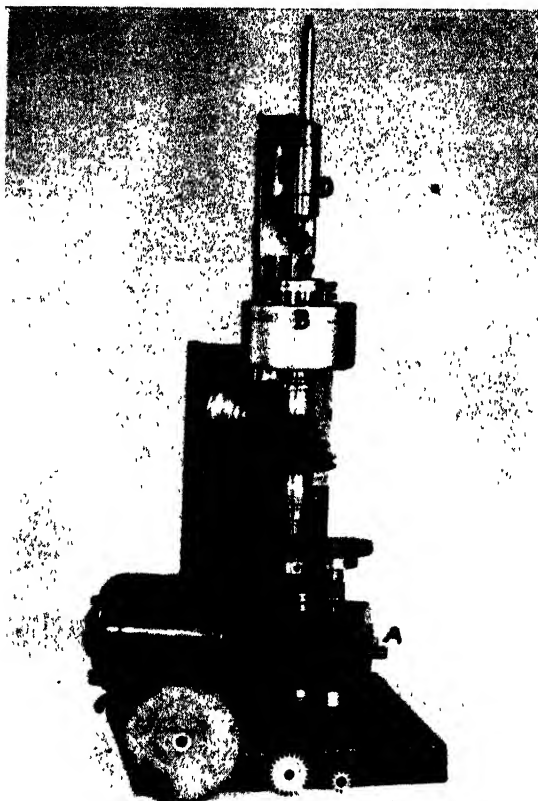


FIG. 1. Viscosimeter with extra gears

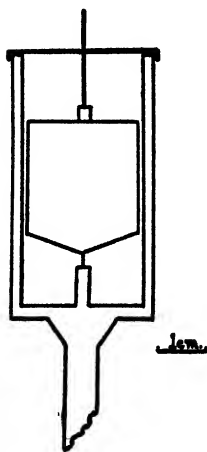


FIG. 2. Cross section of viscosimeter cup containing the larger inner cylinder drawn to scale.

in the synchronous motor were shifted by a lever, and as far as our measurements were concerned the cup could be instantaneously set to rotate at a con-

stant speed. By means of suitably applied lead weights the stray vibrations of the entire apparatus, exclusive of the torsion system, were eliminated.

An illuminated vertical slit and a collimating lens were used as a light source. For visual observations the light was focused on a galvanometer scale. Photographic tracings of the light beam were made in a special camera consisting of a horizontal slit behind which photographic film was passed over a roll at the rate of 18.5 cm. per second. The viscosimeter was calibrated by standard viscosity oils and from the modulus of rigidity of the torsion rod. The end effect was shown to be less than 5 per cent of the total deflection by rough calculation and by the fact that removing the cover so that it no longer touched the gel had no noticeable effect on the torque. A constant-temperature water bath was built around the viscosimeter cup to make measurements at temperatures other than that of the room.

An accessory to this apparatus was constructed to cause the outer cup to rotate through a given angle at a constant speed, reverse its direction, and then return to its original position at the same constant speed. This oscillation of the cup was effected by an arrangement of a heart-shaped cam bearing against a rack with a pinion gear to turn the viscosimeter. Using different combinations of gears, several speeds and amplitudes of oscillation could be obtained. By placing a mirror on the cup of the viscosimeter and taking photographic tracings it was shown that the cup moved at essentially a constant speed from the beginning to the end of each half-cycle.

EXPERIMENTAL RESULTS

The tracings obtained photographically are graphs of stress *vs.* time when a given constant rate of shear is suddenly applied to the material contained between the concentric cylinders. Since the deformation is proportional to time, these curves may be considered as force-deformation curves and are very similar to the stress-strain diagrams commonly used by engineers. In the traces (see figure 3) the horizontal axis represents time and is the same for all traces. The vertical axis is the force axis, and the angular deflection of the torsion wire is proportional to the height of the trace divided by the magnification, which equals the distance in meters from the torsion wire to the camera film. Such a curve for a Newtonian liquid (40 per cent butyl methacrylate in Varsol, a petroleum fraction) is shown at the top of figure 3. The liquid responds at once to the rotation of the outer cup, which started to rotate at point *O*. The line *OA* is due to the twisting of the torsion wire to the position at which the torque due to the wire is exactly balanced by the viscous torque of the liquid. If the torsion wire were turned at the same rate as the outer cylinder, a line like *OA* would result. This means that equilibrium conditions of flow are reached in a time immeasurably small, with respect to this apparatus. When the rotation is stopped, the torsion wire untwists to indicate zero torque. The angle at which this untwisting occurs is less steep than would be expected, as no special provision was made for quickly stopping the rotation of the cup.

A gelatinous, non-homogeneous mixture of soaps in a petroleum base solvent called Formula 241 gave a tracing similar at the origin to that of Newtonian

liquids. However, on rotation the viscous torque diminishes with time. According to the usual rheological concepts this substance is thixotropic and the ap-

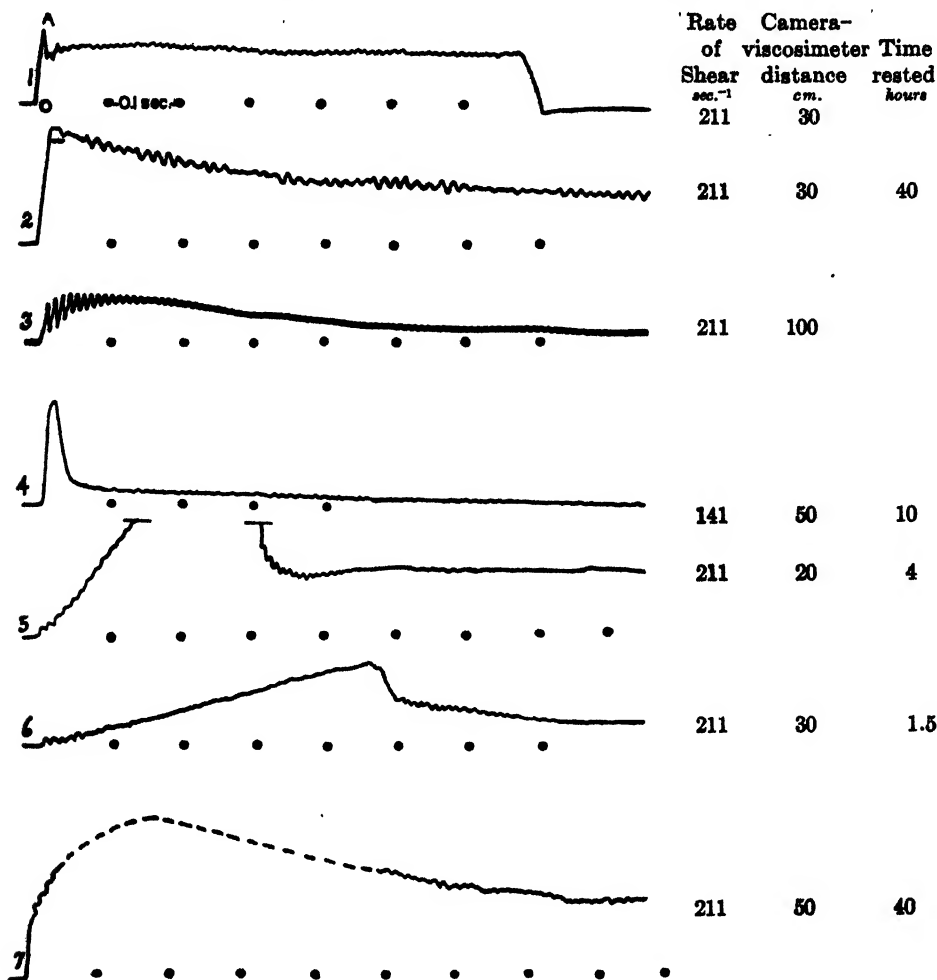


FIG. 3. Some photographic tracings for various fluids. The height of a given trace is proportional to the camera-viscosimeter distance; the greater the distance, the more the trace is magnified.

1. A Newtonian liquid (40 per cent butyl methacrylate monomer in Varsol)
2. A thixotropic pseudoplastic emulsion (Formula 241)
3. A dilute pseudoplastic gel (6 per cent X-104 in Varsol)
4. A dilute gel (4 per cent X-104) thickened with 10 per cent newspaper pulp
5. A gel (5 per cent isobutyl methacrylate acid interpolymers)
6. A gel (3 per cent isobutyl methacrylate acid interpolymers)
7. A gelatinous mixture of 2 per cent isobutyl methacrylate acid interpolymers, 4 per cent fatty acids, 2 per cent rosin, 4 per cent sodium hydroxide, and 0.5 per cent cellulose

* The apparent viscosity coefficient and apparent rate of shear are computed for a fluid by using the equations developed for the viscosimeter filled with a Newtonian liquid. The

parent viscosity coefficient⁴ reaches a constant minimum value after several minutes of shearing at a constant rate. This constant minimum value is plotted in figure 4 as a function of the apparent rate of shear to give a typical curve for a pseudoplastic fluid (8). It is seen that the apparent viscosity coefficient is a function of temperature as well as of shearing rate. If the temperature dependence is given by the equation

$$\eta_{\infty} = e^{-E_{vis}/RT}$$

where η_{∞} is the constant value of the viscosity, T is the absolute temperature, and E_{vis} is an energy term, then $E_{vis} = 7 \pm 3$ kg.-cal.

When the viscosimeter is stopped and then started again after a very short time, the viscous torque upon starting rises only to the value it had just before the rotation ceased. However, if the gel is allowed to rest undisturbed for several hours, the structure will heal and the viscous torque on starting is higher. It has been found that the gel takes about 8 hr. to heal from the state in which the apparent viscosity coefficient has reached the minimum value ($= \eta_{\infty}$) on shearing to that for which the viscosity at the application of shear is a maximum.

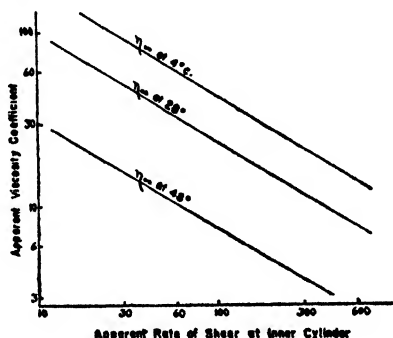


FIG. 4. Pseudoplastic curves for the thixotropic emulsion, Formula 241

Suspensions of bentonite clay in water exhibit the same kind of thixotropy as that found for Formula 241, except that it takes a longer time to reach η_{∞} . On the other hand, several materials have been studied in which the viscous torque gradually increased with time to a constant value at a given rate of shear. This work hardening was shown by several jellied gasoline mixtures. In both cases the initial part of the tracing is similar to that obtained with a Newtonian liquid.

There is another class of gelatinous fluids for which the viscous torque passes through a maximum near the beginning of the rotation (see traces No. 3, 4, and 5 in figure 3). One of these materials, an aluminum soap called X-104 which dissolves in gasoline to form a stringy, translucent, homogeneous gel, was extensively studied. It can be seen in figure 5 that the height of the maximum at a given rate of shear, temperature, and concentration depends on the time

assumption in the integrations used in obtaining these equations is that the viscosity is not a function of the rate of shear. Although the use of these "apparent" values is theoretically unsound, it has some practical value. The term "viscosity" will be used synonymously with "apparent viscosity coefficient" hereafter in this paper.

that the gel is allowed to rest undisturbed or heal before the trace is made. As the rest time, t , increases, the height of the maximum, D_{\max} , asymptotically tends to a constant value, D_{\max}^{∞} , according to the equation:

$$\frac{dD_{\max}}{dt} = -k(D_{\max}^{\infty} - D_{\max})$$

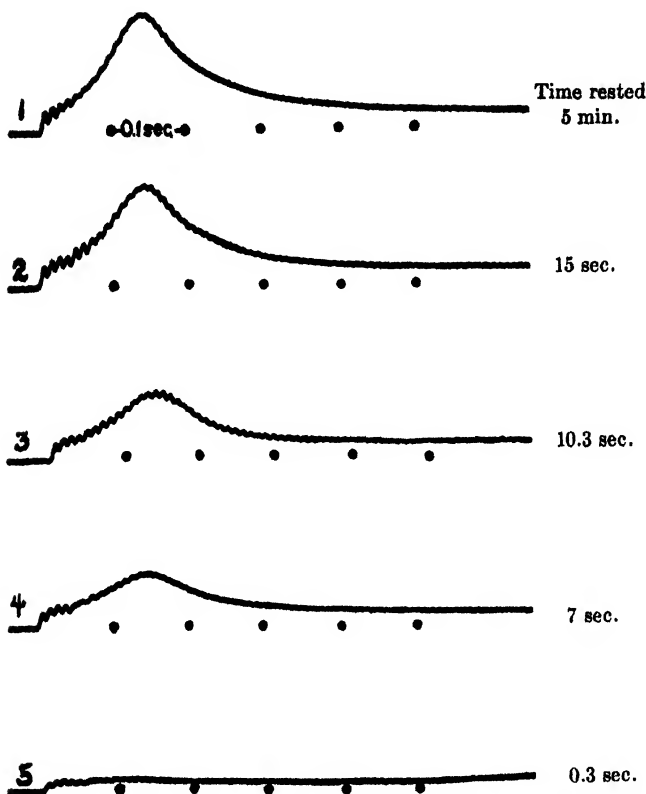


FIG. 5. Photographic tracings for 9 per cent X-104. Variation with rest time. All measurements were taken at a rate of shear of 211 sec^{-1} and at the same camera-to-viscosimeter distance.

As can be seen from figure 6 the healing rate constant does not depend on the rate at which the material has been sheared. The rate constant seems to change with concentration (see inset in figure 6), but this effect may be partially due to the variations from sample to sample. The rate of healing is greatly influenced by temperature; as the temperature increases so does the rate. Thus, from the temperature dependence of the healing rate constant of samples of 9 and 12 per cent X-104 in Varsol, the activation energy associated with this healing process was found to be $9 \pm 1 \text{ kg.-cal.}$

It is apparent in figure 7 that the height of the maximum in the trace and the

time at which the maximum occurs, t_{max} , are functions of the rate of shear. When t_{max} is multiplied by the rate of revolution of the viscosimeter cup, the product is a constant within experimental error at all rates of shear. This means that the maximum always occurs at a given extension (or angle of revolution to be more exact). This idea was tested by means of an arrangement of a cam with rack and pinion so designed that the cup of the jeweler's lathe could be oscillated with a constant speed in both the back and forth motions. The traces obtained with this arrangement are shown in figure 8. As can be seen in table 1, there was no maximum if the angle of the oscillation was less than the

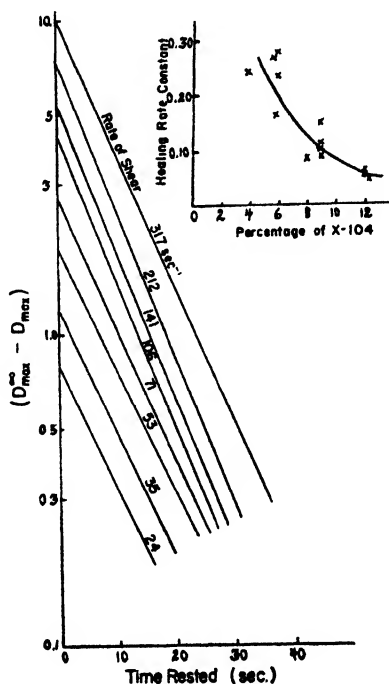


FIG. 6. Healing curves at various rates of shear for 9 per cent X-104. Inset: effect of concentration on healing rate constant.

angle of rotation, θ_{max} , at which the maximum occurred in straight rotation, and θ_{max} is constant for all amplitudes and rates of oscillation. Thus it seems that X-104 gels have a "yield value" for extension, although there is no Bingham yield value.

At low rates of shear the approach to the maximum in the traces (see figure 7) is convex to the force axis, as might be expected from a simple mechanical model (see figure 9). However, at the higher rates of shear the approach to the maximum is concave. The greater the concentration of the X-104, the lower the rate of shear at which the concavity appears (see figure 10).

In the mechanical model of springs and dashpots (figure 9) a concave rise can

only be explained by an increase in the strength of the spring or resistance of the parallel dashpot with time during the first part of the shear at constant rate, or a combination of these two processes. Under certain conditions an increase in the resistance of the series dashpot could also cause this effect. It seems

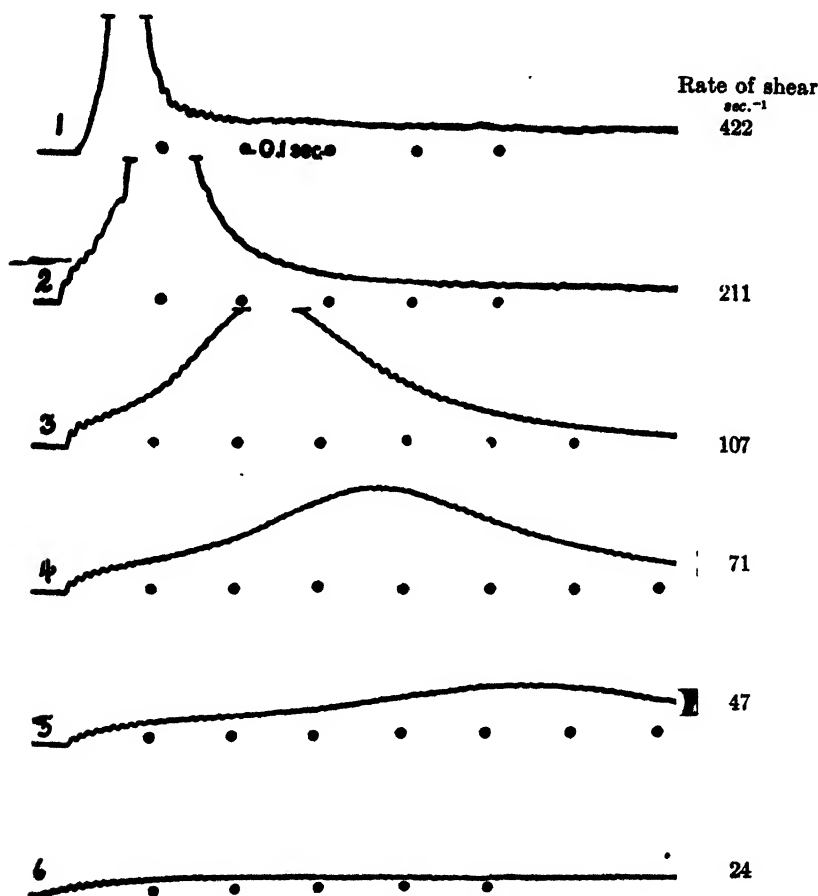


Fig. 7. Photographic tracings for 12 per cent X-104. Variation with rate of shear. All measurements were taken on the completely rested gel and at the same camera-to-viscosimeter distance.

likely to us that increase in rigidity occurs⁵ because of orientation of the elastic elements, probably in the same way that it occurs in rubber (2).

⁵ With the resonance elastometer developed by Goldberg and Sandvik (7) it was found that the shear modulus of 9 and 12 per cent X-104 solutions went through a minimum and then increased with increasing rate of shear, the shear modulus of the 12 per cent solution increasing more quickly than that of the 9 per cent. Although the measurements could not be extended to the higher shearing rates at which the concave approach is found, extrapolation indicates that at these rates the rigidity is greater than that corresponding to zero rate of shear.

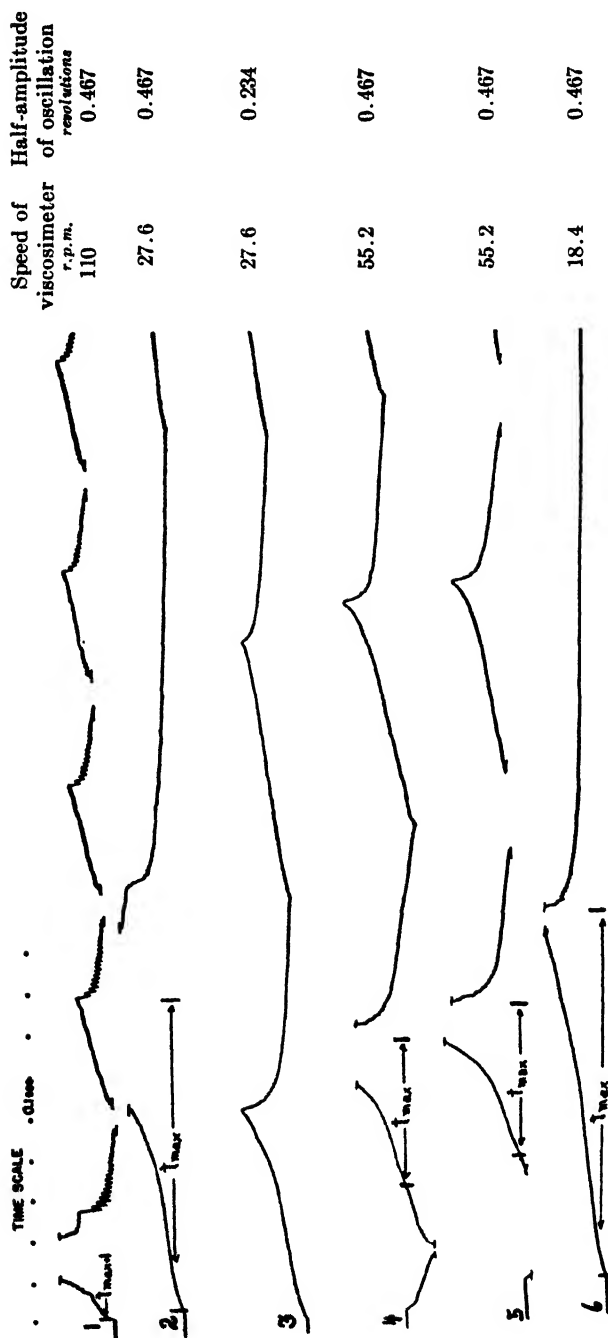


Fig. 8. Oscillational traces for 9 per cent X-104. Traces 4, 5, and 6 were started with the cam off center, so that a fraction of an oscillation of smaller amplitude preceded the regular oscillations.

An interesting qualitative experiment was performed to demonstrate that the approach to the maximum on a tracing could be described in terms of transient

TABLE 1
Position of maximum in traces

TRACE IN FIGURE 8	RATE OF SHEAR	RATE OF REVOLUTION	TIME OF MAXIMUM	ANGLE OF ROTATION AT WHICH MAXIMUM APPEARS
<i>No.</i> (From the regular rotation data)	<i>sec.⁻¹</i> All	<i>r.p.m.</i> All	<i>sec.</i>	<i>revolutions</i> <i>ca. 0.30</i>
1	130	110	0.18	0.33
2	32	27.6	0.73	0.34
3	32	27.6	(No maximum)	(>0.23)
4	65	55.2	0.35	0.32
5	65	55.2	0.35	0.32
6	22	18.4	0.90	0.28

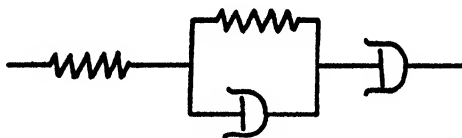


FIG. 9. Mechanical model of a viscous fluid

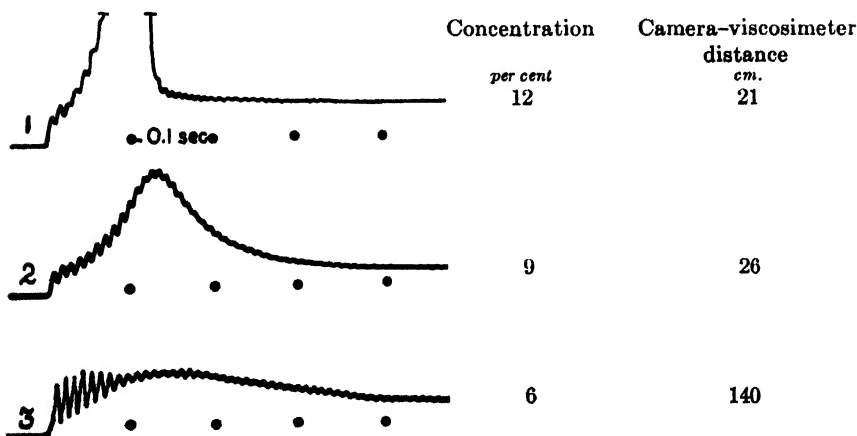


FIG. 10. Photographic tracings for X-104. Effect of concentration on completely rested samples. All measurements were made at a rate of shear of 211 sec^{-1}

elasticity. The top of the torsion rod was suspended from a tiny ball bearing. While the outer cup was turned, the top of the torsion rod was held fixed. When the cup had turned through a given distance, it was stopped and the top of the torsion rod was released, thus allowing the inner cylinder to spring around and

release the elastic tension in the gel. It was found that the inner cylinder traveled nearly as far as the outer cylinder if the outer cylinder had not been turned more than 0.3 revolution (see table 1). By using the formula (5) for elastic shear between two concentric cylinders, a shear modulus can be computed from the angle at which the torque increases to its maximum value for a completely rested gel. These values are compared with the values of the shear modulus determined on the resonance elastometer (7) and the Clark-Hodsmen (1) instrument (see table 2). Since vibration waves are superimposed on the first part of the trace, it is difficult to measure the angle and hence the shear modulus can only be roughly obtained.

All gels that exhibit elastic behavior in the resonance elastometer in shear do not show a maximum in tracings obtained with this apparatus. In fact, we have found several pseudoplastic materials (e.g., Formula 241) that definitely show elasticity but do not give a maximum.

TABLE 2
Elastic data

MATERIAL	SHEAR MODULUS (IN DYNES PER CM. ²)		
	This instrument	Resonance elastometer	Clark-Hodsmen viscosimeter
6% X-104 in Varsol	60	300	550
9% X-104 in Varsol	1200	1400	2200
12% X-104 in Varsol	1300	3400	4300
3% isobutyl methacrylate polymer in gasoline	200	50	
5% isobutyl methacrylate polymer	1000	500	

The apparent viscosity coefficient, η_{∞} , determined for X-104 from the deflection after the maximum, checks with that determined at the same rates of shear on other viscosimeters. Since the viscous resistance is not affected by varying the temperature, $E_{vis} = 0$. It was also noted that the slope of the log viscosity-log shearing rate curve is independent of concentration in the range of 4 to 15 per cent.

DISCUSSION⁶

All the data on X-104 lead to the conclusion that the following molecular model approximates reality. When the gel is resting, a solid-like, three-dimensionally bonded structure is formed. The activation energy for the process by which this structure results is 9 kg.-cal. This process follows a first-order differential equation, as might be expected for a rate-determining step involving events of independent probability. The structure is destroyed on shearing; but,

⁶ It should be noted that the concepts of molecular structure presented in this section have been previously used by many other authors, often with very meager experimental justification.

as the rate of formation of the structure is quite fast, any theoretical flow equation (3) must consider an equilibrium between forming and breaking bonds for every rate of shear. Since the rate of bonding decreases and the internal friction or normal type of viscosity would increase with lowered temperature, the temperature dependence of these components of over-all viscosity will tend to cancel each other. It is likely that this is the reason why E_{vis} is nearly zero. Probably at the higher rates of shear, there is orientation due to flow which causes the shear modulus to increase. When the structure corresponding to the rested X-104 is distorted, the bonds first stretch and then break. If the distortion is less than that needed to break the bonds, the solid-like structure remains whole. At a constant rate of flow the units of flow do not change size, as neither work hardening nor thixotropy is observed.

In comparison with X-104, Formula 241 is non-homogeneous when observed microscopically. Thus it does not have a continuous close-knit structure and would not be expected to exhibit maxima in traces made with our apparatus. The thixotropic behavior and long healing time are due to break-up of the emulsion globules, which are also the flow units. Elasticity can be accounted for by the reversible distortion of the globules held together by the same frictional forces that produce a Bingham yield value in the material.

The information presented in this paper may be useful to those who would classify materials on the basis of their most obvious rheological properties and then draw extended theoretical conclusions from such classified data. A preferred method of approach is to measure the flow resistance and elastic properties as a function of time under as many conditions as possible. The use of our instrument as described here is an attempt in that direction.

SUMMARY

A concentric cylinder viscosimeter which could suddenly be made to rotate at a constant speed is described. Photographic recordings of the variation of shearing force with time were used to differentiate between materials having different rheological structures. An extended study was made of an aluminum soap dissolved in gasoline. The photographic traces of force *vs.* time for this substance exhibit a pronounced maximum near the time rotation was started. From these traces it can be shown that there is a cross-bonded structure which is partially destroyed under shear. An activation energy of 9 kg.-cal. was found for the process by which the structure is re-formed upon standing. The activation energy for flow is zero, but this is explained by assuming that the mechanism of flow is a combination of breaking bonds and the normal type of internal friction.

REFERENCES

- (1) CLARK, A. A., AND HODSMAN, H. J.: *J. Soc. Chem. Ind.* **56**, 67 (1937).
- (2) GUTH, E.: In *Alexander's Colloid Chemistry, Theoretical and Applied*, Vol. 5, p. 286. Reinhold Publishing Corporation, New York (1944).
- (3) KAUFMAN, W., AND EYRING, H.: *J. Am. Chem. Soc.* **62**, 3119 (1940).
- (4) KENDALL, J. M.: *Rheol. Bull.* **12**, 26 (1941).

- (5) POOLE, H. J.: *Trans. Faraday Soc.* **22**, 82 (1926).
- (6) PRYCE-JONES, J.: *J. Oil and Col. Chem. Ass.* **19**, 295 (1936).
- (7) SANDVIK, O., AND GOLDBERG, H.: *Anal. Chem.* **19**, 123 (1947).
- (8) WILLIAMSON, R. V.: *Ind. Eng. Chem.* **21**, 1108 (1929).

ACTIVE MAGNESIA. III

X-RAY *versus* NITROGEN ADSORPTION SURFACE AREAS

A. C. ZETTLEMOYER AND W. C. WALKER

Wm. H. Chandler Chemistry Laboratory, Lehigh University, Bethlehem, Pennsylvania

Received December 10, 1946

The method of Emmett and Brunauer (2) for determining surface areas by nitrogen adsorption at the temperature of liquid nitrogen is well established. The method of determining particle sizes, and consequently surface areas, by the x-ray method has also received extensive development (4) since it was originated by Scherrer (6). There has been, however, no direct comparison between the two methods.

The most extensive application of the x-ray method to the determination of surface areas has been carried out by Hofmann and Wilm (3) on various activated carbons. No gas-adsorption values were obtained on these samples, but for similar materials other investigators have reported areas of the same order of magnitude as was obtained by the x-ray method. In most cases, however, it seems likely that the latter method would indicate higher areas than the former, because aggregates formed by the particles and too small pores would prevent the nitrogen molecules from reaching all crystal faces.

In the course of a series of studies on the nature of active magnesia, x-ray diffraction patterns were obtained on a series of samples which had been carefully examined previously by the nitrogen-adsorption technique (9) and for fluoride adsorption (10). From the broad diffraction bands in the powder diagrams, the half-intensity breadths were estimated, and from these the particle sizes were calculated according to the theoretical equation of Sherrer (6) for cubic crystals. A direct comparison between surface areas as determined by x-ray and by nitrogen adsorption thus became available.

Warren (8) and Birks and Friedman (1) showed that x-ray line broadening could be used in determining the size of magnesium oxide particles. Birks and Friedman concluded that particle sizes above 100 Å. agreed to ± 10 per cent with those estimated from electron micrographs; below 100 Å. these investigators report an accuracy of the measurements on the electron micrographs of the order of ± 25 per cent, so that a comparison with the particle sizes as determined by x-ray measurements was difficult to make in this range. The particle sizes of the samples examined here are mostly below 100 Å., and in

no case was it possible to determine ultimate particle size or shape from electron micrographs.

MATERIALS

The active magnesias were prepared from the hydroxide obtained from sea water (7). Magnesia 2661, although not an active grade, was again included here for comparison. The production conditions and chemical analyses have been summarized elsewhere (9). In table 1 the iodine adsorption numbers, which provide the usual commercial activity test, are presented in the second column. A new sample, Magnesia AS, was added to the series. A preparation of this sample is to be described as part of another study to be reported elsewhere. With this additional sample, as indicated in the third column, the areas as determined by nitrogen adsorption extend from 0.8 to 296 square meters per gram.

TABLE 1
Characteristics of magnesias

GRADE	IODINE NUMBER	AREA		CELL CONSTANT
		Nitrogen	X-ray	
		<i>square meters per gram</i>		<i>A.</i>
AS	202	296	304	4.211
XP	210	230	270	
2642.	150	154	234	4.213
2652-S.	146	146	205	4.206
2652	130	125	189	
2641	76	71	135	4.204
2661	4	0.8	43	4.201

METHODS

Back-reflection x-ray patterns of the various magnesia samples were taken using a General Electric XRD unit, Type 1. Each sample was sifted onto a greased piece of cardboard in such a manner that a fine layer of the powdered sample adhered to the cardboard without falling off when placed in a vertical position. This sample was mounted in a General Electric rotating specimen holder and was placed at a distance of 60.52 mm. from the film, using a calibrated pointer. The specimen and film were rotated in order to give smooth diffraction bands for the larger grained samples and to obtain a more representative diffraction band.

Eastman duplitized non-screen x-ray film was used for registering the diffraction bands. Each pattern was developed for 5 min. in Eastman x-ray developer and fixed for 10 min. in Eastman x-ray fixer. After washing for 30 min., the films were sponged off and dried for 8 hr. before microphotometer measurements were made. This latter precaution was taken to minimize errors due to film shrinkage.

To measure intensities across the diffraction bands a Société Genevoise

microphotometer having a suitably controlled light source and photocell was used.

The equation for the particle size D in terms of the width B at half-maximum of the intensity curve is:

$$D = 0.94 \frac{\lambda}{B \cos \theta} \quad (1)$$

where λ is the wave length of the x-radiation and θ is the Bragg angle. B must be corrected for the instrument width, that is, the width of the half-maximum of the intensity curve for very large particles. For this purpose the intensity curve of a sample of Magnesia 2661 heated for 48 hr. at 1000°C. was measured. This curve showed the two peaks of the Ni $K\alpha_1$ and the Ni $K\alpha_2$ radiation. The average of the widths at the two half-maxima was 0.035525 and this was applied as a correction, b' , in the usual form:

$$B^2 = B'^2 - b'^2 \quad (2)$$

From the value of D , the x-ray surface area can be calculated. This theoretical surface area takes into account each face of each cubic crystallite. If the particle size D is divided by the cell constant for magnesium oxide, 4.20, the length l in terms of unit cells is obtained. The x-ray area, it may be shown, can be calculated from the equation:

$$\text{X-ray area} = 3860/l \quad (3)$$

The apparatus and procedure for determining the areas by nitrogen adsorption have been described previously (9). Nitrogen was adsorbed at liquid-nitrogen temperatures on the evacuated samples. Some minor difficulty was encountered in calculating the areas from the adsorption data. The areas tabulated in the third column of table 1 are the so-called *BET* areas obtained from the *BET* plots. The *BET* plots, however, were not linear, as is usually found, but possessed a slight curvature concave to the pressure axis. Except for Magnesia AS, the nitrogen areas fall in the same order as the iodine numbers. Some of the pores available to nitrogen molecules in the AS sample were apparently too small to accommodate the larger iodine molecules.

The shapes of the nitrogen-adsorption isotherms were explained by hypothesizing a structure consisting of plates of checkerwork of cubic holes and crystallites. The perforated plates were later found on electron micrographs.

RESULTS AND DISCUSSION

The particle sizes of the active grades as determined from the x-ray line broadenings varied from 120 Å. for Magnesia 2641 to 53.4 Å. for Magnesia AS. Magnesia 2661, an inactive grade, had a particle size of 374 Å.

The x-ray areas as calculated from equation 3 are tabulated in the fourth column of table 1. These theoretical areas, representing the surfaces available if none of the particles were touching each other, are all larger than the nitrogen areas. In figure 1 the nitrogen areas are plotted against the x-ray areas. The

dotted line represents the situation that would exist if both methods were to yield equal surface areas. A smooth curve fits the data surprisingly well. As the theoretical surface area increases, the fraction available to the nitrogen

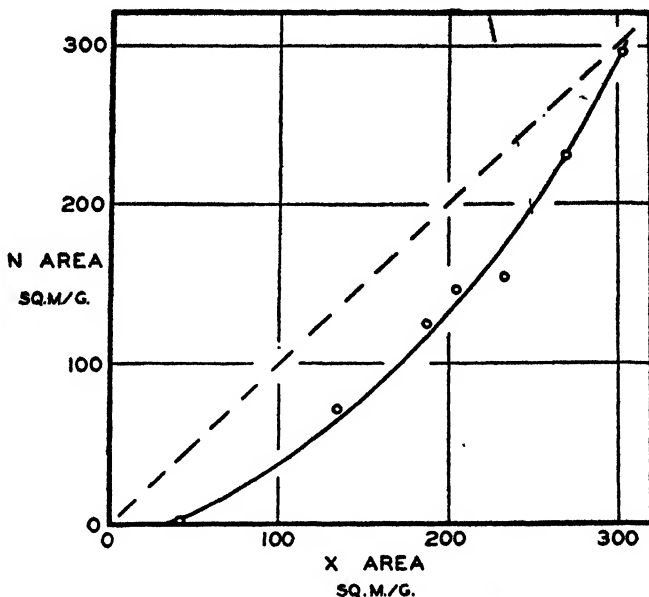


FIG. 1. Nitrogen *versus* x-ray areas

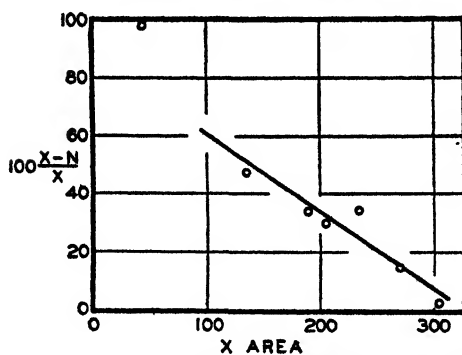


FIG. 2. Per cent deviation *versus* x-ray areas

molecules increases, until for Magnesia AS the nitrogen area very nearly coincides with the x-ray area.

The per cent deviations of the nitrogen area N from the x-ray area X , $\frac{X - N}{X} 100$, were calculated from the smooth curve in figure 1. For x-ray areas above 100 sq.m. per gram, these values, when plotted *versus* the x-ray areas, produce the straight line in figure 2. The equation of this line is:

$$\frac{X - N}{X} 100 = -0.267X + 87.3 \quad (4)$$

Small deviations from the smooth curve of figure 1 yield large deviations from the linear plot in figure 2.

From these results, then, it may be concluded that for active magnesia the x-ray areas and the nitrogen areas agree closely only at the highest areas yet attained. Except for the inactive grade, the x-ray area never exceeds the nitrogen area at any level by more than a factor of two.

The cell constants for the various grades as calculated from the distances between the maxima in the intensity curves are presented in the fifth column of table 1. While these results are not completely consistent, owing to difficulties in estimating the precise positions of the maxima in the smaller-grained samples, the cell constants are generally larger for the samples with the larger areas. In the catalytic decomposition of ethyl alcohol over magnesium oxide, Rubinshtein showed that the cell constant was a critical factor (5).

SUMMARY

X-ray diffraction patterns were obtained on a series of active magnesias prepared from the hydroxide. The particle sizes, and from these the surface areas, were estimated from the broad diffraction bands. The surface areas as determined by x-ray measurements were compared with the surface areas which had been determined previously by nitrogen adsorption. The x-ray areas and the nitrogen areas were found to agree closely at the highest level of 300 sq.m. per gram and to deviate in a regular manner as the particle size decreased.

The cell constants were found to be generally larger for the samples with the larger areas.

REFERENCES

- (1) BIRKS, L. S., AND FRIEDMAN, H.: *J. Applied Phys.* **17**, 687 (1946).
- (2) EMMETT, P. H., AND BRUNAUER, S.: *J. Am. Chem. Soc.* **56**, 35 (1934); **59**, 310 (1937).
- (3) HOFMANN, U. AND WILM, D.: *Z. physik. Chem.* **B18**, 401 (1932); *Z. Elektrochem.* **42**, 504 (1936).
- (4) LAUE, M. VON: *Z. Krist.* **64**, 115 (1926).
BRILL, R.: *Z. Krist.* **68**, 387 (1928).
BRILL, R., AND PELZER, H.: *Z. Krist.* **72**, 398 (1929); **74**, 147 (1930).
JONES, F. W.: *Proc. Roy. Soc. (London)* **A166**, 16 (1938).
- (5) RUBINShteIN, A. M.: *Bull. acad. sci. U.R.S.S.* **1943**, 427-34.
- (6) SCHERRER, P.: *Nachr. Ges. Wiss. Göttingen* **1918**, 98.
- (7) SEATON, M. Y.: *Am. Inst. Mining Met. Engrs.* **148**, 22 (1942); U.S. patents 2,219,725 and 2,219,726.
- (8) WARREN, B. E.: *J. Applied Phys.* **12**, 375 (1941).
- (9) ZETTMLOYER, A. C., AND WALKER, W. C.: *Ind. Eng. Chem.* **39**, 69-74 (1947).
- (10) ZETTMLOYER, A. C., ZETTMLOYER, E. A., AND WALKER, W. C.: To be published.

COLLOIDAL ALUMINUM OXIDE

ARTHUR A. VERNON

*Department of Chemistry, Northeastern University, Boston, Massachusetts**Received July 15, 1946*

A considerable body of literature exists describing methods of preparation of colloidal aluminum oxide hydrates; the available information has been well summarized by Weiser (3) and Weiser and Milligan (4, 5). Bohm and Nielsen (1) reported that evaporation of a dialyzed colloidal aluminum oxide sol to remove the dispersion medium gave a glass-like solid which was redispersible in water. A patent (2) on the formation of such material was obtained in 1937. Neither of the articles gives details of the properties and formation of the reversible solid; as part of a larger program it was necessary to investigate this reversible hydrate or "soluble alumina."

EXPERIMENTAL

Materials: In all the experiments aluminum chloride, ammonium hydroxide, and hydrochloric acid of C.P. grade were used.

Procedure: A slurry was first made by adding 5 *N* ammonium hydroxide to 5 *N* aluminum chloride at 25°C.; it was then centrifuged with successive addition of distilled water until the mother liquor gave only a faint test for chloride ion with silver nitrate. The centrifuged solid was then transferred to a beaker, the peptizing agent was added, and the suspension was evaporated to dryness on a steam bath. Since the prepared hydrates were dispersible up to gel formation, an arbitrary comparison method was used to determine the concentration at the gel point. The hydrate was added to water in a test tube having an inside diameter of $\frac{3}{8}$ in. until a gel was formed which would not flow when the tube was put in a horizontal position. The gel was then removed, weighed, dried, and re-weighed.

RESULTS

Preliminary work: Table 1 gives the method of preparation of some typical sols which were selected from a large number of experiments.

Since the preliminary experiments indicated that a small amount of hydrochloric acid was necessary for reversible sol formation, further work was done to determine the minimum amount necessary. The results are summarized in table 2.

DISCUSSION

Particle size seems to determine to some extent whether a gel is clear or opaque; for example, in table 1 the only difference between samples 202 and 203 is that the latter was dried before the peptizing agent was added. The added heating operation apparently caused agglomeration to larger particles to produce a cloudy gel. Experimental proof of the composition of the product is not available, but the literature would indicate that the hydrate is $\gamma\text{-Al}_2\text{O}_3 \cdot \text{H}_2\text{O}$.

TABLE 1
Preparation and properties of redispersible sols

EXPT. NO.	PREPARATION	NUMBER OF WASHINGS	PEPTIZING AGENT ADDED	REMARKS	SOLID IN GEL <i>per cent</i>	APPEARANCE	
						Of gel	Of dried film
200.	100 cc. $\text{AlCl}_3 \cdot 6\text{H}_2\text{O}$ precipitated with excess NH_4OH	12	None		No gel formed		
201.	Same as 200	12	56 cc. 1 <i>N</i> $\text{AlCl}_3 \cdot 6\text{H}_2\text{O}$ solution		19	Opaque	Continuous
202.	Same as 200	15	56 cc. 1 <i>N</i> $\text{AlCl}_3 \cdot 6\text{H}_2\text{O}$ solution		20	Clear	Continuous
203.	Same as 200	15	56 cc. 1 <i>N</i> $\text{AlCl}_3 \cdot 6\text{H}_2\text{O}$ solution	Dried on steam bath before peptizing agent was added	27	Opaque	Breaks in pieces
204.	50 cc. 5 <i>N</i> $\text{AlCl}_3 \cdot 6\text{H}_2\text{O}$ boiled and excess NH_4OH added	14	28 cc. 1 <i>N</i> $\text{AlCl}_3 \cdot 6\text{H}_2\text{O}$ solution		29	Clear	Breaks in pieces
205.	50 cc. 5 <i>N</i> $\text{AlCl}_3 \cdot 6\text{H}_2\text{O}$ boiled and excess NH_4OH added	14	15 cc. 5 <i>N</i> HCl		23	Clear	Continuous
206.	50 cc. 5 <i>N</i> $\text{AlCl}_3 \cdot 6\text{H}_2\text{O}$ precipitated with excess NH_4OH	12	10 cc. 0.5 <i>N</i> HCl		23	Clear	Breaks in pieces
207.	Same as 206	12	10 cc. 0.5 <i>N</i> HCl		28	Clear	Breaks in pieces
208.	Sample 203 dispersed in water and dried on steam bath	None	None		19	Opaque	Continuous

The minimum amount of hydrochloric acid necessary for redispersion was 0.11 g. per 6.52 g. of $\text{Al}_2\text{O}_3 \cdot \text{H}_2\text{O}$. This corresponds to 0.060 mole of chloride per mole of aluminum oxide.

TABLE 2

Determination of minimum quantity of hydrochloric acid required for reversible sol formation

0.5 N HCl ADDED TO WET SLURRY	SOLID IN GEL	REMARKS
cc.	per cent	
5	No gel	Suspension with about 4 per cent solid
6	27	
8	27	
10	25	
15	23	
20	22	

SUMMARY

1. A peptized hydrated alumina has been prepared which can be dried and redispersed in water.
2. The material forms a gel in water when the solid content is between 20 and 25 per cent.
3. The composition of the sol was 0.06 mole of chloride per mole of aluminum oxide.

REFERENCES

- (1) BOHM AND NICLASSEN: Z. anorg. Chem. **132**, 1 (1924).
- (2) U. S. patent 2,085,129 (June 29, 1927).
- (3) WEISER: J. Phys. Chem. **24**, 521 (1920).
- (4) WEISER AND MILLIGAN: Chem. Rev. **25**, 1-30 (1939).
- (5) WEISER AND MILLIGAN: Advances in Colloid Sci. **1**, 227-46 (1942).

CONTRIBUTIONS TO THE CHEMISTRY OF INDIUM. VIII¹

OBSERVATIONS ON THE FORMATION OF MAGNESIUM INDATE

THERALD MOELLER AND J. GLENN SCHNIZLEIN, JR.²*Noyes Chemical Laboratory, University of Illinois, Urbana, Illinois**Received October 3, 1948*

INTRODUCTION

The comparatively small size and high positive charge of trivalent indium suggest that its oxide and hydroxide might exhibit acidic properties toward sufficiently strong bases. The apparent insolubility of hydrous indium hydroxide in aqueous solutions of sodium and potassium hydroxides (5) may be cited as evidence against such an expectation. On the other hand, early papers by Renz (7, 8) reported the precipitation of magnesium indate, $\text{Mg}(\text{InO}_2) \cdot 3\text{H}_2\text{O}$, when an aqueous solution of indium(III) chloride was treated with magnesium oxide. Frequent summary statements on the amphotericism of indium hydroxide (e.g., 2) are apparently based upon these reports.

The formation of spinel-like indates, $\text{M}(\text{InO}_2)_2$, as a result of sintering magnesium and indium(III) oxides at 1300°C . (1) and as a result of fusing calcium or cadmium nitrate with indium(III) nitrate at 900°C . (6), has been definitely confirmed by x-ray diffraction studies (1, 6). However, direct precipitation of the magnesium compound by the moderately basic magnesium oxide seems open to question. Discounting for the moment the basicity of magnesium oxide, one might expect such an indate to precipitate from alkaline solution only if it were markedly less soluble than hydrous indium hydroxide. The small solubility of the latter (5) suggests the formation of magnesium indate under such conditions to be unlikely.

The report of Renz was based upon excellent agreement between the experimentally determined indium content of his product and that calculated for magnesium indate trihydrate. Although the analytical procedure used by Renz insured a complete separation of indium from magnesium through precipitation of the former in the presence of excess ammonium salts, the conditions under which the original product was dried prior to analysis were not defined. Since the precipitate was undoubtedly hydrous in character and since the possibility of the precipitation of hydrous indium hydroxide, a material which loses its hydrous water only on prolonged heating (4), cannot be overlooked, this may have influenced Renz's results. Furthermore, since his papers cite no analytical evidence for the presence of magnesium in his product, the limited data given cannot be accepted as conclusive evidence for his proposed formulation.

Because of this uncertainty and of its bearing upon the possible amphoteric

¹For the preceding communication in this series, see Moeller: *Ind. Eng. Chem., Anal. Ed.* **15**, 270 (1943).

²Present address: School of Chemistry, University of Minnesota, Minneapolis, Minnesota.

characteristics of indium compounds, a reinvestigation of the formation of magnesium indate seemed justifiable. To this end, the procedure of Renz was repeated and the product studied both analytically and by x-ray diffraction. Comparative diffraction studies were also made upon indium oxide and hydroxide and upon products obtained by high-temperature sintering of magnesium and indium oxides and fusion of magnesium nitrate and indium oxide.

EXPERIMENTAL

A. Materials and apparatus

All indium compounds were prepared from a stock indium(III) chloride solution supplied by the American Smelting and Refining Company. The indium content of this solution was determined to be 1.98 g. mole per liter. All other chemicals used were of analytical reagent quality.

X-ray diffraction patterns were taken in a powder camera of 7 cm. radius, designed in the University of Illinois laboratory and constructed by J. B. Hayes. A Picker x-ray diffraction unit employing a copper tube at 60 k.v.p. and 15 ma. was used. All diffraction pictures were taken with CuK_α radiation and a nickel filter.

B. Procedure

The procedure followed involved preparation of materials by precipitation or by high-temperature reactions, followed by determination of x-ray powder patterns and their evaluation. Specific details pertinent to individual procedures are indicated in the following section.

RESULTS AND DISCUSSION

Included in figure 1 are x-ray diffraction patterns for indium(III) oxide trihydrate, or indium hydroxide (plate I), prepared by precipitating indium(III) chloride solution with aqueous ammonia and drying the well-washed precipitate at 110°C., and anhydrous indium(III) oxide (plate III), prepared by drying the trihydrate at 250°C. These patterns are in essential agreement with those previously reported (3, 4). Both structures are cubic, the unit cell length (a_0) being 5.40 ± 0.07 Å. for the hydrated oxide and 10.12 Å. for the anhydrous.

Repetition of the procedure of Renz by treatment of indium(III) chloride solutions of varying concentrations (0.05, 0.1, 0.5, and 1.0 *M*) with excess magnesium oxide, both at room temperature and at the boiling point, yielded white products (hereafter termed Renz's products), which were washed with ammonium chloride solution and water, dried, and studied by x-ray diffraction. Typical patterns for samples dried at 110°C. (plate II) and at 250°C. (plate IV) are included in figure 1.

The identities in patterns between indium(III) oxide trihydrate and Renz's product dried at 110°C. and between anhydrous indium(III) oxide and Renz's product dried at 250°C. indicate that the procedure of Renz yields hydrous indium hydroxide and not hydrated magnesium indate as precipitate.

This conclusion is substantiated by the results of analyses of products obtained by the Renz procedure. Weighed quantities of these products, which had been dried at 250°C., were dissolved in dilute hydrochloric acid and analyzed for indium by precipitating with aqueous ammonia in the presence of excess ammo-

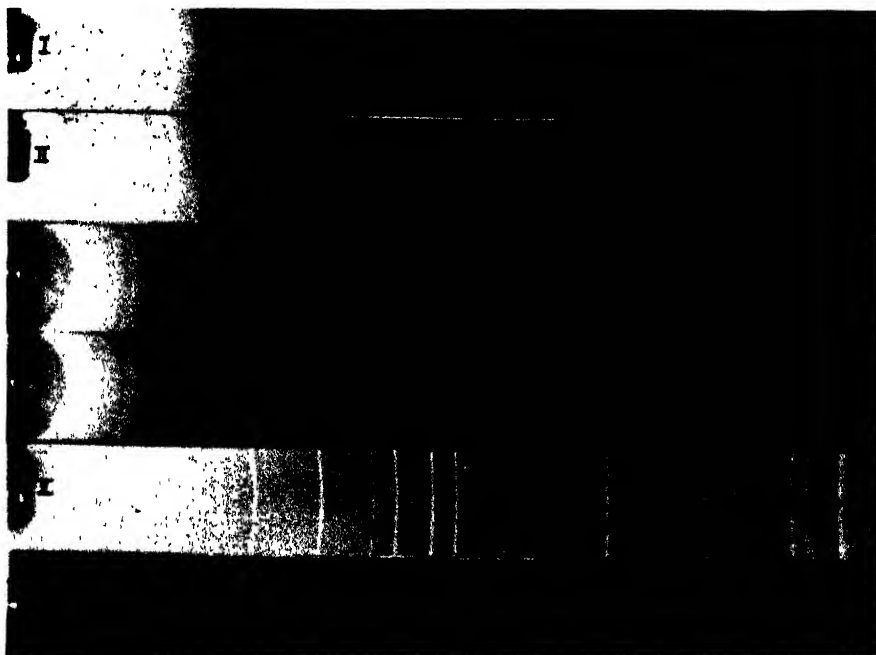


FIG. 1 X-ray diffraction patterns. Plate I, $\text{In}_2\text{O}_3 \cdot 3\text{H}_2\text{O}$ dried at 110°C.; plate II, Renz's product dried at 110°C.; plate III, In_2O_3 dried at 250°C.; plate IV, Renz's product dried at 250°C.; plate V, $\text{Mg}(\text{InO}_2)_2$ plus unreacted In_2O_3 ; plate VI, MgO .

TABLE I
Analytical data on Renz's product

SAMPLE	WEIGHTS AFTER DRYING AT 250°C.	
	Renz's product	In_2O_3 from Renz's product
	grams	grams
1.	0.4619	0.4624
2.	0.5209	0.5209
3.	0.3108	0.3107

nium chloride and drying at 250°C. From the results which are recorded in table 1, it is apparent that the analyzed material was anhydrous indium(III) oxide in every case. Filtrates from indium determinations yielded no precipitates with diammonium orthophosphate and thus contained no magnesium ion.

It may be concluded, therefore, that magnesium oxide is not sufficiently basic in aqueous medium to bring out any latent acidic character in hydrus indium

hydroxide. At 1300°C., however, prolonged sintering (20 hr.) of the component oxides has been shown to yield a well-defined magnesium indate (1). It was of interest to determine whether the compound could be produced under other similar but perhaps less drastic conditions.

A product obtained by sintering a mole-to-mole mixture of magnesium and indium(III) oxides for 20 hr. at 1300°C. yielded the x-ray diffraction pattern shown in plate V of figure 1. A comparison between this pattern and those for indium oxide (plate III) and magnesium oxide (plate VI) indicates the formation of a new structure, although there is also evidence of the presence of unreacted indium oxide. Presumably, unreacted magnesium oxide is also present, but its low scattering power makes its identification difficult. The new structure is a spinel type of "variate atom equipoint" (1) and may be considered to be that of magnesium indate. The calculated unit cell distance (a_0) of 8.81 Å. is in complete agreement with the value reported by Barth and Posnjak (1).

Mixtures of the component oxides heated at 750°C. or 1000°C. for 72 hr. gave no x-ray evidences of indate formation. Fusion of a mixture of hydrated

TABLE 2
Sintering experiments upon MgO-In₂O₃ mixtures

SAMPLE	MOLE RATIO MgO:In ₂ O ₃	PRODUCTS INDICATED BY DIFFRACTION PATTERN
1	1:1	Mg(InO ₂) ₂ + In ₂ O ₃
2	2:1	Mg(InO ₂) ₂
3	1:2	Mg(InO ₂) ₂ + In ₂ O ₃
4	1:3	Trace Mg(InO ₂) ₂ + In ₂ O ₃
5	1:10	In ₂ O ₃

magnesium nitrate and indium oxide followed by heating at 1300°C. for 48 hr. gave a product showing the characteristic patterns of magnesium indate and unreacted indium oxide. Apparently, combination occurs only under extreme temperature conditions, and this observation may be cited as a further refutation of the claims of Renz.

That magnesium oxide has no effect in causing the formation of any new modifications of indium(III) oxide was shown by x-ray diffraction studies upon products obtained by sintering various mixtures of the two oxides at 1250°C. for a total of 82 hr. Data supporting this conclusion are summarized in table 2. All indium(III) oxide patterns were identical.

SUMMARY

1. X-ray diffraction and analytical studies have shown that treatment of an indium(III) salt solution with magnesium oxide precipitates the hydrous hydroxide and not hydrated magnesium indate as previously claimed.

2. Diffraction studies have confirmed reports of the formation of a modified spinel-like magnesium indate as a result of sintering the component oxides for prolonged periods at 1250–1300°C.

3. It has been shown that, except under extreme conditions of temperature and prolonged contact, magnesium and indium(III) oxides are unreactive toward each other.

REFERENCES

- (1) BARTH AND POSNJAK: *Z. Krist.* **A82**, 325 (1932).
- (2) GMELIN: *Handbuch der anorganischen Chemie*, System-Number 37, p. 115. Verlag Chemie, G.M.b.H., Berlin (1936).
- (3) HANAWALT, RINN, AND FREVEL: *Ind. Eng. Chem., Anal. Ed.* **10**, 457 (1938).
- (4) MILLIGAN AND WEISER: *J. Am. Chem. Soc.* **59**, 1670 (1937).
- (5) MOELLER: *J. Am. Chem. Soc.* **63**, 2625 (1941).
- (6) PASSERINI: *Gazz. chim. ital.* **60**, 754 (1930).
- (7) RENZ: *Ber.* **34**, 2763 (1901).
- (8) RENZ: *Ber.* **36**, 4394 (1903).

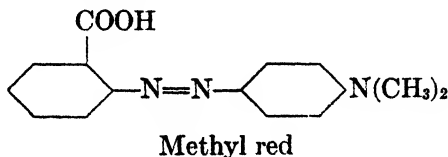
THE CHLOROPHYLL-SENSITIZED PHOTOÖXIDATION OF PHENYLHYDRAZINE BY METHYL RED¹

ROBERT LIVINGSTON, DOROTHY SICKLE², AND AIJI UCHIYAMA

School of Chemistry, Institute of Technology, University of Minnesota, Minneapolis, Minnesota

Received December 3, 1946

The great majority of published studies of photochemical processes sensitized by pigments or dyes are concerned with reactions between reducing agents and molecular oxygen. In the case of chlorophyll-sensitized reactions (*in vitro*), it has even been maintained by one prominent investigator (6, 7) that chlorophyll can transfer its energy of excitation only to molecular oxygen. Quantitative studies on one chlorophyll-sensitized reaction which does not involve molecular oxygen, the oxidation of phenylhydrazine by methyl red



were reported by Ghosh and Sen Gupta in 1934 (4). In view of the importance of this reaction to the theory of photochemical reactions sensitized by solutions of pigments, it is unfortunate that there appear to be three sources of uncertainty in this work. First, the source and purity of the chlorophyll used is not stated.

¹ The authors are indebted to the Graduate School of the University of Minnesota for a grant in aid which made this work possible.

² Present address: Department of Chemistry, College of St. Catherine, St. Paul, Minnesota.

Second, it is not clear whether the authors took into account the profound effect of the alkaline substance, phenylhydrazine, upon the extinction coefficients of the acid-base indicator, methyl red, in the green region of the spectrum. This point is especially important, since the concentration of the methyl red was determined photometrically using green light. Finally, they report that the photochemical reaction was always preceded by a long induction period of unknown origin and of varying duration.

The present work consists of a reëxamination of this photochemical system. It has been demonstrated that the induction period is caused by a side reaction with oxygen. It can be completely prevented by removing dissolved air from the system. Using solutions of pure chlorophyll A or B and making due allowance for the effect of phenylhydrazine upon the absorption of methyl red, quantum yields were obtained about one-fifth as great as those reported by the previous authors (4). These experiments were performed with red light, to avoid the uncertainties due to correction for partial absorptions of the actinic light by methyl red, which is necessary when λ 4358 Å. is used. Otherwise, our results are in general agreement with theirs.

EXPERIMENTAL METHODS

Materials

The methanol used in these experiments was treated with metallic sodium and fractionally distilled. The methyl red was of indicator grade, and was further purified by crystallization from toluene. Its corrected melting point was 182.4°C. The phenylhydrazine was refluxed over zinc dust, vacuum distilled, and stored in the dark at -20°C., out of contact with air.

The chlorophyll A and chlorophyll B solutions were prepared from market spinach by the method of Zscheile (13), using a counter-current extraction system based upon that described by Griffith and Jeffrey (5). The stock solution, in purified ethyl ether, was stored in the dark at -20°C. Solutions in methanol were prepared by adding an excess of the solvent to a sample of the stock solution, and evaporating off (at room temperature or below) the ether and part of the methanol, until a volume corresponding to the desired concentration was obtained.

Apparatus

Light source: The actinic light was a red band, having a maximum at 6200 Å., cutting off sharply at 6000 Å., and tailing off gradually to about 7300 Å. It was obtained from an incandescent source (100-watt, prefocussed projection lamp) with a filter consisting of a Corning filter #241 and 2.5 cm. of 4 per cent cupric sulfate solution. A band of green light, having a maximum at 5000 Å. and extremes at 4750 and 5500 Å., was used to determine the concentration of methyl red photometrically. It was obtained from the incandescent lamp and a filter consisting of Corning filters #401 and #554, Jena #VG3, and 2.5 cm. of 4 per cent cupric sulfate solution.

Optical system: The optical system was similar in principle to that described

by Livingston (9). The light beam was slightly convergent and so defined by circular diaphragms that it just covered the front (plane) face of the cylindrical reaction cell. A Moll, large-surface thermopyle, used without its horn or window, was placed a few millimeters behind the second window of the cell. The galvanometer and thermopyle system was calibrated (and checked at intervals) against a U. S. Bureau of Standards radiation standard lamp, the thermopyle being without its horn or window. Two different standard lamps³ were used, giving results which checked within about 1 per cent. The shutter and either of the two color filters (for actinic or analytical light) could be introduced into the light beam, quickly and reproducibly. The reaction cell and a cell of similar dimensions, but filled with solvent, were mounted on a carriage, which permitted either of them to be introduced into the light beam without otherwise disturbing the system.

Reaction vessels: The reaction vessels were Pyrex-glass cylinders, about 2.8 cm. in diameter and provided with fused-on plane windows. Each vessel was joined through a short section of 6-mm. tubing to a vertical tube about 2 cm. in diameter and 15 cm. long. The top of this tube was provided with a hollow ground-glass stopper, which also served as a stopcock to connect the cell to a short side tube.⁴ Reaction vessels either 12 or 35 mm. in length were used, depending upon the concentration of the dye in the solution. Each reaction vessel was matched with a cell of similar dimensions, but provided with a short side tube and ground-glass stopper in place of the Thunberg tube (12).

Analytical method

The change in concentration of methyl red was followed photometrically. In the majority of the experiments a narrow band of green light having its maximum at 5000 Å. was used. The absorption due to the solution was determined with the thermopyle-galvanometer system. Since the light was not strictly monochromatic, calibration curves ($\log I_0/I_t$ against the molarity of the methyl red) were prepared, using standard solutions in methyl alcohol of the dye in the presence of 0.050 *M* phenylhydrazine and of several concentrations of chlorophyll. A few check experiments were performed, in which the solutions were analyzed for methyl red with the Beckmann spectrophotometer. In these measurements, wave lengths of 5000 and of 4900 Å. were used, since the absorption due to chlorophyll is relatively small (although not negligible) in this region.

The concentration and purity of the chlorophyll A and B solutions were determined spectrophotometrically (1) with the Beckmann instrument.

Routine procedure and computations

The reaction mixtures were prepared volumetrically from stock solutions in methanol. The completed solution was transferred to the reaction vessel, this

³ The authors are indebted to Dr. C. Stacy French of the Department of Botany for placing the second standard lamp at their disposal.

⁴ The design of the upper part of this cell and the technique for its use were adopted from the standard procedure of Thunberg (12).

and subsequent manipulations being performed in a dim light. After the solution had been placed in the cell, it was sealed with a lightly greased, ground-glass stopcock. This stopper was turned to connect the cell to the side tube, and the dissolved gases were removed by evacuation, allowing from 5 to 10 per cent of the solvent to distill off. The second cell was filled with the solvent. Both cells were placed in the carriage on the optical bench, and allowed to come into thermal equilibrium in the dark.

The intensity ($I_0 - I_r$) of the absorbed, red light was determined at the beginning and the end and at least once during the experiment. The relative transmission (I_r/I_0) of the solution for the green (analytical) light was determined just before the start of the illumination (with the red, actinic light), and after each 2-min. period of illumination. The molarities (m_D) of the methyl red were obtained from these measurements by the use of the calibration charts ($\log I_0/I_r$ vs. m_D). From these molarities, the corresponding times, the intensities (in absolute units) of the absorbed red light, and the volume of the solution, the quantum yields were computed in the usual way (9). A mean wave length of the absorbed light of 6600 Å. was used in all computations. This was obtained graphically, using the energy distribution of the incandescent source and the extinction curves for the filter system, and for chlorophyll A.⁵

EXPERIMENTAL RESULTS

The quantum yield with red light

The results of a number of determinations of the quantum yield (in terms of the change in number of molecules of methyl red) are presented in table 1. In all of these experiments, the initial concentrations of phenylhydrazine and methyl red were 0.050 *M* and 1.00×10^{-4} *M*, respectively. The experiments were performed at room temperature, which varied between 27° and 30°C. The values of the quantum yield are based upon an average value of reaction rate for approximately the first 80 per cent of the reaction, over which range the reaction was zero order (cf. curves A of figures 1 and 2).

In agreement with the findings of Ghosh and Sen Gupta (9), the dark reaction is negligibly slow and there is no detectable photochemical reaction in the absence of chlorophyll.

The average value of the quantum yield is 0.12 molecule of methyl red disappearing per quantum absorbed. The probable error of this mean value is very likely less than 20 per cent. Within the limits of accuracy of the experiments, the quantum yield is independent of the concentration of chlorophyll (within the range 1.0×10^{-6} to 1.5×10^{-5} *M*). Chlorophyll A and chlorophyll B appear to be equally efficient sensitizers for this reaction.

To check these results, a few experiments were performed with a modified Warburg respiration monometer⁶ (2), using the chlorophyll-sensitized autooxidation of allylthiourea (3) as an actinometer. To determine the concentration of

⁵ The correction which should be made to the mean wave length when chlorophyll B was used is certainly less than 5 per cent.

⁶ The details of this apparatus will be described elsewhere.

chlorophyll required to produce a maximum rate under the conditions of the experiment, a series of measurements were made with 0.50 *M* of allylthiourea in purified acetone containing different concentrations of chlorophyll. The results given in table 2 were obtained.

Leaving the apparatus and light source unchanged, an oxygen-free solution, containing 0.05 *M* phenylhydrazine, 1.0×10^{-4} *M* methyl red, and 7.5×10^{-5} *M* chlorophyll A in methanol, was placed in the reaction vessel. The air in the

TABLE 1
Summary of the determinations of the quantum yield

CONCENTRATION OF CHLOROPHYLLS		INTENSITY OF ABSORBED LIGHT	QUANTUM YIELD ϕ
A	B		
<i>molarity</i> $\times 10^4$	<i>molarity</i> $\times 10^4$	$\frac{\text{quanta}}{\text{sec.}} \times 10^{-15}$	
75.0	0.0	12.4	0.09
15.2	0.0	13.5	0.11
7.6	0.0	5.9	0.15
7.6	0.0	5.1	0.13
6.1	0.0	11.8	0.11
3.0	0.0	8.7	0.12
1.1	0.0	3.5	0.15
0.0	7.5	6.6	0.09
0.0	7.5	6.2	0.13
1.0	3.8	9.5	0.11
0.5	1.9	9.3	0.12
0.2	1.0	4.3	0.11

TABLE 2
Rate of the allylthiourea reaction

Concentration of chlorophyll A (<i>M</i> $\times 10^5$)	1.0	5.0	7.5	9.5	2.0
Rate (cm. of water per minute)	0.62	1.12	1.27	1.35	1.32

TABLE 3
Rate of the methyl red-phenylhydrazine reaction

Time (minutes)	0	2	4
Concentration of methyl red (<i>M</i> $\times 10^5$)	10.0	5.8	1.1
Rate (moles $\times 10^6$ /l. per minute)....		2.1	2.3

manometer and vessel was displaced with purified nitrogen. After being illuminated for a known time interval, the solution was removed from the vessel and analyzed for methyl red with the Beckmann spectrophotometer, using λ 4900 and λ 5000 Å. The results in table 3 are an average of two such sets of determinations. When a 5-ml. volume is used, this rate corresponds to 1.1×10^{-7} moles per minute. Under similar conditions, the rate (expressed as moles of oxygen consumed per minute) of the allylthiourea reaction is:

$$\frac{\Delta P_{iv}}{RTt} = \frac{1.27 \text{ cm./min.} \times 15.2 \text{ cc.}}{76.0 \text{ cm./atm.} \times 13.5 \text{ gm./cc.} \times 82.1 \frac{\text{cc. atm.}}{\text{degree}} \times 28.1^\circ} = 7.7 \times 10^{-7} \text{ moles per minute}$$

Assuming that Gaffron's (3) value of 1.0 for the quantum yield of the allylthiourea reaction applies to the conditions of the present experiments, the quantum yield for the methyl red-phenylhydrazine reaction is $1.1/7.7 = 0.14$. The (incomplete) data of table 2 indicated that the absorption of the actinic light by the $7.5 \times 10^{-5} M$ chlorophyll solution is not complete; however, this should affect both reactions equally. This value, while slightly larger than that obtained by direct measurement, is in agreement within reasonable limits of experimental error.

During these measurements there was no detectable change in pressure in the manometer. This indicates that, if any nitrogen is formed as a result of the reaction, the number of moles formed is less than 5 per cent of the moles of methyl red reduced.

The quantum yield with λ 4358

Some preliminary measurements (not reported in table 1) gave values of the quantum yield (approximately 0.1) which were independent of the methyl red concentration in the range 5×10^{-5} to $2 \times 10^{-4} M$. A few experiments were performed in which light of λ 4358 Å. was substituted for the red band. The values of the quantum yield, computed from this data upon the assumption that all of the light absorbed was equally effective, were approximately equal to 0.1 and were independent of the fraction of the light absorbed by chlorophyll. Since this latter result was unexpected and appears to be of considerable theoretical interest, these experiments are being repeated under carefully controlled conditions and will be reported later.

The reaction with oxygen

Figures 1 and 2 illustrate the effect of oxygen upon the rate of the photochemical reaction. Each pair of curves represents reactions for which the light intensity was constant and the solutions were identical, except for the oxygen content. The reactions showing no induction period occurred in solutions which had been freed from oxygen. Those exhibiting induction periods were in solutions which were saturated with air (at about $27^\circ C.$), their volumes were 8 ml., and they were confined in contact with approximately 0.3 ml. of air.

In the absence of air, the rate is independent of the concentration of methyl red for values greater than $2 \times 10^{-5} M$. In solutions saturated with air, the rate of disappearance of methyl red is less than 10 per cent of its normal (oxygen-free) rate. The maximum value of the rate of disappearance of methyl red attained after an induction period is always somewhat less than the normal rate (in the present cases about two-thirds of normal). Similar results were obtained in a number of other experiments not reported here. It was also shown that the

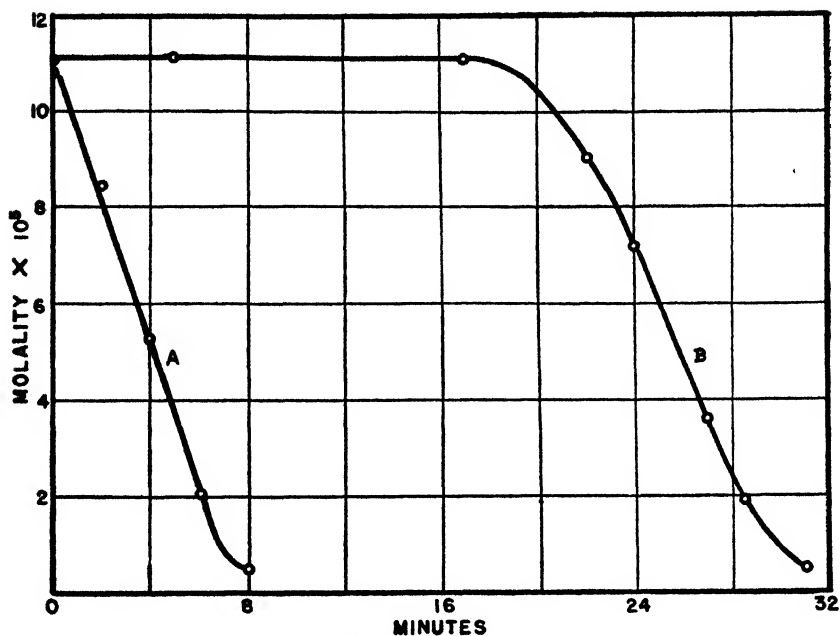


FIG. 1. Experiments illustrating the induction period

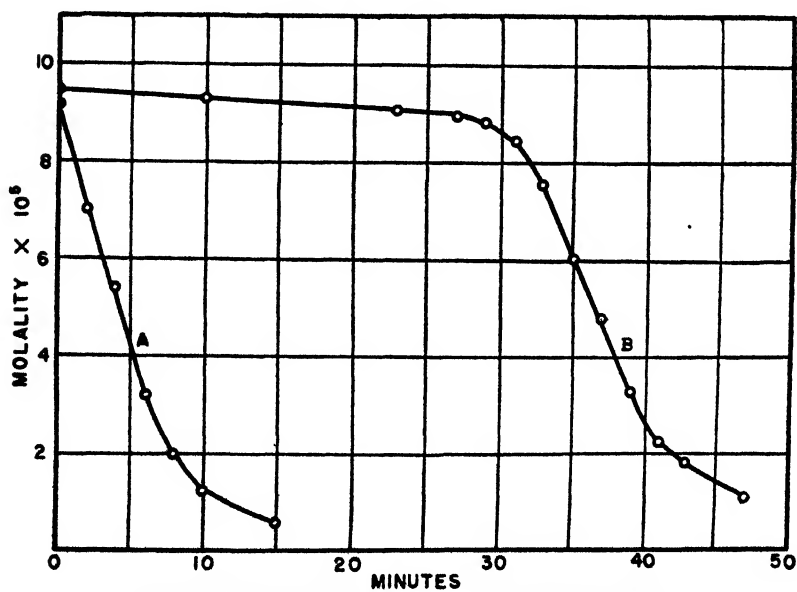


FIG. 2. Experiments illustrating the induction period

length of the induction period increases with an increase in the volume of air in contact with this solution.

The quantum yield for the sensitized reaction between phenylhydrazine and

oxygen may be estimated from the data presented in figures 1 and 2 and the solubility of oxygen in methanol. The solubility of molecular oxygen in methanol at 27°C., expressed as the ratio of the volume of gas dissolved to the volume of the solvent, is 0.228 (8). Since the volume of the solution is 8.0 ml., the number of moles of oxygen in the reaction solution saturated with air is⁷

$$N'_{O_2} = \frac{0.210 \times (745/760) \times 0.228 \times 8.0}{82.1 \times 300} = 1.58 \times 10^{-5} \text{ moles}$$

It is necessary to correct this value for the oxygen contained in an air bubble, of approximately 0.3 ml. volume, which was present in the cell.

$$N''_{O_2} = \frac{0.210 \times (745/760) \times 0.3}{82.1 \times 300} = 0.25 \times 10^{-5} \text{ moles}$$

There were, therefore, approximately 1.83×10^{-5} moles of oxygen present in the cell at the start of the reaction. If we make the probable assumption that the maximum rate of reduction of methyl red is not attained until practically all of the oxygen is used up, we may compute the rates of disappearance of oxygen in experiments IB and IIB as 1.83×10^{-5} moles/20 min. = 9.1×10^{-7} and $1.83 \times 10^{-5}/32 = 5.7 \times 10^{-7}$ moles per minute, respectively. The corresponding rates of reduction of methyl red in the absence of oxygen (experiments IA and IIA) are 1.13×10^{-7} and 5.5×10^{-8} moles per minute. Since the intensities of light and the chlorophyll concentrations were unchanged for each pair of experiments (e.g., IA and IB), the quantum yield, φ_{-O_2} , for the oxygen reaction must be equal to the ratio of the rates multiplied by the quantum yield for the reduction of methyl red, as follows:

$$\text{Figure 1: } \varphi_{-O_2} = \frac{9.1 \times 10^{-7}}{1.13 \times 10^{-7}} \times 0.15 = 1.2$$

$$\text{Figure 2: } \varphi_{-O_2} = \frac{5.7 \times 10^{-7}}{5.5 \times 10^{-8}} \times 0.13 = 1.3$$

Similar analysis of preliminary experiments yields values of φ_{-O_2} between 0.7 and 1.6. While these estimates are admittedly crude, they demonstrate that the quantum yield for the reduction of oxygen by phenylhydrazine is not the same as that for the reduction of methyl red, but is approximately equal to unity.

The reaction between methyl red and allylthiourea

A few experiments were performed to determine the effect of substituting allylthiourea for phenylhydrazine in the reaction mixture. In all of these experiments, the concentrations of methyl red and allylthiourea were 10^{-4} M and 0.50 M, respectively. The solvent was acetone. The cell was evacuated to remove oxygen. In two experiments the solvent contained 2 per cent pyridine (3); in a third it was pyridine-free. A mixture of chlorophylls A and B was

⁷ It is necessary to assume that the solubility of oxygen is unaffected by the presence of 0.050 M phenylhydrazine and of the dilute pigments in the methanol.

used: $5 \times 10^{-6} M$ in one experiment and $5 \times 10^{-5} M$ in two others. In no case was there a detectable reduction of methyl red after 90 min. illumination with red light. With similar light intensity and chlorophyll concentration, the methyl red-phenylhydrazine reaction was more than 50 per cent complete in 10 min.

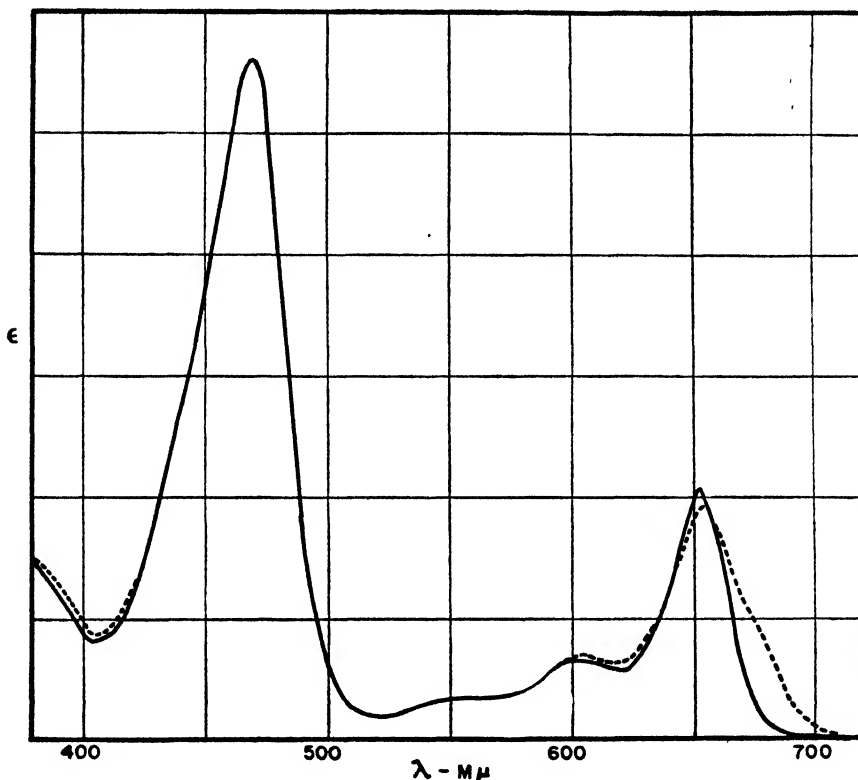


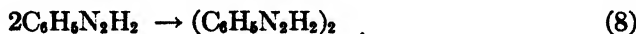
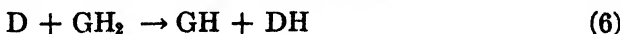
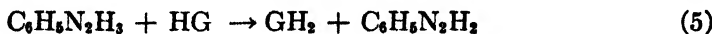
FIG. 3. Absorption spectrum of chlorophyll B in methanol

The absorption spectra of the chlorophylls in the presence of phenylhydrazine

To determine whether 0.05 M phenylhydrazine in methanol had any affect on the absorption spectra of the chlorophylls, the extinction coefficients of pure samples of chlorophyll A and of chlorophyll B, in the presence and absence of phenylhydrazine, were measured with the Beckmann spectrophotometer, at 50 Å. in intervals from λ 3800 to 7500 Å. The curves obtained in pure methanol compare favorably with those published by Zscheile and Harris (14). While 0.05 M phenylhydrazine has no detectable affect upon the absorption spectrum of chlorophyll A in methanol, it distinctly changes that of chlorophyll B, as is illustrated by figure 3. The change occurs chiefly in the red end of the spectrum, it being doubtful if the slight shift which was observed in the violet end is significant.

DISCUSSION

The present data, although incomplete in many respects, can be used to evaluate the merits of the several schemes (11) which have been advanced as mechanisms of chlorophyll-sensitized photooxidations. Any mechanism for the methyl red-phenylhydrazine reaction must be consistent with the following observations: the quantum yield is small (about 0.1) and is independent of the methyl red concentration and (at least over a limited range) of the intensity of the absorbed light; the quantum yields for the oxygen-allylthiourea and the oxygen-phenylhydrazine reactions are near unity; and there is no detectable sensitized reaction between methyl red and allylthiourea. One mechanism which is consistent with these facts, and others previously published (3, 10), can be represented by the following steps. The symbols used have the following significance: GH = chlorophyll, HG = long-lived activated chlorophyll (e.g., tautomer), GH_2 = monohydrogenated chlorophyll, D = methyl red, DH_2 reduced methyl red.



The "follow reactions" (7 and 8) are quite arbitrary. For example, the oxidation product of phenylhydrazine has not been identified, except that its formation does not involve liberation of molecular nitrogen. Making the usual assumption about the existence of a steady state, we obtain the following relation for the quantum yield, φ .

$$\varphi = \frac{k_3}{2(k_2 + k_3)} \times \frac{(\text{C}_6\text{H}_5\text{N}_2\text{H}_2)}{(k_4/k_5) + (\text{C}_6\text{H}_5\text{N}_2\text{H}_2)}$$

The falling off of the yield at higher concentrations of chlorophyll is not taken into account in the preceding mechanism, since it has been adequately discussed elsewhere (11). Additional experiments are planned to test the predicted relation between φ and the concentration of phenylhydrazine.

Since the sensitized reaction between oxygen and phenylhydrazine has a quantum yield near unity, it is very probable that step 5a,



and the appropriate follow reactions replace step 5. Further work is required to show the relative importance of these two steps.

The fact that the quantum yield for the oxidation of allylthiourea by oxygen is about 1, while it is approximately 0 when methyl red is the oxidizing agent, makes it appear very probable that step 5a, rather than an analog to 5, is the dominant one in this reaction.

The shift in the red absorption band of chlorophyll B produced by moderately dilute phenylhydrazine suggests the formation of a compound between phenylhydrazine and presumably the formyl group of chlorophyll B. In this respect, it is interesting that chlorophylls A and B are equally efficient sensitizers under the conditions of our experiments.

SUMMARY

1. The occurrence of the chlorophyll-sensitized photoöxidation of phenylhydrazine by methyl red, which was reported previously by Ghosh and Sen Gupta (4), has been confirmed.

2. In the presence of dissolved oxygen the reaction exhibits an induction period, which can be eliminated by removing the oxygen.

3. A quantum yield of 0.12 (molecules of methyl red disappearing per quantum absorbed) was obtained when a methanol solution containing chlorophyll (either A or B) (10^{-6} to 10^{-5} M), methyl red (10^{-4} M), and phenylhydrazine (0.050 M) was illuminated with red light.

4. Preliminary experiments in which light of λ 4358 Å. was used indicated that light which is absorbed by methyl red as well as by chlorophyll is photochemically active. This result will be studied more carefully and reported later.

5. While the reaction products were not isolated, it was noted that the products were, compared to methyl red, colorless, and that no nitrogen was evolved.

6. Indirect measurements indicate that the quantum yield, for the chlorophyll-sensitized photochemical reaction between oxygen and phenylhydrazine, is approximately equal to unity.

7. The photosensitized reaction with methyl red is negligibly slow when allylthiourea (3) is substituted for phenylhydrazine.

8. Phenylhydrazine, at a concentration of 0.05 M, changes the absorption spectrum of chlorophyll B in methanol, but does not appreciably affect that of chlorophyll A.

REFERENCES

- (1) COMAR, C. L., AND ZSCHEILE, F. P.: *Plant Physiol.* **17**, 198 (1942).
- (2) DIXON, M.: *Manometric Methods*. Cambridge University Press, London (1934).
- (3) GAFFRON, H.: *Ber.* **60B**, 755 (1927).
- (4) GHOSH, J. C., AND SEN GUPTA, S. B.: *J. Indian Chem. Soc.* **11**, 65 (1934).
- (5) GRIFFITH, R. B., AND JEFFREY, R. N.: *Ind. Eng. Chem., Anal. Ed.* **17**, 448 (1945).
- (6) KAUTSKY, H., HIRSCH, A., AND FLESCH, W.: *Ber.* **68**, 152 (1935).
- (7) KAUTSKY, H., AND FLESCH, W.: *Biochem. Z.* **284**, 412 (1936).
- (8) LEVI, M. G.: *Gazz. chim. ital.* **31**, II, 513 (1901).
- (9) LIVINGSTON, R.: *J. Phys. Chem.* **44**, 601 (1940).
- (10) LIVINGSTON, R.: *J. Phys. Chem.* **45**, 1312 (1941).
- (11) RABINOWITCH, E. I.: *Photosynthesis*, Vol. I, Chap. XVIII. Interscience Publishers, Inc., New York (1945).

- (12) THUNBERG, T.: *Handbuch der biologischen Arbeitsmethoden*, Teil I, Heft 7. Urban and Schwarzenberg, Berlin (1920).
(13) ZSCHEILE, F. P., AND COMAR, C. L.: *Botan. Gaz.* **102**, 463 (1941).
(14) ZSCHEILE, F. P., AND HARRIS, D. G.: *Botan. Gaz.* **104**, 515 (1943).

EFFECTS OF HIGH-ENERGY RADIATION ON ORGANIC COMPOUNDS¹

MILTON BURTON²

Monsanto Chemical Company, Clinton Laboratories, Oak Ridge, Tennessee

Received November 8, 1946

I. INTRODUCTION

Organic compounds are hydrogenous materials. Thus, they are particularly effective as moderators for fast neutrons and at the same time become particularly susceptible to their influence. Quite apart from possible usefulness in the production of atomic energy, they definitely belong among those materials which might be introduced in or near a pile for the production of new and interesting chemical effects and chemical products. Furthermore, since piles and other portions of atomic energy plants are operated more or less remotely by human beings, discovery of the effects of all high-energy radiations on materials of which biological systems are composed has become an increasingly important matter.

The practical value of solution of the radiation-chemical problems of organic compounds is by no means the sole justification for their investigation. Just as in reaction kinetics of thermal and photochemical systems, organic compounds offer a very fruitful field for study because so many different aspects of bond type and bond number and of molecular size, complexity, and relative stability (in the thermodynamic sense) can be independently and gradually varied in a manner advantageous for detailed study, for determination of general rules and correlations, and for discovery of underlying principles. The essential information required is knowledge of relative reactivity (under irradiation) of compounds and bonds of various types, of the relative effects of different kinds of radiation, and of the nature of the compounds produced. Much of this information is in the literature prior to the establishment of the Atomic Energy Projects, and some of it has been obtained outside of the projects, notably by the Massachusetts Institute of Technology group (7, 8, 14, 15), even during World War II.

¹Paper presented before the Symposium on Radiation Chemistry, which was held under the auspices of the Division of Physical and Inorganic Chemistry at the 110th Meeting of the American Chemical Society, Chicago, Illinois, September, 1946.

²Present address: Department of Chemistry, University of Notre Dame, Notre Dame, Indiana. The work reviewed is in part taken from studies performed at the Metallurgical Laboratory, University of Chicago.

It is not the purpose of this article to review all the information available on the radiation chemistry of organic compounds. Its subject matter is confined to decomposition processes exclusively. In this limited field, only general principles and hypotheses are offered and a few illustrative examples are selected from both public and project literature.

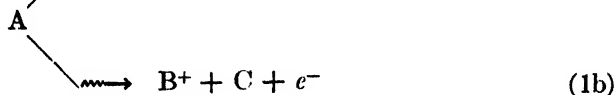
II. SPECIAL FEATURES

All the processes characteristic of photochemistry can occur in radiation chemistry for, apart from the other phenomena associated with high-energy radiation, there are ordinary excitations such as are produced by light of wave length $> 1000 \text{ \AA}$. The processes include fluorescence, simple rupture at the locus of excitation, internal conversion of energy, transfer of energy to another molecule, and reaction with another molecule. Internal conversion is followed by collisional deactivation or by decomposition. In the latter case, the whole process (internal conversion plus decomposition) is called predissociation. Transfer of energy to another molecule may mean merely the conversion of the excitation energy to heat or it may cause reaction of the second molecule. In the latter case, the process is called photosensitization.

In radiation chemistry, the excitation process may occur primarily as the result of action of the radiation on the molecule without ionization or it may occur secondarily after, or as a part of, ionization of the molecule.

The distinctive primary process of radiation chemistry is the process of ionization. A numerically less frequent process is significant in certain special cases; it is an ion(or atom)-ejection process in which a particle is knocked out of lattice or molecular position either by gamma recoil effect (Szilard-Chalmers process) or by fast-neutron impact (Wigner effect). Such an ejection process never occurs alone; it always precedes or is accompanied by the far more extensively occurrent ionization processes. For overall knowledge of what happens to a system in a radiation field we therefore address our attention to the ionization process and its consequences.

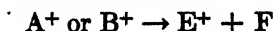
In the ionization process, given sufficient energy or appropriate conditions (as in water), the ion itself may dissociate. Usually, however, the sequence of events in organic chemistry may be represented by the three equations:



*In radiation chemistry the symbol \rightsquigarrow has the same significance as has $\xrightarrow{h\nu}$ in photochemistry. It is intended to show that the consequences of a process (i.e., exposure to high-energy radiation), not its details, are being indicated.

The reactions are successively ionization, ionic discharge, and decomposition (4).

It has been known for a long time (*cf.* Hustrulid, Kusch, and Tate (10)) that the initial ionization step may be by a number of paths. Reaction 1a represents the simplest such step. Reaction 1b represents a group of reactions in which different ionic species and molecules, free radicals, or atoms are formed either in the primary act or stepwise in subsequent acts. For example, Hipple, Fox, and Condon (9) have shown definitely in studies on the ionization of hydrocarbons in the mass spectrograph that ions such as A^+ or B^+ may be metastable and dissociate with production of a variety of products; e.g.,



where F may be a free radical but is usually a stable molecule. In normal butane, for example, $C_4H_{10}^+$ may be produced (by reaction 1a) in the primary act. Thereafter, it can (but does not necessarily) decompose; two reactions are reported for the decomposition of $C_4H_{10}^+$.



Reaction 1 does not stipulate which electron of the molecule is removed nor how much excess energy is conferred on the molecule in the ionization process. In general, because of the nature of the ionization act, the chances are apparently equally good that any one of a large number of electrons in the molecule may be ionized. Thereafter, conceivably, the charge of the molecule may shift to a preferred position to the accompaniment of further excitation of various orbitals. In any event, the Franck-Condon principle applies. The atoms of the molecule do not have an opportunity to shift during the ionization process, but they do shift immediately afterwards to positions of greater stability for the ion. Such a shift is accompanied by processes in which great vibrational excitation of a part of the molecule is dissipated either in collisions with other molecules or to other degrees of freedom in the same molecule. Usually, the final ionic configuration is distended in comparison to that of the parent molecule. It is not apparent whether this distension is over the whole molecule or is localized in the region of ionization. There are certain cases where the molecule is quite symmetrical, as in benzene, in which it is not unreasonable to assume that all the atoms shift and that the missing orbital of the ionic state is, so to speak, "smeared" over the whole ion. This assumption is discussed in further considerations below (Section III, D, (2) and (3)).

Reactions 2 and 3 are prototypical. Actually, B^+ or E^+ may be written for A^+ and B^* or E^* for A^* ; the excited particles can be either excited molecules or excited atoms. Thorough understanding consequently requires detailed consideration, in the particular case under study, of reactions additional or alternative to 2 and 3.

Whatever the details of the situation are, the fact is that the ion which enters

into reaction 2 is distended in comparison with the unexcited molecule A.⁴ The Franck-Condon principle holds also during the process of ionic discharge. The molecule A* formed in reaction 2 has the same configuration as the ion A⁺ from which it was produced. Thus, it is an excited molecule whose excitation may be fairly well localized or may be spread over a number of bonds, depending on the degree of localization of distension of the parent ion. It is sufficient here to say that something in the mechanism makes possible the process of ionic discharge (without immediate subsequent ionization) and that the excess energy consequently liberated in the molecule is far more than sufficient to break any one or two of the bonds in that molecule.

Whether reaction 3 occurs at all depends on whether the excess energy in A* becomes available for a decomposition process before collisional deactivation occurs.⁵ The products X and Y may be either radicals or stable molecules. For occurrence of decomposition into radicals, greater localization of excess energy is required. Perhaps such localization is the more ordinary phenomenon in ionic discharge. In such circumstances a (rearrangement) mechanism involving formation of ultimate molecules in the primary act (i.e., in reaction 3) is improbable. On the other hand, if the excitation energy of A* is distributed over a large number of bonds, the chance of a free-radical split in reaction 3 is reduced and, if collisional deactivation does not occur first, the predominant process in reaction 3 may be an ultimate-molecule split.⁶

III. DECOMPOSITION PRODUCTS

A. Relationship to groups in molecule

In radiation chemistry, as in photochemistry, many decomposition processes involve simple rupture and formation of free atoms or radicals as a first step in the chain. Usually, in photochemistry, at a particular wave length only a special part of the molecule is activated. In radiation chemistry, on the other hand, no part of the molecule should be preferentially ionized⁷ and usually no special part of the molecule is preferentially excited. Thus, in photochemistry

⁴In the ensuing discussion attention will be concentrated on A and its derivatives. A more general discussion requires repeated reference to B⁺ and the possibility that B represents a free radical rather than a stable molecule. In order to avoid unnecessary complication, it is left to the reader mentally to insert the necessary additional analogous statements or to add statements entailed by the reactivity of B in any medium under specific consideration.

⁵The reader will note an analogy here to ordinary thermal and photochemical processes.

⁶A contrast to photochemistry is here notable. In a photochemically excited molecule, the excitation energy is very localized. Nevertheless, under certain conditions (i.e., when the excitation energy is not sufficiently high) decomposition cannot occur at the locus of absorption but must occur in another way. In such circumstances, the ultimate-molecule mechanism may occur (3). In radiation chemistry, on the other hand, the excitation energy is always sufficiently high for bond rupture.

⁷This presumable absence of initially preferential ionization or excitation of a certain part of the molecule in special cases.

it may occur that in a particular class of compounds (e.g., the aldehydes) one single bond is preferentially broken (e.g., the C—C bond adjacent to the carbonyl group (6)). In radiation chemistry such a phenomenon should be exceptional, and we expect that the probability of rupture of a particular bond is more or less closely related to its fractional "concentration" in the molecule. Thus, in a hydrocarbon containing a number of methyl groups, the number of free methyl radical splits should be proportional to their number, just as the number of free hydrogen atoms initially formed should be roughly related to the number of C—H bonds in the molecule.

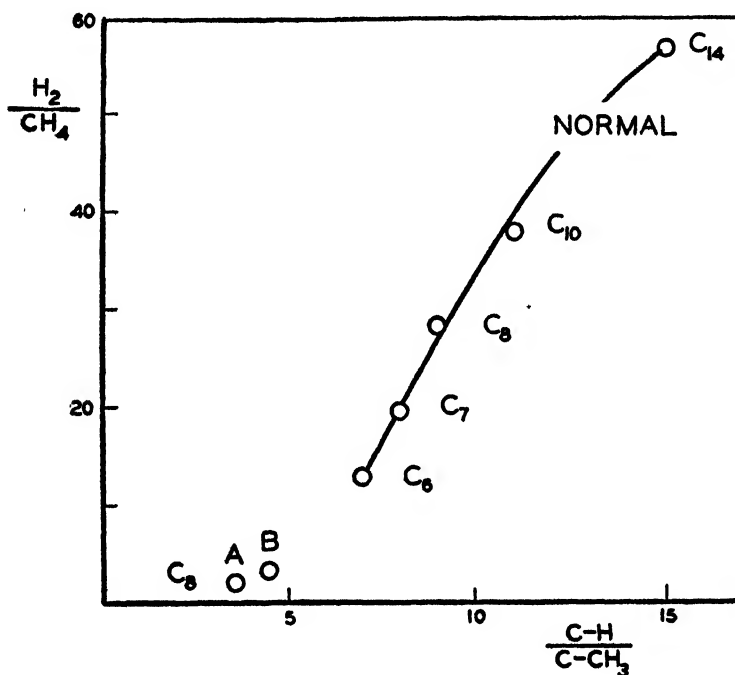


FIG. 1. Relationship between product yield and parent groups in a series of hydrocarbons, according to Schoepfle and Fellows. The curve is through the normal hydrocarbons. Point B is for 2,2-dimethylhexane; point A is for 2,2,5-trimethylpentane

Schoepfle and Fellows (8) offered an interesting example of such a relationship many years ago. Figure 1, taken from their data, shows that the relationship between the ratios (H_2 yield)/(CH_4 yield) and (number of C—H bonds)/(number of C— CH_3 bonds) is nearly linear for a series of normal aliphatic hydrocarbons. However, the points for two isomeric octanes lie distinctly off the curve, with the fraction of hydrogen in the yield much exceeding the expected value. Table 1 is taken from the same set of data as is figure 1. Comparison of 2,5-dimethylhexane with *n*-hexane shows that the yield of methane is nearly what would be expected on the basis of number of C— CH_3 bonds but it is then difficult, on the same basis, to account for the large decrease in hydrogen yield in the former

case. In order to account for the very high H_2/CH_4 ratio in all the cases, Schoepfle and Fellows suggested that a significant portion of the hydrogen yield comes from the decomposition of large radicals. It is sufficient for our purposes here to say that it must come from a process which does not necessarily involve a primary C—H split. As a matter of fact, it is important to note that the type of data summarized by figure 1 cannot be considered evidence for any free-

TABLE 1

Effect of 170-kv. cathode rays (0.3 ma., 30 min.) on some hydrocarbons
(Schoepfle and Fellows: Ind. Eng. Chem. **23**, 1396 (1931))

HYDROCARBON	TOTAL GAS	H ₂	CH ₄	OTHER GAS (CALCULATED)
	cc.	cc.	cc.	cc.
<i>n</i> -Hexane	57.6	38.3	3.1	16.2
<i>n</i> -Heptane	51.4	39.5	2.1	9.8
<i>n</i> -Octane	48.3	38.0	1.4	8.9
<i>n</i> -Decane	41.6	32.8	0.9	7.9
<i>n</i> -Tetradecane	34.9	31.8	0.6	2.5
2,5-Dimethylhexane	49.8	21.0	5.8	23.0
2,2,4-Trimethylpentane	50.3	17.6	7.6	25.1

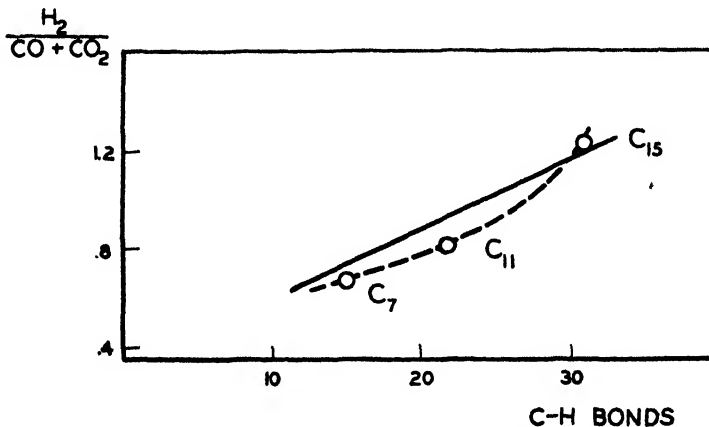


FIG. 2. Relationship between yield of products and number of parent groups in three fatty acids, according to Honig. The solid line is Honig's.

radical or free-atom mechanism at all. Decomposition *via* rearrangement could and should give precisely similar data.

More recently, Honig (8) noted a similar "group to product" relationship between the ratio (H_2 yield)/(CO + CO₂ yield) and number of hydrogen atoms in three fatty acids exposed in the solid state to alpha-particle bombardment. Figure 2, given by Honig, shows a nearly linear relationship. The data are insufficient to indicate whether the departure from linearity is real.

B. Gas production in relation to unsaturation

One of the unfortunate features of many of the data of radiation chemistry is that so little basic quantitative information is given. Very frequently, only gas analyses appear, without any effort to relate amount of product to energy input. However, even when such data appear, they are an inadequate criterion of the degree of decomposition. This situation is particularly true when mechanisms are present for the absorption of free radicals and atoms—as in the decomposition of unsaturated compounds.

The work of Schoepfle and Fellows, already cited, also showed that, as far as gas production is concerned, unsaturated hydrocarbons appear more stable than saturated, and aromatic compounds appear far more stable than aliphatic. Aliphatic side chains on aromatic rings increased the gas yield. In table 2, which comes from project data (2), these facts are very clearly shown, but it is at the same time apparent that many more molecules react than are indicated by gas production alone. In cyclohexene, toluene, and benzene the number of

TABLE 2
Effect of fast-electron irradiation on liquid hydrocarbons
(J. V. Flanagan, C. J. Hochenadel, and R. A. Penneman (2))

HYDROCARBON	G_g (MOLECULES GAS PER 100 E.V.)	G_p (MOLECULES LIQUID CONVERTED TO POLYMER/ 100 E.V.)
Benzene.....	0.04	0.5
<i>n</i> -Heptane.....	4.2	1.7
Cyclohexane.....	4.0	1.2
Cyclohexene.....	1.0	4.2
Methylcyclohexane.....	4.5	4.2
Toluene.....	0.09	0.7

molecules which enter into reaction exceeds the number of molecules of gas produced by a factor ranging from 4.2 to 12.5.

C. Effect of liquid state

Franck and Rabinowitch have pointed out that, in certain photochemical cases, where the same decomposition reaction can be studied both in the gas and in the liquid, the quantum yield of the reaction is generally lower in the liquid (5). Two factors contribute to this decrease in yield: a collisional deactivation effect and a cage effect. The former occurs because the period between collisions in the molecules in a liquid is about 10^{-12} sec. (i.e., about one vibration period) and thus, unless reaction occurs in the interval between collisions (as by rupture), there is a good chance that the excitation energy may be picked off before it becomes effective. The more the excitation energy exceeds the energy required for the reaction, the less is the probability of this process. In the cage effect, radicals produced by rupture collide with the surrounding molecules while they are still within each other's spheres of influence; there is consequently

a probability of primary recombination. The cage effect is enhanced where product radicals and substrate molecules are both large; it would be smaller when a hydrogen atom is a primary product (12). It might be expected that the cage effect would also be reduced when the primary product is travelling with high energy. The cage effect should be without influence on the chance of split into ultimate molecules (11). On the whole, excessive excitation energy will increase yield mainly because of decreased importance of leaking-off of energy rather than because of decreased cage effect. Thus, decomposition yields in radiation-induced reactions in the liquid state should be generally high (as compared with photochemical reactions) and the ultimate-molecule mechanism should be favored. As for the first part of that conclusion, no evidence is readily available now, although we may expect that it will be subjected to test. The conclusion that the ultimate-molecule mechanism should be favored by the liquid state has received support in photochemistry. Some data on the radiation chemistry of fatty acids by Sheppard and Whitehead (15), cited in section III,D,(3), also agree with that conclusion.

D. Reactivity factors

Any factor which increases the lifetime of the excited molecule formed in the act of ionic discharge serves to decrease both decomposition yield and ratio of free radicals to ultimate molecules formed in the primary act. There are several such factors.

(1). Among isomers, greater complexity means longer life of the excited states. Complexity increases the probability of internal conversion of energy from an initial excited state (where energy may be localized in a single part of the molecule) to one of a number of equivalent states in which the energy is fairly well distributed throughout the molecule. While in such a relatively stable state the molecule may lose a critical amount of energy by collision before bond rupture (but not necessarily decomposition by rearrangement) has a chance to occur.

The only experimental data available on this point are those of table 1, relating to the isomeric octanes. The marked decrease in hydrogen yield in going from *n*-octane to its isomers cannot be accounted for on the basis of competition with C—CH₃ splits. An alternative explanation can be based on the notion that the number of C—H splits is reduced from another cause and that the increased yield of methane is not necessarily *via* free CH₃ radicals. According to the point of view of the previous paragraph, the explanation could be that, because of the successively increased complexity of the isomeric octanes, the chance of internal conversion to a state in which the energy is non-localized is increased. Thus, that portion of the decomposition resulting from bond splits is markedly decreased, while rearrangement processes (in which, perhaps, some hydrogen is primarily formed) are not greatly affected. The decrease in hydrogen yield represents then a substantial decrease in C—H splits. Incidentally, small "smearing-out" of excitation energy as in internal conversion should theoretically be reflected first in a decrease in splits of bonds of the greater strength; i.e., C—H bonds as compared with C—C bonds.

In future work it will be desirable to obtain information on the actual quantities of isomeric compounds decomposed as well as on the fractions of products formed *via* free radicals (or atoms) and rearrangements to ultimate molecules.

(2). The more resonance in a molecule (as in benzene), the more likely it is that the state immediately ensuant on ionic discharge will be one in which the excitation energy is distributed throughout the molecule. Thus, the probability is high that the excited molecule may endure without bond rupture until it becomes stabilized by loss of energy in collision processes (or decomposes by rearrangement into ultimate molecules).

(3). The closer the correspondence between ionic and normal-molecular configurations, the less is the molecule ultimately affected by radiation. Benzene may be cited as a possible illustrative extreme case. If, as suggested in Section II, the missing orbital is "smeared" over the whole ion, the ionic and normal-molecular configurations may be so closely alike that the excitation in the molecule caused by discharge of the ion cannot be said to be localized preferably in any single bond. Such a molecule would be rather unreactive, for it would be unlikely that energy so thoroughly distributed among various degrees of freedom would concentrate sufficiently at one bond between collisions (i.e., in about one vibration period in the liquid state) to cause rupture at that bond. Thus, the relative probability either of deactivation or of decomposition by rearrangement would be increased.

For complete understanding of the effects of any radiation on a substance, it would be desirable in the first instance to know what ions are produced by that radiation. Data are in general lacking. There is some information which can be obtained from low-voltage mass-spectroscopic data. It is improper of course to apply such data without reservation or modification in considerations of the effect of high-voltage electrons on liquids, but hints are thereby obtained and in such a way the data are qualitatively instructive.

For example, benzene has been bombarded with electrons at 72 v. in the mass spectrograph and ion abundance ratios have been obtained. Hustrulid, Kusch, and Tate (10) report that, on the scale $C_6H_6^+ = 100$, only seven other species have abundances exceeding 4.0. They are

$C_6H_5^+$	15.2	$C_4H_3^+$	15.7
$C_6H_4^+$	4.6	$C_4H_2^+$	13.3
$C_6H_2^+$	4.0	$C_3H_3^+$	6.6
$C_4H_4^+$	13.5		

An easy hypothesis on the basis of which to account for the low decomposition yield in benzene is that neither the species $C_6H_6^+$, on discharge, nor the simply excited benzene molecules (which might be expected to make the ordinary "photochemical" contribution) lead to decomposition. On the basis of the ideas suggested in this and the previous section, this hypothesis does not appear too strange.

An alternative suggestion which has been offered for the stability of aromatic hydrocarbons is rather special. It finds the explanation in the behavior of the primary products after decomposition of excited $C_6H_6^*$. The suggestion is that the hydrogen atom initially produced reacts with an *adjacent* C_6H_6 molecule to give C_6H_7 , and that that radical back-reacts with the parent C_6H_6 to form two C_6H_6 molecules. A difficulty with this interpretation is that work of Bonhoeffer and Harteck (1) indicates that atomic hydrogen reacts with benzene vapor (not liquid) to split the ring with formation of methane, ethylene, and acetylene—all of which, incidentally, were found in the studies summarized in table 2. However, the early work of Schoepfle and Fellows on mixtures of benzene and cyclohexane indicates a decrease in gas yield best explained in terms of free-atom acceptance by the benzene. More work is clearly required.^{7a}

Another factor which can decrease reactivity (under irradiation) in the way discussed in this section is molecular size. If there is a tendency for spreading of the excitation energy, then the larger the molecule the more nearly will the ionic configuration and molecular configuration correspond. In such a case insufficient energy will be localized at a bond for rupture in that locale and the time required for such localization to occur may, in general, be so large that the decomposition takes place preferentially *via* an ultimate molecule (i.e., rearrangement) mechanism.

The data of Sheppard and Whitehead (15) on the decomposition of fatty acids by radon alphas and high-voltage deuterons have already been cited (2) as illustrative of this principle. The facts are that hydrogen, carbon dioxide, carbon monoxide, and methane are all produced in approximately equal amount in the decomposition of acetic acid but that, when palmitic acid is reached, only the first two are among the major gaseous products and the liquid product is principally pentadecane.

Off-hand, without a principle such as that here offered, one would expect a wider diversity of products with increase of molecular size, particularly if a free-radical mechanism is assumed for the decomposition. The difficulty is well appreciated by Honig (7), who assumes the free-radical mechanism.⁸ He points out that, on his assumption, for every 100 C—H bonds broken, about 45 C—COOH bonds are ruptured, while probably no more than 5 C—C bonds are broken elsewhere in the chain. Honig suggests an explanation of the ratios

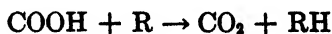
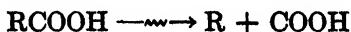
^{7a} *Note added in proof:* Dr. A. O. Allen (private communication, February 24, 1947) calls attention to old work of Linder and Davis (1931) and of Mund (1935), in which substantial decomposition of benzene vapor is reported. Although this result is consonant with the notion that collisional deactivation is an important factor in the non-reactivity of liquid benzene, it does not eliminate the other explanation based on the special cage effect, i.e., that an adjacent C_6H_7 back-reacts with a parent C_6H_6 within a period of about one vibration.

⁸ The data of figure 2 are no proof of an exclusively free-radical mechanism. Increased yield of hydrogen with more hydrogen in the molecule can equally well occur *via* an ultimate-molecule mechanism. However, the important point is the manner of production of pentadecane itself. Even if hydrogen were produced *via* free atoms, the pentadecane could still be formed exclusively *via* rearrangement.

based on relative bond strengths; he concludes that the C—COOH bond is the weakest C—C bond.

Evidently, any straightforward free-radical-mechanism interpretation of the data in the way described leads to a complication resident in the fact that the C—H bonds are certainly stronger than any of the C—C bonds. There is also, however, the difficulty that the excitation energy is far more than sufficient to break any of the bonds in the molecule. If it is spread out over the molecule, then the weakest bonds (i.e., the C—C bonds) should be preferentially broken and the C—H bonds should be barely affected.

The free-radical mechanism attempts to account for the pentadecane by the successive reactions:



If this is the mechanism, some explanation is required. In Section II it is mentioned that the chances are approximately equally good for ionization in the primary act of any one of a large number of electrons in the molecule. If the locus of excitation corresponds precisely to the point of initial ionization, it seems most probable that there should be a wide diversity of products. However, we have no information on the behavior of the ion. It may very well be that, following the ionization step, the charge of the ion (i.e., the missing orbital) will shift to a preferred position; e.g., in palmitic acid the COOH end of the molecule. Thereafter, the break (if rupture is assumed to be the most reasonable process) can occur preferentially in that region.

There is one difficulty with this explanation other than the question of why hydrogen is among the products at all. It is in the question: why should the ultimate ionization tend to be more localized in a large molecule like palmitic acid than in a small one like acetic acid?

For the time being, an explanation of the results on fatty acids based strictly on the matter of molecular size does not appear too unreasonable; but much more quantitative information on a diversity of compounds is necessary before this principle can be considered established.

IV. SUMMARY

All the processes which occur in photochemical reactions of organic compounds occur also in radiation-chemical processes. In addition, there are reactions resultant from the peculiar sequence characteristic of radiation chemistry: i.e., ionization, discharge, and decomposition. In general, any electron in the molecule is equally susceptible to ionization in the initial act; this fact must be constantly recalled in any interpretation of radiation-chemical mechanisms.

Since, in general, the excitation energy lies in any part of the molecule, the yield of a particular product is closely related to the number of parent groups in the molecule. Gas production, particularly in unsaturated compounds, is an inadequate criterion of the resistance of a compound to high-energy radiation.

In the liquid state, the excessive excitation energy tends to minimize the Franck-Rabinowitch effect (i.e., decrease in yield due to collisional deactivation and cage effect). Factors which increase resistance of organic compounds to radiation (and ratio of ultimate molecules to free-radical processes) are molecular complexity, resonance in the molecule, and all properties of the molecule which tend to increase the correspondence between ionic and molecular configurations. Among the latter are molecular symmetry (cf. benzene) and molecular size (cf. palmitic acid). Apparently, increase of molecular size tends to channel the decomposition along a particular path rather than to diversify the products.

REFERENCES

- (1) BONHOEFFER, K. F., AND HARTECK, P.: Z. physik. Chem. **139** (Haber Band), 64 (1928).
- (2) BURTON, M.: J. Phys. Colloid Chem. **51**, 611 (1947).
- (3) BURTON, M., AND ROLLEFSON, G. K.: J. Chem. Phys. **6**, 416 (1938).
- (4) EYRING, H., HIRSCHFELDER, J. C., AND TAYLOR, H. S.: J. Chem. Phys. **4**, 479, 570 (1936).
- (5) FRANCK, J., AND RABINOWITCH, E.: Trans. Faraday Soc. **30**, 120 (1934).
- (6) GARRISON, W. M., AND BURTON, M.: J. Chem. Phys. **10**, 730 (1942).
- (7) HONIG, R. E.: Science **104**, 27 (1946).
- (8) HONIG, R. E., AND SHEPPARD C. W.: J. Phys. Chem. **50**, 119 (1946).
- (9) HIPPLE, J. A., FOX, R. E., AND CONDON, E. U.: Phys. Rev. **69**, 347 (1946).
- (10) HUSTRULID, A., KUSCH, P., AND TATE, J. T.: Phys. Rev. **54**, 1037 (1938).
- (11) NORRISH, R. G. W.: Trans. Faraday Soc. **33**, 1521 (1937).
- (12) ROLLEFSON, G. K., AND BURTON, M.: *Photochemistry and the Mechanism of Chemical Reactions*, p. 357. Prentice-Hall, Inc., New York (1939).
- (13) SCHOEFFLE, C. S., AND FELLOWS, C. H.: Ind. Eng. Chem. **23**, 1396 (1931).
- (14) SHEPPARD, C. W., AND HONIG, R. E.: J. Phys. Chem. **50**, 144 (1946).
- (15) SHEPPARD, C. W., AND WHITEHEAD, W. L.: Bull. Am. Assoc. Petroleum Geol. **30**, 32 (1946).

PHASE BOUNDARIES IN CONCENTRATED SYSTEMS OF
SODIUM OLEATE AND WATER^{1, 2}

ROBERT D. VOLD

*Department of Chemistry, University of Southern California, Los Angeles 7, California**Received December 3, 1946*

Despite extensive investigation (15), knowledge of the behavior of concentrated systems of soap and water is still incomplete. There are three important aspects to the problem. First is the search for phase changes with the object of establishing their occurrence as unambiguously as possible. Second is the ques-

¹Presented before the Division of Colloid Chemistry at the 110th Meeting of the American Chemical Society, Chicago, Illinois, September, 1946.

²Most of the experimental work on which this paper is based was carried out at Stanford University in 1940-41.

tion of the mode of combination of water with soap, whether as stoichiometric hydrates, adsorption complexes, solid solutions, or simply enmeshed in capillary spaces in the soap curd. Finally, there is much interest in the nature of the changes in crystalline or micellar structure occurring at the various transitions.

This paper presents the results of an application of the differential calorimetric method (27) to the determination of phase changes occurring between 150°C. and room temperature in aqueous sodium oleate systems containing more than 60 per cent soap. The data show clearly the existence of several new transitions below 100°C., and supplement the phase diagram (26) proposed in 1939 on the basis of visual observations, dilatometric studies, microscopic investigation, phase separation, and vapor-pressure determinations.³ Additional data have been obtained by vapor-pressure measurements (16), by a freezing-point method (18), by calorimetry (27), and by x-ray diffraction (6, 11), which help to elucidate the very complicated behavior shown by this system. An attempt is made in the present work to correlate the results of all these different investigations.

Sodium oleate was chosen for this detailed study of concentrated aqueous systems, since in this case many of the interesting mesomorphic phases occur at temperatures below 100°C., where they can be investigated conveniently by several different methods. Moreover, sodium oleate is the most important single constituent of commercial soaps, the phase diagram (19) of which resembles that of sodium oleate and water in many respects.

EXPERIMENTAL METHOD AND RESULTS

Materials

The sodium oleate used in this investigation was prepared from oleic acid by neutralization in ethyl alcohol solution with a solution of sodium ethoxide, followed by removal of solvent by evaporation under reduced pressure at 40–60°C. Before use the soap was dried to constant weight by intermittent heating and stirring at 105°C., and thereafter kept in a dark, corked bottle in a desiccator with calcium chloride. All of the work on aqueous systems was carried out using a sodium oleate (III) prepared from an oleic acid purified by the Lapworth method, and further purified by Dr. M. J. Vold by fractional crystallization of acid potassium oleate from ethyl alcohol (17). A few runs were also made on an anhydrous sodium oleate (I) from a specially pure sample of oleic acid (3) which was available in small quantity. This acid, prepared by W. Foreman (2), is believed to be at least 99 per cent pure.

Several other commonly used preparations of sodium oleate were also examined in an effort to evaluate the comparability of results reported from different laboratories. These results are shown in tables 1 and 2, each of the transition tem-

*The vapor-pressure results used in the construction of that diagram were not taken from Dr. Lee's work, as might be inferred from a paper which appeared in *Oil & Soap* **20**, 17 (1943). They were obtained by the author, using an apparatus assembled by Dr. J. L. Porter, before Dr. Lee commenced work by this method.

peratures having been determined by several of the techniques in use in this laboratory, including dilatometric (32), calorimetric (27), microscopic (32), and

TABLE 1
Characteristics of "sodium oleates"

PREPARATION NO.	SOURCE OF ACID	EXCESS ACID OR ALKALI	EQUIVALENT WEIGHT OF ACID	IODINE VALUE OF ACID
		<i>equiv. per mole</i>		
I . . .	Foreman-Brown*	0.000	282.3¶	89.86¶
II† . . .	British Drug Houses, Ltd.	0.0045 (alk.)	284.1§	87.1¶
III‡ . . .	British Drug Houses, Ltd.	0.002 (acid)	288.2§	85.8§
IV	Merck and Co.; pur- chased as sodium oleate	0.013 (alk.)	288.7§	85.5§
V . . .	Kahlbaum's "Olein- saure Kahlbaum"	0.000	287.9¶	86.0¶

* This acid was obtained through the kindness of Professors J. W. McBain and J. B. Brown.

† This acid was made by Lapworth's method. This is the preparation used by R. D. Vold for determination of the phase-rule diagram of sodium oleate and water (*J. Phys. Chem.* **43**, 1213 (1939)).

‡ This acid was supposed to have been the same as II but must have suffered some contamination in transit. It was purified by fractional crystallization of acid potassium oleate from ethyl alcohol as suggested by McBain and Stewart (*J. Chem. Soc.* **1927**, 1392).

§ Determined using the acid recovered from the soap after its preparation. The author is indebted to Dr. M. E. L. McBain for determination of the iodine numbers in this paper.

¶ Determined using the original acid before preparing the soap.

TABLE 2
Average values of reversible transition temperatures of anhydrous "sodium oleates"

TRANSITION	I	II	III	IV	V
A (possibly between two crystal forms)	40 ± 4 (2)*	†	40	Absent	40 ± 1 (3)
Curd fiber-subwaxy . .	65 ± 2 (2)	67 ± 2 (2)	65	68	60
Subwaxy-waxy	115 ± 3 (3)	116 ± 7 (2)	117 ± 2 (2)	107	112 ± 3 (3)
Waxy-superwaxy	180 ± 4 (4)	179	182 ± 3 (3)	183 ± 2 (2)	180 ± 6 (3)
Superwaxy-subneat . .	219 ± 3 (2)	204 ± 3 (2)	242 ± 1 (2)	207 ± 5 (2)	202 ± 0 (3)
Subneat-isotropic liquid	246 ± 3 (4)	242 ± 2 (2)	256 ± 1 (3)	250 ± 5 (3)	243 ± 10 (3)

* The number in parentheses gives the number of methods, average values from which were averaged to arrive at the figure given in the table.

† This sample was not studied in this range of temperature.

hot-wire microscopic methods (25). Lack of precision in the reported temperature of a given transition for a given preparation is due to differences between the results of different techniques, rather than to inexactness of the individual

methods, since duplicate runs by the same method agreed within 4°C. in even the least favorable cases. The difficulty appears to be inherent in the possible chemical instability and the difficulty of ultimate purification of oleic acid, since nearly identical transition temperatures have been reported for the saturated soap, sodium palmitate, from different laboratories (7, 31, 32) using independent materials.

All preparations of sodium oleate studied underwent at least six successive thermally reversible transitions, although all transitions were not always indicated by all methods for every sample. Thus, sodium oleate I showed transitions at 40°C. and 65°C., both dilatometrically and calorimetrically, whereas sodium oleate III underwent transition at 40°C. calorimetrically but not dilatometrically, but at 65°C. showed a transition dilatometrically but not calorimetrically. Such discrepancies may be related to the unsuspected presence of very small amounts of residual water in the supposedly anhydrous samples, since differences in the technique of sample preparation and investigational method may then result in the formation of different low-temperature phases. The finding of Ross and McBain (21) that samples I and III commonly exist at room temperature in different polymorphic forms is also suggestive in this matter.

T_i and T_c curves (26) were determined for aqueous systems of sodium oleates II, III, and IV. The boundaries are qualitatively the same for all three samples. The temperatures of formation of isotropic liquid or middle soap from curd fibers are nearly the same in all cases, with differences in the lower boundary of the soapboiler's neat soap field not greater than 5°C. with the different samples. The boundary of the field of isotropic solution of sodium oleate III at higher temperatures is displaced about 7 per cent in composition toward the water side of the diagram from that of the previously published curve for sodium oleate II (26) and is about 10–15°C. higher in temperature, while that for sodium oleate IV falls between the other two.

Interpretation of differential calorimetric data

This method is based on measurement of the temperature difference between two similar cells, one containing the sample and the other a thermally inert material, as both are uniformly heated at a slow rate. Its application to anhydrous soaps in the present apparatus has already been described (27), and its use further illustrated by application to a series of anhydrous alkali metal palmitates (34) and to low-moisture systems of sodium stearate (28). With pure anhydrous soaps transitions must occur sharply at a single temperature, causing a sharp peak in the curve of differential temperature *vs.* time. Changes of slope in this curve have no phase significance unless the rate of transition is slow relative to the rate of rise of temperature, or on occurrence of a transition of the second kind (28). Application of this method to aqueous systems is considerably more complicated, since here changes of slope in the differential temperature curve are generally of phase significance. This necessitates a very smooth base line

in the absence of transitions which is difficult to achieve, since meaningless changes in slope may be caused by any of a number of instrumental factors (27).

In the anhydrous system the temperature at the top of a peak where the curve starts to drop has no significance, being merely the adventitious point at which the rate of heat input to the sample exceeds the rate of heat absorption due to occurrence of a transition. In the binary system, however, this temperature may be adventitious or may be due to a phase change. Decision between these alternatives may be based on one of several possible considerations. If a given change of slope occurs at about the same temperature independent of rate of heating in duplicate experiments, it is presumably due to a phase change in the sample rather than to a thermal lag or an instrumental vagary. Study of the shape of the curve is sometimes helpful, since the drop in differential temperature is usually much more rapid if merely part of a peak in the curve than if due to a change in slope caused by phase changes in the sample. Least certainly, if the temperature of a given change of slope varies in a regular manner as the composition of the sample is changed, it may be presumed that the change of slope is due to a phase change.

Transformations occurring over a range of temperature will give rise to changes of slope instead of peaks in the differential temperature curve, unless the temperature interval is small. Passage of a sample through a two-phase region with increasing temperature would be expected to cause an increase in the differential temperature on entering the two-phase region and a drop in differential temperature on passing from the two-phase region into a one-phase region. The temperature at the phase boundary is that of the point at which the slope first changes rather than that at which the base-line differential temperature is reestablished, since the latter temperature depends on size of sample, rate of heat transfer, etc. A decrease in slope usually signifies entrance into a one-phase region. However, if one of the phase boundaries of a two-phase region should have a sharp change of slope, it may give rise to a negative change in slope of the differential temperature curve even though the system remains a mixture of two phases.

The application of this method to the study of clay samples in open cells has recently been comprehensively discussed (22). Although there are many analogies between that and the present work, there are also important differences. The soap samples were studied in closed cells under their own partial pressures in order to prevent gross changes in composition. Even so, it is currently impossible to predict the effect any given relative humidity might have on the decomposition of any possible hydrates present in the system despite the possibility of making a rough estimate of the vapor pressure in the cells (16, 29, 33). In the mineralogical work a heating rate of 12°C. per minute was commonly employed, with the result that reported temperatures for the same transition sometimes differ by 50–75°C. In the present work the use of much slower rates of heating insured the correctness of the transition temperatures found. This was established by showing that the same temperature was obtained at heating

ates of both 1.5°C. and 1°C. per minute, even though the peaks were smaller and flatter in the latter case.

The differential thermal curves not only give the temperatures of transitions in the sample but may also help to establish the nature of the changes taking place. A transition involving absorption of a finite quantity of heat at a definite temperature will give rise to a peak in the differential thermal curve, which then can be taken as evidence for the complete disappearance of some phase at that temperature. In a binary system this generally occurs only at eutectic, eutectoid, or peritectoid temperatures, or at the decomposition temperature of a stoichiometric hydrate, although loss of a large amount of adsorbed water over a narrow temperature range would give a peak simulating that due to decomposition of a hydrate. According to the phase rule such peaks must occur at constant temperature independent of gross composition, their areas being proportional to the amount of phase transformation taking place.

In the case of soap systems there is yet one other rather special mechanism which can be advanced to account for the occurrence of a transition at constant temperature in the binary system independent of composition. It is entirely possible that soap crystals may undergo lattice transformations, such as a sharp onset of molecular rotation or a slight change in the packing of the hydrocarbon chains, which would cause a heat effect at temperatures independent of the amount of bound water. This possibility receives support from several x-ray investigations (11, 23) which agree in showing no change in side spacings with water content over a wide range of composition. There may, of course, be simultaneous loss or gain of some bound water at the temperature of the lattice transition due to change in the adsorptive power or capillary porosity of the crystal, the heat effect of which would be superposed on that due to the lattice transition itself.

Experimental procedure and results

The procedure followed in the present work was similar to that already described (27). Systems were prepared by weighing the requisite amounts of dry soap and water into a tube which was then sealed and heated until the contents were completely isotropic. The homogeneous cake formed on cooling was placed on a spot plate, cut into pieces, and these poked through the semicapillary neck of the calorimeter cell as quickly as possible (10 min. to 1 hr.) to minimize changes in composition. The cell was then sealed in two steps, it being allowed to cool after the first constriction of the capillary, thus avoiding any heating of the system which would result in changes in composition along the cell and might also explode it.

The cells were then allowed to stand for about 15 min. at a sufficiently high temperature to insure at least partial fusion and coalescence, so that a coherent cake would be formed in good thermal contact with the glass of the cell. Complete melting was impossible, since the rather fragile calorimeter cells exploded at high temperatures. After having been so heated at temperatures given in table 3, the cells were cooled to room temperature in the calorimeter (from 220°C. to 30°C. in about an hour). The times at room temperature before calorimetric

study were also recorded, since specification of both rate of cooling and aging period may well be necessary to permit subsequent identification of what phase or mixture of phases is likely to have been present initially in each case (28).

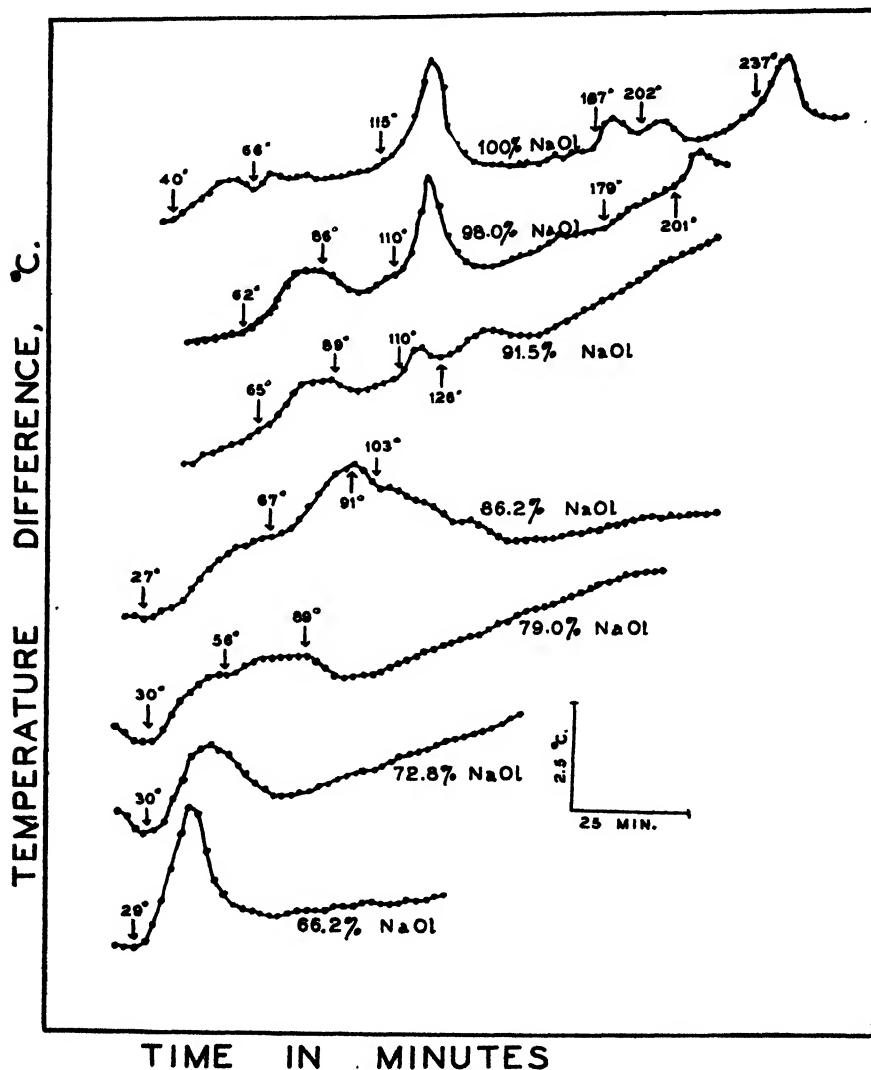


FIG. 1. Characteristic differential calorimetric curves for systems of sodium oleate and water.

Most runs were made at a heating rate of 1.5°C. per minute, as used in calibration of the calorimeter. However, several were carried out at 1°C. per minute, in order to check the reproducibility of the temperatures of peaks in the curve and particularly to assist in establishing the validity of the temperatures at which changes of slope occur. A few runs were also made on samples which had not

TABLE 3
Temperatures of changes in the differential heating curves of sodium oleate-water systems

COMPOSITION: WEIGHT PER CENT SODIUM OLEATE	TEMPERATURE AT END OF RUN	T_c	SHARP INCREASE IN SLOPE	LARGE BROAD PEAK BEGIN- NING AT	SLOPE DROPS STEELY	SHARP HIGH PEAK	OTHER PEAKS	OTHER SLOPE CHANGES	TEMPERATURE AT WHICH CELLS EQUILIBRATED	TIME AT ROOM TEMPERATURE BEFORE RUN BEGAN
Runs at 1.5°C. per minute										
100.00	°C.	°C.	°C.	°C.	°C.	°C.	°C.	°C.	°C.	hours
99.1 ^f	212	— ^a	39 ^a	186, 224	95 (small)	110	202			72
99.1	136	—	37(?)	64	—	106			212	66
98.6	268	—	—	64	—	110		179, 240	270	28
98.6	221	—	—	66	—	106	199		260	18
98.0	220	—	—	65	—	109	202		226	72
96.9	221	—	—	62	86	110	201	155, 179	230	20
		—	—	64	87	114	—	175, 190(?)		
95.7	220	—	—	63	85	112	—	165, 188		20
95.3	220	—	—	67	84	110	—	140, 156, 165, 180, 186	210	3.5
93.9	220	—	—	69	88	112	—	56, 145	230	12
92.2	222	—	—	64	89	111	139 ^d	193	225	14
91.5	221	—	—	65	89	110	—	126, 143	225	71
91.1	219	?	31(?)	67	90	115		137, 127(?), 204	218	5
89.8	221	131	35(?)	67	91	112	125	—	225	64
89.2	218	129	34(?)	70	90	108	126	—	225	44
87.7	205	123	27	62(?)	89	109 ^e		189	225	27
86.2	218	117	27	67	91	—		101, 113, 126	233	24
83.7	219	108	34	70	90	—		—	222	27
81.4	220	99	32	61	87	—		156 ^b , 177 ^b	222	93
79.0	200	90	30	56	89	—		—	221	47
76.5	218	75	30	—	75	—		110 ^b , 159 ^b , 186 ^b	210	21
73.7	158	60	27	—	—	—		87 ^b	163	16

Runs at 1°C. per minute											
72.8	153	55	30	—	—	—	—	—	141	160	21
71.2	150	50	27	—	—	—	—	—	—	160	21
68.9	134	45	27	—	—	—	—	—	—	155	24
66.2	131	41	29	—	—	—	—	—	—	130	48
61.4	110	36	28	—	—	—	—	—	—	115	19
54.6	115	34	28	—	—	—	—	—	76 ^b	115	18
43.5	117	34	29	—	—	—	—	—	80 ^b , 94 ^b	120	4
34.6	80	32	28	—	—	—	—	—	—	98	72
27.3	102	31	28	—	—	—	—	—	—	105	40
Runs at 1°C. per minute											
96.9	73	—	—	58	—	—	—	—	145, 171, 179	210	3.5
95.3	220	—	—	62	—	—	—	—	—	218	18
91.1	219	26(?)	28	63	26(?)	—	127	—	—	233	16
86.2	169	28	28	66	28	—	—	—	105, 121	222	2
81.4	206	33	33	68	33	—	118(?)	—	117 ^b , 150 ^b , 169 ^b , 183 ^b	210	2
76.5	205	29	29	60	29	74	—	—	—	—	48

^a This is the temperature of a peak with the anhydrous soap.

^b Changes so small as to be of questionable validity.

^c — means studied and absent.

^d Might be slope changes at 134, 145.

^e Might be slope changes at 109, 118.

^f This sample not preheated; prepared by dehydration of soapboiler's neat soap at 56°C.

been preheated in the calorimeter cells. In all runs the systems were studied in closed cells under their own aqueous vapor pressure.

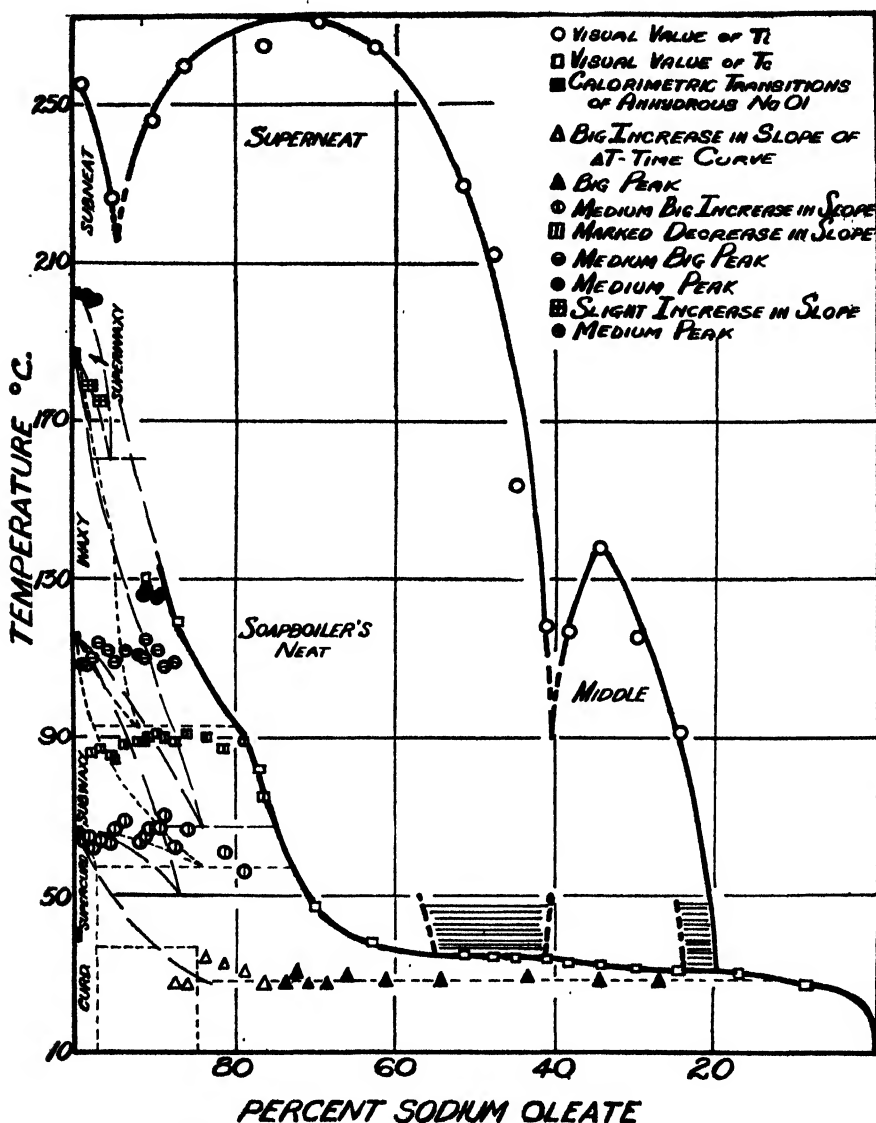


FIG. 2. Phase diagram of the system sodium oleate-water. T_i and T_c curves from Vold (J. Phys. Chem. **43**, 1213 (1939)). Broken lines indicate less certain boundaries from the same reference. Dashed curves from McBain and Lee (Oil & Soap **20**, 17 (1943)).

The data obtained are summarized in tables 3 and 4 and presented graphically in figures 1 and 2. Figure 1 presents typical curves of differential temperature *vs.* time, showing the various peaks and changes of slope which determine the

transition temperatures. Even on this small-scale reproduction the validity of the marked points of changes of slope can be easily demonstrated by laying a straight edge along the curve. This figure also shows clearly the qualitative and sometimes abrupt differences in thermal behavior which result from certain changes in the composition of the system. The numerical data for all samples studied, taken from curves such as these, are assembled in table 3.

Table 4 gives values for the heat of transition at temperatures where peaks occurred in the heating curves, calculated by equation 1 of reference 27. It is evident from the erratic fluctuation that the technique with aqueous systems in the present calorimeter is inadequate to give precision values of transformation energy. However, these results do give an approximate measure of the heat of transition which can be correlated with various possible mechanisms, and they also show qualitatively but very clearly how the energy effect at a transition varies with the water content of the system.

Figure 2 shows the results of the present investigation superposed on the previously accepted phase diagram for the system sodium oleate-water. It is obvious that important revisions are necessary, even though the present data do not suffice to permit construction of a new diagram.

DISCUSSION

The present data are of interest and will be discussed in terms of the possible existence of critical compositions at which other methods have indicated marked changes in the properties of similar systems (10, 11, 18, 30), the problem of whether the various water-containing phases are mixtures of stoichiometric hydrates or contain the water in a solid-solution phase, essentially free in capillary spaces or adsorbed on the surface of the crystallites (5, 9, 12, 16, 18, 28, 29), their relation to previously suggested phase diagrams for the system (16, 26), and conflicting views derived from x-ray investigation as to what crystalline phases may be present (5, 6, 9, 10, 11, 21). The implications of the various transitions detected thermally, shown graphically in figure 2, will be considered successively in order of ascending temperature.

Transition at 28°C.

This transition, resulting in a peak in the differential temperature curve, was found to occur at about 28°C. independent of composition over the range from 74 per cent to 27 per cent sodium oleate. This leads to the presumption that it marks either a peritectoid or eutectoid point or the decomposition temperature of some hydrate. Although the values of the heat of transition as a function of composition are very irregular (*cf.* table 4), they appear to pass through a maximum at about 71 per cent soap, which composition therefore should be that of either the peritectoid or a hydrate. It may possibly be of interest in this connection that a hydrate such as $\text{NaOl} \cdot 6\text{H}_2\text{O}$ would correspond to 73.8 weight per cent sodium oleate.

The behavior undergoes a qualitative change between 73.7 and 76.5 per cent soap, the more concentrated systems showing only a sharp increase in slope of

the differential temperature curve rather than an actual peak. This indicates that whatever change begins at 28°C. occurs at the higher soap concentrations over a range of temperature, although it seems anomalous that the initial temperature of such a transformation should be so nearly independent of composition. Between 87 and 91 per cent sodium oleate there is again a qualitative change in behavior, the more concentrated systems undergoing no thermally evident change until higher temperatures. Strangely, there is no indication in

TABLE 4
Approximate heats of transition

COMPOSITION: WEIGHT PER CENT SODIUM OLEATE	TEMPERATURE	ΔH	TEMPERATURE	ΔH
	°C.	<i>cal. per mole</i>	°C.	<i>cal. per mole</i>
99.1	110	2830		
98.6	106	3320	199	1540
98.6	109	3060	202	1270
98.0	110	2910	201	1090
96.9	114	2410		
95.7	112	2160		
95.3	110	2510		
93.9	112	1310		
92.2	111	1190	139 (doubtful)	412
91.5	110	880		
91.1	115	861		
89.8	112	720	125	983
89.2	108	719	126	663
87.7	109 (doubtful)	518		
86.2	Gone			
73.7	27	3920*		
72.8	30	2540*		
71.2	27	6350		
68.9	27	3670		
66.2	29	4140		
61.4	28	4350		
54.6	28	4080		
43.5	29	2080		
34.6	28	2030		
27.3	28	2680		

* Doubtful whether this is a peak rather than merely two changes in slope.

the aqueous system of the transition found at 40°C. with the anhydrous soap, although this may be related to the existence of more than one room-temperature form of the anhydrous soap (21).

There is a considerable body of confirmatory evidence supporting the existence of a qualitative change in the nature of the system at about 74 per cent sodium oleate. A 79 per cent sample on being pushed through the constriction in the calorimeter cell during filling coalesced and flowed readily but after extrusion

was found to be crumbly and non-adherent. Samples containing 73.7, 72.8, and 68.9 per cent soap flowed similarly, but the extruded material was sticky and moistly homogeneous. Moreover, changes in the degree of binding of water by sodium oleate at different compositions have been reported on the basis of freezing-point determinations (18), the water appearing to be chemically combined between 100 and 94.5 per cent soap, firmly bound between 94.5 and 85 per cent, loosely bound from 85 to 40 per cent, and essentially free at less than 40 per cent sodium oleate. The existence of such compositions is suggestive in the present consideration, despite the difference in temperature between the two sets of data. Finally, x-ray data (10) on commercial soaps, which customarily include a large proportion of sodium oleate, show that agitated soap (synonymous with converter soap of reference 30) of 18.5 per cent water is in the hydrous β -phase at room temperature, while at 15.8 per cent water it is in the ω -form. This difference may be caused by a reversal in the inherent stability of the two phases at room temperature occurring at about this composition, although alternatively it may result merely from a difference in the temperature of mechanical working of the two samples, since this has been shown to have a profound influence on the phases subsequently obtained on cooling to room temperature (1, 20).

It is obvious that the present data are not in agreement with the less certain phase boundaries shown as dotted lines in the earlier diagrams of either Vold (26) or McBain and Lee (16). Consideration of the vapor-pressure curves presented by the latter authors yields little persuasive evidence for the hydrates postulated by them, $\text{NaOl} \cdot 3\text{H}_2\text{O}$ and $\text{NaOl} \cdot 0.43\text{H}_2\text{O}$, with decomposition temperatures respectively of 28°C. and 36°C. The calorimetric evidence is in agreement with the existence of a transition at 28°C. but does not confirm the abrupt change in decomposition temperature from 28°C. to 36°C. at 85 per cent sodium oleate required by the McBain diagram.

No indication is found for the extension to concentrated systems of the eutectoid flats corresponding to simultaneous presence of middle soap-isotropic solution-curd or middle soap-soapboiler's neat soap-curd. It might possibly be thought that the calorimetric transition at 28°C. corresponded to the first of these eutectoids but for the fact that above this temperature all systems had a white waxy appearance entirely unlike that of aqueous middle soap. Moreover, the heat of transition passes through a maximum and then decreases as water content is increased, rather than increasing continuously as would be required if it were due to conversion of isotropic liquid to middle soap. It is also of likely significance that commercial soaps failed to show two changes of slope in their yield value-temperature curves corresponding to these transitions (30). Hence we are inclined to believe that many solid soaps are made up solely of crystalline phases with no free liquid except for that loosely bound in capillaries.

It is also worthwhile wherever possible to compare the present results with the phase picture which has been developed from x-ray work (5, 9, 11). This comparison is made difficult first by the numerous inconsistencies in the published x-ray data and secondly by a slight ambiguity with respect to the initial phase

state of the soap in the present experiments. Samples in the present study were prepared by relatively slow cooling from waxy, soapboiler's neat, or middle soap phases, depending on the composition, whereas much of the x-ray work has been done on samples subjected to intense mechanical agitation at some temperature preceding cooling.

It seems likely that the present samples should be regarded as "unworked," despite the fact that some powdering and compaction occurred on forcing the cake material through the capillary neck of the cell on filling, so that often it flowed through the constriction as a plug of very viscous, white, thixotropic "wax" which apparently set to a harder mass on standing. In all cases, however, the samples were heated sufficiently to form one of the higher-temperature phases prior to the calorimetric run, and then allowed to cool undisturbed. Nevertheless, it is not established whether short periods at such temperatures are sufficient to obliterate completely all effects due to previous processing (14). It consequently becomes of importance to consider the possible effect of an initial mixture of phases on the calorimetric behavior, since to the extent that the filling process constitutes mechanical working or extrusion certain phase changes might be induced which otherwise would not occur (1, 11).

It is possible that in many cases there may be little difference between phase boundaries or transition temperatures due to the presence of different initial crystalline states of a given soap system. Thus, Ferguson reports (9, 11) that ω - and hydrous β -phases of commercial soap melt to soapboiler's neat soap at the same temperature within 2° or 3°C., and that T_c is respectively 65°C. and 61°C. for hydrous β - and δ -phases of a 10 per cent sodium palmitate system. Likewise, λ - and γ -phases of nearly anhydrous sodium stearate transform to super-curd at substantially the same temperature (28).

Further evidence that such differences in phase state need not necessarily affect the transitional behavior is found in the fact that a 99.1 per cent sodium oleate sample prepared by dehydration of soapboiler's neat soap at 56°C. by equilibration with sulfuric acid, and run directly without preliminary melting or heating in the calorimeter cell, gave exactly the same results on successive runs after the sample had been cooled from 212°C. Similarly, in rheological experiments on commercial soaps (30) in many cases the same transition temperatures were found, despite varying thermal and mechanical treatment which would be expected to result in different initial phases in the soap.

Interpretation of the present data in terms of published crystalline soap phases is quite uncertain because of the paucity of data dealing directly with sodium oleate and the impossibility of reasoning by analogy from other soaps as to what crystalline form may be present under a given set of conditions. Many papers have given fragmentary evidence for particular samples (6, 9, 11), but unfortunately sufficient actual data are not presented to permit evaluation of the validity of the various generalizations attempted. Some of the contradictions between different investigators may be due to incorrect designation of phases due to the practice (9, 10, 11, 20) of basing such identification on the presence or absence of one or two supposedly characteristic diffraction rings in the x-ray

pattern. The ambiguity of this method, based on the A.S.T.M. Card Index (13), has been pointed out by Buerger (4, 6) in the case of complicated crystals like the soaps. Another factor which has received inadequate attention in the x-ray work is proper control of relative humidity, since which of several phases may exist may depend predominantly on this variable.

Neither the postulated hydrates of McBain and Lee (16) nor the homogeneous tongue-like phases of Vold (26) are in accord with the present data. Likewise it is clear that no homogeneous phase of continuously variable composition can be temperature-stable between 25° and 35°C., since from 92 per cent to 27 per cent soap a marked transition occurs at 28°C. This result is also difficult to reconcile with the conception that the crystalline soap phase is a solid solution of water in soap existing as a homogeneous phase over a considerable range of composition (9).

Buerger, Smith, Gardiner, *et al.* (6, 12) report the existence of only two phases, η and η' , below T_c in worked systems of aqueous sodium oleate. These are variously reported as the hemihydrate and one-quarter hydrate, or the one-quarter hydrate and the anhydrous soap. Dehydration curves indicate transition from one to the other at 50–60°C. with loss of about 0.25 mole of water per mole of soap. It is also stated that at room temperature the soap is customarily present as η when the system contains more than 6 per cent water and as η' at lower water contents.

The calorimetric data show that this picture is oversimplified, since there are many more transitions than would be possible according to the above scheme. Moreover, it has been shown recently (21) that anhydrous sodium oleate can exist at room temperature in two very different crystalline forms,⁴ with extensive literature references suggesting the possibility of several different polymorphs. The conclusion (6, 12) that a change occurs in the phase state of aqueous systems of sodium oleate at room temperature at 6 per cent water is in interesting agreement with the earlier dilatometric work (18) showing a difference in degree of binding of water at 94.5 per cent sodium oleate. However, the phase picture deduced from this x-ray work (6) makes no provision for the transition found calorimetrically at 28°C., nor for the changes in the nature of the system occurring at about 75 per cent and 91 per cent sodium oleate.

Transition at 66°C.

This change manifests itself by a large, broad peak in the differential temperature-time curves, beginning at a nearly constant temperature of 63–67°C., from 100 per cent to 83.7 per cent soap, the same effect occurring at 61° and 56°C., respectively, in 81.4 and 79.0 per cent systems, but being completely absent when more water is present. The magnitude of the effect decreases continuously with increasing water content, indicating either decreasing heat of transition or a

⁴Recent x-ray studies in this laboratory by Miss Montgomery suggest the possibility that the pattern attributed to form 1 by Ross and McBain may be simply derived from that of form 2 by elimination of impurities.

smaller amount of material undergoing transformation. There might be some question as to whether the values obtained are equilibrium values, in view of the complexity of the phase picture at lower temperatures and the possibility of transformation of a metastable to a stable phase anywhere over a range of temperature, particularly since undercooling prevented examination by cooling curves. However, the reality of the effect and the presumptive validity of the transition temperatures are established, since similar results were obtained in a series of duplicate runs carried out at a different rate of heating (cf. table 3).

The appearance of the differential temperature curve suggests that heat is not absorbed sharply but over a range of temperature, as would be expected on passage through a two-phase region. The temperature difference between the cells does not increase as rapidly as is usual for a "melting" transition, and is maintained over a much longer time than would be expected had the transition occurred completely at 66°C. Nevertheless, the apparent constancy of the transition temperature in this binary system suggests that the change should be of the same nature as that occurring at 28°C., although the accuracy of the data is not sufficient to preclude entirely the possibility of drawing a boundary with a slight dependence of transition temperature on composition.

The existence of this transition, unless it is due to something other than a conventional phase change, makes impossible the position of the homogeneous tongue-like field of subwaxy soap tentatively sketched by Vold (26) from microscopic observations and somewhat differently by McBain and Lee (16) from vapor-pressure measurements. It is likewise in disagreement with the requirements of the theory developed by Gardiner *et al.* (6, 12), who postulate the existence of a hydrate at lower temperatures containing 98.5 per cent or 97.1 per cent sodium oleate, which decomposes on slow heating at a controlled but unspecified pressure at about 50–60°C. On this view systems containing more than 97 per cent sodium oleate should be mixtures of the hydrate and some less hydrous solid phase below 60°C., while those containing more water should be mixtures of the hydrate and soapboiler's neat soap. But this, although it would account for the constancy of transition temperature, requires that as water content increases the heat of transition should pass through a maximum at the composition of the hydrate, whereas actually the heat effect decreases continuously with the increasing water content. This apparent disagreement with earlier work can be lessened only by assuming that the heat effect is due to some other phenomenon than phase change, although it seems strange that no thermal effects were found corresponding to boundaries previously suggested.

One possible explanation is to attribute the thermal effect at 66°C. to some change in crystal structure with no necessary resultant change in hydration and not necessarily involving a phase change of the first kind. Since the heat effect at 66°C. in the anhydrous soap is only 320 cal. per mole, contrasted with 5180 cal. per mole for the curd-subwaxy transition of sodium stearate, it may not correspond to the same transition, as was previously assumed (27). Occurrence of this transition over a range of temperature but commencing at substantially constant temperature might be explained by assuming a second-order phase

change due to a gradual change in crystal structure similar to that at Thiessen's genotypic point (24), which involves only rotation of the chains. The correspondence between the heat of transition of the anhydrous sodium oleate at 66°C. and $\frac{1}{2}RT$ for a rigid rotator is suggestive in this regard. If the water in the system is primarily associated with the molecular heads, it might have but little effect on such a rotational transition temperature, the decrease in heat effect with increasing water content being attributable to the presence in the system of a smaller proportion of the phase capable of undergoing rotational transition. Conner and Smyth (8) have made an interesting although not entirely successful attempt to represent phenomena of this type on a conventional phase diagram.

This whole effect disappears at about 79 per cent sodium oleate, although the region where it occurs at constant temperature ends at 83.7 per cent soap. The approximate agreement in composition with the limiting value for the transition at 28°C. suggests the existence of a perpendicular (hydrate) or nearly perpendicular (solid-solution) phase boundary between these two temperatures at about this composition. More concentrated systems would then contain only "solid" phases, while those more dilute would also contain some soapboiler's neat soap.

Transition at 89°C.

This change appears on the differential temperature curve as a change of slope indicative of a decrease in the temperature difference between sample and reference cell. It occurs at substantially constant temperature (84–91°C.) independent of composition from 98 per cent to 79 per cent sodium oleate, at 75°C. on the T_c curve at 76.5 per cent soap, and is missing at lower concentrations. Since comparable results were obtained in runs made at different rates of heating (*cf.* table 3), the effect must be attributed to a change in the soap rather than to adventitious balance between rate of heat loss by the sample and rate of heat input.

As with the transition at 66°C., so here it is difficult to reconcile this result with previous concepts of the number and nature of the phases of aqueous sodium oleate. If this temperature marks the occurrence or completion of a phase change, it precludes the existence of homogeneous fields of subwaxy and waxy soap between 98 per cent sodium oleate and the boundary of the region of soapboiler's neat soap. The nature of the heating curve suggests a point of completion of a phase change absorbing heat, rather than a phase change occurring sharply at a temperature. Consequently the change cannot be due to a peritectoid or eutectoid or the decomposition of a hydrate. It is most plausibly interpreted as being the temperature of completion of the change which began at 66°C., possibly being the point of complete freedom of rotation of the long soap molecules about their axes. This temperature, in accord with observation, would be expected to be relatively independent of the amount of water present—provided this does not become so great as to result in formation of a phase with a completely different structure—since it is determined primarily by the forces operative between the hydrocarbon chains. The absence of this transition in 99

and 100 per cent systems remains unexplained, unless it is postulated that the presence of water in some way spreads out the transition interval.

Transition at 112°C.

This transition is manifested thermally by a sharp peak in the differential temperature curve of similar aspect to that found with anhydrous sodium oleate at the subwaxy-waxy transition at 115°C. The temperature is substantially constant at about 112°C. independent of composition, the effect being found at all compositions from 99.1 per cent to 87.7 per cent soap. As appears in table 4, the heat of transition rises to a slight maximum at 1.4 per cent water and thereafter decreases continuously as water content increases.

The most likely interpretation of these observations is that this is the temperature of the eutectoid involving waxy, subwaxy, and soapboiler's neat soap of sodium oleate, a conclusion in qualitative accord with previously suggested phase diagrams (16, 26), although placing the temperature considerably higher. Since this transition is not found with an 86.2 per cent system, it is also likely that the field of soapboiler's neat soap extends to a slightly higher soap concentration at this temperature than shown in previous diagrams.

According to this picture, at the transition temperature a mixture of subwaxy soap and soapboiler's neat soap converts into a mixture of subwaxy and waxy phases at water contents lower than the eutectoid composition, and into waxy and soapboiler's neat phases at higher water contents. This interpretation, in accord with the facts, leads to a prediction of large values of the heat of transition at low water contents, falling off very rapidly to the right of the eutectoid composition where the amount of subwaxy soap undergoing transformation decreases, since the heat of transition of anhydrous subwaxy to waxy sodium oleate is large (2890 cal. per mole) (25), and in the case of sodium stearate (28) is made still larger by the presence of 0.75 per cent water in the soap. Since the heat of transition is maximal at 1.4 per cent water, this must be approximately the composition of the eutectoid point. This leads to the interesting and important conclusion that at this temperature the homogeneous solid-solution phase of subwaxy soap cannot incorporate as much as 1.4 per cent water without undergoing transformation to another phase.

Transitions at higher temperatures

As shown in tables 3 and 4, many of the more concentrated systems exhibit a number of transitions at higher temperatures. These transitions are accompanied by a measurable heat effect and appear to be related to those occurring with the anhydrous soap. However, the data are too fragmentary to warrant any detailed discussion.

That such transitions disappear on addition of relatively little water to the system indicates that the boundary of soapboiler's neat or superneat soap runs rather close to the anhydrous axis at elevated temperatures. The small peaks present in the curves of a few samples around 89 per cent sodium oleate at 126°C. may be due to a eutectoid involving waxy, superwaxy, and soapboiler's neat

soap. If this is the case, waxy sodium oleate can incorporate considerable amounts of water into the homogeneous phase, since no indication of this transition is found in systems containing less than 10.8 per cent water. Moreover, this would require the field of homogeneous superwaxy soap to extend as an extremely narrow tongue to a very low eutectoid temperature in the binary system.

SUMMARY

Twenty-nine binary systems of sodium oleate and water were studied in closed cells in a differential calorimeter. From the curves so obtained, values of transition temperatures and heats of transition were deduced. The application of the method of differential calorimetry to binary systems is discussed in detail.

Results obtained indicate the existence of transitions at about 28°, 66°, 89°, and 112°C. in more concentrated sodium oleate systems, which occur at substantially constant temperature independent of composition. The first and last of these appear to be due to phase changes similar to melting of a pure substance, while the middle two seem to mark the beginning and end of some transition occurring over a range of temperature. Changes in the phase nature of the system appear to occur at 74.5 and 89 per cent sodium oleate at 28°C., at 83.5 and 79 per cent at 66°C., at 98 and 79 per cent at 89°C., and at 99 and 87.5 per cent at 112°C.

Possible revisions of previous phase diagrams proposed for this system are discussed. Although the data are inadequate to discriminate between transitions due to peritectoid, eutectoid, or hydrate decomposition, they do not appear to agree with results to be expected from decomposition of any of the stoichiometric hydrates of sodium oleate postulated in the literature. An attempt was also made to relate the various crystalline phases of sodium oleate deduced from x-ray work to the present transitional behavior, with the conclusion that the incompleteness and inconsistency of the published x-ray work prevent any close correlation.

Incidental data are also included showing the transition temperatures of a number of preparations of anhydrous sodium oleate from various standard samples of oleic acid.

REFERENCES

- (1) BODMAN, J. W.: U.S. patent 2,215,539 (September 24, 1940).
- (2) BROWN, J. B.: Chem. Rev. **29**, 33 (1941).
- (3) BROWN, J.B., AND SHINOWARA, G.Y.: J. Am. Chem. Soc. **59**, 6 (1937).
- (4) BUEGER, M.J.: Am. Mineral. **30**, 551 (1945).
- (5) BUEGER, M.J., SMITH, L.B., DE BRETTEVILLE, A., JR., AND RYER, F.V.: Proc. Natl. Acad. Sci. U.S. **28**, 526 (1942).
- (6) BUEGER, M. J., SMITH, L. B., RYER, F. V., AND SPIKE, J. E., JR.: Proc. Natl. Acad. Sci. U. S. **31**, 226 (1945).
- (7) CHESLEY, F.G.: J. Chem. Phys. **8**, 643 (1940).
- (8) CONNER, W.P., AND SMYTH, C.P.: J. Am. Chem. Soc. **63**, 3424 (1941).
- (9) FERGUSON, R.H.: Oil & Soap **21**, 6 (1944).
- (10) FERGUSON, R.H., AND NORDSIECK, H.: Ind. Eng. Chem. **36**, 748 (1944).

- (11) FERGUSON, R.H., ROSEVEAR, F.B., AND STILLMAN, R.C.: *Ind. Eng. Chem.* **35**, 1005 (1943).*
- (12) GARDINER, K.W., BUEGER, M.J., AND SMITH, L.B.: *J. Phys. Chem.* **49**, 417 (1945).
- (13) HANAWALT, J.D., RINN, H.W., AND FREVEL, L.K.: *Ind. Eng. Chem., Anal. Ed.* **10**, 457 (1938).
- (14) LYON, L.L.: Ph. D. Dissertation, University of Southern California, 1944 (available in the Library of the University of Southern California).
- (15) MCBAIN, J.W.: Chap. 5 in Alexander's *Colloid Chemistry*, Vol. I. The Chemical Catalog Co., Inc., New York (1926).
VOLD, R.D.: *Soap* **16**, 31 (1940).
VOLD, R.D., AND VOLD, M.J.: in Alexander's *Colloid Chemistry*, Vol. V. Reinhold Publishing Corporation, New York (1945).
- (16) MCBAIN, J.W., AND LEE, W.W.: *Oil & Soap* **20**, 17 (1943).
- (17) MCBAIN, J.W., AND STEWART, A.: *J. Chem. Soc.* **1927**, 1392.
- (18) MCBAIN, J.W., VOLD, M.J., AND JOHNSTON, S.A.: *J. Am. Chem. Soc.* **63**, 1000 (1941).
- (19) MCBAIN, J.W., VOLD, M.J., AND PORTER, J.L.: *Ind. Eng. Chem.* **33**, 1049 (1941).
- (20) MILLS, V.: U.S. patent 2,295,594 (September 15, 1942).
- (21) ROSS, S., AND MCBAIN, J.W.: *J. Am. Chem. Soc.* **68**, 547 (1946).
- (22) SPIEL, S., BERKELHAMER, L.H., PASK, J.A., AND DAVIES, B.: U.S. Bur. Mines Tech. Paper No. 684 (1945).
- (23) STAUFF, J.: *Kolloid-Z.* **89**, 224 (1939).
- (24) THIESSEN, P.A., AND EHRLICH, E.: *Z. physik. Chem.* **A165**, 453 (1933).
- (25) VOLD, M.J.: *J. Am. Chem. Soc.* **63**, 160 (1941).
- (26) VOLD, R.D.: *J. Phys. Chem.* **43**, 1213 (1939).
- (27) VOLD, R.D.: *J. Am. Chem. Soc.* **63**, 2915 (1941).
- (28) VOLD, R.D.: *J. Phys. Chem.* **49**, 315 (1945).
- (29) VOLD, R.D., AND FERGUSON, R.H.: *J. Am. Chem. Soc.* **60**, 2066 (1938).
- (30) VOLD, R.D., AND LYON, L.L.: *Ind. Eng. Chem.* **37**, 497 (1945).
- (31) VOLD, R.D., ROSEVEAR, F.B., AND FERGUSON, R.H.: *Oil & Soap* **16**, 48 (1939).
- (32) VOLD, R.D., AND VOLD, M.J.: *J. Am. Chem. Soc.* **61**, 808 (1939).
- (33) VOLD, R.D., AND VOLD, M.J.: *J. Am. Chem. Soc.* **61**, 37 (1939).
- (34) VOLD, R.D., AND VOLD, M.J.: *J. Phys. Chem.* **49**, 32 (1945).

A NEW METHOD FOR FORMING SHARP BOUNDARIES IN DIFFUSION EXPERIMENTS

DAVID S. KAHN AND ALFRED POLSON¹

Department of Chemistry, University of Wisconsin, Madison, Wisconsin

Received December 20, 1946

One of the main problems in the performance of optical diffusion experiments is the formation of initial sharp interfaces between solvent and solution. Svedberg (13) formed the interface by flowing in solution from a reservoir, making use of a stopcock to form the boundary between solution and solvent. This interface was then raised to a position in the tube where its blurring could be observed. In order to regulate the flow of the solution better, Polson (8) inserted a capillary

¹ Permanent address: Veterinary Research Laboratories, Onderstepoort, South Africa.

in the tube connecting the reservoir with the solvent side. Also, Lamm (3) has developed various devices for forming initial boundaries. For solutions in which organic solvents are required, the boundary was formed by allowing the solvent to flow through a porous glass plate over the solution. To place the boundary in a position suitable for photography, some of the solution was then emptied from the cell. For aqueous solutions there was developed what is generally known as the Lamm cell. The technique of boundary formation in this cell employs a slide which is pulled out between the solution and solvent, whereby the solution above is levelled onto the solution below the slide. More recently, Loughborough and Stamm (5) and Neurath (6) have devised apparatus in which the interface is formed by sliding solvent over solution. This same principle is made use of in the Tiselius electrophoresis cell.

These classical methods of boundary formation have several disadvantages. With the Svedberg cell, the solution has to be moved in contact with the solvent over a considerable distance. In doing so, the boundary is somewhat distorted and otherwise disturbed. Such distortions are more severe in the case of dilute solutions as compared to more concentrated ones, owing to the smaller density differences of dilute solutions with respect to the solvent.

The porous glass disc method of Lamm has the disadvantage of giving somewhat diffuse boundaries. This is due to mixture of solution and solvent in the glass disc. There is the further distortion of the boundary in moving the solution down the cell to a position such that the boundary can be photographed. The Lamm cell has the disadvantage of always leaving a film of lubricant on the glass surface at the position where the slide is pulled out. This film interferes with the photography of the uniform linear scale through the diffusing column. Some scale lines are entirely cut off and others are deviated from the position that the refractive index of the gradient at that point would require. Since these lost data determine a very important part of the diffusion curve, it is a source of serious error. The same objections can be raised against the Neurath cell. Some grease is left on the glass surface when the two solutions are levelled over each other.

The technique of boundary sharpening has the advantage of placing the boundary at any desired position in the diffusion tube without distortion of the initial interface. The method to be described here has been applied by Polson *et al.* (10, 11) in connection with the sharpening of initial boundaries in the electrophoresis of protein mixtures. The procedure is now applied to diffusion-constant determinations in which a Svedberg type of diffusion cell is used (figure 1). The limb a is filled with the solvent and limb b with the solution. A capillary filled with the solution is dropped into the tube connecting a with b. The cell is then mounted onto a suitable holder and lowered into the thermostat. After temperature equilibration the stopcock is opened and the solution is allowed to flow very slowly. The rate of flow is regulated by means of a manometer. When the boundary has been brought to a suitable position in the tube, the manometer pressure is lowered to such an extent that the boundary remains

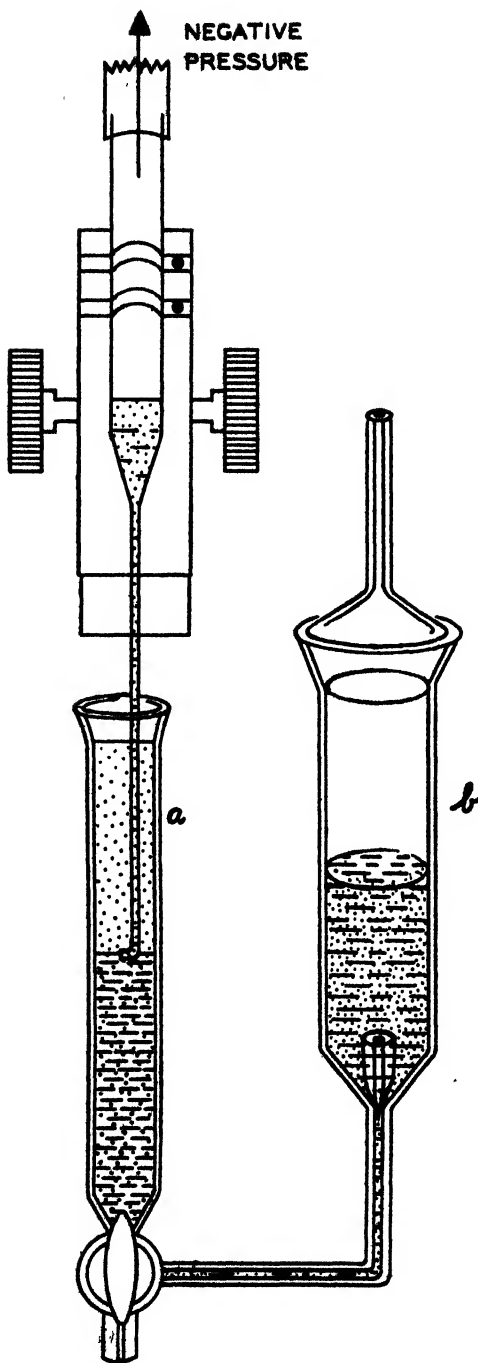


FIG. 1. Illustration of the method of forming a sharp interface between two solutions by means of a fine pipet.

stationary in the tube. A very fine capillary pipet with its orifice bent at right angles is then lowered into the tube a by means of a rack and pinion of a microscope to a level just below the boundary. A negative pressure is applied to the pipet and some solution is sucked up into the pipet. In doing this, the whole diffuse region in the tube can be removed and the solution and solvent move into position to generate a sharp boundary. The degree of sharpness of the boundary can be judged by observing the image projected upon the focal plane of the camera. A boundary is considered sharp if it extends over a distance of less than 0.75 mm. When the boundary is adequately sharpened, the stopcock is closed, the pipet is withdrawn, and a "zero-time" photograph is taken. The open end of the diffusion tube is then closed and the diffusion allowed to proceed.

Once the boundary has been formed, the diffusion experiment proceeds in the conventional manner except for the time interval of photographs. Because of the precise determination of zero time inherent in this technique, earlier and more rapid photographs can give significant data. With a 1 per cent solution of a substance having a diffusion constant of 4×10^{-7} cm.²/sec., the times for photographing the boundary should be 15 min., 30 min., 1 hr., 2 hr., 4 hr., 8 hr., 16 hr., etc. From these data, the refractometric gradient-distance curves are then plotted. The ordinate of maximum height of these curves is very carefully determined. In event of diffusion which is a function of concentration, the ordinate of maximum height for zero time is alone significant. A position of constant concentration is then determined for either the dilute or the concentrated solution side of the curve. The distance between the initial position of the boundary and of the ordinate for a constant concentration of a curve is a measure of the rate of spread of the boundary.

Since, experimentally, the boundary always has finite dimensions, we do not have a true zero time. For the sake of this analysis, a zero-time boundary may be conceived of as being purely two dimensional in character. We can determine a true zero time by plotting the square of the above distance as measured on the ordinate against time. If one extrapolates such a curve to zero thickness (intersecting the time axis), one obtains an approximate zero time. However, such a technique has the disadvantage of a requirement of very large sheets of graph paper and the hazard of the experimenter's guess as to the mean position for a curve through the points, and an analytical procedure is more satisfactory. The spreading of the diffusion boundary can be represented by an equation,

$$x^2 = Kt \quad (1)$$

where x is the distance a boundary corresponding to a definite concentration proceeds from the original interface, t is the time elapsed since the boundary was formed, and K is a constant.

Equation 1 can be written in the form:

$$x_1^2 = K(t_1 + \Delta t) \quad (2)$$

and

$$x_2^2 = K(t_2 + \Delta t) \quad (3)$$

where x_1 and x_2 are the distances a boundary of definite concentration moves in time intervals $(t_1 + \Delta t)$ and $(t_2 + \Delta t)$, respectively. The increment Δt is the error made in the estimation of the initial time. From equations 2 and 3, it can be shown that

$$\Delta t = \frac{x_1^2 t_2 - x_2^2 t_1}{x_2^2 - x_1^2} \quad (4)$$

TABLE 1

Diffusion constant of ovalbumin

Concentration, 1.0 per cent; temperature, 26°C.; medium, 0.15 *M* sodium chloride; error in diffusion time, 126 sec.

TIME	$D \times 10^7$	D^* (STANDARD DEVIATION)
<i>hours</i>	<i>cm.²/sec.</i>	
7.5	8.40	8.92
16.4	8.68	
22.5	8.79	
Average	8.73	

Corrected for diffusion in water at 20°C.: $D = 7.57 \times 10^{-7}$ cm.²/sec.

D (standard deviation) corrected for 20°C.: $D = 7.73 \times 10^{-7}$ cm.²/sec.

(Earlier result obtained by Polson (9); $D = 7.76 \times 10^{-7}$ cm.²/sec.)

* Calculated from the standard deviation of the frequency curve.

For the case where t_1 is set equal to zero (i.e., the zero-time photograph immediately after formation of the boundary) equation 4 reduces to:

$$\Delta t = \frac{x_1^2 t_2}{x_2^2 - x_1^2} \quad (5)$$

Equation 5 is used throughout this work to compute a zero time from the error in the initial time of diffusion of the experiment. The advantages of this mode of extrapolation are that it exploits the precise determination of proximate zero-time characteristics of boundary sharpening and it enables the calculator to get a mathematically exact, average, extrapolated zero time.

In the actual diffusion experiments to test the method the Lamm scale method was used. In the computation of diffusion constants from the diffusion-gradient curves, the inflection-point method was used. The area-height method was tried, but it was found not to be as useful for the calculations, because areas under short-time diffusion curves are too great in terms of their heights, owing to index of refraction effects of second and higher order. These effects become negligible when the refractive-index gradients are small, as in solutions of low

TABLE 2
Diffusion constant of bovine γ_2 -globulin

TIME	$D \times 10^7$	D (STANDARD DEVIATION)
A. Concentration, 0.25 per cent; temperature, 26°C.; medium, 0.15 <i>M</i> sodium chloride; error in diffusion time, 106 sec.		
<i>hours</i>	<i>cm.²/sec.</i>	
0.25	4.80	
0.5	4.83	
1.0	5.00	
3.0	4.90	
Average.....	4.88	

D corrected for diffusion in water at 20°C.: $D = 4.22 \times 10^{-7} \text{ cm.}^2/\text{sec.}$

B. Concentration, 1.0 per cent; temperature, 26°C.; medium, 0.15 *M* sodium chloride; error in diffusion time, 126 sec.

2.4	4.75	
4.083	4.80	
7.40	4.83	
10.73	4.74	
22.36	4.65	4.80
Average.....	4.75	

D corrected for diffusion in water at 20°C.: $D = 4.12 \times 10^{-7} \text{ cm.}^2/\text{sec.}$

D (standard deviation) corrected for diffusion in water at 20°C.: $D = 4.16 \times 10^{-7} \text{ cm.}^2/\text{sec.}$

C. Concentration, 0.3 per cent; temperature, 26°C.; medium, 0.15 *M* sodium chloride; error in diffusion time, 210 sec.

0.52	4.76	
4.366	4.83	
7.233	4.76	
9.30	4.78	
Average	4.78	

D corrected for diffusion in water at 20°C.: $D = 4.14 \times 10^{-7} \text{ cm.}^2/\text{sec.}$

D. Concentration, 1.0 per cent; temperature, 26°C.; medium, 0.15 *M* sodium chloride

6.34	4.71	
10.0	4.74	
22.533	4.81	4.81
Average.....	4.75	

D corrected for diffusion in water at 20°C.: $D = 4.12 \times 10^{-7} \text{ cm.}^2/\text{sec.}$

D (standard deviation) corrected for diffusion in water at 20°C.: $D = 4.17 \times 10^{-7} \text{ cm.}^2/\text{sec.}$

TABLE 3
Diffusion constant of bovine γ_1 -globulin

TIME	$D \times 10^7$	D (STANDARD DEVIATION)
<i>hours</i>	<i>cm.²/sec.</i>	
2.9	4.80	
3.9	4.83	
5.833	4.74	
Average	4.79	

A. Concentration, 0.3 per cent; temperature, 26°C.; medium, 0.15 *M* sodium chloride; error in diffusion time, 16 sec.

D corrected for diffusion in water at 20°C.: $D = 4.15 \times 10^{-7}$ cm.²/sec.

B. Concentration, 1.0 per cent; temperature, 26°C.; medium, 0.15 *M* sodium chloride; error in diffusion time, 115 sec.

3.75	4.30	
9.53	4.74	
13.46	4.68	
21.00	4.62	4.76
Average	4.67	

D corrected for diffusion in water at 20°C.: $D = 4.05 \times 10^{-7}$ cm.²/sec.

D (standard deviation) corrected for diffusion in water at 20°C.: $D = 4.12 \times 10^{-7}$ cm.²/sec.

TABLE 4
Diffusion of human γ -globulin

Concentration, 1.0 per cent; temperature, 26°C.; medium, 0.15 *M* sodium chloride; error in diffusion time, 133 sec.

TIME	$D \times 10^7$	D (STANDARD DEVIATION)
<i>hours</i>	<i>cm.²/sec.</i>	
3.266	4.50	
8.05	4.58	
16.55	4.82	
24.30	4.57	4.61
31.66	4.64	
Average	4.62	

D corrected for diffusion in water at 20°C.: $D = 4.00 \times 10^{-7}$ cm.²/sec.

D (standard deviation) corrected for diffusion in water at 20°C.: $D = 3.99 \times 10^{-7}$ cm.²/sec.
(Earlier result obtained by Pedersen (7): $D = 4.00 \times 10^{-7}$ cm.²/sec.)

concentration or after prolonged diffusion times. In general, short-time diffusion curves are anomalous, and the assumptions upon which diffusion constants may be calculated do not hold. This problem has been discussed by Bridgman and

Williams (1). However, experience has indicated that the inflection-point method may be used earlier than the area-height method to obtain results consistent with those obtained in long-time diffusion experiments. The boundary-sharpening technique provides a more precise determination of time.

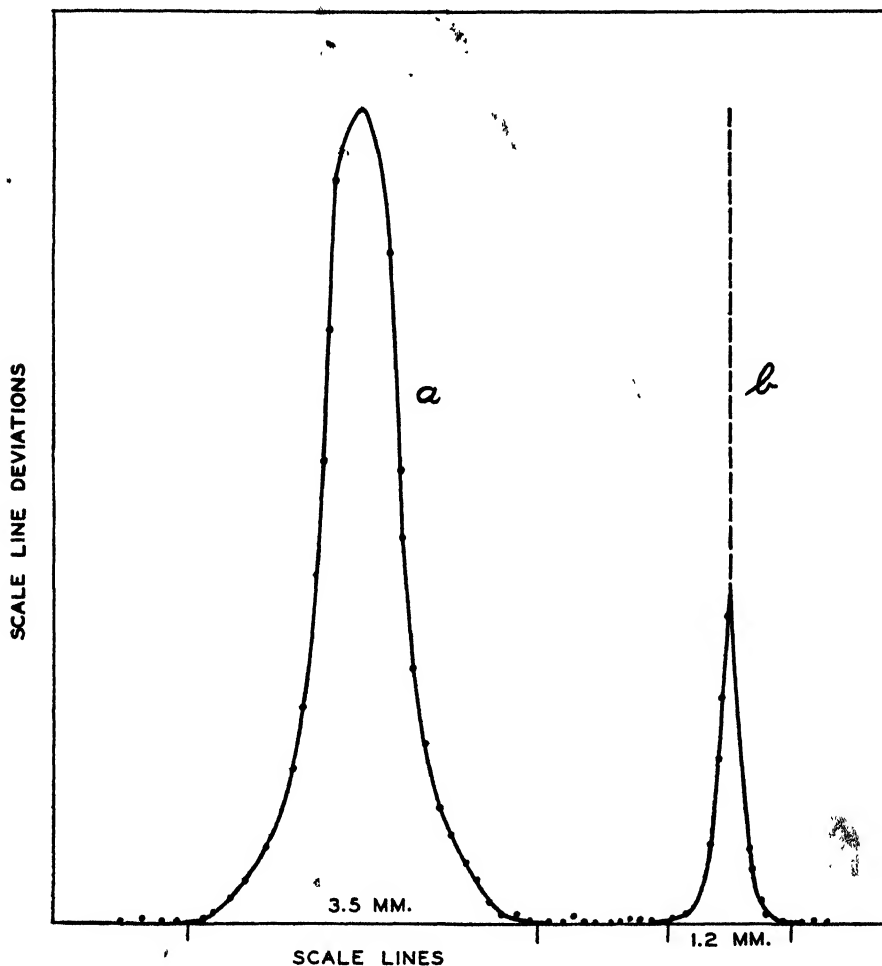


FIG. 2. Concentration gradient curves: (a) gradient curve after formation of the boundary in the usual way; (b) the same gradient curve immediately after being sharpened.

EXPERIMENTAL

The new technique was applied in the determination of the diffusion constants of several representative purified proteins.

Ovalbumin

Ovalbumin was recrystallized six times by using the method of Kekwick and Cannan (2). By electrophoresis at pH 7.6 in phosphate buffer, it was

estimated that the ovalbumin was 95 per cent pure. The impurity was an extra component of slightly higher mobility than the main component. Also, the ovalbumin was tested in the high-velocity ultracentrifuge and found to be essentially homogeneous. Longsworth and MacInnes (4) met with similar difficulties when the attempt was made to obtain electrophoretically homogeneous ovalbumin. Apparently the impurity demonstrated by electrophoresis has a diffusion constant not greatly different from that of the main component, since the diffusion curves fit the normal curve very well.

Bovine γ -globulin

Two fractions of bovine globulin, γ_2 and γ_1 ,² have been investigated. These fractions were analyzed in the electrophoresis apparatus as well as in the high-velocity ultracentrifuge and found to be at least 95 per cent pure by the usual conventions.

In figure 2 are given: (1) a diffusion-gradient curve of a boundary between a solution of γ_2 -globulin and its solvent as it appeared after formation in the Svedberg diffusion cell (the process of formation and raising the boundary to the desired level took 20 min.) and (2) the same boundary immediately after sharpening with the pipet. It is clear that the unsharpened boundary is asymmetrical and diffuse. In direct contrast, the sharpened boundary is sharp and symmetrical. Other experiments with γ_2 - and γ_1 -globulin preparations were carried out at two different concentrations, 0.3 per cent and 1.0 per cent.

DISCUSSION

The above experiments show that the new method, which involves an additional experimental step to sharpen the boundary, has certain definite advantages over previous methods. In the classical experiments long-time diffusion was allowed to eliminate the time error of the initial boundary. Since the initial time in diffusion is now determined with precision, this approach is no longer necessary and short-time diffusion runs can be justified with respect to the time error as being well within the over-all experimental error. However, if the concentration gradient is too high, as it will be after short-time diffusion of concentrated solutions, the assumption as to the relation of index of refraction gradient to concentration gradient no longer may be made. Such short-time curves are anomalous and accurate calculations are not easily made. For this reason, the use of dilute solutions, such as 0.25 per cent, has merit. Under such conditions, the concentration gradient is sufficiently reduced after 15 min. diffusion that a diffusion constant consistent with the ordinary longer time diffusion may be calculated. This experimental fact is significant in several respects. It makes possible a saving of time in determining diffusion constants. It permits the use of smaller amounts of materials which may be difficult to

² For a description of the terms " γ_2 - and γ_1 -globulin" and the method of separation of these two fractions, the reader is referred to a recent article by Deutsch, Alberty, and Gosting (J. Biol. Chem. 165, 21 (1946)).

purify or obtain. It enables a more accurate determination of diffusion constants in dilute solutions, thus making more satisfactory the extrapolation to zero concentration which is often required for molecular-weight calculations. The limiting concentration for previous accurate diffusion determinations was 0.5 per cent. Although the minimum concentration used with the boundary-sharpening technique here is 0.25 per cent, we do not know that this is the limiting concentration. One of the hazards of long-time diffusion of proteins involves the danger that they will change their constitution under these conditions. The probability of denaturation or non-sterility of the solution is reduced with short-time diffusion. In the study of skew curves of concentration-dependent substances, the boundary-sharpening technique suggests itself as a means for a very accurate determination of the zero-time ordinate of the maximum height of the diffusion-gradient curve.

SUMMARY

1. The boundary region of two diffusing liquids can be sharpened by drawing off the diffuse region with a capillary pipet with rectangular tip.
2. The true zero time, approximately 100 sec., can be calculated with a high degree of precision.
3. The boundary-sharpening technique has special merit for use with increasing ly di ute solutions.
4. Specialized applications of this technique are suggested with respect to measurement of diffusion constants at infinite dilution, of concentration-dependent proteins giving skew curves, or of proteins of limited stability under the conditions of diffusion determinations.

It is a great pleasure to acknowledge our gratitude to Professor J. W. Williams for the encouraging interest he has taken in this work and to Mr. Edwin M. Hanson for the help he has given in the construction of the apparatus. We wish also to thank Mr. E. L. Hess, who has been generous enough as to supply us with samples of fractionated bovine globulins.

REFERENCES

- (1) BRIDGMAN, W. B., AND WILLIAMS, J. W.: *Ann. N. Y. Acad. Sci.* **67**, 195 (1942).
- (2) KEKWICK, R. A., AND CANNAN, R. K.: *Biochem. J.* **30**, 227 (1936).
- (3) LAMM, O.: Thesis, University of Upsala, 1937.
- (4) LONGSWORTH, L. G., AND MACINNES, D. A.: *J. Am. Chem. Soc.* **62**, 705 (1940).
- (5) LOUGHBOROUGH, D. L., AND STAMM, A. J.: *J. Phys. Chem.* **40**, 1113 (1936).
- (6) NEURATH, H.: *Science* **93**, 431 (1941).
- (7) PEDERSEN, K. O.: *Ultracentrifugal Studies on Serum and Serum Fractions*. Almquist and Wiksells, Upsala (1945).
- (8) POLSON, A.: *Kolloid-Z.* **87**, 149 (1939).
- (9) POLSON, A.: *Kolloid-Z.* **87**, 149 (1939); **88**, 51 (1939).
- (10) POLSON, A.: *Onderstepoort J. Vet. Sci. Animal Ind.* **20**, 159 (1945).
- (11) POLSON, A., JOUBERT, P. J., AND HAIG, D. A.: *Biochem. J.* **40**, 265 (1946).
- (12) SMITH, E. L., GREENE, R. D., AND BARTNER, E.: *J. Biol. Chem.* **164**, 159 (1946).
- (13) SVEDBERG, T.: *Kolloid-Z. (Zsigmondy Festschrift Ergänz. Band)* **36**, 53 (1925).

THE SURFACE TENSION OF LIQUID CRYSTALS¹WILHELMINA M. SCHWARTZ² AND HAL W. MOSELEY³*Richardson Chemistry Laboratory, Tulane University, New Orleans, Louisiana**Received December 19, 1946*

In spite of the fact that anomalies have been found in the surface tension-temperature curves of liquid crystals, very few investigations of this subject have been reported in the literature. In 1917 F. M. Jaeger (7) measured the surface tension of five liquid crystalline substances as a function of temperature: *p*-azoxyanisole, *p*-azoxyphenetole, anisaldazine and ethyl *p*-ethoxybenzalamino- α -methylcinnamate, which are nematic, and ethyl *p*-azoxybenzoate, which is smectic. He used the maximum bubble pressure method in an atmosphere of nitrogen. Jaeger found that in every case the temperature coefficient of surface tension was abnormally large in the anisotropic phase, and that the surface tension rose suddenly to a maximum at the clearing point. The two latter liquids, ethyl *p*-azoxybenzoate and ethyl *p*-ethoxybenzalamino- α -methylcinnamate, showed an additional maximum in the isotropic phase, but there was some doubt about the purity of these two substances. In 1938 Ferguson and Kennedy (2), using a variation of the capillary-rise method and measuring the surface tension at smaller temperature intervals, confirmed Jaeger's results for *p*-azoxyanisole, *p*-azoxyphenetole, and anisaldazine. They found that the surface tension-temperature curves for these compounds have a van der Waals shape around the clearing point; furthermore, they pointed out that the upward branches of these curves are unique, since in this part of the curve the surface tension increases with temperature. Ferguson (3) later called attention to the fact that this behavior demands further investigation.

In 1943 Naggiar (11) measured the surface tension of *p*-azoxyanisole in the anisotropic phase by a new method, which consisted in observing the radii of curvature of the surfaces of a drop of liquid. Unfortunately, he did not carry his measurements beyond the clearing point. Naggiar found that the surface tension decreases linearly with increasing temperature, and that his results could be expressed by the following equation: $\gamma = 52.1 - 0.110t \pm 0.5$ dynes per centimeter. The temperature coefficient was not, therefore, abnormally large in the anisotropic phase.

This paper reports the measurement of the surface tension of *p*-azoxyanisole, *p*-azoxyphenetole, and ethyl *p*-azoxybenzoate by the wire-ring method. The results obtained are in marked contrast to those of Jaeger and of Ferguson and Kennedy, and in general agreement with the observations of Naggiar.

¹ Based on the thesis submitted by W. M. Schwartz to the Faculty of the Graduate School of Tulane University in partial fulfillment of the requirements for the degree of Master of Science, June, 1933.

² Present address: Southern Regional Research Laboratory, United States Department of Agriculture, New Orleans, Louisiana.

³ Deceased.

PREPARATION AND PURIFICATION OF MATERIALS

In order to avoid any errors due to impurities, the greatest care was taken in the preparation of these compounds. The reagents were purchased from the Eastman Kodak Company and were of reagent grade. All beakers, flasks, etc., used in the preparations were cleaned in hot cleaning solution. The products were purified by repeated recrystallization until they melted sharply at the correct temperatures as given in the literature (6); both the melting and clearing points were determined with a thermometer calibrated by the Bureau of Standards.

p-Azoxyphenetole: This compound was prepared from *p*-nitrophenetole by the method of Gattermann (4). After four recrystallizations from ethyl alcohol with the addition of animal charcoal, the product was obtained as bright yellow needles. It was dried for 2 days in a vacuum desiccator over calcium chloride. Melting point, 137.1–137.4°C.; clearing point, 167.1–167.3°C.

Ethyl p-azoxybenzoate: This was prepared from *p*-nitrobenzoic acid by the method of Meyer and Dahlem (9). After two recrystallizations from ethyl alcohol with animal charcoal, the product was obtained as orange-yellow needles, but as the melting point was not yet sharp, it was recrystallized again from benzene and from ethyl alcohol. It was dried over calcium chloride. Melting point, 114.1–114.6°C.; clearing point, 121.4–122.1°C.

p-Azoxyanisole: This compound was obtained from the Schuschar dt Co., Görlitz, Germany. It was recrystallized from methyl alcohol and dried over calcium chloride. Melting point, 117.5–118.2°C.; clearing point, 134.6–135.0°C.

APPARATUS

The measurements were made with a precision model du Noüy tensiometer, modified for use with the thermostat in which the substances were heated.

The thermostat, based on the design described by Pidgeon and Egerton (12), is shown in figure 1. The tube A is 2.5 cm. in diameter and 24.5 cm. long; it widens out at the end into a flat-bottomed bulb 4 cm. in diameter.⁴ T is a small tube designed to hold a thermometer. The level of the mercury is kept in the tapered end of the control tube by drawing it off through the stopcock S as it rises; this greatly increases the sensitivity of the instrument over wide ranges of temperature. If the contact point is clean, the temperature stays constant to within $\pm 0.05^\circ\text{C}$. for any desired length of time, and can be varied by increments as small as 0.1–0.2°C.

The contact point was made of No. 26 platinum wire and was kept clean by a current of hydrogen. The heating coil was made from 12 ft. of No. 30 nichrome wire, wound non-inductively so that no field should cross A. With a 400-watt lamp in series the temperature rose to 180°C. in about 3 hr., and with 500 watts in series it rose to 200°C. It was found necessary to put in a 2-mfd. condenser to

⁴ The diameter of the bulb should have been larger. It was found impossible to measure substances of high surface tension, such as water, in this apparatus, as the curvature of the surface caused the ring to be pulled over to the side.

keep down the spark at P. The temperature was measured with a thermometer which was graduated in tenths and had been calibrated by the Bureau of Standards.

The thermostat was wrapped on the outside with several layers of asbestos sheet. It was clamped to the tensiometer stage, which was slipped off the base of

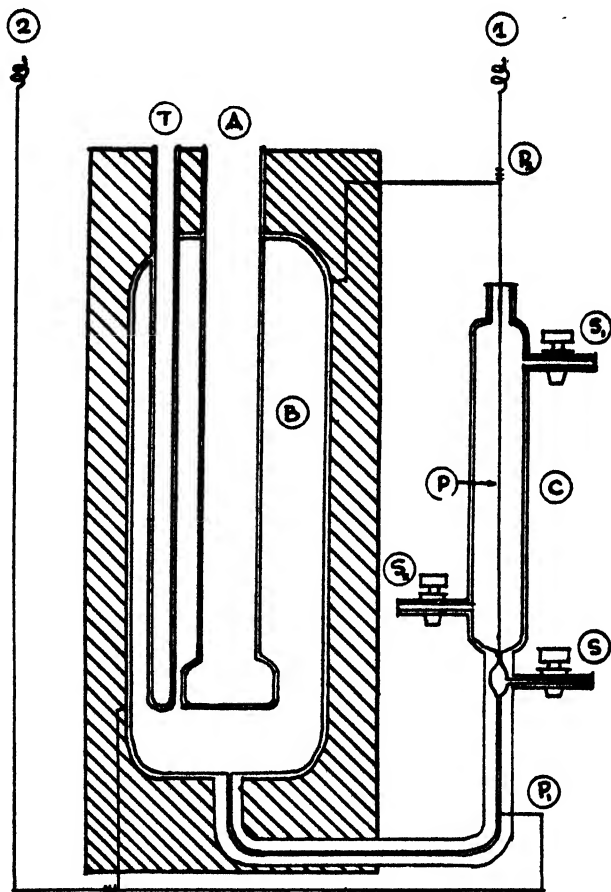


FIG. 1. Thermostat. A, tube in which liquids are measured; B, mercury jacket; T, thermometer well; C, control tube; P, contact point; P₁ and P₂, points at which the control tube is shunted across the heating coil; S, mercury outlet; S₂ and S₁, inlet and outlet for hydrogen.

the tensiometer and mounted separately on a heavy iron base. This was necessary because of its weight, as the mercury jacket held about 25 lb. of mercury. Thus mounted, the thermostat could be placed below the tensiometer so that the arm of the latter hung directly over the tube A, and could be lowered and raised as though it were part of the tensiometer (figure 2). The ring was lengthened by means of an extension to make it reach to the bottom of the tube (A in figure 1) in which the liquids were measured. The extension for the ring was a glass

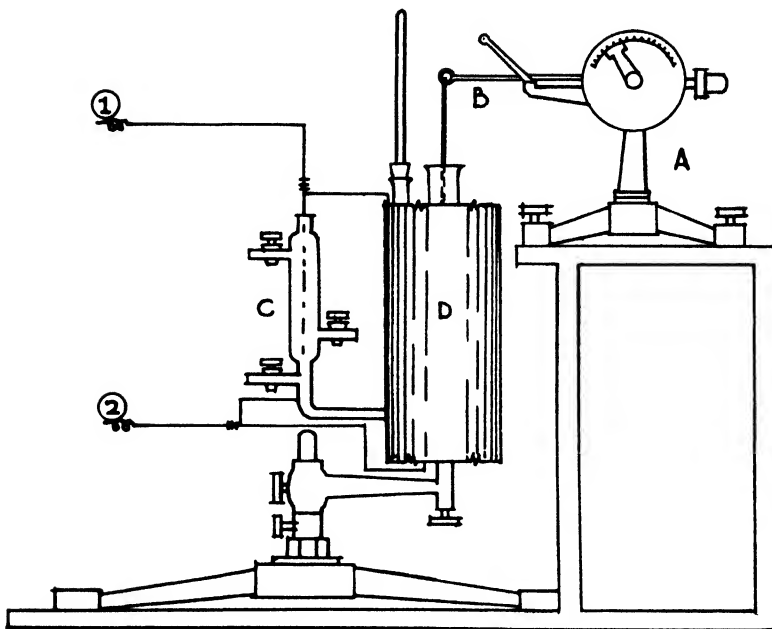


FIG. 2. Thermostat and tensiometer. A, tensiometer; B, arm; C, control tube; D, mercury jacket.

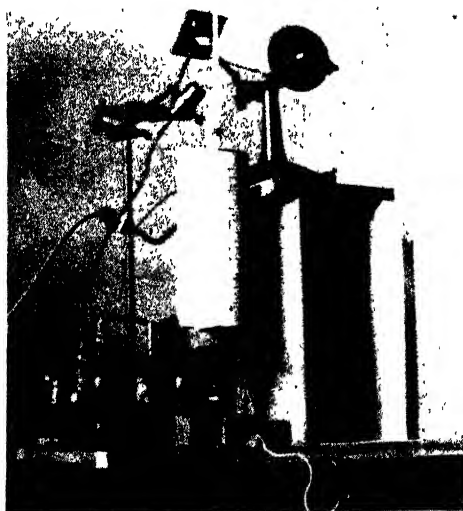


FIG. 3. Photograph of the apparatus

thread, made by drawing out a piece of glass rod and bending a small hook at each end. It had to be of exactly the right length, and approximately 1.2 mm. in diameter. A mirror and light were arranged above the top of the tube A so that the position of the ring during measurements could be observed (1) (figure 3).

EXPERIMENTAL DATA

The surface tension was measured from the beginning of the liquid crystalline phase well into the isotropic phase, great care being taken around the clearing point. The change of phase could be particularly well observed because the mercury surrounding the bulb acted as a reflector, the anisotropic liquid appearing dark while the isotropic liquid was brilliantly clear.

After each substance had been measured, alcohol was poured into the tube, the thermostat was heated, and the hot solution was drawn out by means of an aspirator. The tube was then rinsed several times with alcohol, cleaned with cleaning solution, and rinsed thoroughly with water. It was finally dried by heating up to 180°C. Before each run the compound to be measured was dried overnight

TABLE 1
Surface tension of p-azoxyanisole
Clearing point, 136.1–137.0°C.; $R/r = 40.55$

t °C.	TENSIONMETER READING (ϕ)	DENSITY	R^3/V	F	$\gamma = \phi F$ dynes per cm
120.5	43.0	1.166	0.86	0.9184	39.5
123.1	42.8 ₅	1.163	0.86	0.9184	39.4
127.9	42.3	1.158	0.87	0.9176	38.8
132.7	41.6	1.153	0.87	0.9176	38.2
135.4	41.3	1.147	0.88	0.9168	37.9
136.4	41.0 ₅	1.145	0.88	0.9168	37.6
137.0	41.0	1.144	0.88	0.9168	37.6
137.5	41.0	1.143	0.88	0.9168	37.6
138.0	41.0	1.142	0.88	0.9168	37.6
138.6	41.0	1.141	0.88	0.9168	37.6
139.5	40.9	1.140	0.88	0.9168	37.5
145.7	40.2 ₅	1.135	0.89	0.9157	36.9
150.5	39.8	1.131	0.90	0.9147	36.4
160.1	38.8	1.124	0.92	0.9129	35.4

in a vacuum desiccator over calcium chloride, and the ring and glass extension were cleaned with cleaning solution.

The experimental data are given in tables 1 to 4. The correction factors (F) were calculated by means of the tables of Harkins and Jordan (5). The densities of the liquids were obtained by graphical interpolation from the data of Jaeger (7). The density of air saturated with vapor of liquid, which enters into the formula of Harkins and Jordan for calculating the volume, V , of liquid upheld by the ring, was neglected, since it could not sensibly affect the value of the correction factor. The dimensions of the ring were obtained as follows: the radius of the ring, R , was calculated from the value of the circumference furnished with the ring by the manufacturers; the radius of the wire, r , was measured roughly with a vernier caliper. The data thus obtained, and the value of the ratio, R/r , are compared in table 5 with the data given by Harkins and Jordan for the ring

TABLE 2
Surface tension of p-azoxyphenetole
 Clearing point, 168.3–168.6°C.; $R/r = 40.55$

t °C.	TENSIMETER READING (ϕ)	DENSITY	R^2/V	F	$\gamma = \phi F$ dynes per cm.
141.2	34.7 ₈	1.095	1.00	0.9062	31.5
158.3	33.0	1.078	1.03	0.9038	29.8
159.8	32.9	1.076	1.03	0.9038	29.7
164.2	32.4	1.072	1.05	0.9022	29.2
166.8	32.2	1.069	1.05	0.9022	29.1
168.3	31.9 ₈	1.068	1.06	0.9015	28.8
168.5	31.9	1.068	1.06	0.9015	28.8
168.6	31.9	1.068	1.06	0.9015	28.8
168.8	31.9 ₈	1.067	1.06	0.9015	28.8
169.8	31.9	1.065	1.06	0.9015	28.8
170.7	31.7	1.062	1.06	0.9015	28.6
172.2	31.6	1.059	1.06	0.9015	28.5
174.7	31.4	1.053	1.07	0.9008	28.3
181.9	30.7	1.046	1.08	0.9001	27.6
185.8	30.5	1.043	1.08	0.9001	27.5
190.8	30.0	1.038	1.09	0.8994	27.0
198.0	29.4	1.032	1.11	0.8980	26.4

TABLE 3
Surface tension of ethyl p-azoxybenzoate
 Clearing point, 122.8°C.; $R/r = 40.55$

t °C.	TENSIMETER READING (ϕ)	DENSITY	R^2/V	F	$\gamma = \phi F$ dynes per cm.
123.0	29.8 ₈	1.146	1.21	0.8915	26.6
125.4	30.0	1.144	1.21	0.8915	26.8
127.1	30.3	1.143	1.19	0.8928	27.1
130.5	30.5	1.140	1.18	0.8935	27.3
135.0	30.6	1.138	1.18	0.8935	27.3
140.0	30.6	1.135	1.17	0.8941	27.4
146.3	30.8	1.131	1.16	0.8948	27.6
149.7	30.9	1.128	1.15	0.8954	27.7
155.0	30.9	1.124	1.15	0.8954	27.7
160.2	30.8 ₈	1.121	1.15	0.8954	27.6
166.5	30.8	1.116	1.15	0.8954	27.6
170.8	30.8	1.113	1.14	0.8960	27.6
177.2	30.5	1.110	1.15	0.8954	27.3
181.0	30.3	1.107	1.16	0.8948	27.1
191.4	29.6	1.101	1.18	0.8935	26.5
200.7	29.0	1.095	1.19	0.8928	25.9

furnished with the du Noüy tensiometer. Since the value of R agrees exactly with the value given by these authors, and since the value of r agrees, within the

accuracy of the measurement, with their more exact value, it was concluded that the dimensions of the rings were the same, and that the correct value of the ratio is 40.55 instead of 39.8. The values of γ calculated on this assumption are, in general, 0.1 dyne higher than those obtained if R/r is taken as 39.8; in a few cases they are the same.

TABLE 4
Calibration of apparatus
 $R/r = 40.55$

t	TENSION- ETER READ- ING (ϕ)	DENSITY*	R^3/V	F	$\gamma = \phi F$	γ^\dagger	DEVIATION
1. Surface tension of benzene							
°C.					dynes per cm.		
31.6	29.6	0.8663	0.93	0.9120	27.0	27.4 \pm 0.05	-0.4
34.9	29.1 ₈	0.8628	0.94	0.9112	26.6	26.9 \pm 0.05	-0.3
40.3	28.4	0.8570	0.95	0.9102	25.9	26.2 \pm 0.1	-0.3
50.0	27.0	0.8465	0.99	0.9070	24.5	25.0 \pm 0.1	-0.5
60.0	25.8	0.8356	1.02	0.9046	23.3	23.7 \pm 0.1	-0.4
70.0	24.4	0.8247	1.07	0.9008	22.0	22.5 \pm 0.1	-0.5
2. Surface tension of quinoline							
150.9	32.8 ₈	0.9896	0.95	0.9102	29.9	30.2 \pm 0.3	-0.3
202.3	27.4	0.9446	1.09	0.8994	24.6	24.9 \pm 0.3	-0.3

* *International Critical Tables*, Vol. III, p. 29. McGraw-Hill Book Company, Inc., New York (1926).

† *International Critical Tables*, Vol. IV, pp. 454, 459. McGraw-Hill Book Company, Inc., New York (1926).

‡ Interpolated analytically.

TABLE 5
Values of R , r , and R/r

	EXPERIMENTAL	HARKINS AND JORDAN
R	0.6366 cm.	0.6366 cm.
r	0.016 cm.	0.01570 cm.
R/r	39.8	40.55

The data for ethyl *p*-azoxybenzoate are for the isotropic phase only, as it was found that the liquid crystalline phase of this substance is too viscous to be measured by the ring method.

DISCUSSION

The results are plotted in figures 4 to 7. It will be seen that the surface tension of *p*-azoxyanisole and of *p*-azoxyphenetole, instead of rising to a maximum at the clearing point, decreases approximately 0.1 dyne per degree rise in temperature in

both phases, except for a short distance in the immediate neighborhood of the clearing point, where it remains constant. The curves are linear in both phases, and the slope is only slightly greater in the anisotropic phase than in the isotropic.⁵ In figures 5 and 6, the experimental data for these two substances are compared with the data in the literature. Inspection of these figures reveals that, although the experimental data show good agreement with the data of Jaeger and of Ferguson and Kennedy in the isotropic phase, in the anisotropic phase the curves diverge, those of Jaeger and of Ferguson and Kennedy falling more rapidly and reaching a much lower value, then rising at the clearing point to a point in the neighborhood of the constant value in the experimental curves. This suggests that the anomalies which have been found in these curves are due

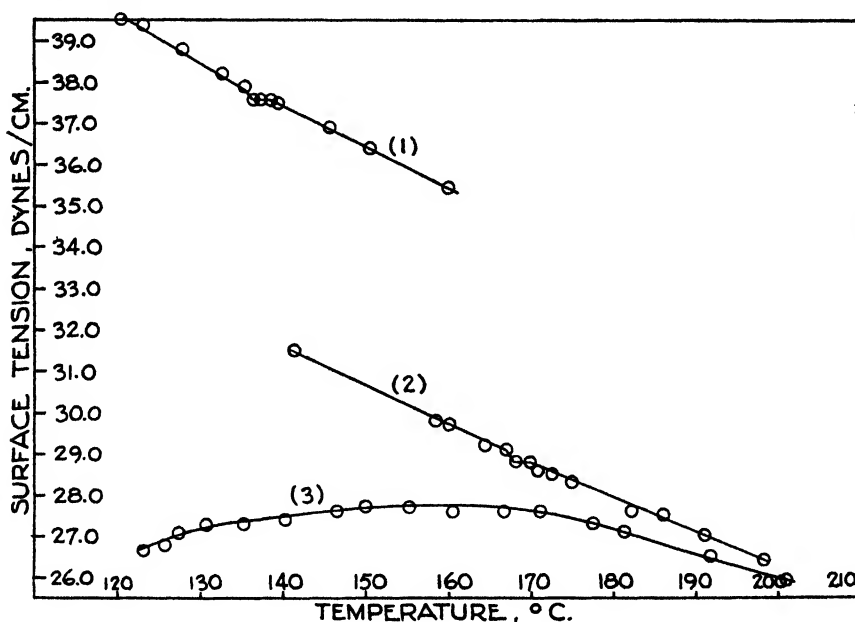
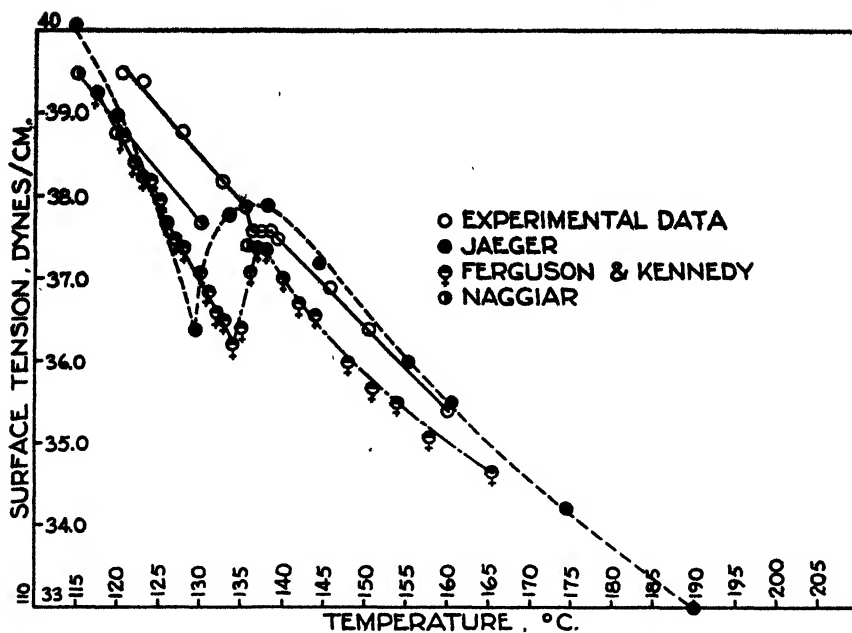
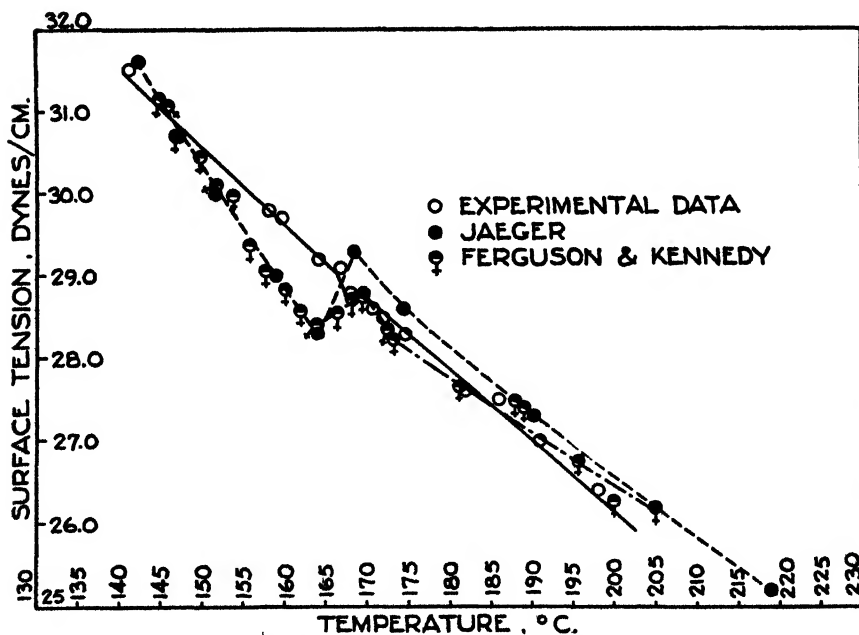


FIG. 4. Surface tension of *p*-azoxyanisole (curve 1), *p*-azoxyphenetole (curve 2), and ethyl *p*-azoxybenzoate (curve 3).

to the fact that the data are not equilibrium values, owing perhaps to superheating. The data of Naggiar for *p*-azoxyanisole appear to confirm this (figure 5). The situation may be similar to that which has recently been found by Matthews (8) to account for minima in interfacial tension-concentration curves. Matthews found that the time factor plays a very important part, the minima becoming less and less pronounced as the age of the interface increases, and he concluded that the minima in these curves are due to the use of data for interfaces that are in different states of rearrangement; they disappear when equilib-

⁵ The curves have the same general trend as those obtained later by Moinet (10), using the same apparatus with slight modifications of design and technique. His data are considerably higher than those reported here.

FIG. 5. Surface tension of *p*-azoxyanisoleFIG. 6. Surface tension of *p*-azoxyphenetole

rium has been attained. The curves plotted in figures 5 and 6 show a similar trend; the anomaly is most pronounced in Jaeger's curves, where the measure-

ments were made at wide temperature intervals, less pronounced in the curves of Ferguson and Kennedy, and least pronounced in the experimental curves. In this connection it should be mentioned that in the present work the thermostatic arrangement was such that the temperature rose very slowly and stayed remarkably constant. Moreover, a number of observations were made at each point, so that the temperature was kept constant at each point for a considerable length of time, as long as 1 hr. in some instances. In the anisotropic phase of ethyl *p*-azoxybenzoate, on the other hand, where measurements were impossible, the temperature was raised more rapidly; the curve for this substance shows marked anomaly in the isotropic phase, the surface tension rising slowly to a maximum at about 160°C. and decreasing from this point on (figure 7).

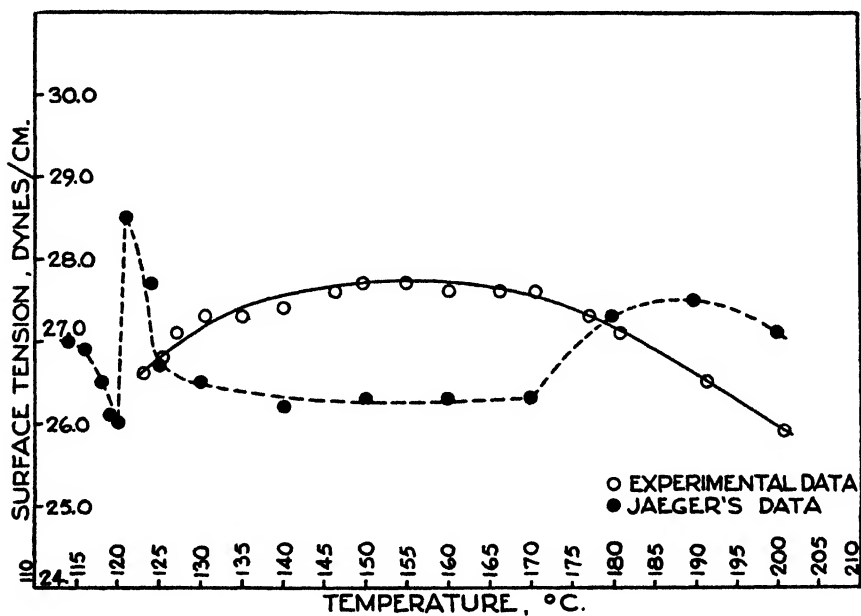


Fig. 7. Surface tension of ethyl *p*-azoxybenzoate

Although Naggiar's curve for *p*-axoxyanisole does not go beyond the clearing point, it is apparent that if extended into the isotropic phase it would show no pronounced anomaly. Naggiar (11) obtained his data by heating the substance up to the clearing point and lowering the temperature for each successive point on the curve; his data are therefore likely to be equilibrium values. This is additional evidence in support of the view that the anomalies in such curves are due to the fact that the data were not obtained under equilibrium conditions.

DISCUSSION OF ERRORS

On calibrating the apparatus with benzene and with quinoline, it was found that at lower temperatures the results were 0.4 ± 0.1 dyne too low, and that at higher temperatures the error was slightly less (see table 4). Harkins and

Jordan (5) give a detailed discussion of the sources of error in the ring method. The most important of these occurs when the plane of the ring is not horizontal. A deviation of 1° from the horizontal lowers the results by 0.43 per cent. A second source of error occurs when the diameter of the vessel which contains the liquid is too small. The error of -0.4 dyne found at lower temperatures could very well be due to one or both of these causes. At higher temperatures, it was found that the observed temperature was $1-2^\circ\text{C}$. higher than the actual temperature of the liquid. This was probably due to convection through the open tube; it introduces an error of $+0.1$ to 0.2 dyne in the results. Hence, at higher temperatures the error of -0.4 dyne is partly compensated by the error in temperature measurement, which is in the opposite direction. The experimental data are therefore believed to be several tenths of a dyne too low throughout.

SUMMARY

1. The surface tensions of *p*-azoxyanisole, *p*-azoxyphenetole, and ethyl *p*-azoxybenzoate were determined by the ring method.

2. The measurements were made with a du Noüy tensiometer modified for use at high temperatures. The substances were heated electrically in a constant-temperature device consisting of a mercury jacket wound with a heating coil and provided with a very sensitive thermostatic arrangement. The temperature was measured by means of a thermometer which had been calibrated by the Bureau of Standards.

3. The surface tension of *p*-azoxyanisole and of *p*-azoxyphenetole was found to decrease approximately 0.1 dyne per degree rise in temperature in both the anisotropic and the isotropic phases, except in the immediate neighborhood of the clearing point, where it remained constant. These results are not in agreement with the results of Jaeger and of Ferguson and Kennedy, who found that the surface tension rises to a maximum at the clearing point, and that the temperature coefficient of surface tension is abnormally large in the anisotropic phase. They confirm Naggiar's curve for *p*-azoxyanisole in the anisotropic phase.

4. Comparison of the experimental curves for *p*-azoxyanisole and *p*-azoxyphenetole with those of Jaeger and of Ferguson and Kennedy suggests that the anomalies in these curves are due to the use of data that are not equilibrium values, owing perhaps to superheating.

5. The experimental data for ethyl *p*-azoxybenzoate are for the isotropic phase only, as the liquid crystalline phase of this substance is too viscous to be measured by the ring method. Marked anomaly was found in the isotropic phase of this substance. This is believed to be due to superheating.

6. On calibrating the apparatus with benzene and with quinoline and comparing the results with the data in the literature, they were found to be 0.4 ± 0.1 dyne too low at temperatures below 100°C .; at higher temperatures the error was slightly less. The probable reasons for this error are discussed.

The surviving author wishes to express her appreciation to Dr. A. B. Cardwell, formerly of the Physics Department of Tulane University, whose help with the

thermostat made this work possible; to J. M. Seitz for suggesting the glass extension for the ring; to Dr. C. J. Likes for his advice and help in interpreting the results; to Dr. T. B. Crumpler for his help in preparing the material for publication; to the Department of Chemical Engineering at Tulane for the drawings of the apparatus; and to many others whose advice and help have been of great value.

REFERENCES

- (1) BOSTON, A. D.: Thesis, Tulane University, 1929 (on file in the Library of Tulane University).
- (2) FERGUSON, A., AND KENNEDY, S. J.: *Phil. Mag.* **26**, 41 (1938).
- (3) FERGUSON, A.: *Endeavour* **2**, 34 (1943).
- (4) GATTERMANN, L., AND RITSCHKE, A.: *Ber.* **23**, 1738 (1890).
- (5) HARKINS, W. D., AND JORDAN, H. F.: *J. Am. Chem. Soc.* **52**, 1751 (1930).
- (6) *International Critical Tables*, Vol. I, p. 315. McGraw-Hill Book Company, Inc., New York (1926).
- (7) JAEGER, F. M.: *Z. anorg. allgem. Chem.* **101**, 1 (1917).
- (8) MATTHEWS, J. B.: *Nature* **157**, 407 (1946).
- (9) MEYER, E., AND DAHLEM, K.: *Ann.* **326**, 331 (1903).
- (10) MOINET, A.: Thesis, Tulane University, 1934 (on file in the Library of Tulane University).
- (11) NAGGIAR, VICTOR: *Ann. phys.* **18**, 5 (1943).
- (12) PIDGEON, L. M., AND EGERTON, A. C.: *J. Sci. Instruments* **8**, 268 (1931); **7**, 172 (1930).

ELECTRONIC INTERPRETATIONS OF ORGANIC CHEMISTRY. II

INTERPRETATION OF THE SOLUBILITY OF ORGANIC COMPOUNDS

SANTI R. PALIT

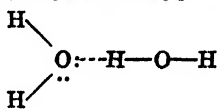
*Department of Chemistry, Polytechnic Institute, Brooklyn, New York**Received October 1, 1946*

It is gradually being realized that physical properties such as dielectric constant or surface tension play a very minor rôle in determining solubility, while hydrogen-bond formation, electronic configuration of groups, and the steric effects are undeniably the chief factors. The importance of hydrogen-bond formation in solubility phenomena has been stressed by Hildebrand (12), and Zellhoeffer, Copley, and Marvel (25) have adduced experimental evidence in its support. Recently, Ewell and coworkers (9) have clearly shown the fallacy of the maxim "like dissolves like," or of using the dielectric constant to serve as a guide to solubility, and have attempted to divide all solvents into five groups depending on their hydrogen-bonding power. We shall probe the question further to see how the presence of complementary chemical groups in the solvent and the solute determine the solubility.

TERMINOLOGY

Before presenting the subject matter it is necessary to clarify the terminology in this field, as a variety of newly coined words are used to convey the same or a similar sense. Though Pauling (19) has pointed out the objection to regarding the hydrogen bond as a bicovalent hydrogen, still it is of advantage to regard such a bond as due to a donation of electrons to hydrogen by a negative atom, for example, by an atom of oxygen in a water molecule to an atom of hydrogen in another molecule of water. We may call oxygen the donor, basic, nucleophilic, or anionoid and hydrogen the acceptor, acidic, electrophilic, or cationoid according to the usage of different authorities, as indicated in table 1. It should be noted that though oxygen is receiving hydrogen for hydrogen-bond formation, it is still to be called a donor, since this hydrogen bond is supposed to operate by donation of a part of the electronic charge of oxygen to the hydrogen. We shall have occasion to use all of these terms according to convenience as they differ slightly in shade of meaning in their

TABLE 1
Hydrogen-bonding process



	IN THE TERMINOLOGY OF				
	Sidgwick	Lewis	Ingold	Lapworth	Brønsted
Oxygen.....	Donor	Base	Nucleophilic	Anionoid	Protophilic
Hydrogen.....	Acceptor	Acid	Electrophilic	Cationoid	Protogenic

usage, but we prefer the terms "donor" and "electrophilic" as being the most expressive and least likely to cause confusion with other terms in standard usage.

WATER AS A SOLVENT

We shall first discuss the solubility of substances in water, which is by far the most important and versatile of all solvents. A molecule of water has both donor and acceptor properties; the donor property owes its origin to the unshared electron pairs in the oxygen and the acceptor or electrophilic property to the hydrogen atoms. Both these properties will necessarily be weak, as a considerable part of the hydrogen atoms and oxygen atoms will become engaged in intermolecular hydrogen-bond formation. The activity of the hydrogen atoms will be further lessened by the fact that if one of the hydrogen atoms in a water molecule is engaged in hydrogen bonding, the hydrogen-bonding power of the other hydrogen will immediately be diminished. This is due to the fact that we might regard the water molecule as being similar in properties to a dibasic

acid, H—O—H , and hydrogen-bond formation as an incipient dissociation process. Just as the second ionization constant of a dibasic acid is usually far less than the first one, similarly the hydrogen-bonding tendency of the second hydrogen will be checked by the formation of a hydrogen bond by the first hydrogen, owing to an inductive electron-pair shift towards the second hydrogen resulting in a diminution of its positive polarity. The oxygen atom being far larger than a hydrogen atom and the angle between the two bonds being about 105° , there is a large negative surface on oxygen, and oxygen being basically a nucleophilic substance, the oxygen atom will have a fair degree of its basic power left over in spite of internal hydrogen bonding. So, we might regard water at lower temperature to have a fair degree of basic or electron-donating power and a weak protogenic (hydrogen-donating) power. Both of these capacities probably increase with an increase in temperature.

Aliphatic alcohols

Comparing the structure of ethane with that of ethyl alcohol, we find that the hydrogens in the $\text{CH}_3\text{CH}_2\text{—}$ group in alcohol will be in a different state of polarity than in ethane, owing to the negative inductive effect of the hydroxyl group. We have reason to believe from a study of acid strength that the inductive effect falls off rapidly with distance and usually almost vanishes beyond the third carbon atom. Hence, though all the hydrogen atoms in ethane are in the same state and of very low polarity (conventionally zero), the alkyl hydrogen atoms in alcohol are more positive, depending upon their distance from the hydroxyl groups. In order to express the idea that the hydrogen atom in a C—H bond is more electropositive than in the paraffins, we shall use the term "polar"; when necessary, we shall indicate the electron displacement and polarity by an arrow placed on the top, $\overset{++}{\text{CH}}$. Now we apply one of our basic assumptions (made in a previous paper of this series) that all hydrogen atoms, including even those in the alkanes, are electrophilic and hence participate in the hydrogen-bonding process, the strength of the hydrogen bonding diminishing with the polarity of the $\overset{++}{\text{CH}}$ bond and practically vanishing with the alkanes. Hence, all the hydrogen atoms in ethyl alcohol will have a weak hydrogen-bonding tendency, as a result of which they will bridge with the oxygen atoms in water, producing a degree of solvation sufficient to make the molecule completely soluble. Similar considerations also apply to *n*-propyl and isopropyl alcohols; therefore we shall expect *n*-propyl alcohol to be less soluble than ethyl alcohol and isopropyl alcohol to be more soluble than *n*-propyl alcohol. However, all of these alcohols are completely soluble in water and so the above deductions cannot be tested.

Considering now the four butyl alcohols, it is easy on the above considerations to predict the order of their solubilities in water. The solubility will decrease parallel to the average C—H bond distance from the electron-attracting group. The average bond distance between the CH—OH , which is a measure of the

average polarity of the hydrogen atoms in the alkyl group, has been calculated for each of the four butyl alcohols, taking the distance of the nearest carbon atom as unity and adding 1 for increase of distance by each successive carbon atom in a chain, as shown in table 2. The numerical figures calculated for the average distance between the CH groups and the OH group in table 2 should not, however, be taken too literally because it is definite that the inductive effect cannot proceed unabated when a branching of the chain occurs, which we do not know how to allow for. It is, however, gratifying to note that the observed values of the solubilities are in the expected order, and this certainly provides confirmation of our basic idea. It should be noted that though there is an equal amount of branching in II and III, III is more soluble, owing to a greater scope of operation of the inductive effect. Tertiary butyl alcohol (IV) is structurally almost like ethyl alcohol as far as the distance of the hydrogen atoms from the OH group is concerned, except that the methyl groups in the tertiary alcohol are probably less polar than in ethyl alcohol, owing to the branching of the attraction of the OH group in three directions. This accounts for the fact that tertiary butyl alcohol is completely soluble in water, as contrasted to the incomplete solubility of its isomers.

Of the eight isomeric amyl alcohols, about which fortunately we have accurate data (10), the solubility is observed to be in the expected order, as shown in table 2. The observed solubility values are, as expected, in the opposite order to the average CH--OH distance. Though this calculation is meant to serve as a rough comparative guide among isomers, it is remarkable that it gives the correct order of the solubility values.

Of the two isomeric alcohols which have the same average CH--OH distance, we can foresee the order of their solubilities from some other considerations. From the fundamental fact that inductive effect falls off rapidly with distance, it follows that the nearer the branching starts to the polar group (in this case the hydroxyl group) the more will be the induced polarity in the hydrogens, and hence the higher the solubility in water. Since there cannot be any branching on the first carbon atom in a primary alcohol and only one branching for the secondary and two for the tertiary, we immediately derive the rule that the solubility will be in the order tertiary > secondary > primary. However, we still require a guide for prediction in cases where the average CH--OH distance is the same for two or more of the same type of alcohols. This can be derived from another consideration. It has been proved that the polarizability of the methyl group is by far higher than that of any other alkyl group; in such cases the compound with a higher number of methyl groups is likely to be more soluble. Also, the nearer the methyl group is to the electron-attracting group, the more will be its effect. Only real methyl groups are to be counted first and not those which are part of groups like ethyl, *n*-propyl, etc., since when the former are present, the latter will contribute much less to the solubility. We can apply this rule between the two amyl alcohols VI and VII, both of which are secondary and have the same average polarity of hydrogens. VII contains three methyl groups (one primary and two secondary),

TABLE 2
Relationship between the solubility of alcohols (20°C.) in water and their average $CH\cdots OH$ distance*

ALCOHOL	FORMULA	AVERAGE $CH\cdots OH$ DISTANCE RECKONING CONTIGUOUS CARBON ATOMS AS OF UNIT DISTANCE	SOLUBILITY IN WATER
Methyl alcohol	CH_3OH	$\frac{3 \times 1}{3} = 3/3$	$\frac{\text{weight}}{\text{per cent}} = 1.00$
Ethyl alcohol	CH_3CH_2OH	$\frac{1}{3} [3 \times 2 + 2 \times 1] = 8/5$	∞
n-Propyl alcohol	$CH_3CH_2CH_2OH$	$\frac{1}{3} [3 \times 3 + 2 \times 2 + 2 \times 1] = 15/7$	∞
Isopropyl alcohol	$CH_3CHOHCH_3$	$\frac{1}{3} [3 \times 2 + 1 \times 1 + 3 \times 2] = 13/7$	∞
<i>C₄ alcohols:</i>			
I. n-Butyl alcohol	$CH_3CH_2CH_2CH_2OH$	$\frac{1}{3} [3 \times 4 + 2 \times 3 + 2 \times 2 + 2 \times 1] = 24/9 = 2.67$	6.4†
II. Isobutyl alcohol	$(CH_3)_2CHCH_2OH$	$\frac{1}{3} [6 \times 3 + 1 \times 2 + 2 \times 1] = 22/9 = 2.44$	8.5†
III. sec-Butyl alcohol	$CH_3CH_2CHOHCH_3$	$\frac{1}{3} [3 \times 3 + 2 \times 2 + 1 \times 1 + 3 \times 2] = 20/9 = 2.22$	20‡
IV. tert-Butyl alcohol	$(CH_3)_3COH$	$\frac{1}{3} [9 \times 2] = 18/9 = 2.00$	∞
<i>C₅ alcohols:</i> ¶			
I. n-Amyl alcohol	$CH_3CH_2CH_2CH_2CH_2OH$	3.18	2.36
II. Isoamyl alcohol	$(CH_3)_2CHCH_2CH_2OH$	3.00	2.85
III. sec-Butyl carbinol	$CH_3CH_2CH(CH_3)CH_2OH$	2.82	3.18
IV. tert-Butyl carbinol	$(CH_3)_3CCH_2OH$	2.64	3.74
V. Methylpropylcarbinol	$CH_3CH_2CH_2CHOHCH_3$	2.64	4.86
VI. Diethylcarbinol	$CH_3CH_2CHOHCH_2CH_3$	2.45	5.61
VII. Methylisopropylcarbinol	$(CH_3)_2CHCHOHCH_3$	2.45	6.07
VIII. Dimethylethylcarbinol	$(CH_3)_2CH_2C(CH_3)_2OH$	2.27	12.15

* All data in this paper for which full reference is not given have been taken from reference 20.

† Data from Jones, who took special precautions to use alkali-free glass (*J. Chem. Soc.* **1929**, 799); other reported values are: Fühner (1924), 7.9 per cent; Hills and Malisoff (1926), 7.81 per cent.

‡ Michels (1922).

§ There are three reported values: Jones (*loc. cit.*), 20 per cent; Alexejew (1886) gives 22.5 per cent; both Lange's *Handbook of Chemistry* and the *Handbook of Chemistry and Physics* (Chemical Rubber Publishing Co.) give 12.5 per cent, without mentioning the source. (Data for the butyl alcohols seems to be very discordant among different sources.)

¶ All values are from Ginnings and Baum: *J. Am. Chem. Soc.* **59**, 1111 (1937).

whereas VI has none; hence VII would be more soluble than VI, a conclusion which agrees with observation. This procedure for determining the order of solubilities of alcohols in water can be summarized in the form of the following three rough guides. The order of their solubilities is:

- (1) Tertiary > secondary > primary.
- (2) Higher average CH---OH distance gives lower solubility among alcohols of the same type.
- (3) Among alcohols of the same type and same CH---OH distance, the one with more methyl groups will be the more soluble.

The above relationships are meant to be rough guides only and depend on a fortunate coincidence of circumstances. The polar group here being highly soluble, the solubility is mainly being conditioned by the solubility of the alkyl group. It should be pointed out that the hydroxyl groups of the three types of alcohols are quite different in character, because by virtue of their exercising their inductive functions, more electronic charge flows towards the tertiary hydroxyl than towards the secondary and so on. This flow of electronic, i.e., negative, charge causes a diminution of the OH polarity; hence the acidity or protogenic power of the alcohols varies in the order primary > secondary > tertiary, and the basic power of the oxygens is in the reverse order. It should also be pointed out that the general notion that the more compact the alcohol the higher is the solubility holds good only in the same type of alcohol, as can be seen by comparing tertiary-butylcarbinol (primary) with methylpropylcarbinol (secondary). The former is far more compact than the latter but is less soluble for reasons of rule 1 above.

We now pass on to the consideration of the hexyl alcohols. The data for only ten isomers are available (11) and are given in table 3 with the calculated average polarity of each. According to rule 1 the solubility is in the order 1, 2, 3 > 4, 5, 6, 7, 8, 9 > 10. Rule 2 gives further distinction among these three groups as 1, 2 > 3 > 4, 5 > 6, 7, 8 > 9 > 10. Rule 3 further differentiates into 2 > 1 > 3 > 4 > 5 > 6 > 8 > 7 > 9 > 10. The observed solubility is in the order 1 > 2 > 3 > 4 > 5 > 6 > 7 > 8 > 9 > 10. Two small violations of rule 3 are noticeable: the first one is 0.17 unit and the second one is 0.04 unit in per cent solubility. We do not really know if the data are to be relied upon to this extent, or if these minor discrepancies are to be expected from the necessarily crude nature of the above guides.

In considering the cyclic alcohols, we should expect them to be more soluble than the open-chain alcohols from which they are derived by ring closure, since any ring closure, in general, heightens the inductive effect by giving it a chance to play along two paths and by a release of the unsymmetrical electronic tension. The data for cyclohexanol, the only cyclic alkanol for which data are obtainable, show the above trend.

Ethers

The same type of consideration can be applied to aliphatic ethers. We can immediately see why dimethyl ether (I) is completely soluble in water, whereas

diethyl ether is only partially soluble; the inductive effect of the ethereal oxygen is not enough, particularly as it is branched out in two directions to make the remote hydrogens in the latter case sufficiently polar.

In table 4 are collected the available solubility data (1, 2) for ethers and also the calculated average polarity of the hydrogen. Of the three C_4 ethers, our expectation according to rule 2 is $1, 2 > 3$ and according to rule 3 is $1 > 2 > 3$, a prediction which agrees with experimental data.

Of the six C_5 ethers, our expectation according to rule 2 is $1, 2 > 3, 4 > 5, 6$; this is found to be true. On further differentiating among these subgroups by rule 3, we get the order $1 > 2 > 3 > 4 > 5 > 6$. The observed results are

TABLE 3
*Solubility of some C_6 alcohols in water (20°C.)**

ALCOHOL	FORMULA	AVERAGE CH—OH DISTANCE	SOLUBILITY per cent
$C_6H_{13}OH$			
<i>Tertiary:</i>			
1. Diethylmethylcarbinol	$(C_2H_5)_2(CH_3)C(OH)$	$32/13 = 2.46$	4.82
2. Dimethylisopropylcarbinol	$(CH_3)_2C(OH)CH(CH_3)_2$	$32/13 = 2.46$	4.65
3. Dimethyl- <i>n</i> -propylcarbinol	$(CH_3)_2C(OH)CH_2CH_2CH_3$	$34/13 = 2.62$	3.63
<i>Secondary:</i>			
4. <i>tert</i> -Butylmethylcarbinol	$(CH_3)_3CCHOHCH_3$	$34/13 = 2.62$	2.64
5. Isopropylethylcarbinol	$(CH_3)_2CHCHOHC_2H_5$	$34/13 = 2.62$	2.24
6. <i>sec</i> -Butylmethylcarbinol	$CH_3CH_2(CH_3)CHCHOHCH_3$	$36/13 = 2.77$	2.09
7. Isobutylmethylcarbinol	$(CH_3)_2CHCH_2CHOHCH_3$	$38/13 = 2.92$	1.79
8. <i>n</i> -Propylethylcarbinol	$CH_3CH_2CH_2CHOHCH_2CH_3$	$36/13 = 2.77$	1.75
9. <i>n</i> -Butylmethylcarbinol	$CH_3CH_2CH_2CH_2CHOHCH_3$	$40/13 = 3.08$	1.51
<i>Primary:</i>			
10. <i>tert</i> -Pentylcarbinol	$(C_2H_5)_3CCH_2OH$	$38/13 = 2.92$	0.82
11. <i>n</i> -Hexyl alcohol†	$CH_3CH_2CH_2CH_2CH_2CH_2OH$	$48/13 = 3.69$	0.59
12. Cyclohexanol‡	$CH_2CH_2CH_2CH_2CH_2CHOH$	$= 2.27$	3.82

* All data unless otherwise mentioned are from Ginnings and Webb (11).

† Fühner (1924).

‡ Sidgwick and Sutton (1930).

$1 > 2 > 4 > 3 > 5 > 6$, i.e., the order is reversed in the case of 3 and 4. On general grounds, however, it also appears that 3 should have less solubility than 4, because the former is a straight-chain ether. However, this only shows the need of more work before a final decision can be made.

Suppose we close the two ethyl groups of diethyl ether to form a closed ring, either by direct carbon-carbon union or through another oxygen atom. In the former case, i.e., with tetrahydrofuran (III) we should expect an increase of solubility not only for the fact that each C—H bond is more affected by the inductive operation acting through two paths but also on account of the average C—H distance from oxygen becoming shorter, as a simple calculation shows.

TABLE 4
Solubility of ethers in water (20°C.)*

ETHER	FORMULA	AVERAGE EC--O DISTANCE	SOLUBILITY per cent
C₂ ethers:			
I. Dimethyl ether.....	CH ₃ OCH ₃	6/6 = 1.0	∞
II. Ethylene oxide.....	CH ₂ OCH ₂	4/4 = 1.0	∞
C₃ ethers:			
1. Methyl isopropyl ether ..	CH ₃ OCH(CH ₃) ₂	3 + 1 + 12 = 16/10 = 1.6	7.4 (20°C.)
2. Diethyl ether†.....	C ₂ H ₅ OC ₂ H ₅	5 + 2 + 2 + 6 = 16/10 = 1.6	6.89 (20°C.)
3. Methyl <i>n</i> -propyl ether ..	CH ₃ OCH ₂ CH ₂ CH ₃	3 + 2 + 4 + 9 = 18/10 = 1.8	3.2 (20°C.)
C₄ ethers:			
1. Methyl <i>tert</i> -butyl ether. .	CH ₃ OC(CH ₃) ₃	21/12 = 1.75	5.16 (25°C.)
2. Ethyl isopropyl ether.....	CH ₃ CH ₂ OCH(CH ₃) ₂	21/12 = 1.75	2.40 (25°C.)
3. Ethyl <i>n</i> -propyl ether ..	CH ₃ CH ₂ OCH ₂ CH ₂ CH ₃	23/12 = 1.92	1.87 (25°C.)
4. Methyl <i>sec</i> -butyl ether ..	CH ₃ OCH(CH ₃)CH ₂ CH ₃	23/12 = 1.92	1.60 (25°C.)
5. Methyl isobutyl ether.....	CH ₃ OCH ₂ CH(CH ₃) ₂	25/12 = 2.08	1.10 (25°C.)
6. Methyl <i>n</i> -butyl ether.....	CH ₃ OCH ₂ CH ₂ CH ₂ CH ₃	27/12 = 2.25	0.89 (25°C.)
Cyclic ethers (five-membered ring):			
III. Tetramethylene oxide (tetrahydrofuran).....	CH ₂ CH ₂ CH ₂ CH ₂ O	12/8 = 1.50	∞ (20°C.)
IV. α -Methyltetramethylene oxide.....	CH ₃ CH ₂ CH ₂ CH(CH ₃)O	17/10 = 1.70	15.05 (20°C.)
V. β -Methyltetramethylene oxide.....	CH ₃ CH ₂ CH(CH ₃)CH ₂ O	19/10 = 1.90	9.50 (20°C.)
Cyclic ethers (six-membered ring):			
VI. Pentamethylene oxide ..	CH ₂ (CH ₂) ₃ CH ₂ O	18/10 = 1.8	8.76 (20°C.)
VII. 1,4-Dioxane	CH ₂ CH ₂ OCH ₂ CH ₂ O	Less than 1.0	∞

* All data except that marked † are from Bennett and Philip (1, 2).

† Seidell (20, page 272).

From similar considerations the latter, i.e., 1,4-dioxane (VII), will be more soluble than dimethyl ether. Both of these compounds have been found to be completely soluble in water. Ethylene oxide (II) also behaves in the expected manner, i.e., its solubility should be higher than that of dimethyl ether (I), from which it is obtained by ring closure. Both of these compounds are found to be completely soluble in water. Propylene oxide compares in structure with methyl ethyl ether, except that there is a ring closure which will in such case tend to increase its solubility in water and a branching of chain which will decrease it. Since the effect due to ring closure is often found to be stronger than branching, we might expect the oxide to have somewhat higher solubility. No data are, however, obtainable for the ether (VII) to examine this point.

We have illustrated enough to show the rôle of the inductive effect in solubility. All other types of compounds showing pure inductive effect can be similarly treated. We might point out that the insolubility of the alkyl halides is chiefly due to the insolubility of the covalently bound halogens caused by their very weak hydrogen-bonding tendency with the hydrogen atoms in water. In other words, the intermolecular hydrogen-bond formation is so strong in water that the covalent halogen atom fails to induce it for its own solvation. We now pass on to the consideration of compounds showing other types of electronic effects.

Aldehydes and ketones

The doubly-bound oxygen in carbonyl groups shows an electromeric effect, i.e., it can serve as a "sink" for electrons when necessary, $C \overset{\curvearrowright}{=O}$. In order that the electromeric shift might take place in the direction of the natural electron affinity, there must also be a source of electrons attached to it. None of the alkyl groups can serve as a good source of electrons except the methyl group; hence the group CH_3CO- should be comparatively highly soluble. Though it is universally agreed that the methyl group in contrast to its homologues serves as a good electron-releasing group, there is some disagreement about the actual mechanism. Effects from pure $+I$ (electron-release) effect at one extreme to pure $+T$ (tautomeric electron-release) effect at the other, leading to what has been termed hyperconjugation, have been postulated. For our purpose we have to imagine it as a joint effort of the three methyl hydrogens to replenish the loss of negative charge on the carbon of the carbonyl caused by an electromeric shift in oxygen. As a result, all the three hydrogens will be more polar and hence contribute towards a higher solubility than usual.

Hence, any aldehyde or ketone having the group CH_3CO will have higher solubility in comparison with similar compounds without this group. This tendency is shown by the complete solubility of acetone and acetaldehyde in water. Also, this effect of the methyl group is clearly noticeable if we compare the solubility of methyl ethyl ketone with that of the alcohol obtained by its reduction (table 5). It will be observed that the ketone in this case is more soluble than the corresponding alcohol. This is rather unusual, as we shall see

TABLE 5
Solubility of aldehydes and ketones

SUBSTANCE	FORMULA	TEMPERATURE	SOLUBILITY	REFERENCE
Acetaldehyde.	CH_3CHO	°C.		
Acetone.....	CH_3COCH_3	20	∞	
		20	∞	
Methyl ethyl ketone.	$\text{CH}_3\text{COCH}_2\text{CH}_3$	20	24.0 per cent	Jones (1929)
sec-Butyl alcohol	$\text{CH}_3\text{CHOHCH}_2\text{CH}_3$	20	20 per cent	Jones (1929)
			12.5 g./100 g. water	Lange's <i>Handbook of Chemistry</i>
Propionaldehyde....	$\text{CH}_3\text{CH}_2\text{CHO}$	20	16.0 per cent	Vaubel (1899), quoted from Seidell, p. 175
Methyl n-propyl ketone.....	$\text{CH}_3\text{COCH}_2\text{CH}_2\text{CH}_3$	30	0.630 mole per cent	Gross, Rintelen, and Saylor: J. Phys. Chem. 43, 197 (1939)
		50	0.515 mole per cent	
Methyl isopropyl ketone.....	$\text{CH}_3\text{COCH}(\text{CH}_3)_2$	30	0.608 mole per cent	
		50	0.594 mole per cent	
Diethyl ketone.....	$\text{CH}_3\text{CH}_2\text{COCH}_2\text{CH}_3$	30	0.576 mole per cent	
		50	0.456 mole per cent	
Propionaldehyde . . .	$\text{CH}_3\text{CH}_2\text{CHO}$	20	16.0 per 100 g. water	Vaubel (<i>loc. cit.</i>)
n-Propyl alcohol.....	$\text{CH}_3\text{CH}_2\text{CH}_2\text{OH}$	20	∞	
Butyraldehyde.....	$\text{CH}_3\text{CH}_2\text{CH}_2\text{CHO}$	20	3.6 per cent	Vaubel (<i>loc. cit.</i>)
n-Butyl alcohol... .	$\text{CH}_3\text{CH}_2\text{CH}_2\text{CH}_2\text{OH}$	20	6.4 per cent	Table 2
Diethyl ketone.....	$\text{CH}_3\text{CH}_2\text{COCH}_2\text{CH}_3$	30	4.69 per 100 g. water	Gross, Saylor, and Gorman: J. Am. Chem. Soc. 55, 650 (1933)
Diethyl carbinol.....	$\text{CH}_3\text{CH}_2\text{CHOHCH}_2\text{CH}_3$	30	4.75 per 100 g. water	Table 2

immediately, and is only attributable to the above property of the methyl group. This power of the methyl group is so strong that the solubility of this compound is higher than that of even the aldehyde with one less carbon atom, i.e., obtained by replacing the methyl group with hydrogen. The same tendency

is observed in methyl propyl (both normal and iso) ketones being more soluble than their isomer diethyl ketone, on all of which we have more reliable data.

The available data with aldehydes and ketones are, however, very scarce and unreliable, but the general behavior of all of them, except for the above special effect of the CH_3CO group, seems to be quite regular. Any aldehyde is less soluble than the corresponding primary alcohol because the electromeric

H
|
 $\text{RC}\overset{\curvearrowright}{=}\text{O}$

effect of the CO group, $\text{RC}\overset{\curvearrowright}{=}\text{O}$ is considerably used up in polarizing the C—H bond; hence the electron-attracting effect is much less felt by the alkyl group. For the same reason, all aldehydes are much less soluble than the corresponding ketones.

If the electromeric effect of the double-bonded oxygen is assumed to be as effective as a hydroxyl group, a ketone will generally be almost as soluble as the secondary alcohol from which it is derived. This is generally found to be the case, as will be seen from the rather unreliable data in table 5.

It should be pointed out, however, that the above comparison of solubilities of liquids is unsound from the thermodynamic point of view. A strict comparison can be made only at the same temperature and also at the same partial pressure of the solutes. However, since our experimental data are very meager in this respect and since partial miscibility between two liquids can arise only out of some strong thermodynamic irregularity which is usually present in most such solvents even under less extreme conditions (for example, see Butler (4)) and since our practical interest is mostly to know the solubility of a liquid as such, our discussion from the standpoint as presented above is justified and useful.

RESONANCE AND SOLUBILITY

Suppose we have a compound AB, which can have two other resonating forms A^+B^- and A^-B^+ . It is usually assumed that this reversal of the polarity in the two forms causes them to compensate each other. This might be true as far as properties like dipole moments are concerned, but not so with some other properties. According to the fundamental concept of resonance, the actual form of the molecule is not a mean of the unperturbed forms, but all these forms contribute to the actual structure. In other words, the observed property of the compound will be such as we should expect from a combination of all the contributing forms, and hence the charged forms will not neutralize each other, but will create an internal charge separation, i.e., one or more buried dipoles in the molecule.

Since dipolar nature means salt-like character, which is characterized by a lack of solubility in organic solvents, we expect that resonance of this kind will tend to decrease the solubility in organic solvents. Hence, among isomers or compounds of very similar structure, the strongest resonating molecule will in general be the least soluble in organic solvents.

Following the above line of reasoning, another experimentally observable deduction can be made. Salts are not only characterized by a lack of solubility

in organic solvents, but they also show a tendency to dissolve in hydroxylic solvents. Hence, the buried dipoles produced by resonance will tend to make the resonating form show a greater affinity for hydroxylic solvents. We want to make clear that we do not mean that the stronger resonance will necessarily create higher solubility in hydroxylic solvents, but it will definitely create such a tendency which can be experimentally tested as follows. If we have two isomers A and B, where A has resonance in its structure much higher than B, we should expect

$$\left(\frac{S_A}{S_B}\right)_{\text{alcohol}} > \left(\frac{S_A}{S_B}\right)_{\text{benzene}}$$

where S represents solubility in the corresponding solvent shown outside the bracket. We now proceed to see how far the above two deductions are supported by available experimental data. However, we should point out that we acknowledge that solubility is a very complex process depending on various factors but our main contention is that the resonance in the structure plays an important rôle in the process, the existence of which can be clearly demonstrated in some simple cases where the other factors play a less dominant rôle.

Dinitrobenzenes

Our first case is that of the three dinitrobenzenes, whose solubilities in many organic solvents are known with a fair degree of accuracy. From one oxygen to another in the second nitro group, there is a conjugated system of double bonds producing a strong resonance between the two nitro groups in the ortho and the para compound, making them simultaneously positive and negative at the two ends, which is reversed by the resonance in the other direction. Since the resonance is stronger, the more extensive is the conjugation, we should expect the para isomer to be the most resonant. Hence, we should expect the solubility in hydrocarbon solvents to decrease in the order meta > ortho > para. This is in agreement with the experimental results (table 6), as compiled by Seidell (20).

A comparative study of the individual solubilities in different solvents as given in table 6 is very illuminating and clarifies the principle of the solvent-solute interaction that we are trying to illustrate. We shall only consider the meta compound, because here the buried dipolarity is the least though not completely absent and hence other factors are more prominent. The solubility of this nitro derivative in organic solvents is evidently conditioned mainly by the solubility of the nitro groups. Hence any compound which has hydrogen to solvate the oxygen will be a good solvent, and the more polar this hydrogen the better is the solubility. This will be seen by comparing benzene with toluene or chloroform with carbon tetrachloride. The benzenoid $\overset{\leftrightarrow}{\text{CH}}$ is certainly more polar than the $\overset{\leftrightarrow}{\text{CH}}$ of toluene, and chloroform has a CH group, whereas carbon tetrachloride or carbon disulfide has none. This explains why benzene is a better solvent than toluene, and chloroform is better than carbon tetra-

chloride or carbon disulfide. However, the alcohols are less powerful solvents than chloroform or benzene, because though alcohols are much stronger hydrogen-bonding solvents, they are far inferior in hydrocarbon-dissolving power, which is also necessary in this case. Further, an optimum electrophilic nature of the hydrogen seems to be necessary; otherwise the hydrogen bonding will be so strong as to create a dipole inside the nitro compound by displacement of electrons towards the oxygen, an effect which will reduce the solubility.

We now proceed to test our second deduction, with regard to the change of solubility in passing to hydroxylic solvents. In table 6 we have also given the values of the ratio of the solubilities para/meta and ortho/meta in various solvents. It will be observed that, in conformity with our expectation, the decrease of solubility in passing from meta to ortho or from meta to para is much lower in benzene or toluene than in the hydroxylic solvents. In fact

TABLE 6
*Solubility of the dinitrobenzenes in various solvents**
(Grams of solute per 100 g. solvent)

SOLVENT	TEMPER- ATURE	ORTHO	META	PARA	ORTHO/ META	PARA/ META
	°C.					
Methyl alcohol	20.5	3.30	6.75	0.69	0.49	0.102
Ethyl alcohol	20.5	1.9	3.5	0.4	0.543	0.114
Propyl alcohol	20.5	1.09	2.4	0.298	0.454	0.124
Benzene	18.2	5.66	39.45	2.56	0.144	0.0654
Toluene	16.2	3.62	30.66	2.36	0.118	0.077
Chloroform	17.6	27.1	32.4	1.82	0.836	0.056
Carbon tetrachloride	16.2	0.143	1.18	0.12	0.121	0.102
Ethyl acetate	18.2	12.96	36.26	3.56	0.36	0.098
Carbon disulfide	17.6	0.236	1.35	0.148	0.175	0.110

* This table is reproduced from Seidell (20, p. 323) and is compiled mainly from the work of de Bruyn (1894).

with one exception (chloroform in ortho/meta), it can be said that the hydroxylic solvents form a class by themselves far different from the rest, showing a tendency towards higher solubility for the more resonating form. The values para/meta for carbon disulfide and carbon tetrachloride are in the range of the alcohols, but the degree of accuracy of the above data is not of such an order as to warrant any reliance on these very small values of the solubility of the para compound in these solvents, which will strongly affect this ratio.

Such data for isomers which differ strongly among themselves in resonance are, however, very scarce in the literature and are of varying degrees of accuracy. Since strong resonance can originate only from the co-existence of a good source and a good sink for electrons, data on compounds containing nitro, carbonyl, and amino groups are most suitable for our purpose. Such data are very scarce, and we quote the very accurate recent data (7) for nitroanilines in table 7. It should be observed that, as expected, the para compound is the least soluble.

However, the ortho compound is consistently more soluble than the meta. This is not owing to a failure of our idea, but is ascribed to the well-known chelation by hydrogen bonding for the ortho derivative, which makes the ortho compound more non-polar. This complication does not enter into the meta and the para compounds; hence we should expect the para compound to be less soluble than the meta and the solubility ratio para/meta to be higher in hydrox-

TABLE 7
*Solubility and solubility ratios of nitroanilines**
(Grams per 100 g. solvent)

SOLVENT	TEMPERATURE °C.	ORTHO	META	PARA	PARA/META
Benzene.	25	20.80	2.718	0.5794	0.21
Chloroform.	25	—	3.216	0.929	0.29
	0	1.17			
Ethyl alcohol (absolute).....	25	27.87	7.778	6.048	0.78
Water.....	25	0.1212	0.0910	0.0568	0.63

* Data from Collet and Johnson (7).

TABLE 8
*Solubility of nitrobenzoic acids**
(Grams per 100 cc. solvent)

SOLVENT	TEMPERATURE °C.	ORTHO	META	PARA	ORTHO/META	PARA/META
Water.....	20	0.682	0.315	0.039	2.16	0.12
Methyl alcohol..	10	42.72	47.34	9.6	0.90	0.20
Ethyl alcohol...	15	37.58	47.26	19.71	0.79	0.42
Acetone.....	10	41.5	41.5	4.54	1.0	0.11
Benzene	10	0.294	0.795	0.017 (12.5°C.)	0.37	<0.021
Carbon disulfide	10	0.012	0.10 (8.5°C.)	0.007	<0.12	<0.07
Chloroform.....	10	0.455 (11°C.)	5.678	0.066	<0.08	0.012
Ether.....	10	21.58	25.175	2.26	0.86	0.09
Lignin	10	Traces	0.013	Traces		

* Compiled by Seidell (20, p. 489).

ylic solvents than in hydrocarbons. The data completely confirm our expectations.

Exactly similar considerations apply to the three nitrobenzoic acids, for which we have much less accurate data. A compilation of the relevant data as given by Seidell (20) is quoted in table 8. It will be observed that the solubilities in all solvents except in water are in the order meta > ortho > para. Also, the ratio para/meta is considerably higher in hydroxylic solvents than in the other organic solvents, a fact which is particularly striking if we compare benzene with ethyl alcohol. The ortho/meta ratio also shows this tendency perceptibly,

though not strikingly, owing to the slight counteracting tendency arising from ortho chelation, as referred to in the foregoing paragraph.

The above conditions are also valid if only one of the disubstituted groups is a source or sink of electrons and the other is an ordinary group, as this will tend to interplay and stabilize the resonance at the para and the ortho positions. Data to the point are available for a few compounds which we discuss below. McCombie and coworkers (17), in an attempt to correlate the solvent effect on reaction kinetics with solubility data, determined the solubilities of the three isomeric nitrobenzyl chlorides in six solvents (see table 9). The variation of the solubility in the order meta > ortho > para is striking. However, it is felt

TABLE 9a
Solubility and solubility ratios of nitrobenzyl chlorides
(Grams per 100 g. solvent)

	ORTHO	META	PARA	ORTHO/META	PARA/META
Ethyl alcohol	26.3	30.4	8.2	0.865	0.27
Benzene... ..	304		74.2		
Nitrobenzene	217	326	68.2	0.665	0.209
Acetone.....	433	644	126.8	0.673	0.197
Ethyl acetate.....	257	394	69.7	0.652	0.177
Ethyl benzoate	171	266	51.2	0.643	0.192

TABLE 9b
Solubility and solubility ratios of hydroxybenzoic acids

	TEMPER- ATURE	ORTHO	META	PARA	PARA/ META	REFERENCE
	°C.					
Benzene.....	25	0.78	0.010	0.0035	0.35	Walker and Wood: J. Chem. Soc. 73, 620 (1898) Seidell (20, pp. 525-30); Savarao: Chem. Ab- stracts 8, 340 (1914)
Acetone.....	23		26.0	22.6	0.87	
Ether	17		9.73	9.43	0.97	
Methyl alcohol...	15		115.2	236.22	2.05	

that the ortho isomer is here somewhat more soluble than expected (though less than meta), owing to a slight tendency toward chelation, as cited in the previous paragraph. Also, the ratio ortho/meta or para/meta significantly increases as we pass to the hydroxylic compound, ethyl alcohol. In fact, all other solvents form a group, while ethyl alcohol stands out separate with a higher value, clearly pointing out the expected effect.

A rather limited amount of data (23) is available for a similar case, the hydroxybenzoic acids, which are also cited in table 9. It will be observed that the para isomer is less soluble than the meta, particularly in benzene, and the ratio para/meta has a strikingly high value in methyl alcohol in comparison with the other three solvents. The reason why the ortho compound has a very

high solubility in benzene is, of course, the ortho chelation by hydrogen bonding. These compounds are of some interest from our viewpoint, because Walker and Wood (23), from whose work the first three data are quoted, were the first to notice in the case of the hydroxybenzoic acids and the toluyl carbamides that the ratio meta/para, meta/ortho, and para/ortho varies considerably from solvent to solvent. Sidgwick and Ewbank (21) observed for the same data that at moderate temperatures "the ratio ortho/para which is very small in water rises as the dielectric constant of the solvent falls, reaching a maximum in

TABLE 9c
Solubility and solubility ratios of chlorobenzoic acids (14–20°C.)
(Grams per 100 cc. saturated solution)

	ORTHO	META	PARA	ORTHO/ META	PARA/ META	REFERENCE
Benzene	0.92	0.66	0.017	1.39	0.0258	Bornwater and Holleman (3)
Carbon tetrachloride.	0.58	0.48	0.04	1.21	0.083	
Carbon disulfide . .	0.52	0.62	0.016	0.84	0.0258	
Ether.	16.96	14	1.72	1.21	0.123	
Water*	2.13	0.385	0.068	5.53	0.177	

* Temperature, 25°C.; grams acid per liter (Osol and Kilpatrick (18)).

TABLE 9d
Solubility of nitrophenols
(Grams per 100 g. solvent)

SOLVENT	TEMPER- ATURE	ORTHO	META	PARA	PARA/META
	°C.				
Benzene*	20	147.2	1.63	0.92	0.56
	30	359.7	2.94	1.13	0.38
Toluene†	70	---	36.1	22.7	0.63
Ethyl alcohol‡	25	46.0	195	189.5	0.97
Water†	40	0.330	3.02	3.28	1.09

* Interpolated from Carrick (6).

† Interpolated from Sidgwick, Spurnell, and Davies (22).

‡ Interpolated from Duff and Bills (8).

benzene which is yet far short of the ratio of the vapour pressures. The ratio para/meta which is very much nearer to unity tends to rise in the same direction."

Available data (3, 18, 20) for a similar case, that of the chlorobenzoic acids, are also given in table 9. It will be observed that the para isomer is consistently much less soluble than the meta. The expected difference in solubility between the ortho and meta isomers is again masked somewhat in most cases by the opposing effect, owing to ortho chelation. The second relation about the ratio of solubilities cannot be tested, owing to a lack of data for alcohols. However, we take recourse to data in water, when it will be observed that the ratio para/

meta is much higher in the hydroxylic solvent, as expected. However, we do not consider water a suitable hydroxylic solvent to test the above relation, because for compounds like acids a complication might arise, owing to unequal dissociation, which might mask the point we are demonstrating.

Nitrophenols come under the same category that we are discussing; hence we should expect the same type of relationship between the para and the meta isomers. Data are very limited, but from the figures cited in table 9, it will be seen that the para isomer is much less soluble than the meta. Also the ratio para/meta is higher in the hydroxylic solvents than in benzene. In fact, the increment in passing to hydroxylic solvents is so much in this case that the para isomer has a higher solubility than the meta in water. These data are obtained by graphical interpolation from the data of Carriek (6) and others (8, 20) for these compounds over a range of temperatures.

THERMODYNAMIC VIEWPOINT

Hildebrand (13) has attributed the above difference in solubility among the three dinitrobenzenes to the difference in their melting points, the compound of the lower melting point being more soluble. This explanation of higher solubility with lower melting point (first observed by Carnally (5)) has been based on thermodynamic reasonings by Hildebrand and others. It may, however, be pointed out that our explanation essentially agrees with the thermodynamic viewpoint, because what we call charge separation by resonance giving a salt-like character and consequent less solubility in organic solvents will also raise the melting point and hence will in general agree with Hildebrand's conclusions.

As far as the three dinitrobenzenes are concerned, Hildebrand has adduced a striking demonstration of the power of the thermodynamic approach. Assuming the solutions of the three dinitrobenzenes in benzene to be thermodynamically "regular", Hildebrand and Carter (15) have calculated the theoretical solubility from the known melting points and heats of fusion of these compounds. For all three compounds, it has been found that their actual solubilities depart from the ideal value and that this departure is the same for all three compounds over the temperature range studied at any given solubility.

Our idea, however, goes farther than this in one respect. It not only gives an electronic interpretation of the above thermodynamically derived rule, but also supplies information about its limitations. Since the decreased solubility of the high-melting isomer is due to an internal charge separation and consequent salt-like character, and since hydroxylic solvents like water, alcohols, etc. are known to be good solvents for some salts, it is conceivable that the reversal of such order might take place in such solvents. We have already come across a few striking cases. For example, the nitrophenols (m.p.: ortho, 45°C.; meta, 96°C.; para, 114°C.) show the expected behavior in benzene and toluene, but in alcohol the para isomer becomes almost as soluble as the meta, and four times more soluble than the ortho, and in water the solubility order reverses itself, being now para > meta > ortho. Even non-resonant compounds

an show wide variance from the melting-point rule, particularly in hydroxylic solvents, and we have already come across one striking case. Tertiary butyl salcohol has a melting point 105°C. higher than that of normal butyl alcohol, but the former is completely soluble in water, whereas the latter has only limited solubility. Another example involves the *o*- and *m*-dihydroxybenzenes, whose melting points are 105°C. and 110°C., respectively. Though their melting points are very close, the order of their solubilities (20) differs widely from solvent to solvent, the order in hydroxylic solvents, e.g., alcohol and water, being the reverse of that in benzene and other organic solvents. The *o*- and *m*-nitrobenzoic acids show the same type of behavior. They have melting points in the same range and the order of their solubilities depends on the solvents. Thus in ether the meta isomer has 22 per cent higher solubility than the ortho isomer; passing to the hydroxylic compound alcohol, it decreases to 18 per cent and in water it completely reverses itself, the ortho isomer becoming more than twice as soluble as the meta.

Incidentally, the foregoing concept explains why dyes are always high-melting solids of low solubility in all solvents in comparison with other organic compounds. The same is probably true as to the cause of high melting point and insolubility in organic solvents of many other organic compounds, e.g., amino acids, proteins, sugars, etc. We should also point out that, according to the above concept, chelation at the ortho position by hydrogen-bond formation is simply an expedient adopted by the molecule to counteract the charge separation due to resonance.

In developing our ideas on solubility, we have been incidentally led to an insight into the melting points of organic compounds. In fact, most of the data on melting points among isomers in disubstituted benzenes can be satisfactorily correlated from such a viewpoint. It may even be that the higher melting point of benzene in comparison with an alkane of the same number of carbon atoms is due to the fact that, owing to a contribution (though small) of the dipolar resonating forms of benzene as also the higher polarity at each $\overset{++}{\text{CH}}$ bond in benzene, a number of internal dipoles are created in it. As soon as a methyl group is substituted in benzene, the electron-release effect of the methyl group upsets the internal equilibria and decreases the polarity at each $\overset{++}{\text{CH}}$ bond in the benzene nucleus, as a result of which the melting point is depressed. However, this does not concern us in the present paper.

Phenanthrene and anthracene

We now consider a very interesting pair of isomers, phenanthrene and anthracene, fairly accurate data for which are available from the work of Hildebrand and coworkers (16) and are collected in table 10.

We do not know with certainty which of the two isomers has stronger resonance. There are no heat of hydrogenation data available for decision on this point. The available combustion data showing a heat of combustion of 1675 and 1685 Cal. for phenanthrene and anthracene, respectively, do not have sufficient

accuracy to lead to an unambiguous decision. General considerations that the resonance becomes stronger the more the contributing forms approach each other in structure would lead us to expect the more symmetrical anthracene to have a stronger resonance than its less symmetrical isomer phenanthrene. This is further supported by the fact that anthracene is more aromatic in chemical properties than phenanthrene, has a much higher melting point, and has a higher density in the solid state. Granting this point, the solubility data (16) become immediately intelligible. It will be observed that, in complete accord with our expectation, anthracene has much lower solubility than phenanthrene and the ratio of their solubilities, anthracene/phenanthrene, is much higher in alcohol than in the hydrocarbon solvents.

The above solubility values are also in agreement with the melting-point rule, as has been pointed out by Hildebrand. He attempted (14) to explain this as due to the fact that anthracene can be easily fitted into a lattice, whereas phenanthrene can not be done so easily, in consideration of their molecular

TABLE 10
*Comparison of the solubilities (20°C.) of phenanthrene and anthracene**

SOLVENT	PHENANTHRENE	ANTHRACENE	RATIO $\frac{\text{ANTHRACENE}}{\text{PHENANTHRENE}}$
Hexane..	4.2	0.18	0.043
Ether	15.1	0.59	0.039
Carbon tetrachloride..	18.6	0.63	0.034
Benzene	20.7	0.81	0.039
Carbon disulfide	25.5	1.12	0.044
Ideal value	22.1	1.07	0.048
Ethyl alcohol	1.25	0.09	0.072

* All data from Hildebrand, Ellefson, and Beebe (16).

Ideal values according to Hildebrand (12, p. 165).

geometry. It may well be that this geometrical factor contributes to the behavior of these two compounds, but it seems that one should not make it alone responsible for it. However, the fact that the density of anthracene is higher than that of phenanthrene, thus showing a more compact structure, is also attributable to the higher resonance in the former. The buried dipoles thus created will tend to attract each other, and this might fit the anthracene molecules into a tighter lattice.

Furan and tetrahydrofuran

Another rather paradoxical solubility behavior can be explained by this resonance concept of solubility. In general, when a double bond is saturated by hydrogen, the compound becomes more paraffinic and hence less soluble in water. Tetrahydrofuran, however, behaves anomalously and the explanation is as follows.

In both compounds there is an inductive effect of the ethereal oxygen (as

explained in the section on ether) which tends to make them soluble in water. In the case of furan, there is superimposed on it an additional effect arising out of the possibility of resonance among the five possible structures (due to the conjugated system) which will produce, as explained in the foregoing cases, a reduction of solubility. The presence of strong resonance in furan is confirmed from an actual calculation of resonance energy from heat of hydrogenation data (24), which shows quite a high value of 17.2 kg.-cal. The interesting point is that the inductive effect of oxygen would have made it more soluble, whereas resonance is making it less soluble; since the latter effect is very strong in this case, it is expected to take precedence over the former and to prevail. Actually, we find furan to be only partially soluble in water, whereas tetrahydrofuran, where only the inductive effect would operate (see the section on ether), is completely miscible with water. We again like to point out that resonance gives an internal charge separation and consequent salt-like character which increases the relative solubility in hydroxylic solvents in comparison to that in a hydrocarbon solvent but does not necessarily give the absolute solubility of a substance.

CONCLUSIONS

We have wholly limited ourselves so far to the treatment of simple systems showing only one type of effect. This is because we wanted to illustrate the applicability of the basic electronic concepts of the organic chemist—the inductive effect, the electromeric effect, and the mesomeric effect (resonance)—which are indeed universally operative but are difficult to demonstrate with complex systems, owing to overlapping of the different effects. It should, however, be made clear that these are only a few of the contributing factors among other equally important factors such as molecular geometry, molecular weight, ionization power, steric factors, etc., the effect of each one of which can be separated and demonstrated in suitable cases. We have here made only a beginning and a long way has yet to be gone with simple compounds and one-type solvents to understand their internal charge distribution and its effect on solubility and melting point, before we can profitably attack the problem on all fronts. Also, lack of reliable data prevents us from discussing many more interesting systems amenable to our treatment, since we believe that the justification of any theory or concept is in its agreement with known facts. The future of our concept clearly depends on the many solubility results yet to be obtained, results which (and only which) can either confirm, extend, or reject this viewpoint.

REFERENCES

- (1) BENNETT AND PHILLIP: *J. Chem. Soc.* **1928**, 1930.
- (2) BENNETT AND PHILLIP: *J. Chem. Soc.* **1928**, 1937.
- (3) BORNWATER AND HOLLEMAN: *Rev. trav. chim.* **31**, 230 (1912).
- (4) BUTLER: *Trans. Faraday Soc.* **33**, 171 (1937).
- (5) CARNALLY AND THOMSON: *J. Chem. Soc.* **53**, 782 (1888).

- (6) CARRICK: J. Phys. Chem. **25**, 628 (1921).
- (7) COLLET AND JOHNSON: J. Phys. Chem. **30**, 70 (1926).
- (8) DUFF AND BILLS: J. Chem. Soc. **1930**, 1331.
- (9) EWELL, HARRISON, AND BERG: Ind. Eng. Chem. **36**, 871 (1944).
- (10) GINNINGS AND BAUM: J. Am. Chem. Soc. **59**, 1111 (1937).
- (11) GINNINGS AND WEBB: J. Am. Chem. Soc. **61**, 1388 (1938).
- (12) HILDEBRAND: *Solubility*, 2nd edition, p. 166. Reinhold Publishing Corporation, New York (1936).
- (13) Reference 12, p. 35.
- (14) HILDEBRAND: Proc. Phys. Soc. (London) **56**, 221 (1944).
- (15) HILDEBRAND AND CARTER: Proc. Natl. Acad. Sci. U. S. **16**, 285 (1930).
- (16) HILDEBRAND, ELLEFSON, AND BEEBE: J. Am. Chem. Soc. **39**, 2301 (1917).
- (17) McCOMBIE, SCARBOROUGH, AND SMITH: J. Chem. Soc. **1927**, 802.
- (18) OSOL AND KILPATRICK: J. Am. Chem. Soc. **55**, 4430 (1933).
- (19) PAULING: *The Nature of the Chemical Bond*, 2nd edition, p. 284. Cornell University Press, Ithaca, New York (1940).
- (20) SEIDELL: *Solubility of Non-electrolytes*, Vol. II. D. Van Nostrand Company, New York (1941).
- (21) SIDGWICK AND EWBANK: J. Chem. Soc. **119**, 979 (1921).
- (22) SIDGWICK, SPURRELL, AND DAVIES: J. Chem. Soc. **107**, 1202 (1915).
- (23) WALKER AND WOOD: J. Chem. Soc. **73**, 618 (1898).
- (24) WHELAND: *The Theory of Resonance*, 1st edition, p. 61. John Wiley and Sons, Inc., New York (1944).
- (25) ZELLMHOEFFER, COPLEY, AND MARVEL: J. Am. Chem. Soc. **60**, 1337 (1938).

THE KINETICS OF DISSOLUTION OF CADMIUM IN HYDROCHLORIC ACID¹

JUNE F. ZIMMERMAN² AND HUGH J. McDONALD

Department of Chemistry, Illinois Institute of Technology, Chicago, Illinois

Received December 20, 1946

The problem of the dissolution of cadmium in various aqueous media has been investigated intermittently over the past two decades (2, 3, 4, 5, 7, 8, 9, 10, 11, 12, 13, 14 and 15), the chief work being that carried out by Centnerszwer and coworkers. The published data appear to be at variance in several places, and in some cases are of doubtful validity. The following work was performed in the hope of clarifying the nature of the reaction between cadmium and hydrochloric acid and suggesting a suitable mechanism for it.

The early procedures for measuring the rate of dissolution of cadmium in hydrochloric acid do not differ radically from those employed in this investigation. The rate was generally followed by measuring the amount of hydrogen

¹ This paper is abstracted from the thesis submitted by June F. Zimmerman to the Faculty of the Graduate School of the Illinois Institute of Technology in partial fulfillment of the requirements for the degree of Master of Science in Chemistry, June, 1945.

² Present address: Bryn Mawr College, Bryn Mawr, Pennsylvania.

evolved and then, as a check, at frequent intervals the weight losses of the cadmium rod were measured. In general, a small bar of cadmium was affixed to a piece of glass and rotated very slowly or not at all in solutions of varying concentration, under conditions of constant temperature. No attempt was made, however, to determine to what order the observed reaction belonged, and the heat of activation was not calculated.

Centnerszwer in 1928 (2) maintained that cadmium belongs to that group of metals whose solution potential is exceeded by the overvoltage of hydrogen in dilute acid solution. For this reason he concluded that pure cadmium is not soluble in dilute acid with measurable velocity and limited his investigation to concentrations of acid of 6, 8, and 10 normal. With acids of this concentration he derived data that indicated the following: (1) The process of solution of cadmium in hydrochloric acid depends upon an induction period, whose duration is greater or less as the acid is more or less dilute. (2) During the induction period the velocity of solution of the cadmium increases steadily, that is to say, the amount of hydrogen evolved per minute increases from minute to minute at these concentrations. (3) The constant of reaction velocity, which becomes apparent after the induction period has run its course, is dependent on the initial concentration of acid and increases greatly with the initial concentration.

Centnerszwer also observed that if the cadmium sample, after being thoroughly cleaned, is activated by immersion for periods of 20–24 hr. in concentrated acid, the induction period decreases and the metal begins to dissolve with constant velocity. This activation of surface may be preserved if the sample is stored overnight in distilled water.

Investigating the effect of stirring the sample at rotation speeds of 300 R.P.M., he observed that the velocity of solution in concentrated acids was markedly changed by varying speeds, while in more dilute solutions agitation had little or no effect. From this he concluded that in dilute solution the reaction is activation controlled, whereas in concentrated solutions it is diffusion controlled. However, calculation of temperature coefficients produced a value which corresponds to that usually found in homogeneous chemical processes where diffusion plays the major rôle. His final comment on the matter may be summed up by saying that in acids of high concentration we are dealing with a process under mixed control, in which both diffusion and activation play important parts.

In 1939 Centnerszwer (3) expressed the belief that the rate of solution could be expressed as a fourth-degree reaction and is purely chemically controlled.

Jablczynski and Wajchselfisz (9) performed the same type of experiment, using Centnerszwer's equipment. Their work led to rather surprising results, in that they observed that when fresh, non-activated cadmium was dissolved in 5 *N* hydrochloric acid, after 40 min. the velocity of attack decreased almost to zero. There was no apparent way to explain this behavior.

When working with activated cadmium surfaces, i.e., surfaces which had been immersed for 24-hr. periods in concentrated or fuming hydrochloric acid, they observed that the amount of activation seemed to be proportional to the depth of color of a light brown coating which formed on the surface. Surpris-

ingly enough, the activation period did not stop abruptly after a 20-hr. exposure to the acid, but rather, crept steadily forward, although the constancy through short periods of time left nothing to be desired. It was the opinion of the above-mentioned workers that the investigations of Centnerszwer had not been extended over a sufficiently long period of time, inasmuch as his "*k*" values were constantly increasing. However, they did agree that this particular solution process is a purely chemical process in which diffusion plays a rather subordinate rôle.

Kimball and Glassner (12), when investigating the rate of solution of cadmium in sulfuric acid, found that the rate could best be expressed by a zero-order equation, and showed that this should be the order on a theoretical basis.

As has already been stated, the equipment used in this study was similar to that used in previous measurements. The course of the reaction was followed by measuring the amount of hydrogen evolved by cadmium—sheet, rod, or electroplate—as it was whirled through a solution of hydrochloric acid of varying concentration. The reaction vessel and the gas-collecting buret were kept at constant temperature throughout by the use of a large water bath and a centrifugal circulating pump. A schematic diagram of the apparatus employed is shown in figure 1.

The cadmium employed for the study was of three types. The bar cadmium of 99.95 per cent purity was supplied by the J. T. Baker Chemical Company in cylinders which were machined to approximate dimensions of 6.4 by 1.2 cm. After machining, the surface was subjected to manual polishing with $\frac{1}{2}$, 00, and 000 emery paper. Subsequent to the polishing the bars were washed with a sodium bicarbonate paste to remove loose metal granules and traces of emery and given final rinses with distilled water to insure removal of all of the bicarbonate paste. In the top of each cadmium bar a threaded brass wedge was sunk in such a fashion that a brass rod could be screwed into it, so that attachment could be made to the stirrer chuck. The upper portion and likewise the lower part were masked with gum-rubber sleeves so that only the center portion, with an area of approximately 15.73 sq. cm., was exposed. The gum rubber tubing employed for this masking had been extracted 20 hr. with c.p. acetone to eliminate the possibility of formation of sulfur-cadmium couples.

Sheet cadmium was also employed in the experimental work. This was supplied at a purity of 99.99 per cent by the Belmont Smelting and Refining Works, Inc., Brooklyn, New York. Small rectangles (4.25 by 2.00 cm.) were cut from the sheet, and holes were punched in the corners, as shown in figure 2, for suspension on the glass S-shaped hook. The total area exposed amounted to approximately 17.90 sq. cm.

Since much of the cadmium used industrially is employed in the form of electroplate, it was felt that an investigation of the behavior of the electroplated cadmium in hydrochloric acid might lead to interesting information. For this purpose cadmium was plated onto a platinum cylinder of approximately the same dimensions given for bar cadmium, using a current density of 0.5 amp. and a 1-volt potential. Prior to plating the platinum was thoroughly degreased,

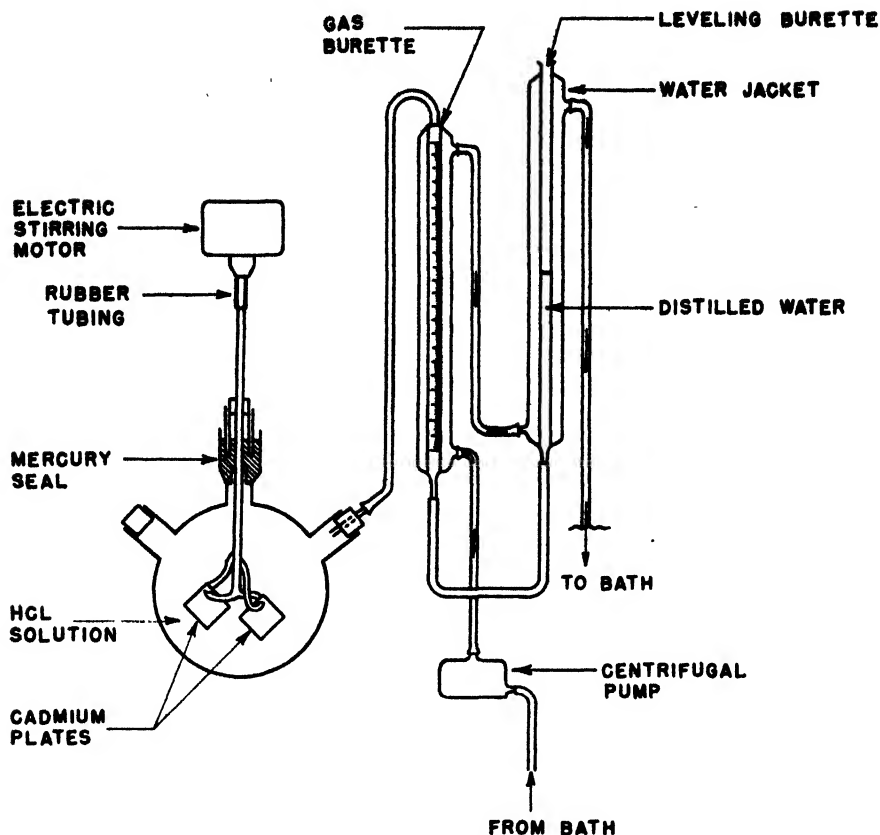


FIG. 1. Schematic diagram of apparatus employed in measuring kinetics of dissolution of cadmium in hydrochloric acid.

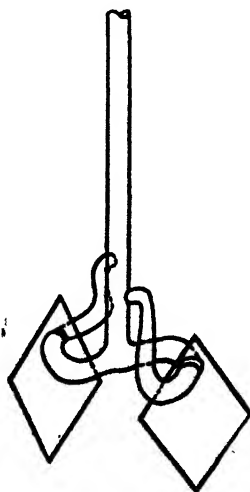


FIG. 2. Schematic diagram of suspension used for sheet cadmium specimens

rinsed, and dried, care being taken to avoid manual contact with the cleaned surface. The plating bath employed was made by dissolving 3.4 ounces per gallon of c.p. cadmium oxide in a solution containing 11.5 ounces per gallon of sodium cyanide. The anode was made of cadmium rod of 99.95 per cent purity. During the plating the cathode was slowly rotated in the bath in order that the

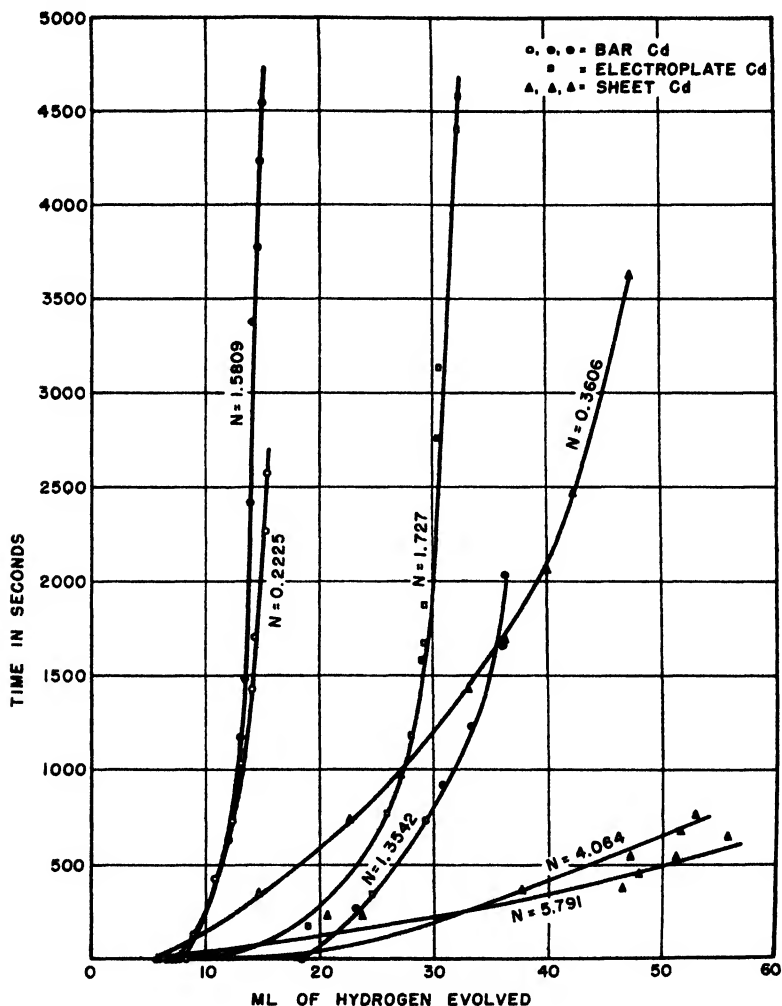


FIG. 3. Hydrogen evolved from bar, electroplated, and sheet cadmium in reaction with hydrochloric acid.

deposit obtained would be even. At frequent intervals the plating operation was interrupted in order that the sodium carbonate residue accumulated might be removed. The plating was continued until a coating of sufficient thickness was obtained. In order that the rate of reaction might be determined, all three types of cadmium were reacted with hydrochloric acid of varying concentration

at a temperature of 25°C. From the graphical evaluation shown in figure 3, it was decided that the reaction could best be represented, after an initial transient period, by the equation for a zero-order reaction: namely,

$$\frac{dx}{dt} = k$$

The k values (specific reaction rate constants) obtained at 25°C. at rotation velocities of 1200 R.P.M. may be summarized in table 1, where N represents the normality of the hydrochloric acid used. From these data it is evident that the type of surface has only a slight effect on the rate of solution of the cadmium. All of the reactions observed were of zero order.

TABLE 1

TYPE OF CADMIUM	HCl	k
	N	
Bar	0.2225	0.00082
	1.3542	0.00086
	1.5809	0.00091
Sheet	0.3606	0.00534
	4.064	0.01915
	5.791	0.03314
Electroplate	1.727	0.00106

Additional calculations were made to determine to what order the hydrochloric acid entered into the reaction, using the expression

$$\frac{(\Delta x/\Delta t)_z}{(\Delta x/\Delta t)_y} = \left(\frac{z}{y}\right)^a$$

where $\Delta x/\Delta t$ represents the velocity constant at concentrations y and z , z being greater than y , and a is the order to which the acid enters into the reaction. Values of a were obtained for cadmium bar equal to 0.0217 and 0.052; for cadmium sheet, 0.513 (fairly concentrated acid). It seems justifiable to conclude from these data that in dilute solutions, at least, variations in the concentration of acid do not measurably affect the rate of dissolution of the metal and, as might be expected, the power to which the acid enters the reaction is very small, probably approaching zero in the case of infinitely dilute solutions.

Work by Warner (16) has shown that the dissolution of metals in aqueous solutions may be classed in two types,—that occurring in the presence of oxygen, and that occurring in its absence. To the former he gives the name "oxygen type"; to the latter, "hydrogen type". Free-energy changes for cadmium reacting in the "hydrogen type" equation are of the order of magnitude of 600 cal. per gram-mole of the metal. On the other hand, the changes involved in the "oxygen type" are -55,600 cal. per gram-mole of the metal employed. It should be expected then that the corrosion of cadmium in hydrochloric acid

would be affected considerably by the presence of oxygen, or by its absence. This expectation was tested by flushing the apparatus and acid used with dry nitrogen. Total flushing and saturation required about 25 min. The results

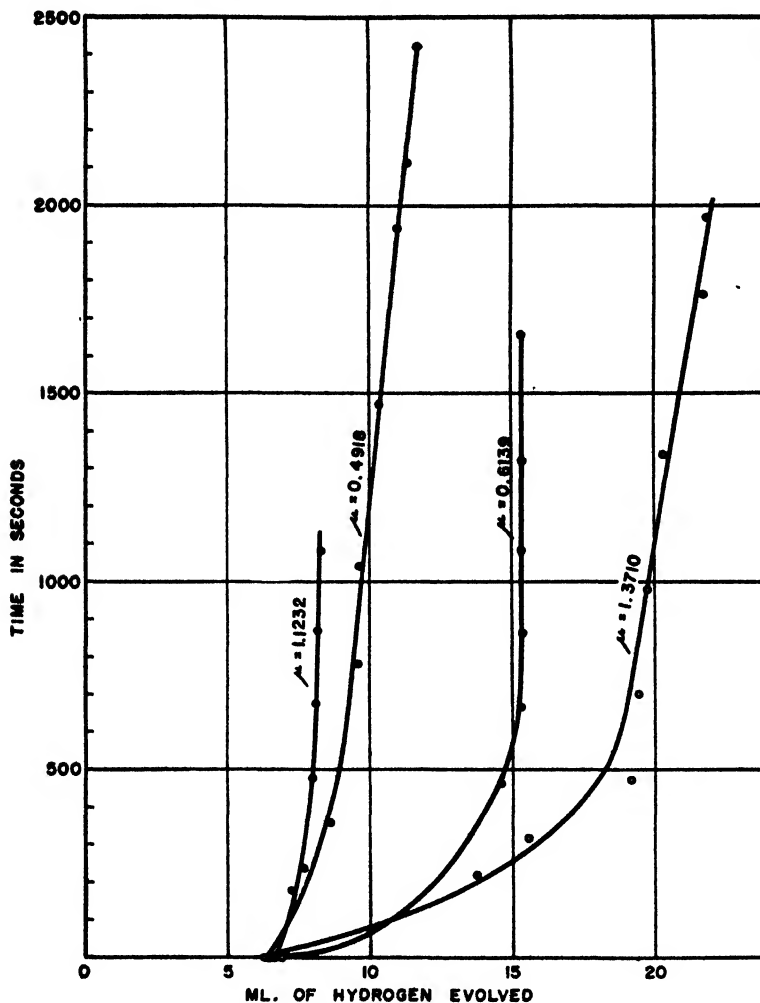


FIG. 4. Hydrogen evolved from acid solutions of varying ionic strength

obtained were rather surprising; although the reaction was not inhibited, the order was found to obey the equation

$$k = \frac{2.303}{t} \log \frac{c_0}{c}$$

where c is the concentration of acid remaining at time t , c_0 the concentration at time t_0 , and k the specific reaction rate constant. The k value obtained for an acid concentration of 1.727 reacting with cadmium sheet at 25°C. and a linear

TABLE 2

IONIC STRENGTH WITH RESPECT TO Cl^-	k
1.3710	0.00379
1.1232	0.00144
0.6139	0.00088
0.4918	0.000206

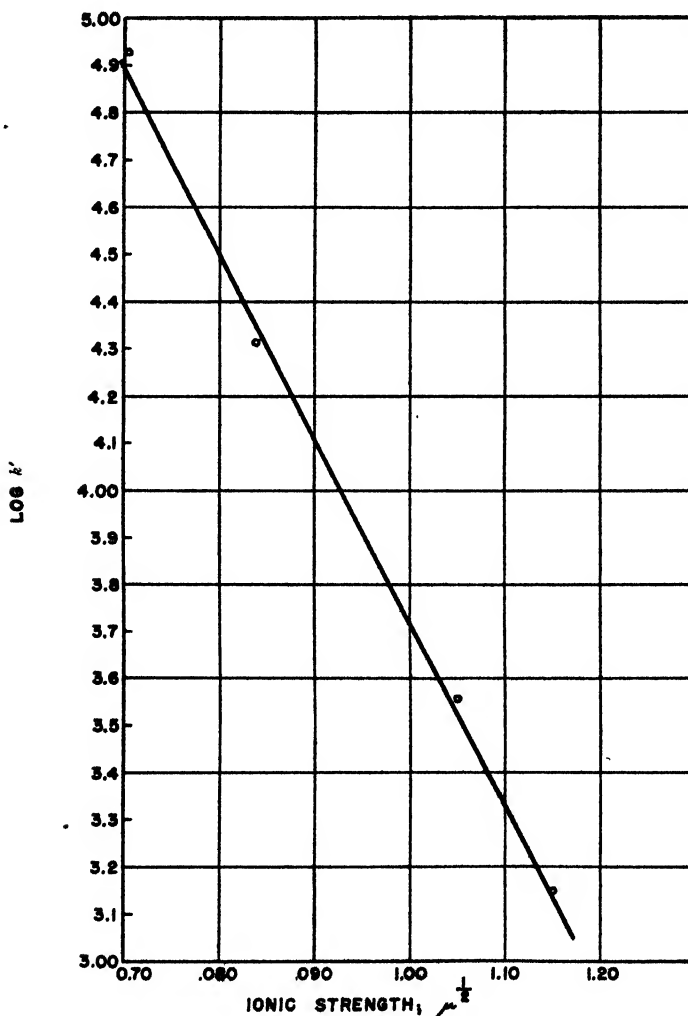


FIG. 5. The change in the velocity constant with change in ionic strength

velocity of 814 R.P.M. was found to be 4.2×10^{-6} . It may be concluded, therefore, that the dissolved oxygen makes the reaction independent of the concentration of acid employed, whereas the absence of oxygen completely changes the

order of the reaction so that it becomes dependent on the concentration of the acid.

The ionic strength, μ , of the hydrochloric acid was varied with respect to chloride ion by the addition of sodium chloride. The reaction rates were determined in the usual fashion. Graphical analysis may be found in figure 4.

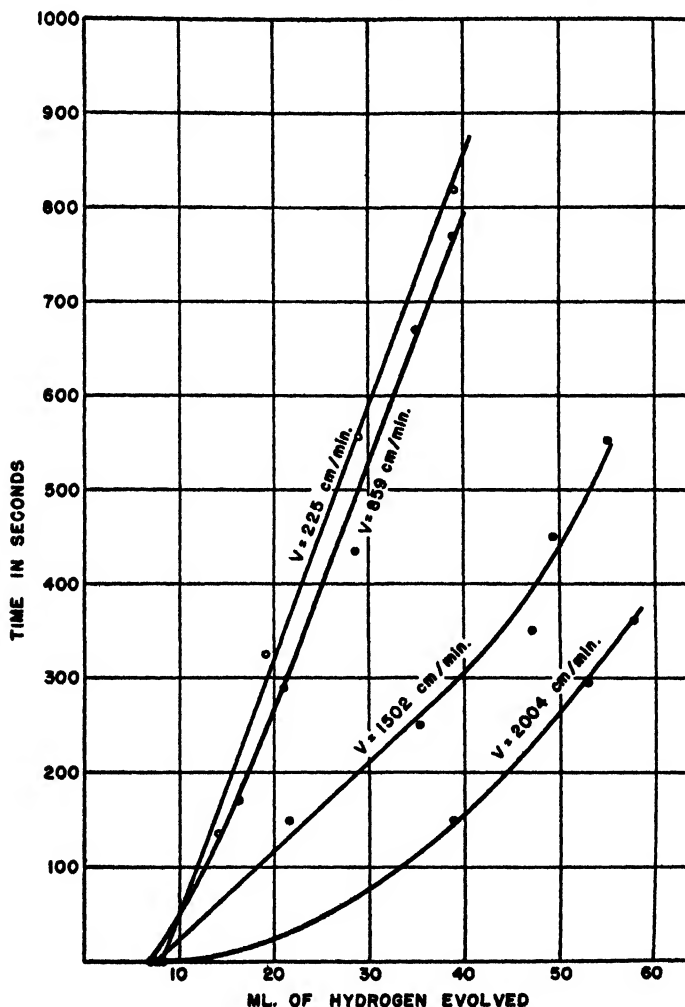


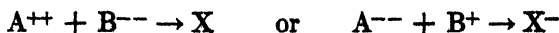
FIG. 6. The effect of linear velocity on the rate of reaction

The calculated values of the velocity constant, k , are shown in table 2. Figure 5 shows a plot of $\log k$ vs. $\mu^{\frac{1}{2}}$. The slope of the line obtained, which according to the Brønsted equation (1),

$$\log k' = -\alpha \Delta(z^2) \mu^{\frac{1}{2}} - \log kK$$

must be equal to $0.5 \Delta(z^2)$, or -2.1 , if k' is the true reaction rate constant, K the equilibrium constant, z the charges on the ions in the rate-determining step,

and α a constant numerically equal to -0.509 in aqueous solutions at 25°C . It must be then, that z^2 is -4 and the rate-determining step is of the type



Of the many possibilities, the reaction which seems most probable is



In order that the effect of changes in the linear velocity of the cadmium plate might be studied, the sheet was whirled through acid solutions at varying speeds.

TABLE 3

LINEAR VELOCITY	VELOCITY CONSTANT k
<i>cm./min.</i>	
225.42	0.0327
859.69	0.0400
1502.80	0.0493
2004.36	0.0672

TABLE 4

HCl	DIELECTRIC CONSTANT*	k
N		
1.3137	57.4	0.0277
0.4978	46.6	0.00872

* Calculated from data published by Harned and Owen (6).

TABLE 5

t	k
$^\circ\text{C}$.	
30	0.0107
35	0.00181
40	0.00011

The graphical analysis of the data obtained is shown in figure 6. The values obtained at 25°C . in $7.3457 N$ hydrochloric acid for varying linear velocities are shown in table 3.

Variations in dielectric constant of the acid employed were produced by the addition of dioxane. The specific reaction rate constants, k , obtained are shown in table 4.

Variations in viscosity were also investigated. It was felt that if diffusion were the controlling factor in determining the velocity of the chemical reaction, the addition of some neutral, non-ionized material such as glucose might upset the diffusion relationships, and changes might be produced in the velocity of the

reaction, or even in the order of the reaction. An attempt to do this experimentally was made by preparing two solutions of 1.3442 and 1.1328 *N* hydrochloric acid and making the former 0.4648 molar with respect to sucrose, the latter, 0.3897 molar. Relative viscosity determinations revealed values of 1.954 and 1.771, respectively. The reaction rate constants were determined in the usual manner. There was no change in the order of the reaction; *k* values found were 0.00152 and 0.00126. From this it might be concluded that variations in viscosity within the range employed do not significantly affect the rate of solution.

It was decided next to determine the effect of variations in temperature on the rate of dissolution of the cadmium. For this purpose, sheet cadmium was reacted with 1.727 *N* hydrochloric acid at temperatures of 30°, 35°, and 40°C. The *k* values found are listed in table 5. Contrary to all expectation, it was observed that the rate of reaction decreased almost by a factor of 10 for every 5-degree rise in temperature. As each reaction proceeded, the surface of the cadmium became darker, until finally, when the surface was nearly black, it was no longer possible to detect any hydrogen given off by the reaction. As the temperature increased, the initiation of the blackening process was hastened. It is tempting to suggest that this layer of material involves the CdCl^+ postulated in the rate-determining step. If this were the case, increase in temperature might increase the dissociation of this complex, according to the equation:



This increased dissociation would then tend to decrease the rate of the reaction. Whatever the phenomena, it was not found possible to determine the actual energy of activation by the method of temperature variation.

SUMMARY

The rate of solution of cadmium in hydrochloric acid may be represented, after an initial transient period, as of zero order, i.e., independent of the concentration of acid employed. The power to which the acid enters the reaction is less than 1, approaching 0 as the acid becomes extremely dilute. Removal of dissolved oxygen from the acid changed the order of the reaction so that it may best be represented as of order 1. The ionic strength of the solution was varied and a rate-determining step postulated. Variations in dielectric constant, in the viscosity of the solution, and in the linear velocity of the cadmium metal were found to have negligible effects on the velocity. It was not possible to determine the energy of activation by the method of temperature variation, inasmuch as the rate decreased by an approximate factor of 10 for each 5-degree rise in temperature. A possible explanation was proposed for this phenomenon.

REFERENCES

- (1) BRØNSTED, J. N.: *Z. physik. Chem.* **102**, 109 (1922); **115**, 337 (1925).
- (2) CENTNERSZWER, M.: *Z. physik. Chem.* **A137**, 352 (1928).
- (3) CENTNERSZWER, M.: *Atti. X Congr. intern. Chem.* **3**, 555 (1939).
- (4) FISHBECK, K., AND SCHMIDT, KARL: *Z. Elektrochem.* **38**, 199 (1932).

- (5) GRONOVER, A., AND WOENLICH, E.: *Z. Untersuch. Lebensm.* **53**, 392 (1927).
- (6) HARNED, H. S., AND OWEN, B. B.: *The Physical Chemistry of Electrolytic Solutions*. Reinhold Publishing Corporation, New York (1943).
- (7) HEDVALL, J. A., BOSTRÖM, N., COLLIANDER, B., AND HAMMARSON, Å.: *Z. anorg. allgem. Chem.* **243**, 231 (1940).
- (8) JABLCEZYNSKI, K., AND PIERSECHALSKI, T.: *Z. anorg. allgem. Chem.* **217**, 298 (1934).
- (9) JABLCEZYNSKI, K., AND WAJCHSELFISZ, H.: *Roczniki Chem.* **9**, 340 (1929).
- (10) JABLCEZYNSKI, K., HERMANOWICZ, E., AND WAJCHSELFISZ, W.: *Z. anorg. allgem. Chem.* **180**, 184 (1904).
- (11) KIMBALL, G. E.: *J. Chem. Phys.* **8**, 199 (1940).
- (12) KIMBALL, G. E., AND GLASSNER, A.: *J. Chem. Phys.* **8**, 820 (1940).
- (13) PLENETEV, S. A., AND SOSUNOV, S.: *J. Phys. Chem. (U.S.S.R.)* **13**, 901 (1939).
- (14) ROETHELI, B., FRANZ, C. J., AND MCKUSICK, B. L. *Metal Ind. (N.Y.)* **30**, 361 (1932).
- (15) WALPERT, G.: *Z. physik. Chem.* **A151**, 219 (1930).
- (16) WARNER, J. C.: *Trans. Electrochem. Soc.* **83**, 319 (1943). See also BROWN, R. H., ROETHELI, B. E., AND FORREST, H. O.: *Ind. Eng. Chem.* **23**, 350 (1931).

THE LONGITUDINAL DISPERSION OF INFRARED RAYS IN POLYSTYRENES

W. W. LEPESCHKIN

U. S. Army Military, Agricultural and Technical school, Weißenstephan, Germany

Received June 3, 1946

I. INTRODUCTION

In some papers published by the author in German journals during the war, it was stated that the so-called longitudinal dispersion of light (discovered by Plotnikov in 1928), in spite of doubts expressed by some physicists, can be easily observed for infrared rays penetrating through substances having carbon chains in their molecules. That the longitudinal dispersion of light can be observed especially easily in this case had been pointed out by previous authors, but their results were not convincing because they did not consider the simultaneously produced Tyndall effect (Splait, 1933; Coban, 1935; Gjuric, 1933, 1939; Jörg, 1937, 1939). Recent experiments by the author on proteins and polystyrenes showed that the Tyndall effect observed in these substances and in their solutions is either absent, or can be made imperceptible by filtration repeated many times, without any effect on the longitudinal dispersion of infrared rays. They proved, moreover, that this dispersion depends upon the molecular weight of the substances. In this paper the latest apparatus used by the author and some results obtained on polystyrenes are described.

II. METHOD AND APPARATUS

In the apparatus used (see figure 1) a low-voltage bulb (6 volts; exactly 5 amp.) with a small incandescent body was the light source. This bulb was enclosed in a

brass shell (Sh) in which two lenses (invisible in the photograph) were properly adjusted in order to concentrate the light on a 1.5-mm. opening of a diaphragm (D_1) where an image of the incandescent body of the bulb appeared (2 mm. in size). Between the lamp and the diaphragm a light filter¹ was placed (F) which let only dark red and infrared rays through. The rays from the image of the incandescent body of the bulb fell on a 5 cm. lens (L) and were made slightly convergent, parallelism of the rays being unattainable; they produced a 15-mm. light circle on another diaphragm (D_2 , at a distance of 21 cm. from the lens), went through the opening of the diaphragm, and then passed through three diaphragms D_3 , D_4 , and D_5 with openings of 1.5, 1, and 1.5 mm. The distances between the diaphragms were 10, 33, and 23 mm. This arrangement was neces-

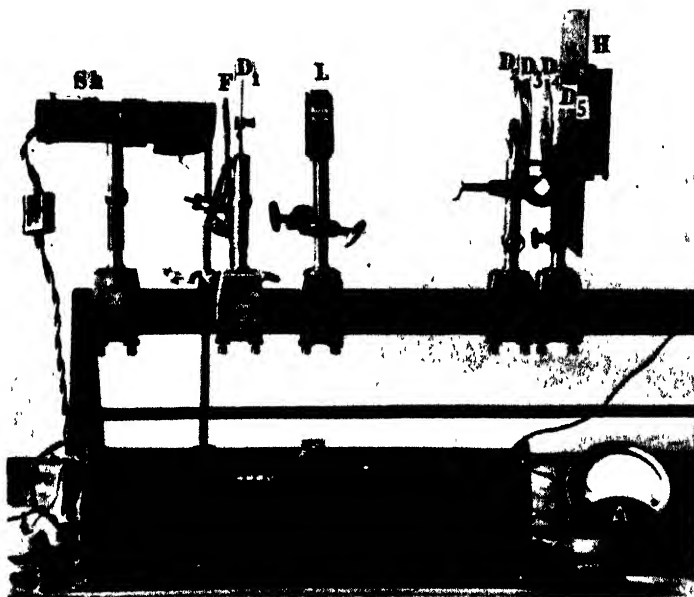


FIG. 1.

sary to make the light beam coming from the diaphragm D_5 completely free from inflection images. The last diaphragm was mounted in a large brass wall to which the holder (H) for a plate case was fastened. The light beam passed in a distance of 5 mm. through a 3-mm. opening in the front wall of the latter and then through a plane-parallel cuvette filled with the solution to be tested (the layer of the solution was always 10 mm.). On the lower edge of the cuvette a horizontal brass strip was pasted with black sealing wax. The light bundle which fell on the strip exactly 2 mm. below its upper edge was partly reflected and di-

¹ This filter was obtained from Schott of Jena and let through all rays of wave length 1050, 950, and 850 $m\mu$, 96 per cent of rays of wave length 775 and 700 $m\mu$, 77 per cent of rays of wave length 690 $m\mu$, 24 per cent of rays of wave length 680 $m\mu$, and 1 per cent of rays of wave length 670 $m\mu$.

rected back to the opening of the diaphragm D_6 , but for the most part it was absorbed by the strip, while the rays dispersed fell above the strip on a photographic plate which was sensitive to infrared rays (Agfa, 800, rapid) and was placed behind the cuvette in the plate case. After development of the plate a dark semicircle appeared above the clear space corresponding to the brass strip. The surface of the semicircle expressed in mm.^2 was measured and corresponded to the relative strength of the dispersion and the Tyndall effect. In the case of polystyrenes the Tyndall effect for dark red rays was not perceptible either in solutions or in solid substances. Thus this light dispersion was in this case and also for infrared rays a pure longitudinal dispersion, the Tyndall effect being inversely proportional to the fourth power of the wave length. In solid polystyrene plates no Tyndall effect was visible even in white light.

It should be emphasized that the photographic plates used for comparing the strength of the longitudinal dispersion in different polystyrenes or their solutions were taken from the same box (these plates gradually lose their sensitivity to infrared rays), and the photographing of the dispersion took place on the same day. Also, the plates were developed in the same bath.

In some experiments the Tyndall effect observed in solutions of polystyrenes in white light was compared with that of rosin suspensions. Two cuvettes of the same shape and size were placed close to each other, perpendicular to the direction of the rays, between the lens and the diaphragm D_2 of the apparatus described above, behind the black wall of a stand having two rectangular openings corresponding to both cuvettes (the distance between the openings was 0.5 mm) and 1 mm. above the level of both liquids. The Tyndall effect was observed from above through a tube the length of which corresponded to clear vision. The standard suspension of colophony (rosin) was obtained by dropping 1 cc. of a 5 per cent solution of rosin in alcohol into 10 cc. of a 0.5 per cent solution of gelatin warmed to 50°C. and then cooling to room temperature. The suspension was added by means of a micropipet to water in the cuvette until the Tyndall effect in both cuvettes became the same. The concentration of rosin in per cent expressed the strength of the Tyndall effect.

Some peculiarities of the method in the case of photographing the longitudinal dispersion of light in solid polystyrenes should be mentioned. In this case the cuvette in the plate case was replaced by an equally large glass plate (1 mm. thick), on the lower edge of which the same brass strip was pasted as on the lower edge of the cuvette. On this glass plate a plate made of solid polystyrenes was placed in such a way as to allow the light beam to penetrate the latter exactly 2 mm. below the upper edge of the brass strip. The polystyrene plates being even enough but not polished were separated from the glass plate by a thin layer of olive oil and fastened by another glass plate of the same size and thickness, which was pressed on by the front wall of the plate case.

The photographing of the dispersion and the observation of the Tyndall effect were made in a dark room. The black semicircles on negatives were measured in the following manner. As they are really not semicircles but segments (the

center of the circle lies 2 mm. below the upper edge of the brass strip), the surface of the semicircles is:

$$F = 0.39B^2 + 6.3 \text{ mm.}^2$$

where B is the width of the segments at the brass strip (in millimeters). The blackness of the segments disappears gradually at their rims; thus B was measured as follows:

In each of two equal-sized rectangular pieces of black cardboard (2 cm. x 1 cm.) a slit (5 mm. x 0.6 mm.) was cut beginning from the short edge of the pieces. One of the latter was glued onto a developed, fixed, and slightly veiled photographic plate of the same size. The plate thus obtained was placed on the negative, whereas the slit was put below the black semicircle and perpendicular to its large axis. The other cardboard piece was also placed on the negative, but the slit was put on the black semicircle itself at its large axis and perpendicular to it. This piece was moved along the axis until the blackness in both

TABLE 1
Molecular weights of the polystyrenes

POLYSTYRENE	MOLECULAR WEIGHT
EF	600,000
III	100,000
IV	210,000
I	55,000
1	102,300
2	452,000
3	143,000

slits became alike. The position of the slit at the axis was marked; after the same manipulation was repeated at the other side of the semicircle, the width B was measured.

III. MATERIAL USED

The molecular weights of the polystyrenes² used were determined according to the Staudinger method (see table 1).

Polystyrenes 1 and 2 were delivered in the form of quite transparent plates (thicknesses 1 mm. and 0.6 mm.), which could be used directly for the determination of the longitudinal dispersion of infrared rays. The light beam went either through two plates (polystyrene 1) or through three plates (polystyrene 2); the whole layer of the substance was therefore in both cases 2 mm. thick. The 1.3-mm. thick, quite transparent plates of polystyrenes EF and IV were

² Some of the polystyrenes were obtained from the I. G. Colour Company, Frankfurt am Main; the others from Prof. Dr. Jenkel, Institute for Physical Chemistry of the Technical Academy in Aachen. The author wishes to express his hearty thanks for these samples.

obtained by the evaporation of their concentrated solutions in benzene. A quite transparent plate of polystyrene III could not be obtained.

Other polystyrenes were used only in their solutions in benzene.

IV. RESULTS

As already mentioned, the solid polystyrenes did not show any Tyndall effect either in dark red or in white light. The light dispersion in their plates was thus a pure longitudinal dispersion. The dispersion measured was as given in table 2 (the exposure to rays lasted 5 min.).

Table 3 shows that the values obtained for the longitudinal dispersion (F) are proportional to the cube roots of the molecular weights of the polystyrenes.

TABLE 2
Dispersion by polystyrenes

POLYSTYRENE	THICKNESS OF POLYSTYRENE LAYER	B	F
	mm.	mm.	mm. ³
EF.....	1.3	31	380
IV.....	1.3	26	269
1.....	1.3	22.5	203
2.....	2	42	693
1.....	2	32.5	418

TABLE 3
Relation between longitudinal dispersion and molecular weight

POLYSTYRENE	MOLECULAR WEIGHT, M	E_n/F_1	$\sqrt[3]{M_n/M_1}$
1	102,300	1	1
IV.	210,000	1.32	1.27
2	452,000	1.69	1.64
EF.....	600,000	1.77	1.80

F_n/F_1 is the ratio between the longitudinal dispersions of polystyrenes IV, 2, and EF and that of polystyrene 1.

Solutions of polystyrenes in benzene, toluene, or carbon disulfide did not show any Tyndall effect in dark red rays. It must therefore be concluded that they do not show any Tyndall effect in infrared rays either, this effect being inversely proportional to the fourth power of the wave length. However they show, as mentioned above, a very weak Tyndall effect in white light, but it has no relation to the molecular weight, and must probably be ascribed to some impurity present in different polystyrenes in a different amount, as is shown in table 4.

The solutions of polystyrenes must evidently be equally concentrated to demonstrate the dependence of the longitudinal dispersion of infrared rays upon the molecular weight. In order to obtain such solutions it should be considered that polystyrenes have thread-like molecules which in the solid state are entangled

with one another, similarly to threads in felt, and stick together. It is therefore comprehensible that the longer the thread-like molecules of polystyrenes (that is, the greater their molecular weight), the more time is necessary to dissolve them. Dissolving polystyrene L requires, for instance, some hours, while dissolving polystyrene EF requires some weeks. It should be pointed out that solutions of polystyrenes can be quite transparent in spite of their containing still solid and swollen particles of the solute. The longitudinal dispersion increases with the concentration, but the greater the latter, the less is the increase of the dispersion. Thus it is smaller in a solution containing 5 per cent of polystyrene only partly dissolved than in a 5 per cent solution in which the polystyrene is dissolved completely. Correspondingly, in the experiments in which the longitudinal dispersion of infrared rays by polystyrenes IV, III, and L was compared, the solutions of polystyrenes IV and III were investigated two months

TABLE 4
Tyndall effect shown by polystyrenes in white light

POLYSTYRENE.	L	I	III	IV	EF
Tyndall effect expressed in per cent concentration of rosin suspension	0.00015	0.00062	0.00041	0.00062	0.00062
Molecular weight	55,000	102,300	100,000	210,000	600,000

TABLE 5
Longitudinal dispersion by solutions of polystyrenes

POLYSTYRENE	LONGITUDINAL DISPERSION		MOLECULAR WEIGHT	MOLECULAR WEIGHT CALCULATED FROM THE FORMULA $F_1/F_2 = \sqrt{M_1/M_2}$
	B	F		
IV	23.5	221	210,000	
III	21	178	100,000	109,000
L	18.5	139	55,000	53,200

after the beginning of the dissolution, while the solution of polystyrene L was photographed 3 days after it was put into benzene, but both solutions were photographed on the same day. The concentration of polystyrene was 5 g. in 100 cc. of solution. The exposure to light lasted 5 min. The results are given in table 5.

The rule of the proportionality between the longitudinal dispersion and the cube root of the molecular weight of the polystyrene is thus valid for solutions of polystyrenes also.

V. INDEX OF REFRACTION OF SOLVENT AND LONGITUDINAL DISPERSION

According to Neugebauer (1), who postulated the theory of the longitudinal dispersion of light, this dispersion results as a deflection of light rays from their direction in consequence of a total internal reflection from the surfaces of bun-

dles of molecules. In the case of polystyrenes this reflection is to be considered as a reflection from the interior surfaces of the molecules, because the latter do not form bundles. The calculations of Neugebauer showed that such deflection of rays must increase with the length of the bundles or, in our case, with the length or weight of the molecules and be especially great for infrared rays. Therefore, the index of refraction of the solvent must be important for the strength of the longitudinal dispersion. This is shown indeed by the experiment in which polystyrene III was mixed with benzene, toluene, and carbon disulfide, and, after 2 weeks, the solutions so obtained were used for the determination of the longitudinal dispersion of infrared rays. The exposure to light lasted 2 min. The results are given in table 6.

As the index of refraction of benzene is greater than that of toluene and smaller than that of carbon disulfide, the results given in table 6 show that the longitudinal dispersion increases with decrease in the index of refraction of the solvent. This fact confirms the theory of Neugebauer. This theory is also confirmed by

TABLE 6

Relation between longitudinal dispersion of infrared rays and refractive index of solvent

SOLVENT	CONCENTRATION OF POLYSTYRENE III <i>g. per 100 cc.</i>	LONGITUDINAL DISPERSION	
		<i>B</i>	<i>F</i>
Benzene.....	5	6.5	22
	10	10	45
Toluene	5	7.5	28
	10	11	53
Carbon disulfide	5	6	20
	10	9	38

the dependence of the longitudinal dispersion upon the orientation of the molecules of polystyrene, as shown by the following experiment:

A 5 per cent solution of polystyrene EF in benzene showed $B = 17.5$ and $F = 125$. The cuvette containing this solution was rotated for 10 min. around its axis so that, after installation in the plate case, it would have the same direction as the light bundle. The polystyrene molecules were thereby oriented in the direction perpendicular to the light bundle. Photographing the longitudinal dispersion gave $B = 23.5$ and $F = 221$. When the cuvette was rotated in the opposite direction, the longitudinal dispersion was $B = 16$ and $F = 105$.

VI. SUMMARY

After describing the latest apparatus used for the determination of the longitudinal dispersion of infrared rays in polystyrenes, the methods of photographing this dispersion in the case of solid polystyrenes and their solutions and of observing the Tyndall effect were described. The solid polystyrenes used in the

shape of transparent plates did not show any Tyndall effect either in dark red or in white light. The solutions of polystyrenes in benzene, toluene, and carbon disulfide did not show any Tyndall effect in dark red and infrared rays but showed a very weak effect in white light, a result which has no connection with the molecular weights of the polystyrenes and must be ascribed to an impurity which is contained in different amounts in different polystyrenes. The dispersion of infrared rays in solid polystyrenes as well as in their solutions is a purely longitudinal dispersion. This dispersion proved to be proportional to the cube root of the molecular weight of the polystyrene in both cases. It also depends upon the index of refraction of the solvent: the greater is the latter, the weaker is the dispersion. The orientation of the polystyrene molecules is important too; the dispersion is stronger if they are oriented perpendicular to the direction of the light bundle than if their orientation is parallel to the same. Both these facts confirm the Neugebauer theory of the longitudinal dispersion of light which considers it as a total internal reflection from the interior surfaces of bundles of molecules or, in our case, from the surfaces of the molecules themselves.

REFERENCE

- (1) NEUGEBAUER, TH.: *Physik. Z.* **41**, 55 (1940).

LONGITUDINAL DISPERSION OF INFRARED RAYS IN OPTICALLY EMPTY AND TURBID MEDIA, AND MOLECULAR WEIGHTS OF SUBSTANCES

W. W. LEPESCHKIN

U. S. Army Military, Agricultural and Technical school, Weihenstephan, Germany

Received June 3, 1946

I. INTRODUCTION

In a series of papers published in German journals during the last years of the war, the author showed that the so-called longitudinal dispersion of light (discovered by Plotnikov in 1928), in spite of some doubts expressed by physicists, can be easily established if infrared rays and substances with long carbon chains in their molecules are used for experiments. In a paper published recently (5) some experiments on polystyrenes were described. These substances are especially suited for use in proving the dispersion mentioned, because they do not show any Tyndall effect either in dark red or in white light if they are in the solid state, and they show only a very weak effect in white light but no effect in dark red rays if they are dissolved in benzene. An important peculiarity of the longitudinal dispersion of infrared rays is its dependence upon the molecular weight of the substance producing the dispersion. It is (within the limits of the exactness of the method) inversely proportional to the cube root

of the molecular weight. This rule allows the determination of the molecular weights of new substances and the testing of already known molecular weights. Especially important was the possibility of applying the rule cited to the determination of the molecular weights, and their changes, of the substances ("vitoids") composing living matter. The corresponding experiments showed that these molecular weights are very high (as high as that of vira), and that they decrease strikingly in the process of death, the vitoids composing living matter disintegrating to ordinary proteins.

In the present paper general methods for the determination of the longitudinal light dispersion, and consequently of the molecular weights, of substances are given, and it is shown that these methods are valid whether the solutions of these substances are optically empty for infrared rays or show a Tyndall effect in these rays.

II. METHOD AND APPARATUS

A detailed description of the apparatus used for photographing the longitudinal dispersion of infrared rays¹ and measuring the surfaces of the dispersion circles obtained has been given in previous papers of the author (7). In the present paper only the general scheme of this apparatus will be described.

A beam of dark red and infrared rays, freed from inflection images by passage through a series of diaphragms, is passed through a plane-parallel cuvette filled with a solution of the substance to be tested and is intercepted by a brass strip pasted on the rear wall of the cuvette at its lower edge. The dispersed rays fall above the brass strip on a photographic plate (sensitive to infrared rays) where, after development, a dark semicircle appears. The latter is really a circle segment, because the main (undiffracted) light beam touches the brass strip 1.5–3 mm. below its upper edge. The surface of the semicircle is computed according to the formula $F = 1.57(a^2 + B^2/4)$, where a is the distance of the light beam from the upper edge of the brass strip and B the width of the segment at the latter (on the plate a clear space below the dark segment). This surface, expressed in mm.², serves as a value proportional to the strength of the dispersion, which, in a general case, results from the sum of the longitudinal dispersion and the Tyndall effect.

In experiments in which the dispersion is very weak, not only the Tyndall effect as additional dispersion but also the light dispersion produced by the rims of the last diaphragm and by the front wall of the cuvette must be considered. To exclude these two latter kinds of dispersion, the cuvette filled with distilled water is photographed. The value of dispersion obtained (expressed in mm.² of the dispersion circles on negatives) is subtracted from the complete dispersion of the solution.

In exact experiments the light absorption by the solution must be considered

¹ The light filter used (RG5, Schott, Jena) let through all rays of wave length 1050, 950, and 750 mμ, 70 per cent of all rays of wave length 690 mμ, 24 per cent of all rays of wave length 680 mμ, and 1 per cent of all rays of wave length 670 mμ.

too. It can be determined by photographing infrared light passing through the solution or suspension and falling on one half of a photographic plate and on its second half without passing through the solution or suspension. After development of the plate the darkness of both halves is compared in a photometer. As to the reflection of light by the walls of the cuvette, it is (in the experiments to be described) always 4 per cent of the incident light.

In the previous papers of the author it was pointed out that in the case of a visible Tyndall effect in dark red rays and presumably also in infrared rays (this effect being inversely proportional to the fourth power of the wave length) $P = S - T$, where P is the longitudinal dispersion, S is the complete (and corrected) dispersion and T is the Tyndall effect, all expressed in mm^2 of the surface of dispersion circles. T was measured by the comparison method (3); a suspension of a substance showing no longitudinal dispersion was found, which had the same Tyndall effect in dark red rays, observed from above, as the solution to be tested and its Tyndall effect was expressed in mm^2 of the dispersion circle by photographing it in the same apparatus. The apparatus in which the Tyndall effects observed from above were compared has been described in previous papers. The selection of suspensions suitable for comparing their Tyndall effects with that of the solution to be tested must be in accordance with the fact that the Tyndall effect in suspensions and emulsions having coarse particles (5 to 300 μ) is produced by light refraction and reflection, while this effect in suspensions with very small particles (100 $\text{m}\mu$ and smaller) is brought about chiefly by light deflection. The ratio (V) of the amount of the Tyndall effect observed from above in the suspensions to the amount of light falling on the photographic plate behind the cuvette consequently depends upon the index of refraction of the particles, but does not depend upon the size of the latter, while in the other case it does not depend upon this index, but depends upon the size of the particles. From the results given in previous papers (6) table 1 can be set up, which shows that the ratio mentioned is, in the case of coarse particles, proportional to the logarithm of the index of refraction.

As is known, if the particles of a suspension are very small, their size influences the color of the Tyndall effect observed in white light; its color becomes more bluish with decreasing size. Also, light going through the suspension becomes more and more yellow and orange with decrease in particle size. Moreover, the turbidity of the suspension increases with increasing particle size. According to these rules it can be concluded that the size of the particles decreases in the following order: rosin, old cholesterol suspension, denatured albumin, fresh cholesterol suspension, colloidal sulfur, colloidal silver. At the same time the ratio of the amount of light observed from above to that photographed increases in the same order. The photographed dispersion becomes therefore relatively weaker with the decreasing size of particles, assuming that the Tyndall effect observed from above is alike in all suspensions. This decrease is seen from table 2.

A suspension can thus be considered as suitable for the comparison of its

Tyndall effect with that of a solution to be tested only if the color of its Tyndall effect and of the white light going through it is similar to that of the solution. Also, the turbidity of both should be similar.

III. TYNDALL EFFECT OF APPARENTLY OPTICALLY EMPTY SOLUTIONS

In a previous paper by the author (4) it was pointed out that many protein solutions can be made optically empty for dark red and consequently for infrared rays by repeated filtration through the same filter, as, for instance, ovalbumin, hemoglobin, *Elodone* hemocyanin, *Homarus* hemocyanin, and genuine tobacco

TABLE 1

KIND OF PARTICLES	INDEX OF REFRACTION, n	LOG n	RATIO OF BOTH LIGHT AMOUNTS, V	V/n
Heat-coagulated albumin	1.380	0.140	1	7.1
Xylene suspended in 50 per cent sugar .	1.398	0.145	1.01	6.9
Xylene suspended in 45 per cent sugar .	1.422	0.153	1.09	7.1
Xylene suspended in 30 per cent sugar .	1.450	0.161	1.14	7.0
Olive oil	1.470	0.167	1.16	8.8
Xylene suspended in 10 per cent sugar .	1.482	0.171	1.29	7.5
Xylene	1.503	0.177	1.32	7.4
Colophony (rosin)	1.510	0.179	1.36	7.5

TABLE 2

SUBSTANCE	TYNDALL EFFECT DISPERSION IN DARK AND INFRARED RAYS		RATIO (V) OF THE AMOUNT OF LIGHT OBSERVED TO THAT PHOTOGRAPHED
	B	F	
	mm.	mm. ²	
Rosin (0.05 per cent)	32	419	1
Old cholesterol*	29	347	1.20
Denatured albumin	27.5	314	1.33
Fresh cholesterol*	23	225	1.86
Colloidal sulfur	22.5	216	1.94
Colloidal silver	4	25	12

* Cholesterol acetate suspension.

mosaic virus. It was emphasized, however, that the solutions of proteins used were optically empty "at the illumination used." In subsequent experiments the latter was increased twelvefold and a very weak Tyndall effect appeared in dark red rays, indicating that the optical emptiness of the solutions used was not complete. But this weak Tyndall effect was unimportant for the determination of the molecular weights of the proteins. Indeed the semicircle of light produced by it was completely masked from the photographic plate placed behind the cuvette by the brass strip, and it could not therefore change the size of the dispersion semicircles on the negatives of the plates. This is true, of course, only if the distance between the light beam and the upper edge of the brass strip is large enough, as is shown by the following experiment.

The Tyndall effect of a 10.4 per cent solution of ovalbumin (pH = 4.8) in white light had a color similar to that of a colloidal sulfur suspension and its intensity corresponded to that of a 0.005 per cent sulfur suspension. In the dark red rays the Tyndall effect disappeared in the albumin solution as well as in the sulfur suspension, a result which can evidently be ascribed to the fact that, besides the influence of the wave length, the light filter used absorbed a great part of the light so that the liquids were illuminated less than before. If the light intensity was increased several times, the Tyndall effect became distinct in dark red rays in the solution as well as in the suspension.

The photographing of the dispersion in ordinary illumination as described in paragraph 2 (liquid layer = 10 mm.; exposure time = 180 sec.; $a = 1.5$) gave: $B_1 = 13.8$ and $F_1 = 77$ in the albumin solution (10.4 per cent) and $B_2 = 12.6$ and $F_2 = 65$ in the sulfur suspension or, considering the absorption of light by both and the reflection by the cuvette walls, $F_1 = 93$ and $F_2 = 68$. As the distance between the light beam and the upper edge of the brass strip was only 1.5 mm., the dispersion produced by the rims of the last diaphragm had to be considered in this case. The albumin solution in the cuvette was replaced by distilled water and the cuvette was photographed again. This time the dispersion was $B_3 = 6.1$ and $F_3 = 17$ or, after considering the reflection, $F_3 = 18$. The photographing of the cuvette which had been filled with the sulfur suspension gave, after replacing the latter with distilled water, $B_4 = 11.6$ and $F_4 = 56$ or, considering the reflection, $F_4 = 58$. Thus the real dispersion in the albumin solution was $F_1 = 93 - 18 = 75$ and in the sulfur suspension $F_2 = 68 - 58 = 10$. The longitudinal dispersion in the albumin solution was therefore $P = 75 - 10 = 65$ and the Tyndall dispersion in this solution was only about 13 per cent of the complete dispersion.

The distance between the light beam and the upper edge of the brass strip was now increased; in one experiment $a = 2.5$ mm., and in another experiment $a = 3.5$ mm. An ovalbumin solution showed the dispersion, in the first experiment, $B_1 = 6$ and $F_1 = 24$ or, after considering absorption and reflection, $F_1 = 26$. In the other experiment the dispersion in a more concentrated solution of ovalbumin was $B_2 = 14.8$ and $F_2 = 103$ and, after considering absorption and reflection, $F_2 = 111$. As the Tyndall dispersion in apparently optically empty ovalbumin solutions is only 13 per cent of the whole dispersion, it was accordingly $0.13 \times 26 = 3.3$ and $111 \times 0.13 = 14.4$. The radii of these semi-

circles are equal to $\sqrt{\frac{2 \times 3.3}{1.57}} = 1.4$ mm. and $\sqrt{\frac{2 \times 13.3}{1.57}} = 2.4$ mm. As the distance

of the light beam from the upper edge of the brass strip was $a_1 = 2.5$ mm. and $a_2 = 3.5$ mm., the whole semicircles of light were in both cases below the upper edge of this strip and consequently could not produce any effect on the photographic plate. We can therefore conclude that, if the distance between the light beam and the upper edge of the brass strip is large enough, the solutions of substances to be tested which do not show any Tyndall effect in dark red rays can be considered as optically empty and the molecular weights computed

from the obtained semicircles of the dispersion are correct without any subtraction of the Tyndall dispersion.

IV. MOLECULAR WEIGHTS OF SUBSTANCES IN TURBID MEDIA

Some protein solutions could not be clarified by filtration many times through the same filter; for instance, solutions of the hemocyanin of *Helix pomatia*. Only if the blood of this snail, after addition of 3 per cent sodium chloride, was centrifuged at a high rate (7000 to 8000 R.P.M.), did it become optically empty in dark red rays. However, the molecular weight of hemocyanin could be determined also in the case when its solutions showed a Tyndall effect in dark red rays, using the method of comparison (see Section II). For comparison a suspension of rosin in water was used which was prepared by dropping 1 cc. of a 5 per cent alcoholic solution of this substance into 10 cc. of 0.5 per cent gelatin (at 40°C.) and diluting the standard suspension thus obtained with water. Using a solution layer 10 mm. thick, 300 sec. exposure to light, and $a = 2.5$ mm., the photographing of the dispersion of dark red and infrared rays in a 2 per cent solution of hemocyanin showed $B = 24$ and $F = 234$ or, after adding the absorption of the rays by the solution which was 51 per cent of incident light, $F = 477$. Considering the loss of light by reflection (4 per cent) the dispersion was $F = 496$. The dispersion produced by the Tyndall effect of rosin suspension which had the same Tyndall effect in dark red rays as the solution of hemocyanin (observed from above) was $B = 29$ and $F = 338$ or, considering reflection (absorption was too weak), $F = 351$. Thus the longitudinal dispersion was $496 - 351 = 145$. An optically empty 2 per cent solution of ovalbumin (pH = 4.8) (thickness of solution layer = 10 mm.; exposure = 300 sec.; $a = 2.5$) showed $B = 6$ and $F = 24$ or, considering absorption and reflection, $F = 26$. The dispersion produced by the diaphragm and cuvette was unimportant. The molecular weight of hemocyanin (M_1) results from the

equation $145/26 = \sqrt[3]{\frac{M_1}{M_2}}$, where M_2 is the molecular weight of ovalbumin,

which was formerly supposed to be 34,000 but according to Polson (8) is 40,000. Thus $M_1 = 6,900,000$. In other experiments it was found to be 7,000,000, 6,800,000, 5,300,000, or on the average 6,200,000. While The Svedberg found this molecular weight to be 5,080,000, according to Polson it is 6,300,000 to 6,700,000. We see therefore that the value found by Polson is more correct than the other.

Some experiments were done with optically empty solutions of hemocyanin. A 2 per cent solution of this protein showed $B = 13.5$ and $F = 81$ or, considering absorption and reflection, $F = 171$. A new 2 per cent solution of ovalbumin (pH = 4.8) showed $B = 6.8$ and $F = 28$ or, after adding the absorption and reflection, $F = 30$. The molecular weight (M_1) of hemocyanin was computed

from the equation: $171/30 = \sqrt[3]{\frac{M_1}{M_2}}$. Thus $M_2 = 7,400,000$.

Some protein substances cannot be freed from particles which show the Tyndall effect in dark red rays. In this case only by applying the comparison method is it possible to determine the molecular weight of proteins. To such proteins belong, for instance, serum proteins. We try now to determine this weight for serum albumin.

According to Adair (1) the molecular weight of serum albumin is 62,000, while Sørensen (9) found it to be smaller (45,000). According to Briggs (2) this molecular weight is 60,000 (cow) or 80,000 (horse), while The Svedberg (10) gave for horse-serum albumin the molecular weight 70,000. In the following experiments two solutions of human-serum albumin were used, one of which was rather turbid, while the other was prepared from other serum and was almost clear. Both albumins were produced by the separation of globulins by adding ammonium sulfate till 42 per cent saturation at pH = 8 and by adjusting the latter to pH 3.9, whereby the albumins were precipitated. After dissolving them and filtering the solutions, the pH was changed to 4.8 (isoelectric point) by adding acetate buffer. After dilution they contained 5 g. of albumin in 100 cc. of solution (determined by drying at 100°C., extracting with water, and drying

TABLE 3

SOLUTIONS	COMPLETE DISPERSION		AFTER CON- SIDERING ABSORPTION AND REFLECTION	TYNDALL EFFECT OF COLLOIDAL SULFUR SUSPENSION		LONGITUDINAL DISPERSION
	B	F		B	F	
Serum albumin, turbid . . .	32	419	452	29.5	358	94
Serum albumin, clear . . .	19	160	176	13	78	98
Ovalbumin	12.7	78	82			82

at 120°C.). Both solutions showed the Tyndall effect in dark red rays. The color of the Tyndall effect in white light was similar to that of a colloidal sulfur suspension. Also, white light going through the solutions and the suspension was similarly orange. Thus, this suspension was used as the comparison suspension. The results of the measurement of the dispersion circles (thickness of solution layer = 10 mm.; exposure to light = 120 sec.; $a = 3.5$ mm.) are given in table 3, where also the dispersion of an optically empty (for dark red rays) ovalbumin solution (pH = 4.8) containing 5 g. of albumin in 100 cc. is given.

According to the cube-root rule we have two equations: $94/82 = \sqrt[3]{\frac{M_1}{M_2}}$ and $98/82 = \sqrt[3]{\frac{M_1}{M_2}}$, where M_2 is the molecular weight of ovalbumin. The molecular weight of serum albumin (M_1) is thus, on the average, 64,000 ($M_2 = 40,000$). This figure is near that found by Adair.

We try now to determine the molecular weight of serum globulins. Accord-

ing to Adair (1) this weight varies between 130,000 and 150,000. The molecular weight of euglobulin was found to be 174,000. Sørensen (9) gives 140,000 as the average molecular weight of globulins. According to the newest results of The Svedberg (10) the latter is equal to 150,000 and 167,000 (for horse serum), while in his earlier experiments it was found equal to 104,000 and 106,800.

In the present experiments euglobulin was produced from human serum by adjusting its pH to 5.3 and precipitating with ammonium sulfate (30 per cent saturation). The precipitate was washed out with the solution of the latter and dissolved in a 5 per cent solution of sodium chloride. By adding acetate buffer the pH of the solution was set at 5.1 (isoelectric point). Euglobulin always contains lipoids and is sometimes considered as a complex of pseudoglobulin and lecithin (17). Consequently, its solution showed in white light a Tyndall effect the color of which is somewhat more yellowish than that of serum albumin and similar to that of a colloidal suspension of cholesterol acetate. Both had also a similar color if white light passed through them. This suspension was thus used as a comparison suspension.

The globulin solution containing 3.4 per cent protein showed (layer thickness = 10 mm.; exposure time to light = 120 sec.; $a = 3.5$) for infrared rays $B = 29$ and $F = 347$. A freshly prepared cholesterol suspension having the same Tyndall effect in dark red rays observed from above showed $B = 20.8$ and $F = 188$. At the same time the optically empty solution of ovalbumin containing 3.4 per cent protein and having a pH of 4.8 showed $B = 14.8$ and $F = 103$. Considering the absorption (for globulin it was 5 per cent, for albumin 4 per cent, for cholesterol 1 per cent) and reflection (40), the longitudinal dispersion was $P = 371 - 198 = 173$ and the molecular weight of euglobulin (M_1) results from the

formula: $173/111 = \sqrt[3]{\frac{M_1}{M_2}}$ or $M_1 = 151,000$ ($M_2 = 40,000$). This figure is

similar to that found in the latest experiments of The Svedberg.

Pseudoglobulin was obtained from human serum by setting the pH of the solution which remained after removing euglobulin at 8 and precipitating with ammonium sulfate (42 per cent saturation). The precipitate was washed out with the same solution of ammonium sulfate, the rest of the latter was pressed away, and the precipitate was dissolved in a 3 per cent solution of sodium chloride. The pH of the solution was set, by addition of acetate buffer, at 5.2 (isoelectric point). The color of the Tyndall effect of the solution in white light was similar to that of a colloidal sulfur suspension; therefore the latter was used as comparison suspension. The complete dispersion of the solution of pseudoglobulin containing 4.8 per cent protein was (layer thickness = 10 mm.; exposure = 120 sec.; $a = 3.5$) $B = 23$ and $F = 224$. The optically empty solution of ovalbumin containing 4.8 per cent protein (pH = 4.8) had $B = 10$ and $F = 58$. The dispersion of the sulfur suspension having the same Tyndall effect in dark red rays (observed from above) was $B = 18$ and $F = 145$. Considering the absorption and reflection we have the longitudinal dispersion $P = 253 - 152 = 101$ and the molecular weight of pseudoglobulin $M_1 = (101/61)^3 \times 40,000 =$

130,000. This figure is in accordance with the figures found by the previous authors.

V. SUMMARY

After a short description of the apparatus and method used for photographing and measuring the light dispersion, which was expressed as the surface in mm.^2 of the dispersion circles on negatives, the longitudinal dispersion of dark red and infrared rays in solutions of different proteins was measured; the absorption of the rays by the solutions and their reflection from the walls of the cuvette containing the latter were considered. In the case of optically empty protein solutions the values obtained express longitudinal dispersion directly, while in the case of turbid solutions the Tyndall effect must be considered. The latter was determined by photographing the dispersion of a suspension which did not show any longitudinal dispersion but had only the Tyndall effect and at the same time this effect observed in dark red rays from above was equal to that of the protein solution to be tested (comparison method). The value obtained was then subtracted from the complete dispersion of the solution to get the longitudinal dispersion. The comparison suspension was selected according to the rule that it must have particles of the same size as the particles producing the Tyndall effect in the solution to be tested and both effects must have therefore the same color in white light. Moreover, white light going through the comparison suspension must have the same color as white light going through the protein solution. Both must show also a similar turbidity in light going through them.

The longitudinal dispersion of dark red and infrared rays determined in optically empty or turbid solution of proteins, like that observed in polystyrenes and their solutions, is proportional to the cube root of the molecular weight of substances producing this dispersion. This rule allowed the examination of the molecular weights of hemocyanin (*Helix pomatia*) and of serum proteins. Some of the solutions of these substances were optically empty, but most of them were turbid. The comparison suspensions used were: rosin suspension in the case of hemocyanin, a colloidal suspension of sulfur in the case of serum albumin and pseudoglobulin, and a freshly made suspension of cholesterol acetate in the case of euglobin. The average molecular weight of hemocyanin was found to be 6,800,000, that of serum albumin 64,000, that of pseudoglobulin 130,000, and that of euglobulin 151,000 (human serum). The computing of these molecular weights was made on the assumption that the molecular weight of ovalbumin is 40,000 (Polson). The pH of each of the protein solutions was set at the isoelectric point. The solution of ovalbumin used in the comparison method was optically empty in dark red rays. If the light intensity was increased several times, the Tyndall effect became visible in these rays too. It appeared as well in the albumin solution as in the colloidal sulfur suspension which had the same Tyndall effect in white light as the albumin solution and did not show it in dark red light. Photographing the light dispersion produced by the Tyndall effect in the same sulfur suspension (dark red and infrared rays) showed that this effect

is very weak and does not influence the values of molecular weights computed from the longitudinal dispersion, assuming that the distance between the light beam and the upper edge of the strip separating it from the photographic plate is great enough (1.5–3.5 mm.) so that the light circle produced by the Tyndall dispersion cannot act on the plate.

REFERENCES

- (1) ADAIR: *Skand. Arch. Physiol.* **49**, 71 (1926).
- (2) BRIGGS, D. R.: *J. Phys. Chem.* **39**, 983 (1935).
- (3) LEPESCHKIN, W. W.: *Protoplasma* **35**, 100 (1940).
- (4) LEPESCHKIN, W. W.: *Biochem. Z.* **309**, 254–69 (1941).
- (5) LEPESCHKIN, W. W.: *Physik. Z.* **43**, 489–96 (1942).
- (6) LEPESCHKIN, W. W.: *Protoplasma* **36**, 422 (1942); **37**, 25 (1943).
- (7) LEPESCHKIN, W. W.: *Kolloid-Z.* **105**, 141 (1943).
- (8) POLSON, A.: *Kolloid-Z.* **87**, 149 (1939).
- (9) SØRENSEN, S. P. L.: *Kolloid-Z.* **53**, 111 (1930).
- (10) SVEDBERG, THE: *Kolloid-Z.* **85**, 119 (1938).
- (11) WENT, ISTVÁN, AND FARAGÓ, F.: *Biochem. Z.* **230**, 238 (1931).

NEW BOOKS

Qualitative Analysis by Spot Tests. Inorganic and Organic Applications. By FRITZ FEIGL. Third, completely revised, English edition, translated by Ralph E. Oesper. xvi + 574 pp. New York-Amsterdam: Elsevier Publishing Company, Inc., 1946. Price: \$8.00.

This edition of Feigl's book differs from the second English edition of 1939 in several respects. New spot reactions have been added (one gets the impression that few important reactions of this type have been developed in the last half-dozen years) and, moreover, the previous text has been subjected to a thorough critical examination. A new feature is the inclusion of a detailed account of the manipulations involved in spot-test analysis. A chapter on the detection of free elements has been added, together with a bibliography of some 140 items on the application of spot tests. The translation has been made in a manner that leaves nothing to be desired, but signs of the British origin of the former translations linger in the use of *felspar* for *feldspar* and *opening up* for *decomposition*. The subject index is exceptionally complete, and the almost entire absence of typographical errors points to careful preparation.

The great value of Feigl's work to the analyst is well known, and further encomiums on the present edition are superfluous. The author, in the preface, asks for coöperation from fellow chemists in the way of suggestions, and the reviewers take advantage of this opportunity to comment on some of the tests which they have used from time to time. On page 50, under the detection of mercury with dithizone, it is implied that antimony interferes by reacting with dithizone; actually antimony does not form a dithizonate. The statement that even low concentrations of acid prevent the reaction of silver with dithizone is not in accord with our experience, which indicates that the reaction is about 90 per cent complete in 6 *N* sulfuric acid solution with a relatively small excess of dithizone. It is hard to believe that it is possible to detect 1 microgram of mercury in the presence of 100,000 times as much silver. Selenium and tellurium should be added to the elements that are precipitated by stannous chloride in the Bettendorf test for arsenic (page 79). On page 100, the prevention of interference of silver in the dimethylaminobenzylidenerhodanine test for gold by precipitation of silver chloride might be pointed out. A saturated solution of silver chloride in

0.1 *N* hydrochloric acid gives no more color with the reagent than 0.1 microgram of gold when the reaction is carried out in a tube of 1 cm.³ cross section. It seems that phosphotungstic acid should be mentioned as a reagent for quinquevalent vanadium, since the yellow color it gives is several times stronger than that produced by hydrogen peroxide. Although the fact is not perhaps of much practical importance, it is worth mentioning under the thiocyanate test for ferric iron (page 124) that trivalent ruthenium also gives a red color with thiocyanate which is strong enough to enable a microgram or so of this element to be detected. No reference is made to the use of thiosulfate as complex former with foreign metals in the detection of zinc with dithizone (page 139). Morin should be added to the reagents listed for beryllium (page 147). As a fluorescence reagent in sodium hydroxide medium it is more sensitive than those now included.

On page 150, under the peroxide test for titanium, it is stated that cerium also gives a color reaction. This is an error which for some strange reason is found in a number of books. Actually, hydrogen peroxide reduces ceric salts to the colorless cerous. The use of 8-hydroxyquinoline for the detection of indium and particularly gallium should be mentioned (page 162). The quinolate complexes of these metals can be extracted with chloroform from solutions having the proper pH. The chloroform layer shows strong fluorescence in ultraviolet radiation. No reaction is given for rhenium. The stannous chloride-thiocyanate test for this element might well be described, especially since we now have a good method for the separation of rhenium from interfering molybdenum.

The part dealing with organic spot tests has been extended from 95 pages in the 1939 edition to 115 pages in the present edition. This part contains sections on the detection of elements in organic compounds, detection of characteristic groups, and identification of specific organic compounds. Again, Feigl has carried out the pioneer work in this field in which only a beginning has been made. It is hardly possible to develop within a short time a complete scheme of "qualitative organic analysis by spot tests." Since qualitative organic analysis is taught in most universities by the organic chemistry departments, it is unlikely that many organic chemists will become acquainted with the organic part of Feigl's book. This is to be deplored and the author might consider the publication of a review of his contributions to qualitative organic chemistry in some periodical which is readily available to organic chemists. With increasing development of spot tests in organic analysis the publication of a separate volume on this subject might deserve consideration. If this is done, a more critical selection of reactions published in the literature would seem advisable. For example, in the part dealing with the detection of nitrogen in organic compounds (page 315) the very sensitive Kjeldahl method could be added. Phosphorus in organic compounds may also be detected by this method. Moreover, the oxidation of nitrogen to nitrate by the procedure of Högl (1933) might be included. Under aldehydes the reaction of Rawnitz (1931), and under glycolic acid the reaction of Dénigès (page 399) might have been mentioned.

E. B. SANDELL.

I. M. KOLTHOFF.

Polarographie. Theoretische Grundlagen, Praktische Ausführung und Anwendungen der Elektrolyse mit der tropfenden Quecksilberelektrode. By J. HEYROVSKY. 514 pp.; 252 fig. Vienna: Springer Verlag, 1941. Lithoprinted by Edwards Brothers, Inc., Ann Arbor, Michigan, 1944.

A book written by Heyrovsky on polarography hardly needs a recommendation. Not only is Professor Heyrovsky the originator of polarography, but he and his associates have developed the theoretical fundamentals, practical performance, and the analytical and other applications of polarography.

The present book is well balanced with regard to presentation of the theory and the practical applications. In the first 210 pages a clear discussion is given of the theory of polarography. In this part more emphasis could have been placed on the significance of exact numerical values of the diffusion coefficient in the Ilkovič equation, especially in the

estimation of the number of electrons involved in polarographic reductions. By ignoring such differences between diffusion coefficients of different ions it is, e.g., wrongly concluded (page 73) that nitrate is polarographically reduced to ammonia.

The theoretical part gives more than an adequate background for the practical part. In eighty pages a detailed discussion of polarographic equipment, performance of the determination of polarograms, and the interpretation of the latter for analytical purposes is given. A chapter of more than one hundred pages is devoted to analytical procedures for the polarographic determination of inorganic and organic compounds alone and in various mixtures. This part could be made more complete. The chapter on the application of polarography to the investigation of proteins and sulfhydryl-containing compounds is outstanding. This chapter should be of special interest to physiologists, biochemists, and pathologists. The pioneer work carried out by Heyrovsky's school should stimulate further research in this important field of medicine.

The last chapter deals with polarographic titrations. On page 424 the author objects to the use of the word "amperometric titrations," which has been coined by the reviewer. Heyrovsky's objection is based upon his statement that the use of a rotating platinum electrode as indicator electrode has no advantages. However, the rotating platinum electrode has established itself in the last six years as a very important electrode for the simple rapid determination of traces of quite a number of constituents.

The last fifty pages give a complete chronological bibliography of polarography until 1941. Such a bibliography is very convenient. In this country there is no need for such a bibliography, because a more up-to-date one has been prepared and is being distributed by E. H. Sargent & Company, Chicago, under the title *Bibliography of Polarographic Literature, 1922-1945*.

Heyrovsky's book is a welcome addition to the literature on polarography.

I. M. KOLTHOFF.

Elastic and Creep Properties of Filamentous Materials and Other High Polymers. By HERBERT LEADERMAN. 278 pp. (mimeographed). Washington, D. C.: Textile Foundation, 1944.

This book is a highly theoretical treatment of the subject from the fundamental point of view of relating the properties of these materials to their structure. The whole of Part I, comprising 103 pages, is devoted to a theoretical and mathematical treatment of primary creep, the superposition principle, and the relation of mechanical models and the structure of high polymers to these properties.

Part II is devoted to the experimental work which Dr. Leaderman carried out as a Fellow of the Textile Foundation on the relationship of the elastic and creep properties of silk, viscose and acetate rayon, and nylon. These materials all show creep properties, i.e., their extension under constant load is not constant but is a function of time, the rate of creep decreasing with time. When the load is removed, elastic contraction takes place followed by a slower creep recovery. Although the latter ceases after a period of time equal to that during which the load was applied—provided the load was below the yield point—a permanent set remains. Such a fibre is said to be "mechanically conditioned," and this conditioning may be removed by treatment with water or steam followed by drying without load. In silk and the rayons the instantaneous or elastic deformation is proportional to the load; however, the delayed deformation (creep) is not, but is a function of time. These materials do not follow the superposition principle. Nylon follows a still different set of laws. It exhibits both types of deformation but the reversible (elastic) deformation is a much larger proportion of the total. Two hundred ten literature references are included in this study, which is for experts in the field rather than laymen.

RALPH E. MONTONNA.

Immuno-catalysis. By M. G. SEVAG. 260 pp. Springfield, Illinois and Baltimore, Maryland: Charles C. Thomas, 1945. Price: \$4.50.

Sevag holds the view that there exists a close analogy between the relationships that enzymes bear to their substrates and reaction products, and the relationships that antigens bear to normal globulin and specific antibodies. Thus, he regards the antigen as being the counterpart of the catalysts in the enzyme reaction, the antibody the counterpart of the reaction product in the enzyme reaction, and normal globin the counterpart of the substrate in the enzyme reaction. The book is devoted to the presentation of data and arguments that tend to substantiate his point of view.

Part 1 of the book is devoted to data and arguments to prove that antigens may be regarded as biocatalysts. Part 2 presents evidence to support the contention that antibodies may be regarded as specific enzyme inhibitors. The balance of the book—parts 3, 4, and 5—is devoted to the presentation of data that are available concerning the production of antibodies against various types of enzymes, part 3 dealing with antibodies against enzymes in general, part 4 with antibodies against bacterial enzymes, and part 5 with antibodies against respiratory enzymes. There is an extensive bibliography of 482 references.

The book is very thought provoking. The reader found it difficult to accept many of the points of view by Sevag; and when the book was reviewed before a group of individuals interested in immunology and enzyme chemistry, it brought about very heated discussions. Nearly everyone found some portion of the book with which he disagreed, but there was no consistency amongst the individuals as to the particular portion of the book to which they took exception.

The subject matter is complex; as a result it requires very careful reading, some sections re-reading, in order to grasp the significance of what the author is presenting. Because of the fact that the subject matter itself is complex, this probably could not be avoided.

Any book that can stimulate thinking and active discussion should be worthwhile. On the basis of such a standard, the book written by Sevag must be regarded as a masterpiece. It should be required reading for anyone who is interested in the field of immunology, and should stimulate new research in this field. People who are interested in enzyme chemistry will find many interesting points of view presented.

H. O. HALVORSON.

Organic Preparations. By CONRAD WEYGAND. 534 pp. New York: Interscience Publishers, Inc., 1945. Price: \$6.00.

This volume is a translation of Part II of Conrad Weygand's *Organisch-Chemische Experimentierkunst*, which was published in 1938. The publishers call attention to one major difference between the original and the translation. The original German edition contains a number of quotations of preparations published in *Organic Syntheses*, but in the present translation these quotations have been replaced by references to the corresponding volumes of *Organic Syntheses*.

There is a great deal of useful information compressed into this volume. An entire volume of the size of the one under review could easily be devoted to each of many of these chapters. As a consequence, one may be disappointed in finding only a few lines devoted to particular topics. Nevertheless, references are cited which will enable the student to expand his information beyond the scope of these short, but usually excellent paragraphs.

This book will be of particular value to students beginning graduate work which requires preparative work in organic chemistry.

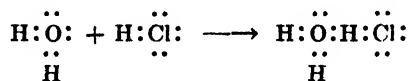
WALTER M. LAUER.

Electronic Theory of Acids and Bases. By W. F. LUDER AND S. ZUFFANTI. 165 pp. New York: John Wiley and Sons, Inc., 1946. Price: \$3.00.

This book is dedicated to the late G. N. Lewis, a fitting tribute to the scholar who was the originator of the electronic theory of acids and bases. In some thirteen chapters the authors present in a clear, concise, and elementary way the fundamentals of the G. N. Lewis theory and its implications. The four phenomenological criteria of acidity and basicity are

described in four separate chapters: Neutralization, Titrations with Indicators, Displacement, and Catalysis. The last three chapters discuss in a more advanced way acid and base catalysis and alkoxides as catalysts. The book is of interest to students in modern inorganic and organic chemistry. The reviewer regrets the unconciliatory attitude of the authors with regard to the Brønsted theory. "The conflict between the two theories has gone on, although the solution to the problem has been at hand since 1923" (page 15). There has not been and there is no conflict between the G. N. Lewis theory and that of Lowry-Brønsted.

The authors are dogmatic in their emphatic rejection of the Brønsted theory in favor of that of Lewis. "Some writers have indicated that hydrogen acids require special consideration in the Lewis terminology. No doubt such a misunderstanding arises from the emphasis of the Brønsted theory upon displacement of one base by another as the only criterion of acid-base phenomena. Actually displacement is only one of the four 'phenomenological criteria' of acids and bases, and the Brønsted type equation is only one of the two types of acid-base displacement. The Brønsted theory is thus included in the Lewis theory and requires no special consideration" (page 99). The reviewer, who is responsible for the advocacy of the treatment of hydrogen acids as a special group, as done in the Brønsted-Lowry theory (see *J. Phys. Chem.* **48**, 51 (1944)), based his defense of the right of existence of the theory that acids are proton donors upon the commonly accepted view that the existence of two-covalent hydrogen is unlikely. Thus, the reaction of a time-honored acid, like HCl, with water cannot be represented by a reaction according to the Lewis theory:



The authors themselves state (page 44) that: "The existence of the hypothetical intermediate addition compound in which the hydrogen bridge between the hydrogen chloride and water molecules involves 2-covalent hydrogen is now regarded as unlikely." Thus, they really represent the reaction between H₂O and HCl as a transfer of the electron from the base chloride to the base water, which is the Brønsted theory. However, in all their discussions in the book they conveniently state that the reaction between hydrogen acids and bases fits in the Lewis theory. In this respect they are "plus royaliste que le roi." Before the reviewer published his proposal to make a distinction between hydrogen acids (Brønsted acids) and all other acids in the Lewis sense and to use both theories he sent the manuscript to the late Professor Lewis, who expressed complete approval with the proposal.

The authors are hardly objective when they deny the right of existence of the Brønsted-Lowry theory, which admittedly is much more limited than the Lewis theory. One does not exclude the other and both theories can be adopted, as the reviewer advocated in his paper in 1944.

In their zeal of defending the sole right of existence of the Lewis theory the authors call an argument against their views a "misunderstanding." We find on page 100: "One familiar example (of displacement reactions) is interesting since it has been the subject of some misunderstanding."

The familiar example is the reaction between silver ions (acid in the theory of Lewis) with hydroxyl ions on the one hand and ammonia on the other. The authors arrive at the conclusion that ammonia is about as strong a base as hydroxyl ion toward silver ion. On the basis of their reasoning the iodate ion would be about as strong a base as hydroxyl ion (towards silver), bromide would be a stronger base, and iodide the strongest. The reviewer maintains that the classification of ionic precipitation reactions ($\text{Ag}^+ + \text{OH}^-$) in the group of acid-base reactions is not only confusing, but is incorrect.

The above critical statements do not detract from the reviewer's appreciation of the good qualities of the book. It is written in a clear and simple way and is thought provoking. It deserves wide circulation among inorganic and organic chemists and among advanced

students in chemistry, provided they are given a more balanced appreciation of the virtues of the Brønsted theory.

I. M. KOLTHOFF.

The Life of a Chemist. Memoirs of VLADIMIR N. IPATIEFF. Edited by XENIA JAUOFF ENDIN, HELEN DWIGHT FISHER, and H. H. FISHER. Translated by V. HAENSEL AND MRS. R. H. LUSHER. 657 pp. Stanford University, California: Stanford University Press, 1946. Price: \$6.00.

These biographical memoirs give an account of the life of the author until 1930, when he left Russia. Shortly afterwards he came to the United States, where he has since continued his distinguished scientific work. This history of Ipatieff's eventful scientific and official career in Russia has an interest far outside the realms of chemistry or science. It gives a revealing insight into the changes that occurred in Russia during one of the most significant periods of modern times.

That Ipatieff succeeded in making the transition from an official and General under the Czarist regime to a highly respected and trusted scientific director and adviser under the Soviet is to be attributed to his singleness of interest in his first and continuing love of chemistry; hence the simple and appropriate title of this book, written in his native Russian and translated by some of his collaborators in this country.

The writer does not state whether he wrote from notes or memory. If the latter, the detailed description of events, researches, and personalities is truly remarkable. His contacts with all prominent scientists in Russia and many in England as well as Germany, where he had part of his chemical education, were extensive. His principal interests were in the field of toxic gases for chemical warfare and in the technique of high-pressure catalysis, in which he made very early and important contributions.

Ipatieff frequently deplors the loss to Russia of valuable scientific men for political causes. The loss of Ipatieff himself is such a case, but fortunately it has been America's gain. His contributions to our supply of high-octane gasoline during the war alone must have compensated Russia in some degree for his loss. And his great love for his native country, which is manifest throughout the book, must have afforded him much satisfaction in his indirect contributions through his adopted country to Russia's success in warfare, in spite of ill-concealed skepticism of her political ideologies and industrial plans.

It is quite evident that although he has found a welcome home in America and assumed an eminent position in its industrial and scientific life, yet his heart remains in his native land, the scene of his early triumphs, which he left reluctantly and would gladly have continued to serve during her years of planning and industrial development. An extensive appendix contains brief historical notes about the principal Russian leaders and organizations mentioned in the text.

S. C. LIND.

A Laboratory Manual of Qualitative Organic Analysis. By H. T. OPENSHAW. 87 pp. Cambridge: The University Press, 1946. New York: The Macmillan Company, 1946. Price: \$1.50.

This small volume presents a laboratory method for the identification of the more common types of organic compounds and includes tables of physical constants for some of these compounds and their derivatives. The procedure put forward is similar to that of other texts, in that it consists of a series of tests for functional groups, which are applied in a definite order, depending upon whether the compound contains carbon, hydrogen and oxygen, nitrogen, sulfur or halogen. The book will serve to acquaint beginning students with a system of analysis; however, it does not contain the theoretical discussion which is necessary for such a comprehensive study of this field as is usual in the typical course given in this country.

WILLIAM E. PARRHAM.

Advances in Enzymology. Vol. 6. Edited by F. F. NORD. x + 563 pp. 215 Fourth Ave., New York: Interscience Publishers, Inc., 1946. Price: \$6.50.

This is the sixth annual review of current advances in enzyme chemistry and related fields of biochemistry. Following an established precedence, the editor has secured articles from men who have contributed to the fields of their several specialties.

The first article treats of the amino acid decarboxylases produced by bacteria; it is by E. F. Gale, who has been active in this field. One of the problems encountered in the use of sulfa drugs and the antibiotics involves the resistance or "adaptation" developed by the organisms. M. G. Sevag discusses this problem particularly as it involves the question of the production of "adaptive enzymes." To complete the picture, D. W. Woolley submits an article on biological antagonisms between structurally related compounds.

In the field of intermediate metabolism, the rôle of myosin is being actively studied. V. A. Engelhardt summarizes the experimental work pointing to the rôle of myosin as an adenosinetriphosphatase. A companion article by C. L. Hoagland considers the altered metabolism in diseases of muscle and points to the possibility that impaired muscle activity may involve reactions which have their origin in other tissues.

Recent work has indicated that the energy-rich bond in acetyl phosphate is of considerable importance, particularly in certain bacterial reactions; a chapter on this field is by F. Lipmann. C. E. Clifton reviews the literature in the extensive field of assimilation of carbon and of nitrogen by microorganisms. A separate chapter by W. G. Frankenburg summarizes the changes produced in the curing of tobacco. The rôle of the tocopherols (vitamin E) as components of certain enzyme systems is surveyed by K. C. D. Hickman and P. L. Harris, who conclude their chapter with a summary of the needs for the tocopherols and the levels at which these are found in foodstuffs.

The amylases are of importance wherever starch is metabolized or used in industrial processes. The actions of the two recognized forms (alpha and beta) are summarized by R. H. Hopkins; this is followed by a complete discussion by W. F. Geddes of the importance of the amylases in the cereal industry.

The current volume maintains the high standard achieved in former years. We are indebted to the authors for the excellent summaries and the critical discussions in these fields where the literature is becoming voluminous. The editor is to be commended for securing three of the eleven articles from scientists in Europe.

W. M. SANDSTROM.

ON THE SOLUBILITY OF PARAFFIN-CHAIN COMPOUNDS

A. BOND¹

International Lubricant Corporation, New Orleans, Louisiana

Received September 17, 1946

The large body of experimental data on the solubility of paraffin-chain compounds of higher molecular weight which has recently become available (9, 12) offered the opportunity to study the thermodynamics of solutions of this interesting group of materials in more detail than has previously been possible.

I. THE FREE ENERGY OF MIXING AS A MEASURE OF THE NON-IDEALITY OF SOLUTIONS

The information which we wish to derive from solubility data is the degree to which the distribution of particles in the solution deviates from randomness and the magnitude of the interaction energy between solvent and solute, or, in short, the degree to which the solutions deviate from Raoult's law.

The solubility of solids—for systems following Raoult's law—is to a good approximation:

$$\ln a_2 = - \frac{\Delta H_f}{R} \left(\frac{1}{T} - \frac{1}{T_f} \right) \quad (1)$$

where ΔH_f = heat of fusion of solute, T_f = melting point of solute in° K., T = temperature (°K.) at which the solubility a_2 is measured, R = gas constant. (The only approximation made here is the neglect of the temperature dependence of ΔH_f , given by the specific-heat difference between the solid and the liquid states of the solute. The few recent specific-heat data (9) of normal paraffins, when applied to this calculation, produce a perceptible reduction in the slope of the "ideal" solubility line at the low-temperature end. The apparently quite low degree of accuracy of the solubility data at the lowest temperatures, as well as the paucity of reliable specific-heat data for most of the compounds to be discussed, militated strongly against the use of a temperature correction for ΔH_f , which would complicate the calculation without benefitting the significance of the results. The magnitude of the error, introduced by this approximation at about 50°C. below the melting point, is of the order of < -30 per cent in a_2 , which will affect $\log \gamma$ only insignificantly.)

Figures 1 and 2 illustrate the manner in which actual solutions follow, or deviate from, equation 1. We obtain a convenient numerical expression for the "non-ideality" of a solution by defining an excess free energy of mixing:

$$\Delta F_m = RT \ln \gamma \quad (2)$$

In figures 3 to 9 ΔF_m is presented in such a manner that one can compare the effect of molecule size and type (of solvent and solute) upon non-ideality at

¹ Present address: Shell Development Company, Emeryville, California.

equal molar concentrations of solute. Before entering into a detailed discussion of these diagrams it should be pointed out that the figures given are not all of equal reliability, mainly because the heat of fusion data in the literature are both scarce and not always consistent. The most plentiful and reliable data are

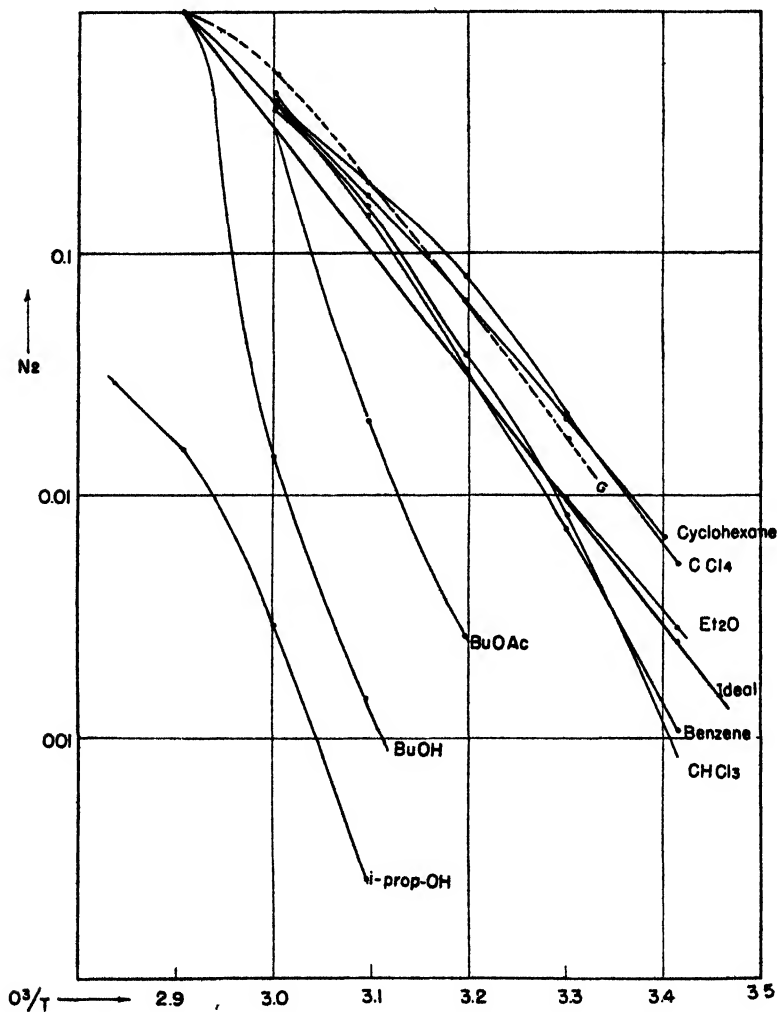


Fig. 1. Solubility of *n*-dotriacontane in various solvents

those on the hydrocarbons (9, 10, 16). The ΔH_f data of the higher fatty acids are available, but not equally reliable. The most probable values were selected by graphical interpolation of materially self-consistent data. The heat of fusion of cetyl alcohol was taken from the recent paper by Parks and Rowe (11), and ΔH_f of monocetylamine was obtained by measurement of the melting-point depression.

While the accuracy of the ΔH_f values used may leave much to be desired, the internal consistency of the results obtained makes it very probable that better ΔH_f values—once they become available—will not materially alter the over-all picture developed.

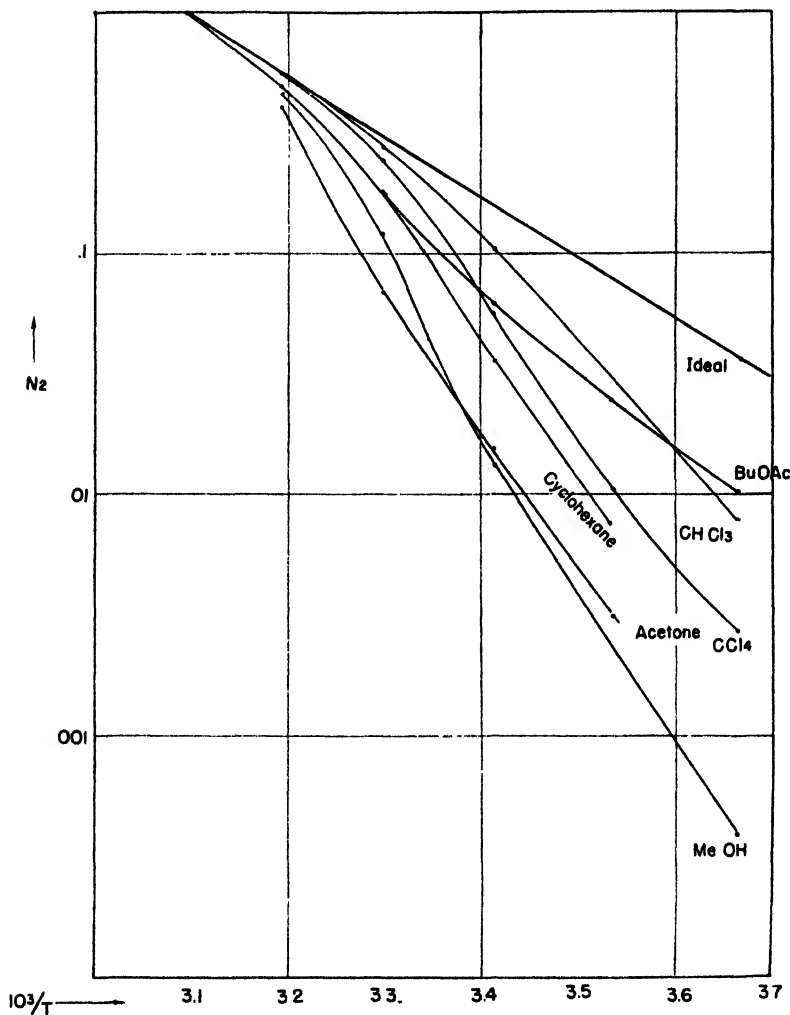


FIG. 2. Solubility of cetyl alcohol in various solvents

The sequence of ΔF_m values² is on the whole about as one would expect. Normal paraffins in "inert" solvents, such as chloroform and carbon tetrachloride, show negative deviations from Raoult's law which increase with their chain length, just as has been observed for the vapor pressure of such solutions (1).

² The ΔF_m graphs are presented in an upside-down fashion in order to be consistent with the direction of the solubility deviation from the "ideal" curve.

In alcoholic solutions the opposite is the case, ΔF_m increasing markedly in the positive direction with increasing chain length, as is easily understandable. Keeping the molecular weight constant and comparing the effect of varying the

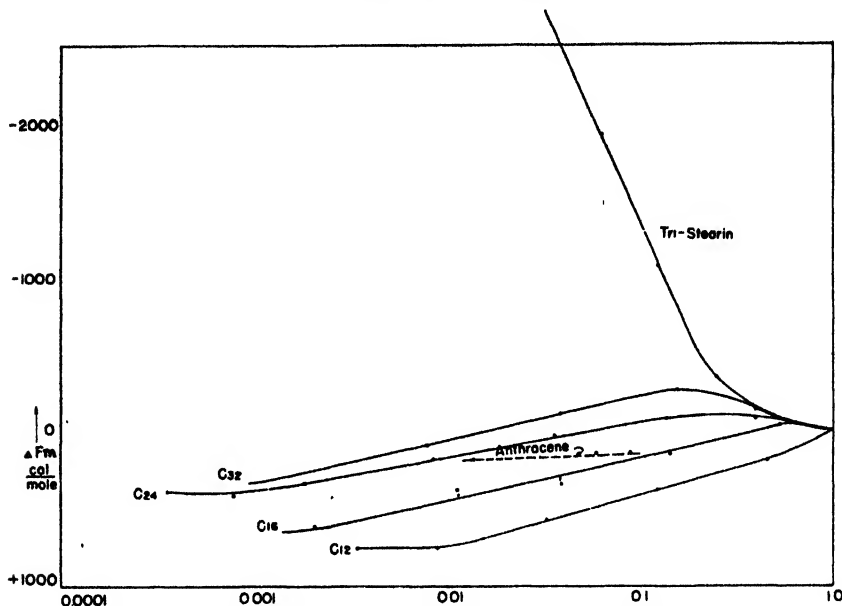


FIG. 3. ΔF_m curves of paraffin hydrocarbons in chloroform

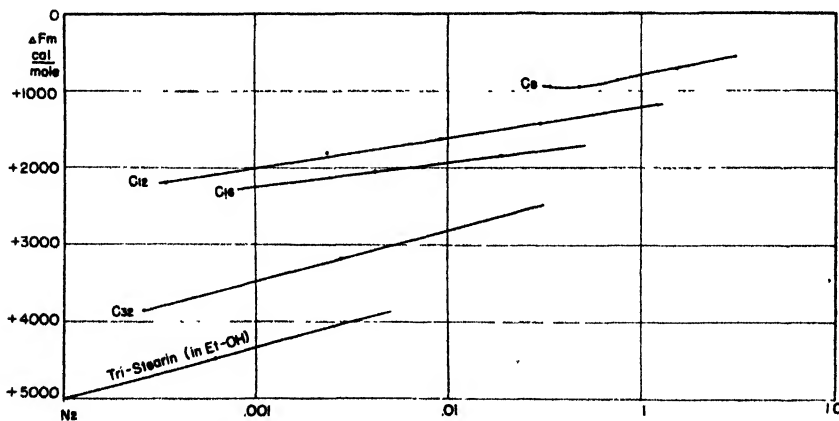


FIG. 4. ΔF_m curves of normal paraffin hydrocarbons in isopropyl alcohol

functional group, we observe in carbon tetrachloride the largest ΔF_m values for the alcohol, the fatty acid and the primary amine following in close succession, while the hydrocarbon alone shows negative deviations from ideality. This observation speaks against the existence of the alcohol, the fatty acid, and the amine as double molecules in solution. In case they existed as double molecules,

the ΔF_m curves of all three compounds should coincide with the curve of dotriacontane, because their functional groups should then not be available for inter-

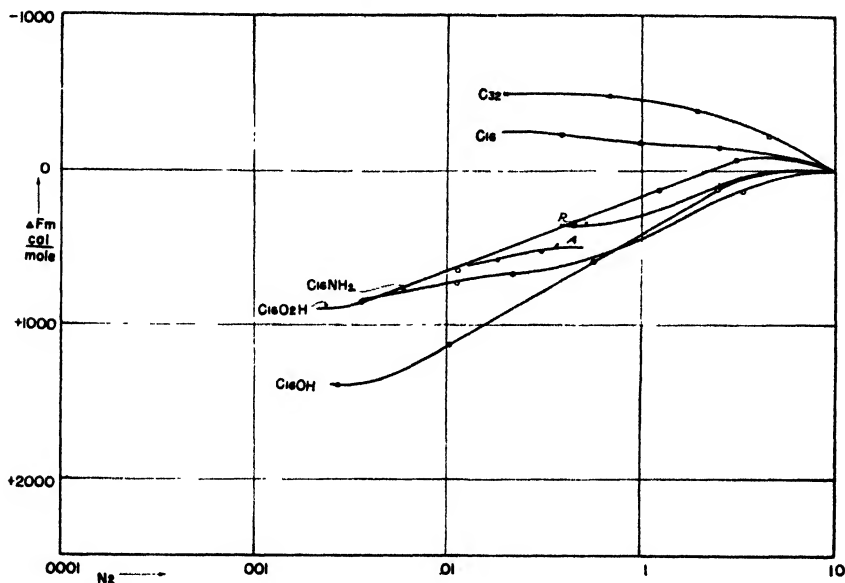


FIG. 5. ΔF_m curves of *n*-hexadecane derivatives in carbon tetrachloride

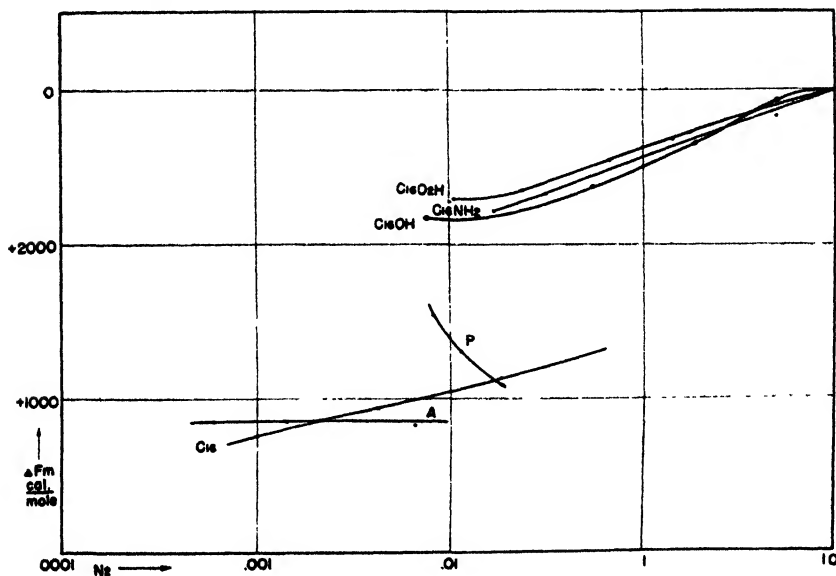


FIG. 6. ΔF_m curves of *n*-hexadecane derivatives in isopropyl alcohol. P = phenanthrene; A = anthracene (for comparison).

action with the solvent. As it is, the curves move in opposite directions. In alcoholic solution we find this situation somewhat reversed. Here the hydro-

carbon has the highest ΔF_m value, but it is rather surprising to observe that the sequence of the other three compounds is the same in isopropyl alcohol as in

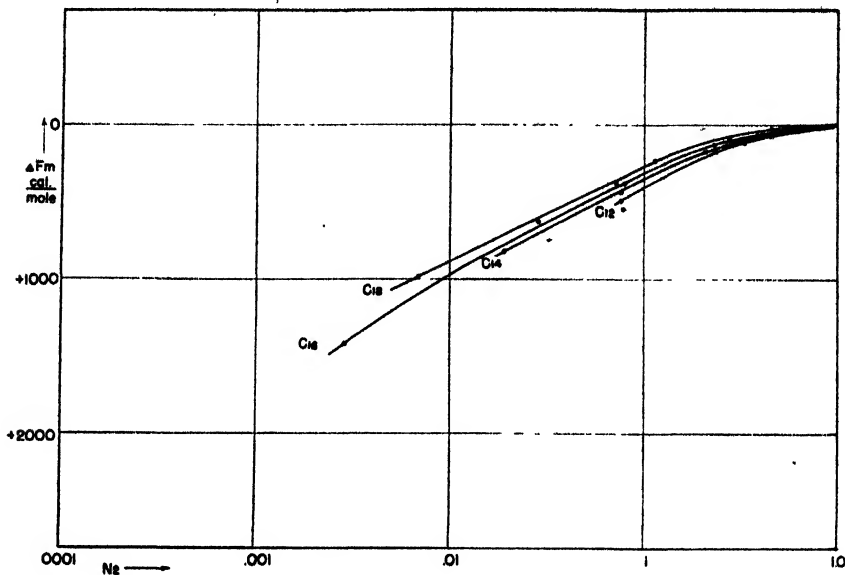


FIG. 7. ΔF_m curves of normal fatty acids in cyclohexane

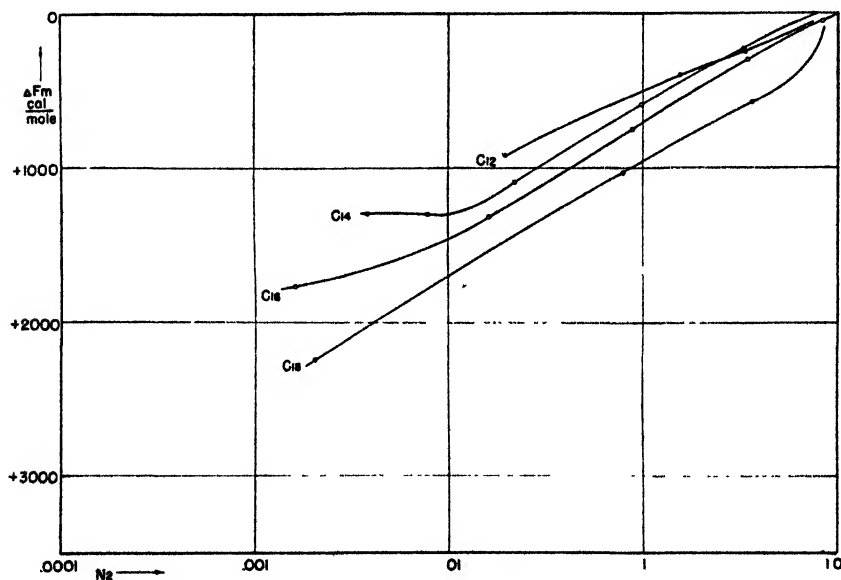


FIG. 8. ΔF_m curves of normal fatty acids in methyl alcohol

carbon tetrachloride. The behavior of the fatty acids in cyclohexane solutions and in methyl alcohol is just as expected, the deviation from ideality *increasing* with the length of the paraffin chain *in the latter*, and *decreasing* in the former.

II. THE ORIGIN OF THE DEVIATIONS FROM RAOULT'S LAW

Negative deviation from Raoult's law, which cannot be accounted for by the cohesive energy difference concept (5), have become of considerable interest during the past decade owing to their frequent occurrence with polymer solutions. Guggenheim (4) proposed a rigorous mathematical treatment of the case of large solute among small solvent molecules, which has recently been applied to the vapor-pressure data of a number of paraffin-chain compound solutions

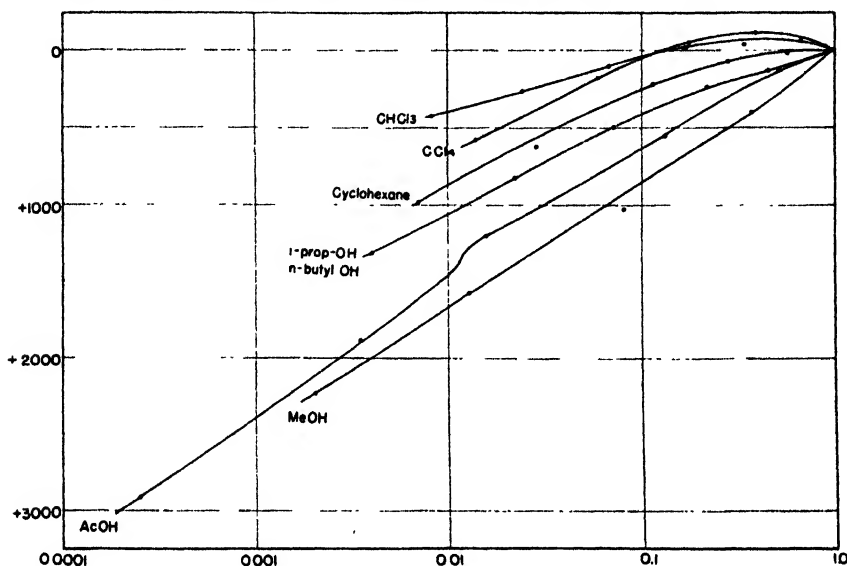


FIG. 9. ΔF_m curves of stearic acid in various solvents

(2). He derives for completely flexible (or completely stiff) chain-like molecules the following equation:

$$a_1 = \frac{N_A}{N_A + \frac{r_B}{r_A} N_B} \left(\frac{N_A + \frac{r_B}{r_A} N_B}{N_A + \frac{q_B}{q_A} N_B} \right)^{\frac{1}{2} z q_A} \cdot \left(\frac{\beta - 1 + 2x}{(\beta + 1)x} \right)^{\frac{1}{2} z q_A} \quad (3)$$

where a_1 = activity of solvent; N_A, N_B = number of molecules of solvent and solute, respectively; r_A, r_B = number of sites occupied by molecules A or B; z = number of nearest neighbors of any one site; $zq_i = r_i(z - 2) + 2$ = number of sites neighbors of the r_i sites which are occupied by a molecule of type i , excluding sites occupied by the next elements of the same molecule, i.e., zq_i is the number of sites which are neighbors of a molecule of type i . The x and β are defined by

$$x = q_A N_A / (q_A N_A + q_B N_B); \quad \beta = \{ (1 - 2x)^2 + 4x(1 - x)e^{2\omega_{AB}/k} \}^{\frac{1}{2}}$$

where ω_{AB} = the contribution of each pair of sites to the intermolecular potential energy, so that the energy of mixing

$$\Delta E_m = z\omega_{AB}(q_A N_A + q_B N_B) \frac{2x(1-x)}{\beta + 1}$$

For the "semi-ideal" case, when $\Delta E_m = 0$, the second bracket term of equation 3 becomes equal to unity.

If we calculate the activity of carbon tetrachloride and cyclohexane³ in the presence of *n*-dotriacontane under the assumption of $\Delta E_m = 0$ by equation 3, we obtain for N_2^0 the curve G in figure 1. The shape and position of this curve suggest that the negative deviation of this solution from Raoult's law can be accounted for without the need of special assumptions of energy (1) or of entropy (15) of mixing effects. The same applies to the *n*-hexadecane systems. The activities calculated from the vapor-pressure data of the same systems (1) are equally well accounted for by use of equation 3 (see reference 2).

In reality, then, not Raoult's law but Guggenheim's modification of it should be accepted for the definition of the reference solution in order to take into account large differences in molecule size between solvent and solute. As in all cases under consideration in this paper, such a change in the reference curve would cause but a small change in ΔF_m (< 500 cal. per mole) and would also leave the relative position of the curves in figures 3-9 essentially unaffected, such recalculation would not reveal any qualitatively new features and was therefore deemed unnecessary at this time.

Negative deviation from Raoult's law due to specific interaction between solvent and solute has been observed in the aliphatic series only for the system amines-chloroform. Monocetylamine in this solvent has at $N_2 \sim 0.02$, $\Delta F_m = -500$ cal. per mole. From Marvel's data (7) one extrapolates for this system $\Delta H_m \sim +1200$ cal. per mole. This would give an entropy change $\Delta S_m \sim +5$ e.u. for the mixing process. Qualitatively all these changes point in the direction of molecular compound formation. They involve such small changes in thermodynamic properties, however, that the association must be a very loose one and hardly comparable with the solvates known among aromatic compounds.

The positive deviations from Raoult's law are for those systems for which $\Delta S_m = 0$ (regular solution), most often explained as due to differences in cohesive energy density ($\Delta E_{vap}/V$) of the pure components. If the premise of the equivalence of all configurations of the segments of all component molecules on any of the available sites, which underlies equation 3, is fulfilled, ω_{AB} should indeed be independent of the molecule-size difference between solvent and solute and should be expressible as a function of

$$\left[\left(\frac{\Delta E_1}{V_1} \right)^{\frac{1}{2}} - \left(\frac{\Delta E_2}{V_2} \right)^{\frac{1}{2}} \right]$$

just as in the case of simple spherical molecules for which the Hildebrand function (5) has been derived. Since in that case the activity coefficient is given by

³ In view of their rigidity, both of these molecules were considered as occupying one site each, the size of which was for geometrical reasons considered as equal to four methylene groups, so that $r_A = 1$, $r_B = 8$; z was taken as 8.

$$RT \ln(N_2^0/N_2) = V \phi_1^2 \left[\left(\frac{\Delta E_1}{V_1} \right)^{\frac{1}{2}} - \left(\frac{\Delta E_2}{V_2} \right)^{\frac{1}{2}} \right]^2 \quad (4)$$

where ϕ_1 = volume fraction of solvent, $N_2^0/N_2 = \gamma_2$ should at a fixed concentration (and in solvents of a narrow molar volume range) be a function of $\Delta E_1/V_1$ only. The plots of $\log \gamma_2$ vs. $(\Delta E_1/V_1)^{\frac{1}{2}}$ in figures 10, 11, and 12 show that this condition is not fulfilled in the solutions under consideration.

The activity coefficient is a function not only of the differences in cohesive energy density but also of molecular structure.⁴ One can, indeed, discern a definite grouping of solvents: (1) The solvents made up of molecules of small polarization anisotropy, such as cyclohexane, carbon tetrachloride, chloroform,

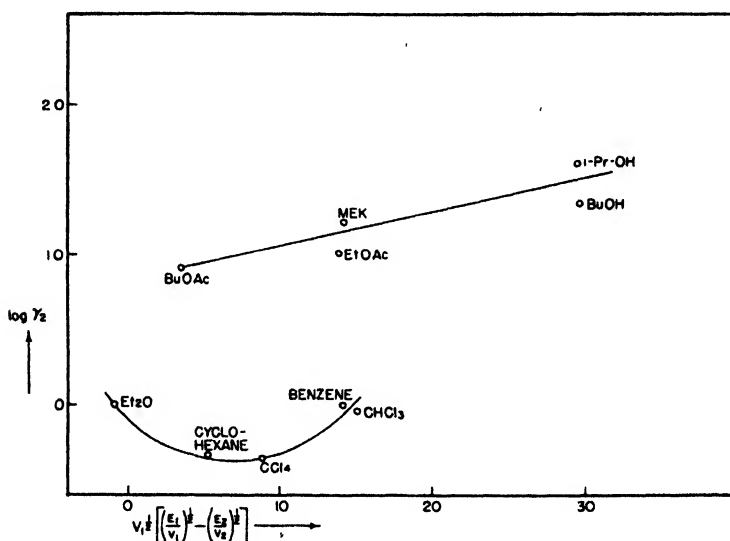


FIG. 10. Plot of activity coefficient γ_2 of *n*-dotriacontane in various solvents (at $N_2 \sim 0.02$) as a function of the cohesive energy density difference.

and benzene; (2) the dipoles containing molecules of considerable polarization anisotropy (strong orientation tendency such as aliphatic ester, ethers, ketones); and (3) the alcohols. This grouping is about what one would expect intuitively from the neglect of entropy changes in the correlation.

We can then calculate the excess entropy of mixing from

$$\Delta S_m = \frac{\Delta H_m - \Delta F_m}{T} \quad (5)$$

⁴ Here, as well as in the following discussions, all comparisons are made at solute concentrations of ~ 2 mole per cent, which is below the concentration at which interpenetration of the randomly configured chains (6) or common possession of one solvent neighbor site by two solute molecules would occur in the case of the largest molecule-size differences of this series.

Most of the presently available data involve alcohols. The recent calorimetric work of Parks and Rowe (11) permits calculation of ΔH_m of cetyl alcohol

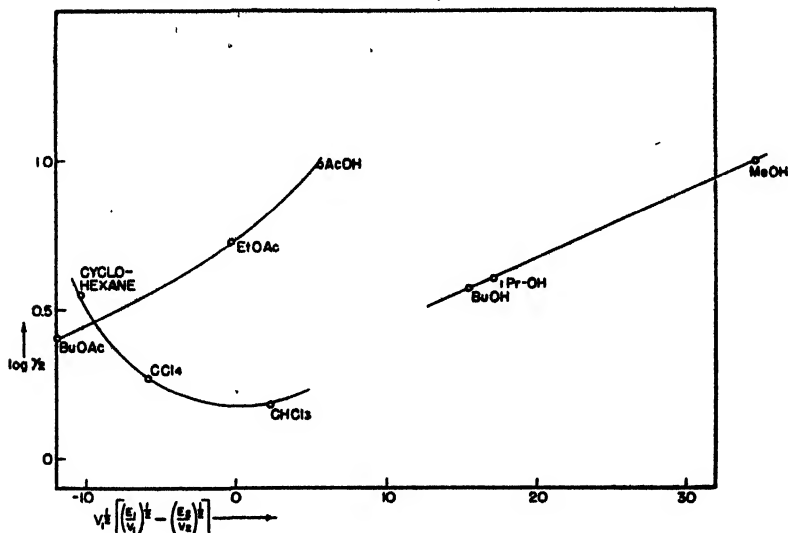


FIG. 11. Plot of activity coefficient γ_2 of stearic acid in various solvents (at $N_2 \sim 0.02$) as a function of the cohesive energy density difference.

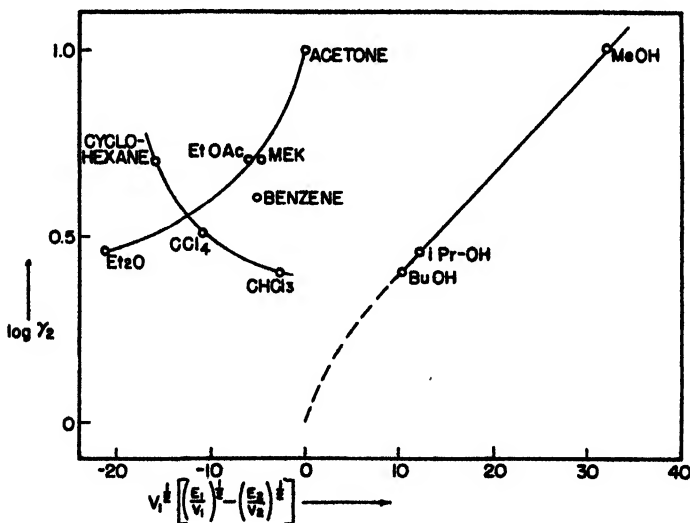


FIG. 12. Plot of activity coefficient γ_2 of cetyl alcohol in various solvents (at $N_2 \sim 0.02$) as a function of the cohesive energy density difference.

in methyl and butyl alcohols. At 25°C. and N_2 of 0.0055 (in methanol) and 0.0109 (in butanol) one obtains from their data $\Delta H_m = -1940$ cal. per mole and -850 cal. per mole, respectively. This gives, after reasonable temperature

correction, at the corresponding saturation line concentration $\Delta S_m \sim -12$ E.U. and ~ -5 E.U., respectively. Extrapolation of K. L. Wolff's (18) data for ΔH_m to cetyl alcohol in cyclohexane gives $\Delta H_m \sim -3$ kg.-cal. per mole and $\Delta S_m \sim -13$ E.U. Reasonable extrapolation of the data for solution of hydrocarbon in alcohol to the system *n*-dotriacontane-isopropyl alcohol leads to $\Delta H_m \sim -2.5$ kg.-cal. and $\Delta S_m \sim -20$ E.U. The pronounced negativity of ΔS_m suggests that in these solutions—or at least in the immediate neighborhood of the solute molecules—there is a more orderly arrangement than in the pure solvent. Such an enhanced state of order can be well visualized to mean that the small alcohol molecules (in the cetyl alcohol-methanol and in the dotriacontane-isopropyl alcohol systems) on the neighbor sites nearest to the paraffin chain are oriented with their alkyl groups toward the paraffin chain in order to minimize the potential-energy differences between each other. This arrangement is similar to Frank's (3) "icebergs" around non-polar solutes in aqueous

TABLE 1

Solubility, excess free energy of mixing, and non-ideal portion of the heat of solution of normal fatty acids in water (calculated from data by Ralston and coworkers (12))

SOLUTE	<i>t</i>	N_2	ΔF_m	$\Delta H'_m$ *
	°C.		cal. per mole	cal. per mole
<i>n</i> -Hexanoic acid	0	1.34×10^{-3}	3590	-930
	60	1.82×10^{-3}	4180	-880
Myristic acid	0	1.02×10^{-6}	5780	+6,850
	60	2.70×10^{-6}	8530	+5,470
Stearic acid	0	1.14×10^{-7}	6000	+9,900
	60	3.16×10^{-7}	9540	+11,000

$$* \Delta H'_m = R(\partial \ln (N_2^0/N_2)/\partial 1/T)_p.$$

systems. The numerical relation between the ΔS_m values and the entropy of fusion of these alcohols suggests, however, that the alcohol molecules in our case do not form "frozen patches" around the solute but should be merely preferentially orientated. Further substantiation of the reality of this picture by additional independent experimental data (such as calorimetric and vapor-pressure measurements) and possibly x-ray diffraction measurements, as well as rigorous analysis, could be interpreted to mean that there is essentially only a quantitative but no qualitative difference between "true" and "micellar" solution.

The solubility of fatty acids in water has an extremely small temperature coefficient. As a result we find $R(\partial \ln \gamma / \partial 1/T)$ to be very strongly positive (table 1). At the extremely small concentrations involved, the term depending on $(\partial \ln f / \partial c)_T$ is probably not very important. We may therefore expect ΔS_m to be either very small—if negative—or even sensibly positive. The latter would indicate that fatty acids, just like other electrolytes, produce an increased

state of disorder in the surrounding water structure (3) by coulombic effects and by their large ion radius.

SUMMARY

Published data of the solubilities of a number of paraffin-chain compounds in common solvents are analyzed for deviations from Raoult's law. These deviations from ideality are expressed as excess free energy of mixing, ΔF_m . Plots of ΔF_m vs. concentration are presented which permit detailed discussion of the relationship between chemical constitution of the solute and its solubility as well as of the specific interactions between solvent and solute.

The negative deviation from Raoult's law (higher than "ideal" solubility) of long-chain paraffin hydrocarbons in cyclohexane and carbon tetrachloride could be accounted for as due to molecule-size differences between solvent and solute alone by application of Guggenheim's solubility theory. This result indicates complete random configuration of the segments of all components in such systems.

The positive deviations from Raoult's law (lower than "ideal" solubility) of most paraffin-chain compounds (alcohols, acids, amines) in the common solvents are shown not to be accountable from differences in cohesive energy density alone, but must also be due to considerable excess entropy of mixing, ΔS_m . Some numerical values of ΔS_m of systems involving alcohols were estimated. All of these were strongly negative, suggesting that insolubility may be proportional to the degree of specific orientation of solvent molecules in the immediate neighborhood of the solute molecule which is required to minimize the potential energy between them.

The solubility data of fatty acids in water differ markedly from those of non-dissociating systems and suggest as the cause both positive heats and positive excess entropy of mixing, closely resembling the behavior of some inorganic ionic systems.

REFERENCES

- (1) BERGER, G.: *Rec. trav. chim.* **57**, 1029 (1938).
- (2) BONDI, A.: To be published.
- (3) FRANK, H. S.: *J. Chem. Phys.* **13**, 507 (1945).
- (4) GUGGENHEIM, E. A.: *Proc. Roy. Soc. (London)* **A183**, 206, 213 (1944).
- (5) HILDEBRAND, J. H.: *The Solubility of Non-electrolytes*. Reinhold Publishing Corporation, New York (1936).
- (6) HULBURT, H. M., *et al.*: *Ann. N. Y. Acad. Sci.* **44**, 371 (1943).
- (7) MARVEL, C. S.: *et al.*: *J. Am. Chem. Soc.* **60**, 1337 (1938).
- (8) MARVEL, C. S., *et al.*: *J. Am. Chem. Soc.* **61**, 3550 (1939); **62**, 2273, 3109 (1940); **63**, 254 (1941).
- (9) MAZEE, R. W.: *T.O.M. Reel No. 79*, p. 2504 et seq.
- (10) PARKS, G. S., AND HUFFMAN, H. M.: *Ind. Eng. Chem.* **23**, 1138 (1931).
- (11) PARKS, G. S., AND ROWE, R. D.: *J. Chem. Phys.* **14**, 507 (1946).
- (12) RALSTON, A. W., AND COWORKERS: *J. Org. Chem.* **7**, 546 (1942); **8**, 344, 473 (1943); **9**, 68, 102, 201, 259, 267, 319, 329 (1944); **10**, 170 (1945).
- (13) ROTHMUND, V.: *Löslichkeit und Löslichkeitsbeeinflussung*. J. A. Barth, Leipzig (1907).

- (14) SEIDELL, A. *Solubilities of Organic Compounds*. D. Van Nostrand Company, New York (1941).
- (15) STAVERMAN, A. J., AND COWORKERS. *Rec. trav. chim.* **60**, 76, 327, 640 (1941).
- (16) UBBELOHDE, A. R., AND OLDHAM, J. W. H.: *Trans. Faraday Soc.* **34**, 282 (1938).
- (17) WILLIAMSON, A. T. *Trans. Faraday Soc.* **40**, 421 (1944).
- (18) WOLFF, K. L., AND COWORKERS: *Z. physik. Chem.* **B36**, 237 (1937), **B46**, 287 (1940).

PHOTOELECTRIC SPECTROPHOTOMETRY

THE PERFORMANCE OF A QUARTZ DOUBLE MONOCHROMATOR IN AN IMPROVED AND MORE VERSATILE PHOTOELECTRIC SPECTROPHOTOMETER¹

F. P. ZSCHEILE²

*Department of Agricultural Chemistry, Purdue University Agricultural Experiment Station
Lafayette, Indiana*

Received December 3, 1946

A photoelectric spectrophotometer was described by Hogness, Zscheile, and Sidwell in 1937 (6) as a much more sensitive, accurate, and rapid instrument than the first of its type reported by Zscheile, Hogness, and Young (21). In 1937 construction was started on a third spectrophotometer, which operates on the same general principles as the second instrument (6) but which embodies certain refinements of construction and arrangement and is much more flexible and versatile in performance. Moreover, it is built about a large quartz Müller-Hilger double monochromator, indicated earlier (6) as the ideal optical instrument for transmittancy measurements. This permits very exhaustive studies on scattered radiant energy and the effect of various slit widths on absorbancy ($\log_{10} I_0/I$) values. This paper describes the performance of this assembly and the results of rigorous tests for scattered radiant energy, with emphasis on the monochromator and photocell employed. Some of this work supplements the report on the earlier assemblies (6, 21).

I. DESCRIPTION OF EXPERIMENTAL EQUIPMENT

Figure 1 shows the entire spectrophotometer except the galvanometer scale, which is back of and above the operator.

Figure 2 shows the contents of the photocell chamber with the vacuum cylinder removed (it appears in figure 1 as a vertical cylinder between the absorption cell chamber and the amplifier control panel). Figure 3 is a diagram of the principal parts of the assembly.

¹ Journal Paper No. 275, Purdue University Agricultural Experiment Station.

² Present address: Division of Agronomy, College of Agriculture, University of California, Davis, California.

A. MONOCHROMATOR AND ACCESSORY LENSES

The large Müller-Hilger Universal Double Spectrometer-Monochromator is wrapped in a black felt cloth to minimize penetration of dust to the optical parts. It has interchangeable glass and crystal-quartz optics. Only the latter were used in this work. The dispersion prism faces are 60 mm. square. The relative aperture for quartz varies from F/4 at 1850 Å. to F/5.8 at 40,000 Å. The focal length is 300 mm. for 5460 Å. At wave lengths 2000, 5500, and 34,000 Å. the dispersion is 6.4, 142, and 218 Å. per millimeter, respectively. Prisms P_1 and Q_1 have aspherical lens surfaces ground on their faces to act as objectives. Prisms



FIG. 1. Photoelectric spectrophotometer

P_2 and Q_2 have highly reflecting aluminized back surfaces. The smaller directive prisms, U_1 , U_2 , V_1 , and V_2 , are constructed of right- and left-handed crystals to compensate polarization effects. Lens surfaces are ground on their faces also. These prisms are all mounted on a single steel carrier which may be easily removed and accurately replaced. A metal partition separates the two halves of the monochromator to obstruct stray radiant energy.

All optical adjustments are made by rotation of the wave-length drum, which moves prisms P_1 and Q_1 toward or away from the directive prisms for focusing and rotates prisms P_2 and Q_2 to change the wave length. The wave-length drum is 12 cm. in diameter and 19 cm. in length. It has two parallel scales: one engraved in black for quartz optics (1,850–40,000 Å.), and one engraved in red for

glass optics (3,600–20,000 Å.). The black scale is 1040 cm. and the red scale 350 cm. in length. From 2200 to 9500 Å. the black scale is 410 cm. long.

The symmetrical slits are 18 mm. in length, their maximum width is 4 mm., and their stainless-steel adjustment dials are calibrated to read directly to 0.01 mm.

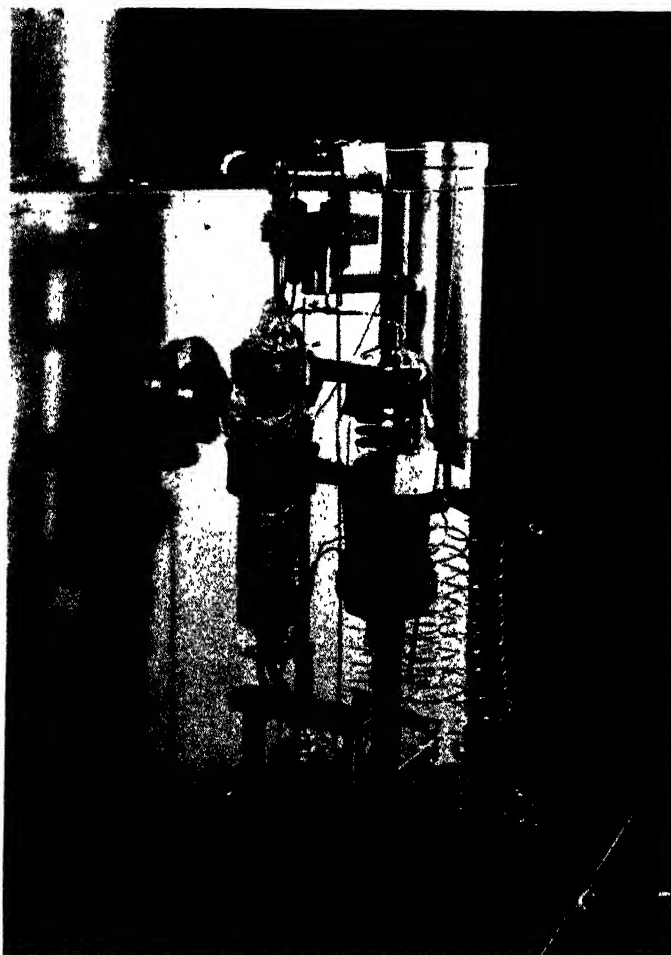


FIG. 2. Photocell chamber with vacuum cylinder removed. Photocell at left. Amplifier tube in brass cylinder at upper right.

The verniers permit width readings to 0.001 mm. Thin crystal-quartz windows (1 mm. thick) protect slits 1 and 3, which are curved to correspond to the straight middle slit. The slit jaws are constructed of stainless steel. The adjustment for slit 2 is easily accessible through a small opening in the top of the monochromator case. The length of slits 1 and 3 is restricted to 6 mm. by wedges to limit the size of the beam of radiant energy striking lens 2 and the photocell.

Lenses 1 and 2 (figure 3) were designed and constructed by Adam Hilger, Ltd.,

especially for this application. Lens 1 is a figured crystal-quartz condensing lens (46 mm. diameter, focal length 8 cm. at 5460 Å.), corrected for spherical

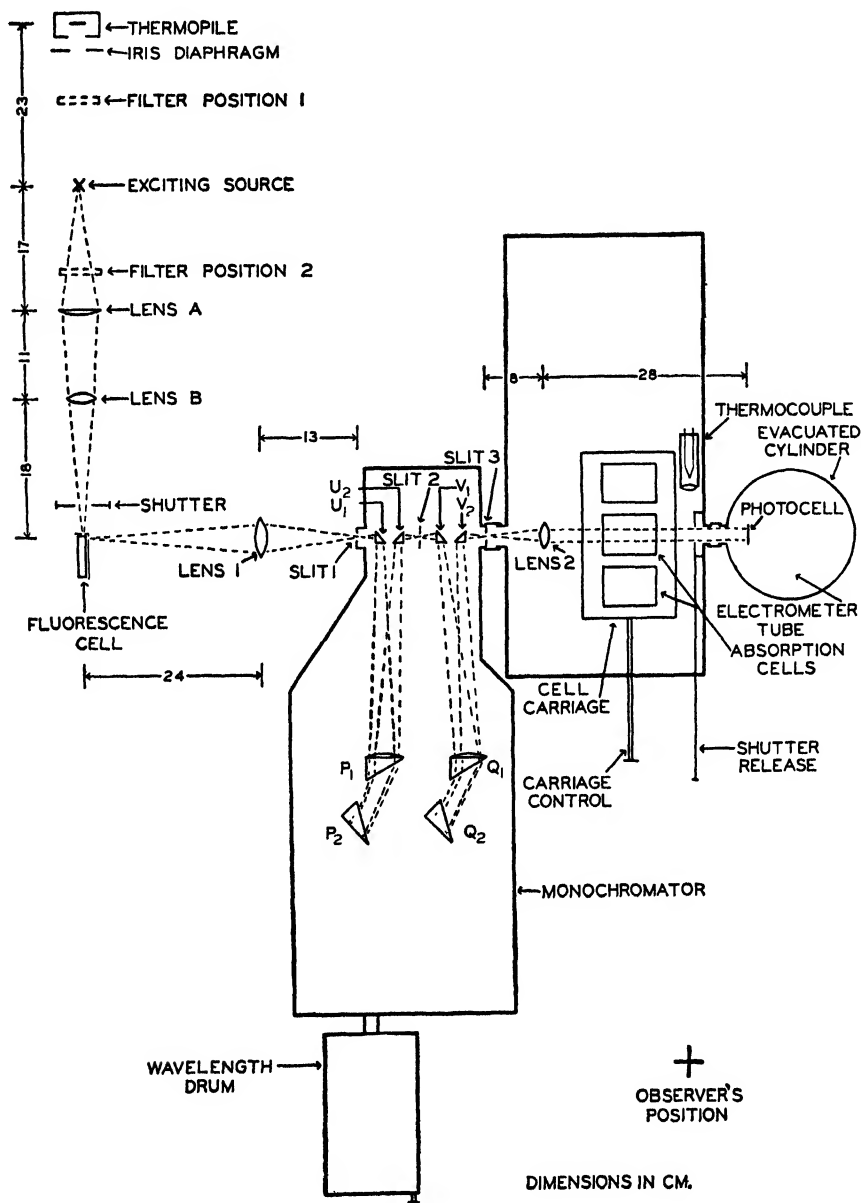


FIG. 3. Diagram of spectrophotometer

aberration, and mounted on a calibrated rack and pinion. This lens and a small crystal-quartz field lens on slit 1 produce a rectangular, evenly irradiated field

on the front face of prism P_1 . The definition of this beam is improved if only the central portion of lens 1 is used.

Lens 2 contains four elements, the two inner ones of crystalline lithium fluoride and the outer two of crystal quartz. Its effective aperture is 24.5 mm. and its focal length 54 mm. It is strictly achromatic at two wave lengths and departures at other wave lengths are negligible. This lens is mounted to produce an image of slit 3 on the cathode of the photocell, slightly out of focus to minimize the effect of possible local variations in sensitivity of the cathode surface. This might be important if the image should be slightly distorted or moved by the absorption cells.

All accessory quartz parts (lenses and windows) were cut perpendicular to the optic axis to minimize polarization.

B. SOURCES OF RADIANT ENERGY

In figure 3 the accessory optical parts are arranged for the study of fluorescence of solutions (19). For absorbancy measurements the source of radiant energy is placed where the fluorescence cell is shown in this figure. A type T10 Mazda incandescent filament lamp, having a single tight upright coil of tungsten wire (coil 6 mm. long), provided the most intense radiant energy through the monochromator among five lamps tested. It operates on 6 volts and 12 amp., provided at constant voltage by six Edison cells (G 6H). The source was satisfactory over the wave-length range 3200 to 9500 Å. with the photocell.

For work in the ultraviolet a hydrogen arc of the Munch type (11) was employed. It was constructed principally of fused quartz, with graded seals for the palladium tube and electrode leads. The source of radiant energy is a slit (3 mm. high and $\frac{3}{8}$ mm. wide) in the shield surrounding the filament cathode. The filament is heated to incandescence by alternating current, but the arc starts on 110 volts D.C. Additional hydrogen must be admitted through the palladium thimble by heating it in a small hydrogen flame each time the arc is struck. This arc is air cooled and operates on low voltages,—two very distinct advantages over the arc used in the earlier instrument (6). Later, the commercially available Beckman hydrogen-discharge lamp was found to be an equally satisfactory source of ultraviolet and more convenient because it does not require the admission of hydrogen to start it. These arcs provide radiant energy from 2200 to 3900 Å. Slits must be varied because of the intensity differences in the hydrogen spectrum and the variation of photocell response with change of wave length. The lower limit of 2200 Å. probably arises from the considerable thickness of quartz in the optical path.

C. PHOTOELECTRIC CELL

A single gas-filled photocell is employed at 90 volts for the entire range used (2200–9500 Å.). It was specially constructed by the R.C.A. Manufacturing Company. In figure 2 it is shown wrapped in tin foil, grounded by a wire to minimize leaks along the outside surface. The principal part of the photocell

tube is fused quartz, with a plane quartz window (1.5 mm. thick, 27 mm. clear diameter) seen in figure 2. The cathode is 31 mm. long and 25 mm. wide. It is flat and is constructed of solid silver. The sensitive surface is rubidium, deposited on the silver. The cathode lead projects from the bottom of the tube through the glass end of a quartz-to-glass graded seal. The anode is a tantalum wire bent to a rectangular shape the dimensions of the cathode. Its lead projects from the top of the tube through the glass end of a smaller graded seal. The anode thus casts no shadow on the cathode. The entire tube is 10 in. long. An internal guard ring is grounded to minimize the dark current. The sensitivity of this tube is 40 microamp. per lumen to 2870°K. color temperature at an anode voltage of 90, as determined by the manufacturers. This rubidium cell was finally chosen because of its excellent stability, and its high sensitivity in the blue region while retaining fair sensitivity in the red. Several cesium-cesium oxide cells of similar construction were not as stable and at times caused pronounced fatigue difficulties.

D. AMPLIFIER

A d.c. amplifier with a Barth circuit as described by Penick (12) was employed. The procedure he described to balance the circuit was very useful. A Western Electric electrometer tube D-96475 was used in a circuit specially fitted to the individual tube by insertion of proper resistance values. The photocell part of the circuit is the same as employed earlier (6). Most of the amplifier circuit is in the aluminum box. Connections between it and the photocell chamber are made by wires shielded with seamless brass flexible tubing. All wires are shielded within solid metal tubes or boxes. Improved stability was achieved by soldering the maximum number of connections and leaving as few of them variable as possible. Switches are Mallory No. 1316L, one-circuit, single-section switches. Variable resistances are Mallory-Yaxley rheostats with Tinnerman nut construction. The two Exide radio receiving batteries (in steel box at the extreme right in figure 1) which supply the voltage for the electrometer tube are continually trickle-charged by the rectifying circuit shown in figure 4. This operates from the 110-volt A.C. main. The amplifier operates continually and after the charging rate is adjusted the assembly is ready for instant use during long periods of time (as long as thirty-four months in practice). Only routine upkeep of batteries, slight adjustments of currents due to temperature changes, and occasional replacement of certain variable resistance units are required.

The galvanometer is seen in the extreme corner (left of center) in figure 1. Leads are in iron pipe for shielding. The illuminated scale is overhead behind the operator, making the total telescope-to-scale distance 18 meters. A 50-power astronomical telescope was substituted for the small transit model shown in the photograph. To obtain a clearer scale image, the galvanometer window was removed and the line of sight then passed through a hole in a protective (against dust) cellophane shield around the galvanometer (Leeds & Northrup Type R. No. 2500-e.; sensitivity, 0.0025 microamp. per millimeter at 1 meter; CDRX, 2400 ohms; resistance, 590 ohms; period, 3.25 sec.). With the shunt

adjustment, the sensitivity of the galvanometer could be varied from 0 to full. The period of the entire system is 6 sec., but varies somewhat depending on the leak employed (table 1).

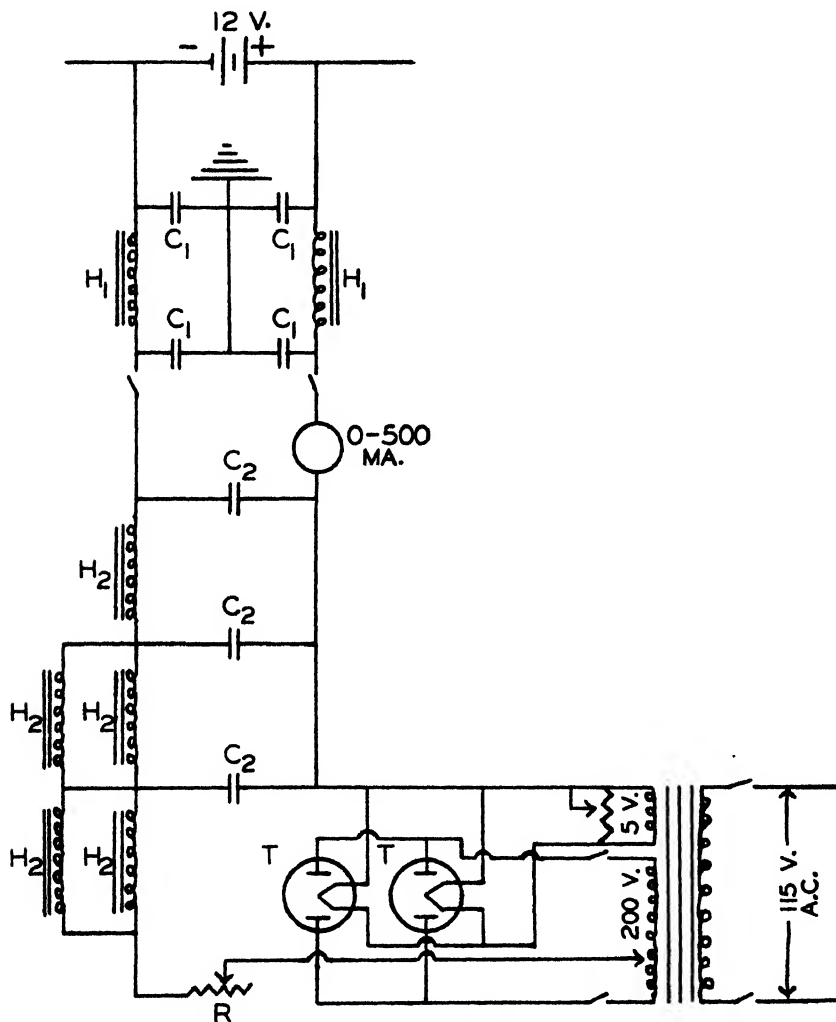


FIG. 4. Rectifier circuit for trickle charger. T = 83v R.C.A. rectifier tubes; C_1 = 2-mfd. condenser; C_2 = 30-mfd. condenser; H_1 = 1 millihenry choke, resistance 6 ohms; H_2 = 12-henry smoothing choke, resistance 105 ohms; R = 225-ohm variable resistor.

The high-resistance leak R can be varied at will by a switch operating by means of the sylphon tubing shown in figure 2 (lower center). This can be done without breaking the vacuum in which the photocell, amplifier tube, and high-resistance leaks are kept. Six leaks, having values of 8.65×10^5 , 8.74×10^7 , 9.30×10^8 , 1.67×10^{10} , 3.25×10^{10} , and 1.18×10^{11} ohms, as well as a ground connection, are available. The switch contact with the leaks is a heavy platinum

wire, connected to the photocell anode by a very fine phosphor-bronze wire of low capacity. The leak leads at the point of contact with the switch are platinum plated on copper. The platinum is insulated from the grounded switch handle by lucite. The tube in the center of figure 2 is a Westinghouse No. WL-756 sputtered-carbon resistor tube (13) (3.25×10^{10} ohms) consisting of a carbon-coated glass spiral sealed in an inert gas, with leads at either end of the tube. The other grid resistors are of the molded type made by S. S. White.

The amplifier tube is shielded inside the brass jacket in figure 2 (upper right). The grid lead projects through a brass tube, filled with ceresin wax near the top to connect as closely as possible with the photocell anode. This shield serves also to keep radiant energy from the amplifier filament from affecting the photocell. The leads from the amplifier tube elements (except the grid) are connected to the sources of voltage supply through the choke coils (twelve turns of wire $1\frac{1}{4}$ in. in diameter, figure 2) and through glass-insulated leads entering the vacuum chamber from below and sealed with beeswax. These coils and condensers are designed to choke out high-frequency surges to which the amplifier tube is sensitive. The choke coils on the filament leads have 0.005-mfd. condensers connecting either end to ground. The coils on the plate and space charge control grid leads have corresponding condensers of 0.0001 mfd.

The photocell-electrometer tube chamber is kept evacuated by a mechanical oil pump. Beeswax-rosin seals at the openings, such as the quartz window and electrical leads, assist in maintaining a sufficient vacuum for several weeks between pumpings. A Pirani gauge indicates the pressure inside.

E. THERMOCOUPLE

A small single-element thermocouple (constructed by L. B. Clark), mounted permanently in vacuum, with a thin bubble-glass window, is set in an adjustable mount inside the absorption cell chamber (figure 3). A small rhodium front-surface mirror may be placed to direct the beam from lens 2 to the thermocouple instead of to the photocell. The receiver is 3 mm. high by $\frac{3}{4}$ mm. wide. Its sensitivity is 4.15 microvolts per microwatt per square millimeter and its resistance is 9 ohms. It is connected directly to a Leeds & Northrup Type HS galvanometer with sensitivity 0.1 microvolt per millimeter at 1 meter, CDRX 15 ohms, period 5.5 sec., and resistance 15.2 ohms, mounted beside the photocell galvanometer on a separate Julius suspension. It has a special chromium-aluminum, front-surface, spherical mirror. A potentiometer circuit permits calibration of the galvanometer. A crystal-quartz adjustable lens (22 mm. diameter, 25 mm. focal length) focuses the radiant energy from the mirror onto the receiver.

A simple movement of the telescope permits use of the same galvanometer scale as used for the photocell circuit.

F. ABSORPTION CELLS

The quartz absorption cells have the same type of metal holders with Pyrex cylinders and quartz windows as those described earlier (6), mounted on the

same kind of holder and carriage. Interchangeable stoppers in all cells are a great advantage. These cells had Pyrex body lengths of 3, 5, 10, 20, 40, 70, and 100 mm.

For work in the Mazda region, fused Pyrex cells (American Instrument Co., Style DX, class 3) were used. They had lengths of 10, 20, 30, 50, 120, and 170 mm. and were 35 mm. in diameter (outside). The beam of radiant energy is essentially parallel, the maximum divergence of any part of the beam from the horizontal path straight through the absorption cell causing a difference of 0.4 per cent from the true cell length. With 0.5-mm. slits at 5460 Å. the beam is 15 x 13 mm. after emerging from lens 2, 11 x 8.5 mm. at the center of the cell carriage, and 9 x 5 mm. at the shutter. The beam is well centered on the photo-cell cathode, with considerable room to spare.

TABLE 1
Typical operating conditions of amplifier circuit

	LEAK RESISTANCE	CURRENT SENSITIVITY*	GALVANOMETER PERIOD
	<i>ohms</i>	<i>amperes per millimeter</i>	<i>seconds</i>
1	8.65×10^6	8.65×10^{-11}	3.25
2	8.74×10^7	1.3×10^{-12}	3.25
3	9.30×10^8	1.2×10^{-14}	3.25
4	1.67×10^{10}	6.8×10^{-16}	3.25
5	3.25×10^{10}	3.5×10^{-16}	6
6	1.18×10^{11}	9.6×10^{-17}	15

* The voltage sensitivity varied over long periods from 80,000 to 95,000 mm. per volt. Current sensitivities are figured from an average value of 88,000 mm. per volt.

The absorption cell chamber is constructed of steel, with a light-tight lid. A small radiator, with cold water flowing through it, a heating element, and a thermostat permit the chamber to be operated at constant temperature (25°C.). This is important for critical work on standard absorption curves (17, 22), because some organic solvents have rather high coefficients of thermal expansion. For such work the volumetric handling of all solutions measured is done with thermostated glassware and solvents.

II. CALIBRATION, TESTING, AND PERFORMANCE OF APPARATUS

A. AMPLIFIER

The response of the amplifier circuit to known voltages impressed on the control grid by means of the calibration potentiometer circuit was shown to be linear, as in the earlier apparatus (6). This is conveniently checked at periodic intervals. Table 1 shows the range of stable operating conditions. All values are for the telescope-to-scale distance of 18 meters.

A more sensitive galvanometer (Type R No. 2500-b) was tried and a considerably higher voltage sensitivity (sixfold) was achieved, but instability and excessively long periods with high-resistance leaks made the present combination

more useful. Whenever possible the 1.67×10^{10} ohm leak was used because of the shorter period required for a reading.

The high-resistance leaks were calibrated at intervals against the Westinghouse resistance, which was assumed to remain constant at 3.25×10^{10} ohms. The procedure was to adjust the source of radiant energy and monochromator slits so that a fairly small galvanometer deflection was obtained at a given wave length. The radiant intensity of the source was assumed to remain constant during a series of rapid measurements with different leaks of higher resistance than the standard (this was checked after the series). Then the deflection with a suitable resistance was obtained for a new setting of the wave-length drum (and usually different galvanometer sensitivity also) to permit a series of measurements on resistors of lower values. Overlapping readings thus established the continuity of the entire group, and from the galvanometer responses the actual resistances of the leaks were calculated. The linearity of responses of the photocell is assumed only

TABLE 2
Measured resistance of White resistors on different dates

LEAK	NOVEMBER 14, 1939	JULY 1, 1940	DECEMBER 1, 1941	MARCH 9, 1944
	<i>ohms</i>	<i>ohms</i>	<i>ohms</i>	<i>ohms</i>
Westinghouse	3.25×10^{10}	3.25×10^{10}	3.25×10^{10}	3.25×10^{10}
White No. 1	1.48×10^{10}	1.67×10^{10}	1.68×10^{10}	1.49×10^{10}
White No. 2	8.68×10^{10}	1.18×10^{11}	1.13×10^{11}	1.27×10^{11}
White No. 3	6.72×10^7	8.74×10^7	3.08×10^7	Unstable
White No. 4		9.30×10^8	1.07×10^9	8.3×10^8
White No. 5		8.65×10^8	4.7×10^8	Unstable

over the range of the galvanometer scale and at two wave lengths (see next section).

The behavior of a few leaks studied over a period of time is shown in table 2.

Over a period of approximately four years, the resistances of White leaks Nos. 1, 2, and 4 changed slightly in relation to the Westinghouse leak. Nos. 3 and 5 changed much more and eventually became unstable.

B. PHOTOCCELL

This photocell is useful in this application over a very wide range of wave lengths (2200 to 9500 Å.) without resorting to the use of very wide slits. For accurate absorbancy measurements at a given wave length the response of the photocell must be linear over a range of irradiance of about eightfold (corresponding to readings of I_0 and I for a density ($\log I_0/I$) range of 0.2 to 0.9). This can be shown easily by means of calibrated screens (6, 15). However, the sensitivity of a photosensitive surface varies widely over the wave-length range employed here. This factor, as well as the emission characteristics of the sources of radiant energy and the absorption characteristics of the optical system, accounts for the necessity for different slit widths in various parts of the spectrum. Different spectral regions isolated (6) result automatically from these consider-

ations, in addition to dispersion. It is thus very desirable that the linearity of response be studied over as wide an irradiance range as practical and at different wave lengths.

Accordingly, the radiant flux striking the photocell cathode was varied over wide ranges. Measurements of transmittance by wire screens with this photocell at several different wave lengths agreed with similar determinations made with an Eppley thermopile (6) (surface type, twelve junctions, copper-constantan element, sensitivity 0.0275 microvolt per microwatt per square centimeter). Identical transmittance values were always obtained when different galvanometer deflections (I_0) were used. To test this further, the transmittance of a screen was measured by use of the 5460 Å. line of the mercury arc. The slits were kept constant in width (0.03 mm.), leaks were varied in resistance 153-fold, and the irradiance was varied by adjustment of the wave-length drum on or slightly off the position for maximum transmittance by the monochromator. For relative irradiancies of 1, 11, and 168, the optical density values were 0.521, 0.521, and 0.523, respectively. When slits were widened to 0.10 mm., the photocell response became very unsteady.

The following ranges of flexibility are available in the variation of irradiance to be measured by the photocell: (1) 1 to 240,000 by changes of high-resistance leaks (this could be extended by use of smaller values than 4.7×10^5 ohms); (2) 1 to 50 by shunt adjustments in the galvanometer circuit; and (3) 1 to 20 by variation of the galvanometer deflection from 10 to 200 cm. When all of these factors are made to operate in one direction, an over-all range of irradiance of 1 to 240,000,000 is available. Probably more than one type of photocell would be necessary to cover this entire range. Experimentally these conditions were combined to produce irradiance ranges of 1 to 28,000 at 4500 Å. and 1 to 550,000 at 6600 Å. with the Mazda source. Throughout these ranges (at five intermediate points), identical values were obtained for the transmittance of a wire screen (density 0.554 ± 1 per cent).

During many years of operation of photocell circuits of this type, the writer has observed an initial instability or fatigue effect characteristic of the photocell when the wave length of radiant energy was rapidly shifted over a fairly large interval (400–500 Å. or more). This effect has not been reported in the literature to his knowledge. Work with this particular photocell over a period of four years permitted an unusual opportunity to observe such behavior. It could always be demonstrated during this period of time. In the routine measurement of absorption spectra, when density readings are made successively at small intervals of 10, 20, or 50 Å., this effect does not appear, but when the wave-length change is large enough, as is often the case in analytical work, the photocell must be irradiated with the shutter open for about 45 sec. until the response becomes steady. This same effect occurs when the shutter is open after a long period of darkness for the cell. The galvanometer first shows an initial response, which then decreases slowly over a short time (ca. 45 sec.) to a steady value about 90 per cent of the initial value. Then, successive operations of the shutter give rise to

reproducible galvanometer deflections and the cell will be reliable for indefinite periods of time so long as it is being continually used. The initial fatigue effect appears to be independent of wave-length region, and was due solely to the photocell, not to galvanometer, amplifier circuit, or source of radiant energy.

Since a potential was maintained on the electrodes of this photocell for periods as long as twenty-seven months, even during the change of batteries, any changes in the dark current could be observed. This was measured by rapidly shifting the amplifier grid (and photocell anode) from ground to a measured high-resistance leak and observing the galvanometer deflection. The operating potential was on the photocell but the shutter was closed. The initial value of the dark current was comparable to that of a cesium-cesium oxide vacuum photocell.

TABLE 3
Change of photocell dark current with time

DATE	DARK CURRENT
	<i>amperes</i>
April 20, 1940	5.90×10^{-13}
April 23, 1940	3.48×10^{-13}
April 24, 1940	3.20×10^{-13}
April 26, 1940	2.10×10^{-13}
April 27, 1940	1.95×10^{-13}
April 29, 1940	1.61×10^{-13}
May 1, 1940	9.2×10^{-14}
May 10, 1940	6.4×10^{-14}
	Potential disconnected here
	Potential connected August 15, 1940
November 14, 1940	1.42×10^{-14}
January 6, 1941	$5-7 \times 10^{-15}$
August 9, 1941	<i>ca.</i> 5×10^{-15}
	Potential disconnected short time on November 11, 1941 for repairs
February 25, 1944	Less than 10^{-16}

(Continental Electric Co.) but the trend with time was to decrease to a negligible value, as shown in table 3. It varied by small amounts from day to day.

The final value could not be measured in this manner. The deflection with a leak of 1.27×10^{11} ohms was less than 1 mm. and could not be detected. These later values are much lower than dark currents reported for cesium-cesium oxide gas-filled cells (4, 6).

C. THERMOCOUPLE

Response of the thermocouple circuit to applied potentials is linear only for deflections of less than 50 cm.

The Mazda incandescent filament lamp is useful in the region 8,000 to 19,000 A. with monochromator slits 0.2 mm. wide, and from 19,000 to 25,000 A. with slits 0.3 mm. wide. The extreme limit for this system is 26,300 A. with 0.3-mm.

slits (deflection 10 cm.). Urgency of other work has prevented the use of the thermocouple for the measurement of absorption spectra.

D. MONOCHROMATOR CALIBRATION

1. Wave-length drum

Monochromatic line sources were used for calibration of the wave-length drum. The automatic focusing mechanism within the monochromator makes this process simpler than with a single monochromator (6), but the large number of prisms complicates their proper rotational settings. The method adopted for setting the prisms was (1) to set those of the second half of the instrument with slit 1 very wide and slits 2 and 3 at a width of 0.05 mm. (length 6 mm.); then (2) to adjust the first half of the monochromator with all slits 0.05 mm. wide. Slit 1 may be as wide as 0.30 mm. without affecting the wave-length correction when slits 2 and 3 are narrow. A microscope accessory system was set in place of lens 2 to permit the easy examination of the image at slit 3 for preliminary visual settings. The U and V prisms were set in the vertical direction so that images of slits were all aligned and the image focused on slit 3 was symmetrical with the slit itself. Prisms P_2 and Q_2 were adjusted visually for wave length. The final rotational settings of prisms U_2 and V_2 were adjusted by use of the photocell. Visual and photoelectric settings do not often agree, owing to errors in the visual method.

The wave-length drum was always rotated clockwise to avoid backlash. Care must be taken that slit widths are equal and that the vernier readings of their closed positions are known accurately. Differences in widths may cause very unsymmetrical slit images of lines when photoelectric readings are plotted against wave length (6).

By this method, the quartz optics have been adjusted so that no wave-length correction was necessary for the drum. However, in practice no adjustment has remained permanent, probably owing in part to temperature changes. In routine work, it is simpler to calibrate the drum with a line source before use and apply small wave-length corrections to the drum scale. With more accurate optical methods it would probably be possible to effect more nearly perfect adjustments.

The following arc lines were symmetrical and well isolated when prisms were in proper adjustment: mercury low-pressure arc, 2893, 3341, 4047, 4358, and 4916 Å.; cadmium arc (Hilger), 4678, 4800, and 5086 Å.; and helium arc (Zeiss), 3889, 4471, 5876, 6678, and 7065 Å. A solution of neodymium chloride in aqueous hydrochloric acid appears promising as a solution for calibration of a wave-length scale, because of its very narrow absorption bands.

2. Spectral region isolated (6)

Spectral regions isolated in practice with nearly transparent solvents are given in table 4. In routine work it is usually more feasible to employ wider slits (if the nature of the absorption bands permits) and use the amplifier at a sensitivity lower than maximum.

III. DISCUSSION OF ERRORS

A. WAVE LENGTH

The accuracy of drum setting with quartz optics is within \pm a fraction of an Ångström unit in the ultraviolet, to ± 1 Å. in the violet, and to ± 2 Å. in the red regions.

TABLE 4
Slit data with quartz optics

	WAVE LENGTH	DISPERSION	REGION ISOLATED	PRACTICAL SLIT WIDTH	CALCULATED REGION ISOLATED
	Å.	Å. per mm.	Å. per mm. slit	mm.	Å.
Hydrogen arc	2200	9.3	18.6	0.90	17
	2300	11	22	0.20	4.4
	2500	15	30	0.15	4.5
	2750	20	40	0.07	2.8
	3000	26	52	0.07	3.6
	3250	33	66	0.10	6.6
	3500	41	82	0.06	5.0
Incandescent filament lamp. . .	3250	33	66	0.12	7.9
	3600	44	88	0.04	3.5
	3800	53	106	0.04	4.3
	4000	62	124	0.03	3.7
	4250	79	158	0.03	4.8
	4500	96	192	0.02	3.8
	5000	130	260	0.02	5.2
	5500	142	284	0.02	5.7
	6000	206	412	0.015	6.2
	6500	246	492	0.015	7.4
	7000	289	578	0.015	8.7
	7500	336	672	0.015	10
	8000	385	770	0.015	12
	8500	427	854	0.03	26
	9000	484	928	0.06	56
	9500	495	990	0.08	79

B. PRECISION OF MEASUREMENT

Precision errors in the measurement of absorbancy have been analyzed mathematically (6). The theoretical error curve (6) of figure 5 is plotted as

$$\log \frac{I_0}{I} \text{ vs. } \frac{\frac{\Delta I}{I_0} \times \frac{I_0}{I}}{2.3 \log \frac{I_0}{I}}$$

using $\Delta I/I_0 = \pm 0.0011$. The latter is an experimentally determined value obtained from the error in reproducing I_0 and is the average of the 420 readings from which curves 2 and 3 were obtained. Comar (2) obtained the data of

figure 5 by measurements of the precision actually attained with this photometer. Precision appears independent of wave length but to avoid such a possible source of error, a glass filter (Corning #243) having an absorption curve with a steep slope was employed so that absorbancy might vary greatly with slight change of wave length. Values of $\log I_0/I$ were 0.150 and 0.850 at 6320 and 6180 Å., respectively. Each point on these curves represents the standard deviation of thirty consecutive absorbancy determinations. Curves 2 and 3 lie close to the theoretical curve.

Curves 3 and 4 indicate the advantage of using large galvanometer scale readings. These two curves were determined at the same time and in such a way as to eliminate all factors except the size of the galvanometer deflection. Thus when large deflections ($I_0 = 175$ to 200 cm.) are used and values of $\log I_0/I$ are

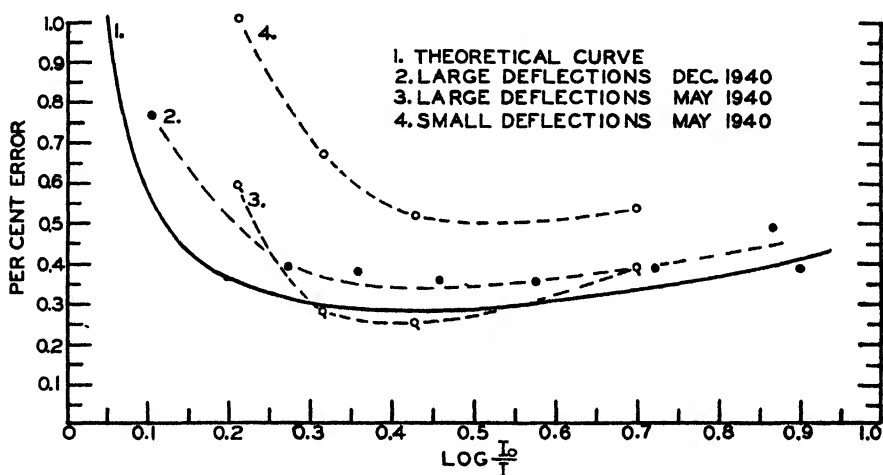


FIG. 5. Precision error curves (2)

kept between 0.2 and 0.9 the error does not exceed ± 0.6 per cent. In practice, total precision errors need not exceed ± 0.6 per cent. No difference was found, either in the precision or value of absorbancy, whether the observation was made by reading, in order I_0 , I , and I_0 , or I , I_0 , and I .

C. STRAY RADIANT ENERGY

The practical elimination of stray or scattered radiant energy is the principal and most fundamental optical improvement over the earlier model (6) possessed by this spectrophotometer. A practical method of comparison of monochromator performance was suggested in the previous study (6). A similar series of measurements was made with the Hilger monochromator but employing a solution of polymerized linseed oil with *one* sharp absorption maximum at 2320 Å. (10). The concentration was constant and the cell length was varied from 1 to 10 cm. The value of S/I_0 (6) or the effective scattered radiant energy at 2320 Å., using the hydrogen arc, was 0.001 or 0.1 per cent. Slits were 0.90 mm. wide. This value is tenfold lower than the most comparable value reported earlier (6),

even though this is a much more rigorous test than given to the single monochromator by use of a potassium chromate solution (6) because of the nature of the ultraviolet-absorption curves.

Several other tests have been applied to this instrument, as described below.

1. Constancy of absorbancy with various slit widths

If scattered radiant energy is passing the exit slit and reaches the photocell, the absorbancy value would be expected to change with various slit widths because the ratio of responses to scattered and monochromatized radiant energy would vary with slit width and wave length. A study was made (22) on the effect of slit width on variation of absorbancy values obtained for a β -carotene solution

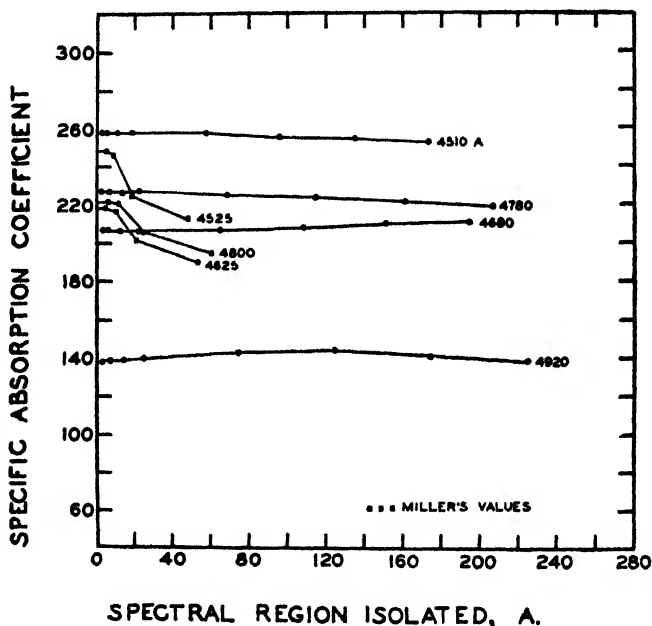


FIG. 6. Effect of width of spectral region isolated on the specific absorption coefficient of β -carotene at selected wave lengths (22).

so that a direct comparison was possible with results reported by Miller (9). He employed a Zeiss single monochromator with glass optics like the one used earlier (6) and found such values extremely sensitive to slit width changes. Figure 6 presents a comparison of the results. A much wider range of slit conditions was covered than in the experiments of Miller, and very different results were obtained. Slits varied in width from 0.015 to 0.90 mm., corresponding to spectral regions isolated of 3 to 225 Å. Results were such as expected from a consideration of the nature of the absorption curve and show no evidence of scattered radiant energy. Changes were small and dependent on the absorbancy over the region considered. With the 4358 Å. mercury line, absorbancy of a β -carotene solution remained constant over a slit width range of 0.06 to 0.50 mm. This latter width is extreme for a source as intense as a mercury arc.

A similar comparison with a single monochromator (Beckman quartz spectrophotometer (1)) is presented in figure 7 for chlorophyll solutions.

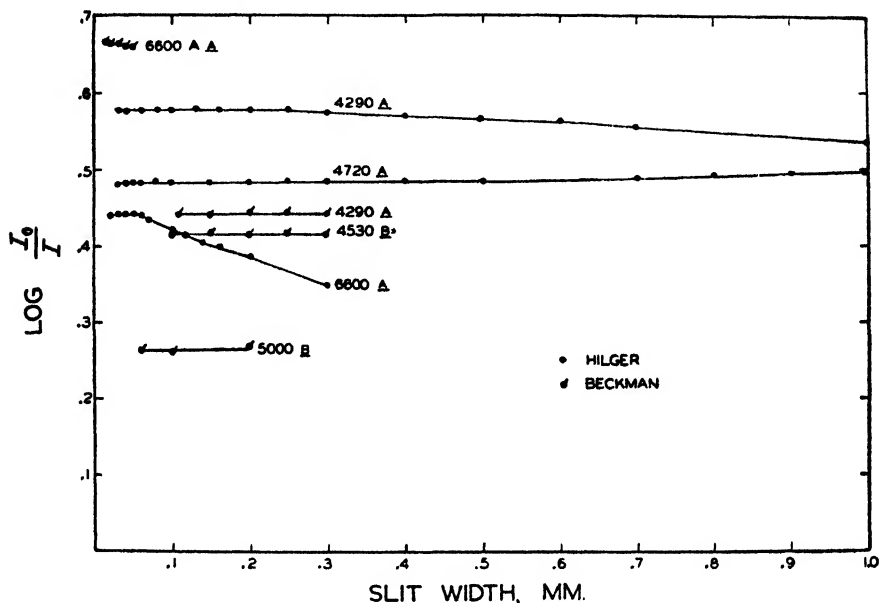


FIG. 7. Effect of width of monochromator slits on optical density values of chlorophyll solutions in ether at selected wavelengths. A = chlorophyll a; B = chlorophyll b. Spectral regions isolated by 0.1-mm. slits are: Hilger monochromator: 17 Å. at 4290 Å., 22 Å. at 4720 Å., and 51 Å. at 6600 Å.; Beckman spectrophotometer: 29 Å. at 4290 Å., 30 Å. at 4530 Å., 42 Å. at 5000 Å., and 86 Å. at 6600 Å.

Chlorophyll a solutions in ether have very intense and sharp absorption bands in the blue and red regions. Zscheile and Comar (17) found constant absorbancy values for such solutions under the following conditions:

	SLITS	SPECTRAL REGION
	mm.	Å.
4290 Å. (maximum)	0.03-0.25	5-40
4720 Å. (minimum)	0.04-0.50	9-110
6600 Å. (maximum)	0.02-0.06	10-30

Also, determinations with narrow slits and radiant energy from a continuous source were identical with those made with the following lines from a mercury arc: 4047, 4078, 4358, 4916, and 5461 Å. One of these (4358 Å.) is on a very steep slope of an intense absorption band. Since the 6600 Å. band of chlorophyll a is very sharp and the dispersion of quartz low in this region, slits must be kept narrow in both instruments. At short wave lengths or in regions of uniform absorption, slits may be much wider.

Mitchell and Kraybill (10) made similar studies in the ultraviolet region. Linseed oil (bodied *in vacuo*) has an absorption maximum at 2320 Å. Constant

absorbancy values were obtained with a hydrogen discharge tube source and slit conditions as follows:

	SLITS	SPECTRAL REGION
	mm.	A.
2320 A. (maximum)	0.20-1.00	2.3-11.4
2680 A. (slope)	0.12-0.60	2.2-11.0

At 2680 A. with slits open to 1.00 mm. and with amplifier sensitivity used for the hydrogen arc at this slit width, the incandescent source caused no galvanometer deflection. At 2320 A. no deflection resulted, even with the amplifier at its most sensitive adjustment. This source is customarily used in the visible region with 0.06-mm. slits. Thus there can be no scattered visible radiant energy transmitted by the monochromator when set for the ultraviolet region.

Zscheile and Henry (20) found constant absorbancy for vitamin A solutions at the maximum as follows: 3280 A. (maximum); slits, 0.06-0.50 mm.; spectral region, 4-34 A. The incandescent source was used. A decrease of only 1 per cent occurred with 0.95-mm. slits.

All of these values are consistent with the assumption of negligible scattered radiant energy.

2. Constancy of absorbancy with accessory filters

Another method of detecting scattered radiant energy is to place colored glass filters in front of slit 1 so that large ranges of *possible* scattered radiant energy never enter the monochromator. If the absorbancy value measured in the usual way differs from that measured with the filter added, the transmission of scattered radiant energy by the monochromator is indicated.

The following series of filter measurements have been made:

β -CAROTENE (22)	FILTER
4500 A. (maximum)	Jena BG 7 (absorbs from 6400 A. to infrared limit of photocell)
4665 A. (minimum)	Corning 385 (absorbs below 3700 A.)
4780 A. (maximum)	Corning 585 (absorbs 5000-6900 A.)
	All three filters combined (absorbs below 3700 A. and above 5000 A.)
CHLOROPHYLL a (17)	FILTER
4290 A. (maximum)	Jena BG 7 Corning 385 Corning 585 All three combined
4720 A. (minimum)	Jena VG 9 (absorbs from 6400 A. to red limit and from 4400 A. to ultraviolet limit of incandescent source) Corning 511 (absorbs from 5000 A. to red limit) Both combined

None of these filters affected the absorbancy values.

3. Constancy of absorbancy with change of source intensity

Comar (2) measured the absorbancy at 6400 Å. of a Corning glass filter (# 243) using constant slits but different irradiancies from the incandescent source (varied by voltage regulation). When I_0 was 54 cm. the absorption coefficient was 0.1021, and when I_0 was 170 cm. the value was 0.1022, each being the average of thirty determinations. Chlorophyll a solutions had constant absorbancy values independent of the color temperature of the incandescent source. Lamp currents were varied from 6.5 to 11 amp., covering a range of color temperature from 2000° to 2950° K. Scattered radiant energy would certainly have varied over this range had it been present in the radiant energy reaching the photocell.

4. Constancy of absorption coefficient with change of $\log I_0/I$

The error due to stray or scattered radiant energy is larger with higher values of $\log I_0/I$ (6). It is seen from figure 5 that no such error is apparent for density values below 0.90. Comar (2) employed chlorophyll a solutions with high $\log I_0/I$ values to determine any possible differences caused by the use of filters, as shown in table 5.

Thus the useful upper limit of $\log I_0/I$ may be considered fixed by the precision error alone, since no appreciable error due to stray radiant energy has been demonstrated.

IV. COMPARISON OF PERFORMANCE WITH THAT OF OTHER INSTRUMENTS

The superiority of this monochromator over the single Zeiss monochromator has been discussed above in relation to carotenoid curves. Valid comparisons for chlorophyll are not available. Unfortunately time did not permit sufficient study with either benzene or potassium chromate solutions to compare with results obtained on the single instrument (6). Practical spectral regions isolated may be compared by reference to table 4 above and tables 2 and 3 (6), which give data for the Zeiss single monochromator. In the ultraviolet the dispersion of the double monochromator with quartz optics is about twice as great as that of the single instrument, whereas in most of the visible region it is less than that of the Zeiss single monochromator with glass optics. The practical spectral regions isolated by the Purdue instrument are comparable in the ultraviolet but wider in the visible region than was the case for the Chicago spectrophotometer.

Excellent agreement of absorbancy values for chlorophyll a was obtained when the same solution was measured (18) with the Hilger instrument and with an instrument employing two separate monochromators in series (15). Recorded transmittancy curves obtained on a General Electric Recording Spectrophotometer, a double monochromator with glass prisms (7), for a solution of chlorophyll a in ether (17) did not have as high maxima or as low minima of absorption as curves obtained the same day on the same solution with the Hilger instrument. The difference in absorption coefficients calculated from transmittancy values at the red peak (6600 Å.) was 17 per cent and at the minimum (4720 Å.) it was 13 per cent. Differences at other wave lengths were intermediate. These differences result from the use of relatively wide spectral bands (100 Å. isolated)

necessary in the recording instrument in comparison with the sharp bands characteristic of the solution employed.

Further comparisons of these instruments were made with a 0.0003 *M* solution of potassium permanganate, using band widths of 5 m μ (100 Å. isolated) with the recording spectrophotometer and slit widths of 0.06 to 0.08 mm. (10 to 35 Å. isolated) with the Hilger instrument. At most wave lengths transmittance values were comparable, but more detail appeared in the curve from the Hilger spectrophotometer. The small minimum at 5300 Å. and inflections at 5080 and 5650 Å. obtained with the recorder were more distinct on the curve from the Hilger monochromator. Narrow spectral regions isolated are thus of im-

TABLE 5
Test for stray radiant energy, chlorophyll a in ether

WAVE LENGTH	SLITS	FILTERS	LOG $\frac{I_0}{I}$
Å.	mm.		
6600 (maximum)	0.08	None	0.868
6600 (maximum)	0.08	Corning 241 + Jena BG 7 (absorbs below 6200 and above 6600 Å.)	0.873
4720 (minimum)	0.06	None	0.320
	0.10	Corning 511 + Jena VG 9 (absorbs below 4400 and above 5000 Å.)	0.322
4290 (maximum)	0.08	None	1.078
	0.08	Corning 511 + 306 (absorbs below 3700 and above 5000 Å.)	1.074

portance also for systems with comparatively broad absorption bands if details are important.

A detailed comparison was made between these two instruments on the transmittancy curve of a didymium glass filter (Jena BG 20). Similar results were obtained on two General Electric Recording Spectrophotometers, one through the courtesy of Dr. S. B. Detwiler of the U. S. Regional Soybean Industrial Products Laboratory, Urbana, Illinois, and one in the laboratory of Dr. M. G. Mellon, Department of Chemistry, Purdue University. The transmittancy curve from the latter instrument (with continuous recording) is presented in figure 8, with that obtained on the same piece of glass with the Hilger monochromator. The improved detail obtained with the instrument capable of using the narrower slits is apparent. Other comparisons of the effect of even wider isolated spectral regions on this curve are presented by Mellon (Figure 36 of reference 7). The amplifier current sensitivity usually employed here is of the

same order as that described by Michaelson (8) for the A.C. amplifier in a General Electric Recording Spectrophotometer. Gibson and Keegan (5) modified one of these automatic instruments to permit the use of 4 and 8 $m\mu$ band widths.

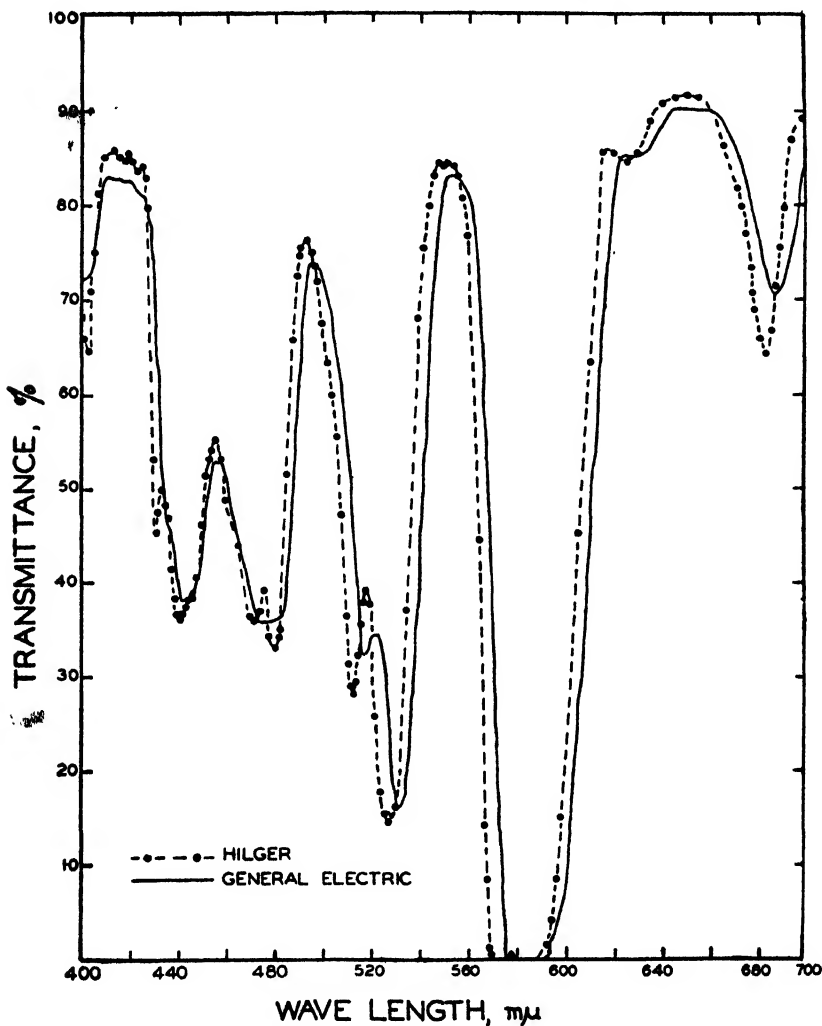


FIG. 8. Transmittance curves of Jena didymium filter, BG 20, #25444, as determined on two double monochromator spectrophotometers.

Their curve for a didymium glass filter taken with a 4 $m\mu$ band width approaches that obtained with the Hilger monochromator in the detail recorded. A curve with intermediate characteristics was obtained on a grating instrument by Sheard and States (14).

Since the announcement of a commercial quartz spectrophotometer (single

monochromator and photoelectric photometer) by Cary and Beckman (1), a great impetus has been given to research problems which involve the accurate measurement of absorption spectra. Insofar as the writer has had an opportunity to study the performance of the Beckman spectrophotometer, his impressions of it are very favorable. A few comparisons of its performance with that of the Hilger double monochromator follow. Narrow slits were used.

A solution of vitamin A alcohol in hexane was studied in the region of 3240–3280 Å. and identical absorbancy values obtained with the two instruments. A solution of α -carotene in hexane was studied from 3800 to 5000 Å., with almost identical results from both instruments. Results for the maxima and minima of hexane solutions of both α - and β -carotenes (all *trans*) reported by Zechmeister and Polgár (16) and measured with the Beckman spectrophotometer are practically identical (± 1 per cent or less) with those reported by Zscheile, White, Beadle, and Roach (22) for similar solutions (but different preparations) studied with the Hilger monochromator. Likewise, identical absorbancy curves in the region 4200–4700 Å. were obtained with the two photometers for a solution of chlorophyll b in ether and in the region 6450–6700 Å. for chlorophyll a. A

TABLE 6
Chlorophyll analysis (6600–6425 Å.)

	TOTAL CHLOROPHYLL	COMPONENT A
	<i>mg per liter</i>	<i>per cent</i>
Hilger	18.9	72.8
Beckman	18.8	73.8

fresh extract from a tomato leaf, prepared for chlorophyll analysis (3), also gave identical curves in the red region and satisfactory agreement on chlorophyll analysis, as shown in table 6.

The absorbing systems discussed above have bands sufficiently broad that they can be resolved with the Beckman spectrophotometer. On account of the greater dispersion of the Hilger monochromator (1.7-fold), smaller dark current (100- to 1000-fold), and higher amplification factor in the Purdue photometer, considerably narrower spectral regions can be utilized and much lower irradiancies can be employed and accurately measured. This would be important in cases of substances very sensitive to photochemical change. The luminous flux to which the absorbing samples are exposed is approximately 10^{-8} lumens, comparable to that of the earlier instrument (6) but with the purity of the radiant energy much higher because of the double monochromator.

Efforts were made to obtain a high irradiance at slit 3 by use of a 40-amp. carbon arc with accessory reflector and lenses. With slits 0.5 mm. wide in the green region an illuminance of 4 to 5 foot candles was obtained, as measured by a Weston photronic cell behind lens 2. With the 72-watt incandescent source usually employed for absorbancy measurements, operating at 10 amp. and with

slits 0.5 mm. wide, the illuminance at slit 3 is not more than 0.2 foot candle, or 0.1 foot candle after passing lens 2.

V. SUMMARY

The performance of a Large Quartz Müller-Hilger Double Monochromator in a photoelectric spectrophotometer assembly is described. The assembly construction is presented with emphasis on differences from other spectrophotometers. A single photocell and thermocouple permit a wide range of wave lengths to be employed.

The high purity of the radiant energy transmitted by the double monochromator was demonstrated in numerous tests for scattered radiant energy including variation of slit width and transmittancy at maxima and minima of absorbance, the use of accessory filters, and use of sources of monochromatic radiant energy.

The sensitivity and flexibility of the d.c. amplifier permit the accurate measurement of absorbancy for narrow spectral regions. Calibration and precision studies are described for amplifier, photocell, and monochromator. The photocell gives a linear response over a great range of irradiancy. Stability of the photocell in relation to wave length was studied under different conditions. The change of dark current was studied in detail.

This spectrophotometer is compared with several others in relation to comparable curves of identical or similar solutions and standards.

It is a pleasure to acknowledge the assistance given by numerous individuals in various phases of the construction and study of this spectrophotometer. The coöperation of J. W. Perry of Adam Hilger Ltd. in the design of the more critical optical parts was indispensable.

The photocell was specially constructed by the R.C.A. Manufacturing Company through the courtesy of Alan M. Glover. The 3- and 5-mm. Pyrex-glass separators for the absorption cells used in the ultraviolet were specially made by the American Instrument Co. R. H. Munch kindly constructed the hydrogen-arc sources of ultraviolet. The thermocouple was constructed by L. B. Clark, of the Smithsonian Institution. Numerous suggestions regarding the photocell and amplifier circuits were given generously by S. W. Barnes of the University of Rochester, W. B. Nottingham of the Massachusetts Institute of Technology, and A. E. Whitford of the University of Wisconsin. Construction of many of the mechanical parts and supports was performed by H. A. Hurd, who also made many helpful suggestions for their design. Assistance in the assembly and testing of parts, as well as in obtaining much of the absorption data presented above, was given by L. F. Green, C. L. Comar, and J. W. White. Coöperation with respect to use of other instruments for comparison curves was generously given by M. G. Mellon and S. B. Detwiler.

REFERENCES

- (1) CARY, H. H., AND BECKMAN, A. O.: *J. Optical Soc. Am.* **31**, 682 (1941).
- (2) COMAR, C. L.: "The Preparation and Absorption Spectra of the Chlorophyll Com-

- ponents; the Chloroplast Substance of Spinach Leaves," Doctoral thesis, Purdue University, Lafayette, Indiana, 1941.
- (3) COMAR, C. L., AND ZSCHEILE, F. P.: *Plant Physiol.* **17**, 198 (1942).
 - (4) DRABKIN, D. L.: *J. Optical Soc. Am.* **35**, 163 (1945).
 - (5) GIBSON, K. S., AND KEEGAN, H. J.: *J. Optical Soc. Am.* **28**, 372 (1938).
 - (6) HOGNESS, T. R., ZSCHEILE, F. P., JR., AND SIDWELL, A. E., JR.: *J. Phys. Chem.* **41**, 379 (1937).
 - (7) MELLON, M. G.: *Colorimetry for Chemists*. The G. Frederick Smith Chemical Co., Columbus, Ohio (1945).
 - (8) MICHAELSON, J. L.: *J. Optical Soc. Am.* **28**, 365 (1938).
 - (9) MILLER, E. S.: *Plant Physiol.* **12**, 667 (1937).
 - (10) MITCHELL, J. H., JR., AND KRAYBILL, H. R.: *Ind. Eng. Chem., Anal. Ed.* **13**, 765 (1941).
 - (11) MUNCH, R. H.: *J. Am. Chem. Soc.* **57**, 1863 (1935).
 - (12) PENICK, D. B.: *Rev. Sci. Instruments* **6**, 115 (1935).
 - (13) RENTSCHLER, H. C., AND HENRY, D. E.: *Rev. Sci. Instruments* **3**, 91 (1932).
 - (14) SHEARD, C., AND STATES, M. N.: *J. Optical Soc. Am.* **31**, 64 (1941).
 - (15) SMITH, JAMES H. C.: *J. Am. Chem. Soc.* **58**, 247 (1936).
 - (16) ZECHMEISTER, L., AND POLGÁR, A.: *J. Am. Chem. Soc.* **65**, 1522 (1943).
 - (17) ZSCHEILE, F. P., AND COMAR, C. L.: *Botan. Gaz.* **102**, 463 (1941).
 - (18) ZSCHEILE, F. P., COMAR, C. L., AND MACKINNEY, G.: *Plant Physiol.* **17**, 666 (1942).
 - (19) ZSCHEILE, F. P., AND HARRIS, D. G.: *J. Phys. Chem.* **47**, 623 (1943).
 - (20) ZSCHEILE, F. P., AND HENRY, R. L.: *Ind. Eng. Chem., Anal. Ed.* **14**, 422 (1942).
 - (21) ZSCHEILE, F. P., JR., HOGNESS, T. R., AND YOUNG, T. F.: *J. Phys. Chem.* **38**, 1 (1934).
 - (22) ZSCHEILE, F. P., WHITE, J. W., JR., BEADLE, B. W., AND ROACH, J. R.: *Plant Physiol.* **17**, 331 (1942).

THE DECOMPOSITION OF BENZOYL PEROXIDE. I

THE KINETICS AND STOICHIOMETRY IN BENZENE

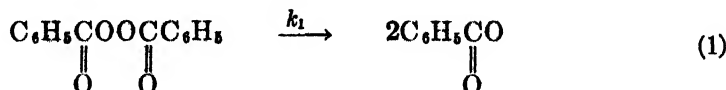
BENJAMIN BARNETT AND WILLIAM E. VAUGHAN

Shell Development Company, Emeryville, California

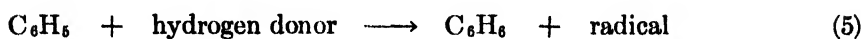
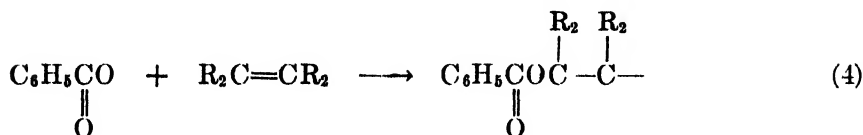
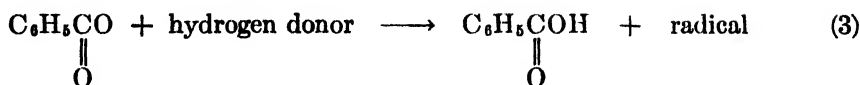
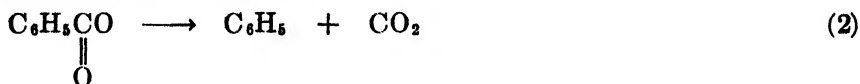
Received March 19, 1947

I. INTRODUCTION AND LITERATURE REVIEW

Although benzoyl peroxide has been extensively used for many years as a polymerization catalyst, the manner of its decomposition under different conditions is still not fully understood. At the concentrations of the peroxide normally used in catalyzed polymerizations, it seems generally accepted (1, 2, 3, 18, 21, 22) that the initial step



is followed by such reactions as:

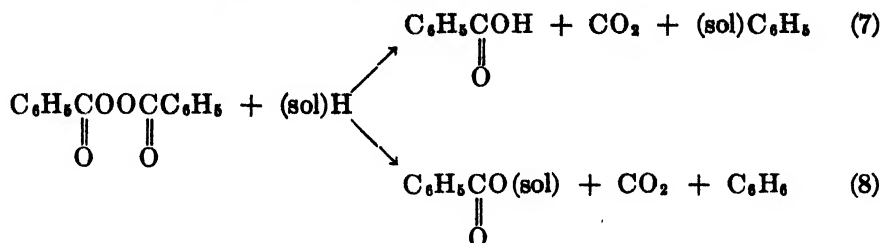


The activation energies reported (5, 20, 21) are of the order of 30–31 kg.-cal. per mole. This may (24) be the energy required to rupture the oxygen-oxygen bond, and consequently equation 1 may represent the rate-determining step. Recent studies (23, 25) indicate that a similar mechanism probably holds for the decomposition of di-*tert*-alkyl peroxides.

On closer study, however, the kinetics are found not to be as straightforward as this scheme would indicate. It has been known for a number of years that the rate of decomposition of benzoyl peroxide is not the same in all solvents (14). The faster rate in mixtures of benzene and vinyl acetate than in benzene alone has been ascribed (18) to the formation of a complex between peroxide and vinyl acetate, more reactive than the peroxide itself; more recently this effect has been interpreted (22) as the disturbance, to a greater degree by vinyl acetate than by benzene, of an equilibrium between benzoyl peroxide and benzoate radicals. The assumption of a primary association step leads to the possibility of subsequent decomposition by a non-radical path of the complex so formed, and some evidence has been presented (10, 29) in support of such a course, particularly in more concentrated solutions. The only free-radical mechanism proposed (17) for these conditions appears to be excluded on energy grounds (26), and in fact no experimental evidence has been obtained (20) for the occurrence of the products to be expected from the radicals assumed.

The stoichiometry of the decomposition of benzoyl peroxide in concentrated solutions has been studied extensively (14), and the participation of the solvent in the reaction is well established (6, 9, 19, 27, 28), although in the higher-boiling solvents, such as nitrobenzene and paraffin wax, rapid decomposition of the peroxide to biphenyl and carbon dioxide (the so-called Kolbe reaction (10)) may result in the entry of only small amounts of the solvent into the final products (9). The Kolbe reaction is the main decomposition path of pure benzoyl

peroxide, both thermally (10, 11, 12, 30) and photochemically (13). For concentrated solutions the earlier "RH" scheme (14) summarizes the stoichiometry in convenient form ("(sol)H" represents solvent):



In benzene equation 7 represents the main reaction (11), in cyclohexane reactions 7 and 8 proceed to about equal extents (16), and in isobutyl alcohol reaction 8 is the main course (15). Not only the rate, therefore, but also the stoichiometry of the decomposition is known to vary from solvent to solvent.

Evidence for a deviation from the simple first-order kinetics represented by equation 1 can be found by examination of the recent literature. There is a distinct trend of the first-order decomposition rate with the concentration of the peroxide in benzene (20), in benzene containing 20 per cent by volume of styrene (8), and in allyl acetate (2). The possibility arises that the nature of the decomposition products may also change with the initial peroxide concentration. No thorough study of either effect has heretofore been made. The problem, however, would appear to be of technical importance, for in those solvents in which the deviation from first-order kinetics is greatest, the peroxide might be decomposing to a large extent by a process which, if non-radical, would be useless for sensitizing polymerization.

The present paper includes the results of a study of the variation of the observed decomposition rate with the initial concentration of benzoyl peroxide in benzene. The change in stoichiometry was followed to the extent of determining the initial rates of formation of carbon dioxide and free acid. The effect of the peroxide concentration on the velocity constant was investigated, and it was also found that the stoichiometry of the decomposition changes steadily as the initial concentration of peroxide is increased. The limiting reaction at low peroxide concentrations is kinetically of the first order, the rate-determining step probably being that represented by equation 1, and the main over-all change is apparently the formation of carbon dioxide and biphenyl. At high concentrations of peroxide, the reaction may be represented by a second-order equation; the mechanism is apparently of a non-radical nature, and the stoichiometry approaches that of reaction 7, the main course of the "RH" scheme in benzene.

To amplify the meager data in the literature on the effect of different solvents on the decomposition rate, a study was also made with a large variety of solvents, in which differences in rate of over twentyfold were obtained at the same peroxide concentration. The results of this study are presented in the following paper (see page 942).

II. EXPERIMENTAL METHODS

The decompositions were carried out in an all-glass apparatus. The reactors, varying in capacity from 100 cc. to 1000 cc., were provided with three openings and an oil-filled thermometer well. A mercury-sealed glass stirrer passed through the middle neck, and at one of the side openings a standard-type, seven-bulb condenser was attached. A capillary sampling tube passed down through the third neck and bore at the top a turned-down enlargement of about 5-cc. capacity closed at each end by a stopcock. This tube permitted removal of samples at any time by application of suction. The system could be flushed with nitrogen or oxygen, as required, by passing the gas in through the sampling tube. From the top of the condenser the evolved gases could be passed to a water-jacketed gas buret for volumetric measurement, to a standard carbon dioxide-absorption train in which the gas was absorbed in Ascarite, or to a reservoir from which samples of the gas could be removed for analysis.

When the thermostated oil bath in which the empty reactor was immersed had attained the proper temperature, the prepared reaction mixture was poured in through the middle opening, and the stirrer then set back in place and started. Tap water, usually at 14–18°C., was used to cool the condenser. When the reaction mixture had reached the desired temperature, as indicated by the calibrated thermometer (accurate to $\pm 0.02^\circ\text{C}.$), a sample of the reaction mixture was removed by means of the sampling tube and at once, at "zero time," a stopcock in the line was opened to permit gas to collect in the buret or to be absorbed in the Ascarite. When the gravimetric method was used, a slow stream of nitrogen was passed through the system throughout the experiment.

In the volumetric determinations of carbon dioxide, a correction was applied for the partial vapor pressure of benzene at the temperature of the tap water used to cool the condenser. The experiments in which evolved gas was determined gravimetrically were run for a maximum of 5 hr., corresponding to decompositions of *ca.* 55 per cent.

Thereafter, to follow the decomposition, samples of the reaction mixture were removed from time to time for analysis, and the amount of gas evolved either read off the buret or determined by weight. Since, when the initial concentration was low, the presence of air or oxygen in the system resulted in slightly too high values for the observed ratio of the number of moles of carbon dioxide formed per mole of peroxide decomposed, the system was always thoroughly flushed with nitrogen at the start.

Total acidity was determined by titration with dilute standard sodium hydroxide. Analyses for oxidizing power were carried out in the following manner: The weighed sample (3–4 g.) was washed into a 500-cc. Erlenmeyer flask with 10 cc. of glacial acetic acid, and after the air in the flask had been removed by sublimation of a few small pieces of dry ice, about a gram of sodium or potassium iodide was added and the mixture refluxed on the steam bath for 15 min. After dilution with about 100 cc. of water, the liberated iodine was titrated with standard thiosulfate solution.

The benzoyl peroxide used was an Eastman White Label product, different

samples of which analyzed from 98.8 to 99.4 per cent peroxide. For a few experiments the White Label material was further purified by dissolving in chloroform and reprecipitating with methyl alcohol; however, this material, which assayed 99.6 per cent, gave no sensibly different results.

III. THE DECOMPOSITION OF BENZOYL PEROXIDE IN BENZENE AT 80°C.

A. KINETICS

The deviation from first-order kinetics was readily observed in any one experiment when the logarithm of the peroxide concentration, P , was plotted against

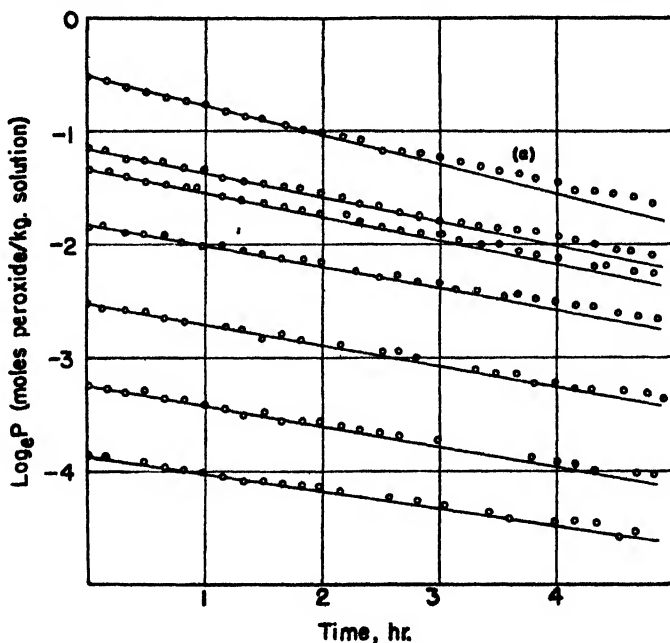


FIG. 1. Decomposition of benzoyl peroxide in benzene. Increasing deviation from first-order kinetics with time. $T = 80^{\circ}\text{C}$.

the time, as in figure 1. Data for a typical run (curve (a) in figure 1) are given in table 1; from this a good idea of the precision of the measurements may be obtained. It is evident that a first-order expression holds only at the start. Since concentrations are expressed as moles per kilogram of solution and since carbon dioxide is evolved, k_1 would normally decrease. Approximately one-tenth of the decrease noted is due to this factor. However, it is difficult to correct for this effect because the stoichiometry changes as the reaction proceeds (see Section B). The pure first-order reaction was isolated by plotting the initial slopes of graphs such as that in figure 1 against the initial concentrations. The initial slopes in figure 1 are:

$$\frac{-d(\log_e P)}{dt} = k_1 (\text{obs.}) \quad (9)$$

and if k_1 (obs.) is a true first-order constant, it obviously should be independent of the concentration of peroxide. The data at 80°C. in table 2, which are plotted in figure 2, show however that this is not the case: even from the start the limiting first-order reaction is accompanied by a *formally* second-order process.¹ For all values of P studied, therefore:

$$\frac{-d(\log_e P)}{dt} = k_1 \text{ (obs.)} = k_1 + k_2 P \quad (10)$$

In figure 2, since k_1 is the intercept at $P=0$, and k_2 the slope,

$$k_1 = 0.158 \text{ hr.}^{-1}$$

$$k_2 = 0.145 \text{ kg./moles-hr.}$$

$$= 0.164 \text{ liters/moles-hr.}$$

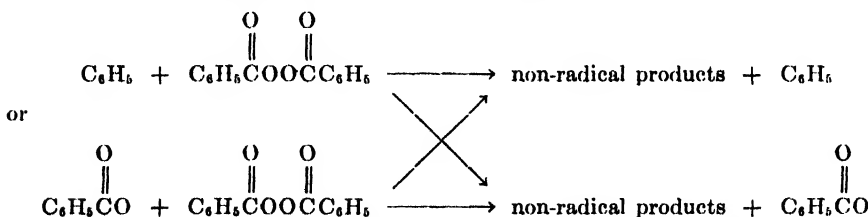
at low peroxide concentrations.

The fraction (see table 2) of the over-all decomposition that is due to the second-order reaction is:

$$f = \frac{k_2 P}{k_1 + k_2 P} = \frac{k_2 P}{k_1 \text{ (obs.)}} \quad (11)$$

and consequently this reaction becomes the major course at concentrations for which $f > 0.5$: namely, for conditions where

¹ Since this paper was written, the authors have conversed with Dr. Kenzie Nozaki, who worked on this same problem with Professor Bartlett at Harvard University prior to joining the staff of the Shell Development Company. Nozaki and Bartlett, an account of whose work is presently appearing (4, 21), have also found a departure from first-order kinetics that is the more observable at higher peroxide concentrations. They feel that under certain conditions the rate of the reaction accompanying the basic first-order change is better expressed by a 3/2-order equation, and ascribe (21) the departure from first-order kinetics to a radical-sensitized decomposition of benzoyl peroxide, thus:



Such a scheme conforms to the 3/2-order rate observed. It is interesting that this interpretation, also, leads to the possibility of "peroxide-wastage": namely, the dissipation of the "catalyst" without forming free radicals which might propagate chains. Under certain conditions, however, these authors concede the possibility of an accompanying second-order reaction.

In support of their conclusion that the side reaction is of the 3/2 order, Nozaki and Bartlett found that certain radical-producing substances, such as hexaphenylethane, increase the decomposition rate of the peroxide. On the other hand, it had previously been found in the present work, in a single experiment, that the oxidizing power of a benzene solution containing 0.2 mole/kg. of benzoyl peroxide and 0.2 mole/kg. of hexaphenylethane decreased at the same rate as that of a solution containing 0.2 mole/kg. of the peroxide alone in benzene.

$$\frac{k_2 P}{k_1 + k_2 P} > 0.5 \quad \text{or} \quad P > \frac{k_1}{k_2} \quad (P > 1.09) \quad (12)$$

This corresponds to concentrations greater than 10.4 mole per cent. It should be noted that the concentrations of benzoyl peroxide used in technical applications are much lower than this (usually of the order of 1–2 per cent), and the participation of the higher-order reaction at these concentrations will be correspondingly less.

The abrupt drop in observed rate near the ordinate axis suggested in figure 2 is not to be interpreted as a deviation from the proposed kinetics, but appears to

TABLE 1

Decomposition of benzoyl peroxide in benzene

P_0 (starting concentration): 0.5861 mole/kg. $T = 80^\circ\text{C}$.

REACTION TIME	CONCENTRATION OF PEROXIDE, P	k_1 (OBS.)	REACTION TIME	CONCENTRATION OF PEROXIDE, P	k_1 (OBS.)
hours	mole/kg.	hr. ⁻¹	hours	mole/kg.	hr. ⁻¹
0	0.5861		3.50	0.2616	0.230
0.33	0.5425	0.233	3.69	0.2512	0.230
0.50	0.5135	0.263	3.83	0.2460	0.227
0.67	0.4954	0.251	4.00	0.2311	0.232
0.83	0.4791	0.243	4.17	0.2229	0.232
1.00	0.4615	0.239	4.33	0.2176	0.226
1.17	0.4441	0.237	4.50	0.2098	0.228
1.33	0.4184	0.253	4.67	0.2076	0.222
1.50	0.4135	0.232	4.83	0.1960	0.227
1.67	0.3941	0.262	5.00	0.1867	0.229
1.83	0.3719	0.249	5.17	0.1807	0.226
2.00	0.3551	0.250	5.33	0.1768	0.223
2.17	0.3541	0.232	5.50	0.1677	0.227
2.33	0.3378	0.236	5.67	0.1600	0.227
2.50	0.3264	0.234	5.83	0.1593	0.223
2.67	0.3063	0.243	6.00	0.1552	0.221
2.83	0.3000	0.237	6.17	0.1483	0.223
3.00	0.2891	0.236	6.33	0.1434	0.222
3.17	0.2806	0.232	6.67	0.1365	0.218
3.33	0.2699	0.233	6.83	0.1303	0.220

be due to the formation of traces of peroxide of the solvent, the effect of which on the rate would be observed only when the total oxidizing power is low from the start. This effect is not very great in benzene even in the presence of oxygen, but in other solvents—such as alcohols, acids, cycloparaffins, and notably, substituted benzenes—the total oxidizing power may increase several fold in the presence of oxygen over that of the initial benzoyl peroxide content. Data illustrating this effect are presented in the following paper.

From the data in table 2, the activation energy of the first-order reaction has been calculated to be 32 kg.-cal./mole (see figure 6), in essential agreement with the literature (18, 20). This point is further discussed in the following paper.

The activation energy of the higher-order reaction can be roughly estimated from the data in table 2. They lead to a value of approximately 28 kg.-cal./

TABLE 2
Decomposition of benzoyl peroxide in benzene
Initial rates as function of initial peroxide concentration, P_0

TEMPERATURE ($\pm 0.1^\circ$)	P_0	k_1 (OBS.)	k_1	k_1	$f = \frac{k_1 P_0}{k_1(\text{OBS.})}$
$^\circ\text{C.}$		hr.^{-1}	hr.^{-1}	kg./moles-hr.	
55	0.07112	0.00411 ± 0.00007	0.0420	0.0450	0.095
60	0.06699	0.00996 ± 0.00031			0.156
70	0.0983	0.0467 ± 0.0018			0.260
	0.1745	0.0504 ± 0.0026			0.348
	0.3304	0.0573 ± 0.0031			0.400
	0.4804	0.0622 ± 0.0027			0.433
	0.6180	0.0696 ± 0.0018			0.445
	0.6955	0.0722 ± 0.0042			0.482
	0.8222	0.0831 ± 0.0020			0.486
	0.8650	0.0808 ± 0.0021			0.542
	0.9454	0.0875 ± 0.0047			0.098
	1.064	0.0883 ± 0.0043			0.099
75	0.1379	0.102 ± 0.005	0.0944	0.0724	0.159
	0.1432	0.105 ± 0.007			0.168
	0.2526	0.115 ± 0.007			0.269
	0.2642	0.114 ± 0.008			0.277
	0.4749	0.128 ± 0.006			0.340
	0.5047	0.132 ± 0.007			0.385
	0.6336	0.135 ± 0.004			0.399
	0.8222	0.155 ± 0.004			0.446
	0.8933	0.162 ± 0.005			0.011
	1.035	0.168 ± 0.004			0.020
80	0.01095	0.150 ± 0.006	0.158	0.145	0.034
	0.02138	0.158 ± 0.008			0.067
	0.03837	0.163 ± 0.006			0.131
	0.07980	0.171 ± 0.005			0.202
	0.1633	0.181 ± 0.004			0.224
	0.2759	0.198 ± 0.005			0.350
	0.3162	0.205 ± 0.006			
	0.5861	0.243 ± 0.008			

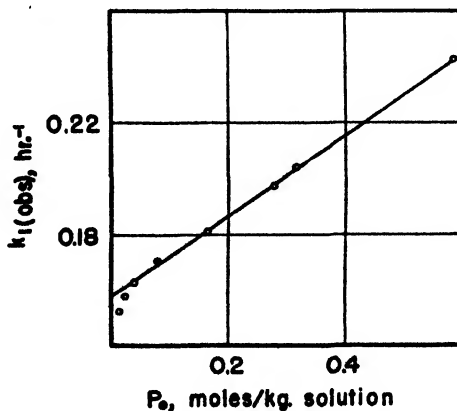


FIG. 2. Decomposition of benzoyl peroxide in benzene. Dependence of observed first-order rate on initial concentration. $T = 80^\circ\text{C.}$

mole. This figure is not accurate, partly because of the small temperature range involved and partly because of the unknown influence of temperature on the solvent effect of the peroxide. Nozaki and Bartlett (21) found an activation energy of 25 kg.-cal./mole for their higher-order process.

The only data in the literature which show the presence of higher-order reactions have been obtained at lower temperatures (see table 3). An analysis of the data of McClure, Robertson, and Cuthbertson (20) for 78°C. gives $k_2 = 0.18$ and for 66°C. $k_2 = 0.06$ for very low peroxide concentrations. The specific rate to be expected at 64°C. from the higher-temperature data of these authors is

TABLE 3
Decomposition of benzoyl peroxide
Evidence from the literature for a simultaneous higher-order reaction

SOLVENT	TEMPERATURE ($\pm 0.1^\circ$)	P_0	k_1	REFERENCE
	$^\circ\text{C.}$		hr.^{-1}	
Benzene*.....	66	0.0772	0.0237	(2b)
		0.126	0.0278	
		0.188	0.0316	
	78	0.0779	0.130	(2b)
		0.124	0.136	
		0.185	0.149	
Benzene containing 3.46 moles styrene per liter.....	64	0.0508	0.0205	(13)
		0.0811	0.0211	
		0.216	0.0257	
Allyl acetate....	80	0.0413	0.191	(13)
		0.0887	0.196	
		0.248	0.227	
		0.413	0.235	

*Brown (7) gives results at 80°C. in benzene, which show a similar trend, but his first-order constants are uniformly lower than those given by other investigators at the same concentrations. It would seem that in these experiments either the peroxide had not completely dissolved at the instant taken as zero time, or that the temperature was actually somewhat less than 80°C. Brown concluded that the first-order decomposition is accompanied by a second-order reaction.

$k_1 = 0.15$ and $k_2 = 0.06$ at low concentrations of peroxide. Cohen's data (8) extrapolate to $k_1 = 0.18$ and k_2 is found to be 0.03 at this temperature. The styrene used in Cohen's experiments may exert a definite solvent effect on k_2 different from that of benzene, but from these data the effect on k_1 would appear to be small. This is in accord with results obtained in this laboratory and to be reported later. If the styrene were displacing an equilibrium between peroxide and benzoate radicals, an appreciably higher limiting rate might be expected under these conditions than in pure benzene (22).

Table 3 also includes data on the decomposition of benzoyl peroxide in allyl

acetate. In this solvent also a higher (apparently second) order process occurs as a side reaction, the rate of which is not greatly different from that of the second-order decomposition in benzene at the same temperature. Other data obtained in this Laboratory indicate that higher-order decomposition reactions accompany the normal first-order decomposition also with other peroxides (23).

TABLE 4

Decomposition of benzoyl peroxide in benzene

Dependence on the initial peroxide concentration of the amounts of carbon dioxide and free acid formed per mole of peroxide decomposed

TEMPERATURE ($\pm 0.1^\circ$)	P_0	α	β	TEMPERATURE ($\pm 0.1^\circ$)	P_0	α	β
$^\circ\text{C.}$				$^\circ\text{C.}$			
55	0.07112	0.72	1.14	80	0.03837		0.25
60	0.06699	0.86	0.81		0.04333	1.61†	
70	0.09827		0.34		0.05668	1.68†	
	0.1745		0.35		0.05788 (a)	1.79	0.67
	0.3319		0.43		0.07508	1.49	
	0.4798		0.43		0.07700	1.56	
	0.6194		0.53		0.07980		0.27
	0.6950		0.52		0.09137 (b)	1.48†	
	0.8241		0.57		0.09457 (a)	1.85	0.44
	0.8590		0.53		0.09708	1.49†	
	0.9485		0.59		0.1051	1.64	
	1.059		0.65		0.1079	1.52	
75	0.1371		0.27		0.1196	1.46†	
	0.1442		0.29		0.1344	1.52	
	0.2650		0.35		0.1473	1.49	
	0.4749		0.46		0.1486 (a)	1.50	0.68
	0.5059		0.47		0.1633		0.37
	0.6353		0.50		0.1738	1.44†	
	0.8308		0.58		0.2022	1.42	
	0.8955		0.58		0.2759	1.33	
	1.035		0.63		0.3162		0.46
80	0.00928		0.24		0.3445	1.30	
	0.01016 (a)*		0.47		0.5861		0.51
	0.01144	1.87			0.6397	1.22†	
	0.01475	1.90	0.36		0.6530	1.28	0.49
	0.01856	1.89			0.7452	1.17	0.50
	0.02138		0.21		1.116	1.17	0.59
	0.03736	1.68			1.237	1.19	0.68

* Atmosphere nitrogen except for cases marked (a) (oxygen) or (b) (air).

† Carbon dioxide determined volumetrically.

B. STOICHIOMETRY OF THE DECOMPOSITION

The stoichiometry of the decomposition has been studied only to the extent of determining the number of moles of carbon dioxide and free acid formed per mole of benzoyl peroxide decomposed. These ratios are represented by α and β , respectively. The co-presence of the second-order reaction should be reflected

increasingly in the observed stoichiometry as the concentration of the peroxide is raised, for it is clear that if the concentration becomes great enough the second-order reaction will become the main path (see equation 12). The data appear in table 4 and are plotted in figure 3. The α - and β -values are clearly dependent on the initial concentrations of peroxide. This is in accord with earlier data by Brown (7), who found that when two solutions of benzoyl peroxide in benzene, 0.1 *M* and 0.8 *M* at the start, were decomposed to the same extent, the carbon

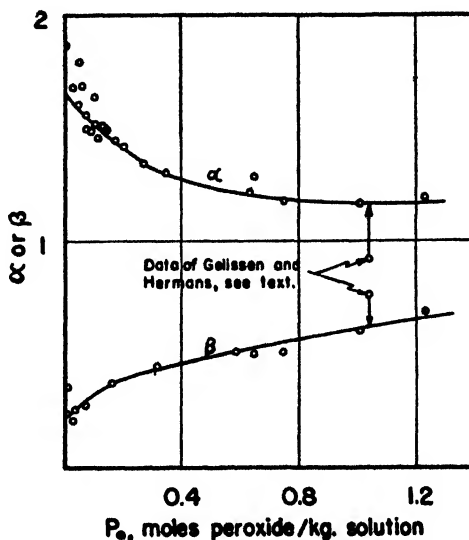


FIG. 3. Decomposition of benzoyl peroxide in benzene. Change in stoichiometry with concentration. $T = 80^{\circ}\text{C}$.

dioxide and benzoic acid appeared in the following proportions (on a solvent-free basis):

	0.1 <i>M</i>	0.8 <i>M</i>
Carbon dioxide.....	20.2 per cent	12.3 per cent
Benzoic acid.....	23.9 per cent	35.5 per cent

The total free acid comprises benzoic and a very small proportion (6, 15) of *p*-phenylbenzoic acid.

The right portions of the curves in figure 3 appear to extrapolate to

$$\alpha = \frac{\text{moles carbon dioxide evolved}}{\text{moles peroxide decomposed}} = 1$$

and

$$\beta = \frac{\text{moles free acid formed}}{\text{moles peroxide decomposed}} = 1$$

but since P may increase indefinitely, no exact value can be estimated for these ratios from the figure. A more useful variable is the fraction f (see table 2), which varies from zero to unity while P increases indefinitely from zero. In the plot in figure 4 of α and β against f , the observed values, α_1 and β_1 , at $f = 0$ are those of the k_1 reaction (since then $P = 0$). As $f \rightarrow 1$, k_1 (obs.) $\rightarrow k_2P$, so that the values, α_2 and β_2 , when $f = 1$ refer essentially to the stoichiometry of the k_2 reaction. The experimentally realizable region in figure 4 is, of course, limited to the interval $0 \leq f < 0.805$, since when $f = 0.805$, P corresponds to pure benzoyl peroxide. Actually, the experimental limit is even lower because of the limited solubility of the peroxide in benzene at 80°C . The realizable

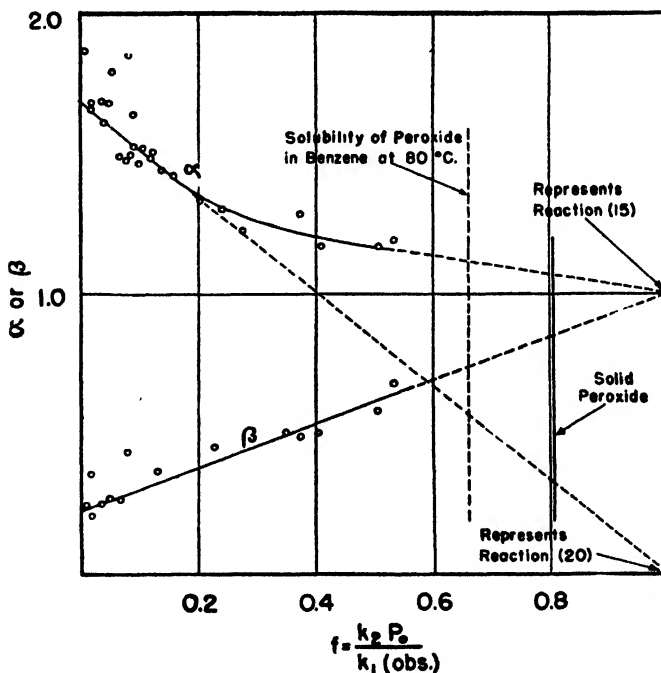


FIG. 4. Decomposition of benzoyl peroxide in benzene. Stoichiometry as function of fraction decomposed in the higher-order reaction. $T = 80^\circ\text{C}$.

range is indicated in figure 4. The data obtained cover a large portion of this interval.

1. Stoichiometry of the first-order reaction

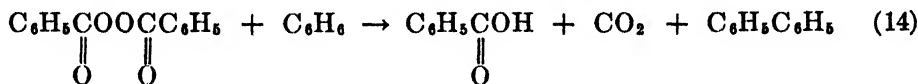
The values of α and β at $P = 0$ are $\alpha_1 = 1.67$ and $\beta_1 = 0.22$, so that $\frac{2 - (1.67 + 0.22)}{2}$ or only some 5.5 per cent of the reacted peroxide is not accounted for by the carbon dioxide and free acid formed. This is in contrast to the results of Gelissen and Hermans (14), who at a concentration of $P = 0.92$ (see figure 3 for comparison) found that about 30 per cent of the reacted peroxide

appeared in the products as a dark, resinous material, and that a large portion of the acid was bound in the form of some unknown ester. Since α_1 does not approximate a whole number, at least two over-all reactions must occur. The major over-all course is almost certainly the formation of biphenyl and carbon dioxide:

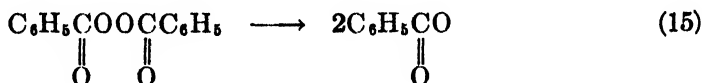


Benzoyl peroxide is known to decompose in the pure state by this path (9, 12, 13, 30) and recently it has been shown (20) to contribute to the carbon dioxide formation at moderate concentrations of the peroxide in benzene.

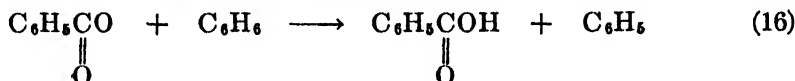
The appearance of acid could be explained, perhaps, on the assumption of another reaction accompanying reaction 13, such as, for example:



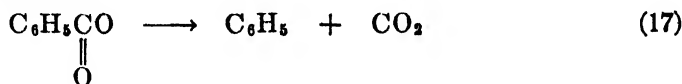
which would appear to be *pseudo* first order under the conditions. However, it seems more probable that only one first-order reaction is involved, the rate step being:



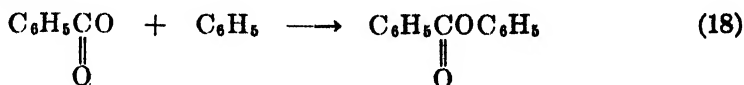
Only $(2 - 1.67)/2$, or 16.5, per cent of the radicals form acid by a reaction such as:



The greater part decomposes:



The fraction of the benzoate radicals formed which react by equation 16 is actually less than 16.5 per cent, because radical combination appears to account for about 5.5 per cent.

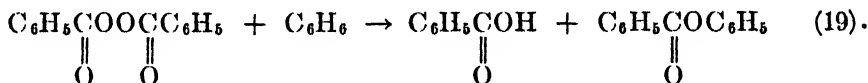


Using these equations and the limiting values of α_1 and β_1 at $P = 0$, it can readily be shown that of the peroxide decomposed, 83.5 per cent forms carbon dioxide and biphenyl, 11.0 per cent forms benzoic acid and, presumably, biphenyl, and 5.5 per cent forms phenyl benzoate. The appearance of phenyl benzoate in the decomposition is well established (14).

2. Stoichiometry of the second-order reaction

While the initial peroxide concentration is varied, or even in a single experiment as the peroxide decomposes, the α - and β -values of the two reactions may also vary, and the values of α_1 and β_1 found will therefore depend on the possibility of variations in α_1 and β_1 . However, the linear curve in figure 4 for β (the value of β actually determined) indicates that both β_1 and β_2 are constants, independent of P .² On the other hand, the curve of α (the over-all value of α for the concurrent reactions) falls rather rapidly, and apparently linearly, at the start; then as f approaches unity, α appears asymptotically to approach unity also. As P increases from zero, the concentration of benzoate radicals would also increase, and since as the concentration of peroxide is raised less solvent becomes available to react with benzoate by reaction 16, the carbon dioxide evolution may be expected to increase as the fraction f increases. Clearly, however, if this effect exists, it is not the factor that determines the shape of the plot of α against f , for otherwise the initial slope of this plot could not be the observed maximum possible slope, that is, the slope for $\alpha_1 = 1.67$ and $\alpha_2 = 0$. Thus it appears that the factor that controls the shape of the α plot is the variation of α_2 with f .

Some 80 per cent of the experimental points in figure 4 fall on the straight line connecting the values $\alpha_1 = 1.67$ and $\alpha_2 = 0$ (at $f = 1$). Combining this requirement of zero carbon dioxide evolution with that of the linear nature of the β plot (namely, $\beta_2 = 1$) gives as the probable initial stoichiometry of the second-order reaction:



At higher values of f , however, the approach of the experimental curve at $f = 1$ to

² If β_2 is the observed value of β , $(\Delta \text{ acid})_1$ and ΔP_1 are, respectively, the number of moles of acid formed and the number of moles of peroxide decomposed in the first-order reaction, and $(\Delta \text{ acid})_2$ and ΔP_2 are the corresponding quantities for the higher-order reaction, then:

$$\beta = \frac{(\Delta \text{ acid})_1 + (\Delta \text{ acid})_2}{\Delta P_1 + \Delta P_2} = \frac{\beta_1 \Delta P_1 + \beta_2 \Delta P_2}{\Delta P_1 + \Delta P_2} = \frac{\beta_1 + \beta_2 \frac{\Delta P_2}{\Delta P_1}}{1 + \frac{\Delta P_2}{\Delta P_1}}$$

But:

$$f = \frac{\Delta P_2}{\Delta P_1 + \Delta P_2} \quad \therefore \frac{\Delta P_2}{\Delta P_1} = \frac{f}{1-f}$$

$$\therefore \beta_2 = \frac{\beta_1 + \beta_2 \frac{f}{1-f}}{1 + \frac{f}{1-f}} = (1-f)\beta_1 + f\beta_2$$

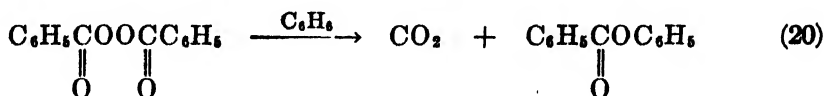
Consequently, when β_1 and β_2 are constants,

$$\frac{d\beta_2}{df} = (\beta_2 - \beta_1)$$

so that the plot of β_2 against f should be linear, with slope $\beta_2 - \beta_1$.

the limiting value $\alpha_2 = 1$ makes it probable that the final stoichiometry of the higher-order reaction is represented by equation 14. Presumably, the stoichiometry of the second-order reaction shifts gradually, as the peroxide concentration is raised, from reaction 19 at the start, to the limiting reaction (14) at high concentrations of peroxide.

Equation 14 represents the main reaction of the "RH scheme" (14) in benzene at high peroxide concentrations. The side reaction of this scheme:



can be accounted for as a summation of reactions 17 and 18.

3. Discussion of the stoichiometries

These results give an insight into the meaning of the accepted "RH scheme" not heretofore possible because of the absence of kinetic data. They show for

TABLE 5
Decomposition of benzoyl peroxide in benzene
Extent of the higher-order reaction at low peroxide concentrations

CONCENTRATION OF PEROXIDE			<i>f</i>
Weight per cent	Mole per cent	<i>P</i> ₂ in moles/kg.	
1.0	0.324	0.0413	0.037
2.0	0.653	0.0826	0.070
4.0	1.32	0.165	0.131
6.0	2.01	0.247	0.185

the first time that the ratio of the main and side reactions (equations 14 and 20) can vary even in the same solvent, taking on different values at different peroxide concentrations.

The changing stoichiometry of the formally second-order reaction is consistent with the assumption of the formation of some intermediate complex, possibly $(\text{C}_6\text{H}_5\text{COO})_2 \cdot \text{C}_6\text{H}_6$, in a preliminary, rapidly reversible step, and its subsequent decomposition in a bimolecular process by different paths. A non-radical process for decomposition has been advanced before, and also the possible formation of a mole-to-mole complex with the solvent (10, 11, 29).

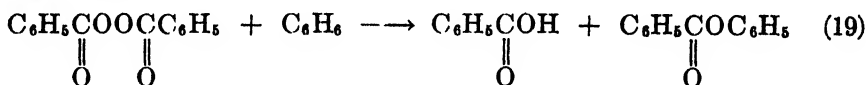
If the concurrent apparent second-order reaction does not involve the formation of free radicals, the fraction of the decomposing peroxide available to form radicals will be correspondingly reduced, and from the practical side it is important to attempt to estimate the effect at peroxide concentrations normally used in technical applications, such as polymerization. For polymerization in benzene at 80°C., if the monomer does not affect the kinetics, table 5 illustrates the extent to which the higher-order reaction enters. The *f*-values given are

the fractions of peroxide which would be "wasted" in not initiating chains, if a non-free-radical decomposition obtains.

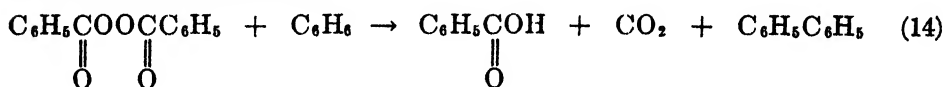
IV. SUMMARY

1. The kinetics of the decomposition of benzoyl peroxide in benzene is strictly first order only at infinite dilution. At all finite concentrations the first-order course is accompanied by a formally second-order reaction. At 80°C. the specific rate of the first-order reaction is $k_1 = 0.158 \text{ hr.}^{-1}$, and of the second-order process, $k_2 = 0.145 \text{ kg./moles-hr.}$ At this temperature the higher-order reaction becomes the major decomposition path at initial peroxide concentrations greater than 1.09 moles per kilogram of solution. The activation energy of the first-order reaction is 32 kg.-cal. per mole (55–80°C.), while that of the side reaction is approximately 28 kg.-cal. per mole (70–80°C.).

2. At 80°C. the over-all stoichiometry of the first-order reaction consists chiefly of the formation of biphenyl and carbon dioxide. Benzoic acid is a minor product. The over-all stoichiometry of the higher-order reaction appears to shift gradually from the initial reaction:



to the final limiting course



as the peroxide concentration is increased.

REFERENCES

- (1) BARTLETT AND ALTSCHUL: *J. Am. Chem. Soc.* **67**, 812 (1945).
- (2) BARTLETT AND ALTSCHUL: *J. Am. Chem. Soc.* **67**, 816 (1945).
- (3) BARTLETT AND COHEN: *J. Am. Chem. Soc.* **65**, 543 (1943).
- (4) BARTLETT AND NOZAKI: *J. Am. Chem. Soc.* **68**, 1495 (1946).
- (5) BEREZOVSKAYA AND VARPHOLOMEEVA: *J. Phys. Chem. (U.S.S.R.)* **14** (2), 936 (1940).
- (6) BOËSEKENS AND HERMANS: *Ann.* **519**, 133 (1935).
- (7) BROWN: *J. Am. Chem. Soc.* **62**, 2657 (1940).
- (8) COHEN: *J. Am. Chem. Soc.* **67**, 17 (1945).
- (9) DIETRICH: *Helv. Chim. Acta* **8**, 149 (1925).
- (10) ERLÉNMEYER: *Helv. Chim. Acta* **10**, 620 (1927).
- (11) FICHTER AND ERLÉNMEYER: *Helv. Chim. Acta* **9**, 144 (1926).
- (12) FICHTER AND FRITSCH: *Helv. Chim. Acta* **6**, 329 (1923).
- (13) FICHTER AND SCHNIDER: *Helv. Chim. Acta* **13**, 1428 (1930).
- (14) GELISSEN AND HERMANS: *Ber.* **58**, 285 (1925) and subsequent papers.
- (15) GELISSEN AND HERMANS: *Ber.* **58**, 765 (1925).
- (16) GELISSEN AND HERMANS: *Ber.* **59**, 662 (1926).
- (17) HEY AND WATERS: *Chem. Rev.* **21**, 186 (1937); see also reference 20.
- (18) KAMENSKAYA AND MEDWEDEV: *Acta Physicochim. U.R.S.S.* **13**, 565 (1940).
- (19) LIPPMANN: *Monatsh.* **7**, 525 (1886); see also references 14 and 27.
- (20) MCCLURE, ROBERTSON, AND CUTHBERTSON: *Can. J. Research* **20B**, 103 (1942).

- (21) NOZAKI AND BARTLETT: J. Am. Chem. Soc. **68**, 1686 (1946).
 (22) PRICE AND TATE: J. Am. Chem. Soc. **65**, 517 (1943).
 (23) RALEY, RUST, AND VAUGHAN: "Kinetics of Vapor-phase Decomposition of Di-*tert*-alkyl Peroxides," J. Am. Chem. Soc., soon to appear.
 (24) RICE AND RICE: *Aliphatic Free Radicals*, p. 165. The Johns Hopkins University Press, Baltimore (1935).
 (25) RUST, SEUBOLD, AND VAUGHAN: "Decomposition of Di-*tert*-alkyl Peroxides and Reactions of the Resulting Free Radicals," J. Am. Chem. Soc., soon to appear.
 (26) VAUGHAN, RUST, AND HEARNE: Nature **156**, 53 (1945).
 (27) WIELAND: Ann. **514**, 145 (1934).
 (28) WIELAND AND MAYER: Ann. **551**, 249 (1942).
 (29) WIELAND AND RASUWAJEW: Ann. **480**, 157 (1930).
 (30) WIELAND, SCHAPIRO, AND METZGER: Ann. **513**, 93 (1934).

THE DECOMPOSITION OF BENZOYL PEROXIDE. II

THE RATES OF DECOMPOSITION IN VARIOUS SOLVENTS

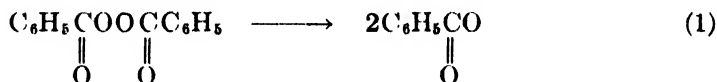
BENJAMIN BARNETT AND WILLIAM E. VAUGHAN

Shell Development Company, Emeryville, California

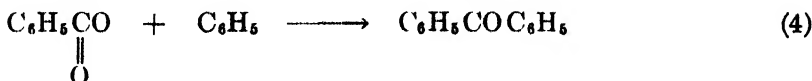
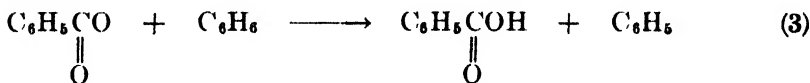
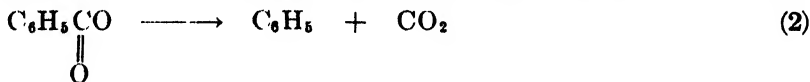
Received March 19, 1947

I. INTRODUCTION

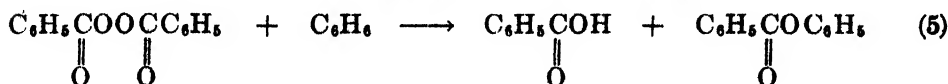
The kinetics and stoichiometry of the decomposition of benzoyl peroxide in benzene have been reported in the preceding paper (1). At infinite dilution the peroxide decomposes in accordance with a first-order equation



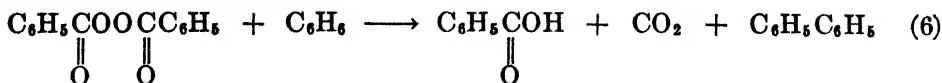
and the benzoate radical undergoes the following independent reactions:



At finite concentrations, however, a formally second-order side reaction is observed, which predominates above a certain critical peroxide concentration. The stoichiometry of this higher-order reaction is initially



but changes gradually as the peroxide concentration is increased, and finally assumes the limiting form:



The work is extended herein to a variety of other solvents and to mixtures of certain solvents. The object of the study was to determine whether the first-order decomposition prevails in all cases at low enough peroxide concentrations, and in passing from solvent to solvent to follow the changes in stoichiometry, as reflected in the amounts of carbon dioxide and free acid formed.

In all cases, a first-order decomposition proceeds at low peroxide concentrations. Particular attention was given to the effect on the decomposition rate of the presence in the solvent of a double bond or a weakly held hydrogen atom, since in accordance with a proposal of Price (13) such solvents may be expected to cause an increase in the rate of decomposition owing to their greater disturbance of an assumed equilibrium between the peroxide and benzoate radicals. No such effect was observed; instead, in agreement with the literature (5, 12), the highest decomposition rates were observed in certain highly polar, associated solvents, such as alcohols and acids. On the other hand, solvents containing a double bond or a weakly held hydrogen atom may affect the stoichiometry strongly. In general such solvents cause the evolution of appreciably less carbon dioxide and the correspondingly increased formation of benzoic acid or a benzoate-olefin radical.

In the presence of oxygen, and in some cases even in an air atmosphere, the decomposing peroxide may sensitize the formation of a relatively stable hydroperoxide of the solvent.

II. EXPERIMENTAL METHODS

The decompositions were carried out in the all-glass apparatus described in the preceding paper (1). The total acidity was determined by titration with dilute standard sodium hydroxide. In most cases the analysis for oxidizing power was carried out by the method previously described, in which the peroxide liberated iodine from a solution of potassium iodide in acetic acid while the mixture was refluxed on the steam bath for 15 min. Certain solvents—for example, allyl alcohol—were found to react with the iodine so formed, however, and for these it was necessary to use a modification of the method of Gelissen and Hermans (6). In this modification a weighed sample of the reaction mixture was washed into the titration flask with *ca.* 10 cc. of acetone, and the flask flushed with carbon dioxide. Twenty-five cubic centimeters of a saturated solution of sodium iodide in acetone were then added and the mixture shaken for 2–3 min. before titrating with standard thiosulfate.

III. RATES OF DECOMPOSITION IN VARIOUS SOLVENTS AT LOW PEROXIDE CONCENTRATIONS

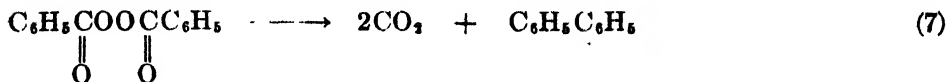
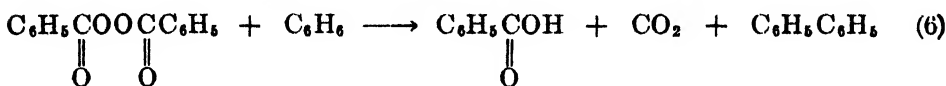
Decomposition rates were measured in a variety of solvents at relatively low peroxide concentrations where the main course is a first-order reaction. The

data are summarized in table 1 in which, for comparison, are included some data for benzene solutions given in the preceding paper. In some of the solvents—for example, benzene, ethylbenzene, cumene, chlorobenzene, benzaldehyde, *n*-heptane, and the ketones—the rates appear to be roughly dependent on their internal pressures (9), as might be expected on the basis of the theory of absolute reaction rates (8), but for most of the solvents no such simple correlation seems to hold. The α - and β -values in columns 5 and 6 of table 1 are respectively the ratios:

$$\frac{\text{moles carbon dioxide evolved}}{\text{moles peroxide decomposed}} \text{ and } \frac{\text{moles free acid formed}}{\text{moles peroxide decomposed}}$$

Comparison of the data in table 1 for the solvents benzene, ethylbenzene, cumene, and benzaldehyde indicates that the availability of more weakly bonded hydrogen atoms in the last three solvents does not increase the rate of decomposition. In fact, the constants at 80°C. for ethylbenzene and cumene are lower than the constant for benzene, and the specific rate in benzaldehyde is only 25 per cent faster than that in benzene. This result appears to weigh against the existence of an equilibrium between peroxide and benzoate radicals which might be rate determining, since solvents with more weakly held hydrogen atoms might be expected to remove the benzoate radicals more rapidly by reaction 3. The higher values of β in such solvents as cumene and ethylbenzene show that this reaction is, in fact, accelerated in these solvents, while the lower values of α show that reaction 2, by which carbon dioxide is evolved, is correspondingly depressed.

The values of α obtained for benzene solutions are plotted in figure 1 against the temperature. The plot includes the data at intermediate temperatures of McClure, Robertson, and Cuthbertson (11). These authors conclude that α can vary only between 1 and 2, corresponding to the limiting stoichiometries:



This, however, would exclude the possibility of independent reaction, in accordance with equations 2, 3, and 4, of the radicals formed in the basic first-order decomposition of the peroxide. Figure 1 shows, in fact, that α does fall below unity at temperatures below ca. 65°C. The apparent limiting values of 1 and 2 for α were found by McClure, Robertson, and Cuthbertson because they worked at temperatures above 65°C., where these limits happen to hold in benzene. The greater variability of α reported in the present work for benzene solutions is consistent with low α -values found in other solvents.

As demonstrated in the preceding paper (1) the first-order decomposition of

TABLE 1
Decomposition of benzoyl peroxide
 Specific decomposition rates in various solvents

SOLVENT	TEMPERATURE ($\pm 0.1^\circ$)	P_0	k_1 (OBS.)	α^*	β^\dagger
	$^\circ\text{C.}$	<i>moles/kg.</i>	<i>hr.⁻¹</i>		
Benzene	55	0.07112	0.00411 ± 0.00007	0.72	1.14
	60	0.06699	0.00996 ± 0.00031	0.86	0.81
	70	0.06792	0.0413 ± 0.0016	1.21	
	75	0.07031	0.0834 ± 0.0042	1.42	
	80	0.06460	0.160 ± 0.002	1.55	0.09
Ethylbenzene	75	0.07203	0.0650 ± 0.0038		
	80	0.08740	0.120 ± 0.008	0.86	0.45
	85	0.07727	0.200 ± 0.019	0.92	0.42
	90	0.06792	0.363 ± 0.023	1.21	
Cumene	80	0.08710	0.133 ± 0.011	0.76	0.54
	85	0.08260	0.230 ± 0.012	0.88	0.38
	90	0.06607	0.429 ± 0.019	1.06	
Chlorobenzene (a)†	80	0.05834	0.167 ± 0.005	0.95	0.28
Benzaldehyde (a)	80	0.06412	0.198 ± 0.010	0.20	
	90	0.07380	0.615 ± 0.020	0.21	
Phenol (a)	80	0.00965	2.25 ± 0.38	0.04	
Nitrobenzene (a)	80	0.05314	0.165 ± 0.012	0.71	
Cyclohexane	80	0.03733	0.278 ± 0.006	0.91	0.91
Methyleyclohexane	80	0.03070	0.189 ± 0.014	0.79	0.57
Tetralin (a)	80	0.06152	0.134 ± 0.014	0.28	0.92
Decalin (a)	80	0.02735	0.812 ± 0.2		0.32
<i>n</i> -Heptane (a)	80	0.03548	0.112 ± 0.004	0.93	
Dioxane (a)	80	0.04820	2.42 ± 0.16	0.28	0.70
Carbon tetrachloride (a)	75	0.04161	0.0384 ± 0.0012	2.4§	0.32
Methyl ethyl ketone	80	0.07586	0.167 ± 0.009	1.66	0.13
Methyl isobutyl ketone	80	0.08570	0.154 ± 0.003	0.83	0.23
<i>n</i> -Butyl alcohol	80	0.02005	2.18 ± 0.30	0.50	1.42
<i>n</i> -Amyl alcohol (a)	80	0.04477	0.534 ± 0.030	0.17	0.93
Benzyl alcohol (a)	80	0.06655	1.60 ± 0.08		1.71
Allyl alcohol (a)	80	0.05200	1.37 ± 0.11	0.06	1.23
Formic acid¶ (a)	80	0.01148	2.50 ± 0.15	0.75	
Acetic acid	75	0.04980	0.271 ± 0.016	0.79	
Propionic acid (a)	80	0.06830	0.115 ± 0.003	1.03	

$$* \alpha = \frac{\text{moles carbon dioxide evolved}}{\text{moles peroxide decomposed}}$$

$$\dagger \beta = \frac{\text{moles free acid formed}}{\text{moles peroxide decomposed}}$$

† Atmosphere nitrogen except for cases marked (a) (air).

§ The gas evolved from carbon tetrachloride solution precipitated silver chloride from solutions of silver nitrate.

¶ The c.p. formic acid used contained *ca.* 10 per cent water.

benzoyl peroxide in benzene is accompanied at all finite concentrations by a higher-order decomposition. In certain cyclic hydrocarbons, such as cyclo-

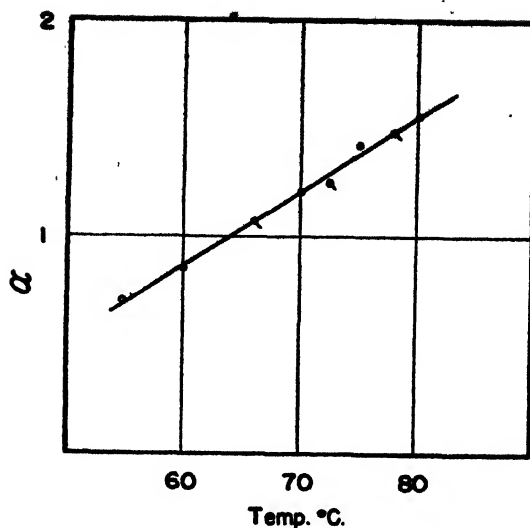


FIG. 1. Decomposition of benzoyl peroxide in benzene. Variation of α (= moles carbon dioxide evolved/moles peroxide decomposed). O, present work; Q, reference 11.

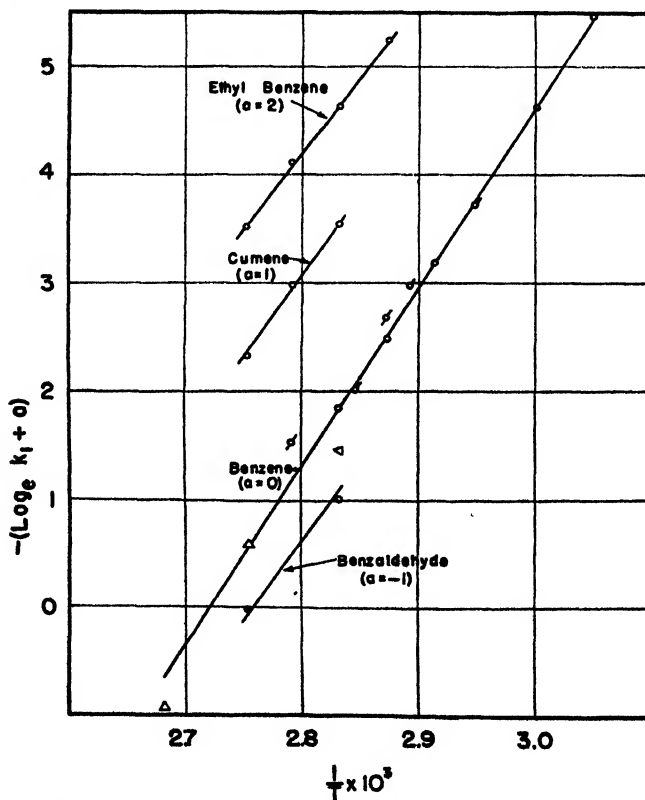


FIG. 2. Decomposition of benzoyl peroxide. Temperature coefficient in various solvents. O, present work, $P_0 = 0.064-0.071$; Q, reference 11, $P_0 = 0.125$; D, reference 10, $P_0 = 0.05$; V, reference 3, $P_0 = 0.26$.

hexane, tetralin, and decalin, the decomposition shows deviation from first-order kinetics much earlier than in benzene. Presumably, in the former solvents the higher-order reactions are more rapid, and consequently participate to a greater extent in the decomposition even at low concentrations. This effect is also evident in the aliphatic acids.

The data for benzene, ethylbenzene, cumene, and benzaldehyde permit estimation of the activation energies in these solvents. From conventional plots of $-\log_e k_1$ against $1/T$ (see figure 2) the values given in table 2 have been obtained.

For clarity of presentation the plots in figure 1 have been displaced an amount α whose value is indicated in each case. Activation energies of from 30 to 33 kg.-cal. per mole have been reported for narrower temperature ranges for the decomposition in benzene (10, 11). All these values appear to approach the bond energy for the O—O linkage in the peroxide (14).¹

TABLE 2
Activation energy of the decomposition of benzoyl peroxide

SOLVENT	<i>E</i>
	<i>kg.-cal./mole</i>
Benzene	32
Ethylbenzene	31
Cumene	31
Benzaldehyde	31

IV. THE RATE OF DECOMPOSITION OF BENZOYL PEROXIDE IN MIXED SOLVENTS

A. DECOMPOSITION RATE IN BENZENE, ETHYLBENZENE, AND CUMENE CONTAINING 20 PER CENT BY VOLUME OF STYRENE

A previous comparison (1) of the available data (4, 11) indicated that at 64°C. the presence of 20 per cent by volume of styrene probably had little effect on the decomposition rate of benzoyl peroxide in benzene. However, Price and Tate (13) have recently concluded that at 80°C. the presence in benzene of this amount of styrene raises the rate of decomposition of tribromobenzoyl peroxide almost sixfold over its value in pure benzene at this temperature. To determine the effect of this proportion of styrene on the rate at higher temperatures, a series of experiments were carried out, not only in benzene, but also in ethyl-

¹ Recently Cass (J. Am. Chem. Soc. **68**, 1976 (1946)) has published on the decomposition of benzoyl peroxide at 30°C. $\pm 0.2^\circ$ in a variety of solvents ranging from aromatic hydrocarbons to polar straight-chain derivatives, such as acetone and butyraldehyde. He also finds a considerable variation in rate and departure from simple first-order kinetics. The activation energy of *ca.* 25 kg.-cal. found by Cass was obtained by combination of his own data at 30°C. with the results of other investigators at higher temperatures. This author has also found that the ratio α depends strongly on the solvent, and may be less than unity.

benzene and in cumene, over a range of temperatures. The benzoyl peroxide concentration used was approximately the same as that of the tribromobenzoyl peroxide in the experiments of Price and Tate. The data appear in table 3, which also includes values of α and β .

The styrene used was prepared just before starting each experiment in which the monomer was to be added. The crude styrene, a Dow product, was washed with 10 per cent sodium hydroxide and then distilled at about 45°C. under a pressure of 20 mm. of mercury.

TABLE 3

Decomposition of benzoyl peroxide

Effect of the presence of 20 per cent by volume styrene on the decomposition rate in certain solvents

SOLVENT	P_0	TEMPERATURE ($\pm 0.1^\circ$)	k_1	α	β
	moles/kg.	°C.	hr. ⁻¹		
Benzene.....	0.0679	70	0.0413 \pm 0.0016	1.19	
	0.0703	75	0.0834 \pm 0.0042	1.37	
	0.0646	80	0.160 \pm 0.002	1.55	
Benzene + styrene.....	0.0720	70	0.0418 \pm 0.0014	0.039	0.09
	0.0714	75	0.0832 \pm 0.0024	0.53	
	0.0594	80	0.160 \pm 0.002	0.92	
Ethylbenzene.	0.0720	75	0.0656 \pm 0.0038		
	0.0679	90	0.363 \pm 0.023	1.21	
Ethylbenzene + styrene	0.0814	75	0.0668 \pm 0.0028	0.48	
	0.0631	90	0.466 \pm 0.023	0.82	
Cumene.....	0.0661	90	0.429 \pm 0.019	1.06	
Cumene + styrene.	0.0619	90	0.422 \pm 0.017	0.73	

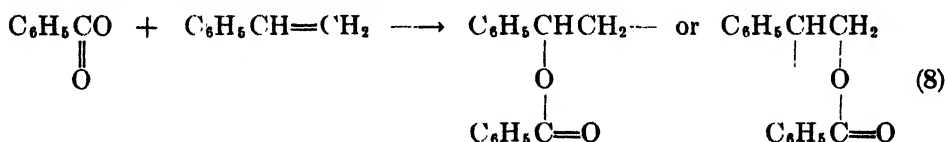
Between 70° and 80°C., as at 64°C., the results show that the presence of styrene in the solvents used has no sensible effect on the rate of decomposition of benzoyl peroxide.

Price and Tate, in carrying out their experiments at 80°C., state that their solutions were refluxed at this temperature. It is evident, however, that their initial temperature must have been considerably higher. A boiling point of *ca.* 93°C. is to be expected for a 20 per cent by volume solution of styrene in benzene, but actually such a solution has been found to boil at 86.2°C. at 762 mm., if boiling chips are present. Otherwise it can overheat to maintain as high a temperature as 93–94°C. On adding an amount of benzoyl peroxide sufficient to give the molar concentration of peroxide used by Price and Tate the boiling point rose to 86.7°C., and thereafter fell off as polymerization progressed:

TIME	BOILING POINT AT 762 MM.
hours	°C.
0	86.7
1.50	85.4
2.50	84.8
4.25	84.4
5.25	84.2
16.5	82.2
23.5	82.1

Consequently, depending on whether overheating occurred, the decomposition rates observed by Price and Tate for their tribromobenzoyl peroxide may have been obtained at temperatures from 6–13°C. higher than that measured in pure benzene at 80°C. On this basis, and assuming the same activation energy for the decomposition of tribromobenzoyl peroxide as for that of benzoyl peroxide, this temperature effect could account for a rate increase of from 2.5- to 4.5-fold in the presence of the added styrene.

The increase in the values of α in each solvent with increasing temperature shows the increasing tendency of benzoate radicals to decompose to carbon dioxide and phenyl radicals by reaction 2. The effect is clearly evident also in the presence of styrene, but in such solutions the values of α are much lower, at the same temperature, than in the pure solvents. Thus, although the monomer does not sensibly affect the rate of decomposition of benzoyl peroxide, it enters intimately into the following reactions of the benzoate radical by rapidly removing it, presumably in accord with the reaction:



which must be faster, particularly at the lower temperatures, than reaction 2. At 70°C., in benzene containing styrene, equation 8 represents the major path for the removal of benzoate radicals, and even at 80°C., in this mixed solvent, the sum of $\alpha + \beta$ is still less than the value of α alone in pure benzene at this temperature. This result appears to comprise the first evidence for the entrance of the benzoate radical itself into the polymerization of styrene, and is in agreement with the finding of Bartlett and Cohen (2) that with certain halogenated benzoyl peroxides polymerization is initiated principally by addition of the halogenated benzoate radicals.

B. EFFECT OF BENZOIC ANHYDRIDE ON THE DECOMPOSITION IN BENZENE

In the preceding section it was shown that the presence in considerable amount of a substance whose structure is somewhat akin to that of the solvents used, results in no sensible increase in the observed rate of decomposition. However,

when benzoic anhydride is added, a considerable decrease in rate is observed even with relatively small additions.

In the determination of the rate of decomposition in benzene, increasing the peroxide concentration may lead not only to higher-order reaction, but also to a decided change in the nature of the solvent. The latter effect alone may cause a shift in the observed first-order constant. The only means of separating these two effects appears to be an indirect one, based on a comparison of the change in the decomposition rate of the peroxide on adding a comparatively inert substance.

When benzoic anhydride is added in increasing proportions at 75°C. to solutions of the peroxide in benzene containing 0.14 mole of peroxide per kilogram of solution after addition of the anhydride, the observed first-order rate falls off steadily, as shown in figure 3. The rate at which the velocity decreases because

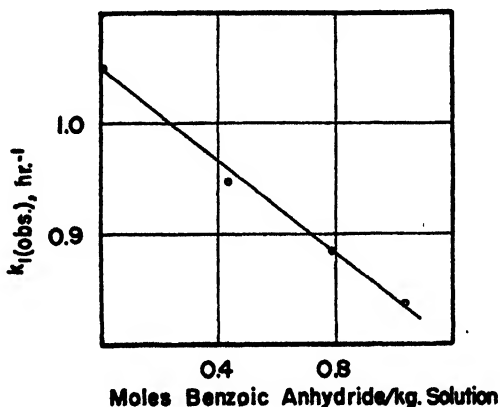


FIG. 3. Decomposition of benzoyl peroxide. Effect of benzoic anhydride on decomposition rate of 0.14 mole/kg. solution of peroxide in benzene. $T = 75^\circ\text{C}$.

of the presence of the anhydride is about one-quarter the rate of increase of k_1 (obs.) with the concentration of peroxide and in the absence of anhydride. In view of the structural similarity between benzoic anhydride and benzoyl peroxide, it is possible that the latter also has a certain inhibiting solvent effect, but if this occurs it is more than offset by the progress of the higher-order reaction.

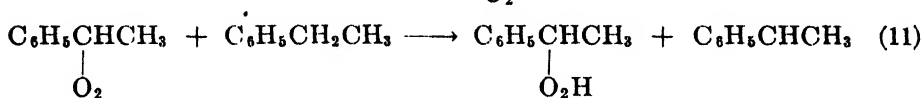
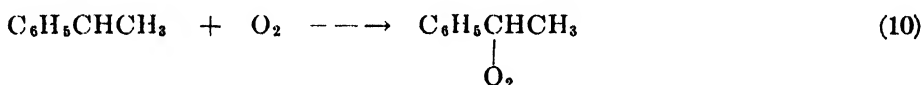
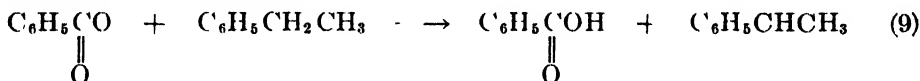
V. RATES OF DECOMPOSITION OF BENZOYL PEROXIDE IN VARIOUS SOLVENTS IN THE PRESENCE OF OXYGEN: PEROXIDE-SENSITIZED FORMATION OF PEROXIDES OF THE SOLVENTS

In certain solvents, such as benzene, aldehydes, and ketones, the rate of decrease of oxidizing power is not sensibly different in an air atmosphere from the rate in one of nitrogen. In other solvents, such as the alcohols, this rate in air is markedly less at the start than later in the reaction. In still another group of solvents, which include the alkyl-substituted benzenes, an atmosphere of oxygen will bring about a considerable perturbation in the initial rate of loss of oxidizing power.

In the cases of alcohols and acids the effect is to simulate an induction period, as is illustrated by figure 4. In substituted benzenes, as in ethylbenzene and cumene, and in cycloparaffins, the oxidizing power actually rises in the presence of oxygen, often quite rapidly, although the benzoyl peroxide is decomposing during this interval. The appearance of more oxidizing power can only be due to the formation of new peroxide, apparently a hydroperoxide of the solvent, by absorption of oxygen by the reacting mixture.

A. FORMATION OF PEROXIDE IN ETHYLBENZENE

The partial pressure of oxygen in air has only a slight effect on the rate of loss of oxidizing power in solutions of benzoyl peroxide in ethylbenzene at 80°C. In the presence of pure oxygen, however, an initial quite rapid *rise* in oxidizing power is observed until the oxygen above the reacting mixture is exhausted. Thereafter, the oxidizing power decreases (see figure 5). The left section of the upper curve in this figure indicates slight autocatalysis, an effect which would probably be more pronounced if it were not for the rapid decrease in the partial pressure of oxygen. Autocatalysis could result by the following path, of a chain character, to hydroperoxide:



Phenyl radicals, as well as benzoate, could initiate this chain.

While the total oxidizing power is rising to a maximum, the benzoyl peroxide presumably is decomposing at the normal rate in the absence of oxygen and, at the maximum the partial pressure of oxygen above the reaction mixture has dropped so low that the difference between the rates of hydroperoxide formation and decomposition is just balanced by the rate of decomposition of benzoyl peroxide. For a short distance beyond the maximum the latter rate predominates, and thereafter the rate of decomposition of benzoyl peroxide is the only measured rate. This is shown by comparing the calculated curve for the decomposition of the peroxide in a nitrogen atmosphere with the right-hand portion of the experimental curve representing total oxidizing power. The two curves become parallel a short distance beyond the maximum, supporting the presumption that during the first 2 hr. the benzoyl peroxide decomposes at the same rate in an atmosphere of oxygen as in a nitrogen atmosphere. On this basis the oxidizing power found at the maximum was corrected for the benzoyl peroxide decomposed up to this point. This correction is indicated in figure 5. The hydroperoxide of ethylbenzene is evidently stable under these conditions.

While the experimental curve was rising to its maximum in this experiment,

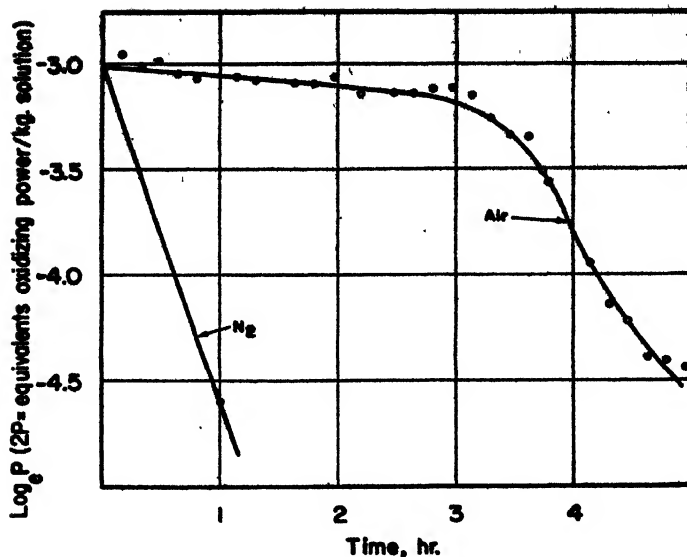


FIG. 4. Decomposition of benzoyl peroxide. Decomposition rate in *n*-butyl alcohol in nitrogen and air atmospheres. $T = 75^{\circ}\text{C}$.

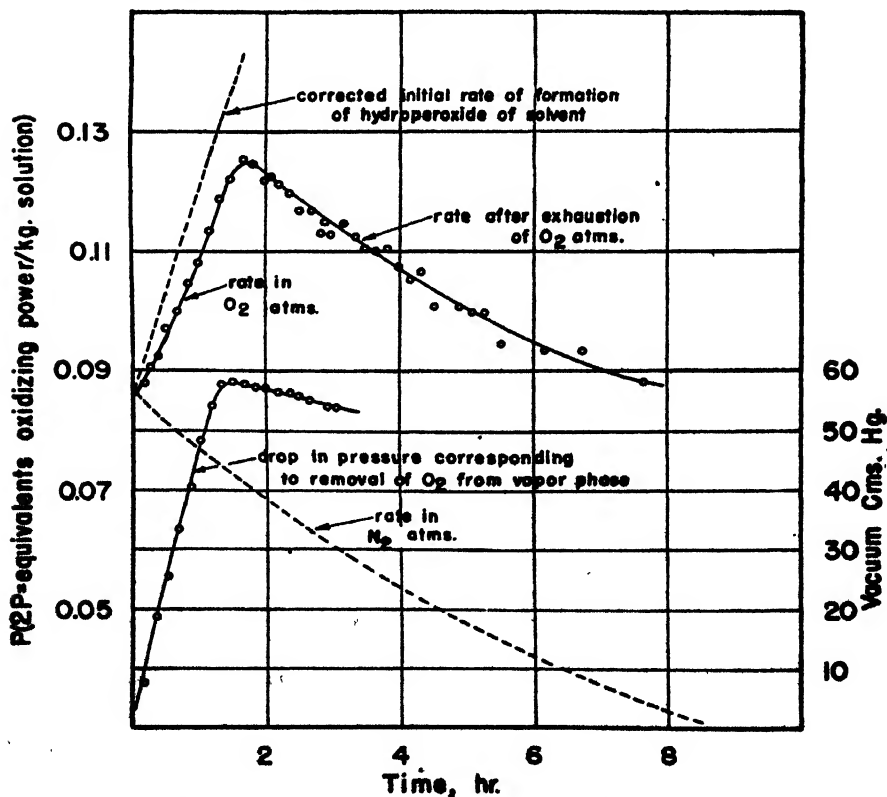


FIG. 5. Decomposition of benzoyl peroxide. Peroxide-sensitized formation of hydroperoxide in ethylbenzene in atmosphere of oxygen at the start. $T = 80^{\circ}\text{C}$.

0.0155 mole of benzoyl peroxide decomposed and 0.0530 mole of hydroperoxide formed. The ratio:

$$\frac{1}{2} \frac{0.0530}{0.0155} = 1.7$$

is the average number of hydroperoxide molecules formed per benzoate radical produced. This is probably a minimum value, for it depends on the rate of diffusion of oxygen into the reaction mixture during the first part of the experiment, or on the mean equilibrium concentration of oxygen in this period. If the former is relatively slow, or the latter low, many of the ethylbenzene radicals formed by reactions 9 and 11 may dimerize or form ester with benzoate radicals before they can encounter an oxygen molecule. By passing air or oxygen continuously through the reaction mixture at atmospheric pressure the above ratio has been raised to 3.6.

The oxygen above the reaction mixture is removed fairly rapidly, perhaps as rapidly as the rate of diffusion of the gas into the reaction mixture will permit. In a closed system there occurs the rapid drop in pressure represented by the lower curve, a minimum pressure being observed at the time the maximum is obtained in the curve representing changes in the oxidizing power of the mixture.

Nozaki and Bartlett (12) state that the effect of oxygen and air is to inhibit *per se* the radical-induced decomposition of benzoyl peroxide.

The use of decomposing peroxides to sensitize peroxide formation is not new. For example, George (7) has used benzoyl peroxide in the air-oxidation of tetralin, and the principle is implicit in such processes as that of catalyzing Diesel fuel oxidation by inoculating with a portion of a previously oxidized batch of fuel (15).

B. FORMATION OF PEROXIDE IN ALCOHOLS

A typical rate curve for the decomposition of benzoyl peroxide in *n*-butyl alcohol at 75°C. in an atmosphere of air is shown in figure 4. The effect of peroxide formation is to give a *pseudo* induction period. Actually this is due to the approximate balance between the rate of formation of new peroxide by absorption of oxygen and the normal rate of decomposition of benzoyl peroxide. Since the absorption of oxygen is probably rapid in both *n*-butyl alcohol and ethylbenzene, the approximate balance observed in the case of the alcohol may be due to the known greater decomposition rate of benzoyl peroxide in this solvent than in ethylbenzene. When the oxygen above the reacting mixture has been largely removed, the rate of loss of oxidizing power in *n*-butyl alcohol approximates that found when a nitrogen atmosphere is present from the start; this is shown by the slopes drawn in figure 4.

A possible course to peroxide in alcohols would appear to be by way of the radical RCHOH , which would eventually lead to hydroperoxide by a mechanism similar to that suggested for ethylbenzene.

The presence of aldehyde has been found to reduce markedly the initial

period of slow change in oxidizing power in solutions of benzoyl peroxide in alcohols decomposing in an atmosphere of air. For example, the effect at 80°C. of adding increasing proportions of propionaldehyde to solutions of benzoyl peroxide in *n*-propyl alcohol is shown in figure 6. The presence of 2.5 per cent by volume of the aldehyde reduces the initial period of slow change to about one-quarter its value in pure *n*-propyl alcohol, and in the presence of 10 per cent by volume of propionaldehyde this interval is completely eliminated. The rate corresponding to the straight-line plot for the mixture containing 10 per cent by volume of aldehyde is sensibly less than the rate in pure *n*-propyl alcohol in

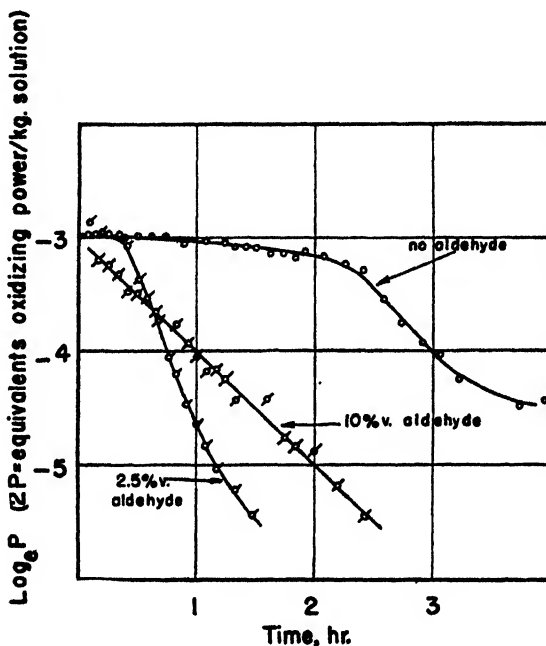


FIG. 6. Decomposition of benzoyl peroxide. Decomposition rate in *n*-propyl alcohol and in *n*-propyl alcohol containing propionaldehyde. Air atmosphere. $T = 80^{\circ}\text{C}$.

the absence of air, but this is in accord with the lower decomposition rates of benzoyl peroxide in aldehydes than in alcohols.

C. FORMATION OF PEROXIDE IN ACETIC ACID AND IN CYCLOPARAFFINS

At 75°C., in an atmosphere of air, acetic acid initially displays a well-defined period of slow change in oxidizing power, but the effect is only about one-quarter that found in *n*-propyl alcohol. Beyond this interval the decomposition of the peroxide is closely first order up to over 70 per cent decomposition. Here also, a rapid contraction occurs in a closed system owing to the absorption of the oxygen above the reaction mixture.

Similar results are obtained when benzoyl peroxide decomposes in an oxygen

atmosphere at 80°C. in cyclohexane and in methylcyclohexane. These hydrocarbons gave a value of *ca.* 2 for the ratio

$$\frac{\text{moles hydroperoxide formed}}{2(\text{moles benzoyl peroxide decomposed})}$$

when a constant stream of air or oxygen was passed through the reacting mixtures at atmospheric pressure.

VI. SUMMARY

1. It is found that at low peroxide concentrations, the decomposition of benzoyl peroxide in twenty-three different solvents is basically first order, although varying some twentyfold in magnitude.

2. The presence of 20 per cent by volume of polymerizing styrene has little effect on the rate of decomposition in benzene at temperatures up to 80°C. This result, together with other evidence presented, appears to weaken the assumption of the existence of an equilibrium between benzoyl peroxide and benzoate radicals.

3. Decomposition rates of benzoyl peroxide in many other solvents indicate that the occurrence of higher-order reactions accompanying a basic first-order change is common to most, if not all, solvents.

4. Many solvents, particularly hydrocarbons, alcohols, and acids, form hydroperoxides when solutions of benzoyl peroxide in these solvents are allowed to decompose in an atmosphere of air or oxygen.

REFERENCES

- (1) BARNETT AND VAUGHAN: *J. Phys. Colloid Chem.* **51**, 926 (1947).
- (2) BARTLETT AND COHEN: *J. Am. Chem. Soc.* **65**, 543 (1943).
- (3) BEREZOVSKAYA AND VARPHOLOMEEVA: *J. Phys. Chem. (U. S. S. R.)* **14**, (2) 936 (1940).
- (4) COHEN: *J. Am. Chem. Soc.* **67**, 17 (1945).
- (5) GELISSEN AND HERMANS: *Ber.* **58**, 765 (1925).
- (6) GELISSEN AND HERMANS: *Ber.* **59**, 63 (1926).
- (7) GEORGE: *Trans. Faraday Soc.* **42**, 210 (1946).
- (8) GLASSTONE, LAIDLER, AND EYRING: *Theory of Rate Processes*, pp. 410-17. McGraw-Hill Book Company, Inc., New York (1941).
- (9) HILDEBRAND: *Solubility*, 2nd edition, Chap. V. The Chemical Catalog Company, Inc., New York (1936).
- (10) KAMENSKAYA AND MEDWEDEV: *Acta Physicochim. U. R. S. S.* **13**, 565 (1940).
- (11) MCCLURE, ROBERTSON, AND CUTHBERTSON: *Can. J. Research* **20B**, 103 (1942).
- (12) NOZAKI AND BARTLETT: *J. Am. Chem. Soc.* **68**, 1686 (1946).
- (13) PRICE AND TATE: *J. Am. Chem. Soc.* **65**, 517 (1943).
- (14) RICE AND RICE: *Aliphatic Free Radicals*, p. 165. The Johns Hopkins University Press, Baltimore (1935).
- (15) U. S. patent 2,365,220 (to Standard Oil Co. of California), December 19, 1944.

SOME PROPERTIES OF THE RADIATION FROM RADIOMANGANESE 54 AND THE ADSORPTION OF MANGANOUS MANGANESE ON HYDROUS FERRIC OXIDE¹

DON H. ANDERSON²

Chemistry Department, The University of Idaho, Moscow, Idaho

Received March 19, 1947

During the course of an investigation to identify an unknown radio element present in an iron disc,³ it was observed that variation in the pH at which the hydrous ferric oxide was precipitated caused a marked change in the amount of radiation of the precipitate. Subsequent determinations of the half-life and the chemical properties indicated that the material was radiomanganese.

There is only one known stable isotope of manganese; this is ^{55}Mn . Several artificial isotopes (3) have been produced. These are radioactive and all but one have quite short half-lives, so short as to make some experimental work rather difficult. Isotopes of mass numbers 51, 52, and 56 have half-lives from 21 min. up to 6.5 days. Radiomanganese 54 has a half-life of about 310 days, which permits experiments to be performed over a period of several days without the need for compensation for decreased activity of the preparation. This isotope was the one used in this work.

The decomposition of radiomanganese 54 results in the formation of stable chromium 54. Two kinds of radiation are observable, one soft and one hard. The mechanism has been demonstrated to be that of *K* electron capture. An electron falls into the manganese nucleus, the atomic number decreases by 1, and an outer electron falls in to replace the missing electron in the *K* shell of the new chromium atom and chromium x-radiation results. The absorption data in aluminum foil corresponds to that of chromium x-radiation excited in the usual manner (3).

EQUIPMENT

The Lauritsen quartz-fiber electroscope is suitable for measuring the radiation from the manganese. The electroscope used had an aluminum-foil window and the samples were placed about 1 cm. below the window. The pH measurements were made by means of a glass electrode and are accurate to ± 0.05 pH unit.

The colorimetric determinations of iron and manganese were made by means of the thiocyanate complex and the oxidation to permanganate, respectively. The colors were compared with standards, using a Cenco Photometer for comparison.

¹ Portions of this paper were presented at the Regional Meeting of the American Chemical Society which was held at Seattle, Washington, on October 20, 1945.

² Present address: Eastman Kodak Company, Color Control Division, Kodak Park Works, Rochester 4, New York.

³ The iron disc, source of radiomanganese, was obtained by Dr. Gerhart Friedlander while he was at the University of Idaho.

EXPERIMENTAL

An iron disc 3 mm. thick with a diameter of 85 mm. was the source of the manganese for this work. Sections cut from the disc possessed a considerable variation in activity; this indicated that the radioactive material might be localized, a conclusion which was confirmed by placing photographic film in contact with the disc. After a 3-day exposure the film was developed and a definite area of intense radioactivity was found. With this record as a guide, drillings were taken from the active area for analysis, and a permanent reference was prepared by mounting some drillings on a piece of cardboard.

This standard preparation was used to determine the ease of absorption of the radiation. The materials that were used were: aluminum, lead, manganese

TABLE 1
Absorption data for aluminum

ALUMINUM	ALUMINUM THICKNESS	ACTIVITY
<i>g./cm.²</i>	<i>mm.</i>	<i>div./min.</i>
0	0.0	0.077*
0.006	0.025	0.040
0.018	0.075	0.023
0.43	1.7	0.020
0.86	3.4	0.018

* This is the average of ten determinations with an average deviation of 0.004.

TABLE 2
Absorption data for lead

LEAD	LEAD THICKNESS	ACTIVITY
<i>g./cm.²</i>	<i>mm.</i>	<i>div./min.</i>
1.36	1.1	0.010
2.32	2.0	0.009
4.0	3.5	0.008
6.96	6.0	0.0065

dioxide, hydrous ferric oxide, and cellophane. Aluminum and lead were chosen to make a comparison with the values in the literature (3) and to assist in identifying the active material. The data for the various materials are readily compared on a plot of activity expressed as divisions per minute against grams of material per square centimeter. The data for aluminum are in table 1.

There is a radiation that is extremely soft, and the absorption in the region 0-0.014 g. of aluminum per square centimeter has been shown by Livingood and Seaborg (3) to be the same as that for the chromium K_{α} radiation.

The region beyond about 0.02 g./cm.² is best investigated with lead, as the absorption of the hard radiation is more pronounced with this material. The data are given in table 2. They yield a value of 9 g./cm.² of lead as being neces-

sary to reduce the radiation by one-half. The value reported by Livingood and Seaborg (3) is 8.4 g./cm.²

The absorption data indicate the need for a careful consideration of the effect of materials present as contaminants or as a matrix to contain the manganese whose activity is to be measured, since small amounts of material can markedly reduce the amount of soft radiation. Aqueous solutions of radio-

TABLE 3
Screening effect of various materials

SCREENING MATERIAL	QUANTITY	ACTIVITY
	ϵ /cm. ²	div./min.
—	—	0.077
MnO ₂	0.012	0.040
MnO ₂ ..	0.025	0.031
MnO ₂	0.059	0.024
MnO ₂	0.066	0.022
MnO ₂	0.085	0.025
MnO ₂	0.160	0.023
MnO ₂	0.296	0.025
Cellophane.....	0.006	0.043
Cellophane.....	0.012	0.033
Cellophane.....	0.030	0.024
Cellophane.....	0.060	0.023
Silver.....	0.00012	0.074

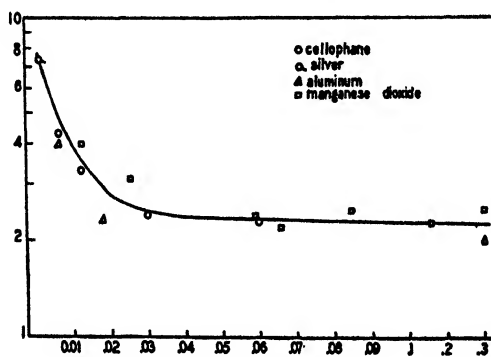


FIG. 1. Absorption of radiation by various materials. Ordinate relative activity expressed as divisions per minute discharge rate of the electroscope. Abscissa, grams per square centimeter of absorbing material. The scale is compressed at the right.

manganese did not produce a significant discharge rate, so all samples used were dried at 110°C. The data for a number of materials are included in table 3 and figure 1. The manganese dioxide was dusted uniformly over a cellophane carrier, and these values of grams per square centimeter include the cellophane.

It is apparent that if a quantitative analysis for manganese is to be undertaken, it is imperative that the conditions be very reproducible with respect to the

presence of foreign material that may exert a screening effect on the radiation. This last imposes some serious limitations on the electroscopic method for determining the absolute amount of manganese present. However, there is a definite advantage in that the electroscope is capable of detecting very small amounts of manganese. Measurements have been made readily on amounts of manganese as small as 0.000011 g. of manganese, giving an activity of 0.015 div./min. which is readily detectable in the presence of a background radiation of 0.010 div./min. The smallest amount detected was 4 γ with an activity of 0.007 div./min., which is still not the lowest limit detectable. This amount was measured in the presence of 0.010 g. of iron, a 10,000-fold excess present as hydrous ferric oxide. Hydrous ferric oxide appears to be a useful agent for

TABLE 4
Screening effect of hydrous ferric oxide

IRON	ACTIVITY
<i>grams</i>	<i>div./min.</i>
0.023	0.065
0.035	0.056
0.051	0.034
0.081	0.034
0.168	0.026
0.260	0.020

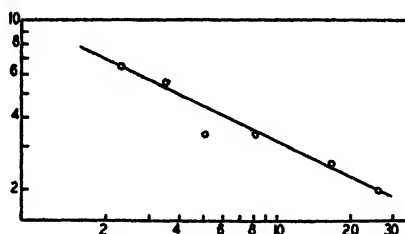


FIG. 2. Absorption of radiation by hydrous ferric oxide, the amount of manganese being constant. Ordinate, relative activity of the preparation. Abscissa, grams of iron present as hydrous ferric oxide times 100.

carrying small amounts of manganese, and it is quite easy to compensate for any screening action.

During the initial phases of the isolation of the manganese, it was observed that the ferric hydroxide would carry down varying amounts of manganese. It seemed desirable to know how complete a separation could be effected. This investigation involved two series of measurements: one on the screening effect of ferric hydroxide, and one on the effect of the H^+ concentration on the adsorption of the manganese.

The screening effect was determined by analyzing a series of hydrous ferric oxide precipitates containing known amounts of iron and identical amounts of manganese. These data are in table 4 and figure 2.

This information may be used to convert the activity readings to a definite amount of iron hydroxide if desired, and it indicates the need for working with as small an amount of carrier as possible when making measurements on the activity of the manganese.

To investigate the adsorption of manganese by hydrous ferric oxide, a series of identical solutions was prepared. These solutions contained about 0.03 g. of iron added as ferric sulfate, 90 γ of manganese, 4 g. of ammonium nitrate, and sufficient ammonia in 100 ml. of solution to bring the pH to the indicated value for each solution. The ammonium nitrate was added to maintain the concentration of the ammonium ion nearly constant. About a third of each preparation was withdrawn an hour after the hydrous ferric oxide was precipitated. This was filtered with mild suction, washed with three changes of water, about 25 ml. of water in all, rinsed with alcohol, and dried overnight at 110°C. A second portion was removed from each solution about one month later and treated in the same manner. The activity of each portion was deter-

TABLE 5
Adsorption of manganese by hydrous ferric oxide

pH	INITIAL DATA			ONE MONTH LATER			
	Iron	Activity	Mn/Fe	Iron	Activity	Mn/Fe	Average Mn/Fe
	grams	div./min.		grams	div./min.		
4.0	0.0097	0.005	0.51	0.0071	0.005	0.71	0.61
4.9	0.0118	0.011	0.93	0.0073	0.005	0.63	0.78
6.0	0.0116	0.016	1.38	0.0110	0.015	1.35	1.37
6.8	0.0118	0.046	3.90	0.0108	0.048	4.45	1.18
7.3	0.0126	0.060	4.76	0.0095	0.042	4.42	4.50
8.0	0.0135	0.066	4.89	0.0097	0.047	4.85	4.87

mined; the data are in table 5. The data indicate that no significant aging took place during one month and that the amount adsorbed was dependent on the H^+ concentration.

Completeness of adsorption at the high pH values was checked by adding a small amount of iron to the filtrate from the sample having a pH of 8.0 and determining the activity of the resulting precipitate. No activity could be detected. The manganese concentration was determined in the stock solution before this was added to the system. The iron content of each portion was determined colorimetrically, using ammonium thiocyanate, after the activity of each had been checked. In table 6 the values have been calculated for the amount adsorbed and the amount in solution. The percentage adsorbed is plotted in figure 3 as a function of the pH. The amount adsorbed is equal to the amount in solution at about pH 6.3. Kolthoff and Overholser (2) in their extensive work on adsorption have reported that the amount of manganese adsorbed increases with an increase in the ammonia concentration and decreases with increasing concentration of ammonium chloride. They did not report the

TABLE 6
Ratio of adsorbed manganese to manganese in solution

pH	AMOUNT ADSORBED	AMOUNT IN SOLUTION	PERCENTAGE ADSORBED
	gammas	gammas	
4.0	11	79	12
4.9	14	76	16
6.0	25	65	28
6.8	77	13	86
7.3	85	5	95
8.0	90		100

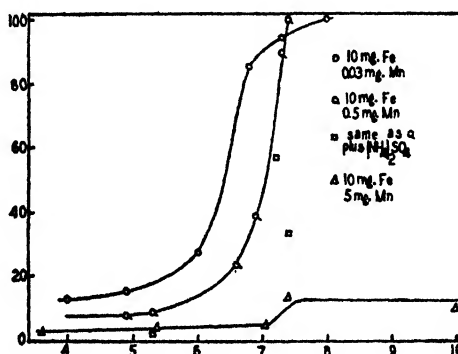


FIG. 3. Adsorption of manganese by hydrous ferris oxide. Ordinate, the percentage of the manganese present that was adsorbed. Abscissa, the pH of the solution.

TABLE 7
Adsorption of manganese as a function of pH and in the presence of ammonium sulfate

IRON PRESENT	(NH ₄) ₂ SO ₄ ADDED	pH	MANGANESE PRESENT	MANGANESE ADSORBED	PERCENTAGE ADSORPTION
grams	grams		grams × 10 ⁴	grams × 10 ⁴	
0.010		4.9	5.1	0.4	8
0.010		5.3	5.1	0.5	9
0.010		6.6	5.1	1.2	24
0.010		6.9	5.1	2.0	39
0.010		7.3	5.1	4.6	90
0.010		7.4	5.1	4.7	(100)
0.010		7.8	5.1	4.9	(100)
0.010	0.5	7.4	5.1	5.2	100
0.010	2	7.2	5.1	2.9	57
0.010	4	7.4	5.1	2.0	33
0.010	1	5.3	5.1	0.1	2
0.010		3.6	50.	1.2	2
0.010		5.4	50.	2.0	4
0.010		7.1	50.	2.2	4
0.010		7.4	50.	6.8	14

hydrogen-ion concentrations or point out whether or not this is due to a buffering action. In order to investigate this and to see if the same type of adsorption curve would be obtained with higher concentrations of manganese, the experiment was repeated using sufficient manganese to permit making an accurate colorimetric determination of manganese.

Solutions were prepared as indicated in table 7, with sufficient ammonia to bring the pH to the values indicated. These data are shown graphically in figure 3; the curves are all of the same general form. From the results it is evident that the ammonium salts actually interfere with the adsorption of the manganese. Apparently a preferential adsorption is taking place. When there is a large excess of manganese the limiting factor is the amount of iron, and up to pH 10 no appreciable precipitation of the manganese takes place. It is possible to state definitely that manganese can be separated from iron by repeated precipitation at a pH in the neighborhood of 4 or 5, at which pH the precipitation of the iron is complete, as reported by Gilchrist (1).

Radiomanganese has been separated from the iron by adding a small amount of a manganese salt and then oxidizing to form manganese dioxide. This reduces the activity of the preparation considerably. Whenever possible, no manganese should be added to the radiomanganese to serve as a carrier. Rather, the manganese should be separated from iron by one or more precipitations at as low a pH as possible. The presence of ammonium sulfate interferes with the adsorption of the manganese and does so even though the hydrogen-ion concentration is maintained constant, as was indicated by Kolthoff and Overholser.

SUMMARY

The adsorption of manganous manganese by hydrous ferric oxide has been studied, using radiomanganese 54 and non-radioactive manganese. The data obtained indicate that at a pH value of 4, which permits the precipitate of hydrous ferric oxide to form, less than 12 per cent of the manganese is precipitated. This relationship holds for ratios of 10 mg. of iron to 5 mg. of manganese and 10 mg. of iron to 0.03 mg. of manganese, in the presence of ammonium nitrate. The effect of ammonium salts has been demonstrated to be related to the adsorption phenomenon and not to a buffer effect that changes the hydrogen-ion concentration of the system and so the solubility of a coprecipitated manganous hydroxide.

The effect of hydrous ferric oxide, manganese dioxide, cellophane, aluminum, and lead on the radiation from radiomanganese has been indicated. The data for aluminum and lead agree with the values in the literature.

REFERENCES

- (1) GILCHRIST, R.: J. Research Natl. Bur. Standards **30**, 95 (1943).
- (2) KOLTHOFF, I. M., AND OVERHOLSER, L. G.: J. Phys. Chem. **43**, 767 (1939).
- (3) LIVINGOOD, J. J., AND SEABORG, G. T.: Phys. Rev. **64**, 391-7 (1938).

STUDIES OF ALUMINUM SOAPS. VIII

WATER SORPTION AND MOISTURE CONTENT¹GEORGE W. SHREVE,² HAROLD H. POMEROY, AND KAROL J. MYSELS³*Department of Chemistry, Stanford University, California**Received February 14, 1947*

Aluminum disoaps such as the dilaurate, $\text{Al}(\text{OH})\text{L}_2$, can be prepared by precipitation by adding a solution of potassium laurate to a large excess of aqueous aluminum chloride solution (7), and extracting the dried precipitate with acetone under conditions minimizing hydrolysis (4). The unextracted precipitate is composed of the disoaps and free as well as sorbed or bound fatty acid.

The soaps thus obtained are slightly hygroscopic. Traces of moisture have a large effect on the behavior of the soap itself and on its dispersion in hydrocarbons. Therefore it is important to obtain information about the sorption of moisture by the soap, its dehydration, and the significance of moisture contents obtained by different methods, including benzene distillation and Karl Fischer reagent.

DEHYDRATION BY MERE EVACUATION

Aluminum dilaurate rapidly and readily reaches a constant weight on evacuation. Even evacuation with an oil pump at room temperature removes moisture, with a loss of weight of 0.6–1.0 per cent within 3 or 4 min. There is no further change of weight in 5 days at room temperature in an evacuated McBain-Bakr sorption balance (2) over water at dry ice temperature (-72°C ., 0.006 mm. of mercury vapor pressure), or in 2 days under the same conditions at 60°C . An identical loss of weight is obtained in 24 hr. either at room temperature in a vacuum desiccator over phosphorus pentoxide or calcium oxide, or in an oven at 105°C . at atmospheric pressure.

When high-grade vacuum grease is not used, an unexpected increase in the weight of the soap can be observed during its dehydration in a desiccator, because the soap avidly sorbs hydrocarbon vapors.

If the conditions of dehydration are sufficiently drastic, however, a further large loss of weight is observed. Thus, in the evacuated sorption balance at 87°C . the loss of weight was 0.7 per cent in 2 hr., and at 100°C . 14.2 per cent in 4 days. In the oven at 105°C . the weight remained constant for 2–3 days after the initial loss, then began to drop at an increasing rate. Here decomposition was obviously occurring, with sintering and later darkening of the fluffy powder and definite formation of laurone.

¹ Study conducted under Contract OEMsr-1057 between Stanford University and the Office of Emergency Management, recommended by Division 11.3 of the National Defense Research Committee, and supervised by Professor J. W. McBain.

² Present address: Department of Chemistry, Kenyon College, Gambier, Ohio.

³ Present address: Department of Chemistry, New York University, University Heights, New York 53, N. Y.

Evacuation for at least 15 min. at room temperature was therefore considered ample for dehydrating the aluminum soap for all this series of studies. The existence of a stable hydrate under these conditions was excluded.

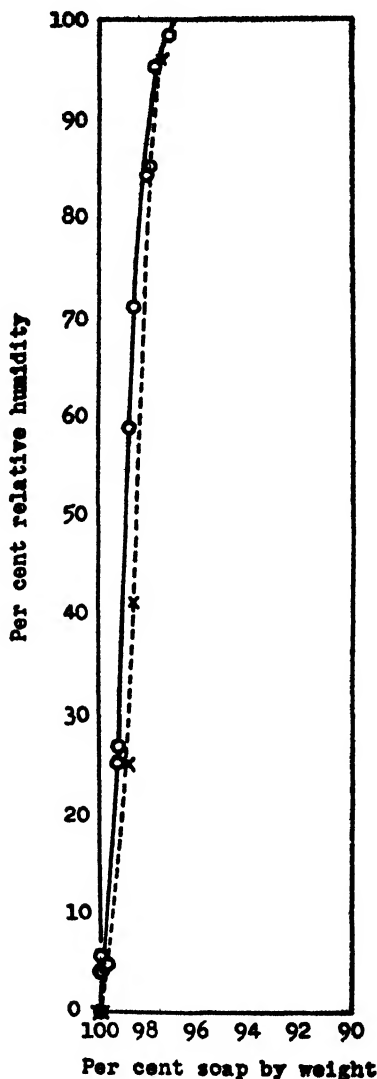


FIG. 1. The sorption^a and desorption of water vapor by aluminum dilaurate, $\text{Al}(\text{OH})\text{L}_3$, at 50°C. O, hydration; X, dehydration.

DEHYDRATION AND HYDRATION IN THE SORPTION BALANCE AT 50°C.

The sorption of water vapor by aluminum dilaurate was determined in a McBain-Bakr sorption balance (2). A single sample of soap was exposed at 50°C. to gradually increasing and decreasing vapor pressures, respectively, from

0.006 mm. of mercury up to saturation and then back. At least 24 hr. was allowed for attainment of constant weight at each set of conditions. This was found to be ample. The whole cycle lasted 23 days. During this time the dry weight of the soap remained unchanged, as shown in figure 1. The uptake of moisture was less than 3 per cent in 100 per cent relative humidity, and most of it occurred between 10 and 25 per cent or above 90 per cent. There is a definite but small hysteresis above 5 per cent relative humidity.

The smooth S-shape of the curve suggests that moisture is held predominantly by surface forces and capillarity. This was confirmed when an x-ray study of the soap, dry and in the presence of saturated water vapor, showed no change of the diffraction pattern (1).

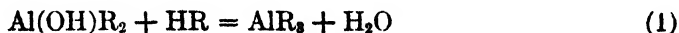
DEHYDRATION OF UNEXTRACTED ALUMINUM SOAPS CONTAINING AN EXCESS OF FATTY ACIDS

Aluminum soaps containing free fatty acid, such as are obtained by precipitation without subsequent extraction, cannot be studied conveniently with the sorption balance. The vapor pressure of fatty acid, particularly of lauric acid, is high enough for the acid to distill from the sample, and a constant weight is not obtained even after 70 days. In the oven at 105°C. the soap sinters and darkens rapidly. Therefore, such soaps were merely dried at room temperature over phosphorus pentoxide in a vacuum desiccator.

DEHYDRATION BY BENZENE DISTILLATION

The moisture content of various aluminum soaps is frequently determined by dispersing the soap in benzene, distilling, and measuring the volume of water carried over by the benzene vapor. This macro method was not suitable for our purposes, but a few experiments were made to determine the significance of such results.

Analysis for moisture may determine either water originally present or, in addition, water formed during the analysis. In a mixture of uncombined fatty acid with aluminum di- and mono-soaps, water might be produced by reactions such as



with the production of 1 mole or 0.5 mole of water per gram-atom of aluminum present. Such reactions do not occur under the conditions of benzene distillation, as was shown when samples of pure dilaurate and of monolaurate (3), once their free moisture had been removed by benzene distillation, failed to produce additional water upon addition of excess lauric acid and redistillation. The amounts of additional moisture found were only 0.40 per cent (instead of 4.06 per cent), and 0.45 per cent (instead of 3.46 or 6.92 per cent), respectively, well within the experimental error.

DEHYDRATION AND REACTION OF HYDROXYL GROUPS
CAUSED BY KARL FISCHER REAGENT (6)

Determination of moisture by means of the Karl Fischer reagent yields consistently much higher results for aluminum soap than do other methods. The "moisture content" of two thoroughly dried samples of soap showing none by benzene distillation was kindly determined by the Shell Development Company of Emeryville, California, using the Fischer method.

The first sample was a pure, dry aluminum dilaurate. The Fischer method gave 2.5 ± 0.4 per cent moisture, corresponding to 0.62 ± 0.11 moles of water per mole $\text{Al}(\text{OH})\text{I}_2$. This shows that the Fischer method gives high misleading values, not only with impure commercial mixtures but also with pure disoaps, because it includes products of reaction brought about during the determination.

The second sample was an unextracted aluminum stearate having an ash content of 3.5 per cent, corresponding to the presence of 4.7 moles of stearic acid per gram-atom of aluminum. The "moisture content" of this soap by the Fischer method was 0.75 per cent to a slowly fading end point, and 0.99 per cent to a stable end point after 80 min. The presence of even this small amount of moisture precludes the possibility that the soap was a mixture of tristearate and stearic acid, because such a mixture could give no moisture at all. A distearate could give from 0.6 per cent to 1.2 per cent of moisture by reaction from its hydroxyl group.

SUMMARY

1. The moisture content of aluminum dilaurate, $\text{Al}(\text{OH})\text{I}_2$, is readily determined gravimetrically.
2. A sorption isotherm of water vapor on aluminum dilaurate at 50°C . is reported, showing less than 3 per cent sorbed, and at moderate humidities only 1 per cent.
3. The formation of water by reactions between fatty acids and basic aluminum soaps or from hydroxyl groups does not occur during moisture determination of aluminum soaps by benzene distillation, but it is brought about by the Karl Fischer reagent.

REFERENCES

- (1) MARSDEN, S. S., JR., MYSELS, K. J., SMITH, G. H., AND ROSS, S.: J. Am. Chem. Soc., submitted for publication.
- (2) MCBAIN, J. W., AND BAKER, A. M.: J. Am. Chem. Soc. **48**, 690 (1926).
- (3) MCGEE, C. G.: Private communication.
- (4) MYSELS, K. J., POMEROY, H. H., AND SMITH, G. H.: J. Am. Chem. Soc., submitted for publication.
- (5) SHREVE, G. W.: Ph.D. Dissertation, Stanford University, 1946.
- (6) SMITH, D. M., BRYANT, W. M. D., AND MITCHELL, J.: J. Am. Chem. Soc. **61**, 2407 (1939); this article contains references to earlier work.
- (7) SMITH, G. H., POMEROY, H. H., MCGEE, C. G., AND MYSELS, K. J.: J. Am. Chem. Soc., submitted for publication.

THE LABORATORY PREPARATION OF ALKALI METAL HYDROXIDES BY ELECTROLYSIS

A. F. WINSLOW, H. A. LIEBHAFSKY, AND H. M. SMITH

*Research Laboratory, General Electric Company, Schenectady, New York**Received January 16, 1947*

From time to time chlorides of cesium and rubidium which have long been in this Laboratory must be converted into other salts, such as azides, chromates, or iodides. In the past, the carbonates served as intermediates for such conversions, and the carbonates were prepared either *via* the sulfate (chloride to sulfate to hydroxide to carbonate) or *via* the oxalate (chloride to nitrate to oxalate to carbonate). Both methods are cumbersome and time consuming. The former, moreover, is liable to give a carbonate contaminated with chloride unless a large excess of sulfuric acid is used—probably the formation of acid sulfates interferes with the elimination of hydrogen chloride.

The preparation of the hydroxides by the electrolysis of alkali metal chloride solution in an oscillating mercury cell seemed to offer an attractive way out of these difficulties. In view of the industrial importance of this process, we were surprised to find relatively little detailed information about cells of the Castner-Kellner type. Fetzer (2) electrolyzed sodium hydroxide in such a cell to eliminate the carbonate. A cell resembling his, except that the joints were fused, was accordingly constructed, studied, and finally operated to prepare the hydroxides of cesium and rubidium from their chlorides.

Since electrolysis of the chlorides involves special problems, preliminary work was done on sodium chloride so that the apparatus could be modified where necessary. In its final form, the cell yielded hydroxides of acceptable purity, but two electrolyses were necessary. No attempt was made to exclude carbon dioxide.

EXPERIMENTAL DETAILS

The various parts of the apparatus are shown in figure 1 (more exact specifications are given on G. E. Drawing M-5917537, dated October 12, 1939). The dimensions are not critical. The troughs to seal the compartments are about 8 mm. wide and 4 mm. deep. The apparatus must meet these requirements: (1) Throughout the oscillations, there must be effective sealing by the mercury to prevent the passing of solution from one chamber to another. (2) In order to reduce the oxidation of mercury in the center compartment, there must be provision for shunting the current past the nickel-mesh cathode (see figure 2). (3) Cooling must be adequate (temperature always below 40°C.) to minimize chlorate formation.

Electrolysis of the chloride

The clean glass cell is firmly clamped to the table, which can tilt through 15°, asbestos pads and tape being used at all points of contact to reduce strain.

In order to minimize creeping of the chloride solutions, a heavy layer of stopcock grease is applied to the cell inside and out over bands extending 2 cm. down from the top. The cam is revolved to give maximum tilt; clean mercury is then poured into the lowest compartment until the liquid extends 2.5 cm. beyond

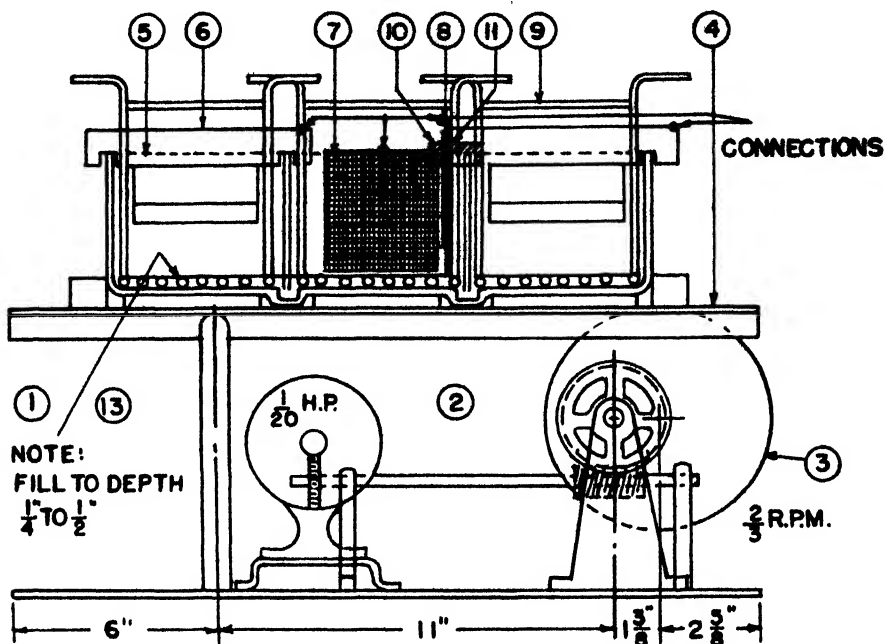


FIG. 1. The apparatus

MATERIALS	PARTS
Mercury (see note)	13 Auxiliary electrode
(see note)	12 Wiring diagram
1 Pyrex 50A3E	11 Insulation tube $\frac{1}{4}$ " x 6"
1 Fibre	10 Bracket
3 Pyrex 50A3E	9 Cooling coil
1 Nickel	8 Cathode by-pass
1 Nickel (18 mesh)	7 Cathode screen
2 Graphite A11A3A	6 Anode
1 Pyrex 50A3E	5 Tank
1 Steel	4 Base— $\frac{1}{4}$ " x 7" x 21" channel
(see note)	3 Cam
	2 Drive
	1 Assembly

the upper seal. Finally, the cell is leveled; the nickel-mesh cathode and the nickel shunt-rod are positioned; water and current connections are made.

The charge of solid chloride is divided, half being placed in each end compartment. With the cell at maximum tilt, distilled water is poured into the upper-

most compartment until one-half of the lower surface of the graphite anode is immersed; the other end compartment is then elevated and treated likewise. (With the anode thus exposed, the escape of chlorine during electrolysis is facilitated; this reduces chlorate formation.) When the center compartment has been filled to about two-thirds its depth with distilled water, the cell is ready to operate. (In a typical run the charge was 2400 g. of cesium chloride; of this, enough remained undissolved to give layers 2 cm. deep on the mercury.)

The motor is now started. The electrolysis circuit is closed with the mesh cathode disconnected and the external resistances adjusted to give 22–25 amp. through the shunt-rod. After about 20 min., the amalgam will be sufficiently concentrated to warrant connecting the mesh cathode so that the electrolytic oxidation of the dissolved alkali metal can begin. In the initial stages of this oxidation the cell is usually quite unstable, owing to the low conductivity of the solution in the center compartment. This instability may be compensated by increasing the proportion of shunted current during this short initial phase, but

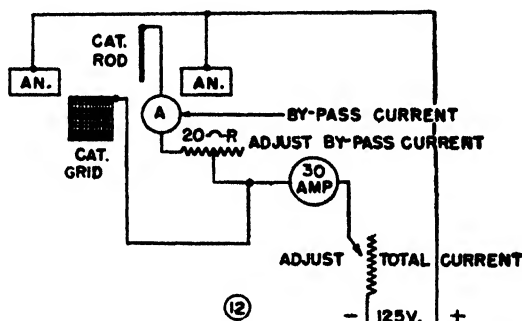


FIG. 2. Provision for shunting the current past the nickel-mesh cathode. For connections, see assembly.

it is better to eliminate it by charging the center compartment with dilute hydroxide solution.

After the initial period, the current is adjusted for stable operation, about one-fifth of the 22–25 amp. being shunted through the nickel rod. Beyond replacing part of the hydroxide solution with distilled water every 8 hr. or so in order to reduce attack of the glass, the apparatus should require little attention until qualitative tests show that virtually no chloride remains in the solutions in the end compartments. At this point the total current is lowered to 10 amp., of which half is shunted. When the appearance of an oxide film on the mercury in the center compartment shows that little dissolved alkali metal remains, 0.7 of this total current is shunted for 10 min.; then all of it for 10 min.; and so on until all the alkali metal has been oxidized, this point being established by shaking samples of mercury from an end compartment with distilled water and phenolphthalein. The cell is then disconnected.

At the end of the run, the solution from the end compartments is usually black with suspended graphite. It contains most of the impurities from the

charge and the chlorate ion (about 4 g. from 2400 g. cesium chloride in a typical case) that has been formed. The center compartment usually seems filled with mercury oxides. The solution and these oxides are sucked out, and the compartment is washed repeatedly with distilled water, the washings being combined with all the hydroxide solutions previously removed.

Electrolysis of the hydroxide

The remaining chloride (in one case, about 1/25 of the charge) is removed by a second electrolysis. After all the mercury oxides have settled out, the crude hydroxide solution is evaporated to a volume that the end compartments can accommodate. For this evaporation, platinum is preferable; nickel (or certain other metals) might do; glass or porcelain introduces risk of contamination. The chief reason for concentrating the solution is to avoid the necessity of withdrawing dilute solutions (from which cesium or rubidium would have to be recovered) during the run.

When hydroxide is being electrolyzed, troublesome "crusts", rich in alkali metal, form on the mercury surface in the end compartments. The tendency to form these crusts, which probably varies inversely with the solubility of the metal in mercury, was much more pronounced with cesium than with sodium. The crusts will not pass into the center compartment, with the result that the mercury there, being soon stripped of dissolved metal, becomes liable to oxidation. Crust formation was reduced by (1) using more mercury to increase turbulence during tilting, (2) stirring the mercury in the end compartments, and (3) decreasing total current and increasing shunted current to reduce oxidation of mercury.

The second electrolysis yields a hydroxide solution, usually near 1 *N*, that is practically free of chloride but contains some carbonate. (Carbonate formation, as Fetzner has shown, can be prevented by covering the cell to protect it from the atmosphere.) As before, suspended mercury oxides must be removed by settling, centrifuging, or filtering. Since the alkaline solution (cesium hydroxide especially) attacks glass, it should be stored in a container of an inert metal or—if permissible—converted to the solid carbonate for storage.

Purity

Considerable purification of the charge ought to result from a double electrolysis. Non-metals should not pass into the mercury. The low concentration of cation impurities militates against the electrodeposition of the corresponding metals even though the standard electrode potentials favor it; moreover, some of these cations tend to be removed as insoluble hydroxides along with the mercury oxides. On the other hand, an increase in sodium content owing to the attack of glass is to be expected.

The results bear out these expectations. Once, with 2400 g. of cesium chloride, the solution from the end compartments contained about 4 g. of calcium ion after the first electrolysis, and a negligible amount after the second. In another case, cesium hydroxide was re-converted to the chloride, which was compared

spectrographically with the starting material. The results follow, those for the starting material being given first: aluminum, present, trace; calcium, low, trace; magnesium, very low, trace; sodium, very low, present; silicon, trace, trace; copper, not found, trace. ("Present" indicates a greater amount than "low".) In every case, the cesium and rubidium salts made from the hydroxides prepared in the cell were pure enough for the applications to which they were put. Had the presence of the sodium derived from glass been objectionable, we should have built the cell of, or lined it with, an alkali-resistant material—perhaps a plastic.

Electrical efficiency

No attempt was made to attain maximum electrical efficiency, which would have entailed operating at low current densities with a minimum of shunted current, lowered the output, and increased the attention required to prevent oxidation. The results in table 1 were obtained in a preliminary investigation. A current of 20 amp. was selected as a reasonable compromise current; additional experiments showed that the shunting of one-fifth of this current during steady operation was satisfactory from the viewpoint of attention required.

TABLE 1
Electrical efficiency in electrolyses of sodium chloride

No.	1	2	3	4	5	6
Total current (amp.)	10	11	20	20	30	30
Time of run (hr.)	4.0	5.7	1.8	5.0	0.5	1.5
Efficiency (per cent)	90	90	80	80	62	67

The lowest electrical efficiency recorded was 20 per cent, which was obtained in an electrolysis of rubidium chloride. Exceptionally large amounts of mercury oxides were formed in this run.

The bottom of one graphite electrode has an area of about 80 sq. cm. The corresponding current density is rather high, a fact which makes good cooling imperative.

Yields

From 2400 g. of cesium chloride, 85 per cent of the theoretical amount of cesium hydroxide, as established by titration with acid, was obtained in the first electrolysis. In the second electrolysis of the same batch, the cesium hydroxide recovered was 98 per cent of that charged. The first percentage is low and the second high, partly because the cesium chloride in the first cesium hydroxide solution was not taken into account.

Shortly after the beginning of the war, cesium chromate was needed in large amount to prepare 16 lb. of phototube pellets for export to Great Britain. The chromate was prepared by reacting cesium hydroxide solution (electrolytically prepared) with cesium dichromate (made by metathesis from the chloride). The over-all yield from 4650 g. of crude cesium chloride was 85 per cent of the

theoretical; the chromate had 99.8 per cent of the theoretical oxidizing power, which was determined iodimetrically by the method of Bray and Miller (1).

Rubidium chromate was prepared from the hydroxide and chromic oxide with an over-all yield of 81 per cent.

SUMMARY

To facilitate the preparation of cesium and rubidium salts from their chlorides, a laboratory-scale oscillating mercury cell has been constructed and operated to make available the pure hydroxides for these preparations. Operating instructions and data are given.

Two electrolyses proved necessary to produce a hydroxide virtually free of chloride, other impurities also being removed to a considerable degree.

Toward the end of an electrolysis, the cell requires close attention if efficient operation is desired. Care is necessary throughout in order to minimize losses whenever expensive materials are being processed.

The chief drawback encountered was a contamination—not serious in the present case—of the hydroxide by sodium ion derived from glass. This contamination could be prevented by building cell and containers of more alkali-resistant materials.

In this work the hydroxides, carbonates, and chromates of cesium and rubidium were prepared, as were also cesium azide and dichromate.

REFERENCES

- (1) BRAY AND MILLER: J. Am. Chem. Soc. **46**, 2204 (1924).
- (2) FETZER: J. Phys. Chem. **32**, 1787 (1928).

HEAT GUARD FOR THE MCBAIN-BAKR SORPTION BALANCE

RENE D. ZENTNER^{1, 2}

Department of Chemistry, Stanford University, California

Received March 11, 1947

Of the numerous techniques presently utilized in the measurement of the weight changes of various materials during sorption, probably the simplest, most reliable, and most accessible is that known as the McBain-Bakr sorption balance (2). By the proper manipulation of this method, isobars, isotherms, and isosteres of various two-component systems may be conveniently, accurately, and reproducibly studied. In general the sorption characteristics of such relatively stable materials as soap (3), textiles, and inorganic materials (1) have been investigated, with respect to both water and liquid hydrocarbons.

¹ Lever Bros. Company Research Assistant to Professor J. W. McBain.

² Present address: Patent Division, Plastics Department, E. I. du Pont de Nemours and Company, Arlington, New Jersey.

The erratic and irreproducible results obtained from studies of dehydrated milk-water and aluminum soap-water systems prompted Dr. Karol J. Mysels of Stanford University to suggest that some factor in the construction of the balance itself was introducing error. It was found that during the sealing and glass-blowing of the balance unit, enough heat was transmitted to affect unstable samples significantly. It was necessary to devise a suitable shield that would guard unstable samples from radiant heat without interfering with the function of the balance itself.

As is known in the literature, the McBain-Bakr sorption balance is customarily employed for investigations and determinations of sorption isotherms for solid-liquid systems. The balance itself consists of five major components: a

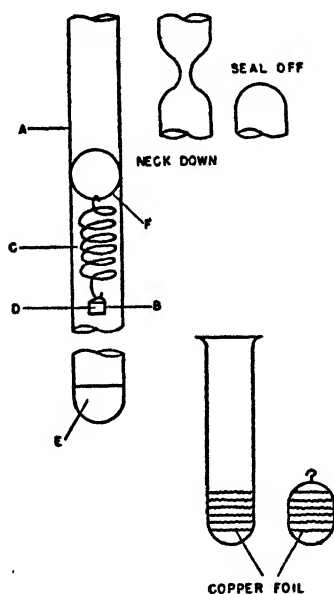


FIG. 1. Heat guard for the McBain-Bakr sorption balance

Pyrex-glass tube (A) sealed at both ends, containing a platinum bucket (B) which contains several milligrams of the sample (D) and is suspended by a helical spring (C) over a reservoir of liquid (E). The entire assembly, evacuated and hermetically sealed, is generally maintained in a two-zone oven (4) provided with suitable windows of such nature that the extension of the spring may be measured at various humidities and temperatures with the aid of a cathetometer and the (sample + sorbed liquid) weight required to produce such extension calculated from Hooke's law.

The last operation in the construction of the balance is that of sealing the top of the balance during evacuation; the neck-down, seal-off, and anneal steps are customarily conducted with an oxyhydrogen torch and at several points the Pyrex glass is worked at white heat. It was discovered that heat radiation

from the heated glass produced changes not only in the weight but also in the appearance of various relatively unstable samples.

The above factors make necessary the use of a protective device that will completely block downward radiation and will be inert, containing no reacting or interfering components. Copper discs sealed within a glass capsule form a satisfactory type of guard. A 6-in. Pyrex test tube whose outside diameter is of such calibre as to fit smoothly inside the 22-mm. Pyrex tube (A) is cleaned and filled to about a half inch in depth with copper discs (cut from copper foil with an old cork-borer). The test tube is "necked down," evacuated to the limits of a Hyvac pump's capacity, and the neck sealed off to yield such a capsule as illustrated. A small glass hook was added to the top of the capsule to facilitate its insertion and removal from the balance.

The capsule is then inserted within the unsealed balance unit to rest on the nichrome wire spring-loop (F); the loop is made with protruding ends to insure its stability within the tube (A).

REFERENCES

- (1) KISTLER, S. S., FISCHER, E. A., AND FREEMAN, I. R.: *J. Am. Chem. Soc.* **65**, 1909 (1943).
- (2) MCBAIN, J. W., AND BAKER, A. M.: *J. Am. Chem. Soc.* **48**, 690 (1926).
- (2) MCBAIN, J. W., AND LEE, W. W.: *Oil & Soap* **20**, 17 (1943); *Ind. Eng. Chem.* **35**, 784 (1943).
- (4) SHREVE, G. W.: Ph.D. thesis, Stanford University, 1946.

ALUMINUM DILAURATE AS ASSOCIATION COLLOID IN BENZENE¹

JAMES W. MCBAIN AND EARL B. WORKING

Department of Chemistry, Stanford University, California

Received March 13, 1947

Ordinary soaps in water are the best known examples of association colloids. In them ions and molecules spontaneously associate to form colloidal particles or micelles, and these micelles are in true reversible equilibrium with the ions and molecules from which they form. It is characteristic of such colloids that the particle weight or apparent molecular weight is a function of concentration and temperature.

The present investigation brings evidence for the existence of an association colloid in a non-aqueous solvent (1): namely, aluminum dilaurate, $\text{Al}(\text{OH})\text{L}_2$, in benzene. This is shown by the change in osmotic pressure with concentration, which contrasts strongly with the behavior of a polymeric colloid, and is confirmed by viscosity measurements.

¹ Study conducted under Contract OEMsr-1057 between Stanford University and the Office of Emergency Management, recommended by Division 11.3 of the National Defense Research Committee and supervised by Professor J. W. McBain.

MATERIALS

The aluminum dilaurate was prepared by precipitation of aluminum trichloride by the addition of 1 mole of potassium laurate (made from Eastman Kodak Company lauric acid) to each mole of aluminum chloride in water at the boiling point, followed by extracting the dried precipitate with acetone dried over Drierite (calcium sulfate). The benzene was Kahlbaum's thiophene free.

THE OSMOTIC PRESSURE OF ALUMINUM DILAURATE IN BENZENE

Direct evidence has been obtained by measuring the osmotic pressure of solutions of aluminum dilaurate in various concentrations in benzene at 20°C. and at 50°C.

The glass osmometers were supplied by the Scientific Apparatus Co., Bloomfield, N. J., as described by R. H. Wagner (4). The cellophane membranes employed for most of the measurements were prepared by soaking cellophane in 62 per cent zinc chloride solution for from 15 to 30 min., washing thoroughly first in dilute hydrochloric acid and then in water, and then transferring through

TABLE 1
Loss of soap from inside to outside of osmometer

MEMBRANE	DURATION OF EXPOSURE	SOAP CON- CENTRATION AT OUTSET	RESIDUE AFTER EVAPORATION	
			Inside	Outside
	<i>weeks</i>	<i>per cent</i>	<i>per cent</i>	<i>per cent</i>
Collodion...	1	1.0	1.0	0.0003
Collodion... ..	2	1.0	1.01	0.0016
Cellophane...	3	0.01	0.0096	0.0005
Cellophane.....	6	1.0	1.01	0.005
Cellophane.....	6	5.0	4.98	0.003

dioxane-water mixtures to pure dioxane, and finally through dioxane-benzene mixtures to pure benzene. Collodion membranes were prepared by swelling the collodion films in benzene-alcohol or benzene-dioxane mixtures and then washing in pure benzene. If they were swollen in alcohol-water mixtures, it was very difficult to transfer them from the water to benzene without destroying the permeability of the collodion.

The membranes have to hold back the aluminum dilaurate while remaining completely porous to benzene. This was tested as follows: At the termination of several of the osmotic-pressure measurements, the solutions were removed from inside and from outside the osmometers and separately evaporated, and the residues were dried and weighed, with the results shown in table 1. Thus it appears that while a distinct trace of soap does pass through either the membrane or the ground joints of the osmometer, or both, the amount is insufficient to affect the osmotic pressure measurably.

The greatest difficulty experienced in the osmotic measurements arose from inaccuracies and failures of the available air thermostat in which the osmometers

were operated. With its large bulb and small bore an osmometer forms a thermometer, and if there is a change in the temperature of the solution in the osmometer, the rise or fall of the column in the stem is much more rapid than can be corrected by the slow diffusion of solvent through the dense membranes used. It should be determined whether membranes of higher permeability could be used to hasten the attainment of equilibrium and still be sufficiently impermeable to the soap.

TABLE 2

Rate of recovery of equilibrium osmotic pressure, 2.4 mm.

Temperature, 20°C.; soap concentration, 0.01 per cent; rise due to capillarity alone, 12.0 mm.

TIME	ZERO LEVEL	COLUMN HEIGHT	APPARENT OSMOTIC PRESSURE
	mm.	mm.	mm.
7:30 A.M.	1.7	16.1	2.4
8:00	1.7	16.1	2.4
8:02	10.3		
8:30	10.3	21.5	-0.8
9:00	10.3	22.6	0.3
9:30	10.3	23.3	1.0
10:00	10.3	23.9	1.6
10:30	10.3	24.4	2.1
11:00	10.3	24.6	2.3
11:30	10.3	24.7	2.4
12:00	10.3	24.7	2.4
1:00 P.M.	10.3	24.7	2.4
1:02	1.7		
1:30	1.7	20.4	6.7
2:00	1.7	19.0	5.3
2:30	1.7	18.0	4.3
3:00	1.7	17.4	3.7
3:30	1.7	16.9	3.2
4:00	1.7	16.4	2.7
4:30	1.7	16.2	2.5
5:00	1.7	16.2	2.5
5:30	1.7	16.1	2.4
6:00	1.7	16.1	2.4

The rate of recovery of equilibrium was tested by adding benzene to the outer cylinder to give a higher zero level, reading at once and from time to time, and then, after equilibrium had apparently been attained, removing benzene to give the original zero level. Meanwhile, special care was exercised to keep the temperature of the thermostat constant. Some results are shown in table 2 for one complete day of operation, the experiment having been in process for several days previously.

Average results of the measurements of osmotic pressure are given in table 3. Because of the difficulties with the thermostat, only those results were included

in the averages where the osmometer had been set up at the desired temperature for at least 2 days, and where neither the temperature nor the osmotic pressure had shown any appreciable change over a period of at least 2 hr. In many instances the pressure readings of freshly made solutions were considerably higher than those given, but the data did not indicate whether this was actually osmotic pressure or merely lack of temperature equilibrium.

To calculate the degree of association of the aluminum dilaurate in benzene, it was assumed that 1 mole (or 442 g.) of $\text{Al}(\text{OH})\text{L}_2$, if present as single separate molecules in 22.4 liters of perfect molecular solution, should give at 0°C . 1 atm. pressure, equal to 10,333 mm. of water or 11,481 mm. of benzene. Then a solution of 1 g. per 100 ml. should give a pressure of $\frac{224 \times 11,481}{442} = 5819$ mm. of

TABLE 3

The osmotic pressures of solutions of aluminum dilaurate in benzene

CONCENTRATION	OSMOTIC PRESSURE OBSERVED AT 20°C .	THEORY FOR SINGLE MOLECULES		OSMOTIC PRESSURE OBSERVED AT 50°C .
		20°C .	50°C .	
<i>g / 100 ml.</i>	<i>mm.</i>	<i>mm.</i>	<i>mm.</i>	<i>mm.</i>
1	10.9	6242	6885	10.1
0.1	2.9	624.2	688.5	
0.01	2.4	62.4	68.9	2.2
0.001	1.0	6.2	6.9	0.6

TABLE 4

Association: molecules of $\text{Al}(\text{OH})\text{L}_2$ per osmotically active particle

Concentration, g. per 100 ml. (per cent).....	1.0	0.1	0.01	0.001
Molecules per particle (at 20°C .)... ..	573	215	26	6
Molecules per particle (at 50°C .)... ..	681		31	10

benzene. Since this is at 0°C ., the pressure at 20°C . should be 6242 mm. and at 50°C . 6885 mm.

The osmotic pressures shown in table 3 correspond to degrees of association as represented in table 4, expressed as the average number of molecules for each osmotically active particle. The smallest observed was six molecules per particle for the most dilute solution at 20°C .

The association particle weights therefore range from 300,000 down to 2600 with change in concentration and temperature. If the density of the aluminum dilaurate in the particle is taken as approximately 1 and the particle is assumed to contain no benzene in its interior, the diameter of a cubical particle of 300,000 particle weight would be about 80 A.

Conclusions from the osmotic data

It must be concluded that aluminum dilaurate in benzene is an association colloid whose association increases rapidly with concentration. The osmotic

pressure divided by the concentration *decreases* very rapidly with concentration. This is in complete contrast the behavior of polymeric colloids; there the osmotic pressure divided by the concentration *increases* with concentration.

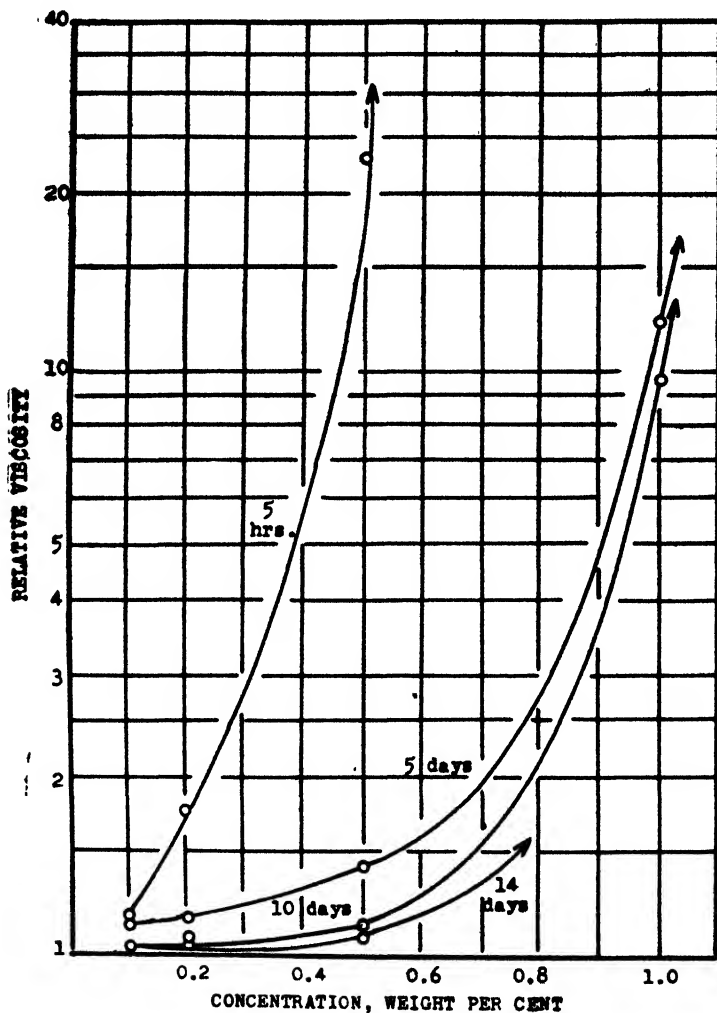


FIG. 1. Variation of the viscosity of benzene solutions of Al(OH)I_2 relative to the viscosity of benzene with changes in concentration and time.

THE VISCOSITY OF BENZENE SOLUTIONS OF ALUMINUM DILAURATE

The viscosity of dilute solutions was measured with Ostwald viscometers at 20°C. and at 40°C. Some of the results, expressed as relative viscosity, η_r —that is, the viscosity of the solution divided by that of pure benzene at the same temperature—are shown graphically in figures 1 and 2. The viscosity of a 1 per cent solution at room temperature when freshly made can be so high as to

be that of a jelly but it decreases with time, as shown in figure 1, and it decreases very rapidly indeed on dilution.

The most striking result obtained is that the viscosity *increases* with temperature, as is seen in figure 2. Thus the relative viscosity of a 1 per cent solution at

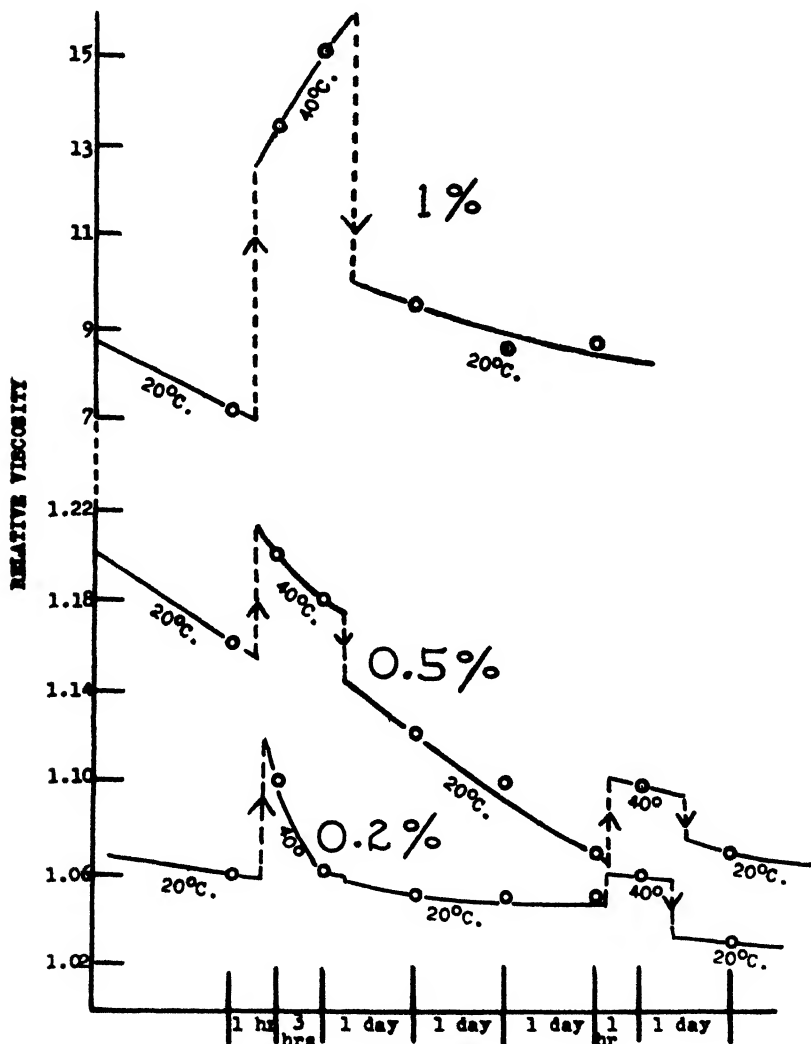


FIG. 2. Variation of relative viscosity of Al(OH)L_3 in benzene with time and change of temperature as indicated by broken lines.

20°C . is doubled by warming to 40°C . Not only does the relative viscosity increase in all cases but even the absolute viscosity increases for the 1 per cent solution. Similar behavior was previously recorded for two well-known systems, nitrocellulose in ethyl alcohol and methyl cellulose in water.

The aging process (decrease in viscosity) is hastened by rise of temperature, as

is apparent in figure 2, but the 1 per cent solution is an exception in that the enhanced viscosity actually increases at the higher temperature.

Conclusions from the viscosity measurements

It is clear that we are here dealing with a structural viscosity (3). This is of the nature of a loose aggregation of the colloidal particles to form a ramifying brush-heap structure which effectively immobilizes much of the free solvent. It may be recalled that Einstein showed that for a given volume, v , of particles in a unit volume of a sol, the relative viscosity $\eta_r = 1 + 2.5v$. Thus for 1 volume per cent solution, the relative viscosity should be 1.025 independent of the degree of dispersion or particle size. Here the relative viscosity is enormously greater and must be recognized as a structural viscosity.

It was shown by Laing and McBain (2) that for sodium oleate and water the actual colloidal particles in a sol and a jelly of the same concentration and temperature are identical and differ only in the degree of their loose ramifying aggregation and resultant structural viscosity. The viscosity behavior of aluminum dilaurate as association colloid may be contrasted with that of polymeric colloids whose polymer size and resultant viscosity are nearly independent of temperature, whereas here the viscosity increases markedly with temperature. In both cases, the specific viscosity, $\eta_r - 1$, divided by concentration, increases with concentration, and it seems inevitable that association must also occur in polymer solutions of finite concentration.

SUMMARY

Aluminum dilaurate, $\text{Al}(\text{OH})\text{L}_2$, is an association colloid in benzene, as shown by osmotic-pressure measurements indicating rapid association with increasing concentration, and by viscosity measurements which show an increase of relative viscosity with increase of temperature, as well as a great dependence of structural viscosity upon concentration and time.

REFERENCES

- (1) GONICK, E.: *J. Colloid Sci.* **1**, 393 (1946).
- (2) LAING, M. E., AND MCBAIN, J. W.: *Trans. Chem. Soc. (London)* **117**, 1507 (1920); *Nature* **125**, 125 (1930).
- (3) MCBAIN, J. W.: *J. Phys. Chem.* **30**, 239 (1926).
- (4) WAGNER, R. H.: *Ind. Eng. Chem., Anal. Ed.* **16**, 520 (1944).

A VAPOR-PHASE SORPTION STUDY OF IODINE AND ACTIVE MAGNESIUM OXIDE UTILIZING THE MCBAIN-BAKR SORPTION BALANCE

R. C. DUNN AND H. H. POMEROY

Department of Chemistry, Stanford University, California

Received March 19, 1947

The sorption of iodine from the vapor phase on magnesium oxide has been explored by very few investigators to date. Guichard (2), as well as Beutel and Kutzetnigg (1), observed the adsorption of iodine from the vapor phase by magnesium oxide but only in a qualitative study. This present work was carried out to examine the quantitative aspects of this problem.

In industry, the activity of magnesium oxide is measured by determining the "iodine number," and by sorption of iodine from carbon tetrachloride solution. The empirical values are relative and depend on the particular iodine number procedure used. Therefore, it is evident that the iodine number alone should not be taken as indicating a definite surface area without standardizing it against other more reliable methods, such as low-temperature nitrogen adsorption (6).

It should be pointed out that the process of taking up iodine from various solutions must be subject to the competition of the respective solvents and any other substances present, and the results could be very different where only iodine and magnesium oxide are involved. The competitive effect of various solvents has been demonstrated in making separations by chromatographic methods, employing magnesium oxide (5).

Sorption of iodine from the vapor phase at room temperature, utilizing the McBain-Bakr sorption balance as here employed, presents a method of determining surface areas unhindered by competitive effects, and is much less complicated than low-temperature nitrogen adsorption. It yields the same quantitative results.

MATERIALS

The iodine used was Merck c.p. resublimed. The magnesium oxide (light-burned) was obtained from the Permanente Metals Corporation (ignition loss, 11.1 per cent).

EXPERIMENTAL TECHNIQUE

The apparatus used for this study was the McBain-Bakr sorption balance (3). It consisted of a vertically placed sealed tube, made of Pyrex glass 18 mm. x 100 cm., in which toward the upper end was placed a quartz spring that suspended a platinum bucket containing the sample, and in the lower end was the sorbate. Iodine crystals were placed in a small evacuated tube, which was sealed off. This sealed-off sorbate capsule, along with a magnetic hammer (used for breaking the capsule), were introduced into the bottom of the tube

before the spring and bucket containing the magnesium oxide sample were suspended in the top. The sorption tube was then evacuated to a pressure of 0.0–0.1 mm. and sealed off. The sorption balance unit was placed in a thermostat, the upper two-thirds being held at about 82°C. in an air bath and the lower one-third at room temperature in an oil bath. The initial reading of the sample weight was checked, using a reading microscope, and the iodine capsule was

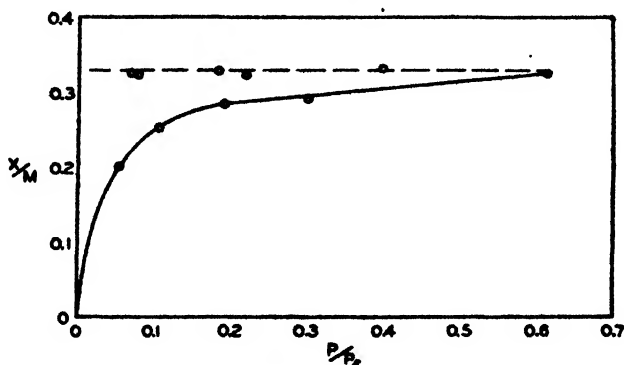


FIG. 1. Sorption of iodine by magnesium oxide. $T = 82^\circ\text{C}$.

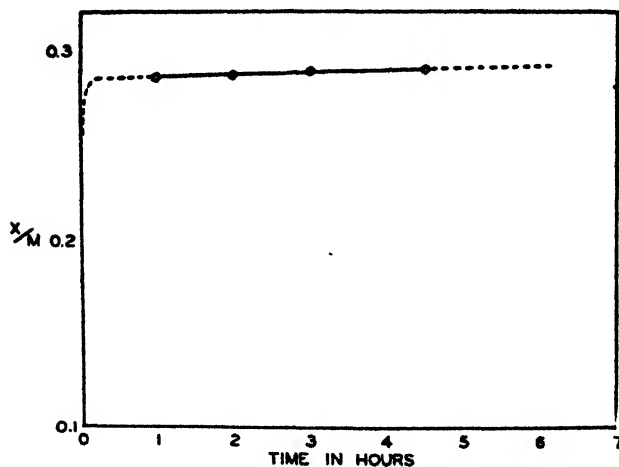


FIG. 2. Rate of sorption. $T = 82^\circ\text{C}$.

then broken by using the hammer. A series of readings were then taken by noting the spring elongation with the reading microscope while holding the air bath at a nearly constant temperature and varying the oil bath over a series of temperatures up to about 82°C.

RESULTS

The results are given in tables 1 and 2. Figure 1 shows the sorption isotherm, while figure 2 shows the rate of sorption. The values for x/m are calculated as milligrams of iodine sorbed per milligram of magnesium oxide.

If the flat portion of the isotherm is interpreted as indicating a monomolecular layer, we would then have approximately 0.33 g. of iodine forming a layer over 1.0 g. of magnesium oxide. Converting this into an apparent surface area based on a value of 1.56×10^{-16} sq. cm. per iodine molecule (4), we would obtain a value of 122 sq. m. per gram.

The surface area of this same sample as determined by low-temperature nitrogen adsorption was found to be 126 ± 10 sq. m. per gram.¹ The sample was outgassed at 250°C. to about 10^{-6} mm. of mercury. Its porosity was found to be 0.43, cc. per gram.

TABLE 1
Sorption of iodine by magnesium oxide at 82°C.

P/P_0	x/m	P/P_0	x/m
0.0555	0.200	0.395 (desorption)	0.334
0.1070	0.254	0.217 (desorption)	0.322
0.193	0.288	0.181 (desorption)	0.334
0.300	0.290	0.155 (desorption)	0.333
0.610	0.327	0.0775 (desorption)	0.327
		0.0671 (desorption)	0.328

TABLE 2
Rate of sorption of iodine by magnesium oxide at 82°C.

TIME	x/m
hours	
1	0.286
2	0.287
3	0.288
4.5	0.289

CONCLUSIONS

1. Sorption of iodine vapor by magnesium oxide is rapid, a maximum value being reached after several hours.
2. The iodine is sorbed irreversibly, possibly indicating chemisorption as the mechanism.
3. Sorption from the vapor phase is a more direct and definitive method than sorption from various solutions and an easier method than low-temperature nitrogen adsorption.

REFERENCES

- (1) BEUTEL AND KUTZETNIGG: *Monatsh.* **63**, 99-116 (1933).
- (2) GUICHARD: *Bull. soc. chim.* [4] **7**, 1017 (1910).

¹ This value was specially determined by Dr. E. E. Roper of the Shell Development Company, Emeryville, California, to check our findings, and to them we wish to express our thanks.

- (3) MCBAIN AND BAKER: *J. Am. Chem. Soc.* **48**, 690 (1926).
- (4) REYERSON AND WISHART: *J. Phys. Chem.* **42**, 683 (1938).
- (5) STRAIN: *Chromatographic Adsorption Analyses*. Interscience Publishers, Inc., New York (1942).
- (6) ZETTMELMOYER AND WALKER: *Ind. Eng. Chem.* **39**, 69 (1947).

TOLERANCE CONCENTRATIONS OF RADIOACTIVE SUBSTANCES

KARL Z. MORGAN

Health Physics Department, Clinton Laboratories, Knoxville, Tennessee

Received April 9, 1947

This paper is a summary of a report scheduled to appear in one of the Health Physics volumes of the Plutonium Project Record, which is expected to be published in the near future. It is to serve as a review of some of the elementary equations and procedures involved in determining tolerance concentrations of radioactive substances when taken into the human system. The expression "tolerance concentration" as used in this report refers to what is sometimes preferably called the "maximum permissible concentration."

I. METHODS OF RADIOACTIVE INTAKE AND ELIMINATION

There are three principal ways in which a radioactive substance may enter the human system: ingestion, inhalation, and incision (or puncture). Part of this radioactive substance remains in the body, where it is subject to various means of distribution by the blood stream; the remainder is eliminated in the exhaled air, in expectoration, in perspiration, in the feces, or in the urine. Some of the radioactivity in the human system is reduced considerably by natural radioactive decay.

II. BACKGROUND RADIATION

All living organisms are subjected at all times to radiation from a certain amount of radioactivity and to other forms of penetrating radiation. The cosmic ray ionizations, which vary considerably with elevation and latitude, may amount to a few thousandths of a milliroentgen per hour (mr./hr.). The natural radioactivity varies considerably from place to place and from time to time. In the air it is caused primarily by radon and thoron and their ABC chain products. Radon concentration in the air over land ranges from $\sim 10^{-16}$ to 10^{-17} curie/cc. of air, and thoron ranges from $\sim 10^{-17}$ to 10^{-19} curie/cc. of air. The background radiation, including cosmic radiation and radiation from the air and ground contamination, usually subjects man continually to a normal radiation of a few hundredths of a milliroentgen per hour. There is some evidence that these low levels of radiation produce certain biological changes in small organisms, but there is no reason to believe that they are harmful to man.

III. TOLERANCE LIMITS OF RADIATION

The problem of determining just how much radiation is harmful to man is rather difficult, because of limited experimental data. Experiments in general seem to indicate that the rate at which radiation is received does not influence the effect of the total daily tolerance dose (i.e., the effect of a dose of 4.17 mr./hr. for 24 hr. is the same as a dose of 400 mr./hr. for 15 min.). However, there are some experimental results which indicate that the rate at which radiation is received does affect the daily tolerance dose under certain conditions. A dose of 36.5 roentgens taken in one day each year, or even 3 roentgens taken in one day each month, is less desirable than limiting one's exposure to a 100-mr. dose each day. The kind of radiation is an important factor, since it determines the ion distribution in tissue. The tolerance dose limits for a 24-hr. exposure as set by Clinton Laboratories and adopted by most of the laboratories associated with the Manhattan Project are 100 mr. for x- and γ -radiation, 100 mrep.¹ for β -radiation, 10 mrep. for α -radiation, 20 mrep. for fast neutrons and protons, and probably about 50 mrep. for thermal neutrons. These are the levels of radiation that are considered to produce no known harmful effects to man when exposed to these levels indefinitely. The factor of safety is probably not more than two or three. There is no factor of safety to give added protection to a person (about one in a thousand) who is supersensitive to radiation. Levels of radiation considerably below the above tolerance values do produce genetic changes in many organisms and some such changes may eventually be observed in human offspring. For these reasons, persons should strive to keep radiation exposure to a minimum and think of "maximum allowable" rather than "tolerance" amounts of radiation.

IV. GENERAL PROCEDURES AND ASSUMPTIONS IN THE SOLUTION OF RADIATION PROBLEMS

The problem of determining the radiation produced by a fixed amount of long-lived radioactive material in a given organ of the body is a relatively simple physical problem, once the distribution of the activity in the organ is observed. The tolerance intake to the human body may be accomplished by any combination of the three methods of intake listed above, and may be by a single dose or by continuous intake. Large doses of external radiation may reduce the tolerance intake dose, or γ -radiation from one organ may reduce the tolerance dose to another organ. Tolerance concentration is difficult to determine because the absorption, distribution, and elimination factors for the human body are not too well known at present. In the following discussion of the effect of radioactive materials in the human body, it is assumed that the only harmful biological effects of radiation are produced by the resulting ionization or that the harmful results are proportional to the amount and distribution of ionization. Future biological experiments may indicate that hydrogen recoil atoms (without ionization) and molecular energy exchanges should be given consideration.

¹ mrep., or milliroentgen equivalent physical, is the amount of radiation that may be absorbed in tissue to the extent of 0.083 erg per gram.

In the case of long-lived radioactive materials deposited in moderate amounts in the organs of the body, it is assumed that it is the prolonged insult of the radiation that produced the main damage, rather than the initial radiation from the primary distribution in the body organs. The body organ is assumed to rid itself of a given radioactive isotope according to a simple exponential function, that is, $dCt/dt = -\lambda Ct$. This simplification gives satisfactory results in most cases, provided one can determine the effective value of the elimination constant. Perhaps more accurate results could be obtained in some cases if one assumed that

$$Ct = C_1 e^{-\lambda_1 t} + C_2 e^{-\lambda_2 t} + \dots$$

in which $C_0 = C_1 + C_2 + \dots$. However, in this report only the simple case is considered in which λ is the sum of the physical and biological decay constants.

For the benefit of those who might wish to make some tolerance determinations for various radioactive elements, a few simple calculations are indicated in this report. Perhaps this method of calculation is partially justified, in that it gives results consistent with experimental observations when applied to radium.

V. NOMENCLATURE

C = microcuries of radioactive element originally in a given organ,

G = micrograms of radioactive element originally in the organ,

Q = microcuries per cubic centimeter,

B = total weight of body in pounds,

f = fraction the organ is of the total body weight = $\frac{\text{weight of organ}}{B}$,

(JB454) = mass of organ in grams,

ρ = ratio of electron volts per ion-pair for the type of radiation used divided by 32,

E = average energy of radiation in Mev.,

R = roentgens (= rep. when applied to α - or β -radiation),

$R = \frac{\text{dis.}}{\mu\text{c. sec.}} \times \frac{\mu\text{c}}{\text{g.}} \times \frac{E}{\text{dis.}} \times \frac{\text{ion-pair}}{E} \times \frac{\text{e.s.u.}}{\text{ion-pair}} \times \text{sec.} \times 0.001293,$

Z = roentgens per day,

P = rate of concentration in μ curies per second,

λ = decay constant.

(If the element in the organ of the body is eliminated exponentially, we may consider $\lambda = \lambda_r + \lambda_e$, in which λ_r = radioactive decay constant and λ_e = body elimination constant.)

T = half-life of radioactive element in seconds,

T_y = half-life of radioactive element in years.

If the element is eliminated exponentially such that the body elimination half-life is T_e and the radioactive half-life is T_r , then

$$\lambda = 0.693 \frac{T_e + T_r}{T_e T_r} \text{ or } T = \frac{T_e T_r}{T_e + T_r}, \quad (1)$$

τ = conversion factor from μ curies to μ grams (= grams per curie),

$$\tau = \frac{\text{at. wt.} \times 3.7 \times 10^{10}}{\text{Avogadro's No.} \times \lambda} = 8.8 \times 10^{-14} \times \text{at. wt.} \times T, \quad (2)$$

In this equation T_r = radioactive half-life in seconds. The curie is herein defined as that amount of material that undergoes 3.7×10^{10} disintegrations per second.

VI. LONG-LIVED RADIOACTIVE ELEMENTS IN THE BODY

The problem is to find the amount, C , of a long-lived radioactive material fixed in an organ of the body, that will produce a specified radiation exposure rate, Z , to that organ of the body. This problem also includes the special case of a short-lived radioactive element in which the rate of fixation of new activity in the organ is equal to the rate of decay or any case in which t/T is very small.

$$Z = \frac{62CE}{(fB454)_\rho} = \frac{0.136CE}{fB_\rho} \text{ roentgens per day} \quad (3)$$

$$C = \frac{Z(fB454)}{62E} \rho = \frac{7.33ZfB}{E} \rho \text{ } \mu\text{curies in organ} \quad (4)$$

$$G = \tau C \text{ } \mu\text{g. in organ} \quad (5)$$

VII. SHORT-LIVED RADIOACTIVE ELEMENTS IN THE BODY

The problem is to find the initial amount, C , of a short-lived radioactive material fixed in an organ of the body that will produce a specified radiation exposure R , in that organ of the body in a given time, t . The initial amount is not maintained by any additional concentration during time t .

$$C = \frac{R(fB454)\lambda\rho 10^4}{7.18E(1 - e^{-\lambda t})} = 6.33 \frac{RfB\lambda\rho 10^5}{E(1 - e^{-\lambda t})} \text{ } \mu\text{curies} \quad (6)$$

$$\text{and since } \lambda = 0.693/T, \quad (7)$$

$$C = 4.38 \frac{RfB\rho 10^5}{TE(1 - e^{-0.693t/T})} \text{ } \mu\text{curies originally in the organ required to produce an exposure } R \text{ in time } t \quad (8)$$

If we set $R = 36.5$ r. of γ -radiation for a time, t , = 365 days, the average exposure may be considered as a tolerance exposure for the year. However, the initial exposure rate is > 0.1 r. per day, and the exposure at the end of the year is < 0.1 (see figure 3A). The exposure rate any time may be found from the initial conditions of this problem or by differentiating equation 8. If this is done, we get

$$Z = \frac{0.136CEe^{-0.693t/T}}{fB_\rho}, \text{ roentgens per day} \quad (9)$$

The time, t , at which Z reduces to tolerance for γ -radiation or 0.1 r. per day and tolerance for α -radiation or 0.01 r. per day is:

$$\begin{array}{ccc} t = 3.32 T \log_{10} \frac{(1.36CE)}{fB_\rho} & \text{and} & t = 3.32 T \log_{10} \frac{(13.6CE)}{fB_\rho} \\ \text{for} & & \text{for} \\ Z = 0.1 \text{ r. per day} & & Z = 0.01 \text{ r. per day} \end{array} \quad (10)$$

The fraction reduction in radiation rate at any time, t , is given by the equation

$$F = e^{-0.693t/T} = 2^{-t/T} \quad (11)$$

VIII. RADIOACTIVE ELEMENT FIXED IN THE BODY AT A CONSTANT RATE

The problem is to find the constant rate of concentration, P , of a radioactive substance in μ curies per second with a half-life, T , which is being fixed in an organ of the body that will have produced a specified radiation exposure, R , in time t . Assume that the radioactive concentration is zero, when $t = 0$. In this case

$$P = 4.38 \frac{RfB\rho 10^5}{TE \left(t + \frac{T}{0.693} e^{-0.693t/T} - \frac{T}{0.693} \right)} \quad \mu\text{curies fixed in organ per second} \quad (12)$$

The daily exposure rate at any time, t , may be found, as in the case of equation 9, and becomes

$$Z = \frac{0.197PET}{fB\rho} (1 - e^{-0.693t/T}) \quad \text{roentgens per day} \quad (13)$$

$$P = \frac{Z(1.61 \times 10^{-7})fB\rho}{ET_v(1 - e^{-0.693t_v/T_v})} \quad \mu\text{curies fixed in organ per second} \quad (14)$$

required to produce a daily exposure, Z , after time t . (Equations 12, 13, and 14 are illustrated in figure 3B)

In this case Z is zero when $t = 0$ and when $t \rightarrow \infty$,

$$Z = \frac{0.197PET}{fB\rho} \quad \text{roentgens per day} \quad (15)$$

The time, t , at which Z increases to 0.1 r. per day and 0.01 r. per day is

$$t = 3.32T \log_{10} \left(\frac{1.97PET}{1.97PET - fB\rho} \right) \quad \text{for} \quad (16)$$

$$Z = 0.1 \text{ r. per day}$$

and

$$t = 3.32T \log_{10} \left(\frac{19.7PET}{19.7PET - fB\rho} \right) \quad \text{for} \quad (16)$$

$$Z = 0.01 \text{ r. per day}$$

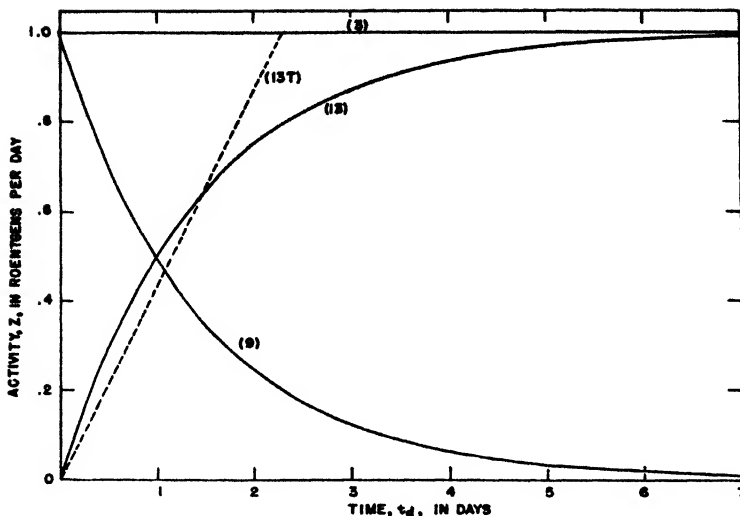


FIG. 1. This figure shows the relationship between the four types of body exposure as follows:

Curve 3 is a plot of equation 3:

$$Z = \frac{0.136CE}{fB\rho}$$

The total exposure or area under this curve is given by equation 3a:

$$R = \frac{0.136CEt_d}{fB\rho}$$

Curve 9 is a plot of equation 9:

$$Z = \frac{0.136CE}{fB\rho} e^{-0.693t_d/T_d}$$

The total exposure is given by equation 9a:

$$R = \frac{0.196CET_d}{fB\rho} (1 - e^{-0.693t_d/T_d})$$

Curve 13 is a plot of equation 13:

$$Z = \frac{0.136PET}{0.693fB\rho} (1 - e^{-0.693t_d/T_d})$$

The total exposure is given by equation 13a:

$$R = \frac{1.7 \times 10^4 PET_d}{fB\rho} \left(t_d + \frac{T_d}{0.693} e^{-0.693t_d/T_d} - \frac{T_d}{0.693} \right)$$

In this example PT is set equal to $0.693C$, so that the sum of equations 13a and 9a is equal to equation 3a.

Curve 13T is a plot of the equation:

$$Z = \frac{0.136 \times 8.64 \times 10^4 PET_d}{fB\rho}$$

This equation is obtained from equation 13 in the limit as $T \rightarrow \infty$. The total exposure is given by equation 13Ta:

$$R = \frac{5.9 \times 10^3 PET_d^2}{fB\rho}$$

It can be shown from equation 13Ta that if $P = C_i/t = C_i/(8.64 \times 10^4 t_d)$ and $C_i = 2C$, the exposure is the same as indicated by equation 3a.

If t is taken as five (or more) times T , we introduce < 1 per cent error by writing equation 12 as

$$P = 4.38 \frac{RfB\rho 10^5}{TE \left(t - \frac{T}{0.693} \right)} \quad \text{or} \quad P = 4.38 \frac{dR/dt fB\rho 10^5}{TE} \quad (17)$$

If t is very large compared to T , then equation 17 may be written

$$Pt = 4.38 \frac{RfB\rho 10^5}{TE} \quad (18)$$

IX. CHAIN PRODUCTS IN THE BODY WHEN THE BODY ELIMINATION DECAY CONSTANT λ_{r_2} IS SMALL COMPARED TO THE RADIATION DECAY CONSTANT λ_{r_2} (i.e., $\lambda_2 \neq \lambda_{r_2}$ AND $T_2 \neq T_{r_2}$)

Let us suppose that an organ of the body has fixed in it C_1^0 μ curies of a parent substance at time $t = 0$ with a decay constant λ_1 , which in turn produces a daughter with a decay constant λ_2 . Then the amount of the parent in curies at time t is $C_1 = C_1^0 e^{-\lambda_1 t}$. The amount in μ curies at time, t , of the daughter is

$$C_2 = \frac{\lambda_2 C_1^0}{\lambda_2 - \lambda_1} (e^{-\lambda_1 t} - e^{-\lambda_2 t}) \quad (19)$$

$$C_1^0 = \frac{6.33 RfB\rho 10^5}{\frac{T_1 E_1}{0.693} (1 - e^{-0.693t/T_1}) + \frac{T_1 E_2}{0.693(T_1 - T_2)} (T_1 - T_1 e^{-0.693t/T_1} - T_2 + T_2 e^{-0.693t/T_2})} \quad (20)$$

in which C_1^0 = curies of parent substance originally in body organ required to produce a radiation exposure, R , in time t . When the time, t , is large compared to T_1 and T_2 ($t > 7T_1$ and $t > 7T_2$), we may simplify equation 20 and write

$$C_1^0 = 4.38 \frac{RfB\rho 10^5}{E_1 T_1 + E_2 T_2} \quad (21)$$

The exposure dose per day may be found by differentiating equation 20:

$$Z = \underbrace{\frac{0.136 C_1^0}{fB\rho} \left[E_1 e^{-0.693t/T_1} \right]}_{\text{r. per day from parent}} + \underbrace{\frac{T_1 E_2}{T_1 - T_2} e^{-0.693t/T_1} - \frac{T_1 E_2}{T_1 - T_2} e^{-0.693t/T_2}}_{\text{r. per day from daughter}} \quad (22)$$

This equation is illustrated by figure 4.

The time when Z is a maximum is found by placing $d^2R/dt^2 = 0$. Then,

$$t_m = \frac{3.32 T_1 T_2}{(T_1 - T_2)} \log_{10} \left(\frac{T_1^2 E_2}{E_1 T_1 T_2 - E_1 T_2^2 + E_2 T_1 T_2} \right) \quad (23)$$

This is the time when there is a maximum energy dissipation rate from the parent plus the daughter.

When $E_1 = E_2$, the above equation becomes:

$$t_m = \frac{3.32 T_1 T_2}{T_1 - T_2} \log_{10} \frac{T_1^2}{2 T_1 T_2 - T_2^2} \quad (24)$$

This is the time when there is a maximum number of disintegrations from the parent plus the daughter.

The time when the energy dissipation rate from the daughter is a maximum is:

$$t_{m_2} = 3.32 \frac{T_1 T_2}{T_1 - T_2} \log_{10} \frac{T_1}{T_2} \quad (25)$$

The time when the radiation rate of the daughter becomes equal to the radiation of the parent is:

$$t_e = 3.32 \frac{T_1 T_2}{T_1 - T_2} \log_{10} \left(\frac{T_1 E_2}{E_1 T_2 - E_1 T_1 + E_2 T_1} \right) \quad (26)$$

The time when the number of disintegrations from the daughter becomes equal to the number of disintegrations from the parent is found by placing $E_1 = E_2$ in the above equation, and

$$t_e' = 3.32 \frac{T_1 T_2}{T_1 - T_2} \log_{10} \frac{T_1}{T_2} \quad (27)$$

But this is the same as found in equation 25 above and indicates that the number of disintegrations of the daughter is equal to the number of disintegrations of the parent when the disintegration rate of the daughter is a maximum. In other words, the two disintegration rate curves intersect at the maximum of the daughter curve (see figure 2).

The maximum radiation rate of the daughter is

$$Z = \frac{0.136 C_1^0 T_1 E_2}{f B \rho (T_1 - T_2)} \left[e^{-\frac{2.3 T_2}{T_1 - T_2} \log_{10} \frac{T_1}{T_2}} - e^{-\frac{2.3 T_1}{T_1 - T_2} \log_{10} \frac{T_1}{T_2}} \right] \quad (28)$$

The time when the slope of the daughter radiation rate curve becomes equal to the slope of the parent radiation rate curve is:

$$t_s = 3.32 \frac{T_1 T_2}{T_1 - T_2} \left[\log_{10} \frac{T_1}{T_2} + \log_{10} \frac{T_1 E_2}{E_1 T_2 - E_1 T_1 + E_2 T_1} \right] \quad (29)$$

or

$$t_s = t_{m_2} + t_e \quad (30)$$

This equation indicates that the daughter and parent radiation rate curves are parallel at a time equal to the sum of $t_{m_2} + t_e$.

If $E_1 = E_2$

$$t_s = 3.32 \frac{T_1 T_2}{T_1 - T_2} \times 2 \log_{10} \frac{T_1}{T_2} = 2 t_{m_2} \quad (31)$$

In other words, equations 29 and 31 express the time required to reach a transient equilibrium between the daughter and the parent, i.e., the time when the parent and daughter radiation rates are changing at the same rate. Equation 29 is for energy equilibrium, and equation 31 is for particle number equilibrium.

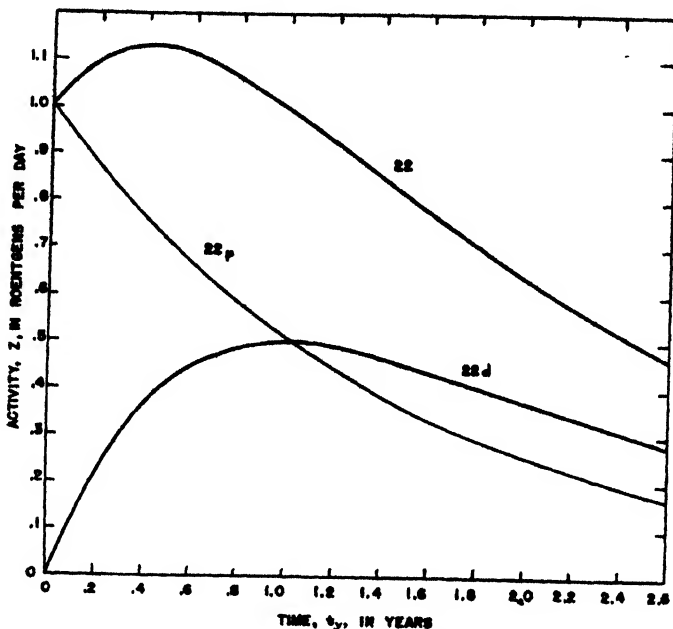


FIG. 2. This figure illustrates the preceding equations. In this example we have let

$$\frac{0.136C_1^0}{fB\rho} = 1, \quad E_1 = E_2 = 1, \quad T_1 = 1 \text{ yr.}, \quad \text{and} \quad T_2 = 1/2 \text{ yr.}$$

Curve 22 is a plot of equation 22 and indicates the variation of Z from the parent plus the daughter during $2\frac{1}{2}$ yr.

Curves 22p and 22d indicate the variation of parent and daughter activity, respectively, during the $2\frac{1}{2}$ yr.

The point of intersection and the maximum of the daughter curve are obtained from either equation 25 or equation 27.

Curves 22p and 22d are parallel at time equals 2 yr. This point is found from equation 31. The ratio of the daughter activity to the parent activity is 1.5 at this time, as given by equation 32.

At transient equilibrium the ratio of the daughter activity to the parent activity is given by the equation:

$$A = \frac{T_1 + T_2}{T_1} \quad (32)$$

It is obvious that initially the parent gives off more particles per second but after the daughter maximum, the daughter gives off more particles per second; this is illustrated in figure 2. In the limit, parent and daughter give off the

same number of particles, but the one with the greater energy per disintegration suffers the greater energy dissipation. A comparative study of graphs 2 and 4 illustrates the difference in behavior of the particle disintegration rate curves and the energy dissipation rate curves.

X. CHAIN PRODUCTS IN THE BODY WHEN THERE MAY BE CONSIDERABLE
BODY ELIMINATION OF THE DAUGHTER SUBSTANCE DURING ITS
RADIOACTIVE HALF-LIFE (i.e., $\lambda_{r_2} \neq \lambda_2$ or $T_{r_2} \neq T_2$)

This is the more general case, and therefore is merely a refinement of the preceding problem. For comparison, several of the preceding equations are repeated in the more general form with similar equation numbers.

In this case the amount in curies of the parent is still

$$C_1 = C_1^0 e^{-\lambda_1 t}$$

but the amount of the daughter becomes

$$C_2 = \frac{\lambda_{r_2} C_1^0}{\lambda_2 - \lambda_1} (e^{-\lambda_1 t} - e^{-\lambda_2 t}) \quad (19.1)$$

Equation 20 becomes

$$C_1^0 = \frac{6.33 R_f B_p 10^5}{\frac{T_1 E_1}{0.693} (1 - e^{-0.693 t / T_1}) + \frac{T_1 T_2 E_2}{T_{r_2} (T_1 - T_2) 0.693} (T_1 - T_1 e^{-0.693 t / T_1} - T_2 + T_2 e^{-0.693 t / T_2})} \quad (20.1)$$

It is to be noted that equation 20.1 is the same as equation 20 except that E_2 is replaced by $E_2 T_2 / T_{r_2}$. Therefore equations 21.1, 22.1, 23.1, 26.1, 28.1, and 29.1 can be obtained immediately by replacing E_2 by $E_2 T_2 / T_{r_2}$ in the corresponding equations 21, 22, 23, 26, 28, and 29. Equations 25.1, 27.1, 30.1, and 31.1 are the same as equations 25, 27, 30, and 31, respectively. Equation 24.1 becomes

$$t_m = \frac{3.32 T_1 T_2}{(T_1 - T_2)} \log_{10} \left(\frac{T_1^2}{T_1 T_{r_2} + T_1 T_2 - T_2 T_{r_2}} \right) \quad (24.1)$$

XI. RADIOACTIVE PARENT FIXED IN THE BODY AT A CONSTANT RATE.
THE PARENT DECAYS INTO A DAUGHTER

This example is similar to cases IX and X except that the radioactive parent is at zero concentration in the body at time $t = 0$, and it is built up in the body at a constant rate of concentration, P . In this case,

$$P = \frac{4.38 R_f B_p 10^5}{T_1 E_1 \left(t + \frac{T_1}{0.693} e^{-0.693 t / T_1} - \frac{T_1}{0.693} \right) + \frac{T_1^2 T_2 E_2}{T_{r_2} (T_1 - T_2)} \cdot \left(\frac{t(T_1 - T_2)}{T_1} - \frac{T_1(1 - e^{-0.693 t / T_1})}{0.693} + \frac{T_2^2(1 - e^{-0.693 t / T_2})}{0.693 T_1} \right)} \quad (33)$$

μ curies fixed in body organ per second that will produce a total exposure, R , in time t .

In terms of daily exposure rate,

$$Z = \frac{0.197PT_1}{fB\rho} \left[\underbrace{E_1(1 - e^{-0.693t/T_1})}_{\text{parent}} + \underbrace{\frac{T_1 T_2 E_2}{T_{r_2}(T_1 - T_2)} \left(\frac{T_1 - T_2}{T_1} - e^{-0.693t/T_1} + \frac{T_2}{T_1} e^{-0.693t/T_2} \right)}_{\text{daughter}} \right] \quad (34)$$

This equation is plotted for Sr^{90} in figure 5. The curve marked $\text{Sr}^{90} + \text{Y}^{90}$ gives the concentration rate of Sr^{90} required to expose the bone to a tolerance rate of exposure of $Z = 0.1$ r. per day after different times of consumption. The curve marked Sr^{90} indicates the concentration rate of Sr^{90} if only Sr^{90} is considered, and the curve marked Y^{90} indicates the concentration rate of Sr^{90} if only the radiation from its daughter Y^{90} is considered.

■ In this equation $Z = 0$ when $t = 0$ and when $t \rightarrow \infty$.

$$Z = \frac{0.197PT_1 \left(E_1 + \frac{T_2 E_2}{T_{r_2}} \right)}{fB\rho} \text{ roentgens per day} \quad (35)$$

Equation 34 does not have a maximum for positive values of time. The μ curie amount, Ct , in the body organ at any time, t , is found from the initial conditions of the problem,

$$C_t = \frac{PT_1}{0.693} \left[\underbrace{(1 - e^{-0.693t/T_1})}_{\text{parent}} + \underbrace{\frac{T_1 T_2}{T_{r_2}(T_1 - T_2)} \left(\frac{T_1 - T_2}{T_1} - e^{-0.693t/T_1} + \frac{T_2}{T_1} e^{-0.693t/T_2} \right)}_{\text{daughter}} \right] \quad (36)$$

The parent and daughter radiations are in transient equilibrium or their curves are parallel when

$$t_e = 3.32 \frac{T_1 T_2}{T_1 - T_2} \log_{10} \left(\frac{T_1 T_2 E_2}{-E_1 T_1 T_{r_2} + E_1 T_2 T_{r_2} + E_2 T_1 T_2} \right) \quad (37)$$

When $E_1 = E_2$ and $T_{r_2} = T_2$, this equation becomes

$$t_e = 3.32 \frac{T_1 T_2}{T_1 - T_2} \log_{10} \left(\frac{T_1}{T_2} \right) \quad (38)$$

XII. SUBMERSION TOLERANCE

Submersion tolerance for beta-gamma activity in a large body of fluid may be determined by assuming that the energy absorbed per cubic centimeter is equal

to the energy emitted per cubic centimeter. Under these conditions

$$Z = \frac{3.7 \times 10^4 Q_a E \times 10^6 \times 4.8 \times 10^{-10} \times 86,400}{32} = 4.8 \times 10^4 Q_a E \quad (39)$$

in which Z = r. per day, Q_a = $\mu\text{c./cc.}$, and E = Mev.

For tolerance of 0.1 r. per day in air when the radiation is from $4\pi^0$,

$$Q_a = \frac{0.1}{4.8 \times 10^4 E} = \frac{2.09 \times 10^{-6}}{E} \mu\text{c./cc. of air} \quad (40)$$

For tolerance of 0.1 r. per day in water when the radiation is from $4\pi^0$,

$$Q_w = \frac{2.09 \times 10^{-6}}{1.293 \times 10^{-3} E} = \frac{1.61 \times 10^{-3}}{E} \mu\text{c./cc. of water} \quad (41)$$

The radiation to the human body, with a few exceptions such as the ear, would be from only $2\pi^0$, and so the values in equations 40 and 41 could be doubled.

XIII. SOME PROBLEMS ILLUSTRATING THE USE OF THE PREVIOUS EQUATIONS

A. General discussion of problems

Some of the general assumptions are as follows:

1. Average mass of body organs in grams (= $fB454$):

a. Total body	70,000	e. Pair lungs	1,000
b. Skeleton	12,000	f. Pair kidneys	300
c. Blood	4,500	g. Pair thyroids	25
d. Skin	4,500		

2. $\rho = 1$ for electron and γ -ray emitters, and $\rho = 1.12$ for α emitters.

3. The 24-hr. tolerance values used here are: 100 mr. for γ , 100 mrep. for β , and 10 mrep. for α . In the following problems tolerance is obtained for continuous exposure unless otherwise indicated. These values should be multiplied by 4.2 to obtain the tolerance value for a 40-hr. per week exposure.

4. Yearly tolerance from daily consumption of radioactive isotopes is considered to deliver a tolerance dose of radiation during the last day of the year for long-lived radioactive substances and to deliver an average daily tolerance dose for each day of the year for short-lived radioactive substances (see figure 3B).

5. The breathing rate is considered as 150 cc. per second. Experiments have indicated that this is about the average for a person standing and moving about in a laboratory. The water consumption rate is taken as 2000 cc. per day.

The effective atomic number is considered to be the same for the body as for air. The assumption would necessitate a small correction for low-energy γ -radiation. The eventually harmful effects of radiation are considered to be due to prolonged radiation from a uniformly distributed and extended source in the organ of the body. Perhaps the tolerance values obtained below should be

reduced by a factor of ten to give added protection against the possible non-uniform distribution of the radioactivity in a given body organ, especially during the early stage of its fixation in the body.

The equations in the preceding sections are derived on the assumption that it requires 32 ev. to produce an ion-pair. This is approximately true for most radiations, but this constant is more nearly 36 ev. per ion-pair for α -particles. In order to correct for this difference, the term ρ in each of the preceding equations is set equal to 1.12 when α -particles are considered.

Two of the problems discussed in the complete report are included in the following section for illustration.

TABLE 1

ISOTOPE	HALF-LIFE	ACTIVITY	ENERGY	MASS	PER CENT PRESENT BY WEIGHT	
	<i>years</i>	<i>per cent</i>	<i>Mev.</i>	<i>grams</i>		
U ²³⁸	4.51 × 10 ⁹	48.9	4.15	1,460,000	99.28±	
U ²³⁵	7.07 × 10 ⁸	2.26	4.52	10,440	0.71±	
U ²³⁴	2.69 × 10 ⁵	48.9	4.71	85.6	0.00583	
Weighted average energy				4.43	1,470,525	99.996

TABLE 2

Tolerance values for natural uranium

TIME IN WHICH THE TOLERANCE AMOUNT OF URANIUM IS BUILT UP IN THE LUNGS	TOLERANCE RATE OF CONCENTRATION, <i>P</i> , IN THE LUNGS	TOLERANCE CONCENTRATION IN AIR	TOLERANCE CONCENTRATION IN AIR
	<i>μc./sec.</i>	<i>μc./cc.</i>	<i>μg./cc.</i>
1 day	475×10^{-9}	12.7×10^{-9}	187×10^{-4}
1 week	70.2×10^{-9}	1.87×10^{-9}	27.5×10^{-4}
1 month	18.4×10^{-9}	0.491×10^{-9}	7.22×10^{-4}
1 year	5.46×10^{-9}	0.145×10^{-9}	2.14×10^{-4}
∞ years	5.37×10^{-9}	0.143×10^{-9}	2.11×10^{-4}

B. Natural uranium

In the case of natural uranium, one curie would be distributed as shown in table 1. It can be shown that the greatest radiation hazard from uranium is probably received by the lungs. In this case, as with plutonium, it is assumed that the lung retains 25 per cent of the inhaled uranium and that the effective half-life is two months. These values depend on the particle size and the chemical form but are probably not far wrong for the uranium oxide and much of the dust. It is assumed in this example that this natural uranium is freed from all its daughter elements.

From equation 14 the inhalation tolerance values in table 2 were obtained.

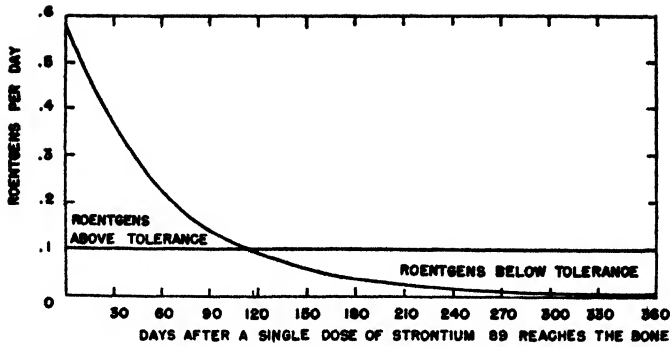


FIG. 3A. A plot of equations 8 and 9

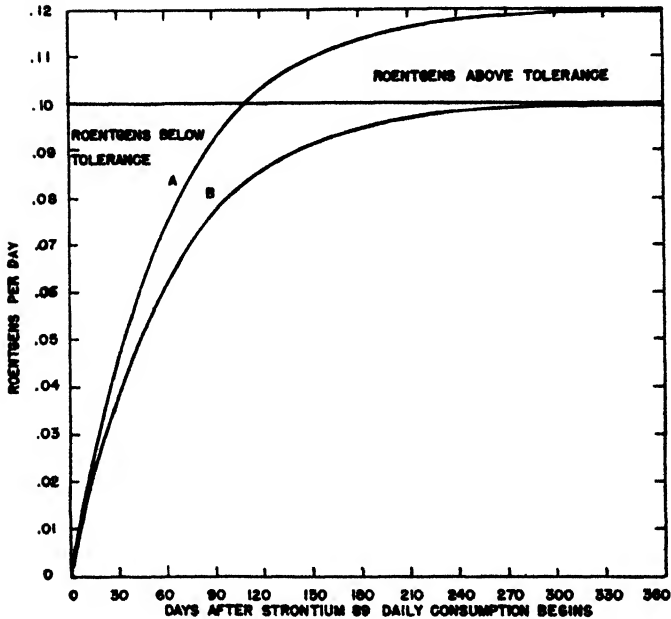


FIG. 3B. A plot of equations 12, 13, and 14 showing the daily exposure rates when Sr^{89} is taken into the bone at a constant rate. Curve A is the case in which the exposure is 36.5 roentgens in a year. Curve B is the case in which the exposure rate is 0.1 roentgen on the 365th day.

C. Strontium⁸⁹

In the case of Sr^{89}

$$\tau = 8.8 \times 10^{-14} \times 89 \times 55 \times 8.64 \times 10^4 = 3.7 \times 10^{-5} \text{ g. per curie}$$

$$E_{\text{av}} = \frac{1.7}{3} = 0.6 \text{ Mev. of } \beta$$

$$T = \frac{T_e T_r}{T_e + T_r} = \frac{200(55)}{255} = 43.2 \text{ days} = 3.74 \times 10^6 \text{ sec.}$$

$$C = \frac{4.38 R_f B_p 10^5}{T E} = 4.38 \frac{36.5(26.4)1 \times 10^5}{3.74 \times 10^6 \times 0.6} = 188 \text{ } \mu\text{curies}$$

$G = 188 \times 3.7 \times 10^{-5} = 7 \times 10^{-3}$ $\mu\text{g.}$ of Sr^{90} when fixed in the bone will give an exposure of 36.5 r. during the first year. If the fraction absorbed from the gastrointestinal tract is 0.15 and the fraction deposited in the bone is 0.5,

$$H = \frac{7 \times 10^{-3}}{0.15(0.5)} = 9.3 \times 10^{-2} \mu\text{g.}$$

of Sr^{90} when taken once orally will expose the bone to 36.5 r. during the first year.

There will be above-tolerance exposure to the bone the first part of the year after the ingestion and a below-tolerance exposure afterwards. The average exposure will be 0.1 r. per day, which is tolerance for β -radiation. This problem is illustrated by a plot of equations 8 and 9 in figure 3A.

From equation 10 the radiation exposure rate ≥ 0.1 r. per day after the 109th day.

TABLE 3
Summary of tolerance data for Sr^{90}

CONCENTRATION OF Sr^{90} IN WATER CONSUMED REGULARLY FOR ONE YEAR		AMOUNT OF Sr^{90} IN WATER CONSUMED AT ONE TIME (FRACTION REACHING BONE = 0.075)		
Which will give an exposure of 36.5 r. during one year (equation 12 or 17)	Which will give an exposure of 0.1 r. on the 365th day (equation 14)	Which will give an exposure of 36.5 r. during one year (equation 8)	Which will give an exposure of 0.1 r. on the 365th day (equation 9)	Which will give an exposure of 0.1 r. per day during the 1st few days (equation 4)
$4.1 \times 10^{-3} \mu\text{c./cc.}$	$3.4 \times 10^{-3} \mu\text{c./cc.}$	2500 $\mu\text{c.}$	$1.5 \times 10^{+6} \mu\text{c.}$ (lethal)	430 $\mu\text{c.}$
$1.5 \times 10^{-7} \mu\text{g./cc.}$	$1.3 \times 10^{-7} \mu\text{g./cc.}$	0.093 $\mu\text{g.}$	5.6 $\mu\text{g.}$	0.016 $\mu\text{g.}$

* It should be noted that it would probably cause serious damage (or even death) if a person ingested 5.6 $\mu\text{g.}$ of Sr^{90} . This would give the gastrointestinal tract serious exposure and the bones an exposure of about 35 roentgens per day for the first few days. Even after 43.2 days the daily exposure rate to the bone would have decreased to only half this value. This shows that although it is safe to ingest daily a concentration of Sr^{90} that will give a tolerance concentration on the 365th day, it is definitely not permissible to take a single dose of Sr^{90} that will give a tolerance concentration on the 365th day.

The rate of exposure when $t \rightarrow 0$ is found from equation 3. In this case,

$$Z = \frac{0.136CE}{fB\rho} = \frac{0.136 \times 188 \times 0.6}{26.4 \times 1} = 0.581 \text{ r. per day}$$

Therefore the radiation exposure is 0.58 r. per day the first few days, and it decreases to 0.1 on the 109th day.

Table 3 summarizes some of the tolerance data for Sr^{90} on the assumption that the bone is the body organ most amenable to damage and that 7.5 per cent of the strontium is absorbed into the bone from the gastrointestinal tract.

XIV. DISCUSSION OF GRAPHS AND TABLES

Figures 1 through 4 illustrate the variation of the daily radiation dose for different types of exposure as a function of the time since the exposure began. Figures 5 and 7 indicate how the tolerance concentration of a substance must be

decreased if the expected time of exposure of a person is increased. If a person plans to work with and be exposed to plutonium or radium inhalation for one year, figure 6 indicates how the tolerance concentration used depends upon the assumed effective half-life, T_v , of the radioactive substance. The circles on the curves indicate the values of T_v that are assumed for plutonium and radium

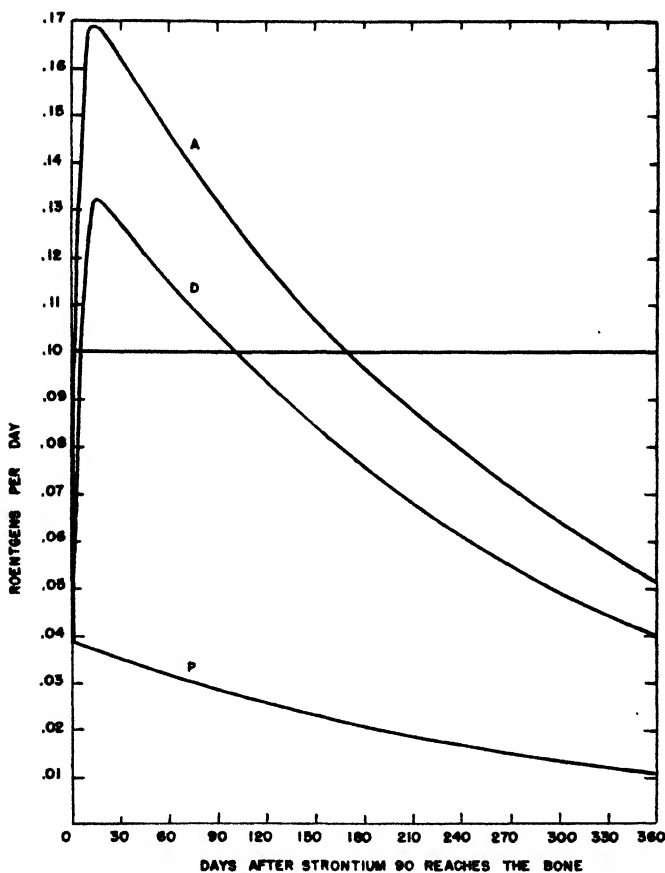


FIG. 4. Radiation to skeleton from the portion of a single dose of Sr^{90} that reaches the skeleton and produces an exposure of 36.5 roentgens during the year. A, total exposure rate; P, parent exposure rate; D, daughter exposure rate.

in this paper. Since T_v is a function of the particle size and the chemical form, one may wish to select other values indicated by these curves.

Table 4 lists the tolerance values for some of the more commonly used radioactive isotopes. The approximate total tolerance amounts of the radioactive isotopes in the human body can be found by dividing the values given in columns 7 or 8 by the fractions in column 5. The methods used here can be applied to tolerance calculations for other radioactive isotopes, provided the physical and

biological constants are known. Some of the biological constants used in these examples were obtained from reports by Dr. J. G. Hamilton. In general, the fractions given in column 6 and the half-lives in column 3 apply to soluble compounds for the ingested elements and to volatile forms where inhalation is considered. In the breathing of uranium, plutonium, and hydrogen, the oxides and dust-borne particles are of principal concern. The chloride of polonium is used in determining the value given in the table. The effective energy of β -radiation was taken as one-third the maximum value. The γ -energy of iodine was neglected, because of the small size of the thyroid.

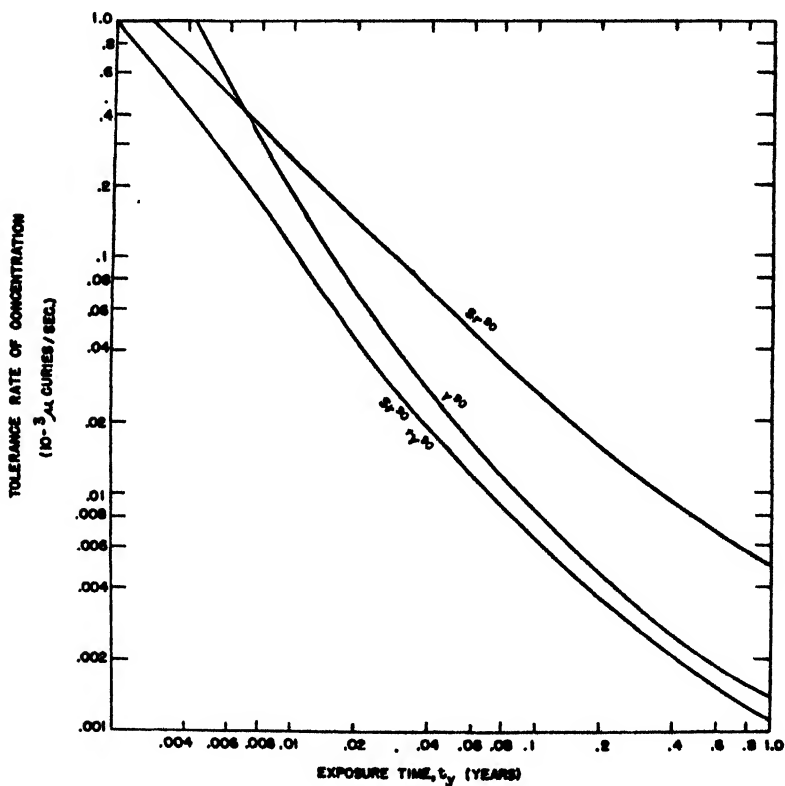


FIG. 5. This figure shows how the tolerance rate of concentration of Sr^{90} in the body varies with exposure time. Curve Sr^{90} indicates the tolerance rate of concentration if only the damage to the bone from Sr^{90} is considered. Curve Y^{90} indicates the tolerance rate of concentration if only the damage to the bone from Y^{90} is considered. Curve $Sr^{90} + Y^{90}$ indicates the tolerance rate of concentration if the total damage is considered.

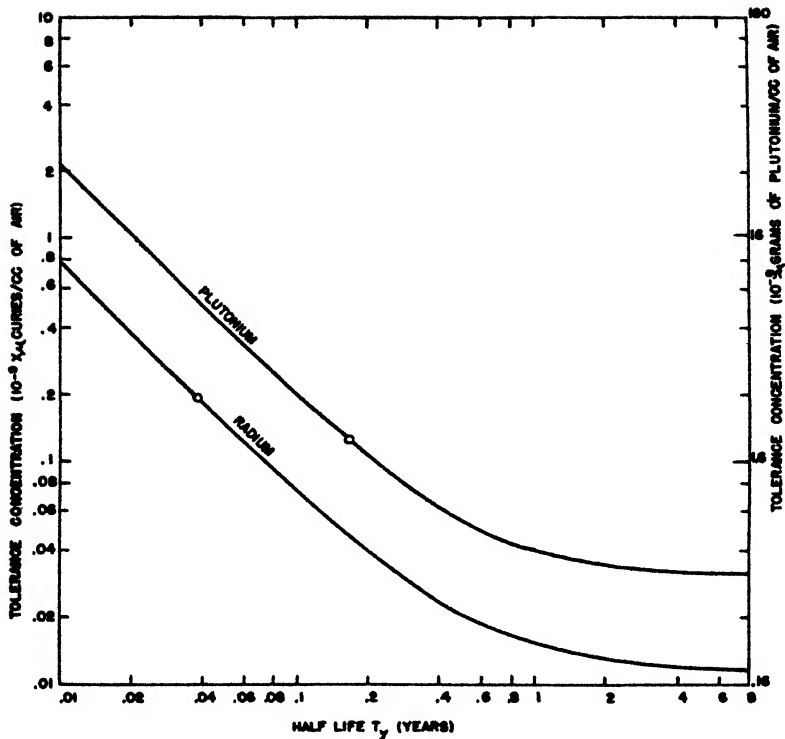


FIG. 6. This figure shows how the tolerance concentrations in air of radium and plutonium vary with the assumed effective half-life. The circles on the curves indicate the values of half-life that are assumed in this report.

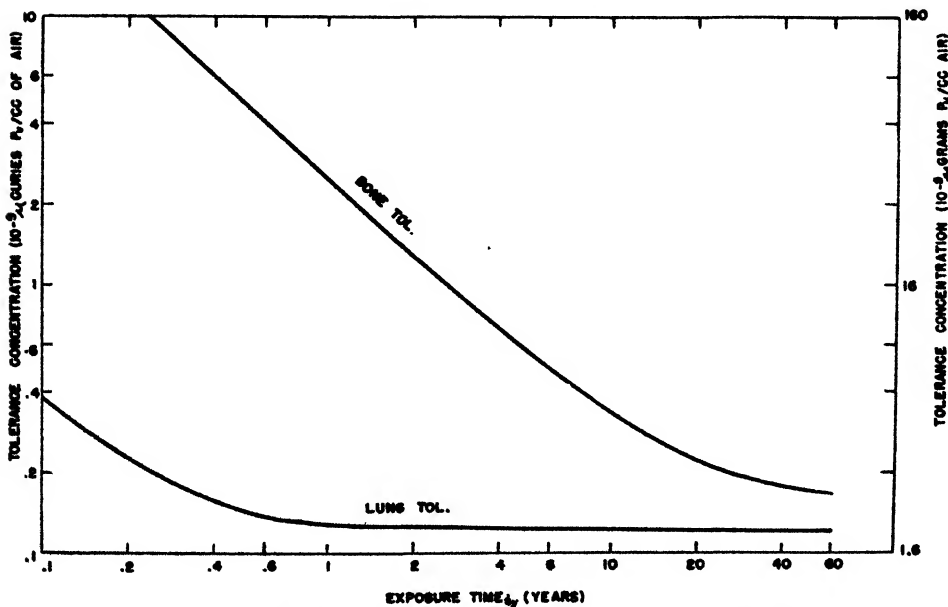


FIG. 7. The curves in this figure illustrate how the tolerance concentration of Pu in the air varies with the exposure time. The upper curve is based on damage to the bone, and the lower curve is based on lung damage.

TABLE 4

A comparative summary of some of the values determined in the preceding examples

(1)	(2)	(3)	(4)	(5)	(6)	(7)	(8)	(9)	(10)	(11)	(12)	(13)	(14)
ELEMENT	GRAMS PER CURIE	ASSUMED EFFECTIVE HALF-LIFE	METHOD OF BODY INTAKE	ORGAN AFFECTED AND FRACTION OF AMOUNT IN BODY THAT IS IN ORGAN	FRACTION TAKEN INTO BODY THAT REACHES ORGAN	$\mu\text{C. IN ORGAN TO PRODUCE AN AVERAGE TOLERANCE RATE WHEN t = 0$	$\mu\text{C. IN ORGAN TO PRODUCE AN AVERAGE TOLERANCE DURING YEAR}$	ONE-YEAR TOLERANCE CONCENTRATION RATE	$\mu\text{C./cc.}$	$\mu\text{g./cc.}$	ONE-YEAR TOLERANCE CONCENTRATION IN AIR	$\mu\text{g./cc.}$	EFFECTIVE ENERGY
Ra^{226} pdts	1	~ 2 weeks	Breathing	Lungs (0.5)	0.25	0.013	0.23	7.5×10^{-3}	2.0×10^{-10}	2.0×10^{-10}	4.4×10^{-3}	4.4×10^{-3}	14 α
Ra^{226} pdts	1	~ 10 yr.	Ingestion	Bone (0.6)	0.06	0.185	0.16	5.1×10^{-3}					14 α
Pu^{239}	16	2 months	Breathing	Lungs (0.3)	0.25	0.035	0.15	4.7×10^{-3}	1.3×10^{-10}	2×10^{-9}			5.10 α
Pu^{239}	16	10 yr.	Ingestion	Bone (0.6)	0.0003	0.42	0.43	1.4×10^{-3}			2.0×10^{-3}	3.1×10^{-2}	5.10 α
Pu^{239}	16	10 yr.	Breathing	Bone (0.6)	0.0375	0.42	0.43	1.4×10^{-3}	2.5×10^{-9}	4.0×10^{-9}			5.10 α
Natural U	1.47×10^4	2 months	Breathing	Lungs (0.3)	0.25	0.041	0.17	5.5×10^{-3}	1.5×10^{-10}	2.1×10^{-10}			4.43 α
Enriched U	2.7×10^4	2 months	Breathing	Lungs (0.3)	0.25	0.039	0.16	5.1×10^{-3}	1.4×10^{-10}	2.3×10^{-10}			4.7 α
U 238		2 months	Breathing	Lungs (0.3)	0.25	0.037	0.166	5.0×10^{-3}	1.3×10^{-10}				
Po^{210}	2.24×10^{-1}	82 days	Breathing	Kidneys (0.05)	0.011	0.010	0.033	1.0×10^{-3}	6.4×10^{-10}	1.4×10^{-10}			5.3 α
Po^{210}	2.24×10^{-1}	82 days	Ingestion	Kidneys (0.05)	0.001	0.010	0.033	1.0×10^{-3}			4.5×10^{-3}	1.0×10^{-3}	5.3 α
Sr^{90}	3.7×10^{-1}	43 days	Ingestion	Bone (0.5)	0.075	32	190	6.0×10^{-3}			3.4×10^{-3}	1.3×10^{-3}	0.5 β
$\text{Sr}^{90} \rightarrow \text{Y}^{90}$	7.74×10^{-1}	Sr-197 days Y-8.49 days	Ingestion	Bone (0.5)	0.075	88 (20)*	34	1.1×10^{-3}			6.2×10^{-3}	4.8×10^{-3}	0.23, 0.5 β
C^{14} (graphite)	0.23	2 months	Breathing	Lungs (0.3)	0.25	32	130	4.3×10^{-3}	1.2×10^{-7}	2.6×10^{-7}			0.06 β
C^{14} (CO_2)	0.23	10 days	Breathing	Total body (1)	0.25	2290	5.7×10^4	1.8×10^{-3}	4.8×10^{-7}	1.1×10^{-7}			0.06 β
I^{131} (water)	3.59×10^{-1}	2 months	Breathing	Lungs (0.02)	0.25	390	4×10^4	1.3×10^{-3}	3.5×10^{-7}	9×10^{-7}			0.005 β
I^{131}	8×10^{-1}	6.3 days	Ingestion or breathing	Thyroid (0.2)	0.20	2.0	81	2.6×10^{-3}	8.5×10^{-8}	6.8×10^{-8}		4.4×10^{-3}	0.2 β
Na^{24}	1.13×10^{-1}	14.8 hr.	Submersion	Body	0.25	2.2	960	3.0×10^{-3}	6.3×10^{-7}	7.1×10^{-7}		5.5×10^{-3}	3.3 β
Na^{24}	1.13×10^{-1}	14 hr.	Ingestion or breathing	Blood (0.25)	0.25				8.1×10^{-7}	9.1×10^{-7}		6.0×10^{-3}	3.3 β

Na ²⁴	1.12 × 10 ⁻⁷	11.5 hr.	Ingestion or breathing	Lungs (0.037)	0.037	0.5	256	8.2 × 10 ⁻⁴	1.5 × 10 ⁻⁴	1.7 × 10 ⁻¹³	9.5 × 10 ⁻³	1.1 × 10 ⁻³	3.3 β _γ
P ³²	3.48 × 10 ⁻⁴	14.3 days	Submersion	Body					4.2 × 10 ⁻⁴	1.5 × 10 ⁻¹¹	3.2 × 10 ⁻³	1.1 × 10 ⁻³	0.5 β
P ³²	3.48 × 10 ⁻⁴	13 days	Ingestion or breathing	Bone (0.9)	0.09	39	750	2.4 × 10 ⁻³	1.8 × 10 ⁻⁴	6.2 × 10 ⁻¹²	0.011	4.0 × 10 ⁻³	0.5 β
B ¹⁰ →La ¹⁴⁰	1.33 × 10 ⁻⁴	B ₀ =11.75 days La=1.51 days	Ingestion	Bone (0.6)	0.06	43	170	5.3 × 10 ⁻³			3.8 × 10 ⁻³	5.1 × 10 ⁻³	0.4, 2.3 β _γ
Sr ⁹⁰	2.3 × 10 ⁻³	25 days	Ingestion or breathing	Skin (0.2)	0.05 (0.1)†	150	1500	4.7 × 10 ⁻³	3.1 × 10 ⁻⁴	7.3 × 10 ⁻¹¹	0.041	9.4 × 10 ⁻⁷	0.05 β
Cs ¹³⁷	6.15 × 10 ⁻⁴	150 days	Ingestion or breathing	Bone (0.99)	0.15 (0.4)†	190	400	1.3 × 10 ⁻³	2.1 × 10 ⁻⁷	1.3 × 10 ⁻¹¹	3.6 × 10 ⁻³	2.2 × 10 ⁻⁷	0.1 β

The tolerance values in columns 9, 10, 11, 12 and 13 are for continuous exposure. If the exposure is for a 40-hr. week, multiply these values by 4.2.

Column 9 is the tolerance concentration rate, P' , in $\mu\text{c./sec.}$, to the body organ that will produce a tolerance rate of exposure after 365 days of consumption.

It should be noted that values given in column 6 depend on the chemical form and in the case of inhalation they depend upon the size of the particles. Until the most likely forms of these elements in a given laboratory are known, it is difficult to assign typical values of tolerance concentration in columns 10, 11, 12, and 13.

Values in column 9 can be obtained directly from equation 14 or by dividing values in column 8 by the seconds in a year.

Column 8 is the $\mu\text{c.}$ in the lung, bone, kidney, or blood required to irradiate the organ with 3.65 roentgens of α or 36.5 roentgens of β in a year. It is the $\mu\text{c.}$ in the thyroid required to irradiate it with 365 roentgens of β in a year.

* The Sr-Y activity reaches a maximum after 15 days. The 88 $\mu\text{c.}$ is required to produce tolerance exposure rate soon after Sr reaches the bone. Only 20 $\mu\text{c.}$ is required to produce tolerance exposure rate on the 15th day. The 34 $\mu\text{c.}$ produces an average yearly tolerance dose. (See figure 4.)

† It is assumed that the fraction reaching the skin by way of the gut is 0.05 and by way of the lungs is 0.1 in the case of Sr. For Cs¹³⁷ it is assumed that 0.15 reaches the bone by way of the gut and 0.4 by way of the lung.

ANALYSIS OF PARTICLE FORMATION AND GROWTH BY SIZE-FREQUENCY DETERMINATIONS OF THE SILVER HALIDE PRECIPITATIONS OF PHOTOGRAPHIC EMULSIONS¹

R. P. LOVELAND AND A. P. H. TRIVELLI

Kodak Research Laboratories, Rochester, New York

Received September 17, 1946

The sizes of the various individual crystals of a precipitate, such as the grains of a photographic emulsion, are usually a result in part of recrystallization, the so-called Ostwald ripening. This is explained by a difference in the solubilities of the smaller and larger crystals in the mother liquor.

I. GROWTH OF THE PRECIPITATED PARTICLES

An investigation of this phase of the process, i.e., the growth of particles by recrystallization of silver bromide after precipitation, has been made by the authors (9, 10). Data were obtained from a series of precipitations made by S. E. Sheppard and R. H. Lambert (14) of these Laboratories, by a method that might be called "stream precipitation," in which the almost instantaneously precipitated particles were formed under the same gross environment throughout the precipitation period. This is, of course, never true with the usual "volume precipitation," where a stream of one component solution is added to a volume of the other solution. Two streams of practically equal volumes of equivalent solutions of silver nitrate and potassium bromide met in a vertical tube so corrugated as to give rapid and intimate mixing. The silver bromide, precipitated as 0.5 molar in 0.65 per cent of gelatin, was ripened at 60°C. as 0.4 molar silver bromide in measured amounts of potassium bromide solutions of varying concentrations: i.e., 0.02, 0.04, 0.06, and 0.08 molar, respectively. Samples were removed from each of the four ripening dispersions after 60, 90, 150, 240, 345, 495, 870, 1110, and 1395 min., respectively, from the start of the ripening.

Particle formation and growth

The particle-size-frequency distribution of practically all of these samples was determined by the photomicrographic method, the size being measured as the projective area of the particles, a method which avoids the complications of the "shape factor," since the size parameters were kept in this dimension rather than being converted to equivalent diameters. On the average, 3720 grains were measured for each size-frequency curve.

Although there was no apparent relation between the size-frequency curves of a ripening series, sampled as mentioned above, and the time of ripening, except an increase in both the average particle size, \bar{x} , and dispersion around that size, σ (figure 1a and table 2), a very fruitful and simplifying relation became evident after a transformation of the variables. It was shown (10) that the size-fre-

¹ Communication No. 1096 from the Kodak Research Laboratories.

quency distribution could be put into an *invariant form*, so that the shape of the graphical curve was unaffected by the principal factors affecting the size distribution of an already formed precipitate, *viz.*, solvent and time of ripening. Although no temperature variation was included in this series, various indications make it probable that that factor would not affect the invariant ripening curve. The latter is formed by plotting the logarithms of both the dependent and the independent variable, or more simply, by the use of commercial log-log graph paper. With samples varying in one of these ripening factors, the result is a series of curves, concave downward and displaced diagonally on the graph paper (see figure 2). That the shape of the curve is unchanged is best shown by sliding individual graph papers along until the observed points of the size distributions lie on the same curve; this is seen to occur well within the errors involved in the frequencies of the "tails" of the size-frequency curves where observations were relatively few and where the relative values are magnified by the use of logarithms. The results for one of the time series (10) are shown in figure 1b.

If there are irregularities in the distribution, such as there definitely are in the particle distributions of photographic emulsions, these "breaks" are reproduced as a specific characteristic essentially unaltered by simple ripening conditions. These "breaks," one of which is observable in figure 1b, will be discussed later.

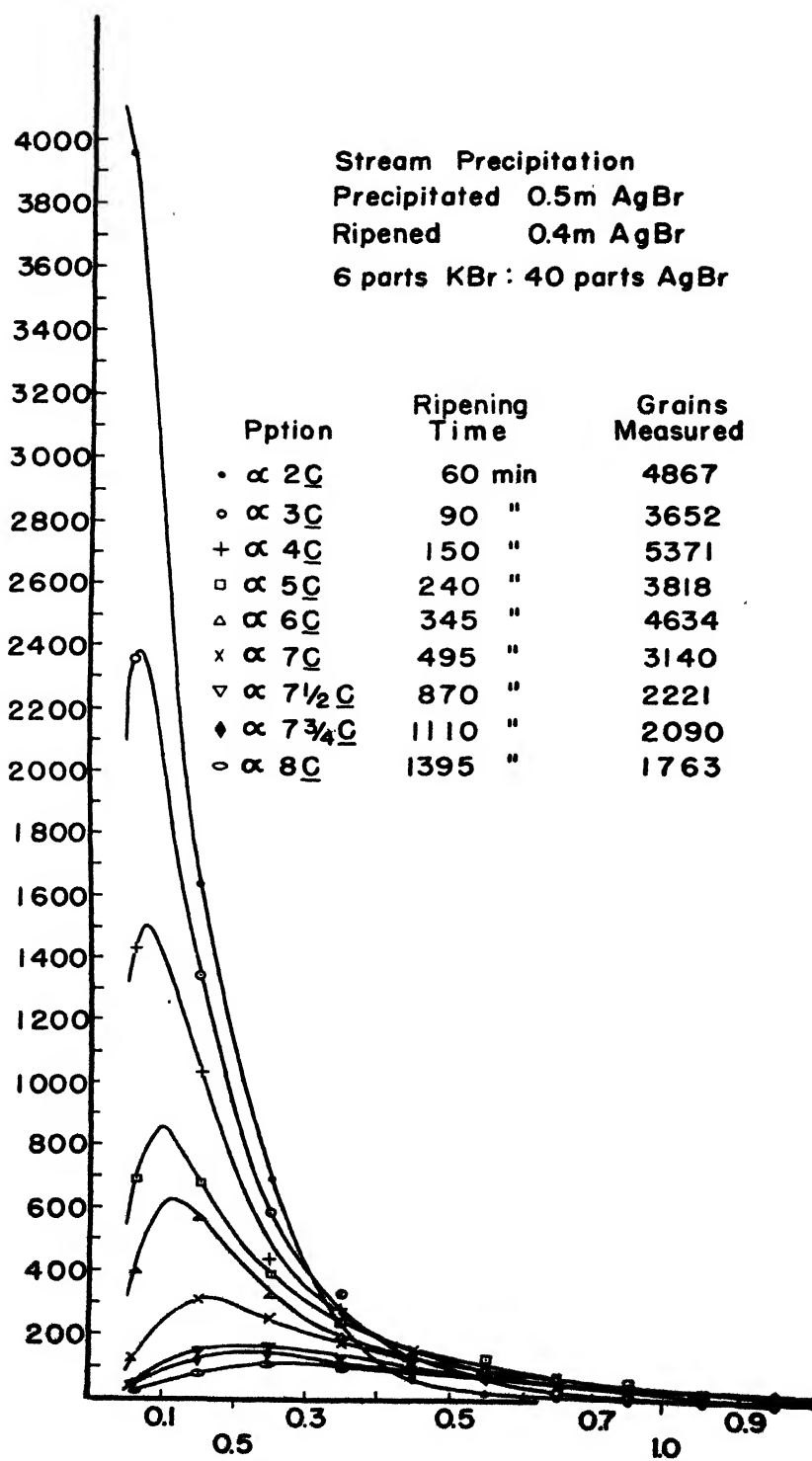
Relationships between distribution characteristics and ripening factors

It was found, moreover, that the shift of the log-log graph papers required to superpose the various curves in a ripening series was along a diagonal straight line. This could be seen by following any coördinate point, as can be noted in figure 1b. In the case of one series (containing 0.04 molar potassium bromide), a parabola was fitted independently and geometrically through the observed points of each size distribution on log-log paper (see figure 2). The shift of the curves was then shown by the location of foci of the series of parabolas and is shown by the diagonal line in figure 2. The relation between the shift of the invariant curve with ripening time (i. e., with the intervals between foci along the diagonal line) is given by line A of figure 3, where the frequency position of the foci of the line of figure 2 is plotted against the time of ripening. A measure of the shift of the log-log curves with ripening time for *each* of the four concentration series can be obtained from the diagonal line of coördinates, such as shown in figure 1b, i. e., by plotting the ordinate locations of the successive positions of any point on the graph papers after superposing the observed points of each log-log frequency curve. This is shown in figure 3, curves B and C. Comparison of the points (for the c distributions) of curve B with those of curve A, made from the same data but after determining the parabolas that gave the best fit, indicates that the latter laborious method is more accurate. The size-distribution curve shifts linearly with ripening time when both variables are transformed to their respective logarithms. Therefore, the relation between the particle-size

No. of Grams $\times 10^{-6}$ per cc Precipitation Solution

Stream Precipitation
Precipitated 0.5m AgBr
Ripened 0.4m AgBr
6 parts KBr : 40 parts AgBr

Pption	Ripening Time	Grains Measured
• α 2C	60 min	4867
◦ α 3C	90 "	3652
+ α 4C	150 "	5371
◻ α 5C	240 "	3818
△ α 6C	345 "	4634
x α 7C	495 "	3140
▽ α 7½C	870 "	2221
◆ α 7¾C	1110 "	2090
◊ α 8C	1395 "	1763



Mean Class Size - $\frac{\text{Area in } \mu^2}{\text{Diam in } \mu}$

characteristics of the whole distribution and the ripening factors is, as previously stated (10):

$$y = cf^a \quad (1)$$

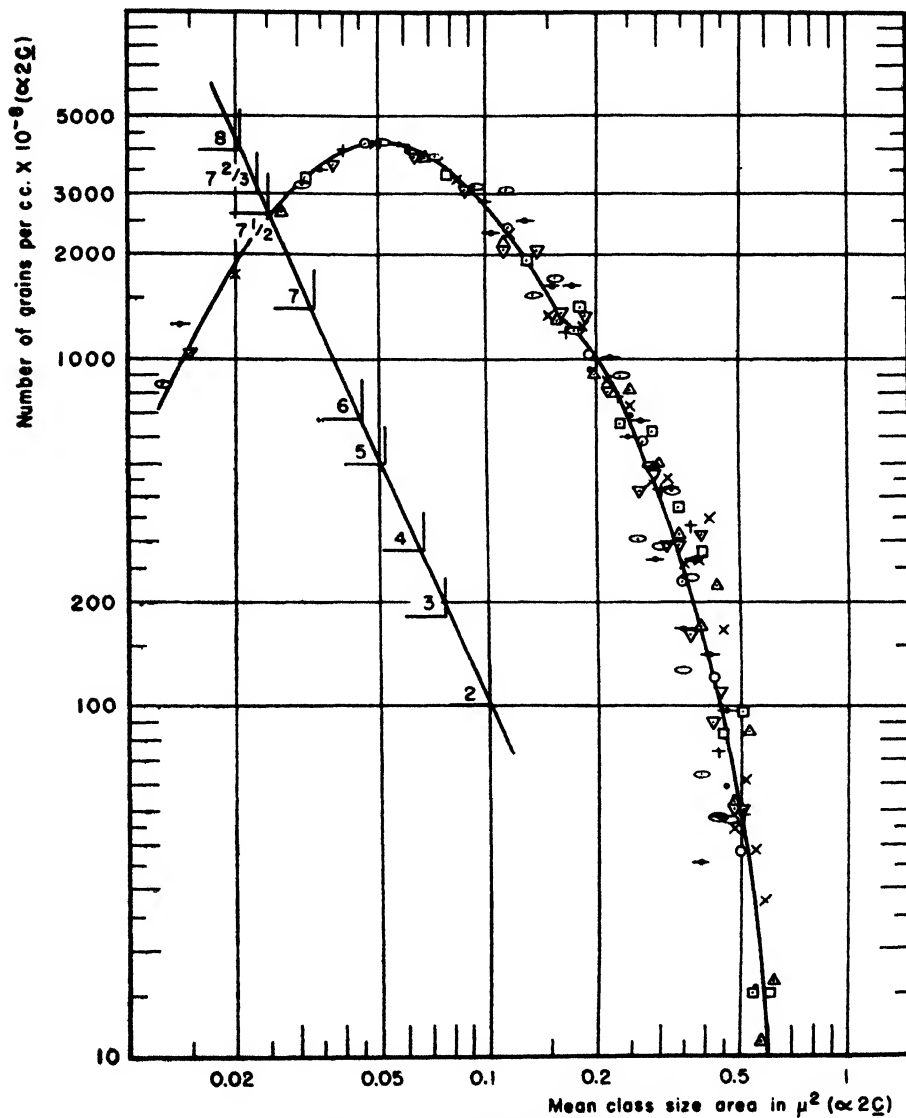


Fig. 1b. $\alpha\epsilon$ precipitations

where y can represent any of the particle-size characteristics dependent on the whole distribution, i. e., N = the total number of particles in the system, \bar{x} = the average particle size, σ = the dispersion around that size, and also the par-

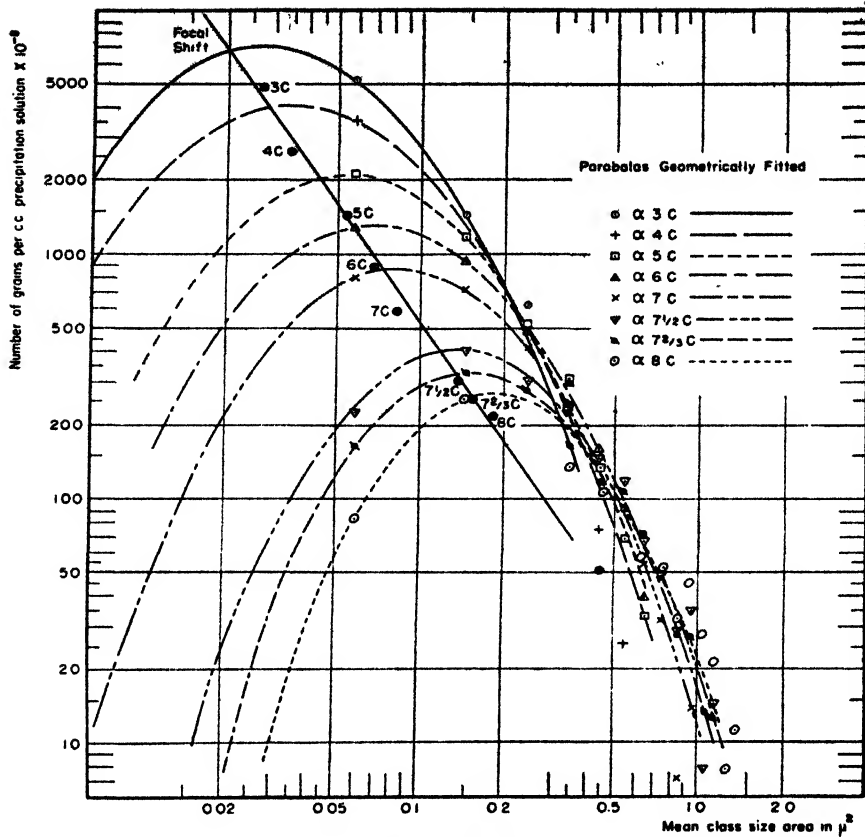


FIG. 2. $\alpha\epsilon$ precipitations

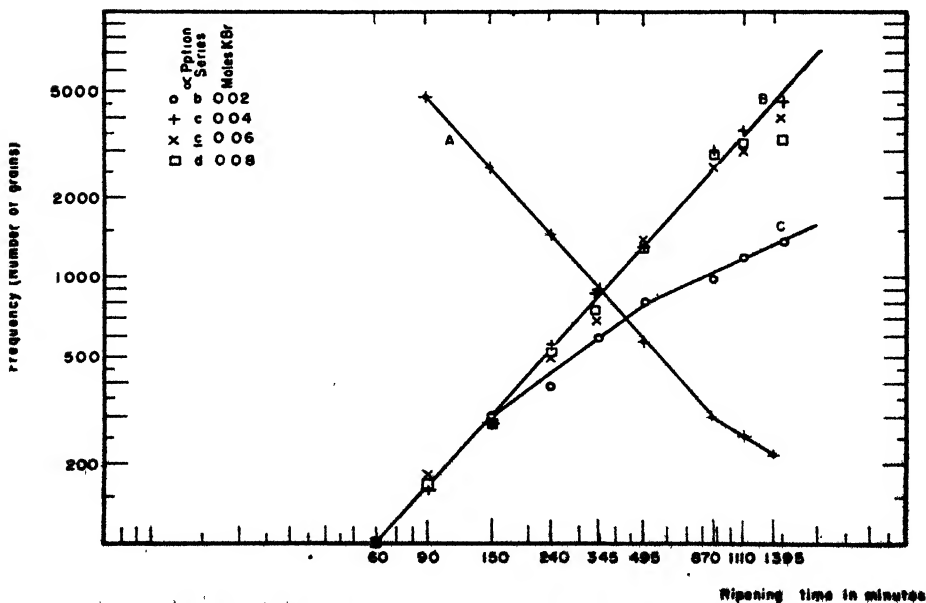


FIG. 3. Shift of invariant curves with ripening time

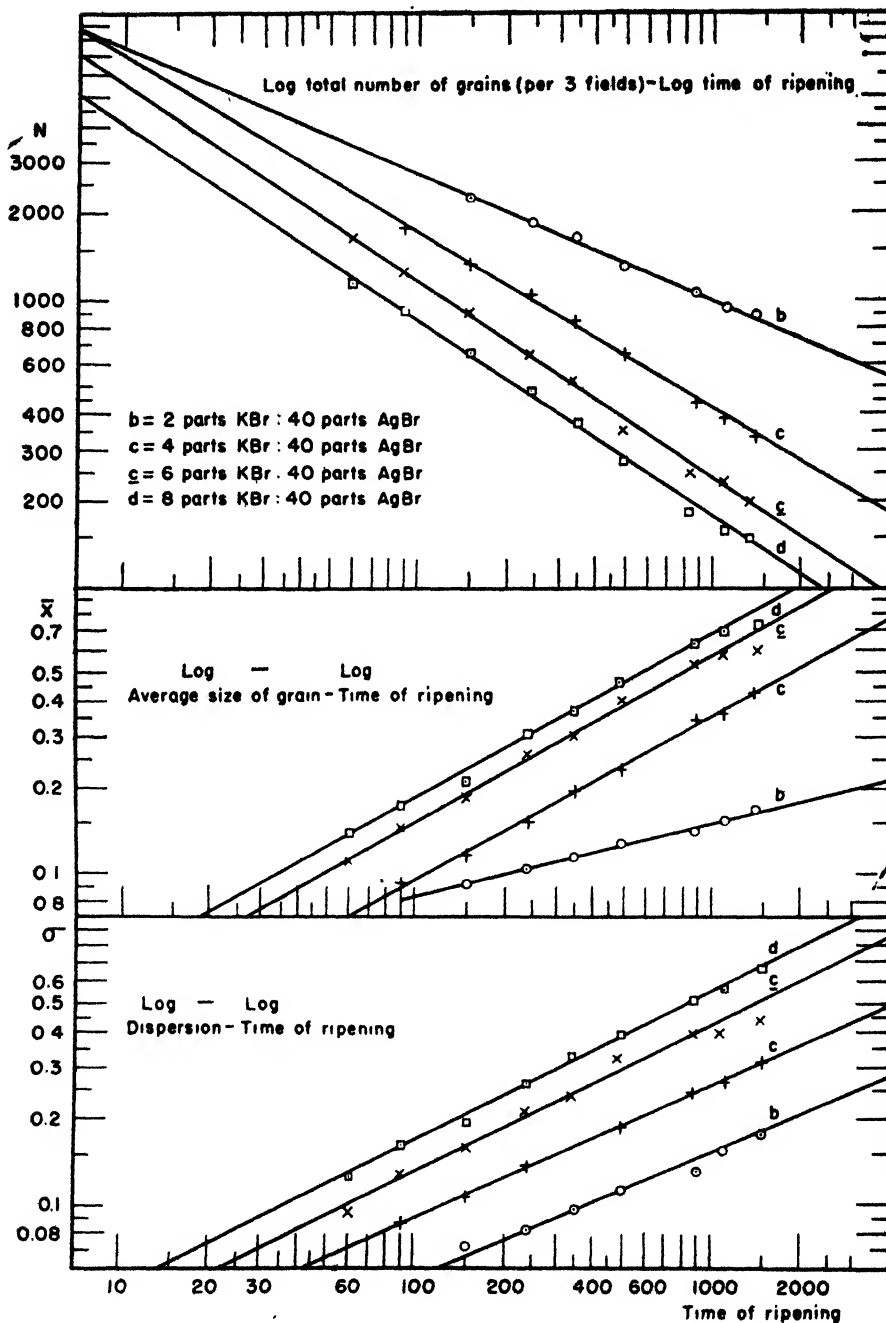
ameters of any mathematical formula used to express the distribution; f can represent either the ripening factor, i. e., the concentration of the solvent, potassium bromide, or the time of ripening; a and c are parameters. a appears to be a constant that is independent of f , at least within a restricted domain. In precipitation series c, g, and d, it has a different value before and after 870 min. ripening time, if the change of the slope in figures 3A and 3B at that value is a significant one. The failure of series b to conform to this condition is discussed below.

These relations can be verified directly by calculation from any adequate size-frequency data obtained from a ripening series, or, more simply, by plotting these variables on log-log paper, whereupon the points should lie along a straight line. Figure 4 shows the graphs of the standard particle-size constants of the four ripening series presented in the previous paper (10) plotted on log-log paper against the time of ripening. The lack of parallelism of the constants for the b series is again evident. There are insufficient data to prove whether this is due to some systematic experimental error or whether the linear relationship fails at very low values of the ripening variable, but there is some evidence of the latter (see page 1019).

If the log-log frequency distribution curve shifts linearly as a whole, then the relationship between the frequency of any *one size* of particles and the ripening time or concentration cannot be linear on the same type of graph paper. This is geometrically evident if one considers, in such a graph as figure 2, the intersection with the invariant curve of any single vertical size ordinate when the whole curve shifts along a diagonal line at a uniform rate, such a uniform shift corresponding to the effect of ripening time. Even the fluctuations and "breaks" in the size-frequency curve must be reflected in the resulting ripening time-frequency curve for a single particle size which can be obtained from such graphs as figure 2, if the frequency values of the successive curves at a single size ordinate are plotted against the ripening times (see figure 5). *These curves represent the number of grains during ripening momentarily having a given size.* In general, for larger particle sizes at relatively short ripening times, the number of grains attaining a given size at successive moments increases with time; for smaller particle sizes, the number of particles of a given size in a silver halide precipitate decreases with time. It probably is not possible, at least with the data available, to formulate an expression covering the whole ripening period for this relation; the inaccuracy of the data for large particle sizes in the "tails" of the size-frequency curve and the breaks in the ripening-frequency curves make this complicated. After the maximum, the curve straightens out quickly and behaves as a rate-of-solution curve; i. e., the number of grains in the size class is a simple exponential function with time,

$$N = Ae^{-kt} \quad (2)$$

and hence are straight lines on semi-log paper. Actually, they consist of broken straight lines, as can be seen from figure 5, because of the breaks already referred to, and as has already been pointed out by Sheppard and Lambert (14). In the

FIG. 4. α precipitations

first three or four class sizes (below $0.5 \mu^2$), the increase in the number of particles with ripening time (and the consequent maximum) occurs at times of ripening so

short that they cannot be obtained in practice; hence these curves appear to be entirely a simple exponential type.

Curves of grain size *vs.* ripening time representing the *history of a grain or group of grains during ripening* would be especially interesting but not simple to obtain.

Normal functions

Another graphical device that simplifies the apparent relationships between grain growth factors and size distribution consists in plotting, instead of the

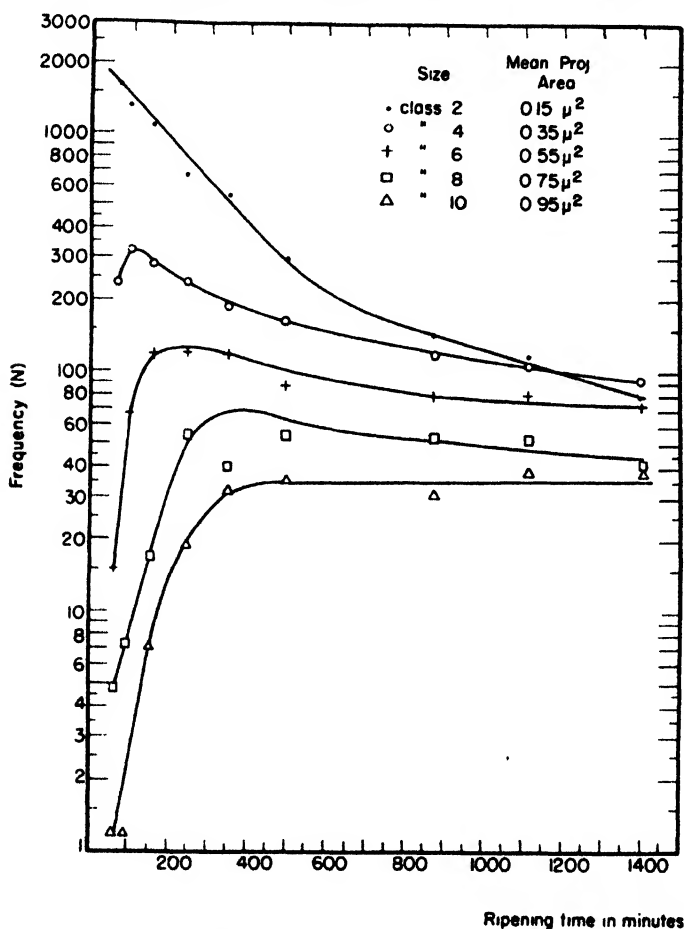


FIG. 5. $\alpha\epsilon$ precipitations

simple frequency values, the linearizing function between the observed frequencies and the so-called "normal frequency law,"

$$y = \frac{1}{\sqrt{2\pi}} e^{-x^2/2} \cdot dx \quad (3)$$

against the logarithms of the particle sizes. The cumulative frequencies and the integral of the error function are used. In practice, it is simplest to accomplish this transformation merely by plotting the cumulative frequencies on commercial "log-probability" paper.

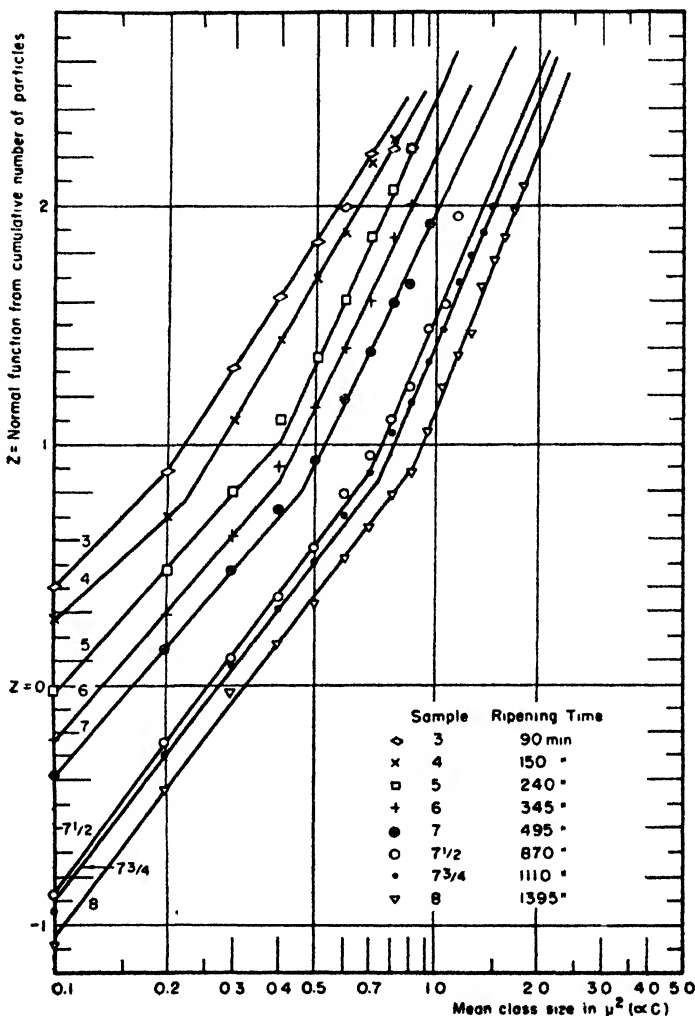


Fig. 6. $\alpha\zeta$ precipitations

An example of this is shown in figure 6, which utilizes the same original data from Lambert's precipitations as figure 2; the simple arithmetic group would be somewhat similar to figure 1a. The unchanged shift of the distribution form, including characteristic irregularities, is just as marked here, again showing that the particle-size-distribution law remains of the same type throughout ripening, in spite of the extreme difference in appearance and skewness at the two extremes.

The use of this transformation as an analytical tool for studying frequency

curves seems to have been first developed by Kapteyn and Van Uven (5, 6, 16) in a series of valuable papers, in which this form was one phase of a general mathematical development of the problem of biological frequency distribution. In these papers they hypothesized that there had originally been a distribution of values according to the "Normal Gauss-LaPlace" law and that the factors of the growth process altered the distribution into its final form. The curve obtained by plotting as described was termed that of the "normal function," $z = f(x)$, and was calculated by means of tables. The function, $\psi(x) = c/f'(x)$, where $f'(x)dx$ represents the first derivative of (x) , was called the "reaction function" and was considered to represent an analysis of the "causes" of growth. If

$$z = \lambda \log x \quad (4)$$

which makes the "normal function" a straight line on semi-log paper, then $\psi(x) = k \cdot x$, and growth, according to this premise, is proportional to the size attained at any time.

It is a well-established fact (1) that the growth of a single crystal is proportional to its surface. It is also a fact (9) that it is an unique property of the logarithmic probability size-frequency function, which must express the particle size distribution if the semi-log normal function is linear, that this same type of function would apply, no matter which size attributes—diameters, areas, volumes, or weights—were measured.

Formula for size-frequency distribution

A linear distribution, upon plotting the cumulative function on log-probability paper, is usually assumed to indicate merely that the arithmetic differential form is that of the usual log-probability formula:

$$y = N \cdot \frac{\lambda}{\sqrt{\pi x}} \cdot e^{-\lambda^2(\ln x - \ln x_m)^2} \cdot dx \quad (5)$$

or

$$y = \frac{A_{-1}}{x} \cdot e^{-k(\log x - a_{-1})^2} \cdot dx \quad (5a)$$

However, both this graph and the parabola on log-log paper can be transformed as strictly to the generic form.²

$$y = A_n x^n \cdot e^{-\kappa(\ln x - \alpha_n)^2} \cdot dx \quad (6)$$

where n is any integer and A_n , κ , and α_n are constants, y is the frequency, and x is the size attribute; also, $\ln x$ is the notation for logarithms to the base e , $\log x$ is that for the common Briggsian system (base 10), and κ is an invariant within the same system of logarithms. Specifically, to convert equation 6 to

$$y = A_{n-r} x^{n-r} \cdot e^{-\kappa(\ln x - \alpha_{n-r})^2} \cdot dx \quad (7)$$

² The notation given here is slightly different from that used originally; it is simpler and allows more consistency in transformation.

where r is any integer and, as before, the subscripts merely consistently identify the constants (in equation 5a, $n = -1$), then:

$$\ln A_{n-r} = \ln A_n + \alpha_n \cdot r + r^2/4\kappa \quad (8)$$

$$\alpha_{n-r} = \alpha_n + r/2\kappa \quad (9)$$

for conversion between the two systems of logarithms,

$$k = \kappa/M^2 \quad a = M \cdot \alpha_n, \text{ where } M = 0.43429 \quad (10)$$

Since the relation between any two measures of size (lengths, volumes, weights, etc.) can be expressed as $z = ax^n$, the mathematical proof for the last statement of the previous section becomes clear. It can also be checked empirically.

Unfortunately, if we have a size-frequency distribution curve with data for one measure, such as a diameter, and for purposes of comparison wish to convert to a different measure, such as projective area or total surface, the conversion will produce a series of unequal class sizes. For this reason it is best to proceed, class by class, with the cumulative data and curve. If u is the size in projective area and x is the size in diameters, then

$$u = \frac{\pi x^2}{4}$$

$$du = \frac{\pi x}{2} \cdot dx$$

If a new constant class width, $\overline{\Delta u}$, is desired for comparison with another determination, a point-by-point multiplication of each class frequency by $\overline{\Delta u}/\Delta u_i$ must be made. If the new midpoints for plotting or calculation are not read from the cumulative graph, they can be calculated for each case as $\frac{u_i + (u_i + 1)}{2}$.

Graphical method for determination of particle-size distribution

The present authors have pointed out (9) that, irrespective of the validity of Kapteyn and Van Uven's theory, this transformation provided a very potent instrument for simplifying the analysis of a particle-size distribution, or series of such distributions, including the determination of the size-frequency curve, and suggested the use of the commercial log-probability paper instead of calculation of the function. The basis of the graphical method proposed was as follows: Consider two functions, the unknown one of the observed data plotted on graph paper, and the one whose curve it is proposed to draw through the points representing the data. It will be found that, unless the two functions are identical or nearly so within the limits of the graph, if the two are simultaneously put through a series of transformations of variable $u = \phi(x)$, $v = \psi(x)$, etc., in some cases the two will undoubtedly seem of different type. In practice, instead of calculating the transformation it is sufficient merely to plot the two on specialized graph papers. Moreover, by carefully choosing the type, relatively few transformations need be made. The authors found that, if the data are plotted on (1) ordinary arithmetic paper, (2) log-log paper, and (3) log-probability paper, and

the proposed curve (which may be entirely empirical and without formula) is plotted more or less simultaneously and consistently on each graph, the result is very similar to a curve obtained by a laborious application of the least-squares method. The log-log paper is especially valuable in determining the locus of the mode and also the curve locus in the "tail" of the distribution.

Later, Hatch and Choate (4) concurred in the use of the log-probability paper for the analysis of size distribution and suggested that the particle-size constants be read directly from the graph. If the distribution on this graph paper is a straight line so that formulas 5 and 6 apply, then the geometric mean, *G.M.*, rather than the usual arithmetic mean, *A.M.* or average, should be the most representative single number to express the distribution, because McAlister (12) obtained this type of formula upon assuming that the *G.M.* was the most representative number. But it should be calculated in the usual way³ rather than by utilizing the 50 per cent line on the cumulative log-probability graph, as recommended by Hatch and Choate, since their procedure strictly determines the median, which equals the *G.M.* only in those cases when the complete distribution is represented by a single straight line on the graph paper. Analogously, the *A.M.* (average) is usually calculated, although it is equal to the median if the plot is linear on cumulative arithmetic probability paper.

Krumbein (7, 8) has particularly developed the procedure of utilizing the cumulative logged graph for graphical analysis and determination of distribution constants. Although his methods, including transformation of variable to a function of $\log_2 x$, are usually applied to the study of sediments, they are equally applicable to distributions of precipitates determined by other means than sedimentation.

Many other particle-size distributions than those of silver halide precipitates are simplified by the use of double log and log-probability papers; in fact, it is now used so generally, including for particle-size distributions formed by comminution, that J. H. Gaddum (2) has recently suggested that systems of this class be called "lognormal distributions." This term will be adopted here as a simplification.

II. STUDY OF VOLUME PRECIPITATION

The more ordinary method of precipitation, wherein one component is run into the bulk of another, is more complex than Lambert's stream type. When, as usual, the addition is gradual, precipitation (particle formation) continues over an appreciable period of time under constantly changing conditions. The complexity is compounded in the case of a reaction like the precipitation of silver halides by addition of silver nitrate solution to a volume of an alkali bromide, such as potassium bromide, since the latter is a solvent for the precipitate. Obviously, growth by ripening will start at once and proceed simultaneously with succeeding particle formation.

Comparison of the two precipitation methods helps the analysis of the factors, although the formation and growth effects cannot be neatly separated in this system.

³ See any handbook of statistics.

The L-1 precipitation experiment

A silver bromide dispersion was prepared by running a solution of 200 g. of silver nitrate in 1 l. of water into a bromide-gelatin solution with 1700 g. of water. The addition of silver nitrate was adjusted to last for 10 min., and was sensibly constant.

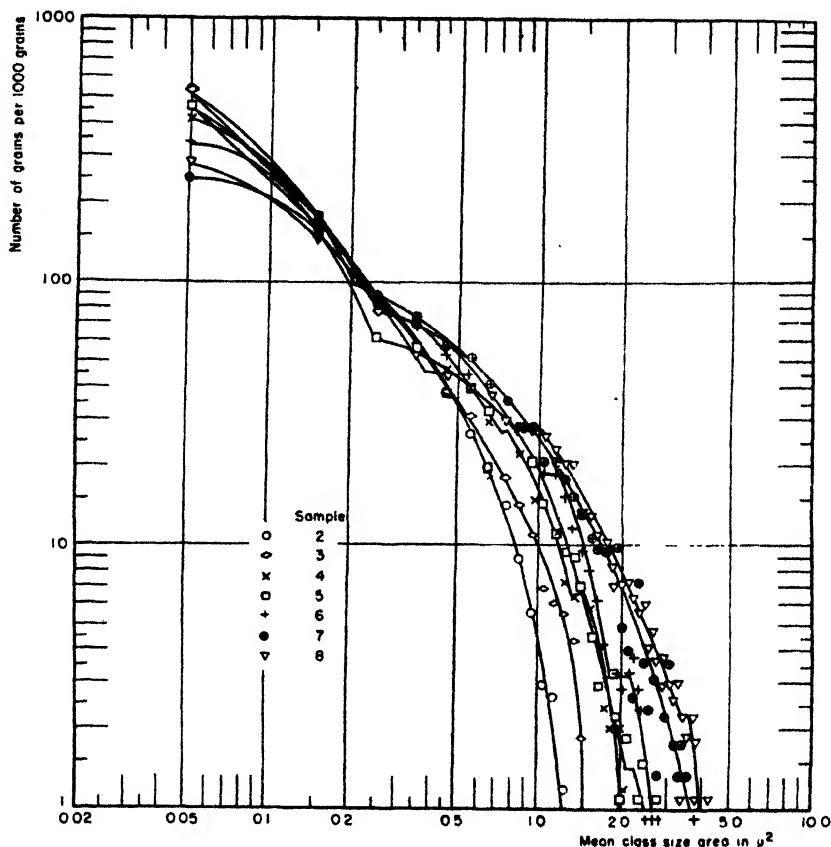


Fig. 7. L-1 precipitation

At given intervals of time (ranging in approximate geometrical progression from a 1-min. period), 5-cc. samples were withdrawn in automatic pipets that had previously been calibrated for the temperature and solutions involved. These samples were immediately diluted and chilled. The data from the particle-size analyses were analyzed by the methods previously discussed.

Particle-size distribution characteristics from volume precipitation

The results of this analysis are best presented for this discussion by the log-log size-frequency curves (figure 7) and the log-size normal functions. It can be seen that the form type of the individual distributions from this more usual type of precipitation is fundamentally the same as that from the simpler stream type of precipitation (*cf.* figures 2 and 6). The individual distributions in this

case are somewhat more complex and the growth relations during the precipitation period are very definitely so, as we should expect. No longer is the width of the log-log curve, corresponding to the basic dispersion of the crystal sizes, a

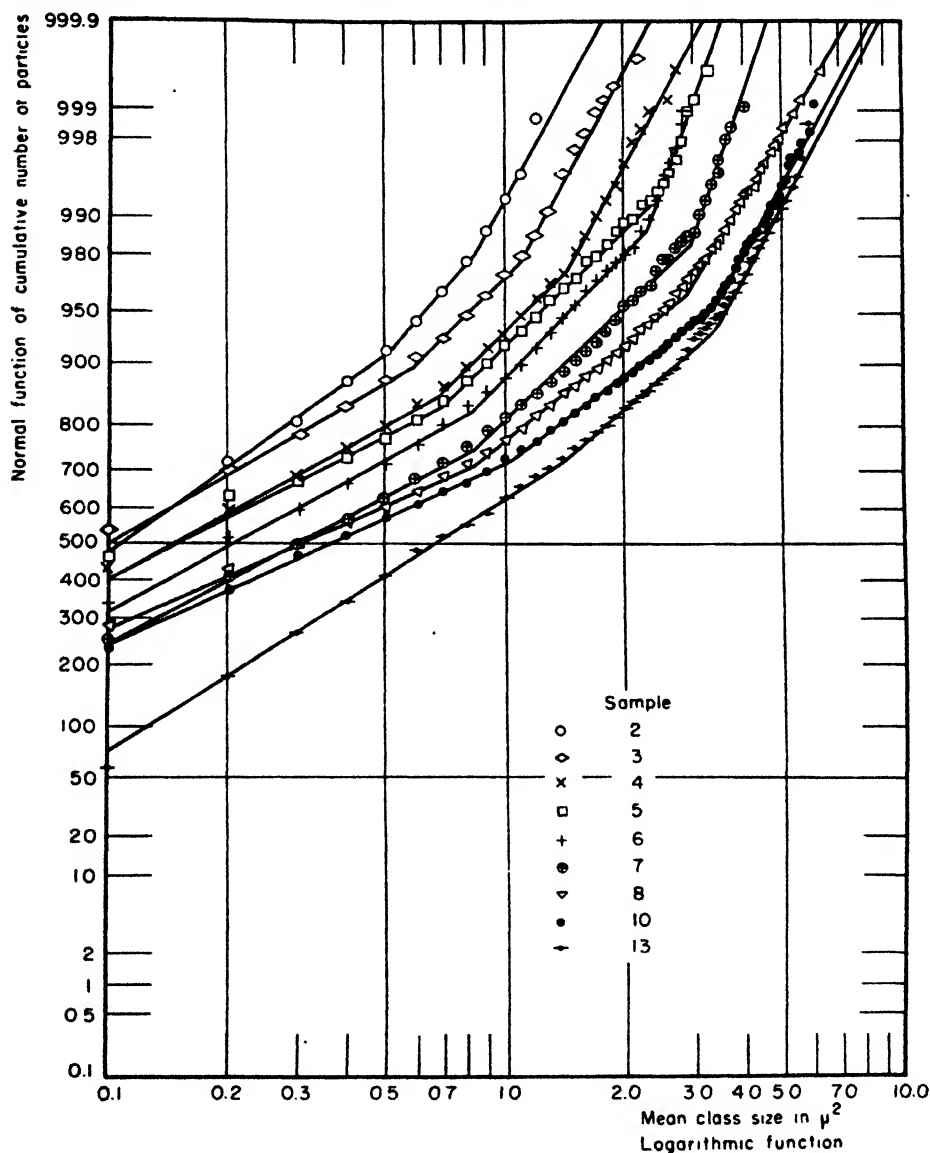


FIG. 8. L-1 precipitation

constant during this period and no longer is formula 1 (page 1007) applicable. When the 10-min. precipitation period is over, the simple growth relations again operate, as can be seen from figure 9 and table 1.

During volume precipitation, the basic dispersion of sizes (width of the log-size-frequency curve), which is not affected by ripening, increases during the

precipitation period. This is substantiated by the data from the size-frequency analyses of another series of volume precipitations where the time of precipitation was constant for each precipitation of the series but the temperature was varied,

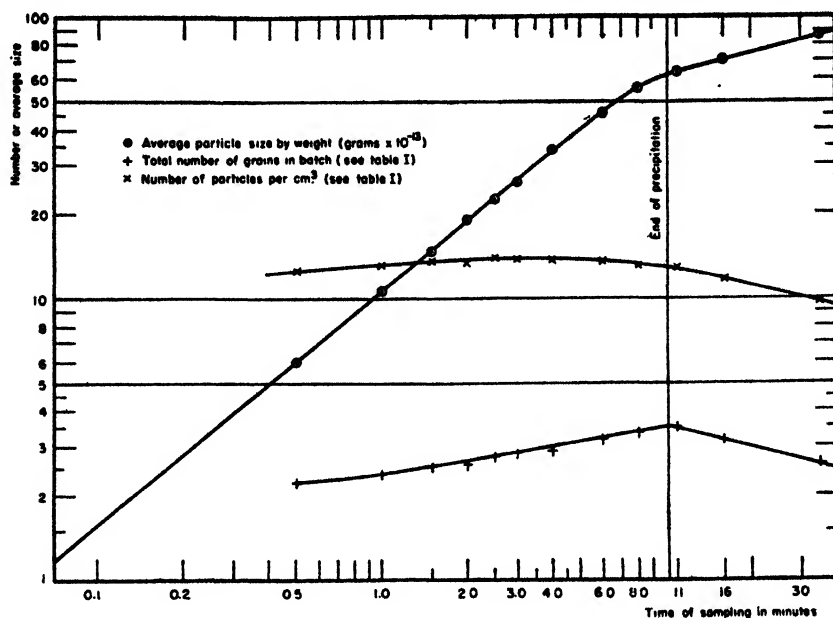


Fig. 9. L-1 precipitation

TABLE 1

Volume precipitation
L-1 precipitation; variable: time

<i>t</i> MINUTES ELAPSED ON SAMPLING	<i>N</i> TOTAL NUMBER $\times 10^{12}$	$[N]$ TOTAL NUMBER PER $\text{CM.}^3 \times 10^{10}$	\bar{g} AVERAGE PARTICLE SIZE PROJECTED AREA IN μ^2	σ DISPERSION AROUND \bar{g} IN μ^2
1.0	118.90	6.55	0.18	0.15
1.5	127.35	6.83	0.21	0.22
2.0	127.85	6.66	0.30	0.32
2.5	138.20	6.98	0.32	0.38
3.0	140.85	6.94	0.41	0.44
4.0	144.45	6.75	0.56	0.61
6.0	158.05	6.74	0.69	0.77
8.0	166.05	6.55	0.80	1.08
11.0	174.40	6.46	0.79	0.97
16.0	157.70	5.84	0.86	1.13
35.0	129.60	4.88	1.12	0.99

that of each successive precipitation from 4 to 8½ being at a higher temperature (figure 14). The greater complexity of this precipitation type is again evident.

The crystal-size distribution form obtained by volume precipitation may be very simple. This is illustrated by the size-frequency distribution curves of the

Seed Lantern emulsion, which were determined very precisely and were presented in the previous paper (9). In this case, the log size-distribution was linear throughout the range, the log-log curve was accurately fitted by a parabola, and consequently, the simple formulas of page 1013 apply rigidly without series expansion.

III. FORMATION OF PARTICLE-SIZE DISTRIBUTIONS

Distribution curve "breaks"

Such a simple size distribution as this is very unusual, however, in silver halide precipitates; indeed, in other precipitates as well. Usually more or less marked discontinuities or "breaks" occur in the distribution curves with the segments of the curves showing the simplified characteristics. As previously pointed out, the breaks have been very useful in showing the nature of the unchanged shift of the distribution curve during crystal growth caused by solvent ripening. These characteristic points can be followed across the graph paper in each succeeding curve formed by the variation of a ripening factor.

If the breaks are merely unchanged indicators during the ripening process, when recrystallization and growth occur, such recrystallization does not produce them and they must be formed during the formation process of the crystals themselves.

Form of the original size distribution

There is little direct evidence, in the data from such precipitation series, as to whether or not the form of the original distribution curve upon precipitation was of a different type, because of the inherent difficulty of obtaining sufficiently early valid samples and the minute size of the particles at this original stage. The lack of parallelism of the lines for the b series of weakest potassium bromide concentration in figure 4 might be considered as indicating that only with this very weak concentration of solvent has the ripening action not come to a saturation limit in its effect.

It will be recalled (cf. page 1018) that the size-frequency distribution of the Seed Lantern emulsion and that of each segment of the other precipitations are strictly of the form that had been derived by Kapteyn and Van Uven (6) on the assumption that an original size distribution had existed that had the "normal" form expressed by the standard Gauss-LaPlace function, but that, with conditions such that growth was proportional to the sizes at each moment, the distribution changed to the lognormal type.

Sheppard and Trivelli (11) have considered that this is consistent with, and can be explained by, the facts that the distributions of velocities of the molecules and ions of a solution as well as the Brownian motions of the particles obey the laws of the kinetic theory and are distributed according to this normal probability law. Since the original crystals are formed by collisions between ions, between ions and particles, and between particles, they considered it reasonable to assume that the initial particle-size distribution of the silver halide crystals was according to this law.

Particle-size distribution of Lippmann emulsions

These assumptions now have independent experimental support in the results of the size-frequency analysis of a Lippmann photographic emulsion.

This type of photographic emulsion is made (13) by volume precipitation but by very rapid addition of the components and without the prolonged solvent effect of a large excess of potassium bromide. As a result, the particles are exceedingly minute, but they are still crystalline (3), although they are so far below microscopic resolution that the coated plates are transparent. Such an emulsion was prepared by E. Yackel, and the size-frequency analysis made by C. E. Hall and A. L. Schoen, of these Laboratories. The measurements made from electron micrographs at 50,000 times magnification were in units of diameter instead of projective area, as were those of the other emulsion. The resultant size-frequency curve is shown in figure 10. Figure 11 shows the data plotted on *arithmetic* probability paper. Obviously the distribution is that of the Gauss-LaPlace law.

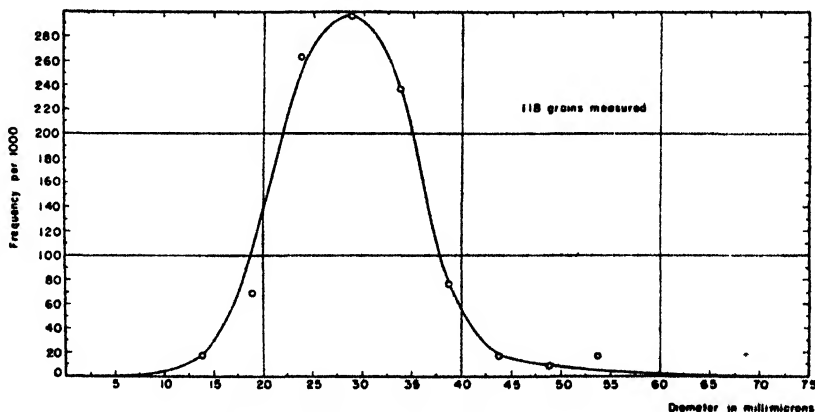


FIG. 10. Regular Lippmann emulsion

It will be noted that there seems to be a break in the distribution near the upper limit of particle size. Previous evidence has indicated that this is not a product of ripening but is a characteristic of the formation of the distribution. This factor is better studied by the analogous curves from another Lippmann emulsion prepared and measured by the same workers (figures 12 and 13). Here we are definitely dealing with a compound "normal curve." Moreover, even without the previous evidence, it is certain that this complexity is not a function of the extremely limited ripening of this type of emulsion.

Theory of formation of size distribution by precipitation

The authors offer the following explanation of these facts: As is well accepted, particle formation by precipitation starts upon nuclei present in the saturated solution. However, there may be various kinds of nuclei, differing in their facility for inducing crystallization, and the readiest will naturally start the process and may become exhausted. The rate of the start of crystallization will then change. Each kind of nuclei would form its own particle-size distribution

which, under ordinary circumstances, may be assumed to be that expressed by the Gauss-LaPlace formula. The breaks in the size distribution observable in its log-log and "normal" functions are caused by this complex nucleation. The crystallization proceeds in the adsorption layer (15) at the surface of the crystal, and hence the velocity of crystallization is very susceptible to impurities.

It might be considered that exhaustion of some impurity during the particle growth phase of the precipitation caused a change of rate which might be reflected as a break in the size distribution. Such a change of rate could only be a speed-

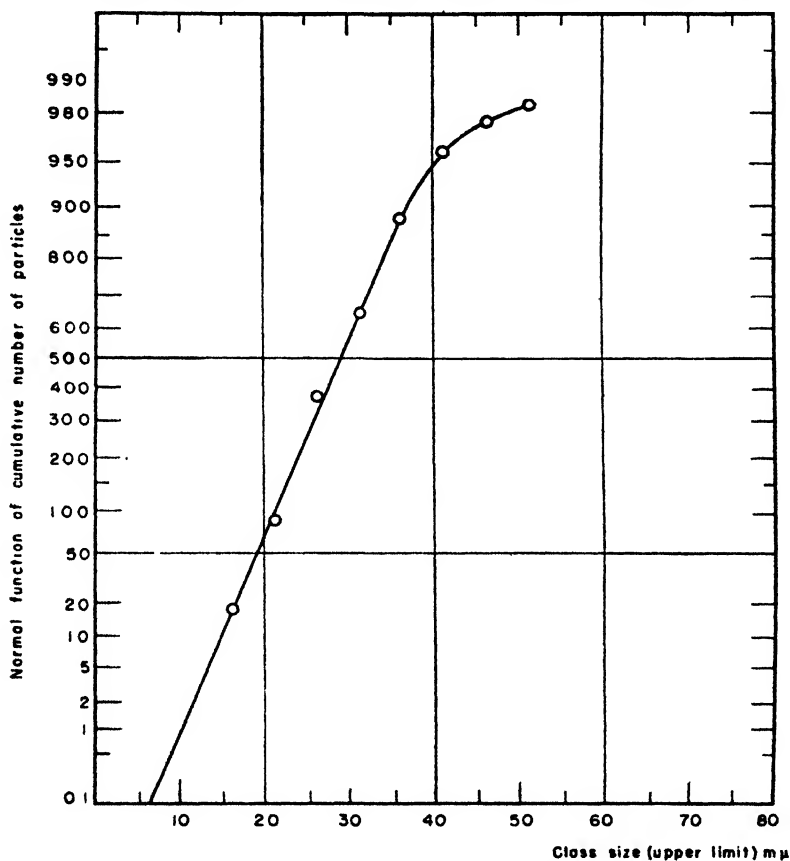


FIG. 11. Regular Lippmann emulsion

ing up, since surface adsorption of impurities can only inhibit crystallization. This is the opposite effect from exhaustion of one kind of nuclei, because that type most easily inducing crystallization will be used up first. Now, when the graphs of the normal functions are examined, such as figures 6 and 8, it must be remembered that the largest particles were formed first. On considering the first derivative of the normal function *but inversely with respect to particle size*, it will be noticed that at each successive break the rate of particle formation decreases. This factor, alone, would invalidate the adsorption of surface impurities as a source of the breaks.

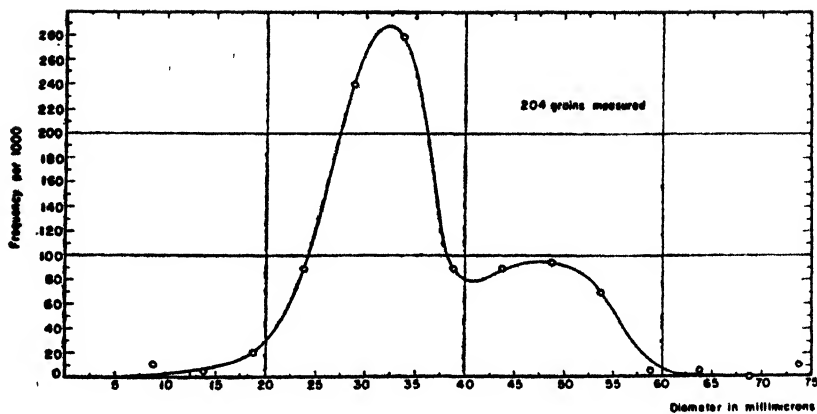


FIG. 12. Lippmann emulsion Y-1432

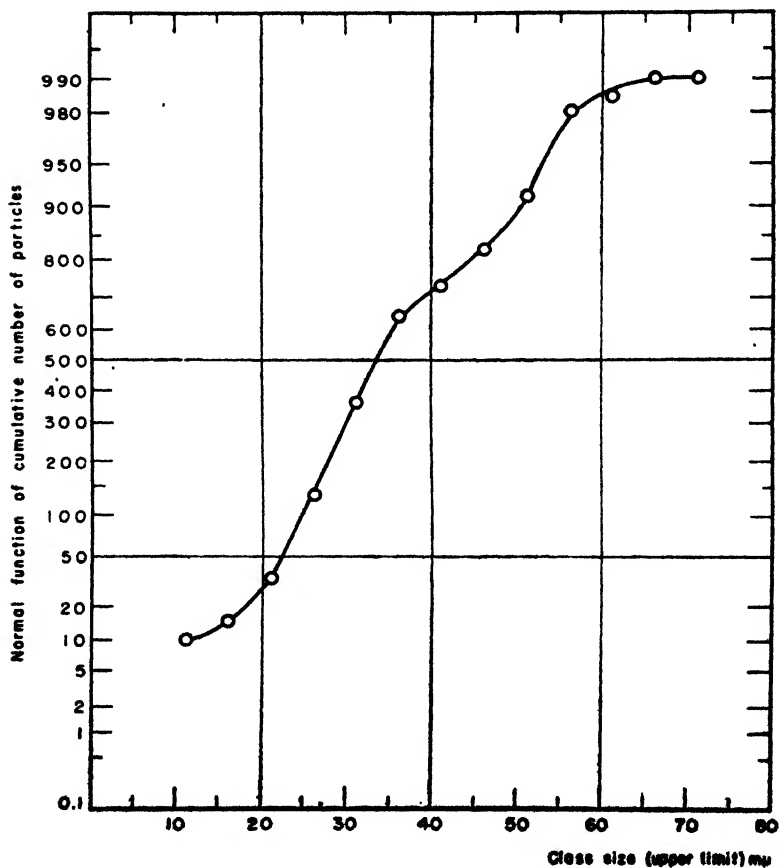


FIG. 13. Lippmann emulsion Y-1432

Formation factors in volume precipitation

With the usual conditions of volume precipitation, especially for silver halides, including the appreciable period of reaction and the presence of solvents of variable concentration, as the excess of the receiving reagent is used up, the picture is even more complicated. The average particle size, $\bar{\alpha}$, and the dispersion around it, σ , are increasing throughout the precipitation, as can be observed

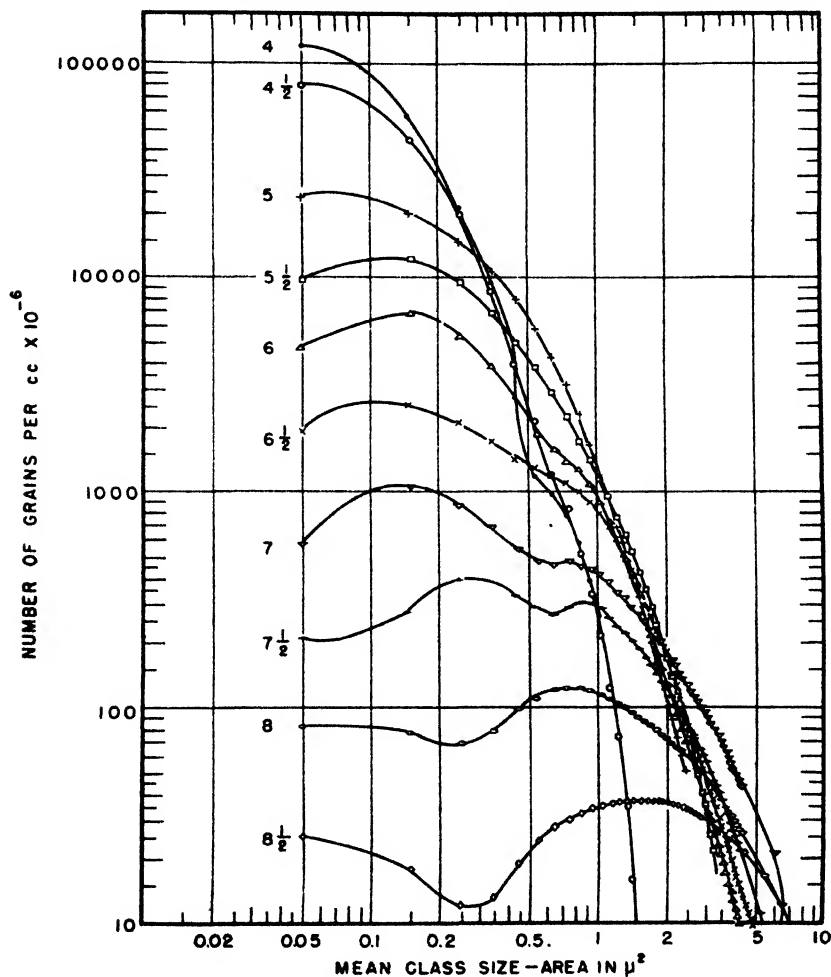


FIG. 14. Volume precipitation

from figure 9 and table 1. These factors, especially the prolonging of the precipitation period, may separate the action of the different types of nuclei still more. In fact, figure 14 represents a case where a so-called "compound curve" was formed during a single straightforward volume precipitation. Each log-log size-frequency curve in figure 14 was obtained from a sample from a precipitation of silver halide lasting about 40 min., each precipitation differing in the temperature which was constant throughout each precipitation.

TABLE 2

Stream precipitation

Series precipitated by R. H. Lambert; precipitated as 0.5 molar AgBr; ripened in KBr as 0.4 molar AgBr

Group b. 2 parts KBr:40 parts AgBr. Number of grains $\times 10^{-3}$ per cc. of solution

CLASS.		1*	1†	2	3	4	5	6	7	8	9	10	11
MEAN CLASS SIZE IN SQUARE MICRONS.		0.06	0.05	0.15	0.25	0.35	0.45	0.55	0.65	0.75	0.85	0.95	1.05
Pre- cipita- tion	Min- utes ripened												
4b	150	6,629.75	6,800.00	1,911.83	641.64	152.67	36.96	14.31	1.18	2.40			
5b	240	4,870.55	5,000.00	1,860.56	681.00	178.90	36.96	16.71	5.98				
6b	345	3,971.58	4,200.00	1,591.03	718.00	230.17	64.40	25.05	9.55	4.76		1.18	
7b	495	2,757.30	2,920.00	1,380.52	647.62	239.73	90.04	44.73	10.14	4.78	3.58	2.38	0.59
7½b	870	2,250.42	2,280.00	1,207.58	421.01	169.36	75.14	45.92	19.68	11.32	5.37	5.96	3.58
7¾b	1110	1,850.13	1,730.00	1,116.93	416.25	173.53	74.55	47.71	22.06	16.10	8.95	8.95	4.17
8b	1395	1,528.84	1,420.00	1,045.97	477.07	179.49	76.93	58.45	20.27	20.27	8.95	11.32	4.17
CLASS.		12	13	14	15	16	17	18	19	20	TOTAL NO. (COR- RECTED)		
MEAN CLASS SIZE IN SQUARE MICRONS.		1.15	1.25	1.35	1.45	1.55	1.65	1.75	1.85	1.95			
Pre- cipita- tion	Min- utes ripened												
4b	150											9,561.0	
5b	240											7,780.1	
6b	345			1.18								6,845.3	
7b	495	1.20	1.20									5,346.5	
7½b	870	2.38	1.20	0.59		0.59						4,249.7	
7¾b	1110	6.57	2.99	2.99		1.20		0.59		0.59		3,634.1	
8b	1395	11.93	2.99	5.96	0.59	1.20	1.20	0.59		1.20		3,348.6	

Group c. 4 parts KBr:40 parts AgBr. Number of grains $\times 10^{-3}$ per cc. of solution

CLASS.		1*	1†	2	3	4	5	6	7	8	9	10
MEAN CLASS SIZE IN SQUARE MICRONS.		0.06	0.05	0.15	0.25	0.35	0.45	0.55	0.65	0.75	0.85	0.95
Pre- cipita- tion	Min- utes ripened											
3c	90	5,067.00	5,820.00	1,429.90	611.80	161.00	50.10	17.90	11.90	1.18		4.76
4c	150	3,440.60	3,800.00	1,085.50	609.40	225.40	74.00	25.00	16.70	2.40		1.18
5c	240	2,061.30	2,050.00	1,130.60	510.40	302.90	130.00	66.80	32.20	9.55	3.58	3.58
6c	345	1,274.60	1,210.00	918.30	474.70	293.40	157.40	88.30	38.20	23.90	5.97	3.58
7c	495	787.87	720.00	701.20	409.10	243.30	136.00	116.90	52.50	31.00	7.16	13.72
7½c	870	224.36	165.00	397.75	296.97	213.48	143.71	116.29	65.60	48.30	28.03	33.99
7¾c	1110	163.98	120.00	323.22	277.89	164.00	116.88	105.55	70.36	48.89	27.43	26.84
8c	1395	82.00	56.00	256.42	248.67	132.39	104.35	103.17	56.66	51.88	31.61	45.32

TABLE 2—Continued

Class.	11	12	13	14	15	16	17	18	19	20	21	22	23	TOTAL NO. (COR- RECTED)
MEAN CLASS SIZE IN SQUARE MICRONS	1.05	1.15	1.25	1.35	1.45	1.55	1.65	1.75	1.85	1.95	2.05	2.15	2.25	
Pre- cipita- tion	Min- utes ripened													
3c	90		1.18											8,109.72
4c	150		1.18	1.18										5,841.94
5c	240													4,239.60
6c	345	1.18	1.18					1.18						3,217.30
7c	495	2.99	2.99	0.59	1.20									2,438.70
7½c	870	7.75	14.31	2.38	1.79									1,535.40
7¾c	1110	13.11	12.52	3.58	2.38	1.79	0.59	0.59		1.79				1,317.40
8c	1395	26.84	21.47	7.75	11.32	3.58	2.38	1.79	1.20	0.59	0.59		0.59	1,164.60

Group g. 6 parts KBr:40 parts AgBr. Number of grains $\times 10^{-8}$ per cc. of solution

CLASS.	1*	1†	2	3	4	5	6	7	8	9	10
MEAN CLASS SIZE IN SQUARE MICRONS	0.06	0.05	0.15	0.25	0.35	0.45	0.55	0.65	0.75	0.85	0.95
Pre- cipita- tion	Min- utes ripened										
2c	60	3,955.16	4,080.00	1,631.57	686.98	234.97	58.43	15.49	7.16	4.76	1.18
3c	90	2,352.54	2,150.00	1,338.17	579.64	324.42	128.81	67.98	21.47	7.16	2.40
4c	150	1,428.98	1,260.00	1,026.89	425.78	279.69	150.88	117.47	26.23	17.28	5.37
5c	240	685.04	540.00	673.86	386.42	238.53	130.01	124.64	71.55	54.87	16.69
6c	345	394.06	315.00	562.51	318.42	190.42	134.37	120.06	71.56	46.12	25.04
7c	495	125.75	91.00	300.14	239.32	166.96	96.21	89.84	62.02	53.67	31.81
7½c	870	41.74	28.00	145.10	151.46	122.04	83.88	81.90	54.86	52.87	32.20
7¾c	1110	42.73	31.80	118.07	139.14	110.91	77.13	83.09	54.47	54.06	31.01
8c	1395	20.87	14.00	80.70	105.34	96.21	78.71	75.13	38.16	42.13	30.21

CLASS	11	12	13	14	15	16	17	18	19	20	21	22	23	24
MEAN CLASS SIZE IN SQUARE MICRONS.	1.05	1.15	1.25	1.35	1.45	1.55	1.65	1.75	1.85	1.95	2.05	2.15	2.25	2.35
Pre- cipita- tion	Min- utes ripened													
2c	60													
3c	90					1.18								
4c	150	1.18	1.79											
5c	240	2.99	2.99	0.59	0.59	0.59	1.79	0.59						
6c	345	7.95	12.32	1.59	2.39	0.80	0.39	0.39	0.39	0.39				
7c	495	18.28	19.08	25.05	11.93	3.18	4.38	2.78	1.99	0.39	1.19			0.39
7½c	870	16.30	18.28	11.13	11.53	6.36	12.32	3.58	4.38	1.19	3.58	1.99	1.99	0.80
7¾c	1110	19.88	22.27	8.74	14.31	5.57	8.74	1.19	4.77	1.59	3.18	1.59	1.59	0.39
8c	1395	19.88	22.66	7.55	12.32	7.16	10.34	3.18	5.96	1.59	8.35	1.19	1.19	0.39

TABLE 2—Continued

CLASS.		25	26	27	28	29	TOTAL NO. (CORRECTED)
MEAN CLASS SIZE IN SQUARE MICRONS		2.45	2.55	2.65	2.75	2.85	
Pre- cipita- tion	Min- utes ripened	0.59	0.39	0.39	0.39	0.39	
2c	60						6,720.54
3c	90						4,622.41
4c	150						3,319.72
5c	240						2,269.38
6c	345						1,842.70
7c	495						1,255.39
7½c	870						877.53
7¾c	1110	828.45					
8c	1395	698.51					

Group d. 8 parts KBr:40 parts AgBr. Number of grains $\times 10^{-8}$ per cc. of solution

CLASS		1*	1†	2	3	4	5	6	7	8	9	10
MEAN CLASS SIZE IN SQUARE MICRONS.		0.06	0.05	0.15	0.25	0.35	0.45	0.55	0.65	0.75	0.85	0.95
Pre- cipita- tion	Min- utes ripened											
2d	60	2,558.27	2,660.00	1,098.45	534.30	277.90	106.16	52.49	14.31	5.98	3.58	3.58
3d	90	1,510.20	1,500.00	980.37	415.05	267.17	152.67	128.81	45.33	20.29	8.34	5.98
4d	150	950.41	910.00	710.82	361.38	195.59	138.95	108.54	49.50	41.74	10.73	13.11
5d	240	412.97	310.00	487.20	291.02	169.36	115.69	101.97	60.83	48.30	33.99	31.61
6d	345	182.37	240.00	342.67	240.11	147.49	108.53	97.40	52.87	55.69	26.63	36.58
7d	495	106.34	78.00	204.73	159.41	120.06	81.10	67.98	51.28	42.93	34.98	33.00
7½d	870	34.29	20.40	80.70	88.25	84.28	55.66	58.44	38.56	37.36	22.27	30.21
7¾d	1110	22.86	13.80	54.47	82.68	76.72	49.29	51.68	34.19	32.00	18.28	23.85
8d	1395	19.88	8.00	40.15	79.11	75.93	43.33	47.70	29.02	30.21	15.90	20.67

CLASS		11	12	13	14	15	16	17	18	19	20	21	22	23	24	25
MEAN CLASS SIZE IN SQUARE MICRONS.		1.05	1.15	1.25	1.35	1.45	1.55	1.65	1.75	1.85	1.95	2.05	2.15	2.25	2.35	2.45
Pre- cipita- tion	Min- utes ripened															
2d	60	1.18	1.18													
3d	90								1.18							
4d	150	3.58	1.79	0.59	1.20	1.20	0.59									
5d	240	12.52	14.31	5.96	6.57	1.79	1.20	1.20			0.59		0.59			
6d	345	16.70	21.07	7.95	9.93	6.76	8.74	1.99	3.58		1.99	0.39				
7d	495	19.08	21.07	11.13	12.73	9.93	10.73	5.57	3.97	2.39	5.16	0.39	0.80			
7½d	870	14.31	15.11	9.93	12.73	5.67	10.34	3.97	5.16	2.39	6.36	3.18	3.58	1.19	3.58	0.39
7¾d	1110	16.70	23.05	7.95	13.51	4.77	9.15	3.97	5.16	3.18	9.15	1.59	2.39	1.19	3.18	0.39
8d	1395	15.50	17.50	7.95	13.12	6.36	8.35	5.96	6.76	1.99	6.36	1.99	2.39	1.99	2.39	1.19

TABLE 2—Continued

CLASS	26	27	28	29	30	31	32	33	34	35	36	37	40	45	TOTAL NO. (COR- RECTED)
MEAN CLASS SIZE IN SQUARE MICRONS..	2.55	2.65	2.75	2.85	2.95	3.05	3.15	3.25	3.35	3.45	3.55	3.65	3.95	4.45	
Pre- cipita- tion	Min- utes ripened														
2d	60														4,760.3
3d	90														3,525.2
4d	150		0.59												2,549.9
5d	240														1,694.7
6d	345														1,427.1
7d	495														976.4
7½d	870	2.78	0.39	1.19	0.39			0.39		0.39					619.6
7¾d	1110	0.80		2.78	3.58		0.39								549.8
8d	1395	3.18	1.59	1.19	0.39	2.39	0.80	0.39	0.80	0.39	0.80	0.39	0.39	0.39	503.7

* The number of particles observed in the first class is that for a class width restricted by the limit of resolution and detection. The latter is taken as $0.02 \mu^2$. The data in this column represent this frequency corrected for graphing by the factor $\Delta x/\Delta x$ ($= 10/8$).

† These values have been corrected to full class width by extrapolation on log-log paper to allow integration and calculation of constants.

REFERENCES

- (1) CAMPBELL, N. P.: J. Chem. Soc. **107**, 475 (Part I, 1915).
- (2) GADDUM, J. H.: Nature **156**, 463 (1945).
- (3) HALL, C. E., AND SCHOEN, A. L.: J. Optical Soc. Am. **31**, 281 (1941).
- (4) HATCH, T., AND CHOATE, S. P.: J. Franklin Inst. **207**, 369 (1929).
- (5) KAPTEYN, J. C.: *Skew Frequency Curves in Biology and Statistics*, 1st paper. P. Noordhoff, Gröningen; E. Steiger Co., New York (1903).
- (6) KAPTEYN, J. C., AND VAN UVEN, M. J.: *Skew Frequency Curves in Biology and Statistics*, 2nd paper. Hoitsema Bros., Gröningen (1916).
- (7) KRUMBEIN, W. C.: "Applications of Logarithmic Moments to Size-Frequency Distributions of Sediments," J. Sedimentary Petrology **6**, 35 (1936).
- (8) KRUMBEIN, W. C.: "The Use of Quartile Measures in Describing and Comparing Sediments," Am. J. Sci. **32**, 98 (1936).
- (9) LOVELAND, R. P., AND TRIVELLI, A. P. H.: J. Franklin Inst. **204**, 193 (1927).
- (10) LOVELAND, R. P., AND TRIVELLI, A. P. H.: J. Franklin Inst. **204**, 377 (1927).
- (11) LÜPFO-CRAMER, H.: "Die Grundlagen der photographischen Negativverfahren," in Eder's *Ausführliches Handbuch der Photographie*, Vol. II, p. 758. W. Knapp, Halle (1927).
- (12) McALISTER, D.: "The Law of the Geometric Mean," Proc. Roy. Soc. (London) **29**, 367 (1879).
- (13) MEES, C. E. K.: *The Theory of the Photographic Process*, p. 34. Macmillan Company, New York (1942).
- (14) SHEPPARD, S. E., AND LAMBERT, R. H.: Colloid Symposium Monograph **6**, 265 (1928).
- (15) TAYLOR, H. S.: *A Treatise on Physical Chemistry*, 2nd edition, Vol. II, p. 1033. D. Van Nostrand Company, New York (1932).
- (16) VAN UVEN, M. J.: "Logarithmic Frequency Distribution," Proc. Acad. Sci. Amsterdam **19**, 533 (1916).

COMMUNICATION TO THE EDITOR

A NOTE ON THE STRENGTH OF ORGANIC BASES

Though the strength of organic acids is fairly well explained and understood from the electronic mechanism, the behavior of organic bases is very anomalous. This has led recently to a rejection by Brown of the thermodynamic dissociation constants of bases in aqueous solution to serve as a measure of base strength, attributing them to "complex solvation effects the importance of which can not yet be estimated"; he takes the strength of binding between a base and a boron trialkyl as a correct measure of base strength. The purpose of the present note is to suggest a new approach, based on classical concepts, which removes some of the anomalies and reconciles the theory and results of Brown with the question of base strength in aqueous solution.

Alkylamines against hydrogen ion: Our main purpose in this note is to draw attention to two hitherto neglected or unnoticed features of the problem. The first point is that the weakness of ammonia is contributed partly by the repulsion of the approaching hydrogen ion by the three positively charged hydrogen atoms around the central nitrogen atom. If one of the hydrogen atoms is replaced by an alkyl group, the approaching hydrogen ion then undergoes repulsion only by the remaining two hydrogen atoms, which are not symmetrically situated about the line of approach. This diminution of the repulsion to the approaching hydrogen ion is the main factor which causes all primary alkylamines to be at least twenty times stronger than ammonia. Of course, the weak electron-donating (+ I) effect of the alkyl groups also contributes partly to this increase of strength.

The second point we want to make is offered to account for the fact that on passing from a secondary to a tertiary alkylamine the base strength invariably falls off very steeply—a fact which is just opposite to what is expected from the classical polar factor considerations. When a basic nitrogen atom captures a proton, it shares some of this positive charge. Now, carbon being electropositive to hydrogen, and an N—C bond being less polarizable than an N—H bond, the tertiary nitrogen atom will have less tendency to capture a proton than a secondary amine has, a fact which will make the former weaker. This idea, which we propose to call 'polarstriction effect', since it arises out of a restrictive effect on an atom to assume a charge owing to the unsuitable electronegativity of the adjoining atoms, is taken from Pauling, who proposed it to explain the unexpected weakness of dialkyl-substituted guanidines. This opposition by the carbon atom is strongest with the methyl group, since the natural tendency of the methyl group is to keep the nitrogen most negative by supplying it electrons by the "hyperconjugation" mechanism; hence, methylamines are the weakest alkylamines. Of course, steric factors depending on the size and shape of the alkyl groups are also operative, but we consider the polarstriction factor to be most important in the matter.

Bases against generalized acids: If the approaching acid is not the positively charged hydrogen ion but is a neutral molecule, e.g., a boron trialkyl, the power-

ful electrical forces arising out of the charged hydrogen ion become practically absent, though not completely absent as formal charges are now involved, and other factors begin to assume more importance. Brown has successfully explained the base strength under such circumstances as due to an interplay between the classical polar factor and a steric factor originating out of the size of the alkyl groups present in the acid and/or the base. Though substantially agreeing with Brown's theory we are inclined to think that his steric factor should also include the polarstriction effect we have discussed, which becomes more probable from the fact observed by Brown that the tertiary amine is invariably weaker than the secondary amine, though the relative strengths of the other amines vary with the nature of the alkyl group present in the acid and/or the base.

SANTI R. PALIT.

Polytechnic Institute of Brooklyn

Brooklyn, New York

April, 1947

NEW BOOKS

Oxidation. A general discussion held by the Faraday Society, September, 1945. 398 pp. London: Gurney and Jackson, 1946. Price: 20 shillings.

The appearance of this volume, containing thirty-two papers presented at a symposium on oxidation, marks a welcome return by the Faraday Society to the policy it had long followed before the war of holding symposia from time to time on subjects of current interest in theoretical chemistry. The subject of oxidation affords a wide spread of topics in many fields of theory and practical application. The general discussions interspersed through the sessions form a most valuable part of the symposium. While the theoretical aspects of oxidation receive full attention, the subject of combustion naturally led to the consideration of fuels and explosive gas reactions.

S. C. LIND.

Abridged Scientific Publications from the Kodak Research Laboratories. Vol. XXVII. 314 pp. Rochester, New York: Eastman Kodak Company, 1945.

This is a continuation of the publication in abridged form of papers which have been previously published in full in English in scientific periodicals. The present volume contains fifty papers published in American and British journals.

S. C. LIND.

Reactions at Carbon-Carbon Double Bonds. By CHARLES C. PRICE. vi + 120 pp. New York: Interscience Publishers, Inc., 1946. Price: \$2.50.

This interesting little book is the result of a group of lectures given by Professor Price at Polytechnic Institute of Brooklyn under the direction of Dr. H. Mark. As stated in the Introduction, this book is the first volume of a series of "Lectures on Progress in Chemistry."

Written in the "eventful summer of 1945," this work constitutes one of the finest reviews of the subject to be found anywhere. While many researchers in physicoorganic chemistry may not share the position taken by Dr. Price in his reluctance to accept the application of

resonance theory to certain aspects of this subject, there is no doubt that his attitude will provoke much new experimental work by the disciples of resonance theory.

Interconversion through hydrogen bonding in the enol forms of β -diketones (page 8) and the dimers of simple carboxylic acids is apparently treated as an application of resonance. This is undoubtedly a case of tautomerism and not resonance, since the hydrogen atom is not situated equidistant from the two oxygen atoms. Hydrogen bonds in general owe their existence to coulombic attraction. There are probably two identical minima in the energy *vs.* internuclear distance curves for these molecules.

A few inconsistencies and small typographical errors are to be noticed. On page 59 it is stated that, "The data thus suggest that primary, secondary, and phenyl radicals are much more reactive than tertiary or benzyl radicals." Yet on page 60 one finds that "The order of reactivity of alkyl free radicals, $I^\circ < II^\circ < III^\circ$," etc. Reference is made on page 31 to the "polarizability of the electrons." Atoms and molecules are polarizable, but the polarization of an electron is probably out of the realm of human imagination. An oxygen atom is missing from the quinone formula on page 86, and formula "B" on page 102 carries a negative charge by mistake.

This book represents a distinct contribution to the chemistry of carbon-carbon double bonds and should be read by all organic chemists. At two cents per page, this volume is certainly not overpriced.

RICHARD T. ARNOLD.

Tables of Spherical Bessel Functions Prepared by the Mathematical Tables Project, Columbia University Press, 1947.

This is one of the series of mathematical projects begun at Columbia University in 1937 and continued at the Bureau of Standards. The tables in the present volume will be of use especially to those interested in the practical application of wave theory in both the old and the new fields in which this type of mathematical analysis is required.

S. C. LIND.

Rarer Metals. By JACK DEMENT AND H. C. DAKE. 392 pp. New York: The Chemical Publishing Company, Inc., 1946. Price: \$7.50.

This publication is primarily intended for those interested in the practical aspects of the mineralogy, chemistry, physical properties, and metallurgy of some of the less familiar elements. Seven groups constitute segregated chapters: beryllium; gallium, indium and thallium; germanium, titanium, zirconium, hafnium, and thorium; vanadium, columbium, and tantalum; molybdenum, tungsten, and uranium; selenium and tellurium; and the six platinum metals.

There are several appendices: an abridged bibliography by R. B. Gordon; a table of atomic weights; the periodic system of the elements; the per cent of about fifty metals in the order of their abundance in igneous rocks, according to Clark and Washington; and an alphabetical subject index. In the opinion of the reviewer uranium (at 8.10^{-2} g. per gram) is ranked about tenfold too high in abundance.

S. C. LIND.

The Chemistry of Free Radicals. By W. A. WATERS. 295 pp. New York: Oxford University Press, 1946. Price: \$6.50.

The chemistry of free radicals is one of the most important topics of present-day science from both the theoretical and the practical points of view.

Dr. Waters has condensed into a relatively small space an excellent survey of gas- and liquid-phase radical reactions which should be of value to all chemists and to organic chemists in particular.

Titles of the twelve chapters are as follows: I. The Discovery of Free Radicals; II. Physical Properties of Free Radicals; III. Triphenylmethyl and its Analogues; IV. Free Radicals Containing Elements other than Carbon; V. Free Atoms and their Gas Reactions;

VI. Photochemical Decompositions; VII. Reactions of Free Alkyl Radicals; VIII. Free Aryl Radicals and their Reactions in Solution; IX. Reactions Catalyzed by Free Radicals; X. Reactions Involving Metals; XI. Some Oxidation Mechanisms; XII. Some Possible Mechanisms for Biochemical Processes.

Certain small and obvious errors or omissions are noticed. The word "bases" (page 111, last line) should probably read "cases". In the first formula on page 112 one sulfur and one oxygen atom are missing. The term "*trans*-dibromocinnamic acid" (page 179) is an unfortunate choice—indeed, its use here is incorrect—in spite of the logic behind its application in this particular case. In view of the recent investigations by Bartlett and Nozaki, as well as those by Marvel, Prill, and DeTar dealing with the polymerization of maleic anhydride and its derivatives, some change is now necessitated at the bottom of page 199.

The clarity of this presentation of data and the critical analysis of alternate possibilities found throughout the text makes this volume a choice item in the reviewer's library.

RICHARD T. ARNOLD.

Helium. By W. H. KEESOM. 494 pp.; 258 illustrations. Amsterdam, London, New York: Elsevier Publishing Company, 1942. Price: \$10.00.

The devotion of an entire book of almost five hundred pages to a single element permits of an admirable thoroughness of treatment, especially when the element has no chemical affinity and attention may be confined to the atomic state. Much of the interest in helium derives from its lightness and chemical inertness and its extremely low melting and freezing points.

Helium was first liquefied in 1908 in the laboratory of Kammerlingh Onnes at Leiden, in which Keesom has been the principal collaborator and of which he has been Director for the past several years. No one could be found more suited to describe the searching studies that have been made of helium from many varied points of interest and nothing has been neglected from its spectacular discovery in the sun down to the latest results in its ejection from the nucleus of heavy atoms in the form of alpha particles. The occurrence, production, and commercial uses are discussed. Even the regulations for the export of helium from the United States are quoted. The gaseous, liquid, and solid states, as well as the properties of the atom such as its spectra and energy, are fully treated. The final chapter is devoted to the helium nucleus.

S. C. LIND.

Nuclear Physics Tables (64 pp.) by J. MATTAUCK and *An Introduction to Nuclear Physics* (109 pp.) by S. FLUEGGE. Translated by Interscience Publishers, Inc. 8 colored plates. New York: Interscience Publishers, Inc., 1946. Price: \$12.00.

This work, as the title indicates, consists of two rather distinct though related parts. The *Tables* contain data collected at the Kaiser Wilhelm Institut up to 1941 for all stable and radioactive isotopes. Full literature references are given. Although the *Tables* are now six years old, they nevertheless contain much material in convenient form which could not be found without wide searches in the literature of several decades just past.

The *Introduction to Nuclear Physics* will also be found valuable, especially to new students of the subject, though it suffers from the lack of any literature references.

S. C. LIND.

German-English Science Dictionary. By LOUIS DeVRIES with the collaboration of members of the Graduate Faculty, Iowa State College. 2nd edition. 558 pp. New York: McGraw-Hill Book Company, Inc., 1946. Price: \$4.50.

This book, very convenient in size and construction, contains 48,000 entries of the English equivalents of German words used in science. The second edition is about 50 per cent larger than the first and has been revised so as to make it more useful to chemists. It also includes words used in the biological, agricultural, and other physical sciences. Several useful tables have been added covering abbreviations, chemical elements, and physical units of measurement.

S. C. LIND.

Inorganic Chemistry. By W. NORTON JONES, JR. 817 pp. Philadelphia, Pa.: The Blakiston Company, 1947. Price: \$4.25.

This book is another addition to the already overcrowded field of general inorganic chemistry texts for the beginning college courses. However, there are a number of features about the book that warrant its publication.

After a brief introduction and a short discussion of the varieties of matter and of measurement and calculation, the reader is introduced to the structure of the atom and then the relation of chemical change to atomic structure. Following this is the chapter on the periodic relation of the elements. In all subsequent descriptive chapters constant reference is made to atomic structure and periodic relationships, and the chemical and physical behavior of each new element or family of elements is discussed in the light of electronic structure, and interrelationships are pointed out. This treatment, for example, certainly gives a clearer and more concrete picture of the number of bonds or valence of an element than the time-honored nebulous definition, "The measure of the combining power of an atom." It is the reviewer's firm conviction that a real understanding of the properties and reactions of the elements and their compounds, mass relationships, theory of acids and bases, etc., can only be obtained by a clear conception of simple atomic structure and electronic configuration,—certainly not from memory.

Except when the more modern theories and laws have had a direct and logical evolution, all historical matter has been omitted. Many times the course of chemical history has been so meandering that it has served only to confuse rather than to clarify. However, in order not to ignore this phase of the subject completely, the book is liberally interspersed with photographs of outstanding scientists, accompanied by brief sketches of their lives and contributions.

The chapters are fairly standard, although they have been thoroughly shuffled to give a different order of presentation. In the early descriptive chapters, the individual elements in the third period are discussed separately, without reference to other members of their family. The latter part of the book then deals with the periodic groups in the standard way. This throws the two elements hydrogen and oxygen, generally introduced first, into chapters 23 and 25, respectively.

Several minor lapses occur in the text: e.g., on page 93, in treating the ionization potential, the statement is made that sodium has the lowest ionizing potential of the elements of period three, whereas on page 251 the statement is made that the $3s$ electron is removed from the atom (of aluminum) more easily than the $3p$ electron of sodium. On page 64 the author states "... oxidation is now considered to be any process by which the valence of an atom is increased." Obviously, he means positive valence.

At the end of each chapter references are given to collateral reading, including such magazines as *Life*, *Fortune*, and *Popular Science*. Forty-nine pages of questions and problems—all without answers—are appended.

Physically, the make-up of the book is good. It is "bound in high grade materials which are sturdy, vermin-proof, and water resisting."

T. D. O'BRIEN.

Kinetic Theory of Liquids. By J. FRENKEL, Physico-technical Institute, Leningrad. xi + 488 pp. London: Oxford University Press, 1946. Price: \$13.00.

This excellent book by Professor Frenkel should be welcomed by all chemists and physicists who are interested in modern theories of matter in a condensed state and who will appreciate a critical discussion of the subject in a volume of moderate compass. In spite of the restrictive title of the treatise, the author devotes a considerable portion of the treatment to matter in the crystalline state.

A list of the chapter headings will perhaps best serve to indicate the main topics treated by the author. These headings are: Real Crystals at Elevated Temperatures; Perturbation of Alternation and Orientation Order in Mixed and Molecular Crystals; Properties of

Liquids and Mechanism of Fusion; Heat Motion in Liquids and their Mechanical Properties; Orientation and Rotational Motion of Molecules in Liquid Bodies; Surface and Allied Phenomena; Kinetics of Phase Transitions; Properties of Solutions; and High Polymeric Substances.

F. H. MACDOUGALL.

Inorganic Syntheses. Vol. II. Edited by W. C. FERNELIUS. xii + 293 pp. New York: McGraw-Hill Book Co., Inc., 1946. Price: \$4.00.

The second volume of *Inorganic Syntheses* follows the general pattern established by the first, but several marked improvements have been introduced. Methods of synthesizing eighty-one varied compounds are presented, the list including some relatively simple substances, such as barium bromate and nitric oxide, as well as such complex materials as triammonium imidodisulfate and dichloro-*bis*-ethylenediamine-cobaltic chloride. Relatively large amounts of space are devoted to the separation and purification of rare earth materials (33 pages) and to derivatives of the less common acids of sulfur (24 pages).

The directions for all of the preparations have been made as specific as possible, and each synthesis has been checked by at least one independent investigator to insure the workability of the procedures and the elimination of directions which might be misinterpreted.

In addition to the experimental part, the volume contains articles on the properties of several of the important types of inorganic compounds for which methods of preparation are given. These include the metal derivatives of the 1, 3-diketones, compounds of the rare earths, and the metal carbonyls.

The nomenclature and indexing used in Volume I have been greatly improved in Volume II, and the book contains a short but excellent article (by Miss Janet D. Scott) on the nomenclature of inorganic compounds. The index is cumulative for both volumes.

The series of volumes on inorganic syntheses is designed to help laboratory workers in the preparation of all sorts of inorganic chemicals, and to outline techniques which may be adapted to inorganic preparations. The need for such help was evidenced by the warm reception accorded to Volume I. The current volume, with its numerous improvements, should be even more valuable.

JOHN C. BAILAR, JR.

Physical Chemistry for Colleges. By E. B. MILLARD. 6th edition. 682 pp. New York and London: McGraw-Hill Book Company, Inc., 1946. Price: \$4.50.

Professor Millard has again undertaken the difficult task of presenting elementary physical chemistry to beginning students. In this, the sixth edition of his widely used text, the greater part of the subject matter has been rewritten, but the selection and order of the topics are essentially the same as in the preceding edition.

The introductory chapter of the previous edition has now been expanded into two chapters: Introduction—Determination of Atomic Weights; and Elementary Thermodynamics. Then follow chapters on: Properties of Substances in the Gaseous State; Properties of Substances in the Liquid State; Crystalline Solids; Solutions; Solutions of Ionized Solutes; Thermochemistry; Equilibrium in Homogeneous Solutions; Heterogeneous Equilibrium; Phase Diagrams (formerly included in the previous chapter); Kinetics of Homogeneous Reactions; Radiation and Chemical Change; Periodic Law of the Elements; Radioactive Changes; Atomic Structure; Colloids—Surface Chemistry; Free Energy of Chemical Changes; and Potentials of Electrolytic Cells. The number of pages has been increased from 600 in the fifth edition to 682 in the present edition; the number of problems has been increased from 327 to 355.

The treatment of topics is, on the whole, quite good. Many of the more difficult concepts are excellently illustrated by the large number of numerical problems worked out in detail in the text. The large number of tabulated data serve not only as a basis for some of the problems for the student, but help him to understand the experimental basis for the laws of

physical chemistry, and, in many cases, the limitations of their validity. The author has wisely kept these numerical data up to date in each new edition, in order that real deviations between experiment and the corresponding law shall not be concealed by the experimental errors. A large number of references to the original literature are given, particularly for the numerical data in the text and in the problems.

The student may, however, find some aspects of this volume a little confusing, and it will be the teacher's duty to help him along. For example the text contains an unnecessarily large number of alternative and sometimes not entirely correct definitions. Heat capacity is defined on page 36 by the relations $C_v = (\partial E/\partial T)_v$ and $C_p = (\partial H/\partial T)_p$, on page 79 by $C_v = (dq/dT)_v$ and $C_p = (dq/dT)_p$, and on page 83 by $C_v = dE/dT$ and $C_p = dH/dT$. It would be well to use only one of these as a definition and derive the others. That given on page 79 is probably to be preferred, because it is not restricted to systems in which the only temperature-dependent work term is that due to expansion work. In any case the important restriction that $(\partial E/\partial \epsilon)_T = 0$ was not stated in connection with the definition given on page 83. Other examples of similar difficulties are the two definitions of the iso-electric point on pages 584 and 585, and the two definitions of free energy on pages 45 and 594.

Some inconsistencies appear in the proof of constant enthalpy in the Joule-Thomson experiment. A change in what constitutes the system occurs during the argument, and as a result some misleading statements are made. Instead of calculating the work done by the original system (the whole sample of gas) on the surroundings, the author divides the gas in the porous plug into thin sections. Then, "The gas in each thin section does work on the section ahead, . . ." This analysis leads to the relation $dw = d(pv)$, even though p varies, and ultimately to "the special thermodynamic equation for the Joule-Thomson effect, $dE = -d(pv)$," which is then integrated.

Several difficulties in the field of molecular structure were noted. The atoms in the oxygen molecule are said to share two pairs of electrons on page 167, but are combined "not merely by sharing two pairs of electrons" on page 562. Actually, the triplet ground state of the oxygen molecule requires two unpaired electrons and these are probably involved in the bond. Cesium chloride is not body-centered cubic (pages 168 and 178) but rather simple cubic; the point at the center of the cube (page 162) must be identical with that at the corner before the lattice on which a structure is based can be called body centered. The author also states on page 155 that "chain hydrocarbons are linear." Of course, they are not linear in the sense that the atoms in carbon dioxide are arranged linearly; the difficulty here may be related to the statements on pages 135 and 139, where it is stated that the carbon-carbon distance as determined from film thicknesses (1.4 Å.) "agrees with" the value as determined by x-ray diffraction (1.54 Å.). The appearance of formulas of the type $(H_2O)_n$ on pages 133 and 134 seems unfortunate in view of the excellent more recent work on the structure of water. In this connection the explanation of the anomalously high conductances of H_3O^+ and OH^- in terms of the structure of water were not found by the reviewer.

A few of the important typographical errors may be worth noting. The dimensions for the acceleration of gravity are given as cm. per sec. on page 22; the first equation on page 69 should read $-d_p = \rho g dh$; the dimensions of pressure are incorrectly given on page 208; the distance 10 Å. corresponds to $1 m\mu$ instead of 1μ as stated on page 567; and a few electrons and symmetry elements are missing from the structural formula for BF_3 (page 561), which has D_{3h} symmetry. Typographical errors such as those on pages 43, 298, 365, 552, and 612 will probably not disturb the student. The binding and the paper on which the text is printed are quite good, in view of present conditions. Naturally, the price has gone up.

I do not wish to emphasize the inaccuracies or errors noted above, or those which I felt were not worth mentioning. This sixth edition of Professor Millard's book is an excellent text for the beginning student, and, under the guidance of a competent teacher, can be most heartily recommended.

WILLIAM N. LIPSCOMB.

Physikalische Chemie in Medizin und Biologie (Physical Chemistry in Medicine and Biology).

By W. BLADERGROEN. 476 pp. Basel, Switzerland: Wepf et Cie Verlag, 1946. Price: 25 francs (Swiss).

This book aims at presenting a cross section of a science which is called by Schade and Habler "physico-chemical medicine." The author has succeeded in presenting concisely the fundamentals of physical chemistry with their significance in biology (including physiology). The chapters are written in an original way, and the book is not a combination of two independent sections on physical chemistry and biophysics and biochemistry brought together in one cover.

In the chapters dealing with the fundamentals the author considers the interests of and stimulates his biological readers by emphasizing the biological significance and applications of many phenomena. It is quite refreshing and enlightening to find in the first chapter on atoms, ions, and molecules a section devoted to the origin of the radiation of the sun.

The following review of titles of chapters shows the wide scope of the book: Atoms, Ions, and Molecules; Thermodynamic Considerations; Aqueous Solutions; Acid-Base Equilibria; Interface Phenomena; Colloids; Structure of the Living Substance; Colloid-chemical Phenomena in the Organism; Important Osmotic Phenomena; Oxidation-Reduction Potential; Problems of Metabolism and Biological Oxidation.

The author states in the preface that he has emphasized especially those topics which are of interest to the student in medicine and the practising physician. The medical doctors and also the medical students in Switzerland must have a background in physical chemistry and even in mathematics which is far more thorough than that of their colleagues in this country. Neither the average American doctor nor the American student of medicine can digest the contents of this excellent book. However, it should be of great value to the student of and scholar in biology, and more specifically biochemistry and biophysics. The book demonstrates clearly that physical chemistry is an integral part of biology and physiology.

The text is quite modern, although certain treatments are outdated. The Nernst derivation of the electrode potential should be replaced by a more modern one; the glass electrode suffers a stepmotherly treatment; a few words might have been said of modern theories of acids and bases; the Langmuir adsorption isotherm certainly should have been discussed with that of Freundlich (page 204). From a chemical view the assumption of the occurrence of the reaction $\text{H}_2\text{CO}_3 + \text{NaCl} \rightarrow \text{NaHCO}_3 + \text{HCl}$ is awkward, even though such a reaction apparently may take place under certain conditions in the body.

The book is eminently suitable as a text in advanced biochemistry and biophysics, and it should stimulate further development of biology on a physicochemical basis.

I. M. KOLTHOFF.

Organic Analytical Reagents. Vol. I. By FRANK J. WELCHER. 442 pp. New York: D. Van Nostrand, Inc., 1947. Price: \$8.00.

As stated in the preface, the main purpose of the book is to assemble in one place a description of all organic compounds used in the analysis of inorganic substances, and to present a discussion of the methods employing these reagents. Three more volumes will follow to complete the work.

The first five chapters (50 pages) are of a general nature; they deal with the electronic theory of valence, coordination compounds, chelate compounds, types of chelate rings, and the effect of structure on solubility. The chapter on coordination compounds is based on the Werner theory, extended by that of Sidgwick. No reference is made to Pauling's work and his well-known book. As far as credit to analytical chemists is concerned, the author has carefully avoided any reference to Feigl's books. Feigl's pioneer theoretical and practical work is still the basis of further developments in the use of organic reagents in inorganic analysis. The omission is deplorable, not only because Feigl deserves universal recognition, but also because in research dealing with organic reagents in inorganic analysis, Feigl's theoretical work is a stimulating guide. It also appears that infrequently the author copies his statements from available texts without acknowledgment.

The other twenty-two chapters in the book deal with the use of hydrocarbons, alcohols, phenols, 8-hydroxyquinoline, ethers, aldehydes, and ketones in qualitative and quantitative inorganic analysis. At one place all the uses of a given reagent are given, irrespective of whether it is a solvent (or precipitant) or a chemical agent. This treatment has definite advantages.

The book comprises a compilation of the literature and is non-critical. As a matter of fact many obviously inferior reagents and methods are included, "since the treatment of the subject is intended to be complete." In the reviewer's opinion the parts dealing with "inferior" reagents could have been condensed considerably and the book would have benefited from it.

At the end of the book there is an index of names and synonyms of organic reagents and an index of uses of organic reagents. The latter is especially valuable, because under a given inorganic constituent to be detected or determined the uses of various reagents are listed, with reference to the corresponding page numbers.

For many years analytical chemists have felt the need for a complete review of the use of organic reagents in inorganic analysis. The author and his assistants deserve praise and gratitude for their painstaking job. No doubt the book will be consulted quite generally by everyone who wishes to obtain a complete account of the determination of an inorganic constituent with an organic reagent.

I. M. KOLTHOFF.

Analytica Chimica Acta. Paul-E. Wenger (8 rue St. Victor, Geneva, Switzerland), *Editor*. G. Charlot, C. Duval, F. Feigl, R. Flatt, J. Gillis, C. J. Van Nieuwenburg, and N. Straford, *Assistant Editors*. No. 1 of Vol. I, January, 1947. Published monthly. New York and Amsterdam: Elsevier Publishing Co., Inc. Price: \$9.50 per year.

This new journal differs from the others covering the analytical field in its avowedly international range. It is subtitled "International journal dealing with every branch of analytical chemistry." Its appearance at this time seems particularly appropriate, because the renowned *Zeitschrift für analytische Chemie* is at present not being published and a notable lacuna thus exists so far as analytical chemistry is concerned in continental Europe, if not the world. In the first number of the *Acta* we find eight papers by French, Belgian, and Swiss authors. Original contributions and review papers are represented.

In the foreword, the editors remark, "When speaking of modern analytical chemistry, it is plain that the term covers the most widely divergent fields of study. The success of our journal accordingly depends on the confidence which research workers in all branches will place in us by sending us their contributions."

E. B. SANDELL.

DIELECTRICS AND RHEOLOGY OF NON-AQUEOUS DISPERSIONS

ANDRIES VOET

Ink Division, Research Department, J. M. Huber Corporation, New York, New York

Received January 31, 1947

I. INTRODUCTION

The object of this investigation was to obtain more information about the state of agglomeration of finely divided particles dispersed in organic liquids. While dispersions made with conventional apparatus, such as roller mills, ball mills, hammer mills, colloid mills, etc., usually show a comparatively small particle size on microscopic observation, there are nevertheless indications that in concentrated dispersions secondary particle agglomeration occurs. A study of the rheology of pigment dispersions, for instance, revealing the existence of plastic and thixotropic systems in many cases, strongly suggests the existence of partly flocculated systems, the structure of which is thought to be destroyed by the application of shearing stresses.

Yet no direct proof of the destruction and rebuilding of such flocculated particle structures has been offered by rheological investigations (5). In addition, the phenomenon of plug flow has rendered a proper interpretation of the rheological behavior of pigment dispersions at very low shearing stresses rather uncertain (2), making our knowledge of particle agglomeration at low shearing stresses very incomplete. Finally, nothing is known about the progressive particle agglomeration in a dispersion at rest.

The method of direct observation by means of optical or electron microscopes¹ of the concentrated dispersions proper, without interference, has hitherto not been possible.

The study of the dielectric properties of pigment dispersions at rest as well as when subjected to varying shearing stresses has made it possible to obtain more direct information regarding the existence of such structures.

The theoretical treatment of the dielectric constant of a dispersion was attempted at the end of the last century. It soon became evident, however, that calculations on the basis of the well-known Clausius-Mosotti relation were totally inadequate when the dielectric constants of dispersion medium and dispersed material were different. This is most likely due to the fact that Mosotti's hypothesis as to the internal field is not fulfilled. The related Lorentz-Lorenz equation is equally invalid (3).

The problem was studied theoretically by Rayleigh (10) and later by O. Wiener (14), Lichtenecker (7), and Bruggeman (1).

An experimental study of the validity of the various theoretical considerations was made by Guillion (6), who investigated the dielectric constant of particles of various materials dispersed in air as well as in organic liquids. The results of this study may be summarized as follows: The dielectric constant ϵ of a disper-

sion of a material of dielectric constant ϵ_1 , dispersed in a volume fraction, V , in a medium with dielectric constant ϵ_2 , depends not only on ϵ_1 , ϵ_2 , and V , but also on the form of the particles, and is independent of the size of the particles. The minimum dielectric constant was found for spherical particles, while a considerable increase was found for non-spherical particles.

For spherical particles an equation proposed by Bruggeman (1) appeared to be covering the experimental data very well, while none of the other proposed equations was satisfactory. The equation:

$$1 - V = \frac{\epsilon_1 - \epsilon}{\epsilon_1 - \epsilon_2} \sqrt[3]{\frac{\epsilon_2}{\epsilon}} \quad (1)$$

holds for any dispersed phase regardless of its own dielectric constant. It is valid even for an infinitely high dielectric constant of the dispersed phase, such as for particles of metals or other conductors. In the latter case the equation is simplified to:

$$1 - V = \sqrt[3]{\frac{\epsilon_2}{\epsilon}} \quad \text{or} \quad \epsilon = \frac{\epsilon_2}{(1 - V)^3}$$

The latter equation may be written as

$$\epsilon = \epsilon_2(1 + 3V) \quad (2)$$

by neglecting the higher terms of V , a procedure which is allowable for smaller values of V .¹

The basis of this investigation is the fact that for non-spherical particles the dielectric constant of a dispersion is very considerably higher than for spherical particles occupying the same volume. In addition, the greater the deviation from the spherical form, the higher is the dielectric constant of the dispersion. Consequently, since particle agglomeration leads to non-spherical chains of particles, these agglomerated particles must show an increase in dielectric constant, which is expected to decrease to the normal value when a shearing stress is applied which breaks up the aggregates. In addition, in a dispersion at rest in which particle structures are in the process of building up, an increase in the dielectric constant is expected, indicating the progressive particle structure formation. A suggestion that such an effect actually exists was found in an observation by Parts (8) that the dielectric constant of a printing ink changed with time.

Both effects were verified experimentally and data were obtained for a number of systems. The quantitative evaluation of the dielectric constant of a dispersion of non-spherical particles is very complicated, owing to the fact that the form factor depends not only on the particle form, but also on the dielectric constants of both phases. It appeared that none of the many theoretical approaches made in the literature leads to a satisfactory equation covering older

¹At a value of $V = 0.10$ the approximation leads to values which are about 5 per cent low, and equation 2 appears therefore to be applicable only for concentrations below 10 per cent by volume.

experiments. While an equation derived by Wiener (10) and modified by Bruggeman (1) was fairly satisfactorily applied in certain experiments by Guillien (6) with dispersed materials of low dielectric constants, all equations led to infinitely high dielectric constants for dispersed conductors, in complete contradiction to observed facts.

Thus, to overcome the discrepancy, we have simply extended Bruggeman's equation by introducing a form factor (f) for non-spherical particles in dispersions where the dielectric constant of the dispersed phase is much larger than the dielectric constant of the medium. Thus the modified Bruggeman equation becomes:

$$\epsilon = \epsilon_2(1 + 3fV) \quad (3)$$

For spherical particles $f = 1$. For non-spherical particles $f > 1$. Without being able to make any definite prediction about particle shape, it is possible to state that the larger the experimentally determined factor f is, the more the particle shape shows deviation from a spherical form. The factor f can never become smaller than 1.

The form factor for plate-like or needle-shaped particles naturally depends on their orientation. According to the theory of Bruggeman (1), the dielectric constant has a minimum for orientation perpendicular to the field, and a maximum for an orientation parallel to the field, while an intermediate factor is valid for random distribution.

II. EXPERIMENTAL PART

A. Dielectric measurements

For the measurement of capacities a series resistance capacity bridge was built in which the bridge arms were chosen in such a way that for the capacities to be measured the bridge becomes an equal ratio bridge.

As generator a transitron oscillator was used, followed by an amplifier which terminated in an isolation transformer with a very small capacity between primary and secondary windings. Thus, capacity variations of the generator did not affect the bridge balance. Potential variations from 5 to 120 volts could be applied at various frequencies.

The null detector used was a vacuum-tube voltmeter preceded by an amplifier. Its sensitivity was variable, permitting the determination of a discrete null point. Both oscillator and null detector were isolated from the bridge and had their own power supply. A schematic representation is given in figure 1. The double cylindrical capacity cell used consisted of a polished nickel-plated brass cup, of 102 mm. inside diameter and 96 mm. inside height, and a nickel-plated brass bob of 90 mm. outside diameter and 90 mm. outside height, provided with a shaft through the center, which was connected with a variable-speed electric motor. The bob was suspended in such a way that it remained 6 mm. from the bottom as well as from the sides of the cup.

The air capacity of the cell was accurately determined by comparison with a

standard capacity cell and checked by means of measurements of the cell capacity when filled with liquids of known dielectric constant.

It was desirable to obtain the dielectric constants of the various dispersions at their static, maximum value, outside of the dispersion range. In order to establish the limiting frequency ranges for each group, the initial measurements were made with frequencies varying from 60 to 20,000 cycles per second. In nearly all cases the value of the dielectric constant remained the same, indicating that the frequencies studied were outside the dispersion range. Only with concentrated suspensions of certain types of carbon black at rest was there a noticeable decrease at 20,000 cycles, but nowhere was a decrease found at 5000 cycles per second. Thus, all measurements were concluded at 5000 cycles per

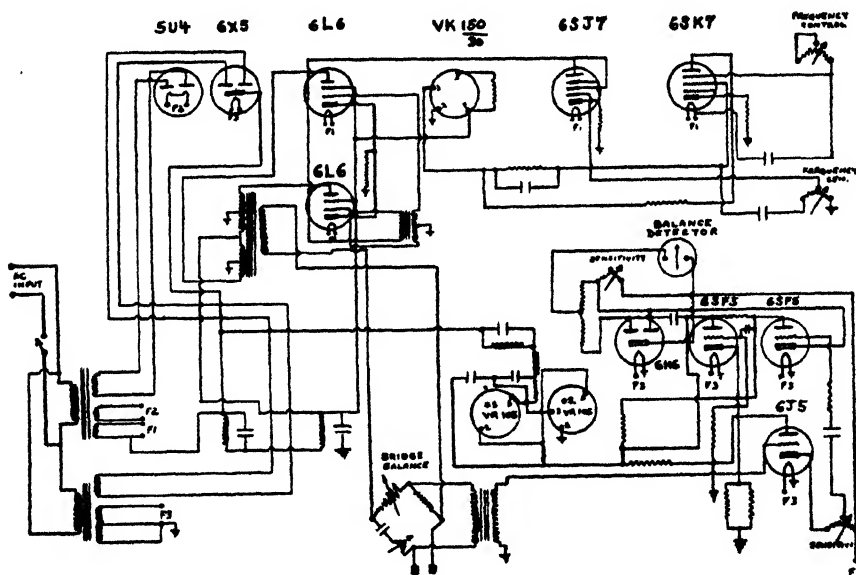


FIG. 1. Capacitance detector

second, corresponding to a wave length of 60,000 meters. The dielectric constants obtained had their maximum, static value corresponding to infinite wave length.

All data were observed at room temperatures, 66–70°F. The temperature effect of the dielectric constant of the dispersions studied is very small.

B. Rheological measurements

While dielectric measurements were made with the described cell at rest as well as at various speeds, rheological data of the dispersion were obtained by means of a standard Gardner mobilometer. For this investigation the yield values were of major importance. They were obtained in a rheological diagram as the intercepts of the straight parts of the force-flow curves, expressed in

are very well represented by linear equations. For both vehicles identical equations were obtained from the experimental data, which are as follows:

$$\epsilon = \epsilon_2(1 + 4.2V)$$

Comparing this equation with equation 3, it may be seen that for zinc powder the form factor is identical under shearing stresses for each of the vehicles used, and has the value $f = 1.4$. In view of the fact that microscopically the particles appear to be approximately spherical, and assuming the validity of equation 2, it must be evident that the form factor f is very sensitive to the shape of the particles.

When the dispersions are allowed to stand, however, it appears that at higher concentration the dielectric constant increases, but returns generally to its original value upon agitation. It is obvious that we have here another change

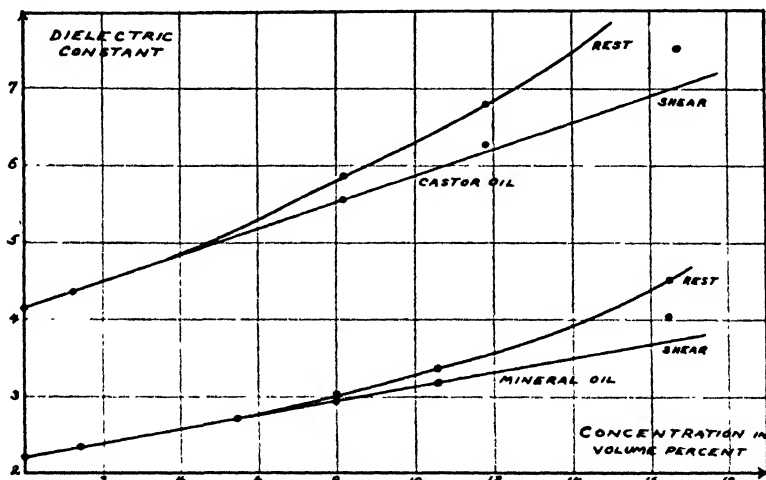


FIG. 3. Change of dielectric constant with concentration for zinc dispersions

of particle shape, which can be explained only by particle agglomeration. Owing to the fact that we have solid zinc particles, occupying a constant volume in the dispersion, no possibility seems to exist for a change in shape of individual particles.

Where particle agglomeration is found to occur, we shall indicate as the agglomeration factor, a_v , the ratio between the experimentally determined form factor at rest at a given concentration and the form factor of the dispersed phase as determined from the linear relationship at lower concentrations and under shearing stresses. Thus,

$$\epsilon'_v = \epsilon_2(1 + 3a_v fV)$$

whereby ϵ'_v is the value of the dielectric constant of the dispersion at rest, characterized by the agglomeration factor a_v at the concentration V . Table 1 indicates values for a_v at various concentrations of zinc powder in both vehicles.

grams of plunger weight. Measurements repeated with a rotary type of viscometer at varying R.P.M. confirmed the character of the rheological diagrams obtained.

III. DATA

A. *Zinc dispersions*

Dispersions were made of zinc powder in a mineral oil as well as in castor oil. The zinc particles had a shape approaching the spherical form, as can be seen from figure 2. Their diameter was between 2-8 microns.



FIG. 2. Shape of particles of zinc powder

In figure 3 the values of the dielectric constant are given for dispersions of various concentrations, both under static conditions and when subjected to shearing stresses. The static data represent values obtained after 10 min. standing, while data under shear represent the limiting lower values of the dielectric constant at the highest obtainable shearing stresses. The dielectric changes are completely reversible and the data may be repeated at will. For lower concentrations both static and shear lines coincide, but in mineral oil for concentrations higher than 6 per cent by volume and for castor oil for concentrations higher than 8 per cent by volume the static and dynamic values differ. These differences increase progressively for high concentrations.

The dynamic values, except perhaps for the value at a very high concentration

From these data it is apparent that particle agglomeration occurs at concentrations above 4 per cent by volume at rest.

Since plasticity generally is believed to be connected with particle agglomeration, force-flow diagrams were established for various concentrations of zinc powder dispersed in mineral oil as well as in castor oil. The yield values are indicated in tables 2 and 3, as intercepts of a force-flow diagram. From these

TABLE 1
Values of σ_y for zinc powder in mineral oil and castor oil

CONCENTRATION BY VOLUME	MINERAL OIL σ_y	CASTOR OIL σ_y
0.02	1.00	1.00
0.04	1.00	1.00
0.06	1.01	1.09
0.08	1.06	1.19
0.10	1.10	1.26
0.12	1.23	1.31
0.14	1.34	1.35
0.16	1.45	1.40

TABLE 2
Zinc in castor oil

CONCENTRATION BY VOLUME	AGGLOMERATION FACTOR	YIELD VALUE	TYPE OF FLOW
0.168	1.42	20	Plastic
0.118	1.29	15	Plastic
0.082	1.19	10	Plastic
0.033	1.00	0	Newtonian
0.010	1.00	0	Newtonian

TABLE 3
Zinc in mineral oil

CONCENTRATION BY VOLUME	AGGLOMERATION FACTOR, σ	YIELD VALUE	TYPE OF FLOW
0.168	1.48	55	Plastic
0.106	1.27	45	Plastic
0.080	1.06	25	Plastic
0.050	1.00	0	Newtonian
0.010	1.00	0	Newtonian

experiments it is evident that Newtonian flow is characterized by absence of particle agglomeration, while a definite particle agglomeration must be associated with plastic flow. Increased particle agglomeration leads to increased yield values.

To study other aspects of plastic flow, the dielectric qualities were determined at low shearing stresses, corresponding to about eight rotations per minute.

It appeared that under these conditions of low shear all zinc powder dispersions investigated showed dielectric constants identical with the value obtained at the highest shearing stresses, corresponding to about 250 R.P.M. Thus it is evident that the forces which act to form particle agglomeration in zinc dispersions are weak and very easily broken up, and it is desirable to study the progression of particle agglomeration at rest. The dielectric qualities of different zinc dispersions were therefore determined at various time intervals after the dispersions had been thoroughly agitated.

Table 4 indicates the variation of the agglomeration factor a_v , calculated from the dielectric data obtained. It can be seen that the particle agglomeration factor changes in dispersions at rest. The upper limit is often not reached in 10 min., and it may sometimes take hours before the final stage of maximum agglomeration is reached. This phenomenon is thus closely connected with thixotropy, which is believed to result from the gradual rebuilding of a previously destroyed particle structure.

The interpretation of rheological data at low shearing stresses fails completely, and no rheological study of systems at rest is possible. The method of this

TABLE 4
Variation of agglomeration factor

TIME	ZINC IN CASTOR OIL		ZINC IN MINERAL OIL	
	$V = 0.082$ av	$V = 0.168$ av	$V = 0.080$ av	$V = 0.165$ av
<i>seconds</i>				
0	1.00	1.29	1.00	1.27
10	1.06	1.30	1.03	1.35
30	1.08	1.33	1.04	1.42
60	1.11	1.37	1.06	1.46
600	1.20	1.42	1.06	1.55

investigation, however, allows a definite conclusion about particle agglomeration, regardless whether the system is subjected to shearing stresses or not.

B. Dispersion of titanium dioxide

Figure 4 shows the dielectric constants of dispersions of titanium dioxide (anatase) in linseed oil as well as in a mineral oil.

The dispersions in linseed oil do not show any change in dielectric constant on being agitated, while mineral oil dispersions having a higher concentration than about 8 per cent by volume show a decrease in dielectric constant. For the dielectric constants of the linseed oil dispersion in general, and for the mineral oil dispersion under shear, the following equation holds:

$$\epsilon = \epsilon_2(1 + 4.5V)$$

Since the dielectric constant of the titanium dioxide used is rather high, about 48, it is possible to use equation 3 as an approximation. Consequently the form factor f for the particles of titanium dioxide appears to be 1.5.

The agglomeration factor, a_v , has been calculated for various concentrations

of the dispersion. Yield values were determined by rheological methods. For all dispersions measured in linseed oil the agglomeration factor is 1.00, while the dispersions all appear to exhibit Newtonian flow, in complete agreement with results obtained with zinc dispersions. Table 5 indicates agglomeration values

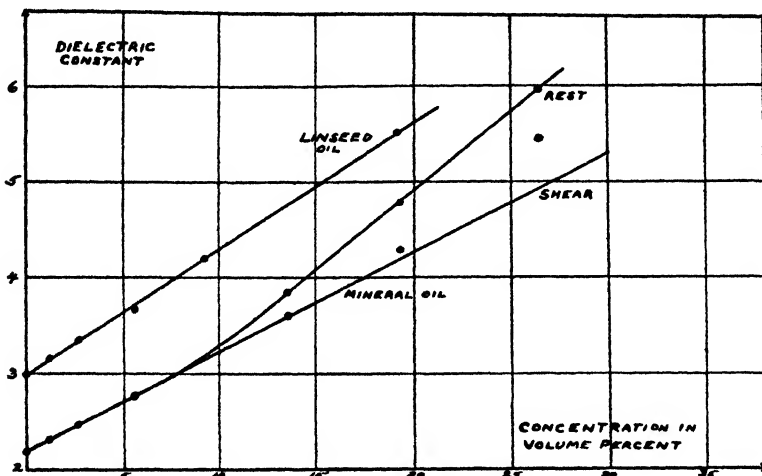


FIG. 4. Change of dielectric constant with concentration for titanium dioxide dispersions

TABLE 5

Values of agglomeration factor for various concentrations

CONCENTRATION BY VOLUME V	AGGLOMERATION FACTOR a_V	YIELD VALUE
0.040	1.00	0
0.080	1.00	0
0.136	1.20	30
0.194	1.31	60
0.264	1.41	95

TABLE 6

Dielectric changes after subsection of dispersions to high shearing stresses

TIME	$V = 0.080$ a_V	$V = 0.136$ a_V	$V = 0.194$ a_V	$V = 0.264$ a_V
<i>seconds</i>				
0	1.00	1.00	1.04	1.20
4	1.00	1.20	1.31	1.36
20	1.00	1.20	1.31	1.38
60	1.00	1.20	1.31	1.41
600	1.00	1.20	1.31	1.41

for dispersions in mineral oil. The time factor for the changes involved appears to be very short. The dielectric changes, after subjecting the dispersion to high shearing stresses, expressed as a variation of agglomeration factors with time, are given in table 6. These data indicate an extremely rapid re-

building of a destroyed particle structure. While for the most concentrated dispersion the process of rebuilding is over in 1 min., for dispersions of lower concentration the process is finished within a few seconds. A rough estimation of the duration of the rebuilding process in the more dilute dispersions, by following the course of the null detector needle of the capacitans bridge, shows that for a concentration $V = 0.136$ the process is finished in about 1 sec., while for $V = 0.194$ the process of rebuilding is completed in about 3 sec.

These observations show beyond doubt that the system requires a short but measurable time for the rebuilding of a destroyed structure. Such short periods of time, however, even if existing at higher shearing stresses, could not be detected by means of rheological measurements.

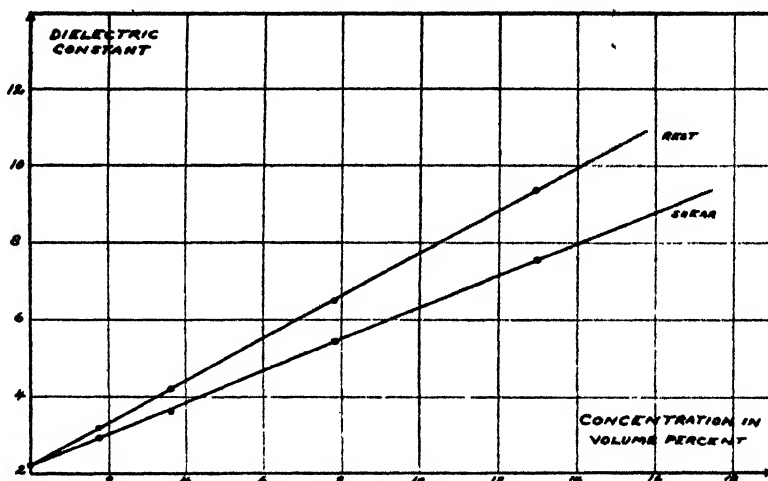


FIG. 5. Change of dielectric constant with concentration for aluminum dispersions

C. Aluminum dispersions in mineral oil

Measurements of the dielectric constant of aluminum powder in mineral oil were made for dispersions both at rest and when subjected to high shearing stresses. The results are given in figure 5, which shows two straight lines, both starting at the dielectric-constant value of the vehicle.

Aluminum powder particles appear microscopically to be comparatively large leaflets, irregularly shaped (figure 6), and it is quite obvious that the differences in static and dynamic dielectric behavior must be explained as differences in particle orientation. Thus, at rest the particles are distributed at random. The following equation holds:

$$\epsilon = \epsilon_2(1 + 24.6V)$$

from which the form factor is calculated as $f = 8.2$, pointing to a very marked deviation from the spherical shape.

The orientated leaflets, however, in accordance with Bruggeman's theory (1), show considerably lower dielectric constants. The data yield the following equation:

$$\epsilon = \epsilon_2(1 + 18.6V)$$

from which a form factor $f = 6.2$ may be calculated.

The orientation of the particles progresses with increasing shearing stresses. This is indicated by the shearing force, proportional to the number of rotations per minute, at which the lower limit of dielectric constant for each concentration

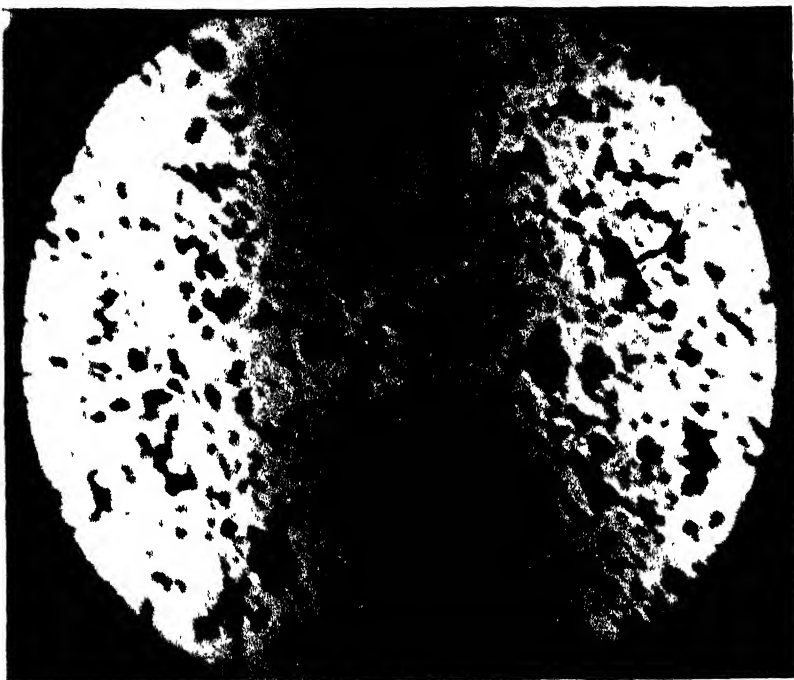


FIG. 6. Shape of particles of aluminum powder

is reached. This value corresponds to a complete orientation perpendicular to the electric lines of force.

When the orientated dispersion is left standing, the aluminum leaflets regain their random distribution after a short period of time, which can be accurately estimated by means of dielectric measurements. The changes are indicated in figure 7 for various dispersions. The yield values, taken as intercepts of the straight parts of the force flow curves, were determined. Table 7 indicates the limiting R.P.M. to obtain complete orientation as well as yield values of dispersions of various concentrations. It must be remarked, however, that on the basis of the data it was difficult to decide whether the systems were "plastic" or "pseudo-plastic."

In order to find out whether particle agglomeration occurs with aluminum leaflets, or whether the differences in static and dynamic dielectric relations must be ascribed solely to particle orientation, a closer examination of the character of the relationship found is desirable. The linear character of the dielectric constant-concentration function at rest suggests that agglomeration does not play an important part, and the decrease in dielectric constant upon application of shear in a direction perpendicular to the measuring field must be ascribed predominantly to particle orientation and not to the breaking up of particle agglomerates. Thus the agglomeration factor a_v must be considered

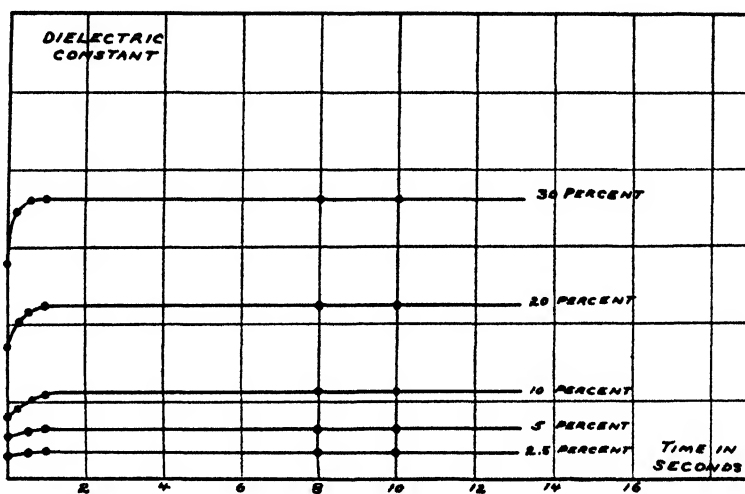


FIG. 7. Change of dielectric constant after discontinuation of agitation for aluminum dispersions.

TABLE 7

Limiting R.P.M. for complete orientation

CONCENTRATION BY VOLUME	0.129	0.070	0.037	0.017	0.008
Yield value.....	55	40	25	20	10
Limiting R.P.M.....	80	50	10	10	10

as equal to unity, notwithstanding differences in dielectric constant at rest and under shear. This is not in disagreement with our definition of agglomeration value, since the latter concept enters only into the picture where dielectric differences are caused by particle agglomeration.

Generally speaking, particle agglomeration is characterized by a linear relationship between dielectric constant and concentration under shear and a curve convex towards the abscissae at rest, although the initial part of this curve, at lower concentrations, may be straight. Particle orientation is characterized by a linear relationship in both cases.

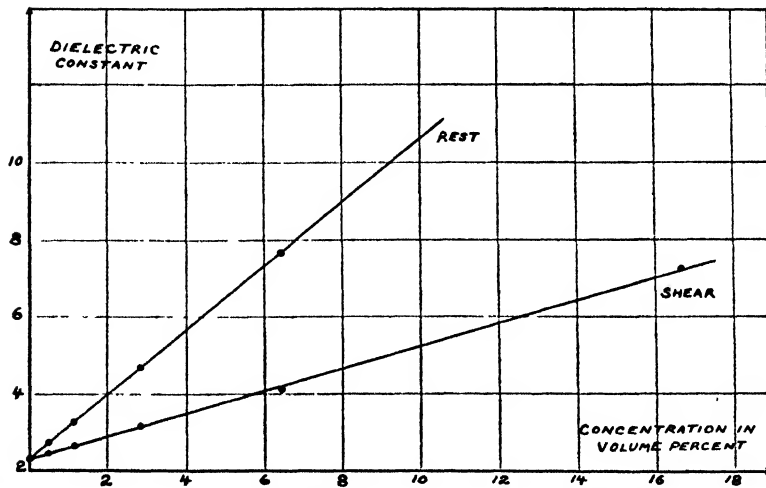


FIG. 8. Change of dielectric constant with concentration for copper dispersions

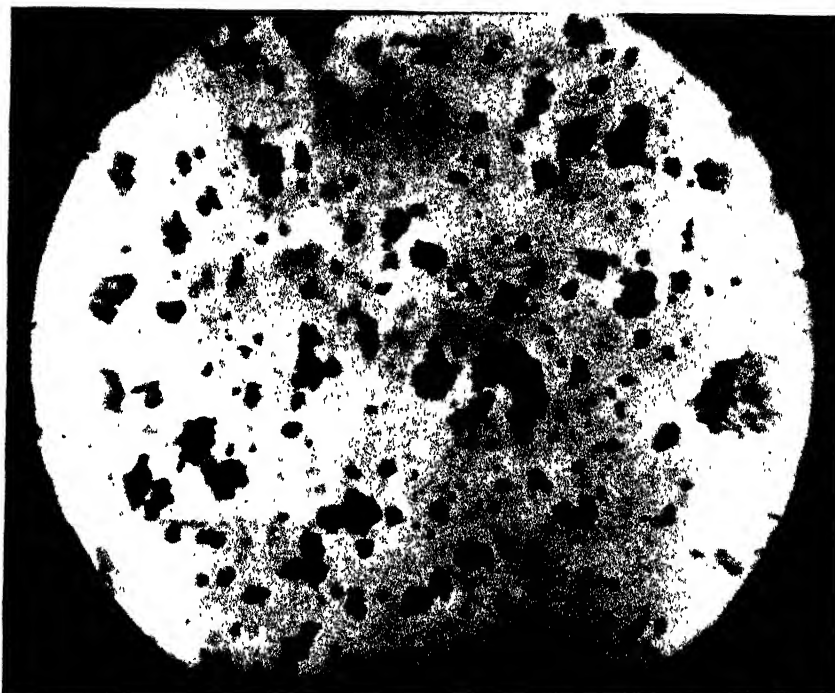


FIG. 9. Shape of particles of copper dust

D. Copper dispersions in mineral oil

Copper dust, electrolytically formed, was studied and dielectric data were obtained under shear and at rest. As with aluminum powder, two straight lines were obtained (figure 8), and microscopic examinations again revealed an irregular leaflet structure of the particles (figure 9).

For random distribution the following equation holds:

$$\epsilon = \epsilon_2(1 + 37.7V)$$

corresponding to a form factor of 12.6, pointing to a very marked deviation of the particle shape from the sphere.

For completely orientated copper leaflets the following equation holds:

$$\epsilon = \epsilon_2(1 + 13.4V)$$

resulting in a decrease of the form factor from 12.6 to 4.5, in agreement with Bruggeman's theory (1).

As with aluminum, the random distribution is reestablished in all dispersions within a few minutes of discontinuation of the application of shearing stress. All dispersions showed, upon rheological investigation, a yield value as intercept

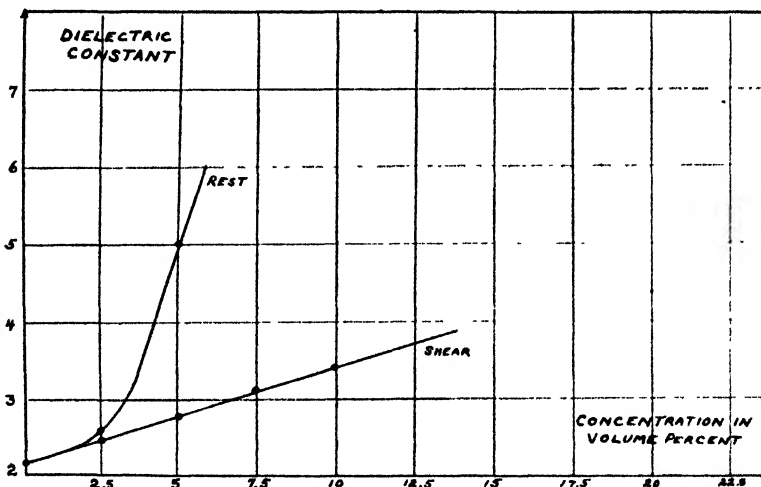


FIG. 10. Change of dielectric constant with concentration for dispersions of 0.5 normal sodium hydroxide in mineral oil.

of the straight part of the force-flow curves. It was not readily possible to decide whether the systems are "plastic" or "pseudo-plastic." Again, a fairly high shearing stress is necessary to obtain a complete orientation of the leaflets, indicated by the limiting value of the shearing stress determined by the progressive decrease of the dielectric constant at increasing R.P.M., which proved to be only slightly lower than with aluminum.

E. Aqueous solutions dispersed in mineral oil

A dispersion of 0.5 *N* aqueous sodium hydroxide, used to obtain conductive particles, was made in a mineral oil with the aid of a conventional dispersing agent. The dielectric data, obtained at rest and when the dispersion was subjected to shearing stresses, are given in figure 10.

As can be seen, the shear line, measured to a concentration up to 10 per cent by volume, is represented by a straight line, the points of which satisfy the following equation:

$$\epsilon = \epsilon_2(1 + 5.91')$$

corresponding to a form factor 2.0.

In addition, it can be seen that at rest an extremely high agglomeration factor exists.

On microscopic observation of the dispersion all particles appear to be perfectly spherical, with diameters varying between 0.1 and 1.5 microns. The deviation of the form factor from 1, the factor for the spherical shape, is easily explained by an elongation of the particles under shear, resulting in ellipsoidal particles instead of spheres.

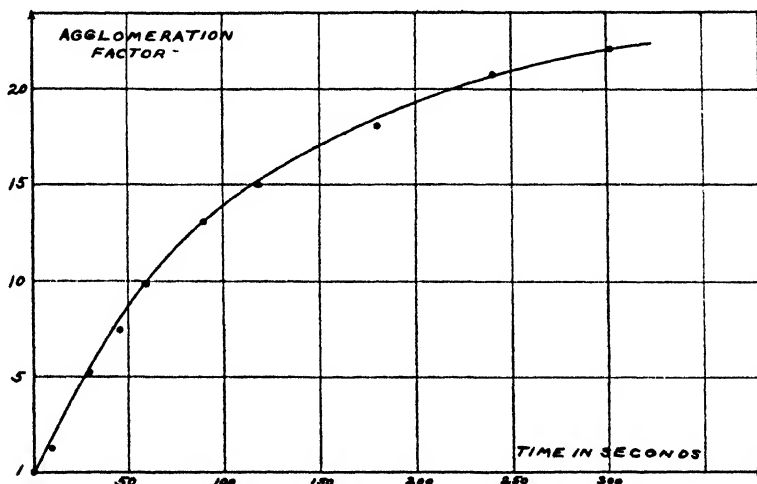


FIG. 11. Change of agglomeration factor with time after discontinued agitation in a 10 per cent by volume dispersion of aqueous 0.5 normal sodium hydroxide in mineral oil.

In very dilute dispersions, particle agglomeration, which is microscopically visible, does not appear to lead generally to coalescence, but merely to the formation of particle chains in which individual particles remain visible.

The changes with time in the dispersion can best be demonstrated by the change of the agglomeration factor with time, calculated by means of equation 4 from the change of the dielectric constant with time, immediately after discontinuing the application of shearing forces. The data are indicated in figure 11, assuming a spherical shape of the particles at rest. After the indicated period of 5 min. the dielectric constant was still going up, but became too high to be measured in the cell used.

Fairly high shearing stresses are needed to break up the particle agglomeration formed; for the 10 per cent dispersion more than 100 R.P.M. are necessary to obtain the minimum dielectric constant.

F. Carbon black

(a) Form factor and agglomeration factor

The dielectric behavior of carbon black dispersions in organic vehicles is completely analogous to the behavior of other dispersions of conductive particles.

Several types of carbon black are known, characterized by different particle sizes. Channel blacks, which are formed by impingement burning of natural gases, have a particle size of 20–30 millimicrons, as determined by electron microscopical investigations. Larger particle sizes are exhibited by furnace

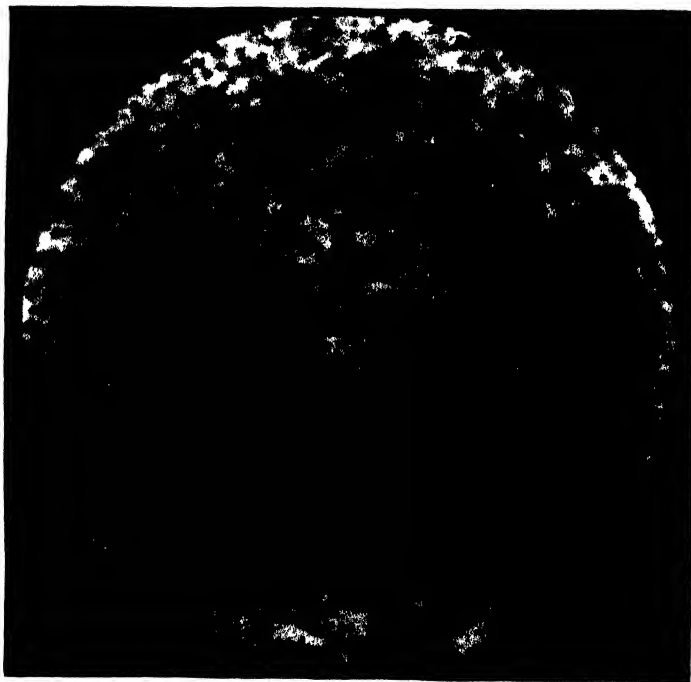


FIG. 12. Shape of particles of carbon black

blacks, which are formed by incomplete combustion of petroleum hydrocarbons at higher temperatures.

While the sizes of the elementary particles of different types of carbon black vary, their shapes are definitely spherical. In dispersions in various organic vehicles, made up with the aid of conventional equipment, such as three-roller mills, colloid mills, or ball mills, the kinetically active particles, however, are not the elementary carbon black particles, but considerably larger particle clusters, easily distinguishable by means of a high-power optical microscope. These particles do not show a spherical shape, as can be seen from figure 12, where a dilute dispersion of channel black in a mineral oil varnish is shown. The greatest particle diameter appears to vary from 0.1 to 1.5 microns.

The dielectric constants of channel black dispersions of varying concentrations in linseed oil, in castor oil, and in a mineral oil varnish, subjected to shear as well as after a 10-min. rest period, are given in figure 13.

From the linear relations revealed by these data, it is seen that for each point of the shear line, regardless of the vehicle, the following equation is valid:

$$\epsilon = \epsilon_2(1 + 11.6V)$$

This equation leads to a form factor of 3.9 in each of the vehicles.

From figure 13 it is seen that in castor oil the dielectric constant at rest differs greatly from its value under shear, a result which points to a large agglomeration factor, greatly increasing at higher concentrations. In the mineral oil varnish there appears to be no agglomeration for lower concentrations of carbon black and only above a concentration of 4 per cent by volume does particle agglomera-

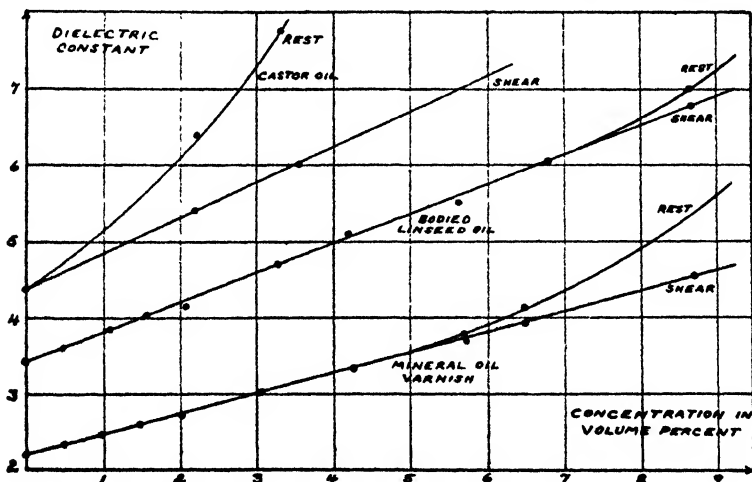


FIG. 13. Change of dielectric constant with concentration for dispersions of channel black

tion occur. In linseed oil agglomerations become apparent only in concentrations higher than 7 per cent by volume of carbon black. Thus we observe clearly that the vehicle, while of no consequence to the form factor, greatly influences the formation of particle agglomerates. This quality of a vehicle has been known by paint and printing ink technologists to exist and has often been referred to as its dispersing or deflocculating characteristics. The significance of this quality actually appears to be the power to prevent agglomeration of already dispersed particles, which may be expressed quantitatively by the method of this investigation as the agglomeration factor at a desired concentration for the given pigment-vehicle combination.

Defining as the index of deflocculation the maximum concentration at which only singular particles exist in the dispersion, this value is given by that concentration by volume of the dispersed phase where the first diversion is found between static and shear value of the dielectric constant. The index of defloc-

culation must thus be considered as the quantitative embodiment of the deflocculating and dispersing characteristics of a vehicle, permitting a quantitative evaluation of the influence of a vehicle or vehicle constituent upon the agglomeration factor, and thus upon the mutually attractive forces between the particles of a dispersion.

Using carbon black as a reference pigment, from figure 13 the index of deflocculation appears to be 0 for castor oil, 4.2 for the mineral oil varnish, and 7.0 for the bodied linseed oil.

It was found that pure mineral oils are not able to prevent an appreciable particle agglomeration of carbon black, even in lower concentrations. A number

TABLE 8
Rheological properties of dispersions of carbon blacks

DISPERSION	PERCENTAGES BY WEIGHT			YIELD VALUE	TYPE OF FLOW
	Carbon black	White mineral oil	Gilsonite		
A.....	4	96.0		38	Plastic
B.....	8	92.0		74	Plastic
C.....	12	87.75	0.25	90	Plastic
D.....	12	87.0	1.00	46	Plastic
E.....	12	85.5	2.50	0	Newtonian
F.....	5	94.75	0.25	0	Newtonian

TABLE 9
Variations of the agglomeration factor at increasing shearing forces

DISPERSIONS	A	B	C	D	E	F
Rest (10 min.).....	6.3	9.2	3.17	1.05	1.00	1.00
10 R.P.M.....	4.1	5.1	2.00	1.02	1.00	1.00
20 R.P.M.....	3.8	4.1	1.67	1.00	1.00	1.00
40 R.P.M.....	3.3	3.0	1.48	1.00	1.00	1.00
60 R.P.M.....	3.1	2.6	1.37	1.00	1.00	1.00
100 R.P.M.....	2.7	2.5	1.20	1.00	1.00	1.00
200 R.P.M.....	2.1	2.4	1.05	1.00	1.00	1.00

of materials, however, when added to the mineral oils, have a very distinct effect of decreasing the agglomeration factor considerably. The most prominent of these agglomeration-preventing materials appear to be of an asphaltic or resinous character and it is possible, on the basis of these experiments, to evaluate their action quantitatively. As an illustration, different dispersions of carbon blacks were made up in a mineral oil and in varnishes consisting of a mineral oil and small quantities of the asphaltic material known as Gilsonite.

Rheological properties are reported in table 8, together with the constituents of the dispersion.

The variations of the agglomeration factor, a_r , at increasing shearing forces, indicated as rotations per minute, are given in table 9.

The change in agglomeration factor with time is given in table 10 for dispersions A, B, C, and D. No change whatsoever was found for dispersions E and F. In all cases the form factor remained 3.9. The results for dispersions A, B, and C are plotted in figure 14, representing the change in particle agglomeration with time upon standing, for various carbon black dispersions.

From these data it is apparent that particle agglomeration is not found in Newtonian liquids, but does occur in plastic systems. Agglomeration gradually breaks down upon increasing the shearing stresses applied to the dispersion.

TABLE 10
Change in agglomeration factor with time

TIME IN SECONDS	0	5	15	30	60	120	300	600	3600
DISPERSION									
A	2.1		5.2	5.5	5.9	6.1	6.2	6.3	6.7
B	2.4	7.8	8.1	8.4	8.7	8.8	9.0	9.1	9.2
C	1.05		2.32	2.44	2.52	2.66	2.79	3.17	3.20
D	1.00				1.005	1.01	1.02	1.05	1.14

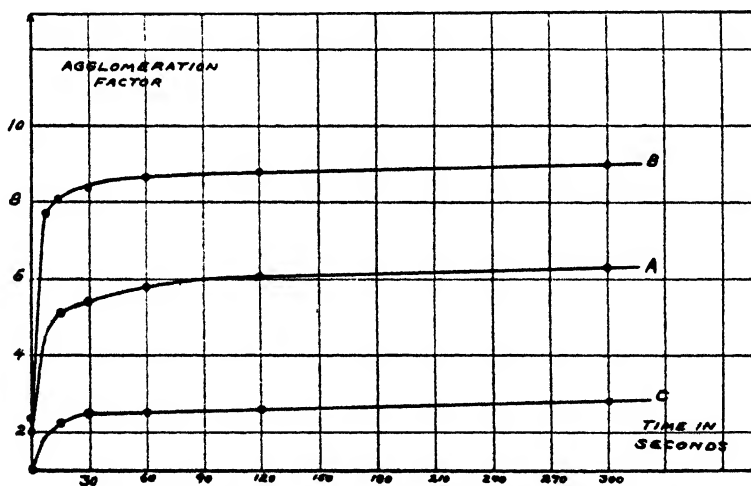


FIG. 14. Change of agglomeration factor with time in different dispersions of carbon black

Contrary to observations with metal powders, in carbon black dispersions comparatively large shearing forces are required to break up the particle aggregates.

(b) Influence of large quantities of resins

The dielectric constant of carbon black dispersed in liquids with a high content of resinous materials was investigated. Table 11 indicates dielectric changes upon application of shear ($\Delta\epsilon$) and the agglomeration factors a_T , after a 12-hr. period of standing, for carbon black dispersions in a petroleum solvent of 240-

270°C. boiling range, in the presence of increasing quantities of a modified rosin. From these data it is apparent that only slight changes in particle agglomeration are found. The dispersions, however, show a marked thixotropy, especially D, E, and F, forming heavy gels upon standing, which turn into thin liquids on agitation and set again into heavy gels in a few hours.

G. Other pigments

A number of pigment dispersions were investigated, the particles of which were non-spherical and non-conductive. The dielectric constants of these particles usually were not known.

In some cases, especially with many organic pigments, the dielectric constants of the dispersion are only slightly different from the dielectric constants of the media. In other cases, especially with inorganic pigments such as Milori Blue, etc., the changes were marked. In general, little change was found upon subjecting these dispersions to shearing stresses, although most dispersions showed plastic flow. The dielectric constants of the dispersions are generally

TABLE 11
Dielectric changes upon application of shear

NO.	PERCENTAGE BY WEIGHT			$\Delta\epsilon$ <i>per cent</i>	AGGLOMERATION FACTOR <i>ay</i>
	Carbon black	Solvent	Modified rosin		
A.....	12	84.7	3.3	1.1	1.02
B.....	12	81.3	6.7	1.4	1.03
C.....	16	67.3	16.7	2.2	1.05
D.....	16	50.5	33.5	3.3	1.08
E.....	16	34.0	50.0	3.7	1.09
F.....	16	27.0	56.4	5.2	1.12

not linearly dependent on the concentration by volume of the dispersed phase. None of the relations proposed in the literature appeared to have general validity (12).

Thus it is apparent that the dielectric method of investigation is not revealing the inner structure in cases where the dielectric constants of dispersed phase and dispersion medium are not very different. The reason must be found in the precision inherent in this method (± 1 per cent), which is not enough to allow conclusions when only slight variations occur.

Other measurements, with improved equipment, are in preparation.

H. The Bruggeman equation

The absolute values of form factors and agglomeration factors derived from the experiments appear to depend on the validity of the factor 3 of the Bruggeman (equation 2) or on its original form:

$$\epsilon = \frac{\epsilon_2}{(1-V)^3}$$

It was therefore felt necessary to check the validity of this equation experimentally for a system of rigid conductive spheres, which had not been done by Guillian (6). After some experimentation an example was found of such a system,—namely, iron powder prepared by thermal decomposition of iron carbonyl in the gas phase. A sample of this powder appeared perfectly spherical upon microscopic examination, with a fairly uniform particle diameter of about 10 microns. Dispersions of varying concentrations were made in a mineral oil as well as in aged linseed oil and the dielectric constants were measured at high shearing stresses.

TABLE 12
Dielectric constants of dispersions of iron at high shearing stresses

PERCENTAGE BY		IN LINSEED OIL	
WEIGHT	VOLUME	CALCULATED	FOUND
60	15.35	6.34	6.62
40	7.42	4.85	5.04
20	2.92	4.20	4.19
10	1.32	4.00	4.00
5	0.51	3.92	3.92
0			3.85

TABLE 13
Dielectric constants of dispersions of iron at high shearing stresses

PERCENTAGE BY		IN MINERAL OIL	
WEIGHT	VOLUME	CALCULATED	FOUND
60	15.50	3.97	4.27
40	7.30	3.02	3.03
20	2.86	2.60	2.59
10	1.29	2.49	2.48
5	0.55	2.43	2.43
0			2.39

The results are given in tables 12 and 13, together with the values calculated from the Bruggeman equation (equation 1), simplified for conductive particles, as shown above.

It can be seen that the data are in agreement with the calculated values up to concentrations of 40 per cent by weight for mineral oil and 20 per cent by weight for linseed oil. For the higher concentrations the calculated values are somewhat lower. Since the iron particles show a strong tendency to form clusters, resulting in a very high dielectric constant at rest, it is quite likely that the maximum shearing stresses applied did not cause a complete freedom from particle agglomeration, resulting in a slightly increased dielectric constant at high concentrations. For the lower concentrations, however, the Bruggeman equation appears to describe the phenomena quantitatively. Thus equation

2, the first approximation of the Bruggeman equation and mathematically justified for lower concentrations, appears to be experimentally confirmed.

The factor 3.0 is thus completely justified for perfectly spherical particles of conductive materials, and the absolute values arrived at for the form factors as well as for the agglomeration factors discussed previously were found to be correct.

IV. DISCUSSION OF RESULTS

In the foregoing sections it has been shown that when particles are dispersed in a liquid of a dielectric constant considerably lower than the dielectric constant of the particles, linear relations exist between the dielectric constant of the dispersion subjected to shear and the concentration by volume of the dispersed particles. A theoretical relation derived by Bruggeman (1) for spherical particles predicted such a linear relationship, characterized by a proportionality factor 3. Actual proportionality factors found varied from 3.0 to considerably higher factors. It was observed that systems having a shape nearest to spherical had the lowest proportionality factor. Consequently a form factor f was introduced which, resting upon the validity of the Bruggeman equation, expressed the experimentally found deviation from the spherical shape. This form factor appeared to be entirely independent of the vehicle and remained constant for a specific dispersed material. Thus, the acceptance of the form factor as a characterization of the shape of the particles of the dispersion is justified. It has not been found possible, however, to relate form factors directly to specific ratios of particle dimensions. Our knowledge at present is limited to the qualification that the larger the form factor, the more deviation there is from the spherical shape.

In addition to a form factor, the experimental evidence pointed to the existence of an agglomeration factor, which takes into account the differences between the dielectric constant of a dispersion when at rest and when subjected to shearing forces. Again, the agglomeration factor does not directly indicate the size of the complex formed, but merely the increased deviation from the spherical shape. Since it has been observed by microscopic examination in dilute suspensions that upon agglomeration particle chains are formed, it is evident that increased agglomeration necessarily leads to increased length of particle chains and is therefore connected with a more distinct deviation from the spherical shape, which in turn causes the measured increase in dielectric constant from which the agglomeration factor may be calculated.

It must be emphasized that, in order to cause an increased dielectric constant of the dispersion, the particles must touch one another directly, forming conductive chains. Particles connected by forces having minima of potential energy at a distance are dielectrically equivalent to totally independent particles. Thus, the experimental evidence indicates that the particle structures are composed of directly connected particles.

From the data it may be observed that on applying shearing stresses, in nearly all cases the agglomeration factor becomes equal to unity. Exceptions are

found at very high concentrations, where values somewhat higher than 1 are found (see, for instance, figures 2 and 3). While it is possible that in some cases the experimentally applied shearing stresses were not high enough to break up the structures entirely, this is decidedly not the reason in other cases, where particle structures are rather loosely bound. In many instances, however, this deviation is a result of the limits of the validity of the mathematical simplification used in equation 2, but differences disappear when applying the original equation 1. When particle agglomerates are subjected to shear, they are partly broken up, but in the presence of strong agglomerating forces, particle chains will still exist at moderate shearing stresses. This will lead to orientation and to a decrease of the dielectric constant, and result in a somewhat decreased agglomeration factor, without breaking up the structure.

Therefore, the most reliable measurements of the actual state of agglomeration are taken at rest. The same difficulty exists with rheological measurements, where the applied forces are used not only for breaking up particle structure, but also for orienting the remnants of the particle chains. The dielectric method, however, allows the elimination of this complication by obtaining data at rest, which is not possible in rheology.

One of the most interesting aspects of this investigation is the relation between particle agglomeration and rheology of the dispersion. We have seen that in all cases of Newtonian flow particle agglomeration was entirely absent. Thus it appears that wherever Newtonian flow is found in a dispersion, the particles move independently. The reverse statement, however, is not true. As was seen with materials such as aluminum and copper powder, the orientation of particles of extreme differences in dimensions under shearing stresses led not only to a difference in dielectric properties, as predicted by Bruggeman (1), but also to a non-Newtonian behavior, resulting from a change in orientation upon a change in shearing stresses.

Thus, it is clear that the rheological evidence of plastic behavior alone is not sufficient to allow conclusions as to the existence of structures of the dispersed phase. Particle agglomeration itself, however, is always connected with plastic flow. It is possible to evaluate the magnitude of the forces necessary to cause a breakdown of the particle structures formed. In table 9, for example, it may be seen that in dispersions A and B comparatively large forces are needed to eliminate particle aggregates in the dispersion, while, for instance, in dispersion D the application of rather weak forces has the same result.

Very important in this respect is the time factor involved in rebuilding the structures upon discontinuation of the applied forces. The time factor in a dispersion at rest, as may be seen from table 10, may vary from a few seconds to an hour, or even longer. Since it is possible to estimate the time factor of the particle agglomeration at various shearing stresses, dielectric measurements have been made at increasing as well as at decreasing R.P.M. The data with plastic dispersions invariably lead to time effects and to hysteresis loops in the curves representing the changes of the dielectric constant or of the agglomeration factors with varying shearing stresses.

Quite similar effects are found when particle agglomeration is entirely absent, but orientation occurs. Such an effect of orientation was found at low shearing stresses with dispersions of aluminum and copper powders.

These effects are also found in rheological investigations, upon measuring flow at varying shearing stresses. The difference, however, is that rheologically only time factors which are comparatively large are easily determined. With time effects lasting only a few seconds it is extremely difficult to establish a hysteresis effect by rheological means, while the dielectric method makes it possible to follow a change in the balance of the capacitans bridge almost instantaneously. In addition, at low shearing stresses and especially at rest, where the most significant changes were found, rheological methods fail completely. Thus, in rheology, it was not surprising to find that a distinction was made between plastic systems showing a time effect and plastic systems in which such effects were absent. The former systems were called thixotropic, while the latter were considered plastic, but not thixotropic.

From our investigations it becomes apparent that all plastic systems show a time effect, irrespective of whether plasticity originates from particle agglomeration or orientation or from both. Thus hysteresis occurs in the curves representing the relationship between dielectric constant, or agglomeration factor, and shearing stresses. By analogy with other plastic systems in which the time effect is pronounced, and detectable by rheological means, the systems with a time effect of short duration must also be considered thixotropic. Consequently all plastic systems appear to be thixotropic. Differences between different types are only quantitative, exhibiting a different magnitude of the time element involved, but no fundamental differences exist between the different plastic systems exhibiting particle agglomeration and orientation.

It was observed that a strong tendency to form particle agglomerates, as witnessed by the large shearing stresses necessary to break down the particle agglomerates, generally leads to a short time factor, while weak binding forces between particles cause a considerably more extended period of time necessary to build up the particle structure. This leads to the seemingly paradoxical statement that with weaker forces between the particles, the thixotropy becomes more apparent. It was observed that strong forces between particles will cause an immediate agglomeration after discontinuation of the applied shearing forces, leading to a rheologically hardly perceptible thixotropy, while weak forces will only slowly rebuild a structure, making thixotropy more apparent. In the absence of any forces between particles, no particle agglomerates are being formed at all. Visualizing the magnitude of the thixotropy as related to its time effect, as is often done, Newtonian dispersions should actually be considered as possessing "infinite" thixotropy, since their rebuilding takes infinitely long. Consequently, the paradox is actually non-existent. For practical reasons thixotropic systems with extremely fast as well as extremely slow time effects have not been recognized as being thixotropic at all, and only systems in which fairly weak agglomerating forces were acting with a "medium" time effect have been recognized as thixotropic by rheological measurements. Thus, Freundlich

(4) stated that thixotropy is connected with a flocculating force which is neither large nor small.

We have seen that carbon black dispersions in which comparatively large quantities of resinous materials are present show only a slight agglomeration, but a very pronounced thixotropy. Examples were given in table 11, where dispersions D, E, and F show a marked thixotropy, but little agglomeration of particles, as measured dielectrically. We must conclude that the thixotropy of these dispersions is due not to particle agglomeration, but to the influence of the resinous compound predominantly present in these dispersions. The thixotropic gel may therefore be visualized as a rigid tactoid structure, consisting of a network of mostly individual carbon black particles having a minimum of potential energy at a short distance from each other, but connected by resin particles. During the formation of this gel, larger resin-carbon black agglomerates are formed. These clusters, however, are not conductive, owing to the fact that the conductive carbon particles are separated from each other by non-conductive resin. Consequently their dielectric effect is equal to the effect of individual, non-agglomerated particles.

Thus, we must recognize two distinctly different types of thixotropy. The first one is caused by the time effect of particle agglomeration, orientation, or both. If large forces are involved, the magnitude effect is large, but the time effect is short and the system is often hardly recognizable as thixotropic. With smaller forces between particles, causing a smaller degree of agglomeration, a perceptible magnitude effect still may exist and is extended over a longer period of time, making the system easily recognizable as thixotropic. Still weaker forces will show a very small effect, drawn out over a longer period of time, and thixotropy is again not recognized.

The second type of thixotropy is caused by minima of the potential energy function of the particles at a distance. In this type of thixotropy the vehicle apparently plays a predominant part, and dispersed particles may be the cornerstones of a network in which the resinous compound is immobilized as a gel. Both time and magnitude effects may be quite large.

The differentiation of thixotropy into two distinctly different types had already been recognized earlier, by the differences in properties and behavior, although the intrinsic factors determining the types were not known. Pryce-Jones (9) distinguishes between systems which solidify slowly and others which exhibit a very rapid rise in consistency. The latter type of thixotropy is called "false-body" thixotropy, being a term taken from the painters' terminology. It is not difficult to identify Pryce-Jones' "false-body" type of thixotropy with the thixotropy connected with time effects of particle agglomeration and orientation, while the slowly solidifying systems are those in which particles at a distance from one another partly immobilize the vehicle.

Roeder (11) extensively describes both types of thixotropy. The slowly solidifying type, with particles at a distance, is called the "ferric oxide" type of thixotropy, by analogy with aqueous ferric oxide sols, which may solidify slowly. The other type of thixotropy is called the "bentonite" type, by analogy

with bentonite clay, dispersions of which solidify within a few minutes. In addition, Roeder mentions certain systems, such as, for instance, quartz powder, rice starch, etc., dispersed in carbon tetrachloride, which behave more or less as a liquid when violently shaken in a test tube, but do not flow at all immediately afterwards, while at rest. These systems, according to Roeder, are extremely thixotropic, but were not recognized as such in rheology, owing to their extremely short time factor. While Green and Weltmann (5) reject such systems as being thixotropic, dielectric evidence is entirely against their opinion. Systems such as dispersion B of table 8 show an exactly similar behavior, accompanied, however, with a great change in the dielectric constant, indicating a large change in particle agglomerations with a very short time factor.

Thixotropy by orientation alone was found to exist with materials such as aluminum and copper leaflets dispersed in organic vehicles. Rheological measurements cannot be used for differentiation between various causes for thixotropy, except under special conditions. Thixotropy by orientation possibly was found for the first time rheologically by Weltmann (13) with mineral oils at very high shearing stresses. This conclusion seems justified by the fact that there appears to be no other reasonable explanation.

V. SUMMARY

The variations in the dielectric constant of a dispersion with the concentration of the dispersed phase have been investigated for a number of dispersions in organic liquids.

Very substantial changes may occur in the dielectric constant of a dispersion of conductive particles and of particles with a relatively high dielectric constant upon subjecting the dispersions to shearing stresses, thus revealing significant changes in the inner structure of the dispersion.

The dielectric constant of a dispersion has been related to the shape of the particles of a dispersion by the introduction of a form factor.

The changes in the dielectric constant of a dispersion upon application of shearing stresses have been related to particle agglomeration and orientation, both of which could be differentiated from each other. The agglomeration factor, related to the shape of the particle agglomerates, is indicative of the forces acting between the particles of the dispersion.

The index of deflocculation of a dispersion, denoting the highest concentration in which a dispersed phase may exist solely as singular particles, is indicative of the deflocculating and dispersing power of a vehicle.

Plastic systems were found to exhibit a time effect either in particle agglomeration or orientation, or in both, although the order of magnitude may be too short to be detected rheologically. Thus, it was found that plastic systems, contrary to conventional opinion, are always thixotropic.

The "false-body" type of thixotropy, characterized by a relatively short time factor, is caused by particle agglomeration and (or) orientation.

The "ferric oxide" type of thixotropy, characterized by a long time factor,

results from a structure in which vehicle constituents are immobilized between particles having minima of potential energy at a distance.

I wish to express my appreciation to Louis R. Suriani for his able assistance in carrying out the experiments and to the J. M. Huber Corporation for their willingness to release the parts of the investigation which are of more general interest.

REFERENCES

- (1) BRUGGEMAN, D. A. G.: *Ann. Physik* **24**, 636 (1935).
- (2) BUCKINGHAM, E.: *Proc. Am. Soc. Testing Materials* **21**, (II), 1154 (1921).
- (3) DEBYE, P.: *Polare Molekeln*, S. Hirzel, Leipzig (1929), for a general discussion of the physical basis of the Lorentz-Lorenz and the Clausius-Mosotti relations.
- (4) FREUNDLICH, H.: "Some Mechanical Properties of Sol's and Gels and their Relation to Protoplasmic Structure", in *The Structure of Protoplasm*, a monograph of the American Society of Plant Physiologists, Iowa State College Press, Ames, Iowa (1942).
- (5) GREEN, H., AND WELTMANN, R. N.: in Alexander's *Colloid Chemistry*, Vol. VI, p. 328. Reinhold Publishing Corporation, New York (1946).
- (6) GUILLJEN, R.: *Ann. phys.* **16**, 205 (1941).
- (7) LICHTENECKER, K.: *Physik. Z.* **27**, 115 (1926).
- (8) PARTS, A.: *Nature* **155**, 236 (1945).
- (9) PRYCE-JONES, J.: *J. Oil Colour Chem. Assoc.* **19**, 295 (1936).
- (10) RAYLEIGH, J. W.: *Phil. Mag.* **1892**, 481.
- (11) ROEDER, H. L.: *Rheology of Suspensions*. Paris, Amsterdam (1939).
- (12) WACHHOLZ, F., AND FRANCESON, A.: *Kolloid-Z.* **92**, 158; **93**, 234 (1940).
- (13) WELTMANN, R. N.: *Ind. Eng. Chem., Anal. Ed.* **15**, 424 (1943).
- (14) WIENER, O.: *Abhandl. math.-phys. Klasse sächs. Akad. Wiss. (Leipzig)* **32**, 509 (1912).

ON A GENERALIZATION IN THE DIFFUSION THEORY

OLE LAMM

Institute of Physical Chemistry, University of Upsala, Upsala, Sweden, and Institute of Theoretical Chemistry, Royal Institute of Technology, Stockholm, Sweden

Received February 14, 1947

I. SYMBOLS

- a = activity,
 n = concentration in mols per cubic centimeter,
 N = mol fraction,
 γ = activity coefficient on the basis of concentration,
 f = activity coefficient on the basis of mol fraction,
 M = molecular weight,
 \bar{v} = partial molar volume,¹

¹ The symbol V was used for this magnitude in earlier papers, except reference 10.

\bar{v}_{12} = mean molar volume of a binary solution (reference equations 4 and 7),

C = linear velocity,

x = diffusion direction,

t = diffusion time,

B_{12} , A_{12} , Q_{12} = thermodynamic factors (equations 1, 17, 47),

φ = frictional coefficient per amount of substance contained in 1 cc.,

Φ = frictional coefficient per mol, and

D = diffusion coefficient.

II. GENERAL REFERENCE EQUATIONS FOR TWO-COMPONENT SYSTEMS

$$(1a) N_1 d \ln a_1 + N_2 d \ln a_2 = 0$$

$$(1b) n_1 d \ln a_1 + n_2 d \ln a_2 = 0$$

$$(1c) N_1 d\bar{v}_1 + N_2 d\bar{v}_2 = 0$$

$$(1d) n_1 d\bar{v}_1 + n_2 d\bar{v}_2 = 0$$

$$(2) n_1 \bar{v}_1 + n_2 \bar{v}_2 = 1$$

$$(3) n_1 = N_1 / \bar{v}_{12}$$

$$(4) \bar{v}_{12} = N_1 \bar{v}_1 + N_2 \bar{v}_2$$

$$(5) \bar{v}_1 dn_1 + \bar{v}_2 dn_2 = 0$$

$$(6) dN_1 = -dN_2$$

$$(7) \bar{v}_{12} = \frac{1}{n_1 + n_2} = \frac{\bar{v}_2}{1 + (\bar{v}_2 - \bar{v}_1)n_1}$$

$$(8) dN_1 = \frac{\bar{v}_{12}^2}{\bar{v}_2} dn_1$$

$$(9) \frac{\partial \bar{v}_{12}}{\partial N_1} = \bar{v}_1 - \bar{v}_2$$

$$(10) N_2 = \frac{n_2 \bar{v}_1}{1 + (\bar{v}_1 - \bar{v}_2)n_2}$$

$$(11) dN_2 = \frac{\bar{v}_1}{[1 + (\bar{v}_1 - \bar{v}_2)n_2]^2} dn_2$$

$$(12) \varphi_{12} = n_1 \Phi_1 = n_2 \Phi_2 = \frac{N_1}{\bar{v}_{12}} \Phi_1 = \frac{N_2}{\bar{v}_{12}} \Phi_2$$

III. A GENERALIZATION OF THE SUTHERLAND-EINSTEIN DIFFUSION EQUATION

The theory of diffusion has been dealt with in some detail in earlier publications (5-10), in which references also to the work of others are to be found. In these treatments of the subject, the diffusion coefficient is referred to coefficients of friction and to thermodynamic factors, the latter for a two-component system being the well-known expression:

$$B_{12} = \frac{\partial \ln a_1}{\partial \ln N_1} = 1 + \frac{\partial \ln f_1}{\partial \ln N_1} \equiv 1 + \frac{\partial \ln f_2}{\partial \ln N_2} \quad (1)$$

The identity follows from the Gibbs-Duhem equation (reference equation 1a). B_{12} is a symmetrical property with respect to the two components, thanks to the

use of mol fractions. The symmetry is the essential point of the present theory. The treatment might be of interest for the kinetic theory of gas diffusion. Although the latter has always been treated in a symmetrical manner, it does not seem to have led to the separation of thermodynamical and frictional factors. The main purpose of the theory is, however, to ensure a rational interpretation of diffusion measurements. For more advanced approaches to diffusion problems, the reader is referred to the works of Onsager (13 and later), and of Meixner (12) on irreversible processes in general, and to the newer "theory of rate processes" (2).

Confining ourselves here to a two-component system (except in Section IX), we begin with a condensed proof of the generalized Sutherland-Einstein relation. The latter expresses a limiting law for ideal, dilute solutions. The diffusion process being a stationary movement, the driving force per cubic centimeter, K_{12} , is the product of the relative velocity, $C_1 - C_2$, between the components and the mutual friction, φ_{12} , per cubic centimeter, so that:

$$K_{12} = (C_1 - C_2)\varphi_{12} \quad (2)$$

In order to determine C_1 and C_2 , the "bulk velocity" x' (compare Onsager and Fuoss (13)) is introduced:

$$x' = C_1 n_1 \bar{v}_1 + C_2 n_2 \bar{v}_2 \quad (3)$$

giving

$$C_1 = K_{12} \frac{n_2 \bar{v}_2}{\varphi_{12}} + x' \quad (4)$$

by elimination of C_2 and considering reference equation 2. The diffusion force *per mol* of component 1 (of activity $a_1 = N_1 f_1$) is:

$$k_1 = -RT \frac{\partial \ln N_1 f_1}{\partial x} = -RT B_{12} \frac{\partial \ln N_1}{\partial x} \quad (5)$$

Now, $K_{12} = n_1 k_1$ and, by reference equation 3, $K_{12} = N_1 k_1 / \bar{v}_{12}$, so we obtain from equations 4 and 5:

$$C_1 = -RT B_{12} \frac{n_2 \bar{v}_2}{\varphi_{12} \bar{v}_{12}} \frac{\partial N_1}{\partial x} + x' \quad (6)$$

The theory of flow provides the equation

$$\frac{\partial n_1}{\partial t} = - \frac{\partial}{\partial x} (C_1 n_1) \quad (7)$$

the time derivative of the concentration equalling the negative derivative of the flow $C_1 n_1$ along the diffusion direction x . Thus

$$\frac{\partial n_1}{\partial t} = RT \frac{\partial}{\partial x} \left[\frac{B_{12}}{\varphi_{12} \bar{v}_{12}} n_1 n_2 \bar{v}_2 \frac{\partial N_1}{\partial x} - n_1 x' \right] \quad (8')$$

and analogously for the second component

$$\frac{\partial n_2}{\partial t} = RT \frac{\partial}{\partial x} \left[\frac{B_{12}}{\varphi_{12} \bar{v}_{12}} n_1 n_2 \bar{v}_1 \frac{\partial N_2}{\partial x} - n_2 x' \right] \quad (8'')$$

Adding left and right members respectively, after an extension of equation 8' by \bar{v}_1 and of equation 8'' by \bar{v}_2 (a procedure due to M. Thiesen (14)), and considering reference equations 2, 5, and 6 we obtain

$$0 = \frac{\partial}{\partial x} (-x') \quad (9)$$

In this operation (the partial molar volumes being inserted within the derivatives) we introduce the restriction that the mixing process is not accompanied by any noticeable volume contraction or expansion. This condition is often fulfilled even in cases of considerable concentration difference between the diffusing liquids, and the volume effect may always be reduced to negligible magnitude by choosing a small concentration difference. Equation 9 means that the velocity in bulk according to equation 3 is independent of x ; as a constant velocity of the diffusion column is of no interest in pure diffusion theory, we may put $x' = 0$. It is concluded that the diffusion process at constant partial molar volumes is characterized by

$$\Sigma C n \bar{v} = 0 \quad (10)$$

In reference 6 the diffusion of the three-component system was treated according to this principle. The physical meaning of this is that the resulting volume transport through an x -level is zero, a rather self-evident statement but here following from a general treatment and the conception of Onsager and Fuoss. Returning to equations 8 we obtain:

$$\frac{\partial n_1}{\partial t} = RT \frac{\partial}{\partial x} \left[\frac{B_{12}}{\varphi_{12} \bar{v}_{12}} n_1 n_2 \bar{v}_2 \frac{\partial N_1}{\partial x} \right] \quad (11)$$

and by reference equations 7 and 8:

$$\frac{\partial n_1}{\partial t} = RT \frac{\partial}{\partial x} \left[\frac{B_{12}}{\varphi_{12}} \frac{n_1 n_2}{n_1 + n_2} \frac{\partial n_1}{\partial x} \right] \quad (12)$$

This is a Wiener-Boltzmann (1) differential equation:

$$\frac{\partial n_1}{\partial t} = \frac{\partial}{\partial x} \left[D_1 \frac{\partial n_1}{\partial x} \right]$$

According to equation 12, D_1 is symmetrical with respect to the two components, so that we may write $D_1 \equiv D_2 \equiv D_{12}$. Considering the reference equations 7 and 12 the following identical formulations of the mutual diffusion coefficient are obtained:

$$D_{12} = RT B_{12} \frac{1}{\Phi_1 + \Phi_2} = RT B_{12} \frac{N_1 N_2}{\varphi_{12} \bar{v}_{12}} = RT B_{12} \frac{n_1 n_2}{\varphi_{12} (n_1 + n_2)} \quad (13)$$

and

$$D_{12} = RTB_{12} \frac{N_1}{\Phi_2} \equiv RTB_{12} \frac{N_2}{\Phi_1} \equiv RTB_{12} \frac{1 - n_2 \bar{v}_2}{\Phi_2[1 + (\bar{v}_1 - \bar{v}_2)n_2]} \quad (14)$$

from which the generalization as compared to the Sutherland-Einstein equation is evident:

$$\lim_{n_1 \rightarrow 1} D_{12} = \frac{RT}{\Phi_2} \quad (15)$$

The partial generalization

$$D_2 = \frac{RT}{\Phi_2} B_{12} \quad (16)$$

is also of interest, as $B_{12} \neq 1$ is quite possible even in very dilute solution, as for electrolytes (equation 43), or in the case of inappropriate choice of component molecular weight (see below). Equations like equation 16 have been proposed by many investigators (for references see 10).

The factor B_{12} may be determined by independent measurements, although this magnitude is undetermined unless we have made suppositions regarding the component molecular weights, i.e., that they be chosen as the smallest possible values consistent with the chemical formulas, or multiples of these. It is, therefore, more satisfactory to introduce A_{12}

$$A_{12} = B_{12} \frac{n_1 n_2}{n_1 + n_2}; \quad D_{12} = RT \frac{A_{12}}{\varphi_{12}} \quad (17)$$

which is unambiguously defined without suppositions, as this is the case with D_{12} , φ_{12} , and RT . Accordingly, the diffusion measurement gives φ_{12} . The distinction is still more enforced in the theory of combined diffusion and sedimentation in a centrifugal field, which the author hopes to publish later, along the same lines as in this work. For the sake of clearness we may discuss a dilute solution, $n_2 \rightarrow 0$. We have, then, $A_{12} \rightarrow B_{12}n_2$, which is independent of the choice of the molecular weight multiple. It might seem self-evident that $B_{12} = 1$, in the limit of dilute solution. But this is true only if we calculate with the smallest actual molecular weight M_2 and not with a multiple nor an integer fraction of this. $B_{12} \rightarrow 1$, only if n_2 represents the actual number of molecules or ions.²

In the next section the thermodynamic factors are discussed for dissociated or associated solutes. It is, in this connection, necessary to recognize the difference between the standard state of the *component* and that of the *molecular species* in which the component may be present in the solution. The latter are always so chosen that activity can be replaced by concentration in the limit of zero concentration. This standard state, say for the double molecules of a dissociable compound, e.g., acetic acid in benzene, is not a realizable one, owing

² The appropriate choice of M_2 is a matter of experience. Thus, for the diffusion of oxygen in water at ordinary temperatures and pressures we cannot choose $M_2 = 16$ and $B_{12} = 1$, as the dissociation of oxygen will be unobservable. $M_2 = 16$ requires $B_{12} = \frac{1}{2}$.

to dissociation into simple molecules upon dilution. It is an imaginary state. The standard state of the *component* may be represented by any one of the actual or possible species in the solution. So, for instance, acetic acid vapor consists mainly of double molecules, and the partial pressure of these may very well represent the activity of the acid as a component (it is supposed that the vapor is sufficiently ideal in other respects except for dissociation). Equally well may we calculate using the partial pressure of the simple molecules and let this represent the activity of the solute. Only the state of simple molecules is, however, realizable as the limit condition of the substance which is reached by increasing dilution. Now, by definition f_2 and B_{12} approach unity when the standard state is approached. Thus, in an actual diffusion experiment, $B_{12} \rightarrow 1$ can be true only if the chosen standard state is approximately realizable and actually is nearly reached in the experiment in question. The question whether the activities of the *different species* in an equilibrium may be represented by their concentrations is not *decisive* of the value of B_{12} .

IV. THE THERMODYNAMIC FACTOR AND ASSOCIATION

In case the solute is associated, B_{12} is directly calculable if the equilibrium according to the mass action law is known (7, 8). Assuming the activity coefficients of the solute molecular species to be unity, we have

$$B_{12} = 1 + \frac{\partial \ln \beta_1}{\partial \ln n_2} = \frac{1}{b} \left(1 + \frac{\partial \ln \beta_b}{\partial \ln n_2} \right) \quad (18)$$

where $\beta_1, \beta_2 \dots \beta_b \dots$ are the fractions of the solute which are present as simple, double, . . . and b -fold molecules, respectively. As discussed in the previous section, B_{12} depends on the choice of component molecular weight. In equations 18 and 19 the lowest value was chosen, corresponding to the fraction β_1 of the component. Let the activity coefficients of the solute molecular species be $\gamma_1, \gamma_2 \dots \gamma_b \dots$; then the more general formula for a dilute solution

$$B_{12} = 1 + \frac{\partial \ln \beta_1 \gamma_1}{\partial \ln n_2} = \frac{1}{b} \left(1 + \frac{\partial \ln \beta_b \gamma_b}{\partial \ln n_2} \right) \quad (19)$$

is valid too, considered in connection with equation 24.

Finally it is, at least in principle, of interest to give up the restriction of dilute solution too. Assume the two-component system to contain, of component 1, among others a molecular species A_a , with the concentration n_a mols per cubic centimeter. The molecular weight of the *component* is counted as corresponding to the formula A_a . We use the notation f for the activity coefficient on the basis of mol fraction, and γ on the basis of mols per cubic centimeter. In the expression for the differential of chemical potential, $d\mu_1 = RT d \ln a_1$, the activity may be written $N_1 f_1$. The activity is also $n_a \gamma_a$, so that $f_1 = n_a \gamma_a / N_1$. Suppose α_a to be the fraction of component 1 present as molecules A_a ; then $n_a = \alpha_a n_1$, where n_1 is the total concentration in mols per cubic centimeter of this component. Thus $f_1 = \alpha_a n_1 \gamma_a / N_1$ and, by reference equation 3,

$$f_1 = \frac{\alpha_a \gamma_a}{v_{12}} \quad (20)$$

For the second component we assume the notation B and consider specially a complexity B_b , analogously characterized by β_b and γ_b . In this way one obtains from equation 1 the general expressions:

$$B_{12} = 1 + \frac{\partial \ln \alpha_a \gamma_a / \bar{v}_{12}}{\partial \ln N_1} \equiv 1 + \frac{\partial \ln \beta_b \gamma_b / \bar{v}_{12}}{\partial \ln N_2} \quad (21)$$

These two expressions for B_{12} have a definite meaning only if the molecular weights A_a and B_b are established for *both* components. Otherwise the mol fractions are undefined.

Returning to the dilute solution, $N_2 \rightarrow 0$ gives (compare reference equations 10 and 11):

$$B_{12} \rightarrow 1 + \frac{\partial \ln \beta_b \gamma_b}{\partial \ln n_2} \quad (22)$$

Here the molecular weight of the solute component corresponds to the chemical formula B_b , so that the right-hand member has to be divided by b to accord with equation 19. The transformation of B_{12} from one molecular weight definition to another (a change of a or b or both) is thus very simple in the limit of dilute solution. In the general case (equation 21) the dependence is most easily seen from equation 17. As A_{12} is independent, B_{12} varies as $(n_1 + n_2)/n_1 n_2$.

Stages of approximation lying between equations 21 and 22 might be of interest too.

V. THE NUMBER OF COMPONENTS

The number of components is essential for the diffusion differential equation; the case of three components (6) is already much more complicated (compare Section IX). In judging the number of components it must be borne in mind that the observation of the diffusion supposes a concentration *gradient*. If in the two-component mixture of hydrogen iodide and nitrogen the hydrogen iodide dissociates into hydrogen and iodine, there is a separation of the latter gases through the diffusion process, so that the composition along the diffusion column can no longer be measured by the number of mols of hydrogen iodide per cubic centimeter. Thus, this is a three-component system when diffusion is considered. In a case like sodium acetate in water, in which the acetate ions are protolyzed by the medium, a partial separation of acetic acid and sodium hydroxide is brought about, the system being a three-component one. On the contrary, a mixture of sulfur trioxide and water remains a two-component system also in relation to diffusion. A further example is a molten mixture of two electrolytically dissociated binary salts, which can, in this connection, be a two-component system only if the salts have one ion in common.

VI. THE FRICTIONAL COEFFICIENTS

(1) As *self-diffusion* is denoted the diffusion of a mixture of components, the latter of which are practically identical in all respects, which influence the diffusion process. The diffusion coefficient of the two-component system is, in this case, independent of the composition of the mixture (*cf.* 9). Also, the three-

component system has in this simple case real diffusion coefficients which are identical (9; equations 23 and 25), whereas in the general case it is characterized by three frictional coefficients in a more complicated way (compare Section IX). Leaving the higher systems aside we return to equation 13, putting $B_{12} = 1$.³ Thus we must have $\Phi_1 + \Phi_2 = \text{constant}$, representing the simplest possible case, from which the experimental function $\Phi_1 + \Phi_2 = F(N_2)$ is a deviation. Owing to the relation (13)

$$\Phi_1 + \Phi_2 = \varphi_{12}\bar{v}_{12}/N_1N_2$$

we also have:

$$\varphi_{12} = \frac{(1 - N_2)N_2}{\bar{v}_1 + (\bar{v}_2 - \bar{v}_1)N_2} (\Phi_1 + \Phi_2) \quad (23)$$

As it is in some respects most obvious to regard the friction per cubic centimeter, it is of value to make clear according to equation 23 (with $\Phi_1 + \Phi_2 = \text{constant}$ and $\bar{v}_1 = \bar{v}_2$) how this depends on the composition even in the simplest case, that of self-diffusion. Incidentally, we also remark that $\Phi_1 + \Phi_2$ is the mutual friction in the volume $(1/n_1 + 1/n_2)$ cc., which may perhaps be called a characteristic volume for the diffusion process.

(2) Returning to the discussion on association or the forming of compounds between the components, the question arises as to the possibility of determining single frictional coefficients of the different molecular species in the mixture. Naturally, the diffusion coefficient depends in a characteristic way on the special frictions between the different species in question, and it should be possible to relate the friction $\Phi_1 + \Phi_2$ or φ_{12} to the single frictional coefficients mentioned. To determine the latter individually our knowledge will not generally be sufficient, apart from the well-known difficulty on the whole of getting a detailed insight into the molecular constitution of the non-dilute mixture in the case of liquids. It will sometimes be possible, however, to take the indirect way of making the simplest possible assumption regarding the constitution,—sufficient to explain the experimental result; the latter being the curve which connects $\Phi_1 + \Phi_2$ or φ_{12} with the composition of the mixture.

If component 2 is in *dilute* solution, and if electrolytic dissociation is not taken into account, a simple relation connects the component coefficient Φ_2 with the coefficients of the different molecular species of the solute (*cf.* 7, 8). We make the same assumption regarding the chemical equilibrium as in Section IV; β_b is the fraction of the solute present as B_b molecules, Φ_b the coefficient of one mol B_b . We have

$$\frac{1}{\Phi_2} = \sum_b \frac{b\beta_b}{\Phi_b} \quad (24)$$

³ How are the component molecular weights to be chosen for an "identical" mixture, in order that $B_{12} = 1$? As an example, ordinary and heavy nitrogen may serve. If the equilibria between the isotopic molecules of nitrogen are very rapidly adjusted, the molecular weights 14 and 15 give the correct answer. If the processes are extremely slow we have three components: N_2^{14} , N_2^{15} , and $N^{14}N^{15}$. Between these extremes, the components are not defined in an ordinary sense, the process requiring a special theory, which involves the chemical velocity constants.

This relation is valid also if the activity coefficients in the mass action equilibrium are different from unity. Φ_2 in equation 24 refers to the molecular weight of simple B molecules.

(3) It is of interest for the general diffusion theory to prove that the component frictions, Φ_1 etc., are functions of the composition and other properties of state, but independent of the gradient property characteristic of diffusion measurements. In the concentration gradient the chemical equilibrium position depends on the linear coördinate x in the direction of the gradient, and it is hardly self-evident that Φ_1 does not change with the magnitude of the gradient. This molar friction equals the molar diffusion force divided by the linear component velocity in centimeters per second. We claim that not only is the frictional coefficient between two definite molecular species a characteristic property of the solution as such, but also the coefficient of one component against a second one, and of one molecular species against the rest of the solution.

The condition for the frictional coefficients to be properties of state in this sense is that the diffusion forces of all molecular species change by the same factor when the magnitude of the gradient changes. If *the diffusion forces retain their relative values*, the mechanical picture is maintained, the time scale changing solely. We shall proceed to prove that this is the case.

Suppose a_a to be the activity of a molecular species A_a of component 1, the activity of which is a_1 . The diffusion force on A_a is $-RT \frac{\partial \ln a_a}{\partial x}$ per mol. We shall prove that the relative change L'_a of the force with the component activity gradient $\frac{\partial a_1}{\partial x}$ is the same for all kinds of molecules. We have

$$L'_a = \frac{1}{\frac{\partial \ln a_a}{\partial x}} \frac{\partial \left(\frac{\partial \ln a_a}{\partial x} \right)}{\partial \left(\frac{\partial a_1}{\partial x} \right)} \quad (25)$$

μ_1 is the chemical potential of component 1, and we write

$$d\mu_1 = RT d \ln a_1 = RT d \ln a_a \quad (26)$$

Owing to this relation we are hereafter bound to regard the molecular weight of component 1 as corresponding to A_a . Equation 26 gives

$$\frac{\partial \ln a_a}{\partial x} = \frac{\partial \ln a_1}{\partial x}$$

thus

$$L'_a = \frac{1}{\frac{1}{a_1} \frac{\partial a_1}{\partial x}} \frac{\partial \left(\frac{1}{a_1} \frac{\partial a_1}{\partial x} \right)}{\partial \left(\frac{\partial a_1}{\partial x} \right)} \quad (27)$$

Now we assume the activity a_1 to be independent of the gradient, so that

$$\frac{\partial \left(\frac{1}{a_1} \frac{\partial a_1}{\partial x} \right)}{\partial \left(\frac{\partial a_1}{\partial x} \right)} = \frac{1}{a_1}$$

and finally

$$L'_a = \frac{1}{\frac{\partial a_1}{\partial x}} \quad (28)$$

For another species A_a with the activity a_a , the mass action law gives $(a_a)^\alpha = k(a_a)^a$, that is,

$$\frac{\partial \ln a_a}{\partial x} = \frac{\alpha}{a} \frac{\partial \ln a_a}{\partial x}$$

The factor α/a vanishes in the expression for L' , and we obtain $L'_a = L'_a$, so that equation 28 is valid for all species of component 1.

Analogously, for all species of component 2 one obtains:

$$L''_b = \frac{1}{\frac{\partial a_2}{\partial x}} \quad (29)$$

This corresponds, however, to the relative change of the diffusion force with the activity gradient $\partial a_2/\partial x$. It is transformed to the derivative with respect to $\partial a_1/\partial x$ by multiplying by

$$\frac{\partial \left(\frac{\partial a_2}{\partial x} \right)}{\partial \left(\frac{\partial a_1}{\partial x} \right)}$$

Reference equation 1b gives:

$$\frac{\partial a_2}{\partial x} = -\frac{n_1 a_2}{n_2 a_1} \frac{\partial a_1}{\partial x} \quad (30)$$

The concentrations and activities being independent of the gradient property, we have

$$\frac{\partial \left(\frac{\partial a_2}{\partial x} \right)}{\partial \left(\frac{\partial a_1}{\partial x} \right)} = -\frac{n_1 a_2}{n_2 a_1} \quad (31)$$

Multiplying equation 29 by this, and again using the reference equation mentioned:

$$L'_b = L''_b \frac{\partial \left(\frac{\partial a_2}{\partial x} \right)}{\partial \left(\frac{\partial a_1}{\partial x} \right)} = \frac{1}{\frac{\partial a_1}{\partial x}} \quad (32)$$

which just conforms to equation 28.

Hitherto, we have not considered compound formation between the components. Supposing an equilibrium



we do not restrict ourselves to one single compound, a , b , p , and q being arbitrary also in this respect. The mass action law gives

$$ab \ln a_{pq} = pb \ln a_a + qa \ln a_b + \ln K \quad (34)$$

thus

$$\frac{\partial \ln a_{pq}}{\partial x} = \frac{p}{a} \frac{\partial \ln a_a}{\partial x} + \frac{q}{b} \frac{\partial \ln a_b}{\partial x} \quad (35)$$

and, considering the expressions previously obtained for L'_a and L'_b ,

$$\frac{\partial \left(\frac{\partial \ln a_{pq}}{\partial x} \right)}{\partial \left(\frac{\partial a_1}{\partial x} \right)} = \frac{1}{\frac{\partial a_1}{\partial x}} \left(\frac{p}{a} \frac{\partial \ln a_a}{\partial x} + \frac{q}{b} \frac{\partial \ln a_b}{\partial x} \right) \quad (36)$$

We have:

$$L'_{pq} = \frac{1}{\frac{\partial \ln a_{pq}}{\partial x}} \frac{\partial \left(\frac{\partial \ln a_{pq}}{\partial x} \right)}{\partial \left(\frac{\partial a_1}{\partial x} \right)} = \frac{1}{\frac{\partial a_1}{\partial x}} \quad (37)$$

the first equality being the definition of L'_{pq} , the second following from equations 35 and 36. The result, again, conforms to equation 28.

It is concluded that the relative diffusion forces are independent of the magnitude of the gradient, if this is the case with activities, a supposition the correctness of which is not questioned for the slow gradients to be met with in this connection. Thus the frictional coefficients are solely determined by the ordinary properties of state, provided the solution or gas mixture is in inner, chemical equilibrium during the diffusion process. The proof is, however, restricted to the two-component system, owing to the use of equation 30.

Problems of this kind are likely to be most efficiently treated by aid of the methods of Onsager or Meixner; nevertheless, the more elementary procedure used here might be of interest.

VII. ELECTROLYTES

In order to calculate the thermodynamic factor for a binary, completely dissociated, and non-protolyzed electrolyte A_aB_b with the ions A^{z+} , B^{z-} , and the concentration n_2 mol A_aB_b per cubic centimeter, we have to transform B_{12} into concentration units (instead of mol fractions). This is reached by derivation of $\gamma_2 n_2 = f_2 N_2$ completely with respect to n_2 and the use of equation 1 and reference equations 10 and 11, an operation which leads to:

$$B_{12} = [1 + (\bar{v}_1 - \bar{v}_2)n_2] \left(1 + \frac{\partial \ln \gamma_2}{\partial \ln n_2} \right) \quad (38)$$

The activity a_{AB} of the electrolyte is:

$$f_2 N_2 = \gamma_2 n_2 = a_+^a b_-^b = n_+^a n_-^b \gamma_+^a \gamma_-^b = a^a b^b n_2^{a+b} \gamma_{\pm}^{a+b} \quad (39)$$

where γ_{\pm} is, by definition, the mean activity coefficient of the electrolyte. Thus,

$$\gamma_2 = a^a b^b n_2^{a+b-1} \gamma_{\pm}^{a+b} \quad (40)$$

and from this,

$$\frac{\partial \ln \gamma_2}{\partial \ln n_2} = a + b - 1 + (a + b) \frac{\partial \ln \gamma_{\pm}}{\partial \ln n_2} \quad (41)$$

Equation 38 gives:

$$B_{12} = [1 + (\bar{v}_1 - \bar{v}_2)n_2](a + b) \left(1 + \frac{\partial \ln \gamma_{\pm}}{\partial \ln n_2} \right) \quad (42)$$

In the limit of ideal, dilute solution, this reduces to

$$B_{12} = a + b \quad (43)$$

The molar frictional coefficient of the solute is, for an electrolyte, the sum of the frictional coefficients of the ions in 1 mol of the salt. This is quite different from the relation 24, owing to the condition of electroneutrality in this case. We do not at all treat the connection of Φ_2 with *conductivity* in this article. It is, however, concluded that equations 16 and 43 lead to a simple proof of the well-known diffusion equation of Nernst-Haskell (4) for the ideal, dilute electrolyte. On the other hand, this confirms the general applicability of the method here developed, especially regarding the treatment of the thermodynamic factor. In concentrated or otherwise not sufficiently ideal solution, equation 43 must be replaced by equation 42 and equation 16 by equation 14, the last alternative. We obtain the simple expression:

$$D_{12} = RT(a + b) \frac{1 - n_2 \bar{v}_2}{\Phi_2} \left(1 + \frac{\partial \ln \gamma_{\pm}}{\partial \ln n_2} \right) \quad (44)$$

The corresponding general equation is

$$D_{12} = RT \frac{1 - n_2 \bar{v}_2}{\Phi_2} \frac{\partial \ln a_2}{\partial \ln n_2} \quad (44')$$

The factor $1 - n_2 \bar{v}_2 = n_1 \bar{v}_1$ is a result of the symmetrical treatment of the two components. Formula 44 supposes (1) a real two-component system of $A_a B_b$ and solvent (compare Section V) in inner equilibrium, and of mechanically normal fluidity⁴; (2) constant partial molar volumes \bar{v}_1 and \bar{v}_2 . The latter is

⁴ The validity of formula 44 does not necessitate that the electrolyte be completely dissociated, nor that it be dissociated according to the scheme $A_a B_b = aA^{a+} + bB^{b-}$, owing to the formal possibility of defining activity as $a^a b^b n_2^{a+b} \gamma_{\pm}^{a+b}$ in any case. On the other hand, it is necessary to choose the molecular weight according to the formula $A_a B_b$ for the calculation of n_2 and Φ_2 .

always true if D_{12} is the real *differential* diffusion coefficient, as obtained with a sufficiently small concentration difference between the diffusing liquids. Thus, the molar volumes by no means need to have the same values at different concentrations n_2 . Diffusion coefficients of this kind have recently been measured by the method of Onsager and Harned (see 3 and later papers).

VIII. GENERAL CONSIDERATIONS IN THE FORMULATION OF THE THERMODYNAMIC FACTOR

According to equations 1 and 17 we have

$$A_{12} = B_{12} \frac{n_1 n_2}{n_1 + n_2} = \frac{\partial \ln a_2}{\partial \ln N_2} \frac{n_1 n_2}{n_1 + n_2} \quad (45)$$

By consequent transformation to units of mols per cubic centimeter one obtains:

$$A_{12} = n_1 n_2 \bar{v}_1 \frac{\partial \ln a_2}{\partial \ln n_2} \quad (46)$$

This coefficient has the advantage of being a direct, unambiguous *property* of the mixture. Dividing this by another property, $n_1 n_2 \bar{v}_1 \bar{v}_2$, and multiplying by RT , we get a new quantity called Q_{12} :

$$\frac{RTA_{12}}{n_1 n_2 \bar{v}_1 \bar{v}_2} = Q_{12} = \frac{RT}{\bar{v}_2} \frac{\partial \ln a_2}{\partial \ln n_2} \quad (47)$$

The differential of the *osmotic pressure* p_1 of component 1 is given by

$$\bar{v}_2 dp_1 + RT d \ln a_2 = 0 \quad (48)$$

We obtain:

$$\frac{\partial p_1}{\partial \ln n_2} = - \frac{RT}{\bar{v}_2} \frac{\partial \ln a_2}{\partial \ln n_2} \quad (49)$$

and equation 47 gives

$$Q_{12} = -n_2 \frac{\partial p_1}{\partial n_2} \quad (50)$$

It is not surprising to find Q_{12} closely related to a directly measurable property of the solution as is the osmotic pressure. The older treatments of liquid diffusion were based on the van't Hoff osmotic-pressure expression. The generalized diffusion theory has a close connection with the more general osmotic pressure interpretation. It should be noticed that Q_{12} is a symmetrical property as indicated by this notation. Writing equation 50:

$$-Q_{12} = n_2 \frac{\partial p_1}{\partial n_2} = n_1 \frac{\partial p_2}{\partial n_1} \quad (51)$$

we see that Q_{12} is a property suitable for the characterization of a binary mixture, although from practical reasons it must generally be measured indirectly.

Finally, we write the values of the magnitudes in question in the limit of zero concentration. $n_2 \rightarrow 0$ gives:

$$\begin{aligned} Q_{12} &\rightarrow \frac{RT}{\bar{v}_2} = \frac{p_2}{n_2 \bar{v}_2} \\ A_{12} &\rightarrow n_2 = \frac{p_2}{RT} \\ B_{12} &\rightarrow 1 \end{aligned} \quad (52)$$

The last equation is the simplest, but supposes the correct molecular weight multiple of component 2 to be chosen. Measuring the other limiting values, Q_{12} or A_{12} , determines this molecular weight.

IX. NOTE ON THE DIFFUSION OF A TERNARY SYSTEM

In previous papers (6, 9) a differential equation for the diffusion of a ternary liquid mixture was written in the form

$$\frac{\partial n_1}{\partial t} = -RT \frac{\partial}{\partial x} \left[\frac{n_1}{\bar{v}_{123} \Sigma \varphi \varphi} \left\{ k_{12} B_2 \frac{\partial N_2}{\partial x} + k_{13} B_3 \frac{\partial N_3}{\partial x} \right\} \right] \quad (53)$$

Two other equations are obtained by cyclic permutation of indices, $1 \rightarrow 2 \rightarrow 3 \rightarrow 1$. The notations are

$$\begin{aligned} \bar{v}_{123} &= N_1 \bar{v}_1 + N_2 \bar{v}_2 + N_3 \bar{v}_3 \\ \Sigma \varphi \varphi &= \varphi_{12} \varphi_{23} + \varphi_{23} \varphi_{31} + \varphi_{31} \varphi_{12} \\ B_1 &= 1 + \frac{\partial \ln f_1}{\partial \ln N_1} \\ k_{12} &= \varphi_{23} (Y_2 + Y_3) + \varphi_{31} Y_2 \\ k_{13} &= \varphi_{23} (Y_2 + Y_3) + \varphi_{12} Y_3 \end{aligned}$$

$Y_1 = n_1 \bar{v}_1$ etc. are the volume fractions, $Y_1 + Y_2 + Y_3 = 1$.

The possibility exists of using mol fractions consistently, but apparently this leads to very complicated expressions. The formulation 53 has the disadvantage of mixed variables, as it contains both mols per cubic centimeter and mol fractions. The best way to avoid this seems to be to introduce *volume fractions* throughout. For this purpose we write activity $Y_1 \Gamma_1$, Γ_1 being the activity coefficient on the basis of volume fraction. We obtain (cf. 6, equation 14)

$$B_1 \frac{\partial N_1}{\partial x} = \frac{\bar{v}_{123}}{\bar{v}_1} O_1 \frac{\partial Y_1}{\partial x} \quad (54)$$

where

$$O_1 = 1 + \frac{\partial \ln \Gamma_1}{\partial \ln Y_1} = \frac{1 + \frac{\partial \ln \gamma_1}{\partial \ln n_1}}{1 + \frac{\partial \ln \bar{v}_1}{\partial \ln n_1}}$$

and

$$\frac{O_1}{\bar{v}_1} \frac{\partial Y_1}{\partial x} + \frac{O_2}{\bar{v}_2} \frac{\partial Y_2}{\partial x} + \frac{O_3}{\bar{v}_3} \frac{\partial Y_3}{\partial x} = 0$$

Equation 54 now gives, more clearly and with disappearing \bar{v}_{123} ,

$$\frac{\partial Y_1}{\partial t} = -RT \frac{\partial}{\partial x} \left[\frac{Y_1}{\Sigma \varphi \varphi} \left\{ k_{12} \frac{O_2}{\bar{v}_2} \frac{\partial Y_2}{\partial x} + k_{13} \frac{O_3}{\bar{v}_3} \frac{\partial Y_3}{\partial x} \right\} \right] \quad (55)$$

The O -values are regarded as empirical functions of the two independent volume concentrations. Besides these, the diffusion process is determined by the frictional coefficients φ_{12} , φ_{23} , and φ_{31} . As the gradient in activity of a component 1 can have a finite value even if $\partial Y_1/\partial x = 0$, owing to the gradient in concentration of the other two components, the functions O incidentally may become infinite. (The connection between the O_1 -values and the B_1 -values cannot be written in concentration variables belonging to component 1 solely.)

The use of concentrations n makes very little difference, related as they are to volume fractions through $Y_1 = n_1 \bar{v}_1$ etc., and \bar{v}_1 here can be regarded as constant, as has already been assumed in the deduction of equation 53. The equation is

$$\frac{\partial n_1}{\partial t} = -RT \frac{\partial}{\partial x} \left[\frac{n_1}{\Sigma \varphi \varphi} \left\{ k_{12} O_2 \frac{\partial n_2}{\partial x} + k_{13} O_3 \frac{\partial n_3}{\partial x} \right\} \right] \quad (56)$$

SUMMARY

The scope and features of a theory of diffusion, detailed in earlier works, have been outlined. A simple proof of a generalized Sutherland-Einstein equation for the diffusion of a binary solution in general is given, and the interpretation of diffusion measurements discussed. The properties of the thermodynamic factor and the frictional coefficients involved are treated in some detail, considering the chemical equilibrium between the components in arbitrary or dilute solutions. An equation for the diffusion of electrolytes is computed. A note is added on the diffusion of a ternary solution, this being most simply described in terms of volume fractions or mols per cubic centimeter.

REFERENCES

- (1) BOLTZMANN, L.: *Wied. Ann. Physik* **53**, 959 (1894).
- (2) GLASSTONE, S., LAIDLER, K. J., AND EYRING, H.: *The Theory of Rate Processes*. McGraw-Hill Book Company, Inc., New York and London (1941).
- (3) HARNED, H. S., AND FRENCH, D. M.: *Ann. N. Y. Acad. Sci.* **46**, No. 5, 267 (1945).
- (4) HASKELL, R.: *Phys. Rev.* **27**, 145 (1908).
- (5) LAMM, O.: *Arkiv Kemi, Mineral. Geol.* **17A**, No. 9 (1943).

- (6) LAMM, O.: Arkiv Kemi, Mineral. Geol. **18A**, No. 2 (1944).
- (7) LAMM, O.: Arkiv Kemi, Mineral. Geol. **18A**, No. 9 (1944).
- (8) LAMM, O.: Arkiv Kemi, Mineral. Geol. **18A**, No. 10 (1944).
- (9) LAMM, O.: Arkiv Kemi, Mineral. Geol. **18B**, No. 5 (1944).
- (10) LAMM, O.: Paper published in honor of T. Svedberg, Uppsala, 1944, p. 182.
- (11) LEWIS, G. N., AND RANDALL, M.: *Thermodynamics and the Free Energy of Chemical Substances*. McGraw-Hill Book Company, Inc., New York (1923).
- (12) MEIXNER, J.: Ann. Physik [5] **39**, 333 (1941); **43**, 244 (1943).
- (13) ONSAGER, L.: Phys. Rev. **37**, 405 (1931).
- ONSAGER, L., AND FUOSS, R. M.: J. Phys. Chem. **36**, 2689 (1932).
- (14) THIESEN, M.: Verhandl. deut. physik. Ges. **4**, 348 (1902).

THE BIOCHEMISTRY OF PLANT PIGMENTS

WILDER D. BANCROFT

Cornell University, Ithaca, New York

Received April 29, 1947

A great deal of work has been done on the chemistry of plant pigments (1), much of it first class. When it comes to the biochemistry of plant pigments our scientific knowledge is still very unsatisfactory. This is apparently because the problem is one which should be attacked by chemists and botanists working jointly. This has not yet happened. It is possible that the botanist could learn enough chemistry to enable him to dispense with the chemist; but no botanist has done that. It is probable that the chemist could learn enough botany to enable him to dispense with the botanist; but no chemist has yet done that.

Lycopene, $C_{40}H_{56}$, is the red pigment of the tomato.

"Lycopene has also been found in hips (*Rosa canina*), in the ripe fruits of *Tamus communis* (Christmas rose), in deadly nightshade (*Solanum dulcamara*), in the fruit of the watermelon (*Cucumis citrullus*), in the berries of *Arum maculatum*, in the apricot (*Prunus armeniaca*), in bryony fruit (*Bryonia dioica*), in the golden flowers of the marigold (*Calendula officinalis*), in the fruit of lily-of-the-valley (*Convullaria majalis*), in Kaki fruit (*Diospyros Kaki*), in tropical fruits, in the dark orange blossom of *Dimorphoteka aurantia*, in *Citrus grandis*, in *Passiflora coerulea*, and in bacteria, as in the *thiocystio bacterium*." (10)

Apart from lycopene the red and many of the blue vegetable pigments are anthocyanins or anthocyan. They are all derivations of 2-phenylbenzopyrylium salts and all, with the exception of a few amino derivatives, are hydroxy derivatives existing in the plant usually as glycosides.

All blue flowers turn red when acidified. Some red flowers, but not all, pass through blue when treated with ammonia. It is not known what stabilizes the blue and whether it is always the same substance or mixture of substances. It is now known that crude extracts of the anthocyanins contain copigments such as tannin, gallic acid, etc., which possess the ability to intensify or modify the color. Thus the glucoside of 2-hydroxyxanthone is an active copigment for cyanin,

and the inner violet parts of the fuchsia flower contain tannin and are thus distinguished from the external red portions. The formation of complexes with organic materials or, for example, with iron, has a greater effect on the color of varying varieties than the acidity of the cell sap, or so say Mayer and Cook. The fact that aluminum sulfate causes hydrangeas to come blue must be because of a marked adsorption of alumina, though this has not yet been shown by the chemist, so far as I can learn. I am hoping that Professor H. B. Weiser of Rice Institute will some day show this to be true. Selective adsorption is colloid chemistry.

I have placed flowers of pink hydrangeas in a saturated solution of alum. The petals turn blue as they should; but it is a slow operation, requiring days. The alum appears to go in through the stems and not through the face of the petals. With a dilute solution of alum there appears to be no change of color; but that may have been because I did not allow enough time. In the growing plant there cannot be a saturated solution of alum, but the time factor is very different. There appears also to be a partial bleaching of the parts of the petals which are still pink, and I cannot offer any explanation for that at present. In hydrangeas grown in a greenhouse some of the petals or parts of them come white or nearly so, without there being any obvious reason for it. I do not like to suggest selective mutations, because I do not know exactly what I mean by the term.

I think that the white hydrangeas are a different variety (1), because they do not turn red or pink even when growing outdoors. There are numerous details about hydrangeas which need studying. I do not know whether alum affects other red flowers, and, if not, why not. I wonder what alum would do with red *Althaea* and with *Geranium maculatum* Linnaeus.

Though it has nothing to do with colors, an interesting fact is cited by the Old Dirt Dobber (20): "The blossom heads of cauliflower should be protected from sunlight in order to develop the desirable white curd. As soon as the head begins to form all of the leaves should be gathered up and tied loosely at the top in order to shut out the light. Tying too tightly is liable to cramp the heads."

People are pretty well agreed that the anthocyanins become more intense in color as one moves up a mountain from sea level. Bonnier (2) says that from studies made in the Austrian Alps he concludes that most flowers are deeper in color the higher they grow and that white flowers tend to become pink. The effect of altitude is very marked with *Myosotis silvatica*, *Campanula rotundifolia*, *Ranunculus silvaticus*, and *Galium Cruciale*. It is very slight with *Thymus Serpyllum* and *Geranium silvaticum*, and practically zero with *Rosa alpina* and *Eritgeron alpinus*. With *Viola tricolor*, *Phyteumas spreatum*, and *Geranium pratense* the differences at the same level were so great as to make impossible any comparison at different levels. The white flowers which became pink at higher levels were *Bellidiastrum Michellii*, *Sirene inflata*, *Silenus rupestris*, and *Bellis perennis*.

Bonnier does not mention any white flowers turning blue with increasing altitude of growth, and I do not know whether the Austrian Alps are or are not unfavorable to the development of blue flowers.

Cockerell (3), when speaking of the Colorado mountains, says that there is a preponderance of blue in the high-mountain flowers.

"The intense blue of some high alpine flowers is most noticeable, and the large number of blue flowers is equally remarkable. I never saw anything equalling in *blueness* the *Omphalodes nana* var. *aretiodes* of the Colorado mountains above timber-line. The brilliancy of these flowers is almost dazzling. The large and beautiful blue flowers of species of *Gentiana*, *Polemonium*, etc. are conspicuous on high mountains. Next to the blues come the pinks. I have shown in the Bulletin of the Torrey Botanical Club how species of *Castilleja*, which are scarlet or yellow at lower altitudes become crimson bracketed as they ascend. Many other examples could be given.

"I have found no one to dispute the reality of this change of colour at least in many groups of plants. The cause of it seemed much more obscure. It is generally agreed that, developmentally, reds come after yellows, crimsons follow red and blue crimson. Further, it is supposed that this series of colours is the result of different degrees of pigmental complexity, perhaps of the nature of, or similar to, various degrees of oxidation. Katabolism, strong metabolism, produces the higher colours—the crimsons, the blues. Moisture, slow development, great growth, with an expansion of the parts—these are favourable to the yellows, and, in a less degree, to the reds; of course the green, the primitive chlorophyll, especially.

"May not all this, therefore, be correlated with the dwarfing? Strong metabolism is necessary; every energy must be thrown into the inflorescence, and, as a side result, we get the crimsons and blues of mountain flowers.

"It may be, even, that all, or nearly all, blue flowers were produced in this way. Very few of those groups of flowers which are never alpine have blue flowers. There will be some exceptions, of course—for instance, I do not know how to account for the blue water-lily—and there are some groups in which a blue flower, however alpine the species, seems to be unproduceable. But even some of the very refractory genera, as *Erysimum* and *Troximon*, do go so far as to produce an occasional purple flower at high altitudes.

"If I am right in my suggestions, the need for selection by bees, made so much of by various authors, no longer exists. My own observations make me very doubtful whether bees do really prefer blue flowers at all, as a general thing—and I can hardly bring myself to believe, though the present hypothesis fell to the ground, that blue in flowers is a result of insect selection."

What Cockerell does not say in his paper is quite as interesting as what he does say. He does not mention that white flowers sometimes turn red or blue at higher altitudes. Bonnier showed that some white flowers turned pink at higher altitudes, and it seems certain that some white flowers must turn blue, though we cannot yet name them. Cockerell does not refer to Bonnier's paper, although it was published about ten years earlier. He does not say whether the red and the blue flowers occur so strikingly on the same mountains or on different mountains, under the same or different soil conditions. My guess is that the red and the blue flowers do not occur under the same soil conditions; but I am only guessing.

Cockerell does not mention that, in Japan, white flowers develop more flavones, as shown by the ammonia test, in the mountains than in the valleys, while nothing is said about the development of either red or blue flowers on the mountains. This may be because the Japanese mountains are lower than the Colorado mountains; but we do not know whether this is so or whether this is the real reason for the apparent difference in behavior.

We also do not know why the edelweiss apparently does not become red or blue at either higher or lower altitudes. We do not know why certain yellows change with high altitudes or why any yellow should change to red. Do dandelions change with altitude? Fischer (8) found that a yellow marigold, *Calendula officinalis*, bleached to a pale yellow when shaded from ultraviolet light; but of course he never tried growing it high on a mountain. The climbing Burmese lily, *Gloriosa superba*, is said to change from yellow to deep crimson as the flowers age.

Any change in external conditions which destabilizes a living plant tends to make the plant change in a way that eliminates the disturbing factors. In a book called *Plant Geography* and published in 1903, A. F. W. Schimper says (page 126),

"... a plentiful water supply favors the development of the vegetative organs as a rule; scarcity of water brings about their reduction. On the contrary, the production of sexual organs is usually impeded by a considerable supply of moisture and favored by drought. This principle, which has long been established by practical operations, has led to various horticultural artifices for the production of a rich supply of blossom. Among these, for instance, is the art of root pruning, in which a trench is dug around the plant and the exposed portion of the root-system cut off. In Ceylon, in order to cause the vine to blossom, the roots are laid partially bare for a time. *Cereus* and other *Cactaceae* bear flowers more plentifully if they have been shrivelled up, than after a period of uninterrupted turgescence. Many plants, for instance, certain species of *Juncus*, blossom only in a relatively dry soil.

"Retarded passage of water through the vessels leads to similar results. If a twig of a coffee plant be broken so that it remains attached to a branch only by a portion of its wood, it produced more flowers and eventually more fruit [11] than an uninjured twig."

Kurz found in the mountains of Burma that increased coolness due to increased altitude expedited the blooming of temperate plants such as *Rhododendron* and *Gentiana*, but delayed that of tropical ones. It is probable, though not so stated, that the tropical plants were destabilized too much.

On p. 418 is the statement that the destructive effects of light on chlorophyll are far less in temperate than in tropical zones. The foliage of Scandinavian vegetation is considered to be of a more intense and pure green than that of Central Europe, although it is illuminated almost continuously during summer. Many effects of light associated with less high intensities are naturally displayed more strikingly as duration of daylight increases. Thus the increased production of pigments in flowers and fruits, as well as of ethereal oils, near the north polar circle, is attributed, probably rightly, to the longer duration of light.

Professor A. J. Heinicke, Director of the Experiment Station at Geneva, New York, and Professor of Pomology at Cornell University, writes me that the same thing is undoubtedly true for red apples and that a Northern Spy apple, for instance, would probably be redder if grown on a mountain than if grown nearer sea level. This does not mean anything in regard to the flavor. Professor Heinicke thinks that one possible factor in the color change would be the generally poorer soil that one would find on the mountain tops. The lower nitrogen content of the soil would tend to make for more brilliant coloring in the flower and fruit parts.

While the effect of altitude is recognized qualitatively by everybody, though we are not clear as to all the details, there is another matter on which there is no agreement. Several people, not botanists or chemists, claim that some flowers growing near the ocean are more intense in color than similar flowers growing a little way back from the sea. They cite, among others, the case of wild roses growing on the coast of Maine. Botanists are sceptical as to this; but I get the impression that they see no reason why such a change should occur and that therefore it does not occur. This line of reasoning does not seem sound to me and I do not yet know what the facts are. We know that salt tends to destroy vegetation and that therefore small amounts of salt might destabilize plants enough to cause more intense coloring. It is a question of fact and not of theory. I have never heard of the alleged effect being claimed as occurring along rivers or lakes, so that it is a question of salts and not of moisture. There seems to be no reason to suppose that we are dealing with copigments. If one planted wild roses in a garden and watered them with a dilute solution of sea salt one should get an experimental answer to the question after one got the conditions worked out.

I tried to get the Garden Gate radio program of Nashville, Tennessee, interested in this problem but without any luck and I do not know why. Evidently there was something wrong in my approach.

When lilacs are allowed to bloom with the blossoms protected from ultraviolet light, there is no failure to develop color. The flowers do not come white or nearly white, as do the flowers of the Japanese quince, *Cydonia japonica*. This means that the anthocyanin is ordinarily developed from a leucoanthocyanin and not from a flavone. Duchartre (6) showed nearly ninety years ago that purple lilacs, cultivated at 33°C. and in darkness, produce white flowers; but any lowering of temperature or exposure to light causes the development of color. This means that at a suitable temperature the pigment in the lilac develops from a flavone. We can now account for the facts said to have been observed by a gardener in Albany, New York. He dug up a lilac bush one winter and brought it indoors. The flowers came white. The temperature indoors was evidently high enough. What we were not told, presumably because the gardener did not appreciate it, was that the indoor light was sufficiently bad so that there was not enough ultraviolet to cause the color change.

Costerus (5) mentions that lilacs often have white flowers when cultivated by florists in the winter. He is not specific as to conditions.

Pearce and Streeter (12) at Cornell University studied the reddening of McIntosh apples in sunlight, which takes place only as the apples get ripe. The wave lengths 3600–4500 Å. are the most effective in causing reddening. Since most flavones and flavonols have a point of maximum absorption somewhere within this range, Pearce and Streeter conclude that a flavone or flavonol is the substance which is converted into an anthocyanin pigment by light. They made no attempt to find out what enzyme makes the flavone photosensitive (19) nor whether other red apples behave like McIntosh apples. So far as we now know, all red apples require ultraviolet light to cause them to turn red.

Professor T. Wallace, Director of the University of Bristol Research Station

at Long Aston, Bristol, writes to Professor Findlay, Professor Emeritus at the University of Aberdeen, and now living in Kent, that

"Whilst we have no special data on the suppression of red colours in fruits, it is a common observation with us in the case of apples that the varieties which develop red colours give these more brightly on fruits exposed to light; whilst in the centre of the tree in the shady positions the fruit may be almost green. I think you could take almost any English apple as an example, but the following would be typical, say Worcester Pearmain, Lord Lawrence, Cox's Orange Pippin, Fortune, Laxton's Superb, all of which colour highly.

"I cannot give you any information regarding the soft fruits, such as raspberries, strawberries, etc.; but should imagine that these, in the main, will develop their colour irrespective of exposure to light.

"Pears and plums may be rather in the same category as apples, though plums may be more liable to develop colour in shady positions than pears. The apple would be the outstanding example."

Dr. W. S. Rogers of the Kent Incorporated Society for Promoting Experiments in Horticulture at Maidstone, Kent, writes to Professor Findlay that

"relatively little work has been done in England on colour in fruit; but I worked on this subject for my Diploma. The thesis was never published in full, but is available at Cambridge University School of Agriculture library. In one small experiment I protected apples of the variety Gladstone from light, by covering them with thick blue paper bags. This variety is normally bright red; but the covered apples remained entirely green. I think that this is a general principle applying to all English coloured apples, except the few ornamental varieties which have a purple sap.

"Black currants will certainly blacken in the shade; but I think strawberries need ultraviolet though I have not tried this."

Since I am not familiar with these English apples I am deeply indebted to Professor Findlay for this information. I think that Dr. Rogers made a bad guess as to strawberries needing ultraviolet light. I do not know of any American apples having red juice; but my guess is that the color of the juice would be independent of light, while the skin of the apple would require ultraviolet light. Miss Spencer, Professor at the Food Technology Research Institute of the University of Texas, Austin, Texas, found that the red color in the skin of the pomegranate did not develop when the fruit was shaded, but that the juice was red.

As has been said, all red American apples which have been studied so far require ultraviolet light to develop the red color; but we have no data on many of these apples. We do not know at all why Porter apples and Rhode Island Greenings do not turn red. I do not know where the russet apple is to be classed.

Laurent (9) says that the red colors of apples, pears, and peaches form only under the influence of the sun's rays, but that blue-black grapes do not require direct sunlight to cause the color to develop. This means that the anthocyanins of these grapes belong predominantly to the leucoanthocyanin type and not predominantly to the flavone type. Nectarines belong undoubtedly with peaches.

I have found no statement as to whether Concord and Delaware grapes color when protected from ultraviolet light, but there is as yet no reason to suppose that American grapes differ fundamentally from European grapes. European grapes can be grown on American stocks to minimize attacks from phylloxera.

The relative uniformity of color in a bunch of grapes indicates that they are predominantly of the leucoanthocyanin type. The same thing is true of Black Hamburg grapes grown under glass in this country.

Laurent does not say what pears he tested, and red pears are not common as red apples are. Day and Young of Santa Clara, California, are growing Comice pears commercially and say that they are very red. I had some sent to me from California. They were of course picked green and shipped in packages. These pears did not turn red when they ripened in the dark. This would seem to confirm Laurent's statement; but Professor McDaniel at Cornell is sceptical about these pears being as red in California as the advertisements imply. There are differences between flowers in one's garden and in the catalogues. It is to be hoped that careful observations will be made on these pears both in California and in Europe.

O. Opoix, in a book published in 1912 and entitled *La culture du poirier*, speaks of the Doyenné du Comice pears and advises that they be kept in cloth or paper sacks until early in the autumn to protect the fruit from worms and insects. If the sacks are taken off early in the autumn the pears color properly. Nothing is said about these pears turning red; but this description applies also to red apples.

In the Ithaca (N. Y.) *Journal* I found a paragraph saying that cotton develops a white blossom which then turns red. I wrote to Professor H. B. Weiser to confirm this; he has informed me that the cotton bloom is white on the first day, pink on the second day, and red on the third day, and falls off on the fourth day. This sounds as though the red comes from a leucoanthocyanin. If this is the case, the white blossoms should turn red when treated with hydrochloric acid solution. If the red develops from a flavone, the blossoms should remain white if kept shaded. It is a perfectly simple matter to determine what happens, but someone must do the experiments and I have not heard that this has yet been done. Obviously it should be done in a cotton country. The trillium or wake-robin also turns red as the flowers age.

With the facts that we have we can now account for some phenomena which bothered Mrs. Muriel W. Onslow (13) a good deal.

"Willstätter's preparation *in vitro* of cyanidin from quercetin, coupled with the fact that most of the flavones and flavonols will produce red pigments on reduction led many investigators to the conclusion that *in the plant* flavone (or flavonol) glucosides are readily converted into anthocyanins by reduction and *vice versa*. This view has been exploited by Shibata [15], Shibata and Kishida [16], Shibata and Nagai [17], Shibata, Nagai and Kishida [18], and Rosenheim [14], who extended the observations already made by other workers that crude extracts from many plants give reactions for flavones and, in such cases, also produce red pigments on reduction.

"The evidence of anthocyanin formation *in the plant* by reduction is, however, slight, being chiefly that provided by Combes [4] already mentioned. Combes prepared artificial anthocyanin by reduction of a flavone pigment from *Ampelopsis*. The artificial and natural products gave the same melting point. Conversely the natural anthocyanin gave, on treatment with hydrogen peroxide, a flavone with the same melting point as the natural product. In no case, as already stated, was any product identified or analyzed.

"On the other hand there exists evidence to this view. We must assume, if the above hypothesis be correct, that the anthocyanins, pelargonidin, cyanidin and delphinidin, are likely to be accompanied in the plant by the corresponding flavonols from which they are

formed by reduction, namely kaempferol, quercitrin and myrcetin. The only plants known where careful investigation has proved the identity of both flavone and anthocyanin present in the same plant are *Delphinium Consolida* and *Viola tricolor*. In the blue flowers of the former, A. G. Perkin was able to find only a glucoside of kaempferol; of the purple variety, Willstätter showed the anthocyanin to be a glucoside of delphinidin. Similarly A. G. Perkin isolated only glucosides of quercitrin from the pansy (*Viola tricolor*) and the purple violet (*V. odorata*), while Willstätter and Weil isolated from the blue-black pansy, violanin, a glucoside of delphinidin—not cyanidin. It is difficult, however, to draw conclusive evidence from the above, since it may be possible, though unlikely, that more than one flavone pigment is present and that one only is reduced to anthocyanin.

"Everest [7] has carried out an investigation designed to elucidate the above problem. He isolated the anthocyanin from *Viola Black Knight*, and found it to be identical with Willstätter's violanin. He claims, too, by qualitative reactions to have shown that two flavones were present, one of which is myrcetin (or, less likely, gossypetin). He did not however isolate either pigment, and the evidence is not by any means conclusive."

Mrs. Onslow is grieved because there are apparently many plants in which the flavones do not correspond with the anthocyanins in the same plants. The alleged difficulty seems to me to be a matter of inadequate chemical knowledge. Mrs. Onslow did not know about leucoanthocyanins and consequently did not consider them in her discussion. If an anthocyanin is derived from a flavone, it must correspond with it unless one postulates an extraordinary rearrangement of structure during the reduction of the flavone to the anthocyanin. Mrs. Onslow does not postulate any such rearrangement and yet does not draw the other necessary conclusion that the so-called abnormal anthocyanins are not formed directly from flavones. If a particular anthocyanin is formed from a leucoanthocyanin, it does not necessarily correspond with a flavone which may occur in the plant but which is not converted into the anthocyanin which we are considering, perhaps because the suitable enzyme is not present. It is evidently necessary to fill the gaps in Mrs. Onslow's knowledge of chemistry.

It must be true that the anthocyanin in the flowers of the Japanese quince corresponds with the flavone which could be but has not yet been isolated from the shaded Japanese quince. Of course the flavones in the white flowers must correspond with the anthocyanin obtained by the reduction of these flavones, but this has not yet been shown experimentally.

My guess is that the pigments in the strawberry and in the skin of the red banana come from leucoanthocyanins, even though a white strawberry and a yellow-skinned banana are known. I do not know anything at first hand about red cherries; but the former Miss Hesse told me that Montmorenci cherries turn red without exposure to ultraviolet light. It is therefore possible, and perhaps probable, that all red cherries will color in the dark and that they therefore belong in the class with grapes and plums and not with apples, pears, peaches, and nectarines.

I am not qualified to tell whether Mrs. Onslow's genetics are as unsatisfactory as her chemistry; but one wonders. We certainly need badly a really good book on the anthocyanins. I do not know where one classes the anthocyanin of the Judas tree, or red bud, as it is called throughout most of the United States.

When the soil is sufficiently low in available iron there is marked chlorosis in vegetation. There is no iron in chlorophyll and no reaction in the synthesis of

chlorophyll is known to involve salts of iron. The chlorosis is therefore still unexplained.

SUMMARY

1. Anthocyanins become more intense in color as one goes up mountains.
2. This increase in color is probably due to a destabilization of the plants. It is not known whether this intensification passes through a maximum at some height, but it probably does at some degree of destabilization.
3. In the Austrian Alps some white flowers become red as one goes up the mountains.
4. It is probable that some white flowers become blue as one goes up mountains, but I have not yet seen any statement to this effect.
5. In Japan white flowers become richer in flavones as one goes up the mountains. I have seen no record of white flowers becoming red or blue in Japan under these conditions; but this must be an oversight.
6. It is not known whether red and blue flowers become white on greater destabilization.
7. It is not known whether the edelweiss changes color at other heights. This must be an oversight.
8. All blue flowers turn red when acidified. Some, but not all, red flowers turn blue when treated with ammonia. The wild geranium, or spotted crane's-bill, *Geranium maculatum* Linnaeus, does turn blue, but the tulip does not.
9. It is not known what stabilizes the blue color.
10. All red colors in the skins of apples, pears, peaches, nectarines, and pomegranates require light to develop the color.
11. It is not known why Porter apples and Greenings do not turn red. I have never seen the Golden Delicious, but it is presumably not red.
12. Grapes, plums, strawberries, red-skinned bananas, and the Montmorenci cherry do not require light to develop the color.
13. At ordinary temperatures the color of lilac blossoms develops from a leucoanthocyanin, but at 35°C. it develops from a flavone.
14. No details are known to me about cotton flowers coming white and later turning red.
15. The anthocyanin in the juice of the pomegranate develops from a leucoanthocyanin.
16. The statement that wild roses and some other flowers are brighter when grown near the ocean than when grown back from the shore has not been confirmed or refuted by any botanist, so far as I know; but it may be true. Salt may destabilize the plants.
17. Mrs. Onslow's difficulty about the flavones not necessarily corresponding with the anthocyanins in the plant is undoubtedly due to her not knowing that some anthocyanins develop from leucoanthocyanins.
18. There are a good many details not yet known about hydrangea flowers.
19. It is very important that botanists and chemists should work in coöperation on borderland problems.

REFERENCES

- (1) BANCROFT: *Science* **98**, 98 (1943).
- (2) BONNIER: *Bull. soc. botan. France* **27**, 103 (1880).
- (3) COCKERELL: *Nature* **43**, 207 (1881).
- (4) COMBES: *Compt. rend.* **157**, 1002 (1914); **158**, 272 (1914).
- (5) COSTERUS: *Nature* **25**, 482 (1882).
- (6) DUCHARTRE: *Bull. soc. botan. Paris* **7**, 152 (1860).
- (7) EVERST: *Proc. Roy. Soc. (London)* **90B**, 251 (1918).
- (8) FISCHER: *Flora* **98**, 380 (1908).
- (9) LAURENT: *Compt. rend. soc. roy. botan. Belg.* **29**, **II**, 71 (1890).
- (10) MAYER AND COOK: *The Chemistry of Natural Coloring Matters*, p. 20. Reinhold Publishing Corporation, New York (1943).
- (11) MÖBIUS: *Biol. Zentr.* **1892**, 48.
- (12) PEARCE AND STREETER: *J. Biol. Chem.* **92**, 743 (1931).
- (13) ONSLOW (MRS.): *The Anthocyanin Pigments of Plants*, 2nd edition, p. 124. University Press, Cambridge (1925).
- (14) ROSENHEIM: *Biochem. J.* **14**, 73 (1920).
- (15) SHIBATA: *Botan. Mag. Tokyo* **29**, 118 (1915).
- (16) SHIBATA AND KISHIDA: *Botan. Mag. Tokyo* **29**, 301 (1915).
- (17) SHIBATA AND NAGAI: *Botan. Mag. Tokyo* **30**, 149 (1916).
- (18) SHIBATA, NAGAI, AND KISHIDA: *J. Biol. Chem.* **28**, 93 (1916).
- (19) WHELDALE: *J. Genetics* **1**, 43 (1911).
- (20) WILLIAMS: *The Old Dirt Dobber's Garden Book*, p. 228. R. M. McBride and Company, New York (1947).

THIN OXIDE FILMS ON ALUMINUM

EARL A. GULBRANSEN AND W. S. WYSONG

*Westinghouse Research Laboratories, East Pittsburgh, Pennsylvania**Received April 11, 1947*

Although aluminum is one of the more reactive metals, the reaction with oxygen at room temperature and even at temperatures up to 600°C. is extremely slow (15). This has led to the view that the oxidation reaction of aluminum is different from that of other metals (1, 15). Since aluminum is found in some heater and other high-temperature alloys, it is of interest to study the reaction kinetics. This communication will present the results of a vacuum microbalance (5, 7) study of the oxidation behavior of aluminum in the temperature range 200–550°C. These results will be correlated with observations on the physical and chemical structure of the oxide film.

If the oxide film theory is accepted as a basis of discussion, there are many favorable factors for the view that the aluminum oxide film is protective. They are the following: (1) the ratio of oxide volume to metal volume is greater than 1; (2) the oxide is very stable thermodynamically in regard to decomposition, reduction, and solid-phase reactions with other metals; (3) the relatively high

melting point and boiling point of the oxide; (4) the fact that alumina is a reduction semiconductor; and (5) the relatively few oxide structures which may form. The unfavorable factors for the oxide on aluminum are the low melting point and the relatively high vapor pressure of the metal.

LITERATURE SURVEY

A number of papers during the last twenty-five years have dealt with the oxidation of aluminum and the structure of the protective film. No critical study has concerned itself with the reaction kinetics. Pilling and Bedworth (15) studied the oxidation at 600°C. by a weight-gain method. One series of measurements showed that the oxidation could be broken down into two distinct stages. The first is the formative stage, during which a thin layer of oxide is formed slowly on the surface, the action lasting 60–80 hr. The second is the protective stage, during which the oxidation ceases. The parabolic rate law is found to hold during the first stage. A value of the rate constant of 0.30×10^{-10} (g./cm.²)² per hour is given. The stable oxide film is 2000 Å. in thickness.

Krylova (11) has studied this reaction by means of the polarization method. Above 400°C. the oxide film on aluminum increased continuously. The details of this work are not available to us at this date.

Numerous workers have studied the thickness of the equilibrium room-temperature film on various types of aluminum specimens, using a variety of techniques. Vernon (21) studied the reaction of aluminum in industrial atmospheres at ambient temperatures, using a weight-gain method. The film reached a thickness of about 100 Å. after 10–14 days. This thickness was found to be independent of the purity of the sample and the nature of the atmosphere. Treadwell and Obrist (20) determined the thickness of the oxide film on aluminum by removing the metal with anhydrous ethereal hydrogen chloride. An estimate of 10–100 Å. is given for the thickness of the air-formed film. Steinheil (18) found somewhat thicker films on specimens of aluminum foil heated gently in a Bunsen flame.

Podgurski (16) has recently measured the air-formed film on a freshly evaporated aluminum film by the use of a vacuum microbalance technique. Assuming a surface roughness ratio of 1, a thickness of 32 Å. after 24 hr. of reaction is calculated.

The structure of the oxide film on aluminum has been studied in some detail by Steinheil (18), Yamaguti (24), Preston and Bircumshaw (17), Darbyshire and Cooper (2), Hass (10), and more recently by de Brouckère (1), using the electron-diffraction technique. The following results are found: The film found on molten aluminum is usually crystalline and corresponds to γ -Al₂O₃. Rapid heating to 700°C. for short times gives a mixture of amorphous Al₂O₃ and γ -Al₂O₃. The α -Al₂O₃ is found on heating the oxide to 1400°C. The room-temperature films are amorphous.

APPARATUS

The microbalance with its auxiliary apparatus is essentially the same as previously described (5, 7). The method is to suspend a 10- or 12-mil sheet of

aluminum from the beam of a sensitive quartz microbalance operating in an all-glass vacuum system. The weight change of the specimen is followed continuously as the several operations are performed upon it. These operations include evacuation to pressures of 10^{-6} mm. of mercury or better, degassing, and oxidation of the metal specimen. Each of these operations can be carried out on aluminum over a temperature range of 25–660°C. (m.p.) and over a pressure range of 10^{-6} mm. to 0.1 atm.

The balance has a sensitivity of 0.86 division (1 division equals 0.001 cm.) per microgram for a sample weight of 0.3659 g. The period of the balance is 8 sec. The balance is checked periodically for a stable zero point and negligible temperature and pressure coefficients. A scale micrometer microscope is used to observe the beam and to record the deflection relative to a fixed point on a quartz supporting frame. The readings are reproducible to $1/4$ of a division or approximately 0.3×10^{-6} g.

METHOD

The weighed aluminum sample is placed on the balance beam and the balance checked for alignment. The specimen glass tube is sealed off. The apparatus is evacuated to 10^{-6} mm. of mercury, liquid air being placed in the traps during the evacuation process. All samples are given a preliminary degassing treatment by heating the quartz specimen tube to 575°C. over a period of 30 min. with an auxiliary furnace. The regular furnace, controlled at the desired temperature, is raised around the specimen tube. After thermal equilibrium is attained, a preliminary set of readings of the balance beam and furnace temperatures is taken. Oxygen is now admitted from the dosing system to the desired pressure. Readings of the balance beam are taken at fixed intervals during the oxidation. At the end of the oxidation the system is evacuated and a final set of readings is taken.

SAMPLES

Four samples of aluminum¹ were used in the experiments. Samples No. 1 and 2 are stated to have an analysis of 99.985 per cent aluminum, as determined on the ingot before rolling. The two samples are taken from different sections of the same sheet roll.

Samples No. 3 and No. 4 are specially prepared. Elaborate precautions are taken to prevent the inclusion of oxide during the rolling processes. Both samples are prepared from blocks 2 in. x 2 in. x 1 in., machined from a high-purity aluminum ingot having the following analysis: silicon, 0.002 per cent; iron, 0.001 per cent; copper, 0.005 per cent; barium, 0.004 per cent; magnesium, 0.008 per cent; sodium, 0.000 per cent; carbon, 0.001 per cent; phosphorus, <0.001 per cent. These blocks are rolled to sheets 0.040 in. thick. Following this reduction, the material is divided into two lots. One lot, sample No. 3, is brightened in Pullen's solution and the second lot, sample No. 4, is brightened in a fluoboric acid solution. This brightening treatment is followed by a reduction

¹ These samples were obtained in a 10-mil sheet form from the Aluminum Company of America, New Kensington, Pennsylvania, through the courtesy of Mr. H. Podgurski.

to 0.030 in. sheet and then annealing at 550°F. for 1 hr. The two lots are again electrolytically brightened in their respective solutions mentioned above. A final reduction to 0.012 in. thick sheet is conducted at the New Kensington foil mill. This stock is again electrolytically brightened. After each of the brightening treatments, the sheets are cleaned in hot phosphoric-chromic acid solution and rinsed with distilled water.

Spectrographic analysis of specimens No. 1 and No. 2 shows iron to be the principal contaminant. Although taken from the same roll, No. 2 contains slightly more iron than No. 1. Small differences are also found for the silicon, magnesium, and calcium impurities.

Sections of the four sheets are polished on a piece of plate glass, using polishing papers 0, 00, and 000, respectively. The last polishing procedure is carried out under a protecting solution of paraffin in kerosene. The sheets are washed with petroleum ether and absolute alcohol. Strips 1.2 cm. in width are cut from the sheets. Specimens are cut to rough weight and trimmed to a weight of 0.3659 g. The samples have an approximate area of 11 cm.² Additional specimens are cut and trimmed to weight after cleaning sections of the original unpolished sheets in petroleum ether and alcohol.

RESULTS

1. Time

The effects of time on the oxidation of different samples of aluminum under widely varying conditions are shown in figures 1 to 7. The weight gain in micrograms per square centimeter is plotted against the time in minutes. The curves in general show that the oxidation rate falls off as the film thickens. At the higher temperatures a nearly linear rate law is observed. The type of rate law will be considered more thoroughly under the section entitled "Discussion." An estimate of the oxide film thickness can be made if we assume a surface roughness ratio of unity and a density of 4.0 for the oxide. The film thickness in Ångströms can be found if the weight gain is multiplied by the factor 53.

2. Temperature

The effect of temperature on the rate of oxidation of polished No. 1 aluminum from 400–500°C. and at a pressure of 7.6 cm. of oxygen is shown in figure 1. A weight gain of about 5 micrograms per square centimeter or 265 Å. is found at 400°C. for a 100-min. oxidation, while a weight gain of 23 micrograms per square centimeter or 1220 Å. is found at 500°C. for a 100-min. oxidation. The calculations are for films formed in addition to the room-temperature oxide film normally present.

The rate measurements on high-purity specimens of polished No. 3 aluminum are shown as a function of temperature in figure 2 from 450–550°C. and at a pressure of 7.6 cm. of oxygen. A weight gain of about 3 micrograms per square centimeter or 159 Å. is found at 500°C. for 100 min. at an oxygen pressure of 7.6 cm. This is to be compared to a value of 23 micrograms per square centimeter or 1220 Å. observed on sample No. 1.

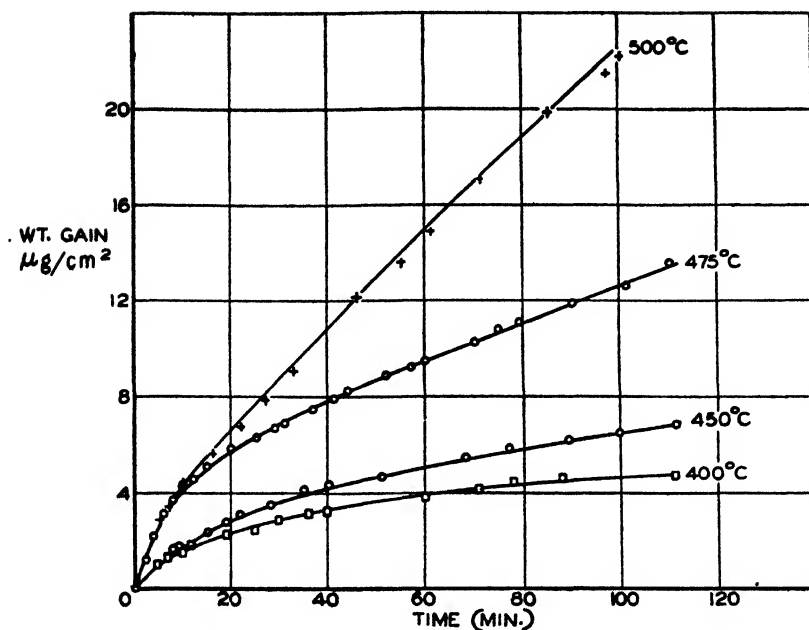


FIG. 1. Effect of temperature on oxidation of No. 1 polished aluminum at 400–500°C and a pressure of 7.6 cm. of oxygen.

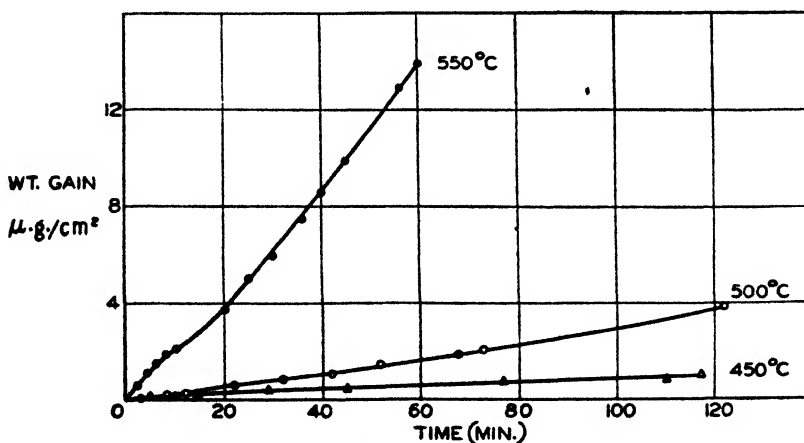


FIG. 2. Effect of temperature on the oxidation of No. 3 polished aluminum at 450–550°C. and a pressure of 7.6 cm. of oxygen.

3. Sample

The oxidation rate at 500°C. and at a pressure of 7.6 cm. of oxygen for the different samples is shown in figure 3. All samples are polished. The oxidation rates vary by a factor of 5 from No. 1 to No. 3. The individual curves are reproducible to 5–10 per cent.

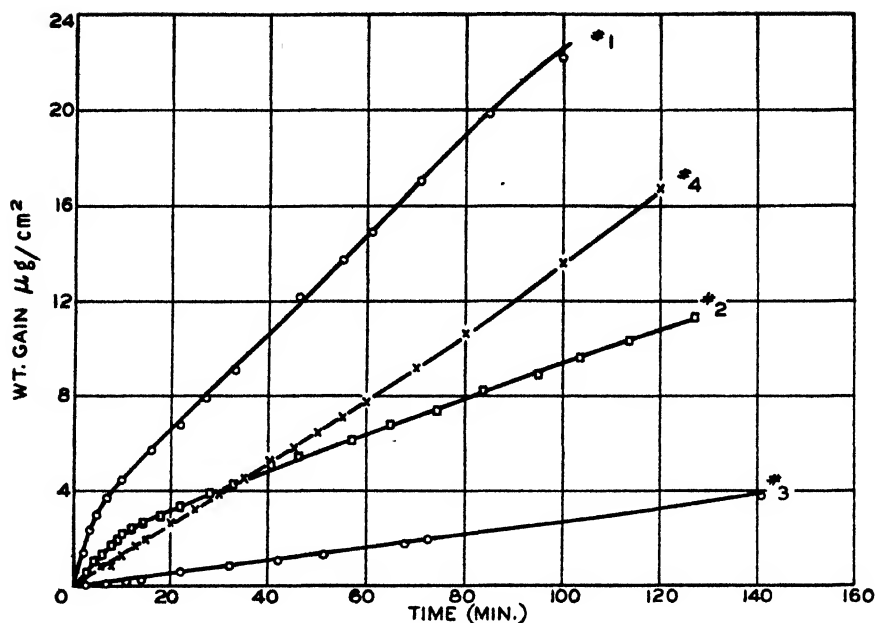


FIG. 3. Effect of samples on the oxidation of aluminum at 500°C. and a pressure of 7.6 cm. of oxygen. All samples polished.

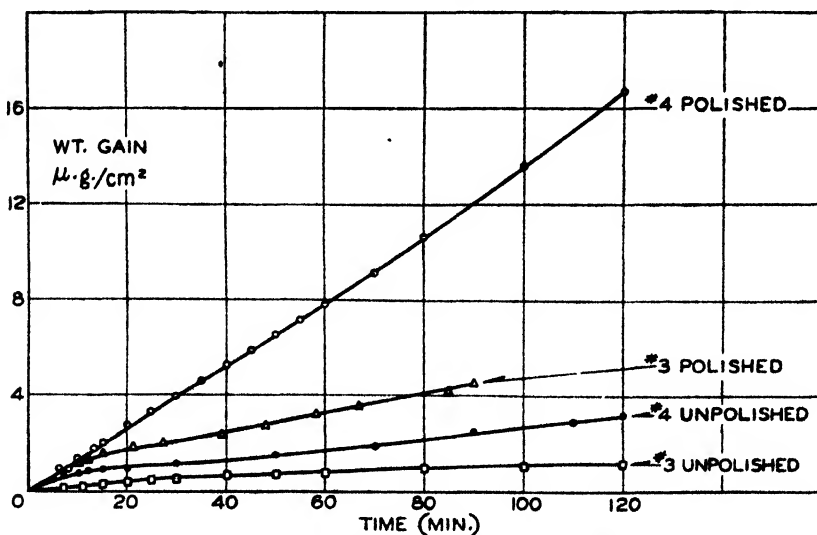


FIG. 4. Effect of abrasion on the oxidation of aluminum at 500°C. and a pressure of 7.6 cm. of oxygen.

4. Abrasion

Figure 4 shows the effect of abrasion (polishing) on the oxidation rates at 500°C. and a pressure of 7.6 cm. of oxygen. Two high-purity samples of alumi-

num are tested. The rate of oxidation of No. 4 polished aluminum is about four times as rapid as that of No. 4 unpolished. A similar behavior is found in the oxidation of No. 3 aluminum.

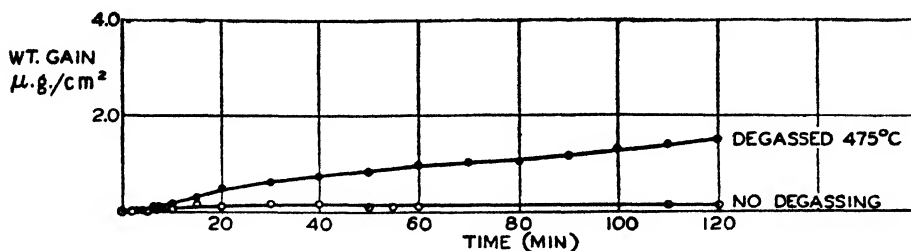


FIG. 5. Effect of degassing of sample on the oxidation of No. 4 polished aluminum at 200°C. and a pressure of 7.6 cm. of oxygen.

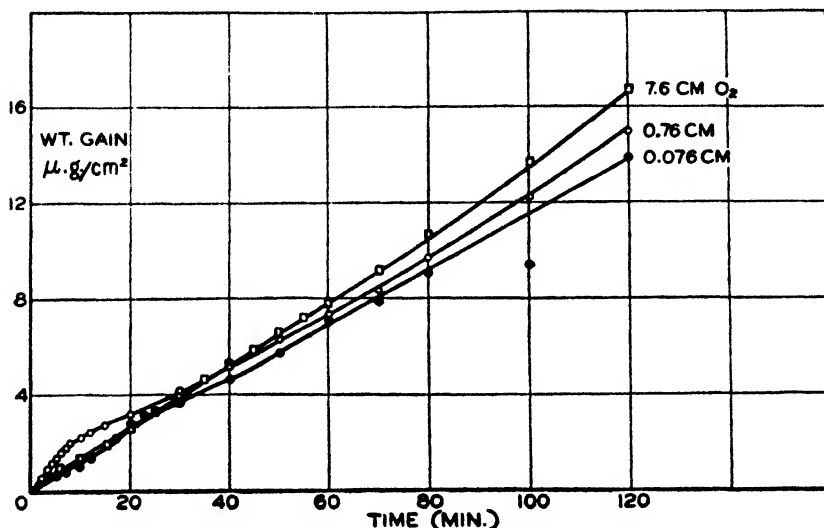


FIG. 6. Effect of pressure on the oxidation of No. 4 polished aluminum at 500°C.

5. Degassing

The effect of degassing the aluminum samples at 475°C. for 30 min. on the oxidation at 200°C. and a pressure of 7.6 cm. of oxygen is shown in figure 5. The effect is quite marked under these conditions.

6. Pressure

A study of the pressure factor is shown in figure 6. The oxidations are made at 500°C. for 120 min. for three pressures—7.6 cm., 0.76 cm., and 0.076 cm. of oxygen. The effect of a pressure change of 100 produces only a minor effect on the oxidation rate. The lower pressures yield a slightly smaller oxidation rate. Measurements on other samples of aluminum show similar effects.

7. Difficulties in measurement

Figure 7 shows an example of what must be avoided in making oxidation measurements. The oxidation is being made on a sample which had not been degassed. The part of the curve on the left shows the degassing of the sample at 450°C. On addition of oxygen at time 0 a weight gain is recorded. As the oxidation proceeds, degassing gradually is overtaking oxidation and a net loss in weight is seen after 80 min. The normal degassing curve is shown at the right after evacuation. The sample appears to contain a large amount of gas.

DISCUSSION

1. General rate equations

Several equations have been proposed to explain the reaction rate of metals in oxygen atmospheres. The most important of these equations are those based on

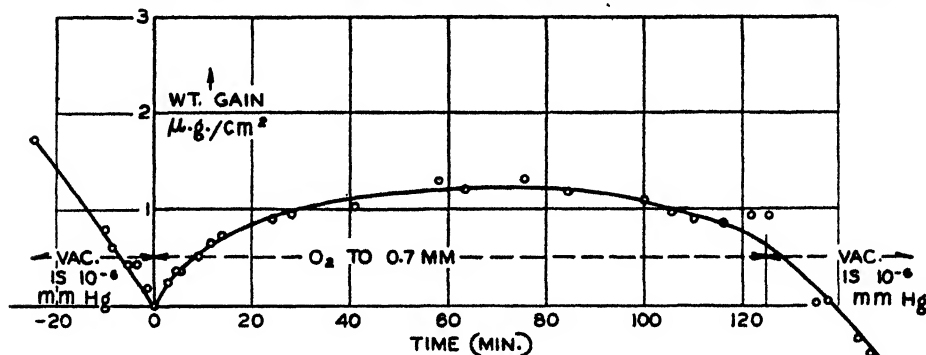


FIG. 7. Oxidation of No. 2 polished aluminum at 450°C. and a pressure of 0.7 mm. of mercury

the diffusion mechanism. This type of analysis leads to the parabolic law or one of its modifications (13, 15, 23). The simple parabolic law states:

$$W = \sqrt{Kt}$$

W is the weight increase per unit area, t is the time, and K is a constant. A modification of the parabolic law to take into account the velocity of the interface reaction was proposed by Wagner and Gr \ddot{u} newald (23). This equation states:

$$aW + \frac{W^2}{2} = K't$$

Here a and K' are constants. Recently Mott (14) has proposed a modification to account for the influence of an electric potential at the oxide-gas interface due to a layer of adsorbed oxygen ions. The growth law is expressed by the equation:

$$\frac{dx}{dt} = \nu a e^{-w/kT} \sinh \left(\frac{eaV}{kT} \cdot \frac{1}{x} \right)$$

W is probably the energy of formation of the ion, a is approximately the interatomic distance, ν is approximately 10^{12} sec.⁻¹, and x is the thickness of the film.

This law reverts to the parabolic law for thick films when $\frac{eaV}{kT} \ll 1$. The potential V creates a field V/x , which aids diffusion of metal ions through the oxide lattice. For thick films the field is negligible and the normal diffusion rate gives the parabolic law.

The logarithmic law has been used to correlate oxidation rate data. The following equation is typical and was devised by Tamman and Köster (19):

$$t = \beta(e^{W/a} - 1)$$

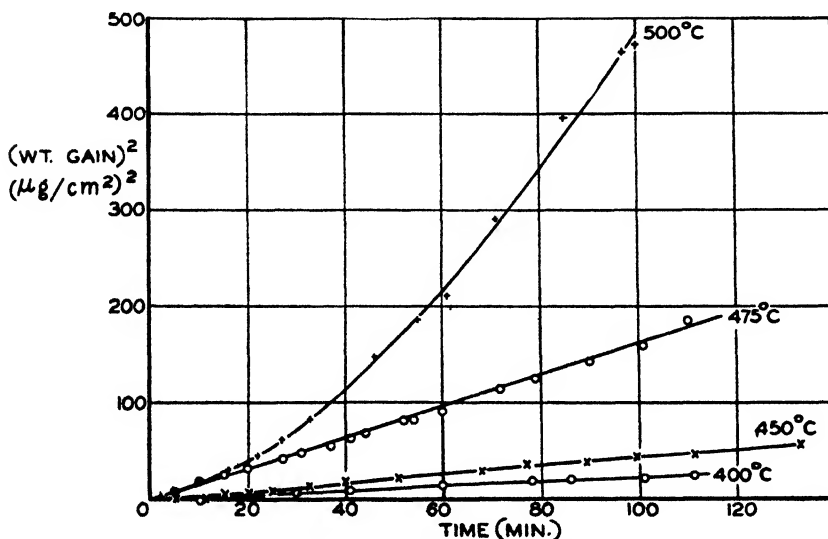


FIG. 8. Effect of temperature on the oxidation of No. 1 polished aluminum at a pressure of 7.6 cm. of oxygen. Parabolic plot.

Here α and β are constants. This equation is empirical in nature, although several rate mechanisms have been suggested (12, 22).

For the case where the film is not protective, a linear rate law is frequently observed. The simplest form of this equation is:

$$W = K''(t)$$

2. Experimental rate equations

To test the data for compliance with the several rate laws, a number of graphs are prepared. Figures 8 and 9 show curves of the square of the weight gain against time for No. 1 polished and No. 3 polished aluminum samples. Figure 8 shows that the parabolic law fits the data for the 400°, 450°, and 475°C. oxidations. The experiment at 500°C. deviates appreciably from the straight line, indicating that a diffusional mechanism is no longer limiting the reaction rate. Mott's (14) modification of the parabolic law predicts a positive deviation for

thin films. This shape of curve is not observed for aluminum, although it has been observed with other metals (9). Figure 9 shows the effect of higher

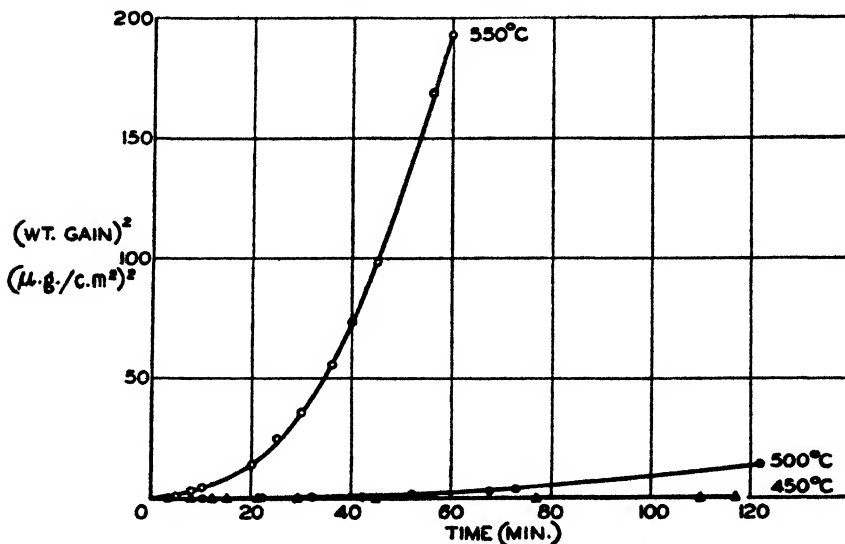


FIG. 9. Effect of temperature on the oxidation of No. 3 polished aluminum at 450–550°C. and a pressure of 7.6 cm. of oxygen. Parabolic plot.

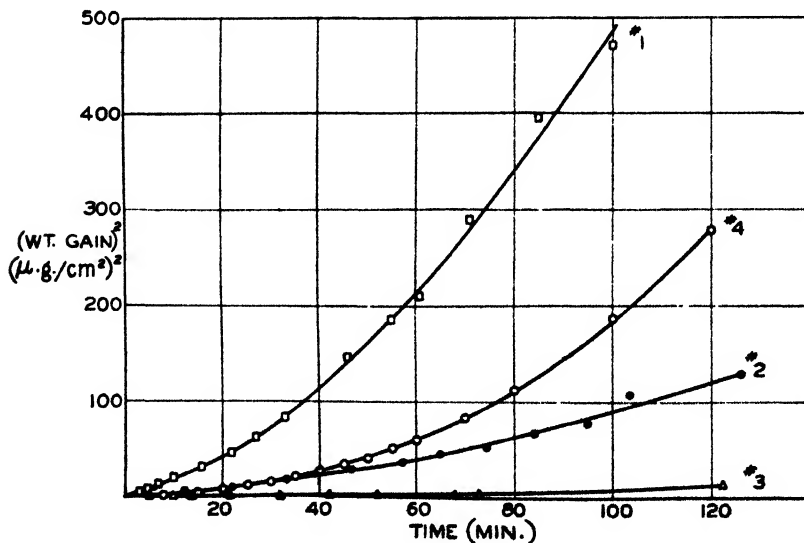


FIG. 10. Effect of sample on oxidation of aluminum at 500°C. and a pressure of 7.6 cm. of oxygen. All samples polished. Parabolic plot.

temperature on the parabolic law plots. The 550°C. curve deviates sharply from the parabolic. In fact, a linear rate law can be seen by referring to figure 2. The transformation of the rate law from the parabolic type to the linear type

occurs over a narrow range in temperature, 475–500°C. This is not observed in the other metals we have studied, with the possible exception of magnesium.

It may be noticed that the deviations from the parabolic rate law occur even during the early stages of the reaction. Figure 6 shows that the oxidation of aluminum obeys the linear rate law during the complete course of the experiment. If one assumes a surface roughness ratio of 1, the film thickness is calculated to be 850 Å. after 2 hr. of oxidation at 500°C. At this temperature the reaction rate is independent of film thickness even for film thicknesses of less than 100 Å. This is a rather thin film to expect to be under sufficient stresses to crack and thus open new metal for reaction. The deviations from conditions normally

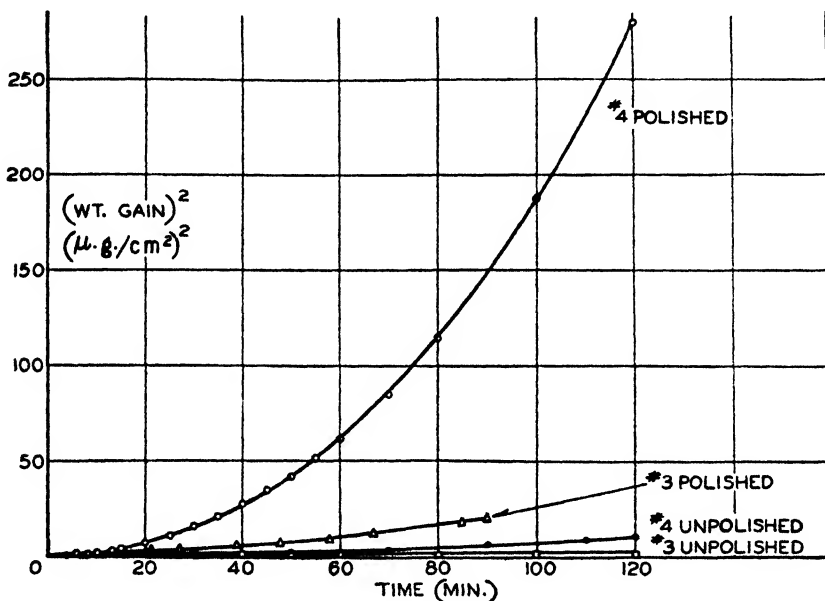


FIG. 11. Effect of abrasion on the oxidation of aluminum at 500°C. and a pressure of 7.6 cm. of oxygen. Parabolic plot.

regarded as protective do not appear to us to be due to stresses in the film but to factors more fundamental in the formation and diffusion of the metal ions in the oxide lattice. If the thickness is no longer rate determining, then the limiting factor is in the rate of formation of ions. This process would give a linear rate law.

The effect of the sample on the deviations from the parabolic law is shown in figure 10 for the oxidations at 500°C. and 7.6 cm. of oxygen. Again, the weight gain squared is plotted against the time in minutes. All of the samples show marked deviations from the parabolic law at 500°C., in spite of their different oxidation rates. The deviations extend to the very thin film range of the curves.

Figure 11 shows the effect of abrasion on the parabolic law plots. Abrasion has no effect on the deviations for the oxidation at 500°C. and 7.6 cm. of oxygen. The effect of pressure on the parabolic plots is shown in figure 12. No effect is

noted. Figures 10 and 12 confirm the point of view that the change from a parabolic rate law to a linear rate law involves a fundamental change in the factors limiting the reaction rate.

The logarithmic rate law is frequently used to correlate oxidation rate data. A plot of the weight gain against the time on a logarithmic scale is shown in figure 13. If the logarithmic rate law is obeyed, a straight line should be found.

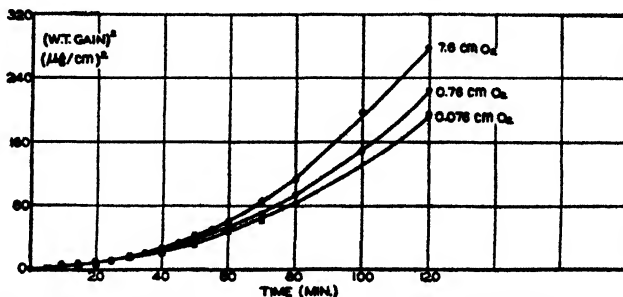


FIG. 12. Effect of pressure on the oxidation of No. 4 polished aluminum at 500°C. Parabolic plot.

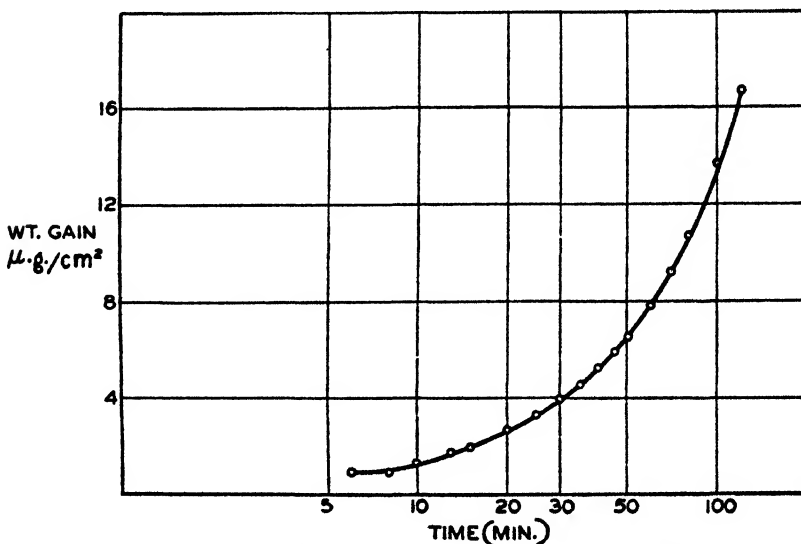


FIG. 13. Oxidation of No. 4 polished aluminum at 500°C. and a pressure of 7.6 cm. of oxygen. Plot of weight gain against the time on a logarithmic scale.

Figure 13 shows that this rate law is not obeyed for a 500°C. oxidation at 7.6 cm. of oxygen. Although correlations may be obtained in certain time and temperature regions of the oxidation process, we have found that serious deviations exist for other conditions of time and temperature. The use of the logarithmic rate law to correlate oxidation-rate measurements suffers from the lack of a plausible physical mechanism.

3. Temperature dependence

The temperature dependence of the parabolic rate law constant was first shown to follow an expression of the Arrhenius type by Dunn (3). Mott (13) has given a physical interpretation of the energy barriers in the reaction mechanism. One of the authors (6) has applied the transition state theory of diffusion developed by Eyring and coworkers (4). The parabolic rate law constant is given by the following equation:

$$K = \frac{2kT}{h} \lambda^2 e^{\Delta S^*/R} e^{-E^*/RT}$$

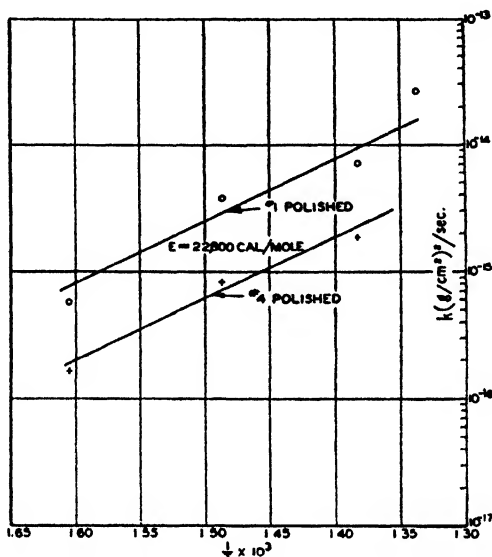


FIG. 14. Plot of the parabolic rate law constant K as a function of $1/T$ on a logarithmic plot for the oxidation of aluminum at 350–475°C. and a pressure of 7.6 cm. of oxygen.

Here, K is Boltzmann's constant, h is Planck's constant, λ is the distance in Ångströms between the aluminum atoms or ions in the oxide lattice (2.74 Å.), ΔS^* is the entropy of activation, and E^* is the energy of activation. The free energy of activation, ΔF^* , of the transition state is given by the equation $\Delta F^* = E^* - T\Delta S^*$, since $P\Delta V^*$ is negligible.

Figure 14 shows a plot of the parabolic rate law constant K as a function of $1/T$ on a logarithmic plot. The results on two specimens of aluminum are shown. Although the data are meager and somewhat scattered, two straight lines appear to fit the data. An energy of activation of 22,800 cal. per mole for both samples is calculated for the temperature range of 350–475°C.

Table 1 shows a comparison of the parabolic law constants and diffusion constants and the entropies, energies, and free energies of activation of the rate-determining process for No. 1 and No. 4 aluminum and for pure iron. The K values are converted to thickness by the use of the density and the stoichio-

metric ratio of oxygen in the particular oxide. A surface roughness ratio of 1 is assumed.

The oxidation processes for the two specimens of aluminum and for iron are very similar. The energy of activation, E^* , for the aluminum oxidation process is 22,800 cal. per mole, while a value of 22,600 cal. per mole is found for iron. Similarly, the entropies of activation, ΔS^* , are negative. The values found for aluminum vary from -25.4 to -28.0 cal. per mole per $^{\circ}\text{C}.$, while the value found for iron is -24.6 . The over-all reaction rate for aluminum is somewhat less than for iron. ΔS^* is a measure of the frequency factor or the probability of an ion with a definite energy getting through the lattice. The free energy of activation is a measure of the effective barrier for the reaction. It is made up of the energy of activation term and the contribution from the entropy of activa-

TABLE 1

Parabolic rate constants and diffusion constants, entropies, energies, and free energies of activation for the oxidation process

MATERIAL	t $^{\circ}\text{C}.$	K $\text{cm}^2/\text{sec}.$	D_0 $\text{cm}^2/\text{sec}.$	ΔS^* $\text{cal.}/\text{mole}/^{\circ}\text{C}.$	E^* $\text{cal.}/\text{mole}$	$T\Delta S^*$ $\text{cal.}/\text{mole}$	ΔF^* $\text{cal.}/\text{mole}$
Aluminum, No. 4 polished.	350	4.7×10^{-16}	2.47×10^{-8}	-25.6	22,800	16,000	38,800
	400	2.34×10^{-16}	3.08×10^{-8}	-25.4	22,800	17,000	39,900
	450	5.29×10^{-16}	2.2×10^{-8}	-26.2	22,800	19,000	41,800
Aluminum, No. 1 polished ...	350	1.7×10^{-16}	0.815×10^{-8}	-27.9	22,800	17,350	40,150
	400	1.08×10^{-16}	1.38×10^{-8}	-26.9	22,800	18,050	40,850
	450	2.01×10^{-16}	0.80×10^{-8}	-28.0	22,800	20,260	43,060
	475	7.53×10^{-16}	1.72×10^{-8}	-26.6	22,800	19,900	42,700
Iron. ...	350	1.2×10^{-16}	5.48×10^{-8}	-24.6	22,600	15,350	37,950
	400	4.09×10^{-16}	4.68×10^{-8}	-24.6	22,600	16,550	39,150
	450	15.25×10^{-16}	5.52×10^{-8}	-24.5	22,600	17,700	40,300

tion, $T\Delta S^*$. For negative values of ΔS^* the term $T\Delta S^*$ adds to the energy of activation and increases the effective barrier to the reaction.

4. Electron-diffraction studies

We have made no systematic study with the electron-diffraction camera (8) of the surface films formed on aluminum. However, during the past few years we have made a number of experiments which are worth presenting at this time. These experiments were made with the specimens in the furnace of our electron-diffraction camera. The reaction was carried out and the patterns taken while the sample was at the elevated temperature. All of the experiments were done with high-purity aluminum (99.985 per cent). The data are shown in table 2. On the left and center of the table are presented the polishing procedures used on the several samples, the temperature at which the reaction was carried out, the nature and pressure of the oxidizing atmosphere, and the time of the reaction.

TABLE 2
Electron-diffraction data on oxide films on aluminum (99.985 per cent pure)

EXPT. NO.	POLISHING PROCEDURE	TEMPERATURE °C	PRESSURE	TIME minutes	DIFFRACTION PATTERN	TYPE OF OXIDE
1.....	No. 1 through 3/0 paper	300 300 300 300	Vacuum Air, 1.5 cm. Air, 1.5 cm. Air, 1.5 cm.	2 7 17	Face-centered cubic aluminum Face-centered cubic aluminum Face-centered cubic aluminum Face-centered cubic aluminum	Amorphous Amorphous Amorphous Amorphous
2.....	No. 1 through 3/0 paper	400 400 400 400	Vacuum Air, 1.5 cm. Air, 1.5 cm. Air, 1.5 cm.	2 7 17	Face-centered cubic aluminum Face-centered cubic aluminum Face-centered cubic aluminum	Amorphous Amorphous Amorphous Amorphous
3.....	No. 1 through 3/0 paper	500 500 500 500	Vacuum Air, 1.5 cm. Air, 1.5 cm. Air, 1.5 cm.	2 7 17	Face-centered cubic aluminum Face-centered cubic aluminum Face-centered cubic aluminum Face-centered cubic aluminum	Amorphous Amorphous Amorphous Amorphous
4.....	No. 1 through 4/0 paper (paraffin + kerosene)	450	O ₂ , 1.1 cm.	11	Face-centered cubic aluminum	Amorphous
5.....	No. 1 through 4/0 paper (paraffin + kerosene)	500*	O ₂ , 2.0 cm.	30	Face-centered cubic aluminum	Amorphous
6. . .	No. 1 through 3/0 paper Nos. 1 and 3 alumina	500 500	Vacuum O ₂ , 7.6 cm.	5	None α -Al ₂ O ₃ † + γ -Al ₂ O ₃	

* Picture taken at 25°C.

† Pattern probably due to polishing alumina.

At the right, under diffraction pattern, is shown the structure found. The type of oxide for the several experiments is also shown. In the experiments numbered 1 to 5 a diffraction pattern of face-centered cubic aluminum is observed. This type of pattern leads to the conclusion that the oxide film is amorphous. Experiment 6 shows a crystalline pattern of $\gamma\text{-Al}_2\text{O}_3$ and $\alpha\text{-Al}_2\text{O}_3$. Considering the fact that this sample is polished with alumina and the fact that this is the only experiment that gave a pattern of the crystalline oxides, we feel that the pattern may be explained as due to alumina picked up during the polishing operation. However, no such pattern is observed on the same sample in the vacuum of the camera before reaction. This experiment does not agree with the results of experiments 1 to 5 and with the results of other investigators (1). In general, the electron-diffraction results confirm the previously observed fact that the oxide film on aluminum up to 500°C. and for short times of reaction with oxygen is amorphous. Even for films of the order of 500 Å. in thickness the film is amorphous.

CONCLUSION

The results shown in this work indicate that aluminum is not unique in its oxidation behavior. The oxidation follows the parabolic rate law in the temperature range of 350–450°C. In this temperature region, an energy of activation of 22,800 cal. per mole and entropies of activation of -25.4 to -28.0 are calculated. Above 475°C. the reaction is shown to deviate from the parabolic rate law, and at temperatures of 500–550°C. the reaction follows a linear rate law. The parabolic rate law constants are similar to those for iron. Aluminum differs from many metals in that the transition zone in temperature, in which the reaction is changing from the parabolic rate law to the linear rate law, is extremely narrow.

The influence of pressure on the reaction rate is small. The effect of the particular sample of high-purity aluminum is very marked. The behavior of a particular sample is determined not only by the impurities present but also by its manner of preparation and the chemical treatment used between and after the several rolling processes.

One of the interesting observations is that the type of rate law that is found is dependent only upon the temperature. The other variables studied have little effect on the fundamental reaction mechanism. This conclusion holds over a wide range of film thickness.

The oxide film is shown from electron-diffraction studies to possess an amorphous structure. This confirms the results of other workers.

REFERENCES

- (1) BROUCKÈRE, L. DE: *J. Inst. Metals* **71**, 131–47 (1945).
- (2) DARBYSHIRE, J. A., AND COOPER, E. R.: *Trans. Faraday Soc.* **30**, 1038 (1934).
- (3) DUNN, J. S.: *J. Chem. Soc.* **1929**, 1149–50.
- (4) GLASSTONE, S., LAIDLER, K. J., AND EYRING, H.: *The Theory of Rate Processes*. McGraw-Hill Book Company, Inc., New York (1941).
- (5) GULBRANSEN, E. A.: *Trans. Electrochem. Soc.* **81**, 187–97 (1942).
- (6) GULBRANSEN, E. A.: *Trans. Electrochem. Soc.* **83**, 301–13 (1943).

- (7) GULBRANSEN, E. A.: *Rev. Sci. Instruments* **15**, 201-4 (1944).
- (8) GULBRANSEN, E. A.: *J. Applied Phys.* **16**, 718-24 (1945).
- (9) GULBRANSEN, E. A.: *Trans. Electrochem. Soc.* **91**, 431-60 (1947).
- (10) HASS, G.: *Verhandl. deut. physik. Ges.* **22**, 1-3 (1941); *cf. Chem. Abstracts* **35**, 7352^a.
- (11) KRYLOVA, T. N.: *Khim. Referat Zhur.* **6**, 122 (1939); *cf. Chem. Abstracts* **34**, 4034^e.
- (12) LUSTMAN, B.: Thesis, Carnegie Institute of Technology, Pittsburgh, Pennsylvania, 1940.
- (13) MOTT, N. F.: *Trans. Faraday Soc.* **36**, 472 (1940).
- (14) MOTT, N. F.: *J. Inst. Metals* **72**, 367-80 (1946).
- (15) PILLING, N. B., AND BEDWORTH, R. E.: *J. Inst. Metals* **29**, 529-82 (1923).
- (16) PODGURSKI, H.: Private communication.
- (17) PRESTON, G. D., AND BIRCUMSHAW, L. L.: *Phil. Mag.* **22**, 654-65 (1936).
- (18) STEINHEIL, A.: *Ann. Physik* **19**, 465 (1934).
- (19) TAMMAN, G., AND KÖSTER, W.: *Z. anorg. allgem. Chem.* **123**, 196 (1922).
- (20) TREADWELL, W. D., AND OBRIST, W.: *Helv. Chim. Acta* **26**, 1816 (1943).
- (21) VERNON, W. H. J.: *Trans. Faraday Soc.* **23**, 117-85 (1927).
- (22) WAGNER, C.: *Angew. Chem.* **49**, 735 (1936).
- (23) WAGNER, C., AND GRÜNEWALD, K.: *Z. physik. Chem.* **40B**, 455 (1938).
- (24) YAMAGUTI, S.: *Sci. Papers Inst. Phys. Chem. Research (Tokyo)* **36**, 463-70 (1939).

A STUDY OF ANHYDROUS CONDITIONS IN THE PREPARATION OF LYOPHOBIC ORGANOSOLS

HARRISON A. NELSON

The Upjohn Company, Kalamazoo, Michigan

Received April 2, 1947

INTRODUCTION

The value of a study of the properties of colloidal suspensions in media other than water has long been recognized, and there are numerous references in the literature to studies on the preparation and properties of ostensibly anhydrous lyophobic organosols. For purposes of obtaining data as a foundation for the postulation of basic kinetic relationships in colloidal suspensions, the advantages of an eminently simple lyophobic sol are apparent. But the organosols that have been studied have in general been complex rather than simple, containing in addition to the disperse phase and medium such complicating factors as dissociated and non-dissociated electrolytes, "protective" agents which may be of somewhat indefinite structure, and diluting solvents, especially water. A close scrutiny of the methods used in the reported anhydrous preparations indicates that in no case have the experimental conditions imposed been sufficiently stringent to assure absolute exclusion of water. The universal distribution and wide solvent range of water result in great practical difficulties in preventing hydration contamination in any anhydrous system not continuously sealed off from contact with atmospheric air. Since some degree of exposure of materials to atmospheric air is disclosed in all preparations previously reported,

none can be considered completely anhydrous and all therefore must exhibit to some slight extent the properties of mixtures and not those of pure organosols.

Thus it would appear that the basic theory of the double layer effect has not been adequately explored with reference to stability in the absence of water. It further appears that conclusions on the mechanism and kinetics of lyophobic organosols may have been improperly based on an assumption of completely anhydrous conditions when these conditions did not actually exist.

Many colloidal suspensions in organic liquids reported in the literature were actually complex mixtures of little value for electrokinetic determinations. Such sols as those reported by Vernon and Nelson (6) obviously contained extraneous compounds introduced in the method of preparation. In these sols, water could have been picked up from the atmosphere, since they were handled in open equipment, or it could have been introduced in crystals of the salts used in the condensation reaction. Protective colloids such as collodion and rubber were present, and electrolytes introduced in the condensation reaction also affected the system. Such sols may quite properly be termed organosols, since the suspension is mainly in an organic liquid, but the study of the true properties of organosols requires a more simplified reproducible system.

Other preparations reported by various investigators have more closely approached the conditions required for the pure organosol, but the possibility for doubt remains in all.

A study of organosols of arsenic trisulfide with respect to methods of preparation and character of stability was made by Bikerman (2). The arsenic trisulfide-nitrobenzene sol prepared by Bikerman was referred to as anhydrous, and the conditions maintained during its formation would be expected to produce a practically anhydrous sol, although the opportunity for exposure of the solvent to atmospheric air left room for a reasonable doubt as to the absolute freedom from water of this preparation.

Several organosols were prepared by Weiser and Mack (7) by chemical condensation methods. Sols of mercuric sulfide in methyl alcohol, acetone, and propyl alcohol, of ferric oxide in methyl alcohol, and of ferric oxide, chromic oxide, and manganic oxide in propyl alcohol were prepared and studied, stability being attributed to preferential adsorption of ions. The procedures used in preparing these sols again indicated opportunities for exposure of the component parts of the sol to atmospheric air. The authors assumed absolutely anhydrous conditions in the preparations studied.

Mechanical and electrical methods of organosol preparation have also been studied to a considerable extent, and these present promising possibilities for development of an adequate procedure for preparing absolutely anhydrous sols. The method of Bredig (3) for the preparation of metal sols by submerged electric arc decomposition was applied by Svedberg to the formation of organosols of alkali metals in ether. In this case freedom from water was fairly well assured, but the presence of miscellaneous compounds due to reaction in the medium was possible. Apparently no very comprehensive effort has been made to utilize the submerged arc for the preparation of anhydrous organosols.

Colloidal suspensions of metals in ethyl alcohol, ether, and xylene were prepared by Andronikashvili and Tsabadse (1) by shaking small filings of the metal with the medium at 800–1400 oscillations per minute. Stability in these sols was obtained by the use of collodion, paraffin, and rubber.

An ingenious method for preparing metal organosols was devised by Torikai and Yamaguti (5), in which molten metal was spun in a centrifuge so as to cause the metal vapors to impinge on the inside wall of a glass cylinder wet with the dispersion medium. In this preparation again the components of the system are apparently allowed to come into some contact with atmospheric air.

A study of the system carbon in xylene was made by Damerell and Urbanic (4). Their sol was prepared by agitating at 650 R.P.M. finely divided carbon in xylene in a beaker. Various protective colloids, such as lecithin and Aerosol OT, were added to stabilize the sols. The addition of small amounts of water was found to decrease stability. Since these sols were prepared in open equipment they cannot be considered anhydrous; here again the observations are not reliable indications of the conditions to be expected in a pure organosol.

It is therefore apparent that no very complete study of anhydrous lyophobic organosols has been made and that as yet no method for the preparation of such sols has been sufficiently refined to provide satisfactory material for such a study. Hence the phenomenon of stability in organosols remains inadequately defined.

Therefore this investigation was undertaken with the following objectives: (1) To review previously reported efforts to produce anhydrous lyophobic organosols with a view to evaluating the proposed stabilizing mechanisms. (2) To determine the possibility of preparing by simple methods an absolutely anhydrous lyophobic organosol.

EXPERIMENTAL

The experimental portion of the investigation was concerned first with attempting to prepare anhydrous organosols according to methods described in the literature and later with the preparation and study of an anhydrous sol of carbon in nitrobenzene.

Considerable attention was given to the problem of producing an anhydrous organosol of arsenic trisulfide in nitrobenzene according to the method of Bikerman (2). Repetition of the Bikerman procedure substantiated the original results, but the introduction of a series of refinements into the original procedure resulted in the development of an apparatus in which it could be shown that completely anhydrous conditions prevent the formation of the Bikerman sol. Several types of experimental apparatus were devised and operated in the attempt to remove the possible sources of water contamination. It was found that the reaction of hydrogen sulfide and arsenic trichloride in nitrobenzene, which is the basis of the Bikerman sol, became increasingly slow with each introduction of an improvement in drying conditions. For example, the use of nitrobenzene distilled twice over phosphorus pentoxide resulted in a slower reaction than was obtained with once-distilled nitrobenzene under conditions otherwise anhy-

drous. It was also found that preparation of fresh arsenic trichloride under very anhydrous conditions and thorough drying of the hydrogen sulfide used were factors capable of slowing the reaction. With the individual components of the reaction under quite rigid control as to water contamination, however, the final reaction was still found possible to complete although quite slow in developing. In the final apparatus, shown in figure 1, the dryness of the individual components of the system was assured and the dryness of the entire system was protected by sealing it in completely, away from atmospheric contamination. Under these conditions the reaction did not take place.

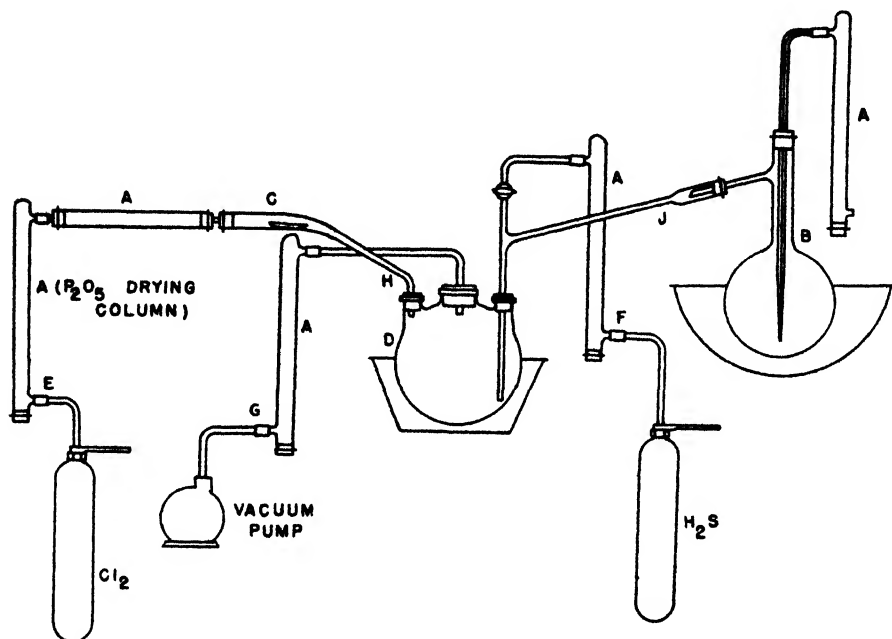


FIG. 1. Apparatus for attempted preparation of arsenic trisulfide-nitrobenzene sol. A, drying column, glass wool, and phosphorus pentoxide; B, nitrobenzene distillation flask; C, platinum boat in ignition tube; D, collection flask in ice bath; E, chlorine inlet; F, hydrogen sulfide inlet; G, vacuum outlet; H, J, seal-off points on inlet tubes.

The apparatus consisted of a sealed glass system containing the reactants or their components in a dried condition and with provision for final dehydration and mixing without contact with atmospheric air. In assembling the apparatus as shown, the drying tubes A were prepared in a dry air box, the nitrobenzene was purified by freezing and double distillation before being placed in the distillation flask B over phosphorus pentoxide, and the arsenic was dried in the platinum boat in a hot-air oven at 150°C. for 1 hr. before installation in the ignition tube C. With all materials in place, all joints and connections, which were as short as possible, were sealed with varnish or sealing wax. The apparatus was then strongly heated for 1 hr. with a direct flame while passing a current of

dry air in through the chlorine inlet tubes E and out through the hydrogen sulfide inlet F and vacuum connection G.

After cooling, the ice bath was placed on the reaction flask D. The arsenic was then burned in a stream of chlorine, and the arsenic trichloride was condensed in the reaction flask. The inlet tube H from the ignition tube was then sealed off and the system evacuated to a vacuum of about 25 in. The nitrobenzene was distilled over into the reaction flask under reduced pressure, and the inlet tube J from the distillation flask was then sealed off.

A clear solution of arsenic trichloride in nitrobenzene was thus formed in the reaction flask. Using the vacuum connection as an outlet, a current of hydrogen sulfide was next bubbled through the solution for 2 hr. There was no apparent reaction in the hydrogen sulfide-arsenic trichloride-nitrobenzene solution, and no change occurred in this system on standing for several days in the reaction flask. The addition of one drop of water or of three drops of ordinary reagent-grade nitrobenzene to the solution in the reaction flask, however, rapidly produced the characteristic yellow Bikerman sol. Repeated runs in this apparatus gave identical results. The nitrobenzene used in these experiments was Eastman Kodak reagent grade. Chlorine and hydrogen sulfide gases were provided in laboratory cylinders. The arsenic was Baker's metallic arsenic, powdered.

An attempt was also made to prepare a sol of mercuric sulfide in nitrobenzene according to the method described by Weiser and Mack as providing an anhydrous sol in propyl alcohol. An apparatus similar to that in figure 1 was used, in which dry mercuric chloride replaced the arsenic metal. In this system, the mercuric chloride was sublimed over into the reaction flask, and the nitrobenzene distilled as for the Bikerman trial. Hydrogen sulfide was then bubbled through the mercuric chloride-nitrobenzene solution for 2 hr. Again there was no apparent reaction and no sol was formed until the system was exposed to atmospheric air for 1 hr., when a gray sol was slowly formed. The mercuric chloride used in these trials was J. T. Baker reagent grade.

Another attempt was made to prepare a completely anhydrous sol according to procedures already described in the literature. Weiser and Mack described as anhydrous a ferric oxide-propyl alcisol. Their preparation depended on the reaction of potassium oxide and ferric chloride in dry propyl alcohol solution. Their procedure was repeated and a sol resulted, but when the refined apparatus described in figure 2 was used, no sol was formed. In this apparatus, also a sealed glass system, dried propyl alcohol was distilled over propyl succinate and sodium, in a method similar to that described by Smith (4), into flasks A and B containing potassium oxide and ferric chloride. The potassium oxide was previously prepared in tube C by burning metallic potassium in a stream of oxygen. The ferric chloride was sublimed from tube D into the reaction flask A.

The potassium oxide was apparently only sparingly soluble in the very dry propyl alcohol, and when the two solutions were mixed in reaction flask A by blowing over the contents of flask B, there was no reaction. The addition of water failed to produce a precipitate.

Since preparations based on chemical precipitation were not successful under

the anhydrous conditions required, a different system was sought for—a system that could preferably be prepared mechanically, so that a more exact control could be maintained over conditions and composition. These requirements were apparently well satisfied by the system carbon in nitrobenzene. For the preparation of this type of sol, the apparatus described in figure 3 was assembled. This was another completely sealed glass apparatus, similar to those previously described, but with simplifications made possible by the purely mechanical nature of the sol preparation. In the operation of this apparatus, the carbon

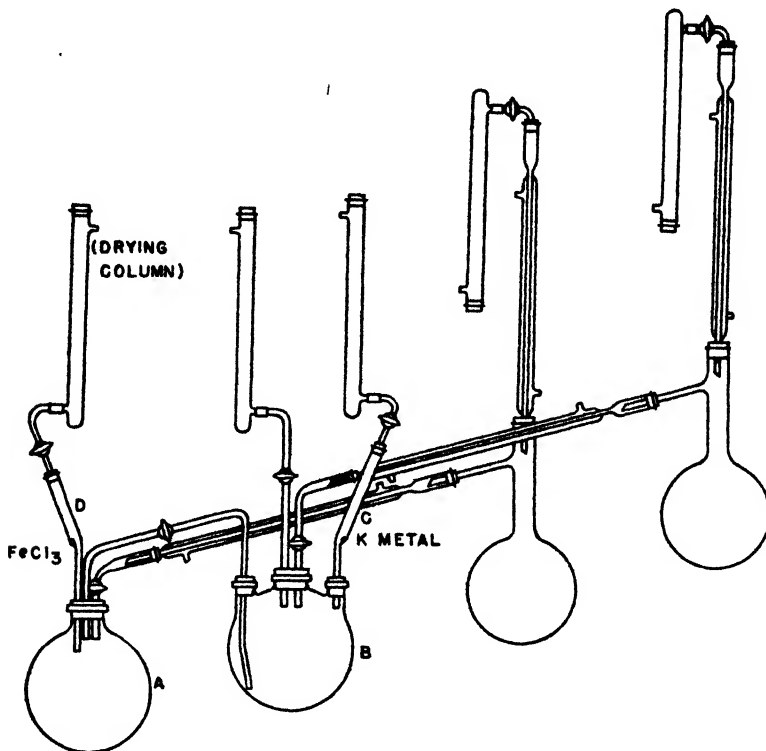


FIG. 2. Apparatus for attempted preparation of ferric oxide-propyl alcisol. A, reaction flask; B, potassium oxide solution flask; C, potassium ignition tube; D, ferric chloride sublimation tube.

was placed in the bottom of flask A, and the nitrobenzene, previously prepared as for the Bikerman trial, was placed in distillation flask B. The apparatus was heated strongly with a direct flame while sweeping a current of dry air through the flask from C to D and E. The nitrobenzene was then distilled over into flask A, and air bubbled through tube C with D as an outlet, to agitate the carbon-solvent mixture. The carbon used in this preparation was gas black prepared directly by incomplete combustion of methane. The carbon black was collected on the inner surface of a Pyrex beaker from which it was scraped by a stainless

steel spatula into the receiver. Before sealing the apparatus, the receiver was heated strongly with the direct flame to drive off any incidental volatile impurities, including residual moisture from the flame. The entire system was then sealed and heated strongly, while passing a stream of dry air in at D and out through F and C. Virtually all of the carbon thus produced was easily taken up into colloidal suspension by the nitrobenzene as it was distilled over. Bubbling dry air through the solution through tube D for a few minutes was sufficient to disperse most of the rest of the carbon. It was possible to filter the sol free of the more coarse particles in suspension by blowing it over into a filter in flask E, which was sealed in the system. The finished sol was collected in a tube which could be sealed immediately on opening the flask.

Dispersions of about 1 g. per liter were possible by this method. In appearance, the sols were a clear amber by transmitted light and a brown gray by

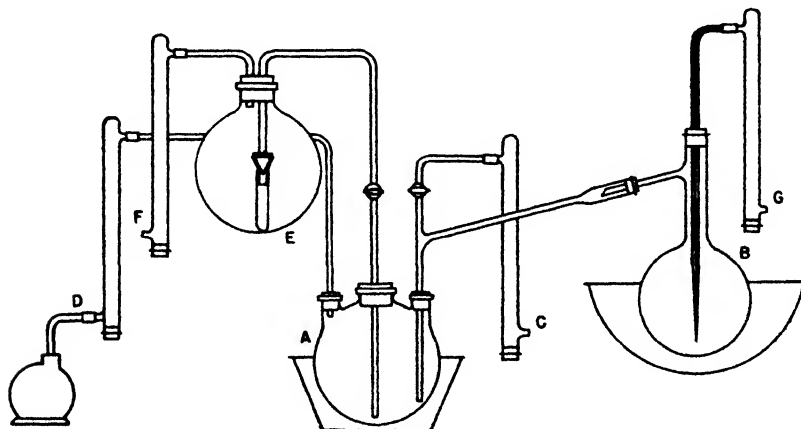


FIG. 3. System for preparing anhydrous carbon-nitrobenzene sol. A, carbon dispersion flask in ice bath; B, nitrobenzene distillation flask; C, air inlet to drying column; D, vacuum outlet; E, receiver for sol, with filter; F, air outlet from drying column; G, air inlet for capillary.

reflected light. Stability of the sols was unaffected by centrifuging at 2500 R.P.M. for 30 min. or by freezing with subsequent thawing. The micelles were negatively charged, as determined by electrophoresis experiments. Determination of particle size in the sols indicated that a range of diameters from $0.01\ \mu$ to $1\ \mu$ was generally present. Somewhat coarser suspensions were also found possible by the same method if the carbon were prepared before dispersion by ignition at a higher temperature. The coarse suspensions prepared contained particles greater than $1\ \mu$ in diameter, exceeding the arbitrary limits defining colloidal dimensions.

DISCUSSION

Throughout the literature references have been made to preparations termed "anhydrous organosols." A study of the literature indicated that only one

group of preparations was based on a control of moisture conditions sufficiently exacting to expect truly anhydrous sols to be formed. Examples of this group were the Bikerman arsenic trisulfide-nitrobenzene sol and the Weiser and Mack ferric oxide-propyl alcohol and mercuric sulfide-propyl alcohol sols. Therefore these preparations were repeated. In order that freedom from water be assured, however, increasingly severe conditions were imposed in the experimental process until it was finally found possible to demonstrate the necessity of water in order to complete the reactions necessary to produce these sols.

In the experimental work on the Bikerman arsenic trisulfide-nitrobenzene sol reported above there is apparent proof that the nitrobenzene was sufficiently free from water to prevent ionization of arsenic trichloride or hydrogen sulfide to take place. Since the same procedure was used in preparing the nitrobenzene for the carbon-nitrobenzene sol preparation, it would follow that the nitrobenzene was in this case also sufficiently water-free to prevent ionization of possible electrolyte impurities. The use of purified materials reduced the incidence of impurities and therefore the conditions in the system were more nearly completely anhydrous than those in other reported sols. Qualitative observations on the carbon-nitrobenzene sol were sufficient to classify the system as a typical stable colloidal suspension. The practical considerations in applying quantitative measurements to the sol are important. For example, the determination of precipitating values of ions is complicated by the fact that water must be excluded to maintain the system and ionization in the solvent is negligible.

In an absolutely anhydrous organosol, the so-called double layer could not be the stabilizing factor, and possibly electrostatic charges would be important. There is incomplete proof, however, that the method of preparation described is capable of producing absolutely anhydrous conditions, and further refinements in the system must be made before a sol can be prepared that irrefutably requires an explanation of stability that differs from the double-layer theory. It is within the scope of this paper only to describe the preparation and observation of a carbon-nitrobenzene sol, anhydrous to a very high degree, and reproducible in simple apparatus.

SUMMARY

1. A study of the references to various lyophobic organosols in the literature has shown that none has been prepared under conditions guaranteeing an absolutely pure two-phase state.

2. Experimental evidence has been presented to show that the arsenic trisulfide-nitrobenzene sol of Bikerman and the ferric oxide-propyl alcohol sol of Weiser and Mack were prepared in the presence of indefinite minute quantities of water.

3. An experimental procedure has been described by the operation of which a stable suspension of carbon in dry nitrobenzene in the practical absence of impurities has been prepared. A study of this lyophobic organosol has shown it to be stable for long periods and to be unaffected by freezing or by centrifuging at 2500 R.P.M. for 30 min.

The first part of this study was carried out at The Rice Institute under the guidance of Dr. H. B. Weiser and Dr. W. O. Milligan, to whom the author wishes to express his sincere appreciation.

REFERENCES

- (1) ANDRONIKASHVILI, E., AND ISABADSE, I.: *Acta Physicochim. U.R.S.S.* **13**, 369-78 (1940).
- (2) BIKERMAN, J. J.: *Z. physik. Chem.* **115**, 261-72 (1925).
- (3) BREDIG, G.: *Z. physik. Chem.* **32**, 127 (1900).
- (4) DAMERELL, V. R., AND URBANIC, A.: *J. Phys. Chem.* **48**, 125-33 (1944).
- (5) TORIKAI, R., AND YAMAGUTI, Z.: *Electrochem. J. (Japan)* **5**, 63-6 (1941).
- (6) VERNON, A. A., AND NELSON, H. A.: *J. Phys. Chem.* **44**, 12-25 (1940).
- (7) WEISER, H. B., AND MACK, G. L.: *J. Phys. Chem.* **34**, 86-100 (1930).

RATES OF ANION EXCHANGE IN ION-EXCHANGE RESINS

ROBERT KUNIN AND ROBERT J. MYERS

*Resinous Products and Chemical Company, Philadelphia, Pennsylvania**Received April 23, 1947*

Though considerable information is available for the various equilibria involved in ion-exchange reactions, comparatively very little data exist for the kinetics of these reactions. Some investigators (12, 15, 17) have indicated the rate of cation exchange to be exceedingly rapid, whereas others (3, 16) have found that although the rate of cation exchange is rapid for some exchange substances, it is exceedingly slow for others. Wiegner and Müller (16) and Cernescu (3) have shown the rate of exchange of cations in various silicates to be dependent upon the structure of the silicate. The time necessary for attainment of equilibrium at room temperature for clay, permutit, and chabazite (a natural zeolite) was shown by Cernescu to be 5 min., 10 days, and 92 days, respectively. The differences in these rates were attributed to the differences in accessibility of the exchange sites. Since most of the clays swell in water and have most of the exchange sites at the immediate surfaces, their ion-exchange rates are quite rapid. However, since natural zeolites do not swell and have exchange sites in the inner portions of the crystal that are only accessible by means of fine pores, their exchange rates are extremely low. This is in apparent agreement with the results of Emmett and DeWitt (5) and of Barrer and Ibbitson (2) on the rate of gas adsorption for chabazite. Nachod and Wood (12), in a recent study of the rates of ion exchange, have concluded that the exchange reactions for several cation and anion exchangers were second-order, bimolecular reactions. They have also concluded that the low activation energy for the exchange of ions on a sulfonated coal implies that diffusion is not the rate-determining step. However, the results of Nachod and Wood on the rates of exchange in greensand, synthetic gel silicates, and resinous exchangers appear to imply that diffusion plays an

important rôle. du Domaine, Swain, and Hougen (4) have found the rate of exchange of ions in a synthetic gel silicate water softener to be dependent upon particle size.

With respect to the kinetics of anion exchange, very little data have been reported outside of the data of Myers *et al.* (11), Nachod and Wood (12), and Martin and Wilkinson (9). From the data that do exist, conclusions as to the rate-determining steps, temperature coefficient, effect of extent of surface, etc. are quite difficult to make. Since many of the previous kinetic studies have been quite sketchy, have not included the evaluation of such factors as extent of surface, ion species, state of hydration of exchange substance, diffusion, etc., and have been incidental to other work, a rather extensive study has been undertaken on the rates of anion exchange in anion-exchange resins. Although the existence of cation exchange has been widely demonstrated and accepted, the existence of the exchange of anions in many colloidal systems has not been as widely accepted. Many results have been interpreted as the molecular adsorption of acid rather than the exchange of anions. Although Mattson (10), Jenny (6), and Stout (13) have demonstrated the existence of anion exchange in

TABLE 1
Description of resins

RESIN	WATER CONTENT	NITROGEN CONTENT	APPARENT DENSITY
	<i>per cent</i>	<i>per cent</i>	<i>grams per cc.</i>
Amberlite IR-4B.....	38.5	14.0	0.64
Resin A.....	60.4	14.4	0.67
Resin B.....	77.1	13.2	0.57
Resin C.....	53.0	17.9	0.69

silicates, the exchange of anions in resinous "anion exchangers" has not been as ably demonstrated until recently. However, the data of Jenny (7) and Sussman (14) and the most recent excellent work of Wiklander (17) apparently indicate that resinous anion exchangers function as true ion exchangers. The data of of these investigators apparently indicate that the amine type of anion-exchange resins contains amine groups which are capable of accepting a proton or oxonium ion and thereby becoming positively charged. In order to satisfy the law of electroneutrality, this charge is balanced by an anion which may be replaced or exchanged by other anions.

EXPERIMENTAL

Materials

The four commercially available anion-exchange resins employed in this study are partially described in table 1. Except when otherwise indicated, the particle size of the resins was 20-50 mesh. The resins were first thoroughly "regenerated" (hydroxyl form) with a 1 *N* solution of sodium hydroxide and rinsed with distilled water until an aqueous suspension remained neutral after 24 hr. For all

runs (except those involving the effect of the degree of hydration) the resins were kept in a moist condition.

Apparatus

The apparatus employed in this study consisted of a 1-liter, three-neck, round-bottom flask containing a thermometer, stirrer, and a pipet sampling device. The stirrer was motor driven with a device for varying the stirring rate. Since the reaction was found to be rather insensitive to small changes in temperature, no precautions were taken to thermostat the flask. However, for the experiments in which the effect of temperature was determined, the low-temperature runs were made in an ice bath and the room-temperature effect study at $30^{\circ}\text{C} \pm 0.5^{\circ}$. The stirring rates chosen for this study were 200 and 400 R.P.M. For all other runs the temperature was $30^{\circ}\text{C} \pm 2^{\circ}$.

Technique

The rates of exchange were obtained from runs in which the concentration in the liquid phase was followed as a function of time. Ten-gram samples were first placed in the flask and the stirring initiated. At a predetermined time, 500 ml. of the desired solution was rapidly added (about 5–10 sec.), and at various time intervals samples (5 or 10 ml.) were withdrawn for analysis. The analyses for acid and base were performed in the usual manner with either standard acid or base, using phenolphthalein as the indicator. Chloride analyses were performed volumetrically according to the Mohr method. The course of the reaction was followed until equilibrium was reached. Equilibrium was usually attained within 24 hr. The rates of exchange were obtained by measuring the slopes along the curve formed on plotting milliequivalents (y) exchanged per gram *versus* time in minutes (t). Slopes (dy/dt) were measured at several points along the curve and the concentration and amount exchanged recorded for each slope. By such a procedure it was possible to obtain the relationship between rate and concentration at a constant fraction exchanged and the relationship between rate and the extent of exchange at a constant concentration. The initial rates were obtained on extrapolation to zero amount absorbed. Although a considerable amount of heat is liberated upon reaction between the hydroxyl form of the anion-exchange resin and acid, the ratio of resin to liquid phase was such that the variation of temperature during any one run was less than 1°C .

The reproducibility of the rate measurements was first checked by performing several runs under very similar conditions. The results presented in figure 1 indicate that the reproducibility was quite good. The slight difference between the runs at 200 R.P.M. may easily be accounted for by the slight difference in the initial concentration. The effect of the stirring rate was investigated by comparing the rate curves obtained for two runs which were identical except for the fact that the stirring rate of one was 200 R.P.M. and that of the other 400 R.P.M. It is quite evident from the results presented in figure 1 that the effect of the stirring rate in the range studied was but slight.

Variables studied

In this investigation the effects of concentration, anion species, particle size, neutral salts, temperatures, amount exchanged, stirring rate, and state of hydration upon rate of exchange were studied. Anion systems were studied which included the anion-exchange processes commercially designated as *acid adsorption*, *regeneration*, and *anion interchange*. For the acid adsorption cycle, hydrochloric, sulfuric, phosphoric, and acetic acids were studied in the range 0.01–1.0 *N*. The regeneration rates were studied using sodium hydroxide (0.1 *N*) as regenerant for a resin which had previously adsorbed chloride. Rates of anion interchange were obtained for the interchange of chloride and sulfate ions by following the rate of exchange on the addition of sodium sulfate to a resin saturated with chloride.

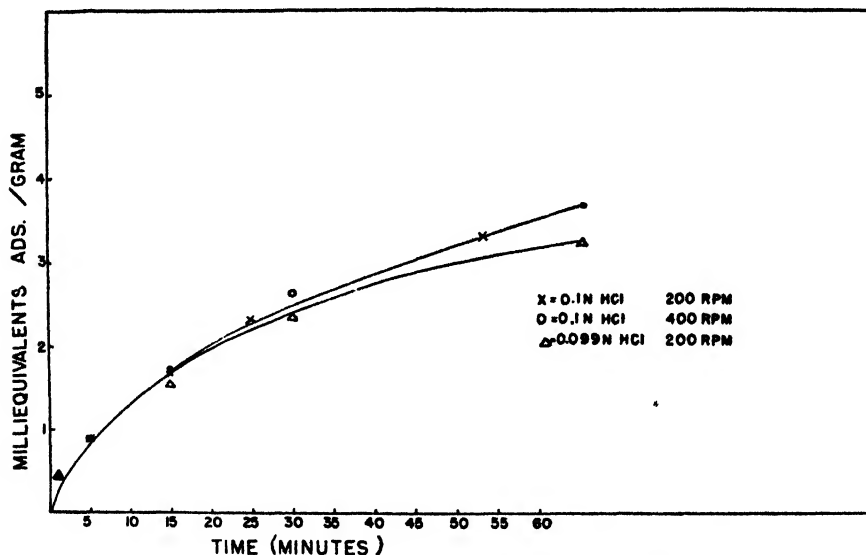


FIG. 1. Effect of stirring rate and reproducibility on the adsorption of hydrochloric acid by Amberlite IR-4B.

RESULTS

Effect of resin pretreatment upon rate of exchange

The effect of the particle size of the resin upon the rate of anion exchange was investigated by determining the rate of hydrochloric acid adsorption by three closely sieved (20–28, 28–35, and 35–40 mesh) fractions of Amberlite IR-4B at room temperature. The rate curves for these runs that are reproduced in figures 2 and 3 indicate a marked effect of particle size upon rate. On applying the “parabolic” diffusion law (1),

$$\frac{y_t}{y_\infty} = k\sqrt{t}$$

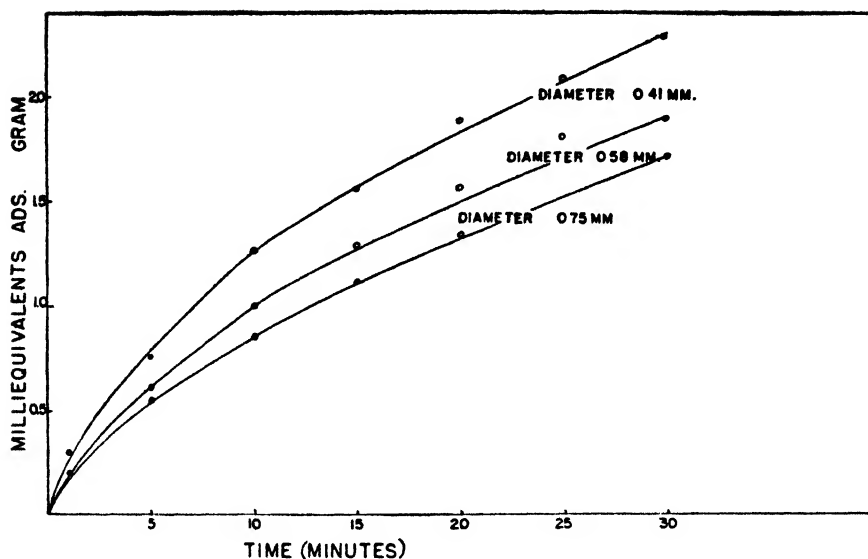


FIG. 2. Effect of particle size on rate of adsorption of hydrochloric acid by Amberlite IR-4B

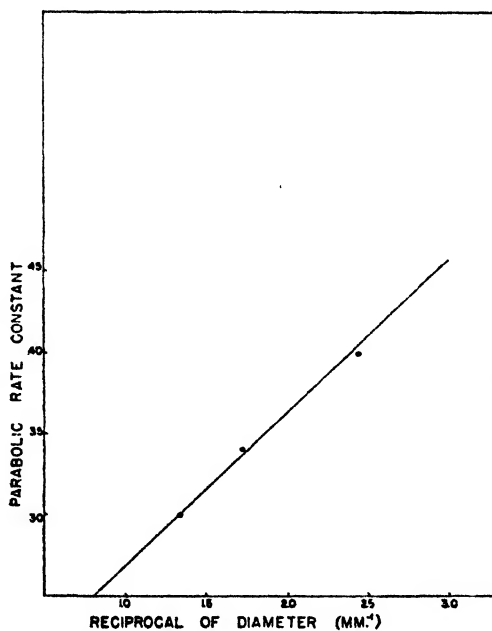


FIG. 3. Effect of particle size on parabolic rate constant

(where y_t and y_∞ are the number of milliequivalents adsorbed at time t and at equilibrium, respectively, and where k is a constant), by plotting $\frac{y_t}{y_\infty}$ against \sqrt{t} , one finds that fair agreement is obtained and that the slopes of these lines are pro-

portional to the reciprocal of the diameter of the particles. This is in perfect agreement with the diffusional theory and is quite similar to the results obtained by Barrer and Ibbitson (2) on the diffusion of gases in zeolites.

In order to determine the effect of the state of hydration of the resin gel upon the rate of exchange, the rate of exchange for an air-dry sample of Amberlite IR-4B was compared with the rate of exchange for an identical sample that had been pre-soaked in water for several hours. The air-dried sample of resin contained less than 5 per cent moisture, whereas the pre-soaked resin contained approximately 60 per cent moisture. The rates of anion exchange were compared with 0.1 normal hydrochloric acid at room temperature. The data for this experiment, as shown in figure 4, indicate that initially the rate of exchange

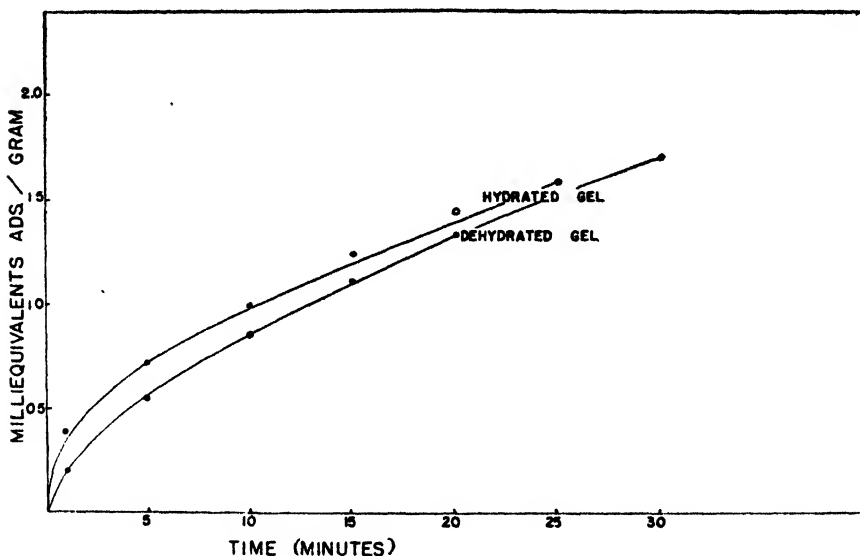


FIG. 4. Effect of state of hydration on rate of adsorption of hydrochloric acid by Amberlite IR-4B.

for the pre-soaked sample was much higher than for the air-dried sample. However, after the first 5 min. the differences became much smaller, indicating that for resins that were not fully hydrated, the initial rate of exchange would depend markedly upon the rate of hydration. In view of these results all resins were kept fully hydrated for subsequent rate measurements.

Effect of concentration and amount exchanged upon the rate of exchange

The effects of concentration and the amount exchanged were investigated by determining the rate curves for varying concentrations of acids. In order that the effects of concentration and extent of exchange could be separated, the rates (as determined by the slopes of the exchange-time curves) were obtained at various concentrations for a fixed concentration. This was determined for

several acids (acetic, hydrochloric, sulfuric, and phosphoric), using Amberlite IR-4B. For the remaining resins, rate curves were obtained for two concentra-

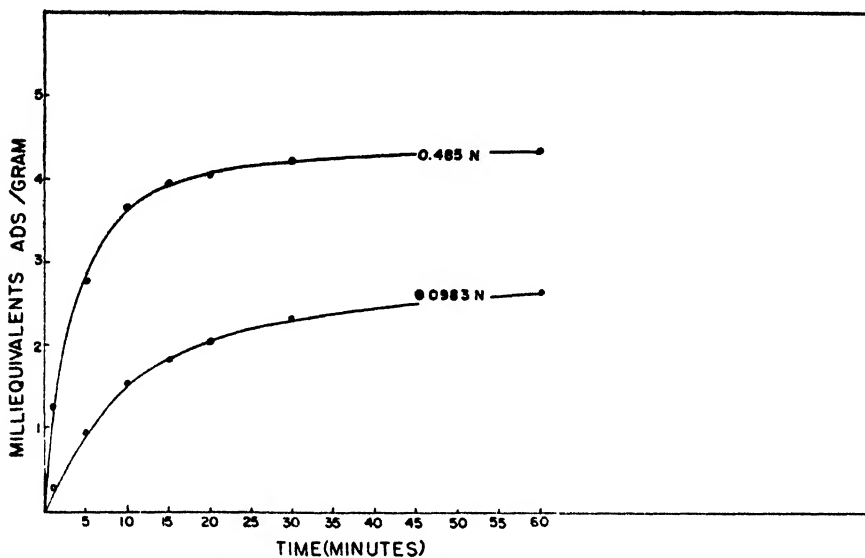


FIG. 5. Rates of adsorption of acetic acid by Amberlite IR-4B

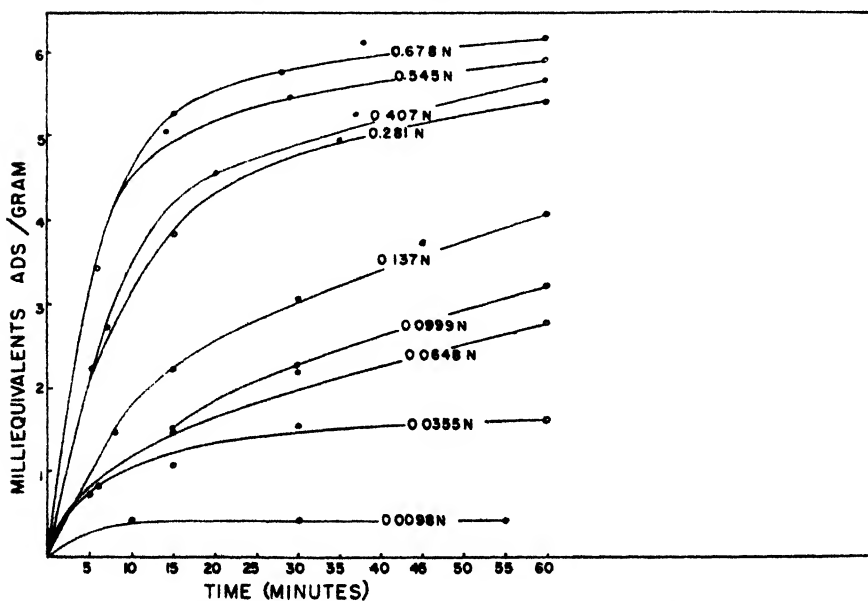


FIG. 6. Rates of adsorption of hydrochloric acid by Amberlite IR-4B

tions of hydrochloric acid. The rate curves for these experiments may be seen in figures 5, 6, 7, 8. If the rates are taken for various degrees of adsorption or

exchange, the rates are directly proportional to the concentration for a fixed quantity exchanged. This is quite evident from the plots in figures 9, 10, 11.

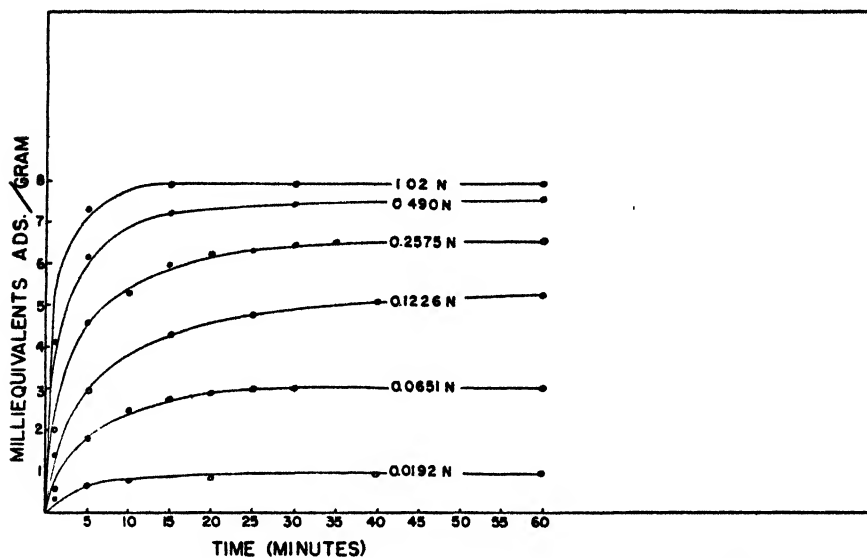


FIG. 7. Rates of adsorption of sulfuric acid by Amberlite IR-4B

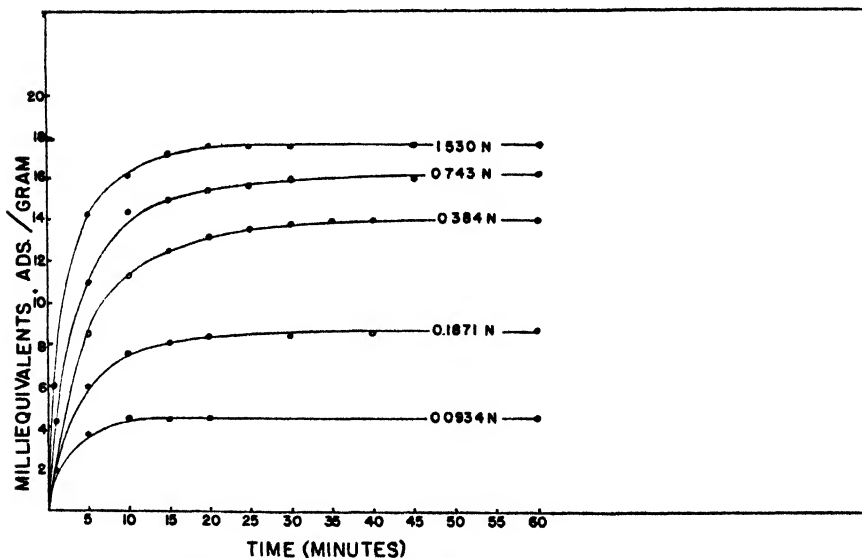


FIG. 8. Rates of adsorption of phosphoric acid by Amberlite IR-4B

As might be expected for a diffusional process, at any fixed concentration the rate is dependent upon the extent of exchange. This is in accord with the diffusion theory. It is quite interesting to note that the rates of exchange for

the various acids on Amberlite IR-4B are $\text{HCl} = \text{CH}_3\text{COOH} < \text{H}_2\text{SO}_4 < \text{H}_3\text{PO}_4$. Whereas the initial rates, $\left(\frac{dy}{dt}\right)_0$, may be expressed by the equation $\left(\frac{dy}{dt}\right)_0 = kC$ (figure 12), the rates as a function of the extent or degree of exchange cannot be

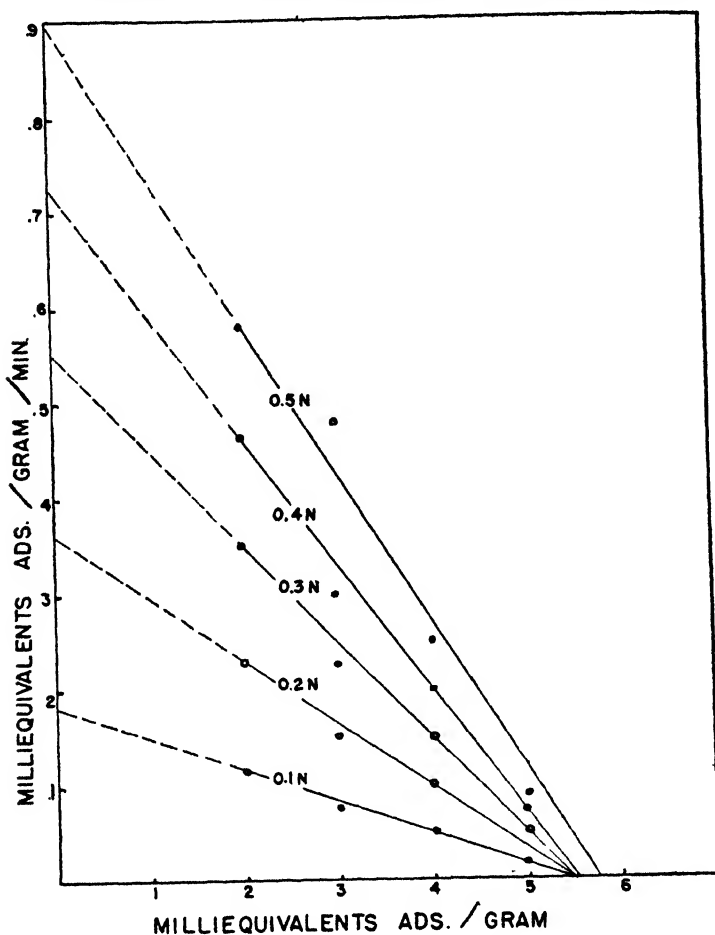


FIG. 9. Rates of adsorption of hydrochloric acid by Amberlite IR-4B

expressed by the same equations. However, the following equations appear to describe the relationships:

$$\begin{aligned} \left(\frac{dy}{dt}\right)_{\text{HCl or CH}_3\text{COOH}} &= kC(y_\infty - y_t) \\ \left(\frac{dy}{dt}\right)_{\text{H}_2\text{SO}_4}^{1/2} &= kC^{1/2}(y_\infty - y_t) \\ \log \left(\frac{dy}{dt}\right)_{\text{H}_3\text{PO}_4} &= k \log C(y_\infty - y_t) \end{aligned}$$

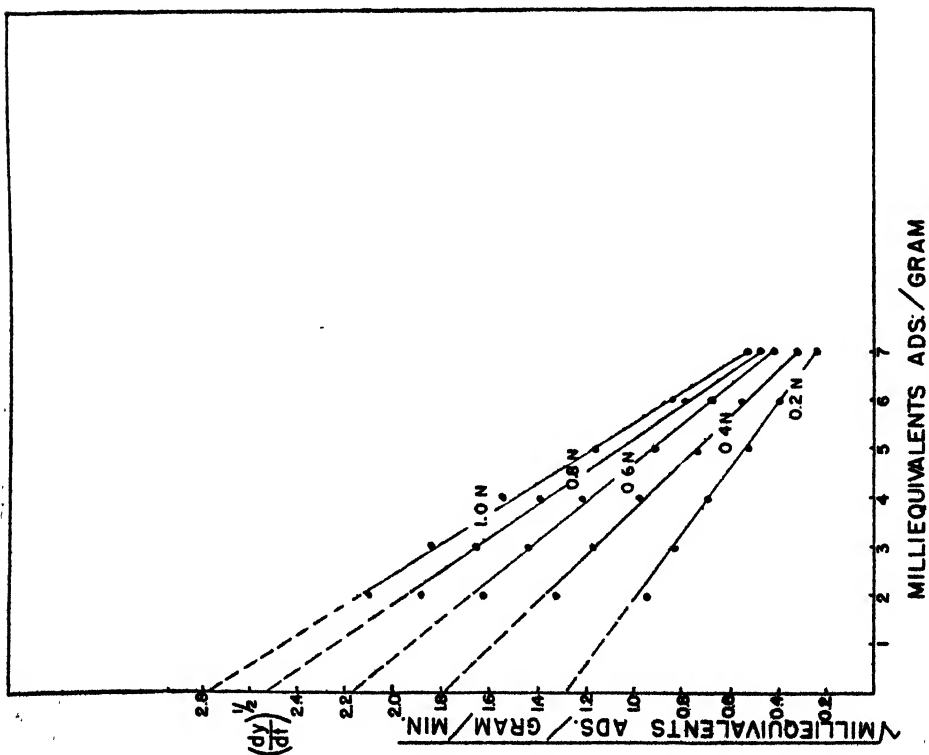


Fig. 10. Rates of adsorption of sulfuric acid by Amberlite IR-4B

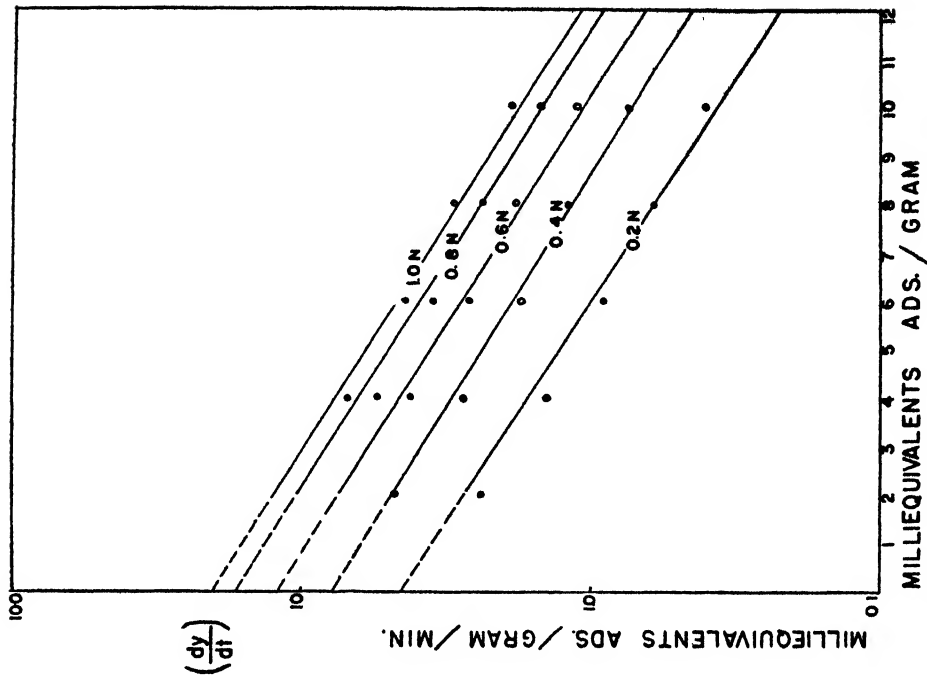


Fig. 11. Rates of adsorption of phosphoric acid by Amberlite IR-4B

It is quite interesting to note that with the exception of Resin A, all resins apparently behaved quite similarly, although there are variations in exchange capacities. Application of the diffusion equation, $\frac{y_t}{y_\infty} = k\sqrt{t}$ (figures 13, 14), to these resins apparently indicates that the rate-determining step is one of diffusion for the resins other than Resin A. Resin A yields results which indicate that an appreciable fraction of the exchange is somewhat independent of diffusion and

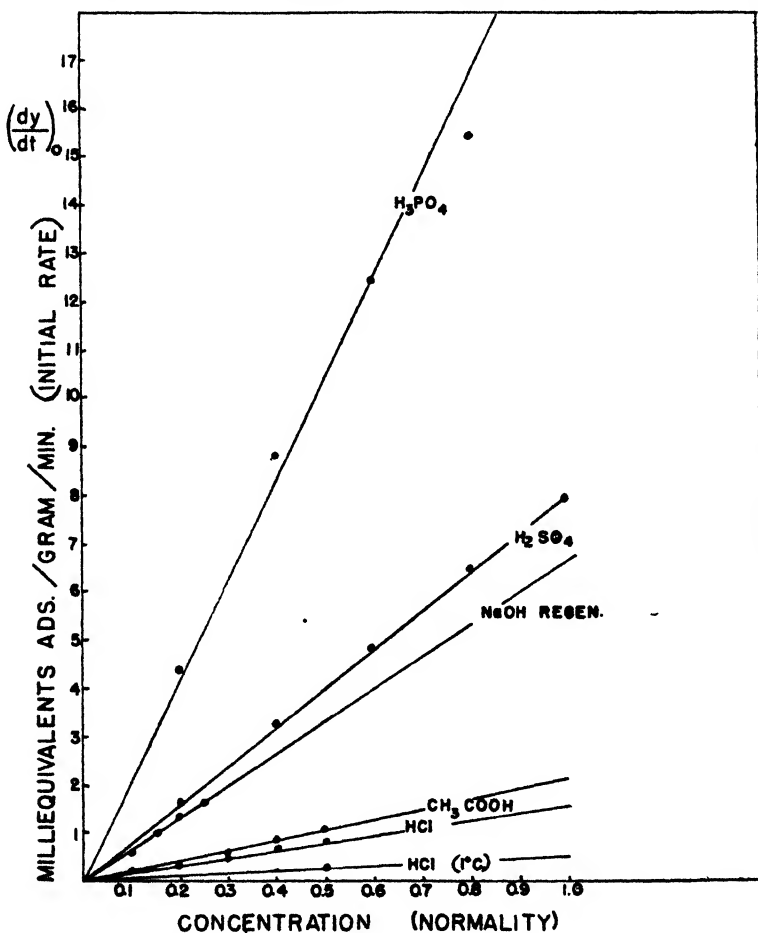


FIG. 12. Initial rates of acid adsorption by Amberlite IR-4B

takes place at the surface. This is in agreement with the fact that this resin is supposedly prepared on a porous base.

Mobility of exchangeable ions

In figure 15 is shown the effect of interrupting a rate study prior to attainment of equilibrium by separation of the liquid and solid phases. On resuming the reaction, it is quite evident that the rate of exchange is much greater than it

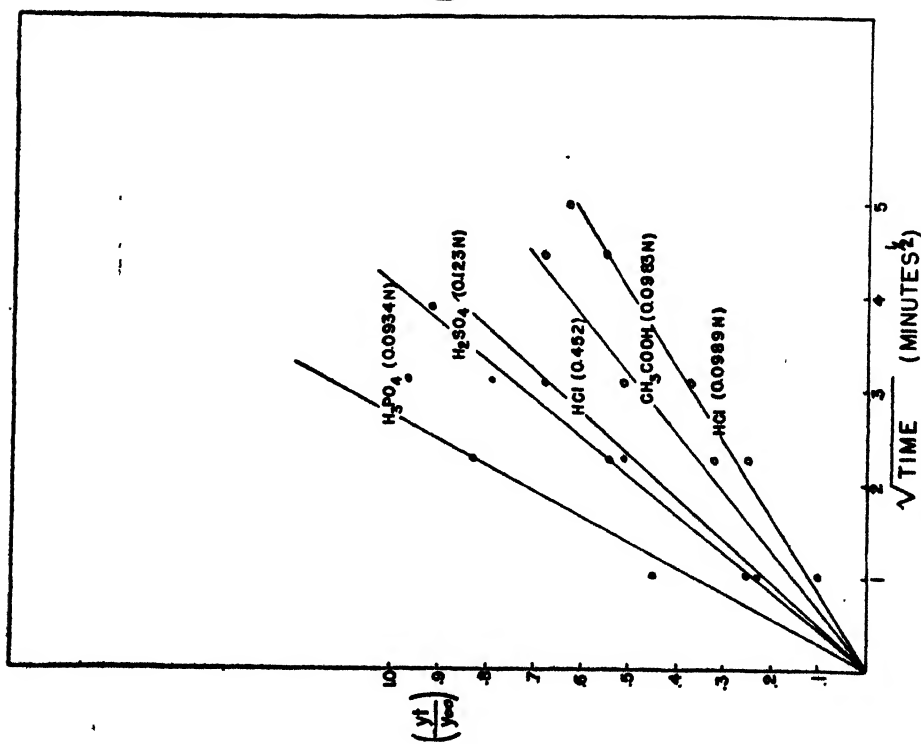


Fig. 13. Rates of adsorption of various acids by Amberlite IR-4B

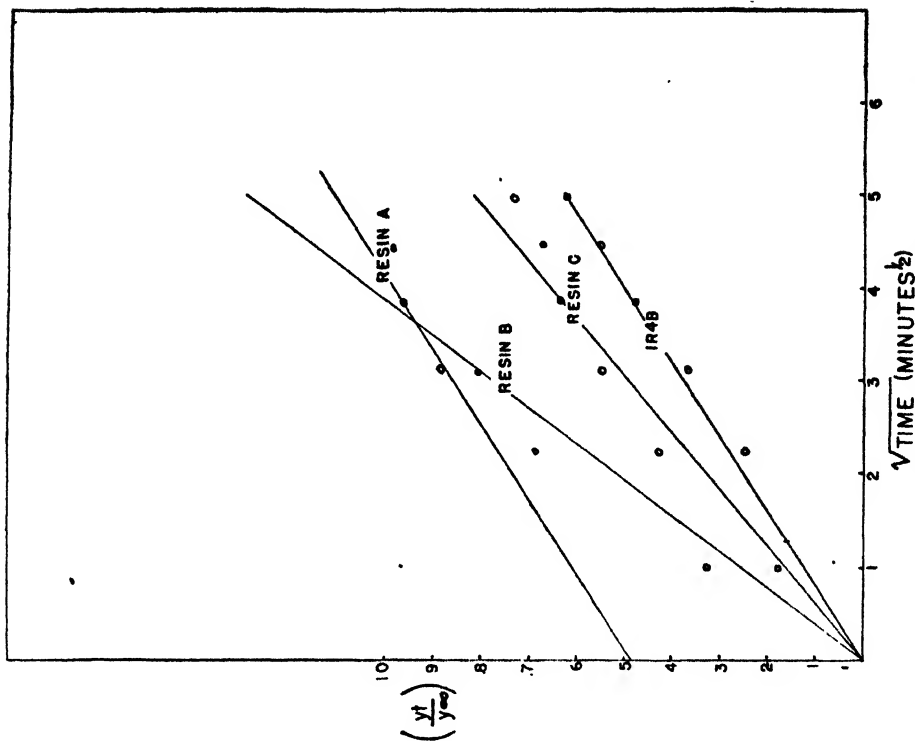


Fig. 14. Rates of adsorption of hydrochloric acid by various resins

would have been had no interruption taken place. This effect is undoubtedly due to a dilution of the surface chloride ions, brought about by exchange with some of the internal hydroxyl ions.

Effect of temperature

The effect of temperature (figure 16) was investigated by lowering the temperature to 1°C. and following the rate of exchange, utilizing 0.1 *N* and 0.5 *N* hydrochloric acid on Amberlite IR-4B. Although an appreciable lowering of the rate was observed for both concentrations, the calculated energy of activation as obtained from the slope of the plot of log rate *vs.* $1/T$ was 6600 cal. This value is approximately equal to that obtained for the diffusion of hydrochloric acid in water.

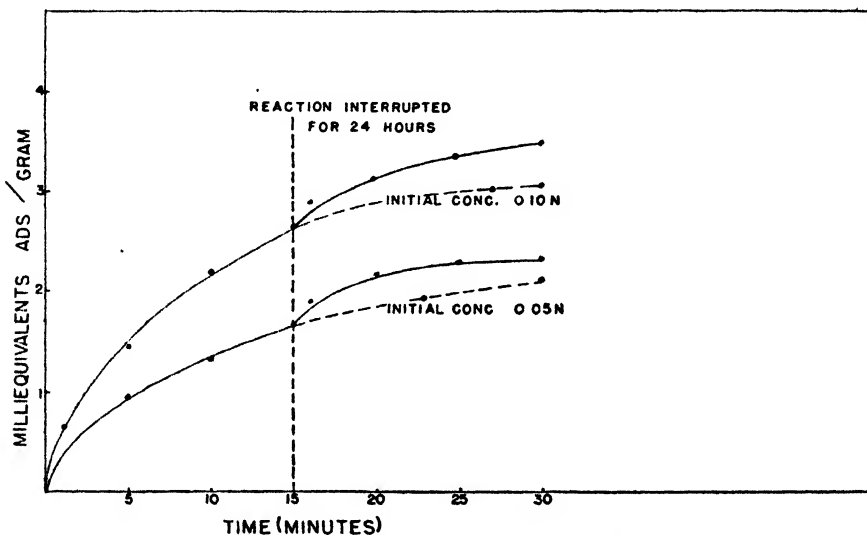


FIG. 15. Effect of reaction interruption on the rate of adsorption of hydrochloric acid by Amberlite IR-4B.

Effect of salt concentration

The addition of sodium chloride to the hydrochloric acid appeared to have a noticeable effect on the rate of exchange. The results (figure 17) indicate that the rate increases with increasing concentration of sodium chloride. Although some exchange is evident on the addition of sodium chloride without hydrochloric acid, the extent of the neutral salt exchange is negligible. This is evident from the equilibrium values obtained for the hydrochloric acid-sodium chloride mixtures. It is apparent then that the weakness of the basicity of the hydroxyl form of the exchanger is such that exchange of anions other than OH^- is negligible at neutral pH's. Utilizing the diffusion equation of MacDougall (8),

$$\frac{D \text{ in NaCl}}{D \text{ in H}_2\text{O}} = \frac{\frac{[\text{HCl}]}{[\text{NaCl}]} + 1}{\frac{[\text{HCl}]}{[\text{NaCl}]} + \frac{U_{\text{Na}} + U_{\text{Cl}}}{U_{\text{H}} + U_{\text{Cl}}}}$$

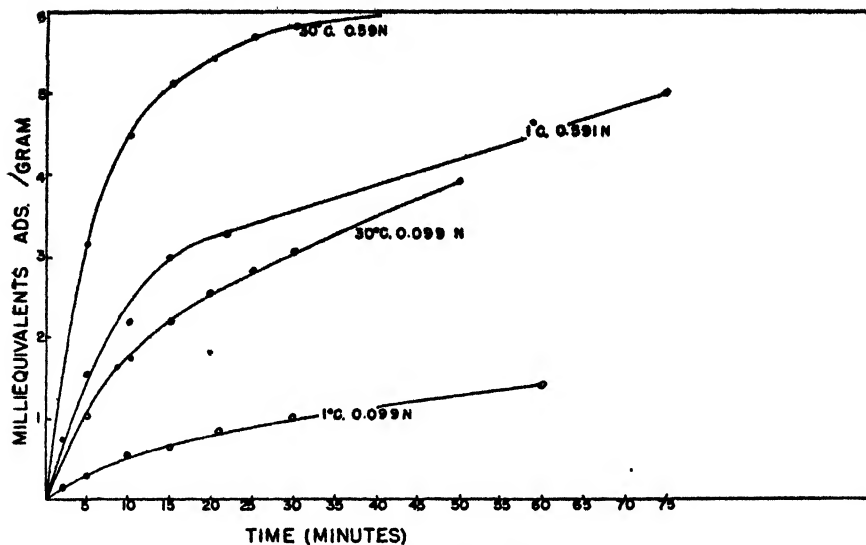


FIG. 16. Effect of temperature on rates of adsorption of hydrochloric acid by Amberlite IR-4B.

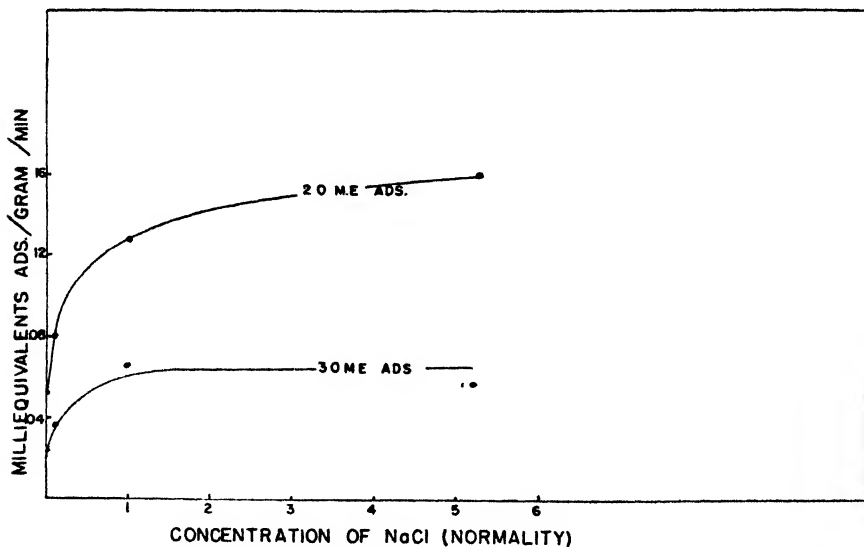


FIG. 17. Effect of sodium chloride on rates of adsorption of hydrochloric acid by Amberlite IR-4B.

where D = diffusion coefficient,

$[\]$ = concentration, and

U = mobility,

one obtains excellent agreement (see table 2) between the calculated and experi-

mental rates of exchange in various sodium chloride solutions. This is further evidence for the theory that diffusion is the rate-determining step in the exchange reactions being studied.

Effect of stirring rate

The results (figure 1) obtained on varying the rate of stirring from 200–400 R.P.M. during the rate of exchange studies indicated that this factor had little effect on the rate of exchange. This is further evidence for the diffusional mechanism. Although the results obtained on the effect of stirring in this study apparently disagree with the results obtained by Martin and Wilkinson (9), the results obtained by these investigators are apparently due to the presence of some soluble alkali that had not been rinsed from the resin. Their data apparently indicate this.

TABLE 2

A comparison of the rates of anion exchange in water and in sodium chloride solutions (Hydrochloric acid on Amberlite IR-4B)

CONCENTRATION OF NaCl <i>moles per liter</i>	RATE IN NaCl/RATE IN H ₂ O	
	Experimental	Calculated from MacDougall's equation (8)
0.1	1.43	1.75
1.0	2.30	2.95
5.2	3.10	3.27

Regeneration rate

The rates of exchange for the regeneration of an "exhausted" anion-exchange resin are shown in figure 18. In these experiments, the chloride ions of Amberlite IR-4B were exchanged for hydroxyl ions, using 0.1 *N* sodium hydroxide. The kinetics of this system appears to be quite similar to that for the reverse process, and the results apparently indicate that the initial rates for the regeneration cycle are faster than for the reverse cycle. Since the exhausted form of the resin (Amberlite IR-4B) is less dense than the regenerated state, these results are in apparent agreement with the diffusional mechanism.

Chloride-sulfate exchange rates

The rate of the chloride-sulfate (figure 19) exchange was studied by following the rate of exchange of chloride bound by Amberlite IR-4B upon the addition of an equivalent quantity of sodium sulfate. On comparing the rates of the chloride-sulfate exchange with the exchange of hydroxyl ions (the acid-adsorption cycle) it is quite evident that the chloride-sulfate exchange is much more rapid and is comparable to the regeneration rates. Again, one may attribute the difference in rates to the fact that the chloride and sulfate forms of Amberlite IR-4B are less dense than the hydroxyl form and therefore permit a more rapid diffusion of ions.

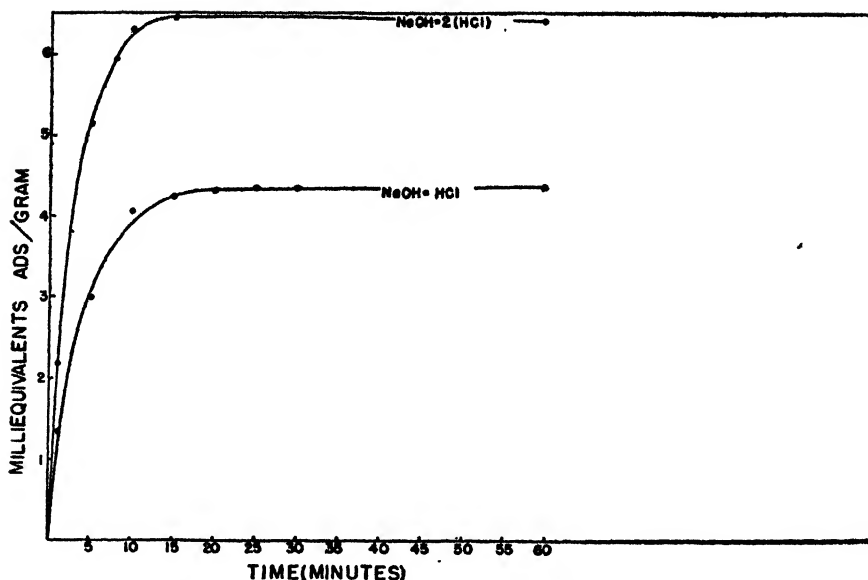


FIG. 18. Rate of hydroxyl-chloride anion exchange on Amberlite IR-4B

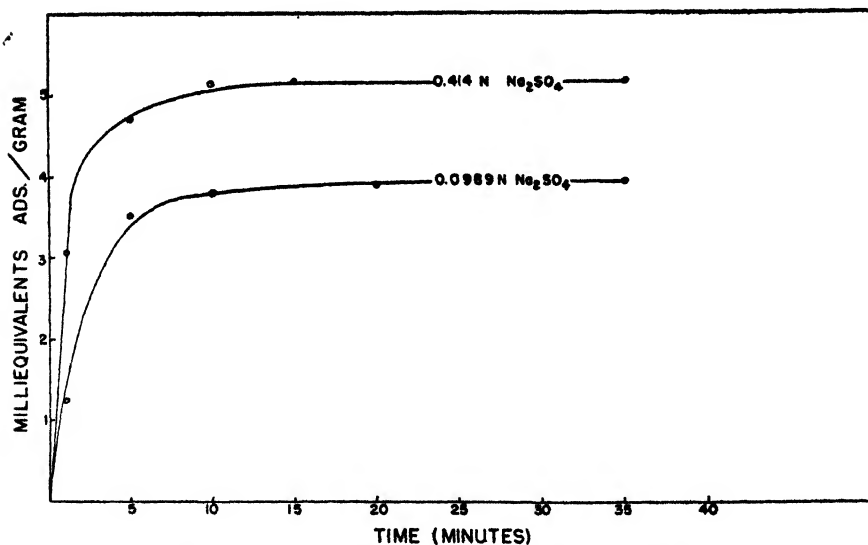


FIG. 19. Rate of chloride-sulfate anion exchange on Amberlite IR-4B

Equilibrium results

Since all rate measurements were continued until equilibrium apparently had been attained, adsorption or exchange isotherms (figures 20, 21) were obtained for hydrochloric, sulfuric, and phosphoric acids on the hydroxyl form of

Amberlite IR-4B. However, since only two points (equilibrium) were obtained for the other resins, complete equilibrium isotherms were not obtained. A

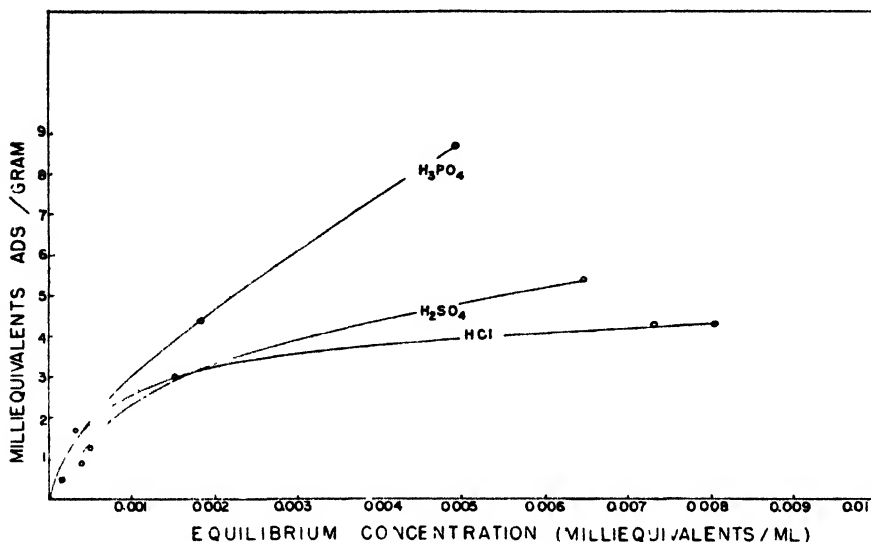


FIG. 20. Adsorption isotherms for Amberlite IR-4B in dilute range

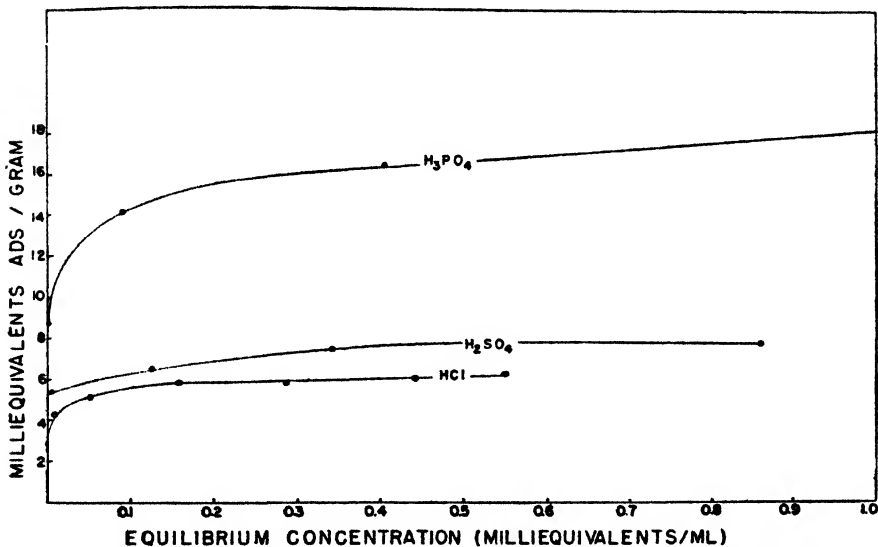


FIG. 21. Adsorption isotherms for Amberlite IR-4B in concentrated range

comparison of the equilibrium capacities of the various resins and the variation of capacity with acid species are shown in table 3. Owing to the fact that the equilibrium capacity was dependent upon concentration, the comparison of

equilibrium capacities was made at a concentration at which the isotherms apparently leveled off. The variations in the exchange capacity with respect to the various acids are quite similar to the results obtained by Myers *et al.* (11); however, the data do indicate that with sulfuric acid there exists an exchange for both SO_4^{--} and HSO_4^- . The adsorption or exchange in the case of phosphoric acid proceeds as if H_2PO_4^- were the only ion exchanged. Neither the Freundlich nor the Langmuir isotherm was able to fit the data over the concentration range investigated.

Heat of adsorption or exchange

The heat of adsorption as calculated from the data obtained for the reaction between hydrochloric acid and Amberlite IR-4B at 1°C. and 30°C. is 8.1 kg.-cal. per mole. The heat of adsorption as measured calorimetrically was found to be 8.7 kg.-cal. per mole.

TABLE 3
Equilibrium capacities of several resins

RESIN	ACID	ACID CONCENTRATION	CAPACITY	
		normality	milliequiv./ gram	milliequiv./ ml.*
Amberlite IR-4B	HCl	0.5	9.20	3.60
Amberlite IR-4B	CH_3COOH	0.5	6.45	2.53
Amberlite IR-4B	H_2SO_4	0.5	11.6	4.55
Amberlite IR-4B	H_3PO_4	0.5	27.7	10.9
Resin B	HCl	0.5	9.29	1.49
Resin A	HCl	0.5	7.00	2.00
Resin C	HCl	0.5	7.43	2.44

* Apparent volume of resin corresponding to a bed volume.

DISCUSSION OF RESULTS

The results obtained in this study indicate that the rate-determining step for the exchange of anions in most exchange resins is apparently the rate of diffusion of the ions through the gel structure. Considerable evidence is available to support this theory: (1) The fact that the rate of exchange is dependent upon the particle size of the resin is in excellent agreement with the "diffusion theory." According to the parabolic diffusion law (1):

$$\frac{y_t}{y_\infty} = k\sqrt{t}$$

k is a function of the diameter of the particle. The data presented in figures 2 and 3 illustrate this effect quite well. (2) The fact that the rate of stirring had but a negligible effect on the rate agrees with the theory that diffusion is the rate-determining step and not the rate of acid supply to the resin surface. (3) The kinetics of the exchange appears to support the diffusion theory quite well, since the rate is dependent upon the degree of saturation of the resin particle

as well as upon the concentration. (4) The dependence of the rate upon the age of the partially saturated resin also supports the diffusion theory, in that this effect can only be explained by the diffusion and exchange of ions from the outer portion of the resin into the inner portion of the resin, thereby permitting the outer portion to exchange anions at a greater rate. This evidence, as shown in figure 14, also indicates the exchangeable ions to be quite mobile. (5) The fact that the activation energy of the exchange for the reaction between hydrochloric acid and the hydroxyl form of the Amberlite resin is of the order of the activation energy for the diffusion of hydrochloric acid in water is in good agreement with diffusion being the rate-determining step. (6) The effect of neutral salts upon the reaction rate between hydrochloric acid and the hydroxyl form of the resin is also in agreement with the diffusion theory, in that the effect of anion concentration upon the rate agrees with the diffusion equation of MacDougall (8).

In view of the results obtained in this study, it is quite apparent that the rates of anion exchange in most commercial anion-exchange resins are dependent upon the particle size, the temperature, the concentration, the degree of resin saturation, the ionic species entering the exchange, and the gel structure of the resin, and that the actual ion-exchange process is practically instantaneous as the ions diffuse into the sphere of the exchange site. These conclusions are essentially identical with those of Wiegner and Müller (16) and Cernescu (3) on the rates of cation exchange in silicates. Were all the exchange positions located at the surface of the gel particles the exchange rate would no longer be dependent upon the diffusional process but would depend only upon the rate of supply of ions to the resin surface and upon the rate of diffusion of ions from the resin surface. All resins studied, with one exception, apparently exhibited very little surface exchange. The exception, Resin A, appears to have a larger fraction of its total exchange at the surface than the other resins. However, since the particle-size distributions of the various resins were not identical, it is difficult to compare the various rate constants quantitatively.

The effect of anion species on the rate of exchange is quite interesting and is indicative of anion exchange rather than molecular acid adsorption. Were hydrochloric, acetic, sulfuric, and phosphoric acids adsorbed molecularly, one would expect hydrochloric acid to have the faster rate because of its higher diffusion coefficient. The increase in rate with increasing functionality of the acid may possibly be due to the greater charge on the anion and therefore a greater attractive force. Although one may argue that phosphoric acid and possibly sulfuric acid at higher degrees of acidity are only monobasic, in the intermicellar liquid of the resin particle (especially where a large concentration of hydroxyl ions is still available) the system may be sufficiently alkaline for complete neutralization of the polybasic acids. The fact that acetic acid and hydrochloric acid (both monobasic acids) exhibit similar rates, although they have widely different ionization constants, is in agreement with this concept. The weakly acid nature of acetic acid is exhibited in the final equilibrium capacity.

SUMMARY

A study of the rates of anion exchange in resinous exchangers has indicated the rate-determining step to be the diffusion of ions through the gel structure and has shown that the rate is dependent upon factors such as (1) particle size, (2) ion species, (3) concentration, (4) temperature, (5) degree of exchange saturation, (6) degree of hydration of resin, and (7) degree of mixing of exchangeable ions.

The authors are indebted to Mr. Edward Kyser for his extensive assistance in the laboratory during the course of the study.

REFERENCES

- (1) BARRER, R. M.: *Diffusion in and through Solids*. University Press, Cambridge (1941); Macmillan Company, New York (1941).
- (2) BARRER, R. M., AND IBITTS, D. A.: *Trans. Faraday Soc.* **40**, 206-16 (1944).
- (3) CERNESCU, N.: *Anuar. inst. geol. Romaniei* **16**, 777-859 (1931).
- (4) DU DOMAINE, J., SWAIN, R. L., AND HOUGEN, O. A.: *Ind. Eng. Chem.* **35**, 546-53 (1943).
- (5) EMMETT, P. H., AND DEWITT, T. W.: *J. Am. Chem. Soc.* **65**, 1253-62 (1943).
- (6) JENNY, H.: *Kolloidchem. Beihefte* **23**, 428-72 (1927).
- (7) JENNY, H.: *J. Colloid Sci.* **1**, 33 (1946).
- (8) MACDOUGALL, F. II.: *J. Phys. Chem.* **38**, 945 (1938).
- (9) MARTIN, G. J., AND WILKINSON, J.: *Gastroenterology* **6**, 315 (1946).
- (10) MATTSO, S., AND WIKLANDER, L.: *Soil Sci.* **49**, 109-53 (1940).
- (11) MYERS, R. J., EASTES, J. W., AND URQUHART, D.: *Ind. Eng. Chem.* **33**, 12-70 (1941).
- (12) NACHOD, F. C. AND WOOD, W.: *J. Am. Chem. Soc.* **66**, 1380-4 (1944).
- (13) STOUT, P. P.: *Proc. Soil. Sci. Soc. Am.* **4**, 177 (1939).
- (14) SUSSMAN, S., NACHOD, F. C., AND WOOD, W.: *Ind. Eng. Chem.* **37**, 618 (1945).
- (15) WALTON, H. F.: *J. Franklin Inst.* **232**, 318 (1941).
- (16) WIEGNER, G., AND MÜLLER, K. W.: *Trans. 3rd Intern. Congr. Soil Sci.* **3**, 5-28 (1936).
- (17) WIKLANDER, L.: *Ann. Roy. Agr. Coll. Sweden* **14**, 1-171 (1946).

ON THE HETEROGENEOUS CATALYTIC ACTIVITY OF COLLOIDAL SILVER IN THE REDUCTION OF SILVER ACETATE

BAL KRISHNA AND SATYESHWAR GHOSH

Physical Chemistry Laboratory, University of Allahabad, Allahabad, India

Received October 16, 1946

Revised copy received April 16, 1947

The rôle of silver as catalyst in the reduction of silver salts has been studied by Sheppard (10) in the silver nitrate-sodium sulfite reaction. Livingston and Lingane (8) have observed catalysis by silver in the reduction of silver ions by hydroquinone. Much valuable work has been done in this connection by James, who has studied the reduction of silver ions (2, 3, 4, 5) and of precipitates of silver chloride (6). Chakarvarti and Ghosh (1) have observed catalysis by

silver in the reduction of the organic salts of silver by hydrogen. In a recent communication (7) Krishna and Ghosh studied the reduction of silver tartrate by resorcinol, wherein it has been pointed out that the reaction is unimolecular with respect to each reactant separately and the total order of the reaction is 2, but that it is greatly affected by colloidal silver and the change in hydrogen-ion concentration brought about during the progress of the reaction. In the present paper, the authors have studied the influence of colloidal silver and hydrogen ions on the kinetics of reduction of silver acetate by resorcinol. The hydrogen ions were controlled by using buffers ranging from pH 3.72 to pH 7.00.

EXPERIMENTAL

A precipitate of silver acetate is prepared by adding a solution of sodium acetate to a solution of silver nitrate. This precipitate is washed several times with distilled water to free it from adsorbed ions. After washing, it is dissolved in water. The strength of the solution is determined by titrating it against a standard potassium chloride solution with potassium chromate as indicator. Twenty-five cubic centimeters of the solution is taken and poured into a dark bottle kept in a water bath which is regulated electrically. To this 25 cc. of distilled water is added. When the solution has attained the temperature of the bath, 50 cc. of resorcinol solution of known strength is added to it. In cases where starch solution, colloidal silver, and buffer solutions are used, the volume and concentrations are so chosen that the total volume is always 100 cc.

From this reaction mixture 10-cc. portions are taken out at different intervals of time and added to $N/25$ potassium chloride solution. To this a few crystals of potassium nitrate are added to precipitate silver particles completely. This mixture is filtered through two or three gravimetric filter papers. From this filtrate, which contains an excess of potassium chloride 5 cc. is taken and titrated against a standard silver nitrate solution.

Standard buffers

Buffer solutions are prepared from sodium acetate and acetic acid. The volume and concentration of the buffers employed are so chosen as to yield the given pH on dilution to 100 cc.

A perusal of table 1 shows that in the earlier stages of the reaction the unimolecular velocity constants are small, gradually increase to a maximum, and then again begin to decrease. With the lowest concentration of resorcinol (1.75 per cent) reduction does not start before 7 min. or more, but the constants obtained between 20 and 80 min. are in fair agreement. This is also true with resorcinol of 2.5 per cent concentration. But in the case where 5 per cent resorcinol solution is used, the unimolecular velocity constants quickly fall after the reaction has progressed for 20 min.

These results show that there exists an induction period, suggesting autocatalysis due to the formation of small particles of silver. With the progress of reaction, the particles grow larger and larger, owing to coalescence with

one another. As the particles increase in size the catalytic activity decreases, and the values of the velocity constants begin to fall. This fall in velocity constant is also due, to some extent, to an increase in hydrogen-ion concentration (see below).

TOTAL ORDER OF THE REACTION

The total order of the reaction is calculated according to Ostwald's isolation method. For this the highest values of the velocity constants obtained at different concentrations of resorcinol (5 per cent and 2.5 per cent) are employed. Assuming that the reaction is unimolecular with respect to silver salt, the total order of the reaction works out to be 2.

TABLE 1
Temperature, 35°C.

TIME	UNIMOLECULAR VELOCITY CONSTANTS		
	Resorcinol (5%)..... 50 cc. Silver acetate (<i>N</i> /16.5). 25 cc. Water..... 25 cc.	Resorcinol (2.5%)..... 50 cc. Silver acetate (<i>N</i> /16.5). 25 cc. Water..... 25 cc.	Resorcinol (1.75%)..... 50 cc. Silver acetate (<i>N</i> /16.5). 25 cc. Water..... 25 cc.
<i>minutes</i>			
0			
5	0.007130	0.003496	0.000000
10	0.007464	0.003519	0.000943
20	0.007555	0.003576	0.001426
40	0.006154	0.003973	0.001443
60	0.004692		
80		0.003309	0.001461
100	0.003663		
120		0.002871	0.001225
140	0.002886		
160		0.002553	0.001220

TEMPERATURE COEFFICIENT

The reaction is repeated at 45°C. with 5 per cent resorcinol. The highest value of the velocity constant at this temperature is 0.018722. The highest value of the constant at 35°C. is 0.007555. Comparing these values we find that the temperature coefficient of the reaction for 10° is 2.4, approximately.

The following points emerge from table 2: (a) In the presence of starch the induction period persists and the values of the velocity constants increase slightly. (b) The values of the velocity constants increase four to five times in the presence of colloidal silver and the induction period disappears. (c) The rate of decrease of velocity constant is greater where colloidal silver has been used.

INFLUENCE OF HYDROGEN IONS

As the reaction proceeds, the acidity of the reaction mixture increases, owing to oxidation of resorcinol. Hydrogen ions act as the retarding agent, and the

fall in the velocity constant can also be ascribed to this factor. We shall see later on that the fall in the velocity constant is due, to a greater extent, to a gradual precipitation of colloidal silver.

TABLE 2
Temperature, 35°C.

UNIMOLECULAR VELOCITY CONSTANTS			
TIME	Resorcinol (1.75%) . . . 50 cc. Silver acetate (<i>N</i> /15) . . . 25 cc. Water 22 cc. Starch (1%) 3 cc.	Resorcinol (1.75%) . . . 50 cc. Silver acetate (<i>N</i> /15) . . . 25 cc. Colloidal silver 22 cc. Starch (1%) 3 cc.	Resorcinol (2.5%) . . . 50 cc. Silver acetate (<i>N</i> /15) . . . 25 cc. Colloidal silver 22.5 cc. Starch (1%) 2.5 cc.
minutes			
0			
5	0.000000	0.013338	0.017510
10	0.000966	0.011718	0.014150
20	0.002967	0.008555	0.011057
40	0.003335	0.006081	0.006411
80	0.002814	0.004223	0.005430
120	0.002397	0.003490	0.003695
160	0.002124	0.003074	0.003037

TABLE 3

Temperature	35°C.
Resorcinol (10%)	25 cc.
Buffer	25 cc.
Starch (1%)	3 cc.
Water	22 cc.
Silver acetate (N/14.25)	25 cc.

TIME	UNIMOLECULAR VELOCITY CONSTANTS		
	pH = 3.72	pH = 4.27	pH = 4.99
minutes			
0			
20	0.0000000	0.0000000	0.0000000
40	0.0000000	0.0000000	0.0002303
80	0.0000000	0.0003483	0.0005872
120			0.0005528
160	0.0001741	0.0002936	
200			0.0007127
320	0.0001166	0.0003008	
400			0.0008688
545		0.0002911	
570	0.0000824		
600			0.0007309
1170	0.0000909	0.0002420	

It is worth while to mention here that oxidation-reduction reactions in general are negatively catalyzed by hydrogen ions. Palit and Dhar (9) found that oxidation of fats, carbohydrates, and urea by air takes place more quickly in an

alkaline solution. A solution of sodium formate is more effective as reducing agent than formic acid itself. This also explains why silver nitrate is less susceptible to reduction than organic salts of silver.

Researches of James (2, 3, 4) also have shown that reduction of silver salts is faster, the higher the pH value of the mixture. Krishna and Ghosh (7) pointed out that during the reduction of silver tartrate by resorcinol the value of the velocity constant increases if to the reaction mixture are added salts which hydrolyze to give excess hydroxyl ions. They have further pointed out that if to a solution of silver tartrate a few drops of sodium hydroxide are added, silver hydroxide is at first precipitated and is then reduced by the tartrate ions. In this way beautiful sols of silver can be produced.

Table 3 shows that (a) the greater the concentration of hydrogen ions the greater the induction period, and (b) the smaller the concentration of hydrogen ions the greater the value of the velocity constants.

TABLE 4
Temperature, 35°C.; pH, 5.57

TIME	UNIMOLECULAR VELOCITY CONSTANTS		
	Resorcinol (10%). 25 cc. Buffer 25 cc. Water 25 cc. Silver acetate (<i>N</i> /17.75). 25 cc.	Resorcinol. 25 cc. Buffer 25 cc. Water. 22 cc. Starch (1%) 3 cc. Silver acetate (<i>N</i> /17.75). 25 cc.	Resorcinol. 25 cc. Buffer. 25 cc. Starch (1%). 5 cc. Colloidal silver 20 cc. Silver acetate (<i>N</i> /17.75). 25 cc.
<i>minutes</i>			
0			
5	0.0000000	0.0000000	0.0253790
10	0.0000000	0.0031090	0.0280449
20	0.0024411	0.0063447	0.0250911
40	0.0011743	0.0074214	0.0189882
100	0.0005665	0.0081032	0.0125738
200	0.0003811	0.0043135	0.0085029
300		0.0031846	0.0063936

IMPORTANCE OF PROTECTIVE COLLOID

We have found that if we do not add starch between the pH range 3.72–4.99, the reaction does not take place appreciably even if the solution is kept for days. The fact is that in the presence of buffer of a high hydrogen-ion concentration the colloidal silver formed is precipitated. The time of precipitation and coagulation is greatly delayed by starch; hence the reaction takes place to an appreciable extent. This points to the catalytic activity of colloidal silver. Although no quantitative measurements have been made, yet we have found qualitatively that protective colloids like agar agar and gelatin behave in the same way as starch.

Table 4 shows that protective colloids and colloidal silver can influence the reaction to a considerable extent. It also shows that with the increase of pH, the velocity constant has increased to a great extent but there is always a fall in the velocity constant after a certain time.

Tables 5 and 6 show, as usual, the increase in velocity constant with an increase in pH.

TABLE 5

Temperature.....	35°C.
pH.....	6
Resorcinol (10%).....	25 cc.
Silver acetate (<i>N</i> /17.75).....	25 cc.
Water.....	20.8 cc.
Sodium acetate (0.5 <i>N</i>).....	20 cc.
Acetic acid (0.1 <i>N</i>).....	4.2 cc.
Starch (1%).....	5 cc.

TIME	UNIMOLECULAR VELOCITY CONSTANTS
<i>minutes</i>	
0	
5	0.005272
10	0.012543
20	0.017691
40	0.013161
100	0.008902
200	0.006576
300	0.006303

TABLE 6

Temperature, 35°C.; pH, 7

TIME	UNIMOLECULAR VELOCITY CONSTANTS	
	Resorcinol (10%)..... 25 cc. Silver acetate (<i>N</i> /17.75) 25 cc. Acetic acid (0.1 <i>N</i>) 0.43 cc. Starch 5 cc. Sodium acetate (0.4 <i>N</i>) 25 cc. Water 20 cc.	Resorcinol (10%)..... 25 cc. Silver acetate (<i>N</i> /17.75) 25 cc. Acetic acid (0.1 <i>N</i>) 0.43 cc. Sodium acetate (0.4 <i>N</i>) 25 cc. Water 25 cc.
<i>minutes</i>		
0		
1½	0.0389538	
2		0.0129619
2½	0.0580120	
5	0.0526430	0.0125223
10	0.0325210	0.0219050
20	0.0333738	0.0191121
40	0.0244420	0.0103955
100	0.0152916	0.0063416

FALL IN VELOCITY CONSTANT

We notice that, in spite of using buffer solution, the values of the velocity constants go on falling after a certain time. Now this fall must be ascribed to a gradual precipitation of colloidal silver and not to a decrease in pH.

CONCLUSION AND DISCUSSION

From the foregoing it is apparent that the kinetics of reduction of silver acetate by resorcinol is influenced mainly by two factors: (a) the catalytic activity of colloidal silver and (b) the retarding influence of hydrogen ions. The true values of the velocity constants are masked by these influences.

Further, it appears that colloidal silver is almost absolutely indispensable in the pH range 3.72–4.99. At higher pH values the reaction can take place in the absence of starch but to a slightly lesser extent. These things point to the fact that the catalytic activity of silver is much more marked at a higher hydrogen-ion concentration.

In order to explain the fall in catalytic activity and the rate of fall of this activity even in the presence of buffer we propose the following mechanism of reaction: As soon as the reaction starts, fine particles of silver in the colloidal state are formed. These fine particles autocatalyze the reaction. But since silver acetate is an electrolyte, it neutralizes the electrical charge of the colloidal silver. This neutralization of charge is also brought about by sodium acetate, which is used in buffers. After being discharged these particles collide with one another and agglomeration begins, with consequent increase in the size of the particles. A particle of silver is able to exert catalytic activity only so long as it does not coalesce to become a larger one. As soon as the diameter of the particle increases, its catalytic activity becomes less.

The primary particles which exert catalytic action form doublets, triplets, etc., by virtue of Brownian motion. These doublets or triplets exert little or no catalytic activity. The rate of decrease of catalytic action will be proportional to the rate of decrease of primary particles, or

$$\frac{d(\text{catalysis})}{dt} = K \cdot \frac{dn}{dt}$$

where n represents the number of primary particles, say, in a unit volume. The rate of decrease of primary particles will depend upon the number of collisions that occur at any instant. The number of collisions in itself will be inversely proportional to the mean free path. The latter in its turn will depend on the number of particles present at any instant. Now in cases where the velocity of the reaction is very great or where colloidal silver has been added, the number of the particles present at any instant will be greater; hence in such cases the rate of fall of catalysis will be greater. We find, for example, that at pH 7 the value of the velocity constant is reduced to one-third or one-fourth of its highest value in about 100 min.

SUMMARY

1. The total order of the reaction between resorcinol and silver acetate is 2. The reaction is unimolecular with respect to each reactant separately.
2. The reaction is catalyzed positively by colloidal silver and negatively by hydrogen ions.

3. The fall in velocity constant is to be ascribed to a gradual precipitation of colloidal silver rather than a decrease in the pH.

4. Protective colloids like starch, agar agar, and gelatin, which stabilize colloidal silver, enhance the value of the velocity constant. In the pH range 3.72–4.99 the presence of a protective colloid is almost indispensable for the reaction to take place appreciably.

REFERENCES

- (1) CHAKARVARTI: Doctoral Thesis, Allahabad University, 1945.
- (2) JAMES: J. Am. Chem. Soc. **61**, 648 (1939).
- (3) JAMES: J. Phys. Chem. **45**, 223 (1941).
- (4) JAMES: J. Am. Chem. Soc. **61**, 2379 (1939).
- (5) JAMES: J. Chem. Phys. **10**, 464, 744 (1942).
- (6) JAMES: J. Am. Chem. Soc. **62**, 536, 1649, 1654 (1940).
- (7) KRISHNA AND GHOSH: Paper read at the joint session of Indian and National Academies of Sciences, India, December, 1946.
- (8) LIVINGSTON AND LINGANE: J. Chem. Education **15**, 320 (1938).
- (9) PALIT AND DHAR: J. Phys. Chem. **32**, 1663 (1928).
- (10) SHEPPARD: Phot. J. **59**, 135 (1919).

ELECTROPHORETIC MOBILITIES AND FRACTIONATION OF SODIUM PECTINATES

WILFRED H. WARD, HAROLD A. SWENSON, AND HARRY S. OWENS

Western Regional Research Laboratory¹, Albany, California

Received April 29, 1947

Experience has shown that decrease in esterification of pectinic acids decreases their apparent ionization constants (1, 4, 6). The interaction effect between carboxyl groups so indicated may manifest itself in other electrochemical properties of pectinic acids. For that reason, the electrophoretic mobilities and equivalent conductivities of various pectinic acids have been measured. Methods of fractionation according to degree of esterification have been studied and are presented here.

MATERIALS

The pectinic and pectic acids used in this investigation were prepared and analyzed according to procedures already published (see references 4 and references after table 1). Quantitative data of interest to this work are given in table 1.

Mobilities were measured in a Tiselius apparatus, using the optical system of Philpot (2) and Svensson (8). The temperature at which mobilities were

¹ Bureau of Agricultural and Industrial Chemistry, Agricultural Research Administration, U. S. Department of Agriculture.

measured was between 0.5° and 1.5°C. Values for the mobilities were calculated from measurements of the movement of the descending boundary and were referred to 0°C. by multiplying by the ratio of viscosity of water at the temperature of the measurement to the viscosity at 0°C. Cacodylate, acetate, or glycine buffers were used and were adjusted to an ionic strength of 0.1 with sodium chloride.

Conductivities were measured in a bridge circuit containing a 1000-cycle tuning-fork oscillator, an amplifier with filter, and an oscilloscope, in addition

TABLE 1
Analytical data on pectinic and pectic acids used in this investigation

SAMPLE IDENTIFICATION*	SOURCE	DEGREE OF ESTERIFICATION	URONIC ANHYDRIDE
		<i>per cent</i>	<i>per cent</i>
10.5.....	Citrus	71.3	83
7.8E.....	Citrus	54.5	82
7.4E.....	Citrus	52.5	81
5.5E.....	Citrus	38.4	81
4.4E.....	Citrus	31.2	80
0.2E.....	Citrus	1.5	80
10.1.....	Citrus	67.3	84
8.0B.....	Citrus	54	85
7.4B.....	Citrus	50	86
6.2B.....	Citrus	41.9	87
3.5B.....	Citrus	23.7	88
0.0B cold ..	Citrus	0.0	90
10.2.....	Apple	69.0	84
1.0A.....	Apple	6.6	92
14†.....	Citrus	93.3	84
15.2†.....	Citrus	96.8	90

* The number refers to the methoxyl content, the letter to the method of deesterification. A = acid (Hills, C. H., White, J. W., and Baker, G. L.: *Proc. Inst. Food Tech.* **1942**, 47). B = base (McCready, R. M., Owens, H. S., and Maclay, W. D.: *Food Ind.* **16**, 749 (1944)). E = enzyme (Owens, H. S., McCready, R. M., and Maclay, W. D.: *Ind. Eng. Chem.* **36**, 936 (1944)).

† Esterification with hydrogen chloride-methanol (Morell, S., Baur, L., and Link, K. P.: *J. Biol. Chem.* **105**, 1 (1934)). Samples supplied by J. F. Carson and by E. F. Jansen of this Laboratory.

to the usual resistors and capacitors. Cells were kept at 25°C. \pm 0.03° and the rest of the apparatus was at 25°C. \pm 0.5°. Precision of \pm 0.2 per cent was possible with solutions having specific conductances greater than 5×10^{-6} mhos cm.⁻¹ Corrections which were from 1.2 to 1.8×10^{-6} mhos cm.⁻¹ were made for the conductivity of the water used. For the conductivity measurements, 0.2 per cent solutions of pectinic acid were titrated to pH 6.7-6.8 with carbon dioxide-free sodium hydroxide solutions. Subsequent dilutions were made without further adjustment of pH. No corrections were made for the contribution to the conductivities of the resulting solutions made by the hydronium ion remaining unneutralized, because they were smaller than the number of significant figures carried in the calculations.

RESULTS

The effect of degree of esterification on the electrophoretic mobility of sodium pectinate is shown in figure 1. As expected, the mobility is inversely related to esterification. The relation is not the linear one suggested by Speiser and coworkers (7) and will be discussed later.

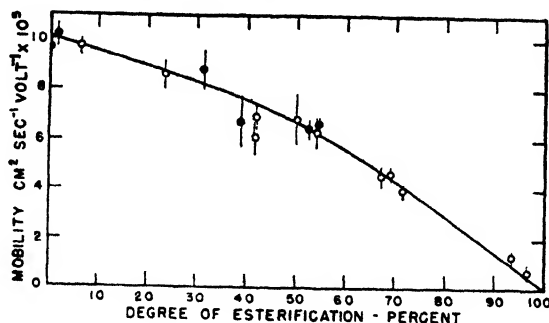


FIG. 1. Mobility *versus* degree of esterification of pectinic acids. Closed circles refer to enzymatically deesterified samples; open circles to remaining samples.

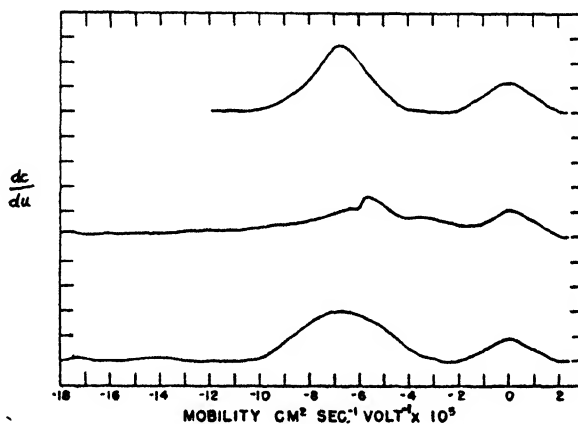


FIG. 2. Electrophoresis records for samples 7.4B at 10,400 sec. (top), 7.4E at 7000 sec. (middle), and 7.8E at 8000 sec. (bottom). The area defined by any pair of abscissas is an approximate measure of the fraction of the sample having mobilities between the chosen limits.

Figure 2 presents *quasi*-distribution diagrams derived by copying electrophoresis photographs to give corresponding scales for displacement of the boundaries (proportional to the mobilities) and equal areas under the curves. No corrections for diffusion have been applied, so that the spread is greater than for the true distribution. The diagrams indicate that deesterification by citrus pectinesterase acting *in situ* produced a more heterogeneous product with respect to degree of esterification than that produced by alkali. A similar difference exists between the action of tomato pectinesterase and that of acid (6, 7).

Some of the mobility curves obtained with the enzymatically deesterified products indicate that the major portion of pectinic acid deesterified by citrus pectinesterase contains less methoxyl than that corresponding to the peak in the electrophoretic diagram. This was tested by fractionation experiments, one of which is recorded here. Sample No. 4.4E was precipitated from a 1 per cent solution, using sodium chloride at a final concentration of 4 per cent. The filtrate was concentrated *in vacuo*; the first fraction was precipitated in acidified acetone, washed three times in acetone-water mixtures, and finally in acetone before drying *in vacuo*. The first precipitate from the salt solution, which contained some of the mother liquor, was suspended in water for 2 hr. and filtered. The filtrate was treated as before to produce fraction 2. The

TABLE 2
Fractionation of sample No. 4.4E according to methoxyl content

FRACTION NO.	METHOXYL	YIELD
	<i>per cent</i>	<i>per cent</i>
1.....	8.4	8
2.....	7.0	7
3.....	5.6	11
4.....	3.3	74

TABLE 3
Effect of pH on mobility of sample No. 8.0B

pH	BUFFER ($\mu = 0.1$)	MOBILITY
		$\text{cm.}^2 \text{ sec.}^{-1} \text{ volt}^{-1} \times 10^4$
6.10	Cacodylate	6.3
4.46	Acetate	6.5
3.80	Acetate	5.0
1.80	Glycine	0.0

whole operation was repeated to produce fraction 3. The residue was called fraction 4. The pertinent data are given in table 2, in which values for the yields were given a proportional correction so that the sum is 100 per cent. The uronic anhydride content remained at 80–82 per cent during the treatments. It is apparent that the bulk of the material has a methoxyl content below the average of 4.4 per cent.

Acid can also be used for fractionation or to increase the sharpness of the fractionation. For example, pectinic acid 5.9E was precipitated at pH 1.5 to yield 1 g. of material containing 9.5 per cent methoxyl and 11 g. containing 4.6 per cent methoxyl. Alternate treatments with acid and salt produced sample 7.8E. The electrophoretic diagram of 7.8E is shown in figure 2 and indicates it to be as homogeneous with respect to methoxyl as sample 7.4B. Fractionation of alkali-deesterified materials has failed to produce fractions differing in methoxyl content by more than 0.5 per cent.

A second interesting observation in figure 2 is the apparent presence of as

much as 10 per cent of migrating material having a mobility of from 10 to $18 \times 10^{-5} \text{ cm.}^2 \text{ sec.}^{-1} \text{ volt}^{-1}$. Since this might be attributed to the presence of some pure polyuronide, the mobility of a sample of alginic acid containing 98 per cent uronic anhydride was determined. Its mobility was $11.9 \times 10^{-5} \text{ cm.}^2 \text{ sec.}^{-1} \text{ volt}^{-1}$, indicating that the rapidly moving boundary was in most instances due to some other factor.

The effect of pH was measured with sample 8.0B, and the data are tabulated in table 3. The decrease in mobility with decrease in pH confirms the findings of S  verborn (3) and of Sookne and Harris (5), and is to be expected from the decreased ionization of pectinic acid.

Concentration changes in the range from 0.5 to 1.0 per cent had no influence on the mobility, showing that the viscosity of the solution had little effect. This is in agreement with the findings of S  verborn (3).

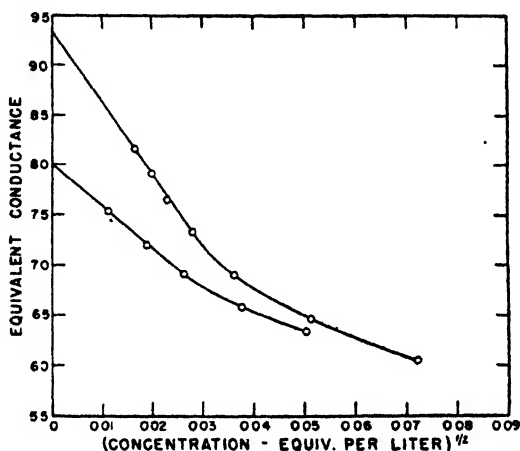


FIG. 3. Equivalent conductance as influenced by equivalent concentration. Top curve is for sodium pectate; bottom curve, sodium pectinate.

Equivalent conductivities of sodium pectinate and sodium pectate as a function of concentration are shown in figure 3. Decrease in degree of esterification increases equivalent conductance. If it is assumed that sodium ion has the same value for its limiting equivalent conductance in each salt solution, the mobility of the pectic ions can be calculated. The value for the pectinate ion is $31.1 \times 10^{-5} \text{ cm.}^2 \text{ sec.}^{-1} \text{ volt}^{-1}$, and for the pectate, $44.7 \times 10^{-5} \text{ cm.}^2 \text{ sec.}^{-1} \text{ volt}^{-1}$. These values are higher than those obtained in the Tiselius apparatus, because of absence of buffer and an increase in temperature to 25°C. The equivalent weights of these samples were 720 and 191, respectively, emphasizing the lack of linearity between mobilities and number of free carboxyl groups.

DISCUSSION

The lack of linear inverse relationship between degree of esterification (or methoxyl content) and mobility of pectinate ion in a buffer solution at pH 6 is unexpected. The concentration of salt should be sufficiently high to prevent

interaction effects between carboxyl groups. The presence of highly ionized sodium salts may tend, however, to decrease the ionization of sodium pectinate. Carboxyl groups on adjoining galacturonide groups are separated by no more than 4.3 Å., even less if orientation of the monomeric units is allowed for. A sodium ion between the groups may be restrained in its movements, and the cumulation of this effect extended over a large ion, like the pectate ion, may be significant. This results in a decrease of the charge on the pectate ion and a decrease in its mobility.

The distribution curve of pectinates of different methoxyl contents in an enzymatically deesterified sample shows that more than half of the material has a methoxyl content below the average and explains in part the difference in values of pH at half-neutralization previously noted for enzyme- and alkali-deesterified pectinic acids (4). The rest of the difference may result from localized, non-random removal of methoxyl groups, as postulated before.

The significance of non-random deesterification to the gelling properties of pectinic acids has been discussed elsewhere (4, 7). Two explanations may be advanced to account for the fast-moving boundaries observed in many instances. One is that the boundary represents a component of the pectinic acids investigated. However, the relatively low mobility of alginate ions makes doubtful the possibility of a pure polyuronide being the component. The presence of a sulfate or phosphate ester seems doubtful, especially after alkaline deesterification, when the rapid boundary also appears. A second possibility is that the boundary is a false one such as described by Svensson (9, 10), who demonstrated such false boundaries with systems analogous to ours with gum arabic, and buffers containing chloride and barbiturate or diethylbarbiturate. The false boundary had a mobility between those of the two buffer anions and approached that of the ion in smaller concentration. It could be suppressed by decreasing the colloid concentration or by increasing the buffer concentration. With pectinate solutions, the fast-moving apparent boundary was decreased by increasing the methoxyl content of the pectinic acid or by decreasing the pH of the buffer. Its mobility approaches that of cacodylate or acetate. The evidence indicates that the fastest-moving boundary is in these instances a false one and does not show the presence of an additional colloidal component.

SUMMARY

The electrophoretic mobility of pectinate ions in buffered solutions at 0°C. increases from near zero at 97 per cent esterification to near 10×10^{-5} cm.² sec.⁻¹ volt⁻¹ at 0 per cent esterification. The increase is not a simple inverse function of degree of esterification.

Mobilities in buffer-free solutions calculated from values for limiting equivalent conductances vary from 31.1 to 44.7×10^{-5} cm.² sec.⁻¹ volt⁻¹ at 25°C. as the equivalent weight is decreased from 720 to 191.

Pectinic acids deesterified *in situ* by citrus pectinesterase are more heterogeneous with respect to methoxyl content than those prepared with alkali *in vitro*.

Enzymatically deesterified pectinic acids were fractionated according to me-

thoxyl content by means of sodium chloride, acid, or a combination of sodium chloride and acid. The data for the fractionation obtained with one sample showed that the majority of the material contained less methoxyl than the average percentage of methoxyl determined for the sample.

REFERENCES

- (1) DEUEL, H.: *Mitt. Lebensm. Hyg.* **34**, No. 1/2, 41 (1943).
- (2) PHILPOT, J. S. L.: *Nature* **141**, 283 (1938).
- (3) SÄVERBORN, S.: Dissertation, Uppsala, 1945: "A contribution to the knowledge of the acid polyuronides" (112 pp.).
- (4) SCHULTZ, T. H., LOTZKAR, H., OWENS, H. S., AND MACLAY, W. D.: *J. Phys. Chem.* **49**, 554 (1945).
- (5) SOOKNE, A. M., AND HARRIS, M.: *J. Research Natl. Bur. Standards* **26**, 65 (1941).
- (6) SPEISER, R., HILLS, C. H., AND EDDY, C. R.: *J. Phys. Chem.* **49**, 328 (1945).
- (7) SPEISER, R., COPLEY, M. J., AND NUTTING, G. C.: *J. Phys. Chem.* **51**, 117 (1947).
- (8) SVENSSON, H.: *Kolloid-Z.* **90**, 141 (1940).
- (9) SVENSSON, H.: *Arkiv Kemi, Mineral. Geol.* **21B**, No. 5 (1946).
- (10) SVENSSON, H.: *Arkiv Kemi, Mineral. Geol.* **22A**, No. 10, 106 (1946).

THE EFFECTS OF TEMPERATURE UPON THE CRITICAL CONCENTRATIONS OF ANIONIC AND CATIONIC DETERGENTS¹H. B. KLEVENS²*Department of Chemistry, University of Chicago, Chicago, Illinois**Received January 2, 1947*

Recently a method involving the determination of the formation of micelles in soap and detergent solutions has been reported (2), based on the change of spectra of a cyanine dye as applied by Sheppard and Geddes (13) to gelatin sols and to a solution of a cationic soap, cetylpyridinium chloride. This method essentially depends on the fact that certain dyes have totally different spectra in polar and in non-polar solvents. Since dyes and oils are solubilized by soap solutions, and are presumably taken into the hydrocarbon atmosphere of the soap micelles (10), the results reported here involve the partition of the dye between the water and the soap micelles. The dye in the presence of soap micelles shows essentially the spectrum of the dye in a non-polar medium or the spectrum of the dye in its monomer form. It was noted that there was a change in the

¹ This is the outcome of some previously reported work released by the Office of Rubber Reserve, Reconstruction Finance Corporation, to which reference is made in the bibliography. This Office has been kind enough to read the manuscript before presentation for publication.

² Present address: Chemical and Physical Research Laboratories, Firestone Tire and Rubber Company, Akron, Ohio.

color of the dye-soap solution upon cooling from 0°C., the temperature at which the preliminary spectra had been determined, to about 18–19°C., i.e., room temperature. These color changes could have been due to a change in the form and constitution of the soap micelle caused by aging, during which hydrolysis could probably occur, or to a temperature dependence of the critical micelle concentration, or to a temperature dependence of the partition of the dye between the water and the soap micelles, or to a change in the aggregation of the dye. Storing of the samples for periods up to 24 hr. at 25°C. in the dark had little or no measurable effect on the spectra. It was later seen that this same change in color with temperature took place when sodium alkyl sulfonates, in which no hydrolysis occurs (8), were used. It was then decided that a more extensive study of the temperature effect would be necessary as a first step in the endeavor to explain this spectral change.

Since most aggregations of macromolecules such as proteins and polymers seem to be temperature dependent, it seemed strange that up to a few years ago most authors have stated that the phase change associated with micelle formation was independent of temperature. Ekwall (3), for example, had reported a single value of the critical micelle concentration (c.m.c.) from conductivity measurements for sodium laurate of 2.8×10^{-2} moles per liter from 17–70°C. and for sodium myristate of 7.0×10^{-3} moles per liter from 17–80°C. Wright, Abbott, Sivertz, and Tarter (17) recalculated Ekwall's data and by the use of specific conductance in place of equivalent conductance showed that there is a temperature effect for sodium myristate. They reported that the c.m.c. increased slightly with temperature from 6.8×10^{-3} at 35°C. to 8.2×10^{-3} *M* at 58°C. Similar plots of the specific conductance of sodium alkyl sulfonate solutions (17) showed a small but definite increase in the c.m.c. with temperature. Wright and Tartar (16) obtained the same temperature effects from density measurements. Bury and Parry (1) measured the c.m.c. of potassium laurate at 25°C. and 35°C. by observing density changes and concluded that the c.m.c. decreased with increasing temperatures.

The c.m.c.'s of three anionic soaps, potassium laurate, potassium myristate, and sodium decyl sulfate, were determined at various temperatures ranging from 15–55°C. by the use of the dye, pinacyanol chloride, and of one cationic soap by the use of acidified indophenol (7) as the dye in the temperature range from 25–55°C. Spectral measurements were made using the spectrophotometer described by Hogness, Zscheile, and Sidwell (4). The soaps were prepared from the corresponding esters, which had been very carefully fractionated, and were the same preparations used previously for the determination of critical micelle formation by the spectral method (2) and by refraction (5). Solutions were made up by weight with water which had been triply distilled and used immediately after final distillation.

A typical series of curves showing the change in spectra of the cyanine solutions upon addition of potassium laurate at 25°C. are shown in figure 1. For comparison, the spectra of the dye in water and in acetone are included. The molal extinction coefficient is here taken as $\log I_0/I$ per centimeter layer thick-

ness per mole per liter. According to Sheppard and coworkers (12), the 6100 Å. band is the molecular or monomer band which starts to appear in solutions of the dye, pinacyanol chloride, at concentrations below 1×10^{-6} molar. The intensity of this band decreases at higher dye concentrations, coupled with an

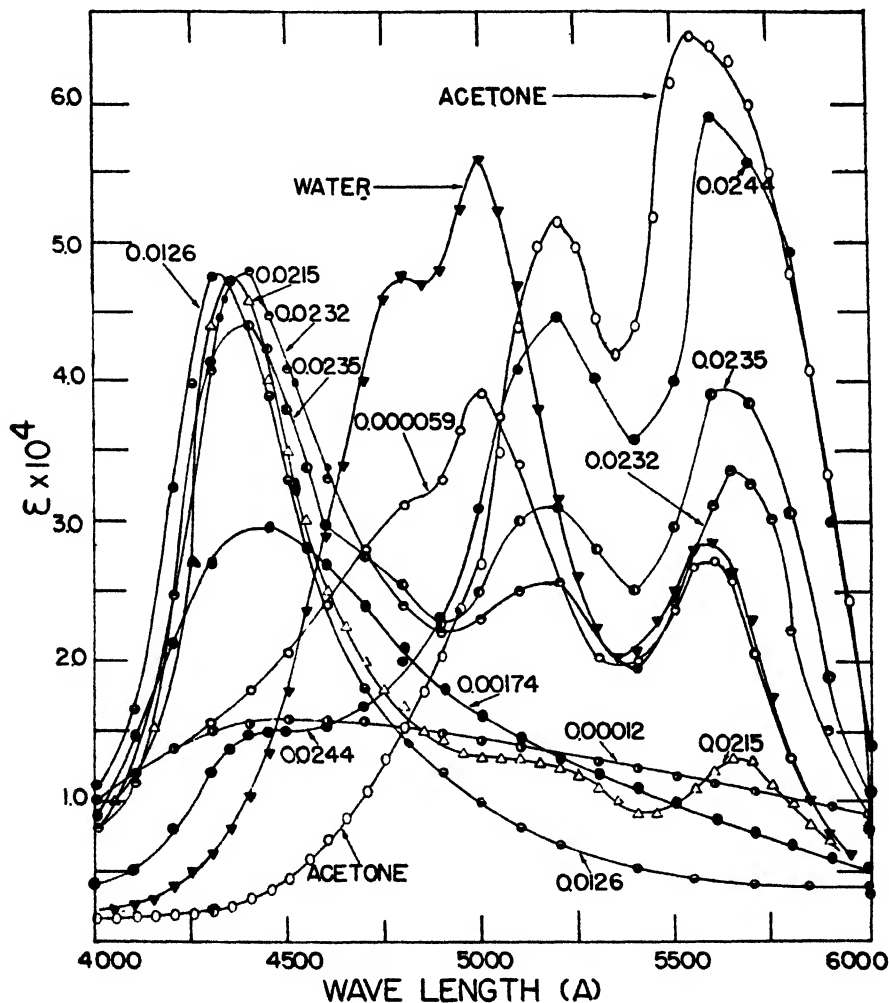


FIG. 1. Effect of the addition of various amounts of potassium laurate (KC_{12}) upon the spectra of pinacyanol chloride ($5 \times 10^{-5}M$, $25.6^{\circ}C.$). Concentration of KC_{12} is given in moles per liter.

increase in the 5400 Å. band, the one associated with the dimer or polymer form of the dye. Addition of small amounts of soap or detergent causes an initial decrease in intensity in both the 5400 Å. and the 6100 Å. bands. Further addition of soap—for example, a concentration of about 1×10^{-4} molar potassium laurate—causes an almost complete loss of intensity of these two bands. At

this concentration, the value of the extinction coefficient, ϵ , is almost independent of the wave length in the region between 4500 and 6000 Å., having however a very diffuse maximum between 4700 and 5500 Å. A new band starts to appear at 4800 Å. upon further addition of potassium laurate to about 2.3×10^{-2} molar. This band seems to be characteristic of detergent-dye solutions at soap concentrations below the c.m.c. It does not appear in dye solutions upon the addition of salt, acid, or base, and seems to be characteristic only of detergent-dye systems. Further evidence will have to be obtained before a definite statement can be made with regard to the type of structure in the detergent at con-

TABLE 1

The effect of potassium laurate on the intensity of band maxima of pinacyanol chloride (1×10^{-5} molar; 25°C.)

SOAP CONCENTRATION molarity	EXTINCTION COEFFICIENT, ϵ , $\left[\frac{\log I_0/I}{\text{cm. (moles/liter)}} \times 10^4 \right]$		
	α	β	γ
2.9×10^{-5}	2.63*	5.19	4.31
5.88×10^{-5}	2.33*	3.84	3.07*
1.22×10^{-4}	1.02*	1.28*	1.56
2.90×10^{-4}	1.03*	1.35*	1.99
1.74×10^{-3}	0.74*	1.27*	2.97
4.25×10^{-3}	0.31*	0.61*	4.27
1.262×10^{-2}	0.35*	0.69*	4.74
1.710×10^{-2}	0.65*	1.26*	4.16
1.930×10^{-2}	0.92	1.18*	3.89
2.225×10^{-2}	2.52	2.09	4.08
2.321×10^{-2}	3.27	2.50	4.72
2.350×10^{-2}	3.90	3.06	4.56
2.394×10^{-2}	5.61	3.94	1.87
2.436×10^{-2}	5.87	4.41	1.43*
2.478×10^{-2}	5.89	4.63	0.29*
4.154×10^{-2}	6.38	5.06	0.17*
2.088×10^{-1}	6.26	4.24	0.31*

* Not band maxima but intensities at wave lengths α , β , and γ .

centrations below the c.m.c. that causes the formation of this spectral band. However, the fact that this band appears at 4900 Å. in dye-saturated fatty acid soap systems, at 5300 Å. in dye-unsaturated fatty acid soap systems, and at both 4900 Å. and 5300 Å. in dye-sulfonate systems (8) seems to indicate that this absorption curve is characteristic of a soap-dye complex of the form $(S_m D_n)_z$, where S = soap and D = dye. In this possible complex, $m \gg n$ but m is not large enough to cause the formation of micelles. It is possible that this band is due to dye with a different aggregation number than the one associated with the 5400 Å. band or to a dye-soap complex.

Addition of more detergent causes a subsequent decrease in the 4800 Å. band, coupled with a simultaneous increase in the 5700 and 6100 Å. bands. This

change in intensity of these three bands has been utilized to show the phase changes associated with the formation of micelles at the critical micelle concentration. Further addition of detergent causes no further change in the position or the intensity of the maxima, and these latter spectra coincide within experimental accuracy with those obtained with the dye dissolved in a non-polar solvent. Figure 2(a) is a plot of the maxima of the various bands, termed α , β , and γ after Sheppard (13), in order of decreasing wave length and shows more strikingly the change in spectra associated with the dye going from a polar to a non-polar environment or from a polymer to a monomer form. These data are collected in table 1.

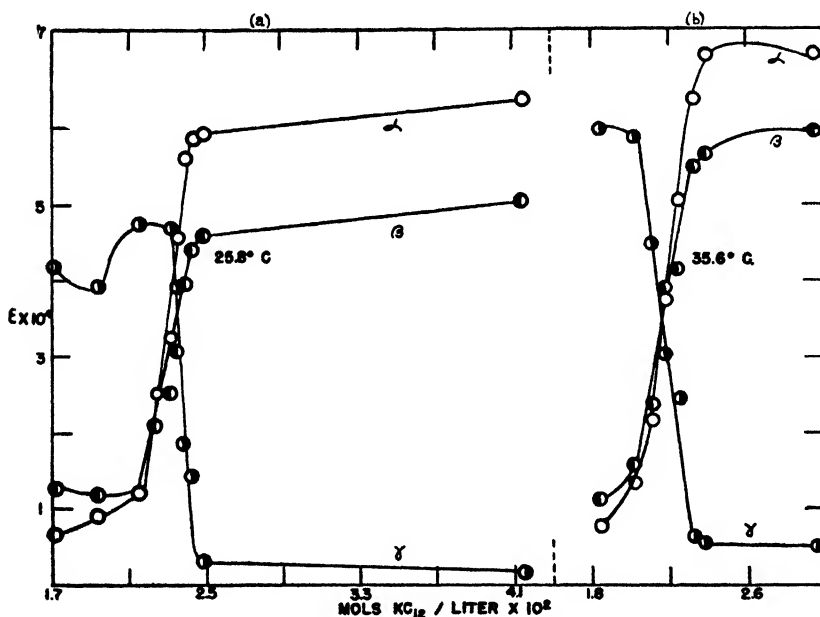


FIG. 2. The effect of the addition of potassium laurate (KC_{12}) upon the band maxima of pinacyanol chloride ($5 \times 10^{-5}M$) at various temperatures.

A choice of the c.m.c. is an arbitrary one and could be defined as the concentration at which the influence of the micelle formation on the dye spectra is first noted. This value would correspond to that concentration at which the 4800 Å. band starts to decrease in intensity, coupled with a simultaneous increase in the 5700 and 6100 Å. bands. Another c.m.c. might be chosen, i.e., that concentration beyond which the formation of additional or the increase in size of the existing micelles would have no further influence on the intensity of the dye. This concentration is the one at which the α and β bands reach maximum values and the γ band a minimum. A further value might be used which would correspond to an average of the other two mentioned above, and would approximately equal that at which the intensities of all three bands are equal.

TABLE 2

The effect of potassium laurate on the intensity of band maxima of pinacyanol chloride
(5×10^{-3} molar)

SOAP CONCENTRATION	EXTINCTION COEFFICIENT, ϵ , $\left[\frac{\log I_0/I}{\text{cm. (moles/liter)}} \times 10^4 \right]$		
	α	β	γ
35.6°C.			
molarity $\times 10^3$			
1.847	0.76	1.13	6.00
2.019	1.35	1.59	5.88
2.109	2.68	2.37	4.49
2.197	3.80	3.04	3.91
2.247	5.06	4.15	2.45
2.329	6.41	5.52	0.65
2.395	7.10	5.72	0.54
2.960	7.00	6.00	0.50
45°C.			
1.885	0.95	2.09	5.21
1.952	0.71	1.64	5.78
2.010	0.70	1.28	5.64
2.046	1.50	1.66	4.63
2.145	4.29	4.03	2.40
2.155	6.65	5.50	0.50
2.245	6.75	5.63	0.45
2.280	6.83	5.77	0.30
55°C.			
1.981	1.76	1.67	2.63
2.000	1.98	2.06	2.66
2.010	2.24	2.03	2.58
2.040	2.14	1.77	2.75
2.055	2.15	1.74	2.80
2.108	3.05	2.45	2.25
2.142	3.77	2.69	1.73
2.202	5.23	3.95	0.35
2.231	5.33	3.97	0.14
15°C.			
2.142	0.43	0.83	5.93
2.179	0.56	0.78	6.24
2.229	0.59	0.94	6.33
2.248	0.72	1.03	6.32
2.271	1.51	1.69	5.65
2.373	4.62	4.43	2.43
2.422	6.68	5.83	0.85
2.445	7.37	6.41	0.20
2.534	7.41	6.46	0.14

In the various tables presented here, the c.m.c. are those covering the entire range from the minimum to the maximum values of the α , β , and γ bands.

The values for the α , β , and γ bands for the pinacyanol chloride-potassium laurate system at 35°C. are plotted in figure 2(b) and tabulated in table 2; those for 45°C., 55°C., and 15°C. are shown in figures 3(a), 3(b), and 3(c) and in table 2. Similar data for potassium myristate are presented in table 3.

The effect of temperature on the c.m.c., as determined by the spectral change of pinacyanol chloride in solutions of potassium laurate from 15–55°C. and in solutions of potassium myristate and sodium decyl sulfate from 25–55°C., is shown in table 4. Included also are the data for the laurylamine hydro-

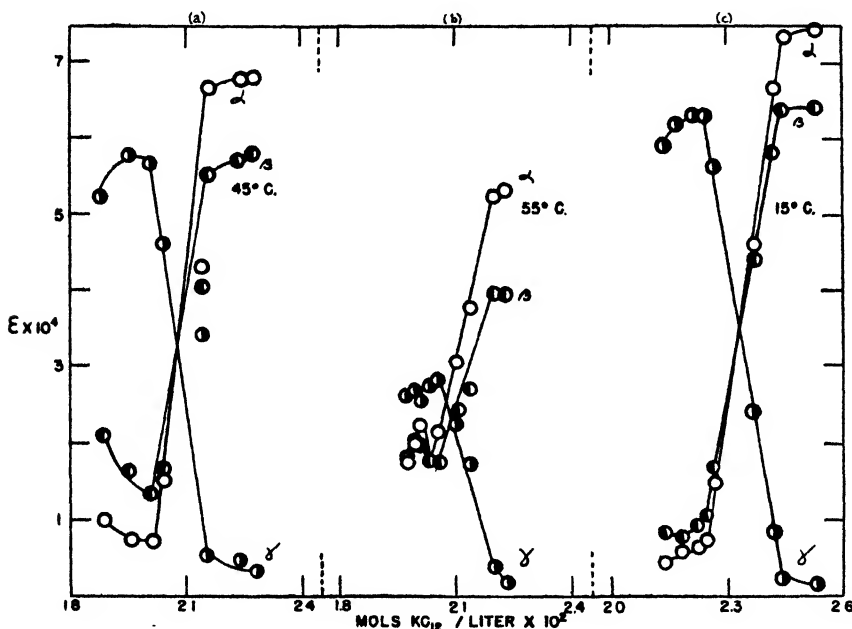


FIG. 3. The effect of the addition of potassium laurate (KC_{12}) upon the band maxima of pinacyanol chloride ($5 \times 10^{-5}M$) at various temperatures.

chloride-indophenol system from 25–55°C. If there were no change in the partition of the dye between water and the soap micelles, or if there were no change in the dye aggregation number, then it could be said that there is a small but definite decrease in the value of the c.m.c. of these soaps and detergents with increase in temperature from 15–55°C. This statement does not agree with the results on the temperature effect obtained by Tartar and his coworkers (17) nor with those obtained by Ralston and Hoerr (11). It then follows that the observed change with temperature must involve not an actual change in the c.m.c. but rather a change in the partition of the dye or the aggregation number of the dye. It has been shown that the equilibrium molecular form \rightleftharpoons dimer of the dye pinacyanol chloride is temperature dependent, proceeding toward

TABLE 3

The effect of potassium myristate on the intensity of band maxima of pinacyanol chloride
(5×10^{-5} molar)

SOAP CONCENTRATION	EXTINCTION COEFFICIENT, ϵ , $\left[\frac{\log I_0/I}{\text{cm. (moles/liter)}} \times 10^4 \right]$		
	α	β	γ

25°C.			
<i>molarity</i> $\times 10^3$			
5.312	0.96	1.13	6.74
5.821	1.62	1.63	6.68
6.020	1.66	1.85	7.25
6.314	4.21	3.80	3.70
6.651	7.02	6.55	1.19
10.483	6.94	6.43	0.59

35.6°C.			
4.240	0.66	1.07	6.48
5.164	1.56	1.57	5.52
5.392	1.31	1.53	6.15
5.605	2.58	2.32	5.55
5.732	3.50	2.88	4.34
6.046	6.04	4.83	2.54
6.621	6.90	6.10	0.56
6.854	6.88	6.11	0.56
7.505	6.85	6.26	0.58

45°C.			
5.022	0.85	1.08	3.76
5.328	1.21	1.60	4.55
5.411	1.74	1.93	4.69
5.430	2.48	2.42	3.34
5.550	4.75	4.05	1.55
5.644	6.83	5.24	0.40
6.080	6.12	5.07	0.23

55°C.			
4.798	0.54	0.77	3.58
5.022	0.77	1.11	4.06
5.332	1.30	1.49	3.52
5.414	1.30	1.50	3.05
5.475	1.46	1.64	2.33
5.616	3.13	2.33	1.60
5.715	5.08	4.00	0.75
6.016	5.26	4.09	0.25

the molecular form with increase in temperature. This would involve a slight increase in the intensity of the 6100 A. band in water solution of the dye, coupled with a corresponding decrease in the intensity of the 5400 A. band, as seen in

figure 4. If there were no change in the partition of the dye between the soap micelle and the water, a similar change could be expected in the soap-dye system with increase in temperature.

TABLE 4

Effect of temperature on the critical micelle concentration, as shown by changes in pinacyanol chloride and in acidified indophenol spectra
(5×10^{-4} molar)

TEMPERATURE °C.	C.M.C. IN MOLES PER LITER $\times 10^3$			
	KC ₁₂	KC ₁₄	NaC ₁₂ sulfate	C ₁₂ amine hydrochloride
15.0	2.25-2.45			
25.6	2.15-2.35	0.60-0.67	0.50-0.57	1.29-1.33
35.8	2.05-2.20	0.54-0.60	0.47-0.52	1.22-1.27
45.0	2.00-2.15	0.53-0.57	0.44-0.48	1.18-1.24
55.0	2.00-2.15	0.53-0.57	0.43-0.47	1.17-1.22

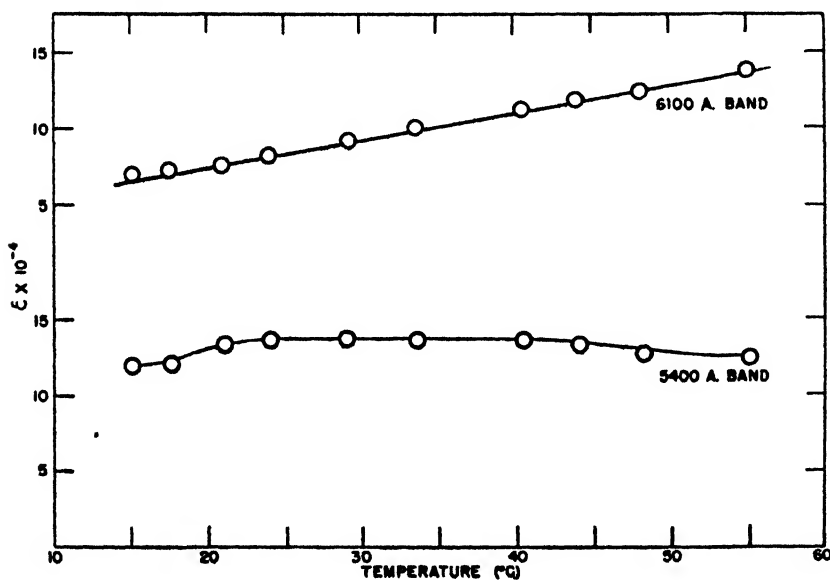


FIG. 4. Change in monomer \rightleftharpoons polymer equilibrium of pinacyanol chloride with temperature, as shown by variations in band maxima.

The formation of aggregates of soap molecules or micelles is accompanied by an increase in the ionic strength of the soap solution and is the explanation which has been advanced (8) for the appearance of the monomer form of the dye, pinacyanol chloride, when micelles are formed in the soap-dye system. This increase in the ionic strength is, of course, dependent on the type of micelle that one assumes, for it is a function of the excess surface charges. From numerous

conductivity data of soap solutions at concentrations above the c.m.c. one must assume that in the case of a micelle the ratio of the surface charges of one sign to the effective charges of opposite sign in the immediate vicinity of the highly charged micelle must be larger than a similar ratio found in soap molecules below the c.m.c.

As shown in figure 4, an increase in temperature will cause a shift dimer \rightarrow molecular form in the soap-free dye system, due to thermal agitation set up within the dye aggregate. This latter explanation would seem at the present time to be the most logical one to explain the observed changes in the c.m.c. with temperature, as determined by the dye method. There are not now sufficient data on the partition of the dye between water and the soap micelles to enable one to endeavor to use the idea of partition to explain these observed phenomena.

TABLE 5

Critical concentrations (moles per liter) for the formation of micelles in sodium alkyl sulfonate solutions as determined by various methods

	SOLUBILITY-TEMPERATURE*	CONDUCTIVITY* (60°C.)	REFRACTION	DYE METHOD
C ₈			1.5-1.55 $\times 10^{-1}$ (25°C.)	1.4-1.5 $\times 10^{-1}$ (25°C.)
C ₁₀	4 $\times 10^{-3}$ (22.5°C.)	4.3 $\times 10^{-3}$	4.1-4.3 $\times 10^{-3}$ (25°C.)	3.7-3.9 $\times 10^{-3}$ (25°C.)
C ₁₂	9.8 $\times 10^{-3}$ (31.5°C.)	1.2 $\times 10^{-3}$	1.0-1.1 $\times 10^{-3}$ (35°C.)	8.8-9.5 $\times 10^{-3}$ (33.5°C.)
C ₁₄	2.7 $\times 10^{-3}$ (39.5°C.)	3.3 $\times 10^{-3}$	3.1-3.2 $\times 10^{-3}$ (45°C.)	2.35-2.6 $\times 10^{-3}$ (42.5°C.)
C ₁₆	1.05 $\times 10^{-3}$ (47.5°C.)		1.1-1.2 $\times 10^{-3}$ (52°C.)	7.5-8.5 $\times 10^{-4}$ (50°C.)

* H. V. Tartar and coworkers.

The determination of the c.m.c. by conductivity and by the use of the spectral changes in dye solutions involves the use of external effects which may have some influence on the c.m.c. The application of a small amount of current in the measurement of conductivity may cause a distortion in the shape or a change in the size of a micelle. Measurement of the c.m.c. by the use of various dyes at all times yields values which are smaller than those determined by other methods (8),—for example, by refraction (5), which involves no external effect on micelle formation. The dye method seems to yield results which are similar to those determined when hydrocarbons are added to soap solutions. In these experiments (9) the c.m.c.'s of various soaps and detergents were found to decrease slightly with increment addition of hydrocarbons.

Just as no correlation could be obtained between experimental observations and dielectric constant changes upon the addition of various solvents to soap solutions (15), none can be determined between the experimental results reported here and changes in the dielectric constant of water with temperature. As

Ward has mentioned, the dielectric environment in the region of the polar groups of the soap and detergent molecules in the micelle are important determinants of micelle formation. Since these effects cannot be measured from available data, nothing as to the dielectric effects on the c.m.c. can be determined at present.

In the various determinations of changes observed in the c.m.c. of soaps and detergents by conductimetric measurements, no observable correction has been made for the changes in viscosity which occur with increase in temperature. It is possible that when these corrections are applied, it may be found that the reported increase in the c.m.c. with increase in temperature is not real, and that the true value of the c.m.c. may be temperature independent.

The method used here to determine the c.m.c. has been found to have many useful applications in research and in manufacturing processes, because of the ease and rapidity of the technique. Measurements could be and have been made by titration instead of by spectroscopy. These measurements can be made in a few minutes with a reproducibility within 3 per cent. Some typical applications of this method are (a) the determination of residual detergent in diet mixtures, (b) the rapid measure of the amount of detergent taken up by various fibers in dipping, and (c) the determination of surface areas and particle size and number of various pigments and synthetic latices (6).

These measurements must in certain cases be made at temperatures above room temperature and care must be taken to use the correct value of the c.m.c. Table 5, taken from work reported recently (8), shows the variations in the c.m.c. of some sodium alkyl sulfonates as determined by conductivity (17), by solubility-temperature (14), by refraction (5), and by the dye method. It can be seen that the data diverge more as the temperature at which the measurements are made increases. This seems to be another indication that the observed changes in the c.m.c. with temperature as determined by the dye technique are not characteristic of changes in soap micelles but rather of changes in dye aggregates.

SUMMARY

Increase in temperature causes an apparent decrease in the critical micelle concentrations (c.m.c.) of soaps and detergents, as determined by spectral changes in various dyes. This apparent decrease in the c.m.c. seems not to be a function of micelle formation but rather due to changes in dye aggregation. Reported values of the c.m.c. as determined by the dye method are at all times found to be smaller than those determined by either conductivity or refraction. The application of a titration technique in place of spectroscopic measurements permits rapid determinations of the c.m.c.

REFERENCES

- (1) BURY, C. R., AND PARRY, G. A.: *J. Chem. Soc.* **1935**, 626.
- (2) CORRIN, M. L., KLEVEN, H. B., AND HARKINS, W. D.: *J. Chem. Phys.* **14**, 216, 480 (1946).
- (3) EKWALL, P.: *Kolloid-Z.* **101**, 135 (1942); *Z. physik. Chem.* **161A**, 195 (1932).

- (4) HOGNESS, T. R., ZSCHEILE, F. P., JR., AND SIDWELL, A. E., JR.: *J. Phys. Chem.* **41**, 379 (1937).
- (5) KLEVENS, H. B.: *J. Chem. Phys.* **14**, 567 (1946).
- (6) KLEVENS, H. B.: *J. Colloid Sci.* **2**, 365 (1947).
- (7) KLEVENS, H. B.: *J. Am. Chem. Soc.* **69** (1947), in press.
- (8) KLEVENS, H. B.: Paper presented before the Division of Colloid Chemistry at the 110th Meeting of the American Chemical Society, Chicago, Illinois, September 9-13, 1946.
- (9) LINGAFELTER, E. C., WHEELER, O. L., AND TARTAR, H. V.: *J. Am. Chem. Soc.* **68**, 1490 (1946).
- KLEVENS, H. B.: Unpublished data.
- (10) See, for example, McBAIN, J. W.: In E. O. Kraemer's *Advances in Colloid Science*, Vol. 1, p. 99. Interscience Publishers, Inc., New York (1942).
- (11) RALSTON, A. W., AND HOERR, C. W.: *J. Am. Chem. Soc.* **64**, 772 (1942).
- (12) SHEPPARD, S. E.: *Rev. Modern Phys.* **14**, 303 (1942).
- (13) SHEPPARD, S. E., AND GEDDES, A. L.: *J. Chem. Phys.* **13**, 63 (1945).
- (14) TARTAR, H. V., AND WRIGHT, K. A.: *J. Am. Chem. Soc.* **61**, 539 (1939).
- (15) WARD, A. F. H.: *Proc. Roy. Soc. (London)* **A176**, 412 (1940).
- RALSTON, A. W., AND HOERR, C. W.: *J. Am. Chem. Soc.* **68**, 851 (1946).
- (16) WRIGHT, K. A., AND TARTAR, H. V.: *J. Am. Chem. Soc.* **61**, 544 (1939).
- (17) WRIGHT, K. A., ABBOTT, A. D., SIVERTZ, V., AND TARTAR, H. V.: *J. Am. Chem. Soc.* **61**, 549 (1939).

ADSORPTION ISOTHERMS OF MIXED VAPORS OF CARBON TETRACHLORIDE AND METHANOL ON ACTIVATED CHARCOAL AT 25°C.¹

W. B. INNES² AND H. H. ROWLEY³

Division of Physical Chemistry, State University of Iowa, Iowa City, Iowa

Received March 6, 1946

Measurements of the adsorption of mixed vapors, though of much practical importance, have been very few. These include the work of Bakr and King (1), Richardson and Woodhouse (11), and Klosky and Woo (8).

Adsorption data obtained in cases where the compositions of both the adsorbate and the vapor in equilibrium with it are not known are difficult to interpret and reproduce. For this reason, the apparatus used for this work was designed so that the composition of the adsorbed phase could be known and kept practically constant throughout the isotherm and the composition of the vapor phase in equilibrium with the adsorbate determined.

¹ This article is based upon a thesis submitted by W. B. Innes to the Faculty of the Graduate School of the State University of Iowa in partial fulfillment of the requirements for the degree of Doctor of Philosophy, August, 1941.

² Present address: Stamford Research Laboratories, American Cyanamid Company, Stamford, Connecticut.

³ Present address: Department of Chemistry, University of Oklahoma, Norman, Oklahoma.

MATERIALS

The charcoal used for this work was 12-20 mesh steam-activated unpurified cocoanut charcoal obtained from the National Carbon Company of Nela Park, Ohio. A fresh sample was employed for each isotherm, since carbon tetrachloride adsorbed on charcoal tends to decompose and "poison" the charcoal at the temperature employed for outgassing (525°C.). The average ash content of the individual 1-2 g. samples of charcoal used for the measurements was 6.8 per cent, with an average deviation of 1.5 per cent.⁴ The ash analyzed about 80 per cent siliceous material and 20 per cent oxides and chlorides of sodium, potassium, and calcium. The variations in ash content can be attributed to coarse pieces of siliceous material. The loss of weight on outgassing of the charcoal was found to be 14 per cent. The charcoal weights were corrected for this loss.

The absolute methanol used was a synthetically made product of a high degree of purity obtained from the Commercial Solvents Corporation. It was further purified by drying with sodium and by fractional distillation. The final product (a middle fraction) distilled over a 0.05°C. range and had a refractive index at 25.0°C. of 1.3266.

The carbon tetrachloride (Mallinckrodt analytical grade) was further purified by repeated fractional distillation. The final product (a middle fraction) distilled over a 0.08°C. range and had a refractive index at 25.0°C. of 1.4572.

PROCEDURE

The measurement of an isotherm was carried out in the following manner, referring to figure 1: A relatively large amount of liquid mixture of known composition was introduced into the liquid reservoir by means of tube 8. Considerable excess over the amount actually adsorbed was used, so that the change in composition of the liquid in the reservoir was negligible during an experiment. After sealing off tube 8, the dissolved air was removed by repeated freezing and evacuation and by distillation between tubes 6a and 6b in conjunction with evacuation. The modified McLeod gauge, 1, was employed to test for the presence of air. This was done by compressing a sample of vapor in equilibrium with the liquid which was at approximately room temperature. If the vapor was completely liquefied on compression, the liquid was deemed to be free of air. After the removal of the air the stopcock 7 was closed, and the tube containing the adsorbent, 3, was sealed on to the apparatus. The adsorbent was then outgassed by evacuation at $525^{\circ} \pm 20^{\circ}\text{C.}$ until the McLeod gauge, 1, gave a pressure of 2×10^{-4} mm. of mercury or less.

The introduction of the vapor into the adsorption tube was accomplished by first opening stopcock 7, and allowing the liquid at 20°C. to equilibrate with its

⁴ The use of a charcoal with such high ash content was not originally intended but came about as a result of mistaken identity, which was only discovered after this work was well under way. Time did not permit a repetition of the experiments with a purer charcoal, although a subsequent study carried out by Mr. R. B. Olney deals with the system benzene-methanol on ash-free charcoal.

vapor phase in the vapor reservoir, 4,⁵ at the air-bath temperature (25°C.). The temperature of the liquid reservoir, 6, was maintained at $20^\circ \pm 0.3^\circ\text{C}$. by immersion in a large vacuum bottle containing water at this temperature. The

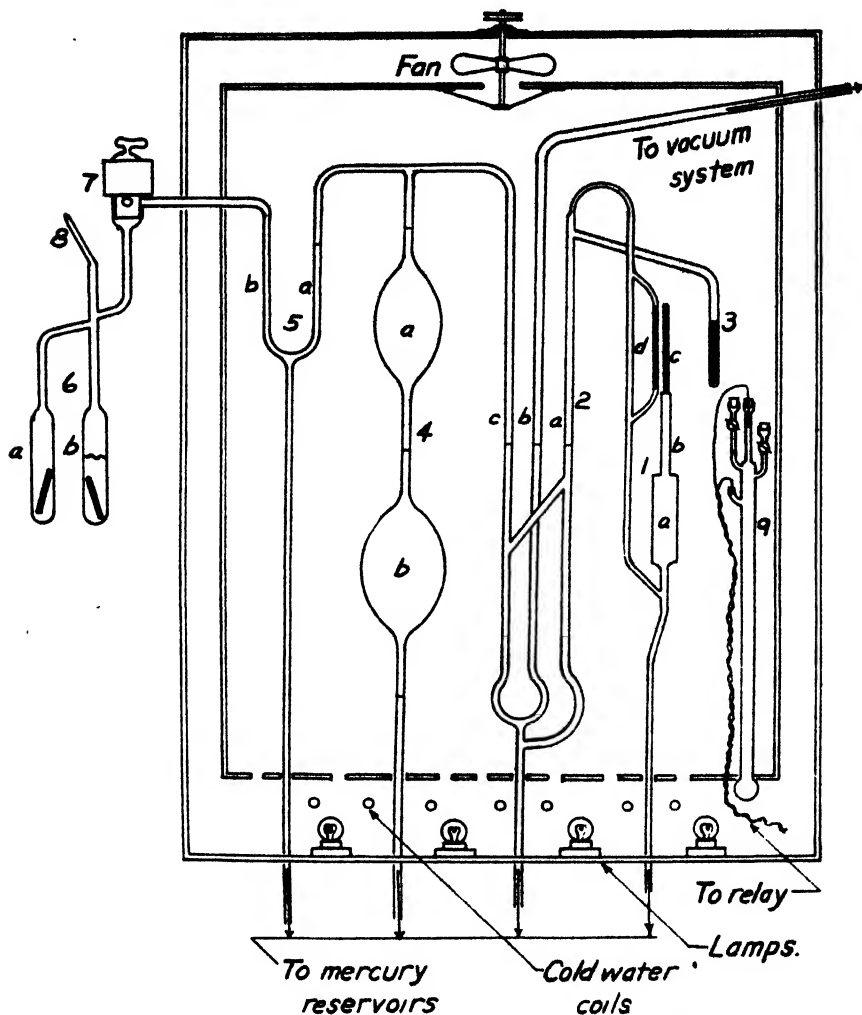


FIG. 1. Schematic diagram of apparatus. 1(a, b, c), McLeod gauge; 2(a, b, c), dead space and connecting tubing; 3, adsorbent tube; 4(a, b), vapor reservoirs; 5(a, b), U tube; 6(a, b), liquid reservoirs; 7, stopcock with mercury seal; 8, tube to admit liquid; 9, mercury thermoregulator.

mercury in the vapor reservoir, 4, was placed at a point corresponding to the amount of vapor to be introduced into the adsorption tube, 3. After equi-

⁵ The composition of the vapor corresponding to a known composition of liquid at 20°C . for the system employed was known from other work (4). However, the vapor composition could also be determined by measurement of the weight of adsorbate after the completion of a run, since the number of moles of adsorbate was known.

librium between liquid and vapor had been established, the mercury in the cut-off 5 was raised and the levels of the mercury in 5, 4, and 2c adjusted to fixed marks, thus confining the vapor sample in a known fixed volume. Since 2b was connected to the vacuum system, the pressure⁶ of the sample in the vapor reservoir, 4, could be determined by measuring the difference between the mercury levels 2c and 2b. For determining mercury levels a cathetometer capable of reading to 0.005 cm. was employed. Since the volume of the vapor reservoir when the levels were at the mark was known from a previous calibration and the pressure had been determined, the number of moles of gas present in the reservoir could be calculated if the perfect gas law was assumed.

To transfer this vapor completely to the adsorbent, the mercury in 2 was lowered until the mercury in c was below the connection piece between c and a. All the vapor, except for negligible amounts in the connecting tubes, was then forced out of the vapor reservoir by displacing it with mercury and immersing the charcoal tube 3 in a carbon dioxide snow-acetone mixture. After completion of this operation the mercury in 2 was raised, the carbon dioxide snow-acetone mixture removed, and the system allowed to equilibrate at bath temperature (25°C.), with the adsorption section open to the modified McLeod gauge. When equilibrium conditions had been reached the pressure in the adsorption chamber was read by measuring the difference between levels 2b and 2a, the levels 2a and 1 being at fixed marks so that the volume of dead space was known. The modified McLeod gauge was employed for measuring pressures less than about 0.100 cm. of mercury.⁷

The amount of dead space was such that the quantity of vapor in the adsorption section was small compared with the amount of material adsorbed on 2 g. of charcoal, varying from 0 to 4 per cent as the equilibrium pressure increased. Hence, except for the last part of the isotherm, it was a good approximation to say that the composition of the adsorbate was the same as that of the introduced vapor. Even at higher pressures of the isotherm this would be a fairly good approximation. If the volume of the dead space, its composition, and the amount of vapor introduced are known, the exact composition of the adsorbate can be calculated if desired.

To determine the composition of the vapor in the dead space the modified McLeod gauge, 1, was employed. The volume in the gauge was a known function of the height of the mercury levels in 1a, 1b, and 1c, and by measuring the heights of the mercury levels in 1a, 1b, 1c, and 1d (making necessary corrections) the pressure of the vapor in the gauge could be determined if the pressure in the adsorption chamber was known. By making a series of measurements and plotting *pv* versus *p* a break was obtained at the condensation pressure which is illus-

⁶ This was purposely kept considerably below saturation in order to avoid appreciable adsorption on the walls or deviation from Boyle's law.

⁷ Though the pressure of a condensable vapor was being measured this procedure was justified, because the pressure in the McLeod gauge during these measurements was considerably less than saturation pressure and compression experiments showed Boyle's law to be obeyed in this range. Adsorption measurements on powdered glass showed that adsorption on the glass walls of the apparatus could be neglected except, possibly, at pressures close to saturation.

trated by the plot in figure 2. A further aid in the determination of the condensation point was the appearance of liquid between the glass walls and the mercury. Since the condensation pressure as a function of the composition of the vapor was known, or could be determined in conjunction with the adsorption experiments, the composition of the vapor could be found if the condensation pressure was known. The composition of the vapor and the total pressures being known, the partial pressures could be calculated if all vapors were assumed to be perfect.

To obtain further points on the adsorption isotherm the process described above was repeated until condensation of the vapor in the vapor phase above the adsorbent was approached. The condensation pressure at this stage makes it possible to determine the composition of both the liquid and the vapor phases that would be in equilibrium with adsorbate of known composition.

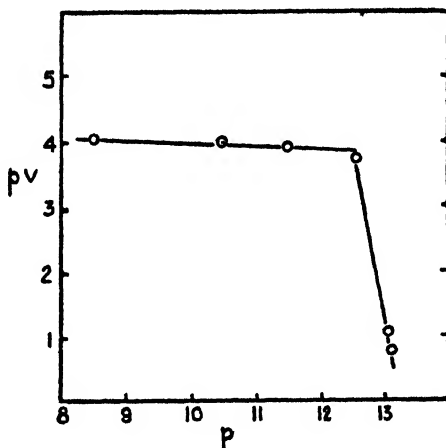


FIG. 2. Illustrative plot used in evaluating condensation pressures

PRECAUTIONS AND SOURCES OF ERROR

In the measurement of the very low pressure range of adsorption isotherms and in the determination of the condensation pressure the principal source of error was due to the presence of small quantities of inert gas, which may be introduced with the vapor if the liquid has not been previously thoroughly outgassed. Also some inert gas may be displaced from the adsorbent (10). This inert gas is not appreciably adsorbed and concentrates in the dead space of the adsorbent section, where it contributes to the total pressure.

The presence of extremely small amounts of inert gas during a run could be conveniently tested for with this apparatus by use of the modified McLeod gauge, as described above. Tests of this nature revealed that, despite the thorough outgassing treatment of the liquid and the adsorbent, very small amounts of inert gas did appear in the dead space. The amount (estimated to be 0.2 cc. at N.T.P. for a complete run) was small enough to affect the percentage accuracy appreciably only at the lower pressures, but was large enough to affect slightly

the value of the condensation pressure obtained over a large part of the pressure range.

In order to get rid of the inert gas, whenever it was thought desirable, advantage was taken of the great difference in the adsorbability of the vapor and of the inert gas. That is, the system was evacuated at a pressure too low^a and for too short a time to permit removal of more than a negligible amount of the vapor, but long enough to effect removal of almost all of the inert gas.

The reproducibility of measurements of the condensation pressure, p_c , was ± 1.0 mm. of mercury, but owing to capillary effects larger errors than this may occasionally have been present. A capillary correction of 0.5 cm. was used when levels were read between tubes 1c and 1d and 0.05 cm. when levels were read between 1b and 1a of figure 1. However, over most of the range the pressures were read by differences in mercury levels in tubing having the same diameter and no correction was applied. The bath temperature was closely watched during these measurements, as the temperature coefficient of p_c is about 1 mm. per 0.1°C . An accuracy in p_c of 1 mm. corresponds to an accuracy of about 0.006 in the mole fraction of the vapor, as can be seen from figure 4. The percentage accuracy of the methanol partial pressures was almost as good as for the total pressures, as in most cases the vapor phase was composed almost entirely of methanol. However, the same cannot be said for the carbon tetrachloride partial pressures because of this reason.

Measurements of the low-pressure range with the McLeod gauge are subject to capillary errors and to deviations from Boyle's law. However, compression measurements showed Boyle's law to be obeyed for the pressures measured. The values obtained were quite reproducible and are believed to be accurate to within 1 per cent except for pressures less than 10^{-3} cm., where the percentage accuracy is somewhat less.

Pressure measurements involving the high-pressure range are estimated to have an accuracy of ± 0.010 cm. of mercury, except near saturation pressures where temperature effects are important.

The reproducibility of the ϕ values (see figure 12) was not all that could be desired in some cases. This was probably due in part to the variation in the ash content of the different samples. Another effect that might arise owing to the ash content might be chemical action between the ash and the adsorbate. However, it is not believed that methanol or carbon tetrachloride will react appreciably with the components of the ash. Another possible effect is a slight lowering of the vapor pressure near the saturation point, owing to the slight solubility of the ash components in alcohol.

In these measurements, pressure equilibria, as evidenced by no measurable change over an hour or more of time, were found to be reached within 1 or 2 hr. in most cases, though occasionally 6 hr. were necessary. However, in a few instances changes in the condensation pressure were observed to occur after pressure equilibrium had been reached. Ample time is believed to have been

^a The pressure was controlled by controlling the temperature of the adsorbent.

allotted for a close approach to both pressure and composition equilibrium in all data reported here. Tests made over periods as long as 24 hr. showed no measurable changes in pressure or composition after it had previously been judged that equilibrium had been reached.⁹ Equilibria appeared to be reached in an even shorter time for the pure components, as might be expected. The speed of its attainment was probably increased by the fact that equilibrium was approached from the desorption side as the charcoal was cooled during each introduction of vapor.

The measuring part of the apparatus has no stopcocks and is isolated from stopcock 7 by the cutoff 5. Hence, absorption of the vapors by grease would not be expected to affect determination of the adsorption equilibrium pressure. Vapor absorption by the grease from stopcock 7 would not be expected to affect vapor-pressure measurements, or the composition of introduced vapor, because of the relatively large amount of liquid used. Nevertheless, care was taken to avoid any excess grease and to keep the liquid about 5° or more below the temperature of the stopcock, in order to avoid excessive absorption of the vapors by the grease.

Another possible source of error was non-attainment of equilibrium between liquid and vapor phases. The apparatus was especially designed to minimize error on this score. That is, stopcock 7 (figure 1) was large enough to have no constrictive effect and the connecting tubing between 6 and 5, which was as short as possible, had a minimum diameter of 0.8 cm. Pressure equilibrium within experimental error was observed to be attained in 20 min. or less, but 30 min. was the minimum time allowed before closing off the vapor reservoir from the liquid. As it appears in this case impossible to realize pressure equilibrium without composition equilibrium, this source of error is not believed to have been important.

VAPOR-PRESSURE MEASUREMENTS

The adsorption measurements offered an opportunity for determining vapor pressures as well. This was done in order to check the data of Fontell (4) at 20°C. and to obtain new data at 25°C. for the system under investigation. The measurements were made by determining the difference in levels between tubes 2c and 2b (figure 1) after equilibrium had been established between the liquid and vapor reservoirs. In carrying out the measurements, an interval of 30 min. or more was allowed for equilibrium, and temperature control of $\pm 0.05^\circ\text{C.}$ was obtained in the manner previously described. An iron nail which was sealed in a glass capsule was present in the liquid reservoir. This was used in conjunction with an external magnet to agitate the solution so as to ensure thermal equilibrium and speed the attainment of liquid-vapor equilibrium. In making

⁹ Consideration of rates of interdiffusion of gases makes it probable that the apparent relatively quick approach to composition equilibrium may have been largely coincidental, owing to the composition of the evaporating adsorbate being close to the final equilibrium composition. The usual criterion for composition equilibrium was no measurable change in condensation pressure over a 3-4 hr. period.

vapor-pressure measurements at 20°C. the air bath was kept at 25°C. A reproducibility of ± 0.05 cm. was obtained. The results of these measurements are given in table 1 and figures 3 and 4. The vapor composition plot at 20°C. was calculated from the data of Nils Fontell (4), while the one at 25°C. was calculated on the assumption that the vapor composition in equilibrium with a given composition of liquid was the same at 25°C. as at 20°C. To justify this assumption experiments were carried out in which the condensation pressure at 25°C. of vapor which had previously been in equilibrium with the liquid at 20°C. was measured in the usual way with the McLeod gauge. The condensation pressure in all cases corresponded to the same vapor composition when calculated on the above assumption as did the vapor pressure at 20°C. The vapor composition

TABLE 1
Vapor-pressure measurements.

MOLE FRACTION OF CCl_4	FONTELL* 20.0°C. cm. Hg	THIS WORK	
		20.0°C. cm. Hg	25.0°C. cm. Hg
0.000	9.60	9.60	12.25
0.015	10.5	10.6	13.8
0.034	11.4	11.4	14.7
0.039	11.6	11.6	14.9
0.072	12.7	12.8	16.2
0.140	14.4		18.4
0.166	14.7	14.5	
0.265	15.7	15.7	19.7
0.500	16.05		
0.910	15.6	15.7	
0.918	15.5	15.6	19.8
0.977	14.5	14.7	18.2
1.000	9.05	9.10	11.40

* From smoothed data.

curve for 25°C. was employed in determining the composition of the vapor in equilibrium with the adsorbate.

The vapor composition could also be determined in the course of adsorption measurements by the simple expedient of sealing off the adsorption tube at the conclusion of the measurement of an isotherm and determining the weight of the vapor plus adsorbate. The number of moles introduced into the adsorption tube, the weight of same, and the molecular weights of the two components being known, the composition of the vapor introduced could be determined. Determining the weight of the introduced vapor necessitates weighing the tube before and after removing the contents and knowing the weight of the adsorbent corrected for loss of weight due to outgassing. However, because of possible variation in this quantity, owing to variable ash content, the probable accuracy of this determination of the mole fraction is about ± 0.02 . Results obtained in this manner agreed satisfactorily with those obtained using the data of Nils Fontell (4).

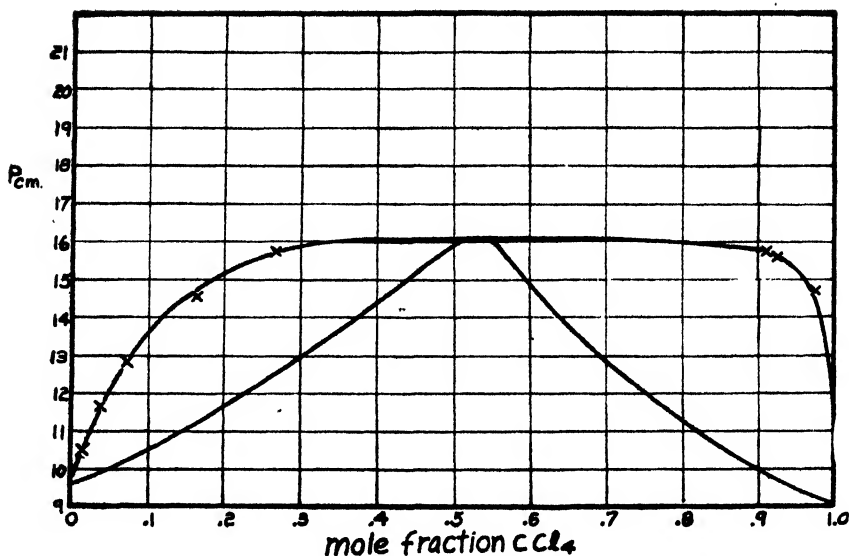


FIG. 3. Liquid and vapor composition *versus* vapor pressure for methanol-carbon tetrachloride at 20°C. Curves according to smoothed data of Nils Fontell; crosses according to data obtained in this work.

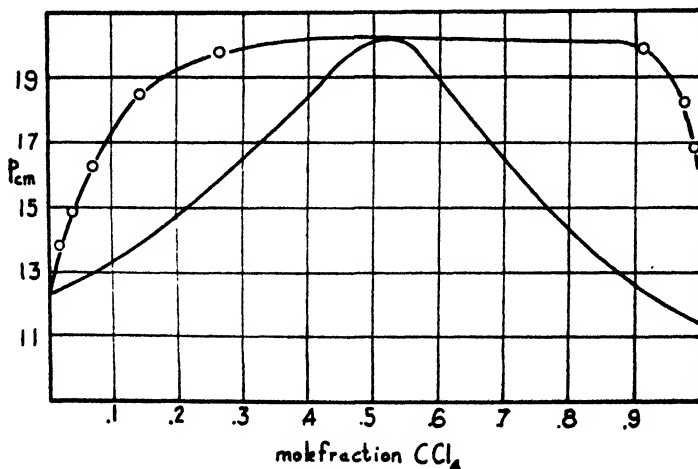


FIG. 4. Liquid and vapor composition *versus* vapor pressure for methanol-carbon tetrachloride at 25°C. Liquid composition-vapor pressure curve according to data (O) obtained in this work. Vapor composition-vapor pressure curve according to assumptions given on page 1161.

RESULTS AND CALCULATIONS

The partial pressure and total pressure adsorption¹⁰ isotherms obtained from these measurements are plotted in figures 5, 6, 7, and 8.

¹⁰ The extrapolated portions (dotted) represent monolayer adsorption only and do not include capillary condensed material.

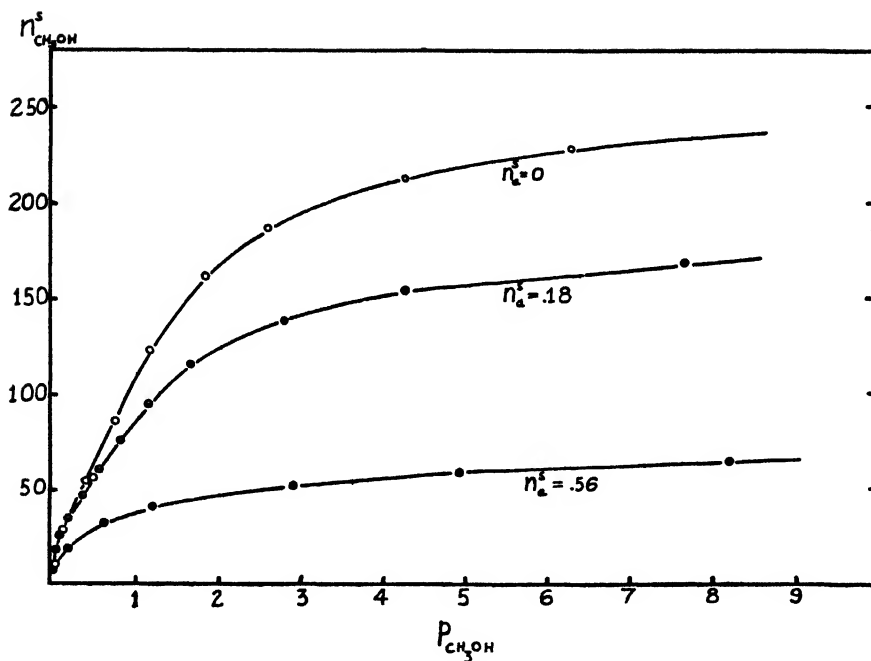


FIG. 5. Partial pressure natural adsorption isotherms for methanol (p in centimeters of mercury; n^s in cubic centimeters at N.T.P. per gram of charcoal).

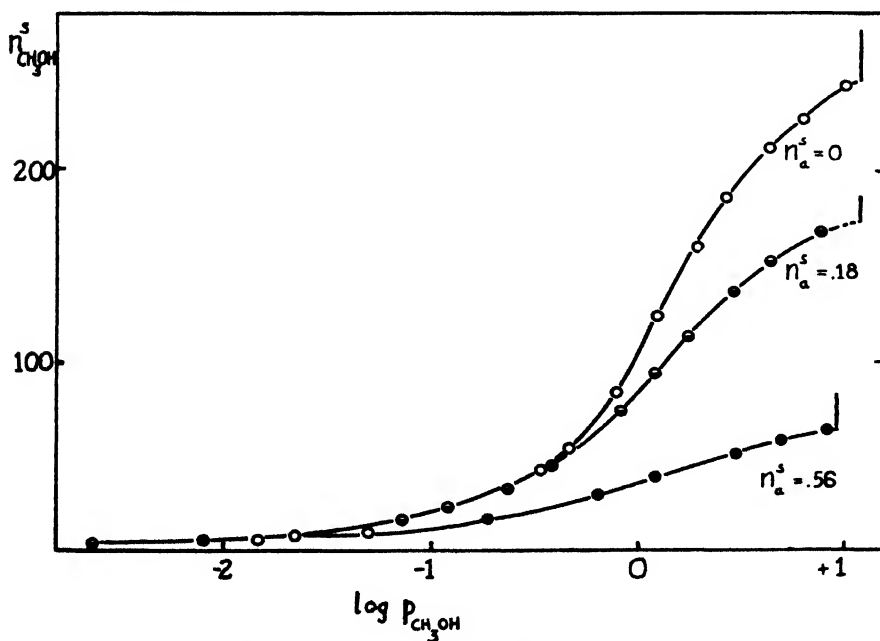


FIG. 6. Partial pressure semi-log adsorption isotherms for methanol (p in centimeters of mercury; n^s in cubic centimeters at N.T.P. per gram of charcoal). Vertical lines at high-pressure extremities indicate saturation pressures. Extrapolated portion (dotted) does not include capillary condensation.

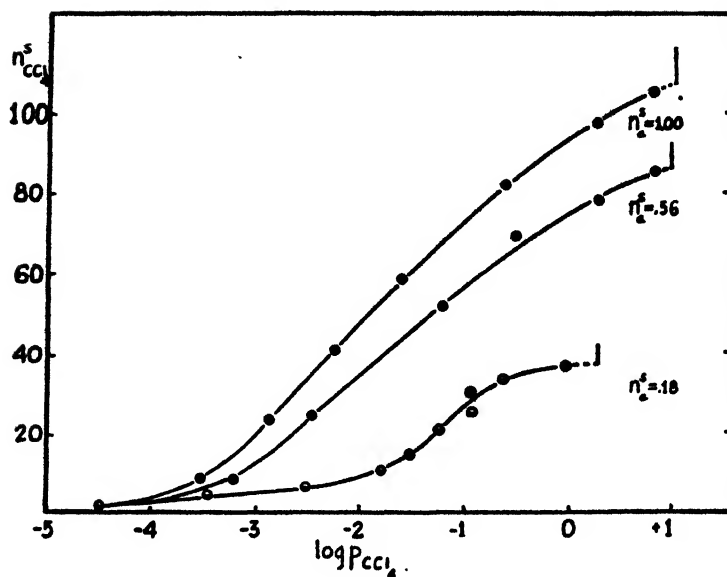


FIG. 7. Partial pressure semi-log adsorption isotherms for carbon tetrachloride (p in centimeters of mercury; n^s in cubic centimeters at N.T.P. per gram of charcoal). Vertical lines at high-pressure extremities indicate saturation pressures. Extrapolated portion (dotted) does not include capillary condensation.

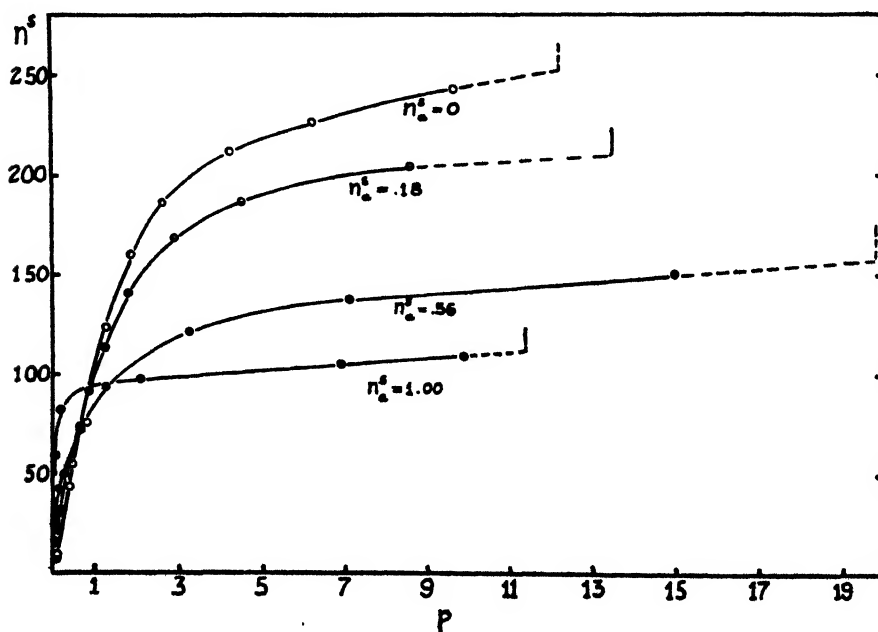


FIG. 8. Total pressure adsorption isotherms for carbon tetrachloride-methanol (p in centimeters of mercury; n^s in cubic centimeters at N.T.P. per gram of charcoal).

By evaluation of areas under the partial pressure semilog isotherms, quantities which might be called partial spreading pressure coefficients ($F_i A / RT$) have been evaluated and are plotted in figures 9 and 10. The total spreading pressure

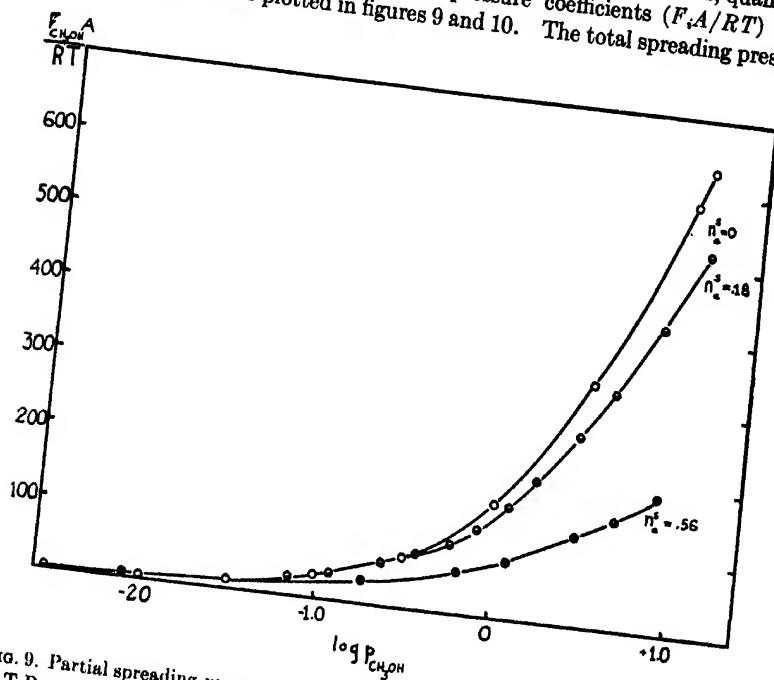


FIG. 9. Partial spreading pressure coefficient of methanol ($F_{CH_3OH} A / RT$ in cubic centimeters at N.T.P. per gram of charcoal) as a function of partial pressure at different surface mole fractions (see equation 1).

coefficient has been shown to be related to these partial spreading pressure coefficients by the following equation (7):

$$\frac{FA}{RT} = \int_0^{p_1} n_1^s d \ln p_1 + \int_0^{p_2} n_2^s d \ln p_2 = \frac{F_1 A}{RT} + \frac{F_2 A}{RT} \quad (1)$$

where A = area of the surface per gram of adsorbent,
 F = total spreading pressure,
 F_1 = partial spreading pressure of first component,
 F_2 = partial spreading pressure of second component,
 n^s = total moles adsorbed per gram of adsorbent,
 n_1^s = moles of carbon tetrachloride adsorbed per gram of adsorbent,
 n_2^s = moles of methanol adsorbed per gram of adsorbent,
 p_1 = partial pressure of carbon tetrachloride, and
 p_2 = partial pressure of methanol.

$$n_a^s = \frac{n_1^s}{n^s} \quad n_b^s = \frac{n_2^s}{n^s}$$

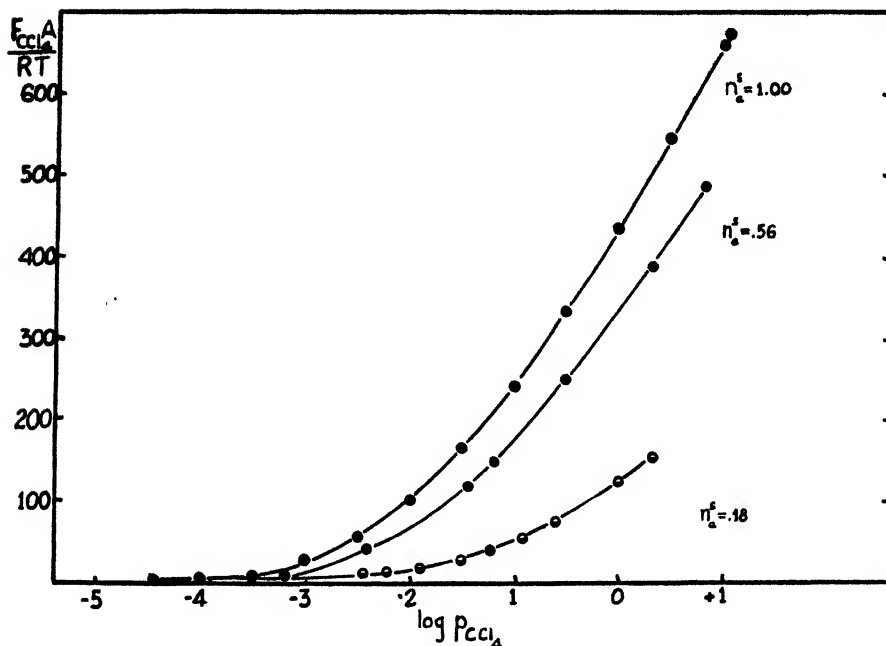


FIG. 10. Partial spreading pressure coefficient of carbon tetrachloride ($F_{\text{CCl}_4}A/RT$ in cubic centimeters at N.T.P. per gram of charcoal) as a function of partial pressure at different surface mole fractions (see equation 1).

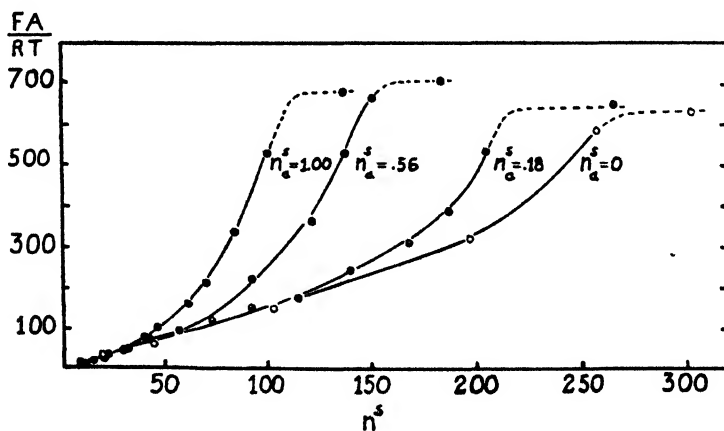


FIG. 11. Total spreading pressure coefficient (FA/RT in cubic centimeters at N.T.P. per gram of charcoal) as a function of total adsorption at different surface mole fractions (see equation 1).

Using equation 1 total spreading pressure coefficients have been evaluated as a function of n^s and are plotted in figure 11.

In the evaluation of spreading pressures a difficulty arises, since measurements

were not carried on down to zero adsorption. However, measurements were made at low enough values so that it is thought that the remaining area is almost negligible. Thus the values given for the spreading pressures to be exact would have to have a small unknown constant added for this area between $n^* = 0$ and $n^* = \text{lowest value measured}$.

Values of the amount adsorbed in cubic centimeters per gram of adsorbent when the surface is completely covered, ϕ , have been estimated¹¹ from isotherms at different values of n_a^* and are given in figure 12. Part of these data were obtained from total pressure isotherms where no attempt was made to measure partial pressures.

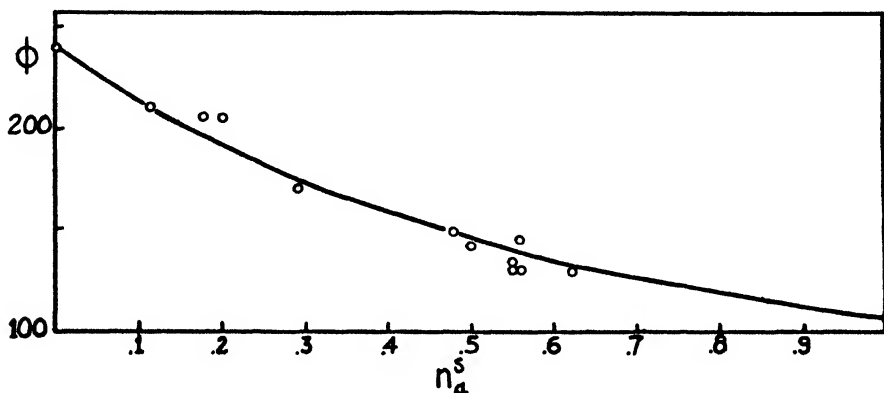


FIG. 12. Amount adsorbed when surface is covered by adsorbate as a function of mole fraction of carbon tetrachloride (see below). ϕ in cubic centimeters at N.T.P. per gram of charcoal.

If the areas occupied by the carbon tetrachloride and methanol molecules were independent of the presence of the other species, the area occupied by a mixture would be an additive function and the following relation would hold true:

$$\frac{1}{\phi} = \frac{n_a^*}{\phi_A} + \frac{n_b^*}{\phi_B}$$

or

$$\frac{1}{\phi} = \frac{n_a^*}{105} + \frac{(1 - n_a^*)}{242} \quad (2)$$

where $\phi_A = \phi$ for $n_a^* = 1.00$,

$\phi_B = \phi$ for $n_b^* = 1.00$,

n_a^* = mole fraction of carbon tetrachloride in the surface phase, and

n_b^* = mole fraction of methanol in the surface phase.

The plot of figure 12 is according to the above equation.

¹¹ Some capillary condensation is indicated at pressures approaching saturation. This is taken into consideration in estimating the ϕ values; i.e., ϕ was evaluated as the amount adsorbed at the point of inflection of the isotherm. The simple B.E.T. equation cannot justifiably be used for determining ϕ , because of porosity, the presence of more than one component, the anomalous adsorption isotherm of methanol, etc.

DISCUSSION

Kinetic considerations

The data appear to indicate that for small amounts adsorbed the partial pressure of one component is not appreciably affected by the presence of the other component, since the partial pressure curves for all values of n_a^* merge as the amount adsorbed becomes small. This is the behavior that would be expected if the adsorbed phase were a two-component perfect gas.

As the amount adsorbed becomes greater, however, the partial pressures for a given amount adsorbed of the component in question are increased more and more by the presence of the second component (see figures 6 and 7). This behavior can be explained on the basis of crowding action of the second component and would be expected for a two-component gas phase under extremely high compression.

Molecular considerations

Methyl alcohol and carbon tetrachloride present quite a contrast in so far as their molecular structure is concerned. Methanol molecules are non-symmetrical and polar with a tendency to associate with the formation of hydrogen bonds (3, 5), while carbon tetrachloride molecules are symmetrical and non-polar with no such tendency. Methanol is a relatively small molecule in comparison with carbon tetrachloride. Carbon tetrachloride gives a normal Langmuir-type adsorption isotherm, while methanol has a somewhat anomalous isotherm, intermediate between the isotherm obtained for pure water on charcoal and the Langmuir type, which would indicate that lateral forces between adsorbed methanol molecules are coming into play.

Because of the symmetry of the carbon tetrachloride molecule, orientation effects can probably be neglected and the assumption made that carbon tetrachloride molecules occupy the area predicted from their molecular volume¹² when adsorbed on charcoal even in the presence of the methanol molecules. If this assumption is made, an idea as to the orientation of the adsorbed methanol molecules can be obtained from the relative ϕ values, which are in proportion to the reciprocal of the area per mole. The value of ϕ for pure methanol is 242 cc. per gram and for pure carbon tetrachloride is 105 cc. per gram; the ratio for the ϕ values, methanol to carbon tetrachloride, is 2.31. However, if normal liquid spacings prevailed, the following inverse relation between molecular volume and ϕ would be expected to hold true:

$$\frac{\phi_B}{\phi_A} = \left[\frac{(V_m)_A}{(V_m)_B} \right]^{2/3}$$

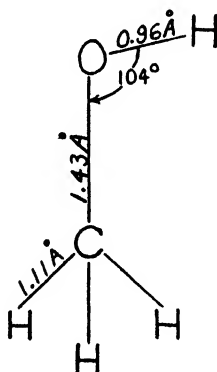
¹² That is,

$$\text{Area per molecule} = (V_m/N)^{2/3} = (M/Nd)^{2/3}$$

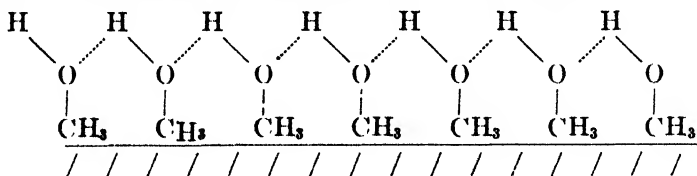
where M = molecular weight, N = Avogadro's number, and d = density of liquid at the same temperature. In other words, the area per molecule assuming the same spacings as present in the liquid.

where $(V_m)_A$ = molecular volume of carbon tetrachloride and $(V_m)_B$ = molecular volume of methanol; the ratio ϕ_B to ϕ_A would be 1.77. The disagreement would appear to indicate that the methanol molecules are oriented so as to occupy considerably less than their normal area. The anomalous isotherm for methanol suggests lateral bonding forces, perhaps involving hydrogen bonds.

The general hydrophobic character of charcoal is illustrated by the almost zero adsorption of water at pressures less than about half of saturation. The organophilic character of charcoal is illustrated by a marked decrease in k (the adsorption equilibrium constant) as the carbon chain is lengthened in a series such as the alkyl chlorides (12). The model of methanol below has been successfully used to explain Raman spectra (9).



The above facts would suggest the following picture¹³ of the methanol molecules as the amount adsorbed approaches a complete monolayer.



If the methanol molecules were oriented as above, it would be expected that their molecular area would be less than predicted from the molecular volume. In fact, the ratio of the actual molecular area to that calculated from the molecular volume of methanol would be expected to be to a good approximation:

$$[\text{molecular volume}^* \text{ of } \text{CH}_4 / \text{molecular volume}^* \text{ of } \text{CH}_3\text{OH}]^{2/3}$$

*Calculated from atomic volumes.

On the basis of the atomic volumes published by LeBas (2) this ratio is 0.765. The calculated ratio of ϕ_B/ϕ_A for oriented adsorption as pictured above then

¹³ This picture is not intended to convey the impression that the surface molecules are fixed on the surface and incapable of lateral movement or that the surface phase can be considered as a condensed phase.

becomes $1.77/0.765 = 2.31$, a value which agrees better than might be expected with the experimental value of 2.31.

The agreement of the ϕ values calculated using equation 2 with the data is within the limits of experimental error. This would indicate that the orientation of the methanol molecules is not appreciably influenced by the presence of the carbon tetrachloride molecules when n^* approaches ϕ .

Thermodynamic considerations

Several thermodynamic relationships have previously been derived for equilibria of this type (7). The present data are not believed extensive or precise enough for more than semiquantitative testing of these relationships. This is particularly true at low pressures where $n_a = 0$ for most of the data.

To evaluate the differential quantities in the following equations the curves $\frac{FA}{RT}$ vs. $\log p_1$, $\frac{FA}{RT}$ vs. $\log p_2$, $\frac{FA}{RT}$ vs. $\log p$, $\log p$ vs. $\log p_1$ at $n_a^* = 0$, $n_a^* = 0.18$, $n_a^* = 0.57$, and $n_a^* = 1.00$ were plotted. Further curves were drawn between these plots at fixed values of the quantities being held constant, and the slopes of the latter curves were determined to obtain the partial differential quantities in question.

Results obtained in testing the equation:

$$\frac{A}{RT} \left(\frac{\partial F}{\partial \ln p} \right)_{p_1} = \frac{n^* n_b^*}{n_b} \quad (6)$$

are given in the following table:

LOG p_1	n_b^*	n^*	n_b	$\frac{n^* n_b^*}{n_b}$	$\frac{A}{RT} \left(\frac{\partial F}{\partial \ln p} \right)_{p_1}$
0	0.43	132	08.4	68	75
-0.5	0.43	123	09.1	58	60
-1.0	0.43	100	09.4	46	50

The equation:

$$A \left(\frac{\partial F}{\partial \ln p_2} \right)_p = \frac{n^* (n_b^* - n_b)}{n_a} \quad (7)$$

has been tested with results given in the following table:

LOG p	n_b^*	n_b	n^*	$\frac{n^* (n_b^* - n_b)}{n_a}$	$\frac{A}{RT} \left(\frac{\partial F}{\partial \ln p_2} \right)_p$
0	0.81	0.970	92	-500	-2170
0.5	0.81	0.950	174	-486	-430
0.8	0.81	0.935	178	-360	-330

The relationship:

$$\left(\frac{\partial \ln p}{\partial \ln p_1}\right)_T = \frac{n_a - n_a^s}{n_b^s} \quad (8)$$

has been tested with the following results:

$\frac{FA}{RT}$	n_a^s	n_a	$\frac{n_a - n_a^s}{n_b^s}$	$\left(\frac{\partial \ln p}{\partial \ln p_1}\right)_T$
300	0.57	0.075	-1.15	-1.1
400	0.57	0.120	-1.05	-1.0
500	0.57	0.239	-0.77	-0.8

The agreement of values calculated using the above equations would appear to be within experimental error.

SUMMARY

A method has been described for the measurement of isothermal adsorption equilibria of mixed vapors, in which the composition of the adsorbed phase is kept constant and the total pressure and composition of the vapor are measured.

This method has been applied to the system carbon tetrachloride-methanol, partial and total pressure isotherms being obtained.

Vapor-pressure and composition data as a function of liquid composition at 20°C. and 25°C. for the system carbon tetrachloride-methanol are given.

The quantity adsorbed when the surface is "completely covered" has been determined as a function of the mole fraction of the adsorbate. The results agree satisfactorily with an equation which assumes that the areas occupied by each molecular species are independent of the areas occupied by the other.

Partial and total spreading pressures have been calculated from the adsorption data.

The results have been discussed from kinetic, molecular, and thermodynamic standpoints.

We are indebted to Mr. R. B. Olney for the measurements of the isotherm at $n_a^s = 0.18$.

REFERENCES

- (1) BAKER, A. M., AND KING, J. E.: J. Chem. Soc. **119**, 454 (1921).
- (2) LeBAS, G.: *The Molecular Volumes of Liquid Chemical Compounds*. Longmans, Green and Company, London (1915).
- (3) DE VRIES, T., AND COLLINS, B. T.: J. Am. Chem. Soc. **63**, 1343 (1941).
- (4) FONTELL, NILS: Soc. Sci. Fennica, Commentationes Phys.-Math. **3**, No. 15 (1936).
- (5) GORDY, W., AND STANFORD, S. C.: J. Chem. Phys. **9**, 204 (1941).
- (6) INNES, W. B.: Master's Thesis, State University of Iowa, Iowa City, 1939.
- (7) INNES, W. B., AND ROWLEY, H. H.: J. Phys. Chem. **49**, 411 (1945).
- (8) KLOSKEY, S., AND WOO, L.: J. Phys. Chem. **32**, 1387 (1928).
- (9) KOEHLER, J. S., AND DENNISON, D. M.: Phys. Rev. **57**, 1006 (1940).
- (10) McBAIN, J. W.: *Sorption of Gases and Vapours by Solids*, p. 93. G. Routledge and Sons, Ltd., London (1932).
- (11) RICHARDSON, L. B., AND WOODHOUSE, J. C.: J. Am. Chem. Soc. **45**, 2647 (1923).
- (12) ROWLEY, H. H., AND INNES, W. B.: Proc. Iowa Acad. Sci. **47**, 165 (1940).

ADSORPTION EQUILIBRIA OF LIQUID MIXTURES OF CARBON TETRACHLORIDE-METHANOL WITH CHARCOAL¹W. B. INNES² AND H. H. ROWLEY³*Division of Physical Chemistry, State University of Iowa, Iowa City, Iowa**Received March 6, 1945*

In investigating equilibria involving a mixed single-phase liquid and an adsorbent the method generally employed is to determine composition before and after adsorption occurs. The quantity

$$\frac{n\Delta n_a}{m}$$

where n = total moles of liquid,

Δn_a = change in the mole fraction of a component of the liquid due to adsorption, and

m = weight of adsorbent,

has been termed the selective adsorption by Bartell and coworkers, who have obtained much data involving its measurement (1-5).

In practice, measurements of $n\Delta n_a$, almost without exception, have been carried out by introducing the adsorbent in contact with a gaseous atmosphere into the liquid and measuring the change in composition of the liquid phase. Since air or other adsorbed materials are present at this time, a question arises as to the effect of these foreign materials. As a matter of fact considerable gas evolution occurs when adsorbents (e.g., charcoal) are introduced into liquid, indicating that the previously adsorbed gases are being displaced, and it would seem likely that for practical purposes the displacement is usually complete, because of the greater adsorbability of the liquid. This displacement, however, does present experimental difficulties, as the displaced gas if removed at room temperature carries with it a considerable amount of vapor, which may in itself change the composition of the liquid phase. Because of these objections some of the present measurements were carried out by using a technique in which the liquid was introduced directly into previously outgassed charcoal, though others were carried out in the customary manner.

The experimental meaning of the previously given definition for selective adsorption is quite clear, but the fundamental significance is not. In previous work, adsorption equilibria have been considered from thermodynamic standpoints, assuming two-dimensional unimolecular surface phases (9, 11). In the case of charcoal, the Langmuir-type isotherm usually obtained is evidence (6)

¹ This article is based upon a thesis submitted by W. B. Innes to the Faculty of the Graduate School of the State University of Iowa in partial fulfillment of the requirements for the degree of Doctor of Philosophy, August, 1941.

² Present address: Stamford Research Laboratories, American Cyanamid Company, Stamford, Connecticut.

³ Present address: Department of Chemistry, University of Oklahoma, Norman, Oklahoma.

that it is impossible as a rule to have more than a single layer, because of steric reasons. Assuming that the adsorbate consists of a single-layer surface phase, the selective adsorption as defined above may be related to the surface quantities as follows: Let n_1^s , n_2^s be the total moles of the first and second components, respectively, in the surface phase after adsorption equilibrium has been reached, and n_1^L , n_2^L be the number of moles of the first and second components, respectively, in the liquid phase after equilibrium has been reached. And let:

$$\begin{aligned} n_1 &= n_1^s + n_1^L & n^L &= n_1^L + n_2^L \\ n_2 &= n_2^s + n_2^L & n^s &= n_1^s + n_2^s \\ n &= n_1 + n_2 \end{aligned}$$

Then:

$$\begin{aligned} n\Delta n_a &= \left(\frac{n_1^L}{n_1^L + n_2^L} - \frac{n_1}{n_1 + n_2} \right) n \\ n\Delta n_a &= \left(\frac{n_1^L}{n_1^L + n_2^L} - \frac{n_1^s + n_1^L}{n_1^s + n_1^L + n_2^s + n_2^L} \right) n \end{aligned}$$

Simplifying:

$$n\Delta n_a = \frac{1}{n^L} [n_2^s n_1^L - n_1^s n_2^L]$$

Letting:

$$\begin{aligned} n_a^L &= \frac{n_1^L}{n^L} & n_b^L &= \frac{n_2^L}{n^L} \\ n_a^s &= \frac{n_1^s}{n^s} & n_b^s &= \frac{n_2^s}{n^s} \end{aligned}$$

And simplifying further:

$$n\Delta n_a = -n^s(n_a^s - n_a^L) \quad (1)$$

The theoretical significance of selective adsorption thus becomes clear. Also, it appears that selective adsorption can be evaluated from a knowledge of n^s , n_a^s , n_a^L , which quantities can be evaluated from mixed-vapor adsorption isotherms (10).

Equilibria between a liquid, vapor, and surface phases for a two-component system have been considered previously (9) and the following relation involving $n^s(n_a^s - n_a^L)$ has been derived:

$$A \left(\frac{\partial F'}{\partial \mu_1} \right)_T = \frac{+ n^s(n_a^s - n_a^L)}{n_b^L} \quad (2)$$

where F' = spreading pressure at specified equilibrium conditions,

μ_1 = chemical potential of the first component, and

A = surface area.

The above equation is similar in form but opposite in sign to Guggenheim and

Adam's (8) version of the Gibbs adsorption equation applying to adsorption at the vapor interface of a binary liquid system. Since spreading pressures can be evaluated from the mixed-vapor adsorption data, this equation offers another means of determining the selective adsorption.

MATERIALS

The materials used for all measurements reported here were the same as described in other work (10). That is, the charcoal was 12-20 mesh, steam-activated, unpurified charcoal obtained from the National Carbon Company of Nela Park, Ohio. The average ash content of the individual 1-2 g. samples was 6.8 per cent, with an average deviation of 1.5 per cent. The loss of weight on

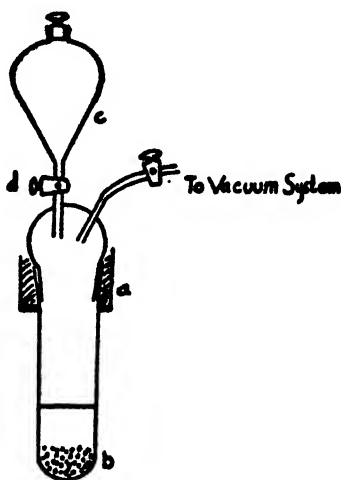


FIG. 1. Schematic diagram of apparatus used for introducing liquid directly into outgassed charcoal.

outgassing was found to be 14 per cent. Values of the weight of charcoal have been corrected for this weight loss. The carbon tetrachloride and methanol used were purified by conventional methods.

MEASUREMENTS OF SELECTIVE ADSORPTION

In the first method employed, liquid was introduced directly into previously evacuated charcoal. This was done by using the setup shown in figure 1. The outgassing was carried out while maintaining the charcoal at $525^\circ \pm 25^\circ\text{C}$. by means of a surrounding electric furnace, until the pressure was 2×10^{-4} mm. of mercury or less, as determined by a McLeod gauge connected to the vacuum system. After outgassing and cooling the adsorbent, the liquid was introduced. The tube was then removed, stoppered, and placed in a 25°C . water bath for 24 hr. or longer.⁴ After this the refractive index at 25°C . was measured, using a temperature-controlled Pulfrich refractometer, and compared with that of the

⁴ No changes greater than experimental error were observed for longer periods of time.

TABLE 1
Values of the refractive index*

MOLE FRACTION OF CCl_4	n_D^{25}	n_D^{20}
0.0	1.3286	1.3291
0.1	1.3532	1.3577
0.2	1.3752	1.3777
0.3	1.3932	1.3958
0.4	1.4071	1.4097
0.5	1.4199	1.4225
0.6	1.4289	1.4305
0.7	1.4377	1.4403
0.8	1.4452	1.4479
0.9	1.4518	1.4547
1.0	1.4572	1.4606

* Smoothed data from large-scale plots.

TABLE 2
Measurements of selective adsorption
(Liquid introduced directly into evacuated charcoal)

$\frac{n}{m}$ (AT N.T.P. PER GRAM OF CHARCOAL)*	Δn_a	$-\frac{n\Delta n_a}{m}$	n_a^L
cc.			
2040	$+0.10 \times 10^{-2}$	-2	0.000
2520	-0.65	18	0.031
1980	-0.76	17	0.035
2410	-0.96	26	0.048
2250	-1.63	42	0.078
1480	-1.98	33	0.080
2050	-1.60	37	0.138
2000	-1.80	41	0.144
1960	-1.57	35	0.156
1840	-1.81	37	0.218
1720	-1.59	31	0.218
1590	-1.25	23	0.375
1450	-1.06	17	0.514
1430	-0.28	4	0.530
1370	-0.10	2	0.600
1330	+1.07	-16	0.763
1220	+2.19	-31	0.836
1210	+1.78	-24	0.860
1110	+0.40	-5	0.980
1090	+1.17	-15	0.980
1159	0.00	0	1.000

* Calculated using the expression $n = 22,400 \times \text{moles of liquid}$.

original liquid. The reproducibility of the refractive-index values obtained was estimated to be ± 0.0001 . The refractive index as a function of the composition was previously determined; the results are given in table 1. They appear to

be in satisfactory relative agreement with those reported by Fontell (7), who reported data at 20°C. in terms of "angles of emergence." The selective adsorption, $n\Delta n_a/m$, was calculated using the expression:

$$\frac{n\Delta n_a}{m} = \frac{n\Delta\alpha}{m} \frac{dn_a}{d\alpha} \quad (3)$$

where n = total moles of liquid introduced,

$\Delta\alpha$ = change in refractive index⁵ due to adsorption,

$\frac{dn_a}{d\alpha}$ = slope of mole fraction-refractive index curve at an intermediate mole fraction value, and

m = mass of charcoal corrected for loss of weight on outgassing.

The results of the measurements are given in table 2 and figure 2.

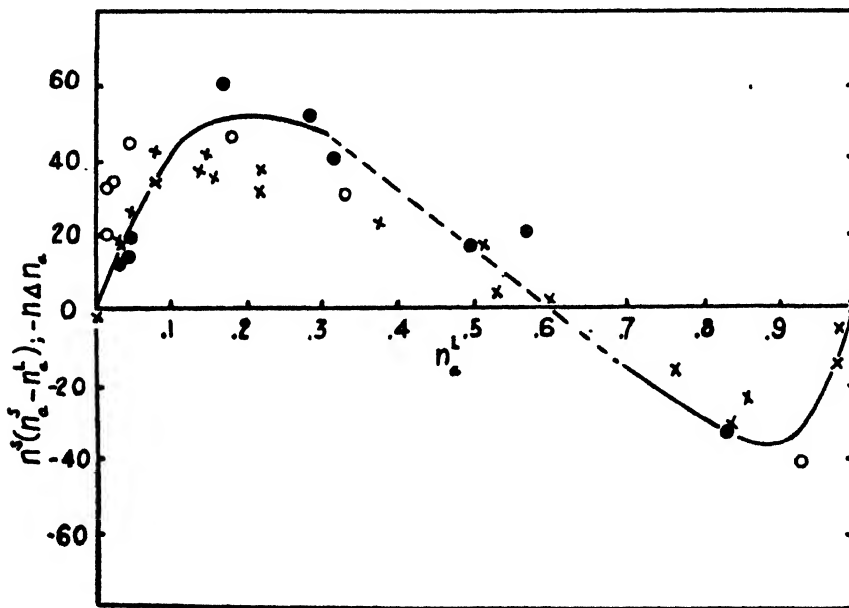


FIG. 2. Selective adsorption of carbon tetrachloride, expressed in cubic centimeters at N.T.P. per gram of charcoal, as a function of the mole fraction of carbon tetrachloride in the liquid phase. X, from measurements of $-n\Delta n_a$ when liquid was introduced directly into outgassed charcoal (see table 2); \odot , from measurements of $-n\Delta n_a$ when charcoal was exposed to dry air before introduction of liquid (see table 3); O, from mixed-vapor adsorption data (see table 4). Plot: thermodynamic evaluation of $n_a^j(n_a^j - n_a^L)$, using equations 2 and 4.

In the second method employed the charcoal was outgassed in the same manner as previously described,⁶ sealed off, weighed, and opened to dry air in a desiccator

⁵ Actually, the angle of emergence was utilized directly in the calculations.

⁶ However, larger samples (5.9 g.) were outgassed and these were split into parts.

before being added to ground-glass-stoppered bottles containing a known weight of liquid of known composition as determined by refractive-index measurements. The bottles were kept loosely stoppered for 5–10 min. to allow the displaced air to escape and then were tightly stoppered. Some loss of vapor was unavoidable. After 48 hr. the composition of the liquid phase was determined by refractive-index measurements. From these data the selective adsorption was calculated. The results are given in table 3 and figure 2.

TABLE 3
Measurements of selective adsorption

(Charcoal exposed to dry air after outgassing before introduction of liquid)

$\frac{n}{m}$ (AT N.T.P. PER GRAM OF CHARCOAL)	Δn_a	$-\frac{n\Delta n_a}{m}$	n_a^L
cc.			
2450	-0.5×10^{-2}	12	0.038
3580	-0.4	14	0.048
2680	-0.7	19	0.049
1760	-3.4	60	0.167
1660	-3.1	52	0.283
1830	-2.2	40	0.311
1380	-1.2	17	0.496
2100	-1.0	21	0.565
1270	+2.5	-32	0.835

EVALUATION OF SELECTIVE ADSORPTION FROM MIXED-VAPOR ADSORPTION
ISOTHERMS

In other work (10) mixed-vapor adsorption isotherms for the system carbon tetrachloride-methanol with the same charcoal were obtained. The values of these data where equilibrium with a liquid phase is being approached make it possible to evaluate the quantities n^* , n_a^* , n_a^L and, hence, also the selective adsorption because of equation 1.

The measurement of the isotherms was carried out in such a manner that n_a^* was known and practically constant throughout the isotherm as long as the amount of vapor introduced into the adsorption tube was not sufficient to bring about liquid condensation.

The values of n^* in this case correspond for practical purposes with the quantity previously termed ϕ , which is the amount adsorbed when the surface is completely covered. The quantity ϕ has been previously evaluated (10) as a function of n_a^* .

As n_a^L is a known function (7) of n_a^V , and values of n_a^V as the saturation pressure is approached were determined during the mixed-vapor adsorption studies, n_a^L can be evaluated. Thus for a given isotherm for which n_a^* is known, both n_a^L and n_a^V can be determined. Using the data obtained from the different isotherms, n_a^* has been plotted as a $f(n_a^L)$ in figure 3. The plot of n_a^V as $f(n_a^L)$ was made

using the data of Fontell (7). Fontell's data were at 20°C., but reasons have been advanced (10) for justifying use of the same curve at 25°C.

Since ϕ , n_a^s , and n_a^L are known for a given isotherm, the selective adsorption can be calculated by use of equation 1. This has been done and the results are presented in table 4 and figure 2.

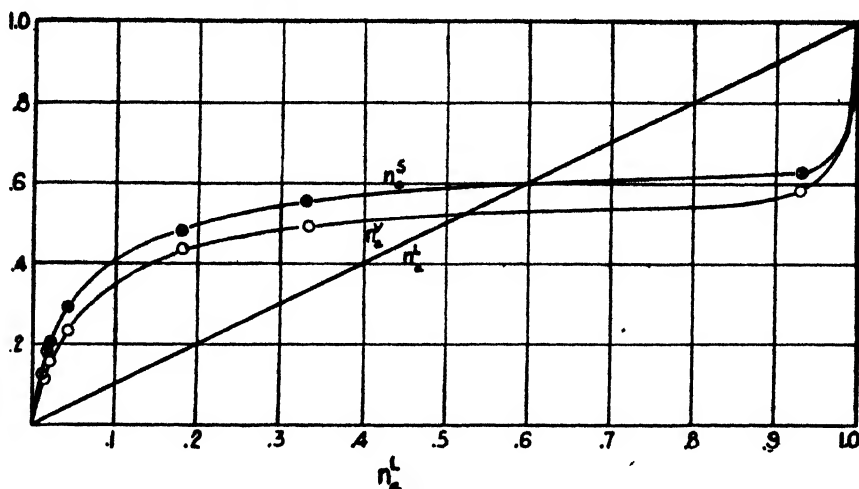


FIG. 3. Mole fraction of carbon tetrachloride in surface, vapor, and liquid phases as a function of the composition of the liquid phase at 25°C.

TABLE 4

Calculations of selective adsorption from mixed-vapor adsorption data

n_a^s	p_0	n_a^L	n_a^V	ϕ^* (AT N.T.P. PER GRAM OF CHARCOAL)	$(n_a^s - n_a^L)$	$\phi(n_a^s - n_a^L)$
	cm. Hg.			cc.		
0.000	12.25	0.000	0.00	242	0.000	0
0.115	13.6	0.015	0.11	212	0.095	20
0.185	13.4	0.017	0.12	196	0.170	33
0.20	14.0	0.022	0.16	192	0.175	34
0.29	15.0	0.044	0.23	176	0.25	44
0.49	19.0	0.176	0.43	148	0.31	46
0.56	20.0	0.33	0.49	140	0.23	32
0.62	19.6	0.93	0.58	134	-0.31	-41
1.00	11.40	1.00	1.00	105	0.00	0

* Values taken from smoothed curve, $\phi(n_a^s)$, given in previous work (10).

p_0 = saturation pressure of vapor in equilibrium with adsorbent when liquid-phase formation is being approached.

THERMODYNAMIC EVALUATION OF SELECTIVE ADSORPTION

Equation 2 was derived with the aid of several assumptions. These were:

$$\frac{V^V}{n_b^V} \gg \frac{V^L}{n_b^L}, \quad V^V \gg V^L, \quad (n_a^s - n_a) \gg (n_a^L - n_a)$$

where V^V and V^L refer to the volume per mole in the vapor and liquid phases, respectively.

The assumption that $V^V \gg V^L$ appears to be a good approximation in the case under consideration. If this is true, examination of the data given in figure 3 shows that $V^V/n_b^V \gg V^L/n_b^L$ is also a good approximation in the range $n_a^L = 0$ to $n_a^L = 0.6$. The assumption

$$(n_a^s - n_a) \gg (n_a^L - n_a^s)$$

would appear to be valid according to the data of figure 3 except in the region where n_a^L is approximately equal to n_a^s , that is, in the neighborhood of $n_a^L = 0.5$. The complementary equation:

$$A \left(\frac{\partial F'}{\partial \mu_2} \right)_T = \frac{-n^s(n_b^L - n_b^s)}{n_a^L} = \frac{-n^s(n_a^s - n_a^L)}{n_b^L} \quad (4)$$

could also be employed. Similar reasoning shows that this equation is a good approximation for values of $n_a^L = 1$ to $n_a^L = 0.6$. It would appear that equation

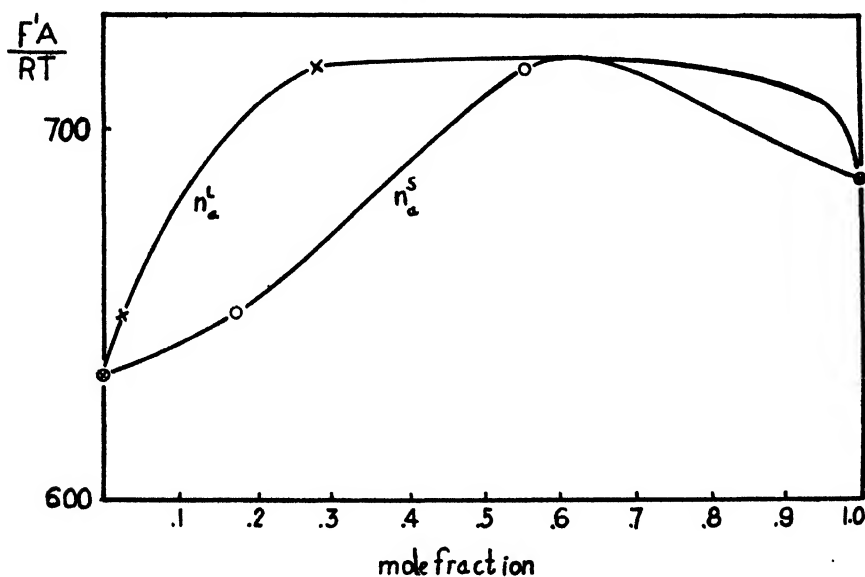


FIG. 4. Total spreading pressure coefficient when equilibrium exists between the surface, vapor, and liquid phases, as a function of the mole fraction of carbon tetrachloride in the liquid and surface phases. ($F'A/RT$) in cubic centimeters at N.T.P. per gram of charcoal.

3 should be employed for values of n_a^L of 0 to 0.5 and equation 4 for values of n_a^L of 0.60 to 1.0 and that neither equation would necessarily be a good approximation in the range $n_a^L = 0.5$ to $n_a^L = 0.6$.

Spreading pressure coefficients have previously (10) been evaluated for complete isotherms up to saturation vapor pressures. The spreading pressure coefficients at the saturation vapor pressure $F'A/RT$ as a function of n_a^s and n_a^V are plotted in figure 4. The partial vapor pressures at saturation are also

known and probably closely approximate fugacities; hence the chemical potentials may be approximately evaluated. The mole fraction in the liquid phase is also known. Therefore, it is possible to calculate the selective adsorption,

$$n^*(n_a^s - n_a^L) = -n\Delta n_a$$

by the use of equations 2 and 4. This has been done and the results obtained are plotted in figure 2, where they are compared with those obtained by other methods. To make the necessary calculations, smoothed curves were made from the limited data. Because of this, the calculated curve for selective adsorption using equations 3 and 4 can only be considered semiquantitative.

DISCUSSION

The agreement between the selective adsorption values obtained by different methods appears to be satisfactory, considering some sources of error that may have been present. Both methods employed for measuring the selective adsorption directly were based on changes in refractive index. After completing the measurements it was discovered that the soluble ash components of the charcoal (almost entirely sodium chloride, potassium chloride) had a measurable effect on the refractive index of methanol but none on that of carbon tetrachloride. This tended to give slightly lower apparent values of selective adsorption of carbon tetrachloride for high alcohol compositions than the true values. This fact is evidenced by the apparent but not real negative selective adsorption for $n_a^L = 0$. In the case of measurements carried out when the liquid was introduced into non-evacuated charcoal, as mentioned above, considerable vapor is lost with the displaced air; this tends to alter the composition of the remaining liquid, and in this case would be expected to give considerably higher values for selective adsorption than the true ones. The fact that some of these data are higher than the other data is therefore not surprising.

The reasonable agreement of the values for selective adsorption calculated using equations 2 and 4 with the values of selective adsorption obtained by other methods is gratifying, even though this curve can only be considered approximate. The fact that zero selective adsorption is found in the region where the spreading pressure is a maximum shows qualitative agreement.

SUMMARY

A relationship between selective adsorption and the magnitude and composition of the adsorbate has been derived. This makes possible the evaluation of selective adsorption from mixed-vapor adsorption isotherms. Calculations of this sort have been made, using previous data for the system carbon tetrachloride-methanol adsorbed on charcoal.

Direct measurements of selective adsorption for the same system were carried out by two methods. In one of these the liquid was introduced directly into outgassed activated charcoal; in the other, outgassed charcoal was exposed to air before addition of the liquid.

The selective adsorption was also determined using a previously derived

thermodynamic relationship which is similar in form to the Guggenheim and Adams version of the Gibbs adsorption equation.

Reasonable agreement between the values for selective adsorption determined by the different methods was obtained.

REFERENCES

- (1) BARTELL, F. E., AND LLOYD, L. E.: J. Am. Chem. Soc. **60**, 2120 (1938).
- (2) BARTELL, F. E., AND SCHEFFLER, G.: J. Am. Chem. Soc. **53**, 2507 (1931).
- (3) BARTELL, F. E., SCHEFFLER, G., AND SLOAN, C. K.: J. Am. Chem. Soc. **53**, 2501 (1931).
- (4) BARTELL, F. E., AND SLOAN, C. K.: J. Am. Chem. Soc. **51**, 1637 (1929).
- (5) BARTELL, F. E., AND SLOAN, C. K.: J. Am. Chem. Soc. **51**, 1643 (1929).
- (6) BRUNAUER, S., EMMETT, P. H., AND TELLER, E.: J. Am. Chem. Soc. **60**, 313 (1938).
- (7) FONTELL, N.: Soc. Sci. Fennica, Commentationes Phys.-Math. **8**, No. 15 (1936).
- (8) GUGGENHEIM, E. A., AND ADAM, N. K.: Proc. Roy. Soc. (London) **A139**, 218 (1933).
- (9) INNES, W. B., AND ROWLEY, H. H.: J. Phys. Chem. **49**, 411 (1945).
- (10) INNES, AND ROWLEY, H. H.: J. Phys. Colloid Chem. **51**, 1154 (1947).
- (11) ROWLEY, H. H., AND INNES, W. B.: J. Phys. Chem. **46**, 537 (1942).

EXPERIMENTAL ARGUMENTS AGAINST THE CONCEPT OF CHROME TANNING AS AN ADSORPTION PROCESS

K. H. GUSTAVSON

Chemical Laboratory, C. J. Lundbergs Läderfabriks A. B., Valdemarsvik, Sweden

Received November 8, 1946

A paper (2) on "The Adsorption Nature of Chrome Tanning" was published in this Journal some nine years ago. The views advanced therein differ in many respects radically from the theoretical concept generally held by active investigators in this field. However, the hypothesis has apparently been accepted by workers not familiar with this special field of colloid chemistry to be the prevailing theory of chrome tanning (30). The aim of the present note is to point out certain inconsistencies, inadvertencies, and misconceptions in the hypothesis of Cameron and McLaughlin in the light of new experimental findings.

The main thesis of the hydrolysis-adsorption concept is that hide protein from a solution of basic chromium sulfate first combines with and removes free acid of the hydrolyzed system. This leads to disturbance of the hydrolysis equilibrium. Insoluble 66 per cent basic chromium sulfate¹ is formed and deposited within the protein structure. Further, it is claimed that chrome tanning is a reversible adsorption process.

The authors' postulate of equilibrium and the reaction mechanism proposed

¹ Per cent basicity = $\frac{\text{equivalents OH}}{\text{equivalents Cr}} \times 100$.

are based on the supposition that the basicity of the chromium compound taken up by collagen is the same as the over-all basicity of the tanning solution employed and that the deposited salt is 66.6 per cent basic. On these assumptions and by means of three sets of experimentally obtained values (content of chromium and acid sulfate of the original chromium sulfate and the chrome content of the tanned pelt), an imposing array of columns of figures is built up which by no means can be considered to form evidence for the postulated mechanism of the reaction. However, the postulates are not generally valid, as evident from data in the paper. In many respects the deductions of the authors appear to verge upon a vicious circle.

A brief résumé of some experimental tests of the adsorption hypothesis will be given in the light of the modern conception of this highly complicated process.

In regard to the pressing technique used by the authors, it has been found both by experiments and from recalculation of data given by the authors in more recent publications (17, 18), that the pressed stock on an average contains 125 per cent water, based on the weight of collagen. The authors have not realized that this "water" consists of (1) *bound* water (about 20 per cent on the weight of collagen), not available as solvent, and (2) *free* water (about 105 per cent) in the form of the solution used for tannage. The amount of Cr and SO_4 present in this solution in uncombined state will be included in the figures of fixed chromium and acid obtained on analysis of pressed leather. Even at moderate chrome concentration, the error in chrome determination will be rather large (10–20 per cent of the chrome content found). As such pressed leather has been used in experiments intended to demonstrate the reversibility of the process, the main part of the chromium compounds removed "in this reversal" probably simply consist of chromium compounds mechanically held in the interstices of the pressed leather. The present author's experiments support such a view, although a slight reversal has in some instances been observed upon prolonged treatment of leather free from soluble chromium compounds. However, a slight reversal of chrome fixation can not be considered as evidence for the reversible nature of the chrome tanning process, as a true reversible system rapidly reaches equilibrium.

Accordingly chrome fixation does not reach a predicted fixed equilibrium but only limiting values, as the requisite of a reversible system is lacking. Further, the hydrolytic system collagen–aqueous solution of basic chromic salt is greatly affected by external factors, such as temperature, in regard to hydrolysis, degree of aggregation of the basic chromic sulfate, its constitution, and its electrochemical behavior (1, 20, 24). Amphoionic structures such as hide protein are further temperature dependent. Thus, the ratio of charged groups to uncharged ones tends to decrease with increasing temperature (3, 23). The final result is that the fixation of chrome by collagen is greatly increased by a rise in temperature (14, 19, 22). The authors have disregarded the cardinal factors of the system, especially the constitutional one, and simply treated the basic chromium salts as chemically *unchangeable* ionic reactants.

They claim a certain equilibrium value of chrome fixation from a given solu-

tion and that the basicity of the chromium salt taken up by collagen, basically of leather, is equal to the basicity of the original chromium compound. The data in table 1 afford a test of these assertions. The data, showing the amount of Cr_2O_3 fixed by collagen and the basicity of the chromium sulfate fixed, were obtained by treating 5.0-g. portions of hide powder in 100-ml. portions of 33 per cent basic chromic sulfate ($\text{Cr}_2(\text{OH})_2(\text{SO}_4)_2 \cdot \text{Na}_2\text{SO}_4$), containing 0.4 equivalent of chromium per liter, at the temperatures given for 4 weeks. Any appreciable fixation of chrome did not occur upon prolonging the interaction beyond this time. The figures of the per cent of basicity of the fixed chromium sulfate (the leather) were obtained by the "difference" method in order to avoid changes in the composition of the leather. From the values of the contents of chromium and hydrolyzable acid present in the original and used solutions, the degree of fixation of these constituents was obtained. With selection of a suitable ratio of hide substrate to solution, as in the present example, the indirect method has proved satisfactory.

Evidently the over-all basicity concept of the authors is not valid; neither is any given equilibrium in chrome fixation established for a certain solution.

TABLE 1

Influence of temperature of tanning upon chrome fixation and basicity of fixed chromium sulfate

Temperature of tanning in °C.	4	20	40
Milliequivalents Cr fixed by 1 g. of collagen	2.64	3.36	4.28
Per cent basicity of fixed chromium sulfate.	32	38	42

If the chrome fixation by hide protein is claimed to be a secondary process, regulated by the acid-binding capacity of collagen, it should be logical to assert that the chrome fixation should be independent of the temperature of the system, since the fixation of strong acids (hydrochloric, sulfuric) by proteins from dilute solutions is temperature independent, providing the treatment does not affect the ionic potency of the protein (hydrolysis, leading to the formation of new acid-binding protein groups) (26).

A few other critical tests will be mentioned. The fixation of strong acids by collagen attains equilibrium within 24 hr. If the chrome fixation is a secondary process, controlled by the primary reaction of the fixation of acid by collagen, it would be expected that chrome fixation should come to a standstill within this time. This is not the case, the limiting values of fixed chrome requiring a period of interaction several times longer (27).

Further, chrome tanning is generally carried out at final pH values of 3-3.5. The combining capacity of collagen for sulfuric acid is in this pH range *ca.* 0.4 milliequivalent of acid per 1 g. of collagen (2 per cent sulfuric acid) (4, 5). The authors evidently consider that collagen in this pH zone possesses its maximum acid-combining capacity, as the indirect figures of protein-bound acid (up to 8.3 per cent sulfuric acid) show values exceeding the amount of acid-binding protein groups of collagen (1.07 milliequivalents per 1 g. of collagen (29)).

This discrepancy is ascribed by the present author to the fact that protein-bound sulfate has chiefly been introduced as sulfate ions, belonging to and compensating the simultaneously fixed cationic chromium complexes, by the attachment to charged basic groups, only a minor part being derived from the free acid of the system (11).

Further, a few lines on the explanation of the chrome fixation by hide pelt, pickled with acid to equilibrium with a solution of sodium sulfate-sulfuric acid of a given pH, e.g., 2.5, from a solution of basic chromic sulfate of a higher pH value, e.g., 3.5. Assuming the acid fixation to be the driving force of chrome fixation, no chrome should be taken up, judged from a physicochemical standpoint. However, large amounts of chromium are fixed in this ordinary process of chrome tanning. The explanation given for this reaction in the paper (2) is hardly compatible with the modern physicochemical concept of reactions between proteins and mineral acids. The industrial practice of chrome tanning is in fact a denouncement of the adsorption hypothesis.

TABLE 2
The acid-binding capacity of proteins and their chrome fixation

	SILK FIBROIN	WOOL KERATIN	COLLAGEN (HIDE POWDER)	ELASTIN	CASEIN	BLOOD FIBROIN	MUSCLE PROTEINS (CHICK- EN)
Milliequivalents HCl fixed by 1 g. of protein	0.16	0.82	0.90	0.34	0.84	1.18	1.29
Milliequivalents Cr fixed by 1 g. of protein	0.16	0.36	6.36	1.28	4.12	12.16	7.92
Ratio of Cr fixation: H ⁺ fixation	1.0	0.4	7.1	3.8	4.9	10.3	6.1

It should be of interest to ascertain the comparative binding capacity of various proteins for hydrogen ions and basic chromium sulfate, since according to the hydrolytic concept, the capacity of proteins for fixation of mineral acids (hydrochloric acid) and their affinity for basic chromic sulfate should be directly related. This is not the case, as evident from the data in table 2. The values of the maximum fixation of hydrochloric acid by various proteins were obtained by treating 1.00 g. of protein in 25 ml. of 0.1 N hydrochloric acid containing 2 per cent sodium chloride by volume, during 24 hr., and determining the acid taken up by the protein by the difference method (methyl red). The values of fixed chrome were obtained by analysis of the washed, chromed proteins which in 2-g. portions were shaken during 120 hr. at room temperature with 100-ml. portions of a solution of 50 per cent basic chrome sulfate liquor, containing 0.8 equivalent of chromium per liter.

It can safely be stated that the number of acidic and basic protein groups, their valency state (the degree of activation), and the molecular organization of the proteins enter as determining factors of chrome fixation by proteins. These factors must be included in the tanning equation.

Further, the authors have not availed themselves of the documentation on

complex formation by basic chromic sulfates (25). Thus, it is evident that the average acidity of the cationic sulfatochromium complexes may vary from 20 to 40 per cent, according to the nature of the chromic compound and the presence of other components, chrome concentration, temperature of solution, etc. In normal systems of moderate concentration and basicities the average acidity of the complexes is in the vicinity of 33 per cent, corresponding to 67 per cent basicity (8). Besides variation in the composition of the positively charged complexes as noted, the electrochemical picture of basic sulfate is easily and fundamentally altered, a fact which especially has been brought out by recent investigation by means of ion-exchanging organolites (13). As an example may be mentioned the composition of the chromic sulfate of table 1 at a concentration of 0.8 equivalent of chromium per liter, kept for 72 hr. at the temperatures given and analyzed by the organolite method (see table 3).

TABLE 3
Composition of basic chromic sulfate as a function of temperature

	4°C.	20°C.	40°C.
Per cent cationic chromium	98	97	71
Per cent uncharged chromium	2	3	22
Per cent anionic chromium	0	0	7

TABLE 4
Electrochemical composition of solutions of basic chromic sulfate at different concentrations

CONCENTRATION OF SOLUTION IN EQUIVALENTS Cr PER LITER	0.8	2.0	4.0	8.0
Per cent cationic chromium complexes . . .	98	88	69	42
Per cent uncharged chromium complexes	2	10	26	49
Per cent anionic chromium complexes	0	2	5	9

Further, the influence of the chrome concentration on the composition of this compound is evident from the data of table 4 (solutions aged 6 weeks).

The affinity of the various chromium complexes for collagen varies widely, and the uncharged ones appear to be independent of the hydrolytic equilibrium of the system. This complication has been entirely disregarded in the adsorption concept.

The importance of the constitution of the chromic salt in its reaction with hide protein is strikingly illustrated by the opposite effect of neutral salts on chromium salts in regard to their affinity for collagen. The addition of large amounts of neutral chlorides (sodium chloride, making the solution 1-2 *M* with respect to the same) to dilute solutions of basic chromic chlorides leads to a decrease in the pH of the system and marked increase in the chrome fixation by collagen, whereas the same addition to more concentrated solutions, giving the same pH effect, markedly retards the reaction with collagen, although in both instances the acid-binding reaction is not materially changed (10). By the

addition of sodium chloride and sodium sulfate to solutions of basic chromic sulfate, the hydrogen-ion concentration is increased and decreased, respectively. However, in both instances chrome fixation is retarded (28, 31).

From solutions of basic chromic sulfate containing certain complex-forming sodium salts of organic acids,—such as formic, oxalic, and phthalic,—collagen fixes large amounts of chromium in the pH range 5–7, corresponding to the isoelectric zone of hide protein or even on its alkaline side, although any fixation of mineral acid cannot occur under these conditions (7).

Even changes in the hide substrate not interfering with its acid-binding function exert a decided influence on the course and extent of the reaction of certain basic chromic sulfates, especially strongly basic ones. By pretreatment of neutral, isoelectric calfskin pelt in strong solutions of lyotropic agents, such as

TABLE 5

The effect of certain pretreatments of calfskin pelt upon its fixation of basic chromic sulfate
Tanning the washed pelt 96 hr. in 60 per cent basic chrome sulfate liquor containing 1.0 equivalent Cr per liter

	Cr FIXED BY 1 G. OF COLLAGEN	HCl FIXED BY 1 G. OF COLLAGEN (pH = 1.0)
	milliequiv.	milliequiv
Pretreatment 14 days at 20°C. in:		
Water (blank)	5.34	0.92
2 M calcium chloride	7.76	0.92
1 M calcium thiocyanate.	8.64	0.90
8 M urea	8.90	0.96
3 M acetic acid	8.37	0.94
Hide powder (blank)	8.13	0.90
Hide powder denatured at 75°C.	12.48	0.90

calcium chloride, calcium thiocyanate, urea, and acetic acid (the treated stock brought to the isoelectric state after pretreatment) or by heat denaturation of hide powder, the affinity of the treated collagen for such chromic compounds is greatly increased, in some instances up to 100 per cent of the value for untreated collagen (9). Table 5 contains some typical data.

The acid-binding capacity of collagen is not changed by these pretreatments. Accordingly, the additional uptake of chromium can not be governed by the fixation of acid by hide protein. In both instances, a part of the chrome fixation probably occurs by coördination on peptide groups.

In regard to the first questions raised in the paper, if the reaction is stoichiometric or adsorptive, it may be said that any simple stoichiometric relationship is not discernible in chrome-tanned collagen. This is not surprising and not conflicting with the concept of the formation of regular chemical compounds, since the possibilities of reaction of proteins and complex salts are numerous and simple stoichiometric ratios are not any more considered as a criterion of

protein reactions (16). An imposing array of findings in support of this view is at hand (6, 12, 15, 16, 21). Secondly, the question of the composition of the chrome compound fixed by collagen is raised. The modern concept of the chrome tanning process (6, 12, 15, 16, 21) considers the main reaction to be an attachment of cationic acidochromium complexes to the charged acidic groups of collagen with a simultaneously occurring coordination of the complexes to the basic groups of adjacent protein chains. The hydrogen ions of the solution compete with the chromium complexes for the free, charged acidic protein groups. With increased pH of the system this competition from the acid is less marked. The sulfate ions belonging to chromium cations are balanced by positively charged protein groups, whereby the electroneutrality of the system is upheld. The chelated chromium complexes act like connecting links or bridges between adjacent protein chains, resulting in a stabilization of the structure (6, 12, 15, 16, 21). This is shown in increased hydrothermal stability (chrome leather will withstand the action of boiling water) and inertness towards proteinases (trypsin). For the existing experimental support of this concept of an internal salt formation, references are given to the literature (6, 12, 15, 16, 21). Regarding the last question, if specific parts of the protein are involved in the reaction and if so, which, any definite information on these points is hardly to be expected in view of our limited knowledge of this special aspect of protein chemistry, although evidences and indications are to be found in the literature and in the concept outlined. The adsorption hypothesis has not added to the knowledge of the problem of how a small amount of a chromic salt incorporated in the protein structure can have such a far-reaching effect on the protein. The internal-complex salt-bridge concept gives an acceptable explanation of the process as well of the nature of the product formed, chrome leather.

SUMMARY

1. The adsorption hypothesis of the fixation of basic chromium sulfates by hide protein (chrome tanning) is based on the supposition that the chromium compound fixed by collagen is 66.6 per cent basic and further, that the "over-all basicity" of the tanned leather is the same as the basicity of the tanning solution employed. These postulates are shown not to be generally valid.

2. The reaction is not a reversible process in the usually accepted meaning of the term.

3. The application of the adsorption concept leads to unacceptable values of protein-bound acid. The reaction kinetics are not in accord with the hypothesis.

4. The governing importance of the constitution of the chromic salts has been entirely disregarded. The influence of temperature of solution upon the complex formation of chromic salts and the effect of concentration changes are demonstrated.

5. The effect of neutral salts on basic chlorides and sulfates of chromium cannot be explained by the concept of Cameron and McLaughlin; neither can the excellent tanning action of certain mixed organosulfatochromium complexes

in a pH range corresponding to the isoelectric zone of collagen or on its alkaline side, in the absence of acid fixation by the protein.

6. The effect of pretreatment of hide protein in solutions of lyotropic agents and heat denaturation of the same, resulting in greatly augmented affinity of such treated collagen for strongly basic chromium sulfates, are directly conflicting with the view of chrome fixation as an acid-regulated process.

7. An outline of the internal-complex salt-bridge concept of the chrome tanning process (the formation of chelate compounds) is presented.

REFERENCES

- (1) BALÁNYI: "Chemie der Chromverbindungen" in Grassmann's *Handbuch der Gerberei-chemie und Lederfabrikation*, Band II, Teil 2, pp. 45-176. J. Springer, Vienna (1939).
- (2) CAMERON AND McLAUGHLIN: J. Phys. Chem. **41**, 961 (1937).
- (3) EBERT: Z. physik. Chem. **121**, 385 (1926). For later literature see reference 23.
- (4) ELÖD AND SIEGMUND: Collegium **1932**, 137 (figures 1 and 2).
- (5) ELÖD AND SILVA: Z. physik. Chem. **137**, 142 (1928).
- (6) GRASSMANN: *Handbuch der Gerberei-chemie und Lederfabrikation*, Band II, Teil 2, pp. 233-6, 266-77. J. Springer, Vienna (1939).
- (7) GUSTAVSON: J. Am. Chem. Soc. **48**, 2963 (1926); J. Soc. Leather Trades Chem. **10**, 203 (1926).
- (8) GUSTAVSON: J. Am. Leather Chem. Assoc. **21**, 559 (1926); **22**, 60 (1927).
- (9) GUSTAVSON: Colloid Symposium Monograph **4**, 79-101; Biochem. Z. **311**, 347 (1942); J. Am. Leather Chem. Assoc. **41**, 47 (1946).
- (10) GUSTAVSON: Ind. Eng. Chem. **19**, 1015 (1927).
- (11) GUSTAVSON: Collegium **1932**, 775.
- (12) GUSTAVSON: *Stiasny Festschrift*, pp. 99-133, E. Roether Verlag, Darmstadt (1937); J. Am. Leather Chem. Assoc. **26**, 635 (1931); Svensk Kem. Tid. **52**, 75 (1940).
- (13) GUSTAVSON: Svensk Kem. Tid. **56**, 14 (1944); **58**, 2 (1946); J. Colloid Sci. **1**, 397 (1946).
- (14) GUSTAVSON AND WIDEN: Collegium **1926**, 103.
- (15) KÜNTZEL: Collegium **1936**, 625.
- (16) KÜNTZEL AND RIESS: Collegium **1936**, 635, 646.
- (17) McLAUGHLIN, ADAMS, AND CAMERON: J. Am. Leather Chem. Assoc. **35**, 694 (1940).
- (18) McLAUGHLIN AND CAMERON: *Stiasny Festschrift*, p. 240. E. Roether Verlag, Darmstadt (1937).
- (19) MERRILL AND SCHROEDER: Ind. Eng. Chem. **21**, 1225 (1929).
- (20) MERRY: *The Chrome Tanning Process*. A. Harvey, London (1936).
- (21) Reference 20, pp. 79-142.
- (22) OTTO: Dissertation, Karlsruhe, 1928, pp. 20-21.
- (23) SCHMIDT: *The Chemistry of the Amino Acids and Proteins*, pp. 872-5. Charles C. Thomas, Baltimore, Maryland (1938).
- (24) STIASNY: *Gerberei-chemie*, pp. 321-487. Steinkopff, Dresden (1931).
- (25) Reference 24, pp. 367-77.
- (26) THEIS AND GOETZ: J. Am. Leather Chem. Assoc. **27**, 570 (1932).
- (27) THOMAS, BALDWIN, AND KELLY: J. Am. Leather Chem. Assoc. **15**, 147 (1920).
- (28) THOMAS AND FOSTER: Ind. Eng. Chem. **14**, 132 (1922).
- (29) VAN SLYKE: J. Biol. Chem. **10**, 15 (1911).
- (30) WEISER: *Inorganic Colloid Chemistry*, Vol. II, Chap. XVII. John Wiley and Sons, Inc., New York (1935).
- (31) WILSON AND GALLUN: J. Am. Leather Chem. Assoc. **15**, 273 (1920).

THE PHASE BEHAVIOR OF SODIUM STEARATE IN ANHYDROUS ORGANIC SOLVENTS

GEROULD H. SMITH¹ AND JAMES W. MCBAIN*Department of Chemistry, Stanford University, California**Received May 20, 1947*

In contrast to the many studies of the phase diagrams of soaps in aqueous systems, very little is known as to the phase behavior of soaps in non-aqueous solvents (2, 6, 8, 10, 11). It is the object of this communication to present data for sodium stearate in twelve different pure hydrocarbon solvents, with special attention given to cyclohexane and toluene.

The relation of these studies to lubricating greases, together with the important effects of water and other additives, will be discussed in a separate publication.

MATERIALS

The sodium stearate was prepared from sodium ethoxide and Eastman Kodak Company stearic acid (White Label; No. 402). It was identified as the γ -form by x-ray diffraction (1, 5). It was found to be neutral to phenolphthalein in boiled-out 95 per cent ethyl alcohol.

Eleven of the hydrocarbon solvents were obtained from the Eastman Kodak Company and used without further purification other than drying and storing over Drierite (anhydrous calcium sulfate): namely, cyclohexane, toluene, *o*-xylene, *m*-xylene, *p*-xylene, 2,2,4-trimethylpentane (isoöctane), *n*-heptane, ethylbenzene, *n*-butylbenzene, cumene, and *p*-cymene. Baker and Adamson reagent-grade, thiophene-free benzene was used. Except for *n*-butylbenzene and *p*-cymene, the solvents showed no tendency to foam when shaken. The *p*-cymene was light yellow in color and may have contained terpenes as an impurity.

EXPERIMENTAL TECHNIQUES

The samples of soap and hydrocarbon were sealed in evacuated Pyrex tubes and studied visually, in a manner similar to the previous investigations by McBain and coworkers on the anhydrous aqueous soap systems. This was supplemented by microscopic examinations under polarized light and by photomicrography. All thermometers and thermocouples were carefully calibrated.

Temperatures, designated by T_i , were those at which, on cooling, anisotropic material began to separate from the single isotropic phase.

Preparation of the samples

Pyrex tubing (6–8 mm. outside diameter), sealed at one end, numbered with a glass-marking pencil and the number fused into the hot glass, was used as sample

¹ Present address: Union Oil Company of California, Oleum, California.

containers. These tubes were sealed to standard taper 12/24 outer cones and cleaned with hot concentrated sulfuric and nitric acids, followed by several rinses with distilled water and dilute ammonia water. They were dried by evacuation and stored in a desiccator over phosphorus pentoxide until use.

Powdered sodium stearate was charged into the sample tubes by extruding tamped plugs of soap from a 3-mm. glass tube 18–20 cm. in length. The soap thus could be deposited at the bottom of the tube without contaminating the walls, preventing decomposition when the tube was sealed. After the soap was dried (described later), the dried solvent was introduced using a hypodermic syringe of 1-ml. capacity, graduated in 0.01 ml. The solvent was deposited directly onto the soap, using a 3-in. needle. During all these operations the tubes were closed tightly with standard-taper ground-glass plugs except for a few seconds when the solvent was being added.

A tube containing the soap and solvent was attached to the vacuum pump and evacuated until the solvent began to boil. Then it was chilled with powdered dry ice. The pressure was reduced below 1 mm. of mercury, and the tube sealed off. Both pieces of the original tube were wiped clean, dried, and weighed. This weight, together with the tare of the tube and the weight of the dried soap, was used to calculate the composition of the sample.

Drying the sodium stearate and solvents

The sodium stearate, after weighing into the tubes before sealing, was dried for 2–6 hr. by heating in an Abderhalden drying pistol over phosphorus pentoxide, using a reduced pressure of less than 1 mm. of mercury. Quinoline was used as the heating medium. Before removal of the samples after drying the apparatus was allowed to cool, and air, dried by slowly passing through a dry ice-cellosolve coldspot, was admitted until it was equal to atmospheric pressure. Then the pistol was opened and the tubes were capped immediately.

Experience demonstrated that even small traces of oxygen resulted in charred soap during the drying. Because of this, the pistol was flushed five times with nitrogen, evacuating between each flush, before heating the soap. The ground-glass pistol cap was sealed with Apiezon grease "L", and it maintained the pressure at less than 1 mm. for 12 hr. or more at the boiling point of quinoline.

The hydrocarbons were dried satisfactorily over Drierite. Indicator-impregnated Drierite changes color in a few days if allowed to stand at the bottom of an open vessel of a hydrocarbon solvent. This change is immediate if water is added to the solvent. Storage of the hydrocarbon solvents and indicator Drierite in stoppered reagent bottles resulted in no color change for the indicator over more than sixteen months.

Observation of the samples

The samples were studied while being heated in a thermostatic bath of white oil, or in a Freas Precision forced-draft oven, or in a Pyrex-tube furnace. The oil bath maintained a temperature regulated to $\pm 0.25^\circ\text{C}$. and could be used over a temperature range of 0° to 200°C .

The Freas oven was equipped with a glass window having three parallel panes, spaced to allow the heated oven air to pass between them, thus minimizing heat losses through the window, but still allowing observation of the samples, which were fastened perpendicularly to a horizontal glass spindle. Wires operating a reel attached to this spindle were led through the air vent of the oven and permitted the samples to be thoroughly rotated and mixed while in the heated oven.

A Pyrex-tube furnace was used for observations at temperatures greater than 310°C. It consisted of five concentric Pyrex tubes which were fastened alternately to two headers, causing an air current passing over a heater between the two outermost shells to pass back and forth inward, until it was vented from the innermost shell which contained the tube under observation. The temperature of the sample was measured with a calibrated, iron-constantan thermocouple, placing the junction next to the sample tube. The entire furnace was rotated to mix the sample. The temperature was varied by controlling both the air flow and the applied voltage to the heater.

Transmitted polarized light was used to illuminate all samples, and was analyzed by manual operation of a second polaroid disk.

GENERAL OBSERVATIONS

1. *Unheated anhydrous systems*

Sodium stearate does not swell in pure anhydrous hydrocarbons at room temperature, but it is capable of soaking up nearly its own volume of solvent. Even when stored for several years in excess of solvent the particles of soap are separate and discrete and are readily redispersed on shaking, although the settled layer looks compact and gelled.

2. *Anhydrous systems on heating*

When sodium stearate is heated in the presence of an excess of solvent, it begins to swell into the solvent at 80–85°C. It needs 5–8 per cent of soap to fill the liquid unless it has been heated so high that all of it dissolves to form isotropic solution.

At 98°C. all anhydrous systems containing below about 45 or 50 per cent of soap exhibit a sharp, sudden change in appearance. The opaque, white, swollen gel becomes translucent and liquid crystalline, transmitting polarized light with bright tan or golden color. A simultaneous structural change at 98°C. results in the engagement of all free liquid if the sample is mixed, distributing the soap during the change. Failure to distribute the soap during the transformation always results in the formation of a compact, gelled layer which is very resistant to dispersion in supernatant liquid. This transformation at 98°C. is reversible only very slowly on cooling, because of undercooling.

Systems containing more than 50 per cent of soap change at about 90°C. to a liquid-crystalline phase which transmits light and is translucent, white, and wax-like in appearance. The samples are dry or wet powder before heating and some difficulty is encountered in observing this change in systems not previously

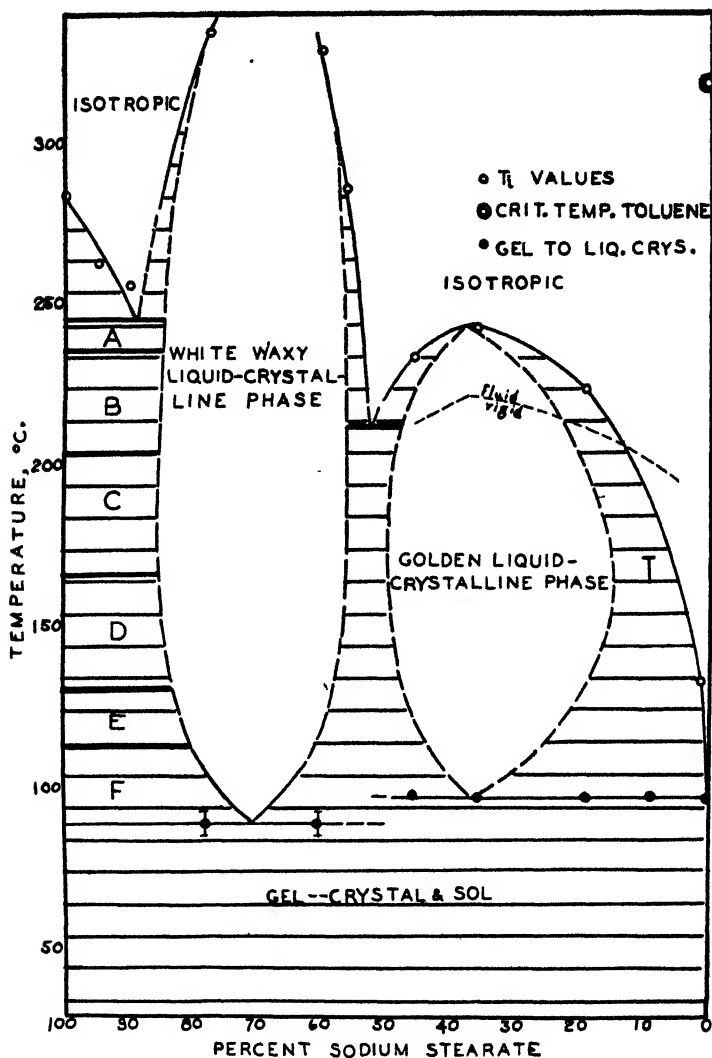


FIG. 1. Phase diagram of anhydrous sodium stearate in dried toluene. Legend for two-phase areas: A, neat soap and liquid-crystalline phase; B, subneat soap and liquid-crystalline phase; C, superwaxy soap and liquid-crystalline phase; D, waxy soap and liquid-crystalline phase; E, subwaxy soap and liquid-crystalline phase; F, supercurd soap and liquid-crystalline phase. (No attempt has been made to represent how the various phases that exist at different temperatures in 100 per cent sodium stearate extend into the phase diagram, although it is known that they do so extend. The black horizontal lines of figure 1 and the corresponding square dots of figure 2 merely represent the phase transitions in the absence of any solvent. Tie-lines adjacent to these phases are devoid of significance.)

melted, because of reflected light. The powdery soap usually sinters to a porous plug at 185–200°C.

Both of the liquid-crystalline phases melt to isotropic sol or jelly at higher

temperatures. The golden, liquid-crystalline phase acquires a "mosaic" pattern a few degrees below the T_i value, which changes to vibrating, dancing particles on a further slight increase in temperature. These dancing and sometimes

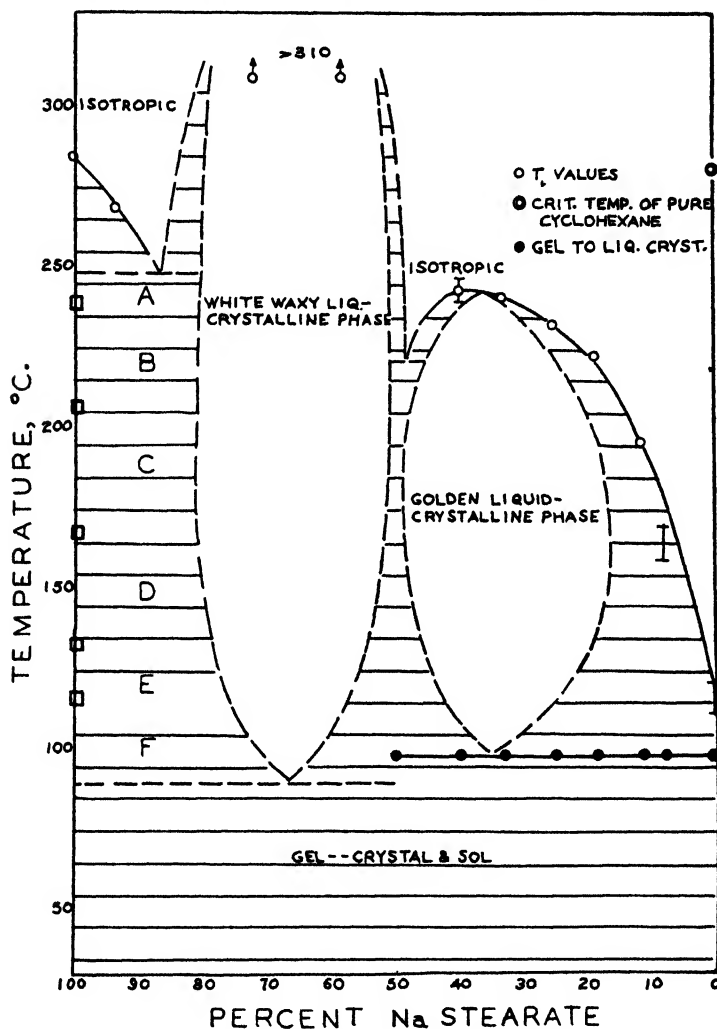


FIG. 2. Phase diagram of anhydrous sodium stearate and dried cyclohexane. A, neat soap and liquid-crystalline phase; B, subneat soap and liquid-crystalline phase; C, superwaxy soap and liquid-crystalline phase; D, waxy soap and liquid-crystalline phase; E, subwaxy soap and liquid-crystalline phase; F, supercurd soap and liquid-crystalline phase. (See note at the end of legend for figure 1.)

brilliantly colored particles settle rapidly in the supernatant, isotropic medium if the sample is not stirred. They dissolve on further heating in the isotropic solution. These changes are reversible. The temperatures at which the disappearance of the last anisotropic, dancing particle, on heating, and the re-

appearance of the first one on cooling the isotropic sol, occur are within 1° for most observations.

The white, wax-like, rigid, liquid-crystalline phase melts to an isotropic liquid at temperatures considerably above the true melting temperature of the pure anhydrous soap, 288°C . White, anisotropic particles separate reversibly from the isotropic melt on cooling, and, concurrently, the system again becomes rigid. Systems containing 85–90 per cent or more of soap melt at about 205°C . to a form resembling the subneat phase of anhydrous sodium stearate. This becomes isotropic below the melting temperature of the anhydrous soap. In figures 1 and 2 the full lines in the figures are those which are carefully authenticated by experimental points; the dashed lines are those whose positions are less accurately determined but nevertheless known to be approximately where indicated. For toluene and cyclohexane the dashed lines around the golden liquid-crystalline phase are corroborated by the experimental points obtained with *p*-xylene.

3. Anhydrous systems during recooling

The systems containing less than 15 per cent of sodium stearate at first become rigid isotropic jellies as they begin to cool from the fluid isotropic sols. This change is not sharp and occurs near 200 – 220°C . Further cooling to 100 – 120°C . usually results in an anisotropic appearance caused by internal strain in the jelly, and is manifested as a flowing pattern with a gradual change of intensity rather than the sharply defined discontinuous anisotropy characteristic of the crystalline and liquid-crystalline forms.

The hot isotropic solutions containing from 15 per cent to about 85 per cent of soap immediately begin to separate out anisotropic particles on cooling. These then solidify to the liquid-crystalline phases. Systems containing more than 85 per cent exhibit the changes characteristic of the pure anhydrous sodium stearate (7).

The appearance of the systems after cooling to room temperature depends on the concentration of the soap and the particular hydrocarbon used in the systems. This appearance may change on storage, giving a measure of the relative stabilities with respect to both the concentration of the soap and the nature of the hydrocarbon.

Systems containing less than 15 per cent of soap, on cooling from the isotropic state first form a jelly which, on further cooling, becomes anisotropic from internal strain without any liquid-crystalline phase being present, until at about 80°C . they contract violently and eject isotropic solvent as a spray. The volume of the resultant opaque gel is comparable with that of the original unheated soap. A portion of such a cooled gel examined by S. Ross, using x-ray diffraction at room temperature with $\text{Cu } K_\alpha$ radiation filtered through nickel foil gave a powder pattern exactly similar to that of the original dried soap, apart from general scattering by solvent (cyclohexane, glycerol, or Nujol). Results with cyclohexane show that even after being heated in hydrocarbon the sodium stearate retains the original crystalline form of pure γ -sodium stearate.

Sorption and desorption isotherms determined by Shreve (9), using the McBain-Bakr sorption balance, show that at 40°C. sodium stearate takes up only 3 per cent by weight of cyclohexane at 100 per cent relative vapor pressure, increasing to 5.5 per cent at 50°C. At 80°C. the sorption amounts to 14 per cent and at 110°C., 33 per cent. At about 110°C. the sorption and desorption is reversible, whereas at lower temperatures hysteresis occurs. The isobaric curves in figure 3 were constructed from the isothermic data, and they showed that marked change in the affinity of the soap for the cyclohexane occurred between 80° and 110°C. This was assumed to be the transformation to the liquid-crystalline phase at 98°C.

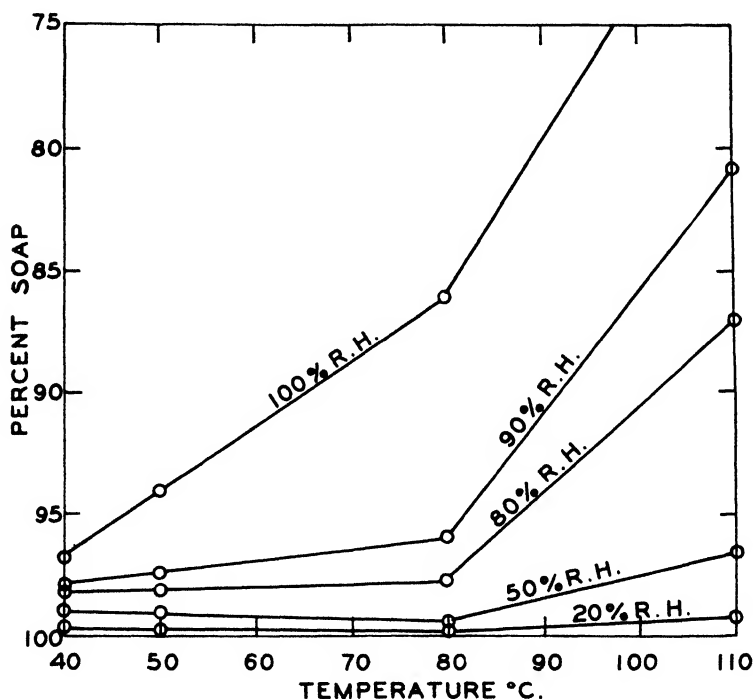


FIG. 3. Isobaric curves for system of pure cyclohexane and sodium stearate

In general, three prominent effects are found to occur on allowing the systems to stand at 24–29°C. after cooling from the isotropic state without stirring. These are syneresis, a decrease in the volume of the rigid portions of the system, and an increase in opalescence or opacity. These changes are more rapid in samples containing less than 20 per cent of soap. In general, the stability of the cooled systems appears to increase from both sides toward the middle of the liquid-crystalline phase areas. All three effects may be exhibited if enough time is allowed for the changes to occur, and the occurrence of syneresis and increased opacity are simultaneous.

TYPICAL EXPERIMENTAL DATA

1. *Sodium stearate in cyclohexane after cooling*

Figure 4 shows changes occurring with increased soap concentration in anhydrous cyclohexane, and exhibits reversion to an opalescent gelled plug up to concentrations of about 10 per cent of soap. Samples 4 and 5 were both synergetic. The latter exhibited a streaked opalescence. Sample 5 was optically

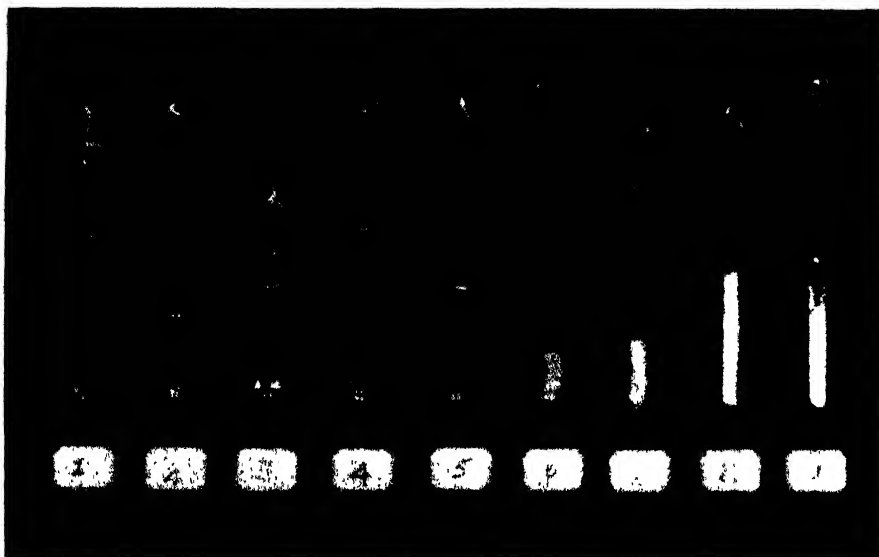


FIG. 4. Appearance of anhydrous systems of sodium stearate in cyclohexane on cooling. Pictures $\frac{1}{2}$ natural size.

TUBE NO.	SOAP	HEATED TO ISOTROPIC
	<i>per cent</i>	
1	0.4	Yes
2	2.9	Yes
3	7.9	Yes
4	18.5	Yes
5	25.1	Yes
6	58.2	No (to 300°C.)
7	72.0	No (to 300°C.)
8	83.0	No (to 300°C.)
9	93.3	Yes

clear to ordinary and polarized light for a year, but then became slightly hazy, and when photographed six months later was progressing toward an opaque, recrystallized gel system. Note the reflections of the light source at the bottom of the first five tubes, only allowing a comparison for relative translucency of contents.

A careful examination of tube 6 will show that parts of the sample are whiter

TABLE 1
Anhydrous systems of sodium stearate in hydrocarbons

PER CENT SOAP		T _i	DESCRIPTION OF COOLED SYSTEMS	
Per cent by weight	Mole per cent		Immediately after cooling	After aging
Cyclohexane (critical temperature, 281°C.)				
0.44	0.2	(115)	Faintly opalescent particles in clear liquid	Opalescent particles in clear liquid
2.9	0.9		Slightly opalescent plug in clear liquid	Slightly opalescent plug in clear liquid
7.9	2.5	(160)	Faint opalescent gel plug in clear liquid	Cloudy plug in clear liquid
11.5	3.8	195	Opalescent gel plug in clear liquid	
18.3	6.2	222	Opalescent gel; slightly synergetic	Opalescent plug; synergetic
25.1	9.1	232	Clear; not synergetic	Opalescent; slightly synergetic
33.2	12.8	240	Slightly opalescent; slightly synergetic	
39.6	16.2	(243)		
45.4	19.8	>310	Waxy-like; tan and white	Waxy-like; tan and white; slightly synergetic
58.2	29.2	>310	White; semitranslucent; not completely sintered	Unchanged
72.0	43.3	>300	White; semitranslucent; not completely sintered	Unchanged
83.0	59.2	>307	White; partly translucent; partly opaque	Unchanged
93.3	80.5	269	Tan; opaque; compact	Unchanged
100.0	100.0	285	Hard; white; opaque; compact	Unchanged
Toluene (critical temperature, 320.6°C.)				
0.93	0.3	(133)	Very slightly opalescent gel in clear liquid	Very slightly opalescent gel particles in clear liquid
9.1	3.14	(165)	Clear gel in clear liquid (opalescent overnight)	Very slightly opalescent gel plug in clear liquid
18.9	6.5	225	Opalescent gel; synergetic	Slightly opalescent plug; synergetic
36.0	15.5	244	Faintly cloudy; no syneresis	Partly cloudy; slightly synergetic
45.4	21.2	235	Slightly opalescent; no syneresis	Opalescent plug; slightly synergetic
55.9	29.0	287	Semitranslucent gel with clear liquid	Unchanged
60.3	33.0	331	Opaque in semitranslucent gel	Opaque in semitranslucent gel; slightly synergetic
77.9	53.3	335	Opaque in semitranslucent gel	Unchanged; no syneresis
89.8	74.1	257	White; opaque	Unchanged
94.6	85.0	264	Hard; white; opaque	Unchanged

TABLE 1—*Continued*

PER CENT SOAP		T_i	DESCRIPTION OF COOLED SYSTEMS	
Per cent by weight	Mole per cent		Immediately after cooling	After aging
<i>p</i> -Xylene (critical temperature, 348.5°C.)				
19.5	8.4	220	Slightly opalescent gel; slightly syneretic	Slightly opalescent plug; syneretic
28.6	13.1	232	Clear jelly; no syneresis	Very slightly opalescent; slightly syneretic
43.7	22.5	244	Cloudy; no syneresis	Cloudy; slight syneresis
56.3	32.6	216	Very slightly opalescent; slightly syneretic	Very slightly opalescent plug; syneretic
61.9	37.8	>280	White; wet; wax-like	Unchanged
87.8	73.0	261	White; wet; compact	Semitranslucent; white; no syneresis
90.8	76.6	263	White; wet; compact	Unchanged
<i>o</i> -Xylene (critical temperature, 363°C.)				
10.2	4.1	(200)	Isotropic; syneretic	Very slightly opalescent plug; syneretic
19.9	8.5	216	Clear; not syneretic	Slightly opalescent plug; syneretic
27.6	12.5	229	Clear; not syneretic	Slightly opalescent plug; syneretic
38.1	18.7	240	Slightly opalescent; slight syneresis	Cloudy; slight syneresis
<i>m</i> -Xylene (critical temperature, 349°C.)				
10.4	4.2		Clear; syneretic	Very slightly opalescent plug; syneretic
20.0	8.6	223	Faintly opalescent; slight syneresis	Unchanged
29.4	13.5	230	Slightly opalescent; not syneretic	Opalescent plug; slightly syneretic
41.1	20.7	244	Slightly opalescent; not syneretic	Opalescent plug; slightly syneretic
Ethylbenzene				
1.36	0.5	(140)	Chunks of opalescent gel in clear liquid	Unchanged
10.3	4.1	(195)	Slightly opalescent gel in clear liquid	Unchanged
19.0	8.1	227	Clear; not syneretic	Very slightly opalescent plug; syneretic
27.8	12.6	236	Slightly opalescent; slightly syneretic	Opalescent plug; slightly syneretic
37.4	18.3	240	Opalescent; not syneretic	Opalescent; very slightly syneretic

TABLE 1—*Continued*

PER CENT SOAP		T _c	DESCRIPTION OF COOLED SYSTEMS	
Per cent by weight	Mole per cent		Immediately after cooling	After aging

<i>Ethylbenzene—Continued</i>				
46.8	24.8	250	Opalescent; translucent	Opalescent; not syneretic
66.1	42.2	>291	White; sintered; opaque; slightly syneretic	Unchanged
78.9	58.4	258	$\frac{1}{2}$ hard white, $\frac{1}{2}$ semitranslucent; not syneretic	Unchanged
88.2	73.6	258	White; semitranslucent; opaque top	Unchanged
95.0	87.5	260	White; opaque	Unchanged

<i>Cumene</i>				
11.3	5.1	(222)	Clear syneretic gel (opalescent after 4 hr.)	Opalescent syneretic gel
23.1	11.2	228	Opalescent syneretic gel	Opalescent syneretic gel plug; syneresis
33.4	17.5	238	Slightly opalescent; very slight syneresis	Slightly opalescent; slightly syneretic
43.7	24.8	245	Cloudy; slightly syneretic	Unchanged

<i>n</i> -Butylbenzene				
9.2	4.5		Very slightly opalescent; not syneretic	Slightly opalescent plug; syneretic
19.9	10.5	193-4	White, fractured gel	White, fractured plug; syneretic
31.1	17.6	226	Light yellow; opalescent; not syneretic	Cloudy; slightly syneretic
38.8	23.2	239	Light yellow; opalescent; not syneretic	Opalescent; not syneretic

<i>p</i> -Cymene (critical temperature, 378°C.)				
9.5	4.7	118	Yellow; slightly opalescent; semitranslucent	Trace of syneresis
19.5	10.3	144	Light yellow; opalescent; not syneretic	Unchanged
27.6	15.2	171	Whiter; opalescent; not syneretic	Unchanged
39.3	23.4		Whiter; opalescent; not syneretic	Unchanged

<i>n</i> -Heptane (critical temperature, 266.8°C.)				
1.48	0.5		Opalescent gel in clear liquid	Opaque gel in clear liquid
9.5	3.2		Opalescent gel in clear liquid	Opaque gel in clear liquid
18.5	7.4		White opaque plug; syneretic	Increased opalescence and syneresis
32.2	14.3	(240)	White; opaque; solid	Unchanged

TABLE 1—*Concluded*

PER CENT SOAP		T;	DESCRIPTION OF COOLED SYSTEMS	
Per cent by weight	Mole per cent		Immediately after cooling	After aging
2,2,4-Trimethylpentane (isooctane) (critical temperature, 296°C.)				
47.4	26.6	°C. (248)	Opalescent syneretic gel	Opalescent syneretic gel
73.3	44.3	(258)	White; opaque; not syneretic	White; opaque; not syneretic
Benzene (critical temperature, 288.5°C.)				
20.1	6.5	222	Clear; not syneretic	Slightly opalescent plug; syneretic
29.9	10.5	>238	Clear; not syneretic	Slightly opalescent plug; slightly syneretic

than the rest. The white patches became the white, wax-like, liquid-crystalline phase on heating, while the remainder was the golden, liquid-crystalline phase. Considerable shrinkage occurred on cooling. The system was metastable at room temperatures and exhibited no syneresis.

The samples in tubes 7 and 8 both were heated to 310°C. without melting, although sintering occurred. It may be pointed out that these systems exhibited a sharp birefringence and were rigid at that temperature, which was 30°C. above the critical temperature of pure cyclohexane and 25°C. above the temperature at which the pure soap melts to isotropic liquid.

The last sample, that in tube 9, exhibited the phase changes observed in the anhydrous soap but became isotropic at a lower temperature than did the pure soap. This showed that a eutectic area was formed between the anhydrous soap and the white, wax-like, liquid-crystalline phase. The cooled system was light tan, opaque, and compact.

2. Selected data on systems of sodium stearate in twelve anhydrous hydrocarbons

Typical individual descriptions of systems of sodium stearate in the twelve anhydrous hydrocarbons are collected in table 1, which includes the values of T_i , the temperature at which, upon cooling the completely homogeneous isotropic solution, the first appearance of heterogeneity or anisotropy occurs. The dipole moments of *n*-heptane, cyclohexane, benzene, *p*-xylene, and *p*-cymene are 0; those of isooctane, toluene, ethylbenzene, *m*-xylene, cumene, and *n*-butylbenzene are 0.4; that of *o*-xylene is 0.7. The critical temperatures of the pure solvents are included in the table.

DISCUSSION

Just as in aqueous systems, the phase rule of Willard Gibbs is found to apply to true equilibria among the phases here recognized, as is illustrated in the phase diagrams for sodium stearate and toluene (figure 1) and sodium stearate and cyclohexane (figure 2).

Two definite phase transformations were observed: namely, from the gel form to one of the two liquid-crystalline phases, and in turn from these liquid-crystalline phases either to an isotropic sol or to a jelly. They were both reversible transformations, although circumstances such as undercooling could cause them to appear irreversible. Further, owing to the defective fluidity of the liquid-crystalline phases, other phases with which they are in equilibrium, such as sol, jelly, crystals, or other liquid crystals, quite frequently cannot separate out or segregate. Many writers include all such systems under the name gels, not reserving "gel," as is done in this Laboratory, for the systems involving a solid crystalline phase, together with a second phase which may be liquid-crystalline, a jelly, or a sol. Sol and jelly constitute a single phase in which there is a gradual change from complete fluidity to that of a typical isotropic, transparent, elastic, thixotropic jelly. Sol and jelly are isotropic when unstrained, but show streaming birefringence. They are reversibly and gradually transformable from one to the other by heating or cooling or by change in concentration. Laing and McBain (4) and Heyman (3) demonstrated for aqueous soap systems that they belong to the same phase.

Figures 1 and 2 depict two liquid-crystalline phases in respect to their composition and the temperature range in which they are the stable phases. Their appearance was characteristic and different. Thus, their coexistence in samples containing about 50 per cent of soap was observed easily, since the samples contained patches of both.

The vapor pressure of the white, wax-like, more concentrated, liquid-crystalline phase was considerably lower than that of the golden liquid-crystalline phase, showing that the association of solvent and soap is considerably stronger for the concentrated liquid-crystalline phase. This is in contrast to a gel phase, where the presence of free solvent asserts its full vapor pressure.

The phase occurring in the lower concentration range was golden and bright, transmitting polarized light with a strong birefringence. In systems which were mobile, the liquid-crystalline material flowed when the tubes were inverted, exhibiting the most exquisite play of pastel colors. Such streaming birefringent effects also were noted in the soft jellies when they were stressed or slowly flowed, but those effects could not compare with the ones occurring in the liquid-crystalline phase for intensity, duration, and numerous brilliant shades of color. The vibrating or dancing particles occurring in the two-phase region between the isotropic and liquid-crystalline phases also exhibited a play of colors, but it was more fleeting because of the lack of oriented flow patterns.

Solubility of sodium stearate and various hydrocarbons

The solubility of dry sodium stearate was found to be remarkably similar in all of the dried, pure hydrocarbon solvents. The temperatures of transformation to the isotropic solution for some of these systems have been plotted in figure 5 (see also figure 6). A curve can be drawn through the points for all but *p*-cymene and *n*-butylbenzene. The deviation among the values for the various hydrocarbons was much less than that which would be caused by even 0.1 per

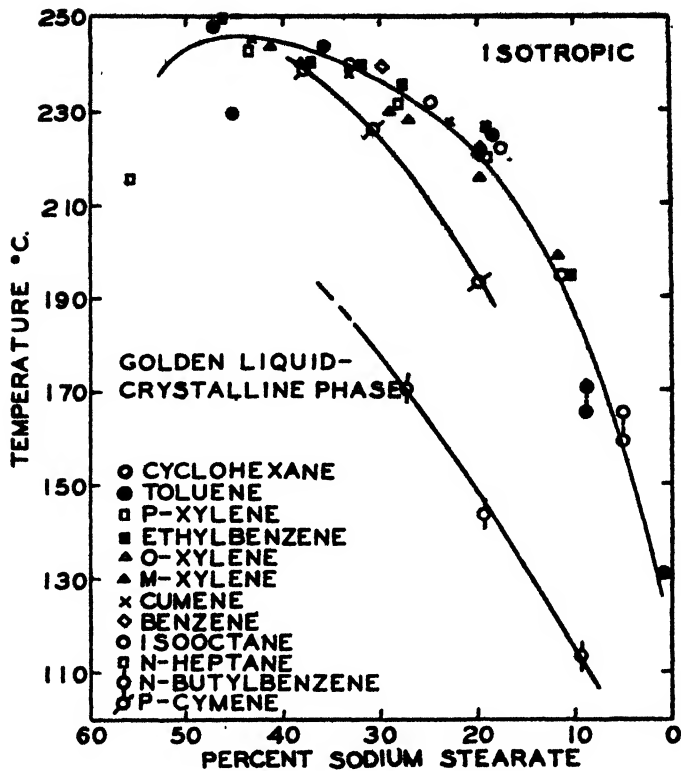


FIG. 5. Solubility of sodium stearate in hydrocarbons

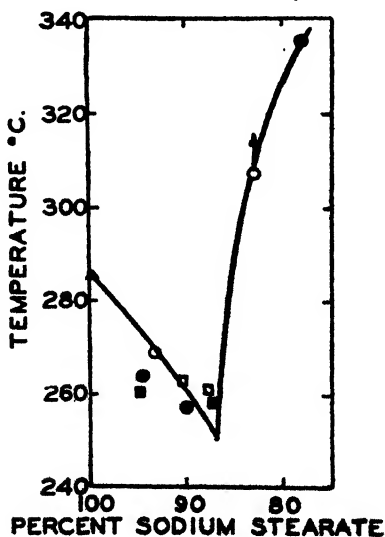


FIG. 6. Solubility of sodium stearate in hydrocarbons. O, cyclohexane; ●, toluene; □, p-xylene; ■, ethylbenzene; △, pure sodium stearate.

cent of water, based on the soap. This attests, in itself, to the purity and dryness of the solvents used, as well as to that of the sodium stearate.

The order of the variation among the temperatures for the solubilities of the soap in these different hydrocarbons was no greater than the range over which phase transformations for the pure anhydrous soap have been reported by various authors.

The general phase diagrams

In view of the similarity of the phase transformations observed for the sodium soap in the various hydrocarbons, the phase diagrams (figures 1 and 2) illustrating the behavior of anhydrous sodium stearate in dry toluene and dry cyclohexane can be considered as generalized diagrams for all the solvents studied.

The critical temperatures of the solvents

The use of solvents such as xylenes and toluene was needed to clarify completely the nature of the phase diagram of sodium stearate in hydrocarbons, because their critical temperatures are sufficiently high to permit all phase changes to be studied. The critical temperatures of *n*-heptane and cyclohexane were too low for complete description of the upper eutectic area between the two liquid-crystalline phases. When systems containing 25–40 per cent of *n*-heptane, cyclohexane, and isoöctane were heated in sealed tubes above 240–245°C., the solvent began to pass rapidly into the vapor phase. The excessive loss of solvent from the condensed phase resulted in a change of concentration that no longer represented the initial condensed system and transformed the contents into the more concentrated, white, wax-like, liquid-crystalline phase.

The vapor pressures were very great, since the glass tubes became anisotropic from strain. In many of these systems the excessive vapor loss began before the systems had a chance to become isotropic. Two samples of cyclohexane, containing 11.5 per cent and 33.2 per cent of sodium stearate, respectively, were taken to 290°C., 9°C. above the critical temperature for the pure solvent, where they exploded. The systems were still fluid and anisotropic, but the volumes of the condensed phase had been reduced to about one-third of the original volume.

SUMMARY

1. The phase behavior of anhydrous systems of sodium stearate and hydrocarbons was studied in sealed tubes by visual observation, employing *n*-heptane, isoöctane, cyclohexane, benzene, toluene, ethylbenzene, *o*-xylene, *m*-xylene, *p*-xylene, cumene, *n*-butylbenzene, and *p*-cymene. These systems are believed to be drier than any hitherto studied.

2. The soap was soluble to the same extent in all of the pure hydrocarbons. The samples of *p*-cymene and *n*-butylbenzene differed, but contained impurities.

3. The phase diagrams are very similar in form for all the hydrocarbons here studied, but differ greatly from that reported elsewhere (2) for cetane.

4. Five general conditions were found to exist in the anhydrous hydrocarbon systems, as follows: (a) A white, opaque *gel* (two-phase) that exhibits limited

swelling as a direct function of temperature; the gel involves more or less dispersed solid *crystalline phase*, together with sol or jelly (see below). (b) A golden or orange, translucent, *liquid-crystalline phase*. (c) A white, wax-like, semi-translucent, *liquid-crystalline phase*, which melts to isotropic liquid at a considerably higher temperature than the pure sodium stearate. (d) An isotropic solution, continuous in *phase* with the jelly (e). (e) In special regions of the sol, not sharply delimited, an isotropic *jelly* which has unlimited swelling, passing to the solution *without* any observed transition or *change of phase*.

5. All phase changes were reversible and obey the phase rule of Willard Gibbs.

REFERENCES

- (1) DE BRETTEVILLE, A., JR., AND MCBAIN, J. W.: J. Chem. Phys. **11**, 426 (1943).
- (2) DOSCHER, T., AND VOLD, R. D.: J. Colloid Sci. **1**, 299 (1946).
- (3) HEYMAN, E.: Trans. Faraday Soc. **34**, 689 (1938).
- (4) LAING, M. E., AND MCBAIN, J. W.: J. Chem. Soc. **117**, 1507 (1920).
- (5) MCBAIN, J. W., DE BRETTEVILLE, A., JR., AND ROSS, S.: J. Chem. Phys. **11**, 179 (1943).
- (6) MCBAIN, J. W., MYSELS, K. J., AND SMITH, G. H.: Trans. Faraday Soc., in press.
- (7) MCBAIN, J. W., VOLD, R. D., AND FRICK, M.: J. Phys. Chem. **44**, 1013 (1940).
- (8) PRASAD, M., HATTIANGDI, G. S., *et al.*: Proc. Indian Acad. Sci. **21**, 1, 56, 90 (1945); **22**, 320 (1945); **24**, 287, 295 (1946); J. Univ. Bombay **14**, 23 (1945); Current Sci. **11**, 300 (1945); J. Soc. Ind. Research (India) **1946**, 489.
- (9) SHREVE, G. W.: Ph.D. Dissertation, Stanford University, 1946.
- (10) VOLD, R. D., LEGGETT, C. W., JR., AND MCBAIN, J. W.: J. Phys. Chem. **44**, 1056 (1940); **46**, 429 (1942).
- (11) VOLD, R. D., AND PHILIPSON, J.: J. Phys. Chem. **50**, 39 (1946).

A DEMONSTRATION OF SOME NEW METHODS OF DETERMINING MOLECULAR WEIGHTS FROM THE DATA OF THE ULTRACENTRIFUGE

W. J. ARCHIBALD

Department of Physics, Dalhousie University, Halifax, Nova Scotia

Received April 8, 1947

The equilibrium method of determining the molecular weights (3) of heavy molecules has many advantages. The formula which is used is based on a sound theory, and with modern centrifuges of the Svedberg or Beams type the measurements required can be obtained with considerable accuracy. The experimental problems of temperature and speed control have been successfully solved, and the study of the optical requirements (which has been largely due to Lamm (3)) has made the determination of the concentration at any point within the cell a matter of routine for any laboratory which possesses the necessary equipment. However, the method has one disadvantage—the time required for the attainment of the equilibrium state is often very long. It is the purpose of the present paper to indicate several procedures by which molecular weights could be determined without waiting for the equilibrium state.

Consider a cell, of the shape indicated by the heavy lines in figure 1, containing a dilute solution of the substance to be studied. It extends from r_a to r_b , subtends an angle θ at the axis of rotation, and has a depth of h cm. Let $n(r, t)$ be the number of dissolved molecules per cubic centimeter at the cylindrical surface

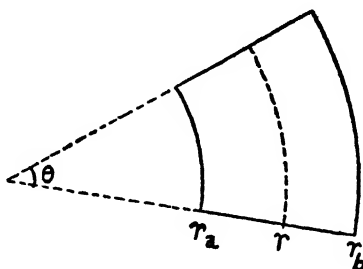


FIG. 1

r at the time t . Then the number of solute molecules crossing the surface at r , per second, in an outward direction (at the time t) is (1):

$$Q(r, t) = \left(\omega^2 s r n - D \frac{\partial n}{\partial r} \right) r \theta h \quad (1)$$

where D is the diffusion constant, s the sedimentation constant of the solute molecules, and ω the angular velocity of the centrifuge. The function $Q(r, t)$ has the property

$$\lim_{t \rightarrow \infty} Q(r, t) = 0 \quad (t \rightarrow \infty)$$

for all values of r . That is, at $t = \infty$ (or when the equilibrium state has been reached) the processes of outward settling and inward diffusion balance exactly at all points. Then

$$\frac{n_2}{n_1} = e^{\frac{\delta}{2}(r_2^2 - r_1^2)} \quad (2)$$

where

$$\delta = \frac{\omega^2 s}{D} = \frac{M(1 - \nu\rho)\omega^2}{RT} \quad (3)$$

However, for all values of t , $Q(r, t)$ is zero for $r = r_a$ and $r = r_b$. This is merely the mathematical statement of the fact that no dissolved molecules can flow out of the cell through either end. The function $n(r, t)$ must always adjust itself so that this condition is fulfilled. This being the case, a study of the curve of concentration *versus* distance near either end of the cell (at any time) would yield a value of M , the molecular weight. But this is just the region in which it is most difficult to measure the concentration accurately, and it would seem that any technique which involves a study of the concentration distribution in this region would present the experimenter with serious difficulties. A method

of procedure which avoids this difficulty will be demonstrated in the following paragraphs.

In figure 2 is to be found a set of curves which give $n(r,t)/n_0$ (where n_0 is the initial uniform concentration) for different values of the time. Unfortunately these are not experimental curves but will serve for purposes of illustration. They are computed curves and the relevant data are as follows: $r_a = 4.160$ cm., $r_b = 4.632$ cm., $\omega = 290\pi$, $V = 0.749$ cc. per gram, $s = 5 \times 10^{-12}$, and $T = 293^\circ\text{K}$. The value of M used in the computations was 68,000; but it will be

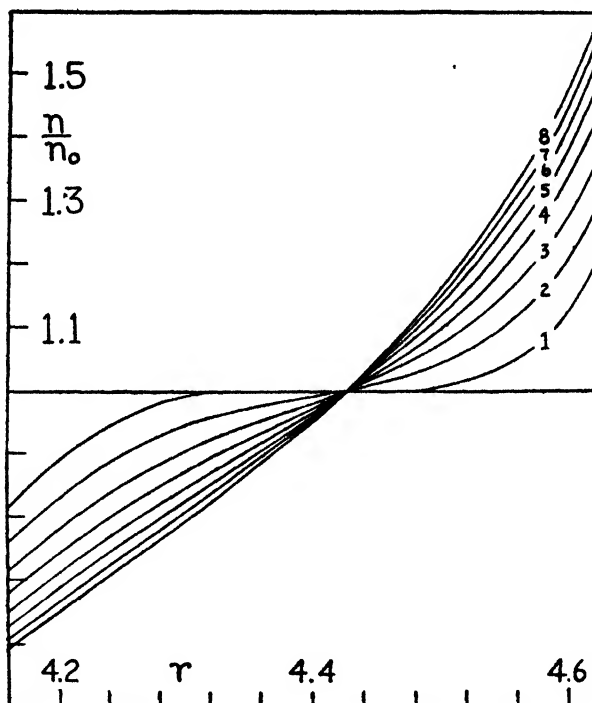


FIG. 2. n/n_0 as a function of r for different values of t . For curve 1, $t = 6,000$ sec.; for curve 2, $t = 12,000$ sec., etc.; for curve 8, $t = 48,000$ sec.

assumed that this is unknown, and it will be shown how the curves may be made to yield this value (without having to know the concentrations accurately at points too near the ends of the cell). It will be observed that the state which existed at $t = 48,000$ sec. is the one nearest equilibrium. The computations show that a period at least 2.5 times as long as this is required to approximate the final state. From each of these curves the function $\frac{1}{rn} \frac{\partial n}{\partial r}$ is calculated at a number of points. Table 1 indicates the manner in which this calculation would be made. It refers to the time $t = 24,000$ sec. and is self explanatory. In actual practice the interval between r_a and r_b would be divided into eight or ten equal intervals; this was not done in compiling table 1, because values of n/n_0 were

known at the points indicated and the data were used as provided without any preliminary interpolation.

TABLE 1
Calculation of $\frac{1}{rn} \frac{\partial n}{\partial r}$ for $t = 24,000$ sec.

r_2	r_1	$\frac{n_2}{n_0}$	$\frac{n_1}{n_0}$	r_{average}	$\frac{1}{n_0} \frac{\partial n}{\partial r}$	$\frac{1}{rn} \frac{\partial n}{\partial r}$
4.201	4.160	0.747	0.681	4.181	1.61	0.538
4.242	4.201	0.804	0.747	4.222	1.39	0.424
4.283	4.242	0.855	0.804	4.263	1.24	0.350
4.323	4.283	0.899	0.855	4.303	1.10	0.292
4.363	4.323	0.938	0.899	4.343	1.00	0.251
4.403	4.363	0.976	0.938	4.383	0.95	0.227
4.442	4.403	1.019	0.976	4.423	1.10	0.249
4.480	4.442	1.068	1.019	4.461	1.29	0.277
4.519	4.480	1.130	1.068	4.500	1.59	0.321
4.557	4.519	1.208	1.130	4.538	2.05	0.387
4.595	4.557	1.308	1.208	4.576	2.63	0.457
4.632	4.595	1.435	1.308	4.614	3.43	0.542

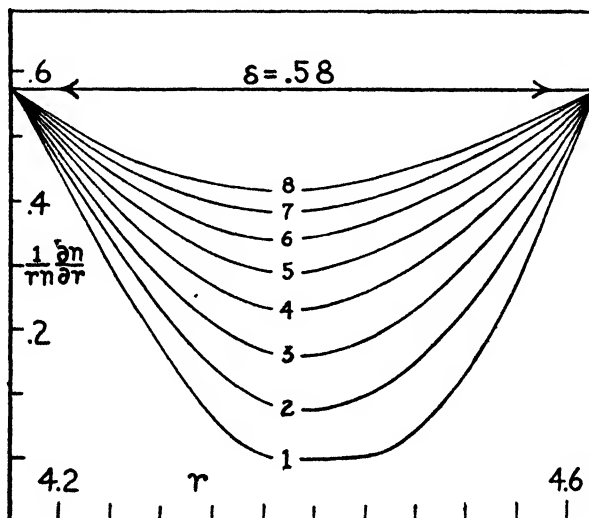


FIG. 3. $\frac{1}{rn} \frac{\partial n}{\partial r}$ as a function of r

In figure 3 the quantity $\frac{1}{rn} \frac{\partial n}{\partial r}$ is plotted as a function of r . There are eight curves in all—one for each of the curves of figure 1. It is to be observed that all these curves when extrapolated to the ends of the cell pass through the same point, and that the numerical value corresponding to this point is the same at

both ends of the cell, *viz.*, 0.58. This is what one would expect, since at r_a and r_b the function $Q(r, t)$ is zero, which means that at these points

$$\frac{1}{rn} \frac{\partial n}{\partial r} = \delta = \frac{M(1 - V\rho)\omega^2}{RT} = \text{Constant} \quad (4)$$

Having determined δ , it is a simple matter to obtain $M = 68,000$ from equation 4.

The value of this procedure lies in the fact that there are several curves to be extrapolated for fixing δ . If there were only one curve available, some doubt might exist as to the validity of any extrapolation which might be made. But having several curves, and knowing that they all must pass through the same point, fixes this point with considerable precision. A further point of importance is that these curves are so simple, being almost straight lines near the ends of the cell. It is clear that there is no need to use as many curves as were used above; three would be almost as good as eight.

There is another method of dealing with the curves in figure 2 which will now be described. It can be shown that $n(r, t)$ must satisfy the following differential equation (2):

$$\frac{\partial}{\partial r} \left\{ \left(\frac{\partial n}{\partial r} - \delta rn \right) r \right\} = \frac{\delta}{\omega^2 s} r \frac{\partial n}{\partial t} \quad (5)$$

Integrating this equation between any two points r_1 and r_2 within the cell, one gets:

$$\left[r \left(\frac{\partial n}{\partial r} - \delta rn \right) \right]_{r_1}^{r_2} = \frac{\delta}{\omega^2 s} \int_{r_1}^{r_2} r \frac{\partial n}{\partial t} dr \quad (6)$$

This equation holds for every value of the time, and in performing the integration on the right-hand side it is necessary to determine $\partial n / \partial t$ at all points between r_1 and r_2 at the particular time considered.

In order to utilize equation 6 it is necessary to obtain a series of values of the function $\partial n / \partial t$. Table 2 indicates how this would be done. It refers to the point $r = 4.343$ cm. Figure 4 enables one to see how this function varies with the time at different points in the cell. Figure 4 contains the data necessary for dealing with equation 6. For the sake of illustration let us study the state of affairs which existed at $t = 24,000$ sec. The manner in which the function $\frac{r}{n_0} \frac{\partial n}{\partial t}$ varies with distance along the cell is indicated in figure 5. (The data for this curve are obtained from figure 4.) The curve extends to the ends of the cell, although only a part of it need be used for fixing the value of δ . An examination of equation 6 shows that if the limits of integration are r_a and r_b , the quantity on the left of the equality sign is zero. Therefore the total area under the curve of figure 5 should be zero. Careful measurement shows that this is actually the case, and this serves as an excellent check on the accuracy of the calculations. The actual area under the curve is 0.07×10^{-6} , while the total area without regard to sign is 9.30×10^{-6} .

TABLE 2
Calculation of $\frac{1}{n_0} \frac{\partial n}{\partial t}$ for $r = 4.343$

t_2	t_1	$\frac{n_2}{n_0}$	$\frac{n_1}{n_0}$	t_{average}	$\frac{1}{n_0} \frac{\Delta n}{\Delta t} \times 10^6$
<i>seconds</i>	<i>seconds</i>				
12,000	6,000	0.970	1.005	9,000	5.83
18,000	12,000	0.941	0.970	15,000	4.83
24,000	18,000	0.919	0.941	21,000	3.83
30,000	24,000	0.900	0.919	27,000	3.17
36,000	30,000	0.884	0.900	33,000	2.67
42,000	36,000	0.872	0.884	39,000	2.00
48,000	42,000	0.860	0.872	45,000	2.00

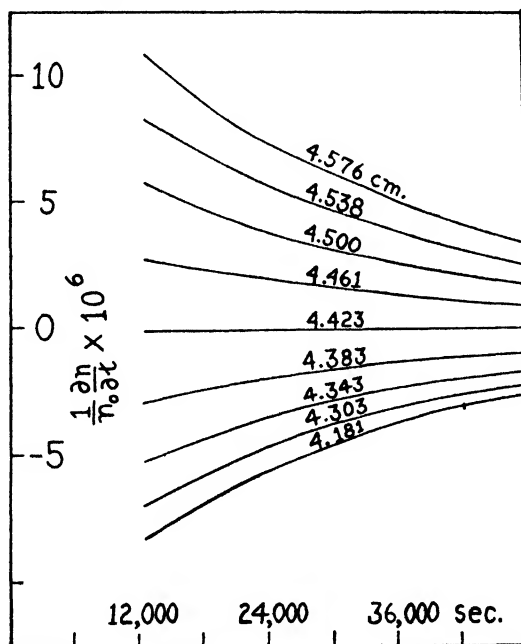


FIG. 4. $\frac{1}{n_0} \frac{\partial n}{\partial t}$ as a function of t for different values of r

From figure 5 it is clear that there are an unlimited number of choices of r_1 and r_2 which will make the integral on the right of equation 6 equal to zero. Suppose that r_1 and r_2 have been so chosen. Then equation 6 becomes

$$\delta = \frac{\left\{ \left(\frac{1}{rn} \frac{\partial n}{\partial r} \right)_{r_2} - \frac{n_1}{n_2} \left(\frac{r_1}{r_2} \right)^2 \left(\frac{1}{rn} \frac{\partial n}{\partial r} \right)_{r_1} \right\}}{1 - \frac{n_1}{n_2} \left(\frac{r_1}{r_2} \right)^2} \quad (7)$$

Since the values of $\frac{1}{rn} \frac{\partial n}{\partial r}$ at r_1 and r_2 , for the time in question, can be obtained from figure 3, we have another method of determining δ . The value of this procedure is that the calculations need not depend on measurements of concentration made near the ends of the cell, because the limits r_1 and r_2 can be picked well within the cell.

If r_1 is taken to be 4.263 cm., then r_2 must be 4.564 in order to make the integral zero. Turning now to figure 3, from the curve for $t = 24,000$ sec. it can be

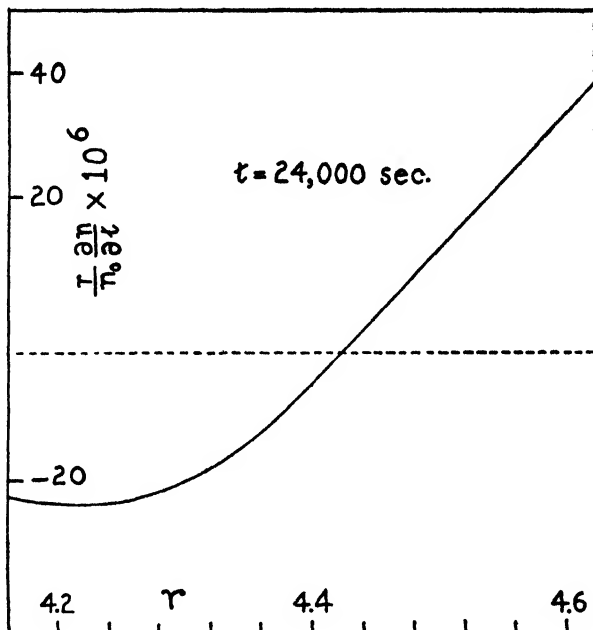


FIG. 5. $\frac{r}{n_0} \frac{\partial n}{\partial r}$ as a function of r for $t = 24,000$ sec.

found that $\frac{1}{rn} \frac{\partial n}{\partial r}$ has the value 0.350 at r_1 and 0.435 at r_2 . Putting these values in equation 7 gives $\delta = 0.56$.

An important feature of this method is that as many determinations of δ as seem necessary can be made and an average taken. Figure 5 can be used in an infinite number of ways by choosing different values of r_1 and r_2 which make the integral zero. But in addition, curves similar to that in figure 5 can be obtained for any value of the time, and these in turn yield further information regarding δ .

We now pass on to describe another manner in which equation 6 can be used. Suppose that the limits are chosen in such a way that the integral is not zero. Then it is possible to determine not only δ but s as well. For example, if we choose $r_1 = 4.263$ and $r_2 = 4.423$ we have:

$$\int_{4.263}^{4.423} \frac{r}{n_0} \frac{\partial n}{\partial r} dr = -2.22 \times 10^{-8} \text{ cm.}^2 \text{ sec.}^{-1}$$

For this case equation 6 becomes

$$\left[\frac{n}{n_0} r^2 \left(\frac{1}{rn} \frac{\partial n}{\partial r} - \delta \right) \right]_{4.263}^{4.423} = \frac{\delta}{s} (-2.68 \times 10^{-12}) \quad (8)$$

since $\omega = 290\pi$. Putting the proper values in the left-hand side of equation 8 (and using $\delta = 0.57$, the average value obtained thus far) one gets $s = 5.1 \times 10^{-13}$, which is to be compared with the value 5×10^{-13} which was assumed in computing the curves of figure 2. It is of interest to note that in finding the values of s

and δ we have at the same time determined D , since $\delta = \frac{\omega^2 s}{D}$. This procedure would be most useful, if the experimental difficulties can be surmounted, because a single run of the ultracentrifuge can be made to yield all three quantities, M , s , and D . Notice that as many determinations of s can be made as seem necessary to give a good average value.

The usefulness of the modern ultracentrifuge is not confined to the study of substances of high molecular weight. With the high rotational speeds obtainable molecules whose weight is less than 1000 can be dealt with. For such light particles it is impossible to measure s by direct means because they settle too slowly. An analysis such as the above would permit s to be measured in such an extreme case. A knowledge of s for small particles might conceivably be of some theoretical interest.

The physical significance of equation 6 can be demonstrated in a simple manner. Consider the region of the cell between the surfaces r_1 and r_2 . The net number of molecules entering this region per second at the time t is $Q(r_1, t) - Q(r_2, t)$. But this is also equal to

$$\int_{r_1}^{r_2} r \theta h \frac{\partial n}{\partial t} dr$$

evaluated at the time t . Equating these two quantities, one has equation 6.

Since many of the substances that one might wish to study do not consist of particles of a single weight, but rather are composed of particles of many different weights, it is important to study the above method in order to see if it is of any value in this case. Suppose there are many groups of molecules present and that the number per cubic centimeter of the i^{th} group at the point r , at the time t , is n_i . Then the number of molecules of this group crossing the surface at r , per second, is:

$$Q_i(r, t) = D_i \left(\delta_i r n_i - \frac{\partial n_i}{\partial r} \right) r \theta h \quad (9)$$

At r_a and r_b this quantity is zero for all groups. Thus at the ends of the cell

$$\frac{M_i(1 - V\rho)\omega^2}{RT} r n_i - \frac{\partial n_i}{\partial r} = 0 \quad (10)$$

for all values of t . Multiplying equation 10 by M_i and summing over all groups, one gets

$$\frac{(1 - V\rho)\omega^2}{RT} r \Sigma(M_i^2 n_i) - \frac{\partial}{\partial r} \Sigma(M_i n_i) = 0 \quad (11)$$

at r_a and r_b for all t . But $\Sigma(M_i n_i) = C$, where C is the concentration in terms of weight of dissolved substance per unit volume. If $\Sigma(M_i^2 n_i)$ is written as $M_w \Sigma(M_i n_i)$, equation 11 becomes

$$\frac{M_w(1 - V\rho)\omega^2}{RT} - \frac{1}{rC} \frac{\partial C}{\partial r} = 0 \quad (12)$$

at r_a and r_b for all t . (The quantity M_w is the weight-average molecular weight and is a function of r and t .) If, as before, the quantity $\frac{1}{rC} \frac{\partial C}{\partial r}$ is computed from an experimental concentration *versus* distance curve at a specific time, this quantity, when plotted against r and extrapolated to the ends of the cell, gives M_w at each end at this particular time. (It is assumed that the optical methods of determining concentrations are applicable and that they give C when the particles are not of uniform size.) This extrapolation will not give the same value at each end of the cell, because M_w will be changing at these points as time goes on. At r_b , the outer boundary, M_w will gradually increase as the fraction of heavier molecules becomes greater, while at r_a , the opposite effect will be observed. If a series of determinations of M_w at r_b and r_a were to be made at different times and plotted, on the same graph, as a function of the time, the two curves obtained should meet when extrapolated back to zero time, and the intersection would be the value of M_w at either end of the cell at $t = 0$, i.e., the weight-average molecular weight of the original substance. It should be pointed out that this treatment assumes that the partial specific volume is independent of the size of the molecule. This is probably a safe assumption when the molecules are all of the same substance.

This latter method, if developed to the point where some precision could be achieved, might possibly have some applications for industry. It is often necessary in the manufacturing process to have the weight-average molecular weight confined between certain limits if the final product is to be acceptable. With a standardized routine and an ultracentrifuge specially built for the purpose, it ought to be possible to fix M_w within narrow limits for many substances in a matter of a few hours.

In a difficult experiment all clues which suggest a value of the quantity sought should be studied. Figure 2 (which, of course, refers to a monodisperse substance) contains a feature which is very noteworthy, *viz.*, that all the curves cross the line $n/n_0 = 1$ at the same point. All the curves for later times up to $t = \infty$ pass through this same point. It might be thought that this is accidental and would not be likely to be true for some other substance. That it is not wholly accidental can be shown by the following considerations. These curves are calculated from the following function (2)

$$\frac{n}{n_0} = \frac{b - a}{e^b - e^a} e^z + \sum_{m=1}^{\infty} A_m M_m(z) e^{(\alpha_m - 1)2\omega^2 z t} \quad (13)$$

which is the solution of equation 5. In equation 13 $z = \delta r^2/2$, $b = \delta r_b^2/2$, $a = \delta r_a^2/2$, the α_m 's are large negative quantities, the A_m 's are constants, and the

M_m 's are rather complicated functions of z . When the equilibrium method is used it is not customary to have the final concentration vary too widely throughout the cell, and $n(r_b)/n(r_a)$ at $t = \infty$ would normally lie between 2.0 and 3.5, which means that $0.7 < b - a < 1.3$. Furthermore, as the cells are of short length (about 0.5 cm.) and placed fairly far from the centre of rotation (about 4.5 cm.), the ratio $b/a = r_b^2/r_a^2 \approx (5.0/4.5)^2 \approx 1.25$, so that a and b will have numerical values in excess of 4.0. This will be true of all experiments aimed at equilibrium performed with centrifuges of the type commonly used. With these restrictions on a and b let us consider equation 13. In a relatively short time after the beginning of the run the higher terms in the summation vanish and

$$\frac{n}{n_0} = \frac{b-a}{e^b - e^a} e^z + A_1 M_1(z) e^{(\alpha_1-1)2\omega^2 s t} \quad (14)$$

The function $M_1(z)$ is not easy to treat analytically, but it can be shown that, subject to the restrictions on b and a pointed out above, it has one root between a and b , and that this root is very close to the value

$$b - 0.45 - 0.40(b - a - 1)$$

Now let us look for the value of z which satisfies

$$\frac{b-a}{e^b - e^a} e^z = 1 \quad (15)$$

This may be written

$$z = b - \ln \left(\frac{x}{1 - e^{-x}} \right) \quad (16)$$

where $x = b - a$. Expanding the right-hand side of this equation about $x = 1$ by Taylor's theorem gives

$$z = b - 0.46 - 0.42(b - a - 1) + \dots$$

Thus the value of z which makes

$$\frac{b-a}{e^b - e^a} e^z$$

equal to unity is almost identical with that which makes $M_1(z)$ equal to zero. This guarantees that all the curves cut the line $n/n_0 = 1$ at practically the same point. Suppose that this point is determined and called r_0 . Then from equation 15:

$$a \left\{ \left(\frac{r_b}{r_a} \right)^2 - 1 \right\} e^a \left\{ \left(\frac{r_0}{r_a} \right)^2 - 1 \right\} = e^a \left\{ \left(\frac{r_b}{r_a} \right)^2 - 1 \right\} \quad (17)$$

The only unknown quantity in this equation is a , which must be found by numerical methods since it is impossible to express it explicitly. From figure 2

we find that $r_0 = 4.425$ cm. and, if the values of r_a and r_b given above are used, equation 17 is satisfied if $a = 4.9$. That is,

$$\delta r_a^2/2 = 4.9 \text{ or } \delta = 0.57$$

This cannot be used as a precision method but should be useful for indicating the order of magnitude of M .

REFERENCES

- (1) ARCHIBALD: *Phys. Rev.* **53**, 746 (1938).
- (2) ARCHIBALD: *Ann. N. Y. Acad. Sci.* **43**, 211 (1942).
- (3) SVEDBERG AND PEDERSEN: *The Ultracentrifuge*. Oxford University Press, London (1940).

NEW BOOKS

Practical Physiological Chemistry. 12th edition. By PHILIP B. HAWK, BERNARD L. OSER, AND WILLIAM H. SUMMERSON. xiv + 1323 pp. Philadelphia: The Blakiston Company, 1947. Price: \$10.00.

The twelfth edition of this well-known book will be welcomed by everyone who is interested in this particular field. All the subjects previously covered have been revised and several new sections have been added. This results in a very complete coverage of the topics which fall within the scope of the title.

The subjects covered, which are presented in the more or less conventional order, are as follows: some physicochemical properties of solutions; the chemistry of carbohydrates, fats, proteins, and nucleic acids; the chemistry of milk; the chemistry of epithelial and connective tissue, teeth, muscular tissue, and nervous tissue; enzymes; the chemistry of digestion; intestinal absorption; putrefaction and detoxication; feces; the chemistry of blood and blood analysis; the chemistry of respiration; energy metabolism; hormones; the constituents of urine and their determination in urine; carbohydrate, fat, protein, and inorganic metabolism; vitamins and deficiency diseases; and antibiotics. In addition there are nine appendices covering such topics as: reagents and solutions; composition of foods; tables of logarithms and atomic weights; analysis of variance; and maintenance of animals for nutrition experiments.

Concerning the new material, the senior author states in the preface, "... new sections have been introduced on the polarograph; on isotopes; on the sulfa drugs; on metabolic antagonists and antibiotics; on the Warburg tissue-slice procedure; on the theory and practice of photometric analysis; on the electrophoretic fractionation of the plasma proteins; on the composition of foods; and on the various vitamins whose importance has become recognized since the last edition together with a fuller discussion of the clinical relationships of certain vitamins. Also many new quantitative procedures for blood and urine have been added."

All the material is presented in a clear manner; the experimental procedures are very detailed and easy to follow. The large number of illustrations (329 text illustrations and 5 color plates) add much to the quality of the book.

With regard to nomenclature and symbols, some changes have been made from previous editions. As an example, the term *milliliter* has been used in place of *cubic centimeter* as a unit of volume. The presentation of numerous chemical formulas is quite useful and enhances the value of the book as a reference.

In format the book is first class, the binding and paper being of high quality.

This book can be easily recommended to anyone in the field of physiological chemistry. As a laboratory text and reference book it is excellent. It should be especially useful to anyone who is teaching laboratory work and to all students doing graduate work in the field.

CHARLES CARR.

Meson Theory of Nuclear Forces. BY WOLFGANG PAULI. 69 pp. New York City: Interscience Publishers, Inc., 1946. Price: \$2.00.

This small volume by one of the most distinguished and active workers in the field of meson physics is based on lectures given at the Massachusetts Institute of Technology in 1944, the notes of which are here published in but slightly amended form. Within the compass of sixty-nine pages Professor Pauli has given the meat of all aspects of the current theory, for both charged and uncharged mesons, and for the so-called weak and strong coupling forms of the theory. The treatment is really only a summary, rather than an exposition, of the theory and is scarcely adapted for a first introduction; for the more sophisticated reader in quantum-mechanical literature it will give an illuminating account of the present state of affairs in the theory of mesons. While the theory is unquestionably a brilliant attempt to extend the electromagnetic theory of photons, and in a certain sense has been vindicated by the discovery of mesons in cosmic rays, the present ambiguous state with respect to nuclear forces and the inherent mathematical difficulties make it difficult to guess in what sense it will remain as a permanent part of our conception of nature. Professor Pauli's discussion gives a balanced account of both the successes and the failures of the theory to date.

EDWARD L. HILL.

Fourier Transforms and Structure Factors. By DOROTHY WRINCH. 96 pp. Monograph No. 2 of the American Society for X-Ray and Electron Diffraction. February, 1946.

Copies of the monograph can be obtained from the Treasurer of the Society, Dr. C. C. Murdock, Department of Physics, Cornell University, Ithaca, New York. Price: \$4.00.

In just the same way that a crystal structure can be represented in terms of a reciprocal lattice every point of which is weighted with its corresponding structure factor, a molecule can be represented in terms of weighted reciprocal space (A. Hettich: *Z. Krist.* **90**, 483 (1935). P. P. Ewald: *Z. Krist.* **90**, 493 (1935). G. Knott: *Proc. Phys. Soc. (London)* **52**, 229 (1940)). Such a representation is called the molecular structure factor, which is very closely related to the Fourier transform of the molecule. This representation has proved particularly useful when the geometry of the molecules or groups comprising a crystal is known and the problem is to determine their relative orientation (A. Charlesby, G. Finch, and H. Wilman: *Proc. Phys. Soc. (London)* **51**, 479 (1939). J. Waser and C. S. Lu: *J. Am. Chem. Soc.* **66**, 2035 (1944); the power of the Fourier transform is illustrated by its use here in reducing the original fifty-four unknown parameters in the biphenylene crystal to four).

In this short and excellent monograph, Dr. Wrinch has recorded the Fourier transforms of a large number of structural types, many of which occur frequently in a wide variety of crystals. These types include points of a lattice (Chapter 3) and, among others, tetrahedral, octahedral, and hexagonal sets of points (Chapter 4). The discussion is extended (Chapter 5) to sets of many points on surfaces and within volumes based on a cubic lattice. The transforms of continuous distributions (Chapter 6) permit a discussion of composite distributions $\delta(D)$, in which continuous distributions D are repeated by parallel displacement at any of the sets of points δ . Three classes of applications are mentioned: (1) When D represents an atom, the composite distribution yields the transform of like or closely similar atoms at the points of one of the sets δ . (2) When D represents the unit of pattern of a crystal and δ the set of points of the lattice, the composite distribution is the crystal, and its transform is defined only at reciprocal lattice points. (3) When δ is a

fragment of a lattice and D is the unit of pattern, the composite distribution is that of a small crystal. The transforms of small cubic crystals bounded by various forms are discussed in Chapter 7.

The possibility of the use of the Fourier transform is mentioned as an aid in the determination of the structures of megamolecular crystals in which the structures and even to some extent the compositions of the molecules are unknown. However, for the present we may expect the principal applications to continue to be in determinations of crystal structures containing molecules whose geometry is known at least approximately. The best information obtained so far concerning the detailed principles upon which the structures of megamolecular crystals are based has come from the relatively few complete structural investigations of simple molecules related to the large molecules.

Mathematically, Dr. Wrinch's book is well presented. The text is expressed in a compact style, which however is not always clear grammatically (e.g., parts of pages 19, 23, 63, 65, 70). The printing, binding, and paper are quite good.

This excellent book can be recommended highly to anyone interested in the ways in which the Fourier transform can be used in structural analysis.

WILLIAM N. LIPSCOMB.

Fundamentals of Semi-micro Qualitative Analysis. By CARL J. ENGELDER. 5½ x 8½ in.; vi+ 385 pp. New York: John Wiley and Sons, Inc., 1947. Price: \$3.50.

This book differs markedly from the earlier conventional book on *Semi-micro Qualitative Analysis* by Engelder, Dunkelberger, and Schiller in that the theoretical material and laboratory directions are not separated. Each of the first five chapters comprising Part I, The Cations, begins with a discussion of some phase of the theory of qualitative analysis, which is followed by a brief discussion of the chemical properties of the ions, preliminary experiments that aid in carrying out the analysis, and a procedure for the analysis of the group. In each chapter, exercises are interposed at suitable points. Advantage is taken of the simpler chemistry of the ions usually placed in Groups IV and V to pass rapidly into the theories fundamental to the proper understanding of qualitative analysis. Discussions of the ions of Groups III, II, and I then follow in that order.

Each of the three chapters comprising Part II, The Anions, contains a discussion of the anions, procedure for the analysis of the ions, and some theory. As in Part I, exercises are placed to enable the student to determine whether he has grasped the subject or not—such as the pH of solutions, the theory of neutralization and hydrolysis, and the electrochemical theory of oxidation.

In Part III, the systematic analysis of liquid and solid samples is discussed for both cations and anions. In the Appendix is a discussion of colloids; the mathematics involved in qualitative analysis; suggestions to the instructor, including a weekly schedule; lists of apparatus and reagents; tables of the concentrations of reagents; logarithms; etc.

The reviewer thinks that the mixing of theory and laboratory directions is apt to confuse the student. Furthermore, if the anions are not studied, the theory in this part will have to be worked into that given with the cations. Some of the statements in the theoretical part are questionable; for example, on page 37 the ionization of sodium chloride is said to be "actually 85.2 per cent," and on page 152 ff. "the per cent of ionization of 0.1- M sodium hydroxide, hydrochloric, and nitric acids is 91–92%, while that of uni-univalent salts is 80–85%, uni-bivalent salts is 65–75%, and that of bi-bivalent salts is 35–45%."

The use of single and double arrows is confusing. On page 62, a single arrow is used in the equation for the precipitation of a difficultly soluble substance, and on page 64 double arrows are used. Similarly, single arrows are found in equations used to write expressions for the appropriate equilibrium constants on pages 68, 135, and 189, and double arrows on pages 184 and 261. The expression for calculating the concentration of an ion, "Molarity \times per cent of ionization" on page 157 is only partly correct. The procedures in general are conventional and are undoubtedly satisfactory.

G. B. HEISIG.

The Problem of Reducing Vulnerability to Atomic Bombs. By AINSLEY J. COALE. 116 pp. Princeton, New Jersey: Princeton University Press, 1947. Price: \$2.00.

Prepared under the direction of the Committee on Social and Economic Aspects of Atomic Energy of the Social Science Research Council, a factual analysis of the problem of dealing with an attack employing atomic bombs is attempted. The writer at the outset wisely discards the possibility that there will be any means of warding off or nullifying such an attack by an enemy possessing atomic weapons. Although the various aspects of amelioration or reduction are studied and expounded at length, one is left with a deep sense of futility.

What is the point of recommending dispersal of centers of production, transportation, communication, and defense without considering the means of putting the proposals into effect within an allowable period of time? The latter, necessarily indefinite, is estimated at 3-15 years. If, then, the proportion of our critical industries and defenses that must be dispersed or go underground is as great as estimated—one-third of our present economy—the question becomes first a practical and economic one: can it be done? and secondly, is there any reasonable likelihood that it will be done?

When one considers the dislocations from the recent war, the difficulty of building, the scarcity and high cost of materials and labor, the maladjustment of distribution and allocation, it seems certain that such a huge program of relocation could not be carried through within the time limit, even if we had the will to do it.

No doubt the Social Science Research Council has also considered all the means of *avoiding* an atomic war. That would seem to the reviewer the much more profitable approach to the problem, the one in which the talents of the Social Science Research Council can best be applied in its own field of human conduct.

S. C. LIND.

Concise Chemical and Technical Dictionary. Edited by H. BENNETT. 6 x 9 in. xxxix + 1055 pp. Brooklyn, New York: The Chemical Publishing Company, Inc., 1947. Price: \$10.00.

"This is a dictionary for both professionals and laymen: chemists and engineers in all industries, technical workers of all trades, manufacturers, importers, brokers, salesmen, teachers, librarians, students of all professions, and every intelligent person who wants to understand what he is reading when he comes across a technical expression in a book, newspaper or advertisement of a chemical product." This quotation from the editor's preface, and another section which states that the volume "... covers every field of scientific and technical development," indicate the wide range of usefulness of the dictionary.

A compilation of thousands of trade-name or proprietary products in many fields is, in the opinion of this reviewer, the most valuable part of the dictionary. The list is strictly up to date, inasmuch as surprisingly few of the names appearing in journals and trade literature fail to show up in the dictionary.

Among the 50,000 definitions included in the volume there are said to be "... descriptions of every common or rare chemical, etc., etc." Surely the editor does not expect the literal acceptance of this statement by an intelligent chemist! Among the thousands of organic and inorganic compounds listed there are too many for which no uses are given and which are therefore out of place in a book of this character. These entries serve to make an unnecessarily large volume which sells at the relatively high price of \$10.00.

Working chemists and research students who wish to have exact information about the physical properties of a particular compound will probably prefer to use one of the standard handbooks rather than a dictionary. This preference might well be dictated after a reading of the following statement: "When properties such as boiling and melting points are given, they may be for commercial rather than for pure products and slight differences must be expected."

The book is well made, the printing is good, and the proofreading has been very carefully done; the reviewer did not notice a single typographical error. The dictionary should prove valuable on many occasions to most of the persons whom the author intends it to serve, and it deserves a place in the libraries of those who can afford the purchase price.

J. LEWIS MAYNARD.

FREE-VOLUME MODELS FOR LIQUIDS

TERRELL L. HILL

Department of Chemistry, The University of Rochester, Rochester, New York

Received April 2, 1947

I. INTRODUCTION

It was found desirable, in another connection, to compare approximately, in the neighborhood of the critical point, the fundamental functions occurring in the van der Waals and Lennard-Jones and Devonshire models of classical liquids with the same functions obtained from experimental data. It is believed that these results, although necessarily of only a semiquantitative nature, might be of interest, and they are presented here. A new approximate free-volume model for classical liquids is discussed briefly in an appendix.

For a classical perfect gas

$$-A/NkT = \ln \left(\frac{2\pi mkT}{h^2} \right)^{3/2} v j(T) + 1 \quad (1)$$

where $v = V/N$ and $j(T)$ is the internal partition function. In passing from a classical perfect gas and equation 1 to the free-volume model of a classical imperfect gas or liquid, we may replace, in equation 1, the volume per molecule, v , by an effective free volume per molecule v_f , and introduce a potential energy of interaction per molecule $-\chi$, evaluated when each molecule is in the center of its cell. In the most general form of this model both v_f and χ would be functions of v and T . Actually, the dependence of χ on T is not very strong. Neglecting this dependence we have, for an imperfect gas or liquid (classical), according to this model:

$$-A/NkT = \ln \left(\frac{2\pi mkT}{h^2} \right)^{3/2} v_f(v, T) j(T) + 1 + \frac{\chi(v)}{kT} \quad (2)$$

The theory of Lennard-Jones and Devonshire (LJD) (7) serves as an illustration of equation 2. We shall actually be concerned primarily with the very crude, but still helpful, simplest free-volume model in which both v_f and χ are taken as functions of v only. The physical picture associated with this latter more restricted model is that each molecule moves freely in a uniform potential field ($-\chi(v)$) over the free volume Nv_f . The remainder of the volume, $V - Nv_f$, is excluded because the potential energy is infinite in this region. The excluded volume arises, of course, owing to the presence of the other molecules. In the more general case (equation 2), each molecule moves in a non-uniform (periodic in three dimensions, on the average) potential field over the entire volume $Nv = V$. The molecules spend most but not all of their time near potential minima (at which the potential energy has the value $-\chi(v)$), following the Boltzmann distribution law. The temperature dependence introduced by the Boltzmann distribution appears in $v_f(v, T)$. Models of this type define "effective" free volumes.

For future use, it will be convenient to define several new quantities (following Fowler and Guggenheim (2) to some extent):

$$\begin{aligned}\Lambda\psi(v) &= \chi(v) \\ vf(v,T) &= v_f(v,T) \\ \Lambda &= z\epsilon \quad (\epsilon, \Lambda > 0) \\ v^* &= r^{*3}/\gamma\end{aligned}\tag{3}$$

We assume that the potential energy of interaction between two molecules, as a function of the distance r between them, is given by

$$V_0(r) = -2\epsilon\left(\frac{r^*}{r}\right)^6 + \epsilon\left(\frac{r^*}{r}\right)^{12}\tag{4}$$

Equation 4 defines ϵ and r^* . Also, z is the average number of nearest neighbors and γ is a geometrical constant depending on the type of packing ($\gamma = \sqrt{2}$ for close packing, and $z = 12$). Λ , $\psi(v)$, $f(v,T)$, and v^* are now defined by equations 3 in terms of ϵ , r^* , γ , z , χ , and v_f . The function $f(v,T)$ is the fraction of the actual volume that is effectively "free."

From equation 2 and

$$\frac{P}{kT} = \frac{\partial}{\partial v} \left(-\frac{A}{NkT} \right)$$

we have

$$\frac{Pv}{kT} = \varphi\left(\frac{v}{v^*}, \frac{\Lambda}{kT}\right) + \frac{\Lambda}{kT} B\left(\frac{v}{v^*}\right)\tag{5}$$

$$\varphi = \frac{\partial \ln v_f}{\partial \ln (v/v^*)} = 1 + \frac{\partial \ln f}{\partial \ln (v/v^*)}\tag{6}$$

$$B = \frac{d\psi}{d \ln (v/v^*)}\tag{7}$$

We expect the functions φ and B to be universal functions, to a good approximation, for suitable gases such as nitrogen, argon, neon, etc. The question now arises as to the correct form of the functions φ and B . Unfortunately there is no satisfactory theory to which to turn, though perhaps the most successful tractable effort is that of LJD. Writing $x = v^*/v$, the LJD model leads to

$$\varphi\left(\frac{v}{v^*}, \frac{\Lambda}{kT}\right) = 1 + 4 \frac{\Lambda}{kT} \left(x^4 \frac{g_l}{g} - x^3 \frac{g_m}{g} \right)\tag{8}$$

$$B\left(\frac{v}{v^*}\right) = 2x^4 - 2.4x^2\tag{9}$$

$$f\left(\frac{v}{v^*}, \frac{\Lambda}{kT}\right) = 2\pi\gamma g\tag{10}$$

$$\psi\left(\frac{v}{v^*}\right) = 1.2x^2 - 0.5x^4\tag{11}$$

where g , g_1 , and g_m are functions of v/v^* and Λ/kT defined by certain integrals. These equations give $\Lambda/kT_c \cong 9$, $v_c/v^* \cong 1.8$, and $P_c v_c/kT_c \cong 0.64$. If we compare these critical constants with experimental values for neon, nitrogen, and argon (see table 1), the first is seen to be quite good (discussed further below) but one should have $v_c/v^* = 2.76$ and $P_c v_c/kT_c = 0.292$.

TABLE 1†

	T_c	$\epsilon \times 10^{15}$ ERGS	z	$\Lambda \times 10^{15}$ ERGS	γ	r^{*3} IN Å ³	v^* IN Å ³	v_c/v^*	$\frac{P_c v_c}{kT_c}$	$\frac{P_c v^*}{kT_c}$
Ne	44.4	4.89	10.42	50.9	1.228	29.2	23.8	2.88	0.293	0.1017
N ₂	126.0	13.25	10.91	144.6	1.286	72.5	56.4	2.64	0.290	0.1098
Ar	151.0	16.5	10.50	173.2	1.237	56.2	45.4	2.75	0.292	0.1062
H ₂	33.2	4.25	(8.96)			35.3			0.294	
He	5.2	0.827	(7.21)			25.7			0.298	

† See pp. 285 and 345 of reference 2; original references are given there.

It is of interest to discuss van der Waals' equation also, from this point of view. We have:

$$(P + a/v^2)(v - b) = kT \quad (12)$$

Using (reference 8)

$$b = \frac{2\pi}{3} r^{*3} = \frac{2\pi}{3} \gamma v^* = K_1 v^* \quad (13)$$

and

$$a = \frac{2\pi}{3} \epsilon r^{*3} = \frac{2\pi}{3} \frac{\Lambda}{z} \gamma v^* = K_2 v^* \quad (14)$$

equation 12 can be rewritten in the form

$$\frac{Pv}{kT} = \varphi(v/v^*) + \frac{\Lambda}{kT} B(v/v^*) \quad (15)$$

with

$$\varphi(v/v^*) = 1 + \frac{K_1}{(v/v^*) - K_1} = \frac{1}{1 - K_1 x} = 1/f(v/v^*) \quad (16)$$

and

$$B(v/v^*) = -K_2/(v/v^*) = -\psi\left(\frac{v}{v^*}\right) \quad (17)$$

The functions f and ψ are found from φ and B by integrating (with respect to x , say), taking $f = 1$ and $\psi = 0$ at $x = 0$. We can also write f as $f = (v - b)/v$. Van der Waals' equation thus follows from a free-volume model with φ , as well as B , taken as a function of v/v^* only. These van der Waals functions (equations 16 and 17) are included in figures 1-4. In these figures, for van der Waals' equation, we take $z = 10.5$ and find γ from equation 20 (see Section II), leading to $K_1 = 2.59$ and $K_2 = 0.247$.

Our object is to compare, in the neighborhood of the critical point, the functions φ , B , f , and ψ of the LJD and van der Waals models with corresponding functions calculated from experimental PVT data (*International Critical Tables*, for example). Unfortunately, the experimental data for argon and nitrogen do not appear to be adequate to study the temperature dependence (of φ and f) satisfactorily, and, for neon, the data seem inadequate even for the volume dependence. In any case the available data restrict one to temperatures slightly above the critical temperature.

In view of the above restrictions, it will be necessary to make the approximation, in examining the experimental data, of neglecting the temperature dependence of φ and f . That is, we assume that the experimental PVT data follow

$$\frac{Pv}{kT} = \varphi\left(\frac{v}{v^*}\right) + \frac{\Lambda}{kT} B\left(\frac{v}{v^*}\right) \quad (18)$$

(in other words, we "force" the experimental data to obey the rather restricted equation 18). This is, of course, a fairly crude assumption, but it should lead to results of semiquantitative significance.

The procedure is then as follows: Suppose Pv/kT is available for approximately the same range in v/v^* , for a gas, at two temperatures, T_1 and T_2 , which do not differ greatly. We may then interpolate (numerically or graphically) $(Pv/kT)_1$ and $(Pv/kT)_2$ for desirable values of v/v^* . From equation 18, we have

$$\begin{aligned} (Pv/kT)_1 &= \varphi(v/v^*) + \frac{\Lambda}{kT_1} B(v/v^*) \\ (Pv/kT)_2 &= \varphi(v/v^*) + \frac{\Lambda}{kT_2} B(v/v^*) \end{aligned} \quad (19)$$

from which we calculate φ and B for each value of v/v^* . In this way, if sufficient data are available, we can obtain the approximate volume dependence of φ and B , near the critical temperature.

II. CALCULATIONS FOR ARGON AND NITROGEN

It is first necessary to make some preliminary calculations concerning γ , v^* , etc. For close packing of either type, $z = 12$ and $\gamma = \sqrt{2}$. Actually, z is probably somewhat less than 12. The only experimental data available are for argon (1, 10), leading to $z = 10.2$ – 10.9 . We adopt $z = 10.5$ here as an average value. In order to estimate z for neon and nitrogen we assume that $\Lambda/kT_c = z\epsilon/kT_c$ has the same value for argon, neon, and nitrogen. For argon (table 1), taking $z = 10.5$ and $\epsilon = 16.5 \times 10^{-15}$ ergs per molecule, we find $\Lambda/kT_c = 8.31$, and we adopt this as an approximate universal value for suitable classical gases. It may be compared with $\Lambda/kT_c \cong 9$ in the LJD theory. Using $\Lambda/kT_c = 8.31$, z is given for neon (the degeneracy in neon should be negligible at its critical temperature) and nitrogen in table 1, and also for hydrogen and helium assuming for the moment that they too are classical. The values of z thus obtained for

hydrogen and helium (in parentheses in the table) are approximate upper limits, since degeneracy aids condensation and hence, with degeneracy, other things being equal, the same critical temperature can obtain with a smaller number of nearest neighbors. The value of z for hydrogen, taking degeneracy into account, is estimated roughly in Appendix II as approximately 8.8. It may be pointed out in this connection that the relatively large discrepancies between T_c (calcd.)¹ and T_c (obsd.) in table 5² of Fowler and Guggenheim (from LJD) for hydrogen and helium are actually of the wrong sign to be explained by degeneracy. This is because z is assumed the same for all gases listed, including hydrogen and helium. From these considerations (table 1), one therefore expects that z should be relatively small for hydrogen and especially for helium. There is some tentative experimental evidence for this ($z = 6$) in the case of helium (6).

In the absence of other information we make the rather reasonable assumption that the values of z in table 1 result from the occurrence of occasional random vacancies in a close-packed lattice. This allows us to estimate γ from z by

$$\gamma = \sqrt{2} z/12 \quad (20)$$

The remainder of the values in table 1 for neon, nitrogen, and argon may then be calculated using γ ³ (see footnote to table 1) and the experimental critical constants. All of the non-experimental values in table 1 should be considered approximate.

Nitrogen

The only suitable data are for $T_1 = 128.64$ (six experimental values of Pv/kT in the approximate range $v/v^* = 1.8$ to 6.0) and $T_2 = 126.78$ (five experimental values in this range). As $T_1 - T_2$ is quite small in this case, numerical interpolation of $(Pv/kT)_1$ and $(Pv/kT)_2$ was used (Lagrange's formula) rather than graphical interpolation. $B(v/v^*)$ and $\varphi(v/v^*)$ were then calculated from table 1 and equations 19. These results are given in table 2 and figures 1 and 2. We also give, in table 2, the critical isotherm ($\Lambda/kT^* = 8.31$) calculated from B , φ , and equation 18.

In order to calculate $f(v/v^*)$ and $\psi(v/v^*)$ we must extrapolate $d \ln f/dx$ and $d\psi/dx$ to $x = 0$. We estimate $(d \ln f/dx)_{x=0}$ and $(d\psi/dx)_{x=0}$ from second virial coefficients, as follows: Assume that, for small x (large v), we can write

$$\frac{Pv}{kT} = \varphi(x) + \frac{\Lambda}{kT} B(x) = 1 - x \frac{d \ln f}{dx} - \frac{\Lambda}{kT} \times \frac{d\psi}{dx} \quad (21)$$

$$= 1 + \frac{B(T)}{v} = 1 + \frac{1}{v} \left(\frac{c_1}{T} + c_2 \right) \quad (22)$$

where $B(T)$ is the second virial coefficient. Hence

$$\left(\frac{d \ln f}{dx} \right)_{x=0} = -\frac{c_2}{v^*} \quad \text{and} \quad \left(\frac{d\psi}{dx} \right)_{x=0} = -\frac{kc_1}{\Lambda v^*} \quad (23)$$

¹ T_c (calcd.) is given incorrectly for helium; it should be 8.0°K.

² Page 345 of reference 2.

TABLE 2
Nitrogen

v/v^*	$\left(\frac{Pv}{kT}\right)_1$	$\left(\frac{Pv}{kT}\right)_2$	$-B$	ϕ	$\frac{Pv}{kT_c}$	$\frac{Pv^*}{kT_c}$	v/v^*	f	ψ
1.847	0.2464	0.2193	0.2268	2.092	0.207	0.112	1.786	0.2218	0.3316
2.308	0.2860	0.2645	0.1803	1.754	0.256	0.111	2.063	0.2587	0.2985
2.770	0.3330	0.3125	0.1716	1.729	0.303	0.109	2.500	0.2979	0.2652
3.232	0.3812	0.3608	0.1709	1.772	0.352	0.109	3.125	0.3510	0.2269
3.694	0.4270	0.4074	0.1643	1.765	0.400	0.108	4.167	0.4365	0.1796
4.155	0.4688	0.4509	0.1500	1.690	0.444	0.107	6.250	0.5434	0.1295
4.617	0.5061	0.4903	0.1327	1.586	0.483	0.105			
5.079	0.5393	0.5251	0.1191	1.508	0.518	0.102			
5.540	0.5690	0.5555	0.1138	1.496	0.550	0.099			
6.002	0.5956	0.5819	0.1142	1.525	0.576	0.096			

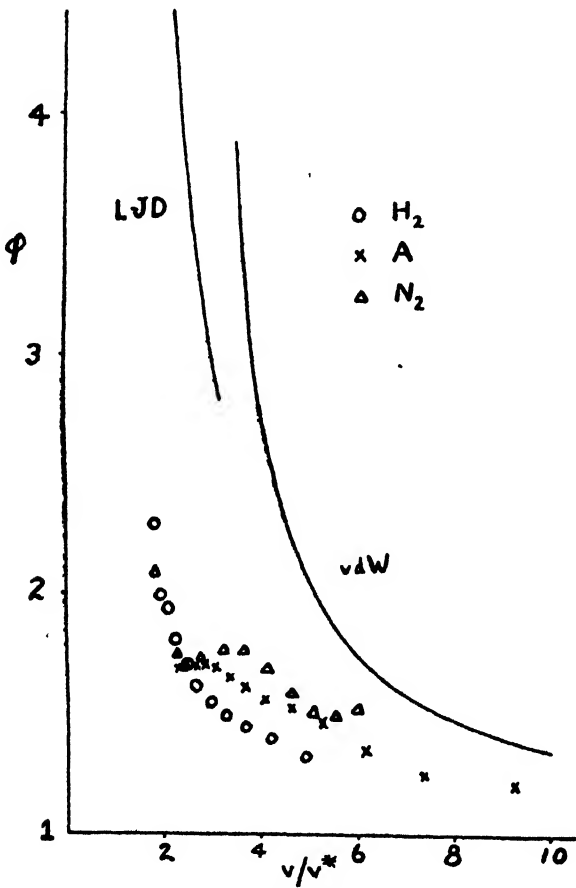


FIG. 1

That is, we assume that $B(T)$ is a linear function of $1/T$ between T_1 and T_2 . For nitrogen, $B(T)$ is available for T_1 and T_2 , and hence c_1 and c_2 may be calculated easily on this assumption. One finds $c_1 = -5.042 \times 10^4 \text{ A}^3\text{-deg.}$ and $c_2 = 229.6 \text{ A}^3$. It may be remarked that the limiting values of the derivatives obtained by equations 23 seem quite reasonable in actually performing the extrapolations. The same is true for argon (and hydrogen). ψ and f may now

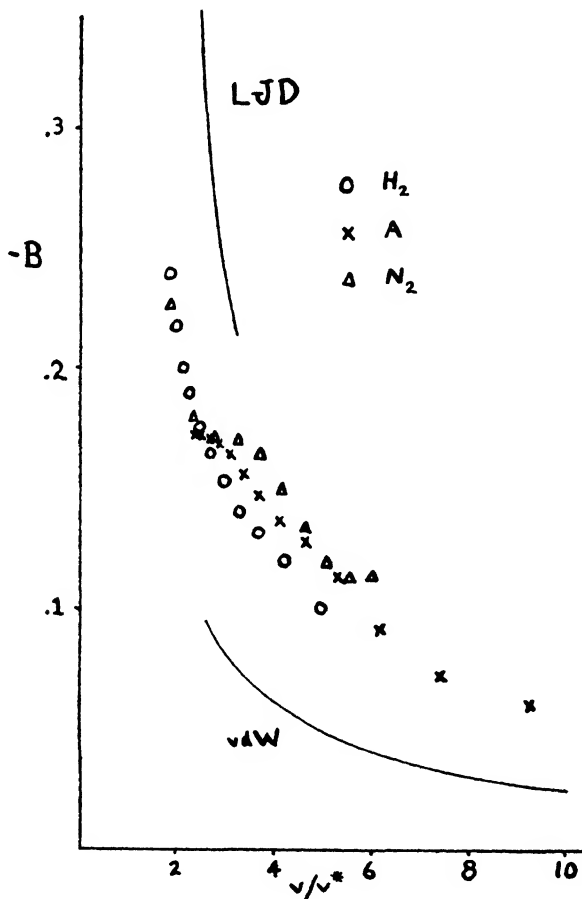


FIG. 2

be calculated by numerical integration, and these functions are also given in table 2, and in figures 3 and 4.

Argon

The temperatures $T_1 = 157.24$ and $T_2 = 152.86$ were used with careful large-scale graphical interpolation of Pv/kT . Values of the second virial coefficient are not available for exactly these temperatures, but a tangent line was used, drawn through the smooth curve of $B(T)$ versus $1/T$ at $(T_1 + T_2)/2 = 155.05$

(the smooth curve had to be extrapolated slightly to this temperature). There is obtained $c_1 = -0.361 \times 10^4 \text{ A.}^3\text{-deg.}$ and $c_2 = 102.8 \text{ A.}^3$. We give in table 3 and figures 1-4 the functions B , φ , f , and ψ , and the calculated critical isotherm in table 3.

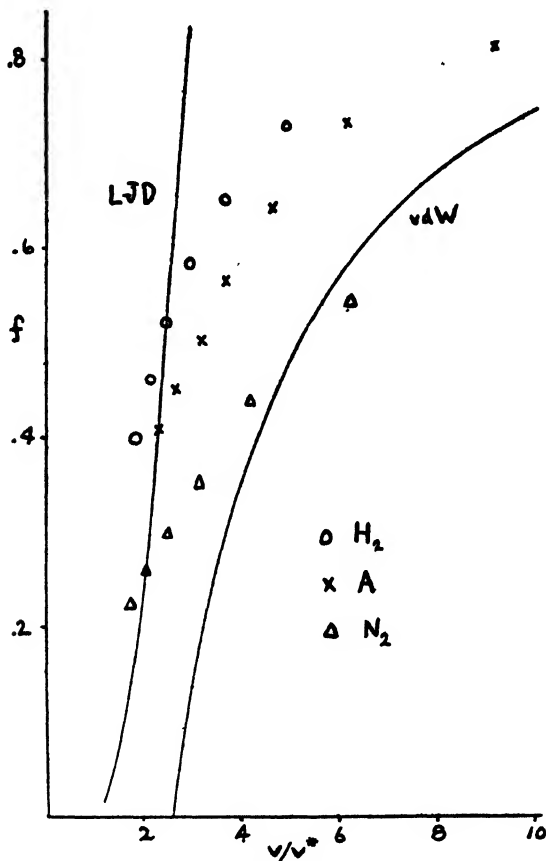


FIG. 3

III. DISCUSSION

The functions φ , B , f , and ψ for argon and nitrogen, and for the van der Waals and LJD models, may be compared in figures 1-4. The curves given for the LJD model are for $\Lambda/kT = 9$ (this is the critical temperature in this model— φ depends on temperature here). It will be observed that neither the van der Waals nor the LJD functions resemble the "experimental" functions very closely, though, rather surprisingly, the van der Waals functions actually seem to be superior in some respects. Apparently the fact that we have, for small x ,

$$\begin{aligned} Pv/kT &= 1 + O(x) \quad \text{van der Waals (and actual gases)} \\ &= 1 + O(x^2) \quad \text{LJD} \end{aligned}$$

is of importance even near the critical point.

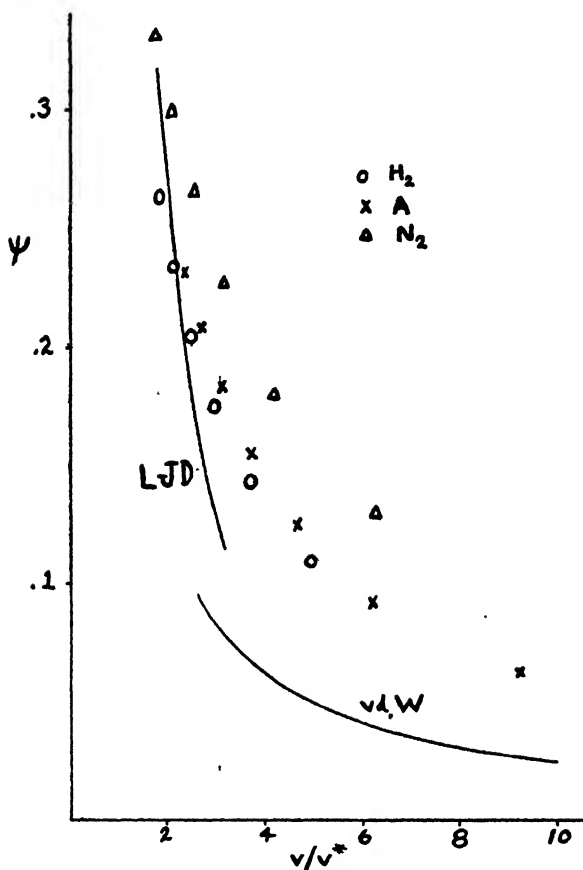


FIG. 4

TABLE 3

Argon

v/v^*	$\left(\frac{Pv}{kT}\right)_1$	$\left(\frac{Pv}{kT}\right)_2$	$-B$	φ	$\frac{Pv}{kT_c}$	$\frac{Pv^*}{kT_c}$	f	ψ
2.308	0.3082	0.2688	0.1723	1.683	0.251	0.109	0.4098	0.2319
2.462	0.3243	0.2849	0.1723	1.699	0.267	0.108		
2.638	0.3423	0.3033	0.1706	1.703	0.285	0.108	0.4497	0.2090
2.841	0.3631	0.3244	0.1693	1.714	0.307	0.108		
3.077	0.3860	0.3485	0.1640	1.695	0.332	0.108	0.5017	0.1830
3.357	0.4128	0.3772	0.1557	1.655	0.361	0.108		
3.693	0.4436	0.4100	0.1470	1.616	0.395	0.107	0.5652	0.1547
4.103	0.4781	0.4469	0.1385	1.567	0.433	0.105		
4.616	0.5178	0.4886	0.1277	1.537	0.476	0.103	0.6417	0.1242
5.276	0.5630	0.5371	0.1133	1.467	0.526	0.100		
6.156	0.6124	0.5914	0.0918	1.345	0.582	0.095	0.7311	0.0917
7.386	0.6660	0.6493	0.0730	1.249	0.642	0.087		
9.233	0.7248	0.7110	0.0603	1.207	0.706	0.076	0.8103	0.0626
12.311	0.7864	0.7761	0.0451	1.146	0.772	0.063		

The discrepancies between nitrogen and argon are rather small in figures 1 and 2, but they are of course considerably magnified in figures 3 and 4 because of the integrations involved.

Although it has been emphasized that the above comparison between experimental and theoretical curves is only semiquantitative, it is felt that the general form of the "experimental" functions φ , B , f , and ψ exhibited in figures 1-4 should be of some value as a test in connection with future work on free-volume models of liquids.

It will be noticed, in figure 3, that at the critical point f is of the order of 0.3-0.5. Earlier work on liquids has given much smaller values (3, 4): $f = 0.003-0.01$. However, the actual discrepancy is not nearly so great as this, for these latter values refer to considerably smaller volumes and temperatures. Let us estimate roughly the magnitude of our f 's for argon and nitrogen at their respective boiling points. We may correct for the volume effect by extrapolating

TABLE 4
LJD functions for $\Lambda/kT = 6$

v/v^*	x^2	ϵ	ϵ_t	ϵ_m	$\frac{P_v}{kT}$	$\frac{P_v^*}{kT}$
1.195	0.7	0.00262	0.00182	0.000333	2.838	2.375
1.291	0.6	0.00395	0.00380	0.000662	2.577	1.996
1.414	0.5	0.00659	0.00865	0.00140	2.133	1.508
1.581	0.4	0.0115	0.0222	0.00325	1.854	1.173
1.826	0.3	0.0213	0.0667	0.00843	1.670	0.915
2.236	0.2	0.0425	0.257	0.0255	1.528	0.683
2.575	0.15	0.0615	0.583	0.0478	1.431	0.556
3.162	0.1	0.0930	1.693	0.1021	1.413	0.447
4.472	0.05	0.1470	7.825	0.2648	1.342	0.300

f , in figure 3, to $f = 0$ at $v/v^* = 0$. We read from these extrapolated curves $f = 0.21$ and 0.14 at the boiling-point values of v/v^* , 1.04 and 1.06. For the temperature dependence we have to assume that it will be about the same as indicated (for g) for the LJD theory (table 7, page 348, of Fowler and Guggenheim (2)). This introduces in our case a factor of about 4.2, which gives $f = 0.05$ and 0.03 . We are interested in temperatures below the boiling points for this comparison, which would give us still smaller values of f than 0.05 and 0.03. In view of the crudeness of the temperature correction, it is therefore hard to say whether there is in fact any actual discrepancy in order of magnitude. It may be noted in this connection that the LJD theory gives $f = 2\pi\gamma g = 0.17$ at the critical point (compared to 0.3-0.5 here).

APPENDIX I

In the course of the present work LJD functions were calculated for $\Lambda/kT = 6$. As these results may be of use to others, they are given in table 4.

APPENDIX II

Hydrogen is probably slightly degenerate (Bose-Einstein) near its critical point. At the present time, no treatment of a degenerate imperfect gas or liquid is available, even for the simplest (hard sphere type) model, owing to mathematical difficulties. However, because the degeneracy in hydrogen at the critical point is only slight, it would seem that one ought to be able to make the necessary small corrections with "order of magnitude" accuracy in this case (but not for helium) by adopting the simplest possible type of assumption: write the well-known (8) expression for the Helmholtz free energy of a perfect Bose-Einstein gas

$$\begin{aligned}
 -A/NkT &= \ln \left(\frac{2\pi mkT}{h^2} \right)^{3/2} \rho v + 1 + \left\{ 0.4618 \frac{v^0(T)}{v} \right. \\
 &\quad \left. + 0.0111 \left[\frac{v^0(T)}{v} \right]^2 + 0.00065 \left[\frac{v^0(T)}{v} \right]^3 + \dots \right\} \quad v > v^0(T) \quad (24) \\
 &= 0.5134 \frac{v}{v^0(T)} \quad v < v^0(T) \\
 v^0(T) &= \frac{1}{2.612\rho} \left(\frac{h^2}{2\pi mkT} \right)^{3/2}
 \end{aligned}$$

where ρ is the degeneracy of the lowest energy level, and then formally replace v by $v_f(v)$ wherever v appears and add a term $\chi(v)/kT$ to both parts of the above equation for $-A/NkT$ (this procedure being in formal analogy with the process: equation 1 \rightarrow equation 2 for a classical liquid). The equation of state then follows immediately.

Some calculations have been made on hydrogen, using the above procedure and experimental PVT data as for argon and nitrogen. A method of successive approximations must be used here to get the "experimental" functions φ , B , f , and ψ . The fact that the experimental data refer to a mixture of ortho- and para-hydrogen was taken into account. It does not seem worthwhile to present these calculations in detail, because they probably have only order-of-magnitude significance. However, a few results might be mentioned: The observed critical temperature of hydrogen is about one-half of a degree lower than it would be if hydrogen were non-degenerate (i.e., classical); z is about 8.8 (instead of the classical value 8.96); the functions φ , B , f , and ψ found for hydrogen agree as well with argon and nitrogen as the argon and nitrogen functions do with each other (figures 1-4). Because of the small amount of degeneracy, these hydrogen functions do not differ much from the results obtained in a classical calculation for hydrogen (as for argon and nitrogen). So the corrected functions for hydrogen should be fairly reliable.

APPENDIX III

We discuss here very briefly a new model of a classical liquid which might be of interest. It has about the same degree of crudeness as the harmonic oscillator

model of a liquid, but it is somewhat more general (it includes the harmonic oscillator model as a special case) and seems more realistic in a sense. It retains, on the one hand, the close connection between a crystal and the harmonic oscillator model of a liquid, and, on the other, it also shows clearly the transition from liquid to gas.

In the harmonic oscillator model, each molecule is considered to be trapped in a cell and performs harmonic oscillations in three dimensions about the center of the cell. As the distance r from the center of the cell increases, the potential energy becomes larger and larger. In the LJD model the potential energy also becomes infinite as r increases, but the form of the potential curve is more complicated than just parabolic (as it is taken to be in the harmonic oscillator model). In both of these models, because of this infinite potential energy property, it is necessary to introduce in a rather arbitrary fashion the possibility of a molecule moving from cell to cell (communal entropy) in the liquid state. The present model avoids this difficulty.

Any given molecule in a liquid may be thought of roughly as being surrounded on the average by a number, z , of nearest neighbors in a close-packed lattice. If z is less than 12, say 10.5, we assume some of the lattice sites are vacant at random. As a molecule moves outward from the center of its cell, the potential energy usually increases. In order for the molecule to continue this outward motion and pass through its own coordinate shell into an adjacent cell it must in general pass over a potential barrier, but *not* an infinite one. If a molecule in a liquid is surrounded by nearest neighbor molecules in a face-centered cubic lattice, there are six most probable places, symmetrically distributed, through which the central molecule can pass in leaving the cell (these are the centers of the six squares formed by groups of four molecules in the coordinate shell). On the time average there is of course spherical symmetry, but for convenience we make use, as an approximation, of the simple cubic symmetry of the six passageways and write for the simplest possible potential function having the desired properties

$$U(x, y, z) = -\chi(v) + \frac{1}{2} [\chi(v) - \chi_s(v)] \left(3 - \cos \frac{2\pi x}{d} - \cos \frac{2\pi y}{d} - \cos \frac{2\pi z}{d} \right) \quad (25)$$

That is, $-\chi(v)$ is the potential energy at the center of a cell (say $x = y = z = 0$), $-\chi_s(v)$ is the potential energy at the side of a cell (top of the potential barrier; say $y = z = 0, x = d/2$), and we assume a cosine curve for intermediate positions. In the picture above, d , the wave length of the potential curve, is $(\sqrt{2}) \times$ (distance between nearest neighbors). However, in the classical treatment used below, d does not appear in the final equations.

The classical partition function for a single molecule in the volume $V = l^3$ is

$$q = \frac{1}{h^3} \iiint \exp(-H/kT) dx dy dz dp_x dp_y dp_z \quad (26)$$

with

$$H = \frac{(p_x^2 + p_y^2 + p_z^2)}{2m} + U(x, y, z) \quad (27)$$

Hence

$$q = \left(\frac{2\pi mkT}{h^2} \right)^{3/2} \exp(\chi/kT) \exp[-\frac{3}{2}(\chi - \chi_s)/kT] \times \left[\int_0^1 \exp\left(\frac{1}{2} \frac{\chi - \chi_s}{kT} \cos \frac{2\pi x}{d}\right) dx \right]^3 \quad (28)$$

The value of the integral is $I_0(u)$, where $I_0(u)$ is a modified Bessel function of the first kind and $u = (\chi - \chi_s)/2kT$. The complete partition function for N molecules is $Q = q^N/N!$. We obtain, finally,

$$-A/NkT = \ln \left(\frac{2\pi mkT}{h^2} \right)^{3/2} v_f(v, T) j(T) + 1 + \frac{\chi(v)}{kT} \quad (29)$$

with

$$v_f(v, T) = v \exp \left\{ -\frac{3}{2}[\chi(v) - \chi_s(v)]/kT \right\} I_0^3 \left(\frac{\chi(v) - \chi_s(v)}{2kT} \right) \\ = v \{ \exp[-u(v, T)] I_0(u(v, T)) \}^3 \quad (30)$$

As $T \rightarrow \infty$ or $V \rightarrow \infty$ ($\chi, \chi_s \rightarrow 0$), $u \rightarrow 0$ and $v_f \rightarrow v$ (perfect gas). As $T \rightarrow 0$ or $V \rightarrow 0$ ($\{\chi - \chi_s\} \rightarrow \infty$), $u \rightarrow \infty$ and

$$v_f \rightarrow v \left[\frac{kT}{\pi(\chi - \chi_s)} \right]^{3/2} \quad (31)$$

since

$$\lim_{u \rightarrow \infty} I_0(u) = \frac{e^u}{(2\pi u)^{1/2}} \quad (32)$$

In the usual harmonic oscillator model

$$v_f(v, T) = \left[\frac{kT}{2\pi m \nu(v)^2} \right]^{3/2} \quad (33)$$

where $\nu(v)$ is the frequency of oscillation. The formal connection between the two models (for large u) is therefore

$$\nu(v) = \left[\frac{\chi(v) - \chi_s(v)}{2m v^{2/3}} \right]^{1/2} \quad (34)$$

In order to proceed further the functions $\chi(v)$ and $\chi_s(v)$ must be specified. It is clear that a more general model of this type could be developed, replacing the arbitrarily assumed cosine form of the potential energy by a function obtained from more fundamental considerations. This would lead to a treatment similar to that of LJD, except that infinite potential barriers would be replaced by finite ones.

It will be noted that there is an obvious connection between the present model of a liquid and the treatment of the problems (5, 9) of (1) hindered rotation in molecules such as ethane and (2) the mobile-localized transition of adsorbed molecules.

SUMMARY

1. The fundamental functions of the van der Waals and Lennard-Jones and Devonshire models of classical liquids are compared with corresponding approximate functions obtained from experimental *PVT* data on nitrogen and argon. Neither of these models is very satisfactory from this point of view. The general form of the "experimental" functions should be useful as an approximate criterion of success of future free-volume models of liquids.

2. Related calculations on hydrogen are discussed very briefly. It is possible to take into account the slight degeneracy in hydrogen near its critical point in only a very approximate manner.

3. A new approximate model of a classical liquid is suggested which retains, on the one hand, the close connection between a crystal and the harmonic oscillator model of a liquid, and which, on the other hand, shows clearly the transition from liquid to gas.

REFERENCES

- (1) EISENSTEIN, A., AND GINGRICH, N. S.: *Phys. Rev.* **62**, 261 (1942).
- (2) FOWLER, R. H., AND GUGGENHEIM, E. A.: *Statistical Thermodynamics*. Cambridge University Press, London (1939).
- (3) FRANK, H. S.: *J. Chem. Phys.* **13**, 478, 493, 507 (1945).
- (4) GLASTONE, S.: *Theoretical Chemistry*, pp. 465-72. D. Van Nostrand Co., Inc., New York (1944).
- (5) HILL, T. L.: *J. Chem. Phys.* **14**, 441 (1946).
- (6) KEESOM, W. H., AND TAKONIS, K. W.: *Physica* **5**, 161, 270 (1938).
- (7) LENNARD-JONES, J. E., AND DEVONSHIRE, A. F.: *Proc. Roy. Soc. (London)* **163A**, 53 (1937); **165A**, 1 (1938).
- (8) MAYER, J. E., AND MAYER, M. G.: *Statistical Mechanics*. John Wiley and Sons, Inc., New York (1940).
- (9) PITZER, K. S., AND GWINN, W. D.: *J. Chem. Phys.* **10**, 428 (1942).
- (10) RICE, O. K.: *J. Chem. Phys.* **7**, 883 (1939).

ADSORPTION OF GASES ON SURFACES OF POWDERS AND METAL FOILS¹

R. T. DAVIS, JR., T. W. DEWITT, AND P. H. EMMETT

Mellon Institute, Pittsburgh 13, Pennsylvania

Received June 11, 1947

During the past ten years many measurements have been made to test the validity for the determination of surface area of an improved method (9) and also a theoretical method (6) for interpreting multilayer adsorption isotherms taken near the boiling points of the gaseous adsorbates. The proposed methods

¹ Presented at the Symposium on the Adsorption of Gases which was held under the auspices of the Division of Colloid Chemistry at the 110th Meeting of the American Chemical Society, Chicago, Illinois, September 11-12, 1946.

have been applied with apparent success to materials having large areas (6, 10, 17) by using gases such as nitrogen as adsorbate at $-195^{\circ}\text{C}.$; to those having very small areas, by using ethylene (18) at $-183^{\circ}\text{C}.$; and to those with medium areas, by using krypton at $-195^{\circ}\text{C}.$ (4).

Within the last three years, one of the authors (T. W. D.) had occasion to measure the surface area of flat metal foil or of bundles of wire, using krypton at $-195^{\circ}\text{C}.$ as adsorbate. He discovered that if 15.5 \AA^2 , the value for the cross-sectional area of krypton as calculated in the usual way, was employed, the surface area obtained was smaller by 30 per cent or so than the geometric area. Even the use of a 1.3 correction factor for the krypton area, as suggested by Beebe (4) and coworkers, yielded a roughness factor equal to or slightly less than unity. Since roughness factors smaller than unity are inconceivable, the present work was undertaken with a view to checking the roughness factor of two foils by krypton and other usable gases. Secondary objectives included obtaining a cross-comparison of area values on a variety of adsorbents with different adsorbates, suggesting new adsorbates to use on samples in the intermediate area range and obtaining, if possible, for the first time, a complete S-shaped isotherm on a surface known to be flat and non-porous.

EXPERIMENTAL

Apparatus

For the adsorption measurements at pressures up to 1 atm. the normal adsorption apparatus was used (8). In some later experiments in which the solution of the gases in stopcock grease became a problem, mercury-activated ball valves were substituted for the stopcocks. For the low-pressure measurements, a separate system with a McLeod gauge having a range of 0.05–18 mm. was employed. The gauge was calibrated in the usual manner and also was checked against a manometer equipped with a travelling microscope; its error was less than 1 per cent. Mercury cut-offs were used instead of stopcocks on this low-pressure apparatus.

Gases

The nitrogen used for adsorption measurements was the prepurified tank grade, the helium, for calibration purposes, was commercial grade and was purified by passage over degassed charcoal at $-195^{\circ}\text{C}.$

n-Butane of 99 per cent purity from the Ohio Chemical Company was liquefied and any low-boiling fraction was pumped off; the remainder was used for adsorption measurements. Its vapor pressure was checked with the data of Aston and Messerly (3). An additional check was made of its purity by infrared and by mass-spectrographic analysis; the results indicated a maximum impurity of 0.3 per cent propane and 0.4 per cent isobutane.

Krypton of a spectroscopically pure grade was obtained from the Linde Air Products Company. An early sample of the gas was found to contain approximately 2 per cent xenon and as such was unsatisfactory. However, additional containers of gas obtained later were found to be free of this impurity.

But the gas was solidified at -195°C . and checked for purity by vapor-pressure measurements.

Freon-21 (dichloromonofluoromethane) from the Matheson Chemical Company and 1-butene of 99 per cent purity from the Phillips Petroleum Company were purified in the same manner as the butane.

Adsorbents

The silver foil was approximately 0.0005 in. thick and 7 in. wide. It was wound on a glass mandrel, and the layers were separated to some extent by silver wires 0.0045 in. in diameter. The geometric surface was 1.56 m.²

The monel ribbon was 0.002 in. thick and 0.125 in. wide. It was wound on a glass mandrel in a number of coils each about 1 in. in diameter. Its geometric area was 0.579 m.²

Two samples of glass spheres were used. They were both prepared by the method of Bloomquist and Clark (5). One sample, very kindly furnished by the Battelle Memorial Institute, had been carefully sized and had a particle diameter of 7 microns. The other sample would pass a 200-mesh screen but was not uniform in size.

The tungsten powder was similar to powder 9799 which had been used by Frankenburg and one of the authors for the study of hydrogen and nitrogen chemisorptions (7, 11).

The zinc oxide was a sample of material sent to us by Dr. C. W. Siller of the New Jersey Zinc Company. It was designated as #F1601.

Activated alumina, in the form of 3/16-in. tablets from the Harshaw Chemical Company, was crushed before use, as it was found to require exceedingly long equilibration times in the original state.

Silica gel from the Davison Chemical Company was likewise crushed before use.

Procedure

Temperature control was accomplished by the use of appropriate baths: namely, ice for 0°C ., dry ice-acetone for -78°C ., and liquid nitrogen for -195°C .

Before adsorption measurements were made, the samples were pumped out at room temperature overnight. Avoiding a higher degassing temperature seemed especially desirable in experiments on the metal foils to guard against the possibility of roughening the surface.

RESULTS AND DISCUSSION

The results of the experimental work are shown in figures 1 to 8. These illustrations give the isotherms for the various gases on the different adsorbents along with the corresponding B.E.T. plots (6) of the data according to the equation

$$\frac{p/p_0}{V(1 - p/p_0)} = 1/V_m C + \frac{(C - 1)}{V_m C} p/p_0 \quad (1)$$

where V is the volume (S.T.P.) of gas adsorbed at relative pressure p/p_0 , V_m is the volume of gas that it would take to form a monolayer on the adsorbent;

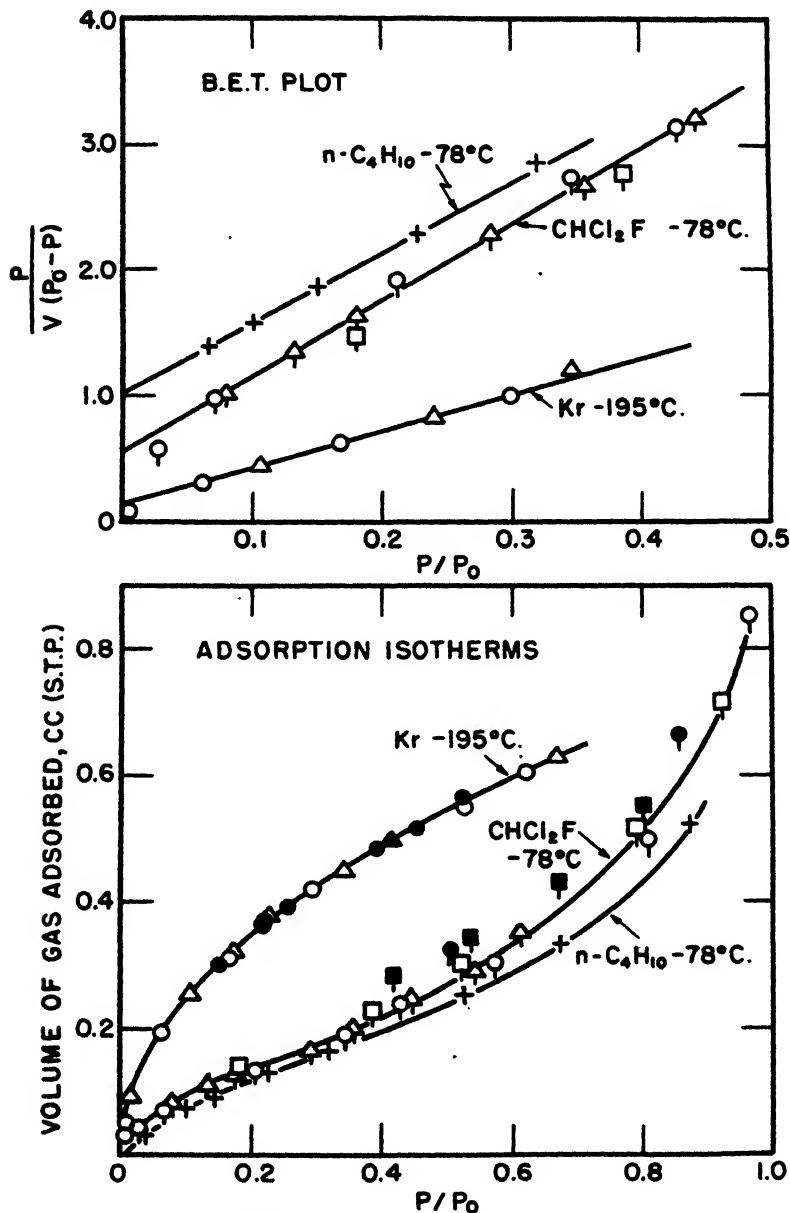


FIG. 1. Adsorption of gases on silver foil; solid symbols are desorption points

and C is a constant that is proportional to $e^{E_1 - E_L/RT}$, where E_1 is the heat of adsorption in the first layer and E_L is the heat of liquefaction.

Figures 1 and 2 are of special interest for two reasons. First, they show that on the surfaces of the flat silver foil and monel ribbon, the isotherms of butane

and Freon-21 are clearly of an S-shaped type. This fact should dispose of any lingering suspicion that the S-shaped adsorption isotherms of gases near their

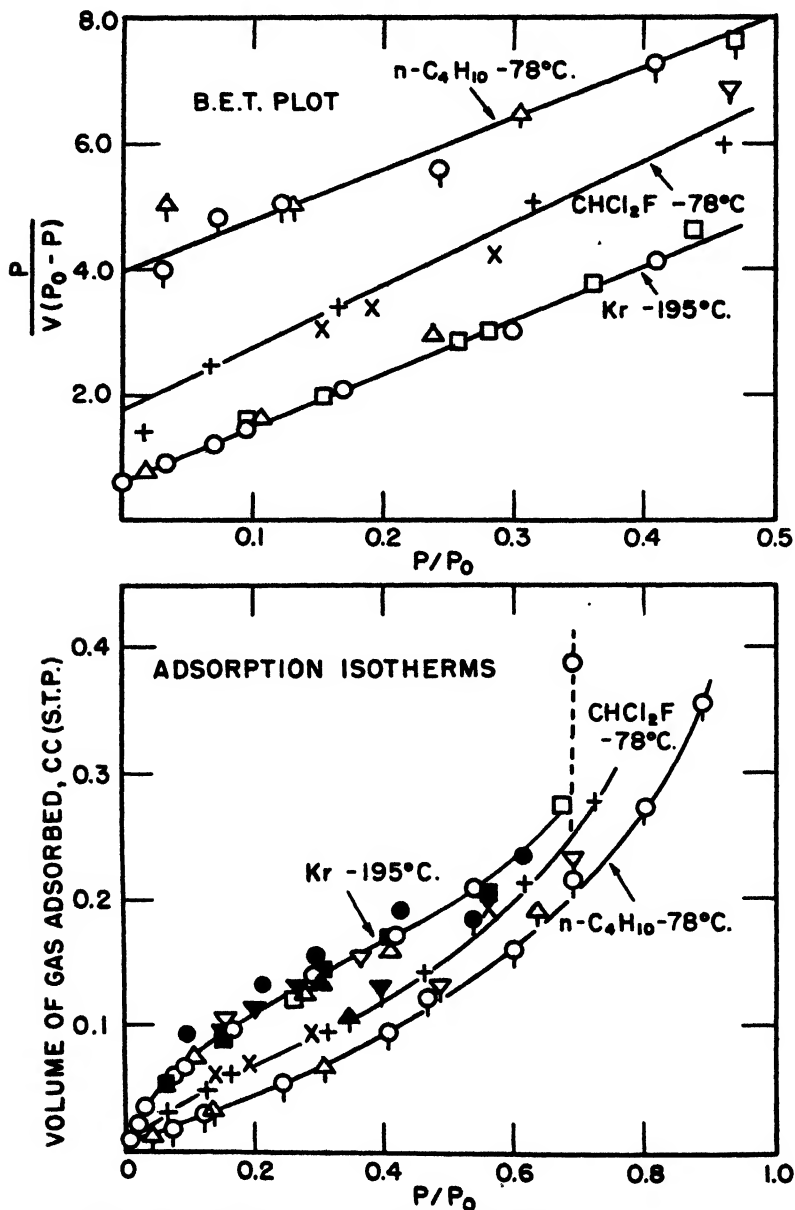


FIG. 2. Adsorption of gases on monel ribbon; solid symbols are desorption points

boiling points are due to monolayer adsorption plus capillary condensation (15, 16) and that flat adsorbents should show only monolayer adsorption (1, 2) The apparent density of the rolls of silver foil and monel ribbon plainly indicates

that the average distance between the layers of metal was of the order of the thickness of the metal (12–15 microns), and hence could not cause capillary condensation in the 0.5–0.99 relative pressure region. The absence of hysteresis in most of the krypton runs on the silver and monel also indicates the absence of capillary condensation between the layers of metal. In this connection, it should be noted that the scattered and irregular desorption points for Freon on silver foil and for butane on monel are probably to be attributed to experimental error, —perhaps to small amounts of less condensible gases in the adsorbate as impurity. The maximum hysteresis observed in these runs amounted to only about 3 per cent of the largest amount of adsorbate in the system.

Doubtless, krypton would also give an S-shaped isotherm if it could be extended to higher p/p_0 values. However, as pointed out by Brunauer, Emmett, and Teller (6) for carbon dioxide at -78°C . and by Beebe (4) and coworkers for krypton at -195°C ., adsorbates appear to be adsorbed in accordance with the p/p_0 ratio based on the extrapolated liquid vapor pressure rather than on that of the solid phase that is stable at the temperatures of the runs. The highest relative pressure to which the data of the krypton isotherm can be extended is p_0/p_{0l} , where p_0 is the normal vapor pressure of the solid and p_{0l} is the extrapolated vapor pressure of the liquid. At this temperature this ratio is 0.67 to 0.69; at these relative pressures there should be little if any tendency for the isotherms to show an S-shape.

The second item of interest in connection with figures 1 and 2 is a comparison between the ratio of the surface areas of the silver and monel as measured by adsorption and the geometric surface area. As shown in column 6 of table 1, the areas calculated from the isotherms using conventional cross-sectional areas of 15.2, 29.7, and 24.7 \AA^2 for the krypton at -195°C ., butane at -78°C ., and Freon-21 at -78°C ., respectively, are too small, for the most part, compared to the geometric areas. In other words, average roughness factors of 0.83 for silver foil and 0.97 for monel are indicated. In view of the fact that the true roughness factors must be at least unity and probably 1.3 or more, it seems necessary to use somewhat larger cross-sectional areas for these adsorbate molecules than those calculated in the usual way from the density of the condensed adsorbates.

The estimated value of these corrected molecular areas will now be discussed in conjunction with data on the other adsorbents.

From the B.E.T. plots of figures 3 to 8, the values of V_m , the volume of gas required to form a monolayer on the surface, have been calculated together with those for C , the other constant of the B.E.T. equation, for the various porous and non-porous adsorbents. These calculations are given in columns 5 and 7 of table 1 for the various gases and adsorbents. From a knowledge of V_m and the cross-sectional area of the molecules of the adsorbed gas (column 4, table 3) the surface areas of the adsorbents have been calculated as listed in column 6 of table 1. The cross-sectional area values of the various gas molecules were obtained in the usual way (9) by means of the equation:

$$\text{Cross-sectional area} = 4 \times 0.866(M/4 \sqrt{2} N d_l)^{2/3}$$

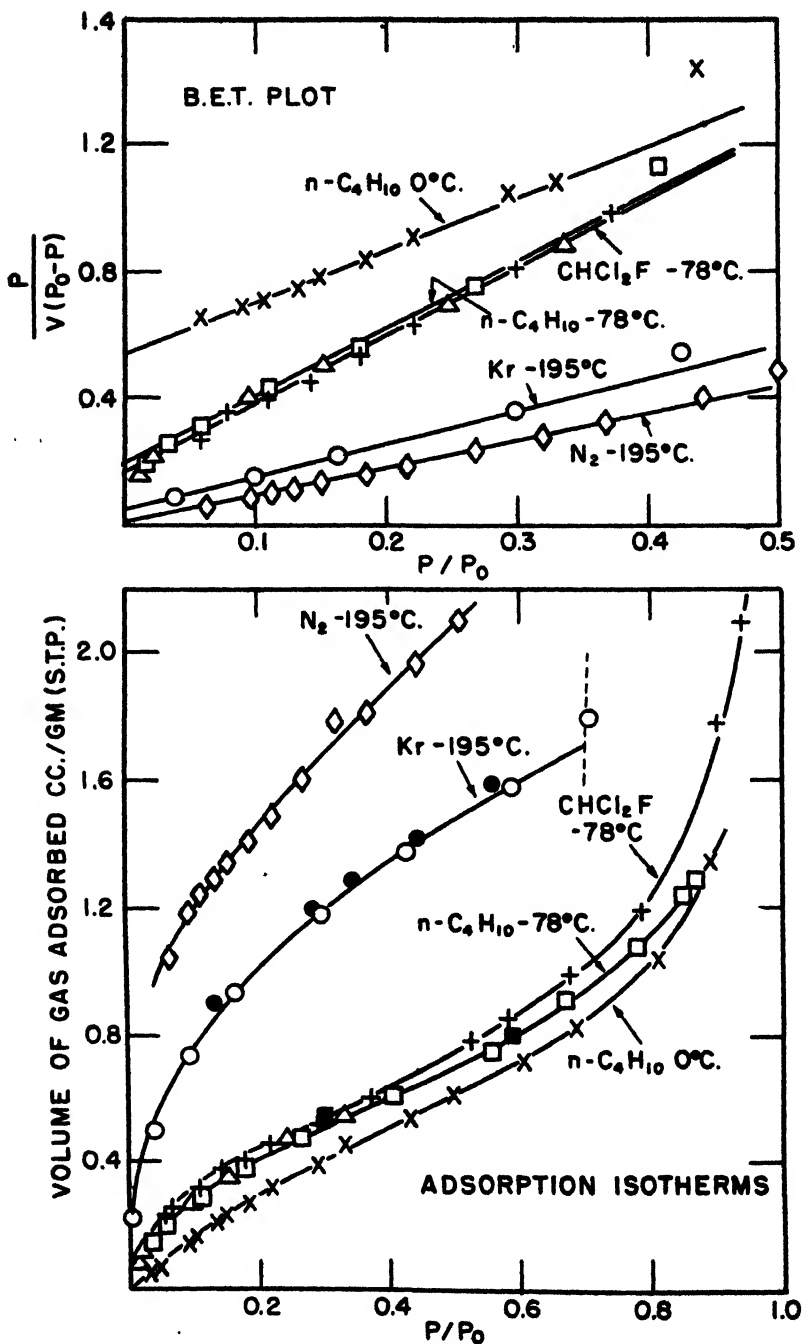


FIG. 3. Adsorption of gases on 200-mesh glass spheres; ●, ■ are for desorption

where M is the molecular weight, N is Avogadro's number, and d_l is the liquid density.

A close examination of table 1 reveals that for the same adsorbent the calculated surface areas vary considerably with the gas used as adsorbate. In table 2 are given the various surface-area ratios for the different gases on the same

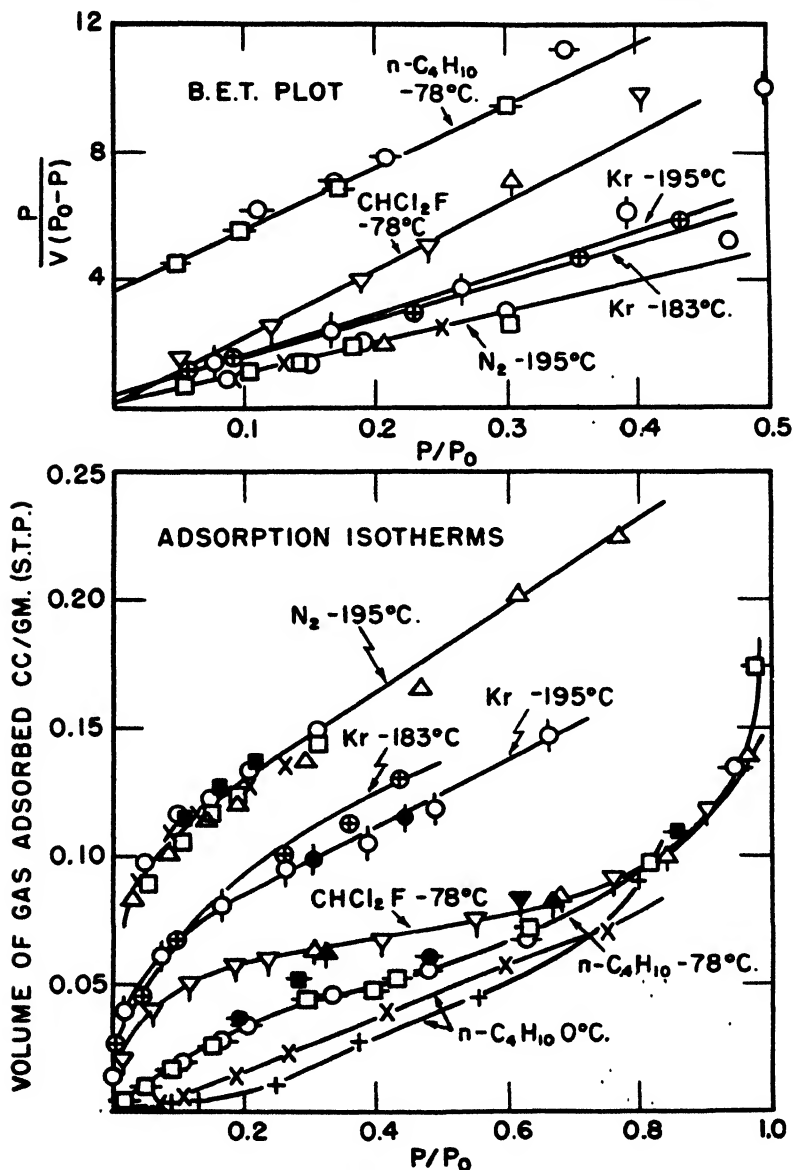


Fig. 4. Adsorption of gases on 7 μ glass spheres; solid symbols are for desorption

adsorbent. With one or two exceptions, the ratio between any two gases is fairly constant and does not seem to be a function of the kind of surface.

From tables 1 and 2 it is apparent that all the surface areas calculated for the finely divided adsorbents by the isotherms for krypton, Freon-21, and butane are

considerably lower than those calculated from the isotherms for nitrogen. This fact and the observation that these same gases lead to a low roughness factor on

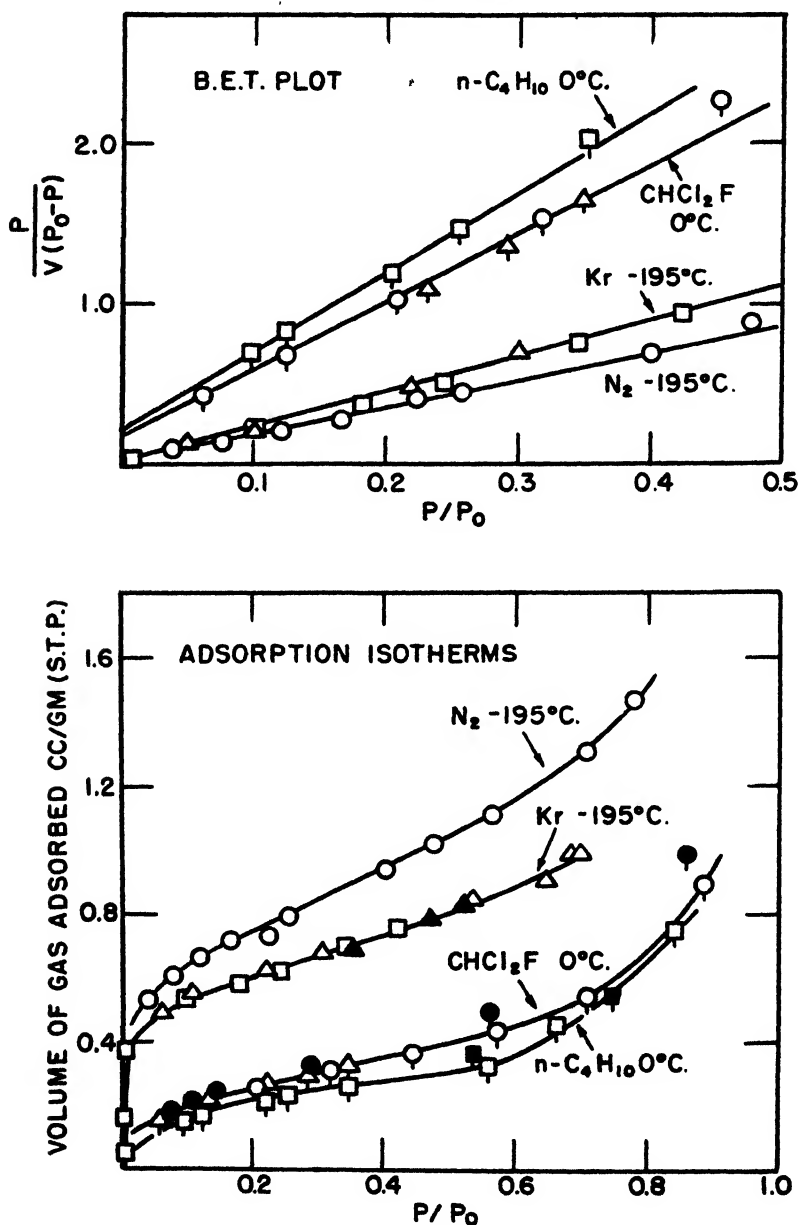


FIG. 5. Adsorption of gases on tungsten powder; solid symbols are for desorption

the metal surfaces make it necessary to use larger cross-sectional areas for krypton, Freon-21, and butane than those calculated from equation 2 above.

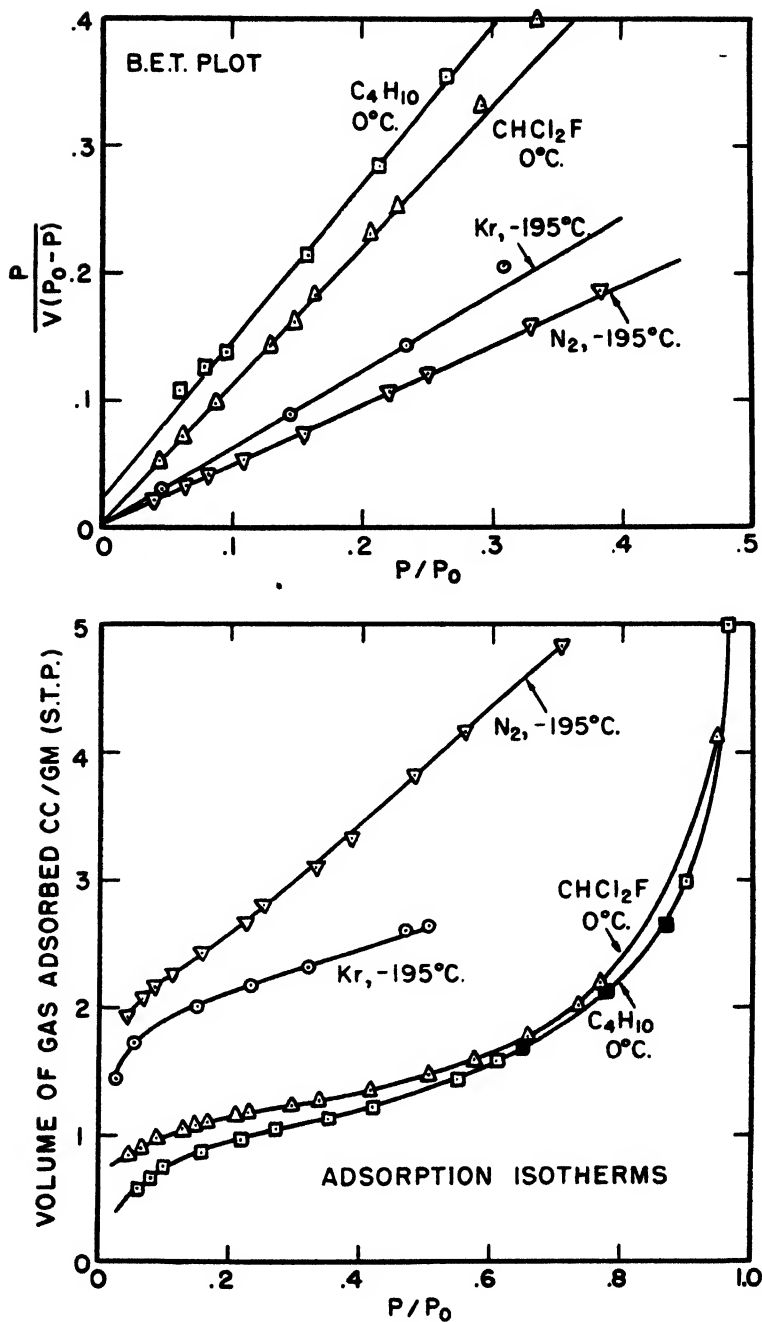


FIG. 6. Adsorption of gases on zinc oxide

In table 3 (column 5) are listed revised molecular areas for the various adsorbates, selected empirically to agree with nitrogen with a view to bringing into agree-

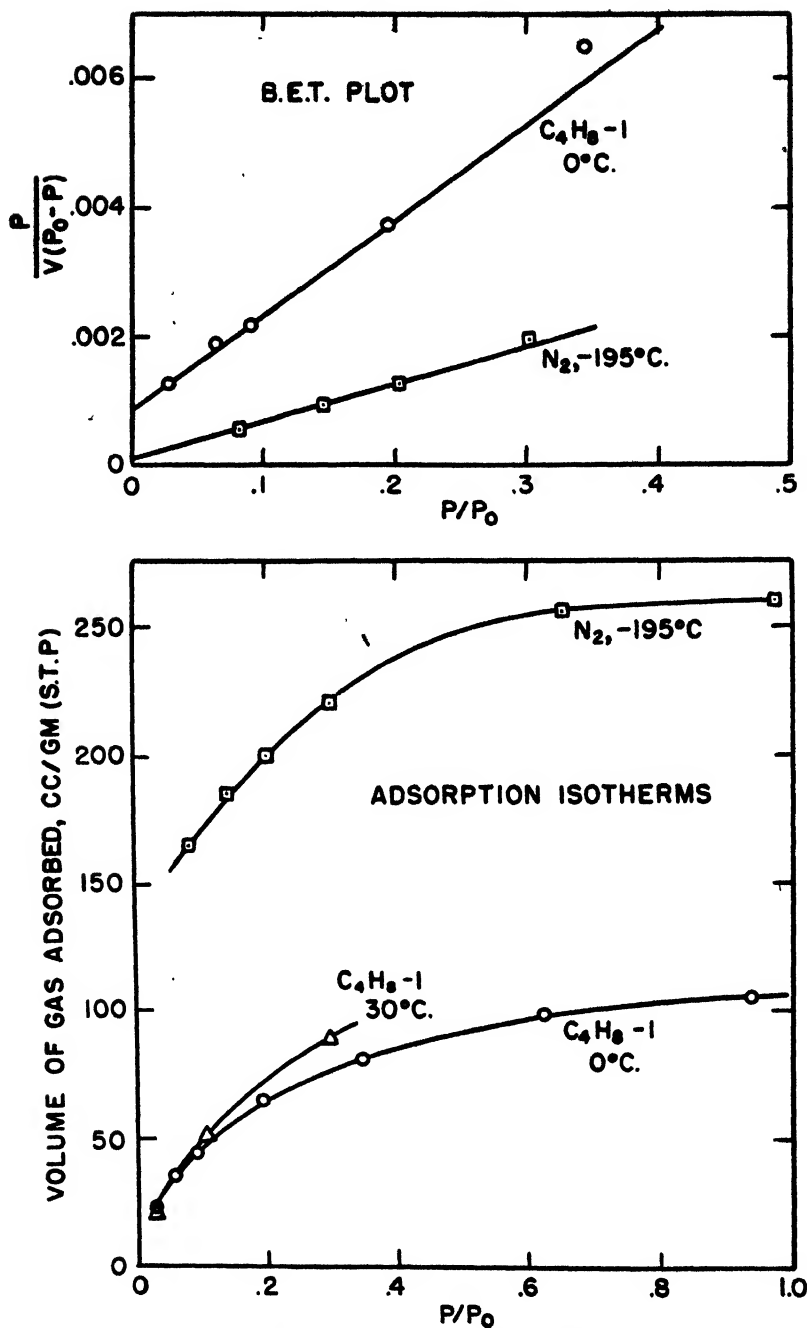


FIG. 7. Adsorption of gases on silica gel

ment the area values for the various adsorbates on the samples set forth in table 1. The last column of this table is a measure of the extent of agreement obtained.

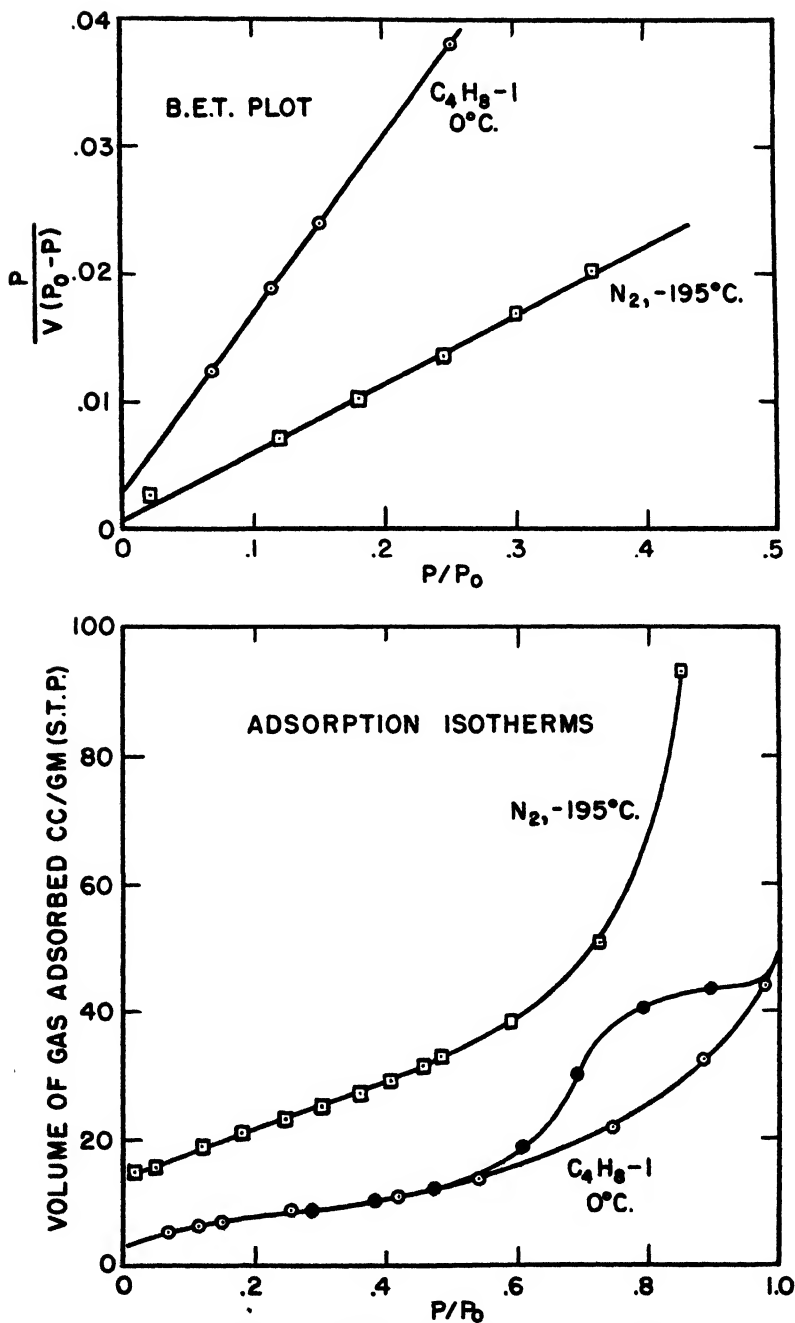


FIG. 8. Adsorption of gases on alumina; ● are for desorption

On all the adsorbents, except the silver foil and the monel metal, the agreement of the areas, as obtained by the various adsorbates, seems to be satisfactory.

The reason for the lack of agreement among the areas given by the various adsorbates for silver foil and monel ribbon is not clear. The ratio of the V_m values for krypton as compared to those for Freon-21 and butane is very differ-

TABLE 1
Adsorption of gases on surfaces of metal foils and powders

ADSORBENT	GAS	T	SAMPLE WEIGHT	V_m /GRAM AT S.T.P.	SURFACE AREA	C	REVISED* SURFACE AREA
		°C.	grams	cc.	m. ² /gram		m. ² /gram
Silver foil (geometric area, 1.56 m. ²)	Kr	-195	92.1	0.379	1.56	18.9	2.14
	C ₄ H ₁₀	-78	92.1	0.152	1.22	6.39	1.78
	CHCl ₂ F	-78	92.1	0.170	1.13	10.9	1.72
Monel ribbon (geometric area, 0.579 m. ²)	Kr	-195	126.8	0.110	0.454	13.5	0.622
	C ₄ H ₁₀	-78	126.8	0.0812	0.652	4.1	0.952
	CHCl ₂ F	-78	126.8	0.0856	0.577	6.6	0.878
Glass spheres (200 mesh)	N ₂	-195	10.50	1.26	5.51	40	5.51
	Kr	-195	3.15	0.927	3.82	22	5.23
	C ₄ H ₁₀	-78	3.15	0.442	3.56	11.6	5.20
	C ₄ H ₁₀	-46	10.50	0.400	3.34	8.47	4.87
	C ₄ H ₁₀	0	10.50	0.389	3.38	5.40	4.93
	CHCl ₂ F	0	10.50	0.440	3.16	13.3	4.8
Glass spheres (7 microns)	N ₂	-195	5.80	0.0986	0.434	150	0.434
	Kr	-195	2.49	0.0783	0.322	32	0.441
	C ₄ H ₁₀	-78	2.49	0.0416	0.333	6.7	0.489
	CHCl ₂ F	-78	2.49	0.0473	0.315	106	0.479
Tungsten powder	N ₂	-195	13.00	0.613	2.69	81	2.69
	Kr	-195	0.597	0.476	1.96	290	2.68
	C ₄ H ₁₀	0	13.00	0.192	1.67	26	2.43
	CHCl ₂ F	0	13.00	0.242	1.73	21	2.62
Zinc oxide	N ₂	-195	12.11	2.15	9.40	155	9.40
	Kr	-195	0.1018	1.66	6.82	150	9.34
	C ₄ H ₁₀	0	12.11	0.837	6.93	52	10.1
	CHCl ₂ F	0	12.11	0.929	6.63	215	10.1
Alumina	N ₂	-195	1.814	18.35	80.4	78	80.4
	1-C ₄ H ₈	0	1.814	7.07	58.1	82	81.3
Silica gel	N ₂	-195	0.287	172	755	57	755
	1-C ₄ H ₈	0	0.146	64.4	531	18	744

* Obtained by using "revised" molecular areas of column 5, table 3.

ent on these two metal surfaces. We can only say that enough duplicate runs were made on each of these surfaces to assure us that the discrepancy is real; the explanation must await further work.

The cross-sectional molecular areas that we have assigned to butane and to krypton are in fair agreement with those assigned by Harkins and Jura (12) and by Beebe and coworkers (4), as illustrated by columns 5 and 6 of table 3. Many more data will be needed before it will be possible to state within close

TABLE 2
Surface-area ratios using various gases

ADSORBENT	$\frac{N_2}{Kr}$	$\frac{N_2}{C_6H_{10}}$	$\frac{N_2}{CHCl_3F}$	$\frac{Kr}{C_6H_{10}}$	$\frac{Kr}{CHCl_3F}$	$\frac{C_6H_{10}}{CHCl_3F}$	$\frac{N_2}{1-C_4H_8}$
Silver				1.28	1.38	1.08	
Monel				0.696	0.787	1.13	
Glass spheres (200 mesh)	1.44	1.60	1.74	1.11	1.21	1.07	
Glass spheres (7 microns)	1.34	1.29	1.37	0.961	1.02	1.06	
Tungsten	1.37	1.61	1.56	1.17	1.13	0.965	
Zinc oxide	1.38	1.35	1.42	0.984	1.03	1.05	
Alumina							1.38
Silica gel							1.42
Average	1.36	1.46	1.52	1.03	1.09	1.06	1.40

TABLE 3
Cross-sectional area of various molecules

GAS	MOLECULAR WEIGHT	TEMPERATURE	CALCULATED AREA	REVISED* AREA	AREAS SUGGESTED BY OTHER WORKERS
		°C.	A^2	A^2	A^2
Nitrogen	28.0	-195	16.2	16.2	16.1 (14) 15.2 (2)
Krypton	83.7	-195	15.2	20.8	19.5 (4)
Butane	58.1	-78 0	29.7 32.1	43.4 46.9	56.6 (14)
Freon-21	102.9	-78 0	24.7 26.4	37.5 40.1	
1-Butene	* 56.1	0	30.5	42.7	

* Revised to yield surface areas by the use of krypton, butane, Freon-21, and 1-butene that agree with those obtained by the use of nitrogen as adsorbate.

limits the molecular area that ought to be used for the various adsorbates. Indeed, it will probably be found that the average area per molecule in a monolayer may vary some from solid to solid.

In making comparisons of the areas of solids as deduced from the isotherms of different adsorbates, it is well to keep in mind the present status of area deter-

minations by nitrogen and to ask particularly whether or not it is possible that the cross-sectional area assigned to the nitrogen molecule may be too low. The most convincing answer to this question will be obtained when and if someone measures the surface area of a metal foil or ribbon using nitrogen as the adsorbate. Only if one then obtains too low a roughness factor for such surfaces will one be able to conclude with certainty that the usual value of 16.2 \AA^2 is too small for the adsorbed nitrogen molecule. The experiments in which Harkins and Jura (12, 14) found that the same area was obtained on a series of non-porous solids, using nitrogen as adsorbate and an area of 16.2 \AA^2 per molecule, as was determined by heat of adsorption measurements with water vapor (13) on one of these same solids, are reassuring but not absolutely conclusive. The possibility of doubt arises from the fact that, in their heat-of-immersion experiments (13), their samples of titanium dioxide were first exposed to water vapor at relative pressures close to unity and then immersed in water. It is evident that the area afforded by the walls of any tiny cracks and capillaries in the surface of the titanium dioxide would have been covered up by capillary condensation prior to the calorimetric measurements. This, in turn, would mean that the area calculated from the heat of immersion would be too small and, therefore, the cross-sectional area that would have to be assigned to nitrogen to yield the true area would have to be greater than the usual 16.2 \AA^2 . Accordingly, in selecting molecular area that will give agreement between the surface areas of the various adsorbents as measured by Freon-21, krypton, and butane and those obtained by the nitrogen isotherms, we are well aware that even the value for the molecular area of nitrogen may eventually have to be changed. For the present, however, it will be assumed that the areas obtained by using 16.2 \AA^2 for nitrogen may be used as a standard in selecting cross-sectional areas for the other adsorbate molecules.

An explanation as to why it is necessary to employ correction factors for the various gases is not yet forthcoming. One of the older explanations was to consider that long narrow butane molecules did not pack well on the surface, and also might be blocked out by very small cracks and pores on the surface. However, this explanation does not seem to be satisfactory. For example, krypton gives a low surface-area value compared to nitrogen and yet its molecular area is less than that of nitrogen, if calculated in the usual way (column 4, table 3) and it is quite symmetrical and, therefore, should pack well on the surface. The molecule of Freon-21 is fairly large in size but should be rather symmetrical and should give no difficulties in packing on the surface; yet it seems to yield a low area just as do butane and krypton. The temperature or the absolute pressure range of the measurements does not seem to be responsible for the low areas, as evidenced by the fact that the butane surface-area values determined for the glass spheres at -78°C . and a pressure of a few millimeters agree very well with those obtained at 0°C . and pressures close to 1 atm. Finally, consideration has been given to the idea that low area values might accompany low C values (equation 1 and table 1). It has been observed many times that the

C value obtained using butane was much lower than that using nitrogen on the same adsorbent. However, this finding does not seem to be the entire explanation, for an examination of table 1 will reveal that there are several instances in which low areas are obtained in runs in which the C values are high and not low. For example, krypton on tungsten, butane, Freon-21, and krypton on zinc oxide, and Freon-21 on the sample of glass spheres (7 microns in diameter) all have C values in the range 50–300 but yield low areas. One very good possibility is that the surface structure of the adsorbent may have considerable influence on the packing of adsorbate molecules on the surface. Operation of such a factor might, qualitatively, provide a reason for poorer agreement among different adsorbates on one material than on another. Of course, it is true that in this work most difficulty was experienced with the samples in the form of sheet or ribbon and the possibility that the physical form of the sample has some influence on the results has not been eliminated; it is hard, however, to imagine why such would be true.

The discussion of the present paper can be summed up by saying that the molecular cross-sectional areas listed in column 5 of table 3 appear to yield surface areas for a variety of finely divided or porous solids in good agreement with those obtained from the nitrogen isotherms with 16.2 \AA^2 as the area occupied by a nitrogen molecule. For silver foil and monel ribbon, these same assignments of molecular area yield reasonable surface areas compared to the measured geometric areas but lead to as much as a 25 per cent deviation from the mean among the area values obtained with Freon-21, krypton, and butane.

SUMMARY

1. The adsorption of nitrogen, krypton, *n*-butane, 1-butene, and Freon-21 has been measured on silver foil, monel ribbon, and a variety of powdered materials.

2. The butane and Freon-21 isotherms on the surfaces of the flat silver foil and monel ribbon are of the S-shaped type.

3. Using the various gases and applying the B.E.T. equation, the surface areas of the materials have been measured.

4. It is found that it is necessary to apply suitable corrections to the surface-area values calculated using the various gases.

The following corrected cross-sectional areas for the various gas molecules are recommended to bring the results in line with those of nitrogen: krypton, 20.8 \AA^2 ; butane, 43.4 \AA^2 at -78°C . and 46.9 \AA^2 at 0°C .; Freon-21, 37.5 \AA^2 at -78°C . and 40.1 \AA^2 at 0°C .; and 1-butene, 42.7 \AA^2 at 0°C .

5. These same area assignments for Freon-21, butane, and krypton yield areas for the silver foil and monel metal that are reasonable compared to geometric areas. However, for this flat metal surface, the agreement among the surface areas as determined by the several adsorbates is not very good, a maximum deviation from the mean of 25 per cent being obtained.

REFERENCES

- (1) ARMBRUSTER: J. Am. Chem. Soc. **64**, 2545 (1942).
- (2) ARMBRUSTER AND AUSTIN: J. Am. Chem. Soc. **66**, 159 (1944).
- (3) ASTON AND MESSERLY: J. Am. Chem. Soc. **62**, 1917 (1940).
- (4) BEEBE, BECKWITH, AND HONIG: J. Am. Chem. Soc. **67**, 1554 (1945).
- (5) BLOOMQUIST AND CLARK: Ind. Eng. Chem., Anal. Ed. **12**, 61 (1940).
- (6) BRUNAUER, EMMETT, AND TELLER: J. Am. Chem. Soc. **60**, 309 (1938).
- (7) DAVIS: J. Am. Chem. Soc. **68**, 1395 (1946).
- (8) EMMETT: Am. Soc. Testing Materials, Symposium on New Methods for Particle Size Determination in Subsieve Range (1941).
- (9) EMMETT AND BRUNAUER: J. Am. Chem. Soc. **59**, 1553 (1937).
- (10) EMMETT AND DEWITT: Ind. Eng. Chem., Anal. Ed. **13**, 28 (1941).
- (11) FRANKENBURG: J. Am. Chem. Soc. **66**, 1827 (1944); **66**, 1838 (1944).
- (12) HARKINS AND JURA: J. Am. Chem. Soc. **66**, 1356 (1944).
- (13) HARKINS AND JURA: J. Am. Chem. Soc. **66**, 1362 (1944).
- (14) HARKINS AND JURA: J. Am. Chem. Soc. **66**, 1366 (1944).
- (15) KISTLER, FISCHER, AND FREEMAN: J. Am. Chem. Soc. **65**, 1909 (1943).
- (16) MCGAVACK AND PATRICK: J. Am. Chem. Soc. **42**, 946 (1920).
- (17) SMITH, THORNHILL, AND BRAY: Ind. Eng. Chem. **33**, 1303 (1941).
- (18) WOOTEN AND BROWN: J. Am. Chem. Soc. **65**, 113 (1943).

ADSORPTION OF ARGON, NITROGEN, AND BUTANE ON
POROUS GLASS¹P. H. EMMETT² AND MARTIN CINES³*Department of Chemical Engineering, The Johns Hopkins University, Baltimore 18, Maryland**Received June 11, 1947*

As an intermediate product in the manufacture of Vycor, the Corning Glass Company (15) produces a porous solid by leaching the boron oxide from a borosilicate glass. These leached glasses appear to have pores that are rather uniform in size for a given sample but can be varied in size from one sample to another by changing the heat-treating and leaching conditions employed. Emmett and DeWitt (13) have already reported a study of the adsorption of oxygen, nitrogen, and argon on one sample of such porous glass. The present paper summarizes the results that have been obtained by studying in more detail the adsorption of argon, nitrogen, and butane on a series of five porous glasses, each of which is characterized by a rather uniform pore size.

EXPERIMENTAL

The adsorption apparatus for the present work was of a standard type (9) that has been employed extensively during the past ten years (2, 4, 10, 11, 12)

¹ Presented at the Symposium on the Adsorption of Gases which was held under the auspices of the Division of Colloid Chemistry at the 110th Meeting of the American Chemical Society, Chicago, Illinois, September 11-12, 1946.

² Present address: Mellon Institute, Pittsburgh 13, Pennsylvania.

³ Present address: Phillips Petroleum Company, Phillips, Texas.

in measuring the surface areas of solids by low-temperature gas adsorption. Nitrogen-of the ordinary tank variety was used without further purification. Argon and butane, each better than 99 per cent pure, were obtained from the Ohio Chemical Company. Both yielded vapor pressures that checked those given in the literature and that, accordingly, indicated a high degree of purity of the adsorbates.

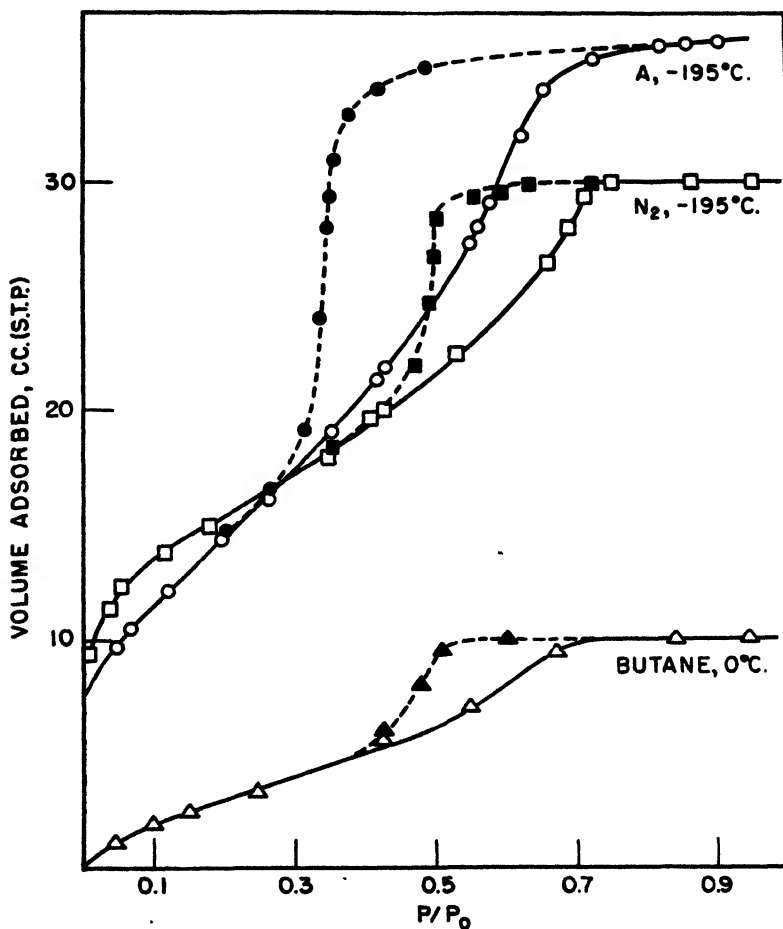


FIG. 1. Adsorption isotherm for argon and nitrogen at $-195^{\circ}\text{C}.$ and for *n*-butane at $0^{\circ}\text{C}.$ on porous glass No. 3. Open symbols, adsorption; solid symbols, desorption.

The various glass samples were ground to a $-100 + 200$ mesh size. The detailed adsorption procedure for most of the runs was the usual one (2, 4, 9, 10, 11, 12). The dead space in the apparatus was calibrated with pure helium.

RESULTS

Figures 1 to 5, inclusive, contain plots of the adsorption data for nitrogen and argon at $-195^{\circ}\text{C}.$ and for butane at $0^{\circ}\text{C}.$ on each of the five porous glasses

studied. The volume of gas (S.T.P.) adsorbed is plotted against the relative pressure in each case. Since argon is a solid at this temperature, the relative pressure has been calculated on the basis of the vapor pressure of the supercooled liquid at -195°C ., as obtained by extrapolating the data from above the triple point. A value of 247 mm. was used for the vapor pressure of this supercooled liquid at -195°C .; its density and surface-tension values were

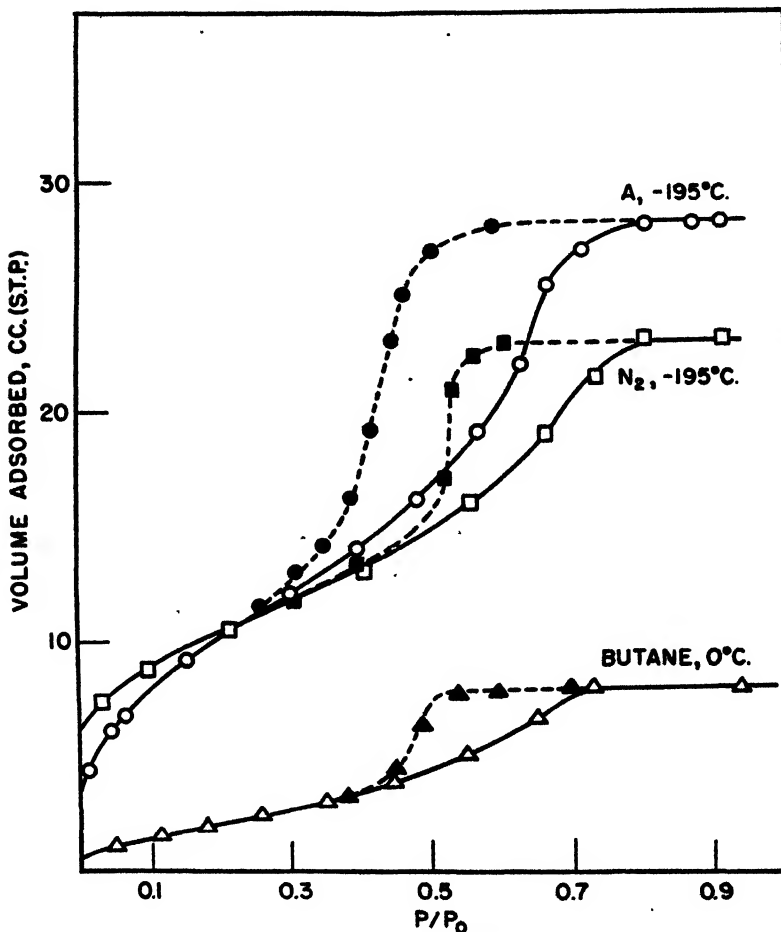


Fig. 2. Adsorption isotherm for argon and nitrogen at -195°C . and for *n*-butane at 0°C . on porous glass No. 4. Open symbols, adsorption; solid symbols, desorption.

also obtained by extrapolation and were 1.42 g./cc. and 14.9 dynes/cm., respectively.

The isotherms in figure 6 are for several other gases that were run on only this one sample. Only water vapor, of these four gases, was extended to sufficiently high pressure to obtain a hysteresis loop. The other gases are useful only in furnishing additional gases from which to calculate the surface area of the glass.

Figure 7 records the data obtained in extensive scanning experiments. A total of ninety-six adsorption points were taken, including five scanning curves for increasing and five for decreasing pressures.

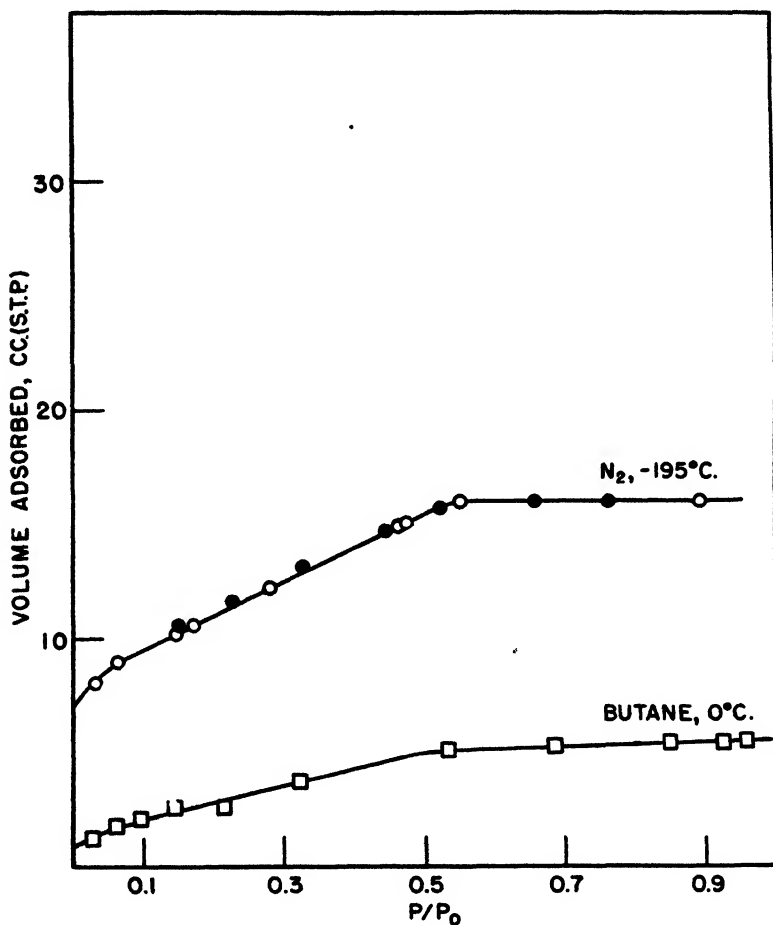


FIG. 3. Adsorption isotherms for nitrogen at $-195^{\circ}\text{C}.$ and for *n*-butane at $0^{\circ}\text{C}.$ on porous glass No. 5. Open symbols, adsorption; solid symbols, desorption.

DISCUSSION

Surface areas by various gases

Within recent years a method (5) has been developed for evaluating V_m , the volume of adsorbate required to form a monolayer on an adsorbent, by plotting adsorption data according to the equation

$$\frac{x}{V(1-x)} = \frac{1}{V_m C} + \frac{(C-1)}{V_m C} x \quad (1)$$

where V is the volume of gas (S.T.P.) adsorbed at the relative pressure x , and C is a constant for a particular adsorbent, adsorbate, and temperature. A multiplication of the number of molecules in V_m by the molecular cross-section as calculated from the density of the liquefied or solidified adsorbate yields an absolute value for the surface area of the adsorbent.

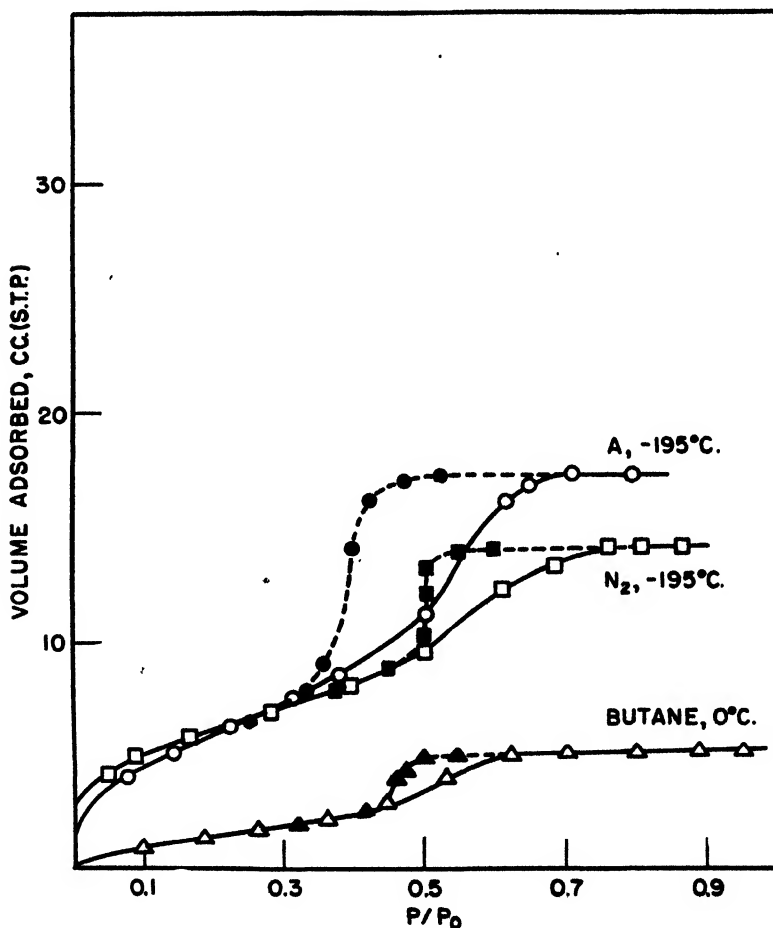


FIG. 4. Adsorption isotherm for argon and nitrogen at $-195^{\circ}\text{C}.$ and for n -butane at $0^{\circ}\text{C}.$ on porous glass No. 6. Open symbols, adsorption; solid symbols, desorption.

Although a number of comparisons have been made between areas obtained by one adsorbate and those obtained by another, new ones are still needed. The present work affords an opportunity to compare nitrogen, argon, and butane on a number of samples of porous glass, and nitrogen, butane, argon, acetylene, carbon dioxide, ammonia, and water vapor on one glass. In table 1 are listed the area values obtained.

As in other recent examples, most of the gases yield areas that are somewhat smaller than those obtained with nitrogen. Actually, the cross-sectional areas that would have to be assigned to the molecules of the various gases to obtain the same area given by the nitrogen isotherm are: argon, 15.4; butane, 49; acetylene, 22.2; carbon dioxide, 20.1; ammonia, 15.4; and water vapor, 19.5 \AA^2 . These compare with values of 13.7, 32, 15.2, 14.2, 13.8, and 10.8 \AA^2 , re-

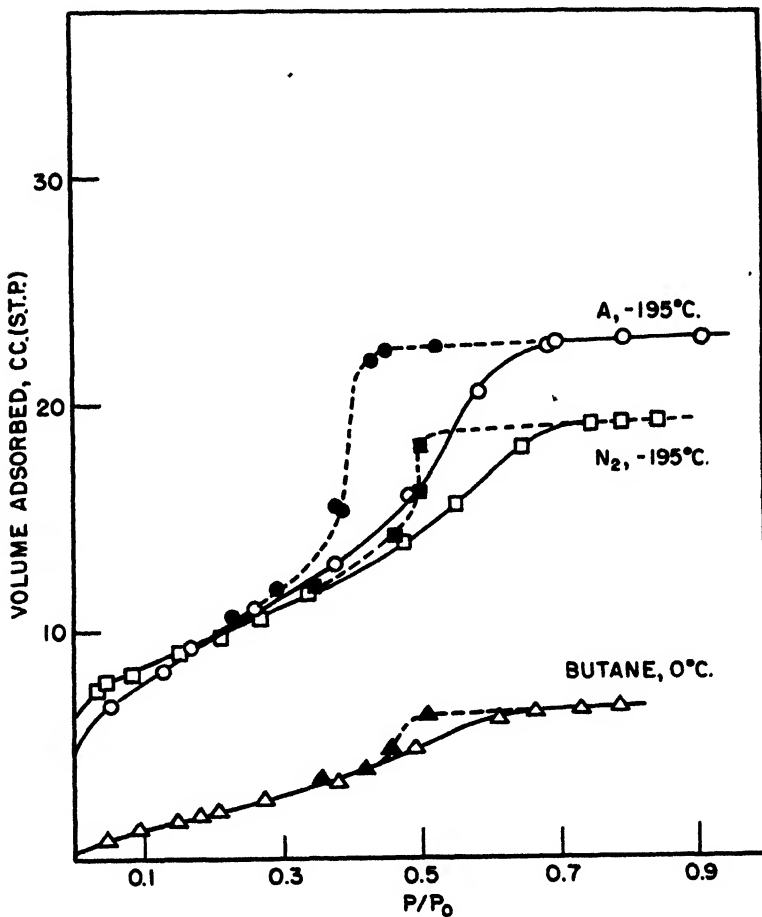


FIG. 5. Adsorption isotherm for argon and nitrogen at $-195^{\circ}\text{C}.$ and for *n*-butane at $0^{\circ}\text{C}.$ on porous glass No. 7. Open symbols, adsorption; solid symbols, desorption.

spectively, calculated from the density of these liquefied gases (11). The reason for the area values being smaller with all the other gases than with nitrogen, using these latter molecular areas, is not yet clear. The low areas with butane might be attributed to screening out the larger butane molecules by some of the capillaries; this could not, however, explain the results obtained with the other gases, since all of them would appear to have molecular cross-sections smaller than that of nitrogen.

Pore-size estimates

All methods for calculating the pore-size distribution for porous materials are subject to a number of uncertainties. For example, it is customary to assume that the pores are cylindrical, in order to simplify the application of equations for calculating pore radii. Furthermore, little progress can be made for the most part in differentiating between the amount of gas held on a surface by multilayer

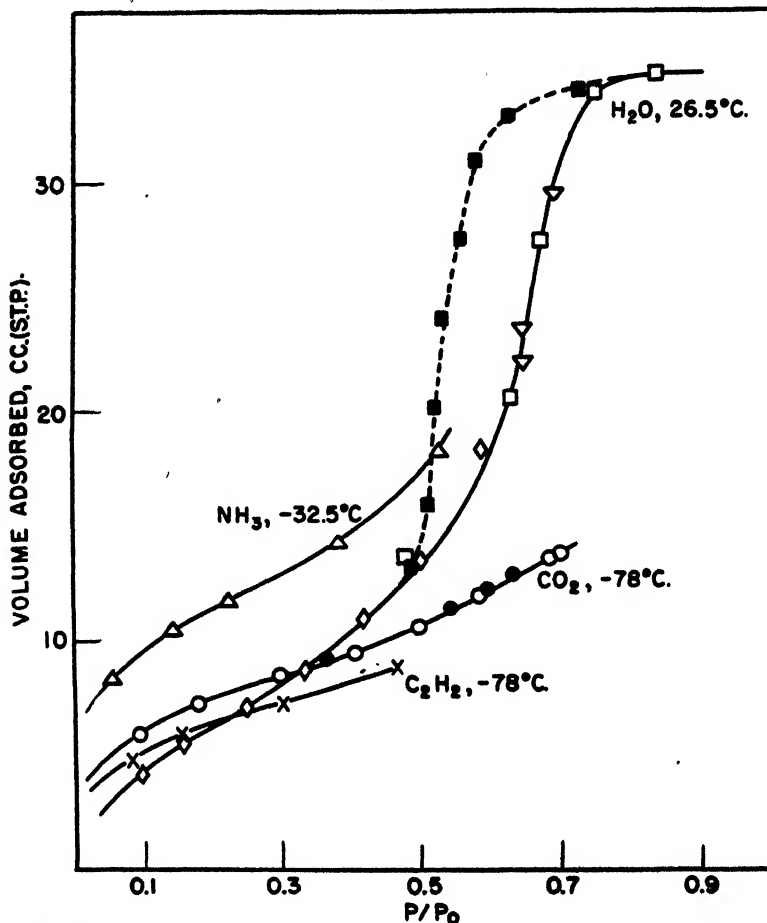


FIG. 6. Adsorption isotherms for acetylene and carbon dioxide at $-78^{\circ}\text{C}.$, ammonia at $-32.5^{\circ}\text{C}.$, and water vapor at $26.5^{\circ}\text{C}.$ on porous glass No. 7. Solid symbols, desorption; other symbols, adsorption.

adsorption and the amount held by capillary condensation without making some assumptions (3) as to the type of size-distribution curve possessed by the pores of the solid and then comparing calculated isotherms based on such curves with the actual isotherms. In the present experiments, the pore distribution is sufficiently sharply defined as to lend itself particularly well to the evaluation of average pore size by several different methods, including the use of the pore volume and area,

the application of the Kelvin equation to the desorption isotherm, and the application of the Kelvin equation and of the Cohan equation to the steepest part of the adsorption isotherm. These will now be considered in turn.

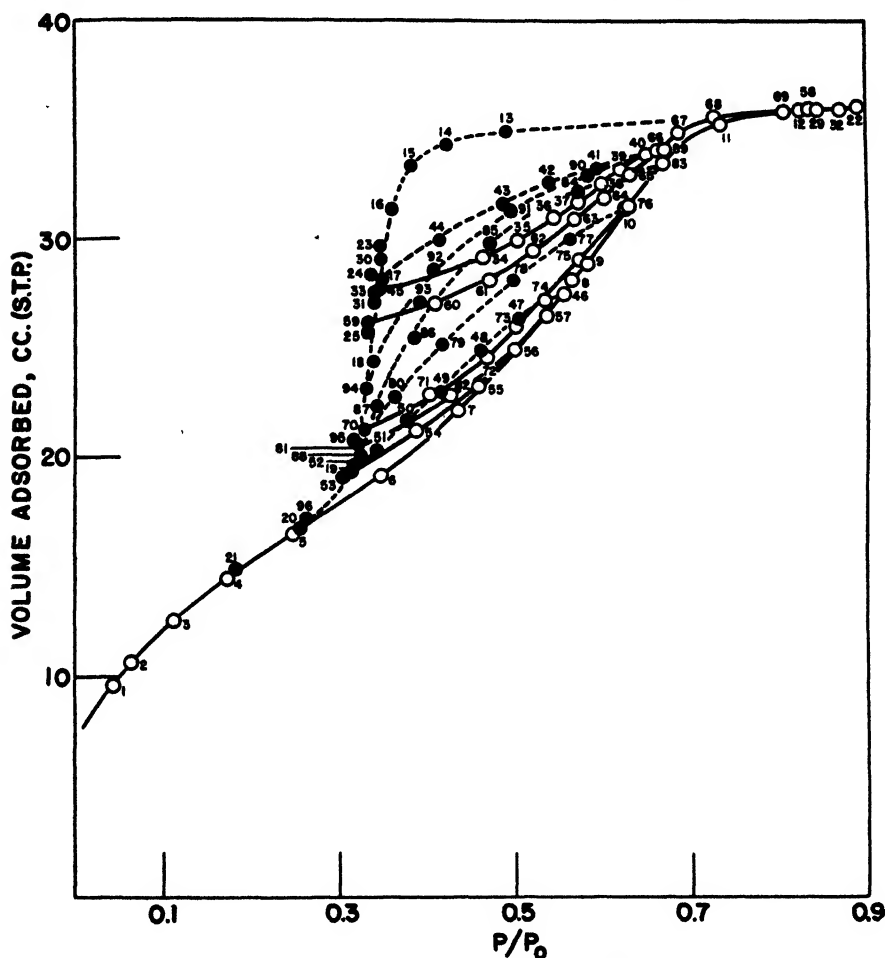


FIG. 7. Scanning curves for argon adsorption on porous glass No. 3. Open circles, adsorption; solid circles, desorption. Points are numbered in the order in which they were obtained.

The most generally accepted method of calculating an average pore distribution is that which involves assuming that the capillaries are cylinders and that, accordingly, the pore size of an average capillary is given by the equation (13)

$$2V/\text{area} = r_v \quad (2)$$

where V is the volume of adsorbate (calculated as cubic centimeters of liquid in each case) taken up close to saturation. Such calculated values for r_v are shown in table 2. Obviously two different values of r_v can be calculated for butane,

TABLE 1
*Surface areas in square meters per gram of porous glass samples as measured
 by isotherms for various gases*

SAMPLE	N ₂ AT -195°C.	C ₄ H ₁₀ AT 0°C.	ARGON AT -195°C.	H ₂ O AT 26.5°C.	CO ₂ AT -78°C.	NH ₃ AT -32.5°C.	C ₂ H ₂ AT -78°C.
Porous glass No. 3.....	221	128	194				
Porous glass No. 4.....	189	118	173				
Porous glass No. 5.....	259						
Porous glass No. 6.....	156	117	136				
Porous glass No. 7.....	232	156	217	128	164	207	159

TABLE 2
*Calculations of pore size and pore volume of porous glass samples
 from adsorption isotherms*

GLASS	GAS	TEMPER- ATURE	ADSORP- TION CAL- CULATED AS VOLUME OF LIQUID PER GRAM	r _p AVERAGE PORE RADIUS CALCU- LATED FROM VOLUME: SURFACE AREA RATIO OF PORES	r _a AVERAGE PORE SIZE BY KELVIN EQUATION† APPLIED TO STEEPEST PART OF ADSORPTION ISOTHERM	r _c AVERAGE PORE SIZE BY COHAN'S EQUATION‡	r _d AVERAGE PORE RADIUS FROM KELVIN EQUATION APPLIED TO STEEPEST PART OF DESORPTION CURVE	r _{max.} RADIUS OF LARGEST PORES PRESENT IN APPRECIABLE NUMBERS BY COHAN EQUATION§
		°C.						
No. 3	N ₂	-195	0.184	16.7	22.9	11.5	13.7	16.6
	A	-195	0.172	17.8 (15.6)*	24.1†	12.1†	11.8†	22.20†
	C ₄ H ₁₀	0	0.171	26.7 (15.5)*	27.8	13.9	16.9	17.2
No. 4	N ₂	-195	0.189	20	29.7	14.9	14.6	18.3
	A	-195	0.177	20.5 (18.7)*	31.7†	15.9†	15.7†	24-29†
	C ₄ H ₁₀	0	0.182	30.9 (19.3)*	29.9	15.0	16.4	19.0
No. 5.....	N ₂	-195	0.158	12.2				7.5
	C ₄ H ₁₀	0	0.146	(13.3)*				~9.0
No. 6. . .	N ₂	-195	0.149	19.1	22	11	13.7	14.9
	A	-195	0.147	21.6 (18.8)*	21.6†	10.8†	13.7†	17.9†
	C ₄ H ₁₀	0	0.156	23.1 (20.0)*	23.6	11.8	16.6	13.4
No. 7. . .	N ₂	-195	0.21	18.1	21	10.5	13.7	13-17
	A	-195	0.193	17.9 (16.3)*	23.7†	11.9†	13.7†	17.9†
	C ₄ H ₁₀	0	0.197	25.3 (17.0)*	20.8	10.4	16.9	13.4
	H ₂ O	26.5	0.194	30.4 (16.7)*	25.9	13.0	16	28

* Values in parentheses were calculated by using the surface area as measured by nitrogen and the pore volume as listed in column 5.

† Extrapolated surface-tension and density values of 14.9 and 1.42, respectively, for supercooled liquid argon at 79.1°K. were used in these calculations. They are accordingly somewhat uncertain.

‡ r_c is equal to r_a/2. However, r_c is, by definition, the radius of the cylindrical space in the capillary after a monolayer of gas is adsorbed on the walls. According to Cohan's theory the radii of the empty capillaries would exceed the values shown in column 7 by one molecular diameter.

§ These values are calculated by equation 4 for the relative pressure at which the adsorption isotherm levels off. 4 A. should be added to get the true maximum radius, since Cohan's equation gives radius to a monolayer.

argon, and water vapor depending on whether, in equation 2, one uses area values found by these respective gases or area values calculated from the nitrogen isotherms. The latter seem to give better agreement.

It is interesting to note that for the various gases the volume calculated as liquid adsorbed at saturation is nearly the same for a given sample of glass. This result would be expected, unless the capillaries are so small as to introduce specific screening effects. It is even true for most charcoals, though charcoals are characterized by much smaller pores than those of glasses No. 3, 4, 6, and 7.

As can be seen in figures 1 to 7, most of the desorption occurs sharply at a given relative pressure. It therefore becomes possible to calculate, from the Kelvin equation, the average pore radius, r_d , corresponding to the relative pressure at this maximum slope in the desorption curve. Such values for the various glasses as determined from desorption curves for nitrogen, argon, butane, and water vapor are listed in table 2. They have been calculated using the usual form of the Kelvin equation (20)

$$r_d = \frac{-2\sigma V \cos \theta}{RT \cdot 2.303 \log p/p_0} \quad (3)$$

where σ is the surface tension in dynes per centimeter, V is the molal volume, R is the gas constant, T is the absolute temperature, θ is the angle of wetting (assumed to be zero in the present calculations), and p/p_0 is the relative pressure for which the radius is being calculated. It seems fairly certain from this and previous work that the Kelvin equation should be considered as giving the radius of the capillary left after at least one molecular layer of adsorbed gas is adsorbed on the glass. Hence it is not surprising that, as is evident in table 2, r_d is usually smaller than r_v by about a molecular diameter.

Another possible pore calculation that is often used makes use of the adsorption isotherm rather than the desorption isotherm and employs some suitable equation. If the Kelvin equation is applied to the steepest part of the adsorption isotherm, values for the radius of an average capillary (r_a in table 2) are all much larger than those obtained by either of the two previously mentioned methods. However, Cohan (6) suggested that the adsorption part of isotherms represented condensation in open-end cylindrical capillaries on a monolayer of adsorbed gas and that the proper equation to use in conjunction with the adsorption part of the isotherms is

$$r_c = \frac{-\sigma V \cos \theta}{RT \ln p/p_0} \quad (4)$$

This differs from equation 3 by a factor of 2 and is derived on the assumption that condensation occurs on a monolayer of adsorbed gas on the cylindrical walls when the pressure p/p_0 is reached. In view of the fact that r_c by definition is smaller than the pore radius by the thickness of a monolayer, it is evident that values obtained by applying the Cohan equation to the adsorption part of the isotherm (table 2) are in fair agreement with the values for r_v .

In table 3 are shown for comparison the values for r_o , $r_o + 4$ A., and $r_d + 4$ A. The 4 A. value is taken as approximately the size of the adsorbate molecules. It is evident that one obtains better general agreement by assuming that the radius calculated by the Kelvin equation is smaller than the true capillary radius by the thickness of one layer (4 A., approximately) rather than by the thickness of two statistical layers. It should be noted, however, that a similar calculation on a sample of another porous glass by Emmett and DeWitt (13) led to the conclusion that one had to assume the presence of two layers of adsorbed gas in order to get good agreement between the values for r_o and r_d . Accordingly, one apparently can merely conclude that the use of the Kelvin equation in calculating average radii from the desorption isotherm of a gas has to assume at least a monolayer of adsorbed gas on the capillary to which the equation is applied. The reason for the one glass requiring two adsorbed layers and the others requiring only one to give agreement is not clear, though it should be noted that the glass requiring two layers of adsorbed gas has an average pore size of about 30 A., compared to the

TABLE 3
Average pore size in Ångström units*

SAMPLE	BY NITROGEN ADSORPTION			BY ARGON ADSORPTION			BY BUTANE ADSORPTION			BY WATER ADSORPTION		
	r_o^*	$r_d + 4$ A.	$r_o + 4$ A.	r_o^*	$r_d + 4$ A.	$r_o + 4$ A.	r_o^*	$r_d + 4$ A.	$r_o + 4$ A.	r_o^*	$r_d + 4$ A.	$r_o + 4$ A.
Porous glass No. 3...	16.3	17.7	15.5	15.6	15.8	16	15.5	20.9	17.9			
Porous glass No. 4...	20	18.6	18.9	18.7	19.7	19.9	19.3	23.0	19.0			
Porous glass No. 6...	19.1	17.7	15	18.8	17.7	14.8	20	20.6	15.8			
Porous glass No. 7...	18.1	17.7	14.5	16.7	17.7	15.9	17	21.9	14.4	16.7	20	16.5

* r_o in each case is calculated from the equation $r_o = 2V/\text{area}$. The area values used are those obtained by nitrogen isotherms. r_d and r_o are taken from table 2, columns 8 and 7.

maximum of 20 A. for the glasses used in the present work, and, therefore, has a desorption relative pressure for most of the gas that is about 0.63 rather than 0.5, found for the glasses used in the present study. This is consistent with there being a larger number of layers of adsorbed gas after the removal of the capillary condensed gas on the sample used by Emmett and DeWitt than on the present samples.

Hysteresis in the desorption isotherms

It has long been noticed that desorption isotherms will, in certain relative pressure ranges for some adsorbents, be considerably different from adsorption isotherms (1, 21). Specifically, the desorption pressure at which a given amount of gas is held by the adsorbent is often much smaller than the adsorption pressure corresponding to the same amount of adsorbate. Various suggestions have been made to explain this hysteresis phenomenon, including the bottle-neck theory of Kraemer (17), the open-pore theory of Cohan (6), and the angle-of-wetting theory

of Zsigmondy (21). However, as has been pointed out on previous occasions (10), for various reasons none of these theories appears to be entirely satisfactory. Truly, the cause of the hysteresis must still be considered as uncertain.

Although it does not appear worthwhile to reiterate the descriptions of the various theories of capillary condensation, it seems necessary to mention certain aspects of the hysteresis explanation proposed by Cohan (6). A comparison of equations 3 and 4 makes it clear, as Cohan has pointed out (7), that when the adsorption curve and the desorption curves meet the radius values for r_c become equal to $r_d/2$; hence, r_d at this point will equal $2D$, where D is the molecular diameter of the adsorbate molecule. This conclusion will be reached only if one assumes that the Kelvin equation gives the entire pore radius without any allowance being made for one or more layers of adsorbed gas and that Cohan's equation gives the radius of the capillary left after the adsorption of a monolayer. As discussed above, however, a comparison of the values of r_d and r_c appears to make it necessary to assume that the Kelvin equation applied to desorption isotherms does not give the true pore radius but the radius of the pore that remains after the taking up of at least a monolayer of adsorbate. How, then, is this discrepancy to be explained? Cohan (7) has cited a long list of examples of adsorption data which he claims are in agreement with the thesis that r_d at the beginning of the hysteresis loop is equal to $2D$, and yet the assumption upon which this calculation is based appears from the data in table 2 to be untenable.

One possible way out of the difficulty might be to assume that the area values calculated in the conventional manner from the nitrogen isotherm by the B.E.T. equation are too small. If this were true, then the values for r_c calculated from the pore volume and the pore area would be too large. By an arbitrary adjustment upward of the area values of the samples, it would thus be possible to bring the calculated values for r_c and r_d into agreement without assuming that r_d has to be calculated from a surface covered with a monolayer rather than from the bare surface of the capillaries. There are, however, serious objections to such a procedure. The excellent agreement between the surface area of titanium dioxide found by the Harkins and Jura (14) heat-of-immersion method and the area calculated from the B.E.T. equation applied to the low-temperature nitrogen isotherm, makes it rather unlikely that the area as measured by the nitrogen isotherm, using 16.2 \AA^2 as the area of each adsorbed nitrogen molecule, can be low by the 20–25 per cent that would be required to lower the r_c values sufficiently to make them agree with the r_d values of tables 2–4. This possibility cannot be completely ruled out, however, since there is the bare possibility that the titanium dioxide used in the heat-of-immersion experiments by Harkins and Jura (14) actually had a certain number of small capillaries that were completely filled with capillary condensed water at the relative pressures with which the samples were presaturated. Any such small capillaries would tend to make the heat-of-immersion results give too low an area and would presumably necessitate the assuming of a nitrogen molecular cross-section larger than 16.2 \AA^2 to bring areas obtained by the nitrogen adsorption and those by the heat of immersion (corrected for capillaries) into agreement.

Another way out of the difficulty would be to assume that r_c , calculated according to the Cohan theory, is the radius of a capillary after two layers of adsorbed molecules are taken up and that r_d is the radius of the capillary left after a single layer is adsorbed. This would lead to the conclusion that r_h , the lower point of juncture of the adsorption and desorption isotherms, is never less than $3D$, rather than $2D$ as postulated by Cohan. Actually, an examination of all of the data by Cohan as well as the data in the present paper show that most of the results would give about as good agreement with r_h equal to $3D$ as with it equal to $2D$, though it must be admitted that for some data r_h is less than $3D$ but is never less than $2D$. However, all such calculations that are based on the application of the Kelvin equation to capillaries of the order of molecular size are open to doubt in general, because of the uncertainty as to the way in which the value of the product $\sigma V \cos \theta$ might change as the capillary size approaches the diameters of molecules. Further discussion of this point at present is probably unwarranted.

Scanning curves

It was hoped that a few scanning curves across the hysteresis loop would throw some light on the significance of capillary condensation. The results make it clear that the adsorption and desorption scanning curves are very different in shape, the former being convex to the pressure axis and the latter concave. Furthermore, the curves make it apparent that on increasing the pressure from a point on the desorption curve, the scanning curve approaches the adsorption isotherm the more closely the higher relative pressure, but probably does not meet it until the adsorption and desorption curves join. Conversely, the desorption scanning curves starting at some point on the adsorption curve appear to merge into the desorption isotherm close to the lower relative pressure at which the adsorption and desorption curves unite. The data are not sufficiently accurate to establish the exact points of juncture of the adsorption and desorption scanning curves but are certainly consistent with these conclusions. These scanning curves are in good agreement with those found by Rao (19) for various gels. They are interesting but still do not furnish the key to explain the existence of the hysteresis phenomenon.

Deitz and Gleysteen (8) have recently suggested that hysteresis possibly can be accounted for by assuming that the heat of desorption is higher than the heat of adsorption. Actually, there are some indications that such is the case (16). In a stricter sense, however, this still does not explain capillary condensation until we know *why* the heat of desorption is greater than the heat of adsorption. Possibly the explanation lies in the fact that most of the molecules going into a capillary during the adsorption part of the hysteresis loop are taken up as multi-layer adsorption having a heat of adsorption close to that of liquefaction, whereas in the desorption part of the loop the escaping molecules by virtue of the curvature of the meniscus from which they evaporate must necessarily entail a higher heat value than was involved in the adsorption process.

In conclusion, it is of interest to point out that the argon adsorption isotherms shown in figures 1-7 are actually taken about 6°C . below the normal melting point

of argon. The curves, however, have the same shape as those taken above the melting point. Presumably one is dealing with condensation to a supercooled liquid in the capillaries rather than with the formation of a solid. In other words, the melting point of the liquid in the capillaries appears to be lower than that of the bulk liquid. It is for this reason that the p_0 values employed in calculating the argon isotherms are taken from the extrapolated curve for the liquefied gas rather than from the curve for the solid-vapor equilibrium. Other examples of this apparent lowering of the freezing point of liquid condensed in capillaries have been noted. For example, water desorption isotherms below the melting point are similar in appearance to those taken above 0°C . (18). Also, in some unpublished work, Brunauer and the author have found that acetylene adsorption curves on iron catalysts for the synthesis of ammonia are the same over the range -78° to -100°C . when plotted on a relative pressure basis (using the extrapolated vapor pressure curve of liquid acetylene for p_0), even though the melting point of acetylene is -81.5°C .

SUMMARY

The values for the surface area of porous glass No. 7, as measured by adsorption isotherms of nitrogen, argon, butane, carbon dioxide, ammonia, water vapor, and acetylene, are 232, 217, 156, 159, 207, 128, and 164, respectively. Adsorption and desorption curves have been obtained for nitrogen and argon at -195°C . and for butane at 0°C . on five different samples of porous glass. Pore radii from the volume to surface area ratio of the pores are compared with values obtained by applying the Kelvin equation to the desorption isotherm and by applying the Cohan equation (equation 4) to the steepest part of the adsorption isotherm.

The authors wish to acknowledge gratefully the help given by Godfrey L. Cabot, Inc., in the form of fellowship funds to defray the cost of this work.

REFERENCES

- (1) ANDERSON: *Z. physik. Chem.* **83**, 191 (1914).
- (2) BEEBE, BECKWITH, AND HONIG: *J. Am. Chem. Soc.* **67**, 1554 (1945).
- (3) BEECK: *Rev. Modern Phys.* **17**, 61 (1945).
- (4) BRUNAUER AND EMMETT: *J. Am. Chem. Soc.* **59**, 2682 (1937).
- (5) BRUNAUER, EMMETT, AND TELLER: *J. Am. Chem. Soc.* **60**, 309 (1938).
- (6) COHAN: *J. Am. Chem. Soc.* **60**, 433 (1938).
- (7) COHAN: *J. Am. Chem. Soc.* **66**, 98 (1944).
- (8) DEITZ AND GLEYSTEEN: *J. Research Natl. Bur. Standards* **29**, 191 (1942).
- (9) EMMETT: American Soc. Testing Materials, Symposium on New Methods for Particle Size Determination in Subsieve Range **1941**, 95.
- (10) EMMETT: In E. O. Kraemer's *Advances in Colloid Science*, pp. 1-36. Interscience Publishers, Inc., New York (1942).
- (11) EMMETT AND BRUNAUER: *J. Am. Chem. Soc.* **59**, 1553 (1937).
- (12) EMMETT AND DEWITT: *Ind. Eng. Chem., Anal. Ed.* **13**, 28 (1941).
- (13) EMMETT AND DEWITT: *J. Am. Chem. Soc.* **65**, 1253 (1943).
- (14) HARKINS AND JURA: *J. Am. Chem. Soc.* **66**, 1362 (1944).
- (15) HOOD AND NORDBERG: U. S. patent 2,106,744.
- (16) JOYNER AND EMMETT: To be published.

- (17) KRAEMER: In *A Treatise on Physical Chemistry*, H. S. Taylor, Editor, Chap. XX, p. 1661. D. Van Nostrand Company, New York (1931).
- (18) MILLIGAN: Paper presented at the Symposium on the Adsorption of Gases which was held under the auspices of the Division of Colloid Chemistry at the 110th Meeting of the American Chemical Society, Chicago, Illinois, September 11-12, 1946.
- (19) RAO: *J. Phys. Chem.* **45**, 500 (1941).
- (20) RIES, VAN NORDSTRAND, JOHNSON, AND BAUERMEISTER: *J. Am. Chem. Soc.* **67**, 1242 (1945).
- (21) ZSIGMONDY: *Z. anorg. Chem.* **71**, 356 (1911).

INVESTIGATION OF LOW-TEMPERATURE NITROGEN ADSORPTION AT HIGH RELATIVE PRESSURES¹

JAMES HOLMES² AND P. H. EMMETT³

Department of Chemical Engineering, The Johns Hopkins University, Baltimore 18, Maryland

Received June 11, 1947

INTRODUCTION

In connection with certain phases of the research on gas mask charcoals conducted by Division 10 of the National Defense Research Committee, it became apparent that pore size and pore-size distribution over the size range from 20 to 160,000 A. diameter might be important factors governing whether a base charcoal would be suitable or not as a catalyst support. The exact extent to which the distribution of large pores proved to be important in such charcoals is, of course, restricted information and cannot be discussed here. Nevertheless, the present method of measuring large pores and some of the pore-size distributions found may be of interest to the manufacturers and users of porous catalytic materials and supports.

Although it was realized that no entirely satisfactory method existed for obtaining pore-size distribution over this wide range, it was decided that low-temperature nitrogen-adsorption isotherms could yield a good deal of information on the subject if they could be carried to sufficiently high pressures (1, 11, 14; 7, see also paper on another porous glass (8)). The present paper describes the technique used in extending the nitrogen isotherms from a maximum relative pressure of about 0.98 usually employed up to a relative pressure of 0.9995. The results here cited should, as a whole, be considered as preliminary and illustrative rather than final, since some of them were obtained before the final technique was perfected.

¹ Presented at the Symposium on the Adsorption of Gases which was held under the auspices of the Division of Colloid Chemistry at the 110th Meeting of the American Chemical Society, Chicago, Illinois, September 11-12, 1946.

² Present address: Houdry Process Corporation, Marcus Hook, Pennsylvania.

³ Present address: Mellon Institute, Pittsburgh 13, Pennsylvania.

EXPERIMENTAL

Materials investigated

The work reported in this paper was carried out upon a number of different charcoals representative of various commercial processes, upon a number of commercial carbon blacks, upon a special laboratory charcoal prepared by carbonizing an ethylidene chloride polymer, and finally upon samples of both porous-glass and sized-glass microspheres.

(a) *Charcoals*: The coconut shell charcoal was a standard product that had been prepared by a combination of calcination and steam treatment.

PCI P58 is a coal charcoal prepared commercially from finely ground coal which had been briquetted, calcined, and, finally, activated with steam at temperatures up to 850–900°C.

The *CFI* charcoal is somewhat similar in its preparation to the *PCI* sample and is likewise a coal charcoal.

Saran charcoal was prepared (10) by a suitable extrusion of an ethylidene chloride polymer, followed by a carbonization step.

(b) *Carbon blacks*:⁴ *Carbolac No. 1* is a black of very intense color. It is prepared by the Godfrey L. Cabot Company by an intensive air after-treatment at 800–1200°F. of a fine-particle-size channel black. From electron-microscope pictures the average particle size appears to be <50 Å. in diameter.

Unspheonized Grade 6 carbon black (Elf 4) is a standard medium-processing channel black produced by the Godfrey L. Cabot Company. Electron-microscope pictures reveal that the average particle size for this black is about 286 Å. diameter.

Spheron Grade 6 is a pelletized medium-processing rubber black made by pelletizing the preceding black into tiny spherical agglomerates approximately 0.1 mm. in diameter. The average size of the individual particles in the pellets is, however, still about 286 Å.

(c) *Glass*: The *porous glass* (9) sample used in the present work is an aliquot of a sample used by Emmett and Cines (7). The sample (porous glass No. 5) was obtained from the Corning Glass Company and is described as having been prepared by leaching out the boron oxide from a borosilicate glass.

The *7-micron glass spheres* have been used previously in several studies carried out by Emmett and coworkers, which are soon to be published. They were prepared by Bloomquist and Clark according to a procedure previously described by them (3).

The *3–5 micron glass spheres* were prepared at The Johns Hopkins University by the general procedure described by Bloomquist and Clark, the average particle size being determined by a microscopic study of the particles.

All of the above samples were evacuated to constant weight at temperatures between 110°C. and 150°C. before the adsorption isotherms were started.

⁴ The various particle-size dimensions given for the different carbon blacks on the basis of either electron microscope or low-temperature nitrogen measurements may be found in references 5 and 15.

EXPERIMENTAL

Adsorption measurements

Nitrogen-adsorption isotherms were made upon the samples at -195°C . The portion of the isotherm up to about 0.95 relative pressure was determined in a standard adsorption apparatus (4, 6). The part of the isotherm above 0.95 relative pressure was determined by using the same apparatus in conjunction with a Pearson differential gauge.

Apparatus

The chief novelty of the present apparatus (figure 1) is the inclusion of the Pearson gauge (2, 12) for determining the high relative pressures.

The principle of the device is readily understood by reference to this figure. As can be seen, arms A and B of the manometer are connected, respectively, to the unknown pressure in equilibrium with the adsorbed nitrogen in the sample tube and to a bulb placed beside it containing liquid nitrogen. An amount of mercury is used such that when the pressure in the two arms of the gauge is the same, the mercury level Y in the capillary tube P is at the lower end of the scale and the mercury in arm A of the manometer is just touching the platinum reference tip. By maintaining the mercury level in arm A always on this reference tip as the pressure difference between the sample bulb and the reference bulb increases, the level in arm B will fall and a volume of mercury proportional to the pressure difference will enter the capillary section. By choosing different ratios in the diameters of the tubing used for arms A and B with respect to the capillary tubing P it is possible to increase or decrease the sensitivity of the gauge to almost any desired extent. In the present apparatus tubing of approximately 10 mm. diameter was used for arms A and B and 1-mm. tubing was used for the capillary section P. The uniformity of the tubing as well as the actual volumes per unit length were carefully determined with mercury and a cathetometer. In this way it was determined that a change of 1 mm. in the mercury level in B was equivalent to a change of 15.4 mm. in P. Since the mercury level in P did not vary more than ± 2 mm. for successive settings on the reference tip, it was possible to measure actual pressure differences to ± 0.13 mm. Of course, if greater accuracy had been desired the setting could have been improved by using a magnifying glass to enlarge the appearance of the platinum tip. Both arms A and B as well as the capillary should be carefully chosen for uniformity throughout their respective working ranges. For the greatest accuracy it would be necessary to calibrate the two sections of tubing against each other, by means of a cathetometer. It is necessary either to eliminate or to correct for temperature changes in the gauge, since changes of several degrees or so in the room temperature will cause a sufficiently large variation in the density (and hence volume) of mercury transferred into P to make the readings differ by more than the experimental error. It is therefore necessary to apply corrections for such changes in temperature or to thermostat the gauge.

RESULTS AND DISCUSSION

Before presenting the results, a short discussion regarding the use of adsorption data for determining pore size and pore-size distribution will be given, as well as

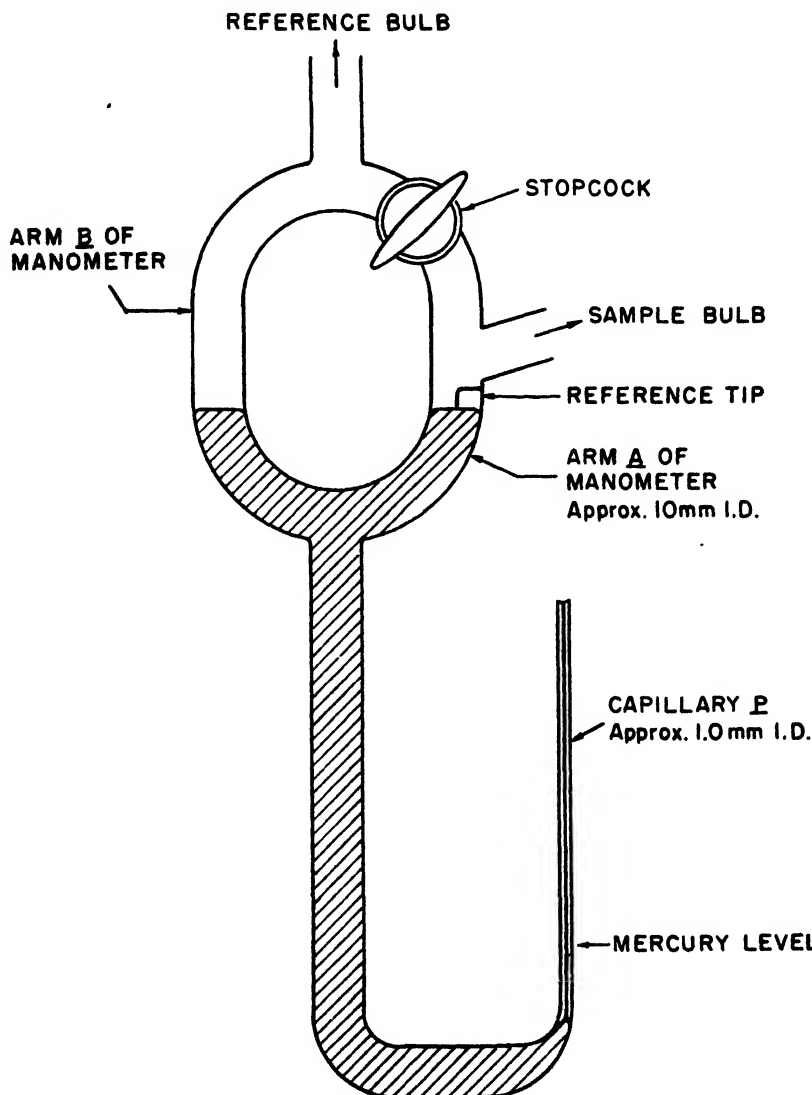


FIG. 1. Sketch of Pearson gauge

a brief discussion of some of the advantages of the Pearson gauge for measurements of high relative pressures.

It is well known that if one assumes that condensation of a vapor takes place

at a relative pressure, p/p_0 , in a cylindrical capillary, the diameter of the capillary, D , can be calculated by the familiar Kelvin equation (16):

$$D = \frac{-4\sigma V \cos \theta}{RT \cdot 2.303 \log p/p_0}$$

where σ is the surface tension of liquid nitrogen, θ is the angle of wetting, V is the molal volume of liquid nitrogen, and T is the temperature of the experiment. However, the application of this equation to a low-temperature nitrogen-adsorption isotherm of a porous solid in calculating the pore size and pore-size distribution is fraught with many difficulties, all of which have been discussed elsewhere (7; see also 8). It will perhaps suffice to point out that the chief complicating factor is the difficulty of distinguishing between the volume of gas taken up by capillary condensation and the volume, V , taken up by multilayer adsorption according to the equation

$$\frac{p/p_0}{V(1 - p/p_0)} = \frac{1}{V_m C} + \frac{C - 1}{V_m C} \frac{p}{p_0} \quad (1)$$

where V_m is the volume of gas required to form a monolayer, C is a constant, and p/p_0 is the relative pressure.

In spite of the confusion arising from the simultaneous occurrence of multilayer adsorption and capillary condensation, some definite conclusions can be drawn relative to pore size and pore-size distribution from the low-temperature nitrogen-adsorption isotherm. For example, at relative pressures lower than about 0.35 it is believed that all the gas taken up is held by adsorption and not by capillary condensation. Furthermore, there is evidence to indicate that multilayer adsorption at relative pressures between about 0.99 and 0.9995 probably reach only such thickness as can be neglected in comparison with the diameter of the capillaries and hence of capillary condensation over this pressure range. Finally, for the special case in which the volume of nitrogen adsorbed at -195°C . does not increase appreciably with pressure above a relative pressure of about 0.4, it seems safe to assume that there are no capillaries present having diameters in excess of the size corresponding to 0.4 relative pressure.

If the solid adsorbent is finely divided but non-porous, one might expect to find only multilayer adsorption and no capillary condensation. However, some capillary spaces must necessarily exist between the small particles. Hence, even for non-porous solids, one may expect some capillary condensation.

There are a number of advantages in using the Pearson gauge in measuring high relative pressures. Perhaps the most outstanding advantage is that the gauge offers a method for measuring the pressure that is far quicker and capable of greater accuracy than would be possible with a cathetometer and the usual type of apparatus. Even if a cathetometer were used with the usual type of apparatus, it would be necessary to adapt the procedure here used of measuring a differential rather than an absolute pressure. One arm of the gauge must be capable of being set at a fixed point and must be exposed to a bulb of adsorbate kept in the same spot in the low-temperature bath as is the adsorption bulb. Even when gaseous nitrogen is used to agitate the liquid-nitrogen bath, it is diffi-

cult to avoid the occurrence of local temperature differences. In the present set-up such effects are largely nullified, since they are transmitted nearly equally to both arms of the gauge. Even with fairly large temperature variations in the bath, only an insignificant change will be produced in the pressure difference itself, once equilibrium has been established.

One of the main difficulties in the present work was encountered only in the measurement of pressures close to unity. It was observed, for instance, that if more gaseous nitrogen were admitted to the sample bulb after saturation had apparently been reached, as judged by the balance of the two arms of the gauge, the added nitrogen would be adsorbed and the gauge arm connected to the sample would remain depressed below the reference arm (thereby indicating a higher pressure over the adsorbent than in the reference arm) when the new equilibrium was established. It is now believed that this is due to the presence of extremely small amounts of impurities in the nitrogen used for the adsorption (the nitrogen used was rated by the producer as 99.99 per cent pure). This impurity is believed to consist mainly of argon, which boils at a somewhat higher temperature than nitrogen. If argon were present in the nitrogen, the pressure in the reference bulb would be somewhat lower than would be normally found for pure nitrogen, owing to the higher boiling point of liquid argon. In the sample tube the argon would be preferentially adsorbed because of its higher boiling point. Once saturation had been reached, however, as more of the gas was added the pressure in equilibrium with the sample should fall gradually and approach that in the reference bulb. It was thus necessary after the gauge arms had become balanced in any run to add small amounts (about 5 cc. at S.T.P. per 0.5 g. of sample) of nitrogen until no change in pressure was found upon successive 5-cc. increments after standing 30 min.

Since equilibrium at very high relative pressures was approached fairly slowly, there was only time to carry out one or two desorption points on a few of the samples.

The results obtained upon the individual samples and a brief discussion of their significance will now be given. For convenience, the solid adsorbents will be divided into two classes: porous and non-porous.

Porous adsorbents

The porous adsorbents were all of such large particle sizes that the capillary volumes at the points of contact were negligible. Accordingly, the shape of the adsorption isotherms up to relative pressures of 0.9995 may be construed as due entirely to the distribution and size of pores within the particles, rather than to condensation between the particles.

(a) *Porous Glass.*⁵ As indicated in figure 2, there is a marked absence of adsorption found for this sample at high relative pressures. It appears certain that there can be little porosity in this sample in pores having radii above about 20 Å.

⁵ Unfortunately these samples were run before it was realized that true saturation was not reached until the gauge indicated a slight excess pressure in the sample bulb as compared to the reference bulb. Accordingly, the values reported for the relative pressures in the high relative pressure range are somewhat too high.

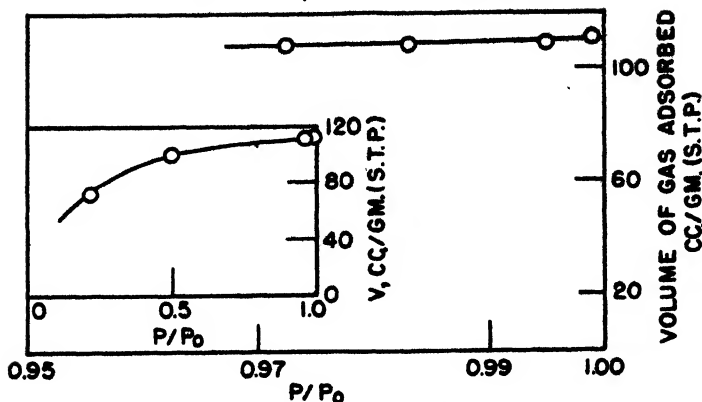


FIG. 2. Nitrogen adsorption isotherm on porous glass No. 5 at -195°C . over the relative pressure range 0.95–1.00. Insert shows entire isotherm.

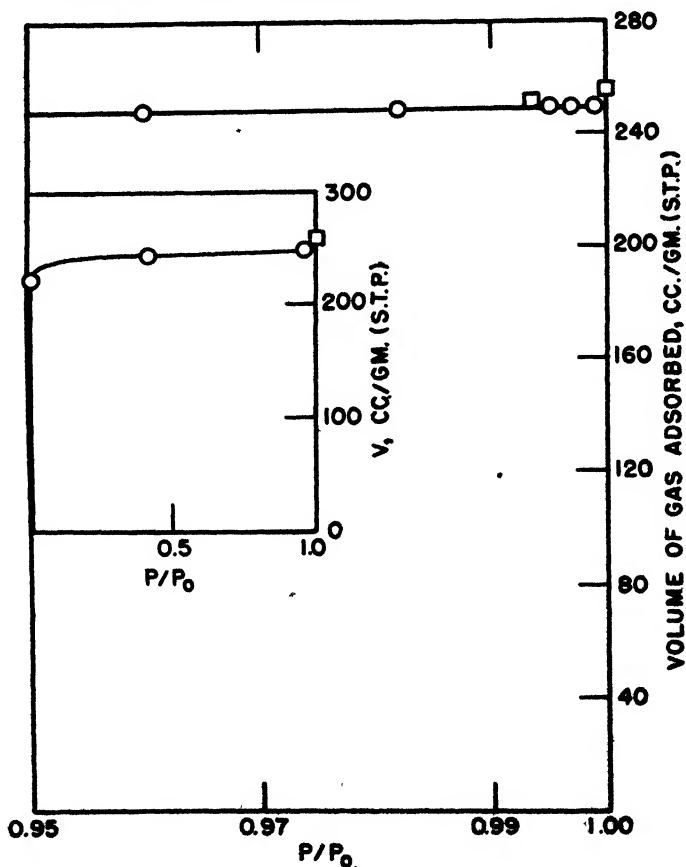


FIG. 3. Nitrogen-adsorption isotherm on Saran charcoal at -195°C . over the relative pressure range 0.95–1.00. Insert shows entire isotherm. Open circles and squares represent adsorption points from two separate runs.

(b) *Saran charcoal*: A comparison of the normal adsorption isotherm carried to 0.95 relative pressure with the Pearson gauge run carried to nearly saturation, both of which are shown in figure 3, reveals that there is remarkably little adsorption above 0.95 p/p_0 , thus indicating an almost complete lack of pores having diameters in excess of 200 Å. This conclusion was further strengthened by the results on mercury penetration⁶ (14), which indicated that there were virtually no pores having openings as large as 10,000 Å. in diameter.

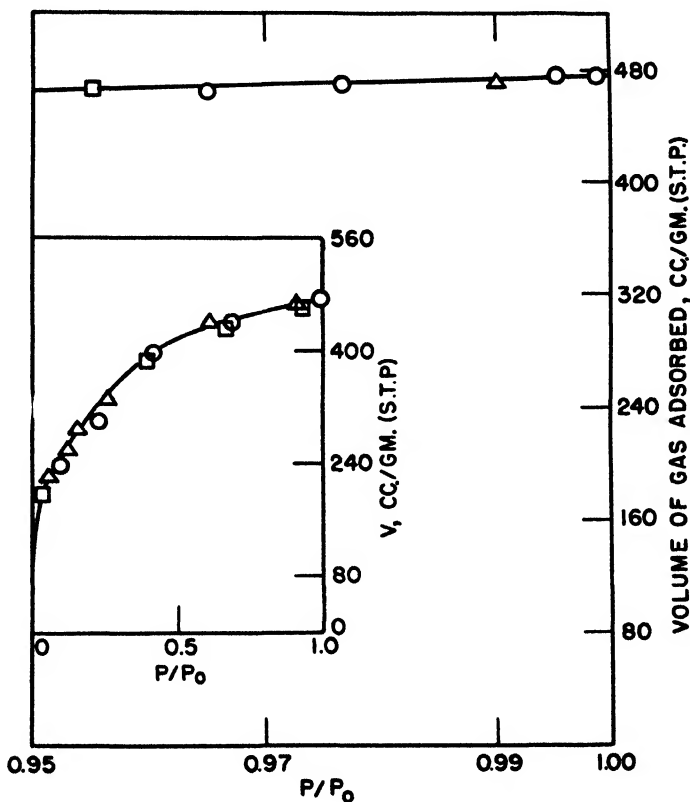


FIG. 4. Nitrogen-adsorption isotherm on CFI "CC" charcoal at $-195^{\circ}\text{C}.$ over the relative pressure range 0.95–1.00. Insert shows entire isotherm. Open circles, squares, and triangles represent adsorption points from three separate runs.

(c) *CFI charcoal*.⁵ This is another case of a sample in which there is an almost complete leveling off of the isotherm, indicative of the absence of large pores. An inspection of the isotherm for this material, shown in figure 4, leads to the

⁵ Measurements made by Corville Mace, Jr., as part of the charcoal research project carried out at The Johns Hopkins University for the National Defense Research Committee. These will be described in a forthcoming publication by one of the authors (P.H.E.), summarizing the adsorption and pore-size studies carried out on charcoal for the National Defense Research Committee.

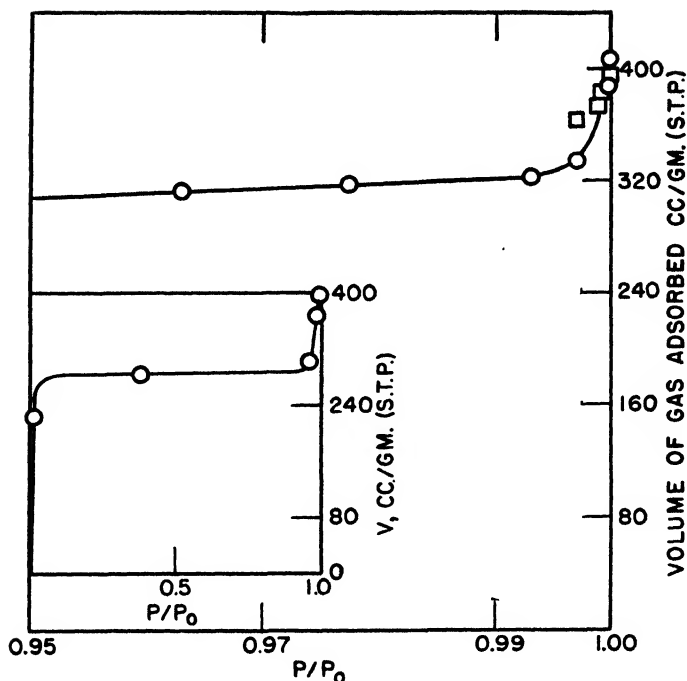


FIG. 5. Nitrogen-adsorption isotherm on PCI P58 charcoal at -195°C . over the relative pressure range 0.95–1.00. Insert shows entire isotherm. Open circles and squares represent adsorption points from two separate runs.

TABLE 1

SAMPLE	V_g VOLUME OF GAS ADSORBED AT 0.999 p/p_0	V_m	V_L VOLUME ADSORBED AT 0.999 p/p_0 CALCU- LATED AS CC OF LIQUID	V_g V_m	APPARENT DENSITY	V_s VOLUME BETWEEN PARTICLES PER GRAM	$V_L \times 100$ V_s
	cc/g.	cc	cc.		g/cc.	cc	
Glass spheres ($7\ \mu$)	45.7	0.12	0.0715	380	?	0.132*	54
Glass spheres ($3\text{--}5\ \mu$)	9.7	0.23	0.01515	42	?	0.132*	11.5
Grade 6 spheronized carbon black	685	23.0	1.07	30	0.352	2.36	45
Grade 6 agitated carbon black	1271	23.0	1.99	55	0.192	4.74	42
Carbolac No 1	3350	230.0	5.25	14.5	0.08	12.0	44

* Values of apparent density were not taken on the glass spheres. The volume, V_s , given for glass is calculated on the assumption of close packing of the glass spheres; hence V_L/V_s in column 8 for the glass spheres represents maximum values.

conclusion that this sample has virtually no pores with diameters in the range 150–40,000 Å. The lack of appreciable mercury penetration⁶ at pressures up to

450 lb. per square inch agrees with this by indicating the absence of pores larger than about 4800 Å.

(d) *PCI P58 charcoal*: This sample forms a striking example of a case in which extrapolation of the isotherm obtained up to a relative pressure of about 0.95 in the conventional way would give a very false indication of large-pore distribution.

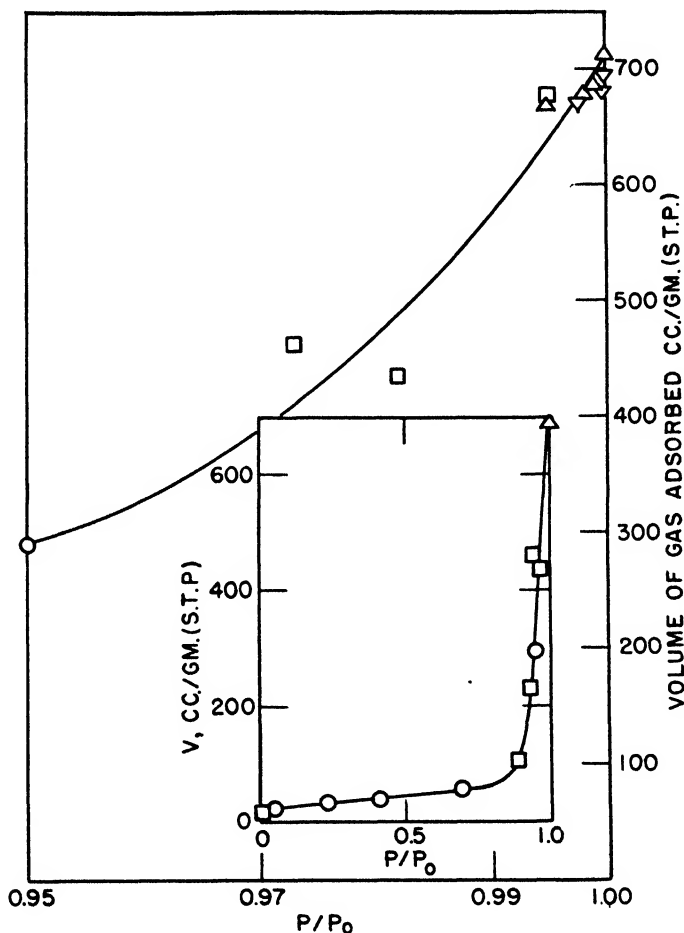


FIG. 6. Nitrogen-adsorption isotherm on Spheron Grade 6 carbon black at -195°C over the relative pressure range 0.95–1.00. Insert shows entire isotherm. Open circles, squares, triangles and inverted triangles represent adsorption points from four separate runs.

As can be seen from figure 5, such an extrapolation would indicate the absence of an appreciable number of large pores, whereas, in actuality, there is considerable porosity in very large pores, as indicated by the increased adsorption with pressure at the higher relative pressures studied with the Pearson gauge as well as by mercury penetration experiments,⁶ which also showed that there was a consider-

able pore volume for pores having openings larger than about 10,000 Å. in diameter.

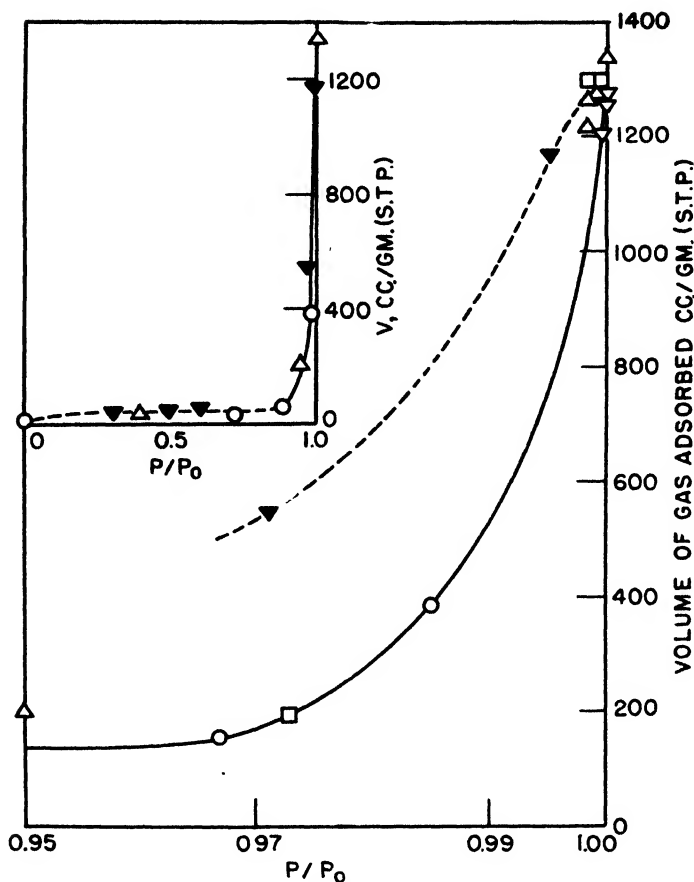


FIG. 7. Nitrogen-adsorption isotherm on Grade 6 carbon black at -195°C over the relative pressure range 0.95–1.00. Insert shows entire isotherm. Open circles, squares, triangles, and inverted triangles represent adsorption points from four separate runs; solid symbols represent desorption points from same runs.

Non-porous adsorbents: 7 μ glass spheres, 3–5 μ glass spheres, Grade 6 Spheron, and Carbolac No. 1

The non-porous adsorbents, covering a size range from 0.005 to 7 microns, are all characterized by a large increase in adsorption at the higher relative pressures. It appears that for all of the following samples, condensation is taking place in the space between the particles. For comparison, the volumes of gas adsorbed at 0.999 relative pressure for the five non-porous solids is summarized in table 1, together with other pertinent data; the detailed isotherms for spheronized Grade 6 carbon black, unspheronized Grade 6 carbon black, and Carbolac No. 1, are shown in figures 6, 7, and 8, respectively.

The question naturally arises as to whether the gas pickup at high relative pressure by these non-porous solids is to be associated with multilayer adsorption or with capillary condensation between the particles. On the one hand, column 5 shows that the statistical number of layers that are adsorbed at a relative pressure of 0.999 if all of the adsorbate is assumed to be held as multilayer adsorption ranges from 14.5 for Carbolac to 380 for the $7\ \mu$ glass spheres. This range in the number of layers adsorbed appears a little unlikely. In this connection it should be pointed out that the apparent difference between the adsorption on the $3\text{--}5\ \mu$ spheres and that on the $7\ \mu$ spheres is open to suspicion. If the adsorption isotherm for the smaller spheres (figure 9) were moved to the left, 0.001 relative

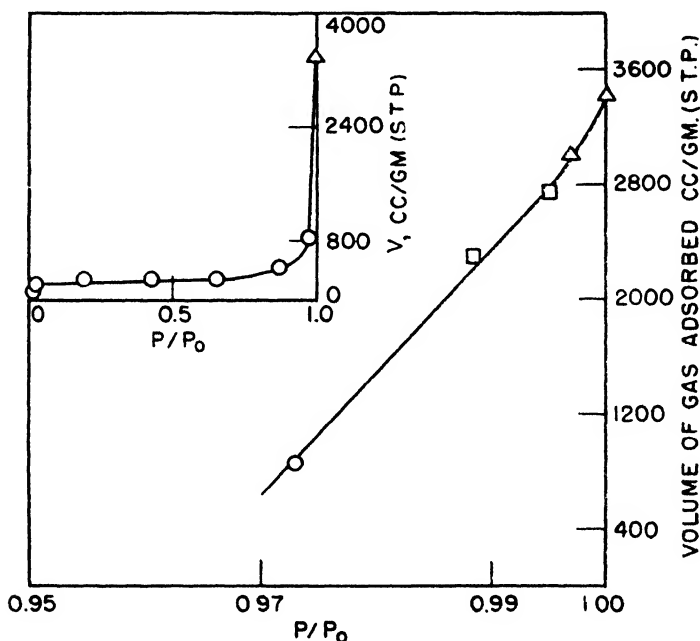


FIG. 8. Nitrogen-adsorption isotherm on Carbolac No. 1 at -195°C . over the relative pressure range 0.95–1.00. Insert shows entire isotherm. Open circles, squares, and triangles represent adsorption points from three separate runs.

pressure unit, it would superimpose on the curve for the $7\ \mu$ spheres (figure 10). This makes the results in figure 9 rather doubtful until checked.

If, on the other hand, one assumes that the large amount of gas pickup at the higher relative pressure is due to capillary condensation in the space between the particles or groups of particles, one finds that the adsorption at 0.999 p/p_0 calculated as liquid is equivalent to 42–54 per cent of the apparent free space except for the $3\text{--}5\ \mu$ sample of glass spheres.

The apparent correlation between the free space between the particles and the amount of gas pickup lends weight to the picture of capillary condensation. It must be realized, however, that if, as the Kelvin equation would indicate, the

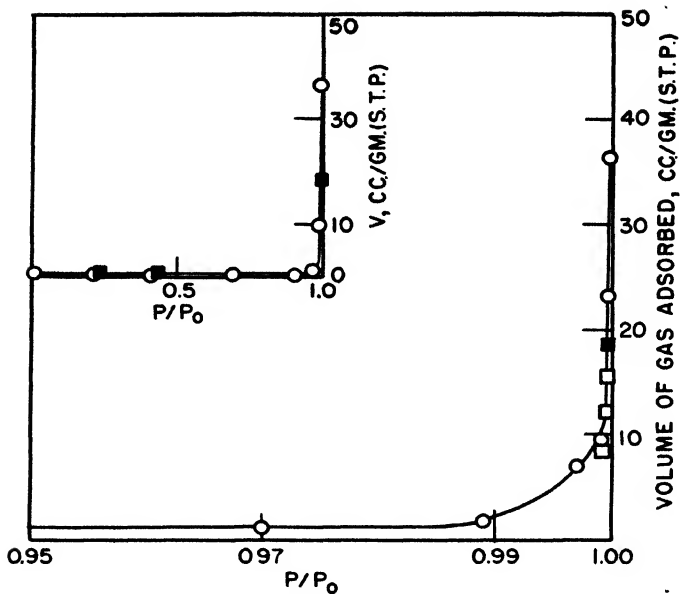


FIG. 9. Nitrogen-adsorption isotherm on 3-5 μ glass spheres at -195°C . over the relative pressure range 0.95-1.00. Insert shows entire isotherm. Open circles and squares represent adsorption points from two separate runs; solid symbols represent desorption points from the same runs

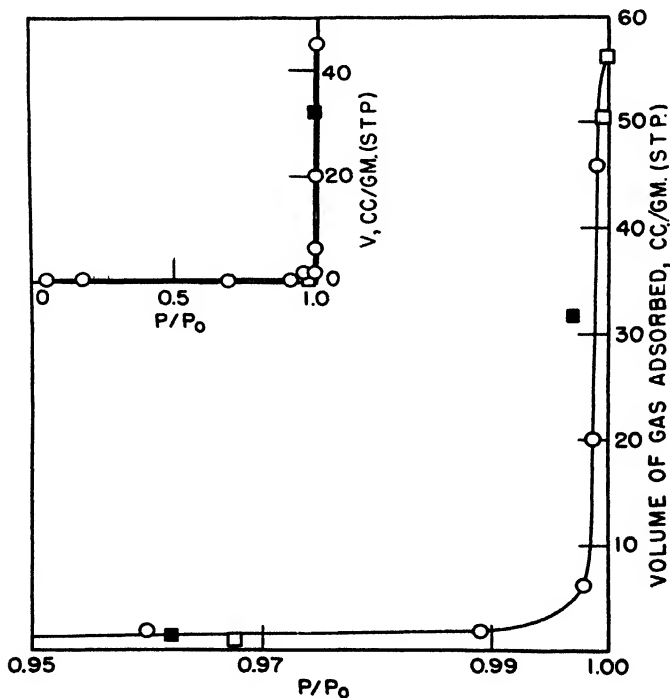


FIG. 10. Nitrogen-adsorption isotherm on 7 μ glass spheres at -195°C . over the relative pressure range 0.95-1.00. Insert shows entire isotherm. Open circles and squares represent adsorption points from two separate runs; solid symbols represent desorption points from the same runs.

space between the particles for condensation at a relative pressure of 0.999 is 18,000 Å., then for the capillary condensation explanation to be valid, one has to postulate that about the same percentage of the free space is located in capillaries or regions 18,000 Å. or less in diameter for the 35–40 Å. particles of Carbolac as well as for the 70,000 Å. glass spheres. This too seems a little improbable, even though admittedly the carbon blacks are very loosely packed and might contain many large concavities in the adsorption tube.

The authors are inclined to favor the view that the large gas pickup is due to capillary condensation between the particles but prefer to defer further discussion until more work has been done.

SUMMARY

An adaptation of a differential manometer is described for the measurement of relative pressures close to unity. Without elaborate thermostating or other precautions, measurements of the adsorption of nitrogen at $-195^{\circ}\text{C}.$ have been carried out up to relative pressures as high as 0.9995 with an accuracy as great as could be obtained with an ordinary cathetometer and with greater simplicity. It is pointed out that even higher relative pressures could probably be obtained with nearly the same ease, provided the present apparatus were carefully thermostated.

Measurements are described on porous glass and a number of charcoals in which there was almost complete absence of any further adsorption of nitrogen above a relative pressure of about 0.95. In terms of capillary adsorption this would indicate the absence of pores in these samples which had diameters of 200 Å. or greater. This was further confirmed by mercury-penetration experiments⁶ in which it was also found that there was an almost complete absence of pores in the range 10,000 to 100,000 Å.

Results on a number of carbon black samples indicate that a very large adsorption occurs above a relative pressure of 0.95. Most of this volume of nitrogen is believed to be condensed in the spaces between the small particles or agglomerates. Measurements upon uniformly sized samples of glass microspheres indicate that, with these samples, all of the space between the spheres has not been filled even at the highest relative pressures measurable with the present gauge. At a relative pressure of 0.999 between 42 and 54 per cent of the space between the particles appears to be filled with liquid adsorbate for four out of the five non-porous solids used.

REFERENCES

- (1) ANDERSON: *Z. physik. Chem.* **88**, 191 (1914).
- (2) BEECK: *Rev. Sci. Instruments* **6**, 399 (1935).
- (3) BLOOMQUIST AND CLARK: *Ind. Eng. Chem., Anal. Ed.* **12**, 61–3 (1940).
- (4) BRUNAUER, EMMETT, AND TELLER: *J. Am. Chem. Soc.* **60**, 309 (1938).
- (5) COLUMBIAN CARBON CO.: *Ind. Eng. Chem., News Ed.* **18**, 492 (1940).
- (6) EMMETT: *American Soc. Testing Materials, Symposium on New Methods for Particle Size Determination in Subsieve Range*, **1941**, 95.
- (7) EMMETT AND CINES: *J. Phys. Colloid Chem.* **51**, 1248 (1947).
- (8) EMMETT AND DEWITT: *J. Am. Chem. Soc.* **65**, 1253 (1943).

- (9) HOOD AND NORDBERG: U. S. patent 2,106,744.
- (10) JOHNSTONE, H. F.: Report to the National Defense Research Committee, Office of Scientific Research and Development, Washington, D. C.
- (11) KUBELKA: Kolloid-Z. **55**, 129 (1931).
- (12) PEARSON: Z. physik. Chem. **A156**, 86 (1931).
- (13) RITTER AND DRAKE: Ind. Eng. Chem. **17**, 782, 787 (1945).
- (14) SCHUCHOWITSKI: Kolloid-Z. **66**, 139 (1934).
- (15) SMITH, THORNHILL, AND BRAY: Ind. Eng. Chem. **33**, 1303 (1941); **35**, 972 (1943).
- (16) THOMSON: Phil. Mag. **42**, 448 (1871).

ALTERATION OF THE SIZE AND DISTRIBUTION OF PORES IN CHARCOALS¹

JAMES HOLMES² AND P. H. EMMETT³

Department of Chemical Engineering, The Johns Hopkins University, Baltimore 18, Maryland

Received June 11, 1947

INTRODUCTION

In the course of some of the research work on charcoal conducted by Division 10 of the National Defense Research Committee, it became apparent that charcoal for gas mask use would have to perform the double function of acting as a good adsorbent and as a suitable catalyst or chemical support. Some poison gases could be removed by adsorption, whereas others that might be employed in gas warfare could be removed only by treating the charcoal with certain chemicals which would operate either by direct reaction or by serving as oxidation catalysts. Much was already known about the adsorptive capacity of charcoals and the way of preparing suitable chars for adsorption work. Comparatively little was known as to the structural characteristics and pore distribution that should be possessed by a charcoal that was to serve as a catalyst support. It was rather evident, however, that pore-size distribution would be an important factor.

In order to supplement quickly the supply of charcoal which by certain processes of manufacturing seemed suitable for the preparation of chemically treated charcoals or "whetlerites" (8), it seemed necessary to undertake a program of studying ways and means of transforming good adsorbent charcoals into suitable chars for "whetlerization." Accordingly, the work reported in the present paper was carried out.

The detailed account of the relation between pore distribution and the suitability of a charcoal for making whetlerite is restricted information and will not

¹ Presented at the Symposium on the Adsorption of Gases which was held under the auspices of the Division of Colloid Chemistry at the 110th Meeting of the American Chemical Society, Chicago, Illinois, September 11-12, 1946.

² Present address: Houdry Process Corporation, Marcus Hook, Pennsylvania.

³ Present address: Mellon Institute, Pittsburgh 13, Pennsylvania.

be included in the present report. Nevertheless, in view of the many and diverse uses of charcoal in industry, it seems of interest to recount the findings as to the method and extent to which pore-size alteration could be brought about on adsorbent charcoals of the types that are generally available commercially.

EXPERIMENTAL

Charcoals used

The work reported here was done on three general types of charcoal: (1) those made by the zinc chloride activation process from wood sawdust, (2) those made by steam activation of coconut shells, and (3) those made by proper calcination and activation of coal. The four charcoals may be described in a little more detail as follows:

CWSN 19 was made by the zinc chloride process; a 0.9 ratio of zinc chloride to wood sawdust was used. It had the unusually low ash content of 0.2 per cent. In the process of manufacture, the sample had been given a final calcination at 850°C. The density of the carbon in the sample as revealed by measurements with helium was 2.09.

CWSN 85 differed from CWSN 19 in that it had an ash content of 6.77 per cent and had not been given a final calcination at 850°C. Furthermore, measurements with helium showed that it had a carbon density of 1.81. The ash content in both of these charcoals was probably mostly zinc oxide or zinc carbonate.

The coconut charcoal was a standard product made by the calcination and steam activation of coconut shells. An ash value and carbon density for it are not available.

Sample PCI P58 was made from coal by a process of calcining the finely ground and briquetted coal, and then activating it with steam at temperatures up to 850° or 900°C. It had an ash content of 19.4 per cent.

Impregnation

The base charcoals were dried in an oven at 125°C. before being impregnated. The total volume of the impregnating solution in cubic centimeters was equal to the weight in grams of charcoal used, when the impregnant was added directly in the form of one of its salts. The solution was added dropwise to the charcoal with vigorous stirring to assure uniform mixing. Sufficient weight of the salt was added so that the charcoal would contain the desired percentage of impregnant calculated on the basis of its oxide. In certain cases, the catalyst was added to the charcoal in the form of a solution of one of its salts and subsequently precipitated in the form of the hydroxide by the addition of an excess of ammonium hydroxide. The ammonium hydroxide solution was always added immediately after the addition of the salt solution; 1 cc. of ammonium hydroxide plus salt solution was used for each gram of charcoal. Following the impregnation, the samples were again dried for several hours at 135°C. in an oven.

Specific details of preparation for the various samples may be summarized with respect to the final form of the impregnant as follows:

Cr_2O_3 : Samples were prepared by (a) the direct addition of chromic nitrate

solution; (b) the addition of chromic nitrate solution followed by the addition of concentrated ammonium hydroxide to the charcoal; and (c) the addition of ammonium chromate solution prepared by the addition of two volumes of concentrated ammonium hydroxide solution to one volume of solution of chromic acid.

Fe_2O_3 : Samples were prepared by (a) the direct addition of ferric nitrate solution; and (b) the addition of ferric nitrate solution followed by concentrated ammonium hydroxide.

NiO : Samples were prepared by (a) the direct addition of nickel nitrate solution; (b) the addition of nickel nitrate solution followed by concentrated ammonium hydroxide; and (c) the direct addition of ammoniacal nickel chloride solution previously prepared by the addition of excess ammonium hydroxide to a solution of nickelous oxide in hydrochloric acid.

Mo_2O_3 : The sample was prepared by the addition of a solution of 85 per cent molybdic acid in water which had been made strongly alkaline with ammonium hydroxide.

Na_2CO_3 : The samples were prepared by the direct addition of a solution of the salt.

Treatment of the samples

All steam, hydrogen, and high-temperature oxygen treatments were carried out in quartz or other inert combustion tubes. The size of the samples for all the small-scale treatments varied from about 3 g. with steam or hydrogen, to 1 g. with oxygen. Large-scale treatments were limited to about 40-g. charges by the size of the combustion tubes accommodated by the furnace. The latter was used in a vertical position with the entering gas passing up through the charcoal bed, which was supported upon a fine chromel screen. The rate of flow of the hydrogen or the oxygen-nitrogen mixture was measured at the exit side by a wet-test flowmeter. For the steam runs, rates of steam passage were obtained by using a small, electrically heated boiler in which the liquid level could be read to about 5 cc.

In most cases, the flow rate of the entering gases was sufficiently large to keep the sample "jiggling." This condition was achieved by passing nitrogen as a diluent through the sample during the steam runs. Nitrogen was passed through the sample while the combustion tube was admitted to the furnace, and a very slow flow of nitrogen was passed through while the temperature of the furnace was brought up to the desired value. Nitrogen was again passed through the sample at the end of the run when the tubes were removed and also during cooling outside of the furnace to room temperature.

The bed thickness and flow rate seemed to have a marked effect upon the final product only for runs in which free oxygen was the oxidizing agent. For such runs, high rates of flow and thick beds both appeared to have a deleterious effect by producing much less specificity in the removal of carbon. It was accordingly desirable to have very slow flow rates and thin beds during oxidation with free

oxygen. In order to prepare the large-scale samples by air oxidation, a special furnace having a very large stainless-steel screen was used. The bed depths never exceeded $\frac{1}{2}$ to $\frac{3}{4}$ cm. in thickness; the flow rates were maintained below 0.5 cc./min./gram of charcoal.

The low-temperature oxygen treatments at 350–500°C. were made with compressed air, whereas the high-temperature oxygen runs were made with tank nitrogen which contained a very small percentage of oxygen as an impurity. In the few runs made at 1000°C., using prepurified nitrogen as the entering gas, the source of oxygen for the treatment was oxygen present as combined oxygen in the impregnant.

Adsorption measurements

The change in the pore distribution and size of the charcoal samples was judged by the change in appearance of the nitrogen-adsorption isotherms, as measured in a standard apparatus (3, 5) at -195°C . The general significance of such adsorption measurements as criteria for pore-size distribution in an adsorbent will be discussed below.

RESULTS

In figures 2 to 20 are shown the nitrogen-adsorption isotherms of the samples before and after the specific treatment listed in the legends of the various figures. Figures 2A to 20A give the adsorption results *per gram* of charcoal, due correction always being made for the weight of impregnating material that may have been added. Whenever density values were determined for the treated sample it became possible to express the results as adsorption per cubic centimeter of sample. The volume in this case is that which one measures by pouring the charcoal sample with appropriate tapping into a graduated cylinder. Figures 2B to 20B give the adsorptions *per cubic centimeter* of sample.

In discussing the result of figures 2 to 20 it will be convenient to subdivide the results into sections relating to steaming, hydrogenation, and air oxidation without impregnation; and into a section in which the effects of each of the impregnating agents will be considered. First, however, the use of nitrogen-adsorption isotherms for estimating pore distribution will be discussed. Also, in connection with figure 1 a few generalizations will be attempted as to the effect of various detailed processes that may reasonably be assumed to occur during experiments on pore-size alteration.

Nitrogen adsorption—the criterion of pore-size changes

It is fully realized that nitrogen-adsorption isotherms do not at the present stage of development permit one to calculate quantitatively the exact pore-size distribution of an adsorbent such as charcoal. It is equally certain, however, that such nitrogen isotherms are reliable means of giving a qualitative indication as to the pore-size distribution and of showing with certainty the absence of pores in certain size ranges.

The isotherms will be discussed in terms of three relative pressure regions: the

section corresponding to relative pressure ranges from 0.0 to 0.4 will, for convenience, be called the *AB* region; that between 0.4 and 0.7 will be referred to as the *BC* region; and that between 0.7 and 0.99 as the *CD* region. The selection of these various regions is somewhat arbitrary, though it also has a certain reasonableness based upon the use that was to be made of the charcoals. It is generally agreed, for example, that capillary condensation will not occur at relative pressures lower than that corresponding to four molecular diameters, as calculated by the Kelvin (13) equation

$$D = \frac{-4\sigma V \cos \theta}{RT \, 2.303 \log p/p_0}$$

where σ is the surface tension of the adsorbate, θ is the angle of wetting of the adsorbate on the solid, V is the molal volume of the liquefied adsorbate, p is the pressure at which the adsorption is being measured, and p/p_0 is the liquefaction pressure of the adsorbate at the temperature of the experiment, T . For nitrogen, this point is at approximately 0.4 relative pressure (actually 0.35 if one uses the value 8.6 (7) for the surface tension of liquid nitrogen at -195°C .) It appears, therefore, that the nitrogen adsorption up to 0.4 relative pressure includes that which is present as a monolayer over the entire surface of small and large capillaries plus such multilayer adsorption (equal to or less than about 0.5 layer) as would be expected at a relative pressure of 0.4 (3). Roughly speaking then, the adsorption up to 0.4 relative pressure should be a measure of the adsorption capacity of a charcoal over the range of relative pressures that might be encountered in any gas mask work. The absolute value of this nitrogen adsorption at 0.4 relative pressure rather than the slope of the adsorption curve will be used, then, in discussing the changes in adsorption capacity brought about by treating the charcoals.

If an adsorption isotherm for nitrogen is flat above 0.4 relative pressure, it appears certain (3) that there is no appreciable number of pores present of a size covered by the relative pressure range 0.4–0.99. The numerical values assigned to pores corresponding to this relative pressure range depend upon assumptions that one makes as to the structure of the charcoal. If one assumes that the capillaries are cylindrical, that the condensed nitrogen has the same density and surface tension as bulk liquid nitrogen, and that the angle of wetting is zero, one finds by equation 1 that the relative pressure range 0.4–0.99 corresponds to pore diameters between about 20 and 1800 Å. On the other hand, if the pores are assumed to consist of cracks with plane parallel walls, distances between the plane parallel walls calculated would be one-half as large as the diameter calculated for the cylindrical capillaries. In the present discussion, any slope in the regions *BC* or *CD* will be attributed to the presence of capillaries in the size ranges that one would calculate from equation 1 (11). No quantitative estimate of the number and distribution of the pores can be made from the nitrogen isotherms, however, because of the difficulty or impossibility of distinguishing between multilayer adsorption in this relative pressure range and the filling of capillaries by capillary condensation. (See, however, the work of Wheeler on silica gels as reported by Beeck (2)).

The reason for breaking the region between 0.4 and 0.99 relative pressure into the two sections *BC* and *CD* has to do with some of the service tests that are applied to charcoal. Many tests on certain poison gases were made at 80 per cent relative humidity, since charcoals behaved differently toward some gases when moist than when dry, and since 80 per cent relative humidity seemed a reasonable upper limit to any humidity that might be encountered frequently in actual use. The exact pore size that would remain filled with water when the relative humidity is dropped to 80 per cent will, of course, depend upon the angle of wetting of the charcoal by water. In some work carried out by Pierce, Blacet, and Juhola (10) there seems reason to believe that in desorption this angle of wetting may be about 0.6 for most charcoals. The adsorption of nitrogen at 0.7 relative pressure should, accordingly, correspond approximately to the filling of all pores that would remain filled with water if the relative pressure were reduced to 80 per cent. Pores larger than this should remain open and, therefore, available as catalyst supports or as chemical supports for any whetlerizing agents that might be present.

The *CD* region corresponds to pores which, according to equation 1 applied to cylindrical capillaries, lie between 70 A. and 1800 A. in diameter. Such pores in all probability are very important as channels through which the larger inner surface of the charcoal particles can be reached by adsorbate gases. Here, too, the slope and not the absolute value of the *CD* region is important, since the slope of this region is a qualitative measure of the volume of pores in this size range.

It is now realized that pores larger than 1800 A. in diameter may also be very important in the performance of a charcoal (10). No indication of the pore size or pore-size distribution above 1800 A. was obtained in the present work, though methods are now known for making such measurements (4, 6, 12, 14).

Generalizations as to separate pore-alteration actions

A little reflection will show that the various possible effects of steam, hydrogen, or other activating agents on the pore size and distribution may be divided into about six separate actions. These six cases will now be briefly described in conjunction with figure 1.

For the sake of simplicity, we shall assume that the isotherm of the original charcoal is flat like that of CWSN 19 in the *N* curve of figure 2. We shall also assume that the charcoal with which we start is already activated to such a point that the walls between the capillaries are only about four carbon layers thick and the capillaries are 20 A. or less in diameter. Under these circumstances about one-half of the carbon atoms are actually on the surface of some of the capillaries. This means that on further activating the charcoal, one might strip off as much as a layer of carbon on each capillary without breaking down the walls between the cracks or capillaries. We shall also assume that large pores belong either to the region that would undergo capillary condensation between 0.4 and 0.7 relative pressure (*BC* region), between 0.7 and 0.99 relative pressure (*CD* region), or at relative pressures greater than 0.99. An increase in pores in the *BC* or *CD* region will be qualitatively indicated in figures 1A and 1B by a uniform posi-

tive slope of the isotherm over the region involved. With these simplifications in mind, we may proceed to consider the adsorption per gram and the adsorption per cubic centimeter for the treated sample (designated by T in figure 1) and the original sample, O, for six possible cases.

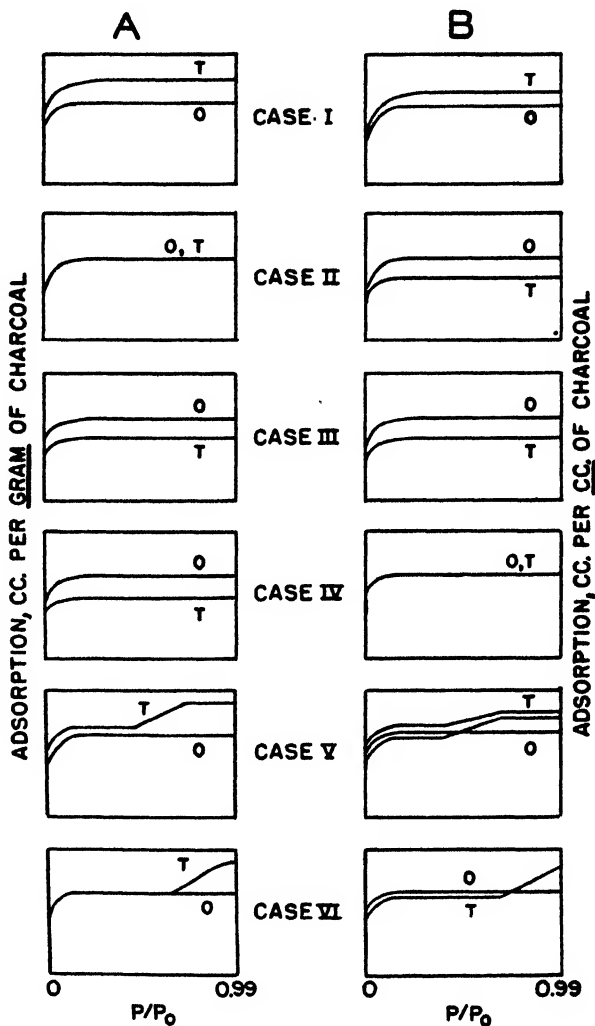


FIG. 1

Case I: Removing a layer of carbon from the smallest pore and opening up new pores without, however, forming any larger than 20 Å. in diameter. The adsorption would increase as indicated in figures 1A and 1B, the increase on a weight basis being somewhat larger than on a volume basis. Figures 1A and 1B are so drawn that the displacement of the isotherms on a weight basis can be

compared directly with the change on a volume basis. This result becomes clearest if one visualizes the 1B figures in terms of a block of charcoal 1 cc. on a

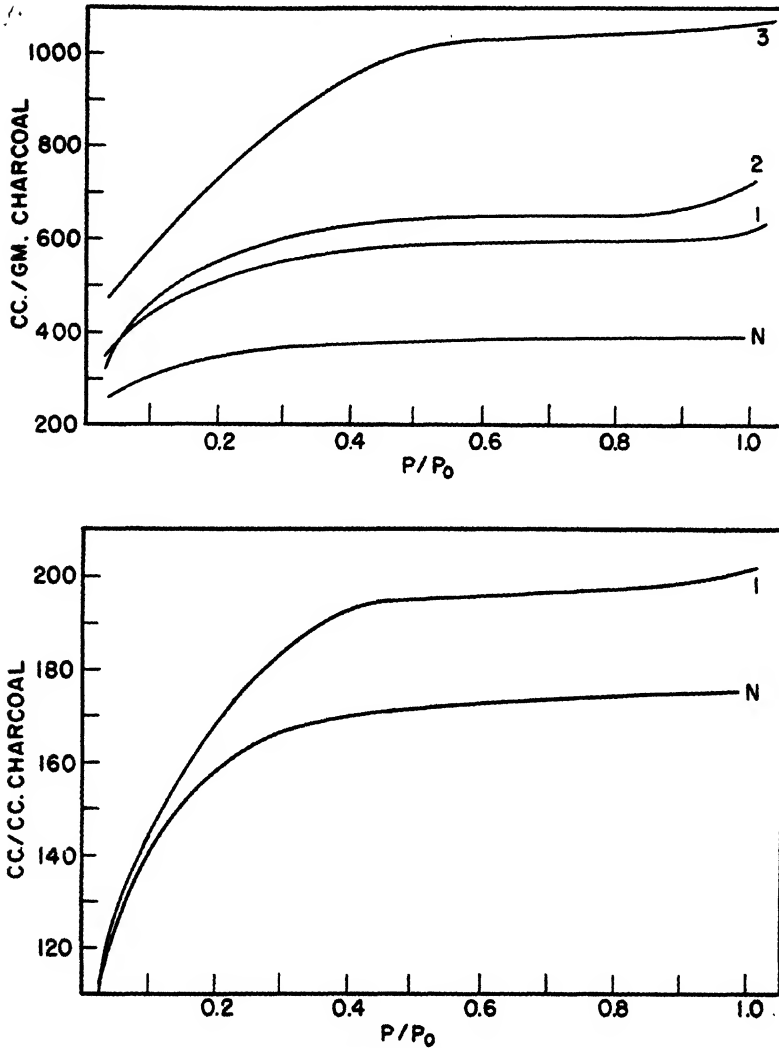


Fig. 2A (upper), 2B (lower). Charcoal CWSN 19

N, untreated base charcoal

1, steamed at 750°C. to 43 per cent loss

2, steamed at 750°C. to 62 per cent loss

3, steamed at 750°C. to 94.5 per cent loss

side as the starting material and then keeps in mind the effect of the treatment on the weight of the sample.

Case II: Small pores are attacked so vigorously as to convert some of them over at least part of their length into capillaries too large to show capillary condensation at 0.99 relative pressure. The adsorption per gram will remain unchanged (neglecting multilayer adsorption on the relatively small surface associated with the large pores), since it is assumed that the average wall thickness of the small capillaries is not altered but that large groups of them by localized attack are converted into very large pores. On the other hand, the adsorption per cubic centimeter is greatly decreased, since large holes having small area are left unfilled by adsorbate at 0.99 relative pressure.

Case III: The impregnant plugs a certain fraction of the small pores. The adsorption on the weight and volume basis will both decrease by the same percentage. This might also result from a closing of small capillaries by growth of graphite crystals during heat treatment.

Case IV: The particles shrink as a result of increase in density of the carbon samples. The adsorption per gram will then decrease, since all pores will become smaller. Calculations indicate that the adsorption per cubic centimeter will probably remain unchanged, since the pore volume per cubic centimeter will be approximately the same as before the particles were shrunk by heat treatment.

Case V: The small pores are converted into pores in the *BC* region by a chemical attack which decreases the thickness of some cell walls and completely removes others. As shown in figure 1B, the total adsorption per cubic centimeter at 0.99 relative pressure will be a little larger than for the original sample, because some carbon will have been removed in the treatment. The total surface area per cubic centimeter will be increased slightly as a result of enlarging pores of any shape by thinning the walls or of producing cylindrical pores in the *BC* region by completely removing pore walls. However, removing pore walls from a structure containing either square or rectangular pores would decrease surface area per cubic centimeter. Accordingly, in Case V, figure 1B, the *AB* region is designated as being subject to either an increase or a decrease when pores less than 20 Å. in diameter are transformed into pores in the 20–70 Å. range. On a weight basis the treatment indicated for Case V would increase the total pore volume filled with adsorbate at 0.99 to a greater extent than on the volume basis by the same reasoning applied to Case I. However, the total surface area per gram of sample would, as indicated in figure 1A, always increase slightly regardless of the shape of the pores.

Case VI: The small pores are converted into pores in the *CD* region without change in thickness of remaining walls. By the same reasoning applied in Case V, the increase in pore volume will be greater on a weight than on a volume basis. The *AB* region will be lower on a volume basis as a result of removal of pore walls, regardless of the capillary shape, and will be practically unchanged on a weight basis.

By suitable combinations of these effects, it is believed that all of the results reported in the present paper can be explained. Attention will be called in the following discussion to examples in figures 2 to 20 that apparently illustrate these, though most of the effects are, as would be expected, combinations of several of these separate cases.

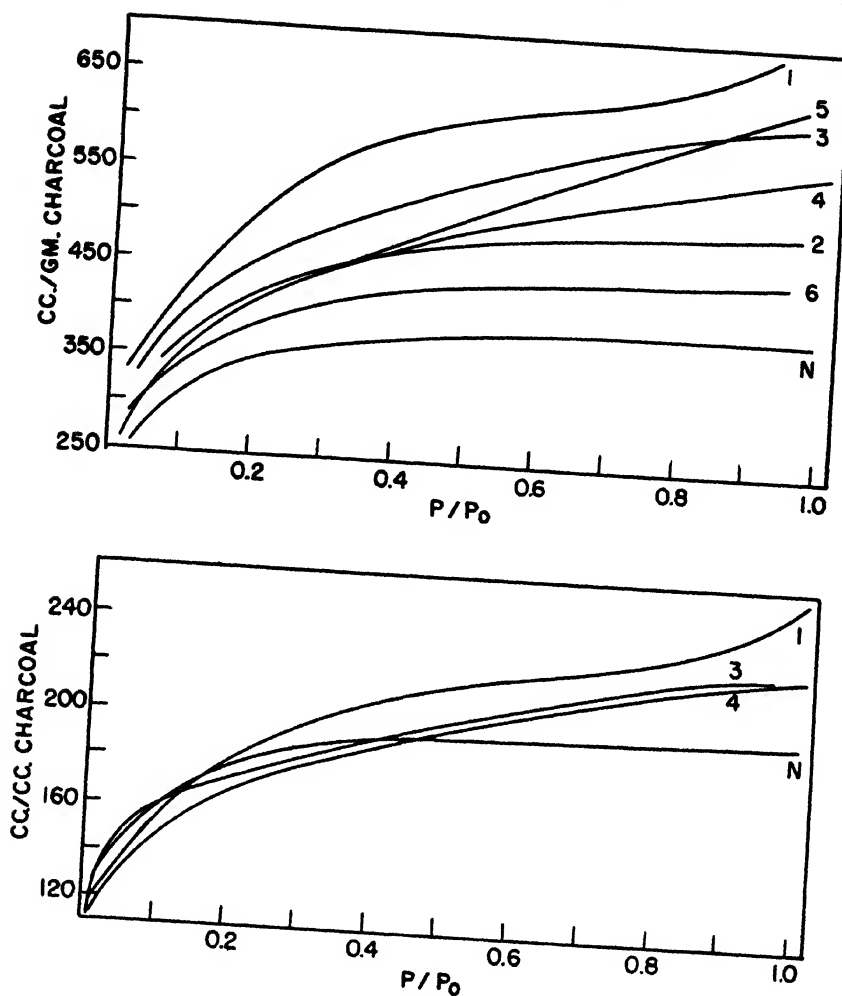


FIG. 3A (upper), 3B (lower). Charcoal CWSN 19
 N, untreated base charcoal
 1, 0.2 per cent Cr_2O_3 (from ammonium chromate), steamed at 750°C . to 58 per cent loss
 2, 1 per cent Cr_2O_3 (from ammonium chromate), steamed at 750°C . to 27 per cent loss
 3, 1 per cent Cr_2O_3 (from ammonium chromate), steamed at 750°C . to 49 per cent loss
 4, 5 per cent Cr_2O_3 (from ammonium chromate), steamed at 750°C . to 46 per cent loss
 5, 5 per cent Cr_2O_3 (from chromic nitrate), steamed at 750°C . to 46 per cent loss
 6, 5 per cent Cr_2O_3 (from chromic nitrate + excess ammonium hydroxide), steamed at 750°C . to 44 per cent loss

Effect of steaming without impregnation

The activation of charcoals by steaming has been a standard procedure for many years (9). It is not surprising therefore that, as shown in figures 2A, 12A, 17A, and 19A, the effect of steaming is predominantly to increase the ad-

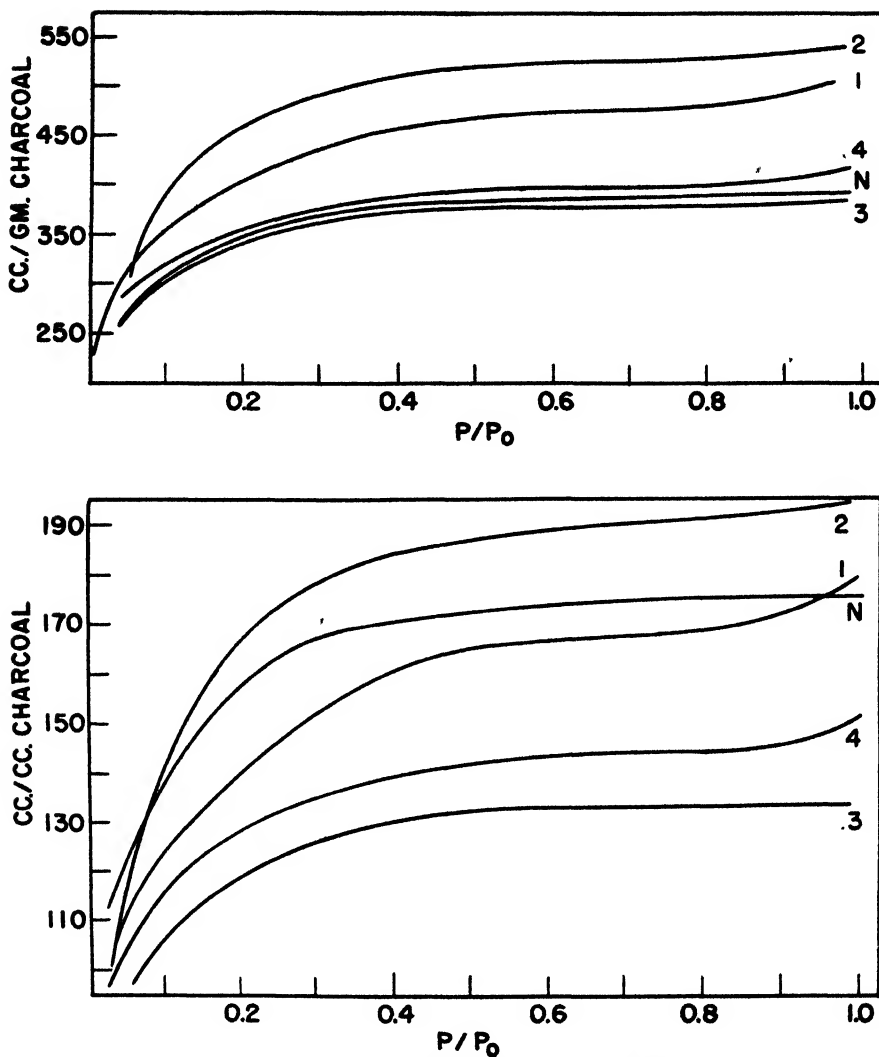


FIG. 4A (upper), 4B (lower). Charcoal CWSN 19

N, untreated base charcoal

1, 5 per cent Fe_2O_3 (from ferric nitrate), steamed at 750°C . to 37 per cent loss

2, 5 per cent Mo_2O_3 (from molybdic acid + excess ammonium hydroxide), steamed at 750°C . to 41 per cent loss

3, 5 per cent NiO (from nickel chloride + excess ammonium hydroxide), steamed at 750°C . to 43 per cent loss

4, Charcoal CWSN 19 TPE-1 (containing cupric oxide), steamed at 750°C . to 26 per cent loss

sorption per gram, as evidenced by the amount of adsorption at 0.4 relative pressure (Case I), without altering materially the slope of the rest of the isotherm.

Such an increase is logically to be expected as resulting from the opening up of new small pores in the charcoal and from slight enlargement of small pores al-

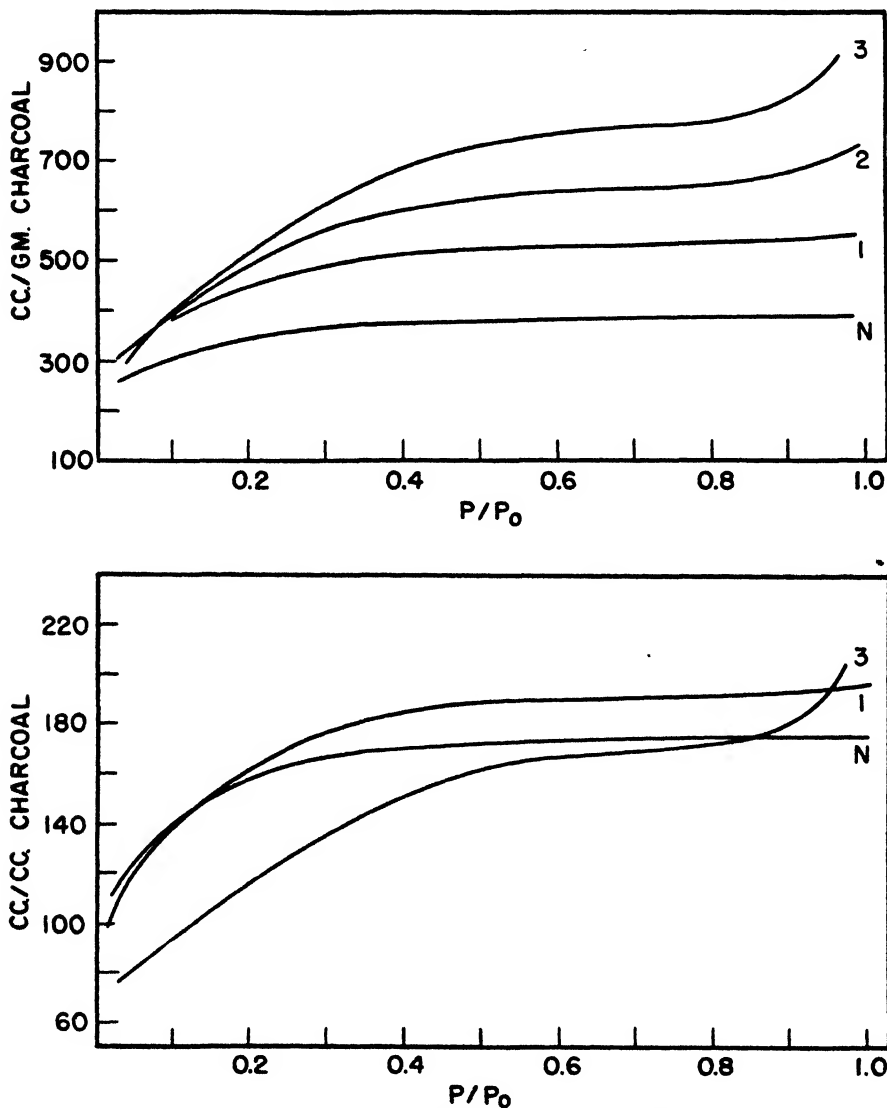


FIG. 5A (upper), 5B (lower). Charcoal CWSN 19

N, untreated base charcoal

1, treated with hydrogen at 1000°C. to 26 per cent loss

2, treated with hydrogen at 1000°C. to 48 per cent loss

3, treated with hydrogen at 1000°C. to 74 per cent loss

ready present. It is likewise not unexpected that, as illustrated by runs 1 and 2, figure 17B, steaming might decrease the adsorption per cubic centimeter. This

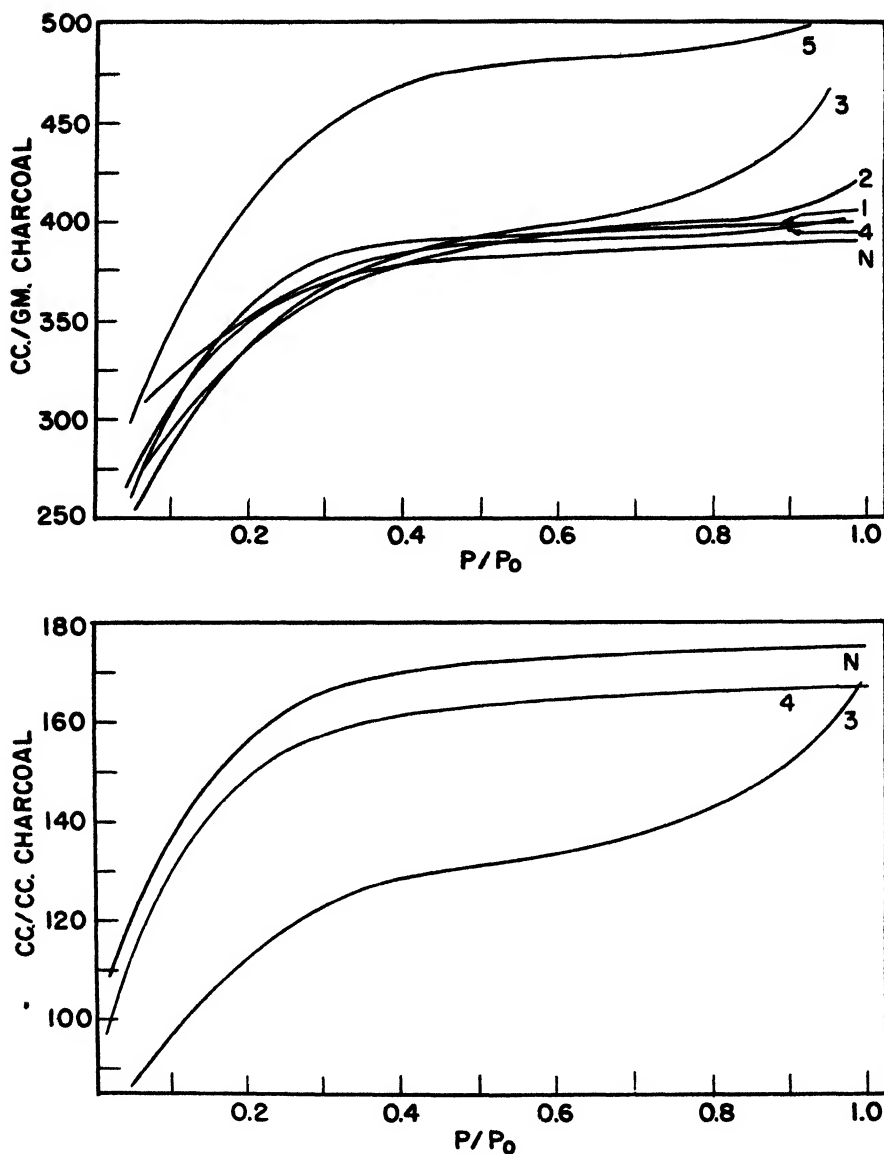


FIG. 6A (upper), 6B (lower). Charcoal CWSN 19

N, untreated base charcoal

1, 1 per cent Cr_2O_3 (from chromic nitrate), treated with hydrogen at 1000°C . to 21 per cent loss

2, 1 per cent Cr_2O_3 (from ammonium chromate), treated with hydrogen at 1000°C . to 40 per cent loss

3, 1 per cent Cr_2O_3 (from ammonium chromate), treated with hydrogen at 1000°C . to 62 per cent loss

4, 5 per cent Mo_2O_3 (from molybdic acid + excess ammonium hydroxide), treated with hydrogen at 1000°C . to 26 per cent loss

5, 5 per cent Na_2O (from sodium carbonate), treated with hydrogen at 1000°C . to 32 per cent loss

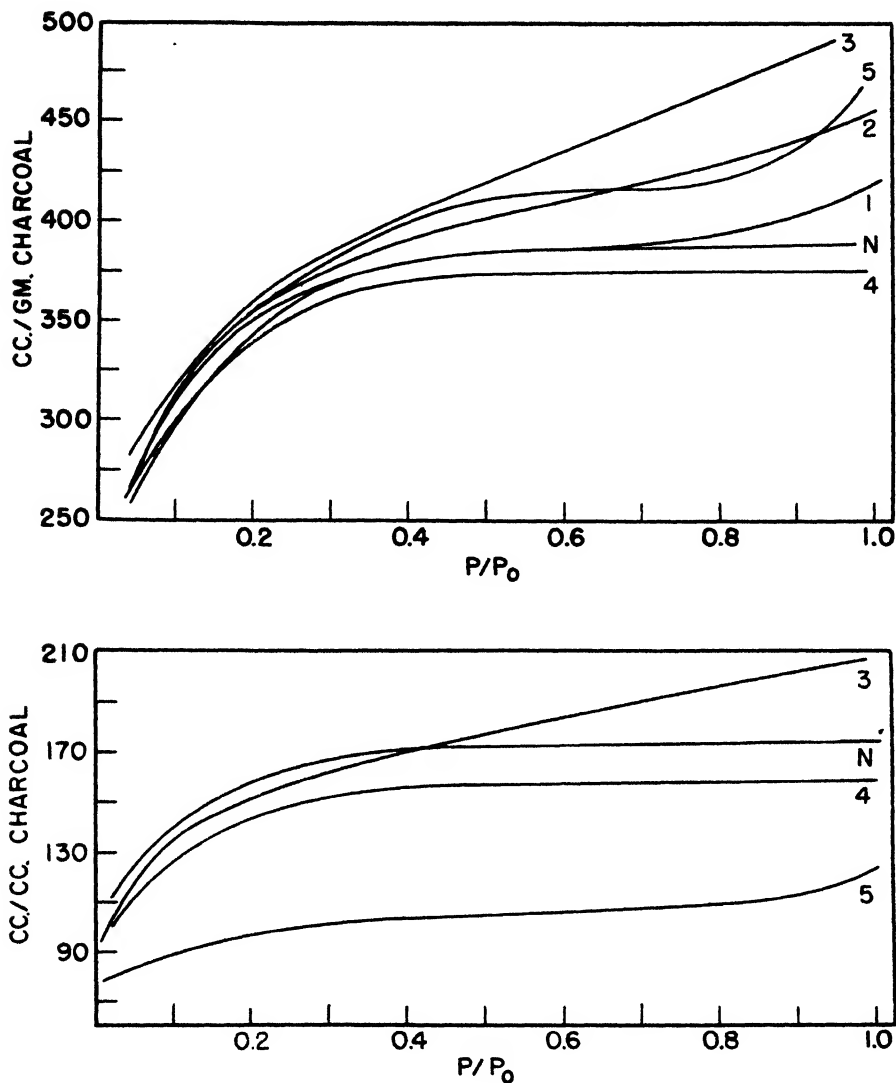


FIG. 7A (upper), 7B (lower). Charcoal CWSN 19

N, untreated base charcoal

- 1, 1 per cent NiO (from nickel nitrate), treated with hydrogen at 1000°C. to 15 per cent loss
- 2, 5 per cent NiO (from nickel nitrate), treated with hydrogen at 1000°C. to 29 per cent loss
- 3, 5 per cent NiO (from nickel nitrate + excess ammonium hydroxide), treated with hydrogen at 1000°C. to 27 per cent loss
- 4, 5 per cent NiO (from nickel chloride + excess ammonium hydroxide), treated with hydrogen at 1000°C. to 25 per cent loss
- 5, 5 per cent NiO (from nickel chloride + excess ammonium hydroxide), treated with hydrogen at 1000°C. to 81 per cent loss

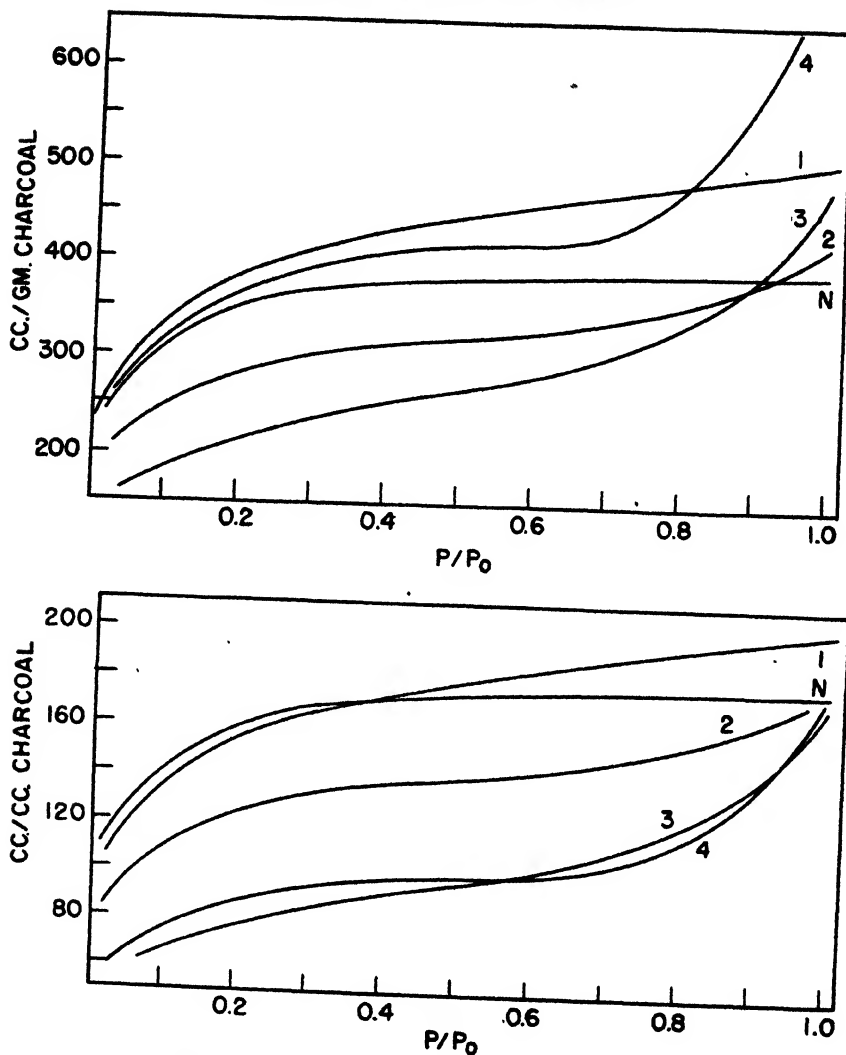


FIG. 8A (upper), 8B (lower). Charcoal CWSN 19
N, untreated base charcoal

- 1, 0.2 per cent Fe_2O_3 (from ferric nitrate + excess ammonium hydroxide), treated with hydrogen at 1000°C . to 15 per cent loss
- 2, 1 per cent Fe_2O_3 (from ferric nitrate), treated with hydrogen at 1000°C . to 15 per cent loss
- 3, 5 per cent Fe_2O_3 (from ferric nitrate), treated with hydrogen at 1000°C . to 32 per cent loss
- 4, 5 per cent Fe_2O_3 (from ferric nitrate + excess ammonium hydroxide), treated with hydrogen at 1000°C . to 50 per cent loss

can result from the removal of pores of all sizes along the sides of major cracks or crevices that are larger than 1800 Å. in diameter (Case II) to an extent more than enough to compensate for the new pores being formed.

Two interesting observations on steaming were made on charcoal CWSN S5. Steaming the original charcoal at the usual temperature of 750°C. produced

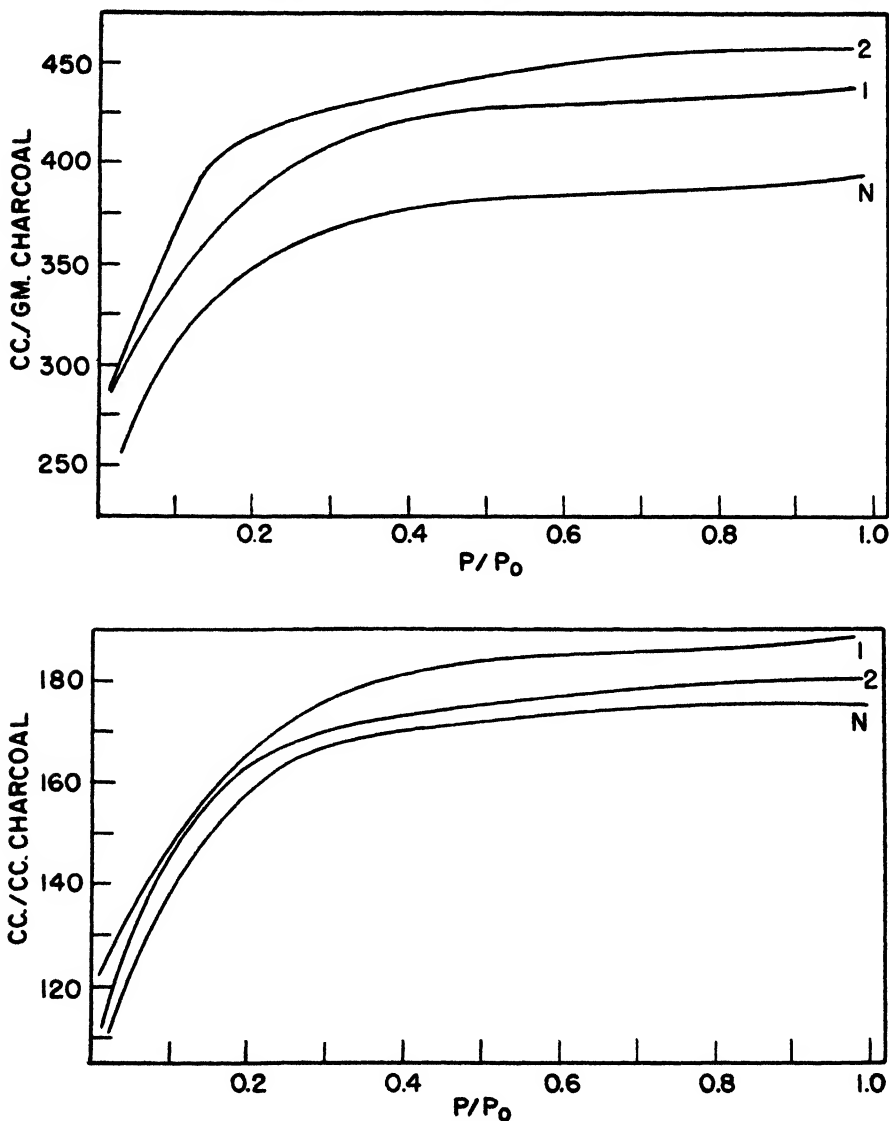


FIG. 9A (upper), 9B (lower). Charcoal CWSN 19

N, untreated base charcoal

1, treated with oxygen-nitrogen mixture at 450°C. to 30 per cent loss

2, treated with oxygen-nitrogen mixture at 750°C. to 40 per cent loss

little change in adsorption on either a volume or a weight basis, as is evidenced by curves 3 and 4 in figures 12A and 12B. When, however, the charcoal was first heat-treated in a stream of nitrogen to 1200°C., with a resulting shrinkage

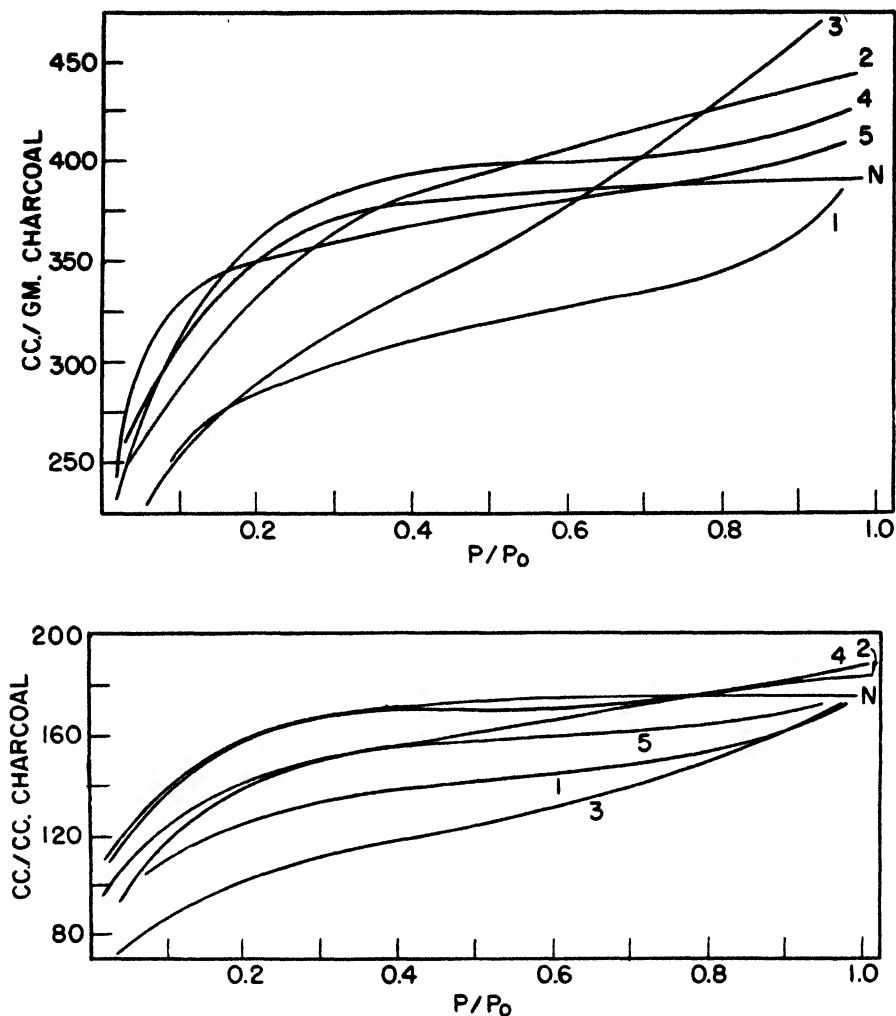


FIG. 10A (upper), 10B (lower). Charcoal CWSN 19

N, untreated base charcoal

- 1, 5 per cent Fe_2O_3 (from ferric nitrate + excess ammonium hydroxide), treated with tank nitrogen at 750°C . to 14 per cent loss
- 2, 5 per cent Fe_2O_3 (from ferric nitrate + excess ammonium hydroxide), treated with tank nitrogen at 500°C . to 28 per cent loss
- 3, 5 per cent Fe_2O_3 (from ferric nitrate + excess ammonium hydroxide), treated with air at 350°C . to 48 per cent loss
- 4, 1 per cent Fe_2O_3 (from ferric nitrate + excess ammonium hydroxide), treated with tank nitrogen at 750°C . to 21 per cent loss
- 5, 5 per cent Cr_2O_3 (from chromic acid + excess ammonium hydroxide), treated with tank nitrogen at 1000°C . to 19 per cent loss

of the particle and increase in the helium density of the carbon from 1.81 to 2.17, the sample became susceptible to further activation by steaming. Curve 5 of figures 12A and 12B shows the adsorption after the 1200°C . sintering (prob-

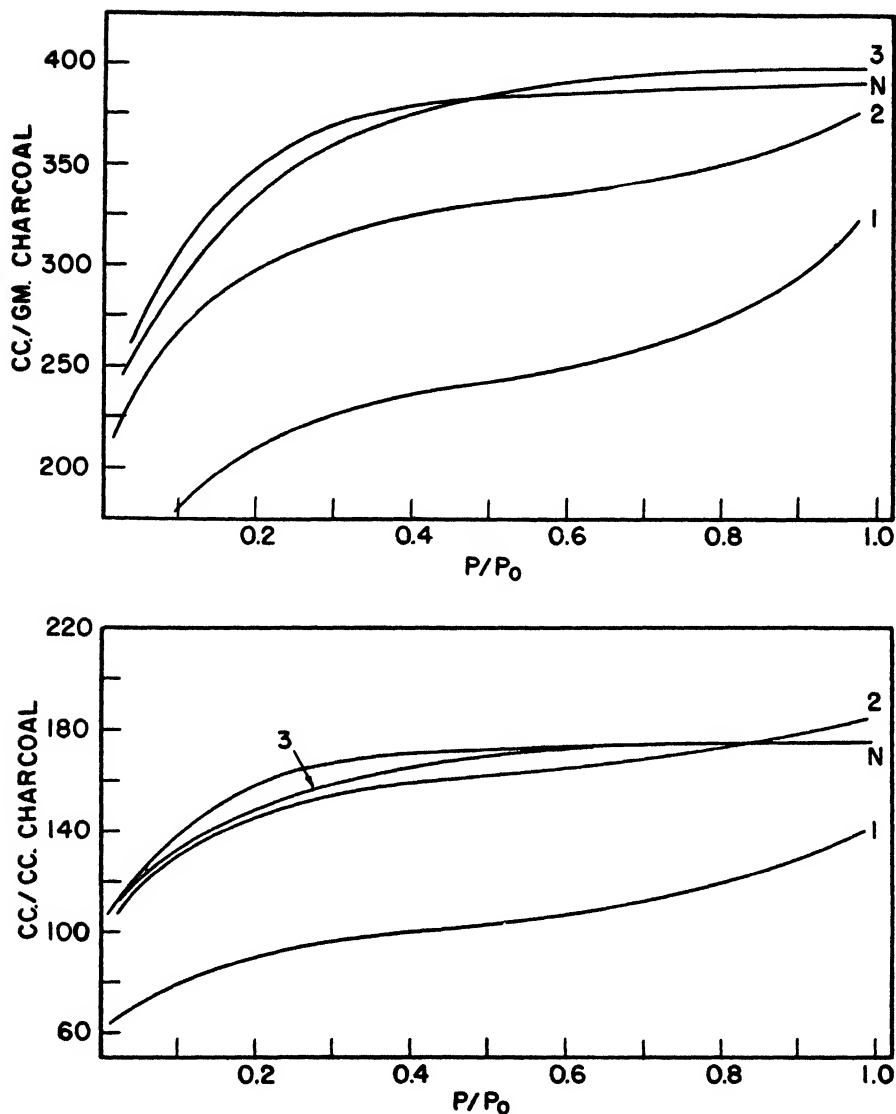


FIG. 11A (upper), 11B (lower). Charcoal CWSN 19

N, untreated base charcoal

- 1, 5 per cent Fe_2O_3 (from ferric nitrate + excess ammonium hydroxide), treated with tank nitrogen at 1000°C . to 13 per cent loss
- 2, 1 per cent Fe_2O_3 (from ferric nitrate + excess ammonium hydroxide), treated with tank nitrogen at 1000°C . to 8 per cent loss
- 3, 5 per cent Fe_2O_3 (from ferric nitrate + excess ammonium hydroxide), treated with tank nitrogen at 500°C . to 12 per cent loss

ably Cases III and IV), and curves 1 and 2 of these figures show the extent of activation by steaming after the heat-treatment at 1200°C .

The second interesting observation on steaming CWSN S5 was the extent to

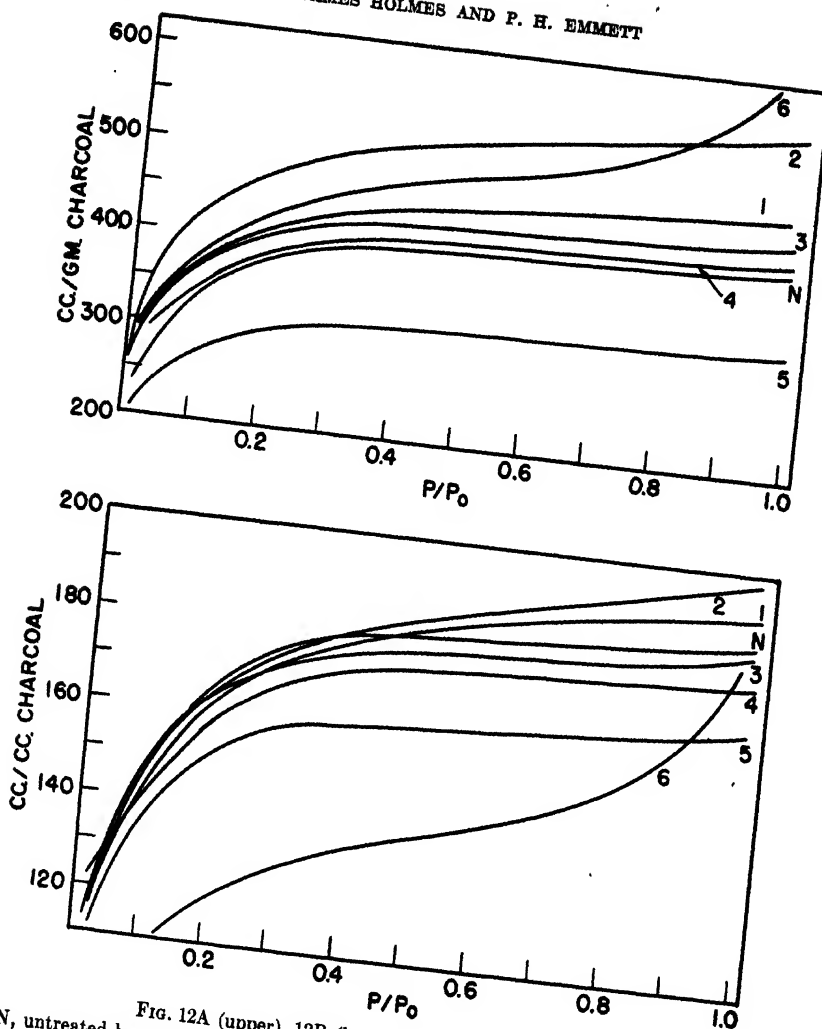


FIG. 12A (upper), 12B (lower). Charcoal CWSN S5
 N, untreated base charcoal
 1, heated at 1200°C. in pure nitrogen, followed by steam treatment at 750°C. to 44 per cent loss
 2, heated at 1200°C. in pure nitrogen, followed by steam treatment at 750°C. to 46 per cent loss
 3, steamed at 750°C. to 46 per cent loss
 4, steamed at 750°C. to 55 per cent loss
 5, heated for 2 hr. in pure nitrogen at 1200°C.
 6, steamed at 1000°C. to 72 per cent loss

which a large number of capillaries in the range 20–1800 Å. in diameter can be opened up if the steaming is sufficiently severe. This is illustrated by curve 6 of figures 12A and 12B. Apparently, the pore walls between the tiny capil-

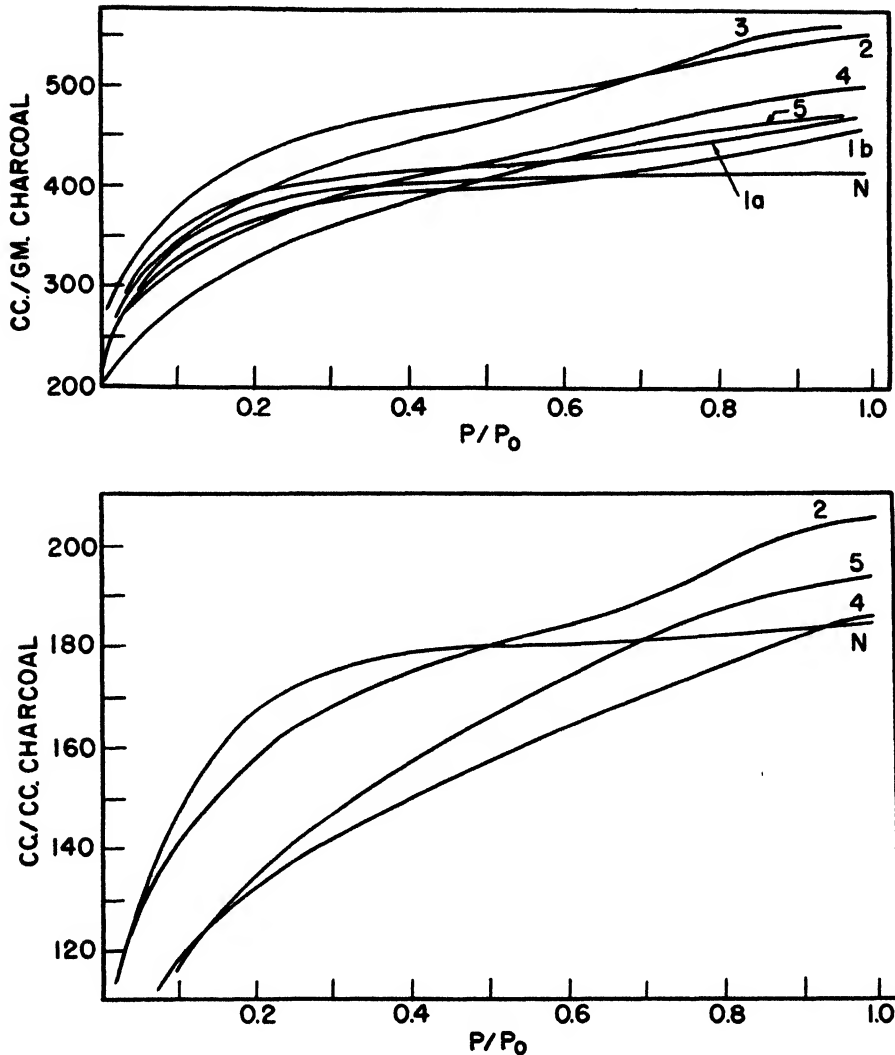


FIG. 13A (upper), 13B (lower). CWSN S5

N, untreated base charcoal

1, large batch of 0.2 per cent Cr_2O_3 (from chromic acid + excess ammonium hydroxide), steamed at 750°C . to (a) 35 per cent and (b) 32 per cent loss

2, 0.2 per cent Cr_2O_3 (from chromic acid + excess ammonium hydroxide), steamed at 750°C . to 39 per cent loss

3, 1 per cent Cr_2O_3 (from chromic acid + excess ammonium hydroxide), steamed at 750°C . to 49 per cent loss

4, 5 per cent Cr_2O_3 (from chromic acid + excess ammonium hydroxide), steamed at 750°C . to 52 per cent loss

5, CWSN S5 TNW 2697 (containing cupric oxide), steamed at 750°C . to 38 per cent loss

laries are eaten away by the strong steaming of the sample at 1000°C ., with a resulting transformation of small pores into those capable of undergoing capillary

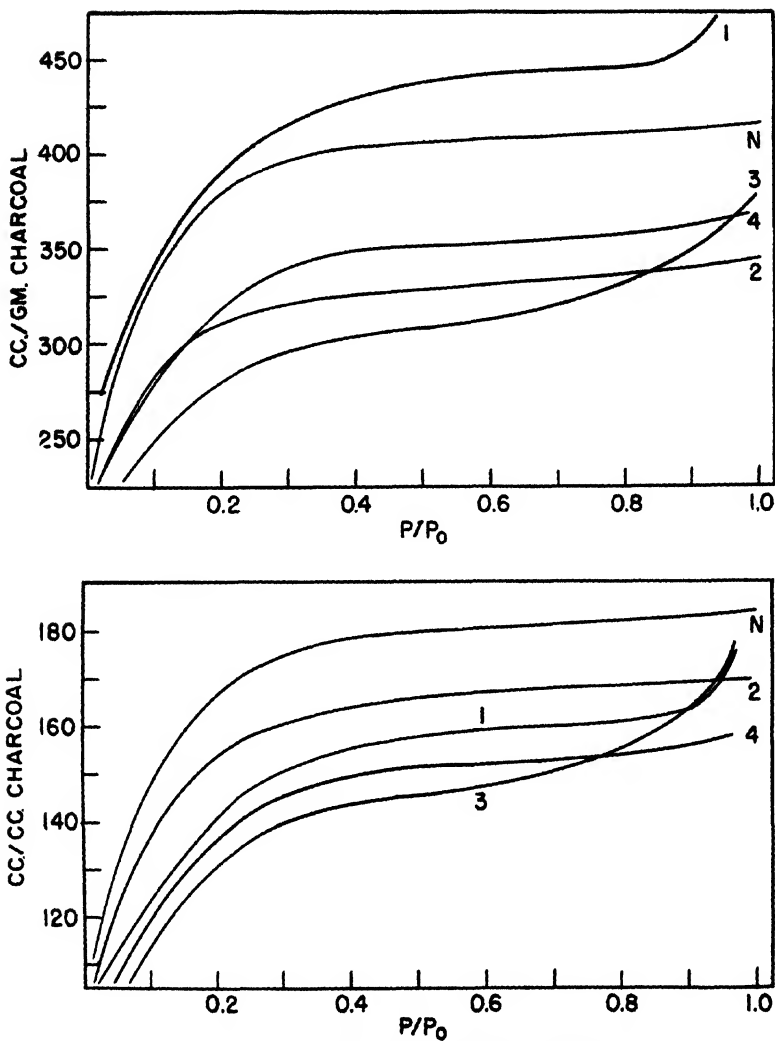


Fig. 14A (upper), 14B (lower). Charcoal CWSN S5

N, untreated base charcoal

1, treated with hydrogen at 1000°C. to 37 per cent loss

2, 1 per cent Cr_2O_3 (from chromic nitrate), treated with hydrogen at 1000°C. to 18 per cent loss

3, 1 per cent Cr_2O_3 (from chromic nitrate), treated with hydrogen at 1000°C. to 29 per cent loss

4, 5 per cent NiO (from nickel nitrate + excess ammonium hydroxide), treated with hydrogen at 1000°C. to 42 per cent loss

condensation in the 0.4–0.99 relative pressure range. It will be noticed that the adsorption at 0.4 relative pressure increased 20 per cent on a weight basis

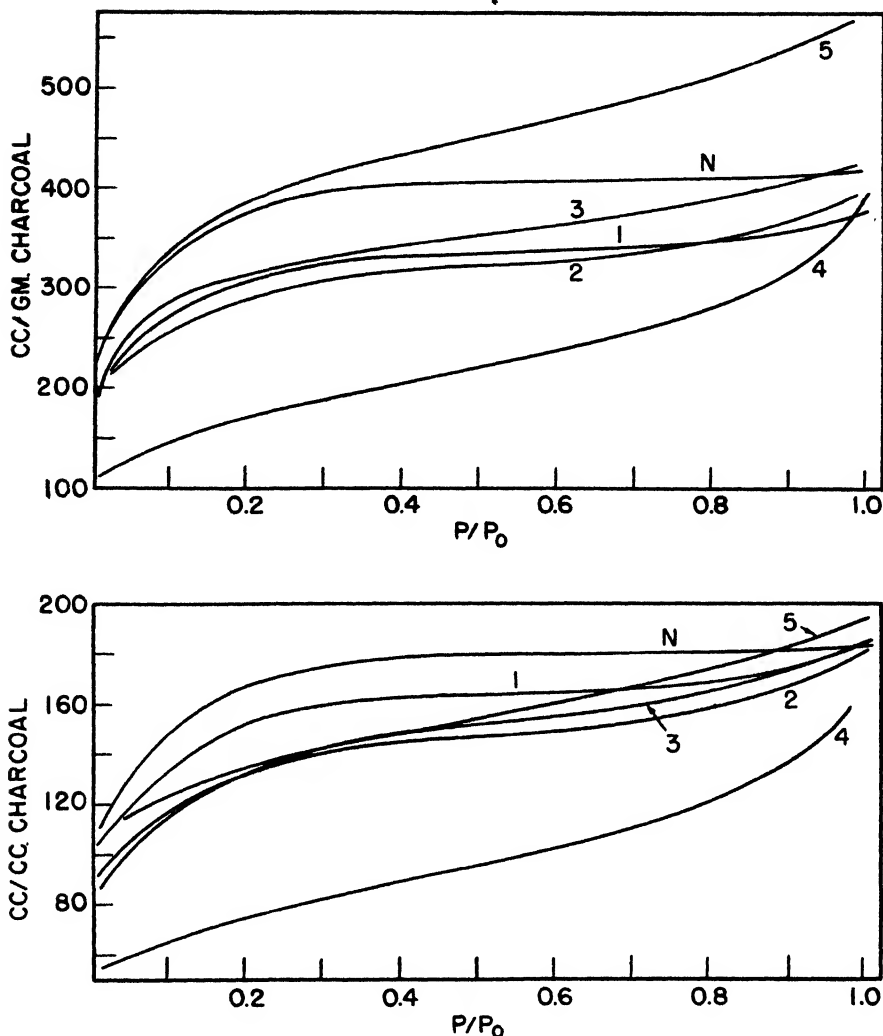


FIG. 15A (upper), 15B (lower). Charcoal CWSN S5

N, untreated base charcoal

1, 1 per cent Fe_2O_3 (from ferric nitrate), treated with hydrogen at 1000°C . to 21 per cent loss

2, 1 per cent Fe_2O_3 (from ferric nitrate), treated with hydrogen at 1000°C . to 34 per cent loss

3, 5 per cent Fe_2O_3 (from ferric nitrate + excess ammonium hydroxide), treated with hydrogen at 1000°C . to 30 per cent loss

4, 5 per cent Fe_2O_3 (from ferric nitrate), treated with hydrogen at 1000°C . to 37 per cent loss

5, 5 per cent Fe_2O_3 (from ferric nitrate + excess ammonium hydroxide), treated with hydrogen at 600°C . to 30 per cent loss

but decreased by about 30 per cent by this very strong steaming at 1000°C . on a volume basis. This is consistent with the transformation of small pores

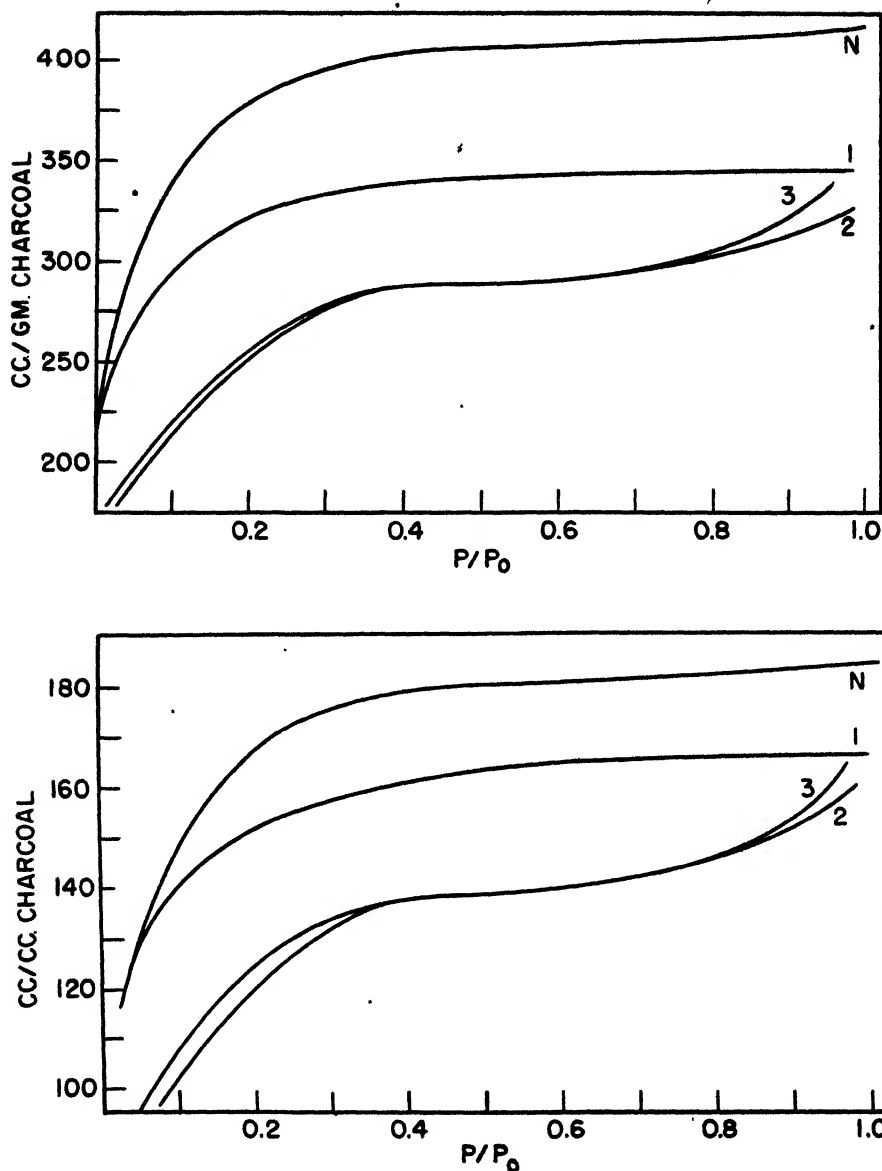


FIG. 16A (upper), 16B (lower). Charcoal CWSN S5

N, untreated base charcoal

1, treated with tank nitrogen at 1000°C. to 19 per cent loss

2, 5 per cent Fe_2O_3 (from ferric nitrate + excess ammonium hydroxide), treated with pure nitrogen at 1000°C. to 15 per cent loss

3, 5 per cent Fe_2O_3 (from ferric nitrate + excess ammonium hydroxide), treated with tank nitrogen at 1000°C. to 25 per cent loss

into those influencing the *BC* and *CD* regions (Cases V and VI) together with the formation of some new pores greater than 1800 Å. in diameter (Case II).

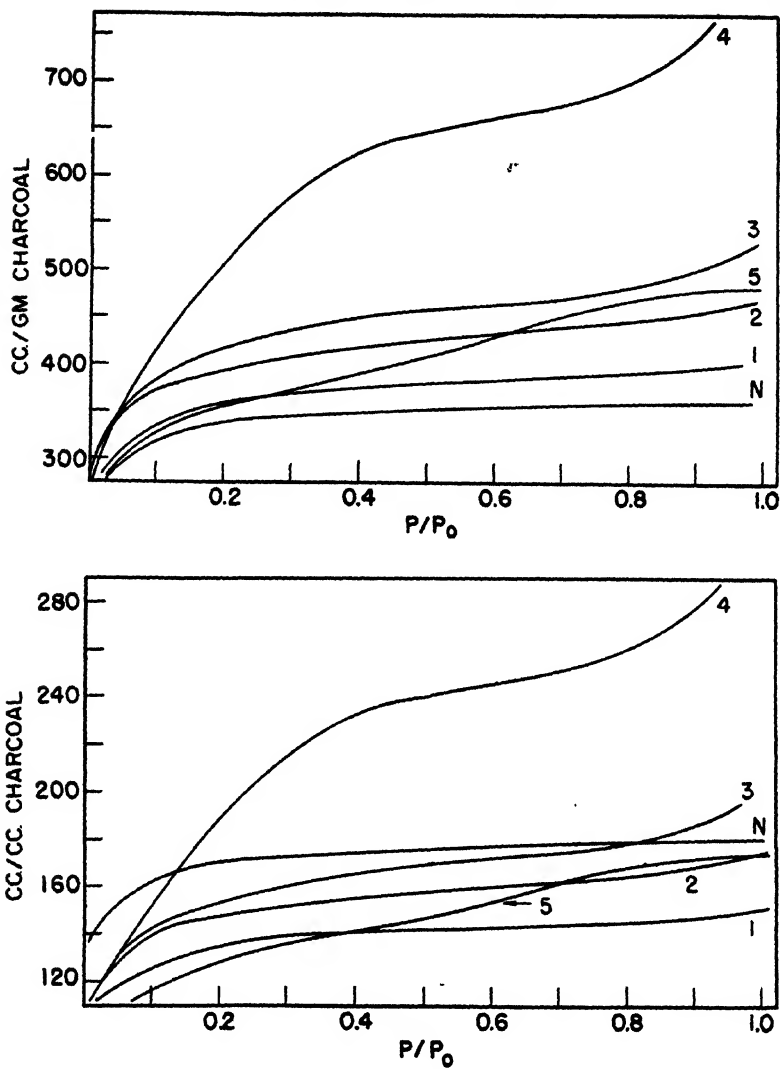


FIG. 17A (upper), 17B (lower). Coconut charcoal

N, untreated base charcoal

1, steamed at 750°C. to 24 per cent loss

2, steamed at 750°C. to 40 per cent loss

3, steamed at 750°C. to 64 per cent loss

4, 0.2 per cent Cr_2O_3 (from chromic acid + excess ammonium hydroxide), steamed at 750°C. to 33 per cent loss5, 5 per cent Cr_2O_3 (from chromic acid + excess ammonium hydroxide), steamed at 750°C. to 39 per cent loss

It is not known with certainty, at present, whether the radical change in the pore distribution illustrated by curve 6 of figure 12 is due to a peculiarity of

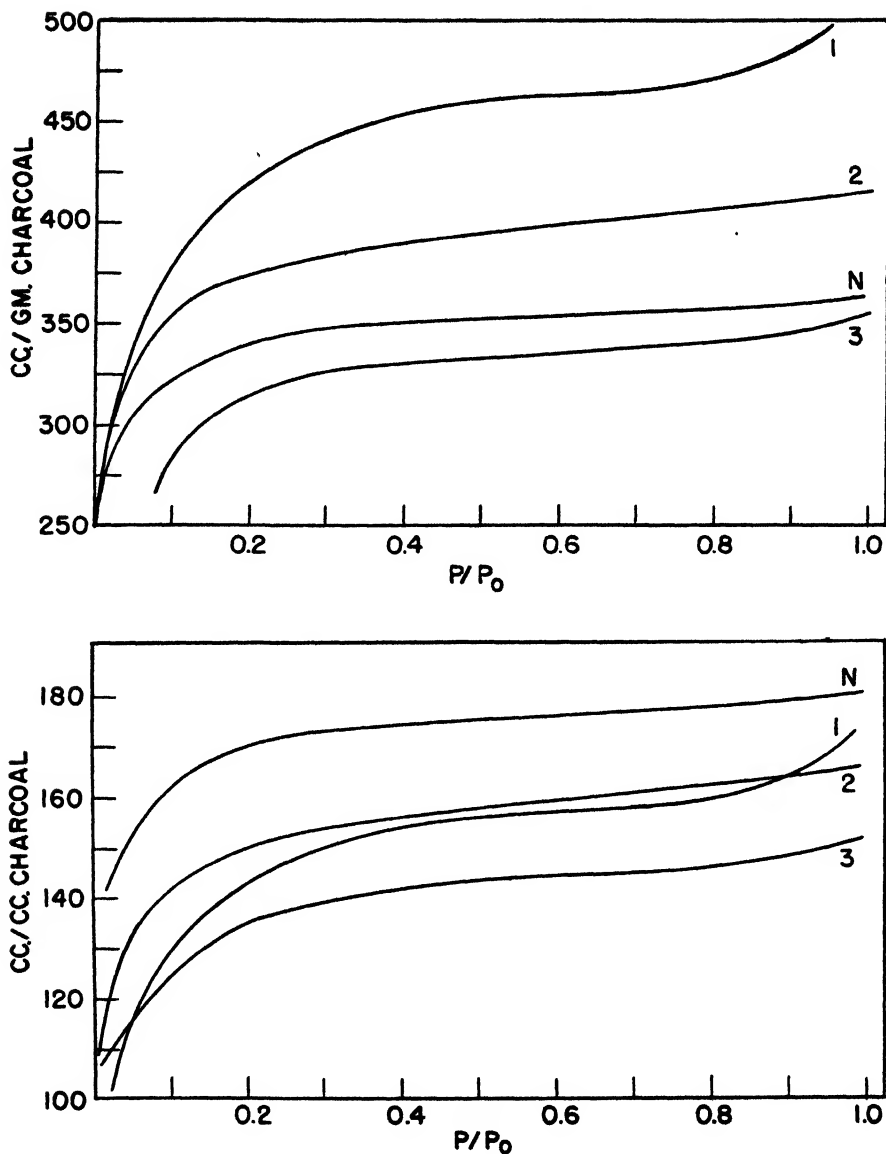


FIG. 18A (upper), 18B (lower). Coconut charcoal

N, untreated base charcoal

1, treated with hydrogen at 1000°C. to 31 per cent loss

2, 0.2 per cent Cr₂O₃ (from chromic acid + excess ammonium hydroxide), treated with hydrogen at 1000°C. to 35 per cent loss

3, 5 per cent Cr₂O₃ (from chromic acid + excess ammonium hydroxide), treated with hydrogen at 1000°C. to 38 per cent loss

CWSN S5 or whether it would have been shown by the other charcoals had they been steamed at 1000°C. instead of the usual 750°C. Usually, steaming any one

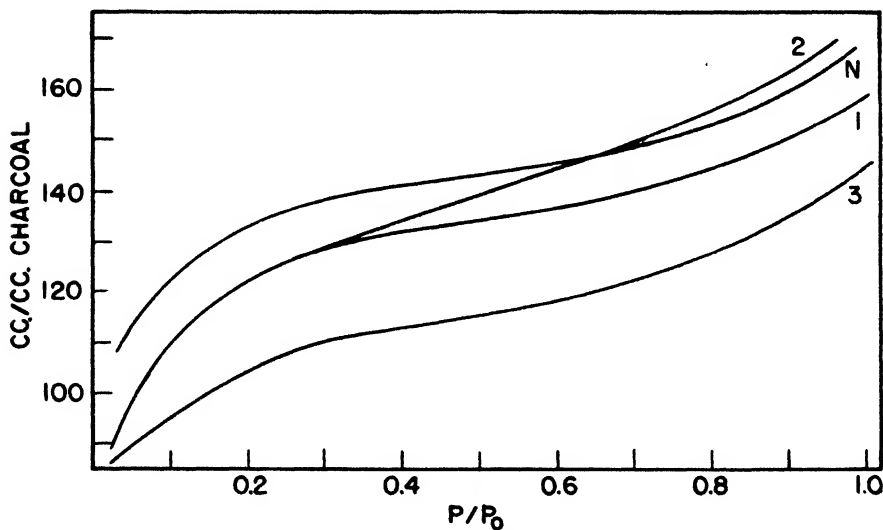
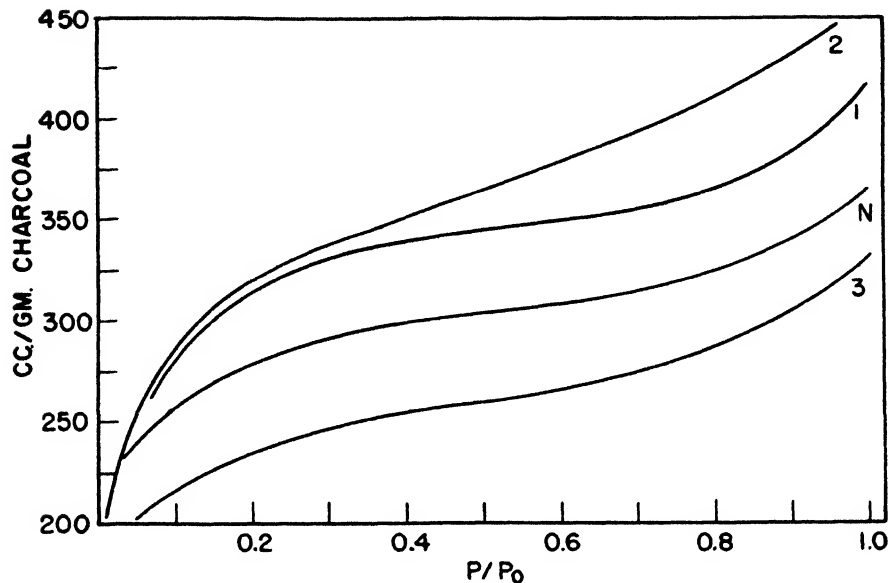


FIG. 19A (upper), 19B (lower). Charcoal PCI P58

N, untreated base charcoal¹

1, steamed at 750°C. to 31 per cent loss

2, 0.2 per cent Cr_2O_3 (from chromic acid + excess ammonium hydroxide), steamed at 750°C. to 39 per cent loss

3, 5 per cent Cr_2O_3 (from chromic acid + excess ammonium hydroxide), steamed at 750°C. to 36 per cent loss

of the four charcoals to as much as 50 per cent weight loss at 750°C. produced practically no alteration in the upper part of the adsorption isotherm, but merely

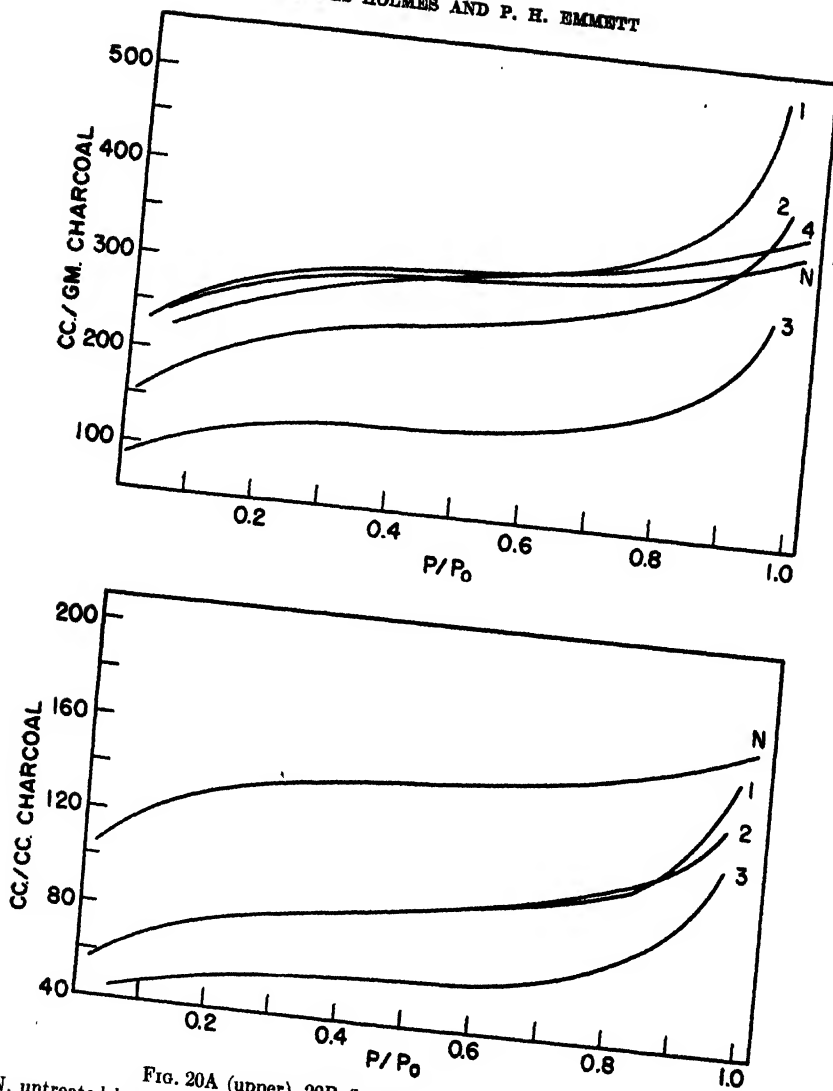


FIG. 20A (upper), 20B (lower). Charcoal PCI P58
 N, untreated base charcoal
 1, treated with hydrogen at 1000°C. to 48 per cent loss
 2, 0.2 per cent Cr_2O_3 (from chromic acid + excess ammonium hydroxide), treated with hydrogen at 1000°C. to 31 per cent loss
 3, 5 per cent Cr_2O_3 (from chromic acid + excess ammonium hydroxide), treated with hydrogen at 1000°C. to 43 per cent loss
 4, activated for 150 min., extracted with hydrofluoric acid, treated with hydrogen at 1000°C. to 28 per cent loss

a shift of the total adsorption to higher adsorption values per gram and either higher or lower adsorptions per cubic centimeter of charcoal.

Hydrogenation without impregnation

It does not seem to have been emphasized in the literature that it is possible to hydrogenate charcoal at temperatures of 1000°C. and to thereby remove as much of the carbon content of the sample as one may wish to do. Actually, however, this behavior might be expected since, as pointed out by Bahr and Jessen (1), carbon deposited on iron carbide can be removed by hydrogen at temperatures greater than 400°C. even though the carbon is present in the free form and not as iron carbide. Mild hydrogenation, like mild steaming, either increases or leaves unchanged the value of the adsorption per gram at 0.4 relative pressure. Furthermore, the slope of the isotherm in the *BC* region is usually unaltered. However, at relative pressures higher than 0.7 and especially at pressures between 0.9 and 0.99, hydrogenated samples have adsorption isotherms that rise very sharply. These facts are illustrated by the curves for hydrogenation without impregnation in figures 5, 14, 18, and 20 (Cases I, II, and VI). Without exception, all of the charcoals that were hydrogenated sufficiently to cause the sharp rise between 0.9 and 0.99 relative pressure showed lower adsorption in the *AB* region per cubic centimeter than did the original charcoal. The results are consistent with the view that the hydrogen attacks the small capillaries and converts them preferentially into capillaries in the range that would have capillary condensation between 0.9 and 0.99, or even into capillaries permitting capillary condensation only at relative pressures higher than 0.99. This latter is strongly suggested by a rather large drop in adsorption per cubic centimeter in the *AB* region induced in some of the samples by the hydrogenation.

Effect of mild oxidation with free oxygen

Mild oxidation with an oxygen-nitrogen mixture was tried on only one of the four charcoals, CWSN 19. On this sample the mild oxidation at either 450° or 750°C. had very much the same effect as steaming at 750°C. in that it increased the low-pressure adsorption (*AB* region) without materially affecting the slope of the isotherm above 0.4 relative pressure (Case I). The single experiment at 1000°C. on CWSN S5 with tank nitrogen (containing its usual small quota of oxygen as an impurity) to a total of 19 per cent loss is confusing, because of the sintering effect that apparently always occurs on this charcoal when it is heated to 1000°C. or 1200°C. The behavior was much the same (curve 1, figure 16) as was observed on heating this charcoal in pure nitrogen for 2 hr. at 1200°C. (curve 5, figure 12). It will be noted, incidentally, in both of these runs, that the percentage decrease in the adsorption per cubic centimeter is less than the per cent decrease per gram (Cases III and IV). This should be true for all those instances in which the particle shrinks in size as a result of the true carbon density increasing and probably loses a few of the smallest pores by virtue of partial graphitization.

Effect of impregnation on heating charcoal in a stream of steam, hydrogen, nitrogen, or a nitrogen-oxygen mixture

It should be realized at the outset that the specificity of the various impreg-

nating agents as regards their influence on the action of the various gases is much less marked and definite than is the general character of steaming, hydrogenating, or oxidizing the samples in the absence of impregnating agents. Frequently, a given impregnating agent has a very different effect on one charcoal than on another; still more confusing is the fact that a given impregnating agent differs in its activity on a particular process as a function of the particular chemical reaction by which it was deposited on the charcoal. Examples of this will appear in the following detailed discussion:

(1) Fe_2O_3 was used as an impregnant only in runs with samples CWSN 19 and CWSN S5, the two charcoals prepared by zinc chloride activation. Of the nineteen runs made, one was with steaming, nine with hydrogenation, eight with either air or tank nitrogen, and one with pure nitrogen. A few generalizations appear possible for the runs, though much more work would be required to make clear all of the details of the manner in which and the mechanism by which iron oxide alters the effects produced by steaming, by hydrogenation, and by the other gas treatments used.

Three characteristics of the use of ferric oxide seem rather definite. In the first place, it seems certain that ferric oxide catalyzes the hydrogenation of CWSN 19 and CWSN S5. For example, curve 4 of figure 8, and curve 5 of figure 15 clearly show a very drastic pore alteration produced by hydrogen at $600^\circ\text{C}.$ in the presence of 5 per cent ferric oxide. Without this impregnant, hydrogen has practically no action on these charcoals at $600^\circ\text{C}.$, whereas with the impregnant a 30 per cent weight loss can be brought about in less than an hour. Secondly, with one exception (curve 3, figure 11), all runs using ferric oxide as impregnant resulted in an increase in slope in the *CD* region corresponding to the building up of pores in the size range 70–1800 Å. in diameter (figures 4, 8, 10, 11, 15, and 16). Finally, in a run with tank nitrogen at $1000^\circ\text{C}.$ to a 13 per cent weight loss, there was observed a 20–40 per cent decrease in adsorption on both a weight and a volume basis (curve 1, figures 11A and 11B), together with the development of a marked slope in the *BC* and *CD* section of the isotherm. This is one of several examples (curve 3, figure 20) of such an effect in the work on impregnation. The effect is consistent with the conclusion that in some way iron blocks off a number of the small pores (Case III) and at the same time converts other small pores into large ones (Cases V and VI).

In a general way, it may be said that ferric oxide tended to drop the adsorption on both a per gram and per volume basis at relative pressures lower than 0.4. As a matter of fact, practically the only treatment that would cause the *AB* region of the adsorption to decrease on CWSN 19 on a gram basis was impregnation with ferric oxide followed by treatment with steam, hydrogen, nitrogen, or a nitrogen-oxygen mixture. Concentrations of impregnant over the entire range from 0.2 to 5.0 per cent were effective, though the catalytic effect of the iron on the reaction of gases with the charcoal increased as a rule with the amount present.

(2) Cr_2O_3 was tried as an impregnating agent for all four charcoals. Its influence is rather different for the various charcoals, so that the results can most effectively be discussed for each charcoal separately.

On CWSN 19, chromic oxide produced comparatively little effect on steaming. A comparison of curves 2 and 6 of figure 3 with curve 1 of figure 2 illustrates the similarity between steaming results with and without chromic oxide. In the other four curves in figure 3, however, it is evident that under some conditions of impregnation, the chromic oxide induces an increase in slope in the isotherms in addition to increasing the absolute adsorption per gram of charcoal. On hydrogenation, chromic oxide appears to eliminate the small pore development that characterized hydrogenation in the absence of impregnant and instead catalyzes the conversion of small pores into those showing adsorption in the *CD* region, as well as to those that are too large to permit capillary condensation even at 0.99 relative pressure (figure 6, curves 2 and 3.)

On charcoal CWSN S5, chromic oxide appears to catalyze the conversion of small pores into larger ones by steaming (Cases V and VI). This is indicated by the decided slope that is given to the isotherms, in contrast to the comparatively flat isotherms obtained on samples that were steamed without impregnation. (Compare curves in figure 13 with curves 3 and 4, figure 12.) The effect of chromic oxide on the hydrogenation of CWSN S5 (curves 2 and 3, figure 14) can perhaps best be described by saying that it appears to catalyze the same type of particle sintering and pore plugging (Cases III and IV) that occurs when a sample is heated in an inert gas to 1200°C. (curve 5, figure 12). In addition to this effect, chromic oxide apparently promotes the attack by the hydrogen on small pores with their conversion into those having condensation in the *CD* region, and at even higher relative pressures (Cases II and VI).

On coconut charcoal, impregnation with 0.2 per cent chromic oxide caused, on steaming, nearly a 100 per cent increase in the adsorption up to 0.4 relative pressure on a weight basis, a 30 per cent increase on a volume basis, and a 15 per cent slope increase in the *CD* region (figures 17A and 17B, curve 4). Strangely enough, steaming a sample impregnated with 5 per cent chromic oxide caused very little change in the amount of adsorption from that of straight steaming, although the slope in the *BC'* and *CD* regions was 10-20 per cent greater after steaming in the presence of the chromic oxide (figure 17, curve 5) than in its absence. Possibly this contrast between the behavior of 5 per cent and 0.2 per cent chromic oxide could result from the larger chromic oxide impregnation superimposing a 40 per cent plugging effect (Case III) on top of an initial increase in pore area and volume analogous to that caused by 0.2 per cent chromic oxide. Hydrogenation of coconut charcoal impregnated with 0.2 or 5 per cent chromic oxide (figure 18, curves 2 and 3) caused none of the slope change characterizing similar runs on CWSN 19 or CWSN S5, the slope of the isotherms being identical with that of the original charcoal; in fact, the marked upturn of the isotherm between 0.9 and 0.99 produced by straight hydrogenation is absent when chromic oxide is present. It should be noted, however, that (curves 2 and 3, figure 18B) the chromic oxide actually was influencing the hydrogenation. For example, as a result of hydrogenation in the presence of 5 per cent chromic oxide, the adsorption decreased about 5 per cent per gram and 20 per cent per cubic centimeter (Case II). It would seem, accordingly, that considerable attack on the

small pores took place with a conversion of many of them to pores too large to be detected by adsorption to 0.99 relative pressure (Case II).

PCI P58 impregnated with chromic oxide behaved little differently on steaming from samples not impregnated as regards the slope of the isotherms; however, the larger (5 per cent) chromic oxide content caused a drop in the absolute adsorption of 15 or 20 per cent on both the weight and volume basis (curve 3, figures 19A and 19B, compared to curve 1) (Case III). Hydrogenation after impregnation with chromic oxide produced the same slope increase in the *CD* region that was obtained without any impregnation; the total pore volume of this charcoal, however, was decreased by the impregnation both on the weight and volume basis (figures 20A and 20B, curve 3). As a matter of fact, the 60 per cent decrease in adsorption on both a weight and a volume basis and the slope change caused by 5 per cent chromic oxide in the hydrogenation experiments suggest that considerable pore plugging (Case III) by the impregnant occurs, together with conversion of small pores into those in the *CD* region.

(3) NiO on CWSN 19 produces (curve 3, figure 4), on steaming, no change in slope of the isotherms, just as was true of straight steaming; however, it appears to drop the total adsorption on both a volume and a weight basis by about 35 per cent, compared to the volume of adsorption after steaming in the absence of nickelous oxide. This behavior might be produced by an extensive pore plugging (Case III) superimposed on the usual new pore formation that is characteristic of straight steaming (Case I). It also might be considered as an example of Case II. For hydrogenation, the nickel results are especially noteworthy in that they show a decided specificity depending on the particular nickel salt used in impregnation. For example, if the nitrate is used and precipitated by ammonium hydroxide, hydrogenation to a weight loss of 27 per cent results in a nitrogen isotherm that is a straight line from 0.4 to 1.0 relative pressure and that has a slope corresponding to a 20 per cent increase in the volume of adsorption over this pressure range (curve 3 in figures 7A and 7B). In contrast to this, the same per cent nickelous oxide produced from nickel chloride plus ammonium hydroxide caused no change in slope and only a few per cent decrease in total adsorption compared to the untreated CWSN 19 (curve 4, figures 7A and 7B). Actually, the nickelous oxide from nickel chloride appears to have very little effect other than to cause a slight pore plugging.

On CWSN S5 in the single experiment in which nickelous oxide was precipitated from the nitrate by an excess of ammonium hydroxide and the sample then hydrogenated at 1000°C. to a 42 per cent loss, there seems to have been little effect other than a decrease of about 15 per cent in the adsorption on both a volume and a weight basis. Again the results are consistent with the nickelous oxide producing a pore plugging (Case III) and at the same time eliminating the usual sharp upturn of the isotherm in the *CD* region that is characteristic of hydrogenation without an impregnant.

(4) A few experiments were made using molybdenum sesquioxide, sodium carbonate, or cupric oxide as impregnants. Neither 5 per cent molybdenum sesquioxide nor 5 per cent sodium carbonate produced any change in slope on the isotherms of CWSN 19 on hydrogenation to a 26 per cent weight loss at 1000°C.;

this was also true of hydrogenation to a similar weight loss in the absence of an impregnant. However, the absolute volume of adsorption in the sample hydrogenated in the presence of the molybdenum sesquioxide was about 20 per cent less than it would have been in the absence of the impregnant; the absolute adsorption after the sodium carbonate treatment was almost exactly the same as it would have been without the sodium carbonate (figures 6A and 6B).

The two experiments on steaming a charcoal containing cupric oxide produced markedly different results. On a CWSN 19 sample containing cupric oxide steaming at 750°C. to a 26 per cent loss produced no change in the slope of the isotherm but an absolute adsorption about 35 per cent smaller on both a weight and a volume basis than it would have been if steamed to a 43 per cent loss in the absence of cupric oxide (curve 4 of figure 4 compared to curve 1 of figure 2). In contrast to this, CWSN S5 containing cupric oxide on being steamed to a 38 per cent loss produced a marked change of its isotherm, the adsorption increasing 20 per cent between 0.4 and 0.99 relative pressure (curve 5, figure 13).

CONCLUSIONS

On the basis of the work here reported, it seems that the following general conclusions are evident:

1. It is possible to tailor-make the pore distributions and pore sizes of charcoals almost at will by suitable combinations of steaming, hydrogen treating, partial oxidation, sintering, and impregnating with ferric oxide, chromic oxide, nickelous oxide, cupric oxide, molybdenum sesquioxide, or sodium carbonate.
2. Much specificity exists as to the action of the impregnating agents, as regards both the particular chemicals from which the oxide is produced and the behavior of one charcoal compared to another.
3. There is some indication that a mere change in the absolute density of carbon in a charcoal as a result of sintering it to 1200°C. in an inert atmosphere may actually increase the ease of pore alteration by steaming at 750°C.

REFERENCES

- (1) BAHR AND JESSEN: Ber. **66B**, 1238 (1933).
- (2) BEECK: Rev. Modern Phys. **17**, 61 (1945).
- (3) BRUNAUER, EMMETT, AND TELLER: J. Am. Chem. Soc. **60**, 309 (1938).
- (4) DRAKE AND RITTER: Ind. Eng. Chem., Anal. Ed. **17**, 787 (1945).
- (5) EMMETT: Am. Soc. Testing Materials, Symposium on New Methods for Particle Size Determination in Subsieve Range **1941**, 95.
- (6) HOLMES AND EMMETT: J. Phys. Colloid Chem. **51**, 1262 (1947).
- (7) *International Critical Tables*, Vol. IV, p. 441. McGraw-Hill Book Company, Inc., New York (1928).
- (8) LAMB, WILSON, AND CHANEY: Ind. Eng. Chem. **11**, 420 (1919).
- (9) MCBAIN: *Sorption of Gases and Vapours by Solids*, pp. 58-79. G. Routledge and Sons, Ltd., London (1932).
- (10) PIERCE, BLACET, AND JUHOLA: Part of the research on charcoal done for the National Defense Research Committee; to be published.
- (11) RIES, VAN NORDSTRAND, JOHNSON, AND BAUERMEISTER: J. Am. Chem. Soc. **67**, 1242 (1945).
- (12) RITTER AND DRAKE: Ind. Eng. Chem., Anal. Ed. **17**, 782 (1945).
- (13) THOMSON: Phil. Mag. [4] **42**, 448 (1871).
- (14) WASHBURN: Phys. Rev. **17**, 273 (1921); Proc. Natl. Acad. Sci. U. S. **7**, 115 (1921).

SURFACE COMPLEXES ON CHARCOAL¹GAS EVOLUTION AS A FUNCTION OF VAPOR ADSORPTION AND OF
HIGH-TEMPERATURE EVACUATIONROBERT B. ANDERSON² AND P. H. EMMETT³*Department of Chemical Engineering, The Johns Hopkins University, Baltimore 18, Maryland**Received June 11, 1947*

As part of the research program undertaken by Division 10 of the National Defense Research Committee on the study of charcoal for gas mask use, a considerable amount of information was obtained relative to the nature and amount of surface complexes on various charcoals. Since such information is of interest to all of those concerned with the employment of activated carbon, charcoals, or carbon black, the present summary of the results is being presented.

The type of work described here is not new. Rhead and Wheeler (8), who studied the oxygen complex on a highly purified charcoal, showed that the complex was not adsorbed or occluded carbon monoxide or dioxide, since these gases did not react with the charcoal at temperatures at which the complex was formed. Lowry and Hulett (5) after World War I presented the results of high-temperature evacuation experiments on a number of American, English, and German charcoals of that war. The work reported here extends the application of the high-temperature evacuation technique to a larger variety of charcoals and to the study of several factors in the activation and oxidation of charcoal or carbon surfaces. In addition, a few data are presented on the question of the extent of gas evolution from surface complexes that occurs as a result of exposure of charcoals to vapors such as carbon tetrachloride.

EXPERIMENTAL

Apparatus

The apparatus for evacuating the samples which is shown in figure 1 was similar to that described by Lowry and Hulett (5). The degassing tube D consisted of a quartz tube of 2.5 cm. inside diameter which was joined by a graded seal to Pyrex tubing. A platinum crucible (J. L. Smith type) containing about 1 g. of charcoal was suspended by platinum wires to a position near the bottom of the quartz tube. The degassing tube was connected to a large stop-cock having a bore 7 mm. in diameter, and this, in turn, to a ground-glass joint so that the tube could be removed from the degassing system for weighing. The degassing tube was connected to a McLeod gauge and to a Stimson mercury pump P (10), which continuously pumped the gas from the sample. This pump

¹ Presented at the Symposium on the Adsorption of Gases which was held under the auspices of the Division of Colloid Chemistry at the 110th Meeting of the American Chemical Society, Chicago, Illinois, September 11-12, 1946.

² Present address: Central Experiment Station, Bureau of Mines, Pittsburgh 13, Pennsylvania.

³ Present address: Mellon Institute, Pittsburgh 13, Pennsylvania.

was designed to operate efficiently against back pressures as high as 10–20 mm. of mercury. From the mercury pump, the gases passed through a liquid-nitrogen trap F to an automatic Toepler pump T of the type described by Urry (12). The gas was collected in bulb S, the mercury being set at N to act as a check valve. When the evacuation was completed, the volume of gas was determined by compressing it into calibrated bulb B by raising mercury to line L, and determining the pressure on the scale M. Then the gas was transferred by an evacuated bulb G to the gas-analysis apparatus.

For temperatures to 1000°C., a resistance furnace was used, the temperatures being measured by a chromel-alumel thermocouple, and controlled automatically to less than $\pm 5^\circ\text{C}$. Above 1000°C. the crucible was heated by an induction furnace, the temperature being measured by an optical pyrometer. The pyrome-

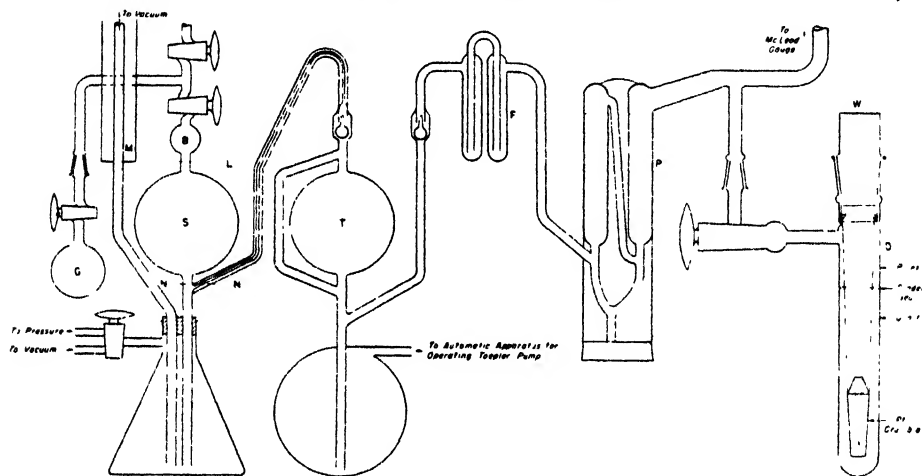


FIG. 1. Apparatus for high-temperature evacuation experiments

ter was sighted through plane Pyrex window W of the degassing tube into the platinum cone within the crucible, the cone approximating black-body conditions. The temperature could be maintained to within $\pm 50^\circ\text{C}$. with the induction furnace.

The gases evolved were separated into three fractions by using liquid nitrogen, dry ice, and warm water in succession on trap F. The fraction that passed through liquid nitrogen contained hydrogen, carbon monoxide, and methane; the part volatile at -78°C . contained carbon dioxide; and that volatile at room temperature contained water, which was determined volumetrically as a vapor by expanding into a large calibrated bulb at about three-fourths of the saturation pressure.

The gases were analyzed by a semimicro method as developed by Taylor and Saunders (11). The method was checked by using known mixtures of gases and found to be satisfactory. Difficulty was encountered in separating carbon dioxide-carbon monoxide mixtures; hence the liquid-nitrogen separation was

used. The analysis of methane by the combustion method gave uncertainties similar to those reported by Taylor and Saunders (11), but since methane was present to only a few per cent, this was not important. Analysis for oxygen was accomplished by using dry yellow phosphorus, the phosphorus being melted and solidified between each analysis to insure a fresh surface. A check on the experimental methods is given in table 1, in which the weights of gases calculated from gas volumes and analyses are compared with weight loss of the degassing tube. The tube was weighed against a counterpoise on a large balance to an accuracy of ± 0.5 mg.

The tube and crucible were washed with dilute hydrochloric acid after each run, rinsed with water, dried, and pumped at $1200^{\circ}\text{C}.$ to a good vacuum. The samples were dried over phosphorus pentoxide for at least 1 day, and then placed in the degassing tube and pumped to a vacuum of 10^{-5} mm. of mercury before gas collection was started.

TABLE 1

Comparison of weight loss of samples by direct weighing with weight loss computed from gas analysis

SAMPLE	WEIGHT LOSS	
	By gas analysis	By direct weighing
	mg	mg.
CWSN S5 extracted with hydrofluoric acid and evacuated to $1200^{\circ}\text{C}.$	242.8	245.8
PCI 1042 extracted with hydrofluoric acid and evacuated to $1200^{\circ}\text{C}.$	125.5	135.5
CWSN 44 evacuated to $900^{\circ}\text{C}.$	63.8	64.7
CWSN 196 B1 evacuated to $900^{\circ}\text{C}.$	49.6	50.2

Nitrogen, steam, and ammonia treatments were carried out in a quartz tube small enough to be weighed on an analytical balance. Transfer of the samples to the degassing tube was done in a stream of pure nitrogen in a manner which precluded the possibility of exposure of the sample to air. For steam treatments, nitrogen saturated with water vapor at $75^{\circ}\text{C}.$ was used.

To control the level of the mercury in the Toepler pump, the apparatus shown in figure 2 was used. The details may be of interest, since the device can be constructed from readily available laboratory supplies. The plugs of the two glass stopcocks are connected by a wooden tube W which fits over the handles of the plugs, the two plugs being set with an angle of about 25° between the open position of each. Lever L attached to the middle of W is connected to an iron core in solenoid S. When the solenoid is not energized, the stopcock B is open to the vacuum line and A is closed. When the solenoid is energized, A is open to atmospheric pressure through a leak with B closed. The solenoid was actuated by a controller of the type described by Rowley and Anderson (9).

Some of the charcoal samples were treated with nitrogen at $1100^{\circ}\text{C}.$ in a

sillimanite tube in a Globar furnace. Samples aged in moist air were prepared at Northwestern University. Analyses of the ash contents of charcoals were made by E. O. Wiig and J. F. Flagg at the University of Rochester.

Nitrogen-adsorption measurements on various charcoals before and after high-temperature evacuation were made on the standard apparatus of the type that has been described many times (3). Samples of evacuated charcoals were transferred in air to the adsorption tube.

For the study of gases displaced during the adsorption of vapors on charcoal a 10- to 20-g. sample of charcoal was evacuated to a pressure of 10^{-5} mm. of mercury. The adsorbate was repeatedly frozen out and pumped to remove dissolved gases. The liquid was then permitted to adsorb on the charcoal and

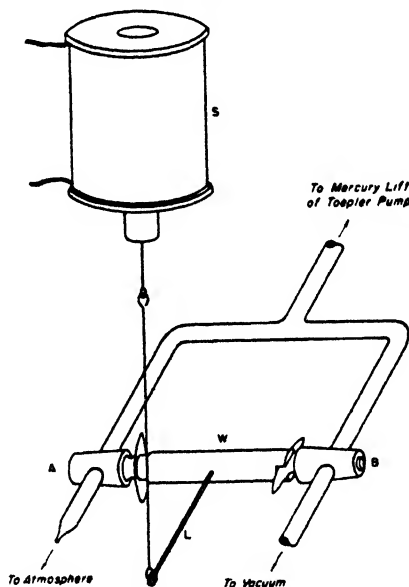


FIG. 2. Apparatus for controlling the level of the mercury in the Toepler pump

to equilibrate for varying lengths of time. The charcoal bulb was then evacuated through a dry-ice trap by the regular gas-collecting system.

Charcoals

The charcoals used include most of the standard varieties upon which research was done in World War II by the National Defense Research Committee. The relative effectiveness of these charcoals for removing gases by adsorption or for acting as supports for chemicals and catalysts that remove gases by chemical means is irrelevant to the present discussion and will not be presented here. The essential information as to the origin and methods of preparation of the charcoals may be summarized as follows:

Charcoals from wood: Charcoals CWSN 19, CWSN S5, CWSN 44, CWSN 196 B1, CWSN 196 B1X were made by the zinc chloride activation process from

wood sawdust. Charcoals CWSN 19, S5, and 44 were obtained by using a dry-weight mixture ratio of 0.90 for zinc chloride: wood sawdust. CWSN 19 was heated to 850°C. in a rotating furnace and was characterized by a low ash content of 0.2 per cent. The ash contents of CWSN S5 and 44 were 6.67 and 3.8 per

TABLE 2
Analyses of ash of typical zinc chloride and coal charcoals in weight per cent

COMPONENT	CWSN S5	PCI 1042
SiO ₂	0.12	10.6
Al ₂ O ₃	0.42	8.2
Fe ₂ O ₃	0.24	2.0
Heavy metals		0.8
CaO	0.45	0.7
ZnO	6.38	

TABLE 3
Degassing experiments on various charcoals

SAMPLE	VOLUME OF GASES EVOLVED, CC. (N.T.P.) PER GRAM														
	25-300°C.			300-600°C.				600-900°C.				900-1200°C			
	CO	CO ₂	H ₂ O	H ₂	CO	CO ₂	H ₂ O	H ₂	CO	CO ₂	H ₂ O	H ₂	CO	(CH ₄)	(CO ₂)
1. N 19	0.2	0.3	0.4	0.3	3.8	1.5	1.3	10.4	11.7	0.5	0.4	46.4	1.0	2.1	0.0
2. NS 5	0.5	2.0	2.3	1.0	4.6	2.3	5.3	92.0	21.7	1.4	6.0	36.9	0.6	0.6	0.0
3. NS 5 (extracted with HIF	0.9	3.0	5.8	2.5	87.2	39.9	1.9	66.9	27.7	1.2	0.2	21.8	0.4	0.6	0.7
4. N 44	0.7	3.3	3.5	1.4	6.6	3.2	4.6	97.5	22.8	1.4	0.5	51.8	2.6	3.0	1.0
5. N 196 B1	0.5	2.7	3.3	1.4	5.5	3.0	4.6	93.0	29.5	0.5	1.8	36.5	0.5	0.8	0.2
6. N 196 B1X	0.2	1.5	1.6	1.0	3.3	6.8	1.6	53.1	11.8	0.2	0.1	33.8	0.1	0.8	0.2
7. C 1242	0.3	0.6	0.9	0.0	0.7	1.2	1.1	5.8	4.0	0.3	0.2	19.3	0.9	0.1	0.2
8. CFI "CC"	0.1	0.2	1.2	0.0	0.7	0.3	1.1	7.8	5.5	0.2	0.2	38.5	6.3	4.0	8.0
9. PCI P58	0.1	0.2	0.9	0.1	1.2	0.7	0.7	16.2	11.4	0.5	0.2	38.3	97.8	4.7	0.0
<hr/>															
	25-120°C.			120-600°C											
	CO	CO ₂	H ₂ O	H ₂	CO	CO ₂	H ₂ O								
10. PCI 25	0.0	0.0	0.5	0.5	2.0	1.0	3.0	10.5	9.9	0.4	0.5	35.3	88.5	2.7	0.3
11. PCI 1042	0.0	0.2	0.6	0.3	2.6	1.2	1.3	7.5	9.6	0.3	0.3	43.2	93.1	2.3	0.4
12. PCI 1042 (extracted with HF)	0.0	0.0	0.7	0.6	51.2	9.4	4.3	20.8	20.9	3.0	0.3	22.3	0.8	0.8	0.4
<hr/>															
	25-300°C.							300-900°C.							
	CO	CO ₂	H ₂ O					H ₂	CO	CO ₂	H ₂ O				
13. B-X2	0.2	3.1	2.3					13.4	7.8	2.2	1.9	36.3	5.4	0.6	0.3

cent, respectively. CWSN 196 B1 and 196 B1X were made by using a zinc chloride: wood sawdust ratio of 1.1:1. They differed primarily in that CWSN 196 B1X had a final calcination in a rotary furnace at 850°C., whereas CWSN 196 B1 was merely dried at 400°C. as a final step. Most of the ash was zinc oxide, as indicated by the analyses of CWSN S5 given in table 2.

CWSC 1242 was made from wood sawdust by calcination and steam activation. CWS B-X2 was a steam-activated charcoal made from nut shells.

Coal charcoals: Samples made from coal include PCI P58, PCI 25, PCI 1042, and CFI "CC." The PCI charcoals were made by briquetting finely ground coal, carbonizing the briquetted material by heating it in two rotary furnaces at a series of temperatures that gradually increased to 515°C., and finally steam activating it in rotary furnaces at temperatures between 870° and 980°C. The details for making CFI "CC" are not available. The samples made from coal

TABLE 4
Summary of degassing experiments on various charcoals

SAMPLE	GASES EVOLVED TO 900°C, CC (NTP) PER GRAM					GASES EVOLVED TO 1200°C, CC (NTP) PER GRAM					WEIGHT PERCENTAGE			
	H ₂	CO	CH ₄	CO ₂	H ₂ O	H ₂	CO	CH ₄	CO ₂	H ₂ O	Hydrogen evolved*	Oxygen evolved*	Ash	Oxygen in ash
1. N 19	10.7	15.7	0.6	2.3	2.1	57.1	16.7	2.7	3.3	2.1	0.58	1.81	0.2	0.04†
2. NS 5	93.0	26.8	0.8	5.7	13.6	129.9	27.4	1.4	5.7	13.6	1.31	3.74	6.67‡	2.0‡
3. NS 5 (ex- tracted with HF)	69.4	115.8	1.2	44.1	9.7	91.2	116.2	1.8	44.8	9.8	0.93	16.10	~0.0	~0.0
4. N 44	97.5	30.1	5.0	7.6	12.1	147.5	32.7	8.3	7.7	12.1	1.5	4.30	3.8	0.8†
5. N 196 B1	94.4	35.5	1.0	6.2	9.7	130.9	36.0	1.8	6.4	9.8	1.29	4.18	3.1	0.6†
6. N 196 B1X	54.1	15.3	0.7	8.5	3.3	87.9	15.7	1.5	8.7	3.4	0.84	2.59	5.0	1.0†
7. C 1242	5.8	5.0	0.1	2.1	2.2	25.1	5.9	0.2	2.3	2.3	0.25	0.91	1.56	
8. CFI "CC"	7.8	6.3	0.0	0.7	2.5	46.3	69.7	0.8	0.9	2.5	0.45	5.28		
9. PCI P58	16.3	12.7	0.3	1.4	1.8	54.6	110.5	5.0	1.4	1.8	0.59	8.22	19.4	
10. PCI 25	11.0	12.0	0.1	1.4	4.0	46.3	100.5	2.8	1.7	4.0	0.40	7.70	20.6	
11. PCI 1042	7.8	9.2	0.2	1.7	2.2	51.0	102.3	2.5	2.1	2.2	0.58	7.76	20.4	10.1‡
12. PCI 1042 (extracted with HF)	21.4	72.1	0.6	12.4	5.3	43.7	72.9	1.2	12.8	5.3	0.46	7.42	0.58	
13. B-X2	13.4	8.0	0.2	5.3	4.2	49.7	13.4	0.8	5.6	4.3	0.50	2.06	8.03	

* The evolved hydrogen was partly free and partly combined; all evolved oxygen was in a combined form.

† Ash assumed to be zinc oxide.

‡ Analyses of E. O. Wiig and J. F. Flagg (see table 2).

had high ash contents. The percentages of ash in PCI P58, PCI 25, and PCI 1042 were 19.4, 20.6, and 20.3, respectively. An analysis of the ash in PCI 1042 is given in table 2. One sample of PCI 1042 that had been extracted with hydrofluoric acid had an ash content of only 0.58 per cent.

RESULTS

In table 3 are presented the results obtained on degassing the various charcoals at temperatures up to 1200°C. The results have been summarized into two groups in table 4: the gas evolution in the range from room temperature to 900°C., and the gas evolution from room temperature to 1200°C. Included in

table 4 also are the values on a weight basis for the per cent of hydrogen evolved (free and combined) and the per cent of combined oxygen evolved. No free oxygen was given off by any of the samples. The ash content of the samples and also the per cent of oxygen in the ash are also shown for comparison. In most of the experiments, the samples were degassed over temperature intervals

TABLE 5

Run 14: Sample of CWSN S5 degassed to 960°C. in 60°C. intervals

TEMPERATURE RANGE °C.	GASES EVOLVED, CC. (N.T.P.) PER GRAM CHARCOAL					FINAL PRESSURE MM $\times 10^4$
	H ₂	CO	* CH ₄	CO ₂	H ₂ O (vapor)	
25- 60	0.00	0.00	0.00	0.00	0.32	0.3
60- 120	0.00	0.01	0.00	0.11	0.67	0.2
120- 180	0.00	0.03	0.00	0.14	0.24	0.6
180- 240	0.00	0.09	0.00	0.50	0.46	1.4
240- 300	0.00	0.19	0.00	0.82	0.82	1.4
Totals... 25- 300	0.00	0.31	0.00	1.55	2.49	
300- 360	0.00	0.21	0.00	0.63	0.73	1.4
360- 420	0.03	0.28	0.00	0.54	0.76	1.0
420- 480	0.03	0.37	0.00	0.34	0.64	1.5
480- 540	0.07	0.84	0.00	0.50	0.98	2.0
540- 600	0.32	2.06	0.10	0.60	1.51	2.3
Totals . 300- 600	0.45	3.79	0.10	2.60	4.62	
600- 660	3.29	4.76	0.00	0.44	3.96	4.5
660- 720	21.48	8.39	0.09	1.22	2.82	8.0
720- 780	30.82	5.86	0.14	0.47	0.41	7.0
780- 840	31.55	2.38	0.00	0.06	0.00	5.0
840- 900	16.41	0.59	0.00	0.03	0.00	5.0
Totals.. 600- 900	105.05	22.18	0.24	2.21	7.19	
900- 960	13.16	0.38	0.00	0.04	0.00	5.0
960-1200	30.49	0.67	0.16	0.04	0.00	5.0
Totals... 900-1200	43.66	1.05	0.16	0.08	0.00	
Totals... 25-1200	147.65	27.08	0.49	6.48	14.30	

of about 300°C., as indicated in tables 3 and 4. However, in one experiment a sample of CWSN S5 was degassed and the gas collected for analysis at intervals of 60°C. The results of this run are summarized in table 5.

In a few experiments with one of the zinc chloride-activated samples, CWSN 196 B1X, an attempt was made to ascertain in detail the effect of exposing a highly degassed sample to oxygen both at room temperature and at 300°C. The final amounts of complex left on the surface after flushing with nitrogen at

1000°C. and at 1110°C. were also desired. All of these results are summarized in table 6 according to the gas evolution at 300° intervals and in table 7 over the range 25–900°C. and 25–1200°C. The weight per cent of evolved hydrogen and

TABLE 6
Effect of heat-treatment on zinc chloride charcoals

SAMPLE	GASES EVOLVED, CC. (N.T.P.) PER GRAM															
	25-300°C			300-600°C.				600-900°C.				900-1200°C.				
	CO	CO ₂	H ₂ O	H ₂	CO	CO ₂	H ₂ O	H ₂	CO	CO ₂	H ₂ O	H ₂	CO	CH ₄	CO ₂	H ₂ O
6. N 196 B1X	0.2	1.5	1.6	1.0	3.3	6.8	1.6	53.1	11.8	0.2	0.1	33.8	0.4	0.8	0.2	0.1
15. N 196 B1X heated in nitrogen at 1000°C.; cooled and transferred in nitrogen	0.0	0.0	0.1	2.1	0.3	0.2	0.8	2.7	0.7	0.1	0.1	33.2	1.3	0.6	0.1	0.0
16. Same as No. 15 exposed to air for one week	0.3	3.5	3.9	1.2	1.5	5.8	2.6	4.5	6.0	0.3	0.1	33.2	1.2	0.7	0.3	0.1
17. N 196 B1X TH 410 heated in nitrogen for 10 hr. at 1100°C.; cooled in nitrogen and then exposed to air	0.3	3.8	1.6	0.9	2.2	4.3	1.0	7.4	4.6	0.2	0.1	12.2	2.0	2.0	0.3	0.0
18. Same as No. 17 exposed to oxygen at 300°C.				25-600°C.												
				0.2	5.7	7.8	1.2	5.1	15.9	0.3	0.0	11.0	0.3	0.2	0.1	0.0
				300-600°C												
19. N 196 B1X exposed to oxygen at 300°C.	0.1	0.4	0.7	0.2	4.1	9.5	1.8	42.9	22.9	1.0	0.4	35.2	0.4	0.4	0.1	0.0
20. N 196 B1X extracted with HF and heated in nitrogen at 1000°C.; cooled and transferred in nitrogen	0.0	0.0	0.6	0.3	0.0	0.1	0.2	1.2	0.1	0.1	0.1	14.1	0.2	0.3	0.4	0.0

oxygen, the ash content, and the weight per cent of oxygen in the ash are also shown.

In the course of developing a chemically treated charcoal called whetlerite for removal of certain gases that would not have been removed by a straight adsorption process, some indication was obtained that the effectiveness of the final product depended upon the extent of exposure of the raw charcoal to air and water vapor prior to the whetlerization. A number of samples of charcoal were therefore artificially "aged" by exposing them to a relative humidity of

80 per cent at 50°C. for an extended period of time. At one stage of the aging work it was reported that heating "aged" samples to 115°C. for an hour restored them to a condition in which they would make satisfactory whetlerites of the type developed in World War II. As a means of ascertaining the extent to which

TABLE 7

Summary of data on effect of heat-treatment of zinc chloride type charcoals

SAMPLE	GASES EVOLVED, CC (N.T.P.) PER GRAM										WIGHT PERCENTAGE			
	Gases evolved to 900°C					Gases evolved to 1200°C.					Hydrogen evolved*	Oxygen evolved*	Ash	Oxygen in ash
	H ₂	CO	CH ₄	CO ₂	H ₂ O	H ₂	CO	CH ₄	CO ₂	H ₂ O				
6. N 196 B1X	54.1	15.3	0.7	8.5	3.3	87.9	15.7	1.5	8.7	3.4	0.84	2.59	5.0	1.0†
15. N 196 B1X heated in nitrogen at 1000°C.; cooled and transferred in nitrogen	4.8	1.0	0.0	0.3	1.0	38.0	2.3	0.6	0.4	1.0	0.36	0.29	5.0	1.0†
16. Same as No. 15 exposed to air for one week	5.7	7.8	0.1	9.6	6.6	38.9	9.0	0.8	9.9	6.7	0.41	2.54	5.0	1.0†
17. N 196 B1X TH 410 heated in nitrogen for 10 hr. at 1100°C.; cooled in nitrogen and then exposed to air	8.3	7.1	0.8	8.3	2.7	20.5	7.3	1.0	8.6	2.7	0.23	1.94	5.0	1.0†
18. Same as No. 17 exposed to oxygen at 300°C. for 30 min.	5.3	21.6	0.6	8.1	1.2	16.3	21.9	0.8	8.2	1.2	0.17	2.82	5.0	1.0†
19. N 196 B1X exposed to oxygen at 300°C. for 30 min.	43.1	27.1	0.2	10.9	2.9	78.3	27.5	0.6	11.0	2.9	0.73	3.74	5.0	1.0†
20. N 196 B1X extracted with HF and heated in nitrogen at 1100°C.; cooled and transferred in nitrogen	1.5	0.1	0.1	0.2	0.9	15.6	0.3	0.4	0.6	0.9	0.15	0.17	0.8	0.2†

* See footnote to table 4.

† Ash assumed to be zinc oxide.

these various aging treatments were reflected in the composition of the surface complex, a series of experiments was carried out on aged and unaged samples of CWSN S5, CWSN 44, and PCI 58. The results are shown in table 8 by 300° intervals between 25° and 900°C., and between 25° and 1200°C.

In tables 3, 6, and 8 the detailed analysis for methane below 900°C. is omitted, since it was usually quite small. The methane content can, however, be obtained

TABLE 8

Effect of aging at 80 per cent relative humidity and 50°C. on oxygen content

SAMPLE	GASES EVOLVED, CC (N.T.P.) PER GRAM														
	25-300°C			300-600°C.			600-900°C.				900-1200°C				
	CO	CO ₂	H ₂ O	H ₂	CO	CO ₂	H ₂ O	H ₂	CO	CO ₂	H ₂ O	H ₂	CO	CH ₄	CO ₂
2. NS 5 original	0.5	2.0	2.3	1.0	4.6	2.3	5.3	92.0	21.7	1.4	6.0	36.9	0.6	0.6	0.0
21. NS 5 aged	0.5	6.7	8.9	1.0	7.1	2.8	6.8	87.2	27.0	1.7	7.2	38.6	0.8	1.1	0.0
22. NS 5 aged and heated in air at 110°C.	0.6	6.9	7.5	1.4	10.4	3.5	7.6	101.1	25.0	1.6	6.4	28.9	0.5	0.8	0.1
4. N 44 original	0.7	3.3	3.5	1.4	6.6	3	24.6	97.5	22.8	1.1	4.0	51.8	2.6	3.3	0.1
23. N 44 aged	0.5	6.2	7.4	1.6	10.7	3.2	7.5	91.5	30.1	1.2	5.5	39.2	1.8	2.5	0.2
9. PCI P58 original	0.1	10.2	0.9	0.1	1.2	0.7	0.7	16.2	11.4	0.5	0.2	38.9	7.8	4.7	0.0
24. PCI P58 aged	0.4	2.3	4.8	0.1	3.6	3.0	1.5	7.6	14.2	0.8	0.7				

Summary of degassing data of aged samples

	GASES EVOLVED TO 900°C, CC (N.T.P.) PER GRAM					GASES EVOLVED TO 1200°C, CC (N.T.P.) PER GRAM					WEIGHT PERCENTAGE			
	H ₂	CO	CH ₄	CO ₂	H ₂ O	H ₂	CO	CH ₄	CO ₂	H ₂ O	Hydrogen evolved*	Oxygen evolved*	Ash	Oxygen in ash
2. NS 5 original	93.0	26.8	0.8	5.7	13.6	129.9	27.4	1.4	5.7	13.6	1.31	3.74	6.67†	2.0†
21. NS 5 aged	88.2	34.6	1.0	11.2	22.9	126.8	35.4	2.1	11.2	23.0	1.37	5.76	6.67†	2.0†
22. NS 5 aged and heated in air at 110°C.	102.5	36.0	2.1	12.0	21.5	131.4	36.5	2.9	12.1	21.5	1.42	5.86	6.67†	2.0†
4. N 44 original	97.5	30.1	5.0	7.6	12.1	147.5	32.7	8.3	7.7	12.1	1.58	4.30	3.8	0.8†
23. N 44 aged	93.1	41.3	1.8	11.2	20.4	132.3	43.1	4.3	11.4	20.4	1.44	6.15	3.8	0.8†
9. PCI P58 original	16.3	12.7	0.3	1.4	1.8	54.6	110.5	5.0	1.4	1.8	0.25	1.23	19.4	
24. PCI P58 aged	7.7	18.2	0.4	6.1	7.0						0.14	2.66	19.4	

* See footnote to table 4.

† Ash assumed to be zinc oxide.

‡

by subtracting the values in column 4 from those in column 9 in tables 4, 6, and the lower half of 8. No appreciable amount of methane was evolved below 600°C.

TABLE 9

Complex formed during steam activation of CWSN 196 B1X extracted with hydrofluoric acid and heated at 1000°C. for 3 hr.

	TEMPERATURE	GASES EVOLVED DURING DEGASSING, CC. (S.T.P.) PER GRAM				
		H ₂	CO	CH ₄	CO ₂	H ₂ O (vapor)
A. Extracted and heated charcoal						
	°C.					
20	25- 300	0.0	0.0	0.0	0.0	0.6
	300- 600	0.3	0.0	0.0	0.1	0.2
	600- 900	1.2	0.1	0.1	0.1	0.1
	900-1200	14.2	0.2	0.3	0.4	0.0
Total		15.6	0.3	0.4	0.6	0.9
B. Treated as in A, then exposed to water vapor at 300°C. for 3½ hr. (weight loss = 0.4 per cent); g. H ₂ O per g. charcoal = 1.22						
25	25- 300	0.0	0.0	0.0	0.1	0.8
	300- 600	0.2	0.1	0.0	0.9	0.8
	600- 900	1.1	0.6	0.1	0.2	0.1
	900-1200	11.4	0.4	0.2	0.2	0.0
Total		12.7	1.1	0.3	1.4	1.7
C. Treated as in A, then exposed to water vapor at 600°C. for 3½ hr. (weight loss = 1.0 per cent); g. H ₂ O per g. charcoal = 0.99						
26. . . .	25- 300	0.0	0.1	0.0	0.0	1.3
	300- 600	0.1	0.0	0.0	0.3	0.6
	600- 900	1.5	1.8	0.0	0.1	0.2
	900-1200	12.3	2.3	0.2	0.3	0.1
Total		13.9	4.2	0.2	0.7	2.2
D. Treated as in A, then exposed to water vapor at 750°C. for 1 hr. (weight loss = 1.6 per cent); g. H ₂ O per g. charcoal = 0.48						
27	25- 600	0.2	0.0	0.0	0.3	1.7
	600- 900	2.7	2.3	0.1	0.3	0.4
	900-1200	16.9	1.9	0.2	0.1	0.0
Total		19.8	4.2	0.3	0.7	2.1
E. Treated as in A, then exposed to water vapor at 900°C. for 3½ hr. (weight loss = 56 per cent); g. H ₂ O per g. charcoal = 1.65						
28	25- 300	0.0	0.0	0.0	0.4	0.6
	300- 600	0.6	0.1	0.0	1.1	1.1
	600- 900	5.8	1.3	0.2	0.2	0.2
	900-1200	40.5	2.2	0.5	0.1	0.1
Total		46.9	3.6	0.7	1.8	2.0

Since most charcoals are activated by treating them with steam it seemed worthwhile to ascertain the influence of steaming upon the composition of the surface complex of a charcoal. A sample of CWSN 196 BIX was used after being extracted with hydrofluoric acid to remove the ash and being heated in nitrogen at 1000°C. for 3 hr. to remove most of the surface complex. Steaming experiments were carried out at 300°C. for 3½ hr. with a 0.4 per cent weight loss; at 600°C. for 3½ hr. with a 1 per cent weight loss; at 750°C. for 1 hr. with a 1.6 per cent weight loss; and at 900°C. for 3½ hr. with a 56 per cent weight loss. Samples from these individual steaming experiments were then degassed and analyzed in the usual way, the gas being collected over 300° temperature intervals. These experiments are summarized in table 9.

A few experiments were made with a view to determining whether or not marked evolution of gas from the surface complex of charcoal occurs when a vapor such as carbon tetrachloride is adsorbed on the sample. Such gas evolu-

TABLE 10
Displacement of complex by adsorption of vapors at 25°C.

CHARCOAL	VAPOR	VOLUME OF LIQUID, CC./G. CHARCOAL	TIME OF ADSORPTION	GASES EVOLVED CC (S.T.P.) PER GRAM	
				CO	CO ₂
			<i>hours</i>		
CWSN 196 B1.....	CCl ₄	0.5	18	0.0028	0.0036
CWSN 196 B1. . .	C ₆ H ₆ Cl	0.4	5	0.00036	0.00039
CWSN 196 B1. .	H ₂ O	0.4	4½	0.0014	0.495
CWSN 196 B1.	H ₂ O	0.2	2½	0.0024	0.205
CWSN 196 B1.....	H ₂ O	0.1	16	0.0016	0.235
PCI P58	C ₆ H ₆ Cl	0.15	3	0.0016	0.00003
PCI P58.	H ₂ O	0.08	1	0.0025	0.0094

tion had been reported in numerous experiments carried out by Allmand (1). Samples of a zinc chloride charcoal, CWSN 196 B1, were treated with carbon tetrachloride, chlorobenzene, and water. After each vapor treatment, the gas that had been evolved was pumped off and analyzed. Similar experiments with PCI P58 were made using chlorobenzene and water vapor, respectively. The results are summarized in table 10.

Finally, in table 11 data are reported on the formation of a nitrogen complex by treating charcoal with ammonia at 600° and 900°C.

The results as summarized in tables 1-11 will now be briefly discussed.

DISCUSSION AND CONCLUSIONS

The experimental results taken as a whole are in agreement with those reported by Lowry and Hulett (5) but are much more extensive. It will be convenient to discuss them under a number of separate headings as follows:

Nature and extent of gas evolution from surface complexes

The carbon monoxide from samples produced by the zinc chloride activation process was evolved primarily at temperatures below 900°C. This is illustrated

by tables 3 and 4 and also by table 5. Simultaneously with the burst of carbon monoxide in the temperature range of 600–840°C. the deposition of a mirror of zinc, formed presumably by the reduction of the zinc oxide present in the ash was observed on the cool parts of the tube. This reduction of zinc oxide by carbon is entirely consistent with known values for the equilibrium constant of the reaction (6):



For this reaction, if the pressures of zinc and carbon monoxide are assumed to be equal, the equilibrium pressures are 0.06 mm. of mercury at 527°C., 1.3 mm.

TABLE 11
*Complex formed during ammonia activation on CWSN 196 BIX,
ash-extracted and heated in nitrogen at 1000°C.*

TEMPERATURE	GASES EVOLVED DURING DEGASSING, CC (S T P) PER GRAM					
	H ₂	CO	N ₂	C ₂ N ₂ HCN	NH ₃	H ₂ O
A. Sample exposed to ammonia at 750°C. for 3 hr.; weight loss = 0.4 per cent						
°C						
25– 600	0.6	0.0	0.1	0.2	0.1	0.5
600– 900	3.3	0.1	0.2	0.1	0.1	0.5
900–1200	26.6	0.4	5.2	2.3	0.3	0.1
Total	30.5	0.5	5.5	2.6	0.5	1.1
B. Sample exposed to ammonia at 900°C. for 3 hr.; weight loss = 17.1 per cent						
25– 300	0.0	0.0	0.0	0.0	0.0	0.6
300– 600	2.3	0.0	0.1	0.2	0.2	0.6
600– 900	5.2	0.1	0.1	0.2	0.2	0.3
900–1200	31.8	0.7	6.3	2.5	0.8	0.2
Total	39.3	0.8	6.5	2.9	1.2	1.7

of mercury at 627°C., and 100 mm. of mercury at 827°C. Since the zinc and carbon monoxide are continually removed to pressures less than 0.1 mm. of mercury, this reaction is thermodynamically possible at temperatures above about 600°C. In zinc smelting, it has been shown that the important reduction reaction is between zinc oxide and carbon monoxide, the reaction of zinc oxide with solid carbon being too slow. However, since the zinc oxide and carbon were very intimately mixed in the charcoals and the carbon monoxide pressure was very low, the reduction probably proceeds by reaction 1. All samples of charcoal made by the zinc chloride process evolve very little carbon monoxide in the temperature range 900–1200°C. This is very much in contrast to all the samples made from coal and having a considerable ash content of silica, alumina, iron oxide, and oxides of other elements. Whereas 94–98 per cent of

the carbon monoxide evolved from the zinc chloride-sawdust charcoals was given off below 900°C., about 90 per cent of the carbon monoxide from the PCI and CFI charcoals was given off above 900°C. This is consistent with the work of Brunner (2), in which the carbon monoxide pressures of the system silica-silicon carbide-carbon were found to be 0.1 mm. of mercury at 900°C. and 10.7 mm. of mercury at 1200°C., and of the system alumina-aluminum carbide-carbon were found to be 10^{-4} mm. of mercury at 900°C. and 0.1 mm. of mercury at 1200°C. With both silicon and alumina, the carbon monoxide pressure was lower for reduction to silicon and aluminum than for the reduction to the carbides.

The evolution of carbon monoxide from charcoals that were prepared in such a way as to have low ash contents (not the samples extracted with hydrofluoric acid, however) appears to have a maximum in the carbon monoxide evolution in the 600-900°C. range. This is illustrated by the data on samples CWSN 19 and CWSC 1242, as shown in tables 3 and 4. This is in general agreement with previous work that has been done on charcoal. It probably also is consistent with the well-known fact that carbon blacks lose most of their volatile matter on being heated to temperatures of about 750° to 800°C. The samples washed with hydrofluoric acid appear to merit special consideration and will be discussed below.

Carbon dioxide evolution seems to reach a maximum in the temperature range 300-600°C. in all of the charcoals. This does not necessarily mean that most of the evolved carbon dioxide is given off over this temperature range, for it is possible that some of the carbon monoxide from the 600-900°C. region results from secondary reaction of carbon dioxide with the hot carbon surface while the gas is passing through the sample. The chance of reaction is minimized by the fact that the gas was continually pumped down to a pressure of 10^{-2} mm. or less, but it cannot be said with certainty that it was entirely eliminated. In almost every experiment, the amount of carbon dioxide was greater than that in equilibrium with carbon monoxide and carbon.

Hydrogen evolution occurs for the most part at a temperature above 900°C. This, too, is in agreement with the findings of Lowry and Hulett. However, a close examination of the data in tables 3 and 4 makes it apparent that samples which, in the process of preparation, were not heated above about 600°C. evolve more hydrogen in the 600-900°C. than in the 900-1200°C. region, the maximum being attained at about 750-800°C. Actually, samples heated to 850°C. during activation evolve about the same amount of hydrogen above 900°C. as those that were not so heated. There is no evidence in the present paper as to the extent to which the evolved hydrogen is surface hydrogen and the extent to which it is hydrogen from carbon-hydrogen complexes deeper within the charcoal particles. When one remembers, however, that the adsorption isotherms of nitrogen on these charcoals correspond to surface areas between 1000 and 2000 sq. m. per gram (see figures 3 and 4), it will be realized that most of the carbon atoms, and hence the carbon-hydrogen complex, must lie in the surface of the charcoal.

Water vapor and methane are both evolved in comparatively small amounts. Water vapor evolution usually reaches a maximum in the 300–600°C. temperature range, though for some of the samples activated with zinc chloride, there is a further evolution of water at about 600–720°C. Perhaps this higher-tempera-

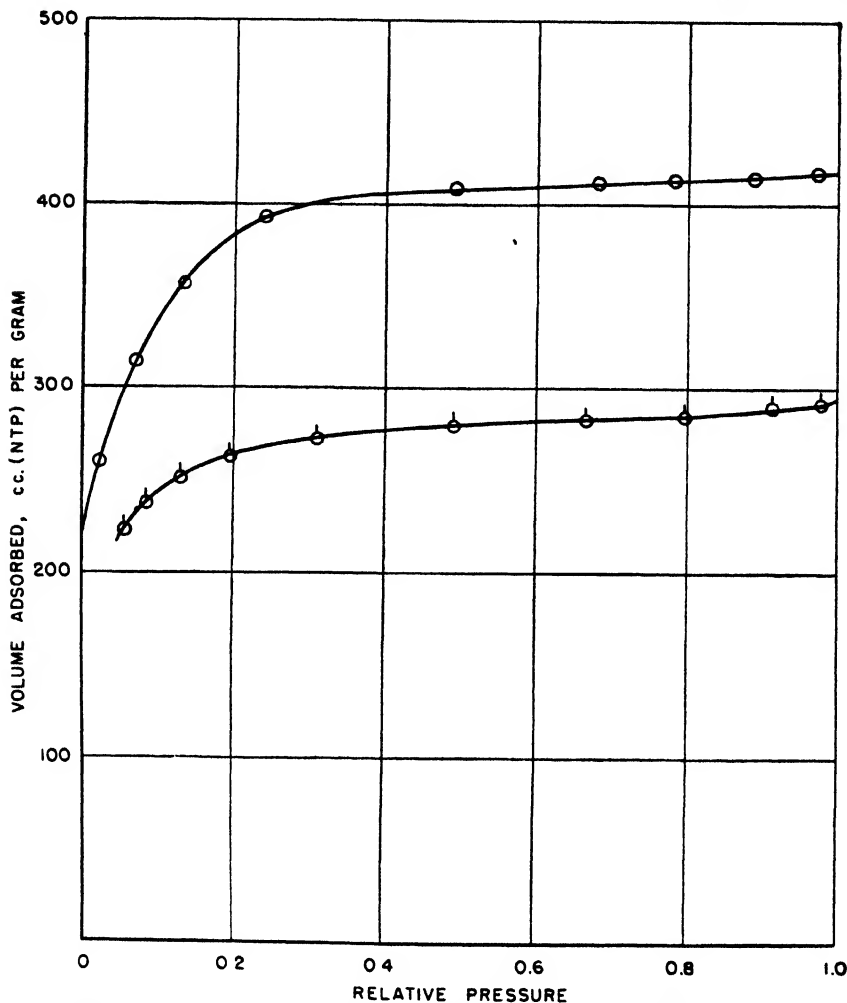


FIG. 3. Nitrogen adsorption isotherms at $-195^{\circ}\text{C}.$ on charcoal CWSN 44. ○, original charcoal; ◊, charcoal after degassing.

ture water is produced by the reduction of some of the zinc oxide ash by the hydrogen that is beginning to be evolved in this same temperature range. Zinc oxide should be reducible by hydrogen under the conditions of the degassing.

Effect of extraction with hydrofluoric acid on the surface complex

Tables 3 and 4 show the results obtained in two experiments in which the ash content of the samples was reduced nearly to zero by the extraction with hydro-

fluoric acid. The gas evolved on heating these extracted samples is very surprising. The amount of complex on the charcoal seems to be greatly increased by the extraction process. For example, CWSN S5 after the washing with hydrofluoric acid evolves 116 cc. of carbon monoxide and 44.8 cc. of carbon di-

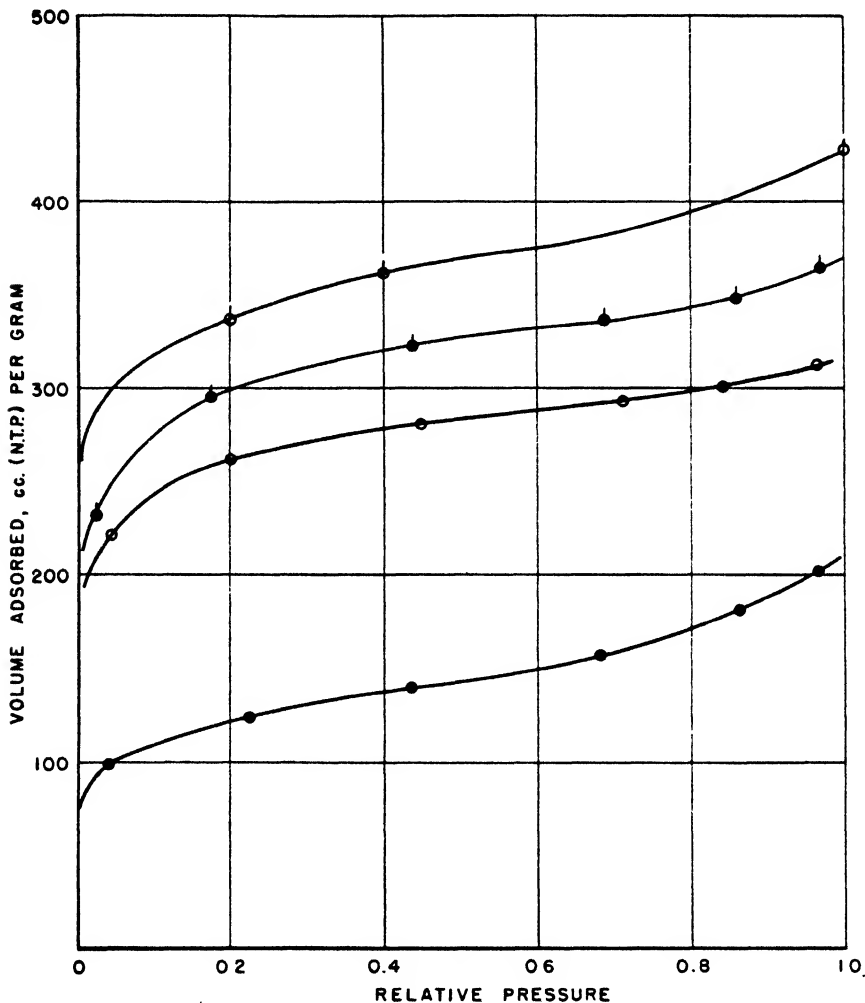


FIG. 4. Nitrogen adsorption isotherms at -195°C . on PCI 1042 charcoals. ○, original PCI 1042; ●, PCI 1042 after degassing; ◐, ash-extracted PCI 1042; ◑, ash-extracted PCI 1042 after degassing.

oxide on being evacuated to 1200°C . compared to 27 and 5.7 cc., respectively, evolved by the unextracted sample. Similarly, PCI 1042 after the washing with hydrofluoric acid evolved 72.1 cc. of carbon monoxide and 12.4 cc. of carbon dioxide on being evacuated to 900°C ., compared to 9.2 and 1.7 cc., respectively, for the unextracted samples. It seems that in some as yet unexplained way the washing process catalyzes the formation of complex on the charcoal surface.

However, these charcoals were not degassed until about two years after their preparation and, although they were kept in stoppered bottles, they may have been able to pick up oxygen slowly over this extended period.

Even below 600°C., surprisingly large quantities of carbon monoxide and carbon dioxide are evolved from the extracted samples. Thus, CWSN S5 evolved 88.1 cc. of carbon monoxide and 45.7 cc. of carbon dioxide below 600°C. after extraction, compared to 5.1 and 4.6 cc., respectively, before extraction. The corresponding figures for PCI 1042 were 51.2 cc. of carbon monoxide and 9.4 cc. of carbon dioxide after extraction, compared to 2.6 cc. of carbon monoxide and 1.4 cc. of carbon dioxide before extraction. In the range 900–1200°C. the extracted sample of PCI 1042 evolved only 0.8 cc. of carbon monoxide, compared with 93.1 cc. for the unextracted sample, confirming our conclusion that most of the carbon monoxide evolution from the original PCI 1042 in this temperature range came from the reduction of ash by carbon.

Changes of adsorption isotherms on degassing

In the high-temperature evacuation the pore structure of the charcoal as evidenced by nitrogen-adsorption isotherms was changed. The interpretation of isotherms as to pore structure has been discussed by Holmes and Emmett (4). Nitrogen isotherms at $-195^{\circ}\text{C}.$ on original and degassed charcoals CWSN 44, PCI 1042, and PCI 1042 ash-extracted, are presented in figures 3 and 4, where the volume of nitrogen adsorbed per gram is plotted against relative pressure. With CWSN 44 in figure 3, the high-temperature evacuation caused the volume adsorbed at a relative pressure of 0.2 to drop from 390 to 264 cc./g. (to 61 per cent of the original), the entire isotherm being decreased by about this ratio. The change in the isotherms is interpreted as a sintering of an equal fraction of all of the pores.

With ash-extracted PCI 1042 in figure 4, the entire isotherm was decreased to a constant fraction (89 per cent) of that of the original extracted sample on high-temperature evacuation. As with CWSN 44, this may be interpreted as the removal of an equal fraction of all the pores by sintering. The degree of sintering is less than with N 44.

The original PCI 1042 sintered to a greater extent than the two other charcoals, and the shape of the isotherm changed to a more pronounced S-type. The degassed charcoal has a lower surface area and probably a smaller number of small pores (less than 16 Å. in diameter) and a larger number of large pores (greater than 50 Å. in diameter) than the original charcoal. Thus, some of the pore walls may have been removed by reduction of the oxides to form larger pores, while probably other pores were sintered.

With CWSN 44 and the ash-extracted PCI 1042 the high temperature caused sintering, but there was little change in the pore distribution. The CWSN 44, which contains zinc oxide, sintered more than the ash-free PCI 1042. With the original PCI 1042 the ash, either because of the large amount or the composition, caused changes in the distribution of the pores. Emmett and Holmes (4) found that certain oxides, such as ferric oxide, nickelous oxide, chromic oxide, and

cupric oxide had pronounced effects in altering pore structure on nitrogen, hydrogen, or steam treatments.

Oxygen pickup by degassed samples

Lowry and Hulett showed that oxygen pickup by charcoal at room temperature is of two distinct types: namely, that which is chemically bound to the charcoal surface and that which is physically bound. The chemically bound oxygen is picked up slowly over a long period of time, whereas the physically adsorbed oxygen is taken up and given off readily by the charcoal at room temperature. Experimental work in the present research confirms these results as regards the chemical adsorption of oxygen; no observations were made relative to physical adsorption. In run 15 of tables 6 and 7 it is shown that the treatment of CWSN 196 B1X with nitrogen at 1000°C. is about as effective in removing oxygen complex and hydrogen as evacuation at 900°C. When this sample in run 15 was exposed to air for a week at room temperature, it picked up sufficient oxygen so that the carbon dioxide evolved on degassing to 1200°C. was as large as that from the original sample and the carbon monoxide evolution was two-thirds as large.

At the same time, more than the original complement of chemisorbed water was picked up by the charcoal, though it is possible that most of this water was held by the 5 per cent ash content that the sample contained. Heating CWSN 196 B1X in a stream of nitrogen even to 1100°C. did not prevent the sample on re-exposure to air at 25°C. from picking up enough oxygen to evolve, on heating, 50 per cent of the original carbon monoxide and 100 per cent of the original carbon dioxide content.

Heating a sample of CWSN 196 B1X TH 410¹ to 300°C. in oxygen for 3 hr. put more complex on it than was present on the original CWSN 196 B1X. The total evolved oxygen given off increased from 2.59 per cent by weight on the original sample to 2.82 per cent on the oxidized sample. The carbon monoxide evolution became 50 per cent greater than on the original sample, whereas the carbon dioxide evolution was approximately the same as on the original. Heating one of the original samples of CWSN 196 B1X in oxygen to 300°C. for 3 hr. (run 19) produced a product similar to that obtained on heating the degassed sample, except that the oxygen in the complex became 3.74 per cent by weight of the sample, in contrast to 2.82 per cent that had been reached by oxygen treatment of a degassed sample (run 19, tables 6 and 7 in comparison to run 18).

Extracting a sample of this same charcoal with hydrofluoric acid and then heating it to 1000°C. in a stream of pure nitrogen produced the most complex-free sample that was encountered. The total free and combined hydrogen evolved on heating this sample to 1200°C. was only 0.15 per cent by weight of the charcoal, and the combined oxygen was 0.17 per cent by weight. Furthermore, the

¹ CWSN 196 BIX TH 410 was prepared by heating sample CWSN 196 BIX in a stream of nitrogen at 1000°C. for 4 hr. to a 4.6 per cent weight loss and then cooling the sample to room temperature in nitrogen.

residual 0.8 per cent ash (presumably zinc oxide) could account for practically all of the combined oxygen evolved from this sample (run 20, tables 6 and 7).

Complex formation by steaming or by aging in moist air

It has been reported a number of times in the literature that charcoal changes its properties as a result of aging. In the aging for 60 days at 50°C. and 80 per cent humidity, the charcoals shown in table 8 increased their oxygen contents by 50 to 120 per cent. The increased oxygen content represents an increase in the volume of evolved carbon monoxide, carbon dioxide, and water vapor. However, on the samples made by the zinc chloride process (CWSN S5 and CWSN 44) care must be used in interpreting this result. There is a sufficiently large ash content on both of these charcoals to account for the entire carbon dioxide content by assuming the ash to be in the form of zinc carbonate after the aging. Furthermore, the total water picked up by these two charcoals is no more than equivalent to the ash holding 2 moles of water per mole of zinc oxide. Accordingly, it is difficult to state with certainty the extent to which the aging has actually changed the composition of the surface complex, in contrast to merely causing an increase in the carbon dioxide and water content of the ash. However, the similarity between the results obtained on the PCI charcoal with 20 per cent ash and the CWSN charcoals with 3.8 and 6.67 per cent ash (probably zinc oxide) makes one believe that a major portion of the added oxygen pickup is in the form of a surface complex.

The drying of an aged sample at 115°C. for 3 hr. produced no significant change in the amount of surface complex.

The results of experiments on the steamed samples shown in table 9 are of considerable interest. For the most part, it is evident that steaming even at temperatures as high as 900°C. produces very little oxygen-carbon complex on the charcoal surface. Steaming at and above 600°C. causes a slight increase in the amount of complex that yields carbon monoxide on heating in the range 600–1200°C., but the total oxygen complex is equivalent to only 1 or 2 per cent of the surface area even after prolonged steaming.

Run E in table 9 indicates that steaming is capable of causing the hydrogen content of the charcoal to increase. After the 900°C. steaming, the hydrogen content evolved to 1200°C. was about 47 cc. per gram compared to 15–20 cc. for the initial samples and for samples steamed to 750°C. It is not certain, however, whether this extra hydrogen is to be attributed to the building up of a surface complex or to the uncovering of a certain amount of hydrogen-carbon complex by the 56 per cent removal of carbonaceous material by steaming. It is also possible that the accumulation of hydrogen might result from the preferential removal of carbon atoms not attached to hydrogen atoms.

In general, the results obtained on the steamed charcoals are in agreement with those reported by Müller and Cobb (7), who studied the chemisorption of water vapor on acid-extracted charcoal at temperatures from 300° to 1100°C. In both their experiments and ours, a small amount of water was chemisorbed and was removed as carbon monoxide, carbon dioxide, or water vapor on degassing

to a high temperature. They noted, as did we, that in the temperature range 700–900°C., steaming results in the fixation of more hydrogen than oxygen.

Displacement of oxygen complex by adsorption

Allmand (1), who studied the sorption of vapors such as carbon tetrachloride, carbon disulfide, and water on charcoal at room temperature and pressures less than 0.1 mm. of mercury (relative pressures less than 0.001), found that in the adsorption process a portion of the oxygen complex was displaced as carbon monoxide and carbon dioxide. This was accompanied by "drifting" of the isotherm, the change in the amount adsorbed being many times the volume of complex displaced. The "drift" could be eliminated only by exposing the sample to the adsorbate at pressures of about 0.1 mm., this procedure being more effective than evacuation at 800°C. In no case have we been able to find any statement by Allmand (1) as to the volume of the displaced gases, but we have noted that the pressure of the evolved gas was reported to be as high as 0.04 mm. in the system.

Our experiments (table 10) show that the amount of complex displaced from our samples in the adsorption of vapors was very small, usually less than 0.006 cc. (S.T.P.) per gram. The carbon monoxide evolution was equivalent to less than 0.001 per cent of a monolayer, and to less than 0.02 per cent of the total carbon monoxide that is evolved on evacuating to 1200°C. Similarly, the carbon dioxide evolution is small in all experiments except those in which water was adsorbed on a charcoal made by the zinc chloride process. It does not seem unreasonable that for these charcoals, the carbon dioxide evolution could be due to the reaction of water vapor with zinc carbonate that might be present in the ash. The largest carbon dioxide evolution was equivalent to only about 8 per cent of the total carbon dioxide that is normally evolved when the sample is evacuated to 1200°C. It is equivalent to only a small fraction of the total zinc oxide in the sample if one assumes, as is usual for samples prepared by the zinc chloride process, that the ash is entirely zinc oxide or some product such as zinc carbonate that could be formed during the contact of the sample with air.

Since the extent of the surface uncovered by displacing the complex was so small, it is probable that no changes in the adsorption isotherms such as reported by Allmand (1) would have been obtained on these samples. It is obvious that adsorption of a vapor to "clean up" the surface has very little effect in these cases on the oxygen complex compared to the effect of evacuating the sample at high temperatures.

Formation of a nitrogen complex

Although, as shown in previous experiments, molecular nitrogen does not react with charcoal, it has been reported (13) that a nitrogen complex can be prepared by passing ammonia over charcoal at 700–900°C. In the process some of the charcoal was gasified, with the formation of hydrogen cyanide. The nitrogen complex was reported to be more stable to thermal decomposition than an oxygen complex; for example, cokes containing nitrogen can be heated to 1100°C. without an appreciable decrease in the nitrogen content.

An extracted CWSN 196 B1X, similar but not identical to the samples used in the steam activation runs of table 10, was exposed to a slow flow of ammonia at 750°C. and 900°C., air being excluded throughout the experiments. The results are given in table 11. In each case some of the sample was gasified and some nitrogen and hydrogen fixed as a complex. In both experiments, about 1 per cent of free and combined nitrogen was removed in the degassing; most of this was evolved in the range 900–1200°C. in the form of nitrogen, and hydrogen cyanide or cyanogen. The gas analysis method was not particularly suitable for these mixtures, but since the gases were fractionated into three parts, it is believed that the errors are not serious. It is interesting to note that the oxygen complex decomposed in the range 600–800°C., whereas the nitrogen complex decomposed principally above 900°C.

SUMMARY

1. Samples of all major types of charcoals studied by the National Defense Research Committee in World War II were evacuated over 300°C. intervals to 1200°C., the evolved gases being collected and analyzed. Oxygen-containing gases, carbon monoxide, carbon dioxide, and water vapor were formed by the decomposition of the oxygen complex and reduction of the oxides in the ash. Large amounts of hydrogen were evolved. In all charcoals, the amount of oxygen evolved would cover less than 50 per cent of the surface.

2. With zinc chloride-wood charcoals, the zinc oxide was reduced in the temperature range 600–900°C., as indicated by the formation of a mirror of metallic zinc in the cooler portions of the degassing tube. The oxides in coal charcoals, silica and alumina, were chiefly reduced in the 900–1200°C. interval. The coal charcoals had less oxygen complex and less hydrogen on them initially than most of the zinc chloride-wood charcoals.

3. Aging of the charcoal in moist air at 50°C. and 80 per cent relative humidity for a month increased their oxygen content by 50–120 per cent.

4. Steam activation was shown to form very little oxygen complex. At 600°C. and below, the sample was not gasified. Above 600°C. gasification occurred, and the hydrogen content of the sample increased.

5. Studies on the amount of oxygen complex displaced on adsorption of carbon tetrachloride, chlorobenzene, or water vapor on charcoal at room temperature indicated that the gas evolved was less than 0.01 cc. per gram of charcoal.

6. While molecular nitrogen does not react with charcoal, ammonia at 750°C. and 900°C. formed a nitrogen complex which was more stable thermally than the oxygen complex.

REFERENCES

- (1) ALLMAND *et al.*: *Proc. Roy. Soc. (London)* **A129**, 235, 252 (1930); **A130**, 610 (1931); **A169**, 25 (1938).
- (2) BRUNNER: *Z. Elektrochem.* **38**, 55 (1932).
- (3) EMMETT: *Advances in Colloid Sci.* **1**, 1–36 (1942).
- (4) HOLMES AND EMMETT: *J. Phys. Colloid Chem.* **51**, 1276 (1947).
- (5) LOWRY AND HULETT: *J. Am. Chem. Soc.* **42**, 1408 (1920).

- (6) MAIER: U. S. Bur. Mines, Bull. No. **324** (1930).
- (7) MÜLLER AND COBB: J. Chem. Soc. **1940**, 177.
- (8) RHEAD AND WHEELER: J. Chem. Soc. **103**, 461, 1210 (1913); Proc. Chem. Soc. **29**, 51, 193 (1913).
- (9) ROWLEY AND ANDERSON: Ind. Eng. Chem., Anal. Ed. **11**, 397 (1939).
- (10) STIMSON: J. Washington Acad. Sci. **7**, 477 (1917).
- (11) TAYLOR AND SAUNDERS: J. Chem. Phys. **9**, 616 (1941).
- (12) URRY: J. Phys. Chem. **36**, 1831 (1932).
- (13) VAN DER LEY AND WIBAUT: Rec. trav. chim. **51**, 1143 (1932).
- (14) BENTE AND WALTON: J. Phys. Chem. **47**, 133, 329 (1943).

SURFACE-AREA MEASUREMENTS ON METAL SPHERES AND ON CARBON BLACKS¹

P. H. EMMETT² AND MARTIN CINES³

Department of Chemical Engineering, The Johns Hopkins University, Baltimore 18, Maryland

Received June 11, 1947

During the past ten years a great many (2, 4, 5, 6, 7, 9, 10, 11, 13, 15) apparently successful measurements have been made of the surface areas of finely divided materials by means of physical adsorption isotherms of nitrogen and other gases near their boiling points.

It seems to have been well established (5, 7) that a plot of the volume of gas, V , adsorbed at the relative pressure p/p_0 according to the equation

$$\frac{p/p_0}{V(1 - p/p_0)} = \frac{1}{V_m C} + \frac{(C - 1)}{V_m C} \frac{p}{p_0} \quad (1)$$

yields a straight line over a sufficiently large relative pressure range to permit the determination of V_m , the volume of gas required to form a monolayer on the solid adsorbent. A simple multiplication of the number of molecules in the monolayer by their average cross-sectional areas yields an absolute surface area value in square meters per gram.

The present paper presents additional evidence of the usefulness of the method in summarizing briefly a number of adsorption results for finely divided porous and non-porous solids that were selected either because of size and shape uniformity or because of the extremely small particle size. The adsorption measurements for the most part have been restricted to the use of nitrogen as an adsorbate at $-195^\circ\text{C}.$, though some runs have been made with carbon disulfide and butane.

¹ Presented at the Symposium on the Adsorption of Gases which was held under the auspices of the Division of Colloid Chemistry at the 110th Meeting of the American Chemical Society, Chicago, Illinois, September 11-12, 1946.

² Present address: Mellon Institute, Pittsburgh 13, Pennsylvania.

³ Present address: Phillips Petroleum Company, Phillips, Texas.

EXPERIMENTAL

The adsorption apparatus and general procedure were the same as used and described on a number of previous occasions (6, 7, 9, 11). The nitrogen was of the ordinary tank variety. Tank butane that was better than 99 per cent pure and C.P. carbon disulfide were fractionated, the middle portions being taken for the experiments.

The uniformly sized and approximately spherical copper and zinc powders, together with the photomicrographs shown in figures 1 and 2, were very kindly furnished by the New Jersey Zinc Company.

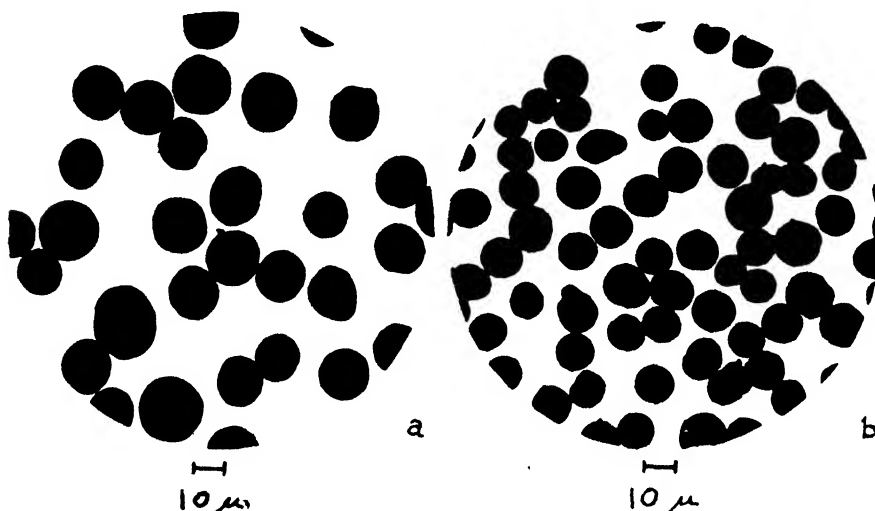


FIG. 1. Photomicrographs of spherical copper powder (a 10-micron scale has been superimposed).

(A) 15-20 MICRON FRACTION		(B) 10-15 MICRON FRACTION	
Area by nitrogen.....	0.039 m. ² /g.	Area by nitrogen.....	0.067 m. ² /g.
Area by count	0.0365 m. ² /g.	Area by count	0.050 m. ² /g.
Roughness factor.....	1.07	Roughness factor.....	1.34

The carbon blacks were supplied by Godfrey L. Cabot, Inc.⁴ Their methods of preparation and general uses and properties have all been described in previous publications (1, 3, 14).

RESULTS

The surface-area values for the metal spheres obtained from the usual B.E.T. plots (5) of the adsorption isotherms for nitrogen, carbon disulfide, and butane according to equation 1 are shown under the photomicrographs in figures 1 and 2.

⁴ The authors wish to express their thanks to Godfrey L. Cabot, Inc., not only for supplying the carbon black samples but also for bearing the cost of the research.

Table 1 gives a complete list of the surface-area values obtained for the various carbon blacks, together with a description of the type of carbon black used. With two exceptions, the calculations of these areas are all made with the help of standard B.E.T. plots (5) of the data of the adsorption isotherms according to equation 1, and need not be described in detail. All results (except those given in parentheses) in table 1 were calculated using for p_0 the normal vapor pressures of the adsorbate.

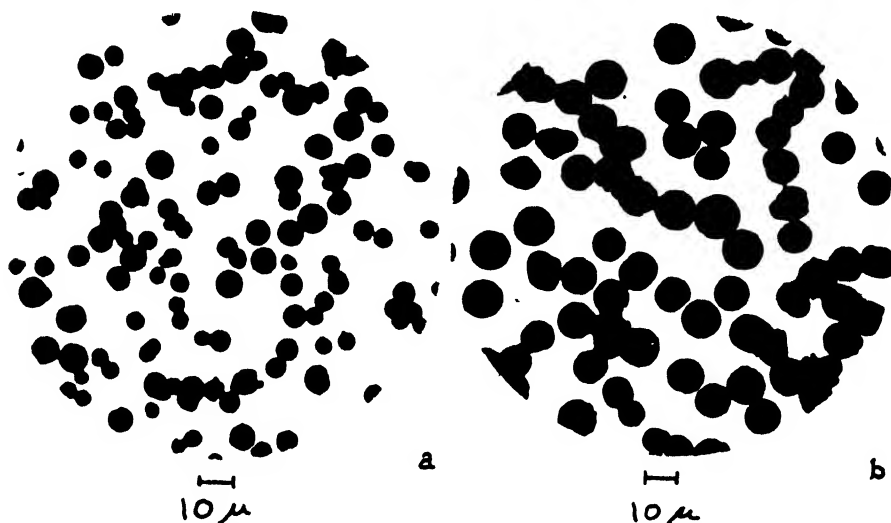


FIG. 2. Photomicrographs of zinc dust (a 10-micron scale has been superimposed)

(A) 5-10 MICRON FRACTION, SAMPLE NJZN 75	(B) 10-15 MICRON FRACTION; SAMPLE NJZN 125
Area by nitrogen 0.233 m. ² /g.	Area by nitrogen 0.134 m. ² /g.
Area by carbon disulfide . . . 0.125 m. ² /g.	Area by carbon disulfide . . . 0.084 m. ² /g.
Area by butane 0.145 m. ² /g.	Area by butane 0.106 m. ² /g.
Roughness factor by nitrogen 1.81	Roughness factor by nitrogen . . 1.76

The two exceptions mentioned above were porous carbon blacks: Mogul, and air after-treated lamp black, LBTT. For these solids containing many fine pores the equation

$$V = \frac{V_m Cx}{(1-x)} \left[\frac{1 - (n+1)x^n + nx^{n+1}}{1 + (c-1)x - cx^{n+1}} \right] \quad (2)$$

was employed, the method of Joyner, Weinberger, and Montgomery (12) being used to evaluate V_m and n , the maximum number of multilayers that can apparently build up on the walls of the narrow pores and capillaries.

The carbon black isotherms have, for convenience, been divided into three general types: *viz.* those for the coarse blacks, those for the very finely divided

TABLE 1
Surface areas of carbon blacks used

SAMPLE NUMBER	DESCRIPTION	SURFACE AREA
		<i>sq. m. per gram</i>
1452	Elf 4—a short ink black; apparent density 12 lb. per cubic foot (a medium-processing rubber black in the fluffy state)	112
1453	Spheron Grade 6—a pelletized medium-processing rubber black; apparent density, 22 lb. per cubic foot	110
1463	Mogul—a long ink black; prepared by the after-treatment in air at 800°F. of a short ink black of the Elf type; apparent density, 12 lb. per cubic foot.	475
1172 .	Carbolac 2—a high-color black prepared from a fine-particle-size channel black by after-treatment in air at 800–1000°F.; apparent density, 7 lb. per cubic foot	772 (814)†
1172-P	Black Pearls* 2—Carbolac 2 in a beaded form; apparent density, about 22 lb. per cubic foot	779 (834)
6204 .	Carbolac 1—a very intense color black; prepared by very intensive air after-treatment at 800–1000°F. of a fine-particle-size channel black; apparent density, 5 lb. per cubic foot.	936 (1023)
6204-P	Black Pearls 1—Carbolac 1 in a pelletized form; apparent density, about 22 lb. per cubic foot	942 (1038)
CRM	The fine-particle channel black used as a raw material in the preparation of Carbolac 1 and 2; apparent density 9 lb. per cubic foot	436 (453)
LBT .	Monsanto lampblack Type T—a rubber grade of lamp-black	26
LBTT.	After-treated Type T lampblack—an experimental sample prepared by air after-treatment at 800°F. of lampblack Type T	218
876 . . .	Monarch 71—a fine-particle-size channel black used as a pigment in the paint and ink industry; apparent density, 12 lb. per cubic foot	398 (418)
880	Black Pearls 71—Monarch 71 in a pelletized form; apparent density, 25 lb. per cubic foot	393
880-100 . . .	An experimental sample of Black Pearls 71 that has been pelletized for 100 hr. rather than the usual $\frac{1}{2}$ hr.	372
879	Spheron Grade 6—a pelletized medium-processing rubber black; apparent density, 22 lb. per cubic foot	112
879-100	Spheron Grade 6 after 100 hr. treatment in the Spheronizing apparatus	114

* All blacks reported in the pelletized or beaded form have been prepared by mechanical agitation by the Spheron process (see U. S. patent 2,120, 541) or by a simple modification thereof involving the addition of small amounts of water.

† Values in parentheses have been obtained by plotting data after correcting p_0 by the Kelvin equation for the small particle size.

blacks, and finally, those for the porous blacks. In figure 3, all of the non-porous black samples having large particles are represented as an average by curve 1, the data having been calculated on the basis of 100 sq. m. surface of each sample. The spread of the points for one isotherm compared to those of another is shown by vertical lines at intervals along the curve. The samples covered by curve 1 are 1452, 1453, CRM, LBT, 879, and 879-100. The absolute surface areas of these carbon black samples vary from 25 to 450 sq. m. per gram.

Curve 2 of figure 3 is an average of four of the very finely divided carbon blacks, samples 1172, 1172P, 6204, and 6204P of table 1. Here again the samples have been put on a 100 sq. m. per sample basis. To avoid confusion, the individual

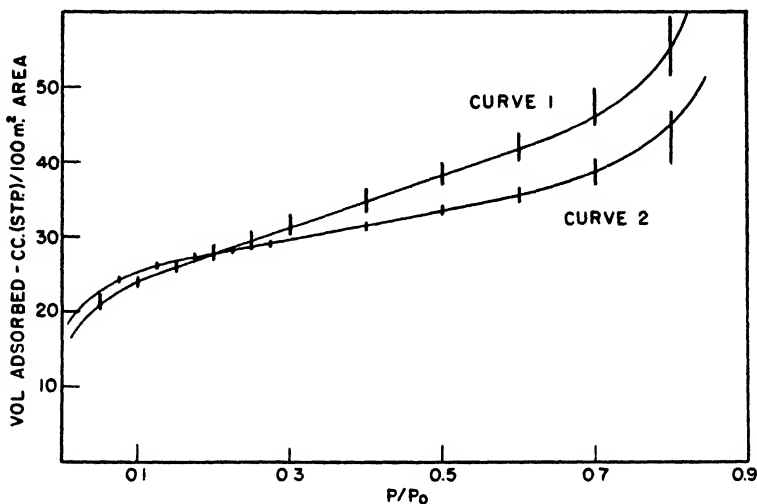


FIG. 3. Average isotherms for nitrogen adsorption at -195°C . per 100 sq. m. area for non-porous carbon blacks. Curve 1 includes isotherms for carbon blacks 1452, 1453, CRM, LBT, 879, and 879-100, all of which have particles in the range extending from about 100 to 1000 Å. in diameter. Curve 2 includes isotherms for samples 1172, 1172P, 6204, and 6204P, the particles being about 35 Å. in diameter if they are assumed to be smooth non-porous spheres. The short vertical lines indicate the spread among the samples for each curve.

points are omitted, but the spread among the four isotherms is indicated by the short vertical lines. The four carbon blacks represented by curve 2 all have areas in the range 800–1000 sq. m. per gram.

The carbon blacks illustrated in figure 3 are believed to be essentially non-porous. In figure 4 are curves for four carbon blacks that have either been so treated during manufacture as to make them porous, or else give some special evidence of porosity. They are samples 1463, LBTT, 876, and 880. Two of these, the Mogul sample No. 1463, and the activated lamp black LBTT have very flat isotherms. On the other hand, curves for samples 876 and 880 of Monarch 71 agree in general with curve 1 of figure 3. The sole evidence for porosity of these latter two blacks is the fact that the surface area by adsorption is several times as great as that calculated from electron micrographs. The

desorption points for only a few isotherms have been obtained in the present work. In figure 4 are included a few such points for the Monarch 71 carbon blacks.

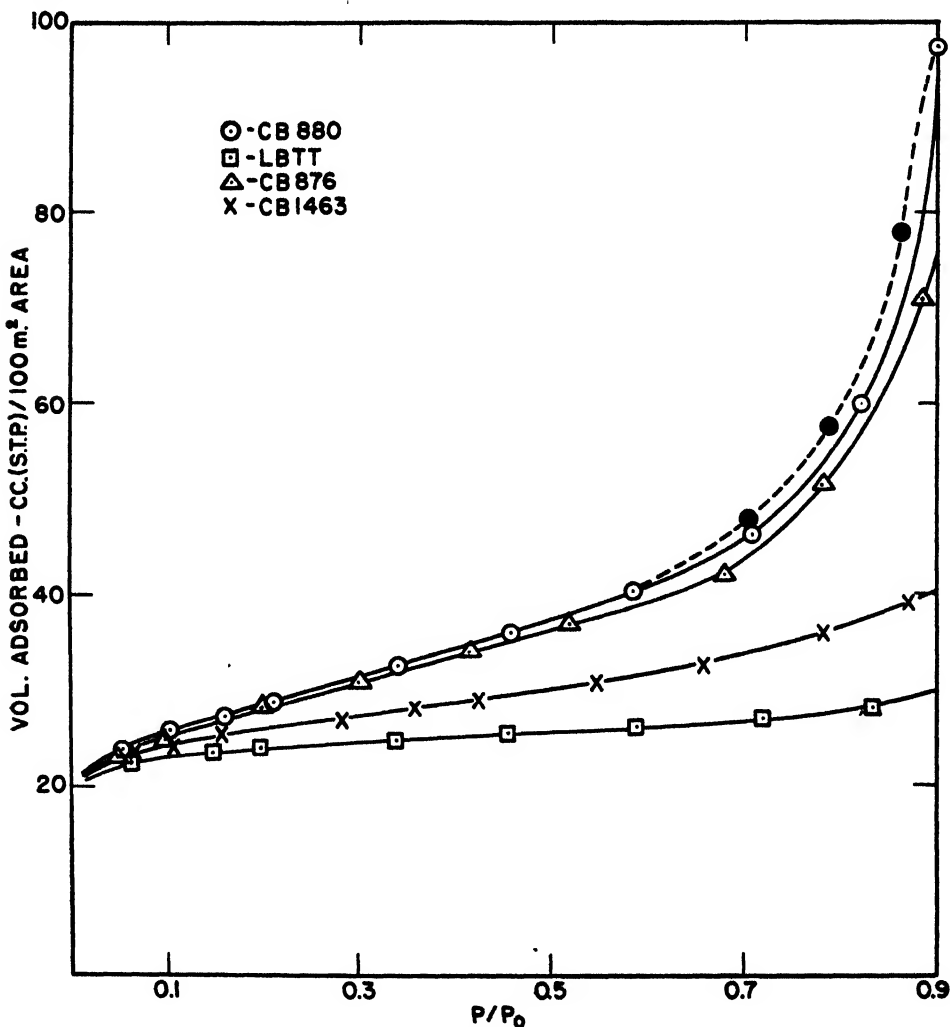


FIG. 4. Adsorption isotherms for nitrogen at $-195^{\circ}\text{C}.$ on porous carbon blacks. Solid circles are desorption points.

The isotherms for the few runs made using carbon disulfide at $0^{\circ}\text{C}.$ or butane at $0^{\circ}\text{C}.$ are shown for sample 1452 in figure 5.

DISCUSSION

Roughness factors and size of the adsorbate molecules

Appended to figures 1 and 2 are the roughness factor calculations for the metal powders for which photomicrographs were available. These roughness

factors are merely the ratios of the surface areas per gram, as measured by the gas-adsorption method, to the geometric area calculated directly from the particle size as shown by the photomicrographs. In calculating the areas by the gaseous adsorbates, the nitrogen, carbon disulfide, and butane molecules were assigned (9) cross-sectional area values of 16.2, 23, and 32 Å², respectively.

The range of these roughness factors as calculated from the nitrogen isotherms is a reasonable one, extending from 1.07 to 1.81. Much less weight should be given the values 1.07 and 1.34 for the two copper powders, since they are based upon nitrogen-adsorption measurements in which the samples gave 0.67 and 0.4 cc. of gas, respectively, as monolayers. Such small V_m values are probably reproducible to no more than 10 or 15 per cent, owing to unavoidable experi-

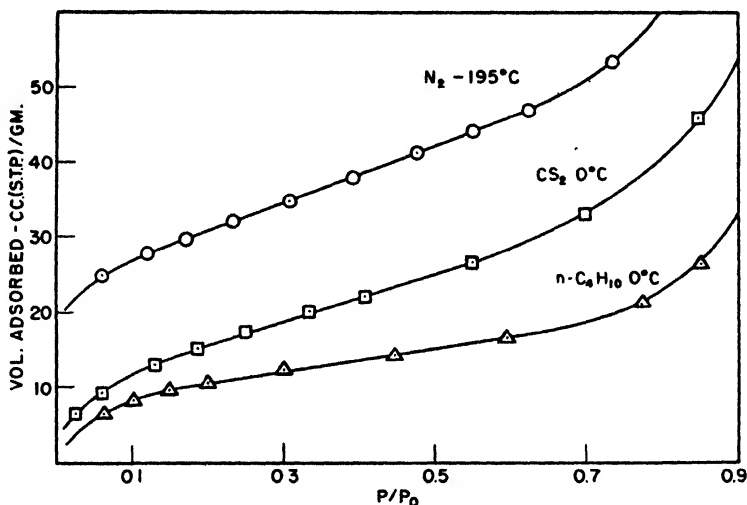


FIG. 5. Adsorption isotherms for nitrogen at -195°C ., carbon disulfide at 0°C ., and *n*-butane at 0°C . on sample 1452.

mental error in the measurements. The isotherms for the zinc dust samples, on the other hand, had V_m values of 2.5 and 4.19 cc., respectively, and are therefore much more accurate than the isotherms for the copper powders.

The surface-area values calculated from carbon disulfide and butane isotherms on the two zinc dust samples and on Grade 6 carbon black are considerably smaller than those obtained for these same materials from nitrogen isotherms. This is consistent with numerous other observations that have appeared in the literature within the last few years (2, 9, 11). For example, Harkins and Jura (11) have pointed out that the area obtained from butane isotherms on a series of six non-porous materials agrees with the area deduced from the nitrogen isotherms only when a value of about 56 Å² is assigned as the cross-sectional area of the butane molecule rather than the 32 Å² assigned by Emmett and Brunauer (4) on the basis of calculations from the density of the liquefied and solidified gas. Actually, on samples NJZN 75, and NJZN 125, and sample 1452

carbon black, areas of 52, 41, and 42 A.² would have to be assigned to the butane molecules to give agreement with the nitrogen area; for carbon disulfide for these three solids, areas of 43, 36.8, and 28.4 A.², respectively, would have to be used in place of the value 23 calculated from the density of the liquid. The cause for the apparent low areas obtained when using certain adsorbate molecules is not clear; there appears to be no question that areas by carbon disulfide and butane are low by 20 to 50 per cent in some cases and that frequently this percentage lowness varies from solid to solid.

Correction of p_0 for small particles

A glance at curves 1 and 2 in figure 3 makes it evident that the isotherms for the most finely divided carbon blacks lie considerably below those for the larger

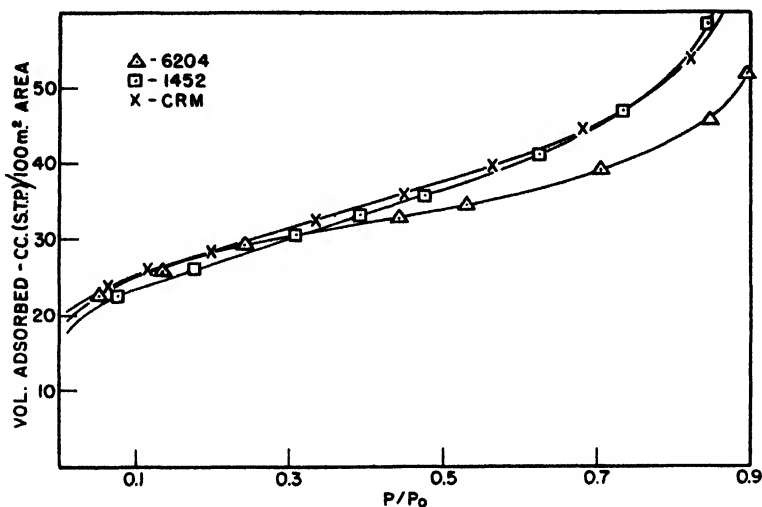


FIG. 6. Adsorption isotherms for nitrogen at -195°C . for samples 1452, CRM, and 6204

particle blacks. It occurred to the writers that this difference in the isotherms might arise from the fact that the extreme curvature of the small particles would increase the value of p_0 for any liquid film that might be approached as the relative pressure increased. To test this hypothesis, an average particle size for the various carbon blacks was calculated from the surface area, using a carbon particle density of 2.1. Then, by the Kelvin equation, a value for p'

$$\ln \frac{p'}{p_0} = \frac{2\sigma V}{rRT} \quad (3)$$

was calculated for liquid droplets having diameters 8 A. greater than those of the average carbon particles. p/p' was then used in new B.E.T. plots and also in new pressure *vs.* volume isotherm plots in place of p/p_0 . The results of these corrections can be illustrated by comparing the isotherms in figures 6 and 7. As is evident, the correction brings the isotherms for a large, a medium, and a

very small diameter carbon black sample into practical superposition over the range of relative pressures between 0.05 and 0.5 when plotted on a 100 sq. m. per sample basis, even though these three blacks cover the range from about 100 to 1000 sq. m. per gram of surface area, or, if the particles are assumed to be non-porous spheres, from a particle size of about 300 to 30 Å. diameter. This hypothesis appears to constitute a reasonable explanation for the fact that the uncorrected isotherms for the black having the smallest particles (figure 6) lie well below those for the blacks having larger particles.

It will also be noted that replotting the adsorption data using the corrected value p' for p_0 yields surface-area values that are somewhat higher than those obtained from the original B.E.T. plots. In table 1, in parentheses, are shown the surface areas obtained from B.E.T. plots that employ the corrected p_0

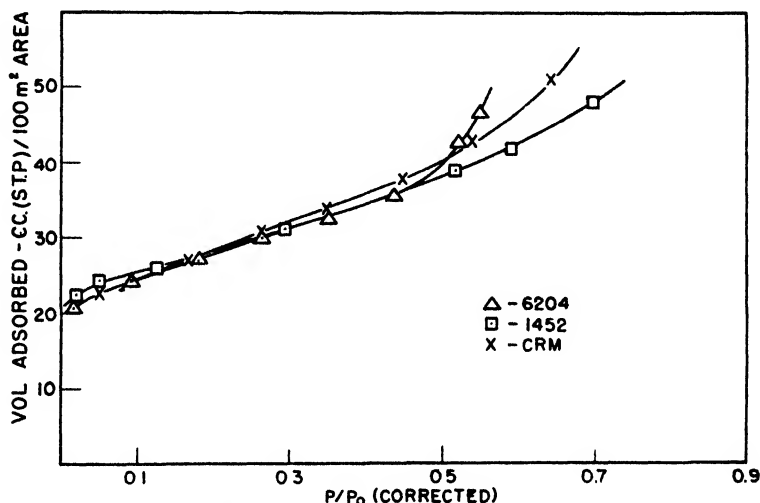


FIG. 7. Isotherms for nitrogen adsorption at $-195^{\circ}\text{C}.$ on samples 1452, CRM, and 6204 after correcting p_0 by the Kelvin equation for the average particle size of the samples.

values. As is evident, this corrected surface area differs from that obtained from the original uncorrected isotherm by less than 5 per cent for non-porous particles having areas of 400 sq. m. per gram or less; it amounts, however, to an increase of 10 or 11 per cent for the very finely divided carbon blacks.

Effect of pelletizing

It was difficult to predict the extent to which pelletizing samples of the various carbon blacks might alter the surface area per gram. Conceivably, considerable blocking out of area might result from forming the tiny carbon black particles into agglomerates by the standard procedures used in producing pellets. To test this point, a sample of Spheron was made up from sample 1452 of Grade 6 carbon black, and samples of Pearls from the finely divided carbon blacks 1172 and 6204. The areas of these pelletized samples were the same as the area of

the original agitated sample from which the Spheron and Pearls were made, as is evident from table 1. If the particles are considered to be non-porous perfect spheres, some screening would be expected for samples 1172 and 6204 even if only a single point of contact existed for each particle. Thus, about 3 per cent of the surface of a sphere would be blocked by a single contact with another sphere of the same size if the spheres are 40 A. in diameter and if all of that portion of the surface closer than 4 A. to the other surface is considered to be blocked out. Actually, it is difficult to imagine fewer than three or four additional points of contact on an average per sphere in the pelletized material compared to the agitated samples, in view of the fact that the density on pelletizing increases from 5 to about 22 lb. per cubic foot. This would mean from 9 to 12 per cent

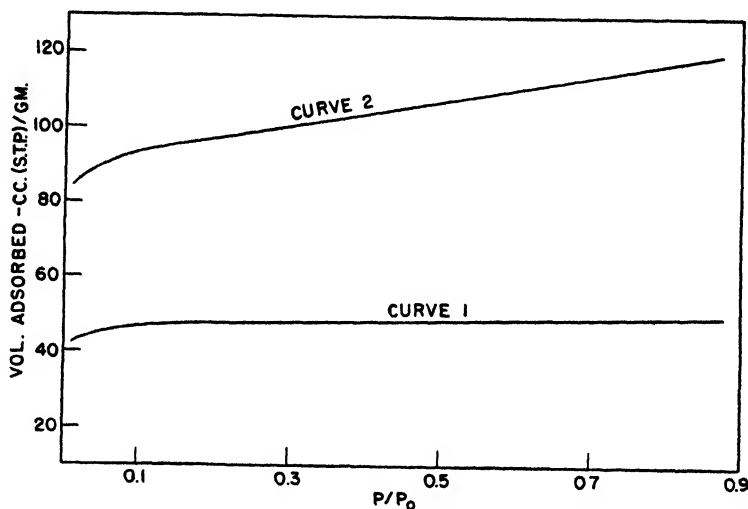


Fig. 8. Increase in the adsorption by Mogul (curve 2) and LBTT (curve 1) resulting from their preparation by air after-treatment from Grade 6 carbon black and LBT, respectively.

blocking of the area of particles 40 A. in diameter. No such added blocking occurs in the pelletized compared to the agitated samples, for the areas of samples 1172P and 6204P are practically the same as the areas of samples 1172 and 6204, respectively. It seems that either most of the tiny carbon black particles within the Spheron or pellets can move with respect to their neighbors sufficiently to permit the adsorbed molecules of nitrogen to form a complete layer over the entire surface or else blocking occurs to the same extent for the agitated and the pelletized samples.

The porous carbon blacks

The air after-treatment used on Mogul and on the activated lamp black LBTT is of such a nature (see table 1) as to produce porosity on the samples. Furthermore, the pores that are formed are of the same order of size as those that exist in ordinary charcoal. This is clearly indicated in figure 8 by the curves formed

by the subtraction of the original adsorption isotherm for the materials from which Mogul and the LBTT were made, from the isotherms of the Mogul and LBTT. These different curves are the same in general appearance as those that have been found for charcoal (5), and confirm the small average size of the pores that are developed in Mogul and LBTT by the activation processes.

The two isotherms in figure 4 for Monarch 71 are quite different from those for the other two porous blacks. Electron-microscope pictures of Monarch 71 are reported to be not too good but, in general, indicate that the geometric surface of the particles is only about one-half or one-third as great as the measured nitrogen area. The actual isotherm of Monarch, however, resembles those of the non-porous carbon blacks represented by the general curve in figure 3 or by the curve for sample 1452 in figure 6. Presumably, therefore, Monarch is suffi-

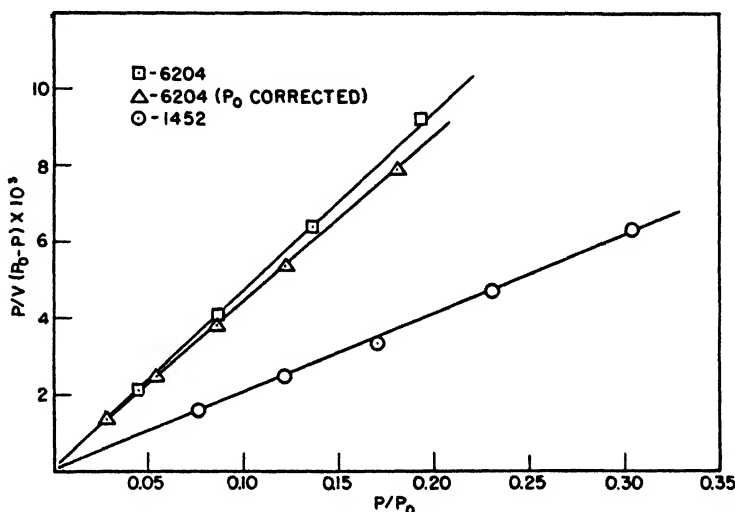


FIG. 9. B.E.T. plots of the adsorption data for samples 1452 and 6204

ciently porous to yield a roughness factor of 2 or 3, but its pores must be much larger than those of Mogul or LBTT. The hysteresis loop obtained for the Monarch sample is consistent with this. It indicates that most of the pores are more than 100 Å. in diameter.

Harkins and Jura plots of adsorption data

In a recent paper, one of the authors (8) pointed out that apparently the exact value for the cross-sectional area of the nitrogen molecule that has to be used in conjunction with the B.E.T. plot of adsorption data to yield the same surface area obtained by the Harkins and Jura method (11) depends strongly on the value of the constant C in equation 1. This constant by definition is

$$C = \frac{a_1 b_1}{b_1 a_2} e^{(E_1 - E_L)/RT}$$

where E_1 is the average heat of adsorption in the first layer and E_L is the heat of liquefaction. To illustrate the effect, the adsorption data for carbon blacks 1452 and 6204 have been plotted both according to equation 1 (figure 9) and according to the Harkins and Jura equation (figure 10):

$$\log p/p_0 = B - \frac{A}{V^2} \quad (2)$$

The C values for samples 6204 and 1452 are, respectively, 665 and 127; the Harkins and Jura plots yield areas agreeing with those obtained from the B.E.T. plots only if a cross-sectional area of 20.6 Å² is used for the nitrogen molecule in the runs on sample 6204, and an area of 17.4 for sample 1452. These data

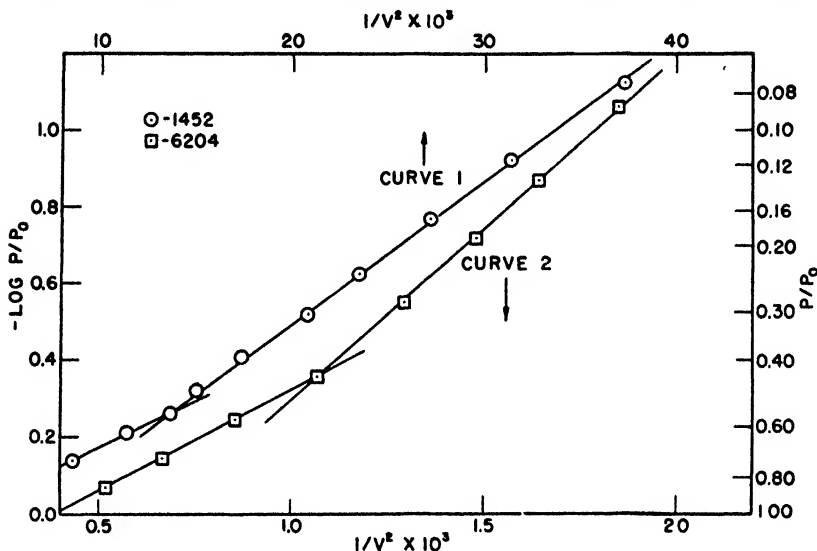


FIG. 10. Harkins and Jura (11) plot of our adsorption data for samples 1452 (curve 1) and 6204 (curve 2).

are not exceptional but are representative of the observations made on the various carbon blacks. Of course, it must be admitted that for the carbon blacks for which the larger C values were obtained, the experimental uncertainty in selecting a C value may be as high as ± 100 units, because of the small value of the intercept $1/V_m C$. Nevertheless, the data definitely conform to the ideas presented previously to the effect that the cross-sectional area of the nitrogen molecule required to bring agreement between surface areas calculated from the B.E.T. plots and those obtained by the Harkins and Jura plots increases with the value of C .

SUMMARY

A comparison of areas obtained by adsorption isotherms for nitrogen at -195°C . with those calculated from photomicrographs yields roughness factors of a reasonable size, in the range 1.1–1.8. Areas determined by using carbon

disulfide or butane are 20–50 per cent lower than those obtained by the use of nitrogen as adsorbate. Pelletizing carbon black produces no appreciable change in its surface area per gram. Evidence is presented for the conclusion that the liquefaction pressure p_0 to be used in applying equation 1 to particles 50 Å. or less in diameter must be corrected to the small diameter by the Kelvin equation.

REFERENCES

- (1) AMON, SMITH, AND THORNHILL: *Ind. Eng. Chem., Anal. Ed.* **15**, 256 (1943).
- (2) BEEBE, BECKWITH, AND HONIG: *J. Am. Chem. Soc.* **67**, 1554 (1945).
- (3) BROWN AND SMITH: *Ind. Eng. Chem.* **34**, 352 (1942).
- (4) BRUNAUER AND EMMETT: *J. Am. Chem. Soc.* **59**, 2682 (1937).
- (5) BRUNAUER, EMMETT, AND TELLER: *J. Am. Chem. Soc.* **60**, 309 (1938).
- (6) EMMETT: *American Soc. Testing Materials, Symposium on New Methods for Particle Size Determination in Subsieve Range* **1941**, 95.
- (7) EMMETT: *Advances in Colloid Sci.* **1**, 1–36 (1942).
- (8) EMMETT: *J. Am. Chem. Soc.* **68**, 1784 (1946).
- (9) EMMETT AND BRUNAUER: *J. Am. Chem. Soc.* **59**, 1553 (1937).
- (10) EMMETT AND DEWITT: *Ind. Eng. Chem., Anal. Ed.* **13**, 28 (1941).
- (11) HARKINS AND JURA: *J. Am. Chem. Soc.* **66**, 1366 (1944).
- (12) JOYNER, WEINBERGER, AND MONTGOMERY: *J. Am. Chem. Soc.* **67**, 2182 (1945).
- (13) SMITH, THORNHILL, AND BRAY: *Ind. Eng. Chem.* **33**, 1303 (1941).
- (14) THORNHILL AND SMITH: *Ind. Eng. Chem.* **34**, 218 (1942).
- (15) WOOTEEN AND BROWN: *J. Am. Chem. Soc.* **65**, 113 (1943).

INTERFACIAL TENSION BY THE RING METHOD: THE BENZENE-WATER INTERFACE

H. L. CUPPLES

*Bureau of Entomology and Plant Quarantine, Agricultural Research Administration,
U. S. Department of Agriculture, Beltsville, Maryland*

Received May 27, 1947

The ring method for the measurement of surface tension has been greatly improved through the researches of Harkins and collaborators (2, 4, 5). Harkins and Jordan (4) present tables of correction factors which are applicable to a wide range of experimental conditions, both as to the properties of the fluids and as to the design of the ring. However, the data upon which these correction factors are based are surface-tension data, and they have published only two preliminary determinations of the benzene–water interfacial tension in support of the applicability of their correction factors to the measurement of interfacial tensions. For the benzene–water interface at 25°C. they reported two values:

RING NO.	R	r	R/r	γ
5.....	1.0142	0.02001	50.69	33.91
7.....	1.2144	0.02913	41.69	34.16

These values are, respectively, 0.77 and 0.52 dynes per centimeter lower than the generally accepted value (34.68) for this interfacial tension (3).

Zuidema and Waters (7) investigated the applicability of the Harkins *F*-factors to the measurement of oil-water interfacial tensions, using the du Nouy tensiometer. They found that the Harkins tables were inadequate, because of an insufficient range of the variables used as arguments, except for the cases of very low scale readings and/or very great differences between the densities of the two phases. For their work they developed a mathematical formula which they used for interpolating and extrapolating values of the Harkins *F*-factor. Then, for eight oils of indefinite composition, and for benzene, they compared the oil-water interfacial tensions as measured by the ring method and by the method of capillary rise. For benzene they obtained the values 34.6 and 34.9 with 4-cm. and 6-cm. rings, respectively. These values are in good agreement with the accepted value for the benzene-water interfacial tension, but they are up to 1.0 dyne per centimeter higher than those reported by Harkins and Jordan (4).

In making preparations to use the du Nouy interfacial tensiometer for the measurement of interfacial tensions, the writer attempted to check the calibration of the instrument by measuring the benzene-water interfacial tension, using A.C.S. reagent-grade benzene. A result several dynes too low was obtained. As interfacial tensions may be lowered by very small amounts of impurities, it was considered to be worth while to make some careful measurements of the benzene-water interfacial tension, using a specially prepared sample of benzene. The results are recorded below.

EXPERIMENTAL

Purified benzene was prepared from thiophene-free, A.C.S. reagent-grade benzene. Starting with 1900 ml., a total of 800 ml. was discarded in three fractional crystallizations. The product was then two times fractionally distilled, with recovery of 430 ml. of an intermediate constant-boiling fraction. A final distillation was made in an all-glass Friedrich recovery still, an intermediate fraction of 300 ml. being collected for use in the interfacial-tension measurements. Application of the isatin-sulfuric acid test confirmed the absence of thiophene. The purified benzene was twice washed with redistilled water, then shaken with redistilled water at 25.0°C., and kept at that temperature in contact with the aqueous phase during the time required to make the interfacial-tension measurements. The water was prepared from the laboratory-distilled water by twice redistilling it subsequent to oxidation with acid permanganate. All glassware used in handling the liquids was carefully cleaned with hot chromic acid cleaning solution. During the period of 8 days in which the interfacial tensions were measured, no drift in values was observed which might be attributed to contamination.

The interfacial tensions were measured with a du Nuoy interfacial tensiometer, using three 6-cm. platinum-iridium rings supplied by the manufacturer of the tensiometer. The ring dimensions supplied by the manufacturer were used

for determining the proper value of the correction factor, F . This value was determined by a graphical extrapolation of the F values published by Harkins and Jordan (4). Their values for rings having $R/r = 50$ include values of R^3/V between 0.30 and 3.50. For rings having R/r values of 52, 54, and 56, the lowest tabulated value of R^3/V is 0.40, but the individual curves are similar in form and are closely spaced. For the rings used in these measurements values of R/r lie between 51.5 and 54.5, and for the benzene-water system R^3/V is approximately 0.29. The amount of extrapolation required is not great, and the extrapolated values should be substantially as accurate as the tabulated values. Further, the appropriate F values have been calculated by the Zuidema and Waters (7) equation, and the calculated values agree well with the values obtained by graphical extrapolation. Data on the three rings, as supplied by the instrument manufacturers, are given in table 1. As a check on ring dimensions, twelve

TABLE 1.
Ring dimensions and factors

RING NO.	R <i>cm.</i>	R/r	F	Z-W	K
1.....	0.9535	54.5	1.066	1.064	1.007
2.....	0.9570	51.5	1.059	1.059	1.011
3.....	0.9562	52.	1.062	1.061	1.007

D_1 (density of lower phase) = 0.9968; D_2 (density of upper phase) = 0.8732

R = radius of ring

r = radius of wire of ring in centimeters

F = Harkins F -factor

Z-W = value calculated from Zuidema-Waters equation

K = the ring-torsion head constant

measurements of R and r of ring No. 3 with a cathetometer gave an average value of $R/r = 52.2$.

The surface tension or interfacial tension, γ , is given by the relation

$$\gamma = \frac{P}{4\pi R} \times F$$

where P is the maximum pull on the ring, in dynes. For a given ring and torsion head this relation may be written $\gamma = KP'F$, where P' is the reading of the torsion scale at maximum pull, and K is a constant which may be evaluated from the dimensions of the ring and a calibration of the torsion wire, or by an over-all calibration of the ring and torsion head against a liquid of known surface tension. The latter method was used for these measurements, the calibrations being made by measuring the maximum torsion scale reading corresponding to the surface tension of benzene at 25.0°C., assuming its value to be 28.22 dynes per centimeter. The experimentally determined values of K are included in table 1. In measuring interfacial tensions the initial or "zero" setting was de-

terminated for the ring immersed in benzene; this gives a small net downward pull corresponding to about 0.2 dyne per centimeter.

Harkins has pointed out that it is important that the wire of the ring should be in a plane, and that the plane of the ring should be parallel to the plane of the interface. Two of the three rings here used were new and the third one was in new-ring condition; all three were checked before use to see that the wire lay in a plane. Each ring after attachment to the tensiometer was leveled by adjustment of the base of the tensiometer so that, when swinging free, its plane was parallel to that of the interface. The leveling was done by leveling the outer

TABLE 2

Interfacial tension of the mutually saturated benzene-water system, at 25.0°C., by the ring method

RING NO.	INTERFACE DIAMETER	P'	KF	γ
	cm.			dynes/cm
2	7	30.0	1.071	32.1
2	7	30.3	1.071	32.5
2	7	30.5	1.071	32.7
2	7	30.4	1.071	32.6
2	7	30.6	1.071	32.8
1	7	30.5	1.073	32.7
1	7	30.6	1.073	32.8
1	7	30.6	1.073	32.8
1	7	30.6	1.073	32.8
1	7	30.5	1.073	32.7
3	7	30.7	1.069	32.8
3	7	30.8	1.069	32.9
3	7	30.6	1.069	32.7
3	7	30.6	1.069	32.7
3	7	30.8	1.069	32.9
3	12	30.8	1.069	32.9
3	12	30.3	1.069	32.4
3	12	30.2	1.069	32.3
Average..				32.67 \pm 0.05

edges of the ring as observed through a cathetometer telescope, and then leveling in a direction at right angles to that first used, repeating the process until satisfactory leveling was obtained in both directions. In preliminary experiments it was found that erratic results were obtained when the ring was pushed downward from the oil into the water, but that consistent results could be obtained by pulling the ring upward from the water to the oil. This finding agrees with that of Leprince-Ringuet (6). It was also found that, after the ring had been in contact with the oil phase, replacing it in the aqueous phase did not completely displace the oil, and an accurate tension measurement could not be made. This agrees with the observation of Alexander and Schulman (1) that "all rings, even platinum, rapidly turn hydrophobic at the interface and consequently need fre-

quent cleaning." However, for this work no attempt was made to make the ring completely hydrophobic and to move it across the interface from the oil to the water. Instead, a procedure was adopted which avoids contact of the ring with the oil. A convenient depth of aqueous phase is placed in the glass container, of 7 or 12 cm. diameter, and the ring, after being cleaned and flamed, is lowered into the aqueous phase and placed about $\frac{1}{8}$ in. below the surface. Then oil phase is carefully added until its surface reaches the sharp bends of the stirrup. At this point a moderate tension is applied to the ring, less than the maximum pull which the interface will exert but sufficient to produce a large part of the maximum vertical displacement of the ring, and additional oil phase is added to again bring the oil surface near the sharp bends of the stirrup. The tension on the ring is then gradually increased to the point of maximum pull, the torsion arm being kept accurately at its "zero" point by continuous adjustment of its vertical position. The tension is increased very slowly when near the maximum value, the final value being reached within 10–15 min. after formation of the interface. Most of the measurements were made in a container having a diameter of 7 cm., but several were made in one having a diameter of 12 cm. During the measurements the room temperature was kept at $25.0^{\circ}\text{C} \pm 0.3^{\circ}$, and the container was partially immersed in water at $25.0^{\circ}\text{C} \pm 0.2^{\circ}$. The liquid was covered to minimize evaporation.

The results are presented in table 2. Average measurements with the several rings agree within a maximum deviation of 0.3 dyne per centimeter, which is reasonably satisfactory. There is no indication that the maximum pull is greater in the larger container. The mean error of a single determination is ± 0.22 dyne per centimeter. The average of the eighteen measurements is 32.67 ± 0.05 dynes per centimeter. This is 2.01 dynes per centimeter lower than the generally accepted value for this interface, and 1.37 dynes per centimeter lower than the average of the two values by the ring method reported by Harkins and Jordan.

SUMMARY

Measurements have been made of the interfacial tension at 25.0°C . of the mutually saturated benzene–water system, using a du Nouy interfacial tensiometer and applying the appropriate Harkins *F*-factor. The average of eighteen measurements, using three rings, is 32.67 dynes per centimeter, a value which is 2.01 dynes lower than the generally accepted value for this interfacial tension.

REFERENCES

- (1) ALEXANDER, A. E., AND SCHULMAN, J. H.: Trans. Faraday Soc. **36**, 960–4 (1940).
- (2) FREUD, B. B., AND FREUD, H. Z.: J. Am. Chem. Soc. **52**, 1772–82 (1930).
- (3) HARKINS, W. D., BROWN, F. E., AND DAVIES, E. C. H.: J. Am. Chem. Soc. **39**, 354–64 (1917).
- (4) HARKINS, W. D., AND JORDAN, H. F.: J. Am. Chem. Soc. **52**, 1751–72 (1930).
- (5) HARKINS, W. D., YOUNG, T. F., AND CHENG, L. H.: Science N.S. **64**, 333–6 (1926).
- (6) LEPRINCE-RINGUET, L.: Pub. sci. tech. ministère air (France) No. **52**, 25 pp. (1934); Chem. Abstracts **31**, 4094 (1937).
- (7) ZUIDEMA, H. H., AND WATERS, G. W.: Ind. Eng. Chem., Anal. Ed. **13**, 312–13 (1941).

EQUILIBRIA IN SILVER ACETATE SOLUTIONS¹F. H. MACDOUGALL AND SIGFRED PETERSON²*School of Chemistry, University of Minnesota, Minneapolis, Minnesota**Received May 27, 1947*

INTRODUCTION

In previous papers from this Laboratory (13, 14) studies were made of the effect of added electrolytes on the solubility of silver acetate in water and in mixed solvents. When the added electrolyte was of the uni-univalent type and contained no ion in common with silver acetate, it was found that the effect could be represented quantitatively by means of a Debye-Hückel equation with a reasonable value for the parameter which, in the theory of Debye, corresponds to an average ionic diameter. In 1931 Larsson and Adell (10) reported that this procedure was unsuccessful when the added electrolyte was an acetate. It seemed reasonable to suppose that this failure could be due to the formation in such cases of appreciable amounts of complex ions. The papers by MacDougall and Allen (14) report the results of solubility measurements when the added electrolyte was either an acetate or a silver salt. These papers present strong evidence in favor of the existence of such complex ions as AgA_2^- and Ag_2A^+ . Estimates were made of the magnitude of the dissociation constants of these complex ions; certain important results obtained in the present investigation enable one to calculate the dissociation constant of AgA_2^- by an independent method.

To obtain additional and, if possible, more exact information about the nature of silver acetate solutions, measurements were made of the electromotive force of suitable cells. Since these measurements lead more or less directly to a determination of the concentration of silver ion in silver acetate solutions, it becomes possible to calculate the amount of dissolved silver which is not in the form of silver ion.

During the progress of our work and after our experiments had shown conclusively that a considerable fraction of dissolved silver acetate is not dissociated, we received a reprint of a valuable paper by Leden (11), who had come to the same conclusion. In order to be able to make some comparison of our results with those obtained by Leden, we found it necessary to determine the solubility of silver acetate in 3 *M* sodium perchlorate.

MATERIALS USED AND METHODS OF ANALYSIS

Most of the materials used were available in a sufficiently high degree of purity to meet the standards given by Rosin (16). Sodium perchlorate was prepared from sodium carbonate and perchloric acid; silver oxide was prepared from silver nitrate and sodium hydroxide.

¹ This paper gives the essential portions of the dissertation presented by Sigfred Peterson to the Graduate Faculty of the University of Minnesota in partial fulfillment of the requirements for the degree of Doctor of Philosophy, March, 1947.

² Du Pont Fellow in the School of Chemistry, University of Minnesota.

Solutions were analyzed for silver by the Volhard method (9). Solutions of potassium thiocyanate were standardized against weighed samples of fused silver nitrate. Solutions containing sodium nitrate or sodium acetate were analyzed by converting the salts to sodium chloride, which was then weighed. Details of the analysis were adapted from Treadwell and Hall (18).

In preparing all solutions, double-distilled "conductivity" water was used.

PREPARATION OF ELECTRODES

For the measurement of equilibria in silver acetate solutions it is necessary to use electrodes reproducible to closer than 0.0001 volt. Many investigators have prepared silver-silver salt (especially halide) electrodes of very high reproducibility; little is said about simple silver electrodes. Lewis (12) found electrodes prepared by the thermal decomposition of silver oxide satisfactory, and electrodes prepared by electrodeposition from cyanide solutions unsatisfactory. The precision needed in this work is greater than that reported by Lewis.

For this investigation the following procedure was used: Platinum wire of 0.36 mm. diameter was sealed through the end of a piece of soft-glass tubing with 5 cm. protruding, and was carefully annealed. The seals were tested for leaks either by immersion for 4 hr. in boiling water and inspection to detect water condensed inside the tube, or by immersion for 2 days in sodium carbonate solution with phenolphthalein indicator solution inside the tubes.³ The protruding wire was fused at the tip and bent into a helix approximately 3 mm. in diameter and approximately 8 mm. in length.

A thick aqueous paste of silver oxide was packed onto the platinum spiral and dried for 45 min. at 100°C. Longer drying causes the oxide to crumble and fall off the electrode; a briefer drying period results in eventual introduction of considerable moisture into the oxide-decomposition chamber. The dried oxide was decomposed to porous silver metal by heating for 6 hr. at 400°C. in a Pyrex tube in an electric furnace. Recombination was prevented by passing purified nitrogen (17) over the electrodes during the last half-hour of the heating and the subsequent cooling. Copper wire was inserted into the tube of the electrode and brought into electrical contact with the platinum by either mercury or Wood's alloy.

Electrodes prepared in this manner were frequently found to differ in potential by several tenths of a millivolt when placed in the same solution. This disagreement often changed with time, usually increasing. An electrolytic purification method was found to reduce the disagreement between almost all electrodes to 0.00002 volt or less. A low current is passed through a dilute perchloric acid solution with a platinum anode and the electrode to be treated as cathode. The conditions for this treatment have not been found critical; 0.5 milliamp. for 3 hr. in 0.02 *M* perchloric acid has been found satisfactory.

After a period of use varying from about two weeks to three months, silver electrodes become negative (in the external circuit) with respect to freshly treated electrodes. A repetition of the electrolytic treatment restores the electrodes

³ Method attributed to T. F. Young by J. E. Wertz.

to agreement. The deterioration of electrodes is much more rapid in acetate solutions than in nitrate solutions.

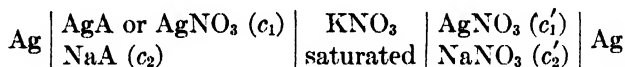
Some study was made of electrodes prepared by electrolytic deposition of silver on platinum. Electrodes formed by deposition from $\text{KAg}(\text{CN})_2$ solution were not reproducible and were decidedly negative (external circuit) to thermally deposited silver electrodes. Rapid electrolysis of 5 per cent silver nitrate solution (0.2 amp. for a few minutes on a 1-cm. length of platinum 0.36 mm. in diameter) gave electrodes which agreed within 0.00002 volt with treated thermal electrodes; however, the silver deposit was so loosely adherent as to make this type of electrode impractical.

To avoid the lack of reproducibility of silver electrodes, other investigators (8, 11) have used silver chloride electrodes. At the suggestion of Professor I. M. Kolthoff, silver iodide electrodes were tried. The silver electrodes described above were electrolytically oxidized for 2–4 hr. with 1.25 milliamp. in 0.05 *M* potassium iodide. The simple platinum cathode was separated from the anode solution by a sintered-glass filter crucible. Mutual agreement among the silver iodide electrodes as well as agreement between these and simple (electrolytically treated) silver electrodes was satisfactory. The iodide electrodes reached equilibrium potentials more slowly than silver electrodes, and also deteriorated with use. The stability of these electrodes appeared greater than that of simple silver electrodes in acetate solution, but less in nitrate solution.

The electrodes were tested by measurement of the electromotive force between them in a multiple-necked cell containing 0.01 *M* silver nitrate.

THE EXPERIMENTAL METHOD

Cells studied were of the type



A very desirable salt bridge for this type of work is that described by Irving and Smith (4). The bridge is of conventional shape with ground-glass plugs at the ends; a film of solution between the plug and its socket conducts sufficient current, while the plug prevents mixing of the bridge and half-cell solutions. To simplify design of the half-cells and assembly of the cells a modification of the ground-glass plug method was adopted. Each half-cell was made with an appendage terminating in a ground-glass plug and fitted with a size No. 4 rubber stopper. The half-cells then dipped into the salt-bridge solution contained in a vessel with two to four necks made to fit size No. 4 stoppers.

The silver electrodes (described in another section) were fitted with size No. 1 natural gum rubber stoppers; all half-cells had necks to fit these stoppers. Most half-cells were made to take two electrodes,—both as an insurance against deterioration of an electrode and to facilitate detection of such deterioration.

The solutions in the cells did not come in contact with the rubber stoppers. All glass-rubber joints were covered with paraffin wax to prevent the leaking in of water from the water bath.

Half-cells were painted black to prevent photochemical reactions in the silver solutions. It was necessary to have a very thorough coat of paint, with no minute gaps; this is especially true for the acetate solutions. A satisfactory paint film both sufficiently light-tight and resistant to long immersion in water was obtained by coating the vessel with varnish, then twice with black paint, and again with varnish.

A Leeds & Northrup Type K-1 potentiometer and a Weston Model 4 standard cell calibrated against a fairly new Eppley No. 100 standard cell were employed in the measurements of electromotive force. The cells studied were immersed in a well-agitated water bath whose temperature fluctuated no more than 0.05°C . about an average temperature known within 0.02°C . The thermostat temperature was measured by a thermometer graduated in tenths of degrees and read to hundredths with the aid of a magnifying glass. It has been calibrated at 25°C . and 35°C . by comparison with copper-constantan thermocouples prepared by J. E. Wertz and calibrated by him at accurately known temperatures.

Cells were measured several times daily over a period of 2-5 days. After a period of 2-20 hr. the measured E.M.F. would become constant with time; later it would drift away from the constant value. The initial variation is without doubt the approach to thermal equilibrium of the cell and electrode equilibrium with the solution (probably the adsorption of silver ion in the pores of the metal). The constant E.M.F. is taken to be the correct value, and the final variation to be due to the deterioration of the electrodes or decomposition of the solutions.

It will be noted that a saturated solution of potassium nitrate was interposed between the two half-cells for the purpose of minimizing the net E.M.F. due to the liquid junctions (15). It is difficult to make even a rough estimate of these E.M.F.'s. To apply the equation given by Henderson (2) it is necessary to know for each solution the equivalent ionic conductances of each species of ion present in the solution. This statement holds for the saturated solution of potassium nitrate as well as for the solutions in the half-cells. If we assume that the Henderson equation is valid for the junctions that occur in the cells whose E.M.F.'s we have measured, a study of the equation shows that the value obtained for any liquid-junction E.M.F. depends markedly on the magnitude of the *difference* between the mobilities of K^+ and NO_3^- in the saturated solution of potassium nitrate and (especially when the other solution contains an electrolyte at a relatively high concentration, such as $0.5\text{ }M$ or $1\text{ }M$) on the *difference* between the mobilities of the positive and negative ions of this electrolyte. The chief source of error is, in general, our uncertainty about the transference number of a saturated solution of potassium nitrate. In using the Henderson equation, we assumed (1) that at 18°C . the equivalent conductance of potassium nitrate in the saturated solution is 61.3 and that the transference number of the cation is 0.51; (2) that in a mixture of two uni-univalent electrolytes the equivalent conductance of each electrolyte is determined by the total concentration; (3) that for solutions other than saturated potassium nitrate we may use transference numbers obtained for dilute solutions of the electrolytes concerned. With these rather uncertain assumptions we calculated the net E.M.F. due to liquid junctions in a number of cells whose compositions are given in a later section of this paper.

NUMBER OF CELL	MEASURED E.M.F.	CALCULATED LIQUID-JUNCTION E.M.F.
	<i>volts</i>	<i>volts</i>
6.....	0.00070	0.00002
17.....	0.00243	0.00023
22.....	0.00720	0.00060

These calculations apparently show that the interposition of a saturated solution of potassium nitrate by no means "eliminates" the liquid-junction E.M.F. Nevertheless, because of the relatively large uncertainty in the calculated values of the liquid-junction E.M.F., the only practicable course for us seemed to be to neglect them entirely. On this basis the measured E.M.F. of a cell is given by the equation

$$E = \frac{RT}{F} \ln \frac{a'}{a}$$

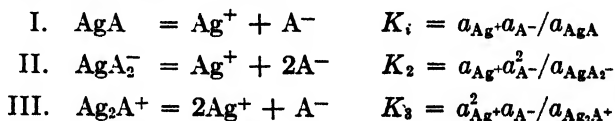
where F is a faraday and where a' and a are the activities of silver ion in the nitrate and acetate solutions, respectively.

It will be noted that the ionic strengths of the two solutions in a given cell (apart from the potassium nitrate solution) were always almost exactly equal. It follows that the mole-fraction activity coefficient of silver ion should be very nearly the same in both solutions up to an ionic strength of 0.1 and approximately the same for higher ionic strengths. A similar statement can be made even if other activity coefficients are used. Thus, if c'_1 is the molar concentration of silver nitrate (assumed to be completely ionized and free from complexes) and if c_{Ag^+} denotes the concentration of free silver ions in the acetate solution, we can write for the E.M.F. of a cell

$$E = \frac{RT}{F} \ln \frac{c'_1}{c_{Ag^+}}$$

THEORETICAL CONSIDERATIONS

In solutions that are unsaturated with respect to solid silver acetate, we suppose the following equilibria to exist:



Let γ_0 be the molal activity coefficient of unionized AgA and let γ be the mean activity coefficient of Ag^+ and A^- . We shall assume that in a given solution the ions A^- and AgA_2^- on the one hand and the ions Ag^+ and Ag_2A^+ on the other hand have equal activity coefficients. If we express the molality of a species by its formula in parentheses, we obtain the following relations:

$$(\text{AgA}) = (\text{Ag}^+)(\text{A}^-)\gamma^2/K_1\gamma_0 \quad (1)$$

$$(\text{AgA}_2^-) = (\text{Ag}^+)(\text{A}^-)^2\gamma^2/K_2 \quad (2)$$

$$(\text{Ag}_2\text{A}^+) = (\text{Ag}^+)^2(\text{A}^-)\gamma^2/K_3 \quad (3)$$

We represent the molalities of total silver and of total acetate in a solution by m_s and m_a , respectively; hence,

$$m_s = (\text{Ag}^+) + (\text{AgA}) + (\text{AgA}_2^-) + 2(\text{Ag}_2\text{A}^+) \quad (4)$$

$$m_a = (\text{A}^-) + (\text{AgA}) + 2(\text{AgA}_2^-) + (\text{Ag}_2\text{A}^+) \quad (5)$$

From equations 4 and 5, one obtains:

$$(\text{A}^-) = m_a - m_s + (\text{Ag}^+) - (\text{AgA}_2^-) + (\text{Ag}_2\text{A}^+) \quad (6)$$

Of the terms on the right-hand side of equation 6, m_a and m_s are known for any solution, since the composition and density are known and the value of (Ag^+) is calculated from the measured electromotive force. Calculations which will be reported later show that (AgA_2^-) is always less (and usually a great deal less) than 1 per cent of (A^-) . From estimates previously made of the values of K_2 and K_3 , it is evident that in the solutions we have investigated the concentration of Ag_2A^+ can only be of the same order of magnitude as that of AgA_2^- when m_a does not greatly exceed m_s . When we come to calculate the concentration of AgA_2^- , we shall find that significant values can be obtained by our methods, only when the concentration of acetate greatly exceeds that of silver. In such a solution the concentration of Ag_2A^+ must be very small, even when compared with that of AgA_2^- . It follows therefore that we may write in place of equation 6 for all our solutions

$$(\text{A}^-) = m_a - m_s + (\text{Ag}^+) \quad (7)$$

and for solutions in which (A^-) is considerably greater than (Ag^+) ,

$$(\text{AgA}_2^-) = m_s - (\text{Ag}^+) - (\text{AgA}) \quad (8)$$

DETERMINATION OF K_i

If we replace in equation 4 the expressions for (AgA) and (AgA_2^-) given by equations 1 and 2, respectively, we find

$$\frac{m_s - (\text{Ag}^+)}{(\text{Ag}^+)(\text{A}^-)\gamma^2} = \frac{1}{K_1\gamma_0} + \frac{(\text{A}^-)}{K_2} = \frac{1}{K'} \quad (9)$$

It has been shown (1) that the activity coefficient of an uncharged molecular species can be frequently represented by the equation

$$\log \gamma_0 = kS \quad (10)$$

For our present purpose, S in equation 10 may be replaced by (A^-) . Moreover, when γ_0 does not greatly exceed unity, equation 10 may be transformed into

$$\frac{1}{\gamma_0} = 1 - 2.3k(\text{A}^-) \quad (11)$$

Substitution of this value of γ_0 in equation 9 results in the expression

$$\frac{1}{K'} = \frac{1}{K_1} + (\text{A}^-) \left(\frac{1}{K_2} - \frac{2.3k}{K_1} \right) \quad (12)$$

If then we can find values of $1/K'$ as a function of (A^-) , we can use a graphical method or the method of least squares to determine the best value of $\frac{1}{K_i}$ and of $\left(\frac{1}{K_2} - \frac{2.3k}{K_i}\right)$. It should be apparent that although this procedure may give a fairly good value of K_i , the value so obtained for K_2 may be more uncertain, partly because of the uncertainty about the correct value of k in equation 10. Because of these considerations, the magnitude of K_2 has also been determined more directly by a quite different method.

It is also clear from equation 9 that evaluation of K' requires a knowledge of γ , the mean activity coefficient of Ag^+ and A^- . To make a satisfactory determination of K_i , K_2 , γ , and γ_0 required the correlation of results obtained in the following investigations: (1) The present paper dealing with the E.M.F. of various cells and reporting also the solubility of silver acetate in 3 molar sodium perchlorate. (2) The solubility of silver acetate in water and in sodium nitrate solutions (13). (3) The paper by Leden (11) which gives the concentration of Ag^+ in solutions containing chiefly sodium acetate and sodium perchlorate to a total molarity of 3.

The paper by MacDougall and Rehner (13) gives an expression for γ as a function of the ionic strength in solutions of sodium nitrate. Applying this equation to our solutions, we are able to obtain a series of values of K' (see equation 9). From this series, we obtain a preliminary value of K_i by the method indicated previously. Using this value of K_i and a value of γ_0 obtained by comparing some of our results with those obtained by Leden, we calculated the concentrations of AgA and hence of Ag^+ and A^- in the nitrate solutions. A new Debye expression was found to fit these results and the new expression for γ was used in equations 9 and 12. As our final expression for γ in aqueous sodium nitrate solutions at 25°C. we found:

$$-\log \gamma^2 = \frac{1.0184S^{\frac{1}{2}}}{1 + S^{\frac{1}{2}}} \quad (13)$$

For 34.7°C. the number 1.0184 becomes 1.0381 on using Wyman's equation (19) for the dielectric constant of water. For the dissociation constant, K_i , of AgA we found:

$$K_i = 0.186 \text{ at } 25^\circ\text{C.}; \quad K_i = 0.179 \text{ at } 34.70^\circ\text{C.} \quad (14)$$

At the same time we were able to correct previously found values (14) for K_1 , the true activity product of silver and acetate ions in aqueous solutions saturated with silver acetate at 25°C. We have found:

$$K_1 = a_{Ag^+}a_{A^-} \text{ (saturated solution)} = 1.95 \times 10^{-3} \quad (15)$$

Moreover, we also found

$$\frac{1}{K_2} - \frac{2.3k}{K_i} = 4.1 \pm 1.0$$

which, with $k = 0.07$ and $K_i = 0.186$, gives

$$K_2 = 0.20 \pm 0.04 \text{ at } 25^\circ\text{C.} \quad (16)$$

For a temperature of 34.7°C. we found by a similar procedure:

$$K_2 = 0.19 \pm 0.04 \text{ at } 34.7^\circ\text{C.}$$

Further discussion will be resumed after presentation of our experimental data.

EXPERIMENTAL DATA

E.M.F. measurements

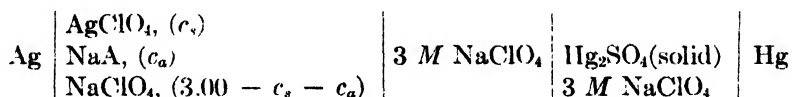
In table 1 are given the molar concentrations and densities of the solutions used, together with the measured E.M.F. in each case. Measurements were made with thirty-four cells at 25°C. and sixteen cells at 34.70°C. Table 2 gives the values of c_{Ag^+} calculated from the E.M.F. and the molalities, m_a , m_s , (Ag^+) , and (A^-) . The molality, (A^-) , was obtained by using equation 7. The seventh column gives the values of $1/K'$ (defined by equation 9) which were obtained by the procedure described previously.

Solubility measurements

Determinations were made of the solubility of silver acetate at 25°C. in water and in 3 *M* sodium perchlorate. The procedure has been described in previous papers (13, 14) from this Laboratory. The solubility found for silver acetate in water ($m = 0.06699$) is somewhat larger than values previously reported from this Laboratory, 0.06674 (14) and 0.0666 (13), but is in the range of other reported values, 0.0668 (5) and 0.0671 (3, 7). Our results are given in table 3.

Experiments of Leden

Leden (11) reports a study of cells of the type



A series of such cells at 20°C. was prepared by adding to the half-cell with $c_a = 0$ successive portions of 3 *M* sodium acetate. Because of the constant ionic strength it was assumed that all activity coefficients remained unchanged. The concentration of free silver ion in a given cell is calculated from the difference between the E.M.F. of the cell and that of the cell in which $c_a = 0$.

Defining B_1 , B_2 , B_3 by the equations

$$B_1 = \frac{c_{\text{AgA}}}{c_{\text{Ag}^+} c_{\text{A}^-}}$$

$$B_2 = \frac{c_{\text{AgA}_2^-}}{c_{\text{Ag}^+} c_{\text{A}^-}^2}$$

$$B_3 = \frac{c_{\text{AgA}_3^{--}}}{c_{\text{Ag}^+} c_{\text{A}^-}^3}$$

TABLE 1

Electromotive force

Cells 1 to 34 at 25°C.; cells 35 to 50 at 34.7°C. For cells 35 to 50, *d* and *c* are for a temperature of 28°C.

CELL	c_1 , AgNO ₃	c_2 , NaNO ₃	c_1 , AgA c_1^* , AgNO ₃	c_2 , NaA	DENSITY	<i>E</i> volts
1	0.04371		0.04371		1.00325	0.00347
2	0.05928		0.05931		1.00461	0.0041
3	0.04147		0.04147		1.00257	0.00342
2	0.05330		0.05331		1.00415	0.00377
5	0.01184	0.04999	0.01184	0.04996	1.00087	0.00466
6	0.005927		0.005928		0.99857	0.0007
7	0.01248		0.01246		0.99889	0.00137
8	0.006224	0.02962	0.006224	0.02961	0.99901	0.003125
9	0.03122		0.03117		1.00157	0.00272
10	0.006226	0.009875	0.006226	0.009874	0.99864	0.00156
11	0.006224	0.01992	0.006224	0.019929	0.99916	0.00242
12	0.003114	0.009912	0.003115	0.009914	0.99761	0.00134
13	0.006236		0.006236		0.99824	0.00066
14	0.006223	0.04999	0.006222*	0.04995	1.00004	0.00387
15	0.05928		0.05931		1.00461	0.00404
16	0.05928		0.05931		1.00461	0.00408
17	0.005925	0.02001	0.005927	0.02000	0.99881	0.00243
18	0.01184		0.01184		0.99904	0.00127
19	0.01184	0.02973	0.01184	0.02974	1.00010	0.00343
20	0.04145		0.04145		1.00281	0.00315
21	0.01184	0.02001	0.01184	0.02000	1.00057	0.00288
22	0.006226	0.10005	0.006225*	0.10006	1.00260	0.00720
23	0.006223	0.1998	0.006222*	0.1998	1.00717	0.0115
24	0.006224	0.4999	0.006223*	0.4998	1.01946	0.02215
25	0.006249	0.7000	0.006248*	0.7001	1.02699	0.02783
26	0.006247	0.9000	0.006246*	0.9001	1.03496	0.03263
27	0.005925	0.4999	0.005927	0.4998	1.01916	0.02248
28	0.01184	0.7000	0.01184	0.6998	1.02809	0.02790
29	0.005924	0.1999	0.005922*	0.1999	1.00715	0.01150
30	0.005925	0.4999	0.005923*	0.4998	1.01892	0.02245
31	0.005914	0.10001	0.005913*	0.10002	1.00218	0.00736
32	0.005914	0.1999	0.005913*	0.1998	1.00604	0.01170
33	0.005905	0.9002	0.005904*	0.9003	1.03457	0.03269
34	0.02961	0.10003	0.02962	0.10003	1.00537	0.00875
35	0.011051		0.011051		0.999856	0.00124
36	0.011056	1.0563	0.011053	1.0562	1.0404	0.03887
37	0.011053	1.9730	0.011056	1.9735	1.0763	0.05645
38	0.011056	0.09974	0.011056	0.09975	1.00296	0.00812
39	0.011053	1.985	0.011053	1.984	1.07684	0.05647
40	0.011051	0.01995	0.011051	0.01993	0.99907	0.00290

TABLE 1—*Concluded*

CELL	c_1, AgNO_3	c_2, NaNO_3	$\frac{c_1, \text{AgA}}{c_1^*, \text{AgNO}_3}$	c_3, NaA	DENSITY	<i>E</i> volts
41	0.011050	0.4984	0.011056	0.4980	1.01897	0.02417
42	0.011051	1.4049	0.011051	1.4051	1.05390	0.04610
43	0.011056	0.1995	0.011056	0.1995	1.00691	0.01270
44	0.011053		0.011053		0.99856	0.00118
45	0.011056	0.02978	0.011056	0.02978	0.99984	0.00387
46	0.011051	0.009873	0.011051	0.00978	0.99916	0.00219
47	0.011053	0.02964	0.011053	0.02964	0.99973	0.00381
48	0.05534		0.05537		1.004	0.00403
49	0.011056	0.04982	0.011056	0.04985	1.00042	0.00522
50	0.02765		0.02765		1.00056	0.00245

Leden finds

$$F(A^-) = \frac{c_s - c_{\text{Ag}^+}}{c_{\text{Ag}^+} + c_{A^-}} = B_1 + B_2 c_{A^-} + B_3 c_{A^-}^2 + \dots \quad (17)$$

This equation is analogous to but more extended than our equation 9. Note that while in equation 9 molal concentrations are used, Leden uses molarities. Note also that B_1 , B_2 , etc. are not true equilibrium constants. Neglecting the very slight difference between molal and molar activities and representing a molar activity coefficient by f , we find the following relations:

$$K_1 = \frac{1}{B_1} \frac{f^2}{f_0}; \quad K_2 = \frac{1}{B_2} \frac{f^2 f_{A^-}}{f_{\text{AgA}_2^-}} \simeq \frac{f^2}{B_2} \quad (18)$$

From the intercept, initial slope, and slight curvature of a plot of $F(A^-)$ against (A^-) , Leden makes the estimates: $B_1 = 2.36 \pm 0.03$, $B_2 = 1.47 \pm 0.05$, and $B_3 = 0.33 \pm 0.1$ at 20°C. We do not think that the curvature of the plot below $(A^-) = 1.0$ is significant. For $(A^-) > 1.0$, the curvature may well be due to other causes (such as change in values of activity coefficients) than the existence of AgA_3^{--} . Accordingly we have confined our attentions to the curve for $(A^-) \leq 1.0$ and have used the method of least squares to find the best straight line. In this way, we find from Leden's data:

$$B_1 = 2.37 \text{ and } B_2 = 1.71$$

Applying these values of B_1 and B_2 to our data in table 3 dealing with the solubility of silver acetate in 2.95 molar sodium perchlorate, we find $c_{\text{AgA}} = 0.00532$, $c_{\text{Ag}^+} = 0.04747$, $c_{A^-} = 0.04729$, $c_{\text{AgA}_2^-} = 0.00018$. The values obtained for c_{AgA} , c_{Ag^+} , and c_{A^-} are virtually independent of the value taken for B_2 . From our values for K_1 and K_2 (see equations 14 and 15) it follows that in all aqueous solutions saturated at 25°C. with silver acetate:

$$a_{\text{AgA}} = \frac{K_1}{K_2} = \frac{0.00195}{0.186} = 0.0105 \quad (19)$$

TABLE 2
Molalities and the function K'

CELL	c_{Ag^+}	m_a	m_s	(Ag^+)	(A^-)	$1/K'$
1	0.0382	0.04388	0.04388	0.0384	0.0384	5.68
2	0.0506	0.05963	0.05963	0.0508	0.0508	5.47
3	0.0363	0.04165	0.04165	0.0365	0.0365	5.78
4	0.0460	0.05356	0.05356	0.0463	0.0463	5.35
5	0.00987	0.06212	0.01190	0.00993	0.0602	5.32
6	0.0058	0.005843	0.005943	0.0058	0.0058	5.68
7	0.01183	0.01250	0.01250	0.01187	0.01187	5.67
8	0.005511	0.03600	0.006252	0.005524	0.03527	5.46
9	0.02809	0.03129	0.03129	0.02819	0.02819	5.58
10	0.005859	0.01615	0.006246	0.005878	0.01578	5.19
11	0.05653	0.02625	0.006246	0.005671	0.02567	5.50
12	0.002956	0.01308	0.003126	0.002965	0.01292	5.36
13	0.006077	0.006253	0.006253	0.006094	0.00609	5.09
14	0.005353	0.05021	0.006254	0.005380	0.04934	5.20
15	0.05065	0.05963	0.05963	0.05092	0.05092	5.37
16	0.05057	0.05963	0.05963	0.05083	0.05083	5.43
17	0.00539	0.02602	0.005949	0.005411	0.02548	5.43
18	0.01127	0.01187	0.01187	0.01130	0.01130	5.66
19	0.01036	0.04176	0.01189	0.01041	0.04027	5.35
20	0.03666	0.04162	0.04162	0.03682	0.03682	5.30
21	0.01059	0.03194	0.01188	0.01059	0.03066	5.68
22	0.004629	0.1007	0.006227	0.004660	0.09912	6.28
23	0.00398	0.2019	0.006287	0.00402	0.1996	6.03
24	0.002628	0.5114	0.006367	0.002688	0.5077	7.45
25	0.002115	0.7229	0.006451	0.002184	0.7186	8.36
26	0.001754	0.9375	0.006506	0.001827	0.9329	9.15
27	0.002470	0.5176	0.006065	0.002528	0.5141	7.52
28	0.003995	0.7346	0.01221	0.004125	0.7265	8.30
29	0.003786	0.2020	0.005983	0.003825	0.1998	6.01
30	0.002473	0.5117	0.006063	0.002531	0.5081	7.60
31	0.004441	0.1007	0.005955	0.004473	0.09925	6.03
32	0.003751	0.2021	0.005981	0.003794	0.1999	6.14
33	0.001655	0.9381	0.006152	0.001724	0.9337	9.15
34	0.02106	0.1307	0.02985	0.02123	0.1221	6.30
35	0.01055	0.01109	0.01109	0.01058	0.01058	5.71
36	0.00255	1.1211	0.01161	0.00268	1.109	10.29
37	0.001315	2.1749	0.01212	0.00144	2.159	15.17
38	0.00814	0.1116	0.01113	0.00820	0.1085	6.09
39	0.001315	2.187	0.01212	0.00144	2.171	15.13
40	0.00991	0.03111	0.01110	0.00995	0.02996	5.56

TABLE 2—*Concluded*

CELL	c_{Ag^+}	m_a	m_s	(Ag^+)	(A^-)	$1/K'$
41	0.00444	0.5215	0.01133	0.00455	0.5147	8.19
42	0.00194	1.5117	0.01180	0.00207	1.498	12.36
43	0.00685	0.2130	0.01118	0.00693	0.2085	6.43
44	0.01057	0.01109	0.01109	0.01061	0.01061	5.42
45	0.00955	0.04101	0.01111	0.00960	0.03950	5.99
46	0.01018	0.02100	0.01109	0.01021	0.02013	5.81
47	0.00957	0.04088	0.01110	0.00962	0.03939	5.91
48	0.0475	0.05566	0.05566	0.04773	0.04773	5.54
49	0.00908	0.06124	0.01112	0.00913	0.0592	5.98
50	0.02521	0.02776	0.02776	0.02531	0.0253	5.42

TABLE 3

Solubility of silver acetate at 25°C.

AgA		NaClO ₄	
Molality	Molarity	Molality	Molarity
0.06699	0.06654	0.	0.
0.06160	0.05304	3.4264	2.9501

For the molar and molal activity coefficients, f_0 and γ_0 , of unionized AgA in 2.95 *M* sodium perchlorate we obtain accordingly

$$f_0 = \frac{0.0105}{0.00532} = 1.97 \quad (20)$$

$$\gamma_0 = 1.70 \quad (21)$$

From equation 10 with $\gamma_0 = 1.7$ and $S = 3$, k is calculated to be about 0.077, which is the basis for our assumption that

$$k = 0.07 \quad (22)$$

It is true that this value may be considerably in error.

We can also find from the previously mentioned data

$$(0.04747) (0.04729) f^2 = K_1 = 0.00195$$

whence

$$f^2 = 0.87 \quad (23)$$

where f is the mean molar activity coefficient of Ag^+ and A^- in 2.95 *M* sodium perchlorate saturated with silver acetate. From this result, the corresponding value of γ^2 is 0.64 or of γ is 0.80. If now we use Leden's value of 1.71 for B_2 , together with $f^2 = 0.87$, we find from the equation $K_2 = f^2/B_2$, a value of K_2

equal to 0.51, more than twice as large as the value we have already found (see equation 14). In this connection it is to be noted, first, that the exact relation between K_2 and B_2 is given by the equation:

$$K_2 = \frac{f^2}{B_2} \frac{f_{A^-}}{f_{AgA_2^-}}$$

secondly, that the rule that all univalent ions in a given solution have equal activity coefficients, though approximately valid in solutions of low or moderate ionic strength, may be greatly in error when the ionic strength is high. As an illustration, consider the values found by Jones (6) for the molal activity coefficient of sodium perchlorate in 3.5 molal sodium perchlorate and of lithium perchlorate in 3.5 molal lithium perchlorate. He finds for γ in these cases 0.619 and 1.89, respectively. It is highly probable that in a 3.5 molal solution containing both sodium perchlorate and lithium perchlorate, the activity coefficient of Li^+ would be much greater than that of Na^+ . Similarly, in a concentrated solution containing sodium perchlorate, sodium acetate, and silver acetate, the ratio f_{A^-} to $f_{AgA_2^-}$ may differ considerably from unity.

A more direct determination of K_2

Using the relations,

$$(AgA) = (Ag^+)(A^-)\gamma^2/K, \gamma_0 \quad (1)$$

$$K, = 0.186 \text{ at } 25^\circ\text{C.}; K, = 0.179 \text{ at } 34.70^\circ\text{C.} \quad (14)$$

$$\log \gamma_0 = 0.07 \text{ } S \text{ for } 25^\circ\text{C. and } 34.70^\circ\text{C.} \quad (23)$$

$$-\log \gamma^2 = \frac{1.0184S^{\frac{1}{2}}}{1 + S^{\frac{1}{2}}} \text{ at } 25^\circ\text{C.} \quad (13)$$

$$-\log \gamma^2 = \frac{1.0381S^{\frac{1}{2}}}{1 + S^{\frac{1}{2}}} \text{ at } 34.7^\circ\text{C.}$$

and the molalities (Ag^+) and (A^-) given in table 2, we can calculate the molality of AgA in the acetate solution of each of the fifty cells studied. By means of the equation

$$(AgA_2^-) = m, - (Ag^+) - (AgA) \quad (8)$$

we can then calculate the molality of the complex ion AgA_2^- in each of the acetate solutions. Now in all the solutions in which (Ag^+) \simeq (A^-), each of these molalities is less than 0.05. Since K_2 is approximately equal to 0.2, it follows from equation 2,

$$(AgA_2^-) = (Ag^+)(A^-)^2\gamma^2/K_2$$

that in all these solutions (AgA_2^-) is less than 0.00040 and frequently much less. To obtain values of (AgA_2^-) which are of any significance we must accordingly restrict ourselves to solutions in which (A^-) is considerably larger than (Ag^+).

This means that we shall consider only cells 24 to 28, 30, 33, 34, 36 to 39, 41, 42 and 43. It may be added that when equation 8 is used to calculate (AgA_2^-) in the acetate solutions of cells 1 to 23 inclusive, the values obtained, most of which are positive, range from -0.00011 to $+0.00037$. From each significant value of (AgA_2^-) , we can calculate K_2 by means of the equation

$$K_2 = \frac{(\text{Ag}^+)(\text{A}^-)^2 \gamma^2}{(\text{AgA}_2^-)} \quad (2)$$

TABLE 4
The equilibrium constant K_2 at 25°C.

CELL	(AgA)	(AgA ₂ ⁻)	K ₂
24	0.00255	0.00113	0.231
25	0.00258	0.00169	0.229
26	0.00252	0.00216	0.235
27	0.00243	0.00111	0.227
28	0.00492	0.00316	0.236
30	0.00240	0.00113	0.218
33	0.00238	0.00205	0.234
34	0.00734	0.00128	(0.133)
Average.....			0.230

TABLE 5
The equilibrium constant K_2 at 34.7°C.

CELL	(AgA)	(AgA ₂ ⁻)	K ₂
36	0.00415	0.00478	0.205
37	0.00312	0.00756	0.219
38	0.00269	0.00024	0.221
39	0.00312	0.00756	0.221
41	0.00445	0.00233	0.191
42	0.00376	0.00597	0.212
43	0.00368	0.00057	0.249
Average.....			0.217

The results of these calculations are tabulated in tables 4 and 5. It is naturally very satisfactory to obtain a series of values of K_2 which agree so well among themselves, at each of the two temperatures. Because of the many assumptions made in the theoretical development of our equations, it is difficult to estimate the uncertainty in the average values obtained for K_2 . However, the values $K_2 = 0.230$ at 25°C. and $K_2 = 0.217$ at 34.70°C. are probably more accurate than those given in equation 16, *viz.*, $K_2 = 0.20 \pm 0.04$ at 25°C. and $K_2 = 0.19 \pm 0.4$ at 34.70°C.

SUMMARY

1. We have measured the E.M.F. at 25°C. and at 34.7°C. of cells in which one of the solutions contained sodium acetate and either silver acetate or silver nitrate.

2. We have determined the solubility of silver acetate at 25°C. in 2.95 *M* sodium perchlorate.

3. In the discussion and interpretation of our results we have made use of previous studies on the solubility of silver acetate in water in the presence of added electrolytes. We have also availed ourselves of a recent investigation of Leden on the E.M.F. of certain cells.

4. The most important result of our work is the determination of the ionization constant, K_i , of silver acetate. For example, in 0.06 molal silver acetate in aqueous solution the degree of ionization is about 85 per cent.

5. We confirmed the existence of the complex ion, AgA_2^- , and determined its dissociation constant, K_2 .

6. Our results enabled us to correct previous estimates of the true activity product, K_1 , of Ag^+ and A^- in saturated aqueous solutions.

7. We give here a list of equilibrium constants expressed in terms of molal activities and the result obtained in a determination of solubility:

(a) For the reaction $\text{AgA} = \text{Ag}^+ + \text{A}^-$,

$$K_i = 0.186 \text{ at } 25^\circ\text{C.}; \quad K_i = 0.179 \text{ at } 34.7^\circ\text{C.}$$

(b) For the reaction $\text{AgA}_2^- = \text{Ag}^+ + 2\text{A}^-$,

$$K_2 = 0.230 \text{ at } 25^\circ\text{C.}; \quad K_2 = 0.217 \text{ at } 34.7^\circ\text{C.}$$

(c) For the equilibria $\text{AgA(s)} = \text{AgA} = \text{Ag}^+ + \text{A}^-$,

$$K_1 = a_{\text{Ag}^+}a_{\text{A}^-} = 0.00195 \text{ at } 25^\circ\text{C.}$$

(d) For the molality, m , and molarity, c , of silver acetate at 25°C. in 2.95 molar sodium perchlorate, saturated with silver acetate, $m = 0.06160$ and $c = 0.05304$.

REFERENCES

- (1) HARNED, H. S., AND OWEN, B. B.: *The Physical Chemistry of Electrolytic Solutions*, pp. 397-405. Reinhold Publishing Corporation, New York (1943).
- (2) HENDERSON, P.: *Z. physik. Chem.* **59**, 118 (1907); **63**, 325 (1908).
- (3) HILL, A. E., AND SIMMONS, J. D.: *J. Am. Chem. Soc.* **31**, 821 (1909).
- (4) IRVING, GEORGE W., JR., AND SMITH, N. R.: *Ind. Eng. Chem., Anal. Ed.* **6**, 480 (1934).
- (5) JAKES, ARTHUR: *Trans. Faraday Soc.* **5**, 235 (1910).
- (6) JONES, J. H.: *J. Phys. Colloid Chem.* **51**, 516-21 (1947).
- (7) KNOX, JOSEPH, AND WILL, H. R.: *J. Chem. Soc.* **115**, 853 (1919).
- (8) KOLTHOFF, I. M., AND BOSCH, W.: *J. Phys. Chem.* **36**, 1702 (1932).
- (9) KOLTHOFF, I. M., AND SANDELL, E. B.: *Textbook of Quantitative Inorganic Analysis*, Chap. XXXV. The Macmillan Company, New York (1937).
- (10) LARSSON, M., AND ADELL, B.: *Z. anorg. allgem. Chem.* **196**, 354 (1931).
- (11) LEDEN, IDO: *Svensk Kem. Tid.* **58**, 129 (1946).

- (12) LEWIS, G. N.: J. Am. Chem. Soc. **28**, 158 (1906).
- (13) MACDOUGALL, F. H.: J. Am. Chem. Soc. **52**, 1390 (1930).
MACDOUGALL, F. H., AND REHNER, JOHN, JR.: J. Am. Chem. Soc. **56**, 368 (1934).
MACDOUGALL, F. H., AND BARTSCH, C. E.: J. Phys. Chem. **40**, 649 (1936).
MACDOUGALL, F. H., AND LARSON, W. D.: J. Phys. Chem. **41**, 417 (1937).
- (14) MACDOUGALL, F. H., AND ALLEN, MARTIN: J. Phys. Chem. **46**, 730 (1942); **46**, 737 (1942); **49**, 245 (1945).
- (15) MACINNES, D. A.: *The Principles of Electrochemistry*, p. 244. Reinhold Publishing Corporation, New York (1939).
- (16) ROSIN, J.: *Chemical Reagents and Standards*. D. Van Nostrand Company, New York (1937).
- (17) TREADWELL, F. P., AND HALL, W. T.: *Analytical Chemistry. Vol. II. Quantitative*, 8th edition, p. 703. John Wiley and Sons, Inc., New York (1935).
- (18) Reference 17, pp. 58, 59, 55.
- (19) WYMAN, J., JR. Phys. Rev. **35**, 623 (1930).

THE SHAPE OF HEAT-CAPACITY AND EQUILIBRIUM COOLING CURVES IN THE REGION OF MELTING OF SOLID SOLUTIONS

KAROL J. MYSELS¹

Department of Chemistry, New York University, University Heights, New York, New York

Received June 4, 1947

Cooling curves are widely used in phase studies to determine the position and shape of solidus and liquidus, the equilibrium lines between solid and liquid phases. It is generally accepted that changes in the slope of cooling curves correspond to beginnings or ends of phase changes, and at the same time it is recognized that lack of equilibrium in phase changes and in thermal conductivity renders interpretation difficult. In view of these difficulties there has been little point heretofore in analyzing more thoroughly the shape of cooling curves, and such analysis seems not to have been made.

The development of adiabatic calorimeters has nowadays removed, in principle at least, the difficulties due to lack of equilibrium and allows the construction of "equilibrium cooling curves" (heat removed *vs.* temperature: $-Q$ *vs.* T) and heat-capacity curves (dQ/dT *vs.* T) from the measured values of heat introduced, Q , and temperature reached, T . These measurements may be made very precisely and reproducibly, but it remains generally difficult to ascertain how closely equilibrium has been approached because of the unidirectional character of the experiments.

Therefore it may be worthwhile to correlate the shapes of these curves with that of the phase diagram and with other properties of the system in order to provide a check on their internal consistency and a help in interpolations.

¹ Present address: Department of Chemistry, University of Southern California, Los Angeles 7, California.

In this paper the general equations for a solid-solution system are first established in a form which allows the calculation of cooling curves in the melting region if other properties of the system are known. Then simplifying assumptions are introduced and cooling curves for some ideal cases presented. After basic concepts are established, lengthy but essentially simple calculations are needed, the details of which will be omitted.²

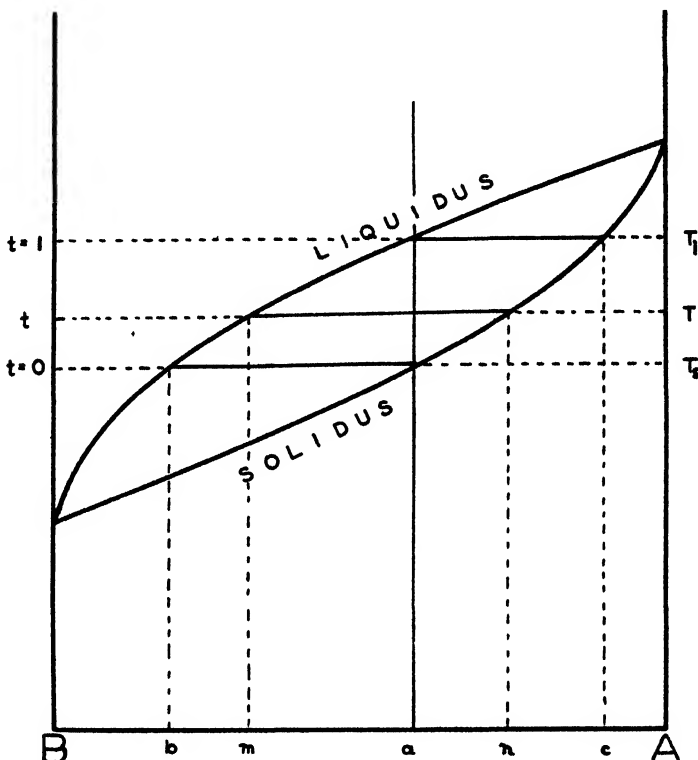


Fig. 1. Schematic phase diagram showing nomenclature used

I. GENERAL EXPRESSION

Let us consider a system of two components *A* and *B* forming a solid solution, as indicated in their phase diagram (figure 1). At temperatures below T_0 the composition containing *a* g. of *A* and $(1 - a)$ g. of *B* corresponds to a solid having a specific heat:

$$\frac{dq}{dT} = H_a \quad (\text{where } T < T_0) \quad (1)$$

Above T_1 it corresponds to a liquid (denoted by ') and having a specific heat:

$$\frac{dq'}{dT} = H'_a \quad (\text{where } T > T_1) \quad (2)$$

² A similar approach has been used by Cohen and Kimball (1) to determine the value $dA/(dA + dB)$.

We are mainly interested in the intermediate zone between T_s and T_l , where a fraction α' of the total is a liquid formed of A' and B' , giving the composition m . The remainder $(1 - \alpha')$ is solid formed of A and B , giving the composition n . The specific heat of this system is the ratio dQ/dT of the heat supplied by the temperature rise accompanied by a change $d\alpha'$, dA' , dB' , dn , and dm occurring in the proportion melted, the amounts A' and B' , and the composition n and m . This total dQ/dT may be considered as the sum of three terms:

(a) A specific-heat term corresponding to the heat necessary to raise the temperature of the solid and liquid without change of composition:

$$\frac{dQ_H}{dT} = \alpha' H'_m + (1 - \alpha') H_n \quad (3)$$

(b) A heat-of-solution term corresponding to the heat necessary to remove dA' of pure solid A from the solid and later (after melting by c) introduce it into the liquid, and the corresponding term for dB' :

$$\frac{dQ_s}{dT} = (1 - \alpha') dS_n - d\alpha' S_n + \alpha' dS'_m + d\alpha' S'_m \quad (4)$$

where S_i is the heat supplied during mixing of i g. of A with $(1 - i)$ g. of B , and dS_i is the change in S when i changes by di corresponding to dT .

(c) A heat-of-melting term corresponding to the melting of pure dA' and pure dB' (intermediate in b).

$$\frac{dQ_M}{dT} = dA' M_A + dB' M_B \quad (5)$$

where M_A and M_B are specific heats of melting of pure A and B . This gives for the specific heat during melting:

$$\begin{aligned} \frac{dQ}{dT} = \frac{dQ_H + dQ_s + dQ_M}{dT} &= H'_m + (1 - \alpha') H_n + \alpha' dS'_m + (1 - \alpha') dS_n \\ &+ d\alpha' (S'_m - S_n) + dA' M_A + dB' M_B \quad (\text{where } T_s < T < T_l) \end{aligned} \quad (6)$$

Now α' , $d\alpha'$, dA' , and dB' can be expressed from the phase diagram as follows:

$$\alpha' = \frac{n - a}{n - m} \quad (7)$$

$$d\alpha' = \frac{(a - m) dn + (n - a) dm}{(n - m)^2} \quad (8)$$

$$A' = \alpha' m \quad (9)$$

$$B' = \alpha' (1 - m) \quad (10)$$

$$dA' = \frac{n(n - a) dm + m(a - m) dn}{(n - m)^2} \quad (11)$$

$$dB' = \frac{(1 - n)(n - a) dm + (1 - m)(a - m) dn}{(n - m)^2} \quad (12)$$

By combining equations 6-12 the heat capacity, dQ/dT , in the melting region of the solution may thus be calculated from independently measurable values n , m , dn , dm of the phase diagram and H , H' , S , S' , M_A , M_B of the thermal properties outside of this region.

The cooling curve — Q vs. T is then obtained by direct integration of the heat capacities given by equations 1, 2, and 6.

II. HEATING OR COOLING OVER THE SOLIDUS AND THE LIQUIDUS

Thus the heat capacity is defined by equation 1 at temperatures below the solidus, by equation 6 between the solidus and liquidus, and by equation 2 above the liquidus. Because of the difference of these expressions, different heat capacities are obtained when the temperature of, for example, the solidus T_s is approached within a small temperature interval, ϵ . Thus if the solidus is approached from below, the heat capacity always remains that of the solid no matter how closely T_s is approached. In other words

$$\lim_{\epsilon \rightarrow 0} \left[\frac{dQ}{dT} \right]_{T=T_s-\epsilon} = H_a \quad (13)$$

Similarly when the solidus is approached from above, the heat capacity is always that of the two-phase system, given by equation 6, no matter how closely T_s is approached. In this equation (equation 6) α' becomes negligible, m approaches b , and dn approaches a specific value (dn_s) as T_s is approached. In other words

$$\begin{aligned} \lim_{\epsilon \rightarrow 0} \left[\frac{dQ}{dT} \right]_{T=T_s+\epsilon} = H_a + M_A \frac{b dn_s}{(a-b)} \\ + M_B \frac{(1-b) dn_s}{(a-b)} + \frac{(S'_b - S_a) dn_s}{(a-b)} + dS_a \end{aligned} \quad (14)$$

The terms following H_a in this last equation give, of course, the value of the difference between these two limits, i.e., the magnitude of the discontinuity in the heat capacity as the solidus is crossed.

These two limits are equal only if

$$\frac{dS_a}{dn_s} = - \frac{bM_A + (1-b)M_B + S'_b - S_a}{a-b} \quad (15)$$

which is certainly highly improbable.

Similarly at T_l the two limits are

$$\lim_{\epsilon \rightarrow 0} \left[\frac{dQ'}{dT} \right]_{T=T_l+\epsilon} = H'_a \quad (16)$$

$$\begin{aligned} \lim_{\epsilon \rightarrow 0} \left[\frac{dQ}{dT} \right]_{T=T_l-\epsilon} = H'_a + M_A \frac{c dm_l}{c-a} \\ + M_B \frac{(1-c) dm_l}{c-a} + \frac{(S'_c - S_a) dm_l}{c-a} + dS'_a \end{aligned} \quad (17)$$

These two limits are equal only if

$$\frac{dS'_a}{dm_l} = -\frac{cM_A + (1 - c)M_B + S'_a - S_c}{c - a} \quad (18)$$

Thus in general (unless relations 15 and 18 are satisfied) there are discontinuities at T_s and T_l in the heat-capacity curve (i.e., there are not two kinks in it but actually it is formed of three unconnected lines).

The cooling curve has corresponding abrupt changes of slope (kinks) at T_s and T_l but is of course continuous.

The heat-capacity curve can be continuous only if both relations 15 and 18 are satisfied. This requires the condition

$$[bM_A + (1 - b)M_B + S'_b - S_a] \frac{dn_s}{dS_a} + [cM_A + (1 - c)M_B + S'_a - S_c] \frac{dm_l}{dS_a} = c - b \quad (19)$$

which is still less probable than relation 15 or 18 above.

III. IDEALIZED CASES

The above considerations make no assumption about the shape of the solidus and liquidus and therefore cannot be carried much further, except in actual cases. The following simplifications, on the other hand, may not apply to any actual system but allow the calculation of these curves in important idealized cases.

To simplify calculations we introduce a reduced temperature t such that

$$t = \frac{T - T_s}{T_s - T_l} \quad (20)$$

Let us now (a) approximate by straight lines the solidus and liquidus in the region concerned³ (from a to c and b , respectively). This gives:

$$n = a + (c - a)t \quad (21)$$

$$m = b + (a - b)t \quad (22)$$

$$\alpha' = \frac{(c - a)t}{(a - b) + (c + b - 2a)t} \quad (23)$$

$$d\alpha' = \frac{(c - a)(a - b) dt}{[(a - b) + (c + b - 2a)t]^2} \quad (24)$$

$$d^2\alpha = \frac{-2(c - a)(a - b)[(c - a) - (a - b)] d^2t}{[(a - b) + (c + b - 2a)t]^3} \quad (25)$$

$$dA' = \frac{(c - a)(a - b)[b + 2(a - b)t + (c + b - 2a)t^2]}{[(a - b) + (c + b - 2a)t]^2} \quad (26)$$

³ This is broader than assuming that all of the solidus and liquidus is straight and extends to the temperature axis (1).

$$dB' = \frac{(c-a)(a-b)[1-b+2(b-a)t-(c+b-2a)t^2]}{[(a-b)+(c+b-2a)t]^2} \quad (27)$$

We can note⁴ that under these conditions α' has no point of inflection, is equal to t at T_1 and T_2 , and is larger or smaller than t at intermediate temperature depending on whether

$$(c-a) > (a-b) \quad (28)$$

or *vice versa*.

Let us furthermore (b) neglect the effects due to heats of solution ($\frac{dQ_s}{dT} = 0$) and (c) neglect changes in the specific-heat term ($\frac{dQ_H}{dt} = H_n = H_m = H_a$).

We have then:

$$\frac{dQ}{dt} = \frac{(c-a)(a-b)\{[b+2(a-b)t+(c+b-2a)t^2](M_A-M_B)+M_B\}}{[(a-b)+(c+b-2a)t]^2} \quad (29)$$

$$\frac{d^2Q}{dt^2} = \frac{2(c-a)(a-b)[(a^2-cb)(M_A-M_B)-M_B(c+b-2a)]}{[(a-b)+(c+b-2a)t]^3} \quad (30)$$

$$\frac{d^3Q}{dt^3} = \frac{-6(c-a)(a-b)[(c-a)-(a-b)]}{[(a-b)+(c+b-2a)t]^4} \quad (31)$$

Thus dQ/dt also has no inflection point and both dQ/dt and d^2Q/dt^2 are either constant or always increasing or decreasing. Their upper and lower values are:

$$\left[\frac{dQ}{dt}\right]_{t=0} = \frac{c-a}{a-b} [bM_A + (1-b)M_B] + H_a \quad (32)$$

$$\left[\frac{dQ}{dt}\right]_{t=1} = \frac{a-b}{c-a} [cM_A + (1-c)M_B] + H_a \quad (33)$$

(The first right-hand term in equations 32 and 33 gives the discontinuity at T_1 and T_2 .)

$$\left[\frac{d^2Q}{dt^2}\right]_{t=0} = \frac{2(c-a)}{(a-b)^2} [(a^2-bc)(M_A-M_B) - (c+b-2a)M_B] \quad (34)$$

$$\left[\frac{d^2Q}{dt^2}\right]_{t=1} = \frac{2(a-b)}{(c-a)^2} [(a^2-bc)(M_A-M_B) - (c+b-2a)M_B] \quad (35)$$

Thus the curvature of Q which depends on equations 32 and 33 will be downward if

$$M_A(a^2-bc) < M_B[(a^2-bc) + (b+c-2a)] \quad (36)$$

and *vice versa*.

This relation in turn depends on the sign of

$$a^2 - bc \quad (37)$$

⁴ Under these assumptions neither dA nor dB is constant and $dA'/(dA' + dB') = b + 2(a-b)t + (c+b-2a)t^2$.

and on the relative value of M_A/M_B and of P , which is defined by

$$P = 1 + \frac{b + c - 2a}{a^2 - bc} \quad (38)$$

It must be noted that the curvature of Q (on a plot of Q vs. t) is opposite of course to that of the heating (or cooling) curve (plot of t vs. Q , figure 2).

The slope of the heat-capacity curve, dQ/dt , depends on the curvature of Q and is also fixed by condition 36. Its curvature however depends on equations 34 and 35 and will be upward if condition 36 is satisfied *and*

$$b + c - 2a \quad (39)$$

is > 0 (and *vice versa*).

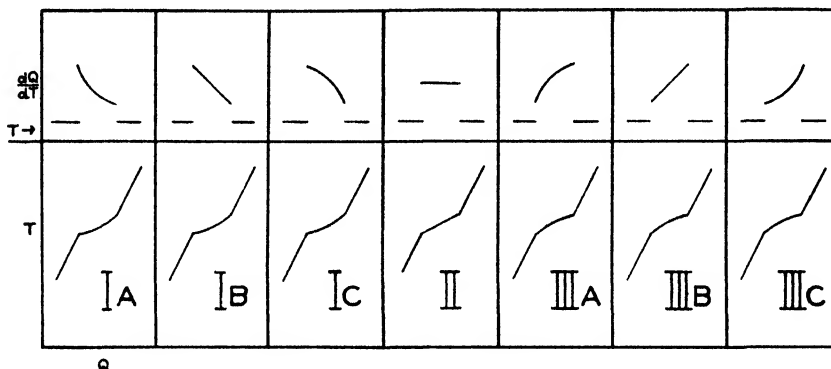


FIG. 2. The seven possible types of heat-capacity and cooling curves in idealized cases

Thus there are seven main types of shapes of cooling and heat-capacity curves, as shown in figure 2. Each is possible only for certain combinations of values of expressions 37, 38, and 39, as shown in table 1 for all possible cases.

Geometrically condition 39 determines the relative direction of solidus and liquidus: when $b + c - 2a = 0$ these are parallel; when it is > 0 they are convergent (right-hand side of the figure).

On the other hand, condition 37 determines the position of the intersection of an extension of the liquidus and solidus: when $a^2 - bc = 0$ the intersection is on the $A = 0$ line; when it is < 0 the intersection is at $A < 0$ or $A > a$ (throughout figure 1 except at $a = 0$ and $a = 1$); when it is > 0 the intersection is at $0 < A < a$, a shape which may be encountered but is not shown in figure 1.

The third condition involves the comparison of P (equation 38) and of the ratio of heats of melting of the pure components M_A/M_B . Now P is completely determined by the value of the above two conditions (37 and 39). When either of these changes sign, P becomes unity or infinity as shown in the third column of table 2.

Thus in order to determine the type of curves throughout the region of solid

solution the value of P , M_A/M_B (conditions 37 and 39) must in general be known as shown in table 1.

In the special case when $M_A/M_B = 1$ it is however not necessary to determine the value of P , because its relation to 1 is determined by conditions 37 and 39 and these latter two variables fully determine the type, as shown in the fifth column of table 2.

TABLE 1
Dependence of type of heat-capacity and cooling curve on the value
of $c + b - 2a$, $a^2 - cb$, and P

$c + b - 2a$	$a^2 - cb$	P		
		$> \frac{M_A}{M_B}$	$= \frac{M_A}{M_B}$	$< \frac{M_A}{M_B}$
> 0	< 0	IIIa	II	Ia
	$= 0$			
	> 0	Ia		IIIa
$= 0$		Ib		IIIb
< 0		Ic		IIIc

TABLE 2
Dependence of the value of P , and of the type of heat-capacity and cooling curves for certain
values of M_A/M_B , on the value of $c + b - 2a$ and of $a^2 - cb$

$c+b-2a$	a^2-cb	P	M_A/M_B		
			<1	$=1$	>1
>0	<0	<1	Ia, II, IIIa	Ia	
	$=0$	$\pm\infty$	II		
	>0	>1	Ia		Ia, II, IIIa
$=0$		$=1$	Ib	II	IIIb
<0		<1	Ic, II, IIIc	IIIc	

When $M_A/M_B \leq 1$ it is possible to determine the type by conditions 37 and 39 without calculating P only through parts of the composition range. In the remainder, when both M_A/M_B and P are ≥ 1 , their actual values have to be compared to distinguish between three possible types of curves. Columns four and six of table 2 illustrate these conditions.

SUMMARY

The heat-capacity and equilibrium cooling curve of a two-component system forming a solid solution is discussed, and its shape in the melting region is cal-

culated completely from properties of the system measurable outside of this region. Conditions for the absence of a discontinuity or change of slope at the solidus and liquidus are examined and simplified idealized cases are presented.

Thanks are due to Professor J. E. Ricci, who called the author's attention to the existence of this problem and kindly reviewed the manuscript.

REFERENCE

- (1) COHEN, M., AND KIMBALL, W. P.: American Documentation Institute Document 1440. Summarized in *Trans. Am. Inst. Min. Met. Engrs., Inst. of Metals. Div.* **143**, 113 (1941).

THE MOLAL VOLUMES OF AQUEOUS SOLUTIONS OF PERCHLORIC ACID

JACOB BIGELEISEN¹

Department of Chemistry, University of California, Berkeley, California and Institute for Nuclear Studies, University of Chicago, Chicago, Illinois

Received February 25, 1947

Perchloric acid is a strong acid in aqueous solution. Perchlorate ion is such a weak base that it forms very few or weak complexes. Furthermore, above 50°C., which is the melting point of perchloric acid monohydrate, solutions are possible which vary in composition continuously from pure water to pure perchloric acid. Thus a study of the thermodynamic properties of perchloric acid solutions is possible over a wide concentration range without the complication of incomplete ionization.² In addition, the degrees of dissociation of perchloric acid solutions have been measured recently by a direct experimental method (18). These degrees of dissociation as determined by the Raman spectra of sodium perchlorate and perchloric acid solutions will aid in the interpretation of the peculiar dependence of the apparent molal volumes of perchloric acid on concentration.

COMPILATION OF EXPERIMENTAL DATA

The apparent molal volumes of perchloric acid in aqueous solution have been calculated and smoothed from the best experimental density data available at 15°C. (7), 25°C. (10, 12, 13),³ and 50°C. (7). The results of the calculations

¹ Present address: Institute for Nuclear Studies, University of Chicago, Chicago, Illinois.

² The vibration spectrum will be used as a criterion to distinguish between the interaction between ions and molecule formation, as discussed by Redlich and Bigeleisen (17) and by Redlich (15).

³ The data of Fajans and Gressmann (3) at 25°C. cover a part of the composition range of those of Kohner and Gressmann (10), and both sets of measurements are in good agreement. Therefore the more complete data of Kohner and Gressmann have been plotted and given additional weight in smoothing all the data.

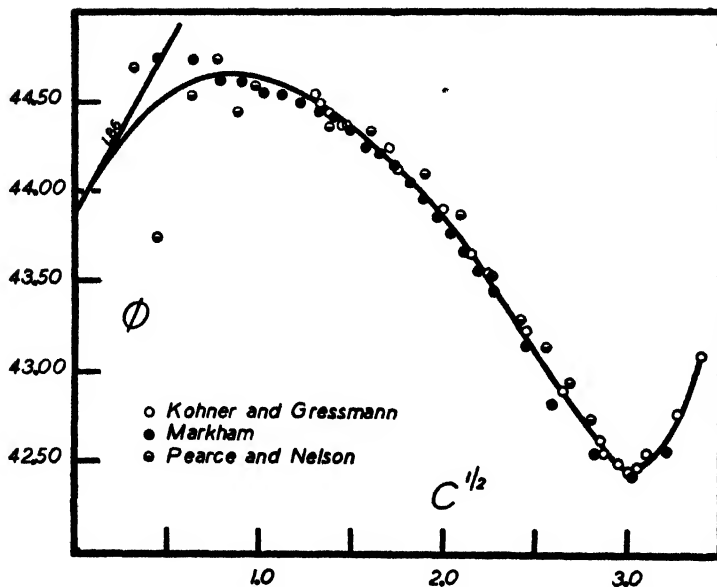


FIG. 1. Apparent molal volumes of perchloric acid at 25°C.

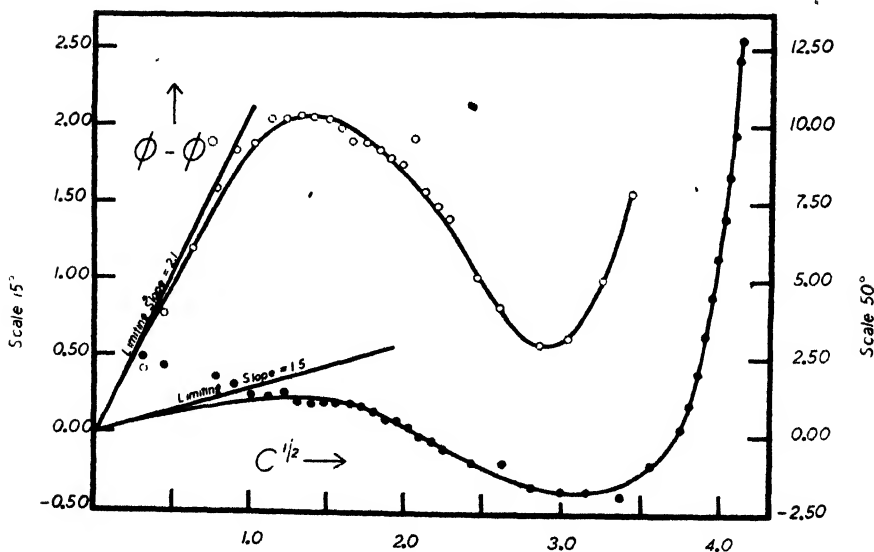


FIG. 2. Apparent molal volumes of perchloric acid at 15°C. (O) and 50°C. (●)

and extrapolations are shown graphically in figures 1 and 2. In table 1 smoothed values read from a large-scale plot are tabulated as a function of the square root of the concentration.⁴ The constants used in the calculations are:

⁴ The data for solutions more dilute than 1 *N* have been tabulated with a precision higher than is warranted by the experimental data. One additional figure is given to facilitate any numerical calculations.

Molecular weight of $\text{HClO}_4 = 100.465$

Density of water: $15^\circ\text{C.} = 0.9991265 \text{ g./ml.}$

$25^\circ\text{C.} = 0.9970739 \text{ g./ml.}$

$50^\circ\text{C.} = 0.98807 \text{ g./ml.}$

The extrapolation to infinite dilution was made with the aid of the limiting law (19),

$$\phi = \phi^0 + kc^{\frac{1}{2}} \quad (1)$$

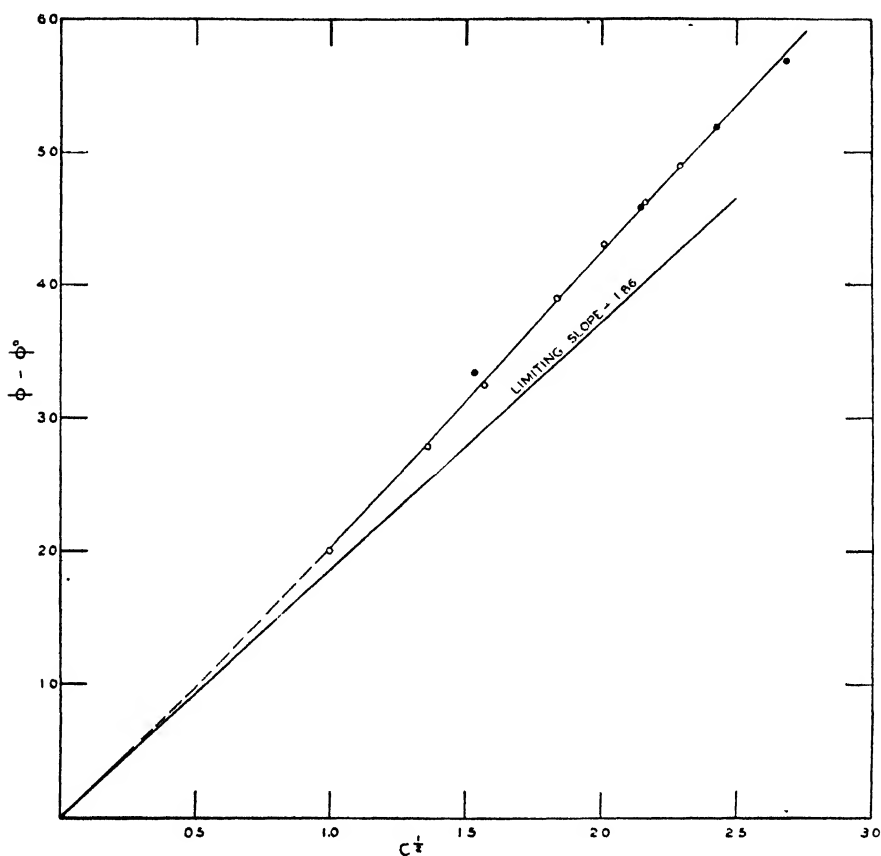


FIG. 3. Apparent molal volumes of sodium perchlorate at 25°C. O, Kohner (9); ●, Hölemann and Kohner (6).

where ϕ is the apparent molal volume at the concentration c (moles per liter), ϕ^0 is the apparent molal volume at $c = 0$, and k is a positive constant which is a function of temperature. The values of k for aqueous solutions as a function of temperature have been derived by Redlich (14). The extrapolation to infinite dilution at 25°C. was facilitated by the data on sodium perchlorate (6, 9). The large deviations between the experimental points and the extrapolated curve in the dilute region at 50°C. are due to the fact that the precision in the 50°C. density data is but 1 in 10^4 . In accord with expectation the scattering is greater at higher dilutions.

TABLE 1

$C^{\frac{1}{2}}$	15°C. $\phi - \phi^0$ $\phi^0 = 41.10 \pm 0.20$	25°C. $\phi - \phi^0$ $\phi^0 = 43.90 \pm 0.20$	50°C. $\phi - \phi^0$ $\phi^0 = 46.0 \pm 0.50$
0.1000	+0.20	+0.184	+0.14
0.2000	0.41	0.350	0.28
0.3000	0.62	0.492	0.42
0.4000	0.81	0.598	0.56
0.5000	0.99	0.673	0.69
0.6000	1.17	0.726	0.81
0.7000	1.36	0.755	0.93
0.8000	1.55	0.766	1.03
0.9000	1.73	0.758	1.10
1.000	1.86	0.736	1.16
1.100	1.97	0.703	1.19
1.200	2.03	0.657	1.20
1.300	2.06	0.600	1.19
1.400	2.06	0.534	1.16
1.500	2.04	0.458	1.11
1.600	1.99	0.376	1.03
1.700	1.92	0.286	0.92
1.800	1.85	0.182	0.76
1.900	1.76	+0.069	0.54
2.000	1.68	-0.060	+0.23
2.100	1.58	0.196	-0.05
2.200	1.48	0.331	0.31
2.300	1.34	0.469	0.58
2.400	1.17	0.611	0.82
2.500	1.01	0.773	1.10
2.600	0.85	0.949	1.32
2.700	0.72	1.112	1.49
2.800	0.62	1.258	1.63
2.900	0.61	1.376	1.72
3.000	0.65	1.404	1.79
3.100	0.76	1.380	1.81
3.200	0.95	1.240	1.75
3.300	1.19	1.048	1.60
3.400	1.52	0.804	1.40
3.500			1.14
3.559			0.95
3.737			0.18
3.798			1.02
3.851			2.06
3.900			3.21
3.944			4.44
3.984			5.70
4.021			7.01
4.055			8.34
4.084			9.71
4.109			11.15
4.125			12.76
$X = \frac{1}{2} = \text{HClO}_4 \cdot \text{H}_2\text{O}$			+2.49

* C = concentration in moles per liter of solution, X = mole fraction perchloric acid, ϕ = apparent molal volume in milliliters per mole.

From the extrapolation of the sodium perchlorate data shown in figure 3, a value of 42.7 ± 0.2 ml. per mole is obtained for ϕ^0 for sodium perchlorate at 25°C . This gives 1.2 ml. per mole for the difference between the apparent molal volumes of hydrogen and sodium ions at 25°C . and infinite dilution, a value which is in good agreement with the more precise value of 1.23 ± 0.04 ml. per mole obtained from the difference between hydrochloric acid and sodium chloride (5, 17, 22).

From the smoothed values in table 1 the densities of perchloric acid solutions can be calculated to an accuracy which is better than any of the present experimental data in the dilute range.

DISCUSSION

Drude and Nernst (1) observed and explained the fact that the dissociation of a molecule into two univalent ions entails a volume decrease of 8–12 cc. per mole. For ions of the same size larger values are to be expected for the more highly charged ones. This volume decrease, called electrostriction by Drude and Nernst, has been confirmed by a sufficient amount of experimental data. Recent values, some of which correct for the effect of electrostatic interaction of the ions, are 11.47 for acetic acid (16), 12 for nitric acid (15), and 20.2 for the dissociation of the bisulfate ion (8) at 25°C . If we assume that anhydrous perchloric acid is practically unionized, which is consistent with the experimental determinations in concentrated solutions (18), and that the molal volume of the unionized acid is independent of the stoichiometric concentration of acid; then the volume change on ionization of perchloric acid at infinite dilution and 50°C . is -12.8 cc. per mole. Interpolation of the density data of pure perchloric acid (7) gives 57.20 cc. per mole for the molal volume of pure perchloric acid at 25°C . and -13.3 cc. per mole for the volume change on ionization at this temperature. This small difference is probably within the limits of error in extrapolations, interpolations, and the assumption of constancy of the molal volume of the undissociated acid.

At a concentration of 9 moles per liter, which is the approximate position of the minima in figures 1 and 2, the degree of dissociation derived from Raman spectra (15, 18) is 0.98. The degree of ionization decreases rapidly at higher concentrations. This decrease produces the sharp rise in the apparent molal volume.

In contrast to these well-established increases in volume upon the formation of unionized molecules, which is in agreement with the Drude–Nernst equation (1, 16), Fajans (2) attributes the decrease in the molal volumes of hydrogen and lithium iodides in aqueous solutions more concentrated than 1.5 *N* and 4 *N*, respectively, to incomplete ionization. Although the volume changes on ionization are expected to be small for iodides,⁵ the conclusion of Fajans is subject to doubt. It is important to point out that Fajans (2) has considered the volume change of dissociation, apart from the electrostriction, in detail and concludes that there is a large decrease in volume in the formation of HI from H_3O^+

⁵ Compare the analogous discussion by Rice (21) for the free energy and entropy of hydration of the alkali halides.

and I^- . According to Fajans, this decrease is larger than the volume increase expected from the removal of electrostriction.

If one attributes the deviation of the apparent molal volume of hydriodic acid from the limiting law to incomplete dissociation and assigns this deviation to electrostriction, then one gets a Born radius which is negative. While the Born radii do not have strict physical significance (11, 16), there are no known cases of negative radii. Thus such deviations from the limiting law must be ascribed to ion-ion and ion-solvent interactions. The alkali halides show both positive and negative deviations from the limiting law (2, 4, 20). Yet there is no evidence against considering them completely dissociated. The deviations of the apparent molal volumes of perchloric acid solutions from the limiting law below $c = 9 N$ are obviously due to such interactions.

SUMMARY

The apparent molal volumes of perchloric acid solutions in water at 15°, 25°, and 50°C. have been calculated and extrapolated to infinite dilution. Smoothed values of the apparent molal volumes have been tabulated as a function of the concentration and permit the calculation of the densities of the solution.

A correlation is made between the dependence of the apparent molal volume on the concentration and the experimentally determined degrees of ionization.

The author wishes to express his gratitude to the late Professor W. C. Bray for his discussions and interest in this investigation.

REFERENCES

- (1) DRUDE, P., AND NERNST, W.: *Z. physik. Chem.* **15**, 79 (1894).
- (2) FAJANS, K.: *J. Chem. Phys.* **9**, 281, 282, 283 (1941).
- (3) FAJANS, K., AND GRESSMANN, M. L.: *Z. physik. Chem.* **A146**, 309 (1930).
- (4) FAJANS, K., AND JOHNSON, O.: *Trans. Electrochem. Soc.* **82**, 273 (1942).
- (5) GEFFCKEN, W., BECKMANN, C., AND KRUIS, A.: *Z. physik. Chem.* **B20**, 398 (1933).
- (6) HÖLEMANN, P., AND KOHNER, H.: *Z. physik. Chem.* **B13**, 388 (1931).
- (7) *International Critical Tables*, Vol. III, p. 55. McGraw-Hill Book Company, Inc., New York (1928).
- (8) KLOTZ, I. M., AND ECKERT, C. F.: *J. Am. Chem. Soc.* **64**, 1878 (1942).
- (9) KOHNER, H.: *Z. physik. Chem.* **B1**, 427 (1928).
- (10) KOHNER, H., AND GRESSMANN, M. L.: *Z. physik. Chem.* **A144**, 137 (1929).
- (11) LATIMER, W. M., PITZER, K. S., AND SLANSKY, C. M.: *J. Chem. Phys.* **7**, 108 (1939).
- (12) MARKHAM, A. E.: *J. Am. Chem. Soc.* **63**, 874 (1941).
- (13) PEARCE, J. N., AND NELSON, A. F.: *J. Am. Chem. Soc.* **55**, 3075 (1933).
- (14) REDLICH, O.: *J. Phys. Chem.* **44**, 619 (1940).
- (15) REDLICH, O.: *Chem. Rev.* **39**, 333 (1946).
- (16) REDLICH, O., AND BIGELEISEN, J.: *Chem. Rev.* **30**, 171 (1942).
- (17) REDLICH, O., AND BIGELEISEN, J.: *J. Am. Chem. Soc.* **65**, 1883 (1943).
- (18) REDLICH, O., HOLT, E. K., AND BIGELEISEN, J.: *J. Am. Chem. Soc.* **66**, 13 (1944).
- (19) REDLICH, O., AND ROSENFELD, P.: *Z. physik. Chem.* **A155**, 65 (1931).
- (20) REDLICH, O., AND ROSENFELD, P.: *Z. Elektrochem.* **37**, 705 (1931).
- (21) RICE, O. K.: *Electronic Structure and Chemical Binding*, Chap. XIX. McGraw-Hill Book Company, Inc., New York (1940).
- (22) WIRTH, H. E.: *J. Am. Chem. Soc.* **62**, 1128 (1940).

SOME MATHEMATICAL RELATIONS INVOLVING THE
SOLUBILITY OF SILVER CYANIDE

JOHN E. RICCI

*Department of Chemistry, New York University, University Heights, New York, New York**Received June 30, 1947*

One of the most interesting processes of analytical chemistry is the argentometric titration of cyanide, the classical Liebig method. The mathematical theory of the end point of this titration involves four equilibrium constants: K_w , the ion-product of water; K_a , the ionization constant of hydrocyanic acid; K , the instability constant of the argentocyanide complex ion, $\text{Ag}(\text{CN})_2^-$; and P , the solubility product of silver cyanide. This assumes that the only species in the solution are H^+ , OH^- , HCN , CN^- , $\text{Ag}(\text{CN})_2^-$, and Ag^+ , besides water, K^+ , and NO_3^- , since potassium hydroxide and nitric acid are assumed to be "strong," or completely ionized, as base and acid, respectively. The modified, Liebig-Dénigès titration, in which the equivalence point is indicated by the appearance of a turbidity of silver iodide in ammoniacal solution, using potassium iodide as indicator, involves in addition three more equilibrium constants: K_b , the ionization constant of ammonia; K' , the instability constant of the silver-ammonia complex ion, $\text{Ag}(\text{NH}_3)_2^+$; and P_{AgI} , the solubility product of silver iodide.

The usual discussion of the mathematical relations at the end points in these processes is scanty and unsatisfactory, not only, however, because of the complexity of the systems, but also because of a certain confusion frequently encountered in regard to the definition of the solubility product of silver cyanide and in regard to the consistency of the numerical values assigned to the several inter-related constants pertaining to silver cyanide. Because of the use of these equilibrium constants in the mathematical treatment of these and related analytical processes involving silver cyanide, it seems important to examine this question of the consistency of the "best" numerical values usually assigned to them in the literature. The result of this examination shows the need of clearer and more uniform definition of the solubility product of silver cyanide and perhaps the necessity of modification of the usually quoted value for this constant, to bring it into conformity with other independently determined quantities on the basis of which it may be calculated.

Following this preliminary consideration, it will be possible, with a consistent set of values of the constants, to derive at least approximate if not exact equations for various problems involving the precipitation of silver cyanide. In these formulas we shall use equilibrium constants which are presumably thermodynamic constants, together with symbols for the concentrations of various species in solution, assuming unity activity coefficients. The introduction of activity coefficients is then best accomplished when a final working equation, exact or approximate, is chosen for use,—as will be illustrated in an example later.

I. ON THE SOLUBILITY PRODUCT OF SILVER CYANIDE

A saturated pure aqueous solution of silver cyanide involves the four equilibrium constants K_w (taken as 1.0×10^{-14} at $25^\circ\text{C}.$), K_a , K , and P . The constants K_a and K may be determined in solutions unsaturated with respect to silver cyanide, and hence without reference either to P or to the solubility, S_0 , of the compound in pure water. Experimentally, then, a further measurement is required, knowing K_w , K_a , and K , to determine either P or S_0 , whereupon the other of these two quantities may be calculated.

For K_a , defined as

$$K_a = [\text{H}^+][\text{CN}^-]/[\text{HCN}] \quad (1)$$

we shall take the value 4×10^{-10} , determined by Harman and Worley (5), and chosen as the best probable value by Latimer in his *Oxidation Potentials* (9).

For the instability constant, K , defined as

$$K = [\text{Ag}^+][\text{CN}^-]^2/[\text{Ag}(\text{CN})_2^-] \quad (2)$$

we use the following equilibrium constant, measured in solutions saturated with respect to silver chloride, by Randall and Halford (17):

$$K_1 = [\text{H}^+]^2[\text{Cl}^-][\text{Ag}(\text{CN})_2^-]/[\text{HCN}]^2 = 1.9 \times 10^{-9} \quad (3)$$

Combined with the solubility product of silver chloride, as $P_{\text{AgCl}} = [\text{Ag}^+][\text{Cl}^-]$, equations 1, 2, and 3 give

$$K = K_a^2 P_{\text{AgCl}}/K_1 \quad (4)$$

Using 1.7×10^{-10} as the value of P_{AgCl} , again as listed by Latimer (10), and the value of K_a already mentioned, we have $K = 1.4 \times 10^{-20.1}$. Most of the analytical texts list values of K ranging from 10^{-23} to 10^{-19} .

The solubility product for silver cyanide may be defined either as

$$P = [\text{Ag}^+][\text{CN}^-] \quad (5)$$

or as

$$P' = [\text{Ag}^+][\text{Ag}(\text{CN})_2^-] \quad (6)$$

Both products are constant for saturation, their relation being

$$P' = P^2/K \quad (7)$$

Unless otherwise noted, the "solubility product of silver cyanide" will here mean P defined as in equation 5; both symbols, as defined in equations 5 and 6, will be used, however, for convenience in the mathematical formulas.

The solubility product may of course be determined without reference to S_0 , the solubility. Thus Randall and Halford (17) found, for solutions saturated with respect to silver cyanide, the following equilibrium constant:

$$K_2 = [\text{H}^+][\text{Ag}(\text{CN})_2^-]/[\text{HCN}] = 3.77 \times 10^{-5} \quad (8)$$

¹ Latimer (10) merely quotes 3.8×10^{-19} , the value calculated by Randall and Halford (17) through still different values of K_a and P_{AgCl} .

Combined with equations 1, 2, and 5, this gives $P = K_2K/K_a$, whence, with equation 4,

$$P = K_2K_aP_{\text{AgCl}}/K_1 \quad (9)$$

Using the values already given for these constants, we have $P = 1.3 \times 10^{-15}$.²

The solubility in pure water, S_0 , with which all the foregoing constants should be consistent, may presumably be determined directly and independently purely as a physical quantity. Such a low solubility, however, is usually determined only indirectly, through assumptions regarding the relative concentrations of the solute ions and species in the saturated solution. The reported values, as listed by Seidell (18), are:

$$3.2 \times 10^{-7} M \text{ at } 17.5^\circ\text{C.}, \text{ by conductivity} \quad (1, \text{ quoting } 14)$$

$$1.6 \times 10^{-6} M \text{ at } 20^\circ\text{C.}, \text{ by conductivity} \quad (2)$$

$$2.1 \times 10^{-7} M \text{ at } 18^\circ\text{C.}, \text{ by potentiometry} \quad (12)$$

The ratio of the solubilities calculated by Bottger (2) for silver chloride and silver cyanide (1.06×10^{-5} and 1.64×10^{-6} , respectively) is very closely equal to the ratio of his reported conductivities (1.33/0.19) for the two substances. Since the number of ions per mole of dissolved silver cyanide tends, with almost complete formation of the complex ion $\text{Ag}(\text{CN})_2^-$, to be half the number for silver chloride, we may perhaps take as a maximum "observed" solubility, or S_0 , at $20\text{--}25^\circ\text{C.}$, $\sim 3 \times 10^{-6} M$. The value usually quoted is $2 \times 10^{-6} M$ (4, 11). Such a value is evidently also understood wherever " P " is given as $S_0^2 \cong 2\text{--}4 \times 10^{-12}$.³ The implication, in such a presentation, seems to be that with such low solubility the salt in its pure saturated solution is "completely ionized",—despite the weakness of hydrocyanic acid as an acid and the great stability of the complex ion $\text{Ag}(\text{CN})_2^-$,—into Ag^+ and CN^- , so that $[\text{Ag}^+] = [\text{CN}^-] = S_0$, and " K_{sp} " = S_0^2 . In reality, the value of P for a given value of S_0 depends upon both K_a and K . P is clearly not equal to S_0^2 , since the dissolved silver, Σ_{Ag} , is in two forms, Ag^+ and $\text{Ag}(\text{CN})_2^-$, and the dissolved cyanide, Σ_{CN} , in three forms, HCN , CN^- , and $\text{Ag}(\text{CN})_2^-$. It will be shown below that a value of P , defined as $[\text{Ag}^+][\text{CN}^-]$, of $\sim 10^{-12}$, is in extraordinary disagreement with values of the order of 10^{-6} for S_0 , 10^{-19} for K , and 10^{-10} for K_a .

Occasionally P' , or $[\text{Ag}^+][\text{Ag}(\text{CN})_2^-]$, is given, instead of P , as the "solubility product"; thus in Fales and Kenny (3), P' is given as 1.1×10^{-11} (referring to Randall and Halford (17)), and $[\text{Ag}^+] = [\text{Ag}(\text{CN})_2^-]$ in the pure solution. This is much more nearly correct than $P \cong 10^{-12}$, although the concentrations of silver ion and argentocyanide ion are not theoretically equal in the pure aqueous

² Latimer (10) gives 7.0×10^{-15} , again as calculated by Randall and Halford (17) with different values of K_a and P_{AgCl} .

³ Kolthoff and Sandell (6): " $[\text{Ag}] = [\text{CN}^-] = \sqrt{4 \times 10^{-12}} = 2 \times 10^{-6}$ " at the "equivalence point."

Willard and Furman (19): By implication, the "solubility product" is here presented as analogous to P_{AgCl} and hence as equal to S_0^2 .

Pearce and Haenisch (15): " $\text{AgCN} = \text{Ag}^+ + \text{CN}^-$, $K_{sp} = 2.2 \times 10^{-12}$."

solution. Incidentally, using the data of Randall and Halford, and $P_{\text{AgCl}} = 1.7 \times 10^{-10}$, we have (combining equations 4, 7, and 9):

$$P' = K_2^2 P_{\text{AgCl}} / K_1 = 1.3 \times 10^{-10} \quad (10)$$

We may list at this point, therefore, as the best available (but not necessarily consistent) values of the quantities involved in the solubility of silver cyanide:

$$S_0 = 2 \times 10^{-6} M$$

$$K_a = 4. \times 10^{-10}$$

$$K = 1.4 \times 10^{-20}$$

$$P = 1.3 \times 10^{-15}$$

$$P' = P^2/K = 1.3 \times 10^{-10}$$

II. ON THE CONSISTENCY OF THE VALUES OF THE CONSTANTS S_0 , P , K , K_a

Given any three of these four quantities, the fourth may be calculated through the following three equations, the first being a statement of the principle of electroneutrality applied to pure aqueous silver cyanide:

$$[\text{H}^+] - K_w/[\text{H}^+] = -[\text{HCN}] \quad (11)$$

$$S_0 = [\text{Ag}^+] + [\text{Ag}(\text{CN})_2^-] \quad (12)$$

$$S_0 = [\text{CN}^-] + 2[\text{Ag}(\text{CN})_2^-] + [\text{HCN}] \quad (13)$$

For convenience, we shall use the simplified symbols H for $[\text{H}^+]$, W for K_w , x for $[\text{Ag}^+]$, and y for $[\text{Ag}(\text{CN})_2^-]$. Then introducing the condition for saturation (equation 5) and the equilibrium constants already defined, these equations become

$$H - W/H = -HP/xK_a = -HPy/K_aP' \quad (14)$$

$$S_0 = x + y = x + P'/x = P'/y + y \quad (15)$$

$$S_0 = P/x + 2P'/x + HP/xK_a = Py/P' + 2y + HPy/K_aP' \quad (16)$$

We shall now consider in turn the calculation of each of the quantities S_0 , P , K , and K_a from the others.

A. To find S_0 from P , K , and K_a

The two expressions for S_0 , of equations 15 and 16, are equated, to eliminate S_0 , giving an expression for x in terms of H and constants:

$$x^2 = P(1 + P/K + H/K_a) \quad (17)$$

When this is then equated with the expression for x obtainable from equation 14, also in terms of H and constants, we obtain an equation in which the only unknown is H , or

$$H^5 + H^4 K_a(1 + P/K - P/K_a^2) - 2H^3 W - 2H^2 K_a W(1 + P/K) + HW^2 + K_a W^2(1 + P/K) = 0 \quad (18)$$

This polynomial may be solved for H by numerical approximation, and then x may be obtained through equation 17. With x known, S_0 may then be found through equation 15 or 16.

This procedure assumes no previous knowledge of the order of magnitude of S_0 . In the actual case of silver cyanide, however, knowing that it is very insoluble and that most of the cyanide is present as $\text{Ag}(\text{CN})_2^-$ rather than as HCN despite the extreme weakness of this acid, we may disregard equation 18 and proceed more simply by assuming that the pure saturated solution is very nearly neutral, and hence that $H \cong \sqrt{W}$. Then equation 17 gives x at once as

$$x \cong \sqrt{P} \sqrt{1 + P/K + \sqrt{W/K_a}} \quad (19)$$

and from equation 16,

$$S_0 \cong \sqrt{P} \left(\frac{1 + 2P/K + \sqrt{W/K_a}}{\sqrt{1 + P/K + \sqrt{W/K_a}}} \right) \quad (20)$$

Since $\sqrt{W} \gg K_a$, this becomes

$$S_0 \cong \sqrt{P} \left(\frac{2P/K + \sqrt{W/K_a}}{\sqrt{P/K + \sqrt{W/K_a}}} \right) \quad (21)$$

Furthermore, since $PK_a \gg K\sqrt{W}$, then, less accurately,

$$S_0 \cong 2P/\sqrt{K}, \text{ or } 2\sqrt{P'} \quad (22)$$

According to the "best" values of P and K already listed, S_0 should therefore be $\cong 2.1 \times 10^{-6}$, instead of 2×10^{-6} , which was already estimated as probably a maximum value from the data.

B. To find P from S_0 , K , and K_a

The expression for x of equation 17 is equated with that from equation 14, or

$$x = H^2 P / K_a (W - H^2) \quad (23)$$

whereupon we may express P in terms of H and other constants. With this result and equation 23, equation 15 then gives an expression defining H as the only unknown, in terms of S_0 and constants:

$$\begin{aligned} H^7(K + K_a^2) + H^6[K_a(K + K_a^2) + S_0(K - K_a^2)] - H^5W(K + 3K_a^2) \\ - H^4K_aW[K + 3K_a^2 - 2S_0K_a] + H^3(3K_a^2W^2) + H^3K_a^2W^2(3K_a - S_0) \\ - H(K_a^2W^3) - K_a^3W^3 = 0 \end{aligned} \quad (24)$$

With H calculated from equation 24, we may then eliminate x from equations 15 and 16, and calculate P in terms of S_0 , K , K_a , and the known H .

But again in the actual case of silver cyanide, we may assume $H \cong \sqrt{W}$, and proceed at once as just indicated. Or, solving equation 21 now for P , we have

$$4P^3 + 4P^2K\sqrt{W}/K_a + PK^2(W/K_a^2 - S_0^2/K) - S_0^2K^2\sqrt{W}/K_a \cong 0 \quad (25)$$

With the numerical values already listed, this gives

$$P \cong \frac{1}{2} S_0 \sqrt{K} \quad (26)$$

or $\cong 1.2 \times 10^{-16}$, instead of 1.3×10^{-15} .

C. To find K from S_0 , P , and K_a

We eliminate K from equations 15 and 16, and introduce equation 23, obtaining

$$H^5 - H^4(S_0 - K_a + 2P/K_a) - 2H^3W \\ + H^2W(S_0 - 2K_a) + HW^2 + K_aW^2 = 0 \quad (27)$$

With H so calculated, x is obtained from equations 15 and 16 with K eliminated; and then K from equation 15.

But if we assume, for silver cyanide, that $H \cong \sqrt{W}$, we may again solve equation 21, now for K , obtaining a simple quadratic:

$$K^2 + K \frac{P \left(\frac{S_0^2 K_a}{\sqrt{W}} - 4P \right)}{S_0^2 - P\sqrt{W}/K_a} - \frac{4P^3 K_a}{\sqrt{W}(S_0^2 - P\sqrt{W}/K_a)} \cong 0 \quad (28)$$

With the numerical values listed, this gives $K = 1.7 \times 10^{-18}$, instead of 1.4×10^{-20} as listed.

D. To find K_a from S_0 , P , and K

Now x may be calculated at once from equation 15. With x known, equations 14 and 16 may then be combined to find the two remaining unknowns, H and K_a .

In the actual case of silver cyanide, the values of S_0 , P , and K listed from the literature are seen at once to be impossible or inconsistent as a group of values, since they give no real value of x in equation 15, which requires that S_0^2 be $> 4P^2/K$. In this case then it is out of the question to evaluate K_a from the given values of S_0 and the other constants.

In the sequel, then, in order to use consistent values, it seems advisable to keep as original data S_0 , K_a , and K , and to use the value of P calculated from these three constants through equation 25. Our numerical values, therefore, will be:

$$S_0 = 2.0 \times 10^{-6}$$

$$K_a = 4.0 \times 10^{-10}$$

$$K = 1.4 \times 10^{-20}$$

$$P = 1.2 \times 10^{-16}$$

$$P' = P^2/K = 1.0 \times 10^{-12}$$

III. EFFECT OF REAGENTS ON THE SOLUBILITY OF SILVER CYANIDE

We shall consider the effect of five separate reagents: A, silver nitrate; B, potassium cyanide; C, nitric acid; D, potassium hydroxide; E, hydrocyanic acid—each at the concentration c —upon the solubility, S , of a suspension of solid silver cyanide in the solution of the reagent.

The calculation depends on the combination of three equations: the electro-neutrality condition, the expression for the total number of equivalents of dissolved silver, Σ_{Ag} , and the similar expression for dissolved cyanide, or Σ_{CN} ; namely,

$$H - W/H = [NO_3^-] - [K^+] + [CN^-] + [Ag(CN)_2^-] - [Ag^+] \quad (29)$$

$$\Sigma_{Ag} = [Ag^+] + [Ag(CN)_2^-]; = S + c \text{ for A; } = S \text{ for B to E} \quad (30)$$

$$\Sigma_{CN} = [CN^-] + 2[Ag(CN)_2^-] + [HCN]; = S \text{ for A, C, E;} \\ = S + c \text{ for B, D} \quad (31)$$

As in the case of finding the solubility, S_0 , of silver cyanide in pure water from the constants, Σ_{Ag} and Σ_{CN} are combined to eliminate S , giving an equation in $\Sigma_{Ag} - \Sigma_{CN}$, which is then combined with equation 29 to obtain an expression for H in terms of constants and x , the $[Ag^+]$ concentration. For cases A and B, i.e., for silver nitrate and potassium cyanide, this expression for H is the same as for pure saturated silver cyanide solution, or

$$H = \sqrt{\frac{xK_a W}{xK_a + P}} \quad (32)$$

For cases C and E (nitric acid and hydrocyanic acid)

$$H = \frac{cxK_a}{2(xK_a + P)} + \sqrt{\left(\frac{cxK_a}{2(xK_a + P)}\right)^2 + \frac{xK_a W}{xK_a + P}} \quad (33)$$

[Note: The symbol $(\quad)^2$ under the root in such a quadratic solution will represent the square of the quantity outside the root.] Equation 33 also holds for case D (potassium hydroxide), but with the sign of c reversed. Such an expression for H is then substituted in the equation for $\Sigma_{Ag} - \Sigma_{CN}$, yielding an equation for x as a function of c and constants,—with the following results:

Case A (silver nitrate)

Writing Σ as the sum $(P' + P)$,

$$y^5 P \Sigma^2 + y^4 P' [2cP \Sigma + K_a \Sigma^2 - P^2 W/K_a] + y^3 (P')^3 [P(c^2 - \Sigma) + 2cK_a \Sigma] \\ - y^2 (P')^3 [2cP - K_a(c^2 - \Sigma)] - y(P')^4 [2cK_a - P] + (P')^5 K_a = 0 \quad (34)$$

For the numerical values applying to silver cyanide, the significant terms are the last three, giving for appreciable values of c ,

$$y \cong P'/c \quad (35)$$

Since $x = P'/y$, then H , from equation 32, $\cong \sqrt{W}$. The solubility is Σ_{CN} ; hence, from equation 31:

$$S = 2y + P/x + HP/xK_a \quad (36)$$

$$\cong [2P' + P + P\sqrt{W}/K_a]/c \cong 2P'/c \quad (37)$$

Case B (potassium cyanide)

The result is the same as equation 34, with the sign of c reversed. In this case the first three terms of the equation are the significant ones, and, approximately,

$$y \cong c \quad (38)$$

Then $S (= \Sigma_{\text{Ag}})$ is

$$S = y + P'/y \cong c \quad (39)$$

Case C (nitric acid—"strong", or completely ionized, acid)

In this case the polynomial corresponding to equation 34 is of the eighth degree, with very cumbersome coefficients. But an approximation is possible since with the actual numerical values applying to silver cyanide, and for all but negligibly small values of c , equation 33 may be taken as

$$H \cong cxK_a/(cxK_a + P) \quad (40)$$

This leads to

$$x^3K_a + x^2P - x(cP + K_a\Sigma) - P\Sigma \cong 0 \quad (41)$$

in which the last term, as well as $K_a\Sigma$ in the third, are negligible. Hence

$$x \cong -\frac{P}{2K_a} + \sqrt{\left(\frac{P}{2K_a}\right)^2 + \frac{cP}{K_a}} \cong \sqrt{cP/K_a} \quad (42)$$

and from Σ_{Ag} ,

$$S = x + P'/x \cong \sqrt{cP/K_a} \quad (43)$$

The effect of strong acid, then, upon the solubility of a substance like silver cyanide is strictly a function of the four equilibrium constants K_a , K , P , and W . The effect of W has already dropped out in the approximation of equation 41; in the final simple formula, equation 43, the effect of P' (or therefore of K) is apparently also absent, but it is implicit in the interconnection of P and the solubility itself. In Kolthoff and Sandell (7), we read that strong acid does not dissolve silver cyanide because it "is a salt of the strong acid $\text{HAg}(\text{CN})_2$." Aside from the fact that we do not know the ionization constant of such a hypothetical "acid," we see here that strong acid does affect the solubility despite the assumption that " $\text{HAg}(\text{CN})_2$ " is a "strong acid." The final approximate formula, equation 43, shows a small but definite effect; in pure water, $x \cong y \cong$

$\sqrt{P'}$; with nitric acid present, x rises to $\sqrt{cP/K_a}$ while y falls to $P'/\sqrt{K_a/cP}$. The relation $P' = P^2/K$ must be kept in mind in interpreting these expressions.

This effect may moreover be compared with that in the absence of complex ion formation. In each case, H is again given by equation 33, and if this is assumed similarly to be simplifiable to equation 40, then

$$x^3 K_a + x^2 P - xP(c + K_a) - P^2 \cong 0 \quad (44)$$

which may also be written directly from equation 41 on setting $P' = 0$ in Σ . Now if K_a and P are comparable in magnitude, the last term may be neglected, and again, as in equations 42 and 43,

$$S = x \cong -\frac{P}{2K_a} + \sqrt{\left(\frac{P}{2K_a}\right)^2 + \frac{cP}{K_a}} \cong \sqrt{cP/K_a} \quad (45)$$

For a given set of values of P and K_a , then, the effect is the same as in the case of silver cyanide (equation 43). But if we compare the salts of two acids of the same value of K_a (in both cases, as in silver cyanide, with $K_a \ll \sqrt{W}$), and of the same value of S_0 (actual water solubility), then in the non-complex case $P \cong S_0^2 K_a / \sqrt{W}$, while in the complex case $P \cong \frac{1}{2} S_0 \sqrt{K}$ (equation 26). Hence the two effects (equation 43 and equation 45) are actually in the ratio $2S_0 K_a / \sqrt{KW}$; in the present case, therefore, the effect is approximately only 1 per cent of what it would be if, with the same value of S_0 and K_a , there were no complex ion formation.

Case D (potassium hydroxide—"strong," or completely ionized, base)

Now equation 33, with $-c$, reduces to

$$H \cong W/c \quad (46)$$

Then

$$x \cong \sqrt{P' + P + PW/cK_a} \cong \sqrt{P'} \quad (47)$$

and

$$S = x + P'/x \cong 2\sqrt{P'} \quad (48)$$

The effect, although practically zero, is in the direction of decreasing the solubility, as is to be expected on the basis of the positive effect of nitric acid. The negative effect may be established by examining dS/dc , using the full expression of equation 47 for x , in equation 48.

Case E (hydrocyanic acid)

Again the full, exact equation defining x or y in terms of c and constants is of the eighth degree, and very cumbersome. But with the approximation indicated in equation 40, which is applicable even in the present case, the result is

$$y^3 P \Sigma + y^2 P' K_a \Sigma - y(P')^2 (cK_a + P) - (P')^3 K_a \cong 0 \quad (49)$$

With appreciable c , the last term may be neglected; since $\Sigma \cong P'$, furthermore, this means

$$y \cong -\frac{P'K_a}{2P} + \sqrt{\left(\frac{P'}{2P}\right)^2 + \frac{cP'K_a}{P}} \cong \sqrt{cP'K_a/P} \quad (50)$$

Hence

$$S = y + P'/y \cong \sqrt{cP'K_a/P} \quad (51)$$

an effect distinctly smaller than that of potassium cyanide.

Finally, equations for the effect of various combinations of these reagents may also be derived by the same general procedure. Thus with nitric acid at concentration c_1 and potassium cyanide at c , $\Sigma_{\text{Ag}} = S$, $\Sigma_{\text{CN}} = S + c$, and H is given by equation 33. Combining Σ_{Ag} and Σ_{CN} , and introducing such an expression for H , simplified again as in equation 40, we obtain

$$y^3P\Sigma - y^2P'[P(c - c_1) - K_a\Sigma] - y(P')^2(cK_a + P) - (P')^3K_a \cong 0 \quad (52)$$

Now if $c > c_1$, the last term may be neglected, and

$$y \cong \frac{c - c_1}{2} + \sqrt{\left(\frac{c - c_1}{2}\right)^2 + \frac{cK_aP'}{P}} \cong c - c_1 \quad (53)$$

as expected from an excess of potassium cyanide. But if $c < c_1$, the only significant terms are the middle two, and

$$y \cong \left(\frac{c}{c_1 - c}\right) \frac{K_aP'}{P} \quad (54)$$

while

$$x \cong \left(\frac{c_1 - c}{c}\right) \frac{P}{K_a} \quad (55)$$

In this case the solution may be said to be one containing nitric acid at the concentration $c_1 - c$, with hydrocyanic acid and potassium nitrate both at the concentration c ; (equation 52 may in fact be considered a combination of equation 41, in terms of y and with nitric acid at $c_1 - c$, and equation 49, for hydrocyanic acid at concentration c). Nevertheless the effect of such a combination on the solubility ($S = x + y$), seen in equations 54 and 55, is smaller than that of either nitric acid (equation 45) or hydrocyanic acid (equation 51) separately.

IV. ON THE ARGENTOMETRIC TITRATION OF CYANIDE

A. The Liebig titration

This is the titration of pure aqueous potassium cyanide with silver nitrate; the concentrations at the equivalence point (practically identical with the end point, which is the appearance of a precipitate of silver cyanide) will be represented as c for potassium cyanide and c_1 for silver nitrate.

(1) The value of x ($= [\text{Ag}^+]$) at the equivalence point, or when $c_1 = c/2$, assuming

no precipitation to have occurred: On combining equations 29, 3, and 31, with $\Sigma_{Ag} = c/2$ and $\Sigma_{CN} = c$, we have

$$[CN^-] = \sqrt{\frac{K}{x} \left(\frac{c}{2} - x \right)} \quad (56)$$

$$H = \sqrt{\frac{W}{1 + [CN^-]/K_a}} \quad (57)$$

and

$$2x - [CN^-] = H[CN^-]K \quad (58)$$

Now if $c/2 \gg x$, $[CN^-] \cong \sqrt{cK/2x}$, and since this is $\gg K$,

$$H \cong \sqrt{K_a W / [CN^-]} \cong \sqrt{2xK_a W / cK}$$

Then equation 58 becomes

$$64x^6 + 8x^3cK - 8x^3cKW/K_a - 2xcKW^2/K_a^2 + c^2K^2 \cong 0 \quad (59)$$

The important terms, for appreciable values of c , are those in x^6 and x ; hence

$$x \cong \frac{1}{2} \sqrt[5]{cKW^2/K_a^2} \quad (60)$$

$\cong 2.5 \times 10^{-8}$ for $c = 0.1$. With this magnitude of c , the solution is therefore supersaturated with respect to silver cyanide, since xy , or $x\left(\frac{c}{2} - x\right)$, $> P'$.

(2) *The value of c_1 at the end point* (saturation with respect to silver cyanide): Now H is given by equation 32, and with $\Sigma_{Ag} = c_1$ while $\Sigma_{CN} = c$, equations 30 and 31 give, with the condition $x[CN^-] = P$:

$$\begin{aligned} x^3cK_a^2 - x^2cK_a[2K_a(2P' + P) - cP] \\ + x[K_a^2(2P' + P)^2 - 2cPK_a(2P' + P) - P^2W] \\ + PK_a(2P' + P)^2 = 0 \end{aligned} \quad (61)$$

From the last three terms, the first being negligible,

$$x^2c^2 - 4xcP' + 4(P')^2 \cong 0 \quad (62)$$

or

$$x \cong 2P'/c \quad (63)$$

Furthermore,

$$c = [CN^-] + 2y + [HCN] \quad (64)$$

and since $[HCN] = H[CN^-]/K_a = HP/xK_a$, then with $x \cong 2P'/c$,

$$y \cong \frac{c}{2} \left[1 - \frac{P}{2P'} \left(1 + \frac{H}{K_a} \right) \right] \quad (65)$$

But with $x \cong 2P'/c$,

$$H \cong \sqrt{2P'K_aW/cP} \quad (66)$$

Hence

$$c_1 = y + x \cong \frac{c}{2} \left[1 + \frac{P}{2P'} \left(1 + \sqrt{\frac{2P'W}{cPK_a}} \right) \right] + 2P'c \quad (67)$$

For appreciable values of c , this means

$$c_1 = \frac{c}{2} [1 + 6 \times 10^{-5} (1 + 0.65/\sqrt{c})] \quad (68)$$

so that the end point occurs slightly early.

B. Treatment of a solution containing both potassium cyanide (c) and potassium chloride (c_2) with silver nitrate (c_1)

The solubility product of silver chloride = P_2 ($= 1.7 \times 10^{-10}$).

If silver cyanide precipitates first, it does so (equation 63) when $x \cong 2P'/c$, while if silver chloride is the first precipitate, it requires $x = P_2/c_2$. Therefore silver chloride cannot precipitate before silver cyanide unless $c_2 > cP_2/2P'$, or $> \sim 85c$.

(1) If $c_2 > cP_2/2P'$, the first precipitate is silver chloride. It appears when, with $\Sigma_{Ag} = c_1$ and $\Sigma_{CN} = c$, H is given by equation 57. But with $x = P_2/c_2$ and $[CN^-] = \sqrt{Ky/x}$,

$$H \cong \sqrt{\frac{K_aW}{\sqrt{c_2yK/P_2}}} \quad (69)$$

Then from Σ_{CN} ,

$$c \cong 2y + [CN^-] \left(1 + \sqrt{\frac{W}{K_a\sqrt{c_2yK/P_2}}} \right) \quad (70)$$

For an approximate solution, we assume that we may set $y = c/2$ in the parenthesis, in which we may furthermore neglect the term 1 since c must here be $< \sim 10^{-2}c_2$, obtaining:

$$y^2 - y \left[c - \frac{W}{K_a} \sqrt{\frac{c_2K}{2cP_2}} \right] + \frac{c^2}{4} \cong 0 \quad (71)$$

$$y \cong \frac{c}{2} - \sqrt{\frac{W}{2K_a}} \sqrt{\frac{cc_2K}{2P_2}} \quad (72)$$

$$\cong \frac{c}{2} - 8.9 \times 10^{-5} (cc_2)^{1/4} \quad (73)$$

Hence the appearance of silver chloride occurs (since $x = P_2/c_2$) when

$$c_1 = y + P_2/c_2 \cong c/2 - 8.9 \times 10^{-5} (cc_2)^{1/4} \quad (74)$$

The second precipitate, silver cyanide, will appear, mixed with the silver chloride, when H , according to equation 32, has the value

$$H \cong \sqrt{xK_aW/P} \quad (75)$$

since x is expected to be very small. From Σ_{CN} , or

$$cx - 2(P' + P) = HP/K_a \quad (76)$$

neglecting P as $\ll 2P'$,

$$y^2 - y \left[c - \frac{PW}{4P'K_a} \right] + \frac{c^2}{4} \cong 0 \quad (77)$$

or

$$y \cong \frac{c}{2} - \sqrt{cPW/8K_aP'} \quad (78)$$

which, for small c , is seen to be larger than the value in equation 73. For the value of c_1 required,

$$c_1 = x + y + c_2 - [Cl^-] \quad (79)$$

and hence, since $x = P'/y$ and $[Cl^-] = P_2/x$,

$$c_1 \cong c_2 + \frac{c}{2} - \sqrt{\frac{cPW}{8K_aP'}} + \frac{2P'}{c} - \frac{c_2P_2}{2P'} \quad (80)$$

which, it must be remembered, applies only for $c_2 \gg c$. For example, if $c_2 = 1$ and $c = 10^{-3}$, silver chloride precipitates (alone) when (from equation 74) $c_1 = 4.98 \times 10^{-4}$, and silver cyanide appears as a second precipitate when (from equation 80) $c_1 = 0.9155$; if $c_2 = 1$ and $c = 10^{-2}$, the corresponding values of c_1 are 4.997×10^{-3} and 0.155.

(2) If $c_2 < cP_2/2P'$, the first precipitate, silver cyanide, appears with the conditions discussed in equations 66–68. For the value of c_1 when silver chloride begins to precipitate, mixed with the silver cyanide, this occurs when

$$[CN^-] = [Cl^-]P/P_2 = c_2P/P_2 \quad (81)$$

Hence, since H is still given by equation 57,

$$H = \sqrt{\frac{P_2K_aW}{c_2P + K_aP_2}} \quad (82)$$

Also,

$$c_1 - c = x - [CN^-] - y - [HCN] \quad (83)$$

and since $x = P/[CN^-]$, $y = P'/x$ and $HCN = H[CN^-]/K_a$, then, exactly,

$$c_1 = c - c_2 \left(\frac{P' + P}{P_2} \right) - \frac{c_2P}{P_2K_a} \sqrt{\frac{P_2K_aW}{c_2P + K_aP_2}} + \frac{P_2}{c_2} \quad (84)$$

(3) Finally, when the solution is saturated with both precipitates and $c_1 =$

$c + c_2$, we have a suspension of silver chloride and silver cyanide in aqueous potassium nitrate, with H again given by equation 32. But since

$$\Sigma_{Ag} = \Sigma_{CN} + [Cl^-] \quad (85)$$

and

$$x + P'/x = P_2/x + P/x + 2P'/x + [HCN] \quad (86)$$

then

$$x^2 - \Sigma = HP/K_a \quad (87)$$

in which $\Sigma = P_2 + P + P'$. Hence

$$x^5 K_a + x^4 P - 2x^3 K_a \Sigma - 2x^2 P \Sigma + x(K_a \Sigma^2 - P^2 W/K_a) + P \Sigma^2 = 0 \quad (88)$$

Approximately,

$$x^4 - 2x^2 + \Sigma^2 \cong 0 \quad (89)$$

and

$$x \cong \sqrt{P_2 + P + P'} \quad (90)$$

Equation 88 is interesting since it may be modified directly according to variations in the system. In the absence of complex ion formation, we simply drop P' from the sum Σ . If the acid "HCN" were strong, though still forming the complex ion, we would divide through by K_a and set $K_a = \infty$, thereby obtaining equation 89, and hence equation 90, as an exact equation.

C. Effect of ammonia (at analytical concentration b) on solubility of silver chloride or silver cyanide

Before treating the Liebig-Dénigès titration of potassium cyanide, we shall first consider the relations involved in the effect of ammonia on the solubility of precipitates such as silver chloride and silver cyanide. We here introduce two other equilibrium constants:

$$K_b = [NH_4^+][OH^-]/[NH_3] = 1.8 \times 10^{-5}$$

and

$$K' = [Ag^+][NH_3]^2/[Ag(NH_3)_2^+] = 6.0 \times 10^{-8}$$

the values again taken from Latimer (10).

(1) *For silver chloride and aqueous ammonia:* Let z represent $[Ag(NH_3)_2^+]$, and $S = [Cl^-]$ = the solubility of silver chloride, or

$$S = x + z \quad (91)$$

For saturation, then,

$$z = S - P_2/S \quad (92)$$

and

$$[NH_3] = \sqrt{K'z/x} = \sqrt{K'(S^2 - P_2)/P_2} = Y \quad (93)$$

Then

$$[\text{OH}^-] - W/[\text{OH}^-] = [\text{NH}_4^+] = K_b Y/[\text{OH}^-] \quad (94)$$

whence

$$[\text{OH}^-] = \sqrt{K_b Y + W} \quad (95)$$

But

$$b = [\text{NH}_3] + [\text{NH}_4^+] + 2z \quad (96)$$

or

$$b = 2[S - P_2/S] + Y + K_b Y/\sqrt{K_b Y + W} \quad (97)$$

with Y defined by equation 93.

This result gives b explicitly and exactly for any specified value of the solubility S . For appreciable values of S , the concentration of ammonia required is approximately

$$b \cong S(2 + \sqrt{K'/P_2}) \quad (98)$$

(a) Equation 97 will now be used to illustrate the introduction of *activity coefficients*. Since the equation is based on the principle of electroneutrality, it holds strictly in terms of concentrations. Hence if the equilibrium constants involved in it are thermodynamic constants, they must be replaced with "mass" constants holding in the ionic atmosphere of the particular solution. The usual simplifying assumption made in such transformation is that if the ionic strength is not too high the activity coefficient of an uncharged species may be taken as unity while the activity coefficients of all univalent ions (the only ones involved in the whole of this discussion), whether positive or negative, are equal to each other. On this basis, equation 97 becomes

$$b = 2 \left[S - \frac{P_2}{\gamma^2 S} \right] + Y + \frac{K_b Y}{\gamma \sqrt{K_b Y + W}} \quad (99)$$

with

$$Y = \sqrt{K' \gamma^2 (S^2 + P_2/\gamma^2)/P_2} \quad (100)$$

If the solution contains only the ammonia and silver chloride, then the ionic strength is

$$\mu = [\text{OH}^-] + [\text{Cl}^-] \quad (101)$$

with $[\text{OH}^-]$ given explicitly by equation 95 and $[\text{Cl}^-] = S$. Hence if the Debye-Hückel limiting law is assumed to apply, so that $\log \gamma = -0.505 \sqrt{\mu}$, equation 99 may be used for a complete calculation. For appreciable S , the approximation 98 becomes

$$b \cong S(2 + \sqrt{K' \gamma^2/P_2}) \quad (102)$$

and $\mu \cong S$. If the solution also contains an indifferent salt such as potassium nitrate at concentration c_i , then

$$\mu = [\text{OH}^-] + S + c_i \quad (103)$$

(b) For an approximate solution for S in terms of b , with appreciable b :

$S \gg P'/S$; $Y \cong S\sqrt{K'/P_2}$ or $\cong SZ$ (with Z defined as $\sqrt{K'/P_2}$); $[\text{OH}^-] > [\text{H}^+]$, or $[\text{OH}^-] \cong \sqrt{K_b}Y \cong \sqrt{K_b}SZ$. Then equation 97 becomes

$$b \cong 2S + SZ + \sqrt{K_b}SZ \quad (104)$$

whence

$$S \cong \frac{2b(2 + Z) + K_b Z}{2(2 + Z)^2} + \sqrt{()^2 - \frac{b^2}{(2 + Z)^2}} \quad (105)$$

But with $b \gg K_b$, this becomes

$$S \cong \frac{b}{(2 + Z)} \cong \frac{b}{2 + \sqrt{K'/P_2}} \quad (106)$$

as from equation 98. For silver bromide and silver iodide, where $K' \gg P_2$,

$$S \cong b\sqrt{P_2/K'} \quad (107)$$

but for silver chloride this final approximation would give $S = b/18.8$, whereas equation 106 gives $S = b/20.8$, an appreciable difference.

(c) A reagent⁴ containing silver nitrate (c_i), potassium nitrate, and ammonia (b) is sometimes used to dissolve silver chloride, and to separate it from silver bromide and silver iodide. To find the solubility of silver chloride in such a solution: if b is appreciable, so that $[\text{NH}_3] \cong b$, then with $z = x[\text{NH}_3]^2/K' \cong xb^2/K'$, and $x = P_2/[\text{Cl}^-] = P_2/S$,

$$S = [\text{Cl}^-] = x + z - c_i \cong \frac{P_2}{s} + \frac{b^2 P_2}{SK'} - c_i \quad (108)$$

$$S + Sc_i - P_2 \left(\frac{K' + b^2}{K'} \right) \cong 0 \quad (109)$$

$$S \cong -\frac{c_i}{2} + \sqrt{\left(\frac{c_i}{2}\right)^2 + \frac{b^2 P_2}{K'}} \quad (110)$$

(2) For silver cyanide and aqueous ammonia we shall assume, for the sake of an approximate formula, that the concentration b is large enough so that $[\text{OH}^-] \cong \sqrt{bK_b}$. From $\Sigma_{\text{CN}} = S$, then,

$$x = (2P' + P + HP/K_a)/S \cong 2P'/S \quad (111)$$

Also, $y = P'/x \cong S/2$; and since $S = x + y + z$, then

$$z \cong S - S/2 - 2P'/S \cong S/2 \quad (112)$$

But

$$b = [\text{NH}_3] + [\text{NH}_4^+] + 2z \quad (113)$$

⁴ Known as Miller's reagent (13).

and

$$[\text{NH}_3] = \sqrt{K'z/x} \cong \frac{S}{2} \sqrt{\frac{K'}{P'}} \quad (114)$$

Hence

$$b \cong \frac{S}{2} \sqrt{\frac{K'}{P'}} \left(1 + \frac{K_b}{[\text{OH}^-]}\right) + 2z \quad (115)$$

$$\cong \frac{S}{2} \sqrt{\frac{K'}{P'}} \left(1 + \frac{K_b}{b}\right) + S \quad (116)$$

Rearranging,

$$b^3 - 2b^2(Q + S) + b(Q + S)^2 - Q^2 K_b \cong 0 \quad (117)$$

with $Q = (S/2)\sqrt{K'P'}$. For any appreciable value of S , $Q \gg S$; hence

$$b \cong Q + S \cong S \left(\frac{\sqrt{K'P'}}{2} + 1 \right) \cong S(123) \quad (118)$$

Conversely, then,

$$S \cong \frac{b}{\left(\frac{\sqrt{K'P'}}{2} + 1 \right)} \cong b/123 \quad (119)$$

D. The Liebig-Dénigès titration

This is the titration of potassium cyanide with silver nitrate, in ammoniacal solution, with potassium iodide as indicator. The concentrations are c_1 for silver nitrate, c for potassium cyanide, c_s for potassium iodide, and b for NH_3 . Now P_s = solubility product of silver iodide = 8.5×10^{-17} (10); the other constants are as already defined.

We shall assume again that b is large enough so that $[\text{OH}^-] \cong \sqrt{bK_b}$.

Disregarding temporarily the presence of the iodide, we shall first consider the effect of ammonia on the usual appearance of a precipitate of silver cyanide as an end point. For the value of $[\text{Ag}^+]$, or x , when silver cyanide would begin to precipitate, the expression for Σ_{CN} gives

$$x = \frac{1}{c} (2P' + P + HP/K_a) \cong \frac{1}{c} (2P' + PW/K_a \sqrt{bK_b}) \quad (120)$$

Then from Σ_{Ag} ,

$$c_1 = x + y + z = x + P'/x + x[\text{NH}_3]^2/K' \quad (121)$$

But with b large enough, we shall assume $[\text{NH}_3] \cong b$. Hence, since $x \cong P'/c$, from equation 120, and $y = P'/x$ and hence $\gg x$,

$$c_1 \cong y + 2b^2 P'/cK' \quad (122)$$

Also,

$$y = P'/x \cong \frac{cP'}{2P' + PW/K_a\sqrt{bK_b}} \cong \frac{c}{2} \left(1 - \frac{PW}{2P'K_a\sqrt{bK_b}} \right) \quad (123)$$

Therefore

$$c_1 \cong \frac{c}{2} \left(1 - \frac{PW}{2P'K_a\sqrt{bK_b}} \right) + \frac{2b^2P'}{cK'} \quad (124)$$

or

$$c_1 \cong \frac{c}{2} \left(1 - \frac{3.4 \times 10^{-7}}{\sqrt{b}} \right) + \frac{3.3 \times 10^{-8}b^2}{c} \quad (125)$$

With $c = 0.1$ and $b = \sqrt{0.1}$, $c_1 = 0.05003$.

The ammonia therefore would cause a slight delay in the appearance of the end point, whereas in the absence of ammonia we found (equations 61–68) that silver cyanide would precipitate just before the equivalence point. However, with potassium iodide also present, the precipitate will not be silver cyanide at all, but silver iodide, precipitating again slightly before the equivalence point.

To find the value of c_1 when the solution becomes saturated with respect to silver iodide: From Σ_{CN} ,

$$c = 2y + [\text{CN}^-](1 + H/K_a) \quad (126)$$

Writing α (= degree of ionization of hydrocyanic acid) for $K_a/(K_a + H)$, and using relations already derived,

$$c = 2y + \sqrt{Ky/x}(1/\alpha) \quad (127)$$

whence, introducing the condition $x = P_3/c_3$,

$$y = \frac{c}{2} + \frac{c_3K}{8P_3\alpha^2} - \sqrt{\frac{c_3K}{8P_3\alpha^2} \left(c + \frac{c_3K}{8P_3\alpha^2} \right)} \quad (128)$$

This is exact and general, but α involves the unknown hydrogen-ion concentration. If the solution is sufficiently alkaline (i.e., if $[\text{OH}^-] \cong \sqrt{bK_b}$) and if b is appreciable, then $\alpha \cong 1$. Also, if z ($= [\text{Ag}(\text{NH}_3)_2^+]$), which equals $x[\text{NH}_3]^2/K'$, is assumed $\cong xb^2/K'$ and hence $\cong b^2P_3/c_3K'$, then we may calculate c_1 from Σ_{Ag} , or $c_1 = x + y + z$, as

$$c_1 \cong \frac{c}{2} - \sqrt{\frac{K}{8P_3}} \sqrt{cc_3} + x + z + \frac{c_3K}{8P_3} \quad (129)$$

the last three terms all being negligible. The end point therefore occurs slightly early, with

$$c_1 \cong \frac{c}{2} - 4.5 \times 10^{-8} \sqrt{cc_3} \quad (130)$$

The conditions usually recommended (8, 16, 20) are $b \cong 0.3$ and $c_3 \cong 0.01$ for $c \cong 0.06$; and then according to equation 130 the error would be ~ -0.4 per

cent, which is considerable. If the error is actually not so great, then something would seem to be wrong with the values of the equilibrium constants appearing in equation 128 and implicit in equation 129.

We may finally evaluate the theoretical value of c_3 (for given values of c and b) for zero error in the titration, or the value required so that $c_1 = c_2/2$ when silver iodide appears as a precipitate. With no precipitation at the equivalence point, when $c_1 = c_2/2$,

$$2\Sigma_{Ag} = x + y + z = \Sigma_{CN} = [CN^-] + 2y + [HCN] \quad (131)$$

Neglecting $[HCN]$ (i.e., assuming $\alpha \cong 1$), and since $[CN^-] = \sqrt{Ky}/x$, while $z \cong xb^2/K'$, this means

$$\sqrt{Ky}/x \cong 2x + 2xb^2/K' \cong 2xb^2/K' \quad (132)$$

Hence

$$y \cong 4x^3b^4/K(K')^2 \quad (133)$$

But from $\Sigma_{Ag} (= c/2)$,

$$y \cong \frac{c}{2} - x - xb^2/K' \cong \frac{c}{2} - \frac{xb^2}{K'} = \frac{c}{2} \quad (134)$$

since $x (= P_3/c_3)$ is extremely small. Finally, therefore, combining with equation 133,

$$x \cong \frac{1}{2}\sqrt[3]{K(K')^2c/b^4} \quad (135)$$

and

$$(c_3)_{\text{required}} = \frac{P_3}{x} \cong 2P_3\sqrt[3]{b^4/cK(K')^2} \quad (136)$$

For $c = 0.06$ and $b = 0.3$, c_3 to give an end point at the equivalence point should then be $\sim 2.2 \times 10^{-5}$.

REFERENCES

- (1) ABEGG, R., AND COX, A. J.: *Z. physik. Chem.* **46**, 11 (1903), quoting reference 14.
- (2) BOTTGER, W.: *Z. physik. Chem.* **46**, 521 (1903).
- (3) FALES, H. A., AND KENNY, F.: *Inorganic Quantitative Analysis*, p. 231. D. Appleton-Century Company, New York (1939).
- (4) *Handbook of Chemistry and Physics*. Chemical Rubber Publishing Company, Cleveland, Ohio (1945).
- (5) HARMAN, R. H., AND WORLEY, F. P.: *Trans. Faraday Soc.* **20**, 502 (1924).
- (6) KOLTHOFF, I. M., AND SANDELL, E. B.: *Textbook of Quantitative Inorganic Analysis*, p. 59. The Macmillan Company, New York (1943).
- (7) Reference 6, p. 62.
- (8) Reference 6, p. 574.
- (9) LATIMER, W. M.: *Oxidation Potentials*, p. 127. Prentice-Hall, Inc., New York (1938).
- (10) Reference 9, p. 177.
- (11) LATIMER, W. M., AND HILDEBRAND, J. H.: *Reference Book of Inorganic Chemistry*, p. 535. The Macmillan Company, New York (1940).

- (12) MASAKI, K.: *Bull. Chem. Soc. Japan* **5**, 345 (1930).
- (13) MILLER, F. W.: *A Laboratory Manual of Qualitative Analysis*, p. 157. The Century Company, New York (1930).
- (14) MORGAN, J. L. R.: *Z. physik. Chem.* **17**, 533 (1895).
- (15) PEARCE, W. C., AND HAENISCH, E. L.: *Quantitative Analysis*, p. 429. John Wiley and Sons, Inc., New York (1940).
- (16) Reference 15, p. 260.
- (17) RANDALL, M., AND HALFORD, J. O.: *J. Am. Chem. Soc.* **52**, 178 (1930).
- (18) SEIDELL, A.: *Solubilities of Inorganic and Metal Organic Compounds*, Vol. I, p. 26. D. Van Nostrand Company, New York (1940).
- (19) WILLARD, H. H., AND FURMAN, N. H.: *Elementary Quantitative Analysis*. D. Van Nostrand Company, New York (1940).
- (20) Reference 19, p. 188.

CATALYTIC OXIDATION OF ANILINE IN THE VAPOR PHASE¹

O. W. BROWN AND W. C. FRISHE²

Department of Chemistry, Indiana University, Bloomington, Indiana

Received June 11, 1947

It has been shown by Brown and coworkers (1, 2, 3, 4) that thallium, lead, bismuth, and their intermetallic compounds are good catalysts for the vapor-phase reduction of nitrobenzene to azobenzene and to aniline. Conversely, it is expected that the oxides of these metals would be good catalysts for the vapor-phase oxidation of aniline to nitrobenzene and to intermediate oxidation products.

The products possibly obtained by the oxidation of aniline through the amino group may be classified according to the number of aniline molecules required to make a molecule of product: (a) monoaniline products such as phenylhydroxylamine, nitrosobenzene, and nitrobenzene; (b) dianiline products such as hydrazobenzene, azobenzene, azoxybenzene, and phenazine; (c) polyaniline products such as aniline black. In this work the production of dianiline products was the chief aim.

In the method used air was mixed with aniline vapor and the mixture was passed over a thallic oxide catalyst at certain temperatures between 250°C. and 500°C. at atmospheric pressure. The alkaline products were absorbed in 1 *N* sulfuric acid. The non-alkaline products, except for permanent gases, were condensed in a glass tube. The pH of the absorbing solution was raised in two steps by adding sodium hydroxide, and the solution was steam distilled in order to recover the amine products. The results are expressed in terms of percentage

¹ This paper is based upon a dissertation submitted by William Christopher Frishe to the Faculty of the Graduate School of Indiana University in partial fulfillment of the requirements for the degree of Doctor of Philosophy, August, 1943.

² Present address: Department of Chemistry, Grove City College, Grove City, Pennsylvania.

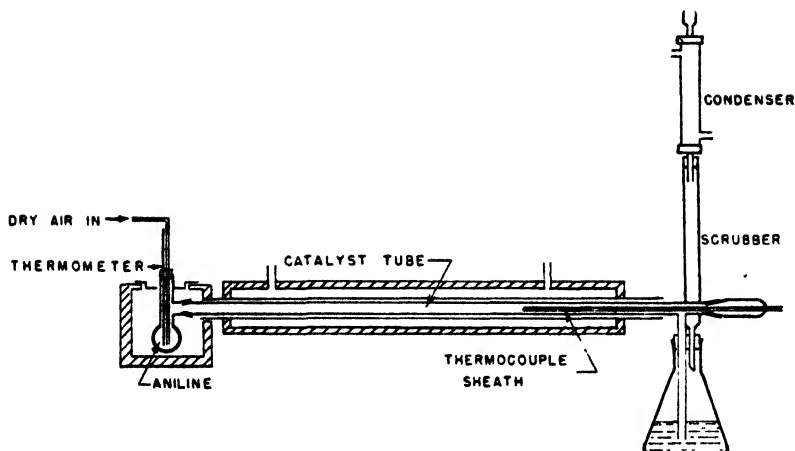


FIG. 1. Horizontal furnace

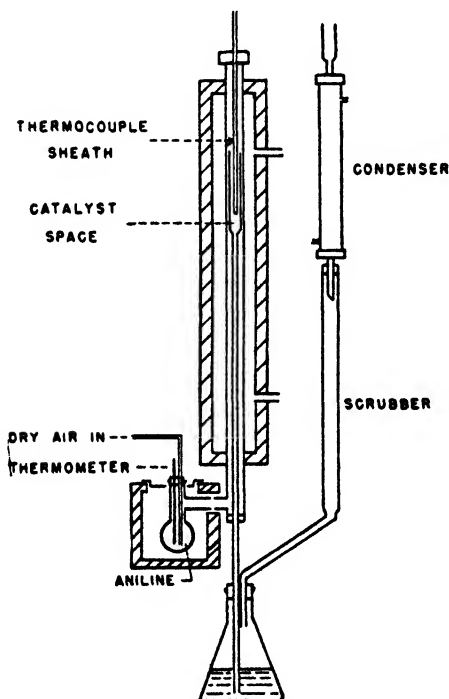


FIG. 2. Vertical furnace

yield of phenazine, percentage yield of azobenzene, and percentage conversion of the aniline passed.

APPARATUS

Figures 1 and 2 are section drawings of the equipment used. The air was metered by passing through an orifice-type flowmeter. The vaporizer consisted

of the heating jacket (a) and the aniline container (b). The heating jacket was made from a wide-mouth sheet-metal can 5 in. x 7 in., which was provided with suitable openings to accommodate the aniline container and was wound with No. 18 chromel wire. The aniline container was made from a 50-ml. Pyrex flask. The neck of the flask was widened so as to receive the stopper holding the thermometer and the air-inlet tube. To the neck was sealed a 19/38 standard-taper joint by which connection was made to the catalyst tube of the horizontal furnace. In the case of the vertical furnace the glass side arm was joined to the iron tee by means of packing. The vaporizer was calibrated by finding the rate of aniline vaporization in grams per hour at several air velocities and vaporizer temperatures. The curves thus obtained were used in determining the mole ratio of oxygen to aniline in the reactant gas stream. The total amount of aniline passed was determined by weighing the aniline container before and after the run. Each furnace was constructed of a 30-in. length of standard 1-in. pipe, two $\frac{1}{8}$ -in. steel discs of $2\frac{7}{8}$ in. outside diameter, each having a centered $1\frac{1}{8}$ -in. hole, and a 22 in. length of standard $2\frac{1}{2}$ -in. iron pipe. The discs were welded to the 1-in. pipe and to the $2\frac{1}{2}$ -in. pipe as shown. The $2\frac{1}{2}$ -in. pipe was tapped on one side to receive two 4-in. lengths of $\frac{1}{2}$ -in. pipe. The outer pipe was lagged and wound with No. 18 chromel wire for heating. The annular space was filled with a tin-lead alloy having a melting point of 180°C . The temperature was controlled by means of a variable resistance in series with the furnace winding. Glass liners were used in all the runs on the horizontal furnace. The liner was constructed from 1.5-cm. Pyrex glass tubing, on the inlet end of which was sealed a 19/38 male standard-taper connection and on the discharge end a 19/38 female standard-taper connection to take the thermocouple as shown. A side arm was sealed onto the tube 3 in. back from the female connection. Through this side arm the product gases went to the absorber. After leaving the vaporizer the gases in the horizontal furnace went successively through a plug of glass wool, 9 in. of pumice (which served as preheater), a plug of glass wool, the catalyst, a plug of glass wool, and then into the side arm and down into the absorber. The catalyst tube in the vertical furnace was made by sealing a long glass tube onto the end of a test tube. In this case the gases were preheated by the iron pipe wall. Some difficulty was experienced with the vertical furnace at the higher temperatures and longer runs on account of sagging of the glass tube. The length and volume of the catalyst space were the same in each furnace.

The temperatures were measured continuously by means of a copper-constantan thermocouple which was sheathed in a glass tube to prevent contamination of the catalyst. The couples were calibrated by running cooling curves on pure electrolytic tin, lead, and zinc, and a calibration curve of temperature *versus* millivolts was obtained. The cold junction was boiling water. In the case of the horizontal furnace the thermocouple sheath was set in to the discharge end of the catalyst tube through a 19/38 standard-taper joint which was connected to the sheath by a ring seal (see figure 1). In the case of the vertical furnace the thermocouple sheath was set in, as shown, through packing. This

latter arrangement has the advantage that the temperatures at various points in the catalyst bed may be measured without taking down the equipment to do it. On leaving the catalyst tube the gases passed into a 1-liter Erlenmeyer flask and bubbled through a boiling 1 *N* sulfuric acid solution. The gases, entrained solid and liquid products, and droplets of sulfuric acid then passed up through a Vigreux-type scrubber countercurrent to the descending acid stream from the reflux condenser. Just inside the lower end of the condenser was a plug of glass wool on which the azobenzene collected.

MATERIALS

The aniline used was Merck's C.P. grade. The air was freed from acid gases and moisture by passage through a soda lime tower.

PREPARATION OF CATALYST

Thallos chloride was treated with concentrated sulfuric acid and nitric acid and the mixture was boiled for several hours. The thallos chloride dissolved and the solution was evaporated until fumes of sulfur trioxide were evolved. This solution was then diluted and neutralized with ammonia. If the brown precipitate was found to contain some white particles of thallos salt, the mixture was made acid and the oxidation was repeated. To the suspension of brown thallic oxide was added shredded asbestos. The intimately mixed thallic oxide and asbestos was then filtered out and dried. The catalyst was 60 per cent thallic oxide and 40 per cent asbestos.

EXPERIMENTAL PROCEDURE

(1) The furnace and the vaporizer jacket were brought up to temperature. (2) The vaporizer flask was weighed and then put into the jacket and brought up to temperature. (3) The cooling water was started and the absorbing solution was heated to boiling and kept boiling gently. (4) The air was turned on to the desired rate. (5) The desired ratio of oxygen to aniline in the reactant gas was determined by adjusting the vaporizer temperature and the air velocity. (6) After the run the vaporizer flask was allowed to cool to room temperature and was then weighed. (7) The absorption flask was removed and a sample was taken from it for the determination of the unconverted aniline.

The diazotization reaction was employed. In dilute acid solution the aniline was titrated with 0.20 molar sodium nitrite solution, and starch-iodide paper was used as the outside indicator. The sodium nitrite solution was standardized by titration against pure *o*-aminophenol. If any aniline was present in the flask, sodium hydroxide solution was added to reduce the sulfuric acid concentration to approximately 0.1 *N*. The phenazine was then removed by steam distillation, filtered from the condensate, dried at 50°C., and weighed. The azobenzene was removed from the glass wool plug in the reflux condenser and dried at room temperature.

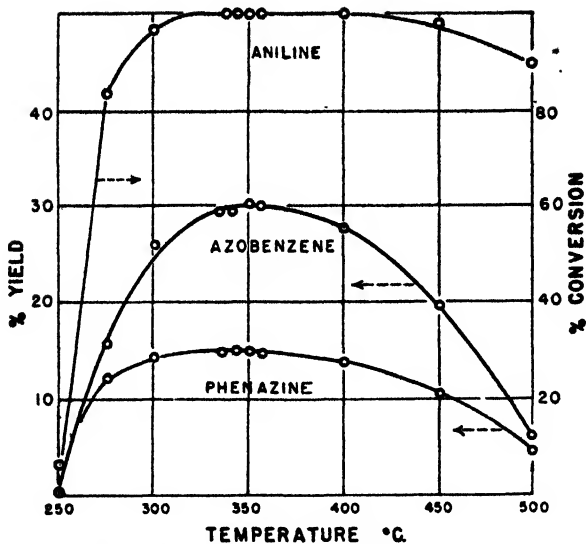


FIG. 3. Effect of temperature of the catalyst space. Concentration of reactants, 8.0 moles of oxygen per mole of aniline. Rate of flow of air, 8.0 standard liters per hour.

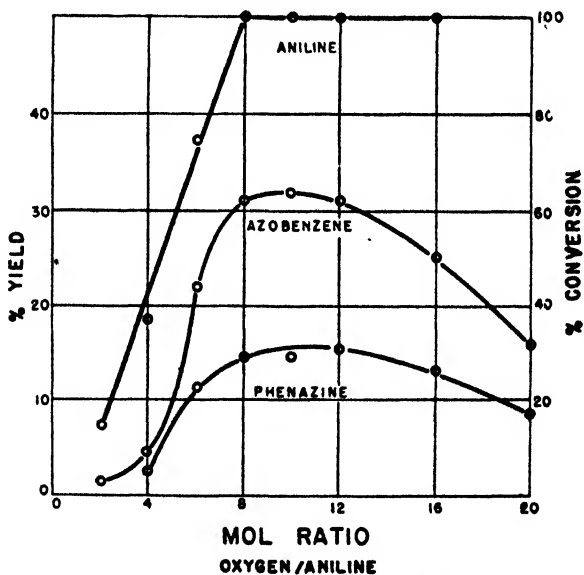


FIG. 4. Effect of concentration of reactants. Temperature of catalyst space, 340°C. Rate of flow of air, 8.0 standard liters per hour.

EXPERIMENTAL RESULTS

The variables studied were: (1) temperature of catalyst space; (2) space velocity; (3) reactant concentration. The space velocity was expressed as stand-

ard (0°C. and 760 mm.) volumes of air passed per hour per volume of catalyst space. The reactant concentration was expressed as the ratio, moles oxygen/mole aniline, in the reactant gas stream. In figures 3, 4, and 5 are shown the effects of the temperature of the catalyst space, the space velocity, and the reactant concentration on the percentage yields of azobenzene and phenazine (left-hand ordinate) and on the percentage conversion of the aniline (right-hand ordinate). The percentage yields are based on the aniline passed.

The percentage conversion of the aniline is:

$$100 - \frac{\text{grams aniline remaining in absorption flask}}{100 \text{ g. aniline charged}}$$

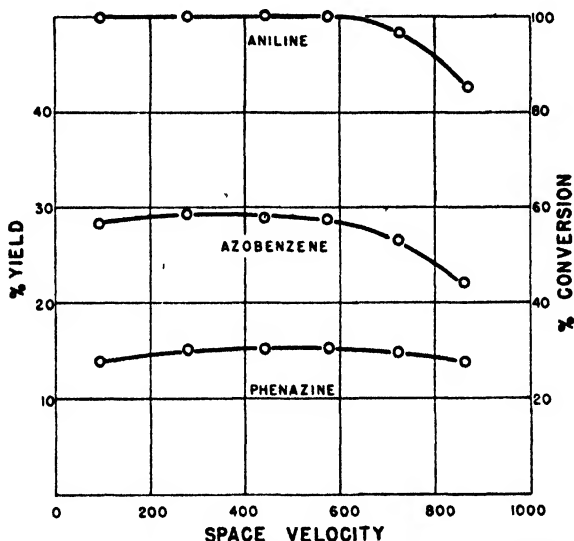


FIG. 5. Effect of space velocity. Temperature of catalyst space, 350°C. Concentration of reactants, 8.0-10.0 moles of oxygen per mole of aniline.

The study of the temperature of the catalyst space (figure 3) contains data from both the vertical and the horizontal reactors. The iron wall in the vertical reactor had no noticeable catalytic effect. The optimum temperature in each type of reactor was found to be about 350°C. At temperatures below 275°C. some aniline black and tar were formed. Small amounts of diphenylamine, ammonia, and benzonitrile were also noticed.

The study of reactant concentration (figure 4) shows rather sharp maxima. The optimum value of moles oxygen/mole aniline is between 8 and 12. Below a mole ratio of 6 the conversion of the aniline dropped off and tar deposited on the catalyst.

The study of space velocity (figure 5) showed a rather broad range of space velocities for maximum yield from 287 to 570 volumes of air per volume of catalyst space per hour.

The average length of an experimental run in all the work was about 12 hr.

SUMMARY

Catalytic vapor-phase oxidation of aniline by air over a thallic oxide catalyst has been studied, and optimum conditions for the production of azobenzene and phenazine have been determined. Two types of catalytic reactor are described.

REFERENCES

- (1) BROWN, BORLAND, JOHNSTON, AND GRILLS: *J. Phys. Chem.* **43**, 805 (1939).
- (2) BROWN, BROTHERS, AND ETZEL: *J. Phys. Chem.* **32**, 457 (1928).
- (3) HENKE AND BROWN: *J. Phys. Chem.* **26**, 324 (1922).
- (4) HENKE AND BROWN: *J. Phys. Chem.* **26**, 631 (1922).

COORDINATION COMPOUNDS OF BORON TRICHLORIDE. V
RELATIONSHIP OF DIPOLE MOMENT OF CHLORIDES TO COMPOUND FORMATION¹

DONALD RAY MARTIN

Noyes Chemical Laboratory, University of Illinois, Urbana, Illinois

Received November 26, 1946

In thermal analysis studies conducted in this Laboratory of systems composed of alkyl chlorides and boron trichloride, it was found that there seemed to be a correlation between the dipole moments of the alkyl chlorides and the ability of the alkyl chlorides to form compounds with boron trichloride. Further, it was observed that the stability of the resulting compounds increases as the dipole moment of the alkyl chloride increases. On the assumption that the C—Cl bond dipole is proportional to the dipole moment of the molecule, it appears that the donating ability of the chlorine atom of the alkyl chloride to the boron atom of boron trichloride is related to the ionic character of the C—Cl bond. For evidence to substantiate this hypothesis a survey of the literature was made of the molecular compounds of boron trichloride in which the donor atom is thought to be chlorine.

Stock and Preiss (14) found that chlorine, with practically no dipole moment, and boron trichloride do not react at room temperature nor at -80°C . Graff (5) made a thermal analysis of the system chlorine-boron trichloride and found only a eutectic point at 65.5 weight per cent boron trichloride and -135.4°C . He obtained a similar result in his study of the system hydrogen chloride-boron trichloride (6). Hydrogen chloride in the vapor phase has a dipole moment of 1.03 D (18). The eutectic point in this system occurs at 44 weight per cent boron trichloride and -134.5°C .

This particular system is of interest, inasmuch as there is no evidence for the existence of chloroboric acid, even at these low temperatures. On the other hand, fluoboric acid and the fluoborates are well known. This fact may be

¹ Presented before the Division of Physical and Inorganic Chemistry at the 110th Meeting of the American Chemical Society, Chicago, Illinois, September 12, 1946.

explained on the basis of the hypothesis being presented. The ionic character of the H—F bond is 43 per cent (7), whereas it is only about 17 per cent for the H—Cl bond (13). Therefore, if the ionic character of the halogen bond to the remainder of the molecule is responsible for the donor properties exhibited by the halogen atom, it follows that the fluorine atom in hydrogen fluoride should be a much better donor than the chlorine atom in hydrogen chloride.

A second factor to be considered is the relative positive nature of the boron atom in boron trifluoride as compared with the boron atom in boron trichloride. Inasmuch as the fluorine atom is more electronegative than the chlorine atom, it follows that the boron atom in boron trifluoride is more positive than the boron atom in boron trichloride. Therefore the boron atom in boron trifluoride should have a greater affinity for the donor halogen atom. However, this second factor is not as important as the first, as is shown by the results of Booth and Martin (3) in a study of the system hydrogen chloride–boron trifluoride. In this system there is no evidence for compound formation. The eutectic point lies at 72.3 mole per cent boron trifluoride and -134.2°C . Thus it is seen that the chlorine atom of hydrogen chloride does not coördinate with the boron atom of boron trifluoride. Wiberg and Sütterlin (17) observed that hydrogen fluoride fluorinates boron trichloride, forming hydrogen chloride and boron trifluoride. It has been observed also that fluorides in general coördinate more readily with boron trifluoride than do chlorides (2).

Thus it is observed that with molecules such as chlorine and hydrogen chloride, in which the chlorine bond is predominantly covalent, no tendency for compound formation with boron trichloride is displayed.

The studies with the alkyl chlorides and boron trichloride mentioned above were undertaken by Martin and Hicks (10) to determine the effect on the donor property of the chlorine atom when it is attached to a methyl group instead of a hydrogen atom. It was thought that a coördination compound might be formed in this case, inasmuch as the dipole moment of methyl chloride is larger than that of hydrogen chloride. The dipole moment for methyl chloride in the liquid state is 1.84 D (1). However, the thermal analysis indicated only a eutectic point at 51.8 mole per cent boron trichloride and -125.1°C .

Inasmuch as the dipole moment of ethyl chloride in the liquid state is 2.01 D (1), Martin and Hicks (10) studied the system ethyl chloride–boron trichloride by thermal analysis. A very flat maximum occurs at 67 mole per cent boron trichloride, corresponding to a compound having a composition most simply expressed at $\text{C}_2\text{H}_5\text{Cl}:(\text{BCl}_3)_2$. Evidently the compound is highly dissociated above its melting point, and therefore the donating ability of the chlorine atom is not very pronounced.

Martin and Humphrey (11) extended this study to the propyl chlorides. The dipole moments in the liquid state of *n*-propyl and isopropyl chlorides are calculated to be 1.97 and 2.02, respectively.² A maximum in the phase rule diagram

² Audsley and Goss (1), in referring to the research of Stuart (Physik. Z. **31**, 80–3 (1930)), state that the dipole moment of liquid *n*-propyl chloride is less than that of liquid ethyl chloride and that as one ascends the homologous series the dipole moment decreases 0.07 D per additional CH_2 group. Inasmuch as the moments for ethyl chloride and *n*-butyl

at 25 mole per cent boron trichloride indicates the presence of a compound most simply expressed as $(i\text{-C}_3\text{H}_7\text{Cl})_3\text{:BCl}_3$. This maximum is much sharper than in the case of ethyl chloride, indicating a more stable compound, and as predicted from dipole-moment data, the donor properties of the chlorine atom are somewhat more pronounced.

Although the difference is quite small, the melting point of the isopropyl compound is higher than that of the ethyl compound, the values being -105.2° and -115.8°C. , respectively (10, 11).

In the study of *n*-propyl chloride, only a eutectic point was found at 41.8 mole per cent boron trichloride and -141.8°C. Inasmuch as the dipole moment of *n*-propyl chloride is less than that of ethyl chloride, compound formation would not be expected.

Admittedly the differences between the dipole moments for the alkyl chlorides that do coöordinate with boron trichloride and those that do not are very small. However, the above studies may be summarized by stating that it appears that the dipole moment of an alkyl chloride must be at least 2.00 D if the alkyl chloride is to coöordinate with boron trichloride.

There is additional evidence to be found among other compounds of boron trichloride with molecules containing chlorine in which the chlorine bond is more ionic in character and the resulting coördination compound more stable. Triphenylchloromethane reacts with boron trichloride at room temperature or at 0°C. to form yellow crystals, which upon analysis were found to have a composition corresponding with the formula $(\text{C}_6\text{H}_5)_3\text{CCl:BCl}_3$ (16). Upon being heated to 200°C. these crystals turn brown but do not melt. They distil with decomposition at 80°C. in a vacuum. Such physical properties indicate a much more stable compound than any of those described above.

Tarible (15) has prepared the compound $\text{PCl}_5\text{:BCl}_3$ by allowing chlorine to displace the bromine from $\text{PBr}_3\text{:BBr}_3$ at room temperature, and the bromine from $\text{PBr}_5\text{:BBr}_3$ in the cold. The existence of this compound supports the hypothesis that an ionic character to the chlorine bond enhances the donor property of the chlorine atom, inasmuch as solid PCl_5 is considered to be comprised of the ions PCl_4^+ and PCl_6^- (4).

Similarly, Lowry and Jessop (9) consider SCl_4 to be composed of the ions SCl_3^+ and Cl^- . This compound reacts with boron trichloride to form the molecular compound $\text{SCl}_4\text{:BCl}_3$. Moissan (12) synthesized this compound in two ways. He allowed boron trisulfide to react with chlorine, and he allowed chlorine to pass into a solution containing sulfur monochloride and boron trichloride. The molecular compound has a melting point of -23°C.

The chlorides of iron and manganese have been reported to form molecular compounds with boron trichloride. Certainly these metallic chlorides have a

chloride are listed as 2.01 and 1.90 D, respectively, it is estimated that a fair value for *n*-propyl chloride would be 1.97 D. In the vapor state, Groves and Sugden (J. Chem. Soc. 1937, 158-62) have reported isopropyl chloride to have a dipole moment 0.05 D higher than that of *n*-propyl chloride. Therefore, in the liquid state, isopropyl chloride probably has a dipole moment around 2.02 D.

higher percentage of ionic character in the metal-to-chlorine bond than is exhibited in any of the chlorides of the non-metals previously discussed. Hoffman (8) allowed chlorine gas to pass over the borides of iron and manganese which were heated to glowing. Under these conditions, colored solids were obtained which upon analysis were found to have compositions corresponding to $(\text{FeCl}_3)_4:\text{BCl}_3$, $(\text{FeCl}_2)_3:\text{BCl}_3$, and $(\text{MnCl}_2)_2:\text{BCl}_3$.

SUMMARY

Experimental evidence seems to support the hypothesis that the ability of a chlorine atom in a compound to act as a donor to the boron atom of boron trichloride is related to the amount of ionic character in the bond attaching the chlorine atom to its molecule. As seen in table 1, the dipole moment seems to be a good criterion by which to predict if a coordination compound with boron trichloride will be formed with the alkyl chlorides (i.e., an alkyl chloride having

TABLE 1

COMPOUND	DIPOLE MOMENT	COMPOUND WITH BCl_3	MELTING POINT OF COMPOUND
	<i>D</i>		$^{\circ}\text{C}$
Cl_3	0	None	
HCl	1.03	None	
CH_3Cl	1.84	None	
$\text{C}_2\text{H}_5\text{Cl}$	2.01	$\text{C}_2\text{H}_5\text{Cl}:(\text{BCl}_3)_2$	-115.8
<i>n</i> - $\text{C}_3\text{H}_7\text{Cl}$	1.97	None	
<i>i</i> - $\text{C}_3\text{H}_7\text{Cl}$	2.02	$(i\text{-C}_3\text{H}_7\text{Cl})_3:\text{BCl}_3$	-105.2
$(\text{C}_6\text{H}_5)_3\text{CCl}$		$(\text{C}_6\text{H}_5)_3\text{CCl}:\text{BCl}_3$	Above 200
$\text{PCl}_5 (\text{PCl}_4^+, \text{PCl}_6^-)$		$\text{PCl}_5:\text{BCl}_3$	
$\text{SCl}_4 (\text{SCl}_3^+, \text{Cl}^-)$...		$\text{SCl}_4:\text{BCl}_3$	-23
FeCl_3		$(\text{FeCl}_3)_4:\text{BCl}_3$ }	Heated to glowing
FeCl_2		$(\text{FeCl}_2)_3:\text{BCl}_3$ }	
MnCl_2		$(\text{MnCl}_2)_2:\text{BCl}_3$ }	

a dipole moment of 2.00 D will coordinate, while one having a moment less than 2.00 D will not coordinate).

Boron trichloride also forms molecular compounds with sulfur tetrachloride and phosphorus pentachloride, which are considered to form ions, and with the metallic chlorides ferric chloride, ferrous chloride, and manganous chloride.

REFERENCES

- (1) AUDSLEY, A., AND GOSS, F. R.: J. Chem. Soc. **1942**, 497-500, 358-66.
- (2) BOOTH, H. S., AND MARTIN, D. R.: "The Coordinating Power of Boron Trifluoride", Paper No. 16, 6th Annual Symposium of the Division of Physical and Inorganic Chemistry, Columbus, Ohio, December 31, 1941.
- (3) BOOTH, H. S., AND MARTIN, D. R.: J. Am. Chem. Soc. **64**, 2198-2205 (1941).
- (4) CLARK, D., POWELL, H. M., AND WELLS, A. F.: J. Chem. Soc. **1942**, 642-5.
- (5) GRAFF, W.: Compt. rend. **196**, 1390-2 (1933).
- (6) GRAFF, W.: Compt. rend. **197**, 754-5 (1933).
- (7) HANNAY, N. B., AND SMYTH, C. P.: J. Am. Chem. Soc. **68**, 171-3 (1946).

- (8) HOFFMAN, J.: *Z. angew. Chem.* **21**, 2545-6 (1908); *Z. anorg. allgem. Chem.* **66**, 361-99 (1910).
- (9) LOWRY, T. M., AND JESSOP, G.: *J. Chem. Soc.* **1931**, 323-9.
- (10) MARTIN, D. R., AND HICKS, W. B.: *J. Phys. Chem.* **50**, 422-7 (1946).
- (11) MARTIN, D. R., AND HUMPHREY, A. S.: *J. Phys. Colloid Chem.* **51**, 425-30 (1947).
- (12) MOISSAN, H.: *Compt. rend.* **115**, 103-8 (1892).
- (13) PAULING, L.: *The Nature of the Chemical Bond and the Structure of Molecules and Crystals*, p. 46. Cornell University Press, Ithaca, New York (1938).
- (14) STOCK, A., AND PREISS, O.: *Ber.* **47**, 3109-13 (1914).
- (15) TARIBLÉ, J.: *Compt. rend.* **116**, 1521-4 (1893).
- (16) WIBERG, E., AND HEUBAUM, U.: *Z. anorg. allgem. Chem.* **222**, 98-106 (1935).
- (17) WIBERG, E., AND SÜTTERLIN, W.: *Z. anorg. allgem. Chem.* **202**, 37-48 (1931).
- (18) ZAHN, C. T.: *Phys. Rev.* **59**, 400-17 (1924).

THE CHEMICAL EROSION OF STEEL BY HOT GASES UNDER PRESSURE¹

RICHARD C. EVANS,² F. HUBBARD HORN,³ ZALMAN M. SHAPIRO,
AND RICHARD L. WAGNER

Department of Chemistry, The Johns Hopkins University, Baltimore, Maryland
and

Ballistic Research Laboratories, Aberdeen Proving Ground, Aberdeen, Maryland

Received June 11, 1947

INTRODUCTION

The destructive effect on steel of hot, high-pressure gases such as are ordinarily found as products of combustion is a problem difficult to solve because of the complexity of those gases. This paper describes an attempt to simplify the problem by studying the two gases largely constituting the products of combustion, carbon monoxide and carbon dioxide, and then adding to them one by one gases often found as traces, such as hydrogen sulfide, sulfur dioxide, ammonia, nitrous oxide, and hydrogen. Quite obviously, great care must be exercised to prevent the melting of the surface of the sample from becoming appreciable and masking the chemical effects. The first part of the paper will therefore survey the conditions present when the temperature is higher and erosion is principally a melting phenomenon and will attempt to set the limits to such a state; the second part will consider the peculiar chemical effects present when the temperature is lower and melting is negligible.

¹ The results reported here are largely from studies begun under NDRC contract OEMsr-463 and continued under contract W-36-034-ORD-4126 between the Army Service Forces and The Johns Hopkins University.

² Present address: Ballistic Research Laboratories, Aberdeen Proving Ground, Maryland.

³ Present address: Research Laboratory, General Electric Company, Schenectady, New York.

PART I

When mixtures of oxygen and excess carbon monoxide are ignited, carbon dioxide and monoxide are obtained at some high instant temperature. The relative concentration of carbon monoxide to carbon dioxide is conveniently expressed as the ratio CO/CO_2 . A 10 per cent mixture, which is near the lower explosive limit, yields after burning a mixture having a CO/CO_2 ratio of 3.5 at a maximum calculated flame temperature of 2160°K . If the concentration of

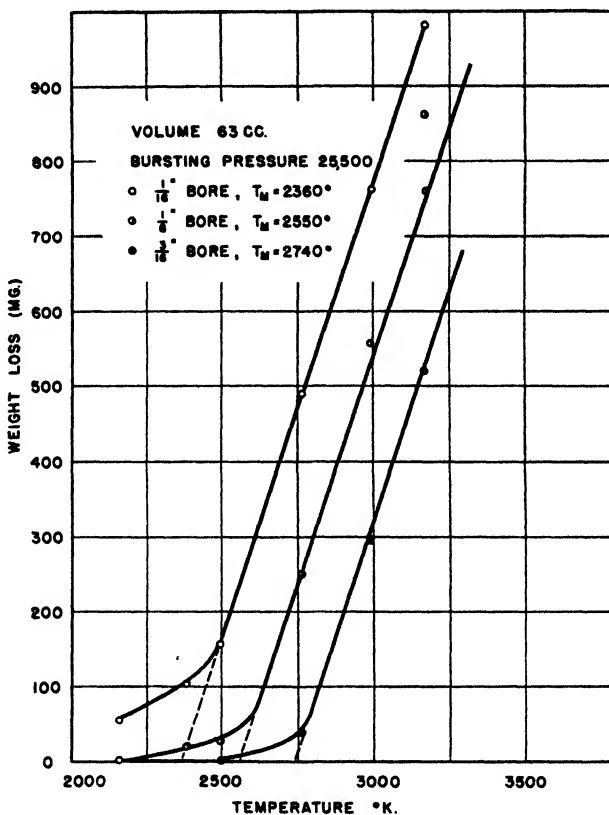


FIG. 1. Erosion as a function of gas temperature at variable gas composition

oxygen be increased, the flame temperature as well as the concentration of carbon dioxide will be increased.

Now, if these hot exploded gases be led across the surface of steel vent plugs (steel similar to SAE 4140), the loss in weight of the vents may be taken as a measure of the erosive effect of the gases. In figure 1 (see table 1) are plotted curves showing weight loss as a function of flame temperature at variable CO/CO_2 ratio and constant number of moles, each curve representing a different vent diameter. Each curve consists of two parts: a linear portion at higher flame temperatures and a curved region at lower flame temperatures, the linear por-

TABLE 1
Erosion as a function of gas temperature at variable gas composition

FLAME TEMPERA- TURE	EXPLODED GAS COMPOSITION CO/CO ₂	FIGURE 1: $P = 25,500$ LB./IN. ² $N = 0.625$ MOLE WEIGHT LOSS			FIGURE 2: $P = 25,500$ LB./IN. ² $N = 0.312$ MOLE WEIGHT LOSS			FIGURE 3: $P = 13,000$ LB./IN. ² $N = 0.312$ MOLE WEIGHT LOSS		
		$\frac{1}{16}$ in.	$\frac{1}{8}$ in.	$\frac{1}{4}$ in.	$\frac{1}{16}$ in.	$\frac{1}{8}$ in.	$\frac{1}{4}$ in.	$\frac{1}{16}$ in.	$\frac{1}{8}$ in.	$\frac{1}{4}$ in.
°K.		mg.	mg.	mg.	mg.	mg.	mg.	mg.	mg.	mg.
2160	3.5	56.6	0.9		13.1	+0.2		0.2	+0.4	
2380	2.95	102.8	19.6		62.0	5.3		5.8	0.3	
2495	2.5	158.2	25.5	0.4	134.9	19.5	4.4	54.9	6.2	
2765	1.89	489.9	249.8	39.0	254.5	150.5	104.0	162.0	51.2	6.3
2990	1.45	763.3	539.2	295.3	365.0	238.5	163.9	274.6	125.1	77.0
3170	1.15	982.3	760.4	520.0		387.0	309.7	406.4	240.7	163.0
3320	0.84						397.6		426.7	351.5
3450	0.58								717.1	

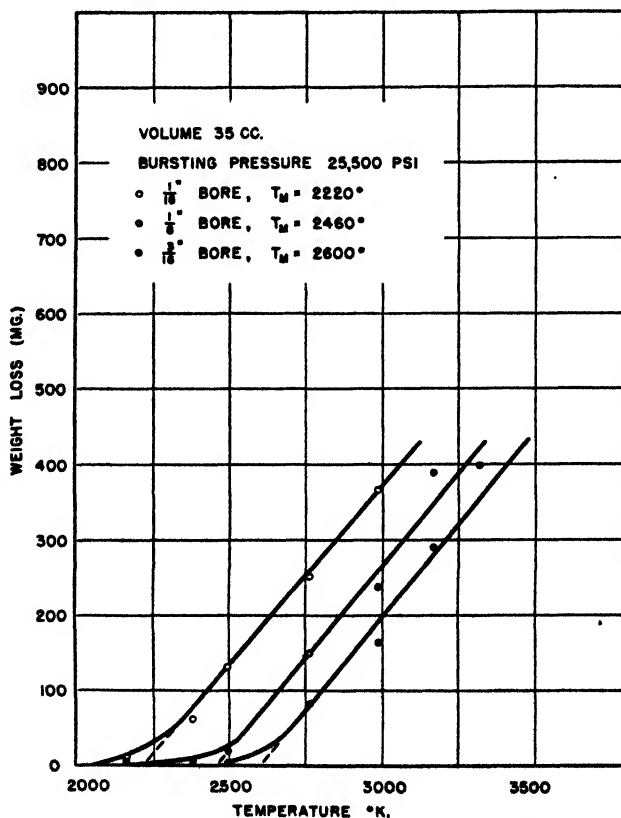


FIG. 2. Erosion as a function of gas temperature at variable gas composition

tions having practically the same slopes. Erosion is greater the smaller the bore. The work of Wiegand (6) on erosion by powder gases indicates that the loss in weight along the linear portion of the curves is due primarily to melting. And

as a rule of thumb, we might extrapolate, as Wiegand has done, to a zero weight loss to obtain an arbitrary temperature (T_m) to divide the chemical from melting regions for a given vent diameter. That the straightness of the curve is somehow related to melting is further indicated by experiments performed on half the number of moles of gas at the same final pressure (figure 2) and at half the previous final pressure (figure 3). In these cases, a straight line becomes a steadily worse approximation to the experimental points as the bore surface conditions

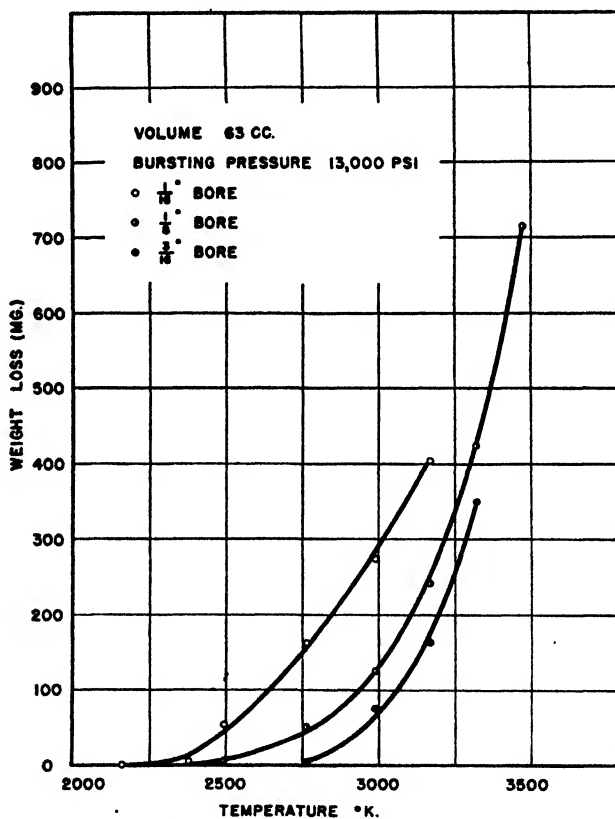


FIG. 3. Erosion as a function of gas temperature at variable gas composition

become milder. Cutting down the number of moles of gas without altering the final pressure produces an effect roughly proportional in magnitude.

These curves, however, are somewhat misleading, for they do not represent a constant CO/CO₂ ratio and therefore do not definitely separate chemical from thermal effects. The experimental procedure may be elaborated to correct for this by adding carbon dioxide to the initial oxygen-carbon monoxide mixture in such a manner as to give a constant CO/CO₂ ratio over a series of temperatures, or a constant temperature over a series of CO/CO₂ ratios. A very brief résumé of the mathematical procedure for selection of individual gas pressures is given in the experimental section. The results of using 0.625 mole of such adjusted

TABLE 2
Erosion as a function of gas composition for various temperatures

EXPLODED GAS COMPOSITION CO/CO ₂	EROSION AT 2160°K. WEIGHT LOSS		EROSION AT 2380°K. WEIGHT LOSS		EROSION AT 2495°K. WEIGHT LOSS		EROSION AT 2630°K. WEIGHT LOSS		EROSION AT 2765°K. WEIGHT LOSS		EROSION AT 3170°K. WEIGHT LOSS	
	mg.	mg.	mg.	mg.	mg.	mg.	mg.	mg.	mg.	mg.	mg.	mg.
0.58									560.9	450.8	928.7	
0.84					191.7	280.3	200.4	325.5	389.3	354.3	929.8	
1.15	34.5	89.0	106.9	75.2	178.0	120.9	316.4	326.6	351.7	400.0	665.0	697.6
1.45	19.3	39.7	87.1	67.2	154.1	194.8	155.5	154.4	372.9	380.0		
1.89	46.2	14.6	27.2	81.9	69.0	62.0	81.2	135.9	249.8	207.8		
2.14	52.8	57.2	78.6	88.1	65.8	35.1	69.1					
2.50	11.7	5.8	46.3	23.1	25.5	33.2						
2.95	0	18.5	19.6	2.9								
3.50	0.9	0.3										

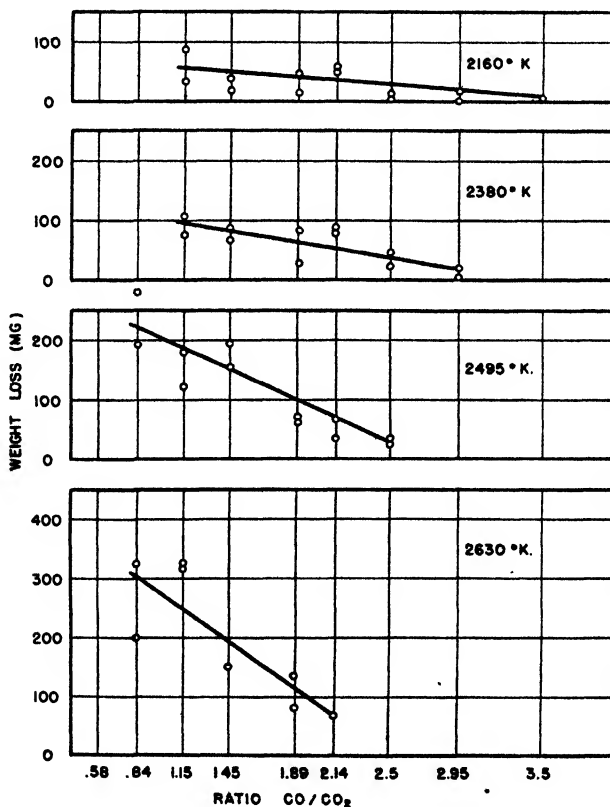


FIG. 4 (first part)

FIG. 4. Erosion as a function of gas composition for various temperatures

gas mixtures in experiments in which the vent bore was $\frac{1}{8}$ in. in diameter are given in table 2 and figure 4. It will be seen that a straight line approximating

the mean distribution of the points shows a greater dependence upon CO/CO_2 ratio as the temperature increases. Now, if the point of intersection of these lines with the various ordinates be plotted on a graph showing weight loss as a function of flame temperature, a family of curves will be obtained for each of which the CO/CO_2 ratio is a constant. This is shown in figure 5. Since this family of curves has been obtained using a constant number of moles of burned gas at prescribed compositions, the regions of weight loss by melting—the linear

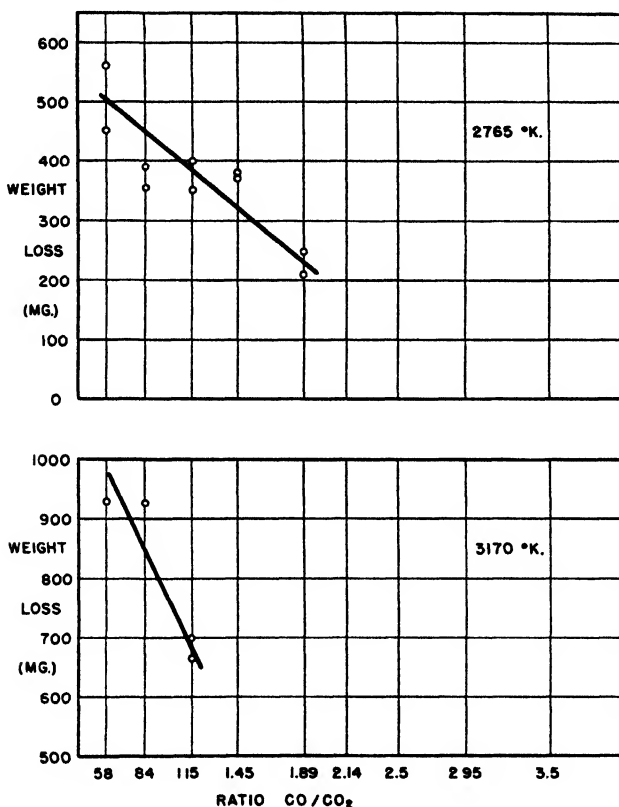


FIG. 4 (second part)

FIG. 4. Erosion as a function of gas composition for various temperatures

part of the curves—are more accurately separated from the regions due to other effects such as chemical.

Forward-reflection x-ray analysis of the bore surface showed the presence of α -iron, austenite, and ferrous oxide in that order as to quantity. No dependence of these products upon CO/CO_2 ratio was observed, though in some cases increased carbon dioxide permitted traces of Fe_3O_4 to be detected.

In trying to determine the chemical interaction of gases and the steel sample, the temperature of the gases is far less important than the temperature to which the steel surface becomes heated. If the eroding gases all possessed the same thermal properties, particularly heat content, then a given number of moles of

different gases would heat the bore surface to a temperature which was a simple function of the temperature of the gas. However, when the eroding gas is a mixture which may interact with the steel and the components of the mixture have different thermal properties, there are at least three factors which complicate any simple dependence of bore surface temperature on the gas temperature:

- (1) The accommodation coefficient, or the fraction of the gas particles which may remain on the bore surface long enough to transfer heat, may be quite different for each of the gases in the eroding mixture. It may also be con-

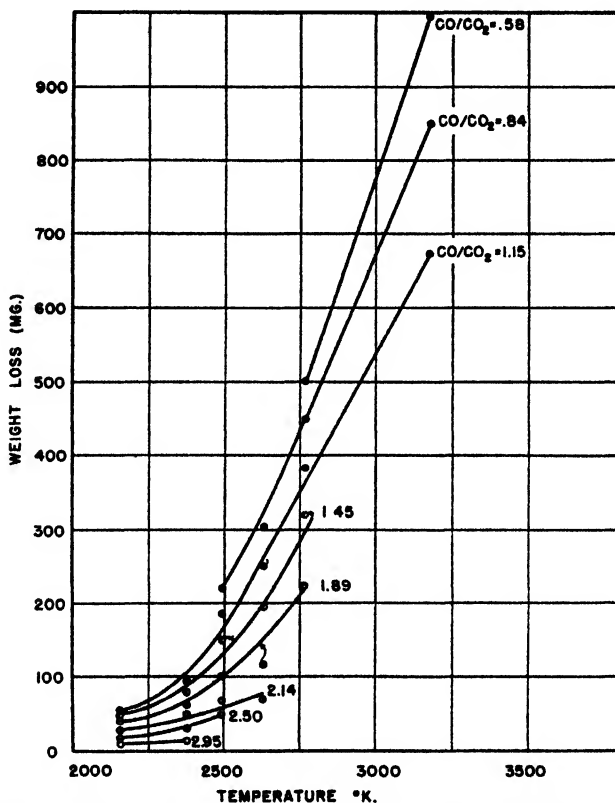


FIG. 5. Erosion as a function of gas temperature for a series of constant gas compositions

siderably altered by the formation of an erosion product, such as oxide, on the bore surface.

- (2) The heat capacities of the gases may be quite different. In the case of carbon monoxide and carbon dioxide at the same temperature, the latter gas possesses about twice the heat capacity per mole as does carbon monoxide. The heat content of a mixture of carbon monoxide and dioxide is therefore greater as the concentration of carbon dioxide increases.
- (3) If the reaction takes place between the steel and the gases, the heat of reaction (presumably exothermic) will serve to increase the temperature of the bore surface.

Since there is no known manner for accounting for all these factors, we must be content with only a partial separation of chemical from thermal effects. Under these harsh conditions of temperature and composition, then, erosion is evidently the result of melting and oxidation. Even so, and regardless of whether the increase in erosion is dependent on an increase in the intensity of thermal factors or chemical factors, the following qualitative conclusions are apparent from the work reported: (1) For a fixed number of moles of a mixture of carbon monoxide and carbon dioxide at a given composition, erosion increases as the calculated adiabatic flame temperature is increased. (2) For a fixed number of moles of mixtures of carbon monoxide and carbon dioxide at a constant calculated adiabatic flame temperature, erosion increases as the concentration of the carbon dioxide is increased. (3) The increase in erosion produced by mixtures of carbon monoxide and carbon dioxide is more strongly dependent on the adiabatic flame temperature of the mixture as the concentration of carbon dioxide in the mixture becomes higher.

PART II

The sulfur gases in bulk have long been known to be destructive of steel and this effect need hardly be discussed here. However, the effect of traces of sulfur gases in vastly increasing the erosive action of carbon monoxide and carbon dioxide mixtures has been but little studied previously. This action in certain cases is so marked that it gives rise to a number of questions: What form of sulfur is really doing the damage; is it hydrogen sulfide, elemental sulfur, or sulfur dioxide? Or are the other gases present after combustion of primary importance? And what is the influence of concentration of the trace gas? Is the action of the sulfur gases direct, or do they merely catalyze the erosive effect of other gases present in the mixture of combustion products? Do nitrogenous gases show a similar effect when present in traces? What is the effect of repeated explosions? The work reported here was undertaken to answer these questions.

The data may be most conveniently presented in the form of a graph where in the first instance (figures 6 and 7 and table 3) the weight loss caused by a gas mixture of $\text{CO}/\text{CO}_2 = 3.5$ and flame temperature of 2160°K . fired ten times is compared with that caused by the same mixture to which had been added 0.71 mole per cent of hydrogen sulfide or sulfur dioxide. It may be seen from figure 5 that such a condition is well below the region of marked melting. It is apparent from the curves that while the factor of increase of erosiveness of the sulfur-bearing gases is great, about 4, for the first firing, it is significantly greater for the tenth, about 8 in the case of hydrogen sulfide and almost 16 for sulfur dioxide. In the second case (figures 8 and 9 and table 4) weight loss from single firings is studied as a function of concentration of the sulfurous gas. Here both gases show an increase in erosiveness as their percentage is increased, sulfur dioxide being somewhat the more active for any given mole per cent. The control, of course, is the point on the zero ordinate. In an attempt to correlate the surface products with the eroding gas mixture, x-ray diffraction photographs of the bore surface by forward reflection indicate in all cases the presence of α -iron and a trace of austenite; where no sulfur is present, some ferrous oxide is found but

this is replaced by ferrous sulfide in experiments using hydrogen sulfide or sulfur dioxide. There is no apparent dependence of these surface products upon number of firings nor upon the concentration of the sulfur-bearing gas.

Of all the nitrogenous gases which might profitably be studied with respect to their influence on erosion, only three—ammonia, nitrous oxide, and nitrogen—have boiling points in a usable range for these experiments and are commercially

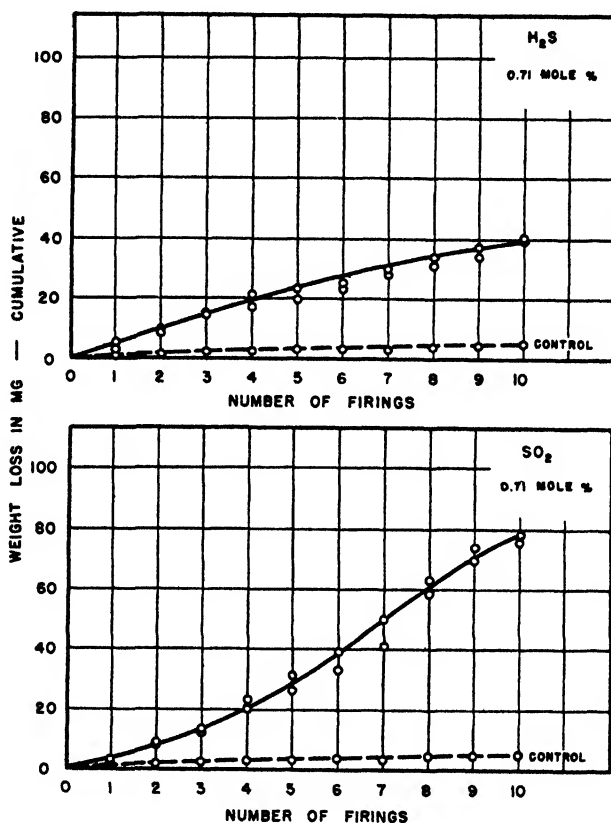


FIG. 6. Erosion as a function of number of firings with added hydrogen sulfide

FIG. 7. Erosion as a function of number of firings with added sulfur dioxide

available. While the likelihood of finding nitrous oxide among the products of combustion is certainly less than that of finding the higher oxides, it is thought that this gas would be transformed during the explosion into the more probable substance. While the data are less reproducible than in the case of the sulfur-bearing gases, nevertheless there are certain consistencies which may be observed from figures 10, 11, 12, and 13 and tables 5 and 6. In the case of ammonia, the addition of a small amount significantly augments erosion, yet increasing the

concentration does not cause a corresponding increase in weight loss. This peculiarity is not at all true in the case of nitrous oxide, though here the presence of available oxygen from the dissociation of nitrous oxide must be kept in mind. Repeated firings showed a nearly constant factor of increase over the control, for a given gas and concentration, as far as the experiments were carried: about 2 for nitrous oxide and the higher concentration of ammonia, and almost 8 for the lower concentration of ammonia. As might have been expected, nitrogen itself has no effect when used in similar quantities.

An examination of the bore surfaces by x-ray methods reveals the presence of α -iron as the principal product and austenite in much smaller amounts in all cases. Fe_3N occurred when ammonia-containing gas was fired ten times and Fe_4N where single firings were made, though a minute quantity of ferrous oxide was identified where Fe_4N was absent. Where nitrous oxide was the added gas,

TABLE 3

Effect on erosion of repeated firings with hydrogen sulfide and sulfur dioxide
 $\text{CO}/\text{CO}_2 = 3.5$; $T = 2160^\circ\text{K}$.

NUMBER OF FIRINGS	CUMULATIVE WEIGHT LOSS						AVERAGE FACTOR OF INCREASE OVER CONTROL	
	0.71 mole per cent H_2S added		Control		0.71 mole per cent SO_2 added		0.71 mole per cent H_2S	0.71 mole per cent SO_2
	mg.	mg.	mg.	mg.	mg.	mg.		
1	3.2	5.2	1.1	0.8	2.5	3.6	4.4	3.2
2 . . .	8.8	9.7	1.7	1.2	7.6	9.0	6.4	5.7
3 . .	15.4	14.6	2.3	1.6	11.9	13.4	7.7	6.5
4 . . .	21.2	17.2	2.4	2.0	23.4	20.4	8.7	9.9
5 . .	23.4	19.9	3.2	2.7	31.8	26.8	7.4	9.9
6	25.6	23.8	3.3	2.9	39.4	33.5	7.9	11.8
7 . . .	30.1	28.4	3.6	3.2	50.2	41.4	8.6	13.5
8 .	34.1	31.7	4.4	4.4	63.5	59.1	7.5	13.9
9	37.7	34.5	5.0	4.7	70.5	74.8	8.0	16.2
10	40.7	39.6	5.0	5.1	76.4	78.9	7.9	15.3

no nitrides were found; nor was there any apparent consistent alteration of the erosion products as a function of its concentration. Lines were found for which there is no identification currently listed. With ammonia, these have d/n values of 2.27–2.31 and 1.57–1.62; with nitrous oxide the values are 2.36–2.39, 2.21–2.29, 1.94–1.95, and 1.86–1.88. They may represent cementite but the identification is not at all positive.

The behavior of hydrogen when added to carbon monoxide-dioxide mixtures is startling: It is not particularly erosive below 2 per cent nor above 5 per cent; however, in the neighborhood of 3.5 per cent there is a maximum weight loss which is far greater than that caused by any of the trace gases already considered, as may be seen in figure 15 and table 8. It should be pointed out that the commercial carbon monoxide used contained a small amount of hydrogen, so the actual values of hydrogen percentage should be somewhat higher than those

given. When the sample was subjected to ten firings with a mixture containing less than 1 per cent hydrogen (figure 14 and table 7), there was only a slight increase in erosiveness over the control even at the tenth round. The bore surfaces of the samples were examined by x-ray diffraction methods, but it is difficult to say whether or not hydrogen has altered the residual products; certainly the effect is slight.

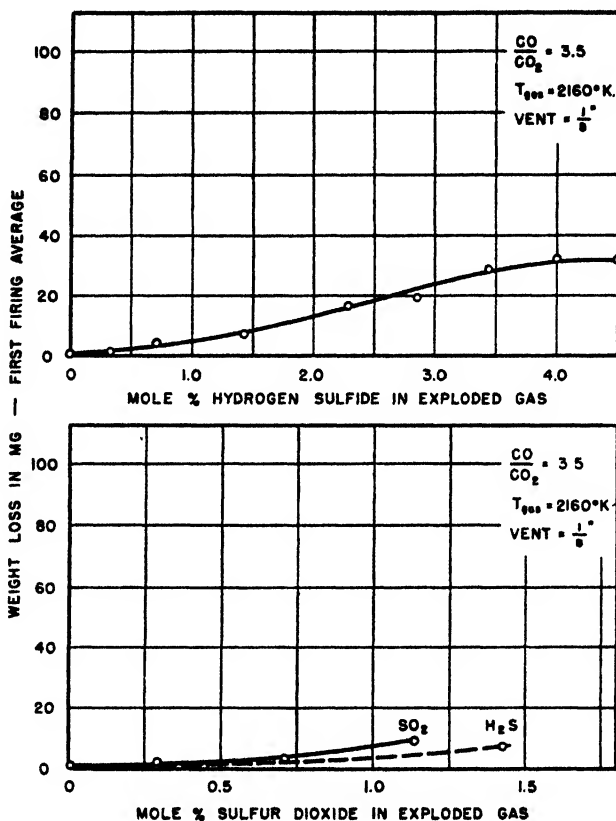


FIG. 8. Erosion as a function of the concentration of hydrogen sulfide

FIG. 9. Erosion as a function of the concentration of sulfur dioxide

When the vent plugs used in these experiments are sectioned transversely, polished, and etched, a ring of hardened steel may be noted surrounding the bore. Since this ring may be largely obliterated by heating the sample and allowing it to cool, it may be assumed that the origin of altered layer is related to the heating of the bore by the eroding gases. Its depth might, therefore, offer a standard for estimating relatively the surface temperature of the bore. Experiments undertaken with this in mind have shown a strong dependence of the altered layer thickness upon the calculated heat content of the gases and a much weaker

dependence upon their temperature and carbon dioxide concentration. In other words, this effect is largely thermal and not chemical.

When the trace gases were added to the explosive mixture, the total heat content might be increased if we assume that they burned, and this added heat

TABLE 4
Effect on erosion of concentration of hydrogen sulfide and sulfur dioxide
 $\text{CO}/\text{CO}_2 = 3.5$; $T = 2160^\circ\text{K}$.

MOLE PER CENT H_2S	AVERAGE WEIGHT LOSS mg.	INDIVIDUAL WEIGHT LOSSES			
		mg.	mg.	mg.	mg.
0.0	0.9	1.1	0.8	0.9	0.3
0.29	1.7	2.1	1.3		
0.71	4.4	7.0	2.2	3.2	5.2
1.43	7.3	11.8	4.6	5.3	7.3
2.28	16.5	14.8	18.4	16.1	
2.86	19.3	19.3	13.4	25.3	
3.43	28.2	33.4	23.3	27.8	
4.00	32.2	44.5	26.7	25.5	
4.58	31.7	33.3	21.8	40.0	

MOLE PER CENT SO_2	AVERAGE WEIGHT LOSS mg.	INDIVIDUAL WEIGHT LOSSES			
		mg.	mg.	mg.	mg.
0.0	0.9	1.1	0.8	0.9	0.3
0.29	1.9	1.8	2.0		
0.71	3.1	2.5	3.6		
1.14*	9.0	10.8	7.2		

* This concentration corresponds to maximum tank pressure at room temperature.

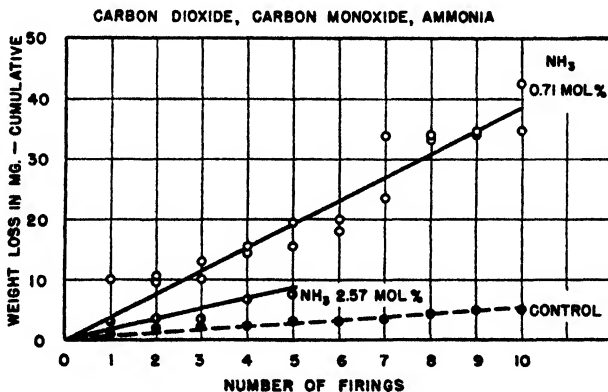


FIG. 10. Erosion as a function of number of firings with added ammonia

content would raise the bore surface temperature. Could this not, then, be the explanation in part for their erosiveness? Measurement of the thickness of the altered layer in such cases indicates otherwise, for except in the case of nitrous oxide, the thickness steadily decreases as the concentration of the trace gas in-

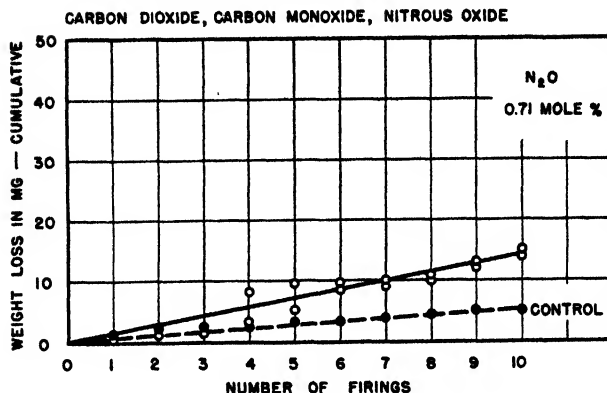


FIG. 11. Erosion as a function of the number of firings with added nitrous oxide

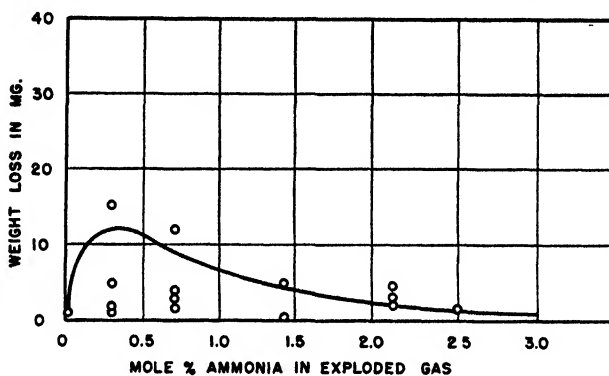


FIG. 12. Erosion as a function of the concentration of ammonia in the exploded gas

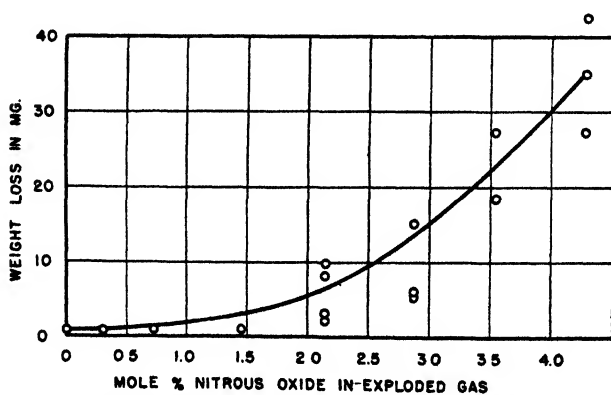


FIG. 13. Erosion as a function of the concentration of nitrous oxide in the exploded gas

creases. The increase in thickness with nitrous oxide is to be expected when its tendency to dissociate is considered.

TABLE 5

Effect on erosion of repeated firings with ammonia and nitrous oxide $\text{CO}/\text{CO}_2 = 3.5; T = 2160^\circ\text{K}.$

NUMBER OF FIRINGS	CUMULATIVE WEIGHT LOSS							
	Control		0.71 mole per cent NH ₃ added		2.57 mole per cent NH ₃ added		0.71 mole per cent N ₂ O added	
	mg.	mg.	mg.	mg.	mg.	mg.	mg.	mg.
1	1.1	0.8	3.0	10.1	3.0	0.2	0.4	0.0
2	1.7	1.2	9.5	10.5	3.6	0.2	1.2	1.0
3	2.3	1.6	10.1	12.8	3.6	0.3	1.6	1.4
4	2.4	2.0	14.6	15.3	6.8	0.3	2.7	8.2
5	3.2	2.7	19.3	15.4	7.4	0.6	5.0	9.4
6	3.3	2.9	20.2	18.1			8.4	9.6
7	3.6	3.2	33.9	23.4			8.8	9.9
8	4.4	4.4	34.0	33.4			10.0	10.6
9	5.0	4.7	34.6	33.8			12.3	13.1
10	5.0	5.1	34.4	42.6			14.8	13.7

TABLE 6

Effect on erosion of ammonia and nitrous oxide concentration $\text{CO}/\text{CO}_2 = 3.5; T = 2160^\circ\text{K}.$

MOLE PER CENT NH_3	AVERAGE WEIGHT LOSS	INDIVIDUAL WEIGHT LOSSES			
	mg.	mg.	mg.	mg.	mg.
0.0	0.7	0.6	0.8		
0.29	5.7	15.4	1.8	1.0	4.7
0.71	5.0	3.8	2.8	1.4	11.9
1.43	0.8	4.6	+0.1	+0.5	+0.6
2.14	2.8	4.3	1.9	2.0	2.8
2.57*	1.1	1.4	0.8		

MOLE PER CENT N_2O	AVERAGE WEIGHT LOSS	INDIVIDUAL WEIGHT LOSSES			
	mg.	mg.	mg.	mg.	mg.
0.0	0.7	0.6	0.8		
0.29	0.3	0.5	0.1		
0.71	0.2	0.3	0.0		
1.43	0.9	0.3	0.7	1.8	0.6
2.14	8.3	8.2	11.8	2.1	3.3
2.86	8.9	15.1	6.1	5.7	
3.58	30.8	27.4	46.6	18.4	
4.29	35.0	27.5	42.5	35.0	

* This concentration corresponds to maximum tank pressure at room temperature.

There are a number of hypotheses which would explain the existence of erosion under conditions thought to be too mild for melting of the steel surface to take place and other hypotheses to interpret the rôle of the trace gases in intensifying erosion. It is possible that surface oxides are formed which are less erosion-

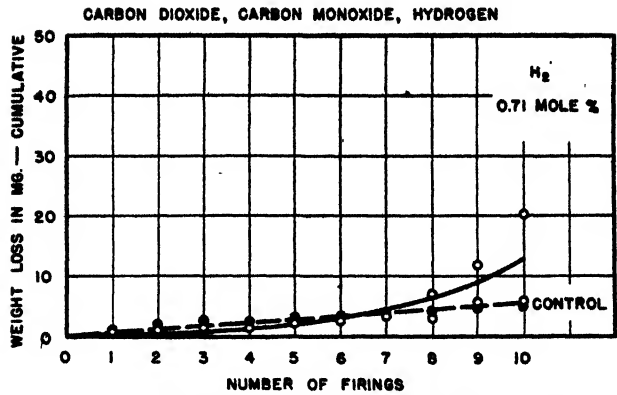


FIG. 14. Erosion as a function of the number of firings with added hydrogen

TABLE 7
Effect on erosion of repeated firings with hydrogen
 $\text{CO}/\text{CO}_2 = 3.5; T = 2160^\circ\text{K}.$

NUMBER OF FIRINGS	CUMULATIVE WEIGHT LOSS			
	Control		0.71 mole per cent H ₂ added	
	mg.	mg.	mg.	mg.
1	1.1	0.8	0.1	0.7
2.	1.7	1.2	0.8	1.5
3.....	2.3	1.6	1.1	1.5
4	2.4	2.0	1.2	1.8
5	3.2	2.7	2.6	2.0
6.	3.3	2.9	3.2	2.7
7	3.6	3.2	3.4	3.0
8	4.4	4.4	7.0	3.1
9.	5.0	4.7	12.2*	5.5
10 .. .	5.0	5.1	20.4*	5.5

* Firings irregular due to excessive erosion of vent plug holder.

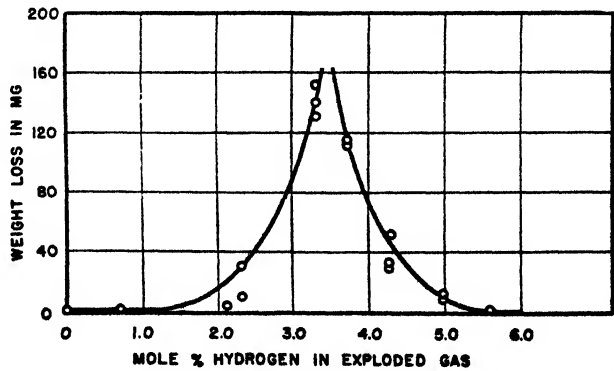
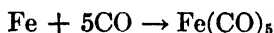


FIG. 15. Erosion as a function of the concentration of hydrogen in the exploded gas

resistant than the parent metal. The surface steel may become plastic at a temperature below its melting point and be physically deformed. The sulfides are known to have melting points lower than those of steel or the oxides of iron. Even nitrogen and carbon enrichment and consequent weakening of the metal at the grain boundaries should be considered.

The authors, however, wish to propose a single hypothesis that will rationalize the greater part of the experimental work presented: specifically, the reaction of carbon monoxide and steel to form volatile iron carbonyl according to the equation:



This reaction is catalyzed by traces of sulfide, ammonia, or hydrogen (5). The reaction is poisoned by oxygen and carbon dioxide. That the magnitude of erosion should be so profoundly influenced by minute quantities of hydrogen

TABLE 8
Effect on erosion of hydrogen concentration
 $\text{CO}/\text{CO}_2 = 3.5; T = 2160^\circ\text{K}.$

MOLE PER CENT H_2	AVERAGE WEIGHT LOSS	INDIVIDUAL WEIGHT LOSSES		
	mg.	mg.	mg.	mg.
0.0	0.7	0.6	0.8	
0.71	0.5	0.1	0.7	0.8
2.13	2.3	3.1	2.0	1.9
2.32	13.5	9.0	1.9	29.6
3.29	142.1	153.9	131.9	140.6
3.72	113.0	112.6	113.5	
4.26	40.0	54.8	30.3	34.8
4.97	12.6	14.1	11.2	
5.60	2.2	0.6	0.6	5.3

sulfide, sulfur dioxide, ammonia, nitrous oxide, or hydrogen is behavior typical of catalysts.

It should be emphasized here that the carbonyl mechanism would not be expected to be operative where carbon dioxide is present in quantity even in the chemical regions of erosion, and, therefore, under such conditions the catalyst gases should have small effect.

While this hypothesis does not require that the iron carbonyl formed during the erosion process have more than momentary existence under such severe temperature and pressure conditions, nevertheless an experiment was devised to test the hypothesis by isolating the substance. The apparatus, described more fully in the experimental section, was simply a very long vent plug connected to an evacuated chamber where products of combustion and erosion could be collected and traps where volatile substances, such as iron carbonyl, could be frozen out. Warming the traps and passing the gas evolved through a hot capillary tube decomposed any iron carbonyl into a dark deposit at the tube

entrance. This deposit as well as black substances remaining in the traps were analyzed for iron. The results are assembled in table 9. Some iron carbonyl was isolated where sulfur was absent; however, a trace of hydrogen sulfide produced a five- to ten-fold increase in the amount. The quantity of carbonyl found is obviously minute, but it should be borne in mind that the other iron

TABLE 9

Iron analyses of deposits in carbonyl isolation experiments

- A. 11 per cent oxygen in carbon monoxide; total initial pressure 4000 lb./in.²; each analysis the sum of five rounds
 B. Addition of 0.125 per cent hydrogen sulfide to A
 C. Addition of 0.25 per cent hydrogen sulfide to A
 D. Addition of 0.50 per cent hydrogen sulfide to A

	IRON ON WALLS OF EVACUATED CHAMBER	IRON IN COLD TRAPS	IRON IN DEPOSITION TUBE (I.E., FROM CARBONYL)
	mg.	mg.	mg.
A.	0.44	3.02	0.0068
B.	0.87	3.52	0.031
C.	1.40	5.72	0.063
D.	1.56	8.53	0.046

TABLE 10

Equilibrium products and adiabatic flame temperatures at 1500 atm. for explosion of carbon monoxide-oxygen mixtures

INITIAL MIXTURE		REACTED MIXTURE			
Moles	Per cent O ₂	Moles CO ₂ * Moles O ₂	Moles CO* Moles O ₂	CO CO ₂	Flame temperature
					°K.
1/3	25.0	1.923	1.116	0.58	3450
1/3.444	22.5	1.900	1.596	0.84	3320
1/4	20.0	1.888	2.168	1.148	3170
1/4.714	17.5	1.938	2.803	1.446	2990
1/5.667	15.0	1.970	3.712	1.885	2765
1/7	12.5	2	5	2.5	2495
1/9	10.0	2	7	3.5	2160

* These values have been corrected, when necessary, for the dissociation of carbon dioxide. The correction involved evaluation of the degree of carbon monoxide oxidation for each of the gas mixtures at each of the temperatures under consideration from the equilibrium constant.

deposits may have had their origin in the decomposition of carbonyl and consequently should not be dismissed from consideration.

It is clear that the mechanism of the gaseous erosion of steel will vary as the temperature, pressure, and gas composition vary in each separate case; nevertheless, the iron carbonyl mechanism has proved useful even in cases where a preliminary survey would indicate the conditions to be severe.

TABLE 11

Initial composition of gases at 0.625 mole for 63-cc. pressure vessel to modify flame temperatures at prescribed composition of combustion products

TEMPER- ATURE	CALORIES	q	q·n(CO ₂)	q·m(CO)	TOTAL MOLES		FILLING MIXTURE		
					Initial	Final	P _{O₂}	P _{CO₂}	P _{O₂ + CO₂ + CO}
25 per cent oxygen series									
°K.									
3450	124,420	0	0	0	4.000	3.039	1170	0	4680
3320	117,290	0.0606	0.1169	0.0676	4.184	3.223	1090	130	4600
3170	109,950	0.1318	0.2532	0.1468	4.400	3.439	1030	260	4520
2990	101,200	0.232	0.446	0.2582	4.704	3.743	945	420	4440
2765	90,050	0.382	0.734	0.425	5.159	4.198	845	620*	4360
2495	77,840	0.600	1.152	0.669	5.821	4.860	730	840	4240
2160	63,240	0.968	1.861	1.079	6.940	5.979	590	1100	4080
22.5 per cent oxygen series									
3320	125,500	0	0	0	4.444	3.496	1020	0	4520
3170	117,900	0.0848	0.1612	0.1355	4.741	3.793	940	150	4440
2990	108,400	0.1578	0.300	0.252	4.996	4.048	870	260	4360
2765	96,800	0.2963	0.563	0.473	5.480	4.532	780	440	4280
2495	83,900	0.4960	0.942	0.792	6.178	5.230	675	635	4160
2160	68,300	0.837	1.590	1.337	7.371	6.423	550	875	4040
20.0 per cent oxygen series									
3170	127,900	0	0	0	5.000	4.056	870	0	4360
2990	117,800	0.0859	0.1619	0.1858	5.348	4.404	810	130	4320
2765	105,500	0.2123	0.401	0.4600	5.861	4.917	725	290	4240
2495	91,600	0.3963	0.749	0.860	6.609	5.665	625	470	4120
2160	74,800	0.7100	1.342	1.540	7.882	6.938	510	680	4000
17.5 per cent oxygen series									
2990	131,000	0	0	0	5.714	4.741	740	0	4240
2765	117,500	0.0870	0.1685	0.2439	6.120	5.154	690	110	4200
2495	102,150	0.2825	0.547	0.792	7.053	6.080	580	315	4080
2160	83,670	0.5645	1.091	1.580	8.385	7.412	475	515	3960
15.0 per cent oxygen series									
2765	133,100	0	0	0	6.687	5.682	620	0	4120
2495	115,900	0.1487	0.2925	0.551	7.511	6.526	540	160	4040
2160	95,250	0.3978	0.784	1.476	8.937	7.942	445	350	3960
12.5 per cent oxygen series									
2495	135,100	0	0	0	8.000	7.000	500	0	4000
2160	111,300	0.2125	0.426	1.063	9.489	8.489	410	180	3920

* Sample computation:

$$P_{\text{CO}_2} = \left(\frac{\text{moles CO}_2}{\text{total initial moles}} \right) \left(\frac{\text{initial moles}}{\text{final moles}} \right) \frac{nRT \text{ (lb./in.}^2 \text{ atm.)}}{V}$$

$$= \frac{0.734}{5.159} \times \frac{5.159}{4.198} \times \frac{0.625 \times 82.06 \times 293 \times 14.7}{63.0} = 620 \text{ lb./in.}^2$$

EXPERIMENTAL

The selection of gas pressures to determine flame temperature or composition.

Reduction in flame temperature without altering composition may be readily effected by diluting the reagent gases with the product gas mixture. If $n\text{CO}_2 + m\text{CO}$ needed $\Sigma\Delta H_1$ cal. to raise its temperature to T_1 , then the same mixture will require some smaller amount of heat, $\Sigma\Delta H_2$, to raise its temperature to some lower value, T_2 . We may ignore the oxygen formed by the dissociation of car-

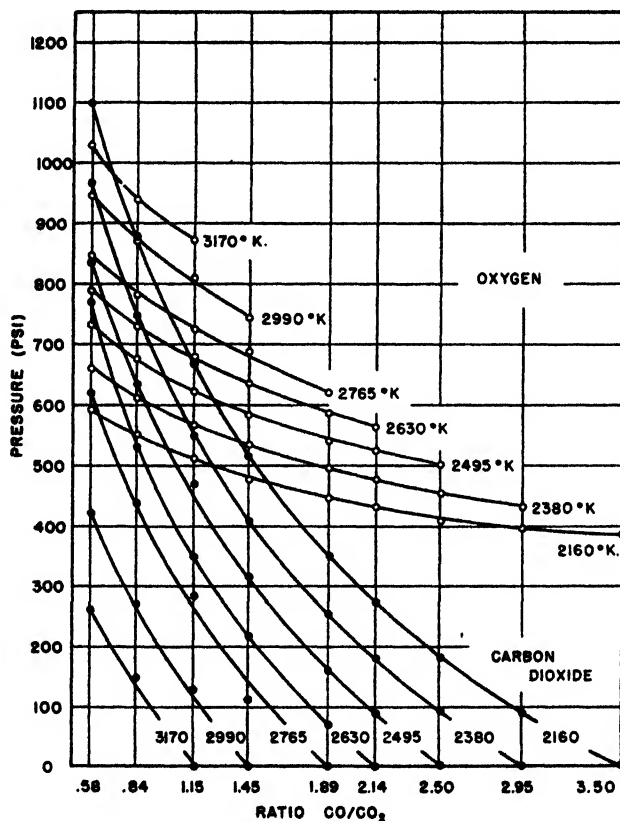


FIG. 16. Chart for the selection of pressures of carbon dioxide and oxygen to obtain specified temperatures and compositions.

bon dioxide and make only a small error. This process may be accomplished by adding to the original mixture an amount of gas $q(n\text{CO}_2 + m\text{CO})$ which must absorb an amount of heat $\Sigma\Delta H_1 - \Sigma\Delta H_2$ in order to reduce the temperature of the exploded mixture from T_1 to T_2 . The value of q may be obtained from

$$q = \frac{\Sigma\Delta H_1 - \Sigma\Delta H_2}{\Sigma\Delta H_2}$$

and is the fraction of the explosion gases necessary to absorb the difference in

heat at the lower temperature, T_2 . The heat content of the mixture was calculated from thermal equations of the following type (2, 4):

$$\Sigma \Delta H = (\text{moles CO}_2) \int_{290}^T (6.688 + 4.23 \times 10^{-3} T - 0.648 \times 10^{-6} T^2) dT +$$

$$(\text{moles CO}) \int_{290}^T (4.98 + 0.21 \times 10^{-3} T + 0.055 \times 10^{-6} T^2) dT$$

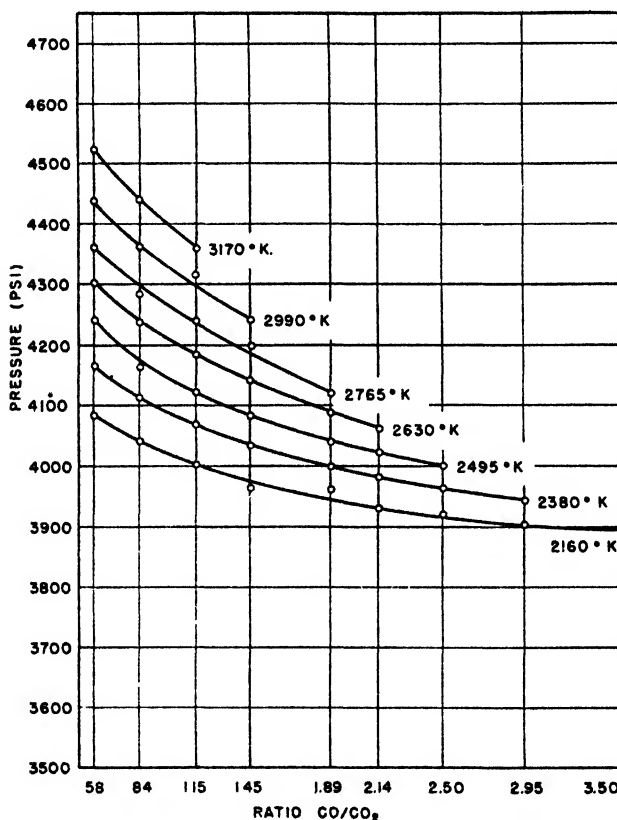
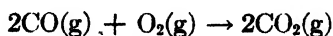
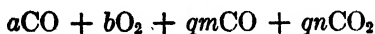


FIG. 17. Chart for the selection of total pressures of carbon monoxide, carbon dioxide and oxygen.

and the equations were corrected for changes in pressure (3, 4, 7). The value of ΔH for the reaction



of $-135,220$ cal. at 1 atm. and 298°K . was taken from Bichowski and Rossini (1). The number of moles of carbon dioxide and carbon monoxide which must be added is given by $q \cdot n\text{CO}_2$ and $q \cdot m\text{CO}$, and the total relative initial quantities involved in the reaction by:



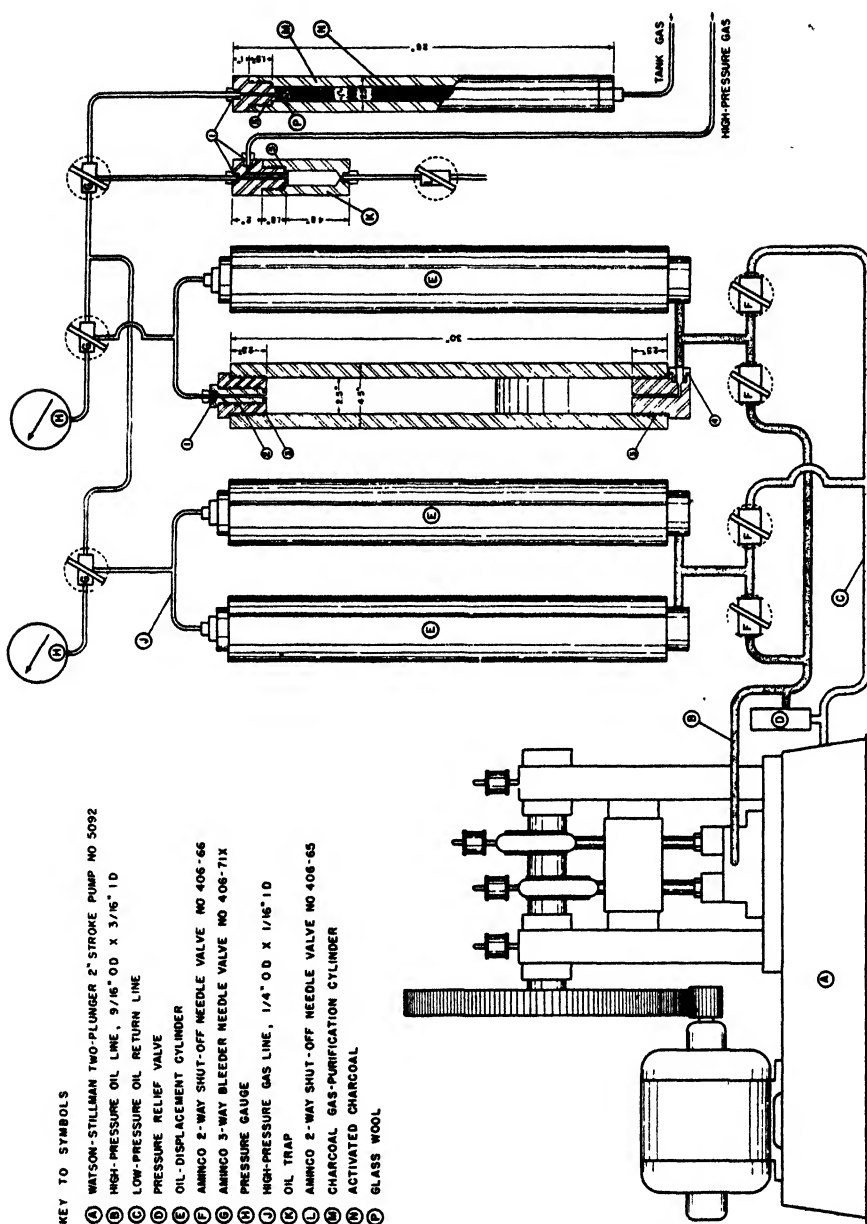


Fig. 18. Carbon monoxide pressure booster apparatus. Screw thread chart: 1, 1 1/8 in. No. 18 Aminco coupling (406-95); 2, 1 1/4 in. No. 12 N.F.; 3, 2 1/4 in. No. 12 N.F.; 4, 1 1/4 in. No. 12 Aminco coupling (406-98); 5, 1 1/4 in. No. 12 N.F.

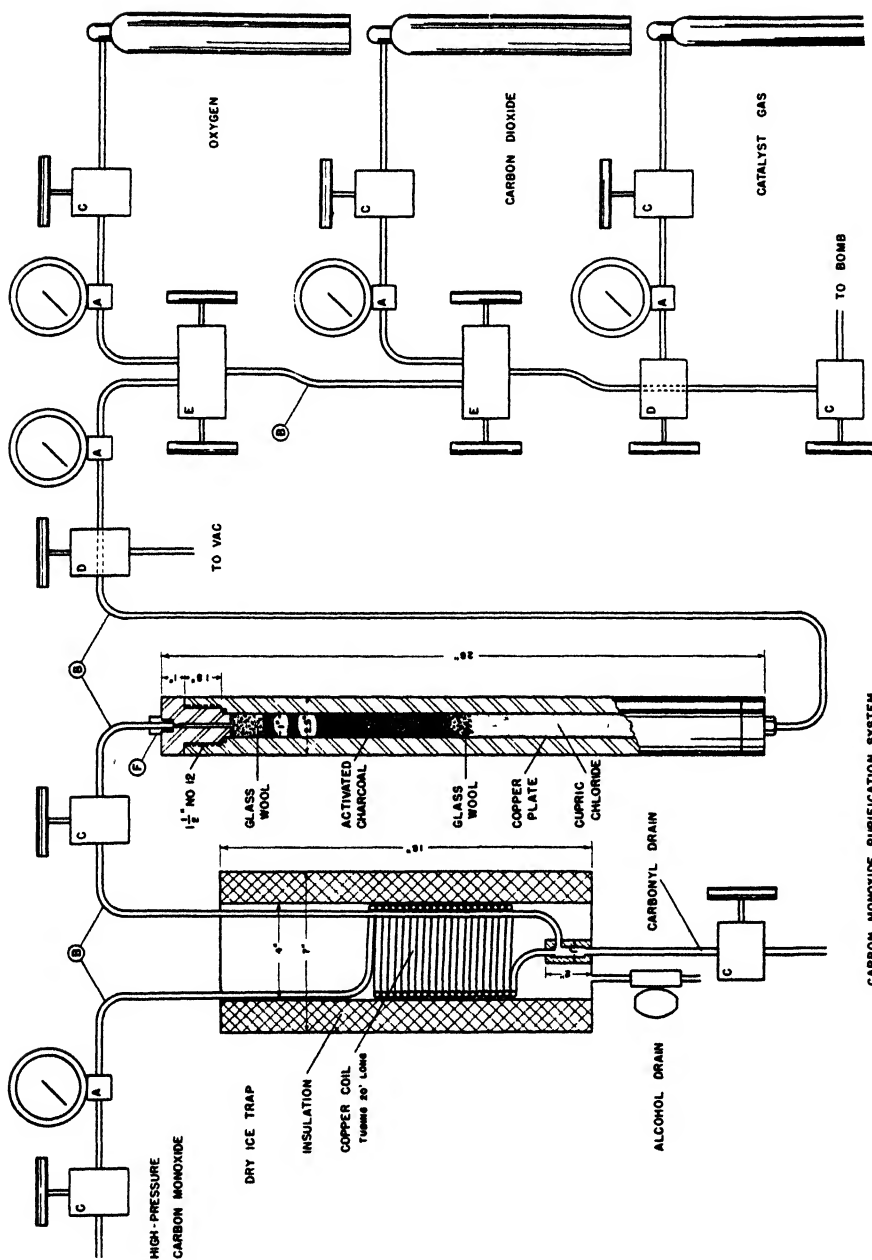


FIG. 19. Gas-mixing system. A, pressure gauge; B, copper tubing, hard, 0.25 in. x 0.040 in.; C, brass Aminco-type valve (406-65X); D, brass Aminco-type valve (406-74A); E, brass Aminco-type valve (406-74A); F, $\frac{3}{16}$ in. No. 18 Aminco coupling (406-95).

It was decided to keep the total number of moles of gas passing over the sample constant, at 0.625 mole. It was therefore only necessary to find the sum of the relative number of moles of reagents, from this the fraction of the total which

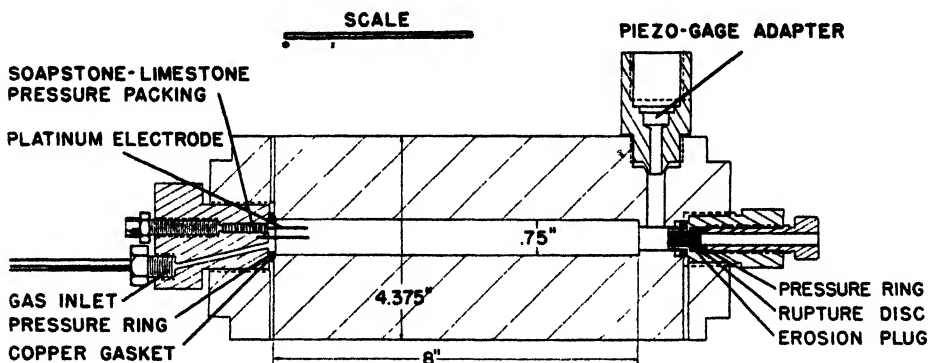


FIG. 20. Diagram of high-pressure bomb (volume = 62.5 ml.)

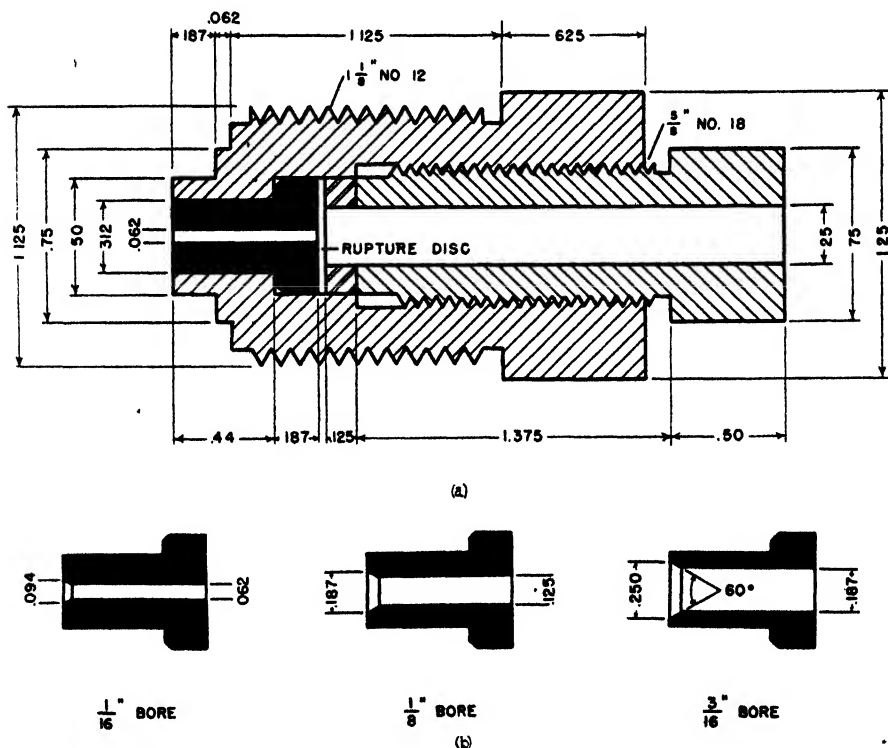


FIG. 21. (a) Holder for vent plugs and (b) detail of vent plugs

each gas comprises, and then the pressure of each gas to be used. For convenience, these values have been tabulated in tables 10 and 11, and plotted in figures 16 and 17.

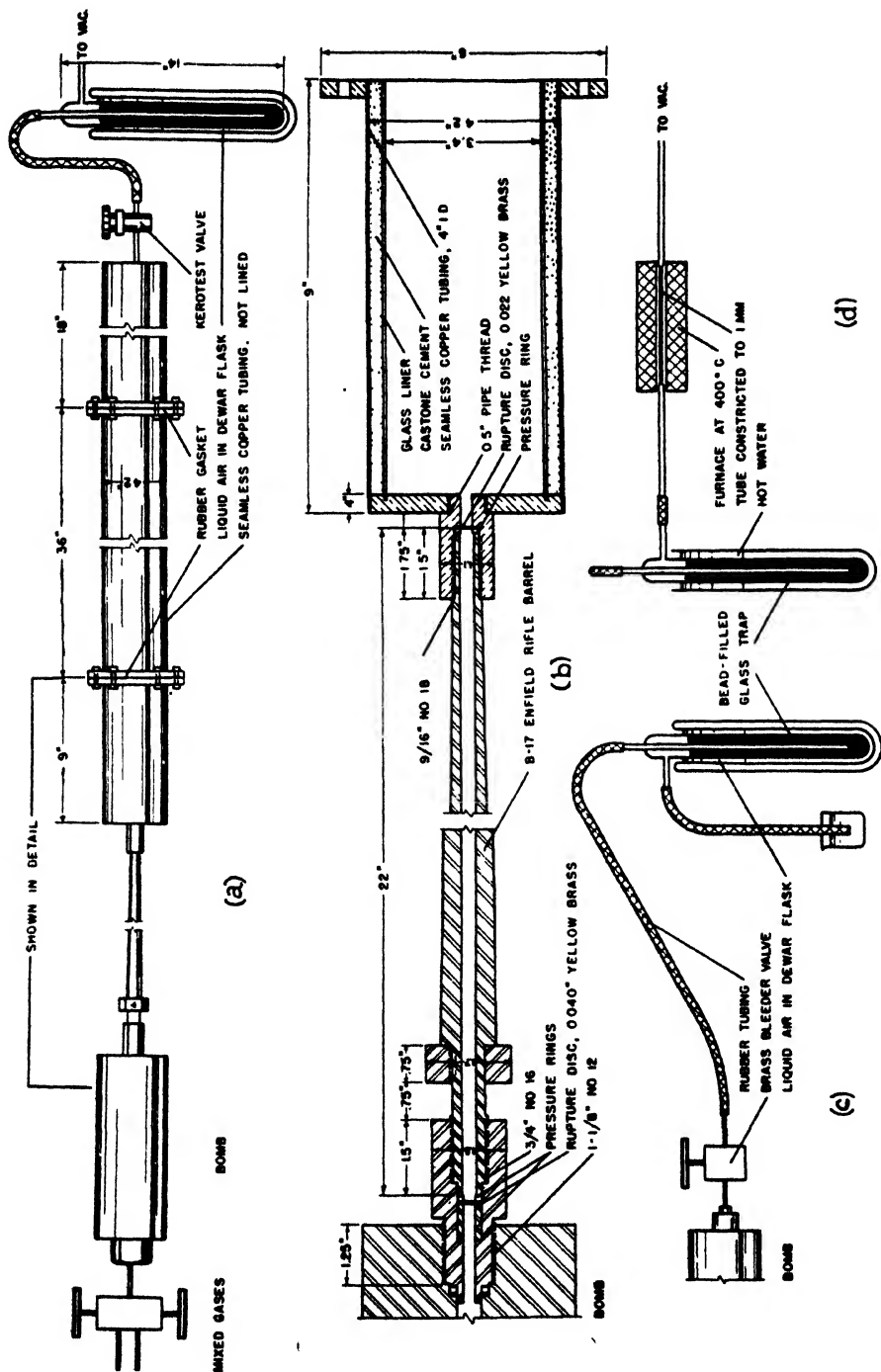


FIG. 22. (a) Apparatus used in the collection of gaseous products of erosion. (b) Detail of rifle barrel adapted to vent plug experiments. (c) Isolation of iron carbonyl from carbon monoxide control experiment. (d) Deposition tube for the decomposition of iron carbonyl.

Apparatus

The apparatus used in these experiments consisted of, first, an oil compression pump and oil displacement cylinders for boosting the tank pressure of commercial carbon monoxide from the customary 800 lb./in.² to the required 6000 lb./in.² (see figure 18); second, a carbon monoxide purification system composed of a coil immersed in a dry ice-alcohol bath followed by steel cylinders packed with charcoal, and finally solid cupric chloride dihydrate, found by experiment to be very effective in removing completely the last traces of iron carbonyl in gases; third, a system of valves, shown in figure 19, to permit the successive introduction into the high-pressure bomb of the three or four gases required for the tests; and fourth, the high-pressure bomb itself where the explosive gas mixtures were ignited and where the erosion vent plug was held. Because the configuration of the bomb probably exerted a considerable effect on the experiments, a drawing of the bomb is given in figure 20, and the vent plug holder in figure 21. The explosions were initiated by a hot wire between the electrodes and the maximum pressures determined by the thickness of the yellow-brass rupture disc. In all cases except those otherwise designated, the bore of the vent plug was $\frac{1}{8}$ in. and the number of moles of burned gas 0.625.

The collection of the gaseous products of erosion involved several additions, shown in figure 22, to the apparatus as used previously: the short vent plug was replaced by a steel tube nearly 2 ft. long—a cal. .30 Enfield rifle barrel served the purpose admirably; to this was connected an evacuated copper cylinder partially glass-lined to facilitate collection and analysis of the products of combustion and erosion. Following the cylinder were bead-filled glass traps immersed in liquid air through which these products were pumped and where carbonyl was frozen out. It was necessary to obstruct partially the gas flow at the time of explosion to prevent destruction of the traps, but this was readily accomplished by a partially closed valve. By heating the glass trap and distilling the collected carbonyl and other gases through a hot capillary, an iron deposit whose origin must have been iron carbonyl was obtained. Such an arrangement is shown in the lower part of figure 22. To prevent ambiguity, frequent control tests were made to detect any carbonyl in the reagent gas by passing it through the cold trap as in the actual experiments. The iron analyses were accomplished by dissolving the deposits in hot dilute hydrochloric acid to which had been added a small amount of nitric acid or bromine water, and after evaporation of the acid, subjecting the residue to the conventional α, α' -dipyridyl procedure.

SUMMARY

The erosion of steel vent plugs by the products of explosion of gas mixtures gives rise to the following qualitative conclusions:

1. For a fixed number of moles of a mixture of carbon monoxide and carbon dioxide at a given composition, erosion increases as the calculated adiabatic flame temperature is increased.
2. For a fixed number of moles of mixtures of carbon monoxide and carbon dioxide at a constant calculated adiabatic flame temperature, erosion increases as the concentration of the carbon dioxide is increased.

3. The increase in erosion produced by mixtures of carbon monoxide and dioxide is more strongly dependent on the adiabatic flame temperature of the mixture as the concentration of carbon dioxide in the mixture becomes higher.

4. When small amounts of hydrogen sulfide or sulfur dioxide are added to the explosive mixture, that mixture becomes vastly more erosive both as a function of concentration of sulfurous gas at a single firing and as a function of number of firings at a single low concentration.

5. When traces of nitrous oxide are added, the increase in erosive effect is somewhat less than that noted for the sulfurous gases.

6. When minute quantities of ammonia are added to the eroding gases, the increase is greater at lower concentrations of ammonia.

7. Hydrogen added in low concentrations to the basic carbon monoxide-carbon dioxide mixture gives rise to a singular maximum in erosive action, the peak of which greatly overshadows the effect of the other trace gases studied.

8. It is proposed that the erosive action outlined in paragraphs 4, 5, 6, and 7 might be rationalized by assuming the reaction of carbon monoxide and steel to form iron carbonyl under the influence of the trace gases as catalysts. Since carbon dioxide when present in quantity probably inhibits the carbonyl reaction, some other mechanism such as oxidation or melting must be used to explain the results of paragraphs 1, 2, and 3.

9. X-ray diffraction analysis of the bore surfaces yielded, in addition to α -iron, austenite, and ferrous oxide, d/n values for which no identification is currently listed.

The authors wish to acknowledge their great indebtedness in conceiving the fundamental basis of the problem and planning the experimental approach to Professor J. C. W. Frazer, who directed the work up to the time of his death; and to thank their able assistants, Mrs. Wm. B. Burford III, Mrs. F. Michael Krouse, Dr. S. S. Hubard, and Mr. Talbott F. Ruby, without whose competent work the problem would have been vastly more difficult.

REFERENCES

- (1) BICHOWSKI, F. R., AND ROSSINI, F. D.: *Thermochemistry of the Chemical Substances*, p. 232. Reinhold Publishing Corporation, New York (1936).
- (2) *International Critical Tables*, Vol. V, p. 82. McGraw-Hill Book Company, Inc., New York (1929).
- (3) MICHELS, A.: Proc. Roy. Soc. (London) **A153**, 214 (1935).
- (4) MICHELS, A.: Proc. Roy. Soc. (London) **A160**, 374 (1937).
- (5) MITTASCH, A.: Z. angew. Chem. **41**, 827 (1928).
- (6) WIEGAND, JAMES H.: Erosion in Vent Plugs: The Effect of Vent Diameter. J. Franklin Inst., in press.
- (7) WORKMAN, E.: Phys. Rev. **37**, 1345 (1937).

HYDROLYSIS OF WOOD CELLULOSE AND DECOMPOSITION
OF SUGAR IN DILUTE PHOSPHORIC ACID¹

ELWIN E. HARRIS AND BILL G. LANG

*Forest Products Laboratory,² Forest Service, U. S. Department of Agriculture**Received May 8, 1947*

INTRODUCTION

The rate of hydrolysis of cellulose and the rate of the decomposition of the hydrolytic products are of great importance in a study of the saccharification of wood. The ideal conditions would be those in which cellulose would be hydrolyzed at a satisfactory rate with minimum decomposition of the hydrolytic products. Economic considerations limit the conditions to the use of dilute acid for the hydrolysis. In earlier investigations, Lüers (8) showed that the rate of hydrolysis of a hydrocellulose in dilute sulfuric acid was approximately equal to the rate of the decomposition of the hydrolytic products and that both reactions were unimolecular reactions. Neuman (9) had previously carried on similar hydrolytic work, but he contended that the rate of decomposition of the hydrolytic products at temperatures above 175°C. was so great that it was useless to study hydrolysis above that temperature. More recent work at the Forest Products Laboratory (12, 14) on the hydrolysis of wood in dilute sulfuric acid indicated that the rate of hydrolysis of wood cellulose increased more rapidly than the rate of decomposition of the hydrolytic products when either the temperature or the acid concentration was increased.

The complexity of the problem of hydrolysis when dealing with wood is increased because wood contains a mixture of carbohydrate materials called hemicellulose, in addition to the stable alpha cellulose. The hemicellulose hydrolyzes very rapidly, its rate of hydrolysis being dependent upon easily hydrolyzable linkages and upon molecules that are relatively smaller in size. When hydrolysis had proceeded sufficiently to hydrolyze the hemicellulose in the Laboratory study, the cellulosic material remaining had lost most of its fibrous structure. Under conditions drastic enough to cause the hydrolysis of the resistant cellulose to occur in a few hours' time, the hydrolysis of the hemicellulose and the loss of fibrous properties occurred in periods of time too short for the usual methods of measurement.

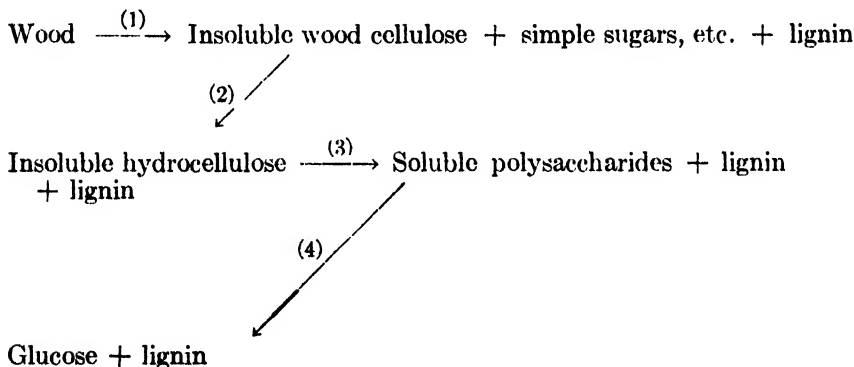
Several investigators, in working with cellulosic fibers, have assumed that the difference in rate of reactivity between the highly reactive and the more resistant carbohydrate material is due to a greater reactivity of the amorphous portion of the molecule. Hess and Trogus (7), Nickerson (10), and Conrad and Scroggie (2) employed hydrolysis and oxidation. Goldfinger, Mark, and Siggia (6) oxidized cellulose with periodic acid, and Azzaf, Haas, and Purves (1) subjected

¹ Presented before the Division of Cellulose Chemistry at the 111th Meeting of the American Chemical Society, which was held at Atlantic City, New Jersey, April 14-18, 1947.

² Maintained at Madison 5, Wisconsin, in cooperation with the University of Wisconsin.

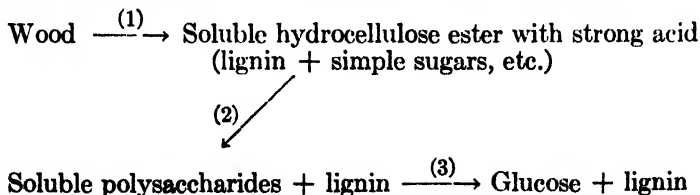
cellulose to thallation in efforts to throw light upon the relationship between amorphous and crystalline cellulose. They did not consider the possibility of the presence of hemicellulose or of modified cellulose that would hydrolyze at a more rapid rate. Pacsu and coworkers (11) explained the differences in the reactivity of cellulose as being due to hemiacetal linkages and hydrogen bonding in the reactive portion, and to hydrolysis of true 1,4-linkages in the resistant portion of cellulose fibers. The latter factor appears to account for the reactions that occur when wood is hydrolyzed. A difference in the energies of activation of the hydrolysis of cellulose in concentrated acids and in dilute acids may be accounted for by assuming a difference in the type of reactive groups. In concentrated acid the energy of activation has been shown to be between 27,800 and 29,800 cal. (3, 4, 16), while the value in dilute sulfuric acid has been found to be between 42,000 and 44,000 cal. (12, 14). Concentrated acid with its higher reactivity toward hydrogen bonds and also acetal groupings puts cellulose into solution, and therefore the energy due to these reactions changes before the measurements are made. With dilute acid both solvation and hydrolysis occur and give higher values.

The reaction occurring in the presence of dilute acid may be expressed as follows:



Reactions 1, 2, and 4 are rapid in dilute solution and incapable of measurement under the conditions of the experiment. Reaction 3 is slow and is measured by the rate of hydrolysis. The energy of activation, however, includes both 3 and 4.

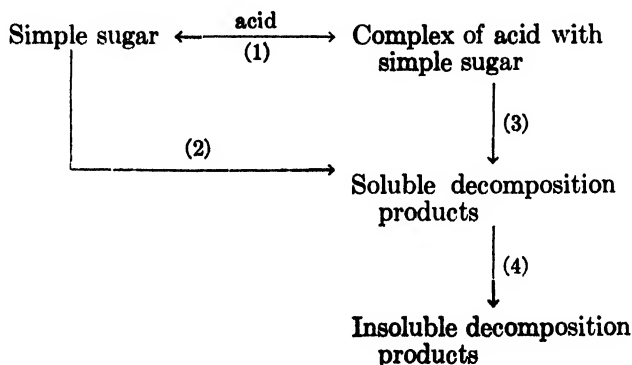
With concentrated acid the reaction may be expressed as follows:



Reaction 1 occurs very rapidly and before the measurements are made. Reactions 2 and 3 take place slowly at low temperatures. Stamm and Cohen (17)

found that both of these reactions occur very slowly at room temperature in 85 per cent phosphoric acid. Wolfrom and coworkers (18) found that hydrolysis with strong hydrochloric acid in the presence of ethyl mercaptan did not produce the glucose mercaptan derivative until the reaction had proceeded for long periods of time. Similar results were found by Gladding and Purves (5) in their work with hydroxylamine and hydrogen chloride on cellulose.

The rate of decomposition of the glucose controls the simple sugars that will be available after periods of hydrolysis. Decomposition is also catalyzed by the presence of acid. The rate of decomposition will be dependent upon the hydrogen-ion concentration, but will not necessarily be the same with all types of acid because the nature of the acid will also influence the type of reaction involved. The tendency to form complex derivatives with the acid increases with the complexity of the acid. The decomposition of the sugars may be expressed as follows:



It may be assumed that the loss in reducing power is represented by reaction 2, which is the one measured by the conditions of the experiment, although in more concentrated solutions the reaction may also proceed by reactions 1 and 3, which may result in a lower rate of decomposition in higher concentrations of complex acids.

MATERIAL USED FOR EXPERIMENTAL WORK

The present work describes the hydrolysis of wood cellulose and the decomposition of simple sugars in the presence of phosphoric acid in concentrations from 0.2 to 3.2 per cent at temperatures from 180°C. to 195°C. A measurement of the pH of the phosphoric acid solutions with a pH meter gave the following values at 20°C.: 3.2 per cent solution, pH 1.4; 1.6 per cent, pH 1.57; 0.8 per cent, pH 1.73; 0.4 per cent, pH 1.91; and 0.2 per cent, pH 2.10. The sulfuric acid solutions used in previous work when tested in a similar manner gave for 1.6 per cent solution, pH 0.5; for 0.8 per cent, pH 0.8; and for 0.4 per cent, pH 1.12. On the basis of hydrogen-ion concentration, the 3.2 per cent phosphoric acid should have less reactivity than the 0.4 per cent sulfuric acid.

The wood used for the hydrolysis tests was air-dried Douglas fir that had been

ground until it remained on an 80-mesh screen and passed a 40-mesh screen. The samples were kept sealed, except when sampling, and were used in air-dried form to eliminate the possibility of decomposition during drying.

The cotton used for the tests was a sample of purified linters that had been obtained commercially.

ANALYSIS

In order to eliminate from results errors that might arise from the use of different analytical procedures, all measurements were designed so that the same method of analysis would be used for all results. In tests of the decomposition of sugar, pure glucose was used for the experiments, and its decomposition was measured by determining the loss in reducing power as determined by the Schaffer and Somogyi (14, 15) method for sugar analyses. The rate of hydrolysis was determined by converting to sugar the cellulosic material in the residue remaining after the hydrolysis (13) and measuring the sugar by the Schaffer and Somogyi method. In this manner it was possible to avoid corrections for decomposition products.

EXPERIMENTAL

Samples for experiments on the hydrolysis of wood and on the decomposition of sugars were sealed in glass tubes and heated by direct steam in a rotating digester. About $1\frac{1}{2}$ min. was required to reach the desired temperature, and about the same length of time was allowed for it to drop back so that no appreciable amount of hydrolysis or decomposition would occur. Pressure was maintained at ± 1 lb. per square inch with the pressure under manual control. The digester was preheated for at least 1 hr. before the test so as to minimize errors due to failure to heat the equipment in a short time. All samples were run in duplicate or triplicate. Samples usually checked within 0.5 per cent.

Decomposition of sugars

Since glucose is the principal sugar in the Douglas-fir hydrolyzate, it was chosen for determination of the rate of decomposition. Ten-milliliter samples of 5 g. of glucose in 100 ml. of solutions containing 0.2, 0.4, 0.8, 1.6, and 3.2 per cent phosphoric acid were heated at three temperatures for various periods of time. The results of these experiments are shown in figure 1. The straight lines indicate that at the temperatures and acid concentrations used the reactions were of the first order. Table 1 gives the calculated first-order reaction constant and the half-life of glucose, both based on the loss of reducing power. When the logarithms of the reaction rates were plotted as a function of pH, the series of straight lines shown in figure 2 was obtained. The reaction rate increased by a constant multiple when the pH was decreased by a constant multiple. The values for the slope M of the lines in figure 2 for a constant temperature were obtained by the following equation:

$$\frac{\log k_2 - \log k_1}{\text{pH}_1 - \text{pH}_2} = M$$

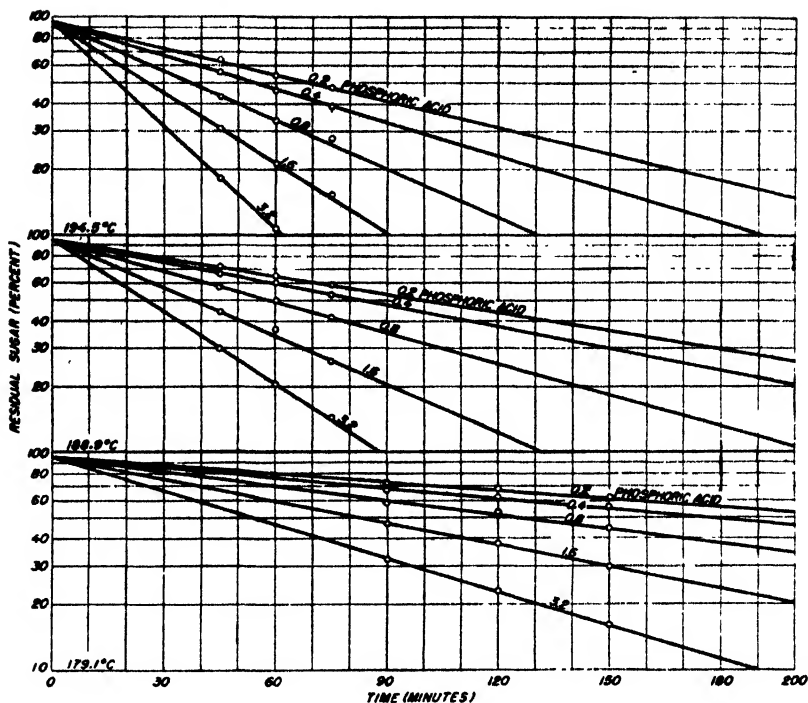


Fig. 1. Decomposition of glucose in dilute phosphoric acid at various temperatures

TABLE 1

The decomposition of glucose in 0.2, 0.4, 0.8, 1.6, and 3.2 per cent phosphoric acid at various temperatures

TEMPERATURE	PHOSPHORIC ACID CONCENTRATION	k FIRST-ORDER REACTION CONSTANT BASED ON LOSS OF REDUCING POWER	HALF-LIFE BASED ON LOSS OF REDUCING POWER
°C.	per cent	minutes ⁻¹	minutes
179.1	0.2	0.0029	238
	0.4	0.0036	192
	0.8	0.0052	133
	1.6	0.00775	89.0
	3.2	0.0120	57.5
188.9	0.2	0.0064	108
	0.4	0.0076	90.5
	0.8	0.0110	62.5
	1.6	0.0169	41.0
	3.2	0.0254	27.2
194.5	0.2	0.0092	74.5
	0.4	0.0118	58.5
	0.8	0.0171	40.5
	1.6	0.0247	28.0
	3.2	0.0360	19.0

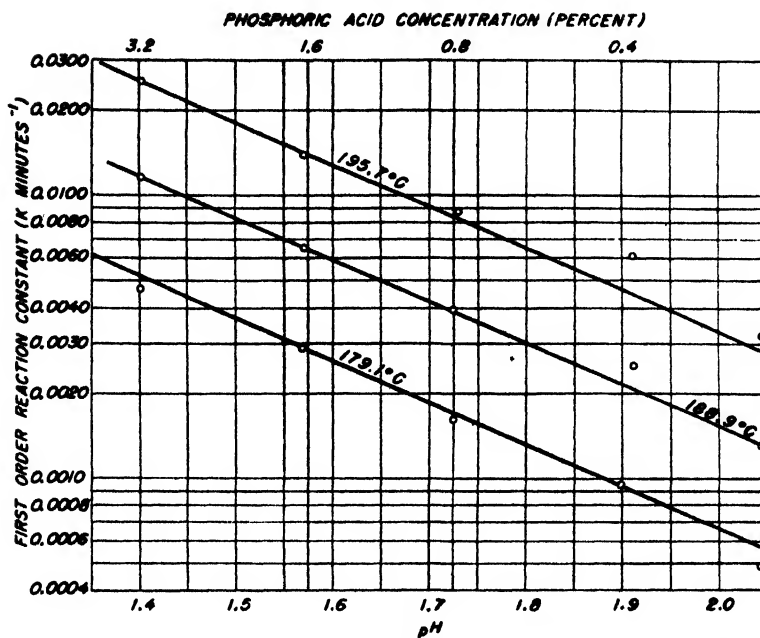


FIG. 2. Relation of first-order reaction constant k to pH in the decomposition of glucose in the presence of phosphoric acid at various temperatures.

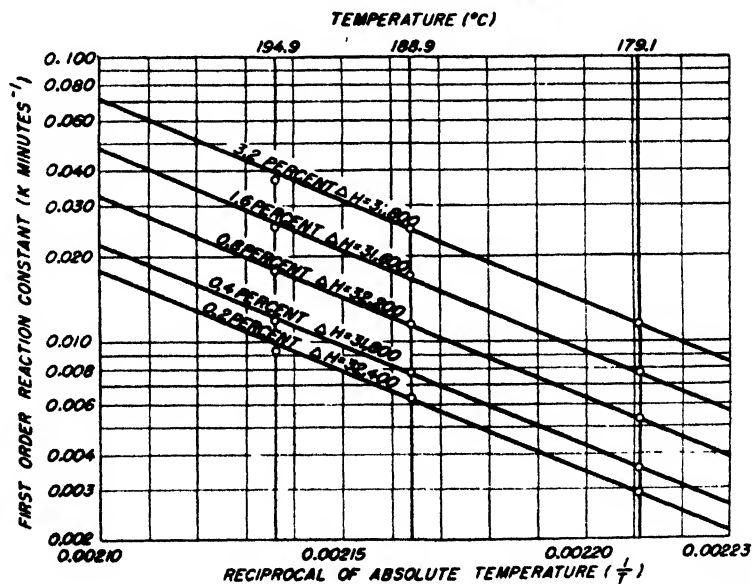


FIG. 3. Relation of first-order reaction constant k to the temperature in the decomposition of glucose with phosphoric acid of various strengths.

where M had an average value of 1.007 over the temperature range 180–195°C. This corresponds to a 26 per cent increase in the rate of decomposition for a decrease of 0.1 in pH.

When the logarithms of the reaction constants in table 1 were plotted against the reciprocal of the absolute temperature, a series of straight lines was obtained, as shown in figure 3. The energy of activation was obtained by multiplying the slope of the lines in figure 3 by -4.56 . The average of the values for the energy of activation for the various acid concentrations was approximately 32,000 cal. At temperatures of 180–195°C. the rate of decomposition increased 114 per cent for an increase of 10°C.

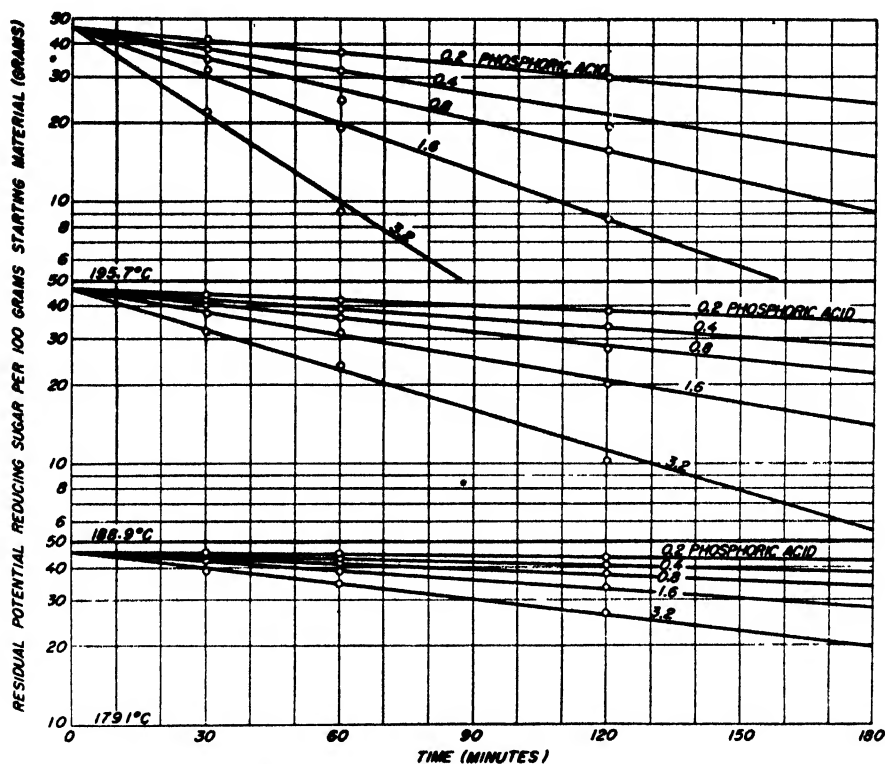


FIG. 4. Hydrolysis of Douglas fir in dilute phosphoric acid at various temperatures

Hydrolysis of Douglas-fir wood

Douglas-fir sawdust, 40 to 80 mesh, was sealed in tubes with solutions of 0.2, 0.4, 0.8, 1.6, or 3.2 per cent phosphoric acid, using a liquid-solid ratio of 10 to 1 at 179.1°, 188.9°, and 195.7°C. for various lengths of time. Figure 4 shows a plot of the logarithms of the residual potential sugar as a function of time. Table 2 gives the calculated values for the first-order reaction constants k and for the half-life of the hydrolysis of the resistant cellulose in Douglas-fir wood, both based upon loss of reducing power.

When the logarithms of the first-order reaction constants were plotted as a function of the pH of the solutions used for hydrolysis, the series of lines shown in figure 5 was obtained. By using the equation

TABLE 2

The hydrolysis of Douglas fir in 0.2, 0.4, 0.8, 1.6, and 3.2 per cent phosphoric acid at various temperatures

TEMPERATURE	PHOSPHORIC ACID CONCENTRATION	k FIRST-ORDER REACTION CONSTANT BASED ON LOSS OF REDUCING POWER	HALF-LIFE BASED ON LOSS OF REDUCING POWER
°C.	per cent	minutes ⁻¹	minutes
179.1	0.2	0.00047	1470
	0.4	0.00097	712
	0.8	0.00161	428
	1.6	0.00291	237
	3.2	0.00474	146
188.9	0.2	0.00160	432
	0.4	0.00256	268
	0.8	0.00395	175
	1.6	0.00670	103
	3.2	0.0117	59
195.7	0.2	0.0036	198
	0.4	0.0062	115
	0.8	0.0088	81
	1.6	0.0142	50
	3.2	0.0250	28

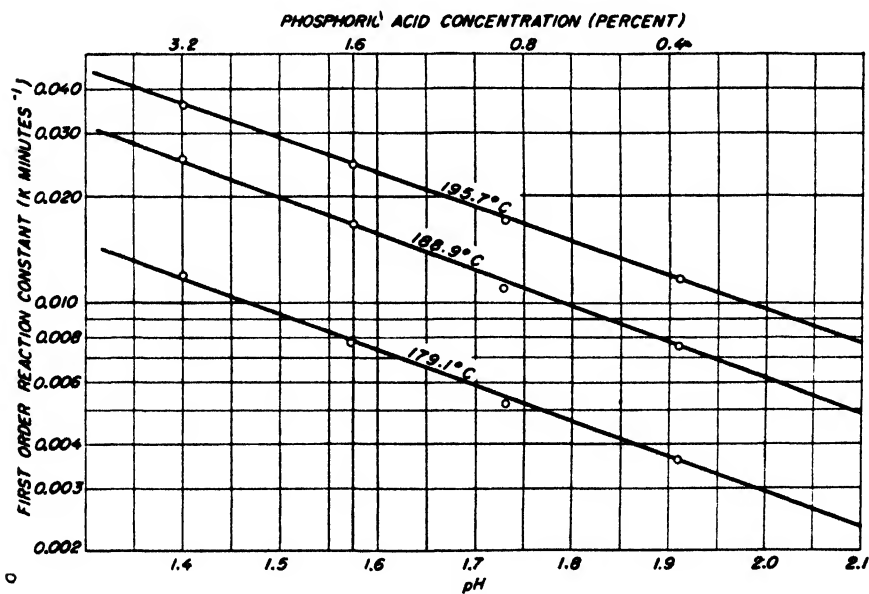


FIG. 5. Relation of first-order reaction constant k to pH in the hydrolysis of Douglas fir with phosphoric acid at various temperatures.

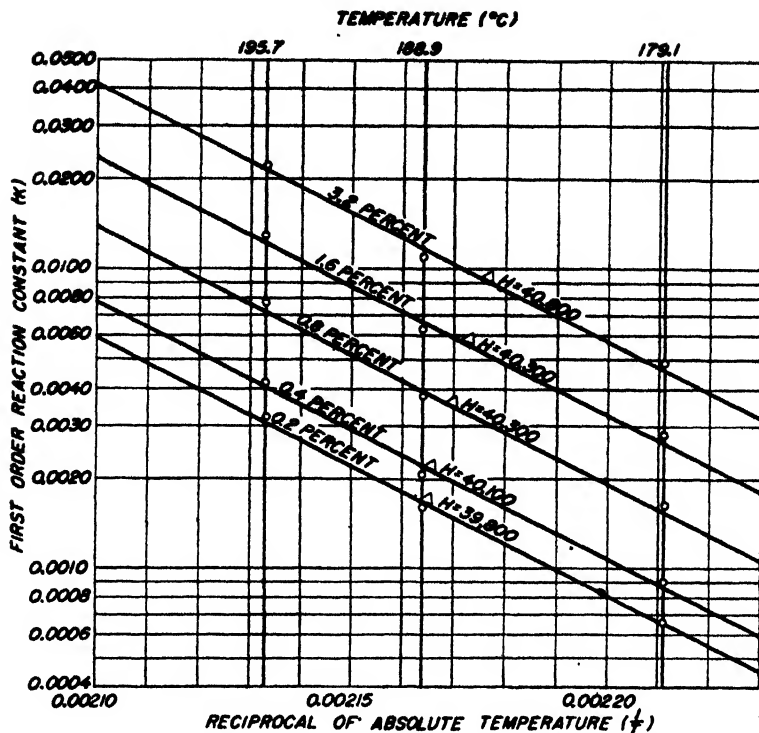


FIG. 6. Relation of first-order reaction constant k to the temperature in the hydrolysis of Douglas fir with phosphoric acid of various strengths.

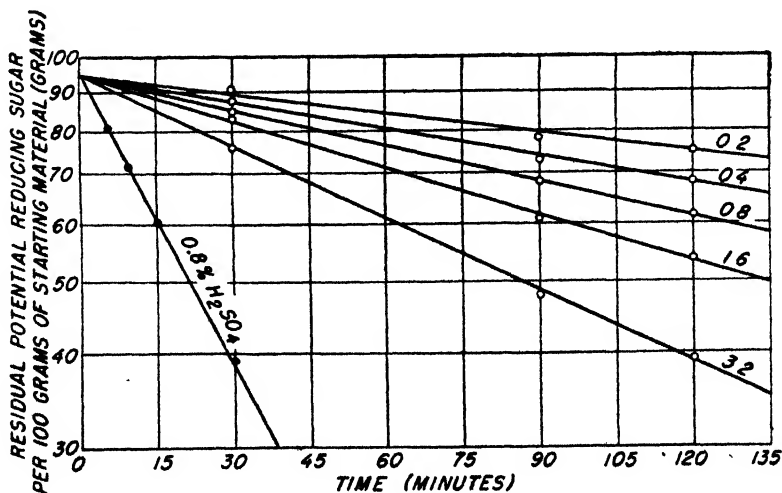


FIG. 7. A comparison between the hydrolysis of cotton cellulose in dilute phosphoric acid and in sulfuric acid at 190°C.

$$\frac{\log k_2 - \log k_1}{\text{pH}_1 - \text{pH}_2} = M$$

the slope of the lines was obtained. The average values for the slope for the three lines is about 1.46. This corresponds to an increase of 40 per cent in the rate of hydrolysis for each drop of 0.1 in the pH of the solution.

Plotting the logarithm of the first-order reaction constants, $-k$, against the reciprocal of the absolute temperature, $1/T$, gave the curves shown in figure 6. From the slope of these curves an average value of 40,300 cal. was obtained for the energy of activation of the reaction for the various concentrations of dilute phosphoric acid. For each 10°C. rise in temperature in the range of 180–195°C., the rate of reaction was increased 158 per cent.

The rate of hydrolysis of a purified cotton cellulose was determined at 190°C. with 0.2, 0.4, 0.8, 1.6, and 3.2 per cent solutions of phosphoric acid. The values for the residual sugars at various intervals of time are shown in figure 7. The value for resistant cellulose extrapolates to 94 per cent. The half-life of the resistant cellulose at 190°C. for 3.2 per cent acid was 110 min.; for 1.6 per cent acid, 182 min.; for 0.8 per cent acid, 223 min.; and for 0.4 per cent acid, 288 min.

DISCUSSION

The decomposition of glucose in dilute phosphoric acid has approximately the same energy of activation, 32,000 cal., as that found previously for its decomposition in dilute sulfuric acid, 32,700 cal., for a similar temperature range, a fact that indicates a similar relationship of the acidity of the solution to the rate of decomposition.

The energy of activation for the hydrolysis of Douglas-fir wood cellulose is slightly lower, 40,300 cal., in dilute phosphoric acid than in sulfuric acid, in which it was found to be 43,900 cal. This difference would indicate that the factors controlling the rate are not the same in the two cases. The value for phosphoric acid is intermediate between the value for dilute sulfuric acid and that for concentrated acid (27,800 to 29,800 cal.) found by Freudenberg and others. It is generally assumed that a reaction occurs between the concentrated acid and the carbohydrate, and it is possible that there was some tendency for similar reactions here.

A comparison of the half-life of the Douglas-fir cellulose with the decomposition of glucose in dilute sulfuric acid and in dilute phosphoric acid as a function of the pH of the solutions, shown in figure 8, thus reveals that the disappearance of the cellulose and the decomposition of the glucose are controlled by the pH of the solution. It also reveals that an increase in acidity or decrease in pH makes the relationship of hydrolysis to decomposition more favorable. Concentrations of phosphoric acid from 0.2 to 3.2 per cent did not provide conditions where the rate of hydrolysis equaled the rate of decomposition. Dilute sulfuric acid in concentrations from 0.4 to 1.6 per cent did produce conditions where the rate of hydrolysis was equal to the rate of decomposition at temperatures from 180°C. to 190°C.

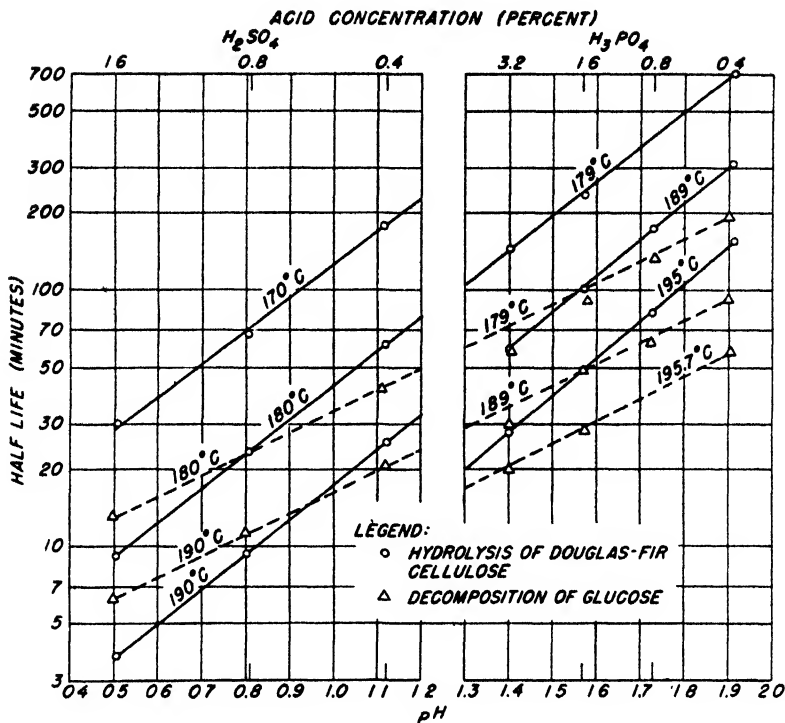


FIG. 8. Relationship of the half-life of cellulose and glucose to the pH of solutions of sulfuric and phosphoric acids at various temperatures.

CONCLUSIONS

It may be concluded from the results of this study that within the temperature range of 180–195°C., phosphoric acid in concentrations of 0.2 to 3.2 per cent is not as suitable for hydrolysis as sulfuric acid.

The rate of hydrolysis of cellulose and of the decomposition of glucose is a function of the pH and not of the acid concentration.

Yields of sugars in wood hydrolysis should be higher with the use of higher concentrations of acids.

Equal yields may be obtained at lower temperatures with higher concentrations of acid.

Provided means can be obtained to remove the sugars as soon as they are produced in wood saccharification, higher yields of sugar should result from the use of higher temperatures for hydrolysis.

REFERENCES

- (1) AZSAF, A. G., HAAS, R. H., AND PURVES, C. B.: J. Am. Chem. Soc. **66**, 59, 66 (1944).
- (2) CONRAD, C. C., AND SCROGGIE, A. G.: Ind. Eng. Chem. **37**, 592 (1945).
- (3) EISENHUT, O., AND SCHWARTZ, E.: Die Chemie **55**, 380 (1942).
- (4) FREUDENBERG, K., AND BLOMQVIST, G.: Ber. **68B**, 2070 (1935).
- (5) GLADDING, E. K., AND PURVES, C. B.: Paper Trade J. **116**, 261 (1943).

- (6) GOLDFINGER, G., MARK, H., AND SIGGIA, S.: *Ind. Eng. Chem.* **35**, 1083 (1943).
- (7) HESS, K., AND TROGUS, C.: *Z. physik. Chem.* **B15**, 157 (1931); *Kolloid-Z.* **68**, 168 (1934).
- (8) LÜERS, H.: *Z. angew. Chem.* **43**, 455 (1930); **45**, 399 (1932).
- (9) NEUMAN, J.: Dissertation, Polytechnic Institute, Dresden, 1910.
- (10) NICKERSON, R. F.: *Ind. Eng. Chem., Anal. Ed.* **13**, 423 (1941); *Ind. Eng. Chem.* **33**, 1022 (1941); **34**, 85, 1480 (1942).
- (11) PACSU, E., AND COWORKERS: *Textile Research J.* **16**, 243, 318, 490, 564 (1946).
- (12) SAEMAN, J. F.: *Ind. Eng. Chem.* **37**, 43 (1945).
- (13) SAEMAN, J. F., BUBL, J. L., AND HARRIS, E. E.: *Ind. Eng. Chem., Anal. Ed.* **17**, 35 (1945).
- (14) SAEMAN, J. F., HARRIS, E. E., AND KLINE, A. A.: *Ind. Eng. Chem., Anal. Ed.* **17**, 95 (1945).
- (15) SCHAFER, P. A., AND SOMOGYI, N.: *J. Biol. Chem.* **100**, 695 (1923).
- (16) SCHULTZ, G. V., AND LOHMAN, H. J.: *J. prakt. Chem.* **157**, 238 (1941).
- (17) STAMM, A. J., AND COHEN, W. E.: *J. Phys. Chem.* **42**, 921 (1938).
- (18) WOLFROM, M. L., AND COWORKERS: *J. Am. Chem. Soc.* **59**, 282 (1937); **60**, 1026, 3009 (1938); **61**, 1072 (1939).

THE SOLUBILITY OF THORIUM NITRATE TETRAHYDRATE IN ORGANIC SOLVENTS AT 25°C.¹

CHARLES C. TEMPLETON AND NORRIS F. HALL

Department of Chemistry, University of Wisconsin, Madison, Wisconsin

Received July 14, 1947

Preliminary to research into the liquid-liquid extraction of thorium salts from aqueous solutions, an investigation has been made of the solubility of thorium nitrate tetrahydrate in a wide range of organic solvents. No such comprehensive study has been previously reported. Misciattelli (4) made a complete study of the system thorium nitrate-diethyl ether-water. Wells (5) measured the ether solubilities of the nitrates of thorium, zirconium, and seven of the rare earths to determine if they interfered with a method of Hillebrand (1) for dissolving uranyl nitrate in ether to separate from it the last traces of the rare earths. Imrie (2) extracted thorium nitrate from aqueous solution with ether, and Misciattelli (3) used ether to extract uranyl nitrate from an aqueous nitric acid solution also containing thorium.

The solubility of the tetrahydrate, rather than that of the anhydrous salt, was investigated because it was desired to use the data to make qualitative predictions concerning extraction from aqueous solution. The anhydrous salt was prepared in Misciattelli's work, but it was necessary to use nitrogen pentoxide.

¹ This paper is based upon the thesis submitted by C. C. Templeton to the Graduate Faculty of the University of Wisconsin in partial fulfillment of the requirements for the degree of Master of Science, April, 1947.

Presented before the Meeting-in-Miniature of the Wisconsin Section of the American Chemical Society, April 26, 1947.

EXPERIMENTAL

Materials

Thorium nitrate tetrahydrate, Baker's C.P. Analyzed, was used for all solutions. The various organic liquids were in each case of Eastman Kodak Company "practical" grade or of better purity. No further purifications were made because of the desire to investigate a large number of solvents in a reasonable length of time.

Method

Suitable amounts of thorium nitrate tetrahydrate and solvent were mixed in a 6-in. test tube. The corked tube was tied with string and sealed with DeKhotinsky cement. Agitation, end over end, in a specially constructed device rotating at 35 R.P.M., was begun immediately in a $25^{\circ}\text{C.} \pm 0.05^{\circ}$ water thermostat and continued for 5 days. After the solution had settled, a portion was pipetted into a platinum crucible for weighing. The covered crucibles were heated with a small flame to evaporate or burn away the solvent. Later, ignition to thorium dioxide was made. Solubilities were calculated as grams of anhydrous thorium nitrate per 100 g. of solution.

Separate experiments showed the evaporation losses on weighing to be less than 0.25 per cent for any solvent boiling above 80°C. , and negligible with respect to the usual gravimetric errors for solvents boiling above 100°C. The gravimetric errors amounted to less than 0.2 per cent.

The method of approaching equilibrium was settled upon after an extended study of the effects of time, agitation, and heating upon the solubility and the stability of the solutions. It was immediately apparent that wide temperature ranges could not be used because of the evolution of gases from the solutions, and also that a long period of continuous agitation was necessary to get the nitrate into solution. Solutions in isoamyl alcohol, propiophenone, and ethyl butyrate were agitated for over 20 days at 25°C. , with periodic determinations of the solubility, in order to investigate the effects of isothermal agitation. For the alcohol and ketone, the solubility was constant after 4 days. No signs of instability had been noted in the alcohol solution after 24 days of continuous agitation; the ketone solution showed gas evolution only on the eighteenth day. The ester solution, however, never attained a constant solubility. An upward inflection point in the solubility-agitation-time curve was noted on the fourteenth day, along with the first evolution of gas. Afterward the solubility continued to increase until the twentieth day, when the gas pressure became great enough to break the cement seal. From the above it was concluded that equilibrium could be reached by isothermal agitation for all the solvents other than esters.

That equilibrium was attained by this method was actually demonstrated in the case of methyl isobutyl ketone by preparing four different solutions with varying proportions of solvent and nitrate. All yielded results which averaged at 42.20, the total spread being only 0.15.

The conventional method of approaching equilibrium from both a higher and a lower temperature was not applicable here because of the small change of the solubility with temperature. For isoamyl alcohol, methyl isobutyl ketone, methyl *n*-amyl ketone, and methyl *n*-hexyl ketone, the values at 25°C. and 35°C. differed by less than 0.5 per cent.

TABLE 1

Solubilities of thorium nitrate tetrahydrate in selected extraction solvents at 25°C. \pm 0.05°

SOLVENT	Th(NO ₃) ₄ PER 100 G. OF SOLUTION	AVERAGE VALUE
	<i>grams</i>	<i>grams</i>
Diisopropyl ketone	20.44 21.24	20.8
Acetophenone	37.05 37.08	37.06
Propiophenone	18.59 19.09 19.28 18.73	18.9
Methyl isobutyl ketone	42.13 42.28 42.18 42.20	42.20
Methyl <i>n</i> -amyl ketone	36.58 36.80 36.65 36.70	36.68
Methyl <i>n</i> -hexyl ketone	30.85 31.25 31.08	31.06
Isoamyl alcohol	37.85 37.80	37.8
<i>n</i> -Hexyl alcohol	33.64 33.36 33.15	33.4

RESULTS AND DISCUSSION

Sixty-five solvents were investigated in all. Table 1 lists the solubilities in eight solvents which are regarded as being promising extraction solvents, owing to their physical properties. These have been determined from two or more separate solution samples. Table 2 contains most of the other solvents besides esters which showed appreciable dissolving power for thorium nitrate tetrahy-

TABLE 2

Other solvents (excluding esters) showing appreciable solvent action on thorium nitrate tetrahydrate at 25°C. \pm 0.05°

SOLVENT	Th(NO ₃) ₄ PER 100 G. OF SOLUTION	SOLVENT	Th(NO ₃) ₄ PER 100 G. OF SOLUTION
	grams		grams
Acetone	59.3	<i>n</i> -Butyl alcohol	44.6
Methyl ethyl ketone	55.7	Isobutyl alcohol	39.9
Ethyl alcohol (absolute)	55.6	Cyclohexanol	35.9
Ethyl alcohol (95%)	56.0	Benzyl alcohol	20.9
Methyl alcohol	65.7	Diethyl ether	42.8
Ethylene chlorohydrin	44.4	Di- <i>n</i> -butyl ether	2.69, 0.53, 0.33*
<i>n</i> -Propyl alcohol	47.0	Diisoamyl ether	1.12, 0.14, 0.14*
Allyl alcohol	45.8	Dioxane	42.9
Isopropyl alcohol	44.4		

* Values determined 1, 2, and 4 days, respectively, after agitation was ceased.

TABLE 3

Solvents showing negligible solvent action on thorium nitrate tetrahydrate

SOLVENT	ThO ₂ PER 100 ML. OF SOLUTION
	grams
Methylene chloride	0.00
Chloroform	0.01
Carbon tetrachloride	0.05
Methylchloroform	0.01
Trichloroethylene	0.02
Ethylene dichloride	0.05
Ethyl bromide	0.02
<i>p</i> -Chlorotoluene	0.00
Chlorobenzene	0.03
Bromobenzene	0.00
Turpentine	0.04
Petroleum ether (four cuts), all below	0.03
2-Pentene	0.00
Benzene	0.00
Toluene	0.02
Tetrahydronaphthalene	0.00
Nitrobenzene	0.02
Aniline	0.04
Dimethylaniline	0.07
<i>o</i> -Toluidine	0.09
Piperidine	0.01
<i>m</i> -Cresol	0.10

drate. These values represent average values from determinations on single solution samples. Table 3 gives the solvents which showed negligible solvent action. Table 4 records the highest observed values for the esters and certain solvents which yielded very viscous solutions; it does not contain true equilibrium values.

Plots have been made of the solubility, within a homologous series of solvents, as a function of the number of carbon atoms in the solvent molecule. Figure 1 shows ketones and ethers, while figure 2 is for alcohols.

The oxygen-containing solvents, in general, dissolved thorium nitrate tetrahydrate appreciably, while the other solvents did not. Thus, the alcohols,

TABLE 4
Thorium nitrate solutions in esters and miscellaneous solvents

SOLVENT	HIGHEST OBSERVED QUANTITY OF Th(NO ₃) ₄ PER 100 G. OF SOLUTION	COMPOSITION OF SOLIDIFIED SYSTEM: PER CENT Th(NO ₃) ₄
	grams	
Ethyl formate	32.5	Solidified
Methyl acetate	Approx. 50.0	75.4
Ethyl acetate	43.4	Solidified
Ethyl propionate	67.1	70.08
Ethyl butyrate	56.9	62.26
Ethyl caproate	28.6	
Ethyl benzoate	6.3	
Ethyl phenylacetate	18.42	(Just before solidification)
Ethyl acrylate	12.6	Solidified
Methyl salicylate	2.4	
Ethylene glycol	44.4	Very viscous
Diethylene glycol	47.3	Very viscous
Hexamethylene glycol	13.5	Very viscous
Glycerol	45.6	Very viscous
Ethylene glycol monomethyl ether	59.2	Very viscous
Ethylene glycol monoethyl ether	54.6	Very viscous
Cyclohexanone	28.5	Solidified
Diethyl carbonate	8.88	Solidified
Isoquinoline	10.5	Solidified

ketones, esters, and ethers showed solvent action, while hydrocarbons, halogenated hydrocarbons, nitro compounds, and amino compounds did not. Exceptions are isoquinoline, which does dissolve, and *m*-cresol, which does not dissolve the nitrate.

The solution phenomenon apparently is dependent upon some property of the oxygen-containing grouping in the solvent molecule. Two generalizations may be drawn from the results. First, within a homologous series, the dissolving power decreases with increase in the molecular weight of the solvent. Secondly, the effectiveness of the dissolving group is decreased as the steric hindrance around it is increased.

The curve for the methyl ketones in figure 1 illustrates the decrease with in-

creasing molecular weight. The decrease due to steric hindrance may be seen from a comparison of diisopropyl ketone with methyl *n*-amyl ketone, which have equal molecular weights. In the case of acetophenone and propiophenone, steric hindrance again comes into play as the decrease caused by an additional $-\text{CH}_2-$ grouping is greater than that caused along the methyl ketone curve where the $-\text{CH}_2-$ is added at the more distant end of the molecule.

The ethers show a much greater decrease in dissolving power with increasing molecular weight than do other solvents. This would be expected, since the values are for a series of symmetrical ethers, the ether linkage being continually more "boxed in" from both sides as methylene groups are added. If a series

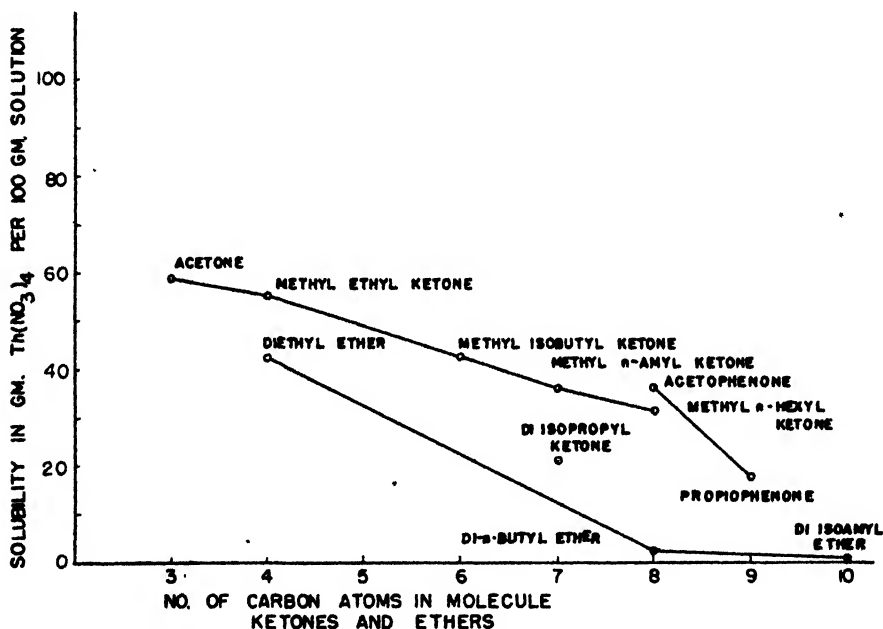


FIG. 1. Solubility of thorium nitrate in ketones and ethers as a function of the nature of the solvent molecule.

of methyl ethers were available, the expected decrease with increasing molecular weight should be less.

The decrease in dissolving power with increasing molecular weight for saturated normal alcohols may be seen in figure 2. The solubilities in the iso alcohols are in each case slightly less than those in their normal isomers. This also may be ascribed to steric hindrance, but when the number of carbon atoms in the alcohol molecule exceeds six, the difference becomes very small. In the latter case, the branching is probably too far away from the hydroxyl group to affect its properties appreciably.

Equilibrium solubilities were not attained for esters by this method, and in fact it appears to be possible to prepare by sufficient agitation a solution of

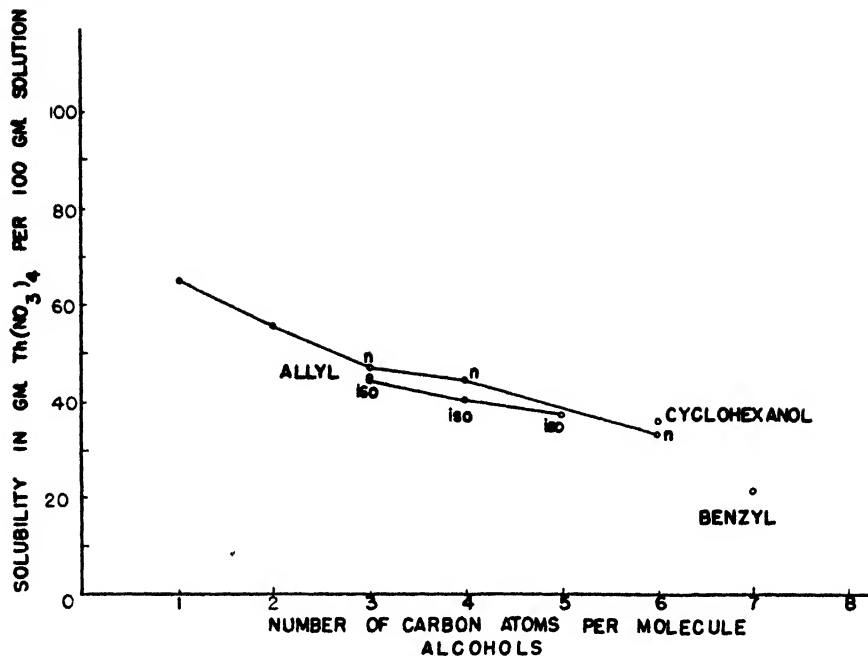


FIG. 2. Solubility of thorium nitrate in alcohols as a function of the nature of the solvent molecule.

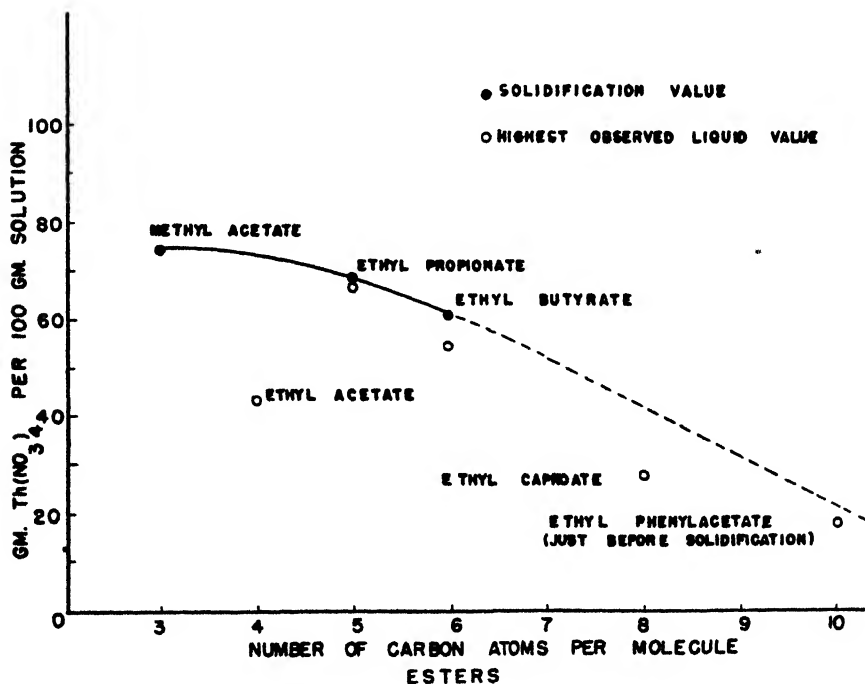


FIG. 3. Trends of the solubility of thorium nitrate in esters as a function of the nature of the solvent molecule.

thorium nitrate in an ester of any concentration up to that at which the entire system solidifies. Thus in figure 3 there have been plotted these solidification concentrations, as well as the highest observed liquid concentrations, of several ester solutions against the size of the solvent molecule. The curve represents the limit beyond which liquid solutions cannot be prepared. As this limit is approached, the solutions become very viscous and show large evolutions of gas. This instability is probably due to some mechanism involving the hydrolysis of the ester by the water of crystallization of the nitrate as a step.

Plots of all these data when expressed as mole ratios or mole fractions exhibit the same trends as those pointed out above for the data expressed as grams of thorium nitrate per 100 g. of solution.

Several glycols, glycol ethers, and other miscellaneous solvents were investigated but failed to give equilibrium solubilities, owing either to their solutions becoming unmanageably viscous or solid, or to their exhibiting very slow rates of solution.

A peculiar behavior was noted for the solutions in di-*n*-butyl and diisooamyl ethers. After the 5 days of agitation was over, the nitrate content of the solution decreased progressively during the first 4 days of standing. This has not been thoroughly investigated, and the highest values have been taken for the solubility comparisons.

A wide variety of side phenomena, such as precipitates, color changes, and gas evolution, have been noted for certain of the systems, after they have stood for long periods of time or undergone considerable agitation. These should be interesting subjects for separate investigations.

Other work on the solubilities of alkali, calcium, zirconyl, and rare earth nitrates in alcohols and ketones indicates that the use of higher alcohols or ketones (such as *n*-hexyl alcohol or methyl *n*-hexyl ketone) to extract thorium nitrate from aqueous solutions also containing the above cations has a definite probability of success. Work is in progress in this laboratory on such a process and also on the determination of the distribution expressions for thorium nitrate between water and these solvents.

SUMMARY

1. Oxygen-containing organic solvents will generally dissolve thorium nitrate tetrahydrate, while other organic solvents will not. Equilibrium may be attained in solutions in alcohols, ketones, and some ethers, but not in esters.

2. Dissolving power decreases with increasing molecular weight of the solvent, and with increased steric hindrance around the oxygen-containing group in the solvent molecule.

This research was supported in part by the Research Committee of the University of Wisconsin Graduate School from funds supplied by the Wisconsin Alumni Research Foundation. In the early phases of the work, Misses Beth Stube and Margaret Susor ably assisted in the analytical work.

OXIDATION OF ACETOIN

REFERENCES

- (1) HILLEBRAND: U. S. Geol. Survey Bull. **78**, 47 (1891).
- (2) IMRIE: Z. anorg. Chem. **164**, 214 (1927); **166**, 1-15 (1927)
- (3) MISCIATTELLI: Phil. Mag. [7] **7**, 670-4 (1929).
- (4) MISCIATTELLI: Gazz. chim. ital. **60**, 833-42 (1930).
- (5) WELLS: J. Washington Acad. Sci. **20**, 146-8 (1930).

COMMUNICATION TO THE EDITOR

A NOTE ON THE OXIDATION OF ACETOIN

Acetoin, acetylmethylcarbinol, exists at ordinary temperatures in the liquid state and in a solid (polymerized) form (Pound and Wilson: J. Phys. Chem. **39**, 1135 (1935)). It is known to oxidize to biacetyl. The solid polymer does not undergo oxidation in air or oxygen; one solid sample was kept for 227 days in oxygen (over mercury) without any diminution in the volume of the gas. The liquid acetoin, however, slowly and continually absorbed oxygen under these conditions. Three experiments were done, the liquid acetoin being initially spread out on filter paper at the top of the eudiometer, but in time the liquid condensed over the tube and on top of the mercury. The room temperatures

TABLE 1

FXPT.	ACETOIN	ORIGINAL GAS		AFTER DAYS	FINAL GAS			O ₂ AB-SORBED	O ₂ FOR BIACETYL FORMATION	EXCESS O ₂ / CO ₂
		O ₂	N ₂		O ₂	N ₂	CO ₂			
	grams	cc	cc.		cc.	cc.	cc.			
1....	0.196	58.5	12	1570	20.5	12		38	25	1.9
2 . . .	0.13	57.6	2.5	351	33.0	2.5	7.4	24.6	16.5	1.1
3	0.116	42.3	2.6	180	23.5	2.6	2.5	18.8	14.8	1.6
Biacetyl	0.2	60.4	10.4	52	42.8	10.4	7.5	17.6		2.3

varied from about 7° to 25°C. The gas volumes were reduced to N.T.P. without any correction for the vapor pressures of the organic liquids present.

The absorption of the oxygen is proportional to the time, though the rate slackens later, i.e., after 100 to 300 days; this initial absorption was approximately 0.085 cc. of oxygen per day. With sample No. 1 after various days the volumes of gas were (days, cc.): 0, 70.6; 100, 61.8; 200, 56.6; 400, 50.4; 600, 45.7; 1000, 42.0; 1400, 40.4; 1600, 39.6. With samples No. 2 and 3 the rate of absorption was just slackening from the initial linear rate in the times shown. As carbon dioxide was formed during the oxidation, the absorption of oxygen is more than the decrease in the volume of the gas. A sample of biacetyl oxidizing under the same conditions, the decrease in the gas volume being initially 0.28 cc. per day, formed ultimately 1 volume of carbon dioxide for 2.3 volumes of oxygen absorbed.

If the first action is the oxidation of the acetoin to biacetyl:



the second action may be



when the oxygen: carbon dioxide ratio by volume is 1.25:1. In the experiments with acetoin it is somewhat greater than this figure, and in the oxidation of the biacetyl it is twice this figure; but it is very probable that some biacetyl is oxidized to acetic acid, without the formation of carbon dioxide.

Undoubtedly the direct oxidation of acetoin proceeds beyond the stage of biacetyl by several reactions, which in these experiments were not further investigated.

JAMES R. POUND.

School of Mines
Ballarat
Victoria, Australia
July 23, 1947

NEW BOOKS

Characterization of Organic Compounds. By F. WILD. viii + 306 pp. Cambridge: The University Press, 1946. New York: The Macmillan Company, 1946. Price: \$3.75.

This book was written to summarize the methods and to give practical details for the preparation of suitable derivatives which are useful for the identification of organic compounds. The author is to be congratulated for this worthwhile contribution to the field of organic chemistry. The more important general methods described in the literature previous to 1946 have been summarized, and full experimental details for the preparation of the derivatives as well as the necessary reagents are described. The author discusses the advantages and disadvantages of the various methods and has included comprehensive tables for the derivatives of the more common organic compounds.

Since the book does not deal to any great extent with the other phases generally used in a systematic identification of organic compounds (i.e., solubility considerations, the classification reagents, etc.) it will not serve to replace other books in this field; however, it should find wide application not only for students but for those engaged in organic research work as well.

WILLIAM E. PARHAM.

Fatty Acids, Their Chemistry and Physical Properties. By K. S. MARKLEY. x + 668 pp. New York: Interscience Publishers, Inc., 1947. Price: \$10.00.

This is a comprehensive treatise on the organic chemistry, and physical properties, of the fatty acids and their derivatives. Even aliphatic amines are included, although these are not, in the usual sense, considered to be derivatives of fatty acids.

The main subdivisions of the book include an introduction dealing with the nature and history of fats and waxes; this is followed by sections on classification, nomenclature, and isomerism; physical properties (crystal properties, spectral properties, thermal properties,

solubility, properties in the liquid state); chemical reactions (salts, esterification, and inter-esterification, alkylation, pyrolysis, halogenation, hydrogenation and hydrogenolysis, oxidation and hydroxylation, autooxidation, biological oxidation, nitrogen derivatives, sulfur derivatives); synthetic methods—*in vitro* and *in vivo*; isolation, separation, and identification of individual fatty acids.

In connection with the presentation of the physical data, the author has made an effort to evaluate critically those in the literature although, as he says, this is a matter of some difficulty, for many of the data were recorded at a time when pure materials could not possibly have been available.

The reviewer thinks that the book suffers because of the obvious attempt at inclusiveness. Even very elementary organic chemistry of the acids is considered, and it would probably have made a more readable book if the writing had been directed toward the specialist who, presumably, already has a thorough knowledge of elementary organic chemistry. This tendency to go back to "first things" gets the author into difficulties once in a while—as, for example, on pages 431–2 where there is confusion as to the meaning of the terms geometric and optical isomers as applied to the dihydroxybehenic acids.

These are, however, minor criticisms and on the whole the book is well written. What is more, it is the only book of its kind published hitherto, and as such it will be of great value as a reference. There are good subject and author indexes.

The book-making is good. The work is attractively printed on good paper, and the binding is first rate.

LEE IRVIN SMITH.

Actions of Radiations on Living Cells. By D. E. LEA. 400 pp. London: Cambridge University Press, 1947. Price: \$4.50.

The effect of radiation on living cells is a subject of fundamental importance in medicine, biology, and genetics. The author shows full recognition of the necessity of understanding the underlying principles of physics, chemistry, and biology in approaching his subject. Thoroughly equipped with this knowledge, he has applied it with admirable effectiveness.

The book is intended for the student and research worker rather than for the radiologist or practitioner. Nevertheless, much of the data and other material would be of great practical use in the hands of one equipped to understand and apply it.

After discussing the physical properties and the chemical effects of various ionizing radiations, the possible mechanism of biological action is presented. Detailed attention is given to the genetic effects, to the structural changes produced in chromosomes by radiation, to mutation, and to lethal effects.

It is with great regret that one learns of the recent untimely death of the author. It is fortunate that he leaves this splendid work which, quite beyond its direct usefulness, is a monument to his genius and a guide for future progress.

S. C. LIND.

The Terpenes. Vol. I. By J. L. SIMONSEN AND L. N. OWEN. Second edition. x + 479 pp. Cambridge: The University Press; New York: The Macmillan Company, 1947. Price: \$6.50.

This is the first volume of the second edition of a standard work—indeed, about the only comprehensive work—covering the field of the terpenes. Sixteen years have elapsed since the first edition of the work appeared, and in the intervening times much work in the field has been done. The plan and scope of the second edition follow closely those of the first. In fact, this may be considered more of a reprinting, with some additions, of the first edition than a truly new edition, for many of the sections are merely reprints of those occurring in the first edition. The literature "has been consulted up to the end of 1945, and it has proved possible to include also some work of a later date."

This edition is a much better job of book making than was the original edition. Although

the new Volume I contains some 50 pages more than the old, it is about half as thick; the quality of the paper and the binding are much improved. There are author and subject indexes.

LEE IRVIN SMITH.

Essays in Rheology. vii + 103 pp. New York: Pitman Publishing Corporation, 1947. Price: \$3.00.

This little book is a compilation of a series of papers presented at the 1944 Oxford Conference of the British Rheologists Club. The Club was established in 1940 under the presidency of Professor Sir Geoffrey Taylor for the discussion of problems relating to the deformation and flow of matter.

The first chapter, "The Rheology of Metals, Polymers and Liquids," was prepared by G. W. Scott Blair on the basis of papers read by E. Orowan ("The Plasticity of Metals"), R. F. Tuckett ("The Rheology of Polymers"), and A. G. Ward ("The Liquid State"). The present status of inquiry in these fields is reviewed in a simple and easily understandable form, with emphasis on the descriptive and qualitative aspects, rather than on the more difficult mathematical and physical aspects, although the latter receive adequate attention for a book of this scope.

Other interesting chapters include "The Relationship Between Compression and Shear Tests"; "The Time Variations of Stress and Strain"; "Rheological Nomenclature and Symbols"; "Theology and Medical Science"; "Rheology and Naval Problems"; "Rheology in the Fine Arts." An appendix on the "Ordinate Method of Exponential Analysis" should prove useful for those interested in the quantitative analysis of relaxation phenomena.

This easily readable little book is a contribution of value not only for the specialist, but also for the non-specialist who wishes to orient himself in the field of rheology.

JOHN G. KIRKWOOD.

Handbook of Chemistry. By N. A. LANGE. Sixth edition. xiv + 1767 + 271 pp. of mathematical tables and formulas. Sandusky, Ohio: Handbook Publishers, Inc., 1946. Price: \$7.00.

The first edition of this book was published in September, 1934, and contained 1556 pages. The present edition contains 2038 pages of material of use to chemists with 16 pages of prefaces, acknowledgments, and table of contents, and an index of 28 pages.

In order to appreciate the extent of the material in this sixth edition and the care and work required to get this material together, one must spend many hours browsing through the book. After these hours have been well spent, the reader will come to the conclusion that Lange's *Handbook of Chemistry* is to the chemist what the unabridged edition of the dictionary is to the student of English literature. To compile a book of the scope of this handbook without error would not fall within the realm of probability, but one has to search diligently to find errors. For instance, on p. 662 the compound vinylamine, $\text{CH}_2 \cdot \text{CH} \cdot \text{NH}_2$, is listed, and a footnote is given that this product is actually ethylene imine, $\text{CH}_2 \cdot \text{CH}_2 \cdot \text{NH}$.

The formula for this latter compound should be written $\text{CH}_2 \cdot \text{CH}_2 \cdot \text{NH}$. The compound vinylamine has not been prepared and should be omitted from the list of organic compounds. The printing, the paper, and the binding are excellent.

H. H. BARBER.

Methods of Vitamin Assay. Prepared and edited by the Association of Vitamin Chemists, Inc. 189 pp. New York: Interscience Publishers, Inc., 1947. Price: \$3.50.

This book admirably fills the need for a compilation of tested methods of vitamin assay applicable to and tested with a great variety of materials. As stated in the preface, "the methods described here are the result of the pooling and interchange of information on analytical technics, and thus represent the combined knowledge and experience of many persons. Only such methods have been included as have been successfully applied to a

variety of foods and other materials by several committee members." As a result of such collaborative effort the methods given can be used with confidence. In addition, various sections of the book have been reviewed by men in whose laboratories analytical work on the various vitamins is in progress.

The first chapter deals with sampling for vitamin analyses. One chapter each is devoted to the following: calorimetric and ultraviolet absorption methods for vitamin A; chromatographic and solvent partition methods for physiologically active carotinoids; thiochrome and fermentation methods for thiamine; fluorometric and microbiological methods for riboflavin; microbiological method for niacin; visual titration method and colorimetric methods with 2,6-dichlorophenolindophenol and 2,4-dinitrophenylhydrazine, respectively, for ascorbic acid. For each of the various methods one procedure is outlined in great detail, including sample calculations. Comments on individual steps are extensively interspersed between the directions for the various manipulations of the procedures. At the end of each chapter there is a brief section on the applications of the given methods to various biological materials, followed by a selected bibliography. Methods of bioassay for vitamins have apparently been purposely omitted from this volume. Methods for vitamins D, E, K, for biotin, folic acid, *p*-aminobenzoic acid, inositol, choline pantothenic acid, and pyridoxine are referred to only through a selected bibliography.

The methods presented in this volume are given in such detail that personnel with relatively limited analytical training should be able to apply them for routine work. Few errors or misprints have been noted: on p. 100 the statement that "riboflavin is reversibly reduced to a leuco base, a *dehydro compound*," should be corrected to read "a dihydro compound"; on p. 119 reference (48) is given to an important paper by Strong but this reference is not included in the bibliography.

In view of the extensive use of photometric and spectrophotometric measurements in the methods published, a brief discussion of photometry and spectrophotometry would be a desirable addition to this book. Also, in the section on the chromatography of carotinoids it would be well to state clearly the relative position on the adsorption column of the various carotinoids:

Methods of Vitamin Assay is well organized and clearly written. It should be available in every laboratory where work on vitamins is in progress. It is to be hoped that future editions of this book will include methods on other vitamins.

M. O. SCHULTZE.

Monographs on the Progress of Research in Holland. The Wet Purification of Coal Gas and Similar Gases by the Staatsmijnen Otto Process. By H. A. PIETERS AND D. W. VAN KREVELLEN. 55 pp. Amsterdam and New York: The Elsevier Publishing Company, Inc., 1947. This volume is No. 15 in a series of Monographs on the Progress of Research in Holland During World War II.

This book deals with past and current methods of removing hydrogen sulfide from manufactured gases and presents developments of the Otto process, which uses an ammonium hydroxide solution as a scrubbing medium plus a newly employed method of regeneration of elemental sulfur from the hydrogen sulfide so removed from the gas.

In eight chapters it presents, successively, a review of liquid purification processes, with comparative flow diagrams; a description of the Staatsmijnen-Otto process; the constitution and properties of the iron cyanide complex which is employed as the catalyst or oxygen carrier in the second stage of the S.M.O. process, for the conversion of the HS^- ion to sulfur and H^+ ions; the general principles of gas absorption largely as outlined in T. K. Sherwood's *Absorption and Extraction* (1937); experimental data and discussion of the velocity of absorption of hydrogen sulfide in the S.M.O. process; a discussion of the velocity of oxidation of the absorbed hydrogen sulfide, in terms of the HS^- concentration, the concentration of the catalyst, the oxygen pressure, and the concentration of dissolved salts $[(\text{NH}_4)_2\text{SO}_4, \text{NH}_4\text{Cl}]$ in the absorption medium, with a comparison of laboratory and industrial plant values for capacity factors; a discussion of by-reactions leading to polysulfide, thiocyanate

and to thiosulfate in terms of the operating variables; and a summary of results and conclusions together with a tabulation of results obtained on oven gas at an industrial installation at Tetre, Belgium. A bibliography of literature on the liquid purification of gas follows Chapter 1.

The description of the S.M.O. process as applied is good. The composition of the oxidation catalyst—"Prussian blue"—is complete, with lattice diagrams illustrating Prussian blue and Prussian white; a coagulated suspension of the two serves as the actual catalyst. The theoretical discussion of the principles of absorption is adequate, although the authors' contributions to the whole theory might have been more clearly indicated. They state, "... our own experiments have enabled us to derive dimensionless relations with the aid of which the values of the transfer coefficients can be calculated (Tables 5 and 6)" and on the rate of absorption of the hydrogen sulfide they summarize as follows: "the absorption effect rises with

- (a) increasing ammonia and decreasing salt concentration of the solution;
- (b) increasing irrigation (liquor flow) and decreasing gas velocity;
- (c) increasing height of the washer.

The temperature has only a slight effect."

They state that "for every experiment the values of k_1 and k_e in the general relations

$$N = K_g A (P_g - P_1)_m$$

$$\frac{1}{K_g} = \frac{1}{k_g} + \frac{1}{H k_1}$$

$$k_g = 0.1 \frac{D}{d} \left(\frac{u d q}{n} \right)^{0.8} \left(\frac{n}{q D} \right)^{1/3}$$

$$k_1 = k_e C_1 \left(\frac{1 q}{a n} \right)^{0.75} \left(\frac{n}{q D} \right)^{1/2}$$

were derived and summarized in Table 7, p. 32. As a mean value we found:

$$k_e = 8 \times 10^{-5} \text{ kmol}^{-1} \text{ sec}^{-1} \text{ m}^4$$

For technical washers the constants C_1 and k_e are mostly smaller (2 to 5 times) than for laboratory scrubbers, as a result of insufficient wetting and channelling effects of the liquid in big scrubbers."

Relative to reaction rate ("oxidation velocity") of the oxidation of the hydrogen sulfide, the authors summarize in these words: "The time of oxidation is directly proportional to the initial concentration of HS' ions and inversely proportional to the partial oxygen pressure; it increases with the salt content of the solution (decreasing H), with the temperature (decreasing H), when the diameter (d) of the bubbles increases, and when the quantity of air (u) which passes through the aerator diminishes; it is not dependent on the concentration of the suspended 'white', and 'the time of oxidation as a function of the temperature is characterized by a minimum at 30°C. This can be explained as follows: Below 10°C. the HS' is oxidized to S . Between 10 and 30°C. a secondary reaction occurs (the formation of polysulphide and its oxidation to thiosulphate) which draws part of the HS' from the main reaction with the result that the time of oxidation diminishes. At 30°C. the influence of the secondary reaction has reached a maximum. Above that temperature the time of oxidation increases with the temperature in agreement with our theory.

"The products of the parasitic secondary reactions (formation of thiosulphate and sulphocyanate) are derived from polysulphide which in its turn is the reaction product of

¹ The value of the dimensionless constant C_1 was derived from separate experiments on the absorption of ammonia in dilute sulfuric acid.

ammonium sulphide and sulphur. In those parts of the S.M.O. installation where the liquid is in the reduced state (i.e., in the washer, the tanks and part of the aerator) so that the HS' ions can react with finely divided sulphur, polysulphide is formed" and "polysulphide solutions greedily absorb oxygen. The oxidation product is thiosulphate. This means the degradation of a corresponding quantity of sulphur which we want to minimize."

"The oxidation is not only limited to the polysulphide but (especially at low P_H values) the HS' is involved as well. Experiments proved that in the absence of polysulphide, HS' is involved as well. Experiments proved that in the absence of polysulphide, HS' is much less sensitive to oxygen. This is obviously a case of induced oxidation."

The reactions of the cyanide ion with polysulfide, thiosulfate, and nascent sulfur are discussed, but the authors project the separate removal of hydrogen cyanide.

The summary provides quantitative values for the power factors, services, and efficiency of hydrogen sulfide removal suitable for cost estimations. Metric units are used throughout the book.

R. L. BROWN.

Microcalorimetry. By W. SWIETOSLAWSKI. x + 199 pp.; 56 fig. New York: Reinhold Publishing Corporation, 1947.

Microcalorimetry is the measurement of small amounts of heat in which the temperature change or the rate of temperature change of the calorimeter is very small. While this book reviews the whole field of microcalorimetry, the work of the Institute of Technology in Warsaw, Poland, where the author was Professor of Physical Chemistry before World War II, is described in greater detail. Professor Swietoslawski is not as well known in this country for his work in microcalorimetry as for his work in ebulliometry and the comparative method of measurement by which properties are determined by comparison with standard substances. Because of the considerable work in the field of microcalorimetry by Professor Swietoslawski and his colleagues, this volume will be especially interesting and valuable to those concerned with calorimetry.

This book covers methods of microcalorimetry rather than results. Types of microcalorimeters are discussed, among them twin calorimeters, the Bunsen ice calorimeter, the adiabatic calorimeter, and a labyrinth flow calorimeter. Accessories, such as thermostats, calorimeter jackets, and thermometers, and methods of correction for heat losses are included. Applications to some important problems are discussed also. The application discussed most extensively is to the measurement of the energy of radioactive radiations, including α -, β -, and γ -rays. There is a bibliography of about 200 references at the end of the book.

F. G. BRICKWEDDE.

SUBJECT INDEX

- Acetoin, oxidation of, 1449
- Acetone, moist, conductivity of some salts in, 708
- Acetylene, polymerization by bombardment with charged particles, 654
- Acetylmethylcarbinol, vapor pressure and heat of vaporization of, 480
- Adsorption equilibria of liquid mixtures of carbon tetrachloride-methanol with charcoal, 1172
 - of gases on porous glass, 1248
 - of gases on surfaces of powders and metal foils, 1232
 - isotherms of carbon tetrachloride-methanol vapors on activated charcoal, 1154
 - of nitrogen at low temperatures and high relative pressures, 1262
- Air bubbles, rise in lubricating oils, 431
- Albumin, serum, mandelate as stabilizer of, 229
- Aluminum, aluminum oxide films on, 1087
- Aluminum dilaurate, as association colloid in benzene, 974
 - oxide, colloidal, 768
 - soaps, 963
- Amino acids, solubility in aqueous solutions
 - of amino acids and peptides, 648
 - acid systems, solubility relations in, 648
- Amylose, helical structure of, 107
- Amylose acetate, ultracentrifugal studies of, 107
 - acetate, viscometric studies of, 107
- Aniline, catalytic oxidation in the vapor phase, 1394
- Aniline formate, changes on storage, 378
- Antoine vapor-pressure equation for mononuclear aromatic hydrocarbons, 528
- Argon, adsorption on porous glass, 1248
- Association, molecular, effect on gelation of pectin, 117
 - of polymer molecules in dilute solution, 32
- Attapulgite, colloid chemistry of, 311
- Balance, sorption. *See* Sorption balance
- Bases, organic, strengths of, 1028
- Benzoyl peroxide, decomposition of, 926, 942
 - peroxide, kinetics of decomposition in benzene, 926
 - peroxide, rates of decomposition in various solvents, 942
- Blood, clotting of, protein interactions in, 198
- Bond energy in diatomic molecules, 407
- Boron trichloride, coordination compounds of, 1400
 - trichloride, coordination compounds with propyl chlorides, 425
- Boundaries, phase, in sodium oleate-water systems, 797
 - sharp, method for formation in diffusion experiments, 816
- Butane, adsorption on porous glass, 1248
- Cadmium, kinetics of dissolution in hydrochloric acid, 857
- Calcium chloride, concentrated solutions of, E.M.F. and conductance measurements in, 704
- Carbon blacks, surface-area measurements on, 1329
 - tetrachloride-methanol, adsorption isotherms on charcoal, 1154
 - tetrachloride-methanol, liquid mixtures with charcoal, adsorption equilibria of, 1172
- Cavitation in absence of gas nuclei, 556
- Cellulose (wood), hydrolysis in dilute phosphoric acid, 1430
- Cellulose acetate, relation of molecular weight to viscosity, 58
 - molecule, physical chemistry of, 1
- Charcoals, adsorption by, 1232, 1248, 1262, 1276, 1308, 1329
 - measurements of surface area on, 1329
 - pores in, alteration of distribution of, 1276
 - pore size in, alteration of, 1276
 - surface complexes on, 1308
- Chlorophyll, in sensitization of photooxidation of phenylhydrazine by methyl red, 775
- Chrome tanning, nature of, 1181
- Chromic oxide-ferrous oxide system, x-ray diffraction studies in, 521
- Clay mineral, attapulgite, colloid chemistry of, 311
- Collodion membranes, permselective, electrochemistry of, 299
- Colloid, association, aluminum dilaurate as, 974

- Colloidal dispersions, effect of freezing on stability of, 415
- Colloids, lyophobic, theory of stability of, 631
- Conductivity of salts in moist acetone, 708
- Coördination compounds of boron trichloride, 1400
- compounds of boron trichloride with propyl chlorides, 425
- Coprecipitation, 483
- Corrosion of lead by solutions of organic acids in hydrocarbon solvents, 681
- Crystallization, induction period of, 382
- Crystals, liquid, surface tension of, 826
- oxygen-containing, energy additivity in, 438
- Cyanogen, polymerization by bombardment with charged particles, 654
- Detergents, anionic, effect of temperature on critical concentrations of, 1143
- cationic, effect of temperature on critical concentrations of, 1143
- solubilization of dyes by, 286
- Diffusion experiments, method for formation of sharp boundaries in, 816
- theory, a generalization in, 1063
- in wood, 240
- Dipole moment, relation to formation of coördination compounds, 1400
- Discoloration of halogen-containing polymers, theory for, 80
- Dispersions, colloidal, effect of freezing on stability of, 415
- non-aqueous, dielectrics and rheology of, 1037
- Dye ions, spectral changes in, relation to the protein error in indicators, 666
- Dyes, water-insoluble, solubilization by soaps and detergents of different types, 286
- Elasticity of polychloroprenes, measurement of, 70
- Electrodes, membrane, use in study of soap solutions, 636
- Electrokinetic potentials of precipitates, 321
- Electrolytes, colloidal, micelle structure in aqueous solutions of, 262
- Electron microscope, in observation of morphology of gases polymerized by charged-particle bombardment, 654
- Electrophoretic patterns of proteins, quantitative interpretation of, 171
- Energy additivity in oxygen-containing crystals and glasses, 438
- Erosion of steel by hot gases under pressure, 1404
- Explosives, propellant, thermochemistry of, 580
- Fetuin, electrophoretic studies on, 164
- ultracentrifugal studies on, 164
- Flow systems, kinetics of gaseous reactions in, 505
- Fluids, anomalous, application of constant shearing motion to, 751
- Foaming capacity of alpha soybean protein dispersions, effect of electrolytes on, 661
- Formaldehyde, reaction with urea, kinetics of, 369
- Gases, adsorption on porous glass, 1248
- adsorption on surfaces of powders and metal foils, 1232
- polymerization by charged-particle bombardment, 654
- Gastropods, hemocyanins of, 206
- Gel, silica. *See* Silica gel
- Glass (porous), adsorption of gases on, 1248
- Glasses, oxygen-containing, energy additivity in, 438
- Heat of combustion of nitroglycerin, 593
- Hemicellulose fractions, molecular properties of, 134
- Hemocyanins of Gastropods, 206
- Hormone, pituitary growth, electrophoretic patterns of, 218
- pituitary growth, physicochemical characteristics of, 218
- Hydrocarbons, aromatic, Antoine vapor-pressure equation for, 528
- Hydrogen cyanide, polymerization by bombardment with charged particles, 654
- Hydroxides, alkali metal, preparation by electrolysis, 967
- Indicators, protein error in, 666
- Indium, chemistry of, 771
- Influenza virus, sedimentation constants of, 148
- Interface, liquid, unusual, 567
- Interfacial tension by the ring method, 1341
- Iodine, sorption on magnesium oxide, 981
- Lead, rate of corrosion by hydrocarbon solutions of organic acids, 681

- Light, scattering of, determination of molecular weight by, 18
- Lipoprotein, low-density, in human plasma, 156
- Liquids, free-volume models for, 1219
 - heat of evaporation of, relation to surface tension, 747
 - organic, amphipathic, equilibrium spreading coefficient on water, 359
 - surface tension, relation to heat of evaporation, 747
- Lithium perchlorate, osmotic and activity coefficients at 25°C., 516
- Lyogels, morphology of, 278
- Magnesia, active, determination of surface areas of, 763
- Magnesium indate, formation of, 771
- Mandelate, as stabilizer of serum albumin, 229
- Manganese, adsorption on hydrous ferric oxide, 956
- Melting point, as function of particle size, 382
- Membranes, collodion, as electrodes in study of soap solutions, 636
 - collodion, permselective, electrochemistry of, 299
- Metal foils, adsorption of gases on surfaces of, 1232
- Micelle structure in aqueous solutions of colloidal electrolytes, 262
- Milk, proteins of, spectroturbidimetric study of, 460
- Molal volumes of aqueous solutions of perchloric acid, 1369
- Molecular weight, determination by light scattering, 18
 - weight, determination by longitudinal dispersion of infrared rays, 875
 - weight, determination from ultracentrifuge data, 1204
- Neoprene latex, coagulation by freezing, 451
- latex, thickening at low temperatures, 443
- Nitrocellulose, molecular heterogeneity of, 574
 - molecular properties of, 569, 574
 - thermochemical constants of, 593
 - viscosity of, 569
- Nitrogen, adsorption at low temperatures and high relative pressures, 1262
 - adsorption on porous glass, 1248
- Nitroglycerin, heat of combustion of, 593
- Oils, lubricating, rise of air bubbles in, 431
- Organic compounds, solubility of, interpretation on an electronic basis, 837
- Organosols, lyophobic, anhydrous conditions in the preparation of, 1103
- Osmometry, dynamic, 474
- Oxidation, catalytic, of aniline in the vapor phase, 1394
- Particles, formation and growth of, 1004
- Particle size, solubility and melting point as functions of, 382
- Pectic acid, x-ray diffraction study of, 710
- Pectin, gelation of, effect of molecular association and charge distribution on, 117
- Pectinic acid, x-ray diffraction study of, 710
- Perchloric acid, molal volumes of aqueous solutions of, 1369
- Phase boundaries in concentrated systems of sodium oleate and water, 797
- Phenylhydrazine, photooxidation by methyl red, sensitization by chlorophyll, 775
- Phosphoric acid, in hydrolysis of wood cellulose, 1430
- Pigments, plant, biochemistry of, 1078
- Pituitary growth hormone, physicochemical characteristics of, 218
- Plant pigments, biochemistry of, 1078
- Plasma, human, lipoprotein of low density from, 156
 - human, proteins of, physical-chemical characteristics of, 184
 - human, X-protein from, 156
- Plasma proteins (human), physical-chemical characteristics of, 184
- Polychloroprenes, elasticity measurements on, 70
- Polymer molecules, association in dilute solution, 32
- Polymers, formation from gases by bombardment with charged particles, 654
 - fractional precipitation of molecular-weight species from, 721
 - halogen-containing, statistical theory of discoloration for, 80
- Polystyrenes, longitudinal dispersion of infrared rays in, 868
- Potentials, electrokinetic, of precipitates, 321
- Powders, adsorption of gases on surfaces of, 1232
- Precipitates, aging of, 483
 - electrokinetic potentials of, 321

- Propellant explosives, thermochemistry of, 580
- Proteins, electrophoretic patterns of, quantitative interpretation of, 171
interaction in clotting of blood, 198
- Proteins of milk, spectroturbidimetric study of, 460
of plasma (human), physical-chemical characteristics of, 184
- Radiation, high-energy, effect on organic compounds, 786
- Radiation chemistry, 611
- Radioactive substances, tolerance concentrations of, 984
transformations and unimolecular reactions, 513
- Radiomanganese 54, properties of radiation from, 956
- Rays, infrared, longitudinal dispersion in polystyrenes, 868
infrared, longitudinal dispersion in turbid media, 875
- Reaction mechanisms, mathematical approach to, 540
- Reactions (gaseous) in flow systems, kinetic of, 505
unimolecular, and radioactive transformations, 513
- Resins, ion-exchange, rates of anion exchange in, 1111
- Rheology of non-aqueous dispersions, 1037
- Rubber dispersions, synthetic, stability of, 443, 451
- Sedimentation constants of influenza virus, 148
- Serum albumin, stabilization with mandelate, 229
- Shearing motion, application to anomalous fluids, 751
- Silica gel, sorption-desorption characteristics of, effect of heat treatment on, 333
sols, effect of freezing on stability of, 415
- Silver, colloidal, catalytic activity in reduction of silver acetate, 1130
- Silver acetate, catalytic activity of colloidal silver in reduction of, 1130
acetate solutions, equilibria in, 1346
bromide powders, compressibility of, 483
cyanide, solubility of, mathematical relations involving, 1375
halide, particles of, size-frequency determination of, 1004
- Soaps, aluminum, moisture content of, 963
aluminum, water sorption by, 963
rates of solution in water, 391
solubilization of dyes by, 236
- Soap solutions, membrane electrodes in study of, 636
- Sodium oleate-water systems, phase boundaries in, 797
pectinates, electrophoretic mobilities of, 1137
pectinates, fractionation of, 1137
perchlorate, osmotic and activity coefficients at 25°C., 516
stearate, phase behavior in anhydrous organic solvents, 1189
- Solid solutions, shape of heat-capacity and equilibrium cooling curves in the region of melting of, 1361
- Sols, silica, effect of freezing on stability of, 415
- Solubility, as function of particle size, 382
- Solubility of amino acids in aqueous solutions of amino acids and peptides, 648
of organic compounds, electronic interpretation of, 837
of paraffin-chain compounds, 891
of silver cyanide, mathematical relations involving, 1375
of thorium nitrate tetrahydrate in organic solvents, 1441
- Sorption balance, McBain-Bakr, heat guard for, 972
balance, McBain-Bakr, in study of sorption of iodine on magnesium oxide, 981
-desorption characteristics of silica gel, effect of heat treatment on, 333
- Soybean, alpha protein from, effect of electrolytes on foaming capacity of, 661
- Spectrophotometer, photoelectric, 903
- Spectrophotometry, photoelectric, 903
- Spreading coefficient, equilibrium, of amphipathic organic liquids on water, 359
- Steel, chemical erosion by hot gases under pressure, 1404
- Sugar, decomposition in dilute phosphoric acid, 1430
- Surface area, determination by point *B* method, 644
area, measurement on metal spheres and carbon blacks, 1329
tension of liquid crystals, 826
- System ferric oxide-chromic oxide, x-ray diffraction studies in, 521

- Tanning, chrome, nature of, 1181
Thorium nitrate tetrahydrate, solubility in
organic solvents, 1441
Ultracentrifuge data, in determination of
molecular weights, 1204
Urea, reaction with formaldehyde, kinetics
of, 369
Virus, influenza, sedimentation constants
of, 148
Viscosity-molecular weight relationship for
cellulose acetate, 58
Wood, diffusion in, 240
dimensional stabilization of, 493
Zinc chloride, concentrated solutions of,
E.M.F. and conductance measurements
in, 704

AUTHOR INDEX

- ALEXANDER, MARY. *See* Corbin, Nancy
- ANDERSON, DON H. Some properties of the radiation from radiomanganese 54 and the adsorption of manganous manganese on hydrous ferric oxide, 956
- ANDERSON, ROBERT B., AND EMMETT, P. H. Surface complexes on charcoal. Gas evolution as a function of vapor adsorption and of high-temperature evacuation, 1308
- ANTONOFF, GEORGE. On unimolecular reactions and radioactive transformations, 513
- ARCHIBALD, W. J. A demonstration of some new methods of determining molecular weights from the data of the ultracentrifuge, 1204
- BADGER, RICHARD M. *See* Blaker, Robert H. *See* Doyle, George J.
- BADGLEY, W. J., AND MARK, H. Viscosity-molecular weight relationship for cellulose acetate, 58
- BALLANTYNE, M. *See* Palmer, K. J.
- BANCROFT, WILDER D. The biochemistry of plant pigments, 1078
- BARNETT, BENJAMIN, AND VAUGHAN, WILLIAM E. The decomposition of benzoyl peroxide. I. The kinetics and stoichiometry in benzene, 926
- AND VAUGHAN, WILLIAM E. The decomposition of benzoyl peroxide. II. The rates of decomposition in various solvents, 942
- BECKMANN, CHARLES O. *See* Dombrow, Bernard A.
- BIGEISEN, J. The molal volumes of aqueous solutions of perchloric acid, 1369
- BLAKER, ROBERT H., BADGER, RICHARD M., AND NOYES, RICHARD M. Molecular properties of nitrocellulose. II. Studies of molecular heterogeneity, 574
- BLINKS, L. R. *See* Pease, Daniel C.
- BLOM, RUSSELL H. *See* Efron, Aaron
- BONDI, A. On the solubility of paraffin-chain compounds, 891
- BOYER, R. F. A statistical theory of discoloration for halogen-containing polymers and copolymers, 80
- BROHULT, SVEN. Hemocyanins of the Gastropoda, 206
- BROWN, A. *See* Oncley, J. L.
- BROWN, O. W., AND FRISHE, W. C. Catalytic oxidation of aniline in the vapor phase, 1394
- BURR, H. K., AND STAMM, ALFRED J. Diffusion in wood, 240
- BURTON, MILTON. Effect of high-energy radiation on organic compounds, 786
- Radiation chemistry, 611
- CALDWELL, O. G. *See* Marshall, C. E.
- CARR, C. W., JOHNSON, W. F., AND KOLTHOFF, I. M. The use of membrane electrodes in the study of soap solutions, 636
- CARVER, EMMETT K., AND VAN WAZER, JOHN R. The sudden application of a constant shearing motion to anomalous fluids, 751
- CINES, MARTIN. *See* Emmett, P. H.
- COAD, KIETH. *See* Reyerson, L. H.
- COOK, MELVIN. Bond energy in diatomic molecules from the force constants, nuclear distances, and classical model theory, 407
- COPLEY, M. J. *See* Speiser, R.
- CORBIN, NANCY, ALEXANDER, MARY, AND EGLOFF, GUSTAV. The Antoine vapor-pressure equation for mononuclear aromatic hydrocarbons, 528
- CUPPLES, H. L. Interfacial tension by the ring method: the benzene-water interface, 1341
- DAVIS, R. T., JR., DEWITT, T. H., AND EMMETT, P. H. Adsorption of gases on surfaces of powders and metal foils, 1232
- DEBYE, P. Molecular-weight determination by light scattering, 18
- DE WIJS, J. C. Note on the relation between the heat of evaporation and the surface tension of liquids, 747
- DEWITT, T. H. *See* Davis, R. T., Jr.
- DOMBROW, BERNARD A., AND BECKMANN, CHARLES O. Ultracentrifugal and viscometric studies of amylose acetates. Further evidence for the helical structure of amylose, 107
- DOTY, PAUL, WAGNER, HERMAN, AND SINGER,

- SEYMOUR. The association of polymer molecules in dilute solution, 32
- DOYLE, GEORGE J., HARBOTTLE, GARMAN, BADGER, RICHARD M., AND NOYES, RICHARD M. Molecular properties of nitrocellulose. I. Studies of viscosity, 569
- DUNN, MAX S. *See* Sexton, Edwin L.
- DUNN, R. C., AND POMEROY, H. H. A vapor-phase sorption study of iodine and active magnesium oxide utilizing the McBain-Bakr sorption balance, 981
- EFRON, AARON, AND BLOM, RUSSELL H. Vapor pressure and heat of vaporization of acetylmethylcarbinol, 480
- EGLOFF, GUSTAV. *See* Corbin, Nancy
- EMMETT, P. H., AND CINES, MARTIN. Adsorption of argon, nitrogen, and butane on porous glass, 1248
- AND CINES, MARTIN. Surface-area measurements on metal spheres and on carbon blacks, 1329
- See* Anderson, Robert B.
- See* Davis, R. T., Jr.
- See* Holmes, James
- EVANS, R. C., HORN, F. HUBBARD, SHAPIRO, ZALMAN M., AND WAGNER, RICHARD L. The chemical erosion of steel by hot gases under pressure, 1404
- FARRELLY, R. O. *See* Robinson, R. A.
- FREY, DELTON R. *See* Turnbull, David
- FRISHE, W. C. *See* Brown, O. W.
- GHOSH, SATYESHWAR. *See* Krishna, Bal
- GOLDBLUM, K. B. Notes on dynamic osmometry, 474
- GREEN, AGNES ANN, AND MCBAIN, JAMES W. Solubilization of water-insoluble dye by pure soaps and detergents of different types, 286
- GREGOR, HARRY F. *See* Sollner, Karl
- GULBRANSEN, EARL A., AND WYSONG, W. S. Thin oxide films on aluminum, 1087
- GUSTAVSON, K. H. Experimental arguments against the concept of chrome tanning as an adsorption process, 1181
- HALL, C. R. L. *See* Taylor, James
- HALL, NORRIS F. *See* Templeton, C. C.
- HALLER, HARRISON S. *See* Leviton, Abraham
- HARBOTTLE, GARMAN. *See* Doyle, George J.
- HARBURY, LAWRENCE. Solubility and melting point as functions of particle size. II. The induction period of crystallization, 382
- HARRIS, ELWIN E., AND LANG, BILL G. Hydrolysis of wood cellulose and decomposition of sugar in dilute phosphoric acid, 1430
- HARRIS, G. M. Kinetics of homogeneous gaseous reactions in flow systems, 505
- HAUSER, ERNST A., AND LE BEAU, D. S. The morphology of lyogels, 278
- HAZEL, FRED. Effect of freezing on the stability of colloidal dispersions. Silica sols—a preliminary report, 415
- See* Perri, Joseph M., Jr.
- HEYMANN, E., AND YOFFE, A. The equilibrium spreading coefficient of amphipathic organic liquids on water, 359
- HILDEBRAND, J. H. *See* Olson, A. R.
- HILL, TERRELL L. Free-volume models for liquids, 1219
- HOLMES, JAMES, AND EMMETT, P. H. Alteration of the size and distribution of pores in charcoals, 1276
- AND EMMETT, P. H. Investigation of low-temperature nitrogen adsorption at high relative pressures, 1262
- HORN, F. HUBBARD. *See* Evans, Richard C.
- HUGGINS, MAURICE L. *See* Sun, Kuan-Han
- HUMPHREY, ALBERT S. *See* Martin, Donald Ray
- INNES, W. B., AND ROWLEY, H. H. Adsorption equilibria of liquid mixtures of carbon tetrachloride-methanol with charcoal, 1172
- INNES, W. B., AND ROWLEY, H. H. Adsorption isotherms of mixed vapors of carbon tetrachloride and methanol on activated charcoal at 25°C., 1154
- JOHNSON, W. F. *See* Carr, C. W.
- JONES, JAMES HOMER. Isotonic solutions: osmotic and activity coefficients of lithium and sodium perchlorates at 25°C., 516
- KAHN, DAVID S., AND POLSON, ALFRED. A new method for forming sharp boundaries in diffusion experiments, 816
- KINELL, PER-OLOF. Elasticity measurements on polychloroprenes, 70
- KLEVENS, H. B. The effect of temperature

- upon the critical concentrations of anionic and cationic detergents, 1143
- KLOTZ, IRVING M., AND WALKER, F. MARIAN. Spectral changes in some dye ions and their relation to the protein error in indicators, 666
- KOLTHOFF, I. M. *See* Carr, C. W.
See Reyerson, L. H.
See Shapiro, I.
- KRISHNA, BAL, AND GHOSH, SATYESHWAR. On the heterogeneous catalytic activity of colloidal silver in the reduction of silver acetate, 1130
- KUNIN, ROBERT, AND MYERS, ROBERT J. Rates of anion exchange in ion-exchange resins, 1111
- LAMM, OLE. On a generalization in the diffusion theory, 1063
- LANG, BILL G. *See* Harris, Elwin E.
- LAUFFER, M. A. *See* Stanley, W. M.
- LE BEAU, D. S. *See* Hauser, Ernst A.
- LEPESCHKIN, W. W. Longitudinal dispersion of infrared rays in optically empty and turbid media, and molecular weights of substances, 875
The longitudinal dispersion of infrared rays in polystyrenes, 868
- LEVITON, ABRAHAM, AND HALLER, HARRISON S. A spectroturbidimetric study of the proteins of milk, 460
- LI, CHOH HAO. Physicochemical characterization of pituitary growth hormone, 218
- LIEBHAFSKY, H. A. *See* Winslow, A. F.
- LIVINGSTON, H. K. Stability of synthetic rubber dispersions. I. Low-temperature thickening of Neoprene latex, 443
- LIVINGSTON, ROBERT, SICKLE, DOROTHY, AND UCHIYAMA, ANI. The chlorophyll-sensitized photooxidation of phenylhydrazine by methyl red, 775
- LONGSWORTH, L. G. The quantitative interpretation of the electrophoretic patterns of proteins, 171
- LOVELAND, R. P., AND TRIVELLI, A. P. H. Analysis of particle formation and growth by size-frequency determinations of the silver halide precipitations of photographic emulsions, 1004
- LUCK, J. MURRAY. Mandelate as a stabilizer of serum albumin, 229
- McBAIN, JAMES W., AND WORKING, EARL B. Aluminum dilaurate as association colloid in benzene, 974
- See* Green, Agnes Ann
See Smith, Gerould H.
- MCDONALD, HUGH J. *See* Zimmerman, June F.
- MACDOUGALL, F. H., AND PETERSON, SIGFRED. Equilibria in silver acetate solutions, 1346
- MARK, H. *See* BADGLEY, W. J.
- MARSHALL, C. E., AND CALDWELL, O. G. The colloid chemistry of the clay mineral attapulgite, 311
- MARTIN, DONALD RAY. Coordination compounds of boron trichloride. V. Relationship of dipole moment of chlorides to compound formation, 1400
AND HUMPHREY, ALBERT S. Coordination compounds of boron trichloride. IV. Systems with the propyl chlorides, 425
- MERRILL, R. C. *See* Palmer, K. J.
- MERTEN, L. *See* Milligan, W. O.
- MILES, GILBERT D. *See* Shedlovsky, Leo
- MILLETT, MERRILL, A., AND STAMM, ALFRED J. Molecular properties of hemicellulose fractions, 134
- MILLIGAN, W. O., AND MERTEN, L. X-ray diffraction studies in the system $\text{Fe}_2\text{O}_3\text{-Cr}_2\text{O}_3$, 521
AND RACHFORD, HENRY H., JR. The effect of heat-treatment on the sorption-desorption hysteresis characteristics of silica gel, 333
- MOELLER, THERALD, AND SCHNIZLEIN, J. GLENN, JR. Contributions to the chemistry of indium. VIII. Observations on the formation of magnesium indate, 771
- MOREY, D. R., AND TAMBLYN, J. W. The fractional precipitation of molecular-weight species from high polymers, 721
- MORGAN, KARL Z. Tolerance concentrations of radioactive substances, 984
- MOSELEY, HAL W. *See* Schwartz, Wilhelmina M.
- MYERS, ROBERT J. *See* Kunin, Robert
- MYSELS, KAROL J. Conductivity of some salts in moist acetone, 708
The shape of heat-capacity and equilibrium cooling curves in the region of melting of solid solutions, 1311
See Shreve, George W.
- NELSON, HARRISON A. A study of anhydrous conditions in the preparation of lyophobic organosols, 1103
- NOYES, RICHARD M. *See* Blaker, Robert H.

- NOYES, RICHARD M. *See* Doyle, George J.
NUTTING, G. C. *See* Speiser, R.
- OLSON, A. R., AND HILDEBRAND, J. H. An unusual liquid interface, 567
- ONCLEY, J. L., SCATCHARD, G., AND BROWN, A. Physical-chemical characteristics of certain of the proteins of normal human plasma, 184
- OWENS, H. S. *See* Palmer, K. J.
See Ward, Wilfred H.
- PALIT, SANTI R. Electronic interpretations of organic chemistry. II. Interpretation of the solubility of organic compounds, 837
A note on the strengths of organic bases, 1028
- PALMER, K. J., MERRILL, R. C., OWENS, H. S., AND BALLANTYNE, M. An x-ray diffraction investigation of pectinic and pectic acids, 710
- PEASE, DANIEL C., AND BLINKS, L. R. Cavitation from solid surfaces in the absence of gas nuclei, 556
- PEDERSEN, KAI O. On a low-density lipoprotein appearing in normal human plasma, 156
Ultracentrifugal and electrophoretic studies on fetuin, 164
- PERRI, JOSEPH M., JR., AND HAZEL, FRED. Effect of electrolytes on the foaming capacity of alpha soybean protein dispersions, 661
- PETERSON, SIGFRED. *See* MacDougall, F. H.
- POLSON, ALFRED. *See* Kahn, David S.
- POMEROY, H. H. *See* Dunn, R. C.
See Shreve, George W.
- POUND, JAMES R. Aniline formate and its changes on keeping, 378
A note on the oxidation of acetoin, 1449
- RACHFORD, HENRY H., JR. *See* Milligan, W. O.
- REYERSON, L. H., KOLTHOFF, I. M., AND COAD, KIETH. The electrokinetic potentials of precipitates, 321
- RICCI, JOHN E. Some mathematical relations involving the solubility of silver cyanide, 1375
- ROBINSON, J. V. The rise of air bubbles in lubricating oils, 431
- ROBINSON, R. A., AND FARRELLY, R. O. Some E.M.F. and conductance measurements in concentrated solutions of zinc and calcium chlorides, 704
- ROWLEY, H. H. *See* Innes, W. B.
- SCATCHARD, G. *See* Oncley, J. L.
- SCHNIZLEIN, J. GLENN, JR. *See* Moeller, Therald
- SCHWARTZ, WILHELMINA M., AND MOSELEY, HAL W. The surface tension of liquid crystals, 826
- SCOTT, GEORGE V. *See* Shedlovsky, Leo
- SEEGERS, WALTER H. Multiple protein interactions as exhibited by the blood-clotting mechanism, 198
- SEXTON, EDWIN L., AND DUNN, MAX S. Solubility of certain amino acids in aqueous solutions of amino acids and peptides, 648
- SHAPIRO, I., AND KOLTHOFF, I. M. Studies on the aging of precipitates and coprecipitation. XXXVIII. The compressibility of silver bromide powders, 483
- SHAPIRO, ZALMAN M. *See* Evans, Richard C.
- SHEDLOVSKY, LEO, MILES, GILBERT D., AND SCOTT, GEORGE V. Rates of solution of soaps in water, 391
- SHREVE, GEORGE W., POMEROY, HAROLD H., AND MYSELS, KAROL J. Studies of aluminum soaps. VIII. Water sorption and moisture content, 963
- SICKLE, DOROTHY. *See* Livingston, Robert
- SINGER, SEYMOUR. *See* Doty, Paul
- SMITH, GEROULD H., AND MCBAIN, JAMES W. The phase behavior of sodium stearate in anhydrous organic solvents, 1189
- SMITH, H. M. *See* Winslow, A. F.
- SMYTHE, LLOYD E. A kinetic study of the urea-formaldehyde reaction, 369
- SOLLNER, KARL, AND GREGOR, HARRY P. The electrochemistry of permselective collodion membranes. II. Experimental studies on the concentration potential across various types of permselective collodion membranes with solutions of several electrolytes, 299
- SPEISER, R., COPLEY, M. J., AND NUTTING, G. C. Effect of molecular association and charge distribution on the gelation of pectin, 117
- STAMM, ALFRED J., AND TARKOW, HAROLD. Dimensional stabilization of wood, 493
See Burr, H. K.
See Millett, Merrill A.
- STANLEY, W. M., AND LAUFFER, M. A. Sedi-

- mentation constants of purified preparations of strains of influenza virus, 148
- SUN, KUAN-HAN, AND HUGGINS, MAURICE L. Energy additivity in oxygen-containing crystals and glasses; 438
- SVEDEBERG, THE. The cellulose molecule.. Physical-chemical studies, 1
- SWENSON, HAROLD A. *See* Ward, Wilfred H.
- TAMBLYN, J. W. *See* Morey, D. R.
- TARKOW, HAROLD. *See* Stamm, Alfred J.
- TAYLOR, JAMES, AND HALL, C. R. L. Determination of the heat of combustion of nitroglycerin and the thermochemical constants of nitrocellulose, 593
- HALL, C. R. L., AND THOMAS, H. The thermochemistry of propellant explosives, 580
- TEMPLETON, C. C., AND HALL, NORRIS F. The solubility of thorium nitrate tetrahydrate in organic solvents at 25°C., 1441
- THIE, JOSEPH. A mathematical approach to reaction mechanisms, 540
- THOMAS, H. *See* Taylor, James
- TRIVELLI, A. P. H. *See* Loveland, R. P.
- TURNBULL, DAVID, AND FREY, DELTON R. Rate of corrosion of lead by hydrocarbon solutions of organic acids, 681
- UCHIYAMA, ALI. *See* Livingston, Robert
- VAN WAZER, JOHN R. *See* Carver, Emmett K.
- VAUGHAN, WILLIAM E. *See* Barnett, Benjamin
- VERNON, ARTHUR A. Colloidal aluminum oxide, 768
- VERWEY, E. J. W. Theory of the stability of lyophobic colloids, 631
- VETTER, R. J. Micelle structure in aqueous solutions of colloidal electrolytes, 262
- VOET, ANDRIES. Dielectrics and rheology of non-aqueous dispersions, 1037
- VOLD, ROBERT D. Phase boundaries in concentrated systems of sodium oleate and water, 797
- WAGNER, HERMAN. *See* Doty, Paul
- WAGNER, RICHARD L. *See* Evans, Richard C.
- WALKER, F. MARIAN. *See* Klotz, Irving M.
- WALKER, H. W. Stability of synthetic rubber dispersions. II. Coagulation of Neoprene latices by freezing, 451
- WALKER, W. C. *See* Zettlemoyer, A. C.
- WARD, WILFRED H., SWENSON, HAROLD A., AND OWENS, HARRY S. Electrophoretic mobilities and fractionation of sodium pectinates, 1137
- WATSON, JOHN H. L. Electron microscope observations of the morphology of several gases polymerized by charged-particle bombardment, 654
- WHITE, LOCKE, JR. A limitation of the determination of surface area by the "Point B" method, 644
- WINSLOW, A. F., LIEBHAFSKY, H. A., AND SMITH, H. M. The laboratory preparation of alkali metal hydroxides by electrolysis, 967
- WORKING, EARL B. *See* McBain, James W.
- WYSONG, W. S. *See* Gulbrandsen, Earl A.
- YOFFE, A. *See* Heymann, E.
- ZENTNER, RENE D. Heat guard for the McBain-Bakr sorption balance, 972
- ZETZLEMOYER, A. C., AND WALKER, W. C. Active magnesia. III. X-ray *versus* nitrogen adsorption surface areas, 763
- ZIMMERMAN, JUNE F., AND McDONALD, HUGH J. The kinetics of dissolution of cadmium in hydrochloric acid, 857
- ZSCHEILE, F. P. Photoelectric spectrophotometry. The performance of a quartz double monochromator in an improved and more versatile photoelectric spectrophotometer, 903

INDEX TO BOOK REVIEWS

- Abridged Scientific Publications from the Kodak Research Laboratories. Vol. XXVII, 1029
- ANDERSON, J. ANSEL (*Editor*). Enzymes and their Rôle in Wheat Technology, 365
- BELCHER, R., AND WILSON, CECIL L. Qualitative Inorganic Microanalysis, 363
- BENNETT, H. (*Editor*). Concise Chemical and Technical Dictionary, 1217
- BLADERGROEN, W. Physikalische Chemie in Medizin und Biologie, 1035
- COALE, AINSLEY J. The Problem of Reducing Vulnerability to Atomic Bombs, 1217
- COONS, K. W. *See* Young, C. B. F.
- COOPER, HERBERT J. Scientific Instruments, 365
- CORK, J. M. Radioactivity and Nuclear Physics, 366
- DAKE, H. C. *See* Dement, Jack
- DEMENT, JACK, AND DAKE, H. C. Rarer metals, 1030
- DEVRIES, LOUIS, *et al.* German-English Science Dictionary, 1031
- DU NOUY, LECOMTE. Studies in Biophysics: The Critical Temperature of Serum (56°), 363
- ENGELDER, CARL J. Fundamentals of Semi-micro Qualitative Analysis, 1216
- Essays in Rheology, 1452
- Faraday Society. General discussion on oxidation, 1029
- FEIGL, FRITZ. Qualitative Analysis by Spot Tests. Inorganic and Organic Applications, 884
- FERNELIUS, W. C. (*Editor*). Inorganic Syntheses. Vol. II, 1033
- FLUEGGE, S. An Introduction to Nuclear Physics, 1031
- FRENKEL, J. Kinetic Theory of Liquids, 1032
- GLASSTONE, SAMUEL. Textbook of Physical Chemistry, 628
- GREEN, DAVID E. (*Editor*). Currents in Biochemical Research, 629
- HAVINGA, E., JULIUS, H. W., VELDSTRA, H., AND WINKLER, K. C. Monographs on the Progress of Research In Holland during the War. Modern Development of Chemotherapy, 366
- HAWK, PHILIP B., OSER, BERNARD C., AND SUMMERSON, WILLIAM H. Practical Physiological Chemistry, 1214
- HERMANS, P. Monographs on the Progress of Research in Holland. Contribution to the Physics of Cellulose Fibres, 367
- HEYROVSKY, J. Polarographie. Theoretische Grundlagen, Praktische Ausführung und Anwendungen der Elektrolyse mit der tropfenden Quecksilberelektrode, 885
- IPATIEFF, VLADIMIR N. The Life of a Chemist, 889
- JACOBSON, C. A. (*Editor*). Encyclopedia of Chemical Reactions, 626
- JONES, W. NORTON, JR. Inorganic Chemistry, 1032
- JULIUS, H. W. *See* Havinga, E.
- KARRER, PAUL. Organic Chemistry, 627
- KEESOM, W. H. Helium, 1031
- LANGE, N. A. Handbook of Chemistry, 1452
- LEA, D. E. Actions of Radiations on Living Cells, 1451
- LEADERMAN, HERBERT. Elastic and Creep Properties of Filamentous Materials and Other High Polymers, 886
- LUDER, W. F., AND ZUFFANTI, S. Electronic Theory of Acids and Bases, 887
- MARKLEY, K. S. Fatty Acids, Their Chemistry and Physical Properties, 1450
- MATTAUCK, J. Nuclear Physics Tables, 1031
- Methods of Vitamin Assay, 1452
- MILLARD, E. B. Physical Chemistry for Colleges, 1033
- NATHANSON, JEROME (*Editor*). Science for Democracy, 363
- NIER, A. O. C. *See* Wilson, D. Wright
- NORD, F. F. (*Editor*). Advances in Enzymology. Vol. 6, 800

- OPENSHAW, H. T. A Laboratory Manual of Qualitative Organic Analysis, 889
- OSER, BERNARD L. *See* Hawk, Philip B.
- OWEN, L. N. *See* Simonsen, J. L.
- PAULI, WOLFGANG. Meson Theory of Nuclear Forces, 1215
- PRICE, CHARLES C. Reactions at Carbon-Carbon Double Bonds, 1029
- PIETERS, H. A., AND VAN KREVELEN, D. W. Monographs on the Progress of Research in Holland. The Wet Purification of Coal Gas and Similar Gases by the Staatsmijnen Otto Process, 1453
- REIMANN, STANLEY P. *See* Wilson, D. Wright
- ROSIN, JOSEPH. Reagent Chemicals and Standards, 626
- SEMAT, HENRY. Fundamentals of Physics, 362
- SEVAG, M. G. Immuno-catalysis, 886
- SIMONSEN, J. L., AND OWEN, L. N. The Terpenes. Vol. I, 1451
- SUMMERSON, WILLIAM H. *See* Hawk, Philip B.
- SWIETOSLAWSKI, W. Microcalorimetry, 1455
- Tables of Fractional Powers, 366
- Tables of Spherical Bessel Functions, 1030
- VAN KREVELEN, D. W. *See* Pieters, H. A.
- VAN SCHELVEN, THEODORE. Steroid Chains as Components of Protein and Carbon Molecules, 627
- VELDSTRA, H. *See* Havinga, E.
- WATERS, W. A. The Chemistry of Free Radicals, 1030
- WELCHER, FRANK J. Organic Analytical Reagents. Vol. I, 1035
- WENGER, PAUL-E. (*Editor*). Analytica Chimica Acta, 1036
- WEYGAND, CONRAD. Organic Preparations, 887
- WILD, F. Characterization of Organic Compounds, 1450
- WILSON, CECIL L. *See* Belcher, R.
- WILSON, D. WRIGHT, NIER, A. O. C., AND REIMANN, STANLEY P. Preparation and Measurement of Isotopic Tracers, 366
- WINKLER, K. C. *See* Havinga, E.
- WRINCH, DOROTHY. Fourier Transforms and Structure Factors, 1215
- YOUNG, C. B. F., AND COONS, K. W. Surface Active Agents, 361
- ZUFFANTI, S. *See* Luder, W. F.

Indian Agricultural Research Institute (Pusa)
LIBRARY, NEW DELHI-110012

This book can be issued on or before.....

Return Date	Return Date